Third Edition

Meteorology for Scientists and Engineers

Roland Stull

Meteorology

for Scientists and Engineers

Third Edition

ROLAND STULL

The University of British Columbia

Vancouver, Canada

Meteorology for Scientists and Engineers, 3rd Edition

Copyright © 2011, 2015 by Roland Stull
Dept. of Earth, Ocean & Atmospheric Sciences
University of British Columbia
2020-2207 Main Mall
Vancouver, BC, Canada V6T 1Z4

This work is available at
http://www.eos.ubc.ca/books/Practical_Meteorology/

ISBN-13: 978-0-88865-178-5

This work is licensed under a
Creative Commons Attribution-NonCommercial-ShareAlike 4.0 International License.
To view a copy of the license, visit
http://creativecommons.org/licenses/by-nc-sa/4.0/ .

Under this license, you are free to:

Share — copy and redistribute the material in any medium or format;

Adapt — translate into different languages, transform, remix, and build upon the material.

Under the following terms:

Attribution — You must give appropriate credit to Roland Stull, provide a link to the license, and indicate if changes were made. You may do so in any reasonable manner, but not in any way that suggests that Stull endorses you or your use.

NonCommercial — You may not use the material for commercial purposes.

ShareAlike — If you translate, transform, remix, or build upon the material, you must distribute your contributions under the same license as the original.

Not covered under this Creative Commons license are images copyright by Warren Faidley (on the front cover and spine), Gene Moore (Fig. 15.3), and Gene Rhoden (Figs. 14.1, 14.3, 14.5 and the figure in the solved example on page 484). While these images may be used with copies of this book, they may not be extracted and used separately from this book without permission of the copyright holders.

•

Cover photograph copyright © by Warren Faidley / weatherstock.com,
used with permission.
Scene is a July 1996 thunderhead over southern Arizona, USA.

•

Copyright © 2011, 2015 by Roland Stull. *Meteorology for Scientists and Engineers, 3rd Ed.*

CONTENTS

CONTENTS SUMMARY

Preface XIII

Chapter 1 • The Atmosphere 1
Chapter 2 • Radiation 27
Chapter 3 • Heat 53
Chapter 4 • Moisture 87
Chapter 5 • Stability 119
Chapter 6 • Clouds 159
Chapter 7 • Precipitation 185
Chapter 8 • Remote Sensing 219
Chapter 9 • Weather Reports & Map Analysis 267
Chapter 10 • Dynamics 289
Chapter 11 • Global Circulation 329
Chapter 12 • Airmasses & Fronts 389
Chapter 13 • Extratropical Cyclones 425
Chapter 14 • Thunderstorms 481
Chapter 15 • Thunderstorm Hazards 545
Chapter 16 • Hurricanes 603
Chapter 17 • Local Winds 645
Chapter 18 • Atmospheric Boundary Layer 687
Chapter 19 • Air Pollution Dispersion 723
Chapter 20 • Numerical Weather Prediction (NWP) 745
Chapter 21 • Natural Climate Processes 793
Chapter 22 • Optics 833

Appendix A • Fundamentals of Science 869
Appendix B • Constants & Conversion Factors 879

Index • 881

"Meteorology for Scientists and Engineers, 3rd Edition" by Roland Stull is licensed under a Creative Commons Attribution-NonCommercial-ShareAlike 4.0 International License. To view a copy of the license, visit http://creativecommons.org/licenses/by-nc-sa/4.0/ . This work is available at http://www.eos.ubc.ca/books/Practical_Meteorology/ .

CHAPTER 1 • THE ATMOSPHERE 1

Introduction 1
Meteorological Conventions 2
Earth Frameworks Reviewed 3
  Cartography 4
  Azimuth, Zenith, & Elevation Angles 4
  Time Zones 5
Thermodynamic State 6
  Temperature 6
  Pressure 7
  Density 10
Atmospheric Structure 11
  Standard Atmosphere 11
  Layers of the Atmosphere 13
  Atmospheric Boundary Layer 13
Equation of State– Ideal Gas Law 14
Hydrostatic Equilibrium 15
Hypsometric Equation 17
Process Terminology 17
Pressure Instruments 19
Summary 19
  Threads 19
  Tips 20
Exercises 21
  Numerical Problems 21
  Understanding & Critical Evaluation 23
  Web-Enhanced Questions 24
  Synthesis Questions 25

CHAPTER 2 • RADIATION 27

Orbital Factors 27
  Planetary Orbits 27
  Orbit of the Earth 27
  Seasonal Effects 30
  Daily Effects 32
  Sunrise, Sunset & Twilight 33
Flux 34
Radiation principles 36
  Propagation 36
  Emission 36
  Distribution 39
  Average Daily Insolation 40

Absorption, Reflection & Transmission 41
Beer's Law 43
Surface Radiation Budget 44
Solar 44
Longwave (IR) 45
Net Radiation 45
Actinometers 45
Summary 47
Threads 47
Exercises 47
Numerical Problems 47
Understanding & Critical Evaluation 49
Web-Enhanced Questions 51
Synthesis Questions 51

CHAPTER 3 • HEAT 53

Sensible and Latent Heats 53
Sensible 53
Latent 56
Lagrangian Heat Budget – Part 1: Unsaturated 57
Air Parcels 57
First Law of Thermodynamics 58
Lapse Rate 59
Adiabatic Lapse Rate 60
Potential Temperature 61
Thermodynamic Diagrams –Part 1: Dry Adiabatic Processes 63
Eulerian Heat Budget 64
First Law of Thermo. – Revisited 64
Advection 65
Molecular Conduction & Surface Fluxes 67
Turbulence 69
Radiation 71
Internal Source: Latent Heat 72
Net Heat Budget 72
Surface Heat Budget 73
Heat Budget 73
Bowen Ratio 74
Apparent Temperatures 76
Wind Chill 76
Heat Index and Humidex 77
Temperature Sensors 78
Summary 79
Threads 79
Exercises 80
Numerical Problems 80
Understanding & Critical Evaluation 83
Web-Enhanced Questions 84
Synthesis Questions 85

CHAPTER 4 • MOISTURE 87

Saturation Vapor Pressure 87
Vapor Pressure 87
Saturation 87
Humidity Variables 91
Mixing Ratio 91
Specific Humidity 91
Absolute Humidity 91
Relative Humidity 92
Dew-Point Temperature 92
Saturation Level or Lifting Condensation Level (LCL) 93
Wet-Bulb Temperature 94
More Relationships Between Moisture Variables 96
Total Water 97
Liquid and Solid Water 97
Total-Water Mixing Ratio 97
Precipitable Water 98
Lagrangian Budgets 99
Water Conservation 99
Heat Conservation for Saturated Air 101
Eulerian Water Budget 107
Horizontal Advection 107
Precipitation 107
Surface Moisture Flux 108
Turbulent Transport 109
Humidity Instruments 111
Summary 112
Threads 112
Exercises 113
Numerical Problems 113
Understanding & Critical Evaluation 115
Web-Enhanced Questions 117
Synthesis Questions 118

CHAPTER 5 • STABILITY 119

Building a Thermo-diagram 119
Components 119
Pseudoadiabatic Assumption 121
Complete Thermo Diagrams 121
Types Of Thermo Diagrams 122
Emagram 122
Stüve & Pseudoadiabatic Diagrams 122
Skew-T Log-P Diagram 122
Tephigram 122
Theta-Height (θ-z) Diagrams 122
More on the Skew-T 124
Guide for Quick Identification of Thermo Diagrams 126
Thermo-diagram Applications 127
Thermodynamic State 128
Processes 129

Parcels vs. Environment 134
Soundings 134
Buoyancy 135
Brunt-Väisälä Frequency 136
Flow Stability 138
Static Stability 138
Dynamic Stability 141
Turbulence Determination 142
Finding Tropopause Height & Mixed-layer Depth 143
Tropopause 143
Mixed-Layer 144
Summary 145
Threads 145
Exercises 145
Numerical Problems 145
Understanding & Critical Evaluation 148
Web-Enhanced Questions 149
Synthesis Questions 150
Large-size Thermo Diagrams 151
Emagram 152
Stüve Diagram 153
Skew-T Log-P Diagram 154
Tephigram 155
Theta-Z Diagram 156
Skew-T Log-P Diagram (ABL) 157
Theta-Z Diagram (ABL) 158

CHAPTER 6 • CLOUDS 159

Processes Causing Saturation 159
Cooling and Moisturizing 159
Mixing 160
Cloud Identification & Development 161
Cumuliform 161
Stratiform 162
Stratocumulus 164
Others 164
Cloud Organization 167
Cloud Classification 168
Genera 168
Species 168
Varieties 169
Supplementary Features 169
Accessory Clouds 169
Sky Cover (Cloud Amount) 170
Cloud Sizes 170
Fractal Cloud Shapes 171
Fractal Dimension 171
Measuring Fractal Dimension 172
Fog 173
Types 173
Idealized Fog Models 173
Summary 178
Threads 178
Exercises 179
Numerical Problems 179
Understanding & Critical Evaluation 181
Web Enhanced Questions 183
Synthesis Questions 183

CHAPTER 7 • PRECIPITATION 185

Supersaturation and Water Availability 186
Supersaturation 186
Water Availability 186
Number and Size of Hydrometeors 187
Nucleation of Liquid Droplets 188
Cloud Condensation Nuclei (CCN) 188
Curvature and Solute Effects 189
Critical Radius 192
Haze 192
Activated Nuclei 193
Nucleation of Ice Crystals 194
Processes 194
Ice Nuclei 195
Liquid Droplet Growth by Diffusion 196
Ice Growth by Diffusion 198
Ice Crystal Habits 198
Growth Rates 200
The Wegener-Bergeron-Findeisen (WBF) Process 201
Collision and Collection 202
Terminal Velocity of Hydrometeors 202
Collection & Aggregation Processes 204
Precipitation Formation 205
Precipitation Characteristics 207
Rain-Drop Size Distribution 207
Rainfall Rates 208
Snowfall Rates & Snow Accumulation 208
Precipitation Distribution 209
Precipitation Measurement 210
Summary 211
Threads 211
Exercises 212
Numerical Problems 212
Understanding & Critical Evaluation 214
Web-Enhanced Questions 217
Synthesis Questions 217

CHAPTER 8 • REMOTE SENSING 219

Radiative Transfer for Satellites 220
Signals 220
Transmittance and Windows 220
Planck's Law & Brightness Temperature 221
Radiative Transfer Equation 224
Weighting Functions 226
Weather Satellites 227

Orbits 227
Geostationary Satellites 227
Polar Orbiting Satellites 228
Imager 230
Visible 230
Infrared (IR) 230
Water-vapor 231
Other Channels 231
Image Examples & Interpretation 231
Sounder 235
Illustration of Retrieval Corollary 1 236
Illustration of Retrieval Corollary 2 236
Weather Radars 240
Fundamentals 240
Maximum Range 241
Scan and Display Strategies 241
Radar Bands 242
Beam Propagation 243
Reflectivity 245
The Radar Equation 245
Rainfall Rate Estimated by Radar Reflectivity 247
Bright Band 248
Hail 248
Other Uses for Reflectivity Data 248
Doppler Radar 249
Radial Velocities 249
Maximum Unambiguous Velocity 250
Velocity Azimuth Display (VAD) 252
Identification of Storm Characteristics 253
Spectrum Width 254
Difficulties 254
Polarimetric Radar 255
Phased-Array Radars & Wind Profilers 257
Summary 260
Threads 260
Exercises 260
Numerical Problems 260
Understanding & Critical Evaluation 262
Web-Enhanced Questions 265
Synthesis Questions 266

CHAPTER 9 • WEATHER REPORTS & MAP ANALYSIS 267

Sea-level Pressure Reduction 267
Weather Observations, Reports 268
Weather Codes 268
METAR and SPECI 270
Weather Observation Locations 271
Synoptic Weather Maps 274
Station Plot Model 274
Map Analysis, Plotting & Isoplething 280
Summary 281
Threads 281
Exercises 282
Numerical Problems 282
Understanding & Critical Evaluation 285
Web-Enhanced Questions 285
Synthesis Questions 287

CHAPTER 10 • DYNAMICS 289

Winds and Weather Maps 290
Height Contours on Isobaric Surfaces 290
Plotting Winds 291
Newton's Second Law of Motion 292
Lagrangian Momentum Budget 292
Eulerian Momentum Budget 293
Horizontal Forces 294
Advection 294
Pressure-Gradient Force 295
Centrifugal Force 296
Coriolis Force 297
Turbulent-Drag Force 300
Summary of Forces 301
Equations of Horizontal Motion 301
Horizontal Winds 302
Geostrophic Wind 302
Gradient Wind 304
Boundary Layer Wind 307
Boundary-Layer Gradient (BLG) Wind 309
Cyclostrophic Wind 311
Inertial Wind 312
Antitriptic Wind 312
Summary of Horizontal Winds 313
Horizontal Motion 314
Equations of Motion — Revisited 314
Scales of Horizontal Motion 315
Vertical Forces and Motion 315
Mass Conservation 317
Continuity Equation 317
Incompressible Continuity Equation 318
Boundary-Layer Pumping 319
Kinematics 320
Measuring Winds 321
Summary 322
Threads 322
Exercises 322
Numerical Problems 322
Understanding & Critical Evaluation 324
Web-Enhanced Questions 326
Synthesis Questions 327

CHAPTER 11 • GLOBAL CIRCULATION 329

Nomenclature 330
A Simplified Description of the Global Circulation 330
Near-surface Conditions 330
Upper-tropospheric Conditions 331
Vertical Circulations 332
Monsoonal Circulations 333
Differential Heating 334
Meridional Temperature Gradient 335
Radiative Forcings 336
Radiative Forcing by Latitude Belt 338
Heat Transport by the Global Circulation 338
Pressure Profiles 340
Non-hydrostatic Pressure Couplets 340
Hydrostatic Thermal Circulations 341
Geostrophic Wind & Geostrophic Adjustment 343
Ageostrophic Winds at the Equator 343
Definitions 343
Geostrophic Adjustment - Part 1 344
Thermal Wind Relationship 345
Thickness 345
Thermal Wind 346
Case Study 348
Thermal Wind & Geostrophic Adjust. - Part 2 349
Explaining the Global Circulation 350
Low Latitudes 350
High Latitudes 352
Mid-latitudes 352
Monsoon 356
Jet Streams 357
Baroclinicity & the Polar Jet 359
Angular Momentum & Subtropical Jet 360
Vorticity 362
Relative Vorticity 362
Absolute Vorticity 363
Potential Vorticity 363
Isentropic Potential Vorticity 364
Horizontal Circulation 365
Mid-latitude Troughs And Ridges 367
Barotropic Instability & Rossby Waves 367
Baroclinic Instability & Rossby Waves 371
Meridional Transport by Rossby Waves 374
Three-band General Circulation 376
A Measure of Vertical Circulation 377
Effective Vertical Circulation 377
Ekman Spiral In The Ocean 378
Summary 379
Threads 379
Exercises 380
Numerical Problems 380
Understanding & Critical Evaluation 382
Web-Enhanced Questions 386
Synthesis Questions 388

CHAPTER 12 • AIRMASSES & FRONTS 389

Anticyclones or Highs 390
Characteristics & Formation 390
Vertical Structure 391
Airmasses 391
Creation 392
Movement 397
Modification 397
Surface Fronts 399
Horizontal Structure 400
Vertical Structure 403
Geostrophic Adjustment – Part 3 404
Winds in the Cold Air 404
Winds in the Warm Over-riding Air 407
Frontal Vorticity 407
Frontogenesis 408
Kinematics 408
Thermodynamics 411
Dynamics 411
Occluded Fronts and Mid-tropospheric Fronts 413
Upper-tropospheric Fronts 414
Drylines 416
Summary 417
Threads 418
Exercises 418
Numerical Problems 418
Understanding & Critical Evaluation 419
Web-Enhanced Questions 421
Synthesis Questions 423

CHAPTER 13 • EXTRATROPICAL CYCLONES 425

Cyclone Characteristics 426
Cyclogenesis & Cyclolysis 426
Cyclone Evolution 427
Cyclone Tracks 430
Stacking & Tilting 432
Other Characteristics 433
Case Study of an Extratropical Cyclone Over North America 433
Overview and Storm Track 433
Storm Data 434
Surface Charts 438
85 kPa Charts 439
70 kPa Charts 439
100 - 50 kPa Thickness 439
50 kPa Charts 440
20 kPa Charts 440
20 kPa Hemispheric Chart 441

Isentropic Charts 441
Lee Cyclogenesis 443
Stationary Planetary Waves 443
Conservation of Potential Vorticity 445
Equatorward Propagation Along the Lee Side 446
Cyclone Spin-up 446
Vorticity Tendency 447
Quasi-Geostrophic Approximation 449
Application to Idealized Weather Patterns 450
Upward Motion 451
Continuity Effects 452
Omega Equation 456
Q-Vectors 460
Sea-level-pressure Tendency 463
Mass Budget 463
Diabatic Heating due to Condensation 465
Net Pressure Tendency 466
Self Development of Cyclones 468
Condensation 468
Temperature Advection 468
Propagation of Cyclones 469
Creation of Baroclinic Zones 469
Propagation of Cold Fronts 470
Summary 470
Threads 471
Exercises 473
Numerical Problems 473
Understanding & Critical Evaluation 475
Web-Enhanced Questions 478
Synthesis Questions 479

CHAPTER 14 • THUNDERSTORMS 481

Thunderstorm Characteristics 481
Appearance 482
Clouds Associated with Thunderstorms 482
Cells & Evolution 484
Thunderstorm Types & Organization 486
Thunderstorm Formation 496
Convective Conditions 496
Key Altitudes 496
High Humidity in the ABL 499
Instability, CAPE & Updrafts 503
CAPE 503
Updraft Velocity 508
Wind Shear in the Environment 509
Hodograph Basics 510
Using Hodographs 514
Triggering vs. Convective Inhibition 522
Convective Inhibition (CIN) 523
Trigger Mechanisms 525
Thunderstorm Forecasting 527
Outlooks, Watches & Warnings 528
Stability Indices for Thunderstorms 530
Storm Case Study 532
Summary 532
Threads 533
Exercises 533
Numerical Problems 533
Understanding & Critical Evaluation 536
Web-Enhanced Questions 541
Synthesis Questions 542

CHAPTER 15 • THUNDERSTORM HAZARDS 545

Precipitation and Hail 545
Heavy Rain 545
Hail 548
Downbursts and Gust Fronts 554
Characteristics 554
Precipitation Drag 555
Evaporative Cooling 556
Downdraft CAPE (DCAPE) 557
Pressure Perturbation 559
Outflow Winds & Gust Fronts 560
Lightning And Thunder 563
Origin of Electric Charge 564
Lightning Behavior & Appearance 566
Lightning Detection 568
Lightning Hazards and Safety 569
Thunder 571
Tornadoes 577
Tangential Velocity & Tornado Intensity 577
Types of Tornadoes & Other Vortices 582
Evolution as Observed by Eye 583
Tornado Outbreaks 583
Storm-relative Winds 584
Origin of Tornadic Rotation 586
Mesocyclones and Helicity 587
Tornadoes and Swirl Ratio 592
Summary 593
Threads 593
Exercises 594
Numerical Problems 594
Understanding & Critical Evaluation 597
Web-Enhanced Questions 600
Synthesis Questions 601

CHAPTER 16 • HURRICANES 603

Hurricane Structure 604
Intensity and Geographic distribution 605
Saffir-Simpson Hurricane Wind Scale 607
Typhoon Intensity Scales 607
Other Tropical-Cyclone Scales 607
Geographic Distribution and Movement 607

Evolution 608
Requirements for Cyclogenesis 608
Hurricane Triggers 610
Life Cycle 613
Movement/Track 615
Tropical Cyclolysis 616
Dynamics 617
Initial Spin Up 617
Subsequent Development 617
Inflow and Outflow 618
Thermodynamics 620
Fuel Creation and Intake 620
Exhaust 620
Warm Core 621
Carnot-cycle Heat Engine 624
A Hurricane Model 626
Pressure Distribution 626
Tangential Velocity 626
Radial Velocity 627
Vertical Velocity 628
Temperature 629
Composite Picture 629
Climatology 630
Seasonality 630
Locations of Strongest Cyclones 631
Natural Cycles & Changes in Activity 631
Hazards 631
Human Population and Zoning 631
Storm Surge 632
Surface Wind-waves 634
Inland Flooding 637
Thunderstorms, Lightning & Tornado Outbreaks 637
Hurricane Forecasting 637
Prediction 637
Safety 638
Summary 639
Threads 639
Exercises 640
Numerical Problems 640
Understanding & Critical Evaluation 641
Web-Enhanced Questions 644
Synthesis Questions 644

CHAPTER 17 • LOCAL WINDS 645

Wind Frequency 645
Wind-speed Frequency 645
Wind-direction Frequency 646
Wind-Turbine Power Generation 647
Thermally Driven Circulations 648
Thermals 648
Cross-valley Circulations 649
Along-valley Winds 653
Sea breeze 654
Open-Channel Hydraulics 657
Wave Speed 658
Froude Number - Part 1 659
Conservation of Air Mass 660
Hydraulic Jump 660
Gap Winds 661
Basics 661
Short-gap Winds 661
Long-gap Winds 662
Coastally Trapped Low-level (Barrier) Jets 664
Mountain Waves 666
Natural Wavelength 666
Lenticular Clouds 666
Froude Number - Part 2 667
Mountain-wave Drag 668
Streamlines, Streaklines, and Trajectories 668
Bernoulli's Equation 669
Principles 669
Some Applications 672
Downslope Winds 675
Bora 675
Foehns and Chinooks 676
Canopy Flows 677
Forests and Crops 677
Cities 678
Summary 679
Exercises 680
Numerical Problems 680
Understanding & Critical Evaluation 682
Web-Enhanced Questions 684
Synthesis Questions 686

CHAPTER 18 • ATMOSPHERIC BOUNDARY LAYER 687

Static Stability — A Review 687
Explanation 687
Rules of Thumb for Stability in the ABL 689
Boundary-layer Formation 689
Tropospheric Constraints 689
Synoptic Forcings 690
ABL Structure and Evolution 692
Temperature 693
Cumulative Heating or Cooling 693
Stable-ABL Temperature 696
Mixed-Layer (ML) Temperature 697
Wind 699
Wind Profile Evolution 699
Drag, Stress, Friction Velocity, and Roughness Length 700
Log Profile in the Neutral Surface Layer 702
Log-Linear Profile in Stable Surf. Layer 702
Profile in the Convective Radix Layer 703
Turbulence 705
Mean and Turbulent Parts 705

Variance and Standard Deviation 706
Isotropy 707
Turbulence Kinetic Energy 708
Free and Forced Convection 710
Turbulent Fluxes and Covariances 711
Turbulence Closure 713
Summary 716
Exercises 717
Numerical Problems 717
Understanding & Critical Evaluation 719
Web-Enhanced Questions 721
Synthesis Questions 722

CHAPTER 19 • AIR POLLUTION DISPERSION 723

Dispersion Factors 724
Air Quality Standards 725
Turbulence Statistics 726
Review of Basic Definitions 726
Isotropy (again) 727
Pasquill-Gifford (PG) Turbulence Types 728
Dispersion Statistics 728
Snapshot vs. Average 728
Center of Mass 729
Standard Deviation – Sigma 729
Gaussian Curve 730
Nominal Plume Edge 730
Taylor's Statistical Theory 731
Passive Conservative Tracers 731
Dispersion Equation 731
Dispersion Near & Far from the Source 732
Dispersion In Neutral & Stable Boundary Layers 732
Plume Rise 732
Gaussian Concentration Distribution 734
Dispersion In Unstable Boundary Layers (Convective Mixed Layers) 735
Relevant Variables 735
Plume Centerline 736
Crosswind Integrated Concentration 736
Concentration 737
Summary 737
Threads 738
Exercises 739
Numerical Problems 739
Understanding & Critical Evaluation 741
Web-Enhanced Questions 742
Synthesis Questions 743

CHAPTER 20 • NUMERICAL WEATHER PREDICTION (NWP) 745

Scientific Basis of Forecasting 746
The Equations of Motion 746
Approximate Solutions 749
Dynamics, Physics and Numerics 749
Models 751
Grid Points 752
Nested and Variable Grids 752
Staggered Grids 753
Finite-Difference Equations 754
Notation 754
Approximations to Spatial Gradients 754
Grid Computation Rules 756
Time Differencing 757
Discretized Equations of Motion 758
Numerical Errors & Instability 759
Round-off Error 759
Truncation Error 760
Numerical Instability 760
The Numerical Forecast Process 762
Balanced Mass and Flow Fields 763
Data Assimilation and Analysis 765
Forecast 768
Case Study: 22-25 Feb 1994 768
Post-processing 770
Nonlinear Dynamics And Chaos 773
Predictability 773
Lorenz Strange Attractor 773
Ensemble Forecasts 776
Probabilistic Forecasts 777
Forecast Quality & Verification 777
Continuous Variables 777
Binary / Categorical Events 780
Probabilistic Forecasts 782
Cost / Loss Decision Models 784
Summary 786
Threads 786
Exercises 787
Numerical Problems 787
Understanding & Critical Evaluation 789
Web-Enhanced Questions 790
Synthesis Questions 791

CHAPTER 21 • NATURAL CLIMATE PROCESSES 793

Radiative Equilibrium 793
Greenhouse Effect 795
Atmospheric Window 796
Average Energy Budget 797
Astronomical Influences 797

Milankovitch Theory 797
Solar Output 803
Tectonic Influences 804
Continent Movement 804
Volcanism 804
Feedbacks 806
Concept 806
Idealized Example 807
Infrared Radiative (IR) Feedback 810
Water-vapor Feedback 810
Lapse-rate Feedback 810
Cloud Feedback 811
Ice–albedo (Surface) Feedback 811
Ocean CO_2 Feedback 812
Biological CO_2 Feedback 812
Daisyworld 813
Physics 813
Equilibrium and Homeostasis 815
GCMs 815
Present Climate 816
Definition 816
Köppen Climate Classification 817
Natural Oscillations 818
El Niño - Southern Oscillation (ENSO) 818
Pacific Decadal Oscillation (PDO) 820
North Atlantic Oscillation (NAO) 824
Arctic Oscillation (AO) 824
Madden-Julian Oscillation (MJO) 824
Other Oscillations 824
Summary 825
Threads 826
Exercises 826
Numerical Problems 826
Understanding & Critical Evaluation 828
Web-Enhanced Questions 831
Synthesis Questions 832

CHAPTER 22 • OPTICS 833

Ray Geometry 833
Reflection 833
Refraction 834
Huygens' Principle 837
Critical Angle 837
Liquid-Drop Optics 837
Primary Rainbow 839
Secondary Rainbow 840
Alexander's Dark Band 841
Other Rainbow Phenomena 841
Ice Crystal Optics 842
Parhelic Circle 844
Subsun 844
22° Halo 845
46° Halo 846
Halos Associated with Pyramid Crystals 847
Circumzenith & Circumhorizon Arcs 848
Sun Dogs (Parhelia) 850
Subsun Dogs (Subparhelia) 851
Tangent Arcs 851
Other Halos 853
Scattering 856
Background 856
Rayleigh Scattering 857
Geometric Scattering 857
Mie Scattering 858
Diffraction & Interference 858
Corona, Iridescence and Glory 859
Supernumerary Bows 860
Mirages 861
Summary 863
Threads 863
Exercises 863
Numerical Problems 863
Understanding & Critical Evaluation 865
Web-Enhanced Questions 867
Synthesis Questions 868

APPENDIX A • FUNDAMENTALS OF SCIENCE 869

Dimensions and Units 870
Standards 870
Unit Conversion 871
Functions and Finite Difference 872
Relationships and Graphs 873
Linear 873
Logarithmic 873
Power 874
Errors 875
Systematic Error & Accuracy 875
Random Error & Precision 875
Reporting Observations 875
Error Propagation 876
On Doing Science 877
Summary 878
Exercises 878
Numerical Problems 878
Understanding & Critical Evaluation 878
Web Enhanced Questions 878
Synthesis Questions 878

APPENDIX B • CONSTANTS & CONVERSION FACTORS 879

Universal Constants 879
Math Constants 879

Earth Characteristics 879
Air and Water Characteristics 880
Conversion Factors & Combined Parameters 880

INDEX 881

Copyright © 2011, 2015 by Roland Stull. *Meteorology for Scientists and Engineers, 3rd Ed.*

PREFACE

PREFACE

This is a book on practical meteorology. I wrote it for students and professionals in science and engineering who want to understand basic concepts, but who don't need to derive equations.

To make this book more accessible, I converted all the equations into algebra. With algebraic approximations to the atmosphere, you can see the physical meaning of each term, and you can plug in numbers to get usable answers.

No previous knowledge of meteorology is needed — I start from the basics. Your background should include basic algebra, trig, and classical physics. This book could serve the fields of Atmospheric Science, Meteorology, Environmental Science and Engineering, Air Quality Meteorology, Climatology, and Geography.

Readers like you have asked to see solved examples of the concepts, to enhance your understanding and speed your ability to apply them to your own situations. To fill this need, I have added "Solved Example" boxes for almost every equation in the book.

This book is designed to be both a textbook and a reference. As a textbook, the end of each chapter includes extensive homework exercises in the following categories: Numerical Exercises, Understanding & Critical Evaluation, Web-Enhanced Questions, and Synthesis Questions.

Although a hand calculator can be used for some of the homework exercises, other exercises are best solved on a computer spreadsheet such as Excel or using a mathematical program such as Matlab, Mathematica, or Maple. I used Excel for my solved examples and most of my graphs.

As a reference, I included in this book many tables, figures and graphs, and have a detailed index. Also, appendices include values of key constants and conversion factors.

This third edition has a new format. The body of the text runs mostly in the inside columns of each page. The outside columns on each page contain the supporting figures, graphs, tables, and solved examples. Other special boxes in these outside columns include Focus, On Doing Science, and Science Graffito. At the request of some readers, I've added Beyond Algebra boxes that use calculus, differential equations and other advanced techniques, but you may safely ignore these boxes if you wish.

New to this edition is a chapter entitled Remote Sensing, which covers weather radar and satellites. Also new is a chapter on Weather Reports & Map Analysis. Many other chapters are greatly expanded and updated. I intentionally omitted large color photographs and maps from this book, partly to keep the price down, and partly because most readers can access such images via the internet.

For instructors, I inserted a bullet next to the most important equations, to help focus the learning. Also, the book contains too much material to cover in one term, so instructors should select the subset of chapters to cover.

ACKNOWLEDGEMENTS

A large number of students have used earlier drafts, allowing me to fix typos and make clarifications thanks to their careful scrutiny. I am indebted to the following additional experts for their suggestions to this 3rd edition: Phil Austin, William Beasley, Allan Bertram, Brian Black, Dominique Bourdin, Brian Cheng, Luca Delle Monache, Xingxiu Deng, Dennis Driscoll, Charlotte Gabites, Paul Greeley, William Hsieh, Katelyn Janzen, Chris Jeffery, Alison Jolley, Doug McCollor, Mathias Mueller, Laurie Neil, Lorne Nelson, Thomas Nipen, Robert Nissen, Anders Persson, Chris Pielou, Robert Rabin, Curt Rose, Alyson Shave, John Spagnol, Gert-Jan Steeneveld, David Stensrud, Haizhen Sun, Bruce Thomson, Greg West, May Wai San Wong, Yongmei Zhou, and Jeff Zong.

The 3rd edition builds upon the earlier editions. As stated in the 2nd edition, I am grateful to the following additional experts: Susan Allick Beach, Larry Berg, Bob Bornstein, David Finley, Maria Furberg, Josh Hacker, Phoebe Jackson, Scott Krayenhoff, Stephanie Meyn, Scott Shipley, Zbigniew Sorbjan, George Taylor, and Dave Whiteman.

Suggestions for the 1st edition came from: Horst Böttger, John Cassano, Judy Curry, C. Dale Elifrits, Jon Foley, Kit Hayden, Jim Hoke, Ed Hopkins, Dave Houghton, Jon Kahl, Ian Lumb, Mankin Mak, Jon Martin, Paul Menzel, Richard Peterson, Robert Sica, Greg Tripoli, and Pao Wang.

I thank the faculty and staff at the University of Wisconsin - Madison and the University of British Columbia - Vancouver, who were very supportive while I wrote the three editions during my tenures as professor. Storm photographs are reproduced with permission of the copyright holders: Warren Faidley, Gene Moore, and Gene Rhoden. I apologize for any names that I forgot. Any remaining errors are my own.

I especially thank my wife Linda for her patience and understanding.

Roland Stull

FOCUS • About the Author

Roland Stull holds a Bachelor's degree in Chemical Engineering and a Ph.D. in Atmospheric Science. He is a Certified Flight Instructor (CFI) and a Certified Consulting Meteorologist (CCM).

Stull is a professor of Atmospheric Science at the University of British Columbia, Canada. He is a fellow of both the American Meteorological Society (AMS) and the Canadian Meteorological and Oceanographic Society (CMOS). He is author or co-author over over 95 scientific journal papers, and he wrote two single-author books.

"Meteorology for Scientists and Engineers, 3rd Edition" by Roland Stull is licensed under a Creative Commons Attribution-NonCommercial-ShareAlike 4.0 International License. To view a copy of the license, visit http://creativecommons.org/licenses/by-nc-sa/4.0/ . This work is available at http://www.eos.ubc.ca/books/Practical_Meteorology/ .

Copyright © 2011, 2015 by Roland Stull. *Meteorology for Scientists and Engineers, 3rd Ed.*

THE ATMOSPHERE

CONTENTS

Introduction 1
Meteorological Conventions 2
Earth Frameworks Reviewed 3
  Cartography 4
  Azimuth, Zenith, & Elevation Angles 4
  Time Zones 5
Thermodynamic State 6
  Temperature 6
  Pressure 7
  Density 10
Atmospheric Structure 11
  Standard Atmosphere 11
  Layers of the Atmosphere 13
  Atmospheric Boundary Layer 13
Equation of State– Ideal Gas Law 14
Hydrostatic Equilibrium 15
Hypsometric Equation 17
Process Terminology 17
Pressure Instruments 19
Summary 19
  Threads 19
  Tips 20
Exercises 21
  Numerical Problems 21
  Understanding & Critical Evaluation 23
  Web-Enhanced Questions 24
  Synthesis Questions 25

"Meteorology for Scientists and Engineers, 3rd Edition" by Roland Stull is licensed under a Creative Commons Attribution-NonCommercial-ShareAlike 4.0 International License. To view a copy of the license, visit http://creativecommons.org/licenses/by-nc-sa/4.0/ . This work is available at http://www.eos.ubc.ca/books/Practical_Meteorology/ .

1 Classical Newtonian physics can be used to describe atmospheric behavior. Namely, air motions obey Newton's laws of dynamics. Heat satisfies the laws of thermodynamics. Air mass and moisture are conserved. When applied to a fluid such as air, these physical processes describe **fluid mechanics**. **Meteorology** is the study of the fluid mechanics, physics, and chemistry of Earth's atmosphere.

The **atmosphere** is a complex fluid system — a system that generates the chaotic motions we call **weather**. This complexity is caused by myriad interactions between many physical processes acting at different locations. For example, temperature differences create pressure differences that drive winds. Winds move water vapor about. Water vapor condenses and releases heat, altering the temperature differences. Such feedbacks are nonlinear, and contribute to the complexity.

But the result of this chaos and complexity is a fascinating array of weather phenomena — phenomena that are as inspiring in their beauty and power as they are a challenge to describe. Thunderstorms, cyclones, snow flakes, jet streams, rainbows. Such phenomena touch our lives by affecting how we dress, how we travel, what we can grow, where we live, and sometimes how we feel.

In spite of the complexity, much is known about atmospheric behavior. This book presents some of what we know about the atmosphere, for use by scientists and engineers.

INTRODUCTION

In this book are five major components of meteorology: (1) thermodynamics, (2) physical meteorology, (3) observation and analysis, (4) dynamics, and (5) weather systems (cyclones, fronts, thunderstorms). Also covered are air-pollution dispersion, numerical weather prediction, and natural climate processes.

Starting into the thermodynamics topic now, the state of the air in the atmosphere is defined by its pressure, density, and temperature. Changes of state associated with weather and climate are small perturbations compared to the average (standard)

ON DOING SCIENCE • Descartes and the Scientific Method

From René Descartes we get more than the name "Cartesian". In 1637 he published a book *Discours de la Méthode*, in which he defined the principles of the modern scientific method:

- Accept something as true only if you know it to be true.
- Break difficult problems into small parts, and solve each part in order to solve the whole problem.
- Start from the simple, and work towards the complex. Seek relationships between the variables.
- Do not allow personal biases or judgements to interfere, and be thorough.

This method formed the basis of the scientific renaissance, and marked an important break away from blind belief in philosophers such as Aristotle.

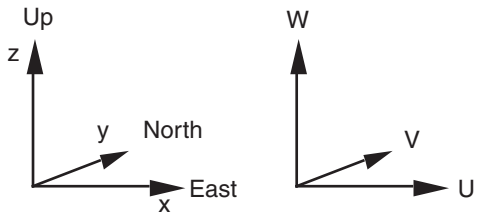

Figure 1.1
Local Cartesian coordinates and velocity components.

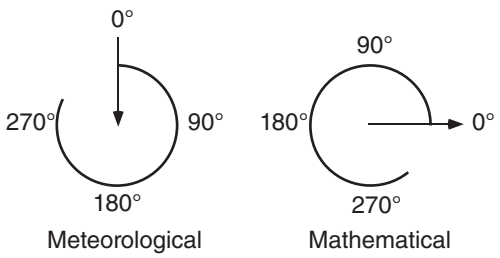

Figure 1.2
Comparison of meteorological and mathematical angle conventions.

atmosphere. These changes are caused by well-defined processes.

Equations and concepts in meteorology are similar to those in physics or engineering, although the jargon and conventions might look different when applied within an Earth framework. For a review of basic science, see Appendix A.

METEOROLOGICAL CONVENTIONS

Although the Earth is approximately spherical, you need not always use spherical coordinates. For the weather at a point or in a small region such as a town, state, or province, you can use local right-hand **Cartesian** (rectangular) **coordinates**, as sketched in Fig. 1.1. Usually, this coordinate system is aligned with x pointing east, y pointing north, and z pointing up. Other orientations are sometimes used.

Velocity components U, V, and W correspond to motion in the x, y, and z directions. For example, a positive value of U is a velocity component from west to east, while negative is from east to west. Similarly, V is positive northward, and W is positive upward (Fig. 1.1).

In polar coordinates, horizontal velocities can be expressed as a direction (α), and speed or magnitude (M). Historically, horizontal wind directions are based on the compass, with 0° to the north (the positive y direction), and with degrees increasing in a **clockwise** direction through 360°. Negative angles are not usually used. Unfortunately, this differs from the usual mathematical convention of 0° in the x direction, increasing **counter-clockwise** through 360° (Fig. 1.2).

Historically winds are named by the direction **from** which they come, while in mathematics angles give the direction toward which things move. Thus, a **west** wind is a wind <u>from</u> the west; namely, from 270°. It corresponds to a positive value of U, with air moving in the positive x direction.

Because of these differences, the usual trigonometric equations cannot be used to convert between (U, V) and (α, M). Use the following equations instead, where α is the compass direction <u>from</u> which winds come.

<u>Conversion to Speed and Direction:</u>

$$M = \left(U^2 + V^2\right)^{1/2} \qquad \bullet(1.1)$$

$$\alpha = 90° - \frac{360°}{C}\cdot\arctan\left(\frac{V}{U}\right) + \alpha_o \qquad \bullet(1.2a)$$

where $\alpha_0 = 180°$ if $U > 0$, but is zero otherwise. C is the angular rotation in a full circle ($C = 360° = 2\cdot\pi$ radians).

*[**NOTE**: Bullets • identify key equations that are fundamental, or are needed for understanding later chapters.]*

Some computer languages and spreadsheets allow a two-argument arc tangent function (atan2):

$$\alpha = \frac{360°}{C}\cdot\text{atan2}(V, U) + 180° \qquad (1.2b)$$

*[**CAUTION**: in the C and C++ programming languages, you might need to switch the order of U & V.]*

Some calculators, spreadsheets or computer functions use angles in degrees, while others use radians. If you don't know which units are used, compute the arccos(–1) as a test. If the answer is 180, then your units are degrees; otherwise, an answer of 3.14159 indicates radians. Use whichever value of C is appropriate for your units.

Conversion to U and V:

$$U = -M\cdot\sin(\alpha) \qquad \bullet(1.3)$$

$$V = -M\cdot\cos(\alpha) \qquad \bullet(1.4)$$

In three dimensions, **cylindrical coordinates** (M, α, W) are sometimes used for velocity instead of Cartesian (U, V, W), where horizontal velocity components are specified by direction and speed, and the vertical component remains W (see Fig. 1.3).

Most meteorological graphs are like graphs in other sciences, with **dependent** variables on the **ordinate** (vertical axis) plotted against an **independent** variable on the **abscissa** (horizontal axis). However, in meteorology the axes are often switched when height (z) is the independent variable. This axis switching makes locations higher in the graph correspond to locations higher in the atmosphere (Fig. 1.4).

EARTH FRAMEWORKS REVIEWED

The Earth is slightly flattened into an **oblate spheroid of revolution** (Fig. 1.5). The distance from the center of the Earth to the north (**N**) and south (**S**) poles is roughly 6356.755 km, slightly less than the 6378.140 km distance from the center to

Solved Example

Find wind speed and direction, given eastward component 3 m/s, and northward 4 m/s.

Solution

(Problem-solving methods are given in Appendix A.)

Given: $U = 3$ m/s. eastward wind component.
$V = 4$ m/s. northward wind component.

Find: M = ? m/s. wind speed
α = ? degrees. wind direction

Sketch:

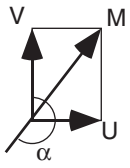

Use eq. (1.1):

$M = [\, U^2 + V^2 \,]^{1/2}$
$= [\, (3\text{ m/s})^2 + (4\text{ m/s})^2 \,]^{0.5}$
$= (9 + 16)^{0.5} \cdot [(\text{m/s})^2]^{0.5}$
$= (25)^{0.5}$ m/s = **5 m/s**.

Use eq. (1.2a):

$\alpha = 90° - (360°/C)\cdot\arctan(V/U) + 180°$
$= 90° - (360/360)\cdot\arctan[(4\text{ m/s})/(3\text{ m/s})]+180°$
$= 90° - \tan^{-1}(1.333) + 180°$
$= 90° - 53.13° + 180° =$ **216.87°**.

Check: Units OK. Sketch OK. Values physical.
Discussion: Thus, the wind is from the south-southwest (SSW) at 5 m/s.

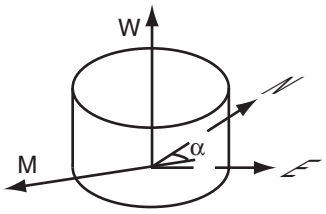

Figure 1.3
Notation used in cylindrical coordinates for velocity.

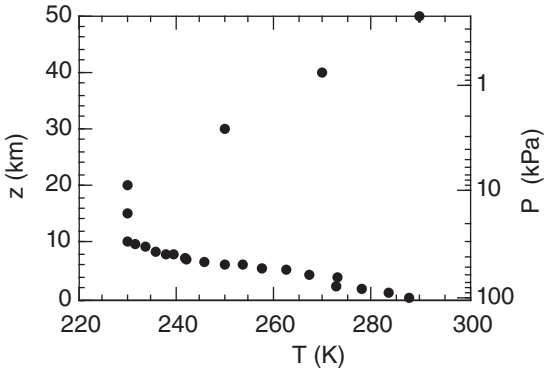

Figure 1.4
Hypothetical temperature T profile in the atmosphere, plotted such that locations higher in the graph correspond to locations higher in the atmosphere. The independent variable can be height z (left axis) or pressure P (right axis).

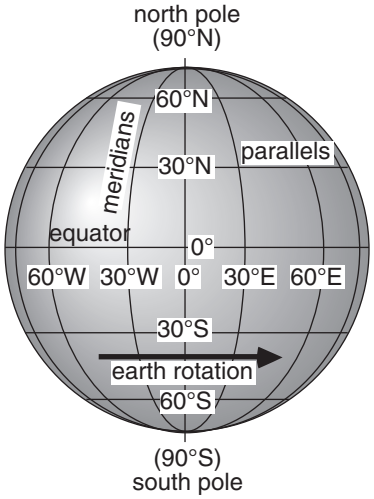

Figure 1.5
Earth cartography.

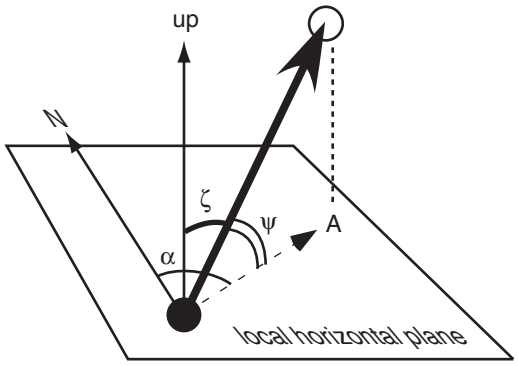

Figure 1.6
Elevation angle Ψ *, zenith angle* ζ *, and azimuth angle* α *.*

Solved Example

A thunderstorm top is at azimuth 225° and elevation angle 60° from your position. How would you describe its location in words? Also, what is the zenith angle?

Solution:

Given: $\alpha = 225°$
$\Psi = 60°$.

Find: Location in words, and find ζ .
(continued next page).

the equator. This 21 km difference in Earth radius causes a north-south cross section (i.e., a **slice**) of the Earth to be slightly elliptical. But for all practical purposes you can approximate the Earth a sphere (except for understanding Coriolis force in the Dynamics chapter).

Cartography

Recall that north-south lines are called **meridians**, and are numbered in degrees **longitude**. The **prime meridian** (0° longitude) is defined by international convention to pass through **Greenwich**, Great Britain. We often divide the 360° of longitude around the Earth into halves relative to Greenwich:

- **Western Hemisphere**: 0 – 180°W,
- **Eastern Hemisphere**: 0 – 180°E.

Looking toward the Earth from above the north pole, the Earth rotates counterclockwise about its axis. This means that all objects on the surface of the Earth (except at the poles) move toward the east.

East-west lines are called **parallels**, and are numbered in degrees **latitude**. By convention, the **equator** is defined as 0° latitude; the **north pole** is at 90°N; and the **south pole** is at 90°S. Between the north and south poles are 180° of latitude, although we usually divide the globe into the:

- **Northern Hemisphere:** 0 – 90°N,
- **Southern hemisphere:** 0 – 90°S.

On the surface of the Earth, each **degree of latitude** equals 111 km, or 60 **nautical miles**.

Azimuth, Zenith, & Elevation Angles

As a meteorological observer on the ground (black circle in Fig. 1.6), you can describe the local angle to an object (white circle) by two angles: the **azimuth angle** (α), and either the **zenith angle** (ζ) or **elevation angle** (ψ). The object can be physical (e.g., sun, cloud) or an image (e.g., rainbow, sun dog). By "local angle", we mean angles measured relative to the Cartesian **local horizontal** plane (e.g., a lake surface, or flat level land surface such as a polder), or relative to the local vertical direction at your location. Local **vertical** (**up**) is defined as opposite to the direction that objects fall.

Zenith means "directly overhead". Zenith angle is the angle measured at your position, between a conceptual line drawn to the zenith (up) and a line drawn to the object (dark arrow in Fig. 1.6). The elevation angle is how far above the horizon you see the object. Elevation angle and zenith angle are related by: $\psi = 90° - \zeta$, or if your calculator uses radians, it is $\psi = \pi/2 - \zeta$. Abbreviate both of these forms by $\psi = C/4 - \zeta$, where $C = 360° = 2\pi$ radians.

For the azimuth angle, first project the object vertically onto the ground (*A*, in Fig. 1.6). Draw a conceptual arrow (dashed) from you to *A*; this is the projection of the dark arrow on to the local horizontal plane. Azimuth angle is the compass angle along the local horizontal plane at your location, measured clockwise from the direction to north (N) to the direction to *A*.

Time Zones

In the old days each town defined their own local time. Local noon was when the sun was highest in the sky. In the 1800s when trains and telegraphs allowed fast travel and communication between towns, the railroad companies created standard time zones to allow them to publish and maintain precise schedules. Time zones were eventually adopted worldwide by international convention.

The Earth makes one complete revolution (relative to the sun) in one day. One revolution contains 360° of longitude, and one day takes 24 hours, thus every hour of elapsed time spans 360°/24 = 15° of longitude. For this reason, each time zone was created to span 15° of longitude, and almost every zone is 1 hour different from its neighboring time zones. Everywhere within a time zone, all clocks are set to the same time. Sometimes the time-zone boundaries are modified to follow political or geographic boundaries, to enhance commerce.

Coordinated Universal Time (UTC) is the time zone at the prime meridian. It is also known as **Greenwich Mean Time (GMT)** and **Zulu time (Z)**. The prime meridian is in the middle of the UTC time zone; namely, the zone spreads 7.5° on each side of the prime meridian. UTC is the official time used in meteorology, to help coordinate simultaneous weather observations around the world.

Internationally, time zones are given letter designations A - Z, with Z at Greenwich, as already discussed. East of the UTC zone, the local time zones (A, B, C, ...) are ahead; namely, local time of day is later than at Greenwich. West of the UTC zone, the local time zones (N, O, P, ...) are behind; namely, local time of day is earlier than at Greenwich.

Each zone might have more than one local name, depending on the countries it spans. Most of western Europe is in the Alpha (A) zone, where A = UTC + 1 hr. This zone is also known as Central Europe Time (CET) or Middle European Time (MET). In N. America are 8 time zones P* - W (see Table 1-1).

Near 180° longitude (in the middle of the Pacific Ocean) is the **international date line**. When you fly from east to west across the date line, you lose a day (it becomes tomorrow). From west to east, you gain a day (it becomes yesterday).

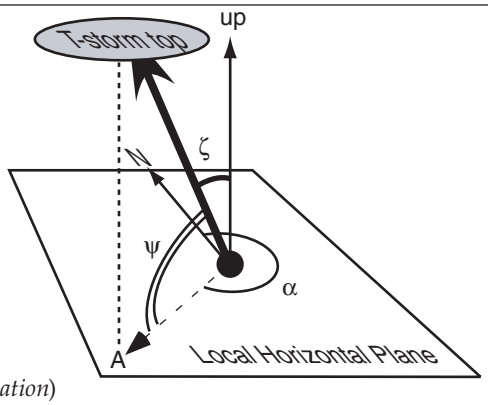

(*continuation*)
Sketch: (see above)
Because south has azimuth 180°, and west has azimuth 270°, we find that 225° is exactly halfway between south and west. Hence, the object is southwest (SW) of the observer. Also, 60° elevation is fairly high in the sky. So **the thunderstorm top is high in the sky to the southwest of the observer**.

Rearrange equation [$\Psi = 90° - \zeta$] to solve for zenith angle: $\zeta = 90° - \psi = 90° - 60° =$ **30°** .

Check: Units OK. Locations reasonable. Sketch good.
Discussion: This is a bad location for a storm chaser (the observer), because thunderstorms in North America often move from the SW toward the northeast (NE). Hence, the observer should quickly seek shelter underground, or move to a different location out of the storm path.

Science Graffito

"It gets late early out there." – Yogi Berra

Table 1-1. Time zones in North America.
ST = standard time in the local time zone.
DT = daylight time in the local time zone.
UTC = coordinated universal time.
For conversion, use:
ST = UTC – α , DT = UTC – β

Zone	Name	α (h)	β (h)
P*	Newfoundland	3.5 (NST)	2.5 (NDT)
Q	Atlantic	4 (AST)	3 (ADT)
R	Eastern	5 (EST)	4 (EDT)
S	Central, and Mexico	6 (CST) 6 (MEX)	5 (CDT) 5
T	Mountain	7 (MST)	6 (MDT)
U	Pacific	8 (PST)	7 (PDT)
V	Alaska	9 (AKST)	8 (AKDT)
W	Hawaii-Aleutian	10 (HST)	9 (HDT)

Solved Example

A weather map is valid at 12 UTC on 5 June. What is the valid local time in Reno, Nevada USA?
Hint: Reno is at roughly 120°W longitude.

Solution:
Given: UTC = 12 , Longitude = 120°W.
Find: Local valid time.

First, determine if standard or daylight time:
Reno is in the N. Hem., and 5 June is after the start date (March) of DT, so it **is** daylight time.
Hint: each 15° longitude = 1 time zone.
Next, use longitude to determine the time zone.
120° / (15° / zone) = 8 zones.
But 8 zones difference corresponds to the Pacific Time Zone. (using the ST column of Table 1-1, for which α also indicates the difference in time zones from UTC)
Use Table 1-1 for Pacific Daylight Time: β = 7 h
PDT = UTC – 7 h = 12 – 7 = **5 am PDT**.

Check: Units OK. 5 am is earlier than noon.
Discussion: In the USA, Canada, and Mexico, 12 UTC maps always correspond to morning of the same day, and 00 UTC maps correspond to late afternoon or evening of the previous day.
Caution: The trick of dividing the longitude by 15° doesn't work for some towns, where the time zone has been modified to follow geo-political boundaries.

FOCUS • Escape Velocity

Fast-moving air molecules that don't hit other molecules can escape to space by trading their kinetic energy (speed) for potential energy (height). High in the atmosphere where the air is thin, there are few molecules to hit. The lowest escape altitude for Earth is about 550 km above ground, which marks the base of the **exosphere** (region of escaping gases). This equals 6920 km when measured from the Earth's center, and is called the critical radius, r_c.

The escape velocity, v_e , is given by

$$v_e = \left[\frac{2 \cdot G \cdot m_{\text{planet}}}{r_c}\right]^{1/2}$$

where $G = 6.67\text{x}10^{-11}\ \text{m}^3\cdot\text{s}^{-2}\cdot\text{kg}^{-1}$ is the gravitational constant, and m_{planet} is the mass of the planet. The mass of the Earth is 5.975×10^{24} kg. Thus, the escape velocity from Earth is roughly v_e = **10,732 m/s.** Using this velocity in eq. (1.5) gives the temperature needed for average-speed molecules to escape: 9,222 K for H_2, and 18,445 K for the heavier He. Temperatures in the exosphere (upper thermosphere) are not hot enough for average-speed H_2 and He to escape, but some are faster than average and do escape.

Heavier molecules such as O_2 have unreachably high escape temperatures (147,562 K), and have stayed in the Earth's atmosphere, to the benefit of life.

Many countries utilize **Daylight Saving Time** (DT) during their local summer. The purpose is to shift one of the early morning hours of daylight (when people are usually asleep) to the evening (when people are awake and can better utilize the extra daylight). At the start of DT (often in March in North America), you set your clocks one hour ahead. When DT ends in Fall (November), you set your clocks one hour back. The mnemonic "Spring ahead, Fall back" is a useful way to remember.

Times can be written as two or four digits. If two, then these digits are hours (e.g., 10 = 10 am, and 14 = 2 pm). If four, then the first two are hours, and the last two are minutes (e.g., 1000 is 10:00 am, and 1435 is 2:35 pm). In both cases, the hours use a 24-h clock going from 0000 (midnight) to 2359 (11:59 pm).

THERMODYNAMIC STATE

The thermodynamic state of air is measured by its pressure (P), density (ρ), and temperature (T).

Temperature

When a group of molecules (microscopic) move predominantly in the same direction, the motion is called wind (macroscopic). When they move in random directions, the motion is associated with temperature. Higher temperatures T are associated with greater average molecular speeds v :

$$T = a \cdot m_w \cdot v^2 \qquad (1.5)$$

where $a = 4.0\text{x}10^{-5}\ \text{K}\cdot\text{m}^{-2}\cdot\text{s}^2\cdot\text{mole}\cdot\text{g}^{-1}$ is a constant. Molecular weights m_w for the most common gases in the atmosphere are listed in Table 1-2.

*[**CAUTION**: symbol "a" represents different constants for different equations, in this textbook.]*

Solved Example

What is the average random velocity of nitrogen molecules at 20°C ?

Solution:
Given: $T = 273.15 + 20 = 293.15$ K.
Find: v = ? m/s (=avg mol. velocity)
Sketch:
Get m_w from Table 1-2. Solve eq. (1.5) for v:
$v = [T/a \cdot m_w]^{1/2}$
$= [(293.15\ \text{K})/(4.0\text{x}10^{-5}\ \text{K}\cdot\text{m}^{-2}\cdot\text{s}^2\cdot\text{mole/g}) \cdot (28.01\text{g/mole})]^{1/2}$ = **511.5 m/s** .

Check: Units OK. Sketch OK. Physics OK.
Discussion: Faster than a speeding bullet.

Absolute units such as Kelvin (K) must be used for temperature in all thermodynamic and radiative laws. Kelvin is the recommended temperature unit. For everyday use, and for temperature differences, you can use degrees Celsius (°C).

*[**CAUTION**: degrees Celsius (°C) and degrees Fahrenheit (°F) must always be prefixed with the degree symbol (°) to avoid confusion with the electrical units of coulombs (C) and farads (F), but Kelvins (K) never take the degree symbol.]*

At **absolute zero** (T = 0 K = –273.15°C) the molecules are essentially not moving. Temperature conversion formulae are:

$$T_{\circ F} = [(9/5)\cdot T_{\circ C}] + 32 \qquad \bullet(1.6a)$$

$$T_{\circ C} = (5/9)\cdot[T_{\circ F} - 32] \qquad \bullet(1.6b)$$

$$T_K = T_{\circ C} + 273.15 \qquad \bullet(1.7a)$$

$$T_{\circ C} = T_K - 273.15 \qquad \bullet(1.7b)$$

For temperature differences, you can use ΔT(°C) = ΔT(K), because the size of one degree Celsius is the same as the size of one unit of Kelvin. Hence, only in terms involving temperature differences can you arbitrarily switch between °C and K without needing to add or subtract 273.15.

Standard (average) sea-level temperature is

T = 15.0°C = 288 K = 59°F.

Actual temperatures can vary considerably over the course of a day or year. Temperature variation with height is not as simple as the curves for pressure and density, and will be discussed in the Standard Atmosphere section a bit later.

Pressure

Pressure P is the force F acting perpendicular (normal) to a surface, per unit surface area A:

$$P = F / A \qquad \bullet(1.8)$$

Static pressure (i.e., pressure in calm winds) is caused by randomly moving molecules that bounce off each other and off surfaces they hit. In a vacuum the pressure is zero.

In the **International System of Units** (**SI**), a **Newton** (N) is the unit for force, and m^2 is the unit for area. Thus, pressure has units of Newtons per square meter, or $N{\cdot}m^{-2}$. One Pascal (Pa) is defined to equal a pressure of 1 $N{\cdot}m^{-2}$. The recommended unit for atmospheric pressure is the **kiloPascal** (**kPa**). The average (standard) pressure at sea level is P = 101.325 kPa. Pressure decreases nearly exponentially with height in the atmosphere, below 105 km.

Table 1-2. Characteristics of gases in the air near the ground. Molecular weights are in g/mole. The volume fraction indicates the relative contribution to air in the Earth's lower atmosphere. EPA is the USA Environmental Protection Agency.

Symbol	Name	Mol. Wt.	Volume Fraction%
Constant Gases			
N_2	Nitrogen	28.01	78.08
O_2	Oxygen	32.00	20.95
Ar	Argon	39.95	0.93
Ne	Neon	20.18	0.0018
He	Helium	4.00	0.0005
H_2	Hydrogen	2.02	0.00005
Xe	Xenon	131.30	0.000009
Variable Gases			
H_2O	Water vapor	18.02	0 to 4
CO_2	Carbon dioxide	44.01	0.035
CH_4	Methane	16.04	0.00017
N_2O	Nitrous oxide	44.01	0.00003
EPA National Ambient Air Quality Standards (NAAQS. 1990 Clean Air Act Amendments)			
CO	Carbon monoxide	28.01	
	(8 h average)		0.0009
	(1 h average)		0.0035
SO_2	Sulfur dioxide	64.06	
	(annual average)		0.000003
	(24 h average)		0.000014
O_3	Ozone (8 h average)	48.00	0.0000075
	(1 h average)		0.000012
NO_2	Nitrogen dioxide	46.01	
	(annual average)		0.0000053
	(1 h average)		0.00001
Mean Condition for Air			
	air	28.96	100.0

Table 1-3. Standard (average) sea-level **pressure**.

Value	Units
101.325 kPa	kiloPascals (recommended)
1013.25 hPa	hectoPascals
101,325. Pa	Pascals
101,325. $N{\cdot}m^{-2}$	Newtons per square meter
101,325 $kg_m{\cdot}m^{-1}{\cdot}s^{-2}$	kg-mass per meter per s^2
1.033227 $kg_f{\cdot}cm^{-2}$	kg-force per square cm
1013.25 mb	millibars
1.01325 bar	bars
14.69595 psi	pounds-force /square inch
2116.22 psf	pounds-force / square foot
1.033227 atm	atmosphere
760 Torr	Torr
Measured as height of fluid in a barometer:	
29.92126 in Hg	inches of mercury
760 mm Hg	millimeters of mercury
33.89854 ft H_2O	feet of water
10.33227 m H_2O	meters of water

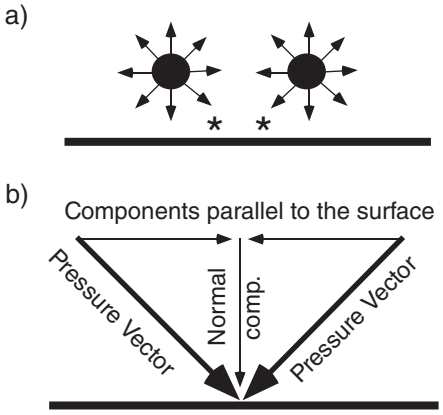

Figure 1.7
*(a) Pressure is isotropic. (b) Dark vectors correspond to those marked with * in (a). Components parallel to the surface cancel, while those normal to the surface contribute to pressure.*

Solved Example

The picture tube of an old TV and the CRT display of an old computer are types of vacuum tube. If there is a perfect vacuum inside the tube, what is the net force pushing against the front surface of a big screen 24 inch (61 cm) display that is at sea level?

Solution

Given: Picture tube sizes are quantified by the diagonal length d of the front display surface. Assume the picture tube is square. The length of the side s of the tube is found from: $d^2 = 2\,s^2$. The frontal surface area is

$A = s^2 = 0.5 \cdot d^2 = 0.5 \cdot (61\text{ cm})^2 = 1860.5\text{ cm}^2$
$= (1860.5\text{ cm}^2)\cdot(1\text{ m}/100\text{ cm})^2 = 0.186\text{ m}^2$.

At sea level, atmospheric pressure pushing against the outside of the tube is 101.325 kPa, while from the inside of the tube there is no force pushing back because of the vacuum. Thus, the pressure difference across the tube face is

$\Delta P = 101.325\text{ kPa} = 101.325\text{x}10^3\text{ N/m}^2$.

Find: ΔF = ? N,
the net force across the tube.
Sketch:

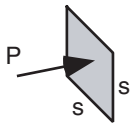

$\Delta F = F_{outside} - F_{inside}$, but $F = P \cdot A$. from eq. (1.8)
$= (P_{outside} - P_{inside})\cdot A$
$= \Delta P \cdot A$
$= (101.325\text{x}10^3\text{ N/m}^2)\cdot(0.186\text{ m}^2)$
$= 1.885\text{x}10^4\text{ N} = \underline{\mathbf{18.85\text{ kN}}}$

Check: Units OK. Physically reasonable.
Discussion: This is quite a large force, and explains why picture tubes are made of such thick heavy glass. For comparison, a person who weighs 68 kg (150 pounds) is pulled by gravity with a force of about 667 N (= 0.667 kN). Thus, the picture tube must be able to support the equivalent of 28 people standing on it!

While kiloPascals will be used in this book, standard sea-level pressure in other units are given in Table 1-3 for reference. Ratios of units can be formed to allow unit conversion (see Appendix A). Although meteorologists are allowed to use **hectoPascals** (as a concession to those meteorologists trained in the previous century, who had grown accustomed to millibars), the prefix "hecto" is non-standard. If you encounter weather maps using millibars or hectoPascals, you can easily convert to kiloPascals by moving the decimal point one place to the left.

In fluids such as the atmosphere, pressure force is **isotropic**; namely, at any point it pushes with the same force in all directions (see Fig. 1.7a). Similarly, any point on a solid surface experiences pressure forces in all directions from the neighboring fluid elements. At such solid surfaces, all forces cancel except the forces normal (perpendicular) to the surface (Fig. 1.7b).

Atmospheric pressure that you measure at any altitude is caused by the weight of all the air molecules above you. As you travel higher in the atmosphere there are fewer molecules still above you; hence, pressure decreases with height. Pressure can also compress the air causing higher density (i.e., more molecules in a given space). Compression is greatest where the pressure is greatest, at the bottom of the atmosphere. As a result of more molecules being squeezed into a small space near the bottom than near the top, ambient pressure decreases faster near the ground than at higher altitudes.

Pressure change is approximately exponential with height, z. For example, if the temperature (T) were uniform with height (which it is not), then:

$$P = P_o \cdot e^{-(a/T)\cdot z} \qquad (1.9a)$$

where a = 0.0342 K/m, and where average sea-level pressure on Earth is P_o = 101.325 kPa. For more realistic temperatures in the atmosphere, the pressure curve deviates slightly from exponential, as discussed in the section on atmospheric structure. *[**CAUTION** again: symbol "a" represents different constants for different equations, in this textbook.]*

Equation (1.9a) can be rewritten as:

$$P = P_o \cdot e^{-z/H_p} \qquad (1.9b)$$

where H_p = 7.29 km is called the **scale height** for pressure. Mathematically, H_p is the **e-folding distance** for the pressure curve.

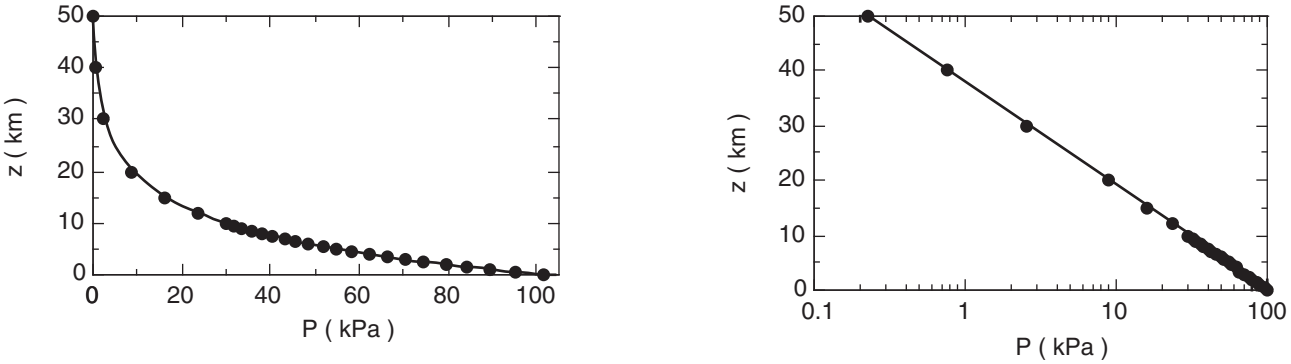

Figure 1.8
Height z vs. pressure P in the atmosphere, plotted on linear (left) and semi-log (right) graphs. See Appendix A for a review of relationships and graphs.

Fig. 1.8 shows the relationship between P and z on linear and semi-log graphs, for $T = 280$ K. [Graph types are reviewed in Appendix A.] In the lowest 3 km of the atmosphere, pressure decreases nearly linearly with height at about (10 kPa)/(1 km).

Because of the monotonic decrease of pressure with height, pressure can be used as a surrogate measure of altitude. (**Monotonic** means that it changes only in one direction, even though the rate of change might vary.) Fig. 1.4 shows such an example, where a reversed logarithmic scale (greater pressure at the bottom of the axis) is commonly used for P. Aircraft also use pressure to estimate their altitude.

In the atmosphere, the pressure at any height z is related to the mass of air above that height. Under the influence of gravity, air mass m has weight $F = m \cdot |g|$, where $|g| = 9.8$ m·s^{-2} is gravitational accel-

Solved Example

Compare the pressures at 10 km above sea level for average temperatures of 250 and 300 K.

Solution

Given: $z = 10$ km $= 10^4$ m
(a) $T = 250$ K, (b) $T = 300$ K
Find: (a) P = ? kPa, (b) P = ? kPa

(a) Use eq. (1.9a):
P=(101.325kPa)·exp[(–0.0342K/m)·(10^4m)/250K]
P = **25.8 kPa**

(b) P=(101.325kPa)·exp[(–0.0342K/m)·(10^4m)/300K]
P = **32.4 kPa**

Check: Units OK. Physically reasonable.
Discussion: Pressure decreases slower with height in warmer air because the molecules are further apart.

FOCUS • e-folding Distance

Some curves never end. In the figure below, curve (a) ends at $x = x_a$. Curve (b) ends at $x = x_b$. But curve (c), the exponentially decreasing curve, asymptotically approaches $y = 0$, never quite reaching it. The area under each of the curves is finite, and in this example are equal to each other.

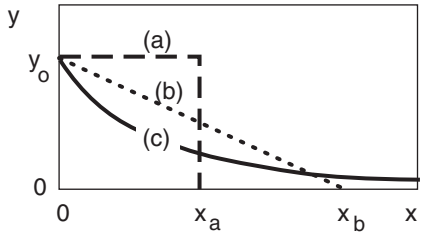

Although the exponential curve never ends, there is another way of quantifying how quickly it decreases with x. That measure is called the e-folding distance (or e-folding time if the independent variable is t instead of x). This is the distance x at which the curve decreases to $1/e$ of the starting value of the dependent variable, where $e = 2.71828$ is the base of natural logarithms. Thus, $1/e = 0.368$.

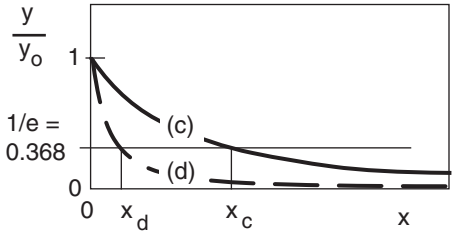

In the example above, both curves (c) and (d) are exponentials, but they drop off at different rates, where x_c and x_d are their respective e-folding distances. Generically, these curves are of the form:

$$y / y_o = e^{-x / x_{efold}} = \exp(-x / x_{efold})$$

Another useful characteristic is that the area A under the exponential curve is $A = y_o \cdot x_{efold}$.

Solved Example

Over each square meter of Earth's surface, how much air mass is between 80 and 30 kPa?

Solution:
Given: P_{bottom} = 80 kPa, P_{top} = 30 kPa, A = 1 m^2
Find: Δm = ? kg

Use eq. (1.11): Δm = [(1 m^2)/(9.8 ms^{-2})]·(80 – 30 kPa)·[(1000 kg·m^{-1}·s^{-2})/(1 kPa)] = **5102 kg**
Check: Units OK. Physics OK. Magnitude OK.
Discussion: About 3 times the mass of a car.

Table 1-4. Standard atmospheric **density** at sea level, for a standard temperature 15°C.

Value	Units
1.2250 kg·m^{-3}.	kilograms per cubic meter (recommended)
0.076474 lb$_m$/ft^3	pounds-mass per cubic foot
1.2250 g/liter	grams per liter
0.001225 g/cm^3	grams per cubic centimeter

Solved Example

At sea level, what is the mass of air within a room of size 5 m x 8 m x 2.5 m ?

Solution
Given: L = 8 m room length, W = 5 m width
H = 2.5 m height of room
ρ = 1.225 kg·m^{-3} at sea level
Find: m = ? kg air mass

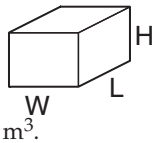

The volume of the room is
$Vol = W{\cdot}L{\cdot}H$ = (5m)·(8m)·(2.5m) = 100 m^3.
Rearrange eq. (1.12) and solve for the mass:
m = ρ·Vol. = (1.225 kg·m^{-3})·(100 m^3) = **122.5 kg**.

Check: Units OK. Sketch OK. Physics OK.
Discussion: This is 1.5 to 2 times a person's mass.

Solved Example

What is the air density at a height of 2 km in an atmosphere of uniform temperature of 15°C?

Solution
Given: z =2000 m, ρ_o =1.225 kg/m^3 , T =15°C =288.15 K
Find: ρ = ? kg/m^3

Use eq. (1.13):
ρ=(1.225 kg/m^3)· exp[(–0.04 K/m)·(2000 m)/288 K]
ρ = **0.928 kg/m**^{3}

Check: Units OK. Physics reasonable.
Discussion: This means that aircraft wings generate 24% less lift, and engines generate 24% less thrust because of the reduced air density.

eration at the Earth's surface. This weight is a force that squeezes air molecules closer together, increasing both the density and the pressure. Knowing that $P = F/A$, previous two expressions are combined to give

$$P_z = |g|{\cdot}m_{above\ z} / A \qquad (1.10)$$

where A is horizontal cross-section area. Similarly, between two different pressure levels is mass

$$\Delta m = (A/|g|){\cdot}(P_{bottom} - P_{top}) \qquad (1.11)$$

Density

Density ρ is defined as mass m per unit volume Vol.

$$\rho = m / Vol \qquad \bullet(1.12)$$

Density increases as the number and molecular weight of molecules in a volume increase. Average air density at sea level is given in Table 1-4. The recommended unit for density is kg·m^{-3} .

Because gases such as air are compressible, air density can vary over a wide range. Density decreases roughly exponentially with height in an atmosphere of uniform temperature.

$$\rho = \rho_o{\cdot}e^{-(a/T){\cdot}z} \qquad (1.13a)$$

or

$$\rho = \rho_o{\cdot}e^{-z/H_\rho} \qquad (1.13b)$$

where a = 0.040 K/m, and where average sea-level density is ρ_o = 1.2250 kg·m^{-3}, at a temperature of 15°C = 288 K. The shape of the curve described by eq. (1.13) is similar to that for pressure, (see Fig. 1.9). The scale height for density is H_ρ = 8.55 km.

Although the air is quite thin at high altitudes, it still can affect many observable phenomena: twilight (scattering of sunlight by air molecules) up to

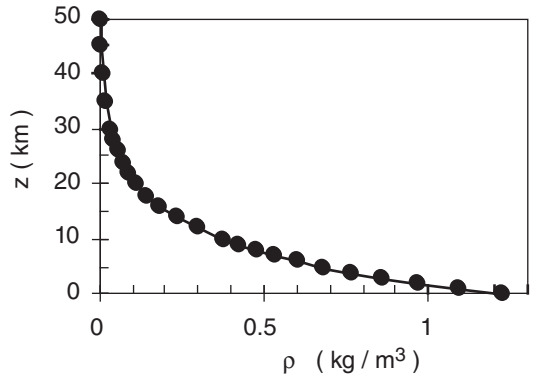

Figure 1.9
Density ρ *vs. height z in the atmosphere.*

63 km, meteors (incandescence by friction against air molecules) from 110 to 200 km, and aurora (excitation of air by solar wind) from 360 to 500 km.

The **specific volume** (α) is defined as the inverse of density ($\alpha = 1/\rho$). It has units of volume/mass.

ATMOSPHERIC STRUCTURE

Atmospheric structure refers to the state of the air at different heights. The true vertical structure of the atmosphere varies with time and location due to changing weather conditions and solar activity.

Standard Atmosphere

The "1976 U.S. Standard Atmosphere" (Table 1-5) is an idealized, dry, steady-state approximation of atmospheric state as a function of height. It has been adopted as an engineering reference. It approximates the average atmospheric conditions, although it was not computed as a true average.

A **geopotential height**, H, is defined to compensate for the decrease of gravitational acceleration magnitude $|g|$ above the Earth's surface:

$$H = R_o \cdot z \,/ (R_o + z) \qquad \bullet(1.14a)$$

$$z = R_o \cdot H \,/ (R_o - H) \qquad \bullet(1.14b)$$

where the average radius of the Earth is $R_o = 6356.766$ km. An **air parcel** (a group of air molecules moving together) raised to **geometric height** z would have the same potential energy as if lifted only to height H under constant gravitational acceleration. By using H instead of z, you can use $|g| = 9.8$ m/s^2 as a constant in your equations, even though in reality it decreases slightly with altitude.

The difference ($z - H$) between geometric and geopotential height increases from 0 to 16 m as height increases from 0 to 10 km above sea level.

Sometimes g and H are combined into a new variable called the **geopotential**, Φ:

$$\Phi = |g| \cdot H \qquad (1.15)$$

Geopotential is defined as the work done against gravity to lift 1 kg of mass from sea level up to height H. It has units of m^2/s^2.

BEYOND ALGEBRA • Geopotential Height

What is "Beyond Algebra"?

These boxes contain supplementary material that use calculus, differential equations, linear algebra, or other mathematical tools beyond algebra. They are not essential for understanding the rest of the book, and may be skipped. Science and engineering students with calculus backgrounds might be curious about how calculus is used in atmospheric physics.

Geopotential Height

For gravitational acceleration magnitude, let $|g_o| = 9.8$ m/s^2 be average value at sea level, and $|g|$ be the value at height z. If R_o is Earth radius, then $r = R_o + z$ is distance above the center of the Earth.

Newton's Gravitation Law gives the force $|F|$ between the Earth and an air parcel:

$$|F| = G \cdot m_{Earth} \cdot m_{air\ parcel} / r^2$$

where $G = 6.67\text{x}10^{-11}$ m^3·s^{-2}·kg^{-1} is the gravitational constant. Divide both sides by $m_{air\ parcel}$, and recall that by definition $|g| = |F|/m_{air\ parcel}$. Thus

$$|g| = G \cdot m_{Earth} / r^2$$

This eq. also applies at sea level ($z = 0$):

$$|g_o| = G \cdot m_{Earth} / R_o^2$$

Combining these two eqs. give

$$|g| = |g_o| \cdot [\, R_o / (R_o + z) \,]^2$$

Geopotential height H is defined as the work per unit mass to lift an object against the pull of gravity, divided by the gravitational acceleration value for sea level:

$$H = \frac{1}{|g_o|} \int_{Z=0}^{z} |g| \cdot dZ$$

Plugging in the definition of $|g|$ from the previous paragraph gives:

$$H = R_o^2 \cdot \int_{Z=0}^{z} (R_o + Z)^{-2} dZ$$

This integrates to

$$H = \left. \frac{-R_o^2}{R_o + Z} \right|_{Z=0}^{z}$$

After plugging in the limits of integration, an putting the two terms over a common denominator, the answer is:

$$H = R_o \cdot z \,/ (R_o + z) \qquad (1.14a)$$

Solved Example

Find the geopotential height and the geopotential at 12 km above sea level.

Solution

Given: z = 12 km, R_0 = 6356.766 km
Find: H = ? km, Φ = ? m^2/s^2

Use eq. (1.14a): H = (6356.766km)·(12km) / (6356.766km + 12km) = **11.98 km**
Use eq. (1.15): Φ = (9.8 m/s^2)·(11,980 m) = **1.17x10^5** m^2/s^2

Check: Units OK.
Discussion: $H \le z$ as expected, because you don't need to lift the parcel as high for constant gravity as you would for decreasing gravity, to do the same work.

Solved Example

Find std. atm. temperature & pressure at H=2.5 km.

Solution

Given: H = 2.5 km. Find: T = ? K, P = ? kPa
Use eq. (1.16): T = 288.15 –(6.5K/km)·(2.5km) = **271.9 K**
Use eq. (1.17): P =(101.325kPa)·(288.15K/271.9K)$^{-5.255877}$
= (101.325kPa)· 0.737 = **74.7 kPa**.
Check: T = –1.1°C. Agrees with Fig. 1.10 & Table 1-5.

Table 1-5. Standard atmosphere.

H (km)	T (°C)	P (kPa)	ρ (kg/m^3)
-1	21.5	113.920	1.3470
0	15.0	101.325	1.2250
1	8.5	89.874	1.1116
2	2.0	79.495	1.0065
3	-4.5	70.108	0.9091
4	-11.0	61.640	0.8191
5	-17.5	54.019	0.7361
6	-24.0	47.181	0.6597
7	-30.5	41.060	0.5895
8	-37.0	35.599	0.5252
9	-43.5	30.742	0.4664
10	-50.0	26.436	0.4127
11	-56.5	22.632	0.3639
13	-56.5	16.510	0.2655
15	-56.5	12.044	0.1937
17	-56.5	8.787	0.1423
20	-56.5	5.475	0.0880
25	-51.5	2.511	0.0395
30	-46.5	1.172	0.0180
32	-44.5	0.868	0.0132
35	-36.1	0.559	0.0082
40	-22.1	0.278	0.0039
45	-8.1	0.143	0.0019
47	-2.5	0.111	0.0014
50	-2.5	0.076	0.0010
51	-2.5	0.067	0.00086
60	-27.7	0.02031	0.000288
70	-55.7	0.00463	0.000074
71	-58.5	0.00396	0.000064
80	-76.5	0.00089	0.000015
84.9	-86.3	0.00037	0.000007
89.7	-86.3	0.00015	0.000003
100.4	-73.6	0.00002	0.0000005
105	-55.5	0.00001	0.0000002
110	-9.2	0.00001	0.0000001

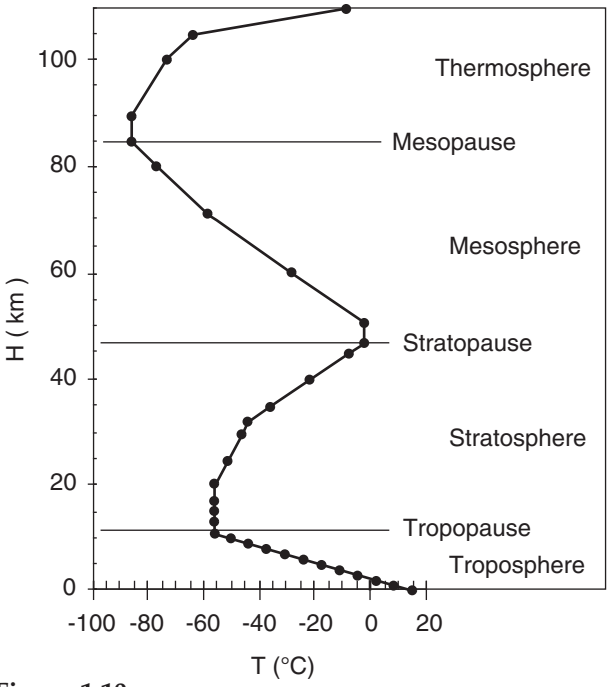

Figure 1.10
Standard temperature T profile vs. geopotential height H.

Table 1-5 gives the standard temperature, pressure, and density as a function of geopotential height H above sea level. Temperature variations are linear between key altitudes indicated in boldface. Standard-atmosphere temperature is plotted in Fig. 1.10.

Below a geopotential altitude of 51 km, eqs. (1.16) and (1.17) can be used to compute standard temperature and pressure. In these equations, be sure to use absolute temperature as defined by T(K) = T(°C) + 273.15 . (1.16)

T = 288.15 K – (6.5 K/km)·H for $H \le 11$ km

T = 216.65 K $11 \le H \le 20$ km

T = 216.65 K +(1 K/km)·(H–20km) $20 \le H \le 32$ km

T = 228.65 K +(2.8 K/km)·(H–32km) $32 \le H \le 47$ km

T = 270.65 K $47 \le H \le 51$ km

For the pressure equations, the absolute temperature T that appears must be the standard atmosphere temperature from the previous set of equations. In fact, those previous equations can be substituted into the equations below to make them a function of H rather than T. (1.17)

P = (101.325kPa)·(288.15K/T) $^{-5.255877}$ $H \le 11$ km

P = (22.632kPa)·exp[–0.1577·(H–11 km)] $11 \le H \le 20$ km

$$P = (5.4749\text{kPa})\cdot(216.65\text{K}/T)^{34.16319} \qquad 20 \le H \le 32 \text{ km}$$

$$P = (0.868\text{kPa})\cdot(228.65\text{K}/T)^{12.2011} \qquad 32 \le H \le 47 \text{ km}$$

$$P = (0.1109\text{kPa})\cdot\exp[-0.1262\cdot(H-47\text{ km})] \qquad 47 \le H \le 51 \text{ km}$$

These equations are a bit better than eq. (1.9a) because they do not make the unrealistic assumption of uniform temperature with height.

Knowing temperature and pressure, you can calculate density using the ideal gas law eq. (1.18).

Layers of the Atmosphere

The following layers are defined based on the nominal standard-atmosphere temperature structure (Fig. 1.10).

Thermosphere	$84.9 \le H$ km
Mesosphere	$47 \le H \le 84.9$ km
Stratosphere	$11 \le H \le 47$ km
Troposphere	$0 \le H \le 11$ km

Almost all clouds and weather occur in the **troposphere**.

The top limits of the bottom three spheres are named:

Mesopause	$H = 84.9$ km
Stratopause	$H = 47$ km
Tropopause	$H = 11$ km

On average, the tropopause is lower (order of 8 km) near the Earth's poles, and higher (order of 18 km) near the equator. In mid-latitudes, the tropopause height averages about 11 km, but is slightly lower in winter, and higher in summer.

The three relative maxima of temperature are a result of three altitudes where significant amounts of solar radiation are absorbed and converted into heat. Ultraviolet light is absorbed by ozone near the stratopause, visible light is absorbed at the ground, and most other radiation is absorbed in the thermosphere.

Atmospheric Boundary Layer

The bottom 0.3 to 3 km of the troposphere is called the **atmospheric boundary layer** (**ABL**). It is often turbulent, and varies in thickness in space and time (Fig. 1.11). It "feels" the effects of the Earth's surface, which slows the wind due to surface drag, warms the air during daytime and cools it at night, and changes in moisture and pollutant concentration. We spend most of our lives in the ABL. Details are discussed in a later chapter.

Solved Example

Is eq. (1.9a) a good fit to standard atmos. pressure?

Solution

Assumption: Use $T = 270$ K in eq. (1.9a) because it minimizes pressure errors in the bottom 10 km.

Method: Compare on a graph where the solid line is eq. (1.9a) and the data points are from Table 1-5.

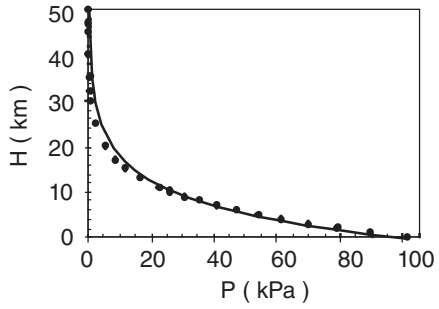

Discussion: Over the lower 10 km, the simple eq. (1.9a) is in error by no more than 1.5 kPa. If more accuracy is needed, then use the hypsometric equation (see eq. 1.26, later in this chapter).

Science Graffito

"Tradition [is] an illusion, an afterimage — comfortable, yes, but unjustified in itself." Mark Helprin, 2004: "Perfection", in *The Pacific & Other Stories*.

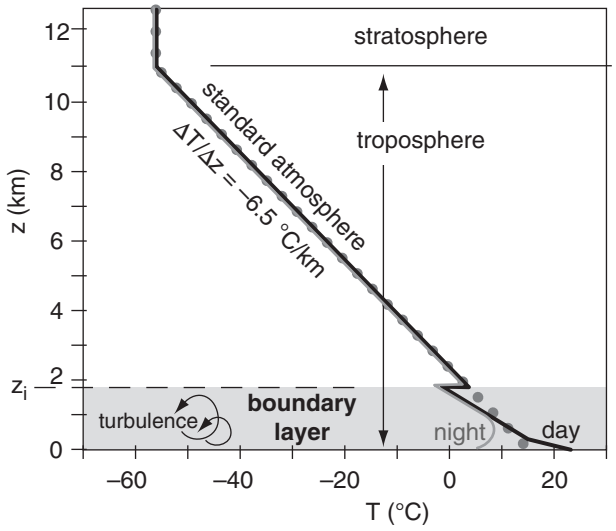

Figure 1.11

Boundary layer (shaded) within the bottom of the troposphere. Standard atmosphere is dotted. Typical temperature profiles during day (black line) and night (grey line) Boundary-layer top (dashed line) is at height z_i.

Solved Example

What is the average (standard) surface temperature for dry air, given standard pressure and density?

Solution:
Given: P = 101.325 kPa, ρ = 1.225 kg·m^{-3}
Find: T = ? K

Solving eq. (1.18) for T gives: $T = P / (\rho \cdot \Re_d)$

$$T = \frac{101.325 \text{ kPa}}{(1.225 \text{ kg·m}^{-3}) \cdot (0.287 \text{ kPa·K}^{-1}\text{·m}^3\text{·kg}^{-1})}$$

= 288.2 K = **15°C**

Check: Units OK. Physically reasonable.
Discussion: The answer agrees with the standard surface temperature of 15°C discussed earlier, a cool but pleasant temperature.

Solved Example

What is the absolute humidity of air of temperature 20°C and water vapor pressure of 2 kPa?

Solution:
Given: e = 2 kPa, T = 20°C = 293 K
Find: ρ_v = ? kg$_{\text{water vapor}}$·m^{-3}

Solving eq. (1.19) for ρ_v gives: $\rho_v = e / (\Re_v \cdot T)$

ρ_v = (2 kPa) / (0.4615 kPa·K^{-1}·m^3·kg^{-1} · 293 K)
= **0.0148** kg$_{\text{water vapor}}$·m^{-3}

Check: Units OK. Physically reasonable.
Discussion: Small compared to the total air density.

Solved Example

In an unsaturated tropical environment with temperature of 35°C and water-vapor mixing ratio of 30 g$_{\text{water vapor}}$/kg$_{\text{dry air}}$, what is the virtual temperature?

Solution:
Given: T = 35°C, r = 30 g$_{\text{water vapor}}$/kg$_{\text{dry air}}$
Find: T_v = ? °C

First, convert T and r to proper units
T = 273.15 + 35 = 308.15 K.
r =(30 g$_{\text{water}}$/kg $_{\text{air}}$)·(0.001 kg/g) = 0.03 g$_{\text{water}}$/g $_{\text{air}}$

Next use eq. (1.21):
T_v = (308.15 K)·[1 + (0.61 · 0.03)]
= 313.6 K = **40.6°C**.

Check: Units OK. Physically reasonable.
Discussion: Thus, high humidity reduces the density of the air so much that it acts like dry air that is 5°C warmer, for this case.

EQUATION OF STATE– IDEAL GAS LAW

Because pressure is caused by the movement of molecules, you might expect the pressure P to be greater where there are more molecules (i.e., greater density ρ), and where they are moving faster (i.e., greater temperature T). The relationship between pressure, density, and temperature is called the **Equation of State**.

Different fluids have different equations of state, depending on their molecular properties. The gases in the atmosphere have a simple equation of state known as the **Ideal Gas Law**.

For dry air (namely, air with the usual mix of gases, except no water vapor), the ideal gas law is:

$$P = \rho \cdot \Re_d \cdot T \qquad \bullet(1.18)$$

where $\Re_d$ = 0.287053 kPa·K^{-1}·m^3·kg^{-1}
= 287.053 J·K^{-1}·kg^{-1} .

$\Re_d$ is called the **gas constant** for dry air. Absolute temperatures (K) must be used in the ideal gas law. The total air pressure P is the sum of the partial pressures of nitrogen, oxygen, water vapor, and the other gases.

A similar equation of state can be written for just the water vapor in air:

$$e = \rho_v \cdot \Re_v \cdot T \qquad (1.19)$$

where e is the partial pressure due to water vapor (called the **vapor pressure**), ρ_v is the density of water vapor (called the **absolute humidity**), and the gas constant for pure water vapor is

$\Re_v$ = 0.4615 kPa·K^{-1}·m^3·kg^{-1}
= 461.5 J·K^{-1}·kg^{-1} .

For moist air (normal gases with some water vapor),

$$P = \rho \cdot \Re \cdot T \qquad (1.20)$$

where density ρ is now the total density of the air. A difficulty with this last equation is that the "gas constant" is NOT constant. It changes as the humidity changes because water vapor has different molecular properties than dry air.

To simplify things, a **virtual temperature** T_v can be defined to include the effects of water vapor:

$$T_v = T \cdot [1 + (a \cdot r)] \qquad \bullet(1.21)$$

where r is the water-vapor mixing ratio [r = (mass of water vapor)/(mass of dry air), with units $g_{water\ vapor}/g_{dry\ air}$, see the Moisture chapter], a = 0.61 $g_{dry\ air}/g_{water\ vapor}$, and all temperatures are in absolute units (K). In a nutshell, moist air of temperature T behaves as dry air with temperature T_v. T_v is greater than T because water vapor is less dense than dry air, and thus moist air acts like warmer dry air.

If there is also liquid water or ice in the air, then this virtual temperature must be modified to include the **liquid-water loading** (i.e., the weight of the drops falling at their terminal velocity) and **ice loading**:

$$T_v = T \cdot [1 + (a \cdot r) - r_L - r_I] \qquad \bullet(1.22)$$

where r_L is the liquid-water mixing ratio ($g_{liquid\ water}$ / $g_{dry\ air}$), r_I is the ice mixing ratio (g_{ice} / $g_{dry\ air}$), and a = 0.61 ($g_{dry\ air}$ / $g_{water\ vapor}$). Because liquid water and ice are heavy, air with liquid-water and/or ice loading acts like colder dry air.

With these definitions, a more useful form of the ideal gas law can be written for air of any humidity:

$$P = \rho \cdot \Re_d \cdot T_v \qquad \bullet(1.23)$$

where $\Re_d$ is still the gas constant for dry air. In this form of the ideal gas law, the effects of variable humidity are hidden in the virtual temperature factor, which allows the dry "gas constant" to be used (nice, because it really is constant).

Solved Example

In a tropical environment with temperature of 35°C, water-vapor mixing ratio of 30 $g_{water\ vapor}/kg_{dry\ air}$, and 10 $g_{liquid\ water}/kg_{dry\ air}$ of raindrops falling at their terminal velocity through the air, what is the virtual temperature?

Solution:

Given: T = 35°C, r = 30 $g_{water\ vapor}/kg_{dry\ air}$
r_L = 10 $g_{liquid\ water}/kg_{dry\ air}$
Find: T_v = ? °C

First, convert T, r and r_L to proper units
T = 273.15 + 35 = 308.15 K.
r =(30 g_{vapor}/kg_{air})·(0.001 kg/g) = 0.03 g_{vapor}/g_{air}
r_L =(5 g_{liquid}/kg_{air})·(0.001 kg/g) = 0.01 g_{liquid}/g_{air}

Next use eq. (1.22):
T_v = (308.15 K)·[1 + (0.61 · 0.03) – 0.01]
= 310.7 K = **37.6°C**.

Check: Units OK. Physically reasonable.
Discussion: Compared to the previous solved example, the additional weight due to falling rain made the air act like it was about 3°C cooler.

HYDROSTATIC EQUILIBRIUM

As discussed before, pressure decreases with height. Any thin horizontal slice from a column of air would thus have greater pressure pushing up against the bottom than pushing down from the top (Fig. 1.12). This is called a **vertical pressure gradient**, where the term **gradient** means change with distance. The net upward force acting on this slice of air, caused by the pressure gradient, is $F = \Delta P \cdot A$, where A is the horizontal cross section area of the column, and $\Delta P = P_{bottom} - P_{top}$.

Also acting on this slice of air is gravity, which provides a downward force (weight) given by

$$F = m \cdot g \qquad \bullet(1.24)$$

where g = – 9.8 m·s^{-2} is the gravitational acceleration. (See Appendix B for variation of g with latitude and altitude.) Negative g implies a negative

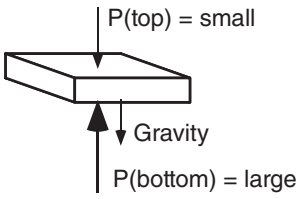

Figure 1.12.
Hydrostatic balance of forces on a thin slice of air.

Solved Example

What is the weight (force) of a person of mass 75 kg at the surface of the Earth?

Solution

Given: m = 75 kg
Find: F = ? N

Sketch:
Use eq. (1.24)
F = $m \cdot g$ = (75 kg)·(– 9.8 m·s^{-2})
= – 735 kg·m·s^{-2} = **– 735 N**

Check: Units OK. Sketch OK. Physics OK.
Discussion: The negative sign means the person is pulled toward the Earth, not repelled away from it.

Solved Example

Near sea level, a height increase of 100 m corresponds to what pressure decrease?

Solution

Given: $\rho = 1.225$ kg·m^{-3} at sea level

$\Delta z = 100$ m

Find: ΔP = ? kPa

Sketch:

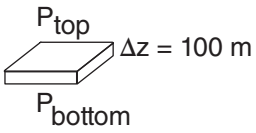

Use eq. (1.25a):

$\Delta P = \rho \cdot g \cdot \Delta z$

$= (1.225 \text{ kg·m}^{-3}) \cdot (-9.8 \text{ m·s}^{-2}) \cdot (100 \text{ m})$

$= -1200.5 \text{ kg·m}^{-1}\text{·s}^{-2}$

$= \underline{\mathbf{-1.20 \text{ kPa}}}$

Check: Units OK. Sketch OK. Physics OK.

Discussion: This answer should not be extrapolated to greater heights.

Science Graffito

Spray painted on a sidewalk of a large university campus was:

"Obey gravity. It's the law."

ON DOING SCIENCE • Check for Errors

As a scientist or engineer you should always be very careful when you do your calculations and designs. Be precise. Check and double check your calculations and your units. Don't take shortcuts, or make unjustifiable simplifications. Mistakes you make as a scientist or engineer can kill people and cause great financial loss.

Be careful whenever you encounter any equation that gives the change in one variable as a function of change of another. For example, in equations (1.25) P is changing with z. The "change of" operator (Δ) MUST be taken in the same direction for both variables. In this example $\Delta P/\Delta z$ means $[\, P(\text{at } z_2) - P(\text{at } z_1)\,] \,/\, [\, z_2 - z_1\,]$. We often abbreviate this as $[\, P_2 - P_1\,] \,/\, [\, z_2 - z_1\,]$.

If you change the denominator to be $[\, z_1 - z_2\,]$, then you must also change the numerator to be in the same direction $[\, P_1 - P_2\,]$. It doesn't matter which direction you use, so long as both the numerator and denominator (or both Δ variables as in eq. 1.25a) are in the same direction.

To help avoid errors in direction, you should always think of the subscripts by their relative positions in space or time. For example, subscripts 2 and 1 often mean top and bottom, or right and left, or later and earlier, etc. If you are not careful, then when you solve numerical problems using equations, your answer will have the wrong sign, which is sometimes difficult to catch.

(downward) force. (Remember that the unit of force is 1 N = 1 kg·m·s^{-2}, see Appendix A). The mass m of air in the slice equals the air density times the slice volume; namely, $m = \rho \cdot (A \cdot \Delta z)$, where Δz is the slice thickness.

For situations where pressure gradient force approximately balances gravity force, the air is said to be in a state of **hydrostatic equilibrium**. The corresponding **hydrostatic equation** is:

$$\Delta P = \rho \cdot g \cdot \Delta z \qquad (1.25a)$$

or

$$\frac{\Delta P}{\Delta z} = -\rho \cdot |g| \qquad \bullet(1.25b)$$

The term **hydrostatic** is used because it describes a stationary (static) balance in a fluid (hydro) between pressure pushing up and gravity pulling down. The negative sign indicates that pressure decreases as height increases. This equilibrium is valid for most weather situations, except for vigorous storms with large vertical velocities.

BEYOND ALGEBRA • Physical Interpretation of Equations

Equations such as (1.25b) are finite-difference approximations to the original equations that are in differential form:

$$\frac{dP}{dz} = -\rho \cdot |g| \qquad (1.25c)$$

The calculus form (eq. 1.25c) is useful for derivations, and is the best description of the physics. The algebraic approximation eq. (1.25b) is often used in real life, where one can measure pressure at two different heights [i.e., $\Delta P/\Delta z = (P_2 - P_1)/(z_2 - z_1)$].

The left side of eq. (1.25c) describes the infinitesimal change of pressure P that is associated with an infinitesimal local change of height z. It is the vertical gradient of pressure. On a graph of P vs. z, it would be the slope of the line. The derivative symbol "d" has no units or dimensions, so the dimensions of the left side are kPa/m.

Eq. (1.25b) has a similar physical interpretation. Namely, the left side is the change in pressure associated with a finite change in height. Again, it represents the slope of a line, but in this case, it is a straight line segment of finite length, as an approximation to a smooth curve.

Both eqs. (1.25b & c) state that rate of pressure decrease (because of the negative sign) with height is greater if the density ρ is greater, or if the magnitude of the gravitational acceleration $|g|$ is greater. Namely, if factors ρ or $|g|$ increase, then the whole right hand side (RHS) increases because ρ and $|g|$ are in the numerator. Also, if the RHS increases, then the left hand side (LHS) must increase as well, to preserve the equality of LHS = RHS.

HYPSOMETRIC EQUATION

When the ideal gas law and the hydrostatic equation are combined, the result is an equation called the **hypsometric equation**. This allows you to calculate how pressure varies with height in an atmosphere of arbitrary temperature profile:

$$z_2 - z_1 \approx a \cdot \overline{T_v} \cdot \ln\left(\frac{P_1}{P_2}\right) \qquad \bullet(1.26a)$$

or

$$P_2 = P_1 \cdot \exp\left(\frac{z_1 - z_2}{a \cdot \overline{T_v}}\right) \qquad \bullet(1.26b)$$

where $\overline{T_v}$ is the average virtual temperature between heights z_1 and z_2. The constant $a = \Re_d / |g| =$ 29.3 m/K. The height difference of a layer bounded below and above by two pressure levels P_1 (at z_1) and P_2 (at z_2) is called the **thickness** of that layer.

To use this equation across large height differences, it is best to break the total distance into a number of thinner intervals, Δz. In each thin layer, if the virtual temperature varies little, then you can approximate by T_v. By this method you can sum all of the thicknesses of the thin layers to get the total thickness of the whole layer.

For the special case of a dry atmosphere of uniform temperature with height, eq. (1.26b) simplifies to eq. (1.9a). Thus, eq. (1.26b) also describes an exponential decrease of pressure with height.

Solved Example (§)

What is the thickness of the 100 to 90 kPa layer, given [P(kPa), T(K)] = [90, 275] and [100, 285].

Solution

Given: observations at top and bottom of the layer
Find: $\Delta z = z_2 - z_1$
Assume: T varies linearly with z. Dry air: $T = T_v$.

Solve eq. (1.26) on a computer spreadsheet (§) for many thin layers 0.5 kPa thick. Results for the first few thin layers, starting from the bottom, are:

P(kPa)	T_v (K)	$\overline{T_v}$ (K)	Δz(m)
100	285	284.75	41.82
99.5	284.5	284.25	41.96
99.0	284	etc.	etc.

Sum of all Δz = **<u>864.11 m</u>**

Check: Units OK. Physics reasonable.
Discussion: In an aircraft you must climb 864.11 m to experience a pressure decrease from 100 to 90 kPa, for this particular temperature sounding. If you compute the whole thickness at once from Δz = (29.3m/K)·(280K)·ln(100/90) = 864.38 m, this answer is less accurate than by summing over smaller thicknesses.

PROCESS TERMINOLOGY

Processes associated with constant temperature are isothermal. For example, eqs. (1.9a) and (1.13a) apply for an **isothermal** atmosphere. Those occurring with constant pressure are **isobaric**. A line on a weather map connecting points of equal temperature is called an **isotherm**, while one connecting points of equal pressure is an **isobar**. Table 1-6 summarizes many of the process terms.

Solved Example

Name the process for constant density.

Solution:

From Table 1-6: It is an **<u>isopycnal</u>** process.

Discussion: Isopycnics are used in oceanography, where both temperature and salinity affect density.

Table 1-6.Process names. (tendency = change with t.)

Name	Constant or equal
adiabat	entropy (no heat exchange)
contour	height
isallobar	pressure tendency
isallohypse	height tendency
isallotherm	temperature tendency
isanabat	vertical wind speed
isanomal	weather anomaly
isentrope	entropy or potential temp.
isobar	pressure
isobath	water depth
isobathytherm	depth of constant temperature
isoceraunic	thunderstorm activity or freq.
isochrone	time
isodop	(Doppler) radial wind speed
isodrosotherm	dew-point temperature
isoecho	radar reflectivity intensity
isogon	wind direction
isogram	(generic, for any quantity)
isohel	sunshine
isohume	humidity
isohyet	precipitation accumulation
isohypse	height (similar to contour)
isoline	(generic, for any quantity)
isoneph	cloudiness
isopleth	(generic, for any quantity)
isopycnic	density
isoshear	wind shear
isostere	specific volume (1/ρ)
isotach	speed
isotherm	temperature

BEYOND ALGEBRA • Hypsometric Eq.

To derive eq. (1.26) from the ideal gas law and the hydrostatic equation, one must use calculus. It cannot be done using algebra alone. However, once the equation is derived, the answer is in algebraic form.

The derivation is shown here only to illustrate the need for calculus. Derivations will NOT be given for most of the other equations in this book. Students can take advanced meteorology courses, or read advanced textbooks, to find such derivations.

Derivation of the hypsometric equation:
Given: the hydrostatic eq:

$$\frac{\mathrm{d}P}{\mathrm{d}z} = -\rho \cdot |g| \qquad (1.25c)$$

and the ideal gas law:

$$P = \rho \cdot \Re_d \cdot T_v \qquad (1.23)$$

First, rearrange eq. (1.23) to solve for density:

$$\rho = P / (\Re_d \cdot T_v)$$

Then substitute this into (1.25c):

$$\frac{\mathrm{d}P}{\mathrm{d}z} = -\frac{P \cdot |g|}{\Re_d \cdot T_v}$$

One trick for integrating equations is to separate variables. Move all the pressure factors to one side, and all height factors to the other. Therefore, multiply both sides of the above equation by dz, and divide both sides by P.

$$\frac{\mathrm{d}P}{P} = -\frac{|g|}{\Re_d \cdot T_v}\,\mathrm{d}z$$

Compared to the other variables, g and $\Re_d$ are relatively constant, so we will assume that they are constant and separate them from the other variables. However, usually temperature varies with height: $T(z)$. Thus:

$$\frac{\mathrm{d}P}{P} = -\frac{|g|}{\Re_d} \cdot \frac{\mathrm{d}z}{T_v(z)}$$

Next, integrate the whole eq. from some lower altitude z_1 where the pressure is P_1, to some higher altitude z_2 where the pressure is P_2:

$$\int_{P_1}^{P_2} \frac{\mathrm{d}P}{P} = -\frac{|g|}{\Re_d} \cdot \int_{z_1}^{z_2} \frac{\mathrm{d}z}{T_v(z)}$$

(continues in next column)

BEYOND ALGEBRA • Hypsometric Eq.

(Continuation)

where $|g|/\Re_d$ is pulled out of the integral on the RHS because it is constant.

The left side of that equation integrates to become a natural logarithm (consult tables of integrals).

The right side of that equation is more difficult, because we don't know the functional form of the vertical temperature profile. On any given day, the profile has a complex shape that is not conveniently described by an equation that can be integrated.

Instead, we will invoke the mean-value theorem of calculus to bring T_v out of the integral. The overbar denotes an average (over height, in this context).

That leaves only dz on the right side. After integrating, we get:

$$\ln(P)\Big|_{P_1}^{P_2} = -\frac{|g|}{\Re_d} \cdot \overline{\left(\frac{1}{T_v}\right)} \cdot z\Big|_{z_1}^{z_2}$$

Plugging in the upper and lower limits gives:

$$\ln(P_2) - \ln(P_1) = -\frac{|g|}{\Re_d} \cdot \overline{\left(\frac{1}{T_v}\right)} \cdot (z_2 - z_1)$$

But the difference between two logarithms can be written as the ln of the ratio of their arguments:

$$\ln\left(\frac{P_2}{P_1}\right) = -\frac{|g|}{\Re_d} \cdot \overline{\left(\frac{1}{T_v}\right)} \cdot (z_2 - z_1)$$

Recalling that $\ln(x) = -\ln(1/x)$, then:

$$\ln\left(\frac{P_1}{P_2}\right) = \frac{|g|}{\Re_d} \cdot \overline{\left(\frac{1}{T_v}\right)} \cdot (z_2 - z_1)$$

Rearranging and approximating $\overline{1/T_v} \approx 1/\overline{T_v}$ (which is NOT an identity), then one finally gets the hypsometric eq:

$$(z_2 - z_1) \approx \frac{\Re_d}{|g|} \cdot \overline{T_v} \cdot \ln\left(\frac{P_1}{P_2}\right) \qquad (1.26)$$

PRESSURE INSTRUMENTS

Atmospheric-pressure sensors are called **barometers**. Almost all barometers measure the pressure difference between atmospheric pressure on one side of the sensor, and a reference pressure on the other side. This pressure difference causes a net force that pushes against a spring or a weight. For most barometers, the reference pressure is a **vacuum** (zero pressure).

Aneroid barometers use a corrugated metallic can (the **aneroid element**) with a vacuum inside the can. A spring forces the can sides outward against the inward-pushing atmospheric-pressure force. The relative inflation of the can is measured with levers and gears that amplify the minuscule deflection of the can, and display the result as a moving needle on a barometer or a moving pen on a **barograph** (a recording barometer). The scale on an aneroid barometer can be calibrated to read in any pressure units (see Table 1-3).

Mercury (Hg) barometers (developed by Evangelista Torricelli in the 1600s) are made from a U-shaped tube of glass that is closed on one end. The closed end has a vacuum, and the other end is open to atmospheric pressure. Between the vacuum and the air is a column of mercury inside the tube, the weight of which balances atmospheric pressure.

Atmospheric pressure is proportional to the height difference Δz between the top of the mercury column on the vacuum side, and the height on the side of the U-tube open to the atmosphere. Typical Δz scales are **millimeters of mercury** (**mm Hg**), **centimeters of mercury** (**cm Hg**), or **inches of mercury** (**in Hg**). To amplify the height signal, **contra-barometers** (developed by Christiaan Huygens in the 1600s) use mercury on one side of the U-tube and another fluid (e.g., alcohol) on the other.

Because mercury is a poison, modern **Torricelli** (U-tube) barometers use a heavy silicon-based fluid instead. Also, instead of using a vacuum as a reference pressure, they use a fixed amount of gas in the closed end of the tube. All Torricelli barometers require temperature corrections, because of thermal expansion of the fluid.

Electronic barometers often have a small can with a vacuum or fixed amount of gas inside. Deflection of the can can be measured by strain gauges, or by changes in capacitance between the top and bottom metal ends of an otherwise non-conductive can. **Digital barometers** are electronic barometers that include analog-to-digital circuitry, so that the pressure signals can be sent to digital computers.

SUMMARY

Pressure, temperature, and density describe the thermodynamic state of the air. These state variables are related to each other by the ideal gas law. Change one, and one or both of the others must change too. Ambient pressure decreases roughly exponentially with height, as given by the hypsometric equation. The vertical pressure gradient is balanced by the pull of gravity, according to the hydrostatic eq.

Density variation is also exponential with height. Temperature, however, exhibits three relative maxima over the depth of the atmosphere, caused by absorption of radiation from the sun. Thermodynamic processes can be classified. The standard atmosphere is an idealized model of atmospheric vertical structure, and is used to define atmospheric layers such as the troposphere and stratosphere. Atmospheric pressure is measured with mercury, aneroid, or electronic barometers.

Threads

Have you ever discovered a loose thread on your clothes, and upon pulling it, found that it leads you to places you didn't expect? With this analogy, a "Threads" section will appear at the end of each chapter, to tie new concepts to past and future chapters, and to wrap things up.

In this chapter, we introduced the special meteorological coordinate system used in all other chapters to convert wind information into everyday terms that people such as sailors and pilots can understand and use. UTC time is used by many organizations that conduct business across time zones. Meteorologists use UTC on weather maps (Chapters 9, 12 and 13).

The standard atmosphere temperature structure determines the ability of storms to grow (Chapters 14 to 16), and confines many weather circulations to the bottom 11 km of the atmosphere, on the average (Chapters 11, 12 and 13).

The hydrostatic equation is used in Chapter 10 to explain why vertical winds are often weaker than horizontal winds. Virtual temperature is used in Chapters 4 to 6, 14 and 15 to help define buoyancy and cloud formation. The hypsometric relationship helps explain the jet stream, and allows a "thermal wind" relationship to be defined in Chapter 11. The ideal gas law and the hydrostatic equation are used in Chapter 3 to show why air parcels become colder as they rise — important for condensation and rain. Process terminology is used in weather maps and thermodynamic diagrams (Chapters 5 and 9).

ON DOING SCIENCE • Be Meticulous

Format Guidelines for Your Homework

Good scientists and engineers are not only creative, they are methodical, meticulous, and accurate. To encourage you to develop these good habits, many instructors require your homework to be written in a clear, concise, organized, and consistent format. Such a format is described below, and is illustrated in all the Solved Examples in this book. The format below closely follows steps you typically take in problem solving (Appendix A).

Format:

1. Give the exercise number, & restate the problem.
2. Start the solution section by listing the "Given" known variables (WITH THEIR UNITS).
3. List the unknown variables to find, with units.
4. Draw a sketch if it clarifies the scenario.
5. List the equation(s) you will use.
6. Show all your intermediate steps and calculations (to maximize your partial credit), and be sure to ALWAYS INCLUDE UNITS with the numbers when you plug them into eqs.
7. Put a box around your final answer, or underline it, so the grader can find it on your page amongst all the coffee and pizza stains.
8. Always check the value & units of your answer.
9. Briefly discuss the significance of the answer.

Example:

Problem : What is air density at height 2 km in an isothermal atmosphere of temperature 15°C?

Solution

Given: $z = 2000$ m
$\rho_o = 1.225$ kg/m^3
$T = 15°C = 288.15$ K
Find: $\rho = ?$ kg/m^3

Use eq. (1.13a): $\rho = (1.225 \text{ kg/m}^3) \cdot \exp[(-0.040\text{K/m}) \cdot (2000\text{m})/288\text{K}]$

$\rho = \underline{\mathbf{0.928}}$ kg/m^3

Check: Units OK. Physics reasonable.

Discussion: $(\rho_o - \rho)/\rho_o \approx 0.24$. This means that aircraft wings generate 24% less lift, aircraft engines generate 24% less power, and propellers 24% less thrust because of the reduced air density. This compounding effect causes aircraft performance to decrease rapidly with increasing altitude, until the **ceiling** is reached where the plane can't climb any higher.

Fig. 1.13 shows the solution of this problem on a computer spreadsheet.

Tips

At the end of each chapter are four types of homework exercises:

- Numerical
- Understanding & Critical Evaluation
- Web Enhanced
- Synthesis

Each of these types are explained here in Chapter 1, at the start of their respective subsections. I also recommend how you might approach these different types of problems.

One of the first tips is in the "On Doing Science" box. Here I recommend that you write your exercise solutions in a format very similar to the "Solved Examples" that I have throughout this book. Such meticulousness will help you earn higher grades in most science and engineering courses, and will often give you partial credit (instead of zero credit) for exercises you solved incorrectly.

Finally, most of the exercises have multiple parts to them. Your instructor need assign only one of the parts for you to gain the skills associated with that exercise. Many of the numerical problems are similar to Solved Examples presented earlier in the chapter. Thus, you can try to do the solved example first, and if you get the same answer as I did, then you can be more confident in getting the right answer when you re-solve the exercise part assigned by your instructor. Such re-solutions are trivial if you use a computer spreadsheet (Fig. 1.13) or other similar program to solve the numerical exercises.

	A	B	C	D	E
1					
2	N21)	What is air density at height			
3		2 km in an atmosphere of			
4		uniform T of 15 °C?			
5					
6		**Given:**	z =	2000	m
7			rho_o=	1.225	kg/m3
8			T =	15	°C
9		**Find:**	rho =	?	kg/m3
10					
11		First convert T to Kelvin.			
12			T =	288.15	K
13		Then use eq (1.13a), where			
14			a =	0.040	K/m
15			rho =	**0.928**	kg/m3
16					
17		**Check:** Units OK. Physics OK.			
18		**Discussion:** This means that			
19		aircraft wings generate			
20		0.928/ 1.225 = 76% of the lift			
21		they would at sea level.			
22					
23	Note to students: the eq used in				
24	cell D15 was: =D7*EXP(-D14*D6/D12)				

Figure 1.13
Example of a spreadsheet used to solve a numerical problem.

EXERCISES

Numerical Problems

These are essentially "plug & chug" exercises. They are designed to ensure that you are comfortable with the equations, units, and physics by getting hands-on experience using them. None of the problems require calculus.

While most of the numerical problems can be solved using a hand calculator, many students find it easier to compose all of their homework answers on a computer spreadsheet. It is easier to correct mistakes using a spreadsheet, and plotting graphs of the answer is trivial.

Some exercises are flagged with the symbol **(§)**, which means you should use a Spreadsheet or other more advanced tool such as Matlab, Mathematica, or Maple. These exercises have tedious repeated calculations to graph a curve or trend. To do them by hand calculator would be painful. If you don't know how to use a spreadsheet (or other more advanced program), now is a good time to learn.

Most modern spreadsheets also allow you to add objects called text boxes, note boxes or word boxes, to allow you to include word-wrapped paragraphs of text, which are handy for the "Problem" and the "Discussion" parts of the answer.

A spreadsheet example is given in Fig. 1.13. Normally, to make your printout look neater, you might use the page setup or print option to turn off printing of the row numbers, column letters, and grid lines. Also, the borders around the text boxes can be eliminated, and color could be used if you have access to a color printer. Format all graphs to be clear and attractive, with axes labeled and with units, and with tic marks having pleasing increments.

N1. Find the wind direction (degrees) and speed (m/s), given the (U, V) components:

a. (-5, 0) knots b. (8, -2) m/s
c. (-1, 15) mi/h d. (6, 6) m/s
e. (8, 0) knots f. (5, 20) m/s
g. (-2, -10) mi/h h. (3, -3) m/s

N2. Find the U and V wind components (m/s), given wind direction and speed:

a. west at 10 knots b. north at 5 m/s
c. 225° at 8 mi/h d. 300° at 15 knots
e. east at 7 knots f. south at 10 m/s
g. 110° at 8 mi/h h. 20° at 15 knots

N3. Convert the following UTC times to local times in your own time zone:

a. 0000 b. 0330 c. 0610 d. 0920
e. 1245 f. 1515 g. 1800 h. 2150

N4. (i). Suppose that a typical airline window is circular with radius 15 cm, and a typical cargo door is square of side 2 m. If the interior of the aircraft is pressured at 80 kPa, and the ambient outside pressure is given below in kPa, then what are the magnitudes of forces pushing outward on the window and door?

(ii). Your weight in pounds is the force you exert on things you stand on. How many people of your same weight standing on a window or door are needed to equal the forces calculated in part a. Assume the window and door are horizontal, and are near the Earth's surface.

a. 30 b. 25 c. 20 d. 15
e. 10 f. 5 g. 0 h. 40

N5. Find the pressure in kPa at the following heights above sea level, assuming an average T = 250K:

a. -100 m (below sea level) b. 1 km
c. 11 km d. 25 km e. 30,000 ft
f. 5 km g. 2 km h. 15,000 ft

N6. Use the definition of pressure as a force per unit area, and consider a column of air that is above a horizontal area of 1 square meter. What is the mass of air in that column:

a. above the Earth's surface.
b. above a height where the pressure is 50 kPa?
c. between pressure levels of 70 and 50 kPa?
d. above a height where the pressure is 85 kPa?
e. between pressure levels 100 and 20 kPa?
f. above height where the pressure is 30 kPa?
g. between pressure levels 100 and 50 kPa?
h. above a height where the pressure is 10 kPa?

N7. Find the virtual temperature (°C) for air of:

	a.	b.	c.	d.	e.	f.	g.
T (°C)	20	10	30	40	50	0	–10
r (g/kg)	10	5	0	40	60	2	1

N8. Given the planetary data in Table 1-7.

(i). What are the escape velocities from a planet for each of their main atmospheric components? (For simplicity, use the planet radius instead of the "critical" radius at the base of the exosphere.).

(ii). What are the most likely velocities of those molecules at the surface, given the average surface temperatures given in that table? Comparing these answers to part (i), which of the constituents (if any) are most likely to escape? a. Mercury b. Venus c. Mars d. Jupiter e. Saturn f. Uranus g. Neptune h. Pluto

Table 1-7. Planetary data.

Planet	Radius (km)	T_{sfc} (°C) (avg.)	Mass relative to Earth	Main gases in atmos.
Mercury	2440	180	0.055	H_2, He
Venus	6052	480	0.814	CO_2, N_2
Earth	6378	8	1.0	N_2, O_2
Mars	3393	–60	0.107	CO_2, N_2
Jupiter	71400	–150	317.7	H_2, He
Saturn	60330	–185	95.2	H_2, He
Uranus	25560	–214	14.5	H_2, He
Neptune	24764	–225	17.1	H_2, He
Pluto*	1153	–236	0.0022	CH_4, N_2, CO

** Demoted to a "dwarf planet" in 2006.*

N9. Convert the following temperatures:

a. 15°C = ?K b. 50°F = ?°C
c. 70°F = ?K d. 15°C = ?°F
e. 303 K = ?°C f. 250K = ?°F
g. 2000°C = ?K h. –40°F = ?°C

N10. a. What is the density (kg·m^{-3}) of air, given P = 80 kPa and T = 0 °C ?

b. What is the temperature (°C) of air, given P = 90 kPa and ρ = 1.0 kg·m^{-3} ?

c. What is the pressure (kPa) of air, given T = 90°F and ρ = 1.2 kg·m^{-3} ?

d. Give 2 combinations of pressure and density that have a temperature of 30°C.

e. Give 2 combinations of pressure and density that have a temperature of 0°C.

f. Give 2 combinations of pressure and density that have a temperature of –20°C.

g. How could you determine air density if you did not have a density meter?

h. What is the density (kg·m^{-3}) of air, given P = 50 kPa and T = –30 °C ?

i. What is the temperature (°C) of air, given P = 50 kPa and ρ = 0.5 kg·m^{-3} ?

j. What is the pressure (kPa) of air, given T = –25°C and ρ = 1.2 kg·m^{-3} ?

N11. At a location in the atmosphere where the air density is 1 kg/m^3, find the change of pressure (kPa) you would feel if your altitude increases by ___ km.

a. 2 b. 5 c. 7 d. 9 e. 11 f. 13 g. 16
h. –0.1 i. –0.2 j. –0.3 k. –0.4 l. –0.5

N12. At a location in the atmosphere where the average virtual temperature is 5°C, find the height difference (i.e., the thickness in km) between the following two pressure levels (kPa):

a. 100, 90 b. 90, 80 c. 80, 70 d. 70, 60
e. 60, 50 f. 50, 40 g. 40, 30 h. 30, 20
i. 20, 10 j. 100, 80 k. 100, 70 l. 100, 60
m. 100, 50 n. 50, 30

N13. Name the isopleths that would be drawn on a weather map to indicate regions of equal

a. pressure b. temperature
c. cloudiness d. precipitation accumulation
e. humidity f. wind speed
g. dew point h. pressure tendency

N14. What is the geometric height and geopotential, given the geopotential height?

a. 10 m b. 100 m c. 1 km d. 11 km

What is the geopotential height and geopotential, given the geometric height?

e. 500 m f. 2 km g. 5 km h. 20 km

N15. What is the standard atmospheric temperature, pressure, and density at each of the following geopotential heights?

a. 1.5 km b. 12 km c. 50 m d. 8 km
e. 200 m f. 5 km g. 40 km h. 25 km

N16. What are the geometric heights (assuming a standard atmosphere) at the top and bottom of the:

a. troposphere b. stratosphere
c. mesosphere d. thermosphere

N17. Is the inverse of an average of numbers equal to the average of the inverses of those number? (Hint, work out the values for just two numbers: 2 and 4.) This question helps explain where the hypsometric equation given in this chapter is only approximate.

N18(§). Using the standard atmosphere equations, re-create the numbers in Table 1-5 for $0 \le H \le 51$ km.

Understanding & Critical Evaluation

These questions require more thought, and are extensions of material in the chapter. They might require you to combine two or more equations or concepts from different parts of the chapter, or from other chapters. You might need to critically evaluate an approach. Some questions require a numerical answer — others are "short-answer" essays.

They often require you to make assumptions, because insufficient data is given to solve the problem. Whenever you make assumptions, justify them first. A sample solution to such an exercise is at right.

U1. What are the limitations of the "standard atmosphere"?

U2. For any physical variable that decreases exponentially with distance or time, the e-folding scale is defined as the distance or time where the physical variable is reduced to 1/e of its starting value. For the atmosphere the e-folding height for pressure decrease is known as the scale height. Given eq. (1.9a), what is the algebraic and numerical value for atmospheric scale height (km)?

U3(§). Invent some arbitrary data, such as 5 data points of wind speed M vs. pressure P. Although P is the independent variable, use a spreadsheet to plot it on the vertical axis (i.e., switch axes on your graph so that pressure can be used as a surrogate measure of height), change that axis to a logarithmic scale, and then reverse the scale so that the largest value is at the bottom, corresponding to the greatest pressure at the bottom of the atmosphere.

Now add to this existing graph a second curve of different data of M vs. P. Learn how to make both curves appear properly on this graph because you will use this skill repeatedly to solve problems in future chapters.

U4. Does hydrostatic equilibrium (eq. 1.25) always apply to the atmosphere? If not, when and why not?

U5. a. Plug eqs. (1.1) and (1.2a) into (1.3), and use trig to show that $U = U$. b. Similar, but for $V = V$.

U6. What percentage of the atmosphere is above a height (km) of : a. 2 b. 5 c. 11 d. 32
e. 1 f. 18 g. 47 h. 8

U7. What is the mass of air inside an airplane with a cabin size of 5 x 5 x 30 m, if the cabin is pressurized to a cabin altitude of sea level? What mass of outside air is displaced by that cabin, if the aircraft is flying at an altitude of 3 km? The difference in those two masses is the load of air that must be carried by the aircraft. How many people cannot be carried because of this excess air that is carried in the cabin?

U8. Given air of initial temperature 20°C and density of 1.0 kg/m^3.
a. What is its initial pressure?
b. If the temperature increases to 30°C in an isobaric process, what is the new density?
c. If the temperature increases to 30°C in an isobaric process, what is the new pressure?
d. For an isothermal process, if the pressure changes to 20 kPa, what is the new density?

Solved Example – Understanding and Critical Evaluation Questions (U)

What are the limitations of eq. (1.9a), if any? How can those limitations be eliminated?

Solution

Eq. (1.9a) for P vs. z relies on an average temperature over the whole depth of the atmosphere. Thus, eq. (1.9a) is accurate only when the actual temperature is constant with height.

As we learned later in the chapter, a typical or "standard" atmosphere temperature is NOT constant with height. In the troposphere, for example, temperature decreases with height. On any given day, the real temperature profile is likely to be even more complicated. Thus, eq. (1.9a) is inaccurate.

A better answer could be found from the hypsometric equation (1.26b):

$$P_2 = P_1 \cdot \exp\left(-\frac{z_2 - z_1}{a \cdot \overline{T_v}}\right) \qquad \text{with } a = 29.3 \text{ m/K.}$$

By iterating up from the ground over small increments $\Delta z = z_2 - z_1$, one can use any arbitrary temperature profile. Namely, starting from the ground, set $z_1 = 0$ and $P_1 = 101.325$ kPa. Set $z_2 = 0.1$ km, and use the average virtual temperature value in the hypsometric equation for that 0.1 km thick layer from $z = 0$ to 0.1 km. Solve for P_2. Then repeat the process for the layer between $z = 0.1$ and 0.2 km, using the new T_v for that layer.

Because eq. (1.9a) came from eq. (1.26), we find other limitations.

1) Eq. (1.9a) is for **dry air**, because it uses temperature rather than virtual temperature.

2) The constant "a" in eq. (1.9a) equals = (1/29.3) K/m. Hence, on a different planet with different gravity and different gas constant, "a" would be different. Thus, eq. (1.9a) is limited to **Earth**.

Nonetheless, eq. (1.9a) is a reasonable first-order approximation to the variation of pressure with altitude, as can be seen by using standard-atmosphere P values from Table 1-5, and plotting them vs. z. The result (which was shown in the solved example after Table 1-5) is indeed close to an exponential decrease with altitude.

e. For an isothermal process, if the pressure changes to 20 kPa, what is the new T?
f. In a large, sealed, glass bottle that is full of air, if you increase the temperature, what if anything would be conserved (P, T, or ρ)?
g. In a sealed, inflated latex balloon, if you lower it in the atmosphere, what thermodynamic quantities if any, would be conserved?
h. In a mylar (non stretching) balloon, suppose that it is inflated to equal the surrounding atmospheric pressure. If you added more air to it, how would the state change?

U9(§). Starting from sea-level pressure at $z = 0$, use the hypsometric equation to find and plot P vs. z in the troposphere, using the appropriate standard-atmosphere temperature. Step in small increments to higher altitudes (lower pressures) within the troposphere, within each increment. How is your answer affected by the size of the increment? Also solve it using a constant temperature equal to the average surface value. Plot both results on a semi-log graph, and discuss meaning of the difference.

U10. Use the ideal gas law and eq. (1.9) to derive the equation for the change of density with altitude, assuming constant temperature.

U11. What is the standard atmospheric temperature, pressure, and density at each of the following geopotential heights (km)?

a. 75 b. 65 c. 55 d. 45 e. 35
f. 25 g. 15 h. 5 i. –0.5

U12. The ideal gas law and hypsometric equation are for compressible gases. For liquids (which are incompressible, to first order), density is not a function of pressure. Compare the vertical profile of pressure in a liquid of constant temperature with the profile of a gas of constant temperature.

U13. At standard sea-level pressure and temperature, how does the average molecular speed compare to the speed of sound? Also, does the speed of sound change with altitude? Why?

U14. For a standard atmosphere below $H = 11$ km:
a. Derive an equation for pressure as a function of H.
b. Derive an equation for density as a function of H.

U15. Use the hypsometric equation to derive an equation for the scale height for pressure, H_p.

Web-Enhanced Questions

These questions allow you to solve problems using current data, such as satellite images, weather maps, and weather observations that you can download through the internet. With current data, exercises can be much more exciting, timely, and relevant. Such questions are more vague than the others, because we can't guarantee that you will find a particular weather phenomenon on any given day.

Many of these questions are worded to encourage you to acquire the weather information for locations near where you live. However, the instructor might suggest a different location if a better example of a weather event is happening elsewhere. Even if the instructor does not suggest alternative locations, you should feel free to search the country, the continent, or the globe for examples of weather that are best suited for the exercise.

Web URL (universal resource locator) addresses are very transient. Web sites come and go. Even a persisting site might change its web address. For this reason, the web-enhanced questions do not usually give the URL web site for any particular exercise. Instead, you are expected to become proficient with internet search engines. Nonetheless, there still might be occasions where the data does not exist anywhere on the web. The instructor should be aware of such eventualities, and be tolerant of students who cannot complete the web exercise.

In many cases, you will want to print the weather map or satellite image to turn in with your homework. Instructors should be tolerant of students who have access to only black and white printers. If you have black and white printouts, use a colored pencil or pen to highlight the particular feature or isopleths of interest, if it is otherwise difficult to discern among all the other black lines on the printout.

You should always list the URL web address and the date you used it from which you acquired the data or images. This is just like citing books or journals from the library. At the end of each web exercise, include a "References" section listing the web addresses used, and any comments regarding the quality of the site.

ON DOING SCIENCE • Give Credit

Part of the ethic of being a good scientist or engineer is to give proper credit to the sources of ideas and data, and to avoid plagiarism. Do this by citing the author and their book, journal paper, or web address.

W1. Download a map of sea-level pressure, drawn as isobars, for your area. Become familiar with the units and symbols used on weather maps.

W2. Download from the web a map of near-surface air temperature, drawn is isotherms, for your area. Also, download a surface skin temperature map valid at the same time, and compare the temperatures.

W3. Download from the web a map of wind speeds at a height near the 200 or 300 mb (= 20 or 30 kPa) jet stream level . This wind map should have isotachs drawn on it. If you can find a map that also has wind direction or streamlines in addition to the isotachs, that is even better.

W4. Download from the web a map of humidities (e.g., relative humidities, or any other type of humidity), preferably drawn is isohumes. These are often found at low altitudes, such as for pressures of 850 or 700 mb (85 or 70 kPa).

W5. Search the web for info on the standard atmosphere. This could be in the form of tables, equations, or descriptive text. Compare this with the standard atmosphere in this textbook, to determine if the standard atmosphere has been revised.

W6. Search the web for the air-pollution regulation authority in your country (such as the EPA in the USA), and find the regulated concentrations of the most common air pollutants (CO, SO_2, O_3, NO_2, volatile organic compounds VOCs, and particulates). Compare with the results in Table 1-2, to see if the regulations have been updated in the USA, or if they are different for your country.

W7. Search the web for surface weather station observations for your area. This could either be a surface weather map with plotted station symbols, or a text table. Use the reported temperature and pressure to calculate the density.

W8. Search the web for updated information on the acceleration due to gravity, and how it varies with location on Earth.

W9. Access from the web weather maps showing thickness between two pressure surfaces. One of the most common is the 1000 - 500 mb thickness chart (i.e., the 100 - 50 kPa thickness chart). Comment on how thickness varies with temperature (the most obvious example is the general thickness decrease further away from the equator).

W10. Access from the web an upper-air sounding (e.g., Stuve, Skew-T, Tephigram, etc.) that plots temperature vs. height or pressure for a location near you. We will learn details about these charts later, but for now look at only temperature vs. height. If the sounding goes high enough (up to 100 mb or 10 kPa or so) , can you identify the troposphere, tropopause, and stratosphere.

W11. Often weather maps have isopleths of temperature (isotherm), pressure (isobar), height (contour), humidity (isohume), potential temperature (adiabat or isentrope), or wind speed (isotach). Search the web for weather maps showing other isopleths. (Hint, look for isopleth maps of precipitation, visibility, snow depth, cloudiness, etc.)

Synthesis Questions

These are "what if" questions. They are often hypothetical — on the verge of being science fiction. By thinking about "what if" questions you can gain insight about the physics of the atmosphere, because often you cannot apply existing paradigms.

"What if" questions are often asked by scientists, engineers, and policy makers. For example, "What if the amount of carbon dioxide in the atmosphere doubled, then how would world climate change?"

For many of these questions, there is not a single right answer. Different students could devise different answers that could be equally insightful, and if they are supported with reasonable arguments, should be worth full credit. Often one answer will have other implications about the physics, and will trigger a train of related ideas and arguments.

A solved example of a synthesis question is presented in the next page. This solution might not be the only correct solution, if it is correct at all.

S1. What if the meteorological angle convention is identical to that shown in Fig. 1.2, except for wind directions which are given by where they blow towards rather than where they blow from. Create a new set of conversion equations (1.1 - 1.4) for this convention, and test them with directions and speeds from all compass quadrants.

S2. Find a translation of Aristotle's *Meteorologica* in your library. Discuss one of his erroneous statements, and how the error might have been avoided if he had following the Scientific Method as later proposed by Descartes.

S3. As discussed in a solved example, the glass on the front face of CRT and old TV picture tubes is

Solved Example – A Synthesis (S) Question

What if liquid water (raindrops) in the atmosphere caused the virtual temperature to increase [rather than decrease as currently shown by the negative sign in front of r_L in eq. (1.22)]. What would be different about the weather?

Solution

More and larger raindrops would cause warmer virtual temperature. This warmer air would act more buoyant (because warm air rises). This would cause updrafts in rain clouds that might be fast enough to prevent heavy rain from reaching the ground.

But where would all this rain go? Would it accumulate at the top of thunderstorms, at the top of the troposphere? If droplets kept accumulating, they might act sufficiently warm to rise into the stratosphere. Perhaps layers of liquid water would form in the stratosphere, and would block out the sunlight from reaching the surface.

If less rain reached the ground, then there would be more droughts. Eventually all the oceans would evaporate, and life on Earth as we know it would die.

But perhaps there would be life forms (insects, birds, fish, people) in this ocean layer aloft. The reason: if liquid water increases virtual temperature, then perhaps other heavy objects (such as automobiles and people) would do the same.

In fact, this begs the question as to why liquid water would be associated with warmer virtual temperature in the first place. We know that liquid water is heavier than air, and that heavy things should sink. One way that heavy things like rain drops would not sink is if gravity worked backwards.

If gravity worked backwards, then all things would be repelled from Earth into space. This textbook would be pushed into space, as would your instructor. So you would have never been assigned this exercise in the first place.

Life is full of paradoxes. Just be careful to not get a sign wrong in any of your equations — who knows what might happen as a result.

thick in order to withstand the pressure difference across it. Why is the glass not so thick on the other parts of the picture tube, such as the narrow neck near the back of the TV?

S4. Eqs. (1.9a) and (1.13a) show how pressure and density decrease nearly exponentially with height.

a. How high is the top of the atmosphere?

b. Search the library or the web for the effective altitude for the top of the atmosphere as experienced by space vehicles re-entering the atmosphere.

S5. What is "ideal" about the ideal gas law? Are there equations of state that are not ideal?

S6. What if temperature as defined by eq. (1.5) was not dependent on the molecular weight of the gas. Speculate on how the composition of the Earth's atmosphere might have evolved differently since it was first formed.

S7. When you use a hand pump to inflate a bicycle or car tire, the pump usually gets hot near the outflow hose. Why? Since pressure in the ideal gas law is proportional to the inverse of absolute virtual temperature ($P=\rho\cdot\Re_d/T_v$), why should the tire-pump temperature warmer than ambient?

S8. In the definition of virtual temperature, why do water vapor and liquid water have opposite signs?

S9. How should equation (1.22) for virtual temperature be modified to also include the effects of airplanes and birds flying in the sky?

S10. Meteorologists often convert actual station pressures to the equivalent "sea-level pressure" by taking into account the altitude of the weather station. The hypsometric equation can be applied to this job, assuming that the average virtual temperature is known. What virtual temperature should be used below ground to do this? What are the limitations of the result?

S11. Starting with our Earth and atmosphere as at present, what if gravity were to become zero. What would happen to the atmosphere? Why?

S12. Suppose that gravitational attraction between two objects becomes greater, not smaller, as the distance between the two objects becomes greater.

a. Would the relationship between geometric altitude and geopotential altitude change? If so, what is the new relationship?

b. How would the vertical pressure gradient in the atmosphere be different, if at all?

c. Would the orbit of the Earth around the sun be affected? How?

Copyright © 2011, 2015 by Roland Stull. *Meteorology for Scientists and Engineers, 3rd Ed.*

RADIATION

CONTENTS

Orbital Factors 27
- Planetary Orbits 27
- Orbit of the Earth 27
- Seasonal Effects 30
- Daily Effects 32
- Sunrise, Sunset & Twilight 33

Flux 34

Radiation principles 36
- Propagation 36
- Emission 36
- Distribution 39
- Average Daily Insolation 40
- Absorption, Reflection & Transmission 41
- Beer's Law 43

Surface Radiation Budget 44
- Solar 44
- Longwave (IR) 45
- Net Radiation 45

Actinometers 45

Summary 47
- Threads 47

Exercises 47
- Numerical Problems 47
- Understanding & Critical Evaluation 49
- Web-Enhanced Questions 51
- Synthesis Questions 51

"Meteorology for Scientists and Engineers, 3rd Edition" by Roland Stull is licensed under a Creative Commons Attribution-NonCommercial-ShareAlike 4.0 International License. To view a copy of the license, visit http://creativecommons.org/licenses/by-nc-sa/4.0/ . This work is available at http://www.eos.ubc.ca/books/Practical_Meteorology/ .

2 Solar energy powers the atmosphere. This energy warms the air and drives the air motion you feel as winds. The seasonal distribution of this energy depends on the orbital characteristics of the Earth around the sun.

The Earth's rotation about its axis causes a daily cycle of sunrise, increasing solar radiation until solar noon, then decreasing solar radiation, and finally sunset. Some of this solar radiation is absorbed at the Earth's surface, and provides the energy for photosynthesis and life.

Downward **infrared** (IR) radiation from the atmosphere to the Earth is usually slightly less than upward IR radiation from the Earth, causing net cooling at the Earth's surface both day and night. The combination of daytime solar heating and continuous IR cooling yields a **diurnal** (daily) cycle of **net radiation**.

ORBITAL FACTORS

Planetary Orbits

Johannes Kepler, the 17th century astronomer, discovered that planets in the solar system have elliptical orbits around the sun. For most planets in the solar system, the eccentricity (deviation from circular) is relatively small, meaning the orbits are nearly circular. For circular orbits, he also found that the time period Y of each orbit is related to the distance R of the planet from the sun by:

$$Y = a_1 \cdot R^{3/2} \tag{2.1}$$

Parameter $a_1 \approx 0.1996$ d·(Gm)$^{-3/2}$, where d is Earth days, and Gm is gigameters = 10^6 km.

Figs. 2.1a & b show the orbital periods vs. distances for the planets in our solar system. These figures show the duration of a year for each planet, which affect the seasons experienced on the planet.

Orbit of the Earth

The Earth and the moon rotate with a **sidereal** (relative to the stars) period of 27.32 days around their common center of gravity, called the Earth-moon **barycenter**. (Relative to the moving Earth,

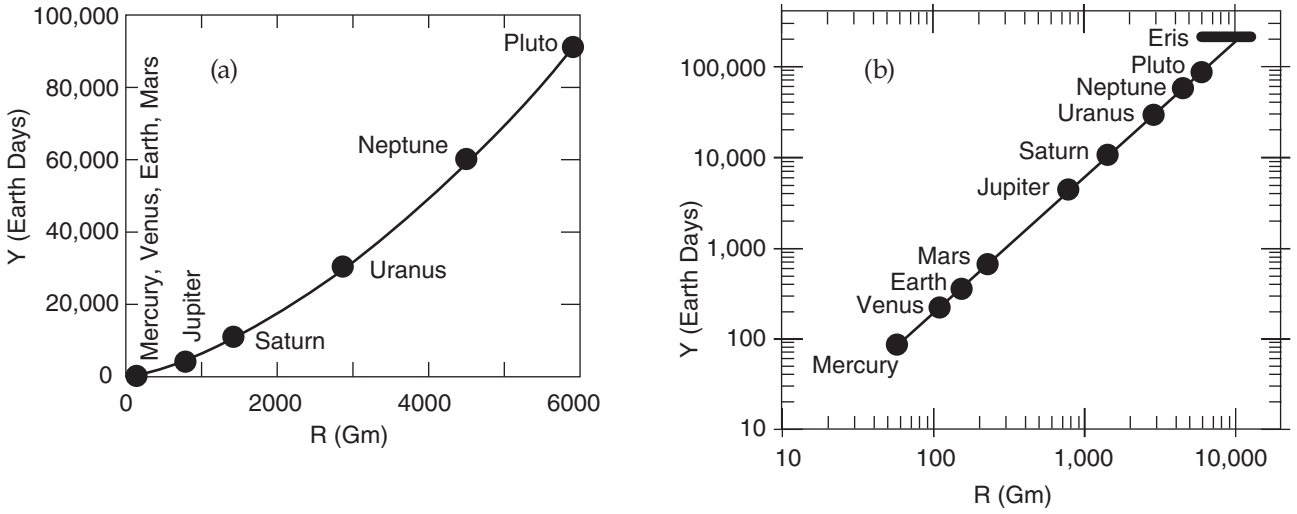

Figure 2.1 a (linear) & b (log-log)
Planetary orbital periods versus distance from sun. Eris (136199) and Pluto (134340) are dwarf planets. Eris, larger than Pluto, has a very elliptical orbit. (a) Linear graph. (b) Log-log graph. (See Appendix A for comparison of various graph formats.)

Solved Example

Verify that eq. (2.1) gives the correct orbital period of one Earth year.

Solution:
Given: R = 149.6 Gm avg. distance sun to Earth.
Find: Y = ? days, the orbital period for Earth

Use eq. (2.1):
$Y = (0.1996\ \text{d}\cdot(\text{Gm})^{-3/2}) \cdot [(149.6\ \text{Gm})^{1.5}]$
= **365.2 days**.

Check: Units OK. Sketch OK. Almost 1 yr.
Discussion: In 365.0 days, the Earth does not quite finish a complete orbit. After four years this shortfall accumulates to nearly a day, which we correct using a leap year with an extra day (see Chapter 1).

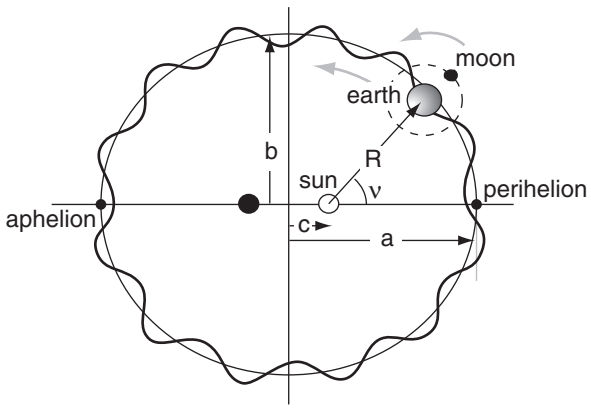

Figure 2.2
Geometry of the Earth's orbit, as viewed from above Earth's North Pole. (Not to scale.) Dark wavy line traces the Earth-center path, while the thin smooth ellipse traces the barycenter path.

the time between new moons is 29.5 days.) Because the mass of the moon ($7.35\text{x}10^{22}$ kg) is only 1.23% of the mass of the Earth (Earth mass is $5.9742\text{x}10^{24}$ kg), the barycenter is much closer to the center of the Earth than to the center of the moon. This barycenter is 4671 km from the center of the Earth, which is below the Earth's surface (Earth radius is 6371 km).

To a first approximation, the Earth-moon barycenter orbits around the sun in an **elliptical** orbit (Fig. 2.2, thin-line ellipse) with sidereal period of P = 365.256363 days. Length of the **semi-major axis** (half of the longest axis) of the ellipse is a = 149.457 Gm, which is the definition of one **astronomical unit** (au).

Semi-minor axis (half the shortest axis) length is b = 149.090 Gm. The center of the sun is at one of the foci of the ellipse, and half the distance between the two foci is c = 2.5 Gm, where $a^2 = b^2 + c^2$. The orbit is close to circular, with an **eccentricity** of only about $e \approx c/a = 0.0167$ (a circle has zero eccentricity).

The closest distance (**perihelion**) along the major axis between the Earth and sun is $a - c$ = 146.96 Gm and occurs at about $d_p \approx$ 4 January. The farthest distance (**aphelion**) is $a + c$ = 151.96 Gm and occurs at about 5 July. The dates for the perihelion and aphelion jump a day or two from year to year because the orbital period is not exactly 365 days. Figs. 2.3 show these dates at the **prime meridian** (Greenwich), but the dates will be slightly different in your own time zone. Also, the dates of the perihelion and aphelion gradually become later by 1 day every 58 years, due to **precession** (shifting of the location of the major and minor axes) of the Earth's orbit around the sun (see the Climate chapter).

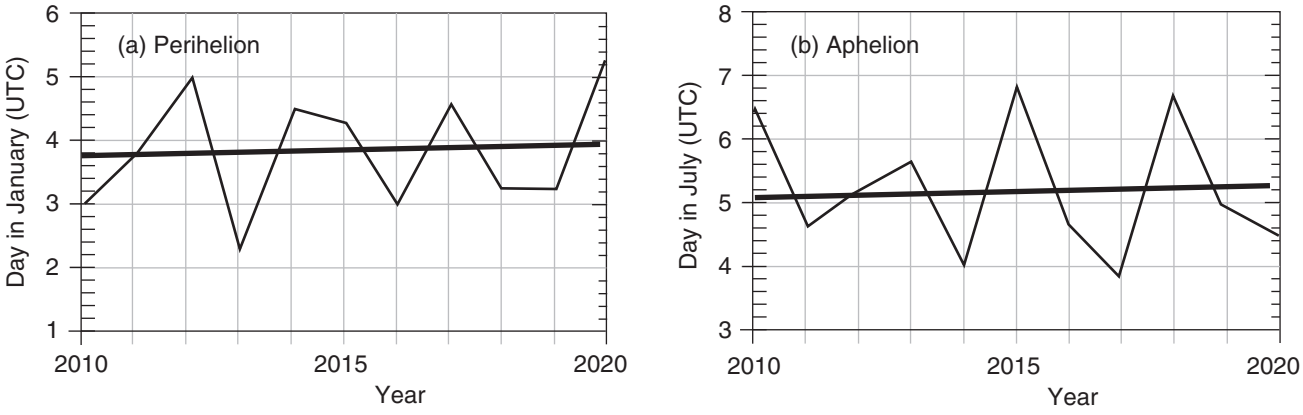

Figure 2.3
Dates of the (a) perihelion and (b) aphelion, & their trends (thick line).

Because the Earth is rotating around the Earth-moon barycenter while this barycenter is revolving around the sun, the location of the center of the Earth traces a slightly wiggly path as it orbits the sun. This path is exaggerated in Fig. 2.2 (thick line).

Define a relative **Julian Day**, d, as the day of the year. For example, 15 January corresponds to d = 15. For 5 February, d = 36 (which includes 31 days in January plus 5 days in February).

The angle at the sun between the perihelion and the location of the Earth (actually to the Earth-moon barycenter) is called the **true anomaly** ν (see Fig. 2.2). This angle increases during the year as the day d increases from the perihelion day (about d_p = 4; namely, about 4 January). According to **Kepler's second law**, the angle increases more slowly when the Earth is further from the sun, such that a line connecting the Earth and the sun will sweep out equal areas in equal time intervals.

An angle called the **mean anomaly** M is a simple, but good approximation to ν. It is defined by:

$$M = C \cdot \frac{d - d_p}{P} \qquad (2.2)$$

where P = 365.256363 days is the (sidereal) orbital period and C is the angle of a full circle ($C = 2\cdot\pi$ radians = 360°. Use whichever is appropriate for your calculator, spreadsheet, or computer program.)

Because the Earth's orbit is nearly circular, $\nu \approx M$. A better approximation to the **true anomaly** for the elliptical Earth orbit is

$$\nu \approx M + [2e - (e^3/4)]\cdot\sin(M) + [(5/4)\cdot e^2]\cdot\sin(2M) + [(13/12)\cdot e^3]\cdot\sin(3M) \qquad (2.3a)$$

or

$$\nu \approx M + 0.0333988\cdot\sin(M) + 0.0003486\cdot\sin(2\cdot M) + 0.0000050\cdot\sin(3\cdot M) \qquad (2.3b)$$

for both ν and M in radians, and e = 0.0167.

Solved Example(§)

Use a spreadsheet to find the true anomaly and sun-Earth distance for several days during the year.

Solution

Given: d_p = 4 Jan. P = 365.25 days.
Find: ν = ?° and R = ? Gm.

Sketch: (same as Fig 2.2)
For example, for 15 Feb, d = 46
Use eq. (2.2):
$M = (2 \cdot 3.14159)\cdot(46-4)/\ 365.256363 =$ **0.722 radians**
Use eq. (2.3b):
$\nu = 0.722 + 0.0333988\cdot\sin(0.722) + 0.0003486\cdot\sin(1.444) + 0.000005\cdot\sin(2.166) =$ **0.745 radians**
Use eq. (2.4):
$R = (149.457\text{Gm})\cdot(1 - 0.0167^2)/[1+0.0167\cdot\cos(0.745)]$
$= (149.457\text{Gm}) \cdot 0.99972 \ / \ 1.012527 =$ **147.60 Gm**

Repeating this calculation on a spreadsheet for several days, and comparing M vs. ν and R(M) vs. R(ν) , gives:

Date	d	M (rad)	ν (rad)	R(M) (Gm)	R(ν) (Gm)
4 Jan	4	0	0	146.96	146.96
18 Jan	18	0.241	0.249	147.03	147.04
1 Feb	32	0.482	0.497	147.24	147.25
15 Feb	46	0.722	0.745	147.57	147.60
1 Mar	60	0.963	0.991	148.00	148.06
15 Mar	74	1.204	1.236	148.53	148.60
29 Mar	88	1.445	1.487	149.10	149.18
12 Apr	102	1.686	1.719	149.70	149.78
26 Apr	116	1.927	1.958	150.29	150.36
21 Jun	172	2.890	2.898	151.87	151.88
23 Sep	266	4.507	4.474	149.93	150.01
22 Dec	356	6.055	6.047	147.02	147.03

Check: Units OK. Physics OK.
Discussion: Because M and ν are nearly equal, you can use M instead of ν in eq. (2.4), with good accuracy.

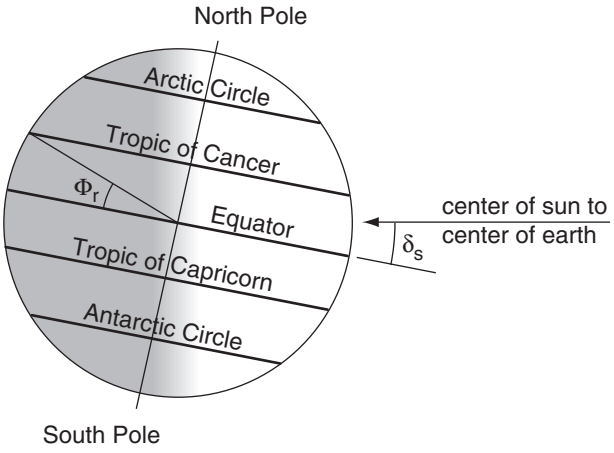

Figure 2.4
Relationship of declination angle δ_s to tilt of the Earth's axis, for a day near northern-hemisphere summer.

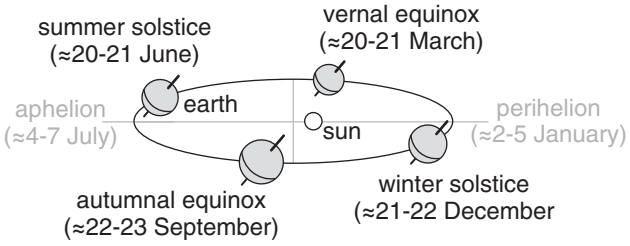

Figure 2.5
Dates (UTC) of northern-hemisphere seasons relative to Earth's orbit.

Table 2-1 . Dates and times (UTC) for northern hemisphere equinoxes and solstices. Format: dd hhmm gives day (dd), hour (hh) and minutes (mm). *From the US Naval Observatory. http://aa.usno.navy.mil/data/docs/EarthSeasons.html*

Year	Spring Equinox (March)	Summer Solstice (June)	Fall Equinox (Sept.)	Winter Solstice (Dec.)
2010	20 1732	21 1128	23 0309	21 2338
2011	20 2321	21 1716	23 0904	22 0530
2012	20 0514	20 2309	22 1449	21 1111
2013	20 1102	21 0504	22 2044	21 1711
2014	20 1657	21 1051	23 0229	21 2303
2015	20 2245	21 1638	23 0820	22 0448
2016	20 0430	20 2234	22 1421	21 1044
2017	20 1028	21 0424	22 2002	21 1628
2018	20 1615	21 1007	23 0154	21 2222
2019	20 2158	21 1554	23 0750	22 0419
2020	20 0349	20 2143	22 1330	21 1002

The distance R between the sun and Earth (actually to the Earth-moon barycenter) as a function of time is

$$R = a \cdot \frac{1 - e^2}{1 + e \cdot \cos(\nu)} \tag{2.4}$$

where e = 0.0167 is eccentricity, and a = 149.457 Gm is the semi-major axis length. If the simple approximation of $\nu \approx M$ is used, then angle errors are less than 2° and distance errors are less than 0.06%.

Seasonal Effects

The tilt of the Earth's axis relative to a line perpendicular to the **ecliptic** (i.e., the orbital plane of the Earth around the sun) is presently Φ_r = 23.44° = 0.409 radians. The direction of tilt of the Earth's axis is not fixed relative to the stars, but wobbles or precesses like a top with a period of about 25,781 years. Although this is important over millennia (see the Climate chapter), for shorter time intervals (up to a century) the precession is negligible, and you can assume a fixed tilt.

The **solar declination angle** δ_s is defined as the angle between the ecliptic and the plane of the Earth's equator (Fig. 2.4). Assuming a fixed orientation (tilt) of the Earth's axis as the Earth orbits the sun, the solar declination angle varies smoothly as the year progresses. The north pole points partially toward the sun in summer, and gradually changes to point partially away during winter (Fig. 2.5).

Although the Earth is slightly closer to the sun in winter (near the perihelion) and receives slightly more solar radiation then, the Northern Hemisphere receives substantially less sunlight in winter because of the tilt of the Earth's axis. Thus, summers are warmer than winters, due to Earth-axis tilt.

The solar declination angle is greatest (+23.44°) on about 20 to 21 June (**summer solstice** in the Northern Hemisphere, when daytime is longest) and is most negative (–23.44°) on about 21 to 22 December

(**winter solstice**, when nighttime is longest). The **vernal equinox** (or **spring equinox**, near 20 to 21 March) and **autumnal equinox** (or **fall equinox**, near 22 to 23 September) are the dates when daylight hours equal nighttime hours ("eqi nox" literally translates to "equal night"), and the solar declination angle is zero.

Astronomers define a **tropical year** (= 365.242190 days) as the time from vernal equinox to the next vernal equinox. Because the tropical year is not an integral number of days, the **Gregorian calendar** (the calendar adopted by much of the western world) must be corrected periodically to prevent the seasons (dates of summer solstice, etc.) from shifting into different months.

To make this correction, a **leap day** (29 Feb) is added every 4th year (i.e., **leap years**, are years divisible by 4), except that years divisible by 100 don't have a leap day. However, years divisible by 400 do have a leap day (for example, year 2000). Because of all these factors, the dates of the solstices, equinoxes, perihelion, and aphelion jump around a few days on the Gregorian calendar (Table 2-1 and Figs. 2.3), but remain in their assigned months.

The solar declination angle for any day of the year is given by

$$\delta_s \approx \Phi_r \cdot \cos\left[\frac{C\cdot(d-d_r)}{d_y}\right] \qquad \bullet(2.5)$$

where d is Julian day, and d_r is the Julian day of the summer solstice, and d_y = 365 (or = 366 on a leap year) is the number of days per year. For years when the summer solstice is on 21 June, d_r = 172. This equation is only approximate, because it assumes the Earth's orbit is circular rather than elliptical. As before, $C = 2\cdot\pi$ radians = 360° (use radians or degrees depending on what your calculator, spreadsheet, or computer program expects).

By definition, Earth-tilt angle (Φ_r = 23.44°) equals the latitude of the **Tropic of Cancer** in the Northern Hemisphere (Fig. 2.4). Latitudes are defined to be positive in the Northern Hemisphere. The **Tropic of Capricorn** in the Southern Hemisphere is the same angle, but with a negative sign. The **Arctic Circle** is at latitude $90° - \Phi_r$ = 66.56°, and the **Antarctic Circle** is at latitude −66.56° (i.e., 66.56°S). During the Northern-Hemisphere summer solstice: the solar declination angle equals Φ_r ; the sun at noon is directly overhead (90° elevation angle) at the Tropic of Cancer; and the sun never sets that day at the Arctic Circle.

Science Graffito

A weather forecast that appeared for northern Yukon Territory (north of the Arctic Circle), Canada, during mid summer:

"Sunny today, sunny tonight, sunny tomorrow."

Solved Example

Find the solar declination angle on 5 March.

Solution

Assume: Not a leap year.
Given: d = 31 Jan + 28 Feb + 5 Mar = 64.
Find: δ_s = ?°
Sketch:

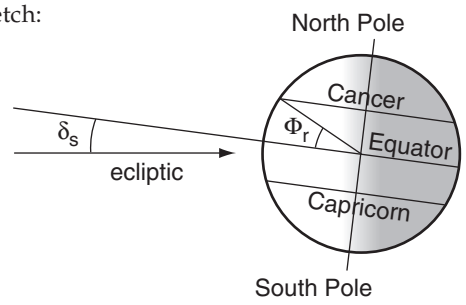

Use eq. (2.5):

δ_s = 23.44° · cos[360°·(64–172)/365]

= 23.44° · cos[–106.521°] = **–6.67°**

Check: Units OK. Sketch OK. Physics OK.
Discussion: On the **vernal equinox** (21 March), the angle should be zero. Before that date, it is winter and the declination angle should be negative. Namely, the ecliptic is below the plane of the equator. In spring and summer, the angle is positive. Because 5 March is near the end of winter, we expect the answer to be a small negative angle.

Solved Example

Find the local elevation angle of the sun at 3 PM local time on 5 March in Vancouver, Canada.

Solution

Assume: Not a leap year. Not daylight savings time.
Also, Vancouver is in the Pacific time zone, where $t_{UTC} = t + 8$ h during standard time.
Given: t = 3 PM = 15 h. Thus, t_{UTC} = 23 h.
ϕ = 49.25°N, λ_e = 123.1°W for Vancouver.
δ_s = –7.05° from previous solved example.
Find: Ψ = ?°

Use eq. (2.6): $\sin(\Psi)$ =
= $\sin(49.25°)\cdot\sin(-7.05°)$ –
$\cos(49.25°)\cdot\cos(-7.05°)\cdot\cos[360°\cdot(23h/24h) - 123.1°]$
= $0.7576 \cdot (-0.1227) - 0.6527 \cdot 0.9924 \cdot \cos(221.9°)$
= $-0.09296 + 0.4821 = 0.3891$
$\Psi = \arcsin(0.3891) =$ **22.90°**

Check: Units OK. Physics OK.
Discussion: The sun is above the local horizon, as expected for mid afternoon.
Beware of other situations such as night that give negative elevation angle.

Daily Effects

As the Earth rotates about its axis, the **local elevation angle** Ψ of the sun above the local horizon rises and falls. This angle depends on the latitude ϕ and longitude λ_e of the location:

$$\sin(\Psi) = \sin(\phi)\cdot\sin(\delta_s) - \cos(\phi)\cdot\cos(\delta_s)\cdot\cos\left[\frac{C\cdot t_{UTC}}{t_d} - \lambda_e\right] \quad \bullet(2.6)$$

Time of day t_{UTC} is in UTC, $C = 2\pi$ radians = 360° as before, and the length of the day is t_d. For t_{UTC} in hours, then t_d = 24 h. Latitudes are positive north of the equator, and longitudes are positive west of the prime meridian. The $\sin(\Psi)$ relationship is used later in this chapter to calculate the daily cycle of solar energy reaching any point on Earth.
[CAUTION: Don't forget to convert angles to radians if required by your spreadsheet or programming language.]

Solved Example(§)

Use a spreadsheet to plot elevation angle vs. time at Vancouver, for 22 Dec, 23 Mar, and 22 Jun. Plot these three curves on the same graph.

Solution

Given: Same as previous solved example, except d = 355, 82, 173.
Find: Ψ = ?°

A portion of the tabulated results are shown below, as well as the full graph.

	Ψ (°)		
t (h)	22 Dec	23 Mar	22 Jun
3	0.0	0.0	0.0
4	0.0	0.0	0.0
5	0.0	0.0	6.6
6	0.0	0.0	15.6
7	0.0	7.8	25.1
8	0.0	17.3	34.9
9	5.7	25.9	44.5
10	11.5	33.2	53.4
11	15.5	38.4	60.5
12	17.2	40.8	64.1
13	16.5	39.8	62.6

(continues in next column)

Solved Example *(continuation)*

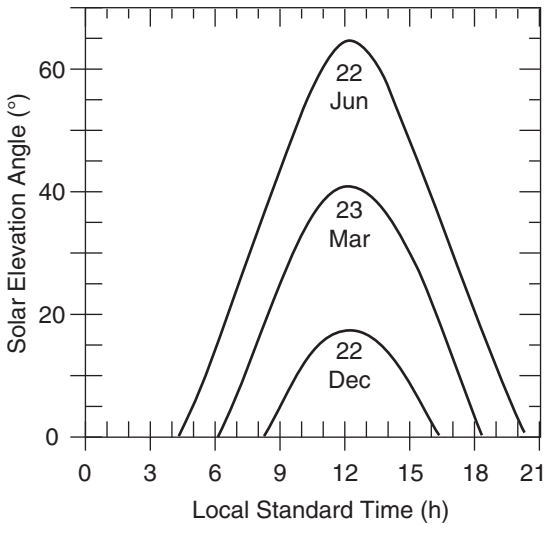

Check: Units OK. Physics OK. Graph OK.
Discussion: Summers are pleasant with long days. The peak elevation does not happen precisely at local noon, because Vancouver is not centered within its time zone.

The local **azimuth angle** α of the sun relative to north is

$$\cos(\alpha) = \frac{\sin(\delta_s) - \sin(\phi)\cdot\cos(\zeta)}{\cos(\phi)\cdot\sin(\zeta)} \qquad (2.7)$$

where $\zeta = C/4 - \Psi$ is the **zenith angle**. After noon, the azimuth angle might need to be corrected to be $\alpha = C - \alpha$, so that the sun sets in the west instead of the east. Fig. 2.6 shows an example of the elevation and azimuth angles for Vancouver (latitude = 49.25°N, longitude = 123.1°W) during the solstices and equinoxes.

Sunrise, Sunset & Twilight

Geometric sunrise and sunset occur when the center of the sun has zero elevation angle. **Apparent sunrise/set** are defined as when the top of the sun crosses the horizon, as viewed by an observer on the surface. The sun has a finite radius corresponding to an angle of 0.267° when viewed from Earth. Also, **refraction** (bending) of light through the atmosphere allows the top of the sun to be seen even when it is really 0.567° below the horizon. Thus, apparent sunrise/set occurs when the center of the sun has an elevation angle of –0.833°.

When the apparent top of the sun is slightly below the horizon, the surface of the Earth is not receiving direct sunlight. However, the surface can still receive indirect light scattered from air molecules higher in the atmosphere that are illuminated by the sun. The interval during which scattered light is present at the surface is called **twilight**. Because twilight gradually fades as the sun moves lower below the horizon, there is no precise definition of the start of sunrise twilight or the end of sunset twilight.

Arbitrary definitions have been adopted by different organizations to define twilight. **Civil twilight** occurs while the sun center is no lower than –6°, and is based on the ability of humans to see objects on the ground. **Military twilight** occurs while the sun is no lower than –12°. **Astronomical twilight** ends when the skylight becomes sufficiently dark to view certain stars, at solar elevation angle –18°.

Table 2-2 summarizes the solar elevation angle Ψ definitions used for sunrise, sunset and twilight. All of these angles are at or below the horizon.

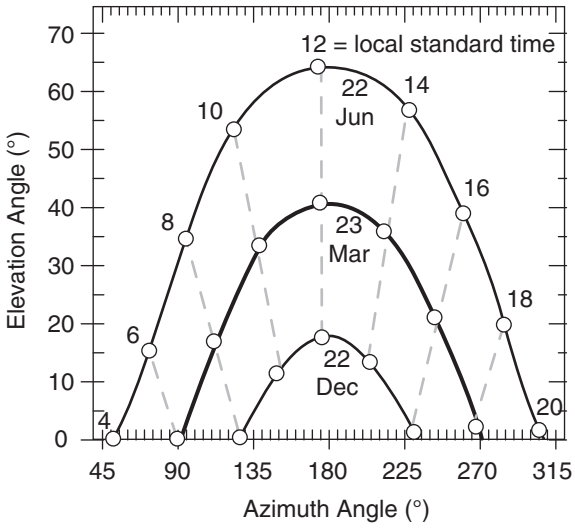

Figure 2.6
Position (solid lines) of the sun for Vancouver, Canada for various seasons. September 21 and March 23 nearly coincide. Isochrones are dashed. All times are Pacific standard time.

Solved Example(§)

Use a spreadsheet to find the Pacific standard time (PST) for all the events of Table 2-2, for Vancouver, Canada, during 22 Dec, 23 Mar, and 22 Jun.

Solution

Given: Julian dates 355, 82, & 173.
Find: t = ? h (local standard time)
Assume: Pacific time zone: $t_{UTC} = t + 8$ h.

Use eq. (2.8a) and Table 2-2:

	22Dec	23Mar	22Jun
Morning:		PST (h)	
geometric sunrise	8.22	6.20	4.19
apparent sunrise	8.11	6.11	4.09
civil twilight starts	7.49	5.58	3.36
military twilight starts	6.80	4.96	2.32
astron. twilight starts	6.16	4.31	n/a
Evening:			
geometric sunset	16.19	18.21	20.22
apparent sunset	16.30	18.30	20.33
civil twilight ends	16.93	18.83	21.05
military twilight ends	17.61	19.45	22.09
astron. twilight ends	18.26	20.10	n/a

Check: Units OK. Physics OK.
Discussion: During the summer solstice (22 June), the sun never gets below –18°. Hence, it is astronomical twilight all night in Vancouver in mid summer.

During June, Vancouver is on daylight time, so the actual local time would be one hour later.

Table 2-2. Elevation angles for diurnal events.

Event	Ψ (°)	Ψ (radians)
Sunrise & Sunset:		
Geometric	0	0
Apparent	–0.833	–0.01454
Twilight:		
Civil	–6	–0.10472
Military	–12	–0.20944
Astronomical	–18	–0.31416

FOCUS • Astronomical Values for Time

The constants $a = 2{\cdot}e/\omega_E$, $b = [\tan^2(\varepsilon/2)]/\omega_E$, and $c = 2{\cdot}\varpi$ in the Equation of Time are based on the following astronomical values: $\omega_E = 2\pi/24\text{h} = 0.0043633$ radians/minute is Earth's rotation rate about its axis, $e = 0.01671$ is the eccentricity of Earth's orbit around the sun, $\varepsilon = 0.40909$ radians = 23.439° is the obliquity (tilt of Earth's axis), $\varpi = 4.9358$ radians = 282.8° is the angle (in the direction of Earth's orbit around the sun) between a line from the sun to the vernal (Spring) equinox and a line drawn from the sun to the moving perihelion (see Fig. 2.5, and Fig. 21.10 in Chapter 21).

Solved Example (§)

Plot time correction vs. day of the year.

Solution:
Given: $d = 0$ to 365
Find: Δt_a = ? minutes

Use a spreadsheet. For example, for $d = 45$ (which is 14 Feb), first use eq. (2.2) find the mean anomaly:

$M = 2\pi{\cdot}(45\text{-}4)/365.25 = 0.705$ rad = 40.4°

Then use the **Equation of Time** (2.8b) in

$\Delta t_a = -(7.659\text{ min}){\cdot}\sin(0.705\text{ rad})$
$+ (9.836\text{ min}){\cdot}\sin(2{\cdot}\ 0.705\text{ rad} + 3.588\text{ rad})$

$\Delta t_a = -4.96 - 9.46 =$ **–14.4 minutes**

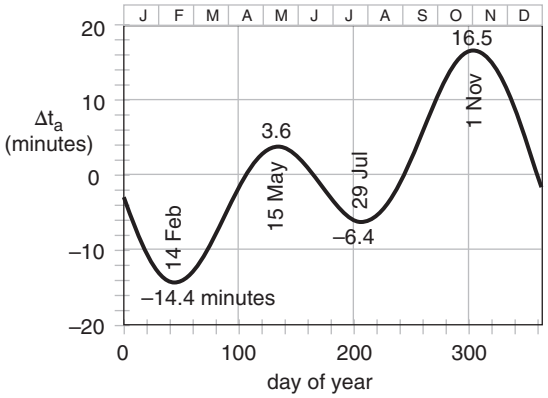

Check: Units OK. Magnitude OK.

Discussion: Because of the negative sign in eq. (2.8c), you need to **ADD** 14.4 minutes to the results of eq. (2.8a) to get the correct sunrise and sunset times.

Approximate (sundial) time-of-day corresponding to these events can be found by rearranging eq. (2.6):

$$t_{UTC} = \frac{t_d}{C}\cdot\left\{\lambda_e \pm \arccos\left[\frac{\sin\phi\cdot\sin\delta_s - \sin\Psi}{\cos\phi\cdot\cos\delta_s}\right]\right\} \qquad (2.8a)$$

where the appropriate elevation angle is used from Table 2-2. Where the ± sign appears, use + for sunrise and – for sunset. If any of the answers are negative, add 24 h to the result.

To correct the time for the tilted, elliptical orbit of the earth, use the approximate **Equation of Time**:

$$\Delta t_a \approx -a\cdot\sin(M) + b\cdot\sin(2M + c) \qquad (2.8b)$$

where $a = 7.659$ minutes, $b = 9.863$ minutes, $c = 3.588$ radians = 205.58°, and where the mean anomaly M from eq. (2.2) varies with day of the year. This time correction is plotted in the solved example. The corrected (mechanical-clock) time t_{eUTC} is:

$$t_{eUTC} = t_{UTC} - \Delta t_a \qquad (2.8c)$$

which corrects sundial time to mechanical-clock time. Don't forget to convert the answer from UTC to your local time zone.

FLUX

A **flux density**, $\mathbb{F}$, called a **flux** in this book, is the transfer of a quantity per unit area per unit time. The area is taken perpendicular (normal) to the direction of flux movement. Examples with metric (SI) units are mass flux (kg·m^{-2}·s^{-1}) and heat flux, (J·m^{-2}·s^{-1}). Using the definition of a watt (1 W = 1 J·s^{-1}), the heat flux can also be given in units of (W·m^{-2}). A flux is a measure of the amount of inflow or outflow such as through the side of a fixed volume, and thus is frequently used in Eulerian frameworks (Fig. 2.7).

Because flow is associated with a direction, so is flux associated with a direction. You must account for fluxes $\mathbb{F}_x$, $\mathbb{F}_y$, and $\mathbb{F}_z$ in the x, y, and z directions, respectively. A flux in the positive x-direction (eastward) is written with a positive value of $\mathbb{F}_x$, while a flux towards the opposite direction (westward) is negative.

The total amount of heat or mass flowing through a plane of area A during time interval Δt is given by:

$$Amount = \mathbb{F}\cdot A\cdot\Delta t \qquad (2.9)$$

For heat, $Amount \equiv \Delta Q_H$ by definition.

Fluxes are sometimes written in **kinematic form**, F, by dividing by the air density, ρ_{air} :

$$F = \frac{\mathbb{F}}{\rho_{air}} \qquad (2.10)$$

Kinematic mass flux equals the wind speed, M. Kinematic fluxes can also be in the 3 Cartesian directions: F_x, F_y, and F_z.

[CAUTION: Do not confuse the usage of the symbol M. Here it means "wind speed". Earlier it meant "mean anomaly". Throughout this book, many symbols will be re-used to represent different things, due to the limited number of symbols. Even if a symbol is not defined, you can usually determine its meaning from context.]

Heat fluxes $\mathbb{F}_H$ can be put into kinematic form by dividing by both air density ρ_{air} and the specific heat for air C_p, which yields a quantity having the same units as temperature times wind speed (K·m·s^{-1}).

$$F_H = \frac{\mathbb{F}_H}{\rho_{air} \cdot C_p} \qquad \text{for heat only} \qquad (2.11)$$

For dry air (subscript "$_d$") at sea level:

$$\rho_{air} \cdot C_{pd} = 1231\ (\text{W·m}^{-2}) \,/\, (\text{K·m·s}^{-1})$$

$$= 12.31\ \text{mb·K}^{-1}$$

$$= 1.231\ \text{kPa·K}^{-1}\ .$$

The reason for sometimes expressing fluxes in kinematic form is that the result is given in terms of easily measured quantities. For example, while most people do not have "Watt" meters to measure the normal "dynamic" heat flux, they do have thermometers and anemometers. The resulting temperature times wind speed has units of a kinematic heat flux (K·m·s^{-1}). Similarly, for mass flux it is easier to measure wind speed than kilograms of air per area per time.

Heat fluxes can be caused by a variety of processes. **Radiative fluxes** are radiant energy (electromagnetic waves or photons) per unit area per unit time. This flux can travel through a vacuum. **Advective flux** is caused by wind blowing through an area, and carrying with it warmer or colder temperatures. For example a warm wind blowing toward the east causes a positive heat-flux component F_{Hx} in the x-direction. A cold wind blowing toward the west also gives positive F_{Hx}. **Turbulent fluxes** are caused by eddy motions in the air, while **conductive fluxes** are caused by molecules bouncing into each other.

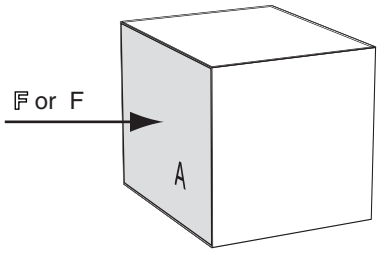

Figure 2.7
Flux F through an area A into one side of a volume.

Solved Example

The mass flux of air is 1 kg·m^{-2}·s^{-1} through a door opening that is 1 m wide by 2.5 m tall. What amount of mass of air passes through the door each minute, and what is the value of kinematic mass flux?

Solution

Given: area A = (1 m) · (2.5 m) = 2.5 m^2
$\mathbb{F}$ = 1 kg·m^{-2}·s^{-1}
Find: (a) Amount = ? kg, and (b) F = ? m·s^{-1}
Sketch: (see Fig. 2.7)

(a) Use eq. (2.9):
Amount = (1 kg·m^{-2}·s^{-1})·(2.5 m^2)·
(1 min)·(60 s/min) = **<u>150 kg</u>**.

(b) Assume: ρ = 1.225 kg·m^{-3} at sea-level
Use eq. (2.10):
F = (1 kg·m^{-2}·s^{-1}) / (1.225 kg·m^{-3})
= **<u>0.82 m·s</u>**$^{-1}$.

Check: Units OK. Sketch OK. Physics OK.
Discussion: The kinematic flux is equivalent to a very light wind speed of less than 1 m/s blowing through the doorway, yet it transports quite a large amount of mass each minute.

Solved Example

If the heat flux from the sun that reaches the Earth's surface is 600 W/m^2, find the flux in kinematic units.

Solution:

Given: $\mathbb{F}_H$ = 600 W/m^2
Find: F_H = ? K·m/s
Assume: sea level.

Use eq. (2.11)
F_H = (600 W/m^2) / [1231 (W·m^{-2}) / (K·m·s^{-1})]
= 0.487 K·m/s

Check: Units OK. Physics OK.
Discussion: This amount of radiative heat flux is equivalent to an advective flux of a 1 m/s wind blowing air with temperature excess of about 0.5°C.

Solved Example

Red light has a wavelength of 0.7 μm. Find its frequency, circular frequency, and wavenumber in a vacuum.

Solution

Given: c_o = 299,792,458 m/s, λ = 0.7 μm
Find: ν = ? Hz, ω = ? s^{-1}, σ = ? m^{-1}.

Use eq. (2.12), solving for ν:
$\nu = c_o/\lambda = (3x10^8 \text{ m/s}) / (0.7x10^{-6} \text{ m/cycle})$
$= \underline{\mathbf{4.28x10}}^{14} \underline{\mathbf{Hz}}$.

$\omega = 2\pi\cdot\nu = 2\cdot(3.14159)\cdot(4.28x10^{14} \text{ Hz})$
$= \underline{\mathbf{2.69x10}}^{15} \text{ s}^{-1}$.

$\sigma = 1/\lambda = 1 / (0.7x10^{-6} \text{ m/cycle})$
$= \underline{\mathbf{1.43x10}}^{6} \text{ m}^{-1}$.

Check: Units OK. Physics reasonable.
Discussion: Wavelength, wavenumber, frequency, and circular frequency are all equivalent ways to express the "color" of radiation.

Solved Example

Find the blackbody monochromatic radiant exitance of green light of wavelength 0.53 μm from an object of temperature 3000 K.

Solution

Given: λ = 0.53 μm, T = 3000 K
Find: E_λ^* = ? $W\cdot m^{-2}\cdot \mu m^{-1}$.

Use eq. (2.13):

$$E_\lambda^* = \frac{c_1}{\lambda^5 \cdot \left[\exp(c_2/(\lambda\cdot T)) - 1\right]}$$

$$E_\lambda^* = \frac{(3.74x10^8 \text{ W}\cdot\text{m}^{-2}\cdot\mu\text{m}^4)/(0.53\mu\text{m})^5}{\exp\left[(1.44x10^4 \text{ K}\cdot\mu\text{m})/(0.53\mu\text{m}\cdot 3000\text{K})\right] - 1}$$

$= \underline{\mathbf{1.04 \text{ x } 10}}^{6} \text{ W}\cdot\text{m}^{-2}\cdot\mu\text{m}^{-1}$

Check: Units OK. Physics reasonable.
Discussion: Because 3000 K is cooler than the sun, about 50 times less green light is emitted. The answer is the watts emitted from each square meter of surface per μm wavelength increment.

RADIATION PRINCIPLES

Propagation

Radiation can be modeled as electromagnetic waves or as photons. Radiation propagates through a vacuum at a constant speed: c_o = 299,792,458 $m\cdot s^{-1}$. For practical purposes, you can approximate this **speed of light** as $c_o \approx 3x10^8 \text{ m}\cdot\text{s}^{-1}$. Light travels slightly slower through air, at roughly c = 299,710,000 $m\cdot s^{-1}$ at standard sea-level pressure and temperature, but the speed varies slightly with thermodynamic state of the air (see the Optics chapter).

Using the wave model of radiation, the **wavelength** λ ($m\cdot cycle^{-1}$) is related to the **frequency**, ν (Hz = $cycles\cdot s^{-1}$) by:

$$\lambda\cdot\nu = c_o \qquad (2.12)$$

Wavelength units are sometimes abbreviated as (m). Because the wavelengths of light are so short, they are often expressed in units of micrometers (μm).

Wavenumber is the number of waves per meter: σ ($cycles\cdot m^{-1}$) = $1/\lambda$. Its units are sometimes abbreviated as (m^{-1}). **Circular frequency** or **angular frequency** is ω (radians/s) = $2\pi\cdot\nu$. Its units are sometimes abbreviated as (s^{-1}).

Emission

Objects warmer than absolute zero can emit radiation. An object that emits the maximum possible radiation for its temperature is called a **blackbody**. **Planck's law** gives the amount of blackbody monochromatic (single wavelength or color) radiant flux leaving an area, called **emittance** or **radiant exitance**, E_λ^*:

$$E_\lambda^* = \frac{c_1}{\lambda^5 \cdot \left[\exp(c_2/(\lambda\cdot T)) - 1\right]} \qquad \bullet(2.13)$$

where T is absolute temperature, and the asterisk indicates blackbody. The two constants are:
c_1 = 3.74 x 10^8 $W\cdot m^{-2}\cdot\mu m^4$, and
c_2 = 1.44 x 10^4 $\mu m\cdot K$.

Eq. (2.13) and constant c_1 already include all directions of exiting radiation from the area. E_λ^* has units of $W\cdot m^{-2}/\mu m$; namely, flux per unit wavelength. For radiation approaching an area rather than leaving it, the radiant flux is called **irradiance**.

Actual objects can emit less than the theoretical blackbody value: $E_\lambda = e_\lambda\cdot E_\lambda^*$, where $0 \le e_\lambda \le 1$ is **emissivity**, a measure of emission efficiency.

The Planck curve (eq. 2.13) for emission from a blackbody the same temperature as the sun (T =

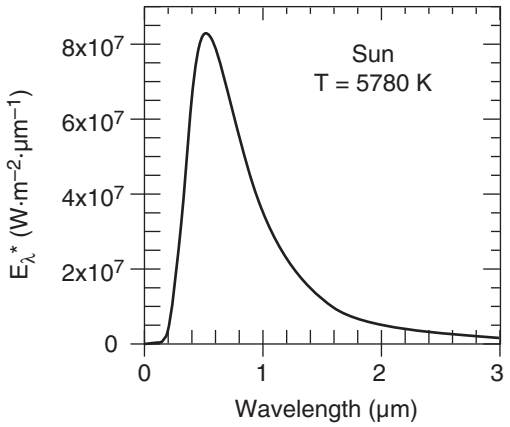

Figure 2.8
Planck radiant exitance, E_λ^*, from a blackbody approximately the same temperature as the sun.

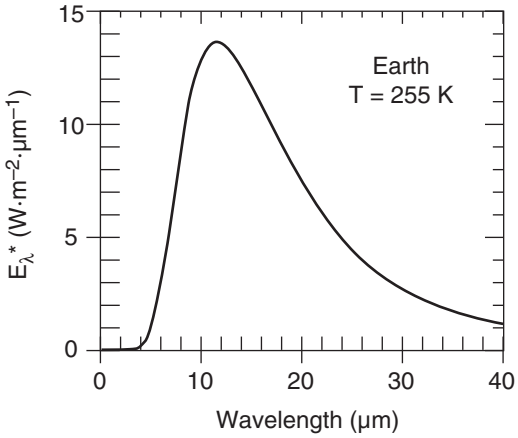

Figure 2.9
Planck radiant exitance, E_λ^*, from a blackbody approximately the same temperature as the Earth.

5780 K) is plotted in Fig. 2.8. Peak emissions from the sun are in the visible range of wavelengths (0.38 – 0.74 μm, see Table 2-3). Radiation from the sun is called **solar radiation** or **short-wave radiation**.

The Planck curve for emission from a blackbody that is approximately the same temperature as the whole Earth-atmosphere system ($T \approx 255$ K) is plotted in Fig. 2.9. Peak emissions from this idealized average Earth system are in the infrared range 8 to 18 μm. This radiation is called **terrestrial radiation**, **long-wave radiation**, or infrared (**IR**) radiation.

The wavelength of the peak emission is given by **Wien's law**:

$$\lambda_{max} = \frac{a}{T} \qquad (2.14)$$

where $a = 2897$ μm·K.

The total amount of emission (= area under Planck curve = total emittance) is given by the **Stefan-Boltzmann law**:

$$E^* = \sigma_{SB} \cdot T^4 \qquad \bullet(2.15)$$

where $\sigma_{SB} = 5.67 \times 10^{-8}$ W·m^{-2}·K^{-4} is the **Stefan-Boltzmann constant**, and E^* has units of W·m^{-2}. More details about radiation emission are in the Remote Sensing chapter in the sections on weather satellites.

Table 2-3. Ranges of wavelengths λ of visible colors. Approximate center wavelength is in **boldface**.

Color	λ (μm)
Red	0.625 - **0.650** - 0.740
Orange	0.590 - **0.600** - 0.625
Yellow	0.565 - **0.577** - 0.590
Green	0.500 - **0.510** - 0.565
Cyan	0.485 - **0.490** - 0.500
Blue	0.460 - **0.475** - 0.485
Indigo	0.425 - **0.445** - 0.460
Violet	0.380 - **0.400** - 0.425

Solved Example

What is the total radiant exitance (radiative flux) emitted from a blackbody Earth at $T = 255$ K, and what is the wavelength of peak emission?

Solution

Given: $T = 255$ K

Find: $E^* = ?$ W·m^{-2} , $\lambda_{max} = ?$ μm

Sketch:

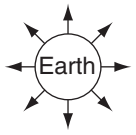

Use eq. (2.15):

$E^* = (5.67 \times 10^{-8}$ W·m^{-2}·K$^{-4}) \cdot (255$ K$)^4$ = **240 W·m^{-2}**.

Use eq. (2.14):

$\lambda_{max} = (2897$ μm·K$) / (255$ K$) =$ **11.36 μm**

Check: Units OK. λ agrees with peak in Fig. 2.9.

Discussion: You could create the same flux by placing a perfectly-efficient 240 W light bulb in front of a parabolic mirror that reflects the light and IR radiation into a beam that is 1.13 m in diameter.

For comparison, the surface area of the Earth is about 5.1×10^{14} m^2, which when multiplied by the flux gives the total emission of 1.22×10^{17} W. Thus, the Earth acts like a large-wattage IR light bulb.

BEYOND ALGEBRA • Incremental Changes

What happens to the total radiative exitance given by eq. (2.15) if temperature increases by 1°C? Such a question is important for climate change.

Solution using calculus:

Calculus allows a simple, elegant way to find the solution. By taking the derivative of both the left and right sides of eq. (2.15), one finds that:

$$dE^* = 4 \cdot \sigma_{SB} \cdot T^3 dT$$

assuming that σ_{SB} is constant. It can be written as

$$\Delta E^* = 4 \cdot \sigma_{SB} \cdot T^3 \cdot \Delta T$$

for small ΔT.

Thus, a fixed increase in temperature of $\Delta T = 1°C$ causes a much larger radiative exitance increase at high temperatures than at cold, because of the T^3 factor on the right side of the equation.

Solution using algebra:

This particular problem could also have been solved using algebra, but with a more tedious and less elegant solution. First let

$$E_2 = \sigma_{SB} \cdot T_2^4 \qquad \text{and} \qquad E_1 = \sigma_{SB} \cdot T_1^4$$

Next, take the difference between these two eqs:

$$\Delta E = E_2 - E_1 = \sigma \cdot \left[T_2^4 - T_1^4 \right]$$

Recall from algebra that $(a^2 - b^2) = (a - b) \cdot (a + b)$

$$\Delta E = \sigma_{SB} \cdot \left(T_2{}^2 - T_1{}^2 \right) \cdot \left(T_2{}^2 + T_1{}^2 \right)$$

$$\Delta E = \sigma_{SB} \cdot \left(T_2 - T_1 \right) \cdot \left(T_2 + T_1 \right) \cdot \left(T_2{}^2 + T_1{}^2 \right)$$

Since $(T_2 - T_1) \,/\, T_1 \ll 1$, then $(T_2 - T_1) = \Delta T$, but $T_2 + T_1 \approx 2T$, and $T_2{}^2 + T_1{}^2 \approx 2 \cdot T^2$. This gives:

$$\Delta E = \sigma_{SB} \cdot \Delta T \cdot 2T \cdot 2T^2$$

or

$$\Delta E \approx \sigma_{SB} \cdot \left[4T^3 \Delta T \right]$$

which is identical to the answer from calculus.

We were lucky this time, but it is not always possible to use algebra where calculus is needed.

Science Graffito

"The great tragedy of science — the slaying of a beautiful hypothesis by an ugly fact." – Aldous Huxley

ON DOING SCIENCE • Scientific Laws – The Myth

There are no scientific laws. Some theories or models have succeeded for every case tested so far, yet they may fail for other situations. Newton's "Laws of Motion" were accepted as laws for centuries, until they were found to fail in quantum mechanical, relativistic, and galaxy-size situations. It is better to use the word "relationship" instead of "law". In this textbook, the word "law" is used for sake of tradition.

Einstein said "No amount of experimentation can ever prove me right; a single experiment can prove me wrong."

Because a single experiment can prove a relationship wrong, it behooves us as scientists to test theories and equations not only for reasonable values of variables, but also in the limit of extreme values, such as when the variables approach zero or infinity. These are often the most stringent tests of a relationship.

Example

Query: The following is an approximation to Planck's law.

$$E_\lambda^* = c_1 \cdot \lambda^{-5} \cdot \exp[\, -c_2 \,/\, (\lambda \cdot T)\,] \qquad \text{(a)}$$

Why is it not a perfect substitute?

Solution: If you compare the numerical answers from eqs. (2.13) and (a), you find that they agree very closely over the range of temperatures of the sun and the Earth, and over a wide range of wavelengths. But...

a) What happens as temperature approaches absolute zero? For eq. (2.13), T is in the denominator of the argument of an exponential, which itself is in the denominator of eq. (2.13). If $T = 0$, then $1/T = \infty$. $\text{Exp}(\infty) = \infty$, and $1/\infty = 0$. Thus, $E_\lambda^* = 0$, as it should. Namely, no radiation is emitted at absolute zero (according to classical theory).

For eq. (a), if $T = 0$, then $1/T = \infty$, and $\exp(-\infty) = 0$. So it also agrees in the limit of absolute zero. Thus, both equations give the expected answer.

b) **What happens as temperature approaches infinity?** For eq. (2.13), if $T = \infty$, then $1/T = 0$, and $\exp(0) = 1$. Then $1 - 1 = 0$ in the denominator, and $1/0 = \infty$. Thus, $E_\lambda^* = \infty$, as it should. Namely, infinite radiation is emitted at infinite temperature.

For eq. (a), if $T = \infty$, then $1/T = 0$, and $\exp(-0) = 1$. Thus, $E_\lambda^* = c_1 \cdot \lambda^{-5}$, which is not infinity. Hence, this approaches the wrong answer in the ∞ T limit.

Conclusion: Eq. (a) is not a perfect relationship, because it fails for this one case. But otherwise it is a good approximation over a wide range of normal temperatures.

Distribution

Radiation emitted from a spherical source decreases with the square of the distance from the center of the sphere:

$$E_2^* = E_1^* \cdot \left(\frac{R_1}{R_2} \right)^2 \qquad \bullet(2.16)$$

where R is the radius from the center of the sphere, and the subscripts denote two different distances from the center. This is called the **inverse square law**.

The reasoning behind eq. (2.16) is that as radiation from a small sphere spreads out radially, it passes through ever-larger conceptual spheres. If no energy is lost during propagation, then the total energy passing across the surface of each sphere must be conserved. Because the surface areas of the spheres increase with the square of the radius, this implies that the energy flux density must decrease at the same rate; i.e., inversely to the square of the radius.

From eq. (2.16) we expect that the radiative flux reaching the Earth's orbit is greatly reduced from that at the surface of the sun. The solar emissions of Fig. 2.8 must be reduced by a factor of 2.167×10^{-5}, based on the square of the ratio of solar radius to Earth-orbital radius from eq. (2.16). This result is compared to the emission from Earth in Fig. 2.10.

The area under the solar-radiation curve in Fig. 2.10 is the **total** (all wavelengths) **solar irradiance (TSI)**, S_o, reaching the Earth's orbit. We call it an irradiance here, instead of an emittance, because relative to the Earth it is an incoming radiant flux. This quantity was formerly called the **solar constant** but we now know that it varies slightly. The average value of solar irradiance measured at the Earth's orbit by satellites is about

$$S_o = 1366 \ (\pm 7) \ \mathrm{W \cdot m^{-2}} \ . \qquad (2.17)$$

In kinematic units (based on sea-level density), the solar irradiance is roughly $S_o = 1.11$ K·m/s.

About ±4 W·m^{-2} of the ±7 W·m^{-2} error bars are due to radiometer calibration errors between the various satellites. Also, during the 11-year sunspot cycle the solar irradiance normally varies by about 1.4 W·m^{-2}, with peak values during sunspot maxima. One example of a longer term variation in solar activity is the **Maunder Minimum** in the late 1600s, during which the solar irradiance was perhaps 2.7 to 3.7 W·m^{-2} less than values during modern solar minima. Such irradiance changes could cause subtle changes (0.3 to 0.4°C) in global climate. See the Climate chapter for more info on solar variability.

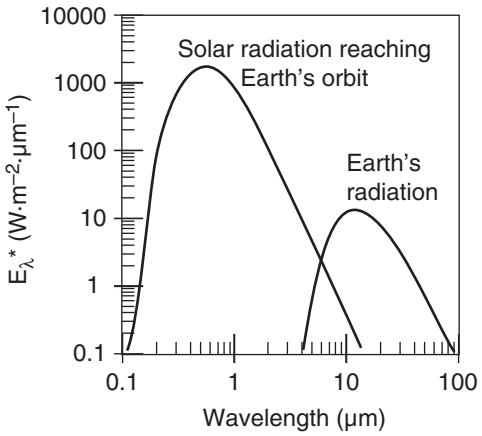

Figure 2.10
Blackbody radiance E reaching top of Earth's atmosphere from the sun and radiance of terrestrial radiation leaving the top of the atmosphere, plotted on a log-log graph.*

Solved Example

Estimate the value of the solar irradiance reaching the orbit of the Earth, given a sun surface temperature (5780 K), sun radius (6.96×10^5 km), and orbital radius (1.495×10^8 km) of the Earth from the sun.

Solution

Given: $T_{sun} = 5780$ K
$R_{sun} = 6.96 \times 10^5$ km = solar radius
$R_{Earth} = 1.495 \times 10^8$ km = Earth orbit radius
Find: $S_o = ?$ W·m^{-2}
Sketch:

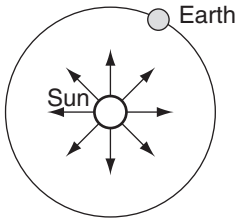

First, use eq. (2.15):
$E_1^* = (5.67 \times 10^{-8} \ \mathrm{W \cdot m^{-2} \cdot K^{-4}}) \cdot (5780 \ \mathrm{K})^4$
$= 6.328 \times 10^7$ W·m^{-2}.
Next, use eq. (2.16), with $R_1 = R_{sun}$ & $R_2 = R_{Earth}$
$S_o = E_2^* = (6.328 \times 10^7 \ \mathrm{W \cdot m^{-2}}) \cdot$
$(6.96 \times 10^5 \ \mathrm{km} / 1.495 \times 10^8 \ \mathrm{km})^2$ = **1372 W·m^{-2}**.

Check: Units OK, Sketch OK. Physics OK.
Discussion: Answer is nearly equal to that measured by satellites, as given in eq. (2.17). The error is due to a poor estimate of effective sun-surface temperature.

Solved Example(§)

Using the results from an earlier solved example that calculated the true anomaly and sun-Earth distance for several days during the year, find the solar radiative forcing for those days.

Solution

Given: R values from previously solved example
Find: S = ? W·m^{-2}

Sketch: (same as Fig 2.2)
Use eq. (2.18).

Date	d	R(ν) (Gm)	S (W/m^2)
4 Jan	4	146.96	1418
18 Jan	18	147.04	1416
1 Feb	32	147.25	1412
15 Feb	46	147.60	1405
1 Mar	60	148.06	1397
15 Mar	74	148.60	1386
29 Mar	88	149.18	1376
12 Apr	102	149.78	1365
26 Apr	116	150.36	1354
21 Jun	172	151.88	1327
23 Sep	266	150.01	1361
22 Dec	356	147.03	1416

Check: Units OK. Physics OK.
Discussion: During N. Hemisphere winter, solar radiative forcing is up to 50 W·m^{-2} larger than average.

Solved Example

During the equinox at noon at latitude ϕ =60°, the solar elevation angle is Ψ = 90° – 60° = 30°. If the atmosphere is perfectly transparent, then how much radiative flux is absorbed into a perfectly black asphalt parking lot?

Solution

Given: Ψ = 30° = elevation angle
$E = S_o$ = 1366 W·m^{-2}. solar irradiance
Find: $\mathbb{F}_{rad}$ = ? W·m^{-2}
Sketch:

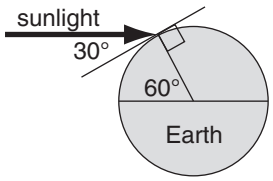

Use eq. (2.19):
$\mathbb{F}_{rad}$ = (1366 W·m^{-2})·sin(30°) = **683 W·m^{-2}**.

Check: Units OK. Sketch OK. Physics OK.
Discussion: Because the solar radiation is striking the parking lot at an angle, the radiative flux into the parking lot is half of the solar irradiance.

According to the inverse-square law, variations of distance between Earth and sun cause changes of the **solar radiative forcing**, S, that reaches the top of the atmosphere:

$$S = S_o \cdot \left(\frac{\bar{R}}{R} \right)^2 \tag{2.18}$$

where S_o = 1366 W·m^{-2} is the average total solar irradiance measured at an average distance $\bar{R}$ = 149.6 Gm between the sun and Earth, and R is the actual distance between Earth and the sun as given by eq. (2.4). Remember that the solar irradiance and the solar radiative forcing are the fluxes across a surface that is perpendicular to the solar beam, measured above the Earth's atmosphere.

Let irradiance E be any radiative flux crossing a unit area that is perpendicular to the path of the radiation. If this radiation strikes a surface that is not perpendicular to the radiation, then the radiation per unit surface area is reduced according to the **sine law**. The resulting flux, $\mathbb{F}_{rad}$, at this surface is:

$$\mathbb{F}_{rad} = E \cdot \sin(\Psi) \tag{2.19}$$

where Ψ is the **elevation angle** (the angle of the sun above the surface). In kinematic form, this is

$$F_{rad} = \frac{E}{\rho \cdot C_p} \cdot \sin(\Psi) \tag{•2.20}$$

where $\rho \cdot C_p$ is given under eq. (2.11).

Average Daily Insolation

The acronym "**insolation**" means "incoming solar radiation" at the top of the atmosphere. The average daily **insolation** $\bar{E}$ takes into account both the solar elevation angle (which varies with season and time of day) and the duration of daylight. For example, there is more total insolation at the poles in summer than at the equator, because the low sun angle near the poles is more than compensated by the long periods of daylight.

$$\bar{E} = \frac{S_o}{\pi} \cdot \left(\frac{a}{R} \right)^2 \cdot \left[h_o' \cdot \sin(\phi) \cdot \sin(\delta_s) + \cos(\phi) \cdot \cos(\delta_s) \cdot \sin(h_o) \right] \tag{2.21}$$

where S_o =1366 W/m^2 is the solar irradiance, a = 149.457 Gm is Earth's semi-major axis length, R is the actual distance for any day of the year, from eq.

(2.4). In eq. (2.21), h_o' is the sunset and sunrise hour angle in radians.

The hour angle h_o at sunrise and sunset can be found using the following steps:

$$\alpha = -\tan(\phi)\cdot\tan(\delta_s) \qquad (2.22a)$$

$$\beta = \min[1, (\max(-1, \alpha)] \qquad (2.22b)$$

$$h_o = \arccos(\beta) \qquad (2.22c)$$

Eq. (2.22b) truncates the argument of the arccos to be between –1 and 1, in order to account for high latitudes where there are certain days when the sun never sets, and other days when it never rises.
[CAUTION. When finding the arccos, your answer might be in degrees or radians, depending on your calculator, spreadsheet, or computer program. Determine the units by experimenting first with the arccos(0), which will either give 90° or π/2 radians. If necessary, convert the hour angle to units of radians, the result of which is h_o'.]

Fig. 2.11 shows the average incoming solar radiation vs. latitude and day of the year, found using eq. (2.21). For any one hemisphere, $\overline{E}$ has greater difference between equator and pole during winter than during summer. This causes stronger winds and more active extratropical cyclones in the winter hemisphere than in the summer hemisphere.

Absorption, Reflection & Transmission

The emissivity, e_λ, is the fraction of blackbody radiation that is actually emitted (see Table 2-4) at any wavelength λ. The absorptivity, a_λ, is the fraction of radiation striking a surface of an object that is **absorbed** (i.e., stays in the object as a different form of energy). **Kirchhoff's law** states that the **absorptivity** equals the **emissivity** of a substance at each wavelength, λ. Thus,

$$a_\lambda = e_\lambda \qquad (2.23)$$

Some substances such as dark glass are semi-**transparent** (i.e., some radiation passes through). A fraction of the incoming (incident) radiation might also be **reflected** (bounced back), and another portion might be **absorbed**. Thus, you can define the efficiencies of reflection, absorption, and transmission as:

$$r_\lambda = \frac{E_{\lambda\ reflected}}{E_{\lambda\ incident}} = \textbf{reflectivity} \qquad (2.24)$$

$$a_\lambda = \frac{E_{\lambda\ absorbed}}{E_{\lambda\ incident}} = \textbf{absorptivity} \qquad (2.25)$$

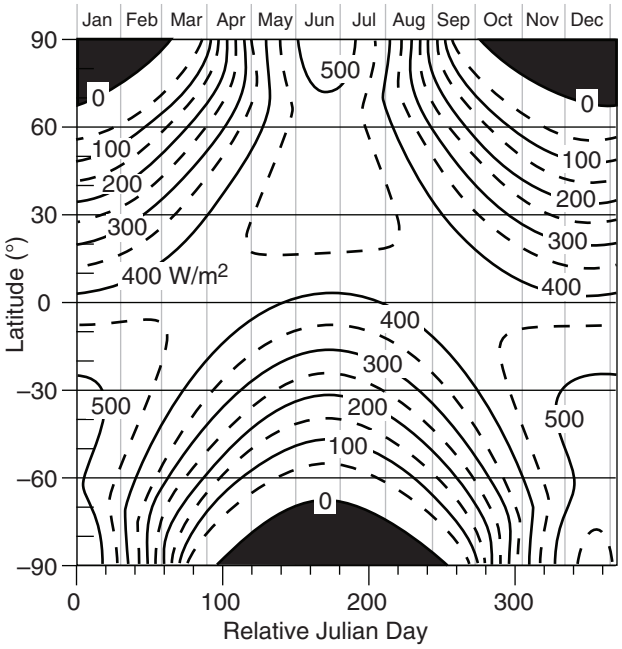

Figure 2.11
Average daily insolation $\overline{E}$ (W/m²) over the globe.

Solved Example

Find the average daily insolation over Vancouver during the summer solstice.

Solution:
Given: $d = d_r = 173$ at the solstice,
$\phi = 49.25°$N, $\lambda_e = 123.1°$W for Vancouver.
Find: $\overline{E}$ = ? W/m²

Use eq. (2.5): $\delta_s = \Phi_r = 23.45°$
Use eq. (2.2): $M = 167.55°$, and assume $\nu \approx M$.
Use eq. (2.4): $R = 151.892$ Gm.
Use eq. (2.22):
$h_o = \arccos[-\tan(49.25°)\cdot\tan(23.45°)] = 120.23°$
$h_o' = h_o \cdot 2\pi/360° = 2.098$ radians
Use eq. (2.21):

$$\overline{E} = \frac{(1368\text{W}\cdot\text{m}^{-2})}{\pi}\cdot\left(\frac{149\text{Gm}}{151.892\text{Gm}}\right)^2 \cdot$$
$$[2.098\cdot\sin(49.25°)\cdot\sin(23.45°) +$$
$$\cos(49.25°)\cdot\cos(23.45°)\cdot\sin(120.23°)]$$

$$\overline{E} = (1327\ \text{W/m}^2)\cdot[2.098(0.3016)+0.5174]$$

$$= \underline{\textbf{486 W/m}}^2$$

Check: Units OK. Physics OK. Agrees with Fig. 2.11.
Discussion: At the equator on this same day, the average daily insolation is less than 400 W/m² .

Table 2-4. Typical infrared emissivities.

Surface	e	Surface	e
alfalfa	0.95	iron, galvan.	0.13-0.28
aluminum	0.01-0.05	leaf 0.8 μm	0.05-0.53
asphalt	0.95	leaf 1 μm	0.05-0.6
bricks, red	0.92	leaf 2.4 μm	0.7-0.97
cloud, cirrus	0.3	leaf 10 μm	0.97-0.98
cloud, alto	0.9	lumber, oak	0.9
cloud, low	1.0	paper	0.89-0.95
concrete	0.71-0.9	plaster, white	0.91
desert	0.84-0.91	sand, wet	0.98
forest, conif.	0.97	sandstone	0.98
forest, decid.	0.95	shrubs	0.9
glass	0.87-0.94	silver	0.02
grass	0.9-0.95	snow, fresh	0.99
grass lawn	0.97	snow, old	0.82
gravel	0.92	soils	0.9-0.98
human skin	0.95	soil, peat	0.97-0.98
ice	0.96	urban	0.85-0.95

Solved Example

If 500 W/m^2 of visible light strikes a translucent object that allows 100 W/m^2 to shine through and 150 W/m^2 to bounce off, find the transmissivity, reflectivity, absorptivity, and emissivity.

Solution

Given: $E_{\lambda\ incoming} = 500$ W/m^2,
$E_{\lambda\ transmitted} = 100$ W/m^2, $E_{\lambda\ reflected} = 150$ W/m^2
Find: $a_\lambda = ?$, $e_\lambda = ?$, $r_\lambda = ?$, and $t_\lambda = ?$

Use eq. (2.26): $t_\lambda = (100\text{ W/m}^2) / (500\text{ W/m}^2) =$ **0.2**
Use eq. (2.24): $r_\lambda = (150\text{ W/m}^2) / (500\text{ W/m}^2) =$ **0.3**
Use eq. (2.27): $a_\lambda = 1 - 0.2 - 0.3 =$ **0.5**
Use eq. (2.23): $e_\lambda = a_\lambda =$ **0.5**

Check: Units dimensionless. Physics reasonable.
Discussion: By definition, **translucent** means partly transparent, and partly absorbing.

$$t_\lambda = \frac{E_{\lambda\ transmitted}}{E_{\lambda\ incident}} = \textbf{transmissivity} \qquad (2.26)$$

Values of e_λ, a_λ, r_λ, and t_λ are between 0 and 1.

The sum of the last three fractions must total 1, as 100% of the radiation at any wavelength must be accounted for:

$$1 = a_\lambda + r_\lambda + t_\lambda \qquad (2.27)$$

or

$$E_{\lambda\ incoming} = E_{\lambda\ absorbed} + E_{\lambda\ reflected} + E_{\lambda\ transmitted} \qquad (2.28)$$

For opaque ($t_\lambda = 0$) substances such as the Earth's surface, you find: $a_\lambda = 1 - r_\lambda$.

The reflectivity, absorptivity, and transmissivity usually vary with wavelength. For example, clean snow reflects about 90% of incoming solar radiation, but reflects almost 0% of IR radiation. Thus, snow is "white" in visible light, and "black" in IR. Such behavior is crucial to surface temperature forecasts.

Instead of considering a single wavelength, it is also possible to examine the net effect over a range of wavelengths. The ratio of total reflected to total incoming solar radiation (i.e., averaged over all solar wavelengths) is called the **albedo**, A :

$$A = \frac{E_{reflected}}{E_{incoming}} \qquad \bullet(2.29)$$

The average global albedo for solar radiation reflected from Earth is $A = 30\%$ (see the Climate chapter). The actual global albedo at any instant varies with ice cover, snow cover, cloud cover, soil moisture, topography, and vegetation (Table 2-5). The Moon's albedo is only 7%.

The surface of the Earth (land and sea) is a very strong absorber and emitter of radiation.

Table 2-5. Typical albedos (%) for sunlight.

Surface	A (%)	Surface	A (%)
alfalfa	23-32	forest, decid.	10-25
buildings	9	granite	12-18
clay, wet	16	grass, green	26
clay, dry	23	gypsum	55
cloud, thick	70-95	ice, gray	60
cloud, thin	20-65	lava	10
concrete	15-37	lime	45
corn	18	loam, wet	16
cotton	20-22	loam, dry	23
field, fallow	5-12	meadow, green	10-20
forest, conif.	5-15	potatoes	19

Table 2-5 *(continuation)*. Typical albedos (%).

Surface	A (%)	Surface	A (%)
rice paddy	12	soil, red	17
road, asphalt	5-15	soil, sandy	20-25
road, dirt	18-35	sorghum	20
rye winter	18-23	steppe	20
sand dune	20-45	stones	20-30
savanna	15	sugar cane	15
snow, fresh	75-95	tobacco	19
snow, old	35-70	tundra	15-20
soil, dark wet	6-8	urban, mean	15
soil, light dry	16-18	water, deep	5-20
soil, peat	5-15	wheat	10-23

Within the air, however, the process is a bit more complicated. One approach is to treat the whole atmospheric thickness as a single object. Namely, you can compare the radiation at the top versus bottom of the atmosphere to examine the total emissivity, absorptivity, and reflectivity of the whole atmosphere. Over some wavelengths called **windows** there is little absorption, allowing the radiation to "shine" through. In other wavelength ranges there is partial or total absorption. Thus, the atmosphere acts as a filter. Atmospheric windows and transmissivity are discussed in detail in the Remote Sensing and Climate chapters.

Beer's Law

Sometimes you must examine radiative **extinction** (reduction of radiative flux) across a short path length Δs within the atmosphere (Fig. 2.12). Let n be the **number density** of radiatively important particles in the air (particles/m^3), and b be the **extinction cross section** of each particle (m^2/particle), where this latter quantity gives the area of the shadow cast by each particle.

Extinction can be caused by absorption and scattering of radiation. If the change in radiation is due only to absorption, then the absorptivity across this layer is

$$a = \frac{E_{incident} - E_{transmitted}}{E_{incident}} \qquad (2.30)$$

Beer's law gives the relationship between incident radiative flux, $E_{incident}$, and transmitted radiative flux, $E_{transmitted}$, as

$$E_{transmitted} = E_{incident} \cdot e^{-n \cdot b \cdot \Delta s} \qquad (2.31a)$$

Beer's law can be written using an **extinction coefficient**, k:

$$E_{transmitted} = E_{incident} \cdot e^{-k \cdot \rho \cdot \Delta s} \qquad (2.31b)$$

where ρ is the density of air, and k has units of m^2/g$_{air}$. The total extinction across the whole path can be quantified by a dimensionless **optical thickness** (or **optical depth** in the vertical), τ , allowing Beer's law to be rewritten as:

$$E_{transmitted} = E_{incident} \cdot e^{-\tau} \qquad (2.31c)$$

To simplify these equations, sometimes a **volume extinction coefficient** γ is defined by

$$\gamma = n \cdot b = k \cdot \rho \qquad (2.32)$$

Visual range (V, one definition of **visibility**) is the distance where the intensity of transmitted light has decreased to 2% of the incident light. It estimates the max distance Δs (km) you can see through air.

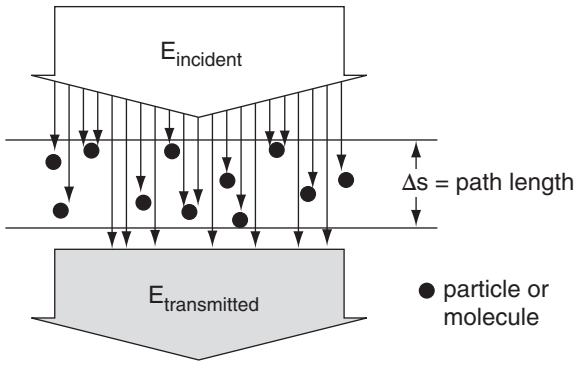

Figure 2.12
Reduction of radiation across an air path due to absorption and scattering by particles such as air-pollution aerosols or cloud droplets, illustrating Beer's law.

Solved Example

Suppose that soot from a burning automobile tire has number density $n = 10^7$ m^{-3} , $b = 10^{-9}$ m^2 , $\Delta s = 20$ m. (a) Find the radiative flux that was not attenuated (i.e., reduction from the solar constant) across the 20 m diameter smoke plume. Assume the incident flux equals the solar constant. (b) Find the optical depth. (c) If this soot fills the air, what is the visual range?

Solution

Given: $n = 10^7$ m^{-3} , $b = 10^{-9}$ m^2 , $\Delta s = 20$ m
$E_{incident} = S = 1366$ W·m^{-2} solar constant
Find: E_{tran} =? W·m^{-2}, τ =? (dimensionless), V =? km
Sketch:

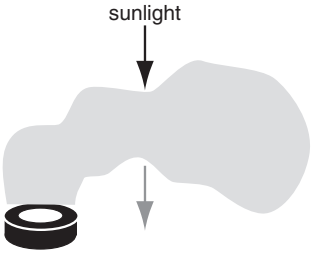

Use eq. (2.32): $\gamma = (10^7 \text{ m}^{-3}) \cdot (10^{-9} \text{ m}^2) = 0.01 \text{ m}^{-1}$

(a) Use eq. (2.31a)
$E_{tran} = 1366 \text{ W·m}^{-2} \cdot \exp[-(0.01 \text{ m}^{-1}) \cdot (20 \text{ m})]$
$= 1366 \text{ W·m}^{-2} \cdot \exp[-0.2] = \underline{\mathbf{1118 \text{ W·m}^{-2}}}$

(b) Rearrange eq. (2.31c):
$\tau = \ln(E_{in}/E_{transmitted}) = \ln(1366/1118) = \underline{\mathbf{0.20}}$

(c) Rearrange eq. (2.31a): $\Delta s = [\ln(E_{incident}/E_{trans})]/\gamma$.
$V = \Delta s = [\ln(1/0.02)]/0.01 \text{ m}^{-1} = \underline{\mathbf{0.391 \text{ km}}}$

Check: Units OK. Sketch OK. Physics OK.
Discussion: Not much attenuation through this small smoke plume; namely, 1366 – 1118 = 248 W·m^{-2} was absorbed by the smoke. However, if this smoke fills the air, then visibility is very poor.

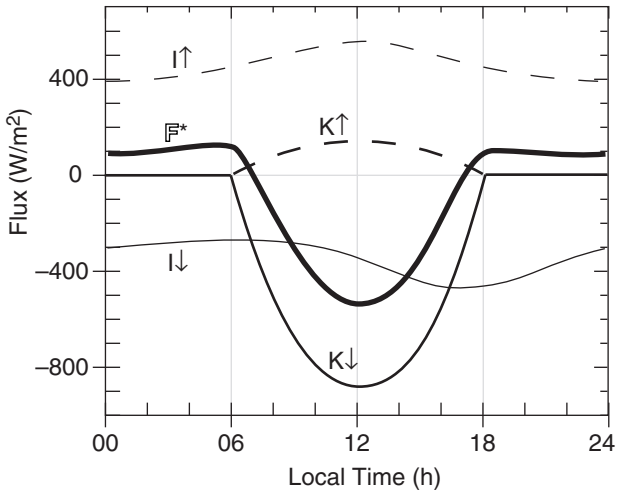

Figure 2.13
Typical diurnal variation of radiative fluxes at the surface. Fluxes are positive upward.

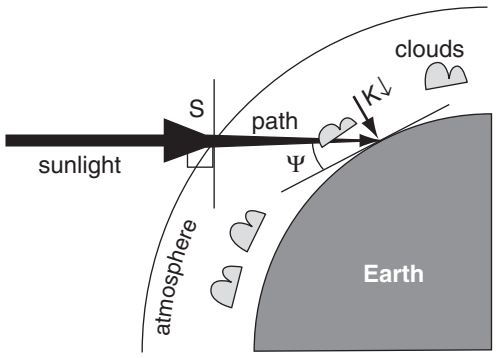

Figure 2.14
Fate of sunlight en route to the Earth's surface.

Solved Example

Downwelling sunlight shines through an atmosphere with 0.8 net sky transmissivity, and hits a ground surface of albedo 0.5, at a time when sin(Ψ) = 0.3. The surface emits 400 W/m^2 IR upward into the atmosphere, and absorbs 350 W/m^2 IR coming down from the atmosphere. Find the net radiative flux.

Solution

Given: $Tr = 0.8$, $S_o = 1366$ W/m^2, $A = 0.5$.
$I\uparrow = 400$ W/m^2, $I\downarrow = 350$ W/m^2
Find: $\mathbb{F}^* = ?$ W/m^2

Use eq. (2.34):
$K\downarrow = -(1366\text{ W/m}^2)\cdot(0.8)\cdot(0.3) = -381$ W/m^2
Use eq. (2.36): $K\uparrow = -(0.5)\cdot(-381\text{ W/m}^2) = 164$ W/m^2
Use eq. (2.33): $\mathbb{F}^* = (-381)+(164)+(-350)+(400)$ W/m^2
$\mathbb{F}^* =$ **–167 W/m**^{2}

Check: Units OK. Magnitude and sign OK.
Discussion: Negative sign means net inflow to the surface, such as would cause daytime warming.

SURFACE RADIATION BUDGET

Define $\mathbb{F}^*$ as the **net radiative flux** (positive upward) perpendicular to the Earth's surface. This net flux has contributions (Fig. 2.13) from **downwelling solar** radiation $K\downarrow$, reflected **upwelling solar** $K\uparrow$, **downwelling longwave** (**IR**) radiation emitted from the atmosphere $I\downarrow$, and **upwelling longwave** emitted from the Earth $I\uparrow$:

$$\mathbb{F}^* = K\downarrow + K\uparrow + I\downarrow + I\uparrow \qquad \bullet(2.33)$$

where $K\downarrow$ and $I\downarrow$ are negative because they are downward.

Solar

Recall that the solar irradiance (i.e., the solar constant) is $S_o \approx 1366 \pm 7$ W·m^{-2} (equivalent to 1.11 K·m/s in kinematic form after dividing by $\rho \cdot C_p$) at the top of the atmosphere. Some of this radiation is attenuated between the top of the atmosphere and the surface (Fig. 2.14). Also, the sine law (eq. 2.19) must be used to find the component of downwelling solar flux $K\downarrow$ that is perpendicular to the surface. The result for daytime is

$$K\downarrow = -S_o \cdot T_r \cdot \sin(\Psi) \qquad (2.34)$$

where T_r is a **net sky transmissivity**. A negative sign is incorporated into eq. (2.34) because $K\downarrow$ is a downward flux. Eq. (2.6) can be used to find sin(Ψ). At night, the downwelling solar flux is zero.

Net transmissivity depends on path length through the atmosphere, atmospheric absorption characteristics, and cloudiness. One approximation for the net transmissivity of solar radiation is

$$T_r = (0.6 + 0.2\sin\Psi)(1 - 0.4\sigma_H)(1 - 0.7\sigma_M)(1 - 0.4\sigma_L) \qquad (2.35)$$

where cloud-cover fractions for high, middle, and low clouds are σ_H, σ_M, and σ_L, respectively. These cloud fractions vary between 0 and 1, and the transmissivity also varies between 0 and 1.

Of the sunlight reaching the surface, a portion might be reflected:

$$K\uparrow = -A \cdot K\downarrow \qquad (2.36)$$

where the surface albedo is A.

Longwave (IR)

Upward emission of IR radiation from the Earth's surface can be found from the Stefan-Boltzmann relationship:

$$I\uparrow = e_{IR} \cdot \sigma_{SB} \cdot T^4 \qquad (2.37)$$

where e_{IR} is the surface emissivity in the IR portion of the spectrum (e_{IR} = 0.9 to 0.99 for most surfaces), and σ_{SB} is the Stefan-Boltzmann constant (= 5.67×10^{-8} W·m^{-2}·K^{-4}).

However, downward IR radiation from the atmosphere is much more difficult to calculate. As an alternative, sometimes a **net longwave flux** is defined by

$$I^* = I\downarrow + I\uparrow \qquad (2.38)$$

One approximation for this flux is

$$I^* = b \cdot (1 - 0.1\sigma_H - 0.3\sigma_M - 0.6\sigma_L) \qquad (2.39)$$

where parameter b = 98.5 W·m^{-2}, or b = 0.08 K·m·s^{-1} in kinematic units.

Net Radiation

Combining eqs. (2.33), (2.34), (2.35), (2.36) and (2.39) gives the **net radiation** ($\mathbb{F}^*$, defined positive upward):

$$\mathbb{F}^* = -(1-A) \cdot S \cdot T_r \cdot \sin(\Psi) + I^* \quad \text{daytime} \bullet (2.40a)$$

$$= I^* \quad \text{nighttime} \bullet (2.40b)$$

Solved Example

Find the net radiation at the surface in Vancouver, Canada, at noon (standard time) on 22 Jun. Low clouds are present with 30% coverage.

Solution

Assume: Grass lawns with albedo A = 0.2 .
No other clouds.
Given: σ_L = 0.3
Find: $\mathbb{F}^*$ = ? W·m^{-2}

Use ψ = 64.1° from an earlier solved example.
Use eq. (2.35) to find the transmissivity:
$T_r = [0.6+0.2\cdot\sin\psi]\cdot(1-0.4\cdot\sigma_L)$
$= [0.6 + 0.2\cdot\sin(64.1°)]\cdot[1-(0.4\cdot0.3)]$
$= [0.80]\cdot(0.88) = 0.686$

Use eq. (2.39) to find net IR contribution:
$I^* = b\cdot(1 - 0.6\cdot\sigma_L)$
$=$ (98.5 W·m^{-2})·[1–(0.6·0.3)] = 80.77 W·m^{-2}

Use eq. (2.40a):
$\mathbb{F}^* = -(1-A) \cdot S \cdot T_r \cdot \sin(\psi) + I^*$
$= -(1-0.2) \cdot (1366$ W·m$^{-2}) \cdot 0.686 \cdot \sin(64.1°)$
$+ 80.77$ W·m^{-2}
$=(-674.36 + 80.77)$ W·m^{-2} = **–593.59 W·m**$^{-2}$

Check: Units OK. Physics OK.
Discussion: The surface flux is only about 43% of that at the top of the atmosphere, for this case. The negative sign indicates a net inflow of radiation to the surface, such as can cause warming during daytime.

ACTINOMETERS

Sensors designed to measure electromagnetic radiative flux are generically called **actinometers** or **radiometers**. In meteorology, actinometers are usually oriented to measure downwelling or upwelling radiation. Sensors that measure the difference between down- and up-welling radiation are called **net actinometers**.

Special categories of actinometers are designed to measure different wavelength bands:

- **pyranometer** – broadband solar (short-wave) irradiance, viewing a hemisphere of solid angle, with the radiation striking a flat, horizontal plate (Fig. 4.15).
- **net pyranometer** – difference between top and bottom hemispheres for short-wave radiation.

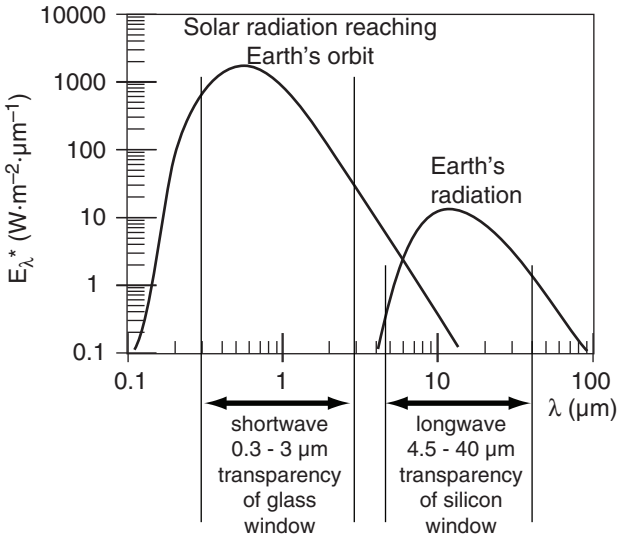

Figure 4.15
The wavelength bands observed by pyranometers (shortwave radiation) and pyrgeometers (longwave radiation) depends on the transparency of the windows used in those instruments.

ON DOING SCIENCE • Seek Solutions

Most differential equations describing meteorological phenomena cannot be solved analytically. They cannot be integrated; they do not appear in a table of integrals; and they are not covered by the handful of mathematical tricks that you learned in math class.

But there is nothing magical about an analytical solution. **Any reasonable solution is better than no solution.** Be creative.

While thinking of creative solutions, also **think of ways to check your answer**. Is it the right order of magnitude, right sign, right units, does it approach a known answer in some limit, must it satisfy some other physical constraint or law or budget?

Example

Find the irradiance that can pass through an atmospheric "window" between wavelengths λ_1 and λ_2.

Solution:

Approach: Integrate Planck's law between the specified wavelengths. This is the area under a portion of the Planck curve.

Check: The area under the whole spectral curve should yield the Stefan-Boltzmann (SB) law. Namely, the answer should be smaller than the SB answer, but should increase and converge to the SB answer as the lower and upper λ limits approach 0 and ∞, respectively.

Methods:

• Pay someone else to get the answer (Don't do this in school!), but be sure to check it yourself.
• Look up the answer in a Table of Integrals.
• Integrate it using the tricks you learned in math class.
• Integrate it using a symbolic equation solver on a computer, such as Mathematica or Maple.
• Find an approximate solution to the full equation. For example, integrate it numerically on a computer. (Trapezoid method, Gaussian integration, finite difference iteration, etc.)
• Find an exact solution for an approximation to the eq., such as a model or idealization of the physics. Most eqs. in this textbook have used this approach.
• Draw the Planck curve on graph paper. Count the squares under the curve between the wavelength bands, and compare to the value of each square, or to the area under the whole curve. (We will use this approach extensively in the Thunderstorm chapter.)
• Draw the curve, and measure area with a planimeter.
• Draw the Planck curve on cardboard or thick paper. Cut out the whole area under the curve. Weigh it. Then cut the portion between wavelengths, & weigh again.
• ...and there are probably many more methods.

- **pyrheliometer** – solar (short wave) direct-beam radiation normal to a flat surface (and shielded from diffuse radiation).
- **diffusometer** – a pyranometer that measures only diffuse solar radiation scattered from air, particles, and clouds in the sky, by using a device that shades the sensor from direct sunlight.
- **pyrgeometer** – infrared (long-wave) radiation from a hemisphere that strikes a flat, horizontal surface (Fig. 4.15).
- **net pyrgeometer** – difference between top and bottom hemispheres for infrared (long-wave) radiation.
- **radiometer** – measure all wavelengths of radiation (short, long, and other bands).
- **net radiometer** – difference between top and bottom hemispheres of radiation at all wavelengths.
- **spectrometers** – measures radiation as a function of wavelength, to determine the spectrum of radiation.

Inside many radiation sensors is a **bolometer**, which works as follows. Radiation strikes an object such as a metal plate, the surface of which has a coating that absorbs radiation mostly in the wavelength band to be measured. By measuring the temperature of the radiatively heated plate relative to a non-irradiated reference, the radiation intensity can be inferred for that wavelength band. The metal plate is usually enclosed in a glass or plastic hemispheric chamber to reduce error caused by heat conduction with the surrounding air.

Inside other radiation sensors are **photometers**. Some photometers use the **photoelectric effect**, where certain materials release electrons when struck by electromagnetic radiation. One type of photometer uses **photovoltaic cells** (also called **solar cells**), where the amount of electrical energy generated can be related to the incident radiation. Another photometric method uses **photoresistor,** which is a high-resistance semiconductor that becomes more conductive when irradiated by light.

Other photometers use **charge-coupled devices** (**CCD**s) similar to the image sensors in digital cameras. These are semiconductor integrated circuits with an array of tiny capacitors that can gain their initial charge by the photoelectric effect, and can then transfer their charge to neighboring capacitors to eventually be "read" by the surrounding circuits.

Simple spectrometers use different filters in front of bolometers or photometers to measure narrow wavelength bands. Higher spectral-resolution spectrometers use **interferometry** (similar to the Michelson inteferometer described in physics books), where the fringes of an interference pattern can be

measured and related to the spectral intensities. These are also sometimes called **Fourier-transform spectrometers**, because of the mathematics used to extract the spectral information from the spacing of the fringes.

You can learn more about radiation, including the radiative transfer equation, in the weather-satellite section of the Remote Sensing chapter. Satellites use radiometers and spectrometers to remotely observe the Earth-atmosphere system. Other satellite-borne radiometers are used to measure the global radiation budget (see the Climate chapter).

SUMMARY

The variations of temperature and humidity that you feel near the ground are driven by the diurnal cycle of solar heating during the day and infrared cooling at night. Both diurnal and seasonal heating cycles can be determined from the geometry of the Earth's rotation and orbit around the sun. The same orbital mechanics describes weather-satellite orbits, as is discussed in the Remote Sensing chapter.

Short-wave radiation is emitted from the sun and propagates through space. It illuminates a hemisphere of Earth. The portion of this radiation that is absorbed is the heat input to the Earth-atmosphere system that drives Earth's weather.

IR radiation from the atmosphere is absorbed at the ground, and IR radiation is also emitted from the ground. The IR and short-wave radiative fluxes do not balance, leaving a net radiation term acting on the surface.

Instruments to measure radiation are called actinometers or radiometers. Radiometers and spectrometers can be used in remote sensors such as weather satellites.

Threads

Just a reminder that the "threads" section at the end of each chapter is designed to highlight linkages to material in the other chapters. It is included to help you develop a coherent picture of atmospheric science, and to anticipate your question of "Why is this material important?".

Radiation affects motions on a wide range of scales, and it affects thermodynamics. Excess solar radiation near the equator, and excess IR cooling at the poles is the driving force for the global circulation (Chapter 11). It ultimately creates the synoptic weather patterns of high and low pressure systems and fronts (Chapter 12 and 13). Averaged over the whole globe, it controls the Earth's climate (Chapter 21).

Radiative heating at different heights creates a vertical atmospheric structure quantified by a standard atmosphere (Chapter 1), and affects static stability and cloud growth (Chapters 5 and 6). On a smaller scale, IR radiative cooling drives downslope drainage winds at night (Chapter 17). Also, sunlight interacts with ice crystals and raindrops to create beautiful optical phenomena such as rainbows (Chapter 22).

Planck's law shows the peak wavelength of solar emissions to be in the visible portion of the spectrum. Sunlight drives the diurnal cycle of the surface heat budget described in Chapter 3, which mostly affects air near the ground, in the atmospheric boundary layer (Chapter 18).

Orbital mechanics dictates the optimum weather satellite altitudes for observing such storms (Chapter 8).

EXERCISES

Numerical Problems

(Students, don't forget to put a box around each answer.)

N1. Given distances R between the sun and planets compute the orbital periods (Y) of:

a. Mercury (R = 58 Gm)
b. Venus (R = 108 Gm)
c. Mars (R = 228 Gm)
d. Jupiter (R = 778 Gm)
e. Saturn (R = 1,427 Gm)
f. Uranus (R = 2,869 Gm)
g. Neptune (R = 4,498 Gm)
h. Pluto (R = 5,900 Gm)
i. Eris: given Y = 557 Earth years, estimate the distance R from the sun assuming a circular orbit.

(Note: Eris' orbit is highly eccentric and steeply tilted at 44° relative to the plane of the rest of the solar system, so our assumption of a circular orbit was made here only to simplify the exercise.)

N2. This year, what is the date and time of the:

a. perihelion b. vernal equinox
c. summer solstice d. aphelion
e. autumnal equinox f. winter solstice

N3. What is the relative Julian day for:

a. 10 Jan	b. 25 Jan	c. 10 Feb	d. 25 Feb
e. 10 Mar	f. 25 Mar	g. 10 Apr	h. 25 Apr
i. 10 May	j. 25 May	k. 10 Jun	l. 25 Jun

m. 10 Jul n. 25 Jul o. 10 Aug p. 25 Aug
q. 10 Sep r. 25 Sep s. 10 Oct t. 25 Oct
u. 10 Nov v. 25 Nov w. 10 Dec x. 25 Dec
y. today's date z. date assigned by instructor

N4. For the date assigned from exercise N3, find:
(i) mean anomaly
(ii) true anomaly
(iii) distance between the sun and the Earth
(iv) solar declination angle
(v) average daily insolation

N5(§). Plot the local solar elevation angle vs. local time for 22 December, 23 March, and 22 June for the following city:
a. Seattle, WA, USA
b. Corvallis, OR, USA
c. Boulder, CO, USA
d. Norman, OK, USA
e. Madison, WI, USA
f. Toronto, Canada
g. Montreal, Canada
h. Boston, MA, USA
i. New York City, NY, USA
j. University Park, PA, USA
k. Princeton, NJ, USA
l. Washington, DC, USA
m. Raleigh, NC, USA
n. Tallahassee, FL, USA
o. Reading, England
p. Toulouse, France
q. München, Germany
r. Bergen, Norway
s. Uppsala, Sweden
t. DeBilt, The Netherlands
u. Paris, France
v. Tokyo, Japan
w. Beijing, China
x. Warsaw, Poland
y. Madrid, Spain
z. Melbourne, Australia
aa. Your location today.
bb. A location assigned by your instructor

N6(§). Plot the local solar azimuth angle vs. local time for 22 December, 23 March, and 22 June, for the location from exercise N5.

N7(§). Plot the local solar elevation angle vs. azimuth angle (similar to Fig. 2.6) for the location from exercise N5. Be sure to add tic marks along the resulting curve and label them with the local standard times.

N8(§). Plot local solar elevation angle vs. azimuth angle (such as in Fig. 2.6) for the following location:
a. Arctic Circle b. 75°N c. 85°N d. North Pole
e. Antarctic Circle f. 70°S g. 80°S h. South Pole
for each of the following dates:
(i) 22 Dec (ii) 23 Mar (iii) 22 Jun

N9(§). Plot the duration of evening civil twilight (difference between end of twilight and sunset times) vs. latitude between the south and north poles, for the following date:
a. 22 Dec b. 5 Feb c. 21 Mar d. 5 May
e. 21 Jun f. 5 Aug g. 23 Sep h. 5 Nov

N10. On 15 March for the city listed from exercise N5, at what local standard time is:
a. geometric sunrise
b. apparent sunrise
c. start of civil twilight
d. start of military twilight
e. start of astronomical twilight
f. geometric sunset
g. apparent sunset
h. end of civil twilight
i. end of military twilight
j. end of astronomical twilight

N11. Calculate the Eq. of Time correction for:
a. 1 Jan b. 15 Jan c. 1 Feb d. 15 Feb e. 1 Mar
f. 15 Mar g. 1 Apr h. 15 Apr i. 1 May j. 15 May

N12. Find the mass flux ($kg \cdot m^{-2} \cdot s^{-1}$) at sea-level, given a kinematic mass flux (m/s) of:
a. 2 b. 5 c. 7 d. 10 e. 14 f. 18 g. 21
h. 25 i. 30 j. 33 k. 47 l. 59 m. 62 n. 75

N13. Find the kinematic heat fluxes at sea level, given these regular fluxes ($W \cdot m^{-2}$):
a. 1000 b. 900 c. 800 d. 700 e. 600
f. 500 g. 400 h. 300 i. 200 j. 100
k. 43 l. –50 m. –250 n. –325 o. –533

N14. Find the frequency, circular frequency, and wavenumber for light of color:
a. red b. orange c. yellow d. green
e. cyan f. blue f. indigo g. violet

N15(§). Plot Planck curves for the following blackbody temperatures (K):
a. 6000 b. 5000 c. 4000 d. 3000 e. 2500
f. 2000 g. 1500 h. 1000 i. 750 j. 500
k. 300 l. 273 m. 260 n. 250 h. 240

N16. For the temperature of exercise N15, find:
(i) wavelength of peak emissions
(ii) total emittance (i.e., total amount of emissions)

N17. Estimate the value of solar irradiance reaching the orbit of the planet from exercise N1.

N18(§). a. Plot the value of solar irradiance reaching Earth's orbit as a function of relative Julian day.

b. Using the average solar irradiance, plot the radiative flux (reaching the Earth's surface through a perfectly clear atmosphere) vs. latitude. Assume local noon.

N19(§). For the city of exercise N1, plot the average daily insolation vs. Julian day.

N20. What is the value of IR absorptivity of:

a. aluminum b. asphalt c. cirrus cloud
d. conifer forest e. grass lawn f. ice
g. oak h. silver i. old snow
j. urban average k. concrete average
l. desert average m. shrubs n. soils average

N21. Suppose polluted air reflects 30% of the incoming solar radiation. How much (W/m^2) is absorbed, emitted, reflected, and transmitted? Assume an incident radiative flux equal to the solar irradiance, given a transmissivity of:

a. 0 b. 0.05 c. 0.1 d. 0.15 e. 0.2 f. 0.25
g. 0.3 h. 0.35 i. 0.4 j. 0.45 k. 0.5 l. 0.55
m. 0.6 n. 0.65 o. 0.7

N22. What is the value of albedo for the following land use?

a. buildings b. dry clay c. corn d. green grass
e. ice f. potatoes g. rice paddy h. savanna
i. red soil j. sorghum k. sugar cane
l. tobacco

N23. What product of number density times absorption cross section is needed in order for 50% of the incident radiation to be absorbed by airborne volcanic ash over the following path length (km)?

a. 0.2 b. 0.4 c. 0.6 d. 0.8 e. 1.0 f. 1.5 g. 2
h. 2.5 i. 3 j. 3.5 k. 4 l. 4.5 m. 5 n. 7

N24. What fraction of incident radiation is transmitted through a volcanic ash cloud of optical depth:

a. 0.2 b. 0.5 c. 0.7 d. 1.0 e. 1.5 f. 2 g. 3
h. 4 j. 5 k. 6 l. 7 m. 10 n. 15 o. 20

N25. What is the visual range (km) for polluted air that has volume extinction coefficient (m^{-1}) of:

a. 0.00001 b. 0.00002 c. 0.00005 d. 0.0001
e. 0.0002 f. 0.0005 g. 0.001 h. 0.002
i. 0.005 j. 0.01 k. 0.02 l. 0.05

N26. (i) What is the value of solar downward direct radiative flux reaching the surface at the city from exercise N5 at noon on 4 July, given 20% coverage of cumulus (low) clouds.

(ii) If the albedo is 0.5 in your town, what is the reflected solar flux at that same time?

(iii) What is the approximate value of net longwave radiation at that time?

(iv) What is the net radiation at that time, given all the info from parts (i) - (iii)?

N27. For a surface temperature of 20°C, find the emitted upwelling IR radiation (W/m^2) over the surface-type from exercise N20.

Understanding & Critical Evaluation

U1. At what time of year does the true anomaly equal:

a. 45° b. 90° c. 135° d. 180° e. 225°
f. 270° g. 315° h. 360°

U2(§) a. Calculate and plot the position (true anomaly and distance) of the Earth around the sun for the first day of each month.

b. Verify Kepler's second law.

c. Compare the elliptical orbit to a circular orbit.

U3. What is the optimum angle for solar collectors at your town?

U4. Design a device to measure the angular diameter of the sun when viewed from Earth. (Hint, one approach is to allow the sun to shine through a pin hole on to a flat surface. Then measure the width of the projected image of the sun on this surface divided by the distance between the surface and the pin hole. What could cause errors in this device?)

U5. For your city, plot the azimuth angle for apparent sunrise vs. relative Julian day. This is the direction you need to point your camera if your want to photograph the sunrise.

U6. a. Compare the length of daylight in Fairbanks, AK, vs Miami, FL, USA.

b. Why do vegetables grow so large in Alaska?

c. Why are few fruits grown in Alaska?

U7. How would Fig. 2.6 be different if daylight (summer) time were used in place of standard time during the appropriate months?

U8(§). Plot a diagram of geometric sunrise times and of sunset times vs. day of the year, for your location.

U9(§). Using apparent sunrise and sunset, calculate and plot the hours of daylight vs. Julian day for your city.

U10. a. On a clear day at your location, observe and record actual sunrise and sunset times, and the duration of twilight.

b. Use that information to determine the day of the year.

c. Based on your personal determination of the length of twilight, and based on your latitude and season, is your personal twilight most like civil, military, or astronomical twilight?

U11. Given a flux of the following units, convert it to a kinematic flux, and discuss the meaning and/or advantages of this form of flux.

a. Moisture flux: $g_{water} \cdot m^{-2} \cdot s^{-1}$

b. Momentum flux: $(kg_{air} \cdot m \cdot s^{-1}) \cdot m^{-2} \cdot s^{-1}$

c. Pollutant flux: $g_{pollutant} \cdot m^{-2} \cdot s^{-1}$

U12. a. What solar temperature is needed for the peak intensity of radiation to occur at 0.2 micrometers?

b. Remembering that humans can see light only between 0.38 and 0.74 microns, would the sun look brighter or dimmer at this new temperature?

U13. A perfectly black asphalt road absorbs 100% of the incident solar radiation. Suppose that its resulting temperature is 50°C. How much visible light does it emit?

U14. If the Earth were to cool 5°C from its present radiative equilibrium temperature, by what percentage would the total emitted IR change?

U15(§). Evaluate the quality of the approximation to Planck's Law [see eq. (a) in the "On Doing Science • Scientific Laws — the Myth" box] against the exact Planck equation (2.13) by plotting both curves for a variety of typical sun and Earth temperatures.

U16. Find the solar irradiance that can pass through an atmospheric "window" between $\lambda_1 = 0.3$ μm and $\lambda_2 = 0.8$ μm. (See the "On Doing Science • Seek Solutions" box in this chapter for ways to do this without using calculus.)

U17. How much variation in Earth orbital distance from the sun is needed to alter the solar irradiance by 10%?

U18. Solar radiation is a diffuse source of energy, meaning that it is spread over the whole Earth rather than being concentrated in a small region. It has been proposed to get around the problem of the inverse square law of radiation by deploying very large mirrors closer to the sun to focus the light as collimated rays toward the Earth. Assuming that all the structural and space-launch issues could be solved, would this be a viable method of increasing energy on Earth?

U19. The "sine law" for radiation striking a surface at an angle is sometimes written as a "cosine law", but using the zenith angle instead of the elevation angle. Use trig to show that the two equations are physically identical.

U20. Explain the meaning of each term in eq. (2.21).

U21. a. Examine the figure showing average daily insolation. In the summer hemisphere during the few months nearest the summer solstice, explain why the incoming solar radiation over the pole is nearly equal to that over the equator.

b. Why are not the surface temperatures near the pole nearly equal to the temperatures near the equator during the same months?

U22. Using Table 2-5 for the typical albedos, speculate on the following:

a. How would the average albedo will change if a pasture is developed into a residential neighborhood.

b. How would the changes in affect the net radiation budget?

U23. Use Beer's law to determine the relationship between visual range (km) and volume extinction coefficient (m^{-1}). (Note that extinction coefficient can be related to concentration of pollutants and relative humidity.)

U24(§). For your city, calculate and plot the noontime downwelling solar radiation every day of the year, assuming no clouds, and considering the change in solar irradiance due to changing distance between the Earth and sun.

U25. Consider cloud-free skies at your town. If 50% coverage of low clouds moves over your town, how does net radiation change at noon? How does it change at midnight?

U26. To determine the values of terms in the surface net-radiation budget, what actinometers would you use, and how would you deploy them (i.e., which directions does each one need to look to get the data you need)?

Web-Enhanced Questions

(Don't forget to cite each web address you use.)

W1. Access a full-disk visible satellite photo image of Earth from the web. What visible clues can you use to determine the current solar declination angle? How does your answer compare with that expected for your latitude and time of year.

W2. Access "web cam" camera images from a city, town, ski area, mountain pass, or highway near you. Use visible shadows on sunny days, along with your knowledge of solar azimuth angles, to determine the direction that the camera is looking.

W3. Access from the web the exact time from military (US Navy) or civilian (National Institute of Standards and Technology) atomic clocks. Synchronize your clocks at home or school, utilizing the proper time zone for your location. What is the time difference between local solar noon (the time when the sun is directly overhead) and the official noon according to your time zone. Use this time difference to determine the number of degrees of longitude that you are away from the center of your time zone.

W4. Access orbital information about one planet (other than Earth) that most interests you (or a planet assigned by the instructor). How elliptical is the orbit of the planet? Also, enjoy imagery of the planet if available.

W5. Access runway visual range reports from surface weather observations (METARs) from the web. Compare two different locations (or times) having different visibilities, and calculate the appropriate volume extinction coefficients and optical thickness. Also search the web to learn how runway visual range (RVR) is measured.

W6. Access both visible and infrared satellite photos from the web, and discuss why they look different. If you can access water-vapor satellite photos, include them in your comparison.

W7. Search the web for information about the sun. Examine satellite-based observations of the sun made at different wavelengths. Discuss the structure of the sun. Do any of the web pages give the current value of the solar irradiance (i.e., the solar constant)? If so, how has it varied recently?

W8. Access from the web daytime visible photos of the whole disk of the Earth, taken from geostationary weather satellites. Discuss how variations in the apparent brightness at different locations (different latitudes; land vs. ocean, etc.) might be related to reflectivity and other factors.

W9. Some weather stations and research stations report hourly observations on the web. Some of these stations include radiative fluxes near the surface. Use this information to create surface net radiation graphs.

W10. Access information from the web about how color relates to wavelength. Also, how does the range of colors that can be perceived by eye compare to the range of colors that can be created on a computer screen?

W11. Search the web for information about albedos and IR emissivities for substances or surfaces that are not already listed in the tables in this chapter.

W12. Find on the web satellite images of either forest-fire smoke plumes or volcanic ash plumes. Compare the intensity of reflected radiation from the Earth's surface as it shines through these plumes with earlier satellite photos when the plumes were not there. Use these data to estimate the extinction coefficient.

W13. Access photos and diagrams from the web that describe how different actinometers are constructed and how they work. Also, list any limitations of these instruments that are described in the web.

Synthesis Questions

(Don't forget to state and justify all assumptions.)

S1. What if the eccentricity of the Earth's orbit around the sun changed to 0.2 ? How would the seasons and climate be different than now?

S2. What if the tilt of the Earth's axis relative to the ecliptic changed to 45° ? How would the seasons and climate be different than now?

S3. What if the tilt of the Earth's axis relative to the ecliptic changed to 90° ? How would the seasons and climate be different than now?

S4. What if the tilt of the Earth's axis relative to the ecliptic changed to 0° ? How would the seasons and climate be different than now?

S5. What if the rotation of the Earth about its axis matched its orbital period around the sun, so that one side of the Earth always faced the sun and the other side was always away. How would weather and climate be different, if at all?

S6. What if the Earth diameter decreased to half of its present value? How would sunrise and sunset time, and solar elevation angles change?

S7. Derive eq. (2.6) from basic principles of geometry and trigonometry. This is quite complicated. It can be done using plane geometry, but is easier if you use spherical geometry. Show your work.

S8. What if the perihelion of Earth's orbit happened at the summer solstice, rather than near the winter solstice. How would noontime, clear-sky values of insolation change at the solstices compared to now?

S9. What if radiative heating was caused by the magnitude of the radiative flux, rather than by the radiative flux divergence. How would the weather or the atmospheric state be different, if at all?

S10. Linearize Planck's Law in the vicinity of one temperature. Namely, derive an equation that gives a straight line that is tangent to any point on the Planck curve. (Hint: If you have calculus skills, try using a Taylor's series expansion.) Determine over what range of temperatures your equation gives reasonable answers. Such linearization is sometimes used retrieving temperature soundings from satellite observations.

S11. Suppose that Kirchhoff's law were to change such that $a_\lambda = 1 - e_\lambda$. What are the implications?

S12. What if Wien's law were to be repealed, because it was found instead that the wavelength of peak emissions increases as temperature increases.
a. Write an equation that would describe this. You may name this equation after yourself.
b. What types of radiation from what sources would affect the radiation budget of Earth?

S13. What if the solar "constant" were even less constant than it is now. Suppose the solar constant randomly varies within a range of ±50% of its present value, with each new value lasting for a few years before changing again. How would weather and climate be different, if at all?

S14. What if the distance between sun and Earth was half what it is now. How would weather and climate be different, if at all?

S15. What if the distance between sun and Earth was double what it is now. How would weather and climate be different, if at all?

S16. Suppose the Earth was shaped like a cube, with the axis of rotation perpendicular to the ecliptic, and with the axis passing through the middle of the top and bottom faces of the cube. How would weather and climate be different, if at all?

S17. Suppose the Earth was shaped like a narrow cylinder, with the axis of rotation perpendicular to the ecliptic, and with the axis passing through the middle of the top and bottom faces of the cylinder. How would weather & climate be different, if at all?

S18. Derive eq. (2.21) from the other equations in this chapter. Show your work. Discuss the physical interpretation of the hour angle, and what the effect of truncating it is.

S19. Suppose that the Earth's surface was perfectly reflective everywhere to short-wave radiation, but that the atmosphere absorbed 50% of the sunlight passing through it without reflecting any. What percentage of the insolation would be reflected to space? Also, how would the weather and climate be different, if at all?

S20. Suppose that the atmosphere totally absorbed all short wave radiation that was incident on it, but also emitted an exactly equal amount of short wave radiation as it absorbed. How would weather and climate be different, if at all?

S21. Consider Beer's law. If there are n particles per cubic meter of air, and if a vertical path length in air is Δs, then multiplying the two gives the number of particles over each square meter of ground. If the absorption cross section b is the area of shadow cast by each particle, then multiplying this times the previous product would give the shadowed area divided by the total area of ground. This ratio is just the absorptivity a. Namely, by this reasoning, one would expect that $a = n \cdot b \cdot \Delta s$.

However, Beer's law is an exponential function. Why? What was wrong with the reasoning in the previous paragraph?

S22. What if the atmosphere were completely transparent to IR radiation. How would the surface net radiation budget be different?

S23. Existing radiometers are based on a bolometer, photovoltaic cell, or charge-coupled device. Design a new type of actinometer that is based on a different principle. Hint, think about what is affected in any way by radiation or sunlight, and then use that effect to measure the radiation.

Copyright © 2011, 2015 by Roland Stull. *Meteorology for Scientists and Engineers, 3rd Ed.*

HEAT

CONTENTS

Sensible and Latent Heats 53
- Sensible 53
- Latent 56

Lagrangian Heat Budget – Part 1: Unsaturated 57
- Air Parcels 57
- First Law of Thermodynamics 58
- Lapse Rate 59
- Adiabatic Lapse Rate 60
- Potential Temperature 61
- Thermodynamic Diagrams –Part 1: Dry Adiabatic Processes 63

Eulerian Heat Budget 64
- First Law of Thermo. – Revisited 64
- Advection 65
- Molecular Conduction & Surface Fluxes 67
- Turbulence 69
- Radiation 71
- Internal Source: Latent Heat 72
- Net Heat Budget 72

Surface Heat Budget 73
- Heat Budget 73
- Bowen Ratio 74

Apparent Temperatures 76
- Wind Chill 76
- Heat Index and Humidex 77

Temperature Sensors 78

Summary 79
- Threads 79

Exercises 80
- Numerical Problems 80
- Understanding & Critical Evaluation 83
- Web-Enhanced Questions 84
- Synthesis Questions 85

"Meteorology for Scientists and Engineers, 3rd Edition" by Roland Stull is licensed under a Creative Commons Attribution-NonCommercial-ShareAlike 4.0 International License. To view a copy of the license, visit http://creativecommons.org/licenses/by-nc-sa/4.0/ . This work is available at http://www.eos.ubc.ca/books/Practical_Meteorology/ .

3 Energy cannot be created or destroyed, according to classical physics. However, it can change form. Heat is one form.

Energy enters the atmosphere predominantly as short-wave radiation from the sun. Once here, some of the energy becomes sensible heat, and some evaporates water. The energy can change form many times while driving the weather. It finally leaves as long-wave terrestrial radiation.

An energy-conservation relationship known as the **First Law of Thermodynamics** forms the basis of a heat budget. We can apply this budget within two frameworks: Lagrangian and Eulerian.

Lagrangian means that we follow an air parcel as it moves in the atmosphere. This is useful for determining the temperature of a rising air parcel, and anticipating whether clouds form.

Eulerian means that we examine a volume fixed in space, such as over a farm or town. This is useful for forecasting temperature at any location, such as at your house. Eulerian methods must consider the transport (flux) of energy to and from the fixed volume. Transport can be via radiation, advection, turbulence, and conduction.

SENSIBLE AND LATENT HEATS

Sensible

Sensible heat ΔQ_H (in units of J) can be sensed by humans; namely, it is that portion of total heat content of air associated with temperature change ΔT at constant pressure. The sensible heat per unit mass of air m_{air} is given by

$$\frac{\Delta Q_H}{m_{air}} = C_p \cdot \Delta T \qquad \bullet(3.1)$$

Sensible heat is also known as **enthalpy** (see focus box in the subsection on the First Law of Thermo.).

The **specific heat at constant pressure**, C_p, depends on the material being heated. For dry air, C_{pd} = 1004 J·kg^{-1}·K^{-1}. For moist air (namely, for a gas consisting of a mixture of dry air molecules plus water vapor molecules), the specific heat is

Solved Example

How much sensible heat is needed to warm 2 kg of dry air by 5°C?

Solution

Given: m_{air} = 2 kg , ΔT = 5°C
C_{pd} = 1004.67 J·kg^{-1}·K^{-1}.
Find: ΔQ_H = ? J

Rearrange eq. (3.1)
$\Delta Q_H = m_{air} \cdot C_{pd} \cdot \Delta T$
= (2 kg)·(1004.67 J·kg^{-1}·K^{-1})·(5°C) = **10.046 kJ**

Check: Units OK. Physics reasonable.
Discussion: This amount of air takes up a space of about 2.45 m^3 — the size of a small closet.

Science Graffito

"He who can no longer pause to wonder and stand rapt in awe is as good as dead; his eyes are closed."
- Albert Einstein.

Science Graffito

"Virtual particles are composed entirely of math and exist solely to fill otherwise embarrassing gaps in physics."
- Bruno Maddox.

FOCUS • Internal Energy

In thermodynamics, **internal energy** consists of the sum of microscopic kinetic and potential energy associated with matter. Microscopic kinetic energy is associated with random motions of masses, while microscopic potential energy is associated with forces that bind masses together.

Microscopic kinetic energies include random movement (translation) of molecules, molecular vibration and rotation, electron motion and spin, and nuclear spin. The sum of these kinetic energies is called **sensible energy**, which we humans can sense and measure as **temperature**.

For binding energies, it takes energy to pull two masses apart and break their bonds. This is analogous to increasing the microscopic potential energy of the system. When the two masses snap back together, their microscopic potential energy is released back into other energy forms. Three forms of binding energy are:
• **latent** — bonds between molecules
• **chemical** — bonds between atoms
• **nuclear** — sub-atomic bonds
We will ignore chemical reactions and nuclear explosions here.

Latent energy is associated with the phase change (solid, liquid, gas). In solids, the molecules are bound closely together in a somewhat rigid lattice. In liquids, molecules can more easily move relative to each other, but are still held close together. In gases, the molecules are further apart and have much weaker bonds.

For example, when you add energy to ice (a process shown by the big arrow in Fig. 3F.1), initially the ice warms (sensible energy increases). Then, energy is consumed to break the bonds of the solid to melt the ice (latent energy increases), after which the liquid can warm (sensible). Next, energy is used to vaporize the liquid (latent), after which the gas can warm (sensible).

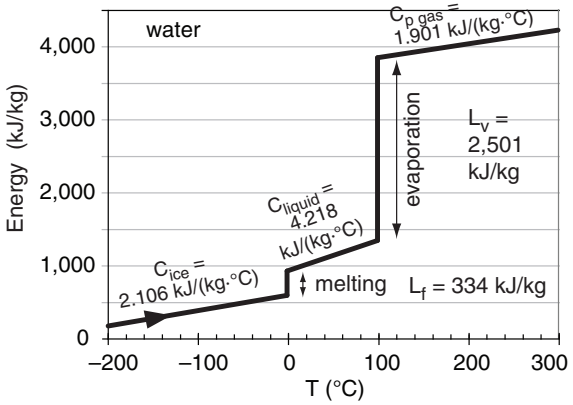

Fig. 3F.1. *Sensible and latent energy for water.*

FOCUS • Cp vs. Cv

C_v — Specific Heat at Constant Volume

Consider a sealed box of fixed volume V filled with air, as sketched in Fig. 3F.2a below. The number of air molecules (idealized by the little spheres) can't change, so the air density ρ is constant. Suppose that initially, the air temperature T_o is cool, as represented by the short arrows denoting the movement of each molecule in box 3F.2a. When each molecule bounces off a wall of the container, it imparts a small force. The sum of forces from all molecules that bounce off a wall of area A results in an air pressure P_o.

If you add Δq thermal energy to air in the box, the temperature rises to T_2 (represented by longer arrows in Fig. 3F.2b). Also, when each molecule bounces off a wall, it imparts a greater force because it is moving faster. Thus, the pressure P_2 will be larger. This is expected from the ideal gas law under constant density, for which

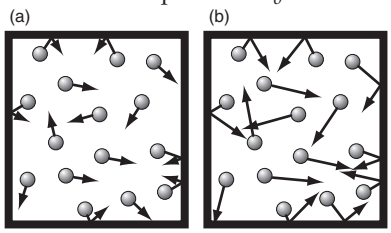

Fig. 3F.2. *Molecules in a fixed volume.*

$$P_o/T_o = P_2/T_2 = \text{constant} = \rho \cdot \Re \qquad (3F.1)$$

Different materials warm by different amounts when you add heat. If you know how much thermal energy Δq you added per kilogram of material, and you measure the resulting increase in temperature $T_2 - T_o$, then you can empirically determine the **specific heat at constant volume:**

$$C_v = \Delta q/(T_2 - T_o) \qquad (3F.2)$$

which is about $C_v = 717\ \text{J}\cdot\text{kg}^{-1}\cdot\text{K}^{-1}$ for dry air.

C_p — Specific Heat at Constant Pressure

For a different scenario, consider a box (Fig. 3F.3c) with a frictionless moveable piston at the top. The weight of the stationary piston is balanced by the pressure of the gas trapped below it. If you add Δq thermal energy to the air, the molecules will move faster (Fig. 3F.3d), and exert greater pressure against the piston and against the other walls of the chamber. But the weight of the piston hasn't changed, so the increased pressure of the gas causes the piston to rise.

But when any molecule bounces off the piston and helps move it, the molecule loses some of its microscopic kinetic energy. (An analogy is when a billiard ball bounces off an empty cardboard box sitting in the middle of the billiard table. The box moves a bit when hit by the ball, and the ball returns more slowly.) The result is that the gas temperature T_1 in Fig. 3F.3e is not as warm as in Figs. 3F.2b or 3F.3d, but is warmer than the initial temperature; namely, $T_o < T_1 < T_2$.

(continues in next column)

(continuation of Focus on Cp vs. Cv)

The molecules spread out within the larger volume in Fig. 3F.3e. Thus, air density ρ decreases, causing fewer molecules near the piston to push against it. The combined effects of decreasing density and temperature cause the air pressure to decrease as the piston rises. Eventually the piston stops rising at the point where the air pressure balances the piston weight, as shown in Fig. 3F.3e.

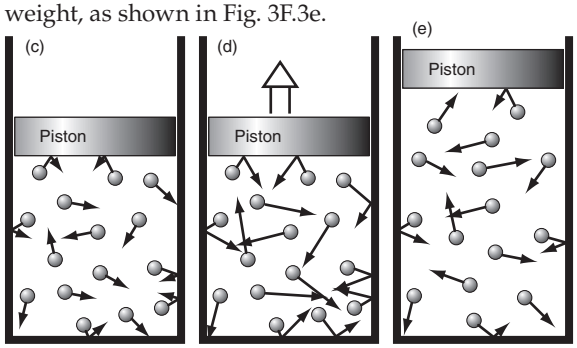

Fig. 3F.3. *Molecules in a constant-pressure chamber.*

Hence, this is an isobaric process (determined by the weight of the piston in this contrived example). The ideal gas law for constant pressure says:

$$\rho_o \cdot T_o = \rho_1 \cdot T_1 = \text{constant} = P / \Re \qquad (3F.3)$$

If you know how much thermal energy Δq you added per kilogram of material, and you measure the resulting increase in temperature $T_1 - T_o$, then you can empirically determine the **specific heat at constant pressure:**

$$C_p = \Delta q/(T_1 - T_o) \qquad (3F.4)$$

which is about $C_p = 1004\ \text{J}\cdot\text{kg}^{-1}\cdot\text{K}^{-1}$ for dry air.

C_p vs. C_v

Thus, in a constant pressure situation, the addition of Δq thermal energy results in less warming [$(T_1 - T_o) < (T_2 - T_o)$] than at constant volume. The reason is that, for constant pressure, some of the random microscopic kinetic energy of the molecules is converted into the macroscale **work** of expanding the air and moving the piston up against the pull of gravity. Such conservation of energy is partly described by the First Law of Thermodynamics.

In the atmosphere, the pressure at any altitude is determined by the weight of all the air molecules above that altitude (namely, the "piston" is all the air molecules above). If you add a small amount of thermal energy to air molecules at that one altitude, then you haven't significantly affected the number of molecules above, hence the pressure is constant. Thus, for most atmospheric situations it is appropriate to use C_p , not C_v , when forecasting temperature changes associated with the transfer of thermal energy into or from an air parcel.

Solved Example

Find the specific heat at constant pressure for humid air holding 10 g of water vapor per kg of dry air.

Solution

Given: $r = 10 g_{vapor}/1000 g_{dry\ air} = 0.01$ g/g
Find: C_p = ? J·kg^{-1}·K^{-1}

Use eq. (3.2):

$C_p = (1004\ \text{J·kg}^{-1}\text{·K}^{-1}) \cdot [\ 1 + (1.84 \cdot (0.01\ \text{g/g}))\ ]$

$= \underline{\mathbf{1022.5\ J·kg}}^{-1}\text{·K}^{-1}$

Check: Units OK. Magnitude reasonable.
Discussion: Even a modest amount of water vapor can cause a significant increase in specific heat. See Chapter 4 for typical ranges of r in the atmosphere.

FOCUS • Specific Heat Cp for Air

The specific heat at constant pressure C_p for air is the average of the specific heats for its constituents, weighted by their relative abundance:

$$m_T \cdot C_p = m_d \cdot C_{pd} + m_v \cdot C_{pv} \qquad (3F.5)$$

where $m_T = m_d + m_v$ is the total mass of air (as a sum of mass of dry air m_d and water vapor m_v), and C_{pd} and C_{pv} are the specific heats for dry air and water vapor, respectively.

Define a mixing ratio r of water vapor as $r = m_v / m_d$. Then eq. (3F.5) becomes:

$$C_p = (1 - r) \cdot C_{pd} \cdot [1 + r \cdot C_{pv} / C_{pd}] \qquad (3F.6)$$

Given: C_{pd} = 1004 J·kg^{-1}·K^{-1} at 0°C for dry air, and C_{pv} = 1850 J·kg^{-1}·K^{-1} for water vapor, eq. (3F.6) becomes

$$C_p \approx C_{pd} \cdot [1 + 1.84 \cdot r] \qquad (3.2)$$

Even for dry air, the specific heat varies slightly with temperature, as shown in figure 3F.4, below:

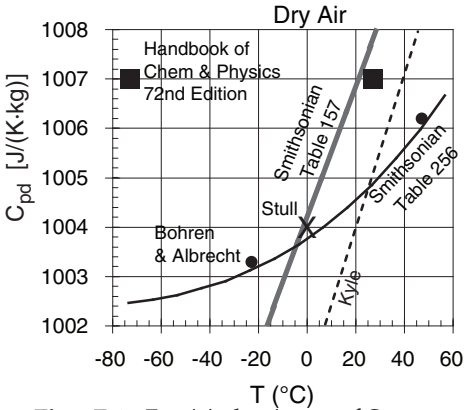

Fig. 3F.4. *Empirical estimates of C_{pd}.*

In this book, we will use C_{pd} = 1004 J·kg^{-1}·K^{-1} , and will approximate it as being constant.

$$C_p \approx C_{pd} \cdot [1 + 1.84 \cdot r] \qquad (3.2)$$

where r is the mixing ratio of water vapor, in units of $g_{vapor}/g_{dry\ air}$. The specific heat of liquid water is much greater: $C_{liq} \approx 4200$ J·kg^{-1}·K^{-1}.

Latent

Latent heat is a hidden heat related to water **phase changes**. Evaporation of liquid-water droplets cools the air by removing sensible heat and storing it as latent heat. The following list summarizes those water phase changes that cool the air:

vaporization: liquid to vapor
melting: solid (ice) to liquid
sublimation: solid to vapor

Phase changes of water in the opposite direction cause sensible warming of the air by releasing latent heat:

condensation: vapor to liquid
fusion: liquid to solid (ice)
deposition: vapor to ice

When air parcels or fixed volumes contain moist air, there is the possibility that water phase changes can alter the temperature, even without heat transport across the volume boundaries. The amount of heat ΔQ_E per mass of phase-changed water Δm_{water} is defined to be

$$\frac{\Delta Q_E}{\Delta m_{water}} = L \qquad \bullet(3.3)$$

where L is known as the **latent-heat** factor.

Values of the latent-heat factor for water are:

$L_v = \pm\ 2.5\text{x}10^6$ J·kg^{-1} $= L_{\ condensation\ \ or\ vaporization}$

$L_f = \pm\ 3.34\text{x}10^5$ J·kg^{-1} $= L_{\ fusion\ or\ \ melting}$

$L_d = \pm\ 2.83\text{x}10^6$ J·kg^{-1} $= L_{\ deposition\ or\ sublimation}$

where the sign depends on the direction of phase change, as described above. See Appendix B for tables of geophysical constants.

LAGRANGIAN HEAT BUDGET – PART 1: UNSATURATED

Air Parcels

Consider a hypothetical blob of air that we follow and examine as it moves through the atmosphere. We can think of it as a very large air-filled balloon about the diameter of two city blocks, but without any latex skin. This lack of a latex skin leaves the air blob unprotected.

When these air blobs move through the atmosphere, myriad eddies (swirls of turbulent motion) tend to mix some of the outside air with the air just inside the blob (such as the mixing you see in smoke rising from a campfire). Thus, warmer or colder air could be added to (**entrained** in through the sides of) the blob, and some air from inside could be lost (**detrained**) to the surrounding atmosphere. Also, in the real atmosphere, atmospheric radiation can heat or cool the air blob. These processes combine to make thermodynamic study of real air blobs extremely difficult.

But to gain some insight into the thermodynamics of air, we can imagine a simplified situation where radiative effects are relatively small, and where the turbulent entrainment/detrainment happens only in the outer portions of the air blob, leaving an inner core somewhat protected. This is indeed observed in the real atmosphere. So consider the protected inner core (about the diameter of a city block) as an **air parcel**.

As the parcel moves we can compute its thermodynamic and dynamic state, based on work done on it, changes within it, fluxes across its surface, and mixing with its surrounding environment. This concept is often employed in **Lagrangian** studies.

In Part 1 of this Lagrangian description, we will study only those situations where there is NO condensation or evaporation of water; namely, **unsaturated** conditions. This does not mean that the air is dry — only that any water vapor within the air is not undergoing phase changes.

Historically, these processes with no phase changes are called "**dry**" processes, even though there may be water vapor in the air. In the Moisture chapter, after moisture variables are introduced, the analysis will continue in a section called " Lagrangian Heat Budget – Part 2: Saturated", where "**moist**" (saturated) processes are included.

Solved Example

How much latent heat is released when 2 kg of water vapor condenses into liquid?

Solution

Given: $m_{vapor} = 2$ kg , $L_v = 2.5 \times 10^6$ J·kg^{-1} .
Find: ΔQ_E = ? J

Rearrange eq. (3.3)

$\Delta Q_E = (2.5 \times 10^6 \text{ J·kg}^{-1}) \cdot (2 \text{ kg}) =$ **5,000 kJ**

Check: Units OK. Physics reasonable.
Discussion: This amount of liquid water would fill a typical bathtub to only a depth of 2 mm. Thus, a small amount of water can hold a large amount of latent heat. Water vapor is a very important source of energy to drive storms.

Solved Example

How much dew must condense on the sides of a can of soda for it to warm the soda from 1°C to 16°C?

Hints: Neglect the heat capacity of the metal can. The density of liquid water is 1000 kg·m^{-3}. Assume the density of soda equals that of pure water. Assume the volume of a can is 354 ml (milliliters), where 1 l = 10^{-3} m^3.

Solution

Given: $\rho_{water} = 1000$ kg·m^{-3}.
$C_{liq} = 4200$ J·kg^{-1}·K^{-1}
Volume (*Vol*) in Can = 354 ml
$L_{cond} = +2.5 \times 10^6$ J·kg^{-1}
$\Delta T = 15$ K
Find: Volume of Condensate
Sketch:

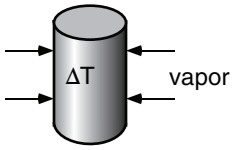

Equate the latent heat release by condensing water vapor (eq. 3.3) with the sensible heat gained by fluid in the can (eq. 3.1)

$$\Delta Q_E = \Delta Q_H$$

$$\rho_{condensate} \cdot (\Delta Vol\ of\ Condensate) \cdot L_{cond} = \rho_{soda} \cdot (Vol\ of\ Can) \cdot C_{liq} \cdot \Delta T$$

Assume the density of condensate and soda are equal, so they cancel. The equation can then be solved for $\Delta Volume\ of\ Condensate$.

$\Delta Volume\ of\ Condensate = (Vol\ of\ Can) \cdot C_{liq} \cdot \Delta T / L_{cond}$
$= (354 \text{ ml}) \cdot (4200 \text{ J·kg}^{-1}\text{·K}^{-1}) \cdot (15 \text{ K}) / (2.5 \times 10^6 \text{ J·kg}^{-1})$
= **8.92 ml**

Check: Units OK. Sketch OK. Physics OK.
Discussion: Latent heats are so large that an amount of water equivalent to only 2.5% of the can volume needs to condense on the outside to warm the can by 15°C. Thus, to keep your can cool, insulate the outside to prevent dew from condensing.

FOCUS • Enthalpy vs. Heat

Let Δq (J/kg) be the amount of thermal energy you add to a stationary mass m of air. Some of this energy warms the air. But as air warms, its volume expands by amount ΔV and pushes against the surrounding atmosphere (which to good approximation is pushing back with constant pressure P). The **work** W done on the atmosphere is $W = P{\cdot}\Delta V$. (To see this, recall that pressure is force F per unit area A. Thus work $W = P{\cdot}\Delta V = F{\cdot}\Delta V/A = F{\cdot}\Delta d$ = force times distance, where volume ΔV divided by area A is distance Δd.)

The **First Law of Thermodynamics** says that energy is conserved, thus the thermal energy input must balance the sum of warming and work done per unit mass:

$$\Delta q = C_v{\cdot}\Delta T + P{\cdot}(\Delta V/m) \qquad (3.4a)$$

where C_v (J·kg^{-1}·K^{-1}) is the **specific heat of air** at constant volume.

But $P{\cdot}(\Delta V/m) = \Delta(P{\cdot}V/m) - V{\cdot}\Delta P/m$ (from the chain rule of calculus). Also, $P{\cdot}V/m = P/\rho = \Re{\cdot}T$ from the ideal gas law, where $\rho = m/V$ is air density and $\Re$ is the gas *constant*. Using this in eq. (3.4a) gives:

$$\Delta q = C_v{\cdot}\Delta T + \Re{\cdot}\Delta T - \Delta P/\rho \qquad (3.4b)$$

By definition for an ideal gas: $C_v + \Re = C_p$. Thus, you can combine the first two terms on the right to give a form of the **First Law of Thermodynamics** that you can use for the atmosphere:

$$\underset{heat}{\Delta q} = \underset{enthalpy}{C_p{\cdot}\Delta T} - \Delta P/\rho \qquad (3.4)$$

In engineering thermodynamics, the word **heat** always refers to the amount the thermal energy transferred to or from a system; namely, heat per unit mass is Δq. However, the amount of thermal energy possessed by a mass of air at constant pressure is given the name **enthalpy**, h. Thus, $h = C_p{\cdot}T$, and $\Delta h = C_p{\cdot}\Delta T$ is the change in enthalpy associated with a temperature change. Engineers carefully discriminate between the words **heat** (heat transferred to/from an object) and **enthalpy** (heat possessed by an object).

This same careful definition should also be used in meteorology. However, by tradition, meteorologists often use the word **sensible heat** in place of the word enthalpy, to describe the heat possessed by an object. Hence, we must be very careful when we talk about "heat". With this in mind, the First Law of Thermo can be annotated as follows:

$$\underset{\substack{heat\\transferred}}{\Delta q} = \underset{\substack{sensible\\heat}}{C_p{\cdot}\Delta T} - \Delta P/\rho \qquad (3.4)$$

This form is useful in meteorology, when rising air parcels experience a decrease in surrounding atmospheric pressure, hence, the last term is non-zero.

First Law of Thermodynamics

The temperature of an air parcel of mass m_{air} changes by amount ΔT when heat (Δq) is transferred to or from the parcel. The temperature also changes when work is done on or by the parcel. This relationship, called the **First Law of Thermodynamics**, can be written (see the Focus box at left) as:

$$C_p \cdot \Delta T = \Delta q + \frac{\Delta P}{\rho} \qquad \bullet(3.4)$$

Heat transferred Δq has units of J/kg. ΔP is the pressure change of air in the parcel, and ρ is air density. The pressure of the parcel usually equals that of its surrounding environment, which decreases exponentially with height. The last term will be non-zero for a rising or sinking air parcel as its pressure changes to match the pressure of its environment.

The first law of thermodynamics can be reformulated using the hydrostatic equation to yield the temperature change of a rising or sinking air parcel

$$\Delta T = -\left(\frac{|g|}{C_p}\right)\cdot\Delta z + \frac{\Delta q}{C_p} \qquad \bullet(3.5)$$

Solved Example

What is the temperature change of a 10 kg air parcel when heated at rate $H = 100$ W for 10 minutes? Water-vapor mixing ratio is $r = 0.01\ g_{vapor}/g_{air}$, and the air parcel is stationary.

Solution

Given: $H = 100$ W, $m_{air} = 10$ kg, $\Delta z = 0$,
$r = 0.01\ g_{vapor}/g_{air}$, $\Delta t = 10$ min
Find: ΔT = ? K

First, calculate the specific heat from eq. (3.2):
$C_p = (1004.67\ J{\cdot}kg^{-1}{\cdot}K^{-1}){\cdot}[1 + 0.84 \cdot 0.01]$
$= 1013.11\ J{\cdot}kg^{-1}{\cdot}K^{-1}$.

Next, calculate the total heat added:
$\Delta Q_H = H{\cdot}\Delta t = (100\ W){\cdot}(10\ min)$
$= (100\ J/s){\cdot}(600\ s) = 6x10^4$ J.

Finally, use eq. (3.5):
$\Delta T = (6x10^4\ J) / [(10\ kg) \cdot (1013.11\ J{\cdot}kg^{-1}{\cdot}K^{-1})]$
$= \mathbf{5.92\ K}$.

Check: Units OK. Physics reasonable.
Discussion: Air density is about 1.225 kg/m^3 at sea level. Thus, 10 kg occupies 8.16 m^3, which is about the size of a large closet. According to the first law of thermodynamics, the air in this closet would be warmed by almost 6 °C if we turned on a 100 W electric light bulb and left it on for 10 minutes, assuming no heat is lost to the walls of the closet.

The heat-transfered-per-mass term (Δq) on the right can be caused by radiative heating, latent heating during condensation, dissipation of turbulence energy into heat, heat from chemical reactions, and convective or turbulent interactions between air inside and outside of the parcel. Advection and convection do not transport heat to/from the parcel, but they do move the parcel about (Fig. 3.1).

The first law of thermodynamics is also called the **conservation of heat**. It says that the temperature of an air parcel will not change, unless heat is added or removed, or unless the pressure of the parcel changes. Thus, even without adding heat to a parcel, its temperature can change during vertical parcel motion. Vertical motion is very important in atmospheric circulations and cloud development.

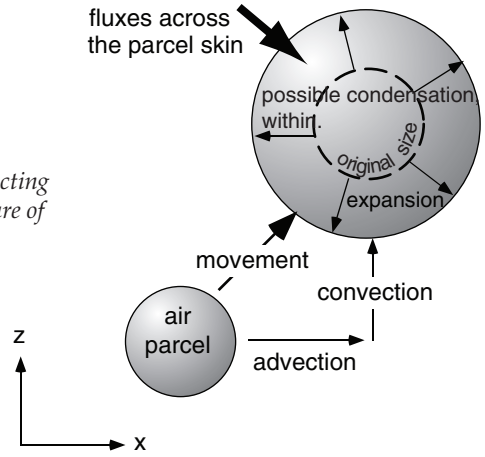

Figure 3.1
Processes affecting the temperature of an air parcel.

Lapse Rate

The decrease of temperature with height is known as the **lapse rate**, Γ. Namely,

$$\Gamma = -\frac{T_2 - T_1}{z_2 - z_1} = -\frac{\Delta T}{\Delta z} \tag{3.6}$$

Two types of lapse rate are **environmental** lapse rates and **process** lapse rates (Fig. 3.2).

When the existing temperature-state of the environment is measured with aircraft, weather balloons, or remote sensors, the resulting graph of temperature vs. height is called an **environmental temperature profile**, or an **environmental sounding**. The temperature decrease within this sounding gives the **environmental lapse rate** as a function of height. It is a static measure of the state of the environment.

Fig. 1.10 is an example of an environmental sounding based on standard-atmosphere conditions. The actual environmental sounding on any day might differ. A wide range of soundings is possible.

A **process lapse rate** gives the temperature decrease associated with some action or process. Examples are the temperature changes with height inside rising air parcels, inside rising cloud parcels, and due to external processes such as radiative heating or cooling. The change of temperature with height for a process is usually defined by a physical relationship, such as the first law of thermodynamics. One common process is the adiabatic process, described next.

Solved Example

Find the lapse rate in the troposphere for a standard atmosphere.

Solution

Given: Std. Atmos. Table 1-5 in Chapter 1, , where
T= –56.5°C at z = 11 km, and T = +15°C at z = 0 km.
Find: Γ = ? °C/km
Use eq. (3.6): Γ = – (–56.5 – 15) /(11–0) = **+6.5 °C/km**

Check: Positive Γ, because T decreases with z.
Discussion: This is the environmental lapse rate of the troposphere.

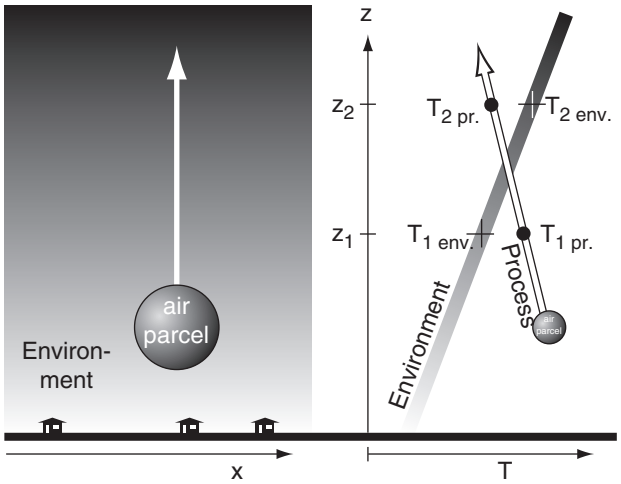

Figure 3.2
Left: Sketch of a physical situation, showing an air parcel moving through an environment. In the environment, darker colors indicate warmer air. Right: Temperature profiles for the environment and the air parcel. The environmental air is not moving. In it, air at height z_1 has temperature $T_{1\ env}$, and air at z_2 has $T_{2\ env}$. The air parcel has an initially warm temperature, but its temperature changes as it rises: becoming $T_{1\ pr}$ at height z_1, and later becoming $T_{2\ pr}$ at height z_2. In the environment of this example, temperature increases as height increases, implying a negative environmental lapse rate. However, the air parcel's temperature decreases with height, implying a positive parcel lapse rate.

Solved Example
A 15°C air parcel at $z = 0$ rises to 2 km. Find final T.

Solution
Given: $T_{initial} = 15°C$, $\Delta z = 2$ km
Find: $T_{final} = ?$ °C

Assume: dry adiabatic process. Use eq. (3.7):
$\Delta T/\Delta z = (T_{final} - T_{init.}) / (z_{final} - z_{init.}) = -9.8$ °C/km
$T_{final} = T_{initial} - (9.8\ °C/km) \cdot \Delta z$
$= 15\ °C - (9.8\ °C/km) \cdot (2\ km) = \underline{\mathbf{-4.6\ °C}}$.

Check: Units OK. Physics reasonable.
Discussion: Sufficient cooling to freeze water.

BEYOND ALGEBRA • Adiabatic Lapse Rate

Calculus can be used to get eq. (3.10) from (3.4). First, write the First Law of Thermo. in its more-accurate differential form, for an adiabatic process ($\Delta q = 0$):

$$dP = \rho \cdot C_p \cdot dT_v$$

Then substitute for density using the ideal gas law $\rho = P / (\Re_d \cdot T_v)$, to give:

$$dP = \frac{P \cdot C_p \cdot dT_v}{\Re_d \cdot T_v}$$

Move pressures to the LHS, and temperatures to the RHS:

$$\frac{dP}{P} = \frac{C_p}{\Re_d} \cdot \frac{dT_v}{T_v}$$

Integrate between pressure P_1 where temperature is T_1, to pressure P_2 where temperature is T_2:

$$\int_{P_1}^{P_2} \frac{dP}{P} = \frac{C_p}{\Re_d} \cdot \int_{T_{v1}}^{T_{v2}} \frac{dT_v}{T_v}$$

where $C_p / \Re_d$ is relatively constant, and was moved out of the integral on the RHS. The result is:

$$\ln(P)\Big|_{P_1}^{P_2} = (C_p / \Re_d) \cdot \ln(T_v)\Big|_{T_{v1}}^{T_{v2}}$$

Plug in the limits, and use $\ln(a) - \ln(b) = \ln(a/b)$:

$$\ln\left(\frac{P_2}{P_1}\right) = (C_p / \Re_d) \cdot \ln\left(\frac{T_{v2}}{T_{v1}}\right)$$

Move $C_p / \Re_d$ to the LHS:

$$(\Re_d / C_p) \cdot \ln\left(\frac{P_2}{P_1}\right) = \ln\left(\frac{T_{v2}}{T_{v1}}\right)$$

Recall that $a \cdot \ln(b) = \ln(b^a)$, thus:

$$\ln\left[\left(\frac{P_2}{P_1}\right)^{\Re_d / C_p}\right] = \ln\left(\frac{T_{v2}}{T_{v1}}\right)$$

Finally, take the anti-log of both sides ($e^{LHS} = e^{RHS}$):

$$\left(\frac{P_2}{P_1}\right)^{\Re_d / C_p} = \frac{T_{v2}}{T_{v1}} \qquad (3.10)$$

Adiabatic Lapse Rate

An **adiabatic** process is one where there is no heat transfer to or from the air parcel ($\Delta q = 0$). This is reasonable if we remember that the air parcel is the protected inner core of a larger blob of air. An air parcel that rises "dry adiabatically" (with no cloud formation) experiences a temperature change given by eq. (3.5), which can be rearranged as:

$$\frac{\Delta T}{\Delta z} = -\left(\frac{|g|}{C_p}\right) = -9.8\ \text{K/km} \qquad \bullet(3.7)$$

Thus, the **"dry" adiabatic lapse rate** Γ_d for a rising air parcel is

$$\Gamma_d = 9.8\ \text{K/km} = 9.8\ °\text{C/km} \qquad (3.8)$$

and it is a process lapse rate. (Degrees K and °C are interchangeable in this equation, because it represents a temperature change with height.) As mentioned earlier, "dry" adiabatic processes also apply to humid air, but only if there is no condensation, clouds, or precipitation in it (i.e., only if the air is unsaturated).

The adiabatic lapse rate can also be found in terms of pressure instead of height. Substituting the ideal gas law into the first law of thermodynamics for an adiabatic process yields:

$$\frac{\Delta T}{T} = \frac{\Re_d}{C_p} \cdot \left(\frac{\Delta P}{P}\right) \qquad (3.9)$$

or

$$\frac{T_2}{T_1} = \left(\frac{P_2}{P_1}\right)^{\Re_d / C_p} \qquad \bullet(3.10)$$

where $\Re_d / C_p = 0.28571$ (dimensionless) for dry air, and where temperatures are in Kelvin.

A different adiabatic lapse rate ("moist" lapse rate) must be used if there is liquid or solid water in the air parcel. This is discussed later in the Moisture chapter.

Solved Example
An air parcel with initial (P, T) = (100 kPa, 20°C) rises adiabatically to $P = 80$ kPa. Find its new T.

Solution
Given: $P_1 = 100$ kPa, $P_2 = 80$ kPa, $T_1 = 20°C = 293K$
Find: $T_2 = ?$ °C

Use eq. (3.10): $T_2 = (293K) \cdot [(80kPa)/(100kPa)]^{0.28571}$
$T_2 = 293K \cdot 0.9382 = 274.9\ K = \underline{\mathbf{1.9°C}}$

Check: Units OK. Value good, since 80 kPa is about 2 km above 100 kPa, we expect about 20°C cooling.

When calculating temperature differences, units of °C and K are interchangeable, because a change of ΔT = 1°C equals a change of ΔT = 1 K. However, when extracting a temperature from such a difference, always convert it to K before using it in a radiative or ideal gas law.

Potential Temperature

When an air parcel rises/sinks "dry" adiabatically into regions of lower/higher pressure, its temperature changes due to work done by/on the air, even though no thermal energy has been removed/added. Define a new temperature variable called the **potential temperature** θ that is proportional to the sensible heat contained in the parcel, but which is unaffected by work done by/on the parcel.

Namely, the potential temperature is constant (i.e., is a **conserved variable**) for adiabatic processes (i.e., $\Delta q = 0$) such as air-parcel ascent, but can increase/decrease when sensible heat is added/removed. Such **diabatic** (non-adiabatic) heat transfer processes include turbulent mixing, condensation, and radiative heating (i.e., $\Delta q \neq 0$).

If height is used as the vertical coordinate, then you can calculate the value of potential temperature θ from:

$$\theta(z) = T(z) + \Gamma_d \cdot z \qquad \bullet(3.11)$$

The units (°C or K) of θ(z) are the same as the units of T(z).

For pressure coordinates, find the value of θ from:

$$\theta = T \cdot \left(\frac{P_o}{P} \right)^{\Re_d / C_p} \qquad \bullet(3.12)$$

where P_o is a reference pressure, $\Re_d/C_p = 0.28571$ (dimensionless) and where absolute temperatures (K) must be used. The word "potential" arises because θ corresponds to the temperature T that a parcel would potentially have if it were moved adiabatically to the ground or to a reference pressure.

It is common practice to use a reference level of P_o = 100 kPa in eq. (3.12), but this is not a strict definition. For example, boundary-layer meteorologists often use eq. (3.11) where z is height above local ground level, not above the 100 kPa altitude.

To include the buoyant effects of water vapor and liquid water in air, we can define a **virtual potential temperature** for air with no liquid water or ice (3.13), and for air containing liquid water and/or ice (3.14) such as cloud or rain drops, or snow:

$$\theta_v = \theta \cdot [1 + (a \cdot r)] \qquad (3.13)$$

$$\theta_v = \theta \cdot [1 + (a \cdot r) - r_L - r_I] \qquad \bullet(3.14)$$

Solved Example

Find θ for air at z = 500 m with T = 10°C?

Solution

Given: z = 500 m, T = 10°C
Find: θ = ? °C

Assume no liquid water, and use eq. (3.11)
θ = 10°C + (9.8 °C/km)· (0.5 km) = **14.9 °C**

Check: Units OK. Physics reasonable.
Discussion: This is the T that air would have when lowered dry adiabatically to the surface. θs are always greater than the actual T, for z above the ref. level.

Solved Example

Find θ for air at P = 70 kPa with T = 10°C?

Solution

Given: P = 70 kPa , T = 10°C = 283 K, P_o = 100 kPa
Find: θ = ? °C

Use eq. (3.12): θ = (283 K) · [(100 kPa) / (70 kPa)]$^{0.28571}$
θ = 313.6 K = **40.4 °C**

Check: Physics OK. θ is always greater than the actual T, for P smaller than the reference pressure.

Solved Example

What is the virtual potential temperature of air at having potential temperature 15°C, mixing ratio 0.008 $g_{water\ vapor}/g_{air}$, and liquid water mixing ratio of: a) 0 ; b) 0.006 $g_{liq.water}/g_{air}$?

Solution

Given: θ =15°C = 288 K, r = 0.008 $g_{water\ vapor}/g_{air}$,
a) r_L = 0 ; b) r_L =0.006 $g_{liq.water}/g_{air}$ ·
Find: θ_v = ? °C
Abbreviate "water vapor" with "wv" here.

a) Use eq (3.13): θ_v = (288K)·
[1 + (0.61 g_{air}/g_{wv}) · (0.008 g_{wv} /g_{air})] .
Thus, θ_v = 289.4 K. Or subtract 273 to get Celsius: θ_v = **16.4 °C**.

a) Use eq (3.14): θ_v = (288K)·
[1 + (0.61 g_{air}/g_{wv}) · (0.008 g_{wv}/g_{air}) −
0.006 $g_{liq.}/g_{air}$] = 287.7 K.
Subtract 273 to get Celsius: θ_v = **14.7°C**.

Check: Units OK. Physics reasonable.
Discussion: When no liquid water is present, virtual pot. temperatures are always warmer than potential temperatures, because water vapor is lighter than air.

However, liquid water is heavier than air, and has the opposite effect. This is called **liquid-water loading**, and makes the air act as if it were colder.

Solved Example

Given cloudy air at P = 70 kPa with T = –1°C, r_s = 5 $g_{water\ vapor}/kg_{air}$, r_L = 2 $g_{liq\ water}/kg_{air}$. Find θ_v.

Solution

Given: P = 70 kPa , T = –1°C = 272K,
$r_s = 5\ g_{water\ vapor}/kg_{air} = 0.005\ g_{wv}/g_{air}$
$r_L = 2\ g_{liq\ water}/kg_{air} = 0.002\ g_{liq}/g_{air}$
Find: θ_v = ? °C

First, use eq. (3.12) to find the potential temperature
$\theta = (272K) \cdot [(100\ kPa)/(70\ kPa)]^{0.28571} = 301\ K$

Next, use eq. (3.15):
$\theta_v = (301\ K) \cdot [\ 1 + (0.61\ g_{air}/g_{wv}) \cdot (0.005\ g_{wv}/g_{air}) - (0.002)\ ] = 301K \cdot (1.001) =$ **301.3 K**
θ_v = 301.3 K – 273 K = **28.3°C**

Check: Units OK. Physics reasonable.
Discussion: For this example, there was little effect of the vapor and liquid water. However, for situations with greater water vapor or liquid water, the virtual potential temperature can differ by a few degrees, which can be important for estimating thunderstorm intensity.

where r is mixing ratio of water vapor, r_L is the mixing ratio of liquid water (cloud and rain drops), r_I = ice mixing ratio, a = 0.61 $g_{air}/g_{water\ vapor}$, and both θ values must be in units of Kelvin. Mixing ratio is described in the Moisture chapter; it is the ratio of grams of water per gram of air. θ_v is used to determine how high air parcels can rise, or how quickly they sink. θ_v is constant only when there is no phase changes and no heat transfer; namely, no latent or sensible heat is absorbed or released.

For air that is rising within clouds, with water vapor condensing, it is usually the case that the air is saturated (= 100% relative humidity; see the Moisture chapter for details). As a result, the water-vapor mixing ratio r can be replaced with r_s , the saturation mixing ratio.

$$\theta_v = \theta \cdot [1 + (a \cdot r_s) - r_L] \qquad \bullet(3.15)$$

where a = 0.61 $g_{air}/g_{water\ vapor}$, as before.

However, there are other situations where the air is NOT saturated, but contains liquid water. An example is the non-cloudy air under a cloud base, through which rain is falling at its terminal velocity. For this case, eq (3.14) should be used with an unsaturated value of water-vapor mixing ratio. This situation occurs often, and can be responsible for damaging downbursts of air (see the Thunderstorm chapters).

Why use potential temperature? Because it makes it easier to compare the temperatures of air parcels at two different heights — important for determining if air will buoyantly rise to create thunderstorms. For example, suppose air parcel A has temperature T_A = 20°C at z = 0, while air parcel B has T_B = 15°C at z = 1 km. Parcel A is warmer than parcel B.

Does that mean that parcel A is buoyant (warmer and wants to rise) relative to parcel B? The answer is no, because when parcel B is moved dry adiabatically to the altitude of parcel A, then parcel B is 5°C warmer than parcel A due to adiabatic warming. In fact, you can move parcels A and B to any common altitude, and after considering their adiabatic warming or cooling, parcel B will always be 5°C warmer than parcel A.

The easiest way to summarize this effect is with potential temperature. Using eq. (3.11), we find that θ_A = 20°C and θ_B = 25°C approximately. θ_A and θ_B keep their values (because θ is a conserved variable) no matter to what common altitude you move them, thus θ_B is always 5 °C warmer than θ_A in this illustration.

Another application for potential temperature is to label lines on a thermodynamic diagram, such as described next.

Thermodynamic Diagrams –Part 1: Dry Adiabatic Processes

It is often necessary to compare environmental lapse rates with process or parcel lapse rates, in order to determine parcel buoyancy, cloudiness and storm growth. Sometimes it is easier to utilize a diagram that already indicates the proper thermodynamic relationships, rather than recalculating the thermodynamic equations for every situation. Such a diagram is called a **thermodynamic diagram**, or **thermo diagram** for short.

These diagrams usually include relationships between so many variables that they become quite cluttered with lines and numbers. We will develop our own thermodynamic diagrams little by little as the book progresses. In this first part, we will include only "dry" adiabatic processes.

Most thermodynamic diagrams have temperature along the horizontal axis, and pressure or height along the vertical axis. We will use pressure with a reversed logarithmic scale along the vertical, as an approximation to height. Fig. 3.3 is an example of such a diagram.

To this background chart, we will add diagonal lines showing the temperature decrease with height associated with air parcels rising adiabatically from the surface. These lines are called **"dry" adiabats**. They are also sometimes called **isentropes**.

We can draw different lines for parcels starting at the bottom of the graph (bottom of the atmosphere) with different temperatures. Fig. 3.3 shows the result, as calculated using a computer spreadsheet (see the Focus box).

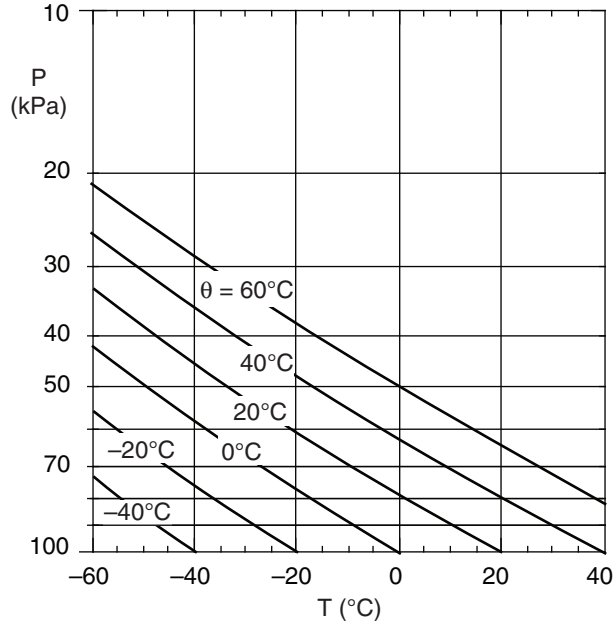

FOCUS • Spreadsheet Thermodynamics

Thermodynamic diagrams can be produced with spreadsheet programs on personal computers. To calculate the dry adiabats, first type in the following row and column headers. Also shown in the spreadsheet below is the first set of temperature values representing the dry adiabats for air parcels starting at four of the different temperatures. These temperatures were just typed in as numbers.

	A	B	C	D	E
1	Dry Adiabat Example				
2					
3	P(kPa)	T(°C)	T(°C)	T(°C)	T(°C)
4	100.0	60.0	40.0	20.0	0.0

Next, in cell A5, increment to the next pressure by typing equation: =A4 – 10 .

In cell B5, enter eq. (3.10) for the temperature along a dry adiabat: =((B$4+273)*($A5/A4)^0.28571) – 273 The dollar sign implies an absolute reference; namely one that is not changed as the equation is auto-filled down or across.

Next select cell B5, and fill it across C5 and D5 to E5:

	A	B	C	D	E
1	Dry Adiabat Example				
2					
3	P(kPa)	T(°C)	T(°C)	T(°C)	T(°C)
4	100.0	60.0	40.0	20.0	0.0
5	90.0	50.1	30.7	11.3	-8.1

Then, select cells A5 through E5. Fill down to row 12

	A	B	C	D	E
1	Dry Adiabat Example				
2					
3	P(kPa)	T(°C)	T(°C)	T(°C)	T(°C)
4	100.0	60.0	40.0	20.0	0.0
5	90.0	50.1	30.7	11.3	-8.1
6	80.0	39.4	20.7	1.9	-16.9
7	70.0	27.7	9.7	-8.4	-26.4
8	60.0	14.8	-2.5	-19.8	-37.1
9	50.0	0.2	-16.2	-32.6	-49.0
10	40.0	-16.7	-32.1	-47.5	-62.9
11	30.0	-36.9	-51.1	-65.3	-79.5
12	20.0	-62.7	-75.4	-88.0	-100.6

Finally, select all the cells holding numbers, and make a graph. Switch the axes such that pressure is on the vertical axis, reverse the order so pressure decreases upward, and finally make the vertical axis logarithmic. The result should look like Fig. 3.3.

Figure 3.3 (at left)
Thermodynamic diagram showing the temperature change of air parcels of several different initial surface (at P = 100 kPa) temperatures, as they rise dry adiabatically. Recall from Chapter 1 that a logarithmic pressure decrease corresponds to roughly a linear height increase. Thus, height increases upward in this diagram. The thick diagonal lines are called "dry" adiabats, and are labeled with potential temperature.

Solved Example

Given air at P = 70 kPa with T = –1°C. Find θ using the thermo diagram of Fig. 3.3.

Solution

Given: P = 70 kPa , T = –1°C
Find: θ = ? °C

First, use the thermo diagram to find where the 70 kPa isobar and the –1°C isotherm intersect. (Since the –1°C isotherm wasn't drawn on this diagram, we must mentally interpolate between the lines that are drawn.) The adiabat that passes through this intersection point indicates the potential temperature (again, we must interpolate between the adiabats that are drawn). By extending this adiabat down to the reference pressure of 100 kPa, we can read off the temperature 28°C, which corresponds to the potential temperature θ = **28°C** .

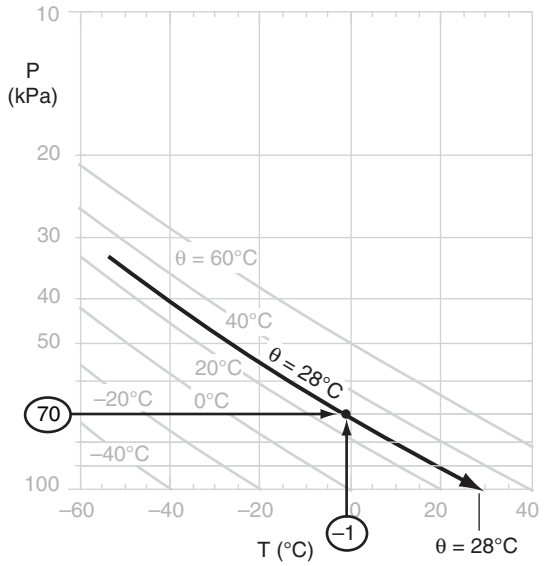

Check: Units OK. Physics reasonable.

Discussion: This exercise is the same as the first part of the previous exercise, for which we calculated θ = 301 K = 28°C. Yes, the answers agree.

The advantage of using an existing printed thermo diagram is that we can draw a few lines and quickly find the answer without doing any calculations. So it can make our lives easier, once we learn how to use it.

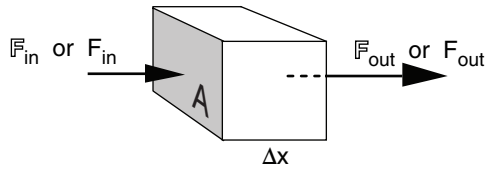

Figure 3.4
Change of flux F across distance Δx can cause changes within the volume. A is area of the face of the cube through which the flux flows. F is a kinematic flux, and $\mathbb{F}$ is a dynamic flux.

Potential temperature is constant along these diagonal lines, so the lines are usually labeled with θ. Sometimes the labeling is implicit; namely, by the temperature near the bottom of the graph where the adiabat intercepts P = 100 kPa. For example, the diagonal line third from the left in Fig. 3.3 is the θ = 0°C adiabat.

To use this diagram, plot the initial temperature and pressure of the air parcel as a point on the graph. If that air parcel rises or descends to a new pressure, draw a line parallel to the diagonal lines, starting at the initial point, and ending at the final pressure. This line shows how the parcel temperature changes, and what its final temperature is. This approach is easier than solving equations, but not as accurate.

EULERIAN HEAT BUDGET

First Law of Thermo. – Revisited

If the heat flux into one side of a fixed volume is less than the flux out of the opposite side (Fig. 3.4), then some amount of heat Δq is obviously removed from the volume. According to the first law of thermodynamics eq. (3.5), a heat loss causes a temperature decrease (assuming no other work is done).

Thus, it is not the flux itself, but the **gradient of flux** (i.e., the change of kinematic flux ΔF_x or dynamic flux $\Delta\mathbb{F}_x$ across distance Δx) that causes temperature change within the volume. The gradient of flux is also known as a **flux divergence**. A positive value of $\Delta F_x/\Delta x$ gives a positive divergence (more flux leaving the volume than entering). Negative flux divergence is possible, which is sometimes called a **flux convergence**.

Considering the fluxes in all three dimensions, the first law of thermodynamics can be rewritten in Eulerian form as a **heat budget**, **heat balance** , or **heat conservation equation** for a stationary volume (e.g., $Vol = A \cdot \Delta x$ in Fig. 3.4):

(3.16)

$$\frac{\Delta T}{\Delta t} = -\frac{1}{\rho \cdot C_p}\left[\frac{\Delta \mathbb{F}_x}{\Delta x} + \frac{\Delta \mathbb{F}_y}{\Delta y} + \frac{\Delta \mathbb{F}_z}{\Delta z}\right] + \frac{\Delta So}{C_p \cdot \Delta t}$$

where ΔS_o is the internal source of heat per unit mass (e.g., J·kg^{-1}), such as caused by **latent heating**, radioactive decay, and exothermal chemical reactions. ΔS_o is negative for net cooling.

The kinematic-flux (F) form of the budget is:

$$\frac{\Delta T}{\Delta t} = -\left[\frac{\Delta F_x}{\Delta x} + \frac{\Delta F_y}{\Delta y} + \frac{\Delta F_z}{\Delta z}\right] + \frac{\Delta So}{C_p \cdot \Delta t} \qquad \bullet(3.17)$$

In these equations, Δx, Δy, and Δz represent the length of sides of the volume, not movement of the volume. Finally, the heat budget can be rewritten using potential temperature:

$$\frac{\Delta\theta}{\Delta t} = -\left[\frac{\Delta F_x}{\Delta x} + \frac{\Delta F_y}{\Delta y} + \frac{\Delta F_z}{\Delta z}\right] + \frac{\Delta So}{C_p \cdot \Delta t} \qquad \bullet(3.18)$$

As discussed in Appendix A, you must be careful when using gradients to ensure that the numerator and denominator are in the same direction. Thus, the flux gradient in the *x*-direction is:

$$\frac{\Delta F_x}{\Delta x} = \frac{F_{x\ right} - F_{x\ left}}{x_{right} - x_{left}} \qquad (3.19)$$

Flux gradients are similar in the other directions. Gradients are like slopes, when plotted.

Equations (3.16 - 3.18) are important because they are used to make temperature forecasts. To solve these equations, we must determine the flux gradients. The flux gradients that appear in eqs. (3.16 - 3.18) can be caused by **advection** (*adv*), **conduction** (*cond*), **turbulence** (*turb*), and **radiation** (*rad*):

$$\frac{\Delta F_x}{\Delta x} = \left.\frac{\Delta F_x}{\Delta x}\right|_{adv} + \left.\frac{\Delta F_x}{\Delta x}\right|_{cond} + \left.\frac{\Delta F_x}{\Delta x}\right|_{turb} + \left.\frac{\Delta F_x}{\Delta x}\right|_{rad} \qquad (3.20)$$

$$\frac{\Delta F_y}{\Delta y} = \left.\frac{\Delta F_y}{\Delta y}\right|_{adv} + \left.\frac{\Delta F_y}{\Delta y}\right|_{cond} + \left.\frac{\Delta F_y}{\Delta y}\right|_{turb} + \left.\frac{\Delta F_y}{\Delta y}\right|_{rad} \qquad (3.21)$$

$$\frac{\Delta F_z}{\Delta z} = \left.\frac{\Delta F_z}{\Delta z}\right|_{adv} + \left.\frac{\Delta F_z}{\Delta z}\right|_{cond} + \left.\frac{\Delta F_z}{\Delta z}\right|_{turb} + \left.\frac{\Delta F_z}{\Delta z}\right|_{rad} \qquad (3.22)$$

We will describe each of these processes next. Finally, the source term ΔS_o will be estimated, and all the results will be put back into the Eulerian heat budget equation.

Advection

The word advect means "to be transported by the mean wind". **Temperature advection** relates to heat being blown to or from a region by the wind. The amount of **advective flux** of heat increases linearly with mean temperature, and with mean wind speed:

$$F_{x\ adv} = U \cdot T \qquad (3.23)$$

$$F_{y\ adv} = V \cdot T \qquad (3.24)$$

$$F_{z\ adv} = W \cdot T \qquad (3.25)$$

Solved Example

Given a cube of dry air at sea level, with side 20 m. An eastward moving heat flux of 3 W·m^{-2} flows in through the left, while a westward moving heat flux of 4 W·m^{-2} flows in through the right. There are no other fluxes or internal sources of heat. What is the kinematic heat flux through each side, and at what rate will temperature change inside the cube?

Solution

Given: $\mathbb{F}_{x\ right} = -4$ W·m^{-2} (negative because it is moving in the negative *x* direction)
$\mathbb{F}_{x\ left} = 3$ W·m^{-2}, $\Delta x = 20$ m

Find: $F_{x\ right}$ = ? K·m/s, $F_{x\ left}$ = ? K·m/s
$\Delta T/\Delta t$ = ? K/s

Sketch:

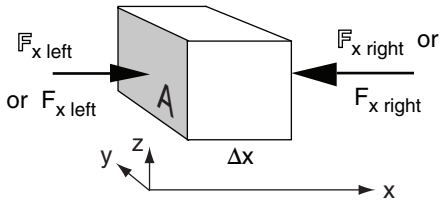

Use eq. (2.11): $F = \mathbb{F} / (\rho \cdot C_p)$

$F_{x\ left}$ = (3 W·m^{-2}) / [1231 (W·m^{-2}) / (K·m·s^{-1})]
= **2.437x10^{-3} K·m·s^{-1}** .

$F_{x\ right}$ = (–4 W·m^{-2}) / [1231 (W·m^{-2})/(K·m·s^{-1})]
= **– 3.249x10^{-3} K·m·s^{-1}** .

The flux gradient (eq. 3.19) is thus:

$$\frac{\Delta F_x}{\Delta x} = \frac{\left[(-3.249\times10^{-3}) - (2.437\times10^{-3})\right](\mathrm{K\cdot m\cdot s^{-1}})}{[20-0]\,(\mathrm{m})}$$

$= -2.843\text{x}10^{-4}$ K·s^{-1}.

Plugging this flux gradient into (3.17) gives
$\Delta T/\Delta t$ = **+ 2.843x10^{-4} K·s^{-1}**.

Check: The sign is positive implying warming with time, because heat is flowing into both sides of the cube.

Discussion: The heating rate is equivalent to 1 K/h.

Solved Example

Given a cube of air with winds as sketched in Fig 3.4. Let the mean wind speed be 10 m/s from west to east, but the temperature entering from the left is 20°C while that leaving on the right is 18°C. If the cube has side 20 km, then what is the advective flux gradient? (That is, what is the temperature-tendency contribution from advection.)

Solution

Given: $U = 10$ m/s, $\Delta T = 18 - 20°C = -2°C$,
$\Delta x = 20$ km
Find: $\Delta F_{x\,adv} / \Delta x$ = ? °C/s

Use (3.26): $\Delta F_{x\,adv} / \Delta x = U \cdot (\Delta T/\Delta x)$
= (10 m/s) · [–2°C / 20000 m] = **– 0.001 °C/s**.
= **–3.6 °C/h**

Check: Units OK. Sketch OK. Physics OK.
Discussion: If this flux gradient were used in the heat-budget equation (3.17), the warming rate would be +3.6 °C/h due to advection. This is called **warm-air advection**, because warmer air is entering the region than is leaving.

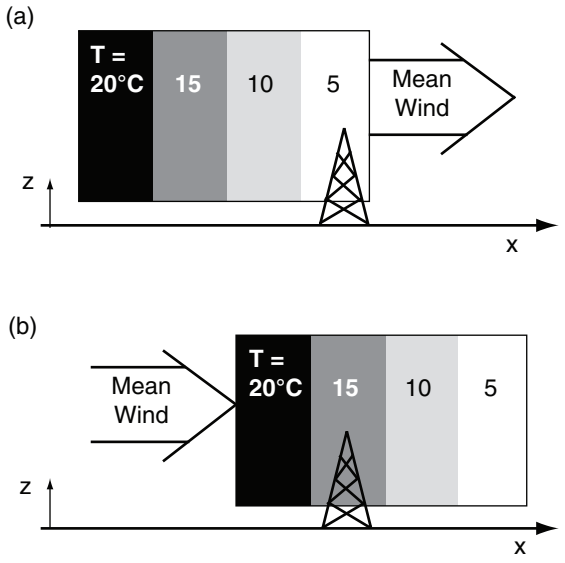

Figure 3.5
Advection illustration. (a) Initial state of the air with an east-west temperature gradient. (b) Later, after the air moves east.

Solved Example

Suppose the average air temperature gets colder with height, such that T = 15°C at z = 200 m and T = 10°C at z = 1000 m, with a linear change in between. If the mean vertical velocity is blowing the cold air downward from aloft, then what is the advective cooling rate at z = 600 m, given a vertical velocity of W = –0.1 m/s? There are no other heat-transfer processes.

Solution

Given: $W = -0.1$ m/s, $z = 600$ m
$\Delta T/\Delta z$ = (10–15°C)/(1000–200 m)
= –0.00625 °C/m
Find: $\Delta T/\Delta t$ = ? °C/s

This is a trick question. Although the air is colder aloft, we anticipate that it will warm as it descends due to the adiabatic compression discussed in the previous sections. When the air gets to the height of interest (600 m), it might be so hot as to cause warming rather than cooling. So we must be careful in solving this.

Plugging (3.28) into (3.17), and neglecting all other heat-transfer processes, we find

$\Delta T/\Delta t = -W\,(\Delta T/\Delta z + \Gamma_d)$
= – (–0.1 m/s) · (–0.00625+ 0.0098°C/m)
= **+ 3.55x10^{-4} °C/s**

Check: Units OK. Physics reasonable.
Discussion: The positive sign indicates a warming rate, not cooling. This advective warming rate is the same at all heights between 200 and 1000 m, not just at 600 m. The warming rate is equivalent to 1.28 °C/hour, which could cause a significant temperature increase if it continues for many hours.

Vertical motion is also called **advection** if by the mean wind, but is called **convection** if caused by buoyancy.

The heat budget (eqs. 3.16 - 3.18), however, uses the flux gradient, not the raw flux. As illustrated in Fig. 3.5a, the temperature at a fixed point such as at the top of a tall tower might initially be 5 °C. However, if the air temperature is greater in the west than the east, and if the wind is blowing from the west, then after a while the warmer air will be over the tower (Fig. 3.5b). Thus, the temperature increases with time at the fixed point for a situation with positive mean wind (blowing from west to east) and a negative horizontal temperature gradient (temperature decreasing from west to east).

Although Fig. 3.5 illustrates only horizontal advection in one direction, we need to consider advective effects in all directions, including vertical. If the mean wind speed varies little across the region of interest, then

$$\frac{\Delta F_{x\,adv}}{\Delta x} = \frac{U \cdot \left(T_{right} - T_{left}\right)}{x_{right} - x_{left}} = U \cdot \frac{\Delta T}{\Delta x} \qquad (3.26)$$

Similarly:

$$\frac{\Delta F_{y\,adv}}{\Delta y} = V \cdot \frac{\Delta T}{\Delta y} \qquad (3.27)$$

and

$$\frac{\Delta F_{z\,adv}}{\Delta z} = W \cdot \left[\frac{\Delta T}{\Delta z} + \Gamma_d\right] \qquad (3.28)$$

The dry adiabatic lapse rate Γ_d = 9.8 °C/km is added to the last term to compensate for the adiabatic temperature change that normally accompanies vertical motion as parcels move into regions of different pressure. This correction term must always be added to temperature whenever vertical motions (vertical advections) are considered.

Substituting eq. (3.11) into eqs. (3.26 - 3.28) allows potential temperature to be used for advection:

$$\frac{\Delta F_{x\ adv}}{\Delta x} = U \cdot \frac{\Delta \theta}{\Delta x} \qquad \bullet(3.29)$$

$$\frac{\Delta F_{y\ adv}}{\Delta y} = V \cdot \frac{\Delta \theta}{\Delta y} \qquad \bullet(3.30)$$

$$\frac{\Delta F_{z\ adv}}{\Delta z} = W \cdot \frac{\Delta \theta}{\Delta z} \qquad \bullet(3.31)$$

Solved Example

The potential temperature of the air increases 5°C per 100 km distance north. If a north wind of 20 m/s is blowing, find the advective flux gradient, and the temperature change associated with this advection.

Solution

Given: $\Delta\theta/\Delta y$ = 5°C/100 km = 5×10^{-5} °C/m
V = – 20 m/s (a north wind comes from the north)
Find: $\Delta F/\Delta y$ = ? °C/s, and $\Delta T/\Delta t$ = ? °C/s

Use eq. (3.30): $\Delta F/\Delta y = (-20\ \text{m/s}) \cdot (5 \times 10^{-5}\ ^\circ\text{C/m})$
= **–0.001 °C/s**
Use eq. (3.17) neglecting all other terms:
$\Delta T/\Delta t = -\Delta F/\Delta y = -(-0.001^\circ\text{C/s}) =$ **+0.001 °C/s**

Check: Physics reasonable. Sign appropriate, because we expect warming as the warm air is blown toward us from the north in this example.
Discussion: $\Delta T/\Delta t$ = 3.6°C/h, a rapid warming rate.

Molecular Conduction & Surface Fluxes

Heat can be transported by individual molecules bouncing into each other. This conduction process works in solids, liquids and gases, and works with or without any mean or turbulent wind. It is the primary way heat is transferred from the Earth's surface to the atmosphere, and also the primary way that heat is transported deeper into the ground.

The amount of conductive heat flux in the vertical is

$$\mathbb{F}_{z\ cond} = -k \cdot \frac{\Delta T}{\Delta z} \qquad (3.32)$$

where the molecular conductivity k is a property of the material through which heat flows. For air at standard conditions near sea level, $k = 2.53 \times 10^{-2}$ W·m^{-1}·K^{-1}.

Temperature gradients $\Delta T/\Delta z$ in most interior parts of the troposphere are relatively small, and k is very small. Thus, molecular conduction is negligible in those regions. Thus, for simplicity we will use

$$\frac{\Delta F_{x\ cond}}{\Delta x} \approx \frac{\Delta F_{y\ cond}}{\Delta y} \approx \frac{\Delta F_{z\ cond}}{\Delta z} \approx 0 \qquad (3.33)$$

in the heat budget equation (3.17) everywhere except at the ground.

Within the bottom few millimeters of air near the surface, vertical temperature gradients can be quite large (Fig. 3.6). For example, on a sunny summer day, the sun might heat the surface of an asphalt road to temperatures greater than 50°C, while the adjacent air temperatures are about 20 or 30°C. Such a large gradient is sufficient to drive a substantial heat flux.

Solved Example

What vertical temperature difference is necessary across the bottom 1 mm of atmosphere to conduct 300 W·m^{-2} of heat flux?

Solution

Given: $\mathbb{F}_{z\ cond}$ = 300 W·m^{-2}, Δz = 0.001 m
$k = 2.53 \times 10^{-2}$ W·m^{-1}·K^{-1}
Find: ΔT = ? °C
Sketch: (see Fig. 3.6)

Rearrange eq. (3.32) to solve for ΔT:
$\Delta T = -\Delta z \cdot \mathbb{F}_{z\ cond} / k$
$\Delta T = -(10^{-3}\ \text{m}) \cdot (300\ \text{W·m}^{-2}) / (2.53 \times 10^{-2}\ \text{W·m}^{-1}\text{·K}^{-1})$
$\Delta T =$ **– 11.9°K**

Check: Units OK. Physics OK.
Discussion: The air 1 mm above ground must be almost 12°C cooler than the surface to conduct the required heat flux. Such large temperature differences are often observed in the real atmosphere very near the ground, especially on sunny days when the ground becomes very hot.

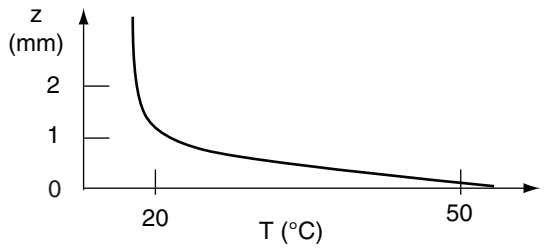

Figure 3.6
Strong temperature gradients within a few millimeters of the ground on a sunny day can drive strong conductive heat fluxes there, but higher in the atmosphere conduction is negligible.

Solved Example

Find the effective surface kinematic heat flux over a forest when the wind speed is 5 m·s^{-1} at a height of 10 m, the surface temperature is 25°C, and the air temperature at 10 m is 20°C.

Solution

Given: M = 5 m/s, z = 10 m
$T_{sfc} - T_{air}$ = 25 – 20°C = 5 °C
Find: F_H = ? K·m·s^{-1}

Use eq. (3.35):
$F_H = (2\text{x}10^{-2})\cdot(5\text{ m/s})\cdot(5°\text{C}) = \underline{\mathbf{0.5\ °C\cdot m\cdot s}}^{-1}$

Check: Units OK. Physics OK.
Discussion: Using conversion (2.11), the dynamic heat flux is 615.5 W·m^{-2}, which is almost half of the solar constant of roughly 1366 W·m^{-2}. This suggests that 50% of the incoming solar radiation heats the air, while the remainder causes evaporation, is conducted into the ground, or is reflected, for this example.

When conduction and turbulence are considered together, we see that turbulence is zero at the ground where conduction can be important, while turbulence is important in the rest of the lower atmosphere where conduction is negligible. For this reason, turbulence and conduction are often combined into an **effective surface turbulent heat flux**, F_H.

In practice, it is virtually impossible to use eq. (3.32) directly, because the temperature gradient across the bottom few millimeters of air is rarely measured or predicted. However, on **windy** days the combination of conduction and turbulence causes the effective surface heat flux to be:

$$F_H = C_H \cdot M \cdot (\theta_{sfc} - \theta_{air}) \qquad \bullet(3.34)$$

or

$$F_H \cong C_H \cdot M \cdot (T_{sfc} - T_{air}) \qquad \bullet(3.35)$$

M is the mean wind speed at 10 m, T_{air} is the air temperature at a height of 10 m, T_{sfc} is the surface skin temperature, and θ_{air} and θ_{sfc} are the corresponding potential temperatures.

C_H is the **bulk heat transfer coefficient**. This coefficient is unfortunately not constant, but varies with surface conditions and turbulence intensity. It has a dimensionless value in the range of 2x10^{-3} over smooth surfaces to 2x10^{-2} over rough or forested surfaces. Eqs. (3.34 - 3.35) are useful during strong advection.

The bottom 1 to 2 km of the troposphere is called the **atmospheric boundary layer** (**ABL**, see the ABL chapter). During **calm** days with strong solar heating and convection, warm rising **thermals** (buoyant air parcels) often occur within the ABL. This type of ABL is called a **mixed layer** (**ML**). The rising thermals cause a substantial effective surface heat flux. Instead of using eqs. (3.34 - 3.35) on these calm sunny days, the surface flux can be found from:

$$F_H = b_H \cdot w_B \cdot (\theta_{sfc} - \theta_{ML}) \qquad \bullet(3.36)$$

or

$$F_H = a_H \cdot w_* \cdot (\theta_{sfc} - \theta_{ML}) \qquad \bullet(3.37)$$

where θ_{ML} is the potential temperature of the air at a height of about 500 m, in the middle of the mixed layer. The empirical **mixed-layer transport coefficient** is a_H = 0.0063, and the **convective transport coefficient** is b_H = 5x10^{-4}. Both are independent of surface roughness.

A **buoyancy velocity scale** w_B gives the effectiveness of thermals in producing vertical heat transport:

$$w_B = \left[\frac{|g| \cdot z_i}{T_{v\,ML}} \cdot (\theta_{v\,sfc} - \theta_{v\,ML}) \right]^{1/2} \qquad \bullet(3.38)$$

where z_i is the depth of the convective ABL (i.e., the mixed layer), and $|g| = 9.8\ \text{m/s}^2$ is gravitational acceleration. Virtual temperatures and virtual potential temperatures (both in absolute units of K) are used in this last expression, but not in eqs. (3.36 - 3.37). Typical vertical velocities are about $w \approx 0.02 \cdot w_B$. To good approximation, the denominator in eq. (3.38) can be approximated by $\theta_{v\,ML}$ (also in units of K).

The **Deardorff velocity** w_* is another convective velocity scale, and is defined as

$$w_* = \left[\frac{|g| \cdot z_i}{T_v} \cdot F_{Hsfc} \right]^{1/3} \qquad \bullet(3.39)$$

where T_v is an average absolute virtual temperature in the ABL, and $F_{Hsfc} = F_H$ is surface kinematic heat flux. Typical values are $w_* = 1$ to 2 m·s^{-1}, and $w_* \approx 0.08 \cdot w_B$.

Another way to find F_H is with a surface heat budget or a Bowen ratio, as described later in this chapter. You could also write an expression similar to eqs. (3.36 - 3.37), except for surface moisture flux in terms of the difference in water-vapor mixing ratio between the surface and the mid-mixed layer.

Solved Example

On a calm sunny day, a 2 km thick mixed layer is dry with θ = 295 K. If T_{sfc} = 325 K, find the effective surface kinematic heat flux.

Solution

Given: $\theta_{ML} = 295$ K, $\theta_{sfc} = 325$ K
$z_i = 2000$ m, $|g| = 9.8\ \text{m·s}^{-2}$
Find: $F_{z\,eff.sfc.}$ = ? K·m·s^{-1}

For dry air: $\theta = \theta_v$ (see eq. 3.13).
Use eq. (3.38) first, then eq. (3.36):

$$w_B = \left[\frac{|9.8\text{m/s}^2| \cdot 2000\text{m}}{295\text{K}} \cdot (325\text{K} - 295\text{K}) \right]^{1/2}$$

$= (\ 1993\ \text{m}^2/\text{s}^2\ )^{1/2} = 44.6\ \text{m·s}^{-1}$

$F_H = (5\text{x}10^{-4}) \cdot (44.6\ \text{m·s}^{-1}) \cdot (325\ \text{K} - 295\ \text{K})$
$= \underline{\mathbf{0.67\ K·m·s^{-1}}}$

Check: Units OK. Physics reasonable.
Discussion: Greater surface-atmosphere temperature differences drive more vigorous thermals, and each thermal then transports more heat.

Turbulence

Turbulence is the quasi-random movement of air by small (order of 2 mm to 2 km) swirls of motion called **eddies**. Although the amount of air leaving one region is always replaced by the same amount returning from somewhere else (conservation of air mass), the departing air might have a different temperature than the arriving air. By moving temperature around, the net result is a heat flux.

Because there are so many eddies of all sizes moving in such a complex fashion, meteorologists do not even try to describe the heat flux contribution from each individual eddy. Instead, meteorologists use statistics to describe the average heat flux caused by all the eddies within a region (see the Atmos. Boundary Layer chapter). The expressions below represent such statistical averages.

The net effect of turbulence is to mix together air from different initial locations. Thus, turbulence tends to homogenize the air. Potential temperature, wind, and humidity gradually become mixed toward more uniform states by the action of turbulence. The amount of mixing varies with time and location, as turbulence intensity changes.

Solved Example

Given an effective surface kinematic heat flux of 0.67 K·m·s^{-1} , find the Deardorff velocity for a dry, 1 km thick boundary layer of temperature 25°C

Solution

Given: $F_H = 0.67\ \text{K·m·s}^{-1}$, $z_i = 1$ km = 1000 m ,
$T_v = T$ (because dry) = 25°C = 298 K.
Find: w_* = ? m/s

Use eq. (3.39):
$w_* = [\ (9.8\ \text{m·s}^{-2}) \cdot (1000\text{m}) \cdot (0.67\ \text{K·m·s}^{-1}) / (298\text{K})]^{1/3}$
$= \underline{\mathbf{2.8\ m/s}}$

Check: Units OK. Physics reasonable.
Discussion: Over land on hot sunny days, warm buoyant thermals often rise with a speed of the same order of magnitude as the Deardorff velocity.

Fair Weather (no thunderstorms)

During fair-weather, turbulence is strong during daytime over non-snowy ground, and can cause significant heat transport within the atmospheric

Solved Example

On a sunny fair-weather day with effective surface kinematic heat flux of 0.1 K·m·s^{-1}, what is the vertical flux divergence across an atmospheric boundary layer of depth 1 km?

Solution

Given: $F_H = 0.1$ K·m·s^{-1}, $z_i = 1000$ m
Find: $\Delta F_{z\ turb}/\Delta z$ = ? (K/s)

Use eq. (3.41):

$$\frac{\Delta F_{z\ turb}}{\Delta z} \approx \frac{-1.2 \cdot F_H}{z_i}$$

$$\frac{\Delta F_{z\ turb}}{\Delta z} \approx \frac{-1.2 \cdot (0.1\ \mathrm{K \cdot m/s})}{1000\mathrm{m}}$$

$$= \underline{\mathbf{-0.00012\ K{\cdot}s}}^{-1}$$

Check: Units OK. Physics OK.

Discussion: The negative sign on the gradient implies heating with time according to eq. (3.17), which makes sense during daytime.

The answer is equivalent to 0.43°C·h^{-1}, or about 5°C/12 h. This seems a bit small, compared to typical amounts of warming during the daylight hours. Thus, one would guess that daytime effective surface heat fluxes can be larger than 0.1 K·m·s^{-1}, and/or ABLs can be shallower than 1 km.

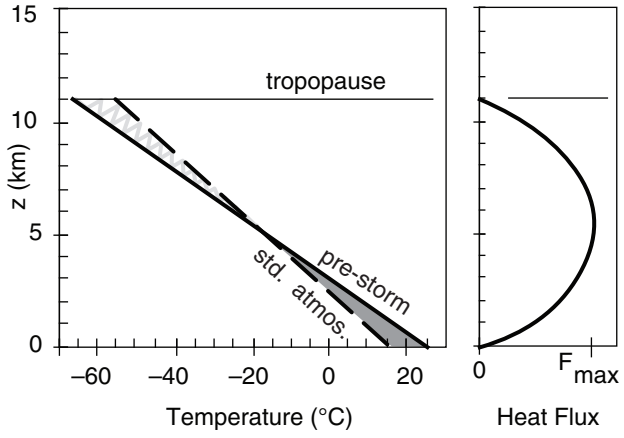

Figure 3.7
Pre-storm air at the bottom of the troposphere that is warmer (shaded dark grey) than the standard atmosphere tends to rise and exchange places with cooler air aloft (hatched light grey) during a thunderstorm. The result is a vertical heat flux.

boundary layer (ABL). [Reasons for different turbulence intensities are explained in the Atmospheric Boundary Layer chapter.] Due to the turbulent homogenization, turbulent fluxes vary roughly linearly with height, and can be estimated from the fluxes at the top and bottom of the ABL.

In fair weather (**wx**) during daytime, the heat flux at the top of the ABL is often roughly 20% of the magnitude of the surface heat flux, but has opposite sign. The flux at the bottom of the ABL is associated with conduction, and was given in the previous subsection as an effective turbulent surface flux F_H. This gives a turbulent flux divergence of:

$$\frac{\Delta F_{z\ turb}}{\Delta z} \approx \frac{F_{z\ top} - F_{z\ bottom}}{z_i} \qquad (3.40)$$

$0 < z < z_i$, fair wx

$$\frac{\Delta F_{z\ turb}}{\Delta z} \approx \frac{-1.2 \cdot F_H}{z_i} \qquad (3.41)$$

where z_i is the depth of the ABL (typically of order 200 m to 3 km).

Above the ABL during fair weather, turbulence is often negligible:

$$\frac{\Delta F_{z\ turb}}{\Delta z} \approx 0 \qquad \text{for } z > z_i \text{, fair wx} \quad (3.42)$$

At night, turbulence is often much weaker. Thus, vertical flux divergence is often quite small during fair-weather nights, and can be neglected everywhere except in the bottom 100 m or so.

Stormy Weather

During stormy weather, deep cumulus clouds and thunderstorms can cause vigorous turbulent mixing throughout the depth of the troposphere. Such convective clouds form in response to warm, buoyant air underlying cooler air (Fig. 3.7). This type of pre-storm environment is said to be unstable, as will be discussed in more detail in the chapters on Stability and Thunderstorms. The atmosphere tries to re-stabilize itself by letting the warm air rise and the cold air sink. This mixing process is called **moist convective adjustment**. Such mixing causes a vertical heat flux.

The mixing continues until some equilibrium profile of temperature is reached. As a first approximation, the **standard atmospheric lapse rate** ($\Gamma_{sa} = -\Delta T/\Delta z = +6.5$ K/km) is used here for the equilibrium profile. If the pre-storm lapse rate is $\Gamma_{ps} = -\Delta T/\Delta z$, then the vertical turbulent flux gradient is approximately:

$$\frac{\Delta F_{z\ turb}}{\Delta z} \approx \frac{z_T}{\Delta t} \cdot \left[\Gamma_{ps} - \Gamma_{sa}\right] \cdot \left(\frac{1}{2} - \frac{z}{z_T}\right) \qquad \text{stormy wx} \quad (3.43)$$

where Δt is the lifetime of the thunderstorms (order of 1 h) , and z_T is depth of the troposphere (order of 11 km). The term in square brackets is positive for an unstable pre-storm environment.

As shown in Fig. 3.7, the heat flux profile is shaped like a parabola. The turbulent vertical heat flux is zero at the top and bottom of the troposphere, and reaches a maximum of

$$F_{\max} = z_T{}^2 \cdot \left[\Gamma_{ps} - \Gamma_{sa} \right] / (8 \cdot \Delta t) \qquad \text{stormy wx} \tag{3.44}$$

in the middle of the troposphere.

The convective adjustment effect of cooling at low altitudes and heating aloft must be added to the precipitation effect (see the source term) of latent heating at all heights, to find the net affect of the thunderstorm. An even more accurate accounting would include IR longwave radiation divergence from the top of the thunderstorm anvil cloud.

In those regions where turbulence exists, turbulent transport in any horizontal direction often cancels transport in the opposite direction, yielding negligible net flux gradients. Also, in non-turbulent regions there is obviously no turbulent flux gradient. Thus, as an idealized approximation, we can assume the following everywhere:

$$\frac{\Delta F_{x\ turb}}{\Delta x} \approx \frac{\Delta F_{y\ turb}}{\Delta y} \approx 0 \tag{3.45}$$

Radiation

Air in the troposphere is relatively opaque to most wavelengths of infrared (IR) radiation, causing radiation emitted at one altitude to be reabsorbed into the air at a neighboring altitude, some of which is re-radiated back to the first level. The net result of this very complex process is a relatively small vertical IR flux gradient within the air, and a nearly zero horizontal flux gradient:

$$\frac{\Delta F_{x\ rad}}{\Delta x} \approx \frac{\Delta F_{y\ rad}}{\Delta y} \approx 0 \tag{3.46}$$

$$\frac{\Delta F_{z\ rad}}{\Delta z} \approx 0.1 \text{ to } 0.2 \text{ (K/h)} \tag{3.47}$$

In the absence of clouds, haze, or smoke, direct radiative warming of the air due to solar radiation is negligible. However, sunlight warms the air indirectly by heating the surface, which then transfers and distributes its heat to the air by conduction and turbulent convection. There can also be substantial solar warming of clouds during daytime.

Solved Example

What is the vertical turbulence flux gradient in stormy weather at 2 km altitude, if the pre-storm vertical temperature gradient was –10 °C/km? Also, what is the maximum value of vertical heat flux near the middle of the troposphere?

Solution

Given: $\Gamma_{ps} = -\Delta T/\Delta z = +10$ K/km, $\Gamma_{sa} = 6.5$ K/km
Find: $\Delta F_{z\ turb}/\Delta z$ = ? (K/s) , F_{max} = ? K·m/s
Assume: $z_T = 11$ km, $\Delta t = 1$ h = 3600 s.

Use eq. (3.43):

$$\frac{\Delta F_{z\ turb}}{\Delta z} \approx \frac{z_T}{\Delta t} \cdot \left[\Gamma_{ps} - \Gamma_{sa} \right] \cdot \left(\frac{1}{2} - \frac{z}{z_T} \right)$$

$$\frac{\Delta F_{z\ turb}}{\Delta z} \approx \frac{11\text{km}}{3600\text{s}} \cdot \left[(10 - 6.5) \frac{\text{K}}{\text{km}} \right] \cdot \left(\frac{1}{2} - \frac{2\text{km}}{11\text{km}} \right)$$

$\Delta F_{z\ turb}/\Delta z$ = **0.0034 K/s**

Use eq. (3.44):

F_{max} =(11,000m)·(11km)·[(10–6.5)K/km)]/[8·(3600s)]
= **14.7 K·m/s**

Check: Units OK. Physics OK.

Discussion: The positive flux gradient implies cooling over time, because of the negative sign on the flux gradient terms in eq. (3.17). This makes sense, because $z = 2$ km is in the bottom half of the troposphere, where the initially-warm air is becoming cooler with time due to mixing with the colder air from above.

The magnitude of the max heat flux due to thunderstorms is much greater than the heat flux due to thermals in fair weather. Thunderstorms move large amounts of heat upward in the troposphere.

ON DOING SCIENCE • Expert vs. Novice

Expert scientists and engineers often solve problems, organize knowledge, and perceive structure differently than students and other novices.

Problem Solving	Novice	Expert
... is ...	a recall task	a process
... begins with ...	hunt for "the equation"	qualitative analysis
... uses classification based on ...	surface features	deep structure
...tools include ...	"the equation"	graphs, limits, diagrams, conservation laws, etc.

Organizing Knowledge	Novice	Expert
Memory recall is ...	piecemeal	effortless retrieval of relevant collected facts
Reasoning by ...	jumping to hasty, unfounded conclusions	fast mental scan through a chain of possibilities
Conflicting data, ideas & conclusions are...	not recognized	recognized, pointing to need for more info
Related ideas are...	memorized as separate facts	integrated into a coherent big picture

Structure Perception	Novice	Expert
Cues about the structure are ...	missed	recognized and trigger new lines of thought
Disparate instances are...	separately classified based on surface features	recognized as having the same underlying structure
Tasks are performed...	before thinking about the organization	after data is organized to find structure
Theories that don't agree with data ...	are used without revision	identify ideas ripe for revision

(Paraphrased from Wendy Adams, Carl Wieman, Dan Schwartz, and Kathleen Harper.)

Internal Source: Latent Heat

The amount of latent heat given to the air during condensation of $\Delta m_{condensing}$ grams of water vapor that are already contained in the Eulerian volume is $L_v \cdot \Delta m_{condensing}$. When distributed throughout the mass of air m_{air} within the volume, the net latent heating rate for the source term is:

$$\frac{\Delta So}{C_p \cdot \Delta t} = \frac{L_v}{C_p} \cdot \frac{\Delta m_{condensing}}{m_{air} \cdot \Delta t} \tag{3.48}$$

For evaporation of existing liquid water, the sign is negative (to cool the air).

Consider a column of air equal to the troposphere depth of roughly z_{Trop} = 11 km, which is appropriate for thunderstorms. The average condensational heating rate of the whole column is proportional to the amount of precipitation that falls out of the bottom. If *RR* denotes **rainfall rate** measured as the change of depth of water in a rain gauge with time, then the latent heating source term is:

$$\frac{\Delta So}{C_p \cdot \Delta t} = \frac{L_v}{C_p} \cdot \frac{\rho_{liq}}{\rho_{air}} \cdot \frac{RR}{z_{Trop}} \tag{3.49}$$

where ρ_{liq} = 1000 kg·m^{-3} is the approximate density of liquid water, ρ_{air} is air density averaged over the whole column, and L_v / C_p = 2500 K·kg$_{air}$·kg$_{liq}^{-1}$ is the ratio of latent heat of condensation to specific heat at constant pressure.

Utilizing the standard atmosphere with a tropopause depth of 11 km gives an **average tropospheric density** of ρ_{air} = 0.689 kg·m^{-3}. Thus, eq. (3.49) can be rewritten as:

$$\frac{\Delta So}{C_p \cdot \Delta t} = a \cdot RR \tag{3.50}$$

where *a* = 0.33 K/(mm of rain), and for *RR* in (mm of rain)/s. Divide by 3600 for *RR* in mm/h.

Net Heat Budget

The net Eulerian heat budget is found by combining the first law of thermodynamics eqs. (3.17 or 3.18) with the definition of all the flux gradients eqs. (3.20 - 3.22). The long messy equation that results can be simplified for many atmospheric situations as follows.

Assume negligible vertical mean temperature advection. Assume negligible horizontal turbulent transport. Assume negligible conduction. Neglect direct solar heating of the troposphere, but approximate IR cooling as a small constant.

The resulting simplified Eulerian net heat budget equation is:

$$\left.\frac{\Delta T}{\Delta t}\right|_{x,y,z} = -\underbrace{\left[U\cdot\frac{\Delta T}{\Delta x}+V\cdot\frac{\Delta T}{\Delta y}\right]}_{\text{advection}} \underbrace{-0.1\frac{\text{K}}{\text{h}}}_{\text{radiation}}$$

$$\underbrace{-\frac{\Delta F_{z\ turb}(\theta)}{\Delta z}}_{\text{turbulence}} \underbrace{+\frac{L_v}{C_p}\cdot\frac{\Delta m_{condensing}}{m_{air}\cdot\Delta t}}_{\text{latent heat}} \quad \bullet(3.51)$$

where the θ in the turbulence term is to remind us that this turbulence flux divergence is for heat. In later chapters we will see similar turbulence flux divergences, but for moisture or momentum. If there is no condensation or evaporation (i.e., for non-cloudy air), the source-sink (latent-heat) term can be set to zero.

The net heat budget is important because you can use it to forecast air temperature at any altitude. Or, if you already know how the air temperature changes with time, you can use the net heat budget to see which processes are most important in causing this change.

The net heat budget applies to a blob of air having a finite volume and mass. For the special case of the Earth's surface (infinitesimally thin; having no mass), you can write a simplified heat budget, as described next.

SURFACE HEAT BUDGET

While the Lagrangian and Eulerian heat budgets give the temperature change and fluxes for a volume (moving or stationary, respectively), we can also examine the fluxes across the Earth's surface. Because the surface has zero thickness, all fluxes must sum to zero. This holds for both heat and moisture.

Heat Budget

During daytime, the net radiative heat-flux to the surface is $-\mathbb{F}^*$, which is balanced by three output fluxes from the surface. They are: turbulent sensible-heat transport into the air (**sensible heat flux** $\mathbb{F}_H$, sometimes called the heat flux), turbulent latent-heat transport into the air (**latent heat flux** $\mathbb{F}_E$ associated with evaporation from the surface), and **molecular conduction** flux from the ground $\mathbb{F}_G$. At night, the directions (signs) of the fluxes are reversed. Regardless of the surface scenario (Fig. 3.8), the fluxes toward the surface must balance the fluxes away from the surface.

Solved Example

Find the tropospheric average latent heating for a rainfall rate of 5 mm·h^{-1} from a thunderstorm.

Solution

Given: RR = 5 mm·h^{-1}.
Find: $\Delta S_o/(C_p\cdot\Delta t)$ = ? K·h^{-1}

Use eq. (3.50): $\Delta S_o/(C_p\cdot\Delta t)$ = 0.33 (K/mm)·(5 mm/h) = **1.65 K·h^{-1}**

Check: Units OK. Physics OK.
Discussion: This is the same order of magnitude as other terms in the Eulerian heat budget.

Solved Example

Find the temperature change during one hour at a fixed point, given U = 5 m/s, V = 0, $\Delta T/\Delta x$ = 1°C/10 km, $\Delta m_{cond}/m_{air}$ = 2 g_{water}/kg_{air} , for a daytime 800 m thick ABL with effective surface kinematic flux of 0.2 K·m/s. Use L_v/C_p = 2.5 K/(g_{water}/kg_{air}).

Solution

Given: (see above)
Find: ΔT = ? °C

Use eq. (3.51). Do each term separately, times Δt:

$$\text{Adv}\cdot\Delta t = -\left[(5\text{m/s})\cdot\left(\frac{1°\text{C}}{10^4\text{m}}\right)\right]\cdot(3600\text{s}) = -1.8°\text{C}$$

$$\text{Lat.Heat\_Source}\cdot\Delta t = \left(2.5\frac{\text{K}\cdot\text{kg}_{\text{air}}}{\text{g}_{\text{water}}}\right)\cdot\left(2\frac{\text{g}_{\text{water}}}{\text{kg}_{\text{air}}}\right) = +5.0°\text{C}$$

$$\text{Rad}\cdot\Delta t = \left(-0.1\frac{\text{K}}{\text{h}}\right)\cdot(1\text{h}) = -0.1°\text{C}$$

$$\text{Turb}\cdot\Delta t = -\frac{-1.2\cdot(0.2\text{K}\cdot\text{m/s})}{800\text{m}}\cdot(3600\text{s}) = +1.1°\text{C}$$

where (3.41) was used for the turbulence term.

Thus: ΔT = (Adv + Latent + Rad + Turb) · Δt
= (–1.8 + 5.0 – 0.1 + 1.1)°C = **4.2 °C**

Check: Units OK. Physics OK.
Discussion: Many processes act simultaneously, some adding and some subtracting from the total. This is one of the complexities of weather forecasting.

During daytime, direct radiative heating of the air is small, and can be neglected. However, strong heating of the ground by solar radiation allows the warm ground to heat the air via the surface heat flux. Thus, radiative heating from the sun is getting to the air indirectly via conduction of sensible heat from the ground, and via surface evaporation of water that transports latent heat. Latent heating was quite important here.

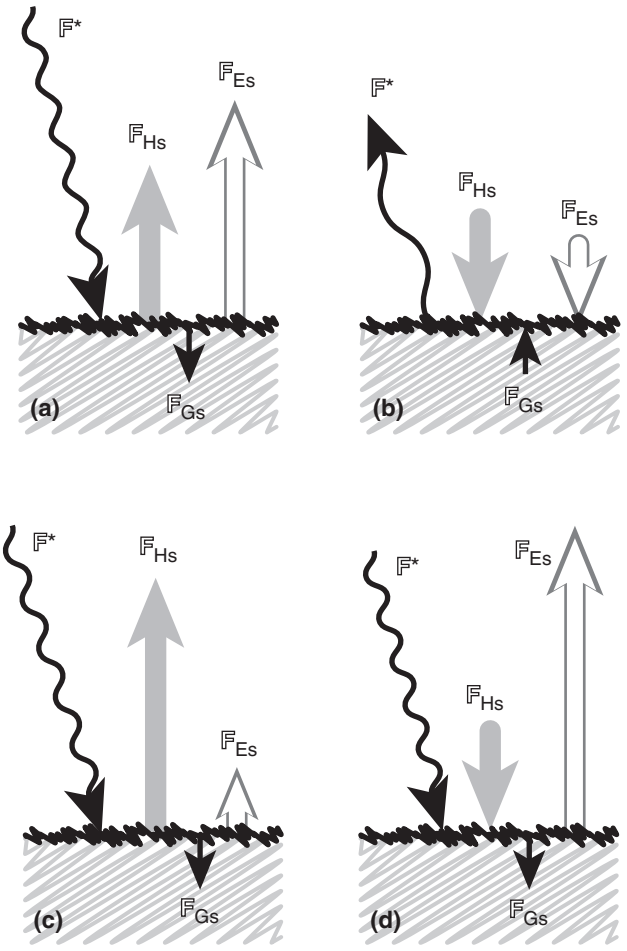

Figure 3.8
Fluxes affecting the surface heat budget. (a) Daytime over vegetated surface. (b) Nighttime over vegetated surface. (c) Daytime over a desert. (d) Oasis effect of warm, dry air advection over a cool, moist surface. $\mathbb{F}^*$ = net radiative flux, $\mathbb{F}_{Hs}$ = sensible heat flux, $\mathbb{F}_{Es}$ = latent heat flux, $\mathbb{F}_{Gs}$ = conductive heat flux into the ground, and subscript s refers to values at Earth's surface.

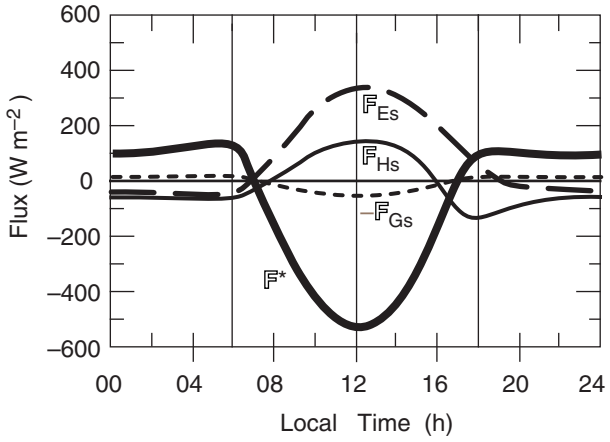

Figure 3.9
Typical diurnal variation of the surface heat budget. The $\mathbb{F}^*$ net radiation curve comes from Chapter 2. Fluxes are positive upward, as defined in the previous caption.

For an infinitesimally thin surface, this balance is

$$-\mathbb{F}^* = \mathbb{F}_H + \mathbb{F}_E - \mathbb{F}_G \qquad \bullet(3.52)$$

or in kinematic form (after dividing by $\rho_{air} \cdot C_p$):

$$-F^* = F_H + F_E - F_G \qquad \bullet(3.53)$$

where all fluxes are defined positive upward. All terms have units of $W \cdot m^{-2}$ in the first equation, and $K \cdot m \cdot s^{-1}$ in the second. Also, Fig. 3.9 shows an example of the daily variation of these fluxes for a moist vegetated surface.

One can think of the net radiation as a forcing on the system, and the other fluxes in eqs. (3.52 - 3.53) as the responses. Namely, all of the radiation absorbed at the surface must go somewhere.

To good approximation, the flux into the ground is proportional to the net radiative flux, which in dynamic and kinematic forms are:

$$\mathbb{F}_G \approx X \cdot \mathbb{F}^* \qquad (3.54)$$

$$F_G \approx X \cdot F^* \qquad (3.55)$$

where $X = 0.1$ during the day, and $X = 0.5$ at night.

Expressions for the effective sensible heat flux at the surface were presented in eqs. (3.34 - 3.37). Similar expressions can be used in the Moisture chapter for the latent heat flux. A Bowen-ratio method for measuring the sensible and latent flux is described in the next subsection.

Note the difference between the heat budget across the surface (eq. 3.53) where the fluxes must balance, and the heat budget within a volume of air (eq. 3.17) where any imbalance of the fluxes causes a net heating or cooling within the volume.

Bowen Ratio

The ratio of the sensible to latent heat fluxes is called the **Bowen ratio**, B:

$$B = \frac{\mathbb{F}_H}{\mathbb{F}_E} = \frac{F_H}{F_E} \qquad (3.56)$$

The Bowen ratio can be 0.1 over the sea, 0.2 over irrigated crops, 0.5 over grassland, 5 over semi-arid regions, and 10 over deserts.

Many observations have confirmed that the sensible heat flux is proportional to the vertical gradient of potential temperature $\Delta\theta$ in the bottom 20 m of the atmosphere. Namely, $F_H = -K_H \cdot \Delta\theta / \Delta z$, where K_H is an eddy diffusivity (see the Atmos. Boundary Layer chapter), and the negative sign says that the

heat flux flows down the local gradient (from hot toward cold air). Similarly, the moisture flux is proportional to the vertical gradient of mixing ratio Δr (grams of water vapor in each kilogram of dry air, as will be described in detail in the Moisture chapter). Namely, $F_E = -K_E \cdot \Delta r / \Delta z$.

By forming a ratio (the Bowen ratio) of these two fluxes and assuming $K_E = K_H$, the result is:

$$B = \gamma \cdot \frac{\Delta\theta}{\Delta r} \tag{3.57}$$

where $\gamma = C_p/L_v = 0.4$ ($g_{water\ vapor}/kg_{air}$)$\cdot K^{-1}$ is called the **psychrometric constant**.

Thus, the Bowen ratio can easily be measured using **thermometers** and **hygrometers**. The potential temperature $\Delta\theta$ and mixing ratio Δr differences must be measured between the same pair of heights z to use this approach (see Fig. 3.10). This gives, $\Delta\theta = T_2 - T_1 + (0.0098\ K/m)\cdot(z_2 - z_1)$, and $\Delta r = r_2 - r_1$.

When eq. (3.56) is combined with the surface energy balance eq. (3.52) and the approximation for ground flux eq. (3.54), the result for sensible heat flux is:

$$\mathbb{F}_H = \frac{-0.9 \cdot \mathbb{F}^*}{\frac{\Delta r}{\gamma \cdot \Delta\theta} + 1} \tag{3.58}$$

or kinematically:

$$F_H = \frac{-0.9 \cdot F^*}{\frac{\Delta r}{\gamma \cdot \Delta\theta} + 1} \tag{3.59}$$

Similarly, for latent heat flux associated with the evaporation or condensation of water at the surface:

$$\mathbb{F}_E = \frac{-0.9 \cdot \mathbb{F}^*}{\frac{\gamma \cdot \Delta\theta}{\Delta r} + 1} \tag{3.60}$$

or

$$F_E = \frac{-0.9 \cdot F^*}{\frac{\gamma \cdot \Delta\theta}{\Delta r} + 1} \tag{3.61}$$

Instead of calculating both equations, one can save time by calculating the first, and then using the surface energy balance to find the other:

$$\mathbb{F}_E = -0.9 \cdot \mathbb{F}^* - \mathbb{F}_H \tag{3.62}$$

or

$$F_E = -0.9 \cdot F^* - F_H \tag{3.63}$$

Solved Example

Given a net radiative surface flux of –600 W·m^{-2} over grassland, find the other terms of the surface heat budget.

Solution

Given: $\mathbb{F}^* = -600$ W·m^{-2} (probably daytime)
$B = 0.5$ for grassland
Find: $\mathbb{F}_G$, $\mathbb{F}_H$, $\mathbb{F}_E$ = ? W·m^{-2}

Use eq. (3.54) with $X = 0.1$ for day:
$\mathbb{F}_G = 0.1 \cdot \mathbb{F}^* = 0.1 \cdot (-600\ W\cdot m^{-2}) =$ **–60 W·m**$^{-2}$

Combine eqs. (3.52) & (3.56):
$\mathbb{F}_H = B \cdot (\mathbb{F}_G - \mathbb{F}^*) / (1 + B)$
$\mathbb{F}_E = (\mathbb{F}_G - \mathbb{F}^*) / (1 + B)$
Thus,
$\mathbb{F}_H = 0.5 \cdot (-60 + 600\ W\cdot m^{-2}) / (1 + 0.5)$
$=$ **180 W·m**$^{-2}$

$\mathbb{F}_E = (-60 + 600\ W\cdot m^{-2}) / (1 + 0.5)$
$=$ **360 W·m**$^{-2}$

Check: Units OK. Physics OK.
Discussion: Does the energy budget really balance? To answer this, use eq. (3.52):

$-\mathbb{F}^* = \mathbb{F}_H + \mathbb{F}_E - \mathbb{F}_G$
$600 = 180 + 360 + 60$ W·m^{-2} Yes, it balances.

The Bowen ratio is quite variable, even over a single type of surface such as grassland. For example, some grasses might be more moist or might be transpiring more than other grasses, depending on the maturity of the grass, insolation, air temperature, and soil moisture. For this reason, it is usually impossible to use the technique in this example to find the sensible and latent heat fluxes. A better alternative is to measure the Bowen ratio first, such as shown by Fig. 3.10 and eq. (3.57).

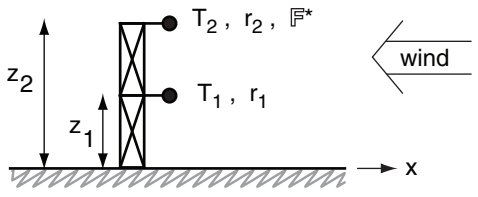

Figure 3.10
Instrumented tower for measuring temperature T and humidity r at two heights, z_1 and z_2. Net radiation is $\mathbb{F}^*$.

Solved Example

Given the following measurements from an instrumented tower, find the sensible and latent heat fluxes. Also, $\mathbb{F}^* = -500\ \mathrm{W{\cdot}m^{-2}}$.

index	z (m)	T (°C)	r (g_{vapor}/kg_{air})
2	10	15	8
1	2	18	10

Solution

Given: the table above.

Find: $\mathbb{F}_H$ and $\mathbb{F}_E$ = ? $\mathrm{W{\cdot}m^{-2}}$

First step is to find $\Delta\theta$:

$$\Delta\theta = T_2 - T_1 + (0.0098\ \mathrm{K/m})\cdot(z_2 - z_1)$$
$$= 15\ \mathrm{K} - 18\ \mathrm{K} + (0.0098\ \mathrm{K/m})\cdot(10\mathrm{m} - 2\mathrm{m})$$
$$= -3\ \mathrm{K} + 0.0784\ \mathrm{K} = -2.92\ \mathrm{K}$$

Use eq. (3.58)

$$\mathbb{F}_H = \frac{-0.9\cdot(-500\mathrm{W\cdot m^{-2}})}{\dfrac{(-2g_{vap}/kg_{air})}{[0.4(g_{vap}/kg_{air})\cdot K^{-1}]\cdot(-2.92\mathrm{K})} + 1}$$

$$\mathbb{F}_H = \underline{\mathbf{165.91\ W{\cdot}m^{-2}}}$$

Next, use eq. (3.62):

$$\mathbb{F}_E = -0.9\cdot\mathbb{F}^* - \mathbb{F}_H$$
$$= -0.9\cdot(-500\ \mathrm{W{\cdot}m^{-2}}) - 165.91\ \mathrm{W{\cdot}m^{-2}}$$
$$= \underline{\mathbf{284.09\ W{\cdot}m^{-2}}}$$

Check: Units OK. Physics OK.

Discussion: Sensible heat flux is roughly 50% of the latent heat flux (i.e., $B = 0.5$). Thus, we can guess that these observations were made over moist grassland.

Solved Example

What is the wind chill index for air temperature of –50°C and wind of 70 km/h.

Solution

Given: $T_{air} = -50°C$, $M = 70$ km/h

Find: $T_{wind\ chill}$ = ? °C.

Use eq. (3.64a):

$$T_{wind\ chill} = \left[0.62\cdot(-50°C) + 13.1°C\right] + \left[0.51\cdot(-50°C) - 14.6°C\right]\cdot\left(\frac{70\mathrm{km/h}}{4.8\mathrm{km/h}}\right)^{0.16}$$

$$= [-17.9°C] + [-40.1°C]\cdot(1.535) = \underline{\mathbf{-79.5°C}}$$

Check: Units OK. Physics OK.

Discussion: This is well in the danger zone. Stay indoors in front of the fireplace and read a good book. I can recommend the book "Meteorology for Scientists and Engineers" — it will put you right to sleep.

In the equations above, recall that kinematic fluxes F have units of (K·m/s), while dynamic fluxes $\mathbb{F}$ have units of (W/m^2).

Measurements of temperature and humidity at two heights (Fig. 3.10) along with measurements of the net radiation near the surface are thus sufficient to determine the vertical effective fluxes of heat and moisture. In the Moisture chapter are equations for converting latent-heat fluxes into water fluxes.

APPARENT TEMPERATURES

Humans and livestock are warm blooded (**homeothermic**). Our metabolism generates heat, while our perspiration evaporates to keep us cool. Our bodies attempt to regulate our metabolism and perspiration to maintain a relatively constant internal temperature of about 37°C (= 98.6°F). Our skin is normally cooler — about 33.9°C (= 93°F).

Whether we feel warm or cool depends not only on air temperature, but on wind speed and humidity. During winter, faster wind makes the air feel colder, because it removes heat from our bodies faster. Wind chill is a measure of this effect.

During summer, higher humidity makes the air feel hotter, because it reduces evaporation of our perspiration. The humidex and heat index measure this effect. These indices are given as **apparent temperatures**; namely, how warm or cold it feels.

Wind Chill

The **wind-chill temperature index** is a measure of how cold the air feels to your exposed face. The official formula, as revised in 2001 by the USA and Canada, for wind chill in °C is:

$$T_{wind\ chill} = \left(a\cdot T_{air} + T_1\right) + \left(b\cdot T_{air} - T_2\right)\cdot\left(\frac{M}{M_o}\right)^{0.16} \quad \text{for } M > M_o \qquad (3.64a)$$

$$T_{wind\ chill} = T_{air} \quad \text{for } M \le M_o \qquad (3.64b)$$

where $a = 0.62$, $b = 0.51$, $T_1 = 13.1°C$, $T_2 = 14.6°C$, and where $M_o = 4.8$ km/h is the average speed that people walk. M is the wind speed measured at the official anemometer height of 10 m. For $M < M_o$, the wind chill equals the actual air temperature. This index applies to non-rainy air.

The air feels colder with colder temperatures and with stronger winds. Table 3-1 shows wind chills computed using this equation on a computer spreadsheet, with the results plotted in Fig. 3.11. The

data used to create eq. (3.64) was from volunteers in Canada who sat in refrigerated wind tunnels, wearing warm coats with only their face exposed.

At wind chills colder than –27°C, exposed skin can freeze in 10 to 30 minutes. At wind chills colder than –48°C: WARNING, exposed skin freezes in 2 to 5 min. At wind chills colder than –55°C: DANGER, exposed skin freezes in less than 2 minutes. In this danger zone is an increased risk of **frostbite** (fingers, toes, ears and nose numb or white), and **hypothermia** (drop in core body temperature).

Heat Index and Humidex

More humid air feels warmer and more uncomfortable than the actual temperature. **Heat index** (or **apparent temperature** or **temperature-humidity index**) is one measure of heat discomfort and heat-stress danger.

The equation-set below approximates Steadman's temperature-humidity index of sultriness:

$$T_{heat\ index}(°C) = T_R + [T - T_R] \cdot \left(\frac{RH \cdot e_s}{100 \cdot e_R} \right)^p \qquad (3.65a)$$

where e_R = 1.6 kPa is reference vapor pressure, and

$$T_R(°C) = 0.8841 \cdot T + (0.19°C) \qquad (3.65b)$$

$$p = (0.0196°C^{-1}) \cdot T + 0.9031 \qquad (3.65c)$$

$$e_s(\text{kPa}) = 0.611 \cdot \exp\left[5423 \left(\frac{1}{273.15} - \frac{1}{(T + 273.15)} \right) \right] \qquad (3.65d)$$

The two input variables are T (dry bulb temperature in °C), and RH (relative humidity percentage, with values of 0 to 100). Also, T_R (°C), and p are parameters, and e_s is the saturation vapor pressure, discussed in the Moisture chapter. Eqs. (3.65) assume that you are wearing a normal amount of clothing for warm weather, are in the shade or indoors, and a gentle breeze is blowing.

Table 3-2 shows the solution to this equation. For low relative humidities (at and below the bold-face underlined numbers in the table), the air feels cooler than the actual air temperature because perspiration evaporates effectively, keeping humans cool. However, for high relative humidity, the apparent temperature is warmer than the actual air temperature.

In Canada, a **humidex** is defined as

$$T_{humidex}(°C) = T(°C) + a \cdot (e - b) \qquad (3.66a)$$

where T is air temperature, a = 5.555 (°C/kPa), b = 1 kPa, and

Table 3-1. Wind-chill temperatures (°C) approx.

Wind Speed		Air Temperature (°C)					
km/h	m/s	–40	–30	–20	–10	0	10
60	16.7	–64	–50	–36	–23	–9	5
50	13.9	–63	–49	–35	–22	–8	6
40	11.0	–61	–48	–34	–21	–7	6
30	8.3	–58	–46	–33	–20	–6	7
20	5.6	–56	–43	–31	–18	–5	8
10	2.8	–51	–39	–27	–15	–3	9
0	0	–40	–30	–20	–10	0	10

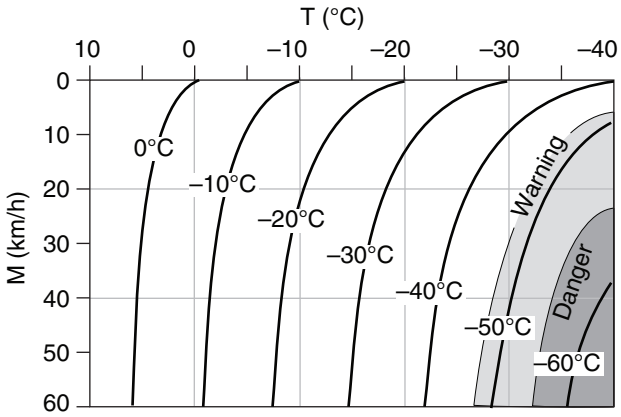

Figure 3.11
Curves are wind chill temperature index (°C), as a function of actual air temperature (T) and wind speed (M).

Table 3-2. Heat Index Apparent Temperature (°C)

RH	Actual Air Temperature (°C)						
(%)	20	25	30	35	40	45	50
100	21	29	41	61			
90	21	29	39	57			
80	21	28	37	52			
70	20	27	35	48			
60	20	26	34	45	62		
50	**19**	25	32	41	55		
40	19	**24**	30	38	49	66	
30	19	24	**29**	36	44	56	
20	18	23	28	**33**	40	48	59
10	18	23	27	32	**37**	**42**	**48**
0	18	22	27	31	36	40	44

Solved Example

Use the equations to find the heat index and humidex for an air temperature of 38°C and a relative humidity of 75% (which corresponds to a dew-point temperature of about 33°C).

Solution

Given: $T = 38°C$, $RH = 75\%$, $T_d = 33°C$

Find: $T_{heat\ index}$ = ? °C , $T_{humidex}$ = ? °C

For heat index, use eqs. (3.65):

$T_R = 0.8841 \cdot (38) + 0.19 = 33.8°C$ (3.65b)

$p = 0.0196 \cdot (38) + 0.9031 = 1.65$ (3.65c)

$e_s = 0.611 \cdot \exp[5423 \cdot (\{1/273.15\} - \{1/(38+273.15)\})]$
$= 6.9$ kPa (3.65d)

$T_{heat\ index} = 33.8 + [38-33.8] \cdot (0.75 \cdot 6.9/1.6)^{1.65}$
$= \underline{\mathbf{62.9°C}}$ (3.65a)

For humidex, use eqs. (3.66):

$e = 0.611 \cdot \exp[5418 \cdot (\{1/273.16\} - \{1/(33+273.16)\})]$
$= 5.18$ kPa (3.66b)

$T_{humidex} = 38 + 5.555 \cdot (5.18-1) = \underline{\mathbf{61.2°C}}$ (3.66a)

Check: Units OK. Values agree with extrapolation of Table 3-2.

Discussion: These values are in the danger zone, meaning that people are likely to suffer heat stroke. The humidex and heat index values are nearly equal for this case.

Table 3-3. **Humidex** apparent temperature (°C)

T_d	Actual Air Temperature T (°C)						
(°C)	20	25	30	35	40	45	50
50							118
45						96	101
40					77	82	87
35				62	67	72	77
30			49	54	59	64	69
25		37	42	47	52	57	62
20	28	33	38	43	48	53	58
15	24	29	34	39	44	49	54
10	21	26	31	36	41	46	51
5	19	24	29	34	39	44	49
0	18	23	28	33	38	43	48
-5	17	22	27	32	37	42	47
-10	16	21	26	31	36	41	46

(3.66b)

$$e(\text{kPa}) = 0.611 \cdot \exp\left[5418\left(\frac{1}{273.16} - \frac{1}{[T_d(°C) + 273.16]}\right)\right]$$

T_d is dew-point temperature, a humidity variable discussed in the Moisture chapter.

Humidex is also an indicator of summer discomfort due to heat and humidity (Table 3-3). Values above 40°C are uncomfortable, and values above 45°C are dangerous. **Heat stroke** is likely for humidex ≥ 54°C.

TEMPERATURE SENSORS

Temperature sensors are generically called **thermometers**. Anything that changes with temperature can be used to measure temperature. Many materials expand when warm, so the size of the material can be calibrated into a temperature. Classical **liquid-in-glass thermometers** use either mercury or a dyed alcohol or glycol fluid that can expand from a reservoir or **bulb** up into a narrow tube.

House **thermostats** (temperature controls) often use a **bimetalic strip**, where two different metals are sandwiched together, and their different expansion rates with temperature causes the metal to bend as the temperature changes. Car thermostats use a wax that expands against a valve to redirect engine coolant to the radiator when hot. Some one-time use thermometers use wax that melts onto a piece of paper at a known temperature.

Many electronic devices change with temperature, such as resistance of a wire, capacitance of a capacitor, or behavior of various transistors (**thermistors**). These changes can be measured electronically and displayed. **Thermocouples** (such as made by a junction between copper and constantan wires, where constantan is an alloy of roughly 60% copper and 40% nickel) generate a small amount of electricity that increases with temperature. **Liquid crystals** change their orientation with temperature, and can be designed to display temperature.

Sonic thermometers measure the speed of sound through air between closely placed transmitters and receivers of sound. Radio Acoustic Sounder Systems (**RASS**) transmit a loud pulse of sound upward from the ground, and then infer temperature vs. height via the speed that the sound wave propagates upward, as measured by a radio or microwave profiler.

Warmer objects emit more radiation, particularly in the infrared wavelengths. An **infrared thermometer** measures the intensity of these emis-

sions to infer the temperature. Satellite remote sensors also detect emissions from the air upward into space, from which temperature profiles can be calculated (see the Remote Sensing chapter).

Even thick layers of the atmosphere expand when they become warmer, allowing the **thickness** between two different atmospheric pressure levels to indicate average temperature in the layer.

SUMMARY

Air parcels that move through the atmosphere while conserving heat are said to be adiabatic. When parcels rise adiabatically, they cool due to the change of pressure with height. The change of temperature with height is called the adiabatic lapse rate, and indicates a physical process. The ambient environmental air through which the parcel moves might have a different lapse rate. Thermodynamic diagrams are convenient for determining how the temperature varies with height or pressure, and for comparing different lapse rates.

Once heat from the sun is in the Earth-atmospheric system, it is redistributed by advection, radiation, turbulence, and conduction. Some of the sensible heat is converted to/from latent heat by water phase change. Eventually, heat is lost from the system as infrared radiation to space.

At the Earth's surface, net radiation is balanced by turbulent fluxes into the atmosphere and conduction into the ground. Turbulent fluxes consist of sensible heat flux, and latent heat flux associated with evaporation of water. The ratio of sensible to latent heat flux is the Bowen ratio. All of these fluxes vary with the diurnal cycle.

Warm blooded animals and humans feel heat loss rather than temperature. On cold, windy days, the heat loss is quantified as a wind chill temperature. During humid hot days, the apparent temperature can be warmer than actual.

Threads

The conversion between latent and sensible heat provides energy that drives thunderstorms (Chapters 14 and 15) and hurricanes (Chapter 16). These thunderstorms stabilize the atmosphere by moist convective adjustment. The transport of moisture by the wind is thus equivalent to a transport of energy, and affects the global energy budget (Chapters 11 and 21).

Latent heat flux (i.e., evaporation driven by the incoming sunlight or other heat source) provides the moisture (Chapter 4) for clouds (Chapter 6) and precipitation (Chapter 7). Surface heat and moisture fluxes drive atmospheric boundary-layer evolution (Chapter 18) and contribute to the Eulerian budget of moisture (Chapter 4).

The Eulerian heat budget is one of the governing equations that is solved as part of a numerical weather forecast (Chapter 20). The Lagrangian heat budget associated with rising air parcels is used to determine cloud formation (Chapter 6), atmospheric turbulence (Chapter 18) and air-pollutant dispersion (Chapter 19). Thermodynamic diagrams (Chapter 5) combine potential temperature, latent heat, and the Lagrangian heat budget. Moist convective adjustment is caused by thunderstorms (Chapters 14 and 15).

EXERCISES

Numerical Problems

N1. Find the change in sensible heat (enthalpy) (J) possessed by 3 kg of air that warms by __°C.

a. 1 b. 2 c. 3 d. 4 e. 5 f. 6 g. 7
h. 8 i. 9 j. 10 k. 11 m. 12

N2. Find the specific heat C_p of humid air having water-vapor mixing ratio ($g_{vapor}/g_{dry\ air}$) of:

a. 0.010 b. 0.012 c. 0.014 d. 0.016 e. 0.018
f. 0.020 h. 0.022 i. 0.024 j. 0.026 k. 0.028
m. 0.030

N3. Find the change in latent heat (J) for condensation of ___ kg of water vapor.

a. 0.2 b. 0.4 c. 0.6 d. 0.8 e. 1.0 f. 1.2 g. 1.4
h. 1.6 i. 1.8 j. 2.0 k. 2.2 m. 2.4

N4. Find the temperature change (°C) of air given the following values of heat transfer and pressure change, assuming air density of 1.2 kg/m^3.

	Δq (J/kg)	ΔP (kPa)
a.	500	5
b.	1000	5
c.	1500	5
d.	2000	5
e.	2500	5
f.	3000	5
g.	500	10
h.	1000	10
i.	1500	10
j.	2000	10
k.	2500	10
m.	3000	10

N5. Find the change in temperature (°C) if an air parcel rises the following distances while experiencing the heat transfer values given below.

	Δq (J/kg)	Δz (km)
a.	500	0.5
b.	1000	0.5
c.	1500	0.5
d.	2000	0.5
e.	2500	0.5
f.	3000	0.5
g.	500	1
h.	1000	1
i.	1500	1
j.	2000	1
k.	2500	1
m.	3000	1

N6. Given the following temperature change ΔT (°C) across a height difference of Δz = 4 km, find the lapse rate (°C/km):

a. 2 b. 5 c. 10 d. 20 e. 30 f. 40 g. 50
h. –2 i. –5 j. –10 k. –20 m. –30

N7. Find the final temperature (°C) of an air parcel with the following initial temperature and height change, for an adiabatic process.

	$T_{initial}$ (°C)	Δz (km)
a.	15	0.5
b.	15	–1.0
c.	15	1.5
d.	15	–2.0
e.	15	2.5
f.	15	–3.0
g.	5	0.5
h.	5	–1.0
i.	5	1.5
j.	5	–2.0
k.	5	2.5
m.	5	–3.0

N8. Using the equations (not using the thermo diagram), find the final temperature (°C) of dry air at a final pressure, if it starts with the initial temperature and pressure as given. (Assume adiabatic)

	$T_{initial}$ (°C)	$P_{initial}$ (kPa)	P_{final}(kPa)
a.	5	100	80
b.	5	100	50
c.	5	80	50
d.	5	80	100
e.	0	60	80
f.	0	60	50
g.	0	80	40
h.	0	80	100
i.	–15	90	80
j.	–15	90	50
k.	–15	70	50
m.	–15	70	100

N9. Same as previous question, but use the thermo diagram Fig. 3.3.

N10. Using equations (and show your work) rather than a thermo diagram, what is the potential temperature of air at:

	z (m)	T (°C)
a.	200	20
b.	1,000	5
c.	200	5
d.	1,000	20
e.	300	10
f.	6,000	–50
g.	10,000	–90
h.	–30	35

i.	700	3
j.	1,300	–5
k.	400	5
m.	2,000	–20

N11. Same as the previous exercise, but find the virtual potential temperature for humid air. Use a water-vapor mixing ratio of 0.01 $g_{vapor}/g_{dry\ air}$ if the air temperature is above freezing, and use 0.002 $g_{vapor}/g_{dry\ air}$ if air temperature is below freezing. Assume no liquid water or ice suspended in the air.

N12. Using equations (and show your work) rather than a thermo diagram, what is the potential temperature of air at:

	P (kPa)	T (°C)
a.	90	20
b.	80	5
c.	110	5
d.	70	20
e.	85	10
f.	40	–50
g.	20	–90
h.	105	35
i.	75	3
j.	60	–5
k.	65	5
m.	50	–20

N13. Same as previous exercise, but use the thermo diagram Fig. 3.3.

N14. Use the thermodynamic diagram (Fig. 3.3) to answer the following.

	Given:		Find:
a.	T = 0°C,	P = 70 kPa	θ (°C)
b.	T = 20°C,	P = 100 kPa	θ (°C)
c.	T = –20°C,	P = 40 kPa	θ (°C)
d.	θ = 40°C,	P = 40 kPa	T (°C)
e.	θ = –20°C,	P = 90 kPa	T (°C)
f.	θ = 40°C,	P = 80 kPa	T (°C)
g.	θ = 40°C,	T = 0 °C	P (kPa)
h.	θ = 60°C,	T = –20 °C	P (kPa)

N15(§). Create a thermodynamic diagram on a spreadsheet like the one plotted in Fig. 3.3, only print it with more lines. Namely, draw isotherm grid lines every 10°C, and draw dry adiabats for every 10°C from –50°C to 80°C.

N16. Find the rate of temperature change (°C/h) in an Eulerian coordinate system with no internal heat source, given the kinematic flux divergence values below. Assume $\Delta x = \Delta y = \Delta z = 1$ km.

	ΔF_x (K·m/s)	ΔF_y (K·m/s)	ΔF_z (K·m/s)
a.	1	2	3
b.	1	2	–3
c.	1	–2	3
d.	1	–2	–3
e.	–1	2	3
f.	–1	2	–3
g.	–1	–2	3
h.	–1	–2	–3

N17. Given the wind and temperature gradient, find the value of the kinematic advective flux gradient (°C/h).

	V (m/s)	$\Delta T/\Delta y$ (°C/100 km)
a.	5	–2
b.	5	2
c.	10	–5
d.	10	5
e.	–5	–2
f.	–5	2
g.	–10	–5
h.	–10	5

N18. Given the wind and temperature gradient, find the value of the kinematic advective flux gradient (°C/h).

	W (m/s)	$\Delta T/\Delta z$ (°C/km)
a.	5	–2
b.	5	2
c.	10	–5
d.	10	–10
e.	–5	–2
f.	–5	2
g.	–10	–5
h.	–10	–10

N19. Find the value of the conductive flux $\mathbb{F}_{z\ cond}$ (W/m^2) given a vertical temperature gradient of __ °C per meter.

a. –1 b. –2 c. –3 d. –4 e. –5 f. –6 g. –7
h. 1 i. 2 j. 3 k. 4 m. 5 n. 6 o. 7

N20. Find the effective surface turbulent heat flux (°C·m/s) over a forest for wind speed of 10 m/s, air temperature of 20°C, and surface temperature (°C) of

a. 21 b. 22 c. 23 d. 24 e. 25 f. 26 g. 27
h. 19 i. 18 j. 17 k. 16 m. 15 n. 14 o. 13

N21. Find the effective kinematic heat flux at the surface on a calm day, for a buoyant velocity scale of 50 m/s, a mixed-layer potential temperature of 25°C, and with a surface potential temperature (°C) of:

a. 26 b. 28 c. 30 d. 32 e. 34 f. 36 g. 38
h. 40 i. 42 j. 44 k. 46 m. 48 n. 50

N22. Find the effective kinematic heat flux at the surface on a calm day, for a Deardorff velocity of 2

m/s, a mixed-layer potential temperature of 24°C, and with a surface potential temperature (°C) of:

a. 26 b. 28 c. 30 d. 32 e. 34 f. 36 g. 38
h. 40 i. 42 j. 44 k. 46 m. 48 n. 50

N23. For dry air, find the buoyancy velocity scale, given a mixed-layer potential temperature of 25°C, a mixed-layer depth of 1.5 km, and with a surface potential temperature (°C) of:

a. 27 b. 30 c. 33 d. 36
e. 40 f. 43 g. 46 h. 50

N24. For dry air, find the Deardorff velocity w_* for an effective kinematic heat flux at the surface of 0.2 K·m/s, air temperature of 30°C, and mixed-layer depth (km) of:

a. 0.4 b. 0.6 c. 0.8 d. 1.0
e. 1.2 f. 1.4 g. 1.6 h. 1.8

N25. Find the value of vertical divergence of kinematic heat flux, if the flux at the top of a 200 m thick air layer is 0.10 K·m/s, and flux (K·m/s) at the bottom is:

a. 0.2 b. 0.18 c. 0.16 d. 0.14
e. 0.12 f. 0.10 g. 0.08 h. 0.06

N26. Find the vertical turbulent flux gradient, for the following surface effective flux values and ABL depths, assuming fair-weather during daytime:

	F_H (K·m·s^{-1})	z_i (km)
a.	0.2	1.0
b.	0.1	2.0
c.	0.3	1.5
d.	0.05	0.2
e.	0.08	0.3
f.	0.12	0.8
g.	0.15	1.0
h.	0.25	1.5

N27. Just before thunderstorms form in a stormy troposphere, the air is 10°C warmer than standard near the ground, and is 5°C cooler than standard near the top of the troposphere (11 km), with a linear temperature variation in between. Find the vertical turbulent flux gradient (K/s) at height (km):

a. 0 b. 0.5 c. 1 d. 1.5 e. 2 f. 2.5 g. 3
h. 3.5 i. 4 j. 5 k. 6 m. 7 n. 8 o. 11

N28. Find the mid-tropospheric maximum value of heat flux (K·m/s) for a stormy atmosphere, where the troposphere is 11 km thick, and the air temperature at the top of the troposphere equals the air temperature of a standard atmosphere. But the air temperature (°C) at the ground is:

a. 16 b. 17 c. 18 d. 19 e. 20 f. 21 g. 22
h. 23 i. 24 j. 25 k. 26 m. 27 n. 28 o. 29

N29. Find the latent-heating rate (°C/h) averaged over the troposphere for a thunderstorm when the rainfall rate (mm/h) is:

a. 0.5 b. 1 c. 1.5 d. 2 e. 2.5 f. 3 g. 3.5
h. 4 i. 4.5 j. 5 k. 5.5 m. 6 n. 6.5 o. 7

N30. Given below the net radiative flux (W/m^2) reaching the surface, find the sum of sensible and latent heat fluxes (W/m^2) at the surface. (Hint: determine if it is day or night by the sign of the radiative flux.)

a. –600 b. –550 c. –500 d. –450 e. –400
f. –350 g. –300 h. –250 i. –200 j. –150
k. –100 m. –50 n. 50 o. 100 p. 150

N31. Same as the previous problem, but estimate the values of the sensible and latent heat fluxes (W/m^2) assuming a Bowen ratio of:

(1) 0.2 (2) 5.0

N32. Given the following measurements of temperature, and specific humidity, find the sensible and latent heat-flux values. Net radiation is –400 W/m^2.

index	z(m)	T(°C)	r (g_{vap}/kg_{air})
2	20	T_2	8
1	10	14	10

where T_2 (°C) is:

a. 13.5 b. 13 c. 12.5 d. 12 e. 11.5 f. 11
g. 10.5 h. 10 i. 9.5 j. 9 k. 8.5 m. 8

N33. Assume you ride your bicycle at a speed given below, during a calm day of temperature given below. What wind chill temperature to your feel?

a. 10 m/s, 20°C b. 5 m/s, 20°C c. 15 m/s, 20°C
d. 10 m/s, –5°C e. 5 m/s, –5°C f. 15 m/s, –5°C

N34(§). Use eqs. (3.64) to create a wind-chill table or graph similar to Table 3-1 and Fig. 3.11, but for wind speeds in miles per hour and temperatures in °F.

N35. Find the heat index apparent temperature (°C) for an actual air temperature of 33°C and a relative humidity (%) of:

a. 5 b. 10 c. 20 d. 30 e. 40 f. 50 g. 60
h. 70 i. 75 j. 80 k. 85 m. 90 n. 90

N36. Find the humidex apparent air temperature (°C) for an actual air temperature of 33°C and a dewpoint temperature (°C) of:

a. 32.5 b. 32 c. 31 d. 30 e. 29 f. 28 g. 27
h. 26 i. 25 j. 23 k. 20 m. 15 n. 10 o. 5

Understanding & Critical Evaluation

U1. Suppose you are given 1 kg of ice at 0°C. If the ice is placed in 1 kg of liquid water initially at 20°C, what will be the final temperature after all the ice melts?

U2. Explain in your own words why the units for specific heat C_p ($J \cdot kg^{-1} \cdot K^{-1}$) are slightly different than the units for the latent heat factor L ($J \cdot kg^{-1}$). (Hint: read the Focus box on Internal Energy.)

U3. Explain in your own words why the magnitude of C_p should be larger than the magnitude of C_v. (Hint: read the Focus box on C_p vs. C_v).

U4. Consider the Focus box on C_p vs. C_v, with Fig. 3F.3c representing an initial state at equilibrium. Suppose you add some weight to the piston in Fig (c) causing the piston to become lower to reach a new equilibrium. Describe what would happen to: (a) the molecules on average, (b) the gas temperature in the cylinder, (c) the air density in the cylinder, and (d) the air pressure in the cylinder.

U5. For the First Law of Thermodynamics (eq. 3.4) which term(s) is/are zero for a process that is:
a. adiabatic b. isothermal c. isobaric

U6. Derive eq. (3.5) from eq. (3.4), showing your steps. (Calculus is not needed to do this.) Show all your work and state any assumptions and limitations of the result.

U7. For Fig. 3.1, speculate on other processes not listed that might affect the air-parcel temperature.

U8. Using Fig. 3.2, explain in your own words the difference between a process lapse rate and an environmental lapse rate. Can both exist with different values at the same height? Why?

U9. Eq. (3.7) tells us that temperature of an adiabatically rising air parcel will decrease linearly with increasing height. In your own words, explain why you would NOT expect the same process to cause temperature to decrease linearly with decreasing pressure.

U10. If an air parcel rises isothermally (namely, heat is added or subtracted to maintain constant temperature), then what would happen to the potential temperature of the air parcel as it rises?

U11. Chinook winds (also known as foehn winds) consist of air descending down the lee slope of a mountain and then continuing some distance across the neighboring valley or plain. Why are Chinook winds usually warm when they reach the valley? (Hint: consider adiabatic descent of an air parcel.)

U12. In the definition of virtual potential temperature, why do liquid water drops and ice crystals cause the air to act heavier (i.e., colder virtual potential temperature), even though these particles are falling through the air?

U13. On a copy of Fig. 3.3 plot the standard-atmosphere temperature profile. If an air parcel from this standard atmosphere at $P = 100$ kPa is lifted dry adiabatically to a height where $P = 50$ kPa, how does its final (process) temperature compare with the standard (environmental) temperature at the same height?

U14(§). Use the equations for the standard atmosphere from Chapter 1, and convert temperatures into potential temperatures every km within the troposphere and stratosphere. Plot the resulting θ vs z.

U15(§). Create a semi-log graph of log P vs. T similar to Fig. 3.3, however do not plot the dry adiabats. Instead, solve the hypsometric equation to plot curves corresponding to the following heights:
z = 1, 2, 3, 4, 5, 6, 7, 8, 9, and 10 km. In other words there will be one curve corresponding to z = 1 km, and another for z = 2 km, etc.

U16. Explain why a positive flux gradient in the presence of a positive wind is associated with cooling and not warming.

U17. Given a 1 km thick mixed layer in the air over the ocean, with sea surface temperature 30°C and air temperature 25°C at z = 10 m, and calm winds. If the mixed layer potential temperature is 20°C and the water-vapor mixing ratio is 0.015 g_{vapor}/g_{air}, then what is the convective effective surface heat flux?

U18. Light travels faster in warm air than in cold. Use this info, along with Fig. 3.6, to explain why **inferior mirages** (reflections of the sky) are visible on hot surfaces such as asphalt roads. (Hint: Consider a wave front that is moving mostly horizontally, but also slightly downward at a small angle relative to the road surface, and track the forward movement of each part of this wave front — an optics method known as Huygens' Principle. See details in the atmospheric Optics chapter.)

U19. Under what conditions would eqs. (3.34 - 3.35) be expected to fail? Why?

U20. Use eqs. (3.37) and (3.39) to solve for the heat flux as a function of the temperature difference.

U21. In Fig. 3.7, the heat flux is greatest at the height where there is no change in the vertical temperature profile from before to after a storm. Why should that be the case?

U22. If no other heating process was acting except radiative divergence in the vertical, what would be the heating rate of air. This typically occurs on calm nights at altitudes roughly 500 m above ground.

U23. In a thunderstorm, the amount of water condensation in the troposphere is often much greater than the amount of rain reaching the ground. Why is that, and how might it affect the heat budget averaged over the whole thunderstorm depth?

U24. What are the limitations of the net heat budget equation (3.51)?

U25. Given a situation where a wind speed of U = 10 m/s is blowing air with horizontal (east-west) temperature gradient of 2°C/100 km. Also suppose that 2 g of water per 1 kg of air is condensing every 15 minutes. Neglect turbulence. Compare the magnitudes of each term in the net heat budget equation (3.51).

U26. Sketch and discuss a figure such as Fig. 3.8, except for nighttime over a desert.

U27. Speculate why the X factor for ground flux is different from day to night. Discuss limitations of that expression for ground flux.

U28. Given a layer of air 1 km thick advecting over a sea surface of 20°C at wind speed U = 20 m/s. The initial air temperature is 10°C. The layer of air experiences bulk turbulent heat transfer into the bottom of it, but no heat transfer across the top, and no radiative heating. Assume the heat from the sea surface is mixed instantaneously in the vertical across the whole air layer. For a steady-state situation with only advection and the effective turbulent surface heat flux, derive an equation for the change of temperature with horizontal distance $\Delta T/\Delta x$.

U29. Use the flux estimates from eqs. (3.58 - 3.61) in the surface heat budget equation to show that they do indeed balance the budget. Also, what are the limitations of those equations?

U30. (§). An alternative equation for wind chill temperature index, based on a modified version of the heat transfer equation (3.35) is:

(3.67)

$$T_{wind\ chill} = T_s + \left(T_{air} - T_s\right) \cdot \left[b + a \cdot \left(\frac{M + M_o}{M_o} \right)^{0.16} \right] + T_c$$

where T_s = 34.6°C is an effective skin temperature, and where, a = 0.5 , b = 0.62 , T_c = 4.2°C, and M_o = 4.8 km/h. Create a table or graph of wind chills using this formula, and compare to wind chills from Table 3-1 or Fig. 3.11.

U31. In Fig. 3.11, where does a small increase in wind speed cause the greatest decrease in wind-chill temperature? Why might you expect this to be the case?

U32. Here is an alternative expression for heat index (*HI*) apparent temperature. Create tables or curves of heat index, and compare with the table in this chapter (after converting the results to Celsius). This expression is designed for use in a spreadsheet, where the (*Tf*) and (*RH*) factors must be replace with the appropriate cell references for temperature in Fahrenheit and relative humidity (0 - 100) in percent.

HI (°F) = -42.379
+ 2.04901523*(*Tf*)
+ 10.14333127*(*RH*)
– 0.22475541*(*Tf*)*(*RH*)
– (6.83783*10^(-3))*(*Tf*^(2))
– (5.481717*10^(-2))*(*RH*^(2))
+ (1.22874*10^(-3))*(*Tf*^(2))*(*RH*)
+ (8.5282*10^(-4))*(*Tf*)*(*RH*^(2))
– (1.99*10^(-6))*(*Tf*^(2))*(*RH*^(2))

where "^" means "raised to the power of". This eq. is adapted from web site http://www.usatoday.com/weather/whumcalc.htm.

Web-Enhanced Questions

W1(§). Access today's actual temperature sounding from the web for a rawinsonde station close to you (or for another sounding station specified by your instructor). Convert the resulting temperatures to potential temperatures, and plot the resulting θ vs. z.

W2. Access upper-air soundings from the web for a rawinsonde launch site near you (or for another sounding station specified by your instructor). What type of thermodynamic diagram is it plotted on? Can you identify which lines are the isobars; the isotherms, the dry adiabats? There are many

different types of thermodynamic diagrams in use around the world, so it is important to learn how to identify the isopleths in each type.

W3. Access the current temperature and wind at your town or location (or for another place as specified by your instructor). Then access the temperature from a town upwind of you. Calculate the portion of heating or cooling rate at your location due only to advection.

W4. Access from the web a weather map or other weather report that shows the observed near-surface air temperature just before sunrise at your location (or at another location specified by your instructor). For the same location, find a map or report of the temperature in mid afternoon. From these two observations, calculate the rate of temperature change over that time period. Also, qualitatively describe which terms in the Eulerian heat budget might be largest. (Hint: if windy, then perhaps advection is important. If clear skies, then heat transfer from the solar-heated ground might be important. Access other weather maps as needed to determine which physical process is most important for the temperature change.)

W5. During winter, access a web report of wind chill for your location (or a different location as specified by your instructor). Can you find on the web a weather map that plots the wind chill? In addition to checking official weather agencies, also check local and network TV web pages.

W6. During summer, access a web report of heat index, temperature-humidity index, or apparent temperature for your location (or a different location specified by your instructor). Can you find on the web a weather map that plots any of these? In addition to checking official weather agencies, also check local and network TV web pages.

Synthesis Questions

S1. What if the sign of the latent heat of condensation or vaporization were opposite. Namely, when liquid water evaporates it heats the air, and when it condenses it cools the air. What would happen to the Earth's oceans as water evaporates from the surface?

S2. Suppose that zero latent heat was associated with the phase changes of water. How would the weather and climate be different, if at all?

S3. Suppose the adiabatic lapse rate had the opposite sign, so that air parcels become warmer as they rise adiabatically. Assuming a standard atmosphere in the troposphere, what would happen to an air parcel from the middle of the troposphere that would be displace slightly up or down?

S4. Suppose that for each 1 km rise of an air parcel, the parcel mixes with an equal mass of surrounding environmental air. How would the process lapse rate for this rising air parcel be different (if at all) from the lapse rate of an adiabatically rising air parcel (having no mixing).

S5. Macro thermodynamics (the kind we've used in this chapter) considers the statistical state of a large collection of molecules that frequently collide with each other, and how they interact on average with their surroundings. Can this same macro thermodynamics be used in the exosphere, where individual air molecules are very far apart (i.e., have a large mean-free path) and rarely interact? Why? Also, explain if/how heat budgets can be used in the exosphere.

S6. Could there be situations where environmental and process lapse rates are equal? If so, give some examples.

S7. Suppose that the virtual potential temperature was not affected by the amount of solid or liquid water in the air. How would weather and climate change, if at all?

S8. The background of the thermo diagram of Fig. 3.3 is an orthogonal grid, where the isotherms are plotted perpendicular to the isobars. Suppose you were to devise a new thermo diagram with the dry adiabats perpendicular to the isobars. On such a diagram, how would the isotherms be drawn? To answer this, draw a sketch of this new diagram, showing the isobars, adiabats, and isotherms. (Do this as a conceptual exercise, not by solving equations to get numbers.)

S9. What if the Earth's crust and surface were made of a metal such a aluminum many hundreds of meters thick. Speculate about the importance of conduction on the surface heat budget, and other implications about the weather.

S10. Lagrangian frameworks follow air parcels as they move. Eulerian frameworks remain fixed relative to the Earth's surface.

What if you were on a cruise ship moving at constant speed from east to west across the ocean.

Devise a heat budget equation relative to this framework. You may name this equation after yourself. Check that it works for any wind direction, and in the limits of zero ship speed.

S11. For the real Earth during cloud-free conditions, most visible light is absorbed by the Earth's surface, while the troposphere is mostly transparent. Suppose that the troposphere were translucent to visible light, but opaque enough that the absorption of sunlight was spread uniformly over the depth of the troposphere, with no sunlight reaching the surface. How would atmospheric structure and weather be different, if at all?

S12. Suppose that the thermometers and hygrometers on the instrumented tower sketched in Fig. 3.10 had random errors of 10% of their magnitudes. Would this error affect the surface flux estimate using the Bowen ratio method? If so, what is the sensitivity (what percentage error does the flux have, compared to the percentage error that the input measurements had)?

S13. The wind-chill concept shows how it feels colder when it is winder. For situations where the wind chill is much colder than the actual air temperature, to what temperature will an automobile engine cool after it is turned off? Why? (Assume the car is parked outside and is exposed to the wind.)

Copyright © 2011, 2015 by Roland Stull. *Meteorology for Scientists and Engineers, 3rd Ed.*

MOISTURE

CONTENTS

Saturation Vapor Pressure 87
- Vapor Pressure 87
- Saturation 87

Humidity Variables 91
- Mixing Ratio 91
- Specific Humidity 91
- Absolute Humidity 91
- Relative Humidity 92
- Dew-Point Temperature 92
- Saturation Level or Lifting Condensation Level (LCL) 93
- Wet-Bulb Temperature 94
- More Relationships Between Moisture Variables 96

Total Water 97
- Liquid and Solid Water 97
- Total-Water Mixing Ratio 97
- Precipitable Water 98

Lagrangian Budgets 99
- Water Conservation 99
  - Lagrangian Water Budget 99
  - Thermo Diagrams – Part 2: Isohumes 100
- Heat Conservation for Saturated Air 101
  - Saturated Adiabatic Lapse Rate 101
  - Thermo Diagrams – Part 3: Saturated Adiabats 102
  - Liquid-Water, Equivalent, and Wet-Bulb Potential Temperatures 104

Eulerian Water Budget 107
- Horizontal Advection 107
- Precipitation 107
- Surface Moisture Flux 108
- Turbulent Transport 109

Humidity Instruments 111

Summary 112
- Threads 112

Exercises 113
- Numerical Problems 113
- Understanding & Critical Evaluation 115
- Web-Enhanced Questions 117
- Synthesis Questions 118

"Meteorology for Scientists and Engineers, 3rd Edition" by Roland Stull is licensed under a Creative Commons Attribution-NonCommercial-ShareAlike 4.0 International License. To view a copy of the license, visit http://creativecommons.org/licenses/by-nc-sa/4.0/ . This work is available at http://www.eos.ubc.ca/books/Practical_Meteorology/ .

Water vapor is one of the gases in air. Unlike nitrogen and oxygen, water-vapor concentration can vary widely in time and space. Most people are familiar with relative humidity as a measure of water-vapor concentration because it affects our body's moisture regulation. But other humidity variables are much more useful in other contexts.

Storms get much of their energy from water vapor, because when water vapor condenses or freezes it releases latent heat. For this reason we carefully track water vapor as it rises in buoyant thermals or is carried by horizontal winds. The amount of moisture available to a storm also regulates the amount of rain or snow precipitating out.

What allows air to hold water as vapor in one case, but forces the vapor to condense in another? This depends on a concept called "saturation".

SATURATION VAPOR PRESSURE

Vapor Pressure

All the gases in air contribute to the total pressure. The pressure associated with any one gas in a mixture is called the **partial pressure**. The partial pressure of water vapor in air is called **vapor pressure**. Symbol e is used for water-vapor pressure. Units are pressure units, such as kPa.

Saturation

Air can hold any proportion of water vapor. However, for humidities greater than a threshold called the **saturation humidity**, water vapor tends to condense into liquid faster than it re-evaporates. This condensation process lowers the humidity toward the equilibrium (saturation) value. The process is so fast that humidities rarely exceed the equilibrium value. Thus, while air can hold any portion of water vapor, the threshold is rarely exceeded by more than 1% in the real atmosphere.

Air that contains this threshold amount of water vapor is **saturated**. Air that holds less than that amount is **unsaturated**. The equilibrium (saturation) value of vapor pressure over a flat surface of

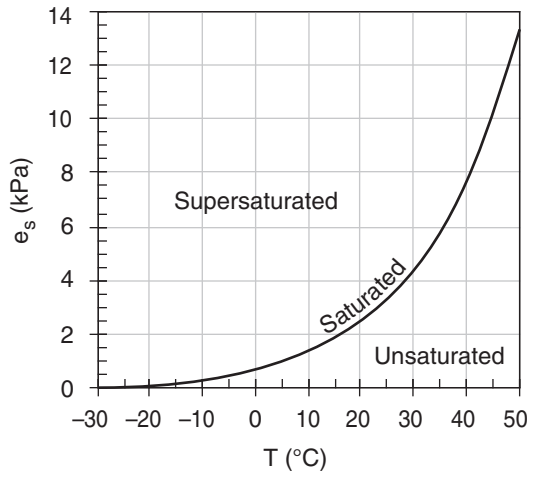

Figure 4.1
Saturation vapor pressure over a flat surface of pure water. A blowup of the portion of this curve colder than 0°C is given in the next figure.

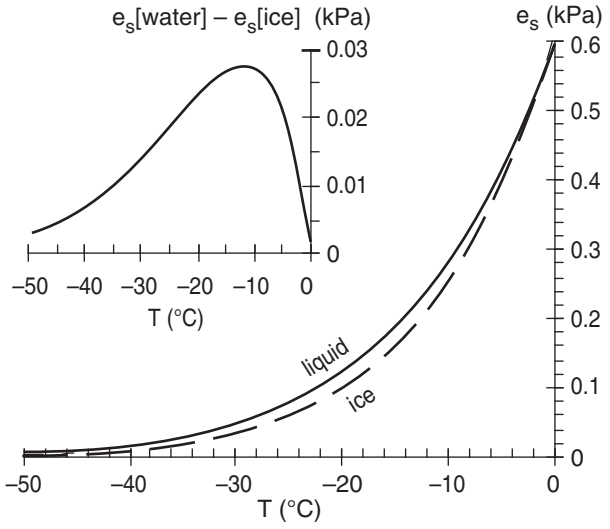

Figure 4.2
Saturation vapor pressure over flat surfaces of pure liquid water and ice, at temperatures below 0°C. The insert shows difference between saturation vapor pressures over water and ice.

Solved Example
Find the saturation vapor pressure for T = 21°C?

Solution
Given: T = 21°C = 294 K
Find: e_s = ? kPa. Use eq. (4.1) for liquid water.

$$e_s = (0.611\text{kPa})\cdot\exp\left[(5423\text{K})\cdot\left(\frac{1}{273\text{K}}-\frac{1}{303\text{K}}\right)\right]$$

$$= (0.611\text{ kPa})\cdot\exp(1.419) = \underline{\mathbf{2.525\text{ kPa}}}$$

Check: Units OK. Physics OK. Agrees with Table 4-1.
Discussion: Compared to average sea-level pressure P = 101.3 kPa, this is roughly 2.5% of the total.

pure liquid water is given the symbol e_s. For unsaturated air, $e < e_s$.

Air can be slightly **supersaturated** ($e > e_s$) when there are no surfaces upon which water vapor can condense (i.e., unusually clean air, with no cloud condensation nuclei, and no liquid or ice particles). Temporary supersaturation might occur when the threshold value drops so quickly that condensation does not remove water vapor fast enough. However, photographs of air flow over aircraft wings for both subsonic and supersonic flight through humid air indicate that condensation to form cloud droplets occurs almost instantly.

Even at saturation, there is a continual exchange of water molecules between the liquid water and the air. The evaporation rate depends mostly on the temperature of the liquid water. The condensation rate depends mostly on the humidity in the air. At equilibrium these two rates balance.

If the liquid water temperature increases, then evaporation will temporarily exceed condensation, and the number of water molecules in the air will increase until a new equilibrium is reached. Thus, the equilibrium (saturation) humidity increases with temperature. The net result is that <u>warmer air can hold more water vapor at equilibrium than cooler air</u>.

The **Clausius-Clapeyron** equation describes the relationship between temperature and saturation vapor pressure, which is approximately:

$$e_s \approx e_o \cdot \exp\left[\frac{L}{\Re_v}\cdot\left(\frac{1}{T_o}-\frac{1}{T}\right)\right] \qquad \bullet(4.1a)$$

where e_o = 0.611 kPa and T_o = 273.15 K are constant parameters, and $\Re_v$ = 461 J·K^{-1}·kg^{-1} is the gas constant for water vapor. Absolute temperature in Kelvin must be used for T in eq. (4.1).

Because clouds can consist of liquid droplets and ice crystals suspended in air, you must consider saturations with respect to water and ice. Over a flat water surface, use the latent heat of vaporization $L = L_v$ = 2.5x10^6 J·kg^{-1} in eq. (4.1), which gives $L_v/\Re_v$ = 5423 K. Over a flat ice surface, use the latent heat of deposition $L = L_d$ = 2.83x10^6 J·kg^{-1}, which gives $L_d/\Re_v$ = 6139 K.

Saturation vapor pressure is listed in Table 4-1 and plotted in Figs. 4.1 and 4.2. These were produced by solving eq. (4.1) on a computer spreadsheet. The exponential-like increase of water-vapor holding capacity with temperature has tremendous impact on clouds and storms. **Supercooled** (unfrozen) liquid water can exist between temperatures of 0 to –40°C, hence, the curve for saturation over water includes temperatures below 0°C.

The Clausius-Clapeyron equation also describes the relationship between water-vapor pressure e and dew-point temperature (T_d, to be defined later):

$$e = e_o \cdot \exp\left[\frac{L}{\Re_v}\cdot\left(\frac{1}{T_o}-\frac{1}{T_d}\right)\right] \qquad (4.1b)$$

Table 4-1. (1) Saturation values of humidity vs. actual air temperature (T). -or-
(2) Actual humidities vs. dew-point temperature (T_d).

Values are for over a flat surface of liquid water. Mixing ratio r and specific humidity q values are for sea-level pressure. Vapor-pressure e and absolute humidity ρ_v values are for any pressure. Subscript s denotes a saturation value.

		For P = 101.325 kPa		
T	**e_s**	**r_s**	**q_s**	**ρ_{vs}**
		or		
T_d	**e**	**r**	**q**	**ρ_v**
(°C)	**(kPa)**	**(g/kg)**	**(g/kg)**	**(g/m³)**
–20	**0.127**	**0.78**	**0.78**	**1.09**
–18	0.150	0.92	0.92	1.28
–16	0.177	1.09	1.09	1.50
–14	0.209	1.28	1.28	1.75
–12	0.245	1.51	1.51	2.04
–10	**0.287**	**1.77**	**1.76**	**2.37**
–8	0.335	2.07	2.06	2.75
–6	0.391	2.41	2.40	3.18
–4	0.455	2.80	2.80	3.67
–2	0.528	3.26	3.25	4.22
0	**0.611**	**3.77**	**3.76**	**4.85**
2	0.706	4.37	4.35	5.57
4	0.814	5.04	5.01	6.37
6	0.937	5.80	5.77	7.28
8	1.076	6.68	6.63	8.30
10	**1.233**	**7.66**	**7.60**	**9.45**
12	1.410	8.78	8.70	10.73
14	1.610	10.05	9.95	12.17
16	1.835	11.48	11.35	13.77
18	2.088	13.09	12.92	15.56
20	**2.371**	**14.91**	**14.69**	**17.55**
22	2.688	16.95	16.67	19.76
24	3.042	19.26	18.89	22.22
26	3.437	21.85	21.38	24.94
28	3.878	24.76	24.16	27.94
30	**4.367**	**28.02**	**27.26**	**31.27**
32	4.911	31.69	30.72	34.93
34	5.514	35.81	34.57	38.96
36	6.182	40.43	38.86	43.40
38	6.921	45.61	43.62	48.27
40	**7.736**	**51.43**	**48.91**	**53.62**
42	8.636	57.97	54.79	59.47
44	9.627	65.32	61.31	65.88
46	10.717	73.59	68.54	72.87
48	11.914	82.91	76.56	80.51
50	**13.228**	**93.42**	**85.44**	**88.84**

BEYOND ALGEBRA • Clausius-Clapeyron

Historical Underpinning

To build better steam engines during the industrial revolution, engineers were working to discover the thermodynamics of water vapor. Steam engineers B.-P.-E. Clapeyron in 1834 and R. Clausius in 1879 applied the principles of S. Carnot (early 1800s), to study isothermal compression of pure water vapor in a cylinder. They measured the saturation vapor pressure at the point where condensation occurred.

Variation of Vapor Pressure with Temperature

By repeating the experiment for various temperatures, they empirically found that:

$$\frac{de_s}{dT} = \frac{L_v}{T}\left[\frac{1}{\rho_v}-\frac{1}{\rho_L}\right]^{-1}$$

where ρ_v is the density of water vapor, and ρ_L is the density of liquid water. But $\rho_L >> \rho_v$ (see Appendix B and Table 4-1), thus $1/\rho_L << 1/\rho_v$, allowing us to neglect the ρ_L term:

$$\frac{de_s}{dT} \cong \frac{L_v}{T}\rho_v$$

The ideal gas law can be used to relate the water vapor pressure to the vapor density: $e_s = \rho_v \cdot \Re_v \cdot T$, where $\Re_v$ is the gas constant for water vapor. Solving for ρ_v and plugging the result into the eq. above gives:

$$\frac{de_s}{dT} \cong \frac{L_v \cdot e_s}{\Re_v \cdot T^2}$$

Use the Separation of Variables method: move all e_s terms to the left, all T terms to the right:

$$\frac{de_s}{e_s} \cong \frac{L_v}{\Re_v}\frac{dT}{T^2}$$

Then integrate, taking care with the limits:

$$\int_{e_o}^{e_s}\frac{de_s}{e_s} \cong \frac{L_v}{\Re_v}\int_{T_o}^{T}\frac{dT}{T^2}$$

where e_o is a known vapor pressure at reference temperature T_o. The integration result is:

$$\ln\left(\frac{e_s}{e_o}\right) \cong -\frac{L_v}{\Re_v}\left[\frac{1}{T}-\frac{1}{T_o}\right]$$

Taking the antilog (exp) of both sides gives eq. (4.1).

$$e_s = e_o \cdot \exp\left[\frac{L}{\Re_v}\cdot\left(\frac{1}{T_o}-\frac{1}{T}\right)\right] \qquad (4.1)$$

See C. Bohren and B. Albrecht [1998: *Atmospheric Thermodynamics*, Oxford, 402pp] for details, and for an interesting historical discussion.

FOCUS • Boiling

Definition:

Boiling is the state where ambient atmospheric pressure equals the equilibrium (saturation) vapor pressure:

$$P = e_s$$

Derivation of Boiling T vs. z:

Because ambient pressure decreases roughly exponentially with height, we can use (1.9b) to replace the left hand side (LHS) of the equation above by $P = P_o \cdot \exp(-z/H_p)$, where $P_o = 101.325$ kPa is sea level pressure (at $z = 0$), and $H_p \approx 7.29$ km is the scale height for pressure. The right hand side (RHS) can be replaced with the Clausius-Clapeyron eq. (4.1), which describes how this boiling pressure is related to T. The net result is:

$$P_o \cdot \exp\left[-\frac{z}{H_p}\right] = e_o \cdot \exp\left[\frac{L_v}{\Re_v} \cdot \left(\frac{1}{T_o} - \frac{1}{T}\right)\right]$$

where $L_v / \Re_v = 5423$ K. Dividing both sides by P_o, and using the trick that $e_o/P_o = \exp[\ln(e_o/P_o)]$, gives:

$$\exp\left[-\frac{z}{H_p}\right] = \exp\left[\ln\left(\frac{e_o}{P_o}\right) + \frac{L_v}{\Re_v}\left(\frac{1}{T_o}\right) - \frac{L_v}{\Re_v}\frac{1}{T}\right]$$

But the first two terms in square brackets on the RHS are constants, and can be grouped as a dimensionless constant a. Taking the *ln* of both sides gives:

$$\frac{z}{H_p} = \frac{L_v}{\Re_v}\frac{1}{T} - a$$

Rearranging to solve for temperature T (which equals $T_{boiling}$ because we had set $P = e_s$):

$$\boxed{T_{boiling} = \frac{L_v / \Re_v}{a + z / H_p}}$$

By definition of the Celsius temperature scale, $T = 100°C = 373.15$ K for boiling at sea level $z = 0$. Using these values of z and T in the eq. above allows us solve for a, yielding $a = 14.53$ (dimensionless).

Discussion:

At $z = 1$ km, the eq. above gives $T_{boiling} = 96.6°C$, and at $z = 2$ km, $T_{boiling} = 93.2°C$. This is an average decrease of 3.4°C / km.

To soften vegetables to the desired tenderness or to prepare meats to the desired doneness, foods must be cooked at a certain temperature over a certain time duration. Slightly cooler cooking temperatures must be compensated with slightly longer cooking times. Thus, boiled foods take longer to cook at higher altitude because the boiling temperature is cooler.

Tetens' formula is an empirical expression for saturation vapor pressure e_s with respect to liquid water:

$$e_s = e_o \cdot \exp\left[\frac{b \cdot (T - T_1)}{T - T_2}\right] \qquad (4.2)$$

It includes the variation of latent heat with temperature, where $e_o = 0.611$ kPa, $b = 17.2694$, $T_1 = 273.15$ K, and $T_2 = 35.86$ K. Although this formula depends on temperature differences (for which °C or K can normally be used), absolute temperature T in units of Kelvins must be used here because the parameters T_1 and T_2 are given in Kelvins.

Solved Example

Compare Tetens' formula with the Clausius-Clapeyron equation for a variety of temperatures

Solution

Use eqs. (4.1) and (4.2) in a spreadsheet.

The result below on a semi-log graph shows the Clausius-Clapeyron equation as a solid line, and Tetens' formula as a dashed line.

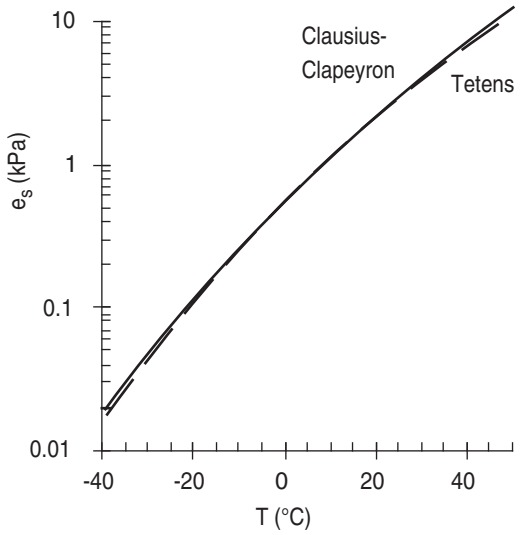

Check: Units OK. Physics OK. Agrees with Table 4-1.
Discussion: Both formulae are extremely close over a wide range of temperatures.

Science Graffito

"I think, therefore I am." — René Descartes.

HUMIDITY VARIABLES

Mixing Ratio

The ratio of mass m of water vapor to mass of dry air is called the mixing ratio, r:

$$r = \frac{m_{water\ vapor}}{m_{dry\ air}} \tag{4.3}$$

where $m_{dry\ air} = m_{total\ air} - m_{water\ vapor}$. To put this into a more useful form, divide the numerator and denominator by a common volume to get a ratio of densities, substitute the ideal gas law for each gas, and assume a common temperature for all gases. The result is:

$$r = \frac{\varepsilon \cdot e}{P - e} \tag{4.4}$$

where $\varepsilon = \Re_d/\Re_v = 0.622\ g_{vapor}/g_{dry\ air} = 622$ g/kg is the ratio of gas constants for dry air to that for water vapor. Eq. (4.4) says that r is proportional to the ratio of partial pressure of water vapor (e) to partial pressure of the remaining gases in the air ($P - e$), where P is total air pressure.

The **saturated mixing ratio**, r_s, is similar to eq. (4.4), except with saturation vapor pressure e_s in place of e.

$$r_s = \frac{\varepsilon \cdot e_s}{P - e_s} \tag{4.5}$$

Examples of mixing ratio values are given in Table 4-1, for air at sea level, where the Clausius-Clapeyron equation or Tetens' formula is used to find e_s.

Although units of mixing ratio are "g/g" (i.e., grams of water vapor per gram of dry air), it is usually presented as "g/kg" (i.e., grams of water vapor per kilogram of dry air) by multiplying the "g/g" value by 1000. By convention in meteorology we don't reduce the ratio "g/g" to 1, because the numerator and denominator represent masses of different substances that must be discerned in mass budgets.

Specific Humidity

The ratio of mass m of water vapor to mass of total (moist) air is called the specific humidity, q, and to a good approximation is given by:

$$q = \frac{m_{water\ vapor}}{m_{total\ air}} \tag{4.6}$$

or

$$q = \frac{\varepsilon \cdot e}{P_d + \varepsilon \cdot e} = \frac{\varepsilon \cdot e}{P - e \cdot (1 - \varepsilon)} \tag{4.7}$$

where $\varepsilon = 0.622$ g/g = 622 g/kg, and P is pressure. Specific humidity q has units of g/g or g/kg.

For **saturation specific humidity**, q_s:

$$q_s = \frac{\varepsilon \cdot e_s}{P_d + \varepsilon \cdot e_s} \tag{4.8}$$

Both the saturation mixing ratio and saturation specific humidity depend on ambient pressure, but the saturation vapor pressure does not. Thus, in Table 4-1 the vapor pressure numbers are absolute numbers that can be used anywhere, while the other humidity variables are given at sea-level pressure and density. The saturation values of mixing ratio and specific humidity can be calculated for any other ambient pressure using eqs. (4.5) and (4.8).

Absolute Humidity

The concentration ρ_v of water vapor in air is called the absolute humidity, and has units of grams of water vapor per cubic meter of air (g/m^3). Absolute humidity is essentially a partial density:

$$\rho_v = \frac{m_{water\ vapor}}{Volume} \tag{4.9}$$

where m is mass and Vol is volume. Absolute humidity can be reformulated using the ideal gas law for water vapor:

$$\rho_v = \frac{e}{\Re_v \cdot T} \tag{4.10}$$

where $\Re_v = 4.61 \times 10^{-4}$ kPa·K^{-1}·m^3·g^{-1} is the gas constant for water vapor. Alternately, by replacing temperature T using the ideal gas law for dry air:

$$\rho_v = \frac{e \cdot \varepsilon \cdot \rho_d}{P - e} \approx \frac{e}{P} \cdot \varepsilon \cdot \rho_d \tag{4.11}$$

where ρ_d is the density of dry air, e is the vapor pressure, $\varepsilon = \Re_d/\Re_v = 622$ g/kg, and P is total air pressure. As discussed in Chapter 1, dry-air density is roughly $\rho_d = 1.225$ kg/m^3 at sea level, and varies with altitude, pressure, and temperature according to the ideal gas law.

The **saturated** value of **absolute humidity**, ρ_{vs}, is found by using e_s in place of e in the equations above:

$$\rho_{vs} = \frac{e_s}{\Re_v \cdot T} \tag{4.12}$$

or

$$\rho_{vs} = \frac{e_s \cdot \varepsilon \cdot \rho_d}{P - e_s} \approx \frac{e_s}{P} \cdot \varepsilon \cdot \rho_d \tag{4.13}$$

Solved Example

Find the saturation values of mixing ratio, specific humidity, and absolute humidity for air of temperature 0°C and pressure 50 kPa.

Solution

Given: T = 0°C, P = 50 kPa

Find: r_s = ? g/kg, q_s = ? g/kg, ρ_{vs} = ? g/m^3

e_s = 0.611 kPa was found directly from Table 4-1 because it does not depend on P.

Use eq. (4.5) for r_s:

r_s = [0.622·(0.611 kPa)] / [50 kPa - 0.611 kPa]
= 0.00770 g/g
= **7.70 g/kg**

Use eq. (4.8) for q_s:

q_s = 0.622·(0.611 kPa)/50 kPa = 0.00760 g/g
= **7.60 g/kg**

Use eq. (4.12) for ρ_{vs}:

ρ_{vs} = (0.611 kPa)/[(461 J·K^{-1}·kg^{-1})·(273 K)]
= **0.00485** kg·m^{-3} = **4.85** g·m^{-3} .

Check: Units OK. Physics OK.

Discussion: The first two values are roughly double those for sea-level pressure (see Table 4-1). The reason is that although the partial pressure of water vapor held in the air is the same, partial pressure of dry air is less. The last value equals the value in Table 4-1, because there is no P dependence.

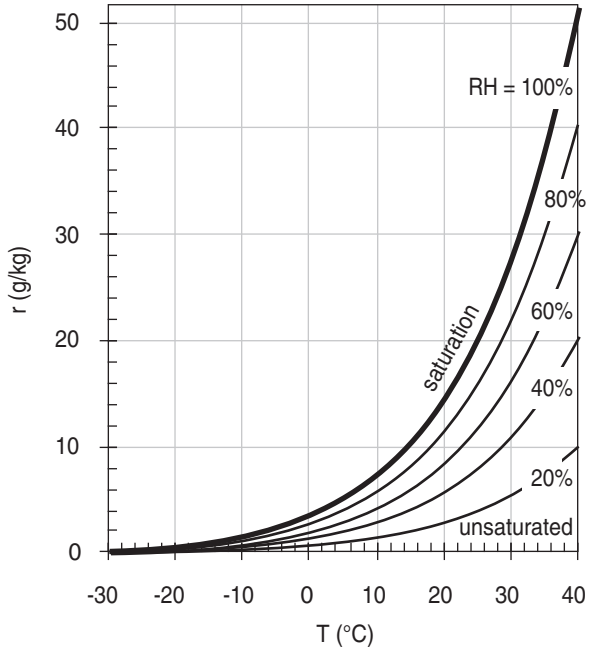

Figure 4.3
Mixing ratio at sea level vs. relative humidity and temperature.

Relative Humidity

The ratio of the actual amount of water vapor in the air compared to the equilibrium (saturation) amount at that temperature is called the relative humidity, RH:

$$\frac{RH\%}{100\%} = \frac{q}{q_s} = \frac{\rho_v}{\rho_{vs}} \approx \frac{r}{r_s} \qquad \bullet(4.14)$$

where e is vapor pressure, q is specific humidity, ρ_v is absolute humidity, r is mixing ratio, and subscript s indicates saturation.

Relative humidity regulates the amount of net evaporation that is possible into the air, regardless of the temperature. At RH = 100% no net evaporation occurs because the air is already saturated. Variation of mixing ratio with RH is shown in Fig. 4.3.

Dew-Point Temperature

The temperature to which air must be cooled in order to become saturated at constant pressure is called the **dew-point temperature**, T_d , (also known as the **dew point**). It is given by eq. (4.1) or found from Table 4-1 by using vapor pressure e in place of e_s and T_d in place of T. Making those substitutions and solving for T_d yields:

$$T_d = \left[\frac{1}{T_o} - \frac{\Re_v}{L}\cdot\ln\left(\frac{e}{e_o}\right)\right]^{-1} \qquad (4.15a)$$

with e_o =0.611 kPa, T_o =273 K, $\Re_v/L_v$ =1.844x10^{-4} K^{-1}.

Eq. (4.15a) can be combined with the definition of mixing ratio r to give:

$$T_d = \left[\frac{1}{T_o} - \frac{\Re_v}{L}\ln\left(\frac{r\cdot P}{e_o\cdot(r+\varepsilon)}\right)\right]^{-1} \qquad \bullet(4.15b)$$

where $\varepsilon = \Re_d/\Re_v = 0.622\ g_{vapor}/g_{dry\ air}$.

Saturation (equilibrium) with respect to a flat surface of liquid water occurs at a slightly colder temperature than saturation with respect to a flat ice surface. With respect to liquid water, use $L = L_v$ in the equation above, where T_d is called the **dew-point temperature**. With respect to ice, $L = L_d$, and T_d is called the **frost-point temperature** (see the "Saturation" subsection for values of L).

If $T_d = T$, the air is saturated. The **dew-point depression** or **temperature-dew-point spread** ($T - T_d$) is a relative measure of the dryness of the air. T_d is usually less than T (except during supersaturation, where it might be a fraction of a degree warmer). If air is cooled below the initial dew-point temperature, then the dew-point temperature drops to remain equal to the air temperature, and

Solved Example

Find the relative humidity for air of T = 20°C and e = 1 kPa.

Solution

Given: T = 20°C , e = 1 kPa
Find: RH = ? %

From Table 4-1 at T = 20°C : e_s = 2.371 kPa.
Use eq. (4.14):
RH = 100% · (1 kPa / 2.371 kPa) = **42%**.

Check: Units OK. Physics OK.
Discussion: The result does not depend on P.

the excess water condenses or deposits as dew, frost, fog, or clouds (see the Cloud and Precip. chapters).

Dew-point temperature is easy to measure and provides the most accurate humidity value, from which other humidity variables can be calculated (see Humidity Instruments section at the end of this chapter). When dew (sweat) forms on the outside of a cold beverage can or bottle, you know that the outside of the beverage container is colder than the dew-point temperature of the surrounding air.

Saturation Level or Lifting Condensation Level (LCL)

When unsaturated air is lifted, it cools at the dry adiabatic lapse rate. If lifted high enough, the temperature will drop to the dew-point temperature, and clouds will form. Dry air (air of low relative humidity) must be lifted higher than moist air. Saturated air needs no lifting at all. Hence, LCL is a measure of humidity.

When lifting non-cloudy air, the height at which saturation just occurs (with no supersaturation) is the **saturation level** or the **lifting condensation level** (**LCL**). For convective (cumuliform) clouds, **cloud base** occurs there. LCL height (distance above the height where T and T_d are measured) for cumuliform clouds is very well approximated by:

$$z_{LCL} = a \cdot (T - T_d) \qquad \bullet(4.16a)$$

where a = 0.125 km/°C.

The pressure P_{LCL} at the LCL is

$$P_{LCL} = P \cdot \left[1 - b \cdot \left(\frac{T - T_d}{T} \right) \right]^{C_p / \Re} \qquad (4.16b)$$

where $b = a \cdot \Gamma_d$ = 1.225 (dimensionless), $C_p/\Re$ = 3.5 (dimensionless), and P is the pressure at the initial

Solved Example

Given desert conditions with a temperature of 30°C and pressure of 100 kPa, find the dew-point temperature for a relative humidity of 20%.

Solution

Given: T = 30°C , P = 100 kPa, RH = 20%
Find: T_d = ? °C

From Table 4-1, e_s = 4.367 kPa.
Use eq. (4.14): e = 0.2·(4.367 kPa)= 0.8734 kPa
We could use eq. (4.15) to solve for T_d, but it is easier to look up the answers in Table 4-1. T_d = **5°C**.

Check: Units OK. Physics OK.
Discussion: The result does not depend on P. This dry air would need to be cooled 25°C before condensation would occur.

Solved Example

Find the dew point for r = 10 g/kg and P = 80 kPa.

Solution

Given: r = 0.01 g_{vapor}/g_{air}, P = 80 kPa
Find: T_d = ? °C

Use eq. (4.15b): $T_d = [(1/(273\text{K}) - (1.844\text{x}10^{-4}\ \text{K}^{-1}) \cdot \ln\{ [(80\text{kPa}) \cdot (0.01 g_{vapor}/g_{air})] / [(0.611\text{kPa}) \cdot ((0.01 g_{vapor}/g_{air}) + (0.622 g_{vapor}/g_{air})] \}]^{-1}$
$= [(1/(273\text{K}) - (1.844\text{x}10^{-4}\ \text{K}^{-1}) \cdot \ln(2.07)]^{-1} = 283.4\text{K}$.
Thus, T_d = 283.4 – 273 = or **10.4°C**

Check: Units OK. Magnitude OK.
Discussion: This humidity might occur in the tropics, with a surface temperature warmer than 30°C.

Solved Example

Find the LCL height and pressure, if T = 20°C and T_d = 10°C at P = 95 kPa.

Solution

Given: T = 20°C, T_d = 10°C, P = 95 kPa.
Find: z_{LCL} = ? km , P_{LCL} = ? kPa

Use eq. (4.16a)
z_{LCL} = (0.125km/°C)·(20 – 10°C)
= **1.25 km above the starting height**

Use eq. (4.16b)
P_{LCL} = (95 kPa)·[1 – 1.225·(20–10°C)/293K]$^{3.5}$
= **81.8 kPa**

Check: Units OK. Physics OK.
Discussion: Reasonable height for cumulus cloud base. Also, since pressure decreases about 10 kPa for each increase of 1 km of altitude near the surface, the pressure answer is also reasonable.

Solved Example

At a pressure of 100 kPa, what is the mixing ratio if the dry and wet-bulb temperatures of a psychrometer are 20°C and 14°C, respectively? Use the equations here, not the look-up tables or graphs.

Solution

Given: $T = 20°C$, $T_w = 14°C$, $P = 100$ kPa
Find: $r = ?$ g/kg

First, solve eq. (4.18): $r_w =$

$$\frac{622\text{g/kg}}{(1.631\text{kPa}^{-1})\cdot(90\text{kPa})\cdot\exp\left(\frac{-17.67\cdot 18°C}{18°C+243.5°C}\right)-1}$$

$r_w =$ 10.13 g/kg.

Then solve eq. (4.19):
r = (10.13g/kg) – [0.40224 (g/kg)/°C]·(20–14°C)
= **7.72 g/kg**.

Check: Units OK. Physics OK.
Discussion: Now we can compare our answer with the data in graph (Fig. 4.4). Using $T_w = 14°C$ along the ordinate, and $T - T_w = 20 - 14 = 6°C$ as the dew-point depression along the abscissa, we find that our answer agrees with the graph. Obviously, for every-day use, it is easier to use the psychrometric graph, or the corresponding psychrometric tables that are published in other books.

Solved Example

For the previous solved example, use its inputs and result to calculate the relative humidity. Again, don't use the look-up tables or graphs yet.

Solution

Given: $T = 20°C$, $r = 7.72$ g/kg, $P = 100$ kPa
Find: $RH = ?$ %

First, use Tetens' formula (4.2) , with the trick that $\Delta T = T(\text{K}) - T_1(\text{K}) = [T(°C)+273] - 273 = T(°C)$, and remembering that for temperature differences: 1°C = 1 K .

$$e_s = 0.611(\text{kPa})\cdot\exp\left[\frac{17.2694\cdot(20\text{K})}{(20+273.16)\text{K}-35.86\text{K}}\right]$$

$e_s = 2.34$ kPa.

Next, use this in eq. (4.5):

$$r_s = \frac{(622\text{g/kg})\cdot 2.34\text{kPa}}{[101.325-2.34]\text{kPa}} = 14.7\text{g/kg}$$

Finally, use eq. (4.14): $RH = 100\%\cdot(r/r_s)$
$RH = 100\% \cdot (7.72/14.7) =$ **52.5%**

Check: Units OK. Physics OK.
Discussion: What a lot of work. If we instead had used psychrometric graph (Fig. 4.5) with $T_w = 14°C$ $T - T_w = 6°C$, we would have found almost the same relative humidity much more easily.

height where temperature T and dew-point T_d are measured, such as at the surface. Don't forget to use Kelvin for the T in the denominator.

These expressions do not work for stratiform (advective) clouds, because these clouds are not formed by air rising vertically from the underlying surface. Air in these clouds blows at a gentle slant angle from a surface hundreds to thousands of kilometers away.

Regardless of whether cumuliform clouds exist, the LCL or saturation level can be used as a measure of humidity. It also serves as a measure of total water content for saturated (cloudy) air. For cloudy air, the saturation level is the altitude to which one must lower an air parcel for all of the liquid or solid water to just evaporate. Eqs. (4.16) do not apply to this situation.

Wet-Bulb Temperature

When the bulb of a glass thermometer is covered by a cloth sleeve that is wet, this **wet bulb** becomes cooler than the actual (**dry bulb**) air temperature T because of the latent heat associated with evaporation of water. Drier ambient air allows more evaporation, causing the wet-bulb temperature T_w to cool significantly below the air temperature. For saturated air there is no net evaporation and the wet-bulb temperature equals that of the dry bulb. You can find the humidity from the difference between the dry and wet-bulb temperatures. This difference, called the **wet-bulb depression** ($T - T_w$), is a measure of the relative dryness of the air.

To work properly, the sleeve or wick must be wet with clean or distilled water. The wet bulb should be well ventilated by blowing air past it (**aspirated psychrometer**) or by moving the thermometer through the air by twirling it around on the end of a short chain (**sling psychrometer**). Usually psychrometers have both wet and dry-bulb thermometers mounted next to each other.

Let T_w represent the wet-bulb temperature, and r_w represent the wet-bulb mixing ratio in the air adjacent to the wet-bulb after water has evaporated into it from the sleeve. Because the latent heat used for evaporation comes from the sensible heat associated with cooling, a simple heat balance gives:

$$C_p\cdot(T - T_w) = -L_v\cdot(r - r_w) \qquad (4.17)$$

where T and r are ambient (dry-bulb) air temperature and mixing ratio, respectively, C_p is the specific heat of air at constant pressure, and L_v is the latent heat of vaporization.

If the wet and dry-bulb temperatures and ambient pressure P are measured or otherwise known, the desired mixing ratio r can be found by first finding r_w:

$$r_w = \frac{\varepsilon}{b \cdot P \cdot \exp\left(\frac{-c \cdot T_w(°C)}{T_w(°C) + \alpha}\right)} \quad (4.18)$$

Then:

$$r = r_w - \beta \cdot (T - T_w) \quad (4.19)$$

where temperatures must have units of °C, and where ε = 622 g/kg, b = 1.631 kPa^{-1}, c = 17.67, α = 243.5°C, and β = 0.40224 (g/kg)/°C. Knowing r, any other moisture variable is easily found.

The easiest way for you to find humidity from dry and wet-bulb temperature is to look-up the humidity in tables called **psychrometric tables**, which are often published in meteorology books. Figures 4.4 and 4.5 present the look-up information as **psychrometric graphs**, which were computed from the equations in this Chapter.

Solved Example

Find the mixing ratio and relative humidity for air temperature of 12°C and wet-bulb temperature of 10°C. Yes, you may use the graphs this time.

Solution

Given: T = 12°C , T_w = 10°C
Find: r = ? g/kg , and RH = ? %

Assume P = 101.3 kPa, so we can use the Figs.
The wet-bulb depression is 12 – 10 = 2°C
Use Fig. 4.4. r = **7 g/kg**.
Use Fig. 4.5. RH = **78%** .

Check: Units OK. Physics OK.
Discussion: Much easier than the solved examples on the previous page. Notice that in Fig. 4.4, r depends mostly on T_w, because the mixing-ratio lines are mostly horizontal. However, RH depends mostly on $T - T_w$, because the lines in Fig. 4.5 are mostly vertical.

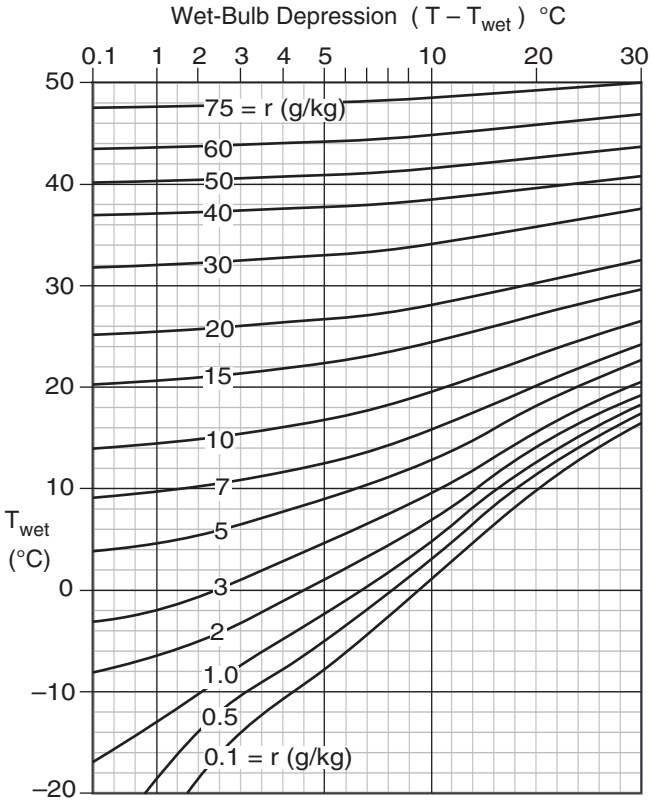

Figure 4.4
Psychrometric graph, to find mixing ratio r from wet and dry-bulb temperatures. Based on P = 101.325 kPa. Caution, the darker vertical lines mark scale changes along the abscissa.

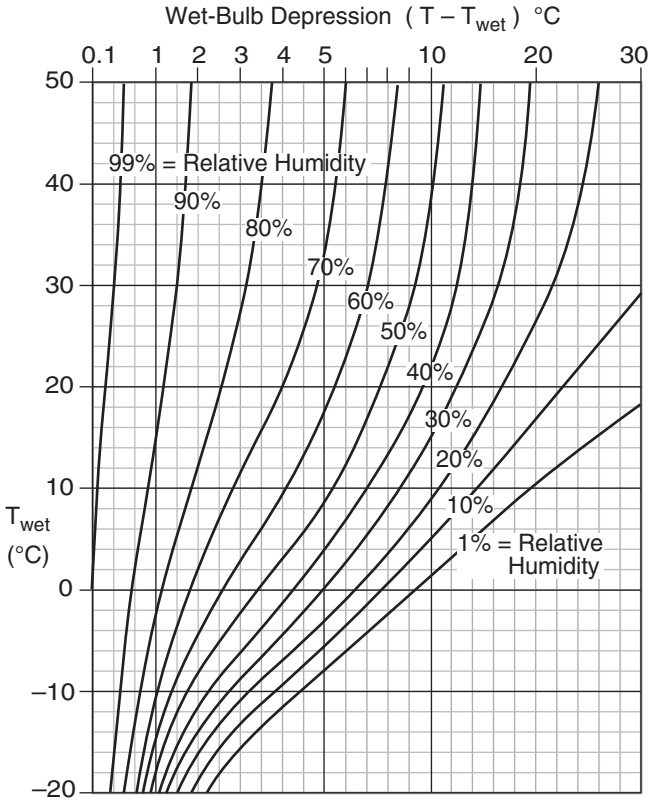

Figure 4.5
Psychrometric graph, to find relative humidity from wet and dry-bulb temperatures. Based on P = 101.325 kPa. Caution, the darker vertical lines mark scale changes along the abscissa.

Solved Example

Find the wet-bulb temperature for air at sea level with temperature 30°C and dew point 24°C. Assume Γ_s = 3.78 °C/km for this case.

Solution

Given: T = 30°C , T_d = 24°C , P = 101.3 kPa
Find: T_w = ?°C

Use Normand's Rule:
Step 1, solve eq. (4.16):
z_{LCL} = (0.125 km/°C)·(30 – 24°C) = 0.75 km.
Step 2, solve eq. (4.20):
T_{LCL} = 30 – (9.8 K/km)·(0.75 km) = 22.65 °C.
Step 3, solve eq. (4.21):
T_w = 22.65 + (3.78 °C/km)·(0.75 km) = **25.5°C**.

Check: Units OK. Physics OK.
Discussion: The resulting wet-bulb depression is ($T - T_w$) = 4.5°C.

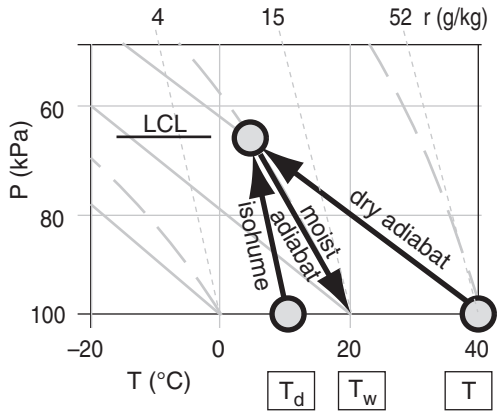

Figure 4.6
Demonstration of Normand's rule on a thermo diagram. It shows how to find wet-bulb temperature T_w, given T and T_d.

FOCUS • Why So Many Moisture Variables?

Vapor pressure, mixing ratio, specific humidity, absolute humidity, relative humidity, dew point depression, saturation level, and wet bulb temperature are different ways to quantify moisture in the air. Why are there so many?

Some variables are useful because they can be measured. Others are useful in conservation equations for water substance, for describing physical characteristics of the air, or for describing how life is affected by humidity. Often we are given or can measure one moisture variable, but must convert it to a different variable to use it.

(continues on next page)

To create your own psychrometric tables or graphs, first generate a table of mixing ratios in a spreadsheet program, using eqs. (4.18) and (4.19). I assumed a standard sea-level pressure of P = 101.325 kPa for the figures here. Then contour the resulting numbers to give Fig. 4.4. Starting with the table of mixing ratios, use eqs. (4.2), (4.5), and (4.14) to create a new table of relative humidities, and contour it to give Fig. 4.5. All of these psychrometric tables and graphs are based on Tetens' formula (eq. 4.2).

Finding T_w from T_d is a bit trickier, but is possible using **Normand's Rule**:

- Step 1: Find z_{LCL} using eq. (4.16).
- Step 2: $T_{LCL} = T - \Gamma_d \cdot z_{LCL}$ (4.20)
- Step 3: $T_w = T_{LCL} + \Gamma_s \cdot z_{LCL}$ (4.21)

where Γ_s is the moist lapse rate described later in this chapter, Γ_d = 9.8 K/km is the dry rate, and T_{LCL} is the temperature at the LCL. Normand's Rule tells us that $T_d \le T_w \le T$.

Normand's rule is easy to implement on a thermo diagram. Although isohumes and moist adiabats on thermo diagrams are not introduced until later in this chapter, I demonstrate Norman's rule here for future reference. Follow a dry adiabat up from the given dry-bulb temperature T, and follow an isohume up from the given dew point T_d (Fig. 4.6). At the *LCL* (where these two isopleths cross), follow a moist adiabat back down to the starting pressure to give the wet-bulb temperature T_w.

More Relationships Between Moisture Variables

Units of g/g must be used for r and q in the relationships below:

$$q = \frac{r}{1+r} \tag{4.22}$$

$$q = \frac{\rho_v}{\rho_d + \rho_v} \tag{4.23}$$

$$q = \left(\frac{\varepsilon \cdot e_o}{P}\right) \cdot \exp\left[\frac{L}{\Re_v} \cdot \left(\frac{1}{T_o} - \frac{1}{T_d}\right)\right] \tag{4.24}$$

$$e = \frac{r}{\varepsilon + r} \cdot P \tag{4.25}$$

$$r = \frac{\rho_v}{\rho_d} \tag{4.26}$$

For air that is not excessively humid:

$$r \approx q \qquad \bullet(4.27a)$$

$$r_s \approx q_s \qquad \bullet(4.27b)$$

TOTAL WATER

Liquid and Solid Water

In clouds, fog, or air containing falling precipitation, one measure of the amount of liquid water in the air is the **liquid water content** (**LWC**). It is defined as

$$\rho_{LWC} = \frac{m_{liq.water}}{Vol} \qquad (4.28)$$

where $m_{liq.water}$ is mass of liquid water suspended or falling through the air, and *Vol* is the air volume. Typical values in cumulus clouds are $0 \le \rho_{LWC} \le 5$ g/m^3. It can also be expressed in units of $kg_{liq.water}/m^3$. LWC is the liquid-water analogy to the absolute humidity for water vapor.

Another measure is the **liquid-water mixing ratio**:

$$r_L = \frac{m_{liq.water}}{m_{dry\ air}} \qquad (4.29)$$

where $m_{liq.water}$ is the mass of liquid water that is imbedded as droplets within an air parcel that contains $m_{dry\ air}$ mass of dry air. A similar **ice mixing ratio** can be defined:

$$r_i = \frac{m_{ice}}{m_{dry\ air}} \qquad (4.30)$$

Both mixing ratios have units of kg_{water}/kg_{air}, or g_{water}/kg_{air}.

Liquid water content is related to liquid-water mixing ratio by

$$r_L = \frac{\rho_{LWC}}{\rho_{air}} \qquad (4.31)$$

where ρ_{air} is air density.

Total-Water Mixing Ratio

Define **total-water mixing ratio** r_T as the mass of water of all phases (vapor, liquid, and ice) per mass of dry air:

$$r_T = r + r_L + r_i \qquad \bullet(4.32a)$$

FOCUS • Why So Many Moisture Variables? *(continuation)*

Directly and easily measurable variables include wet-bulb temperature and dew-point temperature. Wet-bulb temperature is easy to measure by putting a wet cloth sleeve around the bulb of a thermometer, and ventilating the wet bulb. However, it is difficult to convert this into other humidity variables, which is why psychrometric tables and graphs have been developed. Dew point is measured by chilling a mirror until dew forms on it. It is one of the most accurate measurements of humidity.

Absolute humidity can be measured by shining electromagnetic radiation (infrared, ultraviolet, or microwave) across a path of humid air. The attenuation of the signal is a measure of the number of water vapor molecules along the path.

Relative humidity can be measured by: 1) expansion or contraction of organic fibers such as human hairs; 2) the change in electrical conductivity of a carbon powder emulsion on a glass slide; and 3) by how it affects the capacitance across a plastic dielectric. Relative humidity is extremely important because it affects the rate of evaporation from plants, animals, and the soil.

Mixing ratio or specific humidity are not usually measured directly, but are extremely useful because they are conserved within air parcels moving vertically or horizontally without mixing. Namely, heating, cooling, or changing the pressure of an air parcel will not change the mixing ratio or specific humidity in unsaturated air.

Lifting condensation level, or saturation level, can be used to estimate the altitude of cloud base for convective (cumulus) clouds.

Vapor pressure is neither easily measured nor directly useful. However, it is important theoretically because it describes from first principles how saturation humidity varies with temperature.

Solved Example

Find the liquid water mixing ratio in air at sea level, given a liquid water content of 3 g/m^3.

Solution

Given: $\rho_{LWC} = 3\ g_{water}/m^3$. Sea level.
Find: $r_L = ?\ g_{water}/kg_{dry\ air}$.
Assume standard atmosphere, and use Table 1-5 from Chapter 1 to get: $\rho_{air} = 1.225\ kg_{air}/m^3$ at sea level.

Use eq. (4.31):

$r_L = (3\ g_{water}/m^3)/(1.225\ kg_{air}/m^3)$
$= 2.45\ g_{water}/kg_{dry\ air}$. = **2.45 g/kg**

Check: Units OK. Physics OK. Magnitude reasonable.
Discussion: Liquid, solid and water vapor might exist together in a cloud.

Solved Example

Saturated air at sea level with T = 10°C contains 3 g/kg liquid water. Find the total water mixing ratio.

Solution

Given: T = 10°C, r_L = 3 g/kg
Find: r_T = ? g/kg.
Assume: No ice.

Use Table 4-1 because it applies for sea level. Otherwise, solve equations or use thermo diagram.
At T = 10°C: r_s = 7.66 g/kg from the table.

Use eq. (4.32c):
$r_T = r_s + r_L + r_i$ = 7.66 + 3 + 0 = **10.66 g/kg**

Check: Units OK. Physics OK.
Discussion: According to Table 4-1, the air would need to warm to 15°C to evaporate all liquid water

where r is the **water-vapor mixing ratio**, r_L is the **liquid-water mixing ratio**, and r_i is the **ice mixing ratio**. All these mixing ratios have units of kg_{water}/kg_{air}, or g_{water}/kg_{air}. Similar total-water variables are defined in terms of specific humidity and absolute humidity.

Liquid-water cloud droplets can exist unfrozen in air of temperature less than 0°C. Thus, it is possible for ice and liquid water to co-exist in the same air parcel at the same time, along with water vapor.

For negligible precipitation, eq. (4.32a) is approximately:

$$r_T = r \qquad \text{for unsaturated air} \quad \bullet(4.32b)$$

$$r_T = r_s + r_L + r_i \qquad \text{for saturated air} \quad \bullet(4.32c)$$

where the water-vapor mixing ratio is assumed to equal its saturation value r_s when liquid or ice is present. The words **saturated air** means cloudy air, and **unsaturated air** means non-cloudy air.

Total water is nearly conserved, in the sense that the amount of water lost or created via chemical reactions is small compared to the amounts advected with the wind or associated with precipitation. Thus, the change of total water in a volume can be calculated by the amount of water of all phases that enters or leaves the volume.

Recall that saturation water-vapor mixing ratio decreases as temperature decreases (see Table 4-1). Thus, given some initial amount of total water r_T, eq. (4.32c) says that liquid or solid water must increase as temperature and r_s decrease, in order that the sum of all water phases remain constant in saturated air.

Clouds or fog form when the total water content of the air exceeds the saturation (equilibrium) value. Because total water is an important factor in cloud and precipitation formation, budget equations for total water are presented in the next main section.

Solved Example

If an average of 5 g/kg of total water existed in the troposphere, between 100 kPa and 30 kPa, what is the precipitable water depth?

Solution

Given: r_T = 0.005 kg/kg, P_B = 100 kPa, P_T = 30 kPa
Find: d_W = ? m

Use eq. (4.33): and recall from Appendix A that
1 kPa = 1000 $kg_{air}{\cdot}m{\cdot}s^{-2}$. Thus,

d_w = { (0.005 kg/kg) / [(9.8 $m{\cdot}s^{-2}$)·(1000 $kg{\cdot}m^{-3}$)] }
· (100 – 30 kPa) · (1000 $kg_{air}{\cdot}m{\cdot}s^{-2}$ /kPa)
= 0.036 m = **3.6 cm** (≈ 1.4 inches).

Check: Units OK. Physics OK.
Discussion: Why so much precipitation? Because we used an unrealistically large mixing ratio over the whole depth of the troposphere. Although 5 g/kg is reasonable near the surface, higher in the troposphere the air is much colder and can hold much less water vapor.

Precipitable Water

If all the vapor, liquid, and solid water within a column of air in the atmosphere were to precipitate out, the resulting depth of water on the Earth's surface (or in a rain gauge) is called the precipitable water, d_W. It is given by

$$d_W = \frac{r_T}{|g|\cdot\rho_{liq}}\cdot(P_B - P_T) \qquad \bullet(4.33)$$

where r_T is average total-water mixing ratio, P_B and P_T are ambient air pressures at the bottom and top of the column segment, $|g|$ = 9.8 $m{\cdot}s^{-2}$ is gravitational acceleration magnitude, and ρ_{liq} = 1000 $kg{\cdot}m^{-3}$ is density of liquid water.

If the mixing ratio varies with height, then the full column can be broken into smaller column segments of near-uniform mixing ratio. The resulting precipitable-water depths per segment can be summed to give the total precipitable-water depth.

Precipitable water is sometimes used as a humidity variable. The bottom of the atmosphere is warmer than the mid and upper troposphere, and can hold the most water vapor. In a pre-storm cloudless environment, contributions to the total-column precipitable water thus come mostly from the boundary layer. Hence, precipitable water can serve as one measure of boundary-layer total water that could serve as the fuel for thunderstorms later in the day. See the Thunderstorm chapters for a sample map of precipitable water.

In the real atmosphere, winds can advect moisture into a column to replace that lost from precipitation. Consequently, the total rainfall amount observed at the surface after storm passage is often much greater than the precipitable water at any instant. Some microwave and infrared sensors on satellites (see the Remote Sensing chapter) measure precipitable water averaged over large depths of the troposphere.

Science Graffito

"The best way to have a good idea is to have lots of ideas." — Linus Pauling.

LAGRANGIAN BUDGETS

Moist air parcels have two additional properties that were unimportant for dry air. One is the amount of water in the parcel, which is important for determining cloud formation and precipitation amounts. The second is the latent heat released or absorbed when water changes phase, which is critical for determining the buoyancy of air parcels and the energy of thunderstorms.

Water Conservation

Lagrangian Water Budget

If you follow an air parcel as it moves, and assume no turbulent mixing with the environment, then the Lagrangian water budget is

$$\frac{\Delta r_T}{\Delta t} = S^{**} \tag{4.34}$$

where S** is a Lagrangian net source of water. This source could be evaporation from adjacent liquid water, or it could be a loss of water falling from the parcel as precipitation (causing negative S**).

If there is no source or loss, then there is no change of total water content. Phase changes must

Science Graffito

"Great ideas often receive violent opposition from mediocre minds." — Albert Einstein.

Solved Example

An air parcel at sea level has a temperature of 20°C and a mixing ratio of 10 g/kg. If the air is cooled to 10 °C, what is the liquid water content?

Solution

Given: $T = 20°C$, $r = 10$ g/kg
Find: $r_L = ?\ g_{liq}/g_{air}$ at $T = 10°C$

Use Table 4-1 because it applies for sea level. Otherwise, solve equations or use a thermo diagram. Assume no other sources or sinks.

Initially:
$r_s = 14.91$ g/kg from the table, at $T = 20°C$.
Air is initially unsaturated, because $r < r_s$.
Unsaturated air has no liquid water: $r_L = 0$.
Assume no ice at these warm temperatures.

$(r + r_L)_{initial} = (10 + 0)$ (g/kg) = 10 g/kg

Finally:
After cooling the air to 10°C, Table 4-1 shows that the max amount of vapor that can be held in the air at equilibrium is $r = r_s = 7.66$ g/kg. However, total water must be constant if it is conserved. Use eq. (4.35b):

10 g/kg = $(r + r_L)_{final}$ = 7.66 g/kg + $r_{L\,final}$

Thus,

$r_{L\,final}$ = 10 g/kg − 7.66 g/kg = **2.34 g/kg**

Check: Units OK. Physics OK.
Discussion: Some liquid water has formed in the air parcel, so it is now a cloud or fog.

Solved Example

Use Fig. 4.7 to answer (**A**) these questions (**Q**).

Solution

Q: What is the saturation mixing ratio for air of temperature 0°C and pressure 40 kPa?
A: Follow the $T = 0°C$ isotherm vertically, and the $P = 40$ kPa isobar horizontally, to find where they intersect. The saturation mixing ratio (dotted diagonal) line that crosses through this intersection is the one labeled: $r_s \approx$ **10 g/kg**.

Q: What is the actual mixing ratio for air of dew point 0°C and pressure 40 kPa?
A: This is the same intersection point yielding the same numerical answer, but because dew-point temperature was used, the answer represents the actual mixing ratio. $r \approx$ **10 g/kg**.

Q: What is the dew-point temperature for air of mixing ratio 20 g/kg and pressure 80 kPa?
A: From the intersection of the diagonal dotted line for $r = 20$ g/kg and the horizontal isobar for $P = 80$ kPa, go vertically straight down to find $T_d \approx$ **21°C**.

compensate each other to maintain constant total water. Thus, for no net source:

$$(r + r_i + r_L)_{initial} = (r + r_i + r_L)_{final} \qquad \bullet(4.35a)$$

For the special case of no ice, this reduces to:

$$(r + r_L)_{initial} = (r + r_L)_{final} \qquad \bullet(4.35b)$$

On a thermodynamic diagram, conservation of total water corresponds to following an isohume of constant mixing ratio as a parcel rises or descends. Thus, it is total water mixing ratio that is conserved, not dew-point temperature.

Thermo Diagrams – Part 2: Isohumes

Two classes of information are included on thermo diagrams: **states** and **processes**. State of the air is defined by **temperature**, **pressure**, and **moisture**. Two processes are **unsaturated** (**dry**) and **saturated** (**moist**) adiabatic vertical movement, such as experienced by air parcels rising through the atmosphere. Processes can change the state.

The chart background of vertical **isotherms** and horizontal **isobars** was introduced in Chapters 1 (Fig. 1.4) and 3 (Fig. 3.3). Here we will overlay **isohumes** of constant saturation-mixing-ratio state over the background (Fig. 4.7).

To use the thermo-diagram background of P vs. T for isohumes, we need to describe r_s as a function of P and T [abbreviate as $r_s(P, T)$]. Eq. (4.5) gives $r_s(P, e_s)$ and the Clausius-Clapeyron eq. (4.1) gives $e_s(T)$. So combining these two equations gives $r_s(P, T)$.

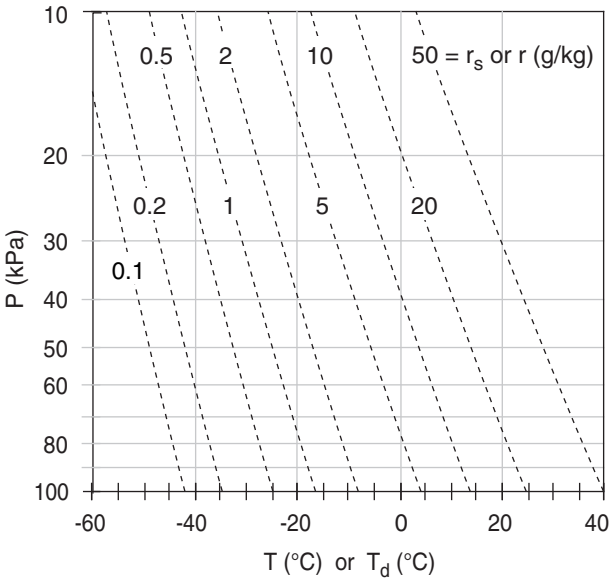

Figure 4.7
Thermodynamic diagram with isohumes of mixing ratio.

But to draw any one isohume (i.e., for any one value of r_s), we need to rearrange the result to give $T(P, r_s)$:

$$T = \left[\frac{1}{T_o} - \frac{\Re_v}{L_v} \cdot \ln\left\{ \frac{r_s \cdot P}{e_o \cdot (r_s + \varepsilon)} \right\} \right]^{-1} \qquad (4.36)$$

where e_o = 0.611 kPa, T_o = 273 K, ε = 0.622 g/g, and $\Re_v/L$ = 0.0001844 K^{-1}. Be sure to use g/g and not g/kg for r_s. The answer is in Kelvin.

Thus, pick any fixed r_s to plot. Then, for a range of P from the bottom to the top of the atmosphere, solve eq. (4.36) for the corresponding T values. Plot these T vs. P values as the isohume line on a thermo diagram. Use a spreadsheet to repeat this calculation for other values of r_s, to plot the other isohumes.

Eqs. (4.36) with (4.15b) are similar. Thus, you can use isohumes of $T(P, r_s)$ to also represent isohumes of $T_d(P, r)$. Namely, you can use isohumes to find the saturation state r_s of the air at any P and T, and you can also use the isohumes to describe the process of how T_d changes when an air parcel of constant r rises or descends to an altitude of different P.

Solved Example

Calculate the dew point of air at pressure 80 kPa and mixing ratio 1 g/kg.

Solution

Given: P = 80 kPa, r = 1 g/kg
Find: T_d = ?°C

Use eq. (4.15b):

$$T_d = \left[\frac{1}{273\text{K}} - 0.000184\text{K}^{-1} \cdot \ln\left\{ \frac{(0.001\text{g/g}) \cdot (80\text{kPa})}{0.611\text{kPa} \cdot (0.001 + 0.622\text{g/g})} \right\} \right]^{-1}$$

$$= [0.003663 - 0.0001844 \cdot \ln\{0.210\}]^{-1}$$
$$= 253.12 \text{ K} = \underline{\mathbf{-20°C}}$$

Check: Units OK. Physics OK. Agrees with Fig. 4.7.
Discussion: We would have found the same numerical answer if we asked for the temperature corresponding to air at 80 kPa that is saturated with r_s = 1 g/kg with r_L = 0. For this situation, we would have used eq. (4.36).

Heat Conservation for Saturated Air

Saturated Adiabatic Lapse Rate

The unsaturated (dry) adiabatic lapse rate, Γ_d = 9.8 K/km, was discussed earlier. It is the temperature decrease ($-\Delta T/\Delta z = \Gamma_d$) an air parcel would experience as it moves vertically in the atmosphere into regions of lower pressure. No mixing or heat transfer across the skin of the parcel can occur for an adiabatic process. Although the word "dry" appears, this lapse rate applies to moist as well as dry air, but only if the air is unsaturated (i.e., not cloudy). Air cools adiabatically as it rises, and warms as it descends.

Saturated (cloudy) air also cools as it rises and warms as it descends, but at a lesser rate than a dry parcel. The reason is that, by definition, a saturated parcel is in equilibrium with the liquid drops. If the parcel then rises and cools, it is no longer in equilibrium, and some of the water-vapor molecules condense as a new equilibrium is approached. During condensation, latent heat is released into the air, partially compensating the adiabatic cooling.

The opposite is true during descent. Some of the cloud droplets evaporate and remove heat from the air, partially compensating the adiabatic warming.

For saturated air, the decrease of temperature with height ($-\Delta T/\Delta z = \Gamma_s$) in clouds and fog is given by the **saturated-adiabatic lapse rate**, Γ_s:

Solved Example

Find the moist adiabatic lapse rate near sea level for T = 26°C, using (a) the actual specific heat, and (b) the specific heat for dry air. (c) Also find $\Delta T/\Delta P$ for a rising saturated air parcel.

Solution

Given: T = 26°C = 299 K , P = 101.325 kPa
Find: Γ_s = ? °C/km

In general, we would need to calculate the saturation mixing ratio using eqs. (4.5) and (4.1). However, for this scenario, we can use Table 4-1 for simplicity, because sea-level pressure was specified. Thus: r_s = 21.85 g/kg = 0.0219 g/g.

(a) Using eq. (3.2), the actual specific heat is:
C_p = 1023 J·kg^{-1}·K^{-1}.
Thus: $|g|/C_p$ = 9.58 K/km
L_v/C_p = 2444 K.
$L_v/\Re_d$ = 8711 K.
Plugging these into eq. (4.37a) gives:

$$\Gamma_s = \frac{(9.58\frac{\text{K}}{\text{km}})\cdot\left[1+\frac{(0.0219\text{g/g})\cdot(8711\text{K})}{299\text{K}}\right]}{\left[1+\frac{(2444\text{K})\cdot(8711\text{K})\cdot(0.0219\text{g/g})\cdot 0.622}{(299\text{K})^2}\right]}$$

= (9.58 K/km)·[1.638]/[4.307] = **3.70 K/km**

(b) Eq. (4.37b) uses C_p for dry air:

$$\Gamma_s = \frac{(9.8\frac{\text{K}}{\text{km}})\cdot\left[1+\frac{(0.0219\text{g/g})\cdot(8711\text{K})}{299\text{K}}\right]}{\left[1+\frac{(1.35\times10^7\,\text{K}^2)\cdot(0.0219\text{g/g})}{(299\text{K})^2}\right]}$$

= (9.8 K/km)·[1.638] / [4.307] = **3.73 K/km**.

(c) Use eq. (4.38b):

$$\frac{\Delta T}{\Delta P} = \frac{\left[0.28571\cdot(299\text{K})+(2488.4\text{K}\cdot(0.0219\text{g/g}))\right]}{P\cdot\left[1+[1.35\times10^7\,K^2\cdot(0.0219\text{g/g})/(299\text{K})^2]\right]}$$

= (32.49K) / P

Assume P = 101.325 kPa at sea level:
$\Delta T/\Delta P$ = **0.32 K/kPa**

Check: Units OK. Physics OK.
Discussion: Don't forget for answers (a) and (b) that lapse rates are the rate of cooling with altitude. As expected the rate of cooling of a rising cloudy air parcel is less than the 9.8 K/km of a dry parcel. Also, method (b) is accurate enough for many situations.

Normally, pressure decreases as altitude increases, thus answer (c) also gives cooling for negative ΔP.

$$\Gamma_s = \frac{|g|}{C_p}\cdot\frac{\left(1+\frac{r_s\cdot L_v}{\Re_d\cdot T}\right)}{\left(1+\frac{{L_v}^2\cdot r_s\cdot\varepsilon}{C_p\cdot\Re_d\cdot T^2}\right)} \qquad (4.37a)$$

This is sometimes called the **moist adiabatic lapse rate**. The value of specific heat C_p is a function of humidity, and can be found using eq. (3.2).

If the variation of specific heat with humidity is neglected for simplicity, then (4.37a) simplifies to:

$$\Gamma_s = \Gamma_d\cdot\frac{\left[1+(a\cdot r_s/T)\right]}{\left[1+(b\cdot r_s/T^2)\right]} \qquad \bullet(4.37b)$$

where Γ_d = 9.8 K/km, a = 8711 K, and b = 1.35x10^7 K^2. As shown in the solved example, eq. (4.37b) differs from (4.37a) by roughly 1%, so it is often accurate enough for most applications. In both equations the saturation mixing ratio r_s varies with temperature, and must be used in units of g/g. Also, temperature must be Kelvin.

Near the ground in humid conditions, the value of the moist adiabatic lapse rate is near 4 K/km, and often changes to 6 to 7 K/km in the middle of the troposphere. At high altitudes where the air is colder and holds less water vapor, the moist rate nearly equals the dry rate of 9.8 K/km.

Instead of a change of temperature with height, the moist lapse rate can be written as a change of temperature ΔT with change of pressure ΔP:

$$\frac{\Delta T}{\Delta P} = \frac{\left[\left(\Re_d/C_p\right)\cdot T+\left(L_v/C_p\right)\cdot r_s\right]}{P\cdot\left(1+\frac{{L_v}^2\cdot r_s\cdot\varepsilon}{C_p\cdot\Re_d\cdot T^2}\right)} \qquad (4.38a)$$

where saturation mixing ratio r_s varies with T.
The corresponding simplified form is:

$$\frac{\Delta T}{\Delta P} = \frac{\left[a\cdot T+c\cdot r_s\right]}{P\cdot\left[1+(b\cdot r_s/T^2)\right]} \qquad \bullet(4.38b)$$

where a = 0.28571, b = 1.35x10^7 K^2 , c = 2488.4 K.

Thermo Diagrams – Part 3: Saturated Adiabats

Recall that two processes shown in thermo diagrams are unsaturated (**dry**) and saturated (**moist**) adiabatic vertical movement, such as experienced by air parcels rising through the atmosphere. Un-

saturated processes were previously indicated by overlaying isentropes (**dry adiabats**) on the background (Chapter 3, Fig. 3.3). Here we will add **saturated adiabats**, also known as **moist adiabats**.

Moist adiabats show how cloudy air changes temperature as it rises or sinks. Unfortunately, eq. (4.38) does not directly give the temperature of a parcel at any pressure height. Instead, one must solve the equation recursively, stepping upward in altitude (toward decreasing P) from an initial temperature at $P = 100$ kPa. Each step must take a small-enough pressure-height increment that the moist lapse rate does not change significantly from one step to the next. For each step, compute:

$$T_2 = T_1 + \frac{\Delta T}{\Delta P} \cdot (P_2 - P_1) \qquad (4.39)$$

where $(\Delta T/\Delta P)$ is from eq. (4.38).

For example, use pressure height increments of $\Delta P = (P_2 - P_1) = -0.1$ kPa all the way from $P = 100$ kPa up to $P = 10$ kPa. Repeat the calculations starting from five initial temperatures at $P = 100$ kPa: $T_1 =$ 40, 20, 0, –20, and –40°C. Fig. 4.8 shows the results of such calculations on a spreadsheet. The calculations were done in units of Kelvin, and then converted to Celsius for plotting. The moist adiabats are labeled with their starting temperature at $P = 100$ kPa, as discussed next. [The solved example at right uses coarser vertical increments of $\Delta P = -2$ kPa. This is too coarse, and can cause 5°C errors at 20 kPa.]

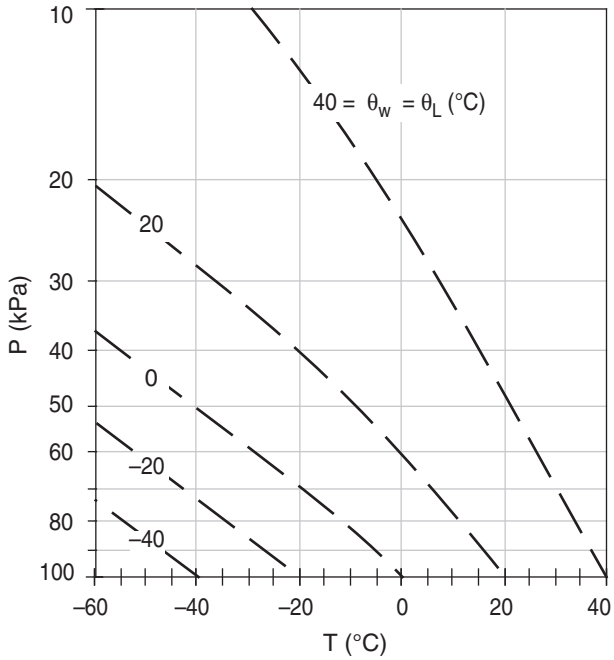

Figure 4.8
Thermodynamic diagram with moist adiabats, labeled by wet-bulb potential temperature θ_w, or by liquid-water potential temperature θ_L.

FOCUS • Spreadsheet Thermodynamics

Saturated (Moist) Adiabatic Lapse Rate

The iteration process of computing the $\theta_w = 20$°C moist adiabat is demonstrated here.

First, set up a spreadsheet with the following row and column headers:

	A	B	C	D	E
1	**Moist Adiabat Example**				
2	ΔP(kPa)=	2			
3					
4	P (kPa)	T(°C)	e_s(kPa)	r_s(g/g)	ΔT/ΔP
5	100	20.0			

where the starting pressure and temperature have been entered as numbers, and where the pressure increment of $\Delta P = 2$ kPa has also been entered.

Because $\Delta T/\Delta P$ in eq. (4.38b) depends on r_s, which in turn depends on e_s, there are the two extra columns C and D in the spreadsheet above. Two typical mistakes are to forget to convert T into Kelvins before using it, or to forget to use g/g for r.

In cell C5, you can enter eq. (4.1), which is:
=0.611*EXP(5423*((1/273.15)-(1/(B5+273.15))))
Then, in cell D5, enter eq. (4.5): =0.622*C5/(A5-C5)
Next, in cell E5, enter eq. (4.38b): =(0.28571*(B5+273.15) +(2488.4*D5)) / (A5*(1+(13500000*D5/((B5+273.15)^2))))
In cell A6, increment the pressure: =A5-B2
Finally, in cell B6 enter eq. (4.39): =B5-(E5*B2)
where the previous 2 eqs referred to B2 as an absolute reference (B2 on some spreadsheets).

Finally, select cells C5:E5 and fill them down one row. Then, select all of row 6; namely cells A6:E6, and fill down about 45 rows. The result is shown below, where we have not shown rows 8 to 43 to save space:

	A	B	C	D	E
1	**Moist Adiabat Example**				
2	ΔP(kPa)=	2			
3					
4	P (kPa)	T(°C)	e_s(kPa)	r_s(g/g)	ΔT/ΔP
5	100	20.00	2.368	0.0151	0.360
6	98	19.28	2.262	0.0147	0.369
7	96	18.54	2.158	0.0143	0.379
...	...	...	...	...	...
44	22	–52.28	0.006	0.0002	2.766
45	20	–57.82	0.003	0.0001	3.007

Discussion: Columns A and B can be plotted as the 20°C moist adiabat. For other moist adiabats, duplicate these cells, but with different starting T in cell B5.

The vertical pressure increment $\Delta P = 2$ kPa is much too coarse to give an accurate value near the top of the graph (i.e., at low pressures). When I repeat the calculation with $\Delta P = 0.1$ kPa, I find $T = -60.93$ at $P = 20$ kPa. Even smaller increments would be better.

Solved Example

Compare on a thermo diagram dry and moist adiabats starting at T = 20°C at P = 100 kPa.

Solution

Given: T = 20°C at P = 100 kPa.
Plot: θ = 20°C and θ_w = 20°C.

Use curves from Fig. 4.8 and Fig. 3.3.

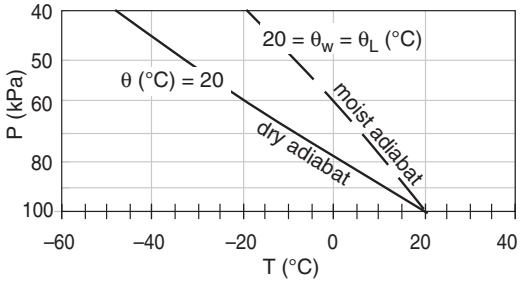

Check: Slopes look reasonable. Labels match.
Discussion: Moist-adiabat temperature decreases more slowly than dry, because condensational latent heating partially compensates for adiabatic cooling.

Solved Example

Air at pressure 80 kPa and temperature 0°C is saturated, & holds 2 g/kg of liquid water. Find θ_e and θ_L.

Solution:

Given: P = 80 kPa, T = 0°C = 273K , r_L = 2 g/kg.
Find: θ_e = ? °C, θ_L = ? °C

First, do preliminary calculations shared by both eqs:
Rearrange eq. (3.12) to give:
$(\theta/T) = (P_o/P)^{0.28571} = (100\text{kPa}/80\text{kPa})^{0.28571} = 1.066$
Thus, θ = 291K = 18°C
At 80 kPa and 0°C, solve eq. (4.5) for r_s = 4.7 g/kg
Then use eq. (3.2):
$C_p = C_{pd}\cdot(1 + 1.84\cdot r) = (1004.67\ \text{J}\cdot\text{kg}^{-1}\cdot\text{K}^{-1})$
$\cdot[1+1.84\cdot(0.0047\ \text{g/g})] = 1013.4\ \text{J}\cdot\text{kg}^{-1}\cdot\text{K}^{-1}$.
Thus, L_v/C_p = 2467 K/(g_{water}/g_{air})
and $(L_v/C_p)\cdot(\theta/T)$ = 2630 K/(g_{water}/g_{air})

Use eq. (4.40):
θ_e = (18°C) + (2630 K/(g_{water}/g_{air}))·(0.0047)
= **30.4 °C**

Use eq. (4.41):
θ_e = (18°C) – (2630 K/(g_{water}/g_{air}))·(0.002)
= **12.7 °C**

Check: Units OK. Physics OK. Magnitudes OK.
Discussion: The answers are easier to find using a thermo diagram (after you've studied the Stability chapter). For θ_e , find the θ value for the dry adiabat that is tangent at the diagram top to the moist adiabat. For θ_L, follow a moist adiabat down to where it crosses the (2 + 4.7 = 6.7 g/kg) isohume, and from there follow a dry adiabat to P = 100 kPa.

Liquid-Water, Equivalent, and Wet-Bulb Potential Temperatures

Recall from the Heat chapter that potential temperature θ is conserved during unsaturated adiabatic ascent or descent. However, if an air parcel containing water vapor is lifted above its LCL, then condensation will add latent heat, causing θ to increase. Similarly, if the air contains liquid water such as cloud drops, when it descends some of the drops can evaporate, thereby cooling the air and reducing θ.

However, we can define new variables that are conserved for adiabatic ascent or descent, regardless of any evaporation or condensation that might occur. One is the **equivalent potential temperature** θ_e:

$$\theta_e \approx \theta + \left(\frac{L_v\cdot\theta}{C_p\cdot T}\right)\cdot r \approx \theta + \frac{L_v}{C_{pd}}\cdot r \qquad \bullet(4.40)$$

Another is **liquid water potential temperature**, θ_L:

$$\theta_L \approx \theta - \left(\frac{L_v\cdot\theta}{C_p\cdot T}\right)\cdot r_L \approx \theta - \frac{L_v}{C_{pd}}\cdot r_L \qquad \bullet(4.41)$$

where L_v = 2.5x10^6 J·kg^{-1} is the latent heat of vaporization, C_p is the specific heat at constant pressure for air (C_p is not constant, see the Heat chapter), T is the absolute temperature of the air, and mixing ratios (r and r_L) have units of (g_{water}/g_{air}). The last approximation in both equations is very rough, with L_v/C_{pd} = 2.5 K·(g_{water}/kg_{air})$^{-1}$.

Both variables are conserved regardless of whether the air is saturated or unsaturated. Consider unsaturated air, for which θ is conserved. In eq. (4.40), water-vapor mixing ratio r is also conserved during ascent or descent, so the right side of eq. (4.40) is constant, and θ_e is conserved. Similarly, for unsaturated air, liquid water mixing ratio r_L = 0, hence θ_L is also conserved in eq. (4.41).

For saturated air, θ will increase in a rising air parcel due to latent heating, but r will decrease as some of the vapor condenses into liquid. The two terms in the right side of eq. (4.40) have equal but opposite changes that balance, leaving θ_e conserved. Similarly, the two terms on the right side of eq. (4.41) balance, due to the minus sign in front of the r_L term. Thus, θ_L is conserved.

By subtracting eq. (4.41) from (4.40), we can see how θ_e and θ_L are related:

$$\theta_e \approx \theta_L + \left(\frac{L_v\cdot\theta}{C_p\cdot T}\right)\cdot r_T \qquad (4.42)$$

where the total water mixing ratio (g/g) is $r_T = r + r_L$. Although θ_e and θ_L are both conserved, they are not equal to each other.

We can use θ_e or θ_L to identify and label moist adiabats. Consider an air parcel starting at P = 100 kPa that is saturated but contains no liquid water ($r = r_s = r_T$). For that situation θ_L is equal to its initial temperature T (which also equals its initial potential temperature θ at that pressure). A rising air parcel from this point will conserve θ_L, hence we could label the moist adiabat with this value (Fig. 4.9).

An alternative label starts from same saturated air parcel at P = 100 kPa, but conceptually lifts it to the top of the atmosphere (P = 0). All of the water vapor will have condensed out at that end point, heating the air to a new potential temperature. The potential temperature of the dry adiabat that is tangent to the top of the moist adiabat gives θ_e (Fig. 4.9). [*CAUTION: On some thermo diagrams, equivalent potential temperature is given in units of Kelvin.*]

In other words, θ_L is the potential temperature at the bottom of the moist adiabat (more precisely, at P = 100 kPa), while θ_e is the potential temperature at the top. Either labeling method is fine — you will probably encounter both methods in thermo diagrams that you get from around the world.

Wet-bulb potential temperature (θ_w) can also be used to label moist adiabats. For θ_w, use Normand's rule on a thermo diagram (Fig. 4.10). Knowing temperature T and dew-point T_d at initial pressure P, and plot these points on a thermo diagram. Next, from the T point, follow a dry adiabat up, and from the T_d point, follow an isohume up. Where they cross is the lifting condensation level LCL.

From that LCL point, follow a saturated adiabat back down to the starting altitude, which gives the **wet-bulb temperature** T_w. If you continue to follow the saturated adiabat down to a reference pressure (P = 100 kPa), the resulting temperature is the **wet-bulb potential temperature** θ_w (see Fig. 4.10). Namely, θ_w equals the θ_L label of the moist adiabat that passes through the LCL point. Labeling moist adiabats with values of wet-bulb potential temperature θ_w is analogous to the labeling scheme for the dry adiabats, which is why I use θ_w here.

To find θ_e(K) for a moist adiabat if you know its θ_w(K), use:

$$\theta_e = \theta_w \cdot \exp(a_3 \cdot r_s / \theta_w)_o \qquad (4.43a)$$

where a_3 = 2491 K·kg$_{air}$/kg$_{vapor}$, and r_s is initial saturation mixing ratio (kg$_{vapor}$/kg$_{air}$) at $T = \theta_w$ and P = 100 kPa (as denoted by subscript "o"). You can approximate (4.43a) by

$$\theta_e(\text{K}) \approx a_o + a_1 \cdot \theta_w(°\text{C}) + a_2 \cdot [\theta_w(°\text{C})]^2 \qquad (4.43b)$$

where a_o = 282, a_1 = 1.35, and a_2 = 0.065, for θ_w in the range of 0 to 30°C (see Fig. 4.11). Also the θ_L label for

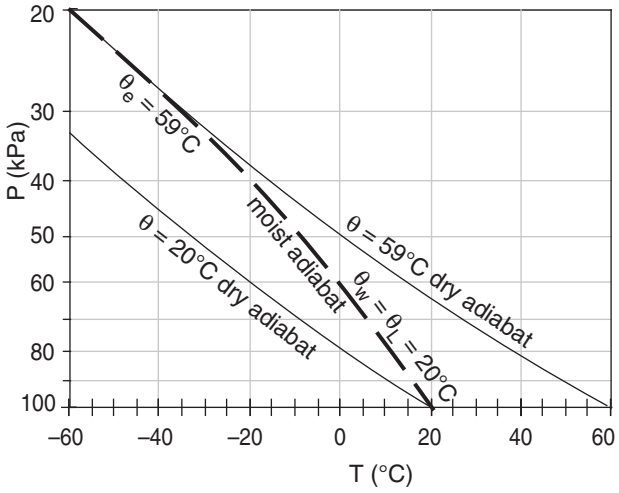

Figure 4.9
Comparison of θ_L, θ_w and θ_e values for the same moist adiabat.

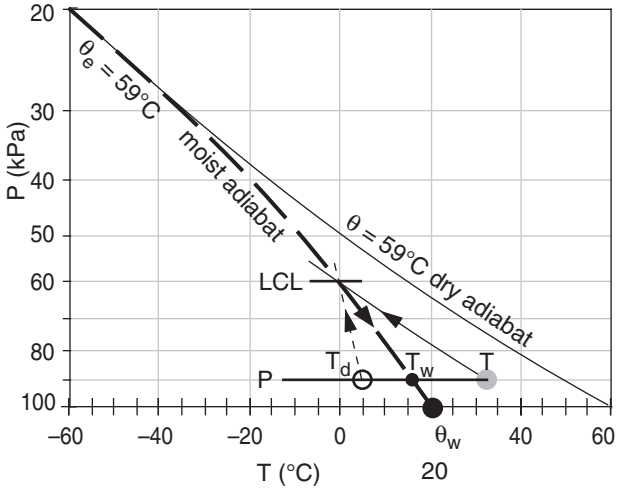

Figure 4.10
Thermo diagram showing how to use Normand's Rule to find wet-bulb potential temperature θ_w, and how it relates to θ_e.

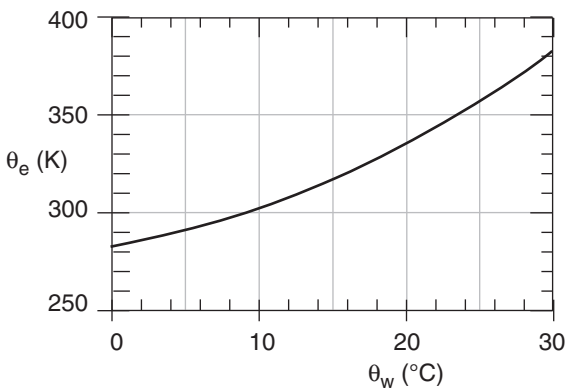

Figure 4.11
Approximate relationship between θ_w and θ_e.

Solved Example

Verify the labels on the moist adiabat that passes through the LCL in Fig. 4.10, given starting conditions T = 33°C and T_d = 5.4°C at P = 90 kPa.

Solution

Given: T = 33°C = 306K, T_d = 5.4°C = 278.4K
Find: θ_e , θ_w and θ_L labels (°C) for the moist adiabat

First, find the initial θ, using eq. (3.12)

$\theta = T{\cdot}(P_o/P)^{0.28571} = (306\text{K}){\cdot}(100\text{kPa}/90\text{kPa})^{\,0.28571}$
$= 315.4\text{K} = 42.4°\text{C}$

Next, find the mixing ratio using eq. (4.1b) & (4.4):

$e = 0.611\text{kPa}{\cdot}\exp[5423{\cdot}(1/273.15 - 1/278.4)] = 0.8885\text{kPa}$
$r = (622\text{g/kg}){\cdot}(0.8885\text{kPa})/[90 - 0.8885\text{kPa}] = 6.2\text{g/kg}$

Next, use eq. (3.2) to find $C_p = C_{pd}{\cdot}(1 + 1.84{\cdot}r)$

$C_p = (1004.67\ \text{J}{\cdot}\text{kg}^{-1}{\cdot}\text{K}^{-1}) \cdot [1 + 1.84{\cdot}(0.0062\ \text{g/g})]$
$C_p = 1016.1\ \text{J}{\cdot}\text{kg}^{-1}{\cdot}\text{K}^{-1}$

Solve the more accurate version of eq. (4.40):

$\theta_e = (42.4°\text{C}) + \{(2500\ \text{J/g}_{\text{water}}){\cdot}(315.4\text{K})/$
$[(1016.1\ \text{J}{\cdot}\text{kg}^{-1}{\cdot}\text{K}^{-1}){\cdot}(306\text{K})]\} \cdot (6.2\ \text{g}_{\text{water}}/\text{kg}_{\text{air}})$
$= (42.4°\text{C}) + (2.536\ \text{K}{\cdot}\text{kg}_{\text{air}}/\text{g}_{\text{water}}){\cdot}(6.2\ \text{g}_{\text{water}}/\text{kg}_{\text{air}})$
$= \underline{\mathbf{58.1°C}} = 331.1\text{ K}$

The approximate version of eq. (4.40) gives almost the same answer, and is much easier:

$\theta_e = (42.4°\text{C}) + (2.5\ \text{K}{\cdot}\text{kg}_{\text{air}}/\text{g}_{\text{water}}){\cdot}(6.2\ \text{g}_{\text{water}}/\text{kg}_{\text{air}})$
$= \underline{\mathbf{57.9°C}}$

Eq. (4.43b) is a quadratic eq. that can be solved for θ_w. Doing this, and then plugging in θ_e = 331.1 K gives:

$\theta_w \approx \underline{\mathbf{19°C}}$. , which is the label on the moist adiabat.

Using $\theta_L \approx \theta_w$:

$\theta_L \approx \underline{\mathbf{19°C}}$.

Check: Units OK. Physics OK.
Discussion: These values are within a couple degrees of the labels in Fig. 4.10. Disappointing that they aren't closer, but the θ_e results are very sensitive to the starting point.

Solved Example

For a moist adiabat of θ_w = 14°C , find its θ_e.

Solution

Given: θ_w = 14°C = 287 K
Find: θ_e = ? K

First get r_s from Fig. 4.7 at P = 100 kPa and T = 14°C:

r_s = 10 g/kg = 0.010 kg/kg.

Next, use eq. (4.43a):

$\theta_e = (287\text{K}) \cdot \exp[2491(\text{K}{\cdot}\text{kg}_{\text{air}}/\text{kg}_{\text{vapor}}) \cdot$
$(0.010\ \text{kg}_{\text{vapor}}/\text{kg}_{\text{air}}) / (287\text{K})] = \underline{\mathbf{313K}}$

Check: Units OK. Agrees with Fig. 4.11.
Discussion: This θ_e = 40°C. Namely, if a saturated air parcel started with $\theta_w = T$ = 14°C, and then if all the water vapor condensed, the latent heat released would warm the parcel to T = 40°C.

Solved Example

Use Normand's rule (in reverse) on a thermodynamic diagram to find the mixing ratio and dew point temperature, given dry and wet-bulb observations of 40°C and 20°C, respectively, from a psychrometer near the surface (where P = 100 kPa).

Solution

Given: T = 40°C, T_w = 20°C, P = 100 kPa.
Find: T_d = ?°C, r = ? g/kg

Combining all the components of the thermo diagram (which will be covered in more detail in the Stability chapter) yields the figure below, for which all the background lines are gray. Thick diagonal lines on this diagram are dry adiabats, and curved dashed lines are moist adiabats, while horizontal and vertical lines are isobars and isotherms, respectively. Isohumes are the nearly-vertical dotted lines.

First, the given values of T and T_w at the given P are plotted as the two circles at the bottom of the Figure. Starting from the T observation, follow a dry adiabat upward. Simultaneously, starting from the T_w observation, follow a moist adiabat upward. They intersect at the LCL at about 65 kPa, which is marked by another circle.

From the LCL, follow (or go parallel to) the isohumes back down to the starting pressure to find the T_d. Alternately, from the intersection point, follow the isohumes upward to find r (interpolating if necessary between the printed values).

The results are roughly r = **7.5 g/kg**, and T_d = **10°C**. (These were actually found from a more precise thermo diagram, as provided in the Stability chapter.)

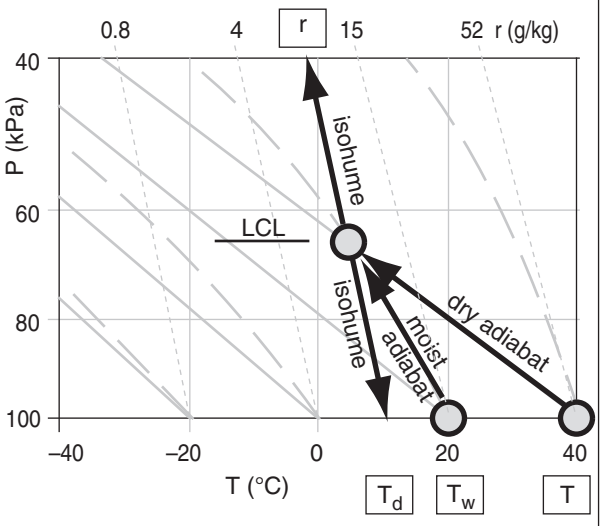

Check: Units OK. Physics OK.
Discussion: Using r_s = 52 g/kg from the starting T, the relative humidity is RH = 8/52 = 15%.

the moist adiabat passing through the LCL equals this θ_w.

EULERIAN WATER BUDGET

Any change of total water content within a fixed Eulerian volume such as a cube of moist air must be explained by transport of water through the sides. Transport processes include advection by the mean wind, turbulent transport, and precipitation of liquid and solid water.

As was done for the heat budget, the moisture budget can be simplified for many atmospheric situations. In particular, the following terms are usually small except in thunderstorms, and will be neglected: vertical advection by the mean wind, horizontal turbulent transport, and conduction (except for effective moisture fluxes near the Earth's surface). The net Eulerian total water (r_T) budget is:

•(4.44)

$$\frac{\Delta r_T}{\Delta t} = -\left[U \cdot \frac{\Delta r_T}{\Delta x} + V \cdot \frac{\Delta r_T}{\Delta y} \right] + \left(\frac{\rho_L}{\rho_d} \right) \frac{\Delta Pr}{\Delta z} - \frac{\Delta F_{z\ turb}(r_T)}{\Delta z}$$

storage *horiz. advection* *precipitation* *turbulence*

where (U, V) are the horizontal wind components in the (x, y) Cartesian directions, z is height, Pr is precipitation rate, and $F_{z\ turb}$ (r_T) is the kinematic turbulent flux of total water.

Most of these terms are similar to those in the heat budget eq. (3.51). The ratio of liquid-water density to dry-air density is ρ_L/ρ_d = 836.7 kg_{liq}/kg_{air} at STP. **Standard Temperature and Pressure** (**STP**) is T = 0°C and P = 101.325 kPa. The liquid water density is close to ρ_L = 1000 kg_{liq}/m^3 (see Appendix B).

Each term is examined next. Surface moisture flux is also discussed because it contributes to the turbulence term for a volume of air on the surface.

Horizontal Advection

Horizontal advection of total water is similar to that for heat. Within a fixed volume, moisture increases with time if air blowing into the volume contains more water than air leaving. The advected water content includes water vapor (i.e., humidity), liquid, and solid cloud particles and precipitation.

Precipitation

Liquid water equivalent is the depth of liquid water that would occur if all solid precipitation were melted. For example, 10 cm depth of snow accumulated in a cylindrical container might be equivalent to only 1 cm of liquid water when melted.

ON DOING SCIENCE • Look for Patterns

Suppose you know that $A = C$, and $C = E$. You can use this knowledge to yield new understanding, by various methods of reasoning.

Deductive reasoning combines known relationships in new ways to allow new applications. For example, using the knowns from the previous paragraph, you could deduce that $A = E$.

Inductive reasoning goes from the particular to the general. It does this by looking for patterns. By such reasoning, you could state that $E = G$. The pattern is as follows: A equals a value that is two letters later in the alphabet, and C equals a value two letters later. By extension, you might hope that any letter of the alphabet equals a value that is two letters later in the alphabet.

Inductive reasoning is riskier than deductive. If the knowns you use as a starting point are unrepresentative of the whole situation, then you will get a biased (i.e., wrong) result. For example: given that I have a sister, and that my best friend has a sister, therefore by inductive reasoning everyone has a sister. To avoid such blunders, it helps to get a large sample of knowns before you extend the pattern into the unknown.

Inductive reasoning usually gives the greatest advances in science, while deductive reasoning gives the greatest utility to engineering. Both forms of reasoning are encouraged.

Regardless of the form of reasoning, you should test your conclusions against independent data. Isaac Newton used inductive reasoning to develop his concepts of motion and gravity, based on observations he made near his home in England. To test his theories with independent data, he built telescopes to watch the motion of planets. Because his theories were found to be **universal** (i.e., they worked elsewhere in the universe), Newton's theories were accepted as the Laws of Motion.

Similarly, engineers might use deductive reasoning to design a bridge, dam, or airplane. However, they first test their design with prototypes, scale models, or computer simulations to support their deductions before they construct the final products.

As an example, we can use reasoning with the Eulerian budgets for heat and moisture. From the Heat chapter, the Eulerian heat budget (eq. 3.51) was:

$$\left.\frac{\Delta T}{\Delta t}\right|_{x,y,z} = -\left[U \cdot \frac{\Delta T}{\Delta x} + V \cdot \frac{\Delta T}{\Delta y} \right] - \frac{\Delta F_{z\ turb}}{\Delta z} + \frac{L_v}{C_p} \cdot \frac{m_{condensing}}{m_{air} \cdot \Delta t} - 0.1\ \frac{\mathrm{K}}{\mathrm{h}}$$

where the first term on the right describes the effects of advection, the second is turbulence, the third term is latent heating, and the last is radiation. The last

(continues in page after next)

Solved Example

Consider a 9 km deep thunderstorm, and examine the bottom 1 km layer of the cloud. Rain from higher in the thunderstorm falls into the top of this layer at rate 0.9 cm/h. From the bottom of the layer, the precipitation rate is 1 cm/h. What is the rate of total water change in the layer?

Solution

Given: Pr_{top} = 0.9 cm/h = 2.5x10^{-5} m/s,
Pr_{bot} = 1.0 cm/h = 2.78x10^{-5} m/s,
Δz = 1 km = 1000 m
Find: $\Delta r_T/\Delta t$ = ? (g/kg)/s.
Assume: No advection or turbulence. Assume the average air density is 1 kg/m^3 in lower troposphere.

Use eq. (4.44):
$\Delta r_T/\Delta t = (\rho_L/\rho_d)\cdot(Pr_{top}-Pr_{bot})/(z_{top}-z_{bot})$ =

$$= \frac{(1.0\times10^6 g_{water}/m^3)}{(1\ kg_{air}/m^3)}\cdot\frac{[(2.5-2.78)\times10^{-5} m/s]}{1000m}$$

= **–0.0028 (g/kg)/s** = –10.1 (g/kg)/h

Check: Units OK. Physics OK.
Discussion: Thus, water is lost from this part of the cloud. If there is no advection of moisture to replace that lost as rain, then this part of the cloud will rain itself dry in several hours if loss continues at a constant rate.

Solved Example

Given a latent heat flux of 300 W·m^{-2} , find the evaporation rate.

Solution

Given: $\mathbb{F}_E$ = 300 W·m^{-2}
Find: *Evap* = ? mm/day

Use eq. (4.49): $Evap = a\cdot\mathbb{F}_E$
= [0.0346 (m^2/W)·(mm/day)]·(300 W/m^2)
= **10.38 mm/day**

Check: Units OK. Physics OK.
Discussion: Evaporation of about 1 cm of water per day could cause significant drying of soil and lowering of water levels in lakes unless replenished by precipitation.

Precipitation rate *Pr* has units of depth of liquid water equivalent per time (e.g., mm/h, or m/s). It tells us how quickly the depth of water in a hypothetical rain gauge would change.

Precipitation rate is a function of altitude, as if the rain gauge could be hypothetically mounted at any altitude in the atmosphere. Some precipitation might evaporate when falling through the air, or condensation might increase the precipitation rate on the way down. If more precipitation falls into the top of a volume than falls out of the bottom, then total water within the volume must increase. At the Earth's surface, precipitation rate equals **rainfall rate** *RR* by definition.

Surface Moisture Flux

The latent heat flux described in the Heat chapter is, by definition, associated with a flux of water. Hence, the heat and moisture budgets are coupled. Methods to calculate the latent heat flux were described in that chapter under the topic of the surface heat budget. Knowing the **surface latent heat flux**, you can use the equations below to transform it into a water flux.

The **vertical flux of water vapor** $\mathbb{F}_{water}$ ($kg_{water}\cdot m^{-2}\cdot s^{-1}$) is related to the latent heat flux $\mathbb{F}_E$ (W/m^2) by:

$$\mathbb{F}_{water} = \mathbb{F}_E / L_v \qquad \bullet(4.45)$$

$$\mathbb{F}_{water} = \rho_{air}\cdot(C_p/L_v)\cdot F_E \qquad (4.46)$$

$$= \rho_{air}\cdot\gamma\cdot F_E \qquad (4.47)$$

where the latent heat of vaporization is L_v = 2.5x10^6 J/kg, $\gamma = C_p/L_v$ = 0.4 (g_{water}/kg_{air})·K^{-1} is the **psychrometric constant**, and where the kinematic latent heat flux F_E has units of K·m·s^{-1} .

Eq. (4.45) can be put into kinematic form by dividing by air density, ρ_{air}.

$$F_{water} = \mathbb{F}_E / (\rho_{air}\cdot L_v) = \gamma\cdot F_E \qquad (4.48)$$

where F_{water} is like a mixing ratio times a vertical velocity, and has units of (kg_{water}/kg_{air})·(m·s^{-1}).

Sometimes, this moisture flux is expressed as an **evaporation rate** *Evap* in terms of depth of liquid water that is lost per unit time (e.g., mm/day):

$$Evap = \mathbb{F}_{water}/\rho_L = \mathbb{F}_E/(\rho_L\cdot L_v) = a\cdot\mathbb{F}_E \qquad (4.49)$$

$$Evap = (\rho_{air}/\rho_L)\cdot F_{water} = (\rho_{air}/\rho_L)\cdot\gamma\cdot F_E \qquad \bullet(4.50)$$

where $a = 4.0\text{x}10^{-10}$ $m^3 \cdot W^{-1} \cdot s^{-1}$ or $a = 0.0346$ $(m^2/W) \cdot (mm/day)$, and $\rho_L = 1000$ kg_{liq}/m^3.

If the latent heat flux is not known, you can estimate F_{water} from the mixing-ratio difference between the surface (r_{sfc}) and the air (r_{air}). For windy, overcast conditions, use:

$$F_{water} = C_H \cdot M \cdot \left(r_{sfc} - r_{air} \right) \tag{4.51}$$

where C_H is the dimensionless **bulk transfer coefficient** (moisture and heat are nearly identical, see the Heat chapter), and M is wind speed. Both r_{air} and M are measured at $z = 10$ m. C_H varies from $2\text{x}10^{-3}$ over smooth surfaces to $2\text{x}10^{-2}$ over rough surfaces.

During free convection of sunny days and light or calm winds:

$$F_{water} = b_H \cdot w_B \cdot \left(r_{sfc} - r_{ML} \right) \tag{4.52}$$

where r_{ML} is the mixing ratio in the middle of the mixed layer, and $b_H = 5\text{x}10^{-4}$ is the **convective transport coefficient** for heat (assumed to be identical to that for moisture, see the Heat chapter). The buoyancy velocity scale w_B was given in the Heat chapter for convective conditions.

These formulas are difficult to use because r_{sfc} is not usually measured. Over oceans, lakes, rivers, and saturated ground, you can assume that the air touching the surface is nearly saturated; thus, $r_{sfc} \approx r_s(T_{sfc})$, where T_{sfc} is the water-surface (skin) temperature. Over drier ground the value is less than saturated, but is not precisely known.

Turbulent Transport

Turbulent transport tends to homogenize moisture by mixing moist and dry regions of air to create a larger region of average humidity. $\Delta F_{z\ turb}(r_T)/\Delta z$ is the change of turbulent flux of total water across distance Δz, and is analogous to the turbulence heat flux discussed in the Heat chapter. $\Delta F/\Delta z$ is called the **flux divergence**.

In the fair-weather, daytime, convective boundary layer (i.e., for $0 < z < z_i$), turbulence causes a flux divergence in the vertical:

$$\frac{\Delta F_{z\ turb}(r_T)}{\Delta z} = \frac{F_{z\ turb\ at\ zi}(r_T) - F_{z\ turb\ at\ surface}(r_T)}{z_i - z_{surface}} \tag{4.53}$$

or

$$\frac{\Delta F_{z\ turb}(r_T)}{\Delta z} = -\frac{\left[0.2 \cdot (\Delta_{z_i} r_T \,/\, \Delta_{z_i} \theta) \cdot F_H \right] + F_{water}}{z_i} \tag{4.54}$$

Solved Example

Find the kinematic water flux over a lake with saturation mixing ratio of $r_{sfc} = 15$ g/kg. The air is overcast with $M = 10$ m/s and $r = 8$ g/kg at height 10 m

Solution

Given: $r_{sfc} = 15$ g/kg, $M = 10$ m/s,
$r_{air} = 8$ g/kg
Find: $F_{water} = ?$ $(kg_{water}/kg_{air}) \cdot (m \cdot s^{-1})$
Assume: smooth lake surface: $C_H = 2\text{x}10^{-3}$ (from paragraph after eq. 3.35).

Use eq. (4.51): $F_{water} = C_H \cdot M \cdot (r_{sfc} - r_{air})$

$F_{water} = (\ 2\text{x}10^{-3}\ ) \cdot (10\ m/s\ ) \cdot (15 - 8\ g/kg)$
$= 0.14\ (g_{water} \cdot kg_{air}) \cdot (m \cdot s^{-1})$
$= \underline{\mathbf{0.00014}}\ (kg_{water}/kg_{air}) \cdot (m \cdot s^{-1})$

Check: Units OK. Physics OK.
Discussion: Eq. (4.50) says this is equivalent to $1.72\text{x}10^{-7}$ m/s of evaporation, or 14.8 mm/day, which is a strong evaporation rate.

ON DOING SCIENCE (continuation)

two terms are source and sink terms of heat.

The Eulerian moisture budget (eq. 4.44) is:

$$\frac{\Delta r_T}{\Delta t} = -\left[U \cdot \frac{\Delta r_T}{\Delta x} + V \cdot \frac{\Delta r_T}{\Delta y} \right] - \frac{\Delta F_{z\ turb}(r_T)}{\Delta z} + \left(\frac{\rho_L}{\rho_d} \right) \frac{\Delta Pr}{\Delta z}$$

Again, the first term on the right describes advection, the second gives turbulence, and the last is a source term associated with precipitation.

Both equations above have the same pattern; namely, a time-tendency term on the left. On the right are advection, turbulence, and source/sink terms. **Inductive reasoning** would allow us to state that Eulerian conservation or budget equations in general should be of the form:

$$\frac{\Delta \Psi}{\Delta t} = -\left[U \cdot \frac{\Delta \Psi}{\Delta x} + V \cdot \frac{\Delta \Psi}{\Delta y} \right] - \frac{\Delta F_{z\ turb}(\Psi)}{\Delta z} + S_\Psi$$

where Ψ is any variable, and S_Ψ represents the source and sink terms. Mean vertical motion and horizontal turbulence flux divergence were neglected.

Given the equation above, we could use **deductive reasoning** to apply it to a new variable, such as the U component of velocity:

$$\frac{\Delta U}{\Delta t} = -\left[U \cdot \frac{\Delta U}{\Delta x} + V \cdot \frac{\Delta U}{\Delta y} \right] - \frac{\Delta F_{z\ turb}(U)}{\Delta z} + S_U$$

Before accepting this, it should be tested and verified against observations. (This was already done by others. The new equation indeed works, as will be shown in the Dynamics chapter.)

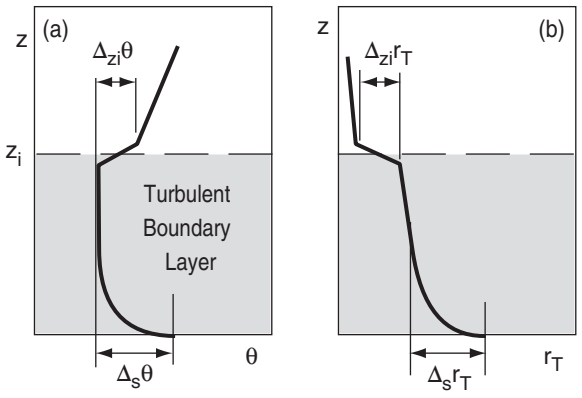

Figure 4.12
Method of estimating jumps in (a) potential temperature $\Delta\theta$, and in (b) total water Δr_T at the top and bottom of a turbulent boundary layer of depth z_i, given the sounding (thick lines). For moisture, the jump $\Delta_{zi} r_T$ can be positive or negative depending on whether the air aloft is moister or drier than the boundary layer. Only the case of drier air aloft is shown in (b).

Solved Example

Given measurements of a 1 km thick boundary layer as shown in Fig. 4.12, with $|\Delta_s\theta| = 8°C$, $|\Delta_{zi}\theta| = 3°C$, $|\Delta_s r_T| = 5$ g/kg, and $\Delta_{zi} r_T = -4$ g/kg. The convective transport coefficient times buoyancy velocity is 0.025 m/s on this calm day. What is the vertical flux divergence of total water due to turbulence, and how does that contribute to moistening the boundary layer?

Solution

Given: $|\Delta_s\theta| = 9°C$, $|\Delta_{zi}\theta| = 3°C$,
$|\Delta_s r_T| = 5$ g/kg, $\Delta_{zi} r_T = -4$ g/kg,
$z_i = 1$ km = 1000 m, $b_H w_B = 0.025$ m/s.
Find: $\Delta r_T/\Delta t = -\Delta F_{z\ turb}(r_T)/\Delta z = ?$ (g/kg)/s
Assume: No advection or precipitation.

Use eq. (4.56):

$$\frac{\Delta F_{z\ turb}(r_T)}{\Delta z} = -\frac{b_H \cdot w_B}{z_i}\left[0.2 \cdot \left(\Delta_{z_i} r_T\right) \cdot \left|\frac{\Delta_s\theta}{\Delta_{z_i}\theta}\right| + \left|\Delta_s r_T\right|\right]$$

$$= -\frac{(0.025\text{m/s})}{(1000\text{m})}\left[0.2 \cdot \left(-4\,\frac{\text{g}}{\text{kg}}\right) \cdot \left|\frac{9°\text{C}}{3°\text{C}}\right| + \left(5\,\frac{\text{g}}{\text{kg}}\right)\right]$$

$$= \underline{\mathbf{-0.000065\ (g/kg)/s}}$$

Thus:
$\Delta r_T/\Delta t = -\Delta F_{z\ turb}(r_T)/\Delta z = = \underline{\mathbf{+0.000065\ (g/kg)/s}}$

Check: Units OK. Physics OK.
Discussion: *(continues on next page)*

where F_H is the kinematic effective surface heat flux (units of K·m/s), and F_{water} is the kinematic effective surface water-vapor flux [units of $(\text{kg}_{\text{water}}/\text{kg}_{\text{air}})\cdot$ (m/s)]. The operator $\Delta_{zi} = (\ )_{zi+} - (\ )_{zi-}$ is the difference between the value of any variable ( ) just above (+) the top of the boundary layer, minus the value just below (–) the top (Fig. 4.12), where the average top of the boundary layer is at height z_i.

Because surface moisture flux F_{water} is directly related to the surface latent heat flux F_E (eq. 4.48), rewrite (4.54) as:

$$\frac{\Delta F_{z\ turb}(r_T)}{\Delta z} = -\frac{0.2 \cdot (\Delta_{z_i} r_T\ /\ \Delta_{z_i}\theta) \cdot F_H + \gamma \cdot F_E}{z_i}$$

$$\text{for } 0 < z < z_i \qquad (4.55)$$

for the convective boundary layer, where $\gamma = 0.4$ $(\text{g}_{\text{water}}/\text{kg}_{\text{air}})\cdot\text{K}^{-1}$ is the psychrometric constant.

Another version can be written using the effective surface heat-flux parameterization of the Heat chapter:

$$\frac{\Delta F_{z\ turb}(r_T)}{\Delta z} = -\frac{b_H \cdot w_B}{z_i}\left\{\left[0.2 \cdot \left(\Delta_{z_i} r_T\right) \cdot \left|\frac{\Delta_s\theta}{\Delta_{z_i}\theta}\right|\right] + \left|\Delta_s r_T\right|\right\}$$

$$\text{for } 0 < z < z_i \qquad (4.56)$$

where b_H is the convective transport coefficient (see the Heat chapter), w_B is the buoyancy velocity scale, and operator $\Delta_s(\ ) = (\ )_{surface} - (\ )_{mid\ mixed\text{-}layer}$ The four equations above are equivalent — use the version that is most convenient for the values on hand.

Above the fair-weather boundary layer (i.e., for $z > z_i$), turbulence is often negligible:

$$\frac{\Delta F_{z\ turb}(r_T)}{\Delta z} \approx 0 \qquad (4.57)$$

Also, within the nighttime boundary layer, the equation above is valid at all heights.

For some situations, the moisture flux (F_{water}) at the Earth's surface into or out of the bottom of a volume of air might be known. A cube of air sitting on a lake surface might gain total water by evaporation from the lake, resulting from an upward or positive flux of water at the surface. Alternately, a cube of humid air sitting over a snow surface might lose water by condensation onto the snow, corresponding to a negative or downward flux of water at the surface. If the flux at the top of the volume is near zero, then the vertical flux divergence is approximately

$\Delta F_{z\ turb}(r_T)/\Delta z = - F_{bottom}(r_T) / d$, where d is depth of the volume.

Turbulent mixing of moisture by thunderstorms is vigorous and complex. Prior to the storm, a humid boundary layer underlies a dry layer of air in the middle troposphere. The thunderstorm lifts and consumes the humid air from the boundary layer, and replaces it with drier air from aloft. However, much of the moisture from the former boundary layer is squeezed out as precipitation, and is accounted for in the precipitation term of the Eulerian moisture budget. The net result is that the humid, prestorm boundary layer becomes drier after the storm.

Solved Example *(continuation)*

Discussion: This is equivalent to a rate of +0.234 (g/kg)/h increase of water in the boundary layer. The air is getting juicier with time.

Water evaporates from the surface to increase the humidity, but dry air entrained into the top of the boundary layer tends to decrease humidity. For this example, the moistening from the surface was greater than the drying from aloft, but it could differ from day to day in real life. Also, there can be other situations where moistening happens from both the top and bottom of the boundary layer, such as when a dry boundary layer is growing into a cloud layer aloft.

HUMIDITY INSTRUMENTS

Instruments that measure humidity are called **hygrometers**. Don't confuse the word with "hydrometers", which are used to measure specific gravity of fluids such as battery acid.

Dew-point hygrometers, also known as **chilled-mirror hygrometers**, reflect a beam of light off a tiny metal mirror. When the mirror is cooled to the dew-point temperature, dew forms on the mirror and the light beam scatters instead of reflecting into a detector. Electronics in the instrument cool or heat the mirror to maintain the surface precisely at the dew point temperature, which is provided as an output. These are accurate instruments with relatively slow response. For cold temperatures and low humidities, **frost-point hygrometers** are used instead.

Hair hygrometers use organic fibers such as long hairs, anchored at one end and attached at the other end by amplifying levers to a dial that reads out relative humidity. As the RH increases, the hairs get longer, causing the dial to turn. These are inaccurate, but are inexpensive and are the most common hygrometers for home use. Other hygrometers use other materials that also change their dimensions when they absorb water molecules.

Psychrometers are instruments with two liquid-in-glass thermometers attached to a board or frame. The bulb of one thermometer is surrounded by a sleeve or wick of cloth that is saturated with distilled water, while the other bulb remains dry. After both thermometers are actively ventilated [by whirling the instrument through the air on a hand-held axel (**sling psychrometer**), or by using a spring or electrically driven fan to blow air past the thermometers (**aspirated psychrometer**)], the two thermometers are read to give the **wet and dry-bulb temperatures**. The wet-bulb is cooler than the dry, because of the latent heat absorbed when water evaporates. This thermodynamic information can be used with psychrometric tables or charts (Figs. 4.4 & 4.5) to determine the humidity. These instruments are extremely slow response, but relatively simple. Modern psychrometers replace the liquid-in-glass thermometers with electronic thermometers such as thermistors.

In old **radiosondes** (balloon-borne weather instruments), the electrical resistance across a carbon-coated glass slide was measured. In more humid air, this **carbon-film hygrometer** becomes more resistive. Modern radiosondes often measure the capacitance across a very thin dielectric plastic that is coated on both sides with a porous metallic grid. Both approaches are small and light enough to be carried aloft, but both sensors can be easily contaminated by chemical vapors that change their electrical properties.

Microwave refractometers draw air into a small chamber filled with microwaves. The refraction (bending) of these microwave beams depends on humidity (see the radar section of the Remote Sensing chapter), and can be measured. These are very fast-response sensors.

Spectral absorption hygrometers, also known as **optical hygrometers**, transmit frequencies of electromagnetic radiation that are strongly absorbed by water vapor. By passing the beam of radiation across a short path of air to a detector, the amount of attenuation can be measured to allow calculation of the absolute humidity. One such instrument, the **Lyman-alpha hygrometer,** uses ultraviolet light of wavelength 0.121567 μm, corresponding to an absorption/emission line of hydrogen. Another, the **krypton hygrometer**, uses emissions at 0.12358 μm, generated by glow tube filled with the noble gas krypton. Other instruments use absorption of infrared light (**infrared hygrometers**). These are

all fast-response instruments. See the Remote Sensing chapter for absorption spectra across the atmosphere.

Some **lidars** (laser radars) have been developed to transmit two neighboring wavelengths of electromagnetic radiation, one of which is affected by water vapor and the other which is not. Such **differential absorption lidars** (**DIAL**) can remotely measure humidity along vertical or slant paths, and can scan the atmosphere to measure the humidity in a volume or in a plane.

Weather radars and other microwave profilers can be used to measure profiles of humidity in the atmosphere, because the speed and/or polarity of microwaves through air depends on humidity.

Some sensors measure path-averaged humidity. One example is the **water-vapor channel on weather satellites**, which measures infrared emissions from water vapor in the air. As discussed in the Remote Sensing chapter, such emissions come from a layer of air several kilometers thick in the top third of the troposphere. These instruments have the advantage of remotely sampling the atmosphere at locations that are difficult to reach otherwise, such as over the oceans. A disadvantage is that they have difficulty seeing through clouds.

Transmissions from **Global Positioning System** (**GPS**) satellites are slightly delayed or refracted by humidity along the path of the beam through the atmosphere. However, data from many such crossing beams from the constellation of GPS satellites can be computationally inverted to yield vertical profiles of humidity, similar to the medical X-ray tomography methods used for brain scans.

SUMMARY

The saturation (equilibrium) vapor pressure of warm air is greater than that of cool air. The Clausius-Clapeyron equation and Tetens' formula quantify this relationship.

Some relative moisture variables compare the actual amount of water vapor in the air to the saturation amount for that temperature: relative humidity, temperature dew-point spread, wet-bulb depression, and condensation level. Other variables measure the concentration of water in the air: vapor pressure, mixing ratio, specific humidity, and absolute humidity.

The amount of water in the air is described by a total water budget. Budgets can be formed following a cloud or air parcel (Lagrangian), or for a fixed volume (Eulerian). As saturated (cloudy) air rises, its temperature cools at the moist adiabatic lapse rate, which is less than the dry rate. These moist adiabats can be drawn on thermodynamic diagrams. Using such diagrams is quicker than calculating complex recursive equations for the moist lapse rate.

Isohumes can also be drawn on thermodynamic diagrams, to show the actual or maximum amount of moisture in the air. For many formulae and for thermodynamic diagrams, actual air temperature is related to equilibrium (saturation) amount of water vapor. Alternately, dew-point temperature is related to actual amount of water vapor in the air.

Threads

Isohumes and moist adiabats are used in Chapters 5 and 6 to create more detailed thermodynamic diagrams to help understand cloud growth. Saturation mixing ratio and vapor pressure determine the growth of individual cloud particles leading to precipitation (Chapter 7). Some of the energy for cyclones (Chapter 13), thunderstorms (Chapters 14 and 15) and hurricanes (Chapter 16) comes from latent heat release, which again depends on the humidity and saturation values in the air. Global warming associated with climate change (Chapter 21) might affect the cloud-cover amount and albedo via changes in humidity.

Temperature and pressure of the standard atmosphere of Chapter 1 were used to find boiling temperatures. The thermodynamic diagram of Chapter 3 was extended here to include isohumes and moist adiabats. Routine forecasts of humidity are made using numerical weather prediction (Chapter 20).

EXERCISES

Numerical Problems

N1. Compare the saturation vapor pressure (with respect to liquid water) calculated with the Clausius-Clapeyron equation and Tetens' formula, for T (°C):

a. 45 b. 40 c. 35 d. 30 e. 25 f. 20 g. 15
h. 10 i. 5 j. 0 k. –5 l. –10 m. –15 n. –20

N2. Calculate the saturation vapor pressures with respect to both liquid water and flat ice, for T (°C) =

a. –3 b. –6 c. –9 d. –12 e. –15 f. –18
g. –21 h. –24 i. –27 j. –30 k. –35 l. –40

N3. Find the boiling temperature (°C) of pure water at altitudes (km) of:

a. 0.2 b. 0.4 c. 0.6 d. 0.8 e. 1.2 f. 1.4
g. 1.6 h. 1.8 i. 2.2 j. 2.4 k. 2.6 l. 2.8

N4. Find e_s (kPa), T_d (°C), r and r_s (g/kg), q and q_s (g/kg), ρ_v and ρ_{vs} (g/m^3), RH (%), LCL (km), and T_w (°C) for the situations below:

	T (°C)	P (kPa)	e (kPa)
a.	30	101.3	1.5
b.	10	80.0	1.0
c.	0	90.0	0.5
d.	5	50.0	0.4
e.	8	101.3	1.0
f.	40	70.0	5.0
g.	10	85.0	0.5
h.	20	90.0	2.0

N5(§). Generate a table similar to Table 4-1, but for an altitude where P (kPa) =

a. 95 b. 90 c. 85 d. 80 e. 75 f. 70 g. 65
h. 60 i. 55 j. 50 k. 45 l. 40 m. 35 n. 30

N6. Saturated outside air of T = 0°C is drawn into your house to replace hot air going up the chimney. If this induced air is heated in the house to 20°C, what is the relative humidity inside?

N7. Find the mixing ratio at P = 100 kPa?

a. T = –10°C with RH = 100%
b. T = +20°C with RH = 20%
c. T = +5°C with RH = 50%
d. T = –10°C with RH = 20%
e. T = +20°C with RH = 50%
f. T = +5°C with RH = 100%
g. T = +50°C with RH = 100%
h. T = +50°C with RH = 2%

N8. What is the LCL height for air with the following conditions at the surface. This is the cloud-base height for convective (cumuliform) clouds.

	T (°C)	T_d (°C)		T (°C)	T_d (°C)
a.	30	10	e.	20	14
b.	10	10	f.	40	35
c.	0	–5	g.	–20	–20
d.	30	0	h.	–10	–40

N9. Psychrometer measurements give the dry-bulb temperatures, T, and wet-bulb temperatures, T_w, listed below. What is the mixing ratio, dew point and relative humidity? Use the equations for this exercise.

	T (°C)	P (kPa)	T_w (°C)
a.	30	101.3	20
b.	10	80.0	10
c.	0	90.0	–5
d.	30	100.0	15
e.	20	90.0	14
f.	0	95.0	–5
g.	20	100.0	6
h.	40	100.0	20

N10. Same as the previous exercise, but you may use the psychrometric graphs (Figs. 4.4 or 4.5).

N11. Given the following temperatures and dew-point temperatures, use the equations of Normand's Rule to calculate the wet-bulb temperature.

	T (°C)	T_d (°C)
a.	30	10
b.	10	10
c.	0	–5
d.	30	0
e.	20	14
f.	40	35
g.	–20	–20
h.	–10	–40

N12. Same as the previous exercise, but you may use a thermo diagram

N13. What is the total-water mixing ratio at sea level, given:

a. r = 5 g/kg, r_L = 1 g/kg
b. r = 5 g/kg, r_L = 3 g/kg
c. T = 10°C, r_L = 2 g/kg
d. r = 10 g/kg, r_L = 5 g/kg
e. T = 5°C, r_L = 5 g/kg
f. T = 3°C, r_L = 3 g/kg
g. T = 0°C, r_L = 4 g/kg
h. T = 20°C, r_L = 5 g/kg

N14. What is the liquid water mixing ratio at sea level for: a. T = 30°C, r_T = 35 g/kg
b. T = 20°C, r_T = 25 g/kg
c. T = 30°C, r_T = 30 g/kg
d. T = 20°C, r_T = 30 g/kg
e. T = 10°C, r_T = 20 g/kg
f. T = 10°C, r_T = 10 g/kg
g. T = 0°C, r_T = 5 g/kg
h. T = 0°C, r_T = 7 g/kg

N15. Using the appropriate equation, calculate the dew-point temperature for air at P = 50 kPa, given a mixing ratio (g/kg) of
a. 30 b. 25 c. 20 d. 15 e. 10 f. 5 g. 3
h. 2 i. 1 j. 0.5 k. 0.3 l. 0.2 m. 0.1 n. 0.05

N16. Same as the previous exercise, but you may use Fig. 4.7.

N17. Using Fig. 4.7, what is the dew point temperature of air parcels ending at a pressure height of 50 kPa, if they start at 100 kPa with dew-point temperatures (°C) of
a. 40 b. 35 c. 30 d. 25 e. 20 f. 15 g. 10
h. 5 i. 0 j. –5 k. –10 l. –15 m. –20 n. –25

N18. Using Fig. 4.7, find the relative humidity for air at

	P (kPa)	T (°C)	T_d (°C)
a.	70	20	0
b.	70	10	10
c.	70	30	–10
d.	90	30	30
e.	90	30	20
f.	90	30	10
g.	100	20	–20
h.	100	–20	–30

N19. Using the equations, what is the value of the moist adiabatic lapse rate (°C/km) at P = 100 kPa for the following temperatures (°C)?
a. 40 b. 30 c. 20 d. 10 e. 0 f. –10 g. –20
Same, but at P = 50 kPa:
h. 20 i. 15 j. 10 k. 5 l. 0 m. –5 n. –10

N20. Same as the previous exercise, but find the moist adiabatic lapse rate as a change of temperature with pressure (°C/kPa).

N21. Using Fig. 4.8, what is the final temperature of a saturated air parcel at P = 70 kPa if lifted moist adiabatically from P = 100 kPa with the following initial temperatures (°C):
a. –30 b. –25 c. –20 d. –15 e. –10 f. –5 g. 0
h. 5 i. 10 j. 15 k. 20 l. 25 m. 30

N22. Same as the previous exercise, but starting at P = 50 kPa and lowering moist adiabatically to P = 80 kPa.

N23. Identify the liquid-water and equivalent potential temperatures for the air parcels in the previous two exercises, using Fig. 4.8 and other figures for dry adiabats in the Heat chapter.

N24. At height 1 km, the temperature is 5°C, the water vapor mixing ratio is 6 g/kg, and liquid-water mixing ratio is 2 g/kg. Use the equations to find the: a. liquid water potential temperature
b. equivalent potential temperature

N25. An unsaturated air parcel from sea level has r = 15 g/kg and T = 30°C. If it rises to a height where it is saturated with r_L (g/kg) as given below, what is its new value of r?
a. 0.5 b. 1 c. 1.5 d. 2 e. 2.5 f. 3 g. 3.5
h. 4 i. 4.5 j. 5 k. 5.5 l. 6 m. 6.5 n. 7

N26. A horizontally uniform wind given below is advecting air of r_T = 10 g/kg at the west side of a region. The other side of the region is 100 km further east, and has a humidity of r_T = 15 g/kg. How does this advection alter the total water mixing ratio across that 100 km-wide region? U (m/s) =
a. 2 b. 4 c. 5 d. 7 e. 10 f. 12 g. 15
h. 18 i. 20 j. 21 k. 23 l. 25 m. 27 n. 30

N27. Precipitation of rate 4 mm/h enters a volume of air at altitude z = 100 m, but only the amount given below (mm/h) reaches the ground at z = 0. How does this precipitation gradient alter the total water mixing ratio within that 100 m-thick layer?
a. 6 b. 5.5 c. 5 d. 4.5 e. 4.3 f. 4.2 g. 4.1
h. 4 i. 3.9 j. 3.8 k. 3.7 l. 3.5 m. 3 n. 2.5

N28. Given below the value of latent heat flux ($W \cdot m^{-2}$) at the surface. Find the kinematic value of latent flux ($K \cdot m/s$), the vertical flux of water vapor ($kg_{water} \cdot m^{-2} \cdot s^{-1}$), the vertical flux of water vapor in kinematic form ($kg_{water}/kg_{air}) \cdot (m/s)$, and the evaporation rate (mm/d).
a. 100 b. 150 c. 200 d. 250 e. 300 f. 350
g. 80 h. 75 i. 70 j. 60 k. 50 l. 40 m. 25

N29. For windy, overcast conditions, estimate the kinematic latent heat flux at the surface, assuming $C_H = 5x10^{-3}$.

	M (m/s)	r_{sfc} (g/kg)	r_{air} (g/kg)
a.	2	25	10
b.	2	20	10
c.	2	15	10
d.	5	25	10
e.	5	20	10
f.	5	15	10
g.	12	25	10
h.	12	20	10
i.	12	15	10

N30. For sunny, free-convective conditions, estimate the kinematic latent heat flux at the surface.

	w_B (m/s)	r_{sfc} (g/kg)	r_{ML} (g/kg)
a.	5	25	10
b.	5	20	10
c.	5	15	10
d.	12	25	10
e.	12	20	10
f.	12	15	10
g.	25	25	10
h.	25	20	10
i.	25	15	10

N31. A radiosonde balloon launched during daytime fair-weather shows vertical profiles in a 1 km thick boundary layer as shown in Fig. 4.12, with $|\Delta_s\theta| = 10°C$, $|\Delta_{zi}\theta| = 2°C$, $|\Delta_s r_T| = 4$ g/kg, and $\Delta_{zi} r_T$ (g/kg) as given below. The convective transport coefficient times buoyancy velocity is 0.025 m/s on this calm day. What is the vertical flux divergence of total water due to turbulence, and how does that contribute to moistening the air?

a. –10 b. –8 c. –5 d. –3 e. –2 f. –1 g. 0
h. +1 i. 2 j. 4 k. 6 l. 7 m. 9 n. 12

Understanding & Critical Evaluation

U1. Vapor pressure *e* represents the partial pressure of water vapor in air. Namely, the total pressure in air can be thought of as consisting as the sum of partial pressures from each of the individual gases within the air.

If total air pressure remains constant, but if evaporation of liquid water into the air causes the humidity to increase (i.e., the vapor pressure increases), then what happens to the other gases in air? Where do they go, if total pressure remains constant?

U2(§). a. Use a spreadsheet to calculate saturation vapor pressure over ice (not over water) for temperatures between –50 and 0°C. Plot the resulting ice curve together with the water curve on the same graph, as in Fig. 4.2. Also, plot a curve of the difference between the ice and water curves, as shown in the inset in Fig. 4.2.

b. Replot the results as semi-log and log-log.

c. Why are the saturation vapor pressures different over water vs. ice?

U3. The Clausius-Clapeyron equation is based on an assumption of air over a flat surface of pure liquid water, and assumes that the liquid water and the air are of the same temperature. However, sometimes in the atmosphere there is warm rain falling into a region of colder air. Explain what would happen in this situation. (Neglect droplet surface curvature.)

U4. In Table 4-1, why can the same columns of numbers be used for actual temperature with saturation values of humidity (the top set of column labels), and for the dew point temperature with actual values of humidity (the bottom set of column labels)?

U5(§). a. Plot a curve of boiling temperature vs. height over the depth of the troposphere.
b. The purpose of pressure cookers is to cook boiled foods faster. Plot boiling temperature vs. pressure for pressures between 1 and 2 times $P_{sea\ level}$.

U6(§). It is often assumed that specific humidity is approximately equal to mixing ratio. How good is that assumption? Create a graph comparing the two values over a range of temperatures. Do this for a few different pressures.

U7(§). On a graph of T vs. T_d, plot curves for different values of RH.

U8. Why is it important to keep thermometers dry (i.e., placing them in a ventilated enclosure such as a **Stevenson screen**) when measuring outside air temperature?

U9(§). Check whether eq. (4.16a) or (4.16b) is a reasonable approximation to the lifting condensation level (LCL). The exact definition is the height of a rising air parcel where temperature and dew point become equal.

a. Do this check using the thermo diagram, for a variety of T and T_d values at the same starting height. For T, follow a dry adiabat upward from the starting temperature and height. For T_d, follow an line of constant mixing ratio up from the starting T_d and height. Where the two lines cross is the LCL.

b. Do the check using the equations for adiabatic temperature change from an earlier chapter, and using the equation for dew point temperature as a function of height or pressure.

U10. Create a table that lists the max and min values allowed for vapor pressure, mixing ratio, specific humidity, absolute humidity, relative humidity, dew-point temperature, LCL, and wet-bulb temperature.

U11. In arid regions (hot, dry), an inexpensive form of air conditioning (sometimes known as a **swamp cooler**) is possible where liquid water is evaporated into the dry air. The result is cooler air (due to latent heat effects) that is more humid.
a. For air of initial temperature T = 40°C, how effective are swamp coolers for different initial relative humidities?
b. At what initial humidity would a swamp cooler not cause the air to be more comfortable? (Hint, use the heat index info from the Heat chapter.)

U12. a. Rearrange the T_w equations to find the T_w value corresponding to r = 0, for arbitrary T and P.
b. Test these values from part (a) for a variety of temperatures at P = 100 kPa.

U13(§). Use a spreadsheet program to generate a table that gives dew point temperatures from measurements of wet and dry bulb temperatures. Check that your results are consistent with Figs. 4.4 & 4.5.

U14(§). For **Normand's Rule**, verify that eqs. (4.20) and (4.21) describe the same process as shown graphically in Fig. 4.6, and compare the numerical value of T_w using thermo-diagram vs. equation methods, for several different starting values of T and T_d.

U15. Use the definitions of mixing ratio eq. (4.4), specific humidity eq. (4.7), and absolute humidity eq. (4.10) to verify relationships (4.22) - (4.27).

U16. Consider a Lagrangian, cloudy air parcel.
a. Suppose precipitation falls into the top of the air parcel, passes through the air parcel, and falls out of the bottom at the same rate that it entered. Discuss what happens with respect to eqs. (4.35).
b. What if no precipitation enters the top or sides of the air parcel, but some falls out of the bottom. Discuss what happens with respect to eqs. (4.35).

U17(§). Use a spreadsheet program to draw dry adiabats and mixing ratio lines on the same thermodynamic diagram, and plot as a semi-log graph. That is, combine Figs. 3.3 and 4.7.

U18. a. Derive eq. (4.36) from the Clausius-Clapeyron equation.
b. Derive a similar equation for dew-point temperature, but using Tetens' formula.

U19. What is the behavior of eq. (4.37b) in the limit of zero absolute temperature, and in the limit of very high temperature?

U20(§). Use a spreadsheet to draw dry and moist adiabats on the same thermodynamic diagram, and plot as a semi-log graph similar to Fig. 4.8.

U21(§). (Very time-consuming but important problem, resulting in a complete thermodynamic diagram.)
a. Use a spreadsheet program to draw dry and moist adiabats and mixing ratio lines on the same thermodynamic diagram. If you can draw graphs in color, use red lines for the dry adiabats, blue lines for the moist adiabats, and green lines for the mixing ratios. The background isotherm and isobar grid lines can be black. Plot the isotherms and adiabats for (T, θ, θ_w) = –60, –40, –20, 0, 20, 40 °C. Plot the isohumes for r = 0.1, 0.2, 0.5, 1, 2, 5, 10, 20, 50 g/kg.
b. (Optional) Also, compute and plot on the same graph lines of constant altitude (m) vs. $T_{surface}$ and P, using the hypsometric equation. If you have color, draw these lines in brown or tan. Assume a dry adiabatic lapse rate from the surface.

U22. In eqs. (4.40) and (4.41) is a factor θ/T. Why is it in those equations? Do they cancel because they are both absolute temperatures?

U23. Let $r_T = r + r_L$ be the total water mixing ratio, which is the sum of the water vapor r plus any liquid water r_L (cloud droplets) present in the air. Consider a rising air parcel with initially no liquid water that is unsaturated, starting from near the surface. Thus the total water equals the initial water vapor mixing ratio.
a. As the air parcel rises toward its LCL, is θ_L conserved? Explain.
b. Above the LCL, a rising air parcel does not conserve θ, because condensation of water releases latent heat into the air and increases the liquid water content. Is θ_L conserved for this rising air parcel that is above its LCL? Explain.

U24. If air starting from near the surface (at P = 100 kPa) is initially just saturated, find the values of equivalent potential temperature θ_e for each of the moist adiabats drawn in Fig. 4.8.
Explanation: $\theta_e > \theta_L$, because θ_e represents the potential temperature of the air after being heated by condensation of ALL the water vapor in the air, while θ_L represents the potential temperature of the air after being cooled by evaporation of all the liquid water present in the air.

U25. Rewrite eq. (4.44) to include vertical advection by mean wind W, and to include evaporation from the ocean. Assume that you are considering a fixed Eulerian volume (such as a hypothetical cube of air) that rests on the sea surface.

U26. Without the simplifying assumptions, write the full Eulerian water budget equation (i.e., like eq. 4.44, but including the missing terms). (Hint, look at the full heat budget equation from the Heat chapter.)

U27. In the Eulerian budget eq. for total water (4.44), there is a precipitation term. In the Eulerian budget eq. for heat (in the Heat chapter), there is a latent heat term that depends on condensation. Condensation and precipitation are related, yet the terms in those two eqs. are different. Why must they be different?

U28(§). Plot curves kinematic latent flux vs. evaporation rate for different altitudes.

U29. Derive eq. (4.54), assuming that $F_{water\ zi} = w_e \cdot \Delta_{zi} r_T$, and $F_{H\ zi} = 0.02 \cdot F_H$, and $F_{H\ zi} = w_e \cdot \Delta_{zi} \theta$, where w_e is entrainment velocity.

U30. Derive eq. (4.56) from (4.55).

U31. Which humidity sensors would be best suited for measuring the rapid fluctuations of humidity in the turbulent boundary layer? Why?

Web-Enhanced Questions

W1. Access the surface weather data for a weather station close to your location (or at some other location specified by your instructor). What is the current humidity (value and units)?

W2. Find a weather map on the web that shows either colored or contoured values of humidity over your country for a recent observation time. Where are the humidities the greatest; the smallest?

W3. Do the humidity formulas presented in the El Paso NWS web page agree with those in this textbook? Compare and discuss. http://www.srh.noaa.gov/epz/?n=wxcalc

W4. Search the web for weather calculator tools (other than the one listed above from the NWS) for calculating or converting humidities, temperatures, and/or pressures between various units.

W5. Search the web to create a catalog or table of the different types of instruments that can be used for measuring humidity. Don't give brand names here, but instead list the type of instrument (such as sling psychrometer). For each type of instrument, briefly explain the physical process that it utilizes to measure humidity, and state which humidity variable it measures.

W6. Search the web for tables or graphs or definitions of various indices that measure discomfort or heat-stress danger for humans and/or livestock as a function of hot air temperature and high humidity. (Hint, Two traditional sources of info are: Houghton, D.D., 1985: Handbook of Applied Meteorology, Wiley Interscience, p786. Weiss, M. H., 1983: Quantifying summer discomfort, Bulletin American Meteor. Soc., 64, 654-655.)

There are a variety of such indices:

- **apparent temperature**,
- **discomfort index**,
- **effective temperature**,
- **heat index** (also known as the R. G. **Steadman Heat Index**),
- **humidex**,
- **humisery**,
- **humiture**,
- **index of thermal stress**.
- **livestock weather safety index**,
- **summer simmer index**,
- **temperature-humidity index** (THI),
- **wet-bulb globe temperature**,

W7. Search the web to find a current weather map analysis that shows isohumes (surface, or at 85 kPa, or at 70 kPa) over your state, province, or country (as assigned by the instructor). Locate your town or school on this map. Search for related current weather info that gives the wind speed and direction at that same altitude over your town.

a. Compute the moisture advection term of the Eulerian moisture budget, and discuss whether the result will cause the air at your location to become more or less humid with time.

b. What precipitation or evaporation rate would be needed to compensate for the advection from part (a), which would result in no change to total water mixing ratio (neglecting turbulence)?

W8. Access the current surface weather data near you every hour, and plot humidity vs. time. Alternately, a web site might already have a plot of humidity vs. time that you could use directly. Plots of weather variables vs. time are called **meteograms**.

W9. Search the web for web sites that plot upper-air soundings on thermodynamic diagrams. In particular, look for different types of thermo diagrams (not for different soundings on the same type of diagram). Print out a sample of each different type of thermo diagram.

In almost all thermo diagrams, the moist adiabats are curved lines that gradually become tangent to the dry adiabats at high altitudes. Use this behavior to identify the moist and dry adiabats in each type of diagram. Then, also identify the isotherms, isobars, and isohumes. You should be able to interpret any type of thermo diagram.

Synthesis Questions

S1. Suppose that saturation vapor pressure decreases as air temperature increases. Assume that clouds, fog, and precipitation can still form in air that becomes saturated. How would cloudiness and fogginess near the ground vary during a daily cycle? How would it vary seasonally?

S2. Suppose that dew-point temperature did not depend on pressure or altitude. Would the lines in a thermo diagram be different? If so, describe them.

S3. Suppose you were to design a new humidity sensor that measured absorption of radiation across a path of humid air. Assume that the path length through which the radiation propagates, and the absorption coefficient for water vapor for the wavelength of interest, are both known. Which principle or law would you utilize to convert radiation absorption into a humidity, and which humidity variable would you get from this instrument?

S4. What if the amount of latent heat released in a rising, saturated air parcel was greater than the adiabatic cooling of the parcel as it expands into lower pressure.

a. What would be different in a thermo diagram?

b. How would this difference affect the weather and climate, if at all?

S5. What if the evaporation rate of water from the surface was constant, and did not depend on surface humidity, air humidity, wind speed, or solar heating (i.e., convection). How would the weather and climate be different, if at all?

S6. Suppose the whole troposphere was saturated with water vapor (100% relative humidity), but there were no cloud droplets or ice crystals in the air.

a. Assuming a standard atmosphere temperature profile, how many kg of water vapor are there over each square meter of Earth surface?

b. How many kg of water vapor would there be in the troposphere total, when summed around the whole surface of the Earth?

c. If all this water were to rain out (leaving the atmosphere completely dry) and flow into the oceans, which cover roughly 70.8% of the Earth's surface, how many meters would sea level rise?

d. Repeat questions a-c, but for the stratosphere.

S7. a. Rewrite the Clausius-Clapeyron equation in the form $e_s = C{\cdot}\exp[-(L/\Re_v){\cdot}(1/T)]$, where C is a constant. What is C equal to?

b. The gas constant for water vapor is $\Re_v \approx k_B/m_v$, where m_v is the mass of a water molecule, and $k_B = 1.3806\text{x}10^{-23}\ \text{J}{\cdot}\text{K}^{-1}{\cdot}\text{molecule}^{-1}$ is the **Boltzmann constant**. Rewrite the eq. from part (a) after substituting for the water-vapor gas constant.

c. The result from (b) contains an exponent of an argument, where that argument is a ratio. The numerator represents the energy needed to separate one molecule from liquid water to allow it to become a vapor molecule in the neighboring air, while the denominator represents the average energy available (as a kinetic energy associated with temperature). Discuss the implications of this interpretation, and why it is relevant to determining equilibrium saturation vapor pressure.

S8. Devise an equation to estimate surface water flux that works for a sunny windy day, which reduces to eqs. (4.51 & 4.52) in the limits of zero convection and zero mean wind, respectively.

Copyright © 2011, 2015 by Roland Stull. *Meteorology for Scientists and Engineers, 3rd Ed.*

STABILITY

CONTENTS

Building a Thermo-diagram 119
- Components 119
- Pseudoadiabatic Assumption 121
- Complete Thermo Diagrams 121

Types Of Thermo Diagrams 122
- Emagram 122
- Stüve & Pseudoadiabatic Diagrams 122
- Skew-T Log-P Diagram 122
- Tephigram 122
- Theta-Height (θ-z) Diagrams 122

More on the Skew-T 124

Guide for Quick Identification of Thermo Diagrams 126

Thermo-diagram Applications 127
- Thermodynamic State 128
- Processes 129

Parcels vs. Environment 134
- Soundings 134
- Buoyancy 135
- Brunt-Väisälä Frequency 136

Flow Stability 138
- Static Stability 138
- Dynamic Stability 141
- Turbulence Determination 142

Finding Tropopause Height & Mixed-layer Depth 143
- Tropopause 143
- Mixed-Layer 144

Summary 145
- Threads 145

Exercises 145
- Numerical Problems 145
- Understanding & Critical Evaluation 148
- Web-Enhanced Questions 149
- Synthesis Questions 150

Large-size Thermo Diagrams 151
- Emagram 152
- Stüve Diagram 153
- Skew-T Log-P Diagram 154
- Tephigram 155
- Theta-Z Diagram 156
- Skew-T Log-P Diagram (ABL) 157
- Theta-Z Diagram (ABL) 158

"Meteorology for Scientists and Engineers, 3rd Edition" by Roland Stull is licensed under a Creative Commons Attribution-NonCommercial-ShareAlike 4.0 International License. To view a copy of the license, visit http://creativecommons.org/licenses/by-nc-sa/4.0/ . This work is available at http://www.eos.ubc.ca/books/Practical_Meteorology/ .

5 A **sounding** is the vertical profile of temperature and other variables in the atmosphere over one geographic location. **Stability** refers to the ability of the atmosphere to be turbulent. Stability is determined by temperature, humidity, and wind profiles. Turbulence and stability vary with time and place because of the corresponding variation of the soundings.

We notice the effects of stability by the: wind gustiness, dispersion of smoke, refraction of light and sound, strength of thermal updrafts, size of clouds, and intensity of thunderstorms.

Thermodynamic diagrams have been devised to help us plot soundings and determine stability. They look complicated at first, but with a bit of practice they can make thermodynamic analysis much easier than solving sets of coupled equations. In this chapter, we first discuss the different types of thermodynamic diagrams, and then use them to determine stability and turbulence.

BUILDING A THERMO-DIAGRAM

Components

In previous chapters, we learned how to compute **isohumes** (the Moisture chapter), **dry adiabats** (the Heat chapter), and **moist adiabats** (the Moisture chapter). We plotted these isopleths on a background graph having temperature along the abscissa and log of pressure along the ordinate. These are reproduced here as Figs. 5.1a-d.

When these isopleths are combined on a single graph, the result is called a **thermodynamic diagram**, or **thermo diagram** for short (Fig. 5.1e). At first glance, Fig. 5.1e looks like a confusing nest of lines; however, you can use the pattern-recognition capability of your mind to focus on the components as shown in Fig. 5.1a-d. Your efforts to master thermo diagrams now will save you time in the future.

Several types of thermo diagrams are used in meteorology. They all can show the same information, and are used the same way. The thermo diagram we learned so far is called an **Emagram**. We learned this one first because it was easy to create using a computer spreadsheet.

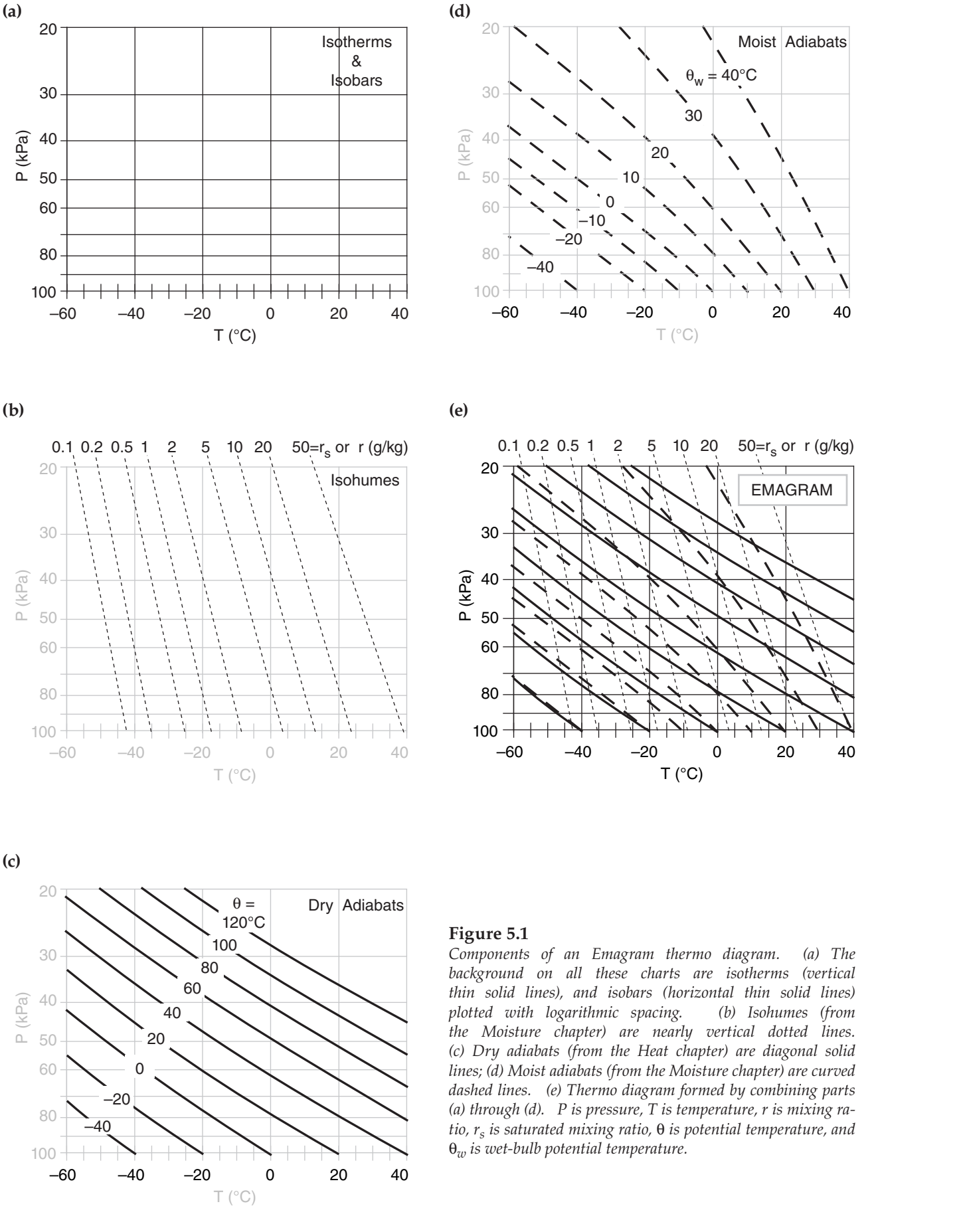

Figure 5.1
Components of an Emagram thermo diagram. (a) The background on all these charts are isotherms (vertical thin solid lines), and isobars (horizontal thin solid lines) plotted with logarithmic spacing. (b) Isohumes (from the Moisture chapter) are nearly vertical dotted lines. (c) Dry adiabats (from the Heat chapter) are diagonal solid lines; (d) Moist adiabats (from the Moisture chapter) are curved dashed lines. (e) Thermo diagram formed by combining parts (a) through (d). P is pressure, T is temperature, r is mixing ratio, r_s is saturated mixing ratio, θ is potential temperature, and θ_w is wet-bulb potential temperature.

On every thermo diagram, including the Emagram in Fig. 5.1e, are plotted at least five types of lines: three give the **state** of the air (**isobars**, **isotherms**, and **isohumes**) and two show how the state changes by a **process** of vertical movement of air (**dry** and **moist adiabats**). Additional state lines for **height contours** are left out of this introductory thermo diagram to avoid clutter, but are included in full thermo diagrams at the end of this chapter.

Pseudoadiabatic Assumption

In the Moisture chapter, we assumed an adiabatic process (no heat transfer or mixing to or from the air parcel) when computing the moist adiabats. However, for any of the thermo diagrams, the moist adiabats can be computed assuming either:

- **adiabatic processes** (i.e., **reversible**, where all liquid water is carried with the air parcels), or
- **pseudoadiabatic processes** (i.e., **irreversible**, where all condensed water is assumed to fall out immediately).

Air parcels in the real atmosphere behave between these two extremes, because small droplets and ice crystals are carried with the air parcel while larger ones precipitate out.

When liquid or solid water falls out, it removes from the system some of the sensible heat associated with the temperature of the droplets, and also changes the heat capacity of the remaining air because of the change in relative amounts of the different constituents. The net result is that an air parcel lifted pseudoadiabatically from 100 kPa to 20 kPa will be about 3°C colder than one lifted adiabatically. This small difference between adiabatic and pseudoadiabatic can usually be neglected compared to other errors in measuring soundings.

Complete Thermo Diagrams

Color thermo diagrams printed on large-format paper were traditionally used by weather services for hand plotting of soundings, but have become obsolete and expensive compared to modern plots by computer. The simplified, small-format diagrams presented so far in this chapter are the opposite extreme – useful for education, but not for plotting real soundings. Also, some weather stations have surface pressure greater than 100 kPa, which is off the scale for the simple diagrams presented so far.

As a useful compromise, full-page, black-and-white thermo diagrams in several formats are included at the end of this chapter. They are optimized for you to reproduce on a copy machine.

[*Hint: Keep the original thermo diagrams in this book clean and unmarked, to serve as master copies.*]

FOCUS • Why so many thermo diagrams?

Meteorological thermo diagrams were originally created as optimized versions of the P vs. α diagrams of classical physics (thermodynamics), where α is the **specific volume** (i.e., α = volume per unit mass = $1/\rho$, where ρ is air density). A desirable attribute of the P vs. α diagram is that when a cyclic process is traced on this diagram, the area enclosed by the resulting curve is proportional to the specific work done by or to the atmosphere. The disadvantage of P vs. α diagram is that the angle between any isotherm and adiabat is relatively small, making it difficult to interpret atmospheric soundings.

Three meteorological thermo diagrams have been devised that satisfy the "area = work" attribute, and are optimized for meteorology to have greater angles between the isotherms and adiabats:

- Emagram,
- Skew-T Log-P Diagram
- Tephigram.

Meteorologists rarely need to utilize the "area = work" attribute, so they also can use any of three additional diagrams:

- Stüve Diagram,
- Pseudoadiabatic (Stüve) Diagram,
- Theta-Height (θ-z) Diagram.

Why are there so many diagrams that show the same things? Historically, different diagrams were devised somewhat independently in different countries. Nations would adopt one as the "official" diagram for their national weather service, and teach only that one to their meteorologists. For example, the tephigram is used in British Commonwealth countries (UK, Canada, Australia, New Zealand). To this day, many meteorologists feel most comfortable with the diagram they learned first.

For many readers, this myriad of diagrams might make an already-difficult subject seem even more daunting. Luckily, all the diagrams show the same thermodynamic state (T, P, r_s) and process lines (θ, θ_w), but in different orientations. So once you have learned how to read one diagram, it is fairly easy to read the others.

The skill to read diverse thermo diagrams will serve you well when acquiring weather data via the internet, because they can come in any format. The internet is the main reason I cataloged the different thermo diagrams in this book.

Of all these diagrams, the Skew-T and Tephigram have the greatest angle between isotherms and adiabats, and are therefore preferred when studying soundings and stability. These two diagrams look similar, but the Skew-T is growing in popularity because it is easier to create on a computer.

TYPES OF THERMO DIAGRAMS

Emagram

"Emagram" is a contraction for "Energy-per-unit-mass diagram." This semi-log diagram (Fig. 5.3a) has temperature (T) along the abscissa, and pressure (P) decreasing logarithmically upward along the ordinate. The isotherms and isobars are straight lines that are perpendicular to each other, and form the orthogonal basis for this diagram.

Dry adiabats (θ) are nearly-straight, diagonal lines slanted up towards the left, and curve slightly concave upward. Moist adiabats (θ_w) curve concave downward, but become parallel to the dry adiabats at cold temperatures and high altitudes. Isohumes (r) are nearly-straight, nearly-vertical lines (with a slight tilt upward to the left).

Height contours (on the large Emagram at the end of this chapter) are approximate, and are provided as a rough guide to users. These contours are nearly horizontal (tilting downward slightly to the right) and nearly straight (slightly concave upward). They are often not drawn in thermo diagrams, and indeed are not shown in Fig. 5.3.

Stüve & Pseudoadiabatic Diagrams

The Stüve diagram (Fig. 5.3b) has T along the abscissa, and pressure decreasing upward along the ordinate according to $(P/P_o)^{\Re d/C_{pd}}$, where $\Re_d/C_{pd}$ = 0.28571 (dimensionless) and P_o = 100 kPa. Stüve diagrams look virtually identical to Emagrams, except that the dry adiabats are perfectly straight. These dry adiabats converge to a point at P = 0 kPa and T = 0 K, which is usually well off of the upper left corner of the graph.

Any thermo diagram can be computed using the pseudoadiabatic assumption for the moist adiabats. However, the particular diagram that is known as a "Pseudoadiabatic Diagram" is often a Stüve plot.

Skew-T Log-P Diagram

Fig. 5.3c is a Skew-T. Although T is labeled linearly along the abscissa, the isotherms are parallel, straight, diagonal lines tilting upward to the right. The Skew-T gets its name because the isotherms are not vertical, but skewed. Pressure decreases logarithmically upward along the ordinate, and the isobars are parallel, horizontal, straight lines.

Dry adiabats are diagonal lines slanted up towards the left, with a pronounced curve concave upward. Moist adiabats are more sharply curved concave left near the bottom of the diagram, changing to less curved, concave to the right, as they merge into the dry adiabats at higher altitudes and colder temperatures. Isohumes are almost straight lines, tilting upward to the right.

This diagram is designed so that the isotherms and dry adiabats are nearly (but not perfectly) perpendicular to each other.

Tephigram

The name Tephigram is a contraction of Tee-Phi Diagram. The logarithm of potential temperature θ physically represents the **entropy** (ϕ = Greek letter Phi) change, and is plotted along the ordinate of Fig. 5.2. Temperature T is along the abscissa. Thus, it is a temperature-entropy diagram, or T-ϕ diagram. Isobars are curved lines in Fig. 5.2.

The range of meteorological interest is shown with the bold rectangle in this figure. When this region is enlarged and tilted horizontally, the result is the tephigram as plotted in Fig. 5.3d.

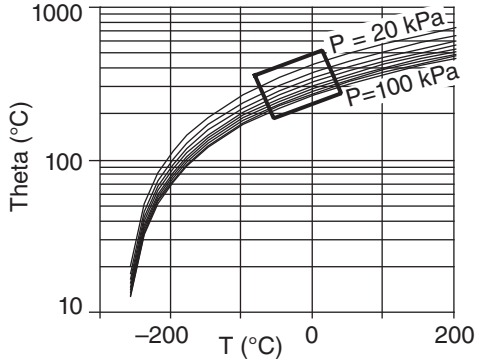

Fig. 5.2
Rectangle shows portion of thermo diagram used for tephigram.

The tephigram looks similar to the Skew-T, with isotherms as straight diagonal lines tilting upward to the right. Dry adiabats are perfectly straight diagonal lines tilting upward left, and are exactly perpendicular to the isotherms. Moist adiabats have strong curvature concave left, and become parallel to the dry adiabats at cold temperatures and high altitudes. Isobars are gently curved (concave down) nearly-horizontal lines. Isohumes are nearly straight diagonal lines tilting upward right.

Theta-Height (θ-z) Diagrams

The orthogonal basis for this diagram are heights (z) plotted along the ordinate and potential temperature (θ) along the abscissa (Fig. 5.3e). Moist adiabats curve to the right of the dry adiabats, but become parallel to the dry adiabats at high altitudes and cold temperatures. Heights are accurate in this diagram, but the isobars are only approximate. Isohumes tilt steeply upward to the right. This diagram is used extensively in boundary-layer meteorology.

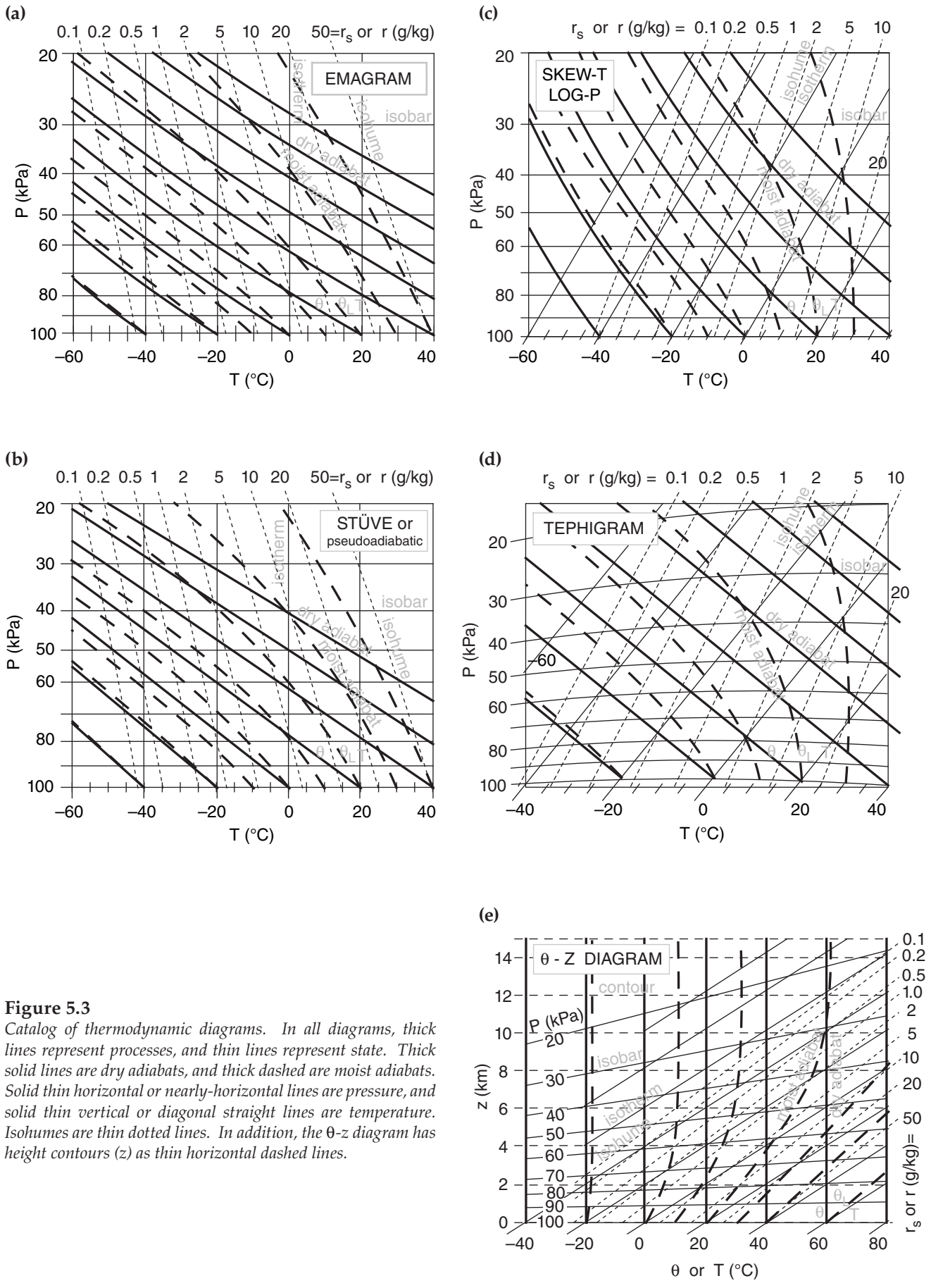

Figure 5.3
Catalog of thermodynamic diagrams. In all diagrams, thick lines represent processes, and thin lines represent state. Thick solid lines are dry adiabats, and thick dashed are moist adiabats. Solid thin horizontal or nearly-horizontal lines are pressure, and solid thin vertical or diagonal straight lines are temperature. Isohumes are thin dotted lines. In addition, the θ-z diagram has height contours (z) as thin horizontal dashed lines.

MORE ON THE SKEW-T

Because of the popularity of the Skew-T, we dissect it in Fig. 5.4, to aid in its interpretation. Tephigram users should find this equally useful, because the only noticeable difference is that the isobars are slightly curved, and increase in slope higher in the tephigram.

The Skew-T diagram is trivial to create, once you have already created an Emagram. The easiest way is to start with a graphic image of an Emagram, and skew it into a parallelogram (Fig. 5.5) using a graphics or drawing program.

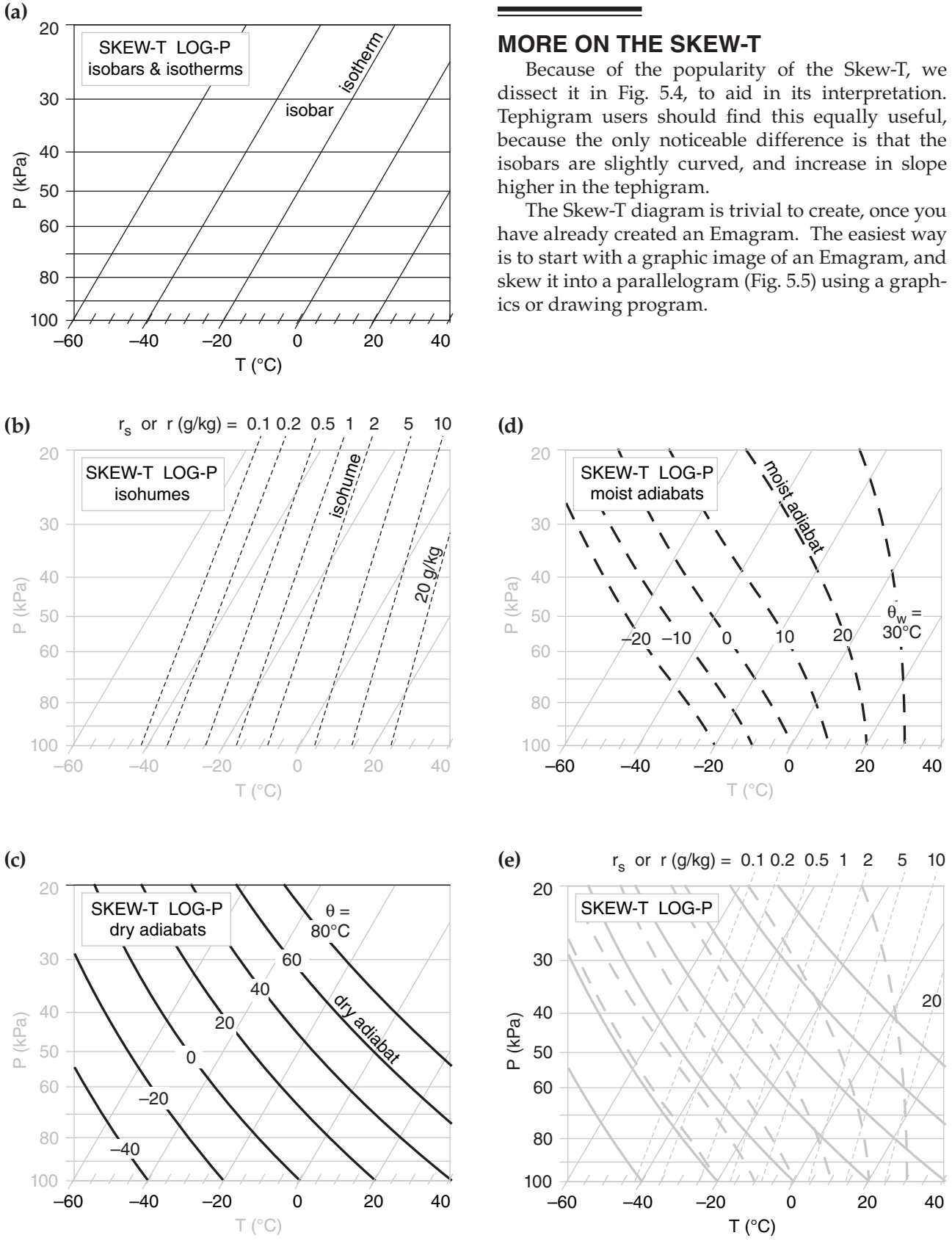

Fig. 5.4

(a)-(d) Components of Skew-Ts, drawn to the same scale so they can be superimposed as a learning aid. The state of the air: (a) isobars and isotherms; (b) isohumes as thin dotted lines. Processes: (c) dry adiabats; (d) moist adiabats. (e) Full Skew-T Log-P, shaded grey to make it easier to write on. The "Skew-T Log-P" diagram is often called a "Skew-T" for short.

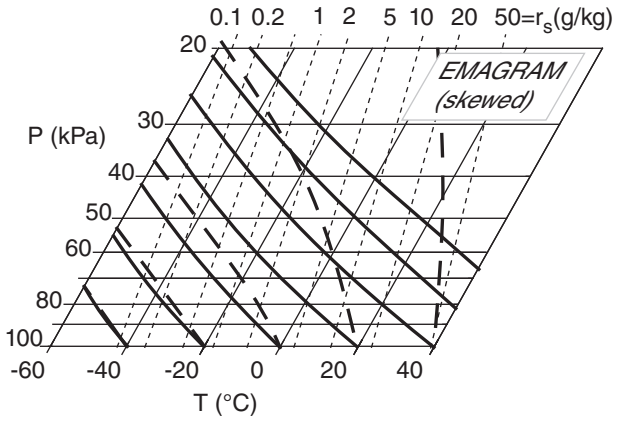

Fig. 5.5
A Skew-T is nothing more than a skewed Emagram.

It is equally simple to draw a Skew-T with a spreadsheet program, especially if you start with the numbers you already calculated to create an Emagram. Let X (°C) be the abscissa of a Cartesian graph, and Y (dimensionless) be the ordinate. Let K be the skewness factor, which is arbitrary. A value of K = 35°C gives a nice skewness (such that the isotherms and adiabats are nearly perpendicular), but you can pick any skewness you want.

The coordinates for any point on the graph are:

$$Y = \ln\left(\frac{P_o}{P}\right) \tag{5.1a}$$

$$X = T + K \cdot Y \tag{5.1b}$$

To draw isotherms, set T to the isotherm value, and find a set of X values corresponding to different heights Y. Plot this one line as an isotherm. For the other isotherms, repeat for other values of T. [Hint: it is convenient to set the spreadsheet program to draw a logarithmic vertical axis with the max and min reversed. If you do this, then use P, not Y, as your vertical coordinate. But you still must use Y in the equation above to find X.]

For the isohumes, dry adiabats, and moist adiabats, use the temperatures you found for the Emagram as the input temperatures in the equation above. For example, the θ = 20°C adiabat has the following temperatures as a function of pressure (recall Thermo Diagrams-Part 1, in the Heat chapter), from which the corresponding values of X can be found.

P(kPa)= 100 , 80 , 60 , 40 , 20
T(°C) = 20 , 1.9 , –19.8, –47.5 , –88
X = 20 , 9.7 , –1.9 , –15.4 , –31.7

Solved Example
Create a Skew-T diagram with one isotherm (T = 20°C), one dry adiabat (θ = 20°C), one moist adiabat (θ_w = 20°C), and one isohume (r = 5 g/kg). Use as input the temperatures from the Emagram (as calculated in earlier chapters). Use K = 35°C, and P_o = 100 kPa.

Solution
Given: The table of Emagram numbers below.
Use eq. (5.1) in a spreadsheet to find X and Y.

	A	B	C	D	E
1	Create Skew-T from Emagram Numbers				
2					
3		Iso-	Dry	Moist	Iso-
4		therm	Adiabat	Adiabat	hume
5		T=20°C	θ=20°C	θ_w=20C	r=5g/kg
6	Emagram (Given):				
7	P (kPa)	T (°C)	T (°C)	T (°C)	T (°C)
8	100	20	20	20	3.7
9	90	20	11.3	16	2.3
10	80	20	1.9	11.4	0.7
11	70	20	-8.4	6	-1.2
12	60	20	-19.8	-0.3	-3.2
13	50	20	-32.6	-8.8	-5.6
14	40	20	-47.5	-20	-8.5
15	30	20	-65.3	-37	-12
16	20	20	-88	-60	-17
17					
18	Skew-T:				
19	Let K=	35°C		Let P_o=	100kPa
20	P	Y	X	X	X	X
21	100	0.00	20	20	20	3.7
22	90	0.11	23.7.	15.0	19.7	6.0
23	80	0.22	27.8	9.7	19.2	8.5
24	70	0.36	32.5	4.1	18.5	11.3
25	60	0.51	37.9	-1.9	17.6	14.7
26	50	0.69	44.3	-8.3	15.5	18.7
27	40	0.92	52.1	-15.4	12.1	23.6
28	30	1.20	62.1	-23.2	5.1	30.1
29	20	1.61	76.3	-31.7	-3.7	39.3

Using the spreadsheet to plot the result gives:

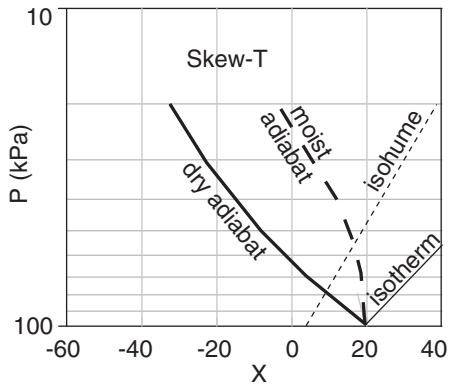

Check: Sketch OK. Matches Fig. 5.4e.
Discussion: Experiment with different values of K starting with K = 0°C, and see how the graph changes from an Emagram to a Skew-T.

Solved Example

For each thermo diagram numbered below, identify its name.

1)

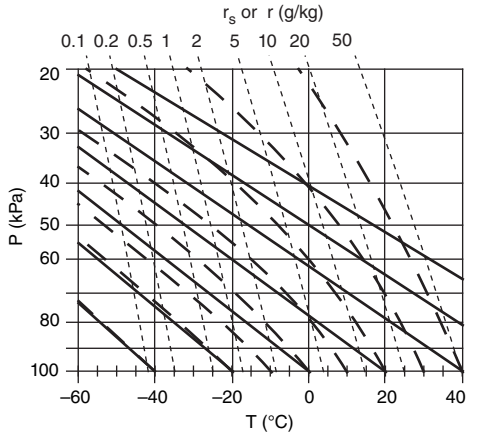

2)

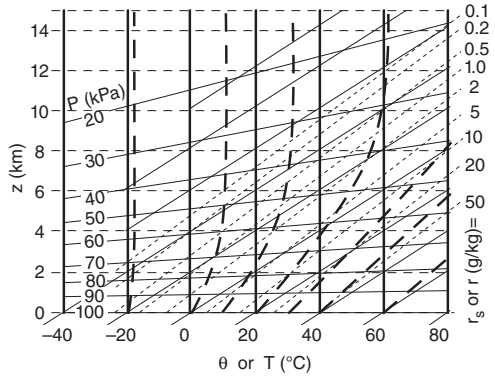

3)

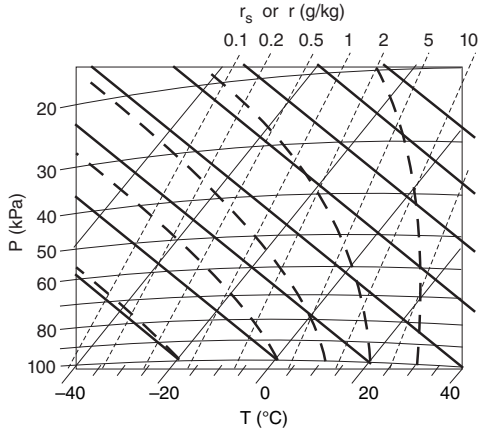

(continued next page)

GUIDE FOR QUICK IDENTIFICATION OF THERMO DIAGRAMS

If you receive a thermo diagram via the internet without any labels identifying the diagram type, use the following procedure to figure it out:

1) if there are some lines from lower left to upper right, then either Skew-T, Tephigram, or θ-*Z* .
   a) if the isobars are exactly horizontal and straight, then Skew-T,
   b) else if the strongly curved lines (moist adiabats) asymptotically approach vertical near the top of the diagram, then θ-*Z*,
   c) else Tephigram,
2) else either Emagram or Stüve .
   a) if dry adiabats are slightly curved, then Emagram,
   b) else Stüve (including Pseudoadiabatic version of Stüve).

When you encounter an unfamiliar thermo diagram, you can take steps to help segregate and identify the various lines. First, identify the isobars, which are horizontal and straight, or nearly so, on virtually all diagrams. Isobars are usually spaced roughly logarithmically with height, and are labeled as either 100, 90, 80, 70 kPa etc., or as 1000, 900, 800, 700 mb or hPa etc. These serve as a surrogate measure of height.

Next, identify the dry and moist adiabats. These are the lines that converge and become parallel at cold temperatures and high altitudes. In all the diagrams, the moist adiabats are the most curved. The adiabats are spaced and labeled roughly linearly, such as 0, 10, 20, 30 °C etc, or often in Kelvin as 273, 283, 293, 303 K, etc. While the dry adiabats are always labeled as potential temperature θ, the moist adiabats can be labeled as either equivalent potential temperature θ_e , liquid-water potential temperature θ_L , or wet-bulb potential temperature θ_w .

An alternative for identifying adiabats is to look at any labeled temperature at the bottom of the graph. Usually at 100 kPa (1000 mb or hPa), you will find that T , θ_w , and θ lines all radiate from the same

Hint: For viewing thermo diagrams: hold the page so you view it from near its edge, rather than perpendicular to the page as is usually done for reading. This allows the curvature of lines to be more apparent. This is the same trick used by carpenters, sighting along a piece of lumber to detect warps and other imperfections.

points. For all diagrams, the T line is rightmost, θ is leftmost, and θ_w is in the middle.

Finally, identify the isotherms and isohumes. These lines cross each other at a small angle, and extend from the bottom to the top of the graph. The isohumes always tilt to the left of the isotherms with increasing height. The isotherms increment linearly (e.g., 0, 10, 20 , 30, °C etc.), while the isohumes usually increment logarithmically (e.g., 1, 2, 5, 10, 20 g/kg, etc.). Isotherms are either vertical, or tilt upward to the right.

THERMO-DIAGRAM APPLICATIONS

Fig. 5.6 shows a complete, but simplified, Emagram. We use this as the common background for the demonstrations that follow.

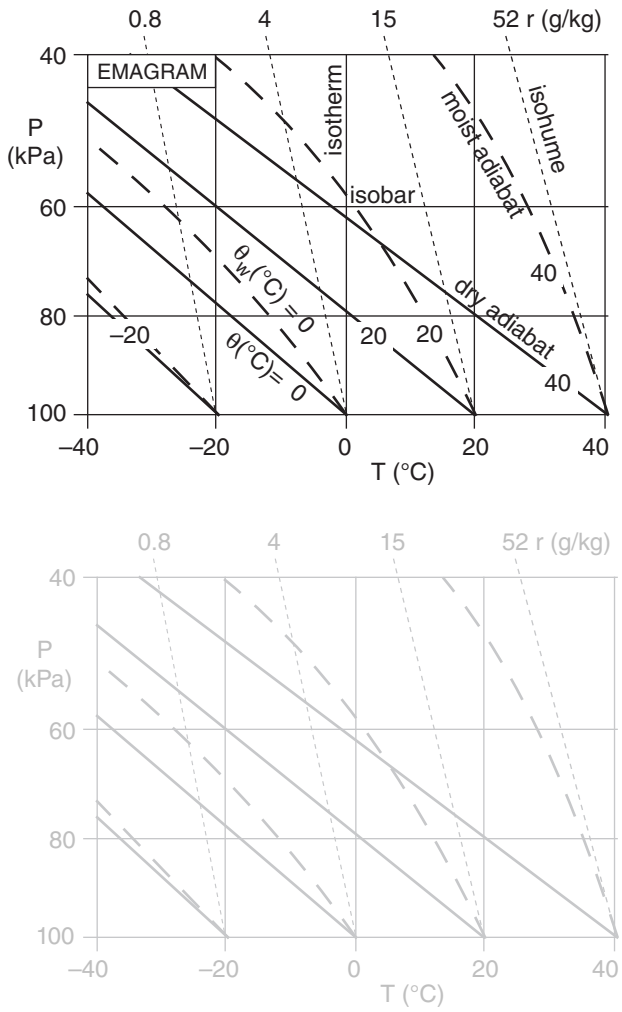

Figure 5.6
Simplified Emagrams. Top: with isopleths labeled. Bottom: with isopleths shaded grey to serve as a background for future discussions.

Solved Example *(continuation)*

4)

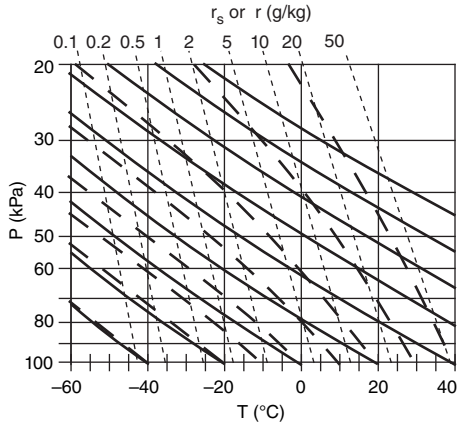

5)

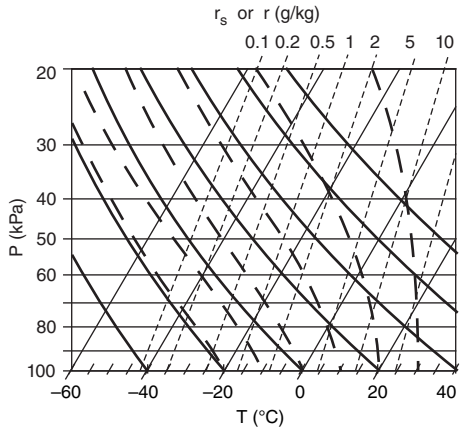

Solution: Use the quick guide.

1) **Stüve**, because satisfies item 2b in the guide.
2) **θ-Z diagram**, because satisfies item 1b.
3) **Tephigram**, because satisfies item 1c.
4) **Emagram**, because satisfies item 2a.
5) **Skew-T**, because satisfies item 1a.

Check: OK, agrees with Fig. 5.3.

Discussion: For practice, pick any one of the diagrams above, and without looking back in Fig. 5.3, try to identify which lines are which.

[Hint: in this book, all thermo diagrams use the same format for the same types of lines: isotherms and isobars are thin solid, isohumes are thin dotted, dry adiabats are thick solid, moist adiabats are thick dashed, and heights are thin dashed (if plotted at all). *CAUTION: Thermo diagrams printed or published by others do NOT follow any standard format of line style or color.*]

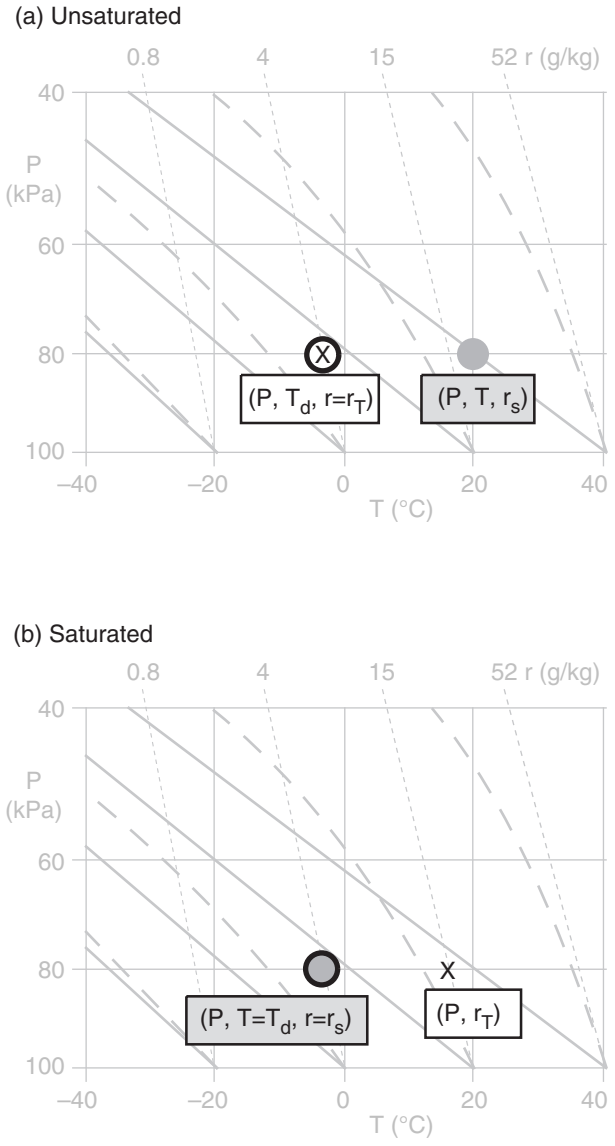

Figure 5.7
In general, three points are needed to represent one air parcel: the right circle (filled with grey) indicates air temperature, and the left circle (black outline) indicates dew-point temperature (as a measure of the amount of water vapor in the air). The X indicates total water content. (a) Unsaturated air. (b) Saturated air. (See the Solved Example for details)

Thermodynamic State

For any one air parcel, three points are needed to describe its state (i.e., its temperature, pressure, and humidity) on a thermo diagram. For this one air parcel at one height, all three points are always plotted on the same isobar (P).

One point represents T, the actual air temperature (grey filled circle in Fig. 5.7). Its coordinates in the thermo diagram are given by (P, T, r_s). Note that r_s is redundant, because it can be determined from P and T. But we include it for convenience, because we use the r_s value for many calculations.

Another point represents T_d, the dew-point temperature (black circle outline). Its coordinates are (P, T_d, r). Again, r is redundant.

The third point gives r_T, the total water mixing ratio in the air parcel (designated by "X" on the thermo diagram). Its coordinates are (P, r_T).

Often, two of these three points coincide. One example is for unsaturated air (Fig. 5.7a) with no rain falling through it. For this case, the temperature and dew-point circles are plotted as before. However, the X is plotted inside the dew-point circle because the total water in the air parcel equals the water-vapor mixing ratio ($r_T = r$), which is fully specified by the dew point. Namely, the isohume that passes through the dew-point circle indicates the actual amount of water vapor in the air, and there are no other phases of water in that air parcel.

The isohume that passes through the actual air temperature gives the saturation mixing ratio (r_s, the maximum equilibrium amount of moisture that could be held as vapor). A separate symbol is NOT plotted on the thermo diagram for r_s for two reasons. One, it does not indicate the actual state of the air parcel. Two, it is fully specified as the isohume that passes through the temperature point.

For saturated (cloudy or foggy) air parcels (Fig. 5.7b), the two temperature points coincide ($T = T_d$ and $r = r_s$). In this figure, the grey-filled circle still represents air temperature, and the black circle outline still represents the dew-point temperature (for water vapor). However, the total water X is usually to the right of the temperature circles, because clouds contain liquid water and/or ice in addition to water vapor. This is explained later.

[***Tip***: *On these figures, we use large size circles and X's to make them easier to see. However, when you plot them on your own thermo diagram, use smaller circles and X's that you write very precisely on the diagram. Also, you may use different colors for each symbol, such as red for temperature and blue for dew-point.*]

Processes

Dry (Unsaturated) Lifting

Suppose that an unsaturated air parcel rises without mixing with the surrounding environment, and with no radiative or other heat transfer to or from it. For this idealized situation, the temperature cools dry adiabatically due to the decreasing pressure, and any molecules (water and air) in the parcel stay in the parcel. Hence, both potential temperature θ and mixing ratio r are conserved.

On the thermodynamic diagram, this corresponds to moving the temperature point (grey filled circle) along the "dry" adiabat that passes through its initial position, and moving the moisture points (black outline circle and "X") along the isohume of constant r (NOT along a T_d line). Always move all three points together to the same pressure (see Fig. 5.8).

If the points don't lie directly on a drawn isopleth (which is usually the case), then imagine a new isopleth that goes through your point, and which is parallel to (and maintains its relative distance from) the neighboring drawn isopleths. You can do this by eye, or you may use a straight-edge to draw on the diagram a new isopleth that goes through your point of interest. Then, move the air parcel along this imaginary isopleth. Namely, move the temperature point in a direction parallel to the dry adiabats, and move the humidity point parallel to the isohumes.

Likewise, for descending air parcels that are unsaturated (and no mixing with the environment and no liquid water present), the temperature point follows the "dry" adiabat and the humidity points follow the isohume.

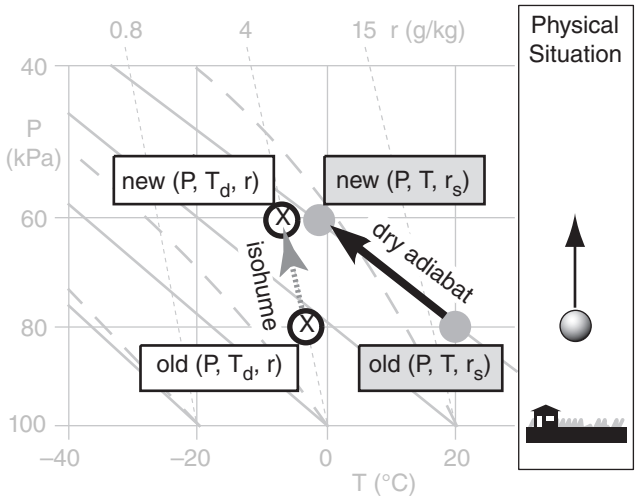

Figure 5.8
Potential temperature and mixing ratios are constant for rising unsaturated air. The new points still represent the one parcel. The new r equals the old r, although new r_s does not equal old r_s.

Solved Example

For the air parcel of Fig. 5.7a, find its temperature, dew point, pressure, mixing ratio, total water mixing ratio, saturation mixing ratio, and relative humidity.

Solution

Given: Fig. 5.7a. Estimate points by eye.
Find: T = ? °C, T_d = ? °C, P = ? kPa
r = ? g/kg, r_T = ? g/kg, r_s = ? g/kg,
RH = ? %

The grey circle on the right is directly on the **T = 20°C** isotherm. The temperature for the white circle on the left must be interpolated between the 0°C and –20°C isotherms. I estimate by eye roughly T_d = **–2.5°C**. The pressure, which must be the same for both points, is **P = 80 kPa** based on the isobar that passes through them.

Interpolating the right circle between isohumes gives roughly r_s = **19 g/kg**, while the actual mixing ratio using the left circle is **r = 4 g/kg**. For this unsaturated air parcel, the total water mixing ratio is $r_T = r$ = **4 g/kg**. Relative humidity is $RH = (100\%)\cdot(r/r_s) = (100\%)\cdot(4/19)$ = **21%**.

Check: Units OK. Physics OK.
Discussion: I actually used the larger thermo diagram at the end of this chapter to get these answers, because it is more accurate. The air is fairly dry.

If the two temperature points would have coincided, such as on a different day with fog (Fig. 5.7b), then $T - T_d$ = 0 °C, and $r_s - r$ = 0 g/kg.

Solved Example

Given Fig. 5.8, what is the new state of the air after being lifted dry adiabatically to P = 60 kPa?

Solution

Given: Fig. 5.8. Estimate points by eye.
Find: T & T_d = ? °C,
r, r_s & r_T = ? g/kg, and RH = ?%

The temperature, when moved along (or parallel to) the dry adiabats, has cooled to about **T = –3°C** at P = 60 kPa. The dew point temperature (X), when moved along (or parallel to) the isohumes, decreases slightly to T_d = **–6.5°C**.

Mixing ratio and total-water mixing ratio are still $r_T = r$ = **4 g/kg**, but saturation mixing ratio has decreased to r_s = 5 g/kg because the actual air temperature decreased. The new relative humidity is: $RH = (100\%)\cdot(4/5)$ = **80%**.

Check: Units OK. Physics OK.
Discussion: Although not yet saturated (i.e., not cloudy), the RH is increasing as the air parcel rises.

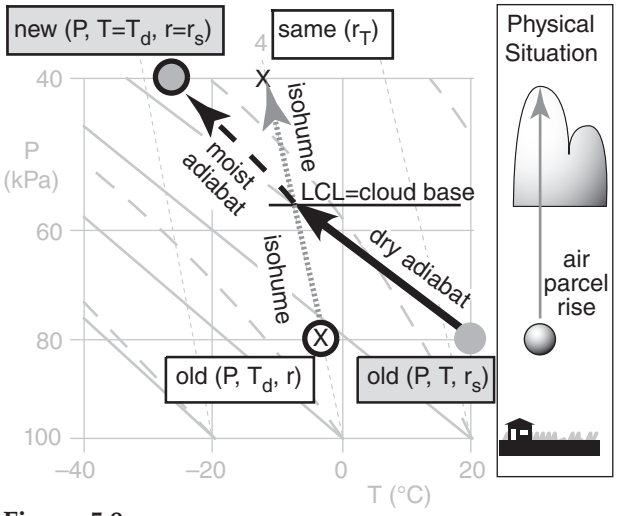

Figure 5.9

The height where the two points converge is the lifting condensation level (LCL). This is cloud base. As the saturated parcel continues to rise, the temperature points coincide and follow the moist adiabat. If no precipitation falls out of the parcel, then total water continues to follow the original isohume (indicated by X at same height as parcel).

Solved Example

Given the example in Fig. 5.9:

(a) At what pressure height is the LCL, and what is the state of the air parcel at that pressure?

(b) What is the state of the air parcel when it reaches a pressure height of 40 kPa?

(c) How much liquid water has been condensed out at that final height?

Solution

Given: Fig. 5.9. Estimate points by eye.

Find: (a) P_{LCL} = ? kPa, $T = T_d$ = ?°C, $r = r_s = r_T$ = ? g/kg

(b) $T = T_d$ = ?°C, $r = r_s$ = ? g/kg, r_T = ? g/kg

(c) r_L = ? g/kg

Using the diagram:

(a) The LCL is at roughly P_{LCL} = **57 kPa**. The parcel is just barely saturated, with temperature and dew points of roughly $T = T_d$ = **–7°C**. The mixing ratio is still $r = r_s = r_T$ = **4 g/kg**.

(b) Moving parallel to the moist adiabat, from the LCL up to P = 40 kPa, the final state is $T = T_d$ = **–25.5°C**. The saturation mixing ratio is now only $r = r_s$ = **1.2 g/kg**. If no precipitation, then total water is unchanged at r_T = **4 g/kg**.

(c) $r_L = r_T - r_s = 4 - 1.2 =$ **2.8 g/kg**.

Check: Units OK. Physics OK.

Discussion: Liquid water amount not only indicates the amount of rainfall possible, but for conditions below freezing it indicates the rate of ice formation on aircraft wings, a hazard to flight. Most commercial jet aircraft heat the leading edge of the wing to prevent ice formation.

Moist (Saturated) Lifting & Liquid Water

Adiabats and isohumes converge with increasing height. Thus, for a rising air parcel there will be some height where the temperature and dew-point coincide. At this altitude or pressure, the air is just saturated. Hence this altitude corresponds to convective (cumulus) cloud base. It is called the **lifting condensation level** (**LCL**), (Fig. 5.9). At this point, all three marks (grey filled circle, black outline circle, and "X") representing the air parcel coincide. Namely, $T_d = T$, and $r = r_s = r_T$ at the LCL.

For air rising above its LCL, T and T_d cool together moist adiabatically, maintaining $T_d = T$. Thus, on the thermo diagram we do not need two circles because there is only one temperature. In Fig. 5.9, this one temperature is represented by the black circle filled with grey. However, we still need to keep track of total water, as indicated by the X in Fig. 5.9. If all water molecules stay in the parcel (i.e., if cloud droplets move with the air and do not precipitate out), then total water mixing ratio r_T remains constant.

The difference between the actual mixing ratio in the cloudy air (using the isohume associated with the parcel's temperature) and the original mixing ratio before the parcel was lifted (indicated by the total water) gives the amount of liquid or solid water that has condensed or deposited. Namely, $r_L = r_T - r_s$. In Fig. 5.9, this is the difference between the X and the grey circle representing the new state of the parcel.

For descending saturated air, follow the total water mixing ratio (from point X) down the isohume, and follow the temperature state down the moist adiabat until they intersect. This intersection point indicates cloud base (LCL) for descending air. At the LCL, split the parcel temperature point into two points representing temperature and dew point, and follow them down the dry adiabat and isohume respectively. The total water (X) coincides with the dew-point below the LCL. The result is exactly as sketched in Fig. 5.9 except all arrows would be in the opposite direction. The reason is that below the LCL, the descending air has warmed sufficiently to hold all the water as vapor.

Precipitation

When liquid or solid water precipitates out, the X point representing total water moves to the left along an isobar on the thermo diagram (Fig. 5.10).

If all the liquid or solid water falls out, then the X on the thermo diagram would move all the way to the circle representing the parcel temperature. If the parcel were to then descend, it would do so dry adiabatically, with T following a dry adiabat, and total water and T_d following the isohume.

If only some of the rain or ice falls out, then the X would move only part way toward the parcel tem-

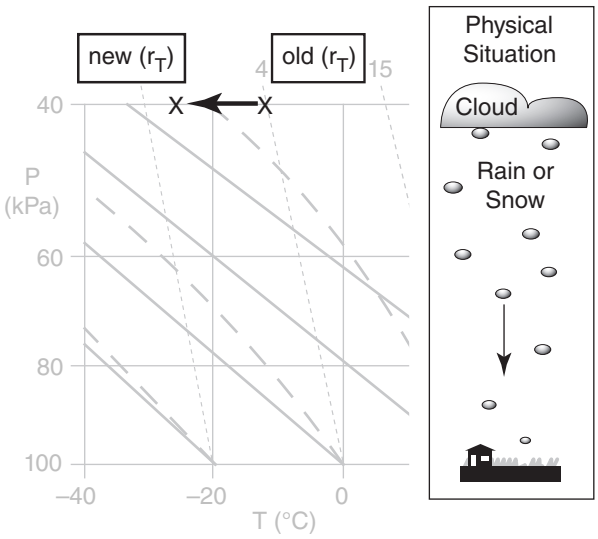

Figure 5.10
Reduction of total water due to precipitation. The new X point cannot be further left than the temperature of the air parcel.

perature. The new X must then be used as the starting point for total water if the parcel rises further or descends. Namely, the X-point stays on its new isohume during vertical parcel movement. If this parcel descends, it will reach its new LCL at a height greater than its original LCL.

The rain or snow that falls out of the parcel implies net heating. It is an irreversible process. Namely, the latent heating of condensation that occurred in the rising air is not balanced by evaporation in the descending air, because there is now less liquid or solid water to evaporate.

Radiative Heating/Cooling

Clouds are opaque to IR radiation, and translucent to visible light. This can warm or cool the cloudy air, but it does not alter the total-water mixing ratio. Such warming or cooling is said to be **diabatic**, because there is heat transfer across the "skin" of the cloudy air parcel. (Recall that "adiabatic" means no heat transfer.)

There is net heat loss by IR radiation upward from cloud top toward space, both day and night. Also, cloud base will exchange IR radiation with the ground and with the underlying air. If the ground is warmer than cloud base, then cloud base will warm if the cloud is low enough.

Sunlight can penetrate into the cloud top (and sides of cumuliform clouds) during daytime, with an e-folding extinction distance on the order of meters. The absorption of sunlight warms the cloudy air parcel. Not all the sunlight is absorbed by the cloud droplets. Some scatters and rescatters off the

Solved Example

From the previous solved example, suppose that 1 g/kg of liquid water falls out, leaving the remaining liquid water as cloud droplets that stay with the parcel. If this parcel descends, what is its new LCL and thermo state back at P = 80 kPa?

Solution

Given: Fig. 5.10, $r_{T\,old}$ = 4 g/kg, and r_{precip} = 1 g/kg
Find: P_{LCL} = ? kPa, r = ? g/kg, T & T_d = ? °C.

The amount of total water remaining in the cloud is $r_{T\,new} = r_{T\,old} - r_{precip} = 4 - 1 = 3$ g/kg.
Follow the r_T = 3 g/kg isohume down until it crosses the moist adiabat of the parcel. The intersection pressure height is the new LCL: about P_{LCL} = **52 kPa**.

Starting from this intersection, create two points, where the temperature point follows the dry adiabat down to P = 80 kPa, and the dew-point point follows the mixing ratio down. This gives: **r ≈ 3 g/kg**, $T_d \approx$ **–6.5 °C**, and **T ≈ 23°C**.

Check: Units OK. Physics OK.
Discussion: The parcel is warmer and drier than when it started (in the first solved example), because the precipitation removed some water, and caused net latent heating due to condensation.

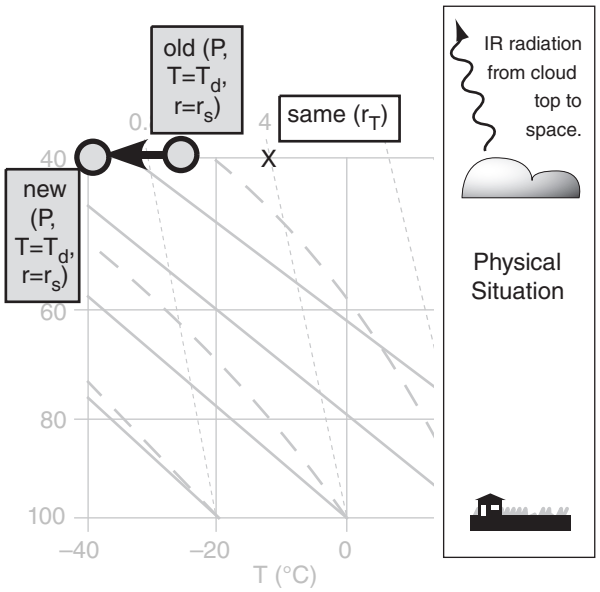

Figure 5.11
Radiative cooling of cloud top. The total water mixing ratio (X) does not change, but temperature and dew point decrease. As less of the total water can be held as vapor at equilibrium, the remainder condenses into additional liquid water.
Thus, $r_{L\,new} = r_T - r_{s\,new}$.

Solved Example

Given the example in Fig. 5.11 with initial $T = –25°C$ and $r_T = 4$ g/kg at cloud top ($P = 40$ kPa). What is the new state of the air in cloud top after IR radiation has cooled the air to –40°C? Also find the liquid water mixing ratio.

Solution

Given: Fig. 5.11, $T = –25°C$, $r_T = 4$ g/kg
Find: T & T_d = ? °C, r & r_s = ? g/kg, r_L = ? g/kg

Initially:
Because the air is saturated, $T_d = T = –25°C$.
Also, $r_T = 4$ g/kg .
Using a large thermo diagram from the end of this chapter, $r = r_s = 1.3$ g/kg.
Thus, $r_L = r_T – r_s = 4 – 1.3 = 2.7$ g/kg.

Finally:
The air is still saturated, $T_d = T =$ **–40°C**.
Total water is unchanged: $r_T =$ **4 g/kg**.
Using a large thermo diagram, $r = r_s =$ **0.3 g/kg**.
Thus, $r_L = r_T – r_s = 4 – 0.3 =$ **3.7 g/kg**.

Check: Units OK. Physics OK.
Discussion: Liquid water mixing ratio has increased as temperature decreased at cloud top.

At $T = –40°C$, any supercooled liquid water will spontaneously freeze into ice particles (see the Precipitation chapter). When this happens, first set $r_{ice\ new} = r_{L\ new}$, and then reset $r_{L\ new} = 0$.

droplets, eventually leaving the cloud. This is why clouds look white during daytime.

At night, when IR cooling from cloud top dominates, cloud top becomes colder, and the cold parcels of cloudy air sink through the cloud and cause turbulence and mixing. The whole cloud becomes colder this way, even though only the top few centimeters experience the direct IR net radiative loss to space.

Fig. 5.11 illustrates net IR cooling at cloud top. As temperature decreases, so must dew point, because the air is saturated and $T_d = T$. However, the colder air can hold less water vapor at equilibrium than before, thus $r = r_s$ decrease. Although total water remains constant, the liquid water mixing ratio increases: $r_{L\ new} = r_T – r_{s\ new}$.

During daytime, the top few centimeters of the cloud are still cooled by net IR radiative loss, but the top few meters are warmed by sunlight. The sum could be either positive or negative when averaged over the whole cloud. However, with cooling happening at the top of the cloud while warming occurs lower in the cloud, turbulence is set up by the cold sinking air and warm rising air.

In short-lived cumulus clouds, the buoyancy of the thermal updraft rising from the ground often dominates, allowing radiative effects to be neglected. However, for stratiform clouds, and longer-lived thunderstorms and hurricanes, radiative effects can be important.

FOCUS • LeChatelier's Principle

LeChatelier examined a few reacting chemicals in equilibrium with each other in a beaker. By adding more of one of the chemicals, he disturbed the equilibrium. Reactions then occurred to partially eliminate the excess chemical, thereby bringing the reagents in the beaker to a new equilibrium.

LeChatelier's notions of chemical equilibria are easily generalized to describe circulations in the atmosphere. When solar heating induces static instabilities in the atmosphere, the atmosphere generates circulations (i.e., convection) to eliminate the instability and reach a new equilibrium.

For situations where the atmosphere is continuously being destabilized by solar heating of the ground, the atmosphere reacts by creating continuous convection (thermals, or cumulus). Similarly, continuous dynamic destabilization creates continuous turbulence, as a reaction that reduces wind shear by mixing.

Science Graffito

"If you come to a fork in the road, take it."
– Yogi Berra.

Science Graffito

"...the purpose of knowledge is to appreciate wonders [of nature] even more."
– Richard Feynman, 1999: *The Pleasure of Finding Things Out: The Best Short Works of Richard Feynman*.

Solved Example

Air initially at 100 kPa has temperature 40°C and dew-point temperature of 20°C. It rises to a height where the pressure is 50 kPa. Precipitation reduces the total water by 5 g/kg, and the parcel radiatively cools by 11°C while at cloud top. Finally, the parcel descends back to 100 kPa. What is the final relative humidity?

Solution

Given: $T = 40°C$ and $T_d = 20°C$ at $P = 100$ kPa.
Find: $RH = ?\%$ at $P = 100$ kPa after all processes.

Method: Use a large thermo diagram from the end of this chapter, for better accuracy. (Fig. 5.6 is shown below to illustrate what was actually accomplished with the larger thermo diagram.)

The initial condition is plotted as the two points initially at $P = 100$ kPa, in the Fig below. The initial temperature happens to be on the $\theta = 40°C$ dry adiabat, and the initial dew point happens to be on the $r = 15$ g/kg isohume.

Follow the dry adiabat (black arrow) and isohume (dotted arrow) up from their starting points, until those isopleths cross. This crossing point is the upward- bound LCL (i.e., cloud base) and is at $P_{LCL} = 75$ kPa and $T_{LCL} = 15°C$ for this example.

This LCL point happens to lie on the $\theta_w = 25°C$ moist adiabat. Above the LCL, follow this moist adiabat up to the pressure of 50 kPa. The parcel temperature is roughly $T = 1°C$. Also, continue tracking the total water (indicated by the X) as it follows the $r_T = 15$ g/kg isohume up.

At the cloud top, the temperature drops by 11°C, from 1°C to –10°C. This puts the temperature near the $\theta_w = 18°C$ moist adiabat (interpolating by eye between the $\theta_w = 15$ and 20°C moist adiabats) on the large thermo diagram. Precipitation removes 5 g/kg, leaving the total water content at $r_T = 15 - 5 = 10$ g/kg (see gray X's).

(continued next column)

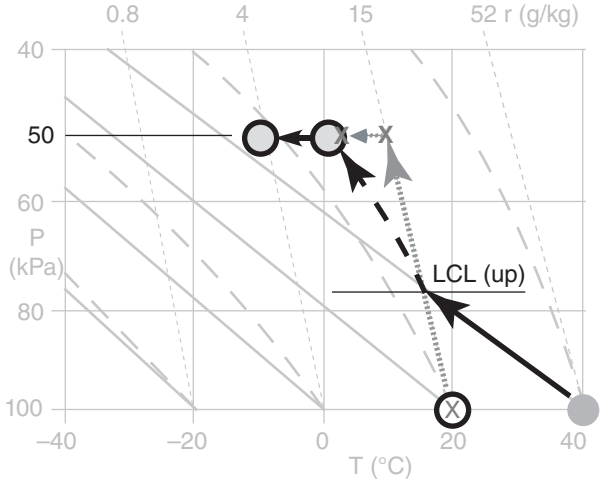

Solved Example (continuation)

Then the parcel descends. From the new temperature point at the cloud top ($T = –10°C$ at $P = 50$ kPa), follow the new moist adiabat down (see Fig. below). From the new total water point ($r_T = 10$ g/kg at $P = 50$ kPa), follow the isohume down.

Where they cross is the LCL for the descending air. $P_{LCL} = 80$ kPa, which is different than the initial LCL because of the irreversible diabatic processes that acted on the parcel (i.e., radiative cooling, and loss of water). The temperature at this new LCL is roughly $T = 10°C$.

Continuing down below the LCL, temperature follows a dry adiabat down to $P = 100$ kPa. The final temperature is roughly $T = 28°C$. Mixing ratio follows the 10 g/kg isohume, which gives a final dew point of $T_d = 14°C$.

At the final temperature, the saturation mixing ratio is roughly $r_s = 25$ g/kg (interpolating by eye between the 20 and 30 g/kg isohumes on the large thermo diagram). Thus, the final relative humidity is:

$RH = r/r_s = (10 \text{ g/kg}) / (25 \text{ g/kg}) =$ **40%**.

Check: Units OK. Physics OK.

Discussion: It helps to use different colors for the temperature and the mixing ratio lines, to avoid confusion. The initial humidity was $RH = 15/52 = 29\%$. So the final air parcel is cooler, with larger RH but smaller T_d.

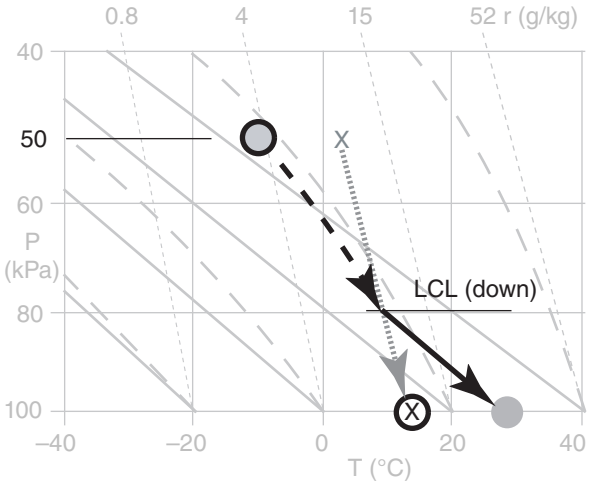

Solved Example

Plot the following sounding on (a) an emagram; and (b) a Skew-T, and discuss the differences.

P (kPa)	T_d (°C)	T (°C)
40	–40	–20
50	–30	–10
60	–5	–5
70	0	0
80	–5	10
90	9	10
99	9	19
100	11	25

Solution

a) Emagram: Using black points and solid lines for T, and white points and dashed lines for T_d:

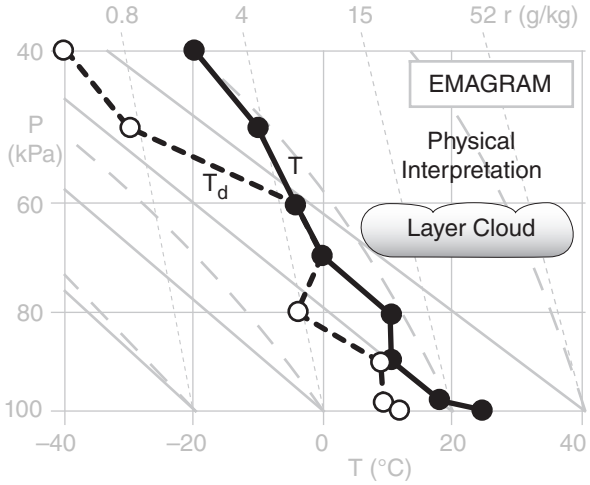

b) Skew-T.

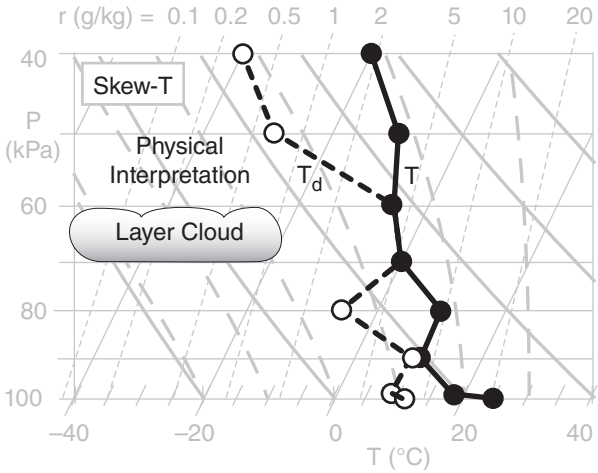

Check: Sketches OK. It is always true that $T_d \leq T$.

Discussion: The kinks in the Skew-T are more apparent than in the Emagram, making it easier to interpret the layers. Both indicate the layer of air between P = 70 and 60 kPa is cloudy, because the temperature and dew points are equal. These are mid-level clouds, and would be identified as altostratus or altocumulus. Air aloft near 40 kPa is very dry, because the temperature - dewpoint spread is large. Near 90 kPa the air is almost saturated; namely, the relative humidity is very high because the temperature - dewpoint spread is small.

PARCELS VS. ENVIRONMENT

Air parcels do not move through a vacuum. They are moving through air that is already present at all heights and locations in the atmosphere. We call this omnipresent air the **environment**. Of course much of the air in the environment got there by moving from somewhere else; however, for simplicity we will assume in this chapter that environmental movement is small compared to the movement of parcels through it.

Soundings

As stated at the start of this chapter, the vertical profile of environmental conditions is called an **upper-air sounding**, or just a **sounding**. The word "sounding" is used many ways. It is the:

- activity of collecting the environment data (as in "to make a sounding").
- data that was so collected (as in "to analyze the sounding data").
- resulting plot of these data on a thermo diagram (as in "the sounding shows a deep unstable layer").

Traditionally, a sounding is collected from an expendable instrument (called a **sonde**) hanging on a **weather balloon** that rises through the ambient environment and radios back its observations to a receiving station. In addition to such **radiosondes** (and **rawinsondes** that also give winds) there are **rocketsondes** lofted by small sounding rockets, and **dropsondes** dropped by parachute from aircraft. **Remote sensors** are also used to observe the atmosphere from the ground or from satellite (see the Remote Sensing chapter).

Regardless of the mechanics of acquiring a sounding, the purpose is to determine the state of the environmental air at various heights at some instant in time. The end result is a **vertical profile** of temperature, pressure, humidity, and winds in the environment. Density is rarely measured directly, but can easily be computed using the ideal gas law. Constituents such as ozone and other pollutants can also be measured. At any height, the decrease of temperature with height is called the **environmental lapse rate**.

Plotting an environmental sounding is similar to that for individual parcels. Each measurement of environmental temperature and humidity at any one height (pressure) is plotted as two points on the thermo diagram for unsaturated air. For cloudy air, the T_d points coincide with the T points. Usually, straight lines are drawn connecting the temperature points (see Focus box on **mandatory** and **significant levels**), and separate straight lines are drawn for the humidity points for unsaturated air. Liquid

or ice mixing ratios are not usually measured by the radiosondes, but can be obtained by **research aircraft** flying slant ascent or descent soundings.

The "standard atmosphere" (see Chapter 1) is an example of a hypothetical environmental sounding.

Buoyancy

As Archimedes discovered, an object that is immersed in a fluid displaces some of the fluid, resulting in buoyant forces on the object. The gravitational force minus the buoyant force gives the net specific force F (i.e., force/mass) acting on an object in a fluid:

$$\frac{F}{m} = \frac{\rho_o - \rho_f}{\rho_o} \cdot g = g' \qquad (5.2)$$

where m is the mass of the object, ρ_o and ρ_f are the densities of the object and fluid, respectively, and g = –9.8 m·s^{-2} is the gravitational acceleration, where the negative sign implies a downward acceleration. The right hand side of eq. (5.2) is called the **reduced gravity**, g', where the sign of g' can be different than the sign of g, depending on whether the net buoyant force is up or down.

The force F is the weight of the object, and is defined to be positive in the same direction that g is positive. Negative F implies a downward force (sinking), and positive implies an upward force (floating). Zero force is said to be **neutrally buoyant**.

Air parcels can also be considered as objects within a fluid of the surrounding environmental air. Plugging the ideal gas law into eq. (5.2) and rearranging gives the reduced gravity for an air parcel:

$$\frac{F}{m} = \frac{T_{ve} - T_{vp}}{T_{ve}} \cdot g = g' \qquad (5.3a)$$

where T_{ve} and T_{vp} are the absolute virtual temperatures (Kelvin) of the environment and parcel at the same altitude or same pressure. For relatively dry air, the approximation that $T_v \approx T$ is often used.

$$\frac{F}{m} \approx \frac{T_p - T_e}{T_e} \cdot |g| = g' \qquad (5.3b)$$

Warm air rises, as given in eq. (5.3). More precisely, a parcel that is warmer than its environment experiences an upward buoyant force.

On a thermodynamic diagram, buoyancy is determined by comparing the temperature of an air parcel against the temperature of the environment at the same height or pressure. An air parcel is assumed to move vertically in the direction of the buoyant force. Of course, as it moves its temperature changes according to the appropriate moist (cloudy) or dry (non-cloudy) process (Fig. 5.12).

Thus, at each new height, the new parcel temperature must be compared to the environment temperature at its new altitude, and the new buoy-

FOCUS • Mandatory & Significant Levels

Rising rawinsondes record the weather at $\Delta z \approx 5$ m increments, yielding data at about 5000 heights. To reduce the amount of data transmitted to weather centers, straight-line segments are fit to the sounding, and only the end points of the line segments are reported. These points, called **significant levels**, are at the kinks in the sounding (as plotted in the previous solved example). Additional **mandatory levels** at the surface and 100, 92.5, 85, 70, 50, 40, 30, 25, 20, 15, 10, 7, 5, 3, 2, & 1 kPa are also reported, to make it easier to analyze upper-air charts at these levels.

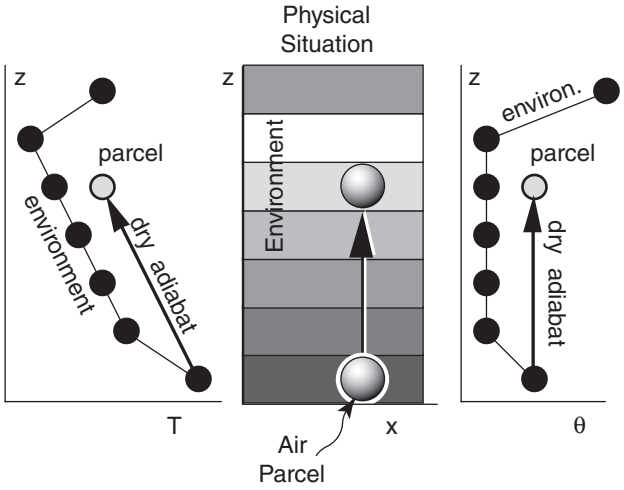

Figure 5.12
Comparison of temperature T(z) methods and potential-temperature θ(z) methods of representing parcel movement through the environment. Darker shades in the center sketch represent warmer temperatures T. Horizontal distance is x. Thin lines in the left and right plots show the environmental sounding. Thick lines show the adiabatic process for the rising air parcel.

Solved Example

Find the buoyant force per mass acting on an air parcel of temperature T_p = 20°C in an environment of temperature T_e = 15°C.

Solution

Given: T_p = 20+273 = 293 K , T_e = 15+273 = 288 K
Find: F/m = ? m·s^{-2}

Assume dry air, so $T_v = T$. Use eq. (5.3a):
F/m = (288 K – 293 K)·(–9.8 m·s^{-2}) / 288 K
= **0.17 m·s^{-2}**

Check: Physics OK. Units don't look like a force per unit mass, but using conversions from Appendix A, the answer can also be written as 0.17 N/kg. Thus, acceleration is equivalent to force per unit mass in classical physics.

Discussion: The positive sign of the answer means an upward buoyant force. Hot air indeed rises.

Solved Example

a) Convert the following sounding to potential temperatures, and plot on a linear graph.

b) If a piece of the environment at P = 100 kPa separates from the rest and rises as an air parcel, what is the resulting potential temperature difference between the parcel and environment at P = 90 kPa?

P (kPa)	T (°C)
80	10
90	10
99	19
100	25

Solution

Given: Sounding above

Find: $\theta(z)$ and plot it.

$\Delta\theta$ at P = 90 kPa

Method

a) You could use equations from the Heat chapter to convert from T to θ, but it is easier to pick off these numbers from the large thermo diagram at the end of this Chapter.

P (kPa)	θ (°C)
80	28.5
90	18.5
99	20
100	25

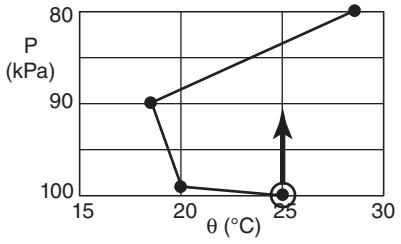

b) Air parcel retains θ = 25°C as it rises. Thus at P = 90 kPa: $\Delta\theta$ = 25 – 18.5°C = **6.5°C**.

Check: Units OK. Physics OK.

Discussion: You would find the same temperature difference using a thermo diagram, without any calculation of potential temperature. Namely, $\Delta T = \Delta\theta$.

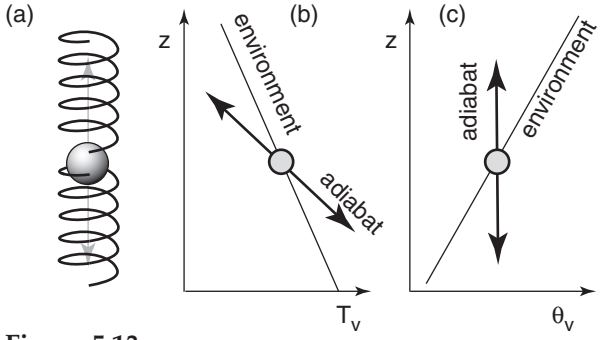

Figure 5.13

(a) A mass constrained between two springs will oscillate up and down if displaced from its equilibrium height. The same will happen for an air parcel displaced vertically in a statically stable environment, regardless of whether it is plotted as (b) virtual temperature T_v or (c) virtual potential temperature θ_v.

ant force can then be estimated to determine if the parcel continues to rise or not. Similar procedures must be used for downward moving parcels.

Virtual potential temperatures (see eqs. 3.13 and 3.14) can be used instead of virtual temperature for plotting soundings and determining buoyancy.

$$\frac{F}{m} = \frac{\theta_{ve} - \theta_{vp}}{T_{ve}} \cdot g = g' \qquad (5.3c)$$

Do not forget that g is negative in eqs. (5.3). Thus, parcels that are warmer than their environment cause a negative ratio on the RHS, which when multiplied by the negative gravity gives a positive (upward) force (i.e., warm air wants to move upward). If you use gravitational acceleration as a magnitude:

$$\frac{F}{m} = \frac{\theta_{vp} - \theta_{ve}}{T_{ve}} \cdot |g| = g' \qquad (5.3d)$$

An example is sketched in Fig. 5.12. The left diagram represents the parcel and environment as it would be plotted on a thermo diagram such as the Emagram of Fig. 5.3a. The air parcel cools as it rises. The right diagram represents the same situation, but in terms of potential temperature θ vs. height z (Fig. 5.3e). The center sketch shows the parcel rising through the environment, where the darker shading represents warmer temperatures T.

Thermo diagrams such as Fig. 5.3 also give θ, so instead of solving equations we can pick-off θ from the graph. The buoyancy of an air parcel at any height is proportional to the potential temperature difference between the parcel and the environmental sounding at the same height or pressure.

The advantage of using potential temperature is that the parcel maintains constant θ as it moves dry adiabatically. That is, it moves vertically on a θ-Z graph. It is for this reason that the θ-Z thermo diagram of Fig. 5.3e is designed. Also, as a conserved variable it is convenient to use in numerical weather-prediction models (see the NWP chapter).

Brunt-Väisälä Frequency

In a statically stable environment, an air parcel behaves like a mass hanging between two springs (Fig. 5.13a). When displaced vertically from its rest position, the mass experiences a restoring force. As it accelerates back toward its equilibrium point, inertia causes it to overshoot. During this overshoot, the net spring force is in the opposite direction. The mass decelerates and changes direction. It overshoots again and again, giving an oscillation.

When an air parcel is lifted from its starting equilibrium height, it becomes colder than the environment due to adiabatic cooling (Fig. 5.13b & c), and

the buoyancy force acts downwards. The parcel accelerates downward but overshoots below its starting point, adiabatically warming during its descent to become hotter than the environment, thereby causing a buoyancy force that acts upward. Thus, buoyancy force acts to restore the parcel to its starting point, but inertia causes it to overshoot, the net result being an oscillation.

The frequency of oscillation is called the Brunt-Väisälä frequency, N_{BV}:

$$N_{BV} = \sqrt{\frac{|g|}{T_v} \cdot \left(\frac{\Delta T_v}{\Delta z} + \Gamma_d \right)} \qquad \bullet(5.4a)$$

or

$$N_{BV} = \sqrt{\frac{|g|}{T_v} \cdot \frac{\Delta \theta_v}{\Delta z}} \qquad \bullet(5.4b)$$

where virtual temperature must be in Kelvin in the denominator, and where the frequency has units of radians/s. For relatively dry air, it is often assumed that $T_v \approx T$, and $\theta_v \approx \theta$. Frequency increases as static stability increases, analogous to stiffening of the spring. The frequency is undefined for unstable air.

The period of oscillation (time to complete one full oscillation) is

$$P_{BV} = \frac{2\pi}{N_{BV}} \qquad (5.5)$$

As the static stability approaches neutral, the period of oscillation approaches infinity. In the real atmosphere, frictional drag on the parcel rapidly damps the oscillation.

Solved Example

Find the period of oscillation of a displaced air parcel in an isothermal environment of 300 K.

Solution

Given: $\Delta T/\Delta z = 0$, $T = 300$ K.
Find: $P_{BV} = ?$ s

Assume dry air. Combine eqs. (5.4a) and (5.5):

$$P_{BV} = \frac{2\pi}{\sqrt{\frac{|g|}{T} \cdot \left(\frac{\Delta T}{\Delta z} + \Gamma_d \right)}}$$

$$P_{BV} = \frac{2\pi}{\sqrt{\frac{(9.8\text{m}\cdot\text{s}^{-2})}{300\text{K}} \cdot (0 + 0.0098\text{K/m})}} = \underline{\mathbf{351\ s}}$$

Check: Units OK. Physics OK.
Discussion: This period equals 5.9 minutes, which is greater than most water-surface wave periods you might see from a ship. Atmospheric oscillations are so slow that you usually cannot see them by eye. However, a time-lapse camera captures these oscillations quite easily, using smoke as a tracer. Wave clouds (lenticular) are caused by these oscillations (Chapters 6 & 17).

BEYOND ALGEBRA
• Brunt-Väisälä Frequency

Setting up the Problem

An air parcel that moves up and down during an oscillation is governed by Newton's second law, $F = m \cdot a$, which will be covered in the Dynamics chapter. F is force, m is mass, and a is acceleration. Dividing both sides by m, and using the definition of acceleration as change of velocity w with time t gives:

$$F/m = \mathrm{d}w/\mathrm{d}t$$

Buoyant F/m is given by eq. (5.3d), and vertical velocity is defined as change of height z with time; namely, $w = \mathrm{d}z/\mathrm{d}t$. Thus:

$$\frac{\theta_{v\,p} - \theta_{v\,e}}{T_{v\,e}} \cdot |g| = \frac{\mathrm{d}^2 z}{\mathrm{d}t^2}$$

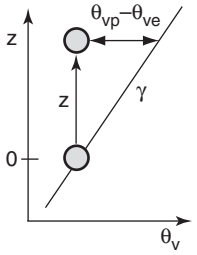

For simplicity, consider the environment shown at right, where environmental virtual potential temperature θ_{ve} increases linearly with height at rate $\gamma = \partial\theta_v / \partial z$. Define $z = 0$ at the initial (rest) height of the air parcel. From the geometry shown in the diagram, a parcel displaced upward by distance z will be cooler than the environment by: $\theta_{vp} - \theta_{ve} = -z \cdot \gamma$. Using this in the eq. above gives:

$$-|g| \cdot \gamma \cdot z / T_{v\,e} = \mathrm{d}^2 z / \mathrm{d}t^2$$

Define $|g| \cdot \gamma / T_{ve} = N_{BV}^2$ (see eq. 5.4b). Thus:

$$\boxed{\mathrm{d}^2 z / \mathrm{d}t^2 = -N_{BV}^2 \cdot z} \qquad (a)$$

This is a simple 2nd-order differential equation.

The Solution

From the bag of tricks learned in Diff. Eqs. class, assume a solution of the form:

$$z = A \cdot \sin(f \cdot t) \qquad (b)$$

where A and f are unknown amplitude (in units of m) and oscillation frequency (in radians/s). Plugging (b) into (a) gives:

$$-f^2 \cdot A \cdot \sin(f \cdot t) = -N_{BV}^2 \cdot A \cdot \sin(f \cdot t)$$

Canceling the A and sine terms leaves: $\boxed{f = N_{BV}}$. Thus, the variation of air-parcel height with time is:

$$\boxed{z = A \cdot \sin(N_{BV} \cdot t)} \qquad (c)$$

Discussion

N_{BV} is the frequency of air-parcel oscillation in radians/s. Use (5.5) to rewrite (c) as:

$$z = A \cdot \sin(2\pi \cdot t / P_{BV})$$

As t increases from 0 to P_{BV}, the argument of the sine goes from 0 to 2π, causing one full cycle.

FLOW STABILITY

Flow stability indicates whether the atmosphere will develop turbulence or will allow waves to grow. We will focus on turbulence of all scales here, from the smallest eddies near the ground to deep convection and thunderstorms filling the troposphere.

- **Unstable** air becomes, or is, turbulent (irregular, gusty).
- **Stable** air becomes, or is, **laminar** (non-turbulent, smooth).
- **Neutral** air has no tendency to change (i.e., is neither stable nor unstable).

Flow stability is controlled by ALL the processes acting on the flow. However, to simplify our understanding of flow, we sometimes focus on just a subset of processes. **Static stability** considers only buoyancy to estimate flow stability, and ignores shears in the mean wind. "Static" means not-moving. **Dynamic stability** considers both wind shears and buoyancy.

Static Stability

One way to estimate static stability is by hypothetically moving a small air parcel through a horizontally-large quasi-stationary environment. Another is to lift whole environmental layers. We will look at both methods.

Parcel Method for Static Stability

To determine static stability, a small portion of the environmental air can be conceptually displaced from its starting point and tracked as an air parcel, such as sketched in the middle part of Fig. 5.12. When conceptually moving this air parcel, follow a dry adiabat while the air is unsaturated (i.e., below its LCL), otherwise follow a moist adiabat. At any height, the buoyant force is based on the temperature difference between the parcel and the environment surrounding it.

> • Rule for Determining Static Stability •
> First, find unstable domains using the nonlocal method described next. Then find neutral and stable layers using the local lapse rate, but only in the remaining regions that were not unstable.

Statically Unstable (U): If the buoyant force on a displaced parcel is in the same direction as the displacement, then the air between the initial parcel height and the displaced height is unstable (see Fig. 5.14). Because of this instability, the parcel will continue accelerating in the direction of its initial movement. This results in **convective** circulations (vertical motions driven by buoyancy), and perhaps convective clouds.

In some environments, it is possible for such an unstable parcel to move across large vertical distances before reaching a height where there is no net buoyancy force. In such a case, the whole vertical domain of buoyant movement of the air parcel is statically unstable. Thus, statically unstable air must be determined by **nonlocal** air parcel movement.

> • Rule for Determining Unstable Regions •
> Parcels from each relative θ maximum in the environmental sounding should be conceptually lifted adiabatically until they hit the sounding, and those from each relative minimum should be lowered adiabatically, until they hit the sounding or hit the ground (Fig. 5.14). The domains spanned by these conceptual parcel movements define the statically unstable regions.

For this rule, remember to follow a dry adiabat below the LCL of the conceptual parcel, but follow a moist adiabat above the LCL. Each parcel from each relative max or min will have its own LCL.

A **relative maximum** is a height with warmer θ than the neighboring environmental points just above and below it. Similarly, a **relative minimum** is a height with cooler θ than the neighboring points just above and below it. Using large size thermo diagrams, it is easy to identify by eye the relative max and min θ points, and easy to conceptually raise or lower air parcels until they hit the sounding.

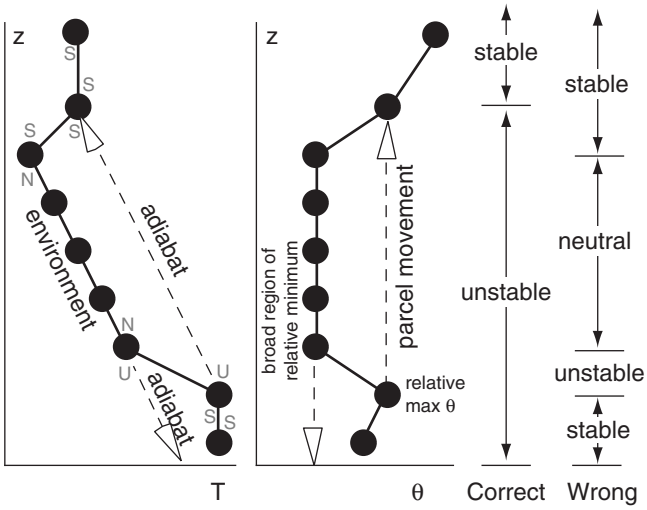

Figure 5.14
Example of correct static stability determination using parcel displacement. Incorrect determination utilizes lapse rates only. If the displaced parcel becomes saturated, follow a moist adiabat instead of a dry adiabat. Grey U, N, S are for the "apex" method of determining nonlocal static stability.

Statically Neutral (N): Those portions of the sounding where the environmental lapse rate approximately equals the adiabatic lapse rate, *and which are* not *otherwise nonlocally unstable*, are approximately statically neutral. A parcel displaced in this environment will feel no buoyant forces. The equations describing this lapse rate (in terms of either temperature T or potential temperature θ), are:

$$\frac{\Delta T}{\Delta z} \approx -\begin{cases}\Gamma_d & \text{if unsaturated}\\ \Gamma_s & \text{if saturated}\end{cases} \quad \bullet(5.6a)$$

or

$$\frac{\Delta \theta}{\Delta z} \approx \begin{cases}0 & \text{if unsaturated}\\ \Gamma_d - \Gamma_s & \text{if saturated}\end{cases} \quad \bullet(5.6b)$$

where Γ_d = 9.8 K/km is the dry adiabatic lapse rate, and Γ_s is the saturated (or moist) adiabatic lapse rate (which varies, see the Moisture chapter), but which is always a positive number.

Statically Stable (S): Those portions of the sounding where the temperature does not decrease with height as fast as the adiabatic rate (including isothermal layers, and **temperature inversion** layers where temperature increases with height), *and which are* not *otherwise nonlocally unstable*, are statically stable. A parcel displaced in this environment will experience buoyant forces opposite to the direction of displacement.

$$\frac{\Delta T}{\Delta z} > -\begin{cases}\Gamma_d & \text{if unsaturated}\\ \Gamma_s & \text{if saturated}\end{cases} \quad \bullet(5.7a)$$

or

$$\frac{\Delta \theta}{\Delta z} > \begin{cases}0 & \text{if unsaturated}\\ \Gamma_d - \Gamma_s & \text{if saturated}\end{cases} \quad \bullet(5.7b)$$

Equation (5.7b) states that unsaturated air is statically stable if potential temperature increases with height (unless it was previously determined to be nonlocally unstable).

The Apex Method for Determining Nonlocal Static Stability: (1) At every apex (kink in the sounding), write a small U, N, or S above that apex if an air parcel displaced upward a small distance from that point is unstable, neutral, or stable, respectively. Similarly, below each apex, write U, N, or S for air displaced downward. (2) For each U above an apex, extend it adiabatically upward until it hits the sounding. Similarly, extend each U below an apex downward. (3) All domains spanned by U are unstable. (4) Any non-U domains are stable or neutral.

Solved Example

Determine the static stability of the sounding in the solved example from the "Parcel vs. Environment" section, earlier in this chapter.

Solution

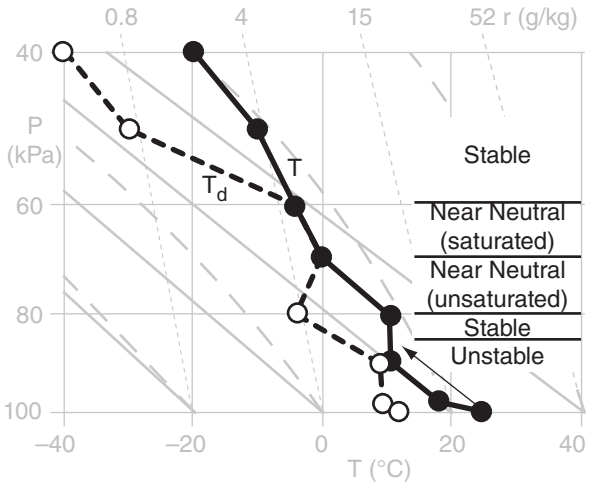

Check: Sketch OK.

Discussion: The unstable layer is turbulent. The near-neutral layers could become turbulent given the slightest wind shear.

FOCUS • A holistic approach to stability

Consider an environmental air parcel in the middle of the mixed layer (at a middle height in Fig. 5.14). If you raise it or lower it a small amount, it will have the same temperature and potential temperature as its new environment. Therefore, you might incorrectly think that the flow is statically neutral, implying only moderate amounts of turbulence and smoke-plume envelopes that cone (see the Air-Pollution chapter).

However, something else is ALSO happening in the middle of the mixed layer that is NOT associated with the middle air parcel. Namely, there are buoyant air parcels rising through the mid-mixed layer from the warmer surface-layer air below. These rising air parcels are creating strong convective turbulence. The vigorous up- and down-drafts in these thermals cause smoke plumes to loop up and down in the mid-mixed layer.

Such a holistic approach is not new. Thunderstorm forecasters usually use the whole sounding, and consider air parcels rising from the surface to the top of the storm to estimate the potential severity of storms. They don't focus on only the local lapse rate in the mid troposphere to estimate thunderstorm intensity.

"Lapse rate" (subadiabatic, adiabatic, superadiabatic) is **not** synonymous with "static stability" (stable, neutral, unstable). If the purpose of a stability definition is to determine whether flow becomes turbulent, then you must consider the whole sounding.

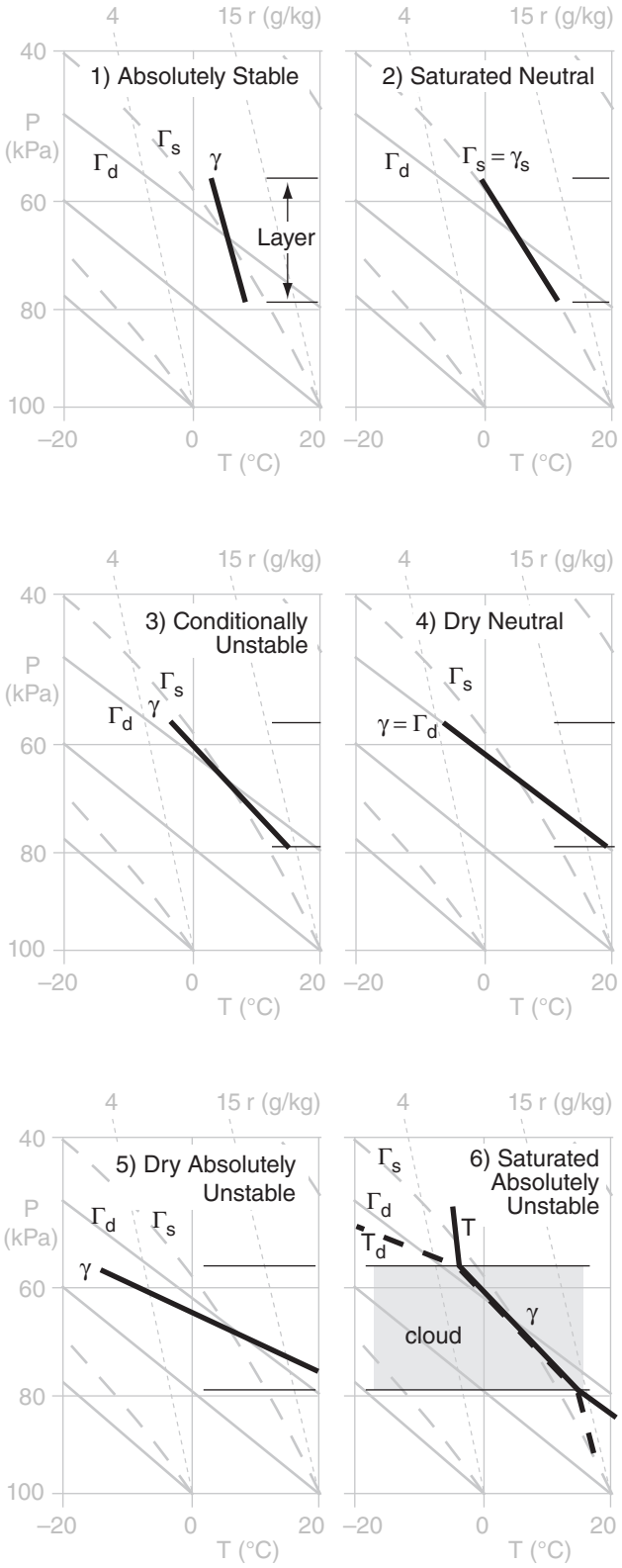

Figure 5.15
Layer stabilities, shown on a portion of a thermo diagram. The thick solid line is environmental air temperature within one layer of air (i.e., a line segment from a complete sounding), and the thick dotted line is environmental dew-point temperature. Γ_d *and* Γ_s *are the dry and saturated adiabatic lapse rates.*

Layer Method for Static Stability

Sometimes a whole layer of environmental air is lifted or lowered by an outside process. Synoptic-scale warm and cold fronts (see the Airmasses and Fronts chapter) and coherent clusters of thunderstorms (**mesoscale convective complexes**, see the Thunderstorm chapters) are examples of layer-lifting processes. In these cases we cannot use the parcel method to determine static stability, because it assumes a quasi-stationary environment.

The lapse rate γ of an environmental layer is defined as the temperature decrease with height:

$$\gamma = -\Delta T / \Delta z \qquad (5.8)$$

Lapse rates are named as shown in Table 5-1, where isothermal and inversion are both subadiabatic.

Table 5-1. Names of environmental lapse rates, where Γ_d is the dry adiabatic lapse rate.

Name	Layer Lapse Rate	Fig.
adiabatic	$\gamma = \Gamma_d = 9.8$°C/km	5.15(4)
superadiabatic	$\gamma > \Gamma_d$	5.15(5)
subadiabatic	$\gamma < \Gamma_d$	5.15(1)
• **isothermal**	T = constant with z	
• **inversion**	T = increases with z	

Layer Stability Classes: Six classes of layer stability are listed in Table 5-2. For a layer of air that is already saturated (namely, it is a layer of clouds, with $T = T_d$), then the environmental lapse rate γ, which is still defined by the equation above, is indicated as γ_s to remind us that the layer is saturated. As before, the word "dry" just means unsaturated here, so there could be moisture in the air.

Table 5-2. Layer static stability, where $\Gamma_d = 9.8$°C/km is the dry adiabatic lapse rate, and Γ_s is the saturated adiabatic lapse rate. Γ_s is always $\le \Gamma_d$.

Name	Layer Lapse Rate
1) absolutely stable	$\gamma < \Gamma_s$
2) saturated neutral	$\gamma_s = \Gamma_s$
3) conditionally unstable	$\Gamma_s < \gamma < \Gamma_d$
4) dry neutral	$\gamma = \Gamma_d$
5) dry absolutely unstable	$\gamma > \Gamma_d$
6) saturated absolutely unstable	$\gamma_s > \Gamma_s$

Fig. 5.15 illustrates these stabilities. The layer of air between the thin horizontal lines has a linear lapse rate shown by the thick line. The slope of this thick line relative to the slopes of the dry Γ_d and moist Γ_s adiabats determines the layer stability class.

Conditional Stability: One of the types of layer stability listed in Table 5-2 is conditional stability. A layer of conditionally unstable air has lapse rate between the dry and moist adiabatic lapse rates. This layer is stable if the air is unsaturated, but is unstable if the air is saturated (cloudy). Hence, the "condition" refers to whether the air is cloudy or not.

The 6th stability class is also just a special case of conditional instability. Namely, it satisfies the condition of being cloudy, so it is unstable.

Conditionally unstable air, if over a deep enough layer, is a favorable environment for thunderstorms to grow. A special set of **thunderstorm stability indices** has been developed to determine if thunderstorms will form, and how intense they might be. These are discussed in the Thunderstorm chapters of this book. The presence of thunderstorms indicate violently unstable air that extends throughout the depth of the troposphere.

When a whole layer is lifted, the temperature at each level within that layer will change according to whether those levels are saturated or not. Fig. 5.16 shows a sample sounding, and how temperatures change following dry adiabats until reaching their local LCL, above which they follow the moist adiabat. This particular example shows how a layer that starts as conditionally unstable can become absolutely unstable if the bottom of the layer reaches saturation sooner than the top.

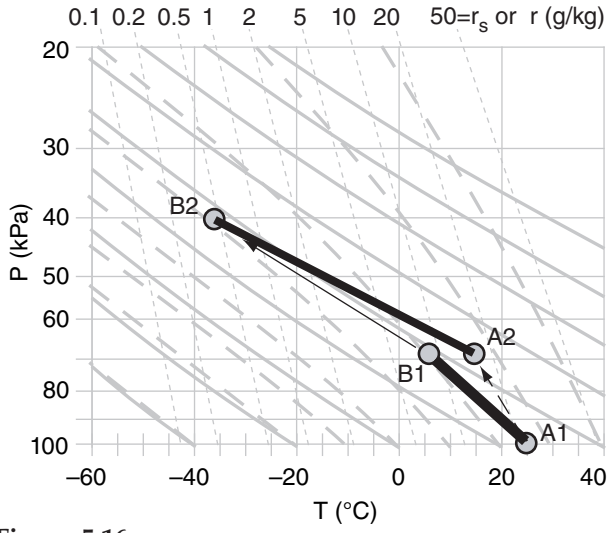

Figure 5.16
Example of lifting a layer to determine layer stability. Conditionally unstable layer (thick black line between points A1 and B1) is lifted 30 kPa. Suppose that the bottom of the layer is already saturated, but the top isn't. Upon lifting, the bottom of the layer will follow a moist adiabat from A1 to A2, while the top follows a dry adiabat from B1 to B2. The layer at its new height (black line A2 to B2) has become absolutely unstable.

Dynamic Stability

Flow can become turbulent in statically stable air if the **wind shear** (change of wind speed or direction with height) is strong enough. Such dynamic stability is indicated by the dimensionless **bulk Richardson number**, *Ri*:

$$Ri = \frac{|g| \cdot (\Delta T_v + \Gamma_d \cdot \Delta z) \cdot \Delta z}{T_v \cdot \left[(\Delta U)^2 + (\Delta V)^2 \right]} \qquad \bullet(5.9a)$$

or

$$Ri = \frac{|g| \cdot \Delta\theta_v \cdot \Delta z}{T_v \cdot \left[(\Delta U)^2 + (\Delta V)^2 \right]} \qquad \bullet(5.9b)$$

where ΔT_v, ΔU, and ΔV represent virtual temperature and wind differences across a height $\Delta z = z_2 - z_1$. The dry adiabatic lapse rate is $\Gamma_d = 9.8$ ·K/km. Temperature in the denominator must be in Kelvin. For relatively dry air, it is often assumed that $T_v \approx T$, and $\theta_v \approx \theta$.

For the special case of statically stable air:

$$Ri = \frac{{N_{BV}}^2 \cdot (\Delta z)^2}{(\Delta U)^2 + (\Delta V)^2} \qquad (5.9c)$$

Solved Example

Given air at $z = 2$ km with $U = 13$ m/s, $V = 0$, and $T = 10$°C, while air at 1.8 km has $U = 5$ m/s, $V = 0$, and $T = 10$°C. a) Find the bulk Richardson number. b) Is the air turbulent? Assume relatively dry air.

Solution

Given: $\Delta T = 0$, $\Delta V = 0$, $\Delta U = 8$ m/s, $\Delta z = 0.2$ km
Find: Ri = ? (dimensionless), and turbulence.

a) Remembering to take all differences (Δ) in the same direction, use eq. (5.9a):

$$Ri = \frac{(9.8\text{m}\cdot\text{s}^{-2}) \cdot [0 + (9.8\text{K/km}) \cdot (0.2\text{km})] \cdot (200\text{m})}{(283\text{K}) \cdot \left[(8\text{m/s})^2 + (0)^2 \right]}$$

$$= \underline{\mathbf{0.21}} .$$

b) The flow is **dynamically unstable** and **turbulent** because $Ri < 0.25$.

Check: Units OK. Physics OK.

Discussion: Isothermal air is strongly statically stable. However, the wind shear is strong enough to overpower the stability, giving a small Richardson number, dynamic instability, and turbulence.

As turbulence causes mixing of temperature and winds, ΔT, ΔU, and ΔV all approach zero. Thus, the denominator of *Ri* becomes smaller faster than the numerator, because velocities are squared in the denominator. As a result, *Ri* increases above the critical value, and turbulence ceases. Thus, turbulence tends to eliminate itself (per **LeChatelier's Principle**, see Focus Box), unless other processes continue to strengthen the wind shear to maintain turbulence.

Solved Example

For the following sounding, determine the regions of turbulence.

z (km)	T (°C)	U (m/s)	V (m/s)
2	0	15	0
1.5	0	12	0
1.2	2	6	4
0.8	2	5	4
0.1	8	5	2
0	12	0	0

Solution:
Given: The sounding above.
Find: a) Static stability (parcel method),
b) dynamic stability, & (c) identify turbulence.
Assume dry air, so $T = T_v$.

Method: Use spreadsheet to compute θ and *Ri*. Note that *Ri* applies to the layers between sounding levels.

z (km)	θ (°C)	z_{layer} (km)	*Ri*
2	19.6		
1.5	14.7	1.5 to 2.0	9.77
1.2	13.8	1.2 to 1.5	0.19
0.8	9.8	0.8 to 1.2	55.9
0.1	9.0	0.1 to 0.8	5.25
0	12	0 to 0.1	–0.358

Next, plot these results:

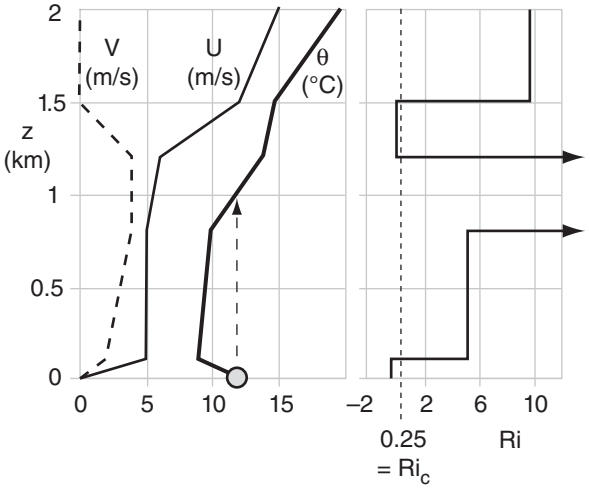

a) Static Stability: Unstable & turbulent for z = 0 to 1 km, as shown by air-parcel rise in the θ sounding.
b) Dynamic Stability: Unstable & turbulent for z = 0 to 0.1 km, & for z = 1.2 to 1.5 km, where $Ri < 0.25$.
c) Turbulence exists where the air is statically OR dynamically unstable, or both. Therefore:
Turbulence at 0 - 1 km, and 1.2 to 1.5 km.

Check: Sketch OK. Physics OK. Units OK.
Discussion: At z = 0 - 1 km is the mixed layer. At z = 1.2 - 1.5 is **clear-air turbulence** (**CAT**) and K-H waves.

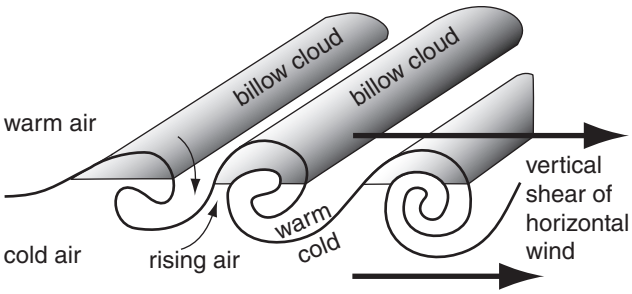

Figure 5.17
Kelvin-Helmholtz (K-H) waves with sufficient moisture to create rows of billow clouds perpendicular to the wind shear.

N_{BV} is undefined for air that is not statically stable.

To a good approximation when Δz is small, the flow is **dynamically unstable** and **turbulent** whenever

$$Ri < Ri_c \qquad \bullet(5.10)$$

The **critical Richardson number** is $Ri_c = 0.25$.

When condition (5.10) is met, the flow is called **dynamically unstable**. Otherwise, for larger *Ri*, the flow is dynamically stable. Statically unstable air results in negative Richardson numbers, which are also dynamically unstable.

Flow that is just becoming dynamically unstable often forms **Kelvin-Helmholtz (K-H) waves** in the air, which look like ocean waves breaking on shore (Fig. 5.17). When there is sufficient moisture in the air to make these waves visible, they appear as parallel bands of narrow clouds called **billow clouds**, filling the crest of each wave. Non-thunderstorm turbulence at altitudes above the top of the atmospheric boundary layer is called **clear-air turbulence** (**CAT**).

Turbulence Determination

Both dynamic instability and static instability give incomplete measures of the existence of turbulence. Static stability does not include the effects of shear in turbulence generation. Dynamic stability does not include the nonlocal processes that can generate turbulence. Thus, to determine whether the flow in any region is turbulent, you must compute both the static stability (using the nonlocal parcel methods given in this chapter), and the dynamic stability (using the Richardson number).

• Turbulence Determination Rule •
1) To be turbulent, the flow must be either statically OR dynamically unstable.
2) To be **laminar** (non-turbulent), the flow must be both statically AND dynamically stable.

FINDING THE TROPOPAUSE HEIGHT AND MIXED-LAYER DEPTH

Tropopause

Recall from Chapter 1 (Fig 1.10) that the standard-atmosphere temperature decreases with height within the troposphere, but is isothermal with height in the bottom part of the stratosphere. Isothermal layers are very strongly statically stable. The strong and deep statically stable layer in the stratosphere discourages vertical motion through it, which is why most of our weather (including thunderstorms and hurricanes) is trapped below it. The base of the stratospheric isothermal layer is the tropopause.

Real soundings are more complex than the simple standard atmosphere, and can have many different stable layers (and isothermal layers) at different heights (Fig. 5.18). Nonetheless, if the radiosonde balloon rises high enough before bursting, then it often can enter the stratosphere. To locate the tropopause, we just need to look for the bottom of the very thick isothermal layer that is near a pressure altitude of 40 to 20 kPa.

Fig. 5.19 illustrates a hypothetical vertical slice through the atmosphere, showing the **isentropes** (lines of equal potential temperature, θ). The spacing between isentropes is a measure of the static stability. Tight packing (i.e., small spacing) between isentropes indicates strong stability. Large spacing between isentropes indicates weak stability. Thus, you can locate the tropopause at the bottom of the region of tight isentrope packing, as sketched in Fig. 5.19. *[**CAUTION**: The tropopause usually does NOT follow any single isentrope.]*

To illustrate the relationship between stability and isentrope spacing, let the circle in Fig. 5.19 represent a weather balloon that is filled with helium, and which is rising through the environment. On the way up, its attached radiosonde measures temperature and pressure, from which potential temperature can be calculated.

The radiosonde would have first risen through relatively cold air with large spacing between isentropes, indicating weak static stability (near neutral). However, as it rises across the 280 K and the 290 K isentropes, the tight packing there indicates stronger static stability, perhaps marking the top of a frontal surface or the inversion at the top of the mixed layer. Higher still in the troposphere, the medium spacing between isentropes indicates moderately stable air. Finally the balloon enters the stratosphere, where very tight packing of isentropes indicates very strong static stability.

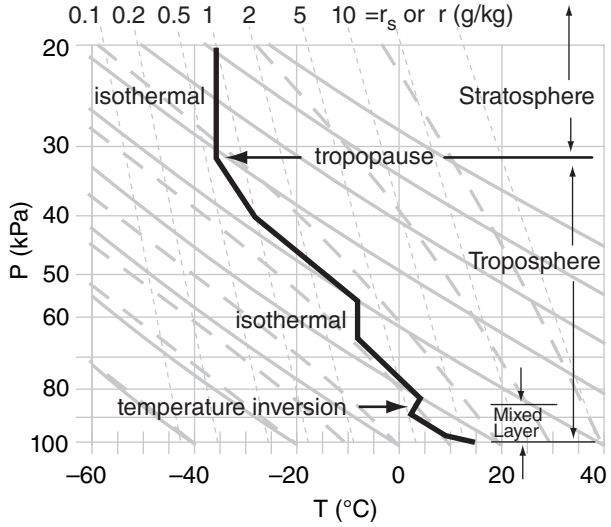

Figure 5.18
Sample atmospheric sounding having two isothermal layers and one temperature inversion.

Solved Example

What is the tropopause height (or pressure) in the sounding of Fig. 5.18, and how is it identified?

Solution

Given: the plotted sounding.
Find: P_{Trop} = ? kPa

The base of the deep isothermal layer near the top of this sounding is at P_{Trop} = **32 kPa**.
The other isothermal and inversion layers are too low, and too thin.

Check: Sketch OK.
Discussion: The tropopause is lower near the poles and higher near the equator. It is lower in winter, higher in summer (see Table 6-1 in the Cloud chapter), but varies considerably from day to day.

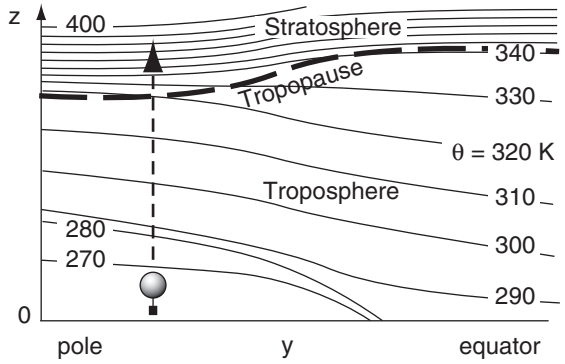

Figure 5.19
Simplified vertical slice through the atmosphere, showing isentropes (lines of equal potential temperature, θ). Heavy dashed line is the tropopause. Grey circle represents a radiosonde balloon rising through the environment.

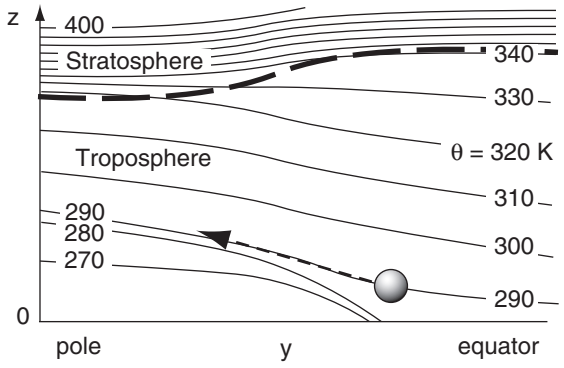

Figure 5.20
Same as Fig. 5.19, but now the grey circle represents an air parcel of potential temperature 290 K, which rides along the environmental 290 K isentrope as the parcel is advected poleward. Thick dashed line indicates the tropopause. Thin dashed line shows the path of the air parcel.

Solved Example

Given the following potential temperature measurements. Plot them on the T vs. log P diagram, and on the θ vs. z diagram.

Indicate the static stability of each layer, and find the location of z_i using the exact method.

z (km)	θ (°C)
3.0	35
2.0	28
1.5	28
1.3	25
1.0	24
0.2	24
0	26

Solution

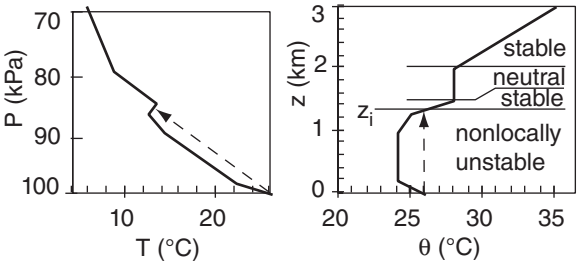

$z_i \approx$ **1.37 km**

Check: Physics OK. Sketch reasonable.

Discussion: θ vs. z is often easier to use than T vs. log(P). Note that z_i is not at the base of the subadiabatic region, but slightly above it due to nonlocal air-parcel rise.

Because of buoyant forces, air parcels tend to follow isentropic surfaces as they advect. In Fig. 5.20, suppose that the circle represents an air parcel, not a weather balloon. Further suppose that the potential temperature of that parcel is 290 K. Because that air parcel is surrounded by an environment of the same potential temperature (as indicated by the 290 K isentrope), the parcel experiences no buoyant forces on it. Namely, it is at its equilibrium height.

Let the parcel be blown horizontally toward the pole. If we assume (incorrectly) that it maintains a constant altitude above sea level, then it finds itself surrounded by an environment of colder air (of θ = 270 K). Thus, the parcel of θ = 290 K is buoyant, and rises through the environment until it reaches its equilibrium 290 K isentrope. In the real atmosphere, such rise happens concurrently with its horizontal motion, so that the parcel path (thin dashed line in Fig. 5.20) follows the sloping surface of the 290 K isentrope. Similarly, if the parcel were blown equatorward, it would follow the same isentrope and descend. The study of forces, motions, and thermodynamics along surfaces of constant potential temperature is called **isentropic analysis**.

Mixed-Layer

When the ground is warmer than the air, a convective mixed layer is created that is nonlocally unstable. The height z_i of the top of this mixed layer is defined as the top of the nonlocally unstable region. The easiest way to determine this height is to use a thermo diagram. The θ vs. z thermo diagram is ideal for mixed-layer studies.

First, obtain a sounding of temperature or potential temperature vs. height. By plotting the sounding on a thermo diagram and conceptually lifting an air parcel from the surface, z_i is found as the height where this rising parcel hits the sounding.

A less accurate, but quick approach, is to look for the temperature inversion (or similar layer that is statically stable) that is near the ground, but not touching it. A **temperature inversion** is where T increases with height. The top of the mixed layer is usually somewhere within this temperature inversion. In Fig. 5.18, the average height of the temperature inversion is about z_i = 85 kPa.

Sometimes thermodynamic information is needed for the boundary layer, to study thermal rise, turbulence, low-cloud and fog formation, and smoke dispersion. Enlargements of the bottom portion of thermo diagrams, focusing on the boundary layer, are provided at the end of this chapter.

Other measures of stability, and applications of the mixed layer, are given in the Atmospheric Boundary Layer and Air-Pollution Dispersion chapters.

SUMMARY

You can use the thermodynamic diagram as a tool to simplify analyses of stability and thermodynamics. There are many different types of thermo diagrams: Emagram, Skew-T, Stüve (or Pseudoadiabatic Diagram), Tephigram, and θ-Z diagram. They all serve the same purpose, and all have isotherms, isobars, isohumes, dry and moist adiabats, and height contours (in some cases).

The state of the air (i.e., its temperature, pressure, and water content), as well as processes that can change the state, can be described via thermo diagrams. Processes include rising or sinking air, condensation/evaporation, precipitation, and radiative heating/cooling. With a thermo diagram you can find the saturation characteristics of air, the amount of liquid water in a cloud, the height of cloud base, potential temperatures, and cloud depth.

Thermo diagrams are often used to plot upper-air soundings. You will also find them valuable to analyze thunderstorms and hurricanes, and to help anticipate their intensity, as will be described in later chapters.

As winds and turbulence move the air from place to place, an air parcel of one temperature can become immersed in an environment of different temperatures. Such a parcel experiences buoyant forces, which causes it to rise or sink. Parcels displaced from their starting location will accelerate further away in a statically unstable environment, but will tend to return to their starting height in a statically stable environment.

In a statically stable environment, air parcels can oscillate vertically at the Brunt-Väisälä frequency. When wind shear, the change of wind speed or direction with height, is considered, statically stable air can be dynamically unstable and turbulent, as estimated using the Richardson number.

Threads

The growth of thunderstorms (Chapters 14 and 15) fueled by warm humid air, and the energy available to hurricanes (Chapter 16) are analyzed using thermo diagrams. Thermo diagrams are used to study the vertical structure of the atmosphere (Chapter 1), the boundary layer (Chapter 18), dispersion of air pollutants (Chapter 19), and frontogenesis (Chapter 12).

The wavelength of mountain waves (Chapter 17) and formation of lenticular clouds depend on the Brunt-Väisälä frequency. Anabatic and katabatic winds (Chapter 17) are driven by buoyant forces.

EXERCISES

Numerical Problems

N1. Identify the thermo diagram type.

a.

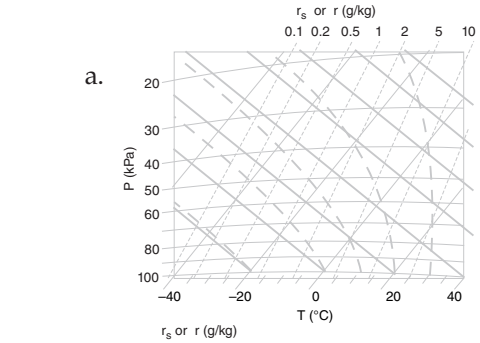

b.

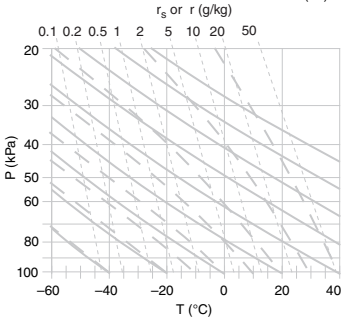

c.

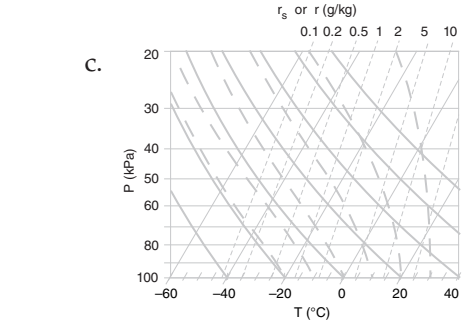

d.

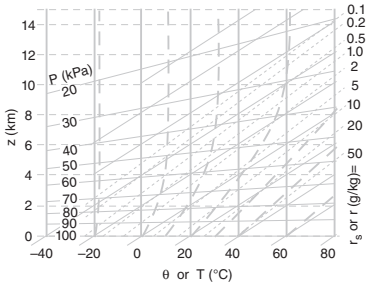

e.

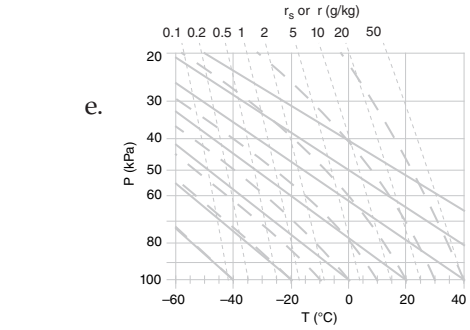

N2. On copies of ALL 5 thermo diagrams from N1, find and label one of the:

a. dry adiabats b. isohumes c. isobars
d. isentropes e. saturated adiabats
f. isotherms g. moist adiabats

N3(§). Use a spreadsheet to create the Skew-T, as given in the Solved Example in the Skew-T section of this Chapter, except do it for isopleths listed below. Describe the results of your experiments with different values of the coefficient *K*, which determines the amount of skewness.

	T, θ, & θ_w (°C)	r (g/kg)
a.	30	50
b.	25	20
c.	15	10
d.	10	2
e.	5	1
f.	0	0.5
g.	–5	0.2
h.	–10	0.1
i.	–15	15
j.	–20	25

N4. On copies of ALL 5 thermo diagrams from N1, plot the following air-parcel state. Hint: The data below represent individual air parcels, NOT a sounding, NOT a vertical profile.

	P(kPa)	T(°C)	T_d(°C)
a.	40	0	–20
b.	90	–5	–5
c.	45	–20	–40
d.	85	20	18
e.	50	10	–5
f.	80	15	15
g.	55	–30	–45
h.	75	–5	–40
i.	60	8	3
j.	70	17	12
k.	65	–7	–13

N5. Repeat N4, but on copies of ALL 5 of the LARGE thermo diagrams from the end of this chapter (but do not use the special ABL diagrams).

N6. For one assigned air-parcel state from question N4, find each of the following using only a Skew-T or Tephigram to answer these questions. Do not solve equations (except for relative humidity).

i) potential temperature
ii) wet-bulb potential temperature
iii) mixing ratio
iv) saturation mixing ratio
v) relative humidity vi) LCL
vii) equivalent potential temperature
viii) wet-bulb temperature

N7. Same as N6, but use only an Emagram or Stüve.

N8. Starting with one assigned air-parcel with state from question N4:

i) lower it to a pressure of 100 kPa, and find its new temperature and dew point. Use only a tephigram or Skew-T.

ii) lower it to a pressure of 100 kPa, and find its new temperature and dew point. Use only a Stüve or Emagram.

iii) raise it to a pressure of 20 kPa, and find its new temperature and dew point. Use only a tephigram or Skew-T.

iv) raise it to a pressure of 20 kPa, and find its new temperature and dew point. Use only a Stüve or Emagram.

N9. Which thermo diagrams from Fig. 5.3 have

a. straight isobars?
b. straight dry adiabats?
c. straight moist adiabats?
d. have the greatest angle between isotherms and dry adiabats?
e. moist adiabats that asymptotically approach dry adiabats near the top of the diagram?
f. moist adiabats that asymptotically approach dry adiabats near the left of the diagram?

N10. Given the initial state of an air parcel below, lift it to a final pressure of 30 kPa, and determine its final values of T, T_d, r_T, r_s, and r_L. Use a copy of the large thermo diagram from the end of this chapter, as specified below.

	P(kPa)	T(°C)	T_d(°C)	Thermo Diagram
a.	100	35	20	Skew-T
b.	100	30	20	Stüve
c.	100	25	10	Tephigram
d.	100	20	–5	Emagram
e.	90	30	25	Skew-T
f.	90	30	15	Stüve
g.	90	25	15	Tephigram
h.	90	20	5	Emagram
i.	80	20	15	Skew-T
j.	80	20	10	Stüve
k.	80	15	0	Tephigram
l.	80	10	–5	Emagram

N11. For the air parcel specified for exercise N10, find its LCL pressure, using the specified thermo diagram.

N12. Starting with the FINAL state of the air parcel specified from exercise N10, allow all of the liquid water to rain out (except if the liquid water from the

final state of N10 was greater than 1 g/kg, then allow only 1 g/kg of liquid water to rain out). Then lower the air parcel back to its starting pressure, and determine its new temperature and dew point. Use the specified thermo diagram from N10.

N13. Starting with the FINAL state of the air parcel specified from exercise N10, allow radiative cooling to change the air parcel temperature by $\Delta T = -8°C$. Then lower the air parcel back to its starting pressure, and determine its new temperature and dew point. Use the specified thermo diagram from N10.

Use the following environmental sounding to answer the exercises below. Assume $V = 0$ everywhere.

P(kPa)	T(°C)	T_d(°C)	U (m/s)
20	–30	–60	40
40	–30	–30	40
60	–5	–30	40
70	–5	–20	40
80	2	0	10
87	7	4	5
98	16	6	5
100	20	9	0

Assume that these pressures are **significant levels** (i.e., altitudes where there is a kink or bend in the profile, with straight line segments between each significant level). Use the word "**layer**" to represent the air between two adjacent significant levels.

N14. Plot the above sounding on a large thermodynamic diagram from the end of this chapter. Use solid dots (of red color if possible) for the temperature and mark an open circle (blue color if available) for the dew points. Draw a solid (red, if possible) line to connect the temperature dots, starting from the bottom up, and draw a dashed (blue, if possible) line for the dew points. Use a/an:

a. Emagram b. Skew-T c. Stüve
d. Tephigram e. θ-Z diagram

N15. Using the sounding above:

a. Find the potential temperature at each height, and plot it on a linear graph of θ vs P.

b. Calculate and plot θ_v vs P.

N16. If an air parcel from the sounding above moves up one level, what buoyancy force per mass acts on it in this new layer. Use a starting air parcel from the layer at P (kPa) =

a. 100 b. 98 c. 87 d. 80 e. 70 f. 60 g. 40

N17. Calculate the Brunt-Väisälä frequency and the corresponding period of oscillation for one layer from the sounding above, where the base of the layer is at level P (kPa) =

a. 100 b. 98 c. 87 d. 80 e. 70 f. 60 g. 40

N18. Using the sounding above as plotted for exercise N14, determine the static stability using the parcel method for the one environmental layer, where the bottom of that one layer is at P (kPa) =

a. 100 b. 98 c. 87 d. 80 e. 70 f. 60 g. 40

Hints: Neglect moisture & condensation. Also, the stability in any one layer could depend on nonlocal effects from other layers.

N19. Same as N18, but find the layer stability.

N20. Using the sounding above, determine the Richardson number and the dynamic stability for the layer that has a layer base at level P (kPa) =

a. 100 b. 98 c. 87 d. 80 e. 70 f. 60 g. 40

N21. Indicate which portions of the sounding above are likely to be turbulent, and explain why.

N22. Using the sounding above:

a. Determine if there is a mixed layer. If so, find the mixed-layer depth z_i.

b. Determine the height of the tropopause.

c. Locate any layer (stratiform) clouds that might be present in the environment.

N23. With the sounding above:

a. Use the thermo diagram to determine the pressure-height of the LCL for an air parcel rising from 100 kPa. How does this compare to the height using a formula (see the Moisture chapter) for the LCL?

b. For a parcel rising from 100 kPa, at what pressure-heights are cloud base and cloud top? What is the mixing ratio of water vapor in the cloud at cloud top? What is the value of liquid water mixing ratio in the cloud at cloud top?

c. Starting with the answer from part (b), assume that all of the liquid water falls out as precipitation from the air parcel at cloud top. Then, if the cloud-top parcel is lowered to 100 kPa, what is its temperature, dew point, and relative humidity? How does that relative humidity compare to the initial relative humidity of the parcel at 100 kPa?

N24. At $P = 100$ kPa, $z = 0$ km, an air parcel has initial values of $T = 30°C$ and $T_d = 0°C$. Use each of the large thermo diagrams at the end of this chapter to find the LCL. How do these LCL values compare to the theoretical value from the equation in the Moisture chapter?

Understanding & Critical Evaluation

U1. Why does the humidity of an unsaturated, rising air parcel follow a line of constant mixing ratio in a thermo diagram, rather than a line of constant dew-point temperature?

U2. Under what conditions would a rising, unsaturated air parcel not follow a dry adiabat in a thermo diagram?

U3. In the full-size Emagram, why do the lines of constant height tilt up to the left, rather than up to the right? If warmer air has greater thickness than colder, then wouldn't the height lines be pushed up on the right side of the diagram? Explain.

U4. In the thermodynamic diagram, the labels at the top of the diagram for mixing ratio are not linear from left to right. Namely, as you look from left to right, the mixing ratio increment between neighboring lines gets larger and larger. Why?

U5. On the full-size Emagram, notice that the dry adiabats are slightly curved. Why are they not straight?

U6. a. Why do you need two points to represent one air parcel for unsaturated air?

b. Why do you need two points to represent one air parcel for saturated air?

c. If only two points are needed for parts (a) and (b), then why do we track three points for each one air parcel as it rises adiabatically?

U7. If you know the starting temperature and pressure of an unsaturated air parcel, and you know its LCL instead of its mixing ratio, is that sufficient information to represent its full thermodynamic state (regarding its temperature and humidity)?

U8. The method of moving air parcels up and down in a thermo diagram assumes that the background environment is steady. Is that a good assumption? When might that assumption be violated? Also, when an air parcel moves from its starting point, what happens to the hole it leaves behind?

U9. Suppose an air parcel is surrounded by an environment that has the same density. The net buoyant force on the parcel would be zero. Yet gravity is still acting on the parcel. Why doesn't gravity pull the parcel downward?

U10. Metal ships float in water. Is it possible for metal to float in air, even if it is not moving? Discuss.

U11. Eq. (5.2) gives buoyant force in terms of object density minus surrounding fluid density. Yet eq. (5.3a) gives the force in terms of fluid (environment) minus object (the air parcel) . Why the sign change? Is it a mistake? Derive (5.3a) from (5.2).

U12. On the θ-Z thermo diagram, why do the moist adiabats tilt to the right with increasing altitude, while the same moist adiabats tilt to the left on the Emagram?

U13. Start with T = 25°C and T_d = 20°C for an air parcel at P = 100 kPa (assumed to be at z = 0). Plot this starting condition on copies of all versions of the boundary-layer thermodynamic diagram.

a. Lift the parcel to the LCL on all diagrams, and compare the LCL heights. At this point, compare the values of T, r, and θ on all diagrams.

b. Continue lifting to a height of 2 km, and compare the values of T, r, r_T, and θ on both diagrams. Discuss.

U14. Fig. 5.14 shows correct and incorrect methods of determining static stability. Why is the wrong method wrong?

U15. The Brunt-Väisälä frequency is undefined for statically unstable air. Why? If θ decreases with increasing z, calculate the Brunt-Väisälä frequency.

U16. Why is the factor 2π in the numerator of eq. (5.5), rather than a factor of 1 ?

U17. a. Verify that eqs. (5.9) are dimensionless.

b. For zero wind shear, the denominator of eqs. (5.9) are zero, causing Ri to be infinite. Does that mean that there can never be any turbulence when the wind shear is zero? Explain.

U18. The small thermo diagrams in this chapter indicate a surface pressure of 100 kPa for demonstration purposes. However, the standard atmospheric pressure at sea-level is 101.325 kPa, and pressures on any given day can be greater than average. How can you plot a pressure greater than 100 kPa on the thermo diagram?

U19. Explain the last sentence in the Fig. 5.8 caption.

U20(§). (This exercise is lengthy.)
Use a computer spreadsheet to create a:

a. Stüve diagram. [Hint: use $(P_o/P)^{\Re_d/C_{pd}}$ as vertical coordinate.]

b. Skew-T diagram.

c. Tephigram. [Hint: plot it in tilted form, as in Fig. 5.2, but with moist adiabats and isohumes add-

ed to the other lines in that figure. This is a very difficult exercise.]

d. θ-Z diagram. [Hint, plot all the isopleths except the isobars.]

U21(§). Use a computer spreadsheet to create an Emagram, but utilize pressures in the range of 110 kPa to 10 kPa.

U22. Suppose the parcel in Fig. 5.12 gradually mixes with its environment as it rises. Plot the path of such a parcel on a T vs. z graph similar to that figure.

U23. What does it mean if the numerator of the Richardson number is negative?

U24. Compare the bulk Richardson number with the flux Richardson number from the Atmospheric Boundary Layer chapter. Hint, consider K-theory, as explained in that chapter.

U25. Create a new conceptual algorithm different from the "Guide" in this chapter to help you identify different thermo diagram types. Test it to ensure that it doesn't falsely identify some diagrams.

U26(§). Use a spreadsheet to reproduce Fig. 5.2, using the relationship for potential temperature as a function of T and P as given in the Heat chapter.

U27. All the dry adiabats in a Stüve diagram converge to a point above the top left of the diagram. Explain why or why not the dry adiabats in an Emagram converge to a point.

U28. Suppose that turbulent mixing in a dynamically unstable, but statically stable, environment causes both $\Delta T/\Delta z$ and $\Delta U/\Delta z$ to be reduced by the same fraction, b. Show how the Richardson number increases as b decreases. Use this to explain why turbulence acts to reduce the dynamic instabilities that caused it, analogous to LeChatelier's principle. (Hint: Assume $V = 0$ for simplicity.)

U29. Fig. 5.10 indicates state changes due to fallout of precipitation.

a. Can the opposite happen? Namely, can precipitation fall INTO an air parcel, with all of the water staying in the air? If so, give an example and show how that process would be plotted on a thermo diagram.

b. What happens if rain from above falls through an air parcel with zero or partial evaporation? Namely, the rainfall does not change during its passage through the air parcel. Indicate this on a thermo diagram.

Web-Enhanced Questions

W1. Search the web for a map of the locations of all the rawinsonde (i.e., upper-air) sites in your country. What are the three sites closest to your location, and what are the station identifiers for those sites?

W2. Search the web for a site that allows you to find the name, abbreviation, latitude and longitude, altitude, and other characteristics of rawinsonde sites.

a. Type in the name of a major city, and determine if it has a rawinsonde launch site.

b. Compare the **WMO** (**World Meteorological Organization**) and **ICAO** (**International Civil Aviation Organization**) identification codes for several stations.

W3. Search the web for soundings plotted on various types of thermodynamic diagrams (e.g., pseudoadiabatic diagrams, tephigrams, Stüve diagrams, Skew-T Log-P diagrams, etc.). Instead of focusing on the particular sounding, look at the background diagram, and identify each type of line in it (dry adiabats, moist adiabats, isobars, isotherms, isohumes, height contours, etc.). How many different types of thermo diagrams can you find on the web? Indicate the URLs for these sites.

W4. Get from the web the current surface T and T_d for the weather station closest to you (or to a station specified by your instructor).

a. Plot those values on a thermo diagram, and determine the LCL height and pressure.

b. If there are cumuliform clouds at the time of this data observation, also get cloud-base height from the web, and compare with the computed LCL. (Hint: search the web for METAR reports of cloud-base altitudes for the airport closest to you.)

W5. Get from the web the current sounding in text form for the rawinsonde (upper-air) site closest to you (or to an upper-air site specified by your instructor). Plot this by hand on one of the large thermo diagrams copied from the end of this chapter, using different colors for T and T_d. For air lifted from the surface, find the LCL. If this lifted air at the LCL is buoyant, continue lifting it until it becomes neutrally buoyant, and mark this height as cloud-top height.

W6. Get from the web a sequence of soundings (once every 12 h if available, otherwise every 24 h) from the past few days for a rawinsonde (upper-air) site near you (or a site specified by your instructor).

a. Compare these soundings, to see how the weather evolves.

b. If you have appropriate software, put each sounding as a frame in a movie, and play the movie

to see the soundings evolve.

c. Check the weather maps to see if frontal passage will happen during the next several days at your rawinsonde site. If so, download and save soundings from just before, during, and after frontal passage, and compare and discuss the results.

W7. Get from the web a sounding from just before a rain event in your area (or for a region specified by your instructor). From this sounding, conceptually lift an air parcel from the boundary layer to a reasonable height for cloud top. Calculate the liquid-water mixing ratio for water that would have condensed during the rise of an air parcel from the surface. Compare this to the amount of precipitation that fell, and discuss why they are different.

W8. On some soundings plotted on the web, other information is also plotted (such as winds). Also, sometimes tables of information such as LCL and many stability indices are given. The web sites that serve such detailed soundings will often have an information page that you can select to learn the definitions of the other terms in such a table. Access and print those definitions, and use them to interpret the info table that is given with the sounding.

W9. Get the most recent sounding from the rawinsonde site closest to you (or a site specified by your instructor).

a. Determine the domains of different parcel static stability in that sounding, and indicate them on or next to the sounding similar to that shown in Fig. 5.14 (using the correct version only, please).

b. For the statically stable regions of the sounding, determine the Brunt-Väisälä frequency for each of those regions. (For simplicity, you can neglect the moisture contribution to virtual temperature for this exercise, and just use the air temperature in the calculation. However, normally you should not neglect the moisture contribution to virtual temperature when you calculate stabilities and Brunt-Väisälä frequencies, especially in the tropics.)

c. For each layer in the sounding, calculate the Richardson number, using the winds and temperatures at the top and bottom of each layer. The resulting Richardson numbers would apply across the whole layer between the top and bottom heights from which temperature and winds were obtained. But each different layer probably has a different Richardson number.

d. Using both (b) and (c), determine the ranges of heights that are likely to be turbulent.

W10. Get the most recent early morning sounding from the rawinsonde site closest to you (or a site specified by your instructor). How warm must the surface temperature be later in the day in order to allow cumuliform cloud tops to reach an altitude where the pressure is 50 kPa? Do you think that such warming is possible on this day?

W11. Get the most recent sounding from the rawinsonde site closest to you (or a site specified by your instructor), and determine the depth of the boundary layer and the height of the tropopause.

W12. Search for images of Kelvin-Helmholtz waves and billow clouds. Print two examples of each, along with their URLs.

Synthesis Questions

S1. The denominator of eq. (5.9c) looks something like a **kinetic energy** per unit mass (ignoring the missing factor of 1/2). Could the numerator be interpreted as a potential energy per unit mass? Explain.

S2. Why did **Archimedes** run naked through the streets of Syracuse when he discovered the principle of displacement and buoyancy? [Note: Archimedes also devised city defenses using lenses to blind the enemy and cranes to capsize their ships, but the Romans conquered Syracuse anyway and killed him.]

S3. Sketch lines in a thermo diagram for a world where condensation of water causes cooling of the air instead of warming. How would the weather and climate be different, if at all? Why?

S4. What if buoyancy depended on the temperature of an air parcel instead of the temperature difference between the parcel and its environment. How would weather and climate be different, if at all? Why?

S5. The Brunt-Väisälä frequency implies oscillations, and oscillations imply waves in the air. Could there really be waves in the air? If so, where do they "come ashore" and "break"?

S6. Why isn't vertical velocity included in the definition of the Richardson number?

S7. What if **global warming** caused the atmosphere to warm, but the Earth's surface stayed about the same temperature. How would static stability and vertical cloud growth be affected, and how would the resulting weather and climate be different, if at all?

S8. In a **nuclear winter** scenario (after nuclear bombs have destroyed the Earth, and had sprayed bits of Earth into the atmosphere), the stratosphere would be filled with fine dust and dark soot particles. Given the short and long wave radiation characteristics that you have studied in earlier chapters, how might the static stability of the troposphere change, and what effect would it have on weather and climate? (Hint: Assume that you are a cockroach, because all other life forms would have been destroyed, so you are the only species left to do this important calculation – as if you would care.)

S9. An isentropic chart shows the altitude (either z or P) of a constant θ surface. Describe how you would use upper-air soundings from different weather stations to get the data needed to draw an isentropic chart.

S10. Devise a new type of thermo diagram that has log(r) along the abscissa, and log(P) along the ordinate with scale reversed (max and bottom and min at top). Plot the isotherms and dry adiabats in this diagram. Name the diagram after yourself, and explain the virtues and utility of your diagram.

S11. What if T_d could be greater than T in a sounding. Explain how that might be possible, and describe how convective clouds might be different, if at all.

S12. Suppose the tropopause was touching the ground everywhere on Earth. How would the weather or climate be different, if at all?

LARGE-SIZE THERMO DIAGRAMS

You have our permission to freely reproduce the following seven thermo diagrams for your own personal use, or for education (but not for commercial resale), so long as you retain the author, title, and publisher citations in the copies. We recommend that you do NOT write on the following seven pages, so that they remain as clean master copies.

These diagrams share common line formats: thin lines representing state of the air; thick lines representing adiabatic processes that change the state.

- Isotherms (temperature: T) and isobars (pressure: P) are thin solid,
- Isohumes (mixing ratio: r) are thin dotted,
- Dry adiabats (potential temperature: θ) are thick solid,
- Moist adiabats (wet-bulb potential temperature: θ_w) are thick dashed, and
- Contours (height: z) are thin dashed (if plotted at all).

The height contours are only approximate. Potential temperatures use a reference pressure of P = 100 kPa, and heights are set to zero at that pressure.

The line labels also follow a common format (except for the θ-Z diagram):

- Isobars are labeled at left. Units are kPa.
- Isohumes are labeled at top (and right in one case). Units are g/kg.
- Heights are labeled at right. Units are km.
- Isotherms and both dry and moist adiabats are labeled at the bottom. Units are °C.

For this last item, the three isopleths sprout from each temperature label like branches from a bush. The branches are always in the same order, although their angles differ from graph to graph. Dry adiabats are the left branch, moist adiabats are the center branch, and isotherms are the right branch.

Two versions of the Skew-T and θ-Z Diagram are included. The standard version spans the range P = 105 to 20 kPa. The other version [with "(ABL)" added to the title] is designed for **atmospheric boundary-layer** and air-pollution work, and gives more detail in the bottom third of the troposphere.

On the next pages (152-158) are these thermo diagrams:

- Emagram
- Stüve Diagram
- Skew-T Log-P Diagram
- Tephigram
- Theta-Z Diagram
- Skew-T Log-P Diagram (ABL)
- Theta-Z Diagram (ABL).

Copyright © 2011, 2015 by Roland Stull. *Meteorology for Scientists and Engineers, 3rd Ed.*

CLOUDS

CONTENTS

Processes Causing Saturation 159
- Cooling and Moisturizing 159
- Mixing 160

Cloud Identification & Development 161
- Cumuliform 161
- Stratiform 162
- Stratocumulus 164
- Others 164
  - Clouds in unstable air aloft 164
  - Clouds associated with mountains 165
  - Clouds due to surface-induced turbulence 165
  - Anthropogenic Clouds 166

Cloud Organization 167

Cloud Classification 168
- Genera 168
- Species 168
- Varieties 169
- Supplementary Features 169
- Accessory Clouds 169

Sky Cover (Cloud Amount) 170

Cloud Sizes 170

Fractal Cloud Shapes 171
- Fractal Dimension 171
- Measuring Fractal Dimension 172

Fog 173
- Types 173
- Idealized Fog Models 173
  - Advection Fog 173
  - Radiation Fog 175
  - Dissipation of Well-Mixed (Radiation and Advection) Fogs 176

Summary 178
- Threads 178

Exercises 179
- Numerical Problems 179
- Understanding & Critical Evaluation 181
- Web Enhanced Questions 183
- Synthesis Questions 183

"Meteorology for Scientists and Engineers, 3rd Edition" by Roland Stull is licensed under a Creative Commons Attribution-NonCommercial-ShareAlike 4.0 International License. To view a copy of the license, visit http://creativecommons.org/licenses/by-nc-sa/4.0/ . This work is available at http://www.eos.ubc.ca/books/Practical_Meteorology/ .

6 Clouds have immense beauty and variety. They show weather patterns on a global scale, as viewed by satellites. Yet they are made of tiny droplets that fall gently through the air. Clouds can have richly complex fractal shapes, and a wide distribution of sizes. Clouds are named according to an international cloud classification scheme.

Clouds form when air becomes saturated. Saturation can occur by adding water, by cooling, or by mixing; hence, Lagrangian water and heat budgets are useful. The buoyancy of the cloudy air and the static stability of the environment determine the vertical extent of the cloud.

Fogs are clouds that touch the ground. Their location in the atmospheric boundary layer means that turbulent transport of heat and moisture from the underlying surface affects their formation, growth, and dissipation.

PROCESSES CAUSING SATURATION

Clouds are saturated portions of the atmosphere where small water droplets or ice crystals have fall velocities so slow that they appear visibly suspended in the air. Thus, to understand clouds we need to understand how air can become saturated.

Cooling and Moisturizing

Unsaturated air parcels can reach saturation by three processes: cooling, adding moisture, or mixing. The first two processes are shown in Fig. 6.1, where saturation is reached by either **cooling** until the temperature equals the dew point temperature, or **adding moisture** until the dew point temperature is raised to the actual ambient temperature.

The temperature change necessary to saturate an air parcel by cooling it is:

$$\Delta T = T_d - T \tag{6.1}$$

Whether this condition is met can be determined by finding the actual temperature change based on the first law of thermodynamics (see the Heat chapter).

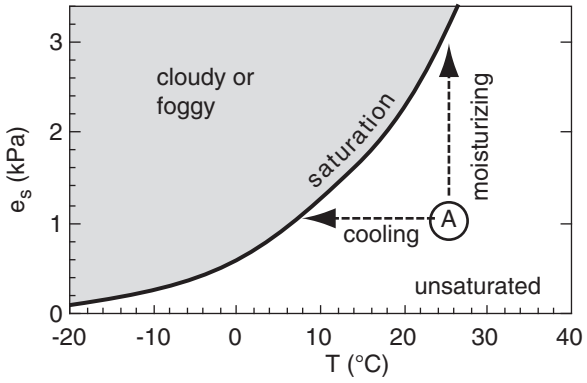

Figure 6.1
Unsaturated air parcel "A" can become saturated by the addition of moisture, or by cooling. The curved line is the saturation vapor pressure from the Moisture chapter.

The moisture addition necessary to reach saturation is

$$\Delta r = r_s - r \tag{6.2}$$

Whether this condition is met can be determined by using the moisture budget to find the actual humidity change (see the Moisture chapter).

In the real atmosphere, sometimes both cooling and moisturizing happen simultaneously. Schematically, this would correspond to an arrow from parcel *A* diagonally to the saturation line of Fig. 6.1.

Clouds usually form by adiabatic cooling of rising air. Air can be rising due to its own buoyancy (making **cumuliform** clouds), or can be forced up over hills or frontal boundaries (making **stratiform** clouds). Once formed, infrared radiation from cloud top can cause additional cooling to help maintain the cloud.

Solved Example

Air at sea level has a temperature of 20°C and a mixing ratio of 5 g/kg. How much cooling OR moisturizing is necessary to reach saturation?

Solution

Given: $T = 20°C$, $r = 5$ g/kg
Find: $\Delta T = ?$ °C, $\Delta r = ?$ g/kg.

Use Table 4-1 because it applies for sea level. Otherwise, solve equations or use a thermo diagram.
At $T = 20°C$, the table gives $r_s = 14.91$ g/kg .
At $r = 5$ g/kg, the table gives $T_d = 4$ °C .

Use eq. (6.1): $\Delta T = 4 - 20 =$ **–16°C** needed.
Use eq. (6.2): $\Delta r = 14.91 - 5 =$ **9.9 g/kg** needed.

Check: Units OK. Physics OK.
Discussion: This air parcel is fairly dry. Much cooling or moisturizing is needed.

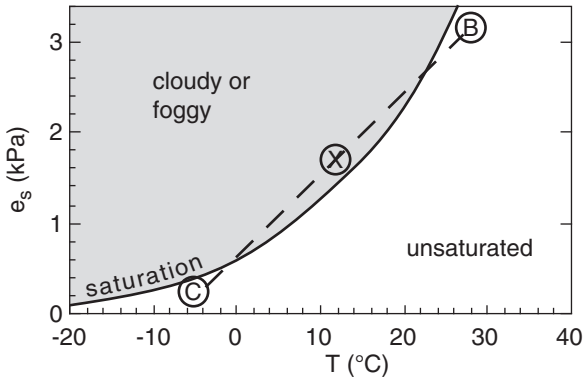

Figure 6.2
Mixing of two unsaturated air parcels B and C, which occurs along a straight line (dashed), can cause a saturated mixture X. The curved line is the saturation vapor pressure from the Moisture chapter.

Mixing

Mixing of two unsaturated parcels can result in a saturated mixture, as shown in Fig. 6.2. Jet contrails and your breath on a cold winter day are examples of clouds that form by the mixing process.

Mixing essentially occurs along a straight line in this graph connecting the thermodynamic states of the two original air parcels. However, the saturation line (given by the Clausius-Clapeyron equation) is curved, so a mixture can be saturated even if the original parcels are not.

Let m_B and m_C be the original masses of air in parcels *B* and *C*, respectively. The mass of the mixture (parcel *X*) is :

$$m_X = m_B + m_C \tag{6.3}$$

The temperature and vapor pressure of the mixture are the weighted averages of the corresponding values in the original parcels:

$$T_X = \frac{m_B \cdot T_B + m_C \cdot T_C}{m_X} \tag{6.4}$$

$$e_X = \frac{m_B \cdot e_B + m_C \cdot e_C}{m_X} \tag{6.5}$$

Specific humidity or mixing ratio can be used in place of vapor pressure in eq. (6.5).

Instead of using the actual masses of the air parcels in eqs. (6.3) to (6.5), you can use the relative portions that mix. For example, if the mixture consists of 3 parts B and 2 parts C, then you can use $m_B = 3$ and $m_C = 2$ in the equations above.

Solved Example

Suppose that the state of parcel B is T = 30°C with e = 3.4 kPa, while parcel C is T = –4°C with e = 0.2 kPa. Both parcels are at P = 100 kPa. If each parcel contains 1 kg of air, then what is the state of the mixture? Will the mixture be saturated?

Solution

Given: B has T = 30°C, e = 3.4 kPa, P = 100 kPa
C has T = –4°C, e = 0.2 kPa, P = 100 kPa
Find: T = ? °C and e = ? kPa for mixture (at X).

Use eq. (6.3): $m_X = 1 + 1 = 2$ kg
Use eq. (6.4): T_X =
[(1kg)·(30°C) + (1kg)·(–4°C)]/(2kg) = **13°C**.
Use eq. (6.5): e_X =
[(1kg)·(3.4 kPa) + (1kg)·(0.2 kPa)]/(2kg) = **1.8 kPa**
P hasn't changed. P = **100 kPa**.

Check: Units OK. Physics OK.
Discussion: At T = 13°C, Table 4-1 gives e_s = 1.5 kPa. Thus, the mixture **is saturated** because its vapor pressure exceeds the saturation vapor pressure. This mixture would be cloudy/foggy.

CLOUD IDENTIFICATION & DEVELOPMENT

You can easily find beautiful photos of all the clouds mentioned below by pointing your web-browser search engine at "cloud classification", "cloud identification", "cloud types", or "International Cloud Atlas". You can also use web search engines to find images of any named cloud. To help keep the cost of this book reasonable, I do not include any cloud photos.

Cumuliform

Cumuliform clouds form vertically in updrafts, and look like fluffy puffs of cotton, cauliflower, rising castle turrets, or in extreme instability as anvil-topped thunderstorms that look like big mushrooms. These clouds have diameters roughly equal to the height of their cloud tops above ground (Fig. 6.3). Thicker clouds look darker when viewed from underneath, but when viewed from the side, the cloud sides and top are often bright white during daytime. The individual clouds are often surrounded by clearer air, where there is compensating **subsidence** (downdrafts).

Cumulus clouds frequently have cloud bases within 1 or 2 km of the ground (in the boundary layer). But their cloud tops can be anywhere within the troposphere (or lower stratosphere for the strongest thunderstorms).

Cumuliform clouds are named by their thickness, not by the height of their base (Fig. 6.3). Starting from the thinnest (with lowest tops), the clouds are **cumulus humilis** (**fair-weather cumulus**),

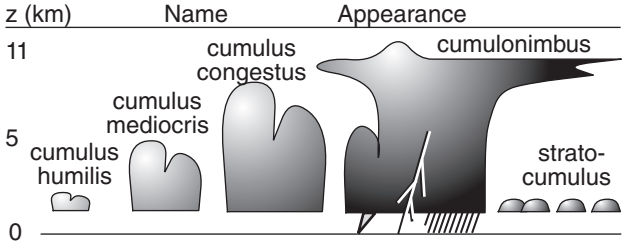

Figure 6.3
Cloud identification: **cumuliform.** *These are lumpy clouds caused by convection (updrafts) from the surface.*

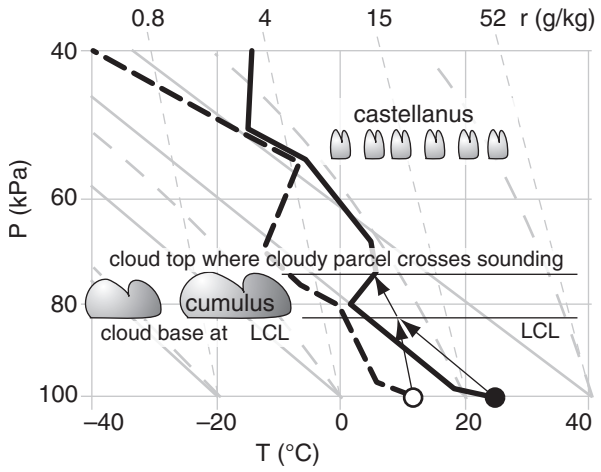

Figure 6.4
Characteristic sounding for cumulus humilis and altocumulus castellanus clouds. Solid thick black line is temperature; dashed black line is dew point; LCL = lifting condensation level. The cumulus humilis clouds form in thermals of warm air rising from the Earth's surface. The altocumulus castellanus clouds are a special stratiform cloud (discussed later in this chapter) that are not associated with thermals rising from the Earth's surface.

Solved Example

Use the sounding in the solved example on the same page as the start of the "Parcel vs. Environment" section of the Stability chapter. Where is cloud base and top for an air parcel rising from the surface?

Solution

Given: sounding from the Stability chapter.
Find: P_{base} = ? kPa, P_{top} = ? kPa

First, plot the sounding on a large thermo diagram from the Stability chapter. Then conceptually lift a parcel dry adiabatically from the surface until it crosses the isohume from the surface. That LCL is at P_{base} = 80 kPa.

However, the parcel never gets there. It hits the environment below the LCL, at roughly P = 83 kPa. Neglecting any inertial overshoot of the parcel, it would have zero buoyancy and stop rising 3 kPa below the LCL. Thus, there is **no cloud** from rising surface air.

Check: Units OK. Physics OK.
Discussion: This was a trick question. Also, the presence of mid-level stratiform clouds is irrelevant.

cumulus mediocris, **cumulus congestus** (**towering cumulus**), and **cumulonimbus** (**thunderstorms**).

Cumuliform clouds develop in **statically unstable air**. The unstable air tries to turbulently stabilize itself by creating convective updrafts and downdrafts. Cumuliform clouds can form in the tops of warm updrafts (**thermals**) if sufficient moisture is present. Hence, cumulus clouds are **convective clouds**. These clouds are dynamically **active** in the sense that their own internal buoyancy-forces (associated with latent heat release) enhance and support the convection and their vertical growth.

If the air is continually destabilized by some external forcing, then the convection persists. Some favored places for destabilization and small to medium cumulus clouds are:

- behind cold fronts,
- on mostly clear days when sunshine warms the ground more than the overlying air,
- over urban and industrial centers that are warmer than the surrounding rural areas,
- when cold air blows over a warmer ocean or lake.

Cold fronts trigger deep cumuliform clouds (thunderstorms) along the front, because the advancing cold air strongly pushes up the warmer air ahead of it, destabilizing the atmosphere and triggering the updrafts (see Thunderstorm chapters).

Also mountains can trigger all sizes of cumulus clouds including thunderstorms. One mechanism is **orographic lift,** when horizontal winds hit the mountains and are forced up. Another mechanism is **anabatic circulation**, where mountain slopes heated by the sun tend to organize the updrafts along the mountain tops (see Local Winds chapter).

Once triggered, cumulus clouds can continue to grow and evolve somewhat independently of the initial trigger. For example, orographically-triggered thunderstorms can persist as they are blown away from the mountain.

On a thermo diagram, **cloud top** is where the buoyant cloud parcel crosses the environmental sounding, and loses its positive buoyancy (Fig. 6.4). **Cloud base** is the lifting condensation level (LCL).

Stratiform

Stratiform clouds are horizontally layered clouds that look like sheets or blankets covering wide areas (Fig. 6.5). Clouds ahead of warm fronts are typically stratiform, including: **cirrus**, **cirrostratus**, **cirrocumulus**, **altostratus**, **altocumulus**, **stratus**, and **nimbostratus**.

Layered clouds are often grouped (high, middle, low) by their relative altitude or level within the

troposphere. However, troposphere thickness and **tropopause height** vary considerably with latitude (high near the equator, and low near the poles, see Table 6-1). It also varies with season (high during summer, low during winter).

Thus, low, middle and high clouds can have a range of altitudes. Table 6-1 lists cloud levels and their altitudes as defined by **World Meteorological Organization** (**WMO**). These heights are only approximate, as you can see from the overlapping values in the table.

High, layered clouds have the prefix "cirro" or "cirrus". The cirrus and cirrostratus are often wispy or have diffuse boundaries, and indicate that the cloud particles are made of ice crystals. In the right conditions, these ice-crystal clouds can cause beautiful **halos** around the sun or moon. See the last chapter for a discussion of atmospheric optics.

Mid-level, layered clouds have the prefix "alto". These and the lower clouds usually contain liquid water droplets, although some ice crystals can also be present. In the right conditions (relatively small uniformly sized drops, and a thin cloud) you can see an optical effect called **corona**. Corona appears as a large disk of white light centered on the sun or moon (still visible through the thin cloud). Colored fringes surround the perimeter of the white disk (see the Optics chapter).

Cirrostratus and altostratus are particularly smooth looking, which implies little or no turbulence within them. Cirrocumulus and altocumulus are layers of lumpy clouds, but the lumps are small and the edges are often sharply defined, suggesting that they are predominantly composed of liquid water droplets. We infer from these small sizes that the turbulent eddies causing these lumps are locally generated within the cloud layer, and are not associated with updrafts from the ground.

Stratus is a thick, smooth, cloud layer at low altitudes, but this type of cloud is not turbulently coupled with the underlying surface. Nimbostratus clouds are thick enough to allow drizzle or rain to form and fall out.

The prefix "**nimbo**" or suffix "**nimbus**" originally designated a precipitating cloud, but such a meaning is no longer prescribed in the international cloud atlas. Nimbostratus usually have light to moderate rain or snow over large horizontal areas, while cumulonimbus (thunderstorm) clouds have heavy rain (or snow in winter) and sometimes hail in small areas or along narrow paths on the ground called **swaths** (e.g., hail swaths or snow swaths).

Stratiform clouds form in **statically stable** air. These are dynamically **passive**, in the sense that buoyant forces suppress their vertical growth. These clouds exist only while some external process causes lifting to overcome the buoyancy.

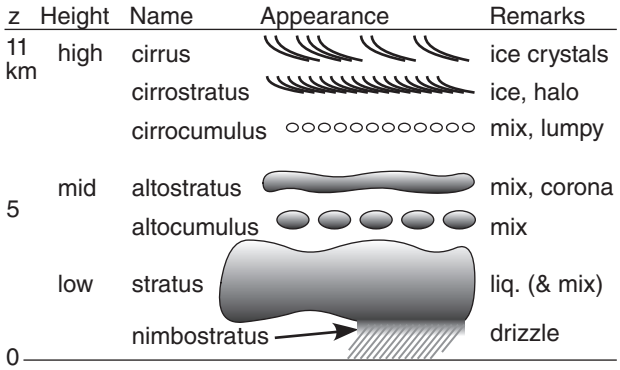

Figure 6.5
Cloud identification: **stratiform.** *Layered clouds caused by nearly horizontal advection of moisture by winds. "Mix" indicates a mixture of liquid and solid water particles. Heights "z" are only approximate — see Table 6–1 for actual ranges.*

Table 6-1. Heights (*z*) and pressures (*P*) of clouds and the tropopause. Tropopause values are average typical values, while cloud heights (*z*) are as defined by the WMO. Pressures are estimated from the heights.
sfc. = Earth's surface.

Region:	**Polar**	**Mid-latitude**	**Tropical**
Tropopause:			
z (km)	8	11	18
P (kPa)	35	22	8
High Clouds:			
z (km)	3 - 8	5 - 13	6 - 18
P (kPa)	70 - 35	54 - 16	47 - 8
Middle Clouds:			
z (km)	2 - 4	2 - 7	2 - 8
P (kPa)	80 - 61	80 - 41	80 - 35
Low Clouds:			
z (km)	sfc. - 2	sfc. - 2	sfc. - 2
P (kPa)	P_{sfc} - 80	P_{sfc} - 80	P_{sfc} - 80

For most stratiform clouds, the external forcing is horizontal **advection** (movement by the mean wind), where humid air is blown up a gently-inclined warm-frontal surface from moisture sources hundreds to thousands of kilometers away.

This process is illustrated in Fig. 5.20. Let the circle in that figure represent a humid air parcel with potential temperature 290 K. If a southerly wind were tending to blow the parcel toward the pole, the parcel would follow the 290 K isentrope like a train on tracks, and would ride up over the colder surface air in the polar portion of the domain. The gentle rise of air along the isentropic surface creates sufficient cooling to cause the condensation.

Stratiform clouds can be inferred from soundings (Fig. 6.6), in the layers above the boundary layer where environmental temperature and dew point are equal (i.e., where the sounding lines touch). Due to inaccuracies in some of the sounding instruments, sometimes the T and T_d lines become close and parallel over a layer without actually touching. You can infer that these are also stratiform cloud layers.

All of the stratiform clouds listed above are not convectively coupled with the ground directly underneath them. Hence, their cloud base cannot be calculated using the LCL for air directly under them. In spite of their lumpiness, cirrocumulus and altocumulus are formed primarily by advection, and are passive layer (i.e., stratiform) clouds. Do not let the suffix "cumulus" in those cloud names fool you.

In North America the nimbostratus clouds often have low bases, and are considered to be a low cloud. However, as we will see in the international cloud classification section, nimbostratus clouds are traditionally listed a mid-level clouds. In this book, we will treat **nimbostratus** as stratiform rain clouds with low cloud base.

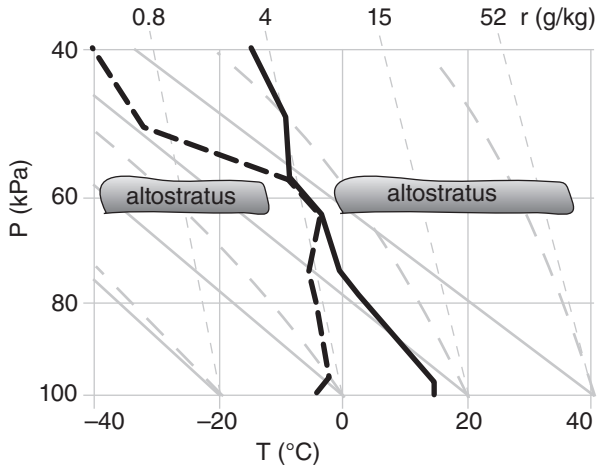

Figure 6.6
Characteristic sounding for stratiform clouds.

Stratocumulus

Stratocumulus clouds are low layers of lumpy clouds, often covering 5/8 or more of the sky (Fig. 6.3). They are somewhat different from either active and passive clouds. Unlike passive clouds, they can be formed by updrafts by air rising from near the surface. Unlike active clouds, these updrafts are sometimes not caused by buoyancy, but can be caused by turbulence generated by wind shear. The larger eddy circulations in the turbulence can lift air parcels from the ground up to the LCL, allowing the clouds to form. Unlike stratus clouds, stratocumulus clouds are turbulently coupled with the underlying surface, and their cloud bases can be estimated using the LCL for near-surface air.

In the real atmosphere, both buoyancy and shear often contribute to the updrafts into the base of stratocumulus clouds. Also, IR radiation emitted upward from cloud top can cool the cloud top, creating cool air parcels that sink as upside-down thermals (i.e., convection driven by cooling from the top, instead of by heating from below). The resulting turbulent circulations can contribute to the lumpiness of the stratocumulus deck (cloud layers are sometimes called **cloud decks**).

Others

There are many beautiful and unusual clouds that do not fit well into the cumuliform and stratiform categories. A few are discussed here: castellanus, lenticular, cap, rotor, banner, contrails, fumulus, billow clouds, pileus, and fractus. Again, you can find pictures of these using your web browser.

Other clouds associated with thunderstorms are described in the Thunderstorm chapters. These include funnel, wall, mammatus, arc, shelf, flanking line, beaver tail, and anvil.

Clouds in unstable air aloft

Two types of clouds can form in layers of statically or dynamically unstable air aloft: castellanus and billow clouds.

Castellanus clouds are distinctive because their diameters are small compared to their height above ground, making them look like castle turrets (Fig. 6.4). They can form in layers of statically unstable air aloft. These layers are forced by **differential advection**; namely, by wind blowing in air of different temperatures from different directions at different heights. For castellanus clouds, differential advection creates a layer of relatively warm air under colder air, which is statically unstable.

If these form just above the top of the boundary layer, they are called **cumulus castellanus**. When slightly higher, in the middle of the troposphere, they are called **altocumulus castellanus**. Alto-

cumulus castellanus are sometimes precursors to thunderstorms (because they indicate an unstable mid-troposphere), and are a useful clue for storm chasers.

Billow clouds (discussed in the Stability chapter) are a layer of many parallel, horizontal lines of cloud that form in the crests of **Kelvin-Helmholtz** (**K-H**) waves (Fig. 5.17). They indicate a layer of turbulence aloft caused by wind shear and dynamic instability. Pilots avoid these turbulent layers. When similar turbulent layers form with insufficient moisture to be visible as billow clouds, the result is a layer of **clear-air turbulence** (**CAT**), which pilots also try to avoid. Sometimes instead of a layer of billows, there will be only a narrow band of breaking wave clouds known as **K-H wave clouds**.

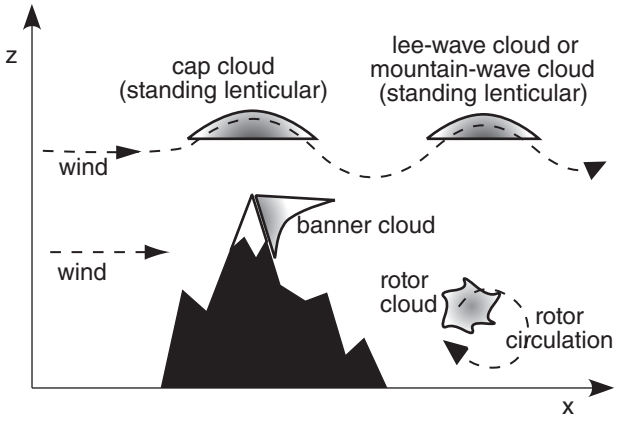

Figure 6.7
Some clouds caused by mountains, during strong winds.

Clouds associated with mountains

In mountainous regions with sufficient humidity, you can observe lenticular, cap, rotor, and banner clouds. The Local Winds chapter discusses others.

Lenticular clouds have smooth, distinctive lens or almond shapes when viewed from the side, and they are centered on the mountain top or on the crest of the lee wave (Fig. 6.7). They are also known as **mountain-wave clouds**, and are dynamically passive clouds that form in hilly regions. If a lenticular cloud forms directly over a mountain, it is sometimes called a **cap cloud**. Cap clouds are caused by updrafts forced when statically-stable air, blown horizontally by the wind, hits sloping terrain or mountains. Lenticular clouds can form in the crest of vertical oscillations in the air called mountain waves that form downwind of mountains.

They are a most unusual cloud, because the cloud remains relatively stationary while the air blows through it. Hence, they are known as **standing lenticular**. The uniformity of droplet sizes in lenticular clouds create beautiful optical phenomena called **iridescence** when the sun appears close to the cloud edge. See the Local Winds chapter for mountain wave details, and the Optics chapter for more on atmospheric optics.

Rotor clouds are violently turbulent balls or bands of ragged cloud that rapidly rotate along a horizontal axis (Fig. 6.7). They form relatively close to the ground under the crests of mountain waves (e.g., under standing lenticular clouds), but much closer to the ground. Pilots flying near the ground downwind of mountains during windy conditions should watch out for, and avoid, these hazardous clouds, because they indicate severe turbulence.

The **banner cloud** is a very turbulent streamer attached to the mountain top that extends like a banner or flag downwind (Fig. 6.7). It forms on the lee side at the very top of high, sharply pointed, mountain peaks during strong winds. As the wind separates to flow around the mountain, low pressure forms to the lee of the mountain peak, and counter-rotating vortices form on each side of the mountain. These work together to draw air upward along the lee slope, causing cooling and condensation. These strong turbulent winds can also pick up previously fallen ice particles from snow fields on the mountain surface, creating a **snow banner** that looks similar to the banner cloud.

Clouds due to surface-induced turbulence

The most obvious clouds formed due to surface-induced turbulence are the **cumuliform** (convective) clouds already discussed. However, there are two others that we haven't covered yet: pileus and fractus.

The **pileus cloud** looks like a thin hat just above, or scarf around, the top of the rising cumulus clouds (Fig. 6.8). It forms in mid-tropospheric humid (nearly saturated) layers of statically stable air that are forced upward above the tops of rapidly rising cumulus congestus clouds (hence, the indirect influence from surface heating). These are very short lived, because the cloud towers quickly rise through the pileus and engulf them.

Fractus clouds are ragged, shredded, often low-altitude clouds that form and dissipate quickly (Fig. 6.8). They can form during windy conditions in the turbulent, boundary-layer air near rain showers, under the normal nimbostratus or cumulonimbus cloud base. These clouds do not need mountains to form, but are often found along the sides of mountains during rainy weather. The falling rain from the cloud above adds moisture to the air, and the updraft portions of turbulent eddies provide the lifting to reach condensation.

Sometimes fractus clouds form in non-rainy conditions, when there is both strong winds and strong

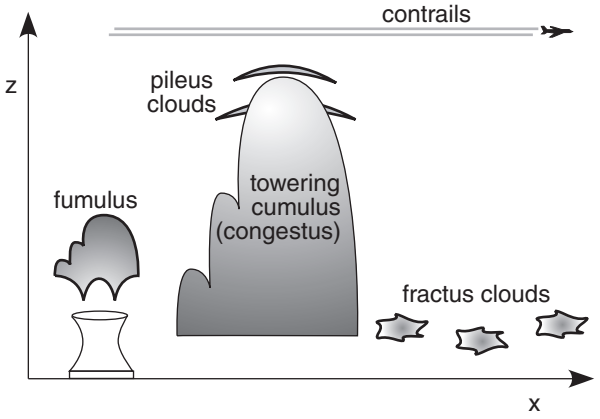

Figure 6.8
Other clouds.

FOCUS • Strato- & Mesospheric Clouds

Although almost all our clouds occur in the troposphere, sometimes higher-altitude thin stratiform (cirrus-like) clouds can be seen. They occur poleward of 50° latitude during situations when the upper atmosphere temperatures are exceptionally cold.

These clouds are so diffuse and faint that you cannot see them by eye during daytime. These clouds are visible at night for many minutes near the end of evening twilight or near the beginning of morning twilight. The reason these clouds are visible is because they are high enough to still be illuminated by the sun, even when lower clouds are in the Earth's shadow.

Highest are **noctilucent clouds**, in the mesosphere at heights of about 85 km. They are made of tiny H_2O ice crystals (size ≈ 10 nm), and are nucleated by meteorite dust. Noctilucent clouds are **polar mesospheric clouds (PMC)**, and found near the polar mesopause during summer.

Lower (20 to 30 km altitude) are **polar stratospheric clouds (PSC)**. At air temperatures below –78°C, nitric acid trihydrate (**NAT-clouds**) can condense into particles. Also forming at those temperatures can be particles made of a supersaturated mixture of water, sulphuric acid, and nitric acid (causing **STS clouds**).

For temperatures colder than –86°C in the stratosphere, pure H_2O ice crystals can form, creating PSCs called **nacreous clouds**. They are also known as **mother-of-pearl clouds** because they exhibit beautiful iridescent fringes when illuminated by the sun. These stratospheric clouds form over mountains, due to mountain waves that propagate from the troposphere into the stratosphere, and amplify there in the lower-density air. They can also form over extremely intense tropospheric high-pressure regions.

solar heating. In this case, the rising thermals lift air to its LCL, while the intense turbulence in the wind shear shreds and tears apart the resulting cumulus clouds to make **cumulus fractus**.

Anthropogenic Clouds

The next two clouds are **anthropogenic** (man-made). These are contrails and fumulus.

Fumulus is a contraction for "fume cumulus". They form in the tops of thermal plumes rising from cooling towers, forest fires, or smokestacks (Fig. 6.8). Modern air-quality regulations often require that industries scrub the pollutants out of their stack gasses by first passing the gas through a scrubber (i.e., a water shower). Although the resulting effluent much is less polluted, it usually contains more water vapor, and thus can cause beautiful white clouds of water droplets within the rising exhaust plume. Similarly, cooling towers do their job by evaporating water to help cool an industrial process, while forest fires produce water vapor and smoke as combustion products when wood burns.

Contrail is a contraction for "condensation trail", and is the straight, long, narrow, horizontal pair of clouds left behind a high-altitude aircraft (Fig. 6.8). Aircraft fuel is a hydrocarbon, so its combustion in a jet engine produces carbon dioxide and water vapor. Contrails form when water vapor in the exhaust of high-altitude aircraft mixes with the cold environmental air at that altitude (see mixing subsection earlier in this chapter). If this cold air is already nearly saturated, then the additional moisture from the jet engine is sufficient to form a cloud. On drier days aloft, the same jet aircraft would produce no visible contrails.

Regardless of the number of engines on the aircraft, the exhaust tends to be quickly entrained into the horizontal **wing-tip vortices** that trail behind the left and right wing tips of the aircraft. Hence, jet contrails often appear initially as a pair of closely-spaced, horizontal parallel lines of cloud. Further behind the aircraft, environmental wind shears often bend and distort the contrails. Turbulence breaks apart the contrail, causes the two clouds to merge into one contrail, and eventually mixes enough dry ambient air to cause the contrail to evaporate and disappear.

Contrails might have a small effect on the global-climate heat budget by reflecting some of the sunlight. Contrails are a boon to meteorologists because they are a clue that environmental moisture is increasing aloft, which might be the first indication of an approaching warm front. They are a bane to military pilots who would rather not have the enemy see a big line in the sky pointing to their aircraft.

CLOUD ORGANIZATION

Clouds frequently become organized into patterns during stormy weather. This organization is discussed in the chapters on Fronts, Midlatitude Cyclones, Thunderstorms, and Hurricanes. Also, sometimes large-scale processes can organize clouds even during periods of fair weather, as discussed here.

Cloud streets or **cloud lines** are rows of fair-weather cumulus-humilis clouds (Fig. 6.9) that are roughly parallel with the mean wind direction. They form over warm land in the boundary layer on sunny days, and over water day or night when cold air advects over warmer water. Light to moderate winds in the convective boundary layer cause **horizontal roll vortices**, which are very weak counter-rotating circulations with axes nearly parallel with the mean wind direction. These weak circulations sweep rising cloud-topped thermals into rows with horizontal spacing of roughly twice the boundary-layer depth (order of 1 km).

Mesoscale cellular convection (**MCC**) can also form in the boundary layer, but with a much larger horizontal scale (order of 5 to 50 times the boundary layer depth; namely, 10 to 100 km in diameter). These are so large that the organization is not apparent to observers on the ground, but is readily visible in satellite images. **Open cells** consist of a honeycomb or rings of cloud-topped updrafts around large clear regions (Fig. 6.9). **Closed cells** are the opposite — a honeycomb of clear-air rings around cloud clusters. Cloud streets changing into MCC often form when cold continental air flows over a warmer ocean. [*WARNING: Abbreviation **MCC** is also used for **Mesoscale Convective Complex**, which is a cluster of deep thunderstorms.*]

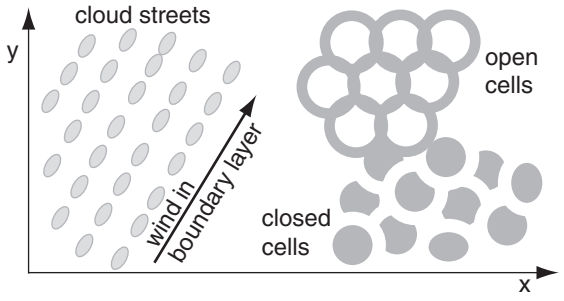

Figure 6.9
Organized boundary-layer clouds, such as are seen in a satellite image. Grey = clouds.

ON DOING SCIENCE • Cargo Cult Science

"In the South Seas there is a cargo cult of people. During the war they saw airplanes land with lots of good materials, and they want the same thing to happen now. So they've arranged to make things like runways, to put fires along the sides of the runways, to make a wooden hut for a man to sit in, with two wooden pieces on his head like headphones and bars of bamboo sticking out like antennas – he's the controller – and they wait for the airplanes to land. They're doing everything right. The form is perfect. It looks exactly the way it looked before. But it doesn't work. No airplanes land. So I call these things cargo cult science, because they follow the apparent precepts and forms of scientific investigation, but they're missing something essential, because the planes don't land."

"Now it behooves me, of course, to tell you what they're missing. ... It's a kind of scientific integrity, a principle of scientific thought that corresponds to a kind of utter honesty... For example, if you're doing an experiment, you should report everything that you think might make it invalid – not only what you think is right about it: other causes that could possibly explain your results; and things you thought of that you've eliminated by some other experiment, and how they worked – to make sure the other fellow can tell they have been eliminated."

"Details that could throw doubt on your interpretation must be given, if you know them. You must do the best you can – if you know anything at all wrong, or possibly wrong – to explain it. If you make a theory, ... then you must also put down all the facts that disagree with it, as well as those that agree with it. There is also a more subtle problem. When you have put a lot of ideas together to make an elaborate theory, you want to make sure when explaining what it fits, that those things it fits are not just the things that gave you the idea for the theory; but that the finished theory makes something else come out right, in addition."

"In summary, the idea is to try to give all the information to help others to judge the value of your contribution; not just the information that leads to judgement in one particular direction or another."

– Richard P. Feynman, 1985: *"Surely You're Joking, Mr. Feynman!". Adventures of a Curious Character.* Bantam. 322pp.

Science Graffito

"Science is the belief in the ignorance of experts."
– Richard Feynman.

CLOUD CLASSIFICATION

Cloud morphology is the study and classification of cloud shapes. The classification method introduced in 1803 by Luke Howard is still used today, as approved by the World Meteorology Organization (WMO).

WMO publishes an *International Cloud Atlas* with photos to help you identify clouds. As mentioned, you can easily find similar photos for free by pointing your web search engine at "cloud classification", "cloud identification", "cloud types", or "International Cloud Atlas".

The categories and subcategories of clouds are broken into:

- **genera** - main characteristics of clouds
- **species** - peculiarities in shape & structure
- **varieties** - arrangement and transparency
- **supplementary features** and **accessory clouds** - attached to other (mother) clouds
- **mother clouds** - clouds with attachments
- **meteors** - precipitation (ice, water, or mixed)

Most important are the genera.

Genera

The ten cloud **genera** are listed in Table 6-2, along with their official abbreviations and symbols as drawn on weather maps. These genera are mutually exclusive; namely, one cloud cannot have two genera. However, often the sky can have different genera of clouds adjacent to, or stacked above, each other.

Table 6-2. Cloud genera.

Genus	Abbreviation	WMO Symbol	USA Symbol
cirrus	Ci		
cirrostratus	Cs		
cirrocumulus	Cc		
altostratus	As		
altocumulus	Ac		
nimbostratus	Ns		
stratus	St		
stratocumulus	Sc		
cumulus	Cu		
cumulonimbus	Cb		

Species

Subdividing the genera are cloud **species**. Table 6-3 lists the official WMO species. Species can account for:

- forms (clouds in banks, veils, sheets, layers, etc.)
- dimensions (horizontal or vertical extent)
- internal structure (ice crystals, water droplets, etc.)
- likely formation process (orographic lift, etc.)

Species are also mutually exclusive. An example of a cloud genus with specie is "Altocumulus castellanus (Ac cas)", which is a layer of mid-level lumpy clouds that look like castle turrets.

Table 6-3. WMO cloud species. (Ab. = abbreviation)

Specie	Ab	Description
calvus	cal	the top of a deep Cu or Cb that is starting to become fuzzy, but no cirrus (ice) anvil yet
capillatus	cap	Cb having well defined streaky cirrus (ice) anvil
castellanus	cas	small turrets looking like a crenellated castle. Turret height > diameter. Can apply to Ci, Cc, Ac, Sc.
congestus	con	very deep Cu filling most of troposphere, but still having crisp cauliflower top (i.e., no ice anvil). Often called **Towering Cu** (TCU).
fibratus	fib	nearly straight filaments of Ci or Cs.
floccus	flo	small tufts (lumps) of clouds, often with virga (evaporating precip.) falling from each tuft. Applies to Ci, Cc, Ac, Sc.
fractus	fra	shredded, ragged, irregular, torn by winds. Can apply to Cu and St.
humilis	hum	Cu of small vertical extent. Small flat lumps.
lenticularis	len	having lens or almond cross section, often called mountain wave clouds. Applies to Cc, Ac, Sc.
mediocris	med	medium size Cu
nebulosus	neb	Cs or St with veil or layer showing no distinct details
spissatus	spi	thick Ci that looks grey.
stratiformis	str	spreading out into sheets or horizontal layers. Applies to Ac, Sc, Cc.
uncinus	unc	hook or comma shaped Ci

Varieties

Genera and species are further subdivided into **varieties** (Table 6-4), based on:

- transparency (sun or moon visible through cloud)
- arrangement of visible elements

These varieties are NOT mutually exclusive (except for translucidus and opacus), so you can append as many varieties to a cloud identification that apply. For example, "cumulonimbus capillatus translucidus undulatus" (Cb cap tr un).

Table 6-4. WMO cloud varieties.

Variety	Ab.	Description
duplicatus	du	superimposed cloud patches at slightly different levels. Applies to Ci, Cs, Ac, As, Sc.
intortus	in	Ci with tangled, woven, or irregularly curved filaments
lacunosus	la	honeycomb, chessboard, or regular arrangement of clouds and holes. Applies to Cc, Ac, and Sc.
opacus	op	too thick for the sun or moon to shine through. Applies to Ac, As, Sc, St.
perlucidus	pe	a layer of clouds with small holes between elements. Applies to Ac, Sc.
radiatus	ra	very long parallel bands of clouds that, due to perspective, appear to converge at a point on the horizon. Applies to Ci, Ac, As, Sc, and Cu.
translucidus	tr	layer or patch of clouds through which sun or moon is somewhat visible. Applies to Ac, As, Sc, St.
undulatus	un	cloud layers or patches showing waves or undulations. Applies to Cc, Cs, Ac, As, Sc, St.
vertebratus	ve	Ci streaks arranged like a skeleton with vertebrae and ribs, or fish bones.

Supplementary Features

Table 6-5. WMO cloud supplementary features, and the **mother** clouds to which they are attached. (Ab. = abbreviation.)

Feature	Ab.	Description
arcus	arc	a dense horizontal roll cloud, close to the ground, along and above the leading edge of Cb gust-front outflows. Usually attached to the Cb, but can separate from it as the gust front spreads. Often has an arch shape when viewed from underneath, and a curved or arc shape in satellite photos.
incus	inc	the upper portion of a Cb, spread out into an (ice) anvil with smooth, fibrous or striated appearance.
mamma	mam	hanging protuberances of pouch-like appearance. Mammatus clouds are often found on the underside of Cb anvil clouds.
praecipitatio	pra	precipitation falling from a cloud and reaching the ground. Mother clouds can be As, Ns, Sc, St, Cu, Cb.
tuba	tub	a cloud column or funnel cloud protruding from a cloud base, and indicating an intense vortex. Usually attached to Cb, but sometimes to Cu.
virga	vir	visible precipitation trails that evaporate before reaching the ground. They can hang from Ac, Cu, Ns or Cb clouds.

Accessory Clouds

Smaller features attached to other clouds.

Table 6-6. WMO **accessory clouds**, and the **mother** clouds to which they are attached. (Ab.=abbreviation.)

Name	Ab.	Description
pannus	pan	ragged shreds, sometimes in a continuous layer, below a mother cloud and sometimes attached to it. Mother clouds can be As, Ns, Cu, Cb.
pileus	pil	a smooth thin cap, hood, or scarf above, or attached to, the top of rapidly rising cumulus towers. Very transient, because the mother cloud quickly rises through and engulfs it. Mother clouds are Cu con or Cb.
velum	vel	a thin cloud veil or sheet of large horizontal extent above or attached to Cu or Cb, which often penetrate it.

Table 6-7. Sky cover. Oktas= eighths of sky covered.

Sky Cover (oktas)	Symbol	Name	Abbr.	Sky Cover (tenths)
0	○	Sky **Clear**	SKC	0
1	◴	**Few*** Clouds	FEW*	1
2	◔			2 to 3
3	◕	**Scattered**	SCT	4
4	◑			5
5	◒	**Broken**	BKN	6
6	◕			7 to 8
7	◐			9
8	●	**Overcast**	OVC	10
unknown	⊗	Sky **Obscured**	**	unknown

** "Few" is used for (0 oktas) < coverage ≤ (2 oktas).*

*** See text body for a list of abbreviations of various obscuring phenomena.*

Solved Example

Use a spreadsheet to find and plot the fraction of clouds ranging from X = 50 to 4950 m width, given ΔX = 100 m, S_X =0.5, and L_X = 1000 m.

Solution

Given: ΔX = 100 m, S_X =0.5, L_X = 1000 m.
Find: $f(X)$= ?

Solve eq. (6.6) on a spreadsheet. The result is:

X (m)	f(X)
50	2.558×10^{-8}
150	0.0004
250	0.0068
350	0.0252
450	0.0495
550	0.0710
etc.	etc.
Sum of all f =	0.999

Check: Units OK. Physics almost OK, but the sum of all f should equal 1.0, representing 100% of the clouds. The reason for the error is that we should have considered clouds even larger than 4950 m, because of the tail on the right of the distribution. Also smaller ΔX would help.

Discussion: Although the dominant cloud width is about 800 m for this example, the long tail on the right of the distribution shows that there are also a small number of large-diameter clouds.

SKY COVER (CLOUD AMOUNT)

The fraction of the sky (celestial dome) covered by cloud is called **sky cover**, **cloud cover**, or **cloud amount**. It is measured in eights (**oktas**) according to the World Meteorological Organization. Table 6-7 gives the definitions for different cloud amounts, the associated symbol for weather maps, and the abbreviation for aviation weather reports (**METAR**).

Sometimes the sky is **obscured**, meaning that there might be clouds but the observer on the ground cannot see them. Obscurations (and their abbreviations) include: **mist** [BR; horizontal visibilities ≥ 1 km (i.e., ≥ 5/8 of a statute mile)], **fog** [FG; visibilities < 1 km (i.e., < 5/8 statute mile)], **smoke** (FU), **volcanic ash** (VA), **sand** (SA), **haze** (HZ), **spray** (PY), widespread **dust** (DU).

For aviation, the altitude of cloud base for the lowest cloud with coverage ≥ 5 oktas (i.e., lowest broken or overcast clouds) is considered the **ceiling**. For obscurations, the **vertical visibility** (VV) distance is reported as a ceiling instead.

CLOUD SIZES

Cumuliform clouds typically have diameters roughly equal to their depths, as mentioned previously. For example, a fair weather cumulus cloud typically averages about 1 km in size, while a thunderstorm might be 10 km.

Not all clouds are created equal. At any given time the sky contains a spectrum of cloud sizes that has a **lognormal distribution** (Fig. 6.10, eq. 6.6)

$$f(X) = \frac{\Delta X}{\sqrt{2\pi} \cdot X \cdot S_X} \cdot \exp\left[-0.5 \cdot \left(\frac{\ln(X / L_X)}{S_X} \right)^2 \right] \quad (6.6)$$

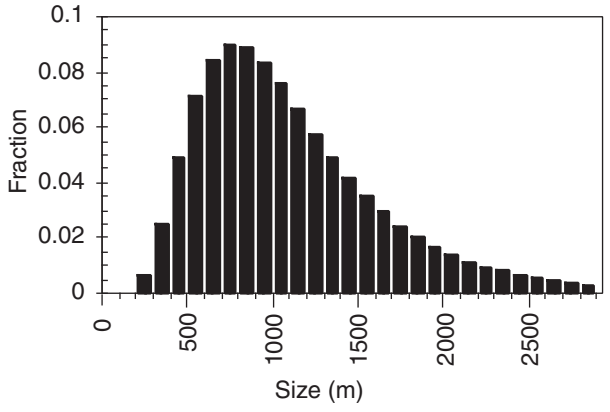

Figure 6.10
Lognormal distribution of cloud sizes.

where X is the cloud diameter or depth, ΔX is a small range of cloud sizes, $f(X)$ is the fraction of clouds of sizes between X–0.5ΔX and X+0.5ΔX, L_x is a location parameter, and S_x is a dimensionless spread parameter. These parameters vary widely in time and location.

According to this distribution, there are many clouds of nearly the same size, but there also are a few clouds of much larger size. This causes a skewed distribution with a long tail to the right (see Fig. 6.10).

Science Graffito

"... look to the failed answers to find in them a route to success."
– Mark Helprin, 2004: *A Brilliant Idea and His Own*.

FRACTAL CLOUD SHAPES

Fractals are patterns made of the superposition of similar shapes having a range of sizes. An example is a dendrite snow flake. It has arms protruding from the center. Each of those arms has smaller arms attached, and each of those has even smaller arms. Other aspects of meteorology exhibit fractal geometry, including lightning, turbulence, and clouds.

Fractal Dimension

Euclidian geometry includes only integer dimensions; for example 1-D, 2-D or 3-D. Fractal geometry allows a continuum of dimensions; for example $D = 1.35$.

Fractal dimension is a measure of space-filling ability. Common examples are drawings made by children, and newspaper used for packing cardboard boxes.

A straight line (Fig. 6.11a) has fractal dimension $D = 1$; namely, it is one-dimensional both in the Euclidian and fractal geometry. When toddlers draw with crayons, they fill areas by drawing tremendously wiggly lines (Fig. 6.11b). Such a line might have fractal dimension $D \approx 1.7$, and gives the impression of almost filling an area. Older children succeed in filling the area, resulting in fractal dimension $D = 2$.

A different example is a sheet of newspaper. While it is flat and smooth, it fills only two-dimensional area (neglecting its thickness), hence $D = 2$. However, it takes up more space if you crinkle it, resulting in a fractal dimension of $D \approx 2.2$. By fully wadding it into a tight ball of $D \approx 2.7$, it begins to behave more like a three-dimensional object, which is handy for filling empty space in cardboard boxes.

A **zero set** is a lower-dimensional slice through a higher-dimensional shape. Zero sets have fractal dimension one less than that of the original shape (i.e., $D_{zero\ set} = D - 1$). Sometimes it is easier to mea-

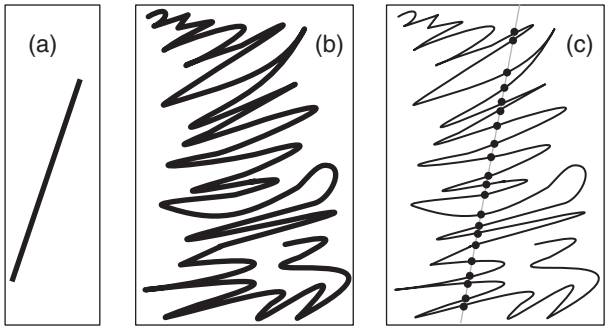

Figure 6.11
(a) A straight line has fractal dimension D = 1. (b) A wiggly line has fractal dimension 1 < D < 2. (c) The zero-set of the wiggly line is a set of points with dimension 0 < D < 1.

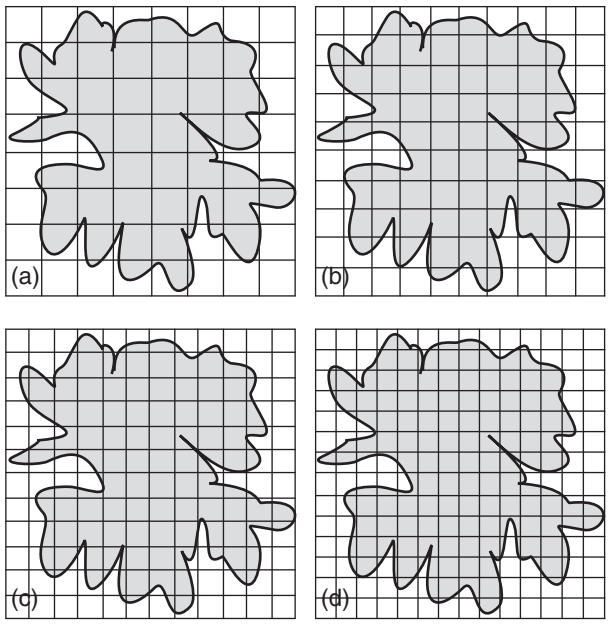

Figure 6.12
Cloud shadow overlaid with small tiles. The number of tiles M per side of domain is: (a) 8, (b) 10, (c) 12, (d) 14.

Solved Example

Use Fig. 6.12 to measure the fractal dimension of the cloud shadow.

Solution

For each figure, the number of boxes is:

	M	N
(a)	8	44
(b)	10	53
(c)	12	75
(d)	14	88

(You might get a slightly different count.)

Plot the result on a log-log graph, & fit a straight line.

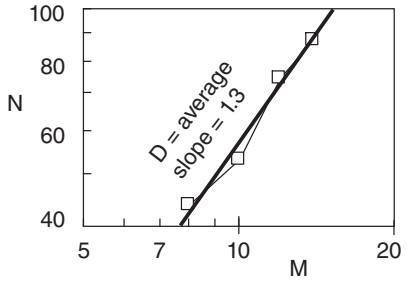

Use the end points of the best-fit line in eq. (6.7):

$$D = \frac{\log(100 / 40)}{\log(15 / 7.5)} = \underline{\mathbf{1.32}}$$

Check: Units OK. Physics OK.

Discussion: About right for a cloud. The original domain size relative to cloud size makes no difference. Although you will get different M and N values, the slope D will be almost the same.

sure the fractal dimension of a zero set, from which we can calculate the dimension of the original.

For example, start with the wad of paper having fractal dimension $D = 2.7$. It would be difficult to measure the dimension for this wad of paper. Instead, carefully slice that wad into two halves, dip the sliced edge into ink, and create a print of that inked edge on a flat piece of paper. The wiggly line that was printed (Fig. 6.11b) has fractal dimension of $D = 2.7 - 1 = 1.7$, and is a zero set of the original shape. It is easier to measure.

To continue the process, slice through the middle of the print (shown as the grey line in Fig. 6.11c). The wiggly printed line crosses the straight slice at a number of points (Fig. 6.11c); those points have a fractal dimension of $D = 1.7 - 1 = 0.7$, and represent the zero set of the print. Thus, while any one point has a Euclidian dimension of zero, the set of points appears to partially fill a 1-D line.

Measuring Fractal Dimension

Consider an irregular-shaped area, such as the shadow of a cloud. The perimeter of the shadow is a wiggly line, so we should be able to measure its fractal dimension. Based on observations of the perimeter of real-cloud shadows, $D = 1.35$. If we assume that this cloud shadow is a zero set of the surface of the cloud, then the cloud surface dimension is $D = D_{zero\ set} + 1 = 2.35$.

A **box-counting** method can be used to measure fractal dimension. Put the cloud-shadow picture within a square domain. Then tile the domain with smaller square boxes, with M tiles per side of domain (Fig. 6.12). Count the number N of tiles through which the perimeter passes. Repeat the process with smaller tiles.

Get many samples of N vs. M, and plot these as points on a log-log graph. The fractal dimension D is the slope of the best fit straight line through the points. Define subscripts 1 and 2 as the two end points of the best fit line. Thus:

$$D = \frac{\log(N_1 / N_2)}{\log(M_1 / M_2)} \qquad (6.7)$$

This technique works best when the tiles are small. If the plotted line is not straight but curves on the log-log graph, try to find the slope of the portion of the line near large M.

FOG

Types

Fog is a cloud that touches the ground. The main types of fog are:

- upslope
- radiation
- advection
- precipitation or frontal
- steam

They differ in how the air becomes saturated.

Upslope fog is formed by adiabatic cooling in rising air that is forced up sloping terrain by the wind. Namely, it is formed the same way as clouds. As already discussed in the Moisture chapter, air parcels must rise or be lifted to their lifting condensation level (LCL) to form a cloud or upslope fog.

Radiation fog and advection fog are formed by cooling of the air via conduction from the cold ground. **Radiation fog** forms during clear, nearly-calm nights when the ground cools by IR radiation to space. **Advection fog** forms when initially-unsaturated air advects over a colder surface.

Precipitation fog or **frontal fog** is formed by adding moisture, via the evaporation from warm rain drops falling down through the initially-unsaturated cooler air below cloud base.

Steam fog occurs when cold air moves over warm humid surfaces such as unfrozen lakes during early winter. The lake warms the air near it by conduction, and adds water by evaporation. However, this thin layer of moist warm air near the surface is unsaturated. As turbulence causes it to mix with the colder air higher above the surface, the mixture becomes saturated, which we see as steam fog.

Idealized Fog Models

By simplifying the physics, we can create mathematical fog models that reveal some of the fundamental behaviors of different types of fog.

Advection Fog

For formation and growth of advection fog, suppose a fogless mixed layer of thickness z_i advects with speed M over a cold surface such as snow covered ground or a cold lake. If the surface potential temperature is θ_{sfc}, then the air potential temperature θ cools with downwind distance according to

$$\theta = \theta_{sfc} + (\theta_o - \theta_{sfc}) \cdot \exp\left(-\frac{C_H}{z_i} \cdot x \right) \qquad (6.8)$$

Solved Example

Fog formation: A layer of air adjacent to the surface (where P = 100 kPa) is initially at temperature 20°C and relative humidity 68%. (a) To what temperature must this layer be cooled to form **radiation** or **advection** fog? (b) To what altitude must this layer be lifted to form **upslope** fog? (c) How much water must be evaporated into each kilogram of dry air from falling rain drops to form **frontal** fog? (d) How much evaporation (mm of lake water depth) from the lake is necessary to form **steam** fog throughout a 100 m thick layer? [Hint: Use eqs. from the Moisture chapter.]

Solution

Given: P = 100 kPa, T = 20°C, RH = 68%, Δz = 100 m
Find: a) T_d=?°C, b) z_{LCL}=?m, c) r_s=?g/kg d) d=?mm

Using Table 4-1: e_s = 2.371 kPa.
Using eq. (4.14): $e = (RH/100\%) \cdot e_s$
= (68%/100%)·(2.371 kPa) = 1.612 kPa

(a) Knowing e and using Table 4-1: T_d = **14°C**.

(b) Using eq. (4.16):
$z_{LCL} = a \cdot [T - T_d]$ = (0.125 m/K)·
[(20+273)K – (14+273)K] = **0.75 km**

(c) Using eq. (4.4), the initial state is:
$r = \varepsilon \cdot e/(P-e)$ = 0.622 · (1.612 kPa) / (100 kPa – 1.612 kPa) = 0.0102 g/g = 10.2 g/kg
The final mixing ratio at saturation (eq. 4.5) is:
$r_s = \varepsilon \cdot e_s/(P-e_s)$ = 0.622·(2.371 kPa) / (100 kPa – 2.371 kPa) = 0.0151 g/g = 15.1 g/kg.
The amount of additional water needed is
$\Delta r = r_s - r$ = 15.1 – 10.2 = **4.9** g_{water}/kg_{air}

(d) Using eqs. (4.11) & (4.13) to find absolute humidity
$\rho_v = \varepsilon \cdot e \cdot \rho_d / P$
= (0.622)·(1.612 kPa)·(1.275 kg·m^{-3})/(100 kPa)
= 0.01278 kg·m^{-3}
$\rho_{vs} = \varepsilon \cdot e_s \cdot \rho_d / P$
= (0.622)·(2.371 kPa)·(1.275 kg·m^{-3})/(100 kPa)
= 0.01880 kg·m^{-3}
The difference must be added to the air to reach saturation: $\Delta\rho = \rho_{vs} - \rho_v$ =
$\Delta\rho$ = (0.01880–0.01278) kg·m^{-3} = 0.00602 kg·m^{-3}
But over A =1 m^2 of surface area, air volume is
$Vol_{air} = A \cdot \Delta z$ = (1 m^2)·(100 m) = 100 m^3.
The mass of water needed in this volume is
$m = \Delta\rho \cdot Vol_{air}$ = 0.602 kg of water.
But liquid water density ρ_{liq} = 1000 kg·m^{-3}: Thus,
$Vol_{liq} = m / \rho_{liq}$ = 0.000602 m^3
The depth of liquid water under the 1 m^2 area is
$d = Vol_{liq} / A$ = 0.000602 m = **0.602 mm**

Check: Units OK. Physics OK.
Discussion: For many real fogs, cooling of the air and addition of water via evaporation from the surface happen simultaneously. Thus, a fog might form in this example at temperatures warmer than 14°C.

BEYOND ALGEBRA • Advection Fog

Derivation of eq. (6.8):

Start with the Eulerian heat balance, neglecting all contributions except for turbulent flux divergence:

$$\frac{\partial \theta}{\partial t} = -\frac{\partial F_{z\ turb}(\theta)}{\partial z}$$

where θ is potential temperature, and F is heat flux. For a mixed layer of fog, F is linear with z, thus:

$$\frac{\partial \theta}{\partial t} = -\frac{F_{z\ turb\ zi}(\theta) - F_{z\ turb\ sfc}(\theta)}{z_i - 0}$$

If entrainment at the top of the fog layer is small, then $F_{z\ turb\ zi}(\theta) = 0$, leaving:

$$\frac{\partial \theta}{\partial t} = \frac{F_{z\ turb\ sfc}(\theta)}{z_i} = \frac{F_H}{z_i}$$

Estimate the flux using bulk transfer eq. (3.21). Thus:

$$\frac{\partial \theta}{\partial t} = \frac{C_H \cdot M \cdot (\theta_{sfc} - \theta)}{z_i}$$

If the wind speed is roughly constant with height, then let the Eulerian volume move with speed M:

$$\frac{\partial \theta}{\partial t} = \frac{\partial \theta}{\partial x}\frac{\partial x}{\partial t} = \frac{\partial \theta}{\partial x} \cdot M$$

Plugging this into the LHS of the previous eq. gives:

$$\frac{\partial \theta}{\partial x} = \frac{C_H \cdot (\theta_{sfc} - \theta)}{z_i}$$

To help integrate this, define a substitute variable $s = \theta - \theta_{sfc}$, for which $\partial s = \partial \theta$. Thus:

$$\frac{\partial s}{\partial x} = -\frac{C_H \cdot s}{z_i}$$

Separate the variables: $\frac{ds}{s} = -\frac{C_H}{z_i}dx$

Which can be integrated (using the prime to denote a dummy variable of integration):

$$\int_{s'=s_o}^{s} \frac{ds'}{s'} = -\frac{C_H}{z_i}\int_{x'=0}^{x} dx'$$

Yielding:

$$\ln(s) - \ln(s_o) = -\frac{C_H}{z_i} \cdot (x - 0)$$

or

$$\ln\left(\frac{s}{s_o}\right) = -\frac{C_H}{z_i} \cdot x$$

Taking the antilog of each side (i.e., exp):

$$\frac{s}{s_o} = \exp\left(-\frac{C_H}{z_i} \cdot x\right)$$

Upon rearranging, and substituting for s:

$$\theta - \theta_{sfc} = (\theta - \theta_{sfc})_o \cdot \exp\left(-\frac{C_H}{z_i} \cdot x\right)$$

But θ_{sfc} is assumed constant, thus:

$$\boxed{\theta = \theta_{sfc} + (\theta_o - \theta_{sfc}) \cdot \exp\left(-\frac{C_H}{z_i} \cdot x\right)} \qquad (6.8)$$

where θ_o is the initial air potential temperature, C_H is the heat transfer coefficient (see the Heat chapter), and x is travel distance over the cold surface. This assumes an idealized situation where there is sufficient turbulence caused by a brisk wind speed to keep the boundary layer well mixed.

Advection fog forms when the temperature drops to the dew-point temperature T_d. At the surface (more precisely, at z = 10 m), $\theta \approx T$. Thus, setting $\theta \approx T = T_d$ at saturation and solving the equation above for x gives the distance over the lake at which fog first forms:

$$x = \frac{z_i}{C_H} \cdot \ln\left(\frac{T_o - T_{sfc}}{T_d - T_{sfc}}\right) \qquad (6.9)$$

Surprisingly, neither the temperature evolution nor the distance to fog formation depends on wind speed.

For example, advection fog can exist along the California coast where warm humid air from the

Solved Example

Air of initial temperature 5°C and depth 200 m flows over a frozen lake of surface temperature –3°C. If the initial dew point of the air is –1°C, how far from shore will **advection** fog first form?

Solution

Given: T_o = 5°C, T_d = –1°C,
T_{sfc} = –3 °C, z_i =200 m
Find: x = ? km.
Assume smooth ice: C_H = 0.002 .

Use eq. (6.9): x = (200 m/0.002)·
ln[(5–(–3))/(–1–(–3))] = **138.6 km**
Sketch, where eq. (6.8) was solved for T vs. x:

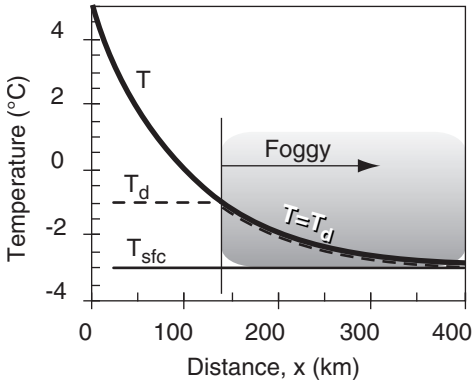

Check: Units OK. Physics OK.
Discussion: If the lake is smaller than 138.6 km in diameter, then no fog forms. Also, if the dew-point temperature needed for fog is colder than the surface temperature, then no fog forms.

west blows over the cooler "Alaska current" coming from further north in the Pacific Ocean.

Advection fog, once formed, experiences radiative cooling from fog top. Such cooling makes the fog more dense and longer lasting as it can evolve into a well-mixed radiation fog, described in the next subsection.

Dissipation of advection fog is usually controlled by the synoptic and mesoscale weather patterns. If the surface becomes warmer (e.g., all the snow melts, or there is significant solar heating), or if the wind changes direction, then the conditions that originally created the advection fog might disappear. At that point, dissipation depends on the same factors that dissipate radiation fog. Alternately, frontal passage or change of wind direction might blow out the advection fog, and replace the formerly-foggy air with cold dry air that might not be further cooled by the underlying surface.

Radiation Fog

For formation and growth of radiation fog, assume a stable boundary layer forms and grows, as given in the Atmospheric Boundary Layer chapter. For simplicity, assume that the ground is flat, so there is no drainage of cold air downhill (a poor assumption). If the surface temperature T_s drops to the dew-point temperature T_d then fog can form (Fig. 6.13). The fog depth is the height where the nocturnal temperature profile crosses the initial dew-point temperature T_{do}.

The time t_o between when nocturnal cooling starts and the onset of fog is

$$t_o = \frac{a^2 \cdot M^{3/2} \cdot (T_{RL} - T_d)^2}{(-F_H)^2} \qquad (6.10)$$

where a = 0.15 $m^{1/4}.s^{1/4}$, T_{RL} is the residual-layer temperature (extrapolated adiabatically to the surface), M is wind speed in the residual layer, and F_H is the average surface kinematic heat flux. Faster winds and drier air delay the onset of fog. For most cases, fog never happens because night ends first.

Once fog forms, evolution of its depth is approximately

$$z = a \cdot M^{3/4} \cdot t^{1/2} \cdot \ln\left[(t / t_o)^{1/2} \right] \qquad (6.11)$$

where t_o is the onset time from the previous equation. This equation is valid for $t > t_o$.

Liquid water content increases as a saturated air parcel cools. Also, visibility decreases as liquid water increases. Thus, the densest (lowest visibility)

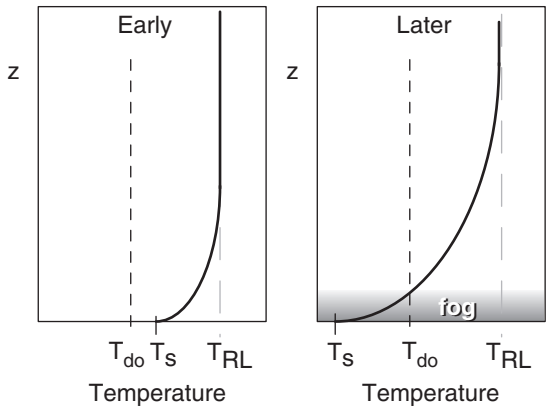

Figure 6.13
Stable-boundary-layer evolution at night leading to radiation fog onset, where T_s is near-surface air temperature, T_{do} is original dew-point temperature, and T_{RL} is the original temperature. Simplified, because dew formation on the ground can decrease T_d before fog forms, and cold-air downslope drainage flow can remove or deposit cold air to alter fog thickness.

Solved Example

Given a residual layer temperature of 20°C, dew point of 10°C, and wind speed 1 m/s. If the surface kinematic heat flux is constant during the night at –0.02 K·m/s, then what is the onset time and height evolution of **radiation** fog?

Solution

Given: T_{RL} = 20°C, T_d = 10°C, M = 1 m/s
F_H = –0.02 K·m/s
Find: t_o = ? h, and z vs. t.

Use eq. (6.10):

$$t_o = \frac{(0.15 m^{1/4} \cdot s^{1/4})^2 \cdot (1 m/s)^{3/2} \cdot (20 - 10°C)^2}{(0.02°C \cdot m/s)^2}$$

= **1.563 h**

The height evolution for this wind speed, as well as for other wind speeds, is calculated using eq. (6.11):

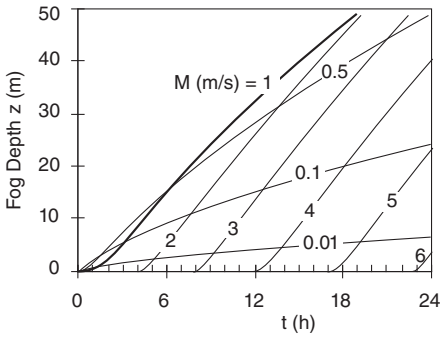

Check: Units OK. Physics OK.
Discussion: Windier nights cause later onset of fog, but stimulates rapid growth of the fog depth.

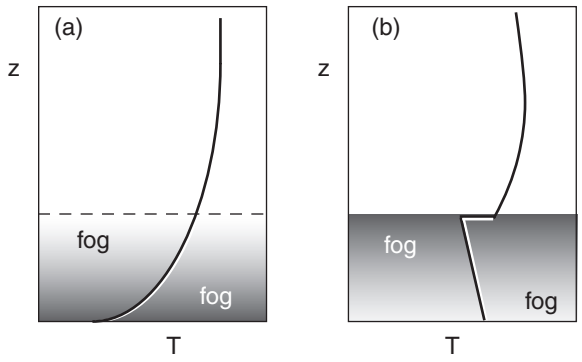

Figure 6.14
(a) Stratified fog that is more dense and colder at ground. (b) Well-mixed fog that is more dense and colder at the top due to IR radiative cooling.

Solved Example

Initially, total water is constant with height at 10 g/kg, and wet-bulb potential temperature increases with height at rate 2°C/100m in a stratified fog. Later, a well-mixed fog forms with depth 100 m. Plot the total water and θ_W profiles before and after mixing.

Solution

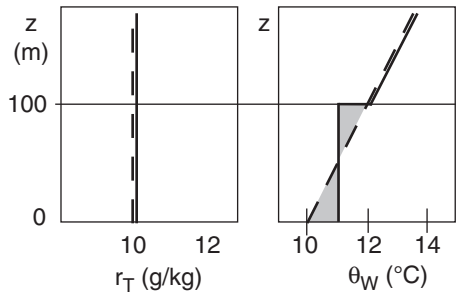

Check: Units OK. Physics OK.

Discussion: Dashed lines show initial profiles, solid are final profiles. For θ_W, the two shaded areas must be equal for heat conservation. This results in a temperature jump of 1°C across the top of the fog layer for this example. Recall from the Moisture and Stability chapters that actual temperature within the saturated (fog) layer decreases with height at the moist adiabatic lapse rate (lines of constant θ_W).

part of the fog will generally be in the coldest air, which is initially at the ground.

Initially, fog density decreases smoothly with height because temperature increases smoothly with height (Fig. 6.14a). As the fog layer becomes optically thicker and more dense , it reaches a point where the surface is so obscured that it can no longer cool by direct IR radiation to space.

Instead, the height of maximum radiative cooling moves upward into the fog away from the surface. Cooling of air within the nocturnal fog causes air to sink as cold thermals. Convective circulations then turbulently mix the fog.

Very quickly, the fog changes into a **well-mixed fog** with wet-bulb-potential temperature θ_W and total-water content r_T that are uniform with height. During this rapid transition, total heat and total water averaged over the whole fog layer are conserved. As the night continues, θ_W decreases and r_L increases with time due to continued radiative cooling.

In this fog the actual temperature decreases with height at the moist adiabatic lapse rate (Fig. 6.14b), and liquid water content increases with height. Continued IR cooling at fog top can strengthen and maintain this fog.

Dissipation of Well-Mixed (Radiation and Advection) Fogs

During daytime, solar heating and IR cooling are both active. Fogs can become less dense, can thin, can lift, and can totally dissipate due to warming by the sun.

Stratified fogs (Fig. 6.14a) are optically thin enough that sunlight can reach the surface and warm it. The fog albedo can be in the range of A = 0.3 to 0.5 for thin fogs. This allows the warm ground to rapidly warm the fog layer, causing evaporation of the liquid drops and dissipation of the fog.

For optically-thick well-mixed fogs (Fig. 6.14b), albedoes can be A =0.6 to 0.9. What little sunlight is not reflected off the fog is absorbed in the fog itself. However, IR radiative cooling continues, and can compensate the solar heating. One way to estimate whether fog will totally dissipate at time t in the future is to calculate the sum Q_{Ak} of accumulated cooling and heating (see the Atmospheric Boundary Layer chapter) during the time period $(t - t_o)$ since the fog first formed:

$$Q_{Ak} = F_{H.night} \cdot (t - t_o) + (1 - A) \cdot \frac{F_{H.\max} \cdot D}{\pi} \cdot \left[1 - \cos\left(\frac{\pi \cdot (t - t_{SR})}{D} \right) \right] \quad (6.12)$$

where $F_{H.night}$ is average nighttime surface kinematic heat flux (negative at night), and $F_{H.max}$ is the amplitude of the sine wave that approximates surface kinematic sensible heat flux due to solar heating (i.e., the positive value of insolation at local noon). D is daylight duration hours, t is hours after sunset, t_o is hours after sunset when fog first forms, and t_{SR} is hours between sunset and the next sunrise.

The first term on the right should be included only when $t > t_o$, which includes not only nighttime when the fog originally formed, but the following daytime also. This approach assumes that the rate $F_{H.night}$ of IR cooling during the night is a good approximation to the continued IR cooling during daytime.

The second term should be included only when $t > t_{SR}$, where t_{SR} is sunrise time. (See the Atmospheric Boundary Layer Chapter for definitions of other variables). When Q_{Ak} becomes positive, fog dissipates (neglecting other factors such as advection, and assuming no fog initially).

While IR cooling happens from the very top of the fog, solar heating occurs over a greater depth in the top of the fog layer. Such heating underneath cooling statically destabilizes the fog, creating convection currents of cold thermals that sink from the fog top. These upside-down cold thermals continue to mix the fog even though there might be net heating when averaged over the whole fog. Thus, any radiatively heated or cooled air is redistributed and mixed vertically throughout the fog by convection.

Such heating can cause the bottom part of the fog to evaporate, which appears to an observer as **lifting** of the fog (Fig. 6.15a). Sometimes the warming during the day is insufficient to evaporate all the fog. When night again occurs and radiative cooling is not balanced by solar heating, the bottom of the elevated fog lowers back down to the ground (Fig. 6.15b).

In closing this section on fogs, please be aware that the equations above for formation, growth, and dissipation of fogs were based on very idealized situations, such as flat ground and horizontally uniform heating and cooling. In the real atmosphere, even gentle slopes can cause katabatic drainage of cold air into the valleys and depressions (see the Local Winds chapter), which are then the favored locations for fog formation. The equations above were meant only to illustrate some of the physical processes, and should not to be used for operational fog forecasting.

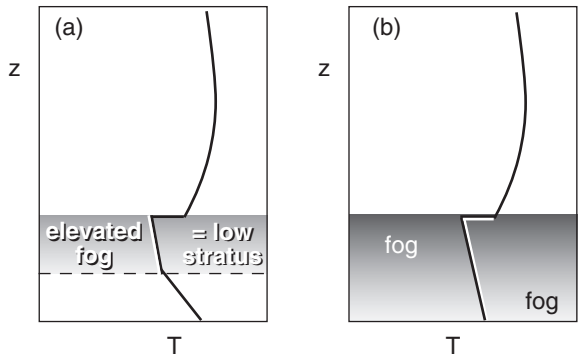

Figure 6.15
*(a) Heating during the day can modify the fog of Fig. 6.14b, causing the base to **lift** and the remaining elevated fog to be less dense (b) If solar heating is insufficient to totally dissipate the fog, then nocturnal radiative cooling can re-strengthen it.*

Solved Example(§)

When will fog dissipate if it has an albedo of A = (a) 0.4; (b) 0.6; (c) 0.8 ? Assume daylight duration of D = 12 h. Assume fog forms at t_o = 3 h after sunset. Given: $F_{H\ night}$ = –0.02 K·m/s, and $F_{H\ max\ day}$ = 0.2 K·m/s. Also plot the cumulative heating.

Solution

Given: (see above) Let t = time after sunset.
Use eq. (6.12), & solve on a spreadsheet:

(a) t = 16.33 h = 4.33 h after sunrise = **10:20 AM**
(b) t = 17.9 h = 5.9 h after sunrise = **11:54 AM**
(c) **Fog never dissipates**, because the albedo is so large that too much sunlight is reflected off of the fog, leaving insufficient solar heating to warm the ground and dissipate the fog.

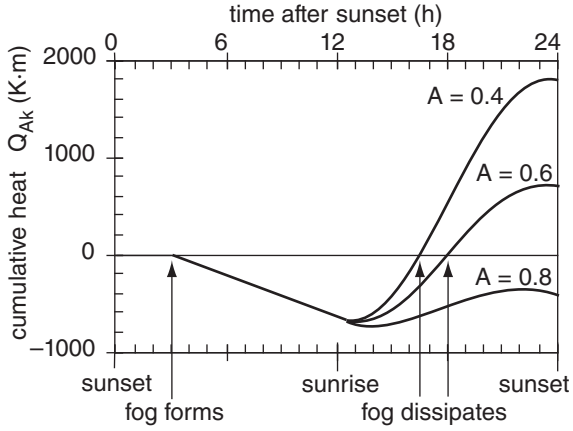

Check: Units OK. Physics OK.
Discussion: Albedo makes a big difference for fog dissipation. There is evidence that albedo depends on the type and number concentration of fog nuclei.

SUMMARY

Condensation of water vapor occurs by cooling, adding moisture, or mixing. Cooling and moisturizing are governed by the Eulerian heat and water budgets, respectively. Turbulent mixing of two nearly-saturated air parcels can yield a saturated mixture. We see the resulting droplet-filled air as clouds or fog.

If clouds are buoyant (i.e., the cloud and subcloud air is statically unstable), thermals of warm air actively rise to form cumuliform clouds. These have a lognormal distribution of sizes, and have fractal shapes. Active clouds are coupled to the underlying surface, allowing thermo diagrams to be used to estimate cloud base and top altitudes.

If the clouds are not buoyant (i.e., the cloud layer is statically stable), the clouds remain on the ground as fog, or they are forced into existence as stratiform clouds by advection along an isotropic surface over colder air, such as at a front.

Clouds can be classified by their altitude, shape, and appearance. Special symbols are used on weather maps to indicate cloud types and coverage.

While almost all clouds are created in rising air and the associated adiabatic cooling, fogs can form other ways. IR radiative cooling creates radiation fogs, while cooling associated with advection of humid air over a cold surface causes advection fogs. Precipitation and steam fog form by adding moisture to the air that touches a liquid water surface (e.g., raindrops, or a lake), followed by mixing with the surrounding cooler air to reach saturation.

Although fog forms in a layer of cold air resting on the ground, that cold-air can be either statically stable or unstable depending on whether continued cooling is being imposed at the bottom or top of the layer, respectively. Heat and moisture budget equations can be used to forecast fog onset, development, and dissipation for some idealized situations.

Threads

Clouds of many different sizes and fractal shapes shade the ground, thereby altering the Earth's radiation budget and climate (Chapters 2 and 21). In turn, heat (Chapter 3) and moisture (Chapter 4) budgets are used to determine if saturation is reached.

Cloud depth depends on static stability (Chapter 5), for which thermo diagrams are useful. Radiation (Chapter 2) causes radiation fog. Droplet growth (Chapter 7) determines fog visibility, and precipitation rates from clouds. Condensation of water vapor can occur in rising plumes from smoke stacks and cooling towers (Chapter 19).

Adiabatic cooling process also causes condensation in tornado funnel clouds (Chapter 15). Advection fog is one example of air-mass transformation (Chapter 12). All fogs are within the boundary layer (Chapter 18). Ice crystal clouds (cirrostratus) and some liquid-water droplet clouds (lenticular) in front of the sun create beautiful optical phenomena such as halos and iridescence (Chapter 22).

EXERCISES

Numerical Problems

N1. Given the following temperature and vapor pressure for an air parcel. (i) How much moisture Δe (kPa) must be added to bring the original air parcel to saturation? (ii) How much cooling ΔT (°C) must be done to bring the original parcel to saturation? Original [T (°C) , e (kPa)] =

a. 20, 0.2 b. 20, 0.4 c. 20, 0.6 d. 20, 0.8 e. 20, 1.0
f. 20, 1.5 g. 20, 2.0 h. 20, 2.2 i. 10, 0.2 j. 10, 0.4
k. 10, 0.6 l. 10, 0.8 m. 10, 1.0 n. 30, 1.0 o. 30, 3.0

N2. On a winter day, suppose your breath has T = 30°C with T_d = 28°C, and it mixes with the ambient air of temperature T = –10°C and T_d = –11°C. Will you see your breath? Assume you are at sea level, and that your breath and the environment mix in proportions of (breath : environment):

a. 1:9 b. 2:8 c. 3:7 d. 4:6 e. 5:5
f. 6:4 g. 7:3 h. 8:2 i. 9:1

N3(§). A jet aircraft is flying at an altitude where the ambient conditions are P = 30 kPa, T = –40°C, and T_d = –42°C. Will a visible contrail form? (Hint, assume that all possible mixing proportions occur.)

Assume the jet exhaust has the following conditions: [T (°C) , T_d (°C)] =

a. 200, 180 b. 200, 160 c. 200, 140 d.200, 120
e. 200, 100 f. 200, 80 g. 200, 60 h. 200, 40
i. 400, 375 j. 400, 350 k. 400, 325 l. 400, 300
m. 400, 275 n. 400, 250 o. 400, 200 p. 400, 150

N4. Given the following descriptions of ordinary clouds. (i) First classify as cumuliform or stratiform. (ii) Then name the cloud. (iii) Next, draw both the WMO and USA symbols for the cloud. (iv) Indicate if the cloud is made mostly of liquid water or ice (or both). (v) Indicate the likely altitude of its cloud base and top. (vi) Finally, sketch the cloud similar to those in Figs. 6.3 or 6.5.

a. Deep vertical towers of cloud shaped like a gigantic mushroom, with an anvil shaped cloud on top. Flat, dark-grey cloud base, with heavy precipitation showers surrounded by non-precipitating regions. Can have lightning, thunder, hail, strong gusty winds, and tornadoes. Bright white cloud surrounded by blue sky when viewed from the side, but the cloud diameter is so large that when from directly underneath it might cover the whole sky.
b. Sheet of light-grey cloud covering most of sky, with sun or moon faintly showing through it, casting diffuse shadows on ground behind buildings and people.
c. Isolated clouds that look like large white cotton balls or cauliflower, but with flat bases. Lots of blue sky in between, and no precipitation. Diameter of individual clouds roughly equal to the height of their tops above ground.
d. Thin streaks that look like horse tails, with lots of blue sky showing through, allowing bright sun to shine through it with crisp shadows cast on the ground behind trees and people.
e. Thick layer of grey cloud with well poorly-defined cloud base relatively close to the ground, and widespread drizzle or light rain or snow. No direct sunlight shining through, and no shadows cast on the ground. Gloomy.
f. Isolated clouds that look like small, white cotton balls or popcorn (but with flat bases), with lots of blue sky in between. Size of individual clouds roughly equal to their height above ground.
g. Thin uniform veil covering most of sky showing some blue sky through it, with possibly a halo around a bright sun, allowing crisp shadows cast on the ground behind trees and people.
h. Layer of grey cloud close to the ground, but lumpy with some darker grey clouds dispersed among thinner light grey or small clear patches in a patchwork or chessboard pattern. Not usually precipitating.
i. Thin veil of clouds broken into very small lumps, with blue sky showing through, allowing bright sun to shine through it with crisp shadows cast on the ground behind trees and people.
j. Sheet of cloud covering large areas, but broken into flat lumps, with sun or moon faintly showing through the cloudy parts but with small patches of blue sky in between the lumps, casting diffuse shadows behind buildings and people.
k. Deep towers of cloud with bright white sides and top during daytime, but grey when viewed from the bottom. Clouds shaped like stacks of ice-cream balls or turrets of cotton balls with tops extending high in the sky, but with flat bases relatively close to the ground. Usually no precipitation.
l. Thick layer of grey cloud with well defined cloud base relatively close to the ground. No direct sunlight shining through, and no shadows cast on the ground. No precipitation.

N5. Use a thermo diagram to plot the following environmental sounding:

P (kPa)	T (°C)
20	–15
25	–25
35	–25
40	–15
45	–20
55	–15
70	0
80	9
85	6
95	15

Determine cloud activity (active, passive, fog, none), cloud-base height, and cloud-top height, for the conditions of near-surface (P = 100 kPa) air parcels given below: [T (°C) , T_d (°C)] =

a. 20, 14 b. 20, 7 c. 20, 17 d. 20, 19
e. 15, 15 f. 30, 0 g. 30, 10 h. 30, 24
i. 25, 24 j. 25, 20 k. 25, 16 l. 25, 12
m. 25, 10 n. 25, 6 o. 15, 10 p. 22, 22

N6. The buoyancy of a cloudy air parcel depends on its virtual temperature compared to that of its environment. Given a saturated air parcel of temperature and liquid-water mixing ratio as listed below. What is its virtual temperature, and how would it compare to the virtual temperature with no liquid water?

[T(°C), r_L(g/kg)] = a. 20, 1 b. 20, 2 c. 20, 5
d. 20, 10 e. 10, 1 f. 10, 3 g. 10, 7 h. 10, 12
i. 0, 2 j. 0, 4 k. 0, 8 l. 0, 15 m. 5, 1
n. 5, 2 o. 5, 4 p. 5, 6 q. 5, 8 r. 5, 10

N7. On a large thermo diagram from the end of the Stability chapter, plot a hypothetical sounding of temperature and dew-point that would be possible for the following clouds.

a. cirrus b. cirrostratus c. cirrocumulus
d. altostratus e. altocumulus f. stratus
g. nimbostratus h. fog

N8. Name these special clouds.

a. Parallel bands of clouds perpendicular to the shear vector, at the level of altocumulus.
b. Parallel bands of cumulus clouds parallel to the wind vector in the boundary layer.
c. Two, long, closely-spaced parallel cloud lines at high altitude.
d. Clouds that look like flags or pennants attached to and downwind of mountain peaks.
e. Look like altocumulus, but with more vertical development that causes them to look like castles.
f. Clouds that look like breaking waves.
g. Look like cumulus or cumulus mediocris, but relatively tall and small diameter causing them to look like castles.
h. Clouds that look lens shaped when viewed from the side, and which remain relatively stationary in spite of a non-zero wind.
i. A low ragged cloud that is relatively stationary and rotating about a horizontal axis.
j. Ragged low scattered clouds that are blowing rapidly downwind.
k. Low clouds that look like cotton balls, but forming above industrial cooling towers or smoke stacks.
l. A curved thin cloud at the top of a mountain.
m. A curved thin cloud at the top of a rapidly rising cumulus congestus.

N9. Discuss the difference between cloud genera, species, varieties, supplementary features, accessory clouds, mother clouds, and meteors.

N10. Given the cloud genera abbreviations below, write out the full name of the genus, and give the WMO and USA weather-map symbols.

a. Cb b. Cc c. Ci d. Cs e. Cu
f. Sc g. Ac h. St i. As j. Ns

N11. For the day and time specified by your instructor, fully classify the clouds that you observe in the sky. Include all of the WMO-allowed classification categories: genera, specie, variety, feature, accessory cloud, and mother cloud. Justify your classification, and include photos or sketches if possible.
[HINT: When you take **cloud photos**, it is often useful to include some ground, buildings, mountains, or trees in the photo, to help others judge the scale of the cloud when they look at your picture. Try to avoid pictures looking straight up. To enhance the cloud image, set the exposure based on the cloud brightness, not on the overall scene brightness. Also, to make the cloud stand out against a blue-sky background, use a polarizing filter and aim the camera at right angles to the sunbeams. Telephoto lenses are extremely helpful to photograph distant clouds, and wide-angle lenses help with widespread nearby clouds. Many cloud photographers use zoom lenses that span a range from wide angle to telephoto. Also, always set the camera to focus on infinity, and never use a flash.]

N12. Draw the cloud coverage symbol for weather maps, and write the METAR abbreviation, for sky cover of the following amount (oktas).

a. 0 b. 1 c. 2 d. 3 e. 4
f. 5 g. 6 h. 7 i. 8 j. obscured

N13.(§). Use a spreadsheet to find and plot the fraction of clouds vs. size. Use ΔX = 100 m, with X in

the range 0 to 5000 m.
(i) For fixed S_x = 0.5, plot curves for L_X (m) =
a. 200 b. 300 c. 400 d. 500 e. 700 f. 1000 g. 2000
(ii) For fixed L_X = 1000 m, plot curves for S_X =
h. 0.1 i. 0.2 j. 0.3 k. 0.4 l. 0.5 m. 0.6 n. 0.8

N14. In Fig. 6.12, divide each tile into 4 equal quadrants, and count N vs. M for these new smaller tiles to add data points to the solved-example figure for measuring fractal dimension. Do these finer-resolution tiles converge to a different answer? Do this box-counting for Fig. 6.12 part:
a. (a) b. (b) c. (c) d. (d)

N15. Use the box counting method to determine the fractal dimensions in Fig. 6.11b. Use M =
a. 4 b. 5 c. 6 d. 7 e. 8 f. 9
g. 10 h. 12 i. 14 j. 16 k. 18 l. 20

N16. For air starting at sea level:
(i) How high (km) must it be lifted to form upslope fog?
(ii) How much water (g_{liq}/kg_{air}) must be added to cause precipitation fog?
(iii) How much cooling (°C) is necessary to cause radiation fog?
Given the following initial state of the air
[T (°C) , RH (%)] =
a. 10, 20 b. 10, 40 c. 10, 60 d. 10, 80 e. 10, 90
f. 20, 20 g. 20, 40 h. 20, 60 i. 20, 80 j. 20, 90
k. 0, 20 l. 0, 40 m. 0, 60 n. 0, 80 o. 0, 90

N17(§). In spring, humid tropical air of initial temperature and dew point as given below flows over colder land of surface temperature 2 °C. At what downwind distance will advection fog form? Also plot the air temperature vs. distance. Assume z_i = 200 m, and C_H = 0.005 .
The initial state of the air is [T (°C), T_d (°C)] =
a. 20, 15 b. 20, 10 c. 20, 5 d. 20, 0 e. 20, –5
f. 20, –10 g. 20, –15 h. 10, 8 i. 10, 5 j. 10, 2
k. 10, 0 l. 10, –2 m. 10, –5 n. 10, –8 o. 10, –10

N18(§). Given F_H = –0.02 K·m·s^{-1} . (i) When will radiation fog form? (ii) Also, plot fog depth vs. time.
Given residual-layer initial conditions of
[T (°C) , T_d (°C) , M (m/s)] =
a. 15, 13, 1 b. 15, 13, 2 c. 15, 13, 3 d. 15, 13, 4
e. 15, 10, 1 f. 15, 10, 2 g. 15, 10, 3 h. 15, 10, 4
i. 15, 8, 1 j. 15, 8, 2 k. 15, 8, 3 l. 15, 8, 4
m. 15, 5, 1 n. 15, 5, 2 o. 15, 5, 3 p. 15, 5, 4

N19(§). (i) When will a well-mixed fog dissipate? Assume: albedo is 0.5, fog forms 6 h after sunset, and daylight duration is 12 h. (ii) Also, plot the cumulative heat vs. time.

Given the following values of surface kinematic heat flux: [$F_{H.night}$ (K·m/s) , $F_{H.max\ day}$ (K·m/s)] =
a. –0.02, 0.15 b. –0.02, 0.13 c. –0.02, 0.11
d. –0.02, 0.09 e. –0.02, 0.07 f. –0.02, 0.17
g. –0.015, 0.15 h. –0.015, 0.13 i. –0.015, 0.11
j. –0.015, 0.09 k. –0.015, 0.07 l. –0.015, 0.17

Understanding & Critical Evaluation

U1. What processes in the atmosphere might simultaneously cool and moisturize unsaturated air, causing it to become saturated?

U2. Cumulus humilis clouds often have flat bases at approximately a common altitude over any location at any one time. Cumulus fractus clouds do not have flat bases, and the cloud-base altitudes vary widely over any location at one time. What causes this difference? Explain.

U3. Can you use darkness of the cloud base to estimate the thickness of a cloud? If so, what are some of the errors that might affect such an approach? If not, why not?

U4. Fig. 6.4 shows that the LCL computed from surface air conditions is a good estimate of cloud-base altitude for cumulus humilis clouds, but not for cloud-base altitude of altocumulus castellanus. Why?

U5. What methods could you use to estimate the altitudes of stratiform clouds by eye? What are the pitfalls in those methods? This is a common problem for weather observers.

U6. Should stratocumulus clouds be categorized as cumuliform or stratiform? Why?

U7. List all the clouds that are associated with turbulence (namely, would cause a bumpy ride if an airplane flew through the cloud).

U8. What do pileus clouds and lenticular clouds have and common, and what are some differences?

U9. Cloud streets, bands of lenticular clouds, and Kelvin-Helmholtz billows all consist of parallel rows of clouds. Describe the differences between these clouds, and methods that you can use to discriminate between them.

U10. The discrete cloud morphology and altitude classes of the official cloud classification are just points along a continuum of cloud shapes and altitudes. If you observe a cloud that looks halfway

between two official cloud shapes, or which has an altitude between the typical altitudes for high, middle, or low, clouds, then what other info can you use as a weather observer to help classify the cloud?

U11 (full term project). Build your own cloud chart with your own cloud photos taken with a digital camera. Keep an eye on the sky so you can try to capture as many different cloud types as possible. Use only the best one example of each cloud type corresponding to the clouds in Figs. 6.3 and 6.5. Some clouds might not occur during your school term project, so it is OK to have missing photos for some of the cloud types.

U12. List all of the factors that might make it difficult to see and identify all the clouds that exist above your outdoor viewing location. Is there anything that you can do to improve the success of your cloud identification?

U13(§). a. On a spreadsheet, enter the cloud-size parameters (S_X, L_X, ΔX) from the solved example into separate cells. Create a graph of the lognormal cloud distribution, referring to these parameter cells.

b. Next, change the values of each of these parameters to see how the shape of the curve changes. Can you explain why L_X is called the location parameter, and S_X is called the spread parameter? Is this consistent with an analytical interpretation of the factors in eq. (6.6)? Explain.

U14. The box-counting method can also be used for the number of points on a straight line, such as sketched in Fig. 6.11c. In this case, a "box" is really a fixed-length line segment, such as increments on a ruler or meter stick.

a. Using the straight line and dots plotted in Fig. 6.11c, use a centimeter rule to count the number of non-overlapping successive 1 cm segments that contain dots. Repeat for half cm increments. Repeat with ever smaller increments. Then plot the results as in the fractal-dimension solved example, and calculate the average fractal dimension. Use the zero-set characteristics to find the fractal dimension of the original wiggly line.

b. In Fig. 6.11c, draw a different, nearly vertical, straight line, mark the dots where this line crosses the underlying wiggly line, and then repeat the dot-counting procedure as described in part (a). Repeat this for a number of different straight lines, and then average the resulting fractal dimensions to get a more statistically-robust estimate.

U15. a. Crumple a sheet of paper into a ball, and carefully slice it in half. This is easier said than done. (A head of cabbage or lettuce could be used instead.) Place ink on the cut end using an ink pad, or by dipping the paper wad or cabbage into a pan with a thin layer of red juice or diluted food coloring in the bottom. Then make a print of the result onto a flat piece of paper, to create a pattern such as shown in Fig. 6.11b. Use the box counting method to find the fractal dimension of the wiggly line that was printed. Using the zero-set characteristic, estimate the fractal dimension of the crumpled paper or vegetable.

b. Repeat the experiment, using crumpled paper wads that are more tightly packed, or more loosely packed. Compare their fractal dimensions.
(P.S. Don't throw the crumpled wads at the instructor. Instructors tend to get annoyed easily.)

U16. Can precipitation fog form when cold raindrops fall through warmer air? Explain.

U17. A fog often forms near large waterfalls. What type of fog is it usually, and how does it form?

U18. In this chapter we listed some locations and seasons where advection fog is likely. Describe 3 other situations (locations and seasons) when advection fog would be likely. (If possible, use locations close to home.)

U19. Derive eq. (6.10), based on the exponential temperature profile for a stable boundary layer (see the Atmospheric Boundary Layer chapter). State and justify all assumptions. [This requires calculus.] Be critical of any simplifications that might not be appropriate for real fogs.

U20. Derive eq. (6.11) from (6.10), and justify all assumptions. Be critical of any simplifications that might not be appropriate for real fogs.

U21. Derive eq. (6.12) using info from the Atmospheric Boundary Layer chapter, and justify all assumptions. Be critical of any simplifications that might not be appropriate for real fogs.

U22. Use the data in the solved example for fog dissipation, but find the critical albedo at which fog will just barely dissipate.

U23. During possible frost events, some orchard and vineyard owners try to protect their fruit from freezing by spraying a mist of water droplets or burning smudge pots to make smoke in and above their plants. Why does this method work, and what are its limitations?

Web Enhanced Questions

W1. Search the web or consult engineering documents that indicate the temperature and water vapor content of exhaust from aircraft jet engines. What ambient temperature and humidity of the atmosphere near the aircraft would be needed such that the mixture of the exhaust with the air would just become saturated and show a jet contrail in the sky. (You might need to utilize a spreadsheet to experiment with different mixing proportions to find the one that would cause saturation first.)

W2. Search the web for cloud-classification images corresponding to the clouds in Figs. 6.3 and 6.5. Copy the best example of each cloud type to your own page to create a cloud chart. Be sure to also record and cite the original web site for each cloud photo.

W3. Search the web for thermo diagrams showing soundings for cases where different cloud types were present (e.g., active, passive, fog). Estimate cloud base and cloud top altitudes from the sounding, and compare with observations. Cloud base observations are available from the METAR surface reports made at airports. Cloud top observations are reported by aircraft pilots in the form of PIREPS.

W4. Search the web to identify some of the instruments that have been devised to determine cloud-base altitude?

W5. Search the web for cloud images corresponding to the "Other Clouds" discussed near the start of this chapter. Copy the best example of each cloud type to your own page. Be sure to also record and cite the original web site for each cloud photo.

W6. Search the web for satellite and ground-based images of cloud streets, open cells, and closed cells. Create a image table of these different types of cloud organization.

W7. Search the web for a surface weather map that plots surface observations for locations near you. For 3 of the stations having clouds, interpret (describe in words) the sky cover and cloud genera symbols (using Tables 6-7 and 6-2) that are plotted.

W8. Table 6-2 shows only a subset of the symbols used to represent clouds on weather maps. Search the web for map legends or tables of symbols that give a more complete list of cloud symbols.

W9. a. Search the web for fractal images that you can print. Use box counting methods on these images to find the fractal dimension, and compare with the fractal dimension that was specified by the creator of that fractal image.

b. Make a list of the URL web addresses of the ten fractal images that you like the best (try to find ones from different research groups or other people).

W10. Search the web for satellite images that show fog. (Hints: Try near San Francisco, or try major river valleys in morning, or try over snowy ground in spring, or try over unfrozen lakes in Fall). For the fog that you found, determine the type of fog (radiation, advection, steam, etc.) in that image, and justify your decision.

W11. a. Search the web for very high resolution visible satellite images of cumulus clouds or cloud clusters over an ocean. Display or print these images, and then trace the edges of the clouds. Find the fractal dimension of the cloud edge, similar to the procedure that was done with Fig. 6.12.

W12. Search the web for a discussion about which satellite channels can be used to discriminate between clouds and fog. Summarize your findings.

W13. Search the web for methods that operational forecasters use to predict onset and dissipation times of fog. Summarize your findings. (Hint: Try web sites of regional offices of the weather service.)

Synthesis Questions

S1. What if the saturation curve in Fig. 6.1 was concave down instead of concave up, but that saturation vapor pressure still increased with increasing temperature. Describe how the cooling, moisturizing, and mixing to reach saturation would be different.

S2. Suppose that descending (not ascending) air cools adiabatically. How would cloud shapes be different, if at all? Justify.

S3. Cloud classification is based on morphology; namely, how the cloud looks. A different way to classify clouds is by the processes that make the clouds. Devise a new scheme to classify clouds based on cloud processes; name this scheme after yourself; and make a table showing which traditional cloud names fall into each category of your new scheme, and justify.

S4. Clouds in the atmospheres of other planets in our solar system have various compositions:
- Venus: sulfuric acid
- Mars: water

• Jupiter: ammonia, sulfur, water
• Saturn: ammonia, ammonia hydrosulfide, water
• Uranus & Neptune: methane.

Would the clouds on these other planets have shapes different than the clouds on Earth? If so, then develop a cloud classification for them, and explain why. If not, why not?

S5. Utilize the information in (a) and (b) below to explain why cloud sizes might have a lognormal distribution.

a. The **central-limit theorem** of statistics states that if you repeat an experiment of adding N random numbers (using different random numbers each time), then there will be more values of the sum in the middle of the range than at the extremes. That is, there is a greater probability of getting a middle value for the sum than of getting a small or large value. This probability distribution has the shape of a **Gaussian curve** (i.e., a **bell curve** or a **"normal" distribution**; see the Air Pollution chapter for examples).

For anyone who has rolled **dice**, this is well known. Namely, if you roll one die (consider it to be a **random number generator** with a uniform distribution) you will have an equal chance of getting any of the numbers on the die (1, 2, 3, 4, 5, or 6).

However, if you roll two dice and sum the numbers from each die, you have a much greater chance of getting a sum of 7 than of any other sum (which is exactly half way between the smallest possible sum of 2, and the largest possible sum of 12). You have slightly less chance of rolling a sum of 6 or 8. Even less chance of rolling a sum of 5 or 9, etc.

The reason is that 7 has the most ways (6 ways) of being created from the two dice (1+6, 2+5, 3+4, 4+3, 5+2, 6+1). The sums of 6 and 8 have only 5 ways of being generated. Namely, 1+5, 2+4, 3+3, 4+2, and 5+1 all sum to 6, while 2+6, 3+5, 4+4, 5+3, 6+2 all sum to 8. The other sums are even less likely.

b. The logarithm of a product of numbers equals the sum of the logarithms of those numbers.

S6. Build an instrument to measure relative sizes of cumulus clouds as follows. On a small piece of clear plastic, draw a fine-mesh square grid like graph paper. Or take existing fine-mesh graph paper and make a transparency of it using a copy machine. Cut the result to a size to fit on the end of a short tube, such as a toilet-paper tube.

Hold the open end of the tube to your eye, and look through the tube toward cumulus clouds. [CAUTION: Do NOT look toward the sun.] Do this over relatively flat, level ground, perhaps from the roof of a building or from a window just at tree-top level. Pick clouds of medium range, such that the whole cloud is visible through the tube.

For each cloud, record the relative diameter (i.e., the number of grid lines spanned horizontally by the cloud), and the relative height of each cloud base above the horizon (also in terms of number of grid lines). Then, for each cloud, divide the diameter by the cloud-base height to give a normalized diameter. This corrects for perspective, assuming that cumulus cloud bases are all at the same height.

Do this for a relatively large number of clouds that you can see during a relatively short time interval (such as half an hour), and then count the clouds in each bin of normalized cloud diameter.

a. Plot the result, and compare it with the lognormal distribution of Fig. 6.10.

b. Find the L_X and S_X parameters of the lognormal distribution that best fit your data. (Hint: Use trial and error on a spreadsheet that has both your measured size distribution and the theoretical distribution on the same graph. Otherwise, if you know statistics, you can use a method such a Maximum Likelihood to find the best-fit parameters.)

S7. Suppose that you extend Euclidian space to 4 dimensions, to include time as well as the 3 space dimensions. Speculate and describe the physical nature of something that has fractal dimension of 3.4 .

S8. For advection fog, eq. (6.8) is based on a well-mixed fog layer. However, it is more likely that advection fog would initially have a temperature profile similar to that for a stable boundary layer (Atmospheric Boundary Layer chapter). Derive a substitute equation in place of eq. (6.8) that includes this better representation of the temperature profile. Assume for simplicity that the wind speed is constant with height, and state any other assumptions you must make to get an answer. Remember that any reasonable answer is better than no answer, so be creative.

S9. Suppose that fog was transparent to infrared (longwave) radiation. Describe how radiation fog formation, growth, and dissipation would be different (if at all) from real radiation fogs?

S10. Suppose that clouds were transparent to solar radiation, and couldn't shade the ground. Describe and explain the possible differences in cloud morphology, coverage, duration, and their effects on weather and climate, if any.

S11. Find a current weather map (showing only fronts and winds) for your continent. Use your knowledge to circle regions on the map where you expect to find different types of fog and different types of clouds, and label the fog and cloud types.

Copyright © 2011, 2015 by Roland Stull. *Meteorology for Scientists and Engineers, 3rd Ed.*

PRECIPITATION

CONTENTS

Supersaturation and Water Availability 186
- Supersaturation 186
- Water Availability 186
- Number and Size of Hydrometeors 187

Nucleation of Liquid Droplets 188
- Cloud Condensation Nuclei (CCN) 188
- Curvature and Solute Effects 189
- Critical Radius 192
- Haze 192
- Activated Nuclei 193

Nucleation of Ice Crystals 194
- Processes 194
- Ice Nuclei 195

Liquid Droplet Growth by Diffusion 196

Ice Growth by Diffusion 198
- Ice Crystal Habits 198
- Growth Rates 200
- The Wegener-Bergeron-Findeisen (WBF) Process 201

Collision and Collection 202
- Terminal Velocity of Hydrometeors 202
  - Cloud Droplets 202
  - Rain Drops 203
  - Hailstones 204
- Collection & Aggregation Processes 204
  - Warm-cloud Process 204
  - Cold-cloud Processes 205
- Precipitation Formation 205
  - Warm Clouds 205
  - Cold Clouds 206

Precipitation Characteristics 207
- Rain-Drop Size Distribution 207
- Rainfall Rates 208
- Snowfall Rates & Snow Accumulation 208
- Precipitation Distribution 209

Precipitation Measurement 210

Summary 211
- Threads 211

Exercises 212
- Numerical Problems 212
- Understanding & Critical Evaluation 214
- Web-Enhanced Questions 217
- Synthesis Questions 217

"Meteorology for Scientists and Engineers, 3rd Edition" by Roland Stull is licensed under a Creative Commons Attribution-NonCommercial-ShareAlike 4.0 International License. To view a copy of the license, visit http://creativecommons.org/licenses/by-nc-sa/4.0/ . This work is available at http://www.eos.ubc.ca/books/Practical_Meteorology/ .

7 **Hydrometeors** are liquid and ice particles that form in the atmosphere. Hydrometeor sizes range from small cloud droplets and ice crystals to large hailstones. **Precipitation** occurs when hydrometeors are large and heavy enough to fall to the Earth's surface. **Virga** occurs when hydrometers fall from a cloud, but evaporate before reaching the Earth's surface.

Precipitation particles are much larger than cloud particles, as illustrated in Fig. 7.1. One "typical" raindrop holds as much water as a million "typical" cloud droplets. How do such large precipitation particles form?

The **microphysics** of cloud- and precipitation-particle formation is affected by super-saturation, nucleation, diffusion, and collision.

Supersaturation indicates the amount of excess water vapor available to form rain and snow.

Nucleation is the formation of new liquid or solid hydrometeors as water vapor attaches to tiny dust particles carried in the air. These particles are called cloud condensation nuclei or ice nuclei.

Diffusion is the somewhat random migration of water-vapor molecules through the air toward existing hydrometeors. Conduction of heat away from the droplet is also necessary to compensate the latent heating of condensation or deposition.

Collision between two hydrometeors allows them to combine into larger particles. These processes affect liquid water and ice differently.

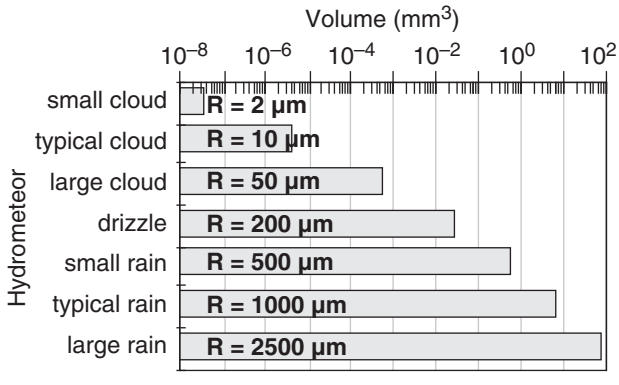

Figure 7.1
Drop volumes and radii, R.

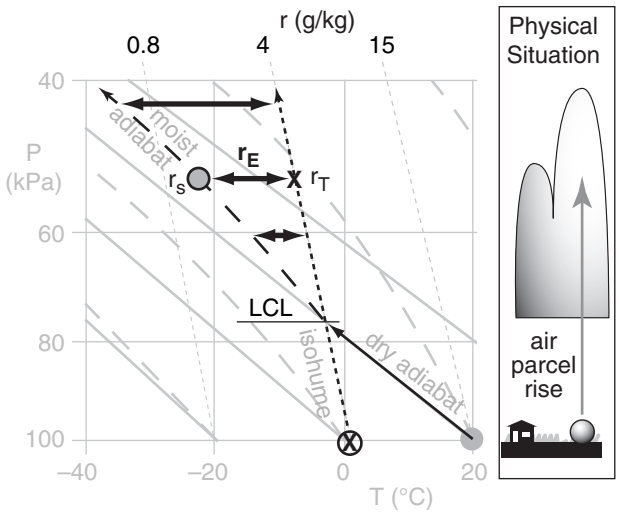

Figure 7.2
Thermo diagram (emagram) showing how excess-water mixing ratio r_E (thick line with arrows at each end) increases with increasing height above cloud base (LCL) for an air parcel rising adiabatically. r_T = total water mixing ratio; r_s = saturation mixing ratio for water vapor. r_E is the amount of water that can form hydrometeors.

Solved Example

An air parcel starts at 100 kPa with temperature 20°C and mixing ratio 4 g/kg. Use a thermo diagram to find the adiabatic value of excess-water mixing ratio when the parcel reaches a pressure of 60 kPa, and find the max available supersaturation.

Solution

Given: Initially $r = r_T = 4$ g/kg, $T = 20$°C, $P = 100$ kPa
Finally: $P = 60$ kPa.
Find: r_E = ? g/kg, S_A = ? (dimensionless)

Use a full size thermo diagram from the Stability chapter. Starting with the initial conditions, and following the air parcel up dry-adiabatically from the surface, we find the LCL is at $P = 75$ kPa and $T = –3$°C, which marks cloud-base. Above the LCL, follow the moist adiabat, which gives $T \approx –15$°C at $r_s = 2$ g/kg at $P = 60$ kPa. Assuming no entrainment and mixing, $r_T = 4$ g/kg.

Use eq. (7.5): $r_E = (4 – 2)$ g/kg = **2 g/kg**.
Then use eq. (7.7): $S_A = r_E/r_s =$ **1** = **100%**.

Check: Units OK. Physics OK. Agrees with Figs. 7.2 & 7.3)

Discussion: A supersaturation of 100% corresponds to a relative humidity of $RH = 200\%$ from eq. (7.2). Thus, there is twice as much water in the air as can be held at equilibrium. This excess water vapor drives condensation. For real clouds, we expect r_E in the range of 0.5 to 1.5 g/kg, based on the curves in Fig. 7.3.

SUPERSATURATION AND WATER AVAILABILITY

Supersaturation

When there is more water vapor in the air than it can hold at equilibrium, the air is said to be **supersaturated**. Supersaturated air has relative humidity *RH* greater than 100%. Define this excess relative humidity as a **supersaturation** fraction *S*:

$$S = RH - 1 \qquad \bullet(7.1)$$

or as a supersaturation percentage *S*%:

$$S\% \;=\; 100\% \cdot S \;=\; RH\% - 100\% \qquad \bullet(7.2)$$

Using the definition of relative humidity from the Moisture chapter, rewrite supersaturation in terms of total vapor pressure *e* and saturation vapor pressure e_s:

$$S = \frac{e}{e_s} - 1 \qquad \bullet(7.3)$$

for $e > e_s$. It can also be approximated using mixing ratios:

$$S \approx \frac{r}{r_s} - 1 \qquad \bullet(7.4)$$

for $r > r_s$.

Water Availability

Suppose that an initially-unsaturated air parcel has total water mixing ratio of r_T. If the air parcel rises adiabatically (i.e., no mixing with the environment, and no precipitation in or out), then it cools and its saturation mixing ratio decreases. You can use a thermo diagram (from the Stability chapter) to find these changing mixing ratios, as sketched here in Fig. 7.2.

Above the parcel's lifting condensation level (LCL) the saturation mixing ratio r_s is less than r_T. This supersaturated air has an **excess water mixing ratio** r_E of:

$$r_E = r_T - r_s \qquad \bullet(7.5)$$

The excess water is available to condense onto liquid drops and to deposit onto ice crystals:

$$r_L + r_i = r_E \qquad (7.6)$$

where r_L is liquid-water mixing ratio, and r_i is ice mixing ratio. At temperatures *T* in the range $–40 < T < 0$°C, supercooled liquid water and ice crystals can co-exist in the air.

Available supersaturation fraction is defined as:

$$S_A = \frac{r_E}{r_s} = \frac{r_T}{r_s} - 1 \qquad (7.7)$$

As hydrometeors grow and remove water vapor, r becomes less than r_T, and S becomes less than S_A. Droplets and ice crystals stop growing by condensation and deposition when they have consumed all the available supersaturation (i.e., when $r \to r_s$ and $S \to 0$).

The adiabatic estimate of r_E increases with height above the LCL, as sketched in Figs. 7.2 and 7.3. However, in many real clouds, **diabatic** (i.e., non-adiabatic) processes such as entrainment and mixing of clear drier air into the top and sides of the cloud cause the total-water mixing ratio to not be conserved with height. As a result, typical amounts of excess-water mixing ratio are less than adiabatic (dashed lines in Fig. 7.3).

Beware that the adiabatic r_E curve varies from situation to situation, depending on the thermodynamic initial conditions of the air parcel. So Fig. 7.3 is just one example (based on the Fig. 7.2 scenario).

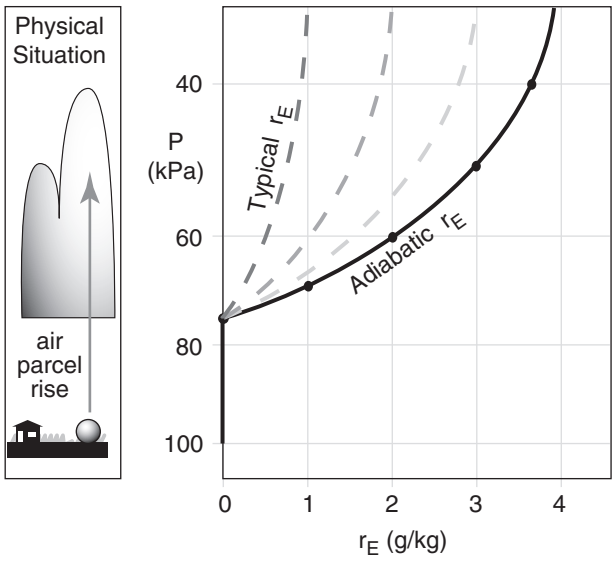

Figure 7.3
Example of the increase of excess water mixing ratio r_E vs. height above cloud base for the scenario in the previous figure. The adiabatic value (solid line) represents the max likely value in non-precipitating clouds, while the dashed curves show ranges of actual max values. P is pressure.

Number and Size of Hydrometeors

Suppose we partition the available excess water equally between all hydrometeors (for example, for all liquid water droplets). In this way, we can estimate the average radius R for each droplet due only to condensation (i.e., before collisions between droplets allow some to merge and grow into larger drops):

$$R = \left[\frac{3}{4\pi} \cdot \frac{\rho_{air}}{\rho_{water}} \cdot \frac{r_E}{n} \right]^{1/3} \qquad \bullet(7.8)$$

where excess-water mixing ratio r_E is in kg_{water}/kg_{air}, ρ is density, and n is the number density of hydrometeors (the count of hydrometeors per cubic meter of air). Typical values are R = 2 to 50 μm, which is small compared to the 1000 μm separation between droplets, and is too small to be precipitation.

This is an important consideration. Namely, even if we ignore the slowness of the diffusion process (described later), the hydrometeors stop growing by condensation or deposition before they become precipitation. The reason is that there are too many hydrometeors, all competing for water molecules, thus limiting each to grow only a little.

The number density n of hydrometeors is initially controlled by the number density of nuclei upon which they can form, as described next.

Solved Example

Within a cloud, suppose air density is 1 kg/m^3 and the excess water mixing ratio is 4 g/kg. Find the final drop radius for hydrometeor counts of (a) $10^8/m^3$, and (b) $10^9/m^3$.

Solution

Given: r_E = 0.004 kg_{water}/kg_{air}, ρ_{air} = 1 kg/m^3
n = (a) $10^8/m^3$, and (b) $10^9/m^3$.
Find: R = ? μm
Assume: ρ_{water} = 1000 kg/m^3, as listed in Appendix A.

Use eq. (7.8). Part (a),:

$$R = \left[\frac{3 \cdot (1 kg_{air}/m^3) \cdot (0.004 kg_{water}/kg_{air})}{4\pi \cdot (10^3 kg_{water}/m^3) \cdot (10^8 m^{-3})} \right]^{1/3}$$

$$= 2.12 \times 10^{-5} \text{ m} = \underline{\mathbf{21.2\ \mu m}}.$$

(b) Similarly, R = **9.8 μm**.

Check: Units OK. Physics OK.
Discussion: Both of these numbers are well within the range of "typical" cloud droplets. Thus, the final drop size is NOT large enough to become precipitation.

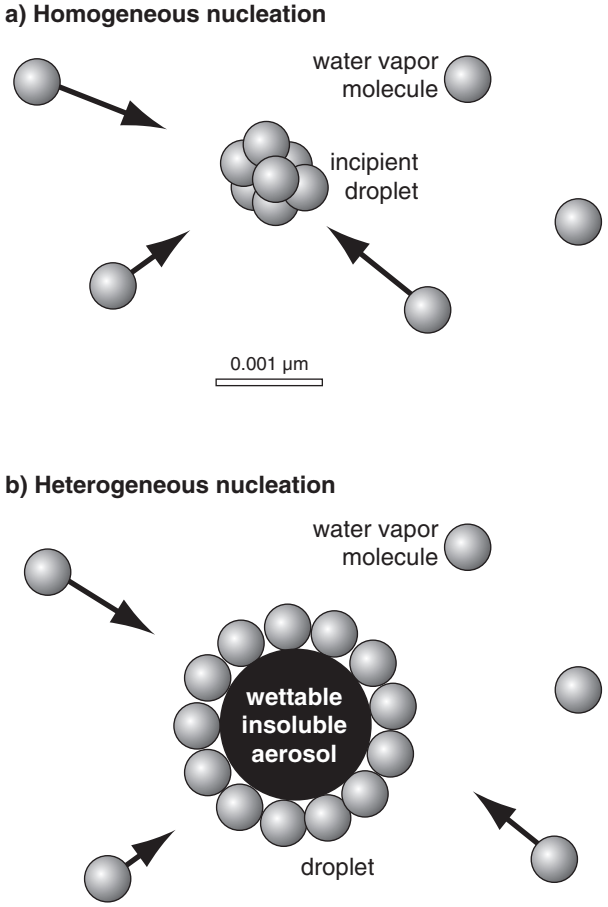

Figure 7.4
Sketch of differences between (a) homogeneous nucleation of cloud droplets and (b) heterogeneous nucleation around a wettable insoluble aerosol particle.

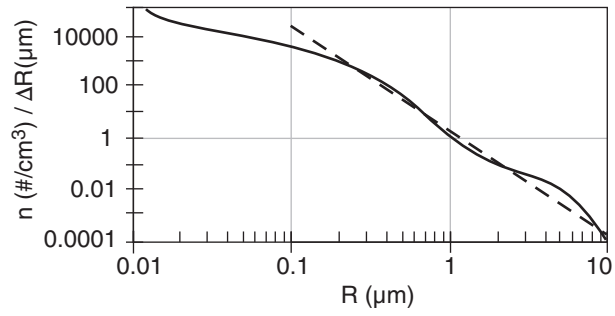

Figure 7.5
CCN particle count n vs. radius R, for c = 2,000,000 μm³·m⁻³.

NUCLEATION OF LIQUID DROPLETS

Nucleation (the creation of new droplets) in clean air is called **homogeneous nucleation** (Fig. 7.4a). We will show that homogeneous nucleation is virtually impossible in the real atmosphere and can be neglected. Nucleation of cloud droplets by water vapor condensing on tiny dust particles in the air is called **heterogeneous nucleation** (Fig. 7.4b). Even with heterogeneous nucleation, there is a barrier to droplet formation that must first be overcome.

Cloud Condensation Nuclei (CCN)

An **aerosol** is any tiny solid or liquid particle suspended in the air. The subset of aerosol particles that can nucleate cloud droplets are called **cloud condensation nuclei** (**CCN**). To nucleate a droplet, a solid aerosol either must be soluble in water (such as various salt particles), or be sufficiently large in diameter (radius > 0.1 μm) and have a wettable surface (i.e., be **hydrophilic**).

Boundary-layer air over oceans has smaller concentrations of aerosols than continental air. Over oceans, of the 150 to 1000 total aerosol particles/cm^3 of air, only about 90 to 200 particles/cm^3 are CCN at normal values of relative humidity ($RH \approx 101\%$) inside clouds. Over continents, of the 2,000 to 70,000 total aerosol particles/cm^3 of air, only about 200 to 700 particles/cm^3 are CCN. At higher relative humidities, larger percentages of aerosols act as CCN. Exceptionally clean air over the Arctic can have only 30 CCN particles/cm^3, while over industrial cities the CCN count can approach 10^6 particles/cm^3.

CCN particles can form when pollutant gases (of molecular size: 10^{-4} to 10^{-3} μm) in the air cluster to form **ultrafine aerosols** (size 10^{-3} to 10^{-2} μm) or are oxidized in the presence of sunlight. Over the oceans, sulfate and sulfuric acid CCN can form this way from gases such as dimethyl sulfide and methane sulfonic acid, produced by **phytoplankton** (microscopic drifting plant life in the ocean).

Further condensation of more pollutant gases and **coagulation** (sticking together) cause the aerosols to quickly grow to 0.01 to 1 μm size, called **fine aerosols**. Beyond this size range they grow more slowly. As a result, aerosols in this size range tend to accumulate — a process called **accumulation mode**. At larger 1 to 10 μm sizes, **coarse mode** CCN can form by other processes, such as strong winds that pick up fine dirt from the ground.

Small nuclei are much more abundant than larger ones (thin wiggly line in Fig. 7.5). Instead of a smooth decrease in number of particles as their size increases, the aerosol curve often has two or three

peaks corresponding to the ultrafine, accumulation, and coarse modes.

Over continental regions, the **number density** (n = count of particles per volume of air) of particles with radius between $R - 0.5{\cdot}\Delta R$ and $R + 0.5{\cdot}\Delta R$ can be approximated by:

$$n(R) = c \cdot R^{-4} \cdot \Delta R \qquad (7.9)$$

for particles larger than 0.2 μm, and for small ΔR. Constant c depends on the total concentration of particles. This distribution, called the **Junge distribution**, is the dashed straight line in Fig. 7.5.

Curvature and Solute Effects

Both droplet curvature and chemical composition affect the evaporation rate, which affect the fate of the droplet.

Curvature Effect

The evaporation rate from the curved surface of a droplet is greater than that from a flat water surface, due to surface tension. But droplet growth requires condensation to exceed evaporation. Thus, to be able to grow, smaller droplets need greater RH in the air than larger drops. The resulting equilibrium RH in the air as a function of droplet radius R is described by **Kelvin's equation**

$$RH\% = 100\%{\cdot}\exp\left[\frac{2{\cdot}\sigma}{\rho_m{\cdot}k_B{\cdot}T{\cdot}R}\right] \qquad (7.10a)$$

where $\sigma = 0.076$ N/m is **surface tension** of pure water at 0°C, $\rho_m = 3.3\text{x}10^{28}$ molecules/m^3 is the number density of water molecules in liquid at 0°C, $k_B = 1.38\text{x}10^{-23}$ J·K^{-1}·molecule^{-1} is Boltzmann's constant, and T is absolute temperature (in Kelvin) of the droplet. Kelvin's equation can be abbreviated as

$$RH\% = 100\%{\cdot}\exp\left[\frac{c_1}{T{\cdot}R}\right] \qquad (7.10b)$$

where $c_1 = 0.3338$ μm·K $= 2\sigma/(\rho_m{\cdot}k_B)$.

Fig. 7.6 illustrates the curvature effect described by Kelvin's equation, where conditions above the line allow droplets to grow. For example, droplets of radius smaller than 0.005 μm need an environment having $RH > 128\%$ to grow. But larger droplets of radius 0.1 μm need only $RH > 101\%$ to grow.

For homogeneous nucleation in clean air (no aerosols), incipient droplets form when several water-vapor molecules merge (Fig. 7.4a). The resulting droplet has extremely small radius (≈0.001 μm), causing it to evaporate quickly, given the typical humidities in clouds of ≈101% (grey shaded band in Fig. 7.6). How-

Solved Example

If $c = 5\text{x}10^7$ μm^3·m^{-3} for the Junge distribution, then how many CCN are expected within radii ranges of (a) 0.45 - 0.55 μm and (b) 0.95 - 1.05 μm?

Solution

Given: $R = 0.5$ μm & 1.0 μm, $\Delta R = 0.1$ μm for both ranges, and $c = 5\text{x}10^7$ μm^3·m^{-3}
Find: n = ? #/m^3

Use eq. (7.9):
(a) $n = (5\text{x}10^7 \mu\text{m}^3{\cdot}\text{m}^{-3}){\cdot}(0.5\ \mu\text{m})^{-4}\ {\cdot}(0.1\mu\text{m}) = \underline{\mathbf{8\ x\ 10}}^7/\text{m}^3$.
(b) $n = (5\text{x}10^7\ \mu\text{m}^3{\cdot}\text{m}^{-3}){\cdot}(1\ \mu\text{m})^{-4}\ {\cdot}(0.1\ \mu\text{m}) = \underline{\mathbf{5\ x\ 10}}^6/\text{m}^3$.

Check: Units OK. Physics OK.
Discussion: Doubling the particle radius reduces the number density by more than tenfold. If each CCN nucleates a cloud droplet, then each m^3 of cloudy air contain tens of millions of cloud droplets. Concentrations in real clouds can be 10s to 1000s of times greater.

Solved Example

What humidity in a cloud at 0°C is needed to allow a droplet of radius 0.03 μm to grow?

Solution:

Given: $R = 0.03$ μm. $T = 273$ K
Find: RH = ? %
Use eq. (7.10b)
$RH\% = 100\% \cdot \exp[(0.334\ \mu\text{m}{\cdot}\text{K}) / (273\text{K} \cdot 0.03\ \mu\text{m})]$
$= \underline{\mathbf{104.16\%}}$
Check: Units OK. Magnitude OK.
Discussion: A stable droplet this small is unlikely in a real cloud, where typically $RH \approx 101\%$ or less.

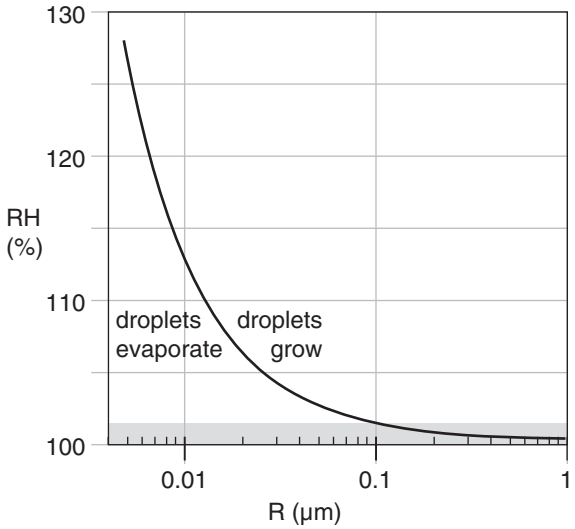

Figure 7.6
Curvature effect, showing the relative humidity (RH) needed in air for a droplet of radius R to grow. The curve is given by Kelvin's equation, for pure water at 0°C. Shaded region highlights the range of RH typically found in clouds.

Table 7-1. Properties of some solutes. M_s is molecular weight, i is approximate ion count.

Solute	Chemistry	M_s	i
salt	NaCl	58.44	2
ammonium sulfate	$(NH_4)_2SO_4$	132.13	3
hydrogen peroxide	H_2O_2	34.01	2
sulfuric acid	H_2SO_4	98.07	3
nitric acid	HNO_3	63.01	2

Solved Example

Find the equilibrium relative humidity over a droplet of radius 0.2 µm, temperature 20°C, containing 10^{-16} g of ammonium sulfate.

Solution

Given: $R = 0.2$ µm, $T = 293$ K, $m_s = 10^{-16}$ g
Find: $RH\% = 100\% \cdot (e_s^*/e_s) =$? %

From Table 7-1 for ammonium sulfate:
$M_s = 132.13$, and $i = 3$.
Use eq. (7.11):

$$\frac{e_s^*}{e_s} \approx \frac{\exp\left(\frac{0.3338\text{K}\cdot\mu\text{m}}{(293\text{K})\cdot(0.2\mu\text{m})}\right)}{1+\frac{(4.3\times10^{12}\mu\text{m}^3\cdot\text{g}^{-1})\cdot 3\cdot(10^{-16}\text{g})}{(132.13)\cdot(0.2\mu\text{m})^3}}$$

$= 1.00571 / (1+0.00122) = 1.00448$
$RH\% = 100\% \cdot (e_s^*/e_s) =$ **100.448%**

Check: Units OK. Physics OK.
Discussion: Fig. 7.7b gives a value of about 100.49% for a temperature of 0°C. Thus, warmer temperatures require less supersaturation of water vapor in the air to prevent the droplet from vaporizing.

Solved Example

In fog at 10°C, the vapor pressure is 1.4 kPa. Find the supersaturation fraction and percentage.

Solution

Given: $T = 10$°C , $e_s^* = 1.4$ kPa
Find: $S =$? , and $S\% =$?

First, use Table 4-1 in the Moisture chapter to find the saturation vapor pressure at 10°C: $e_s = 1.233$ kPa.
Next, use eq. (7.12):
$S = (1.4 \text{ kPa} / 1.233 \text{ kPa}) - 1 = 1.135 - 1 =$ **0.135**
$S\% = 100\% \cdot S =$ **13.5%**

Check: e_s^* is indeed > e_s, thus supersaturated.
Discussion: Unrealistically large, given typical supersaturations in clouds and fog of order S%=1%.

ever, for heterogeneous nucleation the small number of water molecules can coat the outside of the aerosol particle (Fig. 7.4b), with a resulting radius that is relatively large. Droplets formed by heterogeneous nucleation grow and remove water-vapor molecules from the air, thereby lowering the RH and eliminating the chance for homogeneous nucleation.

Solute Effect

Solutions (i.e., water containing dissolved chemicals) evaporate water molecules at a slower rate than does pure water. Solutions occur when condensation occurs on impurities such as certain cloud condensation nuclei (CCN) that dissolve in the nascent water droplet. This can partially compensate the curvature effect.

Recall that the saturation vapor pressure e_s over a flat surface of pure water was given in the Moisture chapter by the Clausius-Clapeyron equation. The two opposing effects of curvature and solute can be combined into one equation (**Köhler equation**) for the ratio of actual saturation vapor pressure e_s^* in equilibrium over a solution with a curved surface, to vapor pressure over a flat surface of pure water e_s:

$$RH = \frac{e_s^*}{e_s} \approx \frac{\exp\left(\frac{c_1}{T\cdot R}\right)}{1+\frac{c_2\cdot i\cdot m_s}{M_s\cdot R^3}} \qquad \bullet(7.11)$$

where RH is the relative humidity fraction, T is absolute temperature, R is drop radius, i is number of ions per molecule in solution (called the **van't Hoff factor**), m_s is mass of solute in the droplet, and M_s is molecular weight of solute. The two parameters are: $c_1 = 0.3338$ K·µm, and $c_2 = 4.3\text{x}10^{12}$ µm^3·g^{-1}. Table 7-1 gives properties for common atmospheric solutes.

In eq. (7.11) the relative humidity RH can be greater than 1, corresponding to a relative-humidity percentage ($RH\% = 100\% \cdot e_s^*/e_s$) that is greater than 100%. Similar to eq. (7.3), **supersaturation** relative to the hydrometeor can be defined as a fraction:

$$S = (e_s^*/e_s) - 1 \qquad \bullet(7.12)$$

or as a percentage, $S\% = 100\% \cdot S$:

$$S\% = 100\% \cdot [(e_s^*/e_s) - 1] \qquad \bullet(7.13)$$

Thus, the left hand side of eq. (7.11) can be easily rewritten as supersaturation.

The numerator of eq. (7.11) describes the **curvature effect**, and together with the left hand side is the **Kelvin equation**. The denominator describes the **solute effect** of impurities in the water. Eq. (7.11) was solved in a spreadsheet to produce the **Köhler**

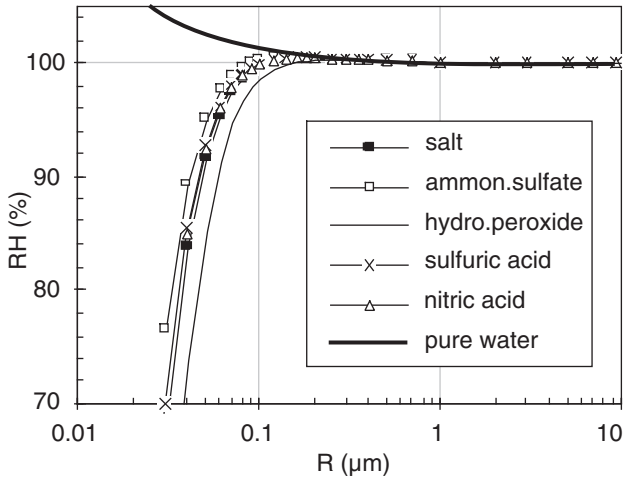

Figure 7.7a
Köhler curves, showing equilibrium relative humidities over droplets of different radius with various solutes. T = 0°C. Solute mass = 10^{-16} g.

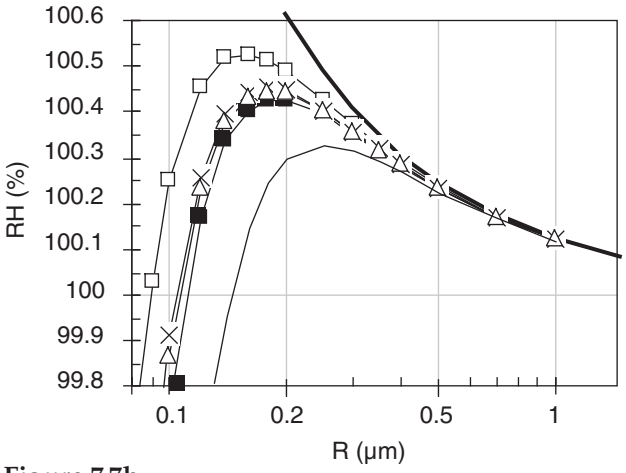

Figure 7.7b
Blow-up of Fig. 7.7a.

curves in Fig. 7.7. Using these Köhler curves, we can study nucleation.

First, the curve in Fig. 7.7 for pure water increases exponentially as drop radius becomes smaller. This curve was already shown in Fig. 7.6, computed from Kelvin's equation. It was used to explain why homogeneous nucleation is unlikely, because when the first several water-vapor molecules come together to form a condensate, their droplet radius is so small that the droplet instantly explodes.

Second, solutions of some chemicals can form small droplets even at humidities of less than 100%. Such **hygroscopic** (water attracting) pollutants in the air will grow into droplets by taking water vapor out of the air.

Third, if humidities become even slightly greater than the peaks of the Köhler curves, or if droplet radius becomes large enough (see Focus box), then

FOCUS • Droplet Growth

To help interpret Fig. 7.7b, consider a droplet containing just one chemical such as salt, in a cloud having a known humidity, such as *RH* = 100.3%. This is redrawn below.

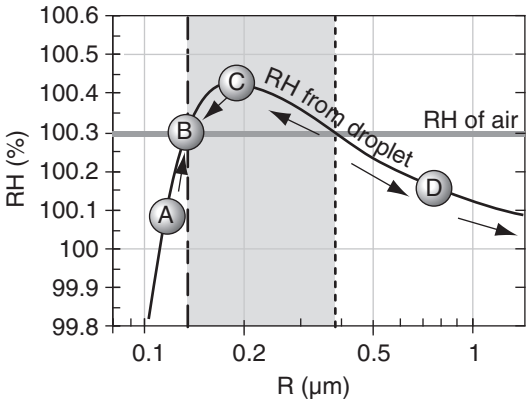

Figure 7.a. *Interpretation of a Köhler curve.*

Think of the Köhler curve as the *RH* associated with the droplet, which is trying to drive evaporation from the droplet. The *RH* in air (horizontal grey line) is trying to drive condensation to the droplet.

If $RH_{droplet} > RH_{air}$, then evaporation > condensation, and the droplet radius becomes smaller as water molecules leave the droplet. This is the situation for any droplet in the light grey band; namely, droplet C suffers net evaporation, causing its radius to decrease toward B.

If $RH_{droplet} < RH_{air}$, then evaporation < condensation, and droplet radius increases due to net condensation. Droplet D has this state, and as its radius increases it moves to the right in the graph, causing $RH_{droplet}$ to decrease further and driving even faster droplet growth. Activated droplets such as these continue growing (shown by right-pointing arrows) until they consume the excess humidity (driving the RH_{air} down toward 100%). Such droplet growth is a first stage in formation of precipitation in warm clouds.

Droplet A also has $RH_{droplet} < RH_{air}$, and would tend to increase in radius due to net condensation. But in this part of the Köhler curve, increasing radius causes increasing $RH_{droplet}$, and causes the net condensation to diminish until the droplet radius reaches that at B.

Thus, the vertical dotted line in Fig. 7.a is an unstable equilibrium. Namely, a droplet on the Köhler curve at the dotted line would either grow or shrink if perturbed slightly from its equilibrium point.

However, the vertical dashed line is a stable equilibrium point. Droplets approach this radius and then stop growing. Namely, they stay as small haze particles, and do not grow into larger cloud or precipitation particles.

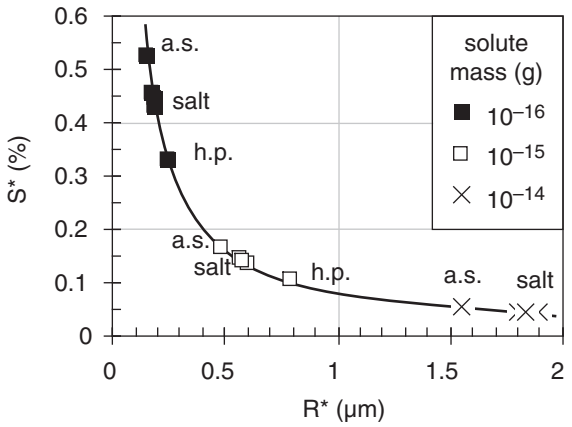

Figure 7.8
Critical values of supersaturation S vs. critical drop radius R*, for various solute masses and chemicals. a.s. = ammonium sulfide, salt = sodium chloride, h.p. = hydrogen peroxide. Nitric acid and sulfuric acid are near the salt data points.*

droplets can grow unimpeded. CCN reaching this state are said to be **activated**. Growth of droplets from activated nuclei continues until enough vapor (i.e., r_E) is consumed to reduce the supersaturation back toward 100%. Pure droplets cannot form or co-exist in an environment with neighboring solution droplets, because of the low supersaturation remaining in the air after much of the vapor has condensed out onto the solution droplets. That is another reason why homogeneous nucleation can be neglected for practical purposes.

Fourth, although not shown in these curves, the equations allow droplets to form at lesser supersaturations if the mass of dissolved solute is greater. Hence, larger CCN can grow into droplets earlier and can grow faster than smaller CCN.

Critical Radius

The location of the peak of the Köhler curves marks the barrier between the larger, activated droplets that can continue to grow, from the smaller **haze** droplets that reach an equilibrium at small size. The drop radius R^* at this peak is called the **critical radius**, and the corresponding **critical supersaturation** fraction is $S^* = e_s^*/e_s - 1$. They are given by:

$$R^* = \sqrt{\frac{c_3 \cdot i \cdot m_s \cdot T}{M_s}} \qquad \bullet(7.14)$$

and

$$S^* = \sqrt{\frac{c_4 \cdot M_s}{i \cdot m_s \cdot T^3}} \qquad \bullet(7.15)$$

where $c_3 = 3.8681\text{x}10^{13}$ μm^2·K^{-1}·g^{-1}, and $c_4 = 1.278\text{x}10^{-15}$ K^3·g. For critical supersaturation as a percentage, use S%* = 100%·S*.

Critical conditions are plotted in Fig. 7.8 for various masses of different chemicals. Obviously S^* is inversely related to R^*, so as solute mass increases, smaller supersaturations are necessary to reach the critical point, and at that point the droplets will be larger. Also, notice that different chemicals will grow to different sizes, which is one factor causing a range of drop sizes in the cloud.

Haze

For conditions left of the peak on any Köhler curve (i.e., $R < R^*$), CCN rapidly grow into small droplets that stop growing at an equilibrium size determined by the humidity, temperature, and solute (see previous Focus box). These small droplets are called **haze** droplets. Thus, tiny droplets can exist even at relative humidities below 100%.

Solved Example

Find the critical radius and supersaturation value for 10^{-15} g of ammonium sulfate at 0°C.

Solution

Given: $m_s = 10^{-15}$ g, $T = 273$ K
Find: $R^* = ?$ μm, $S\%^* = ?$ %.

Use eq. (7.14) & Table 7-1. $R^* =$

$$\sqrt{\frac{(3.8681\times10^{13}\,K^{-1}\cdot g^{-1}\mu m^2)\cdot 3\cdot(10^{-15}\,g)\cdot(273K)}{132.13}}$$

$R^* =$ **0.49 μm**

Use eq. (7.15) & Table 7-1. $S^* =$

$$S^* = \sqrt{\frac{(1.278\times10^{-15}\,\text{K}^3\cdot\text{g})\cdot 132.13}{3\cdot(10^{-15}\,\text{g})\cdot(273\text{K})^3}} = 0.00166$$

$S\%^* =$ **0.166%**

Check: Units OK. Physics OK.
Discussion: Agrees with the point (white square) plotted in Fig. 7.8 for "a.s.". Thus, the larger mass nucleus needs less supersaturation to become activated.

For a parcel of rising air with increasing supersaturation, the larger nuclei will become activated first, followed by the smaller nuclei if the parcel keeps cooling and if the excess vapor is not removed by the larger nuclei first.

Solved Example

For 10^{-16} g of ammonium sulfate at 0°C, how does haze droplet radius change as *RH* increases from 70 to 80%? Also, how many molecules are in each aerosol?

Solution

Assume: Same conditions as in Fig. 7.7a.
Given: RH = 70%, 80%.
Find: R = ? μm, n = ? molecules

Solve eq. (7.11), or use Fig. 7.7a. I will use the Fig.
$R \approx$ **0.027 μm** at 70%; $R \approx$ **0.032 μm** at 80%.

The number of molecules is $n = \rho_m \cdot [(4/3) \cdot \pi \cdot R^3]$
$n =$ **2.72x10**^{6} molecules; $n =$ **4.53x10**^{6} molecules

Check: Units OK. Physics OK.
Discussion: Haze particles indeed become larger as relative humidity increases, thereby reducing visibility. Scattering of light by this size of particles is called **Mie scattering** (see the Optics chapter).

Haze droplets are aerosols. When a tiny, dry CCN grows to its equilibrium size by the condensation of water molecules, this process is called **aerosol swelling**. Aerosol swelling is responsible for reducing **visibility** in polluted air as humidities increase above about 75%.

Even haze particles contain many water molecules. Liquid water contains about $\rho_m = 3.3\text{x}10^{28}$ molecules/m^3. Thus, the smallest haze particles of radius 0.02 μm contain roughly $n = \rho_m \cdot [(4/3) \cdot \pi \cdot R^3] =$ 1.1 million molecules.

The word **smog** is a contraction of "smoke" and "fog", which is a reasonable lay description of haze. Many urban smogs are a stew of ingredients including ozone, volatile hydrocarbons such as evaporated gasoline, and various oxides of nitrogen. These react in the atmosphere, particularly in the presence of sunlight, to create sulfates, nitrates, and hydrogen peroxide CCNs. Aerosol swelling and reduced visibilities are quite likely in such urban smogs, particularly when the air is humid.

Activated Nuclei

For conditions to the right of the peak on any Köhler curve (i.e., $R > R^*$), CCN are activated and can continue growing. There is no equilibrium that would stop their growth, assuming sufficient water vapor is present. These droplets can become larger than haze droplets, and are called **cloud droplets**.

Because atmospheric particles consist of a variety of chemicals with a range of masses, we anticipate from the Köhler curves that different CCN will become activated at different amounts of

BEYOND ALGEBRA • Critical Radius

Derivation of the critical radius, eq. (7.14).

The critical radius is at e_s^*/e_s = maximum. But at the maximum, the slope is zero: $d(e_s^*/e_s)/dR = 0$. By finding this derivative of eq. (7.11) with respect to R, and setting it to zero, we can solve for R at the maximum. This is R^* by definition.

The right side of eq. (7.11) is of the form a/b. A rule of calculus is:

$$d(a/b)/dR = [b \cdot (da/dR) - a \cdot (db/dR)] \; / \; b^2.$$

Also, a is of the form $a = \exp(f)$, for which another rule is:

$$da/dR = a \cdot (df/dR).$$

Combining these 2 rules and setting the whole thing to zero gives:

$$0 = \frac{a}{b}\left[\frac{df}{dR} - \frac{1}{b}\frac{db}{dR}\right]$$

But (a/b) is just the original right side of eq. (7.11), which we know is close to 1.0 at the max, not close to 0. Thus, the eq. above equals 0 only if:

$$\frac{df}{dR} = \frac{1}{b}\frac{db}{dR}$$

Plugging in for f and b and differentiating yields:

$$\frac{-c_1}{T \cdot R^2} = \frac{1}{\left[1 + \dfrac{c_2 \cdot i \cdot m_s}{M_s \cdot R^3}\right]} \frac{(-3) \cdot c_2 \cdot i \cdot m_s}{M_s \cdot R^4}$$

Multiply both sides by $(-R^4 \cdot T/c_1)$:

$$R^2 = (3 \cdot T / c_1) \cdot \frac{\left[\dfrac{c_2 \cdot i \cdot m_s}{M_s}\right]}{\left[1 + \dfrac{c_2 \cdot i \cdot m_s}{M_s \cdot R^3}\right]}$$

Multiply the numerator and denominator of the right side by $M_s \; / \; (c_2 \cdot i \cdot m_s)$, which gives:

$$R^2 = (3 \cdot T / c_1) \cdot \frac{1}{\left[\dfrac{M_s}{c_2 \cdot i \cdot m_s} + \dfrac{1}{R^3}\right]}$$

By plugging in typical values, we can show that the $1/R^3$ term is small enough to be negligible compared to the other term in square brackets. This leaves:

$$R^2 \cong \left(\frac{3 \cdot c_2}{c_1}\right) \cdot \left(\frac{T \cdot i \cdot m_s}{M_s}\right)$$

Define $c_3 = 3 \cdot c_2 \; / c_1$, set $R = R^*$, and take the square root of both sides to get the final answer:

$$\boxed{R^* \cong \sqrt{\frac{c_3 \cdot i \cdot m_s \cdot T}{M_s}}} \qquad (7.14)$$

Solved Example

How many nuclei would be activated in continental air of supersaturation percentage 0.5%? Also, how much air surrounds each droplet, and what is the distance between drops?

Solution

Given: $S = 0.005$

Find: n_{CCN} = ? particles/m^3,
Vol = ? mm^3, x = ? mm.

(a) Use eq. (7.16):
$n_{CCN} = (6\text{x}10^8\ \text{m}^{-3})\cdot(0.5)^{0.5} =$ **4.24x10**^{8} /m^3

(b) Also:
$Vol = 1/n_{CCN} =$ **2.36 mm**^{3} /droplet

(c) Using eq. (7.17): $x = Vol^{1/3} =$ **1.33 mm**.

Check: Units OK. Physics OK.

Discussion: If all of these nuclei become cloud droplets, then there are over 40 million droplets within each cubic meter of cloud. But there is a relatively large distance between each drop.

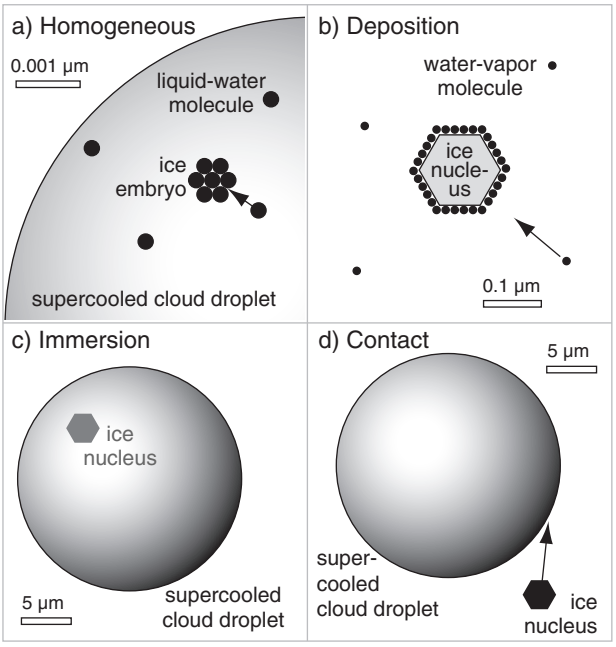

Figure 7.9
Sketch of (a) homogeneous, and (b-d) heterogeneous ice nucleation processes.

supersaturation. The number density n_{CCN} (# of CCN per m^3) activated as a function of supersaturation fraction S is roughly:

$$n_{CCN} = c \cdot (100 \cdot S)^k \qquad (7.16)$$

but varies widely. In maritime air, $c \approx 1\text{x}10^8$ m^{-3} and $k \approx 0.7$. In continental air $c \approx 6\text{x}10^8$ m^{-3} and $k \approx 0.5$. The number of activated nuclei is in the range of 10^8 to 10^9 m^{-3}, which is usually just a small fraction of the total number of particles in the air.

The distance x between cloud droplets is on the order of 1 mm, and is given by

$$x = n_{CCN}^{-1/3} \qquad (7.17)$$

NUCLEATION OF ICE CRYSTALS

Ice cannot survive at temperatures above 0°C at normal atmospheric pressures. Below that temperature, ice crystals can exist in equilibrium with air that is supersaturated with respect to ice. The saturation curve for ice was plotted in Fig. 4.2, and is close to, but slightly below, the curve for supercooled liquid water.

There is a thermodynamic barrier to ice formation, analogous to the barrier for droplet growth. This barrier can be overcome with either very cold temperatures (colder than –40°C), high supersaturation in the air, or by the presence of ice nuclei.

Processes

Homogeneous freezing nucleation is the name for the spontaneous freezing that occurs within supercooled liquid-water droplets as temperature decreases to near –40°C. No impurities are needed for this. Instead, ice embryos form by chance when clusters of water molecules happen to come together with the correct orientations (Fig. 7.9a). At –40°C, the cluster needs only about 250 molecules. At slightly warmer temperatures the critical embryo size is much larger, and thus less likely to occur. Because larger supercooled droplets contain greater numbers of molecules, they are more likely to form an ice embryo and freeze.

Heterogeneous freezing nucleation can occur a variety of ways (Fig. 7.9b-d), but all require an impurity (Table 7-2), which is generically called an **ice nucleus**. These processes are described next.

Deposition nucleation (Fig. 7.9b) occurs when water vapor deposits directly on a **deposition nucleus**. While the solute effect was important for liq-

uid droplet nucleation, it does not apply to ice nucleation because salts are excluded from the ice-crystal lattice as water freezes. Thus, the size and crystal structure of the ice nucleus is more important. Deposition is unlikely on particles of size 0.1 μm or less. Colder temperatures and greater supersaturation increases deposition nucleation.

Immersion freezing (Fig. 7.9c) occurs for those liquid drops already containing an undissolved ice nucleus called a **freezing nucleus**. Each nucleus has a critical temperature below 0°C at which it triggers freezing. Thus, as external processes cause such a contaminated drop to cool, it can eventually reach the critical temperature and freeze.

Larger drops contain more freezing nuclei, and have a greater chance of containing a nucleus that triggers freezing at warmer temperatures (although still below 0°C). To freeze half of the drops of radius R, the temperature must drop to T, given statistically by

$$T \approx T_1 + T_2 \cdot \ln(R/R_o) \qquad (7.18)$$

where R_o = 5 μm, T_1 = 235 K, and T_2 = 3 K.

Condensation freezing is a cross between deposition nucleation and immersion freezing. In this scenario, which occurs below 0°C, nuclei are more attractive as condensation nuclei than as deposition nuclei. Thus, supercooled liquid water starts to condense around the nucleus. However, this liquid water immediately freezes due to the immersion-nucleation properties of the nucleus.

Contact freezing (Fig. 7.9d) occurs when an uncontaminated supercooled liquid drop happens to hit an external **contact nucleus**. If the droplet is cooler than the critical temperature of the ice nucleus, then it will freeze almost instantly. This also happens when (supercooled) **freezing rain** hits and instantly freezes on trees and power lines. Ice crystals in the air are also good contact nuclei for supercooled water.

Ice Nuclei

Only substances with similar molecular structure as ice can serve as ice nuclei. Such substances are said to be **epitaxial** with ice.

Natural ice nuclei include fine particles of clay such as kaolinite stirred up from the soil by the wind. Certain bacteria and amino acids such as l-leucine and l-tryptophan from plants also can nucleate ice. Combustion products from forest fires contain many ice nuclei. Also, ice crystals from one cloud can fall or blow into a different cloud, triggering continued ice formation.

Other substances have been manufactured specifically to seed clouds, to intentionally change the amount or type (rain vs. hail) of precipitation. Silver

Table 7-2. Listed are the warmest ice nucleation threshold temperatures (°C) for substances that act as ice nuclei. Processes are: 1 contact freezing, 2 condensation freezing, 3 deposition, and 4 immersion freezing. (x = not a process for this substance.)

Substance	Process			
	1	2	3	4
silver iodide	–3	–4	–8	–13
cupric sulfide	–6	x	–13	–16
lead iodide	–6	–7	–15	x
cadmium iodide	–12	x	–21	x
metaldehyde	–3	–2	–10	x
1,5-dihydroxynaphlene	–6	–6	–12	x
phloroglucinol	x	–5	–9	x
kaolinite	–5	–10	–19	–32

Solved Example

What cloud temperature is needed to immersion-freeze half of the droplets of 100 μm radius?

Solution

Given: R = 100 μm. Find: T = ? K

Use eq. (7.18)

T = 235K + (3K)·ln(100μm/5μm) = 244K = **–29°C**

Check: Units OK. Physics OK.

Discussion: Smaller droplets can remain unfrozen at much colder temperatures than larger drops, which are thus available to participate in the WBF precipitation growth process described later.

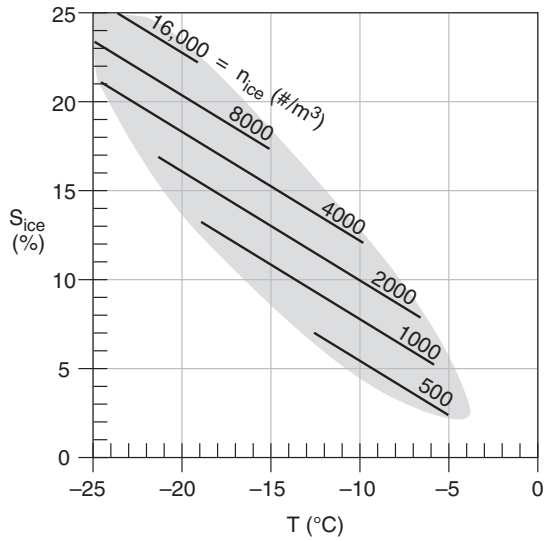

Figure 7.10

Number density n_{ice} of active ice nuclei per m^3 of air as a function of ice supersaturation S and temperature T. Shaded region encloses typically observed combinations of S and T.

Solved Example

Given a supersaturation gradient of 1% per 2 μm near a droplet in a cloud at 4 km altitude where saturated mixing ratio is 1.5 g/kg and the diffusivity is $2\text{x}10^{-5}$ $m^2 \cdot s^{-1}$. Find (a) the mixing-ratio gradient, (b) the kinematic moisture flux, and (c) the dynamic moisture flux.

Solution:

Given: $\Delta S\%/\Delta x = 1\% / 2\ \mu m$, $r_s = 0.0015\ kg_{water}/kg_{air}$
$D = 2\text{x}10^{-5}\ m^2 \cdot s^{-1}$.

Find: (a) $\Delta r/\Delta x$ = ? $(kg_{water}/kg_{air})/m$, (b) F = ? $(kg_{water}/kg_{air}) \cdot (m/s)$, (c) $\mathbb{F}$ = ? $kg_{water} \cdot m^{-2} \cdot s^{-1}$.

First, convert units in the saturation gradient:

$\Delta S/\Delta x = [1\%/2\ \mu m] \cdot (10^6 \mu m/1m)/100\% = 5000\ m^{-1}$.

Next, use eq. (7.21):

$\Delta r/\Delta x = (0.0015 kg/kg) \cdot (5000 m^{-1})$
$= \underline{7.5}\ (kg_{water}/kg_{air}) \cdot m^{-1}$.

Then use eq. (7.20):

$F = -(2\text{x}10^{-5}\ m^2 \cdot s^{-1}) \cdot (7.5\ (kg/kg) \cdot m^{-1})$
$= \underline{\mathbf{-1.5x10}}^{-4}\ (kg_{water}/kg_{air}) \cdot (m/s)$.

Finally, use the definition of kinematic flux from the Radiation chapter: $F = \mathbb{F} / \rho_{air}$. As a first guess for density, assume a standard atmosphere at z = 2 km, and use Table 1-5 in Chapter 1 to estimate $\rho_{air} \approx 0.82\ kg_{air}/m^3$. Thus: $\mathbb{F} = (\rho_{air}) \cdot (F)$
$= (0.82 kg_{air}/m^3) \cdot [-1.5\text{x}10^{-4} (kg_{water}/kg_{air}) \cdot (m/s)]$
$= \underline{\mathbf{-1.23x10}}^{-4}\ kg_{water} \cdot m^{-2} \cdot s^{-1}$.

Check: Units OK. Physics OK.

Discussion: Diffusive fluxes are very small, which is why it can take a couple hours for droplets to grow to their maximum drop radius. The negative sign means water vapor flows from high to low humidity.

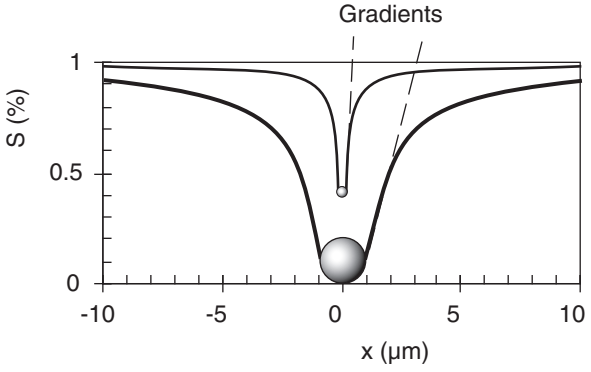

Figure 7.11
Humidity gradients in supersaturated environment near growing droplets. S% is supersaturation percentage, x is distance. The nucleus for both droplets is salt of mass 10^{-16} g. Background supersaturation is 1%, the small droplet has radius 0.2 μm, and the large drop 1.0 μm. Equilibrium supersaturation adjacent to the droplets is taken from Fig. 7.7b. Nearest neighbor droplets are roughly 1000 μm distant.

iodide has been a popular chemical for cold-cloud seeding. Other cold-cloud-seeding chemicals are lead iodide, cupric sulfide, phloroglucinol, and metaldehyde. Table 7-2 lists some ice nuclei and their critical temperatures. Because contact nucleation occurs at the warmest temperatures for most substances, it is the most likely process causing ice nucleation.

Air usually contains a mixture of ice nuclei having a variety of ice nucleation processes that become active at different temperatures and supersaturations. The number density n_{ice} of active ice nuclei per cubic meter of air is shown in Fig. 7.10.

LIQUID DROPLET GROWTH BY DIFFUSION

In a supersaturated environment, condensation onto a growing droplet removes water vapor from the adjacent air (Fig. 7.11). This lowers the humidity near the droplet, creating a humidity gradient down which water vapor can diffuse.

Diffusion is the process where individual water-vapor molecules meander through air via Brownian motion (i.e., random walk). The net direction of diffusion is always down the humidity gradient toward drier air.

The diffusive moisture flux $\mathbb{F}$ in $kg_{water} \cdot m^{-2} \cdot s^{-1}$ is

$$\mathbb{F} = -D \cdot \frac{\Delta \rho_v}{\Delta x} \qquad \bullet(7.19)$$

where x is distance, D is diffusivity, and ρ_v is absolute humidity (water-vapor density) in kg_{water}/m^3. To rewrite this in kinematic form, divide by dry-air density ρ_{air} to give:

$$F = -D \cdot \frac{\Delta r}{\Delta x} \qquad \bullet(7.20)$$

where r is water-vapor mixing ratio, and kinematic flux F has units of mixing ratio times velocity $[(kg_{water}/kg_{air}) \cdot (m/s)]$. Larger gradients cause larger fluxes, which cause droplets to grow faster.

The mixing ratio gradient is $\Delta r/\Delta x$. This is related to the supersaturation gradient $\Delta S/\Delta x$ by:

$$\frac{\Delta r}{\Delta x} = \frac{\Delta\left[(1+S) \cdot r_s\right]}{\Delta x} \approx r_s \cdot \frac{\Delta S}{\Delta x} \qquad (7.21)$$

where r_s is the saturation mixing ratio over a flat water surface. For this expression, the supersaturation fraction is defined by eq. (7.4), and supersaturation percentage by eq. (7.2).

Larger drops create a more gentle gradient than smaller drops. The humidity profile is given by:

$$S \approx S_\infty + \frac{R}{|x|} \cdot (S_R - S_\infty) \qquad (7.22)$$

where S is supersaturation fraction at distance x from the center of the drop, S_∞ is background supersaturation at a large distance from the droplet, S_R is equilibrium supersaturation adjacent to the drop, and R is droplet radius. Eq. (7.22) was solved on a spreadsheet to create Fig. 7.11.

The **diffusivity** D is approximately

$$D = c \cdot \frac{P_o}{P} \cdot \left(\frac{T}{T_o} \right)^{1.94} \qquad (7.23)$$

where $c = 2.11\text{x}10^{-5}$ m^2·s^{-1} is an empirical constant, $P_o = 101.3$ kPa, and $T_o = 273.15$ K. This molecular diffusivity for moisture is similar to the thermal conductivity for heat, discussed in the Heat chapter.

During droplet growth, not only must water vapor diffuse through the air toward the droplet, but heat must conduct away from the drop. This is the latent heat that was released during condensation. Without conduction of heat away from the drop, it would become warm enough to prevent further condensation, and would stop growing.

Droplet radius R increases with the square-root of time t, as governed by the combined effects of water diffusivity and heat conductivity:

$$R \approx c_4 \cdot \left(D \cdot S_\infty \cdot t \right)^{1/2} \qquad \bullet(7.24)$$

where S_∞ is the background supersaturation fraction far from the drop. Also, dimensionless constant c_4 is:

$$c_4 = (2 \cdot r_\infty \cdot \rho_{air} / \rho_{liq.water})^{1/2} \qquad (7.25)$$

where background mixing ratio is r_∞. Small droplets grow by diffusion faster than larger droplets, because of the greater humidity gradients near the smaller drops (Fig. 7.11 and eq. 7.22). Thus, the small droplets will tend to catch up to the larger droplets.

The result is a drop size distribution that tends to become **monodisperse**, where most of the drops have approximately the same radius. Also, eq. (7.24) suggests that time periods of many days would be necessary to grow rain-size drops by diffusion alone. But real raindrops form in much less time (tens of minutes), and are known to have a wide range of sizes. Hence, diffusion cannot be the only physical process contributing to rain formation.

Solved Example

Find the water vapor diffusivity at $P = 100$ kPa and $T = -10$°C.

Solution

Given: $P = 100$ kPa and $T = 263$ K.
Find: $D = ?$ m^2·s^{-1}.

Use eq. (7.23):

$$D = (2.11 \times 10^{-5}\,\text{m}^2\text{s}^{-1}) \left(\frac{101.3\text{kPa}}{100\text{kPa}} \right) \left(\frac{263\text{K}}{273.15\text{K}} \right)^{1.94}$$

$$= \underline{\mathbf{1.99x10}}^{-5}\ \text{m}^2\cdot\text{s}^{-1}.$$

Check: Units OK. Physics OK.
Discussion: Such a small diffusivity means that a large gradient is needed to drive the vapor flux.

Solved Example

Find and plot drop radius vs. time for diffusive growth, for the same conditions as the previous solved example. Assume 1% supersaturation.

Solution

Given: $P = 100$ kPa, $T = 263$ K, $D = 2\text{x}10^{-5}$ m^2·s^{-1}.
Find: R(μm) vs. t

First get ρ_{air} from the ideal gas law:

$$\rho_{air} = \frac{P}{\Re_d \cdot T} = \frac{100\text{kPa}}{(0.287\text{kPa}\cdot\text{K}^{-1}\cdot\text{m}^3\cdot\text{kg}^{-1})\cdot(263\text{K})}$$

$$= 1.325\ \text{kg}\cdot\text{m}^{-3}\ .$$

$r_s \approx 1.8$ g/kg $= 0.0018$ kg/kg from thermo diagram in Ch. 5. But supersaturation $S = 1\% = 0.01 = [\, r_\infty / r_s \,] - 1$.
Thus $r_\infty = [\, 1 + S \,] \cdot r_s$
$= 1.01 \cdot (0.0018\ \text{kg/kg}) = 0.00182$ kg/kg.

Using this in eq. (7.25): $c_4 = [2 \cdot (0.00182\ \text{kg}_w/\text{kg}_a) \cdot (1.325\ \text{kg}_a\cdot\text{m}^{-3}) / (1000\ \text{kg}_w\cdot\text{m}^{-3})]^{1/2}$
$c_4 = 0.0022$ (dimensionless)

Finally solve eq. (7.24) on a spreadsheet:
$R \approx 0.0022 \cdot [(2\text{x}10^{-5}\ \text{m}^2/\text{s}) \cdot (0.01) \cdot t\,]^{1/2}$

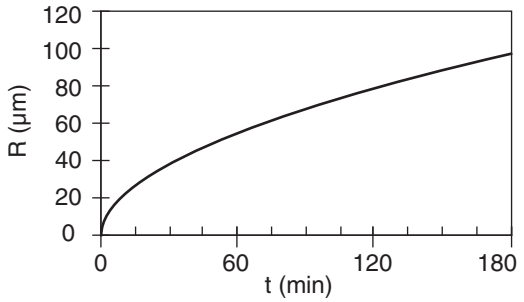

Check: Units OK. Physics OK.
Discussion: The droplet radius increases with the square root of time — fast initially and slower later. After 3 hours, it has a size on the borderline between cloud and rain drops. Thus, it is virtually impossible to grow full-size rain drops solely by diffusion.

FOCUS • Cubic Ice

Fourteen **phases** of ice have been identified, and are labeled using Roman numerals I–XIV (see Fig. 7.b). More phases might be discovered in the future. Each phase is a preferred arrangement of molecules having uniform chemical composition and physical state.

At normal atmospheric temperatures and pressures, ice I is most prevalent. However, it comes in two variants: **hexagonal ice** (**Ih**), and **cubic ice** (**Ic**). Ice Ih is the form that is thermodynamically stable in the troposphere. Both forms of ice I have a tetrahedral arrangement of water molecules.

Hexagonal ice Ih forms crystals that are hexagonal plates, hexagonal columns with flat ends, hexagonal columns with pyramidal ends, and **dendrites** (snowflakes with 6 arms). Samples of these crystal shapes have been collected in the atmosphere, and are frequently observed. This is the normal ice that we see.

Cubic ice Ic is believed to be able to form as cubes, square columns capped by pyramids, and octahedrons (equal to two pyramids with their bases merged). Natural crystals of ice Ic have been detected in the lower stratosphere, but never been successfully captured in the lower troposphere partly because it is metastable with respect to ice Ih, and at warmer temperatures ice Ic rapidly converts to Ih. Cubic ice has been created in the lab under atmospheric conditions, and its existence in the atmosphere has been inferred from certain halos observed around the sun (because ice crystals act like prisms; see the Optics chapter).

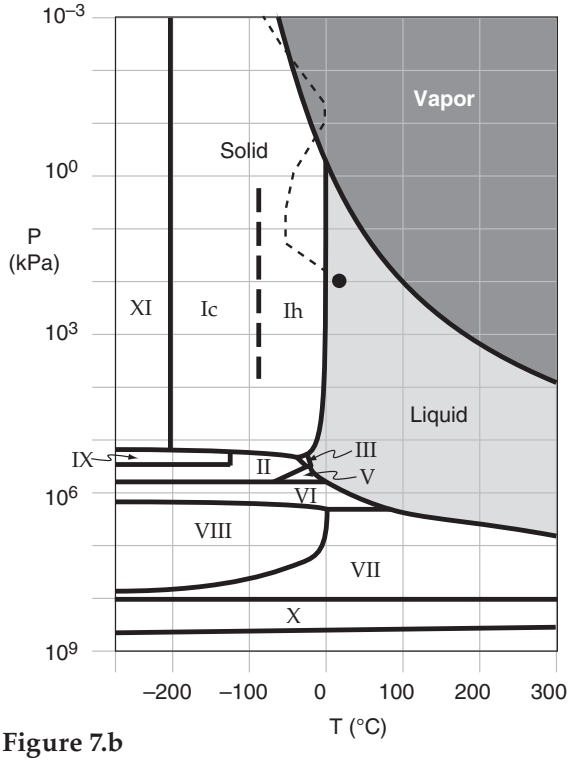

Figure 7.b
Phase diagram for water, as a function of temperature (T) and pressure (P). Standard atmosphere is thin dotted line, with circle at Earth-surface standard conditions. (Not all phases are plotted.) See exercise U26 and Table 7-7.

ICE GROWTH BY DIFFUSION

Ice Crystal Habits

In the troposphere, the normal ice crystal shape that forms from direct deposition of water vapor is hexagonal (see Focus Box at left). The particular hexagonal shape that grows depends on temperature and supersaturation (Fig. 7.12). These shapes are called **habits**. Supersaturation is sometimes given as **water-vapor density excess** $\rho_{ve} = \rho_v - \rho_{vs}$, where ρ_v is absolute humidity and ρ_{vs} is the saturation value of absolute humidity.

As ice crystals fall and move by wind and turbulence, they pass through regions of different temperature and vapor-density excess in the cloud. This allows individual crystals to grow into complex combinations of habits (Fig. 7.13). For example, a crystal that starts growth as a column might later be capped on each end by large plates. Because each crystal travels through a slightly different path through the cloud, each snowflake has a unique shape.

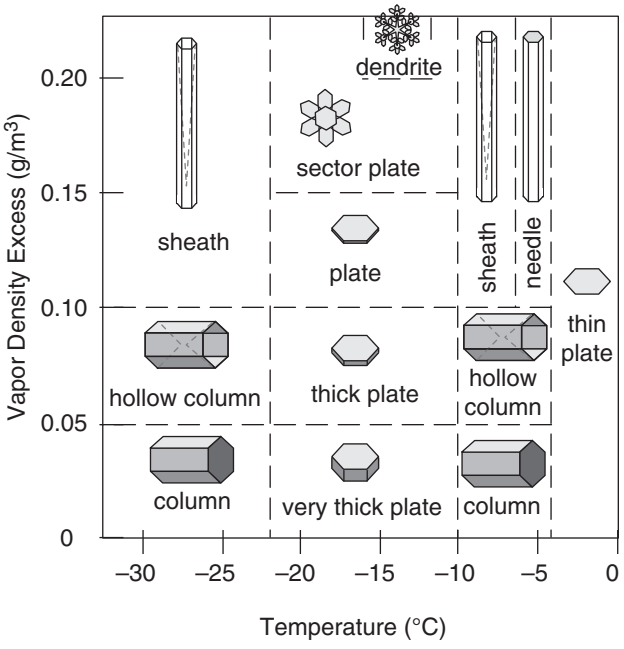

Figure 7.12
Ice crystal habits (idealized). Sheaths are hollow needles, and needles are long, narrow, solid columns. Outside the range of this figure, solid-column rosettes are found at temperatures below –40°C.

Figure 7.13
Some of the observed ice crystal shapes. [Courtesy of Kenneth Libbrecht, www.SnowCrystals.com.]

Solved Example
For each snow crystal class in Table 7-A (see Focus Box at right), identify (by row and column label) all crystal shapes from Fig. 7.13 that are in that class.

Solution

Class	Shapes
1a Columns:	1A, 1B, 2B, 5D
1b Needles:	1C, 5B, 6B, 7B
1c Plates:	1E, 2A, 3A, 3D, 4A, 4D, 6C, 7C, 7D
1d Stellars:	2E, 3A, 3D, 4A, 4D, 4E, 5A, 6A,
1e Irregular:	1D, 1E, 2C, 2D, 3C, 3E, 4C, 5C, 5E, 6D
1f Graupel:	6E, 7E
1g Hail:	(none)
1h Ice Pellets:	(none)

Discussion: Identifying ice-crystal class is somewhat subjective. Different experts might give a slightly different classification than the solution above.

FOCUS • Snow Grain Classification

Snow avalanches are often associated with weak snow layers buried under stronger layers of snow. Field observations of snow crystal shape and size are important for detecting the different snow layers. The International Commission on Snow and Ice (ICSI) developed in 1990 a standard symbology (Table 7-A & Table 7-B) to use when logging snow data.

Table 7-A. Morphological (shape-based) classification of precipitation particles. T = temperature, ρ_{ve} = excess water vapor density.
[Colbeck et al, 1990: *The International Classification for Seasonal Snow on the Ground*, ICSI. 37pp. Available from http://www.crrel.usace.army.mil/techpub/CRREL_Reports/reports/Seasonal_Snow.pdf]

	Name	Symbol	Shape & Formation
1a	Columns		Short, prismatic crystal, solid or hollow. See Fig. 7.12 for T & ρ_{ve} conditions.
1b	Needles		Needle-like, approximately cylindrical. See Fig. 7.12 for T & ρ_{ve} conditions.
1c	Plates		Plate-like, mostly hexagonal. See Fig. 7.12 for T & ρ_{ve} conditions.
1d	Stellars, Dendrites		Six-fold start-like, planar or spatial. See Fig. 7.12 for T & ρ_{ve} conditions.
1e	Irregular Crystals		Clusters of very small crystals. Polycrystals growing at varying environmental conditions.
1f	Graupel		Heavily rimed particles. Caused by accretion of supercooled water.
1g	Hail		Laminar internal structure, translucent or milky, glazed surface. Growth by accretion of supercooled water.
1h	Ice Pellets		Transparent, mostly small spheroids. Frozen rain.

Table 7-B. Snow-grain classification (ICSI).

Term	Size (mm)
Very fine	< 0.2
Fine	0.2 to 0.5
Medium	0.5 to 1.0
Coarse	1.0 to 2.0
Very coarse	2.0 to 5.0
Extreme	> 5.0

Solved Example

Given a mixed-phase cloud (i.e., having both ice crystals and supercooled liquid water droplets) at –14°C that is saturated with respect to water (and thus supersaturated with respect to ice; see Fig. 4.2 in the Moisture chapter). If the water vapor diffusivity is $1.5\text{x}10^{-5}$ m^2 s^{-1}, then what is the relative mass of ice crystals after 1 hour of growth, for (a) a 3-D crystal and (b) a 2-D crystal that is 15 μm thick?

Solution

Given: $D = 1.5\text{x}10^{-5}$ m^2 s^{-1}, t = 1 h = 3600 s, T = 259K
d = 15 μm = $1.5\text{x}10^{-5}$ m.
Find: m = ? kg
Assume: initial mass m is negligible

First, use Fig. 4.2 in the Moisture chapter to estimate the supersaturation. The insert in that fig. shows that $(e_{water} - e_{ice}) \approx 0.0275$ kPa at T = –14°C, and $e_{ice} \approx 0.175$ kPa. The supersaturation is:

$S = (e_{water} - e_{ice}) / e_{ice}$ = (0.0275 kPa)/(0.175 kPa)
S = 0.157 (dimensionless)

Use the ideal gas law for water vapor (eq. 4.10) to estimate vapor density from vapor pressure (which for this case equals $e_{water} \approx 0.20$ kPa, from previous paragraph):

$\rho_v = e_{water}/(\Re_v \cdot T)$ =
= (0.2 kPa) /[(0.461 kPa·K^{-1}·m^3·kg^{-1})·(259 K)]
= 1.68×10^{-3} kg/m^3

(a) Use eq. (7.26). The factor in parenthesis is
$(\rho_v{}^3/\rho_i)^{1/2} = [(1.68\text{x}10^{-3}\text{ kg/m}^3)^3/(916.8\text{ kg/m}^3)]^{1/2}$
$= 2.27\text{x}10^{-6}$ kg/m^3
and the term in square brackets of eq. (7.26) is
[ ] = [(1.5x10^{-5} m^2 s^{-1})·(0.157)·(3600s)]$^{3/2}$
[ ] = (8.478x10^{-3} m^2)$^{3/2}$ = 7.8x10^{-4} m^3

Thus, solving eq. (7.26):
m = 11.85·(2.27x10^{-6} kg/m^3)·(7.8x10^{-4} m^3)
= 2.1x10^{-8} kg = **2.1x10**$^{-5}$ g

(b) Use eq. (7.27):

$$m = \frac{5.09}{1.5\text{x}10^{-5}\text{m}} \cdot \left(\frac{(0.00168\text{kg/m}^3)^2}{916.8\text{kg/m}^3} \right) \cdot [8.478\text{x}10^{-3}\text{m}^2]^2$$

= 7.51x10^{-8} kg = **7.51x10**$^{-5}$ g

Check: Units OK. Physics OK. Agrees with Fig. 7.14.
Discussion: Typically observed ice-crystal mass is about 3x10^{-5} g. Typical **snowflakes** that fall to Earth are often aggregates of hundreds of ice crystals stuck together, with a total mass of about 3 mg/snowflake.

Growth Rates

Because of the diversity of shapes, it is better to measure crystal size by its mass m rather than by some not-so-representative radius. Rate of growth by diffusion depends on crystal habit.

Columns and very thick plates have **aspect ratio** (height-to-width ratio) of roughly 1. If the aspect ratio remains constant during growth, then the growth equation is:

$$m \approx c_3 \cdot (\rho_v{}^3 / \rho_i)^{1/2} \cdot [D \cdot S \cdot t]^{3/2} \qquad (7.26)$$

where c_3 = 11.85 (dimensionless), ρ_v is the density of water vapor (=absolute humidity, see eq. 4.10), ρ_i is ice density (= 916.8 kg/m^3 at 0°C), D is diffusivity, S is supersaturation fraction, and t is time. If the crystal were spherical with radius R, then its mass would be $m = \rho_{liq.water} \cdot (4 \cdot \pi/3) \cdot R^3$. Taking the cube root of both sides of eq. (7.26) gives an equation similar to eq. (7.24). Thus growth rate of a 3-D crystal is very similar to growth of a liquid droplet.

For 2-D growth, such as dendrites or plates of constant thickness d, the growth equation changes to

$$m \approx \frac{c_2}{d} \cdot \left(\frac{\rho_v{}^2}{\rho_i} \right) \cdot [D \cdot S \cdot t]^2 \qquad (7.27)$$

where c_2 = 5.09 (dimensionless). For 1-D growth of needles and sheaths of constant diameter, the growth equation is

$$m \propto \exp\left[(D \cdot S \cdot t)^{1/2} \right] \qquad (7.28)$$

These three growth rates are sketched in Fig. 7.14.

Evidently 2-D crystals increase mass faster than 3-D ones, and 1-D crystals increase mass faster still. Those crystals that gain the mass fastest are the ones that will precipitate first.

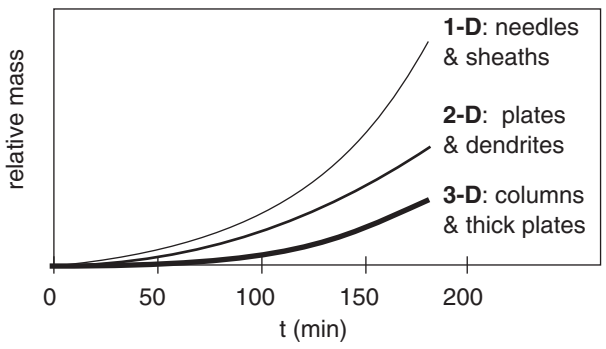

Figure 7.14
Relative growth rates of crystals of different habits.

The Wegener-Bergeron-Findeisen (WBF) Process

Recall from the Moisture chapter that ice has a lower saturation vapor pressure than liquid water at the same temperature. Fig. 7.15 shows an enlargement of the saturation vapor-pressure curves for liquid water and ice.

Suppose that initially (time 1, on the time line in Fig. 7.15) there are only supercooled liquid water droplets in a cloudy air parcel. These droplets exist in a supersaturated environment and therefore grow as the excess water vapor diffuses toward the droplets. As the air parcel rises and cools within the cloud, some ice nuclei might become activated at time 2, causing ice crystals to form and grow. The excess water vapor now deposits on both the liquid and solid hydrometeors.

Both the ice crystals and liquid droplets continue to grow, because both are in a supersaturated environment (time 3). However, the ice crystal grows a bit faster because it is further from its ice saturation line (i.e., more supersaturated) than the liquid droplet is from liquid saturation line.

As both hydrometeors grow, water vapor is removed from the air, reducing the supersaturation. Eventually, near point 4 on the time line, so much vapor has been consumed that the relative humidity has dropped below 100% with respect to liquid water. Hence, the liquid droplet begins to evaporate into the unsaturated air. However, at point 4 the ice crystal continues to grow because the air is still supersaturated with respect to ice.

The net result is that the ice crystals grow at the expense of the evaporating liquid droplets, until the liquid droplets disappear (point 5). This is called the **Wegener-Bergeron-Findeisen** (**WBF**) process.

The difference between ice and liquid saturation vapor pressures is greatest in the range –8°C to –16°C, as shown in Fig. 7.16 (from the insert in Fig. 4.2). This is the temperature range where we expect the maximum effect from the WBF growth process, also known as the **cold-cloud process** because temperatures below freezing are needed.

If a large number of ice nuclei exist in the air, then a large number of ice crystals will form that are each too small to precipitate. For a very small number of ice nuclei, those few ice crystals will rapidly grow and precipitate out, leaving behind many small liquid cloud droplets in the cloud. Both of these scenarios lead to relatively little precipitation.

Only with a medium concentration (1 to 10) ice nuclei per liter (compared to about a million liquid droplets in the same volume) will the ice nuclei be able to scavenge most of the condensed water before precipitating out. This scenario causes the maximum precipitation for the WBF processes. But a

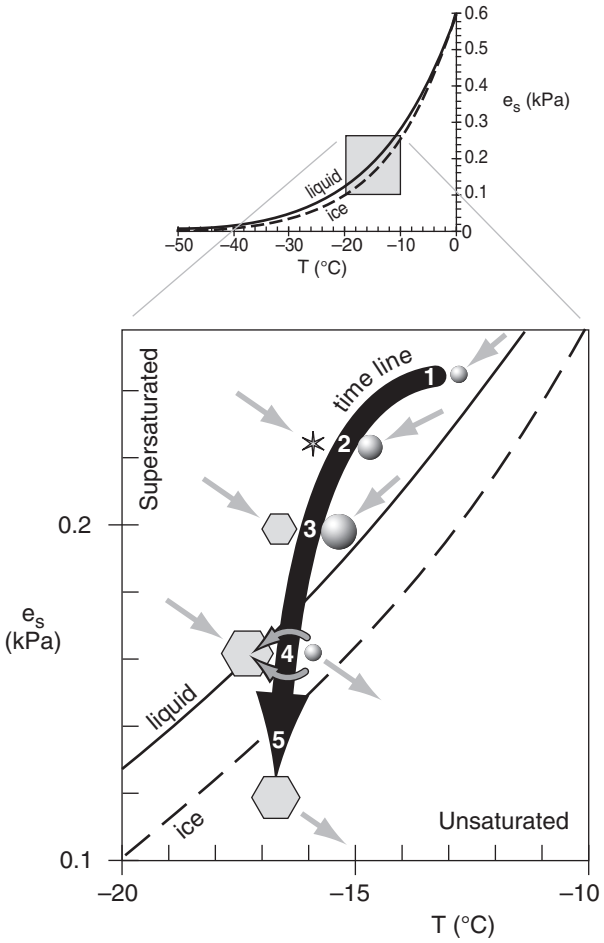

Figure 7.15
Enlargement of part of the saturation curve from Fig. 4.2, illustrating the WBF (cold-cloud) ice-growth process in a rising, cooling air parcel. Shown are saturation vapor pressure (e_s) vs. temperature (T) over liquid water and ice. Spheres represent cloud droplets, and hexagons represent ice crystals. Small grey arrows indicate movement of water vapor toward or away from the hydrometeors. Thick black arrow indicates time evolution.

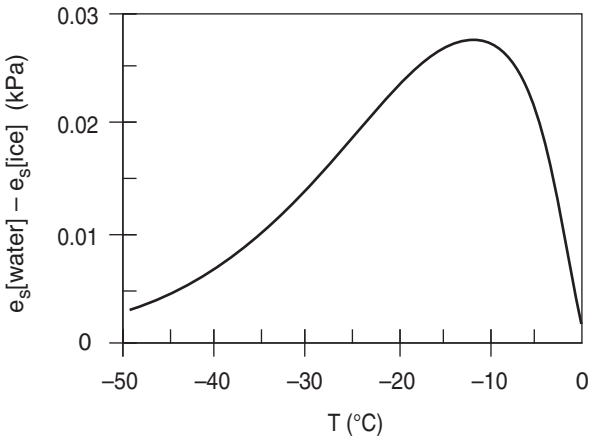

Figure 7.16
Saturation vapor pressure difference over water vs. over ice (copied from Fig. 4.2).

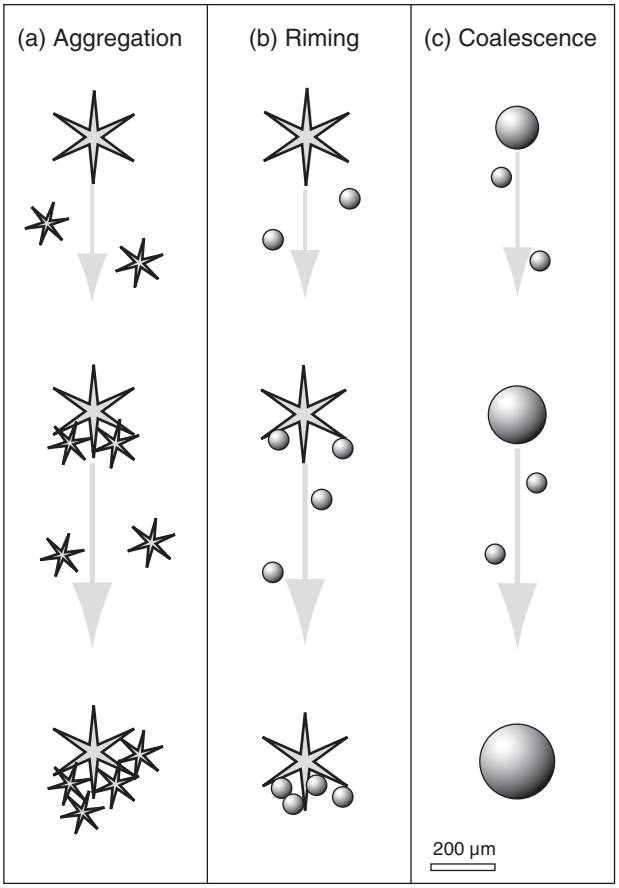

Figure 7.17
Collision and collection of hydrometeors in (a) very cold clouds with no liquid water; (b) cold clouds with both supercooled liquid-water droplets that freeze quickly when they hit ice crystals; and (c) warm clouds. Grey arrows show the fall velocity of the larger hydrometeor relative to the smaller ones.

Solved Example

What updraft wind is needed to keep a typical cloud droplet (R = 10 µm) from falling?

Solution

Given: R = 10 µm

Find: w_T = ? m/s, and use: $w_{up} = -w_T$

Use eq. (7.29):

$w_T = (-1.19 \times 10^8\ \text{m}^{-1}\ \text{s}^{-1}) \cdot (10 \times 10^{-6}\ \text{m})^2 =$

$= -0.012$ m/s = **–1.2 cm/s**

w_{up} = **1.2 cm/s**

Check: Units OK. Physics OK.

Discussion: The required updraft velocity is positive 1.2 cm/s, which is a very gentle movement of air. Recalling that most clouds form by adiabatic cooling within updrafts of air, these updrafts also keep cloud droplets aloft.

restriction on this precipitation formation process is that it happens only in cold clouds (clouds colder than 0°C).

As was discussed in the nucleation sections, there are indeed fewer ice nuclei than CCN, hence the cold-cloud process can be an important first step in getting hydrometeors large enough to begin to fall out of the cloud as precipitation.

The cold-cloud process can occur even in summer, but higher in the troposphere where the air is colder. As these ice particles fall into warmer air at lower altitude, they melt into raindrops to create summer convective rain showers (see Fig. 7.21 later in this chapter).

COLLISION AND COLLECTION

Larger hydrometeors (ones with a greater mass/drag ratio) fall the fastest. As a result, different hydrometeors move at different speeds, allowing some to **collide** (hit each other). Not all collisions result in the merging of two hydrometeors. Those particles that do merge form a particle that is even heavier, falls faster, and collides with even more particles (Fig. 7.17). Hence, this positive feedback can cause hydrometeors to rapidly grow large enough to precipitate.

Terminal Velocity of Hydrometeors

Everything including cloud and rain drops are pulled by gravity. The equilibrium velocity resulting when gravity balances frictional drag is called the **terminal velocity**.

Cloud Droplets

For particles of radius $R < 40$ µm, which includes most cloud droplets and aerosols, **Stokes Drag Law** gives the terminal velocity w_T as

$$w_T \approx -k_1 \cdot R^2 \qquad (7.29)$$

where $k_1 = 1.19 \times 10^8\ \text{m}^{-1} \cdot \text{s}^{-1}$. The negative sign on indicates the droplets are falling.

When drops fall at their terminal velocity, the gravitational pull on the drops is transmitted by frictional drag to the air. In other words, the weight of the air includes the weight of the drops within it. Hence, droplet-laden air is heavier than cloud-free air, and behaves as if it were colder (see virtual temperature, eq. 1.22). Falling rain also tends to drag air with it.

Typical terminal velocities of these smallest droplets and aerosols are mm/s to cm/s relative to the air. However, the rising air in clouds often has updraft velocities (cm/s to m/s) that are greater than the terminal velocity of the particles. The net result is that cloud droplets and aerosols are carried upward inside the cloud.

Rain Drops

Rain drops are sufficiently large and fall fast enough that Stokes drag law is not appropriate. If raindrops were perfect spheres, then

$$w_T \approx -k_2 \cdot \left(\frac{\rho_o}{\rho_{air}} \cdot R \right)^{1/2} \qquad (7.30)$$

where $k_2 = 220\ \mathrm{m^{1/2} \cdot s^{-1}}$, $\rho_o = 1.225\ \mathrm{kg \cdot m^{-3}}$ is air density at sea level, and ρ_{air} is air density at the drop altitude. Again, the negative sign in the equation means a downward velocity.

However, the larger raindrops become flattened as they fall due to the drag (see polarimetric radar section of the Remote Sensing chapter). They do not have a tear-drop shape. This flattening increases air drag even further, and reduces their terminal velocity from that of a sphere. Fig. 7.18 shows raindrop terminal velocities. For the smallest drops, the curve has a slope of 2, corresponding to Stokes law. For intermediate sizes R = 500 to 1000 μm, the slope is 0.5, which corresponds to eq. (7.30). At the larger sizes about R = 2.5 mm, the terminal velocity curve has near zero slope as the droplet becomes so deformed that it begins to look like a parachute. Drops larger than about 2.5 mm radius tend to break up. The largest raindrops rarely exceed 4 mm radius.

Let R be the **equivalent radius** of a sphere having the same volume as the deformed drop. An empirical curve for terminal velocity (relative to air) over range $20 \le R \le 2500$ μm is:

$$w_T = -c \cdot \left[w_o - w_1 \cdot \exp\left(\frac{R_o - R}{R_1} \right) \right] \qquad \bullet(7.31)$$

where w_o = 12 m/s, w_1 = 1 m/s, R_o = 2500 μm, and R_1 = 1000 μm. This curve gives a maximum terminal velocity of 11 m/s for the largest drops. The density correction factor is $c = (\rho_{70kPa}/\rho_{air})^{1/2} \approx (70\ \mathrm{kPa}/P)^{1/2}$, where P is ambient pressure. Rain falls faster where the air is thinner (less dense).

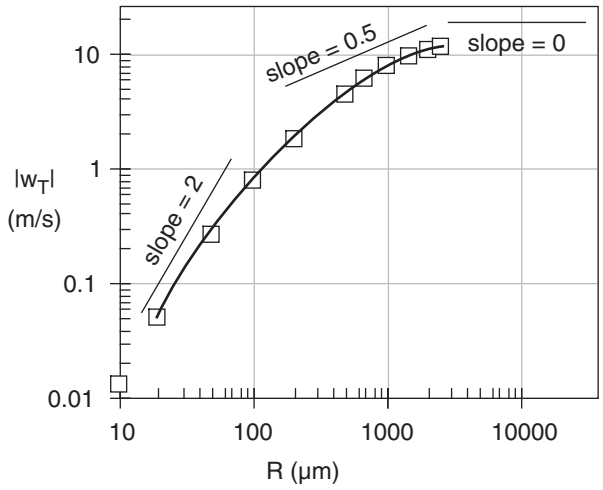

Figure 7.18
Raindrop terminal speed $|w_T|$ at P = 70 kPa and T = 0°C. R is the equivalent radius of a spherical drop. Curve is eq. (7.31).

Solved Example

Find the terminal velocity of a droplet of equivalent radius 1500 μm, at P = 70 kPa.

Solution

Given: R = 1500 μm, c = 1 at P = 70 kPa.
Find: w_T = ? m/s.

Use eq. (7.31):

$w_T = -1 \cdot [(12\mathrm{m/s}) - (1\mathrm{m/s}) \cdot \exp\{(2500\mu\mathrm{m} - 1500\mu\mathrm{m})/(1000\mu\mathrm{m})\}]$

$= \underline{\mathbf{-9.3\ m/s}}$

Check: Units OK. Physics OK. Agrees with Fig. 7.18. Negative sign means falling downward.

Discussion: This $w_T \approx 34$ km/h. Updrafts in thunderstorms are fast, and keep these large drops aloft.

Solved Example

Plot the terminal velocity of hailstones vs. equivalent diameter (0.01 to 0.1 m) at 5 km altitude.

Solution

Given: z = 5 km

Find: w_T (m/s) vs. D (m), where $D = 2{\cdot}R$.

Assume: std. atmosphere. Thus ρ_{air} = 0.7361 kg/m^3 at z = 5 km, from Chapter 1.

Assume: C_D = 0.55, and ρ_i = 900 kg/m^3 , calm air.

Use a spreadsheet to solve eq. (7.32).

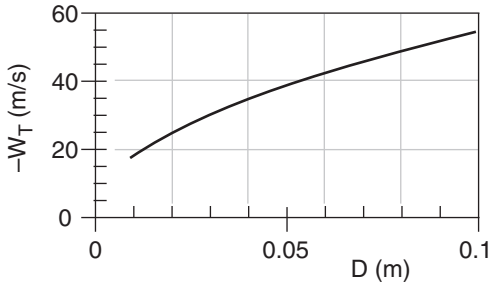

Check: Magnitudes agree with plot in the Thunderstorm chapters. Sign is negative (implying downward fall).

Discussion: Massive hailstones falling at these fast velocities can kill people, strip foliage and small branches off trees, destroy crops, and kill animals.

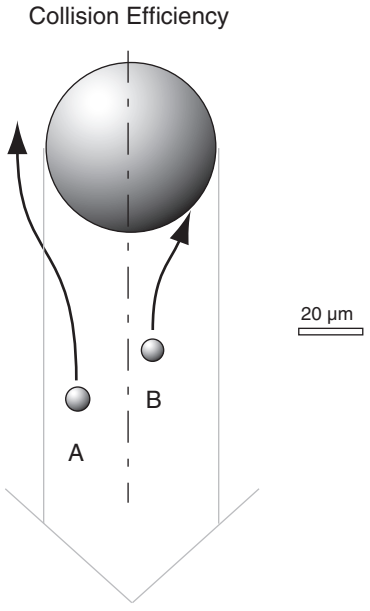

Figure 7.19

Smaller droplets A & B are both in the path of the falling larger drop. Relative to the large drop, small droplet A is pushed aside by the air flowing around the large drop, and does not collide. But droplet B, closer to the centerline of the larger drop, does collide.

Hailstones

The terminal velocity w_T of a hailstone relative to the air is approximated by:

$$w_T = -\left[\frac{8}{3}\frac{|g|}{C_D}\frac{\rho_i}{\rho_{air}}R\right]^{1/2} \qquad \bullet(7.32)$$

where $|g|$ = 9.8 m/s^2 is gravitational acceleration magnitude, $C_D \approx 0.55$ (dimensionless) is a **drag coefficient** of the hailstone through air, $\rho_i \approx 900$ kg/m^3 is the density of the hailstone, ρ_{air} is air density, and R is hailstone radius. The negative sign means the hailstone falls downward.

The drag coefficient varies between 0.4 and 0.8, because hailstones have different shapes, surface roughnesses, and tumblings. The hailstone ice density can be less than the density of pure ice, because of varying amounts of imbedded air bubbles. Air density decreases with increasing altitude (see Chapter 1); hailstones fall faster in thinner air. For non-spherical hailstones, R is taken as the equivalent radius of a sphere that has the same volume as the actual hailstone.

Large hailstones form only in thunderstorms with strong updrafts. Thus, the hailstone terminal velocity relative to the ground is the sum of the air updraft speed (a positive number) and the hailstone terminal velocity relative to the air (a negative number).

Collection & Aggregation Processes

Warm-cloud Process

The merging of two liquid droplets (Fig. 7.17c) is called **coalescence**. This is the only process for making precipitation-size hydrometeors that can happen in warm clouds (clouds warmer than 0°C), and is thus called the **warm-cloud process**.

When droplets of different size approach each other, they do not always merge. One reason is that the smaller droplet partly follows the air as it flows around the larger droplet, and thus may not collide with the larger drop (Fig. 7.19). This is quantified by a **collision efficiency** (E), which is small ($0.02 < E < 0.1$) when the smaller droplet is very small ($2 < R < 5$ µm). But if both droplets are relatively large (such as when the smaller droplet has $R > 10$ µm, and the larger droplet has $R > 30$ µm), then efficiencies can be $0.5 \le E \le 1$.

Even if two droplets collide, they might not merge because a thin layer of air can be trapped between the two droplets (Fig. 7.20b). For this situation, the two droplets bounce off of each other and do not coalesce. The **coalescence efficiency** (E') is

very small ($0.1 \le E' \le 0.3$) when both drops are large ($300 \le R \le 500$ μm). The efficiency is greater ($E' > 0.8$) when both droplets are small ($R < 150$ μm, as in Fig. 7.20a).

The product of both efficiencies is the **collection efficiency**: $E_c = E \cdot E'$. The maximum efficiency possible is 1.0, but usually efficiencies are smaller.

Cold-cloud Processes

When ice particles collide and stick to other ice particles (Fig. 7.17a), the process is called **aggregation**. Such aggregation is aided if the colliding particles are dendrites, for which the snowflake arms can interlock. Also, if the ice particles are warmer than –5°C, then the ice surface becomes sticky, allowing multiple ice crystals to aggregate into soft little irregular clumps of snow.

The growth of ice particles by collection and instant freezing of supercooled liquid droplets (Fig. 7.17b) in mixed-phase clouds is called **accretion** or **riming**. Hydrometeors that become so heavily rimed as to completely cover and mask the original habit are called **graupel**. Graupel has the consistency of a sugar cube (i.e., many separate solid grains stuck together), but often in the shape of a cone or a sphere. For an aggregate to be called graupel, it's diameter must be no larger than 5 mm.

If the collected water does not freeze instantly upon contacting the ice particle, but instead flows around it before freezing, then **hail** can form. Graupel contains a lot of air trapped between the frozen droplets on the graupel, and thus is often softer and less dense than hail. See the Thunderstorm chapters for more information about hail.

Precipitation Formation

Warm Clouds

How do terminal velocity and collection efficiency relate to the formation of large, precipitation-size particles in warm clouds? Recall that: (1) the atmosphere has an excessively large number of CCN; (2) this causes the available condensate in a rising cooling air parcel to be partitioned into a large number of small droplets (droplets too small to rain out); (3) droplets tend to become monodisperse (nearly the same size) due to diffusion; (4) droplets of the same size have the same terminal velocity, and thus would be unlikely to collide with each other as they are kept aloft in the updraft; and (5) with no collisions we would not expect larger precipitation drops to form in warm clouds.

Yet warm-cloud rain happens quite nicely in the real atmosphere, especially in the tropics. Why?

Five factors can help make warm-cloud rain:

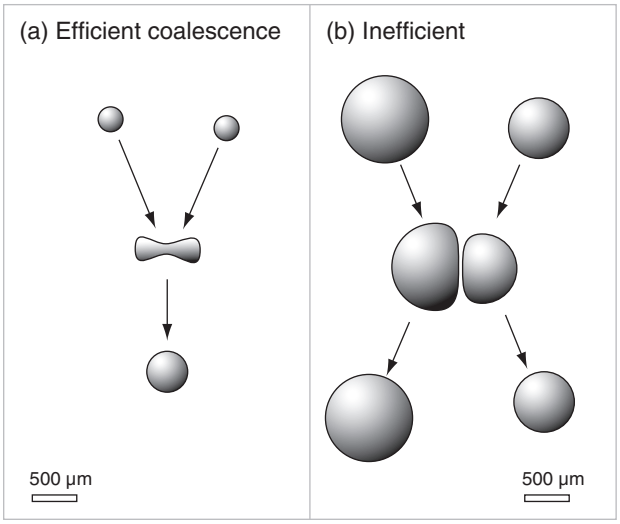

Figure 7.20
Colliding small droplets in (a) coalesce into a single drop. Colliding larger droplets in (b) do not coalesce, because of a film of air trapped between them that cannot completely escape before the two droplets bounce off of each other.

FOCUS • Meteors and Meteorology

Ancient Greeks defined "meteors" as anything in the sky. They were particularly concerned about missiles the gods might toss down, such as bits of rock, ice, or lightning bolts.

Only much later did scientists discriminate between missiles from space (bits of rock called **meteoroids**) and missiles from the atmosphere (bits of just about anything else from the sky). But by then "**meteorology**" was firmly entrenched as the name for **atmospheric science**.

According to the *Glossary of Meteorology*, meteorologists study the following meteors:

- **hydrometeors** – wet: clouds, rain, snow, fog, dew, frost, etc.
- **lithometeors** – dry: dust, sand, smoke, haze
- **igneous meteors** – lightning, corona
- **electrometeors** – lightning (again), thunder
- **luminous meteors** – rainbows, halos, etc.

Except for "hydrometeors", these terms are seldom used any more.

Science Graffito

"Bemused locals [in Stroud, Gloucestershire, UK] were not only stunned to witness frogs raining from the sky [in October 1987], but these frogs were also pink. Scientists identified them as a rare albino strain indigenous to southern Spain and North Africa."

"Minnows and sticklebacks fell over Glamorganshire in 1959, and sand eels rained down on Sunderland in August 1918. Crabs, starfish, flounder, and periwinkles have also fallen on the peaceful English countryside."

"Falls of fish are common in India,...[and have included] shrimps, squid, and herring." "At Acapulco, Mexico, a heavy October rain shower during the 1968 Olympics was accompanied by falling maggots."

"Mr. Alfred Wilson of Bristol [was] caught in a shower of hazel nuts." "In Gorky, USSR, in 1940, a treasure chest was whipped into the air by a whirlwind, and the ... residents were treated to an inundation of silver coins."

"Other reports of curious offerings from above include water lizards, snails, snakes, worms, cannon balls, turtles, ducks, and an alligator which fell on Charleston, Mississippi, in 1893. More gruesomely, it rained skulls, skeletons, and coffins when a tornado ripped up the vaults of a cemetery in New Orleans in the nineteenth century."

{ Roberts, S.K., 1999: Raining cats and frogs, *Weather*, **54**, p126. }

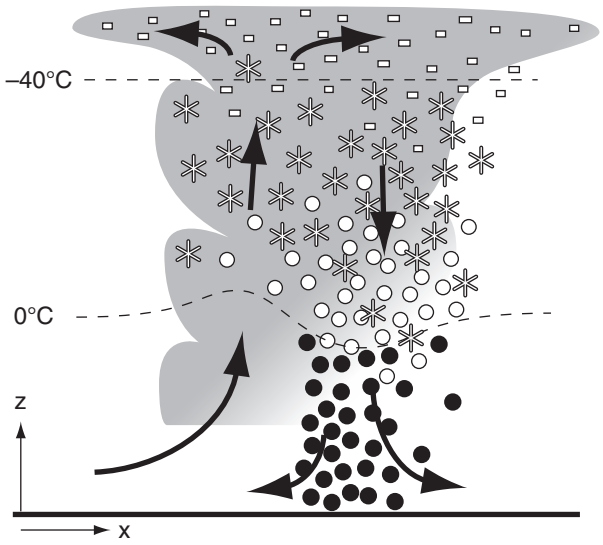

Figure 7.21
Thunderstorms can have cold-cloud tops and warm-cloud bases, allowing efficient growth of ice precipitation that can melt into large raindrops on the way down.

• First, by random chance a small number of collisions do occur, which starts to broaden the spectrum of drop sizes. This broadens the range of terminal velocities to allow more collisions, which accelerates via positive feedback (with help from breakup of larger drops).
• Second, not all CCN are the same size — some are called **giant CCN** (particles > 3 μm radius, with a wettable surface) and can create a small number of larger cloud droplets that fall relative to (and collide with) the other cloud droplets.
• Third, turbulence can entrain outside clear air into the top and sides of a cloud, causing some droplets to partly evaporate, thereby broadening the spectrum of droplet sizes, again allowing collisions.
• Fourth, IR radiation from individual drops near cloud top and sides can cool the drops slightly below the ambient air temperature, allowing greater condensation growth of those drops relative to interior drops.
• Fifth, electrical charge build-up in cumuliform clouds (see the Thunderstorm chapters) can draw droplets together of different charge, and can cause sparks between nearby droplets to allow them to coalesce more efficiently.

Cold Clouds

In cold clouds ($T < 0$°C), the smaller number of ice nuclei in the atmosphere allows the available condensate to deposit onto a small number of larger ice particles. Even in mixed-phase clouds, the WBF process can remove water molecules from the large number of droplets and deposit them onto a small number of ice crystals. Thus, the ice crystals are larger, and can fall as precipitation. Also, the crystals often have a wide range of sizes and shapes so they can collide and aggregate easily, which also creates large-enough particles to fall as precipitation.

Cumuliform clouds including thunderstorms can be deep enough to have their bases in warm air and their tops in cold air (Fig. 7.21). Thus, ice particles can grow to large size (order of 1-5 mm) via the WBF process, aggregation, and riming in the cold part of the cloud, and then melt into large raindrops as they pass through warmer air closer to the ground. Most rain from mid-latitude thunderstorms forms this way. See the Thunderstorm chapters for more information about heavy rain.

Also, on those rare occasions when thunderstorms can be triggered in late Fall or early Spring, boundary-layer temperatures can be cold enough to allow snow from thunderstorms to reach the ground as large snow clusters (snow balls) without totally melting, accompanied by lightning and thun-

der from the storm. This is sometimes nicknamed **thundersnow**.

Regardless of whether clouds are warm or cold, a simple rule of precipitation is that thicker clouds can cause heavier precipitation rates with larger size drops. The main reason is that hydrometeors take a longer time to fall the greater distance through thicker clouds, giving them more time to grow.

PRECIPITATION CHARACTERISTICS

Rain-Drop Size Distribution

Small raindrops outnumber large ones. Classically, the rain-drop spectrum has been fit by an exponential function, known as the **Marshall-Palmer distribution**:

$$N = \frac{N_o}{\Lambda} \exp(-\Lambda \cdot R) \qquad \bullet(7.33)$$

where N is the number of drops of radius greater than R within each cubic meter of air, and $N_o \approx 1.6\text{x}10^7\ \text{m}^{-4}$. Parameter $\Lambda(\text{m}^{-1}) = 8200 \cdot (RR)^{-0.21}$, where RR is rainfall rate in mm/h. Fig. 7.22 shows the Marshall-Palmer distribution. While there are on the order of 1000 drops of drizzle size and larger in each cubic meter of air, there are only tens of drops of typical raindrop size and larger.

Fig. 7.23 shows rain-drop distributions for a variety of rain rates. Larger drop diameters are associated with heavier rainfall rates. Drop diameters in the range of 4 to 8 mm diameters have been observed for the heaviest rain events. Because large liquid drops tend to break up into smaller ones as they fall, it is possible that some of the largest-diameter drops reported in Fig. 7.23 consisted of still-melting graupel or aggregated/rimed snow.

Beware that these curves vary significantly from storm to storm. Many thunderstorms have much greater numbers of large 1000 to 2500 μm radius drops. Real clouds are very heterogeneous in their generation of rain, causing a patchiness in the rainfall rates. This patchiness causes the raindrop size distributions to continually change with time and place; namely, they are not the simplistic, steady distributions given above. This patchiness is also observed by weather radar (see the Remote Sensing chapter), and in the rainfall observed by rain gauges on the ground. You probably also experienced it when driving or walking through rain.

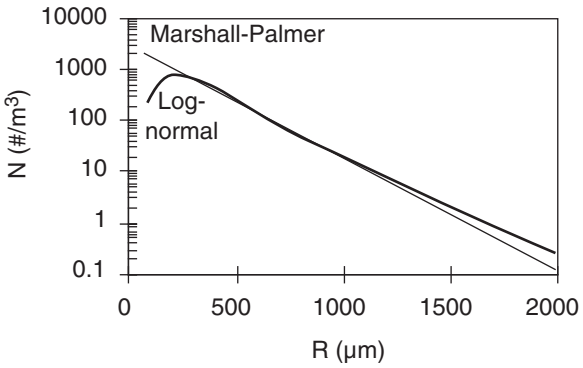

Figure 7.22
Rain drop size distributions. Rainfall rate was RR = 10 mm/h.

Solved Example

Find the number of raindrops larger than 1000 μm, using the parameters given below.

Solution

Given: $RR = 10$ mm/h, $N_o = 1.6\text{x}10^7\ \text{m}^{-4}$, $R = 1000$ μm

Find: $N = ?\ \text{m}^{-3}$.

First, find $\Lambda = 8200 \cdot (10\ \text{mm/h})^{-0.21} = 5056\ \text{m}^{-1}$.

Next, use eq. (7.33) for Marshall-Palmer:

$N = [(1.6\text{x}10^7\ \text{m}^{-4})/(5056\ \text{m}^{-1})] \cdot \exp[-(5056\ \text{m}^{-1}) \cdot (10^{-3}\ \text{m})]$

$= \underline{\mathbf{20.2\ m}}^{-3}$.

Check: Units OK. Physics OK. Agrees with Fig. 7.22.

Discussion: Don't forget that N is like 1 – cumulative distribution. It doesn't give the count of drops of size equal to R, but counts all drops of size R and greater.

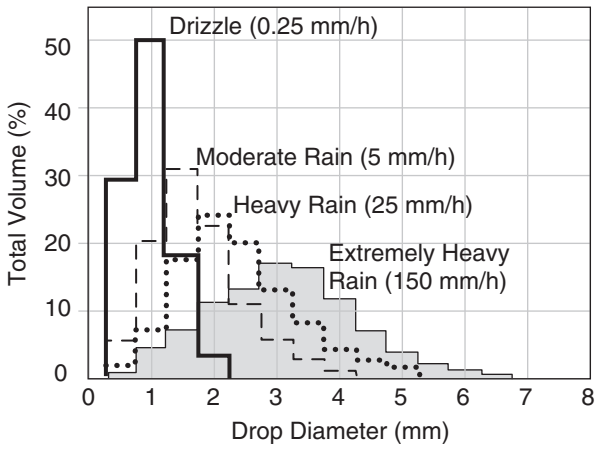

Figure 7.23
Typical distribution of rain-drop sizes during different rain rates. Area under each curve equals 100% of the total volume of rain accumulated in the rain gauge for that rain rate.

Table 7-3. Rain intensity criteria (from USA *Fed. Meteor. Handbook No. 1*, Sep 2005), and their corresponding weather-map symbols and Meteorological Aviation Report (METAR) codes for continuous, non-freezing rain.

Rain Intensity	Rainfall rate		Symbol on Map
	inches/h	≈mm/h	METAR code
heavy	> 0.30	> 7.6	
			+RA
moderate	0.11 – 0.30	2.6 – 7.6	
			RA
light	0* – 0.10	0* to 2.5	• •
			–RA
trace	< 0.005	<0.1	

Solved Example

Is the record rainfall envelope valid for these other actual observations: (a) 206 mm/20 min at Curtea-de-Arges, Romania on 7 July 1889; (b) 304.8 mm/42 min at Holt, MO, USA on 22 July 1947?

Solution

Given: (a) d_{obs} = 206 mm, P_{rain} = 20 minutes = 0.333 h
(b) d_{obs} = 304.8 mm , P_{rain} = 42 min = 0.7 h
Find: if d_{obs} is approx. equal or less than $d_{max\ rain}$

Use eq. (7.34): (a) $d_{max\ rain}$ = **209.6 mm**
(b) $d_{max\ rain}$ = **303.7 mm**

Discussion: Yes, envelope is approx. valid for both.

Table 7-4. Drizzle and snow intensity criteria (from USA *Fed. Meteor. Handbook No. 1*, Sep 2005), and their weather-map symbols and Meteorological Aviation Report (METAR) codes for continuous precipitation.

Precip. Intensity	Visibility (x_v)		Symbol on Map	
			METAR Code	
	miles	≈km	Drizzle	Snow
heavy	$x_v \le 0.25$	$x_v \le 0.4$		
			+DZ	**+SN**
moderate	$0.25 < x_v \le 0.5$	$0.4 < x_v \le 0.8$		
			DZ	**SN**
light	$x_v > 0.5$	$x_v > 0.8$	, ,	* *
			–DZ	**–SN**

Rainfall Rates

Sometimes **rainfall rate** (i.e., **precipitation intensity**) is classified as **light** (or **slight**), **moderate**, or **heavy**. Different countries set different thresholds for these rainfall categories. Table 7-3 shows rainfall intensity criteria used in the USA to determine weather symbols in station plots on surface weather maps. A **trace** amount of precipitation is a very small amount of rain that might wet the ground, but is too small to be detected in a rain gauge (i.e., < 0.1 mm). See the Thunderstorm chapters for more information about very heavy rain and downpours from thunderstorms.

Drizzle is precipitation of very small drops (diameter < 0.5 mm) that are closely spaced and uniform. Although precipitation rates (mm/h) from drizzle are usually very small, drizzle can reduce visibility (Table 7-4).

World-record rainfall total accumulated depth $d_{max.rain}$ in a rain gauge over any storm period P_{rain} is approximately contained under the following envelope:

$$d_{max.rain} = a \cdot P_{rain}^{1/2} \qquad (7.34)$$

where a = 363 $mm_{rain} \cdot h^{-1/2}$. For example, on 25 May 1920 Fussen, Germany received 126 mm in 8 minutes. On 18 July 1942 Smethport, PA, USA received 780 mm in 6 hours. On 15 March 1952, Cilaos, La Re Union Island received 1,830 mm in 1 day. Cherraounji, India received 9,300 mm for the month of July 1861, and received 26,461 mm over the year ending 31 July 1861.

Snowfall Rates & Snow Accumulation

Snowfall rates in the US are classified using the same visibility criterion as drizzle (Table 7-4). Low visibility due to heavy snowfall or blowing loose snow, when accompanied by strong winds, is classified as a **blizzard** if it persists for 3 to 4 hours (Table 7-5). If you are outside in a blizzard, you could easily get disoriented and not be able to return to a shelter, because of **white-out** conditions, where the snow makes the ground and sky look uniformly white so you cannot discern any features or landmarks.

When it is snowing, the precipitation rate is usually measured as **liquid-water equivalent** in units of mm/h. Namely, it is the precipitation rate after all precipitation is melted. Heated rain gauges accomplish this.

You can also estimate the snowfall rate by periodically measuring the depth of snow on the ground using a meter stick or other metric. However, melting of the snow on warm ground, and compression of snow by the weight of snow above cause large errors in these estimates. Thus, liquid-water equivalent is used instead as a more accurate measure.

New fallen snow has a density roughly 10% of that of liquid water. Thus, a rough first guess is that new-fallen snow depth is about 10 times the liquid-water equivalent depth.

Actual snow densities vary widely, as listed in Table 7-6. The density of freshly falling dry snow is very small because of the air between branches of each ice crystal, and because of air trapped between ice crystals as they accumulate on the ground. After snow has fallen, **metamorphosis** takes place where the tips of the crystals evaporate and redeposit near the crystal centers. Such snow gradually changes into **snow grains** (similar to sugar grains), and becomes more compact and dense. Snow can be further modified by partial melting and refreezing (on a diurnal cycle, and also on an annual cycle for glacier snow). The weight of additional snow on top can further compact deeper older snow.

Piste is the name for a ski run where the snow has been compacted by grooming machines. Density and strength can be increased by mechanically chopping and compacting the snow, by adding liquid water (that later freezes), and by adding chemicals such as nitrate fertilizers or urea.

Precipitation Distribution

Combining rain-gauge data over land with satellite observations over oceans gives the annual precipitation distribution shown in Fig. 7.24. The heaviest rain is in the tropics, where the warm sea surface causes copious amounts of evaporation (Fig. 7.25), where the warm air can hold a large amount of precipitable water, and where the general circulation contains updrafts. Rain is suppressed at 30° north and south due to extensive regions of downdraft in the Hadley-cell circulation. This circulation is discussed in the Global Circulation chapter.

Table 7-5. Blizzard criteria.

Weather Condition	Criteria (all must be met)	
	USA	Canada
visibility	≤ 0.25 mile	≤ 1 km
wind speed	≥ 35 mi/h	≥ 40 km/h
duration	≥ 3 h	≥ 4 h

Table 7-6. Snow density.

Density (kg/m^3)	Characteristics
50 - 100	Fresh falling snow.
100 - 200	New top snow. Uncompacted. Called "**powder**" by skiers.
200 - 300	Settled snow on ground. Self-compacted after several days.
300 - 500	Compacted snow by grooming machines. Some target densities (kg/m^3) for groomed ski slopes are: 450 for cross-country (**nordic**) tracks, 530-550 for snowboard and downhill (**alpine**) runs, and 585 - 620 for slalom. Also forms naturally in deep layers of snow, such as during glacier formation.
500 - 550	Called "**névé**". Snow that has been partially melted, refrozen, & compacted.
550 - 830	Called "**firn**". Naturally compacted and aged over 1 year. A form of ice still containing air channels, observed during glacier formation.
830 - 917	Ice with bubbles, typical in the top 1000 m of old glaciers.
917	Solid ice (no bubbles). Typical of glacier ice below 1000 m depth.

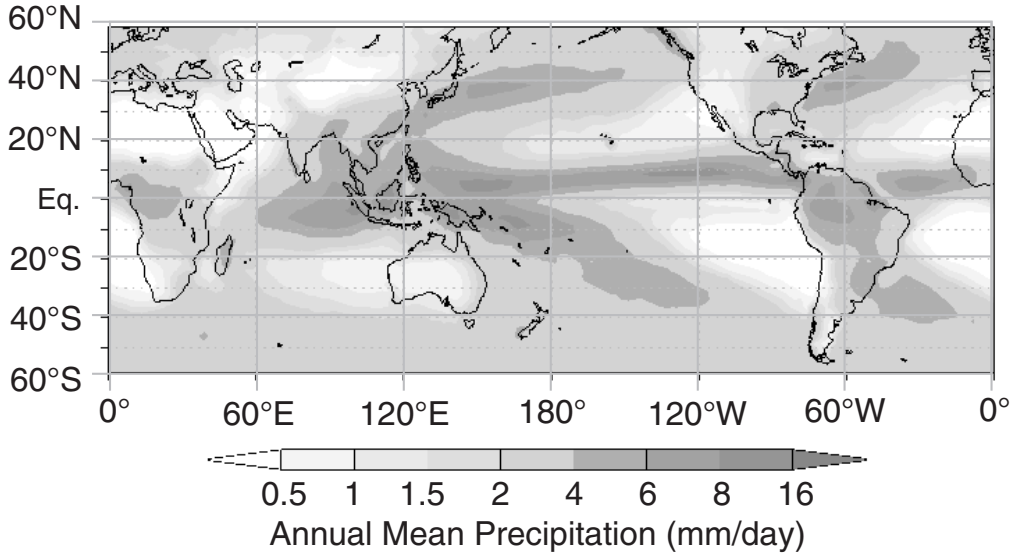

Figure 7.24
Annual mean precipitation during years 1979 to 2000.
[Adapted from image courtesy of US Climate Prediction Center (NOAA/ National Weather Service, National Centers for Environmental Prediction). http://www.cpc.ncep.noaa.gov/products/precip/CWlink/wayne/annual.precip.html]

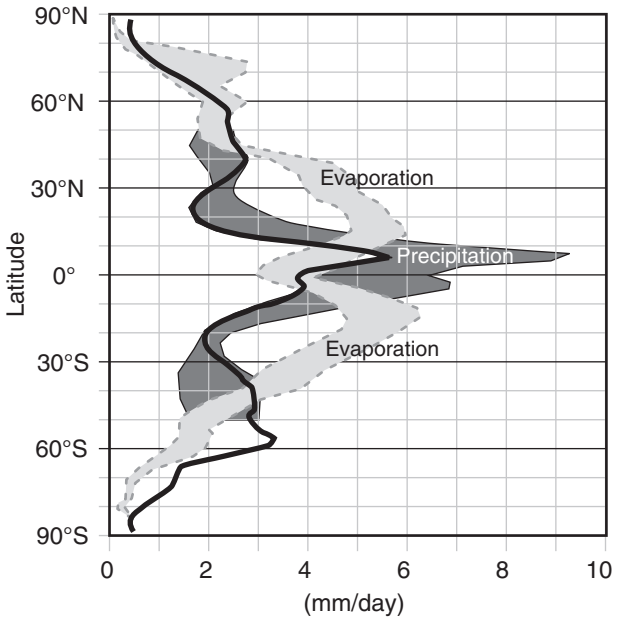

Figure 7.25
Zonally averaged rates of evaporation (light grey with dotted outline) and precipitation (dark grey with solid black outline). Estimated from a combination of satellite observations, numerical simulations, and surface observations. Spread of the grey areas indicates uncertainty (disagreement among the different methods). Data courtesy of NASA GSFC and the Global Precipitation Climatology Project (plotted as the thick black line).

PRECIPITATION MEASUREMENT

The simplest precipitation instrument is a **rain gauge**, which is a cylindrical bucket into which the rain falls. By using a measuring stick to manually read the water depth in the bucket at successive times such as every hour, you can determine rainfall rate. For greater sensitivity, a funnel can be placed over the bucket to collect rain faster, but the depth of water in the bucket must be reduced by the ratio of the horizontal cross-section areas of the bucket to the funnel opening. To get the **liquid-water equivalent** of the snowfall, some rain gauges are heated to melt snow, and others are painted black to passively melt snow by absorbing sunlight. Some gauges are surrounded by a segmented **wind shield** to reduce errors due to blowing precipitation.

Automated rain gauges exist. **Weighing rain gauges** weigh the rain-filled bucket over successive intervals, inferring rain accumulation by weight increase, knowing the density of liquid water.

Tipping-bucket rain gauges direct the captured rain into a tiny bucket on one side of a lever. When the bucket gets full, it tips the lever like a seesaw (teeter-totter), emptying that bucket while simultaneously moving under the funnel an empty bucket from the other end of the lever. Each tip can be counted digitally, and the frequency of tips during an hour gives the rainfall rate.

An **evaporative rain gauge** has two metal plates, one above the other, each oriented horizontally (one facing up, and the other facing down). Each plate is heated electrically to maintain the same specified temperature warmer than ambient air. Precipitation falling on the hot top plate evaporates quickly, thereby removing heat from that plate. By measuring the amount of extra electricity needed to keep the top plate at the same temperature as the bottom, and knowing the latent heat of vaporization, the rainfall rate can be determined.

Attenuation rain gauges have a light beam that shines horizontally across an open air path exposed to precipitation. The attenuation of the light beam is related to precipitation intensity, but errors can be due to air pollution, fog, and different absorption cross-sections of liquid vs. solid precipitation.

A **disdrometer** measures size distribution of rain drops via the momentum imparted to a horizontal plate by each falling drop. Another method is a particle imager that sends light from an array of light-emitting diodes to an array of tiny photodetectors. Each hydrometeor casts a shadow that can be detected, where the size and the shape of the shadows are used together to estimate precipitation rate, hydrometeor type and size. A **Knollenberg probe** uses this imaging method, and can be mounted on aircraft flying through clouds and precipitation.

A **liquid-water content (LWC) probe** consists of an electrically heated wire. When mounted on an aircraft flying through a cloud, the rain and cloud droplets evaporate upon hitting the hot wire. By measuring the electrical power needed to maintain a constant wire temperature against the evaporative cooling, the LWC can be inferred.

Snow amount on the ground can be measured by placing a liquid antifreeze-filled thin-skin metal **snow pillow** on the ground before the winter snow season. As snow accumulates during the season, the weight of the snow squeezes the pillow and displaces some of the fluid. Pressure sensors measure the weight of the displaced fluid to infer snow weight.

Downward-pointing **ultrasonic snow-depth sensors** mounted on a tall pole measure the travel time for an emitted pulse of sound to reach the ground and echo back to the sensor on the pole. This gives the distance between the top of the snow and the sensor, which can be subtracted from the sensor height above bare ground to give the snow depth. Similar sensors use travel time for IR or visible light pulses.

Remote sensors (see the Remote Sensing chapter) can also be used to measure rain rate or accumulation. Ground-based **weather radar** actively emits microwaves, and can estimate rainfall rate from the echo intensity and polarization characteristics of the microwave signal that is scattered back to the radar from the precipitation particles. **Passive microwave sensors** on some weather satellites can measure the **brightness temperature** of the minute amounts of microwaves emitted from the Earth's surface and atmosphere. With this info one can infer the atmospheric total water content in a column of the atmosphere (used to estimate **tropical rainfall** over the oceans), and can infer snow depth on the ground (over high-latitude regions).

SUMMARY

Cloud droplets that form on cloud condensation nuclei (CCN) overcome a formation barrier caused by the surface tension of the curved surface. However, because there are so many CCN between which the available water is partitioned, the result is a large number of very small droplets. These drops grow slowly by diffusion, and develop a monodisperse droplet-size distribution. Such a distribution reduces droplet collisions, and does not favor droplet growth into precipitation hydrometeors. Hence, we get pretty clouds, but no rain.

Warm-cloud ($T > 0°C$) rain can happen in the tropics, particularly over oceans where there are fewer CCN allow formation of a smaller number of larger drops. Several other processes can cause the droplet sizes to have more diversity, resulting in different terminal velocities for different drops. This encourages collision and coalescence to merge smaller droplets into ones that are large enough to precipitate out.

In clouds colder than 0°C, ice nuclei trigger ice crystals to grow. Ice crystals can exist in the air along with supercooled liquid drops. Because of the difference between liquid and ice saturation humidities, the ice can grow at the expense of evaporating liquid droplets. If the ratio of water to ice hydrometeors is about a million to one, then most of the water will be transferred to ice crystals, which are then heavy enough to fall as precipitation.

As larger ice particles fall and hit smaller supercooled liquid droplets, the droplets can freeze as rime onto the ice crystals, causing the hydrometeors to grow even faster. This process can create graupel and hail. Also, ice crystals can aggregate (collide and stick together) to make larger clumps of snow. Most rain at midlatitudes results from melted snow that form from this "cold cloud" process.

Threads

Larger precipitation particles form in deeper clouds, where cloud depth (Chapter 6) depends on atmospheric stability (Chapter 5). Thunderstorms (Chapters 14 and 15) produce the largest rain droplets and ice crystals, including hail.

Air pollution (Chapter 19) near urban areas often becomes cloud and ice nuclei, causing precipitation over and downwind of large cities to be altered from the background rural average. Precipitation and clouds are important feedback factors in global climate (Chapter 21).

Total rainfall out of severe thunderstorms (Chapters 14 and 15) and hurricanes (Chapter 16) is often much greater than calculated precipitable water, primarily due to the strong inflow of humid air that fuels these storms. Precipitation intensity can be observed with weather radar (Chapter 8).

Ice crystals and liquid droplets in the air cause beautiful halos, rainbows, and other optical phenomena (Chapter 22). Droplet size distribution is very uniform in lenticular clouds (Chapter 17).

The supersaturation (Chapter 4) needed to cause droplet and ice-crystal formation occurs in air that rises and cools adiabatically (Chapter 3), due to the decrease of atmospheric pressure with height (Chapter 1). However, the condensation that forms droplets also releases latent heat (Chapter 3), which causes rising air parcels to cool at the moist rather than the dry adiabatic rate (Chapters 3 and 4).

EXERCISES

Numerical Problems

N1. Using Fig. 7.1, how many of the following droplets are needed to fill a large rain drop.
a. small cloud droplet
b. typical cloud droplet
c. large cloud droplet
d. drizzle droplet
e. small rain droplet
f. typical rain droplet

N2. Find the supersaturation fraction and supersaturation percentage, given relative humidities (%) of: a. 100.1 b. 100.2 c. 100.4 d. 100.5 e. 100.7
f. 101 g. 101.2 h. 101.8 i. 102 j. 102.5
k. 103.3 l. 104.0 m. 105 n. 107 o. 110

N3. For air at T = –12°C, find the supersaturation fraction, given a vapor pressure (kPa) of:
a. 0.25 b. 0.26 c. 0.28 d. 0.3 e. 0.31
f. 0.38 g. 0.5 h. 0.7 i. 0.9 j. 1.1
k. 1.2 l. 1.4 m. 1.6 n. 1.8 o. 1.9
Hint. Get saturation vapor pressure from the Moisture chapter.

N4. For air at P = 80 kPa and T = –6°C, find the supersaturation percentage, given a mixing ratio (g/kg) of: a. 6 b. 5.8 c. 5.6 d. 5.4 e. 5.2 f. 5.1 g. 5
h. 4.9 i. 4.7 j. 4.5 k. 4.3 l. 4.1 m. 3.8 n. 3.6
Hint. Get saturation mixing ratio from a thermo diagram (at the end of the Stability chapter).

N5. For the previous problem, assume the given mixing ratios represent total water mixing ratio. Find the excess water mixing ratio (g/kg).

N6. For an air parcel with excess water mixing ratio of 10 g/kg at a geopotential height of 5 km above mean sea level, find the average radius (μm) of the hydrometeor assuming growth by condensation only, given a hydrometeor number density (#/m^3) of: a. $1x10^8$ b. $2x10^8$ c. $3x10^8$ d. $4x10^8$ e. $5x10^8$
f. $6x10^8$ g. $7x10^8$ h. $8x10^8$ i. $9x10^8$ j. $1x10^9$
k. $2x10^9$ l. $3x10^9$ m. $4x10^9$ n. $5x10^9$ o. $8x10^9$

N7. If $c = 5x10^6$ μm^3·m^{-3}, use the Junge distribution to estimate the number density of CCN (#/m^3) within a ΔR = 0.2 μm range centered at R (μm) of:
a. 0.2 b. 0.3 c. 0.4 d. 0.5 e. 0.6 f. 0.8 g. 1.0
h. 2 i. 3 j. 4 k. 5 l. 6 m. 8 n. 10

N8. For pure water at temperature –20°C, use Kelvin's equation to find the equilibrium RH% in air over a spherical droplet of radius (μm):
a. 0.005 b. 0.006 c. 0.008 d. 0.01 e. 0.02
f. 0.03 g. 0.04 h. 0.05 i. 0.06 j. 0.08
k. 0.09 l. 0.1 m. 0.2 n. 0.3 o. 0.5

N9 (§). Produce Köhler curves such as in Fig. 7.7b, but only for salt of the following masses (g) at 0°C:
a. 10^{-18} b. 10^{-17} c. 10^{-16} d. 10^{-15} e. 10^{-14}
f. 10^{-13} g. 10^{-12} h. 10^{-11} i. $5x10^{-18}$ j. $5x10^{-17}$
k. $5x10^{-16}$ l. $5x10^{-15}$ m. $5x10^{-14}$ n. $5x10^{-13}$

N10(§). Produce Köhler curves for a solute mass of 10^{-16} g of salt for the following temperatures (°C):
a. –35 b. –30 c. –25 d. –20 e. –15
f. –10 g. –5 h. 2 i. 5 j. 10 k. 15
l. 20 m. 25 n. 30

N11. Find the critical radii (μm) and supersaturations at a temperature of –10°C, for
a. $5x10^{-17}$ g of hydrogen peroxide
b. $5x10^{-17}$ g of sulfuric acid
c. $5x10^{-17}$ g of nitric acid
d. $5x10^{-17}$ g of ammonium sulfate
e. $5x10^{-16}$ g of hydrogen peroxide
f. $5x10^{-16}$ g of sulfuric acid
g. $5x10^{-16}$ g of nitric acid
h. $5x10^{-16}$ g of ammonium sulfate
j. $5x10^{-15}$ g of hydrogen peroxide
k. $5x10^{-15}$ g of sulfuric acid
l. $5x10^{-15}$ g of nitric acid
m. $5x10^{-15}$ g of ammonium sulfate
n. $5x10^{-14}$ g of hydrogen peroxide
o. $5x10^{-14}$ g of sulfuric acid
p. $5x10^{-14}$ g of nitric acid
q. $5x10^{-14}$ g of ammonium sulfate

N12. For the nuclei of the previous exercise, find the equilibrium haze droplet radius (μm) for the following relative humidities (%):
(i) 70 (ii) 72 (iii) 74 (iv) 76 (v) 78
(vi) 80 (vii) 82 (viii) 84 (ix) 86 (x) 88
(xi) 90 (xii) 92 (xiii) 94 (xiv) 96 (xv) 98

N13. How many CCN will be activated in maritime air at supersaturations (%) of
a. 0.2 b. 0.3 c. 0.4 d. 0.5 e. 0.6 f. 0.8 g. 1.0
h. 2 i. 3 j. 4 k. 5 l. 6 m. 8 n. 10

N14. Find the average separation distances (μm) between cloud droplets for the previous problem.

N15. What temperature is needed to immersion-freeze half the droplets of radius (μm)
a. 10 b. 20 c. 30 d. 40 e. 50 f. 60 g. 70

h. 80 i. 90 j. 125 k. 150 l. 200 m. 200 n. 300

N16. Estimate the number density of active ice nuclei for the following combinations of temperature and supersaturation [T(°C), S_{ice}(%)].

a. –5, 3 b. –5, 5 c. –10, 5 d. –10, 10
e. –15, 10 f. –10, 12 g. –15, 12 h. –20, 13
i. –15, 18 j. –20, 20 k. –25, 20 l. –20, 23
m. –25, 23 n. –23, 25

N17. For a supersaturation gradient of 1% per 2 μm, find the kinematic moisture flux due to diffusion. Given T = –20°C, and P = 80 kPa. Use D ($m^2 \cdot s^{-1}$) of:

a. $1x10^{-6}$ b. $2x10^{-6}$ c. $3x10^{-6}$ d. $4x10^{-6}$
e. $5x10^{-6}$ f. $6x10^{-6}$ g. $7x10^{-6}$ h. $8x10^{-6}$
i. $9x10^{-6}$ j. $1x10^{-5}$ k. $3x10^{-5}$ l. $4x10^{-5}$
m. $5x10^{-5}$ n. $6x10^{-5}$ o. $7x10^{-5}$ p. $8x10^{-5}$

N18 (§). Compute and plot supersaturation (%) vs. distance (μm) away from drops of the following radii , given a background supersaturation of 0.5%

a. 0.15 μm containing 10^{-16} g of salt
b. 0.15 μm containing 10^{-16} g of ammon.sulfate
c. 0.15 μm containing 10^{-16} g of sulfuric acid
d. 0.15 μm containing 10^{-16} g of nitric acid
e. 0.15 μm containing 10^{-16} g of hydrogen perox.
f. 0.3 μm containing 10^{-16} g of salt
g. 0.3 μm containing 10^{-16} g of ammon.sulfate
h. 0.3 μm containing 10^{-16} g of sulfuric acid
i. 0.3 μm containing 10^{-16} g of nitric acid
j. 0.3 μm containing 10^{-16} g of hydrogen perox.
k. 0.5 μm containing 10^{-16} g of salt
l. 0.5 μm containing 10^{-16} g of ammon.sulfate
m. 0.5 μm containing 10^{-16} g of sulfuric acid
n. 0.5 μm containing 10^{-16} g of nitric acid
o. 0.5 μm containing 10^{-16} g of hydrogen perox.
p. 2 μm containing 10^{-16} g of salt
q. 1 μm containing 10^{-16} g of ammon.sulfate
r. 1 μm containing 10^{-16} g of sulfuric acid
s. 1 μm containing 10^{-16} g of nitric acid
t. 1 μm containing 10^{-16} g of hydrogen perox.

N19. Find the diffusivity ($m^2 \cdot s^{-1}$) for water vapor, given [P(kPa) , T(°C)] of:

a. 80, 0 b. 80, –5 c. 80, –10 d. 80, –20
e. 70, 0 f. 70, –5 g. 70, –10 h. 70, –20
i. 60, 0 j. 60, –5 k. 60, –10 l. 60, –20
m. 50, 0 n. 50, –5 o. 50, –10 p. 50, –20

N20 (§). For the previous exercise, plot droplet radius (μm) vs. time (minutes) for diffusive growth.

N21. What phase (I - XIV) of ice is expected at the following locations in a standard atmosphere?

a. Earth's surface b. mid-troposphere
c. tropopause d. mid stratosphere
e. stratopause f. mid-mesosphere
g. mesopause

N22. What phase (I - XIV) of ice is expected for the following conditions of [P(kPa) , T(°C)]?

a. 1, –250 b. 1, –150 c. 1, –50 d. 1, 50
e. 10^3, –250 f. 10^3, –150 g. 10^3, –50 h. 10^3, 50
i. $5x10^5$, –250 j. $5x10^5$, –150 k. $5x10^5$, –30
l. $5x10^5$, 50 m. 10^7, –250 n. 10^7, –50 o. 10^7, 50

N23. What crystal habit could be expected for the following combinations of [ρ_{ve} (g/m^3) , T(°C)]:

a. 0.22, –25 b. 0.22, –20 c. 0.22, –13
d. 0.22, –8 e. 0.22, –5 f. 0.22, –2
g. 0.12, –25 h. 0.12, –20 i. 0.12, –13
j. 0.12, –8 k. 0.12, –5 l. 0.12, –2
m. 0.08, –25 n. 0.08, –20 o. 0.08, –13
p. 0.08, –8 q. 0.08, –5 r. 0.08, –2

N24. Suppose the following ice crystals were to increase mass at the same rate. Find the rate of increase with time of the requested dimension.

a. effective radius of column growing in 3-D
b. diameter of plate growing in 2-D
c. length of needle growing in 1-D

N25 (§). Given D = $2x10^{-5}$ $m^2 \cdot s^{-1}$ and ρ_v = 0.003 $kg \cdot m^{-3}$, plot ice-crystal mass (g) vs. time (minutes) for 3-D growth such as a hexagonal column. Use the following supersaturation fraction:

a. 0.001 b. 0.002 c. 0.003 d. 0.004 e. 0.005
f. 0.006 g. 0.007 h. 0.008 i. 0.009 j. 0.01
k. 0.012 l. 0.014 m. 0.016 n. 0.018 o. 0.020

N26 (§). Same as the previous problem, but for 2-D growth of a thin flat plate of thickness 10 μm.

N27 (§). Use the Clausius-Clapeyon equation from the Moisture chapter to calculate the saturation vapor pressure over liquid water and ice for $-50 \le T \le 0$°C, and use that data to calculate and plot the difference. Namely, reproduce Fig. 7.16 with your own calculations.

N28. Find the terminal velocity of cloud droplets of radius (μm): a. 0.2 b. 0.4 c. 0.6 d. 0.8
e. 1.0 f. 2 g. 3 h. 4 i. 5 j. 7
k. 10 l. 15 m. 20 n. 30 o. 40 p. 50

N 29. Find the terminal velocity of rain drops of radius (μm): a. 100 b. 150 c. 200 d. 300
e. 400 f. 500 g. 600 h. 700 i. 800
j. 900 k. 1000 l. 1200 m. 1500 n. 2000

N30. Calculate the terminal velocity of hailstones of radius (cm): a. 0.25 b. 0.5 c. 0.75 d. 1 e. 1.25

f. 1.5 g. 1.75 h. 2 i. 2.5 j. 3 k. 3.5
l. 4 m. 4.5 n. 5 o. 5.5 p. 6

N31. What type of "meteor" is:
a. a rainbow b. lightning c. corona
d. dust e. a cloud f. a halo g. sand
h. rain i. smoke j. snow k. fog
l. haze m. dew n. frost

N32. For a Marshall-Palmer rain-drop size distribution, if the rainfall rate is
(i) 10 mm/h, or (ii) 20 mm/h,
how many droplets are expected of radius (μm) greater than:
a. 100 b. 200 c. 300 d. 400 e. 500
f. 700 g. 1000 h. 1200 i. 1500 j. 2000

N33. What is the rain intensity classification and the weather map symbol for rainfall rates (mm/h) of:
a. 0.02 b. 0.05 c. 0.1 d. 0.2 e. 0.5
f. 1.0 g. 2 h. 3 i. 4 j. 5
k. 6 l. 7 m. 8 n. 9 o. 10

N34. For precipitation in the form of
(i) drizzle, or (ii) snow,
what is the precipitation intensity classification and weather map symbol for visibility (km) of:
a. 0.1 b. 0.2 c. 0.3 d. 0.4 e. 0.5 f. 0.6 g. 0.7
h. 0.8 i. 0.9 j. 1.0 k. 1.2 l. 1.5 m. 2 n. 5

N35. For a liquid-water equivalent precipitation value of 5 cm, find the snow depth if the snow density (kg/m^3) is: a. 50 b. 75 c. 100 d. 150 e. 200
f. 250 g. 300 h. 350 i. 400 j. 450 k. 500
l. 550 m. 600 n. 650 o. 700 p. 800 q. 900

N36. Find the mean annual precipitation for the following locations, given their longitudes, latitudes:
a. 120°W, 50°N b. 120°W, 25°N c. 120°W, 10°N
d. 120°W, 10°S e. 120°W, 30°S f. 60°W, 0°N
g. 60°W, 20°N h. 60°W, 40°N i. 0°W, 50°N
j. 0°W, 25°N k. 0°W, 5°N l. 0°W, 20°S
m. 120°E, 25°S n. 120°E, 0°N o. 120°E, 30°N

N37. What are the values of zonally averaged evaporation and precipitation rates at latitude:
a. 70°N b. 60°N c. 50°C d. 40°N e. 30°N
f. 20°N g. 10°N h. 0° i. 10°S j. 20°S
k. 30°S m. 40°S n. 50°S o. 60°S p. 70°S

Understanding & Critical Evaluation

U1. If saturation is the maximum amount of water vapor that can be held by air at equilibrium, how is supersaturation possible?

U2. Fig. 7.2 shows how excess-water mixing ratio can increase as a cloudy air parcel rises. Can excess-water mixing ratio increase with time in a cloudy or foggy air parcel that doesn't rise? Explain.

U3. What can cause the supersaturation S in a cloud to be less than the available supersaturation S_A?

U4. Fig. 7.3 applies to cumulus clouds surrounded by clear air. Would the curves be different for a uniform stratus layer? Why?

U5. An air parcel contains CCN that allow 10^9 m^{-3} hydrometeors to form. If the air parcel starts at P = 100 kPa with T = 20°C and T_d = 14°C, find the average radius of cloud droplets due to condensation only, after the air parcel rises to P (kPa) of:
a. 85 b. 82 c. 80 d. 78 e. 75 f. 72 g. 70
h. 67 i. 63 j. 60 k. 58 l. 54 m. 50 n. 45
Hint. Use a thermo diagram to estimate r_E.

U6. Derive eq. (7.8), stating and justifying all assumptions. (Hint: consider the volume of a spherical drop.)

U7. Rewrite eq. (7.8) for hydrometeors that form as cubes (instead of spheres as was used in eq. 7.8). Instead of solving for radius R, solve for the width s of a side of a cube.

U8. In Fig. 7.5, consider the solid curve. The number density (#/cm^3) of CCN between any two radii R_1 and R_2 is equal to the average value of $n/\Delta R$ within that size interval times ΔR (=$R_2 - R_1$). This works best when R_1 and R_2 are relatively close to each other. For larger differences between R_1 and R_2, just sum over a number of smaller intervals. Find the number density of CCN for droplets of the following ranges of radii (μm):
a. $0.02 < R < 0.03$ b. $0.03 < R < 0.04$
c. $0.04 < R < 0.05$ d. $0.05 < R < 0.06$
e. $0.06 < R < 0.08$ f. $0.08 < R < 0.1$
g. $0.2 < R < 0.3$ h. $0.3 < R < 0.4$
i. $0.4 < R < 0.5$ j. $0.5 < R < 0.6$
k. $0.6 < R < 0.8$ l. $0.8 < R < 1$
m. $0.1 < R < 0.2$ n. $1 < R < 2$
o. $0.1 < R < 1$ p. $0.1 < R < 10$
q. $0.02 < R < 0.1$ r. $0.02 < R < 10$

U9. a. Find a relationship between the number density of CCN particles n, and the corresponding mass concentration c ($\mu g \cdot m^{-3}$), using the dashed line in Fig. 7.5 and assuming that the molecular weight is M_s.
b. Use Table 7-1 to determine the molecular weight of sulfuric acid (H_2SO_4) and nitric acid

(HNO_3), which are two contributors to acid rain. Assuming tiny droplets of these acids are the particles of interest for Fig. 7.5, find the corresponding values or equations for mass concentration of these air pollutants.

U10. a. From the solid curve in Fig. 7.5, find the number density of CCN at R = 1 μm, and use this result to determine the value and units of parameter c in the CCN number density eq. (7.9)

b Plot the curve resulting from this calibrated eq. (7.9) on a linear graph, and on a **log-log graph**.

c. Repeat (a) and (b), but for R = 0.1 μm.

d. Repeat (a) and (b), but for R = 0.01 μm.

e. Why does eq. (7.9) appear as a straight line in Fig. 7.5? What is the slope of the straight line in Fig. 7.5? [Hint: for log-log graphs, the **slope** is the number of decades along the vertical axis (ordinate) spanned by the line, divided by the number of decades along the horizontal axis (abscissa) spanned by the line. **Decade** means a factor of ten; namely, the interval between major tic marks on a logarithmic axis.]

f. For number densities less than 1/cm^3, what does it mean to have less than one particle (but greater than zero particles)? What would be a better way to quantify such a number density?

g. As discussed in the Optics chapter, air molecules range in diameter between roughly 0.0001 and 0.001 mm. If the dashed line in Fig. 7.5 were extended to that small of size, would the number density indicated by the Junge distribution agree with the actual number density of air molecules? If they are different, discuss why.

U11. Show how the Köhler equation reduces to the Kelvin equation for CCNs that don't dissolve.

U12 (§). Surface tension σ for a cloud droplet of pure water squeezes the droplet, causing the pressure inside the droplet to increase. The resulting pressure difference ΔP between inside and outside the droplet can be found from the **Young-Laplace equation** ($\Delta P = \sigma \cdot dA/dV$, where A is surface area and V is volume of the droplet). For a spherical droplet of radius R this yields:

$$\Delta P = 2 \cdot \sigma \; / \; R$$

Plot this pressure difference (kPa) vs. droplet radius over the range $0.005 \le R \le 1$ μm.

U13. a. Using the equation from the previous exercise, combine it with Kelvin's equation to show how the equilibrium relative humidity depends on the pressure excess inside the droplet.

b. If greater pressure inside the drop drives a greater evaporation rate, describe why RH greater than 100% is needed to reach an equilibrium where condensation from the air balances evaporation from the droplet.

U14. Using the full Köhler equation, discuss how supersaturation varies with:

a. temperature.
b. molecular weight of the nucleus chemical.
c. mass of solute in the incipient droplet.

U15. Consider a Köhler curve such as plotted in the Focus box on Droplet Growth. But let the RH = 100.5% for air. Starting with an aerosol with characteristics of point A on that figure, (a) discuss the evolution of drop size, and (b) explain why haze particles are not possible for that situation.

U16. Considering Fig. 7.7, which type of CCN chemical would allow easier formation of cloud droplets: (a) a CCN with larger critical radius but lower peak supersaturation in the Köhler curve; or (b) a CCN with smaller critical radius but higher supersaturation? Explain.

U17. What is so special about the critical radius, that droplets larger than this radius continue to grow, while smaller droplets remain at a constant radius?

U18. The Kelvin curve (i.e., the Köhler curve for pure water) has no critical radius. Hence, there is no barrier droplets must get across before they can grow from haze to cloud droplets. Yet cloud droplets are easier to create with heterogeneous nucleation on solute CCN than with homogeneous nucleation in clean air. Explain this apparent paradox.

U19. In air parcels that are rising toward their LCL, aerosol swelling increases and visibility decreases as the parcels get closer to their LCL. If haze particles are at their equilibrium radius by definition, why could they be growing in the rising air parcel? Explain.

U20. How high above the LCL must air be lifted to cause sufficient supersaturation to activate CCN for liquid-droplet nucleation?

U21. Suppose a droplet contained all the substances listed in Table 7-2. What is the warmest temperature (°C) that the droplet will freeze due to:

a. contact freezing b. condensation freezing
c. deposition freezing d. immersion freezing

U22. Discuss the differences in nucleation between liquid water droplets and ice crystals, assuming the air temperature is below freezing.

U23. Discuss the differences in abundance of cloud vs. ice nuclei, and how this difference varies with atmospheric conditions.

U24. Can some chemicals serve as both water and ice nuclei? For these chemicals, describe how cloud particles would form and grow in a rising air parcel.

U25. If droplets grow by diffusion to a final average radius given by eq. (7.8), why do we even care about the diffusion rate?

U26. In the focus box on Cubic Ice, a phase diagram was presented with many different phases of ice. The different phases have different natural crystal shapes, as summarized in the table below. In the right column of this table, draw a sketch of each of the shapes listed. (Hint, look in a geometry book or on the internet for sketches of geometric shapes.)

Table 7-7. Crystal shapes for ice phases.

Shape	Phases	Sketch
hexagonal	Ih	
cubic	Ic, VII, X	
tetragonal	III, VI, VIII, IX, XII	
rhombic	II, IV	
ortho-rhombic	XI	
monoclinic	V	

U27. The droplet growth-rate equation (7.24) considers only the situation of constant background supersaturation. However, as the droplet grows, water vapor would be lost from the air causing supersaturation to decrease with time. Modify eq. (7.24) to include such an effect, assuming that the temperature of the air containing the droplets remains constant. Does the droplet still grow with the square root of time?

U28. If ice particles grew as spheres, which growth rate equation would best describe it? Why?

U29. Verify that the units on the right sides of eqs. (7.26) and (7.27) match the units of the left side.

U30. Manipulate the mass growth rate eq. (7.26) to show that the effective radius of the ice particle grows as the square root of time. Show your work.

U31. Considering the different mass growth rates of different ice-crystal shapes, which shape would grow fastest in length of its longest axis?

U32. If the atmosphere were to contain absolutely no CCN, discuss how clouds and rain would form, if at all.

U33. In Fig. 7.15 the thick black line follows the state of a rising air parcel that is cooling with time. Why does that curve show e_s decreasing with time?

U34. If both supercooled liquid droplets and ice crystals were present in sinking cloudy air that is warming adiabatically, describe the evolutions of both types of hydrometeors relative to each other.

U35. On one graph similar to Fig. 7.18, plot 3 curves for terminal velocity. One for cloud droplets (Stokes Law), another for rain drops, and a third for hail. Compare and discuss.

U36. Can ice crystals still accrete smaller liquid water droplets at temperatures greater than freezing? Discuss.

U37. Large ice particles can accumulate smaller supercooled liquid water drops via the aggregation process known as accretion or riming. Can large supercooled liquid water drops accumulate smaller ice crystals? Discuss.

U38. Is it possible for snow to reach the ground when the atmospheric-boundary-layer temperature is warmer than freezing? Discuss.

U39. Compare CCN size spectra with raindrop size spectra, and discuss.

U40. For warm-cloud precipitation, suppose that all 5 formation factors are working simultaneously. Discuss how the precipitation drop size distribution will evolve with time, and how it can create precipitation.

U41. Is it possible to have blizzard conditions even with zero precipitation rate? Discuss.

U42. Precipitation falling out of a column of atmosphere implies that there was net latent heating in that column. Use the annual mean precipitation of Fig. 7.24 to discuss regions of the world having the greatest latent heating of the atmosphere.

U43. According to Fig. 7.25, some latitudes have an imbalance between evaporation and precipitation. How can that be maintained?

U44. Suppose that a disdrometer gives you information on the size of each hydrometeor that falls, and how many of each size hydrometer falls per hour. Derive an equation to relate this information to total rainfall rate.

Web-Enhanced Questions

W1. Search the web for any journal articles, conference papers, or other technical reports that have pictures of droplet or ice-crystal growth or fall processes (such as photos taken in vertical wind tunnels).

W2. Can you find any satellite photos on the web showing haze? If so, which satellites and which channels on those satellites show haze the best? Do you think that satellites could be used to monitor air pollution in urban areas?

W3. Search the web for microphotographs of ice crystals and snow flakes with different habits. What habits in those photos were not given in the idealized Fig. 7.12?

W4. Find on the web a clear microphotograph of a dendrite snow flake. Print it out, and determine the fractal dimension of the snow flake. (Hint, see the Clouds chapter for a discussion of fractals.)

W5. Search various government air-pollution web sites (such as the U.S. Environmental Protection Agency: http://www.epa.gov/) for sizes of aerosol pollutants. Based on typical concentrations (or on concentrations specified in the air-quality standards) of these pollutants, determine the number density, and compare with Fig. 7.5.

W6. Search the web for information about surface tension, and how it relates to **Gibbs free energy**.

W7. Search the web for information about snow and snowflakes.

W8. Search the web for climate statistics of actual annual precipitation last year worldwide (or for your country or region), and compare with Fig. 7.24.

W9. Search the web for photos and diagrams of precipitation measurement instruments, and discuss their operation principles.

Synthesis Questions

S1. What if the saturation vapor pressure over supercooled water and ice were equal.

a. Discuss the formation of clouds and precipitation.

b. Contrast with those processes in the real atmosphere.

c. Discuss how the weather and climate might change, if at all.

S2. In Fig. 7.15, suppose that the saturation vapor pressure over ice were greater, not less, than that over water. How would the WBF process change, if at all? How would precipitation and clouds change, if at all?

S3. What if you were hired to seed warm ($T > 0°C$) clouds (i.e., to add nuclei), in order to create or enhance precipitation. Which would work better: (a) seeding with 10^5 salt particles/cm^3, each with identical of radius 0.1 μm; or (b) seeding with 1 salt particle/cm^3, each with identical radius of 0.5 μm; or (c) seeding with a range of salt particles sizes? Discuss, and justify.

S4. What if you were hired to seed cold ($T < 0°C$) clouds (i.e., to add nuclei), in order to create or enhance precipitation. Would seeding with water or ice nuclei lead to the most precipitation forming most rapidly? Explain and justify.

S5. Is it possible to seed clouds (i.e., add nuclei) in such a way as to reduce or prevent precipitation? Discuss the physics behind such weather modification.

S6. What if all particles in the atmosphere were **hydrophobic** (i.e., repelled water). How would the weather and climate be different, if at all?

S7. What if the concentration of cloud nuclei that could become activated were only one-millionth of what currently exists in the atmosphere. How would the weather and climate change, if at all?

S8. Eq. (7.29) indicates that smaller droplets and aerosol particles fall slower. Does Stoke's law apply to particles as small as air molecules? What other factors do air molecules experience that would affect their motion, in addition to gravity?

S9. What if Stoke's law indicated that smaller particles fall faster than larger particles. Discuss the nature of clouds for this situation, and how Earth's weather and climate might be different.

S10. What if rain droplet size distributions were such that there were more large drops than small drops. Discuss how this could possibly happen, and describe the resulting weather and climate.

S11. Suppose that large rain drops did not break up as they fell. That is, suppose they experienced no drag, and there was no upper limit to rain drop size. How might plant and animal life on Earth have evolved differently? Why?

S12. What if cloud and rain drops of all sizes fell at exactly the same terminal velocity. Discuss how the weather and climate might be different.

S13. What if condensation and deposition absorbed latent heat (i.e., caused cooling) instead of releasing latent heat. How would clouds, precipitation, weather and climate be different, if at all.

S14. Weather modification is as much a social issue as a scientific/technical issue. Consider a situation of **cloud seeding** (adding nuclei) to enhance precipitation over arid farm land in county X. If you wanted to make the most amount of money, would you prefer to be the:

a. meteorologist organizing the operation,
b. farmer employing the meteorologist,
c. company insuring the farmer's crop,
d. company insuring the meteorologist, or
e. lawyer in county Y downwind of county X, suing the meteorologist, farmer, and insurance companies?

Justify your preference.

S15. Suppose that you discovered how to control the weather via a new form of cloud seeding (adding nuclei). Should you ...

a. keep your results secret and never publish or utilize them, thereby remaining impoverished and unknown?

b. publish your results in a scientific journal, thereby achieving great distinction?

c. patent your technique and license it to various companies, thereby achieving great fortune?

d. form your own company to create tailored weather, and market weather to the highest bidders, thereby becoming a respected business leader?

e. modify the weather in a way that you feel is best for the people on this planet, thereby achieving great power?

f. allow a government agency to hold hearings to decide who gets what weather, thereby achieving great fairness and inefficiency?

g. give your discovery to the military in your favorite country, thereby expressing great patriotism? (Note: the military will probably take it anyway, regardless of whether you give it willingly.)

Discuss and justify your position. (Hint: See the "On Doing Science" box at the end of this chapter before you answer this question.)

ON DOING SCIENCE • Consequences

The scenario of exercise S15 is not as far-fetched as it might appear. Before World War II, American physicists received relatively little research funding. During the war, the U.S. Army offered a tremendous amount of grant money and facilities to physicists and engineers willing to help develop the atomic bomb as part of the Manhattan Project.

While the work they did was scientifically stimulating and patriotic, many of these physicists had second thoughts after the bomb was used to kill thousands of people at the end of the war. These concerned scientists formed the "Federation of Atomic Scientists", which was later renamed the "Federation of American Scientists" (FAS).

The FAS worked to discourage the use of nuclear weapons, and later addressed other environmental and climate-change issues. While their activities were certainly worthy, one has to wonder why they did not consider the consequences before building the bomb.

As scientists and engineers, it is wise for us to think about the moral and ethical consequences before starting each research project.

Copyright © 2011, 2015 by Roland Stull. *Meteorology for Scientists and Engineers, 3rd Ed.*

REMOTE SENSING

CONTENTS

Radiative Transfer for Satellites 220
- Signals 220
- Transmittance and Windows 220
- Planck's Law & Brightness Temperature 221
- Radiative Transfer Equation 224
- Weighting Functions 226

Weather Satellites 227
- Orbits 227
  - Geostationary Satellites 227
  - Polar Orbiting Satellites 228
- Imager 230
  - Visible 230
  - Infrared (IR) 230
  - Water-vapor 231
  - Other Channels 231
- Image Examples & Interpretation 231
- Sounder 235

Weather Radars 240
- Fundamentals 240
  - Maximum Range 241
  - Scan and Display Strategies 241
  - Radar Bands 242
  - Beam Propagation 243
- Reflectivity 245
  - The Radar Equation 245
  - Rainfall Rate Estimated by Radar Reflectivity 247
  - Bright Band 248
  - Hail 248
  - Other Uses for Reflectivity Data 248
- Doppler Radar 249
  - Radial Velocities 249
  - Maximum Unambiguous Velocity 250
  - Velocity Azimuth Display (VAD) 252
  - Identification of Storm Characteristics 253
  - Spectrum Width 254
  - Difficulties 254
- Polarimetric Radar 255
- Phased-Array Radars & Wind Profilers 257

Summary 260

Exercises 260
- Numerical Problems 260
- Understanding & Critical Evaluation 262
- Web-Enhanced Questions 265
- Synthesis Questions 266

"Meteorology for Scientists and Engineers, 3rd Edition" by Roland Stull is licensed under a Creative Commons Attribution-NonCommercial-ShareAlike 4.0 International License. To view a copy of the license, visit http://creativecommons.org/licenses/by-nc-sa/4.0/ . This work is available at http://www.eos.ubc.ca/books/Practical_Meteorology/ .

8 To understand and predict the weather, we first must measure it. **In-situ** or **direct** weather instruments must physically touch, or be exposed to, the air being measured. Examples include **thermometers** (temperature), **barometers** (pressure), **hygrometers** (humidity), **anemometers** (wind speed), **wind vanes** (wind direction), **pyranometers** (solar radiation), and **rain gauges** (precipitation).

Remote sensors infer the weather conditions by detecting the characteristics of waves propagating from distant regions. The waves can be electromagnetic (light, infrared, microwaves, etc.) or sound. **Active** remote instrument systems such as **radar** (RAdio Detection And Ranging) transmit their own waves toward the object and then receive the signal bouncing back to the sensors. **Passive** ones, such as some satellite sensors, receive waves naturally emanating from the object.

Clouds, precipitation, and air molecules can totally or partially **absorb** electromagnetic radiation (Fig. 8.1a), **scatter** it into many directions (Fig. 8.1b), or **reflect** it (Fig. 8.1c). Objects also **emit** radiation (Fig. 8.1d) according to Planck's law. Interactions of radiation with the Earth, air, and clouds create the **signals** that satellites and radar use.

This chapter covers the basics of **weather satellites** and radar. Other remote-sensor systems, not covered here, include **lidar** (LIght Detection And Ranging), and **sodar** (SOund Detection And Ranging).

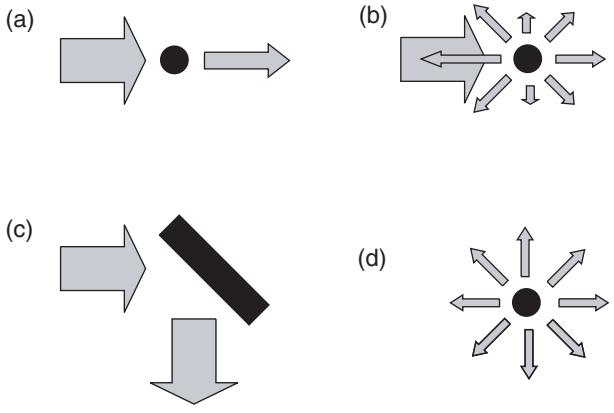

Figure 8.1
(a) Partial absorption, (b) scattering, (c) reflection, and (d) emission of electromagnetic radiation (arrows) by objects (black).

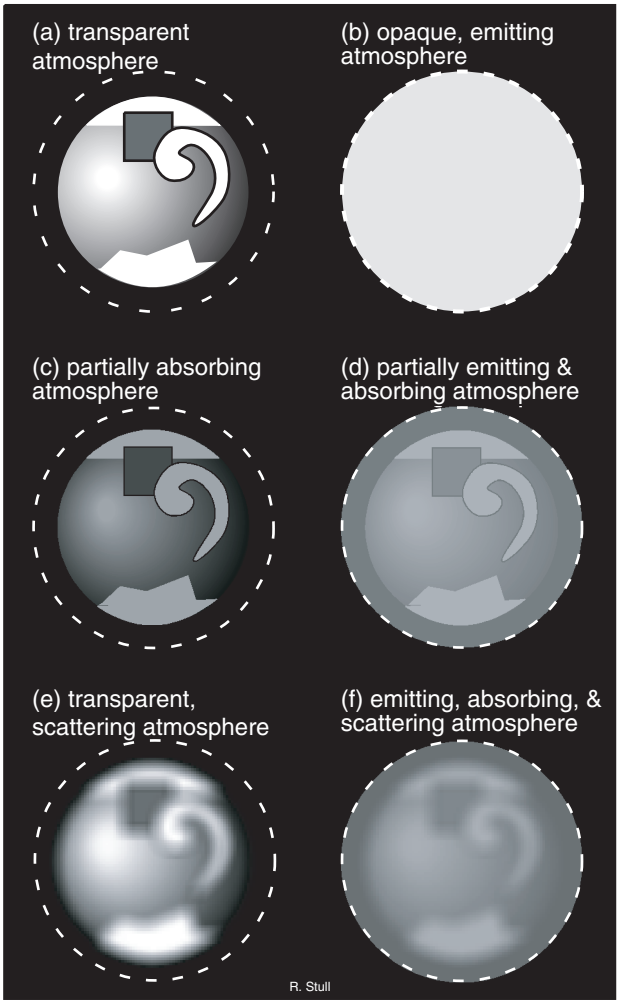
(a) transparent atmosphere
(b) opaque, emitting atmosphere
(c) partially absorbing atmosphere
(d) partially emitting & absorbing atmosphere
(e) transparent, scattering atmosphere
(f) emitting, absorbing, & scattering atmosphere
R. Stull

Figure 8.2
Illustration of visibility of the Earth and atmosphere as viewed by satellite. Figure (d) is overly simplistic, because variations in atmospheric constituents in the mid and upper atmosphere will cause atmospheric emissions (glowing) to be uneven.

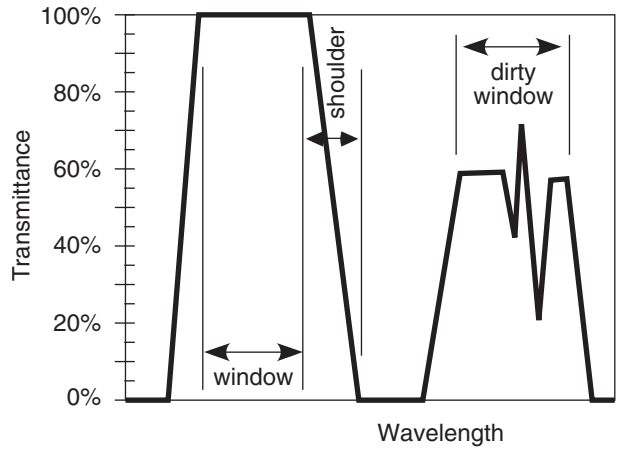

Figure 8.3
Windows in the electromagnetic spectrum.

RADIATIVE TRANSFER for Satellites

Signals

Weather satellites have sensors called **radiometers** that passively measure upwelling electromagnetic radiation from the Earth and atmosphere. **Infrared** (**IR**, **long-wave**) and **microwave** radiation are emitted by the Earth, atmosphere, clouds, and the sun (see the Radiation chapter). **Visible** light (**short-wave** or **solar radiation**) is emitted by the sun and reflected and absorbed by the Earth system. Additional portions of the **electromagnetic spectrum** are useful for remote sensing.

What the satellite can "see" in any one wavelength depends on the transparency of the air at that wavelength. A perfectly transparent atmosphere allows the upwelling radiation from the Earth's surface or highest cloud top to reach the satellite. Thus, wavelengths for which the air is transparent (Fig. 8.2a) are good for observing clouds and land use.

If air molecules strongly absorb upwelling radiation at another wavelength, then none of the signal at that wavelength from the Earth and clouds will reach the satellite (i.e., an opaque atmosphere). But according to Kirchhoff's law (see the Radiation chapter), absorptivity equals the emissivity at that wavelength. This atmosphere will emit its own spectrum of radiation according to Planck's law, causing the atmosphere to glow like an infrared light bulb (Fig. 8.2b). Wavelengths with this characteristic are good for observing the top of the atmosphere, but are bad for remote sensing of the Earth and clouds.

For other wavelengths, the atmosphere partially absorbs the upwelling radiation, causing the Earth and clouds to look dimmer (Fig. 8.2c). But this usually never happens alone, because Kirchhoff's law says that the atmosphere will also partially emit in the same wavelengths. The result is a dim view of the Earth, partially masked by a dimly glowing atmosphere (Fig. 8.2d).

For wavelengths scattered by air molecules, the signal from the Earth and clouds becomes blurred (Fig. 8.2e). For some wavelengths, this blurring is so extreme that no useful signal reaches the satellite, other than noise from all the scattered light rays. Finally, there are other wavelengths where all of the processes happen: atmospheric scattering, absorption, and emission (Fig. 8.2f).

Transmittance and Windows

Of the electromagnetic energy that is upwelling through any height, the percentage of it that comes out the top of the atmosphere is called **transmittance**. Transmittance varies with wavelength.

Portions of the spectrum where transmittances are large are called **windows** (Fig. 8.3), by analogy to visible light passing through clear glass windows. At wavelengths near the window, there can be **shoulder** regions where transmittance rapidly changes. Portions of the spectrum having partial transmittance are sometimes called **dirty windows**. By designing satellite-borne radiometers that are sensitive to different window and non-window wavelengths, you can measure different characteristics of the Earth and atmosphere.

Figures 8.4 (next 2 pages) show the transmittance at different wavelengths. Different gases in the atmosphere have different molecular vibration and rotation modes, causing them to absorb at discrete wavelengths called **absorption lines**. In Fig. 8.4, the windows are regions with transmittance of about 80% or higher.

These transmittance curves are not physical laws and are not constant, but can change slightly with atmospheric conditions. The **absorption bands** (i.e., non-window regions) shift wavelength very slightly with temperature and pressure.

The amount of absorption and transmission depend strongly on the concentration of absorbing gas along the path length of the radiation (see Beer's Law, in the Radiation chapter). Some gas concentrations vary with season (carbon dioxide CO_2), some vary hourly depending on the weather (water vapor H_2O, ozone O_3), while others are relatively constant. Additional gases indicated in these figures are molecular oxygen (O_2), methane (CH_4), carbon monoxide (CO), and nitrous oxide (N_2O).

Water vapor is a major absorber, so more humid conditions and deeper moist layers cause greater absorption. Recall from Chapter 1 that most of our storms and most of the atmosphere's humidity are trapped within the troposphere. Thus, transmittance is weakest in the tropics (high humidity and deep troposphere) and strongest near the poles (low absolute humidity and shallow troposphere). At mid latitudes, transmittance is greatest in winter (low humidity, shallow troposphere) and weakest in summer (higher humidity and deeper troposphere). Transmittance can easily vary by plus or minus 20% between these different locations and seasons in some portions of the spectrum, especially for wavelengths greater than 5 μm.

Another factor that reduces transmittance is **scattering** by air molecules and **aerosols** (e.g., air-pollution particles). Scattering increases (causing transmittance to decrease) as wavelength gets shorter (dashed curve in Fig. 8.4a). For cleaner air, the dashed curve is higher and transmittance is greater, but the opposite occurs for heavily polluted, aerosol-laden air. The visible light portion of the spectrum is a **dirty window** region. Fig. 8.4 shows that the atmosphere is clearer in some of the IR windows than in the visible light portion of the spectrum that you see every day with your eyes.

Solved Example

Wavelength 1.85 μm has: (a) what transmittance, and (b) corresponds to which sketch in Fig. 8.2 of Earth visibility as viewed from space?

Solution

Given: $\lambda = 1.85$ μm

Find: (a) transmittance = ? % , (b) Earth visibility = ?

(a) From Fig. 8.4b, **transmittance = 10%** approx., mostly due to strong absorption by water vapor.

(b) It would **look like Fig. 8.2b** in the infrared.

Check: (no easy check for this)

Discussion: Most water vapor is in the troposphere. Satellites would see it glow like an IR light bulb.

So far, we examined atmospheric transmittance (the left column of images in Fig. 8.2). Next, we look at atmospheric emissions (right column of Fig. 8.2).

Planck's Law & Brightness Temperature

In the Radiation chapter, Planck's law allowed computation of total energy flux radiating from a blackbody object per unit wavelength ($W \cdot m^{-2} \cdot \mu m^{-1}$) as a function of temperature. Emissions from a flat surface are in all directions, illuminating a hemisphere around the object.

But a satellite cannot measure the total radiation coming out of the Earth or atmosphere — it can measure only the portion of radiation that happens to be coming toward the satellite within the solid angle intercepted by the radiometer. Assuming the radiation is uniform in all directions (i.e., **isotropic**), then the portion of radiative flux per unit wavelength λ per unit **steradian** (sr) of solid angle is Planck's Law equation divided by π:

$$B_\lambda(T) = \frac{c_{1B} \cdot \lambda^{-5}}{\exp\left(\frac{c_2}{\lambda \cdot T}\right) - 1} \qquad \bullet(8.1)$$

where B is the **blackbody radiance** in units of $W \cdot m^{-2} \cdot \mu m^{-1} \cdot sr^{-1}$, and

$$c_{1B} = 1.191\ 042\ 82 \times 10^8\ W \cdot m^{-2} \cdot \mu m^4 \cdot sr^{-1}$$

$$c_2 = 1.438\ 775\ 2 \times 10^4\ \mu m \cdot K\ .$$

Thus, $c_{1B} = c_1/\pi$, where c_1 was from eq. (2.13). Don't forget that T must be in units of Kelvin. A steradian is the solid angle with vertex at the center of a sphere

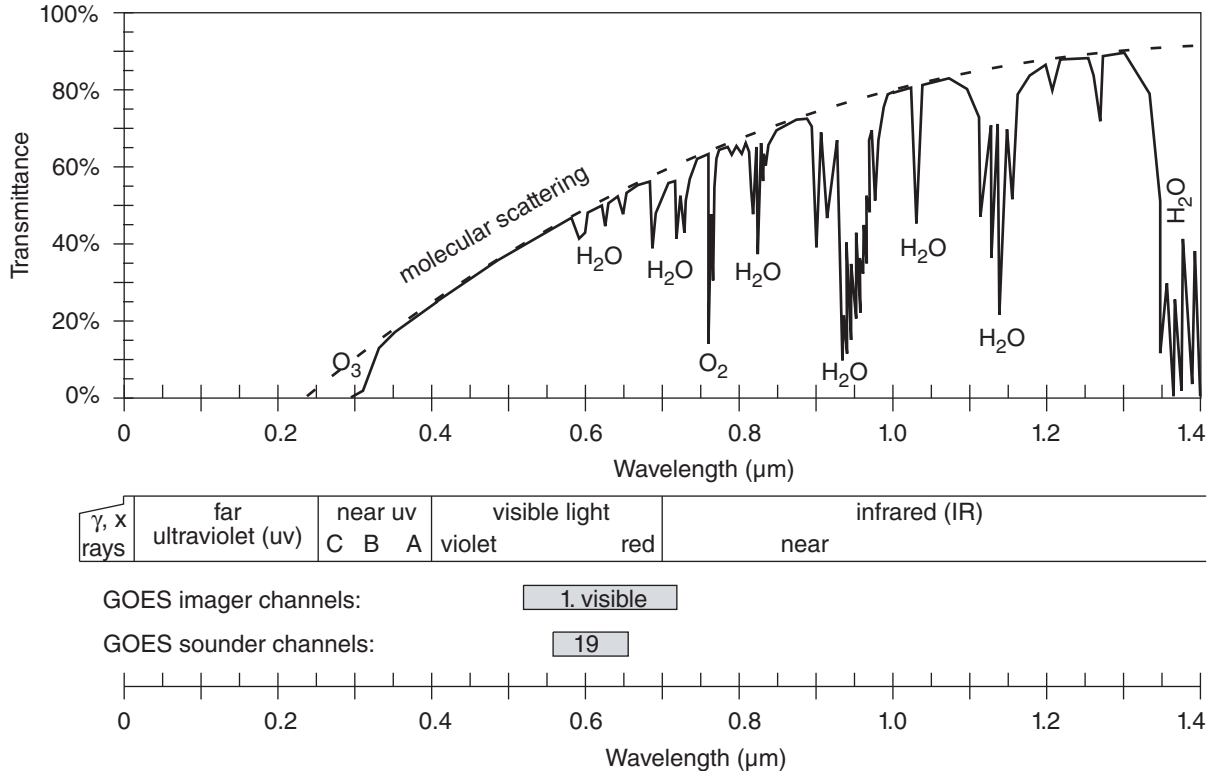

Fig. 8.4a.

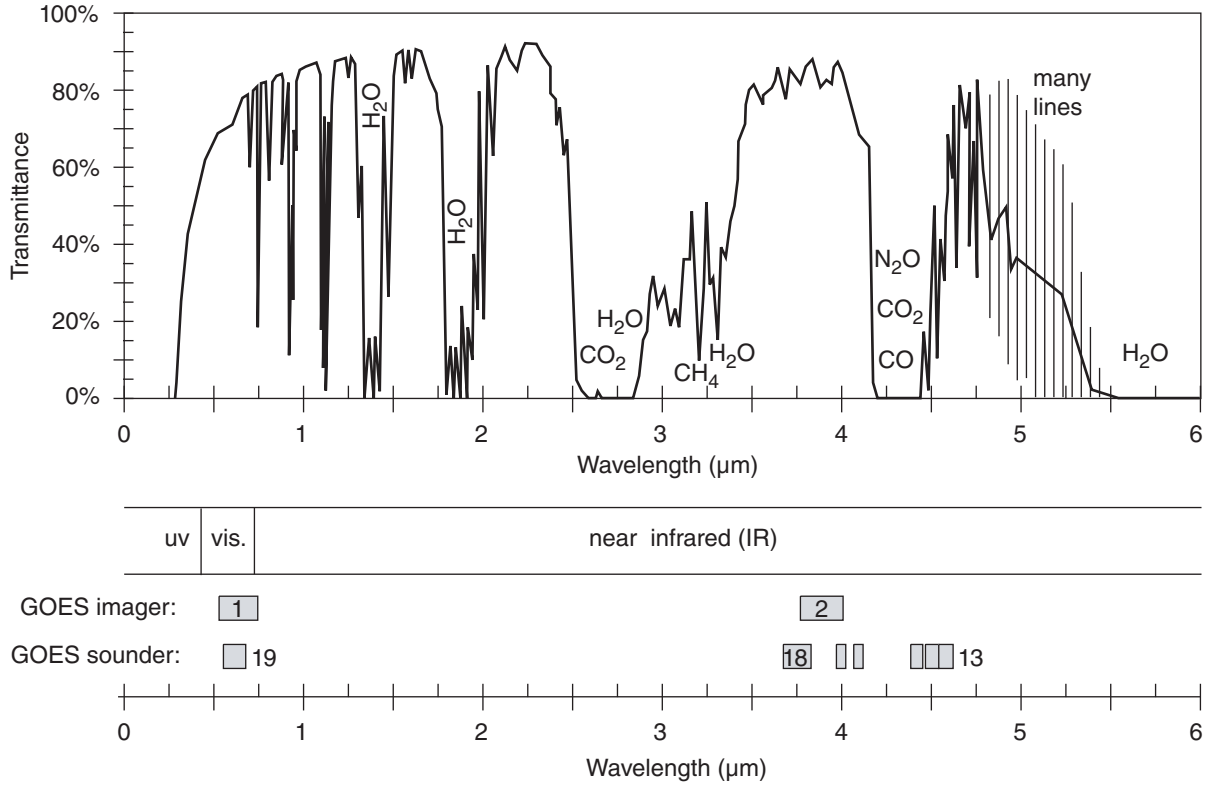

Fig. 8.4b.

Figure 8.4 (this page and next)
Atmospheric transmittance of electromagnetic radiation. Wavelength bands: (a) 0 to 1.4 μm; (b) 0 to 6 μm; (c) 5 to 30 μm; and (d) 30 μm to 100 cm (logarithmic scale). For regions of strong absorption (i.e., low transmittance) the dominant absorbing chemical is given. The name of the spectral bands, and satellite radiometer channels are indicated.

Fig. 8.4c.

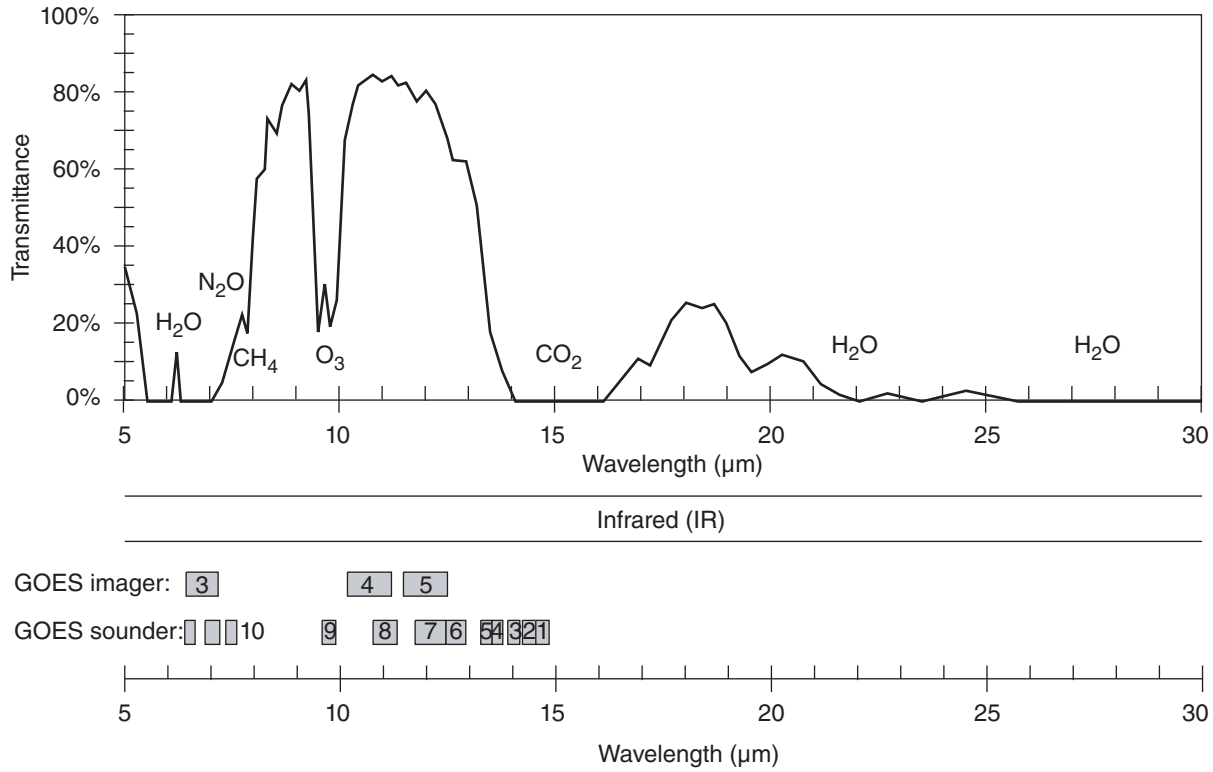

Fig. 8.4d.

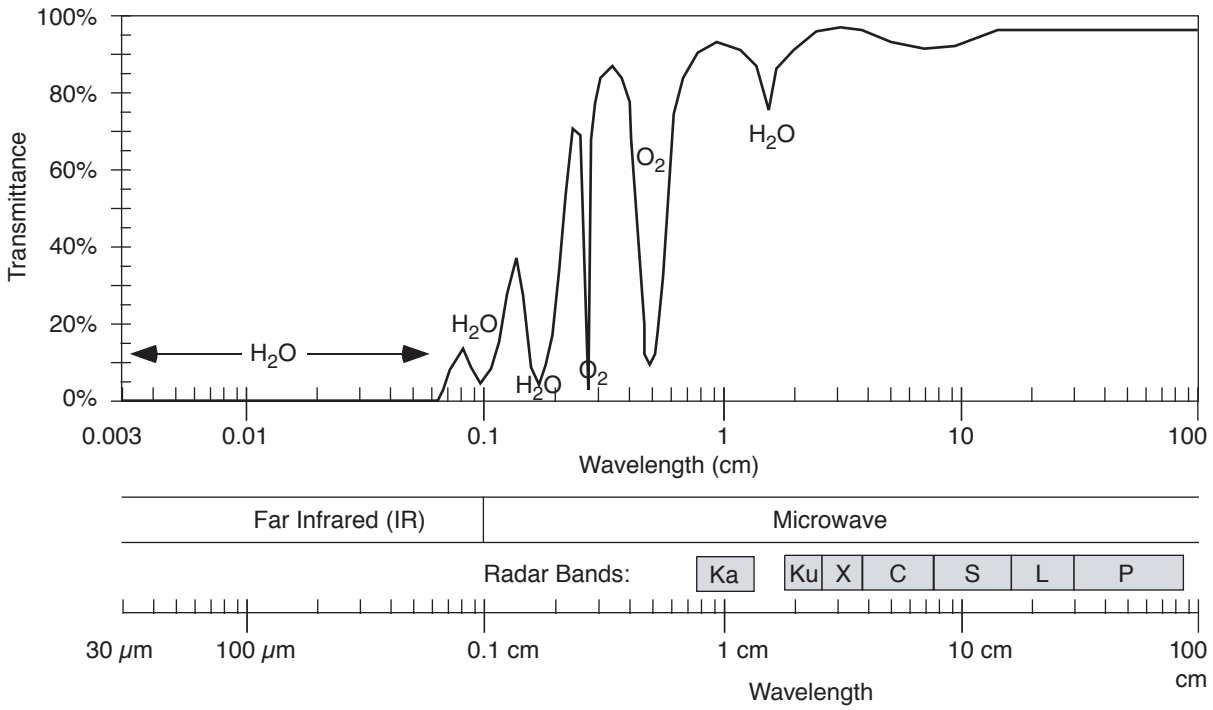

Figure 8.4 (continuation)
See Chapter 2 for wavelengths emitted by sun and Earth. Upwelling radiation can be either terrestrial radiation emitted from the atmosphere and the Earth's surface, or solar radiation reflected upward from the Earth's surface and from within the atmosphere.

Solved Example

What is the blackbody radiance at wavelength 10.9 μm from a cloud top of temperature –20°C ?

Solution

Given: T = –20°C = 253 K, λ = 10.9 μm
Find: $B_\lambda(T)$ = ? W · m^{-2} · μm^{-1} · sr^{-1}

Use eq. (8.1):

$$B_\lambda(T) = \frac{(1.191\text{x}10^8 \text{W}\cdot\text{m}^{-2}\mu\text{m}^4\text{sr}^{-1})\cdot(10.9\mu\text{m})^{-5}}{\left[\exp\left(\frac{1.44\text{x}10^4\mu\text{m}\cdot\text{K}}{(10.9\mu\text{m})\cdot(253\text{K})}\right)\right]-1}$$

$$= \underline{\mathbf{4.22}}\ \text{W}\cdot\text{m}^{-2}\cdot\mu\text{m}^{-1}\cdot\text{sr}^{-1}$$

Check: Units OK. Physics OK.
Discussion: 10.9 μm is an IR wavelength in an atmospheric window region of the spectrum (Fig. 8.4). Thus, these emissions from the cloud would be absorbed only little by the intervening atmosphere, and could be observed by satellite.

Solved Example

A satellite measures a radiance of 1.1 W·m^{-2} ·μm^{-1} · sr^{-1} at wavelength 6.7 μm. What is the brightness temperature?

Solution

Given: $B_\lambda(T)$= 1.1 W·m^{-2} ·μm^{-1} ·sr^{-1}, λ = 6.7 μm
Find: T_B = ? K

Use eq. (8.2) :

$$T_B = \frac{(1.44\text{x}10^4\mu\text{m}\cdot\text{K})/(6.7\mu\text{m})}{\ln\left(1+\frac{1.191\text{x}10^8\text{W}\cdot\text{m}^{-2}\mu\text{m}^4\text{sr}^{-1}\cdot(6.7\mu\text{m})^{-5}}{1.1\text{W}\cdot\text{m}^{-2}\mu\text{m}^{-1}\text{sr}^{-1}}\right)}$$

$$= \underline{\mathbf{239\ K}}$$

Check: Units OK. Physics OK.
Discussion: 6.7 μm is an IR wavelength in a water-vapor absorption (=emission) part of the spectrum (Fig. 8.4). The atmosphere is partly opaque in this region, so the radiation received at the satellite was emitted from the air. This brightness temperature is about –34°C. Such temperatures are typically found in the upper troposphere. Thus, we can infer from the standard atmosphere that this satellite channel is "seeing" the upper troposphere.

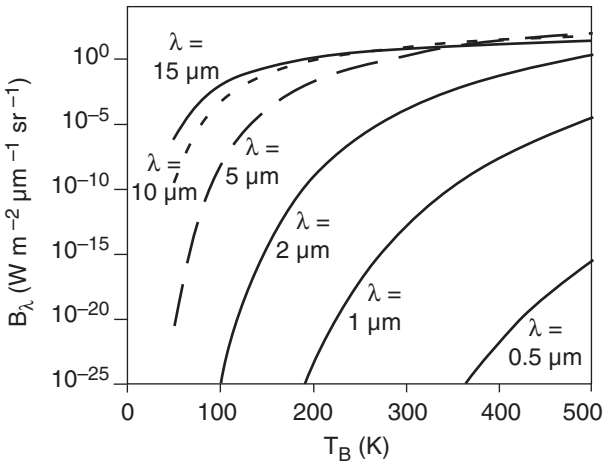

Figure 8.5
Planck's law emissions vs. brightness temperature.

(of radius r) that encompasses an area of r^2 on the surface of the sphere; 4π sr cover the whole surface.

Fig. 8.5 shows Planck's law plotted differently; namely, blackbody radiance vs. temperature. Blackbody radiance increases monotonically with increasing temperature. Hotter objects emit greater radiation (assuming a blackbody emissivity of 1.0).

You can also use Planck's law in reverse. Plug a measured radiance into eq. (8.1), and solve for temperature. This temperature is called the **brightness temperature** (T_B), which is the temperature of a hypothetical blackbody that produces the same radiance as the measured radiance:

$$T_B = \frac{c_2/\lambda}{\ln\left(1+\frac{c_{1B}\cdot\lambda^{-5}}{B_\lambda}\right)} \qquad \bullet(8.2)$$

Radiative Transfer Equation

Recall from Fig. 8.2 that surface emissions might be partially or totally absorbed by the atmosphere before reaching the satellite. The atmosphere emits its own radiation, some of which might also be lost by absorption before reaching the satellite.

These effects are summarized by the **radiative transfer equation**:

$$L_\lambda = B_\lambda(T_{skin})\cdot\hat{\tau}_{\lambda,sfc} + \sum_{j=1}^{n} e_\lambda(z_j)\cdot B_\lambda(T_j)\cdot\hat{\tau}_{\lambda,j} \qquad (8.3)$$

where L_λ is the radiance at wavelength λ that exits the top of the atmosphere and can be observed by satellite. T_{skin} is the temperature of the top few molecules of the Earth's surface, NOT the standard meteorological "surface" temperature measured 2 m above ground. $\hat{\tau}$ is transmittance; e is emissivity. This equation is called **Schwarzchild's equation**.

The first term on the right hand side (RHS) gives the blackbody emissions from the Earth's surface, reduced by the overall transmittance $\hat{\tau}_{\lambda,\,sfc}$ between the surface and the top of the atmosphere (from Fig. 8.4). Namely, satellites can see the Earth's surface at wavelengths for which the air is not totally opaque.

The second term on the RHS is a sum over all atmospheric layers ($j = 1$ to n), representing the different heights z_j in the atmosphere. The net emissions from any one layer j are equal to the emissivity $e_\lambda(z_j)$ of the air at that height for that wavelength, times the blackbody emissions. However, the resulting radiance is reduced by the transmittance $\hat{\tau}_{\lambda,j}$ between that height and the top of the atmosphere.

Transmittance $\hat{\tau} = 0$ if all of the radiation is absorbed before reaching the top of the atmosphere. Transmittance = 1 – **absorptance**; namely, $\hat{\tau} = 1 - a$.

To help understand the second term, consider a hypothetical or "toy" profile of transmittance (Fig. 8.6). For the air below 5 km altitude, $\hat{\tau} = 0$, thus $a = (1 - \hat{\tau}) = 1$. But if $a = 1$, then $e = 1$ from Kirchhoff's Law (see the Radiation chapter). Hence, the layers of air below 5 km are efficient emitters of radiation, but none of this radiation reaches the top of the atmosphere because it is all absorbed by other air molecules along the way, as indicated by zero transmissivity. So a satellite cannot "see" the air at this range of heights.

Above 10 km altitude, although the atmosphere is transparent in this toy profile, it has zero emissivity. So no radiation is produced from the air at these altitudes, and again the satellite cannot see this air.

But for heights between 5 and 10 km, the atmosphere is partially emitting (has nonzero emissivity), and the resulting upwelling radiation is not totally absorbed (as indicated by nonzero transmissivity). Thus, radiation from this layer can reach the satellite. The satellite can see through the atmosphere down to this layer, but can't see air below this layer.

Thus, with the right wavelength, satellites can measure brightness temperature at an elevated layer of cloudless air. At other wavelengths with different transmittance profiles, satellites can measure temperature in different layers, at the top of the atmosphere, at cloud top, or at the Earth's surface.

In general, heights where transmittance changes are heights for which the air can be remotely observed. After a bit of math, the **radiative transfer equation** can be rewritten in terms of transmittance change $\Delta\hat{\tau} = [\,\hat{\tau}_{\text{top of layer j}} - \hat{\tau}_{\text{bottom of layer j}}\,]$:

$$L_\lambda = B_\lambda(T_{skin})\cdot\hat{\tau}_{\lambda,sfc} + \sum_{j=1}^{n} B_\lambda(T_j)\cdot\Delta\hat{\tau}_{\lambda,j} \qquad (8.4)$$

If the full atmospheric depth is black (i.e., no surface emissions to space), then $\sum_{j=1}^{n}\Delta\hat{\tau}_{\lambda,j} = 1$.

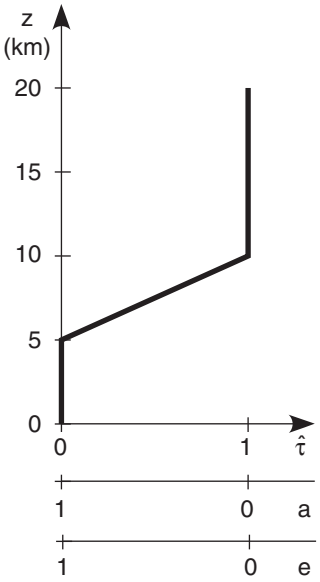

Figure 8.6
Hypothetical variation of atmospheric transmittance ($\hat{\tau}$), absorptance (a), and emissivity (e) with height (z).

Solved Example

Given the IR transmittance profile of Fig. 8.6, for λ = 6.7 μm. Suppose the vertical temperature profile in the atmosphere is:

z (km)	T (°C)
15 to 20	–40
10 to 15	–30
5 to 10	–20
0 to 5	0

and the Earth's surface (skin) temperature is 15°C. Find the upwelling IR radiation at the top of the atmosphere.

Solution

Given: the data above.

Find: L_λ = ? $\text{W}\cdot\text{m}^{-2}\cdot\mu\text{m}^{-1}\cdot\text{sr}^{-1}$.

You can save some work by thinking about the problem first. From Fig. 8.6, the transmittance τ is 0 at the surface ($z = 0$). Thus, none of the surface emissions will reach the top of the atmosphere, so T_{skin} is irrelevant, and the first term on the RHS of eq. (8.4) is zero.

Also, as discussed, the satellite can't see the layers between 0 to 5 km and 10 to 20 km for this toy profile, so the temperatures in these layers are also irrelevant. Thus, all terms in the sum in eq. (8.4) are zero except the one term for the one layer at 5 to 10 km.

In this layer, the absolute temperature is T = 273 – 20°C = 253 K. Across this layer, the change of transmittance is $\Delta\hat{\tau} = [\,1 - 0\,]$. Thus, the only nonzero part of eq. (8.4) is:

$L_\lambda = 0 + B_\lambda(253\text{ K})\cdot[\,1 - 0\,]$

where you can solve for B_λ using eq. (8.1).

$L_\lambda = B_\lambda =$ **1.82** $\text{W}\cdot\text{m}^{-2}\cdot\mu\text{m}^{-1}\cdot\text{sr}^{-1}$.

Check: Units OK. Physics OK.

Discussion: A lot of work was saved by thinking first.

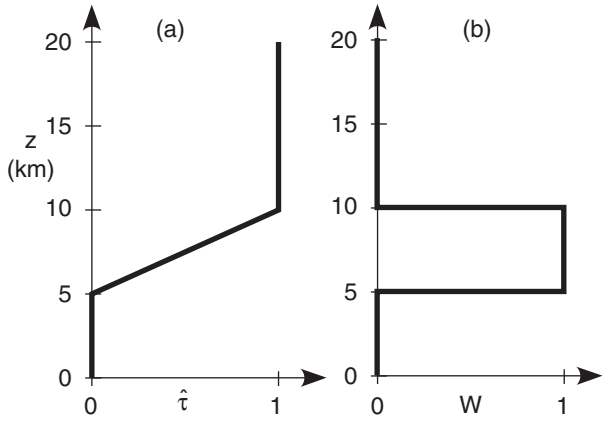

Figure 8.7
Hypothetical transmittance $\hat{\tau}$ *and weighting function W (z) .*

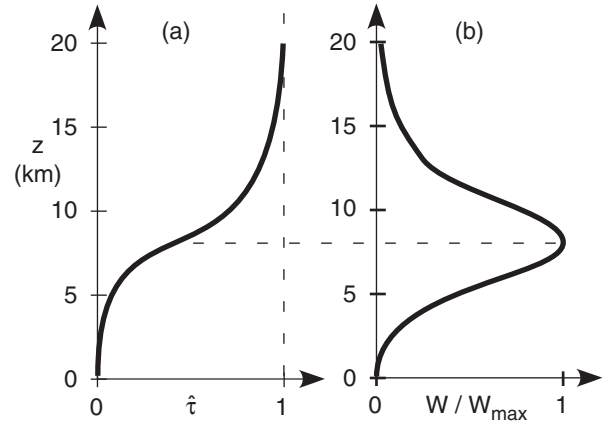

Figure 8.8
Transmittance $\hat{\tau}$ *and weighting function W (z) at* $\lambda = 6.7\ \mu m$. *This is the GOES-8 imager* **water-vapor channel** *(IR channel 3). The weight is normalized by its maximum value.*

Weighting Functions

In eq. (8.4) the factor $\Delta\hat{\tau}$ within the sum acts as a weight, determining the relative contribution of each layer to the total radiance out the top of the atmosphere at that wavelength. Use the symbol $W_{\lambda,j}$ for these weights (i.e., $W_{\lambda,j} = \Delta\hat{\tau}_{\lambda,j}$). With this trivial notation change, the **radiative transfer equation** is:

$$L_\lambda = B_\lambda(T_{skin})\cdot\hat{\tau}_{\lambda,sfc} + \sum_{j=1}^{n} B_\lambda(T_j)\cdot W_{\lambda,j} \qquad \bullet(8.5)$$

where $\Sigma_j W_j = 1$ for any one wavelength.

For the toy profile of Fig. 8.7a, the corresponding vertical profile of weights, called the **weighting function**, is shown in Fig. 8.7b. The weights are proportional to the slope of the transmittance line. (Any vertical line segment in Fig. 8.7a has zero slope, remembering that the independent height variable is along the ordinate in this meteorological graph).

In reality, the weighting function for any wavelength is a smooth curve. Fig. 8.8 shows the curve at $\lambda = 6.7\ \mu m$, for which water vapor is the emitter.

In essence, the weighting function tells you the dominant height-band seen by a satellite channel. For Fig. 8.8, all moist layers in the height range of roughly 5 to 12 km (mid to upper troposphere) are blurred together to give one average moisture value. Hence, this **water-vapor channel** can see tops of deep thunderstorms, but not the boundary layer.

By utilizing many wavelengths with weighting functions that peak at different heights, the satellite can focus on different overlapping height bands. Heights of peak *W* change where $\hat{\tau}$ in Fig. 8.4 changes with λ. Figs. 8.9 show the weighting functions for the sounder channels (Fig. 8.4) on the GOES-8 satellite. Newer satellites use interferometer methods, giving a nearly infinite suite of weighting functions that peak at a wide range of different altitudes.

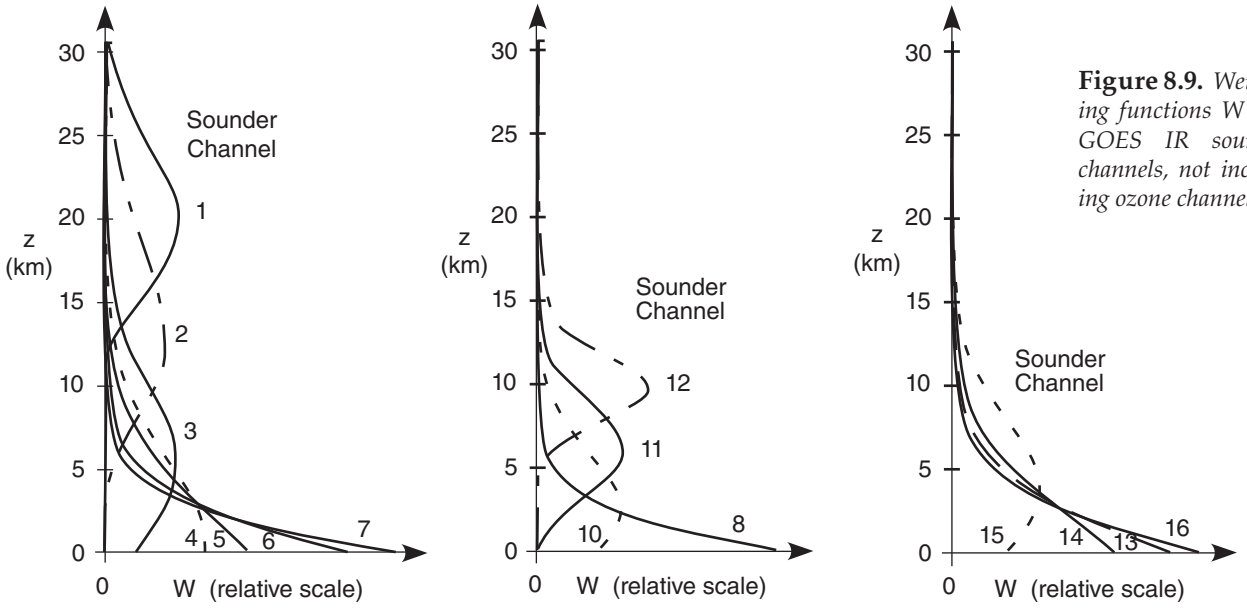

Figure 8.9. *Weighting functions W for GOES IR sounder channels, not including ozone channel 9.*

WEATHER SATELLITES

Orbits

Artificial satellites such as weather satellites orbiting the Earth obey the same orbital mechanics as planets orbiting around the sun. For satellites in near-circular orbits, the pull by the Earth's gravity f_G balances centrifugal force f_C :

$$f_G = \frac{G \cdot M \cdot m}{R^2} \qquad \bullet(8.6)$$

$$f_C = \left(\frac{2\pi}{t_{orbit}} \right)^2 \cdot m \cdot R \qquad \bullet(8.7)$$

where R is the distance between the center of the Earth and the satellite, m is the mass of the satellite, M is the mass of the Earth (5.9742×10^{24} kg), and G is the gravitational constant (6.6742×10^{-11} $N \cdot m^2 \cdot kg^{-2}$). See Appendix B for lists of constants.

Solve for the orbital time period t_{orbit} by setting $f_G = f_C$:

$$t_{orbit} = \frac{2\pi \cdot R^{3/2}}{\sqrt{G \cdot M}} \qquad \bullet(8.8)$$

Orbital period does not depend on satellite mass, but increases as satellite altitude increases.

Weather satellite orbits are classified as either **polar-orbiting** or **geostationary** (Fig. 8.10). Polar-orbiters are **low-Earth-orbit** (**LEO**) satellites.

Geostationary Satellites

Geostationary satellites are in high Earth orbit over the equator, so that the orbital period matches the Earth's rotation. Relative to the fixed stars, the Earth rotates 360° in 23.934 469 6 h, which is the duration of a **sidereal day.** With this orbital period, geostationary satellites appear parked over a fixed point on the equator. From this vantage point, the satellite can take a series of photographs of the same location, allowing the photos to be combined into a repeating movie called a **satellite loop**.

Disadvantages of geostationary satellites include: distance from Earth is so great that large magnification is needed to resolve smaller clouds; many satellites must be parked at different longitudes for imagery to cover the globe; imaging is interrupted during nights near the equinoxes because the solar panels are in darkness — eclipsed by the Earth; and polar regions are difficult to see.

Satellites usually have planned lifetimes of about 3 to 5 years, so older satellites must be continually replaced with newer ones. Lifetimes are limited partly because of the limited propellant storage needed to make orbital corrections. Satellites are also hurt by tiny meteoroids that frequently hit the satellite

Solved Example

At what (a) distance above the Earth's center, & (b) altitude above the Earth's surface, must a geostationary satellite be parked to have an orbital period of exactly one sidereal day? Use Appendix B for Earth constants.

Solution

Given: $t_{orbit} = 23.934\,469\,6$ h = 86,164 s.
$M = 5.973\,6 \times 10^{24}$ kg
$G = 6.674\,28 \times 10^{-11}$ $m^3 \cdot s^{-2} \cdot kg^{-1}$
Find: (a) R = ? km, (b) z = ? km

(a) Rearrange eq. (8.8):
$R = (t_{orbit} / 2\pi)^{2/3} \cdot (G \cdot M)^{1/3}$ = **42,167.5 km**
(b) From this subtract Earth radius at equator (R_o = 6,378 km) to get height above the surface:
$z = R - R_o$ = **35,790 km**

Check: Units OK. Physics OK.
Discussion: Compares well with real satellites. As of June 2009, the GOES-12 satellite was at R = 42,165.9 km. It was slightly too low, orbiting slightly too fast, causing it to gradually get ahead of the Earth's rotation. Namely, it drifts 0.004°/day toward the east relative to the Earth.

Such drift is normal for satellites, which is why they carry propellant to make orbital adjustments, as commanded by tracking stations on the ground.
More Discussion: For a calendar day (24 h from sun overhead to sun overhead), the Earth must rotate 360.9863°, because the position of the sun relative to the fixed stars changes as the Earth moves around it.

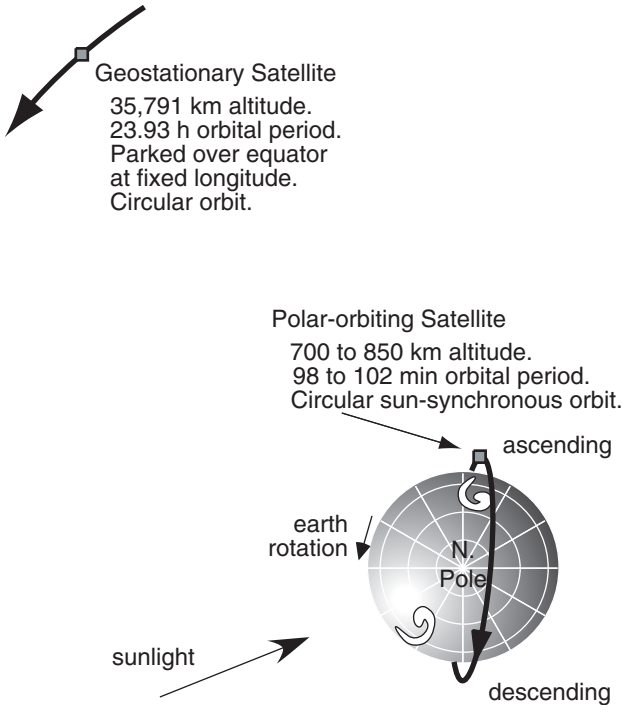

Figure 8.10
Sketch (to scale) of geostationary and polar-orbiting weather satellite orbits.

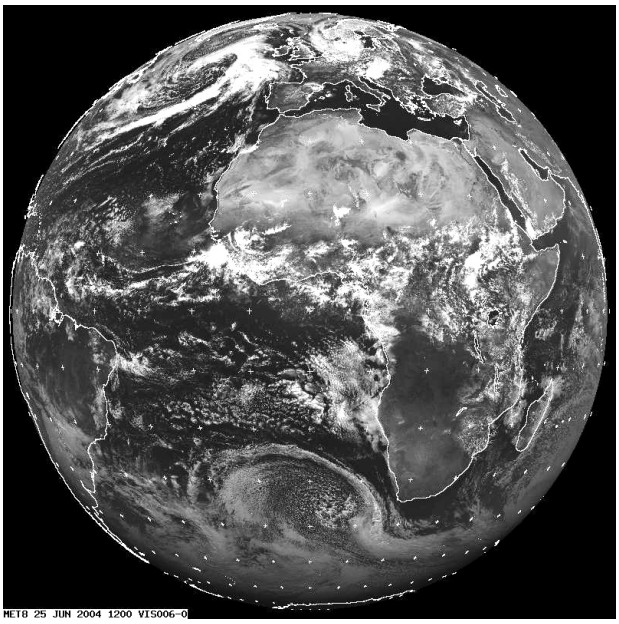

Figure 8.11
Example of Earth disk image from Meteosat-8 (MSG-1). Parked at 0° longitude. Began routine operations on 29 Jan 2004. Copyright © 2004 by EUMETSAT. Used with permission. http://oiswww.eumetsat.org/IDDS-cgi/listImages

Science Graffito

"You can observe a lot just by watching."
– Yogi Berra.

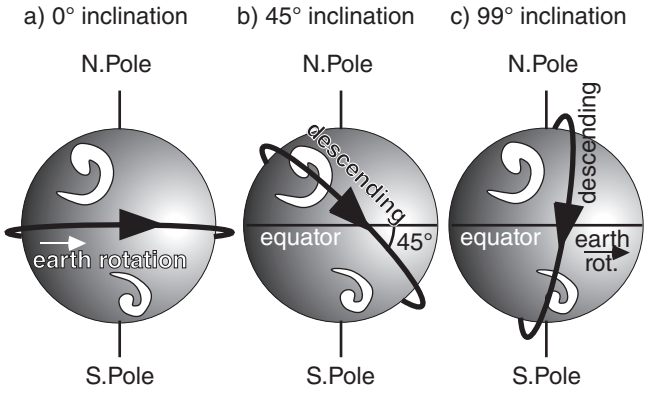

Figure 8.12
Examples of inclinations of satellite orbits. Sun-synchronous satellites use orbit (c).

at high speed, and by major solar storms. For this reason, most meteorological satellite agencies try to keep an in-orbit spare satellite nearby.

The USA has a series of **Geostationary Operational Environmental Satellite** (**GOES**). They usually park one satellite at 75°W to view the N. American east coast and western Atlantic, and another at 135°W to view the west coast and eastern Pacific — named **GOES-East** and **GOES-West**.

The European Organization for the Exploitation of Meteorological Satellites (EUMETSAT) operate **Meteosat** satellites (Fig. 8.11). They try to keep one parked near 0° longitude, to view Europe, Africa, the Mediterranean Sea, and the eastern Atlantic Ocean.

The Japan Meteorological Agency (JMA) operates Multi-functional Transport Satellites (**MT-SAT**), with one parked at 140°E to give a good view of Japan and approaching Pacific typhoons. The China Meteorological Administration has a series of **Fengyun** (FY, "Wind & cloud") geostationary satellites parked at 86.5°E, 105°E, and 123.3°E. Russia had Geostationary Operational Meteorological Satellites (**GOMS**) in orbit, and plans to launch some in the future. The India Space Research Organization (ISRO) operates **INSAT** satellites in the 60° to 95°E range of longitudes.

Thus, there are usually sufficient geostationary satellites around the equator to view all parts of the Earth except the poles.

Polar Orbiting Satellites

If geostationary positioning is not required, then weather satellites could be placed at any altitude with any orbital inclination. However, there is a special altitude and inclination that allows satellites to view the Earth at roughly the same local time every day. Advantages are consistent illumination by the sun, lower altitude to better resolve the smaller clouds, and good views of high latitudes.

To understand this special orbit, consider the following. When the orbital plane of the satellite is along the Earth's equator, AND the direction of satellite orbit is the same as the direction of Earth's rotation, then the orbit is defined to have 0° **inclination** (Fig. 8.12a). Greater inclination angles (Fig. 8.12b) indicate greater tilt of the orbit relative to the equator. For inclinations greater than 90°, the satellite is orbiting opposite to the Earth's rotation (Fig. 8.12c). For an inclined orbit, the **ascending node** is the side of the orbit where the satellite crosses the equator northbound (behind the Earth in Fig. 8.12b & c). The **descending node** is where it crosses the equator southbound (in front of the Earth in Fig. 8.12b & c).

Polar orbiting weather satellites are designed so that the locations of the ascending and descending nodes are **sun synchronous**. Namely, the satellite

always observes the same local solar times on every orbit. For example, Fig. 8.13a shows a satellite orbit with descending node at about 10:20 AM local time. Namely, the local time at city A directly under the satellite when it crosses the equator is 10:20 AM.

For this sun-synchronous example, 100 minutes later, the satellite has made a full orbit and is again over the equator. However, the Earth has rotated 25.3° during this time, so it is now local noon at city A. However, city B is now under the satellite (Fig. 8.13b), where its local time is 10:20 AM. 100 minutes later, during the next orbit, city C is under the satellite, again at 10:20 AM local time (Fig. 8.13c).

For the satellite orbits in Fig. 8.13, on the back side of the Earth, the satellite always crosses the equator at 10:20 PM local time during its ascension node.

Sun-synchronous polar-orbiting satellites are nicknamed by the time of day when they cross the equator during daylight. It does not matter whether this daylight crossing is during the ascent or descent part of the orbit. For the example of Fig. 8.13, this is the **morning** or **AM satellite**.

Many countries have polar orbiting weather satellites. The USA's **Polar Orbiting Environmental Satellites** (**POES**) are designated **NOAA**-*X*, where X is the satellite ID number. NOAA-19, launched in Feb 2009, is the last POES. Each satellite has a design life of about 4 years in space. The next series of USA polar-orbiting weather satellites is called the **Joint Polar Satellite System** (**JPSS**).

For the polar orbit to remain sun synchronous during the whole year, the satellite orbit must precess 360°/year as the Earth orbits the sun; namely, 0.9863° every day. This is illustrated in Fig. 8.14. Aerospace engineers, astronomers and physicists devised an ingenious way to do this without using their limited supply of onboard propellant. They take advantage of the pull of the solar gravity and the resulting slight tidal bulge of the "solid" Earth toward the sun. As the Earth rotates, this bulge (which has a time lag before disappearing) moves eastward and exerts a very small gravitational pull on the satellite in the direction of the Earth's rotation.

This applies a torque to the orbit to cause it to gradually rotate relative to the fixed stars, so the orbit remains synchronous relative to the sun. The combination of low Earth orbit altitude AND inclination greater than 90° gives just the right amount of precession to maintain the sun synchronous orbit.

The result is that polar-orbiting weather satellites are usually placed in low Earth orbit at 700 to 850 km altitude, with short orbital period of 98 to 102 minutes, and inclination of 98.5° to 99.0°. Polar orbiting satellites do not go directly over the poles, but intentionally miss the poles by 9°. This is still close enough to get good images of the poles.

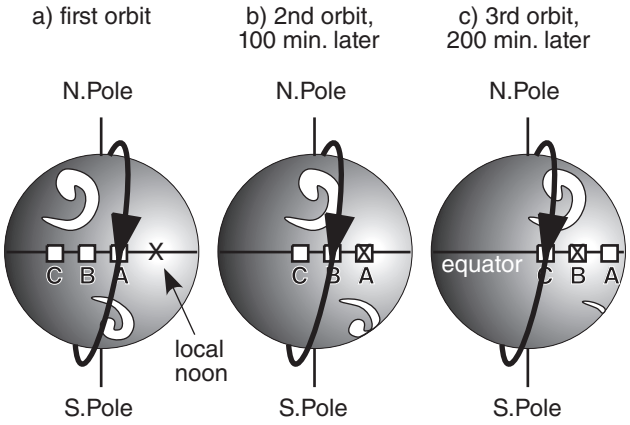

Figure 8.13
Rotation of the Earth under a sun-synchronous satellite orbit. X marks local noon.

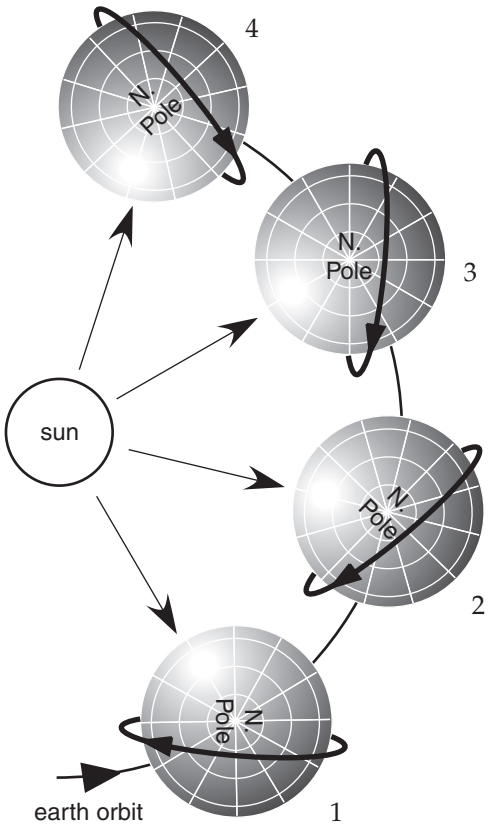

Figure 8.14
Precession of polar satellite orbit (thick lines) as the Earth orbits around the sun (not to scale). The page number at the top of this textbook page can represent a "fixed star".

Table 8-1. Imager channels on USA GOES weather satellites. All channels except #3 are in atmospheric windows. Channel wavelengths vary slightly from satellite to satellite. •Indicates important channels.

Channel #	Name	Center Wavelength (μm)	Wavelength Range (μm)
1 •	visible	0.65	0.52 - 0.72
2	short-wave IR window	3.9	3.78 - 4.03
3 •	water vapor	6.7	6.47 - 7.02
4 •	long-wave IR window	10.7	10.2 - 11.2
5	IR dirty window		
	(for GOES 10-11)	12	11.5 - 12.5
	(for GOES 12-13)	13.3	13.0 - 13.7

Table 8-2. Imager channels on European MSG Meteosat-8 weather satellite.

Channel #	Name	Center Wavelength (μm)	Wavelength Range (μm)
1	VIS 0.6 (visible green)	0.635	0.56 - 0.71
2	VIS 0.8 (visible red)	0.81	0.74 - 0.88
3	NIR 1.6 (near IR)	1.64	1.50 - 1.78
4	IR 3.9	3.90	3.48 - 4.36
5	WV 6.2 (water vapor: high trop.)	6.25	5.35 - 7.15
6	WV 7.3 (water vapor: mid-trop.)	7.35	6.85 - 7.85
7	IR 8.7	8.70	8.30 - 9.10
8	IR 9.7 (ozone)	9.66	9.38 - 9.94
9	IR 10.8	10.80	9.80 - 11.8
10	IR 12.0	12.00	11.0 - 13.0
11	IR 13.4 (high-troposphere)	13.40	12.4 - 14.4
12	HRV (high-resolution visible)	broad-band	0.4 - 1.1

FOCUS • Some Other Satellite Systems

Scatterometer sensors on satellites can detect capillary waves on the ocean, allowing near-surface wind speeds to be estimated. Passive and active Special Sensor Microwave Imagers (**SSM/I**) can retrieve precipitation and precipitable water over the ocean. Combining a series of observations while a satellite moves allows small onboard antennas to act larger, such as via **synthetic aperture radar** (SAR).

Imager

Modern weather satellites have many capabilities, one of which is to digitally photograph (make images of) the clouds, atmosphere, and Earth's surface. Meteorologists use these photos to help identify and locate weather patterns such as fronts, thunderstorms and hurricanes. Pattern-recognition programs can also use sequences of photos to track cloud motions, thereby inferring the winds at cloud-top level. The satellite instrument system that acquires the digital data to construct these photos is called the **imager**.

As of year 2010, USA geostationary (GOES) weather satellites have 5 imager channels (wavelength bands) for viewing the Earth system (Fig. 8.4). Most of the spectral bands were chosen specifically to look through different transmittance windows to "see" different atmospheric and cloud features. These channels are summarized in Table 8-1.

Imager channels for the European Meteosat-8 are listed in Table 8-2. This satellite has 12 channels. Included are more visible channels to better discern colors, including vegetation greenness (important for weather and climate modeling). Future USA satellites will also have more channels. The discussion below is for the most-used GOES imager channels.

Visible

Visible satellite images (GOES channel 1) show what you could see with your eyes if you were up in space. All cloud tops look white during daytime, because of the reflected sunlight. In cloud-free regions the Earth's surface is visible. At night, this channel is useless on present-day civilian satellites; however, special low-light visible-channel imagers on military satellites and future civilian satellites can see city lights, and see the clouds by moonlight.

Infrared (IR)

Infrared satellite images (GOES channel 4) use long wavelengths in a transmittance window, and can clearly see through the atmosphere to the surface or the highest cloud top. There is very little solar energy at this wavelength to be reflected from the Earth system to the satellite; hence, the satellite sees mostly emissions from the Earth or cloud. The advantage of this channel is it is useful both day and night, because the Earth never cools to absolute zero at night, and thus emits IR radiation day and night.

Images made in this channel are normally grey shaded such that colder temperatures look whiter, and warmer looks darker. But in the troposphere, the standard atmosphere gets colder as height increases (Chapter 1). Thus, white colored clouds in this image indicate high clouds (cirrus, thunderstorm anvils, etc.), and darker grey clouds are low

clouds (stratus, fog tops, etc.) Medium grey shading implies middle clouds (altostratus, etc.).

Fig. 8.15 demonstrates the principles behind this IR shading. At any one spot in the field of view, (a) a radiance L is measured by the satellite radiometer — for example: 7.6 $W \cdot m^{-2} \cdot \mu m^{-1} \cdot sr^{-1}$, as shown by the dashed line. The picture element (**pixel**) in the image that corresponds to this location is shaded darker (b) for greater L values, mimicking photographic film that becomes darker when exposed to more light. Not knowing the emissivity of the emitting object viewed at this spot, you can (c) assume a black body, and then use the Planck curve (d) for this IR channel to infer (e) brightness temperature T_B (= 283 K in this example). But for any normal temperature profile in the troposphere, such as the standard atmosphere (f), warmer temperatures are usually (g) closer to the ground (z = 0.9 km in this example).

The net result for this IR window channel is that the darker shading (from b, redrawn in h) corresponds to lower clouds (i). Similarly, following the dotted curve, lesser values of observed radiance correspond to colder temperatures and higher clouds, and are shown as whiter pixels.

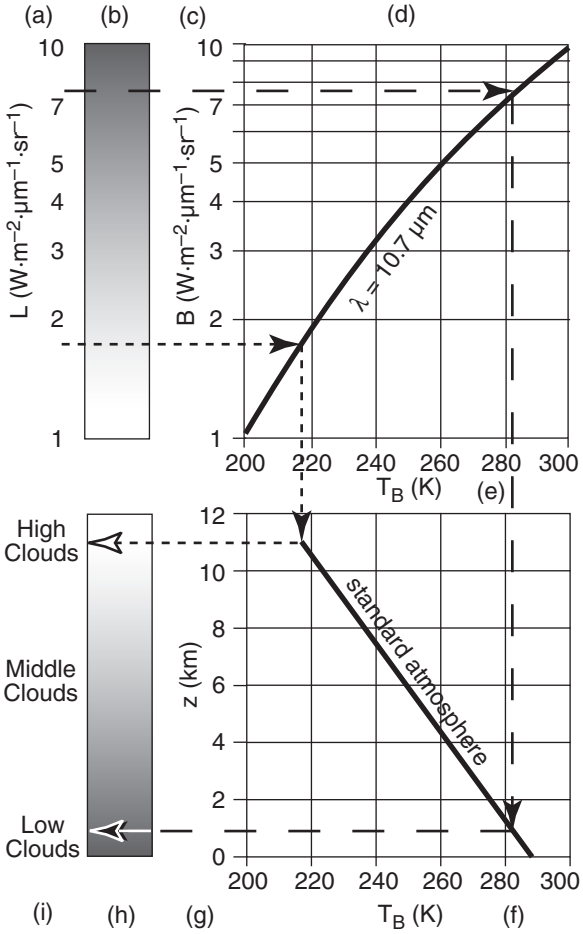

Figure 8.15
Imaging principles for the IR window channel.

Water-vapor (WV)

Water-vapor images are obtained by picking a wavelength (channel 3) that is NOT in a window. In this part of the spectrum, water (as vapor, liquid, or ice) in the atmosphere can absorb radiation. If little water is present in the mid to upper troposphere (Fig. 8.8b), then most of the IR radiation from the Earth can reach the satellite. The warm brightness temperature associated with emissions from the Earth's surface is displayed as dark grey in a water-vapor satellite image — indicating drier air aloft.

For higher concentrations of water in air, most of the surface emissions do not reach the satellite because they are absorbed by the water in the mid to upper troposphere. Kirchhoff's law tells us that this atmospheric layer is also an effective emitter. The colder brightness temperatures associated with strong emissions from this cold layer of air are displayed as light grey — indicating moist air aloft.

Water-vapor images are useful because: (1) they provide data day and night; (2) animations of image sequences show the movement of the air, regardless of whether clouds are present or not; and (3) they give average conditions over a thick layer in the upper troposphere. Because of item (2), pattern recognition programs can estimate average winds in the upper troposphere by tracking movement of blobs of humid air, with or without clouds being present.

Other Channels

Channels 2 and 5 are used less by forecasters, but they do have some specialized uses. Channel 2 sees both reflected solar IR and emitted terrestrial IR, and can help detect fog and low stratus clouds. It is sometimes called the **fog channel**. It can also help to discriminate between water-droplet and ice-crystal clouds, and to see hot spots such as forest fires.

Channel 5 is near the IR longwave window of channel 4, but slightly shifted into a shoulder region (or dirty window) where there are some emissions from low-altitude water vapor. Computerized images of the difference between channels 4 & 5 can help identify regions of greater humidity in the boundary-layer, which is useful for forecasting storms.

Image Examples & Interpretation

Figures 8.16a-c show visible (Vis), infrared (IR) and water vapor (WV) images of the same scene. You can more successfully interpret cloud type when you use and compare all three of these image channels. The letters below refer to labels added to the images. Extra labels on the images are used for a solved example and for homework exercises.

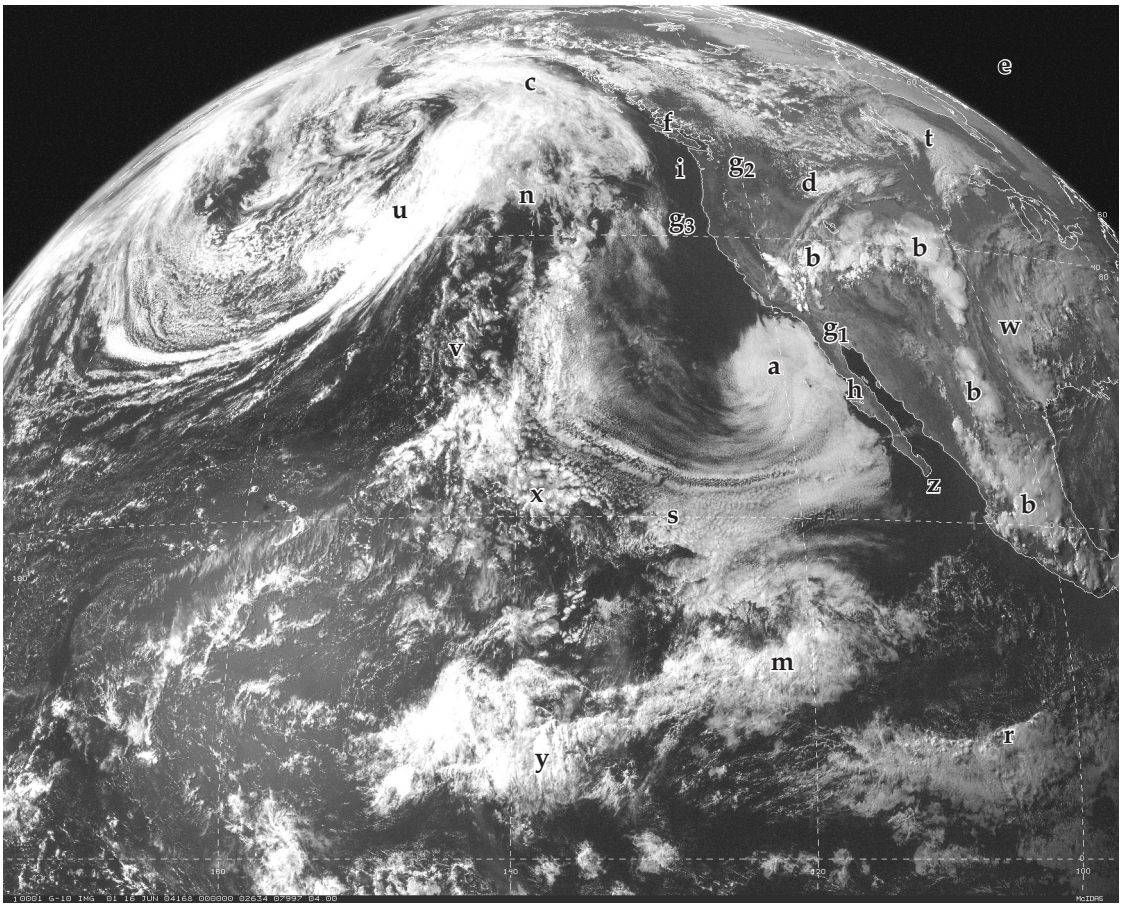

Figure 8.16a
Visible satellite image.

To aid image interpretation, letter labels a-z are added to identical locations in all 3 satellite images.

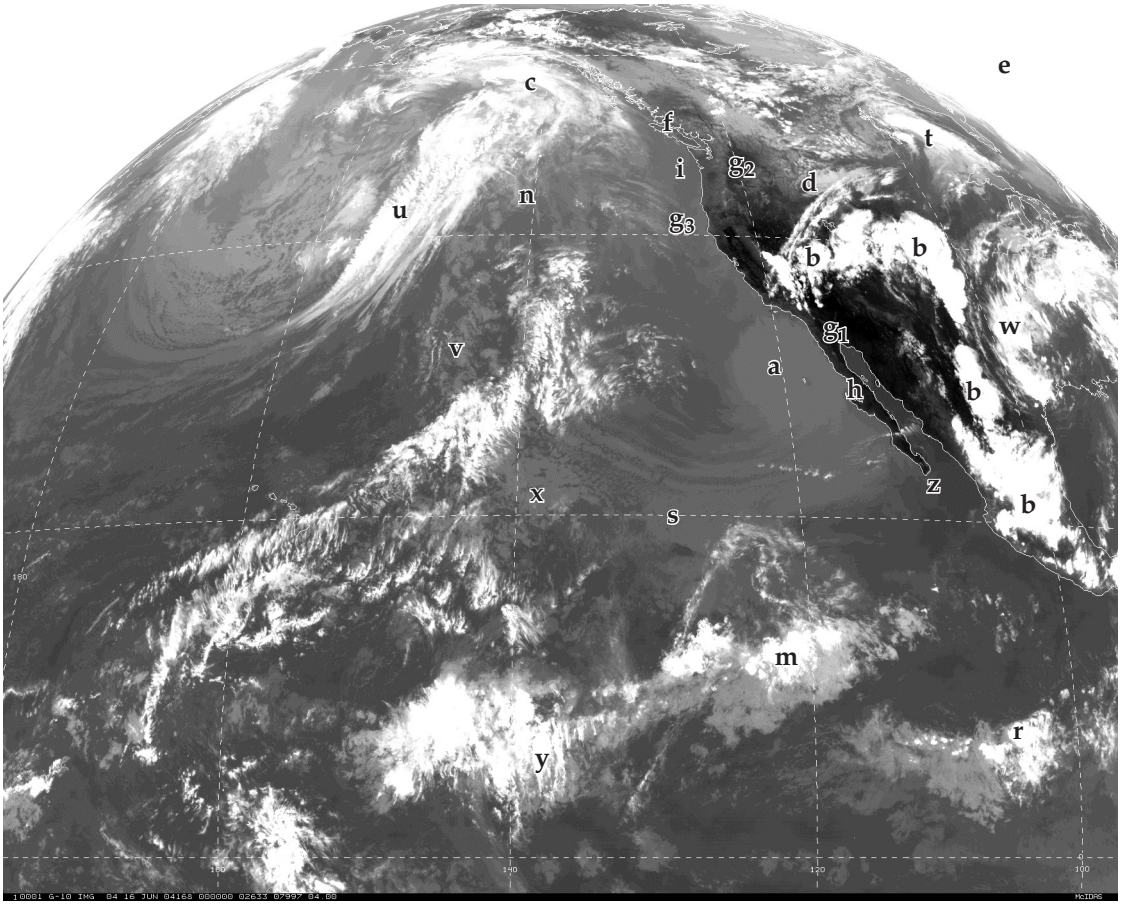

Figure 8.16b
Infrared (IR) satellite image.

[Images a-c courtesy of Space Science & Engineering Center, Univ. of Wisconsin-Madison. Valid time for images: 00 UTC on 16 June 2004.]

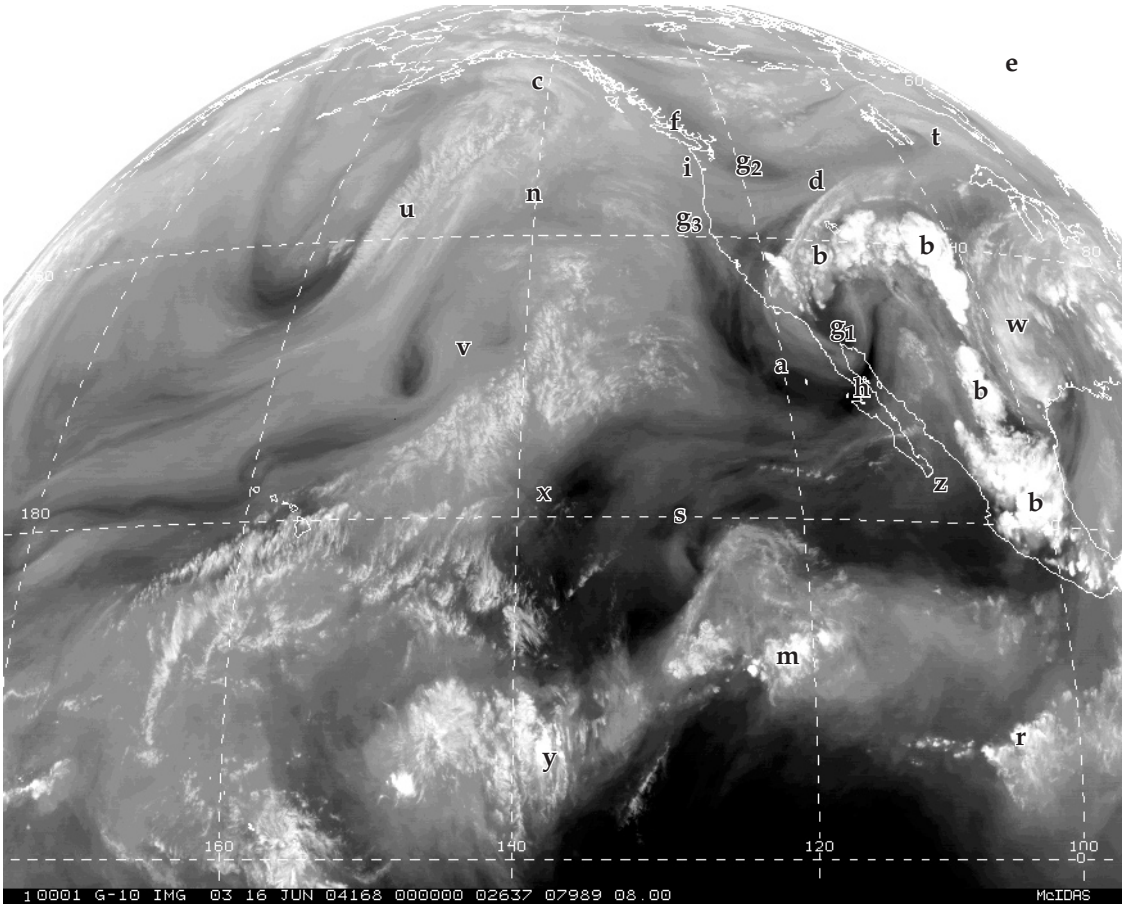

Figure 8.16c
Water-vapor satellite image.

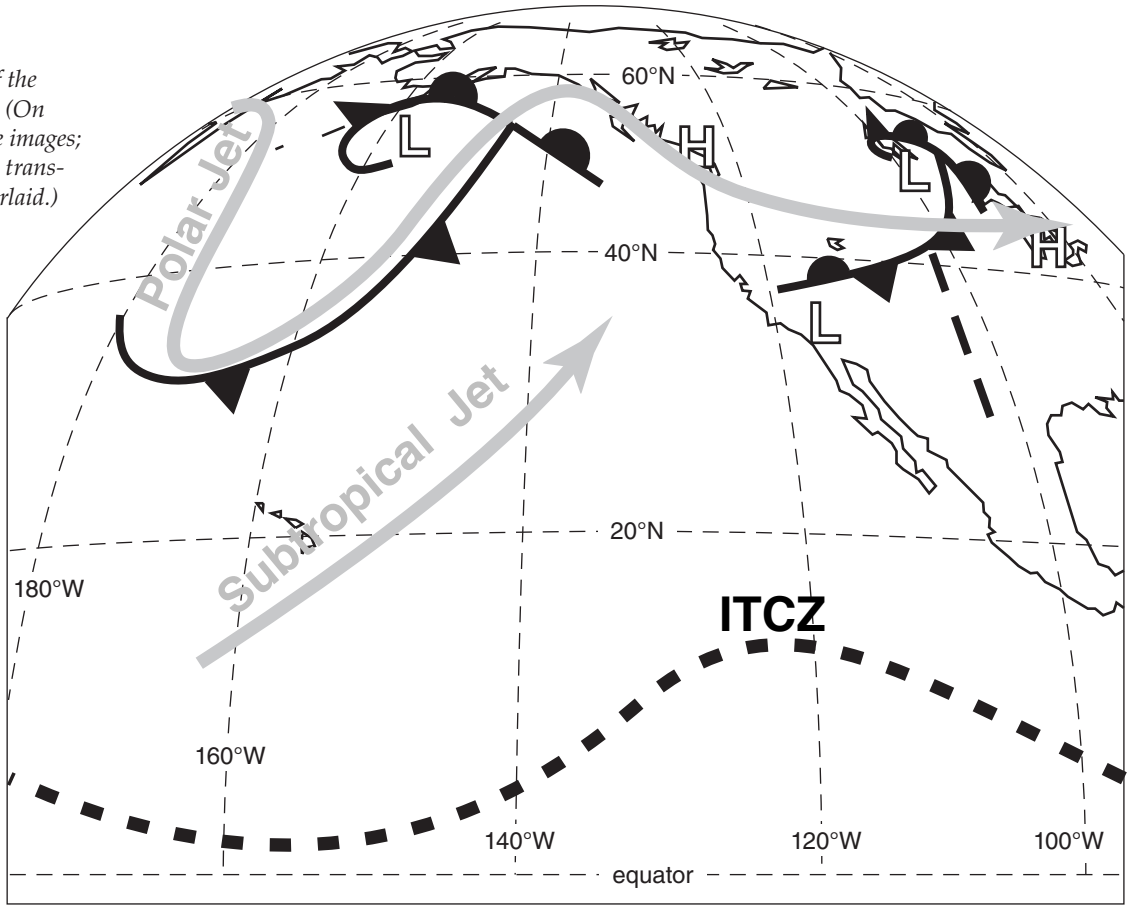

Figure 8.16d
Interpretation of the satellite images. (On same scale as the images; can be copied on transparency and overlaid.) Symbols and acronyms will be explained in later chapters.

a. Fog or low stratus:
Vis: White, because it is a cloud.
IR: Medium to dark grey, because low, warm tops.
WV: Invisible, because not in upper troposphere. Instead, WV shows amount of moisture aloft.

b. Thunderstorms:
Vis: White, because it is a cloud.
IR: Bright white, because high, cold anvil top.
WV: Bright white, because copious amounts of water vapor, rain, and ice crystals fill the mid and upper troposphere. Often the IR and WV images are enhanced by adding color to the coldest temperatures and most-humid air, respectively, to help identify the strongest storms.

c. Cirrus, cirrostratus, or cirrocumulus:
Vis: White, because cloud, although can be light grey if cloud is thin enough to see ground through it.
IR: White, because high, cold cloud.
WV: Medium to light grey, because not a thick layer of moisture that is emitting radiation.

d. Mid-level cloud tops:
Could be either a layer of altostratus/altocumulus, or the tops of cumulus mediocris clouds.
Vis: White, because it is a cloud.
IR: Light grey, because mid-altitude, medium-temperature.
WV: Medium grey. Some moisture in cloud, but not a thick enough layer in mid to upper troposphere to be brighter white.

e. Space:
Vis: Black (unless looking toward sun).
IR: White, because space is cold.
WV: White, because space is cold.

f. Snow-capped Mountains (not clouds):
Vis: White, because snow is white.
IR: Light grey, because snow is cold, but not as cold as high clouds or outer space.
WV: Maybe light grey, but almost invisible, because mountains are below the mid to upper troposphere. Instead, WV channel shows moisture aloft.

g. Land or Water Surfaces (not clouds):
g_1 is in very hot desert southwest in summer, g_2 is in arid plateau, and g_3 is Pacific Ocean.
Vis: Medium to dark grey. Color or greyshade is that of the surface as viewed by eye.
IR: g_1 is black, because very hot ground.
g_2 is dark grey, because medium hot.
g_3 is light grey, because cool ocean.
WV: Light grey or invisible, because below mid to upper troposphere. Instead, sees moisture aloft.

h. Tropopause Fold or Dry Air Aloft.
Vis: Anything.
IR: Anything.
WV: Dark grey or black, because very dry air in the upper troposphere. Occurs during tropopause folds, because dry stratospheric air is mixed down.

i. High Humidities Aloft.
Vis: Anything.
IR: Anything.
WV: Light grey. Often see meandering streams of light grey, which can indicate a jet stream. (Might be hard to see in this copy of a satellite image.)

"**Image Interpretation**" means the use of satellite images to determine weather features such as fronts, cyclones, thunderstorms and the global circulation. This is a very important part of manual weather forecasting. Whole books are devoted to the subject, and weather forecasters receive extensive training in it. In this book, image interpretation of cyclones, fronts, and thunderstorms is covered in the later chapters on those topics.

Solved Example
Determine cloud type at locations "m" and "n" in satellite images 8.16a-c.

Solution
Given: visible, IR, and water vapor images
Find: cloud type

m: vis: White, therefore cloud, fog, or snow.
IR: White, thus high cloud top (cirrus or thunderstorm, but not fog or snow).
wv: White, thus copious moisture within thick cloud layer. Thus, not cirrus.
Conclusion: **thunderstorm**.

n: vis: White, therefore cloud, fog, or snow. (Snow cover is unlikely on unfrozen Pacific).
IR: Medium grey, roughly same color as ocean. Therefore warm, low cloud top.
wv: Medium grey (slightly darker than surrounding regions), therefore slightly drier air aloft. But gives no clues regarding low clouds.
Conclusion: **low clouds or fog**

Check: Difficult to check or confirm now. But after you learn synoptics you can check if the cloud feature makes sense for the weather pattern that it is in.
Discussion: This is like detective work or like a medical diagnosis. Look at all the clues, and rule out the clouds that are not possible. Be careful and systematic. Use other info such as the shape of the cloud or its position relative to other clouds or relative to mountains or oceans. Interpreting satellite photos is somewhat of an art, so your skill will improve with practice.

However, for future reference, Fig. 8.16d shows my interpretation of the previous satellite photos. This particular interpretation shows only some of the larger-scale features. See the Fronts, Cyclones, and Global Circ. chapters for symbol definitions.

Sounder

The sounder radiometer measures radiances at different wavelength channels (Table 8-3) that have different weighting functions (Fig. 8.9), in order to estimate vertical temperature profiles (i.e., temperature soundings). These weighting functions peak at different altitudes, allowing us to estimate a **sounding** (temperatures at different altitudes). We will examine the basics of this complex **retrieval** process.

There is a limit to our ability to retrieve sounding data, as summarized in two corollaries. **Corollary 1** is given at right. To demonstrate it, we will start with a simple weighting function and then gradually add more realism in the subsequent illustrations.

Consider the previous idealized transmittance profile (Fig. 8.7), but now divide the portion between $z = 5$ and 10 km into 5 equal layers. As shown in Fig. 8.17a, the change in transmittance across each small layer is $\Delta\hat{\tau} = 0.2$ (dimensionless); hence, the weight (Fig. 8.17b) for each layer is also $W = 0.2$. Assume that this is a crude approximation to sounder channel 3, with central wavelength of $\lambda = 14.0$ μm.

Suppose the "actual" temperature of each layer, from the top down, is $T = -20, -6, -14, -10$, and 0°C, as illustrated by the data points and thin line in Fig. 8.17c. (We are ignoring the portions of the sounding below 5 km and above 10 km, because this weighting function cannot "see" anything at those altitudes, as previously discussed.)

Using Planck's Law (eq. 8.1), find the blackbody radiance from each layer from the top down: $B = 3.88$, 4.82, 4.27, 4.54, and 5.25 $W{\cdot}m^{-2}{\cdot}\mu m^{-1}{\cdot}sr^{-1}$. Weight each by $W = 0.2$ and then sum according to radiative transfer eq. (8.5) to compute the weighted average. This gives the radiance observed at the satellite: $L = 4.55$ $W{\cdot}m^{-2}{\cdot}\mu m^{-1}{\cdot}sr^{-1}$. The surface (skin) term in eq. (8.5) was neglected because the transmittance at the surface is zero, so no surface information reaches the satellite for this idealized transmittance profile.

This satellite-observed radiance is communicated to ground stations, where automatic computer programs retrieve the temperature using eq. (8.2). When we do that, we find $T_B = 263.18$ K , or **T = –9.82°C**. This is plotted as the thick line in Fig. 8.17c.

Detailed temperature-sounding structure is not retrieved by satellite, because the retrieval can give only one piece of temperature data per weighting function. Vertically broad weighting functions tend to cause significant smoothing of the retrieved temperature sounding.

Table 8-3. Sounder channels on GOES weather satellites. (Also see Fig. 8.4.)

Channel #	Center Wavelength (μm)	Channel #	Center Wavelength (μm)
1	14.7	11	7.0
2	14.4	12	6.5
3	14.0	13	4.6
4	13.7	14	4.5
5	13.4	15	4.4
6	12.7	16	4.1
7	12.0	17	4.0
8	11.0	18	3.8
9	9.7	19	0.6
10	7.5		

Retrieval Corollary 1: The sounder can retrieve (at most) one piece of temperature data per channel. The temperature it gives for that channel is the average brightness temperature weighted over the depth of the weighting function.

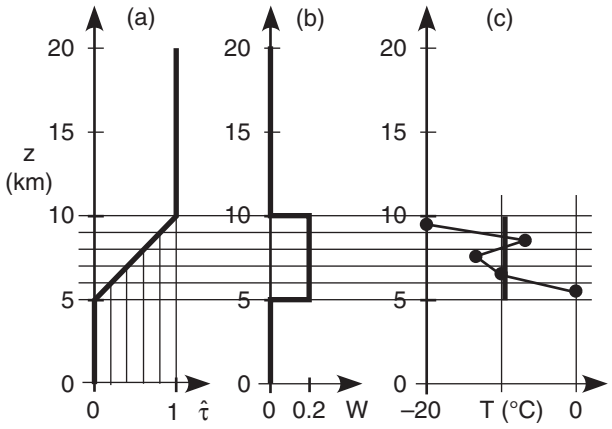

Figure 8.17
Retrieval of temperature from one channel (idealized). (a) transmittance; (b) weighting function; (c) original (thin line with data points) and satellite retrieved (thick line) temperatures.

Science Graffito

"It is not the *result* of scientific research that ennobles humans and enriches their nature, but the *struggle to understand* while performing creative and open-minded intellectual work." – Albert Einstein, 1930.

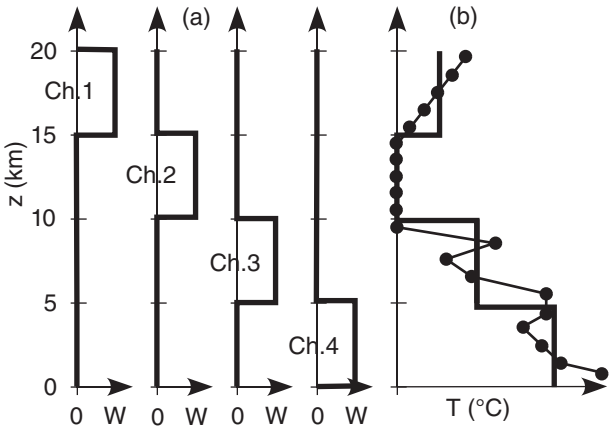

Figure 8.18
(a) Weighting functions for four idealized channels (Ch. 1 – 4). (b) Actual (thin line) and retrieved (thick line) temperature sounding.

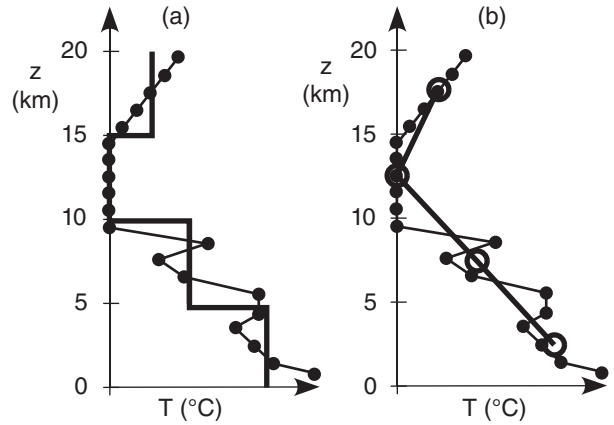

Figure 8.19
Retrieved soundings (a, thick line), are usually plotted as (b) single data points (open circles) for each channel, connected by straight lines.

Retrieval Corollary 2: If weighting functions from different channels have significant overlap in altitude and similar shapes, then they do not provide independent observations of the atmosphere. For this situation, if there are also measurement errors in the radiances or the weighting functions, then the sounding can retrieve **fewer** than one piece of temperature data per sounder channel. (See the "Beyond Algebra" box later in this section for a demonstration.)

Science Graffito

"Facts do not cease to exist because they are ignored." – Aldous Huxley.

Illustration of Retrieval Corollary 1 (Non-overlapping Weighting Functions)

Consider a slightly more realistic illustration of a perfect (idealized) case where the weighting functions do not overlap vertically between different channels (Fig. 8.18a). The relationship between actual temperatures (thin line) and the resulting temperature retrievals are sketched. Namely, the weighting functions are independent of each other, allowing the four channels to retrieve four independent temperatures, as plotted by the thick line (Fig. 8.18b). The thick line is the retrieved sounding.

Instead of plotting the retrieved sounding as a sequence of vertical line segments as shown in Fig. 8.19a, it is often plotted as data points. For our four independent channels, we would get four data points (large, open circles), and the resulting sounding line is drawn by connecting the circles (Fig. 8.19b). The retrieved sounding (thick line in Fig. 8.19b) does a good job of capturing the gross-features of the temperature profile, but misses the fine details such as sharp temperature inversions.

Illustration of Retrieval Corollary 2 (Overlapping Weighting Functions)

With non-overlapping weighting functions the sounding-retrieval process was easy. For more realistic overlapping weighting functions, it becomes very difficult, as summarized in **Retrieval Corollary 2**, given in the left column.

We can first study this as a **forward problem**, where we pretend we already know the temperature profile and want to find the radiances that the satellite would see. This approach is called an **Observing System Simulation Experiment** (**OSSE**), used by instrument designers to help anticipate the radiances arriving at the satellite, so that they can fix problems before the satellite is launched. We anticipate that the radiance received in one channel depends on the temperatures at many heights. Easy!

Later, we will approach this more realistically; i.e., as an **inverse problem** where we have satellite-measured radiances and want to determine atmospheric temperatures. The inverse problem for overlapping weighting functions requires us to solve a set of coupled nonlinear equations. Nasty!

To illustrate the forward problem, suppose that idealized weighting functions of Fig. 8.20 and Table 8-4 approximate the actual GOES weighting functions for sounder channels 1 – 4. For any one channel, the sum of the weights equals one, as you can check from the data in the figure. Each weighting function peaks at a different height. For simplicity, look at only the atmospheric contribution to the radiances and ignore the surface (skin) term.

For this forward example, suppose the temperatures for each layer (from the top down) are $T = -40$, -60, -30, and $+20$°C, as plotted in Fig. 8.21. Namely, we are using a coarse-resolution T profile, because we already know from Corollary 1 that retrieval methods cannot resolve anything finer anyway.

For each channel, we can write the radiative transfer equation (8.5). To simplify these equations, use $\lambda = 1, 2, 3, 4$ to index the wavelengths of sounder channels 1, 2, 3, 4. Also, use $j = 1, 2, 3, 4$ to index the four layers of our simplified atmosphere, from the top down. The radiative transfer equation for our simple 4-layer atmosphere, without the skin term, is:

$$L_\lambda = \sum_{j=1}^{4} B_\lambda(T_j) \cdot W_{\lambda,j} \tag{8.9}$$

After expanding the sum, this equation is:

$$L_1 = B_1(T_1)\cdot W_{1,1} + B_1(T_2)\cdot W_{1,2} + B_1(T_3)\cdot W_{1,3} + B_1(T_4)\cdot W_{1,4} \tag{8.10a}$$

$$L_2 = B_2(T_1)\cdot W_{2,1} + B_2(T_2)\cdot W_{2,2} + B_2(T_3)\cdot W_{2,3} + B_2(T_4)\cdot W_{2,4} \tag{8.10b}$$

$$L_3 = B_3(T_1)\cdot W_{3,1} + B_3(T_2)\cdot W_{3,2} + B_3(T_3)\cdot W_{3,3} + B_3(T_4)\cdot W_{3,4} \tag{8.10c}$$

$$L_4 = B_4(T_1)\cdot W_{4,1} + B_4(T_2)\cdot W_{4,2} + B_4(T_3)\cdot W_{4,3} + B_4(T_4)\cdot W_{4,4} \tag{8.10d}$$

j: layer 1 layer 2 layer 3 layer 4

Because of the wide vertical spread of the weights, the radiance in each channel depends on the temperature at many levels, NOT just the one level at the peak weight value. But the radiative transfer equations are easy to solve; namely, given T and W, it is straight forward to calculate the radiances L, because we need only solve one equation at a time. I did this on a spreadsheet — the resulting radiances for each channel are in Table 8-5.

Now consider the more realistic **inverse** problem. To find the temperature T for each layer, knowing the radiance L from each sounder channel, you must solve the whole set of coupled equations (8.10a-d). These eqs. are nonlinear in temperature, due to the Planck function B. The number of equations equals the number of sounder channels. The number of terms in each equation depends on how finely discretized are the sounder profiles from Fig. 8.9,

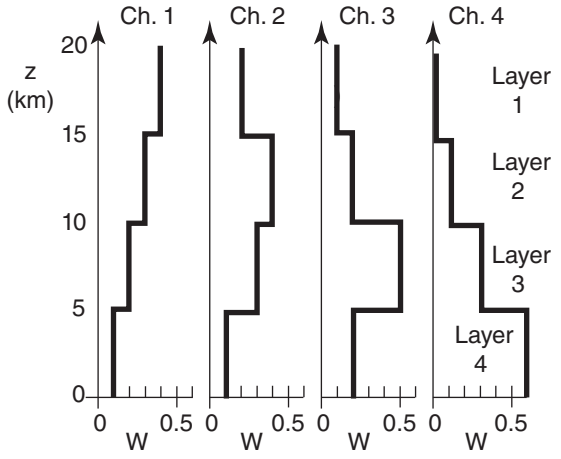

Figure 8.20
Idealized weighting functions for sounder channels Ch. 1 – 4 .

Table 8-4. Idealized sounder weights $W_{\lambda,j}$.

Vector	Channel (λ)	Layer in Atmosphere (j)			
		1 (top)	2	3	4 (bottom)
A	1	0.4	0.3	0.2	0.1
B	2	0.2	0.4	0.3	0.1
C	3	0.1	0.2	0.5	0.2
D	4	0	0.1	0.3	0.6

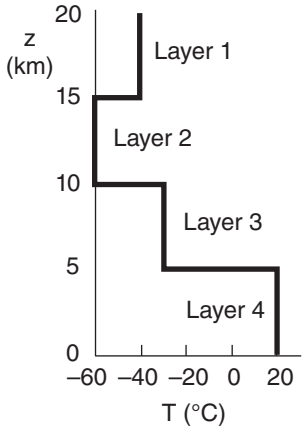

Figure 8.21
Hypothetical atmospheric temperature profile.

Table 8-5. Solution of the forward radiative transfer equation for the 4-layer illustrative atmosphere. The actual wavelengths λ for each channel were copied from Table 8-3.

Channel	λ (μm)	L ($W \cdot m^{-2} \cdot \mu m^{-1} \cdot sr^{-1}$)
1	14.7	2.85
2	14.4	2.87
3	14.0	3.64
4	13.7	5.40

Solved Example
Given a 4-channel sounder with weighting functions in Fig. 8.20 & Table 8-4. The satellite observed radiances are: $L_1 = 2.85$, $L_2 = 2.87$, $L_3 = 3.64$, & $L_4 = 5.4$ W·m^{-2} ·μm^{-1} ·sr^{-1} . Retrieve the temperature sounding.

Solution:
Given: *L(obs)* above; weights *W* from Table 8-4.
Find: Temperatures T_1 to T_4 (K), where $()_1$ is top layer.

I did this manually by trial and error on a spreadsheet — a bit tedious, but it worked.

• First, guess a starting sounding of *T(guess)* = –20°C everywhere (= 253K). See Table 8-6.
• Use eqs. (8.10) to compute radiances *L(guess)* for each channel.
• For Ch.1: $error^2_1 = (L_{1\ guess} - L_{1\ obs})^2$; etc. for Ch.2-4.
• Compute *Sum of error*^{2} = $error^2_1 + error^2_2$ + etc.
This initial total error was very large (= 3.7255).
• Experiment with different values of T_4 (temperature of layer 4) to find the "best" value that gives the least *Sum of error*^{2} so far. Then, keeping this "best" T_4 value, experiment with T_3 , finding its best value. Proceed similarly for layers 2 & 1. This completes iteration 1, as shown in Table 8-6.
• Keeping the best T_1 through T_3, experiment with T_4 again — you will find a different "best" value. Then do layers 3, 2, & 1 in succession. This ends iteration 2.
• Keep iterating for layers 4, 3, 2, 1. Boring. But each time, the *Sum of error*^{2} becomes less and less.

I eventually got tired and gave up. The answer is *T(final guess)* in Table 8-6.

Check: The actual *T* is given in Fig. 8.21, & listed here:

Height:	1 (top)	2	3	4 (bot.)
T (actual)	–40	–60	–30	+20
T (final guess)	**–45**	**–50.1**	**–33.6**	**+20.1**

Discussion: Not a perfect answer, which we know only because this exercise was contrived from an earlier illustration where we knew the actual temperature.

Why was it not perfect? It was very difficult to get the temperatures for layers 1 and 2 to converge to a stable solution. Quite a wide range of temperature values for these layers gave virtually the same error, so it was difficult to find the best temperatures. This is partly related to the close similarity in weighting functions for Channels 1 and 2, and the fact that they had large spread over height with no strong peak in any one layer. The radiances from these two channels are not independent of each other, resulting in a solution that is almost singular (not well behaved in a mathematical sense; not allowing a solution).

These difficulties are typical. See the "Focus Box" on the next page.

Table 8-6. Approximate solution to the Solved Ex. inverse problem. *T* (°C) is air temperature. *L* (W·m^{-2}·μm^{-1}·sr^{-1}) is radiance. Error = *L(obs) – L(guess).*

Height:	1 (top)	2	3	4 (bot.)
T (initial guess)	–20	–20	–20	–20
T (1st iteration)	–32.9	–42.9	–43.3	+2.5
T (final guess)	**–45**	**–50.1**	**–33.6**	**+20.1**

Channel:	1	2	3	4
L (obs)	2.85	2.87	3.64	5.40
L (from T initial guess)	3.70	3.78	3.88	3.95
error^2	0.7189	0.8334	0.0591	2.114
sum of error^2	3.7255			
L (from T final guess)	2.84	2.93	3.60	5.39
error^2	0.00009	0.00367	0.00155	0.00019
sum of error^2	0.0055			

which is related to the number of retrieval altitudes. From Retrieval Corollary 1 there is little value to retrieve more altitudes than the number of sounder channels. For example, the current GOES satellite has 19 channels; hence, we need to solve a coupled set of 19 equations, each with 19 nonlinear terms.

Solving this large set of coupled nonlinear equations is tricky; many different methods are used by government forecast centers and satellite institutes. Here is a simple approach that you can solve on a spreadsheet, which gives an approximate solution:

Start with an initial guess for the temperature of each layer. The better the first guess, the quicker you will converge toward the best answer. Use those temperatures to solve the much easier forward problem; namely, calculate the radiances L_λ from each eq. (8.10) separately. Calculate the squared error ($L_{\lambda\ calc} - L_{\lambda\ obs}$)^2 between the calculated radiances and the observed radiances from satellite for each channel, and then sum the errors to get an overall measure of the quality of the guessed temperature sounding.

Next, try to reduce the overall error by modifying the temperature guesses. For example, vary the guessed temperature for only one atmospheric layer, until you find the temperature that gives the least total error. Then do the same for the next height, and continue doing this for all heights. Then repeat the whole process, from first height to last height, always seeking the minimum error. Keep repeating these steps (i.e., keep **iterating**), until the total error is either zero, or small enough (considering errors in the measured radiances).

Some of the difficulties in sounding retrievals are listed in the Focus Box below. In spite of these difficulties, satellite-retrieved soundings are steadily improving, and make an important positive contribution to weather-forecast quality.

FOCUS • Satellite Retrieval Difficulties

- Radiance is an average from a deep layer, often overlapping with other layers.
- Radiance observations (in different channels) are not independent of each other.
- It is difficult to separate the effects of temperature and water-vapor variations in radiance signal.
- There is not a unique relationship between the spectrum of outgoing radiance and atmospheric temperature and humidity profiles.
- Temperatures are nonlinearly buried within the Planck function (but linear approximations are often used).
- Radiance observations have errors, caused by instrument errors, sampling errors, interference by clouds, and errors in the estimation of the weighting functions.
- Because of all these factors, there are an infinite number of temperature profiles that all satisfy the observed radiances within their error bars. Thus, statistical estimates must be used.
- To help pick the best profile, a good first guess and boundary conditions are critical. (**Retrieval Corollary 3: The retrieved profile looks more like the first guess than like reality.**)
- Satellite-retrieved soundings are most useful in regions (such as over the oceans) lacking other in-situ observations, but in such regions it is difficult to provide a good first guess. Often numerical weather forecasts are used to estimate the first guess, but such forecasts usually deviate quite significantly from reality over ocean data-voids.

BEYOND ALGEBRA • Info Projection

By representing weighting functions as vectors, inner (dot •) products show how much information from one vector is contained in (projected on) the other vectors. This helps demonstrate satellite Retrieval Corollary 2: The amount of retrieved info can be less than the number of weighting functions.

To illustrate, consider a 2-layer atmosphere and let each height represent an orthogonal axis in 2-D space. The discrete weight values at each height within any one weighting function give corresponding coordinates for that vector in the 2-D space.

For example, row 1 of the Fig. at right shows weighting functions for two channels, *A* and *B*, which are represented as vectors in the last Fig. of that row. For this special case of non-overlapping weighting functions, *A* and *B* give completely independent

(continues in the next column)

BEYOND ALGEBRA • Info Projection *(continuation)*

pieces of info, as indicated by the orthogonal vectors. The total information value = 2.

Row 2 of the Fig illustrates two identical weighting functions. Their vector representations perfectly coincide in the 2-D space. While the one weighting function gives us information, the second function tells us nothing new. Thus, total info value = 1.

Row 3 of the Fig. shows two different, but broadly overlapping, weighting functions. When plotted in vector space, we see that much of *B* projects onto *A*. Namely, much of *B* tells us nothing new. The only new contribution from vector *B* is the component that is orthogonal to *A*. For this example, only 30% of *B* gives new info (B_{new}); therefore, the total info value is 1.3 (= 1.0 from *A* + 0.3 from *B*).

In a sum of squares sense, the fraction of vector *B* = (W_{B1}, W_{B2}, W_{B3}, ...) that is NOT explained by (i.e., not projected onto) vector *A* = (W_{A1}, W_{A2}, W_{A3}, ...) is:

$$f = 1 - \frac{(A \bullet B)^2}{|A|^2 \ |B|^2} = 1 - \frac{(\Sigma_j \ W_{A,j} \ W_{B,j})^2}{(\Sigma_j \ W_{A,j}^2)(\Sigma_j \ W_{B,j}^2)} \qquad (8.11)$$

For higher-order vector spaces, we can use (8.11) to successively find the fraction of vector *C* that provides new info; namely, the portion of *C* that is orthogonal both to *A* and to the new-info part of *B*.

The vector representing the new-info part of *B* (the portion of *B* not projecting on *A*) is:

$$B_{new} = B_{\perp A} = B - \frac{(A \bullet B)}{|A|^2} A \qquad (8.12)$$

Using this info projection method on the weights of Fig. 8.20 (with vectors *A* to *D* identified in Table 8-4) give: *A*: 1 , B_{new}: 0.19 , $C_{additional\ contrib.\ to\ Bnew}$ = 0.267 , C_{new} = 0.258, $D_{contrib.\ to\ Bnew}$ = 0.115 , $D_{contrib.\ to\ Cnew}$ = 0.303 , D_{new} = 0.419 .

The total info value sums to **2.55**. Thus, the 4 weighting functions give fewer than 4 independent pieces of info about the temperature profile.

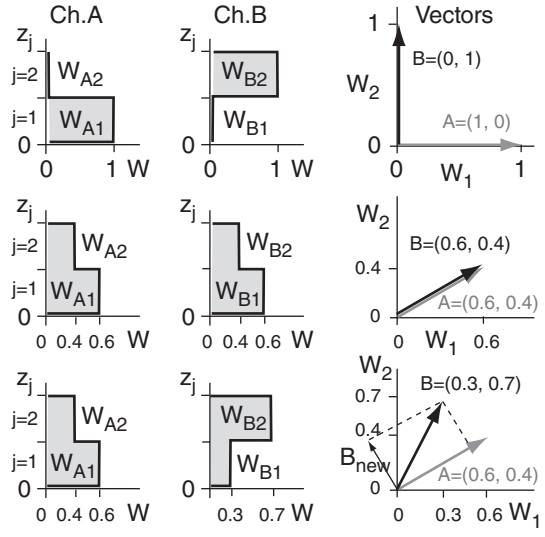

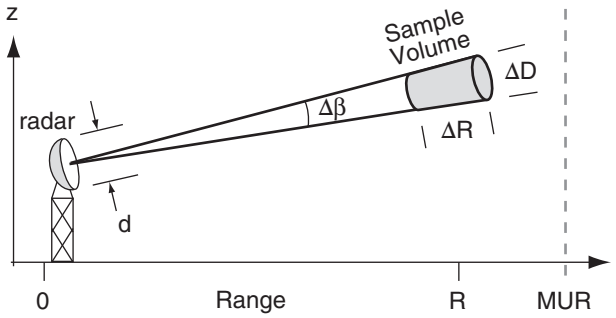

Figure 8.22
Radar beam. MUR is maximum unambiguous range.

Solved Example
Given a 10 cm wavelength radar with a 9 m diameter antenna dish, find the beamwidth.

Solution:
Given: $\lambda = 10$ cm $= 0.1$ m , $d = 9$ m.
Find: $\Delta\beta = ?°$

Use eq. (8.13): $\Delta\beta = (71.6°)\cdot(0.1\text{m})/(9\text{m}) =$ **0.8°**

Check: Units OK. Physics OK. Reasonable value.
Discussion: This large dish and wavelength are used for the USA WSR-88D operational weather radars.

Solved Example
Find the round-trip travel time to a target at R=20 km.

Solution:
Given: $R = 20$ km $= 2\text{x}10^4$ m, $c = 3 \text{ x } 10^8$ m/s.
Find: $t = ?$ μs

Rearrange eq. (8.16): $t = 2\,R\,/\,c$
$t = 2 \cdot (2\text{x}10^4\text{m}) \,/\, (3\text{x}10^8\text{m/s}) = 1.33\text{x}10^{-4}$ s = **133 μs**

Check: Units OK. Physics OK.
Discussion: The typical duration of an eye blink is 100 to 200 ms. Thus, the radar pulse could make 1000 round trips to 20 km in the blink of an eye.

WEATHER RADARS

Fundamentals

Weather radars are active sensors that emit pulses of very intense (250 - 1000 kW) microwaves generated by magnetron or klystron vacuum tubes. These transmitted pulses, each of $\Delta t = 0.5$ to 10 μs duration, are reflected off a parabolic **antenna dish** that can rotate and tilt, to point the train of pulses toward any azimuth and elevation angle in the atmosphere. **Pulse repetition frequencies** (PRF) are of order 50 to 2000 pulses per second.

The microwaves travel away from the radar at the speed of light through the air ($c \approx 3\text{x}10^8$ m/s), focused by the antenna dish along a narrow beam (Fig. 8.22). The angular thickness of this beam, called the **beamwidth** $\Delta\beta$, depends on the wavelength λ of the microwaves and the diameter (d) of the parabolic antenna:

$$\Delta\beta = a\cdot\lambda/d \qquad (8.13)$$

where $a = 71.6°$. Larger-diameter antennae can focus the beam into narrower beamwidths. For many weather radars, $\Delta\beta < 1°$.

The volume sampled by any one pulse is shaped like a slightly tapered cylinder (i.e., the frustum of a cone; Fig. 8.22). Typical pulse lengths ($c\cdot\Delta t$) are 300 to 500 m. However, the sampled length ΔR is half the pulse length, because of the round trip the energy must travel in and out of the sample volume.

$$\Delta R = c\cdot\Delta t/2 \qquad (8.14)$$

The diameter (ΔD) is:

$$\Delta D = R\cdot\Delta\beta \qquad (8.15)$$

for beamwidth $\Delta\beta$ in radians (= degrees $\cdot\,\pi/180°$). $\Delta D \approx 0.1$ km at close range (R), and increases to 10 km at far range. Thus, the resolution of the radar decreases as range increases.

A very small amount (10^{-5} to 10^{-15} W) of the transmitted energy is **scattered** back towards the radar when the microwave pulses hit objects such as **hydrometeors** (rain, snow, hail), insects, birds, aircraft, buildings, mountains, and trees. The radar dish collects these weak **returns** (**echoes**) and focuses them onto a detector. The resulting signal is amplified and digitally processed, recorded, and displayed graphically.

The **range** (radial distance) R from the radar to any target is easily calculated by measuring the round-trip time t between transmission of the pulse and reception of the scattered signal:

$$R = c \cdot t/2 \qquad \bullet(8.16)$$

Also, the azimuth and elevation angles to the target are known from the direction the radar dish was pointing when it sent and received the signals. Thus, there is sufficient information to position each target in 3-D space within the volume scanned.

Weather radar cannot "see" each individual rain or cloud drop or ice crystal. Instead, it sees the average energy returned from all the hydrometeors within a finite size pulse subvolume. This is analogous to how your eyes see a cloud; namely, you can see a white cloud even though you cannot see each individual cloud droplet.

Weather radars look at three characteristics of the returned signal to help detect storms and other conditions: **reflectivity**, **Doppler shift**, and **polarization**. These will be explained in detail, after first covering a few more radar fundamentals.

Maximum Range

The maximum range that the radar can "see" is limited by both the **attenuation** (absorption of the microwave energy by intervening hydrometeors) and pulse-repetition frequency. In heavy rain, so much of the radar energy is absorbed and scattered that little can propagate all the way through (recall Beer's Law from the Radiation chapter). The resulting **radar shadows** behind strong targets are "blind spots" that the radar can't see.

Even with little attenuation, the radar can "listen" for the return echoes from one transmitted pulse only up until the time the next pulse is transmitted. For those radars where the microwaves are generated by klystron tubes (for which every pulse has exactly the same frequency, amplitude, and phase), any echoes received after this time are erroneously assumed to have come from the second pulse. Thus, any target greater than this **maximum unambiguous range** (**MUR**, or R_{max}) would be erroneously displayed a distance R_{max} closer to the radar than it actually is (Fig. 8.35). MUR is given by:

$$R_{max} = c \;/\; [\, 2 \cdot PRF \,] \qquad \bullet(8.17)$$

Magnetron tubes produce a more random signal that varies from pulse to pulse, which can be used to discriminate between subsequent pulses and their return signals, thereby avoiding the MUR problem.

Scan and Display Strategies

Modern weather radars are programmed to automatically sweep 360° in azimuth α, with each successive scan made at different elevation angles ψ (called **scan angles**). For any one elevation angle, the radar samples along the surface of a cone-shaped region of air (Fig. 8.23). When all these scans are merged into one data set, the result is called a **volume scan**. The radar repeats these volume scans roughly every 5 to 10 minutes to sample the air around the radar.

Data from volume scans can be digitally sliced and displayed on computer in many forms. Animations of these displays over time are called **radar loops**. Typical 2-D displays are:

Solved Example

A 5 cm wavelength radar with 5 m diameter antenna dish transmits 1000 pulses per second, each pulse lasting 1 μs. (a) What are the sample-volume dimensions for a pulse received 100 μs after transmission. (b) Is the range to this sample volume unambiguous?

Solution:

Given: $\lambda = 5$ cm, $d = 5$ m, $PRF = 1000$/s,
$\Delta t = 1$ μs, $t = 100$ μs.

Find: (a) ΔR = ? m, and ΔD = ? m. (b) R_{max} = ? km.

(a) Use eq. (8.14): $\Delta R = (3\text{x}10^8\text{m/s})\cdot(10^{-6}\text{s})/2 =$ **150 m**.
To use eq. (8.15) for ΔD, we first need R and $\Delta\beta$.
From eq. (8.13): $\Delta\beta = (71.6°)\cdot(0.05\text{m})/(5\text{m}) = 0.72°$
From eq. (8.16): $R = (3\text{x}10^8\text{m/s})\cdot(10^{-4}\text{s})/2 = 15$ km.
Use eq. (8.15): $\Delta D = (15000\text{m})\cdot(0.72°)\cdot\pi/(180°) =$ **188 m**.

(b) Use eq. (8.17): $R_{max} = (3\text{x}10^8\text{m/s})/[2\cdot1000/\text{s}] = 150$km
But $R = 15$ km from (a).
Yes, range IS unambiguous because $R < R_{max}$.

Check: Units OK. Physics OK.
Discussion: If the range to the rain shower had been $R = 160$ km, then the target would have appeared on the radar display at an erroneous range of $R - R_{max} = 160 - 150$ km = 10 km from the radar, and would be superimposed on any echoes actually at 10 km range.

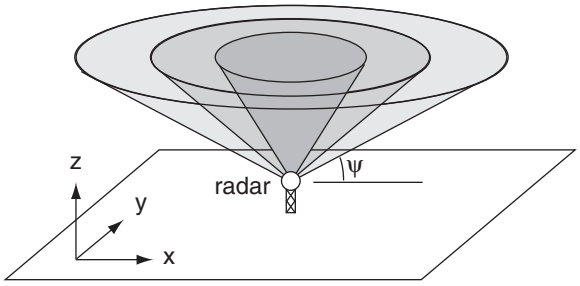

Figure 8.23
Scan surfaces at different elevation angles ψ .

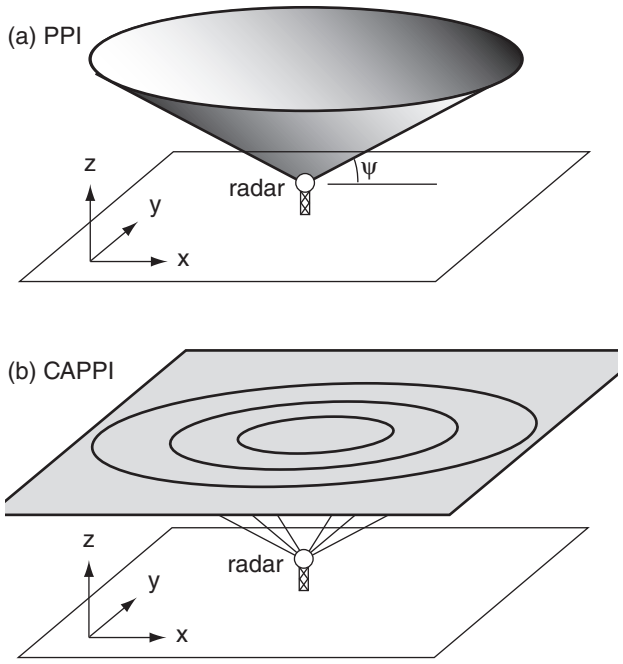

Figure 8.24
(a) Plan-Position Indicator (PPI) display. (b) Constant Altitude Plan Position Indicator (CAPPI) display.

- **PPI** (**plan position indicator**), which shows the radar echoes around 360° azimuth, but at only one elevation angle. Namely, this data is from a cone that spans many altitudes (Fig. 8.24a). These displays are often superimposed on background maps showing towns, roads and shorelines.

- **CAPPI** (**constant-altitude plan position indicator**), which gives a horizontal slice at any altitude (Fig. 8.24b). These displays are also superimposed on background maps (Fig. 8.26). At long ranges, the CAPPI is often allowed to follow the PPI cone from the lowest elevation-angle scan.

- **RHI** (**range-height indicator**, see Fig. 8.25a), which is a vertical slice along a fixed azimuth (α) line (called a **radial**) from the radar. It is made by physically keeping the antenna dish pointed at one azimuth while stepping the elevation angle up and down.

- **AVCS** (**arbitrary vertical cross section**) which gives a vertical slice in any horizontal direction through the atmosphere (Fig. 8.25b).

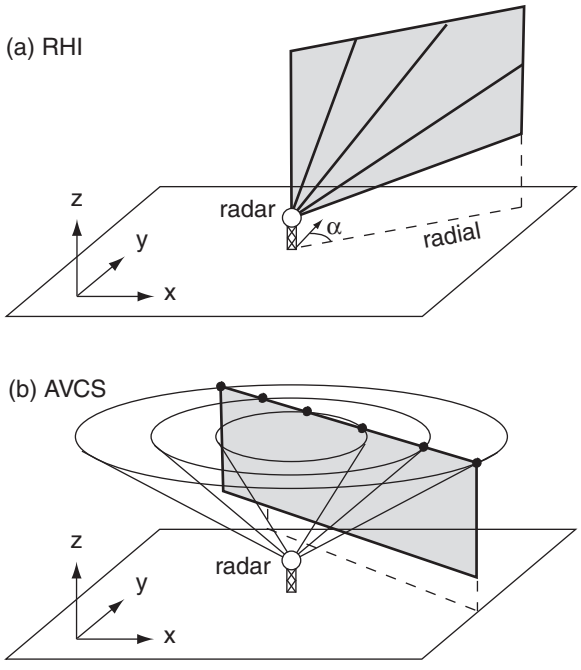

Figure 8.25
(a) Range Height Indicator (RHI) display. (b) Arbitrary Vertical Cross Section (AVCS) display.

Radar Bands

In the microwave portion of the electromagnetic spectrum are wavelength (λ) bands that have been assigned for use by radar (Fig. 8.4d). Each band is given a letter designation:

- **L band**: λ = 15 to 30 cm. Used in air traffic control and to study **clear-air turbulence** (**CAT**).
- **S band**: λ = 7.5 to 15 cm. Detects precipitation particles, insects, and birds. Long range (roughly 500 km) capabilities, but requires a large (9 m diameter) antenna dish.
- **C band**: λ = 3.75 to 7.5 cm. Detects precipitation particles and insects. Shorter range (roughly 250 km because the microwave pulses are more quickly attenuated by the precipitation), but requires less power and a smaller antenna dish.
- **X band**: λ = 2.5 to 3.75 cm. Detects tiny cloud droplets, ice crystals and precipitation. Large attenuation; therefore very short range. The radar sensitivity decreases inversely with the 4^{th} power of range.
- **K band** is split into two parts:
  Ku band: λ = 1.67 to 2.5 cm
  Ka band: λ = 0.75 to 1.11 cm.
  Detects even smaller particles, but has even shorter range. (The gap at 1.11 to 1.67 cm is due to

very strong absorption by a water-vapor line, causing the atmosphere to be opaque at these wavelengths; see Fig. 8.4d).

The US National Weather Service's nationwide network of **NEXRAD** (Next Generation Radar) Weather Surveillance Radars (**WSR-88D**) uses the S band (10 cm) to detect storms and estimate precipitation. The Canadian Meteorological Service uses C band (5 cm) radars. Some North American TV stations also have their own C-band weather radars. Europe is moving to a C-band standard for weather radars, although some S band radars are also used in Spain. Weather-avoidance radars on board commercial aircraft are X band, to help alert the pilots to stormy weather ahead. Police radars include X and K bands, while microwave ovens use S band (12.2 cm). All bands are used for weather research.

Beam Propagation

A factor leading to erroneous signals is **ground clutter**. These are undesired returns from fixed objects (tall towers, trees, buildings, mountains). Usually, ground clutter is found closest to the radar where the beam is still low enough to hit objects, although in mountainous regions ground clutter can occur at any range where the beam hits a mountain. Although ground-clutter returns are often strong because these targets are large, the fact that most of them don't move allows them to be filtered out. However, swaying trees and moving traffic on a highway can confuse some ground-clutter filters.

In a vacuum, the radar pulses would propagate at the speed of light in a straight line. However, in the atmosphere, the denser and colder the air, the slower the speed. A measure of this speed reduction is the **index of refraction**, n:

$$n = c_o \,/\, c \qquad \bullet(8.18)$$

where c_o = 299,792,458 m/s is the speed of electromagnetic radiation in a vacuum, and c is the speed in air. The slowdown is very small, giving index of refraction values on the order of 1.000325.

To focus on this small change, a new variable called the **refractivity,** N, is defined as

$$N = (n - 1) \times 10^6 \qquad \bullet(8.19)$$

For example, if n = 1.000325, then N = 325. For radio waves, including microwaves:

$$N = a_1 \cdot \frac{P}{T} - a_2 \cdot \frac{e}{T} + a_3 \cdot \frac{e}{T^2} \qquad \bullet(8.20)$$

where P is atmospheric pressure at the beam location, T is air temperature (in Kelvin), e is water va-

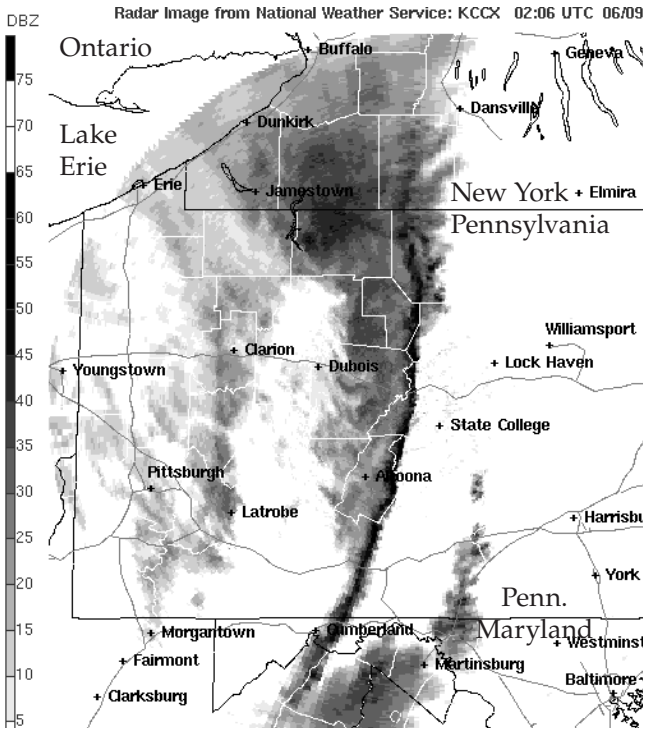

Figure 8.26
CAPPI display of radar reflectivity (related to rainfall intensity) of a violent squall line of thunderstorms (dark curved line through center of image) sweeping across Pennsylvania in 2003. [Courtesy of the US National Weather Service.]

Solved Example

Find the refractivity and speed of microwaves through air of pressure 90 kPa, temperature 10°C, and relative humidity 80%.

Solution:

Given: P = 90 kPa, T = 10°C = 283 K, RH = 80%

Find: N (dimensionless) and c (m/s)

First, convert RH into vapor pressure. Knowing T, get the saturation vapor pressure from Table 4-1: e_s = 1.233 kPa. Then use eq. (4.14): $e = RH \cdot e_s$ = 0.80·(1.233 kPa). e = 0.986 kPa

Next, use P, T, and e in eq. (8.20):

N= (776.89 K/kPa)·(90kPa)/(283K)
– (63.938 K/kPa)·(0.986kPa)/(283K)
+ (3.75463x10^6 K^2/kPa)·(0.986kPa)/(283K)^2
N = 247.067 – 0.223 + 46.224 = **293.068**

Solve eq. (8.18) for c, and plug in n from (8.19):

$c = c_o \,/\, [1 + N\text{x}10^{-6}]$ = (299,792,458 m/s) / 1.000293

c = **299,704,624.2 m/s**

Check: Units OK. Physics OK.

Discussion: The military carefully monitors and predicts vertical profiles of refractivity to determine whether the signal from their air-defense radars would get ducted or trapped, which would prevent them from detecting enemy aircraft sneaking in above the duct.

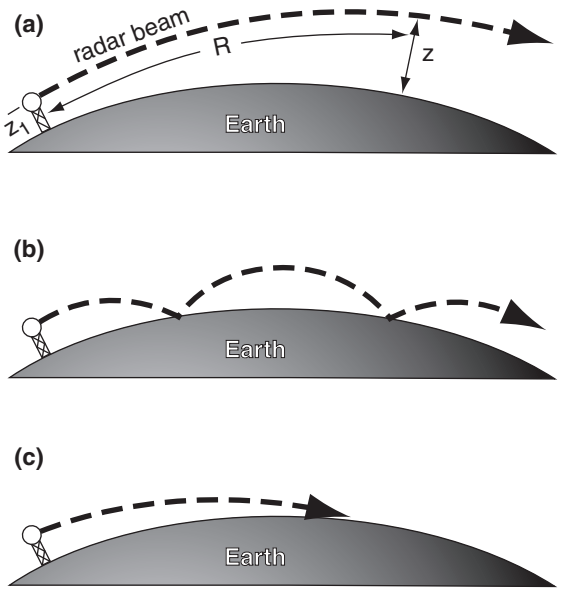

Figure 8.27
(a) Standard refraction of radar beam centerline in Earth's atmosphere. (b) Ducting or trapping over a smooth sea-surface. (c) Trapping over a rough surface.

Solved Example(§)

For a radar on a 10 m tower, plot the centerline height of the beam vs. range for standard refraction, for a 1° elevation angle.

Solution:
Given: $\Delta N/\Delta z = -39$ N/km, $z_1 = 10$ m $= 0.01$ km,
$R_o = 6371$ km
Find: z (km) vs. R (km)

$\Delta N/\Delta z = -39$. Thus $\Delta n/\Delta z = -39\text{x}10^{-6}$ km^{-1} .
Use eq. (8.21):
$R_c = (6371 \text{ km}) \,/\, [1+(6356.766 \text{ km})(-39\text{x}10^{-6} \text{ km}^{-1})]$
$= (6371 \text{ km}) \cdot 1.33 = 8473$ km
Use eq. (8.22): $z = 0.01$ km $-$ 8473 km
$+ [\, R^2 + (8473 \text{ km})^2 + 2R\cdot(8473 \text{ km})\cdot\sin(1°)\,]^{1/2}$
For example, $z =$ **2.35 km** at $R = 100$ km. Using a spreadsheet for many different R values gives:

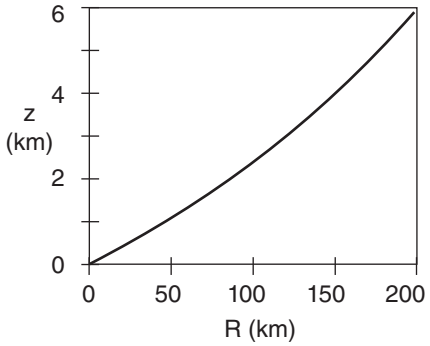

Check: Units OK. Physics OK. Graph reasonable.
Discussion: Why does the line curve up with increasing range? Although the radar beam bends downward, the Earth's surface curves downward faster.

por pressure, $a_1 = 776.89$ K/kPa, $a_2 = 63.938$ K/kPa, and $a_3 = 3.75463\text{x}10^6$ K^2/kPa. In the first term on the RHS, P/T is proportional to air density, according to the ideal gas law. The other two terms account for the polarization of microwaves by water vapor (polarization is discussed later). The parameters in this formula have been updated to include current levels of CO_2 (order of 375 ppm) in the atmosphere.

Although small, the change in propagation speed through air is significant because it causes the microwave beam to **refract** (bend) toward the denser, colder air. Recall from chapter 1 that density decreases nearly exponentially with height, which results in a vertical gradient of refractive index $\Delta n/\Delta z$. This causes microwave beams to bend downward with a radius of curvature R_c of

$$R_c = \frac{R_o}{1 + R_o\cdot(\Delta n / \Delta z)} = k_e \cdot R_o \qquad (8.21)$$

where $R_o = 6371$ km is the average Earth radius.

In the bottom part of the atmosphere, the vertical gradient of refractive index is roughly $\Delta n/\Delta z = -39\text{x}10^{-6}$ km^{-1} (or $\Delta N/\Delta z = -39$ km^{-1}) in a standard atmosphere. The resulting **standard refraction** of the radar beam has a radius of curvature approximately 4/3 of the Earth's radius (Fig. 8.27a); namely, $k_e = 4/3$. The height z of the center of the radar beam above the Earth's surface at any slant range R along the beam can then be found from the **beam propagation equation**:

$$z = z_1 - R_c + \sqrt{R^2 + {R_c}^2 + 2R\cdot R_c\cdot\sin\psi} \qquad (8.22)$$

knowing the height z_1 of the radar above the Earth's surface, and the radar elevation angle ψ.

Superimposed on this first-order effect are second-order effects due to temperature and humidity variations that cause changes in refractivity gradient (Table 8-7). For example, when a cool humid boundary layer is capped by a hot dry temperature inversion, then conditions are right for a type of **anomalous propagation** called **superrefraction**. This is where the radar beam has a smaller radius of curvature than the Earth's surface, and thus will bend down toward the Earth.

With great enough superrefraction, the beam hits the ground and is absorbed and/or causes a ground-

Table 8-7. Radar beam propagation conditions.

$\Delta N/\Delta z$ (N/km)	Refraction
> 0	subrefraction
0 to –79	normal range
–39	standard refraction
–79 to –157	superrefraction
< –157	trapping or ducting

clutter return at large range if the Earth's surface is rough there (Fig. 8.27c). However, for smooth regions of the Earth's surface such as a waveless ocean, the beam can "bounce" repeatedly, which is called **ducting** or **trapping** (Fig. 8.27b).

When cooler, moister air overlies warmer drier air, then **subrefraction** occurs, where the radius of curvature is larger than for standard refraction. This effect is limited by the fact that atmospheric lapse rate is rarely statically unstable over large depths of the mid and upper troposphere.

Reflectivity

The Radar Equation

Recall that the radar transmits an intense pulse of microwave energy with power P_T (≈ 750 kW for WSR-88D radars). Particles in the atmosphere scatter a miniscule amount of this energy back to the radar, resulting in a small received power P_R. The ratio of received to transmitted power is explained by the **radar equation**:

$$\left[\frac{P_R}{P_T}\right] = [b] \cdot \left[\frac{|K|}{L_a}\right]^2 \cdot \left[\frac{R_1}{R}\right]^2 \cdot \left[\frac{Z}{Z_1}\right] \qquad \bullet(8.23)$$

$$\begin{bmatrix}\text{relative}\\ \text{received}\\ \text{power}\end{bmatrix} = \begin{bmatrix}\text{equip–}\\ \text{ment}\\ \text{effects}\end{bmatrix} \cdot \begin{bmatrix}\text{atmos–}\\ \text{pheric}\\ \text{effects}\end{bmatrix} \cdot \begin{bmatrix}\text{range}\\ \text{inverse}\\ \text{square}\end{bmatrix} \cdot \begin{bmatrix}\text{target}\\ \text{reflect–}\\ \text{ivity}\end{bmatrix}$$

where each factor in brackets is dimensionless.

The most important parts of this equation are the **refractive-index magnitude** $|K|$, the range R between the radar and target, and the **reflectivity factor** Z. These are summarized below. The Focus Box has more details on the radar equation.

$|K|$ (dimensionless): Liquid drops are more efficient at scattering microwaves than ice crystals. $|K|^2 \approx 0.93$ for liquid drops, and $|K|^2 \approx 0.208$ for ice (assuming spherical ice particles of the same mass as the actual snow crystal).

R (km): Returned energy from more distant targets is weaker than from closer targets, as given by the inverse-square law (see Radiation chapter).

Z (mm^6/m^3): Larger numbers (N) of larger-diameter (D) drops in a given volume (Vol) of air will scatter more microwave energy. This **reflectivity factor** is given by:

$$Z = \frac{\sum^{N} D^6}{Vol.} \qquad \bullet(8.24)$$

where the sum is over all N drops, and where each drop could have a different D.

FOCUS • Deriving the Radar Equation

The radar transmits a burst of power P_T (W). As this pulse travels range R to a target drop, the energy flux (W/m^2) diminishes as it spreads to cover spherical surface area $4\pi R^2$, according to the inverse square law (see the Radiation chapter). But the parabolic antenna dish focuses the energy, resulting in antenna gain G relative to the normal spherical spread of energy. While propagating to the drop, some of the energy is lost along the way, as described by attenuation factor L_a. The net energy flux E_i (W/m^2) reaching the drop is $E_i = P_T \cdot G \,/\, (4\pi R^2 \cdot L_a)$ (R1)

If that incident "power per unit area" hits a drop that has **backscatter cross-sectional** area σ, then power P_{BS} (W) gets scattered in all directions:

$$P_{BS} = E_i \cdot \sigma \qquad \text{(R2)}$$

This miniscule burst of return power spreads to cover a spherical surface area, and is again attenuated by L_a while en route distance R back to the radar. The returning energy flux E_R (W/m^2) at the radar is

$$E_R = P_{BS} \,/\, (4\pi R^2 \cdot L_a) \qquad \text{(R3)}$$

Eq. (R3) is similar to (R1), except that the drop does not focus the energy, therefore there is no gain G.

But when this flux is captured by the antenna with area A_{ant} and focused with gain G onto a detector, the resulting received power per drop P_R' (W) is

$$P_R' = E_R \cdot A_{ant} \cdot G \qquad \text{(R4)}$$

The effective antenna area depends on many complex antenna factors, but the net result is:

$$A_{ant} = \lambda^2 \,/\, [8\pi \cdot \ln(2)] \qquad \text{(R5)}$$

The radar sample volume is much larger than a single drop, thus the total returned power P_R is the sum over N drops:

$$P_R = \sum^{N} P_R' \qquad \text{(R6)}$$

These N drops are contained in the sample volume Vol of air (Fig. 8.22). Assuming a cylindrical shape of length ΔR (eq. 8.14) and diameter ΔD (eq. 8.15), gives

$$Vol = \pi R^2 \cdot (\Delta\beta)^2 \cdot c \cdot \Delta t \,/\, 8 \qquad \text{(R7)}$$

where $\Delta\beta$ is beam width (radians), c is microwave speed through air, and Δt is the radar pulse duration.

For hydrometeor particle diameters D less than a third of the radar wavelength λ, the backscatter cross-section area σ is well approximated by a relationship known as **Rayleigh scattering**:

$$\sigma = \pi^5 \cdot |K|^2 \cdot D^6 \,/\, \lambda^4 \qquad \text{(R8)}$$

where $|K|$ is the **refractive index magnitude** of the drop or ice particle.

Combining these 8 equations, and using eq. (8.24) to define the reflectivity factor Z, gives the traditional form of the **radar equation**: (R9)

$$P_R = \left[\frac{c \cdot \pi^3}{1024 \cdot \ln(2)}\right] \cdot \left[\frac{P_T \cdot G^2 \cdot (\Delta\beta)^2 \cdot \Delta t}{\lambda^2}\right] \cdot \left[\left(\frac{|K|}{L_a \cdot R}\right)^2 \cdot Z\right]$$

P_R = [*constant*] · [*radar characteristics*] · [*atmos. char.*]

When the right side is multiplied by Z_1/Z_1 and rearranged into dimensionless groups, the result is the version of the radar equation shown as eq. (8.23).

Solved Example

For a 5 cm radar, the energy scattered from a 1 mm diameter drop is how much greater than that from a 0.5 mm drop?

Solution:
Given: $\lambda = 5$ cm, $D_1 = 0.5$ mm, $D_2 = 1$ mm
Find: $\sigma_{scat2} / \sigma_{scat1}$ (dimensionless)

For Rayleigh scattering [see Focus Box eq. (R8)]:
$\sigma_{scat2} / \sigma_{scat1} = (D_2/D_1)^6 = 2^6 = \underline{\mathbf{64}}$.

Check: Units OK. Physics OK.
Discussion: Amazingly large difference. Double the drop size and get 64 times the scattered energy.

Solved Example

WSR-88D radar detects a 40 dBZ rain shower 20 km from the radar, with no other rain detected. Transmitted power was 750 kW, what is the received power?

Solution:
Given: Echo = 40 dBZ, $R = 20$ km, $P_T = 750{,}000$ W, $|K|^2 = 0.93$ for rain (i.e., liquid), $b = 14{,}255$, $R_1 = 2.17\text{x}10^{-10}$ km for WSR-88D.
Find: $P_R = ?$ W
Assume: $L_a = 1.0$ (no attenuation), because there are no other rain showers between the radar and target.

Use eq. (8.27) and rearrange to solve for Z/Z_1 :
$Z/Z_1 = 10^{(dBZ/10)} = 10^{(40/10)} = 10^4$.

Use the radar equation (8.23): $P_R = (7.5\text{x}10^5\text{W})\cdot(14{,}255)\cdot[(0.93)\cdot(2.17\text{x}10^{-10}\text{km})/(20\text{km})]^2\}\cdot[10^4]$
$P_R = \underline{\mathbf{1.09 \text{ x } 10}}^{-8}$ W .

Check: Units OK. Physics OK.
Discussion: With so little power coming back to the radar, very sensitive detectors are needed. WSR-88D radars can detect signals as weak as $P_R \approx 10^{-15}$ W.

Normal weather radars use the same parabolic antenna dish to receive signals as to transmit. But such an intense pulse is transmitted that the radar antenna electrically "rings" after the transmit impact for 1 μs, where this "ringing" sends strong power as a false signal back toward the receiver. To compensate, the radar must filter out any received energy during the first 1 μs before it is ready to detect the weak returning echoes from true meteorological targets. For this reason, the radar cannot detect meteorological echoes within the first 300 m or so of the radar.

Even when looking at the same sample volume of rain-filled air, the returned power varies considerably from pulse to pulse. To reduce this noise, the WSR-88D equipment averages about 25 sequential pulses together to calculate each smoothed reflectivity value that is shown on the radar display for each sample volume.

The other factors in the radar equation are:

$Z_1 = 1$ mm^6/m^3 is the **reflectivity unit factor**.

$R_1 = \text{sqrt}(Z_1 \cdot c \cdot \Delta t/\lambda^2)$ (8.25)
is a **range factor** (km), where c ≈ 3x10^8 m/s is microwave speed through air. For WSR-88D radar, wavelength λ = 10 cm and pulse duration is $\Delta t \approx 1.57$ μs, giving $R_1 \approx 2.17\text{x}10^{-10}$ km.

L_a is a dimensionless **atmospheric attenuation factor** ($L_a \geq 1$) accounting for one-way losses by absorption and scattering as the microwave pulse travels between the radar and the target drop. $L_a = 1$ means no attenuation, and increasing values of L_a imply increasing attenuation. For example, the signal returning from a distant rain shower is diminished (appears weaker than it actually is) if it travels through a nearby shower en route to the radar. If you don't know L_a, then assume $L_a \approx 1$.

$b = \pi^3 \cdot G^2 \cdot (\Delta\beta)^2/[1024 \cdot \ln(2)]$ (8.26)
is a dimensionless **equipment factor**. For WSR-88D, the antenna gain is $G \approx 45.5$ dB = 35,481 (dimensionless), and the beam width is $\Delta\beta \approx 0.95° = 0.0161$ radians, giving $b \approx 14{,}255$.

Of most interest to meteorologists is the reflectivity factor Z, because larger Z is usually associated with heavier precipitation. Because Z has such a wide range of values, the reflectivity is usually expressed as **decibels** (dB) of Z (namely, **dBZ**):

$$\text{dBZ} = 10 \cdot \log(Z/Z_1) \qquad \bullet(8.27)$$

where this is a common logarithm (base 10). Although dBZ is dimensionless, the suffix "dBZ" is added after the number (e.g., 35 dBZ).

dBZ can be calculated from radar measurements of P_R/P_T by using the log form of the radar eq.:

$$dBZ = 10\left[\log\left(\frac{P_R}{P_T}\right) + 2\log\left(\frac{R}{R_1}\right) - 2\log\left|\frac{K}{L_a}\right| - \log(b)\right] \qquad \bullet(8.28)$$

Although the R/R_1 term compensates for most of the decrease echo strength with distance, atmospheric attenuation L_a still increases with range. Thus dBZ still decreases slightly with increasing range.

Reflectivity or **echo intensity** is the term used by meteorologists for dBZ, and this is what is displayed in **radar reflectivity images**. Typical values are –28 dBZ for haze, –12 dBZ for insects in clear air, 25 to 30 dBZ in dry snow or light rain, 40 to 50 dBZ in heavy rain, and up to 75 dBZ for giant hail.

Rainfall Rate Estimated by Radar Reflectivity

A tenuous, but useful, relationship exists between rainfall rate, and radar echo intensity. Both increase with the number and size of drops in the air. However, this relationship is not exact. Complicating factors on the rainfall rate RR include the drop terminal velocity, partial evaporation of the drops while falling, and downburst speed of the air containing the drops. Complicating factors for the echo intensity include the bright-band effect (see next page), and unknown backscatter cross sections for complex ice-crystal shapes.

Nonetheless, an empirically tuned approximation can be found:

$$RR = a_1 \cdot 10^{(a_2 \cdot dBZ)} \qquad \bullet(8.29)$$

where $a_1 = 0.017$ mm/h and $a_2 = 0.0714$ dBZ^{-1} (both a_2 and dBZ are dimensionless) are the values for the USA WSR-88D radars. This same equation can be written as:

$$Z = a_3 \cdot RR^{a_4} \qquad (8.30)$$

where $a_3 = 300$, and $a_4 = 1.4$, for RR in mm/h and Z in mm^6/m^3. Equations such as (8.29) and (8.30) are called **Z-R relationships**.

Some displays of radar echo intensity use six discrete "**levels**", corresponding to descriptive **rainfall categories**. These are easier for the general public to understand than dBZ. The definitions of these levels with respect to dBZ are given in Fig. 8.28. Color-enhanced weather radar displays on TV show these six levels as different colors. Different countries use different thresholds for precipitation levels. For example, in Canada moderate precipitation is defined as 2.5 to 7.5 mm/h.

Z-R relationships can never be perfect, as is demonstrated here. Within an air parcel of mass 1 kg, suppose that $m_L = 5$ g of water has condensed and falls out as rain. If that 5 g is distributed equally among $N = 1000$ drops, then the diameter D of each drop is 2.12 mm, from:

$$D = \left[\frac{6 \cdot m_L}{\pi \cdot N \cdot \rho_{liq}} \right]^{1/3} \qquad (8.31)$$

where $\rho_{liq} = 10^3$ kg/m^3 is the density of liquid water. However, if the same mass of water is distributed among $N = 10{,}000$ droplets, then $D = 0.98$ mm. When these two sets of N and D values are used in eq. (8.24), the first scenario gives 10 times the reflectivity Z as the second, even though they have identical total mass of liquid water m_L and identical rainfall amount. Nonetheless, Z-R relationships are useful at giving a first approximation to rainfall rate.

Solved Example

What is the rainfall rate for an echo of 43 dBZ?

Solution

Given: echo = 43 dBZ
Find: RR = ? mm/h.

Use eq. (8.29):
$RR = (0.017\text{mm/h}) \cdot 10^{[0.0714(1/\text{dBZ}) \cdot 43\text{dBZ}]} =$ **19.9 mm/h**.

Check: Units & physics OK. Agrees with Fig. 8.28.
Discussion: This would be displayed as a level 3 echo on a radar display, corresponding to heavy rain. Pilots utilize intensity levels for flight planning. They try to avoid the intensity levels 3 and higher due to the chance of strong turbulence in thunderstorms.

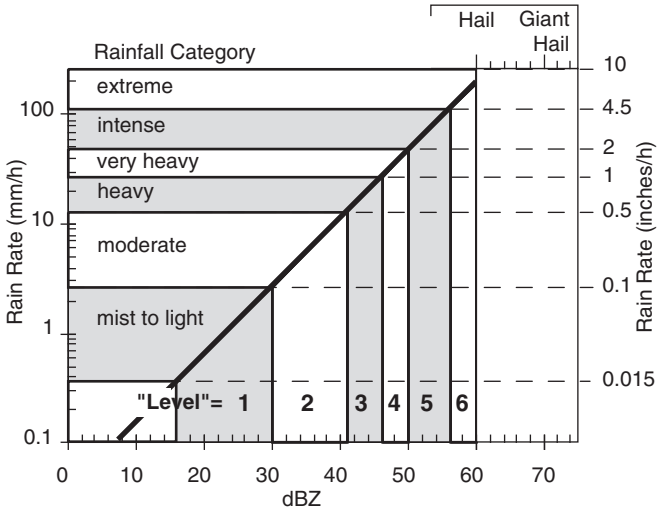

Figure 8.28
Rainfall intensity chart. (Approximate, because dBZ to Rain Rate depends on Z-R relationship.)

Solved Example

Air parcels A and B both have liquid-water mixing ratio 3 g/kg, but A has 1000 active liquid-water nuclei and B has 5,000. Compare the dBZ from both parcels.

Solution:
Given: $r_L = 3$ g/kg, $\rho_L = 10^3$ kg/m^3
$N_A = 1000$, $N_B = 5000$.
Find: dBZ_A and dBZ_B (dimensionless)
Assume air density is $\rho = 1$ kg/m^3. Assume *Vol.*=1 m^3
Assume equal size droplets form on each nucleus, so that $\Sigma D^6 = N \cdot D^6$.

Use eq. (8.31):
$D_A = [6 \cdot (0.003\text{kg}) / (\pi \cdot 1000 \cdot (10^3\ \text{kg/m}^3)]^{1/3}$
$= 0.00179$ m $= 1.79$ mm

(continues on next page)

Solved Example *(continuation)*

D_B=[6·(0.003kg)/(π·5000·(10^3 kg/m^3)]$^{1/3}$
= 0.00105 m = 1.05 mm

Use eq. (8.24), but using $N{\cdot}D^6$ in the numerator:
Z_A = 1000·(1.79 mm)^6 /(1 m^3) = 3.29x10^4 mm^6/m^3
Z_B = 5000·(1.05 mm)^6 /(1 m^3) = 6.70x10^3 mm^6/m^3

Use eq. (8.27):
dBZ_A = 10·log[(3.29x10^4 mm^6/m^3)/(1 mm^6/m^3)]
= **45.2 dBZ**
dBZ_B = 10·log[(6.70x10^3 mm^6/m^3)/(1 mm^6/m^3)]
= **38.3 dBZ**

Check: Units OK. Physics OK.
Discussion: Thus, the same amount of liquid water (3 g/kg) in each parcel would lead to substantially different radar reflectivities. This is the difficulty of *Z-R* relationships. But not all is lost -- the polarization radar section shows how more accurate rainfall estimates can be made using radar.

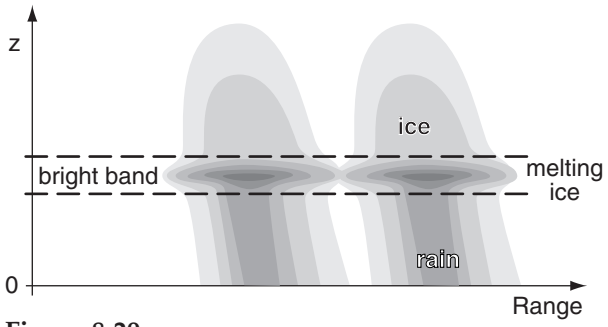

Figure 8.29
RHI sketch of the bright band in two precipitation cells.

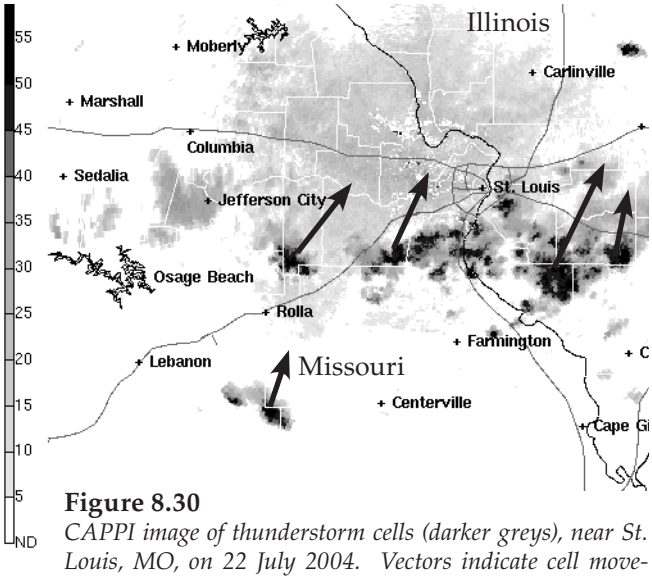

Figure 8.30
CAPPI image of thunderstorm cells (darker greys), near St. Louis, MO, on 22 July 2004. Vectors indicate cell movement. (Courtesy of the US NWS.)

Bright Band

Ice crystals scatter back to the radar only about 20% of the energy scattered by the same amount of liquid water (as previously indicated with the $|K|^2$ factor in the radar equation). However, when ice crystals fall into a region of warmer air, they start to melt, causing the solid crystal to be coated with a thin layer of water. This increases the reflectivity of the liquid-water-coated ice crystals by a factor of 5, causing a very strong radar return known as the **bright band.** Also, the wet outer coating on the ice crystals cause them to stick together if they collide, resulting in a smaller number of larger-diameter snowflake clusters that contribute to even stronger returns.

As the ice crystals continue to fall and completely melt into liquid drops, their diameter decreases and their fall speed increases, causing their drop density and resulting reflectivity to decrease. The net result is that the bright band is a layer of strong reflectivity at the melting level of falling precipitation. The reflectivity in the bright band is often 15 to 30 times greater than the reflectivity in the ice layer above it, and 4 to 9 times greater than the rain layer below it. Thus, Z-R relationships fail in bright-band regions.

In an RHI display of reflectivity (Fig. 8.29) the bright band appears as a layer of stronger returns. In a PPI display the bright band is donut shaped — a hollow circle of stronger returns around the radar, with weaker returns both inside and outside the circle.

Hail

Hail can have exceptionally high radar reflectivities, of order 60 to 75 dBZ, compared to typical maxima of 50 dBZ for heavy rain. Because hailstone size is too large for microwave Rayleigh scattering to apply, the normal Z-R relationships fail. Some radar algorithms diagnose hail for reflectivities > 40 dBZ at altitudes where the air is colder than freezing, with greater chance of hail for reflectivities ≥ 50 dBZ at altitudes where temperature ≤ –20°C.

Other Uses for Reflectivity Data

Radar reflectivity images are used by meteorologists to **identify storms** (thunderstorms, hurricanes, mid-latitude cyclones), track storm movement, find echo-top height and thunderstorm features, indicate likelihood of hail, and estimate rain rate and flooding potential. For example, Fig. 8.30 shows isolated thunderstorm cells, while Fig. 8.26 shows an organized squall line. The radar image typically presented by TV weather briefers is the reflectivity image.

Clear-air reflectivities from bugs can help identify cold fronts, dry lines, thunderstorm outflow (gust

fronts), sea-breeze fronts, and other boundaries (discussed later in this book). Weather radar can also track bird migration. Clear-air returns are often very weak, so radar **clear-air scan** strategies use a slower azimuth sweep rate and longer pulse duration to allow more of the microwave energy to hit the target and to be scattered back to the receiver.

Doppler Radar

Doppler weather radars can not only measure the intensity of rainfall by the amount of scattered microwave energy, they can also measure the speed of the droplet-laden air toward or away from the radar (i.e., **radial velocity**, see Fig. 8.31). This latter feature allows the radar to detect motions within storms that might be associated with tornadoes or damaging straight-line winds from gust fronts.

Radial Velocities

One way to measure radial velocity is to measure the frequency shift $\Delta\nu$ of the received signal compared to the transmitted frequency, ν. When the microwaves from the radar bounce off of droplet-laden air that is moving away from the radar, the frequency becomes slightly lower. Conversely, higher frequencies are found for air moving toward the radar. Such frequency shifts associated with moving targets are called **Doppler shifts**.

The magnitude of frequency shift is given by the Doppler equation:

$$|\Delta\nu| = \frac{2\cdot|M_r|}{\lambda} \qquad \bullet(8.32)$$

where M_r is the radial velocity of the air relative to the radar, and λ is the wavelength of the microwaves (e.g., λ = 10 cm for WSR-88D S-band radars). The wavelength and frequency are related by the speed of light $c = 3\text{x}10^8$ m/s according to:

$$\nu = c \,/\, \lambda \quad . \qquad \bullet(8.33)$$

However, the **frequency shift** is so miniscule that it is very difficult to measure (see solved example).

Solved Example

An S-band radar would measure what Doppler shift for a velocity of 100 m/s around a tornado?

Solution

Given: M_r = 100 m/s, assume λ = 10 cm for S-band.
Find: $\Delta\nu$ = ? s^{-1}
Use eq. (8.32): $\Delta\nu = [2\cdot(100\text{ m/s})] \,/\, (0.1\text{ m}) =$ **2000** s^{-1}
Check: Units OK. Physics OK.
Discussion: The original transmitted frequency (eq. 8.33) is: $\nu = c \,/\, \lambda = (3\text{x}10^8\text{ m/s}) \,/\, (0.1\text{ m}) = 3\text{x}10^9\ s^{-1}$. $\Delta\nu$ is less than one part per million compared to ν.

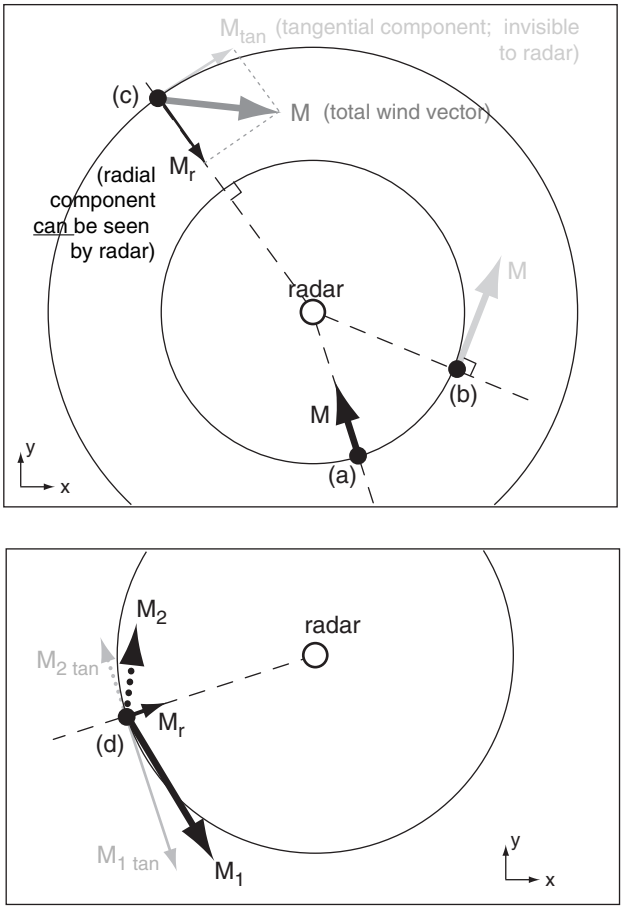

Figure 8.31

Illustration of which velocities can be seen by Doppler radar. For any location where you know the wind vector, mentally draw a circle (centered on the radar) that passes through the location, and draw a radial line (shown dashed in these figs.) from the radar to the location. The radar can see only the component of the wind vector along the radial line, and cannot see the component along the circle. Examples: (a) At point (a) the total wind vector M is along the radial line, hence the radar sees the whole wind. (b) At point (b) the total wind vector M is tangent to the circle, hence the radar sees zero wind there. (c) At point (c) the total wind vector M has a radial component that the radar sees, and a tangential component that is invisible. Hence, only a portion of the total wind is seen there.

Conversely, if you don't know the actual wind but have Doppler radar observations, beware that an infinite number of true wind vectors can create the radial component seen by the radar. For example, at point (d) two completely different wind vectors M_1 and M_2 have the same radial component M_r. Hence, the radar would give you only M_r but you would have no way of knowing the total wind vector. The solution to this dilemma is to have two Doppler radars (i.e., **dual Doppler***) at different locations that can both scan the same wind location from different directions.*

Science Graffito

"Treat people as if they were what they ought to be, and you help them to become what they are capable of being." – J. W. von Goethe.

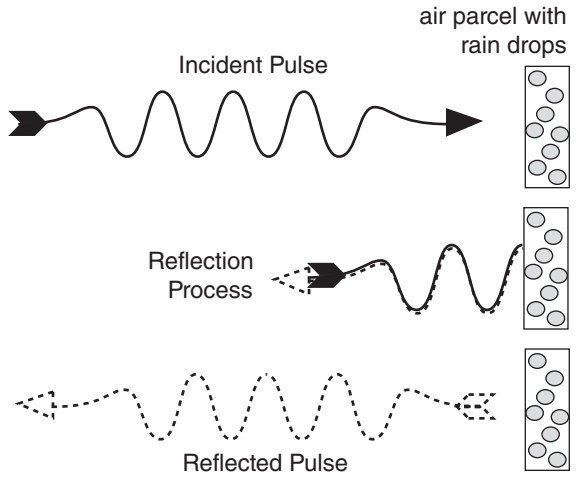

Figure 8.32
A pulse of microwaves scatters off a stationary, droplet-laden air parcel that coincides with the radar sample volume. The same shading (solid for incident pulse, dashed for reflected pulse) is used in the next two figures.

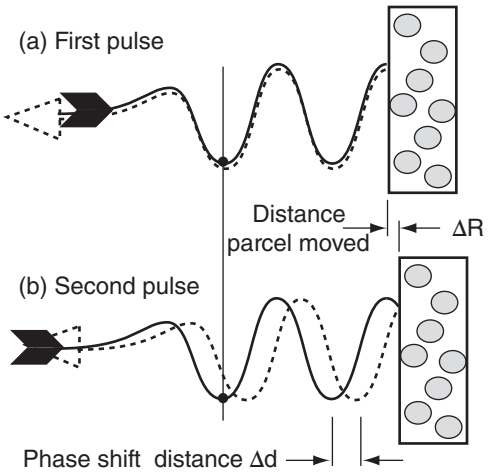

Figure 8.33
Phase shift distance is twice the distance moved by the air parcel.

Table 8-8. Display convention for Doppler velocities.

Sign of M_r	Radial Direction Relative to Radar	Display Color
Positive	AWAY	Red & Orange
Zero	(none)	White, Gray or Black
Negative	TOWARD	Blue & Green

Instead, Doppler radars detect air motion by measuring the **phase shift** of the microwaves. Consider a pulse of microwaves that scatter from a droplet-laden air parcel (Fig. 8.32). When that parcel is at any one location and is illuminated by a radar pulse, there is a measurable phase difference (difference in locations of the wave troughs) between the incident wave and the scattered wave. Fig. 8.33a illustrates a phase difference of zero; namely, the troughs coincide.

If the parcel has moved to a slightly different distance from the radar when the next pulse hits, then there will be a different phase shift compared to that of the first pulse (Fig. 8.33b). As illustrated, the phase shift Δd is just twice the radial distance ΔR that the air parcel moved. You can demonstrate this to yourself by drawing a perfect wave on a thin sheet of tracing paper, folding the paper horizontally a certain distance ΔR from the crest, and then comparing the distance Δd between incident and folded troughs or crests. Knowing the time between successive pulses (= 1/PRF), the radial velocity M_r is:

$$M_r = \Delta R \cdot \text{PRF} = \text{PRF} \cdot \Delta d / 2 \qquad (8.34)$$

Table 8-8 gives the display convention for PPI or CAPPI displays of Doppler radial velocities in North America. Slower speeds are sometimes displayed with less color saturation (lighter, paler, closer to white). The color convention is modeled after the astronomical "red shift" for stars moving away from Earth. In directions from the radar that are perpendicular to the mean wind, there is no radial component of wind (Fig. 8.31); hence, this appears as a white or light grey line (Fig. 8.38a) of zero radial velocity (called the **zero isodop**). In some countries, the zero isodop is displayed with finite width as a black "no-data" line, because the ground-clutter filter eliminates the slowest radial velocities.

Maximum Unambiguous Velocity

The phase-shift method imposes a **maximum unambiguous velocity** $M_{r\,max}$ the radar can measure, given by:

$$M_{r\,max} = \lambda \cdot \text{PRF} / 4 \qquad \bullet(8.35)$$

where λ is wavelength. Fig. 8.34 shows the reason for this limitation. From the initial pulse to the second pulse, if the air parcel moved a quarter wavelength ($\lambda/4$) AWAY from the radar (Fig. 8.34b), then the scattered wave is a half wavelength out of phase from the incident wave. However, if the air parcel moved a quarter wavelength TOWARD the radar (Fig. 8.34c), then the phase shift is also half a wave-

length. Namely, the AWAY and TOWARD velocities give exactly the same phase-shift signal at this critical speed, and the radar phase detector cannot distinguish between them.

Velocities slightly faster than $M_{r\,max}$ AWAY from the radar erroneously appear to the phase detector as fast velocities TOWARD the radar. Similarly, velocities faster than $M_{r\,max}$ TOWARD the radar are erroneously folded back as fast AWAY velocities. The false, displayed velocities $M_{r\,false}$ are:
For $M_{r\,max} < M_r < 2M_{r\,max}$:

$$M_{r\,false} = M_r - 2\,M_{r\,max} \qquad (8.36a)$$

For $(-2M_{r\,max}) < M_r < (-M_{r\,max})$:

$$M_{r\,false} = M_r + 2\,M_{r\,max} \qquad (8.36b)$$

Speeds greater than $2|M_{r\,max}|$ fold twice.

For greater max velocities $M_{r\,max}$, you must operate the Doppler radar at **greater** PRF (see eq. 8.35). However, to observe storms at greater range R_{max}, you need **lower** PRF (see eq. 8.17). This trade-off is called the **Doppler dilemma** (Fig. 8.35). Operational Doppler radars use a compromise PRF.

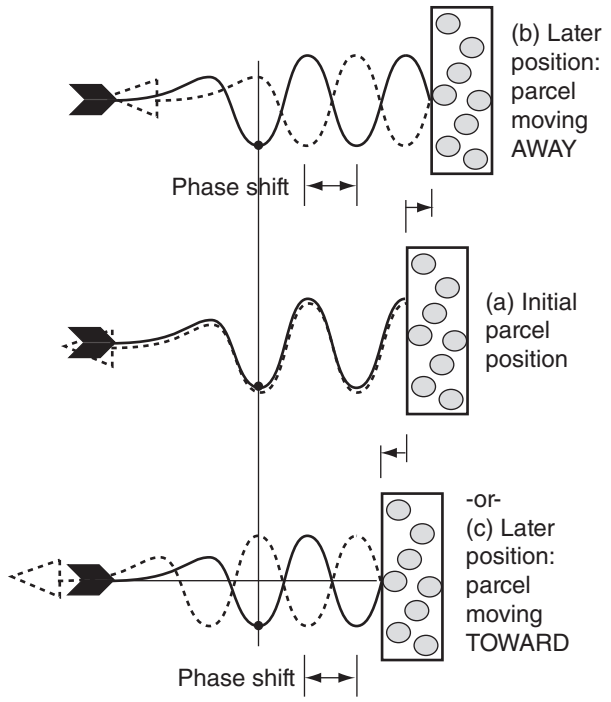

Figure 8.34
Air movement of distance equal to quarter a wavelength toward and away from the radar can yield identical phase shifts, making velocity interpretation ambiguous (i.e., erroneous).

Solved Example

A C-band radar emitting 2000 microwave pulses per second illuminates a target moving 30 m/s away from the radar. What is the displayed radial velocity?

Solution:
Given: PRF = 2000 s^{-1} , M_r = +30 m/s.
Assume λ = 5 cm because C-band.
Find: displayed M_r

Use eq. (8.35):
$M_{r\,max}$ = (0.05 m)·(2000 s^{-1})/4 = **25 m/s**

But $M_r > M_{r\,max}$, therefore velocity folding.
Use eq. (8.36a):
$M_{r\,false}$ = (30 m/s) – 2·(25 m/s) = **–20 m/s** ,
where the negative sign means toward the radar.

Check: Units OK. Physics OK.
Discussion: This is a very large velocity in the wrong direction. Algorithms that automatically detect **tornado vortex signatures** (**TVS**), look for regions of fast AWAY velocities adjacent to fast TOWARD velocities. However, this Doppler velocity-folding error produces false regions of adjacent fast opposite velocities, causing false-alarms for tornado warnings.

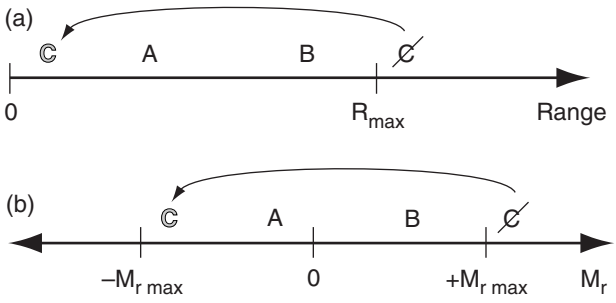

Figure 8.35
(a) Reflectivity targets at ranges A and B from the radar appear in their proper locations. Target C, beyond the max unambiguous range (R_{max}), is not displayed at its actual location, but appears as a false echo ℂ on the radar display closer to the radar. (b) Air parcels with negative or positive radial velocities A and B are displayed accurately. Parcel C with positive velocity greater than $M_{r\,max}$ is falsely displayed ℂ with large negative velocity.

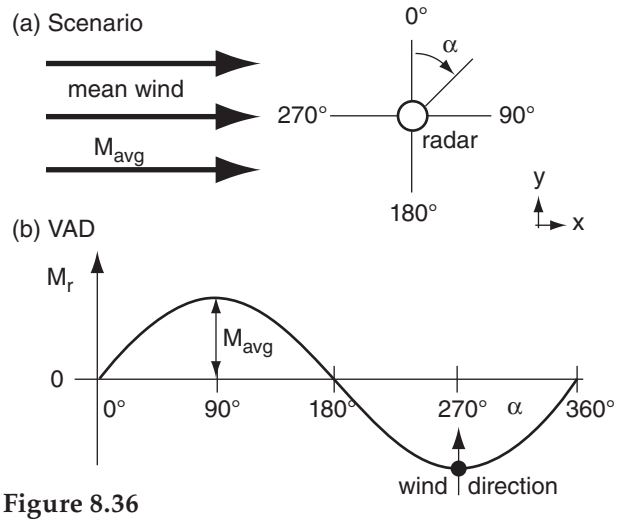

Figure 8.36
(a) Scenario of mean winds relative to radar. (b) Velocity-azimuth display (VAD) of radial wind component.

Solved Example

From a 1 km thick layer of air near the ground, the average radial velocity is –2 m/s at range 100 km from the radar. What is the vertical motion at the layer top?

Solution:
Given: R = 100 km , Δz = 1 km , $M_{r\,avg}$ = –2 m/s.
Find: w = ? m/s at z = 1 km.
Assume: w_{bot} = 0 at the ground (at z = 0).

Use eq. (8.37): Δw = –2·(–2 m/s) · (1 km) / (100 km)
Δw = +0.04 m/s.
But $\Delta w = w_{top} - w_{bot}$. Thus: w_{top} = **+0.04 m/s**

Check: Units OK. Physics OK.
Discussion: This weak upward motion covers a broad 100 km radius circle, and would enhance storms.

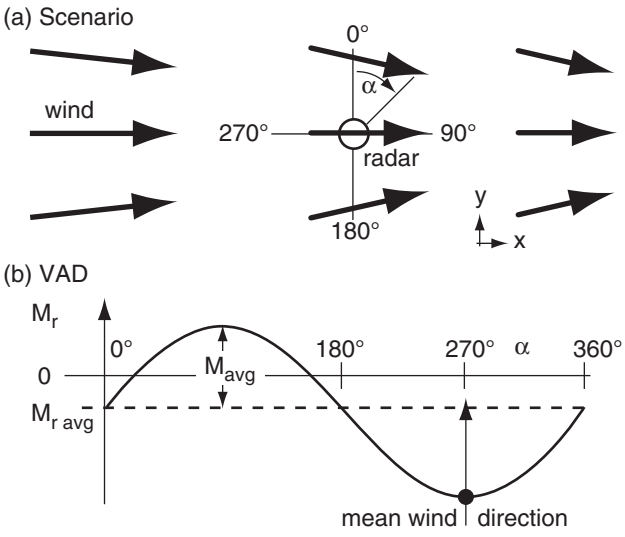

Figure 8.37
(a) Scenario of mean winds AND horizontal convergence. (b) Velocity-azimuth display (VAD) of radial wind component.

Velocity Azimuth Display (VAD)

A plot of radial velocity M_r (at a fixed elevation angle and range) vs. azimuth angle α is called a **velocity-azimuth display** (**VAD**), which you can use to measure the mean horizontal wind speed and direction within that range circle. Fig. 8.36a illustrates a steady mean wind blowing from west to east through the Doppler radar sweep area. The resulting radial velocity component measured by the radar is a sine wave on the VAD (Fig. 8.36b).

Mean horizontal wind speed M_{avg} is the amplitude of the sine wave relative to the average radial velocity $M_{r\,avg}$ (=0 for this case), and the meteorological wind direction is the azimuth at which the VAD curve is most negative (Fig. 8.36b). Repeating this for different heights gives the winds at different altitudes, which you can plot as a wind-profile sounding or as a hodograph (explained in the Thunderstorm chapters). The measurements at different heights are made using different elevation angles and ranges (eq. 8.22).

You can also estimate mean vertical velocity using horizontal divergence determined from the VAD. Picture the scenario of Fig. 8.37a, where there is convergence (i.e., negative divergence) superimposed on the mean wind. Namely, west winds exist everywhere, but the departing winds east of the radar are slower than the approaching winds from the west. Also, the winds have a convergent north-south component. When plotted on a VAD, the result is a sine wave that is displaced in the vertical (Fig. 8.37b). Averaging the slower AWAY radial winds with the faster TOWARD radial winds gives a negative average radial velocity $M_{r\,avg}$, as shown by the dashed line in Fig. 8.37b. $M_{r\,avg}$ is a measure of the divergence/convergence, while M_{avg} still measures mean wind speed.

Due to mass continuity (discussed in the Dynamics chapter), gain of air horizontally into a volume requires upward motion of air out of the volume to conserve mass (i.e., mass flow in = mass flow out). Thus:

$$\Delta w = \frac{-2 \cdot M_{r\,avg}}{R} \cdot \Delta z \qquad (8.37)$$

where Δw is change in vertical velocity across a layer of thickness Δz, and R is range from the radar at which the radial velocity M_r is measured.

Upward vertical velocities (associated with horizontal **convergence** and negative $M_{r\,avg}$) enhance cloud and storm development, while downward vertical velocities (**subsidence**, associated with horizontal **divergence** and positive $M_{r\,avg}$) suppresses clouds and provides fair weather. Knowing that w = 0 at the ground, you can solve eq. (8.37) for

w at height Δz above ground. Then, starting with that vertical velocity, you can repeat the calculation using average radial velocities at a higher elevation angle to find w at this higher altitude. Repeating this gives the vertical velocity profile.

A single Doppler radar cannot measure the full horizontal wind field, because it can "see" only the radial component of velocity. However, if the scan regions of two nearby Doppler radars overlap, then in theory the horizontal wind field can be calculated from this **dual-Doppler** information, and the full 3-D winds can be inferred using mass continuity.

Identification of Storm Characteristics

While the VAD approach averages the winds within the whole scan circle, you can also use the smaller scale patterns of winds to identify storm characteristics. For example, you can use Doppler information to help detect and give advanced warning for **tornadoes** and **mesocyclones** (see the Thunderstorm chapters). Doppler radar cannot see the whole rotation inside the **thunderstorm** — just the portions of the vortex with components moving toward or away from the radar. But you can use this limited information to define a **tornado vortex signature** (**TVS**, Fig. 8.38b) with the brightest red and blue pixels next to each other, and with the zero isodop line passing through the tornado center and following a radial line from the radar.

Hurricanes also exhibit these rotational characteristics, as shown in Fig. 8.39. Winds are rotating counterclockwise around the eye of this Northern Hemisphere hurricane. The zero isodop passes through the radar location in the center of this image, and also passes through the center of the eye of the hurricane. See the Hurricane chapter for details.

Cold-air **downbursts** from thunderstorms hit the ground and **diverge** (spread out) as damaging horizontal **straight-line winds** (Fig. 8.38c). The leading edge of the outflow is the **gust front**. Doppler radar sees this as neighboring regions of opposite moving radial winds, similar to the TVS but with the zero isodop perpendicular to the radial from the radar, and with the blue region always closer to the radar than the red region.

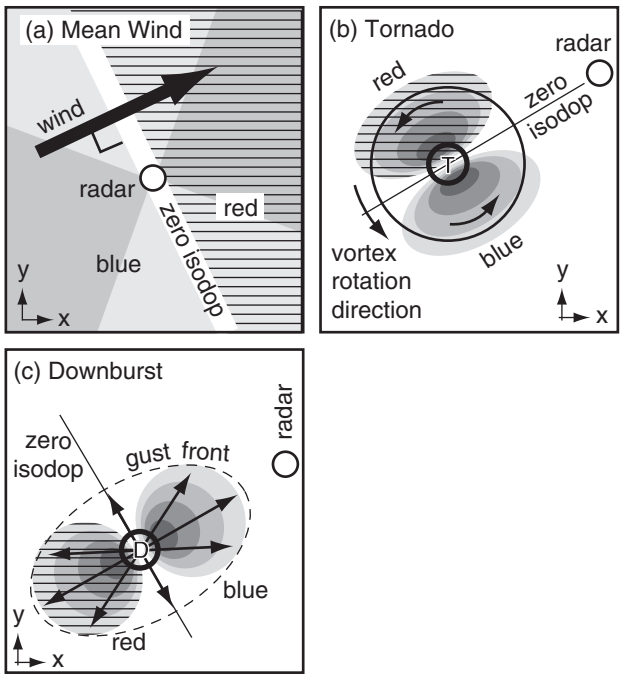

Figure 8.38
PPI or CAPPI radar image interpretation. The white circle indicates the radar location. Hatched shaded regions represent red, and indicate wind components AWAY from the radar. Other shaded regions represent blue, and indicate TOWARD the radar. Darker shadings represent more vivid colors, and mean faster radial winds. Actual wind directions are shown by the black arrows. (a) Uniform mean wind in the domain. (b) Tornado (T) vortex, surrounded by weaker mesocyclone vortex (large circle). (c) Downburst (D) and gust front (dashed line) at the leading edge of outflow air.

Solved Example

A downburst and outflow are centered directly over a Doppler radar. Sketch the Doppler display.

Solution:

Given: Air diverging in all directions from radar
Sketch: Doppler radar display appearance

At every azimuth from the radar, air is moving AWAY. Thus red would be all around the radar, out to the gust front. The fastest outflow is likely to be closest to the radar.

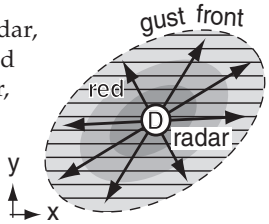

Check: Sketch consistent with display definitions.
Discussion: Meteorologists at the radar might worry about their own safety, and about radome damage. The **radome** is the spherical enclosure that surrounds the radar antenna, to protect the radar from the weather. Also, a wet radome causes extra attenuation, making it difficult to see distant precipitation echoes.

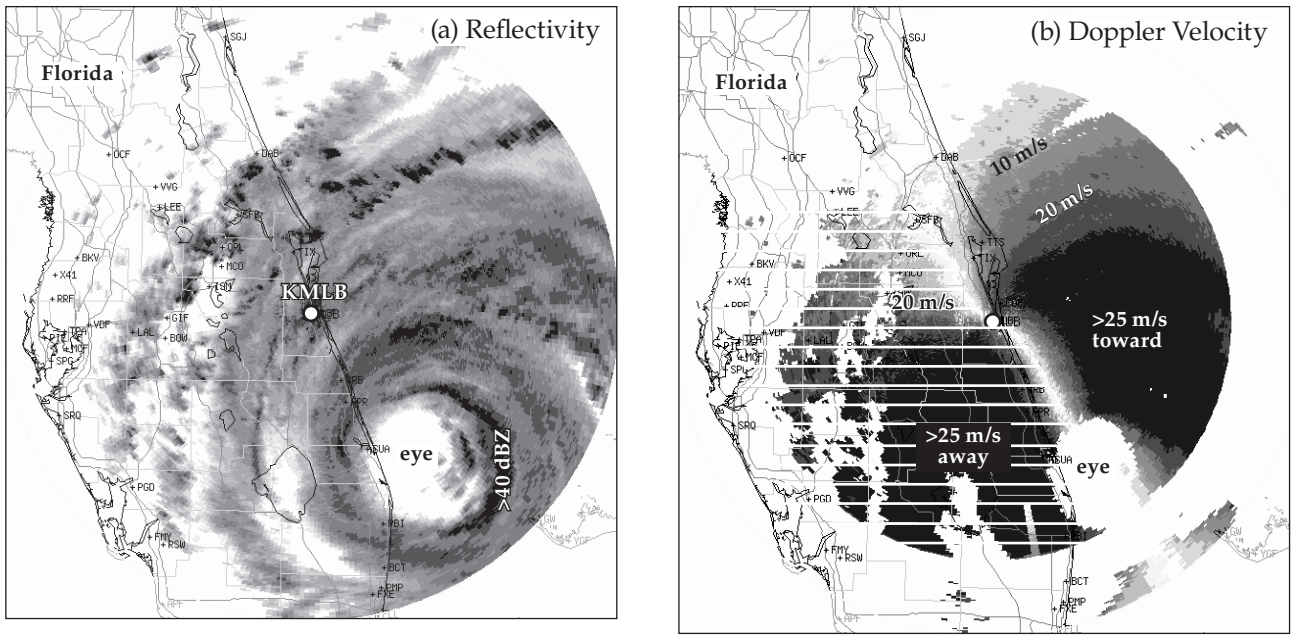

Figure 8.39
Radar images of Hurricane Francis at 0300 UTC on 5 September 2004 as the eye is approaching the coast of Florida, USA. Hurricane intensity at this time was category 2 on the Saffir-Simpson scale, although it had been category 4 before reaching the coast. The Melbourne, FL, radar KMLB is in the center of the radar image. (a) PPI image where darker shading represents greater reflectivity (dBZ). (b) Doppler radial velocities (in the original image velocities toward the radar were colored blue, and away velocities were red). In this black and white image, the AWAY winds are shown with white hatching superimposed. [Adapted from US National Weather Service data as displayed by the Research Applications Program division of the US National Center for Atmospheric Research.]

Solved Example
Explain the "S" curve in the zero isodop of Fig. 8.39b.

Solution:
Given: Doppler velocities in Fig. 8.39b.
Find: Explanation for "S" curve of zero isodop.

For a PPI display, the radar is observing the air along the surface of an inverted scan cone (Fig. 8.24a). Hence, targets at closer range to the radar correspond to targets at lower altitude. Curvature in the zero isodop indicates vertical shear of the horizontal winds (called **wind shear** for short).

Close to the radar the zero isodop is aligned northwest to southeast. The wind direction at low altitude is perpendicular to this direction; namely, from the **northeast at low altitude**.

Further from the radar (but still on the radar side of the eye), the zero isodop is south-southeast of the radar. The winds at this range are perpendicular to a straight line drawn from the radar to the zero isodop; namely, from the **east-northeast at mid altitudes**.

Discussion: As you will see in the Dynamics & Hurricane chapters, boundary-layer winds feel the effect of drag against the ground, and have a direction that spirals in toward the eye. Above the boundary layer, in the middle of the troposphere, winds circle the eye.

Spectrum Width

Another product from Doppler radars is the **spectrum width**. This is the variance of the Doppler velocities within the sample volume, and is a measure of the intensity of atmospheric **turbulence** inside storms. Also, the Doppler signal can be used with reflectivity to help eliminate ground clutter. For high elevation angles and longer pulse lengths, the spectrum width is also large in bright bands, because the different fall velocities of rain and snow project onto different radial velocities. Strong **wind shear** within sample volumes can also increase the spectrum width.

Difficulties

Besides the maximum unambiguous velocity problem, other difficulties with Doppler-estimated winds are: (1) ground clutter including vehicles moving along highways; (2) lack of information in parts of the atmosphere where there are no scatterers (i.e., no rain drops or bugs) in the air; and (3) scatterers that move at a different speed than the air, such as falling raindrops or migrating birds.

Polarimetric Radar

Because *Z-R* relationships are inaccurate and do not give consistent results, other methods are used to improve estimates of precipitation type and rate. One method is to transmit microwave pulses with different **polarizations**, and then compare their received echo intensities. Radars with this capability are called **polarimetric**, **dual-polarization**, or **polarization-diversity** radars.

Recall that electromagnetic radiation consists of perpendicular waves in the electric and magnetic fields. **Polarization** is defined by the direction of the electric field. Radars can be designed to switch between two or three polarizations: **horizontal**, **vertical**, and **circular** (see Fig. 8.40). Air-traffic control radars use circular polarization, because it partially filters out the rain, allowing a clearer view of aircraft. Most weather radars use horizontal and vertical linear polarizations.

Horizontally polarized pulses get information about the horizontal dimension of the precipitation particles (because the energy scattered depends mostly on the particle horizontal size). Similarly, vertically polarized pulses get information about the vertical dimension. By alternating between horizontal and vertical polarization with each successive transmitted pulse, algorithms in the receiver can use echo differences to estimate the average shape of precipitation particles in the sample volume.

Only the smallest cloud droplets are spherical (Fig. 8.41a, equal width and height). These would give returns of equal magnitude for both horizontal and vertical polarizations. However, larger rain drops become more **oblate** (Fig. 8.41b, flattened on the bottom and top) due to air drag when they fall. The largest drops are shaped like a hamburger bun (Fig. 8.41c). This gives greater reflectivity factor Z_H from the horizontally polarized pulses than from the vertically polarized ones Z_V. The amount of oblateness increases with the mass of water in the drop. There is some evidence that just before the largest drops break up, they have a parachute or jelly-fish-like shape (Fig. 8.41d).

Some hydrometeor shapes change the polarization of the scattered pulse. For example, clockwise circular polarized transmitted pulses are scattered with counterclockwise circular polarization by any rain drops that are nearly spherical. Tumbling, partially melted, irregular-shaped, ice crystals can respond to horizontally polarized pulses by returning a portion of the energy in vertical polarization. Different shapes of ice crystals have different reflectivity factors in the vertical and horizontal.

Four variables are often analyzed and displayed on special radar images to help diagnose hydrometeor structure and size. These are:

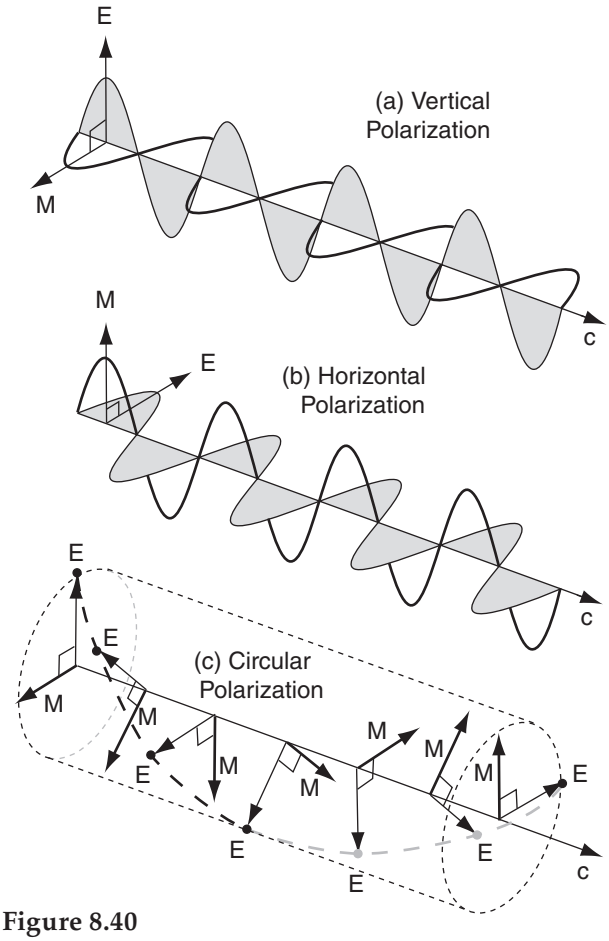

Figure 8.40
Polarization of microwaves, where E = electric field, M = magnetic field, and c = wave propagation at speed of light. (a) Vertical; (b) Horizontal; and (c) Circular polarization.

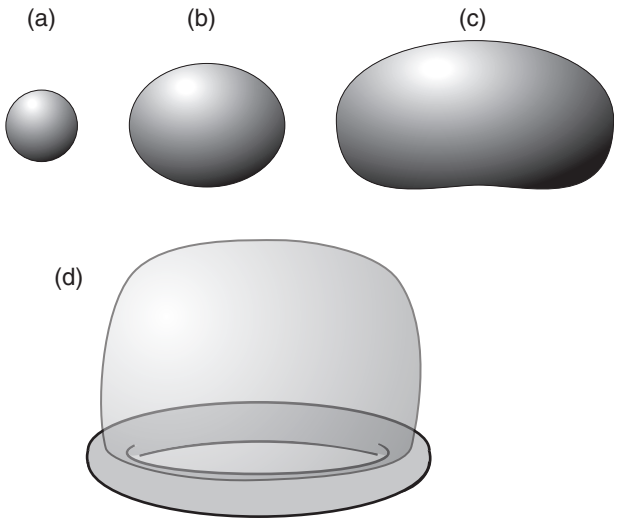

Figure 8.41
Enlargement of raindrop shapes vs. diameter D (approximate). (a) D < 1 mm; (b) 1 mm < D < 3 mm ; (c) 3 mm < D; (d) large (D ≈ 4 mm) jellyfish-like shape just before drop breaks up..

Solved Example

Polarization radar measures reflectivity factors of Z_{HH} = 1000 dBZ , Z_{VV} = 398 dBZ , and Z_{VH} = 0.3 dBZ. (a) Find the differential reflectivity and the linear depolarization ratio. (b) Discuss characteristics of the hydrometeors. (c) What values of specific differential phase and co-polar correlation coefficient would you expect? Why?

Solution:

Given: Z_{HH} = 1000 dBZ, Z_{VV} = 398 dBZ , and Z_{VH} = 0.3 dBZ

Find: Z_{DR} = ? dB, LDR = ? dB

(a) Use eq. (8.38): Z_{DR} = 10·log(1000 dBZ/398 dBZ) = **+4.0** dB

Use eq. (8.39): LDR = 10·log(0.3 dBZ/1000 dBZ) = **–35.2** dB

(b) **Discussion**: The positive value of Z_{DR} indicates a hydrometeor with greater horizontal than vertical dimension, such as **large, oblate rain drops**. The very small value of *LDR* supports the inference of rain, rather than snow or hail.

(c) I would expect K_{DP} = **2 to 4 °/km**, because of large oblate rain drops.

I would also expect ρ_{HV} = **0.95** , because **rain intensity is light to moderate**, based on eq. (8.27):

dBZ = 10·log(Z_{HH}/Z_1)
= 10·log(1000dBZ/1dBZ)
= **30 dBZ**, which is then used to find the intensity classification from Fig. 8.28.

Check: Units OK. Results reasonable for weather.

Discussion: See item (b) above.

In eq. (8.27) I used Z_{HH} because the horizontal drop dimension is the one that is best correlated with the mass of the drop, as illustrated in Fig. 8.41.

- **Differential Reflectivity**: Z_{DR} (unit: dB)

$$Z_{DR} = 10 \cdot \log(Z_{HH}/Z_{VV}) \qquad \bullet(8.38)$$

where the first and second (H, V) subscripts of reflectivity *Z* give the polarization of received and transmitted pulses, respectively.
Typical values: –2 to +6 dB, where negative and positive values indicate vertical or horizontal orientation of the hydrometeor's major axis.
Useful with *Z* for improving rain-rate estimates, and to identify radar attenuation regions.

- **Linear Depolarization Ratio**. LDR (unit: dB)

$$LDR = 10 \cdot \log(Z_{VH}/Z_{HH}) \qquad \bullet(8.39)$$

Typical values: > –10 dB for ground clutter
–15 dB for melting snowflakes.
–20 to –26 dB for melting hail
< –30 dB for rain
Useful for estimating micrometeor type or habit. Can also help remove ground clutter, and identify the bright band.

- **Specific Differential Phase**: K_{DP}
(unit: degrees of phase shift per 1 km path)
Relative amount of phase shift (shift of the crests of the electromagnetic waves) in the returned echoes from the horizontally vs. vertically transmitted pulses.
Typical values: –1 to +6 °/km, where positive values indicate oblate (horizontally dominant) hydrometeors. Tumbling hail appears symmetric on average, resulting in K_{DP} = 0.
Improves accuracy of rain rate estimate, and helps to isolate the portion of echo associated with rain in a rain/hail mixture.

- **Co-polar Correlation Coefficient**: ρ_{HV}
(unit: dimensionless, in range –1 to +1)
Measures the amount of similarity in variation of the time series of received signals from the horizontal vs. vertical polarizations.
Typical values of $|\rho_{HV}|$:
0.5 means very large hail
0.7 to 0.9 means drizzle or light rain
0.90 to 0.95 means hail, or bright-band mix.
≥ 0.95 means rain, snow, ice pellets, graupel
0.95 to 1.0 means rain
Useful for estimating the heterogeneity of micrometeors (mixtures of different-shaped ice crystals and rain drops) in the sampling volume, and radar beam attenuation.

One suggestion for an improved estimate of rainfall rate RR with S-band polarimetric radar is:

$$RR = a_o \cdot K_{DP}^{a_1} \cdot Z_{DR}^{a_2} \qquad \bullet(8.40)$$

where a_o = 90.8 mm/h (see solved example "check" for discussion of units), a_1 = 0.89, and a_2 = –1.69 . Such improved rainfall estimates are crucial for **hydrometeorologists** (experts who predict drought severity, river flow and flood potential).

Based on all the polarimetric information, fuzzy-logic algorithms are used at radar sites to classify the hydrometeors and to instantly display the result on computer screens for meteorologists. Hydrometeor Classification Algorithms (HCA) for WSR-88D radars use different algorithms for summer (warm mode) and winter (cold mode) precipitation.

• Warm Mode: big drops, hail, heavy rain, moderate rain, light rain, no echoes, birds/insects, anomalous propagation.

• Cold Mode: convective rain, stratiform rain, wet snow, dry snow, no echoes, birds/insects, anomalous propagation.

Combinations of polarimetric variables can also help identify graupel and estimate hail size, estimate attenuation of the radar signal, identify storms that might become electrically active (lots of lightning), identify regions that could cause hazardous ice accumulation on aircraft, detect tornado debris clouds, and correct for the bright band.

Solved Example

Polarization radar measures a differential reflectivity of 5 dB and specific differential phase of 4°/km. Estimate the rainfall rate.

Solution:

Given: Z_{DR} = 5 dB , K_{DP} = 4°/km.

Find: RR = ? mm/h

Use eq. (8.40):

$RR = (90.8 \text{ mm/h}) \cdot (4°/\text{km})^{0.89} \cdot (5 \text{ dB})^{-1.69}$

$= (90.8 \text{ mm/h}) \cdot 3.43 \cdot 0.066 =$ **20 mm/h**

Check: Units don't match. The reason is that the units of a_o are not really [mm/h], but are $[(\text{mm/h}) \cdot (°/\text{km})^{-0.89} \cdot (\text{dB})^{+1.69}]$. These weird units resulted from an empirical fit of the equation to data, rather than from first principles of physics.

Discussion: This corresponds to heavy rain (Fig. 8.28), so hydrometeorologists would try to forecast the number of hours that this rain would continue to estimate the **storm-total accumulation** (= rainfall rate times hours of rain). If excessive, they might issue a flood warning.

Phased-Array Radars & Wind Profilers

Phased-array radars steer the radar beam not by rotating the antenna dish, but by using multiple transmitter heads that can transmit at slightly different times. Picture a building (the rectangle in Fig. 8.42a) as viewed from above. On one side of the building are an array of microwave transmitters (black dots in the Fig). When any transmitter fires, it emits a wave front shown by the thin semicircle. If all transmitters fire at the same time, then the superposition of all the waves yield the most energy in an effective wave front (thick gray line) that propagates perpendicularly away from the transmitter building, as shown by the gray arrow. For the example in the figure, the effective wave front moves east.

But these transmitters can also be made to fire sequentially (i.e., slightly out of phase with each other) instead of simultaneously. Suppose transmitter 1 fires first, and then a couple nanoseconds later transmitter 2 fires, and so on. A short time after transmitter 5 fires, its wave front (thin semicircle) has had time to propagate only a short distance, however the wave fronts from the other transmitters have been propagating for a longer time, and are further away from the building (Fig. 8.42b). The superposition of

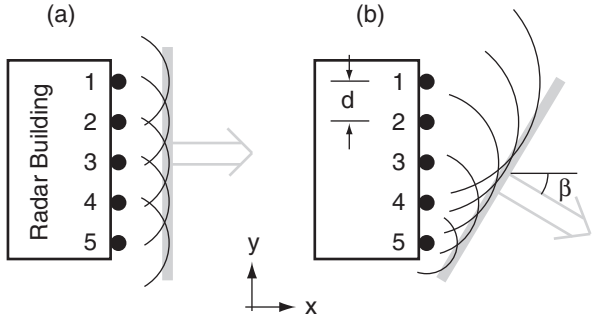

Figure 8.42
Phased array radar concept.

Solved Example

What time delay is needed in phased array radar to steer the beam 30° away from the line normal (perpendicular) to the radar face, if the transmitter elements are 1 m apart?

Solution:
Given: $\beta = 30°$, $d = 1$ m , $c = 3\text{x}10^8$ m/s
Find: Δt = ? s

Use eq. (8.41): $\Delta t = [(1\text{m})/(3\text{x}10^8\ \text{m/s})]\cdot\sin(30°)$
$\Delta t = 1.67\text{x}10^{-9}$ s = **1.67 ns**.

Check: Units OK. Physics OK. Agrees with Fig. 8.40.
Discussion: The larger the angle β, the smaller the effective size of the transmitter face, and the less focused is the beam. This is a disadvantage of phased-array radars used for meteorology: the sample volume changes not only with range but also with direction β. Therefore, the algorithms used to interpret meteorological characteristics (reflectivity, Doppler velocity, spectrum width, polarimetric data) must be modified to account for these variations.

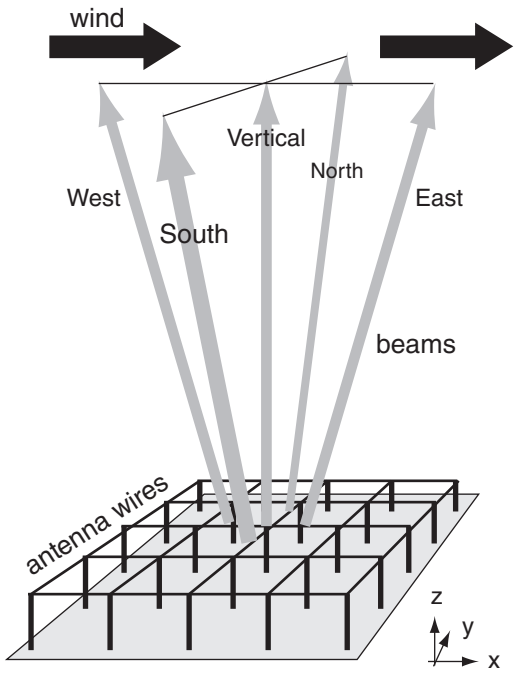

Figure 8.43
Wind profiler concept.

the individual wave fronts now yields an effective wave front (thick gray line) that is propagating toward the southeast.

Let Δt be the time delay between firing of subsequent transmitters. For transmitter elements spaced a distance d from each other, the time delay needed to give an effective propagation angle β (see Fig. 8.42b) is:

$$\Delta t = (d/c)\cdot\sin(\beta) \qquad (8.41)$$

where $c = 3\text{x}10^8$ m/s is the approximate speed of microwaves through air.

By changing Δt, the beam (grey arrow) can be steered over a wide range of angles. Negative Δt steers the beam toward the northeast, rather than southeast in this example. Also, by having a 2-D array of transmitting elements covering the whole side of the building, the beam can also be steered upward by firing the bottom elements first.

Two advantages of this approach are: (1) fewer moving parts, therefore less likelihood of mechanical failure; and (2) the beam angle can be changed instantly from one extreme to the other. However, to see a full 360° azimuth around the radar site, phased-array transmitting elements must be designed into all 4 walls of the building. While the military have used phased array radars for decades to detect aircraft and missiles, these radars are just beginning to be used in civilian meteorology.

Another phased-array application to meteorology is the **wind profiler**. This observes horizontal wind speed and direction at many heights by measuring the Doppler shifts in the returned signals from a set of radio beams tilted slightly off from vertical (Fig. 8.43).

Some wind profilers look like a forest of TV antennas sticking out of the ground, others like window blinds laying horizontally, others like a large trampoline, and others like a grid of perpendicular clothes lines on poles above the ground (Fig. 8.43). Each line is a radio transmitter antenna, and the effective beam can be steered away from vertical by phased (sequential) firing of these antenna wires.

Wind profilers work somewhat like radars — sending out pulses of radio waves and determining the height to the clear-air targets by the time delay between transmitted and received pulses. The targets are turbulent eddies of size equal to half the radio wavelength. These eddies cause refractivity fluctuations that scatter some of the radio-wave energy back to receivers on the ground.

Wind profilers with 16 km altitude range use Very High Frequencies (**VHF**) of about $\nu = 50$ MHz ($\lambda = c / \nu = 6$ m). Other **tropospheric wind profilers**

use an Ultra High Frequency (**UHF**) near 400 MHz (λ = 0.75 m = 75 cm). Smaller **boundary-layer wind profilers** for sampling the lower troposphere use an ultra high frequency near 1 GHz (λ = 30 cm).

Normally, wind profilers are designed to transmit in only 3, 4 or 5 nearly-vertical, fixed beam directions (Fig. 8.43). The fixed zenith angle of the slightly-tilted beams is on the order of ζ = 14° to 24°.

The radial velocities M_{east} and M_{west} measured in the east- and west-tilted beams, respectively, are affected by the U component of horizontal wind and by vertical velocity W. Positive W (upward motion; thick gray vector in Fig. 8.44) projects into positive (away from wind profiler) components of radial velocity for both beams (thin gray vectors). However, positive U (thick black vector) wind contributes positively to M_{east}, but negatively (toward the profiler) to M_{west} (thin black vectors).

Assume the same average U and W are measured by both beams, and design the profiler so that all tilted beams have the same zenith angle. Thus, the two radial velocities measured can be subtracted and added to each other, to yield the desired two wind components:

$$U = \frac{M_{east} - M_{west}}{2 \cdot \sin\zeta} \qquad \bullet(8.42a)$$

$$W = \frac{M_{east} + M_{west}}{2 \cdot \cos\zeta} \qquad \bullet(8.42b)$$

Use similar equations with radial velocities from the north- and south-tilted beams to estimate V and W. Fig. 8.45 shows sample wind-profiler output.

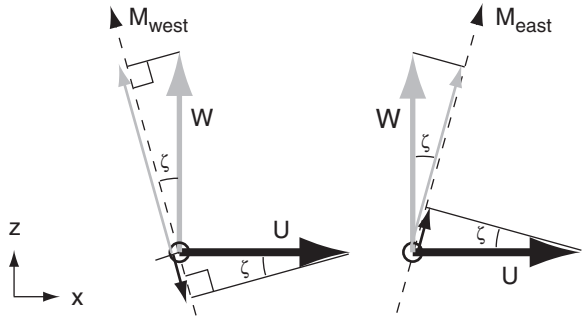

Figure 8.44
Projections of horizontal wind U and vertical velocity W to the radial wind directions M_{west} and M_{east} along wind-profiler west and east tilted beams.

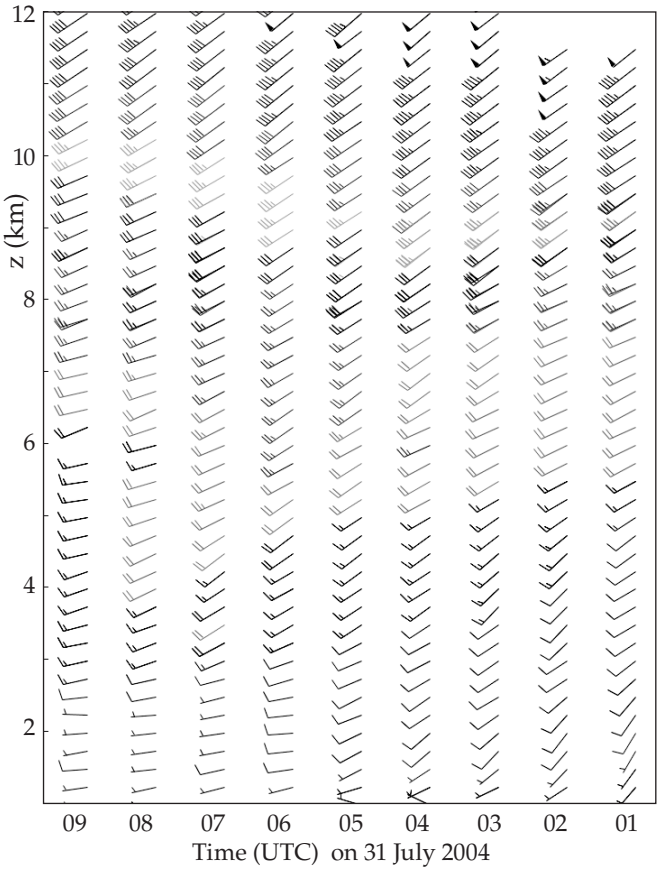

Figure 8.45
Wind profiler observations for Wolcott, IN. Arrow shows horizontal wind direction. Each short wind barb = 5 m/s, long = 10 m/s, & pennant = 50 m/s. (E.g., wind at z = 10 km, t = 02 UTC is 45 m/s from southwest.) Courtesy of US National Oceanic and Atmospheric Admin. (NOAA) Profiler Network (NPN).

Solved Example

A wind profiler with 20° beam tilt uses the Doppler shift to measure radial velocities of 3.326 m/s and –3.514 m/s in the east- and west-tilted beams, respectively, at height 4 km above ground. Find the vertical and horizontal wind components at that height.

Solution:
Given: M_{east} = 3.326 m/s, M_{west} = –3.514 m/s, ζ = 20°
Find: U = ? m/s and W = ? m/s.

Use eq. (8.42a):
U = [(3.326 m/s) – (–3.514 m/s)]/[2·sin(20°)] = **10 m/s**
Use eq. (8.42b):
W = [(3.326 m/s)+(–3.514 m/s)]/[2·cos(20°)] = **–0.1 m/s**

Check: Units OK. Physics OK.
Discussion: The positive U component indicates a west wind (i.e., wind FROM the west) at z = 4 km. Negative W indicates subsidence (downward moving air). These are typical of fair-weather conditions under a strong high-pressure system. Typical wind profilers make many measurements each minute, and then average their results over 5 minutes to 1 hour.

SUMMARY

Passive sensors on weather satellites observe many different wavelengths of electromagnetic radiation upwelling from the Earth-atmosphere-cloud system. Imager sensors take high-quality digital photographs of clouds and air motion, for which the most important wavelength channels are visible, IR, and water-vapor. Sounder radiometers remotely probe different depths in the atmosphere.

For reflected visible sunlight and for wavelengths in IR windows, the satellite sees down to the highest cloud top, or to the ground if no clouds block the view. In IR opaque regions, the satellite cannot see through the atmosphere, and instead measures radiation emitted from the air.

For this latter situation, atmospheric emissions at any one wavelength come from a broad range of altitudes, as defined by weighting functions. By observing many different wavelengths with weighting functions that peak at different altitudes, the data can be inverted to retrieve vertical profiles of temperature. Retrievals are difficult, but provide useful remotely-sensed soundings over the oceans having insufficient in-situ observations.

Two favorite satellite orbits are geostationary (high altitude) and sun-synchronous polar orbiting (low altitude). Weather features and storms can be interpreted from satellite images and movie loops. In IR images, high (cold) clouds are often displayed with the lighter grays and white, while lower clouds are darker gray.

Weather radars are active sensors that transmit strong pulses of microwaves, and then measure the echoes that bounce back from precipitation. Stronger echoes (i.e., large scattering) show regions of more and larger rain and snow particles, which are used to estimate rainfall rate and storm intensity. Movement of these echoes show the storm track.

When the wind carries the hydrometeors in a radial direction relative to the radar, the echo frequency is shifted slightly due to the Doppler effect. Doppler radars analyze this radial velocity by measuring the phase shift of the echoes. Certain wind patterns yield characteristic signatures in the Doppler wind field, which are used to detect incipient tornadoes and other damaging winds.

Polarimetric weather radars transmit and receive microwaves with different polarizations (usually horizontal and vertical). Hydrometeors with different shapes return polarized signals differently, allowing better estimation of rainfall rates and precipitation type. Phased-array radars need no moving parts to can scan the weather. Wind profilers measure horizontal wind speed and directions.

Threads

Satellites and radar measure electromagnetic radiation (Chapter 2) to do remote sensing, and are affected by attenuation according to Beer's Law. They often do not measure the complete thermodynamic state (Chapter 1) and motion (Chapter 17) of the air, but dynamics (Chapter 10) and thermodynamics (Chapter 3) can be used to infer the missing pieces.

Satellite sounders measure the vertical structure of the atmosphere, which deviates day-to-day from the standard atmosphere (Chapter 1). Some wind profilers are specifically designed to measure the atmospheric boundary layer (Chapter 18).

Clouds (Chapter 6) observed by satellite and precipitation (Chapter 7) observed by radar imply large releases of latent heat (Chapter 3) due to condensation (Chapter 4), which alters the static stability (Chapter 5) and triggers storms. Both satellite and radar observations are crucial for measuring thunderstorms, tornadoes, and gust fronts (Chapters 14 and 15) and hurricanes (Chapter 16), and for increasing the lead time for storm warnings.

Geostationary satellites observe the global circulation (Chapter 11), and satellite images can be interpreted to diagnose locations of fronts (Chapter 12) and lows (Chapter 13). Satellite winds, wind-profiler winds, and satellite soundings are important inputs to numerical weather prediction models (Chapter 20). The newer satellites have sufficiently fine resolution to detect air pollution (Chapter 19), and have sensitive radiometers to measure changes in the Earth's radiation budget that might be associated with climate change (Chapter 21).

EXERCISES

Numerical Problems

N1. Using Fig. 8.4, identify whether the following wavelengths (μm) are in a window, dirty window, shoulder, or opaque part of the transmittance spectrum, and identify which sketch in Fig. 8.2 shows how the Earth would look at that wavelength. [Hint: transmittance of ≥ 80% indicates a window.]

a. 0.5	b. 0.7	c. 0.95	d. 1.25	e. 1.33
f. 1.37	g. 1.6	h. 2.3	i. 2.4	j. 5.0

N2. Find the blackbody radiance for the following sets of [λ (μm), T (°C)]:

a. 14.7, –60	b. 14.4, –60	c. 14.0, –30
d. 13.7, 0	e. 13.4, 5	f. 12.7, 15
g. 12.0, 25	h. 11.0, –5	i. 9.7, –15

N3. For the wavelengths in the previous problem, identify the closest GOES sounder channel #, and the altitude of the peak in the weighting function.

N4. Find the brightness temperature for the following wavelengths (μm), given a radiance of 10^{-15} $W \cdot m^{-2} \cdot \mu m^{-1} \cdot sr^{-1}$:

a. 0.6 b. 3.8 c. 4.0 d. 4.1 e. 4.4
f. 4.5 g. 4.6 h. 6.5 i. 7.0 j. 7.5

N5(§). Given the following temperature sounding:

z (km)	T (°C)	z (km)	T (°C)
15 to 20	–50	5 to 10	–5
10 to 15	–25	0 to 5	+5
		Earth skin	+20

Find the radiance at the top of the atmosphere for the following transmittance profiles & wavelengths:
λ (μm): (a) 7.0 , (b) 12.7 , (c) 14.4 , (d) 14.7

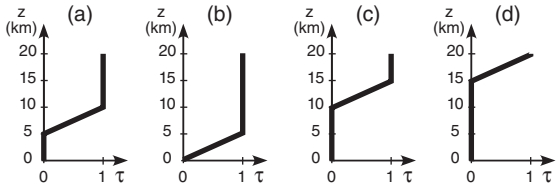

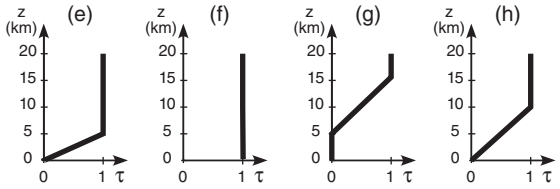

λ (μm): (e) 11.0 , (f) 2.6 , (g) 6.5 , (h) 4.4

N6. For the transmittances of the previous exercise, plot the weighting functions.

N7. For the following altitudes (km) above the Earth's surface, find the satellite orbital periods:

a. 40,000 b. 600 c. 800 d. 2,000 e. 5,000
f. 10,000 g. 15,000 h. 20,000 i. 30,000 j. 50,000

N8. What shade of grey would the following clouds appear in visible, IR, and water-vapor satellite images? a. cirrus b. cirrocumulus c. cirrostratus
d. altocumulus e. altostratus
f. stratus g. nimbostratus h. fog
i. cumulus humilis j. cumulus congestus
k. cumulonimbus l. stratocumulus

N9(§). Do an OSSE to calculate the radiances observed at the satellite, given the weighting functions of Fig. 8.20, but with the following atmospheric temperatures (°C): Layer 1 = –30, Layer 2 = –70, Layer 3 = –20, and Layer 4:

a. 40 b. 35 c. 30 d. 25 e. 20 f. 15 g. 10 h.5

N10. Find the beamwidth angle for a radar pulse for the following sets of [wavelength (cm) , antenna dish diameter (m)]:

a. [20, 8] b. [20, 10] c. [10, 10] d. [10, 5] e. [10, 3]
f. [5, 7] g. [5, 5] h. [5, 2] i. [5, 3] j. [3, 1]

N11. What is the name of the radar band associated with the wavelengths of the previous exercise?

N12. Find the range to a radar target, given the round-trip (return) travel times (μs) of:

a. 2 b. 5 c. 10 d. 25 e. 50
f. 75 g. 100 h. 150 i. 200 j. 300

N13. Find the radar max unambiguous range for pulse repetition frequencies (s^{-1}) of:

a. 50 b. 100 c. 200 d. 400 e. 600
f. 800 g. 1000 h. 1200 i. 1400 j. 1600

N14. Find the Doppler max unambiguous velocity for a radar with pulse repetition frequency (s^{-1}) as given in the previous exercise, for radar with wavelength of: (i) 10 cm (ii) 5 cm

N15. Determine the size of the radar sample volume at a range of 30 km for a 10 cm radar with 5 m diameter antenna dish and pulse duration (μs) of:

a. 0.1 b. 0.2 c. 0.5 d. 1.0 e. 1.5 f. 2 g. 3 h. 5

N16(§). Calculate and plot the microwave refractivity vs. height using P and T of a standard atmosphere, but with vapor pressures (kPa) of:

a. 0 b. 0.05 c. 0.1 d. 0.2 e. 0.5
f. 1.0 g. 2 h. 5 i. 10 j. 20

[Note: Ignore supersaturation issues.]

N17(§). For the previous exercise, plot the vertical gradient $\Delta n/\Delta z$ of refractive index vs. height within the troposphere; determine the average vertical gradient in the troposphere; find the radius of curvature of the radar beam; and find the k_e beam curvature factor.

N18(§). For a radar with 0.5° elevation angle mounted on a 10 m tower, calculate and plot the height of the radar-beam centerline vs. range from 0 to 500 km, for the following beam curvature factors k_e, and name the type of propagation:

a. 0.5 b. 0.8 c. 1.0 d. 1.25 e. 1.33
f. 1.5 g. 1.75 h. 2 i. 2.5 j. 3

N19. Find the rainfall rate, intensity "level", and rainfall category for these radar echo dBZ values, using only the simple Z-R relationship:

a. 10 b. 35 c. 20 d. 45
e. 58 f. 48 g. 52 h. 25

N20. Find reflectivity dBZ for rain 10 km from a WSR-88D, if received power (in 10^{-14} W) is: a. 1 b.2 c. 4 d. 6 e. 8 f. 10 g. 15 h. 20 i. 40 j. 60 k. 80

N21. If weather radar indicates the following reflectivity values during the periods listed, what is the total rainfall at the end of the 40 minutes?

Time (min)	dBZ	Time (min)	dBZ
0 - 20	13	27 - 32	42
20 - 23	25	32 - 35	21
23 - 27	39	35 - 39	6

N22. Find the Doppler shift of 10 cm microwaves for radial velocities (m/s) of: a. –100 b. –75 c. –50 d. –20 e. 100 f. 75 g. 50 h. 20

N23. Given a max unambiguous velocity of 25 m/s, what velocities would be displayed on a Doppler radar for rain-laden air moving with the following real radial velocities (m/s)?
a. 26 b. 28 c. 30 d. 35 e. 20 f. 25 g. 55
h. –26 i. –28 j. –30 k. –35 l. –20

N24. Given a max unambiguous range of 200 km, at what range in the radar display does a target appear if its actual range is:
a. 205 b. 210 c. 250 d. 300 e. 350
f. 400 g. 230 h. 240 i. 390 j. 410

N25. Given the following sets of [average radial velocity (m/s) , range (km)], find the change of vertical velocity across a change of height of 1 km.
a. [–3, 100] b. [–2, 200] c. [–1, 50] d. [–4, 50]
e. [3, 100] f. [2, 200] g. [1, 50] h. [4, 50]

N26. Given polarimetric radar observations of Z_{VV} = 500 and Z_{VH} = 1.0, find the differential reflectivity and linear depolarization ratio for Z_{HH} values of:
a. 100 b. 200 c. 300 d. 400 e. 500
f. 600 g. 700 h. 800 i. 900 j. 1000

N27. Find the rainfall rate for the following sets of [K_{DP} (°/km) , Z_{DR} (dB)] as determined from polarimetric radar:
a. [1, 2] b. [1, 3] c. [1, 4] d. [1, 5]
e. [2, 2] f. [2, 6] g. [3, 2] h. [3, 4]
i. [3, 6] j. [5, 2] k. [5, 4] l. [5, 6]

N28. A wind profiler has transmitters spaced 0.5 m apart. Find the beam zenith angle for Δt (ns) of:
a. 0.2 b. 0.5 c. 1.0 d. 2 e. 3 f. 5

N29. For a wind profiler with 17° beam tilt, find U and W given these sets of [M_{east}(m/s), M_{west}(m/s)]:
a. [4, –4] b. [4, –3] c. [4, –5] d. [–4, 4]
e. [–4, 3] f. [–4, 5] g. [1, 1] h. [–1, –1]

Understanding & Critical Evaluation

U1(§). Create blackbody radiance curves similar to Fig. 8.5, but for the following satellite channels. Does a monotonic relationship exists between brightness temperature and blackbody radiance?
a. GOES imager channels 2 - 5.
b. Meteosat-8 imager channels 3 – 6
c. Meteosat-8 imager channels 7 - 11
d. GOES sounder channels 1 - 4
e. GOES sounder channels 5 - 8
f. GOES sounder channels 9 - 12
g. GOES sounder channels 13 - 16
h. GOES sounder channels 17 - 18
i. Meteosat-8 imager channels 1, 2, and 12

U2. For what situations would the brightness temperature NOT equal the actual temperature?

U3. a. Which GOES sounder channels can see the Earth's surface?
b. For the channels from part (a), how would the brightness temperature observed by satellite be affected, if at all, by a scene that contains scattered clouds of diameter smaller than can be resolved. For example, if the channel can see pixels of size 1 km square, what would happen if some of that 1 km square contained cumulus clouds of diameter 300 m, and the remaining pixel area was clear?

U4. Consider the radiative transfer equation. For an opaque atmosphere, $\hat{\tau}_{\lambda\,sfc} = 0$. What happens to the radiation emitted from the Earth's surface?

U5. Knowing the relationship between transmittance profile and weighting function, such as sketched in Figs. 8.7 or 8.8, sketch the associated transmittance profile for the following GOES sounder channels. [Hint, use the weights as sketched in Fig. 8.9 .]
a. 1 b. 2 c. 3 d. 4 e. 5
f. 7 g. 10 h. 11 i. 12 j. 15

U6(§). Given the following temperature sounding:

z (km)	T (°C)	z (km)	T (°C)
15 to 20	–50	5 to 10	–5
10 to 15	–25	0 to 5	+5
		Earth skin	+20

Find the radiance at the top of the atmosphere for the following transmittance profiles & wavelengths:
λ (μm): (a) 7.0 , (b) 12.7 , (c) 14.4 , (d) 4.4

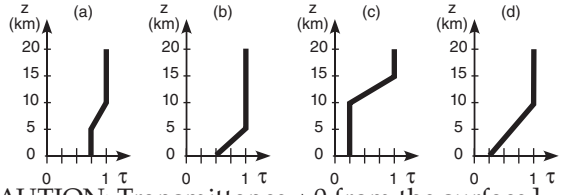

[CAUTION: Transmittance ≠ 0 from the surface.]

U7. For the transmittances of the previous exercise, plot the weighting functions.

U8. a. How low can a LEO satellite orbit without the atmosphere causing significant drag? [Hint, consider the exosphere discussion in the escape-velocity focus box in Chapter 1.]
b. What is the orbital period for this altitude?
c. If the satellite is too low, what would likely happen to it?

U9. a. What is the difference in orbital altitudes for geostationary satellites with orbital periods of 1 calendar day (24 h) and 1 sidereal day?
b. Define a sidereal day, explain why it is different from a calendar day, and discuss why the sidereal day is the one needed for geostationary orbital calculations.

U10. a. Discuss the meanings and differences between geostationary and sun-synchronous orbits.
b. Can satellite loops be made with images from polar orbiting satellites? If so, what would be the characteristics of such a loop?
c. What is the inclination of a satellite that orbits in the Earth's equatorial plane, but in the opposite direction to the Earth's rotation?
d. What are the advantages and disadvantages of sun-synchronous vs. geostationary satellites in observing the weather?

U11. What shade of gray would the following clouds appear in visible, IR, and water-vapor satellite images, and what pattern or shape would they have in the images?

a. jet contrail
b. two cloud layers: cirrus & altostratus
c. two cloud layers: cirrus & stratus
d. three cloud layers: cirrus, altostratus, stratus
e. two cloud layers: fog and altostratus
f. altocumulus standing lenticular
g. altocumulus castellanus
h. billow clouds
i. fumulus
j. volcanic ash clouds

U12. a. Using Fig. 8.8, state in words the altitude range that the water-vapor channel sees.
b. Sometimes water-vapor satellite loops show regions becoming whiter with time, even though there is no advection of water vapor visible in the loop. What might cause this?
c. Why is very dense fog with 100% relative humidity invisible in water-vapor satellite image?

U13. For locations (a) to (f), interpret the following satellite images, taken by GOES-12 at 2115 UTC on 18 Sept 2003, and justify your interpretation.
Top: visible. Middle: IR. Bottom: water vapor.
(Images courtesy of Space Science & Engineering Center.)

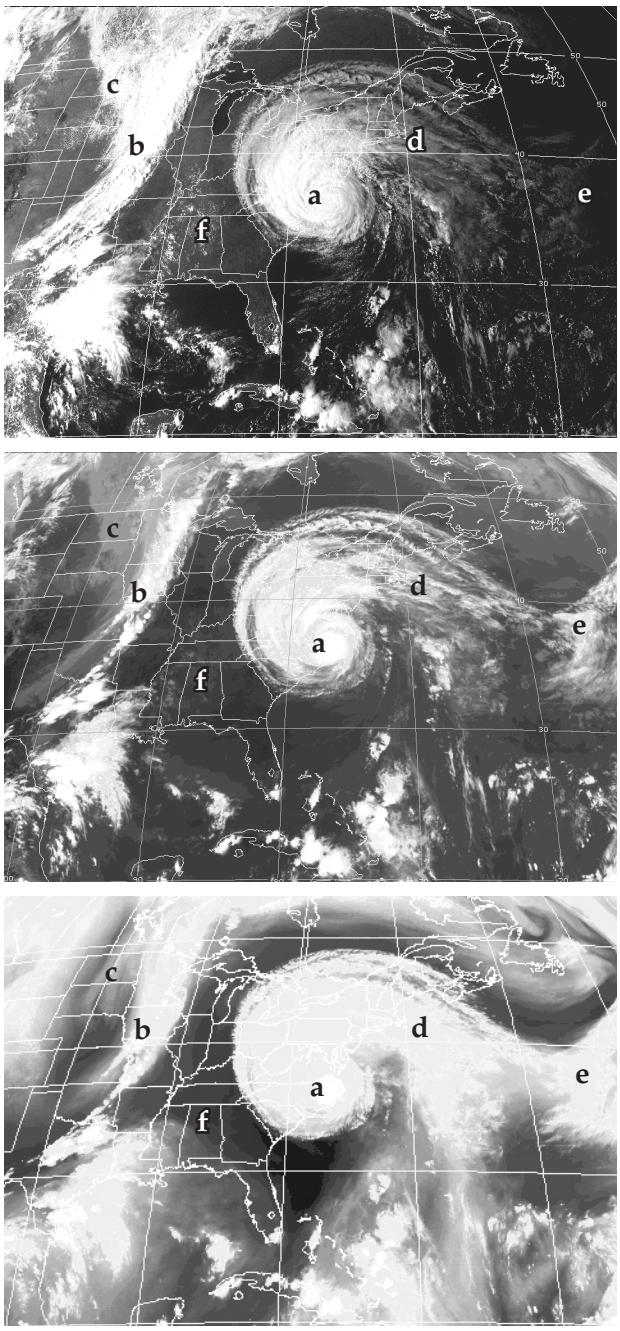

U14(§). Re-do the temperature sounding retrieval exercise of Table 8-6 and its solved example. Iterate through each layer 3 times, and then discuss the answer and its errors. Start with an initial temperature (°C) guess at all heights of:

a. –60 b. –50 c. –40 d. –30 e. 0

f. Instead of an isothermal initial guess, use a different initial guess for each layer based on the standard atmosphere near the center of the layer.

U15(§). Re-do the temperature sounding retrieval exercise of Table 8-6 and its solved example. Iterate through each layer 3 times, and save your answer as a baseline result. Start with the same initial temperature (–45 °C) guess at all heights.

Then repeat the process with the following errors added to the radiances before you start iterating, and discuss the difference between these new results and the results from the previous paragraph. What is the relationship between radiance error measured by satellite and temperature sounding error resulting from the data inversion?

a. Channel 1, add 5% error to the radiance.
b. Channel 1, subtract 5% error from radiance.
c. Channel 2, add 5% error to the radiance.
d. Channel 2, subtract 5% error from radiance.
e. Channel 3, add 5% error to the radiance.
f. Channel 3, subtract 5% error from radiance.
g. Channel 4, add 5% error to the radiance.
h. Channel 4, subtract 5% error from radiance.

U16(§). For Doppler radar, plot a curve of R_{max} vs. $M_{r\,max}$ for a variety of PRFs between 100 and 2000 s^{-1} , identify the problems with the interpretation of velocities and ranges above and below your curve, and discuss the Doppler dilemma. Use the following Doppler radar wavelengths (cm) for your calculations, and identify the name of their radar band:

a. 20 b. 10 c. 5 d. 3 e. 2 f. 1

U17. Discuss the advantages and disadvantages of PPI, CAPPI, RHI, and AVCS displays for observing:

a. thunderstorms b. hurricanes c. gust fronts
d. low-pressure centers e. fronts

U18(§). For P = 90 kPa, calculate a table of values of $\Delta N/\Delta z$ for different values of temperature gradient $\Delta T/\Delta z$ along the column headers, and different values of $\Delta e/\Delta z$ along the row headers. Then indicate beam propagation conditions (superrefraction, etc.) in each part of the table. Suggest when and where the worst anomalous propagation would occur.

U19. Which is more important in creating strong radar echoes: a larger number of small drops, or a small number of larger drops? Why?

U20. Derive eq. (8.31) using the geometry of a spherical drop.

U21. In eq. (8.28), why is the log(range) multiplied by 2 ?

U22. How does radar reflectivity factor Z change when dBZ doubles?

U23. Hong Kong researchers have found that $Z = a_3 \cdot RR^{a4}$, where a_3 = 220 ±12 and a_4 = 1.33 ±0.03, for RR in mm/h and Z in mm^6/m^3. Find the corresponding equation for RR as a function of dBZ.

U24. For a weather radar in good working order, under what conditions might the radar not be able to see cells of heavy rain?

U25. How might the bright band look in the vertical velocities measured with a wind profiler? Why?

U26. For an RHI radar display showing a bright band (see Fig a below), sketch how would the bright-band look in the plan-position indicator (PPI) display (Fig b) for the elevation angle ψ shown in (a). Assume the max range shown in (a) corresponds to the range circle drawn in (b).

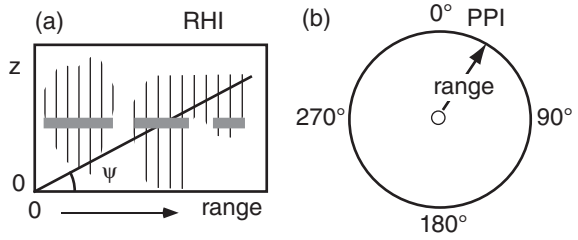

Fig (a) Range height indicator (RHI) radar display, where hatching indicates precipitation, and the darker gray horizontal regions are the "bright bands". Fig (b) Plan position indicator (PPI) display (blank, ready for you to sketch your answer).

U27. What design changes would you suggest to completely avoid the limitation of the max unambiguous velocity?

U28. Interpret the VAD display below to diagnose mean wind speed, direction, & convergence, if any.

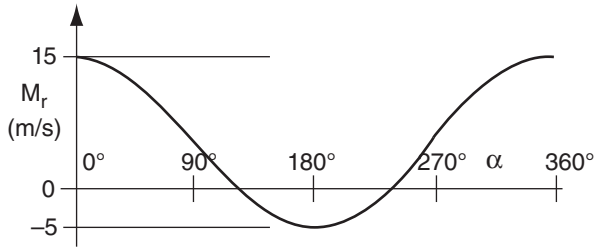

U29(§). Create a table of rainfall rate values, where each column is a different K_{DP} value (within typical range), and each row is a different Z_{DR} value. Draw the isohyets by hand in that table (i.e., draw lines connecting points of equal rainfall rate).

U30. Discuss the advantages and disadvantages of using larger zenith angle for the beams in a wind profiler.

U31. Interpret these weather conditions as observed on a Doppler radar display of radial velocity.

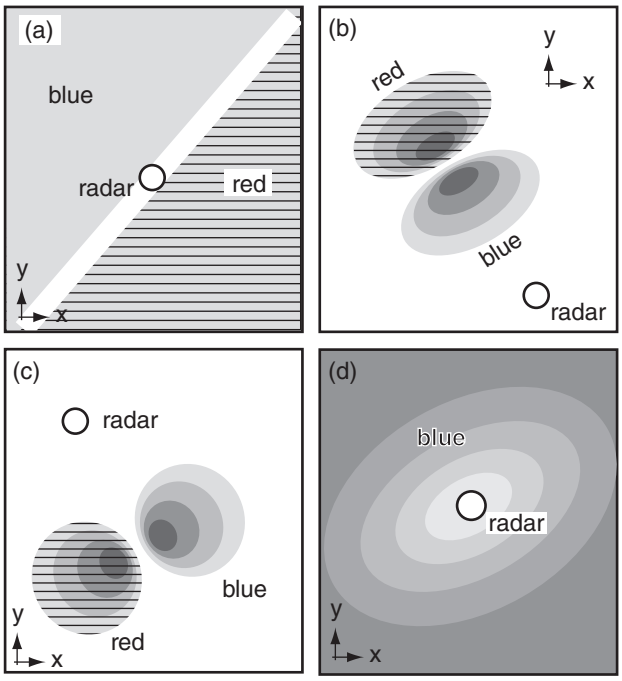

U32. a. Given the vectors drawn in Fig. 8.44, first derive a equations for M_{east} and M_{west} as the sum of the wind vectors projected into the east and west beams, respectively. Then solve those coupled equations to derive eqs. (8.42).
b. Write eqs. similar to eq. (8.42), but for the V and W winds based on M_{north} and M_{south}.

Web-Enhanced Questions

W1. Search the web for graphs of transmittance for wavelengths greater than 100 cm (like Figs. 8.4), and find the names of these regions of the electromagnetic spectrum. Comment on the possibility for remote sensing at these longer wavelengths.

W2. Search the web for graphs of weighting functions for one of the newer weather satellites (for the imager or for the sounder), as specified by your instructor. Discuss their advantages and disadvantages compared to the weighting functions given in this book.

W3. Search the web for current orbital characteristics for the active weather satellites specified by your instructor. Also, look for photos or artist drawings of these satellites.

W4. Search the web for data to create tables that list the currently active weather satellites around the world. Discuss any gaps in worldwide weather-satellite coverage.

W5. Search the web for images from all the different channels (for the imager or for the sounder) for one of the satellites, as specified by your instructor. Discuss the value and utility of each image.

W6. Search the web for satellite loops that cover your location. Compare these images with the weather you see out the window, and make a short-term forecast based on the satellite loop.

W7. Search the web to find the most recent set of visible, IR, and water-vapor images that covers your area. Print these images; label cloud areas as (a), (b), etc.; and interpret the clouds in those images. For the cloud area directly over you, compare you satellite interpretation with the view out your window.

W8. Search the web for thermo diagrams showing temperature soundings as retrieved from satellite sounder radiance data. Compare one of these soundings with the nearest rawinsonde (in-situ) sounding (by searching on "upper air" soundings).

W9. Search the web for tutorials on satellite-image interpretation; learn how to better interpret one type of cloud system (e.g., lows, fronts, thunderstorms); and write a summary tutorial for your classmates.

W10. Search the web for galleries of classical images showing the best examples of different types of clouds systems (e.g., hurricanes, squall lines).

W11. Search the web for tutorials on radar-image interpretation, and learn how to better interpret one type of echo feature (e.g., tornadoes, thunderstorms). Write a summary tutorial for your classmates.

W12. Use the web to access weather radar imagery for your local area (or as given by your instructor).
a. What different types of weather radar information are available (reflectivity, Doppler velocity, polarimetric data, derived products, etc)?
b. How recent are these types of radar images?
c. If radar loops are available, comment on how precipitation cell movement is different or similar to movement of the whole storm system or front.

W13. Some radar imagery available on the web includes a precipitation estimate from the past 24 h. For a current precipitation event, compare these rainfall estimates to those available from conventional rain gauges in the same area.

W14. During certain conditions, weather radar can see insects, birds, and non-precipitating clouds. Can

you find on the web any radar sites displaying any of these conditions? What is the URL web address, and what does it show?

W15. For your country, search the web for a map or list of all weather radar locations. How much of your country is covered by such radar?

W16. Search the web for photos of typical weather radar antenna and/or enclosures. Find and show a table listing the scan rate, elevation angles, and transmitted power for normal operation of these weather radars?

W17. Search the web to compare radar bands used for weather radar, police radar & microwave ovens.

W18. Search the web for examples of radar ducting or trapping.

W19. Search the web for other radar relationships to estimate rainfall rate, including other Z-R relationships and ones that use polarimetric data.

W20. Discuss the bright-band phenomenon by searching the web for info and photos.

W21. Search the web for info & photos on rain droplet & ice crystal shape, as affects polarimetric radar.

W22. Find real-time imagery of polarimetric radar products such as Z_{DR}, *LDR*, K_{DP}, and ρ_{HV}, and discuss their value in weather interpretation.

W23. Search the web for photos of phased-array radars and wind profilers. Compare and discuss.

W24. Search the web for locations in the world having "wind profiler" sites. Examine and discuss real-time data from whichever site is closest to you.

W25. Compare high-resolution satellite images from Earth-observing satellites (Aqua, Terra, and newer) with present-generation weather satellite imagery.

Synthesis Questions

S1. What if substantial cloud coverage could occur at any depth in the stratosphere as well as in the troposphere. Discuss how clouds at different altitudes would look in visible, IR, and water-vapor satellite images. Are there any new difficulties?

S2. What if molecular scattering by air was significant at all wavelengths. How would that affect satellite images and sounding retrievals, if at all?

S3. Suppose that Planck's law and brightness temperature were not a function of wavelength. How would IR satellite image interpretation be affected?

S4. If satellite weighting functions have about the same vertical spreads as plotted in Fig. 8.9, discuss the value of adding more and more channels.

S5. What if gravity on Earth were twice as strong as now. What would be the altitude and orbital period of geostationary satellites?

S6. What if the Earth were larger diameter, but had the same average density as the present Earth. How large would the diameter have to be so that an orbiting geostationary weather satellite would have an orbit that is zero km above the surface? (Neglect atmospheric drag on the satellite.)

S7. Determine orbital characteristics for geostationary satellites over every planet in the solar system.

S8. What if you could put active radar and lidar on weather satellites. Discuss the advantages and difficulties. (Note, this is actually being done.)

S9. Devise a method to eliminate both the max-unambiguous range and max-unambiguous velocity of Doppler radar.

S10. What if pressure and density were uniform with height in the atmosphere. How would radar beam propagation be affected?

S11. Compile (using web searches) the costs of developing, launching, operating, and analyzing the data from a single weather satellite. Compare with analogous costs for a single rawinsonde site.

S12. What if radar reflectivity was proportional only to the number of hydrometeors in a cloud, and not their size. How would radar-echo displays and rainfall-rate calculations be affected?

S13. What if Doppler radars could measure only tangential velocity rather than radial velocity. Discuss how mean wind, tornadoes, and downburst/gust-fronts would look to this radar.

S14. **Radio Acoustic Sounding Systems** (**RASS**) are wind profilers that also emit loud pulses of sound waves that propagate vertically. How can that be used to also measure the temperature sounding?

Copyright © 2011, 2015 by Roland Stull. *Meteorology for Scientists and Engineers, 3rd Ed.*

WEATHER REPORTS & MAP ANALYSIS

CONTENTS

Sea-level Pressure Reduction 267
Weather Observations, Reports 268
- Weather Codes 268
- METAR and SPECI 270
- Weather Observation Locations 271

Synoptic Weather Maps 274
- Station Plot Model 274
- Map Analysis, Plotting & Isoplething 280

Summary 281
- Threads 281

Exercises 282
- Numerical Problems 282
- Understanding & Critical Evaluation 285
- Web-Enhanced Questions 285
- Synthesis Questions 287

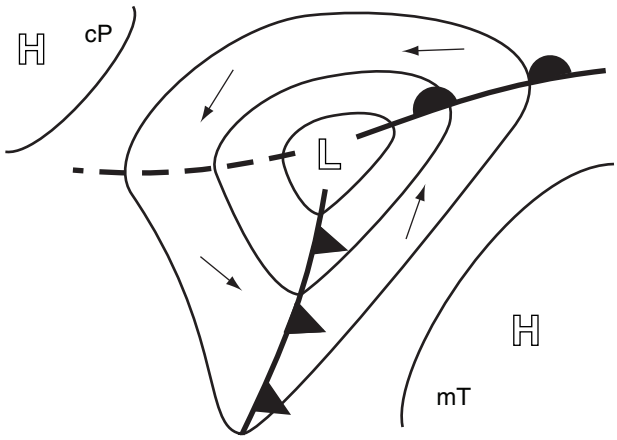

Figure 9.1
Idealized surface weather map showing high (H) and low (L) pressure centers, isobars (thin lines), and fronts (heavy solid lines) in the N. Hemisphere. Vectors indicate near-surface wind. Dashed line is a trough of low pressure. cP indicates a continental polar airmass; mT indicates a maritime tropical airmass.

"Meteorology for Scientists and Engineers, 3rd Edition" by Roland Stull is licensed under a Creative Commons Attribution-NonCommercial-ShareAlike 4.0 International License. To view a copy of the license, visit http://creativecommons.org/licenses/by-nc-sa/4.0/ . This work is available at http://www.eos.ubc.ca/books/Practical_Meteorology/ .

9 Surface weather maps summarize weather conditions that can affect your life. Where is it raining, snowing, windy, hot or humid? More than just plots of raw weather reports, you can analyze maps to highlight key features including high- and low-pressure centers, airmasses, and fronts (Fig. 9.1). In this chapter you will learn how to interpret some surface weather reports, and how to analyze surface weather maps.

SEA-LEVEL PRESSURE REDUCTION

Near the bottom of the troposphere, pressure gradients are large in the vertical (order of 10 kPa/km) but small in the horizontal (order of 0.001 kPa/km). As a result, pressure differences between neighboring surface weather stations are dominated by their relative station elevations z_{stn} (m) above sea level.

However, horizontal pressure variations are important for weather forecasting, because they drive horizontal winds. To remove the dominating influence of station elevation via the vertical pressure gradient, the reported station pressure P_{stn} is extrapolated to a constant altitude such as mean sea level (MSL). Weather maps of **mean-sea-level pressure** (P_{MSL}) are frequently used to locate high- and low-pressure centers at the bottom of the atmosphere.

The extrapolation procedure is called **sea-level pressure reduction**, and is made using the hypsometric equation:

$$P_{MSL} = P_{stn} \cdot \exp\left(\frac{z_{stn}}{a \cdot \overline{T_v^*}} \right) \qquad (9.1)$$

where $a = \Re_d / |g| = 29.3$ m/K, and the average air virtual temperature $\overline{T_v}$ is in Kelvin.

A difficulty is that $\overline{T_v}$ is undefined below ground. Instead, a fictitious average virtual temperature is invented:

$$\overline{T_v^*} = 0.5 \cdot [T_v(t_o) + T_v(t_o - 12\text{ h}) + \gamma_{sa} \cdot z_{stn}] \qquad (9.2)$$

where $\gamma_{sa} = 0.0065$ K/m is the standard-atmosphere lapse rate for the troposphere, and t_o is the time of the observations at the weather station. Eq. (9.2) attempts to average out the diurnal cycle, and it also extrapolates from the station to halfway toward sea level to try to get a reasonable temperature.

Solved Example

Phoenix Arizona (elevation 346 m MSL) reports dry air with T = 36°C now and 20°C half-a-day ago. P_{stn} = 96.4 kPa now. Find P_{MSL} (kPa) at Phoenix now.

Solution

Given: T(now) = 36°C, T(12 h ago) = 20°C,
z_{stn} = 346 m, P(now) = 96.4 kPa. Dry air.
Find: P_{MSL} = ? kPa

$T_v \approx T$, because air is dry. Use eq. (9.2) : $\overline{T_v^*}$ =
= 0.5·[(36°C) + (20°C) + (0.0065 K/m)·(346 m)]
= 29.16·°C (+ 273.15) = 302.3 K
Use eq. (9.1):
P_{MSL} = (96.4 kPa)·exp[(346 m)/((29.3 m/K)·(302.3 K))]
= (96.4 kPa)·(1.03984) = **100.24 kPa**

Check: Units OK. Physics OK. Magnitude OK.
Discus.: P_{MSL} can be significantly different from P_{stn}

Solved Example

Interpret the following METAR code:
METAR KSJT 160151Z AUTO 10010KT 10SM TS FEW060 BKN075 28/18 A2980 RMK AO2 LTG DSNT ALQDS TSB25 SLP068 T02780178

Hint: see the METAR section later in this chapter.

Solution:
Weather conditions at KSJT (San Angelo, Texas, USA) observed at 0151 UTC on 16th of the current month by an automated station: Winds are from the 100° at 10 knots. Visibility is 10 statute miles or more. Weather is a thunderstorm. Clouds: few clouds at 6000 feet AGL, broken clouds at 7500 feet AGL. Temperature is 28°C and dewpoint is 18°C. Pressure (altimeter) is 29.80 inches Hg. REMARKS: Automated weather station type 2. Distant (> 10 statute miles) lightning in all quadrants. Thunderstorm began at 25 minutes past the hour. Sea-level pressure is 100.68 kPa. Temperature more precisely is 27.8°C, and dewpoint is 17.8°C.

Discussion: As you can see, codes are very concise ways of reporting the weather. Namely, the 3 lines of METAR code give the same info as the 12 lines of plain-language interpretation.

You can use online web sites to search for station IDs. More details on how to code or decode METARs are in the Federal Meteor. Handbook No. 1 (2005) and various online guides. The month and year of the observation are not included in the METAR, because the current month and year are implied.

I am a pilot and flight instructor, and when I access METARs online, I usually select the option to have the computer give me the plain-language interpretation. Many pilots find this the easiest way to use METARs. After all, it is the weather described by the code that is important, not the code itself. However, meteorologists and aviation-weather briefers who use METARs every day on the job generally memorize the codes.

WEATHER OBSERVATIONS, REPORTS

The **World Meteorological Organization** (**WMO**), a component of the United Nations, coordinates international weather observing activities and sets observation standards. Weather observations are taken **synoptically**, which means that they are taken at the same time around the world. By international agreement, the time standard is **Coordinated Universal Time** (**UTC**, see Chapter 1).

The greatest number of manual synoptic surface and upper-air observations is obtained at 00 UTC, and nearly as many are taken at 12 UTC every day. Some countries also take upper-air observations at 06 and 18 UTC, as their budgets permit.

Weather Codes

One of the great successes of the WMO is the international sharing of real-time weather data via the **Global Telecommunication System** (**GTS**). To share this data, meteorologists in the world have agreed to speak the same weather language. This is accomplished by using **Universal Observation Codes** and abbreviations. Definitions of some of these codes are in:

World Meteorological Organization: 1995 (revised 2010): *Manual on Codes. International Codes Vol. 1.1 Part A - Alphanumeric Codes*. WMO No. 306 (http://www.wmo.int/pages/prog/www/WMOCodes.html)

Federal Meteorological Handbook No. 1 (Sept 2005): *Surface Weather Observations and Reports*. FCM-H1-2005 (http: www.ofcm.gov/fmh-1/fmh1.htm).

Sharing of real-time data across large distances became practical with the invention of the electric telegraph in the 1830s. Later developments included the teletype, phone modems, and the internet. Because weather codes in the early days were sent and received manually, they usually consisted of human-readable abbreviations and contractions.

Modern table-driven code formats (**TDCF**) are increasingly used to share data. One is **CREX** (Character form for the Representation and EXchange of data). Computer binary codes include **BUFR** (Binary Universal Form for the Representation of meteorological data) and **GRIB** (Gridded Binary).

However, there still are important sets of **alphanumeric codes** (letters & numbers) that are human writable and readable. Different alphanumeric codes exist for different types of weather observations and forecasts, as listed in Table 9-1. We will highlight one code here — the **METAR**.

Table 9-1. List of alphanumeric weather codes.

Name	Purpose
SYNOP	Report of surface observation from a fixed land station
SHIP	Report of surface observation from a sea station
SYNOP MOBIL	Report of surface observation from a mobile land station
METAR	Aviation routine weather report (with or without trend forecast)
SPECI	Aviation selected special weather report (with or without trend forecast)
BUOY	Report of a buoy observation
RADOB	Report of ground radar weather observation
RADREP	Radiological data report (monitored on a routine basis and/or in case of accident)
PILOT	Upper-wind report from a fixed land station
PILOT SHIP	Upper-wind report from a sea station
PILOT MOBIL	Upper-wind report from a mobile land station
TEMP	Upper-level pressure, temperature, humidity and wind report from a fixed land station
TEMP SHIP	Upper-level pressure, temperature, humidity and wind report from a sea station
TEMP DROP	Upper-level pressure, temperature, humidity and wind report from a dropsonde released by carrier balloons or aircraft
TEMP MOBIL	Upper-level pressure, temperature, humidity and wind report from a mobile land station
ROCOB	Upper-level temperature, wind and air density report from a land rocketsonde station
ROCOB SHIP	Upper-level temperature, wind and air density report from a rocketsonde station on a ship
CODAR	Upper-air report from an aircraft (other than weather reconnaissance aircraft)
AMDAR	Aircraft report (Aircraft Meteorological DAta Relay)
ICEAN	Ice analysis
IAC	Analysis in full form
IAC FLEET	Analysis in abbreviated form
GRID	Processed data in the form of grid-point values
GRAF	Processed data in the form of grid-point values (abbreviated code form)

Table 9-1 (continued). Alphanumeric codes.

Name	Purpose
WINTEM	Forecast upper wind and temperature for aviation
TAF	Aerodrome forecast
ARFOR	Area forecast for aviation
ROFOR	Route forecast for aviation
RADOF	Radiological trajectory dose forecast (defined time of arrival and location)
MAFOR	Forecast for shipping
TRACKOB	Report of marine surface observation along a ship's track
BATHY	Report of bathythermal observation
TESAC	Temperature, salinity and current report from a sea station
WAVEOB	Report of spectral wave information from a sea station or from a remote platform (aircraft or satellite)
HYDRA	Report of hydrological observation from a hydrological station
HYFOR	Hydrological forecast
CLIMAT	Report of monthly values from a land station
CLIMAT SHIP	Report of monthly means and totals from an ocean weather station
NACLI, CLINP, SPCLI, CLISA, INCLI	Report of monthly means for an oceanic area
CLIMAT TEMP	Report of monthly aerological means from a land station
CLIMAT TEMP SHIP	Report of monthly aerological means from an ocean weather station
SFAZI	Synoptic report of bearings of sources of atmospherics (e.g., from lightning)
SFLOC	Synoptic report of the geographical location of sources of atmospherics
SFAZU	Detailed report of the distribution of sources of atmospherics by bearings for any period up to and including 24 hours
SAREP	Report of synoptic interpretation of cloud data obtained by a meteorological satellite
SATEM	Report of satellite remote upper-air soundings of pressure, temperature and humidity
SARAD	Report of satellite clear radiance observations
SATOB	Report of satellite observations of wind, surface temperature, cloud, humidity and radiation

METAR and SPECI

METAR stands for Meteorological Aviation Report. It contains a routine (hourly) surface weather observation made at a manual or automatic weather station at an airport. It is formatted as a text message using codes (abbreviations, and a specified ordering of the data blocks separated by spaces) that concisely describe the weather.

Here is a brief summary on how to read METARs. Grey items below can be omitted if not needed.

Format

[METAR or **SPECI]** [corrected] [weather station ICAO code] [day, time] [report type] [wind direction, speed, gusts, units] [direction variability] [prevailing visibility, units] [minimum visibility, direction] [runway number, visual range] [current weather] [lowest altitude cloud coverage, altitude code] [higher-altitude cloud layers if present] [temperature/dewpoint] [units, sea-level pressure code] [supplementary] **RMK** [remarks].

Example (with remarks removed):

METAR KTTN 051853Z 04011G20KT 1 1/4SM R24/6200FT VCTS SN FZFG BKN003 OVC010 M02/M03 A3006 RMK...

Interpretation of the Example Above

Routine weather report for Trenton-Mercer Airport (NJ, USA) made on the 5th day of the current month at 1853 UTC. Wind is from 040° true at 11 gusting to 20 knots. Visibility is 1.25 statute miles. Runway visual range for runway 24 is 6200 feet. Nearby thunderstorms with snow and freezing fog. Clouds are broken at 300 feet agl, and overcast at 1000 ft agl. Temperature minus 2°C. Dewpoint minus 3°C. Altimeter setting is 30.06 in. Hg. Remarks...

SPECI

If the weather changes significantly from the last routine METAR report, then a special weather observation is taken, and is reported in an extra, unscheduled SPECI report. The SPECI has all the same data blocks as the METAR plus a plain language explanation of the special conditions.

The criteria that trigger SPECI issuance are:

Wind direction: changes >45° for speeds ≥ 10 kt.
Visibility: changes across threshold: 3 miles, 2 miles, 1 mile, 0.5 mile or instrument approach minim.
Runway visual range: changes across 2400 ft.
Tornado, Waterspout: starts, ends, or is observed.
Thunderstorm: starts or ends.
Hail: starts or ends.
Freezing precipitation: starts, changes, ends.
Ceiling: changes across threshold: 3000, 1500, 1000, 500, 200 (or lowest approach minimum) feet.
Clouds: when layer first appears below 1000 feet.
Volcanic eruption: starts.

Details of METAR / SPECI Data Blocks

Corrected: COR if this is a corrected METAR.
Weather Station **ICAO** Code is a 4-letter ID specified by the Internat. Civil Aviation Organization.
Day, Time: 2-digit day within current month, 4-digit time, 1-letter time zone (Z = UTC. Chapter 1).
Type: AUTO=automatic; (blank)=routine; NIL= missing.
Wind: 3-digit direction (degrees relative to true north, rounded to nearest 10 degrees). VRB=variable. 2- to 3-digit speed. (000000=calm). G prefixes gust max speed. Units (KT=knots, KMH=kilometers per hour, MPS=meters per second).
Direction Variability only if > 60°. Example: 010**V**090, means variable direction between 010° and 090°.
Prevailing Visibility: 4 digits in whole meters if units left blank. If vis < 800 m, then round down to nearest 50 m. If 800 ≤ vis < 5000 m, then round down to nearest 100 m. If 5000 ≤ vis < 9999 m, then round down to nearest 1000 m. Else "9999" means vis ≥ 10 km. In USA: number & fraction, with SM=statute miles. NDV = no directional variations.
Minimum Visibility: 4 digits in whole meters if units are blank & 1-digit (a point from an 8-point compass)
Runway Visual Range (RVR): **R**, 2-digit runway identifier, (if parallel runways, then: L=left, C=center, R=right), **/** , 4-digit RVR. Units: blank=meters, FT=feet. If variable RVR, then append optional: 4 digits, **V**, 4 digits to span the range of values. Finally, append optional tendency code: U=up (increasing visibility), N=no change, D-down (decreasing visibility).
Weather: see Tables in this chapter for codes. 0 to 3 groups of weather phenomena can be reported.
Clouds: 3-letter coverage abbreviation (see Table 9-10), 3-digit cloud-base height in hundreds of feet agl. TCU=towering cumulus congestus, CB = cumulonimbus. If no clouds, then whole cloud block replaced by CLR=clear or by SKC=sky clear. NSC= no significant clouds below 5000 ft (1500 m) with no thunderstorm and good visibility. NCD if no clouds detected by an automated system.
Higher Cloud Layers if any: 2nd lowest clouds reported only if ≥ SCT. 3rd lowest only if ≥ BRN.
Note: if visibility > 10 SM and no clouds below 5,000 ft (1500 m) agl and no precipitation and no storms, then the visibility, RVR, weather, & cloud blocks are omitted, and replaced with CAVOK, which means ceiling & visibility are OK (i.e., no problems for visual flight). (Not used in USA.)
Temperature/Dew-point: rounded to whole °C. Prefix M=minus.

Sea-level Pressure: 4 digits. Unit code prefix: A = altimeter setting in inches mercury, for which last 2 digits are hundredths. Q = whole hectoPascals hPa). Example: Q1016 = 1016 hPa = 101.6 kPa.

Supplementary: Can include: RE recent weather; WS wind shear; W sea state; runway state (SNOCLO=airport closed due to snow); trend, significant forecast weather (NOSIG=no change in significant weather, NSW=nil significant weather)

Remarks: **RMK**. For details, see the manuals cited three pages earlier.

Although you can read a METAR if you've memorized the codes, it is easier to use on-line computer programs to translate the report into plain language. Consult other resources and manuals to learn the fine details of creating or decoding METARs.

Weather Observation Locations

Several large governmental centers around the world have computers that automatically collect, test data quality, organize, and store the vast weather data set of coded and binary weather reports. For example, Figs. 9.2 to 9.12 show locations of weather observations that were collected by the computers at the European Centre for Medium-Range Weather Forecasts (**ECMWF**) in Reading, England, for a six-hour period centered at 00 UTC on 15 June 2007.

The volume of weather data is immense. There are roughly 1,400,000 locations (manual stations, automatic sites, and satellite obs) worldwide that report weather observations near 00 UTC. At ECMWF, many hundreds of megabytes (MB) of weather-observation data are processed and archived every day. The locations for the different types of weather-observation data are described next.

Surface observations (Fig. 9.2) include manual ones from land (SYNOP) and ship (SHIP) at key synoptic hours. Many countries also make hourly observations at airports, reported as METARs.

Surface automatic weather-observation systems make more frequent or nearly continuous reports. Examples of automatic surface weather stations are **AWOS** (Automated Weather Observing System), and **ASOS** (Automated Surface Observing System) in the USA. Those automatic reports that are near the synoptic hours are also included in Fig. 9.2.

Both moored and drifting buoys (BUOY; Fig. 9.3) also measure near-surface weather and ocean-surface conditions, and relay this data via satellite.

Small weather balloons (Fig. 9.4) can be launched manually or automatically from the surface to make **upper-air soundings**. As an expendable **radiosonde** package is carried aloft by the helium-filled

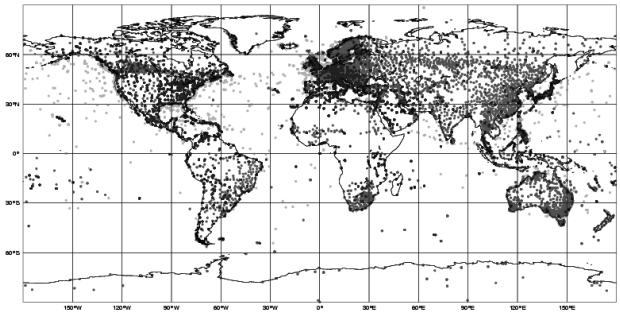

Figure 9.2
Surface data locations for observations of temperature, humidity, winds, clouds, precipitation, pressure, and visibility collected by synoptic weather stations on land and ship. Valid: 00 UTC on 15 Jun 2007. Number of observations: 9,560 METAR (land) + 15,752 SYNOP (land) + 2,179 SHIP = 27,491 surface obs. (From the European Centre for Medium Range Weather Forecasts: ECMWF.)

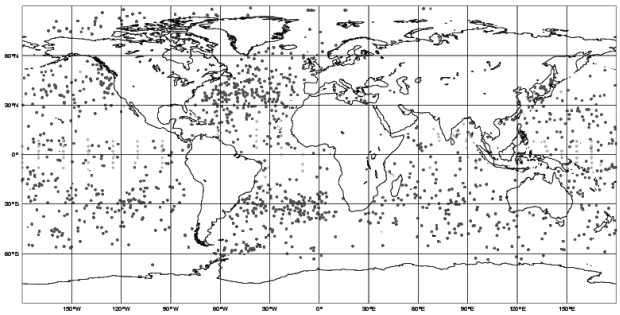

Figure 9.3
Surface data locations for temperature and winds collected by drifting and moored BUOYs. Valid: 00 UTC on 15 Jun 2007. Number of observations: 5,790 drifters + 209 moored = 5,999 buoys. (From ECMWF.)

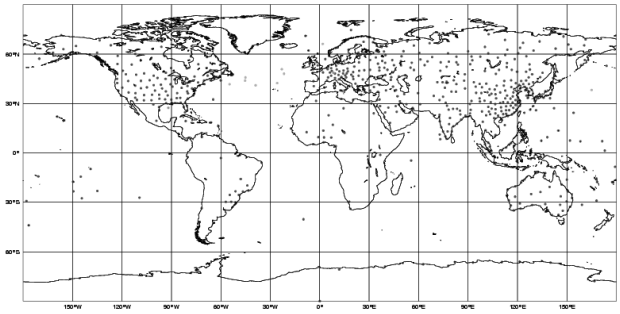

Figure 9.4
Upper-air sounding locations for temperature, pressure, humidity, and winds collected by rawinsonde balloons launched from land and ship, and by dropsondes released from aircraft. Valid: 00 UTC on 15 Jun 2007. Number of observations: 819 land (TEMP) + 9 ship (TEMP SHIP) + 2 dropsondes (TEMP DROP) = 630 soundings. Extra dropsondes are often dropped in Atlantic hurricanes and during strong winter storms over the NE Pacific Ocean (From ECMWF.)

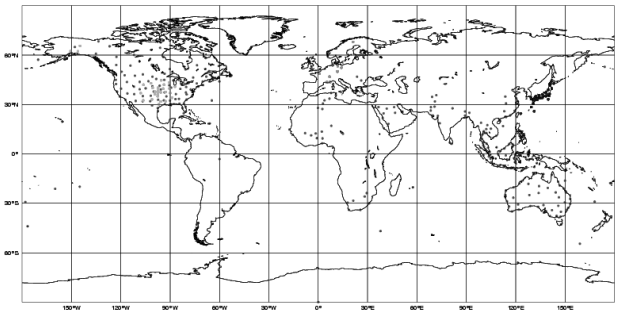

Figure 9.5
Upper-air data locations for winds collected by: PILOT balloons, ground-based wind profilers, and Doppler radars. Valid: 00 UTC on 15 Jun 2007. Number of observations: 290 pilot/rawinsonde balloons + 481 microwave wind profilers = 771 wind soundings. (From ECMWF.)

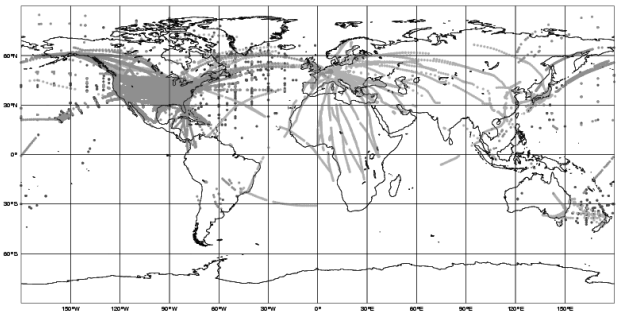

Figure 9.6
Upper-air data locations for temperature and winds collected by commercial aircraft: AIREP manual reports (black), and AMDAR & ACARS (grey) automated reports. Valid: 00 UTC on 15 Jun 2007. Number of observations: 7,099 AIREP + 20,333 AMDAR + 32,734 ACARS = 60,166 aircraft observations, most at their cruising altitude of 10 to 15 km above sea level. (From ECMWF.)

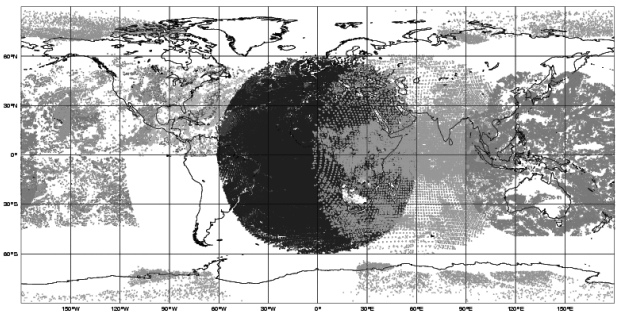

Figure 9.7
Upper-air data locations for winds collected by geostationary satellites (SATOB) from the USA (GOES), Europe (METEOSAT), and others around the world. Based on movement of clouds and water-vapor patterns, using IR, water vapor, and visible channels. Valid: 00 UTC on 15 Jun 2007. Number of observations: 258,738. (From ECMWF.)

latex balloon, and later as it descends by parachute, it measures temperature, humidity, and pressure. These radiosonde observations are called **RAOBs**.

Some radiosondes include additional instruments to gather navigation information, such as from **GPS** (Global Positioning Satellites). These systems are called **rawinsondes**, because the winds can be inferred by the change in horizontal position of the sonde. When a version of the rawinsonde payload is dropped by parachute from an aircraft, it is called a **dropsonde.**

Simpler weather balloons called **PIBALs** (Pilot Balloons) carry no instruments, but are tracked from the ground to estimate winds (Fig. 9.5). Most balloon soundings are made at 00 and 12 UTC.

Remote sensors on the ground include weather radar such as the **NEXRAD** (Weather Surveillance Radar WSR-88D). Ground-based microwave **wind profilers** (Fig. 9.5) automatically measure a vertical profile of wind speed and direction. **RASS** (Radio Acoustic Sounding Systems) equipment uses both sound waves and microwaves to measure virtual temperature and wind soundings.

Commercial aircraft (Fig. 9.6) provide manual weather observations called Aircraft Reports (**AIREPS**) at specified longitudes as they fly between airports. Many commercial aircraft have automatic meteorological reporting equipment such as **ACARS** (Aircraft Communication and Reporting System), **AMDAR** (Aircraft Meteorological Data Relay), & **ASDAR** (Aircraft to Satellite Data Relay).

Geostationary satellites are used to estimate tropospheric winds (Fig. 9.7) by tracking movement of clouds and water-vapor patterns. Surface winds over the ocean can be estimated from satellite using **scatterometer** systems (Fig. 9.8) that measure the scattering of microwaves off the sea surface. Rougher sea surface implies stronger winds.

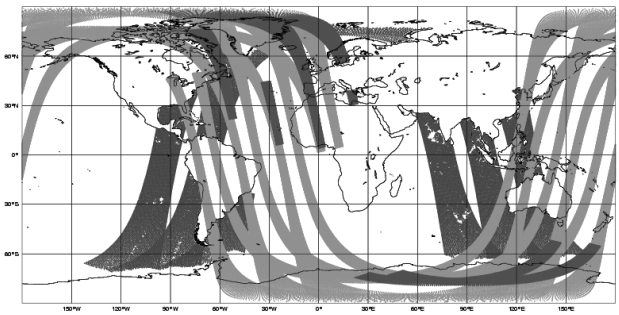

Figure 9.8
Surface-wind estimate locations from microwave scatterometer measurements of sea-surface waves by the polar-orbiting satellites. Valid: 00 UTC on 15 Jun 2007. Number of observations: 285,104. (From ECMWF.)

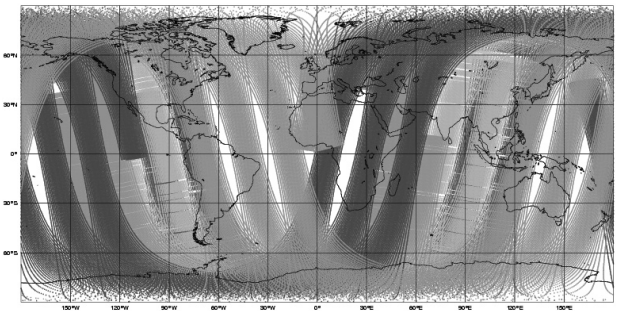

Figure 9.9
Temperature-sounding (SATEM) locations from radiation measurements by polar-orbiting NOAA satellites in cloudless areas, using TOVS (TIROS Operational Vertical Sounder) and AMSU (Advanced Microwave Sounding Unit). Satellites: several NOAA satellites, Aqua, and MetOP. Valid: 00 UTC on 15 Jun 2007. Number of observations: 315,667. (From ECMWF.)

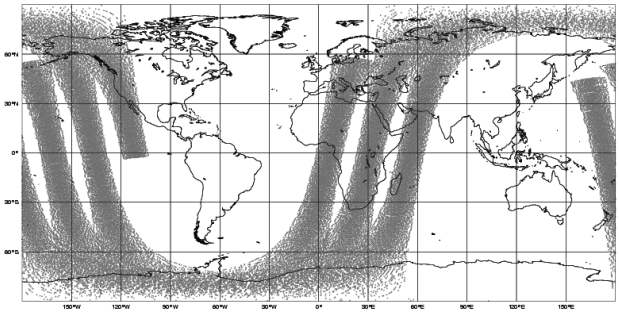

Figure 9.10
Temperature-sounding (SATEM) locations from high-spectral-resolution radiation measurements by polar-orbiting Aqua satellite in cloudless areas, using AIRS (Atmospheric Infrared Sounder). Valid: 00 UTC on 15 Jun 2007. Number of observations: 65,447. (From ECMWF.)

Satellites radiometrically estimate air-temperature to provide remotely-sensed upper-air automatic data (Fig. 9.9). One USA system is the **TOVS** (TIROS Operational Vertical Sounder, where **TIROS** is Television and Infrared Operational System) on the **NOAA** (National Oceanographic and Atmospheric Administration) civilian polar-orbiting satellites. Another is the **AMSU** (Advanced Microwave Sounding Unit), currently flying on NOAA 15, 16, 17, 18, Aqua, and the European MetOp satellites.

Higher spectral-resolution soundings (Fig. 9.10) are made with the **AIRS** (Atmospheric Infrared Sounding) system on a polar-orbiting Aqua satellite.

Humidity profiles are gathered using the **SSM/I** (Special Sensor Microwave Imager) system on the **DMSP** (Defense Meteorological Satellite Program) military polar-orbiting satellites (Fig. 9.11).

Radiance measurements (Fig. 9.12) from geostationary satellites are used to estimate temperature and humidity conditions for numerical forecast models via variational data assimilation in three or four dimensions (**3DVar** or **4DVar**). Tropospheric precipitable water can be estimated by satellite from the amount of microwave or IR radiation emitted from the troposphere.

These synoptically reported data give a snapshot of the weather, which can be analyzed on **synoptic weather maps**. The methods used to analyze the weather data to create such maps are discussed next.

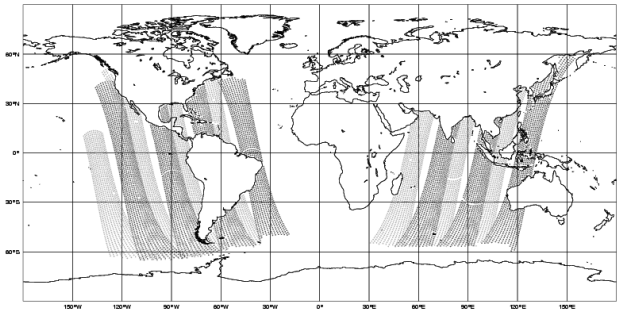

Figure 9.11
Humidity (SATOB) estimate locations from microwave radiances observed by the SSM/I sensor on polar-orbiting DMSP satellites 13, 14 & 15. Valid: 00 UTC on 15 Jun 2007. Number of observations: 11,140. (From ECMWF.)

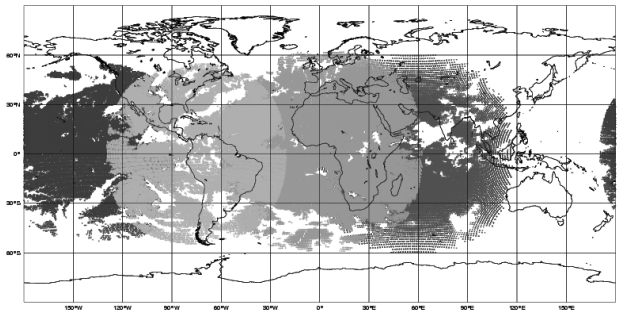

Figure 9.12
Radiance (SATRAD) measurement locations from radiation measurements by geostationary satellites Valid: 00 UTC on 15 Jun 2007. Number of observations: 361,128. (From ECMWF.)

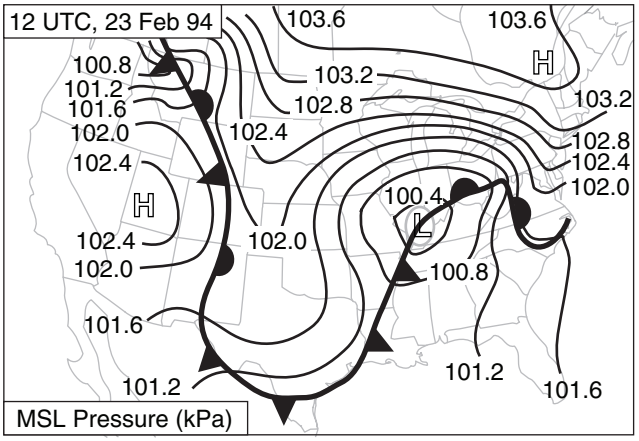

(a)

(b)

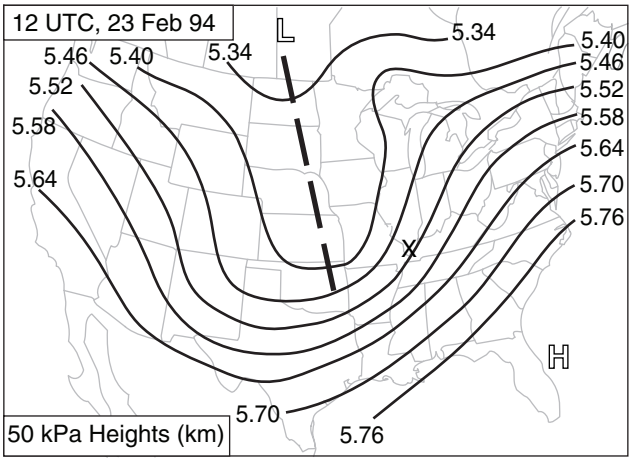

Figure 9.13
Examples of synoptic weather maps showing (a) the pressure pattern at the bottom of the troposphere, and (b) near the middle of the troposphere. The surface weather map (a) shows pressure reduced to mean sea-level (MSL), fronts, and high (H) and low (L) pressure centers. The upper-air map (b) shows height contours for the 50 kPa isobaric surface, and also indicates high and low centers, and the trough axis (dashed line). [Based on original analyses by Jon Martin.]

SYNOPTIC WEATHER MAPS

Although the word "synoptic" literally means "at the same time", the type of weather that can be seen on a synoptic map has come to be known as **synoptic-scale** weather (See Table in Dynamics chapter).

Synoptic weather maps give a snapshot of the weather. Fig. 9.13a shows an example of a synoptic weather map for the surface, based on surface weather observations. Fig. 9.13b shows an upper-air synoptic map valid at the same time, using data from weather balloons, aircraft, satellite, and ground-based remote sensors. By studying both maps, you can get a feeling for the three-dimensional characteristics of the weather.

Three steps are needed to create such maps. First, the weather data must be observed and communicated to central locations. Second, the data is tested for quality, where erroneous or suspect values are removed. These steps were already discussed.

Third, the data is analyzed, which means it is integrated into a coherent picture of the weather. This last step often involves interpolation to a grid (if it is to be analyzed by computers), or drawing of isopleths and identification of weather features (lows, fronts, etc.) if used by humans. Next, we will focus on manual weather-map analysis.

Station Plot Model

On weather maps, the location of each weather station is circled, and that station's weather data is plotted in and around the circle. The standardized arrangement of these data is called a **station plot model** (Fig. 9.14). Before the days of computerized geographic information systems (GIS), meteorologists had to rely on abbreviated codes to pack as much data around each plotted weather station as possible. These codes are still used today.

Unfortunately, different weather organizations/countries use different station plot models and different codes. Here is how you interpret the surface station plot models for USA and Canada:

• **T** is a two-digit **temperature** in whole degrees (°C in most of the world; °F if plotted by the USA).

Example: **18** means 18°F if plotted by a USA organization, but means 18°C if plotted by a Canadian organization.

[CAUTION: On weather maps produced in the USA, temperatures at Canadian weather stations are often converted to °F before being plotted. The opposite happens for USA stations plotted on Canadian weather maps — they are first converted to °C. You

should always think about the temperature value to see if it is reasonable for the units you assume.]

• **T**$_d$ is a two-digit **dew-point temperature** in whole degrees (°C in most of the world; °F if plotted by the USA).

Example: **14** means 14°F if plotted by a USA organization, but means 14°C if plotted by a Canadian organization. [Same CAUTION as for **T**.]

• **P** is the 3 least-significant digits of a 4- or 5-digit metric **mean sea-level pressure** value. To the left of the 3 digits, prefix either "9" or "10", depending on which one gives a value closest to standard sea-level pressure. For kPa, insert a decimal point two places from the right. For hPa, insert a decimal point one place from the right.

Example: **041** means 100.41 kPa, or 1004.1 hPa. New example: **986** means 99.86 kPa, or 998.6 hPa.

[CAUTION: Some organizations report **P** in inches of mercury (in. Hg.) instead of hPa. P_{MSL} (in. Hg.) is an **altimeter setting**, used by aircraft pilots.]

• **past wx** is a glyph (Table 9-2) for **past weather** in the past hour (or past 6 hours for Canada). It is blank unless different from present weather.

• **wx** is a glyph for **present weather** (at time of the weather observation). Tables 9-3 show the commonly used weather glyphs. Examples:

means snow shower; means thunderstorm with moderate rain.

• **vis** is the code for **visibility** (how far you can see objects).

In the USA, visibility is in statute miles.
(a) if visibility ≤ 3 $^1/_8$ miles, then *vis* can include a fraction.
(b) if 3 $^1/_8$ < visibility < 10 miles, then *vis* does not include a fraction.
(c) if 10 ≤ visibility, then *vis* is left blank.

Example: **2** $^1/_4$ means visibility is 2 $^1/_4$ statute miles. New example: **8** means visibility is 8 miles.

In Canada, visibility is in kilometers, but is coded into a two-digit *vis* code integer as follows:
(a) if *vis* ≤ 55, then visibility (km) = 0.1·*vis*
(b) if 56 ≤ *vis* ≤ 80, then visibility (km) ≈ *vis* – 50
(c) if 81 ≤ *vis*, then visibility (km) ≈ 5·(*vis* – 74)

Examples: **24** means 2.4 km. **66** means 16 km. **82** means 40 km. See Fig. 9.15 for a graph.

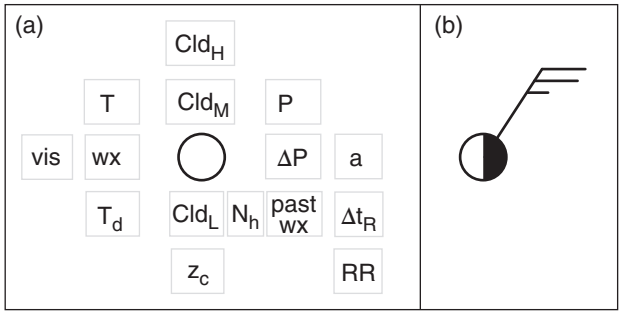

Figure 9.14
Station plot model. (a) Fixed fields (see tables). (b) Total cloud coverage represented by partially filled circle, and wind direction and speed. The circle represents the station location. Normally, (a) and (b) are plotted superimposed.

Table 9-2. Past or recent weather glyphs and codes (past wx).

Glyph	Meaning	METAR
	Drizzle	DZ
	Rain	RA
	Snow	SN
	Shower(s)	SH
	Thunderstorm (thunder is heard or lightning detected, even if no precipitation)	TS
	Fog (with visibility < 5/8 statute mile)	FG
	Sand Storm	SS
	Dust Storm	DS
	Drifting snow	DRSN
	Blowing snow	BLSN

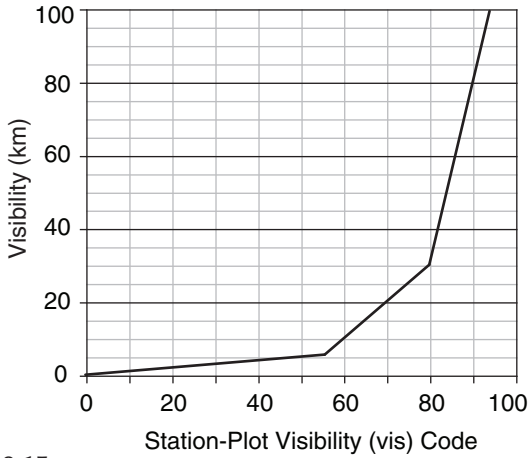

Figure 9.15
Visibility (vis) code for Canada.

Table 9-3a. Basic weather (wx) symbols and codes.

Glyph	Meaning	METAR
Precipitation:		
	Drizzle ‡	DZ
	Rain ‡	RA
	Snow ‡	SN
	Hail (large, diameter ≥ 5 mm)	GR
	Graupel (snow pellets, small hail, size < 5 mm)	GS
	Ice Pellets (frozen rain, called sleet in USA)	PL
	Ice Crystals ("diamond dust")	IC
	Snow Grain	SG
	Ice Needles	
	Unknown Precipitation (as from automated station)	UP
Obscuration:		
	Fog (with visibility < 5/8 statute mile) ‡	FG
	Mist (diffuse fog, with visibility ≥ 5/8 statute mile)	BR
	Haze	HZ
	Smoke	FU
	Volcanic Ash	VA
	Sand in air	SA
	Dust in air	DU
	Spray	PY
Storms & Misc.:		
	Squall	SQ
	Thunderstorm (thunder is heard or lightning detected, even if no precipitation)‡	TS
	Lightning	
	Funnel Cloud	FC
	Tornado or Waterspout	+FC
	Dust Devil (well developed)	PO
	Sand Storm	SS
	Dust Storm	DS

‡ Can be used as a "Past Weather" glyph.

Table 9-3b. Weather-code modifiers.

Glyph	Meaning	METAR prefix
Intensity, Proximity, or Recency: (Grey box ▫ is placeholder for a precipitation glyph from Table 9-3a. For example, ▫▫ means light drizzle.)		
	Light	–
	Moderate	(blank)
	Heavy	+
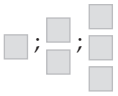	Intermittent and light ; moderate ; heavy	(no code for intermittent)
	In the vicinity. In sight, but not at the weather stn.	VC
	Virga (precip. in sight, but not reaching the ground).	VIRGA
	In past hour, but not now	
	Increased during past hour, and occurring now	
	Decreased during the past hour, and occurring now	
Descriptor:		
	Shower (slight)	–SH
	Shower (moderate)	SH
	Shower (heavy)	+SH
	Thunderstorm	TS
	Thunderstorm (heavy)	+TS
	Freezing. (if light, use left placeholder only) ***	FZ
	Blowing (slight)**	–BL
	Blowing (moderate)**	BL
	Blowing (strong, severe)**	+BL
	Drifting (low) (For DU, SA, SN raised < 2 m agl)	DR
	Shallow*	MI
	Partial*	PR
	Patchy*	BC

(* Prefixes for fog FG only.) (** Prefixes only for DU, SA, SN or PY.)
(*** Prefixes only for FG, DZ, or RN.)

Table 9-4. High Clouds (Cld_H).

Glyph	Meaning
	Cirrus (scattered filaments, "mares tails", not increasing).
	Cirrus (dense patches or twisted sheaves of filament bundles).
	Cirrus (dense remains of a thunderstorm anvil).
	Cirrus (hook shaped, thickening or spreading to cover more sky).
	Cirrus and cirrostratus increasing coverage or thickness, but covering less than half the sky.
	Cirrus and cirrostratus covering most of sky, and increasing coverage or thickness.
	Cirrostratus veil covering entire sky.
	Cirrostratus, not covering entire sky.
	Cirrocumulus (with or without smaller amounts of cirrus and/or cirrostratus).

Table 9-5. Mid Clouds (Cld_M).

Glyph	Meaning
	Altostratus (thin, semitransparent).
	Altostratus (thick), or nimbostratus.
	Altocumulus (thin).
	Altocumulus (thin, patchy, changing, and/or multi-level).
	Altocumulus (thin but multiple bands or spreading or thickening).
	Altocumulus (formed by spreading of cumulus).
	Multiple layers of middle clouds (could include altocumulus, altostratus, and/or nimbostratus).
	Altocumulus castellanus (has turrets or tuffs).
	Altocumulus of chaotic sky (could include multi-levels and dense cirrus).

• **Cld_H** is a glyph for high clouds (see Table 9-4).

• **Cld_M** is a glyph for mid-level clouds (Table 9-5).

• **Cld_L** is a glyph for low clouds (see Table 9-6).

• **N_h** is fraction of sky covered by low and mid clouds only. Units: oktas (eighths).

This can differ from the total sky coverage (see Table 9-10), which is indicated by the shading inside the station circle.

• **z_c** is a single-digit code for cloud-base height of lowest layer of clouds (Table 9-7).

• **ΔP** is 2 digits giving pressure change in the past 3 hours, prefixed with + or –. Units are hundredths of kPa. Example: –28 is a pressure decrease of 0.28 kPa or 2.8 hPa.

Table 9-6. Low Clouds (Cld_L).

Glyph	Meaning
	Cumulus (Cu) humilis. Fair-weather cumulus. Little vertical development.
	Cumulus mediocris. Moderate to considerable vertical development.
	Cumulus congestus. Towering cumulus. No anvil top.
	Stratocumulus formed by the spreading out of cumulus.
	Stratocumulus. (Not from spreading cu)
	Stratus.
	Scud. Fractostratus or fractocumulus, often caused by rain falling from above.
	Cumulus and stratocumulus at different levels (not cause by spreading of Cu.
	Cumulonimbus. Thunderstorm. Has anvil top that is glaciated (contains ice crystals, and looks fibrous).

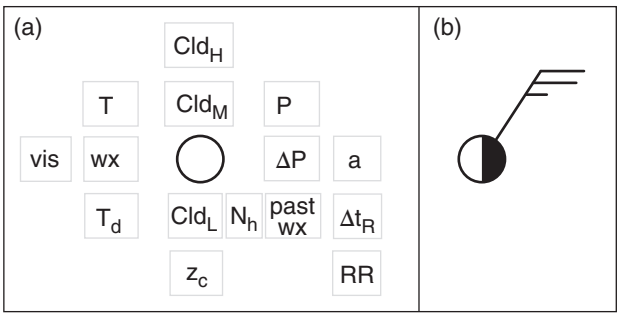

Figure 9.14 (again)
Station plot model.

Table 9-7. Codes for cloud-base height (z_c).

Code	meters agl	feet agl
0	0 to 49	0 to 149
1	50 to 99	150 to 299
2	100 to 199	300 to 599
3	200 - 299	600 to 999
4	300 - 599	1,000 to 1,999
5	600 to 999	2,000 to 3,499
6	1,000 to 1,499	3,500 to 4,999
7	1,500 to 1,999	5,000 to 6,499
8	2,000 to 2,499	6,600 to 7,999
9	≥ 2,500	≥ 8,000

Table 9-8. Symbols for pressure change (barometric tendency) during the past 3 hours. (a)

Glyph	Meaning
	Rising, then falling
	Rising, then steady or rising more slowly
	Rising steadily or unsteadily
	Falling or steady, later rising; or Rising slowly, later rising more quickly
	Steady
	Falling, then rising, but ending same or lower
	Falling, then steady or falling more slowly
	Falling steadily or unsteadily
	Steady or rising, then falling; or Falling, then falling more quickly

• **a** is a glyph representing the pressure change (barometric tendency) during the past 3 hours (Table 9-8). It mimics the trace on a barograph.

• Δt_R is a single-digit code that gives the number of hours ago that precipitation began or ended.

0 means no precipitation
1 means 0 to 1 hour ago
2 means 1 to 2 hours ago
3 means 2 to 3 hours ago
4 means 3 to 4 hours ago
5 means 4 to 5 hours ago
6 means 5 to 6 hours ago
7 means 7 to 12 hours ago
8 means more than 8 hours ago

• **RR** is the accumulated precipitation in past 6 hours. In the USA, the units are hundredths of inches. For example: 45 means 0.45 inches.

• **wind** is plotted as a direction shaft with barbs to denote speed (Fig. 9.14b). Table 9-9, reproduced from the Dynamics chapter, explains how to interpret it.

• **total clouds** is indicated by the portion of the station plot circle that is blackened (Fig. 9.14b). Table 9-10, reproduced from the Cloud chapter, explains its interpretation.

Table 9-9. Interpretation of wind barbs.

Symbol	Wind Speed	Description
	calm	two concentric circles
	1 - 2 speed units	shaft with no barbs
	5 speed units	a half barb (half line)
	10 speed units	each full barb (full line)
	50 speed units	each pennant (triangle)

• The total speed is the sum of all barbs and pennants. For example, indicates a wind from the west at speed 75 units. Arrow tip is at the observation location.
• CAUTION: Different organizations use different speed units, such as knots, m/s, miles/h, km/h, etc. Look for a legend to explain the units. When in doubt, assume knots — the WMO standard. To good approximation, 1 m/s ≈ 2 knots.

In the next subsection you will learn how to analyze a weather map. You can do a **hand analysis** (manual analysis) by focusing on just one meteorological variable. For example, if you want to analyze temperatures, then you should focus on just the temperature data from the station plot for each weather station, and ignore the other plotted data. This is illustrated in Fig. 9.16, where I have highlighted the temperatures to make them easier to see.

[*CAUTION: Do not forget that the plotted temperature represents the temperature at the station location (namely, at the plotted station circle), not displaced from the station circle as defined by the station plot model.*]

Table 9-10. Sky cover. Oktas=eighths of sky covered.

Sky Cover (oktas)	Symbol	Name	Abbr.	Sky Cover (tenths)
0	○	Sky **Clear**	SKC	0
1	◴	**Few*** Clouds	FEW*	1
2	◔			2 to 3
3	◕	**Scattered**	SCT	4
4	◑			5
5	◒	**Broken**	BKN	6
6	◕			7 to 8
7	◐			9
8	●	**Overcast**	OVC	10
unknown	⊗	Sky **Obscured**		unknown

* "Few" is used for (0 oktas) < coverage ≤ (2 oktas).

Solved Example

Decode the (a) station plot and the (b) METAR below, and compare the information they contain.

(a) Station Plot Example

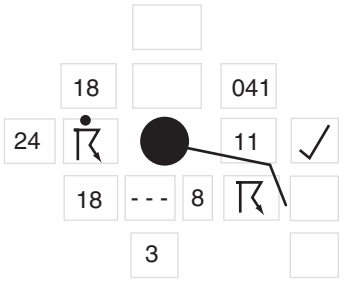

(b) METAR

METAR CYYB
040000Z 11010KT
1 1/2SM TSRA BR
BKN008 OVC020
18/18 A2965 RMK
SF5SC3 CB
ASOCTD PRES
UNSTDY SLP041

(c) Translation of METAR (Info from Stn Plot underlined)

Meteorological Aviation Report for North Bay (CYYB) ON, Canada on 4th day of the month at 0000 UTC.
Wind from 110° true at 10 knots.
Visibility 1.5 statuate miles (= 2.4 km).
Present weather is thunderstorm with moderate rain and mist.
Cloud coverage: broken clouds with base at 800 feet above ground, overcast with base at 2000 feet.
Temperature is 18°C, and dew point is 18°C.
Altimeter is 29.65 inches of mercury.

Remarks:
Stratus fractus clouds with 5/8 coverage, and
Stratocumulus clouds with 3/8 coverage, both associated with cumulonimbus.
Sea-level pressure is unsteady 100.41 kPa.
[Additional info in station plot, but not in METAR: past weather was thunderstorm; pressure first decreased, then increased with net increase of 0.11 kPa in 3 hr.]

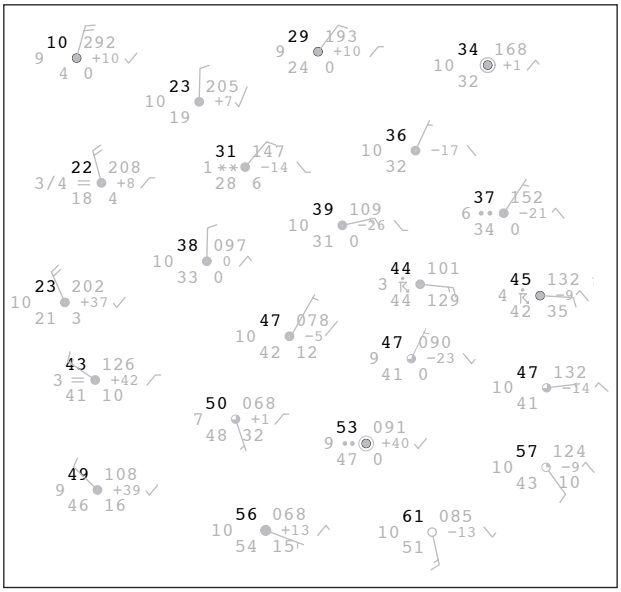

Figure 9.16

A surface weather map with temperatures highlighted. Units: T and T_d (°F), visibility (miles), speed (knots), pressure and 3-hour tendency (see text), 6-hour precipitation (hundredths of inches). Extracted from a "Daily Weather Map" courtesy of the US National Oceanic and Atmospheric Administration (NOAA), National Weather Service (NWS), National Centers for Environmental Prediction (NCEP), Hydrometeorological Prediction Center (HPC). The date/time of this map is omitted to discourage cheating during map-analysis exercises, and the station locations are shifted slightly to reduce overlap.

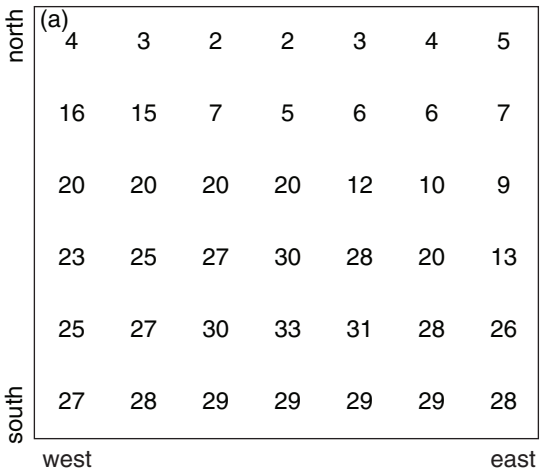

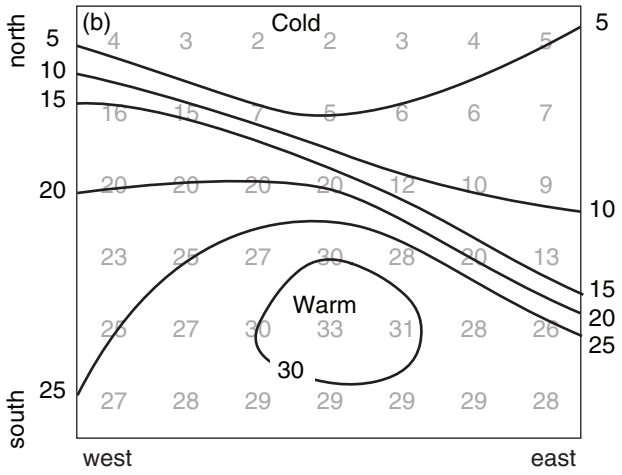

Map Analysis, Plotting & Isoplething

You might find the amount of surface-observation data such as plotted in Fig. 9.16 to be overwhelming. To make the plotted data more comprehensible, you can simplify the weather map by drawing **isopleths** (lines of equal value, see Table 1-6).

For example, if you analyze temperatures, you draw **isotherms** on the weather map. Similarly, if you analyze pressures you draw the **isobars**, or for humidity you draw **isohumes**.

Also, you can identify features such as fronts and centers of low and high pressure. Heuristic models of these features allow you to anticipate their evolution (see chapters on Airmasses, Fronts and Cyclones).

Most weather maps are analyzed by computer. Using temperature as an example, the synoptic temperature observations are interpolated by the computer from the irregular weather-station locations to a regular grid (Fig. 9.17a). Such a grid of numbers is called a **field** of data, and this particular example is a **temperature field**. A discrete temperature field such as stored in a computer array approximates the continuously-varying temperature field of the real atmosphere. The gridded field is called an **analysis**.

Regardless of whether you manually do a **hand analysis** on irregularly-spaced data (as in Fig. 9.16), or you let the computer do an **objective analysis** on a regularly-spaced grid of numbers (as in Fig. 9.17a), the next steps are the same for both methods.

Continuing with the temperature example of Fig. 9.17, draw isotherms connecting points of equal temperature (Fig. 9.17b). The following rules apply to any line connecting points of equal value (i.e., **isopleths**), not just to isotherms:

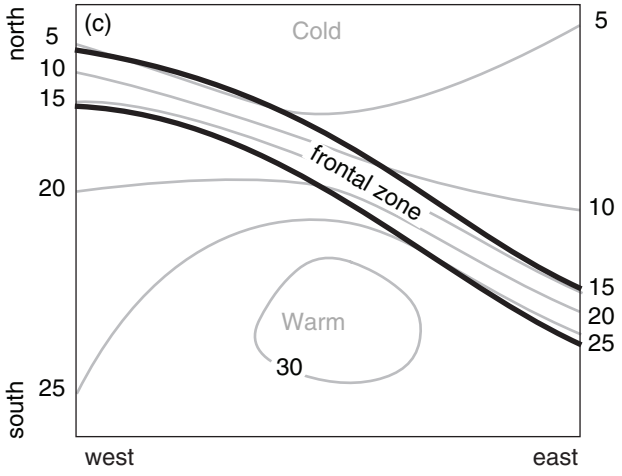

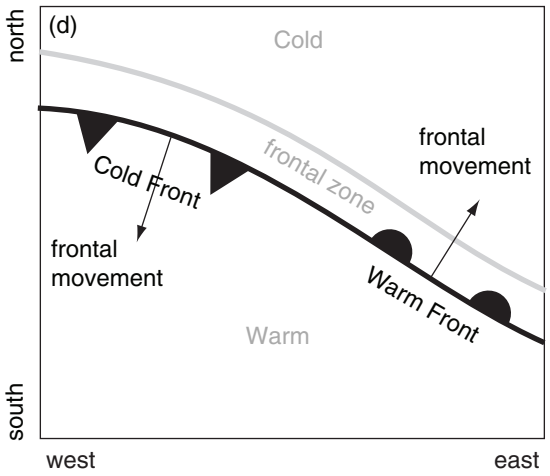

Figure 9.17

Weather map analysis: a) temperature field, with temperature in (°C) plotted on a Cartesian map; b) isotherm analysis; c) frontal zone analysis; d) frontal symbols added. [Note: The temperature field in this figure is for a different location and day than the data that was plotted in Fig. 9.16.]

- draw isopleths at regular intervals (such as every 2°C or 5°C for isotherms)
- interpolate where necessary between locations (e.g., the 5°C isotherm must be equidistant between gridded observations of 4°C & 6°C)
- isopleths never cross other isopleths of the same variable (e.g., isotherms can't cross other isotherms, but isotherms can cross isobars)
- isopleths never end in the middle of the map
- label each isopleth, either at the edges of the map (the only places where isopleths can end), or along closed isopleths
- isopleths have no kinks, except sometimes at fronts or jets

Finally, label any relative maxima and minima, such as the warm and cold centers in Fig. 9.17b.

You can identify **frontal zones** as regions of tight isotherm packing (Fig. 9.17c), namely, where the isotherms are closer together. Note that no isotherm needs to remain within a frontal zone.

Finally, always draw a heavy line representing the front on the warm side of the frontal zone (Fig. 9.17d), regardless of whether it is a cold, warm, or stationary front.

Frontal symbols are drawn on the side of the frontal line toward which the front moves. Draw semicircles to identify warm fronts (for cases where cold air retreats). Draw triangles to identify a cold front (where cold air advances). Draw alternating triangles and semicircles on opposite sides of the front to denote a stationary front, and on the same side for an occluded front. Fig. 9.18 summarizes frontal symbols, many of which will be discussed in more detail in the Airmasses and Fronts chapter.

In Fig. 9.17d, there would not have been enough information to determine if the cold air was advancing, retreating, or stationary, if I hadn't added arrows showing frontal movement. When you analyze fronts on real weather maps, determine their movement from successive weather maps at different times, by the wind direction across the front, or by their position relative to low-pressure centers.

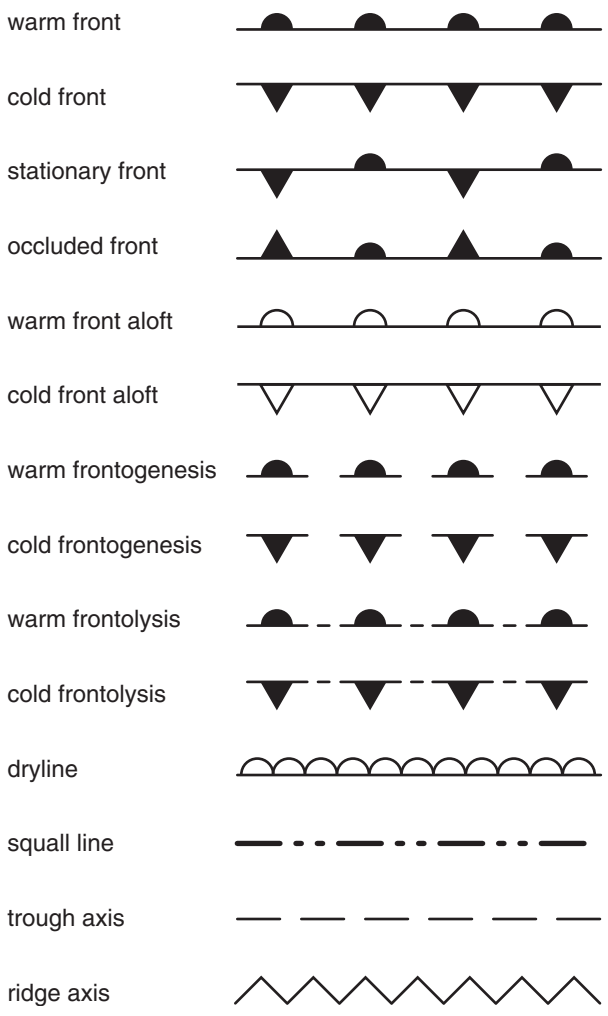

Figure 9.18
Glyphs for fronts, other airmass boundaries, and axes. The suffix "genesis" implies a forming or intensifying front, while "lysis" implies a weakening or dying front. A stationary front is a frontal boundary that does not move very much. Occluded fronts and drylines will be explained in the Fronts chapter.

SUMMARY

Hundreds of thousands of weather observations are simultaneously made around the world at standard observation times. Some of these weather observations are communicated as alphanumeric codes such as the METAR that can be read and decoded by humans. A station-plot model is often used to plot weather data on weather maps. Map analysis is routinely performed by computer, but you can also draw isopleths and identify fronts, highs, lows, and airmasses by hand.

Threads

Fronts and highs, as analyzed on weather maps, are discussed in Chapter 12. Map analysis is also used to identify mid-latitude cyclones (Chapter 13) and tropical cyclones (Chapter 16). Weather maps can summarize average conditions such as the global circulation (Chapter 11). Pressure gradients found from weather maps define the strength of the wind (Chapter 10). Temperature and humidity from weather maps help us to anticipate the threat of severe thunderstorms (Chapters 14 and 15) and local winds (Chapter 17).

EXERCISES

Numerical Problems

N1. Reduce to sea level the pressure the following station observations of pressure, height, and virtual temperature. Assume no temperature change over the past 12 hours.

	P (kPa)	z (m)	T_v(°C)
a.	102	–30	40
b.	100	20	35
c.	98	150	30
d.	96	380	30
e.	94	610	20
f.	92	830	18
g.	90	980	15
h.	88	1200	12
i.	86	1350	5
j	84	1620	5
k.	82	1860	2

N2. Decode the following METAR. Hint: It is not necessary to decode the station location; just write its ICAO abbreviation followed by the decoded METAR. Do not decode the remarks (RMK).

a. KDFW 022319Z 20003KT 10SM TS FEW037 SCT050CB BKN065 OVC130 27/20 A2998 RMK AO2 FRQ LTGICCG TS OHD MOV E-NE

b. KGRK 022317Z 17013KT 4SM TSRA BKN025 BKN040CB BKN250 22/21 A3000 RMK OCNL LTGCCCG SE TS OHD-3SE MOV E

c. KSAT 022253Z 17010KT 10SM SCT034 BKN130 BKN250 28/23 A2998 RMK AO2 RAE42 SLP133 FEW CB DSNT NW-N P0001 T02830233

d. KLRD 022222Z 11015KT M1/4SM TSRA FG OVC001 24/23 A2998 RMK AO2 P0125 PRESRR

e. KELD 022253Z AUTO 14003KT 4SM RA BR OVC024 23/21 A3006 RMK AO2 TSB2153E12 SLP177 T02280211 $

f. KFSM 022311Z 00000KT 10SM TSRA SCT030 22/21 A3004 RMK AO2 P0000

g. KLIT 022253Z 08009KT 7SM TS FEW026 BKN034CB OVC060 27/22 A3003 RMK AO2 RAB28E45 SLP169 OCNL LTGICCC OHD TS OHD MOV N P0000 T02720217

h. KMCB 022315Z AUTO 34010KT 1/4SM +TSRA FG BKN005 OVC035 24/23 A3009 RMK AO2 LTG DSNT ALQDS P0091 $

i. KEET 022309Z AUTO 05003KT 3SM -RA BR SCT024 BKN095 23/23 A3005 RMK AO2 LTG DSNT N AND E AND SW

j. KCKC 022314Z AUTO 20003KT 2SM DZ OVC003 13/11 A3009 RMK AO2

k. CYQT 022300Z 20006KT 20SM BKN026 OVC061 16/11 A3006 RMK SC5AC2 SLP185

l. CYYU 022300Z 23013KT 15SM FEW035 BKN100 BKN200 BKN220 23/08 A3013 RMK CU2AS2CC1CI1 WND ESTD SLP207

m. CYXZ 022300Z 00000KT 15SM -RA OVC035 14/11 A3021 RMK SC8 SLP239

n. KETB 022325Z AUTO 10007KT 009V149 10SM -RA CLR 19/11 A3021 RMK AO2

o. CYWA 022327Z AUTO 33004KT 9SM RA FEW027 FEW047 BKN069 19/12 A3016

Table 9-11. Weather-Glyph Exercises.

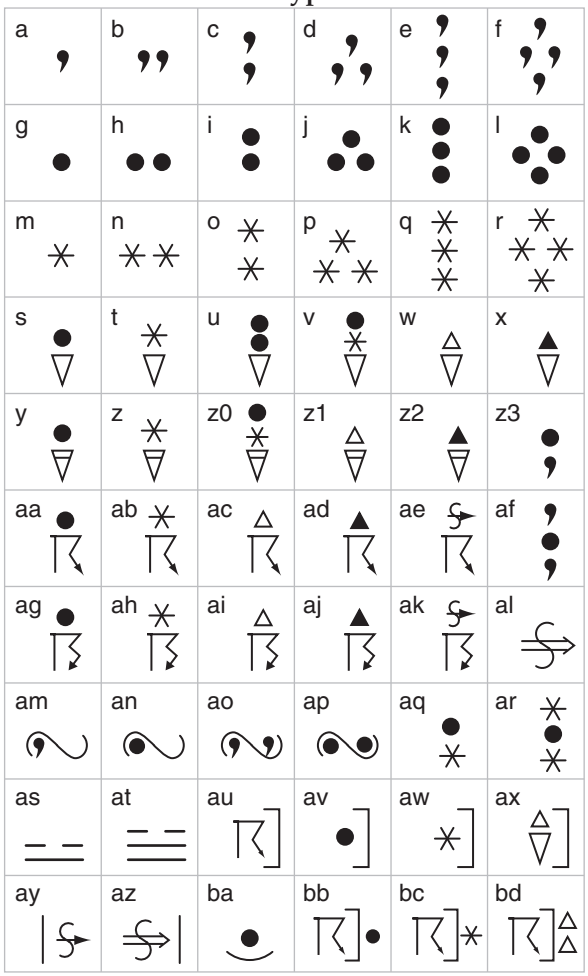

N3. Translate into words a weather glyph assigned from the table on the previous page.

N4 For a weather glyph from the table on the previous page, write the corresponding METAR abbreviation, if there is one.

N5. Using the station plot model, plot the weather observation data around a station circle drawn on your page for one METAR from exercise N2, as assigned by your instructor.

N6. Using the USA weather map below (Fig. 9.19), decode the weather data for the weather station labeled (a) - (w), as assigned by your instructor.

N7. Photocopy the USA weather map below (Fig. 9.19) and analyze it by drawing isopleths for:

a. temperature (isotherms) every 5°F
b. pressure (isobars) every 0.4 kPa
c. dew point (isodrosotherms) every 5°F
d. wind speed (isotachs) every 5 knots
e. pressure change (isallobar) every 0.1 kPa

N8. Using the Canadian weather map (Fig. 9.20) on the next page, decode the weather data for the station labeled (a) - (z), as assigned by your instructor.

N9. Photocopy the Canadian weather map (Fig. 9.20), and analyze it by drawing isopleths for the following quantities.
a. temperature (isotherms) every 2°C
b. dew point (isodrosotherms) every 2°C
c. pressure change (isallobar) every 0.1 kPa
d. total cloud coverage (isonephs) every okta
e. visibility every 5 km

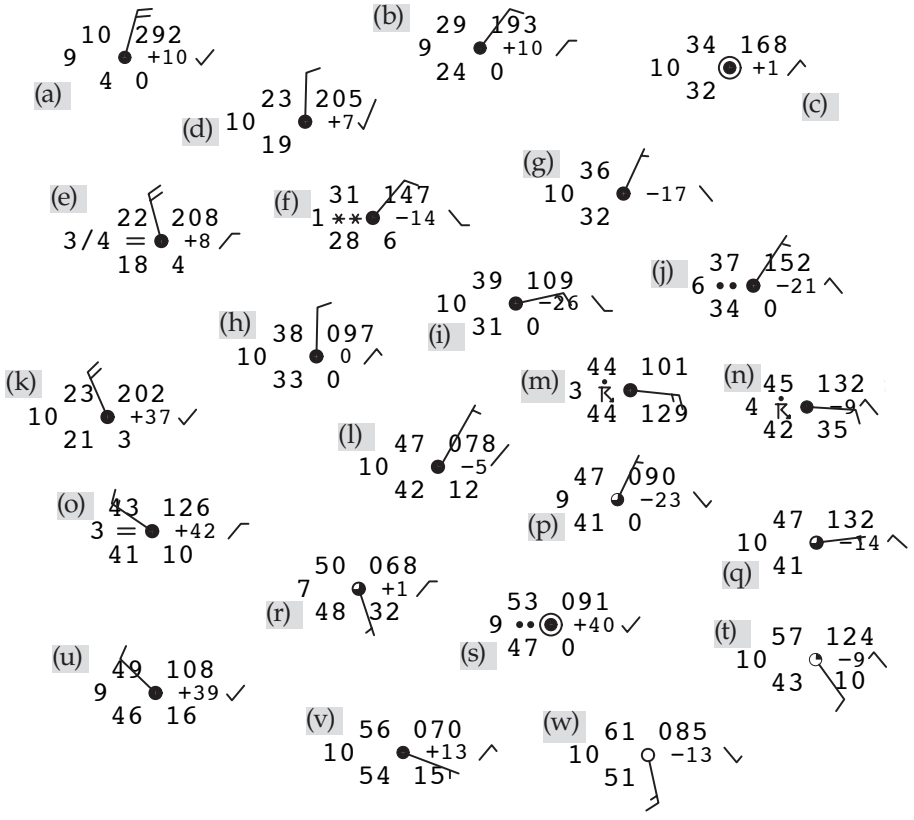

Figure 9.19
USA surface weather map. Units: T and T_d (°F), visibility (miles), speed (knots), pressure and 3-hour tendency (see text), 6-hour precipitation (hundredths of inches). Extracted from a "Daily Weather Map" courtesy of the US National Oceanic and Atmospheric Administration (NOAA), National Weather Service (NWS), National Centers for Environmental Prediction (NCEP), Hydrometeorological Prediction Center (HPC). The date/time of this map is omitted to discourage cheating during map-analysis exercises, and the station locations are shifted slightly to reduce overlap.

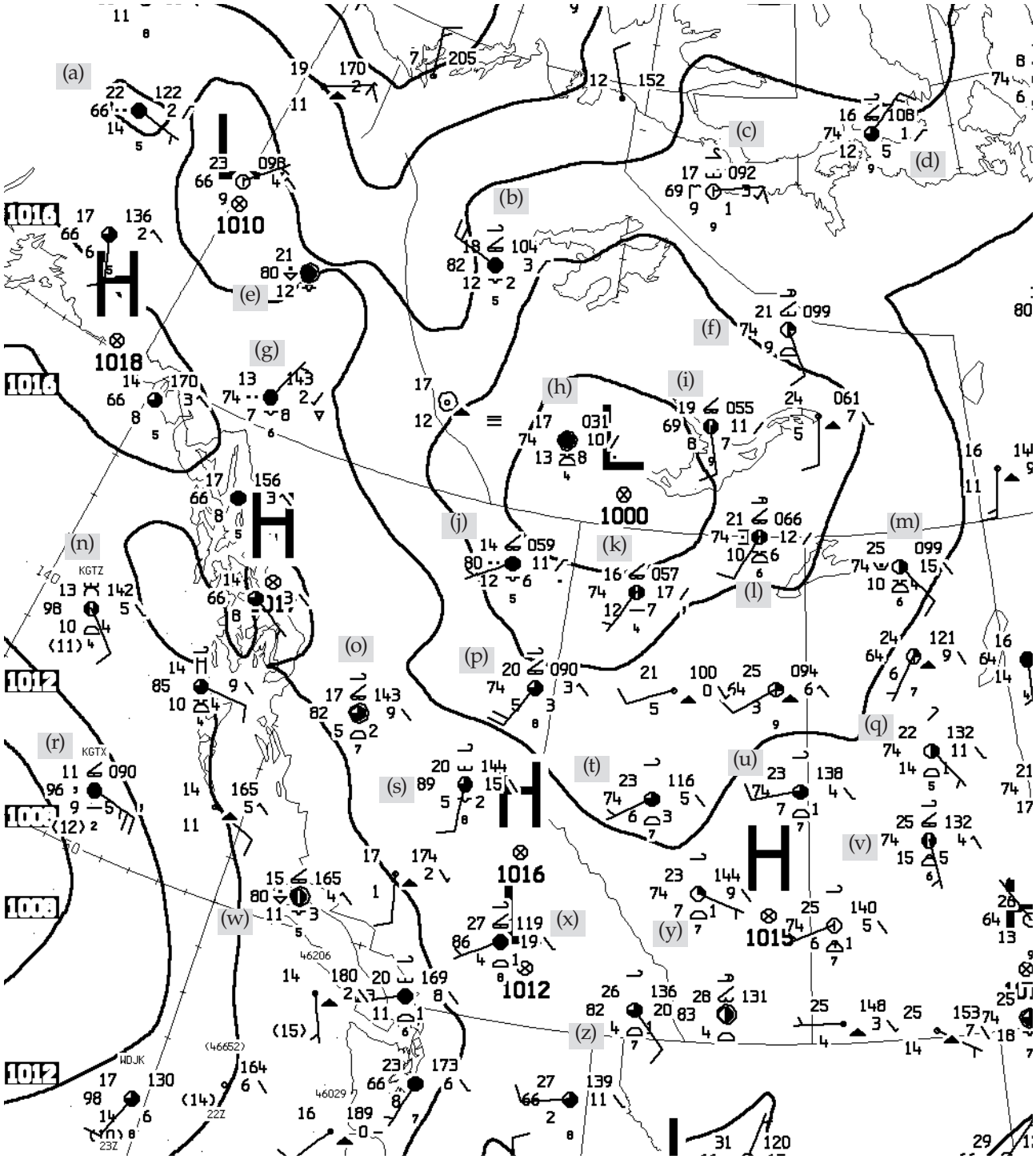

Figure 9.20
Canadian weather map courtesy of Environment Canada. http://www.weatheroffice.gc.ca/analysis/index_e.html

8	9	11	12	13	14	15
7	9	11	13	14	15	16
8	9	14	18	20	20	18
9	9	16	19	22	24	24
10	11	18	20	22	25	25
12	14	19	20	22	24	25
14	18	19	21	22	23	24
18	19	20	21	22	23	23

Figure 9.21-i
Temperature (°C).

9.5	9.4	9.4	9.5	9.6	9.7	9.8
9.4	9.3	9.2	9.3	9.4	9.6	9.7
9.5	9.2	8.9	9.2	9.3	9.4	9.6
9.5	9.4	9.1	9.4	9.5	9.5	9.6
9.6	9.4	9.2	9.5	9.6	9.7	9.7
9.6	9.4	9.4	9.6	9.7	9.8	9.9
9.6	9.4	9.6	9.7	9.8	9.9	0.0
9.6	9.6	9.7	9.8	9.9	0.0	0.1

Figure 9.21-ii
Pressure (kPa). [The first 1 or 2 digits of the pressure are omitted. Thus, 9.5 on the chart means 99.5 kPa, while 0.1 means 100.1 kPa.]

N10. Both of the weather maps of Fig. 9.21 correspond to the same weather. Do the following work on a photocopy of these charts:

a. Draw isotherms and identify warm and cold centers. Label isotherms every 2°C.
b. Draw isobars every 0.2 kPa and identify high and low pressure centers.
c. Add likely wind vectors to the pressure chart.
d. Identify the frontal zone(s) and draw the frontal boundary on the temperature chart.
e. Use both charts to determine the type of front (cold, warm), and draw the appropriate frontal symbols on the front.
f. Indicate likely regions for clouds and suggest cloud types in those regions.
g. Indicate likely regions for precipitation.
h. For which hemisphere are these maps?

Understanding & Critical Evaluation

U1. Are there any locations in the world where you could get a reasonable surface weather map without first reducing the pressure to mean sea level? Explain.

U2. What aspects of mean sea level reduction are physically unsound or weak? Explain.

U3. One of the isoplething instructions was that an isopleth cannot end in the middle of the map. Explain why such an ending isopleth would imply a physically impossible weather situation.

U4. Make a photocopy of the surface weather map (Fig. 9.22) on the next page, and analyze your copy by drawing isobars (solid lines), isotherms (dashed lines), high- and low-pressure centers, airmasses, and fronts.

Web-Enhanced Questions

W1. Access a surface weather map that shows station plot information for Denver, Colorado USA. Decode the plotted pressure value, and tell how you can identify whether that pressure is the actual station pressure, or is the pressure reduced to sea level.

W2. Do a web search to identify 2 or more suggestions on how to reduce station pressure to sea level. Pick two methods that are different from the method described in this chapter.

W3. Search the web for maps that show where METAR weather data are available. Print such a map that covers your location, and identify which 3 stations are closest to you.

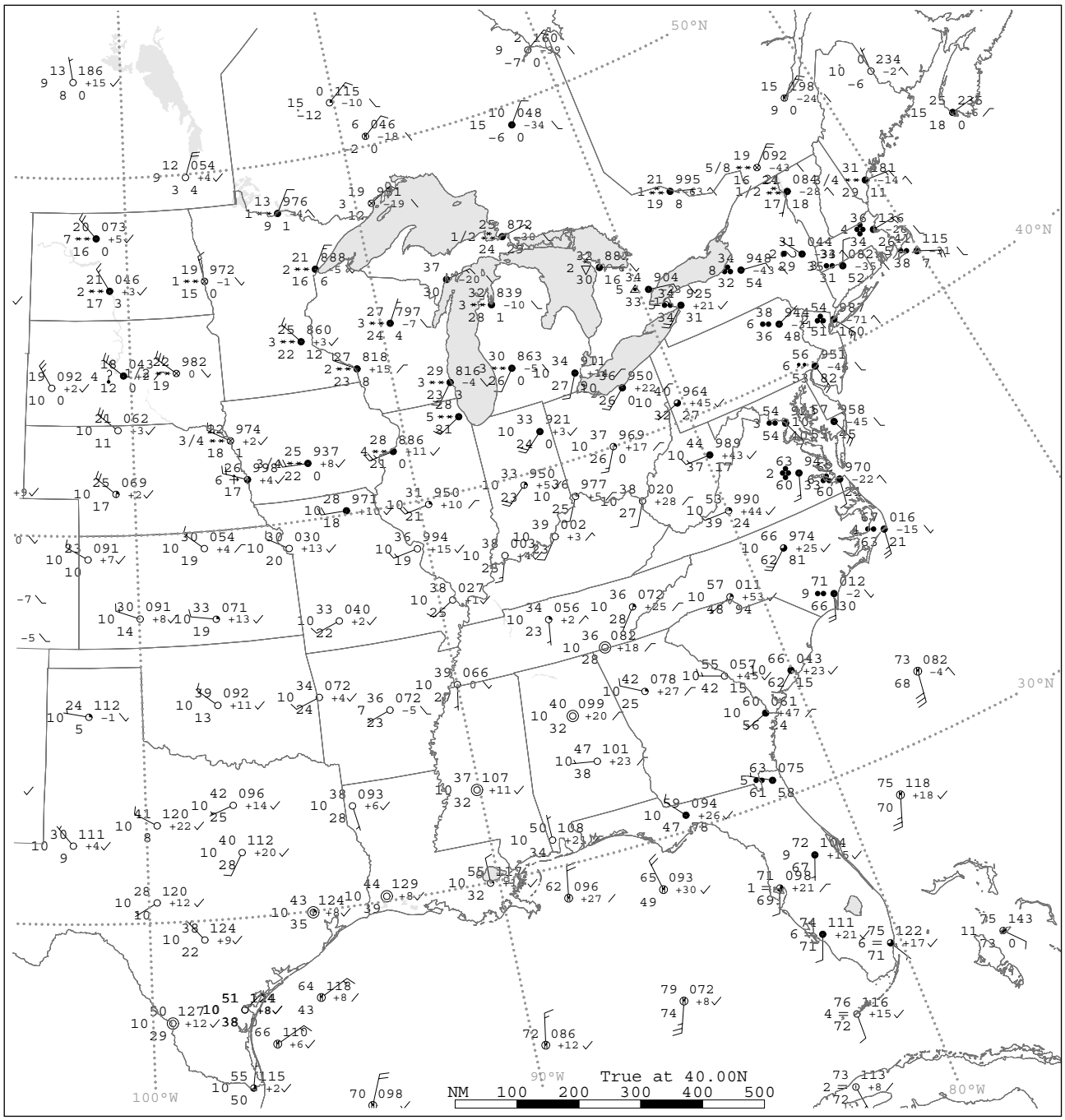

Figure 9.22
A surface weather map of central and eastern N. America. Units: T and T_d (°F), visibility (miles), speed (knots), pressure and 3-hour tendency (see text), 6-hour precipitation (hundredths of inches). Extracted from a "Daily Weather Map" courtesy of the US National Oceanic and Atmospheric Administration (NOAA), National Weather Service (NWS), National Centers for Environmental Prediction (NCEP), Hydrometeorological Prediction Center (HPC). The date/time of this map is omitted to discourage cheating during map-analysis exercises.

W13. Search the web for sites that give the ICAO station ID for different locations. This is the ID used to indicate the name of the weather station in a METAR.

W4. Access the current METAR for your town, or for a nearby town assigned by your instructor. Try to decode it manually, and write out its message in words. Compare your result with a computer decoded METAR if available.

W5. Search the web for maps that show where weather observations are made today (or recently), such as were shown in Figs. 9.2-13.16. Hint: If you can't find a site associated with your own country's weather service, try searching on "ECMWF data coverage" or "Met Office data coverage" or "FNMOC data coverage".

W6. For each of the different sensor types discussed in the section on Weather Observation Locations, use the web to get photos of each type of instrument: rawinsonde, dropsonde, AWOS, etc.

W7. Search the web for a history of ocean weather ships, and summarize your findings.

W8. Access from the web a current plotted surface weather map that has the weather symbols plotted around each weather station. Find the station closest to your location (or use a station assigned by the instructor), and decode the weather data into words.

W9 Access simple weather maps from the web that print values of pressure or temperature at the weather stations, but which do not have the isopleths drawn. Print these, and then draw your own isobars or isotherms. If you can do both isobars and isotherms for a given time over the same region, then identify the frontal zone, and determine if the front is warm, cold, or occluded. Plot these features on your analyzed maps. Identify highs and lows and airmasses.

W10. Use the web to access surface weather maps showing plotted station symbols, along with the frontal analysis. Compare surface temperature, wind, and pressure along a line of weather stations that crosses through the frontal zone. How do the observations compare with your ideas about frontal characteristics?

Synthesis Questions

S1. Suppose that you wanted to plot a map of thickness of the 100 to 50 kPa layer (see the Global Circulation chapter for a review of thickness maps). However, in some parts of the world, the terrain elevation is so high that the surface pressure is lower than 100 kPa. Namely, part of the 100 to 50 kPa layer would be below ground.

Extend the methods on sea-level pressure reduction to create an equation or method for estimating thickness of the 100 to 50 kPa layer over high ground, based on available surface and atmospheric sounding data.

S2 What if there were no satellite data? How would our ability to analyze the weather change?

S3. What if only satellite data existed? How would our ability to analyze the weather change?

S4. a. Suppose that all the weather observations over land were accurate, and all the ones over oceans had large errors. At mid-latitudes where weather moves from west to east, discuss how forecast skill would vary from coast to coast across a continent such as N. America.

b. How would forecast skill be different if observations over oceans were accurate, and over land were inaccurate?

S5. Pilots flying visually (VFR) need a certain minimum visibility and cloud ceiling height. The **ceiling** is the altitude of the lowest cloud layer that has a coverage of broken or overcast. If there is an obscuration such as smoke or haze, the ceiling is the vertical visibility from the ground looking up.

Use the web to access pilot regulations for your country to learn the ceiling and visibility needed to land VFR at an airport with a control tower. Then translate those values into the codes for a station plot model, and write those values in the appropriate box relative to a station circle.

S6. In Fig. 9.4, notice that west of N. America is a large data-sparse region over the N.E. Pacific Ocean. This region, shown in Fig. 9.23 below, is called the **Pacific data void**. Although there is buoy and ship data near the surface, and aircraft data near the tropopause, there is a lack of mid-tropospheric data in that region.

Although Figs. 9.2 - 9.12 show lots of satellite data over that region, satellites do not have the vertical coverage and do not measure all the meteorological variables needed to use as a starting point for accurate weather forecasts.

Suppose you had an unlimited budget. What instruments and instrument platforms (e.g., weather ships, etc.) would you deploy to get dense spatial coverage of temperature, humidity, and winds in the Pacific data void? If you had a limited budget, how would your proposal be different?

[Historical note: Anchored weather ships such as one called **Station Papa** at 50°N 145°W were formerly stationed in the N.E. Pacific, but all these ships were removed due to budget cutbacks. When they were removed, weather-prediction skill over large parts of N. America measurably decreased, because mid-latitude weather moves from west to east. Namely, air from over the data void regions moves over North America.]

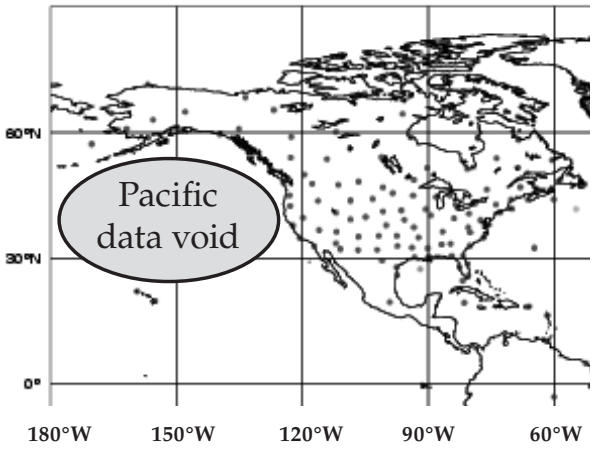

Figure 9.23
The "Pacific data void" & upper-air sounding locations (dots).

ON DOING SCIENCE • Creativity in Engineering

"Just as the poet starts with a blank sheet of paper and the artist with a blank canvas, so the engineer today begins with a blank computer screen. Until the outlines of a design are set down, however tentatively, there can be no appeal to science or to critical analysis to judge or test the design. Scientific, rhetorical or aesthetic principles may be called on to inspire, refine and finish a design, but creative things do not come of applying the principles alone. Without the sketch of a thing or a diagram of a process, scientific facts and laws are of little use to engineers. Science may be the theatre, but engineering is the action on the stage."

"Designing a bridge might also be likened to writing a sonnet. Each has a beginning and an end, which must be connected with a sound structure. Common bridges and so-so sonnets can be made by copying or mimicking existing ones, with some small modifications of details here and there, but such are not the creations that earn the forms their reputation or cause our spirits to soar. Masterpieces come from a new treatment of an old form, from a fresh shaping of a familiar genre. The form of the modern suspension bridge — consisting of a deck suspended from cables slung over towers and restrained by anchorages — existed for half a century before John Roebling proposed his Brooklyn Bridge, but the fresh proportions of his Gothic-arched masonry towers, his steel cables and diagonal stays, and his pedestrian walkway centered above dual roadways produced a structure that remains a singular achievement of bridge engineering. Shakespeare's sonnets, while all containing 14 lines of iambic pentameter, are as different from one another and from their contemporaries as one suspension bridge is from another."

– Henry Petroski, 2005: Technology and the humanities. *American Scientist*, **93**, p 305.

Copyright © 2011, 2015 by Roland Stull. *Meteorology for Scientists and Engineers, 3rd Ed.*

DYNAMICS

CONTENTS

Winds and Weather Maps 290
- Height Contours on Isobaric Surfaces 290
- Plotting Winds 291

Newton's Second Law of Motion 292
- Lagrangian Momentum Budget 292
- Eulerian Momentum Budget 293

Horizontal Forces 294
- Advection 294
- Pressure-Gradient Force 295
- Centrifugal Force 296
- Coriolis Force 297
- Turbulent-Drag Force 300
- Summary of Forces 301

Equations of Horizontal Motion 301

Horizontal Winds 302
- Geostrophic Wind 302
- Gradient Wind 304
- Boundary-Layer Wind 307
- Boundary-Layer Gradient (BLG) Wind 309
- Cyclostrophic Wind 311
- Inertial Wind 312
- Antitriptic Wind 312
- Summary of Horizontal Winds 313

Horizontal Motion 314
- Equations of Motion — Revisited 314
- Scales of Horizontal Motion 315

Vertical Forces and Motion 315

Mass Conservation 317
- Continuity Equation 317
- Incompressible Continuity Equation 318
- Boundary-Layer Pumping 319

Kinematics 320

Measuring Winds 321

Summary 322
- Threads 322

Exercises 322
- Numerical Problems 322
- Understanding & Critical Evaluation 324
- Web-Enhanced Questions 326
- Synthesis Questions 327

"Meteorology for Scientists and Engineers, 3rd Edition" by Roland Stull is licensed under a Creative Commons Attribution-NonCommercial-ShareAlike 4.0 International License. To view a copy of the license, visit http://creativecommons.org/licenses/by-nc-sa/4.0/ . This work is available at http://www.eos.ubc.ca/books/Practical_Meteorology/ .

10 We use winds to power our wind turbines, push our sailboats, cool our houses, and dry our laundry on the clothesline. But winds can also be destructive — in hurricanes, thunderstorms, or mountain downslope windstorms. We design our bridges and skyscrapers to withstand wind gusts. Airplane flights are planned to compensate for headwinds and crosswinds.

Winds are driven by forces acting on air. But these forces can be altered by heat and moisture carried by the air, resulting in a complex interplay we call weather. The relationship between forces and winds is called **atmospheric dynamics**. Newtonian physics describes atmospheric dynamics well.

Pressure, drag, and advection are atmospheric forces that act in the horizontal. Other forces, called apparent forces, are caused by the Earth's rotation (Coriolis force) and by turning of the wind around a curve (centrifugal and centripetal forces).

These different forces are present in different amounts at different places and times, causing large variability in the winds. For example, Fig. 10.1 shows changing wind speed and direction around a low-pressure center. In this chapter we explore forces, winds, and the dynamics that link them.

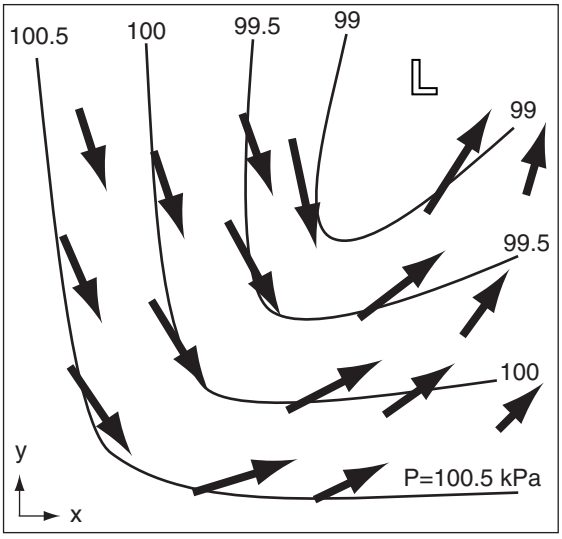

Figure 10.1
Sketch of sea-level pressure (thin lines are isobars) & the resulting near-surface winds (arrows). "L" is low pressure center.

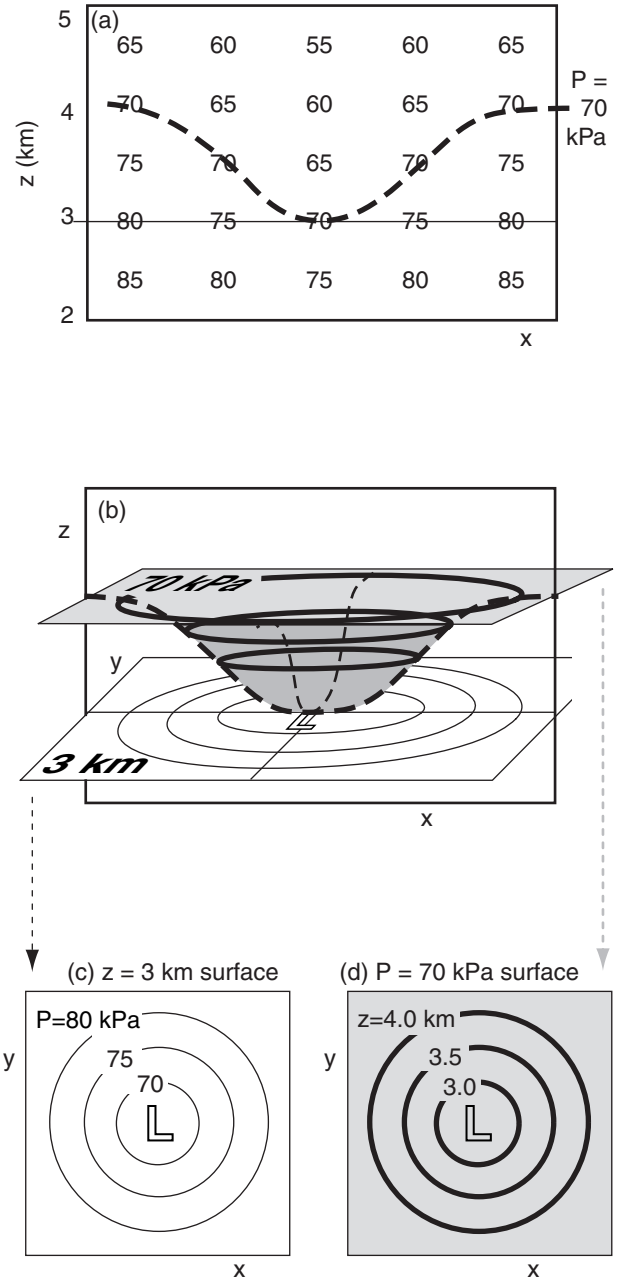

Figure 10.2
(a) Vertical slice through atmosphere, showing pressure values (kPa). Thick dashed line is the 70 kPa isobar. Thin straight line is the 3 km height contour. The location of lowest pressure on the height contour corresponds to the location of lowest height of the isobar. (b) 3-D sketch of the same 70 kPa isobaric surface (shaded), and 3 km height surface (white). (c) Pressures intersected by the 3 km constant height surface. (d) Heights crossed by the 70 kPa surface. The low-pressure center (L) in (c) matches the low-height center in (d).

WINDS AND WEATHER MAPS

Height Contours on Isobaric Surfaces

Pressure-gradient force is the most important force because it is the only one that can drive winds in the horizontal. Other horizontal forces can alter an existing wind, but cannot create a wind from calm air. All the forces, including pressure-gradient force, are explained in the next sections. However, to understand the pressure gradient, we must first understand pressure and its atmospheric variation.

We can create weather maps showing values of the pressures measured at different horizontal locations all at the same altitude, such as at mean-sea-level (MSL). Such a map is called a **constant-height map**. However, one of the peculiarities of meteorology is that we can also create maps on other surfaces, such as on a surface connecting points of equal pressure. This is called an **isobaric map**. Both types of maps are used extensively in meteorology, so you should learn how they are related.

In Cartesian coordinates (x, y, z), height z is geometric distance above some reference level, such as the ground or sea level. Sometimes we use geopotential height H in place of z, giving a coordinate set of (x, y, H) (see Chapter 1). However, an alternative coordinate system can use pressure P as the vertical coordinate, because pressure decreases monotonically with increasing height. **Pressure coordinates** consist of (x, y, P).

A **monotonic** variable is one that changes only in one direction. For example, it increases or is constant, but never decreases. Or it decreases or is constant, but never increases. Pressure in the atmosphere always decreases with increasing height.

A surface connecting points of equal pressure is an **isobaric surface**. In low-pressure regions, this surface is closer to the ground than in high-pressure regions (Fig. 10.2b). Thus, this surface curves up and down through the atmosphere. Although isobaric surfaces are not flat, we draw them as flat weather maps on the computer screen or paper (Fig. 10.2d).

Low pressures on a constant-height map correspond to low heights on a constant-pressure surface. High pressures on a constant height map correspond to high heights on a constant pressure surface. Similarly, regions on a constant-height map that have tight **packing** (close spacing) of isobars correspond to regions on isobaric maps that have tight packing of height contours, both of which are regions of strong pressure gradients that can drive strong winds. This one-to-one correspondence of both types of maps (Figs. 10.2c & d) makes it easier for you to use them interchangeably.

It is impossible for two different isobaric surfaces to cross each other. Also, these surfaces never fold back on themselves, because pressure decreases monotonically with height. However, they can intersect the ground, such as frequently happens in mountainous regions.

Isobaric charts will be used extensively in the remainder of this book when describing upper-air features (mostly for historical reasons; see Focus box). Fig. 10.3 is a sample weather map showing height contours of the 30 kPa isobaric surface.

Plotting Winds

Symbols on weather maps are like musical notes in a score — they are a shorthand notation that concisely expresses information. For winds, the symbol is an arrow with feathers (or barbs and pennants). The tip of the arrow is plotted over the observation (weather-station) location, and the arrow shaft is aligned so that the arrow points toward where the wind is going. The number and size of the feathers indicates the wind speed (Table 10-1, copied from Table 9-9). Fig. 10.3 illustrates wind barbs.

Table 10-1. Interpretation of wind barbs.

Symbol	Wind Speed	Description
◎	calm	two concentric circles
———	1 - 2 speed units	shaft with no barbs
——╲	5 speed units	a half barb (half line)
——╱	10 speed units	each full barb (full line)
——◣	50 speed units	each pennant (triangle)

• The total speed is the sum of all barbs and pennants. For example, ——◣╱╱ indicates a wind from the west at speed 75 units. Arrow tip is at the observation location.
• CAUTION: Different organizations use different speed units, such as knots, m/s, miles/h, km/h, etc. Look for a legend to explain the units. When in doubt, assume knots — the WMO standard. For unit conversion, a good approximation is 1 m/s ≈ 2 knots.

Solved Example

Draw wind barb symbol for winds from the:
(a) northwest at 115 knots; (b) northeast at 30 knots.

Solution

(a) 115 knots = 2 pennants + 1 full barb + 1 half barb.
(b) 30 knots = 3 full barbs

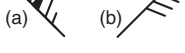

Check: Consistent with Table 10-1.

Discussion: Feathers (barbs & pennants) should be on the side of the shaft that would be towards low pressure if the wind were geostrophic.

FOCUS • Why use isobaric maps?

Constant pressure charts are used for five reasons. First, the old **radiosonde** (consisting of weather sensors hanging from a free helium balloon that rises into the upper troposphere and lower stratosphere) measured pressure instead of altitude, so it was easier to plot their measurements of temperature, humidity and wind on an isobaric surface. For this reason, **upper-air charts** (i.e., showing weather above the ground) traditionally have been drawn on isobaric maps.

Second, aircraft altimeters are really pressure gauges. Aircraft assigned by air-traffic control to a specific "altitude" above 18,000 feet MSL will actually fly along an isobaric surface. Many weather observations and forecasts are motivated by aviation needs.

Third, pressure is a measure of mass in the air, so every point on an isobaric map has the same number of air molecules above it.

Fourth, an advantage of using equations of motion in pressure coordinates is that you do not need to consider density, which is not routinely observed.

Fifth, some weather forecast models use pressure coordinate systems in the vertical.

However, more and more routine upper-air soundings around the world are being made with modern **GPS** (**Global Positioning System**, satellite triangulation method) sondes that can measure geometric height as well as pressure. Also, some of the modern weather forecast models do not use pressure as the vertical coordinate. In the future, we might see the large government weather data centers starting to produce upper-air weather maps on constant height surfaces.

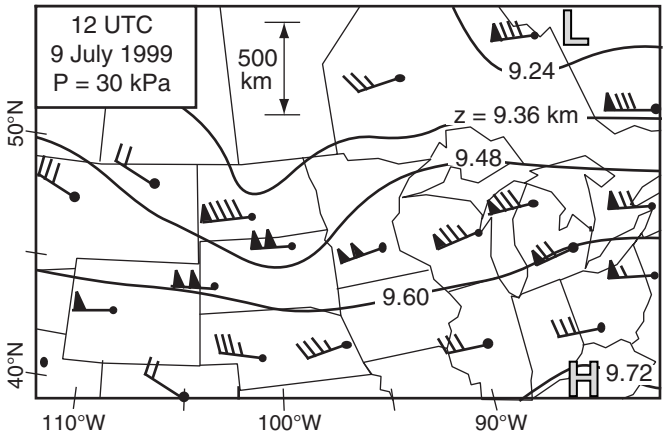

Figure 10.3
Weather map for a 30 kPa constant pressure surface over central N. America. Solid contours show height z (km) of this surface above mean sea level (MSL). Hence, this is called a "30 kPa height chart". Wind barbs (Table 10-1) show wind observations in knots (2 knots ≈ 1 m/s). The relative maxima and minima heights are labeled as H (high heights) and L (low heights).

NEWTON'S SECOND LAW OF MOTION

Lagrangian Momentum Budget

Forces, winds, and acceleration are vectors possessing both magnitude and direction. **Newton's second law of motion** (often shortened to **Newton's second law**) states that a vector force $\vec{F}$ acting on an object such as an air parcel of mass m causes it to accelerate $\vec{a}$ in the same direction as the applied force:

$$\vec{F} = m \cdot \vec{a} \qquad \bullet(10.1)$$

Acceleration is defined as the rate of change of velocity with time t:

$$\vec{a} = \frac{\Delta \vec{V}}{\Delta t} \qquad (10.2)$$

where $\vec{V}$ is the vector wind velocity.

Combining eqs. (10.1) and (10.2) give

$$\vec{F} = m \cdot \frac{\Delta \vec{V}}{\Delta t} \qquad (10.3a)$$

If mass is constant, then the equation can be written as:

$$\vec{F} = \frac{\Delta (m \cdot \vec{V})}{\Delta t} \qquad (10.3b)$$

But mass times velocity equals momentum. Thus, eq. (10.3b) describes the change in momentum with time following the air parcel; namely, it is the **Lagrangian momentum budget**.

Rearranging eq. (10.3a) gives a forecast equation for the wind velocity:

$$\frac{\Delta \vec{V}}{\Delta t} = \frac{\vec{F}_{net}}{m} \qquad (10.4)$$

The subscript "net" implies that there might be many forces acting on the air parcel, and we need to consider the vector sum of all forces in eq. (10.4), as given by Newton's Corollary 1 (see Focus box).

For situations where $\vec{F}_{net}/m = 0$, eq. (10.4) tells us that the flow will maintain constant velocity due to **inertia**. Namely, $\Delta \vec{V} / \Delta t = 0$ implies that $\vec{V}$ = constant (not that $\vec{V} = 0$).

FOCUS • In Newton's Own Words

Newton's laws of motion, in his own words, are given below. Actually, his original words were Latin, the language of natural philosophy (science) at that time (1687). Here is the translation from Newton's *Philosophiæ Naturalis Principia Mathematica* ("Mathematical Principles of Natural Philosophy"):

"**Law I**. Every body perseveres in its state of being at rest or of moving uniformly straight forward, except inasmuch as it is compelled by impressed forces to change its state.

"**Law II**. Change in motion is proportional to the motive force impressed and takes place following the straight line along which that force is impressed.

"**Law III**. To any action, there is always a contrary, equal reaction; in other words, the actions of two bodies each upon the other are always equal and opposite in direction.

"**Corollary 1**. A body under the joint action of forces traverses the diagonal of a parallelogram in the same time as it describes the sides under their separate actions."

Solved Example

A 1500 kg car accelerates from 0 to 60 mph (0 to 96.6 km/h) in 9 seconds, heading south. (a) Find its average acceleration. (b) What magnitude and direction of force acted on it to make it accelerate?

Solution

Given: $\vec{V}_{initial} = 0$, $\vec{V}_{final} = 60$ mph = 27 m/s
$t_{initial} = 0$, $t_{final} = 9$ s. Direction is south.
$m = 1500$ kg.

Find: $\vec{a}$ = ? m·s^{-2} , $\vec{F}$ = ? N

(a) Use eq. (10.2): $\vec{a} = \frac{\Delta \vec{V}}{\Delta t}$

= (27 – 0 m/s) / (9 – 0 s) = **3** m·s^{-2} **to the south**

(b) Use eq. (10.1): $\vec{F}$ = (1500 kg) · (3 m·s^{-2})
= **4500 N to the south**
(From Appendix A, recall that 1 N = 1 kg·m·s^{-2})

Check: Units OK. Physics OK.
Discussion: If the car falls off a cliff, gravity would accelerate it at g = –9.8 m·s^{-2} , where the negative sign denotes the downward direction.

Eulerian Momentum Budget

For wind forecasts over a fixed location such as a town or lake, use an **Eulerian** reference frame. Define a local Cartesian coordinate system with x increasing toward the local East, y toward the local North, and z up (see Chapter 1).

Wind components in a Cartesian framework can be found by rewriting the vector equation (10.4) as three separate scalar equations: one for the west-to-east wind component (U), one for the south-to-north component (V), and one for the vertical component (W):

$$\frac{\Delta U}{\Delta t} = \frac{F_{x\,net}}{m} \qquad \bullet(10.5a)$$

$$\frac{\Delta V}{\Delta t} = \frac{F_{y\,net}}{m} \qquad \bullet(10.5b)$$

$$\frac{\Delta W}{\Delta t} = \frac{F_{z\,net}}{m} \qquad \bullet(10.5c)$$

where subscripts (x, y, z) indicate the component of the net vector force toward the (east, north, up), respectively. Relationships between the horizontal "speed and direction" method of representing a vector wind versus the "U and V component" method were given in Chapter 1.

Recall that $\Delta U/\Delta t = [U(t+\Delta t) - U(t)]/\Delta t$. Thus, we can rewrite eqs. (10.5) as forecast equations:

$$U(t+\Delta t) = U(t) + \frac{F_{x\,net}}{m}\cdot\Delta t \qquad \bullet(10.6a)$$

$$V(t+\Delta t) = V(t) + \frac{F_{y\,net}}{m}\cdot\Delta t \qquad \bullet(10.6b)$$

$$W(t+\Delta t) = W(t) + \frac{F_{z\,net}}{m}\cdot\Delta t \qquad \bullet(10.6c)$$

These equations are often called the **equations of motion**. Together with the continuity equation (later in this chapter), the equation of state (ideal gas law from Chapter 1), and the energy budget equations in the Heat and Moisture chapters, they describe the dynamic and thermodynamic state of the air.

To forecast winds [$U(t+\Delta t)$, $V(t+\Delta t)$, $W(t+\Delta t)$] at some future time, we must know the winds now [$U(t)$, $V(t)$, $W(t)$], and the forces acting on the air. Mathematically, this is known as an **initial-value problem**, because we must know the initial winds to forecast the future winds. Even numerical weather forecast models (see the NWP chapter) must start with an **analysis** of current weather observations.

Average horizontal winds are often 100 times stronger than vertical winds, except in thunderstorms and near mountains. We will focus on horizontal forces and winds first, and return to vertical winds later in this chapter.

Solved Example

If $F_{x\,net}/m = 1\text{x}10^{-4}$ m·s^{-2} acts on air initially at rest, then what is the final wind speed after 10 minutes?

Solution

Given: $U(0) = 0$, $F_{x\,net}/m = 1\text{x}10^{-4}$ m·s^{-2} , $\Delta t = 600$ s
Find: $U(\Delta t) = ?$ m/s. Assume: V=0.

Use eq. (10.6a): $U(t+\Delta t) = U(t) + \Delta t \cdot (F_{x\,net}/m)$
$= 0 + (600\text{s})\cdot(1\text{x}10^{-4}\ \text{m}\cdot\text{s}^{-2})$ = **0.06 m/s**.

Check: Units OK. Physics OK.
Discussion: Not very fast, but over many hours it becomes large. Positive U means it is toward the east.

ON DOING SCIENCE • Be Creative

Isaac Newton grew up on his mother's farm at Woolsthorpe, and built model windmills, clocks, and sundials. His grades in school were OK. He got into fights with his classmates, and carved his name in his desk. His schoolmaster saw a spark of talent in Isaac, and suggested to his mother that Isaac should go to college, because he would never be a good farmer.

At age 18, Isaac Newton went to Cambridge University in England in 1661, and after working at odd jobs to pay his way, finally graduated with a B.A. in 1665. Later that year the plague hit, killing 10% of the London population in three months. For fear that the plague would spread, Cambridge Univ. was closed until 1667. Isaac and the other students went home.

He continued his scientific studies in seclusion at his mother's farmhouse during the 18 months that school was closed. During this period, at age 23 to 24, he laid the groundwork for many of his major discoveries. This included the laws of motion, the study of optics, the invention of the reflecting telescope, the explanation for the orbits of planets, the understanding of gravity, and the co-invention of calculus.

Often the most creative science, music, literature, and art are done by young men and women who have not been biased and (mis)directed by studying the works of others too much. Such knowledge of past work will often subconsciously steer one's research in the directions that others have already taken, which unfortunately discourages novel ideas.

Be creative, and learn from your mistakes. So what if you "re-invent the wheel", and "discover" something that was already discovered a century ago. The freedom to make personal discoveries and mistakes and the knowledge you gain by doing so allows you to be much more creative than if you had just read about the end result in a journal.

So we have a paradox. I wrote this book to help you learn the meteorological advances made by others, but I discourage you from studying the works of others. As a scientist or engineer, you must make your own decision about the best balance of these two philosophies that will guide your future work.

Science Graffito

"If I have been able to see further than others, it was because I stood on the shoulders of giants."
– Sir Isaac Newton.

HORIZONTAL FORCES

To solve the equations of motion for horizontal winds in an Eulerian framework, we need to know the horizontal forces acting on the air. The net "force per unit mass" consists of contributions from **advection** (AD), **pressure-gradient force** (PG), **Coriolis force** (CF), and **turbulent drag** (TD). In addition, imbalances between forces sometimes balance **centrifugal force** (CN):

$$\frac{F_{x\,net}}{m} = \frac{F_{x\,AD}}{m} + \frac{F_{x\,PG}}{m} + \frac{F_{x\,CN}}{m} + \frac{F_{x\,CF}}{m} \cdot \qquad (10.7a)$$

$$\frac{F_{y\,net}}{m} = \frac{F_{y\,AD}}{m} + \frac{F_{y\,PG}}{m} + \frac{F_{y\,CN}}{m} + \frac{F_{y\,CF}}{m} \cdot \qquad (10.7b)$$

Units of force per mass are N/kg, which is identical to units of $m{\cdot}s^{-2}$ (see Appendix A). We will use these latter units.

Advection

Not only can wind blow air of different temperature or humidity into a region, but it can also blow air of different **specific momentum** (i.e., momentum per unit mass). Recall that momentum is defined as mass times velocity, hence specific momentum equals the velocity (i.e., the wind) by definition. Thus, the wind can blow different winds into a region. Namely, winds can change due to advection, in an Eulerian framework.

This is illustrated in Fig. 10.4a. Consider a mass of air (grey box) with slow U wind (5 m/s) in the north and faster U wind (10 m/s) in the south. Thus, U decreases toward the north, giving $\Delta U/\Delta y$ = *negative*. This whole air mass is advected toward the north over a fixed weather station "O" by a mean wind (V = *positive*). At the time sketched in Fig. 10.4b, a west wind of 5 m/s is measured at "O". Later, at the time of Fig. 10.4c, the west wind has increased to 10 m/s at the weather station. The rate of increase of U at "O" is larger for faster advection (V), and is larger if $\Delta U/\Delta y$ is more negative.

Thus, $\Delta U/\Delta t = -V \cdot \Delta U/\Delta y$ for this example. The advection term on the RHS causes an acceleration of U wind on the LHS, and thus acts like a force per unit mass: $\Delta U/\Delta t = F_{x\,AD}/m = -V \cdot \Delta U/\Delta y$.

Advection is not usually considered a force in the traditional Lagrangian sense, but you must always include it when momentum budget equations are rewritten in Eulerian frameworks. You have seen similar advection terms in the Eulerian heat and moisture budget equations earlier in this book.

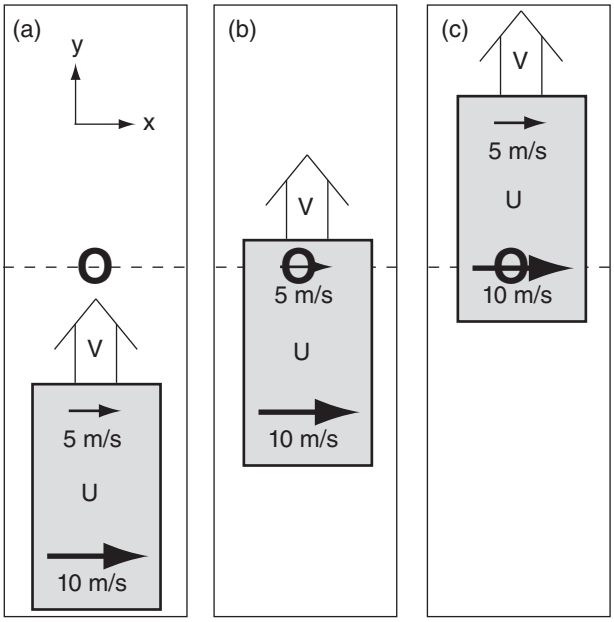

Figure 10.4
Illustration of V advection of U wind. "O" is a fixed weather station. Grey box is an air mass containing a gradient of U wind. Initial state (a) and later states (b and c).

In general, the components of advective force per unit mass are:

$$\frac{F_{x\,AD}}{m} = -U\cdot\frac{\Delta U}{\Delta x} - V\cdot\frac{\Delta U}{\Delta y} \qquad \bullet(10.8a)$$

$$\frac{F_{y\,AD}}{m} = -U\cdot\frac{\Delta V}{\Delta x} - V\cdot\frac{\Delta V}{\Delta y} \qquad \bullet(10.8b)$$

where $\Delta U/\Delta x$ is the gradient of U-wind in the x-direction, and the other gradients are defined similarly. Advection needs a **gradient** (i.e., change across a distance). Without a change of wind with distance, momentum advection cannot cause accelerations

Vertical advection of horizontal wind ($-W\cdot\Delta U/\Delta z$ in eq. 10.8a, and $-W\cdot\Delta V/\Delta z$ in eq. 10.8b) also exists. But W is often very small outside of thunderstorms, so we neglect vertical advection here.

Pressure-Gradient Force

Pressure-gradient force always acts perpendicularly to the isobars (or height contours) on a weather map, from high to low pressure (or heights). This force exists regardless of the wind speed, and does not depend on the wind speed. It starts the horizontal winds and can accelerate, decelerate, or change the direction of existing winds. On a weather map, more closely spaced isobars (i.e., more closely packed, with smaller distance Δd between them) indicate a greater pressure-gradient force (Fig. 10.5).

The components of pressure-gradient force are:

$$\frac{F_{x\,PG}}{m} = -\frac{1}{\rho}\cdot\frac{\Delta P}{\Delta x} \qquad \bullet(10.9a)$$

$$\frac{F_{y\,PG}}{m} = -\frac{1}{\rho}\cdot\frac{\Delta P}{\Delta y} \qquad \bullet(10.9b)$$

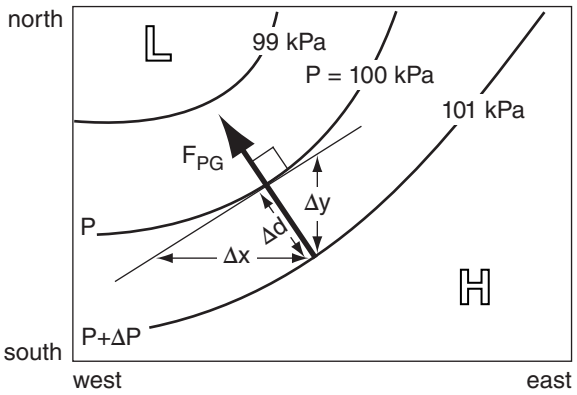

Figure 10.5
Pressure gradient force (heavy line) is perpendicular to isobars (medium lines) from high to low pressure. H and L indicate regions of high and low pressure, respectively.

Solved Example

Vancouver (British Columbia, Canada) is roughly 250 km north of Seattle (Washington, USA). The winds (U, V) are (8, 3) m/s in Vancouver and (5, 5) m/s in Seattle. Find the advective force per unit mass.

Solution

Given: (U, V) = (8, 3) m/s in Vancouver,
(U, V) = (5, 5) m/s in Seattle
Δy = 250 km, Δx = not relevant (unknown)
Find: $F_{x\,AD}/m$ =? m·s^{-2} , $F_{y\,AD}/m$ =? m·s^{-2}

Use the definition of a gradient:
$\Delta U/\Delta y = (8 - 5\text{ m/s})/250{,}000\text{ m} = 1.2\text{x}10^{-5}\text{ s}^{-1}$
$\Delta U/\Delta x = 0$ (unknown in this problem)
$\Delta V/\Delta y = (3 - 5\text{ m/s})/250{,}000\text{ m} = -0.8\text{x}10^{-5}\text{ s}^{-1}$
$\Delta V/\Delta x = 0$ (unknown)
Average U = (8 + 5 m/s)/2 = 6.5 m/s
Average V = (3 + 5 m/s)/2 = 4 m/s

Use eq. (10.8a):
$F_{x\,AD}/m = -(6.5\text{m/s})\cdot 0 - (4\text{m/s})\cdot(1.2\text{x}10^{-5}\text{ s}^{-1})$
$= \underline{\mathbf{-4.8\text{x}10}}^{-5}$ m·s^{-2}
Use eq. (10.8b):
$F_{y\,AD}/m = -(6.5\text{m/s})\cdot 0 - (4\text{m/s})\cdot(-0.8\text{x}10^{-5}\text{ s}^{-1})$
$= \underline{\mathbf{3.2\text{x}10}}^{-5}$ m·s^{-2}

Check: Units OK. Physics OK.
Discussion: The U winds are slower in Seattle than Vancouver, but are being blown toward Vancouver by the southerly flow. Thus, advection is decreasing the U-wind, hence, the negative sign. The V-wind is faster in Seattle, and these faster winds are being blown toward Vancouver, causing a positive acceleration there.

Solved Example

Milwaukee is 100 km east of Madison, Wisconsin, USA. The sea-level pressure at Milwaukee is 100.1 kPa and at Madison is 100 kPa. What is the pressure gradient force per mass? Assume $\rho = 1.2$ kg·m^{-3}.

Solution

Define: Cartesian coord. with $x = 0$ at Madison.
Given: P = 100.1 kPa at x = 100 km,
P = 100.0 kPa at x = 0 km. $\rho = 1.2$ kg·m^{-3}.
Find: $F_{x\,PG}/m$ =? m·s^{-2}

Use eq. (10.9a):

$$\frac{F_{y\,PG}}{m} = -\frac{1}{(1.1\text{kg}\cdot\text{m}^{-3})}\cdot\frac{(101{,}000 - 100{,}000)\text{Pa}}{(400{,}000 - 0)\text{m}}$$

$= \underline{\mathbf{-8.33\text{x}10}}^{-4}$ m·s^{-2}.
where 1 Pa = 1 kg·m^{-1}·s^{-2} was used (Appendix A).

Check: Units OK. Physics OK.
Discussion: The negative answer implies that the force is in the negative x-direction; that is, from Milwaukee toward Madison.

Solved Example

If the height of the 50 kPa pressure surface decreases by 10 m northward across a distance of 500 km, what is the pressure-gradient force?

Solution

Given: $\Delta z = -10$ m, $\Delta y = 500$ km, $|g| = 9.8$ m·s^{-2}.
Find: F_{PG}/m = ? m·s^{-2}

Use eqs. (10.11a & b):
$F_{x\,PG}/m = 0$ m·s^{-2} , because $\Delta z/\Delta x = 0$. Thus, $F_{PG}/m = F_{y\,PG}/m$.

$$\frac{F_{y\,PG}}{m} = -|g|\cdot\frac{\Delta z}{\Delta y} = -\left(9.8\frac{\text{m}}{\text{s}^2}\right)\cdot\left(\frac{-10\text{m}}{500{,}000\text{m}}\right)$$

F_{PG}/m = **0.000196 m·s^{-2}**

Check: Units OK. Physics OK. Sign OK.
Discussion: For our example here, height decreases toward the north, thus a hypothetical ball would roll downhill toward the north. A northward force is in the positive y direction, which explains the positive sign of the answer.

Table 10-2. Sign s for centrifugal-force equations.

Hemisphere	For flow around a	
	Low	High
Northern	+1	–1
Southern	–1	+1

Solved Example

On the back side of a low pressure center in the northern hemisphere, winds are from the north at 10 m/s at distance 250 km from the low center. Find the centrifugal force.

Solution

Given: $R = 2.5\text{x}10^5$ m,
$V = -10$ m/s
Find: $F_{x\,CN}/m$ = ? m·s^{-2}.

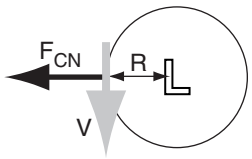

Use eq. (10.13a), with $s = +1$ from Table 10-2.

$$\frac{F_{xCN}}{m} = -1\cdot\frac{(-5\text{m/s})\cdot(5\text{m/s})}{5\times10^5} = \underline{\mathbf{-4x10^{-4}\ m\cdot s^{-2}}}.$$

Check: Units OK. Physics OK. Sketch OK.
Discussion: The negative sign indicates a force toward the west, which is indeed outward from the center of the circle.

where ρ is air density, and ΔP is the change of pressure across distance Δx or Δy. The negative sign makes the force act from high toward low pressure.

The magnitude of pressure-gradient force is

$$\left|\frac{F_{PG}}{m}\right| = \left|\frac{1}{\rho}\cdot\frac{\Delta P}{\Delta d}\right| \qquad (10.10)$$

where Δd is the distance between isobars.

The hydrostatic equation (1.25) can be used to convert the pressure-gradient terms from height to pressure coordinates. On isobaric surfaces, the pressure-gradient terms become:

$$\frac{F_{x\,PG}}{m} = -|g|\cdot\frac{\Delta z}{\Delta x} \qquad (10.11a)$$

$$\frac{F_{y\,PG}}{m} = -|g|\cdot\frac{\Delta z}{\Delta y} \qquad (10.11b)$$

where $\Delta z/\Delta x$ and $\Delta z/\Delta y$ are the slopes of the isobaric surfaces (i.e., change of height with distance), and $|g| = 9.8$ m·s^{-2} is the magnitude of gravitational acceleration. If you could place a hypothetical ball on the isobaric surface plotted in Fig. 10.2b, the direction that it would roll downhill is the direction of the pressure-gradient force, and the magnitude is

$$\left|\frac{F_{PG}}{m}\right| = \left|g\cdot\frac{\Delta z}{\Delta d}\right| \qquad (10.12)$$

where Δd is distance between height contours.

Pressure-gradient force is the ONLY force that can drive the horizontal winds in the atmosphere. The other forces, such as Coriolis, drag, centrifugal, and even advection, disappear for zero wind speed. Hence, these other forces can change the direction and speed of an existing wind, but they cannot create a wind out of calm conditions.

Centrifugal Force

Newton's laws of motion state that an object tends to move in a straight line unless acted upon by a force in a different direction. Such a force, called centripetal force, causes the object to change direction and bend its trajectory. **Centripetal** force is the sum or the imbalance of other forces.

Centrifugal force is an apparent force that is opposite to centripetal force and pulls outward from the center of the turn. The components of centrifugal force are

$$\frac{F_{xCN}}{m} = +s\cdot\frac{V\cdot M}{R} \qquad \bullet(10.13a)$$

$$\frac{F_{yCN}}{m} = -s\cdot\frac{U\cdot M}{R} \qquad \bullet(10.13b)$$

where s is a sign coefficient given in Table 10-2, $M = (U^2 + V^2)^{1/2}$ is wind speed (always positive), and R is the radius of curvature. The sign depends on whether air is circulating around a high or low pressure center, and whether it is in the Northern or Southern Hemisphere.

The total magnitude is:

$$\left|\frac{F_{CN}}{m}\right| = \frac{M^2}{R} \qquad (10.14)$$

Coriolis Force

Coriolis force is an apparent force caused by the rotation of the Earth. It acts perpendicular to the wind direction, to the right in the N. Hemisphere, and to the left in the Southern (Fig. 10.6).

To understand Coriolis force, we need to quantify the rotation rate of the Earth. The Earth rotates one full revolution (2π radians) during a sidereal day (i.e., relative to the fixed stars, $P_{sidereal}$ is a bit less than 24 h, see Appendix B), giving an angular rotation rate of

$$\Omega = 2\cdot\pi / P_{sidereal} \qquad \bullet(10.15)$$

$$= 0.729\ 211\ 6 \times 10^{-4} \text{ radians/s}$$

The units for Ω are often abbreviated as s^{-1}. Using this rotation rate, a **Coriolis parameter** is defined as

$$f_c = 2\cdot\Omega\cdot\sin(\phi) \qquad \bullet(10.16)$$

where $2\cdot\Omega = 1.458423\text{x}10^{-4}$ s^{-1}, and ϕ is latitude. This parameter is constant at any fixed location. At mid-latitudes, the magnitude is on the order of $f_c = 1\text{x}10^{-4}$ s^{-1}.

In the N. Hemisphere, the Coriolis force is:

$$\frac{F_{xCF}}{m} = f_c \cdot V \qquad \bullet(10.17a)$$

$$\frac{F_{yCF}}{m} = -f_c \cdot U \qquad \bullet(10.17b)$$

Thus, there is no Coriolis force when there is no wind. Coriolis force cannot cause the wind to blow; it can only change its direction.

The magnitude of Coriolis force is:

$$| F_{CF}/m | \approx 2 \cdot \Omega \cdot |\sin(\phi)\cdot M| \qquad (10.18a)$$

or

$$| F_{CF}/m | \approx | f_c \cdot M | \qquad (10.18b)$$

as is shown in the 2nd Focus box on Coriolis force.

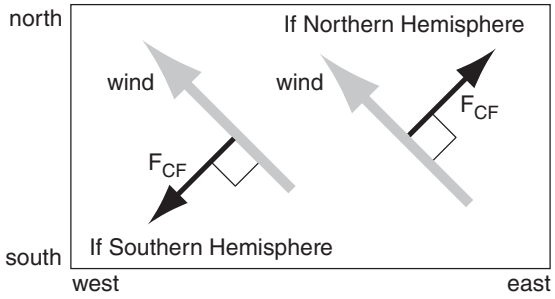

Figure 10.6
Coriolis force (dark lines).

Solved Example
a) Plot Coriolis parameter vs. latitude. b) Find Coriolis force at Norman, OK, USA, for a wind of U = 10 m/s.

Solution
Given: U = 10 m/s, ϕ = 35.2°N at Norman.
Find: Plot f_c vs ϕ. Also: $F_{y\,CF}/m$ = ? m·s^{-2}.

a) Find f_c (s^{-1}) vs. ϕ(°) using eq. (10.16). For example:
$f_c = (1.458\text{x}10^{-4}\ s^{-1})\cdot\sin(35.2°) = 8.4\text{x}10^{-5}\ s^{-1}$.

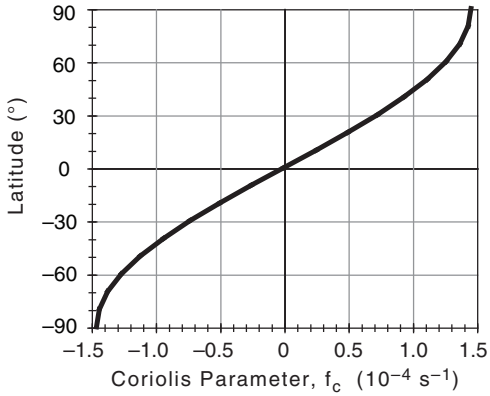

b) Coriolis force in the y-direction (eq. 10.17b) is:
$F_{y\,CF}/m = -(8.4\text{x}10^{-5}\ s^{-1})\cdot(10\text{m/s}) = \underline{\mathbf{-\ 8.4x10}}^{-4}$ m·s^{-2}.

Check: Units OK. Physics OK.
Discussion: The – sign means force is north to south.

FOCUS • Coriolis Force in 3-D

Eqs. (10.17) give only the dominant components of Coriolis force. There are other smaller-magnitude Coriolis terms (labeled *small* below) that are usually neglected. The full Coriolis force in 3-dimensions is:

$$\frac{F_{xCF}}{m} = f_c\cdot V - 2\Omega\cdot\cos(\phi)\cdot W \qquad (10.17c)$$

[*small because often W<<V*]

$$\frac{F_{yCF}}{m} = -f_c\cdot U \qquad (10.17d)$$

$$\frac{F_{zCF}}{m} = 2\Omega\cdot\cos(\phi)\cdot U \qquad (10.17e)$$

[*small relative to other vertical forces*]

FOCUS • What is Coriolis Force?

In 1835, Gaspar Gustave Coriolis used kinetic-energy conservation to explain the apparent force that now bears his name. The following clarification was provided by Anders Persson in 1998 and 2006.

Background

Coriolis force can be interpreted as the difference between two other forces: centrifugal force and gravitational force.

As discussed previously, **centrifugal force** is $F_{CN}/m = (M_{tan})^2/R$, where M_{tan} is the tangential velocity of an object moving along a curved path with radius of curvature R (see Fig. 10.a). This force increases if the object moves faster, or if the radius becomes smaller. The symbol X marks the center of rotation of the object, and the small black circle indicates the object.

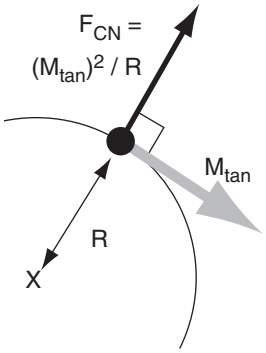

Figure 10.a. *Centrifugal force, F_{CN}.*

Because the Earth is plastic (i.e., deformable), centrifugal force due to the Earth's rotation and **gravitational force** F_G have shaped the surface into an ellipsoid, not a sphere. This is exaggerated in Fig. 10.b. The vector sum of F_G and F_{CN} is the **effective gravity**, F_{EG}. This effective gravity acts perpendicular to the local surface, and defines the direction we call **down**. Thus, a stationary object feels no net force (the downward force is balanced by the Earth holding it up).

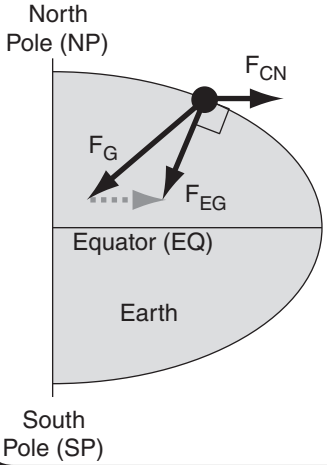

Figure 10.b. *North-south slice through Earth.*

(continues in next column)

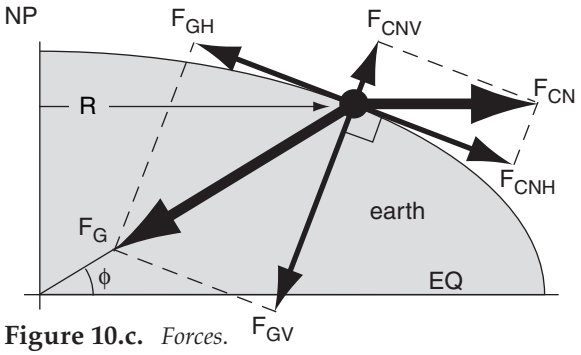

Figure 10.c. *Forces.*

Now that "up" and "down" are identified, we can split centrifugal and actual gravitational forces into local horizontal (subscript H) and vertical (subscript V) components (Fig. 10.c). Because F_{CN} is always parallel to the equator (EQ), trigonometry gives $F_{CNH} \approx F_{CN} \cdot \sin(\phi)$, where ϕ is latitude.

Objects at Rest

The Earth rotates counterclockwise when viewed from above the north pole (NP). During time interval Δt, any single meridian (a longitude line, such as labeled with distance R in Fig. 10.d) will rotate by angle $\Omega\,\Delta t$, where Ω is the angular velocity of Earth (= 360°/ sidereal day).

Suppose an object (the dark circle) is at rest on this meridian. Then during the same time interval Δt, it will move as shown by the grey arrow, at speed $M_{tan} = \Omega \cdot R$. Because this movement follows a parallel (latitude line), and parallels encircle the Earth's axis, the stationary object is turning around a circle. This creates centrifugal force. The horizontal component F_{CNH} balances F_{GH}, giving zero net apparent horizontal force on the object (Fig. 10.d).

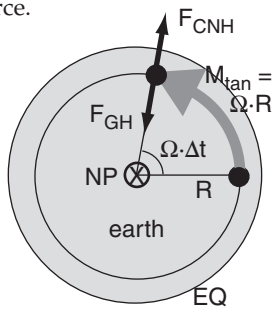

Figure 10.d. *Object at rest.*

Objects Moving East or West

Next, we can ask what happens if the object moves eastward with velocity M relative to the Earth's surface (shown by the thin white arrow in Fig. 10.e). The Earth is rotating as before, as indicated by the thin meridian lines in the figure. Thus, the total movement of the object is faster than before, as shown by the grey arrow. This implies greater total centrifugal force, which results in a greater horizontal component F_{CNH}. However, the gravity component F_{GH} is unchanged.

(continues in next column)

FOCUS • Coriolis Force (continuation)

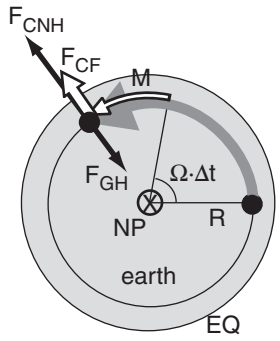

Figure 10.e. *Object moving east.*

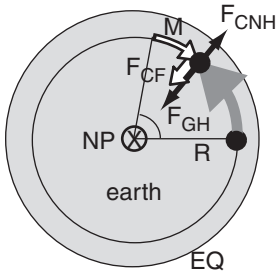

Figure 10.f. *Object moving west.*

Thus, those two forces (F_{CNH} & F_{GH}) do NOT balance. The difference between them is a net force to the right of the relative motion M. This force difference is called **Coriolis force**, F_{CF} , and is indicated by the thick white arrow in Fig. 10.e.

Similarly, for an object moving westward (thin white arrow in Fig. 10.f), the net tangential velocity (grey arrow) is slower, giving an imbalance between F_{CNH} & F_{GH} that acts to the right of M. This is identified as Coriolis force, as shown with the thick white arrow.

Objects Moving North or South

For a northward moving object, the rotation of the Earth (dashed thick grey line) and the relative motion of the object (M, thin white arrow) combine to cause a path shown with the solid thick grey line (Fig. 10.g). This has a smaller radius of curvature (R) about a center of rotation (X) that is NOT on the North Pole (O). The smaller radius causes a greater horizontal component of centrifugal force (F_{CNH}), which points outward from X.

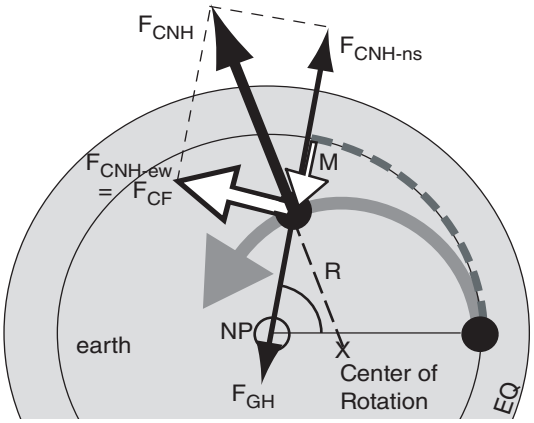

Figure 10.g. *Object moving north.*

We can conceptually divide this horizontal centrifugal force into a north-south component ($F_{CNH\text{-}ns}$) and an east-west component ($F_{CNH\text{-}ew}$). The southward component $F_{CNH\text{-}ns}$ balances the horizontal

(continues in next column)

FOCUS • Coriolis Force (continuation)

gravitational component F_{GH}, which hasn't changed very much relative to the other changes. However, the east-west component is acting to the right of the relative object motion M, and is identified as Coriolis force: $F_{CF} = F_{CNH\text{-}ew}$.

Similarly, a southward moving object has a larger radius of curvature, giving a Coriolis force to the right. In fact, an object moving in any arbitrary direction has Coriolis force acting to the right in the Northern Hemisphere.

Magnitude of Coriolis Force

For an object at rest (Figs. 10.c & d):

$$F_{GH} = F_{CNH} \equiv F_{CNHR} \qquad \text{(C1)}$$

where subscript R denotes "rest". At rest:

$$M_{tan\ rest} = \Omega \cdot R \qquad \text{(C2)}$$

For an eastward moving object (Fig. 10.e), Coriolis force is defined as:

$$F_{CF} \equiv F_{CNH} - F_{GH} \qquad \text{(definition)}$$

$$= F_{CNH} - F_{CNHR} \qquad \text{(from eq. C1)}$$

$$= \sin(\phi) \cdot [F_{CN} - F_{CNR}] \qquad \text{(from Fig. 10.c)}$$

Divide by mass m, and plug in the definition for centrifugal force as velocity squared divided by radius:

$$F_{CF} / m = \sin(\phi) \cdot [\ (M_{tan})^2/R - (M_{tan\ rest})^2/R\ ]$$

Use $M_{tan} = M_{tan\ rest} + M$, along with eq. (C2):

$$F_{CF} / m = \sin(\phi) \cdot [\ (\Omega \cdot R + M)^2/R - (\Omega \cdot R)^2/R\ ]$$

$$= \sin(\phi) \cdot [(2 \cdot \Omega \cdot M) + (M^2/R)]$$

The last term is small & can be neglected compared to the first term. Thus, the magnitude of Coriolis force is:

$$F_{CF}/m \approx 2 \cdot \Omega \cdot \sin(\phi) \cdot M \qquad (10.18)$$

$$\equiv f_c \cdot M \qquad \text{(from eq. 10.16)}$$

This answer is found for motion in any direction.

BEYOND ALGEBRA • Apparent Forces

In vector form, centrifugal force/mass for an object at rest on Earth is $-\boldsymbol{\Omega} \times (\boldsymbol{\Omega} \times \mathbf{r})$, and Coriolis force/mass is $-2\boldsymbol{\Omega} \times \mathbf{V}$, where vector $\boldsymbol{\Omega}$ points along the Earth's axis toward the north pole, $\mathbf{r}$ points from the Earth's center to the object, $\mathbf{V}$ is the object's velocity relative to Earth, and $\times$ is the vector cross product.

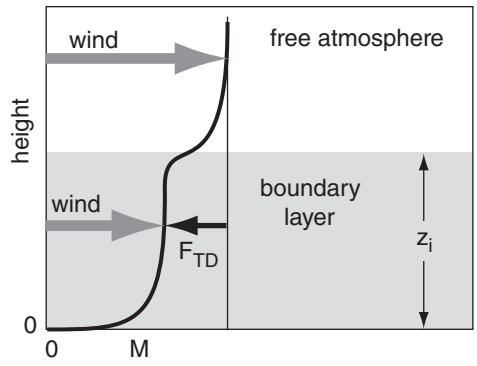

Figure 10.7
Turbulent drag force F_{TD} opposes the wind in the boundary layer.

Solved Example

Find the drag force per unit mass on a wind of U = 10 m/s, V = 0 for a: (a) statically neutral boundary layer over smooth ground; and (b) statically unstable boundary layer with w_B = 45 m/s. The boundary layer is 1 km thick.

Solution

Given: $U = M$ = 10 m/s, z_i = 1000 m,
$C_D = 2\text{x}10^{-3}$, w_B = 45 m/s.
Find: $F_{x\,TD}/m$ = ? m·s^{-2}.

(a) Combine eqs. (10.21) and (10.19a):

$$\frac{F_{xTD}}{m} = -C_D \cdot M \cdot \frac{U}{z_i} = -(0.02) \cdot \frac{(15\text{m/s})^2}{1500\text{m}}$$

$$= \underline{\mathbf{-2x10}}^{-4} \quad \text{m·s}^{-2}.$$

(b) Combine eqs. (10.22) and (10.19a):

$$\frac{F_{xTD}}{m} = -b_D \cdot w_B \cdot \frac{U}{z_i}$$

$$= -(0.00183) \cdot (50\text{m/s}) \cdot \frac{(15\text{m/s})}{1500\text{m}}$$

$$= \underline{\mathbf{-8.24x10}}^{-4} \quad \text{m·s}^{-2}.$$

Check: Units OK. Physics OK.
Discussion: The negative sign means that the drag force is toward the west, which is opposite the wind direction. Both mechanical and buoyant turbulence are equally effective at transporting frictional information to the air.

Turbulent-Drag Force

At the Earth's surface the air experiences drag against the ground. This turbulent-drag force increases with wind speed, and is always in a direction opposite to the wind direction. Namely, drag slows the wind (Fig. 10.7).

Only the **boundary layer** (see the Atmospheric Boundary Layer chapter) experiences this drag. It is not felt by the air in the remainder of the troposphere (except for deep vigorous thunderstorms or for mountain-wave drag, see the Local Winds chapter). The drag force acting on a boundary layer of depth z_i is:

$$\frac{F_{xTD}}{m} = -w_T \cdot \frac{U}{z_i} \qquad \bullet(10.19a)$$

$$\frac{F_{yTD}}{m} = -w_T \cdot \frac{V}{z_i} \qquad \bullet(10.19b)$$

where w_T is a turbulent **transport velocity**.

The total magnitude of turbulent drag force is

$$\left|\frac{F_{TD}}{m}\right| = w_T \cdot \frac{M}{z_i} \qquad (10.20)$$

and is opposite to the wind direction.

During windy conditions of near **neutral** static stability, turbulence is generated primarily by the **wind shear** (change of wind speed or direction with height). This turbulence transports frictional information upward from the ground to the air at rate:

$$w_T = C_D \cdot M \qquad (10.21)$$

where wind speed M is always positive, and C_D is a dimensionless **drag coefficient** in the range of $2\text{x}10^{-3}$ over smooth surfaces to $2\text{x}10^{-2}$ over rough or forested surfaces (see the Atmospheric Boundary Layer chapter). It is similar to the bulk heat transfer coefficient that was discussed in the Heat chapter.

During statically **unstable** conditions of light winds and strong surface heating (e.g., daytime), buoyant thermals transport the frictional information upward at rate:

$$w_T = b_D \cdot w_B \qquad (10.22)$$

where w_B is the **buoyancy velocity scale** (always positive, see the Heat chapter), and $b_D = 1.83\text{x}10^{-3}$ is dimensionless.

Summary of Forces

Table 10-3. Summary of forces.

Item	Name of Force	Direction	Magnitude (N/kg)	Horiz. (H) or Vert. (V)	Remarks ("item" is in column 1; H & V in col. 5)
1	**gravity**	down	$\left\|\frac{F_G}{m}\right\| = \|g\| = 9.8\ \text{m}\cdot\text{s}^{-2}$	V	**hydrostatic equilibrium** when items 1 & 2V balance
2	**pressure gradient**	from high to low pressure	$\left\|\frac{F_{PG}}{m}\right\| = \left\|\frac{1}{\rho}\cdot\frac{\Delta P}{\Delta d}\right\|$	V & H	the only force that can drive horizontal winds
3	**Coriolis** (apparent)	90° to right (left) of wind in Northern (Southern) Hemisphere	$\left\|\frac{F_{CF}}{m}\right\| = 2\cdot\Omega\cdot\|\sin(\phi)\cdot M\|$	H*	**geostrophic wind** when 2H and 3 balance (explained later in horiz. wind section)
4	**turbulent drag**	opposite to wind	$\left\|\frac{F_{TD}}{m}\right\| = w_T\cdot\frac{M}{z_i}$	H*	**boundary-layer wind** when 2H, 3 and 4 balance (explained in horiz. wind section)
5	**centrifugal** (apparent)	away from center of curvature	$\left\|\frac{F_{CN}}{m}\right\| = \frac{M^2}{R}$	H*	centripetal = opposite of centrifugal. **Gradient wind** when 2H, 3 and 5 balance
6	**advection** (apparent)	(any)	$\left\|\frac{F_{AD}}{m}\right\| = M\cdot\left\|\frac{\Delta(U \text{ or } V)}{\Delta d}\right\|$	V & H	neither creates nor destroys momentum; just moves it

**Horizontal is the direction we will focus on. However, Coriolis force has a small vertical component for zonal winds. Turbulent drag can exist in the vertical for rising or sinking air, but has completely different form than the boundary-layer drag given above. Centrifugal force can exist in the vertical for vortices with horizontal axes. Note: units N/kg = m·s^{-2}.*

EQUATIONS OF HORIZONTAL MOTION

Combining the forces from eqs. (10.7, 10.8, 10.9, 10.17, and 10.19) into Newton's Second Law of Motion (eq. 10.5) gives simplified equations of horizontal motion:

•(10.23a)

$$\frac{\Delta U}{\Delta t} = -U\frac{\Delta U}{\Delta x} - V\frac{\Delta U}{\Delta y} - \frac{1}{\rho}\cdot\frac{\Delta P}{\Delta x} + f_c\cdot V - w_T\cdot\frac{U}{z_i}$$

•(10.23b)

$$\frac{\Delta V}{\Delta t} = -U\frac{\Delta V}{\Delta x} - V\frac{\Delta V}{\Delta y} - \frac{1}{\rho}\cdot\frac{\Delta P}{\Delta y} - f_c\cdot U - w_T\cdot\frac{V}{z_i}$$

tendency — *horizontal advection* — *pressure gradient* — *Coriolis* — *turbulent drag*

These are the forecast equations for wind. Centrifugal force is not included because it is the opposite of **centripetal** force, which is the net imbalance of the other forces already included above.

As was shown in the solved examples, each of the terms can be of similar magnitude: $1\text{x}10^{-4}$ to $10\text{x}10^{-4}$ m·s^{-2} (which is equivalent units of N/kg, see Appendix A for review). For some situations, some of the terms are small enough to be neglected compared to the others. For example, above the boundary layer the turbulent-drag term is near zero. Near the equator, Coriolis force is near zero. At the center of high or low pressure regions, the pressure gradient is near zero.

There are other physical processes that have been neglected in the simplified equations just presented. **Molecular friction** is significant in the bottom few millimeters of the ground. **Mountain-wave drag** can be large in mountainous regions (see the Local Winds chapter). Cumulus clouds can cause turbulent **convective mixing** above the boundary layer (see the Atmospheric Boundary Layer and Thunderstorm chapters). Vertical advection of the horizontal wind has been neglected because it often is small. Mean vertical motions (e.g., large-scale subsidence) will be examined later in this chapter.

In the section that follows, the equations of motion are simplified for some special cases, to yield theoretical winds in the horizontal. Where appropriate, the forces and winds will also be given in isobaric coordinates.

Table 10-4. Names of idealized steady-state horizontal winds, and the forces that govern them.

$$0 = -U\frac{\Delta U}{\Delta x} \; -\frac{1}{\rho}\cdot\frac{\Delta P}{\Delta x} \; +f_c\cdot V \; -w_T\cdot\frac{U}{z_i} \; +s\frac{V\cdot M}{R}$$

Forces:	*pressure gradient*	*Coriolis*	*turbulent drag*	*centrifugal*
Wind Name				
Geostrophic	•	•		
Gradient	•	•		•
Boundary Layer	•	•	•	
BL Gradient	•	•	•	•
Cyclostrophic	•			•
Inertial		•		•
Antitriptic	•		•	

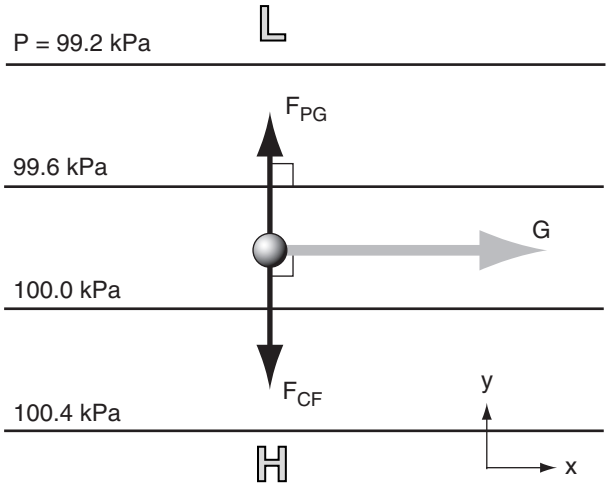

Figure 10.8
Idealized weather map, showing geostrophic wind (G, grey arrow) caused by a balance between two forces (black arrows): pressure-gradient force (F_{PG}) and Coriolis force (F_{CF}). P is pressure, with isobars plotted as thin black lines. L and H are low and high-pressure regions. The small sphere represents an air parcel.

Solved Example

Pressure increases 1 kPa eastward across a distance of 500 km. What is the geostrophic wind speed, given $\rho = 1$ kg/m^3 and $f_c = 10^{-4}$ s^{-1} ?

Solution

Given: ΔP =1 kPa, Δx =500 km, ρ =1 kg/m^3, f_c =10^{-4} s^{-1}.
Find: G = ? m/s

$U_g = 0$, thus $G = V_g$. Use eq. (10.26b):

$$V_g = \frac{-1}{(1.2\text{kg/m}^3)\cdot(1.1\times10^{-4}\text{s}^{-1})}\cdot\frac{(-2[}{(80[} = \underline{\textbf{20 m/s}}$$

Check: Units OK. Physics OK.
Discussion: "Kilo" in the numerator & denominator cancel. Given that $\Delta P/\Delta x$ = 0.002 kPa/km, the answer agrees with Fig. 10.10. The wind is toward the north.

HORIZONTAL WINDS

When air accelerates to create wind, forces such as Coriolis and drag change too, because they depend on the wind speed. This, in turn, changes the acceleration via eqs. (10.23), so there is a **feedback process**. This feedback continues until the forces finally balance each other. At that point, there is no net force, and no further acceleration.

This final condition is called **steady state**:

$$\frac{\Delta U}{\Delta t} = 0, \quad \frac{\Delta V}{\Delta t} = 0 \qquad \bullet(10.24)$$

In steady-state, wind speeds do not change with time, but are not necessarily zero. Only the acceleration is zero.

Under certain idealized conditions, some of the forces in the equations of motion are small enough to be neglected. For these situations, theoretical steady-state winds can be found based on only the remaining larger-magnitude forces. These theoretical winds are given special names, as listed in Table 10-4. These winds are examined next in more detail. The real winds under these special conditions are often close to the theoretical winds.

Geostrophic Wind

The geostrophic wind (U_g , V_g) is a theoretical wind that results from a steady-state balance between pressure-gradient force and Coriolis force (Fig. 10.8). After setting the other forces to zero, eqs. (10.23) become:

$$0 = -\frac{1}{\rho}\cdot\frac{\Delta P}{\Delta x} \; +f_c\cdot V \qquad (10.25a)$$

$$0 = -\frac{1}{\rho}\cdot\frac{\Delta P}{\Delta y} \; -f_c\cdot U \qquad (10.25b)$$

Solving these equations for U and V, and then defining $U \equiv U_g$ and $V \equiv V_g$, gives:

$$U_g = -\frac{1}{\rho\cdot f_c}\cdot\frac{\Delta P}{\Delta y} \qquad \bullet(10.26a)$$

$$V_g = +\frac{1}{\rho\cdot f_c}\cdot\frac{\Delta P}{\Delta x} \qquad \bullet(10.26b)$$

where $f_c = (1.4584\text{x}10^{-4}\text{ s}^{-1})\cdot\sin(\textit{latitude})$ is the Coriolis parameter, ρ is air density, and $\Delta P/\Delta x$ and $\Delta P/\Delta y$ are the horizontal pressure gradients.

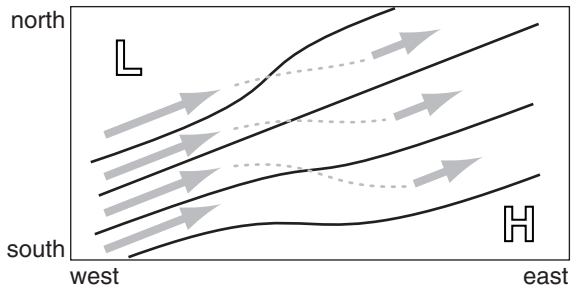

Figure 10.9
Geostrophic winds (grey arrows) are faster (longer arrows) where isobars (thin lines) are closer together. (For N. Hemis.)

In regions of straight isobars above the top of the boundary layer and away from the equator, the actual winds are approximately geostrophic. These winds blow parallel to the isobars or height contours, with low pressure to the left in the Northern Hemisphere (Fig. 10.9). The wind is faster in regions where the isobars are closer together (i.e., where the isobars are tightly packed) and at lower latitudes (Fig. 10.10).

The total geostrophic wind speed G is:

$$G = \sqrt{U_g{}^2 + V_g{}^2} \qquad (10.27)$$

If Δd is the distance between two isobars (in the direction of greatest pressure change; namely, perpendicular to the isobars), then the magnitude of the geostrophic wind is:

$$G = \left| \frac{1}{\rho \cdot f_c} \cdot \frac{\Delta P}{\Delta d} \right| \qquad \bullet(10.28)$$

Above sea level, weather maps are often on isobaric surfaces (constant pressure charts). The geostrophic wind as a function of horizontal distances between height (z) contours on a constant-pressure chart is:

$$U_g = -\frac{|g|}{f_c} \cdot \frac{\Delta z}{\Delta y} \qquad \bullet(10.29a)$$

$$V_g = +\frac{|g|}{f_c} \cdot \frac{\Delta z}{\Delta x} \qquad \bullet(10.29b)$$

where $|g| = 9.8\ \text{m}\cdot\text{s}^{-2}$ is gravitational acceleration magnitude, and f_c is the Coriolis parameter. The corresponding magnitude of geostrophic wind on an isobaric chart is:

$$G = \left| \frac{g}{f_c} \cdot \frac{\Delta z}{\Delta d} \right| \qquad \bullet(10.29c)$$

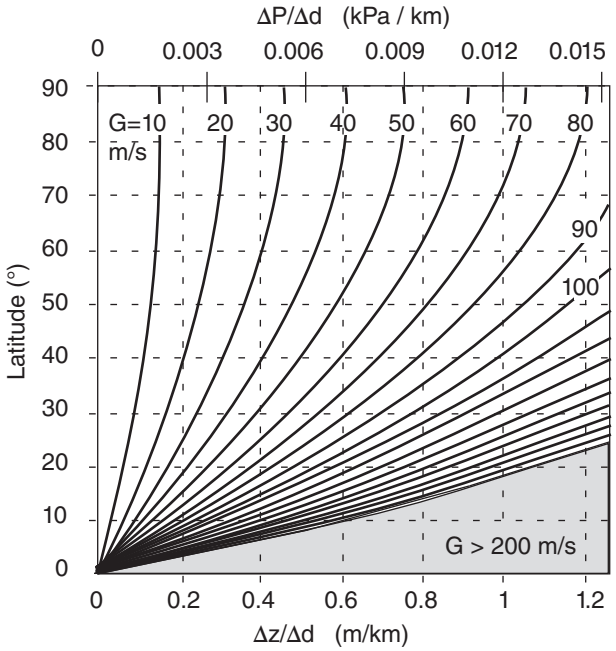

Figure 10.10
Geostrophic wind speed G vs. latitude and height gradient (Δz/Δd) on a constant pressure surface. Top scale is pressure gradient at sea level.

Solved Example

If height increases by 100 m eastward across a distance of 500 km, then what is the geostrophic wind speed, given $f_c = 10^{-4}\ \text{s}^{-1}$?

Solution

Given: $\Delta z = 100$ m, $\Delta x = 500$ km, $f_c = 10^{-4}\ \text{s}^{-1}$.
Find: $G = ?$ m/s

$U_g = 0$, thus $G = V_g$. Use eq. (10.29b):

$$V_g = +\frac{|g|}{f_c} \cdot \frac{\Delta z}{\Delta x} = \left(\frac{9.8\text{m s}^{-2}}{0.00009\text{s}^{-1}} \right) \cdot \left(\frac{50\text{m}}{200{,}000\text{m}} \right) = \underline{\textbf{19.6 m/s}}$$

Check: Units OK. Physics OK.
Discussion: This is nearly the same answer as before. Δz of 100 m on an isobaric surface corresponds to ΔP of roughly 1 kPa on a constant height surface. A hypothetical ball rolling downhill would start moving toward the west, but would be deflected northward by Coriolis force in the Northern Hemisphere.

FOCUS • Approach to Geostrophy

How does an air parcel, starting from rest, approach the final steady-state geostrophic wind speed G sketched in Fig. 10.8?

Start with the equations of horizontal motion (10.23), and ignore all terms except the tendency, pressure-gradient force, and Coriolis force. Use the definition of

continues on next page

FOCUS • Appr. to Geostrophy *(continued)*

geostrophic wind (eqs. 10.26) to write the resulting simplified equations as:

$$\Delta U / \Delta t = -f_c \cdot (V_g - V)$$
$$\Delta V / \Delta t = f_c \cdot (U_g - U)$$

Next, rewrite these as forecast equations:

$$U_{new} = U_{old} - \Delta t \cdot f_c \cdot (V_g - V_{old})$$
$$V_{new} = V_{old} + \Delta t \cdot f_c \cdot (U_g - U_{new})$$

Start with initial conditions (U_{old}, V_{old}) = (0, 0), and then iteratively solve the equations on a spreadsheet to forecast the wind.

For example, consider the conditions given in the previous solved example, where we would anticipate the wind should approach (U_g, V_g) = (0, 20) m/s. The actual evolution of winds (U, V) and air parcel position (X, Y) are shown in Figs. below.

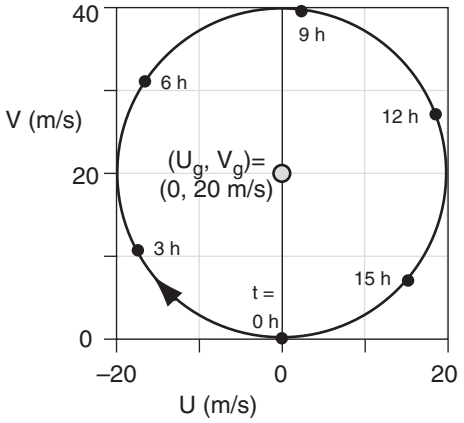

Surprisingly, the winds never reach geostrophic equilibrium, but instead rotate around the geostrophic wind. This is called an **inertial oscillation**, with period of $P = 2 \cdot \pi / f_c$. Twice this period is called a **pendulum day**. For our solved example, P = 17.45 h.

The net result in the figure below is that the wind indeed moves at the geostrophic speed of 20 m/s to the north (≈ 1250 km in 17.45 h), but along the way it staggers west and east with an additional **ageostrophic** (non-geostrophic) part.

Inertial oscillations are sometimes observed at night in the boundary layer, but rarely higher in the atmosphere. Why not? (1) The ageostrophic component of wind (wind from the East in this example) moves air mass, and changes the pressure gradient. (2) Friction damps the oscillation toward a steady wind.

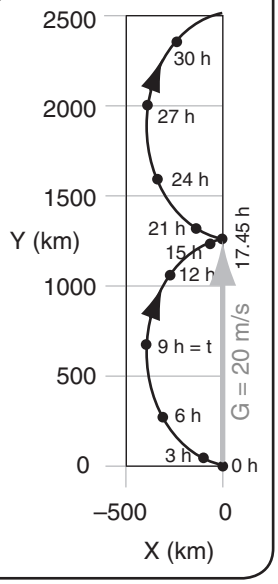

If the **geopotential** $\Phi = |g| \cdot z$ is substituted in eqs. (10.29), the resulting geostrophic winds are:

$$U_g = -\frac{1}{f_c} \cdot \frac{\Delta \Phi}{\Delta y} \qquad (10.30a)$$

$$V_g = \frac{1}{f_c} \cdot \frac{\Delta \Phi}{\Delta x} \qquad (10.30b)$$

Gradient Wind

Around a high or low pressure center, the steady-state wind follows the curved isobars, with low pressure to the left in the Northern Hemisphere. Around lows, the wind is slower than geostrophic, called **subgeostrophic**, regardless of the hemisphere. Around highs, the steady-state wind is faster than geostrophic, or **supergeostrophic**. The curved steady-state wind is called the **gradient wind**.

The gradient wind occurs because of an imbalance (Figs. 10.11 & 10.12) between pressure-gradient (F_{PG}) and Coriolis forces (F_{CF}); namely, the net force (F_{net}) is not zero. This net force is called centripetal force, and is what causes the wind to continually change direction as it goes around a circle. By describing this change in direction as causing an apparent force (centrifugal), we can find the steady-state gradient wind:

$$0 = -\frac{1}{\rho} \cdot \frac{\Delta P}{\Delta x} + f_c \cdot V + s \cdot \frac{V \cdot M}{R} \qquad (10.31a)$$

$$0 = \underbrace{-\frac{1}{\rho} \cdot \frac{\Delta P}{\Delta y}}_{\text{pressure gradient}} \underbrace{- f_c \cdot U}_{\text{Coriolis}} \underbrace{- s \cdot \frac{U \cdot M}{R}}_{\text{centrifugal}} \qquad (10.31b)$$

Because the gradient wind is for flow around a circle, we can frame the governing equations in radial coordinates:

$$\frac{1}{\rho} \cdot \frac{\Delta P}{\Delta R} = f_c \cdot M_{\tan} + \frac{M_{\tan}^2}{R} \qquad (10.32)$$

where R is radial distance from the center of the circle, f_c is the Coriolis parameter, ρ is air density, $\Delta P / \Delta R$ is the radial pressure gradient, and $M_{\tan}$ is the magnitude of the tangential velocity; namely, the gradient wind. The signs of the terms in this equation are for flow around a low.

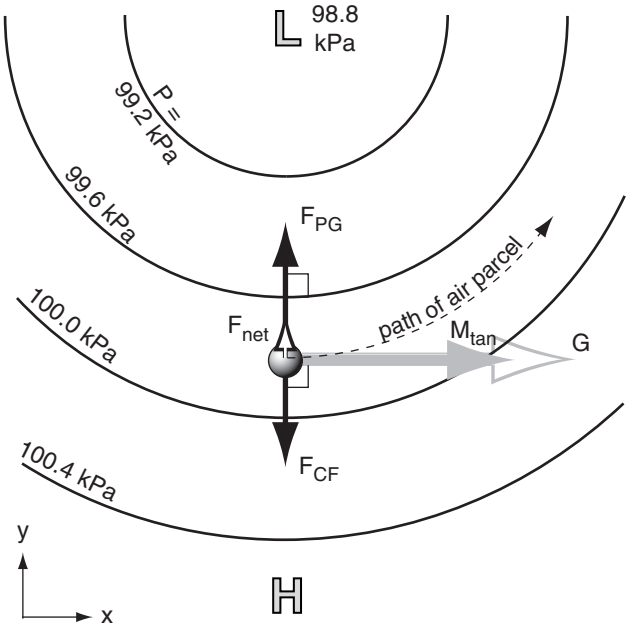

Figure 10.11
Forces (dark arrows) that cause the gradient wind (solid grey arrow, M_{tan}) to be slower than geostrophic (hollow grey arrow) when circling around a low-pressure center (called a cyclone in the N. Hem.). The short white arrow with black outline shows centripetal force (the imbalance between the other two forces). Centripetal force pulls the air parcel (grey sphere) inward to force the wind direction to change as needed for the wind to turn along a circular path.

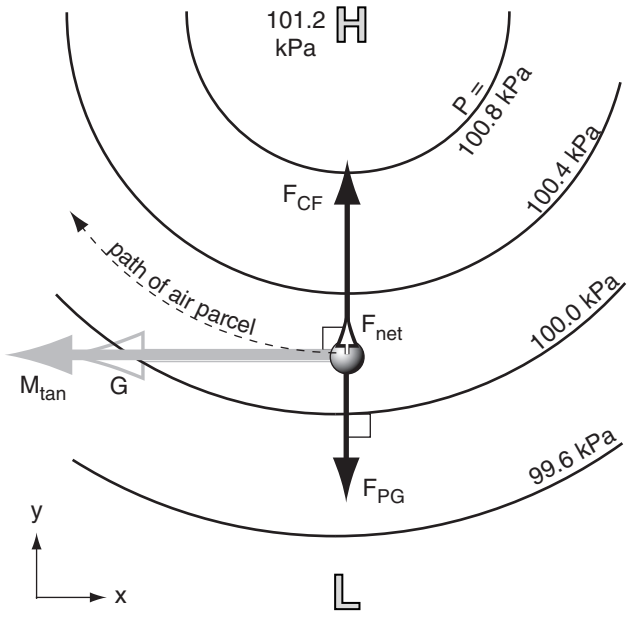

Figure 10.12
Forces (dark arrows) that cause the gradient wind (solid grey arrow, M_{tan}) to be faster than geostrophic (hollow grey arrow) for an air parcel (grey sphere) circling around a high-pressure center (called an anticyclone in the N. Hemisphere).

Define $U_{\tan} \equiv U$ and $V_{\tan} \equiv V$ as the components of gradient wind, with a total gradient wind speed of $M_{\tan} = [U_{\tan}^2 + V_{\tan}^2]^{1/2}$. One solution to eq. (10.32) is

$$M_{\tan} = G \pm \frac{M_{\tan}^2}{f_c \cdot R} \qquad (10.33)$$

where $M_{\tan}$ is the gradient-wind speed, and where the negative sign is used for flow around low pressure centers, and the positive sign for highs. This solution demonstrates that wind is "slow around lows" (Fig. 10.13), meaning slower than geostrophic G. However, the solution is implicit because the desired wind $M_{\tan}$ is on both sides of the equal sign.

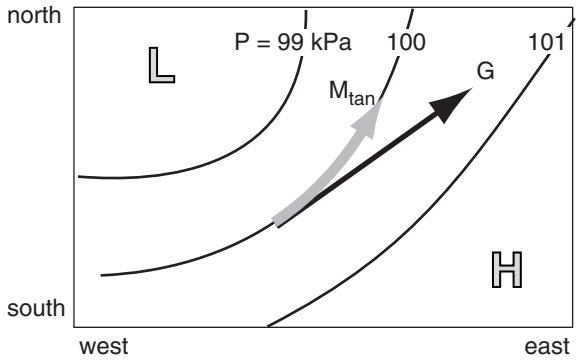

Figure 10.13
Geostrophic wind G and gradient wind M_{tan} around a low pressure center in the Northern Hemisphere.

Solved Example

What radius of curvature causes the gradient wind to equal the geostrophic wind?

Solution

Given: $M_{\tan} = G$ Find: R = ? km

Use eq. (10.33), with $M_{\tan} = G$: $G = G \pm G^2/(f_c \cdot R)$

This is a valid equality $G = G$ only when the last term in eq. (10.33) approaches zero; i.e., in the limit of $\underline{\mathbf{R = \infty}}$.

Check: Eq. (10.33) still balances in this limit. **Discussion**: Infinite radius of curvature is a straight line, which (in the absence of any other forces such as turbulent drag) is the condition for geostrophic wind.

Solved Example

If the geostrophic wind around a low is 10 m/s, then what is the gradient wind speed, given $f_c = 10^{-4}$ s^{-1} and a radius of curvature of 500 km? Also, what is the curvature Rossby number?

Solution

Given: G = 10 m/s, R = 500 km, $f_c = 10^{-4}$ s^{-1}
Find: M_{tan} = ? m/s, Ro_c = ? (dimensionless)

Use eq. (10.34a)

$$M_{tan} = 0.5 \cdot (10^{-4}\text{s}^{-1}) \cdot (500000\text{m}) \cdot \left[-1 + \sqrt{1 + \frac{4 \cdot (10 m/s)}{(10^{-4}\text{s}^{-1}) \cdot (500000\text{m})}} \right]$$

$$= \underline{\mathbf{8.54\ m/s}}$$

Use eq. (10.35):

$$Ro_c = \frac{(10\text{m/s})}{(10^{-4}\text{s}^{-1}) \cdot (5 \times 10^5\text{m})} = \underline{\mathbf{0.2}}$$

Check: Units OK. Physics OK.
Discussion: The small Rossby number indicates that the flow is in geostrophic balance. The gradient wind is indeed slower than geostrophic around this low.

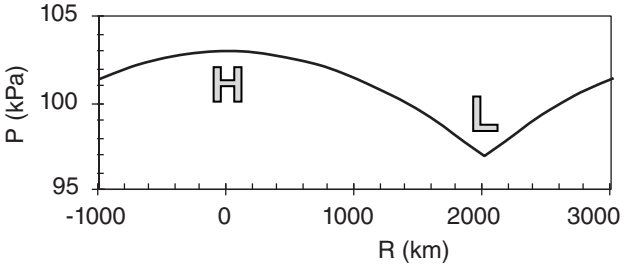

Figure 10.14
Variation of surface pressure across an anticyclone (H) and cyclone (L), showing that the curve can have steep pressure gradients near the low and a cusp at the low, but not at the high. Arbitrary center pressures of 103 kPa and 97 kPa were chosen to illustrate the anticyclone and cyclone, respectively.

Solving the quadratic equation (10.33) for the **cyclonic** flow (around a low-pressure center) yields the gradient wind M_{tan}:

$$M_{tan} = 0.5 \cdot f_c \cdot R \cdot \left[-1 + \sqrt{1 + \frac{4 \cdot G}{f_c \cdot R}} \right] \quad \bullet(10.34a)$$

For **anticyclonic** flow (around a high-pressure center):

$$M_{tan} = 0.5 \cdot f_c \cdot R \cdot \left[1 - \sqrt{1 - \frac{4 \cdot G}{f_c \cdot R}} \right] \quad \bullet(10.34b)$$

A "curvature" **Rossby number** (Ro_c) can be defined that uses the radius of curvature (R) as the relevant length scale:

$$Ro_c = \frac{G}{f_c \cdot R} \quad (10.35)$$

[Neither R nor Ro_c are the "Rossby deformation radius" (see eq. 10.70, and the Airmasses, Fronts, and Extratropical Cyclones chapters).] Small values of the **Rossby number** indicate flow that is nearly in geostrophic balance.

The cyclonic gradient wind (around a <u>low</u>) is:

$$M_{tan} = \frac{G}{2 \cdot Ro_c} \cdot \left[-1 + \left(1 + 4 \cdot Ro_c\right)^{1/2} \right. \quad (10.36a)$$

and anticyclonic gradient wind (around a <u>high</u>) is:

$$M_{tan} = \frac{G}{2 \cdot Ro_c} \cdot \left[1 - \left(1 - 4 \cdot Ro_c\right)^{1/2} \right. \quad (10.36b)$$

where G is the geostrophic wind.

For high-pressure centers, steady-state physical (non-imaginary) solutions exist only for $Ro_c \le 1/4$. Thus, around anticyclones, isobars cannot be both closely spaced and sharply curved. In other words, the pressure cannot decrease rapidly away from high centers. There is no analogous restriction on cyclones, because any value of Ro_c is possible. Thus, pressure gradients and winds <u>must be gentle in highs</u>, but <u>can be vigorous near low centers</u> (Figs. 10.14 and 10.15).

By combining the definition of the Rossby number with that for geostrophic wind, and setting Ro_c = 1/4, we find that the maximum horizontal variations of pressure P or height z near anticyclones are:

$$z = z_c - \left(f_c^2 \cdot R^2 \right. \quad \bullet(10.37a)$$

$$P = P_c - \left(\rho \cdot f_c^2 \cdot R^2 \right) \quad \bullet(10.37b)$$

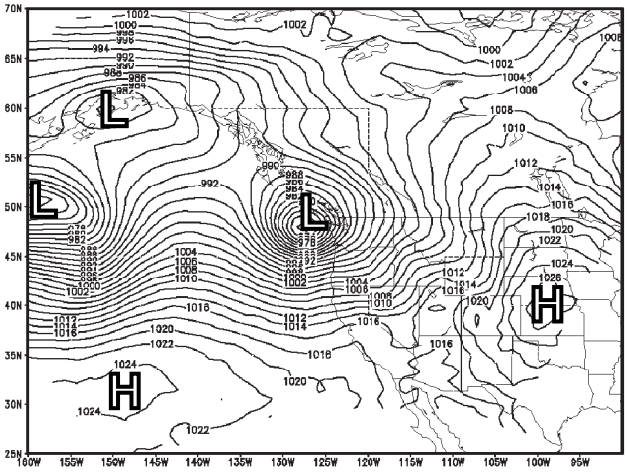

Figure 10.15
Sea-level pressure (contoured every 2 mb= 0.2 kPa), for 00 UTC on 24 Nov 1998. Notice the tight packing of isobars around lows, but looser spacing near high-pressure centers.

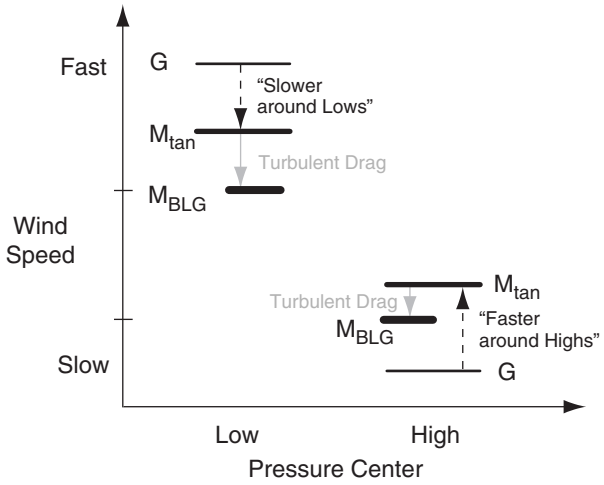

Figure 10.16
Relative magnitudes of different wind speeds around low- and high-pressure centers. G = geostrophic wind, M_{tan} = gradient wind speed, M_{BLG} = boundary-layer gradient wind speed. G is smaller in highs than in lows, because it is not physically possible to have strong pressure gradients to drive strong steady-state winds at high centers.

where z_c and P_c are the reference height or pressure at the center of the anticyclone, f_c is the Coriolis parameter, $|g|$ is gravitational acceleration magnitude, ρ is air density, and R is distance from the center of the anticyclone (Fig. 10.14).

Figs. 10.14 and 10.15 show that pressure gradients, and thus the geostrophic wind, can be large near low centers. However, pressure gradients, and thus the geostrophic wind, must be small near high centers. This difference in geostrophic wind speed G between lows and highs is sketched in Fig. 10.16. The slowdown of gradient wind M_{tan} (relative to geostrophic) around lows, and the speedup of gradient wind (relative to geostrophic) around highs is also plotted in Fig. 10.16. The net result is that gradient winds, and even boundary-layer gradient winds M_{BLG} (described later in this chapter), are usually stronger (in an absolute sense) around lows than highs. For this reason, low-pressure centers are often windy.

Boundary-Layer Wind

Turbulent drag in the boundary layer slows the wind below the geostrophic value, and turns the wind to point at a small angle (α) across the isobars toward low pressure (Fig. 10.17). For flow along straight isobars, the steady-state equations of motion become:

$$0 = -\frac{1}{\rho}\cdot\frac{\Delta P}{\Delta x} + f_c \cdot V - w_T \cdot \frac{U}{z_i} \qquad (10.38a)$$

$$0 = -\frac{1}{\rho}\cdot\frac{\Delta P}{\Delta y} - f_c \cdot U - w_T \cdot \frac{V}{z_i} \qquad (10.38b)$$

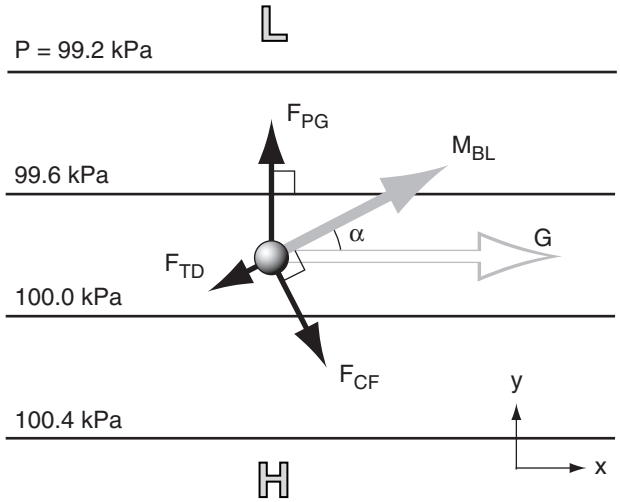

Figure 10.17
Balance of forces (black arrows) creating a boundary-layer wind (M_{BL}, solid grey arrow) that is slower than geostrophic (G, hollow grey arrow). The grey sphere represents an air parcel. Thin black lines are isobars. 𝕃 and 𝕳 are low and high-pressure centers.

Solved Example

Find the boundary-layer winds given U_g = 10 m/s, V_g = 0, z_i = 1 km, C_D = 0.002, and $f_c = 10^{-4}$ s^{-1}. Also, what angle do the winds cross the isobars? This is a statically neutral boundary layer.

Solution

Given: (see above)
Find: U_{BL} =? m/s, V_{BL} =? m/s, M_{BL} =? m/s, α = ? °
Use eqs. (10.41): with $G = (U_g^2 + V_g^2)^{1/2}$ = 10 m/s

$$a = \frac{0.003}{(10^{-4}\,\mathrm{s}^{-1})\cdot(1500\mathrm{m})} = 0.02\ \mathrm{s/m}$$

Check: $a \cdot G$ = (0.02s/m)·(10 m/s) =0.2 (is < 1. Good.)
U_{BL}=[1–0.35·(0.02s/m)·(10m/s)]·(10m/s) ≈ **9.3 m/s**
V_{BL}=[1–0.5·(0.02s/m)·(10m/s)]·
(0.02s/m)·(10m/s)·(10m/s) ≈ **1.8 m/s**

$$M_{ABL} = \sqrt{U_{ABL}^2 + V_{ABL}^2} = \sqrt{13.4^2 +} = \mathbf{9.47\ m/s}$$

The geostrophic wind is parallel to the isobars.
The angle between BL wind and geostrophic is
$\alpha = \tan^{-1}(V_{BL}/U_{BL}) = \tan^{-1}(1.8/9.3)$ = **11°** .

Check: Units OK. Physics OK.
Discussion: The boundary-layer wind speed is indeed slower than geostrophic (9.47 vs. 10 m/s), but only slightly slower because the drag coefficient for this example was very small. Also, it crosses the isobars slightly toward low pressure. (The geostrophic wind toward the east means low pressure is to the north.)

Solved Example

Find the boundary layer winds given U_g = 10 m/s, V_g = 0, z_i = 1 km, w_B = 45 m/s, $b_D = 1.83\times10^{-3}$, and $f_c = 10^{-4}$ s^{-1}. Also, at what angle does the wind cross the isobars? This is a statically unstable boundary layer.

Solution

Given: (see above, for a convective BL)
Find: U_{BL} = ? m/s, V_{BL} = ? m/s, M_{BL} = ? m/s, α = ?°

Use eqs. (10.42):

$$c_1 = \frac{(1.83\times10^{-3})\cdot(50\mathrm{m/s})}{(10^{-4}\,\mathrm{s}^{-1})\cdot(1500\mathrm{m})} = 0.824\ \text{(dimensionless)}$$

$c_2 = 1/[1+(0.8242)^2] = 0.60$ (dimensionless)
$U_{BL} = 0.6\cdot[(10\mathrm{m/s}) - 0\,]$ = **6.0 m/s**
$V_{BL} = 0.6\cdot[0 + (0.824)\cdot(10\mathrm{m/s})]$ = **4.94 m/s**
Use eq. (10.40):
$M_{BL} = [U^2_{BL} + V^2_{BL}\,]^{1/2}$ = **7.77 m/s**
$\alpha = \tan^{-1}(V_{BL}/U_{BL}) = \tan^{-1}(4.94/6.0)$ = **39.5°**

Check: Units OK. Physics OK.
Discussion: As before, the boundary layer winds are subgeostrophic, and cross the isobars toward low pressure. Turbulent drag has similar effects, regardless of whether the turbulence is generated mechanically by wind shear, or by buoyant rising thermals.

Namely, the only forces acting for this special case are pressure gradient, Coriolis, and turbulent drag (Fig. 10.17).

Define $U_{BL} = U$ and $V_{BL} = V$ as components of the boundary-layer wind. An implicit solution of eqs. (10.38) is:

$$U_{ABL} = U_g - \frac{w_T \cdot V_{AB}}{f_c \cdot z_i} \qquad (10.39a)$$

$$V_{ABL} = V_g + \frac{w_T \cdot U_{AB}}{f_c \cdot z_i} \qquad (10.39b)$$

where (U_g, V_g) are geostrophic wind components, f_c is Coriolis parameter, z_i is ABL depth, and w_T is the turbulent transport velocity.

Eqs. (10.39) can be solved by iteration (guess V_{BL} and plug into the first equation, solve for U_{BL} and plug into second equation, solve for V_{BL} and repeat the process). The magnitude of the boundary-layer wind is:

$$M_{BL} = [U^2_{BL} + V^2_{BL}\,]^{1/2} \qquad (10.40)$$

If the boundary layer is statically **neutral** with strong wind shear, then $w_T = C_D \cdot M_{BL}$, where C_D is the drag coefficient (see eq. 10.21). An approximate explicit solution for the wind at most altitudes in the boundary layer is:

$$U_{ABL} \approx (1 - 0.35\cdot a\cdot U_g)\cdot U_g - (1 - 0.5\cdot a\cdot V_g)\cdot a\cdot V_g\cdot G \qquad \bullet(10.41a)$$

$$V_{ABL} \approx (1 - 0.5\cdot a\cdot U_g)\cdot a\cdot G\cdot U_g + (1 - 0.35\cdot a\cdot V_g)\cdot V_g \qquad \bullet(10.41b)$$

for $a \cdot G < 1$, where $a = C_D/(f_c \cdot z_i)$ and G is the geostrophic wind speed. If this condition is not met, or if no reasonable solution can be found using eqs. (10.41), then use the iterative approach described in the next section, but with the centrifugal terms set to zero. Eqs. (10.41) do not apply to the **surface layer** (bottom 10% of the neutral boundary layer).

For a statically **unstable** boundary layer with light winds, use $w_T = b_D \cdot w_B$ (see eq. 10.22). An exact explicit solution for the winds at most altitudes in the boundary layer is:

$$U_{ABL} = c_2 \cdot [U_g - c_1 \cdot V_g \qquad \bullet(10.42a)$$

$$V_{ABL} = c_2 \cdot [V_g + c_1 \cdot U_g \qquad \bullet(10.42b)$$

where $c_1 = \dfrac{b_D \cdot w_B}{f_c \cdot z_i}$, and $c_2 = \dfrac{1}{[1 + c_1^2]}$.

Again, this solution does not apply to the **surface layer** (bottom 5% of convective boundary layer). See the "Forces" section earlier in this chapter for definitions of the factors in c_1.

Thus, for both neutral and unstable static stabilities, boundary-layer winds (for most mid-boundary-layer altitudes) cross the isobars at a small angle (α) toward low pressure. This cross-isobaric flow occurs for both straight and curved isobars.

Boundary-Layer Gradient (BLG) Wind

In regions of curved isobars at the bottom of cyclones and anticyclones, drag force exists in the boundary layer (BL) in addition to pressure gradient and Coriolis force. The imbalance (F_{net}) of these forces creates a centripetal force that causes the air to spiral in towards low-pressure centers (Fig. 10.18) and spiral out from high-pressure centers. Fig. 10.1 shows a sketch of the BL gradient winds in the N. Hemisphere, and the associated isobars.

Assume steady state, neglect advection, and require an imbalance of forces equal to the centrifugal force, to reduce the equations of motion to:

$$0 = -\frac{1}{\rho}\cdot\frac{\Delta P}{\Delta x} + f_c \cdot V - w_T \cdot \frac{U}{z_i} + s\cdot\frac{V\cdot M}{R} \qquad (10.43a)$$

$$0 = -\frac{1}{\rho}\cdot\frac{\Delta P}{\Delta y} - f_c \cdot U - w_T \cdot \frac{V}{z_i} - s\cdot\frac{U\cdot M}{R} \qquad (10.43b)$$

pressure gradient *Coriolis* *turbulent drag* *centrifugal*

Without actually solving these equations, we can anticipate the following from our previous understanding of geostrophic, gradient, and boundary-layer winds. Boundary-layer gradient (BLG) wind speed is slower than the gradient wind speed due to the drag. The BLG winds flow counterclockwise around lows in the N. Hemisphere, and clockwise around highs. Instead of blowing parallel to the curved isobars like the gradient wind, BLG winds cross the isobars at a small angle (α, tens of degrees) toward low pressure (Fig. 10.19).

The turbulent drag term is different for highs and lows. Winds are strong around lows and skies are often overcast, hence the transport velocity is best represented by the statically neutral parameterization:

$$w_T = C_D \cdot M = C_D \cdot [\, U^2 + V^2 \,]^{1/2} \qquad (10.21 \text{ again})$$

which adds even more nonlinearity to eqs. (10.43).

In highs, winds are light and skies are clear, suggesting that transport velocity should be given by the statically unstable parameterization during daytime by:

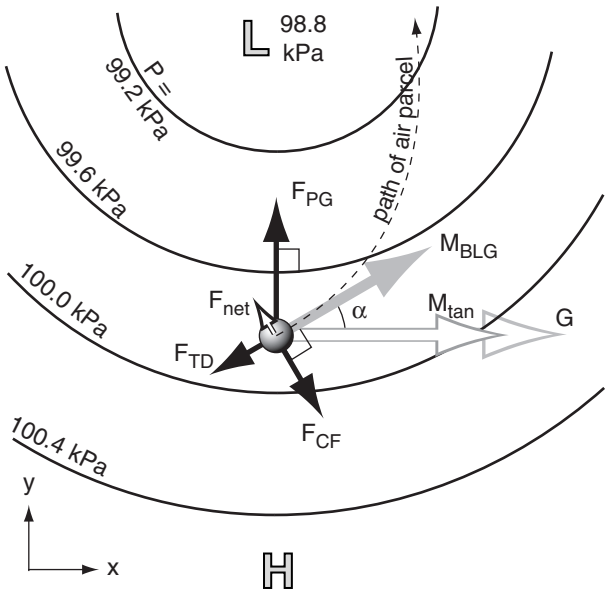

Figure 10.18
Imbalance of forces (black arrows) yield a net centripetal force (F_{net}) that causes the boundary layer gradient wind (M_{BLG}, solid grey arrow) to be slower than both the gradient wind (M_{tan}) and geostrophic wind (G). The resulting air-parcel path crosses the isobars at a small angle α toward low pressure.

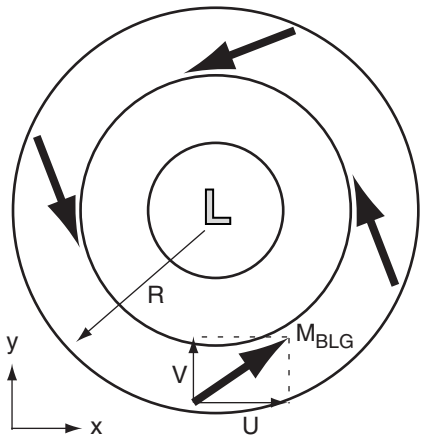

Figure 10.19
Tangential (U) and radial (V) components of the BLG wind in the N. Hemisphere, for that one vector south of the Low.

Solved Example

Find the BLG winds south of a low pressure center in the N. Hemisphere, given G = 20 m/s at radius R = 500 km from the low center, z_i = 1 km, C_D = 0.01, and f_c = 10^{-4} s^{-1}. Also, find the speed.

Solution

Given: (see above)
Find: U_{BLG} = ? m/s, V_{BLG} = ? m/s, M_{BLG} = ? m/s

Use eqs. (1.1) and (10.44) in a spreadsheet. Set the time step to Δt = 1 h. Choose U = 0 and V = 0 as the first guess. Make 20 iterations (see the Focus box).

Boundary Layer Gradient Wind

G (m/s) = 20		zi (km) = 1	
fc (1/s) = 0.0001		CD = 0.01	
R (km) = 500		delta t(s)= 3600	

Iteration	U (m/s)	V (m/s)	M (m/s)	delta U	delta V
0	0.00	0.00	0.00	0.000	7.200
1	0.00	7.20	7.20	2.965	5.334
2	2.97	12.53	12.88	4.300	0.046
3	7.26	12.58	14.53	2.045	-2.754
4	9.31	9.83	13.54	-0.042	-1.847
5	9.27	7.98	12.23	-0.506	-0.465
6	8.76	7.51	11.54	-0.312	0.195
7	8.45	7.71	11.44	-0.070	0.288
8	8.38	8.00	11.58	0.051	0.150
9	8.43	8.15	11.72	0.062	0.015
10	8.49	8.16	11.78	0.029	-0.038
11	8.52	8.12	11.77	0.001	-0.033
12	8.52	8.09	11.75	-0.009	-0.012
13	8.51	8.08	11.74	-0.007	0.002
14	8.51	8.08	11.73	-0.002	0.005
15	8.51	8.09	11.74	0.001	0.003
16	8.51	8.09	11.74	0.001	0.001
17	8.51	8.09	11.74	0.001	-0.001
18	8.51	8.09	11.74	0.000	-0.001
19	8.51	8.09	11.74	0.000	0.000
20	**8.51**	**8.09**	**11.74**	0.000	0.000

U_{BLG} = **8.51 m/s**, V_{BLG} = **8.09 m/s**, M_{BLG} = **11.74 m/s**, where (U_{BLG}, V_{BLG}) are (tangential, radial) parts.

Check: Units OK. Physics OK. Check that the computed wind approaches the: (1) geostrophic wind as R approaches ∞, with C_D = 0; (2) gradient wind when C_D = 0; (3) boundary-layer wind when R approaches ∞.

I performed these checks using a modified spreadsheet that relaxed the results using a weighted average of new and previous winds, and found: (1) for geostrophic: U_{BLG} = G = 20 m/s, V_{BLG} = 0; (2) for gradient: U_{BLG} = 15.31 m/s, V_{BLG} = 0; and (3) for BL: U_{BLG} = 7.81 m/s, V_{BLG} = 9.76 m/s. This BL solution is the exact solution; it is better than approximate eqs. (10.41).

Discussion: The solution converges toward the BLG wind, as if an air parcel started from rest and began accelerating. The Fig. at right used Δt = 1000 s (not 1 h). Starting at zero wind speed, each dot shows the wind forecast for the next time step in the iteration.

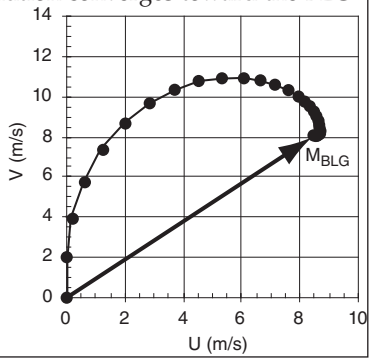

$$w_T = b_D \cdot w_B \qquad \text{(10.22 again)}$$

where w_B is not a function of wind speed. For statically stable conditions at night in fair weather, steady state is unlikely, so eqs. (10.43) are invalid.

While the equations of motion for geostrophic and gradient winds were simple enough to allow an analytical solution, and we could devise an approximate analytical solution for the BL wind, we are not so lucky with the BLG wind. The set of coupled equations (10.43) are nonlinear and nasty to solve.

Nonetheless, we can numerically iterate towards the answer by including the tendency term on the LHS of each equation. For example, LHS = $\Delta U/\Delta t$ = $[U(t+\Delta t) - U(t)]/\Delta t$. Also, rewrite eqs. (10.43) in cylindrical coordinates, letting U be the tangential component, and V be the radial component (Fig. 10.19). Use geostrophic wind G as a surrogate for the radial pressure gradient.

For BLG winds around a low in the N. Hemisphere (i.e., s = +1), equations (10.43) can be rewritten as the following set of coupled equations, which is valid day or night:

$$M = (U^2 + V^2)^{1/2} \qquad \text{(1.1 again)}$$

$$U(t+\Delta t) = U + \Delta t \cdot \left[f_c \cdot V - \frac{C_D \cdot M \cdot U}{z_i} + s\frac{V \cdot M}{R} \right] \qquad \text{(10.44a)}$$

$$V(t+\Delta t) = V + \Delta t \cdot \left[f_c \cdot (G - U) - \frac{C_D \cdot M \cdot V}{z_i} - s\frac{U \cdot M}{R} \right] \qquad \text{(10.44b)}$$

where (U, V) represent (tangential, radial) parts for the wind vector south of the low center.

FOCUS • Solution by Iteration

Equations (10.44) are difficult to solve analytically, but we can iterate as an alternative way to solve for the BLG wind components. To use this approach:

(1) Make a first guess that (U, V) = (0, 0).
(2) Plug in these values everywhere that U, $U(t)$, V, or $V(t)$ appears in eqs. (1.1) and (10.44).
(3) Solve eqs. (10.44) for the new values of $[U(t+\Delta t), V(t+\Delta t)]$.
(4) Repeat steps 2 & 3, but using the new winds.
(5) Continue until the $[U(t+\Delta t), V(t+\Delta t)]$ wind components converge to steady values, which by definition are the (U_{BLG}, V_{BLG}) components that we want.

Iterative approaches are tedious when done on a hand calculator, so use a spreadsheet or computer program instead, such as was done in the solved example.

Similar equations can be derived for convective boundary layers in high-pressure regions.

You can use the iterative method described in the Focus box to solve equations (10.44). In the solved example, notice that the spreadsheet iterations do not proceed directly to the final solution, but spiral toward it. This spiral is called a **damped inertial oscillation**.

Equations (10.44) are also valid for unsteady (time varying) solutions, such as at night. At night when drag is weak, the winds may never reach steady state, and may continue as undamped or weakly-damped **inertial oscillations** (see a previous Focus Box on *Approach to Geostrophy*). Such oscillations can temporarily cause winds to be greater than geostrophic in regions of straight isobars, or greater than gradient in regions of curved isobars. This is one reason for the **supergeostrophic** (faster than geostrophic) **nocturnal jet**, which will be covered in the Atmospheric Boundary Layer chapter.

Cyclostrophic Wind

In intense vortices, strong winds rotate around a very tight circle. Winds in tornadoes are about 100 m/s, and in water spouts are about 50 m/s. As the tornado strengthens and tangential winds increase, centrifugal force increases much more rapidly than Coriolis force. Centrifugal force quickly becomes the dominant force that balances pressure-gradient force (Fig. 10.20). Thus, a steady-state rotating wind is reached at much slower speeds than the gradient wind speed.

For steady state winds, the equations of motion reduce to:

$$0 = -\frac{1}{\rho}\cdot\frac{\Delta P}{\Delta x} + s\cdot\frac{V\cdot M}{R} \qquad (10.45a)$$

$$0 = \underbrace{-\frac{1}{\rho}\cdot\frac{\Delta P}{\Delta y}}_{\text{pressure gradient}} \underbrace{-s\cdot\frac{U\cdot M}{R}}_{\text{centrifugal}} \qquad (10.45b)$$

Because of the cylindrical nature of these flows as they rotate around intense low-pressure centers, it is easier to write and solve the equations for cyclostrophic wind M_{cs} in cylindrical form:

$$M_{cs} = \sqrt{\frac{R}{\rho}\cdot\frac{\Delta P}{\Delta R}} \qquad (10.46)$$

where R is radial distance outward from the center of rotation, $\Delta P/\Delta R$ is the local radial pressure gradient, and M_{cs} is the tangential speed.

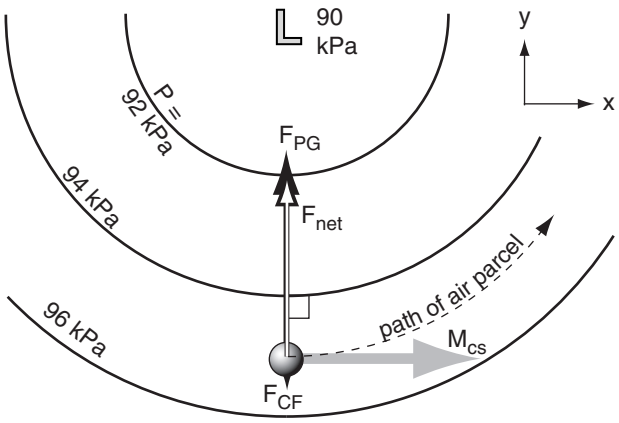

Figure 10.20
Around tornadoes, pressure gradient force is so strong that it greatly exceeds all other forces. The net force (F_{net}) pulls the air around the tight circle at the cyclostrophic wind speed (M_{cs}).

Solved Example

A 10 m radius waterspout has a tangential velocity of 45 m/s. What is the radial pressure gradient?

Solution

Given: M_{cs} = 45 m/s, R = 10 m.
Find: $\Delta P/\Delta R$ = ? kPa/m.

Assume cyclostrophic wind, and ρ = 1 kg/m^3.
Rearrange eq. (10.46):

$$\frac{\Delta P}{\Delta R} = \frac{\rho}{R}\cdot M_{cs}^2 = \frac{(1\text{kg/m}^3)\cdot(45\text{m/s})^2}{10\text{m}}$$

$\Delta P/\Delta R$ = 202.5 kg·m^{-1}·s^{-2} / m = **0.2 kPa/m**.

Check: Units OK. Physics OK.
Discussion: This is 2 kPa across the 10 m waterspout radius, which is 1000 times greater than typical synoptic-scale pressure gradients on weather maps.

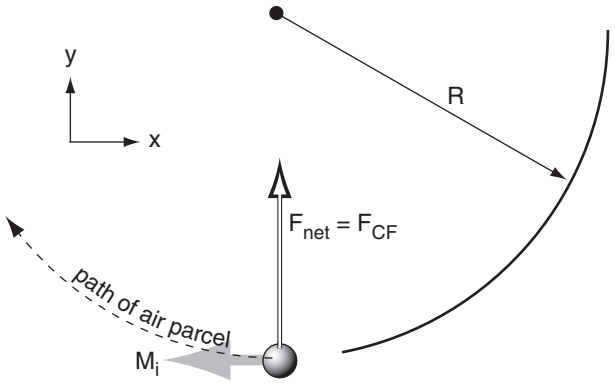

Figure 10.21
Imbalance of forces (F, black arrows) on an air parcel (grey ball), creating an anticyclonic inertial wind M_i, grey arrow). R is radius of curvature, and F_{CF} is Coriolis force.

Solved Example

For an inertial ocean current of 5 m/s, find the radius of curvature and time period to complete one circuit. Assume a latitude where $f_c = 10^{-4}$ s^{-1}.

Solution

Given: $M_i = 5$ m/s, $f_c = 10^{-4}$ s^{-1}.
Find: R = ? km, P = ? h

Use eq. (10.48): $R = -(5 \text{ m/s}) / (10^{-4} \text{ s}^{-1}) =$ **–50 km**
Use $P = 2\pi/f_c = 62832$ s = **17.45 h**

Check: Units OK. Magnitudes OK.
Discussion: The tracks of drifting buoys in the ocean are often **cycloidal**, which is the superposition of a circular inertial oscillation and a mean current that gradually moves the whole circle.

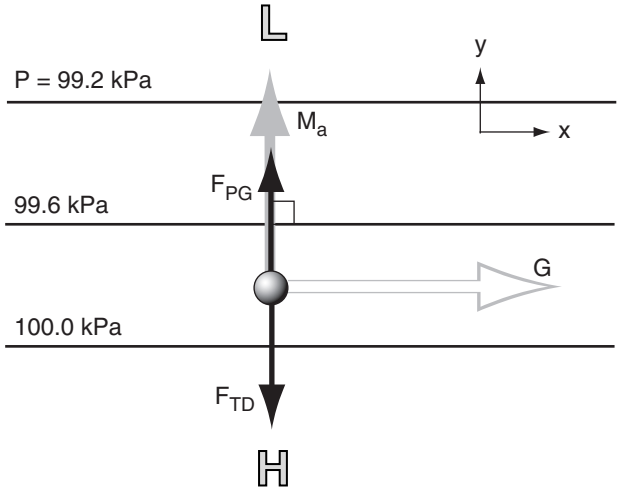

Figure 10.22
Balance of forces (F, black arrows) that create the antitriptic wind M_a (grey arrow). G is the theoretical geostrophic wind. F_{TD} is turbulent drag, and F_{PG} is pressure-gradient force.

Cyclostrophic winds never occur around high pressure centers, because the strong pressure gradients needed to drive such winds are not possible. Around lows, cyclostrophic winds can turn either counterclockwise or clockwise in either hemisphere, because Coriolis force is not a factor.

Inertial Wind

Steady-state **inertial motion** results from a balance of Coriolis and centrifugal forces:

$$0 = f_c \cdot M_i + \frac{M_i^2}{R} \tag{10.47}$$

where M_i is inertial wind speed, f_c is the Coriolis parameter, and R is the radius of curvature. Since both of these forces depend on wind speed, the inertial wind cannot start itself from zero. It can occur only after some additional force first causes the wind to blow, and then that extra force disappears.

The inertial wind coasts around a circular path of radius R,

$$R = -\frac{M_i}{f_c} \tag{10.48}$$

where the negative sign implies anticyclonic rotation (Fig. 10.21). The time period needed for this **inertial oscillation** to complete one circuit is $P = 2\pi/f_c$, which is half of a **pendulum day** (see *Approach to Geostrophy* Focus Box earlier in this chapter).

Although rarely observed in the atmosphere, inertial oscillations are frequently observed in the ocean. This can occur where wind stress on the ocean surface creates an ocean current, and then after the wind dies the current coasts in an inertial oscillation.

Antitriptic Wind

A steady-state antitriptic wind M_a could result from a balance of pressure-gradient force and turbulent drag:

$$0 = -\frac{1}{\rho} \cdot \frac{\Delta P}{\Delta d} - w_T \cdot \frac{M_a}{z_i} \tag{10.49}$$

where ΔP is the pressure change across a distance Δd perpendicular to the isobars, f_c is the Coriolis parameter, w_T is the turbulent transport velocity, and z_i is boundary-layer depth.

This wind blows perpendicular to the isobars (Fig. 10.22), directly from high to low pressure:

$$M_a = \frac{z_i \cdot f_c \cdot G}{w_T} \tag{10.50}$$

For free-convective boundary layers, $w_T = b_D \cdot w_B$ is not a function of wind speed, so M_a is proportional to G. However, for windy forced-convection boundary layers, $w_T = C_D \cdot M_a$, so solving for M_a shows it to be proportional to the square root of G.

This wind would be found in the boundary layer, and occurs as an along-valley component of "long gap" winds (see the Local Winds chapter). It is also sometimes thought to be relevant for thunderstorm cold-air outflow and for steady sea breezes. However, in most other situations, Coriolis force should not be neglected; thus, the boundary-layer wind and BL Gradient winds are much better representations of nature than the antitriptic wind.

Summary of Horizontal Winds

Table 10-5 summarizes the idealized horizontal winds that were discussed earlier in this chapter.

On real weather maps such as Fig. 10.23, isobars or height contours have complex shapes. In some regions the height contours are straight (suggesting that actual winds should nearly equal geostrophic or boundary-layer winds), while in other regions the height contours are curved (suggesting gradient or boundary-layer gradient winds). Also, as air parcels move between straight and curved regions, they are sometimes not quite in equilibrium. Nonetheless, when studying weather maps you can quickly estimate the winds using the summary table.

Solved Example

In a 1 km thick convective boundary layer at a location where $f_c = 10^{-4}$ s^{-1}, the geostrophic wind is 5 m/s. The turbulent transport velocity is 0.02 m/s. Find the antitriptic wind speed.

Solution

Given: $G = 5$ m/s, $z_i = 1000$ m, $f_c = 10^{-4}$ s^{-1}, $w_T = 0.02$ m/s

Find: $M_a = ?$ m/s

Use eq. (10.50):

$M_a = (1000\text{m}) \cdot (10^{-4}\ \text{s}^{-1}) \cdot (5\text{m/s}) \ / \ (0.2\ \text{m/s})$

$= \underline{\mathbf{25\ m/s}}$

Check: Magnitude seems too large. Units OK.

Discussion: Eq. (10.50) can give winds of $M_a > G$ for many convective conditions, for which case Coriolis force would be expected to be large enough that it should not be neglected. Thus, antitriptic winds are unphysical. However, for forced-convective boundary layers where drag is proportional to wind speed squared, reasonable solutions are possible.

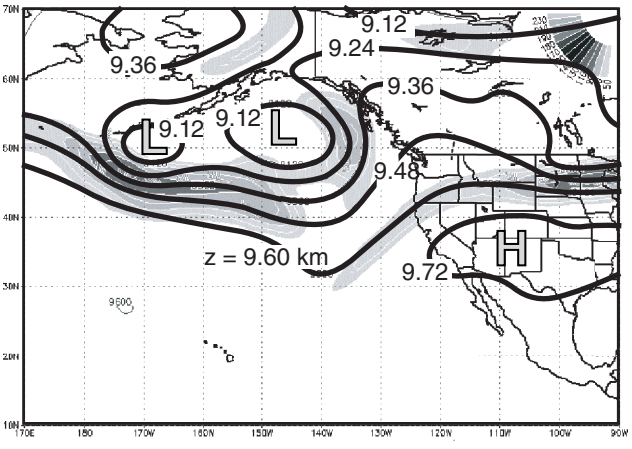

Figure 10.23

Upper-air 30 kPa height chart valid at 12 UTC on 9 July 99. Shading indicates isotachs in the jet stream, where light grey denotes roughly 25 m/s or greater winds, and darker shading is roughly 50 m/s or greater. Thick lines are height contours. Faster winds occur where contours are packed. [Adapted from a US Navy Fleet Numerical Meteor. and Ocean. Ctr. chart.]

FOCUS • The Rossby Number

The **Rossby number** (*Ro*) is a dimensionless ratio defined by

$$Ro = \frac{M}{f_c \cdot L} \qquad \text{or} \qquad Ro = \frac{M}{f_c \cdot R}$$

where M is wind speed, f_c is the Coriolis parameter, L is a characteristic length scale, and R is radius of curvature.

In the equations of motion, suppose that advection terms such as $U \cdot \Delta U/\Delta x$ are order of magnitude M^2/L, and Coriolis terms are of order $f_c \cdot M$. Then the Rossby number is like the ratio of advection to Coriolis terms: $(M^2/L) \ / \ (f_c \cdot M) = M/(f_c \cdot L) = Ro$. Or, we could consider the Rossby number as the ratio of centrifugal (order of M^2/R) to Coriolis terms, yielding $M/(f_c \cdot R) = Ro$.

Use the Rossby number as follows. If $Ro < 1$, then Coriolis force is a dominant force, and the flow tends to become geostrophic (or gradient, for curved flow). If $Ro > 1$, then the flow tends not to be geostrophic.

For example, a midlatitude cyclone (low-pressure system) has approximately $M = 10$ m/s, $f_c = 10^{-4}$ s^{-1}, and $R = 1000$ km, which gives $Ro = 0.1$. Hence, midlatitude cyclones tend to adjust toward geostrophic balance, because $Ro < 1$. In contrast, a tornado has roughly $M = 50$ m/s, $f_c = 10^{-4}$ s^{-1}, and $R = 50$ m, which gives $Ro = 10{,}000$, which is so much greater than one that geostrophic balance is not relevant.

Table 10-5. Summary of horizontal winds**.

Item	Name of Wind	Forces	Direction	Magnitude	Where Observed
1	**geostrophic**	pressure-gradient, Coriolis	parallel to straight isobars with Low pressure to the wind's left*	faster where isobars are closer together. $G = \left\| \frac{1}{\rho \cdot f_c} \cdot \frac{\Delta P}{\Delta d} \right\|$	aloft in regions where isobars are nearly straight
2	**gradient**	pressure-gradient, Coriolis, centrifugal	similar to geostrophic wind, but following curved isobars. Clockwise* around Highs, counterclockwise* around Lows.	slower than geostrophic around Lows, faster than geostrophic around Highs	aloft in regions where isobars are curved
3	**boundary layer**	pressure-gradient, Coriolis, drag	similar to geostrophic wind, but crosses isobars at small angle toward Low pressure	slower than geostrophic (i.e., **subgeostrophic**)	near the ground in regions where isobars are nearly straight
4	**boundary-layer gradient**	pressure-gradient, Coriolis, drag, centrifugal	similar to gradient wind, but crosses isobars at small angle toward Low pressure	slower than gradient wind speed	near the ground in regions where isobars are curved
5	**cyclostrophic**	pressure-gradient, centrifugal	either clockwise or counterclockwise around strong vortices of small diameter	stronger for lower pressure in the vortex center	tornadoes, waterspouts (& sometimes in the eye-wall of hurricanes)
6	**inertial**	Coriolis, centrifugal	anticyclonic circular rotation	coasts at constant speed equal to its initial speed	ocean-surface currents

** For Northern Hemisphere. Direction is opposite in Southern Hemisphere. ** Antitriptic winds are unphysical; not listed here.*

HORIZONTAL MOTION

Equations of Motion — Revisited

The geostrophic wind can be used as a surrogate for the pressure-gradient force, based on the definitions in eqs. (10.26). With this substitution, we can then group this term with the Coriolis term in the **equations of horizontal motion** (10.23):

$$\frac{\Delta U}{\Delta t} = -U\frac{\Delta U}{\Delta x} - V\frac{\Delta U}{\Delta y} + f_c \cdot \left(V - V_g\right) - w_T \cdot \frac{U}{z_i} \qquad \bullet(10.51a)$$

$$\frac{\Delta V}{\Delta t} = -U\frac{\Delta V}{\Delta x} - V\frac{\Delta V}{\Delta y} - f_c \cdot \left(U - U_g\right) - w_T \cdot \frac{V}{z_i} \qquad \bullet(10.51b)$$

tendency | *horizontal advection* | *Coriolis* | *pressure gradient* | *turbulent drag*

To be accurate, an additional vertical advection term should be included in the right-hand side of each equation. Namely, $-W \cdot \Delta U/\Delta z$ in the forecast equation for U wind, and $-W \cdot \Delta V/\Delta z$ in the equation for V wind. For example, fast jet-stream horizontal winds aloft can be advected down toward the surface, causing fast, damaging surface winds. Similarly, slow boundary-layer horizontal winds can be advected upward to spread the effects of surface drag higher into the atmosphere.

A centrifugal term could also be added for winds associated with curved isobars, which is an artifice to account for the continual changing of wind direction caused by an imbalance of the other forces (where the imbalance is the centripetal force).

The third term on the right is called the **geostrophic departure** term. The wind difference is also called the **ageostrophic wind** (U_{ag}, V_{ag}):

$$U_{ag} = U - U_g \qquad \bullet(10.52a)$$

$$V_{ag} = V - V_g \qquad \bullet(10.52b)$$

Scales of Horizontal Motion

In the atmosphere, motions of many scales are superimposed: from small turbulent eddies through thunderstorms and cyclones to large planetary-scale circulations such as the jet stream. Scales of horizontal motion are classified in Table 10-6.

Small atmospheric phenomena of horizontal dimension less than about 10 km are frequently **isotropic**; namely, their vertical and horizontal dimensions are roughly equal. Horizontally-larger phenomena are somewhat pancake-like, because the vertical dimension is generally limited by the depth of the troposphere (about 11 km).

Fig. 10.24 shows that time scales τ and horizontal length scales λ of many meteorological phenomena early follow a straight line on a log-log plot. This implies that

$$\tau/\tau_o = (\lambda/\lambda_o)^b \qquad (10.53)$$

where $\tau_o \approx 10^{-3}$ h, $\lambda_o \approx 10^{-3}$ km, and $b \approx 7/8$. For example, microscale turbulence about 1 m in diameter might last about a 1 s. Boundary-layer thermals of diameter 1 km have circulation lifetimes of about 25 min. Thunderstorms of size 10 km might last a few hours. Cyclones of size 1000 km might last a week.

In the next several chapters, we cover weather phenomena from largest to smallest horiz. scales:

- Chapter 11 Global Circulation (planetary)
- Chapter 12 Airmasses and Fronts (synoptic)
- Chapter 13 Extratropical Cyclones (synoptic)
- Chapter 14 Thunderstorms (meso β)
- Chapter 15 Thunderstorm Hazards (meso γ)
- Chapter 16 Hurricanes (meso α & β)
- Chapter 17 Local Winds (meso β & γ)
- Chapter 18 Atm. Boundary Layers (microscale)

Although hurricanes are larger than thunderstorms, we cover thunderstorms first because they are the building blocks of hurricanes. Similarly, midlatitude cyclones often contain fronts, so fronts are covered before extratropical cyclones.

Table 10-6. Scales of horizontal motion in the troposphere.

Size	Scale	Name	
40,000 km	macro α	planetary scale	
4,000 km	macro β	synoptic scale*	
700 km	meso α	mesoscale**	
300 km	meso β		
30 km	meso γ		
3 km	micro α	microscale***	boundary-layer turbulence
300 m	micro β		surface-layer turbulence
30 m	micro γ		inertial subrange turbulence
3 m	micro δ		
300 mm			fine-scale turbulence
30 mm			
3 mm	viscous	dissipation subrange	
0.3 μm	molecular	mean-free path between molec.	
0.003 μm		molecule sizes	
0			

Note: Disagreement among different organizations.
*Synoptic: AMS: 400 - 4000 km; WMO: 1000 - 2500 km.
**Mesoscale: AMS: 3 - 400 km; WMO: 3 - 50 km.
***Microscale: AMS: 0 - 2 km; WMO: 3 cm - 3 km.
where AMS = American Meteorological Society,
and WMO = World Meteorological Organization.

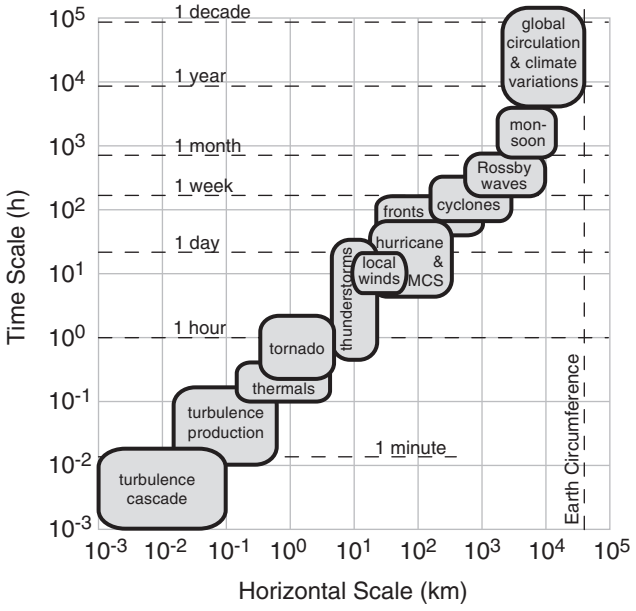

Figure 10.24
Typical time and spatial scales of meteorological phenomena.

VERTICAL FORCES AND MOTION

Forces acting in the vertical can cause or change vertical velocities, according to Newton's Second Law. In an Eulerian framework, the **vertical component of the equations of motion** is:

$$\frac{\Delta W}{\Delta t} = -U\frac{\Delta W}{\Delta x} - V\frac{\Delta W}{\Delta y} - W\frac{\Delta W}{\Delta z} - \frac{1}{\rho}\frac{\Delta P}{\Delta z} - |g| - \frac{F_{z\,TD}}{m} \qquad (10.54)$$

tendency | *advection* | *pressure gradient* | *gravity* | *turb. drag*

Science Graffito

"The book of nature is written in the language of mathematics."

– Galileo, as paraphrased by Alex Stone, 2005. *Discover*, **26**, p77.

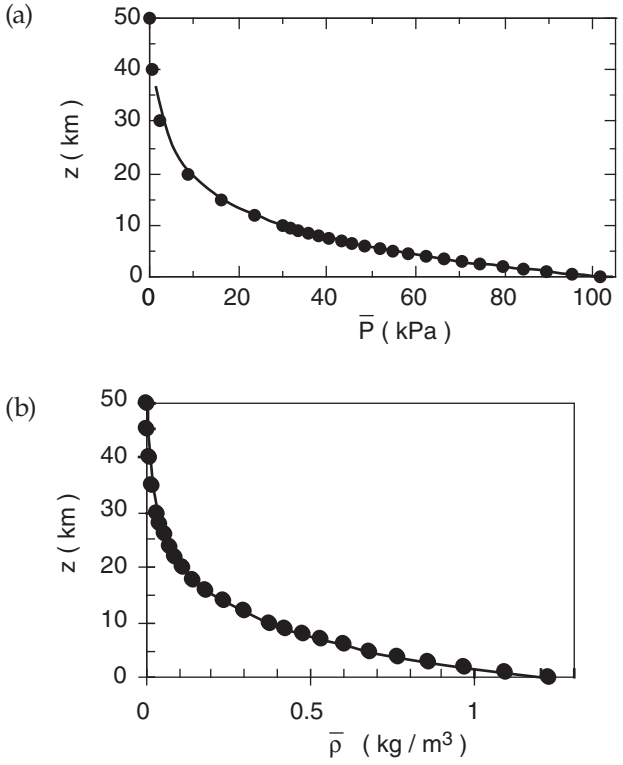

Figure 10.25
Mean background state, showing variations with height z of (a) atmospheric pressure $\overline{P}$ and (b) density $\overline{\rho}$ (from Chapter 1).

Solved Example

An updraft of 8 m/s exists 2 km west of your location, and there is a west wind of 5 m/s. At your location there is zero vertical velocity, but the air is 3°C warmer than the surrounding environment of 25°C. What is the initial vertical acceleration of the air over your location?

Solution

Given: $\Delta\theta$ = 3°C, T_e = 273+25 = 298 K, U= 5m/s
$\Delta W/\Delta x$= (8m/s – 0) / (–2,000m – 0)
Assume: V = 0 . Drag = 0 initially, given W = 0.
Dry air, thus $T_v = T$.
Find: $\Delta W/\Delta t$ = ? m·s^{-2}

Use eq. (10.59): $\dfrac{\Delta W}{\Delta t} = -U\dfrac{\Delta W}{\Delta x} + \dfrac{\theta_p - \theta_e}{\overline{T}_e}\cdot|g|$

= –(5 m/s)·(–8m·s–1/2,000m)+(3/298)·(9.8m·s^{-2})
= 0.020 + 0.099 = 0.119 m·s^{-2}

Check: Units OK. Physics OK.
Discussion: Extrapolated over a minute, this initial acceleration gives W = 7.1 m/s. However, this vertical velocity would not be achieved because as soon as the velocity is nonzero, the drag term also becomes nonzero and tends to slow the vertical acceleration.

where the left hand side is the vertical acceleration, and the right hand side lists the vertical forces per mass. (U, V, W) are the three Cartesian velocity components in the (x, y, z) directions, P is pressure, ρ is air density, t is time, $F_{z\ TD}$ is the turbulent drag force in the vertical, and mass is m. Gravitational acceleration magnitude is $|g|$ = 9.8 m·s^{-2}. Coriolis force is negligible in the vertical (see the Focus box on *Coriolis Force in 3-D*, earlier in this chapter), and is not included in the equation above.

Recall from Chapter 1 that our atmosphere has an extremely large pressure gradient in the vertical, which is almost completely balanced by gravity (Fig. 10.25). Also, there is a large density gradient in the vertical. We can define these large terms as a **mean background state** or a **reference state** of the atmosphere. Use the overbar over variables to indicate their average background state. Define this background state such that it is exactly in **hydrostatic balance** (see Chapter 1):

$$\frac{\Delta \overline{P}}{\Delta z} = -\overline{\rho}\cdot|g| \qquad (10.55)$$

However, small deviations in density and pressure from the background state can drive important **non-hydrostatic** vertical motions, such as in thermals and thunderstorms. To discern these effects, we must first remove the background state from the full vertical equation of motion. Focus on the pressure-gradient and gravity terms of eq. (10.54), rewritten here as:

$$\frac{1}{\rho}\left[-\frac{\Delta P}{\Delta z} - \rho|g|\right] \qquad (10.56)$$

Split the total density ρ into a background ($\overline{\rho}$) and deviation (ρ') part: $\rho = \overline{\rho} + \rho'$. Do the same for pressure: $P = \overline{P} + P'$. The terms above become:

$$\frac{1}{\left(\overline{\rho}+\rho'\right)}\left[-\frac{\Delta \overline{P}}{\Delta z} - \frac{\Delta P'}{\Delta z} - \overline{\rho}|g| - \rho'|g|\right] \qquad (10.57)$$

The first and third terms in square brackets in eq. (10.57) cancel out, due to hydrostatic balance (eq. 10.55) of the background state.

Next, a **Boussinesq approximation** is made that $\rho'|g|/\left(\overline{\rho}+\rho'\right) \approx \left(\rho'/\right.$, which implies that density deviations are important in the gravity term, but negligible for all other terms. This is reasonable because $\rho' << \overline{\rho}$. In the Stability chapter, it was shown that density deviations can be described by virtual temperature T_v deviations (with a sign change because low density corresponds to high temperature):

$$-\frac{\rho'}{\bar{\rho}}\cdot|g| \;=\; \frac{\theta_v'}{\bar{T}_v}\cdot|g| \;=\; \frac{\theta_{v\,p}-\theta_{v\,e}}{\bar{T}_{v\,e}}\cdot|g| \;=\; g' \quad (10.58)$$

where subscript p denotes the air parcel, and subscript e is for the environment, and g' is called the **reduced gravity**. T_{ve} in the denominator must be in Kelvin.

Plugging this back into eq. (10.54) gives:

$$\frac{\Delta W}{\Delta t} = -U\frac{\Delta W}{\Delta x} - V\frac{\Delta W}{\Delta y} - W\frac{\Delta W}{\Delta z} \quad \bullet(10.59)$$

$$-\frac{1}{\bar{\rho}}\frac{\Delta P'}{\Delta z} + \frac{\theta_{v\,p}-\theta_{v\,e}}{\bar{T}_{v\,e}}\cdot|g| - \frac{F_{z\,TD}}{m}$$

Terms from this equation will be used in the Local Winds and Thunderstorms chapters, to explain strong vertical velocities.

Turbulent drag is the resistance of a vertically moving air parcel against other surrounding (stationary environmental) air. This is a completely different effect than drag against the Earth's surface, and is not described by the same drag equations. The nature of $F_{z\,TD}$ is considered in the chapter on Air Pollution Dispersion, as it affects the rise of smoke-stack plumes. Air with no vertical movement relative to its environment has no drag.

MASS CONSERVATION

Barring any nuclear reactions, air molecules are not converted into energy, and air mass is conserved. In an Eulerian framework, mass flowing into a fixed volume minus the mass flowing out gives the change of mass within the volume (Fig. 10.26). The equation describing this mass balance is called the **continuity equation**. The name "continuity" is based on the observation that gases such as air tend to spread smoothly and evenly within a volume.

Continuity Equation

Recall that mass within a unit volume is defined as density, ρ. The **mass budget** is:

$$\frac{\Delta\rho}{\Delta t} = \left\{-U\frac{\Delta\rho}{\Delta x} - V\frac{\Delta\rho}{\Delta y} - W\frac{\Delta\rho}{\Delta z}\right\} - \rho\left[\frac{\Delta U}{\Delta x} + \frac{\Delta V}{\Delta y} + \frac{\Delta W}{\Delta z}\right] \quad (10.60)$$

which is also called the **continuity equation**. The terms in curly braces { } describe advection. Eq. (10.60) can be rearranged (using calculus) to be:

FOCUS • Eötvös Effect

When you move along a path at constant distance R above Earth's center, gravitational acceleration appears to change slightly due to your motion. The measured gravity $|g_{obs}| = |g| - a_r$, where:

$$a_r = 2\cdot\Omega\cdot\cos(\phi)\cdot U \;+\; (U^2 + V^2)/R$$

The first term is the vertical component of Coriolis force (eq. 10.17e in the Focus box on p.297), and the last term is centrifugal force as you follow the curvature of the Earth. Thus, you feel lighter traveling east and heavier traveling west. This is the **Eötvös effect**.

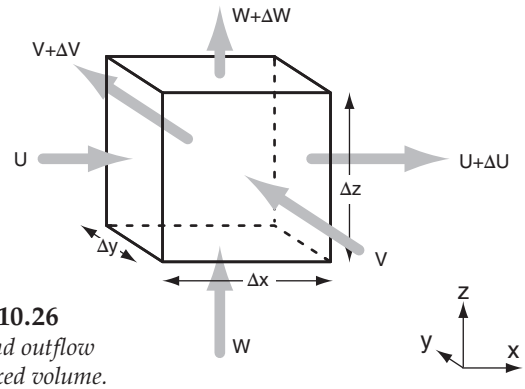

Figure 10.26
Inflow and outflow from a fixed volume.

Solved Example

Just before a tornado strikes your garage, the air density inside is 1 kg/m^3. Winds of 100 m/s enter the open garage from the west, but nothing leaves from the east. Also, your garage is temporarily intact, so the other walls, floor, and ceiling prevent winds in those other directions. The east end of your garage is 8 m from the open west end. What is the density change in your garage during the first 1 s, neglecting advection?

Solution

Given: $U_{door} = 100$ m/s, $U_{end} = 0$ m/s, $\Delta x = 8$ m,
$\rho = 1$ kg/m^3.
Find: $\Delta\rho/\Delta t$ = ? kg·m^3·s^{-1} .

Use eq. (10.60), with $V = W = 0$ because the other walls, roof, and floor prevent winds in those directions:

$$\frac{\Delta\rho}{\Delta t} = -\rho\frac{V_{N.entr.} - V_{S.entr.}}{\Delta y_{tunnel}} = -\left(1.2\frac{\text{kg}}{\text{m}^3}\right)\frac{(-60-0)}{(20)\text{r}}$$

$\Delta\rho/\Delta t$ = **+12.5** kg·m^3·s^{-1} .

Check: Units OK. Physics OK.
Discussion: Due to Bernoulli's principle (Local Winds chapter), you won't have to worry about this high density for long. The pressure inside your garage will increase so fast that it will blow out your walls and roof as if a bomb exploded. So don't leave your garage door (or your windows) open during a tornado.

$$\frac{\Delta\rho}{\Delta t} = -\left[\frac{\Delta(\rho U)}{\Delta x} + \frac{\Delta(\rho V)}{\Delta y} + \frac{\Delta(\rho W)}{\Delta z}\right] \qquad (10.61)$$

where U, V, and W are the wind components in the x, y, and z directions, respectively, and t is time.

Be careful when calculating the wind gradients; calculate them as wind at location 2 minus wind at location 1, divided by distance at location 2 minus distance at location 1. Do not accidently subtract 1 from 2 in the numerator, and then subtract 2 from 1 in the denominator, because it gives the wrong sign.

Incompressible Continuity Equation

Density at any fixed altitude changes only a little with temperature and humidity for most non-violent weather conditions. Therefore, we can neglect mass changes within the volume, compared to the inflow and outflow. The air is said to be **incompressible** when the density does not change ($\Delta\rho \approx 0$). This approximation fails in strong thunderstorm updrafts and tornadoes.

For incompressible flow, the left hand side and the advection terms of eq. (10.60) are zero. This requires inflow to balance outflow:

$$\frac{\Delta U}{\Delta x} + \frac{\Delta V}{\Delta y} + \frac{\Delta W}{\Delta z} = 0 \qquad \bullet(10.62)$$

This continuity equation is illustrated in Fig. 10.26 for an example of inflow and outflow across the faces of a cube. The length of the grey arrows represents the strength of the wind components. Also, for this example $\Delta x = \Delta y = \Delta z$.

In the x-direction of this particular illustration, there is less wind (U) entering the cube than leaving ($U + \Delta U$). This is called **divergence**. For this case, ΔU is positive. In the z-direction (vertical), there is more air entering (W) than leaving ($W + \Delta W$), in Fig. 10.26. This is called **convergence**, and ΔW is negative. In the y-direction, the air entering (V) and leaving ($V + \Delta V$) are equal, so there is no convergence or divergence. For this example, ΔV is zero.

For this example shown in Fig. 10.26, the continuity equation is

(positive) + (0) + (negative) = 0

so we anticipate that mass is conserved. In the real atmosphere, the directions having convergence or divergence might differ from this example, but the sum must always equal zero. Namely convergence in one or two directions must be balanced by divergence in the other direction(s).

Horizontal divergence (D) is defined as

$$D = \frac{\Delta U}{\Delta x} + \frac{\Delta V}{\Delta y} \qquad (10.63)$$

Negative values of D correspond to convergence. Plugging this definition into eq. (10.62) shows that vertical velocities increase with height where there is convergence:

$$\frac{\Delta W}{\Delta z} = -D \qquad (10.64)$$

For situations such as circular isobars around a low pressure center, cylindrical coordinates are easier to use (Fig. 10.27). The continuity equation is then

$$\frac{2 \cdot V_{in}}{R} = \frac{\Delta W}{\Delta z} \qquad \bullet(10.65a)$$

where R is the radius of the cylinder, and Δz is the cylinder depth. We assume that the radial inflow velocities V_{in} through the sides of the cylinder are equal everywhere. When V_{in} is positive (indicating horizontal inflow), then ΔW is also positive (indicating vertical outflow).

If a cylinder of air is at the ground where $W = 0$ at the cylinder bottom, then W at the cylinder top is:

$$W = (2 \cdot V_{in} \cdot \Delta z) \,/\, R \qquad (10.65b)$$

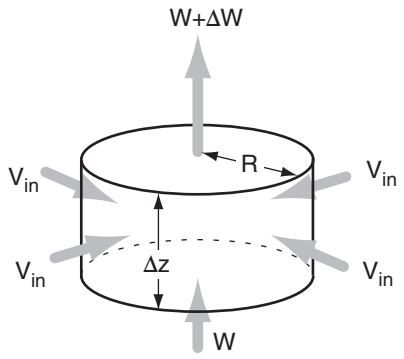

Figure 10.27 *Mass conservation in cylindrical coordinates.*

Solved Example

At a radius of 400 km from a low center, boundary layer winds have a 2 m/s component that crosses the circular isobars inward. If the boundary layer is 1 km thick, estimate the average vertical velocity out of the top of the boundary layer.

Solution

Given: $V_{in} = 2$ m/s, $R = 400$ km, $\Delta z = z_i = 1$ km

Find: $W = ?$ m/s

Use eq. (10.65b): $W = 2 \cdot V_{in} \cdot \frac{\Delta z}{R} = 2 \cdot (3\text{m/s}) \cdot \frac{1\text{km}}{500\text{km}}$

$= \underline{\mathbf{0.01\ m/s}}$

Check: Units OK. Physics OK.

Discussion: For non-thunderstorm conditions, this magnitude of about 1 cm/s is typical for vertical velocities in the atmosphere. Such small velocities allow use of the hydrostatic assumption (see Chapter 1).

Boundary-Layer Pumping

Around low-pressure regions near the surface, turbulent drag causes horizontal inflow (convergence) and slower tangential winds within the boundary layer. There is no vertical air motion ($W = 0$) at the bottom of the boundary layer because of the ground. Thus, horizontal inflow in the boundary layer must be balanced by vertical outflow from the boundary-layer top.

This mechanism for creating mean upward motion is called **Ekman pumping** or **boundary-layer pumping**. The upward motion carries water vapor, which then condenses in the adiabatically cooled air, causing clouds and precipitation. Thus, low-pressure regions generally have foul weather.

Around high-pressure centers, turbulent drag causes horizontal outflow (divergence). This is balanced by downward motion called **subsidence** at the top of the boundary layer. Subsidence warms air adiabatically, thereby evaporating most clouds and causing fair weather in high-pressure regions.

In the section on the BLG wind, we defined V_{BLG} as the radial component of wind, which by definition equals the inflow velocity V_{in} for eq. 10.65 (see Fig. 10.28). Unfortunately, we were unable to find an analytical solution for V_{BLG}. However, there is an analytical solution available for V_{BL} from an earlier section, which is slightly greater than V_{BLG}. For the subsequent analysis, we will use $V_{in} \approx V_{BL}$, knowing that the result will be an upper limit on what are likely slower inflow velocities in the real atmosphere.

Assuming that the winds are relatively strong around lows, and that cloudy conditions preclude strong surface heating or cooling, we can assume that the boundary layer is statically **neutral**. For this situation, the inflow velocity across the isobars is given by eq. (10.41b).

Combining this inflow velocity with the cylindrical form of the continuity equation (10.65) allows us to calculate the vertical velocity W_{BL} at the top of the boundary layer (Fig. 10.28):

$$W_{BL} = \frac{2 \cdot b \cdot C_D}{f_c} \cdot \frac{G^2}{R} \qquad \bullet(10.66)$$

where R is the radius of curvature of the isobars around the low center, G is the geostrophic wind speed, f_c is the Coriolis parameter, and C_D (≈ 0.005 over land) is the drag coefficient for a neutral boundary layer.

The factor $b = \{ 1 - 0.5 \cdot [C_D \cdot G/(f_c \cdot z_i)] \}$ is from eq. (10.41b), where boundary-layer depth is z_i. For simplicity, the statically neutral **boundary-layer depth within a cyclone** can be approximated as

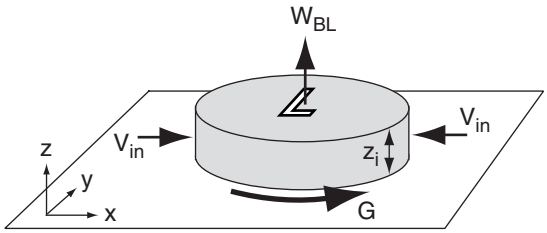

Figure 10.28
Convergence and updrafts in a cyclone.

$$z_i \approx \frac{G}{N_{BV}} \qquad (10.67)$$

where N_{BV} is the Brunt-Väisälä frequency (see the Stability chapter) above the boundary layer. This allows b to be rewritten as: $b = \{ 1 - 0.5 \cdot [C_D \cdot N_{BV}/f_c] \}$. The approximation for boundary-layer cross-isobaric flow is valid only when $[C_D \cdot N_{BV}/f_c] < 1$.

The updraft velocity in eq. (10.66) depends on both the size and rotation speed of the cyclone. Vorticity is one measure of the combined effects of rotation speed and size. **Geostrophic relative vorticity** can be defined as

$$\zeta_g = \frac{2 \cdot G}{R} \qquad (10.68)$$

which is a measure of the rotation of the air. More details of vorticity will be covered in the Global Circulation chapter.

Using the geostrophic vorticity in eq. (10.66) yields an alternative expression for the vertical velocity pumped out of the top of a cyclone:

$$W_{BL} = C_D \cdot \frac{G}{f_c} \cdot \zeta_g \cdot \left[1 - 0.5 \frac{C_D \cdot N_{BV}}{f_c} \right] \qquad (10.69)$$

The terms outside of the brackets suggest that greater vertical velocities (and hence nastier storms) occur for stronger geostrophic winds (i.e., tighter packing of isobars) over rougher terrain, and where there is greater curvature of the cyclonic flow. Also, lower latitudes give smaller Coriolis parameters, which allow greater vertical velocity.

The term in square brackets shows that the fastest vertical velocity is expected in statically neutral flow (where $N_{BV} = 0$) above the boundary layer. Greater static stabilities cause weaker vertical velocities.

By utilizing the approximation for mixed-layer depth (eq. 10.67), an **internal Rossby radius of deformation** can be approximated as

Solved Example

A geostrophic wind of 10 m/s blows cyclonically around a low-center with radius of curvature of 1000 km. The latitude is such that f_c = 0.0001 s^{-1}, and the drag coefficient is 0.005. The tropospheric lapse rate is standard above the BL.

What is the vertical velocity out of the top of the boundary layer? Also, estimate the boundary-layer depth, geostrophic relative vorticity, and internal Rossby radius.

Solution

Given: G = 10 m/s, $R = 10^6$ m, f_c = 0.0001 s^{-1}, C_D = 0.005, N_{BV} = 0.0113 s^{-1} (from a previous solved example using the standard atmos.)

Find: z_i = ? m, ζ_g = ? s^{-1}, λ_R = ? km, W_{BL} = ? m/s

Assume: tropospheric depth z_T = 11 km

Use eq. (10.67):

$z_i \approx G/N_{BV}$ = (10 m/s)/(0.0113 s^{-1}) = **885 m**

Use eq. (10.68):

$$\zeta_g = \frac{2\cdot(15\text{m/s})}{5\times10^5\text{m}} = \mathbf{2x10}^{-5}\ \text{s}^{-1}$$

Use eq. (10.70):

$$\lambda_R \approx \frac{(15\text{m/s})}{(0.0001\text{s}^{-1})}\cdot\frac{11\text{km}}{1.327\text{km}} = \mathbf{1243\ km}$$

First check that $[C_D\cdot N_{BV}/f_c] < 1$.

$[0.005\cdot(0.0113\text{s}^{-1})/(0.0001\text{s}^{-1})] = 0.565 < 1$. OK.

Use eq. (10.71): W_{BL} =

$$0.004\cdot\frac{(1.327\text{km})}{(11\text{km})}\cdot(1.243\times10^6\text{m})\cdot(6\times10^{-5}\text{s}^{-1})\cdot\left[1-0.5\cdot(0.004)\cdot\frac{1243\text{km}}{11\text{km}}\right]$$

= (0.01 m/s) · [0.718] = **0.0072 m/s**

Check: Units OK. Physics OK.

Discussion: This vertical velocity of 7.2 mm/s is typical of synoptic circulations. Although weak, it is sufficient to lift air to cause condensation, releasing latent heat which allows stronger buoyant updrafts within the clouds.

$$\lambda_R \approx \frac{G}{f_c}\cdot\frac{z_T}{z_i} \tag{10.70}$$

where z_i is the boundary-layer depth and z_T is the depth of the troposphere. The internal Rossby radius of deformation is discussed in more detail in the Global Circulation chapter, and an external Rossby radius is given in the Airmasses & Fronts chapter.

Thus, an alternative form for the vertical velocity equation can be written using the Rossby radius of deformation:

$$W_{BL} = C_D\cdot\frac{z_i}{z_T}\cdot\lambda_R\cdot\zeta_g\cdot\left[1-0.5\cdot C_D\cdot\frac{\lambda_R}{z_T}\right] \tag{10.71}$$

KINEMATICS

Kinematics is the study of patterns of motion, without regard to the forces that cause them. We will focus on horizontal divergence, vorticity, and deformation. All have units of s^{-1}.

We have already encountered **divergence**, D, the spreading of air:

$$D = \frac{\Delta U}{\Delta x} + \frac{\Delta V}{\Delta y} \tag{10.72}$$

Figure 10.29a shows an example of pure divergence. Its sign is positive for divergence, and negative for **convergence** (when the wind arrows point toward a common point).

Vorticity describes the rotation of air (Fig. 10.29b). The relative vorticity, ζ_r, is given by:

$$\zeta_r = \frac{\Delta V}{\Delta x} - \frac{\Delta U}{\Delta y} \tag{10.73}$$

The sign is positive for counterclockwise rotation (i.e., cyclonic rotation in the N. Hemisphere), and negative for clockwise rotation. Vorticity is discussed in greater detail in the Global Circulation chapter. Neither divergence nor vorticity vary with rotation of the axes — they are **rotationally invariant**.

Two types of **deformation** are stretching deformation and shearing deformation (Figs. 10.29c & d). **Stretching deformation**, F_1, is given by:

$$F_1 = \frac{\Delta U}{\Delta x} - \frac{\Delta V}{\Delta y} \tag{10.74}$$

The axis along which air is being stretched (Fig. 10.29c) is called the **axis of dilation** (x axis in this

example), while the axis along which air is compressed is called the **axis of contraction** (y axis in this example).

Shearing deformation, F_2, is given by:

$$F_2 = \frac{\Delta V}{\Delta x} + \frac{\Delta U}{\Delta y} \tag{10.75}$$

As you can see in Fig. 10.29d, shearing deformation is just a rotated version of stretching deformation. The **total deformation**, F, is:

$$F = \left[F_1^2 + F_2^2 \right]^{1/2} \tag{10.76}$$

Deformation often occurs along fronts. Most real flows exhibit combinations of divergence, vorticity, and deformation.

MEASURING WINDS

For weather stations at the Earth's surface, wind direction can be measured with a **wind vane** mounted on a vertical axel. **Fixed vanes** and other shapes can be used to measure wind speed, by using strain gauges to measure the minute deformations of the object when the wind hits it.

The generic name for a wind-speed measuring device is an **anemometer**. A **cup anemometer** has conic- or hemispheric-shaped cups mounted on spokes that rotate about a vertical axel. A **propellor anemometer** has a propellor mounted on a horizontal axel that is attached to a wind vane so it always points into the wind. For these anemometers, the rotation speed of the axel can be calibrated as a wind speed.

Other ways to measure wind speed include a **hot-wire** or **hot-film anemometer**, where a fine metal wire is heated electrically, and the power needed to maintain the hot temperature against the cooling effect of the wind is a measure of wind speed. A **pitot tube** that points into the wind measures the dynamic pressure as the moving air stagnates in a dead-end tube. By comparing this dynamic pressure with the static pressure measured by a different sensor, the pressure difference can be related to wind speed.

Sonic anemometers send pulses of sound back and forth across a short open path between two opposing transmitters and receivers of sound. The speed of sound depends on both temperature and wind speed, so this sensor can measure both. Tracers such as smoke, humidity fluctuations, or clouds can be **tracked** photogramatically from the ground

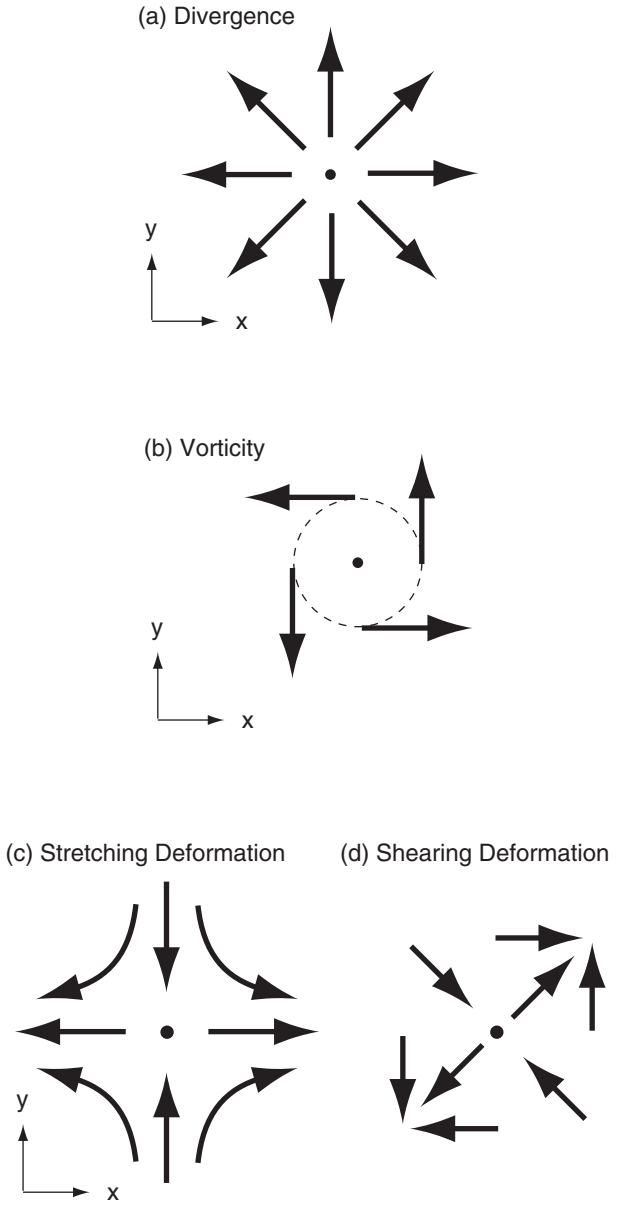

Figure 10.29
Kinematic flow-field definitions. Black arrows represent wind velocity.

or from remote sensors such as laser radars (**lidars**) or satellites, and the wind speed then estimated from the change of position of the tracer between successive images.

Measurements of wind vs. height can be made with **rawinsonde balloons** (using a GPS receiver in the sonde payload to track horizontal drift of the balloons with time), **dropsondes** (like rawinsondes, only descending by parachute after being dropped from aircraft), **pilot balloons** (carrying no payload, but being tracked instead from the ground using radar or theodolites), **wind profilers**, **Doppler weather radar** (see the Remote Sensing chapter), and via anemometers mounted on aircraft.

SUMMARY

Pressure-gradient force can start winds moving, and can change wind direction and speed. This force points from high to low pressure on a constant altitude chart (such as at sea-level), or points from high to low heights on an isobaric chart (such as the 50 kPa chart).

Once the air is moving, other forces such as turbulent drag or Coriolis force also act on the air. Coriolis force is an apparent force that accounts for our moving frame of reference on the rotating Earth. Turbulent drag is important only near the ground, in the boundary layer. The relationship between forces and acceleration of the winds is given by Newton's second law of motion.

When all forces balance, the winds are steady. In regions of straight isobars above the boundary layer, pressure-gradient and Coriolis forces balance to cause winds that are geostrophic. Around highs or lows, there are slight imbalances associated with centrifugal force, which causes steady-state gradient winds. In the boundary layer, winds are slower than either geostrophic or gradient because of turbulent drag. In tornadoes and waterspouts, centrifugal and pressure gradient forces nearly balance to create the intense cyclostrophic wind. In oceans, currents can inertially flow in a circle.

The two most important force balances at mid-latitudes are hydrostatic balance in the vertical, and geostrophic balance in the horizontal.

Outside of thunderstorms, winds are well described by incompressible mass continuity. Thus, mechanisms that cause motion in one direction (horizontal or vertical) will also indirectly cause motions in the other direction as the air tries to maintain continuity, resulting in a circulation. **Kinematics** is the word that describes the behavior and effect of winds (such as given by the continuity equation), while the word **dynamics** describes how forces cause winds (as given by Newton's second law).

Threads

Forces cause winds, and winds flow over mountains to form mountain waves and lenticular clouds (Chapter 17). Winds embody the global circulation (Chapter 11), which moves air masses around to create fronts (Chapter 12), extratropical cyclones (Chapter 13) and our global climate (Chapter 21). The equations of motion are solved every day on large computers to make the daily weather forecasts (Chapter 20). The interplay between buoyancy (Chapter 5) and dynamics creates phenomena such as thunderstorms, tornadoes (Chapters 14 and 15), and hurricanes (Chapter 16). Winds advect air pollutants from place to place (Chapter 19).

Not only do winds advect temperature (Chapter 3), but horizontal temperature variations cause horizontal pressure variations via the hypsometric equation (Chapter 1), thereby driving the jet-stream winds. Winds riding over colder air masses carry water vapor (Chapter 4), some of which can condense to make clouds (Chapter 6) and precipitation (Chapter 7). Clouds imbedded in the air will move horizontally with the air, and can be tracked by satellite (Chapter 8) to estimate the wind speed and direction. The complexity of the atmosphere is becoming apparent.

EXERCISES

Numerical Problems

N1. Plot the wind symbol for winds with the following directions and speeds:

a. N at 5 kt	b. NE at 35 kt	c. E at 65 kt
d. SE at 12 kt	e. S at 48 kt	f. SW at 105 kt
g. W at 27 kt	h. NW at 50 kt	i. N at 125 kt

N2. Find the acceleration of a 75 kg person when pushed by a force (N) of

a. 1	b. 2	c. 5	d. 10	e. 20	f. 50
g. 100	h. 200	i. 500	j. 1000		k. 2000

N3. If the initial velocity of an object is zero, find the final velocity after 100 s for an applied net force per unit mass of:

a. 5 N/kg	b. 10 $m \cdot s^{-2}$
c. 15 N/kg	d. 20 $m \cdot s^{-2}$
e. 25 N/kg	f. 30 $m \cdot s^{-2}$
g. 35 N/kg	h. 40 $m \cdot s^{-2}$
i. 45 N/kg	j. 50 $m \cdot s^{-2}$

N4. Find the advective "force" per unit mass given the following wind components (m/s) and horizontal distances (km):

a. U=10, ΔU=5, Δx=3
b. U=6, ΔU=–10, Δx=5
c. U=–8, ΔV=20, Δx=10
d. U=–4, ΔV=10, Δx=–2
e. V=3, ΔU=10, Δy=10
f. V=–5, ΔU=10, Δy=4
g. V=7, ΔV=–2, Δy=–50
h. V=–9, ΔV=–10, Δy=–6

N5. What is the pressure-gradient force per unit mass between Seattle, WA, and Corvallis, OR (about 340 km south of Seattle), if sea-level pressure is 98.4 kPa in Seattle and has the following pressure (kPa) in Corvallis?

a. 98.6 b. 98.8 c. 99.0 d. 99.2 e. 99.4
f. 99.6 g. 99.8 h. 100.0 i. 100.2 j. 100.4
k. 100.6 l. 100.8 m. 101.0 n. 101.2 o. 101.4

N6. Given U = –5 m/s and V = 10 m/s, find the components of centrifugal force around a 800 km diameter:

a. low in the southern hemisphere
b. high in the northern hemisphere
c. high in the southern hemisphere
d. low in the northern hemisphere

N7. Calculate the Coriolis parameter for

a. Munich, Germany
b. Oslo, Norway
c. Madrid, Spain
d. Chicago, USA
e. Buenos Aires, Argentina
f. Melbourne, Australia
g. Vancouver, Canada
h. Beijing, China
i. Moscow, Russia
j. Tokyo, Japan
k. (your town)

N8. For Chicago, find the Coriolis force per unit mass in the N. Hemisphere for:

a. U = 10 m/s b. V = 5 m/s c. U= 3 m/s
d. U = –10 m/s e. V = –5 m/s f. U = 8 m/s
g. U = –3 m/s h. V = –8 m/s i. V = 40 m/s

N9. For a neutral boundary layer, find the turbulent drag force per unit mass over a forest for

a. U = 5 m/s and V = 25 m/s
b. U = –10 m/s and V = 5 m/s
c. U = 5 m/s and V = –15 m/s
d. U = –5 m/s and V = –5 m/s
e. U = –40 m/s and V = 5 m/s
f. U = 5 m/s and V = 35 m/s
g. U = 25 m/s and V = –2 m/s
h. U = 0 m/s and V = 10 m/s

N10. For a statically unstable boundary layer, find the turbulent drag force per unit mass, given a buoyant velocity scale of 60 m/s and

a. U = 5 m/s and V = 1 m/s
b. U = –1 m/s and V = 3 m/s
c. U = 2 m/s and V = –4 m/s
d. U = –2 m/s and V = –1 m/s
e. U = –4 m/s and V = 0 m/s
f. U = 5 m/s and V = 3 m/s
g. U = 5 m/s and V = –2 m/s
h. U = 0 m/s and V = 2 m/s

N11. Draw a northwest wind of 5 m/s in the S. Hemisphere on a graph, and show the directions of forces acting on it. Assume it is in the boundary layer.

a. pressure gradient b. Coriolis
c. centrifugal d. drag

N12. What is the geostrophic wind speed at a height where ρ = 0.7 kg/m^3, $f_c = 10^{-4}$ s^{-1}, and the pressure gradient (kPa/100 km) magnitude is:

a. 0.1 b. 0.2 c. 0.3 d. 0.4 e. 0.5
f. 0.6 g. 0.7 h. 0.8 i. 0.9 j. 1.0
k. 1.1 m. 1.2 n. 1.3 o. 1.4 p. 1.5

N13. At a latitude of 60°N, find the geostrophic wind given a height gradient (m/km on a constant pressure surface) of:

a. 0.1 b. 0.2 c. 0.3 d. 0.4 e. 0.5
f. 0.6 g. 0.7 h. 0.8 i. 0.9 j. 1.0
k. 1.1 m. 1.2 n. 1.3 o. 1.4 p. 1.5

N14. If the geostrophic wind around a high is 10 m/s, then what is the gradient wind speed, given $f_c = 10^{-4}$ s^{-1} and a radius of curvature of:

a. 800 km b. 500 km c. 600 km
d. 1000 km e. 2000 km f. 1500 km
g. 700 km h. 1200 km i. 900 km

N15. Find the boundary layer winds given U_g = 5 m/s, V_g = 5 m/s, z_i = 1500 m, and $f_c = 10^{-4}$ s^{-1}. Also, what angle do the winds cross the isobars? This is a statically neutral boundary layer. Use C_D =

a. 0.002 b. 0.004 c. 0.006 d. 0.008 e. 0.010
f. 0.012 g. 0.014 h. 0.016 i. 0.018 j. 0.019

N16. Same as previous problem, but for an unstable boundary layer with w_B (m/s) of:

a. 75 b. 100 c. 50 d. 200 e. 150
f. 225 g. 125 h. 250 i. 175 j. 275

N17(§). Recompute M_{BLG} as in the solved example in the Boundary Layer Gradient Wind section, but with the following changes:
a. G = 10 m/s b. z_i = 2 km c. C_D = 0.002
d. R = 1000 km e. $f_c = 2\text{x}10^{-4}$ s^{-1}
f. G = 15 m/s g. z_i = 1.5 km h. C_D = 0.005
i. R = 1500 km j. $f_c = 1.5\text{x}10^{-4}$ s^{-1}

N18. Given a pressure gradient of 0.5 kPa/m, compute the cyclostrophic wind at the following radii (m): a. 10 b. 12 c. 14 d. 16 e. 18
f. 20 g. 22 h. 24 i. 26 j. 28 k 30

N19. For an inertial wind, find the radius of curvature (km) and the time period (h) needed to complete one circuit, given $f_c = 10^{-4}$ s^{-1} and an initial wind speed (m/s) of:
a. 1 b. 2 c. 3 d. 4 e. 6 f. 7 g. 8 h. 9
i. 10 j. 11 k. 12 m. 13 n. 14 o. 15

N20. Find the antitriptic wind for the conditions of exercise N15.

N21. The boundary layer is 2 km thick. At a radius of 200 km from a low center, estimate the average vertical velocity through the top of the boundary layer (BL), given an inward radial wind component (m/s) of: a. 2 b. 1.5 c. 1.2 d. 1.0
e. –0.5 f. –1 g. –2.5 h. 3 i. 0.8 j. 0.2

N22. Estimate boundary layer depth within a cyclone given an isothermal environment above the boundary layer, and a geostrophic wind (m/s) near the surface of: a. 5 b. 10 c. 15 d. 20 e. 25
f. 30 g. 35 h. 40 i. 3 j. 8 k. 2 l. 1

N23(§). For a 1 km thick boundary layer over a surface of drag coefficient 0.003, plot the vertical velocity due to boundary-layer pumping as a function of geostrophic wind speed, but for only wind speeds within the valid range for that eq. Plot separate curves for the following radii (km) of curvature:
(Assume a latitude of 45°, & standard atmosphere)
a. 500 b. 1000 c. 2000 d. 3000 e. 4000
(Assume a latitude of 60°, & standard atmosphere)
f. 500 g. 700 h. 900 i. 1500 j. 2500

N24. Estimate the value of internal Rossby radius of deformation at latitude 60°N for a tropospheric depth of 11 km and geostrophic wind speed of 15 m/s. Assume a boundary-layer depth of
a. 500 m b. 1 km c. 2 km d. 750 m e. 250 m
f. 1.5 km g. 2.5 km h. 3 km i. 3.5 km j. 100 m

N25. Given $\Delta U/\Delta x = \Delta V/\Delta x$ = (5 m/s) / (500 km), find the divergence, vorticity, and total deformation for ($\Delta U/\Delta y$, $\Delta V/\Delta y$) in units of (m/s)/(500 km) as given below:
a. (–5, –5) b. (–5, 0) c. (0, –5) d. (0, 0) e. (0, 5)
f. (5, 0) g. (5, 5) h. (–5, 5) i. (5, –5)

Understanding & Critical Evaluation

U1. Compare eq. (10.1) with (1.24), and discuss.

U2. Can eqs. (10.6) be used to make a forecast if the initial conditions (i.e., the current winds) are not known? Discuss.

U3. If all of the net forces (eq. 10.7) are zero, does that mean that the wind speeds (eq. 10.5) are zero? Explain.

U4. Eqs. (10.8) suggest that winds can advect winds. How is that possible?

U5. In eqs. (10.8), why does advection depend on the gradient of winds (e.g., $\Delta U/\Delta x$) across the Eulerian domain, rather than on just the value of wind that is being blown into the domain?

U6. In Fig. 10.5, and on weather maps, what is the relationship between packing of isobars (i.e., the number of isobars that cross through a square cm of weather map) and the pressure gradient?

U7. In the N. Hemisphere, the pressure gradient points from high to low pressure. Which way does it point in the S. Hemisphere?

U8. Eqs. (10.9) give the horizontal components of the pressure-gradient force. Combine those equations vectorially to show that the vector direction of the pressure-gradient force is indeed perpendicular to the isobars and pointing toward lower pressure, for any arbitrary isobar direction such as shown in Fig. 10.5.

U9. Eqs. (10.13) give the horizontal components of centrifugal force. Combine those equations vectorially to show that the vector direction of centrifugal force is indeed outward from the center of rotation, and is proportional to the square of the tangential velocity.

U10. An air parcel at rest (relative to the Earth) near the equator experiences greater tangential velocity due to the Earth's rotation than do air parcels at higher latitudes. Yet the Coriolis parameter is zero at the equator. Why?

U11. Eqs. (10.17) give the horizontal components of the Coriolis force. Combine those equations vectorially to show that the vector direction of the Coriolis force is indeed 90° to the right of the wind direction, for any arbitrary wind direction such as the two shown in Fig. 10.6.

U12. For the subset of eqs. (10.1 - 10.17) defined by your instructor, rewrite them for the S. Hemisphere.

U13. Eqs. (10.19) give the horizontal components of the turbulent drag force.

a. Combine those equations vectorially to show that the vector direction of the drag force is indeed opposite to the wind direction, for any arbitrary wind direction.

b. Show that the magnitude of the drag force is proportional to the square of the wind speed, M, for statically neutral conditions.

U14. Compare the values of the turbulent transport velocity during windy (statically neutral) and convective (statically unstable) conditions. Discuss.

U15. Plug eqs. (10.26) into (10.27) to find the vector speed and direction (see Chapter 1) of the geostrophic wind as a function of the vector pressure gradient.

U16. Re-derive the geostrophic wind eqs. (10.26) for the S. Hemisphere.

U17. Derive eqs. (10.29) from eqs. (10.26).

U18. The geostrophic wind approaches infinity as the equator is approached (see Fig. 10.10), yet the winds in the real atmosphere are not infinite there. Why?

U19. Verify that eq. (10.33) is indeed a solution to the gradient wind eqs. (10.31).

U20. Verify that eqs. (10.34) are solutions to eq. (10.33).

U21. Imagine an idealized weather map that had a single high pressure center next to a single low pressure center. Further, suppose that if you were to draw a line through those two centers, that the pressure variation along that line would be the same as Fig. 10.14. Given that information, and assuming circular cyclones and anticyclones, draw isobars on the weather map at ±0.5 kPa increments, starting at 100 kPa. Comment on the packing of (i.e., how closely spaced are) isobars near the centers of the cyclone and anticyclone.

U22. a. Is there any limit on the strength of the pressure gradient that can occur just outside of the center of cyclones? (Hint: consider Fig. 10.14)

b. What controls this limit?

c. What max winds are possible around cyclones?

U23. Calculate the geostrophic and gradient winds, as appropriate, at a number of locations using the height contours plotted in Fig. 10.3. Compare them to the observed winds and comment.

U24. What is implicit about the implicit solution (eq. 10.39) for the boundary-layer wind?

U25. How accurate are the approximate boundary layer wind solutions (eq. 10.41)? Under what conditions are the approximate solutions least accurate? (Hint: compare with an iterative solution to the implicit equations 10.39).

U26. Why is an exact explicit solution possible for the steady-state winds in the unstable boundary layer, but not for the neutral boundary layer?

U27. Verify that eqs. (10.42) are indeed exact solutions to (10.39) or (10.38).

U28(§). a. Recreate on a spreadsheet the solved example for the boundary-layer gradient winds.

b. Recreate the checks of that equation for the special cases where it reduces to the geostrophic wind, gradient wind, and boundary-layer wind.

c. Compare the results from (b) against the respective analytical solutions (which you must compute yourself).

d. Can the analytical solutions for the gradient wind and the (neutral) boundary layer wind be combined to yield an approximate analytical solution to the BLG winds. If so, what are the limitations, and the magnitude of the errors. (Hint: Try substituting M_{tan} in place of G in the equations for boundary layer wind.)

U29. Photocopy Fig. 10.13, and enhance the copy by drawing additional vectors for the boundary-layer wind and the BLG wind. Make these vectors be the appropriate length and direction relative to the geostrophic and gradient winds that are already plotted.

U30. Verify that the cyclostrophic winds are indeed a solution to the governing equations (10.45).

U31. Re-derive the equations for cyclostrophic wind, but in terms of height gradient on a constant pressure surface, instead of pressure gradient along a constant height surface. [Hint: Compare eqs. (10.29) to (10.26).]

U32. What aspects of the *Approach to Geostrophy* Focus Box are relevant to the inertial wind? Discuss.

U33. a. Derive eq. (10.66) based on geometry and mass continuity (total inflow = total outflow).

b. For horizontal winds, we know that an increased drag coefficient will reduce wind speed. Why in eq. (10.66) does an increased drag coefficient cause increased vertical wind speed?

c. When considering that factor b in eq. (10.66) is a negative function of the drag coefficient, does your answer to part (b) change?

U34. The paragraph after eq. (10.69) gives a physical interpretation of the equation. Show how that interpretation was reached, by examining each term in the equation and discussing its impact on W.

U35. Given eq. (10.70), determine the physical meaning of the internal Rossby radius of deformation by how it affects the various terms in (10.71).

U36. Regarding horizontal balances of forces, if only Coriolis and turbulent-drag forces were active, speculate on the nature of the resulting wind.

U37. Modify eqs. (10.66) through (10.71) if necessary, to describe the boundary-layer pumping around highs (anticyclones) rather than around lows (cyclones). Discuss the significance of your equations.

U38. Rewrite the total deformation as a function of divergence and vorticity. Discuss.

Web-Enhanced Questions

W1. Search the web for historical discussions of Isaac Newton, and summarize what you find. What did you find most unusual or interesting?

W2. Search the web for "Coriolis Force", to find sites that show animations of the movement of objects in a rotating coordinate system. Tabulate a list of the best sites.

W3. a. Search the web for a current sea-level weather map that covers your area, and which includes isobars. Measure the distance (km) between isobars, and compute the pressure gradient force.

b. Same as (a), but do this for several days in a row. Then plot a graph of how the pressure gradient changes with time over your location.

W4. Search the web for 50 kPa (500 mb) weather maps that cover part of the S. Hemisphere. Compute the geostrophic and gradient wind speeds and directions in regions of straight and curved isobars, respectively, and compare with upper-air observations. Discuss the differences between these winds and corresponding winds in the N. Hemisphere.

W5. Find a current 50 kPa (= 500 mb) weather map (or other map as specified by your instructor) that has height contours already drawn on it. Look for a region in the map where the isobars are nearly straight.

a. Compute the geostrophic wind speed components, and the total geostrophic wind speed vector (speed and direction).

b. If upper-air (rawinsonde) observations are available near your area, compare the measured winds with the geostrophic value computed from part (a).

c. If there are multiple regions of nearly straight isobars at different latitudes in your weather map, see how the observed winds in these regions vary with latitude, and compare with the expected latitudinal variation of geostrophic wind (as from Fig. 10.10).

W6. a. Same as W5, except look for a region on the map where the isobars are curving in a cyclonic (counterclockwise in the N. Hemisphere) direction when following along with the wind direction. Compute the gradient wind for this case.

b. Same as (a) but for anticyclone (clockwise) turning winds.

c. Compare the measured winds from rawinsondes to the theoretical winds from (a) and (b). Confirm that the gradient winds (both theoretical and observed) are slower than geostrophic around lows, and faster around highs.

W7. a. Find a sea-level weather map from the web that has isobars drawn on it. Look for a day or a region where there are neighboring regions of strong high and low pressure. Print this map, and draw a straight line connecting the centers of the high and the low. Extend this line well past the centers of the high and low. Using the isobars that cross your drawn line, find how pressure varies with distance between the high and low, and plot the results similar to Fig. 10.14.

b. If you set the location of the center of the high as the origin of your coordinate system, check

whether the shape of the pressure curve agrees with eq. (10.37b). Confirm that the pressure variation across a low-pressure center can have a cusp, while that across a high center cannot.

W8. Search the web for a weather map at 50 kPa (500 mb) or any other altitude above the boundary layer, that includes the equator. Find a region of relatively straight isobars near the equator, and compute the geostrophic wind speed based on the plotted pressure gradient. Compare this theoretical wind with observed upper-air winds for the same altitude. Why don't the observations agree with the theory?

W9. Find a current sea-level weather map from the web, that shows both wind direction (such as the wind symbol on surface station observations), and isobars.

a. For a region of the map where the isobars are relatively straight, and hopefully over non-mountainous and non-coastal terrain, confirm that the observed boundary-layer winds indeed cross the isobars at some small angle from high to low pressure. What is the average angle?

b. For a region where the isobars are curved around a high or low, confirm that the winds spiral in towards the center of the low, and out from the center of a high.

c. Around either the high or low, estimate the average value of the component of wind that represents inflow or outflow from the low or high. Use that value of V_{in} (or V_{out}) in eq. (10.65) to compute the vertical velocity at the top of the boundary layer.

d. Based on the inward or outward component of velocity from (c), estimate the drag force acting on the air. If this calculation is for flow around a low where the winds are relatively fast, find the value of the drag coefficient C_D for statically neutral conditions.

W10. a. If it is hurricane season, search the web for a weather map that is just above the top of the boundary layer (85 kPa or 850 mb might be good enough), but which is well below the altitude of the 60 kPa pressure. Look for a map (either observed or forecast) that has the height contours around the hurricane on this pressure surface (85 kPa). Find the location just outside of the eye where the height contours are packed closest together, and calculate the pressure gradient there. Then use that pressure gradient to compute the cyclostrophic wind, and compare your theoretical value with the observed upper-air values at that height.

b. Do the same as (a), but using a sea-level weather map showing the isobars. Also comment on the effect of boundary layer drag.

Synthesis Questions

S1. Suppose Newton's second law of motion was not a function of mass. How would the motion of bullets, cannon balls, and air parcels be different, if at all?

S2. What if Newton's second law of motion stated that velocity was proportional to force/mass. How would weather and climate be different, if at all?

S3. What if wind could not advect itself. How would the weather and climate be different, if at all?

S4. Suppose that pressure-gradient force was along isobars, rather than perpendicular to them. Describe how winds would be different, how weather maps would be different, and how this might affect the weather and climate, if at all.

S5. There is some debate in the literature that our understanding of Coriolis force might be incorrect. We think that Coriolis force is an apparent force. Can an apparent force change the momentum and kinetic energy of air parcels? If so, would this violate Newton's laws when viewed from a non-rotating frame? Discuss. (Hint: look for a series of descriptive articles by Anders Persson that appeared in *Weather* magazine starting in year 2000.)

S6. Fig. 10.7 shows wind shear across the top of the boundary layer, where subgeostrophic winds in the boundary layer change to geostrophic winds above the boundary layer. The shear can exist because a strongly statically stable layer of air caps the boundary layer. If such a stable capping inversion did not exist, how might the wind profile be different over the depth of the troposphere?

S7. Suppose that turbulent drag force acted 90° to the right of the wind direction in the boundary layer. Discuss how the boundary-layer winds would work around highs and lows, and in regions of straight isobars. How would the weather and climate be different, if at all?

S8. Suppose that the boundary-layer drag force did not increase with velocity (in the case of an unstable boundary layer) or with velocity squared (in the case of a neutral boundary layer), but was constant regardless of wind speed. How would the boundary layer winds, weather, and climate change, if at all?

S9. What if there were no Coriolis force? How would winds, weather, and climate be different, if at all?

S10. On our present world where we perceive a Coriolis force, are there situations where it is possible for wind to blow directly high to low pressure, rather than more-or-less parallel to the isobars? Describe such scenarios.

S11. What if geostrophic winds could turn around high or low pressure systems without feeling centripetal or centrifugal force. How would the weather and climate be different, if at all?

S12. Suppose that cusps in pressure were allowed at high-pressure centers as well as at low pressure centers (see Fig. 10.14) so that strong pressure gradients could exist near the center of both types of pressure centers. Describe how the winds, weather, and climate might be different, if at all?

S13. Suppose that the Earth's surface were frictionless. How would the weather and climate be different, if at all?

S14. Suppose that the tropopause acted like a rigid lid on the troposphere, and that the air at the top of the troposphere felt frictional drag against this rigid lid. How would the winds, weather, and climate be different, if at all?

S15. What if the Earth were a flat spinning disk instead of a spinning sphere. How would the weather and climate be different, if at all?

S16. Suppose the Earth's rotation were twice as fast as now. How would the weather and climate change, if at all?

S17. Suppose that the axis of the Earth's rotation were along a radial line drawn from the sun (i.e., in the plane of the ecliptic), rather than being more or less perpendicular to the ecliptic plane. How would the weather and climate be different, if at all?

S18. Suppose the Earth did not rotate. How would the winds, weather, and climate be different, if at all?

S19. Why is incompressibility such a good approximation for the real atmosphere? How does the atmosphere react to density changes, that might help ensure little density change? (Hint: consider the first solved example in the continuity equation section.)

S20. Extend the discussion of the Focus box on Coriolis Force by deriving the magnitude of the Coriolis force for an object moving
a. westward b. southward

S21. For zonal (east-west) winds, there is also a vertical component of Coriolis force. Using your own diagrams similar to those in the Focus box on Coriolis Force, show why it can form. Estimate its magnitude, and compare the magnitude of this force to other typical forces in the vertical. Show why a vertical component of Coriolis force does not exist for meridional (north-south) winds.

S22. What if a cyclostrophic-like wind also felt drag near the ground? This describes conditions at the bottom of tornadoes. Write the equations of motion for this situation, and solve them for the tangential and radial wind components. Check that your results are reasonable compared with the pure cyclostrophic winds. How would the resulting winds affect the total circulation in a tornado? As discoverer of these winds, name them after yourself.

S23. The time duration of many weather phenomena are related to their spatial scales, as shown by eq. (10.53) and Fig. 10.24. Why do most weather phenomena lie near the same diagonal line on a log-log plot? Why are there not additional phenomena that fill out the relatively empty upper and lower triangles in the figure? Can the distribution of time and space scales in Fig. 10.24 be used to some advantage?

Copyright © 2011, 2015 by Roland Stull. *Meteorology for Scientists and Engineers, 3rd Ed.*

GLOBAL CIRCULATION

CONTENTS

Nomenclature 330
A Simplified Description of the Global Circulation 330
Near-surface Conditions 330
Upper-tropospheric Conditions 331
Vertical Circulations 332
Monsoonal Circulations 333
Differential Heating 334
Meridional Temperature Gradient 335
Radiative Forcings 336
Radiative Forcing by Latitude Belt 338
Heat Transport by the Global Circulation 338
Pressure Profiles 340
Non-hydrostatic Pressure Couplets 340
Hydrostatic Thermal Circulations 341
Geostrophic Wind & Geostrophic Adjustment 343
Ageostrophic Winds at the Equator 343
Definitions 343
Geostrophic Adjustment - Part 1 344
Thermal Wind Relationship 345
Thickness 345
Thermal Wind 346
Case Study 348
Thermal Wind & Geostrophic Adjust. - Part 2 349
Explaining the Global Circulation 350
Low Latitudes 350
High Latitudes 352
Mid-latitudes 352
Monsoon 356
Jet Streams 357
Baroclinicity & the Polar Jet 359
Angular Momentum & Subtropical Jet 360
Vorticity 362
Horizontal Circulation 365
Mid-latitude Troughs And Ridges 367
Barotropic Instability & Rossby Waves 367
Baroclinic Instability & Rossby Waves 371
Meridional Transport by Rossby Waves 374
Three-band General Circulation 376
A Measure of Vertical Circulation 377
Effective Vertical Circulation 377
Ekman Spiral In The Ocean 378
Summary 379
Exercises 380

"Meteorology for Scientists and Engineers, 3rd Edition" by Roland Stull is licensed under a Creative Commons Attribution-NonCommercial-ShareAlike 4.0 International License. To view a copy of the license, visit http://creativecommons.org/licenses/by-nc-sa/4.0/ . This work is available at http://www.eos.ubc.ca/books/Practical_Meteorology/ .

11 Solar radiation absorbed in the tropics exceeds infrared loss, causing heat to accumulate. The opposite is true at the poles, where there is net radiative cooling. Such radiative **differential heating** between poles and equator creates an imbalance in the atmosphere/ocean system (Fig. 11.1a).

Le Chatelier's Principle states that an imbalanced system reacts in a way to partially undo the imbalance. For the atmosphere of Fig. 11.1a, warm tropical air rises due to buoyancy and flows toward the poles, and the cold polar air sinks and flows toward the equator (Fig. 11.1b).

Because the radiative forcings are unremitting, a ceaseless movement of wind and ocean currents results in what we call the **general circulation** or **global circulation**. The circulation cannot instantly undo the continued destabilization, resulting in tropics that remain slightly warmer than the poles.

But the real general circulation on Earth does not look like Fig. 11.1b. Instead, there are three bands of circulations in the Northern Hemisphere (Fig. 11.1c), and three in the Southern. In this chapter, we will identify characteristics of the general circulation, explain why they exist, and learn how they work.

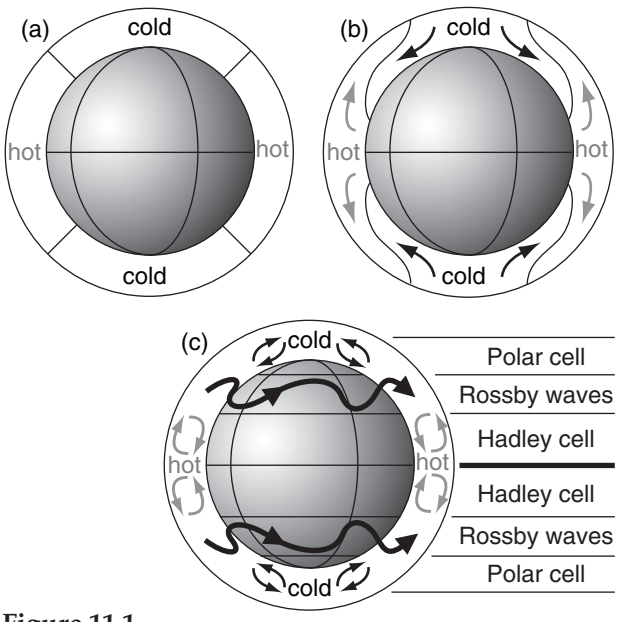

Figure 11.1
Earth/atmosphere system, showing that (a) differential heating by radiation causes (b) atmospheric circulations. Add Earth's rotation, and (c) 3 circulation bands form in each hemisphere.

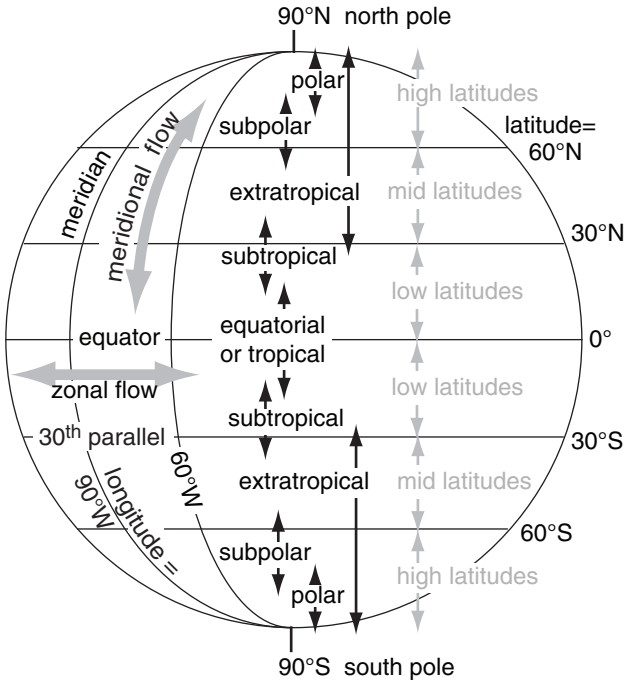

Figure 11.2
Global nomenclature.

NOMENCLATURE

Latitude lines are **parallels**, and east-west winds are called **zonal flow** (Fig. 11.2). Each 1° of latitude = 111 km. Longitude lines are **meridians**, and north-south winds are called **meridional flow**.

Mid-latitudes are the regions between about 30° and 60° latitude. **High latitudes** are 60° to 90°, and **low latitudes** are 0° to 30°.

The **subtropical** zone is at roughly 30° latitude, and the **subpolar** zone is at 60° latitude, both of which partially overlap mid-latitudes. **Tropics** span the **equator**, and **polar** regions are near the Earth's poles. **Extratropical** refers to everything outside of the tropics: poleward from roughly 30°N and 30°S.

For example, **extratropical cyclones** are low-pressure centers — typically called **lows** and labeled with $\mathbb{L}$ — that are found in mid- or high-latitudes. **Tropical cyclones** include **hurricanes** and **typhoons**, and other strong lows in tropical regions.

In many climate studies, data from the months of June, July, and August (**JJA**) are used to represent conditions in N. Hemisphere summer (and S. Hemisphere winter). Similarly, December, January, February (**DJF**) data are used to represent N. Hemisphere winter (and S. Hemisphere summer).

ON DOING SCIENCE • Toy Models

Some problems in meteorology are so complex, and involve so many interacting variables and processes, that they are intimidating if not impossible to solve. However, we can sometimes gain insight into fundamental aspects of the problem by using idealized, simplified physics. Such an approximation is sometimes called a "toy model".

A rotating spherical Earth with no oceans is one example of a toy model. The meridional variation of temperature given later in this chapter is another example. These models are designed to capture only the dominant processes. They are toy models, not complete models.

Toy models are used extensively to study climate change. For example, the greenhouse effect can be examined using toy models in the Climate chapter. Toy models capture only the dominant effects, and neglect the subtleties. You should never use toy models to infer the details of a process, particularly in situations where two large but opposite processes nearly cancel each other.

For other examples of toy models applied to the environment, see John Harte's 1988 book "*Consider a Spherical Cow*", University Science Books. 283 pp.

A SIMPLIFIED DESCRIPTION OF THE GLOBAL CIRCULATION

Consider a hypothetical rotating planet with no contrast between continents and oceans. The **climatological average** (average over 30 years; see the Climate chapter) winds in such a simplified planet would have characteristics as sketched in Figs. 11.3. Actual winds on any day could differ from this climatological average due to transient weather systems that perturb the average flow. Also, monthly-average conditions tend to shift toward the summer hemisphere (e.g., the circulation bands shift northward during April through September).

Near-surface Conditions

Near-surface average winds are sketched in Fig. 11.3a. At low latitudes are broad bands of persistent easterly winds ($U \approx -7$ m/s) called **trade winds**, named because the **easterlies** allowed sailing ships to conduct transoceanic trade in the old days.

These trade winds also blow toward the equator from both hemispheres, and the equatorial belt of convergence is called the **intertropical conver-**

gence zone (**ITCZ**). On average, the air at the ITCZ is hot and humid, with low pressure, strong upward air motion, heavy convective (thunderstorm) precipitation, and light to calm winds except in thunderstorms. This **equatorial trough** (low-pressure belt) was called the **doldrums** by sailors whose sailing ships were becalmed there for many days.

At 30° latitude are belts of high surface pressure called **subtropical highs** (Fig. 11.3a). In these belts are hot, dry, cloud-free air descending from higher in the troposphere. Surface winds in these belts are also calm on average. In the old days, becalmed sailing ships would often run short of drinking water, causing horses on board to die and be thrown overboard. Hence, sailors called these miserable places the **horse latitudes**. On land, many of the world's deserts are near these latitudes.

In mid-latitudes are transient centers of low pressure (**mid-latitude cyclones, L**) and high pressure (**anticyclones, H**). Winds around lows **converge** (come together) and circulate **cyclonically** — counterclockwise in the N. Hemisphere, and clockwise in the S. Hemisphere. Winds around highs **diverge** (spread out) and rotate **anticyclonically** — clockwise in the N. Hemisphere, and counterclockwise in the S. Hemisphere. The cyclones are regions of bad weather (clouds, rain, high humidity, strong winds) and fronts. The anticyclones are regions of good weather (clear skies or fair-weather clouds, no precipitation, dry air, and light winds).

The high- and low-pressure centers move on average from west to east, driven by large-scale winds from the west. Although these **westerlies** dominate the general circulation at mid-latitudes, the surface winds are quite variable in time and space due to the sum of the westerlies plus the transient circulations around the highs and lows.

Near 60° latitude are belts of low surface pressure called **subpolar lows**. Along these belts are light to calm winds, upward air motion, clouds, cool temperatures, and precipitation (as snow in winter).

Near each pole is a climatological region of high pressure called a **polar high**. In these regions are often clear skies, cold dry descending air, light winds, and little snowfall. Between each polar high (at 90°) and the subpolar low (at 60°) is a belt of weak easterly winds, called the **polar easterlies**.

Upper-tropospheric Conditions

The stratosphere is strongly statically stable, and acts like a lid to the troposphere. Thus, vertical circulations associated with our weather are mostly trapped within the troposphere. These vertical circulations couple the average near-surface winds with the average upper-tropospheric (near the tropopause) winds described here (Fig. 11.3b).

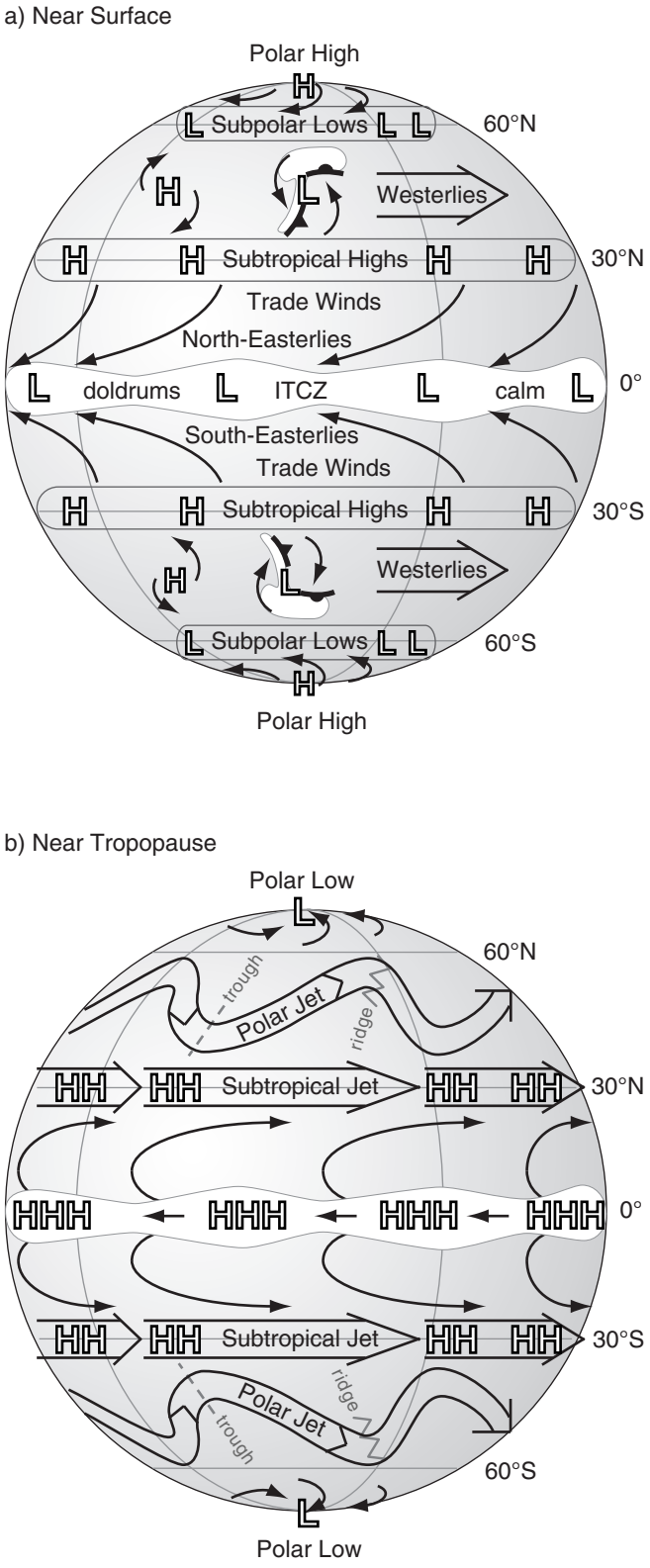

Figure 11.3
Simplified global circulation in the troposphere: (a) near the surface, and (b) near the tropopause. H and L indicate high and low pressures, and HHH means very strong high pressure. White indicates precipitating clouds.

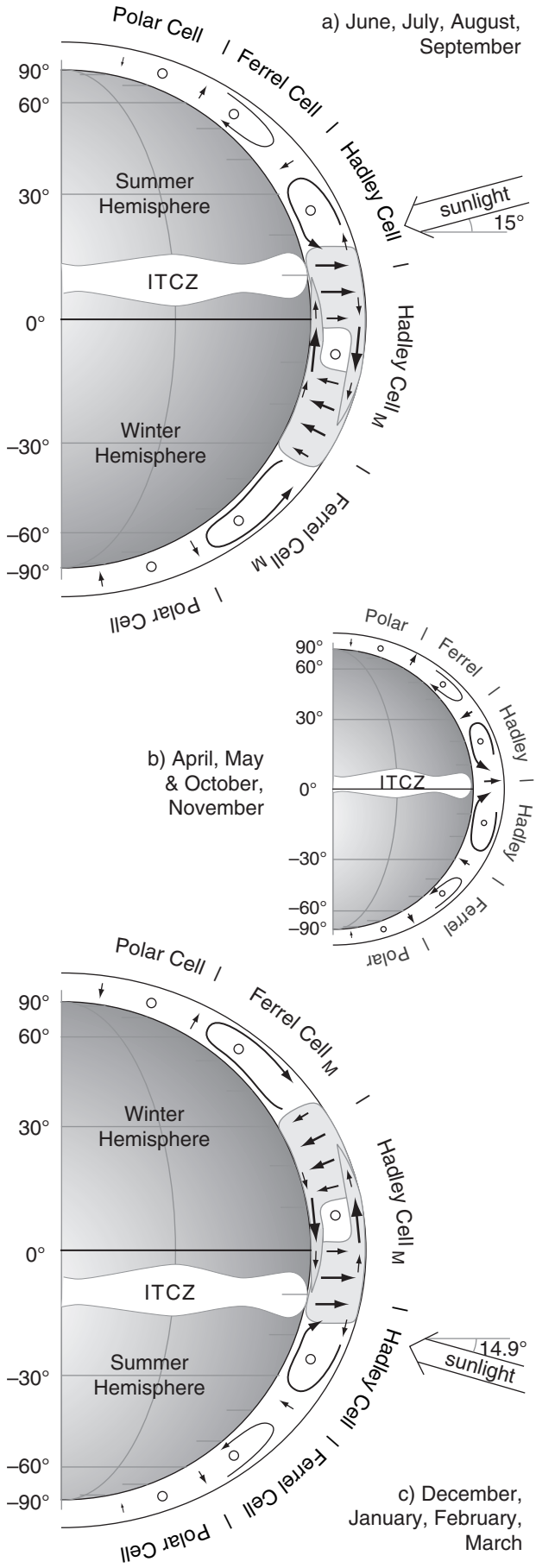

In the tropics is a belt of very strong equatorial high pressure along the tops of the ITCZ thunderstorms. Air in this belt blows from the east, due to easterly inertia from the trade winds being carried upward in the thunderstorm convection. Diverging from this belt are winds that blow toward the north in the N. Hemisphere, and toward the south in the S. Hemisphere. As these winds move away from the equator, they turn to have an increasingly westerly component as they approach 30° latitude.

Near 30° latitude in each hemisphere is a persistent belt of strong westerly winds at the tropopause called the **subtropical jet**. This jet meanders north and south a bit. Pressure here is very high, but not as high as over the equator.

In mid-latitudes at the tropopause is another belt of strong westerly winds called the **polar jet**. The centerline of the polar jet meanders north and south, resulting in a wave-like shape called a **Rossby wave**, as sketched in Fig. 11.1c. The equatorward portions of the wave are known as low-pressure **troughs**, and poleward portions are known as high-pressure **ridges**. These ridges and troughs are very transient, and generally shift from west to east relative to the ground.

Near 60° at the tropopause is a belt of low to medium pressure. At each pole is a low-pressure center near the tropopause, with winds at high latitudes generally blowing from the west causing a cyclonic circulation around the **polar low**. Thus, contrary to near-surface conditions, the near-tropopause average winds blow from the west at all latitudes (except near the equator).

Vertical Circulations

Vertical circulations of warm rising air in the tropics and descending air in the subtropics are called **Hadley cells** or **Hadley circulations** (Fig. 11.4). At the bottom of the Hadley cell are the trade winds. At the top, near the tropopause, are divergent winds. The updraft portion of the Hadley circulation is often filled with thunderstorms and heavy precipitation at the ITCZ. This vigorous convection in the troposphere causes a high tropopause (15 - 18 km altitude) and a belt of heavy rain in the tropics.

The summer- and winter-hemisphere Hadley cells are strongly asymmetric (Fig. 11.4). The major Hadley circulation (denoted with subscript "M") crosses the equator, with rising air in the summer

Figure 11.4 *(at left)*
Vertical cross section of Earth's global circulation in the troposphere. (a) N. Hemisphere summer. (b) Transition months. (c) S. Hemisphere summer. The major (subscript $_M$) Hadley cell is shaded light grey. Minor circulations have no subscript.

hemisphere and descending air in the winter hemisphere. The updraft is often between 0° and 15° latitudes in the summer hemisphere, and has average core vertical velocities of 6 mm/s. The broader downdraft is often found between 10° and 30° latitudes in the winter hemisphere, with average velocity of about –4 mm/s in downdraft centers. Connecting the up- and downdrafts are meridional wind components of 3 m/s at the cell top and bottom.

The major Hadley cell changes direction and shifts position between summer and winter. During June-July-August-September, the average solar declination angle is 15°N, and the updraft is in the Northern Hemisphere (Fig. 11.4a). Out of these four months, the most well-defined circulation occurs in August and September. At this time, the ITCZ is centered at about 10°N.

During December-January-February-March, the average solar declination angle is 14.9°S, and the major updraft is in the Southern Hemisphere (Fig. 11.4c). Out of these four months, the strongest circulation is during February and March, and the ITCZ is centered at 10°S. The major Hadley cell transports significant heat away from the tropics, and also from the summer to the winter hemisphere.

During the transition months (April-May and October-November) between summer and winter, the Hadley circulation has nearly symmetric Hadley cells in both hemispheres (Fig. 11.4b). During this transition, the intensities of the Hadley circulations are weak.

When averaged over the whole year, the strong but reversing major Hadley circulation partially cancels itself, resulting in an annual average circulation that is somewhat weak and looks like Fig. 11.4b. This weak annual average is deceiving, and does not reflect the true movement of heat, moisture, and momentum by the winds. Hence, climate experts prefer to look at months JJA and DJF separately to give **seasonal averages**.

In the winter hemisphere is a **Ferrel cell**, with a vertical circulation of descending air in the subtropics and rising air at high latitudes; namely, a circulation opposite to that of the major Hadley cell. In the winter hemisphere is a modest **polar cell**, with air circulating in the same sense as the Hadley cell.

In the summer hemisphere, all the circulations are weaker. There is a minor Hadley cell and a minor Ferrel cell (Fig. 11.4). Summer-hemisphere circulations are weaker because the temperature contrast between the tropics and poles are weaker.

Monsoonal Circulations

Monsoon circulations are continental-scale circulations driven by continent-ocean temperature contrasts, as sketched in Figs. 11.5. In summer, high-

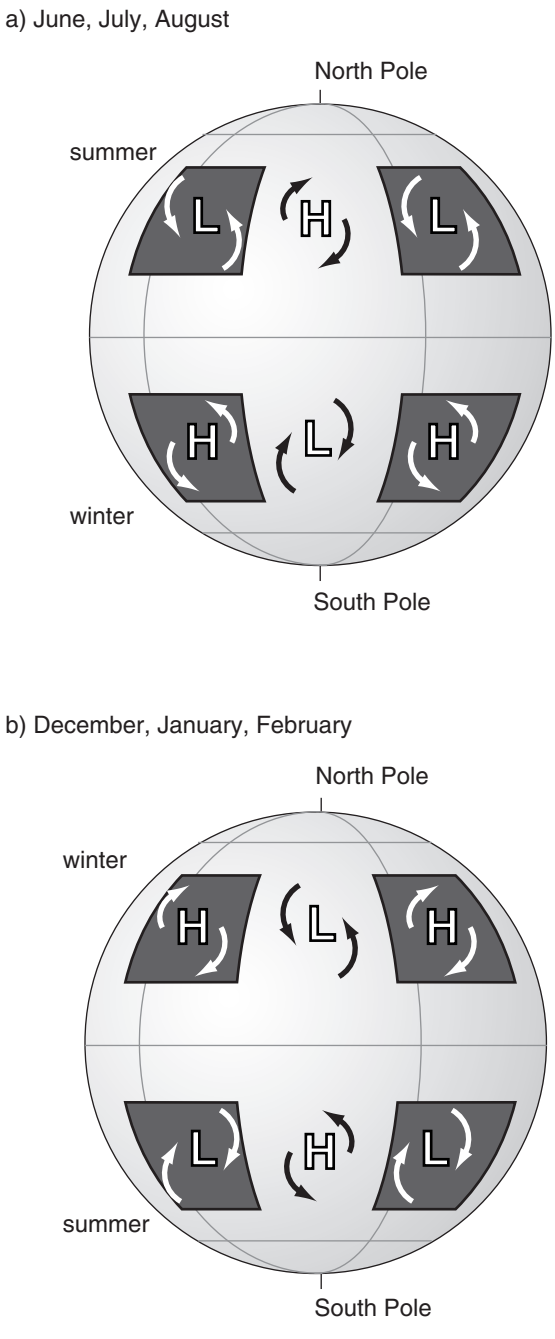

Figure 11.5
Idealized seasonal-average monsoon circulations near the surface. Continents are shaded dark grey; oceans are light grey. H and L are surface high- and low-pressure centers.

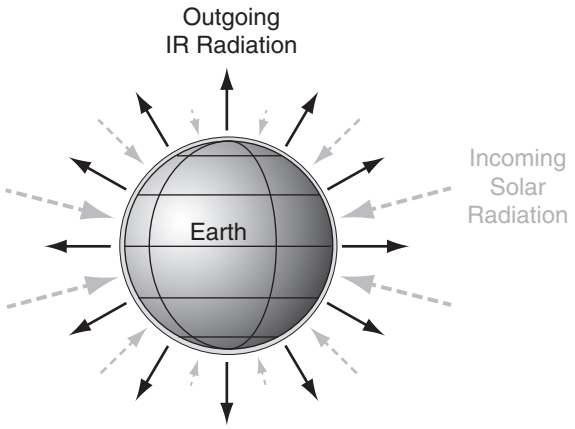

Figure 11.6
Annual average incoming solar radiation (grey dashed arrows) and of outgoing infrared (IR) radiation (solid black arrows), where arrow size indicates relative magnitude. [Because the Earth rotates and exposes all locations to the sun at one time or another, the incoming solar radiation is sketched as approaching all locations on the Earth's surface.]

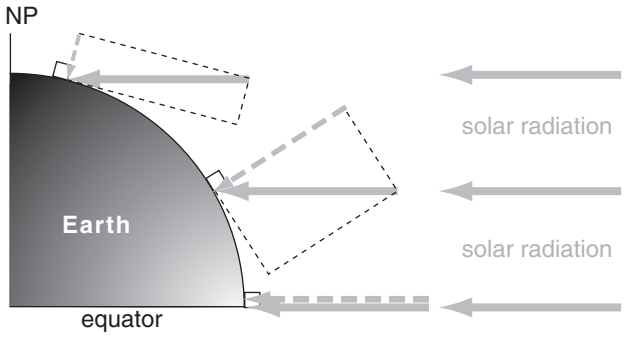

Figure 11.7
Of the solar radiation approaching the Earth (thick solid grey arrows), the component (dashed grey arrow) that is perpendicular to the top of the atmosphere is proportional to the cosine of the latitude (during the equinox).

pressure centers (anticyclones) are over the relatively warm oceans, and low-pressure centers (cyclones) are over the hotter continents. In winter, low-pressure centers are over the cool oceans, and high-pressure centers are over the colder continents.

These monsoon circulations represent average conditions over a season. The actual weather on any given day can be variable, and can deviate from these seasonal averages.

Our Earth has a complex arrangement of continents and oceans. As a result, seasonally-varying monsoonal circulations are superimposed on the seasonally-varying planetary-scale circulation to yield a complex and varying global-circulation pattern.

At this point, you have a descriptive understanding of the global circulation. But what drives it?

DIFFERENTIAL HEATING

Differential heating drives the global circulation. Incoming solar radiation (**insolation**) nearly balances the outgoing infrared (IR) radiation when averaged over the whole globe. However, at different latitudes are significant imbalances (Fig. 11.6), which cause the differential heating.

Recall from the Radiation chapter that the flux of solar radiation incident on the top of the atmosphere depends more or less on the cosine of the latitude, as shown in Fig. 11.7. The component of the incident ray of sunlight that is perpendicular to the Earth's surface is small in polar regions, but larger toward the equator (grey dashed arrows in Figs. 11.6 and 11.7). The incoming energy adds heat to the Earth-atmosphere-ocean system.

Heat is lost due to infrared (IR) radiation emitted from the Earth-ocean-atmosphere system to space. Since all locations near the surface in the Earth-ocean-atmosphere system are relatively warm compared to absolute zero, the Stefan-Boltzmann law from the Radiation chapter tells us that the emission rates are also more or less uniform around the Earth. This is sketched by the solid black arrows in Fig. 11.6.

Thus, at low latitudes, more solar radiation is absorbed than leaves as IR, causing net warming. At high latitudes, the opposite is true: IR radiative losses exceed solar heating, causing net cooling. This differential heating drives the global circulation.

Because the global circulation cannot instantly eliminate the temperature disparity across the globe, there is a residual north-south temperature gradient that we will examine first.

Meridional Temperature Gradient

Sea-level temperatures are warmer near the equator than at the poles, when averaged over a whole year and averaged around latitude belts (Fig. 11.8a). Although the Northern Hemisphere is slightly cooler than the Southern at sea level, an idealization (toy model) of the variation of zonally-averaged temperature T with latitude ϕ is:

$$T \approx a + b \cdot \left[\frac{3}{2} \cdot \left(\frac{2}{3} + \sin^2 \phi \right) \cdot \cos^3 \phi \right] \qquad (11.1)$$

For sea level, the parameters are: $a \approx -12°C$, $b \approx 40°C$. Parameter b represents a temperature difference between equator and pole, so it could also have been written as $b \approx 40$ K.

The magnitude of the equator-to-pole temperature gradient decreases with altitude, and changes sign in the stratosphere. Namely, in the stratosphere, it is cold in the tropics and warmer near the poles. For this reason, parameter b in eq. (11.1) can be generalized as:

$$b \approx b_1 \cdot \left(1 - \frac{z}{z_T} \right) \qquad (11.2)$$

where $b_1 = 40°C$, z is height above sea level, and $z_T \approx 11$ km is the average depth of the troposphere.

A similarly crude but useful generalization of parameter a can be made so that it too changes with altitude z above sea level:

$$a \approx a_1 - \gamma \cdot z \qquad (11.3)$$

where $a_1 = -12°C$ and $\gamma = 3.14$ °C/km.

From Fig. 11.8, we see that in the tropics there is little temperature variation — it is hot everywhere. The reason for this is the very strong mixing and transport of heat by the Hadley circulations. However, in mid-latitudes, there is a significant north-south temperature gradient that supports a variety of storm systems. Although eq. (11.1) might seem unnecessarily complex, it is designed to give sufficient uniformity in the tropics to shift the large temperature gradients toward mid-latitudes.

The temperature gradient associated with eq. (11.1) is

$$\frac{\Delta T}{\Delta y} \approx -b \cdot c \cdot \left[\sin^3 \phi \cdot \cos^2 \phi \right] \qquad (11.4)$$

where $c = 1.18 \times 10^{-3}$ km^{-1} is a constant valid at all heights, b is given by eq. (11.2), and y is distance in the north-south direction. The meridional temperature gradients at sea level and at $z = 15$ km are plotted in Fig. 11.8b.

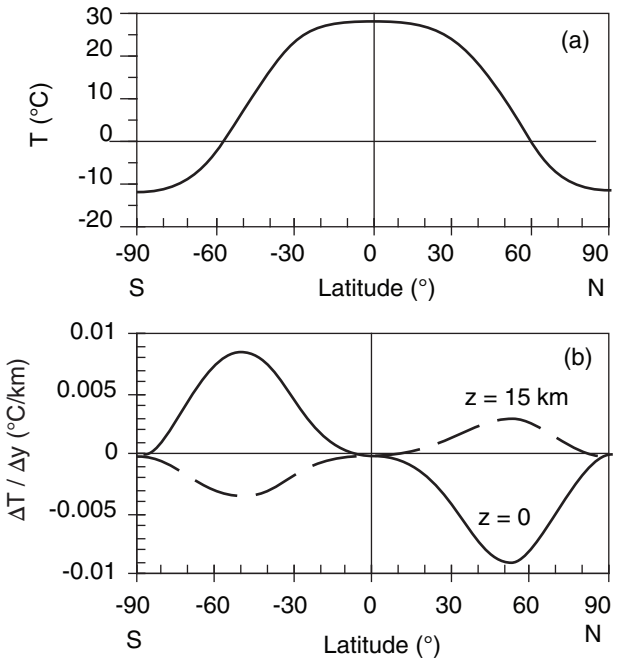

Figure 11.8
Idealized annually and zonally averaged (a) temperature at sea level, and (b) north-south temperature gradient at sea level and at 15 km altitude.

Solved Example

Find the meridional temperature and temperature gradient at 45°N latitude, at sea level (sl).

Solution

Given: $\phi = 45°$

Find: $T_{sl} = ?$ °C, $\Delta T/\Delta y = ?$ °C/km

Use eq. (11.1) with $z = 0$ at sea level:

$$T_{sl} \approx -12°C + (40°C) \cdot \left[\frac{3}{2} \cdot \left(\frac{2}{3} + \sin^2 45° \right) \cdot \cos^3 45° \right]$$

$$= \underline{\mathbf{12.75\ °C}}$$

Use eq. (11.4):

$$\frac{\Delta T}{\Delta y} \approx -(40°C) \cdot (1.18 \times 10^{-3}) \cdot \left[\sin^3 45° \cdot \cos^2 45° \right]$$

$$= \underline{\mathbf{-0.0083\ °C/km}}$$

Check: Units OK. Physics OK. As a quick check, from Fig. 11.8a, the temperature decreases by about 9°C between 40°N to 50°N latitude. But each 1° of latitude equals 111 km of distance y. This temperature gradient of –9°C/(1110 km) from the figure agrees with the numerical answer above.

Discussion: Temperature decreases toward the north in the northern hemisphere, which gives the negative sign for the gradient.

BEYOND ALGEBRA • Temperature Gradient

Problem: Derive eq. (11.4) from eq. (11.1).

Solution: Given:

$$T \approx a + b \cdot \left[\frac{3}{2} \cdot \left(\frac{2}{3} + \sin^2 \phi \right) \cdot \cos^3 \phi \right]$$

Find: $$\frac{\partial T}{\partial y} = \frac{\partial T}{\partial \phi} \cdot \frac{\partial \phi}{\partial y} \qquad (a)$$

The first factor on the right in (a) is: $\frac{\partial T}{\partial \phi} = b \cdot \left(\frac{3}{2} \right) \cdot$

$$\left[(2 \sin \phi \cdot \cos \phi) \cos^3 \phi - 3 \left(\frac{2}{3} + \sin^2 \phi \right) \cos^2 \phi \cdot \sin \phi \right]$$

Taking $\sin\phi \cdot \cos^2\phi$ out of the square brackets:

$$\frac{\partial T}{\partial \phi} = b \left(\frac{3}{2} \right) \sin \phi \cdot \cos^2 \phi \cdot \left[2 \cos^2 \phi - 2 - 3 \sin^2 \phi \right]$$

But $\cos^2\phi = 1 - \sin^2\phi$, thus $2\cos^2\phi = 2 - 2\sin^2\phi$:

$$\frac{\partial T}{\partial \phi} = b \left(\frac{3}{2} \right) \sin \phi \cdot \cos^2 \phi \cdot \left[-5 \sin^2 \phi \right] \qquad (b)$$

Inserting eq. (b) into (a) gives:

$$\frac{\partial T}{\partial y} = -b \cdot \left(\frac{15}{2} \cdot \frac{\partial \phi}{\partial y} \right) \cdot \sin^3 \phi \cdot \cos^2 \phi \qquad (c)$$

Define: $\left(\frac{15}{2} \cdot \frac{\partial \phi}{\partial y} \right) = c$ Thus, the final answer is:

$$\boxed{\frac{\partial T}{\partial y} = -b \cdot c \cdot \sin^3 \phi \cdot \cos^2 \phi} \qquad (11.4)$$

All that remains is to find c. $\partial\phi/\partial y$ is the change of latitude per distance traveled north. The total change in latitude to circumnavigate the Earth from the north pole past the south pole and back to the north pole is 2π radians, and the circumference of the Earth is $2\pi R$ where $R = 6371$ km is the average radius of the Earth. Thus:

$$\frac{\partial \phi}{\partial y} = \frac{2\pi}{2\pi \cdot R} = \frac{1}{R}$$

The constant c is then:

$$c = \left(\frac{15}{2} \cdot \frac{1}{R} \right) = 1.18 \times 10^{-3} \ \text{km}^{-1} \qquad (e)$$

Check: The solved example on the previous page verified that eq. (11.4) is a reasonable answer, given the temperature defined by eq. (11.1).

Caution: Eq. (11.1) is only a crude approximation to nature, designed to be convenient for analytical calculations of temperature gradients, thermal winds, IR emissions, etc. While it serves an education purpose here, more accurate models should be used for detailed studies.

Because the meridional temperature gradient results from the interplay of differential radiative heating and advection by the global circulation, let us now look at radiative forcings in more detail.

Radiative Forcings

Incoming Solar Radiation

Because of the tilt of the Earth's axis and the change of seasons, the actual flux of incoming solar radiation is not as simple as was sketched in Fig. 11.6. But this complication was already discussed in the Radiation chapter, where we saw an equation to calculate the incoming solar radiation (**insolation**) as a function of latitude and day. The resulting insolation figure is reproduced below (Fig. 11.9a).

If you take the spreadsheet data from the Radiation chapter that was used to make this figure, and average rows of data (i.e., average over all months for any one latitude), you can find the annual average insolation E_{insol} for each latitude (Fig. 11.9b). Insolation in polar regions is amazingly large.

The curve in Fig. 11.9b is simple, and in the spirit of a toy model can be nicely approximated by:

$$E_{insol} = E_o + E_1 \cdot \cos(2\,\phi) \qquad (11.5)$$

where the empirical parameters are $E_o = 298$ W/m^2, $E_1 = 123$ W/m^2, and ϕ is latitude. This curve and the data points it approximates are plotted in Fig. 11.10.

But not all the radiation incident on the top of the atmosphere is absorbed by the Earth-ocean-atmosphere system. Some is reflected back into space

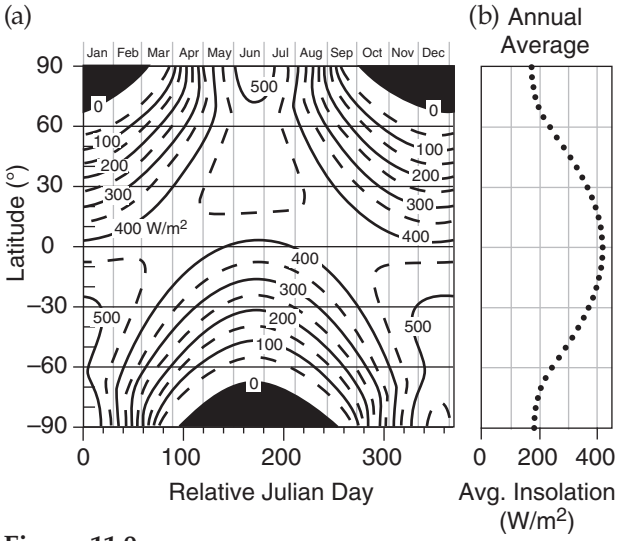

Figure 11.9
(a) Solar radiation (W/m^2) incident on the top of the atmosphere for different latitudes and months (copied from the Radiation chapter). (b) Meridional variation of insolation, found by averaging the data from the left figure over all months for each separate latitude (i.e., averages for each row of data).

from snow and ice on the surface, from the oceans, and from light-colored land. Some is reflected from cloud top. Some is scattered off of air molecules. The amount of insolation that is NOT absorbed is surprisingly constant with latitude at about $E_2 \approx 110$ W/m^2. Thus, the amount that IS absorbed is:

$$E_{in} = E_{insol} - E_2 \qquad (11.6)$$

where E_{in} is the incoming flux (W/m^2) of solar radiation absorbed into the Earth-ocean-atmosphere system (Fig. 11.10).

Outgoing Terrestrial Radiation

As you learned in the Remote Sensing chapter, infrared radiation emission and absorption in the atmosphere are very complex. At some wavelengths the atmosphere is mostly transparent, while at others it is mostly opaque. Thus, some of the IR emissions to space are from the Earth's surface, some from cloud top, and some from air at middle altitudes in the atmosphere.

In the spirit of a toy model, suppose that the net IR emissions are characteristic of the absolute temperature T_m near the middle of the troposphere (at about $z_m = 5.5$ km). Next, idealize the zonally- and annually-averaged outgoing radiative flux E_{out} by the Stefan-Boltzmann law (see the Radiation chapter):

$$E_{out} \approx \varepsilon \cdot \sigma_{SB} \cdot T_m^4 \qquad (11.7)$$

where $\sigma_{SB} = 5.67\text{x}10^{-8}$ W·m^{-2}·K^{-4} is the Stefan-Boltzmann constant, and $\varepsilon \approx 0.9$ is effective emissivity (see the Climate chapter). When you use $z = z_m = 5.5$ km in eqs. (11.1 - 11.3) to get T_m vs. latitude for use in eq. (11.7), the result is E_{out} vs. ϕ, as plotted in Fig. 11.10.

Net Radiation

The net radiative heat flux per vertical column of atmosphere is the input minus the output:

$$E_{net} = E_{in} - E_{out} \qquad (11.8)$$

which is plotted in Fig. 11.10 for our toy model.

Solved Example
What is E_{net} at the Eiffel Tower latitude?

Solution
Given: $\phi = 48.8590°$, $z = 5.5$ km
$E_{in} = 171.5$ W/m^2 from previous solved example.
Find: E_{net} = ? W/m^2
Use eq. (11.2): $b = (40°\text{C})\cdot[1 - (5.5\text{ km}/11\text{ km})] = 20°\text{C}$
Use eq.(11.3): $a = (-12°\text{C}) - (3.14°\text{C/km})\cdot(5.5\text{ km}) = -29.27°\text{C}$
(continued in next column)

Solved Example
Estimate the annual average solar energy absorbed at the latitude of the Eiffel Tower in Paris, France.

Solution
Given: $\phi = 48.8590°$ (at the Eiffel tower)
Find: E_{in} = ? W/m^2

Use eq. (11.5):
$E_{insol} = (298\text{ W/m}^2) + (123\text{ W/m}^2)\cdot\cos(2 \cdot 48.8590°)$
$= (298\text{ W/m}^2) - (16.5\text{ W/m}^2) = 281.5\text{ W/m}^2$
Use eq. (11.6):
$E_{in} = 281.5\text{ W/m}^2 - 110.0\text{ W/m}^2 =$ **171.5 W/m^2**

Check: Units OK. Agrees with Fig. 11.10.
Discussion: The actual annual average E_{in} at the Eiffel Tower would probably differ from this zonal avg.

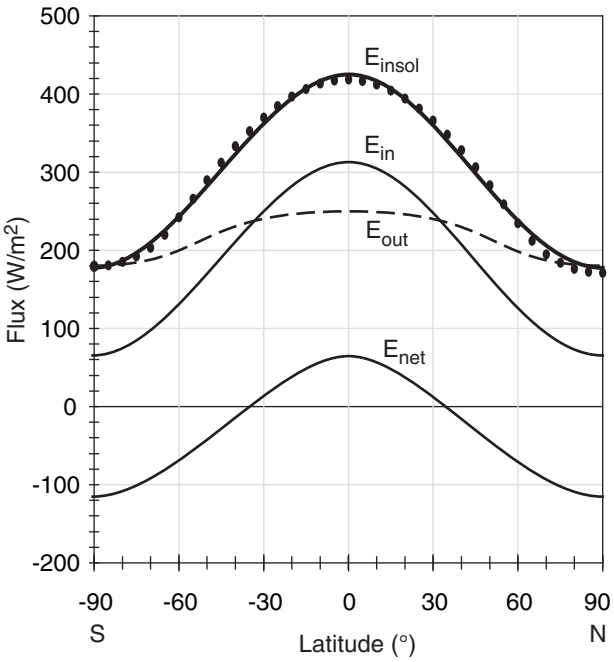

Figure 11.10
Data points are insolation vs. latitude from Fig. 11.9b. Eq. 11.5 approximates this insolation E_{insol} (thick black line). E_{in} is the solar radiation that is absorbed (thin solid line, from eq. 11.6). E_{out} is outgoing terrestrial (IR) radiation (dashed; from eq. 11.7). Net flux $E_{net} = E_{in} - E_{out}$. Positive E_{net} causes heating; negative causes cooling.

Solved Example *(continuation)*
Use eq. (11.1): $T_m = -18.73$ °C = 254.5 K
Use eq.(11.7): $E_{out} = (0.9)\cdot(5.67\text{x}10^{-8}\text{W·m}^{-2}\text{·K}^{-4})\cdot(254.5\text{ K})^4$
$= 213.8$ W/m^2
Use eq. (11.8): $E_{net} = (171.5\text{ W/m}^2) - (213.8\text{ W/m}^2)$
$=$ **−42.3 W/m^2**

Check: Units OK. Agrees with Fig. 11.10
Discussion: Net radiative heat loss at Paris latitude. Must be compensated by winds blowing heat in.

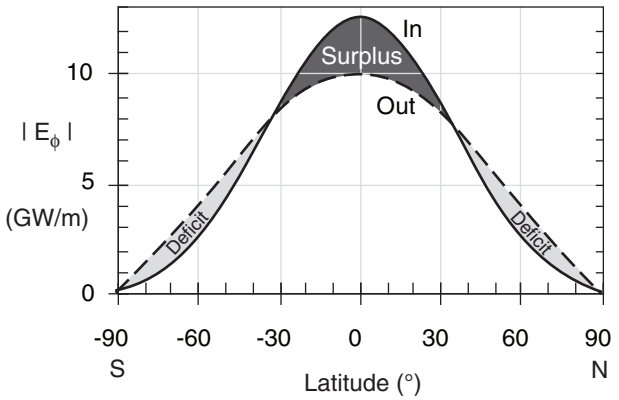

Figure 11.11
Zonally-integrated radiative forcings for absorbed incoming solar radiation (solid line) and emitted net outgoing terrestrial (IR) radiation (dashed line). The surplus balances the deficit.

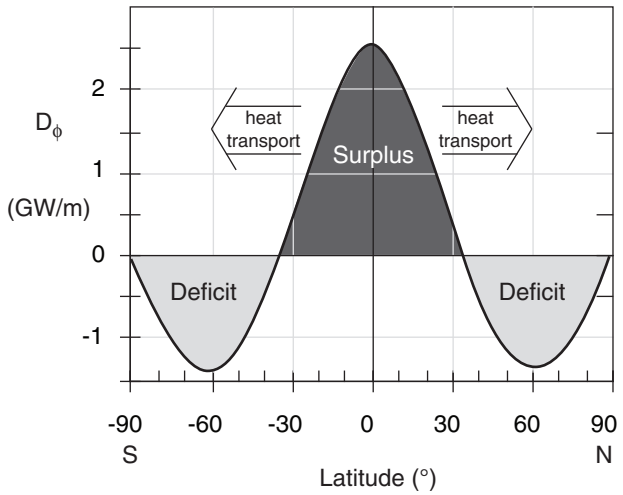

Figure 11.12
Difference between incoming and outgoing zonally-integrated radiative forcings on the Earth. Surplus balances deficits. This differential heating imposed on the Earth must be compensated by heat transport by the global circulation; otherwise, the tropics would keep getting hotter and the polar regions colder.

Solved Example

From the previous solved example, find the zonally-integrated differential heating at $\phi = 48.859°$.

Solution

Given: $E_{net} = -42.3$ W/m^2 , $\phi = 48.859°$ at Eiffel Tower
Find: D_ϕ = ? GW/m

Combine eqs. (11.8-11.10): $D_\phi = 2\pi \cdot R_{Earth} \cdot \cos(\phi) \cdot E_{net}$
$= 2(3.14159) \cdot (6.357 \times 10^6 \text{m}) \cdot \cos(48.859°) \cdot (-42.3 \text{ W/m}^2)$
$= -1.11 \times 10^9$ W/m = **–1.11 GW/m**

Check: Units OK. Agrees with Fig. 11.12.
Discussion: Net radiative heat loss at this latitude is compensated by warm Gulf stream and warm winds.

Radiative Forcing by Latitude Belt

Eq. (11.8) and Fig. 11.10 can be deceiving, because latitude belts have shorter circumference near the poles than near the equator. Namely, there are fewer square meters near the poles that experience the net deficit than there are near the equator that experience the net surplus.

To compensate for the shrinking latitude belts, multiply the radiative flux by the circumference of the belt $2\pi \cdot R_{Earth} \cdot \cos(\phi)$, to give a more appropriate zonally-integrated (i.e., summed over all x around the latitude circle) measure of radiative forcing E_ϕ vs. latitude ϕ:

$$E_\phi = 2\pi \cdot R_{Earth} \cdot \cos(\phi) \cdot E \qquad (11.9)$$

where E is the magnitude of outgoing or incoming radiative flux from eqs. (11.7 or 11.6), and R_{Earth} = 6371 km is the average Earth radius. These E_ϕ values are plotted in Fig. 11.11 in units of GW/m.

The difference D_ϕ between incoming and outgoing values of E_ϕ is plotted in Fig. 11.12.

$$D_\phi = E_{\phi\ in} - E_{\phi\ out} \qquad (11.10)$$

To interpret this curve, picture a sidewalk built around the world along a parallel. If this sidewalk is 1 m wide, then Fig. 11.12 gives the number of gigawatts of net radiative power absorbed by the sidewalk, for sidewalks at different latitudes.

This curve shows the radiative differential heating. The areas under the positive and negative portions of the curve in Fig. 11.12 balance, leaving the Earth in overall equilibrium (neglecting global warming for now).

Heat Transport by the Global Circulation

The radiative imbalance between equator and poles in Fig. 11.12 drives atmospheric and oceanic circulations. These circulations act to undo the imbalance by removing the excess heat from the equator and depositing it near the poles (as per Le Chatelier's Principle). First, we can use the radiative differential heating to find how much global-circulation heat transport is needed. Then, we can examine the actual heat transport by atmospheric and oceanic circulations.

Transport Needed

The net meridional transport is zero at the poles by definition. Starting at the north pole and summing D_ϕ over all the "sidewalks" to any latitude ϕ of interest gives the total transport *Tr* needed for the global circulation to compensate all the radiative imbalances north of that latitude:

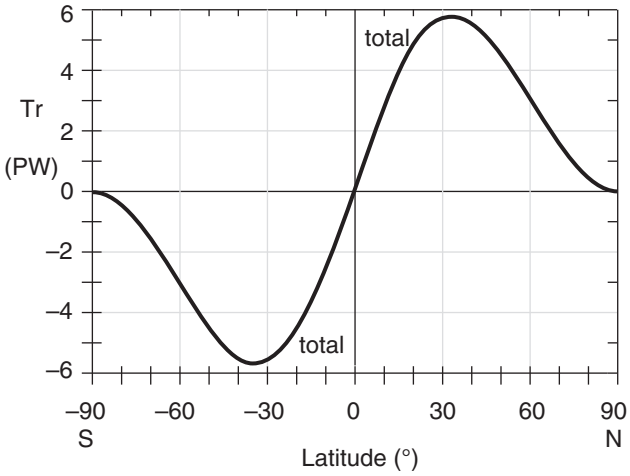

Figure 11.13
Needed heat transport Tr by the global circulation to compensate radiative differential heating, based on a simple "toy model". Agrees very well with achieved transport in Fig. 11.14.

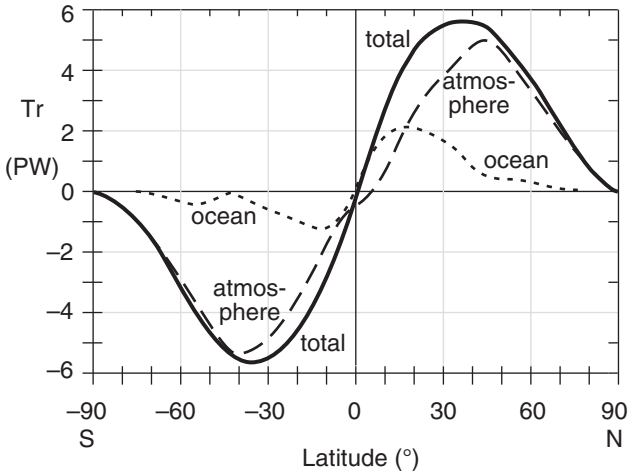

Figure 11.14
*Meridional heat transports: Satellite-observed total (solid line) & ocean estimates (dotted). Atmospheric (dashed) is found as a residual. 1 PW = 1 petaWatt = 10^{15} W. [Data from K. E. Trenberth and J. M. Caron, 2001: "J. Climate", **14**, 3433-3443.]*

$$Tr(\phi) = \sum_{\phi_o = 90°}^{\phi} (-D_\phi) \cdot \Delta y \qquad (11.11)$$

where Δy is the width of the sidewalk.

[Meridional distance Δy is related to latitude change $\Delta\phi$ by: Δy(km) = (111 km/°) · $\Delta\phi$ (°) .]

The resulting "needed transport" is shown in Fig. 11.13, based on the simple "toy model" temperature and radiation curves of the past few sections. The magnitude of this curve peaks at about 5.6 PW (1 petaWatt = 10^{15} W) at latitudes of about 35° North and South (positive *Tr* means northward transport).

Transport Achieved

Satellite observations of radiation to and from the Earth, estimates of heat fluxes to/from the ocean based on satellite observations of sea-surface temperature, and in-situ measurements of the atmosphere provide some of the transport data needed. Numerical forecast models are then used to tie the observations together and fill in the missing pieces. The resulting estimate of heat transport achieved by the atmosphere and ocean is plotted in Fig. 11.14.

Ocean currents dominate the total heat transport only at latitudes 0 to 17°N, and remain important up to latitudes of ± 40°. In the atmosphere, the Hadley circulation is a dominant contributor in the tropics and subtropics, while the Rossby waves dominate atmospheric transport at mid-latitudes.

Knowing that global circulations undo the heating imbalance raises another question. How does the differential heating in the atmosphere drive the winds in those circulations? That is the subject of the next three sections.

Solved Example

What total heat transports by the atmosphere and ocean circulations are needed at 50°N latitude to compensate for all the net radiative cooling between that latitude and the North Pole? The differential heating as a function of latitude is given in the following table (based on the toy model):

Lat (°)	D_ϕ (GW/m)	Lat (°)	D_ϕ (GW/m)
90	0	65	–1.380
85	–0.396	60	–1.403
80	–0.755	55	–1.331
75	–1.049	50	–1.164
70	–1.261	45	–0.905

Solution

Given: ϕ = 50°N. D_ϕ data in table above.
Find: *Tr* = ? PW

Use eq. (11.11). Use sidewalks (belts) each of width $\Delta\phi$ = 5°. Thus, Δy (m) = (111,000 m/°) · (5°) = 555,000 m is the sidewalk width. If one sidewalk spans 85 - 90°, and the next spans 80 - 85° etc, then the values in the table above give D_ϕ along the edges of the sidewalk, not along the middle. A better approximation is to average the D_ϕ values from each edge to get a value representative of the whole sidewalk. Using a bit of algebra, this works out to:

Tr = – (555000 m)· [(0.5)·0.0 – 0.396 – 0.755 – 1.049
– 1.261 – 1.38 – 1.403 – 1.331 – (0.5)·1.164] (GW/m)
Tr = (555000 m)·[8.157 GW/m] = **4.527 PW**

Check: Units OK (10^6 GW = 1 PW). Agrees with Fig. 11.14. **Discussion**: This northward heat transport warms all latitudes north of 50°N, not just one sidewalk. The warming per sidewalk is $\Delta Tr/\Delta\phi$.

ON DOING SCIENCE • Residuals

If something you cannot measure contributes to things you can measure, then you can estimate the unknown as the **residual** (i.e., difference) from all the knowns. This is a valid scientific approach. It was used in Fig. 11.14 to estimate the atmospheric portion of global heat transport.

CAUTION: When using this approach, your residual not only includes the desired signal, but it also includes the sums of all the errors from the items you measured. These errors can easily accumulate to cause a "noise" that is larger than the signal you are trying to estimate. For this reason, **error estimation** and **error propagation** (see Appendix A) should always be done when using the method of residuals.

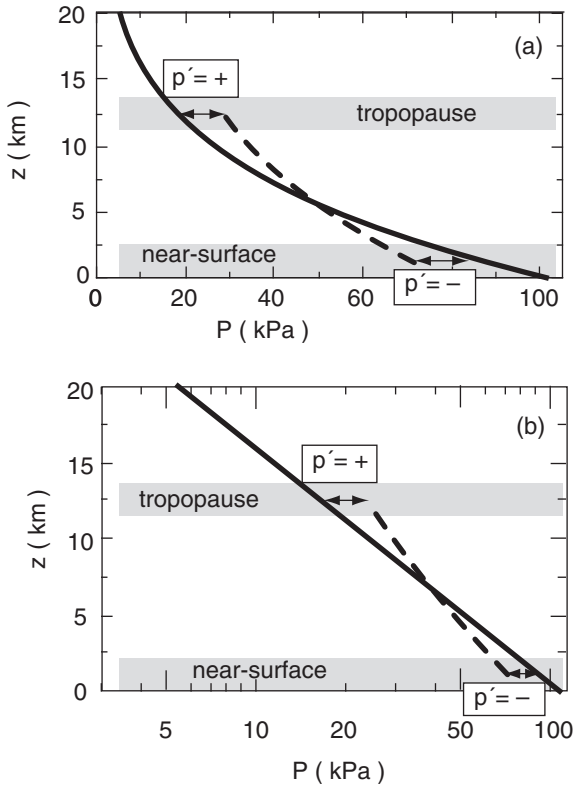

Figure 11.15
Background hydrostatic pressure (solid line), and non-hydrostatic column of air (dashed line) with pressure perturbation p′ that deviates from the hydrostatic pressure $P_{hydrostatic}$ at most heights z. In this example, even though p′ is positive (+) near the tropopause, the total pressure in the column ($P_{column} = P_{hydrostatic} + p'$) at the tropopause is still less than the surface pressure. The same curve is plotted as (a) linear and as (b) semilog.

PRESSURE PROFILES

The following fundamental concepts can help you understand how the global circulation works:

- non-hydrostatic pressure couplets due to horizontal winds and vertical buoyancy,
- hydrostatic thermal circulations,
- geostrophic adjustment, and
- the thermal wind.

The first two concepts are discussed in this section. The last two are discussed in subsequent sections.

Non-hydrostatic Pressure Couplets

Consider a background reference environment with no vertical acceleration (i.e., **hydrostatic**). Namely, the pressure-decrease with height causes an upward pressure-gradient force that exactly balances the downward pull of gravity, causing zero net vertical force on the air (see Fig. 1.12 and eq. 1.25).

Next, suppose that immersed in this environment is a column of air that might experience a different pressure decrease (Fig. 11.15); i.e., **non-hydrostatic pressures**. At any height, let $p' = P_{column} - P_{hydrostatic}$ be the deviation of the actual pressure in the column from the theoretical hydrostatic pressure in the environment. Often a positive p' in one part of the atmospheric column is associated with negative p' elsewhere. Taken together, the positive and negative p's form a **pressure couplet**.

Non-hydrostatic p' profiles are often associated with non-hydrostatic vertical motions through Newton's second law. These non-hydrostatic motions can be driven by horizontal convergence and divergence, or by buoyancy (a vertical force). These two effects create opposite pressure couplets, even though both can be associated with upward motion, as explained next.

Horizontal Convergence/Divergence

If external forcings cause air near the ground to converge horizontally, then air molecules accumulate. As density ρ increases according to eq. (10.60), the ideal gas law tells us that p' will also become positive (Fig. 11.16a).

Positive p' does two things: it (1) decelerates the air that was converging horizontally, and (2) accelerates air vertically in the column. Thus, the pressure perturbation causes **mass continuity** (horizontal inflow near the ground balances vertical outflow).

Similarly, an externally imposed horizontal divergence at the top of the troposphere would lower the air density and cause negative p', which would also accelerate air in the column upward. Hence, we

expect upward motion (W = positive) to be driven by a p' couplet, as shown in Fig. 11.16a.

Buoyant Forcings

For a different scenario, suppose air in a column is positively buoyant, such as in a thunderstorm where water-vapor condensation releases lots of latent heat. This vertical buoyant force creates upward motion (i.e., warm air rises, as in Fig. 11.16b).

As air in the thunderstorm column moves away from the ground, it removes air molecules and lowers the density and the pressure; hence, p' is negative near the ground. This suction under the updraft causes air near the ground to horizontally converge, thereby conserving mass.

Conversely, at the top of the troposphere where the thunderstorm updraft encounters the even warmer environmental air in the stratosphere, the upward motion rapidly decelerates, causing air molecules to accumulate, making p' positive. This pressure perturbation drives air to diverge horizontally near the tropopause, causing the outflow in the anvil-shaped tops of thunderstorms.

The resulting pressure-perturbation p' couplet in Fig. 11.16b is opposite that in Fig. 11.16a, yet both are associated with upward vertical motion. The reason for this pressure-couplet difference is the difference in driving mechanism: imposed horizontal convergence/divergence vs. imposed vertical buoyancy.

Similar arguments can be made for downward motions. For either upward or downward motions, the pressure couplets that form depend on the type of forcing. We will use this process to help explain the pressure patterns at the top and bottom of the troposphere.

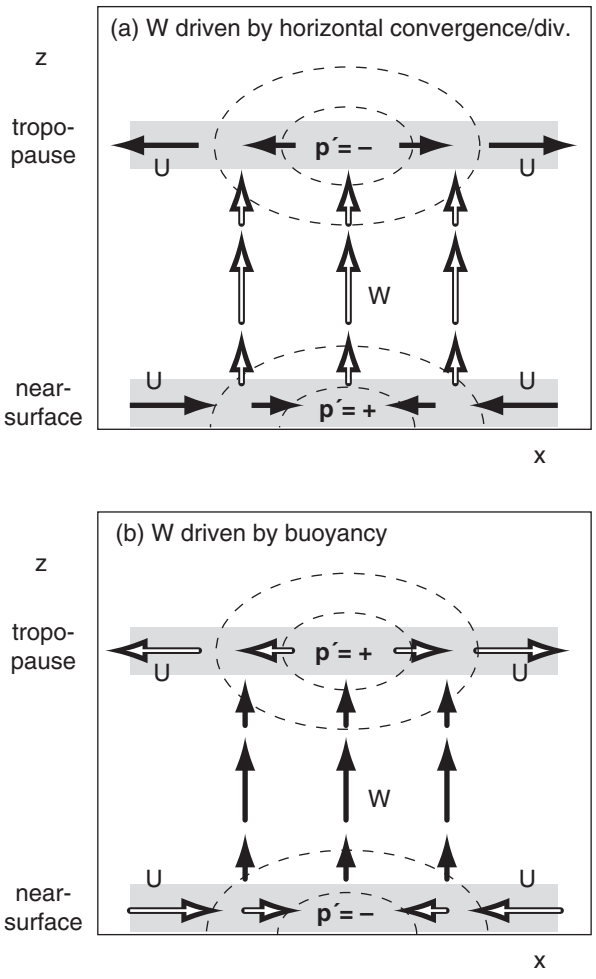

Figure 11.16
(a) Vertical motions driven by horizontal convergence or divergence. (b) Vertical motions driven by buoyancy. In both figures, black arrows indicate the cause (the driving force), and white arrows are the effect (the response). p′ is the pressure perturbation (deviation from hydrostatic), and thin dashed lines are isobars of p′. U and W are horizontal and vertical velocities. In both figures, the responding flow (white arrows) is driven down the pressure-perturbation gradient, away from positive p′ and toward negative p′.

Hydrostatic Thermal Circulations

Cold columns of air tend to have high surface pressures, while warm columns have low surface pressures. Figs. 11.17 illustrate how this happens.

Consider initial conditions (Fig. 11.17i) of two equal columns of air at the same temperature and with the same number of air molecules in each column. Since pressure is related to the mass of air above, this means that both columns A and B have the same initial pressure (100 kPa) at the surface.

Next, suppose that some process heats one column relative to the other (Fig. 11.17ii). Perhaps condensation in a thunderstorm cloud causes latent heating of column B, or infrared radiation cools column A. After both columns have finished expanding or contracting due to the temperature change, they will reach new hydrostatic equilibria for their respective temperatures.

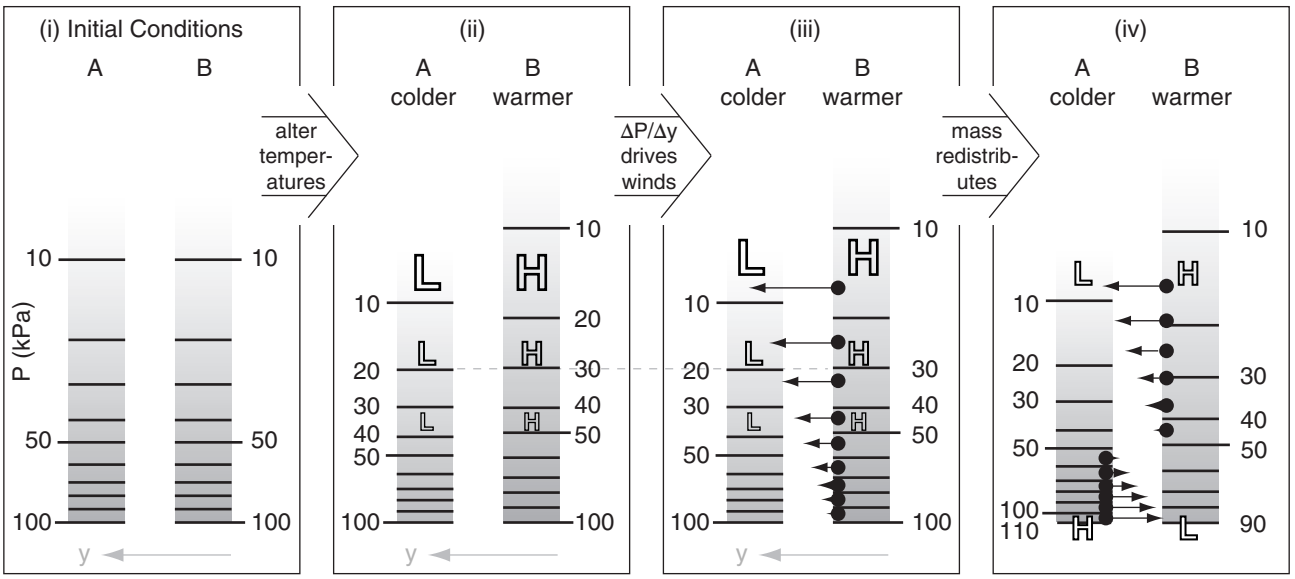

Figure 11.17
Formation of a thermal circulation. The response of two columns of air that are heated differently is that the warmer air column develops a low pressure perturbation at the surface and a high pressure perturbation aloft. Response of the cold column is the opposite. Notation: H = high pressure perturbation, L = low; black dots represents air parcels; thin arrows are winds.

The hypsometric equation (see Chapter 1) says that pressure decreases more rapidly with height in cold air than in warm air. Thus, although both columns have the same surface pressure because they contain the same number of molecules, the higher you go above the surface, the greater is the pressure difference between warm and cold air. In Fig. 11.17ii, the printed size of the "H" and "L" indicate the relative magnitudes of the high- and low-pressure perturbations p'.

The horizontal pressure gradient $\Delta P/\Delta y$ aloft between the warm and cold air columns drives horizontal winds from high toward low pressure (Fig. 11.17iii). Since winds are the movement of air molecules, this means that molecules leave the regions of high pressure-perturbation and accumulate in the regions of low. Namely, they leave the warm column, and move into the cold column.

Since there are now more molecules (i.e., more mass) in the cold column, it means that the surface pressure must be greater in the cold column (Fig. 11.17iv). Similarly, mass lost from the warm column results in lower surface pressure. This is called a **thermal low.**

A result (Fig. 11.17iv) is that, near the surface, high pressure in the cold air drives winds toward the low pressure in warm air. Aloft, high pressure-perturbation in the warm air drives winds towards low pressure-perturbation in the cold air. The resulting **thermal circulation** causes each column to gain as many air molecules as they lose; hence, they are in mass equilibrium.

This equilibrium circulation also transports heat. Air from the warm air column mixes into the cold column, and vice versa. This intermixing reduces the temperature contrast between the two columns, causing the corresponding equilibrium circulations to weaken. Continued destabilization (more latent heating or radiative cooling) is needed to maintain the circulation.

The circulations and mass exchange described above can be realized at the equator. At other latitudes, the exchange of mass is often slower (near the surface) or incomplete (aloft) because Coriolis force turns the winds to some angle away from the pressure-gradient direction. This added complication, due to geostrophic wind and geostrophic adjustment, is described next.

GEOSTROPHIC WIND & GEOSTROPHIC ADJUSTMENT

Ageostrophic Winds at the Equator

Air at the equator can move directly from high (ℍ) to low (𝕃) pressure (Fig. 11.18 - center part) under the influence of pressure-gradient force. Zero Coriolis force at the equator implies infinite geostrophic winds. But actual winds have finite speed, and are thus **ageostrophic** (not geostrophic).

Because such flows can happen very easily and quickly, equatorial air tends to quickly flow out of highs into lows, causing the pressure centers to neutralize each other. Indeed, weather maps at the equator show very little pressure variations zonally. One exception is at continent-ocean boundaries, where continental-scale differential heating can continually regenerate pressure gradients to compensate the pressure-equalizing action of the wind. Thus, very small pressure gradients can cause continental-scale (5000 km) monsoon circulations near the equator. Tropical forecasters focus on winds, not pressure.

If the large-scale pressure is uniform in the horizontal near the equator (away from monsoon circulations), then the horizontal pressure gradients disappear. With no horizontal pressure-gradient force, no large-scale winds can be driven there. However, winds can exist at the equator due to inertia — if the winds were first created geostrophically at nonzero latitude and then coast across the equator.

But at most other places on Earth, Coriolis force deflects the air and causes the wind to approach geostrophic or gradient values (see the Dynamics chapter). Geostrophic winds do not cross isobars, so they cannot transfer mass from highs to lows. Thus, significant pressure patterns (e.g., strong high and low centers, Fig. 11.18) can be maintained for long periods at mid-latitudes in the global circulation.

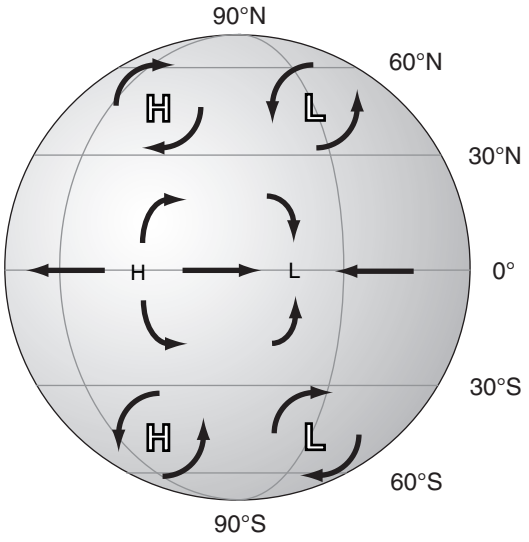

Figure 11.18
At the equator, winds flow directly from high (H) to low (L) pressure centers. At other latitudes, Coriolis force causes the winds to circulate around highs and lows. Smaller size font for H and L at the equator indicate weaker pressure gradients.

Definitions

The spatial distribution of wind speeds and directions is known as the **wind field**. Similarly, the spatial distribution of temperature is called the **temperature field**.

The **mass field** is the spatial distribution of air mass. As discussed in Chapter 1, pressure is a measure of the mass of air above. Thus, the term "mass field" generically means the spatial distribution of pressure (i.e., the **pressure field**) on a constant altitude chart, or of heights (the **height field**) on an isobaric surface.

In **baroclinic conditions** (where temperature changes in the horizontal), the hypsometric equation allows changes to the pressure field to be described

ON DOING SCIENCE •
The Scientific Method Revisited

"Like other exploratory processes, [the scientific method] can be resolved into a dialogue between fact and fancy, the actual and the possible; between what could be true and what is in fact the case. The purpose of scientific enquiry is not to compile an inventory of factual information, nor to build up a totalitarian world picture of Natural Laws in which every event that is not compulsory is forbidden. We should think of it rather as a logically articulated structure of justifiable beliefs about a Possible World — a story which we invent and criticize and modify as we go along, so that it ends by being, as nearly as we can make it, a story about real life."

- by Nobel Laureate Sir Peter Medawar (1982) *Pluto's Republic*. Oxford Univ. Press.

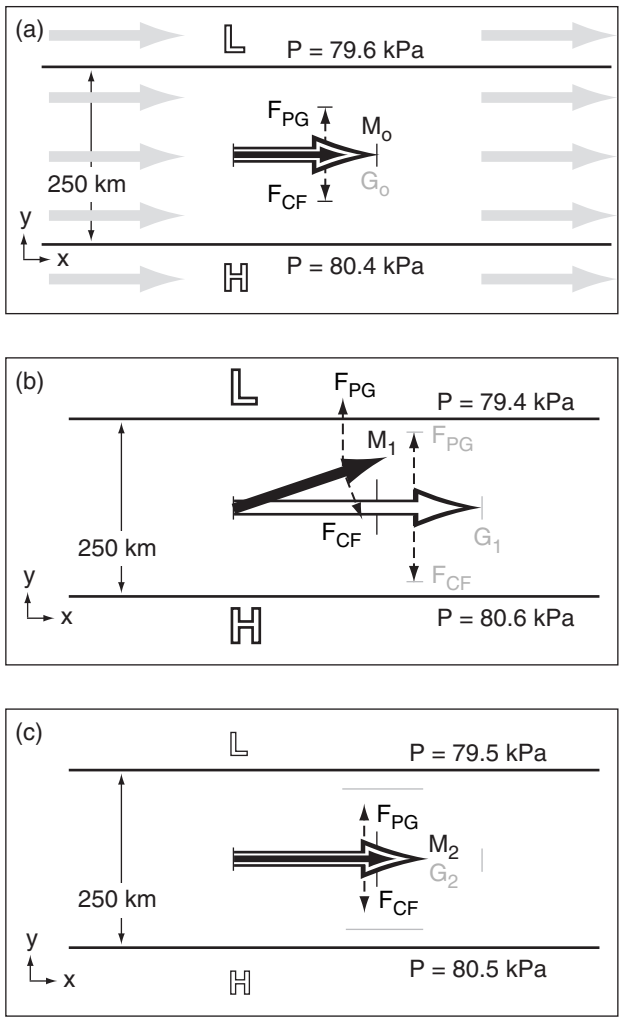

Figure 11.19
Example of geostrophic adjustment in the N. Hemisphere (not at equator). (a) Initial conditions, with the actual wind M (thick black arrow) in equilibrium with (equal to) the theoretical geostrophic value G (white arrow with black outline). (b) Transition. (c) End result at a new equilibrium. Dashed lines indicate forces F. Each frame focuses on the region of disturbance.

Solved Example

Find the internal Rossby radius of deformation in a standard atmosphere at 45°N.

Solution

Given: $\phi = 45°$. Standard atmosphere from Chapter 1:
$T(z = Z_T = 11 \text{ km}) = -56.5°C$, $T(z=0) = 15°C$.
Find: $\lambda_R = ?$ km

First, find $f_c = (1.458 \times 10^{-4} \text{ s}^{-1}) \cdot \sin(45°) = 1.031 \times 10^{-4} \text{ s}^{-1}$

Next, find the average temperature and temperature difference across the depth of the troposphere:
$T_{avg} = 0.5 \cdot (-56.5 + 15.0)°C = -20.8°C = 252$ K
$\Delta T = (-56.5 - 15.0)$ °C = –71.5°C across $\Delta z = 11$ km

(continued on next page)

by changes in the temperature field. Similarly, the thermal wind relationship (described later in this chapter) relates changes in the wind field to changes in the temperature field.

Geostrophic Adjustment - Part 1

The tendency of non-equatorial winds to approach geostrophic values (or gradient values for curved isobars) is a very strong process in the Earth's atmosphere. If the actual winds are not in geostrophic balance with the pressure patterns, then both the winds and the pressure patterns tend to change to bring the winds back to geostrophic (another example of Le Chatelier's Principle). This process is called **geostrophic adjustment**.

Picture a wind field (grey arrows in Fig. 11.19a) initially in geostrophic equilibrium ($M_o = G_o$) at altitude 2 km above sea level (thus, no drag at ground). We will focus on just one of those arrows (the black arrow in the center), but all the wind vectors will march together, performing the same maneuvers.

Next, suppose an external process increases the horizontal pressure gradient to the value shown in Fig. 11.19b, with the associated faster geostrophic wind speed G_1. With pressure-gradient force F_{PG} greater than Coriolis force F_{CF}, the force imbalance turns the wind M_1 slightly toward low pressure and accelerates the air (Fig. 11.19b).

The component of wind M_1 from high to low redistributes air mass (moves air molecules) in the horizontal, weakening the pressure field and thereby reducing the theoretical geostrophic wind (G_2 in Fig. 11.19c). Thus, **the mass field adjusts to the wind field**. Simultaneously the actual wind accelerates to M_2. Thus, **the wind field adjusts to the mass field**. After both fields have adjusted, the result is $M_2 > M_o$ and $G_2 < G_1$, with $M_2 = G_2$.

These adjustments are strongest near the disturbance (i.e., the region forced out of equilibrium), and gradually weaken with distance. The e-folding distance, beyond which the disturbance is felt only a little, is called the **internal Rossby radius of deformation**, λ_R:

$$\lambda_R = \frac{N_{BV} \cdot Z_T}{f_c} \qquad \bullet(11.12)$$

where f_c is the Coriolis parameter, Z_T is the depth of the troposphere, and N_{BV} is the Brunt-Väisälä frequency. This radius relates buoyant and inertial forcings. It is on the order of 1300 km.

For large-scale disturbances (wavelength $\lambda > \lambda_R$), most of the adjustment is in the wind field. For small-scale disturbances ($\lambda < \lambda_R$), most of the adjustment is in the temperature or pressure fields. For mesoscales, all fields adjust a medium amount.

Solved Example *(continuation)*
Find the Brunt-Väisälä frequency (see the Stability chapter). $N_{BV} = \sqrt{\frac{(9.8\text{m/s})}{252\text{K}}\left[\frac{-71.5\text{K}}{11000\text{m}} + 0.0098\frac{\text{K}}{\text{m}}\right]} = 0.0113\text{s}^{-1}$
where the temperature differences in square brackets can be expressed in either °C or Kelvin.
Finally, use eq. (11.12): $\lambda_R = (0.0113\ \text{s}^{-1})\cdot(11\ \text{km}) \ / \ (1.031\text{x}10^{-4}\ \text{s}^{-1}) =$ **1206 km**

Check: Units OK. Magnitude OK. Physics OK.
Discussion: When a cold-front over the Pacific approaches the steep mountains of western Canada, the front feels the influence of the mountains 1200 to 1300 km before reaching the coast, and begins to slow down.

THERMAL WIND RELATIONSHIP

Recall that horizontal temperature gradients cause vertically varying horizontal pressure gradients (Fig. 11.17), and that horizontal pressure gradients drive geostrophic winds. We can combine those concepts to see how horizontal temperature gradients drive vertically varying geostrophic winds. This is called the **thermal wind effect**.

This effect can be pictured via the slopes of isobaric surfaces (Fig. 11.20). If a horizontal temperature gradient is present, it changes the tilt of pressure surfaces with increasing altitude because the thickness between isobaric surfaces is greater in warmer air (see eq. 1.26, the hypsometric equation).

But geostrophic wind (U_g, V_g) is proportional to the tilt of the pressure surfaces (eq. 10.29). Thus, as shown in the Focus box on the next page, the **thermal wind relationship** is:

$$\frac{\Delta U_g}{\Delta z} \approx \frac{-|g|}{T_v \cdot f_c} \cdot \frac{\Delta T_v}{\Delta y} \qquad \bullet(11.13a)$$

$$\frac{\Delta V_g}{\Delta z} \approx \frac{|g|}{T_v \cdot f_c} \cdot \frac{\Delta T_v}{\Delta x} \qquad \bullet(11.13b)$$

where $|g| = 9.8\ \text{m}\cdot\text{s}^{-2}$ is gravitational acceleration magnitude, T_v is the virtual temperature (in Kelvins, and nearly equal to the actual temperature if the air is fairly dry), and f_c is the Coriolis parameter. The north-south temperature gradient alters the east-west geostrophic winds with height, and vice versa.

Because the atmosphere above the boundary layer is nearly in geostrophic equilibrium, the change of actual wind speed with height is nearly equal to the change of the geostrophic wind.

Thickness

The thickness between two different pressure surfaces is a measure of the average virtual temperature within that layer. For example, consider the two different pressure surfaces colored white in Fig.

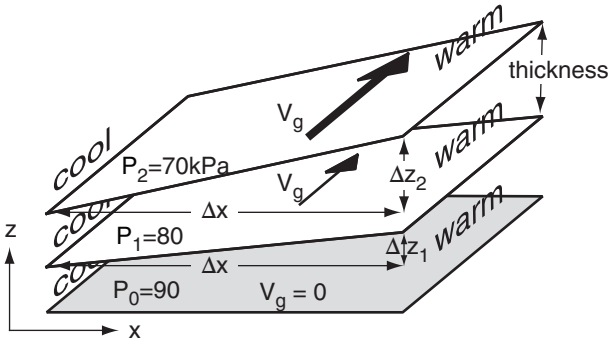

Figure 11.20
The three planes are surfaces of constant pressure (i.e., isobaric surfaces) in the N. Hemisphere. A horizontal temperature gradient tilts the pressure surfaces and causes the geostrophic wind to increase with height. Geostrophic winds are reversed in S. Hemisphere.

Solved Example
Temperature increases from 8°C to 12°C toward the east, across 100 km distance (Fig. 11.20). Find the vertical gradient of geostrophic wind, given $f_c = 10^{-4}\ \text{s}^{-1}$.

Solution
Assume: Dry air. Thus, $T_v = T$
Given: $\Delta T = 12 - 8°\text{C} = 4°\text{C}$, $\Delta x = 100$ km,
$T = 0.5\cdot(8+12°\text{C}) = 10°\text{C} = 283$ K, $f_c = 10^{-4}\ \text{s}^{-1}$.
Find: $\Delta U_g/\Delta z$ & $\Delta V_g/\Delta z$ = ? (m/s)/km

Use eq. (11.13a):

$$\frac{\Delta U_g}{\Delta z} \approx \frac{-(9.8\text{m/s}^2)}{(283K)\cdot(10^{-4}\text{s}^{-1})}\cdot(0°\text{C/km}) = 0\ \text{(m/s)/km}$$

Thus, U_g **= uniform with height**.
Use eq. (11.13b):

$$\frac{\Delta V_g}{\Delta z} \approx \frac{(9.8\text{m/s}^2)}{(283K)\cdot(10^{-4}\text{s}^{-1})}\cdot\frac{(4°\text{C})}{(100\text{km})} = \textbf{13.9 (m/s)/km}$$

Check: Units OK. Physics OK. Agrees with Fig.
Discussion: Each kilometer gain in altitude gives a 13.9 m/s increase in northward geostrophic wind speed. For example, if the wind at the surface is –3.9 m/s (i.e., light from the north), then the wind at 1 km altitude is 10 m/s (strong from the south).

BEYOND ALGEBRA • Thermal Wind Effect

Problem: Derive Thermal Wind eq. (11.13a).

Solution: Start with the definitions of geostrophic wind (10.26a) and hydrostatic balance (1.25b):

$$U_g = -\frac{1}{\rho \cdot f_c}\frac{\partial P}{\partial y} \quad \text{and} \quad \rho \cdot |g| = -\frac{\partial P}{\partial z}$$

Replace the density in both eqs using the ideal gas law (1.20). Thus:

$$\frac{U_g \cdot f_c}{T_v} = -\frac{\Re_d}{P}\frac{\partial P}{\partial y} \quad \text{and} \quad \frac{|g|}{T_v} = -\frac{\Re_d}{P}\frac{\partial P}{\partial z}$$

Use $(1/P)\cdot\partial P = \partial \ln(P)$ from calculus to rewrite both:

$$\frac{U_g \cdot f_c}{T_v} = -\Re_d \frac{\partial \ln(P)}{\partial y} \quad \text{and} \quad \frac{|g|}{T_v} = -\Re_d \frac{\partial \ln(P)}{\partial z}$$

Differentiate the left eq. with respect to z:

$$\frac{\partial}{\partial z}\left(\frac{U_g \cdot f_c}{T_v}\right) = -\Re_d \frac{\partial \ln(P)}{\partial y\ \partial z}$$

and the right eq. with respect to y:

$$\frac{\partial}{\partial y}\left(\frac{|g|}{T_v}\right) = -\Re_d \frac{\partial \ln(P)}{\partial y\ \partial z}$$

But the right side of both eqs are identical, thus we can equate the left sides to each other:

$$\frac{\partial}{\partial z}\left(\frac{U_g \cdot f_c}{T_v}\right) = \frac{\partial}{\partial y}\left(\frac{|g|}{T_v}\right)$$

Next, do the indicated differentiations, and rearrange to get the exact relationship for thermal wind:

$$\boxed{\frac{\partial U_g}{\partial z} = -\frac{|g|}{T_v \cdot f_c}\frac{\partial T_v}{\partial y} + \frac{U_g}{T_v}\left(\frac{\partial T_v}{\partial z}\right)}$$

The last term depends on the geostrophic wind speed and the lapse rate, and has magnitude of 0 to 30% of the first term on the right. If we neglect the last term, we get the approximate thermal wind relationship:

$$\boxed{\frac{\partial U_g}{\partial z} \approx -\frac{|g|}{T_v \cdot f_c}\frac{\partial T_v}{\partial y}} \qquad (11.13a)$$

Discussion: A **barotropic** atmosphere is when the geostrophic wind does not vary with height. Using the exact equation above, we see that this is possible only when the two terms on the right balance.

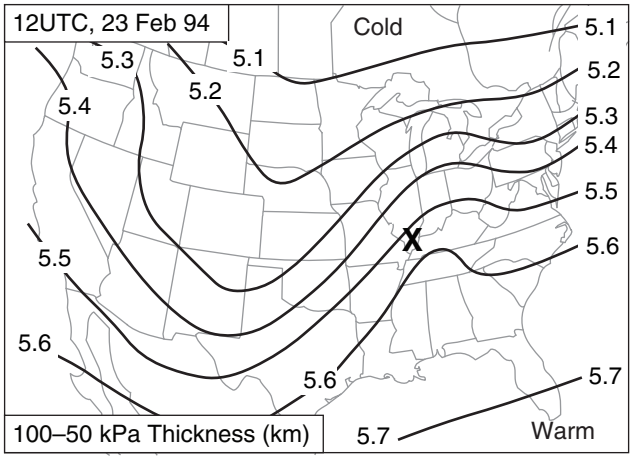

Figure 11.21
100–50 kPa thickness (km), valid at 12 UTC on 23 Feb 94. X marks the location of a surface low-pressure center.

11.20. The air is warmer in the east than in the west. Thus, the thickness of that layer is greater in the east than in the west.

Maps of thickness are used in weather forecasting. One example is the "100 to 50 kPa thickness" chart, such as shown in Fig. 11.21. This is a map with contours showing the thickness between the 100 kPa and 50 kPa isobaric surfaces. For such a map, regions of low thickness correspond to regions of cold temperature, and vice versa. It is a good indication of average temperature in the bottom half of the troposphere, and is useful for identifying airmasses and fronts (discussed in the next chapter).

Define **thickness** TH as

$$TH = z_{P2} - z_{P1} \qquad \bullet(11.14)$$

where z_{P2} and z_{P1} are the heights of the P_2 and P_1 isobaric surfaces.

Thermal Wind

The thermal wind relationship can be applied over the same layer of air bounded by isobaric surfaces as was used to define thickness. By manipulating eqs. (10.29), we find:

$$U_{TH} = U_{G2} - U_{G1} = -\frac{|g|}{f_c}\frac{\Delta TH}{\Delta y} \qquad \bullet(11.15a)$$

$$V_{TH} = V_{G2} - V_{G1} = +\frac{|g|}{f_c}\frac{\Delta TH}{\Delta x} \qquad \bullet(11.15b)$$

where subscripts *G2* and *G1* denote the geostrophic winds on the P_2 and P_1 pressure surfaces, $|g|$ is gravitational-acceleration magnitude, and f_c is the Coriolis parameter.

The variables U_{TH} and V_{TH} are known as the **thermal wind components**. Taken together (U_{TH}, V_{TH}) they represent the vector difference between the geostrophic winds at the top and bottom pressure surfaces. **Thermal wind magnitude** M_{TH} is:

$$M_{TH} = \sqrt{U_{TH}^2 + V_{TH}^2} \tag{11.16}$$

In Fig. 11.20, this vector difference happened to be in the same direction as the geostrophic wind. But this is not usually the case, as illustrated in Fig. 11.22.

Given an isobaric surface P_1 (medium grey in Fig. 11.22), with a height contour shown as the dashed line. The geostrophic wind G_1 on the surface is parallel to the height contour, with low heights to its left (N. Hemisphere). Isobaric surface P_2 (for $P_2 < P_1$) is also plotted (light grey). Cold air to the west is associated with a thickness of TH = 5 km between the two pressure surfaces. To the east, warm air has thickness 7 km. These thicknesses are added to the bottom pressure surface, to give the corner altitudes of the upper surface. On that upper surface are shown a height contour (dashed line) and the geostrophic wind vector G_2. We see that $G_2 > G_1$ be-

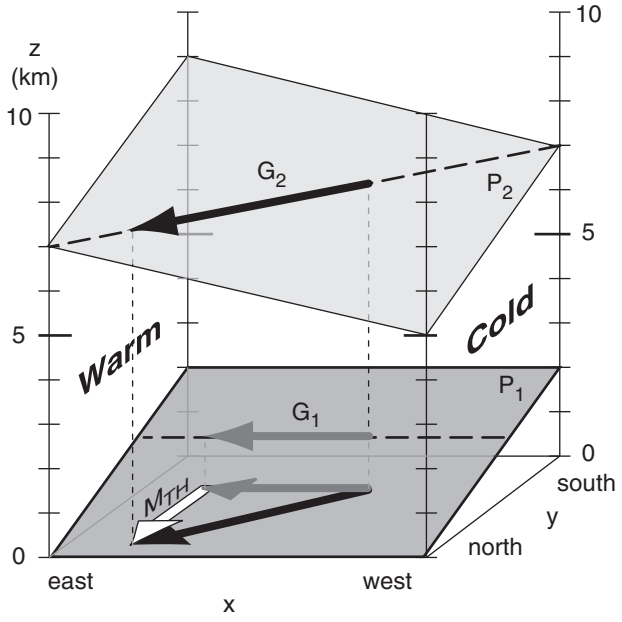

Figure 11.22
Relationship between the thermal wind M_{TH} and the geostrophic winds G on isobaric surfaces P. Viewpoint is from north of the air column.

Solved Example

Suppose the thickness of the 100 - 70 kPa layer is 2.9 km at one location, and 3.0 km at a site 500 km to the east. Find the components of the thermal wind vector, given $f_c = 10^{-4}$ s^{-1}.

Solution

Assume: No north-south thickness gradient.
Given: TH_1 = 2.9 km, TH_2 = 3.0 km,
Δx = 500 km, $f_c = 10^{-4}$ s^{-1}.
Find: U_{TH} = ? m/s, V_{TH} = ? m/s

Use eq. (11.15a): U_{TH} = **0 m/s**.
Use eq. (11.15b):

$$V_{TH} = \frac{g}{f_c}\frac{\Delta TH}{\Delta x} = \frac{(9.8 \text{ms}^{-2})\cdot(3.0-2.9)\text{km}}{(10^{-4}\text{s}^{-1})\cdot(500\text{km})}$$

$$= \textbf{19.6 m/s}$$

Check: Units OK. Physics OK. Agrees with Fig. 11.22.
Discussion: There is no east-west thermal wind component because the thickness does not change in the north-south direction. The positive sign of V_{TH} means a wind from south to north, which agrees with the rule that the thermal wind is parallel to the thickness contours with cold air to its left (west, in this example).

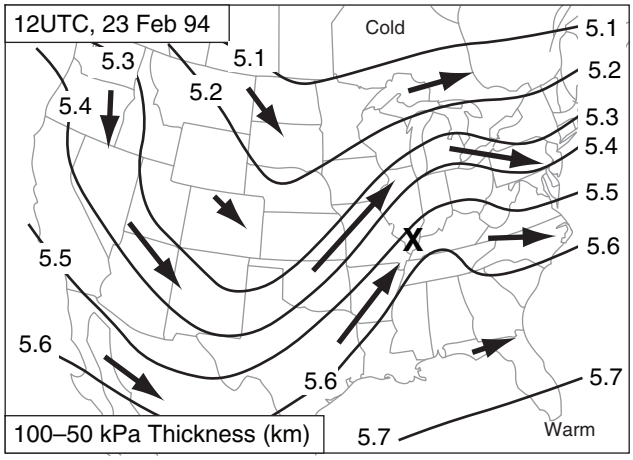

Figure 11.23
100–50 kPa thickness (smooth black curves, in units of km), with thermal wind vectors added. Larger vectors qualitatively denote stronger thermal winds.

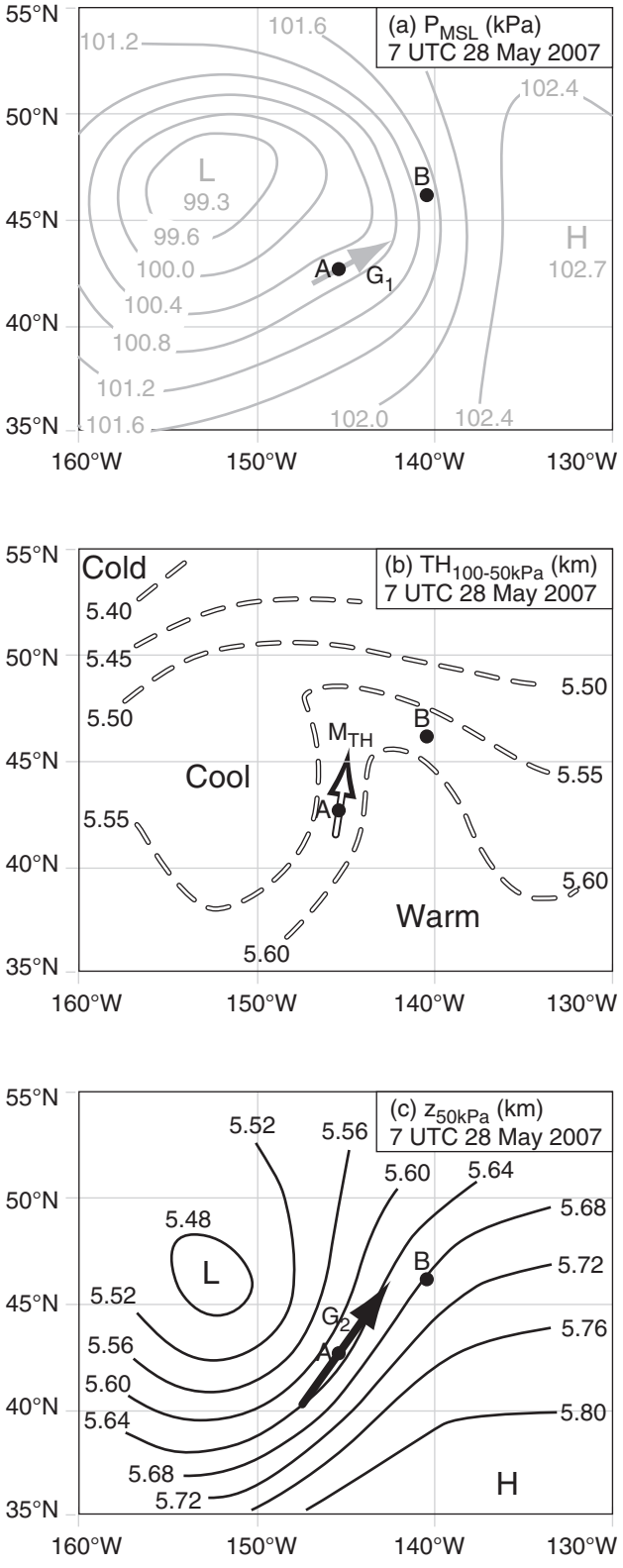

Figure 11.24
Weather maps for a thermal-wind case-study. (a) Mean sea-level pressure (kPa), as a surrogate for height of the 100 kPa surface. (b) Thickness (km) of the layer between 100 kPa to 50 kPa isobaric surfaces. (c) Geopotential heights (km) of the 50 kPa isobaric surface.

cause the top surface has greater slope than the bottom. The thermal wind is parallel to the thickness contours with cold to the left (white arrow). This thermal wind is the vector difference between the geostrophic winds at the two pressure surfaces, as shown in the projection on the ground.

Eqs. (11.15) imply that the thermal wind is parallel to the thickness contours, with cold temperatures (low thickness) to the left in the N. Hemisphere (Fig. 11.23). Closer packing of the thickness lines gives stronger thermal winds because the horizontal temperature gradient is larger there.

Thermal winds on a thickness map behave analogously to geostrophic winds on a constant pressure or height map, making their behavior a bit easier to remember. However, while it is possible for actual winds to equal the geostrophic wind, there is no real wind that equals the thermal wind. The thermal wind is just the vector difference between geostrophic winds at two different heights or pressures.

Case Study

Figs. 11.24 show how geostrophic winds and thermal winds can be found on weather maps, and how to interpret the results. These maps may be copied onto transparencies and overlain.

Fig. 11.24a is a weather map of pressure at sea level in the N. Hemisphere, at a location over the northeast Pacific Ocean. As usual, L and H indicate low- and high-pressure centers. At point A, we can qualitatively draw an arrow (grey) showing the theoretical geostrophic (G_1) wind direction; namely, it is parallel to the isobars with low pressure to its left.

Recall that pressures on a constant height surface (such as at height $z = 0$ at sea level) are closely related to geopotential heights on a constant pressure surface. So we can be confident that a map of 100 kPa heights would look very similar to Fig. 11.24a.

Fig. 11.24b shows the 100 - 50 kPa thickness map, valid at the same time and place. The thickness between the 100 and the 50 kPa isobaric surfaces is about 5.6 km in the warm air, and only 5.4 km in the cold air. The white arrow qualitatively shows the thermal wind M_{TH}, as being parallel to the thickness lines with cold temperatures to its left.

Fig. 11.24c is a weather map of geopotential heights of the 50 kPa isobaric surface. L and H indicate low and high heights. The black arrow at A shows the geostrophic wind (G_2), drawn parallel to the height contours with low heights to its left.

If we wished, we could have calculated quantitative values for G_1, G_2, and M_{TH}, utilizing the scale that 5° of latitude equals 555 km. [*CAUTION: This scale does not apply to longitude, because the meridians get closer together as they approach the poles. However,*

once you have determined the scale (map mm : real km) based on latitude, you can use it to good approximation in any direction on the map.]

Back to the thermal wind: if you add the geostrophic vector from Fig. 11.24a with the thermal wind vector from Fig. 11.24b, the result should equal the geostrophic wind vector in Fig. 11.24c. This is shown in the solved example.

Although we will study much more about weather maps and fronts in the next few chapters, I will interpret these maps for you now.

Point A on the maps is near a cold front. From the thickness chart, we see cold air west and northwest of point A. Also, knowing that winds rotate counterclockwise around lows in the N. Hemisphere (see Fig. 11.24a), I can anticipate that the cool air will advance toward point A. Hence, this is a region of **cold-air advection**. Associated with this cold-air advection is **backing of the wind** (i.e., turning counterclockwise with increasing height), which we saw was fully explained by the thermal wind.

Point B is near a warm front. I inferred this from the weather maps because warmer air is south of point B (see the thickness chart) and that the counterclockwise winds around lows are causing this warm air to advance toward point B. **Warm air advection** is associated with **veering of the wind** (i.e., turning clockwise with increasing height), again as given by the thermal wind relationship. I will leave it to you to draw the vectors at point B to prove this to yourself.

Solved Example

For Fig. 11.24, qualitatively verify that when vector M_{TH} is added to vector G_1, the result is vector G_2.

Solution

Given: the arrows from Fig. 11.24 for point A.
These are copied and pasted here.
Find: The vector sum of $G_1 + M_{TH} = ?$

Recall that to do a vector sum, move the tail of the second vector (M_{TH}) to be at the arrow head of the first vector (G_1). The vector sum is then the vector drawn from the tail of the first vector to the tip (head) of the second vector.

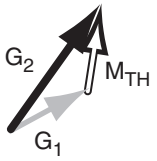

Check: Sketch is reasonable.
Discussion: The vector sum indeed equals vector G_2, as predicted by the thermal wind.

Thermal Wind & Geostrophic Adjustment - Part 2

As geostrophic winds adjust to pressure gradients, they move mass to alter the pressure gradients. Eventually, an equilibrium is approached (Fig. 11.25) based on the combined effects of geostrophic adjustment and the thermal wind. This figure is much more realistic than Fig. 11.17 because Coriolis force prevents the winds from flowing directly from high to low pressure.

With these concepts of:
- differential heating,
- nonhydrostatic pressure couplets due to horizontal winds and vertical buoyancy,
- hydrostatic thermal circulations,
- geostrophic adjustment, and
- the thermal wind,

we can now go back and explain why the global circulation works the way it does.

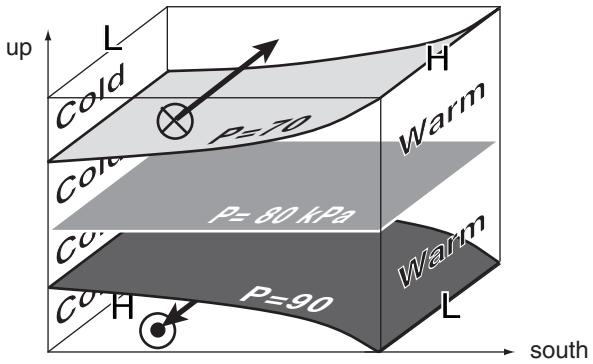

Figure 11.25
Typical equilibrium state after geostrophic adjustment. Isobaric surfaces are shaded, and recall that high heights of isobaric surfaces correspond to regions of high pressure on constant altitude surfaces. Arrows represent geostrophic wind.

Note: High (H) and low (L) pressure labels are relative to the average pressure at the same altitude where the labels are drawn. For example, the pressure at the top right is high relative to the pressure at the top left. Both of these top pressures are lower than both of the surface pressures, because pressure monotonically decreases with increasing height.

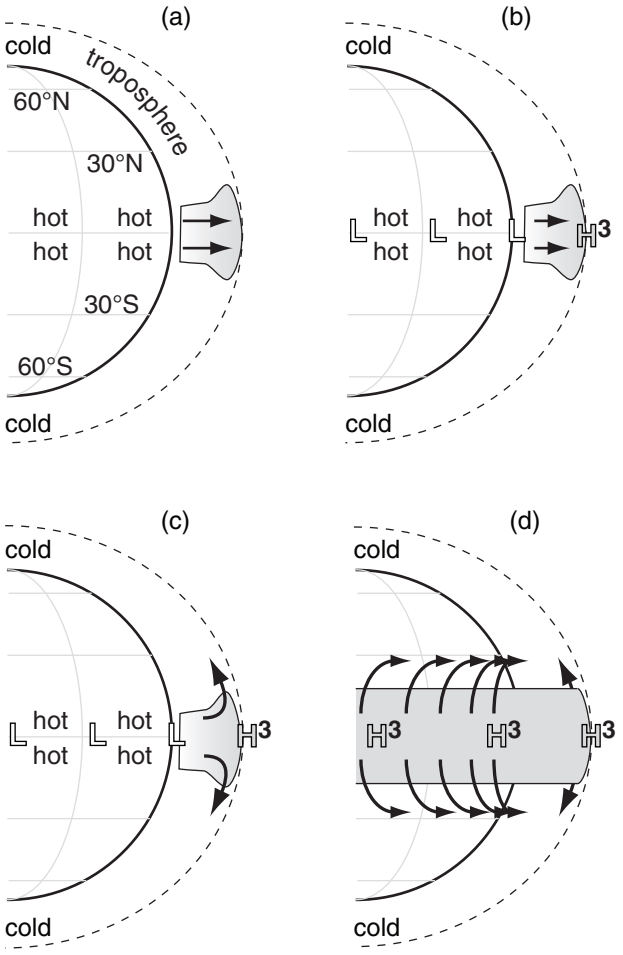

Figure 11.26
Application of physical concepts to explain the general circulation (see text). White-filled H and L indicate surface high and low pressure regions; grey-filled H and L are pressure regions near the tropopause. (continued on next pages)

ON DOING SCIENCE • Model Sensitivity

CAUTION: Whenever you find that a model has high **sensitivity** (i.e., the output result varies by large magnitude for small changes in the input parameter), you should be especially wary of the results. Small errors in the parameter could cause large errors in the result. Also, if the real atmosphere does not share the same sensitivity, then this is a clue that the model is poorly designed, and perhaps a better model should be considered.

Models are used frequently in meteorology — for example: numerical weather prediction models (Chapter 20) or climate-change models (Chapter 21). Most researchers who utilize models will perform careful **sensitivity studies** (i.e., compute the output results for a wide range of parameter values) to help them gauge the potential weaknesses of the model.

EXPLAINING THE GLOBAL CIRCULATION

Low Latitudes

Differential heating of the Earth's surface warms the tropics and cools the poles (Fig. 11.26a). The warm air near the equator can hold large amounts of water vapor evaporated from the oceans. Buoyancy force causes the hot humid air to rise over the equator. As the air rises, it cools and water vapor condenses, causing a belt of thick thunderstorm clouds around the equator (Fig. 11.26a) with heavy tropical precipitation.

The buoyantly forced vertical motion removes air molecules from the lower troposphere in the tropics, and deposits the air near the top of the troposphere. The result is a pressure couplet (Fig. 11.26b) of very high perturbation pressure p' (indicated with HHH or H^3 on the figures) near the tropopause, and low perturbation pressure (L in the figures) at the surface.

The belt of tropical high pressure near the tropopause forces air to diverge horizontally, forcing some air into the Northern Hemisphere and some into the Southern (Fig. 11.26c). With no Coriolis force at the equator, these winds are driven directly away from the high-pressure belt.

But as these high-altitude winds move away from the equator, they are increasingly affected by Coriolis force (Fig. 11.26d). This causes winds moving into the Northern Hemisphere to turn to their right, and those moving into the Southern Hemisphere to turn to their left.

But as the winds move further and further away from the equator, they are turned more and more to the east, creating the subtropical jet (Fig. 11.26e) at about 30° latitude. Coriolis force prevents these upper-level winds from getting further away from the equator than about 30° latitude (north and south), so the air accumulates and the pressure increases in those belts. When simulations of the general circulation impose a larger Coriolis force (as if the Earth spun faster), the convergence bands occur closer to the equator. For weaker Coriolis force, the convergence is closer to the poles. But for our Earth, the air converges at 30° latitude.

This pressure perturbation p' is labeled as HH or H^2 in Fig. 11.26e, to show that it is a positive pressure perturbation, but not as strong as the H^3 perturbation over the equator. Namely, the horizontal pressure gradient between H^3 and H^2 drives the upper-level winds to diverge away from the equator.

The excess air accumulated at 30° latitudes cannot go up into the stratosphere in the face of very

strong static stability there. The air cannot go further poleward because of Coriolis force. And the air cannot move equatorward in the face of the strong upper-level winds leaving the equator. The only remaining path is downward at 30° latitude (Fig. 11.26f) as a nonhydrostatic flow. As air accumulates near the ground, it causes a high-pressure perturbation there — the belt of subtropical highs labeled with H.

The descending air at 30° latitude warms dry-adiabatically, and does not contain much moisture because it was squeezed out earlier in the thunderstorm updrafts. These are the latitudes of the subtropical deserts (Fig. 11.26h), and the source of hot airmasses near the surface.

Finally, the horizontal pressure gradient between the surface subtropical highs near 30° latitude and the equatorial lows near 0° latitude drives the surface winds toward the equator. Coriolis force turns these winds toward the west in both hemispheres (Fig. 11.26g), resulting in the easterly trade winds (winds from the east) that converge at the ITCZ.

The total vertical circulation in the tropics and subtropics we recognize as the Hadley Cell (labeled h.c. in Fig. 11.26f). This vertical circulation (a **thermally-direct circulation**) is so vigorous in its vertical mixing and heat transport that it forces a deeper troposphere in the tropics than elsewhere (Fig. 11.4). Also, the vigorous circulation spreads and horizontally mixes the radiatively warmed air somewhat uniformly between ±30° latitude, as sketched by the temperature plateau in Fig. 11.8a.

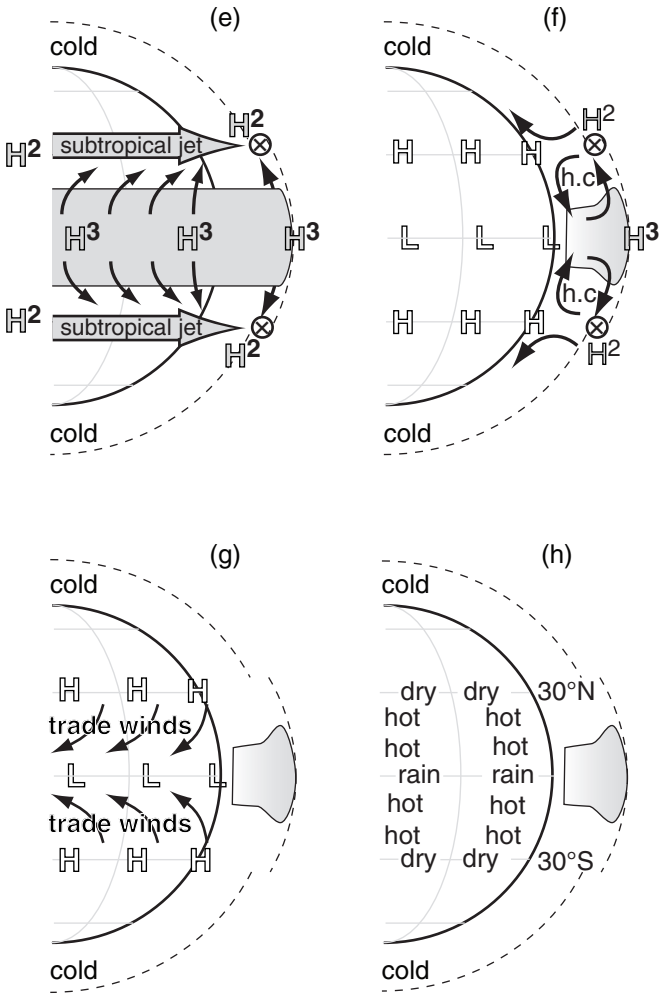

Figure 11.26 (continuation)
Explanation of low-latitude portion of the global circulation. The dashed line shows the tropopause. The "x" with a circle around it (representing the tail feathers of an arrow) indicates the axis of a jet stream that goes into the page.

FOCUS • The Trade Inversion

Descending air in the subtropical arm of the Hadley circulation is hot and dry. Air near the tropical sea surface is relatively cool and humid. Between these layers is a strong temperature inversion called the **trade inversion** or **passat inversion**. This statically stable layer (between the dashed lines in the Figure) creates a lid to the tropical convection below it. The inversion base is lowest (order of 500 m) in the subtropics, and is highest (order of 2,500 m) near the ITCZ. Fair-weather cumulus clouds (**trade cumuli**) between the lifting condensation level (LCL) and the trade inversion are shallowest in the subtropics and deeper closer to the ITCZ.

By capping the humid air below it, the trade inversion allows a latent-heat fuel supply to build up, which can be released in hurricanes and ITCZ thunderstorms.

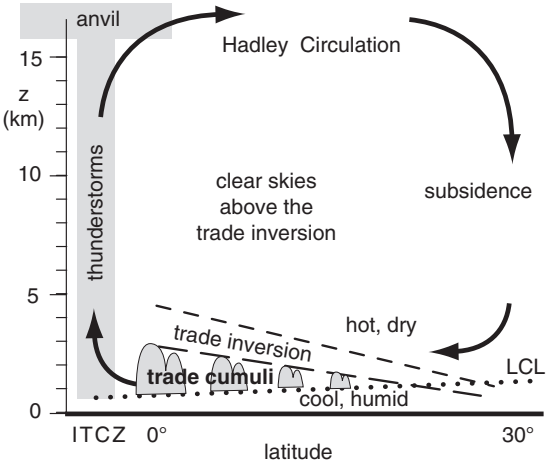

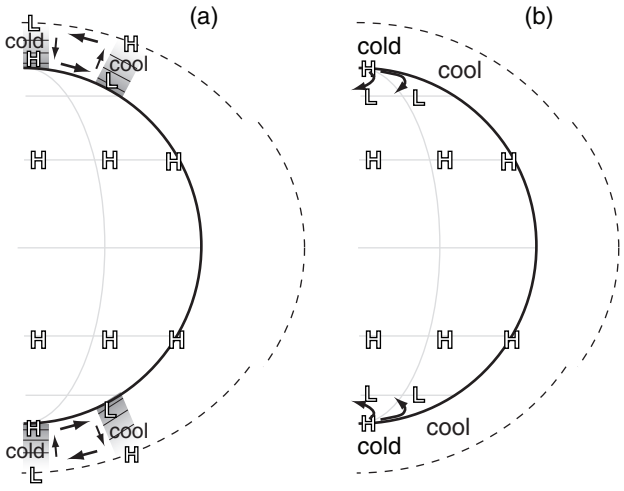

Figure 11.27
Explanation of high-latitude portion of general circulation.

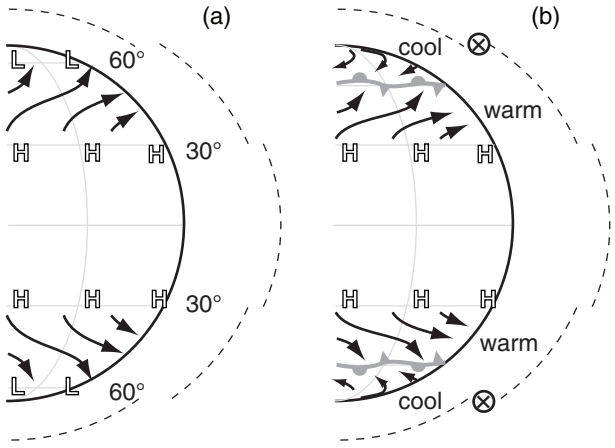

Figure 11.28
Explanation of mid-latitude flow near the Earth's surface. H and L indicate belts of high and low pressure, black arrows are average surface winds, and the polar front is shaded grey. The circle with "x" in it represents the tail feathers of the jet-stream wind vector blowing into the page.

High Latitudes

As sketched in Fig. 11.8a, air temperature is very cold at the poles, and is cool at 60° latitude. The temperature difference between 60° and 90° latitudes creates opposite north-south pressure gradients and winds at the top and bottom of the troposphere, due to the thermal circulation effect (Fig. 11.17). A vertical cross section of this thermal circulation (Fig. 11.27a) shows a weak polar cell. Air generally rises near 60°N and descends near the pole.

At the poles are surface high-pressure centers, and at 60° latitudes are belts of subpolar lows at the surface. This horizontal pressure gradient drives equatorward winds, which are turned toward the west in both hemispheres due to Coriolis force (Fig. 11.27b). Namely, the winds become geostrophic, and are known as **polar easterlies**.

At the top of the shallow (6 to 8 km thick) troposphere are poleward winds that are turned toward the east by Coriolis force. These result in an upper-level westerly flow that circulates around the upper-level polar low (Fig. 11.3b).

Mid-latitudes

Recall that the Hadley cell is unable to mix heat beyond about ±30° latitude. This leaves a very strong meridional temperature gradient in mid-latitudes (Fig. 11.8) throughout the depth of the troposphere. Namely, the temperature change between the equator and the poles has been compressed to a latitude band of about 30 to 60° in each hemisphere.

Between the subtropical high-pressure belt near 30° latitude and the subpolar low-pressure belt near 60° latitude is a weak meridional pressure gradient near the Earth's surface. This climatological-average pressure gradient drives weak boundary-layer winds from the west in both hemispheres (Fig. 11.28a), while the drag of the air against the surface causes the wind to turn slightly toward low pressure.

Near the subpolar belt of low pressure is a region of surface-air convergence, with easterly winds from the poles meeting westerly winds from mid-latitudes. The boundary between the warm subtropical air and the cool polar air at the Earth's surface is called the **polar front** (Fig. 11.28b) — a region of even stronger horizontal temperature gradient.

Recall from the hypsometric equation in Chapter 1 that the height difference (i.e., the thickness) between two isobaric surfaces increases with increasing temperature. As a result of the meridional temperature gradient, isobaric surfaces near the top of the troposphere in mid-latitudes are much more steeply sloped than near the ground (Figs. 11.29 & 11.32). This is related to the thermal-wind effect.

In the Northern Hemisphere this effect is greatest in winter (Fig. 11.32), because there is the greatest temperature contrast between pole and equator. In the Southern Hemisphere, the cold Antarctic continent maintains a strong meridional temperature contrast all year.

Larger pressure gradients at higher altitudes drive stronger winds. The core of fastest westerly winds near the tropopause (where the pressure-gradient is strongest) is called the **polar jet stream**, and is also discussed in more detail later in this chapter. Thus, the climatological average winds throughout the troposphere at mid-latitudes are from the west (Fig. 11.30a) in both hemispheres.

Although the climatological average polar-jet-stream winds are straight from west to east (as in Fig. 11.30a), the actual flow on any single day is unstable. Two factors cause this instability: the variation of Coriolis parameter with latitude (an effect that leads to **barotropic instability**), and the increase in static stability toward the poles (an effect that leads to **baroclinic instability**). Both of these instabilities are discussed in more detail later.

These instabilities cause the jet stream to meander meridionally (north-south) as it continues to blow from the west (Fig. 11.30b). The meanders that form in this flow are called **Rossby waves**. Regions near the tropopause where the jet stream meanders equatorward are called **troughs**, because the lower pressure on the north side of the jet stream is brought equatorward there. Poleward meanders of the jet stream are called **ridges**, where higher pressure extends poleward. The locations of Rossby-wave troughs and ridges usually propagate toward the east with time, as will be explained in detail later in this chapter.

Recall that there is a subtropical jet at roughly 30° latitude associated with the Hadley Cell. Thus, in each hemisphere are a somewhat-steady subtropical jet and an unsteady polar jet (Fig. 11.30b). Both of these jets are strongest in the winter hemisphere, where there is the greatest temperature gradient between cold poles and hot equator.

Troughs and ridges in the jet stream are crucial in creating and killing cyclones and anticyclones near the Earth's surface. Namely, they cause the extremely large weather variability that is normal for mid-latitudes. The field of **synoptic meteorology** comprises the study and forecasting of these variable systems, as discussed in the Airmasses, Fronts, and Extratropical Cyclone chapters.

Figs. 11.31 and 11.32 show actual global pressure patterns at the bottom and top of the troposphere. The next section explains why the patterns over the oceans and continents differ.

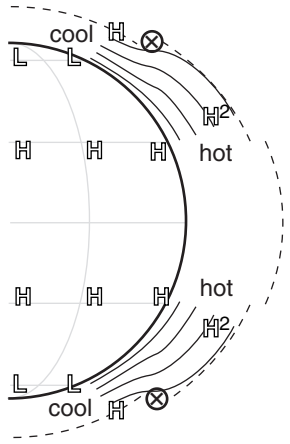

Figure 11.29
Isobaric surfaces (thin solid black lines) are spaced further apart in hot air than in cool air. Regions of steeper slope of the isobars have stronger pressure gradient, and drive faster winds. The jet-stream axis is shown with ⊗.

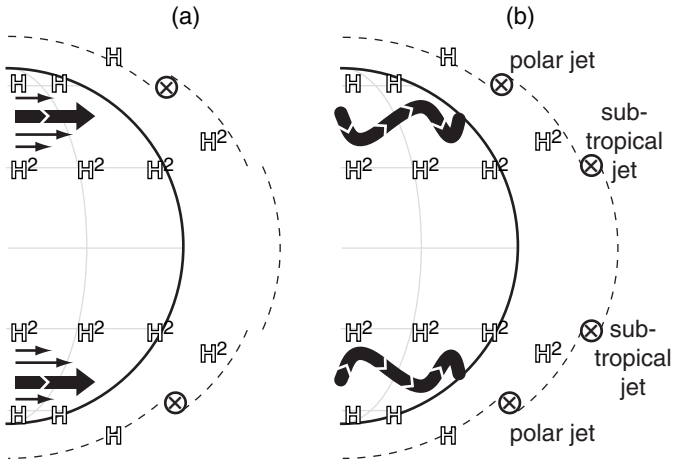

Figure 11.30
Mid-latitude flow near the top of the troposphere. The thick black arrow represents the core or axis of the jet stream: (a) average, (b) snapshot. (See caption in previous two figures for legend.)

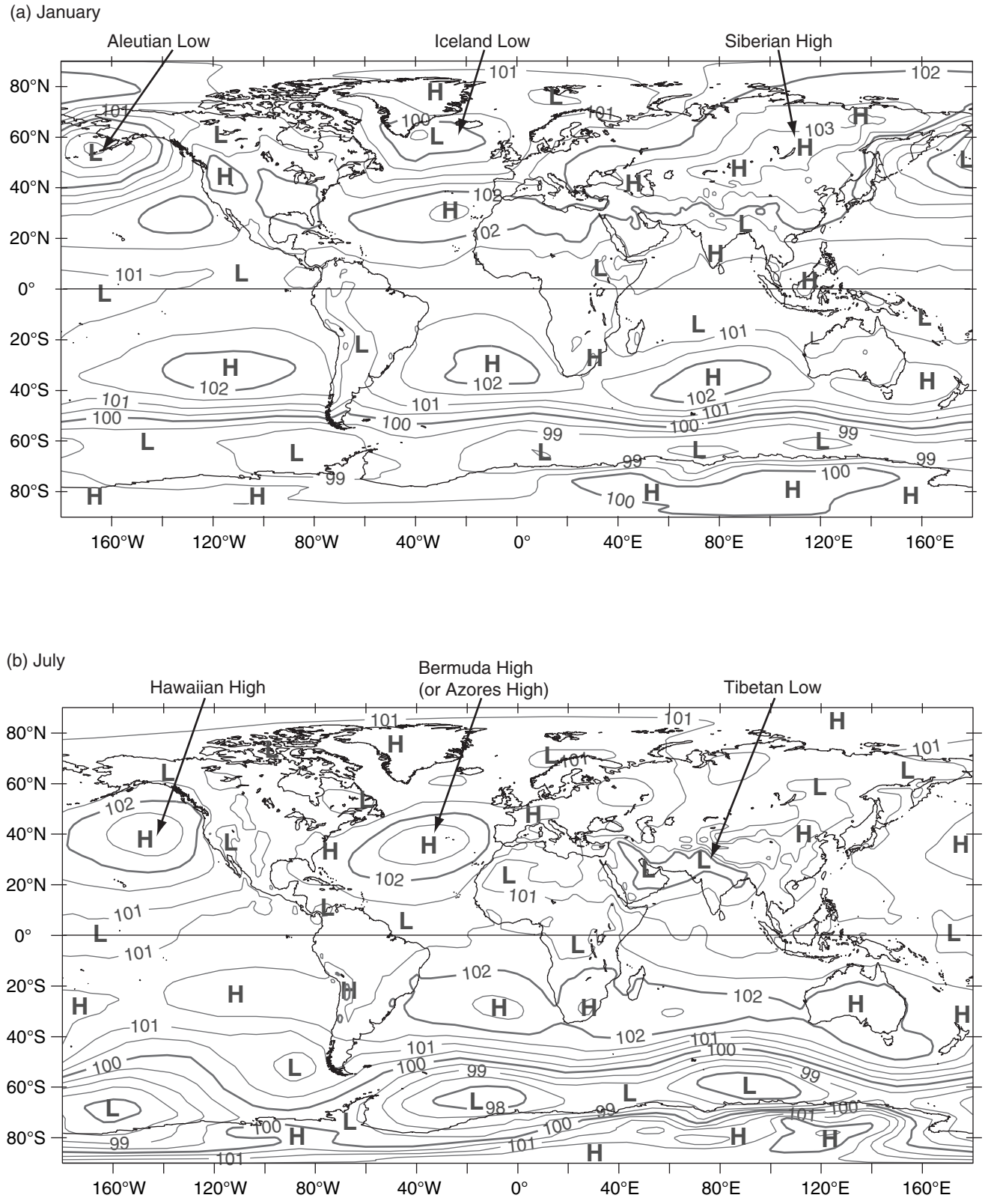

Figure 11.31
Mean sea-level pressure (kPa) for (a) January 2001, and (b) July 2001. [European Centre for Medium Range Weather forecasts (ECMWF) ERA-40 data used in this analysis have been provided by ECMWF, and have been obtained from the ECMWF data server.]

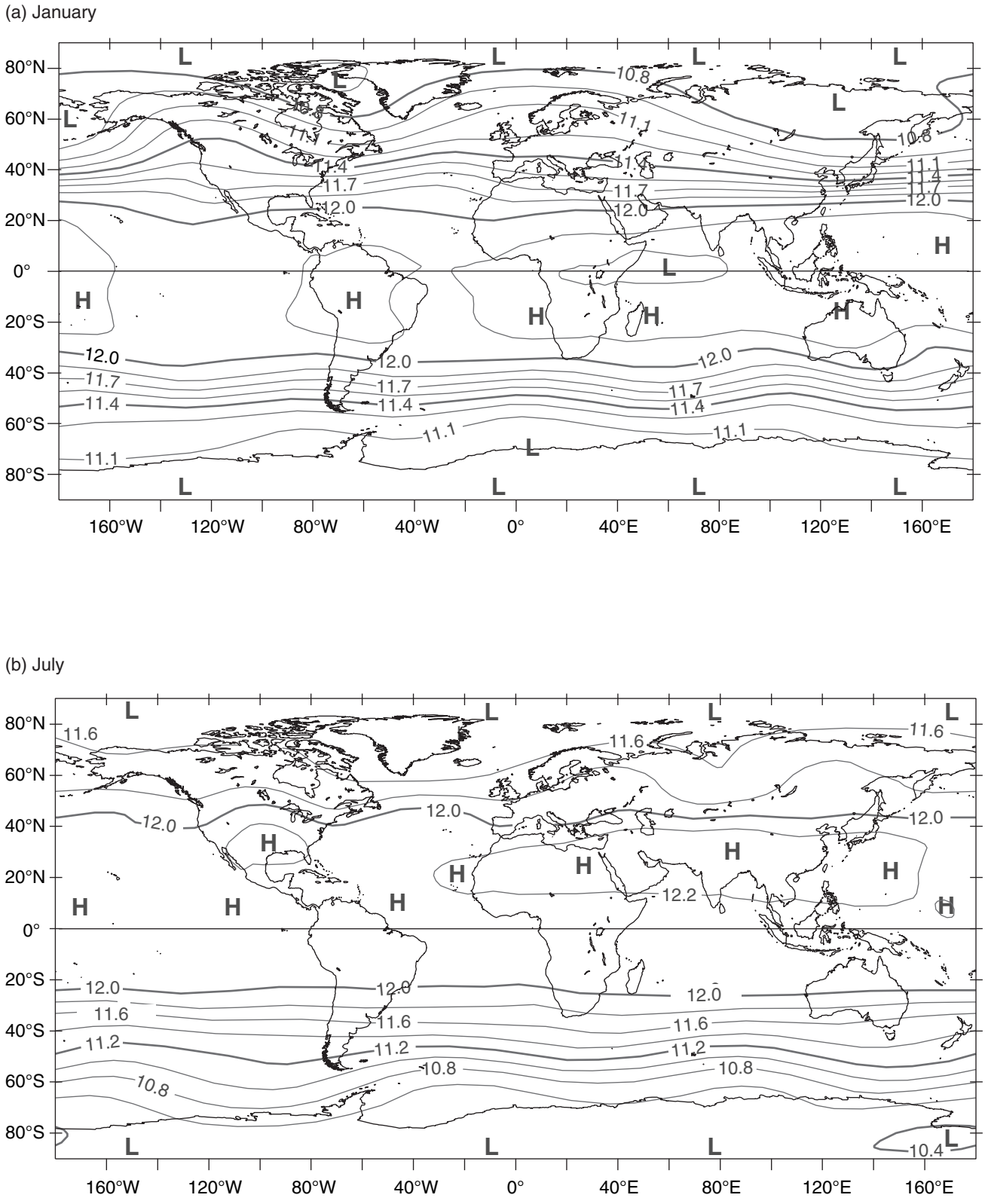

Figure 11.32
Geopotential height (km) of the 20 kPa isobaric surface (near the tropopause) for (a) January 2001, and (b) July 2001. [ECMWF ERA-40 data used in this analysis have been provided by ECMWF, and have been obtained from the ECMWF data server.]

Monsoon

Recall from the Heat chapter that the temperature change of an object depends on the mass of material being heated or cooled, and on the specific heat of the material. If you put the same amount of heat into objects of similar material but differing mass, the smaller masses will warm the most.

Rocks and soil on continents are opaque to sunlight, and are good insulators of heat. Thus, sunlight directly striking the land surface warms only a very thin top layer (mm) of molecules, causing this thin layer to get quite warm. Similarly, longwave (infrared) radiative heat loss at night causes the very thin top layer to become very cold. Namely, there is a large **diurnal** (daily) temperature contrast. Also, because there are more daylight hours in summer and more nighttime hours in winter, continental land surfaces tend to become hot in summer and cold in winter.

Water in the oceans is partially transparent and sometimes turbulent, allowing sunlight to be absorbed and spread over a thick layer (meters to tens of meters) of molecules. Also, water has a large specific heat (see the Heat chapter), hence a large input of heat causes only a small temperature change. Thus, ocean surfaces have very small diurnal temperature changes, and have only a medium amount of seasonal temperature changes.

The net result is that during summer, continents warm faster than the oceans. During winter, continents cool faster than the oceans.

Consider a cold region next to a warm region. Over the cold surface, the near-surface air cools and develops a high-pressure center with anticyclonically rotating winds, as explained by the thermal circulation sketched in Fig. 11.17. Over warm surfaces, the thermal circulation causes near-surface air to warm and develop a low-pressure center with cyclonic winds. As already mentioned, this is called a **thermal low**.

Combining the effects from the previous two paragraphs with the strong tendency of the winds to become geostrophic (or gradient) yields the near-surface monsoonal flows shown in Fig. 11.5. Opposite pressure patterns and circulations would occur near the top of the troposphere. The regions near surface lows tend to have rising air and abundant clouds and rain. Regions near surface highs tend to have dry fair weather with few clouds.

Monsoon circulations occur over every large continent and ocean (Fig. 11.31). Some are given names. Over the Atlantic in summer, winds on the south and west sides of the monsoonal **Bermuda High** (also called the **Azores High**) steer Atlantic hurricanes northward as they near North America. Over the North Pacific in summer is the **Hawaiian High** or **Pacific High** which provides cool northerly breezes and months of fair weather to the west coast of North America.

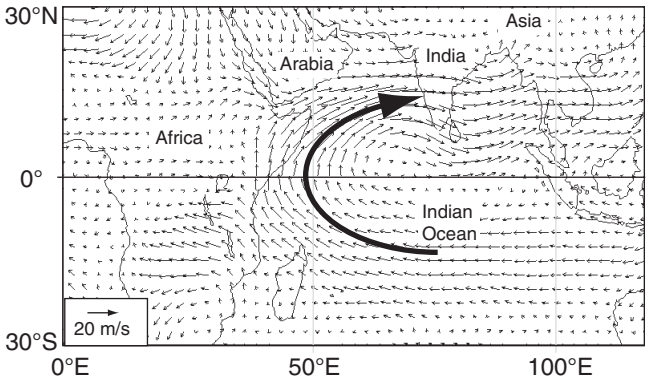

Figure 11.33
Monsoon winds near India on 85 kPa isobaric surface (at z ≈ 1.5 km), averaged over July 2001. Thin arrow length shows wind speed (see legend). Thick arrow shows cross-equatorial flow.

The summer low over northern India is called the **Tibetan Low**. It helps drive strong cross-equatorial flow (Fig. 11.33) that brings the much needed monsoon rains over India. Ghana in West Africa also receives a cross-equatorial monsoon flow.

Winter continental highs such as the **Siberian High** over Asia are formation locations for cold airmasses. Over the North Atlantic Ocean in winter is the **Icelandic Low**, with an average circulation on its south side that steers mid-latitude cyclones toward Great Britain and northern Europe. The south side of the winter **Aleutian Low** over the North Pacific brings strong onshore flow toward the west coast of North America, causing many days of clouds and rain.

The actual global circulation is a superposition of the zonally averaged flows and the monsoonal flows (Fig. 11.31). Also, a snapshot or satellite image of the Earth on any given day would likely deviate from the one-month averages presented here. Other important aspects of the global circulation were not discussed, such as conversion between available potential energy and kinetic energy. Also, monsoons and the whole global circulation are modulated by El Niño / La Niña events and other oscillations, discussed in the Climate chapter.

In the previous sections, we have described characteristics of the global circulation in simple terms, looked at what drives these motions, and explained dynamically why they exist. Some of the phenomena we encountered deserve more complete analysis, including the jet stream, Rossby waves with their troughs and ridges, and some aspects of the ocean currents. The next sections give details about how these phenomena work.

JET STREAMS

In the winter hemisphere there are often two strong jet streams of fast west-to-east moving air near the tropopause: the **polar jet stream** and the **subtropical jet stream** (Figs. 11.34 & 11.35).

The subtropical jet is centered near 30° latitude in the winter hemisphere. This jet: (1) is very steady; (2) meanders north and south a bit; (3) is about 10° latitude wide (width ≈1,000 km); and (4) has seasonal-average speeds of about 45 m/s over the Atlantic Ocean, 55 to 65 m/s over Africa and the Indian Ocean, and 60 to 80 m/s over the western Pacific Ocean. The **core** of fast winds near its center is at 12 km altitude (Fig. 11.35). It is driven by outflow from the top of the Hadley cell, and is affected by both Coriolis force and angular-momentum conservation.

The polar jet is centered near 50 to 60° latitude in the winter hemisphere. The polar jet: (1) is extremely variable; (2) meanders extensively north and south; (3) is about 5° latitude wide; and (4) has widely varying speeds (25 to 100 m/s). The core altitude is about 9 km. This jet forms over the polar front — driven by thermal-wind effects due to the strong horizontal temperature contrast across the front.

When meteorological data are averaged over a month, the subtropical jet shows up clearly in the data (e.g., Fig. 11.36) because it is so steady. However, the polar jet disappears because it meanders and shifts so extensively that it is washed out by the long-term average. Nonetheless, these transient meanders of the polar jet (troughs and ridges in the Rossby waves) are extremely important for mid-latitude cyclone formation and evolution (see the Extratropical Cyclone chapter).

In the summer hemisphere both jets are much weaker (Figs. 11.35b and 11.36), because of the much weaker temperature contrast between the equator and the warm pole. Core wind speeds in the subtropical jet are 0 to 10 m/s in N. Hemisphere summer, and 5 to 45 m/s in S. Hemisphere summer. This core shifts poleward to be centered near 40° to 45° latitude. The polar jet is also very weak (0 to 20 m/s) or non-existent in summer, and is displaced poleward to be centered near 60° to 75° latitude.

FOCUS • Jet Stream Aspect Ratio

Jet streams in the real atmosphere look very much like the thin ribbons of fast-moving air, as sketched in Fig. 11.34. Jet vertical thickness (order of 5 to 10 km) is much smaller than their horizontal width (order of 1000 to 2000 km). Namely, their aspect ratio (width/thickness) is large. Figures such as 11.35 are intentionally distorted to show vertical variations better.

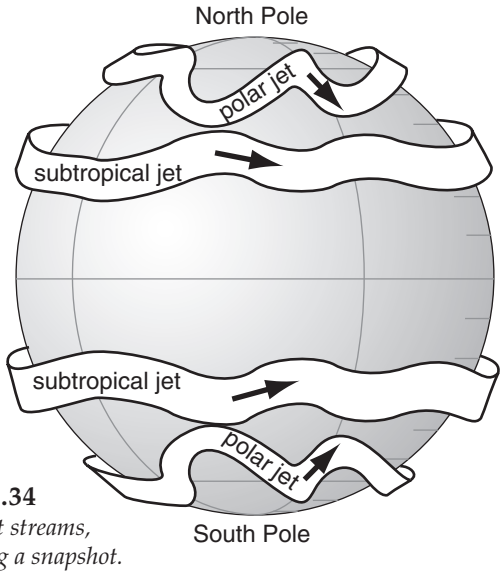

Figure 11.34
Sketch of jet streams, representing a snapshot.

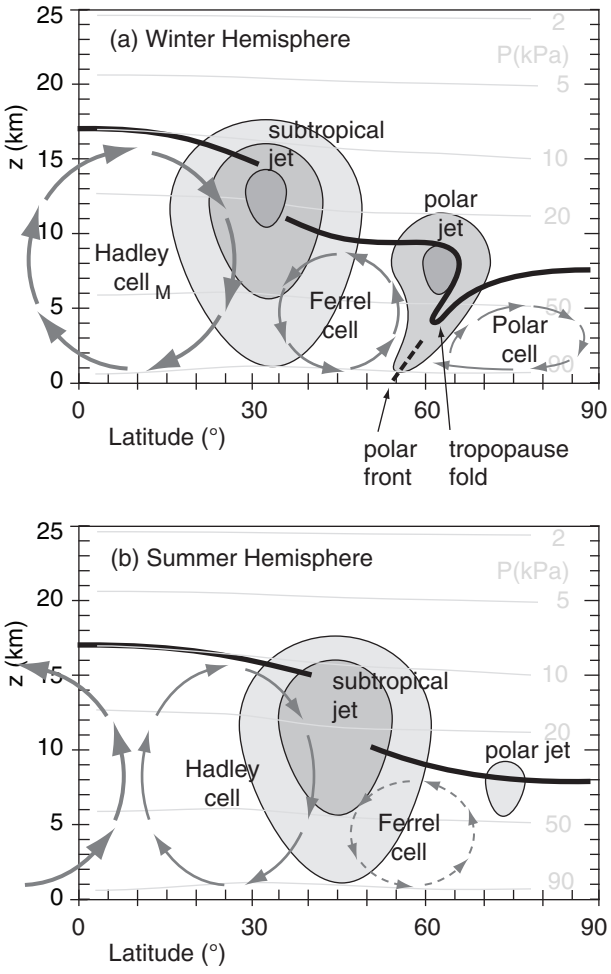

Figure 11.35
Simplified vertical cross-section. Thick solid line is the tropopause. Darker shading indicates faster winds from the west (perpendicular to the page). This is a snapshot, not a climatological average; hence, the polar jet and polar front can be seen.

(a) February

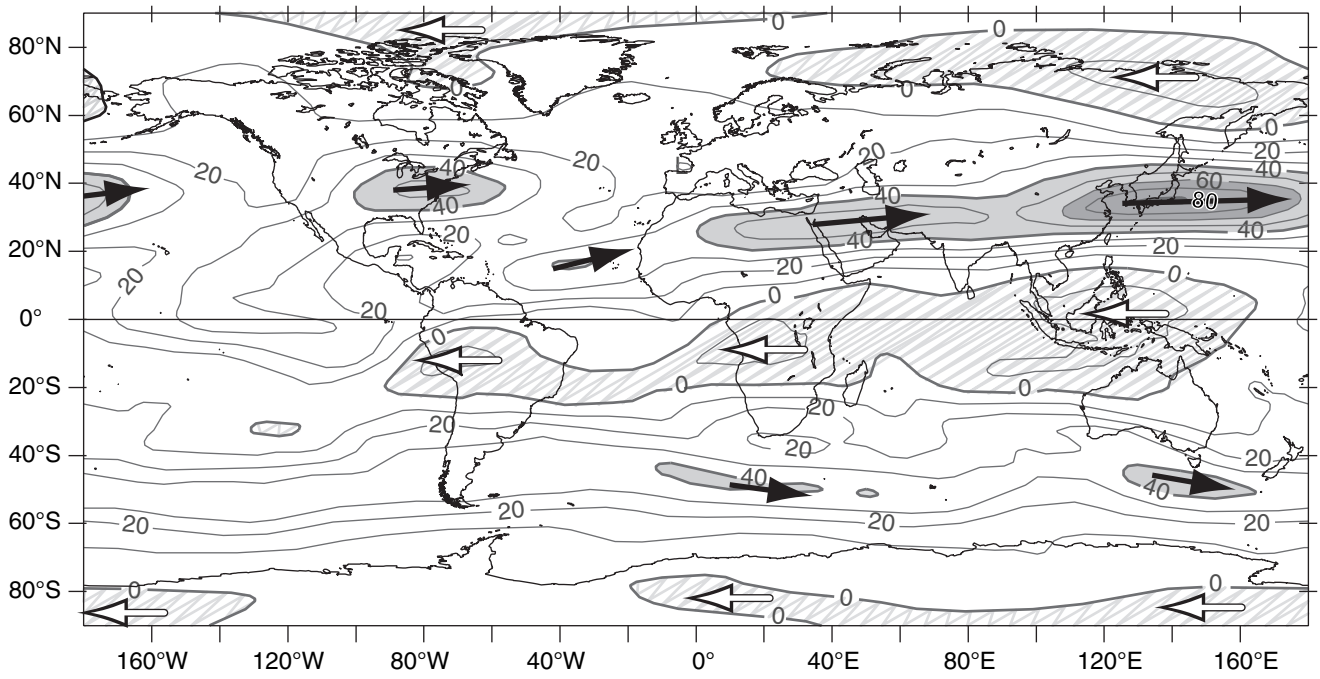

(b) August

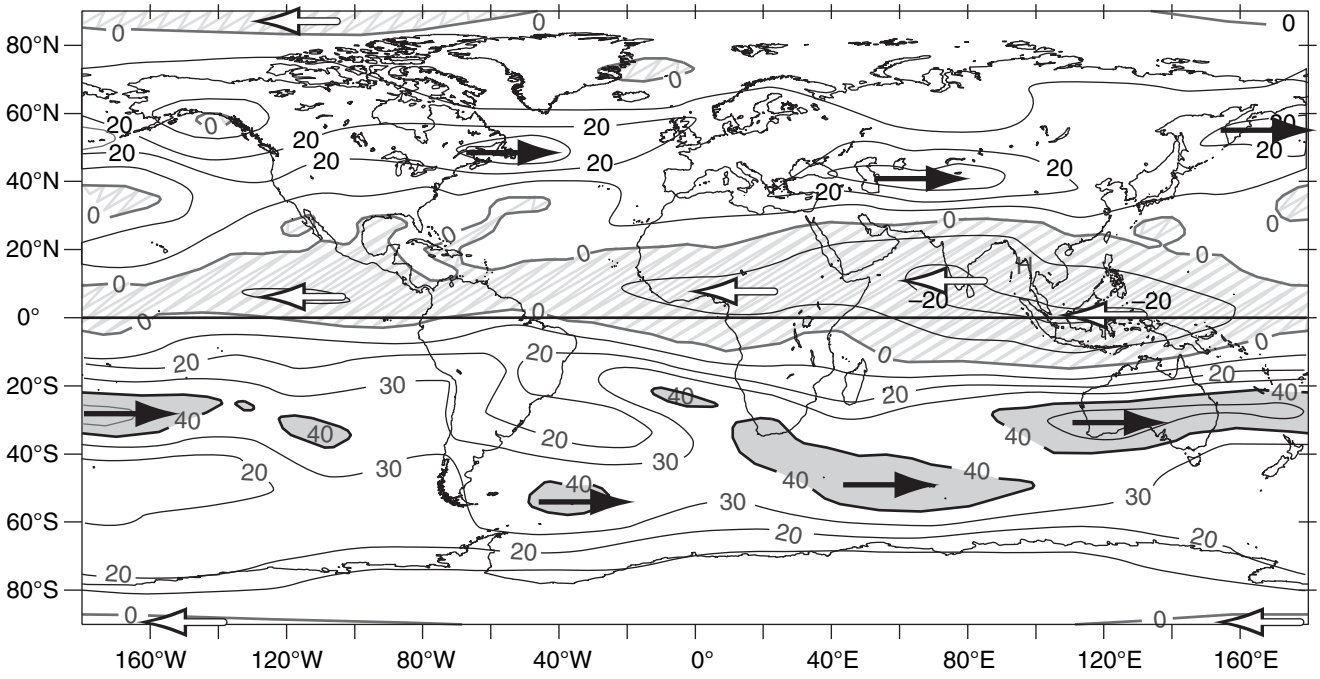

Figure 11.36

Zonal (U) component of winds (m/s) at 20 kPa isobaric surface (near the tropopause) for (a) February, and (b) August 2001. Contour interval is 10 m/s. All negative (east) winds are lightly hatched, and are indicated with white arrows. Positive (west) winds are indicated with black arrows, and are shaded at 40, 60, and 80 m/s. February and August are shown because the jets are stronger than during January and July, respectively. In 2001, polar easterlies were observed at 20 kPa, contrary to the longer-term climate average of polar westerlies as sketched in Fig. 11.3b. [ECMWF ERA-40 data used in this analysis have been provided by ECMWF, and have been obtained from the ECMWF data server.]

Baroclinicity & the Polar Jet

Baroclinicity associated with the meridional temperature gradient drives the west-to-east winds near the top of the troposphere, via the thermal-wind relationship. Fig. 11.37a shows a typical isotherm vertical cross-section for N. Hemisphere winter. Air near the ground is warmer near the equator and colder at the poles. This meridional temperature gradient exists throughout the troposphere.

The temperature at the tropopause at 60°N is warmer than the temperature at the higher-altitude tropopause near the equator. This is associated with a temperature reversal in the stratosphere, where the air is colder over the equator and warmer over 60° latitude. Recall that the spatial distribution of temperature is called the **temperature field**.

Apply the hypsometric equation to the temperature field to give the **pressure field** (the spatial distribution of pressures, Fig. 11.37b). In the troposphere, greater thickness between any two pressure surfaces in the warmer equatorial air than in the colder polar air causes the isobars to become more tilted at mid-latitudes as the tropopause is approached. Above the tropopause, tilt decreases because the meridional temperature gradient is reversed. Although the isobar tilt in Fig. 11.37b is subtle, it is significant.

Regions with the greatest tilt have the greatest meridional pressure gradient, which drives the fastest geostrophic wind (Fig. 11.37c). This maximum of westerly winds at mid-latitudes explains the polar jet stream at the tropopause in mid-latitudes. The center of the jet stream, known as the **jet-stream core**, occurs in a region that can be idealized as a break or fold in the tropopause, as will be discussed in the Fronts and Extratropical Cyclones chapters.

The toy model presented in eq. (11.1) and Fig. 11.8 is a starting point for quantifying the nature of the jet stream. Equations (11.2), (11.4) and (11.13) can be combined to give the wind speed as a function of latitude ϕ and altitude z, where it is assumed for simplicity that the winds near the ground are zero:

$$U_{jet} \approx \frac{|g| \cdot c \cdot b_1}{2\Omega \cdot T_v} \cdot z \cdot \left(1 - \frac{z}{2 \cdot z_T}\right) \cdot \cos^2(\phi) \cdot \sin^2(\phi) \qquad (11.17)$$

where U_{jet} is used in place of U_g to indicate a specific application of geostrophic wind to the polar jet stream, and where $c = 1.18\text{x}10^{-3}$ km^{-1} and $b_1 \approx 40$ K as before. The definition of the Coriolis parameter eq. (10.16) $f_c = 2{\cdot}\Omega{\cdot}\sin\phi$ was used, where $2{\cdot}\Omega = 1.458\text{x}10^{-4}$ s^{-1}. The average troposphere depth is $z_T \approx 11$ km, gravitational acceleration is $|g| = 9.8$ m/s^2, and T_v is the average virtual temperature (in Kelvin).

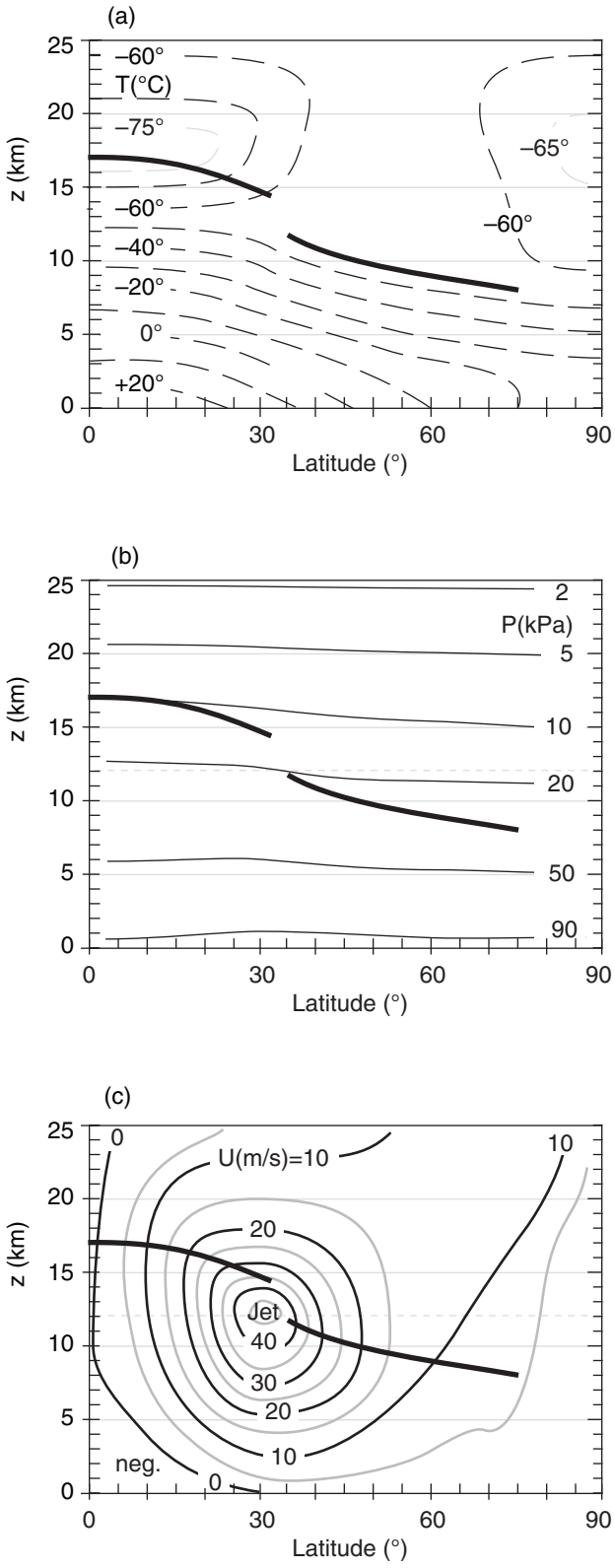

Figure 11.37
Example of vertical slices through the N. Hemisphere atmosphere for January 2003: (a) isotherms T (°C), (b) isobars P (kPa), (c) isotachs of the zonal wind U (m/s). Heavy solid line marks the tropopause. Wind direction of the jet in (c) is from the west (i.e., toward the reader). These figures can be overlain.

Solved Example

Find the geostrophic wind speed at the tropopause at 45° latitude, assuming an idealized temperature structure as plotted in Fig. 11.8. Assume an average temperature of 0°C, and neglect moisture.

Solution

Given: $z = z_T = 11$ km, $\phi = 45°$, $T_v = 273$ K.
Find: $U_g = ?$ m/s

Use eq. (11.17):

$$U_{jet} \approx \frac{(9.8\text{m}\cdot\text{s}^{-2})\cdot(1.18\times10^{-3}\text{km}^{-1})\cdot(40\text{K})}{(1.458\times10^{-4}\text{s}^{-1})\cdot(273\text{K})}\cdot$$

$$(11\text{km})\cdot\left(1-\frac{1}{2}\right)\cdot\cos^2(45°)\cdot\sin^2(45°)$$

$$= \underline{\mathbf{16\ m/s}}$$

Check: Units OK. Physics OK.

Discussion: Actual average wind speeds of about 40 m/s are observed in the jet stream of the winter hemisphere over a three-month average. Sometimes jet velocities as great as 100 m/s are observed on individual days. In the winter hemisphere, the temperature gradient is often greater than that given by eq. (11.4), which partially explains our low wind speed. Also, angular momentum can accelerate the wind.

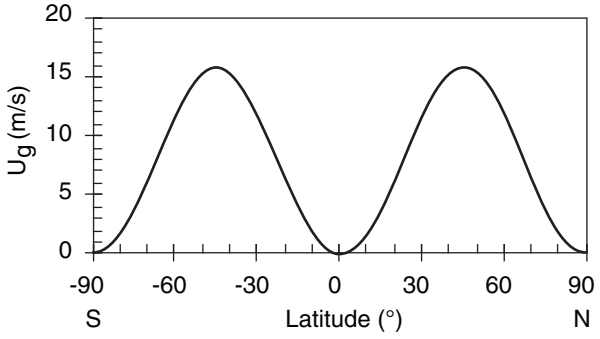

Figure 11.38
Geostrophic winds at 11 km altitude (from toy model).

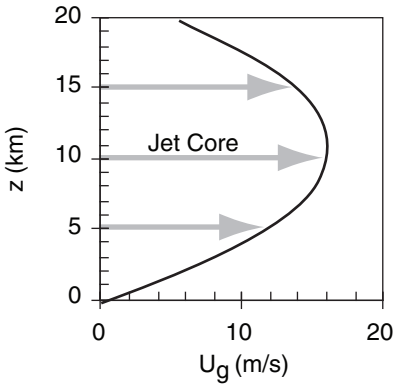

Figure 11.39
Vertical profile of (toy model) geostrophic wind at 45° latitude.

From Fig. 11.8b we see there are two extremes of north-south temperature gradient, one in the northern hemisphere and one in the southern. Those are the latitudes (in this toy model) where we can anticipate to find the strongest jet velocities (Fig. 11.38). Although the temperature gradient in the southern hemisphere has a sign opposite to that in the north, the sign of the Coriolis parameter also changes. Thus, the jet stream velocity is positive (west to east) in both hemispheres.

A spreadsheet solution of eq. (11.17) is shown in Figs 11.38 and 11.39. At the tropopause (z = 11 km), Fig. 11.38 shows the jet-stream velocity, with maxima at 45° north and south latitudes. For 45° latitude, Fig. 11.39 shows the vertical profile of geostrophic wind speed, with the fastest speeds (i.e., the **jet core**) at the tropopause.

The gross features shown in this figure are indeed observed in the atmosphere. However, actual spacing between jets in the northern and southern hemispheres is less than 90°; it is roughly 70° or 75° latitude difference. Also, the centers of both jets shift slightly northward during northern-hemisphere summer, and southward in winter. Jet speeds are not zero at the surface. Nevertheless, the empirical toy model presented here via eq. (11.1) serves as an instructive first introduction.

Angular Momentum & Subtropical Jet

A factor affecting the subtropical jet stream is **angular momentum** (mass times velocity times radius of curvature).

Consider air initially moving at some zonal velocity U_s relative to the Earth's surface at some initial (source) latitude ϕ_s. Because the Earth is rotating, the Earth's surface at the source latitude is moving eastward at velocity U_{Es}. Thus, the total eastward speed of the air parcel relative to the Earth's axis is $(U_s + U_{Es})$.

If there were no forces acting on the air, then conservation of angular momentum as the air moves to a destination latitude ϕ_d (Fig. 11.40) is:

$$m\cdot(U_s + U_{Es})\cdot R_s = m\cdot(U_d + U_{Ed})\cdot R_d \qquad \bullet(11.18)$$

where m is the mass of air, U_d is the tangential velocity of the air relative to the Earth's surface at the destination latitude, and U_{Ed} is the tangential velocity of the Earth's surface at the destination.

The radius from the Earth's axis to the surface at latitude ϕ is $R_\phi = R_E\cdot\cos(\phi)$, where R_ϕ represents source or destination radius (R_s or R_d), and $R_E = 6371$ km is the average Earth radius (Fig. 11.40). Also, the tangential velocity of the Earth at latitude ϕ is $U_\phi = \Omega\cdot R_\phi = \Omega\cdot R_E\cdot\cos(\phi)$, where the rate of rotation is $\Omega = 0.729\text{x}10^{-4}$ s^{-1}.

Solving these equations for the air velocity U_d relative to the Earth at the destination gives:

$$U_d = \left[\Omega \cdot R_E \cdot \cos(\phi_s) + U_s\right] \cdot \frac{\cos(\phi_s)}{\cos(\phi_d)} - \Omega \cdot R_E \cdot \cos(\phi_d) \tag{11.19}$$

As we already discussed, winds at the top of the Hadley cell diverge away from the equator, but cannot move beyond 30° latitude because Coriolis force turns the wind. When we use eq. (11.19) to predict the zonal wind speed for typical trade-wind air that starts at the equator with U_s = –7 m/s and ends at 30° latitude, we find unrealistically large wind speeds (125 m/s) for the subtropical jet (Fig. 11.41). Actual typical wind speeds in the subtropical jet are of order 40 to 80 m/s in the winter hemisphere, and slower in the summer hemisphere.

The discrepancy is because angular momentum is <u>not</u> conserved — due to forces acting on the air. Coriolis force turns the wind, causing air to accumulate and create a pressure-gradient force to oppose poleward motion in the Hadley cell. Turbulent drag force slows the wind a small amount. Also, the jet streams meander north and south, which helps to transport slow angular momentum southward and fast angular momentum northward. Namely, these meanders or synoptic-scale eddies cause mixing of zonal momentum.

Next, the concept of vorticity is discussed, which will be useful for explaining how troughs and ridges develop in the jet stream. Then, we will introduce a way to quantify circulation, to help understand the global circulation.

Solved Example

For air starting at the equatorial tropopause, what would be its zonal velocity at 20°N if angular momentum were conserved?

Solution

Given: ϕ_d = 20°N, ϕ_s = 0°, $\Omega \cdot R_E$ = 463 m/s
Find: U_d = ? m/s
Assume: no turbulence; U_s = –7 m/s easterlies.

Use eq. (11.19): U_d =

$$\left[(463\text{m/s})\cos(0°) + U_s\right]\frac{\cos(0°)}{\cos(20°)} - (463\text{m/s})\cos(20°)$$

U_d = = **<u>50.2 m/s</u>**

Check: Units OK. Physics OK. Agrees with Fig. 11.41
Discussion: Winds in the real atmosphere are much less than this, because forces and momentum mixing prevent conservation of angular momentum.

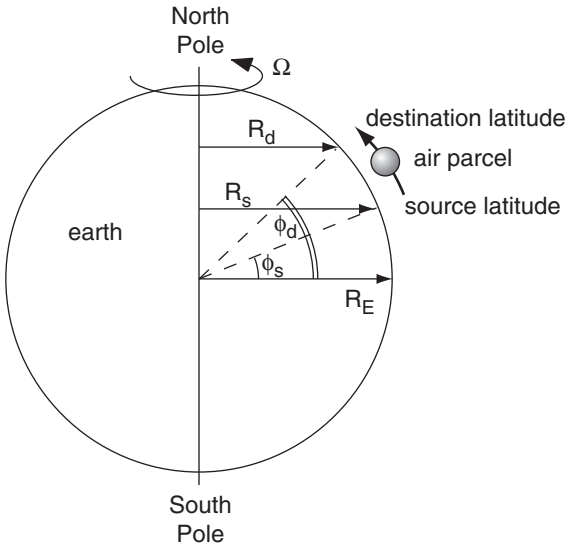

Figure 11.40
Geometry for northward air-parcel movement.

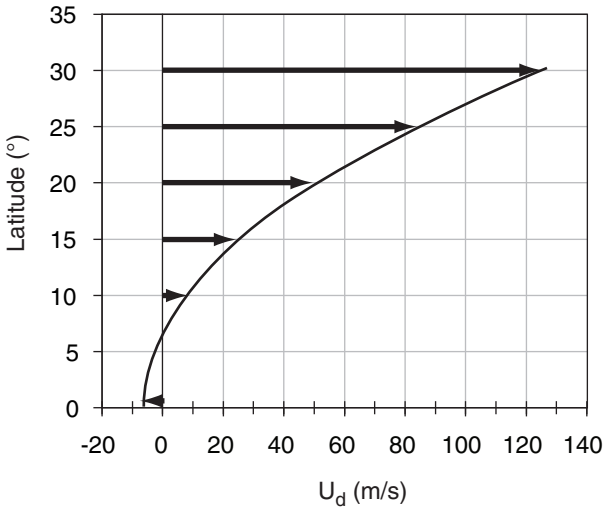

Figure 11.41
Zonal wind speed U_d at various destination latitudes for typical trade-wind air that starts at the equator with U_s = –7 m/s, for the unrealistic case of conservation of angular momentum.

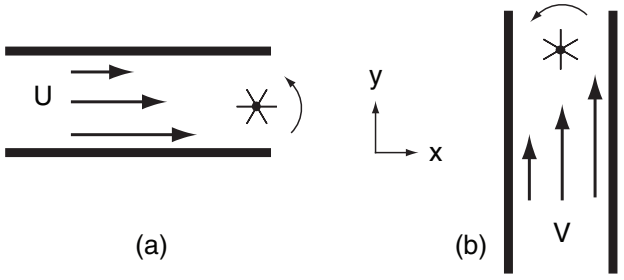

Figure 11.42
Shear-induced relative vorticity. Counter-clockwise turning of the paddle wheels indicates positive vorticity for both examples. (a) ΔU/Δy is negative. (b) ΔV/Δx is positive.

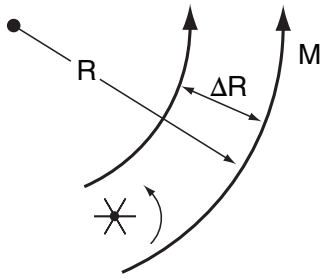

Figure 11.43
Vorticity for flow around a curve, where both the curvature and the shear contribute to positive vorticity in this example (i.e., the paddle wheel rotates counter-clockwise).

VORTICITY

Relative Vorticity

Relative vorticity ζ_r is a measure of the rotation of fluids about a vertical axis relative to the Earth's surface, as introduced in the Dynamics chapter. It is defined as positive in the counter-clockwise direction. The unit of measurement of vorticity is inverse seconds.

The following two definitions are equivalent:

$$\zeta_r = \frac{\Delta V}{\Delta x} - \frac{\Delta U}{\Delta y} \qquad \bullet(11.20)$$

$$\zeta_r = \frac{\Delta M}{\Delta R} + \frac{M}{R} \qquad \bullet(11.21)$$

where (U, V) are the (eastward, northward) components of the wind velocity, R is the radius of curvature traveled by a moving air parcel, and M is the tangential speed along that circumference in a counterclockwise direction.

Fig. 11.42 illustrates eq. (11.20). If fluid travels along a straight channel, but has shear, then it also has vorticity because a tiny paddle wheel carried by the fluid would be seen to rotate. Fig. 11.43 illustrates eq. (11.21), where fluid following a curved path also has vorticity, so long as radial shear of the tangential velocity does not cancel it. Fig. 11.44 shows both shear and rotational relative vorticity.

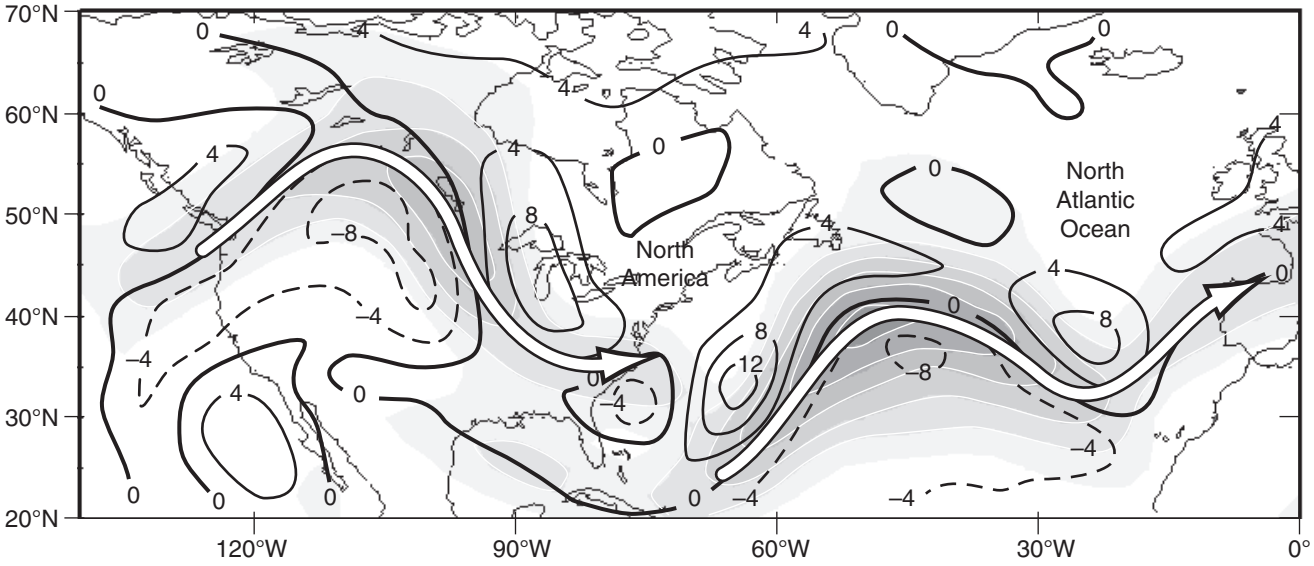

Figure 11.44
Weather map example of relative vorticity (contour lines, with units of 10^{-5} s^{-1}) near the tropopause (at the 20 kPa isobaric surface) at 12 UTC on 5 January 2001. White arrows show jet stream axis of fastest winds over North America and the Atlantic Ocean. Shading gives wind speeds every 10 m/s from 30 m/s (lightest grey) to over 80 m/s (darkest grey). (Based on NCEP/NCAR 40-year reanalysis data, with initial plots produced using the plotting tool by Christopher Godfrey, the University of Oklahoma School of Meteorology.)

FOCUS • Solid Body Relative Vorticity

One can derive eq. (11.22) from either eq. (11.20) or eq. (11.21). Consider the sketch at right, where speed M is tangent to the rotating disk at radius R.

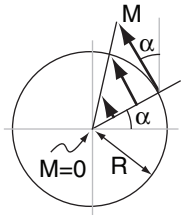

Starting with eq. (11.21):

$$\zeta_r = \frac{\Delta M}{\Delta R} + \frac{M}{R}$$

Thus:

$$\zeta_r = \frac{(M-0)}{R} + \frac{M}{R} = \boxed{\frac{2M}{R}}$$

Or, starting with (11.20):

$$\zeta_r = \frac{\Delta V}{\Delta x} - \frac{\Delta U}{\Delta y} = \frac{(M\cos\alpha - 0)}{R\cos\alpha} - \frac{(-M\sin\alpha - 0)}{R\sin\alpha}$$

Thus:

$$\zeta_r = \frac{M}{R} + \frac{M}{R} = \boxed{\frac{2M}{R}}$$

A special case of the last equation is where the radial shear is just great enough so that winds at different radii sweep out identical angular velocities about the center of curvature. In other words, the fluid rotates as a solid body. For this case, the last equation reduces to

$$\zeta_r = \frac{2M}{R} \qquad \bullet(11.22)$$

Absolute Vorticity

Measured with respect to the "fixed" stars, the total vorticity must include the Earth's rotation in addition to the relative vorticity. This sum is called the absolute vorticity ζ_a:

$$\zeta_a = \zeta_r + f_c \qquad \bullet(11.23)$$

where the Coriolis parameter $f_c = 2\Omega\cdot\sin(\phi)$ is a measure of the vorticity of the planet, ϕ is latitude, and where $2\Omega = 1.458\text{x}10^{-4}\ \text{s}^{-1}$.

Potential Vorticity

Potential vorticity ζ_p is defined as the absolute vorticity divided by the depth Δz of the column of air that is rotating:

$$\zeta_p = \frac{\zeta_r + f_c}{\Delta z} = \text{constant} \qquad \bullet(11.24)$$

It has units of $(\text{m}^{-1}\cdot\text{s}^{-1})$. In the absence of turbulent drag and heating (latent, radiative, etc.), potential vorticity is conserved.

Solved Example

At 50°N is a west wind of 100 m/s. At 46°N is a west wind of 50 m/s. Find (a) relative, (b) absolute vorticity.

Solution

Given: U_2 =100 m/s, U_1 =50 m/s, $\Delta\phi$ =4°lat. V =0 m/s
Find: ζ_r = ? s^{-1} , ζ_a = ? s^{-1}

(a) Use eq. (11.20): Appendix A: 1°latitude = 111 km
ζ_r = – (100 – 50 m/s) / ($4.4\text{x}10^5$ m) = $\underline{\mathbf{-1.14x10^{-4}}}\ \text{s}^{-1}$

(b) Average ϕ = 48°N. Thus, $f_c = (1.458\text{x}10^{-4}\ \text{s}^{-1})\cdot\sin(48°)$
$f_c = 1.08\text{x}10^{-4}\ \text{s}^{-1}$. then, use eq. (11.23):
$\zeta_a = (-1.14\text{x}10^{-4}) + (1.08\text{x}10^{-4})$ = $\underline{\mathbf{-6x10^{-6}}}\ \text{s}^{-1}$.

Check: Units OK. Physics OK.
Discussion: Shear vorticity from a strong jet stream, but its vorticity is opposite to the Earth's rotation.

Solved Example

If wind rotates as a solid body about the center of a low pressure system, and the tangential velocity is 10 m/s at radius 300 km, find the relative vorticity.

Solution

Given: M = 10 m/s (cyclonic), R = 300,000 m.
Find: ζ_r = ? s^{-1}

Use eq. (11.22):
$\zeta_r = 2\cdot(10\text{ m/s}) / (3\text{x}10^5\text{ m}) = \underline{\mathbf{6.67x10^{-5}}}\ \text{s}^{-1}$

Check: Units OK. Physics OK.
Discussion: Relative vorticities of synoptic storms are typically about this order of magnitude.

Solved Example

An 11 km deep layer of air at 45°N latitude has no curvature, but has a shear of –10 m/s across horizontal distance 500 km. What is the potential vorticity?

Solution

Assume the shear is in the cyclonic direction.
Given: Δz = 11000 m, ϕ = 45°N, ΔM = –10 m/s,
ΔR = 500000 m.
Find: ζ_p = ? $\text{m}^{-1}\cdot\text{s}^{-1}$

Use eq. (11.24):

$$\zeta_p = \frac{\frac{(10\text{m/s})}{5\times10^5\text{m}} + (1.458\times10^{-4}\text{s}^{-1})\cdot\sin(45°)}{11000\text{m}}$$

$$= (2+10.31)\text{x}10^{-5} / 11000\text{ m} = \underline{\mathbf{1.12x10^{-8}}}\ \text{m}^{-1}\cdot\text{s}^{-1}$$

Check: Units OK. Physics OK.
Discussion: Planetary vorticity is 5 times greater than the relative vorticity for this case. It cannot be neglected when computing potential vorticity.

Solved Example

Find the IPV for the previous example ($\zeta_a = 1.23\text{x}10^{-4}$ s^{-1}), using $\rho = 0.5$ kg/m^3 and $\Delta\theta/\Delta z = 3.3$ K/km.

Solution

Given: $\zeta_a = 1.23\text{x}10^{-4}$ s^{-1} , $\rho = 0.5$ kg/m^3 ,
$\Delta\theta/\Delta z = 3.3$ K/km , $\Delta z = 11$ km
Find: ζ_{IPV} = ? PVU

Use eq. (11.26):

$$\zeta_{IPV} = \frac{(1.23\times10^{-4}\,\text{s}^{-1})}{(0.5\text{kg}\cdot\text{m}^{-3})}\cdot\left(3.3\text{K}\cdot\text{km}^{-1}\right)$$

$$= 8.12\text{x}10^{-7}\ \text{K}\cdot\text{m}^2\cdot\text{s}^{-1}\cdot\text{kg}^{-1} = \underline{\textbf{0.812 PVU}}$$

Check: Units OK. Physics OK.
Discussion: This is a reasonable value (< 1.5 PVU) in troposphere.

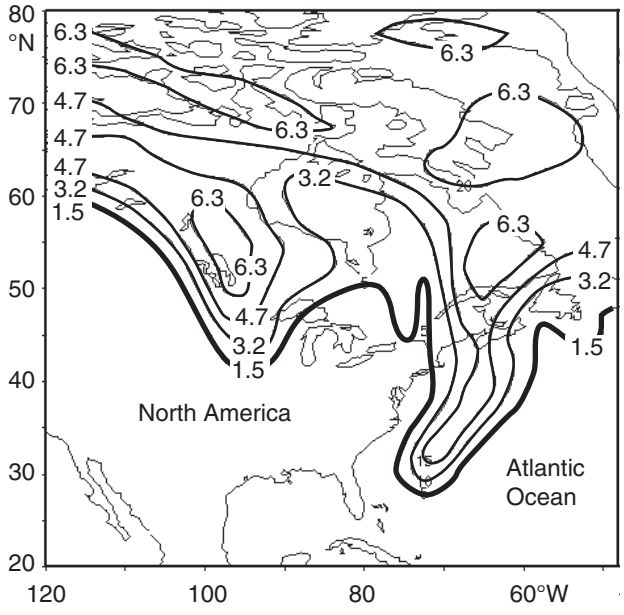

Figure 11.45
Example of isentropic potential vorticity on the 315 K isentropic surface, at 00 UTC on 5 January 2001. Units are PVU. Values greater than 1.5 are in stratospheric air. Because the tropopause is at lower altitude near the poles than at the equator, the 315 K potential temperature surface crosses the tropopause; so it is within the troposphere in the south part of the figure and in the stratosphere in the north part. Tropopause folds are evident by the high PVU values just west of the Great Lakes, and just east of the North American coastline. (Based on NCEP/NCAR 40-year reanalysis data, with initial plots produced using the plotting tool by Christopher Godfrey, the University of Oklahoma School of Meteorology.)

Combining the previous equations yields:

$$-\frac{\Delta M}{\Delta n} + \frac{M}{R} + f_c = \zeta_p\cdot\Delta z \qquad \bullet(11.25)$$

shear curvature planetary stretching

where ζ_p is a constant that depends on the initial conditions of the flow. The last term states that if the column of rotating air is stretched vertically, then its relative vorticity must increase or it must move further north where planetary vorticity is greater.

Isentropic Potential Vorticity

Isentropic potential vorticity (IPV) is

$$\zeta_{IPV} = \frac{\zeta_r + f_c}{\rho}\cdot\left(\frac{\Delta\theta}{\Delta z}\right) \qquad (11.26)$$

where ζ_r is the relative vorticity measured on an isentropic surface (i.e., a surface connecting points of equal potential temperature θ), and ρ is air density. Larger IPVs exist where the air is less dense and where the static stability $\Delta\theta/\Delta z$ is greater. For this reason, the IPV is two orders of magnitude greater in the stratosphere than in the troposphere.

Using the hydrostatic relation (Chapter 1), we can rewrite this as

$$\zeta_{IPV} = -|g|\cdot(\zeta_r + f_c)\cdot\frac{\Delta\theta}{\Delta p} \qquad (11.27)$$

IPV is measured in **potential vorticity units** (**PVU**), defined by 1 PVU = 10^{-6} K·m^2·s^{-1}·kg^{-1} . On average, $\zeta_{IPV} < 1.5$ PVU for tropospheric air, and $\zeta_{IPV} > 1.5$ PVU for stratospheric air (a good atmospheric cross-section example is shown in the Extratropical Cyclone chapter).

Isentropic potential vorticity is conserved for air moving adiabatically and frictionlessly along an isentropic surface (i.e., a surface of constant potential temperature). Thus, it can be used as a tracer of air motion.

Stratospheric air entrained into the troposphere retains its IPV > 1.5 PVU for a while before losing its identity due to turbulent mixing. Thus, IPV is useful for finding tropopause folds and the accompanying intrusions of stratospheric air into the troposphere (Fig. 11.45), which can bring down toward the ground the higher ozone concentrations and **radionuclides** (radioactive atoms from former atomic-bomb tests) from the stratosphere.

Because isentropic potential vorticity is conserved, if static stability ($\Delta\theta/\Delta z$) weakens, then eq. (11.26) says absolute vorticity must increase to maintain constant IPV. For example, Fig. 11.46 shows isentropes for flow from west to east across the

Rocky Mountains. Where isentropes are spread far apart, static stability is low. Because air tends to follow isentropes (for frictionless adiabatic flow), a column of air between two isentropes over the crest of the Rockies will remain between the same two isentropes as the air continues eastward.

Thus, the column of air shown in Fig. 11.46 becomes stretched on the lee side of the Rockies and its static stability decreases (same $\Delta\theta$, but spread over a larger Δz). Thus, absolute vorticity in the stretched region must increase. Such increased cyclonic vorticity encourages formation of low-pressure systems (extratropical cyclones) to the lee of the Rockies — a process called **lee cyclogenesis**.

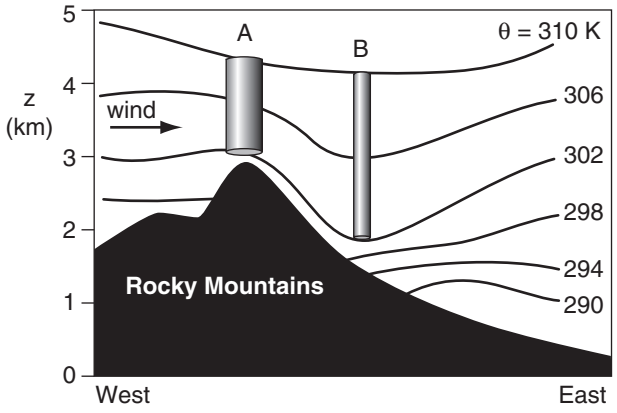

Figure 11.46
Wind blowing from west to east (A) over the Rocky Mountains creates mountain waves and downslope winds, which cause greater separation (B) between the 302 and 310 K isentropes to the lee of the mountains. This greater separation implies reduced static stability and vertical stretching.

HORIZONTAL CIRCULATION

Consider a closed shape of finite area (Fig. 11.47a). Pick any starting point on the perimeter, and hypothetically travel counterclockwise around the perimeter until you return to the starting point. As you travel each increment of distance Δl, observe the local winds along that increment, and get the average tangential component of wind velocity M_t.

The horizontal **circulation** C is defined as the product of this tangential velocity times distance increment, summed over all the increments around the whole perimeter:

$$C = \sum_{i=1}^{n} \left(M_t \cdot \Delta l \right)_i \qquad (11.28)$$

where i is the index of each increment, and n is the number of increments needed to complete one circuit around the perimeter. Take care that the sign of M_t is such that it is positive if the tangential wind is in the same direction as you are traveling, and negative if opposite. The units of circulation are $m^2 \cdot s^{-1}$.

If we approximate the perimeter by Cartesian line segments (Fig. 11.47b), then eq. (11.28) becomes:

$$C = \sum_{i=1}^{n} \left(U \cdot \Delta x + V \cdot \Delta y \right)_i \qquad (11.29)$$

The sign of Δx is (+) if you travel in the positive x-direction (toward the East), and (–) if opposite. Similar rules apply for Δy (+ toward North).

To better understand circulation, consider idealized cases (Figs. 11.48a & b). For winds of tangential velocity M_t rotating counterclockwise around a circle of radius R, the circulation is $C = 2\pi R \cdot M_t$. For clockwise circular rotation, the circulation is $C = -2\pi R \cdot M_t$, namely, the circulation value is negative. From these two equations, we see that a fast speed around a small circle (such as a tornado) can give

Solved Example

Given Fig. 11.46. (a) Estimate $\Delta\theta/\Delta z$ at A and B. (b) if the initial absolute vorticity at A is 10^{-4} s^{-1}, find the absolute vorticity at B.

Solution

Given: $\zeta_a = 10^{-4}$ s^{-1} at A, $\theta_{top} = 310$ K, $\theta_{bottom} = 302$ K.
Find: (a) $\Delta\theta/\Delta z$ = ? K/km at A and B.
(b) ζ_a = ? s^{-1} at B.

$\Delta\theta = 310$ K – 302 K = 8 K at A & B. Estimate the altitudes at the top and bottom of the cylinders in Fig. 11.46.
A: $z_{top} = 4.4$ km, $z_{bottom} = 3.1$ km. Thus $\Delta z_A = 1.3$ km.
B: $z_{top} = 4.2$ km, $z_{bottom} = 1.9$ km. Thus $\Delta z_B = 2.3$ km.

(a) $\Delta\theta/\Delta z$ = 8K / 1.3 km = **6.15 K/km** at A.
$\Delta\theta/\Delta z$ = 8K / 2.3 km = **3.48 K/km** at B.

(b) If initial (A) and final (B) IPV are equal, then rearranging eq. (11.26) and substituting $(\zeta_r + f_c) = \zeta_a$ gives:
$\zeta_{aB} = \zeta_{aA} \cdot (\Delta z_B/\Delta z_A)$
$= (10^{-4}\text{ s}^{-1}) \cdot [(2.3\text{ km})/(1.3\text{ km})] =$ **1.77x 10^{-4} s^{-1}**

Check: Units OK. Sign OK. Magnitude good.
Discussion: Static stability $\Delta\theta/\Delta z$ is much weaker at B than A. Thus absolute vorticity at B is much greater than at A. If the air flow directly from west to east and if the initial relative vorticity were zero, then the final relative vorticity is $\zeta_r = 0.77\text{x}10^{-4}$ s^{-1}. Namely, to the lee of the mountains, cyclonic rotation forms in the air where none existed upwind. Namely, this implies cyclogenesis (birth of cyclones) to the lee (downwind) of the Rocky Mountains.

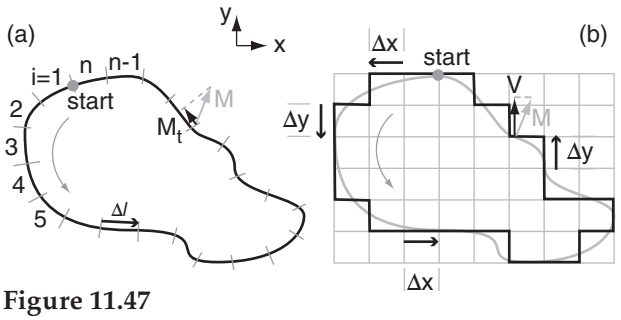

Figure 11.47
Method for finding the circulation. M is the wind vector. M_t and V are projections onto the perimeter. (a) Stepping in increments of Δl around an arbitrary shape. (b) Stepping around a Cartesian (gridded) approximation to the shape in (a).

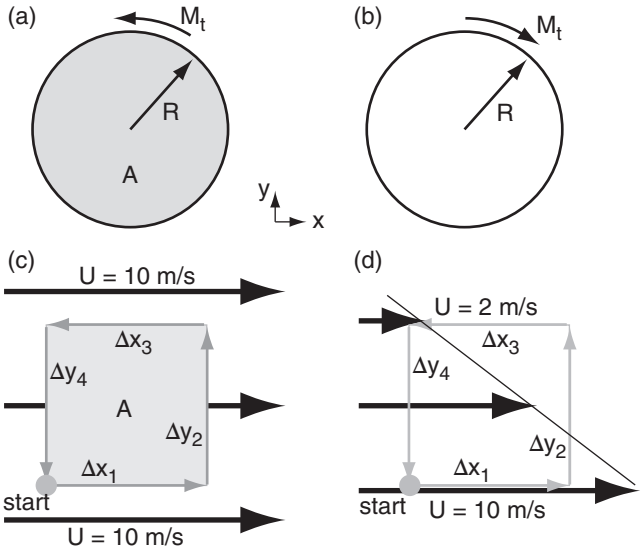

Figure 11.48
Circulation examples. (a) Counterclockwise rotation around a circle. (b) Clockwise rotation around a circle. (c) Uniform wind. (d) Uniform shear. Area A enclosed by circulation is shaded.

Solved Example

Find the horizontal circulation for Fig. 11.48d. Assume $\Delta x = \Delta y = 1$ km. Relate to shear and rel. vorticity.

Solution

Given: U_{bottom}= 10 m/s, U_{top}= 2 m/s, V=0, Δx=Δy=1 km
Find: C = ? m^2/s, ζ_r = ? s^{-1}

Use eq. (11.29) from start point:
$C = (U\cdot\Delta x)_1 + (V\cdot\Delta y)_2 + (U\cdot\Delta x)_3 + (V\cdot\Delta x)_4$
$(10\text{m/s})\cdot(1\text{km}) + 0 + (2\text{m/s})\cdot(-1\text{km}) + 0$
C = 8 (m/s)·km = **8000 m**^{2}/s
Use eq. (11.30): with area $A = \Delta x\cdot\Delta y$ = 1 km^2
$U_{shear} = \Delta U/\Delta y = (U_{top}-U_{bottom})/\Delta y$
= [(2 – 10 m/s)/(1 km)] = –8 (m/s)/km
$C = [0 - U_{shear}]\cdot A = -[-8\text{ (m/s)/km}]\cdot(1\text{ km}^2)$
= 8 (m/s)·km = **8000 m**^{2}/s.
Use eq. (11.31): $\zeta_r = C/A$ = 8 (m/s)/km = **0.008 s**$^{-1}$.

Check: Units OK. Physics OK. Magnitude OK.
Discussion: Strong shear. Large circ. Large vorticity.

the same circulation magnitude as a slower speed around a larger circle (e.g., a mid-latitude cyclone).

Consider two more cases (Figs. 11.48c & d). For a circuit in a constant wind field of any speed, the circulation is $C = 0$. For a circuit within a region of uniform shear such as $\Delta U/\Delta y$, the circulation is $C = -(\Delta U/\Delta y)\cdot(\Delta y\cdot\Delta x)$. Comparing these last two cases, we see that the wind speed is irrelevant for the circulation, but the wind shear is very important.

In the last equation above, $(\Delta y\cdot\Delta x) = A$ is the area enclosed by the circulation. In general, for uniform U and V shear across a region, the horizontal circulation is:

$$C = \left(\frac{\Delta V}{\Delta x} - \frac{\Delta U}{\Delta y}\right)\cdot A \qquad (11.30)$$

But the term in parentheses is the relative vorticity ζ_r. This gives an important relationship between horizontal circulation and vorticity:

$$C = \zeta_r \cdot A \qquad (11.31)$$

Vorticity is defined at any one point in a fluid, while circulation is defined around a finite-size area. Thus, eq. (11.31) is valid only in the limit as A becomes small, or for the special case of a fluid having uniform vorticity within the whole circulation area.

The horizontal circulation C defined by eq. (11.30 & 11.31) is also known as the **relative circulation** C_r. An **absolute circulation** C_a can be defined as

$$C_a = (\zeta_r + f_c)\cdot A \qquad (11.32)$$

where f_c is the Coriolis parameter. The absolute circulation is the circulation that would be seen from a fixed point in space looking down on the atmosphere rotating with the Earth.

For the special case of a frictionless **barotropic atmosphere** (where isopycnics are parallel to isobars), **Kelvin's circulation theorem** states that C_a is constant with time.

For a more realistic **baroclinic atmosphere** containing horizontal temperature gradients, the **Bjerknes circulation theorem:**

$$\frac{\Delta C_r}{\Delta t} = -\sum_{i=1}^{n}\left(\frac{\Delta P}{\rho}\right)_i - f_c\cdot\frac{\Delta A}{\Delta t} \qquad (11.33)$$

says relative circulation varies with the torque applied to the fluid (via the component of pressure forces in the direction of travel, summed around the perimeter of the circulation area) minus the Earth's rotation effects in a changing circulation area. The units of $\Delta P/\rho$ are J/kg, which are equivalent to the m^2·s^{-2} units of $\Delta C_r/\Delta t$. The pressure term in eq. (11.33) is called the **solenoid term**.

MID-LATITUDE TROUGHS AND RIDGES

The jet streams do not follow parallels in zonal flow around the Earth to make perfect circles around the north and south poles. Instabilities in the atmosphere cause the jet stream to meander north and south in a wavy pattern as they encircle the globe (Fig. 11.49). As already mentioned, these waves are called **planetary waves** or **Rossby waves**, and have a wavelength of roughly 3000 to 4000 km (Fig. 11.44). The number of waves around the globe is called the **zonal wavenumber**, and is typically 7 or 8, although they can range from about 3 to 13.

In Fig. 11.49, jet stream winds (shaded) follow the height contours in a general counterclockwise (west to east) circulation as viewed looking down on the North Pole. The jet stream roughly demarcates the boundary between the cold polar air from the warmer tropical air, because this temperature difference generates the jet stream winds due to the thermal-wind relationship.

Regions of relatively low pressure or low height are called **troughs**. The center of the trough, called the **trough axis**, is indicated with a dashed line. Winds turn cyclonically (counterclockwise in the N. Hemisphere) around troughs; hence, troughs and low-pressure centers (lows) are similar.

Ridges of relatively high pressures or heights are between the troughs. **Ridge axes** are indicated with a zig-zag line. Air turns anticyclonically (clockwise in the N. Hemisphere) around ridges; hence, ridges and high-pressure centers (highs) are similar.

Two types of instabilities trigger these waves in the global circulation: barotropic instability and baroclinic instability. Barotropic instability, caused by the Earth's rotation, is described next. Baroclinic instability adds the effects of the north-south temperature gradient.

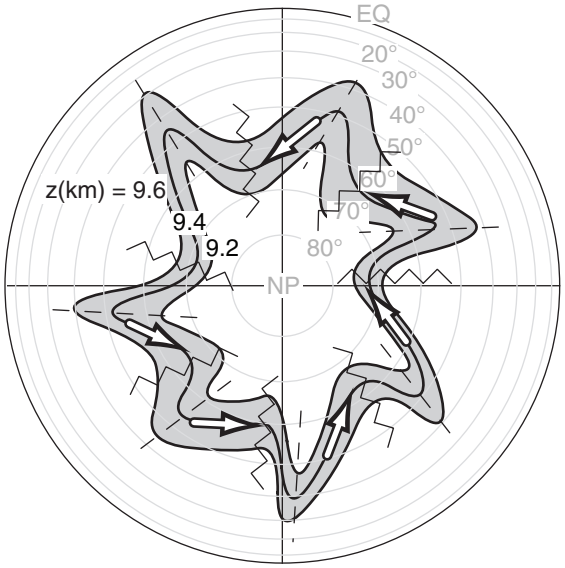

Figure 11.49
Height (z) contours of the 30 kPa pressure surface. View is looking down on the north pole (NP), and circles are parallels labeled with latitude. Dashed lines indicate trough axes; zig-zag lines indicate ridge axes. The jet stream is shaded, with white arrows showing wind direction. EQ is the equator.

Barotropic Instability & Rossby Waves

Picture the jet stream at mid-latitudes, blowing from west to east. If some small disturbance (such as flow over mountains, discussed in the Extratropical Cyclones chapter) causes the jet to turn slightly northward, then conservation of potential vorticity causes the jet to meander north and south. This meander is the **Rossby wave** or **planetary wave**.

To understand this process, picture initially-zonal flow at mid-latitudes, such as sketched in Fig. 11.50 at point 1. Straight zonal flow has no relative vorticity (no shear or curvature; i.e., $M/R = 0$), but there is the planetary vorticity term in eqs. (11.23 - 11.25) related to the latitude of the flow. For the

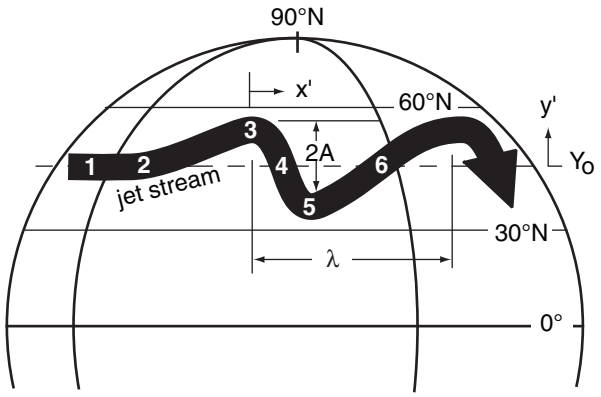

Figure 11.50
Initially zonal flow of the jet stream at point 1, if disturbed at point 2, will develop north-south meanders called Rossby waves. λ = wavelength. A = wave amplitude.

BEYOND ALGEBRA • Vorticity of a Wave

Problem: How does relative vorticity ζ_r vary with distance east (x) in a planetary wave?

Solution: Idealize the planetary wave as a sine wave

$$y = A \cdot \sin(2\pi \cdot x / \lambda) \quad (a)$$

where y is distance north of some reference parallel (such as 45°N), A is north-south amplitude, and λ is east-west wavelength. Assume constant wind speed M following the path of the sine wave. The U and V components can be found from the slope s of the curve. Combining $s = V/U$ and $U^2 + V^2 = M^2$ gives:

$$U = M \cdot (1+s^2)^{-1/2} \quad \text{and} \quad V = M \cdot s \cdot (1+s^2)^{-1/2} \quad (b)$$

But the slope is just the first derivative of eq. (a)

$$s = \partial y / \partial x = (2\pi A / \lambda) \cdot \cos(2\pi \cdot x / \lambda) \quad (c)$$

Write eq. (11.20) in terms of partial derivatives:

$$\zeta_r = \partial V / \partial x - \partial U / \partial y \quad (d)$$

which can be rewritten as:

$$\zeta_r = \partial V / \partial x - (\partial U / \partial x) \cdot (\partial x / \partial y)$$

or

$$\zeta_r = \partial V / \partial x - (\partial U / \partial x) \cdot (1 / s) \quad (e)$$

Plugging eqs. (b) and (c) into (e) gives the answer:

$$\zeta_r = \frac{-2 \cdot M \cdot A \cdot \left(\frac{2\pi}{\lambda}\right)^2 \cdot \sin\left(\frac{2\pi x}{\lambda}\right)}{\left[1 + \left(\frac{2\pi A}{\lambda}\right)^2 \cdot \cos^2\left(\frac{2\pi x}{\lambda}\right)\right]^{3/2}} \quad (f)$$

This is plotted in Fig. 11.a below, for an example where λ = 4000 km, A = 1000 km, and M = 50 m/s.

Discussion: $|\zeta_r| = 2M/R$, where R is the radius of curvature for a sine wave, as is given in many calculus textbooks. Notice the narrow, sharp peaks of vorticity. Increased wave amplitude narrows the vorticity peaks.

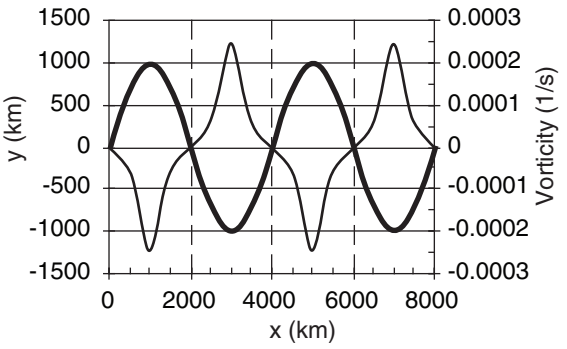

Figure 11.a.
Streamline of an idealized planetary wave (thick), and the corresponding vorticity (thin).

special case of a fluid of fixed depth Δz such as the troposphere (Δz = 11 km), the conservation of potential vorticity simplifies to

$$\left[\frac{M}{R} + f_c\right]_{initial} = \left[\frac{M}{R} + f_c\right]_{later} \quad (11.34)$$

where we will focus on the curvature term as a surrogate to the full relative vorticity.

If this flow is perturbed slightly (at point 2) to turn to the north, the air is now moving into higher latitudes where the Coriolis parameter and planetary vorticity are greater. Thus, a negative shear or curvature (negative R) must form in the flow to compensate the increased planetary shear, in order to keep potential vorticity constant. In plain words, the jet turns clockwise in the N. Hemisphere (anticyclonic) at point 3 until it points southeast.

As it proceeds southward toward its initial latitude (point 4), it has less curvature (i.e., less relative vorticity), but still points southeast. The jet then overshoots south of its initial latitude to a region where planetary vorticity is less (point 5). To preserve potential vorticity, it develops a cyclonic (counterclockwise in N. Hemisphere) curvature and heads back northeast. Thus, initially stable (zonal) flow from point 1 has become wavy, and is said to have become **unstable**.

This Rossby wave requires a variation of Coriolis parameter with latitude to create the instability — an effect called **barotropic instability**. Parameter $\beta = \Delta f_c / \Delta y$ gives the rate of change of Coriolis parameter f_c with distance north y:

$$\beta = \frac{\Delta f_c}{\Delta y} = \frac{2 \cdot \Omega}{R_{earth}} \cdot \cos\phi \quad \bullet(11.35)$$

where R_{Earth} =6371 km is the average Earth radius. Thus, $2 \cdot \Omega / R_{Earth} = 2.29 \times 10^{-11}$ m^{-1}·s^{-1}, and β is on the order of (1.5 to 2)x10^{-11} m^{-1}·s^{-1}.

The path taken by the wave is approximately:

$$y' \approx A \cdot \cos\left[2\pi \cdot \left(\frac{x' - c \cdot t}{\lambda}\right)\right] \quad (11.36)$$

where y' is the north-south displacement distance from the center latitude Y_o of the wave, x' is the distance east from some arbitrary longitude, c is the phase speed (the speed at which the crest of the wave moves relative to the Earth), A is the north-south amplitude of the wave, λ is the wavelength (see Fig. 11.50), and the primes indicate the deviation from a mean background state.

Typical wavelengths are $\lambda \approx 6000$ km, although a wide range of wavelengths can occur. The circumference ($2\pi \cdot R_{Earth} \cdot \cos\phi$) along a parallel at mid-latitudes limits the total number of barotropic waves that can fit around the globe to about 4 to 5. The north-south domain of the wave roughly corresponds to the 30°-60° mid-latitudes where the jet stream is strongest, giving $A \approx 1665$ km.

These waves propagate relative to the mean zonal wind U_o at **intrinsic phase speed** c_o of about

$$c_o = -\beta \cdot \left(\frac{\lambda}{2\pi} \right)^2 \qquad \bullet(11.37)$$

where the negative sign indicates westward propagation relative to the mean background flow. However, when typical values for β and λ are used in eq. (11.37), the intrinsic phase speed is roughly half the magnitude of the eastward jet-stream speed.

A **phase speed** c relative to the ground is defined as:

$$c = U_o + c_o \qquad \bullet(11.38)$$

which gives the west-to-east movement of the wave crest. For typical values of c_o and background zonal wind speed U_o, the phase speed c is positive. Hence, the mean wind pushes the waves toward the east relative to observers on the Earth. Eastward moving waves are indeed observed.

Equation (11.37) is called a **dispersion relation** because waves of different wavelengths propagate at different phase speeds. Waves that initially coincide would tend to separate or disperse with time.

By combining eqs. (11.37) and (11.38), we see that waves of shorter wavelength (**short waves**) travel faster toward the east than **long waves** (Fig. 11.51). Thus, short waves ride the long wave analogous to a car driving along a hilly road (see solved example).

(a) Short Waves

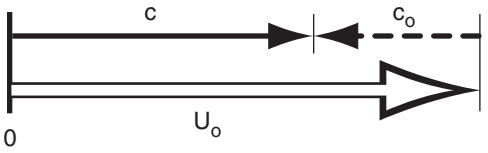

(b) Long Waves

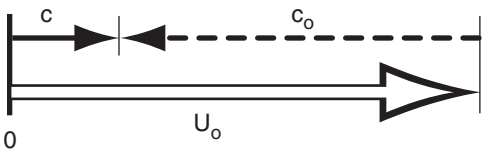

Figure 11.51 *(at left)*
Sum of large background west wind U_o with smaller intrinsic Rossby-wave phase speed c_o from the east gives propagation speed c of Rossby waves relative to the ground.

BEYOND ALGEBRA • The Beta Plane

We can derive β from the definition of f_c. Start with eq. (10.16):

$$f_c = 2\,\Omega \sin\phi$$

where ϕ is latitude.

Since y is the distance along the perimeter of a circle of radius R_{Earth}, recall from geometry that

$$y = R_{Earth} \cdot \phi$$

for ϕ in radians.

Rearrange this to solve for ϕ, and then plug into the first equation to give:

$$f_c = 2\,\Omega \sin(y/R_{Earth})$$

By definition of β, take the derivative to find

$$\beta = \frac{\partial f_c}{\partial y} = \frac{2 \cdot \Omega}{R_{earth}} \cdot \cos\left(\frac{y}{R_{earth}} \right)$$

Finally, use the second equation above to give:

$$\boxed{\beta = \frac{2 \cdot \Omega}{R_{earth}} \cdot \cos\phi} \qquad \bullet(11.35)$$

For midlatitude planetary waves confined to a latitude belt such as sketched in Fig. 11.50, it is often convenient to assume β = constant. This has the same effect as assuming that a portion of the Earth is shaped like a cone (as sketched below in white) rather than a sphere. The surface of the cone is called a **beta plane**, and looks like a lamp shade. Such an idealization allows barotropic effects to be described with slightly simpler math.

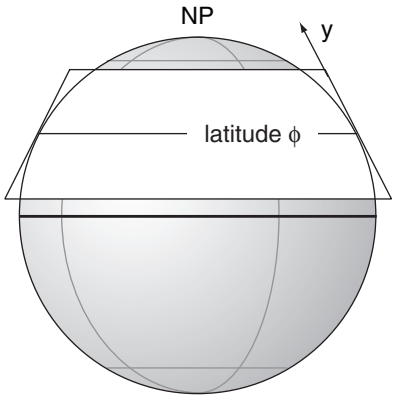

Solved Example (§)

A background jet stream of speed 50 m/s meanders with 6000 km wavelength and 1500 km amplitude, centered at 45°N. Find the beta parameter. Also, plot the path (i.e., the meridional displacement) of the barotropic wave between $0 \le x' \le 10000$ km at some initial time and 6 hours later, and find the phase speeds.

Solution

Given: $\phi = 45°$, $U_o = 50$ m/s, $\lambda = 6000$ km, $A = 1500$ km, $t = 0$ and 6 h

Find: $\beta = ?\ m^{-1}{\cdot}s^{-1}$, $y'(x') = ?$ km, $c_o = ?$ m/s, $c = ?$ m/s

First, use eq. (11.35):

$$\beta = \frac{1.458\times10^{-4}\,s^{-1}}{6371000\,m}\cdot\cos(45°) = \underline{\mathbf{1.62x10}}^{-11}\ m^{-1}{\cdot}s^{-1}.$$

Next, use eq. (11.37):

$$c_o = -(1.62\times10^{-11}\,m^{-1}s^{-1})\left(\frac{6\times10^{6}\,m}{2\pi}\right)^2$$

$$= \underline{\mathbf{-14.7\ m/s}}$$

Use eq. (11.38):

$$c = (50 - 14.7)\ m/s = \underline{\mathbf{35.26\ m/s}}$$

Use eq. (11.36) on a spreadsheet for $t = 0$ & 6 h:

$$y' \approx (1500\text{km})\cdot\cos\left[2\pi\cdot\left(\frac{x' - (35.26\text{m/s})\cdot t}{6\times10^{6}\,m}\right)\right]$$

The results are plotted below:

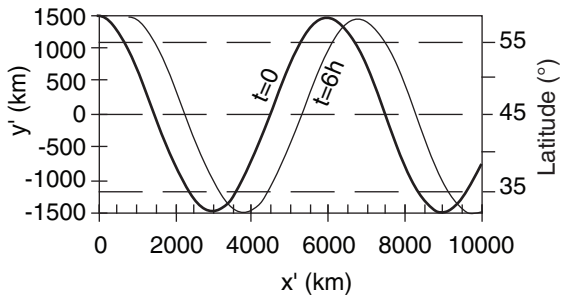

Check: Units OK. Physics OK.

Discussion: The barotropic long wave propagates east about 800 km during the 6 h interval. The jet stream blows along this wavy path at speed 50 m/s.

Although this Rossby-wave phase speed is much slower than a jet airliner, the wave does not need to land and refuel. Thus, during 24 hours, this long wave could travel over 3000 km — greater than the distance between San Francisco, CA and Chicago, IL, USA.

This is why weather systems can move so far in one day.

Solved Example (§)

Same as the previous solved example, except that in addition to the previous long wave, there is also a barotropic short wave of 1000 km wavelength with amplitude 300 km.

Solution

Given: Same, plus $\lambda = 1000$ km, $A = 300$ km.

Find: $c = ?$ m/s, $y'(x') = ?$ km

Use eq. (11.37):

$$c_o = -(1.62\times10^{-11}\,m^{-1}s^{-1})\left(\frac{10^{6}\,m}{2\pi}\right)^2 = \underline{\mathbf{-0.41\ m/s}}$$

Use eq. (11.38):

$$c = (50 - 0.41)\ m/s = \underline{\mathbf{49.6\ m/s}}$$

Use eq. (11.36):

$$y' \approx (300\text{km})\cdot\cos\left[2\pi\cdot\left(\frac{x' - (49.6\text{m/s})\cdot t}{1\times10^{6}\,m}\right)\right]$$

The results are plotted below:

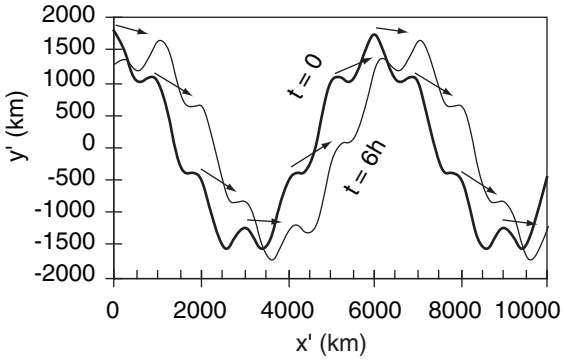

Check: Units OK. Physics OK.

Discussion: The movement of the crest of each short wave is indicated with the arrows. Not only do they move with the propagating background long wave, but they also ride the long wave toward the east at a speed nearly equal to the wind speed in this example.

At this speed, a short wave could travel about 4285 km during 24 hours, more than the distance from San Francisco, CA to New York City, USA. Not only do these short waves travel very fast, but they are in and out of the city very quickly. Thus, they cause rapid changes in the weather.

For this reason, weather forecasters pay particular attention to short waves to avoid surprises. Although short waves are sometimes difficult to spot visually in a plot of geopotential height, you can see them more easily on plots of 50 kPa vorticity. Namely, each short wave has a vorticity that can be highlighted or colorized on a forecast map.

Baroclinic Instability & Rossby Waves

Recall from Figs. 11.1b and 11.37a that, at mid-latitudes, the cold polar air slides under the warmer tropical air. This causes the air to be statically stable, as can be quantified by a Brunt-Väisälä frequency N_{BV}. The development later in this section extends what we learned of barotropic flows to the more complete baroclinic case having both β and N_{BV} effects in an environment with north-south temperature gradient.

First, we take a heuristic approach, and idealize the atmosphere as being a two-layer fluid, with a north-south sloping density interface such as idealized in Fig. 11.52. This will give us a qualitative picture of baroclinic waves.

Qualitative Model

Initially-zonal flow of the jet stream (sketched as the dark-shaded ribbon of air at point 1) has no relative vorticity, but it does have planetary vorticity related to its latitude. The narrow white column in the front left of Fig. 11.52 represents air having such absolute vorticity.

If this jet stream is perturbed northward by some outside influence such as a mountain, it rides up on the density interface over the cold air. The stratosphere is so statically stable that it acts like a lid on the troposphere. Thus, as the ribbon of air meanders northward, it is squeezed between the tropopause and the rising density interface. Namely, Δz shrinks. For this situation, the potential vorticity equation can be written as:

$$\left[\frac{f_c + (M/R)}{\Delta z}\right]_{initial} = \left[\frac{f_c + (M/R)}{\Delta z}\right]_{later} \qquad (11.39)$$

where f_c is the Coriolis parameter, M is the wind speed, and R is the radius of curvature.

The column depth is less at point 3 than initially at point 2; hence, the absolute vorticity at 3 must also be less than that at 2, for the ratio of absolute vorticity to depth to remain constant. The planetary contribution does not help – in fact, it is larger at point 3 because it is at a higher latitude. Hence, the only way to conserve potential vorticity is for the relative vorticity to decrease substantially. As it decreases below its initial value of zero, the jet-stream path curves anticyclonically at point 3.

The jet stream overshoots to the south, develops cyclonic relative vorticity and turns back to the north (not sketched in Fig. 11.52). This breakdown of zonal flow into wavy flow is called **baroclinic instability**. The baroclinic Rossby waves look similar to those in Fig. 11.50, except with shorter wavelength λ than barotropic waves because now both f_c and Δz work together to cause the oscillation.

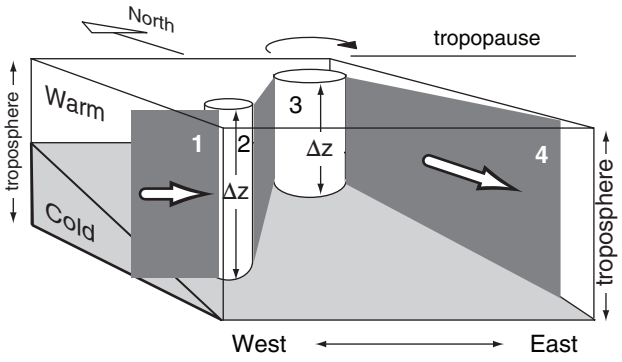

Figure 11.52
Some of the processes involved in baroclinic instability. Dark gray ribbon represents the jet-stream axis, while white columns indicate rotation associated with the absolute vorticity of the jet.

Solved Example(§)

Same as the previous solved example, except for a baroclinic wave in a standard atmosphere, with the one dominant wave. Wave amplitude is 1500 km. Plot results at t = 0 and 6 h for z = 0 and 11 km.

Solution

Given: Same, and use Table 1-5 for std. atmos:

ΔT = –56.5–15 = –71.5°C across Δz = 11 km.

T_{avg} = 0.5·(–56.5+15°C) = –20.8°C = 252 K

Find: λ_R = ? km, λ = ? km, c = ? m/s, $y'(x')$ = ? km

Use eq. (5.4a):

$$N_{BV} = \sqrt{\frac{(9.8\text{m/s})}{252\text{K}}\left(\frac{-71.5\text{K}}{1.1\times10^4\text{m}} + 0.0098\frac{\text{K}}{\text{m}}\right)}$$

N_{BV} = 0.0113 s^{-1}

Use eq. (10.16):

$$f_c = (1.458\times10^{-4}s^{-1})\cdot\sin(45°) = 1.031\text{x}10^{-4}\text{ s}^{-1}$$

Use eq. (11.12):

$$\lambda_R = \frac{(0.0113\text{s}^{-1})\cdot(11\text{km})}{1.03\times10^{-4}\text{s}^{-1}} = \underline{\mathbf{1206\text{ km}}}$$

Use eq. (11.43):

$\lambda = \lambda_d = 2.38\,\lambda_R = \underline{\mathbf{2870\text{ km}}}$

Use eq. (11.41):

$$c_o = \frac{-(1.62\times10^{-11}\text{m}^{-1}\text{s}^{-1})}{\pi^2\cdot\left[\frac{4}{(2870\text{km})^2}+\frac{1}{(1206\text{km})^2}\right]} = \underline{\mathbf{-1.40\text{ m/s}}}$$

Use eq. (11.42):

c = (50 – 1.40)m/s = $\underline{\mathbf{48.6\text{ m/s}}}$

Use eq. (11.40):

$$y' \approx (1500\text{km})\cos\left(\frac{\pi\cdot z}{11\text{km}}\right)\cos\left[2\pi\left(\frac{x'-48.6\text{m/s}\cdot t}{2870\text{km}}\right)\right]$$

The results are plotted below:

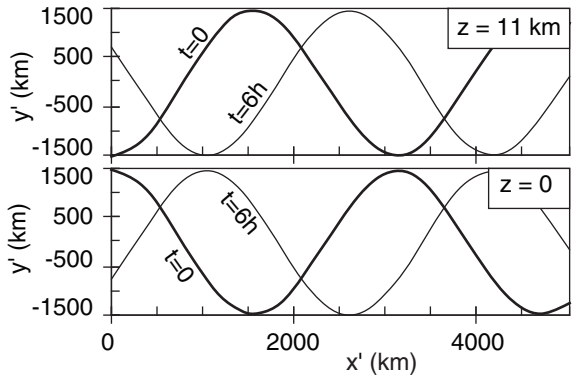

Check: Units OK. Physics OK.

Discussion: The Rossby wave at z = 11 km is indeed 180° out of phase from that at the surface.

Quantitative Approach

To extend this argument, consider the continuous stratification of Fig. 5.20 (reproduced on the next page). Between the 290 K and 340 K isentropes in that illustration, the air is statically stable. A column of air bounded at the bottom and top by these isentropes near the equator shortens as it moves poleward. Thus, we could use the Brunt-Väisälä frequency and the north-south temperature gradient (i.e., the baroclinicity) as a better representation of the physics than the two layer model of Fig. 11.52.

Skipping a long derivation, we end up with a north-south displacement y' of a baroclinic wave that is approximately:

$$y' \approx A\cdot\cos\left(\pi\cdot\frac{z}{Z_T}\right)\cdot\cos\left[2\pi\cdot\left(\frac{x'-c\cdot t}{\lambda}\right)\right] \qquad (11.40)$$

where $Z_T \approx 11$ km is the depth of the troposphere, A is north-south amplitude, c is phase speed, λ is wavelength, x is distance East, and t is time. The extra cosine term containing height z means that the north-south wave amplitude first decreases with height from the surface to the middle of the troposphere, and then increases with opposite sign toward the top of the troposphere. Namely, the planetary wave near the tropopause is 180° out of phase compared to that near the ground.

[*CAUTION: this is an oversimplification. Waves in the real atmosphere aren't always 180° out of phase between top and bottom of the troposphere. Nonetheless, this simple approach gives some insight into the workings of baroclinic waves.*]

The dispersion relation gives intrinsic phase speed c_o as:

$$c_o = \frac{-\beta}{\pi^2\cdot\left[\frac{4}{\lambda^2}+\frac{1}{\lambda_R^2}\right]} \qquad \bullet(11.41)$$

where eq. (11.35) gives β, wavelength is λ, and eq. (11.12) gives the internal Rossby deformation radius λ_R. As before, the phase speed relative to the ground is:

$$c = U_o + c_o \qquad \bullet(11.42)$$

Intrinsic phase speed c_o is negative, with magnitude less than the background jet velocity U_o, allowing the waves to move east relative to the ground.

As for barotropic waves, baroclinic waves have a range of wavelengths that can exist in superposition. However, some wavelengths grow faster than others, and tend to dominate the flow field. For baroclinic waves, this dominant wavelength λ_d is on the order of 3000 to 4000 km, and is given by:

$$\lambda_d \approx 2.38\cdot\lambda_R \qquad (11.43)$$

where λ_R is the internal Rossby radius of deformation (eq. 11.12).

North-south displacement y' is not the only characteristic that is wavy in baroclinic flow. Also wavy are the perturbation velocities (u', v', w'), pressure p', potential temperature θ', and vertical displacement η', where the prime denotes deviation from the mean background state.

To present the wave equations for these other variables, we will simplify the notation by using:

$$a = \pi \cdot z / Z_T \tag{11.44}$$

and

$$b = 2\pi \cdot (x' - c \cdot t) / \lambda \tag{11.45}$$

Thus:

$$\begin{aligned} y' &= \hat{Y} \cdot \cos(a) \cdot \cos(b) \\ \eta' &= \hat{\eta} \cdot \sin(a) \cdot \cos(b) \\ \theta' &= -\hat{\theta} \cdot \sin(a) \cdot \cos(b) \\ p' &= \hat{P} \cdot \cos(a) \cdot \cos(b) \\ u' &= \hat{U} \cdot \cos(a) \cdot \cos(b) \\ v' &= -\hat{V} \cdot \cos(a) \cdot \sin(b) \\ w' &= -\hat{W} \cdot \sin(a) \cdot \sin(b) \end{aligned} \tag{11.46}$$

Symbols wearing the caret hat (^) represent amplitude of the wave. These amplitudes are defined to be always positive (remember c_o is negative) in the Northern Hemisphere:

$$\begin{aligned} \hat{Y} &= A \\ \hat{\eta} &= \frac{A \cdot \pi \cdot f_c \cdot (-c_o)}{Z_T} \cdot \frac{1}{N_{BV}^2} \\ \hat{\theta} &= \frac{A \cdot \pi \cdot f_c \cdot (-c_o)}{Z_T} \cdot \frac{\theta_o}{g} \\ \hat{P} &= A \cdot \rho_o \cdot f_c \cdot (-c_o) \\ \hat{U} &= \left[\frac{A \cdot 2\pi \cdot (-c_o)}{\lambda} \right]^2 \cdot \frac{1}{A \cdot f_c} \\ \hat{V} &= \frac{A \cdot 2\pi \cdot (-c_o)}{\lambda} \\ \hat{W} &= \frac{A \cdot 2\pi \cdot (-c_o)}{\lambda} \cdot \frac{\pi \cdot (-c_o) \cdot f_c}{Z_T \cdot N_{BV}^2} \end{aligned} \tag{11.47}$$

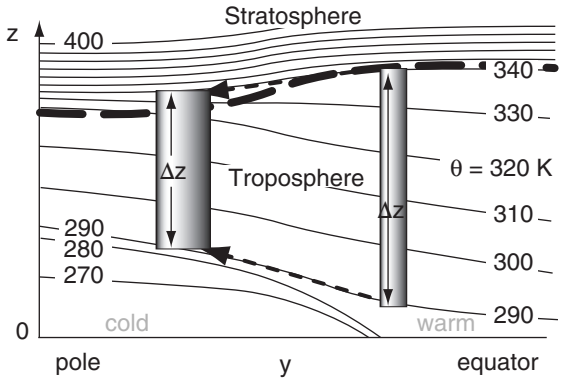

Figure 5.20 (again)
Vertical cross section through the atmosphere, showing isentropes (lines of constant potential temperature θ). The depth Δz of column of air on the right will shrink as the column moves poleward, because air tends to follow isentropes during adiabatic processes. Thus, the same Δθ between top and bottom of the air columns spans a shorter vertical distance for the poleward column, meaning that static stability and Brunt-Väisälä frequency are greater there.

Solved Example

Same as previous solved example, but find the pressure amplitudes at sea level.

Solution

Given: A = 1500 km, $f_c = 1.031 \times 10^{-4}$ s^{-1}, c_o = –1.40 m/s
Find: $\hat{P}$ = ? kPa

Use std. atmosphere for sea level: $\rho_o = 1.225$ kg·m^{-3} .
Use eq. (11.47):

$$\hat{P} = (1500\text{km})\left(1.225 \frac{\text{kg}}{\text{m}^3}\right)(1.031 \times 10^{-4}\text{s}^{-1})\left(1.4 \frac{\text{m}}{\text{s}}\right)$$

= **0.265 kPa**

Check: Units OK. Physics OK.
Discussion: Between high and low pressure is a distance of half a wavelength, which is 1435 km for this case (see previous solved example). The pressure difference between crest and trough of the wave is 2· $\hat{P}$ = 0.53 kPa. Thus, the pressure gradient is order of 0.53/1435 = 0.00037 kPa/km, which is sufficient to drive the winds.

In the real atmosphere, condensation in clouds (which was neglected in eqs. 11.47) contributes to the dynamics to make horizontal pressure gradients even stronger.

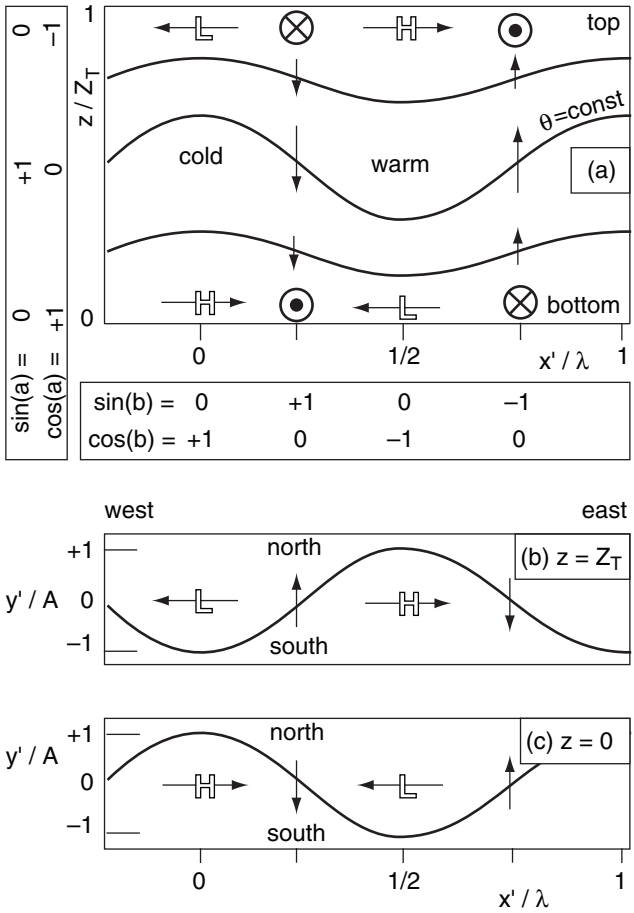

Figure 11.53
Idealized structure of baroclinic wave in N. Hem. (a) West-to-east vertical cross section. (b) Weather map (plan view) at tropopause. (c) Surface weather map. Legend: Arrows show wind. L & H are low & high pressures, dot-circle is southward-pointing vector, x-circle is northward vector. Wavy lines on the cross section are isentropes. Also shown are sine & cosine terms from baroclinic wave equations. (after Cushman-Roisin, 1994)

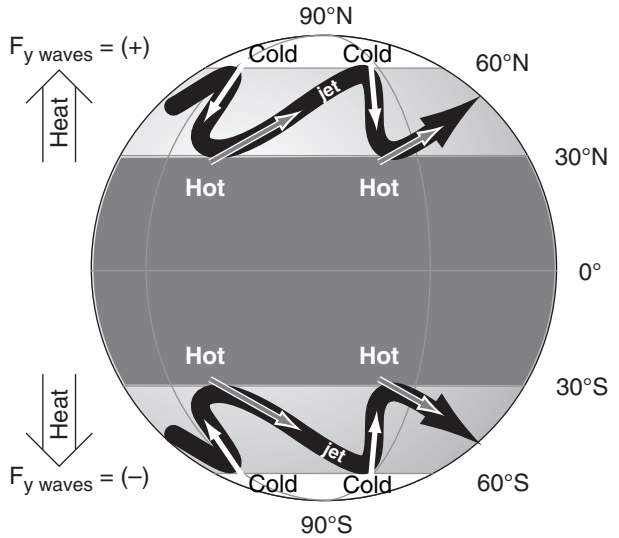

Figure 11.54
Heat transport by Rossby waves (black line) in midlatitudes.

where ρ_o is the average air density at wave altitude z. Each of these amplitudes depends on A, the amplitude of the meridional displacement, which is not fixed but depends on the initial disturbance and wave amplitude.

Fig. 11.53 illustrates the structure of this baroclinic wave in the Northern Hemisphere. Fig. 11.53c corresponds to the surface weather maps used in the previous solved examples. All the variables are interacting to produce the wave. The impact of all these variables on synoptic weather will be discussed in the Extratropical Cyclones chapter.

Actual variables are found by adding the perturbation variables (eqs. 11.46) to the background state. Mean background pressure P_o decreases hydrostatically with height. Thus, the actual pressure is $P = P_o + p'$ at any height.

Mean background potential temperature θ_o increases linearly with height (assuming constant N_{BV}), making the actual potential temperature $\theta = \theta_o + \theta'$. Background meridional and vertical winds are assumed to be zero, leaving $V = v'$ and $W = w'$. Background zonal wind U_o is assumed to be geostrophic and constant, leaving $U = U_o + u'$. Meridional displacement perturbations (y') are relative to the reference latitude (Y_o) used for the Coriolis-parameter calculation. Vertical displacement perturbations (η') are relative to the height variable z that appears in eq. (11.44).

Many other factors affect wave formation in the jet stream, including turbulent drag, clouds and latent heating, and nonlinear processes in large-amplitude waves. Also, the more complete solution to baroclinic instability includes waves propagating meridionally as well as zonally (we focused on only zonal propagation here). However, our description captures most of the important aspects of midlatitude flow that are observed in the real atmosphere.

Meridional Transport by Rossby Waves

Heat Transport

As the jet stream blows along the meandering planetary-wave path (Fig. 11.54), it picks up warm air (T' = deviation from mean temperature = positive) and carries it poleward (v' = + in N. Hem.). Similarly, cold air (T' = –) is carried equatorward (v' = – in N. Hem.). The average meridional kinematic heat flux ($F_{y\ waves}$) is the sum of advective transports divided by the number N of these transports. For the N. Hemisphere, this meridional heat flux is:

$$F_{y\ waves} = (1/N)\cdot\Sigma(v'T') = (+)\cdot(+) + (–)\cdot(–) = \text{positive.}$$

while it is negative in the Southern Hemisphere.

Thus, the north-south meandering jet stream causes a northward heat flux in the N. Hemisphere and a southward heat flux in the S. Hemisphere (Fig. 11.54) without requiring a vertical circulation cell.

The greatest flux is likely to occur where the waves have the most intense v-component (Fig. 11.54), and also where the north-south temperature gradient is greatest (Fig. 11.8). Both of these processes conspire together to create significant wave heat fluxes centered in mid-latitudes (Fig. 11.55 bottom).

Curvature (*Curv*) of a line is defined to be positive when the line bends concave up (shaped like a bowl). Likewise, curvature is negative for concave down (shaped like a hill). The signs of the curvatures of wave heat flux are indicated in the top of Fig. 11.55, which we will use in the next section.

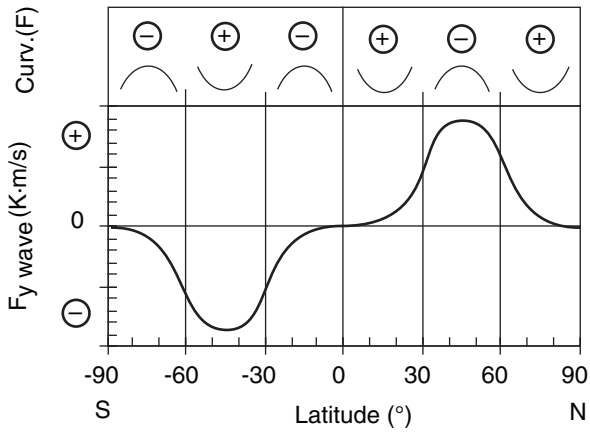

Figure 11.55
Bottom: Sketch of meridional wave flux of heat (F_y, positive northward, in kinematic units). Top: Sketch of sign of curvature of the wave flux.

Momentum Transport

Recall from Fig. 11.41 that tropical air is faster (u' = positive) when moved toward 45° latitude. Similarly, polar air is slower (u' = negative) when moved toward 45° latitude. This was because of angular-momentum conservation, where air near the equator is at a larger distance (larger radius) from the Earth's axis than air near the poles. Thus, the polar and tropical regions serve as reservoirs of slow and fast momentum, respectively, which can be tapped by the meandering jet stream.

Analogous to heat transport, we find that the poleward-moving (v' = + in N. Hem.) portions of Rossby waves carry fast zonal momentum (u'= +) air, and equatorward-moving (v' = – in N. Hem.) portions carry slow zonal momentum (u' = –) (Fig. 11.56). The net meridional transport of zonal momentum $\overline{u'v'}$ for the Northern Hemisphere is positive, and is largest at the center of mid-latitudes.

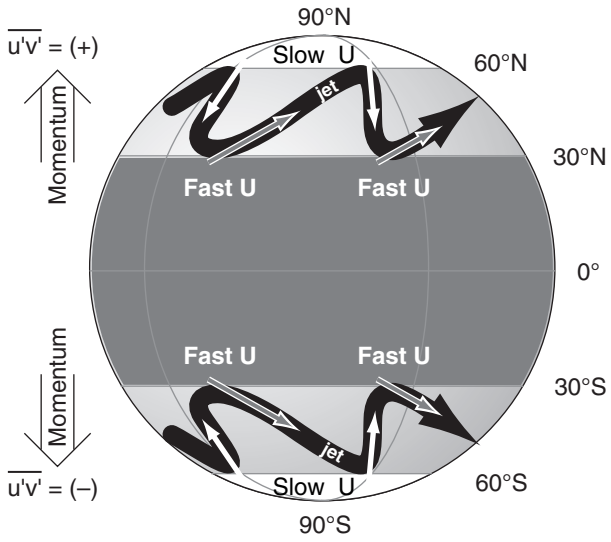

Figure 11.56
Meridional transport of eastward momentum by Rossby waves in the jet stream (black wavy line) in midlatitudes.

$$\overline{u'v'} = (1/N)\cdot\Sigma(v'\cdot u') = (+)\cdot(+) + (-)\cdot(-) = \text{positive}.$$

It is negative for the Southern Hemisphere.

However, the reservoir of tropical momentum is much larger than that of polar momentum because of the larger circumference of latitude lines in the tropics. Hence, tropical momentum can have more influence on midlatitude air. To account for such unequal influence, a weighting factor $a = \cos(\phi_s)/\cos(\phi_d)$ can be included in the angular momentum expression:

$$a\cdot u' \approx \Omega\cdot R_{earth}\cdot\left[\frac{\cos^2\phi_s}{\cos\phi_d} - \cos\phi_d\right]\cdot\frac{\cos\phi_s}{\cos\phi_d} \qquad (11.48)$$

where subscript s represents source location, d is destination, and $\Omega\cdot R_{Earth}$ = 463.4 m/s as before.

Fig. 11.57 shows that the weighted zonal velocity is asymmetric about 45° latitude. Namely, from 60°

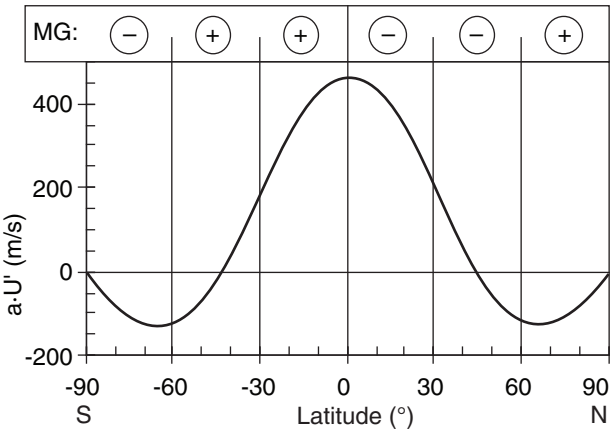

Figure 11.57
Zonal velocity from various source latitudes reaching destination 45°, weighted by the relative amounts of source-region air.

Solved Example

Find the weighted zonal velocity perturbation for air arriving at 50°N from 70°N.

Solution

Given: $\phi_s = 70°N$, $\phi_d = 50°N$

Find: $a{\cdot}u' = ?$ m/s

Use eq. (11.48):

$$a{\cdot}u' = (463.4\text{m/s}){\cdot}\left[\frac{\cos^2(70°)}{\cos(50°)} - \cos(50°)\right]\frac{\cos(70°)}{\cos(50°)}$$

$$= \underline{\textbf{– 113.6 m/s}}$$

Check: Physics OK. Magnitude too large.

Discussion: The negative sign means air from 70°N is moving slower from the west than any point at 50°N on the Earth's surface is moving. Thus, relative to the Earth, the wind is from the east.

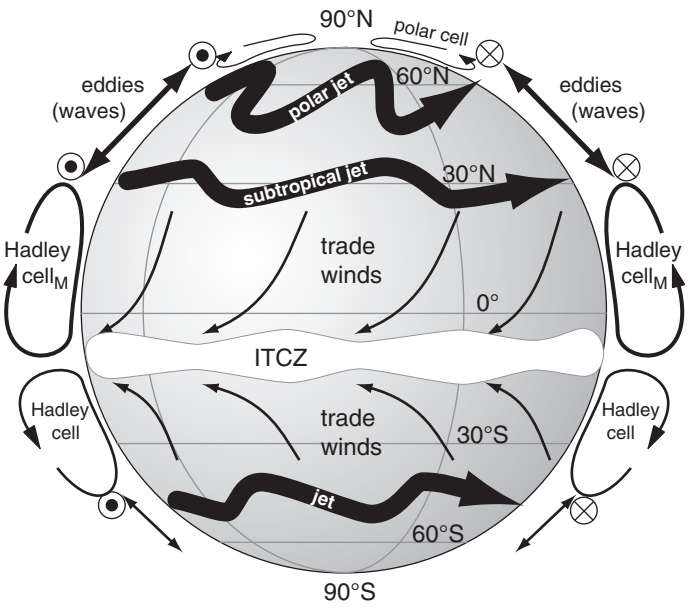

Figure 11.58

Sketch of three-band structure of general circulation for February (N. Hemisphere winter): 1) vertical Hadley cell in tropics, 2) horizontal Rossby waves at midlatitudes, and 3) a weak vertical circulation near the poles. For the jet axes, the dot-circle is wind out of the page, and x-circle is wind into the page.

FOCUS • Torques on the Earth

During high-wind episodes in one of the circulation bands, temporary changes in wind-drag torques are large enough to make measurable changes in the Earth's rotation rate — causing the length of a day to increase or decrease 1 - 3 μs over periods of months. In addition, external influences (lunar and solar tides, solar wind, geomagnetic effects, space dust) cause the Earth to spin ever more slowly, causing the length of a day to increase 1.4 ms/century at present.

latitude the velocity is –100 m/s, but from a source of 30° latitude the velocity is about +200 m/s. Although the momentum transport is positive everywhere, it decreases to the north. Hence, the meridional gradient MG of zonal momentum is negative in the Northern Hemisphere mid-latitudes:

$$MG = \Delta\,\overline{u'v'} / \Delta y = \text{negative}. \qquad (11.49)$$

Although quantitatively the wind magnitudes from angular-momentum arguments are unrealistically large, as discussed earlier, the qualitative picture of momentum transport is valid.

Rossby waves that transport U momentum poleward have a recognizable rounded-sawtooth shape, as was sketched in Fig. 11.56. Specifically, the equatorward-moving portions of the jet stream are aligned more north-south (i.e., are more meridional), and sometimes even tilt backwards (toward the west as it moves toward the equator). The poleward-moving portions of the jet are more zonal (west to east).

THREE-BAND GENERAL CIRCULATION

The preceding sections explained the assertion that was made in the opening paragraphs of this chapter. Namely, Coriolis force causes the thermally-driven planetary circulation to break down into three latitude-bands of circulation (Fig. 11.58) in each hemisphere. These bands are: a strong, asymmetric, **direct** vertical-circulation Hadley cell in the tropics (0° to 30°); a band of mostly horizontal Rossby waves at mid-latitudes (30° to 60°); and a weak direct vertical circulation cell in polar regions (60° to 90°). Fig. 11.58 includes more (but not all) of the details and asymmetries explained in this chapter.

The circulation bands work together to globally transport atmospheric heat (Fig. 11.14), helping undo the differential heating that was caused by solar and IR radiation. The Earth-atmosphere-ocean system is in near equilibrium thermally, with only extremely small trends over time related to global warming.

The circulation bands also work together in the meridional transport of zonal momentum. The trade winds, blowing opposite to the Earth's rotation, exert a **torque** (force times radius) that tends to slow the Earth's spin due to frictional drag against the land and ocean surface. However, in mid-latitudes, the westerlies dragging against the Earth's surface and against mountains apply an opposite torque, tending to accelerate the Earth's spin. On the long term, the opposite torques nearly cancel each other. Thus, the whole Earth-atmosphere-ocean system maintains a near-equilibrium spin rate.

A Measure of Vertical Circulation

Getting back to atmospheric circulations, a measure of vertical-cell circulation *CC* is:

$$CC = \left[\frac{f_c^2}{N_{BV}^2} \frac{\Delta V}{\Delta z} \right] - \frac{\Delta w}{\Delta y} \qquad (11.50)$$

CC is positive for **direct cells** in the N. Hemisphere, as illustrated in Fig. 11.59. Direct cells are ones where the vertical circulation is in the direction that would be expected if there were no Coriolis force. The units for circulation are s^{-1}.

In a direct cell, vertical velocity decreases and even changes sign toward the north, making $\Delta w/\Delta y$ negative. Also, northward velocity *V* increases with height, making $\Delta V/\Delta z$ positive for a direct cell. Both of these terms contribute to positive *CC* in a direct cell. Similarly, *CC* is negative for an **indirect cell** (one that circulates oppositely to a direct cell).

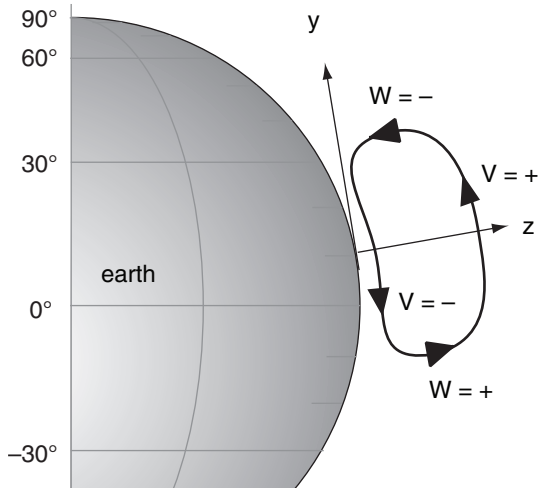

Figure 11.59
Example of a direct-circulation cell in the N. Hemisphere, for the major Hadley cell during N. Hem. winter.

Effective Vertical Circulation

The equations of motion can be combined to yield an equation for the vertical circulation *CC* that can be applied even where vertical cells do not dominate. This circulation equation is written in abbreviated form as eq. (11.51). Buoyancy associated with a heated surface can drive a vertical circulation. But if some of the heating difference is transported by planetary waves, then there will be less heat available to drive a direct circulation.

Based on the previous discussions of radiative differential heating E_{net} from Fig. 11.10, momentum gradient *MG* (proportional to $\Delta U/\Delta z$) from Fig. 11.57, and heat flux curvature $Curv(F_{y\ wave})$ from Fig. 11.55, the contributions of each term to the circulation are listed below the equation. The sign of $\Delta MG/\Delta z$ equals the sign of *MG*, assuming that northward momentum transport is weakest at the ground, and increases with height because the jet-stream winds increase with height.

$$CC \propto -\frac{\Delta E_{net}}{\Delta y} + Curv(F_{y\ wave}) + \frac{\Delta MG}{\Delta z} \qquad (11.51)$$

circulation *radiation* *wave-heat* *wave-momentum*

$CC_{polar} \propto$ positive + positive + positive = <u>positive</u>
$CC_{midlat} \propto$ positive + negative +negative = <u>negative</u>
$CC_{tropics} \propto$ positive + positive + positive = <u>positive</u>

Thus, horizontal planetary waves at mid-latitudes are so effective that they reverse the effective vertical circulation — a result called the **Ferrel cell**.

Solved Example

Suppose the Hadley cell updraft and downdraft velocities are 6 and –4 mm/s, respectively, and the meridional wind speeds are 3 m/s at the top and bottom of the cell. The major Hadley cell is about 17 km high by 3900 km wide, and is centered at about 10° latitude. Temperature in the tropical atmosphere decreases from about 25°C near the surface to –77°C at 17 km altitude. Find the vertical cell circulation.

Solution

Given: $\Delta w = -10$ mm/s = –0.01 m/s , $\Delta y = 3.9 \times 10^3$ km
$\Delta V = 6$ m/s, $\Delta z = 17$ km, $\phi = 10°$, $\Delta T = -102$°C.
Find: $CC = ?\ s^{-1}$.

First, use eq. (10.16):
$f_c = (1.458 \times 10^{-4}\ s^{-1}) \cdot \sin(10°) = 2.53 \times 10^{-5}\ s^{-1}$
Next, for the Brunt-Väisälä frequency, we first need:
$T_{avg} = 0.5*(25 - 77)°C = -26°C = 247$ K
In the tropics $\Delta T/\Delta z = -6$ °C/km = –0.006 K/m
Then use eq. (5.4), and assume $T_v = T$:

$$N_{BV} = \sqrt{\frac{9.8 m/s^2}{247 K}(-0.006 + 0.0098)\frac{K}{m}} = 0.0123\ s^{-1}$$

Finally, use eq. (11.50):

$$CC = \left[\left(\frac{2.53 \times 10^{-5} s^{-1}}{0.0123 s^{-1}} \right)^2 \cdot \frac{6 m/s}{17000 m} \right] - \frac{-0.01 m/s}{3.9 \times 10^6 m}$$

$CC = 1.493 \times 10^{-9} + 2.564 \times 10^{-9}\ s^{-1} = \underline{\mathbf{4.06 \times 10}}^{-9}\ s^{-1}$

Check: Units OK. Physics OK.
Discussion: Both terms contribute positively to the circulation of the major Hadley cell during Northern Hemisphere winter.

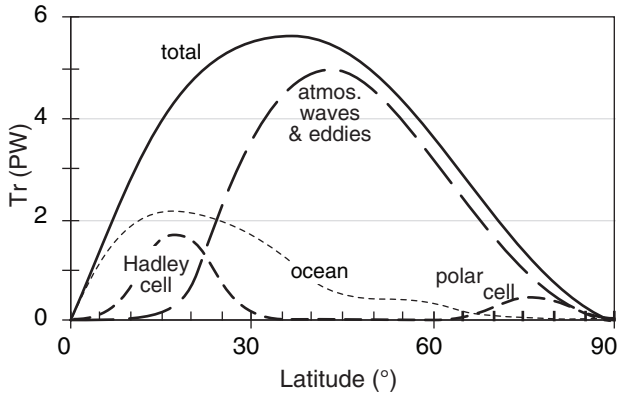

Figure 11.60
Contributions of direct circulations (medium dashed line, for Hadley cell and polar cell) and indirect circulations (long dashed line, for Rossby waves and eddies) to total meridional heat transport Tr in the N. Hemisphere

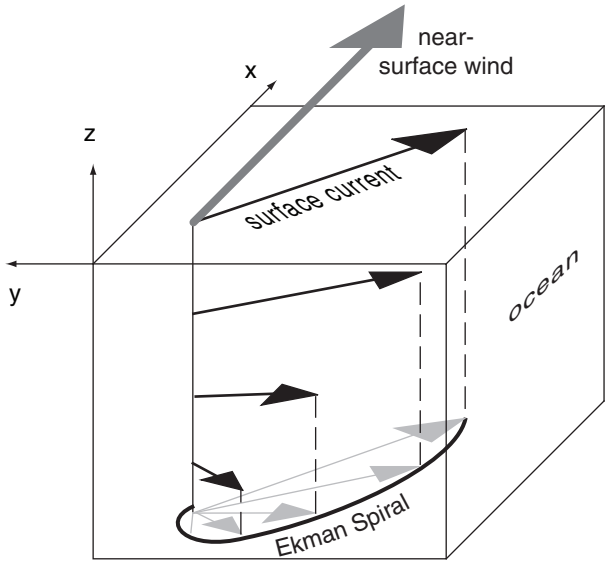

Figure 11.61
Ekman spiral of ocean currents. Black arrows show currents at different depths. Projecting these vectors onto an imaginary plane at the bottom gives the grey vectors, which show the spiral nature of the Ekman currents.

Fig. 11.60 redraws the N. Hemisphere portion of Fig. 11.14, qualitatively highlighting the relative contributions of the direct (Hadley and polar cells) and indirect (Ferrel cell/Rossby waves) atmospheric circulations to the total meridional heat transport. The Rossby wave circulation (and its associated high and low-pressure eddies) dominate at mid-latitudes. Vertically direct circulations dominate elsewhere.

Ocean currents also contribute to global heat redistribution. Although ocean-circulation details are not within the scope of this book, we will introduce one ocean topic here — the Ekman spiral. This describes how wind drag can drive some ocean currents, including hurricane storm surges.

EKMAN SPIRAL IN THE OCEAN

As the wind blows over the oceans, the air drags along some of the water. The resulting ocean currents turn under the influence of Coriolis force (Fig. 11.61), eventually reaching an equilibrium given by:

$$U = \left[\frac{{u_{*water}}^2}{(K \cdot f_c)^{1/2}}\right] \cdot \left[e^{\gamma \cdot z} \cdot \cos\left(\gamma \cdot z - \frac{\pi}{4}\right)\right] \qquad (11.52a)$$

$$V = \left[\frac{{u_{*water}}^2}{(K \cdot f_c)^{1/2}}\right] \cdot \left[e^{\gamma \cdot z} \cdot \sin\left(\gamma \cdot z - \frac{\pi}{4}\right)\right] \qquad (11.52b)$$

where the x-axis and U-current direction point in the direction of the surface wind. When these current vectors are plotted vs. depth (z is positive upward), the result is a spiral called the Ekman spiral.

The friction velocity u_{*water} for water is

$${u_{*water}}^2 = \frac{\rho_{air}}{\rho_{water}} \cdot {u_{*air}}^2 \qquad (11.53)$$

where the friction velocity for air u_{*air} is given in the Boundary Layer Chapter. The **depth parameter** is

$$\gamma = \sqrt{\frac{f_c}{2 \cdot K}} \qquad (11.54)$$

where K is the eddy viscosity (see the Boundary-Layer chapter) in the ocean. The inverse of γ is called the **Ekman layer depth**. Transport of water by Ekman processes is discussed further in the Hurricane chapter.

SUMMARY

Radiation causes differential heating — net heating of the tropics and cooling at the poles. In response, a global circulation develops due to buoyancy, pressure, and geostrophic effects, which moves the excess heat from the equator to the poles.

Near the equator, warm air rises and creates a band of thunderstorms at the ITCZ. The updrafts are a part of the Hadley-cell direct vertical circulation, which moves heat away from the equator. This cell cannot extend beyond about 30° to 35° latitude because Coriolis force turns the upper-troposphere winds toward the east, creating a subtropical jet near 30° latitude at the tropopause. Near the surface are the trade-wind return flows from the east.

A strong meridional temperature gradient remains at mid-latitudes, which drives westerly winds via the thermal-wind effect, and creates a polar jet at the tropopause. This jet stream is unstable, and usually meanders north and south as Rossby waves. Vorticity can help explain these waves.

The waves transport so much heat and angular momentum in mid-latitudes that a reverse (indirect) circulation develops there, called the Ferrel cell. A weak direct cell also exists in polar regions. Atmospheric winds drive ocean currents. All these ceaseless global circulations transport sufficient heat and momentum to keep the Earth in near equilibrium.

Threads

Radiation (Chapter 2) causes the differential heating that drives the global circulation in the troposphere (Chapter 1). This circulation moves both sensible and latent heat (Chapter 3).

The jet stream, caused by various dynamic forces (Chapter 10), meanders north and south creating troughs and ridges. This pattern creates surface high pressure areas and airmasses (Chapter 12), and low pressure areas called cyclones (Chapter 13). Upward motion in troughs and lows causes moist (Chapter 4) and dry (Chapt 3) adiabatic cooling (Chapter 5), which create clouds (Chapter 6) and precipitation (Chapter 7). Downward motion in ridges and highs creates relatively shallow boundary layers (Chapter 18) that can trap air pollutants (Chapter 19) .

Numerical models (Chapter 20) of the general circulation are called **global climate models** (**GCMs**) when used to forecast climate change (Chapter 21). Hurricane tracks (Chapter 16) are steered by monsoon circulations such as the Bermuda high. The ITCZ consists of thunderstorms (Chapters 14 and 15). The Ekman spiral process causes sea level to rise ahead of landfalling hurricanes (Chapter 16), contributing to the destructive storm surge.

Solved Example

Plot the Ekman spiral in the ocean at 45° latitude, using an eddy viscosity of $2\text{x}10^{-3}$ m^2·s^{-1}, and $u_{*water}{}^2 = 4\text{x}10^{-4}$ m^2/s^2.

Solution

Given: $u_{*water}{}^2 = 4\text{x}10^{-4}$ m^2/s^2, $K = 0.002$ m^2·s^{-1}, $\phi = 45°$

Find: U & V (m/s) vs. z (m)

First solve for Coriolis param.: $f_c = 0.0001031$ s^{-1} .
Use eq. (11.54):

$$\gamma = \sqrt{\frac{0.0001031\text{s}^{-1}}{2\cdot(0.002\text{m}^2\text{s}^{-1})}} = 0.1605 \text{ m}^{-1}$$

Solve eqs. (11.52) on a spreadsheet, resulting in:

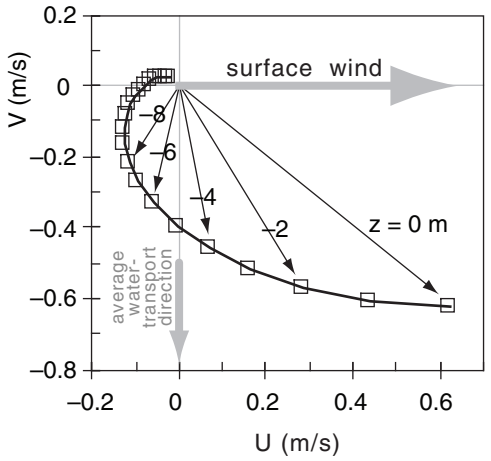

Check: Units OK. Physics OK.

Discussion: The surface current is 45° to the right of the wind direction. Deeper currents decrease in speed and turn further to the right due to Coriolis force. The average water transport is in the $-V$ direction; namely, at right angles to the surface wind.

EXERCISES

Numerical Problems

N1(§). Plot the idealized zonally-averaged temperature (°C) vs. latitude at the following heights (km) above ground (AGL).

a. 0.5 b. 1 c. 1.5 d. 2 e. 2.5 f. 3 g. 3.5
h. 4 i. 4.5 j. 5 k. 5.5 l. 6 m. 6.6 n. 7
o. 8 p. 9 q. 10 r. 11 s. 12 t. 13 u. 14

N2(§). Plot the idealized zonally-averaged meridional temperature gradient (°C/km) vs. latitude at the following heights (km) above ground level.

a. 0.5 b. 1 c. 1.5 d. 2 e. 2.5 f. 3 g. 3.5
h. 4 i. 4.5 j. 5 k. 5.5 l. 6 m. 6.6 n. 7
o. 8 p. 9 q. 10 r. 11 s. 12 t. 13 u. 14

N3. Estimate the annual average insolation (W/m^2) at the following latitude:

a. 90° b. 85° c. 80° d. 75° e. 70° f. 65° g. 60°
h. 55° i. 50° j. 45° k. 40° l. 35° m. 30° n. 25°
o. 20° p. 15° q. 10° r. 5° s. equator

N4. Estimate the annual average amount of incoming solar radiation (W/m^2) that is absorbed in the Earth-ocean-atmosphere system at latitude:

a. 90° b. 85° c. 80° d. 75° e. 70° f. 65° g. 60°
h. 55° i. 50° j. 45° k. 40° l. 35° m. 30° n. 25°
o. 20° p. 15° q. 10° r. 5° s. equator

N5. Using the idealized temperature near the middle of the troposphere (at z = 5.5 km), estimate the outgoing infrared radiation (W/m^2) from the atmosphere at the following latitude:

a. 90° b. 85° c. 80° d. 75° e. 70° f. 65° g. 60°
h. 55° i. 50° j. 45° k. 40° l. 35° m. 30° n. 25°
o. 20° p. 15° q. 10° r. 5° s. equator

N6. Using the results from the previous two exercises, find the net radiation magnitude (W/m^2) that is input to the atmosphere at latitude:

a. 90° b. 85° c. 80° d. 75° e. 70° f. 65° g. 60°
h. 55° i. 50° j. 45° k. 40° l. 35° m. 30° n. 25°
o. 20° p. 15° q. 10° r. 5° s. equator

N7. Using the results from the previous exercise, find the latitude-compensated net radiation magnitude (W/m^2; i.e., the differential heating) at latitude:

a. 90° b. 85° c. 80° d. 75° e. 70° f. 65° g. 60°
h. 55° i. 50° j. 45° k. 40° l. 35° m. 30° n. 25°
o. 20° p. 15° q. 10° r. 5° s. equator

N8. Assuming a standard atmosphere, find the internal Rossby radius of deformation (km) at latitude:

a. 90° b. 85° c. 80° d. 75° e. 70° f. 65° g. 60°
h. 55° i. 50° j. 45° k. 40° l. 35° m. 30° n. 25°
o. 20° p. 15° q. 10° r. 5° s. equator

N9. Given the following virtual temperatures at your location (20°C) and at another location, find the change of geostrophic wind with height [(m/s)/km]. Relative to your location, the other locations are:

	Δx(km)	Δy(km)	T_v(°C)		Δx(km)	Δy(km)	T_v(°C)
a.	0	100	15	k.	100	0	15
b.	0	100	16	l.	100	0	16
c.	0	100	17	m.	100	0	17
d.	0	100	18	n.	100	0	18
e.	0	100	19	o.	100	0	19
f.	0	100	21	p.	100	0	21
g.	0	100	22	q.	100	0	22
h.	0	100	23	r.	100	0	23
i.	0	100	24	s.	100	0	24
j.	0	100	25	t.	100	0	25

N10. Find the thermal wind (m/s) components, given a 100 to 50 kPa thickness change of 0.1 km across the following distances:

Δx(km) =	a. 200	b. 250	c. 300	d. 350
e. 400	f. 450	g. 550	h. 600	i. 650
Δy(km) =	j. 200	k. 250	l. 300	m. 350
n. 400	o. 450	p. 550	q. 600	r. 650

N11. Find the magnitude of the thermal wind (m/s) for the following thickness gradients:

	ΔTH(km) / Δx(km)	&	ΔTH(km) / Δy(km)
a.	–0.2 / 600	and	– 0.1 / 400
b.	–0.2 / 400	and	– 0.1 / 400
c.	–0.2 / 600	and	+ 0.1 / 400
d.	–0.2 / 400	and	+ 0.1 / 400
e.	–0.2 / 600	and	– 0.1 / 400
f.	–0.2 / 400	and	– 0.1 / 400
g.	–0.2 / 600	and	+ 0.1 / 400
h.	–0.2 / 400	and	+ 0.1 / 400

N12. For the toy model temperature distribution, find the wind speed (m/s) of the jet stream at the following heights (km) for latitude 30°:

a. 0.5 b. 1 c. 1.5 d. 2 e. 2.5 f. 3 g. 3.5
h. 4 i. 4.5 j. 5 k. 5.5 l. 6 m. 6.6 n. 7
o. 8 p. 9 q. 10 r. 11 s. 12 t. 13 u. 14

N13. If an air parcel from the starting latitude 5° has zero initial velocity relative to the Earth, then find its U component of velocity (m/s) relative to the Earth when it reaches the following latitude, assuming conservation of angular momentum.

a. 0° b. 2° c. 4° d. 6° e. 8° f. 10° g. 12°
h. 14° i. 16° j. 18° k. 20° l. 22° m. 24° n. 26°

N14. Find the relative vorticity (s^{-1}) given the following changes of (U , V) wind speed (m/s), across distances of Δx = 300 km and Δy = 600 km respectively.

a. 50, 50 b. 50, 20 c. 50, 0 d. 50, –20 e. 50, –50
f. 20, 50 g. 20, 20 h. 20, 0 i. 20, –20 j. 20, –50
k. 0, 50 l. 0, 20 m. 0, 0 n. 0, –20 o. 0, –50
p. –20, 50 q. –20, 20 r. –20, 0 s. –20, –20 t. –20, –50
u. –50, 50 v. –50, 20 x. –50, 0 y. –50, –20 z. –50, –50

N15. Given the following radial shear ($\Delta M/\Delta R$) in [(m/s)/km] and tangential wind speed M (m/s) around radius R (km), find relative vorticity (s^{-1}):

a. 0.1, 30, 300 b. 0.1, 20, 300 c. 0.1, 10, 300
d. 0.1, 0, 300 e. 0, 30, 300 f. 0, 20, 300
g. 0, 10, 300 h. –0.1, 30, 300 i. –0.1, 20, 300
j. –0.1, 10, 300 k. –0.1, 0, 300

N16. If the air rotates as a solid body of radius 500 km, find the relative vorticity (s^{-1}) for tangential speeds (m/s) of:

a. 10 b. 20 c. 30 d. 40 e. 50 f. 60 g. 70
h. 80 i. 90 j. 100 k. 120 l. 140 m. 150

N17. If the relative vorticity is $5x10^{-5}$ s^{-1}, find the absolute vorticity at the following latitude:

a. 90° b. 85° c. 80° d. 75° e. 70° f. 65° g. 60°
h. 55° i. 50° j. 45° k. 40° l. 35° m. 30° n. 25°
o. 20° p. 15° q. 10° r. 5° s. equator

N18. If the absolute vorticity is $5x10^{-5}$ s^{-1}, find the potential vorticity ($m^{-1}{\cdot}s^{-1}$) for a layer of thickness (km) of:

a. 0.5 b. 1 c. 1.5 d. 2 e. 2.5 f. 3 g. 3.5
h. 4 i. 4.5 j. 5 k. 5.5 l. 6 m. 6.6 n. 7
o. 8 p. 9 q. 10 r. 11 s. 12 t. 13 u. 14

N19. The potential vorticity is $1x10^{-8}$ $m^{-1}{\cdot}s^{-1}$ for a 10 km thick layer of air at latitude 48°N. What is the change of relative vorticity (s^{-1}) if the thickness (km) of the rotating air changes to:

a. 9.5 b. 9 c. 8.5 d. 8 e. 7.5 f. 7 g. 6.5
h. 10.5 j. 11 k. 11.5 l. 12 m. 12.5 n. 13

N20. If the absolute vorticity is $3x10^{-5}$ s^{-1} at 12 km altitude, find the isentropic potential vorticity (PVU) for a potential temperature change of ___ °C across a height increase of 1 km.

a. 1 b. 2 c. 3 d. 4 e. 5 f. 6 g. 6.5
h. 7 i. 8 j. 9 k. 10 l. 11 m. 12 n. 13

N21. Find the horizontal circulation associated with average relative vorticity $5x10^{-5}$ s^{-1} over area (km^2):

a. 500 b. 1000 c. 2000 d. 5000 e. 10,000
f. 20,000 g. 50,000 h. 100,000 i. 200,000

N22. Find the beta parameter (m^{-1} s^{-1}) at latitude:

a. 90° b. 85° c. 80° d. 75° e. 70° f. 65° g. 60°
h. 55° i. 50° j. 45° k. 40° l. 35° m. 30° n. 25°
o. 20° p. 15° q. 10° r. 5° s. equator

N23. Suppose the average wind speed is 60 m/s from the west at the tropopause. For a barotropic Rossby wave at 50° latitude, find both the intrinsic phase speed (m/s) and the phase speed (m/s) relative to the ground for wavelength (km) of:

a. 1000 b. 1500 c. 2000 d. 2500 e. 3000
f. 3500 g. 4000 h. 4500 i. 5000 j. 5500
k. 6000 l. 6500 m. 7000 n. 7500 o. 8000

N24. Plot the barotropic wave (y' vs x') from the previous exercise, assuming amplitude 2000 km.

N25. Same as exercise N23, but for a baroclinic Rossby wave in an atmosphere where air temperature decreases with height at 4°C/km.

N26(§). Plot the baroclinic wave (y' vs x') from the previous exercise, assuming amplitude 2000 km and a height (km):

(i) 2 (ii) 4 (iii) 6 (iv) 8 (v) 10

N27. Find the dominant (fastest growing) wavelength for a baroclinic wave in a standard atmosphere at latitude:

a. 90° b. 85° c. 80° d. 75° e. 70° f. 65° g. 60°
h. 55° i. 50° j. 45° k. 40° l. 35° m. 30° n. 25°
o. 20° p. 15° q. 10° r. 5° s. equator

N28. For the baroclinic Rossby wave of exercise N25 with amplitude 2000 km, find the wave amplitudes of the:

(i). vertical-displacement perturbation
(ii). potential-temperature perturbation
(iii). pressure perturbation
(iv). U-wind perturbation
(v). V-wind perturbation
(vi). W-wind perturbation

N29(§). For the previous exercise, plot separate vertical cross sections showing perturbation values for those variables.

N30. Find the latitude-weighted $a{\cdot}u'$ momentum value (m/s) for air that reaches destination latitude 50° from source latitude: a. 80° b. 75° c. 70°
d. 65° e. 60° f. 55° g. 45° h. 40° i. 35°

N31. Suppose the ____ cell updraft and downdraft velocities are ___ and ___ mm/s, respectively, and the meridional wind speeds are 3 m/s at the top and bottom of the cell. The cell is about __ km high by

___ km wide, and is centered at about ___ latitude. Temperature in the atmosphere decreases from about 15°C near the surface to –57°C at 11 km altitude. Find the vertical circulation.

cell	W_{up} (mm/s)	W_{down} (mm/s)	Δz (km)	Δy (km)	ϕ (°)
a. Hadley	6	–4	17	3900	10
b. Hadley	4	–4	15	3500	10
c. Hadley	3	–3	15	3500	5
d. Ferrel	3	–3	12	3000	45
e. Ferrel	2	–2	11	3000	45
f. Ferrel	2	–2	10	3000	50
g. polar	1	–1	9	2500	75
h. polar	1	–1	8	2500	75
i. polar	0.5	–0.5	7	2500	80

N32. Find the friction velocity at the water surface if the friction velocity (m/s) in the air (at sea level for a standard atmosphere) is:

a. 0.05 b. 0.1 c. 0.15 d. 0.2 e. 0.25
f. 0.3 g. 0.35 h. 0.4 i. 0.45 j. 0.5
k. 0.55 l. 0.6 m. 0.65 n. 0.7 o. 0.75

N33. Find the Ekman-spiral depth parameter at latitude 50° for eddy viscosity ($m^2\ s^{-1}$) of:

a. 0.0002 b. 0.0004 c. 0.0006 d. 0.0008 e. 0.001
f. 0.0012 g. 0.0014 h. 0.0016 i. 0.0018 j. 0.002
k. 0.0025 l. 0.003 m. 0.0035 n. 0.004 o. 0.005

N34(§). For the previous exercise, plot the Ekman spiral (U, V) components for depths from the surface down to where the velocities are near zero, for water friction velocity of $u_* = 0.025$ m/s.

Understanding & Critical Evaluation

U1. During the months when the major Hadley cell exists, trade winds can cross the equator. If there are no forces at the equator, explain why this is possible.

U2. In regions of surface high pressure, descending air in the troposphere is associated with dry (non-rainy) weather. These high-pressure belts are where deserts form. In addition to the belts at ±30° latitude, semi-permanent surface highs also exist at the poles. Are polar regions deserts? Explain.

U3. The subtropical jet stream for Earth is located at about 30° latitude. Due to Coriolis force, this is the poleward limit of outflow air from the top of the ITCZ. If the Earth were to spin faster, numerical experiments suggest that the poleward limit (and thus the jet location) would be closer to the equator. Based on the spins of the other planets (get this info from the web or a textbook) compared to Earth, at what latitudes would you expect the subtropical jets to be on Jupiter? Do your predictions agree with photos of Jupiter?

U4. Horizontal divergence of air near the surface tends to reduce or eliminate horizontal temperature gradients. Horizontal convergence does the opposite. Fronts (as you will learn in the next chapter) are regions of strong local temperature gradients. Based on the general circulation of Earth, at what latitudes would you expect fronts to frequently exist, and at what other latitudes would you expect them to rarely exist? Explain.

U5. In the global circulation, what main features can cause mixing of air between the Northern and Southern Hemispheres? Based on typical velocities and cross sectional areas of these flows, over what length of time would be needed for the portion $1/e$ of all the air in the N. Hemisphere to be replaced by air that arrived from the S. Hemisphere?

U6. In Fig. 11.4, the average declination of the sun was listed as 14.9° to 15° for the 4-month periods listed in those figures. Confirm that those are the correct averages, based on the equations from the Radiation chapter for solar declination angle vs. day of the year.

U7. Thunderstorms are small-diameter (15 km) columns of cloudy air from near the ground to the tropopause. They are steered by the environmental winds at an altitude of roughly 1/4 to 1/3 the troposphere depth. With that information, in what direction would you expect thunderstorms to move as a function of latitude (do this for every 10° latitude)?

U8. The average meridional wind at each pole is zero. Why? Also, does your answer apply to instantaneous winds such as on a weather map? Why?

U9. Can you detect monsoonal (monthly or seasonal average) pressure centers on a normal (instantaneous) weather map analysis or forecast? Explain.

U10. Figs. 11.3a & 11.5a showed idealized surface wind & pressure patterns. Combine these and draw a sketch of the resulting idealized global circulation including both planetary and monsoon effects.

U11. Eqs. (11.1-11.3) represent an idealized ("toy model") meridional variation of zonally averaged temperature. Critically analyze this model and discuss. Is it reasonable at the ends (boundaries) of the curve; are the units correct; is it physically justifiable; does it satisfy any budget constraints (e.g., con-

servation of heat, if appropriate), etc. What aspects of it are too simplified, and what aspects are OK?

U12. (a) Eq. (11.4) has the 3rd power of the sine times the 2nd power of the cosine. If you could arbitrarily change these powers, what values would lead to reasonable temperature gradients ($\Delta T/\Delta y$) at the surface and which would not (Hint: use a spreadsheet and experiment with different powers)?

(b) Of the various powers that could be reasonable, which powers would you recommend as fitting the available data the best? (Hint: consider not only the temperature gradient, but the associated meridional temperature profile and the associated jet stream.) Also, speculate on why I chose the powers that I did for this toy model.

U13. Concerning differential heating, Fig. 11.9 shows the annual average insolation vs. latitude. Instead, compute the average insolation over the two-month period of June and July, and plot vs. latitude. Use the resulting graph to explain why the jet stream and weather patterns are very weak in the summer hemisphere, and strong in the winter hemisphere.

U14. At mid- and high-latitudes, Fig. 11.9 shows that each hemisphere has one full cycle of insolation annually (i.e., there is one maximum and one minimum each year).

But look at Fig. 11.9 near the equator.

a. Based on the data in this graph (or even better, based on the eqs. from the Radiation chapter), plot insolation vs. relative Julian day for the equator.

b. How many insolation cycles are there each year at the equator?

c. At the equator, speculate on when would be the hottest "seasons" and when would be the less-hot "seasons".

d. Within what range of latitudes near the equator is this behavior observed?

U15. Just before idealized eq. (11.6), I mentioned my surprise that E_2 was approximately constant with latitude. I had estimated E_2 by subtracting my toy-model values for E_{insol} from the actual observed values of E_{in}. Speculate about what physical processes could cause E_2 to be constant with latitude all the way from the equator to the poles.

U16. How sensitive is the toy model for E_{out} (i.e., eq. 11.7) to the choice of average emission altitude z_m? Recall that z_m, when used as the altitude z in eqs. (11.1-11.3), affects T_m. Hint: for your sensitivity analysis, use a spreadsheet to experiment with different z_m and see how the resulting plots of E_{out} vs. latitude change. (See the "On Doing Science" box about model sensitivity.)

U17(§). Solve the equations to reproduce the curves in figure: a. 11.10 b. 11.11 c. 11.12 d. 11.13

U18. We recognize the global circulation as a response of the atmosphere to the instability caused by differential heating, as suggested by **LeChatelier's Principle**. But the circulation does not totally undo the instability; namely, the tropics remain slightly warmer than the poles. Comment on why this remaining, unremoved instability is required to exist, for the global circulation to work.

U19. In Fig. 11.12, what would happen if the surplus area exceeded the deficit area? How would the global circulation change, and what would be the end result for Fig. 11.12?

U20. Check to see if the data in Fig. 11.12 does give zero net radiation when averaged from pole to pole.

U21. The observation data that was used in Fig. 11.14 was based on satellite-measured radiation and differential heating to get the total needed heat transport, and on estimates of heat transport by the oceans. The published "observations" for net atmospheric heat transport were, in fact, estimated as the difference (i.e., residual) between the total and the ocean curves. What could be some errors in this atmosphere curve? (Hint: see the On Doing Science box about Residuals.)

U22. Express the 5 PW of heat transport typically observed at 30° latitude in other units, such as

a. horsepower b. megatons of TNT

(Hint: 1 Megaton of TNT ≈ 4.2×10^{15} J.)

U23. For Fig. 11.15, explain why it is p' vs. z that drive vertical winds, and not P_{column} vs. z.

U24. a. Redraw Figs. 11.16 for situations that cause downdrafts.

b. Figs. 11.16 both show updraft situations, but they have opposite pressure couplets. As you already found from part (a) both pressure couplets can also be associated with downdrafts. What external information (in addition to the sign of the pressure couplet) do you always need to decide whether a pressure couplet causes an updraft or a downdraft? Explain.

U25. a. For the thermal circulation of Fig. 11.17(iv), what needs to happen for this circulation to be maintained? Namely, what prevents it from dying out?

b. For what situations in the real atmosphere can thermal circulations be maintained for several days or more?

U26. a. Study Fig. 11.18 closely, and explain why the wind vectors to/from the low- and high-pressure centers at the equator differ from the winds near pressure centers at mid-latitudes.

b. Redraw Fig. 11.5a, but with continents and oceans at the equator. Discuss what monsoonal pressures and winds might occur during winter and summer, and why.

U27. a. Redraw Fig. 11.19, but for the case of geostrophic wind decreasing from its initial equilibrium value. Discuss the resulting evolution of wind and pressure fields during this geostrophic adjustment.

b. Redraw Fig. 11.19, but for flow around a low-pressure center (i.e., look at the gradient winds rather than the geostrophic winds). Discuss how the wind and pressure fields adjust when the geostrophic wind is increased above its initial equilibrium value.

U28. How would the vertical potential temperature gradient need to vary with latitude for the "internal Rossby radius of deformation" to be invariant? Assume constant troposphere depth.

U29. In the Local Winds chapter, gap winds and coastally-trapped jets are explained. Discuss how these flows relate to geostrophic adjustment.

U30. At the top of **hurricanes** (see the Hurricanes chapter), so much air is being continuously pumped to the top of the troposphere that a high-pressure center is formed over the hurricane core there. This high is so intense and localized that it violates the conditions for gradient winds; namely, the pressure gradient around this high is too steep (see the Dynamics chapter).

Discuss the winds and pressure at the top of a hurricane, using what you know about geostrophic adjustment. Namely, what happens to the winds and air mass if the wind field is not in geostrophic or gradient balance with the pressure field?

U31. In the thermal-wind relationship (eqs. 11.13), which factors on the right side are constant or vary by only a small amount compared to their magnitude, and which factors vary more (and are thus more important in the equations)?

U32. In Fig. 11.20, how would it change if the bottom isobaric surface were tilted; namely, if there were already a horizontal pressure gradient at the bottom?

U33. Draw a sketch similar to Fig. 11.20 for the thermal-wind relationship for the Southern Hemisphere.

U34. In maps such as Fig. 11.21, explain why thickness is related to average temperature.

U35. Redraw Fig. 11.22 for the case cold air in the east and warm air in the west (i.e., opposite to what is in the existing figure). Assume no change to the bottom isobaric surface.

U36. Copy Fig. 11.24.
a. On your copy, draw the G_1 and G_2 vectors, and the M_{TH} vector at point B. Confirm that the thermal wind relationship is qualitatively satisfied via vector addition. Discuss why point B is an example of veering or backing.
b. Same as (a) but calculate the actual magnitude of each vector at point B based on the spacing between isobars, thickness contours, or height contours, and then using the appropriate equations from this and previous chapters. Again, confirm that the thermal wind relationship is satisfied. (1° latitude = 111 km)

U37. Using a spreadsheet, start with an air parcel at rest at the tropopause over the equator. Assume a realistic pressure gradient between the equator and 30° latitude. Use dynamics to solve for acceleration of the parcel over a short time step, and then iterate over many time steps to find parcel speed and position. How does the path of this parcel compare to the idealized paths drawn in Fig. 11.26d? Discuss.

U38. In the thunderstorms at the ITCZ, copious amounts of water vapor condense and release latent heat. Discuss how this condensation affects the average lapse rate in the tropics, the distribution of heat, and the strength of the equatorial high-pressure belt at the tropopause.

U39. Summarize in a list or an outline all the general-circulation factors that make the mid-latitude weather different from tropical weather.

U40. Explain the surface pressure patterns in Figs. 11.31 in terms of a combination of idealized monsoon and planetary circulations.

U41. Figs. 11.31 show mid-summer and mid-winter conditions in each hemisphere. Speculate on what the circulation would look like in April or October.

U42. Compare Figs. 11.32 with the idealized planetary and monsoon circulations, and discuss similarities and differences.

U43. Based on Figs. 11.32, which hemisphere would you expect to have strong subtropical jets in both summer and winter, and which would not. What factors might be responsible for this difference?

U44. For the Indian monsoon sketched in Fig. 11.33, where are the updraft and downdraft portions of the major Hadley cell for that month? Also, what is the relationship between the trade winds at that time, and the Indian monsoon winds?

U45. What are the dominant characteristics you see in Fig. 11.34, regarding jet streams in the Earth's atmosphere? Where don't jet streams go?

U46. In Figs. 11.35, indicate if the jet-stream winds would be coming out of the page or into the page, for the: a) N. Hemisphere, (b) S. Hemisphere.

U47. Although Figs. 11.36 are for different months than Figs. 11.32, they are close enough in months to still both describe summer and winter flows.

a. Do the near-tropopause winds in Figs. 11.36 agree with the pressure gradients (or height gradients) in Figs. 11.32?

b. Why are there easterly winds at the tropopause over/near the equator, even though there is negligible pressure gradient there?

U48. Describe the mechanism that drives the polar jet, and explain how it differs from the mechanism that drives the subtropical jet.

U49. In Fig. 11.37b, we see a very strong pressure gradient in the vertical (indicated by the different isobars), but only small pressure gradients in the horizontal (indicated by the slope of any one isobar). Yet the strongest average winds are horizontal, not vertical. Why?

U50. Why does the jet stream wind speed decrease with increasing height above the tropopause?

U51. Derive eq. (11.17) for jet stream wind speed, knowing the temperature field given by the toy model earlier in this chapter. Describe the physical meaning of each term in that equation. Also, describe the limitations of that equation.

U52. Why does an air parcel at rest (i.e., calm winds) near the equator possess large angular momentum? What about for air parcels that move from the east at typical trade wind speeds?

U53. At the equator, air at the bottom of the troposphere has a smaller radius of curvature about the Earth's axis than at the top of the troposphere. How significant is this difference? Can we neglect it?

U54. Although angular-momentum conservation is not a good explanation for the jet stream, can it explain the trade winds? Discuss with justification.

U55. Suppose water in your sink is in solid body rotation at one revolution per 5 seconds, and your sink is 1 m in diameter and 0.5 m deep.

a. Find the potential vorticity.

b. If you suddenly pull the stopper and the fluid stretches to depth 1 m in your drain, what is the new relative vorticity and new rotation rate?

U56. In eq. (11.20), why is there a negative sign on the last term? Hint: How does the rotation direction implied by the last term without a negative sign compare to the rotation direction of the first term?

U57. In the Thunderstorm chapters, you will learn that the winds in a portion of the tornado can be irrotational. This is surprising, because the winds are traveling so quickly around a very tight vortex. Explain what wind field is needed to gave **irrotational winds** (i.e., no relative vorticity) in air that is rotating around the tornado. Hint: Into the wall of a tornado, imagine dropping a neutrally-buoyant small paddle wheel the size of a flower. As this flower is translated around the perimeter of the tornado funnel, what must the local wind shear be at the flower to cause it to not spin relative to the ground? Redraw Fig. 11.43 to show what you propose.

U58. Eq. (11.25) gives names for the different terms that can contribute toward vorticity. For simplicity, assume Δz is constant (i.e., assume no stretching). On a copy of Fig. 11.44, write these names at appropriate locations to identify the dominant factors affecting the vorticity max and min centers.

U59. If you were standing at the equator, you would be rotating with the Earth about its axis. However, you would have zero vorticity about your vertical axis. Explain how that is possible.

U60. Eq. (11.26) looks like it has the absolute vorticity in the numerator, yet that is an equation for a form of potential vorticity. What other aspects of that equation make it like a potential vorticity?

U61. Compare the expression of horizontal circulation C with that for vertical circulation CC.

U62. Relate Kelvin's circulation theorem to the conservation of potential vorticity. Hint: Consider a constant Volume = $A \cdot \Delta z$.

U63. The jet stream sketched in Fig. 11.49 separates cold polar air near the pole from warmer air near the equator. What prevents the cold air from extending further away from the poles toward the equator?

U64. If the Coriolis force didn't vary with latitude, could there be Rossby waves? Discuss.

U65. Compare the barotropic and baroclinic relationships for phase speed of planetary waves. Which is fastest (and in what direction) in mid-latitudes?

U66. If the troposphere were isothermal everywhere, find the number of planetary waves that would encircle the Earth at 45°N, using baroclinic theory. How does this differ from barotropic theory?

U67. Once a Rossby wave is triggered, what mechanisms do you think could cause it to diminish (i.e., to reduce the waviness, and leave straight zonal flow).

U68. In Fig. 11.50 at point (4) in the jet stream, why doesn't the air just continue turning clockwise around toward points (2) and (3), instead of starting to turn the other way?

U69. How would you explain the difference between barotropic and baroclinic waves to non-scientists?

U70. What conditions are needed so that Rossby waves have zero phase speed relative to the ground? Can such conditions occur in the real atmosphere?

U71. How does static stability affect the phase speed of baroclinic Rossby waves?

U72. Using eq. (11.40) for the north-south displacement of a baroclinic wave, discuss (and/or plot) how the location of the crest of the wave changes with altitude z within the troposphere.

U73. Where, with respect to the ridges and troughs in a baroclinic wave, would you expect to find the greatest: (a) vertical displacement; (b) vertical velocity; (c) potential temperature perturbation?

U74. In Figs. 11.51 and 11.53 in the jet stream, there is just as much air going northward as there is air going southward across any latitude line, as required by mass conservation. If there is no net mass transport, how can there be heat or momentum transport?

U75. a. What is the sign of CC for a direct circulation in the S. Hemisphere (i.e., for eq. 11.50)?

b. Determine the signs of terms in eq. (11.51) for the S. Hemisphere.

U76. Why does the expression for cell circulation contain the Coriolis parameter and Brunt-Väisälä frequency?

U77. Would there be an Ekman spiral in the ocean if there was no Coriolis force? Explain.

U78. Consider a cyclonic air circulation over an ocean in your hemisphere. Knowing the relationship between ocean currents and surface winds, would you anticipate that the near-surface wind-driven ocean currents are diverging away from the center of the cyclone, or converging toward the center? Explain, and use drawings. Note: Due to mass conservations, horizontally diverging ocean surface waters cause upwelling of nutrient-rich water toward the surface, which can support ocean plants and animals, while downwelling does the opposite.

Web-Enhanced Questions

W1. Download a northern or southern hemispheric map of the winds near the tropopause (or pressures or heights from which winds can be inferred), and identify regions of near zonal flow, near meridional flow, monsoon circulations over the ocean and over continents, and the ITCZ.

W2. Download an animated loop of geostationary satellite photos (IR or water vapor) for the whole Earth disk, and identify regions of near zonal flow, near meridional flow, extratropical cyclones, ITCZ, and tropical cyclones (if any).

W3. From the web, find a rawinsonde sounding at a location in the trade-wind region, and confirm the wind reversal between low and high altitudes.

W4. Download a still, daytime, visible satellite image for the whole disk from a geostationary satellite, and estimate fractional cloudiness over the different latitude belts for that instant. Use this to estimate the incoming solar radiation reaching the ground in each of those belts, and plot the zonally-averaged results vs. latitude.

W5. Download a series of rawinsonde soundings for different latitudes between the equator and a pole. Find the tropopause from each sounding, and then plot the variation of tropopause height vs. latitude.

W6. Download a map of sea-surface temperature (SST), and discuss how SST varies with latitude.

W7. Download an IR satellite image showing the entire Earth (i.e., a whole disk image), and compute the effective radiation temperature averaged around latitude belts. Use this with the Stefan-Boltzmann equation to estimate and plot E_{out} vs. latitude due to IR radiation.

W8. Download satellite-derived images that show the climatological average incoming and outgoing radiation at the top of the atmosphere. How does it relate to the idealized descriptions in this chapter?

W9. Download satellite-derived or buoy & ship-derived ocean currents for the global oceans, and discuss how they transport heat meridionally, and why the oceanic transport of heat is relatively small at mid to high latitudes in the N. Hemisphere.

W10. Use a satellite image to locate a strong portion of the ITCZ over a rawinsonde site, and then download the rawinsonde data. Plot (compute if needed) the variation of pressure with altitude, and discuss how it does or doesn't deviate from hydrostatic.

W11. Search the web for sites where you can plot "reanalysis data", such as the NCEP/NCAR reanalysis or any of the ECMWF reanalyses. Pick a month during late summer from some past year in this data-base, and plot the surface pressure map. Explain how this "real" result is related to a combination of the "idealized" planetary and monsoonal circulations.

W12. Same as the previous exercise, but for monthly average vertical cross sections that can be looped as movies. Display fields such as zonal wind, meridional wind, and vertical velocity, and see how they vary over a year.

W13. Download weather maps of temperature for the surface, and for either the 85 kPa or 70 kPa isobaric surfaces. Over your location, or other location specified by your instructor, use the thermal wind relationship to find the change of geostrophic wind with height between the surface and the isobaric level you chose above the surface.

W14 Download a weather map for the 100-50 kPa thickness, and calculate the components of the thermal-wind vector for that surface. Also, what is the thermal-wind magnitude? Draw arrows on the thickness chart representing the thermal-wind vectors.

W15. Download data from a string of rawinsonde stations arranged north to south that cross the jet stream. Use the temperature, pressure, and wind speed data to produce vertical cross-section analyses of: (a) temperature; (b) pressure; and (c) wind speed. Discuss how these are related to the dynamics of the jet stream.

W16. Download weather maps of height contours for the 20 or 30 kPa isobaric surface, and draw a line within the region of most closely-spaced contours to indicate the location of the jet stream core. Compare this line to weather maps you can download from various TV and weather networks showing the jet stream location. Comment on both the location and the width of the jet stream.

W17. Download a weather forecast map that shows vorticity. What type of vorticity is it (relative, absolute, potential, isentropic)? What is the relationship between vorticity centers and fronts? What is the relationship between vorticity centers and bad weather (precipitation)?

W18. Download surface weather observations for many sites around your location (or alternately, download a weather map showing wind speed and direction), and calculate the following vorticities at your location: (a) relative; (b) absolute; (c) potential.

W19. Download a map of height contours for either the 50, 30, or 20 kPa surface. Measure the wavelength of a dominant planetary wave near your region, and calculate the theoretical phase speed of both barotropic and baroclinic waves for that wavelength. Compare and discuss.

W20. Download maps at a variety of altitudes and for a variety of fields (e.g., heights, temperature, vertical velocity, etc.), but all valid at the same time, and discuss how they are related to each other using baroclinic theory.

W21. View an animation of a loop of IR or water vapor satellite images for the whole disk of the Earth. Identify the three bands of the general circulation, and discuss how they deviate from the idealized picture sketched in this chapter. To hand a result in, print one of the frames from the satellite loop and sketch on it lines that demarcate the three zones. Speculate on how these zones vary with season.

W22. Download a map of recent ocean surface currents, and compare with a map showing the general

circulation winds for the same time. Discuss how the two maps are related.

Synthesis Questions

S1. If the Earth did not rotate, how would the steady-state general circulation be different, if at all?

S2. If our current rotating Earth with current global circulation suddenly stopped rotating, describe the evolution of the global circulation over time. This is called the **spin-down** problem.

S3. If the Earth rotated twice as fast, how would the steady-state global circulation be different, if at all?

S4. If our current rotating Earth with current global circulation suddenly started rotating twice as fast, describe the evolution of the global circulation over time. This is a **spin-up** situation.

S5. If radiative heating was uniform between the equator and the poles, how would the steady-state global circulation be different, if at all?

S6. If the equator were snow covered and the poles were not, how would the global circulation change, if at all?

S7. Suppose that the sun caused radiative cooling of Earth, while IR radiation from space caused warming of Earth. How would the weather and climate be different, if at all?

S8. If an ice age caused the polar ice caps to expand to 50° latitude in both hemisphere, describe how global circulation would change, if at all?

S9. About 250 million years ago, all of the continents had moved together to become one big continent called **Pangaea**, before further plate tectonic movement caused the continents to drift apart. Pangaea spanned roughly 120° of longitude (1/3 of Earth's circumference) and extended roughly from pole to pole. Also, at that time, the Earth was spinning faster, with the solar day being only about 23 of our present-day hours long. Assuming no other changes to insolation, etc, how would the global circulation have differed compared to the current circulation?

S10. If the Earth was dry and no clouds could form, how would the global circulation differ, if at all? Would the tropopause height be different? Why?

S11. Suppose the troposphere were half as deep. How would the global circulation be different?

S12. If potential vorticity was not conserved, how would the global circulation be different, if at all?

S13. Suppose the average zonal winds were faster than the phase speed of short waves, but slower than the phase speed for long waves. Describe how the weather and weather forecasting would be different at mid-latitudes, if at all?

S14. Suppose that short waves moved faster than long waves, how would the weather at mid-latitudes be different, if at all?

S15. Suppose the troposphere was statically unstable everywhere. Could baroclinic waves exist? If so, how would they behave, and how would the weather and global circulation be different, if at all?

S16. If planetary waves did not transport momentum, heat, and moisture meridionally, how would the weather and climate be different, if at all?

S17. If the ocean currents did not transport any heat, how would the atmospheric global circulation and weather be different, if at all?

S18. What if the ocean surface were so slippery that there would be zero wind drag. Would any ocean currents develop? How? Why?

S19. Suppose there was an isolated small continent that was hot relative to the surrounding cooler ocean. Sketch a vertical cross section in the atmosphere across that continent, and use thickness concepts to draw the isobaric surfaces. Next, draw a plan-view map of heights of one of the mid-troposphere isobaric surfaces, and use thermal-wind effects to sketch wind vectors on this same map. Discuss how this approach does or doesn't explain some aspects of monsoon circulations.

S20. If the Rossby wave of Fig. 11.50 was displaced so that it is centered on the equator (i.e., point (1) starts at the equator), would it still oscillate as shown in that figure, or would the trough of the wave (which is now in the S. Hem.) behave differently? Discuss.

S21. If the Earth were shaped like a cylinder with its axis of rotation aligned with the axis of the real Earth, could Rossby waves exist? How would the global circulation be different, if at all?

S22. In the subtropics, low altitude winds are from the east, but high altitude winds are from the west. In mid-latitudes, winds at all altitudes are from the west. Why are the winds in these latitude bands different?

Copyright © 2011, 2015 by Roland Stull. *Meteorology for Scientists and Engineers, 3rd Ed.*

AIRMASSES & FRONTS

CONTENTS

Anticyclones or Highs 390
Characteristics & Formation 390
Vertical Structure 391
Airmasses 391
Creation 392
Movement 397
Modification 397
Surface Fronts 399
Horizontal Structure 400
Vertical Structure 403
Geostrophic Adjustment – Part 3 404
Winds in the Cold Air 404
Winds in the Warm Over-riding Air 407
Frontal Vorticity 407
Frontogenesis 408
Kinematics 408
Thermodynamics 411
Dynamics 411
Occluded Fronts and Mid-tropospheric Fronts 413
Upper-tropospheric Fronts 414
Drylines 416
Summary 417
Threads 418
Exercises 418
Numerical Problems 418
Understanding & Critical Evaluation 419
Web-Enhanced Questions 421
Synthesis Questions 423

12 A high-pressure center, or **high** (H), often contains an **airmass** of well-defined characteristics, such as cold temperatures and low humidity. When different airmasses finally move and interact, their mutual border is called a **front**, named by analogy to the battle fronts of World War I.

Fronts are usually associated with low-pressure centers, or **lows** (L). Two fronts per low are most common, although zero to four are also observed. In the Northern Hemisphere, these fronts often rotate counterclockwise around the low center like the spokes of a wheel (Fig. 12.1), while the low moves and evolves. Fronts are often the foci of clouds, low pressure, and precipitation.

In this chapter you will learn the characteristics of anticyclones (highs). You will see how anticyclones are favored locations for airmass formation. Covered next are fronts in the bottom, middle, and top of the troposphere. Factors that cause fronts to form and strengthen are presented. This chapter ends with a special type of front called a dry line.

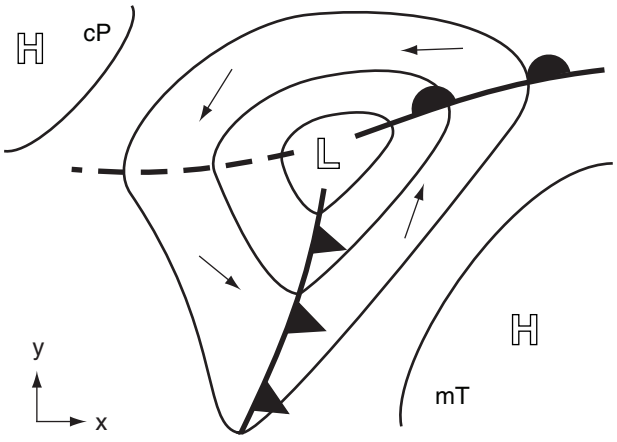

Figure 12.1
Idealized surface weather map (from the Weather Reports & Map Analysis chapter) for the N. Hemisphere showing high (H) and low (L) pressure centers, isobars (thin lines), a warm front (heavy solid line with semicircles on one side), a cold front (heavy solid line with triangles on one side), and a trough of low pressure (dashed line). Vectors indicate near-surface wind. cP indicates a continental polar airmass; mT indicates a maritime tropical airmass.

"Meteorology for Scientists and Engineers, 3rd Edition" by Roland Stull is licensed under a Creative Commons Attribution-NonCommercial-ShareAlike 4.0 International License. To view a copy of the license, visit http://creativecommons.org/licenses/by-nc-sa/4.0/ . This work is available at http://www.eos.ubc.ca/books/Practical_Meteorology/ .

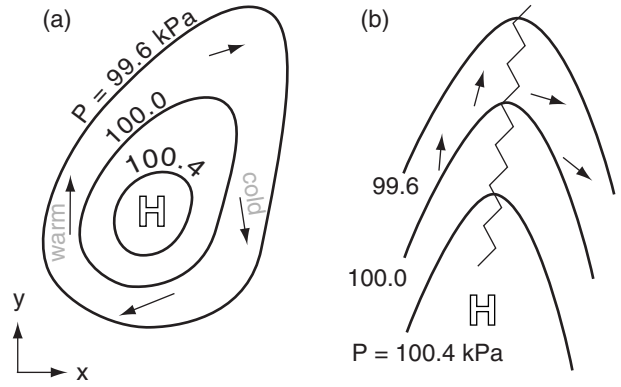

Figure 12.2
Examples of isobars plotted on a sea-level pressure map. (a) High-pressure center. (b) High-pressure ridge in N. Hemisphere mid-latitudes. Vectors show surface wind directions.

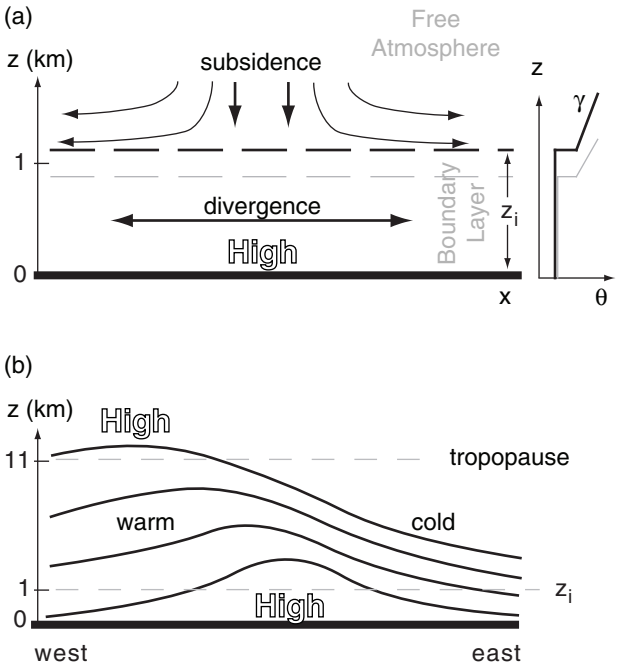

Figure 12.3
(a) Left: vertical circulation above a surface high-pressure center in the bottom half of the troposphere. Black dashed line marks the initial capping inversion at the top of the boundary layer. Grey dashed line shows the top later, assuming no turbulent entrainment into the boundary layer. Right: idealized profile of potential temperature, θ, initially (black line) and later (grey). The boundary-layer depth z_i is on the order of 1 km, and the potential-temperature gradient above the boundary layer is represented by γ.
(b) Tilt of high-pressure ridge westward with height, toward the warmer air. Thin lines are height contours of isobaric surfaces. Ridge amplitude is exaggerated in this illustration.

ANTICYCLONES OR HIGHS

Characteristics & Formation

High-pressure centers, or **highs**, are identified on constant altitude (e.g., sea-level) weather maps as regions of relative maxima in **pressure**. The location of high-pressure center is labeled with "H" (Fig. 12.2a). High centers can also be found on upper-air isobaric charts as relative maxima in **geopotential height** (see the Dynamics chapter, Fig. 10.2).

When the pressure field has a relative maximum in only one direction, such as east-west, but has a horizontal pressure-gradient in the other direction, this is called a high-pressure **ridge** (Fig. 12.2b). The **ridge axis** is labeled with a zigzag line.

The column of air above the high center contains more air molecules than neighboring columns. This causes more weight due to gravity (see Chapter 1), which is expressed in a fluid as more pressure.

Above a high center is often downward motion (**subsidence**) in the mid-troposphere, and horizontal spreading of air (**divergence**) near the surface (Fig. 12.3a). Subsidence impedes cloud development, leading to generally clear skies and fair weather. Winds are also generally calm or light in highs, because gradient-wind dynamics of highs require weak pressure gradients near the high center (see the Dynamics chapter).

The diverging air near the surface spirals outward due to the weak pressure-gradient force. Coriolis force causes it to rotate clockwise (anticyclonically) around the high-pressure center in the Northern Hemisphere (Fig. 12.2a), and opposite in the Southern Hemisphere. For this reason, high-pressure centers are called **anticyclones**.

Downward advection of dry air from the upper troposphere creates dry conditions just above the boundary layer. Subsidence also advects warmer potential temperatures from higher in the troposphere. This strengthens the temperature inversion that caps the boundary layer, and acts to trap pollutants and reduce visibility near the ground.

Subsiding air cannot push through the capping inversion, and therefore does not inject free-atmosphere air directly into the boundary layer. Instead, the whole boundary layer becomes thinner as the top is pushed down by subsidence (Fig. 12.3a). This can be partly counteracted by entrainment of free atmosphere air if the boundary layer is turbulent, such as for a convective mixed layer during daytime over land. However, the entrainment rate is controlled by turbulence in the boundary layer (see the Atmos. Boundary Layer chapter), not by subsidence.

Five mechanisms support the formation of highs at the Earth's surface:

• Global Circulation: Planetary-scale, semi-permanent highs predominate at 30° and 90° latitudes, where the global circulation has downward motion (see the Global Circulation chapter). The **subtropical highs** centered near 30° North and South latitudes are 1000-km-wide belts that encircle the Earth. **Polar highs** cover the Arctic and Antarctic. These highs are driven by the global circulation that is responding to differential heating of the Earth. Although these highs exist year round, their locations shift slightly with season.

• Monsoons: Quasi-stationary, continental-scale highs form over cool oceans in summer and cold continents in winter (see the Global Circulation chapter). They are seasonal (i.e., last for several months), and form due to the temperature contrast between land and ocean.

• Transient Rossby waves: Surface highs form at mid-latitudes, east of high-pressure ridges in the jet stream, and are an important part of mid-latitude weather variability (see the Global Circulation and Extratropical Cyclone chapters). They often exist for several days.

• Thunderstorms: Downdrafts from thunderstorms (see the Thunderstorm chapters) create **meso-highs** roughly 10 to 20 km in diameter at the surface. These might exist for minutes to hours.

• Topography/Surface-Characteristics: Meso-highs can also form in mountains due to blocking or channeling of the wind, mountain waves, and thermal effects (anabatic or katabatic winds) in the mountains. Sea-breezes or lake breezes can also create meso-highs in parts of their circulation. (See the Local Winds chapter.)

The actual pressure pattern at any location and time is a superposition of all these phenomena.

Vertical Structure

The location difference between surface and upper-tropospheric highs (Fig. 12.3b) can be explained using gradient-wind and thickness concepts.

Because of barotropic and baroclinic instability, the jet stream meanders north and south, creating troughs of low pressure and ridges of high pressure, as discussed in the Global Circulation chapter. **Gradient winds** blow faster around ridges and slower around troughs, assuming identical pressure gradients. The region east of a ridge and west of a trough has fast-moving air entering from the west, but slower air leaving to the east. Thus, horizontal convergence of air at the top of the troposphere adds more air molecules to the whole tropospheric column at that location, causing a surface high to form east of the upper-level ridge.

West of surface highs, the anticyclonic circulation advects warm air from the equator toward the poles (Figs. 12.2a & 12.3b). This heating west of the surface high causes the **thickness** between isobaric surfaces to increase, as explained by the hypsometric equation. Isobaric surfaces near the top of the troposphere are thus lifted to the west of the surface high. These high heights correspond to high pressure aloft; namely, the upper-level ridge is west of the surface high.

The net result is that high-pressure regions tilt westward with increasing height (Fig. 12.3b). In the Extratropical Cyclone chapter you will see that deepening low-pressure regions also tilt westward with increasing height, at mid-latitudes. Thus, the mid-latitude tropospheric pressure pattern has a consistent phase shift toward the west as altitude increases.

AIRMASSES

An **airmass** is a widespread (of order 1000 km wide) body of air in the bottom third of the troposphere that has somewhat-uniform characteristics. These characteristics can include one or more of: temperature, humidity, visibility, odor, pollen concentration, dust concentration, pollutant concentration, radioactivity, cloud condensation nuclei (CCN) activity, cloudiness, static stability, and turbulence.

Airmasses are usually classified by their temperature and humidity, as associated with their source regions. These are usually abbreviated with a two-letter code. The first letter, in lowercase, describes the humidity source. The second letter, in upper-

Solved Example

A "**cA**" airmass has what characteristics?

Solution

Given: cA airmass.
Find: characteristics

Use Table 12-1: cA = continental Arctic
Characteristics: **Dry and very cold**.

Check: Agrees with Fig. 12.4.
Discussion: Forms over land in the arctic, under the polar high. In Great Britain, the same airmass is labeled as Ac.

Table 12-1. Airmass abbreviations. **Boldface** indicates the most common ones.

Abbr.	Name	Description
c	**continental**	Dry. Formed over land.
m	**maritime**	Humid. Formed over ocean.
A	Arctic	Very cold. Formed in the polar high.
E	Equatorial	Hot. Formed near equator.
M	Monsoon	Similar to tropical.
P	**Polar**	Cold. Formed in subpolar area.
S	Superior	A warm dry airmass having its origin aloft.
T	**Tropical**	Warm. Formed in the subtropical high belt.
k	colder than the underlying surface	
w	warmer than the underlying surface	
Special (regional) abbreviations.		
AA	Antarctic	Exceptionally cold and dry.
r	returning	As in "rPm" returning Polar maritime [Great Britain]

Note: Layered airmasses are written like a fraction, with the airmass aloft written above a horizontal line and the surface airmass written below. For example, just east of a dryline you might have:

$$\frac{cT}{mT}$$

case, describes the temperature source. Table 12-1 shows airmass codes. [*CAUTION: In Great Britain, the two letters are reversed.*]

Examples are **maritime Tropical** (**mT**) airmasses, such as can form over the Gulf of Mexico, and **continental Polar** (**cP**) air, such as can form in winter over Canada.

After the weather pattern changes and the airmass is blown away from its genesis region, it flows over surfaces with different relative temperatures. Some organizations append a third letter to the end of the airmass code, indicating whether the moving airmass is (**w**) warmer or (**k**) colder than the underlying surface. This coding helps indicate the likely static stability of the air and the associated weather. For example, "mPk" is humid cold air moving over warmer ground, which would likely be statically unstable and have convective clouds and showers.

Creation

An airmass can form when air remains stagnant over a surface for sufficient duration to take on characteristics similar to that surface. Also, an airmass can form in moving air if the surface over which it moves has uniform characteristics over a large area. Surface high-pressure centers favor the formation of airmasses because the calm or light winds allow long residence times. Thus, many of the **airmass genesis** (formation) regions (Fig. 12.4) correspond to the planetary- and continental-scale high-pressure regions described in the previous section.

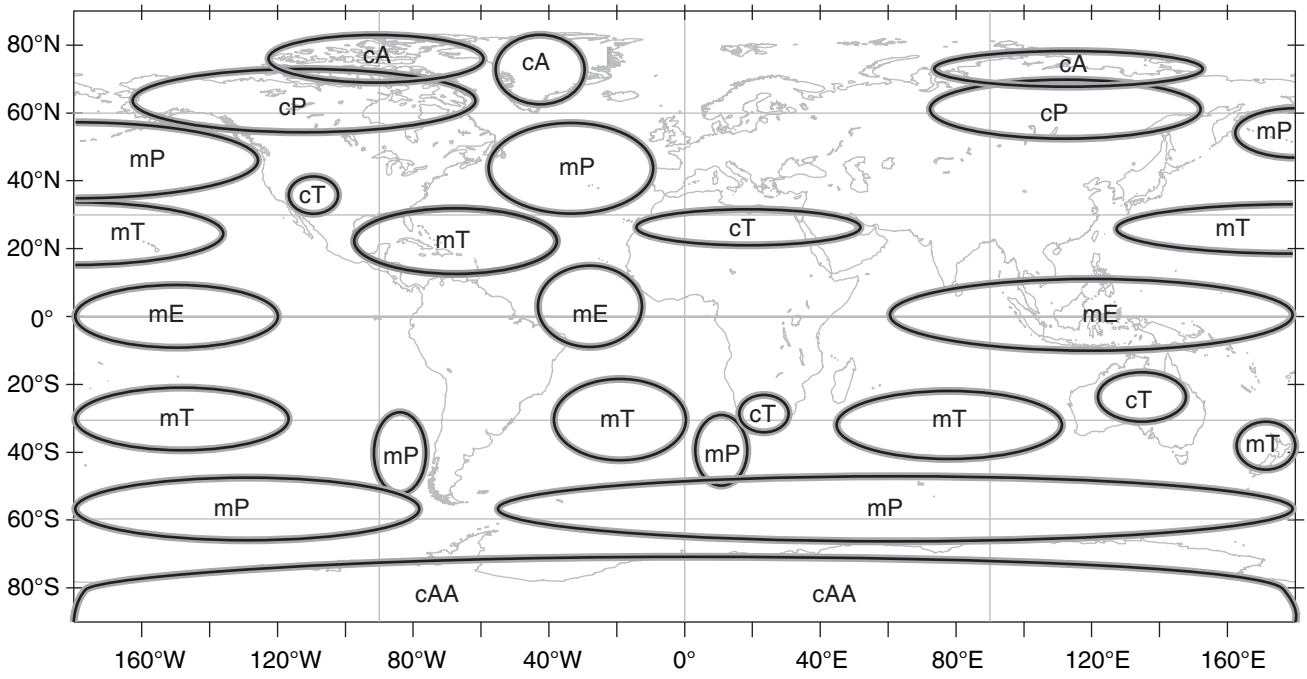

Figure 12.4
Airmass formation regions (symbols are defined in Table 12-1). Some meteorologists change all "mE" to "mT", and "cAA" to "cA".

Airmasses form as boundary layers. During their residence over a surface, the air is modified by processes including radiation, conduction, divergence, and turbulent transport between the ground and the air.

Warm Airmass Genesis

When cool air moves over a warmer surface, the warm surface modifies the bottom of the air to create an evolving, **convective mixed layer** (**ML**). Turbulence — driven by the potential temperature difference $\Delta\theta_s$ between the warm surface θ_{sfc} and the cooler airmass θ_{ML} — causes the ML depth z_i to initially increase (Fig. 12.5). This is the depth of the new airmass. A heat flux from the warm surface into the air causes θ_{ML} to warm toward θ_{sfc}. θ_{ML} is the temperature of the new airmass as it warms.

Synoptic-scale divergence β and subsidence w_s, which is expected in high-pressure airmass-genesis regions, oppose the ML growth. Changes within the new airmass are rapid at first. But as airmass temperature gradually approaches surface temperature, the turbulence diminishes and so does the rate of ML depth increase. Eventually, the ML depth begins to decrease (Fig. 12.5) because the reduced turbulence (trying to increase the ML thickness) cannot counteract the relentless subsidence.

A "toy model" describing the atmospheric boundary-layer processes that create a warm airmass is given in the Focus Box. The nearby Solved Example box uses this toy model to find the evolution of the warm airmass depth (i.e., the ML depth z_i) and its potential temperature θ_{ML} evolution. This is the solution that was plotted in Fig. 12.5.

The e-folding time (see Chapter 1) for the θ_{ML} to approach θ_{sfc} is surprisingly constant — about 1 to 2 days. As a result, creation of this warm **tropical** airmass is nearly complete after about a week. That is how long it takes until the airmass temperature nearly equals the surface temperature (Fig. 12.5). The time τ to reach the peak ML thickness is typically about 1 to 4 days (see another Focus box).

Cold Airmass Genesis

When air moves over a colder surface such as arctic ice, the bottom of the air first cools by conduction, radiation, and turbulent transfer with the ground. Turbulence intensity then decreases within the increasingly statically-stable boundary layer, reducing the turbulent heat transport to the cold surface.

However, direct radiative cooling of the air, both upward to space and downward to the cold ice surface, chills the air at rate 2°C/day (averaged over a 1 km thick boundary layer). As the air cools below the dew point, water-droplet clouds form. Continued radiative cooling from cloud top allows ice crystals

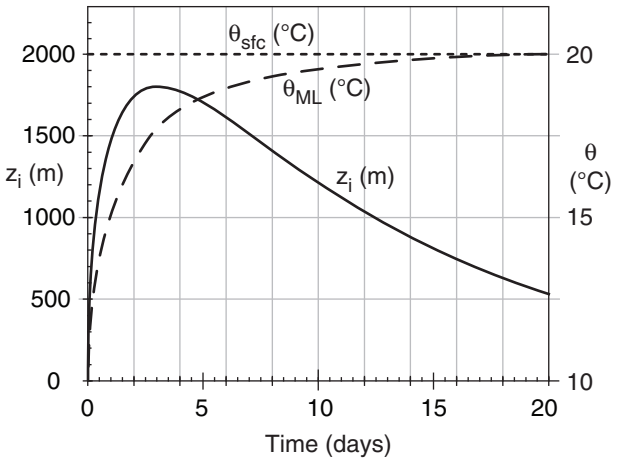

Figure 12.5
Genesis of a warm airmass after cold air comes to rest over a warmer surface. This is an example based on toy-model equations in the Focus Box. Airmass potential temperature is θ_{ML} and depth is z_i. Imposed conditions for this case-study example are: large-scale divergence $\beta = 10^{-6}\ s^{-1}$, potential temperature gradient in vertical $\gamma_o = 3.3$ K/km, initial near-surface air potential temperature $\theta_{ML} = \theta_o = 10°C$, and surface temperature $\theta_{sfc} = 20°C$.

ON DOING SCIENCE • Math Clarity

In math classes, you might have learned how to combine many small equations into a single large equation that you can solve. For meteorology, although we could make such large single-equation combinations, we usually cannot solve them.

So there is no point in combining all the equations. Instead, it is easier to see the physics involved by keeping separate equations for each physical process. An example is the toy model given in the Focus Box on the next page for warm airmass genesis. Even though the many equations are coupled, it is clearer to keep them separate.

FOCUS • Warm Airmass Genesis

Modeling warm airmass creation (genesis) is an exercise in atmospheric boundary-layer (ABL) evolution. Since we do not cover ABLs in detail until a later chapter, the details are relegated to this Focus Box. You can safely skip them now, and come back later after you have studied ABLs.

Define a relative potential temperature θ based on a reference height (z) at the surface (z = 0). Namely, $\theta \approx T + \Gamma_d \cdot z$, where Γ_d = 9.8 °C/km is the dry adiabatic lapse rate.

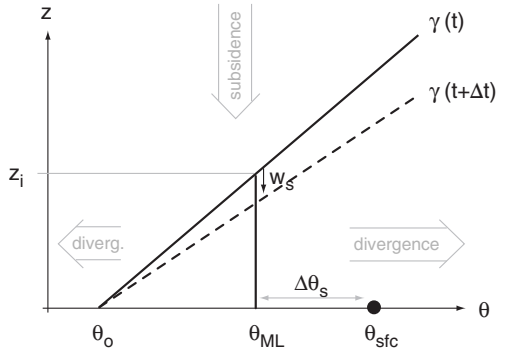

Suppose that a cool, statically stable layer of air initially (subscript o) has a near-surface temperature of θ_o and a linear potential-temperature gradient $\gamma_o = \gamma = \Delta\theta/\Delta z$ before it comes to rest over a warm surface of temperature θ_{sfc} (see Fig. above). We want to predict the time evolution of the depth (z_i) and potential temperature (θ_{ML}) of this new airmass. Because this airmass is an ABL, we can use boundary-layer equations to predict z_i (the height of the convective mixed-layer ,ML), and θ_{ML} (the ML potential temperature).

ML depth increases by amount Δz_{ie} during a time interval Δt due to thermodynamic encroachment (i.e., warming under the capping sounding). This is an entrainment process that adds air to the ML through the ML top. Large scale **divergence** $\beta = \Delta U / \Delta x + \Delta V / \Delta y$ removes air horizontally from the ML and causes a subsidence velocity of magnitude w_s at the ML top:

$$w_s = \beta \cdot z_i^* \tag{7}$$

Thus, a change in ML depth results from the competition of these two terms:

$$z_i = z_i^* + \Delta z_{ie} - w_s \cdot \Delta t \tag{12}$$

where the asterisk * indicates a value from the previous time step.

The amount of heat ΔQ (as an incremental accumulated kinematic heat flux) transferred from the warm surface to the cooler air during time interval Δt under light-wind conditions depends on the temperature difference at the surface $\Delta\theta_s$ and the intensity of turbulence, as quantified by a buoyancy velocity scale w_b:

$$\Delta Q = b \cdot w_b \cdot \Delta\theta_s \cdot \Delta t \tag{10}$$

where $b = 5\text{x}10^{-4}$ (dimensionless) is a convective heat transport coefficient (see the Heat chapter).

(continues in next column)

FOCUS *(continuation)*

The buoyancy velocity scale is:

$$w_b = \left[\frac{|g|}{\theta_{ML}^*} \cdot z_i^* \cdot \Delta\theta_s \right]^{1/2} \tag{9}$$

where $|g|$ = 9.8 m/s^2 is gravitational acceleration.

That heat goes to warming θ_{ML}, which by geometry adds a trapezoidal area under the γ curve :

$$\Delta z_{ie} = \left[\frac{2 \cdot \Delta Q}{\gamma} + \left(z_i^* \right)^2 \right]^{1/2} - z_i^* \tag{11}$$

Knowing the entrainment rate, we get $\Delta\theta_{ML}$ geometrically from where it intercepts the γ curve:

$$\theta_{ML} = \theta_{ML}^* + \gamma \cdot \Delta z_{ie} \tag{13}$$

With this new ML temperature, we can update the surface temperature difference

$$\Delta\theta_s = \theta_{sfc} - \theta_{ML}^* \tag{8}$$

Knowing the large-scale divergence, we can also update the potential temperature profile in the air above the ML:

$$\gamma = \gamma_o \cdot \exp(\beta \cdot t) \tag{6}$$

All that remains is to update the time variable:

$$t = t^* + \Delta t \tag{5}$$

You might have noticed that some of the equations above are initially singular, when the ML has zero depth. So, for the first small time step ($\Delta t \approx$ 6 minutes = 360 s), you should use the following special equations in the following order:

$$t = \Delta t \tag{1}$$

$$\Delta\theta_s = \theta_{sfc} - \theta_o \tag{2}$$

$$z_i = \Delta\theta_s \cdot \left[\frac{2 \cdot b \cdot \Delta t}{\gamma_o} \cdot \left(\frac{|g|}{\theta_o} \right)^{1/2} \right]^{2/3} \tag{3}$$

$$\theta_{ML} = \theta_o + \gamma_o \cdot z_i \tag{4}$$

Then, for all the subsequent time steps, use the set of equations (5 to 13 in the order as numbered) to find the resulting ML evolution. Repeat eqs. (5 to 13) for each subsequent step. As the solution begins to change more gradually, you may use larger time steps Δt. The result is a toy model that describes warm airmass formation as an evolving convective boundary layer.

The solved example on the next page shows how this can be done with a computer spreadsheet. First, you need to specify the imposed constants γ_o , θ_o, β and θ_{sfc}. Next, initialize the values of: $\gamma = \gamma_o$, $z_i = 0$, and $\theta_{ML} = \theta_o$ at $t = 0$. Then, solve the equations for the first step. Finally, continue iterating for subsequent time steps to simulate warm airmass genesis.

These simulations show that greater divergence causes a shallower ML that can warm faster. Greater static stability in the ambient environment reduces the peak ML depth.

Solved Example (§)

Air of initial ML potential temperature 10°C comes to rest over a 20°C sea surface. Divergence is 10^{-6} s^{-1}, and the initial $\Delta\theta/\Delta z = \gamma = 3.3$ K/km. Find and plot the warm airmass evolution of potential temperature and depth.

Solution

Given: $\theta_o = 10°C = 283K$, $\theta_{sfc} = 20°C$, $\gamma_o = 3.3$ K/km, $\beta = 10^{-6}$ s^{-1}.
Find: $\theta_{ML}(t) = ?$ °C, $z_i(t) = ?$ m

For the first time step of $\Delta t = 6$ min (=360 s), use eqs. (1 to 4 from the Focus Box on the previous page). For subsequent steps, repeatedly use eqs. (5 to 13 from that same Focus Box).

t (s)	t (d)	γ (K/m)	w_s (m/s)	$\Delta\theta_s$ (°C)	w_b (m/s)	ΔQ (K·m)	Δz_{ie} (m)	z_i (m)	θ_{ML} (°C)
0	0.000							0	10
360	0.004			10				74	10.2
720	0.008	0.00330	0.00007	9.75	5.0	8.8	29.8	104	10.3
1080	0.013	0.00330	0.00010	9.66	5.9	10.3	26.4	131	10.4
1440	0.017	0.00330	0.00013	9.57	6.6	11.3	24.0	155	10.5
. . .									
259200	3.00	0.00428	0.00179	2.41	12.0	104.3	13.6	1789	17.7
270000	3.13	0.00432	0.00179	2.35	11.9	150.8	19.4	1789	17.7
280800	3.25	0.00437	0.00179	2.26	11.7	142.8	18.2	1788	17.8
. . .									
1684800	19.50	0.01779	0.00057	0.14	1.6	4.9	0.5	542	19.9
1728000	20.00	0.01858	0.00054	0.13	1.5	4.4	0.4	519	19.9

Sample results from the computer spreadsheet are shown above. The final answer is plotted in Fig. 12.5.

Check: Units OK. Physics OK. Fig. 12.5 reasonable.
Discussion: I used small time steps of $\Delta t = 6$ minutes initially, and then as Δz_{ie} became smaller, I gradually increased past $\Delta t = 3$ h to $\Delta t = 12$ h. The figure shows rapid initial modification of the cold, statically stable airmass toward a warm, unstable airmass. Maximum z_i is reached in about $\tau = 3.06$ days (see Focus box), in agreement with Fig. 12.5.

FOCUS • Time of Max Airmass Thickness

The time τ to reach the peak ML thickness for warm airmass genesis is roughly

$$\tau \approx c \cdot \left(\frac{\theta_o}{|g| \cdot \beta \cdot \gamma_o \cdot e^{\beta \cdot \tau}} \right)^{1/3} \qquad \text{(c)}$$

where $c = 140$ (dimensionless), and the other variables are defined in the text. τ is typically about 1 to 4 days. Any further lingering of the airmass over the same surface temperature results in a loss of airmass thickness due to divergence.

Equation (c) is an implicit equation; namely, you need to know τ in order to solve for τ. Although this equation is difficult to solve analytically, you can iterate to quickly converge to a solution in about 5 steps in a computer spreadsheet. Namely, start with $\tau = 0$ as the first guess and plug into the right side of eq. (c). Then solve for τ on the left side. For the next iteration, take this new τ and plug it in on the right, and solve for an updated τ on the left. Repeat until the value of τ converges to a solution; namely, when $\Delta\tau/\tau < \varepsilon$ for $\varepsilon = 0.01$ or smaller.

Solved Example (§)

For the conditions of the previous solved example, find the time τ that estimates when the new warm airmass has maximum thickness.

Solution

Given: $\theta_o = 10°C = 283K$, $\theta_{sfc} = 20°C$, $\gamma_o = 3.3$ K/km, $\beta = 10^{-6}$ s^{-1}.
Find: $\tau = ?$ days

Use eq. (c) from the Focus Box at left. Start with $\tau = 0$. The first iteration is:

$$\tau = 140 \cdot \left[\frac{283\text{K}}{(9.8\text{m/s}^2) \cdot (10^{-6}\text{s}^{-1}) \cdot (0.0033\text{K/m}) \cdot e^0} \right]^{1/3}$$

$= 288498$ s $= 3.339$ days

Subsequent iterations give: $\tau =$
3.033 -> 3.060 -> 3.057 -> 3.058 -> **3.058 days**

Check: Units OK. Physics OK. Agrees with Fig. 12.5.
Discussion: Convergence was quick. From Fig. 12.5, the actual time of this peak thickness was between 3 and 3.125 days, so eq. (c) does a reasonable job.

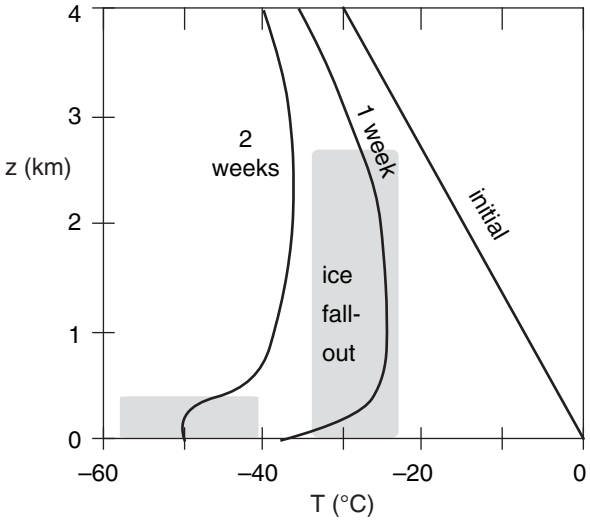

Figure 12.6
Genesis of a continental-polar air mass over arctic ice. The cloud/fog regions are shaded.

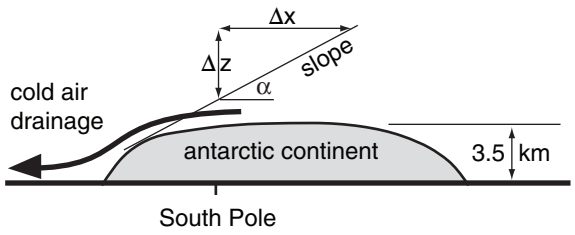

Figure 12.7
Cold katabatic winds draining from Antarctica.

Solved Example

Find the slope force per unit area acting on a katabatic wind of temperature –20°C with ambient air temperature 0°C. Assume a slope of $\Delta z/\Delta x = 0.1$.

Solution

Given: $\Delta\theta = 20$ K, $T_e = 273$ K, $\Delta z/\Delta x = 0.1$
Find: $F_{x\,S}/m = ?$ m·s^{-2}

Use eq. (12.1):

$$\frac{F_{x\,S}}{m} = \frac{(9.8\text{m}\cdot\text{s}^{-2})\cdot(20\text{K})}{273\text{K}}\cdot(0.1)$$

$= \underline{\mathbf{0.072\ m\cdot s}}^{-2}$

Check: Units OK. Physics OK.
Discussion: This is two orders of magnitude greater than the typical synoptic forces (see the Dynamics chapter). Hence, drainage winds can be strong.

to grow at the expense of evaporating liquid droplets, changing the cloud into an ice cloud.

Radiative cooling from cloud top creates cloudy "thermals" of cold air that sink, causing some turbulence that distributes the cooling over a deeper layer. Turbulent entrainment of air from above cloud top down into the cloud allows the cloud top to rise, and deepens the incipient airmass (Fig. 12.6).

The ice crystals within this cloud are so few and far between that the weather is described as cloudless ice-crystal precipitation. This can create some spectacular **halos** and other optical phenomena in sunlight (see the Optics chapter), including sparkling ice crystals known as **diamond dust**. Nevertheless, infrared radiative cooling in this cloudy air is much greater than in clear air, allowing the cooling rate to increase to 3°C/day over a layer as deep as 4 km.

During the two-week formation of this **continental-polar** or **continental-arctic** airmass, most of the ice crystals precipitate out leaving a thinner cloud of 1 km depth. Also, subsidence within the high pressure also reduces the thickness of the cloudy airmass and causes some warming to partially counteract the radiative cooling.

Above the final fog layer is a nearly isothermal layer of air 3 to 4 km thick that has cooled about 30°C. Final air-mass temperatures are often in the range of –30 to –50 °C, with even colder temperatures near the surface.

While the Arctic surface consists of relatively flat sea-ice (except for Greenland), the Antarctic has mountains, high ice-fields, and significant surface topography (Fig. 12.7). As cold air forms by radiation, it can drain downslope as a **katabatic wind** (see the Local Winds chapter). Steady winds of 10 m/s are common in the Antarctic interior, with speeds of 50 m/s along some of the steeper slopes.

As will be shown in the Local Winds chapter, the buoyancy force per unit mass on a surface of slope $\Delta z/\Delta x$ translates into a quasi-horizontal slope-force per mass of:

$$\frac{F_{x\,S}}{m} = \frac{|g|\cdot\Delta\theta}{T_e}\cdot\frac{\Delta z}{\Delta x} \qquad \bullet(12.1)$$

$$\frac{F_{y\,S}}{m} = \frac{|g|\cdot\Delta\theta}{T_e}\cdot\frac{\Delta z}{\Delta y} \qquad \bullet(12.2)$$

where $|g| = 9.8$ m·s^{-2} is gravitational acceleration, and $\Delta\theta$ is the potential-temperature difference between the draining cold air and the ambient air above. The ambient-air absolute temperature is T_e.

The sign of these forces should be such as to accelerate the wind downslope. The equations above work when the magnitude of slope $\Delta z/\Delta x$ is small,

because then $\Delta z/\Delta x = \sin(\alpha)$, where α is the slope angle of the topography.

The katabatic wind speed in the Antarctic also depends on turbulent drag force against the ice surface, ambient pressure-gradient force associated with synoptic weather systems, Coriolis force, and turbulent drag caused by mixing of the draining air with the stationary air above it. At an average drainage velocity of 5 m/s, air would need over 2 days to move from the interior to the periphery of the continent, which is a time scale on the same order as the inverse of the Coriolis parameter. Hence, Coriolis force cannot be neglected.

Katabatic drainage removes cold air from the genesis regions and causes turbulent mixing of the cold air with warmer air aloft. The resulting cold-air mixture is rapidly distributed toward the outside edges of the antarctic continent.

One aspect of the global circulation is a wind that blows around the poles. This is called the **polar vortex**. Katabatic removal of air from over the antarctic reduces the troposphere depth, enhancing the persistence and strength of the antarctic polar vortex due to potential vorticity conservation.

Movement

Airmasses do not remain stationary over their birth place forever. After a week or two, a transient change in the weather pattern can push the airmass toward new locations.

When airmasses move, two things can happen:
(1) As the air moves over surfaces with different characteristics, the airmass begins to change. This is called **airmass modification**, and is described in the next subsection.
(2) An airmass can encounter another airmass. The boundary between these two airmasses is called a **front**, and is a location of strong gradients of temperature, humidity, and other airmass characteristics. Fronts are described in detail later.

Tall mountain ranges can strongly **block** or **channel** the movement of airmasses, because airmasses occupy the bottom of the troposphere. Fig. 12.8 shows a simplified geography of major mountain ranges.

For example, in the middle of North America, the lack of any major east-west mountain range allows the easy movement of cold polar air from Canada toward warm humid air from the Gulf of Mexico. This sets the stage for strong storms (see the Extratropical Cyclone chapter and the chapters on Thunderstorms).

The long north-south barrier of mountains (Rockies, Sierra Nevada, Cascades, Coast Range) along the west coast of North America impedes the easy entry of Pacific airmasses toward the center of that continent. Those mountains also help protect the west coast from the temperature extremes experienced by the rest of the continent.

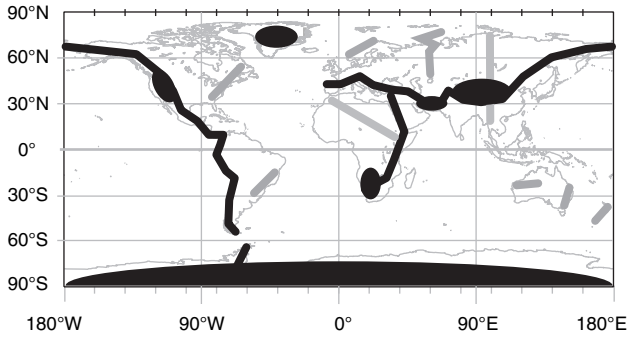

Figure 12.8
Locations of major mountain ranges (black lines), lesser ranges (grey lines), and large plateaus of land or ice (black ovals).

In Europe, the mountain orientation is the opposite. The Alps and the Pyrenees are east-west mountain ranges that inhibit movement of Mediterranean airmasses from reaching northward. The lack of major north-south ranges in west and central Europe allows the easy movement of maritime airmasses from the Atlantic to sweep eastward, bringing cool wet conditions.

One of the greatest ranges is the Himalaya Mountains, running east-west between India and China. Maritime tropical airmasses moving in from the Indian Ocean reach these mountains, causing heavy rains over India during the monsoon. The same mountains block the maritime air from reaching further northward, leaving a very dry Tibetan Plateau and Gobi Desert in its **rain shadow**.

The discussion above focused on blocking and channeling by the mountains. In some situations air can move over mountain tops (Fig. 12.9). When this happens, the airmass is strongly modified, as described next.

Modification

As an airmass moves from its origin, it is modified by the new landscapes under it. For example, a polar airmass will warm and gain moisture as it moves equatorward over warmer vegetated ground. Thus, it gradually loses its original identity.

Via Surface Fluxes

Heat and moisture transfer at the surface can be described with **bulk-transfer relationships** such as eq. (3.34). If we assume for simplicity that wind-induced turbulence creates a well-mixed airmass of quasi-constant thickness z_i, then the change of

Solved Example

An mP airmass initially has T = 5°C & RH = 100%. Use a thermo diagram to find T & RH at: 1 Olympic Mtns (elevation ≈ 1000 m), 2 Puget Sound (0 m), 3 Cascade Mtns (1500 m), 4 the Great Basin (500 m), 5 Rocky Mtns (2000 m), 6 the western Great Plains (1000 m).

Solution

Given: Elevations from west to east (m) = 0, 1000, 0, 1500, 500, 2000, 1000
Initially RH=100%. Thus $T_d = T$ = 5°C
Find: T (°C) & RH (%) at surface locations 1 to 6.
Assume: All condensation precipitates out. No additional heat or moisture transfer from the surface.
Start with air near sea level, where P_{SL} = 100 kPa.

Use Fig. 12.9 and an emagram from the Stability chapter. On the thermo diagram, the air parcel follows the following route: 0 - 1 - 2 - 1 - 3 - 4 - 3 - 5 - 6.

Initially (point 0), $T_d = T$ = 5°C. Because this air is already saturated, it would follow a saturated adiabat from point 0 to point 1 at z = 1 km, where the still-saturated air has $T_d = T$ = –1°C.

If all condensates precipitate out, then air would descend dry adiabatically (with T_d following an isohume) from point 1 to 2, giving T = 9°C and T_d = 1°C.

When this unsaturated air rises, it first does so dry adiabatically until it reaches its LCL at point 1. This now-cloudy air continues to rise toward point 3 moist adiabatically, where it has $T_d = T$ = –4°C. Etc.

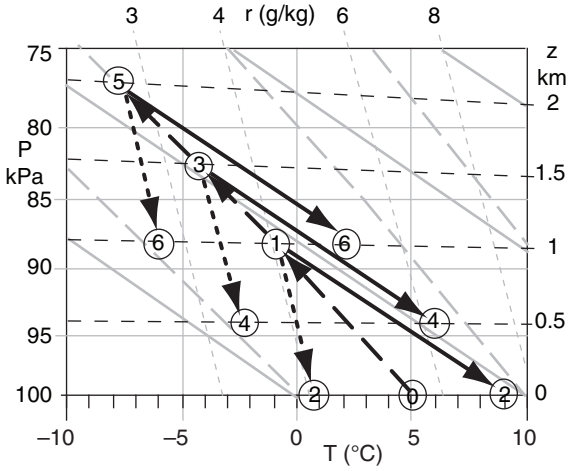

Results, where Index = circled numbers in Fig above.

Index	z (km)	T (°C)	T_d (°C)	RH (%)
0	0	5	5	100
1	1	–1	–1	100
2	0	9	1	55
3	1.5	–4	–4	100
4	0.5	6	–2	54
5	2	–7	–7	100
6	1	2	–6	53

Check: Units OK. Physics OK. Figure OK.
Discussion: The airmass has lost its maritime identity by the time it reaches the Great Plains, and little moisture remains. Humidity for rain in the plains comes from the southeast (not from the Pacific).

airmass potential temperature θ_{ML} with travel-distance Δx is:

$$\frac{\Delta\theta_{ML}}{\Delta x} \approx \frac{C_H \cdot (\theta_{sfc} - \theta_{ML})}{z_i} \qquad (12.3)$$

where $C_H \approx 0.01$ is the bulk-transfer coefficient for heat (see the chapters on Heat and on the Atmospheric Boundary Layer).

If the surface temperature is horizontally homogeneous, then eq. (12.3) can be solved for the airmass temperature at any distance x from its origin:

$$\theta_{ML} = \theta_{sfc} - (\theta_{sfc} - \theta_{ML\,o}) \cdot \exp\left(-\frac{C_H \cdot x}{z_i}\right) \qquad (12.4)$$

where $\theta_{ML\,o}$ is the initial airmass potential temperature at location x = 0.

Solved Example

A polar airmass with initial θ = –20°C and depth = 500 m moves southward over a surface of 0°C. Find the initial rate of temperature change with distance.

Solution

Given: θ_{ML} = –20°C, θ_{sfc} = 0°C, z_i = 500 m
Find: $\Delta\theta_{ML}/\Delta x$ = ? °C/km. Assume no mountains.

Use eq. (12.3):

$$\frac{\Delta\theta_{ML}}{\Delta x} \approx \frac{(0.01)\cdot[0°C - (-20°C)]}{(500\text{m})} = \underline{\mathbf{0.4\ °C/km}}$$

Check: Units OK. Physics OK.
Discussion: Neither this answer nor eq. (12.4) depend on wind speed. While faster speeds give faster position change, they also cause greater heat transfer to/from the surface (eq. 3.34). These 2 effects cancel.

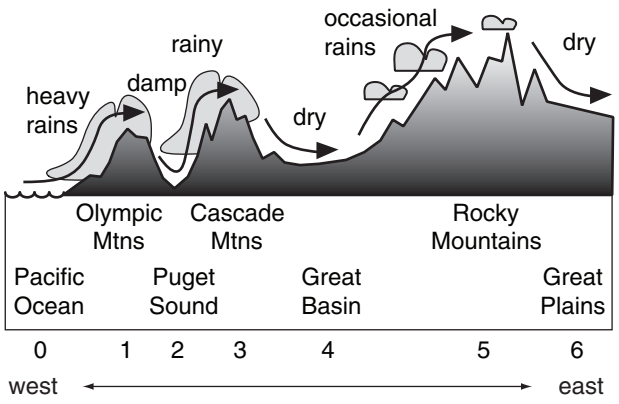

Figure 12.9
Modification of a Pacific airmass by flow over mountains in the northwestern USA. (Numbers are used in the solved example.)

Via Flow Over Mountains

If an airmass is forced to rise over mountain ranges, the resulting condensation, precipitation, and latent heating will dry and warm the air. For example, an airmass over the Pacific Ocean near the northwestern USA is often classified as maritime polar (mP), because it is relatively cool and humid. As the prevailing westerly winds move this airmass over the Olympic Mountains (a coastal mountain range), the Cascade Mountains, and the Rocky Mountains, there is substantial precipitation and latent heating (Fig. 12.9).

SURFACE FRONTS

Surface fronts mark the boundaries between airmasses at the Earth's surface. They usually have the following attributes:

- strong horizontal temperature gradient
- strong horizontal moisture gradient
- strong horizontal wind gradient
- strong vertical shear of the horizontal wind
- relative minimum of pressure
- high vorticity
- **confluence** (air converging horizontally)
- clouds and precipitation
- high static stability
- kinks in isopleths on weather maps

In spite of this long list of attributes, fronts are usually labeled by the surface temperature change associated with frontal passage.

Some weather features exhibit only a subset of attributes, and are not labeled as fronts. For example, a **trough** (pronounced like "trof") is a line of low pressure, high vorticity, clouds and possible precipitation, wind shift, and confluence. However, it often does not possess the strong horizontal temperature and moisture gradients characteristic of fronts.

Another example of an airmass boundary that is often not a complete front is the **dryline**. It is discussed later in this chapter.

Recall from the Weather Reports and Map Analysis chapter that fronts are always drawn on the warm side of the frontal zone. The frontal symbols (Fig. 12.10) are drawn on the side of the frontal line toward which the front is moving. For a stationary front, the symbols on both sides of the frontal line indicate what type of front it would be if it were to start moving in the direction the symbols point.

Fronts are three dimensional. To help picture their structure, we next look at horizontal and vertical cross sections through fronts.

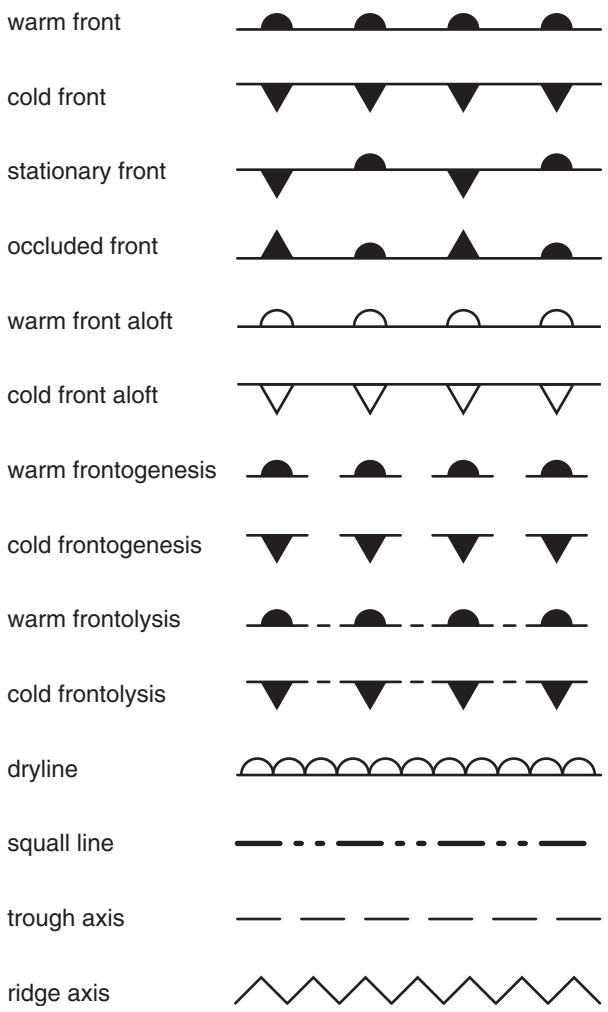

Figure 12.10
Glyphs for fronts, other airmass boundaries, and axes (copied from the Weather Reports and Map Analysis chapter). The suffix "genesis" implies a forming or intensifying front, while "lysis" implies a weakening or dying front. A stationary front is a frontal boundary that doesn't move very much. Occluded fronts and drylines will be explained later.

FOCUS • Bergen School of Meteorology

During World War I, Vilhelm Bjerknes, a Norwegian physicist with expertise in radio science and fluid mechanics, was asked in 1918 to form a Geophysical Institute in Bergen, Norway. Cut-off from weather data due to the war, he arranged for a dense network of 60 surface weather stations to be installed. Some of his students were C.-G. Rossby, H. Solberg, T. Bergeron, V. W. Ekman, H. U. Sverdrup, and his son Jacob Bjerknes.

Jacob Bjerknes used the weather station data to identify and classify cold, warm, and occluded fronts. He published his results in 1919, at age 22. The term "front" supposedly came by analogy to the battle fronts during the war. He and Solberg also later explained the life cycle of cyclones.

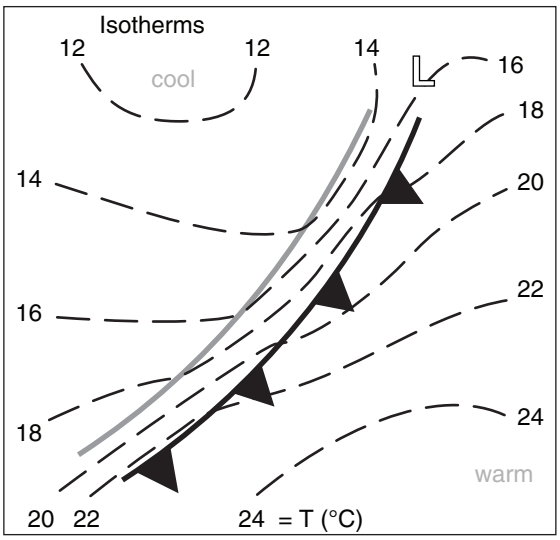

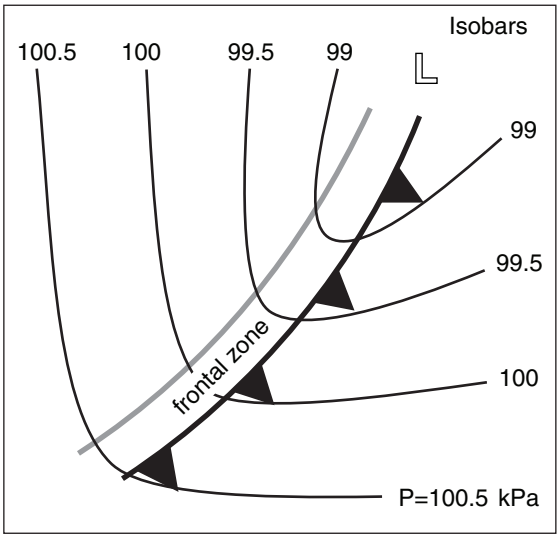

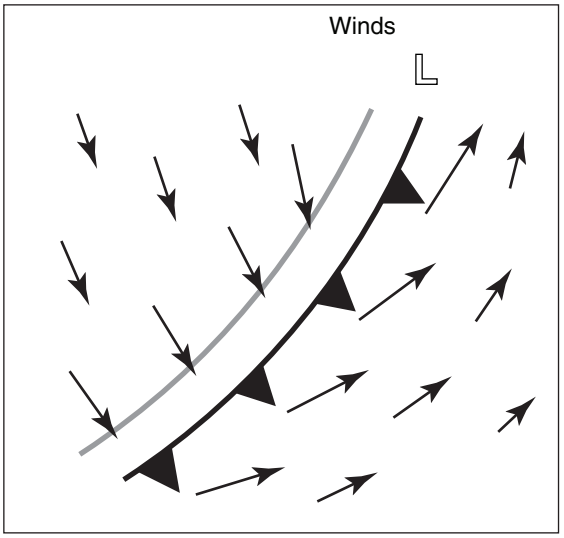

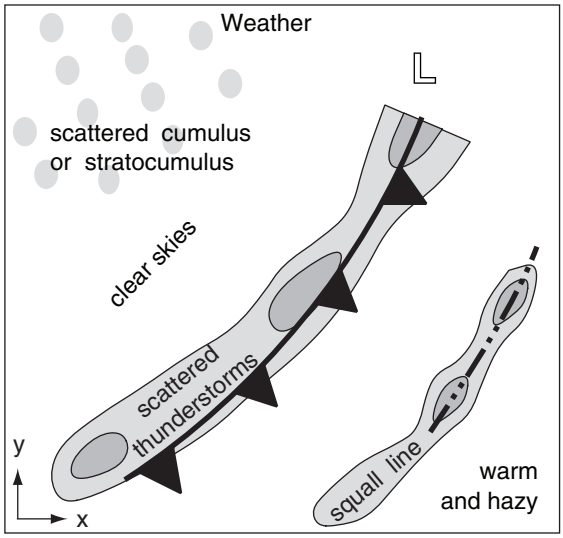

Figure 12.11 (both columns) *Cold front horizontal structure (maps can be overlain).*

Horizontal Structure

Cold Fronts (Fig. 12.11)

In central N. America, winds ahead of cold fronts typically have a southerly component, and can form strong low-level jets at night and possibly during day. Warm, humid, hazy air advects from the south.

Sometimes a **squall line** of thunderstorms will form in advance of the front, in the warm air. These squall lines can be triggered by wind shear and by the kinematics (advection) near fronts. They can also consist of thunderstorms that were initially formed on the cold front, but progressed faster than the front.

Along the front are narrow bands of towering cumuliform clouds with possible thunderstorms and scattered showers. Along the front the winds are stronger and gusty, and pressure reaches a relative minimum. Thunderstorm anvils often spread hundreds of kilometers ahead of the surface front.

Winds shift to a northerly direction behind the front, advecting colder air from the north. This air is often clean with excellent visibilities and clear blue skies during daytime. If sufficient moisture is present, scattered cumulus or broken stratocumulus clouds can form within the cold airmass.

As this airmass consists of cold air advecting over warmer ground, it is statically unstable, convective, and very turbulent. However, at the top of the airmass is a very strong stable layer along the frontal inversion that acts like a lid to the convec-

tion. Sometimes over ocean surfaces the warm moist ocean leads to considerable post-frontal deep convection.

The idealized picture presented in Fig. 12.11 can differ considerably in the mountains.

Warm Fronts (Fig. 12.12)

In central N. America, southeasterly winds ahead of the front bring in cool, humid air from the Atlantic Ocean, or bring in mild, humid air from the Gulf of Mexico.

An extensive deck of stratiform clouds (called a **cloud shield**) can occur hundreds of kilometers ahead of the surface front. In the cirrostratus clouds at the leading edge of this cloud shield, you can sometimes see halos, sundogs, and other optical phenomena. The cloud shield often wraps around the poleward side of the low center.

Along the frontal zone can be extensive areas of low clouds and fog, creating hazardous travel conditions. Nimbostratus clouds cause large areas of drizzle and light continuous rain. Moderate rain can form in multiple **rain bands** parallel to the front. The pressure reaches a relative minimum at the front.

Winds shift to a more southerly direction behind the warm front, advecting in warm, humid, hazy air. Although heating of air by the surface might not be strong, any clouds and convection that do form can often rise to relatively high altitudes because of weak static stabilities throughout the warm airmass.

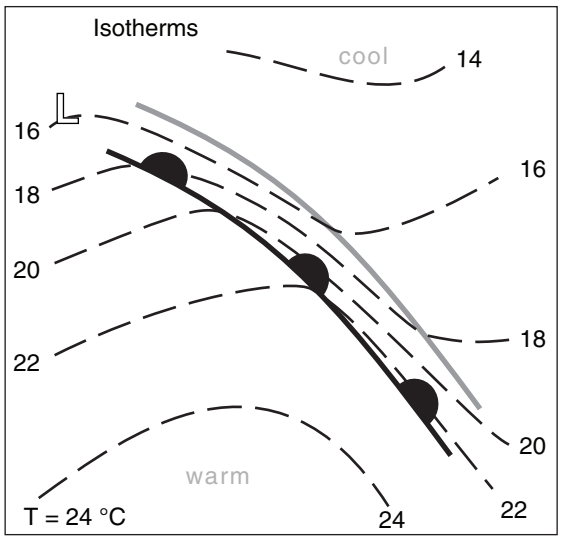

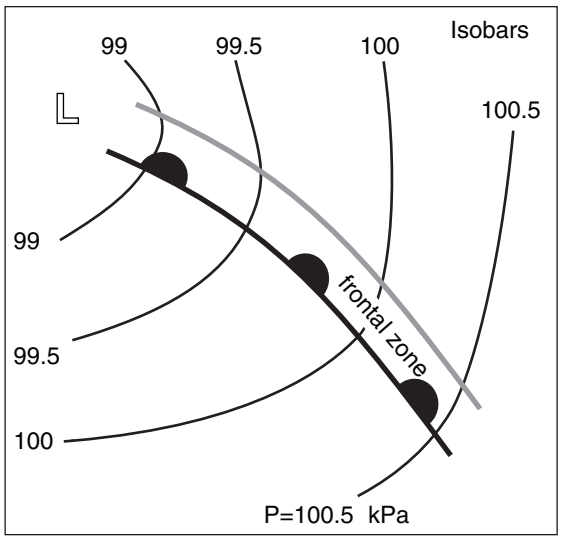

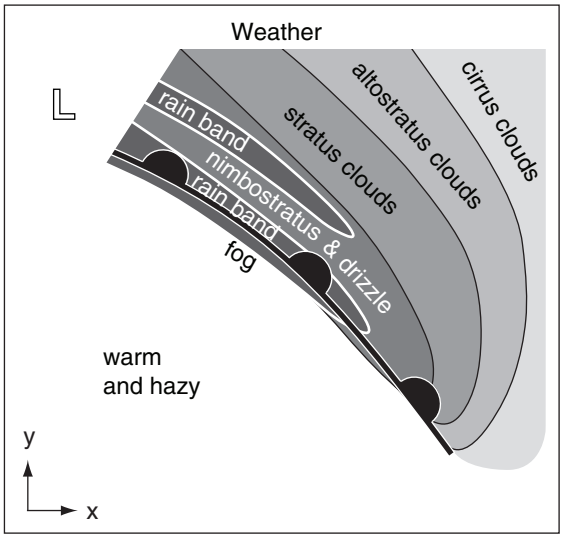

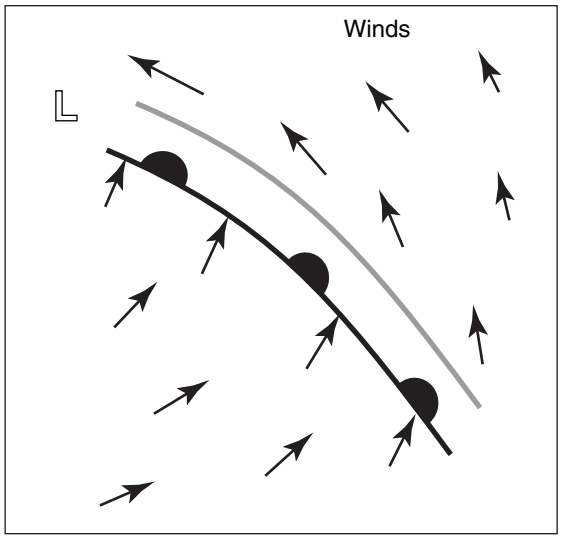

Figure 12.12 (both columns) *Warm front structure (maps can be overlain).*

Solved Example

Given the plotted surface weather data below, analyze it for temperature (50°F and every 5°F above and below) and pressure (101.2 kPa and every 0.4 kPa above and below). Identify high- and low-pressure centers and fronts. Discuss how the winds, clouds and weather compare to the descriptions in Figs. 12.11 & 12.

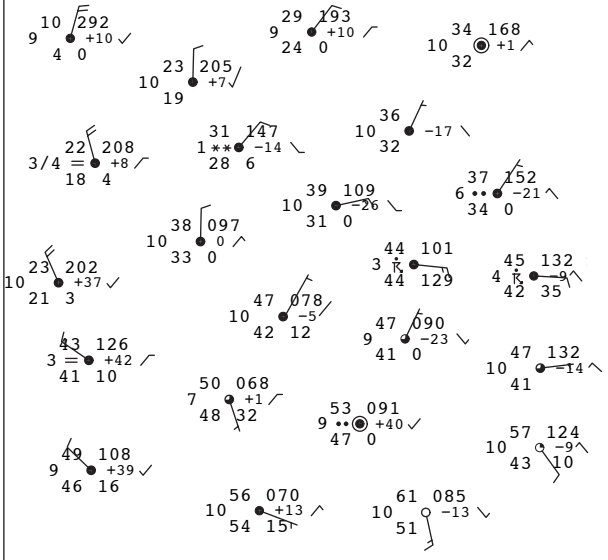

Solution

First, using methods shown in the Weather Reports & Map Analysis chapter, draw the isotherms (°F):

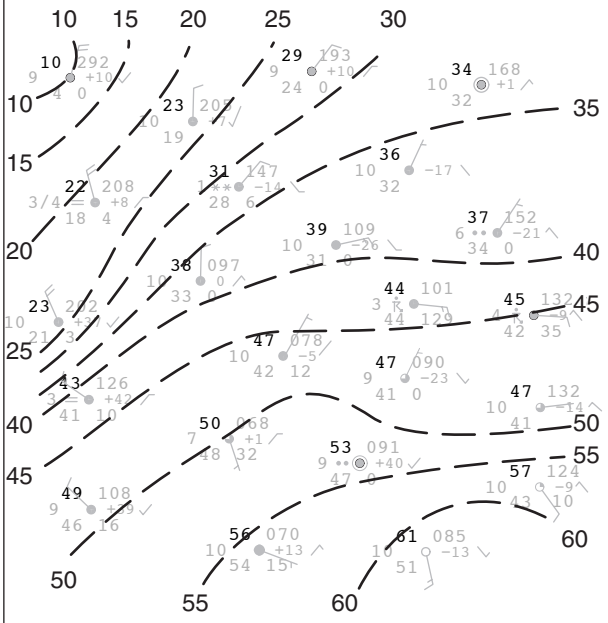

Next, analyze it for pressure. Recall that the plotted pressure is abbreviated. We need to prefix 9 or 10 to the left of the pressure code, and insert a decimal point two places from the right (to get kPa). Choose between 9 and 10 based on which one results in a pressure closest to standard sea-level pressure 101.3 kPa.

(continues in next column)

Solved Example *(continued)*

For the pressure data in this solved example, every prefix is 10. For example, the plotted pressure code 097 means 100.97 kPa. Similarly, 208 means 102.08 kPa. By analyzing pressures, we get the following map of isobars (kPa):

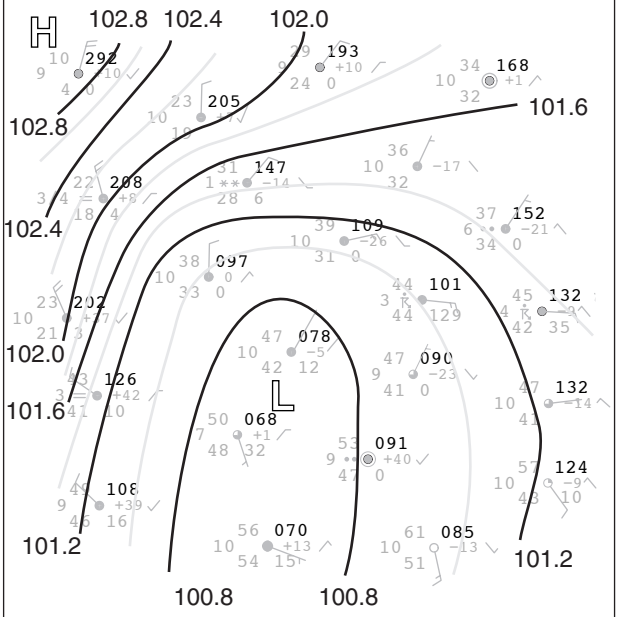

Next, overlay the isobars and isotherms, and find the frontal zones (drawn with the thick black and grey lines) and fronts (thick black line).

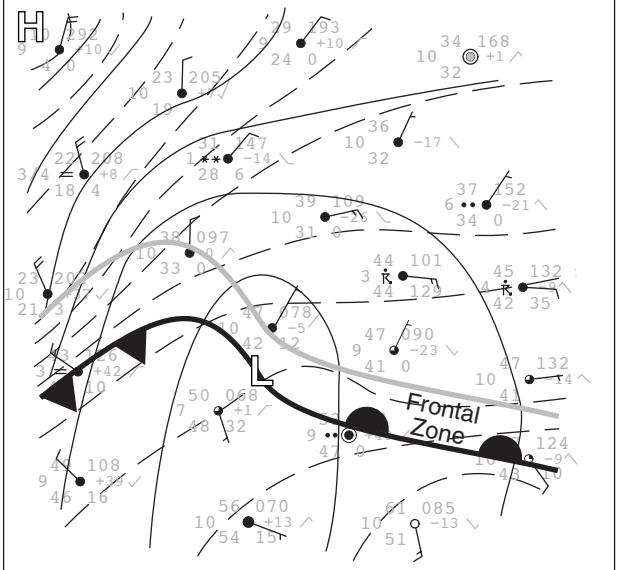

Check: Looks reasonable.

Discussion: Winds are generally circulating counterclockwise around the low center (except the very light winds, which can be sporadic). Overcast skies cover most of the region, with some thunderstorms and rain north of the warm front, and snow further northwest of the low where the air is colder.

Vertical Structure

Suppose that radiosonde observations (**RAOBs**) are used to probe the lower troposphere, providing temperature profiles such as those in Fig. 12.13a. To locate fronts by their vertical cross section, first convert the temperatures into potential temperatures θ (Fig. 12.13b). Then, draw lines of equal potential temperature (**isentropes**). Fig. 12.13c shows isentropes drawn at 5°C intervals. Often isentropes are labeled in Kelvin.

In the absence of diabatic processes such as latent heating, radiative heating, or turbulent mixing, air parcels follow isentropes when they move adiabatically. For example, consider the θ = 35°C parcel that is circled in Fig. 12.13b above weather station B. Suppose this parcel starts to move westward toward C.

If the parcel were to be either below or above the 35°C isentrope at its new location above point C, buoyant forces would tend to move it vertically to the 35°C isentrope. Such forces happen continuously while the parcel moves, constantly adjusting the altitude of the parcel so it rides on the isentrope.

The net movement is westward and upward along the 35°C isentrope. Air parcels that are forced to rise along isentropic surfaces can form clouds and precipitation, given sufficient moisture. Similarly, air blowing eastward would move downward along the sloping isentrope.

In three dimensions, you can picture **isentropic surfaces** separating warmer θ aloft from colder θ below. Analysis of the flow along these surfaces provides a clue to the weather associated with the front. Air parcels moving adiabatically must follow the "topography" of the isentropic surface. This is illustrated in the Extratropical Cyclones chapter.

At the Earth's surface, the boundary between cold and warm air is the **surface frontal zone**. This is the region where isentropes are packed relatively close together (Figs. 12.13b & c). The top of the cold air is called the **frontal inversion** (Fig. 12.13c). The frontal inversion is also evident at weather stations C and D in Fig. 12.13a, where the temperature increases with height. Frontal inversions of warm and cold fronts are gentle and of similar temperature change.

Within about 200 m of the surface, there are appreciable differences in frontal slope. The cold front has a steeper nose (slope ≈ 1 : 100) than the warm front (slope ≈ 1 : 300), although wide ranges of slopes have been observed.

Fronts are defined by their temperature structure, although many other quantities change across the front. Advancing cold air at the surface defines

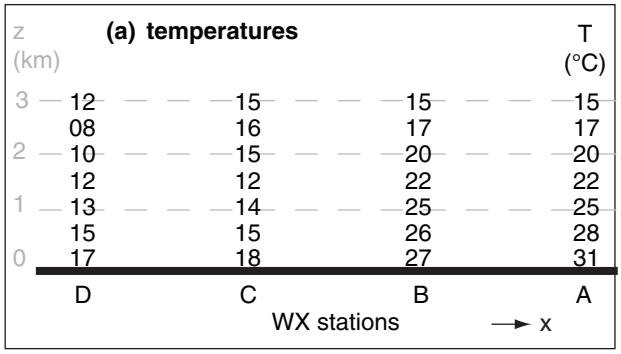

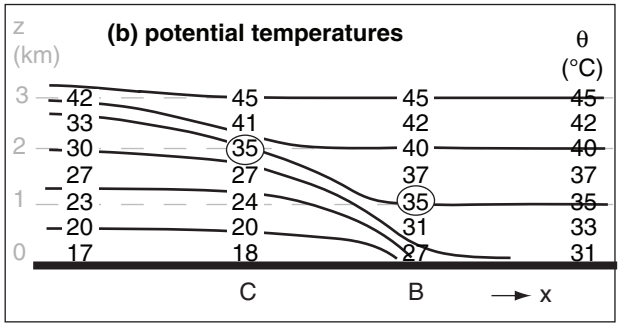

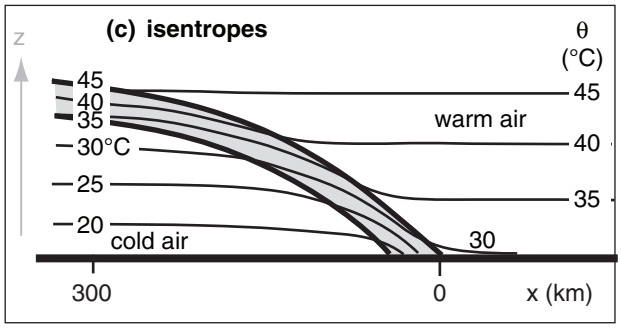

Figure 12.13
Analysis of soundings to locate fronts in a vertical cross section. Frontal zone / frontal inversion is shaded in bottom figure, and is located where the isentropes are tightly packed (close to each other).

Solved Example

What weather would you expect with a warm katafront? (See next page.)

Solution & Discussion

Cumuliform clouds and showery precipitation would probably be similar to those in Fig. 12.16a, except that the bad weather would move in the direction of the warm air at the surface, which is the direction the surface front is moving.

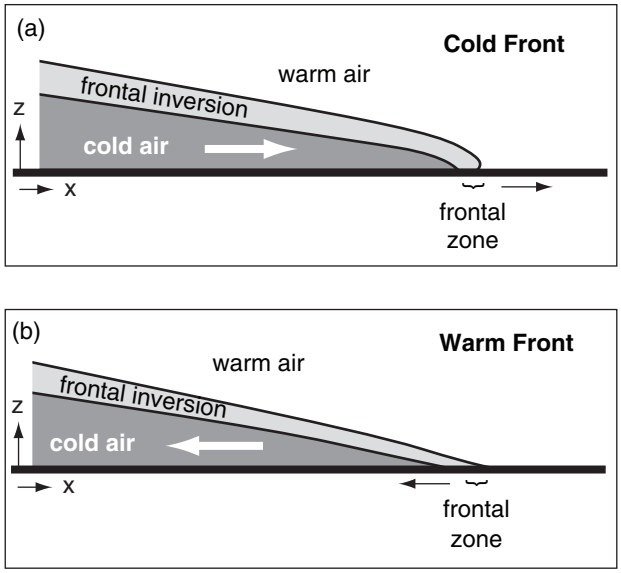

Figure 12.14
Vertical structure of fronts, based on cold air movement.

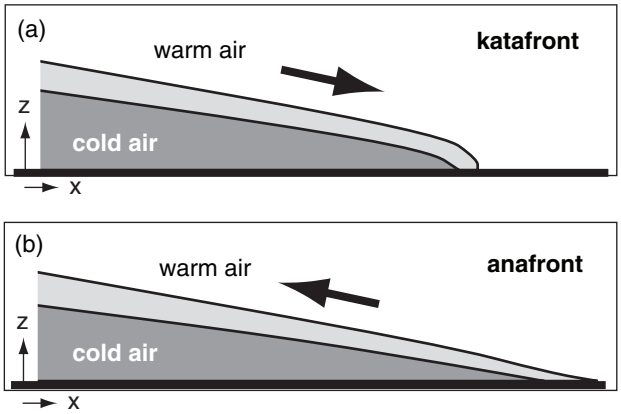

Figure 12.15
Vertical structure of fronts, based on overlying-air movement.

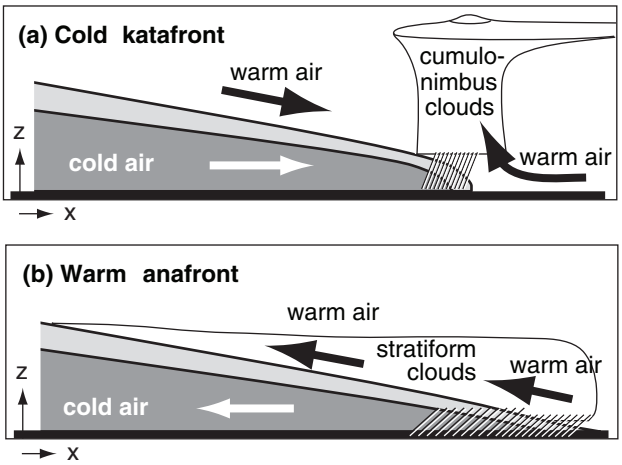

Figure 12.16
Typical fronts in central N. America.

the **cold front**, where the front moves toward the warm airmass (Fig. 12.14a). Retreating cold air defines the **warm front**, where the front moves toward the cold airmass (Fig. 12.14b).

Above the frontal inversion, if the warm air flows down the frontal surface, it is called a **katafront**, while warm air flowing up the frontal surface is an **anafront** (Fig. 12.15). It is possible to have cold katafronts, cold anafronts, warm katafronts, and warm anafronts.

Frequently in central N. America, the cold fronts are katafronts, as sketched in Fig. 12.16a. For this situation, warm air is converging on both sides of the frontal zone, forcing the narrow band of cumuliform clouds that is typical along the front. It is also common that warm fronts are anafronts, which leads to a wide region of stratiform clouds caused by the warm air advecting up the isentropic surfaces (Fig. 12.16b).

A **stationary front** is like an anafront where the cold air neither advances nor retreats.

GEOSTROPHIC ADJUSTMENT – PART 3

Winds in the Cold Air

Why does cold dense air from the poles not spread out over more of the Earth, like a puddle of water? Coriolis force is the culprit, as shown next.

Picture two air masses initially adjacent (Fig. 12.17a). The cold airmass has initial depth H and uniform virtual potential temperature θ_{v1}. The warm airmass has uniform virtual potential temperature $\theta_{v1} + \Delta\theta_v$. The average absolute virtual temperature is $\overline{T_v}$. In the absence of rotation of the coordinate system, you would expect the cold air to spread out completely under the warm air due to buoyancy, reaching a final state that is horizontally homogeneous.

However, on a rotating Earth, the cold air experiences Coriolis force (to the right in the Northern Hemisphere) as it begins to move southward. Instead of flowing across the whole surface, the cold air spills only distance a before the winds have turned 90°, at which point further spreading stops (Fig. 12.17b).

At this quasi-equilibrium, pressure-gradient force associated with the sloping cold-air interface balances Coriolis force, and there is a steady geostrophic wind U_g from east to west. The process of approaching this equilibrium is called **geostrophic adjustment**, as was discussed in the previous chapter. Real atmospheres never quite reach this equilibrium.

At equilibrium, the final spillage distance a of the front from its starting location equals the **external Rossby-radius of deformation**, λ_R:

$$a = \lambda_R = \frac{\sqrt{|g| \cdot H \cdot \Delta\theta_v / \overline{T_v}}}{f_c} \qquad \bullet(12.5)$$

where f_c is the Coriolis parameter and $|g| = 9.8\ \text{m/s}^2$ is gravitational acceleration magnitude.

The geostrophic wind U_g in the cold air at the surface is greatest at the front (neglecting friction), and exponentially decreases behind the front:

$$U_g = -\sqrt{|g| \cdot H \cdot (\Delta\theta_v / \overline{T_v})} \cdot \exp\left(-\frac{y+a}{a}\right) \qquad \bullet(12.6)$$

for $-a \le y \le \infty$. The depth of the cold air h is:

$$h = H \cdot \left[1 - \exp\left(-\frac{y+a}{a}\right)\right] \qquad \bullet(12.7)$$

which smoothly increases to depth H well behind the front (at large y).

Figs. 12.17 are highly idealized, having airmasses of distinctly different temperatures with a sharp interface in between. For a fluid with a smooth continuous temperature gradient, geostrophic adjustment occurs in a similar fashion, with a final equilibrium state as sketched in Fig. 12.18. The top of this diagram represents the top of the troposphere, and the top wind vector represents the jet stream.

This state has high surface pressure under the cold air, and low surface pressure under the warm air (see the Global Circulation chapter). On the cold side, isobaric surfaces are more-closely spaced in height than on the warm side, due to the hypsometric relationship. This results in a pressure reversal aloft, with low pressure (or low heights) above the cold air and high pressure (or high heights) above the warm air.

Horizontal pressure gradients at low and high altitudes create opposite geostrophic winds, as indicated in Fig. 12.18. Due to Coriolis force, the air represented in Fig. 12.18 is in equilibrium; namely, the cold air does not spread any further.

This behavior of the cold airmass is extremely significant. It means that the planetary-scale flow, which is in approximate geostrophic balance, is unable to complete the job of redistributing the cold air from the poles and warm air from the tropics. Yet some other process must be acting to complete the job of redistributing heat to satisfy the global energy budget (in the Global Circulation chapter).

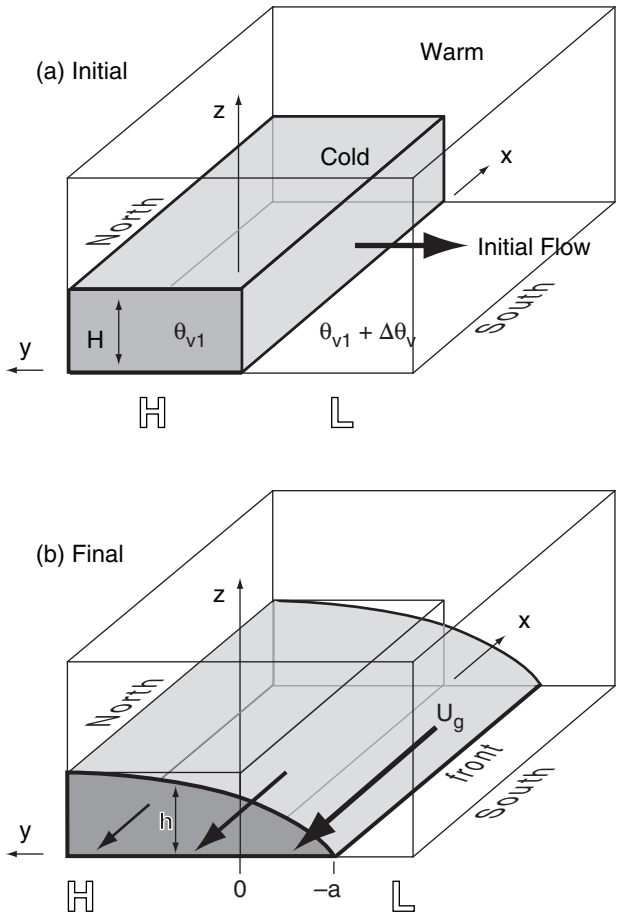

Figure 12.17
Geostrophic adjustment of a cold front. (a) Initial state. (b) Final state is in dynamic equilibrium, which is never quite attained in the real atmosphere.

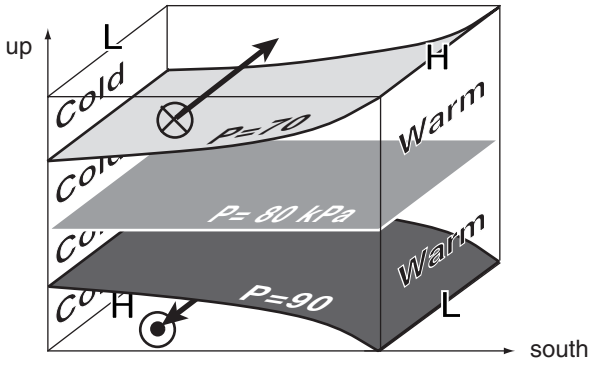

Figure 12.18
Final dynamic state after geostrophic adjustment within an environment containing continuous temperature gradients. Arrows represent geostrophic wind. Shaded areas are isobaric surfaces. H and L indicate high and low pressures relative to surrounding pressures at the same altitude. Dot-circle represents the tip of an arrow pointing toward the reader, x-circle represents the tail feathers of an arrow pointing into the page.

BEYOND ALGEBRA • Geostrophic Adjustment

We can verify that the near-surface (frictionless) geostrophic wind is consistent with the sloping depth of cold air. The geostrophic wind is related to the horizontal pressure gradient at the surface by:

$$U_g = -\frac{1}{\rho \cdot f_c} \cdot \frac{\Delta P}{\Delta y} \qquad (10.26a)$$

Assume that the pressure at the top of the cold airmass in Figs. 12.17 equals the pressure at the same altitude h in the warm airmass. Thus, surface pressures will be different due to only the difference in weight of air below that height.

Going from the top of the sloping cold airmass to the bottom, the vertical increase of pressure is given by the hydrostatic eq: $\Delta P_{cold} = -\rho_{cold} \cdot |g| \cdot h$

A similar equation can be written for the warm air below h. Thus, at the surface, the difference in pressures under the cold and warm air masses is:

$$\Delta P = -|g| \cdot h \cdot (\rho_{cold} - \rho_{warm})$$

multiplying the RHS by $\bar{\rho} / \bar{\rho}$, where $\bar{\rho}$ is an average density, yields:

$$\Delta P = -|g| \cdot h \cdot \bar{\rho} \cdot [(\rho_{cold} - \rho_{warm}) / \bar{\rho}]$$

As was shown in the Buoyancy section of the Stability chapter, use the ideal gas law to convert from density to virtual temperature, remembering to change the sign because the warmer air is less dense. Also, $\Delta T_v = \Delta\theta_v$. Thus: $\Delta P = -|g| \cdot h \cdot \bar{\rho} \cdot [(\theta_{v\,warm} - \theta_{v\,cold}) / \bar{T}_v]$

where this is the pressure change in the negative y direction.

Plugging this into eq. (10.26a) gives:

$$U_g = -\frac{|g| \cdot (\Delta\theta_v / T_v)}{f_c} \cdot \frac{\Delta h}{\Delta y}$$

which we can write in differential form:

$$\boxed{U_g = -\frac{|g| \cdot (\Delta\theta_v / T_v)}{f_c} \cdot \frac{\partial h}{\partial y}} \qquad (b)$$

The equilibrium value of h was given by eq. (12.7):

$$h = H \cdot \left[1 - \exp\left(-\frac{y + a}{a}\right)\right] \qquad (12.7)$$

Thus, the derivative is:

$$\frac{\partial h}{\partial y} = \frac{H}{a} \cdot \exp\left(-\frac{y + a}{a}\right)$$

Plugging this into eq. (b) gives:

$$U_g = -\frac{|g| \cdot (\Delta\theta_v / T_v)}{f_c} \cdot \frac{H}{a} \cdot \exp\left(-\frac{y + a}{a}\right) \qquad (c)$$

But from eq. (12.5) we see that:

$$f_c \cdot a = f_c \cdot \lambda_R = \sqrt{|g| \cdot H \cdot (\Delta\theta_v / T_v)} \qquad (12.5)$$

Eq. (c) then becomes:

$$\boxed{U_g = -\sqrt{|g| \cdot H \cdot (\Delta\theta_v / T_v)} \cdot \exp\left(-\frac{y + a}{a}\right)} \qquad (12.6)$$

Thus, the wind is consistent (i.e., geostrophically balanced) with the sloping height.

That other process is the action of cyclones and Rossby waves. Many small-scale, short-lived cyclones are not in geostrophic balance, and they can act to move the cold air further south, and the warm air further north. These cyclones feed off the potential energy remaining in the large-scale flow, namely, the energy associated with horizontal temperature gradients. Such gradients have potential energy that can be released when the colder air slides under the warmer air (see Fig. 11.1).

Solved Example

A cold airmass of depth 1 km and virtual potential temperature 0°C is imbedded in warm air of virtual potential temperature 20°C. Find the Rossby deformation radius, the maximum geostrophic wind speed, and the equilibrium depth of the cold airmass at $y = 0$. Assume $f_c = 10^{-4}\ s^{-1}$.

Solution

Given: $\overline{T_v} = 280$ K, $\Delta\theta_v = 20$ K, $H = 1$ km, $f_c = 10^{-4}\ s^{-1}$.

Find: a = ? km, U_g = ? m/s at $y = -a$, and h = ? km at $y = 0$.

Use eq. (12.5):

$$a = \frac{\sqrt{(9.8\text{m}\cdot\text{s}^{-2}) \cdot (1000\text{m}) \cdot (20\text{K}) / (280\text{K})}}{10^{-4}\text{s}^{-1}}$$

$$= \underline{\textbf{265 km}}$$

Use eq. (12.6):

$$U_g = -\sqrt{(9.8\text{m}\cdot\text{s}^{-2})(1000\text{m})(20\text{K}) / (280\text{K})} \cdot \exp(0)$$

$$= \underline{\textbf{–26.5 m/s}}$$

Use eq. (12.7):

$$h = (1\text{km}) \cdot [1 - \exp(-1)] \quad = \quad \underline{\textbf{0.63 km}}$$

Check: Units OK. Physics OK.

Discussion: Frontal-zone widths on the order of a = 200 km are small compared to lengths (1000s km).

Winds in the Warm Over-riding Air

Across the frontal zone is a stronger-than-background horizontal temperature gradient. In many fronts, the horizontal temperature gradient is strongest near the surface, and weakens with increasing altitude.

The thermal-wind relationship tells us that the geostrophic wind will increase with height in strong horizontal temperature gradients. If the frontal zone extends vertically over a large portion of the troposphere, then the wind speed will continue to increase with height, reaching a maximum near the tropopause.

Thus, jet streams are associated with frontal zones. The jet blows parallel to the frontal zone, with greatest wind speeds on the warm side of the frontal zone. If the cold air is advancing as a cold front, then this jet is known as a **pre-frontal jet**.

This is illustrated in Fig. 12.19. Plotted are isentropes, isobars, isotachs, and the frontal zone. The cross-frontal direction is north-south in this figure, causing a pre-frontal jet from the West (blowing into the page, in this diagram).

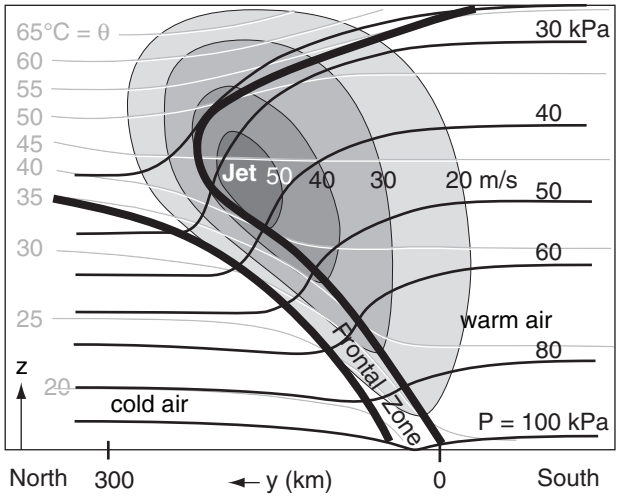

Figure 12.19
Vertical section across a cold front in the N. Hemisphere. Thick lines outline the frontal zone in the troposphere, and show the tropopause in the top of the graph. Medium black lines are isobars. Thin grey lines are isentropes. Shaded areas indicate isotachs, for a jet that blows from the West (into the page).

Frontal Vorticity

Combining the cold-air-side winds from Fig. 12.17b and warm-air-side winds from Fig. 12.19 into a single diagram yields Fig. 12.20. In this sketch, the warm air aloft and south of the front has geostrophic winds from the west, while the cold air near the ground has geostrophic winds from the east.

Thus, across the front, $\Delta U_g/\Delta y$ is negative, which means that the relative vorticity (eq. 11.20) of the geostrophic wind is positive (ζ_r = +) at the front (grey curved arrows in Fig. 12.20). In fact, cyclonic vorticity is found along fronts of any orientation. Also, stronger density contrasts across fronts cause greater positive vorticity.

Also, frontogenesis (strengthening of a front) is often associated with horizontal convergence of air from opposite sides of the front (see next section). Horizontal convergence implies vertical divergence (i.e., vertical stretching of air and updrafts) along the front, as required by mass continuity. But stretching increases vorticity (see the chapters on Stability, Global Circulation, and Extratropical Cyclones). Thus, frontogenesis is associated with updrafts (and associated clouds and bad weather) and with increasing relative vorticity.

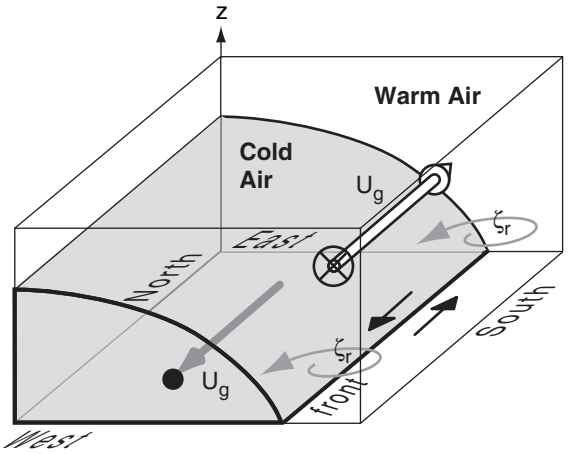

Figure 12.20
Sketch of cold front, combining winds in the cold air (thick straight grey arrow) from Fig. 12.17b with the winds in the warm air (thick white arrow) from Fig. 12.19. These winds cause shear across the front, shown with the black arrows. This shear is associated with positive (cyclonic) relative vorticity of the geostrophic wind (thin curved grey arrows).

FOCUS • The Polar Front

Because of Coriolis force, cold arctic air cannot spread far from the poles, causing a quasi-permanent frontal boundary in the winter hemisphere. This is called the **polar front**.

It has a wavy irregular shape where some segments advance as cold fronts, other segments retreat as warm fronts, some are stationary, and others are weak and cause gaps in the front.

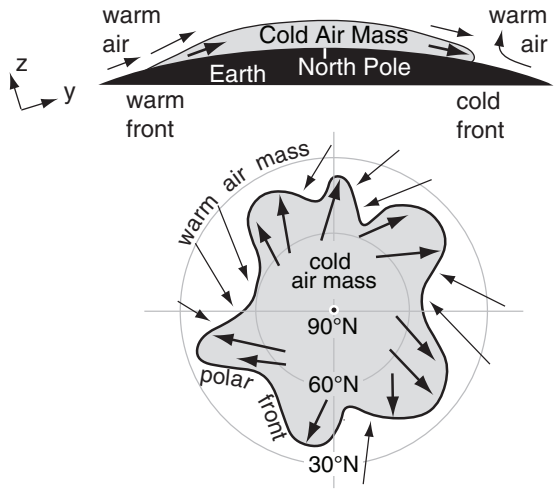

Figure a. *Top: Vertical slice through the North Pole. Bottom: View from space looking down on N. Pole.*

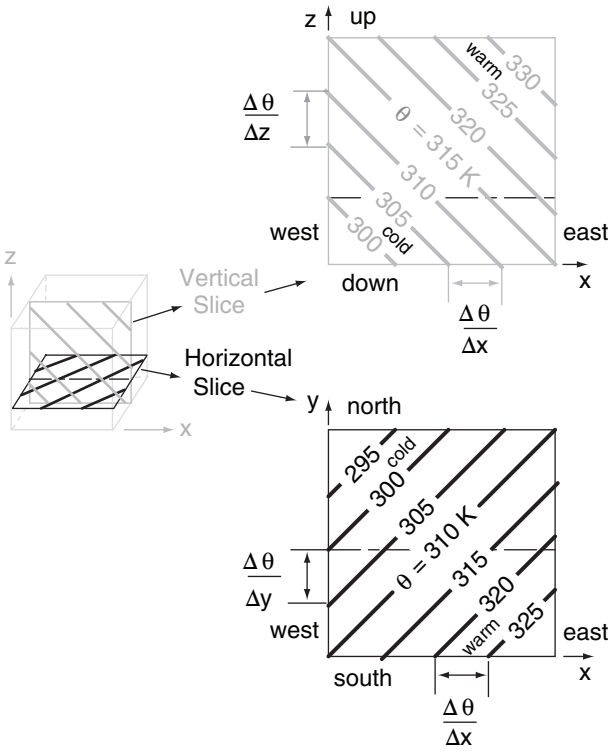

Figure 12.21
Vertical and horizontal slices through a volume of atmosphere, showing initial conditions prior to frontogenesis. The thin horizontal dashed lines show where the planes intersect.

FRONTOGENESIS

Fronts are recognized by the change in temperature across the frontal zone — greatest at the surface. Hence, the horizontal temperature gradient (temperature change per distance across the front) is one measure of frontal strength. Usually potential temperature is used instead of temperature to simplify the problem when vertical motions can occur.

Physical processes that tend to increase the potential-temperature gradient are called **frontogenetic** — literally they cause the birth or strengthening of the front. Three classes of such processes are kinematic, thermodynamic, and dynamic.

Kinematics

Kinematics refers to motion or advection, with no regard for driving forces. This class of processes cannot create potential-temperature gradients, but it can strengthen or weaken existing gradients.

From earlier chapters, we saw that radiative heating causes north-south temperature gradients between the equator and poles. Also, the general circulation causes the jet stream to meander, which creates transient east-west temperature gradients along troughs and ridges. The standard-atmosphere also has a vertical gradient of potential temperature in the troposphere (θ increases with z). Thus, it is fair to assume that temperature gradients often exist, which could be strengthened during kinematic frontogenesis.

To illustrate kinematic frontogenesis, consider an initial potential-temperature field with uniform gradients in the x, y, and z directions, as sketched in Fig. 12.21. The gradients have the following signs (for this particular example):

$$\frac{\Delta\theta}{\Delta x} = + \qquad \frac{\Delta\theta}{\Delta y} = - \qquad \frac{\Delta\theta}{\Delta z} = + \tag{12.8}$$

Namely, potential temperature increases toward the east, decreases toward the north, and increases upward. There are no fronts in this picture initially.

We will examine the subset of advections that tends to create a cold front aligned north-south. Define the strength of the front as the potential-temperature gradient across the front:

$$\text{Frontal Strength} = FS = \frac{\Delta\theta}{\Delta x} \tag{12.9}$$

The change of frontal strength with time due to advection is given by the kinematic frontogenesis equation:

$$\frac{\Delta(FS)}{\Delta t} = -\left(\frac{\Delta\theta}{\Delta x}\right)\cdot\left(\frac{\Delta U}{\Delta x}\right) - \left(\frac{\Delta\theta}{\Delta y}\right)\cdot\left(\frac{\Delta V}{\Delta x}\right) - \left(\frac{\Delta\theta}{\Delta z}\right)\cdot\left(\frac{\Delta W}{\Delta x}\right) \quad \bullet(12.10)$$

Strengthening Confluence Shear Tilting

Confluence

Suppose there is a strong west wind U approaching from the west, but a weaker west wind departing at the east (Fig. 12.22 top). Namely, the air from the west almost catches up to air in the east.

For this situation, $\Delta U/\Delta x = -$, and $\Delta\theta/\Delta x = +$ in eq. (12.10). Hence, the product of these two terms, when multiplied by the negative sign attached to the confluence term, tends to strengthen the front [$\Delta(FS)/\Delta t = +$]. In the shaded region of Fig. 12.22, the isentropes are packed closer together; namely, it has become a frontal zone.

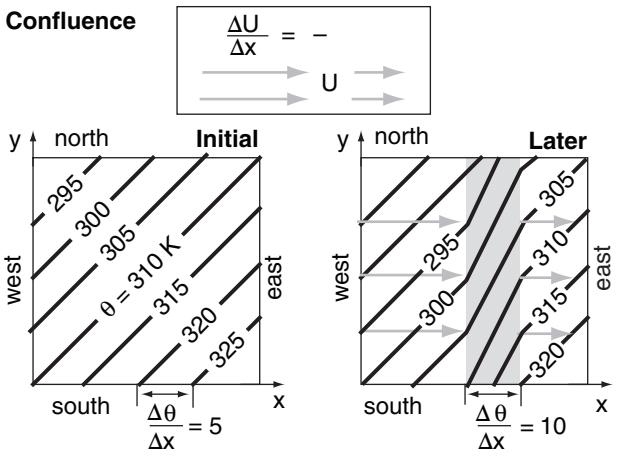

Figure 12.22
Confluence strengthens the frontal zone (shaded) in this case. Arrow tails indicate starting locations for the isotherms.

Shear

Suppose the wind from the south is stronger on the east side of the domain than the west (Fig. 12.23 top). This is one type of wind shear. As the isentropes on the east advect northward faster than those on the west, the potential-temperature gradient is strengthened in-between, creating a frontal zone.

While the shear is positive ($\Delta V/\Delta x = +$), the northward temperature gradient is negative ($\Delta\theta/\Delta y = -$). Thus, the product is positive when the preceding negative sign from the shear term is included. Frontal strengthening occurs for this case [$\Delta(FS)/\Delta t = +$].

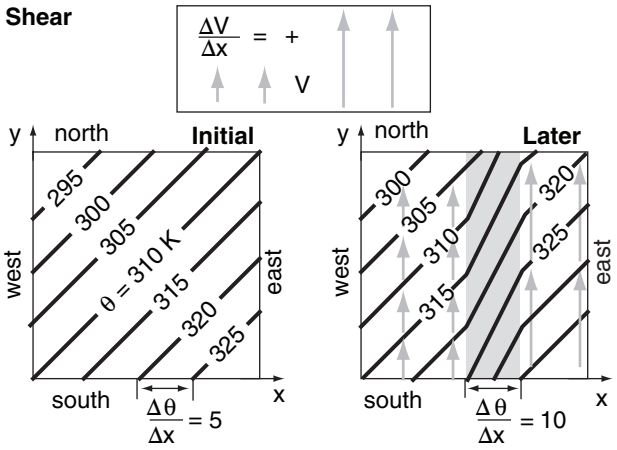

Figure 12.23
Shear strengthens the frontal zone (shaded) in this case. Arrow tails indicate starting locations for the isotherms.

Tilting

If updrafts are stronger on the cold side of the domain than the warm side, then the vertical potential-temperature gradient will be tilted into the horizontal. The result is a strengthened frontal zone (Fig. 12.24).

The horizontal gradient of updraft velocity is negative in this example ($\Delta W/\Delta x = -$), while the vertical potential-temperature gradient is positive ($\Delta\theta/\Delta z = +$). The product, when multiplied by the negative sign attached to the tilting term, yields a positive contribution to the strengthening of the front for this case [$\Delta(FS)/\Delta t = +$].

While this example was contrived to illustrate frontal strengthening, for most real fronts, the tilting term causes weakening. Such **frontolysis** is weakest near the surface because vertical motions are smaller there (the wind cannot blow through the ground).

Tilting is important and sometimes dominant for upper-level fronts, as described later.

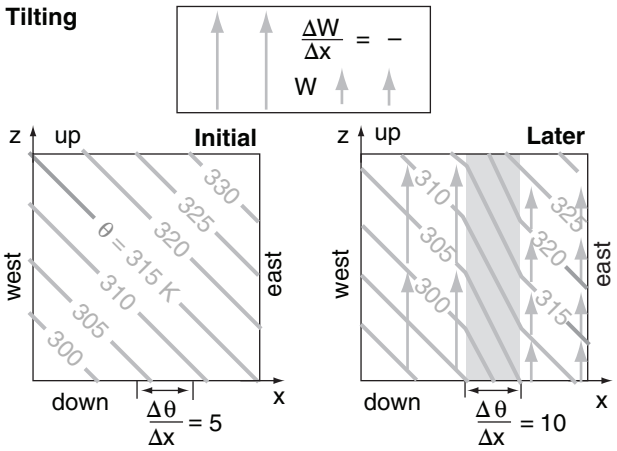

Figure 12.24
Tilting of the vertical temperature gradient into the horizontal strengthens the frontal zone (shaded) in this illustration.

Solved Example

Given an initial environment with $\Delta\theta/\Delta x = 0.01$°C/km, $\Delta\theta/\Delta y = -0.01$°C/km, and $\Delta\theta/\Delta z = 3.3$°C/km. Also, suppose that $\Delta U/\Delta x = -0.05$ (m/s)/km, $\Delta V/\Delta x = 0.05$ (m/s)/km, and $\Delta W/\Delta x = 0.02$ (cm/s)/km. Find the kinematic frontogenesis rate.

Solution

Given: (see above)

Find: $\Delta(FS)/\Delta t$ = ? °C·km^{-1}·day^{-1}

Use eq. (12.10):

$$\frac{\Delta(FS)}{\Delta t} = -\left(0.01\frac{^\circ C}{km}\right)\cdot\left(-0.05\frac{m/s}{km}\right) - \left(-0.01\frac{^\circ C}{km}\right)\cdot \left(0.05\frac{m/s}{km}\right) - \left(3.3\frac{^\circ C}{km}\right)\cdot\left(0.0002\frac{m/s}{km}\right)$$

$$= +0.0005 + 0.0005 - 0.00066\ ^\circ C\cdot m\cdot s^{-1}\cdot km^{-2}$$

$$= \underline{\mathbf{+0.029\ ^\circ C\cdot km^{-1}\cdot day^{-1}}}$$

Check. Units OK. Physics OK.

Discussion: Frontal strength $\Delta\theta/\Delta x$ nearly tripled in one day, increasing from 0.01 to 0.029 °C/km.

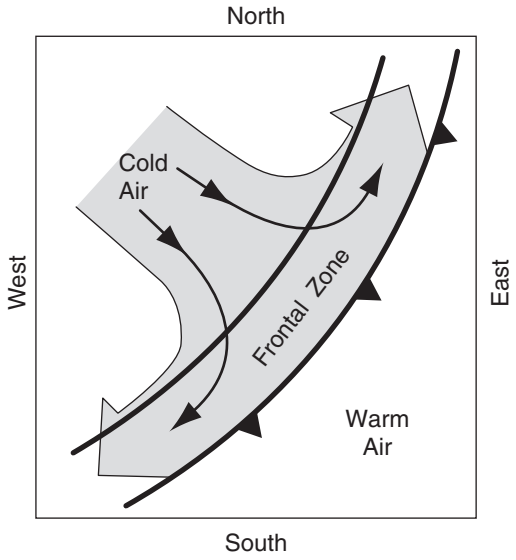

Figure 12.25
An illustration of the near-surface horizontal air-flow pattern at a frontal zone.

Deformation

The previous figures presented idealized kinematic scenarios. Often in real fronts the flow field is a more complex combination of scenarios. For example, Fig. 12.25 shows a **deformation** (change of shape) flow field in the cold air, with **confluence** ($\rightarrow\ \leftarrow$ coming together horizontally) of air perpendicular to the front, and **diffluence** ($\leftarrow\ \rightarrow$ horizontal spreading of air) parallel to the front.

In such a flow field both convergence and shear affect the temperature gradient. For example, consider the two identical deformation fields in Figs. 12.26a & b, where the only difference is the angle of the isentropes in a frontal zone relative to the **axis of dilation** (the line toward which confluence points, and along which diffluence spreads).

For initial angles less than 45° (Fig. 12.26a & a'), the isentropes are pushed closer together (frontogenesis) and tilted toward a shallower angle. For initial angles greater than 45°, the isentropes are spread farther apart (frontolysis) and tilted toward a shallower angle. Using this info to analyze Fig. 12.25 where the isentropes are more-or-less parallel to the frontal zone (i.e., initial angle << 45°), we would expect that flow field to cause frontogenesis.

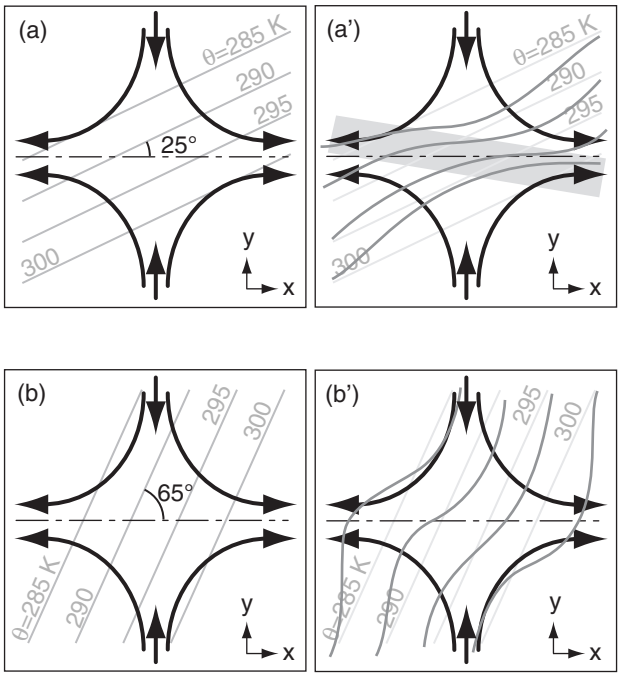

Figure 12.26
Black arrows are wind, and grey arrows are isentropes. Dashed line is the axis of dilation. (a) and (a') are initial and final states for shallow initial angle, showing frontogenesis. The shaded area in (a') highlights the strengthened frontal zone. (b) and (b') are initial and final states for steep initial angle, showing frontolysis. (after J. Martin, 2006: "Mid-Latitude Atmospheric Dynamics: A First Course. Wiley.)

Thermodynamics

The previous kinematic examples showed **adiabatic** advection (potential temperature was conserved while being blown with the wind). However, **diabatic** (non-adiabatic) thermodynamic processes can heat or cool the air at different rates on either side of the domain. These processes include radiative heating/cooling, conduction from the surface, turbulent mixing across the front, and latent heat release/absorption associated with phase changes of water in clouds.

Define the diabatic warming rate (DW) as:

$$\text{Diabatic Warming Rate} = DW = \frac{\Delta\theta}{\Delta t} \qquad \bullet(12.11)$$

If diabatic heating is greater on the warm side of the front than the cold side, then the front will be strengthened:

$$\frac{\Delta(FS)}{\Delta t} = \frac{\Delta(DW)}{\Delta x} \qquad \bullet(12.12)$$

In most real fronts, **turbulent mixing** between the warm and cold sides weakens the front (i.e., causes **frontolysis**). **Conduction** from the surface also contributes to frontolysis. For example, behind a cold front, the cold air blows over a usually-warmer surface, which heats the cold air (i.e., airmass modification) and reduces the temperature contrast across the front. Similarly, behind warm fronts, the warm air is usually advecting over cooler surfaces.

Over both warm and cold fronts, the warm air is often forced to rise. This rising air can cause **condensation** and cloud formation, which strengthen fronts by warming the already-warm air.

Radiative cooling from the tops of stratus clouds reduces the temperature on the warm side of the front, contributing to frontolysis of warm fronts. Radiative cooling from the tops of post-cold frontal stratocumulus clouds can strengthen the front by cooling the already-cold air.

Dynamics

Kinematics and thermodynamics are insufficient to explain observed frontogenesis. While kinematic frontogenesis gives doubling or tripling of frontal strength in a day (see previous solved examples), observations show that frontal strength can increase by a factor of 15 during a day. Dynamics can cause this rapid strengthening.

Because fronts are long and narrow, we expect along-front flow to tend toward geostrophy, while across front flows could be ageostrophic. We can anticipate this by using the **Rossby number** (see Fo-

Solved Example

A thunderstorm on the warm side of a 200 km wide front rains at 2 mm/h. Find the frontogenesis rate.

Solution

Given: $RR = 0$ at $x = 0$,
and $RR = 2$ mm/h at $x = 200$ km
Find: $\Delta(FS)/\Delta t$ = ? °C·km^{-1}·day^{-1}

From the Heat chapter:
$\Delta\theta/\Delta t = (0.33°\text{C/mm})\cdot RR = 0.66°\text{C/h}$.

Combine eqs. (12.11) & (12.12): $\Delta(FS)/\Delta t = \Delta(\Delta\theta/\Delta t)/\Delta x$

$\Delta(FS)/\Delta t$ = [(0.66°C/h)·(24 h/day) – 0] / [200 km – 0]
= (15.84°C/day)/(200km) = **0.079 °C·km^{-1}·day^{-1}**

Check: Units OK. Physics OK. Magnitude good.
Discussion: This positive value indicates thermodynamic frontogenesis.

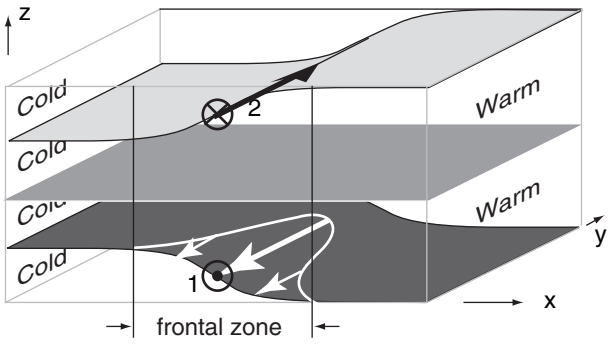

Figure 12.27
Isobaric surfaces near a hypothetical front, before being altered by dynamics. Vectors show equilibrium geostrophic winds, initially (state "o"). Dot-circle (1) represents the tip of an arrow pointing toward the reader; x-circle (2) represents the tail feathers of an arrow pointing into the page.

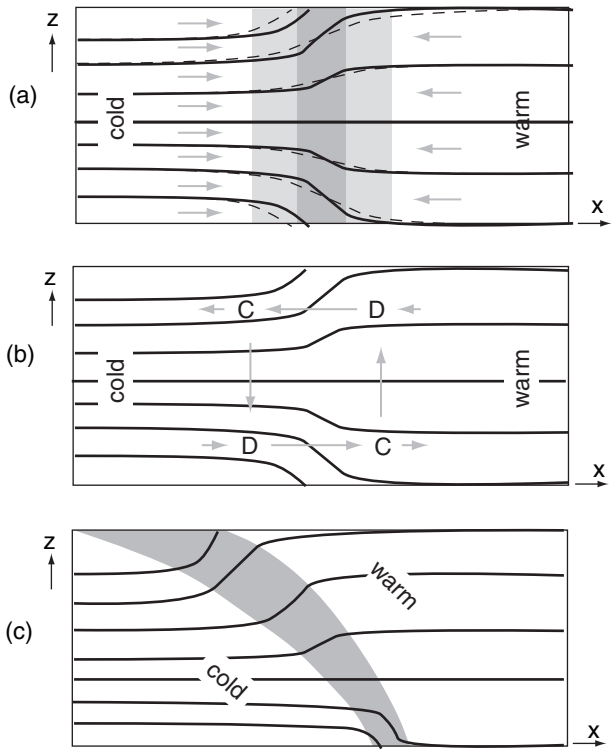

Figure 12.28
Vertical cross section showing dynamic strengthening of a front. The frontal zone is shaded; lines are isobars; and arrows are ageostrophic winds. D and C are regions of horizontal divergence and convergence. (a) Initial state (thin dashed lines) modified (thick lines) by confluence (arrows). (b) Ageostrophic circulation, called a Sawyer-Eliassen circulation. (c) Final equilibrium state.

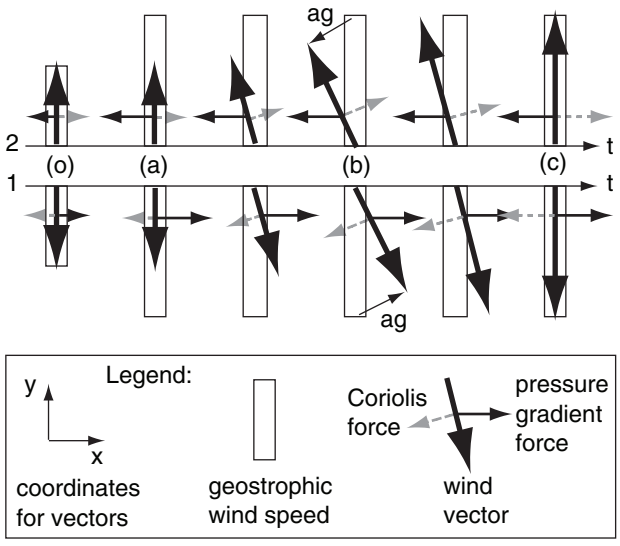

Figure 12.29
Time lines labeled 1 & 2 are for the vectors 1 & 2 in Fig. 12.27. Initial state (o) is given by Fig. 12.27. Later states (a)-(c) correspond to Figs. 12.28(a)-(c). The ageostrophic wind (ag) at time (b) is also indicated. States (o) and (c) are balanced.

cus Box in the Dynamics chapter). Fronts can be of order 1000 km long, but of order 100 km wide. Thus, the Rossby number for along-front flow is of order $Ro = 0.1$. But the across-front Rossby number is of order $Ro = 1$. Recall that flows tend toward geostrophy when $Ro < 1$. Thus, ageostrophic dynamics are anticipated across the front, as are illustrated next.

Picture an initial state in geostrophic equilibrium with winds parallel to the front, as sketched in Fig. 12.27. This figure shows a special situation where pressure gradients and geostrophic winds exist only midway between the left and right sides. Zero gradients and winds are at the left and right sides. A frontal zone is in the center of this diagram.

Suppose some external forcing such as kinematic confluence due to a passing Rossby wave causes the front to strengthen a small amount, as sketched in Fig. 12.28a. Not only does the potential-temperature gradient tighten, but the pressure gradient also increases due to the hypsometric relationship.

The increased pressure gradient implies a different, increased geostrophic wind. However, initially, the actual winds are slower due to inertia, with magnitude equal to the original geostrophic speed.

While the actual winds adjust toward the new geostrophic value, they temporarily turn away from the geostrophic direction (Fig. 12.29) due to the imbalance between pressure-gradient and Coriolis forces. During this transient state (b), there is a component of wind in the x-direction (Fig. 12.28b). This is called **ageostrophic flow**, because there is no geostrophic wind in the x-direction.

Because mass is conserved, horizontal convergence and divergence of the *U*-component of wind cause vertical circulations. These are thermally direct circulations, with cold air sinking and warm air rising and moving over the colder air. The result is a temporary cross-frontal, or **transverse circulation** called a **Sawyer-Eliassen circulation**. The updraft portion of the circulation can drive convection, and cause precipitation.

The winds finally reach their new equilibrium value equal to the geostrophic wind. In this final state, there are no ageostrophic winds, and no cross-frontal circulation. However, during the preceding transient stage, the ageostrophic cross-frontal circulation caused extra dynamic confluence near the surface, which adds to the original kinematic confluence to strengthen the surface front. The transverse circulation also tilts the front (Fig. 12.28c).

In summary, a large and relatively steady geostrophic wind blows parallel to the front (Fig. 12.27). A weak, transient, cross-frontal circulation can be superimposed (Fig. 12.28b). These two factors are also important for upper-tropospheric fronts, as described later.

OCCLUDED FRONTS AND MID-TROPOSPHERIC FRONTS

When three or more airmasses come together, such as in an **occluded front**, it is possible for one or more fronts to ride over the top of a colder airmass. This creates lower- or mid-tropospheric fronts that do not touch the surface, and which would not be signaled by temperature changes and wind shifts at the surface. However, such **fronts aloft** can trigger clouds and precipitation observed at the surface.

Occluded fronts occur when cold fronts catch up to warm fronts. What happens depends on the temperature and static-stability difference between the cold advancing air behind the cold front and the cold retreating air ahead of the warm front.

Fig. 12.30 shows a **cold front occlusion**, where very cold air that is very statically stable catches up to, and under-rides, cooler air that is less statically stable. The warm air that was initially between these two cold airmasses is forced aloft. Most occlusions in interior N. America are of this type, due to the very cold air that advances from Canada in winter.

Observers at the surface would notice stratiform clouds in advance of the front, which would normally signal an approaching warm front. However, instead of a surface warm front, a surface occluded front passes, and the surface temperature decreases like a cold front. The trailing edge of cool air aloft marks the warm front aloft.

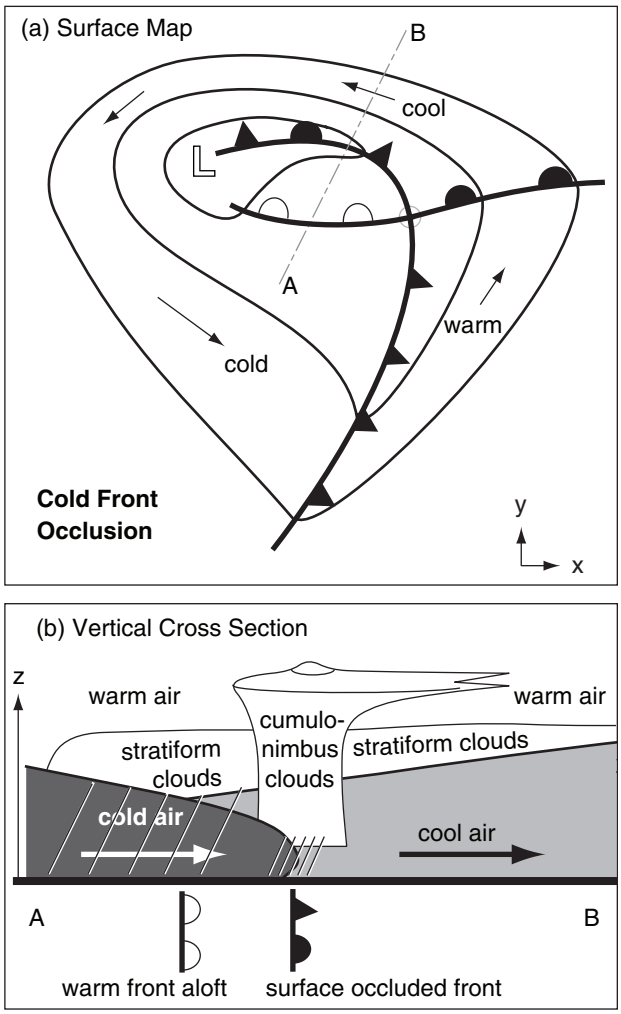

Figure 12.30
Cold front occlusion. (a) Surface map showing position of surface cold front (dark triangles), surface warm front (dark semicircles), surface occluded front (dark triangles and semicircles), and warm front aloft (white semicircles). (b) Vertical cross section along slice A-B from top diagram. Diagonal lines = rain.

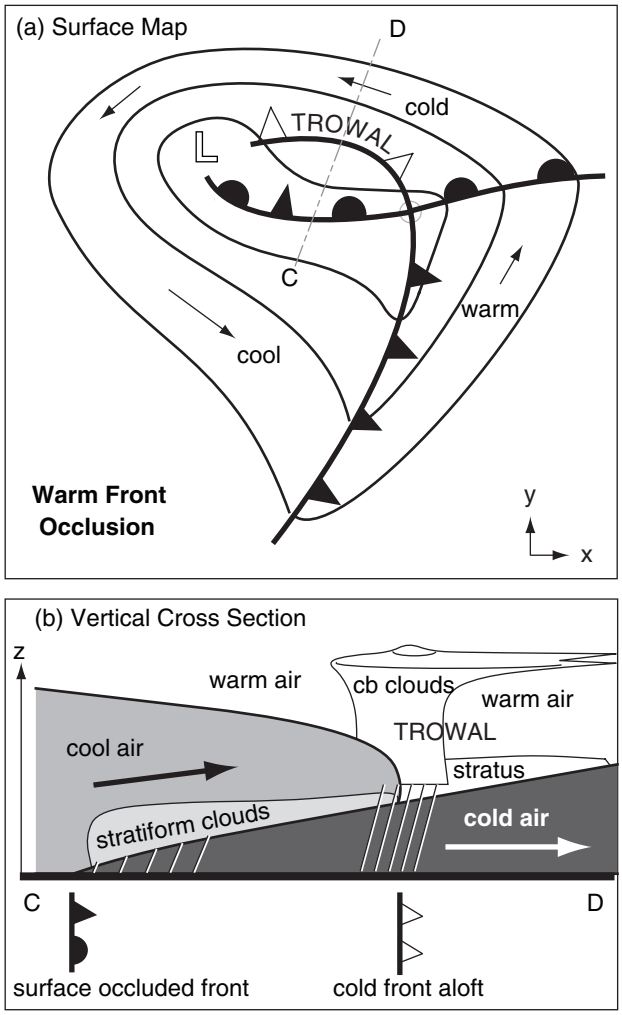

Figure 12.31
Warm front occlusion. (a) Surface map. Symbols are similar to Fig. 12.30, except that white triangles denote a cold front aloft. (b) Vertical cross section along slice C-D from top diagram. TROWAL = trough of warm air aloft. The open grey circle shows the triple-point location (meeting of 3 surface fronts).

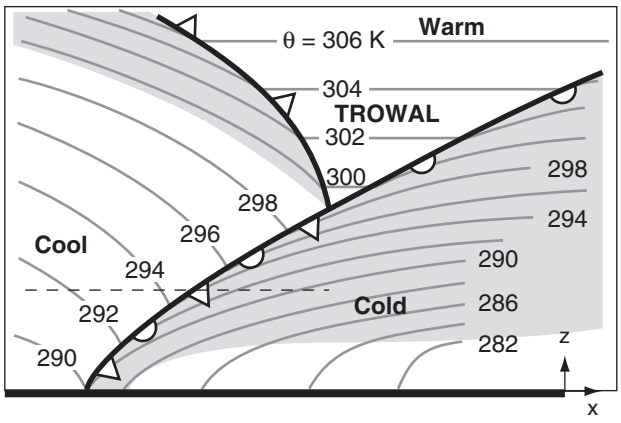

Figure 12.32
Idealized vertical cross-section through a warm front occlusion, showing the bottom 5 km of the troposphere. Dark grey lines are isentropes. Light grey shading indicates strong static stability (regions where the isentropes are packed closer together in the vertical). TROWAL = trough of warm air aloft.

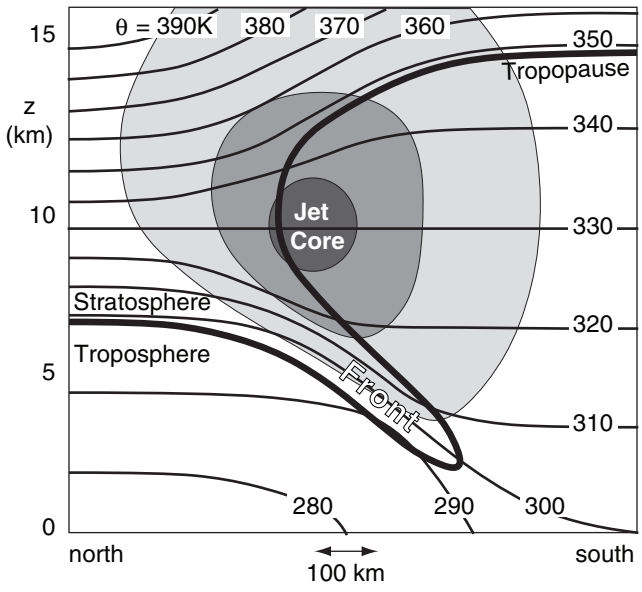

Figure 12.33
Idealized vertical cross-section through the jet stream in N. Hemisphere. Shading indicates west-to-east speeds (into the page): light ≥ 50 m/s, medium ≥ 75 m/s, dark ≥ 100 m/s. Thin lines are isentropes (K). Thick line is the tropopause. "Front" indicates the upper-tropospheric front, where stratospheric air is penetrating into the troposphere.

The location in Figs. 12.30 and 12.31 where the cold, warm, and occluded fronts intersect at the surface is called the **triple point**.

Fig. 12.31 shows a **warm front occlusion**, where cool air that is less statically stable catches up to, and over-rides, colder air that is more statically stable, forcing aloft the warm air that was in-between. Most occlusions in Europe and the Pacific Northwest USA are this type, due to mild cool air that advances from over the cool ocean during winter.

Observers at the surface notice stratiform clouds in advance of the front. But before the surface front arrives, there can be showers or thunderstorms associated with the cool front aloft. Later, a surface occluded front passes with widespread drizzle, and the surface temperature warms.

Fig. 12.32 shows how the static stability relates to the type of occlusion. In this sketch of a warm front occlusion, look at the static stability across the occluded front, at the altitude of the dashed line. To the east of the front in the cold airmass, the air is strongly stable (as shown by the tight packing of the isentropes in the vertical). To the west in the cool airmass, the air is less statically stable (i.e., greater vertical spacing between isentropes). If this had been a cold frontal occlusion instead, the greatest static stability would have been west of the front.

The wedge of warm air (Fig. 12.32) pushed up between the cool and cold airmasses is called a **TROWAL**, an acronym that means "**trough of warm air aloft**." This TROWAL, labeled in Fig. 12.31a, touches the ground at the triple point, but tilts toward higher altitudes further north. Under the TROWAL can be significant precipitation and severe weather at the surface (Fig. 12.31b) — hence it is important for weather forecasting.

The previous sketches are "text-book" examples of prototypical situations. In real life, more complex maps and cross sections can occur. Sometimes more than three airmasses can be drawn together in a low, causing multiple cold or warm fronts, and multiple fronts aloft.

UPPER-TROPOSPHERIC FRONTS

Upper-tropospheric fronts are also called **upper-level fronts**, and are sometimes associated with **folds in the tropopause**. A cross-section through an idealized upper-level front is sketched in Fig. 12.33.

In the lower troposphere, the south-to-north temperature gradient creates the jet stream due to the thermal wind relationship (see the Global Circula-

tion chapter). A reversal of the meridional temperature gradient above 10 km in this idealized sketch causes wind velocities to decrease above that altitude. Within the stratosphere, the isentropes are spaced closer together, indicating greater static stability.

South of the core of the jet stream, the tropopause is relatively high. To the north, it is lower. Between these two extremes, the tropopause can wrap around the jet core, and fold back under the jet, as sketched in Fig. 12.33. Within this fold the isentropes are tightly packed, indicating an **upper-tropospheric front**. Sometimes the upper-level front connects with a surface front (Fig. 12.19).

Stratospheric air has unique characteristics that allow it to be traced. Relative to the troposphere, stratospheric air has high ozone content, high radioactivity (due to former nuclear bomb testing), high static stability, low water-vapor mixing ratio, and high **isentropic potential vorticity**.

The tropopause fold brings air of stratospheric origin down into the troposphere. This causes an injection of ozone and radioactivity into the troposphere. The dry air in the tropopause fold behind the cold front is often clearly visible in water-vapor satellite images of the upper troposphere.

The heavy line in Fig. 12.33 corresponds roughly to the 1.5 PVU (potential vorticity units) isopleth, and is a good indicator of the tropopause. Above this line, PVU values are greater than 1.5, and increase rapidly with height to values of roughly 10 PVU at the top of Fig. 12.33. Below this line, the PVU gradient is weak, with typical values of about 0.5 PVU at mid-latitudes. PVU is negative in the Southern Hemisphere, but of similar magnitude.

Sawyer-Eliassen dynamics help create tropopause folds. Picture a tropopause that changes depth north to south, as in Figs. 11.35 or 11.37 of the Global Circulation chapter, but does not yet have a fold. If the jet core advects colder air into the region, then the thickness between the 10 and 20 kPa isobaric surfaces (Fig. 11.37b) will decrease as described by the hypsometric equation. This will cause greater slope (i.e., greater height gradient) of the 10 kPa surface near the jet core. This temporarily upsets geostrophic balance, causing an ageostrophic circulation above the jet from south to north.

This transient flow continues to develop into a cross jet-stream direct circulation that forms around the jet as sketched in Fig. 12.34 (similar to Fig. 12.28b). Below the fold is an indirect circulation that also forms due to a complex geostrophic imbalance. Both circulations distort the tropopause to produce the fold, as sketched in Fig. 12.34, and strengthen the upper-level front due to the kinematic tilting term.

Science Graffito

"It seems odd that scientists, of all people, would question the search for anything thought to be elusive or even impossible to find. Think of the naysayers who used to scoff every time Carl Sagan said there had to be other planets orbiting other suns in other solar systems; now other planets are discovered so often it's hard to keep track of how many there are.

You'd think that the science establishment, having been proven wrong so many times, would adopt a bit more humility. If there's one thing we keep learning, it's that we don't know as much as we think we do."

– Editors of *Discover Magazine*, Sept. 99 , 20, p 57.

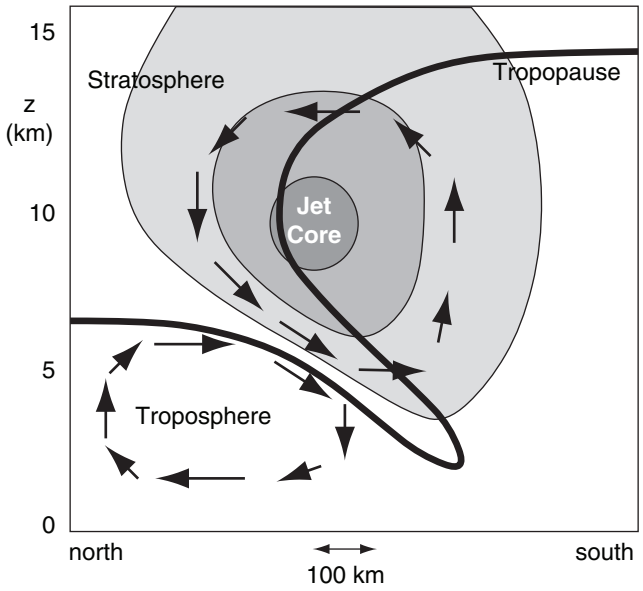

Figure 12.34
Transverse (cross-jet-stream) circulations (arrows) that dynamically form an upper-tropospheric front (i.e., a tropopause fold).

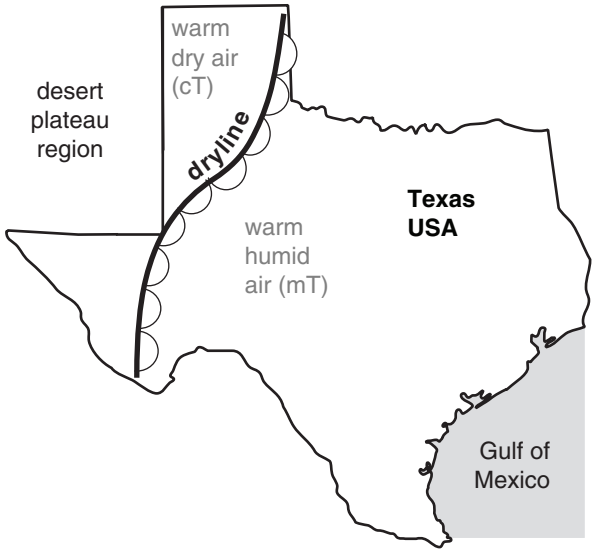

Figure 12.35
Typical location of dryline in the southwestern USA.

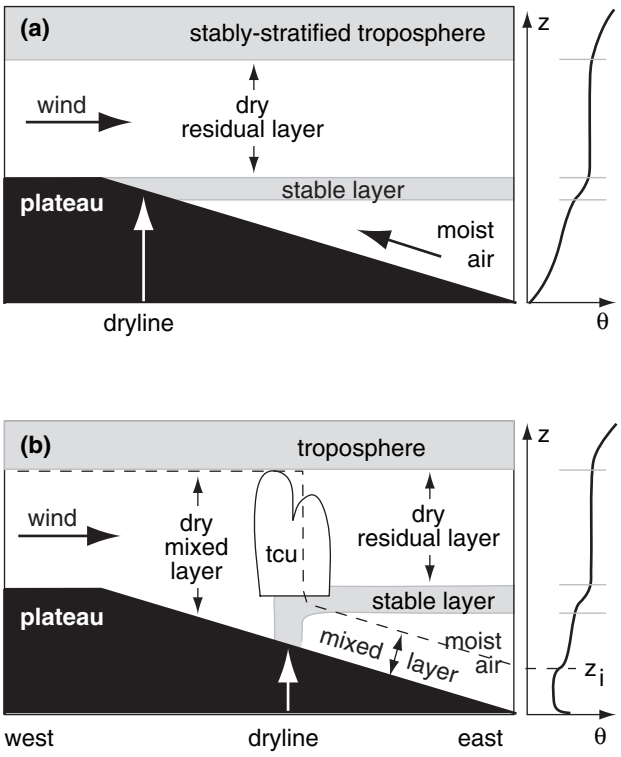

Figure 12.36
Idealized vertical cross section through a dryline (indicated by white arrow). Winds are indicated with black arrows. (a) Early morning. (b) Mid afternoon, with a convective mixed layer of thickness z_i. tcu = towering cumulus clouds. At right of each figure is the potential temperature θ sounding for the east side of the domain.

DRYLINES

In western Texas, USA, there often exists a boundary between warm humid air to the east, and warm dry air to the west (Fig. 12.35). This boundary is called the **dryline**. Because the air is hot on both sides of the boundary, it cannot be labeled as a warm or cold front. The map symbol for a dryline is like a warm front, except with open semicircles adjacent to each other, pointing toward the moist air.

Moist air on the east side comes from the Gulf of Mexico, while the dry air comes from the semi-arid plateaus of Mexico and the Southwestern USA. Drylines are observed during roughly 40 to 50% of all days in spring and summer, in that part of the world. Similar drylines are observed in other parts of the world.

During midday through afternoon, convective clouds are often triggered along the drylines. Some of these cloud bands grow into organized thunderstorm squall lines that can propagate east from the dryline.

Drylines need not be associated with a wind shift, convergence, vorticity, nor with low pressure. Hence, they do not satisfy the definition of a front. However, sometimes drylines combine with troughs to dynamically contribute to cyclone development.

Drylines tend to move eastward during the morning, and return westward during evening. This diurnal cycle is associated with the daily development of a convective mixed layer, interacting with the sloping terrain, via the following mechanism.

Over the high plateaus to the west, deep hot turbulent mixed layers can form in the late afternoon. By night and early morning, after turbulence decays, this thick dry layer of hot air over the plateau becomes a non-turbulent residual layer with nearly adiabatic lapse rate (Fig. 12.36a). Westerly winds advect this dry air eastward, where it overrides cooler, humid air at lower altitudes. Between that elevated residual layer and the moister air below is a strong stable layer such as a temperature inversion.

After sunrise, the warm ground causes a convective mixed-layer to form and grow. The mixed-layer depth is shown by the dashed line in Fig. 12.36b. Because the ground is higher in the west, the top of the mixed layer is able to reach the dry residual-layer air in the west earlier than in the east. When this dry air is entrained downward into the air below, it causes the surface humidity to drop.

Meanwhile, further east, the top of the mixed layer has yet to reach the dry air aloft, so the humidity is still high there. The dryline separates this moist surface air in the east from the dry air to the west.

As the day continues, the mixed layer in the moist air deepens, allowing the region of dry-air entrainment to spread eastward. This causes the dryline to move eastward as the day progresses. At night, convective turbulence ceases, a stable boundary layer develops, and prevailing low-altitude easterlies advect moist air back toward the west (Fig. 12.36a).

If we assume that initially the inversion is level with respect to sea level, then using geometry, we can see that the progression speed of the dryline eastward $\Delta x/\Delta t$ is directly related to the rate of growth of the mixed layer $\Delta z_i/\Delta t$:

$$\frac{\Delta x}{\Delta t} = \frac{\Delta z_i \,/\, \Delta t}{s} \tag{12.13}$$

where $s = \Delta z/\Delta x$ is the terrain slope.

Suppose the early morning stable boundary layer has a linear profile of potential temperature $\gamma = \Delta\theta/\Delta z$, then the mixed-layer growth proceeds with the square-root of accumulated daytime heating Q_{Ak} (see the Atmospheric Boundary Layer chapter):

$$z_i = \left(\frac{2 \cdot Q_{Ak}}{\gamma} \right)^{1/2} \tag{12.14}$$

As a result, the distance Δx that a dryline moves eastward as a function of time is:

$$\Delta x = \frac{1}{s} \cdot \left(\frac{2 \cdot Q_{Ak}}{\gamma} \right)^{1/2} \tag{12.15}$$

Time is hidden in the cumulative heat term Q_{Ak}.

Solved Example (§)

Suppose the surface heat flux during the day is constant with time at 0.2 K·m/s in the desert southwest USA. The early morning sounding has a potential temperature gradient of $\gamma = 10$ K/km. The terrain slope is 1:400. Plot the dryline position with time.

Solution

Given: $\gamma = 10$ K/km, $s = 1/400$, $F_H = 0.2$ K·m/s,
Find: $\Delta x(t) = ?$ km.

For constant surface flux, cumulative heating is:

$$Q_{Ak} = F_H \cdot \Delta t$$

where Δt is time since sunrise.

Thus, eq. (12.15) can be rewritten as:

$$\Delta x = \frac{1}{s} \cdot \left(\frac{2 \cdot F_H \cdot \Delta t}{\gamma} \right)^{1/2}$$

$$= \frac{400}{1} \cdot \left[\frac{2 \cdot (0.2\text{K} \cdot \text{m/s}) \cdot \Delta t}{(0.01\text{K/m})} \right]^{1/2}$$

Plotting this with a spreadsheet program:

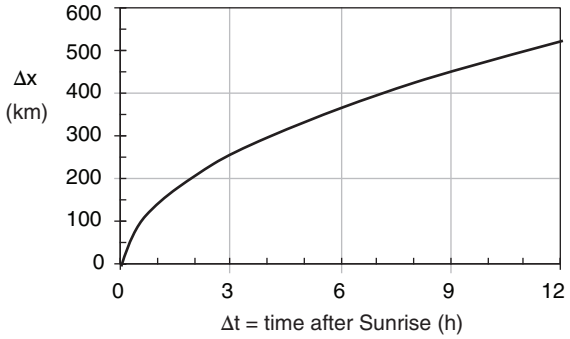

Check: Units OK. Physics OK. Graph reasonable.
Discussion: The dryline moves to the east with the square-root of time. Thus, the further east it gets, the slower it goes.

SUMMARY

Surface fronts mark the boundaries between airmasses. Changes in wind, temperature, humidity, visibility, and other meteorological variables are frequently found at fronts. Along frontal zones are often low clouds, low pressure, and precipitation. Fronts rotate counterclockwise around the lows in the Northern Hemisphere as the lows move and evolve.

Fronts strengthen or weaken due to advection by the wind (kinematics), external diabatic heating (thermodynamics), and ageostrophic cross-frontal circulations (dynamics). One measure of frontal strength is the temperature change across it. The spread of cold air behind a front is constrained by Coriolis force, as winds adjust toward geostrophic.

Airmasses can form when air resides over a surface sufficiently long. This usually happens in high-pressure centers of light wind. Airmasses over cold surfaces take longer to form than those over warmer

surfaces because turbulence is weaker in the statically stable air over the cold surface. As airmasses move from their source regions, they are modified by the surfaces and terrain over which they flow.

Upper-tropospheric fronts can form as folds in the tropopause. Drylines form over sloping terrain as a boundary between dry air to the west and moist air to the east; however, drylines do not usually possess all the characteristics of fronts.

Threads

Mid-latitude highs form because of the meandering jet stream (Chapter 11). Formation and modification of airmasses, and dryline evolution, are caused by boundary layer (Chapter 18) processes such as turbulence. Subsidence and divergence in highs are linked by the continuity equation (Chapter 10). Airmass modification over mountains can be estimated using thermo diagrams (Chapter 5). Geostrophic adjustment is caused by Coriolis force (Chapter 10). Isentropes (Chapter 3) can be used for frontal analysis.

Airmasses are drawn into lows (Chapter 13), which enhances baroclinicity to strengthen the cyclonic circulation. Highs and fronts are predicted numerically (Chapter 20) during routine weather forecasts. Cold and occluded fronts and dry lines can trigger thunderstorms (Chapters 14 and 15). Air pollution (Chapter 19) is trapped in highs, causing air stagnation events and air-pollution alerts.

EXERCISES

Numerical Problems

N1. Identify typical characteristics of the following airmass:

a. cAA	b. cP	c. cT	d. cM	e. cE
f. mA	g. mP	h. mT	i. mM	j. mE
k. cEw	l. cAk	m. cPw	n. mPk	o. mTw

N2. List all the locations in the world where the following airmasses typically form.

a. cAA	b. cA	c. cP	d. mP	e. mT
f. cT	g. mE			

N3.(§) Produce a graph of warm airmass depth z_i and airmass potential temperature θ_{ML} as a function of time, similar to Fig. 12.5. Use all the same conditions as in that figure (γ = 3.3 K/km, $\beta = 10^{-6}$ s^{-1}, initial $\Delta\theta s$ = 10°C; see the solved example on the subsequent page) for genesis of a warm airmass, except with the following changes:

a. initial $\Delta\theta s$ = 5°C	b. initial $\Delta\theta s$ = 15°C
c. initial $\Delta\theta s$ = 20°C	d. initial $\Delta\theta s$ = 15°C
e. $\beta = 0\ s^{-1}$	f. $\beta = 10^{-7}\ s^{-1}$
g. $\beta = 5 \times 10^{-7}\ s^{-1}$	h. $\beta = 5 \times 10^{-6}\ s^{-1}$
i. $\beta = 10^{-5}\ s^{-1}$	j. γ = 5 K/km
k. γ = 4 K/km	l. γ = 3 K/km
m. γ = 2 K/km	n. γ = 1 K/km

N4. Same as the previous exercise, but find the time scale τ that estimates when the peak airmass depth occurs for warm airmass genesis.

N5. For the katabatic winds of Antarctica, find the downslope buoyancy force per unit mass for this location:

Location	$\Delta z/\Delta x$	$\Delta\theta$ (K)	T_e (K)
a. Interior	0.001	40	233
b. Interior	0.002	35	238
c. Interior	0.003	30	243
d. Intermediate	0.004	27	245
e. Intermediate	0.005	25	248
f. Intermediate	0.006	24	249
g. Intermediate	0.007	23	250
h. Coast	0.008	22	251
i. Coast	0.009	21	252
j. Coast	0.010	20	253
k. Coast	0.011	19	254

N6.(§) An Arctic airmass of initial temperature –30°C is modified as it moves at speed 10 m/s over smooth warmer surface of temperature 0°C. Assume constant airmass thickness. Find and plot the airmass (mixed-layer) temperature vs. downwind distance for an airmass thickness (m) of:

a. 100 b. 200 c. 300 d. 400 e. 500
f. 600 g. 700 h. 800 i. 900 j. 1000
k. 1200 l. 1400 m. 1500

N7. Find the external Rossby radius of deformation at 60° latitude for a cold airmass of thickness 500 m and $\Delta\theta$ (°C) of:
a. 2 b. 4 c. 6. d. 8 e. 10 f. 12 g. 14
h. 16 i. 18 j. 20 k. 22 l. 24 m. 26 n. 28
Assume a background potential temperature of 300K.

N8.(§) Find and plot the airmass depth and geostrophic wind as a function of distance from the front for the cases of the previous exercise. Assume a background potential temperature of 300 K.

N9. Suppose that $\Delta\theta/\Delta x$ = 0.02°C/km, $\Delta\theta/\Delta y$ = 0.01°C/km, and $\Delta\theta/\Delta z$ = 5°C/km. Also suppose that $\Delta U/\Delta x$ = – 0.03 (m/s)/km, $\Delta V/\Delta x$ = 0.05 (m/s)/km, and $\Delta W/\Delta x$ = 0.02 (cm/s)/km. Find the kinematic frontogenesis contributions from:
a. confluence b. shear c. tilting
d. and find the strengthening rate.

N10. A thunderstorm on the warm side of a 300 km wide front rains at the following rate (mm/h). Find the thermodynamic contribution to frontogenesis.
a. 0.2 b. 0.4 c. 0.6 d. 0.8 e. 1.0 f. 1.2 g. 1.4
h. 1.6 i. 1.8 j. 2.0 k. 2.5 l. 3.0 m. 3.5 n. 4.0

N11. Plot dryline movement with time, given the following conditions. Surface heat flux is constant with time at kinematic rate 0.2 K·m/s. The vertical gradient of potential temperature in the initial sounding is γ. Terrain slope is $s = \Delta z/\Delta x$.

γ (K/km)	s	γ (K/km)	s
a. 8	1/500	b. 8	1/400
c. 8	1/300	d. 8	1/200
e. 12	1/500	f. 12	1/400
g. 12	1/300	h. 12	1/200
i. 15	1/500	j. 15	1/400

Understanding & Critical Evaluation

U1. Would you expect there to be a physically- or dynamically-based upper limit on the number of warm fronts and cold fronts that can extend from a low-pressure center? Why?

U2. Sketch a low with two fronts similar to Fig. 12.1, but for the Southern Hemisphere.

U3. What are the similarities and differences between a ridge and a high-pressure center? Also, on a weather map, what characteristics would you look for to determine if a weather feature is a ridge or a trough?

U4. In high-pressure centers, is the boundary-layer air compressed to greater density as subsidence pushes down on the top of the mixed layer? Explain.

U5. In Fig. 12.3b, use the hypsometric relationship to explain why the ridge shifts or tilts westward with increasing altitude. Hint: consider where warm and cold air is relative to the surface high.

U6. How would Fig. 12.3b be different, if at all, in Southern Hemisphere mid-latitudes. Hint: Consider the direction that air rotates around a surface high, and use that information to describe which side of the high (east or west) advects in warm air and which advects in colder air.

U7. Consider the global-circulation, monsoon, and topographic mechanisms that can form high-pressure regions. Use information from the chapters on Global Circulation, Extratropical Cyclones, and Local Winds to identify 3 or more regions in the world where 2 or more of those mechanisms are superimposed to help create high-pressure regions. Describe the mechanisms at each of those 3 locations, and suggest how high-pressure formation might vary during the course of a year.

U8. Out of all the different attributes of airmasses, why do you think that the airmass abbreviations listed in Table 12-1 focus on only the temperature (i.e., AA, A, P, T, M, E) and humidity (c, m)? In other words, what would make the relative temperature and humidity of airmasses be so important to weather forecasters? Hint: consider what you learned about heat and humidity in earlier chapters.

U9. Fig. 12.4 shows the genesis regions for many different airmasses. At first glance, this map looks cluttered. But look more closely for patterns and describe how you can anticipate where in the world you might expect the genesis regions to be for a particular airmass type.

U10. In this chapter, I described two very different mechanisms by which warm and cold airmasses are created. Why would you expect them to form differently? Hint: consider the concepts, not the detailed equations.

U11. Fig. 12.5 shows how initially-cold air is transformed into a warm airmass after it becomes parked over a warm surface such as a tropical ocean. It is

not surprising that the airmass temperature θ_{ML} asymptotically approaches the temperature of the underlying surface. Also not surprising: depth z_i of the changed air initially increases with time.

But more surprising is the decrease in depth of the changed air at longer times. Conceptually, why does this happen? Why would you expect it to happen for most warm airmass genesis?

U12. Using the concept of airmass conservation, formulate a relationship between subsidence velocity at the top of the boundary layer (i.e., the speed that the capping inversion is pushed down in the absence of entrainment) to the radial velocity of air within the boundary layer. (Hint: use cylindrical coordinates, and look at the geometry.)

U13. For the toy model in the Focus Box on Warm Airmass Genesis, ΔQ is the amount of heat (in kinematic units) put into the mixed layer (ML) from the surface during one time step. By repeating over many time steps, we gradually put more and more heat into the ML. This heat is uniformly mixed in the vertical throughout the depth z_i of the ML, causing the airmass to warm.

Yet at any time, such as 10 days into the forecast, the amount of additional heat contained in the ML (which equals its depth times its temperature increase since starting, see Fig. 12.5) is less than the accumulated heat put into the ML from the surface (which is the sum of all the ΔQ from time zero up to 10 days).

That discrepancy is not an error. It describes something physical that is happening. What is the physical process that explains this discrepancy, and how does it work?

U14. In the solved example on warm airmass genesis, I iterate with very small time step at first, but later take larger and larger time steps. Why would I need to take small time steps initially, and why can I increase the time step later in the simulation? Also, if I wanted to take small time steps for the whole duration, would that be good or bad? Why?

U15. Suppose that cold air drains katabatically from the center of Antarctica to the edges. Sketch the streamlines (lines that are parallel to the flow direction) that you would anticipate for this air, considering buoyancy, Coriolis force, and turbulent drag.

U16.(§) Assume the katabatic winds of Antarctica result from a balance between the downslope buoyancy force, Coriolis force (assume 70°S latitude), and turbulent drag force at the surface (assume neutral boundary layer with C_D = 0.002). The surface is smooth and the depth of the katabatic layer is 100 m. Neglect entrainment drag at the top of the katabatic flow. The slope, potential temperature difference, and ambient temperature vary according to the table from exercise N5. Find the katabatic wind speed at the locations in the table from exercise N5.

U17. Where else in the world (Fig. 12.8) would you anticipate orographic airmass modification processes similar to those shown in Fig. 12.9? Explain.

U18. For airmass modification (i.e., while an airmass is blowing over a different surface), why do we describe the heat flux from the surface using a bulk transfer relationship ($C_H \cdot M \cdot \Delta\theta$), while for warm airmass genesis of stationary air we used a buoyancy-velocity approach ($b \cdot w_b \cdot \Delta\theta$)?

U19. The Eulerian heat budget from the Heat chapter shows how air temperature change ΔT is related to the heat input over time interval Δt. If this air is also moving at speed M, then during that same time interval, it travels a distance $\Delta x = M \cdot \Delta t$. Explain how you can use this information to get eq. (12.3), and why the wind speed M doesn't appear in that eq.

U20. Look at Fig. 12.9 and the associated solved example. In the solved example, the air passes twice through the thermodynamic state given by point 1 on that diagram: once when going from point 0 to points 2, and the second time when going from points 2 to point 3.

Similarly, air passes twice through the thermodynamic state at point 3 on the thermo diagram, and twice through point 5.

But air can achieve the same thermodynamic state twice only if certain physical (thermodynamic) conditions are met. What are those conditions, and how might they NOT be met in the real case of air traversing over these mountain ranges?

U21. Knowing that the front on a weather map is always drawn on the warm side of the frontal zone at the surface, explain why warming is felt BEFORE a warm front approaches, but cooling is not felt until AFTER a cold front passes.

U22. Overlay Fig. 12.11 with Fig. 12.12 by aligning the low-pressure centers. Do not rotate the images, but let the warm and cold fronts extend in different directions from the low center. Combine the information from these two figures to create a new, larger figure showing both fronts at the same time, extending from the same low. On separate copies of this merged figure, draw:

a. isotherms b. isobars c. winds d. weather

U23. Suppose you saw from your barometer at home that the pressure was falling. So you suspect that a front is approaching. What other clues can you use (by standing outside and looking at the clouds and weather; NOT by looking at the TV, computer, or other weather instruments) to determine if the approaching front is a warm or cold front. Discuss, along with possible pitfalls in this method.

U24. Draw new figures (a) - (d) similar to (a) - (d) in Figs. 12.11 and 12.12, but for an occluded front.

U25. Use the columns of temperature data in Fig. 12.13a, and plot each column as a separate sounding on a thermo diagram (See the Stability chapter for blank thermo diagrams that you can photocopy for this exercise. Use a skew-T diagram, unless your instructor tells you otherwise). Describe how the frontal zone shows up in the soundings.

U26. Draw isentropes that you might expect in a vertical cross-section through a warm front.

U27. Other than drylines, is it possible to have fronts with no temperature change across them? How would such fronts be classified? How would they behave?

U28. What clouds and weather would you expect with a cold anafront?

U29. Why should the Rossby radius of deformation depend on the depth of the cold airmass in a geostrophic adjustment process?

U30. For geostrophic adjustment, the initial outflow of cold air turns, due to Coriolis force, until it is parallel to the front. Why doesn't it continue turning and point back into the cold air?

U31. For geostrophic adjustment, what is the nature of the final winds, if the starting point is a shallow cylinder of cold air 2 km thick and 500 km radius?

U32. Starting with Fig. 12.18, suppose that ABOVE the bottom contoured surface the temperature is horizontally uniform. Redraw that diagram but with the top two contoured surfaces sloped appropriately for the new temperature state.

U33. By inspection, write a kinematic frontogenesis equation (similar to eq. 12.10), but for an east-west aligned front.

U34. Figs. 12.22 - 12.24 presume that temperature gradients already exist, which can be strengthened by kinematic frontogenesis. Is that presumption valid for Earth's atmosphere? Justify.

U35. For the fronts analyzed in the Solved Example in the section on Surface Fronts – Horizontal Structure, estimate and compare magnitudes of any kinematic, thermodynamic, and dynamic processes that might exist across those fronts, based on the plotted weather data (which includes info on winds, precipitation, etc.). Discuss the relative importance of the various mechanisms for frontogenesis.

U36. Speculate on which is more important for dynamically generating ageostrophic cross-frontal circulations: the initial magnitude of the geostrophic wind or the change of geostrophic wind.

U37. What happens in an occluded front where the two cold air masses (the one advancing behind the cold front, and the one retreating ahead of the warm front) have equal virtual temperature?

U38. Draw isentropes that you expect in a vertical cross-section through a cold front occlusion (where a cold front catches up to a warm front), and discuss the change of static stability across this front.

U39. What types of weather would be expected with an upper-tropospheric front that does not have an associated surface front? [Hint: track movement of air parcels as they ride isentropic surfaces.]

U40. Draw a sketch similar to Fig. 12.34 showing the transverse circulations, but for a vertical cross-section in the Southern Hemisphere.

U41. Would you expect drylines to be possible in parts of the world other than the S.W. USA? If so, where? Justify your arguments.

Web-Enhanced Questions

W1. Monitor the weather maps on the web every day for a week or more during N. Hemisphere winter, and make a sketch of each low center with the fronts extending (similar to Fig. 12.1). Discuss the variety of arrangements of warm, cold, and occluded fronts that you have observed during that week.

W2. Same as W1, but for the S. Hemisphere during S. Hemisphere winter.

W3. On a surface weather map, identify high-pressure centers, and identify ridges. Also, on a 50 kPa

(500 hPa) chart, do the same. Look at the ratio of ridges to high centers for each chart, and identify which chart (surface or 50 kPa) has the largest relative number of high centers, and which has the largest relative number of ridges.

W4. From weather maps showing vertical velocity w, find typical values of that vertical velocity near the center of highs. (If $\omega = \Delta P/\Delta t$ is used instead of w, it is acceptable to leave the units in mb/s). Compare this vertical velocity to the radial velocity of air diverging away from the high center in the boundary layer.

W5. Use a sequence of surface weather maps every 6 or 12 h for a week, where each map spanning a large portion of the globe. Find one or more locations that exhibits the following mechanism for formation of a surface high pressure:

a. global circulation b. monsoon
c. Rossby wave d. thunderstorm
e. topographic

W6. Do a web search to find surface weather maps that also include airmass abbreviations on them. Print one of these maps, and suggest how the labeled airmass moved to its present location from its genesis region (where you will need to make a reasonable guess as to where its genesis region was).

W7. Use weather maps on the web to find a location where air has moved over a region and then becomes stationary. Monitor the development of a new airmass (or equivalently, modification of the old airmass) with time at this location. Look at temperature and humidity.

W8. For a weather situation of relatively zonal flow from west to east over western N. America, access upper air soundings for weather stations in a line more-or-less along the wind direction. Show how the sounding evolves as the air flows over each major mountain range. How does this relate to airmass modification?

W9. Access upper air soundings for a line of RAOB stations across a front. Use this data to draw vertical cross-sections of:

a. pressure or height b. temperature
c. humidity d. potential temperature

W10. Same as previous exercise, but identify the frontal inversions (or frontal stable layers) aloft in the soundings.

W11. Access a sequence of weather maps that cover a large spatial area, with temporal coverage every 6 or 12 h for a week. Find an example of a front that you can follow from beginning (frontogenesis) through maturity to the end (frontolysis). Discuss how the front moves as it evolves, and what the time scale for its evolution is.

W12. Print from the web a weather map that shows both the analyzed fronts and the station plot data. On this map, draw your own analysis of the data to show where the frontal zones are. Discuss how the weather characteristics (wind, pressure, temperature, weather) across these real fronts compare with the idealized sketches of Figs. 12.11 and 12.12.

W13. Access a sequence of surface weather maps from the web that show the movement of fronts. Do you see any fronts that are labeled as stationary fronts, but which are moving? Do you see any fronts labeled as warm or cold fronts, but which are not moving? Are there any fronts that move backwards compared to the symbology labeling the front (i.e., are the fronts moving opposite to the direction that the triangles or semicircles point)? [Hint: often fronts are designated by how they move relative to the low center. If a cold front, for example, is advancing cyclonically around a low, but the low is moving toward the west (i.e., backwards in mid-latitudes), then relative to people on the ground, the cold front is retreating.]

W14. Access weather map data that shows a strong cold front, and compare the winds on both sides of that front to the winds that you would expect using geostrophic-adjustment arguments. Discuss.

W15. For a wintertime situation, access a N. (or S.) Hemisphere surface weather map from the web, or access a series of weather maps from different agencies around the world in order to get information for the whole Hemisphere. Draw the location of the polar front around the globe.

W16. Access weather maps from the web that show a strengthening cold or warm front. Use the other weather data on this map to suggest if the strengthening is due mostly to kinematic, thermodynamic, or dynamic effects.

W17. Access a sequence of weather maps that shows the formation and evolution of an occluded front. Determine if it is a warm or cold occlusion (you might need to analyze the weather map data by hand to help you determine this).

W18. Use the web to access a 3-D sketch of a TROWAL. Use this and other web sites to determine other characteristics of TROWALs.

W19. Download upper-air soundings from a station under or near the jet stream. Use the data to see if there is a tropopause fold. [Hint: assuming that you don't have measurements of radioactivity or isentropic potential vorticity, use mixing ratio or potential temperature as a tracer of stratospheric air.]

W20. Search the web for surface weather maps that indicate a dryline in the S.W. USA. If one exists, then search the web for upper-air soundings just east and just west of the dryline. Plot the resulting soundings of potential temperature and humidity, and discuss how it relates to the idealized sketch of a dryline in this textbook.

Synthesis Questions

S1. Fig. 12.2 shows a ridge that is typical of mid-latitudes in the N. Hemisphere. Sketch a ridge for:

a. Southern Hemisphere mid-latitudes
b. N. Hemisphere tropics
c. S. Hemisphere tropics

Hint: Consider the global pressure patterns described in the Global Circulation chapter.

S2. What if there was no inversion at the top of the boundary layer? Redraw Fig. 12.3a for this situation.

S3. What if the Earth had no oceans? What mechanisms could create high-pressure centers and/or high-pressure belts?

S4. For your location, rank the importance of the different mechanisms that could create highs, and justify your ranking.

S5. Airmasses are abbreviated mostly by the relative temperature and humidity associated with their formation locations. Table 12-1 also describes two other attributes: returning airmasses, and airmasses that are warmer or colder than the underlying surface. What one additional attribute would you wish airmasses could be identified with, to help you to predict the weather at your location? Explain.

S6. Fig. 12.4 shows many possible genesis regions for airmasses. But some of these regions would not likely exist during certain seasons, because of the absence of high-pressure centers. For the hemisphere (northern or southern) where you live, identify how the various genesis regions appear or disappear with the seasons. Also, indicate the names for any of the high-pressure centers. For those that exist year round, indicate how they shift location with the seasons. (Hint: review the global circulation info in the Global Circulation chapter.)

S7. What if airmasses remained stationary over the genesis regions forever? Could there be fronts and weather? Explain.

S8. Would it be possible for an airmass to become so thick that it fills the whole troposphere? If so, explain the conditions needed for this to occur.

S9. What if boundary-layer processes were so slow that airmasses took 5 times longer to form compared to present airmass formation of about 3 to 5 days? How would the weather and global circulation be different, if at all?

S10. Cold-air drainage from Antarctica is so strong and persistent that it affects the global circulation. Discuss how this affect is captured (or not) in the global maps in the Global Circulation chapter.

S11. What if Antarctica was flat, similar to the Arctic? How would airmasses and Earth's climate be different, if at all?

S12. Consider Fig. 12.8. How would airmass formation and weather be different, if at all, given:

a. Suppose the Rocky Mountains disappeared, and a new dominant mountain range (named after you), appeared east-west across the middle of N. America.

b. Suppose that the Alps and Pyrenees disappeared and were replaced by a new dominant north-south mountain range (named after you) going through Europe from Copenhagen to Rome.

c. Suppose no major mountain ranges existed.

S13. Suppose a cross-section of the terrain looked like Fig. 12.9, except that the Great Basin region were below sea level (and not flooded with water). Describe how airmass modification by the terrain would be different, if at all.

S14. What if precipitation did not occur as air flows over mountain ranges? Thus, mountains could not modify air masses by this process. How would weather and climate be different from now, if at all?

S15. A really bad assumption was made in eq. (12.3); namely, z_i = constant as the airmass is modified. A better assumption would be to allow z_i to change with time (i.e., with distance as it blows over the new surface). The bad assumption was made because it

allowed us to describe the physics with a simple eq. (12.3), which could be solved analytically to get eq. (12.4). This is typical of many physical problems, where it is impossible to find an exact analytical solution to the full equations describing true physics (as best we know it).

So here is a philosophical question. Is it better to approximate the physics to allow an exact analytical solution of the simplified problem? Or is it better to try to get an approximate (iterated or graphical solution) to the exact, more-complicated physics? Weigh the pros and cons of each approach, and discuss.

S16. For a (a) cold front, or a (b) warm front, create station plot data for a weather station 100 km ahead of the front, and for another weather station 100 km behind the front. Hint: use the sketches in Figs. 12.11 and 12.12 to help decide what to plot.

S17. Suppose the width of frontal zones were infinitesimally small, but their lengths remained unchanged. How would weather be different, if at all?

S18. What if turbulence were always so intense that frontal zones were usually 1000 km in width? How would weather be different, if at all?

S19. Does the geostrophic adjustment process affect the propagation distance of cold fronts in the real atmosphere, for cold fronts that are imbedded in the cyclonic circulation around a low-pressure center? If this indeed happens, how could you detect it?

S20. The boxes at the top of Figs. 12.22 - 12.24 show the associated sign of key terms for kinematic frontogenesis. If those terms have opposite signs, draw sketches similar to those figures, but showing frontolysis associated with:

a. confluence b. shear c. tilting.

S21. Suppose that condensation of water vapor caused air to cool. How would the thermodynamic mechanism for frontogenesis work for that situation, if at all? How would weather be near fronts, if at all?

S22. Suppose that ageostrophic motions were to experience extremely large drag, and thus would tend to dissipate quickly. How would frontogenesis in Earth's atmosphere be different, if at all?

S23. After cold frontal passage, cold air is moving over ground that is still warm (due to its thermal inertia). Describe how static stability varies with height within the cold airmass 200 km behind the cold front. Draw thermo diagram sketches to illustrate your arguments.

S24. Suppose a major volcanic eruption injected a thick layer of ash and sulfate aerosols at altitude 20 km. Would the altitude of the tropopause adjust to become equal to this height? Discuss.

S25. Suppose the slope of the ground in a dryline situation was not as sketched in Fig. 12.36. Instead, suppose the ground was bowl-shaped, with high plateaus on both the east and west ends. Would drylines exist? If so, what would be their characteristics, and how would they evolve?

Copyright © 2011, 2015 by Roland Stull. *Meteorology for Scientists and Engineers, 3rd Ed.*

EXTRATROPICAL CYCLONES

CONTENTS

Cyclone Characteristics 426
- Cyclogenesis & Cyclolysis 426
- Cyclone Evolution 427
- Cyclone Tracks 430
- Stacking & Tilting 432
- Other Characteristics 433

Case Study of an Extratropical Cyclone Over North America 433
- Overview and Storm Track 433
- Storm Data 434
- Surface Charts 438
- Isobaric Charts 439
- Isentropic Charts 441

Lee Cyclogenesis 443
- Stationary Planetary Waves 443
- Conservation of Potential Vorticity 445
- Equatorward Propagation Along the Lee Side 446

Cyclone Spin-up 446
- Vorticity Tendency 447
- Quasi-Geostrophic Approximation 449
- Application to Idealized Weather Patterns 450

Upward Motion 451
- Continuity Effects 452
  - Jet-Stream Curvature 453
  - Jet Streaks 454
- Omega Equation 456
- Q-Vectors 460

Sea-level-pressure Tendency 463
- Mass Budget 463
- Diabatic Heating due to Condensation 465
- Net Pressure Tendency 466

Self Development of Cyclones 468
- Condensation 468
- Temperature Advection 468
- Propagation of Cyclones 469
- Creation of Baroclinic Zones 469
- Propagation of Cold Fronts 470

Summary 470

Exercises 473

13 **Cyclones** are synoptic-scale regions of **low pressure** near the surface (Fig. 13.1), with horizontal winds turning **cyclonically** (counterclockwise in N. Hemisphere) and **upward vertical velocity** in the mid troposphere. The updrafts support clouds, precipitation, and sometimes thunderstorms.

Tropical cyclones are covered separately, in the chapter on hurricanes. **Extratropical cyclones** (cyclones outside of the tropics) are covered here, and include transient **mid-latitude cyclones** and **polar cyclones**. Other names for extratropical cyclones are **lows** or **low-pressure centers**. Table 13-1 compares names for cyclones.

Lows can cause floods, blizzards, strong winds and hazardous travel conditions. They are the large regions of bad weather that come from the west every two to seven days in mid-latitudes.

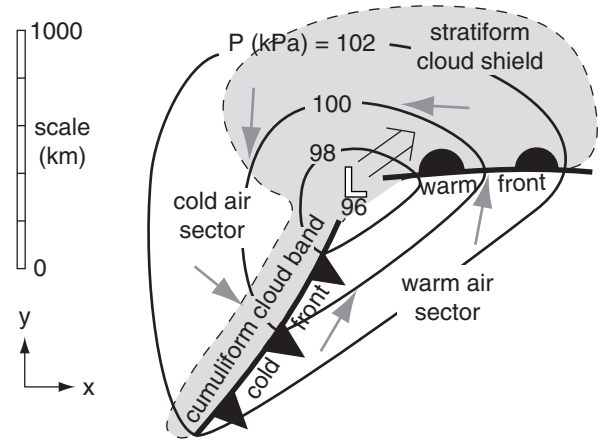

Figure 13.1
Components of a typical extratropical cyclone in the N. Hemisphere. Light grey shows clouds, dark grey arrows are near-surface winds, thin black lines are isobars (kPa), thick black lines are fronts, and the double-shaft arrow shows movement of the low center 𝕃 *.*

"Meteorology for Scientists and Engineers, 3rd Edition" by Roland Stull is licensed under a Creative Commons Attribution-NonCommercial-ShareAlike 4.0 International License. To view a copy of the license, visit http://creativecommons.org/licenses/by-nc-sa/4.0/ . This work is available at http://www.eos.ubc.ca/books/Practical_Meteorology/ .

Table 13-1. Cyclone names. "Core" is storm center. *T* is relative temperature.

Common Name in N. Amer.	Formal Name	Other Common Names	T of the Core	Map Symbol
low	extra-tropical cyclone	mid-latitude cyclone low-pressure center storm system* cyclone *(in N. America)*	cold	L
hurricane	tropical cyclone	typhoon *(in W. Pacific)* cyclone *(in Australia)*	warm	

(Often used by TV meteorologists.)*

CYCLONE CHARACTERISTICS

Cyclogenesis & Cyclolysis

Cyclogenesis is the birth and growth of cyclones. Such intensification can be defined by the:

- sea-level pressure decrease,
- upward-motion increase, and
- vorticity increase.

These characteristics are not independent; for example, upward motion can reduce surface pressure, which draws in lower-tropospheric air that begins to rotate due to Coriolis force. However, you can gain insight into the workings of the storm by examining the dynamics and thermodynamics that govern each of these characteristics. Each of these will be explored in detail later in this chapter.

The following conditions favor rapid cyclogenesis:

- strong baroclinicity – a strong horizontal temperature gradient, such as a frontal zone
- weak static stability – temperature decreasing with height faster than the tropospheric standard atmosphere
- mid- or high-latitude location – Earth's contribution to vorticity increases toward the poles
- large moisture input – latent heating due to cloud condensation adds energy and reduces static stability
- large-amplitude wave in the jet stream – a trough to the west and ridge to the east of the surface low enhance horizontal divergence aloft, which strengthens updrafts
- terrain elevation decrease toward east – cyclogenesis to the lee of mountains

A cyclone that develops extremely fast is called a **cyclone bomb**, and the process is called **explosive cyclogenesis**. To be classified as a bomb, the central pressure of a cyclone must decrease at a rate of 0.1 kPa per hour for at least 24 hours. Explosive cyclogenesis often occurs when cold air moves over the northern edge of a very warm ocean current, such as over the Gulf Stream off the Northeast USA. In these regions, strong evaporation and heat transfer from the sea surface enhances many of the factors listed above for rapid cyclogenesis. Cyclone bombs can cause sudden major winter storms, with high seas, snow and freezing rain that are hazards to shipping and road travel.

The opposite of cyclogenesis is **cyclolysis**. This is literally death of a cyclone.

FOCUS • Southern Hemisphere Lows

Some aspects of mid-latitude cyclones in the Southern Hemisphere are similar to those of N. Hemisphere cyclones. They have low pressure at the surface, rotate cyclonically, form east of upper-level troughs, propagate from west to east and poleward, and have similar stages of their evolution. They often have fronts and bad weather.

Different are the following: warm tropical air is to the north and cold polar air to the south, and the cyclonic rotation is clockwise due to the opposite Coriolis force. The figure below shows an idealized extra-tropical cyclone in the S. Hemisphere.

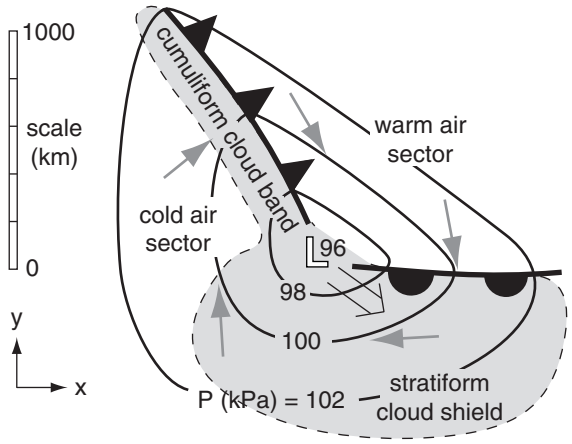

Figure a.
Sketch of mid-latitude cyclone in the Southern Hemisphere.

Cyclone Evolution

Most cyclones go through a life cycle of formation, growth, weakening, and death over a period of about a week at mid-latitudes. However, lifetimes less than a day and greater than two weeks have been observed. While cyclones exist, they are moved by the jet stream and by other large-scale components of the global circulation.

One condition that favors cyclogenesis is a **baroclinic** zone; namely, a region of large temperature change across a short horizontal distance near the surface. Frontal zones such as stationary fronts (Fig. 13.2a) are regions of strong baroclinicity.

Above (near the tropopause) and parallel to this baroclinic zone is often a strong jet stream (Fig. 13.2b), driven by the thermal wind effect (see the chapters on Global Circulation, and Airmasses & Fronts). If conditions are right (as discussed later in this chapter), the jet stream can remove air molecules from a column of air above the front, at location "D" in Fig. 13.2b. This lowers the surface pressure under location "D", causing **cyclogenesis** at the surface. Namely, location "D" is where you would expect a surface low-pressure center to form.

The resulting pressure gradient around the surface low starts to generate lower-tropospheric winds that circulate around the low (Fig. 13.3a, again near the Earth's surface). This is the **spin-up** stage — so named because vorticity is increasing as the cyclone intensifies. The winds begin to advect the warm air poleward on the east side of the low and cold air equatorward on the west side, causing a kink in the formerly stationary front near the low center. The kinked front is wave shaped, and is called a **frontal wave**. Parts of the old front advance as a warm front, and other parts advance as a cold front. Also, these winds begin to force some of the warmer air up over the colder air, thereby generating more clouds.

If jet-stream conditions continue to be favorable, then the low continues to intensify and mature (Fig. 13.3b). As this cyclogenesis continues, the central pressure drops (namely, the cyclone **deepens**), and winds and clouds increase as a **vortex** around the **low center**. Precipitation begins if sufficient moisture is present in the regions where air is rising.

The advancing cold front often moves faster than the warm front for three reasons. (1) The Sawyer-Eliassen circulation tends to push near-surface cold air toward warmer air at both fronts. (2) Circulation around the vortex tends to deform the frontal boundaries and shrink the warm-air region to a smaller wedge shape east and equatorward of the low center. This wedge of warm air is called the **warm-air sector** (Fig. 13.1). (3) Evaporating precipitation cools both fronts (enhancing the cold front

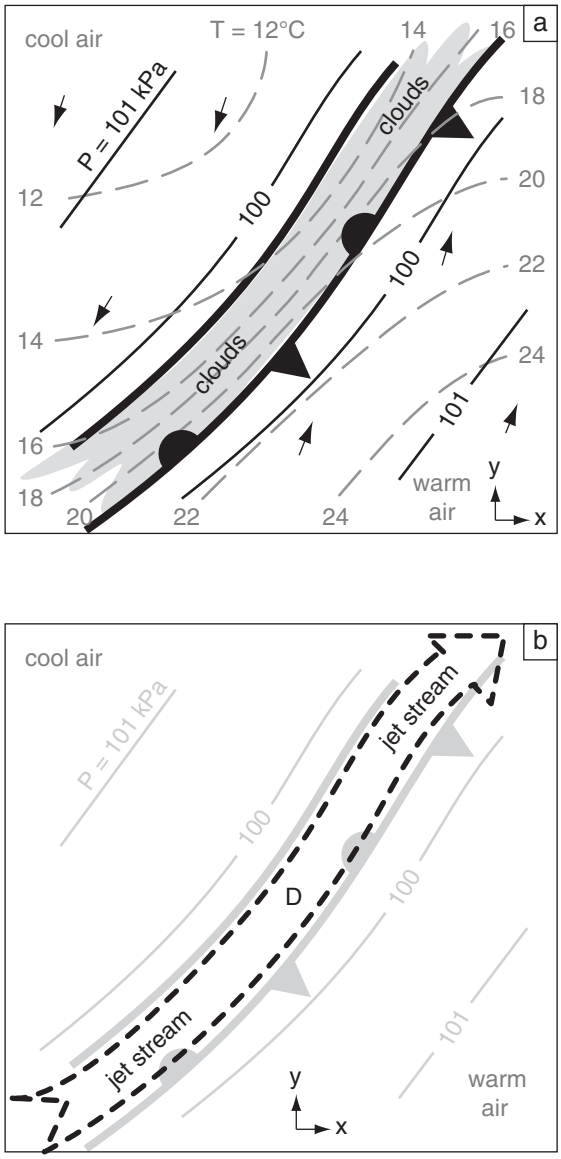

Figure 13.2
Initial conditions favoring cyclogenesis in N. Hemisphere. (a) Surface weather map. Solid thin lines are isobars. Dashed lines are isotherms. The thick black lines mark the leading and trailing edges of the frontal zone. Grey shading indicates clouds. Fig. 13.3 shows subsequent evolution. (b) Upper-air map over the same frontal zone, where the dashed black arrow indicates the jet stream near the tropopause. The grey lines are a copy of the surface isobars and frontal zone from (a), to help you picture the 3-D nature of this system.

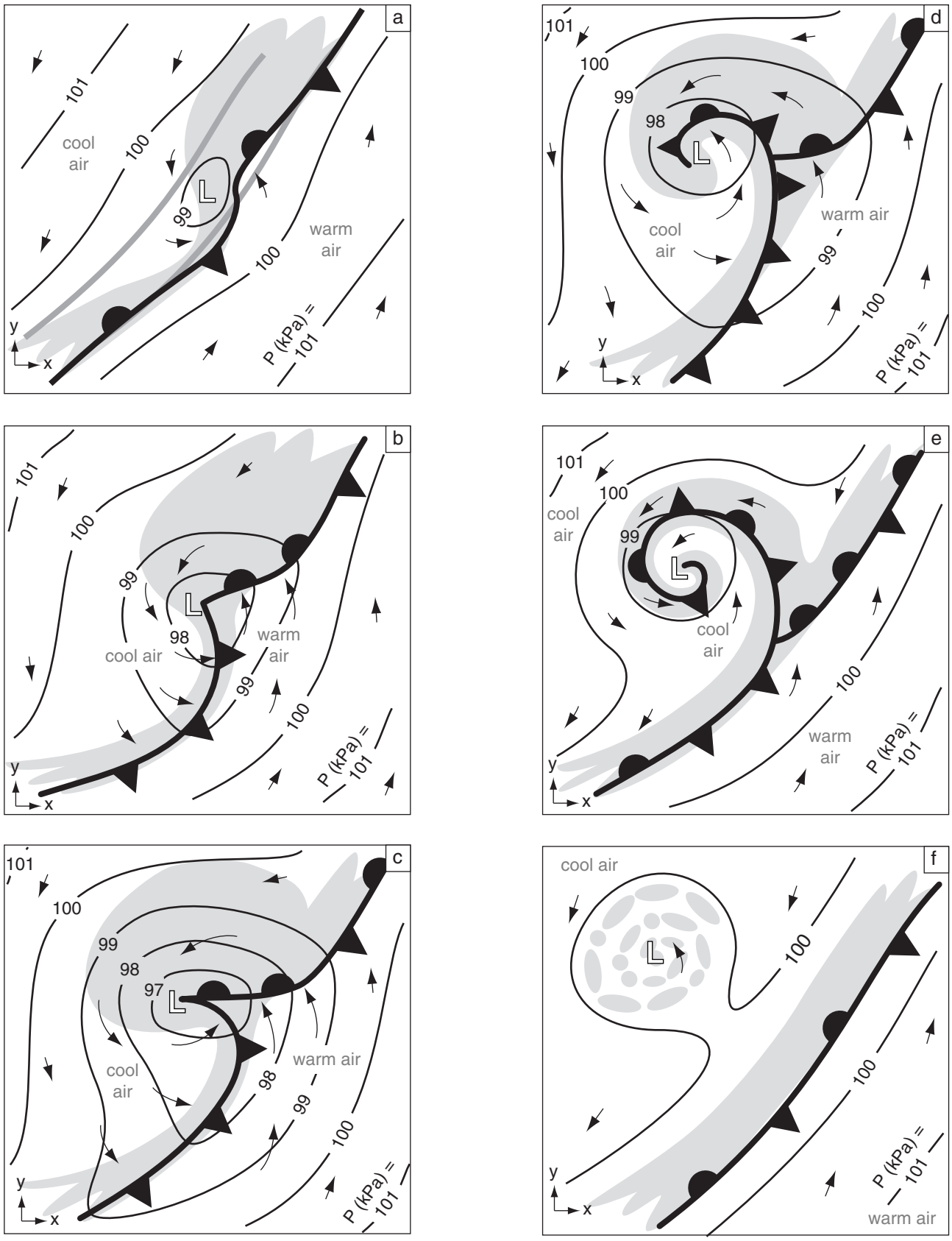

Figure 13.3

Extratropical cyclone evolution in the N. Hemisphere, including cyclogenesis (a - c), and cyclolysis (d - f). These idealized surface weather maps move with the low center. Grey shading indicates clouds, solid black lines are isobars (kPa), thin arrows are near-surface winds, L is at the low center, and medium grey lines in (a) bound the original frontal zone. Fig. 13.2a shows the initial conditions.

but diminishing the warm front). These combined effects amplify the frontal wave.

At the peak of cyclone intensity (lowest central pressure and strongest surrounding winds) the cold front often catches up to the warm front near the low center (Fig. 13.3c). As more of the cold front overtakes the warm front, an occluded front forms near the low center (Fig. 13.3d). The cool air is often drier, and is visible in satellite images as a **dry tongue** of relatively cloud-free air that begins to wrap around the low. This marks the beginning of the **cyclolysis** stage. During this stage, the low is said to **occlude** as the occluded front wraps around the low center.

As the cyclone occludes further, the low center becomes surrounded by cool air (Fig. 13.3e). Clouds during this stage spiral around the center of the low — a signature that is easily seen in satellite images. But the jet stream, still driven by the thermal wind effect, moves east of the low center to remain over the strongest baroclinic zone (over the warm and cold fronts, which are becoming more stationary).

Without support from the jet stream to continue removing air molecules from the low center, the low begins to **fill** with air due to convergence of air in the boundary layer. The central pressure starts to rise and the winds slow as the vorticity **spins down**.

As cyclolysis continues, the low center often continues to slowly move further poleward away from the baroclinic zone (Fig. 13.3f). The central pressure continues to rise and winds weaken. The tightly wound spiral of clouds begins to dissipate into scattered clouds, and precipitation diminishes.

But meanwhile, along the stationary front to the east, a new cyclone might form if the jet stream is favorable (not shown in the figures).

In this way, cyclones are born, evolve, and die. While they exist, they are driven by the baroclinicity in the air (through the action of the jet stream). But their circulation helps to reduce the baroclinicity by moving cold air equatorward, warm air poleward, and mixing the two airmasses together. As described by **Le Chatelier's Principle**, the cyclone forms as a response to the baroclinic instability, and its existence partially undoes this instability. Namely, cyclones help the global circulation to redistribute heat between equator and poles.

Figures 13.3 are in a moving frame of reference following the low center. In those figures, it is not obvious that the warm front is advancing. To get a better idea about how the low moves while it evolves over a 3 to 5 day period, Figs. 13.4 show a superposition of all the cyclone locations relative to a fixed frame of reference. In these idealized figures, you can more easily see the progression of the low center, the advancement of the warm fronts and the advancement of cold air behind the cold fronts.

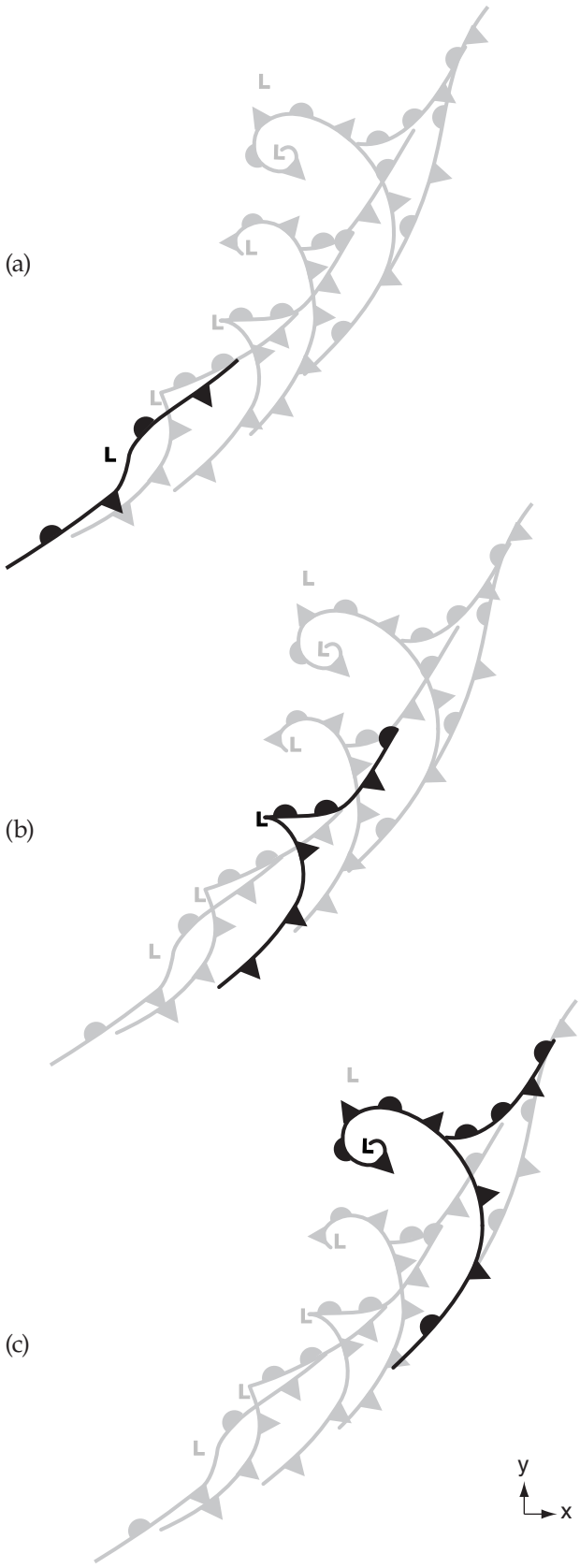

Figure 13.4
Illustration of movement of a low while it evolves. Fronts and low centers are from Figs. 13.3. Every second cyclone location is highlighted in a through c.

Cyclone Tracks

Extratropical cyclones are steered by the global circulation, including the prevailing westerlies at mid-latitudes and the meandering Rossby-wave pattern in the jet stream. Typical **storm tracks** (cyclone paths) of low centers are shown in Fig. 13.5. Multi-year climate variations (see the Climate chapter) in the global circulation, such as associated with the El Niño / La Niña cycle or the North Atlantic Oscillation (NAO), can alter the cyclone tracks. Mid-latitude cyclones are generally stronger, translate faster,

Figure 13.5 (below)
Climatology of extratropical cyclone tracks (lines with arrows) for (a) January and (b) July. Other symbols represent genesis and decay regions, as explained in the text. Circled symbols indicate stationary cyclones.

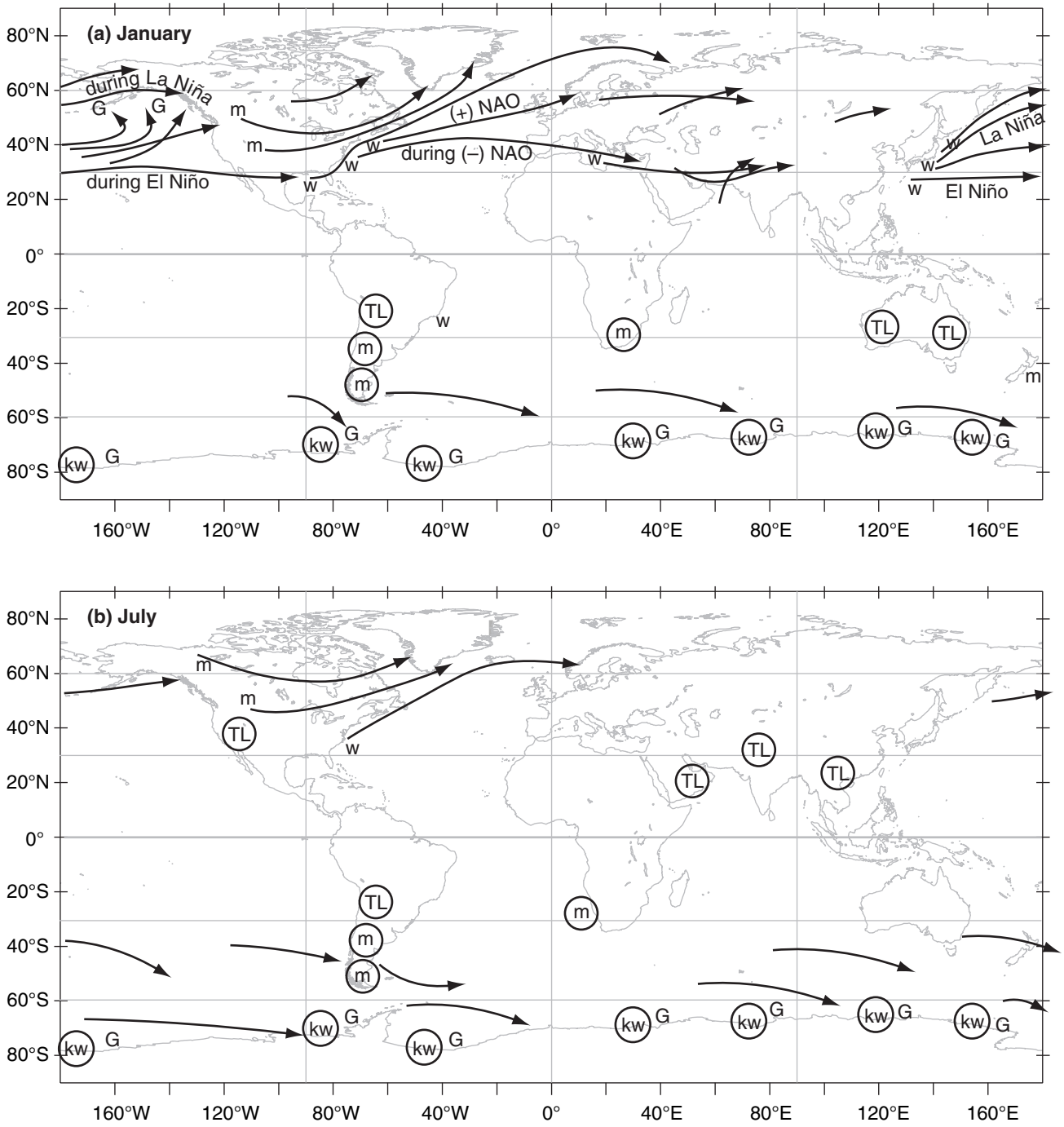

and are further equatorward during winter than in summer.

One favored cyclogenesis region is just east of large mountain ranges (shown by the "m" symbol in Fig. 13.5; see **Lee Cyclogenesis** later in this chapter). Other cyclogenesis regions are over warm ocean **boundary currents** along the western edge of oceans (shown by the symbol "w" in the figure), such as the **Gulf Stream** current off the east coast of N. America, and the **Kuroshio Current** off the east coast of Japan. During winter over such currents are strong sensible and latent heat fluxes from the warm ocean into the air, which adds energy to developing cyclones. Also, the strong wintertime contrast between the cold continent and the warm ocean current causes an intense baroclinic zone that drives a strong jet stream above it due to thermal-wind effects.

Cyclones are often strengthened in regions under the jet stream just east of troughs. In such regions, the jet stream steers the low center toward the east and poleward. Hence, cyclone tracks are often toward the northeast in the N. Hemisphere, and toward the southeast in the S. Hemisphere.

Cyclones in the Northern Hemisphere typically evolve during a 2 to 7 day period, with most lasting 3 - 5 days. They travel at typical speeds of 12 to 15 m/s (43 to 54 km/h), which means they can move about 5000 km during their life. Namely, they can travel the distance of the continental USA from coast to coast or border to border during their lifetime. Since the Pacific is a larger ocean, cyclones that form off of Japan often die in the Gulf of Alaska just west of British Columbia (BC), Canada — a cyclolysis region known as a **cyclone graveyard** (G).

Quasi-stationary lows are indicated with circles in Fig. 13.5. Some of these form over hot continents in summer as a monsoon circulation. These are called **thermal lows** (TL), as was explained in the Global Circulation chapter in the section on Hydrostatic Thermal Circulations. Others form as quasi-stationary lee troughs just east of mountain (m) ranges.

In the Southern Hemisphere (Fig. 13.5), cyclones are more uniformly distributed in longitude and throughout the year, compared to the N. Hemisphere. One reason is the smaller area of continents in Southern-Hemisphere mid-latitudes and subpolar regions. Many propagating cyclones form just north of 50°S latitude, and die just south. The region with greatest cyclone activity (cyclogenesis, tracks, cyclolysis) is a band centered near 60°S.

These Southern Hemisphere cyclones last an average of 3 to 5 days, and translate with average speeds faster than 10 m/s (= 36 km/h) toward the east-south-east. A band with average translation speeds faster than 15 m/s (= 54 km/h; or > 10° lon-

FOCUS • North American Geography

To help you interpret the weather maps, the map and tables give state and province names.

Figure b.

Canadian Postal Abbreviations for Provinces:

AB	Alberta	NT	Northwest Territories
BC	British Columbia	NU	Nunavut
MB	Manitoba	ON	Ontario
NB	New Brunswick	PE	Prince Edward Isl.
NL	Newfoundland & Labrador	QC	Quebec
NS	Nova Scotia	SK	Saskatchewan
		YT	Yukon

USA Postal Abbreviations for States:

AK	Alaska	MD	Maryland	OK	Oklahoma
AL	Alabama	ME	Maine	OR	Oregon
AR	Arkansas	MI	Michigan	PA	Pennsylvania
AZ	Arizona	MN	Minnesota	RI	Rhode Isl.
CA	California	MO	Missouri	SC	South Carolina
CO	Colorado	MS	Mississippi	SD	South Dakota
CT	Connecticut	MT	Montana	TN	Tennessee
DE	Delaware	NC	North Carolina	TX	Texas
FL	Florida	ND	North Dakota	UT	Utah
GA	Georgia	NE	Nebraska	VA	Virginia
HI	Hawaii	NH	New Hampshire	VT	Vermont
IA	Iowa	NJ	New Jersey	WA	Washington
ID	Idaho	NM	New Mexico	WI	Wisconsin
IL	Illinois	NV	Nevada	WV	West Virginia
IN	Indiana	NY	New York	WY	Wyoming
KS	Kansas	OH	Ohio	DC	Wash. DC
KY	Kentucky				
LA	Louisiana				
MA	Massachusetts				

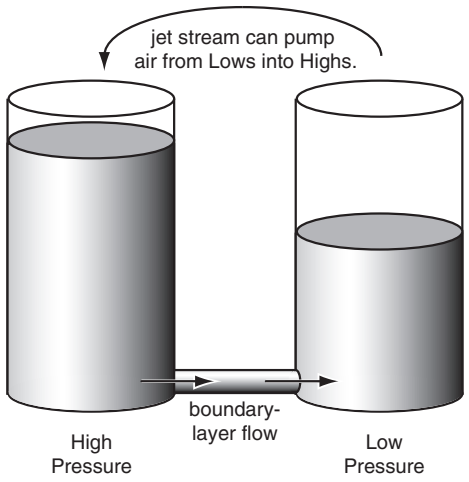

Figure 13.6
Two tanks filled with water to different heights are an analogy to neighboring high and low pressure systems in the atmosphere.

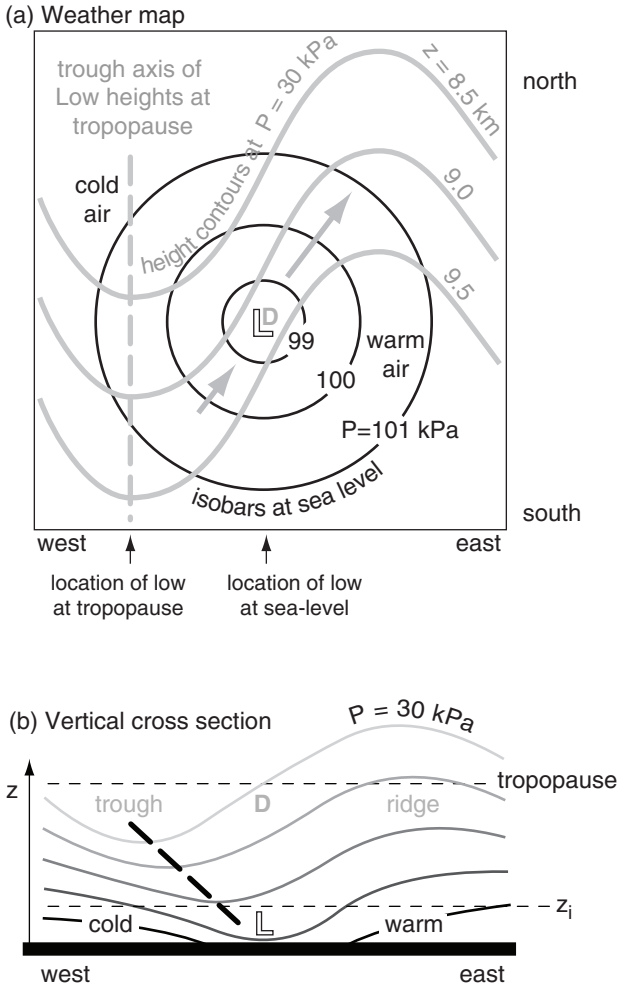

Figure 13.7
(a) Two N. Hemisphere weather maps superimposed: (thin black lines) sea-level pressure, and (grey lines) 30 kPa heights. Jet-stream winds (thick grey arrows) follow the height contours (b) East-west vertical cross section through middle of (a). Heavy dashed line is trough axis. L indicates low center at surface, and D indicates divergence aloft. (Pressure and height variations are exaggerated.)

gitude/day) extends from south of southwestern Africa eastward to south of western Australia. The average track length is 2100 km. The normal **cyclone graveyard** (G, cyclolysis region) in the S. Hemisphere is in the **circumpolar trough** (between 65°S and the Antarctic coastline).

Seven stationary centers of enhanced cyclone activity occur around the coast of Antarctica, during both winter and summer. Some of these are believed to be a result of fast **katabatic** (cold downslope) winds flowing off the steep Antarctic terrain (see the Airmasses & Fronts chapter). When these very cold winds reach the relatively warm unfrozen ocean, strong heat fluxes from the ocean into the air contribute energy into developing cyclones. Also the downslope winds can be channeled by the terrain to cause cyclonic rotation. But some of the seven stationary centers might not be real — some might be caused by improper reduction of surface pressure to sea-level pressure. These seven centers are labeled with "kw", indicating a combination of **k**atabatic winds and relatively **w**arm sea surface.

Stacking & Tilting

Lows at the bottom of the troposphere always tend to kill themselves. The culprit is the boundary layer, where turbulent drag causes air to cross isobars at a small angle from high toward low pressure. By definition, a low has lower central pressure than the surroundings, because fewer air molecules are in the column above the low. Thus, boundary-layer flow will always move air molecules toward surface lows (Fig. 13.6). As a low fills with air, its pressure rises and it stops being a low. Such **filling** is quick enough to eliminate a low in less than a day, unless a compensating process can remove air more quickly.

Such a compensating process often occurs if the axis of low pressure **tilts** westward with increasing height (Fig. 13.7). Recall from the **gradient-wind** discussion in the Dynamics chapter that the jet stream is slower around troughs than ridges. This change of wind speed causes divergence aloft; namely, air is leaving faster than it is arriving. Thus, with the upper-level trough shifted west of the surface low (L), the divergence region (D) is directly above the surface low, supporting cyclogenesis. Details are explained later in this Chapter. But for now, you should recognize that a westward tilt of the low-pressure location with increasing height often accompanies cyclogenesis.

Conversely, when the trough aloft is **stacked** vertically above the surface low, then the jet stream

is not pumping air out of the low, and the low fills due to the unrelenting boundary-layer flow. Thus, vertical stacking is associated with cyclolysis.

Other Characteristics

Low centers often move parallel to the direction of the isobars in the warm sector (Fig. 13.1). So even without data on upper-air steering-level winds, you can use a surface weather map to anticipate cyclone movement.

Movement of air around a cyclone is three-dimensional, and is difficult to show on two-dimensional weather maps. Fig. 13.8 shows the main streams of air in one type of cyclone, corresponding to the snapshot of Fig. 13.3b. Sometimes air in the **warm-air conveyor belt** is moving so fast that it is called a low-altitude **pre-frontal jet**. When this humid stream of air is forced to rise over the cooler air at the warm front (or over a mountain) it can dump heavy precipitation and cause flooding.

Behind the cold front, cold air often descends from the mid- or upper-troposphere, and sometimes comes all the way from the lower stratosphere. This dry air **deforms** (changes shape) into a **diffluent** (horizontally spreading) flow near the cold front.

To show the widespread impact of a winter mid-latitude cyclone, a case-study is introduced next.

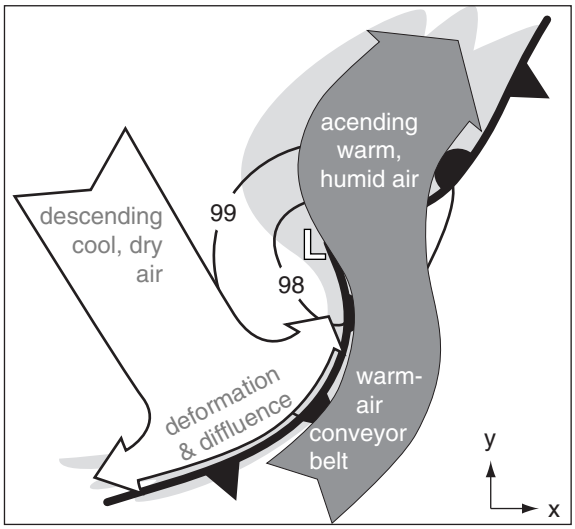

Figure 13.8
Ascending and descending air in a cyclone. Thin black lines with numbers are isobars (kPa). Thick black lines are fronts.

CASE STUDY OF AN EXTRATROPICAL CYCLONE OVER NORTH AMERICA

Overview and Storm Track

On 22 February 1994, an upper-level trough is over the east side of the Rocky Mountains (Fig. 13.9). At the surface, a long stationary front spans from Montana through Texas, and extends northeastward towards Pennsylvania as a dying cold front (Fig. 13.10a). [See the focus box two pages before, for locations of the states.]

Divergence in the upper-tropospheric jet stream between the trough and a ridge east of Texas causes a broad region of upward motion over the southern plains. This **upper-level disturbance** forms a cloud shield and precipitation. As upward motion continues, a surface low (i.e., a cyclone) develops on the stationary front in west Texas in early morning, and moves into east Texas by afternoon (Fig. 13.10a).

As the cyclone tracks northeast toward Illinois (Fig. 13.10b) during 22 to 23 Feb, it intensifies and forms well-developed cold and warm fronts. A squall line of intense thunderstorms with hail and weak tornadoes is triggered in the Southern Plains

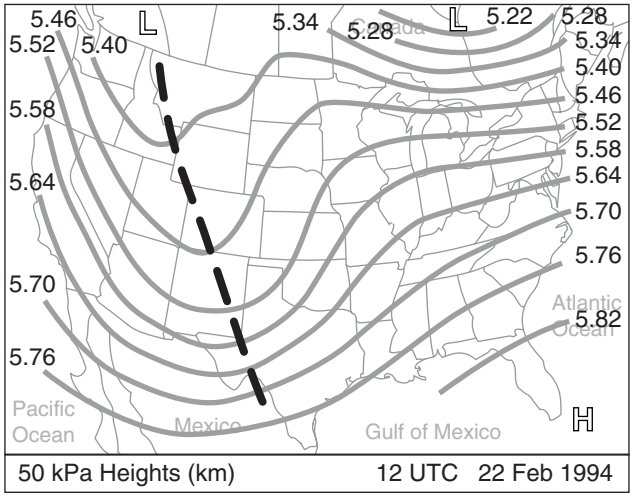

Figure 13.9
Geopotential heights (grey lines) in the mid-troposphere prior to cyclone development. Black dashed line shows the trough axis of low heights (corresponding to low pressure on a constant altitude surface).

(a)

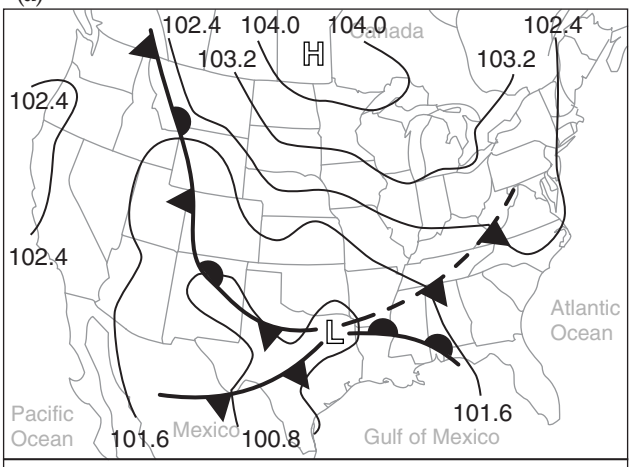

Sea-level Pressure (kPa) & Fronts. 12 UTC, 22 Feb 1994

(b)

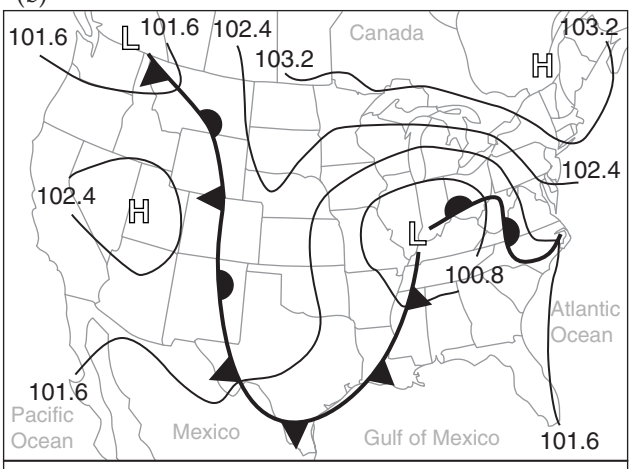

Sea-level Pressure (kPa) & Fronts. 12 UTC, 23 Feb 1994

(c)

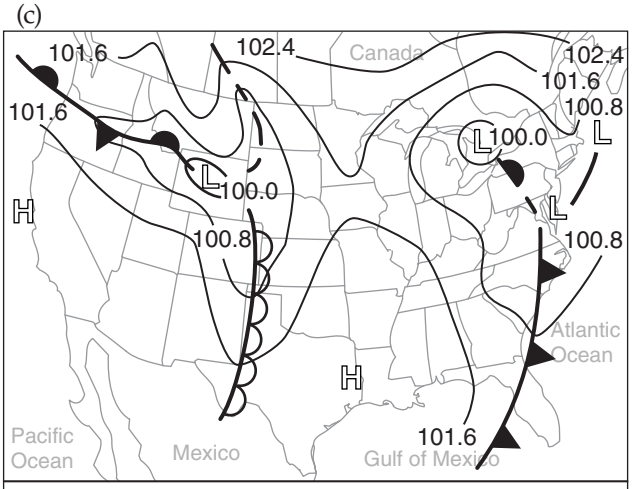

Sea-level Pressure (kPa) & Fronts. 12 UTC, 24 Feb 1994

Figure 13.10
Surface weather maps, showing evolution of a case-study mid-latitude cyclone. 𝕃 = low-pressure center, ℍ = high-pressure center. Thin black lines are isobars. Thick lines are fronts.

along and ahead of the cold front. North of the low, heavy snow falls in the upper plains and midwest.

The main low quickly tracks further northeast (Fig. 13.10c), dropping heavy snow across the Ohio valley. The cyclone occludes and begins to weaken while producing heavy snow and freezing rain over the northeast USA.

Meanwhile, a new secondary cyclone forms off the Carolina coast (Fig. 13.10c, and location "g" in Fig. 13.11), caused in part by support from the upper-level flow. This storm rapidly intensifies over the warm Gulf-stream. During 24 Feb 1994 the old cyclone merges/shifts into the new low (Fig. 13.11 locations f –> h). The combined cyclone deepens rapidly while continuing to move into Canada. It causes blizzard conditions from Washington DC to Prince Edward Island, Canada, in the next three days. A third low forms (not drawn) in Alberta, Canada, east of the Rockies. It quickly sweeps across the northern plains bringing strong winds, which whip up the previously fallen snow creating whiteout conditions and deep snow drifts. Such fast-moving lows are called **Alberta Clippers**.

In summary, the original cyclone is born, completes its full life cycle, and dies within just a few days while causing misery across a large portion of N. America east of the Rockies (Fig. 13.11). Many more weather maps showing characteristics of this cyclone are given in this chapter.

Storm Data

• **20 Feb 94** – Heavy rains (15 cm) cause flooding in south Texas.

• **21 Feb** – Thunderstorms and heavy rain continue in north Texas and southern Oklahoma, with 2 cm diameter hail, an F0 tornado (see Fujita scale in the Thunderstorm chapters), and straight-line winds gusting to 25 m/s. Heavy snow begins in the Colorado Rockies.

• **22 Feb** – Thunderstorms continue in Texas and Oklahoma, with more hail (most 2 cm diameter, but some 5 cm). Lightning starts some fires, and heavy rains cause flash floods that wash out highways and close bridges.

Snow ends in the mountains of Colorado, leaving up to 38 cm of new snow on the ground. Elsewhere, snow and heavy snow fall all day, leaving 20 cm accumulation in Kansas, and 25 cm in Nebraska, causing schools to close early. Heavy snow starts in South Dakota, Iowa, N. Missouri, and Illinois.

Snow mixed with freezing rain begins in southern Missouri, leaving an ice glaze 3.5 cm thick. Snow starts in Ohio, dropping 15 cm, followed by a little freezing rain and gusts to 12 m/s.

• **23 Feb** – Thunderstorms continue in Texas with gusts up to 22 m/s, rolling a mobile home. An F1 tornado damages barns, mobile homes, and an aircraft hangar. Hail 4.5 cm in diameter falls in Texas.

Winds of 38 m/s are reported in ski areas near and east of the continental divide in the Colorado Rockies.

Heavy snow continues in Nebraska (35 cm), South Dakota (30 cm), Kansas (26 cm), Missouri (25 cm), and Illinois (23 cm at O'Hare airport in Chicago, with strong winds and drifting snow). Heavy snow starts in North Dakota.

Thundersnow in Iowa accumulates at a rate of 9 cm/h near Des Moines and Waterloo. A band of convective snow showers leaves up to 28 cm in a 3 h period as it sweeps across N.E. Iowa. Winds of 17 m/s reduce visibilities to 0.1 km, cause drifts up to 1.5 m, resulting in power outages and many closed roads. A dry airmass advects into extreme S.E. Iowa.

Thunderstorm straight-line winds and an F0 tornado damage numerous buildings in Alabama and Ohio. Heavy rains cause flash floods in Tennessee, which wash out bridges and cars, and require evacuation of 5 families.

Heavy wet snow spreads through more of the midwest, starting in SE. Minnesota (23 cm) and S. Wisconsin (40 cm, with 18 m/s winds, whiteout conditions in blowing snow, numerous accidents, schools closed). In Michigan, 33 cm of new snow with winds gusting to 22 m/s cause near blizzard conditions (schools closed in 12 counties).

Heavy snow and freezing rain spreads into New England, including Maine, New Hampshire, Vermont, Massachusetts, New York, and New Jersey.

• **24 Feb** – Mountain downslope winds increase in Colorado, with gusts up to 48 m/s at the National Center for Atmospheric Research in Boulder. A roof blows off a community college in Lakewood, CO, causing evacuation of 1500 people.

Blizzard conditions with heavy snow occurs in North Dakota (23 cm new snow, with gusts to 20 m/s). Near blizzard conditions are in South Dakota as snowfall ends there.

Michigan reports 34 cm total snow, with drifts up to 1 m. A 25-car pileup involves a fully-loaded gasoline tanker on interstate 96, resulting in one death. Heavy snow ends in Wisconsin.

Heavy rains and flash floods end in Tennessee.

Heavy snow and ice storms continue in New England, enhanced by the new cyclone moving up the East Coast. Many states are hit: Maine (38 cm snow in NW., but more freezing rain in SE.), New Hampshire (28 cm), Vermont (45 cm snow, with sleet and freezing rain mixed in S.), Massachusetts (20 cm snow, with sleet and freezing rain along E. coast),

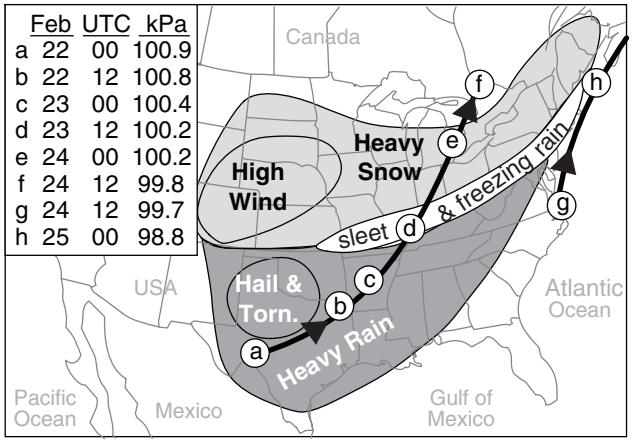

Figure 13.11
Track (thick black line) of the case-study cyclone (a-f), its weather, and central-pressure evolution during Feb 1994. The old cyclone at f merges into a new cyclone at g, which moves to h.

and New York (55 cm snow, with ice storms near coast causing downed power lines).

• **25 Feb** – Strong winds cause a blizzard in N. Illinois, with an additional 15 cm new snow, gusts to 17 m/s, whiteout conditions, dangerous wind chill, and schools closed. Heavy snow in Indiana leaves 25 cm in places.

The "Alberta Clipper" cyclone sweeps across the Plains States, causing a ground blizzard (gusts to 22 m/s with 10 cm new snow), dangerous wind chills, and a convective snow shower of 85 dBZ observed by a WSR-88D radar. Blowing of old snow causes drifts up to 3 m. Strong gusts occur in Kansas and North Dakota. Snow starts again in Wisconsin, with 25 cm new snow, with additional lake-effect snow near Great Lakes. Heavy snow falls in Ohio.

Heavy snow changes to sleet and freezing rain, and ends in New Hampshire, Vermont, New York.

• **26 Feb** – Blizzard ends in N. Illinois with peak gusts 30 m/s, closing 4 interstate highways and leaving hundreds of stranded cars. Similar conditions in N. Indiana, with blowing and drifting snow, whiteout conditions, gusts to 25 m/s, and drifts to 1 m, leave 1400 stranded motorists. A snow emergency declared in 8 counties. In N. Ohio is 15 cm of new snow, gusts to 20 m/s, and convective snowfall rates of 5 cm/h. Heavy snow ends in S. New York, leaving up to 23 cm of new snow.

Next, we will study the characteristics of the cyclone at 12 UTC on 23 Feb 1994 — a time near its peak intensity. A stack of charts at different isobaric surfaces are presented, each valid at the same time. Taken together, these weather maps give us an understanding of the 3-D structure of the storm.

FOCUS • Isosurfaces & Their Utility

Lows and other synoptic features are five-dimensional beasts (3-D spatial structure + 1-D time evolution + 1-D multiple variables). To accurately analyze and forecast the weather, you should try to form in your mind a multi-dimensional picture of the weather. Although some computer-graphics packages can display 5-dimensional data, most of the time we are stuck with flat 2-D weather maps.

Thus, to examine the inner workings of cyclones, look at 2-D atmospheric slices (Fig. c) in the horizontal, vertical, or along special curved surfaces called iso-surfaces. In this way you can study a two-dimensional dissection of these beasts, which often reveals insights into their higher-dimensional physics.

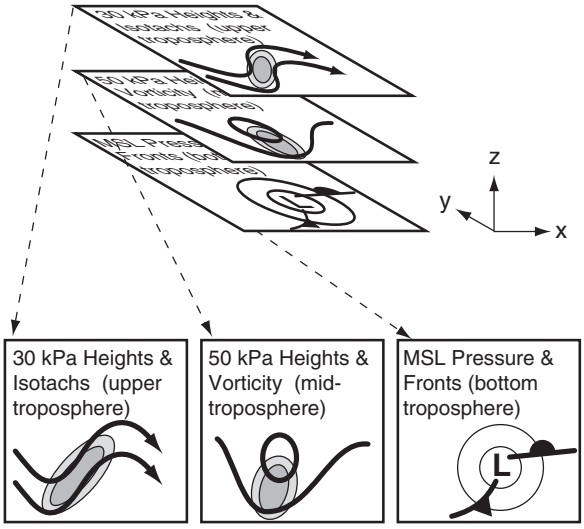

Figure c
A set of weather maps for different altitudes helps you gain a 3-D perspective of the weather. MSL = mean sea level.

Different iso-surfaces have different advantages, as discussed in this Focus Box. See Table 1-6 of Chapter 1 for a comprehensive list of iso-surface names.

Height

The only constant height surface used regularly is the surface at **mean sea level** (**MSL**). Weather maps analyzed on this surface are somewhat fictitious, because sea-level is underground virtually everywhere except at the oceans. (A few land-surface locations are below sea level, such as Death Valley and the Salton Sea USA, or the Dead Sea in Israel and Jordan). Nevertheless, this MSL surface is used to represent the weather where people live. It also represents the bottom boundary on the atmosphere.

A frequently plotted map is MSL pressure with surface fronts.

(continues in next column)

FOCUS • Isosurfaces *(continuation)*

Pressure

Isobaric (equal pressure) surfaces must be identified by their pressure. Commonly-used isobaric charts include the: 95 kPa surface, 85 kPa surface, 70 kPa surface, 50 kPa surface, 30 kPa surface, and 20 kPa surface. Because atmospheric pressure monotonically decreases with height, we know that the 20 kPa surface is at higher altitude than the 50 kPa surface, and so forth.

In mountainous regions such as the Rocky mountains, the 95 kPa and 85 kPa surfaces do not exist because they would be below ground. These surfaces are not usually plotted in that region (unless data is extrapolated to a hypothetical isobaric surface below ground).

On an isobaric chart, we can plot various weather elements (anything except pressure). For example, we can plot temperatures observed on the 50 kPa surface. We could draw lines of equal temperature (isotherms) along this isobaric surface. The meteorological jargon for such an analysis is a chart of "50 kPa isotherms".

An analysis of heights-above-sea-level along a 50 kPa isobaric surface is called a chart of "50 kPa heights". Similarly, we could look at "85 kPa isohumes", "20 kPa isotachs", "50 kPa absolute vorticity", or any other combination of our choosing.

Although confusing at first, sometimes two different weather maps are plotted on the same chart. This is done to illustrate physical relationships between both fields of data. An example is a chart of 50 kPa heights and isotherms. Such a chart tells us about temperature advection by the wind.

Sometimes the two superimposed charts are not on the same atmospheric surface, such as sea-level pressure (a constant height chart) and 95 kPa isotherms (a constant pressure chart). By using perhaps solid lines for isobars and dashed lines for isotherms, the result is hopefully not too cluttered.

Thickness

Often a map of height-thickness between pressures of 100 kPa and 50 kPa is analyzed. Greater thickness corresponds to warmer temperature, according to the hypsometric equation. In meteorological jargon, this map would be called the "100-50 kPa thickness" chart.

Horizontal temperature gradients cause horizontal thickness gradients. The **thermal wind** flows parallel to thickness lines, with low thickness (cold air) to the left of the thermal wind vector in the Northern Hemisphere. Recall that the thermal wind indicates how the geostrophic wind changes with height. Thermal-wind advection of geostrophic vorticity is important for cyclogenesis, as will be explained later in this chapter.

(continues on next page)

FOCUS • Isosurfaces (continued)

Potential Temperature

An **isentropic** surface connects points of equal potential temperature. Such a surface curves up and down. For example, the global average surface temperature decreases from equator to pole, and the average potential temperature increases with altitude in the troposphere. These two effects cause isentropic surfaces to slope downward toward the equator, on average. Any snapshot of an isentropic surface can differ from the average, particularly near fronts.

Isentropic surfaces are identified by their temperature, usually in Kelvin. An example is the "300 K isentropic surface", which is close to sea level near the equator, but rises to 4 to 8 km near the poles. The "350 K isentropic surface" is at a higher altitude, mostly in the stratosphere. Again, we can plot other weather elements on such a surface, such as 300 K heights or isohumes.

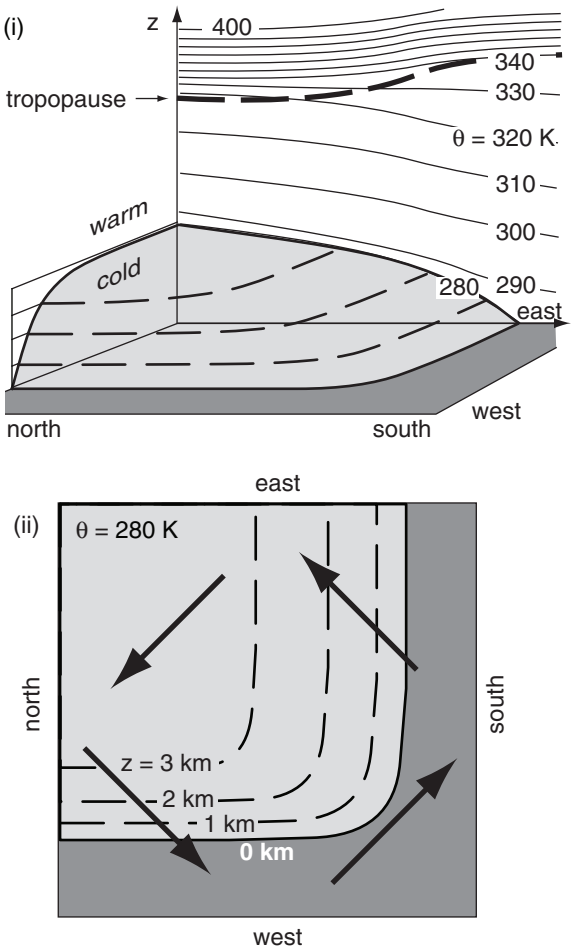

Figure d

Isentropic surface. (i) Three-dimensional sketch of the 280 K isentropic surface, corresponding to Fig. 5.20. (ii) Vertical view of the same scene. This is an isentropic chart. Dashed lines are height contours of the 280 K isentropic surface, and vectors are wind directions along that surface.

(continues in next column)

FOCUS • Isosurfaces (continued)

Isentropic surfaces cannot cross other isentropic surfaces. They can intersect the ground.

Isentropic surfaces are used because air parcels follow them when blown by the wind, under adiabatic conditions (see Figs. 5.20 and 12.13). Diabatic processes such as radiation, turbulence, and condensation can warm or cool the parcel, and cause it to change (jump) to a different isentropic surface.

Fig. d sketches an idealized isentropic surface corresponding to the 280 K isentrope of Fig. 5.20. Fig. d(i) is a 3-D representation, where there is a cold dome of air in the north-east. This could be the cold air behind a cold front. The 280 K surface slopes upward to the north-east. The dashed lines on this figure represent height contours of the isentropic surface above mean sea level.

A vertical view of the same scene is shown in Fig. d(ii). This is an **isentropic chart**. Height contours are shown again as dashed lines. Other variables could also be shown on the isentropic surface, such as temperature, humidity, wind, vorticity, etc.

This figure shows wind vectors on the isentropic surface, for the idealized case of circulation around a low-center in the N. Hemisphere. Because air parcels tend to follow isentropic surfaces as they advect, the wind vector in the upper-right portion of Fig. d(ii) implies that air parcels are rising as they blow toward the higher height contours. From such rising, we would expect adiabatic cooling and clouds to form in that region.

At the lower left side of this figure, air is blowing down the isentropic surface toward lower altitudes, in this hypothetical circulation. Descending air parcels warm adiabatically, and become cloud free.

Potential Vorticity (PVU)

The 1.5 PVU isentropic-potential-vorticity surface can be plotted as a marker for the tropopause. It often is found at high altitude (15 to 18 km) near the equator, and lower altitude (6 km) near the poles. These surfaces can fold back on themselves, such as near fronts. Vertical cross sections of PVU can show intrusions of stratospheric air into the troposphere near fronts – the tropopause folding that was discussed in Fig. 12.34. Another example of such a fold is shown in Fig. 13.19a later in this chapter for the synoptic-storm case study.

Surface

The "**surface weather map**" shows weather at the elevation of the Earth's surface. Namely, it follows the terrain up and down, and is not necessarily at mean sea level.

Surface Charts

Although the cyclone central pressure at southern Illinois is not very low in an absolute sense (Fig. 13.12a), it is quite low relative to the neighboring intense highs. The strong pressure gradient between high and low is sufficient to drive very strong winds (Fig. 13.12e; and storm data given earlier).

Quite a large surface temperature change exists across the frontal zone (Fig. 13.12b). Cold air ($\theta \leq 0°C$) is advecting from the north behind the low, while warm air ($\theta \approx 20°C$) is advecting from the south ahead of the low.

The cold air (see the 0°C isentrope) is dammed-up against the Rockies, causing the western part of the front to become stationary. The Appalachian mountains also slow the northward march of the warm front, resulting in some frontal kinks east of the low center. Humid air (high dew-point temperatures) are in the southeast (Fig. 13.12c), with drier air north.

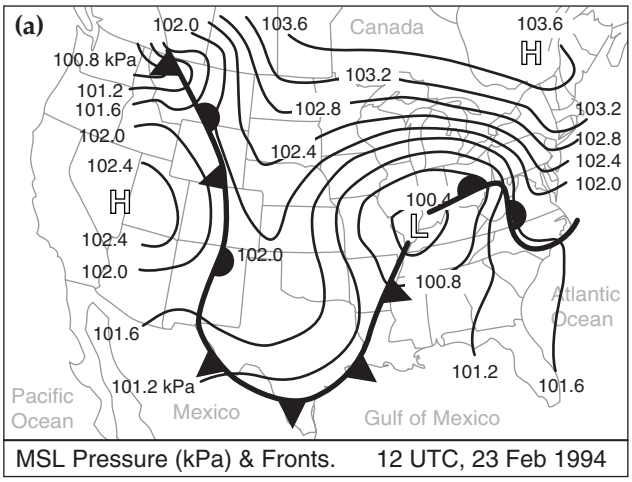

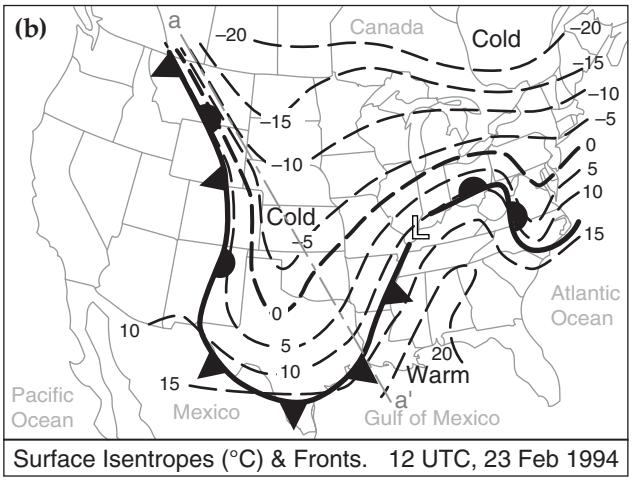

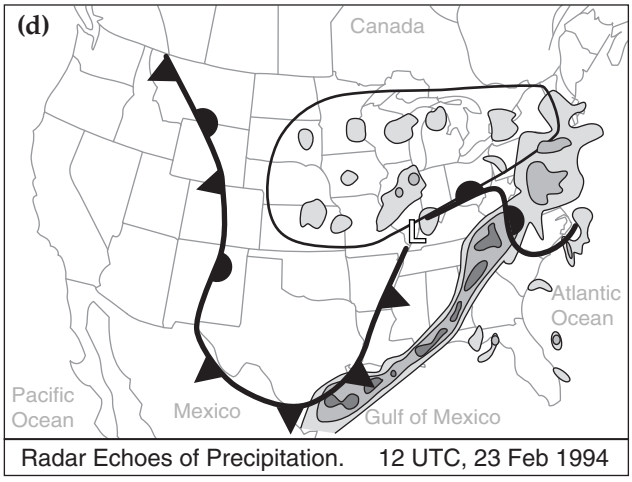

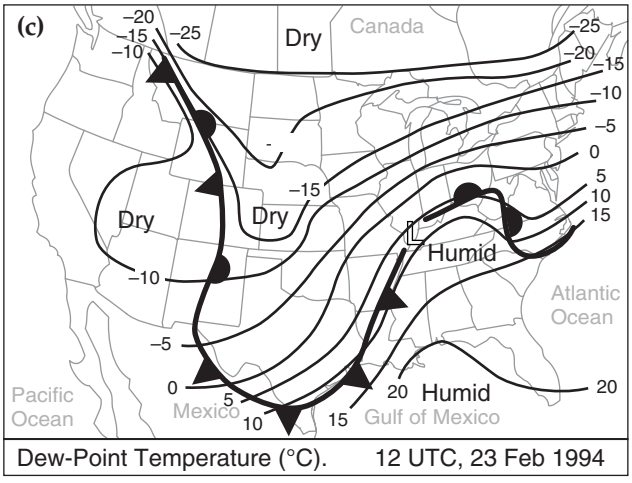

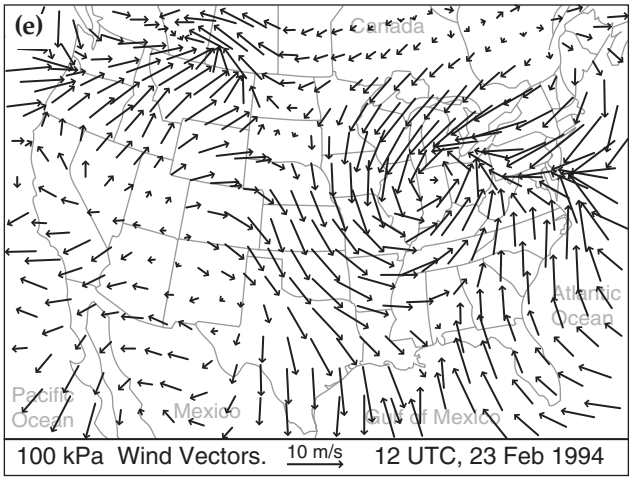

Figure 13.12

Surface weather maps. (a) Mean sea level pressure (P, kPa), & surface fronts. (b) Surface isentropes (θ, °C) & fronts. (c) Humidity (Td, °C) & fronts. (d): Radar echoes of precipitation & fronts. Levels: 1 - light precip. (light gray); 3 - heavy precip. (medium gray); 5 - intense precip. (dark). Black line in (d) encircles snow. (e) Near-surface (100 kPa) wind vectors. [Analysis by Jon Martin.]

85 kPa Charts

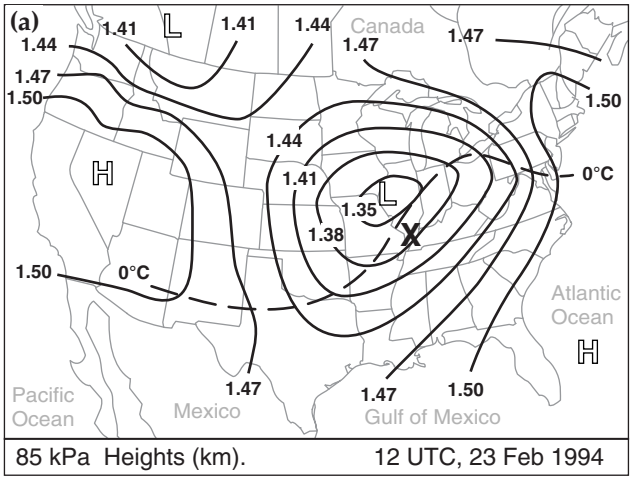

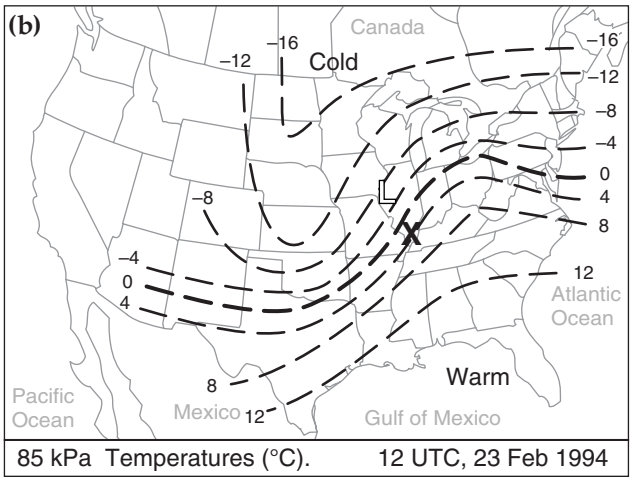

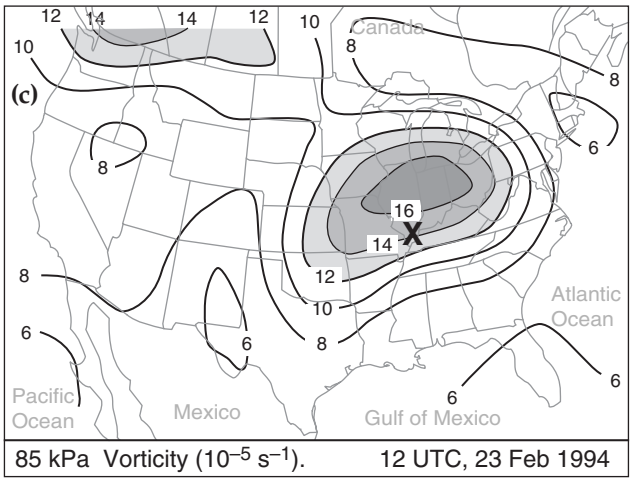

Figure 13.13
85 kPa weather maps. (a) Geopotential height (km). (b) Temperature (°C). (c) Absolute vorticity (10^{-5} s^{-1}). X marks the surface low. [Courtesy of Jon Martin.]

70 kPa Charts

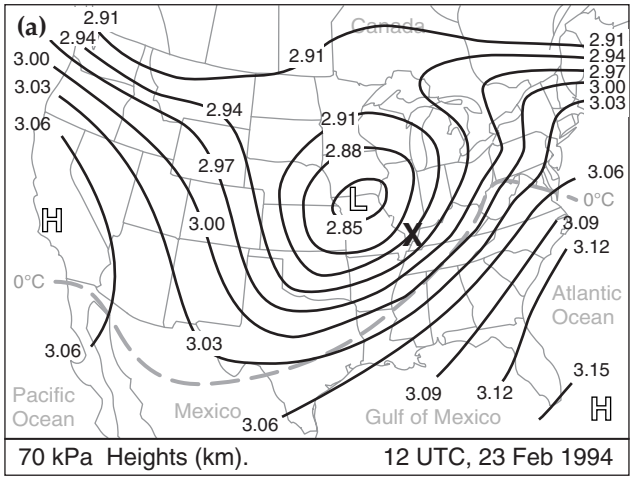

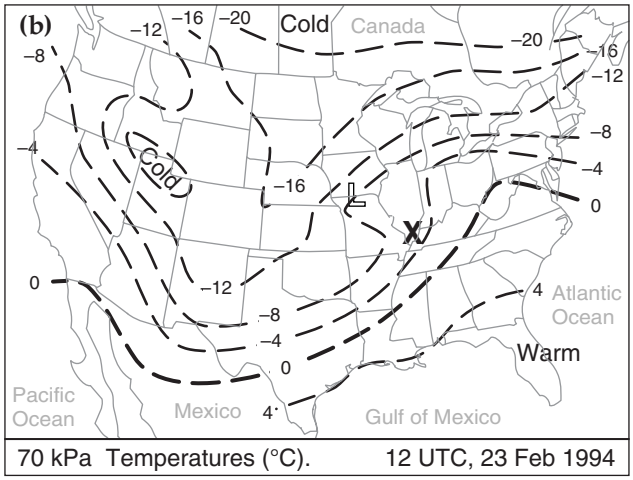

Figure 13.14
70 kPa weather maps. (a) Geopotential heights (km). (b) Temperature (°C). X marks surface low. [Courtesy of Jon Martin.]

100 - 50 kPa Thickness

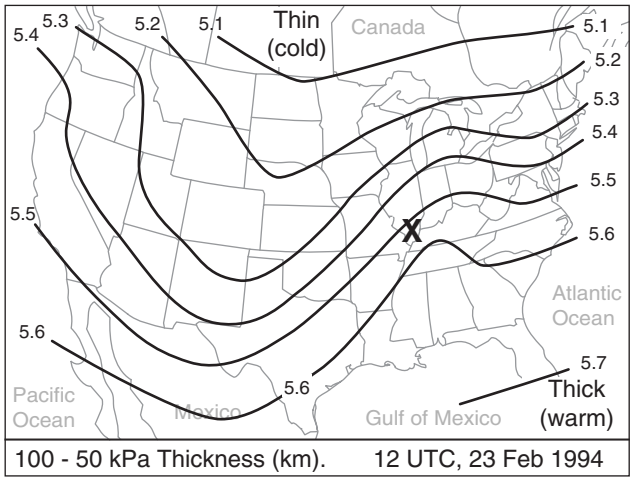

Figure 13.15
100–50 kPa thickness (km), from a 24 h forecast of the NWS NGM, valid at 12 UTC on 23 Feb 94. X marks surface low.

50 kPa Charts

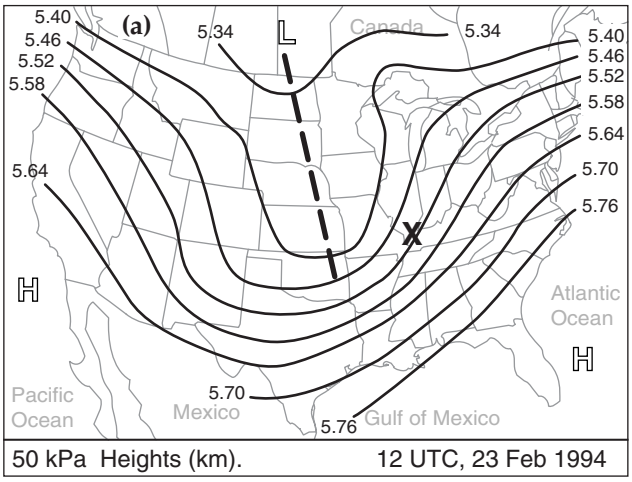

50 kPa Heights (km). 12 UTC, 23 Feb 1994

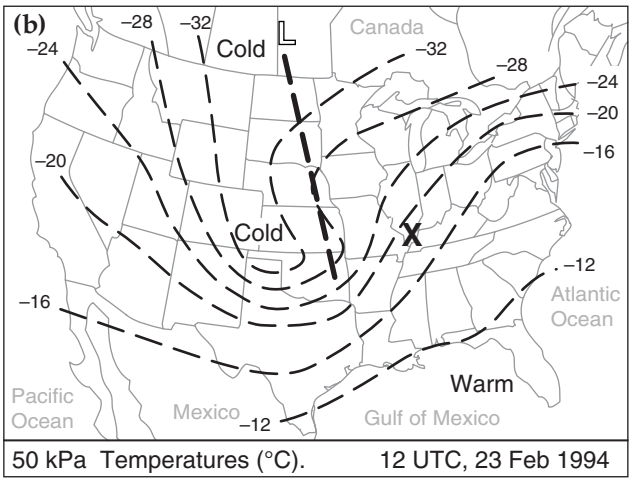

50 kPa Temperatures (°C). 12 UTC, 23 Feb 1994

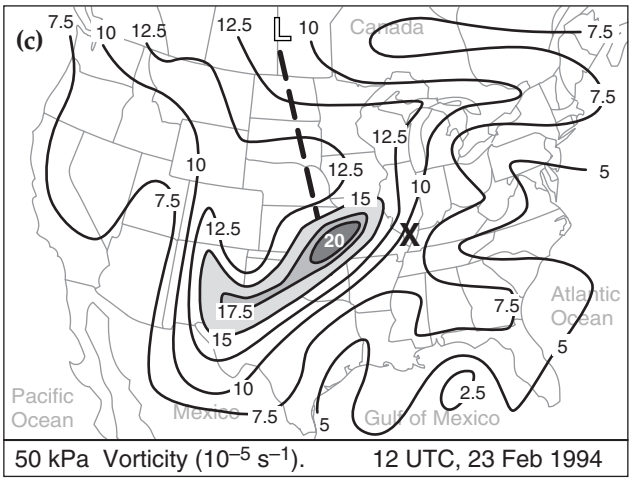

50 kPa Vorticity (10^{-5} s^{-1}). 12 UTC, 23 Feb 1994

20 kPa Charts

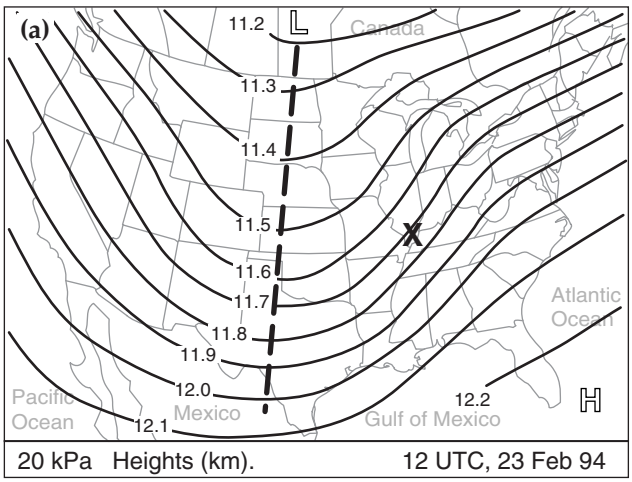

20 kPa Heights (km). 12 UTC, 23 Feb 94

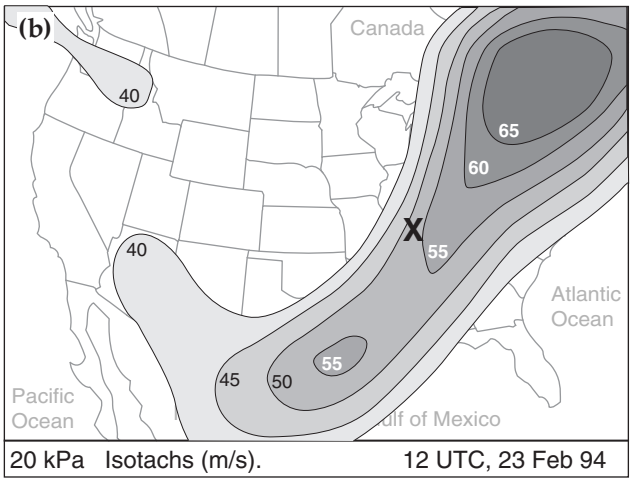

20 kPa Isotachs (m/s). 12 UTC, 23 Feb 94

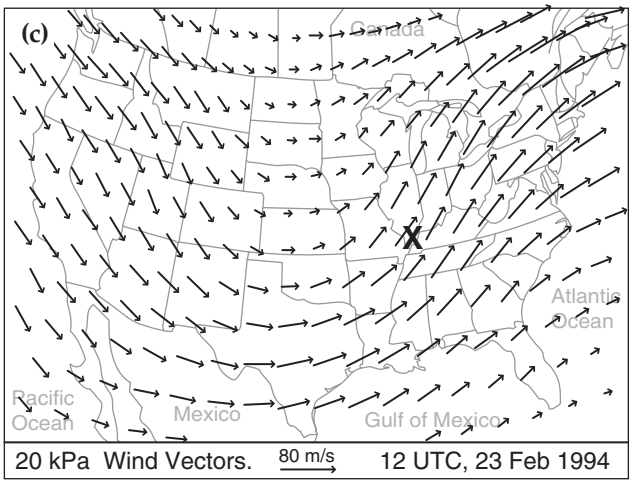

20 kPa Wind Vectors. 12 UTC, 23 Feb 1994

Figure 13.16
50 kPa weather maps. (a) Geopotential heights (km). (b) Temperature (°C). (c) Absolute vorticity (10^{-5} s^{-1}). Thick dashed line is trough axis. X marks the surface low. [courtesy of Jon Martin.]

Figure 13.17
20 kPa weather maps. (a) Geopotential heights (km). (b) Isotachs (m/s). (c) Wind vectors. X marks the surface low. [courtesy of Jon Martin.]

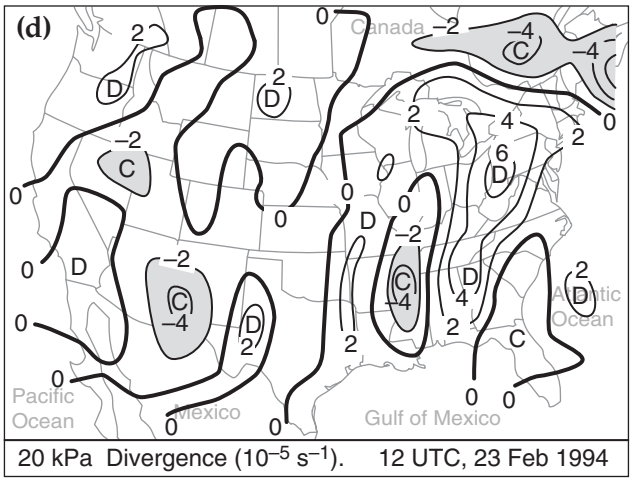

Figure 13.17 *(continued)*
(d) 20 kPa Horizontal divergence (10^{-5} s^{-1}) at the top of the troposphere. D = divergence, C = convergence.

Isentropic Charts

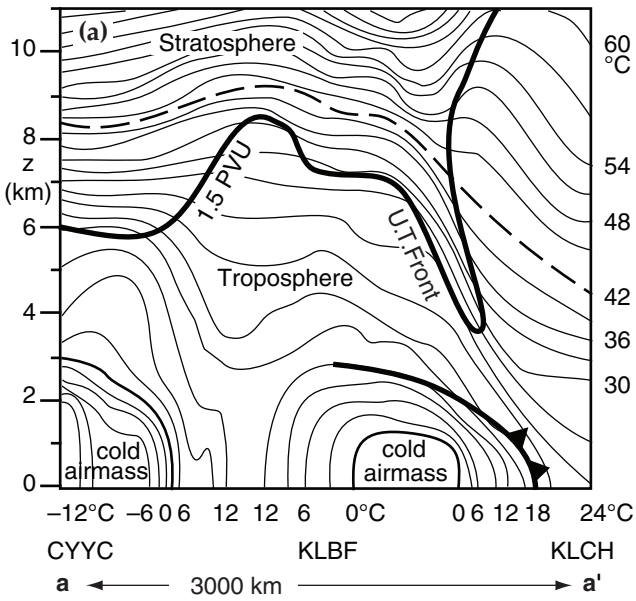

20 kPa Hemispheric Chart

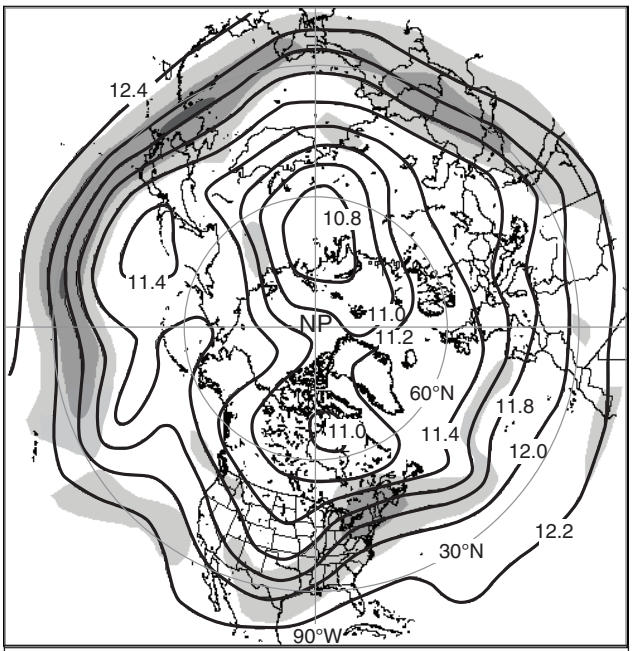

Figure 13.18
20 kPa Northern hemispheric chart centered on the North Pole (NP). Solid lines show geopotential heights, and shading shows isotachs. Light shading has winds ≥ 40 m/s; medium shading has winds ≥ 60 m/s; and dark shading has winds ≥ 80 m/s. Shading highlights the jet stream. [Adapted from NCEP Reanalysis Plotter output, courtesy of Christopher Godfrey, the University of Oklahoma School of Meteorology. Data is from the National Centers for Environmental Prediction/National Center for Atmospheric Research 40-Year Reanalysis Project.]

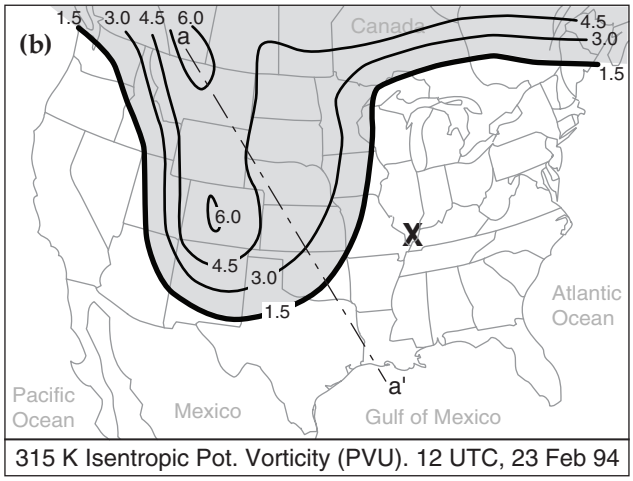

Figure 13.19
(a) Vertical cross section from northwest (CYYC = Calgary, Alberta) through the central USA (KLBF = North Platte, Nebraska) to the southeast (KLCH = Lake Charles, Louisiana). Thin lines are isentropes (θ, °C), labeled at right and bottom. Thick solid line in top half of Fig. is the 1.5 potential vorticity unit (PVU) contour, which indicates the tropopause. Cold-frontal symbols indicate the surface front and frontal inversion top. UT Front indicates upper-tropospheric front. z is height above sea level. Valid 00 UTC 24 Feb 94. [This is 12 h later than the other figs.] (b) Isentropic potential vorticity on the θ = 315 K surface. This surface corresponds to the 42°C dashed line in (a). Shading indicates where the 315 K surface is in the stratosphere. Dash-dot line in (b) shows the cross-section slice in (a). Units are potential vorticity units (PVU), where 1 PVU = 10^{-6} $K{\cdot}m^2{\cdot}s^{-1}{\cdot}kg^{-1}$.

North of the low in the cold air (Fig. 13.12d) is a broad area of light to moderate snow that the radar cannot detect. Imbedded are regions of moderate to heavy snow that the radar can see. Closer to the low, and just east of it where temperatures are near 0°C, sleet and freezing rain are falling.

Well in advance of the cold front in the southeast USA is a squall line of intense thunderstorms. These storms produce heavy rain, hail, and some small tornadoes. The squall line is feeding on latent heat, because of the high humidities near the Gulf of Mexico. The wind field (Fig. 13.12e) shows a strong wind shift near the squall line, suggesting the main dynamic activity is not at the cold front but at the squall line.

85 kPa Charts

Pressure level 85 kPa corresponds to about 1.4 km above sea level. At this height, the low center is over western Illinois (Fig. 13.13a). This is northwest of the surface low. Because winds at this pressure level follow the height contours, expect northerly winds in the Central Plains (Nebraska and Kansas), and southerly winds to the east of the low center.

From Texas to Pennsylvania is a strong baroclinic zone, which is evident by the close spacing between isotherms (Fig. 13.13b). Strong cold-air advection exists in Oklahoma, Texas, Arkansas, and Missouri. This is marked by the height contours crossing the isotherms, with winds advancing the cold air. Warm-air advection occurs east of the low center. Cyclonic rotation around the low creates a vorticity maximum (**vort max**; shaded in Fig. 13.13c) over the midwest.

70 kPa Charts

Pressure level 70 kPa is roughly 3 km above sea level. At this height, the low is centered over northern Missouri (Fig. 13.14a) — significantly northwest of the surface low. The tightly packed height contours from Arkansas through West Virginia suggest a strong southwesterly wind in that region.

Cold-air advection is occurring in Oklahoma, Texas, and New Mexico (Fig. 13.14b). Subsidence and clearing skies are expected in regions of cold-air advection aloft. Warm-air advection is associated with ascending air, clouds, and precipitation, such as over and east of the Great Lakes.

100–50 kPa Thickness Chart

The cold air pushing into the central plains of the USA from Canada has small 100–50 kPa thickness (Fig. 13.15), as expected from the hypsometric equation. A thermal wind parallel to the thickness lines would create a jet stream that dips south toward Texas and then NE. toward Ohio, as is indeed observed.

50 kPa Charts

With nearly equal amount of air mass above and below it, the 50 kPa pressure level is near the mass-weighted middle of the atmosphere. It is roughly 5.5 km above sea level at mid-latitudes.

Instead of a closed low center as in the charts for lower altitudes, the 50 kPa chart shows a trough of low pressure (Fig. 13.16a) through the central plains. This trough axis (heavy dashed line in the figure) is much further west of the surface low. The trough is a portion of the Rossby wave, such as discussed in the Global Circulation chapter.

The region of cold air (Fig. 13.16b) is west of the trough. Hence, you can expect self-development to occur (explained later in this chapter), with strengthening of the wave amplitude.

Fig. 13.16c shows absolute vorticity on the 50 kPa pressure surface. The vorticity maximum (**vort max**) is often at, or just behind, the low center. Winds advect the vort max (**positive vorticity advection**), thereby supporting propagation of the low. This vorticity map is from a 24 h forecast of the U.S. National Weather Service (NWS) Nested Grid Model (NGM), valid at 12 UTC on 23 Feb 94.

20 kPa Charts

The 20 kPa pressure level is roughly at 11.5 km above sea level. In Fig. 13.17a, the trough over central North America is quite evident.

The wind-speed chart (Fig. 13.17b) shows a jet stream from the desert southwest USA through Texas and then northeast over the Great Lakes toward Nova Scotia, Canada. A **jet streak** (relative maximum of wind speed) is over the northeast portion of the figure. Horizontal divergence aloft (Fig. 13.17d) favors cyclone development at the surface near Lake Ontario, near the left entrance region to this jet streak. Such development indeed occurred, as indicated by the storm track of Figs. 13.10 & 13.11.

Winds are nearly geostrophic, as suggested by the fact that the wind vectors in Fig. 13.17c are roughly parallel to the height contours of Fig. 13.17a.

A hemispheric chart at the 20 kPa level is plotted in Fig. 13.18. Superimposed are heights and isotachs. From this N. Hemispheric perspective, you can see that the trough over the USA is part of a global Rossby-wave pattern between about 30° and 50°N latitude around the North Pole. The trough axis at roughly 100°W longitude over the USA is one of about 7 jet-stream troughs in the hemisphere.

Some high-latitude countries use 30 kPa charts instead of 20 kPa, because of the lower tropopause.

Isentropic Charts

Fig. 13.19a shows a **vertical cross section** from northwest to southeast, across North America (along section line **a – a'** in Figs. 13.12b and 13.19b). Plotted are isentropes (equal potential temperature), and a single contour of isentropic potential vorticity.

The cold air mass is evident in Kansas (to the right of KLBF in this plot). The surface front is just northwest of Lake Charles, Louisiana (KLCH), as indicated by the tight packing of the isentropes near the surface.

The 1.5 PVU line marks the tropopause. Above this line, the isentropes are more closely spaced, indicating the greater static stability in the stratosphere.

Between North Platte and Lake Charles is a **tropopause fold**, as indicated by the 1.5 PVU line dipping down from the stratosphere. An upper-level front is evident in this region, based on the close spacing between isentropes.

Fig. 13.19b is a plot of isentropic potential vorticity on the θ = 315 K (= 42°C) isentropic surface. This surface corresponds to the dashed line in Fig. 13.19a. Shading shows where this surface is in the stratosphere, by the values of isentropic potential vorticity that are greater than 1.5 PVU there. The troposphere is shallower near the poles than near the equator. Thus, the 315 K isentropic surface is usually in the stratosphere near the pole (as suggested by the widespread shading at high latitudes in Fig. 13.19b), and in the troposphere near the equator.

In the next sections, we see how dynamics can be used to explain cyclone formation and evolution.

LEE CYCLOGENESIS

Waves in the upper-air (jet-stream) flow can create mid-latitude cyclones at the surface, as sketched in Figs. 13.6 and 13.7. Rossby showed in 1939 that evolution of planetary waves (i.e., **Rossby waves**) can be described by conservation of absolute vorticity, as was discussed in the Global Circulation chapter. One way to create Rossby waves is by topographic modification of the flow, as is described next.

Stationary Planetary Waves

When air flows across a mountain range such as the Rocky Mountains (Fig. 13.20a), planetary-scale Rossby waves that meander north and south are triggered in the atmosphere (Fig. 13.20b). These Rossby waves are stationary relative to the ground. Otherwise, they behave like the barotropic and baroclinic

FOCUS • Multi-field Charts

Most of the weather maps presented in the previous case study contained plots of only one field, such as the wind field or height field. Because many fields are related to each other or work together, meteorologists often plot multiple fields on the same chart.

To help you discriminate between the different fields, they are usually plotted differently. One might use solid lines and the other dashed. Or one might be contoured and the other shaded (see Fig. e or Fig. 13.7a). Look for a legend or caption that describes which lines go with which fields, and gives units.

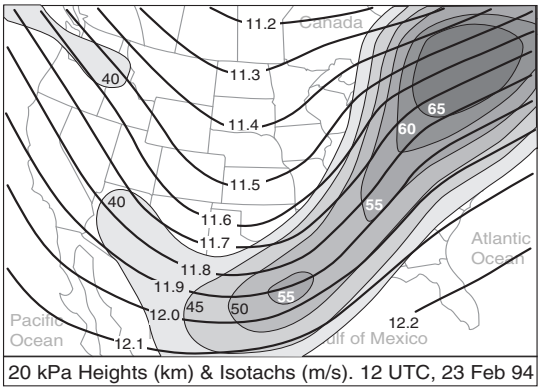

Fig. e.
Geopotential heights (lines) and wind speed (shaded).

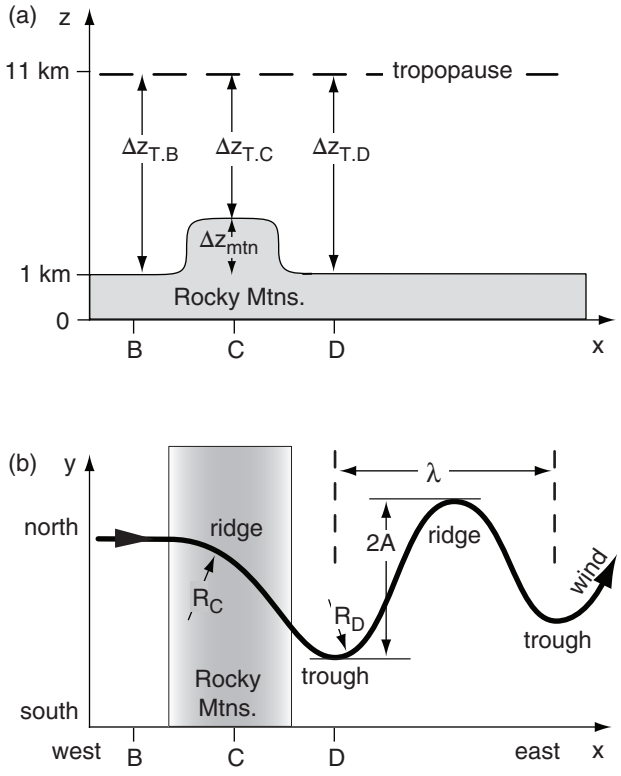

Figure 13.20
Cyclogenesis to the lee of the mountains. (a) Vertical cross section. (b) Map of jet-stream flow. "Ridge" and "trough" refer to the wind, not the topography.

FOCUS • Synoptics

Synoptic meteorology is the study and analysis of weather maps, often with the aim to forecast the weather on horizontal scales of 400 to 4000 km. **Synoptic weather maps** give a snapshot of atmospheric conditions over a large area, as created from weather observations made simultaneously.

Typical weather phenomena at these **synoptic scales** include cyclones (Lows), anticyclones (Highs), and airmasses. Fronts are also included in synoptics because of their length, even though frontal zones are so narrow that they can also be classified as mesoscale. See Table 10-6 and Fig. 10.24 in the Dynamics chapter for a list of different atmospheric scales.

The material in this chapter and in the previous one fall solidly in the field of **synoptics**. People who specialize in synoptic meteorology are called **synopticians**.

The word "synoptics" is from the Greek "synoptikos", and literally means "seeing everything together". It is the big picture.

Solved Example

For wind blowing 16.2 m/s over a 1 km-high mountain range at 45°N, find the wavelength and amplitude of the lee planetary wave. Assume the tropospheric depth is 10 km upstream of the mountains.

Solution

Given: $\phi = 45°N$, $M = 16.2$ m/s, $\Delta z_{mtn} = 1$ km, $\Delta z_T = 10$ km.

Find: $\lambda = ?$ km, $A = ?$ km

First, find β at 45°N, using eq. (13.2):

$\beta = (2.294\text{x}10^{-11}\ \text{m}^{-1}\cdot\text{s}^{-1}) \cdot \cos(45°)$
$= 1.62\text{x}10^{-11}\ \text{m}^{-1}\cdot\text{s}^{-1}$

Next, use eq. (13.1):

$$\lambda \approx 2\cdot\pi\cdot\left[\frac{16.2\text{m}\cdot\text{s}^{-1}}{1.62\times10^{-11}\text{m}^{-1}\cdot\text{s}^{-1}}\right]^{1/2} = \underline{\textbf{6283 km}}$$

Use eq. (13.4):

A = [(1 km) / (10 km)] · (6371 km) = **637 km**

Check: Units OK. Physics OK.

Discussion: The circumference of the 45° meridian is $2\cdot\pi\cdot R_{Earth}\cdot\cos(45°) = 28{,}306$ km. Thus, about 4.5 wavelengths fit round the Earth – it is indeed a planetary-scale wave. Also, the north-south meander of the wave spans $2\cdot A \approx 11°$ latitude.

waves in the global circulation, discussed in the Global Circulation chapter. The north-south (meridional) component of wave-amplitude often decays to the east of the mountains, as boundary-layer turbulence and deep convection cause damping.

At the parts of the wave furthest from the equator, the air is turning anticyclonically (clockwise in the Northern Hemisphere). Hence, over the mountains (location *C* in Fig. 13.20b), one would generally expect to find a predominance of highs.

Just east of the mountain range, a trough forms (location *D* in Fig. 13.20b). This location is to the **lee** (downwind) of the mountains. East of that trough, upper-air divergence can favor **lee cyclogenesis** at the surface.

The dominant wavelength λ of these upper-atmosphere waves is approximately

$$\lambda \approx 2\cdot\pi\cdot\left[\frac{M}{\beta}\right]^{1/2} \qquad (13.1)$$

where M is the average wind speed. As you have seen in an earlier chapter, the rate β of increase of the Coriolis parameter f_c with distance north is:

$$\beta = \frac{\Delta f_c}{\Delta y} = \frac{2\cdot\Omega}{R_{earth}}\cdot\cos\phi \qquad \bullet(13.2)$$

where $2\cdot\Omega = 1.458\text{x}10^{-4}\ \text{s}^{-1}$ is twice the angular rotation rate of the Earth. β is on the order of 1.5 to $2\text{x}10^{-11}\ \text{m}^{-1}\cdot\text{s}^{-1}$ at mid latitudes.

The north-south amplitude A depends on the height of the mountains Δz_{mtn} relative to the upstream depth of the troposphere Δz_T:

$$A \approx \frac{f_c}{\beta}\cdot\frac{\Delta z_{mtn}}{\Delta z_T} \qquad (13.3)$$

The ratio $f_c/\beta = R_{Earth}\cdot\tan(\phi)$, where $R_{Earth} = 6371$ km is the average Earth radius, and ϕ is latitude. At mid-latitudes where $\tan(\phi) \approx 1$, the amplitude is

$$A \approx \frac{\Delta z_{mtn}}{\Delta z_T}\cdot R_{earth} \qquad (13.4)$$

The north-south distance Δy between crest and trough is $\Delta y = 2\cdot A$.

Thus, wavelength depends on wind speed, but not mountain height. Wave amplitude depends on mountain height, but not wind speed.

Conservation of Potential Vorticity

Another way to examine lee-side creation of Rossby waves is by their vorticity. Neglecting shear and assuming constant wind-speed M for simplicity, eq. (11.25) for potential vorticity ζ_p becomes:

$$\zeta_p = \frac{(M/R) + f_c}{\Delta z} = \text{constant} \qquad \bullet(13.5)$$

which states that potential vorticity is conserved.

Suppose air at point B (Fig. 13.20b), west of the Rockies, blows directly from west to east, and initially has no curvature ($M/R = 0$). Thus, at location B eq. (13.5) reduces to

$$\zeta_p = \frac{f_{c.B}}{\Delta z_{T.B}} \qquad (13.6)$$

where $\Delta z_{T.B}$ is the average depth of troposphere at point B. This initial condition sets the constant value of the potential vorticity for this example.

Let Δz_{mtn} be the relative mountain height above the surrounding land (Fig. 13.20a). As the air blows over the mountain range, the troposphere becomes thinner as it is squeezed between mountain top and the tropopause: $\Delta z_{T.C} = \Delta z_{T.B} - \Delta z_{mtn}$. But the latitude of the air hasn't changed much yet, so $f_{c.C} \approx f_{c.B}$. The previous two equations combine (because $\zeta_{p.B} = \zeta_{p.C}$) to give the anticyclonic radius of curvature over the west portion of the mountains (at location C):

$$R_C = \frac{-M}{f_{c.B} \cdot (\Delta z_{mtn} / \Delta z_{T.B})} \qquad (13.7)$$

Namely, in eq. (13.5), when Δz became smaller while f_c was constant, M/R had to also become smaller to keep the ratio constant. But since M/R was initially zero, the new M/R had to become negative. Negative R means anticyclonic curvature.

As the air moves south, the Coriolis parameter decreases, thereby requiring the radius of anticyclonic curvature to increase (i.e., to become less curved). Eventually, the flow is straight, blowing toward the southeast near the east side of the Rocky Mountains. As the air overshoots south, and as the air column stretches as it leaves the mountains, the curvature must become positive (cyclonic) in order to keep potential vorticity constant. The radius of curvature R_D is similar in magnitude to R_C, but of opposite sign. This is the region where a lee trough would form in the jet stream flow. Cyclogenesis is favored just east of the lee trough.

Solved Example

Suppose a noncurving wind blows from the west at 20 m/s (assume constant), at latitude 40°N. Initially, the tropospheric depth is 10 km. Then, the air flows over the Rocky Mountains, where you can assume a relative terrain depth of 1 km above the neighboring plains. Find the potential vorticity, and the radius of curvature over the mountains.

Solution

Given: $\phi = 40°\text{N}$, $M = 20$ m/s, $R_{initial} = \infty$,
$\Delta z_T = 10$ km, $\Delta z_{mtn} = 1$ km.
Find: $\zeta_p = ?\ \text{m}^{-1}\cdot\text{s}^{-1}$, $R_C = ?$ km

Assume: shear can be neglected.

First, find the Coriolis parameter using eq. (10.16):
$f_c = (1.458\text{x}10^{-4}\ \text{s}^{-1})\cdot\sin(40°) = 9.38\text{x}10^{-5}\ \text{s}^{-1}$

Use eq. (13.6):

$$\zeta_p = \frac{9.38\times10^{-5}\,\text{s}^{-1}}{10\text{km}} = \underline{\mathbf{9.38x10}}^{-9}\ \text{m}^{-1}\,\text{s}^{-1}$$

Use eq.(13.7) to find anticyclonic radius of curvature:

$$R_C = \frac{-(20\text{m/s})}{(9.38\times10^{-5}\,\text{s}^{-1})\cdot(1\text{km}/10\text{km})} = \underline{\mathbf{-2132\ km}}$$

Check: Units OK. Physics OK.
Discussion: We expect $R_D \approx -R_C$, namely about 2000 km. Thus, mountains trigger long-wavelength ridges and troughs. Cyclones are favored east of the Rockies, just east of the first lee trough.

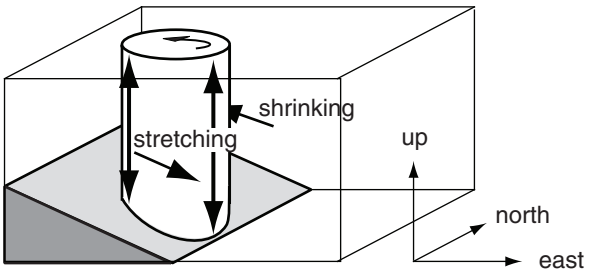

Figure 13.21
Cyclone on the eastern slope of a mountain in N. Hemisphere.

Solved Example

An extratropical cyclone of radius 500 km has potential vorticity of 2×10^{-8} m^{-1}·s^{-1}. It sits on a mountain slope of 1/1000. Find the increase of relative vorticity along the south side of the cyclone in N. Hemisphere.

Solution

Given: R = 500 km, $\zeta_p = 2 \times 10^{-8}$ m^{-1}·s^{-1}, $\alpha = 0.001$
Find: $\Delta\zeta_r$ = ? s^{-1} .
Assumption: Neglect changes of latitude.

Use eq. (13.8):

$$\Delta\zeta_r = 2 \cdot (500{,}000 \text{ m}) \cdot (0.001) \cdot (2 \times 10^{-8} \text{ m}^{-1}\cdot\text{s}^{-1})$$
$$= \underline{\mathbf{2 \times 10}}^{-5} \text{ s}^{-1} .$$

Check: Units OK. Physics OK.
Discussion: This intensification on the cyclone fringe is easily as large as the average relative vorticity within center of the cyclone, resulting in southward cyclone movement toward the region of increasing relative vorticity.

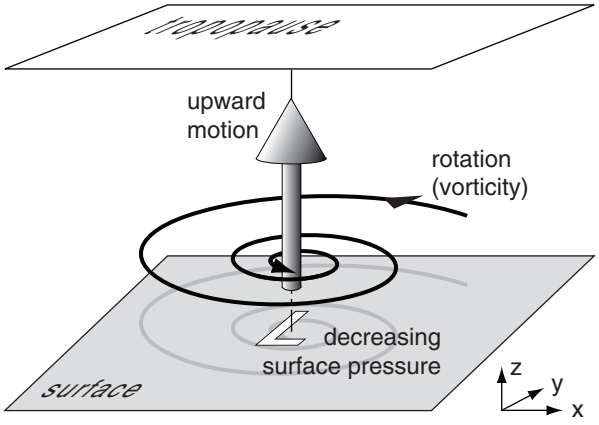

Figure 13.22
Attributes of cyclogenesis. Updrafts remove air molecules from near the ground, which lowers surface pressure. The pressure gradient drives winds, which rotate due to Coriolis force.

Equatorward Propagation Along the Lee Side

Picture a cyclone that already exists at the lee side (i.e., east) of the mountain range (Fig. 13.21). The bottom of this cyclone rests on a sloping surface (slope $\alpha = \Delta z/\Delta x$). Circulation around the low will cause downslope flow on the equatorward side, and upslope on the poleward side.

Rotation about the low will cause vertical columns of air along the equatorward side of the cyclone to stretch. Those on the poleward side shrink. For any potential vorticity ζ_p of the cyclone, stretching intensifies the relative vorticity ζ_r on the equatorward side, according to:

$$\Delta\zeta_r = 2 \cdot R \cdot \alpha \cdot \zeta_p \qquad (13.8)$$

A similar change of opposite sign occurs on the poleward side. This causes the low to propagate equatorward along the eastern side of the mountains, toward the region of greater relative vorticity.

Another way to examine the same process is by the adiabatic warming that occurs at the bottom of the column (on the equatorward side) as it descends down the mountain slope. No warming occurs at the top of the column, because air is not flowing downward there.

This differential heating reduces the overall static stability of the troposphere; namely, $\Delta\theta/\Delta z$ decreases. A decrease of static stability must be accompanied by an increase of relative vorticity, in order to maintain constant isentropic potential vorticity ζ_{IPV} (eq. 11.26). Thus, relative vorticity intensifies on the equatorward side of the cyclone, and decreases on the poleward side. The low tends to propagate equatorward along the eastern side of the mountains, toward the region of greater relative vorticity.

CYCLONE SPIN-UP

Even in the absence of lee effects, baroclinic instability (see the Global Circulation chapter) can cause cyclogenesis. Cyclogenesis is associated with upward motion, decreasing surface pressure, and increasing vorticity. You can gain insight into cyclogenesis by studying all three characteristics, even though they are intimately related (Fig. 13.22). Let us start with vorticity.

Vorticity-increase at low altitudes is one measure of increasing cyclone strength. The equation that forecasts change of vorticity with time is called the **vorticity tendency equation**.

Vorticity Tendency

A forecast equation for relative vorticity ζ_r is:

•(13.9)

$$\frac{\Delta\zeta_r}{\Delta t} = -U\frac{\Delta\zeta_r}{\Delta x} - V\frac{\Delta\zeta_r}{\Delta y} - V\frac{\Delta f_c}{\Delta y} + f_c\frac{\Delta W}{\Delta z}$$

spin-up *horiz. advection* *beta* *stretching*

$$-W\frac{\Delta\zeta_r}{\Delta z} + \zeta_r\frac{\Delta W}{\Delta z} + \frac{\Delta U}{\Delta z}\cdot\frac{\Delta W}{\Delta y} - \frac{\Delta V}{\Delta z}\cdot\frac{\Delta W}{\Delta x} - C_D\frac{M}{z_i}\zeta_r$$

vert.advect. *stretching* *tilting* *turb. drag*

The first term gives the **spin-up** rate of a cyclone, because it indicates the increase of vorticity. This term is also called the **vorticity tendency** term, because it shows how vorticity tends to change with time. A positive tendency corresponds to a strengthening cyclone.

Fig. 13.23 shows a physical interpretation of the other terms. Advection (Fig. 13.23a) changes vorticity by blowing-in air with different vorticity from some other location. **Positive vorticity advection** (**PVA**) occurs when greater vorticity is blown in.

The opposite is **negative vorticity advection** (**NVA**). Advection can work in both horizontal directions and in the vertical direction, although just one horizontal direction is sketched in Fig. 13.23a.

The **beta effect** is named because $\Delta f_c/\Delta y = \beta$ = positive in the N. Hemisphere (see eq. 13.2). If wind moves air northward (i.e., V = positive) to where f_c is larger, then relative vorticity ζ_r becomes smaller (as indicated by the negative sign in front of the beta term) to conserve potential vorticity (Fig. 13.23b).

Stretching has already been discussed in the Global Circulation chapter. As shown in Fig. 13.23c, a short vortex tube will stretch if the top rises faster than the base. This difference in rise is given by $\Delta W/\Delta z$. The two stretching terms account for the Earth's rotation and the relative vorticity.

When such a tube stretches in the vertical, mass conservation requires horizontal convergence (C), which shrinks the tube radius. Because of this convergence/divergence effect, the stretching term is also known as the **divergence term**. Horizontal convergence spins up cyclonic vorticity, and divergence spins up anticyclonic vorticity.

The **tilting term** shows how horizontal vorticity can be tilted into vertical vorticity. For example, Fig. 13.23d shows vorticity associated with the vertical shear of horizontal wind near the ground. The vortex tubes are shown between the U wind vectors. If these tubes were then tilted by a vertical velocity that increases toward the north, then the horizontal vortex tubes would become more vertical, thereby contributing to the vertical vorticity.

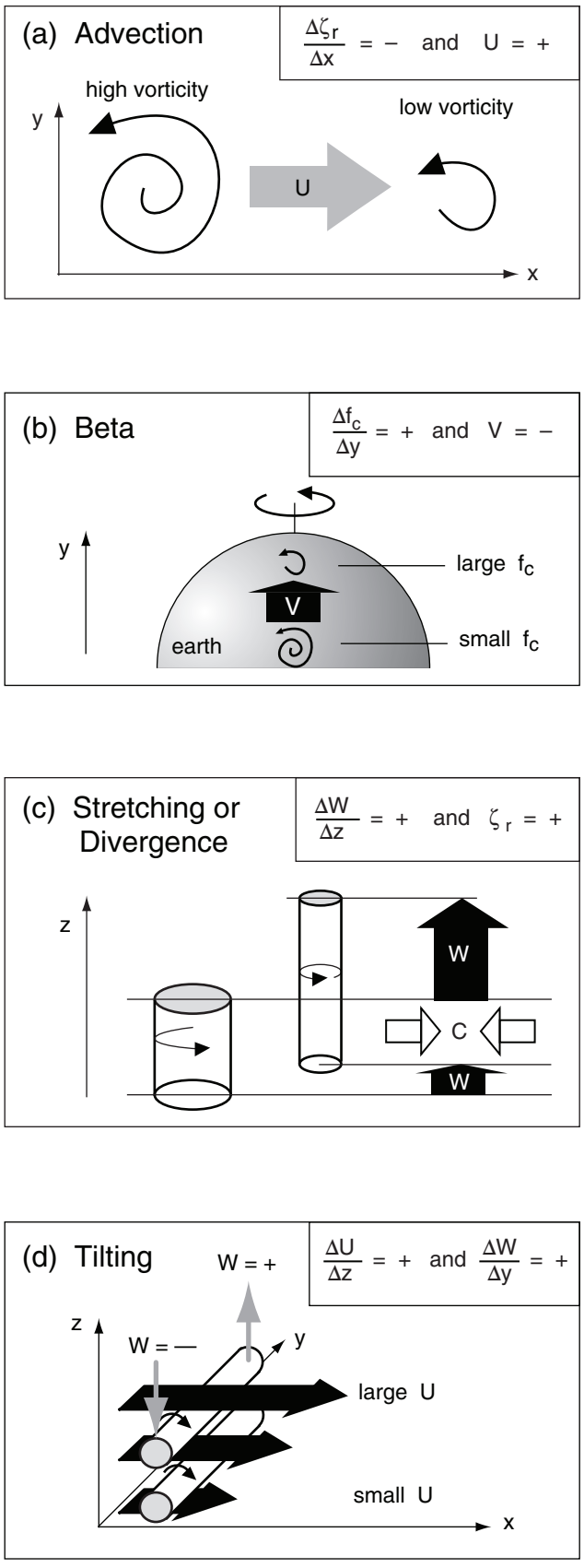

Figure 13.23
Physical interpretation of terms in the vertical vorticity equation (continued next column).

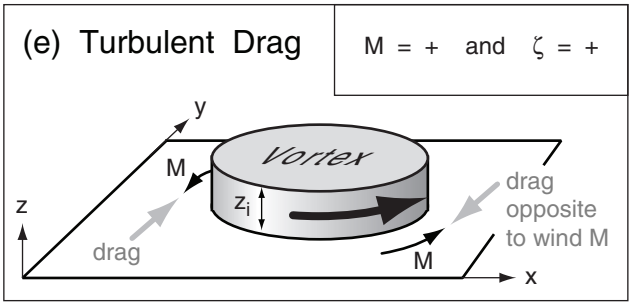

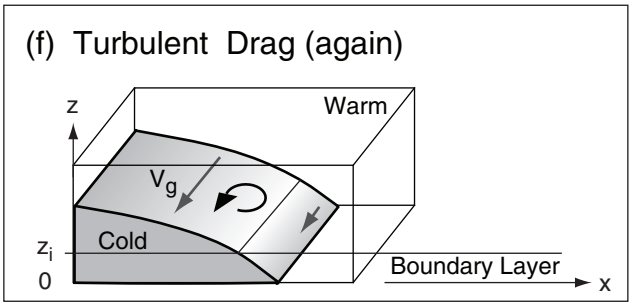

Figure 13.23 *(continuation)*
Physical interpretation of terms in the vertical vorticity equation

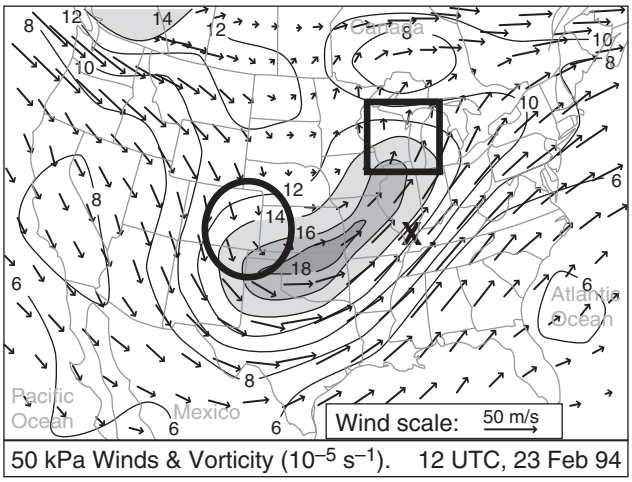

Figure 13.24
Absolute vorticity (shaded) and winds (vectors) at 50 kPa, highlighting regions of positive (square) and negative (oval) vorticity advection for the case-study storm.

Figure 13.25 (at right)
Vertical velocity (m/s) for the case-study storm. At this altitude, a value of w = 0.075 m/s corresponds to ω *= –0.5 Pa/s.*

Finally, the **turbulent-drag** term has two effects. One effect is to reduce rotation regardless of direction, which causes **spin-down** (Fig. 13.23e). This occurs in the turbulent boundary layer (of depth z_i) due to frictional drag against the ground. In the absence of continued spin-up processes, the cyclone will spin-down and die.

The other turbulent-drag effect causes spin up, although it is not apparent from eq. (13.9). Recall from Fig. 12.17 (geostrophic adjustment) that a geostrophic wind forms along sloping isentropic surfaces. If such a surface intersects the boundary layer, then turbulent drag will slow the winds near the ground, but not above the boundary layer (Fig. 13.23f). The resulting shear produces cyclonic relative vorticity.

The net spin-up or spin-down depends on the sum of all these terms.

You can identify the action of some of these terms by looking at weather maps.

Fig. 13.24 shows the wind vectors and absolute vorticity on the 50 kPa isobaric surface (roughly in the middle of the troposphere) for the case-study cyclone. **Positive vorticity advection** (PVA) occurs where wind vectors are crossing the vorticity contours from high toward low vorticity, such as highlighted by the dark box in Fig. 13.24. Namely, higher vorticity air is blowing into regions that contained lower vorticity. This region favors cyclone spin up.

Negative vorticity advection (NVA) is where the wind crosses the vorticity contours from low to high vorticity values (dark oval in Fig. 13.24). By using the absolute vorticity instead of relative vorticity, Fig. 13.24 combines the advection and beta terms.

Fig. 13.25 shows vertical velocity in the middle of the atmosphere. Since vertical velocity is near zero at the ground, regions of positive vertical velocity at 50 kPa must correspond to stretching in the bottom half of the atmosphere. Thus, the updraft regions in the figure favor cyclone spin-up (i.e., cyclogenesis).

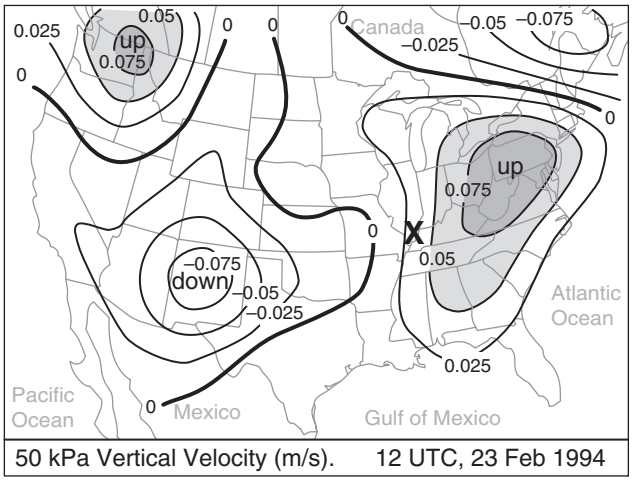

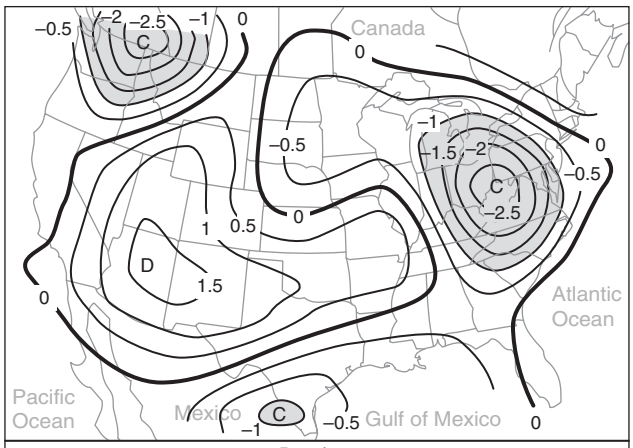

Figure 13.26 (right)
Horizontal divergence ($D = \Delta U/\Delta x + \Delta V/\Delta y$) for the case-study storm. C = horizontal convergence (= – D).

In the bottom half of the troposphere, regions of stretching must correspond to regions of convergence of air, due to mass continuity. Fig. 13.26 shows the **divergence** field at 85 kPa. Negative divergence corresponds to convergence. The regions of low-altitude convergence (shaded) favor cyclone spin-up.

Low-altitude spin-down due to turbulent drag occurs wherever there is rotation. Thus, the positive vorticity regions in Fig. 13.13c (shaded) are where spin-down is occurring for the case-study cyclone. The tilting term will be discussed in the Thunderstorm chapters.

Quasi-Geostrophic Approximation

Above the boundary layer (and away from fronts, jets, and thunderstorms) the terms in the second line of the vorticity equation are smaller than those in the first line, and can be neglected. Also, for synoptic scale, extratropical weather systems, the winds are almost geostrophic (**quasi-geostrophic**).

These weather phenomena are simpler to analyze than thunderstorms and hurricanes, and can be well approximated by a set of equations (quasi-geostrophic vorticity and omega equations) that are less complicated than the full set of **primitive equations** of motion (Newton's second law, the first law of thermodynamics, continuity, and ideal gas law).

As a result of the simplifications above, the vorticity forecast equation simplifies to the following **quasi-geostrophic vorticity equation**:

$$\frac{\Delta\zeta_g}{\Delta t} = -U_g\frac{\Delta\zeta_g}{\Delta x} - V_g\frac{\Delta\zeta_g}{\Delta y} - V_g\frac{\Delta f_c}{\Delta y} + f_c\frac{\Delta W}{\Delta z} \qquad \bullet(13.10)$$

spin-up | *horizontal advection* | *beta* | *stretching*

where the relative geostrophic vorticity ζ_g is defined similar to the relative vorticity of eq. (11.20), except using geostrophic winds U_g and V_g:

$$\zeta_g = \frac{\Delta V_g}{\Delta x} - \frac{\Delta U_g}{\Delta y} \qquad \bullet(13.11)$$

For solid body rotation, eq. (11.22) becomes:

$$\zeta_g = \frac{2\cdot G}{R} \qquad \bullet(13.12)$$

where G is the geostrophic wind speed and R is the radius of curvature.

Solved Example

Suppose an initial flow field has no geostrophic relative vorticity, but there is a straight north to south geostrophic wind blowing at 10 m/s at latitude 45°. Also, the top of a 1 km thick column of air rises at 0.01 m/s, while its base rises at 0.008 m/s. Find the rate of geostrophic-vorticity spin-up.

Solution

Given: $V = -10$ m/s, $\phi = 45°$, $W_{top} = 0.01$ m/s, $W_{bottom} = 0.008$ m/s, $\Delta z = 1$ km.
Find: $\Delta\zeta_g/\Delta_t = ?$ s^{-2}

First, get the Coriolis parameter using eq. (10.16):
$f_c = (1.458\text{x}10^{-4}\ s^{-1})\cdot\sin(45°) = 0.000103\ s^{-1}$

Next, use eq. (13.2):

$$\beta = \frac{\Delta f_c}{\Delta y} = \frac{1.458\times10^{-4}\,s^{-1}}{6.357\times10^{6}\,m}\cdot\cos 45°$$
$$= 1.62\text{x}10^{-11}\ m^{-1}\cdot s^{-1}$$

Use the definition of a gradient (see Appendix A):

$$\frac{\Delta W}{\Delta z} = \frac{W_{top} - W_{bottom}}{z_{top} - z_{bottom}} = \frac{(0.01 - 0.008)\text{m/s}}{(1000 - 0)\text{m}}$$
$$= 2\text{x}10^{-6}\ s^{-1}$$

Finally, use eq. (13.10). We have no information about advection, so assume it is zero. The remaining terms give:

$$\frac{\Delta\zeta_g}{\Delta t} = -(-10\text{m/s})\cdot(1.62\times10^{-11}\,m^{-1}\cdot s^{-1}) + (0.000103 s^{-1})\cdot(2\times10^{-6}\ s^{-1})$$

spin-up | *beta* | *stretching*

$$= (1.62\text{x}10^{-10} + 2.06\text{x}10^{-10})\ s^{-2} = \underline{\mathbf{3.68x10}}^{-10}\ s^{-2}$$

Check: Units OK. Physics OK.
Discussion: Even without any initial geostrophic vorticity, the rotation of the Earth can spin-up the flow if the wind blows appropriately.

BEYOND ALGEBRA • The Laplacian

A Laplacian operator ∇^2 can be defined as

$$\nabla^2 A = \frac{\partial^2 A}{\partial x^2} + \frac{\partial^2 A}{\partial y^2} + \frac{\partial^2 A}{\partial z^2}$$

where A represents any variable. Sometimes we are concerned only with the horizontal (H) portion:

$$\nabla_H^2 (A) = \frac{\partial^2 A}{\partial x^2} + \frac{\partial^2 A}{\partial y^2}$$

What does it mean? If $\partial A/\partial x$ represents the slope of a line when A is plotted vs. x on a graph, then $\partial^2 A/\partial x^2 = \partial[\ \partial A/\partial x\ ]/\partial x$ is the change of slope; namely, the curvature.

How is it used? Recall from the Dynamics chapter that the geostrophic wind is defined as

$$U_g = -\frac{1}{f_c}\frac{\partial \Phi}{\partial y} \qquad V_g = \frac{1}{f_c}\frac{\partial \Phi}{\partial x}$$

where Φ is the geopotential ($\Phi = |g| \cdot z$). Plugging these into eq. (13.11) gives the geostrophic vorticity:

$$\zeta_g = \frac{\partial}{\partial x}\left(\frac{1}{f_c}\frac{\partial \Phi}{\partial x}\right) + \frac{\partial}{\partial y}\left(\frac{1}{f_c}\frac{\partial \Phi}{\partial y}\right)$$

or

$$\boxed{\zeta_g = \frac{1}{f_c}\nabla_H^2(\Phi)} \qquad (13.11b)$$

This illustrates the value of the Laplacian — as a way to more concisely describe the physics.

For example, a low-pressure center corresponds to a low-height center on an isobaric sfc. That isobaric surface is concave up, which corresponds to positive curvature. Namely, the Laplacian of $|g| \cdot z$ is positive, hence, ζ_g is positive. Thus, a low has positive vorticity.

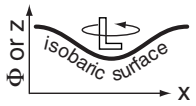

Figure f.

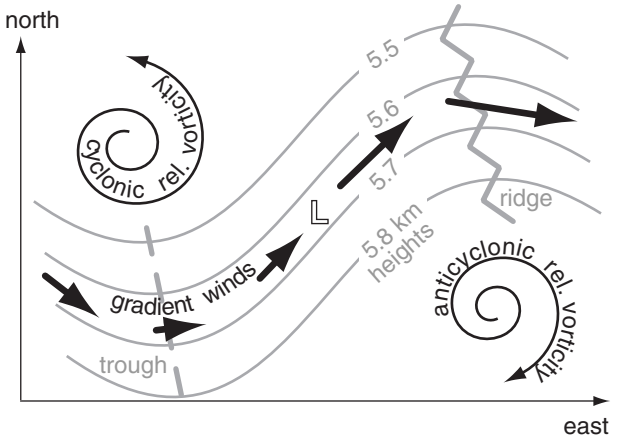

Figure 13.27
An idealized 50 kPa chart with equally-spaced height contours, as introduced by J. Bjerknes in 1937. The location of the surface low L is indicated.

The prefix "quasi-" is used for the following reasons. If the winds were perfectly geostrophic or gradient, then they would be parallel to the isobars. Such winds never cross the isobars, and could not cause convergence into the low. With no convergence there would be no vertical velocity.

However, we know from observations that vertical motions do exist and are important for causing clouds and precipitation in cyclones. Thus, the last term in the quasi-geostrophic vorticity equation includes W, a wind that is not geostrophic. When such an **ageostrophic** vertical velocity is included in an equation that otherwise is totally geostrophic, the equation is said to be **quasi-geostrophic**, meaning partially geostrophic. The quasi-geostrophic approximation will also be used later in this chapter to estimate vertical velocity in cyclones.

Within a quasi-geostrophic system, the vorticity and temperature fields are closely coupled, due to the dual constraints of geostrophic and hydrostatic balance. This implies close coupling between the wind and mass fields, as was discussed in the Global Circulation and Fronts chapters in the sections on geostrophic adjustment. While such close coupling is not observed for every weather system, it is a reasonable approximation for synoptic-scale, extratropical systems.

Application to Idealized Weather Patterns

An idealized weather pattern ("toy model") is shown in Fig. 13.27. Every feature in the figure is on the 50 kPa isobaric surface (i.e., in the mid troposphere), except the 𝕃 which indicates the location of the surface low center. All three components of the geostrophic vorticity equation can be studied.

Geostrophic and gradient winds are parallel to the height contours. The trough axis is a region of cyclonic (counterclockwise) curvature of the wind, which yields a large positive value of geostrophic vorticity. At the ridge is negative (clockwise) relative vorticity. Thus, the **advection** term is positive over the 𝕃 center and contributes to spin-up of the cyclone because the wind is blowing higher positive vorticity into the area of the surface low.

For any fixed pressure gradient, the gradient winds are slower than geostrophic when curving cyclonically ("slow around lows"), and faster than geostrophic for anticyclonic curvature, as sketched with the thick-line wind arrows in Fig. 13.27. Examine the 50 kPa flow immediately above the surface low. Air is departing faster than entering. This imbalance (divergence) draws air up from below. Hence, W increases from near zero at the ground to some positive updraft speed at 50 kPa. This **stretching** helps to spin-up the cyclone.

The **beta** term, however, contributes to spin-down because air from lower latitudes (with smaller Coriolis parameter) is blowing toward the location of the surface cyclone. This effect is small when the wave amplitude is small. The sum of all three terms in the quasigeostrophic vorticity equation is often positive, providing a net spin-up and intensification of the cyclone.

In real cyclones, contours are often more closely spaced in troughs, causing relative maxima in jet stream winds called jet streaks. Vertical motions associated with horizontal divergence in jet streaks are discussed later in this chapter. These motions violate the assumption that air mass is conserved along an "isobaric channel". Rossby also pointed out in 1940 that the gradient wind balance is not valid for varying motions. Thus, the "toy" model of Fig. 13.27 has weaknesses that limit its applicability.

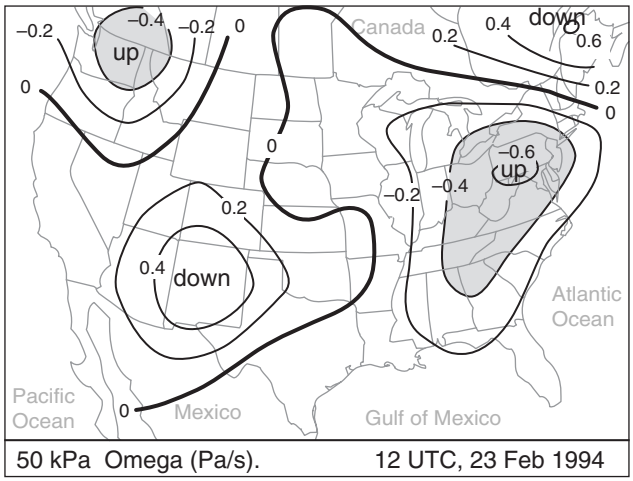

Figure 13.28
Vertical velocity (omega) in pressure coordinates, for the case-study cyclone. Negative omega corresponds to updrafts.

UPWARD MOTION

Upward vertical motion is another measure of cyclone vigor and cloud formation. For the case-study cyclone, Fig. 13.25 shows upward motion near the middle of the troposphere (at 50 kPa).

In height z coordinates, the vertical velocity is defined as $W = \Delta z/\Delta t$, where t is time. An analogous vertical velocity, **omega** (ω), can be defined in pressure coordinates:

$$\omega = \frac{\Delta P}{\Delta t} \qquad \bullet(13.13)$$

where units of omega are Pa/s.

Because pressure decreases with height, ω is negative for updrafts, while W is positive. Using the hydrostatic equation, the relationship between ω and W is:

$$\omega = -\rho \cdot |g| \cdot W \qquad \bullet(13.14)$$

where ρ is air density and $|g| = 9.8\ \text{m}\cdot\text{s}^{-2}$ is gravitational acceleration magnitude. For example, at P = 50 kPa where standard atmospheric density is $\rho \approx 0.69\ \text{kg}\cdot\text{m}^{-3}$, an updraft of W = 1 m/s gives ω = –6.8 Pa/s. Either W or ω can be used to represent vertical motion.

Most numerical weather prediction models (see the NWP chapter) use ω. Fig. 13.28 shows upward motion (ω) near the middle of the troposphere (at 50 kPa).

We will use three approaches to investigate vertical motion: continuity equation, omega equation, and Q-vectors. The continuity approach shows how jet-stream winds diverging horizontally at the top of the troposphere cause vertical motion in the mid

Solved Example

At an elevation of 5 km MSL, suppose (a) a thunderstorm has an updraft velocity of 40 m/s, and (b) the subsidence velocity in the middle of an anticyclone is –0.01 m/s. Find the corresponding omega values.

Solution

Given: (a) W = 40 m/s. (b) W = – 0.01 m/s. z = 5 km.
Find: ω = ? kPa/s for (a) and (b).

To estimate air density, use the standard atmosphere table from Chapter 1: $\rho = 0.7361\ \text{kg/m}^3$ at z = 5 km.

Next, use eq. (13.14) to solve for the omega values:

(a) $\omega = -(0.7361\ \text{kg/m}^3)\cdot(9.8\ \text{m/s}^2)\cdot(40\ \text{m/s})$
$= -288.55\ (\text{kg}\cdot\text{m}^{-1}\cdot\text{s}^{-2})/\text{s} = -288.55\ \text{Pa/s}$
$= \underline{\mathbf{-0.29\ kPa/s}}$

(b) $\omega = -(0.7361\ \text{kg/m}^3)\cdot(9.8\ \text{m/s}^2)\cdot(-0.01\ \text{m/s})$
$= 0.0721\ (\text{kg}\cdot\text{m}^{-1}\cdot\text{s}^{-2})/\text{s} = 0.0721\ \text{Pa/s}$
$= \underline{\mathbf{7.21x10^{-5}\ kPa/s}}$

Check: Units OK. Sign OK.
Discussion: CAUTION. Remember that the sign of omega is opposite that of vertical velocity, because as height increases in the atmosphere, the pressure decreases. As a quick rule of thumb, near the surface where air density is greater, omega (in kPa/s) has magnitude of roughly a hundredth of W (in m/s), with opposite sign.

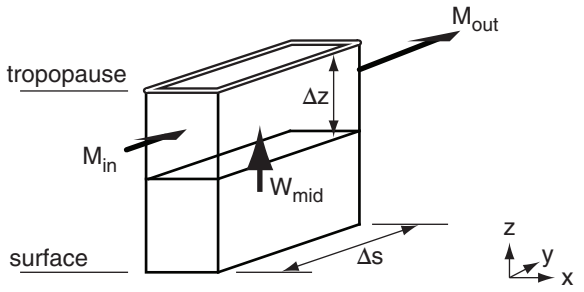

Figure 13.29
A column of tropospheric air, showing that mid-level vertical motion W is related to upper level divergence $M_{out} - M_{in}$, where M is wind speed.

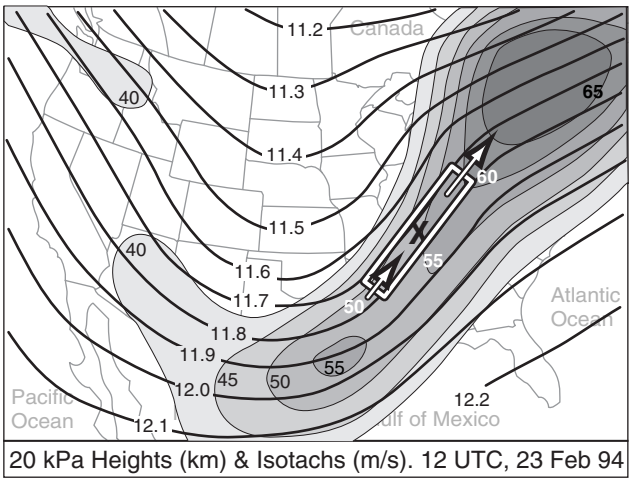

Figure 13.30
Over the surface cyclone (X) is a region (box) with faster jet-stream outflow than inflow (arrows). Isotachs are shaded.

Solved Example

Jet-stream inflow winds are 50 m/s, while outflow winds are 75 m/s a distance of 1000 km further downstream. What updraft is induced below this 5 km thick divergence region? Assume air density is 0.5 kg/m^3.

Solution

Given: M_{in} = 50 m/s, M_{out} = 75 m/s, Δs = 1000 km, Δz = 5 km.
Find: W_{mid} = ? m/s

Use eq. (13.17):
$W_{mid} = [M_{out} - M_{in}]\cdot(\Delta z/\Delta s)$
= [75 - 50 m/s]·[(5km)/(1000km)] = **0.125 m/s**

Check: Units OK. Physics unreasonable, because the incompressible continuity equation assumes constant density — a bad assumption over a 5 km thick layer.
Discussion: Although this seems like a small number, over an hour this updraft velocity would lift air about 450 m. Given enough hours, the rising air might reach its lifting condensation level, thereby creating a cloud or enabling a thunderstorm.

troposphere. The omega equation uses quasi-geostrophic dynamics in the bottom half of the troposphere to diagnose vertical motion from the vorticity and thermal wind. Q-vectors consider ageostrophic motions that help maintain quasi-geostrophic flow. All approaches give complementary insight.

Continuity Effects

Vertical motion in a cyclone is often driven by changes of horizontal wind speed of the upper-tropospheric jet stream. Mass continuity requires that horizontal divergence be compensated by vertical convergence, and vice versa. Namely, air leaving a region horizontally must be balanced by replacement air entering the same region vertically, so as not to leave a vacuum (Fig. 13.29). The jet stream is near the base of the stratosphere, where strong static stability aloft impedes vertical motion above the jet. Thus, most of the compensating vertical motion occurs in the troposphere, beneath the level of the jet.

For the column of air sketched in Fig. 13.29, the incompressible continuity equation becomes

$$W_{mid} = D\cdot\Delta z \tag{13.15}$$

or

$$W_{mid} = \left[\frac{\Delta U}{\Delta x} + \frac{\Delta V}{\Delta y}\right]\cdot\Delta z \tag{13.16}$$

or

$$W_{mid} = \frac{\Delta M}{\Delta s}\cdot\Delta z \tag{13.17}$$

where $\Delta M = M_{out} - M_{in}$ is the change of horizontal wind speed, Δs is horizontal distance between inflow and outflow locations, $\Delta M/\Delta s$ is the upper level **horizontal divergence** ($D = \Delta U/\Delta x + \Delta V/\Delta y$, see Fig. 13.17d), Δz is the thickness of the upper portion of the troposphere (between the 50 kPa surface and the tropopause), and W_{mid} is the vertical velocity across the 50 kPa surface. For simplicity, assume that all of horizontal divergence aloft can be represented by the winds in one direction, as sketched.

Fig. 13.30 shows this scenario for the case-study storm. Geostrophic winds are often nearly parallel to the height contours (solid black lines in Fig. 13.30). Thus, for the region outlined with the white box drawn parallel to the contour lines, the main inflow and outflow are at the ends of the box (arrows). The isotachs (shaded) tell us that the inflow (≈ 50 m/s) is slower than outflow (≈60 m/s).

Two mechanisms that cause jet-stream divergence are examined next: curvature of the jet stream, and jet streaks. The first is a large-scale feature in approximate geostrophic balance. The second is a smaller-scale feature that causes an ageostrophic (non-geostrophic) divergent flow.

Jet-Stream Curvature

Recall that air blows slower around troughs than around ridges, due to centrifugal force (see the Dynamics chapter). Consider a column of air situated east of an upper-level trough. The gradient wind speed horizontally entering the column is less than that leaving (Fig. 13.31). This results in a wind speed difference of ΔM across a distance $\Delta s = d$.

Assume the jet stream oscillates north-south as a sine wave. If the north-south distance between crest and trough is Δy [= 2 · (amplitude of wave)], and the east-west wavelength is λ, then the distance d between crest and trough is:

$$\Delta s = d = \left[(\lambda / 2)^2 + \Delta y^2 \right]^{1/2} \tag{13.18}$$

Gradient wind speeds around anticyclones and cyclones were discussed in the Dynamics chapter. The speed difference between outflow (anticyclonic) and inflow (cyclonic) is

$$\Delta M = 0.5 \cdot f_c \cdot R \cdot \left[2 - \sqrt{1 - \frac{4 \cdot G}{f_c \cdot R}} - \sqrt{1 + \frac{4 \cdot G}{f_c \cdot R}} \right] \tag{13.19}$$

where G is geostrophic wind speed. The radius of curvature R at crests and troughs of sine waves is:

$$R = \frac{1}{2\pi^2} \cdot \frac{\lambda^2}{\Delta y} \tag{13.20}$$

The effect of upper-level divergence due to jet-stream curvature can be found by combining the equations above:

$$W_{mid} = \frac{\dfrac{f_c \cdot \Delta z \cdot \lambda^2}{4\pi^2 \cdot \Delta y} \left[2 - \sqrt{1 - \dfrac{8\pi^2 G \cdot \Delta y}{f_c \cdot \lambda^2}} - \sqrt{1 + \dfrac{8\pi^2 G \cdot \Delta y}{f_c \cdot \lambda^2}} \right]}{[(\lambda / 2)^2 + \Delta y^2]^{1/2}} \tag{13.21}$$

Thus, knowing the wavelength, amplitude, and geostrophic wind speed, it is possible to estimate the vertical motion.

Jet-stream curvature is one of the factors causing cyclogenesis for the case-study storm (Fig. 13.30). Near the trough over Texas, jet stream winds are 40 - 55 m/s. Near the ridge over the eastern Great Lakes, jet-stream winds are 60 - 68 m/s. For this case, the trough-to-crest distance is about Δs = 2200 km.

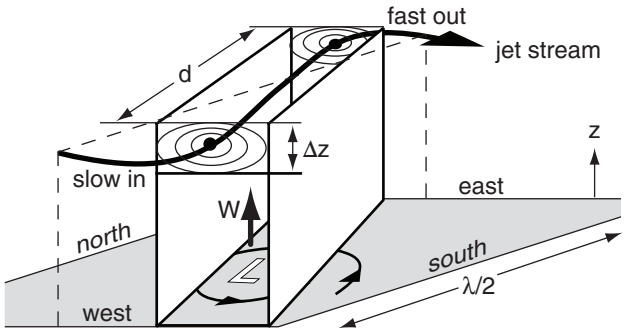

Figure 13.31
Factors affecting total mass within a column of air in the N. Hemisphere. The column is between the two vertical planes that are drawn.

Solved Example

Given a jet stream with thickness 5 km, air density 0.364 kg·m^{-3}, wavelength 6000 km, amplitude 500 km, and average geostrophic wind speed 30 m/s. Find the radius of curvature at the crest, distance d along the flow, inflow vs. outflow wind-speed difference, and mid-level vertical velocity.

Solution

Given: ρ_{top} = 0.364 kg·m^{-3}, G = 30 m/s,
Δz = 5 km, λ = 6000 km,
Δy = 2 · (500 km) = 1000 km.
Find: R = ? km, d = ? km, ΔM= ? m/s, W_{mid} = ? m/s
Assume: f_c = 0.0001 s^{-1}

Use eq. (13.20):

$$R = \frac{1}{2\pi^2} \cdot \frac{(6000\text{km})^2}{(1000\text{km})} = \underline{\textbf{1824 km}}$$

From Chapter 10 use:

$$\frac{G}{f_c \cdot R} = Ro_c = \frac{30\text{m/s}}{(0.0001\text{s}^{-1}) \cdot (1824\text{km})} = 0.164$$

Use eq. (13.19):

$$\Delta M = \frac{10\text{m/s}}{2(0.164)} \cdot \left[2 - \sqrt{1 - 4(0.164)} - \sqrt{1 + 4(0.164)} \right]$$
$$= \underline{\textbf{11.6 m/s}}$$

Use eq. (13.18):
$d = [\ (3000\text{km})^2 + (1000\text{km})^2\ ]^{1/2} = \underline{\textbf{3162 km}}$

Use eq. (13.17):

$$W_{mid} = \left(\frac{11.6\text{m/s}}{3162\text{km}} \right) \cdot 5\text{km} = \underline{\textbf{0.018 m/s}}$$

Check: Units OK. Physics OK.
Discussion: A vertical velocity of a couple cm/s averaged over the whole cyclone is typical, although local updrafts in clouds can be faster.

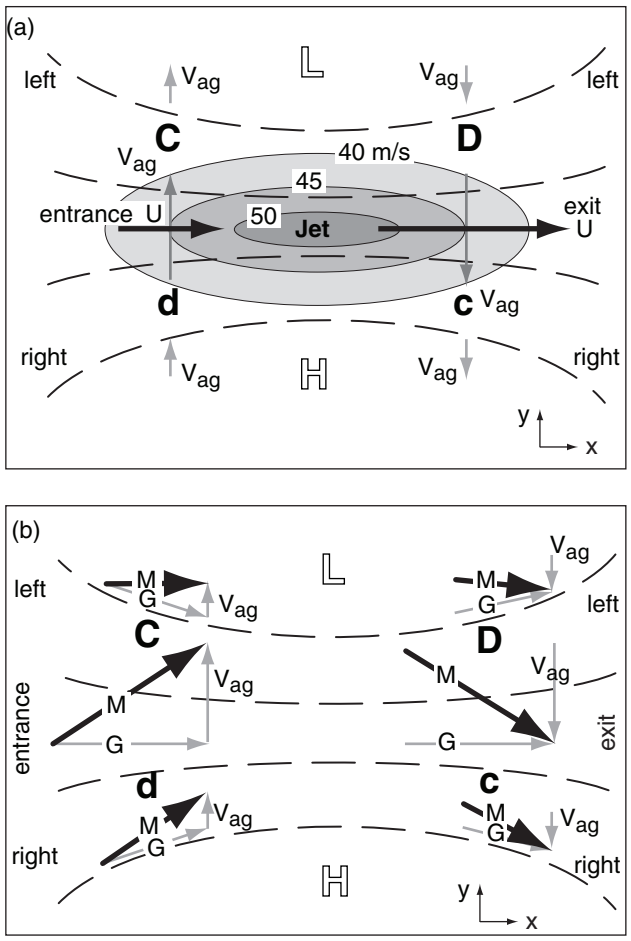

Figure 13.32
Horizontal divergence (D = strong, d = weak) and convergence (C = strong, c = weak) near a jet streak. Shown are isobars or height contours (dashed lines), and ageostrophic components V_{ag} of wind (thin grey arrows) . (a) Isotachs (shaded contours), jet stream wind and jet axis (heavy arrows), (b) Geostrophic wind G is parallel to the isobars (also shown with grey arrows). The vector sum of the gray vectors is the total wind speed M, shown by the heavy black vectors.

Solved Example

A west wind of 60 m/s in the center of a jet streak decreases to 40 m/s in the jet exit region 500 km to the east. Find the exit ageostrophic wind component.

Solution

Given: ΔU = 40–60 m/s = –20 m/s, across Δx = 500 km.
Find: V_{ag} = ? m/s

Use eq. (13.25), and assume $f_c = 10^{-4}$ s^{-1}.
The average wind is U = (60 + 40 m/s)/2 = 50 m/s.

V_{ag} = [(50 m/s) / (10^{-4} s^{-1})] · [(–20 m/s) / (5×10^5 m)]
= **–20 m/s**

Check: Units OK. Sign OK. Physics OK.
Discussion: Negative sign means V_{ag} is north wind.

Jet Streaks

A jet streak is a relative maximum of wind speed within the jet stream. Picture a jet streak as sketched in Fig. 13.32a, blowing from west to east. This forms in the upper-tropospheric jet stream in regions where isobars or height contours are tightly packed (i.e., closely spaced). Wind speed reaches a maximum at the center of the streak.

Wind cannot only advect temperature or humidity, but it can also advect itself. As a result, the wind maximum advects itself eastward. An outcome is that the jet maximum finds itself in a region where the isobars are further apart. Namely, the actual wind speed in the exit region of the streak is faster than the theoretical geostrophic wind. This is a situation that causes an ageostrophic (i.e., not in geostrophic balance) wind to the south.

To quantify this effect, start with the full equations of motion from the Dynamics chapter (eqs. 10.51a). Consider only the equation for U wind (assuming a jet aligned west to east), assume approximate steady state (no time change), and neglect boundary-layer drag. The result is:

$$0 = -U\frac{\Delta U}{\Delta x} + f_c\left(V - V_g\right) \qquad (13.22)$$

Define an **ageostrophic wind** V_{ag} as the difference between the actual wind and the geostrophic wind:

$$V_{ag} = V - V_g \qquad \bullet(13.23)$$

Similarly:

$$U_{ag} = U - U_g \qquad \bullet(13.24)$$

With this definition, the equation of motion becomes

$$V_{ag} = \frac{U}{f_c}\cdot\frac{\Delta U}{\Delta x} \qquad \bullet(13.25)$$

For a north-south aligned jet axis, the corresponding ageostrophic wind would be

$$U_{ag} = -\frac{V}{f_c}\cdot\frac{\Delta V}{\Delta y} \qquad \bullet(13.26)$$

In the **exit region** of a west-east aligned jet, U is positive but $\Delta U/\Delta x$ is negative (wind decreases eastward). Thus, eq. (13.25) says that a negative V_{ag}

ageostrophic wind develops (i.e., blows from north to south). In the **entrance region** the U wind increases in the x direction, causing a positive V_{ag} (i.e., blows from south to north, as sketched in Fig. 13.32a).

The magnitude of ageostrophic wind is largest near the jet axis, it decreases in magnitude further off to the side of the jet. As a result, horizontal divergence of the ageostrophic wind exists in the **left exit region** of the jet, and convergence in the right exit region, regardless of the jet orientation. A similar but opposite convergence-divergence pair occurs in the entrance region. These four regions are called the **four quadrants** of the jet streak (Fig. 13.35).

The total wind speed M is the vector sum of the geostrophic components G parallel to the isobars, and the ageostrophic components V_{ag} as indicated in Fig. 13.32b. Focusing on the total wind speed (thick black vectors in Fig. 13.32 b), one can see strong convergence in the left entrance region (i.e., the vectors come towards each other at a large angle). Similarly, large divergence exists in the left exit region.

In the right entrance and exit regions, however, the total wind vectors are almost parallel to the wind vectors along the center axis of the jet. Thus, divergence and convergence are weaker there.

This ageostrophic behavior can also be seen in the case-study event (Fig. 13.33). This figure overlays wind vectors, isotachs, and geopotential height contours near the top of the troposphere (at 20 kPa). The broad area of shading shows the jet stream. Embedded within it are two relative speed maxima (one over Texas, and the other over New England) that we identify as jet streaks. Recall that if winds are geostrophic (or gradient), then they should flow parallel to the height contours.

In Fig. 13.33 the square highlights the exit region of the Texas jet streak, showing wind vectors that cross the height contours toward the right. Namely, inertia has caused these winds to be faster than geostrophic (**supergeostrophic**), therefore Coriolis force is stronger than pressure-gradient force, causing the winds to be to the right of geostrophic. The oval highlights the entrance region of the second jet, where winds cross the height contours to the left. Inertia results in slower-than-geostrophic winds (**subgeostrophic**), causing the Coriolis force to be too weak to counteract pressure-gradient force.

Fig. 13.34 shows the vertical and horizontal circulations induced by the ageostrophic motion near the exit region of the jet streak. Such a flow is called a **secondary circulation**. The vertical components of this circulation, which are caused by the convergence and divergence regions aloft, also induce a pair of horizontal divergence and convergence at the surface.

FOCUS • Ageostrophic right-hand rule

If the geostrophic winds are accelerating, use your right hand to curl your fingers from vertical toward the direction of acceleration (the acceleration vector). Your thumb points in the direction of the ageostrophic wind.

This right-hand rule also works for deceleration, for which case the direction of acceleration is opposite to the wind direction.

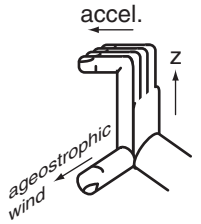

Figure g.

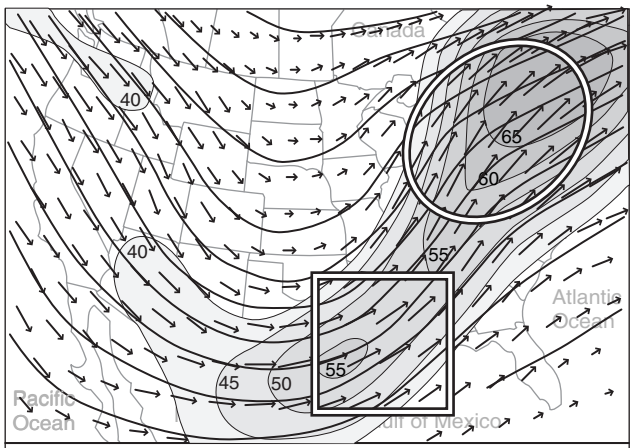

Figure 13.33

Superposition of the 20 kPa charts for geopotential heights (medium-thickness black curved lines), isotachs in m/s (shading), and winds (vectors). The scale for winds and the values for the height contours are identical to those in Figs. 13.17. Regions of relatively darker shading indicate the jet streaks. White/black square outlines the exit region from a small jet streak over Texas, and white/black oval outlines the entrance region for a larger jet streak over the northeastern USA.

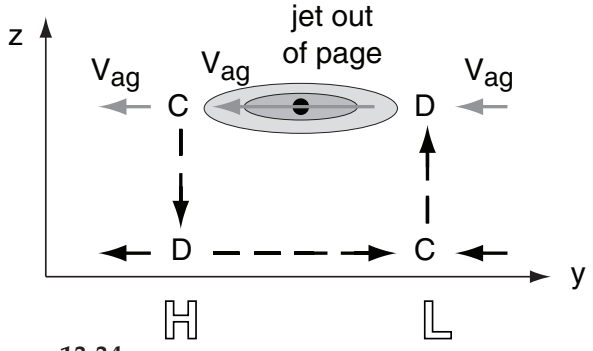

Figure 13.34

Vertical cross-section through the exit region of a jet (shaded), where the jet points out of the page. The V_{ag} ageostrophic winds (thin grey lines) are driven by jet-streak dynamics, while the dashed circulation is driven by mass continuity. Regions of horizontal convergence C and divergence D are indicated. This circulation creates or strengthens low (L) and high (H) pressure centers near the surface.

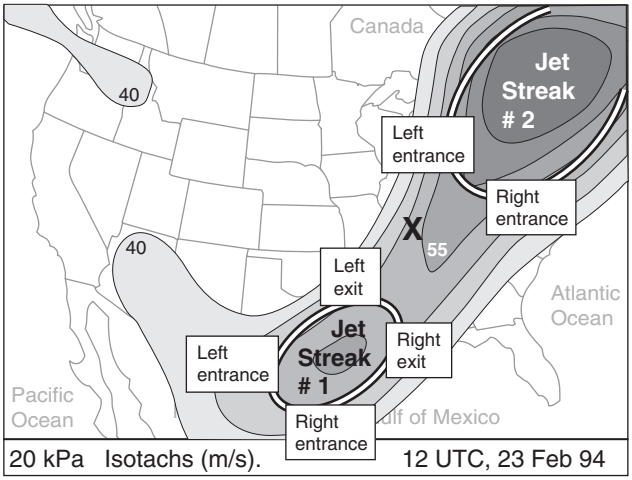

Figure 13.35
Entrance and exit regions of jet streaks (highlighted with ovals). X marks the surface low center.

Solved Example

A jet streak of width 1000 km has a core wind speed of 50 m/s that decreases eastward to 25 m/s across a distance of 1000 km. If the jet region is 5 km thick, find the mid-level vertical velocity. Assume $f_c = 10^{-4}$ s^{-1}.

Solution

Given: $U = 50$ m/s, $\Delta U = 25 - 50 = -25$ m/s,
$\Delta x = \Delta y = 10^6$ m, $\Delta z = 5000$ m.
Find: W_{mid} = ? m/s

Use eq. (13.27):

$$W_{mid} = \frac{(50\text{m/s})\cdot(25\text{m/s})}{(10^{-4}\text{s}^{-1})\cdot(10^6\text{m})}\cdot\frac{(5000\text{m})}{(10^6\text{m})} = \underline{\mathbf{0.0625\ m/s}}$$

Check: Units OK. Physics OK.
Discussion: This is a larger average vertical velocity over a much smaller horizontal area than for the previous solved example. Such a vertical velocity can significantly intensify a cyclone.

FOCUS • Sutcliffe Development Theorem

To help forecast cyclogenesis, Sutcliffe devised

$$D_{top} - D_{bottom} = -\frac{1}{f_c}\left[U_{TH}\frac{\Delta\zeta_{gc}}{\Delta x} + V_{TH}\frac{\Delta\zeta_{gc}}{\Delta y}\right]$$

where **divergence** is $D = \Delta U/\Delta x + \Delta V/\Delta y$, column geostrophic vorticity is $\zeta_{gc} = \zeta_{g\ top} + \zeta_{g\ bottom} + f_c$, and (U_{TH}, V_{TH}) are the thermal-wind components.

This says that if the vorticity in an air column is positively advected by the thermal wind, then this must be associated with greater air divergence at the column top than bottom. When combined with eq. (13.15), this conclusion for upward motion is nearly identical to that from the Trenberth omega eq. (13.29).

The sense (direction) of this circulation below the **exit region** of the jet is **indirect** (opposite to the sense of rotation of a Hadley cell). The sense below the **entrance region** is **direct**.

Regions of divergence aloft remove mass from the column of air, thereby lowering sea-level pressure. Such sea-level pressure drop and associated upward motion cause cyclogenesis. Hence, cyclones are favored below the left exit region and right entrance region of the jet streak.

Looking again at the case-study storm, Fig. 13.35 shows the entrance and exit regions of the two dominant jet streaks in this image (for now, ignore the smaller jet streak over the Pacific Northwest). Thus, you can expect divergence aloft at the left exit and right entrance regions. These are locations that would favor cyclogenesis near the ground. Indeed, a new cyclone formed over the Carolinas (under the right entrance region of jet streak # 2), as was described in the case-study overview. Convergence aloft, favoring cyclolysis (cyclone death), is at the left entrance and right exit regions.

To find the mid-level vertical velocity below the left-exit or right-entrance quadrant, let $\Delta s = \Delta y$ be the north-south half-width of a predominantly west-to-east jet streak. Assume the ageostrophic wind V_{ag} smoothly approaches zero within a distance Δy to the side of the jet. Using eq. (13.25) in eq. (13.16) with V_{ag} in place of M, the upward motion is

$$W_{mid} = \left|\frac{U\cdot\Delta U}{f_c\cdot\Delta x}\right|\cdot\frac{\Delta z}{\Delta y} \qquad (13.27)$$

Omega Equation

The **omega equation** is the name of a diagnostic equation used to find vertical motion in pressure units (omega; ω). We will use a form of this equation developed by K. Trenberth, based on quasi-geostrophic dynamics and thermodynamics.

The full omega equation is one of the nastier-looking equations in meteorology (see the Beyond Algebra box). To simplify it, focus on one part of the full equation, apply it to the bottom half of the troposphere (the layer between 100 to 50 kPa isobaric surfaces), and convert the result from ω to W.

The resulting approximate omega equation is:

$$W_{mid} \cong \frac{-2\cdot\Delta z}{f_c}\left[U_{TH}\frac{\overline{\Delta\zeta_g}}{\Delta x} + V_{TH}\frac{\overline{\Delta\zeta_g}}{\Delta y} + V_{TH}\frac{\beta}{2}\right] \qquad \bullet(13.28)$$

where W_{mid} is the vertical velocity in the mid-troposphere (at $P = 50$ kPa), Δz is the 100 to 50 kPa thickness, U_{TH} and V_{TH} are the thermal-wind components

for the 100 to 50 kPa layer, f_c is Coriolis parameter, β is the change of Coriolis parameter with y (see eq. 13.2), ζ_g is the geostrophic vorticity, and the overbar represents an average over the whole depth of the layer. An equivalent form is:

$$W_{mid} \cong \frac{-2 \cdot \Delta z}{f_c}\left[M_{TH} \frac{\overline{\Delta\left(\zeta_g + (f_c / 2)\right)}}{\Delta s} \right] \qquad \bullet(13.29)$$

where s is distance along the thermal wind direction, and M_{TH} is the thermal-wind speed.

Regardless of the form, the terms in square brackets represent the advection of vorticity by the thermal wind, where vorticity consists of the geostrophic relative vorticity plus a part of the vorticity due to the Earth's rotation. The geostrophic vorticity at the 85 kPa or the 70 kPa isobaric surface is often used to approximate the average geostrophic vorticity over the whole 100 to 50 kPa layer.

A physical interpretation of the omega equation is that greater upward velocity occurs where there is greater advection of cyclonic (positive) geostrophic vorticity by the thermal wind. Greater upward velocity favors clouds and heavier precipitation. Also, by moving air upward from the surface, it reduces the pressure under it, causing the surface low to move toward that location and deepen.

Weather maps can be used to determine the location and magnitude of the maximum upward motion. The idealized map of Fig. 13.36a shows the height (z) contours of the 50 kPa isobaric surface, along with the trough axis. Also shown is the location of the surface low and fronts.

At the surface, the greatest vorticity is often near the low center. At 50 kPa, it is often near the trough axis. At 70 kPa, the vorticity maximum (**vort max**) is usually between those two locations. In Fig. 13.36a, the darker shading corresponds to regions of greater cyclonic vorticity at 70 kPa.

Fig. 13.36b shows the thickness (Δz) of the layer of air between the 100 and 50 kPa isobaric surfaces. Thickness lines are often nearly parallel to surface fronts, with the tightest packing on the cold side of the fronts. Recall that thermal wind is parallel to the thickness lines, with cold air to the left, and with the greatest velocity where the thickness lines are most tightly packed. Thermal wind direction is represented by the arrows in Fig. 13.36b, with longer arrows denoting stronger speed.

Advection is greatest where the area between crossing isopleths is smallest (the Focus Box on the next page explains why). This rule also works for advection by the thermal wind. The dotted lines represent the isopleths that drive the thermal wind.

Solved Example

The 100 to 50 kPa thickness is 5 km and $f_c = 10^{-4}$ s^{-1}. A west to east thermal wind of 20 m/s blows through a region where avg. cyclonic vorticity decreases by 10^{-4} s^{-1} toward the east across a distance of 500 km. Use the omega eq. to find mid-tropospheric upward speed.

Solution

Given: $U_{TH} = 20$ m/s, $V_{TH} = 0$, $\Delta z = 5$ km,
$\Delta\zeta = -10^{-4}$ s^{-1}, $\Delta x = 500$ km, $f_c = 10^{-4}$ s^{-1}.
Find: W_{mid} = ? m/s

Use eq. (13.28):

$$W_{mid} \cong \frac{-2 \cdot (5000\text{m})}{(10^{-4}\text{s}^{-1})}\left[(20\text{m/s})\frac{(-10^{-4}\text{s}^{-1})}{(5\times10^{5}\text{m})} + 0 + 0 \right] = \underline{\mathbf{0.4\ m/s}}$$

Check: Units OK. Physics OK.

Discussion: At this speed, an air parcel would take 7.6 h to travel from the ground to the tropopause.

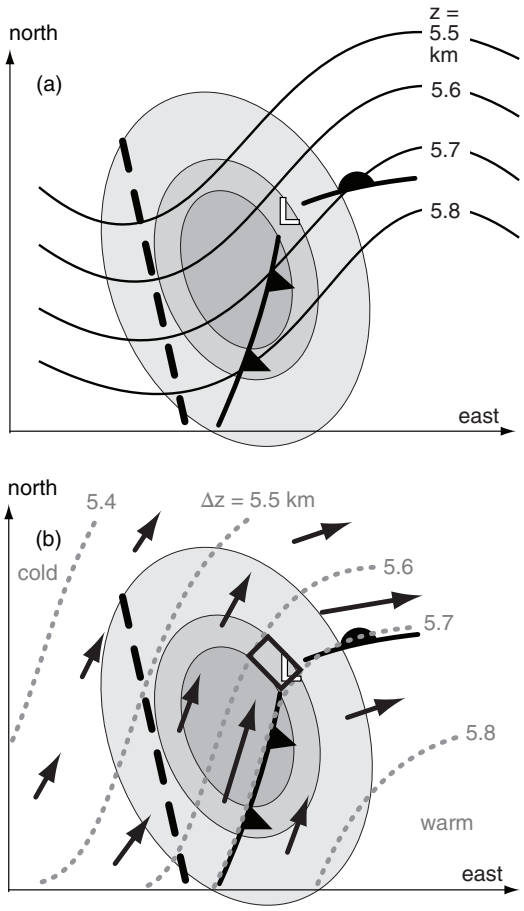

Figure 13.36

(a) Weather at three different pressure heights: (1) 50 kPa heights (solid lines) and trough axis (thick dashed line); (2) surface low pressure center (L) and fronts; (3) 70 kPa vorticity (shaded). (b) Trough axis, surface low and fronts, and vorticity shading are identical to Fig. (a). Added are: 100 to 50 kPa thickness (dotted lines), thermal wind vectors (arrows), and region of maximum positive vorticity advection by the thermal wind (rectangular box). It is within this box that the omega equation gives the greatest updraft speed, which support cyclogenesis.

BEYOND ALGEBRA • The Omega Eq.

Full Omega Equation

The omega equation describes vertical motion in pressure coordinates. One form of the quasi-geostrophic omega equation is:

$$\left\{\nabla_p^2 + \frac{f_o^2}{\sigma}\frac{\partial^2}{\partial p^2}\right\}\omega = \frac{-f_o}{\sigma}\cdot\frac{\partial}{\partial p}\left[-\vec{V}_g \bullet \vec{\nabla}_p\left(\zeta_g + f_c\right)\right] - \frac{\Re}{\sigma\cdot p}\cdot\nabla_p^2\left[-\vec{V}_g \bullet \vec{\nabla}_p T\right]$$

where f_o is a reference Coriolis parameter f_c at the center of a beta plane, σ is a measure of static stability, V_g is a vector geostrophic wind, $\Re$ is the ideal gas law constant, p is pressure, T is temperature, ζ_g is geostrophic vorticity, and • means vector dot product.

$\vec{\nabla}_p(\,) = \partial(\,)/\partial x\big|_p + \partial(\,)/\partial y\big|_p$ is the **del operator**, which gives quasi-horizontal derivatives along an isobaric surface. Another operator is the **Laplacian**:

$$\nabla^2{}_p(\,) = \partial^2(\,)/\partial x^2\Big|_p + \partial^2(\,)/\partial y^2\Big|_p \quad .$$

Although the omega equation looks particularly complicated and is often shown to frighten unsuspecting people, it turns out to be virtually useless. The result of this equation is a small difference between very large terms on the RHS that often nearly cancel each other, and which can have large error.

Trenberth Omega Equation

Trenberth developed a more useful form that avoids the small difference between large terms:

$$\left\{\nabla_p^2 + \frac{f_o^2}{\sigma}\frac{\partial^2}{\partial p^2}\right\}\omega = \frac{2f_o}{\sigma}\cdot\left[\frac{\partial \vec{V}_g}{\partial p} \bullet \vec{\nabla}_p\left(\zeta_g + (f_c/2)\right)\right]$$

For the omega subsection of this chapter, we focus on the vertical (pressure) derivative on the LHS, and ignore the Laplacian. This leaves:

$$\frac{f_o^2}{\sigma}\frac{\partial^2\omega}{\partial p^2} = \frac{2f_o}{\sigma}\cdot\left[\frac{\partial \vec{V}_g}{\partial p} \bullet \vec{\nabla}_p\left(\zeta_g + (f_c/2)\right)\right]$$

Upon integrating over pressure from p = 100 to 50 kPa:

$$\frac{\partial\omega}{\partial p} = \frac{-2}{f_o}\cdot\left[\vec{V}_{TH} \bullet \overline{\vec{\nabla}_p\left(\zeta_g + (f_c/2)\right)}\right]$$

where the definition of thermal wind V_{TH} is used, along with the mean value theorem for the last term.

The hydrostatic eq. is used to convert the LHS: $\partial\omega/\partial p = \partial W/\partial z$. The whole eq. is then integrated over height, with $W = W_{mid}$ at $z = \Delta z$ (= 100 - 50 kPa thickness) and $W = 0$ at $z = 0$.

This gives W_{mid} =

$$\frac{-2\cdot\Delta z}{f_c}\left[U_{TH}\,\overline{\frac{\Delta\left(\zeta_g + (f_c/2)\right)}{\Delta x}} + V_{TH}\,\overline{\frac{\Delta\left(\zeta_g + (f_c/2)\right)}{\Delta y}}\right]$$

But f_c varies with y, not x. The result is eq. (13.28).

FOCUS • Max Advection on Wx Maps

One trick to locating the region of maximum advection is to find the region of smallest area between crossing isopleths on a weather (wx) map, where one set of isopleths must define a wind.

For example, consider temperature advection by the geostrophic wind. Temperature advection will occur only if the winds blow across the isotherms at some nonzero angle. Stronger temperature gradient with stronger wind component perpendicular to that gradient gives stronger temperature advection.

But stronger geostrophic winds are found where the isobars are closer together. Stronger temperature gradients are found where the isotherms are closer together. In order for the winds to cross the isotherms, the isobars must cross the isotherms. Thus, the greatest temperature advection is where the tightest isobar packing crosses the tightest isotherm packing. At such locations, the area bounded between neighboring isotherms and isobars is smallest.

This is illustrated in the surface weather map below, where the smallest area is shaded to mark the maximum temperature advection. There is a jet of strong geostrophic winds (tight isobar spacing) running from northwest to southeast. There is also a front with strong temperature gradient (tight isotherm spacing) from northeast to southwest. However, the place where the jet and temperature gradient together are strongest is the shaded area.

Each of the odd-shaped tiles (**solenoids**) between crossing isobars and isotherms represents the same amount of temperature advection. But larger tiles imply that temperature advection is spread over larger areas. Thus, greatest temperature flux (temperature advection per unit area) is at the smallest tiles.

This approach works for other variables too. If isopleths of vorticity and height contours are plotted on an upper-air chart, then the smallest area between crossing isopleths indicates the region of maximum **vorticity advection** by the geostrophic wind. For vorticity advection by the **thermal wind**, plot isoplets of vorticity vs. **thickness contours**.

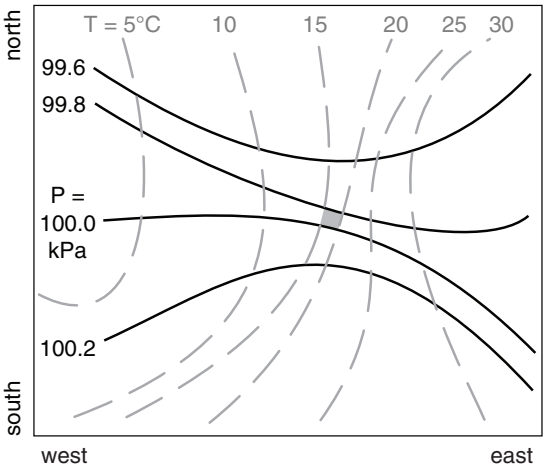

Fig. h. *Solid lines are isobars. Grey dashed lines are isotherms. Greatest temperature advection is at shaded tile.*

Figure 13.37 (right)
Superposition of the vorticity chart (grey lines and shading) at 85 kPa with the chart for thickness (thick black lines) between the 100 and 50 kPa isobaric surfaces, for the case-study storm. The thermal wind (arrows) blows parallel to the thickness lines with cold air to its left. The white box highlights a region of positive vorticity advection (PVA) by the thermal wind, where updrafts, cyclogenesis, and bad weather would be expected.

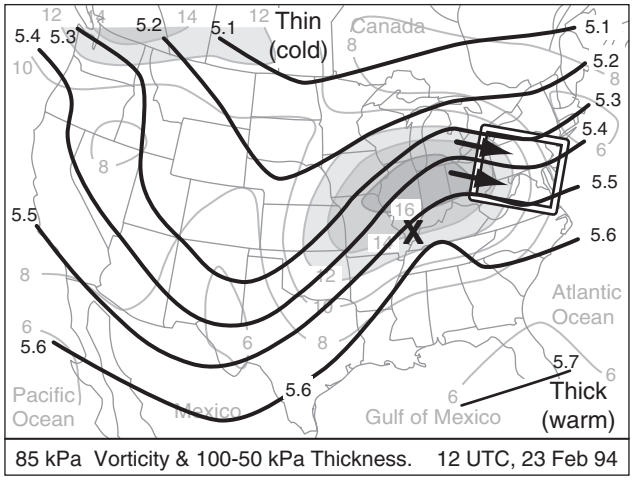

In Fig. 13.36 the thin black lines around the shaded areas are isopleths of vorticity. The solenoid at the smallest area between these crossing isopleths indicates the greatest vorticity advection by the thermal wind, and is outlined by a rectangular box. For this particular example, the greatest updraft would be expected within this box.

Be careful when you identify the smallest area. In Fig. 13.36b, another area equally as small exists further south-south-west from the low center. However, the cyclonic vorticity is being advected away from this region rather than toward it. Hence, this is a region of negative vorticity advection by the thermal wind, which would imply downward vertical velocity and cyclolysis or anticyclogenesis.

To apply these concepts to the case-study storm, Fig. 13.37 superimposes the 85 kPa vorticity chart with the 100 - 50 kPa thickness chart. The white box highlights a region of small solenoids, with the thermal wind blowing from high towards low vorticity. Hence, the white box outlines an area of **positive vorticity advection** (**PVA**) by the thermal wind, so anticipate substantial updrafts in that region. Such updrafts would create bad weather (clouds and precipitation), and would encourage cyclogenesis in the region outlined by the white box.

Near the surface low center (marked by the X in Fig. 13.37) is weak negative vorticity advection. This implies downdrafts, which contribute to cyclolysis. This agrees with the actual cyclone evolution, which began weakening at this time, while a new cyclone formed near the Carolinas and moved northward along the USA East Coast.

The Trenberth **omega equation** is heavily used in weather forecasting to help diagnose synoptic-scale regions of updraft and the associated cyclogenesis, cloudiness and precipitation. However, in the derivation of the omega equation (which we did not cover in this book), we neglected components that describe the role of ageostrophic motions in helping to maintain geostrophic balance. The Focus box on the Geostrophic Paradox describes the difficulties of maintaining geostrophic balance in some situations — motivation for Hoskin's Q-vector approach described next.

FOCUS • The Geostrophic Paradox

Consider the entrance region a jet streak. Suppose that the thickness contours are initially zonal, with cold air to the north and warm to the south (Fig. i(a)). As entrance winds (black arrows in Fig. i(a) converge, warm and cold air are advected closer to each other. This causes the thickness contours to move closer together (Fig. i(b), in turn suggesting tighter packing of the height contours and faster geostrophic winds at location "X" via the thermal wind equation. But the geostrophic wind in Fig. i(a) is advecting slower wind speeds to location "X".

Paradox: advection of the geostrophic wind by the geostrophic wind seems to undo geostrophic balance at "X".

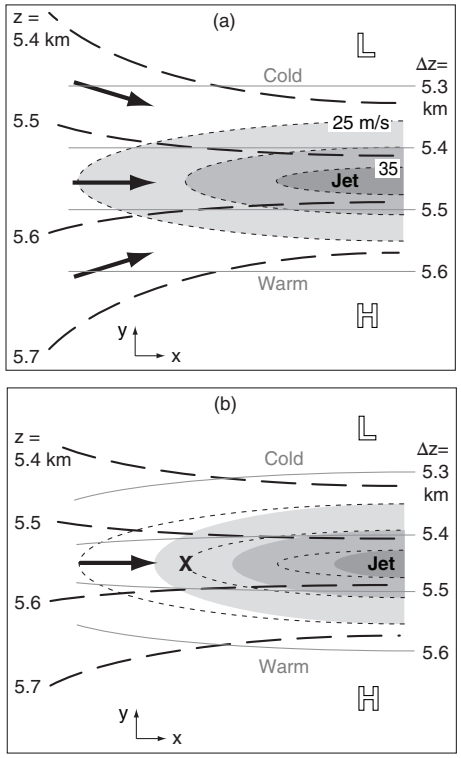

Fig. i. *Entrance region of jet streak on a 50 kPa isobaric surface. z is height (black dashed lines), Δz is thickness (thin grey lines), shaded areas are wind speeds, with initial isotachs as dotted black lines. L & H are low and high heights. (a) Initially. (b) Later.*

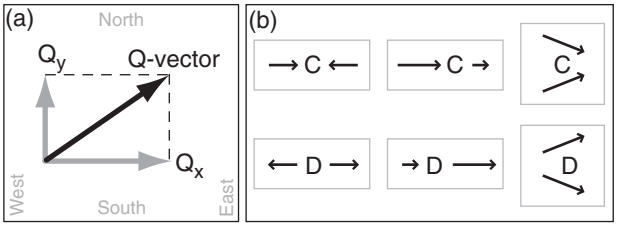

Figure 13.38
(a) Components of a Q-vector. (b) How to recognize patterns of vector convergence (C) and divergence (D) on weather maps.

Solved Example

Given the weather map at right showing the temperature and geostrophic wind fields over the NE USA. Find the Q-vector at the "X" in S.E. Pennsylvania. Side of each grid square is 100 km, and corresponds to G = 5 m/s for the wind vectors.

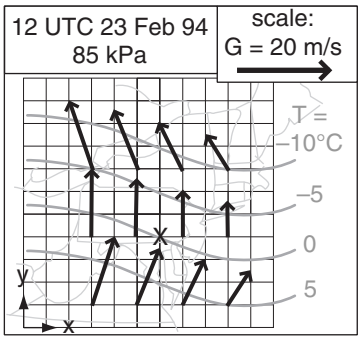

Figure j

Solution

Given: P = 85 kPa, G (m/s) & T (°C) fields on map.
Find: Q_x & Q_y = ? $m^2 \cdot s^{-1} \cdot kg^{-1}$

First, estimate U_g, V_g, and T gradients from the map.
$\Delta T/\Delta x$ = –5°C/600km, $\Delta T/\Delta y$ = –5°C/200km,
$\Delta U_g/\Delta x = 0$, $\Delta V_g/\Delta x$ = (–2.5m/s)/200km
$\Delta U_g/\Delta y$ = (–5m/s)/300km, $\Delta V_g/\Delta y = 0$,
$\Re/P = 0.287/85 = 0.003376\ m^3 \cdot kg^{-1} \cdot K^{-1}$

Use eq. (13.30): $Q_x = -(0.003376\ m^3 \cdot kg^{-1} \cdot K^{-1}) \cdot$
$[(0) \cdot (-8.3) + (-12.5) \cdot (-25)] \cdot 10^{-12}\ K \cdot m^{-1} \cdot s^{-1}$
$Q_x = \mathbf{-1.06x10^{-12}}\ m^2 \cdot s^{-1} \cdot kg^{-1}$

Use eq. (13.31): $Q_y = -(0.003376\ m^3 \cdot kg^{-1} \cdot K^{-1}) \cdot$
$[(-16.7) \cdot (-8.3) + (0) \cdot (-25)] \cdot 10^{-12}\ K \cdot m^{-1} \cdot s^{-1}$
$Q_y = \mathbf{-0.47x10^{-12}}\ m^2 \cdot s^{-1} \cdot kg^{-1}$

Use eq. (13.32) to find Q-vector magnitude:
$|Q| = [(-1.06)^2 + (-0.47)^2]^{1/2} \cdot 10^{-12}\ K \cdot m^{-1} \cdot s^{-1}$
$|Q| = \mathbf{1.16x10^{-12}}\ m^2 \cdot s^{-1} \cdot kg^{-1}$

Check: Units OK. Physics OK. Similar to Fig. 13.40.

Discussion: The corresponding Q-vector is shown at right; namely, it is pointing from the NNE because both Q_x and Q_y are negative. There was obviously a lot of computations needed to get this one Q-vector. Luckily, computers can quickly compute Q-vectors for many points in a grid, as shown in Fig. 13.40. Normally, you don't need to worry about the units of the Q-vector. Instead, just focus on Q-vector convergence zones such as computers can plot (Fig. 13.41), because these zones are where the bad weather is.

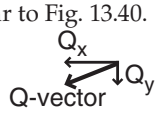

Q-Vectors

Q-vectors allow an alternative method for diagnosing vertical velocity that does not neglect as many terms.

Defining Q-vectors

Define a horizontal Q-vector (units $m^2 \cdot s^{-1} \cdot kg^{-1}$) with x and y components as follows:

$$Q_x = -\frac{\Re}{P}\left[\left(\frac{\Delta U_g}{\Delta x}\cdot\frac{\Delta T}{\Delta x}\right)+\left(\frac{\Delta V_g}{\Delta x}\cdot\frac{\Delta T}{\Delta y}\right)\right] \qquad (13.30)$$

$$Q_y = -\frac{\Re}{P}\left[\left(\frac{\Delta U_g}{\Delta y}\cdot\frac{\Delta T}{\Delta x}\right)+\left(\frac{\Delta V_g}{\Delta y}\cdot\frac{\Delta T}{\Delta y}\right)\right] \qquad (13.31)$$

where $\Re$ = 0.287 $kPa \cdot K^{-1} \cdot m^3 \cdot kg^{-1}$ is the gas constant, P is pressure, (U_g, V_g) are the horizontal components of geostrophic wind, T is temperature, and (x, y) are eastward and northward horizontal distances. On a weather map, the Q_x and Q_y components at any location are used to draw the Q-vector at that location, as sketched in Fig. 13.38a. Q-vector magnitude is

$$|Q| = \left(Q_x^{\,2} + Q_y^{\,2}\right)^{1/2} \qquad (13.32)$$

Estimating Q-vectors

Eqs. (13.30 - 13.32) seem non-intuitive in their existing Cartesian form. Instead, there is an easy way to estimate Q-vector direction and magnitude using weather maps. First, look at direction.

Suppose you fly along an isotherm (Fig. 13.39) in the direction of the thermal wind (in the direction that keeps cold air to your left). Draw an arrow describing the geostrophic wind vector that you observe at the start of your flight, and draw a second arrow showing the geostrophic wind vector at the end of your flight. Next, draw the vector difference, which points from the head of the initial vector to the head of the final vector. The Q-vector direction points 90° to the right (clockwise) from the geostrophic difference vector.

The magnitude is

$$|Q| = \frac{\Re}{P}\left|\frac{\Delta T}{\Delta n}\cdot\frac{\Delta \vec{V}_g}{\Delta s}\right| \qquad (13.33)$$

where Δn is perpendicular distance between neighboring isotherms, and where the temperature difference between those isotherms is ΔT. Stronger baroclinic zones (namely, more tightly packed isotherms) have larger temperature gradient $\Delta T/\Delta n$. Also, Δs

is distance of your flight along one isotherm, and ΔV_g is the magnitude of the geostrophic difference vector from the previous paragraph. Thus, greater change of geostrophic wind in stronger baroclinic zones has a larger Q-vector. Furthermore, Q-vector magnitude increases with the decreasing pressure P found at increasing altitude.

Using Q-vectors / Forecasting Tips

Different locations usually have different Q-vectors, as sketched in Fig. 13.40 for the case-study storm. Interpret Q-vectors on a synoptic weather map as follows:

- Updrafts occur where Q-vectors converge (Fig. 13.41 gives an example for the case-study storm).
- Subsidence (downward motion) occurs where Q-vectors diverge.
- Frontogenesis occurs where Q-vectors cross isentropes (lines of constant potential temperature) from cold toward warm.
- Updrafts in the TROWAL region ahead of a warm occluded front occur during cyclolysis where the along-isentrope component of Q-vectors converge.

Using the tricks for visually recognizing patterns of vectors on weather maps (Fig. 13.38b), you can identify by eye regions of convergence and divergence in Fig. 13.40. Or you can let the computer analyze the Q-vectors directly to plot Q-vector convergence and divergence (Fig. 13.41). Although Figs. 13.40 and 13.41 are analysis maps of current weather, you can instead look at Q-vector forecast maps as produced automatically by numerical weather prediction models (see the NWP chapter) to help you forecast regions of updraft, clouds, and precipitation.

Remember that Q-vector convergence indicates regions of likely synoptic-scale upward motion and associated clouds and precipitation. Looking at Fig. 13.41, see a moderate convergence region running from the western Gulf of Mexico up through eastern Louisiana and southern Mississippi. It continues as a weak convergence region across Alabama and Georgia, and then becomes a strong convergence region over West Virginia, Virginia and Maryland. A moderate convergence region extend northwest toward Wisconsin.

This interpretation agrees with the general locations of radar echoes of precipitation plotted in Fig. 13.12d. Note that the frontal locations, as analyzed in Fig. 13.12d do not correspond to the precipitation regions. This demonstrates the utility of Q-vectors — even when the updrafts and precipitation are not exactly along a front, you can use Q-vectors to anticipate the bad-weather regions.

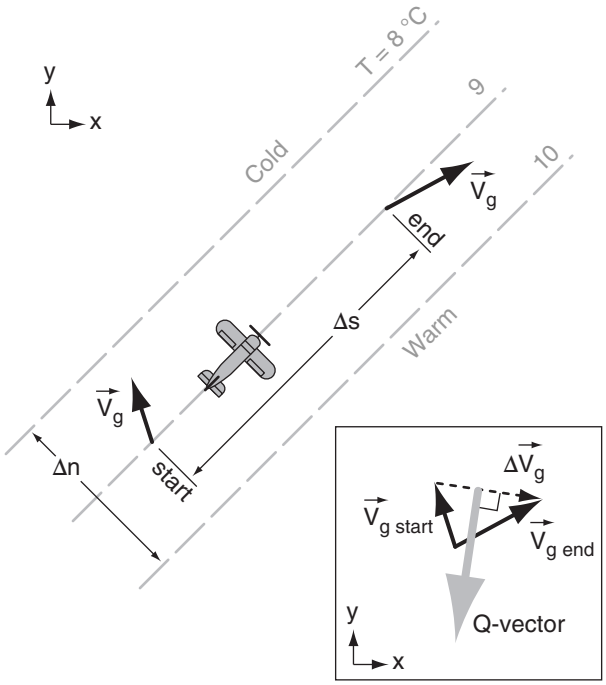

Figure 13.39
Illustration of natural coordinates for Q-vectors. Dashed grey lines are isotherms. Aircraft flies along the isotherms with cold air to its left. Black arrows are geostrophic wind vectors. Grey arrow indicates Q-vector direction (but not magnitude).

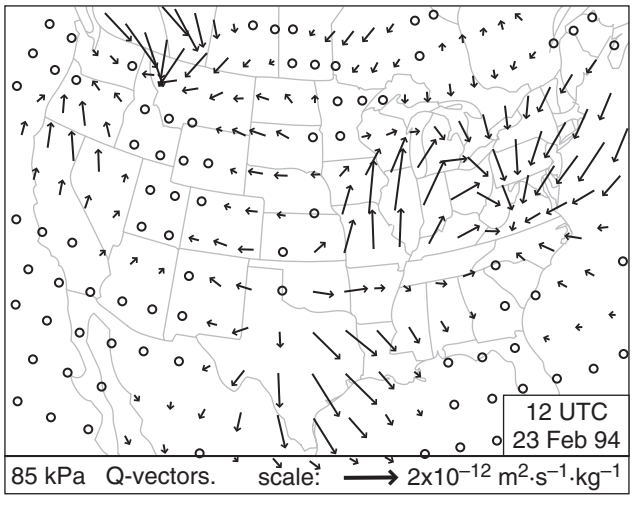

Figure 13.40
*Weather map of Q-vectors. (**o** means small magnitude.)*

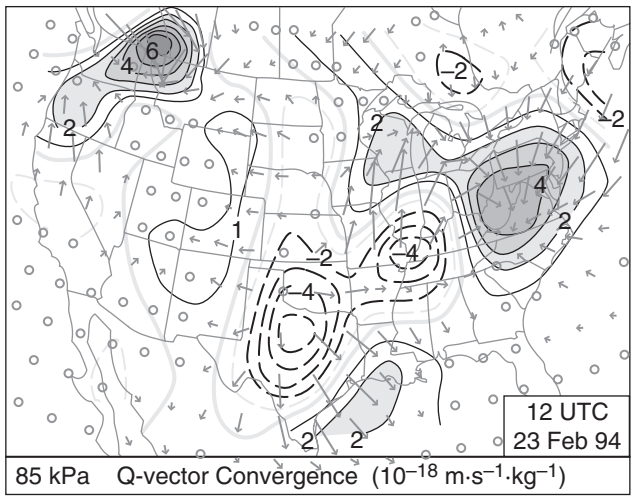

Figure 13.41
Convergence of Q-vectors (shaded). Divergence (dashed lines).

Solved Example

Discuss the nature of circulations and anticipated frontal and cyclone evolution, given the Q-vector divergence region of southern Illinois and convergence in Maryland & W. Virginia, using Fig. 13.41.

Solution

Given: Q-vector convergence fields.
Discuss: circulations, frontal & cyclone evolution

Discussion: From Fig. 13.10b, recall that the low-center is over southern Illinois, right at the location of maximum divergence of Q-vectors in Fig. 13.41. This suggests that: (1) The cyclone is entering the cyclolysis phase of its evolution (synoptic-scale subsidence that opposes any remaining convective updrafts from earlier in the cyclones evolution) as it is steered northeastward toward the Great Lakes by the jet stream (Fig. 13.17b). (2) The cyclone will likely shift toward the more favorable updraft region over Maryland. This shift indeed happened, as discussed in the case-study overview earlier in this Chapter, and as plotted in Figs. 13.10c & 13.11.

The absence of Q-vectors crossing the fronts in western Tennessee and Kentucky suggest no frontogenesis there.

Between Maryland and Illinois, we would anticipate a mid-tropospheric ageostrophic wind from the east-northeast. This would connect the updraft region over western Maryland with the downdraft region over southern Illinois. This circulation would move air from the warm-sector of the cyclone to over the low center, helping to feed warm humid air into the cloud shield over and north of the low.

Also, along the Texas Gulf coast, note that the Q-vectors in Fig. 13.40 are crossing the cold front (Fig. 13.12b) from cold toward warm air. Using the third bullet on the previous page, you can anticipate frontogenesis in this region.

Resolving the Geostrophic Paradox

What about the ageostrophic circulations that were missing from the Trenberth omega equation? Fig. 13.41 suggests updrafts at the Q-vector convergence region over the western Gulf of Mexico, and subsidence at the divergence region of central Texas. Due to mass continuity, expect an ageostrophic circulation of mid-tropospheric winds from the southeast toward the northwest over the Texas Gulf coast, which connects the up- and down-draft portions of the circulation. This ageostrophic wind moves warm pre-frontal air up over the cold front in a **direct circulation** (i.e., a circulation where warm air rises and cold air sinks).

But if you use the 85 kPa height chart of Fig. 13.13a to anticipate geostrophic winds over central Texas, you would expect light winds at 85 kPa from the northwest. These opposing geostrophic and ageostrophic winds agree nicely with the warm-air convergence (creating thunderstorms) for the cold katafront sketch in Fig. 12.16a.

Similarly, over West Virginia and Maryland, Fig. 13.41 shows convergence of Q-vectors at low altitudes, suggesting rising air in that region. This updraft adds air mass to the top of the air column, increasing air pressure in the jet streak right entrance region, and tightening the pressure gradient across the jet entrance. This drives faster geostrophic winds that counteract the advection of slower geostrophic winds in the entrance region. Namely, the ageostrophic winds as diagnosed using Q-vectors help prevent the Geostrophic Paradox (Focus Box).

BEYOND ALGEBRA • Q-vector Omega Eq.

By considering the added influence of ageostrophic winds, the Q-vector omega equation is:

$$\left\{\nabla_p^2 + \frac{f_o^2}{\sigma}\frac{\partial^2}{\partial p^2}\right\}\omega = \frac{-2}{\sigma}\cdot\left[\frac{\partial Q_1}{\partial x} + \frac{\partial Q_2}{\partial y}\right] + \frac{f_o\cdot\beta}{\sigma}\frac{\partial V_g}{\partial p} - \frac{R/C_p}{\sigma\cdot P}\nabla^2(\Delta Q_H)$$

The left side looks identical to the original omega equation (see a previous Beyond Algebra box for an explanation of most symbols). The first term on the right is the convergence of the Q vectors. The second term is small enough to be negligible for synoptic-scale systems. The last term contributes to updrafts if there is a local maximum of sensible heating ΔQ_H.

SEA-LEVEL-PRESSURE TENDENCY

Sea-level pressure is another measure of cyclone intensity. When pressure drops in an intensifying low center, the low is said to **deepen**. In other words, the low becomes lower. This corresponds to **falling** geopotential heights. When sea-level pressure increases, the low **fills** and heights **rise** (i.e., the low weakens).

The pressure change with time is called the **pressure tendency**, and is closely related to the **height tendency** of isobaric surfaces (Fig. 13.42). The amount of air mass in the column of atmosphere above the low center determines the surface pressure in a hydrostatic environment.

Mass Budget

We will approach this subject heuristically. Picture a small cylinder filled with air, as shown in Fig. 13.43a. Near the middle of the cylinder is a massless, frictionless piston. Above and below the piston, the air pressures are identical, and the air densities are identical (i.e., ignore gravity for now).

Suppose that some of the air is withdrawn from the top of the cylinder, as shown in Fig. 13.43b. Pressure in the top of the cylinder will decrease, which will cause the piston to rise until the bottom pressure decreases to equal the top pressure. At that point, the densities above and below the piston are also identical. Similarly, air mass could have been added to the top of the cylinder, causing the pressure to increase and piston to move down.

Thus, you can use the vertical motion of the piston as a surrogate measure of net mass flow and pressure change. Namely, upward motion indicates a decrease in total air mass in the cylinder (summing both above and below the piston), and is associated with pressure decrease in the cylinder. Conversely, downward motion indicates increases in both mass and pressure.

That rule seems simple. However, picture what would happen if air were withdrawn or added to the bottom of the cylinder. Upward piston motion would correspond to an increase in mass and pressure, not a decrease as before. Thus, you can use vertical piston movement as a surrogate measure of pressure change only if you change the sign of the result depending on whether mass is added at the top or bottom of the column.

Extend this reasoning to the atmosphere, where the cylinder of the previous example will now be visualized as a column of air from the ground to the top of the atmosphere. A complication is that atmospheric density decreases with height. Recall that

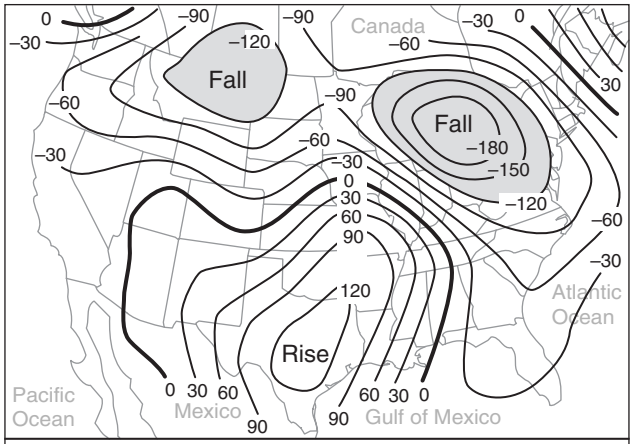

Figure 13.42
Change of geopotential height with time near the surface, for the case-study storm. Shaded regions indicates where heights (and surface pressures) are decreasing (falling); namely, regions of cyclogenesis. Height rises favor anticyclogenesis.

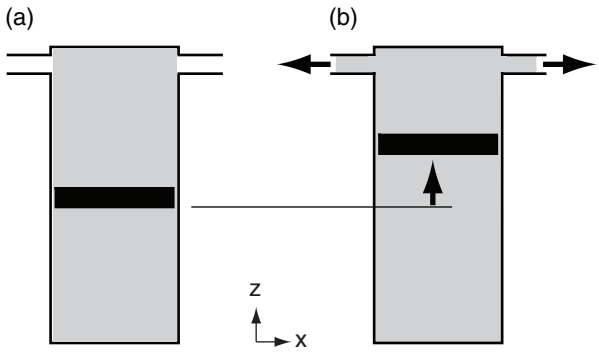

Figure 13.43
(a) Column of air (grey shading) in a cylinder, with a piston (black) in the middle. (b) Piston location changes after some air is withdrawn from the top. Assume that no air leaks past the piston.

Solved Example

If the surface pressure is 100 kPa, how much air mass is in the whole air column above a 1 meter squared surface area?

Solution

Given: $A = 1\ m^2$, $P_s = 100$ kPa
Find: $m = ?$ kg

Rearrange eq. (13.34) to solve for m:
$m = P_s \cdot A / |g| = [(100\ kPa) \cdot (1\ m^2)\ ] / (9.8\ m/s^2)$

But from Appendix A: $1\ Pa = 1\ kg \cdot m^{-1} \cdot s^{-2}$, thus:
$m = [(10^5\ kg \cdot m^{-1} \cdot s^{-2}) \cdot (1\ m^2)\ ] / (9.8\ m/s^2)$
$= \underline{\mathbf{10.2 \times 10^3}}\ \underline{\mathbf{kg}} = 10.2$ Mg

Check: Units OK. Physics OK.
Discussion: This calculation assumed that gravitational acceleration is approximately constant over the depth of the atmosphere.

Eq. 13.34 can be used for the pressure at any height in the atmosphere, but only if m represents the mass of air above that height. For example, if the tropopause is at pressure 25 kPa, then the mass of air above the tropopause is one quarter of the previous answer; namely, 2.55 Mg over each square meter.

Subtracting this value from the previous answer shows that of the total 10.2 Mg of mass in the atmosphere above a square meter, most of the air (7.65 Mg) is within the troposphere.

Solved Example

Divergence of air at the top of the troposphere removes air molecules from the top of a tropospheric column, causing a 0.1 m/s updraft at height 8 km above ground level (AGL). No other processes add or remove air mass. What is the corresponding surface pressure tendency?

Solution

Given: $z = 8$ km, $W_{surrogate}(8\ km) = 0.1$ m/s
Find: $\Delta P_s / \Delta t = ?$ kPa/s

For air density at $z = 8$ km, assume a standard atmosphere. Use $\rho = 0.5252\ kg/m^3$.

Use eq. (13.37) with negative sign because the forcing is at the top of the troposphere:
$\Delta P_s / \Delta t = -(9.8\ m/s^2) \cdot (0.5252\ kg/m^3) \cdot (0.01\ m/s)$
$= -0.0515\ kg \cdot m^{-1} \cdot s^{-3} = -0.0515$ Pa/s
$= \underline{\mathbf{-5.15 \times 10^{-5}\ kPa/s}}$

Check: Units OK. Physics reasonable.
Discussion: The corresponding hourly pressure tendency is $\Delta P_s / \Delta t = -0.185$ kPa/h. If this rapid deepening of the cyclone were to continue for 24 h, we would classify this explosive cyclogenesis as a **cyclone bomb**.

pressure is force per unit area, and that force is mass times acceleration. Recall from Chapter 1 that sea-level pressure P_s is a measure of the total **mass** m **of air in a column** above the surface

$$P_s = \frac{|g|}{A} \cdot m \qquad \bullet(13.34)$$

where $|g| = 9.8\ m \cdot s^{-2}$ is gravitational acceleration magnitude, and A is the horizontal cross-section area under the column.

Changes in sea-level pressure with time t are caused by changes in total air mass above the surface:

$$\frac{\Delta P_s}{\Delta t} = \frac{|g|}{A} \cdot \frac{\Delta m}{\Delta t} \qquad \bullet(13.35)$$

Recall from the definition of density that

$$m = \rho \cdot Volume = \rho \cdot A \cdot z \qquad (13.36)$$

where z is the height of a hypothetical volume containing constant-density air. Thus, $\Delta m / \Delta t$ causes $\Delta z / \Delta t$, where $\Delta z / \Delta t$ is vertical velocity w. Define the change of height of the hypothetical volume with time as a surrogate velocity $W_{surrogate}$ that is analogous to the piston movement.

Thus, if the mass flow in or out of the column occurs at a height z where the air density $\rho(z)$ is known, then the equations above can be combined to give the pressure tendency:

$$\frac{\Delta P_s}{\Delta t} = \pm |g| \cdot \rho(z) \cdot W_{surrogate}(z) \qquad (13.37)$$

The proper sign for the right-hand-side of the equation must be chosen depending on the cause of the surrogate vertical motion (i.e., use the negative sign if it is driven at the top of the troposphere, and positive sign if driven at the bottom). More than one mechanism can add or subtract mass to a column of air, so generalize the right-hand-side of eq. (13.37) to be a sum of terms.

Four mechanisms will be included here in a simplified model for pressure tendency:

- Upper-level divergence
- Boundary-layer pumping
- Advection
- Diabatic heating

Upper-level **Divergence** has just been described in the previous section as a mass-removal process. Namely, sea-level pressure can drop if the jet stream or a jet streak removes mass aloft. That resulting W_{mid} will be used as one of the forcing terms in the

net pressure-tendency equation, to be given later in this section.

Boundary-layer pumping was discussed in the Dynamics chapter. Sometimes lows deepen so rapidly, that the accelerating boundary-layer winds blow directly from high to low pressure as an ageostrophic non-equilibrium flow. Later, if the low persists for a sufficiently-long duration, the winds can turn cyclonically and behave as a classical equilibrium boundary-layer flow, with a vertical velocity as was given in the Dynamics chapter. This W_{BL} will be used later in the net pressure-tendency equation.

Advection describes the movement of cyclones by the steering-level winds. Namely, surface pressure can drop at a fixed point on the ground if the horizontal wind blows in an air column having less total mass than the column of air that is blowing out. Analogous to advection terms in other equations earlier in this book (e.g., heat, moisture, and momentum budget eqs.), the advection term will be approximated as $-M_c \cdot (\Delta P_s/\Delta s)$, where M_c is the speed of movement of the whole column of air along path s, and $\Delta P_s/\Delta s$ is the horizontal surface pressure gradient along that path.

Diabatic (i.e., not adiabatic) **heating** due to condensation is discussed in detail in the next section. Other diabatic effects such as direct radiative heating can also affect the mass budget, but are not discussed here.

Diabatic Heating due to Condensation

When water vapor condenses in clouds, latent heat is released. This heat warms the air in a column, causing it to expand (Fig. 13.44). According to the hypsometric equation, horizontal pressure gradients develop that push the air out of the top of the column. Hence, mass diverges from the column, which lowers the sea-level pressure (see the Hydrostatic Thermal Circulation section of the Global Circulation chapter).

In an overly simplified point-of-view, the heated air expands out of the top of the column and overflows. The amount of overflow out of the top in this simple view equals the amount of mass diverged from the sides in a more realistic view. None-theless, vertical velocity W at the top of the column is a surrogate measure of the mass loss.

If all of the condensation falls as precipitation, then the latent-heating rate is related to the rainfall rate RR:

$$\frac{\Delta T_v}{\Delta t} = \frac{a}{\Delta z} \cdot \frac{L_v}{C_p} \cdot \frac{\rho_{liq}}{\rho_{air}} \cdot RR \qquad (13.38)$$

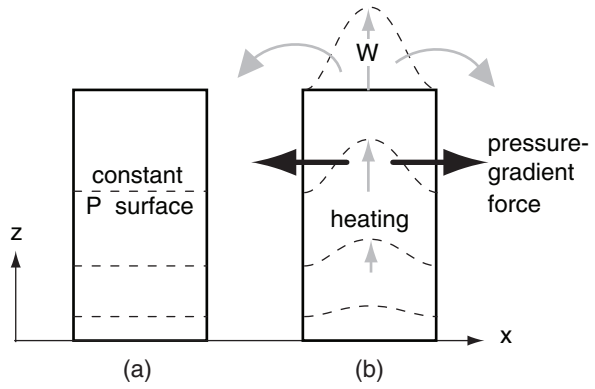

Figure 13.44
(a) Column of air before heating. (b) Column of air after heating, where the air expands and overflows out of the column. P = pressure; W = vertical velocity.

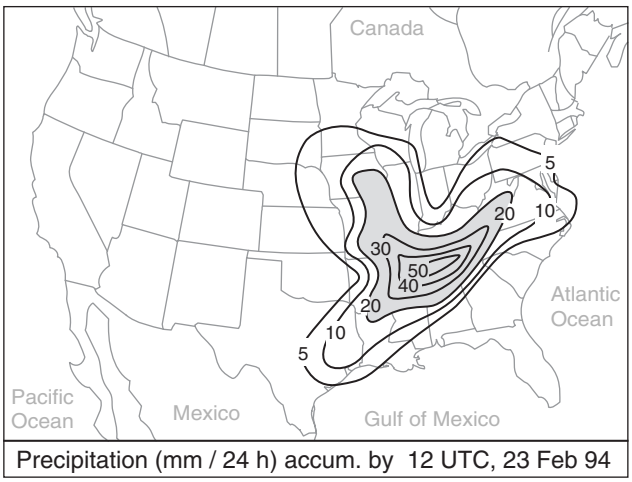

Figure 13.45
Precipitation (liquid equivalent) measured with rain gauges.

Solved Example

For the maximum contoured precipitation rate for the case-study storm (in Fig. 13.45), find the diabatic heating contribution to sea-level pressure tendency.

Solution

Given: RR = 50 mm/24 h
Find: $\Delta P_s/\Delta t$ = ? kPa/h

First, convert RR from 24 h to 1 hr:
RR = 2.1 mm/h

Use eq. (13.40):
$\Delta P_s/\Delta t = -(0.082\ \text{kPa/mm}_{\text{rain}})\cdot(2.1\ \text{mm/h})$
$= \underline{\mathbf{-0.17\ kPa/h}}$

Check: Units OK. Physics OK. Magnitude OK.
Discussion: This deepening rate corresponds to 4.1 kPa/day — not large enough to be classified as a cyclone "bomb".

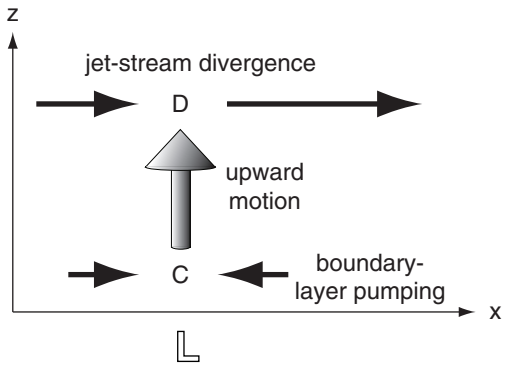

Figure 13.46
Sketch of coupling between convergence (C) in the boundary layer and divergence (D) in the upper atmosphere. Arrows represent winds. L is location of low-pressure center at surface.

where T_v is the virtual temperature in the column, t is time, $a = 10^{-6}$ km/mm, L_v is the latent heat of vaporization, C_p is the specific heat at constant pressure for air, L_v/C_p = 2500 K·kg$_{\text{air}}$ /kg$_{\text{liq}}$, ρ_{liq} is the density of liquid water (1000 kg/m^3), ρ_{air} is the density of air, Δz is the column depth in km, and where RR often has units of mm/h.

The net effect on sea-level pressure can be found by combining the hypsometric equation and the equation above:

$$\frac{\Delta P_s}{\Delta t} = -\frac{|g|}{\overline{T}_v}\cdot\frac{L_v}{C_p}\cdot\rho_{liq}\cdot RR \qquad \bullet(13.39)$$

where $|g|$ = 9.8 m·s^{-2} is the magnitude of gravitational acceleration, RR is rainfall rate (often converted to units of mm/h), and $\overline{T_v}$ is the average virtual temperature in the column (≈ 300 K). Because RR is the net precipitation reaching the ground, the equation above represents the net or average effect of latent heating over the whole cyclone depth.

Although this equation depends on absolute temperature (which can vary), you can approximate the equation as

$$\frac{\Delta P_s}{\Delta t} \approx -b\cdot RR \qquad \bullet(13.40)$$

where $b = \dfrac{|g|}{\overline{T}_v}\cdot\dfrac{L_v}{C_p}\cdot\rho_{liq} \approx 0.082\ \text{kPa/mm}_{\text{rain}}$.

You can estimate rainfall rate with weather radar, or you can measure it with rain gauges. Fig. 13.45 shows measured precipitation liquid-equivalent depth (after melting any snow) for the case-study storm.

Net Pressure Tendency

Combining all of the mechanisms just described using the idealized geometry of Fig. 13.46 yields the following form for the net **sea-level pressure tendency equation**:

$$\frac{\Delta P_s}{\Delta t} = -M_c\frac{\Delta P_s}{\Delta s} + |g|\cdot\rho_{BL}\cdot W_{BL} - |g|\cdot\rho_{mid}\cdot W_{mid} - b\cdot RR \qquad \bullet(13.41)$$

pressure tendency — *horizontal advection* — *boundary-layer pumping (in)* — *upper-level horiz. divergence (out)* — *latent heating*

where (ρ_{BL}, ρ_{mid}) and (W_{BL}, W_{mid}) are the average air densities and vertical velocities at the top of the boundary layer and midpoint of the column, respectively. The horizontal translation speed of the column is M_c measured positive in the direction of movement, along horizontal path s. RR is rainfall

rate at the surface, $|g| = 9.8\ \text{m·s}^{-2}$ is gravitational acceleration magnitude, and $b \approx 0.082\ \text{kPa/mm}_{\text{rain}}$. A negative value of $\Delta P_s/\Delta t$ corresponds to pressure drop and cyclone intensification.

Imagine a scenario where baroclinic instability in the jet stream causes a Rossby wave to move over some location on the Earth that initially lacks any strong highs or lows. If the upper-level trough is west of this location and ridge east, then divergence aloft can begin to suck air out of the column (time *A* in Fig. 13.47). Similarly, the presence of a jet streak at the right location could initiate upper-level divergence.

As sea-level pressure falls, pressure gradient force begins to spin-up the circulation around the low. Initially the circulation is weak, resulting in weak boundary-layer pumping. At this stage the upper level divergence is continuing to withdraw air from the column faster than boundary-layer pumping fills it, allowing the low to intensify (time *B*).

The rising air in the cyclone causes clouds to form, with the resulting precipitation. Latent heating warms the air, which contributes to the loss of mass and decrease of sea-level pressure.

As the low matures, it wraps the cold and warm airmasses further around the low center, thereby modifying the temperature gradients and thermal winds. The low center begins to lag behind the region of maximum divergence aloft. The surface low and associated air masses also interact with and modify the jet-stream aloft.

After the time of maximum divergence (time *C* in Fig. 13.47), withdrawal of air aloft decreases while input of air from the boundary layer increases, eventually reaching the point (time *D*) where input and output match. The cyclone has reached its lowest pressure at this point.

Later as the low occludes, it lags so far behind the upper-air wave that jet-stream divergence ceases over the column. Meanwhile the still-spinning surface low continues to pump boundary-layer air into the column. With the upper-level trough east of the surface low, convergence aloft also pumps air into the column from above. Thus, input of mass is now occurring at both the top and bottom (time *E*), causing the sea-level pressure to rise. The cyclone rapidly fills and spins down as pressure gradients weaken.

Finally at (time *F*), the low has filled completely, and circulations disappear. During its lifetime, the low has done its job of moving warm air poleward and cold air equatorward. Analogous to Le Chatelier's principle, it has partially undone the baroclinic instability that produced it in the first place.

Solved Example

Suppose upper level divergence has an effective vertical velocity of 0.03 m/s over a cyclone, while boundary-layer pumping causes a vertical velocity of 0.01 m/s. The rainfall rate is 5 mm/h. Sea-level pressure increases 1 kPa across a distance of 200 km as you move west of the cyclone, and there is a steering wind from the west at 20 m/s (so *s* is positive toward the east). Find the sea-level pressure tendency.

Solution

Given: $W_{mid} = 0.03$ m/s , $W_{BL} = 0.01$ m/s,
$\Delta P/\Delta s = -1$ kPa/200 km, $RR = 5$ mm/h

Find: $\Delta P_s/\Delta t$ = ? kPa/h

Assume: $\rho_{BL} = 1.112\ \text{kg·m}^{-3}$, $\rho_{mid} = 0.5\ \text{kg·m}^{-3}$

Use eq. (13.41): $\Delta P_s/\Delta t =$

$$-\left(20\frac{\text{m}}{\text{s}}\right)\left(\frac{-1\text{kPa}}{2\times10^5\,\text{m}}\right)+\left(9.8\frac{\text{m}}{\text{s}^2}\right)\left(1.112\frac{\text{kg}}{\text{m}^3}\right)\left(0.01\frac{\text{m}}{\text{s}}\right)$$
$$-\left(9.8\frac{\text{m}}{\text{s}^2}\right)\left(0.5\frac{\text{kg}}{\text{m}^3}\right)\left(0.03\frac{\text{m}}{\text{s}}\right)-\left(0.084\frac{\text{kPa}}{\text{mm}}\right)\left(5\frac{\text{mm}}{\text{h}}\right)$$

$\Delta P_s/\Delta t =$ 0.0001 +0.00011 −0.00015 −0.00012 kPa/s
advect +B.L. – jet diverg. – diabatic

$= -0.00006$ kPa/s $=$ **$\underline{-0.22\ \text{kPa/h}}$**

Check: Units OK. Physics OK. Magnitude OK.
Discussion: The cyclone would continue to deepen, given this scenario. Advection is quite important. Don't forget to convert from Pa to kPa in the boundary-layer (BL) and jet-divergence terms. Also convert the rainfall term to kPa/s from kPa/h.

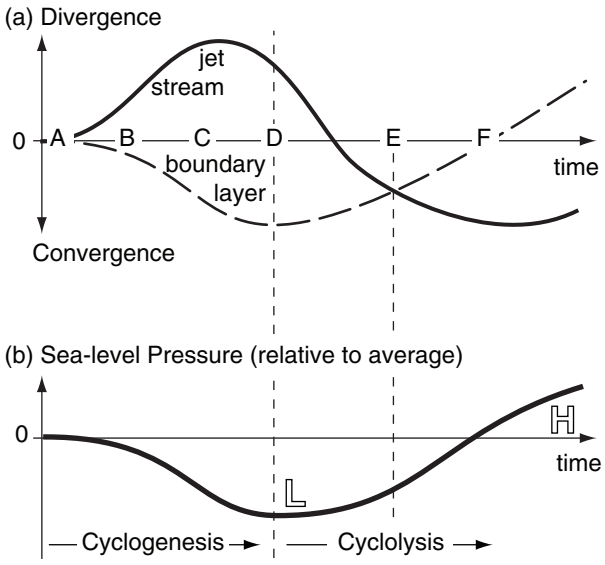

Figure 13.47
(a) Divergence contributions from the jet stream and boundary layer, and (b) their modification of sea-level pressure during cyclone evolution.

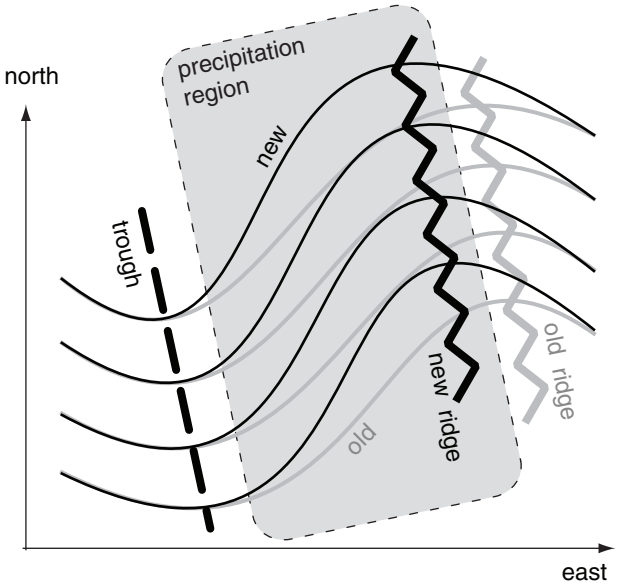

Figure 13.48
50 kPa chart showing cloud and precipitation region in the upper troposphere, causing latent heating and a westward shift of the ridge axis.

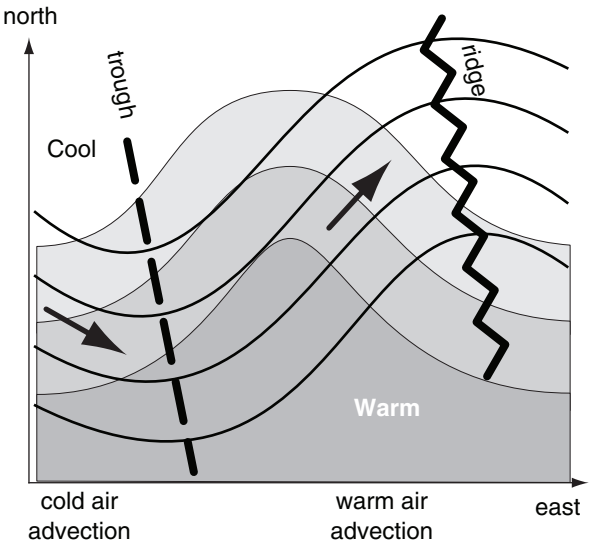

Figure 13.49
50 kPa chart showing a temperature field (shaded) that is 1/4 wavelength west of the wave in the height contours (solid lines).

SELF DEVELOPMENT OF CYCLONES

Up to this point, cyclogenesis has been treated as a response to various external imposed forcings. However, some positive feedbacks allow the cyclone to enhance its own intensification. This is often called **self development**.

Condensation

As discussed in the quasi-geostrophic vorticity subsection, divergence of the upper-level winds east of the Rossby-wave trough (Fig. 13.48) causes a broad region of upward motion there. Rising air forms clouds and possibly precipitation if sufficient moisture is present. Such a cloud region is sometimes called an **upper-level disturbance** by broadcast meteorologists, because the bad weather is not yet associated with a strong surface low.

Latent heating of the air due to condensation enhances buoyancy and increases upward motion. The resulting **stretching** enhances spin-up of the vorticity, and the upward motion withdraws some of the air away from the surface, leaving lower pressure. Namely, a surface low forms.

Diabatic heating also increases the average temperature of the air column, which pushes the 50 kPa pressure surface upward (i.e., increasing its height), according to the hypsometric relationship. This builds or strengthens a ridge in the upper-level Rossby wave west of the initial ridge axis.

The result is a shortening of the wavelength between trough and ridge in the 50 kPa flow, causing tighter turning of the winds and greater vorticity (Fig. 13.48). Vorticity advection also increases.

As the surface low strengthens due to these factors (i.e., divergence aloft, vorticity advection, precipitation, etc.), more precipitation and latent heating can occur. This positive feedback shifts the upper-level ridge further west, which enhances the vorticity and the vorticity advection. The net result is rapid strengthening of the surface cyclone.

Temperature Advection

Cyclone intensification can also occur when warm air exists slightly west from the Rossby-wave ridge axis, as sketched in Fig. 13.49. For this situation, warm air advects into the region just west of the upper-level ridge, causing ridge heights to increase. Also cold air advects under the upper-level trough, causing heights to fall there.

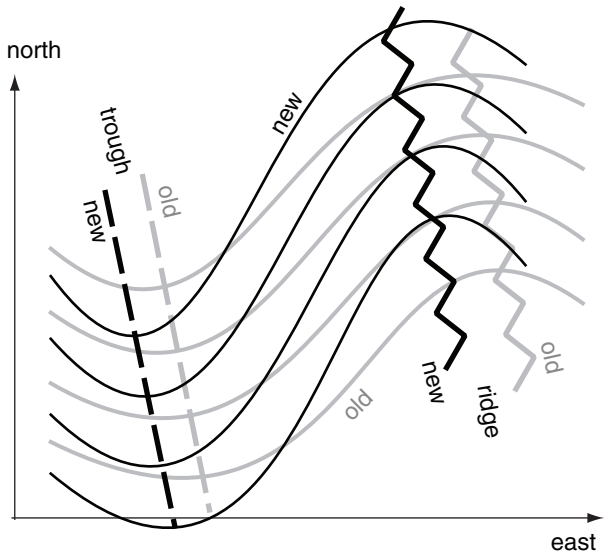

Figure 13.50
50 kPa chart showing the westward shift and intensification of north-south wave amplitude caused by differential temperature advection.

The net result is intensification of the Rossby-wave amplitude (Fig. 13.50) by deepening the trough and strengthening the ridge. Stronger wave amplitude can cause stronger surface lows due to enhanced upper-level divergence.

Propagation of Cyclones

For a train of cyclones and anticyclones along the mid-latitude baroclinic zone (Fig. 13.51a), a Q-vector analysis (Fig. 13.51b) suggests convergence of Q-vectors east of the low, and divergence of Q-vectors west of the low (Fig. 13.51c). But convergence regions imply updrafts with the associated clouds and surface-pressure decrease — conditions associated with cyclogenesis. Thus, the cyclone (𝕃) in Fig. 13.51c would tend to move toward the updraft region indicated by the Q-vector convergence.

The net result is that cyclones tend to propagate in the direction of the thermal wind.

Creation of Baroclinic Zones

Cyclones and anticyclones tend to create or strengthen baroclinic zones such as fronts. This works as follows.

Consider a train of lows and highs in a region with uniform temperature gradient, as shown in Fig. 13.52a. The rotation around the lows and highs tend to distort the center isotherms into a wave, by moving cold air equatorward on the west side of the lows and moving warm air poleward on the east side.

In addition, convergence into lows pulls the isotherms closer together, while divergence around

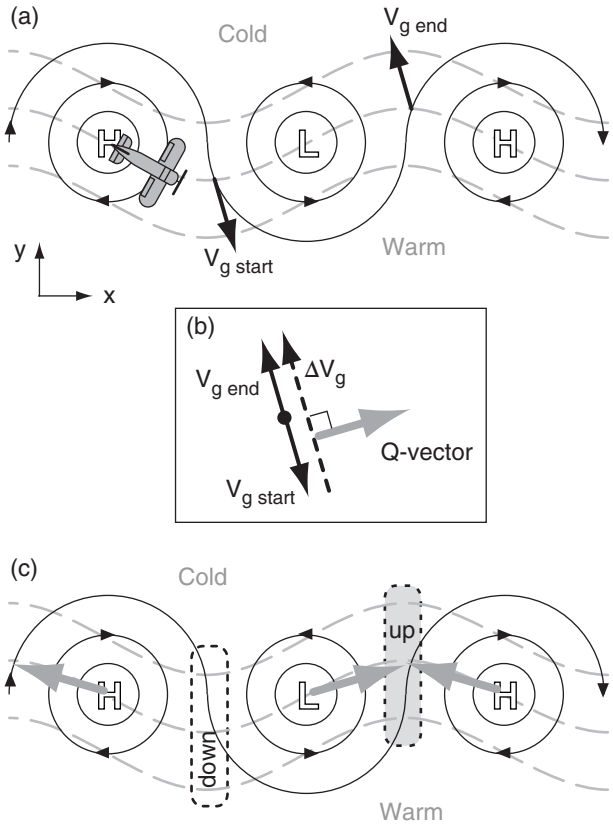

Figure 13.51
Using Q-vectors to estimate cyclone propagation. Grey dashed lines are isotherms (or thickness contours). Thin black lines are isobars (or height contours). (a) Airplane is flying in the direction of the thermal wind. Black arrows are geostrophic wind vectors encountered by the airplane on either side of the cyclone (𝕃). (b) Vector difference (black dashed line) between starting and ending geostrophic-wind vectors (drawn displaced to the right a bit so you can see it) for the portion of aircraft flight across the low. Q-vector (grey thick arrow) is 90° to the right of the dashed vector. (c) Q-vector from (b) is copied back to the cyclone. Similar analyses can be done to find the Q-vectors for the anticyclones (ℍ). Convergence of Q-vectors (grey shaded box with dotted outline) indicates region of updraft. Divergence of Q-vectors (white box with dotted outline) indicates region of downdraft. (for N. Hemisphere.)

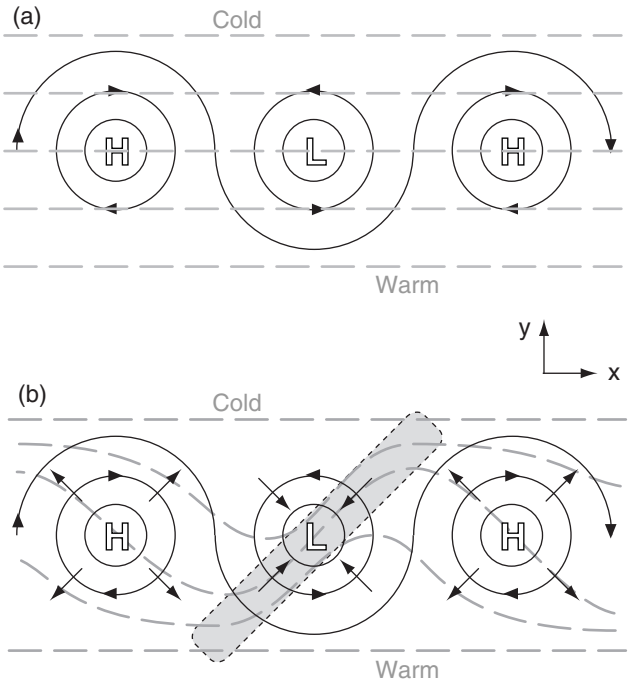

Figure 13.52
Rotational and divergent wind components (thin black arrows) and isotherms (dashed grey lines) in the lower troposphere. (a) Initial train of highs (H) and lows (L) in a uniform temperature gradient in the N. Hemisphere. (b) Later evolution of the isotherms into frontal zones (shaded rectangle is a baroclinic zone).

highs tends to push isotherms further apart. The combination of rotation and convergence/divergence tends to pack the isotherms into frontal zones near lows, and spread isotherms into somewhat homogeneous airmasses at highs (Fig. 13.52b).

Much of the first part of this chapter showed how cyclones can develop over existing baroclinic regions. Here we find that cyclones can help create those baroclinic zones — resulting in a positive feedback where cyclones modify their environment to support further cyclogenesis. Thus, cyclogenesis and frontogenesis often occur simultaneously.

Propagation of Cold Fronts

Recall from Fig. 13.8 that the circulation around a cyclone can include a deformation and diffluence region of cold air behind the cold front. If the diffluent winds in this baroclinic zone are roughly geostrophic, then you can use Q-vectors to analyze the ageostrophic behavior near the front.

Fig. 13.53a on the next page is zoomed into the diffluence region, and shows the isotherms and geostrophic wind vectors. By flying an imaginary airplane along the isotherms and noting the change in geostrophic wind vector, estimate the Q-vectors at the front as drawn in Fig. 13.53b. Further from the front, the Q-vectors are near zero.

Thus, Q-vector convergence is along the leading edge of the cold front (Fig. 13.53c), where warm air is indeed rising over the front. Behind the cold front is Q-vector divergence, associated with downward air motion of cool dry air from higher in the troposphere (Fig. 13.8).

Science Graffito & On Doing Science • Truth vs. Uncertainty

"There are no certainties in science. Scientists do not assert that they know what is immutably 'true' — they are committed to searching for new, temporary theories to explain, as best they can, phenomena." Science is "a process for proposing and refining theoretical explanations about the world that are subject to further testing and refinement." – U.S. Supreme Court.

[*CAUTION: The definition, role, and activities of science cannot be defined or constrained by a legal court or religious inquisition. Instead, science is a philosophy that has gradually developed and has been refined by scientists. The "On Doing Science" boxes in this book can help you to refine your own philosophy of science.*]

SUMMARY

Cyclones are regions of low pressure, cyclonic vorticity, and upward motion. These lows can cause clouds, precipitation and strong winds. Cyclogenesis is the birth or growth of cyclones, while cyclolysis is their decline and death.

Mountain ranges can disturb the planetary flow, causing north-south waves in the otherwise west-to-east jet stream. The troughs of such waves contain cyclonic curvature, and usually exist just east of the mountains. This tends to enhance cyclogenesis in the lee of mountain ranges, such as in Colorado and Alberta just east of the Rocky Mountains.

Vorticity is one measure of cyclone intensity. Vorticity changes with terrain height, advection, stretching, tilting, turbulent drag, and with latitude.

Upward motion is another measure of cyclone intensity. It is often driven by jet streaks, and by curvature in the jet stream. Greater updrafts are possible in environments with weaker static stability, and with closely-packed and tightly-curved isobars on sea-level weather maps. Advection of geostrophic vorticity by the thermal wind also contributes to upward motion, as described by the omega equation and Sutcliffe's development equation. Upward motion can also be found in regions where Q-vectors converge.

Divergence aloft tends to reduce the sea-level pressure, and lows can deepen due to latent heating associated with precipitation. This is partially counteracted by inflow of air due to boundary-layer pumping, which is relentless in trying to cause cyclolysis. Once a surface low exists, it can enhance itself via temperature advection and latent-heat release in clouds. Cyclogenesis and frontogenesis often occur simultaneously.

A variety of weather maps, such as for the 23 February 1994 case-study shown in this chapter, can be used to study extratropical cyclones and other synoptic weather features.

Threads

Almost every chapter preceding this one contributed to the understanding of extratropical cyclones. We utilized concepts of temperature, density, pressure, and the standard atmosphere from Chapter 1. Cyclones form as nature's way to redistribute heat caused by the radiative imbalance (Chapter 2) between the equator and poles. This radiative imbalance causes baroclinicity primarily in the boundary layer (Chapter 18) via the heat budget (Chapter 3).

The bad weather of cyclones includes clouds (Chapters 4 - 6), precipitation (Chapter 7), and strong winds (Chapter 10). Condensation — as detected in precipitation areas by weather radar (Chapter 8) — releases latent heat which can strengthen cyclones. Cyclones are triggered by waves in the jet stream of the global circulation (Chapter 11), and help to transport heat, momentum, and moisture at mid-latitudes. The convergence at cyclones draws together different airmasses (Chapter 12), thereby forming fronts and enhancing baroclinicity.

Cyclones can be predicted numerically by solving the primitive equations (Chapter 20). Thunderstorms and tornadoes (Chapters 14 and 15) are triggered by the frontal weather near cyclones. Extratropical cyclones are **cold core systems**, which differ from warm core tropical cyclones (i.e., hurricanes, Chapter 16). Polluted air (Chapter 19) converges near cyclones and fronts, but pollutants can be washed out by rain. Changes in climate (Chapter 21) might alter the tracks or intensities of cyclones.

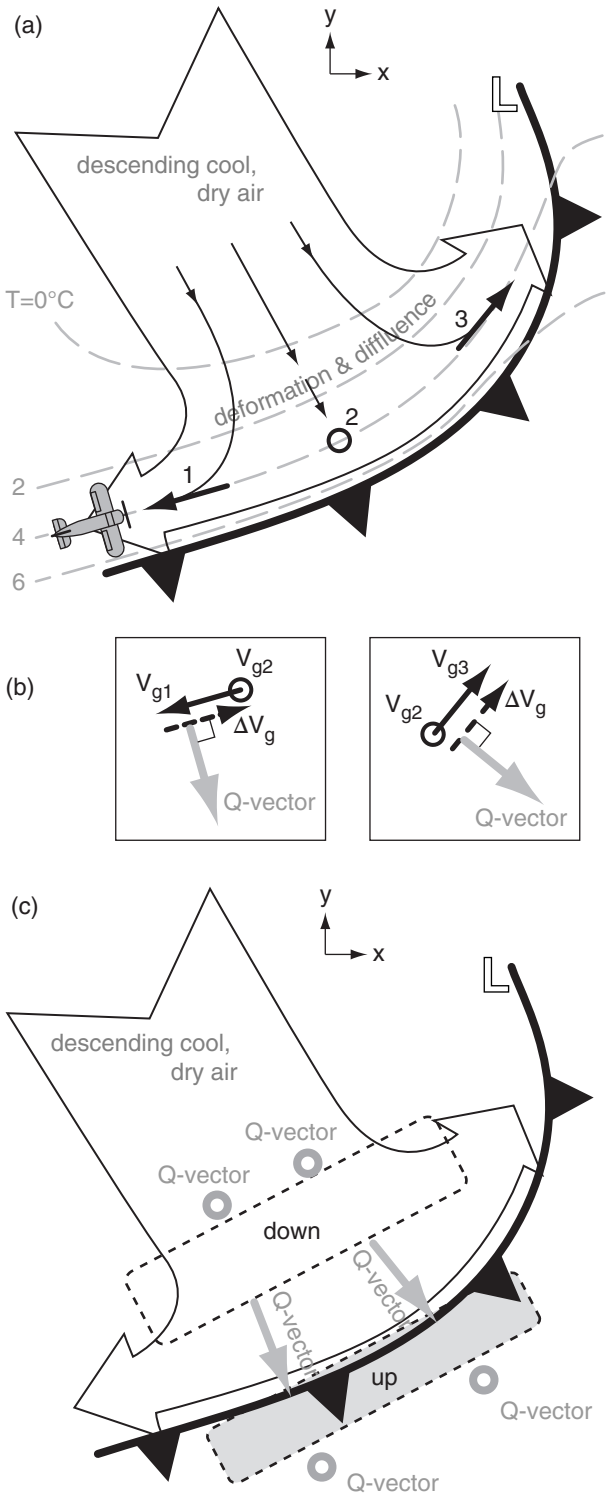

Figure 13.53
Using Q-vectors to locate regions of upward and downward motion due to diffluence of air behind a cold front. (a) Thin black lines are wind direction. Dashed grey lines are isotherms, along which an imaginary airplane flies. Thick black arrows show geostrophic wind vectors, with "o" representing zero wind. (b) Estimation of Q-vectors between points 1 and 2, and also between points 2 and 3. (c) The Q-vectors from (b) plotted in the baroclinic zone, with near-zero Q-vectors (grey "o") elsewhere. Q-vector convergence in grey shaded region suggests updrafts.

FOCUS • Landfalling Pacific Cyclones

Mid-latitude cyclones that form over the warm ocean waters east of Japan often intensify while approaching the dateline (180° longitude). But by the time they reach the eastern North Pacific ocean they are often entering the cyclolysis phase of their evolution. Thus, most landfalling cyclones that reach the Pacific Northwest coast of N. America are already occluded and are spinning down.

The cyclone labeled L_1 in Fig. k has just started to occlude. Satellite images of these systems show a characteristic tilted-"T" (↗) shaped cloud structure (grey shaded in Fig. k), with the cold front, occluded front, and a short stub of a warm front.

As the cyclone translates further eastward, its translation speed often slows and the low center turns northward toward the cold waters in the Gulf of Alaska — a cyclone graveyard where lows go to die. In the late occluded phase, satellite images show a characteristic "cinnamon roll" cloud structure, such as sketched with grey shading for cyclone L_2.

For cyclone L_2, when the cold front progresses over the complex mountainous terrain of the Pacific Northwest (British Columbia, Washington, Oregon), the front becomes much more disorganized and difficult to recognize in satellite and surface weather observations (as indicated with the dashed line over British Columbia).

The remaining portion of L_2's cold front still over the Pacific often continues to progress toward the southeast as a "headless" front (seemingly detached from its parent cyclone L_2).

Sometimes there is a strong "**pre-frontal jet**" of fast low-altitude winds just ahead of the cold front, as shown by the black arrows in Fig. k. If the source

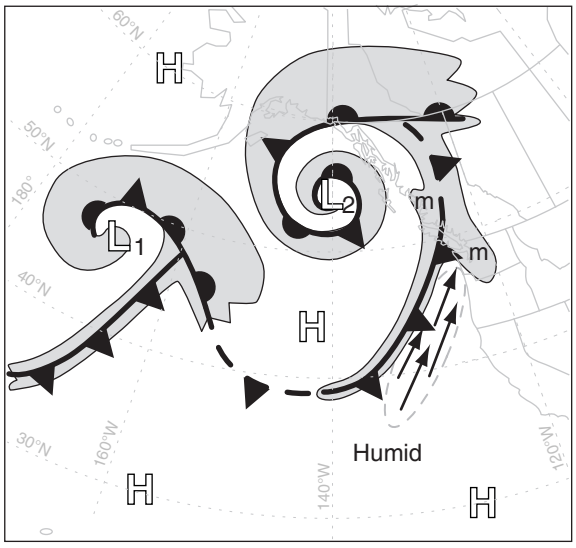

Figure k
Sketch of occluding mid-latitude cyclones approaching the Pacific Northwest coast of N. America.

(continues in next column)

FOCUS • Pacific Cyclones *(continued)*

region of this jet is in the humid sub-tropical air, then copious amounts of moisture can be advected toward the coast. If the source of this jet is near Hawaii, then the conveyor belt of moist air streaming toward N. America is nicknamed the "**Pineapple Express**".

When this humid air hits the coast, the air is forced to rise over the mountains. As the rising air cools adiabatically, clouds and orographic precipitation form over the mountains (indicated by "m" in Fig. k). Sometimes the cold front stalls (stops advancing) while the pre-frontal jet continues to pump moisture toward the mountains. This situation causes extremely heavy precipitation and flooding.

Fig. l shows an expanded view of the Vancouver, Seattle, Victoria region (corresponding to the lower-right "m" from Fig. k). Low-altitude winds split around the Olympic Mountains, only to converge (thick dashed line) in a region of heavy rain or snow called the **Olympic Mountain Convergence Zone** (also known as the **Puget Sound Convergence Zone** in the USA). The windward slopes of mountain ranges often receive heavy orographic precipitation (dotted ovals), while in between is often a **rain shadow** of clearer skies and less precipitation.

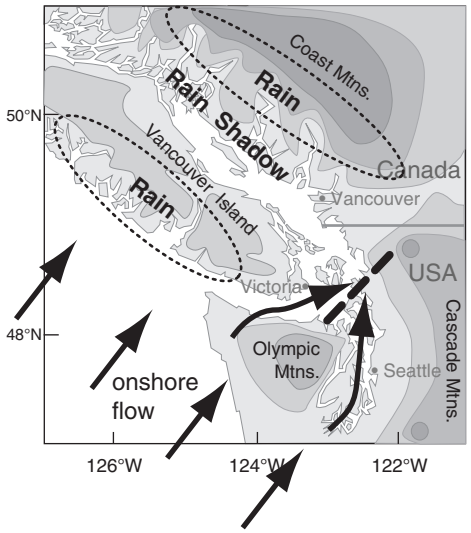

Figure l
Zoomed view of the Pacific Northwest. Pacific Ocean, sounds, and straits are white, while higher terrain is shaded darker. Arrows represent low-altitude wind.

EXERCISES

Numerical Problems

N1. For latitude 50°N, find the approximate wavelength (km) of upper-atmosphere (Rossby) waves triggered by mountains, given an average wind speed (m/s) of:

a. 20 b. 25 c. 30 d. 35 e. 40 f. 45 g. 50
h. 55 i. 60 j. 65 k. 70 l. 75 m. 80 n. 85

N2. Find the rate of increase of the β parameter (i.e., the rate of change of Coriolis parameter with distance north) in units of $m^{-1}s^{-1}$ at the following latitude (°N):

a. 40 b. 45 c. 50 d. 55 e. 60 f. 65 g. 70
h. 80 i. 35 j. 30 k. 25 l. 20 m. 15 n. 10

N3. For latitude 40°N and troposphere of depth 11 km, find the north-south amplitude (km) of upper-atmosphere (Rossby) waves triggered by mountains, given an average mountain-range height (km) of:

a. 0.4 b. 0.6 c. 0.8 d. 1.0 e. 1.2 f. 1.4 g. 1.6
h. 1.8 i. 2.0 j. 2.2 k. 2.4 l. 2.6 m. 2.8 n. 3.0

N4. How good is the approximation of eq. (13.4) to eq. (13.3) at the following latitude (°N)?

a. 40 b. 45 c. 50 d. 55 e. 60 f. 65 g. 70
h. 80 i. 35 j. 30 k. 25 l. 20 m. 15 n. 10

N5. For a troposphere of depth 12 km at latitude 43°N, find the potential vorticity in units of $m^{-1}s^{-1}$, given the following:

[wind speed (m/s) , radius of curvature (km)]
a. 50 , 500
b. 50 , 1000
c. 50 , 1500
d. 50 , 2000
e. 50 , –500
f. 50 , – 1000
g. 50 , –1500
h. 50 , -2000
i. 75 , 500
j. 75 , 1000
k. 75 , 1500
l. 75 , 2000
m. 75 , –1000
n. 75 , – 2000

N6. For air at 55°N with initially no curvature, find the potential vorticity in units of $m^{-1}s^{-1}$ for a troposphere of depth (km):

a. 7.0 b. 7.5 c. 8.0 d. 8.5 e. 9.0 f. 9.5 g. 10.0
h. 10.5 i. 11 j. 11.5 k. 12 l. 12.5 m. 13 n. 13.5

N7. When air at latitude 60°N flows over a mountain range of height 2 km within a troposphere of depth 12 km, find the radius of curvature (km) at location "C" in Fig. 13.20 given an average wind speed (m/s) of: a. 20 b. 25 c. 30 d. 35 e. 40 f. 45 g. 50
h. 55 i. 60 j. 65 k. 70 l. 75 m. 80 n. 85

N8. Regarding equatorward propagation of cyclones on the eastern slope of mountains, if a cyclone of radius 1000 km and potential vorticity of $3x10^{-8}$ $m^{-1}s^{-1}$ is over a slope as given below ($\Delta z/\Delta x$), find the change in relative vorticity (s^{-1}) between the north and south sides of the cyclone.

a. 1/500 b. 1/750 c. 1/1000 d. 1/1250
e. 1/1500 f. 1/1750 g. 1/2000 h. 1/2250
i. 1/2500 j. 1/2750 k. 1/3000 l. 1/3250

N9. Recall from the Dynamics chapter that incompressible mass continuity implies that $\Delta W/\Delta z = -D$, where D is horizontal divergence. Find the Coriolis contribution to the stretching term (s^{-2}) in the relative-vorticity tendency equation, given the average divergence in Fig. 13.26 for the following USA state:

a. AZ b. IL c. OK d. OH e. VA f. CO g. WA
h. WY i. PA j. WI k. central TX l. NY m. IN

N10. Find the spin-up rate (s^{-2}) of quasi-geostrophic vorticity, assuming that the following is the only non-zero characteristic:

a. geostrophic wind of 30 m/s from north within region where geostrophic vorticity increases toward the north by $6x10^{-5}$ s^{-1} over 500 km distance.

b. a geostrophic wind of 50 m/s from west within region where geostrophic vorticity increases toward the east by $8x10^{-5}$ s^{-1} over 1000 km distance.

c. A location at 40°N with geostrophic wind from the north of 25 m/s.

d. A location at 50°N with geostrophic wind from the south of 45 m/s.

e. A location at 35°N with vertical velocity increasing 0.5 m/s with each 1 km increase in height.

f. A location at 55°N with vertical velocity decreasing 0.2 m/s with each 2 km increase in height.

N11. Find the value of geostrophic vorticity (s^{-1}), given the following changes of (U_g, V_g) in m/s with 500 km distance toward the (north, east):

a. (0, 5) b. (0, 10) c. (0, –8) d. (0, –20)
e. (7, 0) f. (15, 0) g. (–12, 0) h. (-25, 0)
i. (5, 10) j. (20, 10) k. (–10, 15) l. (–15, –12)

N12. Find the value of geostrophic vorticity (s^{-1}), given a geostrophic wind speed of 35 m/s with the following radius of curvature (km). Assume the air rotates similar to a solid-body.

a. 450 b. –580 c. 690 d. –750 e. 825 f. –988

g. 1300 h. –1400 i. 2430 j. –2643 k. 2810
l. –2900 m. 3014 n. –3333

N13. What is the value of omega (Pa/s) following a vertically-moving air parcel, if during 1 minute its pressure change (kPa) is:
a. –2 b. –4 c. –6 d. –8 e. –10 f. –12 g. –14
h. –16 i. –18 j. –20 k. 0.00005 l. 0.0004
m. 0.003 n. 0.02

N14. At an altitude where the ambient pressure is 85 kPa, convert the following vertical velocities (m/s) into omega (Pa/s):
a. 2 b. 5 c. 10 d. 20 e. 30 f. 40 g. 50
h. –0.2 i. –0.5 j. –1.0 k. –3 l. –5 m. – 0.03

N15. Using Fig. 13.17d, find the most extreme value horizontal divergence (10^{-5} s^{-1}) at 20 kPa over the following USA state:
a. MI b. NM c. NV d. WV e. TN f. GA
g. ND h. WA i. KY j. PA k. NY l. AR

N16. Find the vertical velocity (m/s) at altitude 9 km in an 11 km thick troposphere, if the divergence (10^{-5} s^{-1}) given below occurs within a 2 km thick layer within the top of the troposphere.
a. 0.2 b. 1 c. 1.5 d. 2 e. 3 f. 4 g. 5 h. 6
i. –0.3 j.–0.7 k. –1.8 l. –2.2 m. –3.5 n. –5

N17. Jet-stream inflow is 30 m/s in a 4 km thick layer near the top of the troposphere. Jet-stream outflow (m/s) given below occurs 800 km downwind within the same layer. Find the vertical velocity (m/s) at the bottom of that layer
a. 35 b. 40 c. 45 d. 50 e. 55 f. 60 g. 65
h. 70 i. 30 j. 25 k. 20 l. 15 m. 10 n. 5

N18. Find the diagonal distance (km) from trough to crest in a jet stream for a wave of 750 km amplitude with wavelength (km) of:
a. 1000 b. 1300 c. 1600 d. 2000 e. 2200
f. 2500 g. 2700 h. 3000 i. 3100 j. 3300
k. 3800 l. 4100 m. 4200 n. 4500

N19. Given the data from the previous exercise, find the radius (km) of curvature near the crests of a sinusoidal wave in the jet stream.

N20. Find the gradient-wind speed difference (m/s) between the jet-stream speed moving through the anticyclonic crest of a Rossby wave in the N. Hemisphere and the jet-stream speed moving through the trough. Use data from the previous 2 exercises, and assume a geostrophic wind speed of 75 m/s for a wave centered on latitude 40°N.

N21. Given the data from the previous 3 exercises. Assuming that the gradient-wind speed difference calculated in the previous exercise is valid over a layer between altitudes 8 km and 12 km, where the tropopause is at 12 km, find the vertical velocity (m/s) at 8 km altitude.

N22. Suppose that a west wind enters a region at the first speed (m/s) given below, and leaves 500 km downwind at the second speed (m/s). Find the north-south component of ageostrophic wind (m/s) in this region. Location is 55°N.
a. (40, 50) b. (30, 60) c. (80, 40) d. (70, 50)
e. (40, 80) f. (60, 30) g. (50, 40) h. (70, 30)
i. (30, 80) j. (40, 70) k. (30, 70) l. (60, 20)

N23. Use the ageostrophic right-hand rule to find the ageostrophic wind direction for the data of the previous problem.

N24. Using the data from N22, find the updraft speed (m/s) into a 4 km thick layer at the top of the troposphere, assuming the half-width of the jet streak is 200 km.

N25. The 100 to 50 kPa thickness is 5.5 km and the Coriolis parameter is 10^{-4} s^{-1}. A west-to-east thermal wind of 25 m/s flows through a region where the average cyclonic vorticity decreases by $2x10^{-4}$ s^{-1} toward the east across a distance (km) given below. Use the omega equation to find the mid-tropospheric upward speed (m/s).
a. 200 b. 300 c. 400 d. 500 e. 600
f. 700 g. 800 h. 900 i. 1000 j. 1100
k. 1200 l. 1300 m. 1400 n. 1400

N26. On the 70 kPa isobaric surface, $\Delta U_g/\Delta x$ = 4m/s/500 km and $\Delta T/\Delta x$ = ___°C/500 km, where the temperature change is given below. All other gradients are zero. Find the Q-vector components Q_x, Q_y, and the magnitude and direction of Q.
a. 1 b. 1.5 c. 2 d. 2.5 e. 3 f. 3.5 g. 4
h. 4.5 i. 5 j. 5.5 k. 6 l. 6.5 m. 7 n. 7.5

N27. Find Q-vector magnitude on the 85 kPa isobaric surface if the magnitude of the horizontal temperature gradient is 5°C/200 km, and the magnitude of the geostrophic-wind difference-vector component (m/s) along an isotherm is __ /200 km, where __ is:
a. 1 b. 1.5 c. 2 d. 2.5 e. 3 f. 3.5 g. 4
h. 4.5 i. 5 j. 5.5 k. 6 l. 6.5 m. 7 n. 7.5

N28. Find the mass of air over 1 m^2 of the Earth's surface if the surface pressure (kPa) is:
a. 104 b. 102 c. 100 d. 98 e. 96 f. 94 g. 92
h. 90 i. 88 j. 86 k. 84 l. 82 m. 80 n. 78

N29. Assume the Earth's surface is at sea level. Find the vertical velocity (m/s) at height 3 km above ground if the change of surface pressure (kPa) during 1 hour is:

a. –0.5 b. –0.4 c. –0.3 d. –0.2 e. –0.1 f. 0.1
g. 0.2 h. 0.4 i. 0.6 j. 0.8 k. 1.0 l. 1.2 m. 1.4

N30. Given the rainfall (mm) accumulated over a day. If the condensation that caused this precipitation occurred within a cloud layer of thickness 6 km, then find the virtual-temperature warming rate (°C/day) of that layer due to latent heat release.

a. 1 b. 50 c. 2 d. 45 e. 4 f. 40 g. 5
h. 35 i. 7 j. 30 k. 10 l. 25 m. 15 n. 20

N31. For the data in the previous exercise, find the rate of decrease of surface pressure (kPa) per hour, assuming an average air temperature of 5°C.

Understanding & Critical Evaluation

U1. Compare the similarities and differences between cyclone structure in the Northern and Southern Hemisphere?

U2. In the Cyclogenesis & Cyclolysis section is a list of conditions that favor rapid cyclogenesis. For any 3 of those bullets, explain why they are valid based on the dynamical processes that were described in the last half of the chapter.

U3. Knowing the acceleration rate for a parcel of air at sea level (given Newton's second law and assuming that you know the horizontal pressure gradient), speculate on if it is possible for air to accelerate so slowly compared to the deepening of a cyclone bomb that the wind speed is not in geostrophic equilibrium. Discuss using order-of-magnitude numbers.

U4. Make a photocopy of Fig. 13.3. For each one of the figure panels on this copy, infer the centerline position of the jet stream and draw it on those diagrams.

U5. Create a 6-panel figure similar to Fig. 13.3, but for cyclone evolution in the Southern Hemisphere.

U6. Justify the comment that cyclone evolution obeys Le Chatelier's Principle.

U7. Refer back to the figure in the Global Circulation chapter that sketches the position of mountain ranges in the world. Use that information to hypothesize favored locations for lee cyclogenesis in the world, and test your hypothesis against the data in Fig. 13.5.

U8. Why are there no extratropical cyclone tracks from east to west in Fig. 13.5?

U9. Contrast the climatology of cyclone formation and tracks in the Northern vs. Southern Hemisphere (using the info in Fig. 13.5), and explain why there is a difference in behaviors based on the dynamical principles in the last half of the chapter.

U10. Justify why the tank illustration in Fig. 13.6 is a good analogy to atmospheric flow between cyclones and anticyclones.

U11. Fig. 13.7 shows the axis of low pressure tilting westward with increasing height. Explain why this tilt is expected. (Hints: On which side of the cyclone do you expect the warm air and the cold air? The hypsometric equation in Chapter 1 tells us how fast pressure decreases with height in air of different temperatures.)

U12. Redraw Fig. 13.7 a & b for the Southern Hemisphere, by extending your knowledge of how cyclones work in the Northern Hemisphere.

U13. Regarding stacking and tilting of low pressure with altitude, make a photocopy of Fig. 13.3, and on this copy for Figs. b and e draw the likely position of the trough axis near the top of the troposphere. Justify your hypothesis.

U14. Fig. 13.8 shows a warm-air conveyor bring air from the tropics. Assuming this air has high humidity, explain how this conveyor helps to strengthen the cyclone. Using dynamical principles from the last half of the chapter to support your explanation.

U15. Fig. 13.10 has coarse temporal resolution when it shows the evolution of the case-study cyclone. Based on your knowledge of cyclone evolution, draw two weather maps similar to Fig. 13.10, but for the times centered between the maps in the book. Namely, draw weather maps for 00 UTC 23 Feb 94 and 00 UTC 24 Feb 94.

U16. Speculate on why the dividing line between snow and rain in Fig. 13.11 is not parallel to the cyclone track.

U17. From the set of case-study maps in Figs. 13.12 through 13.19, if you had to pick 3 maps to give you the best 5-D mental picture of the cyclones, which 3 would you pick? Justify your answer.

U18. Of the following isosurfaces (height, pressure, thickness, and potential temperature), which one seems the most peculiar to you? What questions would you want to ask to help you learn more about that one isosurface?

U19. Starting with a photocopy of Fig. 13.12a, trace onto it the 70 kPa height map (in one color, such as blue) and the 50 kPa height map (in a different color, such as red). Analyze the tilt with height of the axis of low pressure, and explain why such tilt does or does not agree with the state of cyclone evolution at that time.

U20. Compare and contrast the 85 kPa temperature map of Fig. 13.13b with the thickness map of Fig. 13.15 for the case-study storm. Why or why not would you expect them to be similar?

U21. Compare the wind vectors of Fig. 13.17c with the heights in Fig. 13.17a. Use your understanding of wind dynamics to explain the relationship between the two maps.

U22. In the vertical cross section of Fig. 13.19a, why are the isentropes packed more closely together in the stratosphere than in the troposphere? Also, why is the stratosphere missing from the right side of that figure? [Hints: Consider the standard atmosphere temperature profile from Chapter 1. Consider the Global Circulation chapter.

U23. Why are the surface temperatures in Fig. 13.19a much warmer than the temperatures shown along a – a′ in Fig. 13.12b?

U24. In Fig. 13.20, how would lee cyclogenesis be affected if the tropopause perfectly following the terrain elevation? Explain.

U25. In Fig. 13.20, speculate on why the particular set of Rossby waves discussed in that section are known as "stationary" waves.

U26. What is the wavelength of stationary planetary waves near the equator?

U27. Suppose straight west-to-east flow at latitude 60° and initial troposphere depth 11 km encounters a semi-infinite plateau of terrain height 2 km above sea level. Describe mathematically the nature of the flow over the plateau, assuming the tropopause height doesn't change. Would the triggering of cyclones, and the wavelength of planetary waves be different? Why? Can you relate your answer to weather over the Tibetan Plateau?

U28. If cyclones often form to the lee of mountain ranges, do cyclones often weaken near the upwind side of mountain ranges? Why? How can you verify your answer?

U29. Suppose that instead of the Rocky Mountains, there was a trench in the land as wide as the Rockies are wide, and as deep as the Rockies are high. How would the weather and climate be different, if at all?

U30. In the winter, the tropopause is often lower and the wind speeds faster than during summer. How would the triggering of stationary planetary waves be different between winter and summer, if at all?

U31. Is there poleward propagation of cyclones at the upwind slopes of mountain ranges? Describe.

U32. Fig. 13.22 highlights 3 important attributes of cyclones that are discussed in greater detail in the last half of the chapter. Speculate on why we study these attributes separately, even though the caption to that figure discusses how all 3 attributes are related.

U33. Can the vorticity, vertical velocity, and sea-level pressure tendency equations be used to study or predict cyclolysis? Describe.

U34. The tilting effect of the vorticity equation has two terms, but only one term was sketched in Fig. 13.23d. Sketch the other term.

U35. Except for the last term in the full vorticity tendency equation, all the other terms can evaluate to be positive or negative (i.e., gain or loss of relative vorticity). What is it about the mathematics of the turbulent drag term in that equation that always make it a loss of relative vorticity?

U36. Based on what you learned from Fig. 13.24, what tips would you teach to others to help them easily find regions of PVA and NVA.

U37. In Figs. 13.23, no diagram was shown for vertical advection. Draw a sketch to illustrate this process.

U38. Suppose that the only two terms in the vorticity tendency equation were the spin-up term and the turbulent drag term. If there was some initial non-

zero vorticity, describe how the vorticity would evolve with time.

U39. Devise a tilting term for vertical vorticity that is tilted into horizontal vorticity. Could this process happen in nature?

U40. a. Summarize the quasi-geostrophic approximation.

b. What are the limitations of the quasi-geostrophic vorticity equation?

U41. The quasi-geostrophic vorticity equation includes a term related to vorticity advection by the geostrophic wind. The omega equation has a term related to vorticity advection by the thermal wind. Contrast these terms, and how they provide information about cyclogenesis.

U42. Use the case-study weather maps to calculate as many terms as reasonably possible in the vorticity-tendency equation, on the 50 kPa isobaric surface at the location of the "X".

U43. Fig. 13.27 examines flow east of a trough. Draw a similar sketch, except east of a ridge, and indicate the physical effects causing vorticity change. Also, indicate if the result is spin-up or spin-down.

U44. How does the radius of curvature of a planetary wave vary with latitude, everything else being equal?

U45. Why does jet stream curvature contribute to surface cyclogenesis east of the jet trough axis rather than west of the trough axis?

U46. Recall the limitation on the max wind speed and pressure gradient near high-pressure centers, but not near lows. How does that affect the possible strength of the jet-stream curvature effect for cyclogenesis?

U47. Using the case-study weather map (Fig. 13.30) for 20 kPa heights and isotachs, calculate the jet streak and curvature contributions to mid-tropospheric vertical velocity and to sea-level pressure tendency over the Ohio Valley, valid at 12 UTC on 23 Feb 94.

U48. Make a photo copy of Fig. 13.18. Using the jet-stream curvature and jet-streak information in that figure, draw on your copy the locations in the Northern Hemisphere where cyclogenesis is favored.

U49. In Fig. 13.32b, why are some divergence and convergence regions indicated as being stronger than others? Discuss.

U50. Consider a steady, straight jet stream from west to east. Instead of a jet streak of higher wind speed imbedded in the jet stream, suppose the jet streak has lower wind speed imbedded in the jet stream. For the right and left entrance and exit regions to this "slow" jet streak, describe which ones would support cyclogenesis at the surface.

U51. Does the "Ageostrophic right-hand rule" work in the Southern Hemisphere too? Justify your answer based on dynamical principles.

U52. For a jet-streak axis that is aligned from SW to NE, how could you use eqs. (13.25 & 13.26) for this situation?

U53. Fig. 13.34 suggests low-altitude convergence of air toward cyclones (lows), rising motion, and high-altitude divergence. Is this sketch supported by the case-study data from Figs. 13.17d, 13.25, and 13.26?

U54. For Fig. 13.34, what causes the portion of the secondary circulation near the ground? (Remember that Newton's law states that forces are needed to drive winds.)

U55. a. For the set of four maps of horizontal structure of a cold front (in the Airmasses & Fronts chapter), use the "area between crossing isopleths" technique to locate the region of maximum temperature advection.

b. Same, but for the warm-front maps.

U56. Discuss how Fig. 13.37 relates to the omega equation, and how the figure and equation can be used to locate regions that favor cyclogenesis.

U57. Recall that the thermal wind is really the change of geostrophic wind with height, which is proportional to the horizontal temperature gradient. Rewrite the omega equation in terms of:

a. the vertical gradient of geostrophic wind
b. the horizontal temperature gradient.

U58. Show that eq. (13.29) is identical to (13.28). What assumptions are needed to convert between the two equations, if any?

U59. What if there was no baroclinicity (no horizontal temperature gradient). How would that affect the omega eq.?

U60. What role does inertia play in the "geostrophic paradox"?

U61. Suppose that the geostrophic wind vectors are parallel to the height contours in Fig. 13.13a for the case-study storm. Use that information along with the isotherms in Fig. 13.13b to estimate the direction of the Q-vectors at the center of the following USA state:

a. KY b. WV c. WI d. KS e. AR

U62. Use the Q-vector approach to forecast where cyclogenesis might occur in the Pacific Northwest USA (in the upper left quadrant of Figs. 13.40 and 13.41).

U63. What are the limitations on the heuristic arguments of Fig. 13.43, where a vertical velocity was used as a surrogate for terms in the mass budget?

U64. Create a relationship between surface pressure tendency and dBZ values of reflectivity observed by weather radar.

U65. Given that Doppler radar can measure both precipitation rate and radial components of velocity, what quantitative information can be used from it to compute intensification of cyclones?

U66. Is it possible for the latent heating term in the net pressure tendency equation to increase, rather than decrease, the central pressure of a cyclone? Describe the conditions necessary for this to happen.

U67. In Fig. 13.47, describe the dynamics that makes the time of maximum convergence in the boundary layer occur after the time of maximum divergence in the jet stream, during cyclone evolution.

U68. Sketch a figure similar to Fig. 13.49, except for the temperature wave located 1/4 wavelength to the right instead of to the left of the height field. How would that alter the flow (sketch your result similar to Fig. 13.50)? Speculate on how likely it is that the temperature wave is shifted this way.

U69. Would anticyclones have any self development processes analogous to those for cyclones? Describe.

U70. Explain why the Q-vector analysis of Fig. 13.51 indicates the propagation of cyclones is toward the east. Also explain why this relates to self-propagation rather than relating to cyclogenesis driven by the jet-stream flow.

U71. Use Fig. 13.52 to explain why fronts are associated with cyclones and not anticyclones. The same figure can be used to explain why airmasses are associated with anticyclones. Discuss.

U72. Can cyclones form if global baroclinicity is absent (e.g., no air-temperature gradient between the equator and the poles)? Why?

U73. Explain how the up- and down-couplet of air motion in Fig. 13.53c (as diagnosed using Q-vectors), works in a way to strengthen and propagate the cold front.

U74. Use a Q-vector analysis to speculate on the dynamics needed to cause warm fronts to strengthen and propagate.

U75. For the case-study cyclone in this chapter, combine all the information from the vorticity tendency, vertical motion, and surface-pressure tendency to synthesize a coherent description of the dynamics of this storm.

Web-Enhanced Questions

W1. For an exciting storm system that affected you (or a storm assigned by your instructor), develop a case study of weather maps from the web and discuss cyclone evolution based on the physical processes reviewed in this chapter.

W2. Search the web for sources of storm damage data ("Storm Data").

W3. For an intense cyclone, download a set weather maps and upper air maps for a snapshot of the weather. Use this to develop a 5-D image in your mind of the storm, and its dynamics.

W4. Search the web for maps showing typical or historical tracks of extra-tropical cyclones. What are the names of some of the favored cyclone formation sites or tracks (such as the Alberta Clipper)?

W5. Track an intense cyclone as it approaches the west coast of the N. America from the Pacific. Download a sequence of maps showing how the storm changes as it passes over the various mountain ranges in the western part of the continent.

W6. For an exciting storm that caused significant damage, download data from the web to create a summary map of its track and damage, similar to Fig. 13.11.

W7. Search the web for case studies of cyclone bombs, or explosive cyclogenesis. Discuss the evolution of these storms.

W8. From web maps of the jet stream (upper air charts at 20, 25, or 30 kPa), measure the wavelength of the various waves. Also measure the wave amplitude. How do they vary with latitude? With season?

W9. From web maps of the jet stream (upper air charts at 20, 25, or 30 kPa), estimate the vorticity from the radius of curvature and the wind speed.

W10. Download upper-air maps of temperature and height contours for a level such as 85 or 70 kPa. Superimpose these two fields if they are not already on the same map. Use the technique described in the "Advection" focus box to locate the region of maximum temperature advection.

W11. Same as the previous problem, but for a level such as 50 kPa where vorticity and height maps are available to locate the region of maximum vorticity advection. Locate both the regions of max positive and negative vorticity advection by the geostrophic wind. Which region would most likely favor cyclone development?

W12. Download a map of 70 kPa vorticity, and of 100 - 50 kPa thickness contours. From the thickness, determine the thermal wind near a cyclone. Use the result to find the region of max vorticity advection by the thermal wind, which according to the omega equation would favor upward motion and strengthening of cyclones.

W13. Search the web for an isentropic weather map for the current weather. If you cannot find one, then search the web for a map from a previous case study, or from a figure in a paper about isentropic analysis. From this map, discuss the elevation variation of the isentropic surface, state how high it is within the troposphere, and discuss any other info such as if winds are likely to blow up or down the isentropic surface in various regions.

W14. Locate a jet streak on a current weather map, or a past map if necessary, and label the right and left entrance and exit regions. Indicate where on the map you would expect cyclones to develop or strengthen. Given the change of wind velocity at different locations near the entrance or exit of the jet streak, plug those numbers into the formula to estimate upward motion associated with jet streak divergence.

W15. Study the spacing of height contours at a jet stream level (20, 25, or 30 kPa) as the jet stream flows around neighboring ridges and troughs, using a map you download from the web. Does the spacing between contours remain relatively constant around both the ridge and trough? If not, given the changes in spacing, and given what you know about gradient wind speeds (e.g., slow around lows), discuss the variation of actual wind speed around the ridge and trough.

W16. Search the web for radar observations in a cyclone having heavy precipitation. From the dBZ values, estimate the rainfall rate (see an earlier chapter for the relationship). Then, from the rainfall rate, estimate the latent heating contribution to the surface pressure tendency. Also, see if self-development of the cyclone occurs due to latent heating.

W17. Search the web for the site of a major weather map provider, government weather service, university forecasting project, military forecast service, numerical forecast center (NCEP, ECMWF, CMC), or research organization that produces lots of weather maps. In addition to traditional maps on various isosurfaces (e.g., height, pressure, thickness, potential temperature, etc.), what other weird, interesting, and useful maps can you find?

W18. Find a web site that produces maps of Q-vectors or Q-vector divergence. Print this map and a normal surface weather map with fronts, and discuss how you would anticipate the cyclone to evolve based on a Q-vector analysis.

Synthesis Questions

S1. Consider Fig. 13.6. What if frictional drag is zero at the bottom of the atmosphere (in the boundary layer), how would cyclone evolution be different, if at all?

S2. What if the case-study cyclone of Fig. 13.11 occurred in April rather than February, what broad aspects of the storm data would change, if at all?

S3. Suppose no major north-south mountain ranges exist in N. America. How would the weather and climate be different, if at all?

S4. Suppose a major mountain range exists east-west across the center of N. America, and no north-south ranges. How would weather and climate be different, if at all?

S5. What if average temperature decreased toward the east over N. America, rather than toward the north. How would this change in the direction of baroclinicity change the weather and climate, if at all?

S6. What if the Earth rotated twice as fast. How would the triggering of cyclones and the nature of stationary planetary waves be different, if at all?

S7. Most numerical weather prediction (NWP) models use the primitive equations (the conservation equations for heat, moisture, and momentum, along with the continuity eq. and ideal gas law) to make their forecasts (as described in a later chapter).

a. Is it possible to use the quasi-geostrophic vorticity and omega equations to make a forecast instead?

b. How would you get the wind components and temperature from such a forecast?

c. Is such a forecast system simpler or more complicated to solve than the primitive equations?

S8. Suppose the jet stream is at its current altitude, and meanders north and south, and creates horizontal divergence and convergence as it does now. But what if the static stability in the stratosphere equaled that in the troposphere. What change would occur to jet-stream forcing of surface pressure systems, if any? Discuss.

S9. Suppose that the troposphere were as strongly stable as the stratosphere. How would the weather and climate be different, if at all?

S10. Suppose that extratropical cyclones did not exist. How would the weather and climate be different, if at all?

S11. Suppose that Earth was a larger planet that had a very hot core and surface, similar to Jupiter. If the heat from the solid Earth to the atmosphere was the dominant source of heat that balanced net longwave radiative cooling from the atmosphere, how would the weather and climate on Earth be different, if at all?

S12. Re-read this chapter and extract all the forecasting tips to create your own concise synoptic-weather forecast guide.

Copyright © 2011, 2015 by Roland Stull. *Meteorology for Scientists and Engineers, 3rd Ed.*

THUNDERSTORMS

CONTENTS

Thunderstorm Characteristics 481
- Appearance 482
- Clouds Associated with Thunderstorms 482
- Cells & Evolution 484
- Thunderstorm Types & Organization 486
  - Basic Storms 486
  - Mesoscale Convective Systems 488
  - Supercell Thunderstorms 492

Thunderstorm Formation 496
- Convective Conditions 496
- Key Altitudes 496

High Humidity in the ABL 499

Instability, CAPE & Updrafts 503
- CAPE 503
- Updraft Velocity 508

Wind Shear in the Environment 509
- Hodograph Basics 510
- Using Hodographs 514
  - Shear Across a Single Layer 514
  - Mean Wind Shear Vector 514
  - Total Shear Magnitude 515
  - Mean Environmental Wind (Normal Storm Motion) 516
  - Supercell Storm Motion 518
  - Bulk Richardson Number 521

Triggering vs. Convective Inhibition 522
- Convective Inhibition (CIN) 523
- Trigger Mechanisms 525

Thunderstorm Forecasting 527
- Outlooks, Watches & Warnings 528
- Stability Indices for Thunderstorms 530
- Storm Case Study 532

Summary 532
- Threads 533

Exercises 533
- Numerical Problems 533
- Understanding & Critical Evaluation 536
- Web-Enhanced Questions 541
- Synthesis Questions 542

"Meteorology for Scientists and Engineers, 3rd Edition" by Roland Stull is licensed under a Creative Commons Attribution-NonCommercial-ShareAlike 4.0 International License. To view a copy of the license, visit http://creativecommons.org/licenses/by-nc-sa/4.0/ . This work is available at http://www.eos.ubc.ca/books/Practical_Meteorology/ .

14 Thunderstorms are among the most violent and difficult-to-predict weather elements. Yet, thunderstorms can be studied. They can be probed with radar and aircraft, and simulated in a laboratory or by computer. They form in the air, and must obey the laws of fluid mechanics and thermodynamics.

Thunderstorms are also beautiful and majestic. In thunderstorms, aesthetics and science merge, making them fascinating to study and chase.

Thunderstorm characteristics, formation, and forecasting are covered in this chapter. The next chapter covers thunderstorm hazards including hail, gust fronts, lightning, and tornadoes.

THUNDERSTORM CHARACTERISTICS

Thunderstorms are **convective clouds** with large vertical extent, often with tops near the tropopause and bases near the top of the boundary layer. Their official name is **cumulonimbus** (see the Clouds Chapter), for which the abbreviation is **Cb**. On weather maps the symbol ⌈ζ represents thunderstorms, with a dot •, asterisk *, or triangle ▵ drawn just above the top of the symbol to indicate rain, snow, or hail, respectively. For severe thunderstorms, the symbol is ⌈ϟ .

© Gene Rhoden / weatherpix.com

Figure 14.1
Thunderstorm.

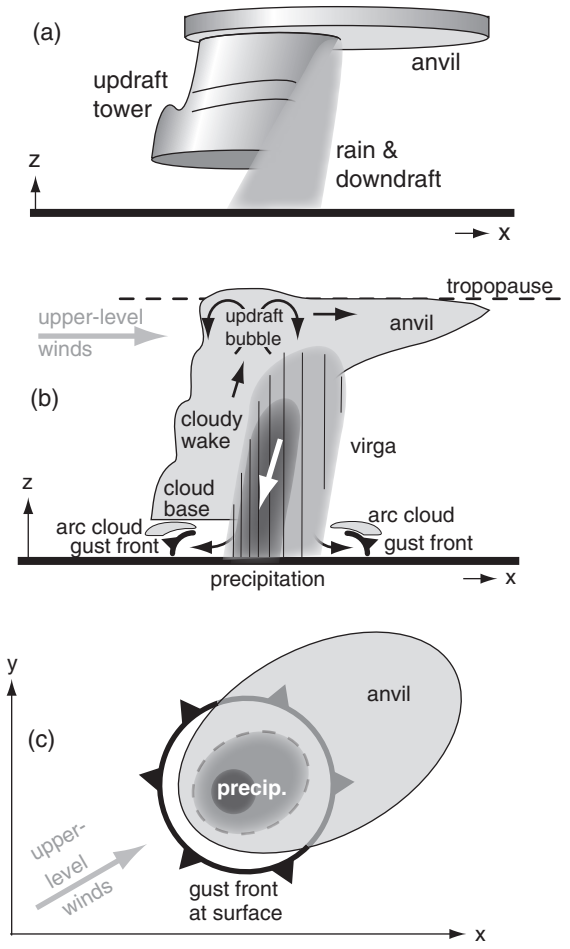

Figure 14.2
(a) Sketch of a basic (airmass) thunderstorm in its mature stage. (b) Vertical slice through the storm. Light shading indicates clouds, medium and dark shadings are moderate and heavy precipitation, and arrows show air motion. (c) Horizontal composite, showing the anvil at storm top (as viewed from above by satellite), the precipitation in the low-to-middle levels (as viewed by radar), and the gust front of spreading winds at the surface.

© Gene Rhoden / weatherpix.com

Figure 14.3
Photo of supercell thunderstorm.

Appearance

A mature thunderstorm cloud looks like a mushroom or anvil with a relatively large-diameter flat top. The simplest thunderstorm (see Figs. 14.1 & 14.2) has a nearly vertical stem of diameter roughly equal to its depth (of order 10 to 15 km). The large top is called the **anvil**, **anvil cloud**, or **thunderhead**, and has the official name **incus** (Latin for anvil). The anvil extends furthest in a direction as blown by the upper-tropospheric winds.

If the thunderstorm top is just starting to spread out into an anvil and does not yet have a fibrous or streaky appearance, then you identify the cloud as **cumulonimbus calvus** (see the Clouds Chapter). For a storm with a larger anvil that looks strongly **glaciated** (i.e., has a fibrous appearance associated with ice-crystal clouds), then you would call the cloud a **cumulonimbus capillatus**.

Within the stem of a mature thunderstorm is the cloudy **main updraft tower** topped by an **updraft bubble** (Fig. 14.2b). When this rising air hits the tropopause, it spreads to make the anvil. Also in the stem is a downdraft with precipitation. When the downdraft air hits the ground it spreads out, the leading edge of which is called the **gust front**. When viewed from the ground under the storm, the main updraft often has a darker cloud base, while the rainy region often looks not as dark and does not have a well-defined cloud base.

Not all cumulonimbus clouds have lightning and thunder. Such storms are technically not thunderstorms. However, in this book we will use the word **thunderstorm** to mean any cumulonimbus cloud, regardless of whether it has lightning.

More complex thunderstorms can have one or more updraft and downdraft regions. The most severe, long-lasting, less-frequent thunderstorms are **supercell thunderstorms** (Figs. 14.3 & 14.4).

Clouds Associated with Thunderstorms

Sometimes you can see other clouds attached to thunderstorms, such as a funnel, wall, mammatus, arc, shelf, flanking line, scud, pileus, dome, and beaver tail (Fig. 14.4). Not all thunderstorms have all these associated clouds.

Arc clouds (official name **arcus**, Fig. 14.2b) or **shelf clouds** form near the ground in boundary-layer air that is forced upward by undercutting cold air flowing out from the thunderstorm. These cloud bands mark the leading edge of **gust-front** outflow from the **rear-flank downdraft** (Fig. 14.4), usually associated with the **flanking line**. Often the undersides of arc clouds are dark and turbulent-looking, while their tops are smooth. Not all gust fronts have arc clouds, particularly if the displaced air is dry. See the Thunderstorm Hazards chapter.

The **beaver tail** (Fig. 14.4) is a smooth, flat, narrow, low-altitude cloud that extends along the boundary between the inflow of warm moist air to the thunderstorm and the cold air from the rain-induced **forward flank downdraft** (**FFD**).

A **dome** of **overshooting** clouds sometimes forms above the anvil top, above the region of strongest updraft. This is caused by the inertia of the upward moving air in the main updraft, which overshoots above its neutrally buoyant **equilibrium level** (**EL**). Storms that have **overshooting tops** are often more violent and turbulent.

The **flanking line** is a band of cumuliform clouds that increase from the medium-size **cumulus mediocris** (**Cu med**) furthest from the storm to the taller **cumulus congestus** (**Cu con**) close to the **main updraft**. Cumulus congestus are also informally called **towering cumulus** (**TCu**). The flanking line forms along and above the gust front, which marks the leading edge of colder outflow air from the **rear-flank downdraft** (**RFD**).

If humid layers of environmental air exist above rapidly rising cumulus towers, then **pileus** clouds can form as the environmental air is pushed up and out of the way of the rising cumulus clouds. Pileus are often very short lived because the rising cloud tower that caused it often keeps rising through the pileus and obliterates it.

The most violent thunderstorms are called **supercell** storms (Figs. 14.3 & 14.4), and usually have a quasi-steady rotating updraft (called a **mesocyclone**). The main thunderstorm updraft in supercells sometimes has curved, helical **cloud striations** (grooves or ridges) on its outside similar to threads of a screw (Fig. 14.4a). Supercells can produce intense **tornadoes** (violently rotating columns of air), which can appear out of the bottom of an isolated cylindrical lowering of the cloud base called a **wall cloud**. The portion of the tornado made visible by cloud droplets is called the **funnel cloud**, which is the name given to tornadoes not touching the ground. Tornadoes are covered in the next chapter. Most thunderstorms are not supercell storms, and most supercell storms do not have tornadoes.

Attached to the base of the wall cloud is sometimes a short, horizontal cloud called a **tail cloud**, which points towards the **forward flank precipitation** area. Ragged cloud fragments called **scud** (**cumulus fractus**) often form near the tip of the tail cloud and are drawn quickly into the tail and the wall cloud by strong winds.

The wall cloud and tornado are usually near the boundary between cold downdraft air and the low-level warm moist inflow air, under a somewhat **rain-free cloud base**. In mesocyclone storms, you can see the wall cloud rotate by eye, while rotation

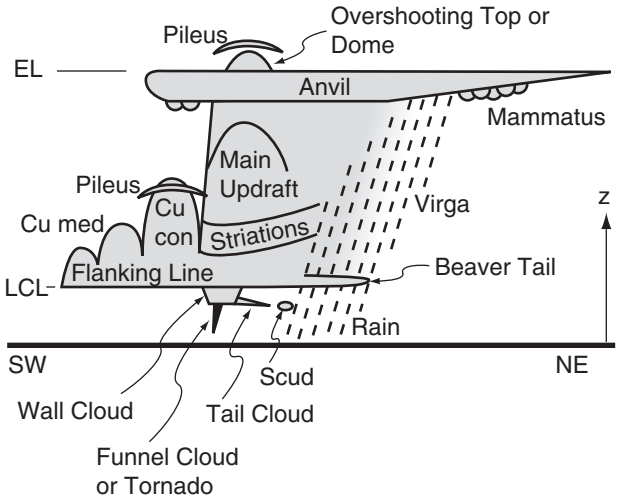

Figure 14.4a
Sketch of a classic supercell thunderstorm (Cb) as might be viewed looking toward the northwest in central North America. The storm would move from left to right in this view (i.e., toward the northeast). Many storms have only a subset of the features cataloged here. Cu med = cumulus mediocris; Cu con = cumulus congestus; LCL = lifting condensation level; EL = equilibrium level (often near the tropopause, 8 to 15 km above ground); NE = northeast; SW = southwest.

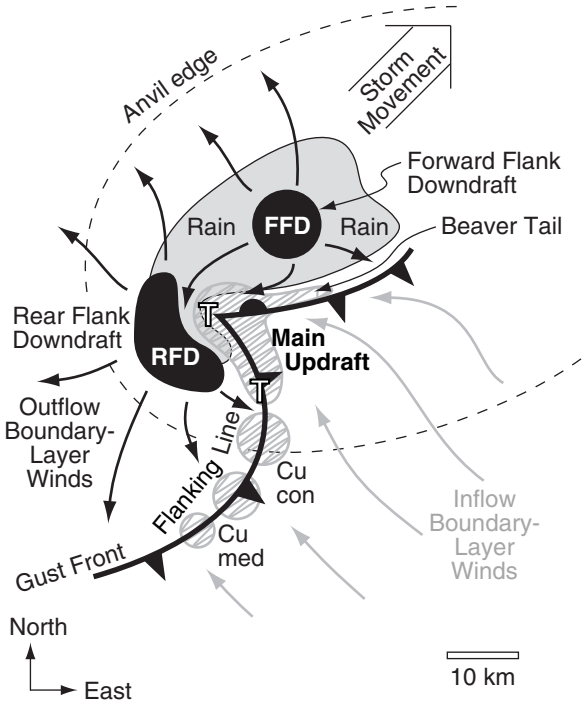

Figure 14.4b
Plan view (top down) sketch of a classic supercell thunderstorm. 𝕋 indicates possible tornado positions; RFD = Rear Flank Downdraft; FFD = Forward Flank Downdraft. Regions of updraft are hatched with grey; downdrafts are solid black; rain is solid light grey. Low surface pressure is found under the updrafts (especially near the "𝕋" locations), and high pressure under the downdrafts. Vectors are near-surface winds: cold are black, warm are grey.

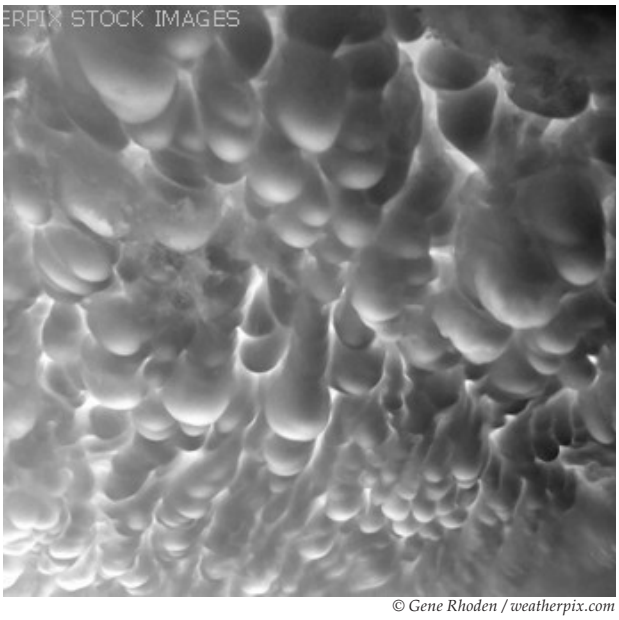

© Gene Rhoden / weatherpix.com

Figure 14.5
Mammatus clouds.

Solved Example

Identify the thunderstorm features, components, and associated clouds that are in Fig. 14.3.

Solution

Given: Photo 14.3, reproduced here.
Find: Cloud features.

Method: Compare photo 14.3 to diagram 14.4a.

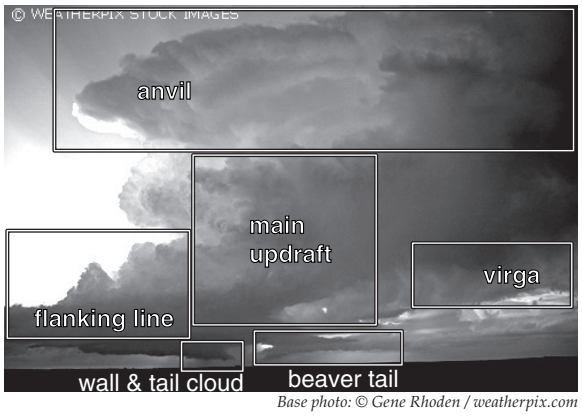

Base photo: © Gene Rhoden / weatherpix.com

Discussion: This cloud is a supercell thunderstorm, because it looks more like the cloud sketched in Fig. 14.4a than the simple single-cell air-mass thunderstorm in Fig. 14.2. The main updraft is tilted from lower left to upper right, a sign of wind shear in the environment. If a tornado exists under the wall cloud, it is too small to see in this figure. Given the orientation of the cloud features (similar to those in Fig 14.4a), the photographer was probably looking toward the northwest, and the thunderstorm is moving toward the northeast (to the right in this figure).

of the larger-diameter supercell is slower and is apparent only in time-lapse movies. Non-rotating wall clouds also occur with non-rotating thunderstorms (i.e., non-supercell storms).

The **rain** portion of a thunderstorm is often downwind of the main updraft, in the forward portion of the storm. Cloud edges and boundaries are often not distinguishable in the rain region. Although thunderstorms are rare in cold weather, when they occur they can cause very heavy snowfall instead of rain. Further downwind of the heavy rain area is a region of **virga**, where the precipitation (rain or snow) evaporates before reaching the ground.

Mammatus clouds look like sacks or protuberances hanging from the bottom of layered clouds, and are sometimes found on the underside of thunderstorm anvils (Fig. 14.5). No correlation exists between the presence of mammatus clouds and the intensity of thunderstorms (i.e., hail, tornadoes, etc.). Not all thunderstorms have mammatus clouds.

One of many theories for mammatus clouds is that the thunderstorm updraft pumps air into the anvil with slightly cooler virtual temperature than environmental air. This anvil air is statically unstable, so the cold air begins sinking as upside-down thermals. Because these sinking air parcels are laden with cloud droplets or ice crystals, the air warms at only the moist adiabatic rate. Thus, evaporation of some of the water helps keep the mammatus clouds cooler than their environment, and the liquid water loading of the remaining droplets contributes to cooler virtual temperatures, so they keep sinking.

In an environment with weak wind shear, the **anvil cloud** in weak thunderstorms can be symmetrical, looking like a mushroom cap (Fig. 14.1). However, for larger, longer lasting thunderstorms in the presence of strong winds aloft, the ice crystals brought up by the main updraft will spread out asymmetrically (Fig. 14.2) in an anvil that can be 100 km wide (crosswind) and 300 km long (downwind).

If you want to chase and photograph isolated storms in N. America, the best place to be is well to the side of the storm's path. As most storms move northeast in N. America, this corresponds to your being southeast of the thunderstorm. This location is relatively safe with good views of the storm and the tornado (see "On Doing Science • Be Safe").

For non-chasers overtaken by a storm, the sequence of events they see is: cirrus anvil clouds, mammatus clouds (if any), gust front (& arc cloud, if any), rain, hail (if any), tornado (if any), and rapid clearing with sometimes a rainbow during daytime.

Cells & Evolution

The fundamental structural unit of a thunderstorm is a **thunderstorm cell**, which is of order 10

km in diameter and 10 km thickness (i.e., its **aspect ratio** = depth/width = 1). Its evolution has three stages: (1) towering-cumulus; (2) mature; and (3) dissipation, as sketched in Fig. 14.6. This life cycle of an individual cell lasts about 30 to 60 min.

The towering cumulus stage consists of only updraft in a rapidly growing cumulus congestus tower. It has no anvil, no downdrafts, and no precipitation. It is drawing warm humid boundary-layer air into the base of the storm, to serve as fuel. As this air rises the water vapor condenses and releases latent heat, which adds buoyancy to power the storm.

In the mature stage (Fig. 14.7), the thunderstorm has an anvil, both updrafts and downdrafts, and heavy precipitation of large-size drops. This often is the most violent time during the storm, with possible lightning, strong turbulence and winds. The precipitation brings cooler air downward as a downburst, which hits the ground and spreads out. In the absence of wind shear, two factors conspire to limit the lifetime of the storm (Fig. 14.6): (1) the storm runs out of fuel as it consumes nearby boundary-layer air; and (2) the colder outflow air chokes off access to adjacent warm boundary-layer air.

In the dissipating stage, the storm consists of downdrafts, precipitation, and a large **glaciated** (containing ice crystals) anvil. The storm rains itself out, and the precipitation rate diminishes. The violent aspects of the storm are also diminishing. With no updraft, it is not bringing in more fuel for the storm, and thus the storm dies.

The last frame in Fig. 14.6 shows the anvil-debris stage, which is not one of the official stages listed in severe-weather references. In this stage all that remains of the former thunderstorm is the anvil and associated virga, which contains many ice crystals that fall and evaporate slowly. No precipitation reaches the ground. The anvil remnant is not very turbulent, and drifts downwind as a thick cirrostratus or altostratus cloud as it gradually disappears.

Meanwhile, the cold outflow air spreading on the ground from the former storm might encounter fresh boundary-layer air, which it lifts along its leading edge (gust front) to possibly trigger a new thunderstorm (labeled "Cu con 2" in the last frame of Fig. 14.6). This process is called **storm propagation**, where the first storm (the "mother") triggers a daughter storm. This daughter storm can go through the full thunderstorm life cycle if conditions are right, and trigger a granddaughter storm, and so forth.

Some thunderstorms contain many cells that are in different stages of their evolution. Other storms have special characteristics that allow the cell to be maintained for much longer than an hour. The types of thunderstorms are described next.

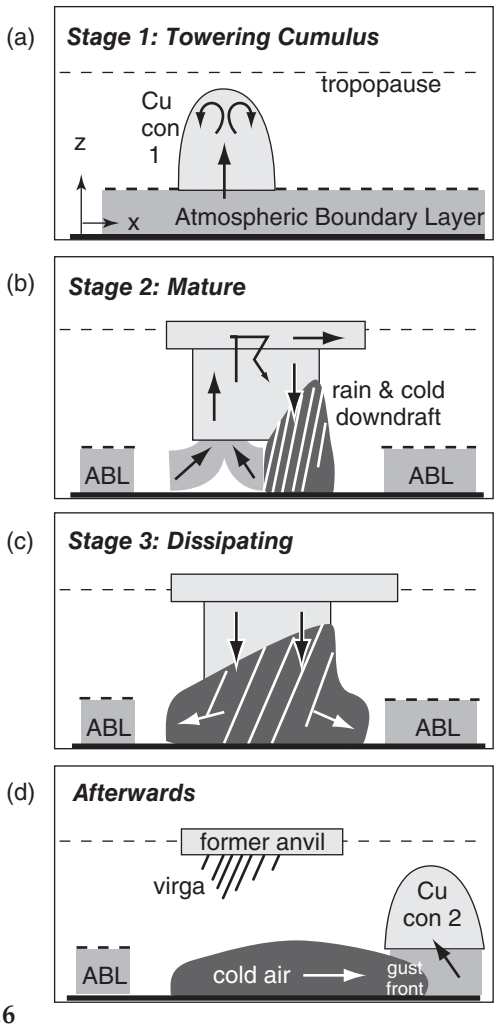

Figure 14.6
Phases of thunderstorm cell evolution. Light grey shading represents clouds, medium grey is pre-storm boundary layer (ABL) of warm humid air that serves as fuel for the storm. Dark shading is colder outflow air. Diagonal white lines represent precipitation. Arrows show air motion. Cu con = cumulus congestus.

ON DOING SCIENCE • Be Safe

In any scientific or engineering work, determine the possible hazards to you and others before you undertake any action. If you are unable to increase the safety, then consider alternative actions that are safer. If no action is relatively safe, then cancel that project.

For example, chasing thunderstorms can be very hazardous. Weather conditions (heavy rainfall, poor visibility, strong winds, hail, lightning, and tornadoes) can be hazardous. Also, you could have poor road conditions and a limited ability to maneuver to get out of harm's way in many places.

Your safety and the safety of other drivers and pedestrians must always be your first concern when storm chasing. Some storm-chase guidelines are provided in a series of "On Doing Science" boxes later in this chapter and continuing into the next chapter.

(continues in later pages)

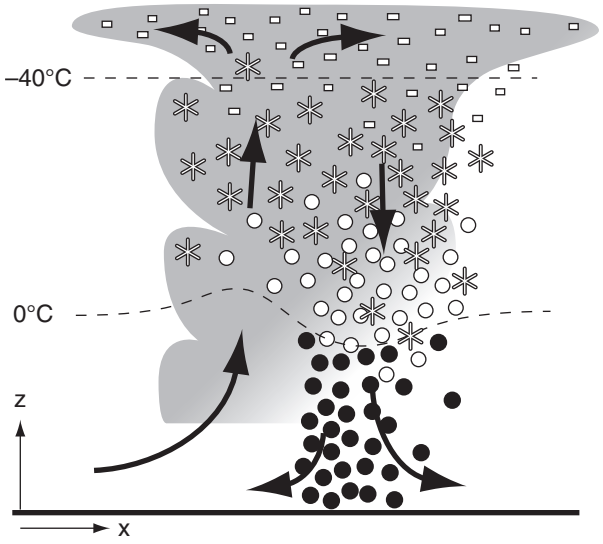

Figure 14.7
Airmass thunderstorm in its mature stage during summer. Grey shading represents cloud droplets (except above the –40°C isotherm, where all hydrometeors are frozen), black dots represent rain, white dots are graupel, dendrite shapes are snow, and small white rectangles are small ice crystals. Arrows show winds, and dashed lines give air temperature.

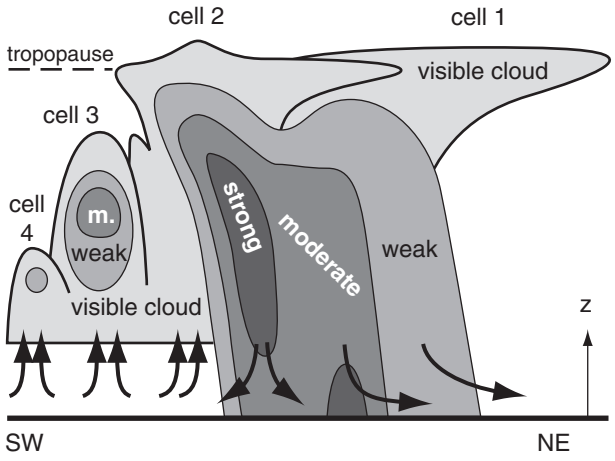

Figure 14.8
Multicell thunderstorm. Cell 1 is the oldest cell, and is in the dissipating stage. Cell 2 is mature. Cell 3 is in the cumulus stage. Cell 4 is the newest and smallest, in an early cumulus stage. Shaded regions indicate where we would see clouds and rain by eye. Medium, dark, and very dark shading indicate weak, moderate (m.), and strong radar echoes inside the clouds, which generally correspond to light, moderate, and heavy precipitation. Arrows show low-altitude winds.

Thunderstorm Types & Organization

Types of thunderstorm organization include:

- basic storms
  - single cell (airmass)
  - multicell
  - orographic
- mesoscale convective systems (MCS)
  - squall line
  - bow echo
  - mesoscale convective complex (MCC)
  - mesoscale convective vortex (MCV)
- supercells
  - classic (CL)
  - low precipitation (LP)
  - high precipitation (HP)

Basic Storms

Single-cell Thunderstorms. An **airmass thunderstorm** (Figs. 14.1, 14.2 & 14.7) is often a single-cell thunderstorm with evolution very similar to Fig. 14.6. It can form in the middle of a warm humid airmass, usually in late afternoon. Satellite images of airmass thunderstorms show that several often exist at the same time, all with somewhat symmetric anvils, and scattered within the airmass analogous to mushrooms in a meadow. These storms can be triggered by thermals of rising warm air (heated at the Earth's surface) that happen to be buoyant enough to break through the capping inversion at the boundary-layer top.

The lifetime of airmass thunderstorms are about the same as that of an individual cell (30 to 60 minutes), but they can spawn daughter storms as sketched in Fig. 14.6. Each can produce a short-duration (15 minutes) rain shower of moderate to heavy intensity that covers an area of roughly 5 - 10 km radius. Airmass thunderstorms that produce short-duration severe weather (heavy precipitation, strong winds, lightning, etc.) during the mature stage are called **pulse storms**.

Multicell Thunderstorms. Most thunderstorms in North America are **multicell storms** (Fig. 14.8). Within a single cloud mass that by eye looks like a thunderstorm, a weather radar can see many (2 to 5) separate cells (Fig. 14.9) by their precipitation cores and their winds. In a multicell storm, the different cells are often in different stages of their life cycle. Given weak to moderate wind shear in the environment, the downburst and gust front from one of the mature cells (cell 2 in Fig. 14.8) can trigger new adjacent cells (namely, cells 3 and 4).

In central North America where warm humid boundary-layer winds often blow from the southeast in the pre-storm environment, new cells often

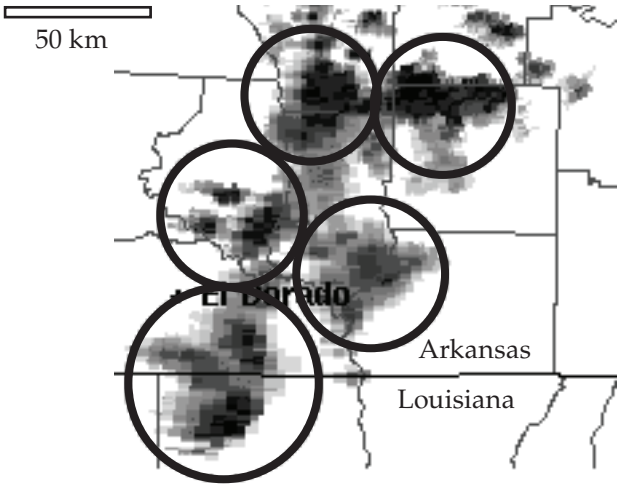

Figure 14.9.
Radar reflectivity PPI image of a multicell thunderstorm in south-central USA, 28 June 2001. Darkest grey indicates > 50 dBZ; namely, the heaviest precipitation. Cells are circled. Courtesy of the US National Weather Service, NOAA.

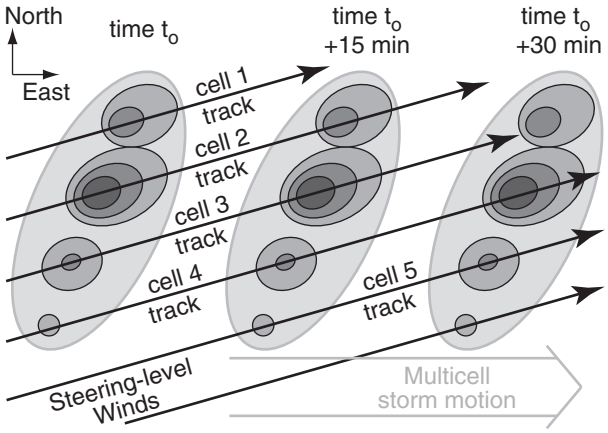

Figure 14.10
Diagram of multicell thunderstorm motion. Grey shading indicates visible clouds and radar echoes corresponding to Fig. 14.8. Black arrows show tracks of individual cells. Double-arrow in grey shows motion of the multicell cloud mass. Each light-grey large oval shows position of the cloud mass every 15 min.

form on the south flank of the storm (closest to the fuel supply), while the northeastward-moving mature cells decay as their fuel supply is diminished (Fig. 14.10). The resulting multicell thunderstorm appears to move to the right of the **steering-level winds** (normal or average winds in the bottom 6 km of the troposphere), even though individual cells within the storm move in the direction of the normal steering-level winds (Fig. 14.10).

Orographic Thunderstorms. Single or multicell storms triggered by mountains or hills are called **orographic thunderstorms**. With the proper environmental wind shear (Fig. 14.11), low-altitude upslope winds can continuously supply humid boundary-layer air. If the upper-level winds are from the opposite direction (e.g., from the west in Fig. 14.11), then these storms can remain stationary over a mountain watershed for many hours, funneling heavy rains into canyons, and causing devastating **flash floods**. One example is the Big Thompson Canyon flood in the Colorado Rockies, which killed 139 people in 1976 (see the discussion in the Thunderstorm Hazards chapter).

Sometimes if winds are right, thunderstorms are triggered over the mountains, but then are blown away to other locations. For example, orographic thunderstorms triggered over Colorado and Wyoming in late afternoon can move eastward during the evening, to hit the USA Midwest (e.g., Wisconsin) between midnight and sunrise.

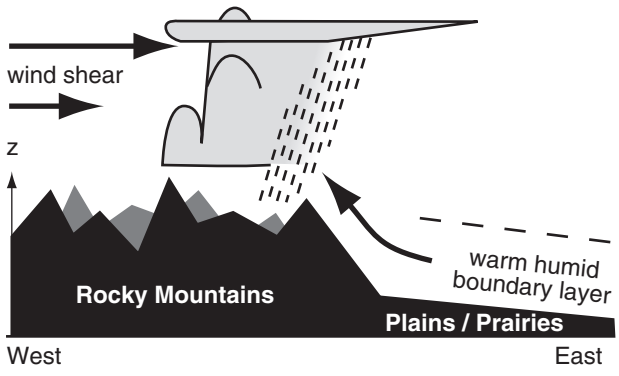

Figure 14.11
Orographic thunderstorm, stationary over the mountains.

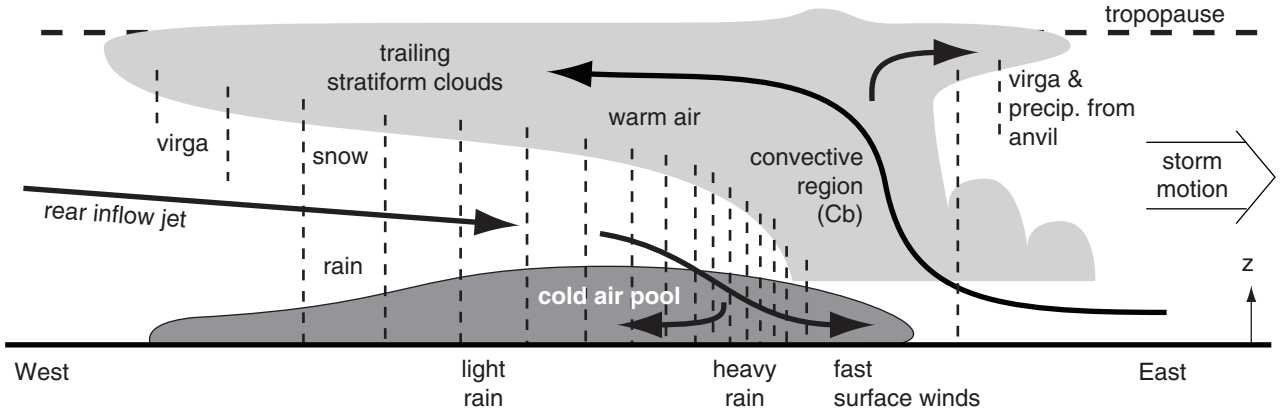

Figure 14.12
Vertical cross section of a mesoscale convective system (MCS).

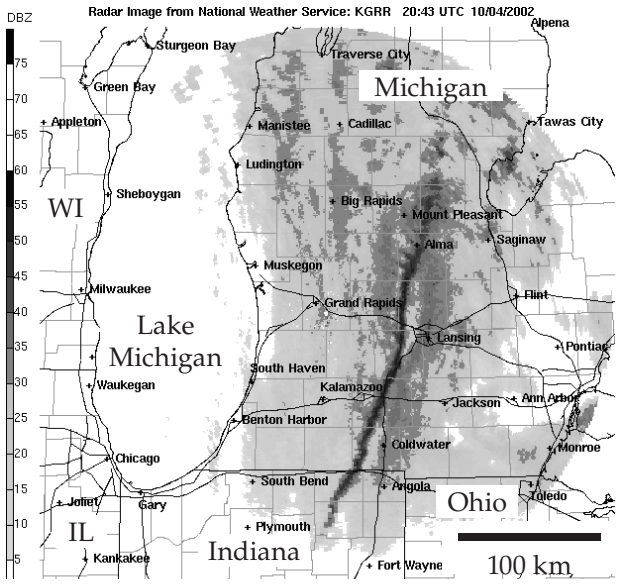

Figure 14.13.
Radar reflectivity PPI image of a mesoscale convective system (MCS) in southern Michigan, USA, on 4 Oct 2002. Dark shading indicates a line of heavy thunderstorm rain associated with radar reflectivities > 50 dBZ. Ahead and behind this squall line are broad regions of lighter, stratiform precipitation with imbedded convective cells. Courtesy of the US National Weather Service, NOAA.

Mesoscale Convective Systems

Another type of multicell-storm organization is a **mesoscale convective system** (**MCS**). This often has a narrow line of thunderstorms with heavy precipitation, followed by additional scattered thunderstorm cells (Figs. 14.12 & 14.13). The anvils from all these thunderstorms often merge into a single, large stratiform **cloud shield** that trails behind. This trailing **stratiform** region has widespread light to moderate precipitation that contributes about 1/3 of the total MCS rainfall.

These systems can be triggered by the terrain (many form just east of the Rocky Mountains), by synoptic systems (such as cold fronts), or by the gust fronts from a smaller number of thunderstorms. To survive, they need large convective instability and large wind shear over a deep layer of the environment. MCSs are responsible for 30 to 70% of precipitation over central N. America during the warm season. Some MCSs reach their peak intensity about midnight.

Ice crystals falling from the trailing stratiform clouds melt or partially sublime, and the resulting rain then continues to partially evaporate on the way down. This produces a broad region of chilled air (due to latent heats of melting, sublimation, and evaporation) that descends to the ground and accumulates as a **cold-air pool** at the surface. The extra weight of the cold air produces a mesoscale high pressure (**meso-high**) at the surface in this region (Fig. 14.14).

Meanwhile, warm humid boundary-layer air ahead of the MCS is drawn into the storm by the combined effects of buoyancy and wind shear. This air rises within the imbedded thunderstorm cells, and releases latent heat as the water vapor condenses. The resulting heating produces a layer of relatively warm air at mid and upper levels in the MCS (Fig. 14.14). The top of the anvil is cooled by IR radiation to space.

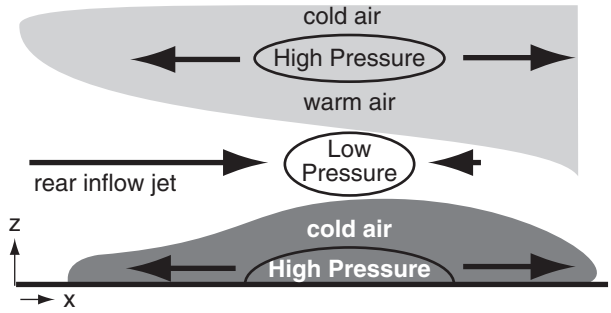

Figure 14.14
Zoomed view of the left half of Fig. 14.12, showing the rear portion of an MCS. Variation of pressure (relative to a standard atmosphere) with altitude caused by layers of warm and cold air in the stratiform portion of an MCS.

The resulting sandwich of relatively warmer and cooler layers causes a mesoscale low-pressure region (a **meso-low**) at mid altitudes (Fig. 14.14) and high pressure aloft (see solved example). The horizontal pressure-gradient force at mid altitudes causes air to converge horizontally. The thunderstorm updraft partially blocks mid-altitude inflow from the front of the storm, so the majority of inflow is from the rear. This is called a **rear inflow jet** (**RIJ**).

As the RIJ approaches the core of the MCS, it passes through the precipitation falling from above, and is cooled. This cooling allows the RIJ to descend as it blows toward the front of the storm, causing damaging **straight-line winds** at the ground. Large damaging straight-line wind events are called **derechos** (see a later Focus Box).

Solved Example

Plot MCS thermodynamics:

(a) Assume a standard atmosphere in the environment outside the MCS, and calculate $P_{std.atm.}$ vs. z.

(b) Inside the MCS, assume the temperature T_{MCS} differs from the $T_{std.atm.}$ by:
–12 K for $9 < z \le 11$ km due to rad. cooling at anvil top;
+8 K for $4 \le z \le 9$ km due to latent heating in cloud;
–12 K for $0 \le z \le 2$ km in the cold pool of air;
0 K elsewhere. Use P_{sfc} = 101.8 kPa in the MCS.
Plot $\Delta T = T_{MCS} - T_{std.atm.}$ vs. z .

(c) Calculate P_{MCS} vs. z in the MCS.

(d)Plot pressure difference $\Delta P = P_{MCS} - P_{std.atm.}$ vs. z

Solution:

Given: T and P data listed above within MCS, and std. atm. in the environment outside the MCS.

Find & plot: ΔT (K) vs. z (km); and ΔP (kPa) vs. z (km)

Method:

(a) In a spreadsheet, use standard-atmosphere eq. (1.16) to find $T_{std.atm.}$ vs. z, assuming $H = z$.

(Continues in next column.)

Solved Example. *(Continuation)*

For this standard atmosphere outside the MCS, use hypsometric eq. (1.26b) to find P vs. z by iterating upward in steps of Δz = 250 m from $P_1 = P_{sfc}$ = 101.325 kPa at $z_1 = 0$. Assume $T_{v\,avg} = T_{avg} = 0.5 \cdot (T_1 + T_2)$ in eq. (1.26b) for simplicity (since no humidity information was given in the problem). Thus (with a = 29.3 m/K):

$$P_2 = P_1 \cdot \exp[\,(z_1 - z_2) \,/\, (a \cdot 0.5 \cdot (T_1 + T_2)\,] \qquad (1.26b)$$

(b) Plot ΔT vs. z, from data given in the problem.

(c) Find $T_{MCS}(z) = T_{std.atm.}(z) + \Delta T(z)$. Do the similar hypsometric P calculations as (a), but inside the MCS.

(d) Find $\Delta P = P_{MCS} - P_{std.atm.}$ from (c) and (a), and plot.

Spreadsheet segments:

	(a)		(b)	(c)		(d)
	Std. Atmos.			MCS		ΔP
z (m)	T (K)	P (kPa)	ΔT (K)	T (K)	P (kPa)	(kPa)
0	288.2	101.3	–12	276.2	101.8	0.5
250	286.5	98.3	–12	274.5	98.7	0.4
500	284.9	95.4	–12	272.9	95.7	0.2
750	283.3	92.6	–12	271.3	92.7	0.1
. . .	. . .	. . .	. . .	. . .	. . .	. . .
2000	275.2	79.5	–12	263.2	79.0	–0.5
2250	273.5	77.1	0	273.5	76.6	–0.5
. . .	. . .	. . .	. . .	. . .	. . .	. . .
3750	263.8	63.7	0	263.8	63.3	–0.4
4000	262.2	61.7	8	270.2	61.3	–0.4
. . .	. . .	. . .	. . .	. . .	. . .	. . .
9000	229.7	30.8	8	237.7	31.3	0.5
9250	228.0	29.6	–12	214.0	30.1	0.5
. . .	. . .	. . .	. . .	. . .	. . .	. . .
11000	216.7	22.7	–12	204.7	22.7	0.0
11250	215.0	21.8	0	215.0	21.8	0.0

(Note: The actual spreadsheet carried more significant digits.)

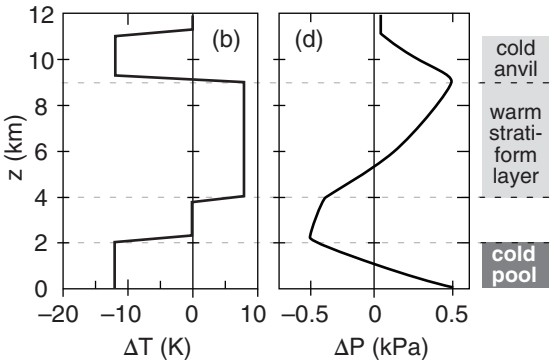

Check: Units OK. Standard atmosphere P agrees with Table 1-5. Graphs are reasonable.

Discussion: High pressure at the surface causes the cold-pool air to spread out, as sketched in Figs. 14.12 & 14.14. The lowest pressure is above the cold pool and below the warm stratiform clouds. This low pressure (relative to the environment) sucks in air as a rear inflow jet. The deep layer of warm stratiform clouds eventually causes high pressure aloft, causing the cloudy air to spread out in the anvil. The cold anvil top then brings the pressure back to ambient, so that above the anvil there are no pressure differences.

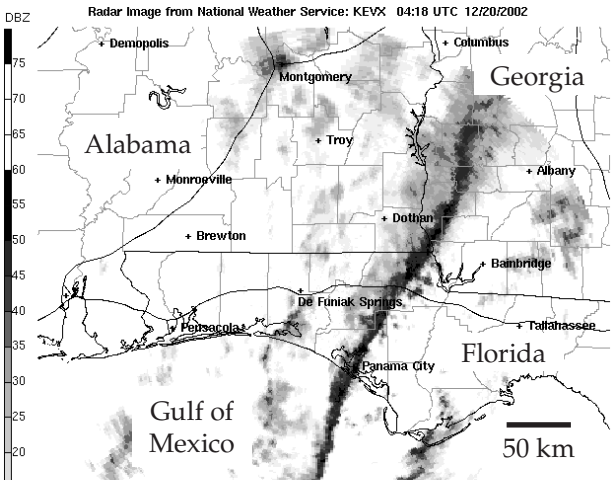

Figure 14.15
Radar reflectivity PPI image of squall line in Florida, Georgia and Alabama, USA, on 20 December 2002. Darkest shading corresponds to thunderstorms with reflectivity > 50 dBZ. Courtesy of the US National Weather Service, NOAA.

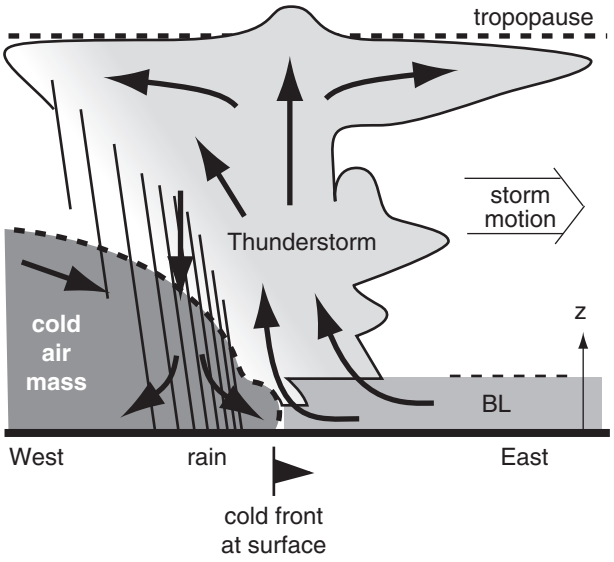

Figure 14.16
Vertical cross section through a squall-line thunderstorm, triggered by a cold front. Boundary-layer (BL) pre-storm air is warm and humid; cold air mass is colder and drier. Dashed lines indicate base of stable layers such as temperature inversions.

Squall Line. One type of MCS is a **squall line**, where a linear triggering mechanism such as a cold front, dry line or gust front causes many neighboring thunderstorms to merge into a long narrow line (Figs. 8.26 & 14.15). Squall lines can be many hundreds (even a thousand) kilometers long, but are usually only 15 to 400 km wide. They can persist for several hours to several days if continuously triggered by the advancing front. Heavy thunderstorm precipitation falls immediately behind the cold front at the surface, and sometimes has weaker stratiform precipitation behind it. Squall line storms can also have prodigious lightning, hail, damaging winds and tornadoes (although the tornadoes tend to be weaker than supercell-thunderstorm tornadoes).

Fig. 14.16 illustrates flow characteristics in a vertical cross section perpendicular to the squall-line axis. Environmental wind shear along the advancing cold front allows the thunderstorms to persist in the mature stage for the lifetime of the squall line. Cold, dry air descends from the west in the cold air mass from behind the squall line. This cold descent is enhanced by cool downburst air in the precipitation region. Both effects help advance the leading edge of the cold front at the ground. Warm, humid boundary-layer air blowing from the east ahead of the front is lifted by the undercutting denser cold advancing air, thereby continuously feeding the main updraft that moves with the advancing front.

A well defined arc or shelf cloud often exists along the leading edge of the cold front, associated with violent straight-line winds. If the gust front from the downburst advances eastward faster than the cold front, then a second line of thunderstorms may be triggered along the gust front in advance of the cold front or the squall line might separate from the front.

Bow Echo. For MCSs with strong buoyancy in the updraft air and moderate to strong wind shear in the bottom 2 to 3 km of the environment, the cold pool becomes deeper and colder, and rear-inflow-jet (RIJ) wind speeds can become stronger. The RIJ pushes forward the center portion of the squall line, causing it to horizontally bend into a shape called a **bow echo** (Fig. 14.17). Bow-echo lines are 20 to 200 km long (i.e., smaller than most other MCSs) and are often more severe than normal MCSs.

Vorticity caused by wind shear along the advancing cold pool causes counter-rotating vortices at each end of the bow-echo line. These are called **line-end vortices** or **bookend vortices** (Fig 14.17), which rotate like an eggbeater to accelerate the RIJ and focus it into a narrower stream. For bow echoes lasting longer than about 3 h, Coriolis force enhances the northern cyclonic vortex in the

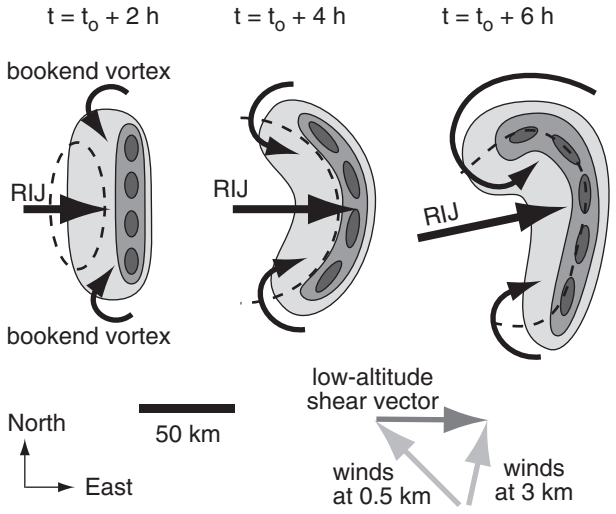

Figure 14.17
Evolution of a bow-echo line of thunderstorms. Shading indicates radar reflectivity, dashed line outlines cold air pool at surface, RIJ is rear inflow jet, t is time, and t_o is formation time.

Northern Hemisphere and diminishes the southern anticyclonic vortex, causing the bow echo to become asymmetric later in its evolution.

Strong straight-line winds near the ground from a bow echo can damage buildings and trees similar to an EF2 tornado (see the "Tornado" section later in this chapter for a description of tornado damage scales). If a sequence of bow echoes causes wind damage along a 400 km path or greater and lasts about 3 hours or more, with wind speeds ≥ 26 m/s with gusts ≥ 33 m/s, then the damaging wind event is called a **derecho** (see Focus Box 3 pages later).

Mesoscale Convective Complex (MCC). If the size of the MCS cloud shield of merged anvils is large (diameter ≥ 350 km), has an overall elliptical or circular shape, and lasts 6 to 12 h, then it is called a **mesoscale convective complex** (**MCC**). An additional requirement to be classified as an MCC is that the top of the cloud shield, as seen in IR satellite images, must have a cold brightness-temperature ≤ –33°C. Within this cold cloud shield must be a smaller region (diameter ≥ 250 km) of higher, colder cloud top with brightness temperature ≤ –53°C.

MCCs can produce heavy rain over large areas, with the most intense rain usually happening first. MCCs are most often observed at night over a statically stable boundary layer, which means that the fuel for these storms often comes from the warm humid air stored in the residual boundary layer from the day before. They can be triggered by: weak warm frontal zones, weak mid-tropospheric short waves, and are often associated with low-level jets of wind.

Solved Example

Estimate the speed of the rear inflow jet (RIJ) wind that is drawn into the MCS mid-tropospheric low-pressure region, for the previous solved example. The MCS has horizontal radius of 175 km, and is located in Oklahoma (latitude 35°N) .

Solution

Given: $\Delta P = -0.5$ kPa at height $z = 2$ km, from previous solved example.
$R = 175$ km = radius of meso-low in mid-troposphere, latitude $\phi = 35°$N
Find: M_{RIJ} = ? m/s

Assume the RIJ is geostrophic ($M_{RIJ} = U_g$). To use eq. (10.26a) for the geostrophic wind, we need:
$\Delta P/\Delta y$, ρ and f_c .
Consider the region just south of the low center.
$\Delta P/\Delta y$ = (–0.5 kPa)/(175 km) = –0.00286 kPa/km
Assuming std. atmosphere. Use Table 1-5 at 2 km
$\rho = 1.0$ kg·m^{-3} .
Use eq. 10.16 to find the Coriolis parameter:
$f_c = (1.458\text{x}10^{-4}\ \text{s}^{-1})\cdot\sin(35°) = 0.836\text{x}10^{-4}\ \text{s}^{-1}$.
Combine these data in eq. (10.26a):
$U_g = -[(1.0\ \text{kg·m}^{-3})\cdot(0.836\text{x}10^{-4}\ \text{s}^{-1})]^{-1}\cdot(-0.00286\ \text{Pa/m})$
$= 34.2$ m/s
Thus,
$M_{RIJ} = U_g$ = **34.2 m/s**

Check: Units OK. Magnitude reasonable. Sign OK.
Discussion: This implies a RIJ from the west, in the region just south of the mid-tropospheric meso-low center. If this RIJ descends down to the surface due to the influence of precipitation cooling, it could cause damaging straight-line wind gusts that exceed the threshold to be classified as a derecho.

One caution: the geostrophic wind assumes steady state. In a rapidly intensifying MCS, steady-state might not be the best assumption. If the wind were accelerating, then it could have an ageostrophic component pointing towards the low center.

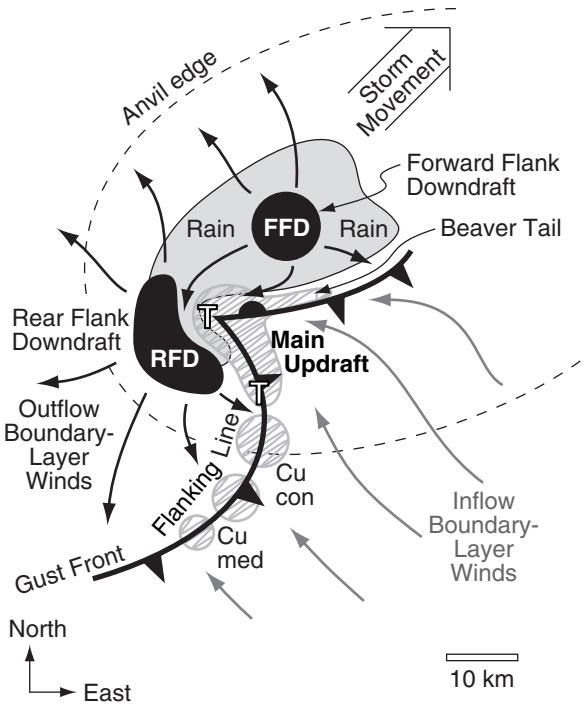

Figure 14.18
Plan view (top down) sketch of a classic supercell in the N. Hemisphere (copied from Fig. 14.4b). T indicates possible tornado positions; RFD = Rear Flank Downdraft; FFD = Forward Flank Downdraft. Regions of updraft are hatched with grey; downdrafts are solid black; rain is solid light grey. Low surface pressure is found under the updrafts (especially near the "T" locations), and high pressure under the downdrafts. Vectors are surface winds: cold are black, warm are grey.

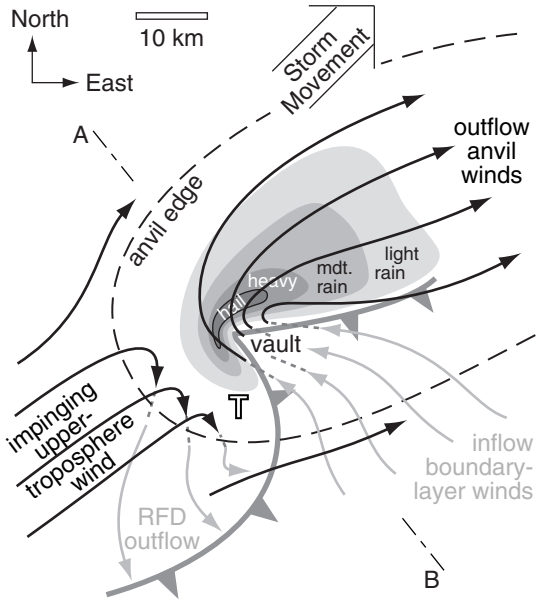

Figure 14.19
Plan view of classic (CL) supercell in the N. Hemisphere. Low altitude winds are shown with light-grey arrows, high-altitude winds with black arrows, and ascending/descending air with short-dashed lines. T indicates tornado location.

Mesoscale Convective Vortex (MCV). Between midnight and sunrise, as the static stability of the boundary layer increases, the thunderstorms within MCSs often weaken and die. Thunderstorms are more difficult to trigger then, because cold nocturnal boundary-layer air resists rising. Also, above the nocturnal layer is a thin residual layer that has only a small capacity to hold the fuel supply of warm humid air from the previous day's mixed layer. As the MCS rains itself out, all that is left by the next morning are mid-level stratiform clouds.

However, the mid-tropospheric mesoscale low-pressure region (Fig. 14.14) in the MCS has existed for about half a day by this time, and has developed cyclonic rotation around it due to Coriolis force. This mesoscale rotation is often visible (by satellite) in the mid-level (former MCS) stratiform clouds, and is called a **mesoscale convective vortex** (**MCV**). The stable boundary layer beneath the MCV reduces surface drag, allowing the rotation to persist for many more hours around the weak low.

Although these weakly rotating systems are not violent and often don't have a circulation at the surface, they can be tracked by satellite during the morning and early afternoon as they drift eastward. They are significant because they can enhance new thunderstorm formation via weak convergence and upward motion. Thus, by evening the dying MCV can change into a new MCS.

Supercell Thunderstorms

A violent thunderstorm having a rotating updraft and persisting for hours is called a **supercell storm** (Figs. 14.3 & 14.4). Its downdraft and surface features (Fig 14.18, a duplicate of Fig. 14.4b) are organized in a way to trigger new thunderstorms nearby along a **flanking line**, and then to entrain these incipient updrafts (cumulus congestus clouds) into the main supercell updraft to give it renewed strength. The main, persistent, rotating updraft, or **mesocyclone**, is 3 to 10 km in diameter, and can extend throughout the whole depth of the thunderstorm.

Supercell storms are responsible for the most violent tornadoes (EF3 - EF5, as defined in the next chapter) and hail, and can have damaging straight-line winds and intense rain showers causing flash floods. To support supercells, the pre-storm environment must have a deep layer of convectively unstable air, and strong wind shear in the bottom 6 km of the troposphere.

Although supercells can have a wide range of characteristics, they are classified into three categories: **low-precipitation** (**LP**) storms, medium precipitation or **classic** (**CL**) supercells, and **high-precipitation** (**HP**) storms. Storms that fall between these categories are called **hybrid storms**.

Classic Supercells. Figures 14.3 and 14.4 show characteristics of a classic supercell. One way to understand how supercells work is to follow air parcels and hydrometeors (precipitation particles) as they flow through the storm.

Warm humid boundary-layer air flowing in from the southeast (Fig. 14.19) rises in the main supercell updraft, and tiny cloud droplets form once the air is above its LCL. So much water vapor condenses that large amounts of latent heat are released, causing large buoyancy and strong updrafts (often ≥ 50 m/s). Cloud droplets are carried upward so quickly in the updraft that there is not yet time for larger precipitation particles to form. Hence, the updraft, while visible by eye as a solid cloud, appears only as a **weak echo region** (**WER**) on radar PPI scans because there are no large hydrometeors. This region is also known as an **echo-free vault** (Fig. 14.19).

As the air reaches the top of the troposphere, it encounters stronger winds, which blows these air parcels and their cloud particles downwind (to the northeast in Fig. 14.19). Since the whole storm generally moves with the mean wind averaged over the bottom 6 km of troposphere (to the northeast in Fig. 14.19), this means that the air parcels in the top part of the storm are flowing to the storm's forward flank. This differs from MCSs, where the updraft air tilts back toward the storm's trailing (rear) flank.

While rising, the air-parcel temperature drops to below freezing, and eventually below –40°C near the top of the thunderstorm (similar to Fig. 14.7), at which point all hydrometeors are frozen. Various microphysical processes (cold-cloud Bergeron process, collision, aggregation, etc.) cause larger-size hydrometeors to form and precipitate out. The larger, heavier hydrometeors (hail, graupel) fall out soonest, adjacent to the updraft (to the north in Fig. 14.19). Medium size hydrometeors are blown by the upper-level winds farther downwind (northeast), and fall out next. Lighter hydrometeors fall more slowly, and are blown farther downwind and fall in a larger area.

In summer, all of these ice particles (except for some of the hail) melts while falling, and reaches the ground as rain. The greatest precipitation rate is close to the updraft, with precipitation rates diminishing farther away. The very smallest ice particles have such a slow fall velocity that they have a long residence time in the top of the troposphere, and are blown downwind to become the anvil cloud.

Meanwhile, the falling precipitation drags air with it and causes it to cool by evaporation (as will be explained in more detail in the next chapter). This causes a downdraft of air called the **forward flank downdraft** (**FFD**, see Fig. 14.18). When this cold air hits the ground, it spreads out. The leading edge of

Solved Example

If a Doppler radar were located near the words "10 km" in the bottom right corner of Fig. 14.18, then sketch the resulting color patterns on the Doppler PPI wind display for near-surface winds.

Solution:

Given: Near-surface winds from Fig. 14.18 are copied below, with radar located southeast of the storm center.

Find: Sketch the Doppler wind display.

Assume sufficient number-density of insects to allow Doppler radar returns even in rain-free areas.

Hatched grey corresponds to red colors, for winds away from the radar. Plain grey corresponds to blues and greens, for winds toward the radar. White is the zero isodop line. Darker shading near the "T" is to suggest a tornado vortex signature.

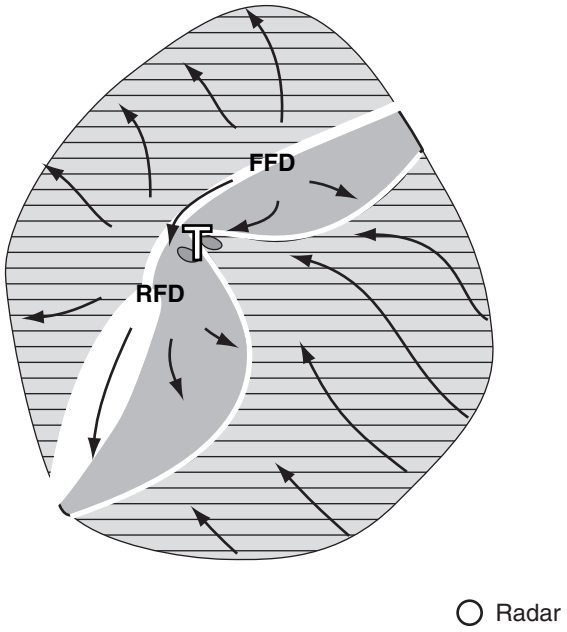

Check: Compares well with info in Chapter 8.

Discussion: Fig. 14.19 already shows the radar reflectivity display. By interpreting the reflectivity and Doppler info together, you can create in your mind a coherent picture of the storm.

The gust fronts show up clearly in the Doppler display. The tornado-vortex signature in the Doppler display and the hook echo in the reflectivity display both suggest the presence of a tornado.

Finally, real thunderstorms are imbedded in an environment that is not usually calm, so there would also be red and blue colors outside of the regions sketched here.

FOCUS • Derecho

A **derecho** is a hazardous event of very strong straight-line (non-tornadic) horizontal winds (≥ 26 m/s) often causing widespread (≥ 400 km length) damage at the surface. It is associated with clusters of downbursts of air from a single moving mesoscale convective system (MCS), which causes localized destruction that sweeps through the event area during several hours to over a day. Within the event area, the wind intensity and damage can be variable.

The word "derecho" is based on a Spanish word for "straight-ahead" or "direct". Derechos occur in the prairies east of the Rocky Mountains (see Fig. below), and were first reported over a century ago. Although derechos can occur during any month, they are most frequent in April through August, with peak frequencies during May and July. Peak wind speeds over 65 m/s have been rarely observed.

In the USA, an average of 21 derechos occur each year, killing 9 and injuring 145 people annually. Most of the deaths are people in cars and boats, while most of the injuries are people in mobile homes and cars. Derechos can blow down trees, destroy mobile homes, and damage other structures and cars.

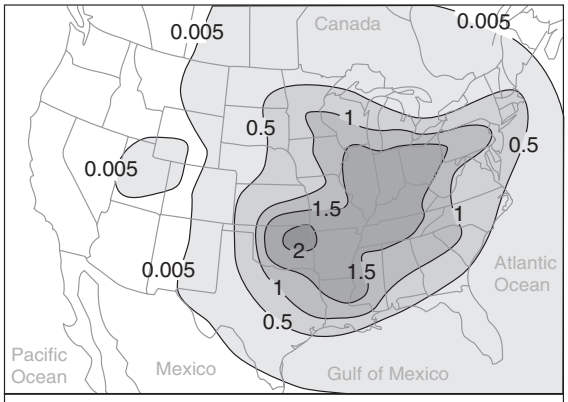

Figure 14.a.
Derecho climatology.

Based on data from Ashley & Mote, 2005: Derecho hazards in the United States. Bull. Amer. Meteor. Soc., 86, 1577-1592.

the spreading cold air is called the (forward-flank) **gust front**, and is often indicated with cold-frontal symbols. This gust front helps to deflect the boundary-layer air upward into the main updraft, and can create a **beaver-tail cloud**, as described earlier.

Due to rotation of the whole updraft (the origin of rotation will be discussed later), the precipitation region is often swept counterclockwise around the updraft for N. Hemisphere supercells. This creates a characteristic curve of the precipitation region that is seen on weather radar as a **hook echo** around the echo-free vault (Fig. 14.19).

In the S. Hemisphere (and for a small portion of N. Hemisphere supercells — see Fig. 14.63), the updrafts rotate clockwise. These supercells can still produce hook echoes, but with the hook projecting in a direction different than that sketched in Fig. 14.19).

The supercell storm is so tightly organized that it acts as an obstacle to fast winds in the upper troposphere. When these ambient winds from the west or southwest hit the supercell, some are deflected downward, creating the **rear-flank downdraft** (**RFD**). As the dry upper-tropospheric air moves down adjacent to the cloudy updraft, it entrains some cloud droplets, which quickly evaporate and cool the air. This negative buoyancy enhances the RFD such that when the air hits the ground it spreads out, the leading edge of which is a (rear-flank) **gust front**.

When warm, humid boundary-layer air flowing into the storm hits the rear-flank gust front, it is forced upward and triggers a line of cumulus-cloud growth called the **flanking line** of clouds. The inflow and circulation around the supercell draws these new cumulus congestus clouds into the main updraft, as previously described. At the cusp of the two gust fronts, there is low surface pressure under the updraft. This **meso-low** (see Table 10-6) and the associated gust fronts look like mesoscale versions of synoptic-scale cyclones, and are the surface manifestation of the **mesocyclone**.

Strong **tornadoes** are most likely to form in one of two locations in a supercell. One is under the largest cumulus congestus clouds just as they are being entrained into the main updraft, due to the rotation between the RFD and the updraft. These form under the rain-free cloud-base portion of the supercell, and are often easy to view and chase. The other location is under the main updraft at the cusp where the two gust fronts meet, due to rotation from the parent mesocyclone. Tornadoes are discussed in more detail in the next chapter.

Low Precipitation Supercells (Fig. 14.20). In drier regions of North America just east of the Rocky Mountains, LCLs are much higher above ground. However, mountains or dry lines can cause sufficient lift to trigger high-base supercell storms. Also, if strong environmental wind shear causes a strongly tilted updraft, then incipient precipitation particles are blown downwind away from the rich supply of smaller supercooled cloud droplets in the updraft, and thus can't grow large by collection/accretion. Most of the hydrometeors that form in these storms evaporate before reaching the ground; hence the name **low-precipitation** (**LP**) **supercells**.

With fewer surrounding low clouds to block the view, LP storms often look spectacular. You can often see the updraft, and can see evidence of its rotation due to cloud striations, curved inflow bands and possibly a rotating wall cloud. If present, the beaver tail is easily visible. Although rainfall is only light to moderate, LP storms can produce great amounts of large-diameter hail. Those LP supercells having exceptionally strong updrafts produce anvils that look like a mushroom cloud from a nuclear bomb explosion.

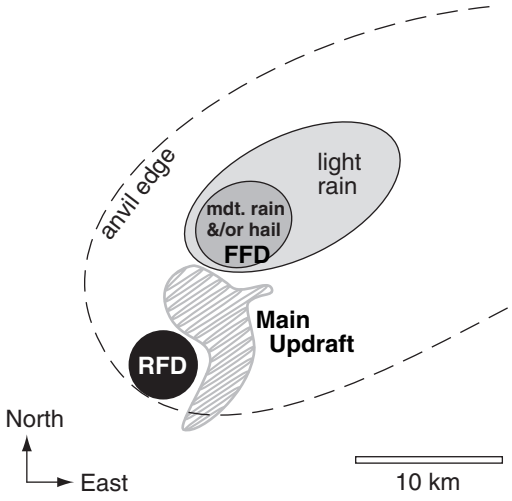

Figure 14.20
Low-precipitation (LP) supercell thunderstorm in the N. Hemisphere. FFD = forward flank downdraft; RFD = rear flank downdraft. Often little or no precipitation reaches the ground. The hatched grey region indicates updrafts.

High Precipitation Supercells (Fig. 14.21). In very warm humid locations such as southeastern North America, some supercell storms can produce widespread heavy precipitation. These are known as **high-precipitation** (**HP**) **supercells**. Precipitation falls from most of the cloud-base areas, often filling both the FFD and the RFD. So much rain falls upstream in the rear-flank region of the storm that the main mesocyclone is sometimes found downstream (forward) of the main precipitation region.

Some storms have curved inflow bands and cloud striations on the updraft that you can see from a distance. Also, the smooth-looking beaver-tail clouds are most common for HP storms, near the forward-flank gust front. Much more of the surrounding sky is filled with low and mid-level clouds, which together with low visibilities makes it difficult to get good views of this storm.

As this type of storm matures, the heavy-rain region of the hook echo can completely wrap around the updraft vault region. Storm chasers call this region the **bear's cage**, because of the high danger associated with tornadoes and lightning, while being surrounded by walls of torrential rain and hail with poor visibility and hazardous driving/chasing conditions.

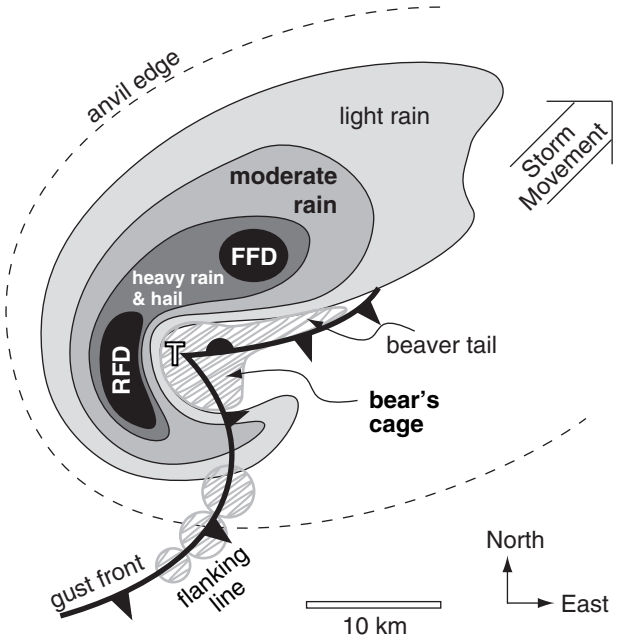

Figure 14.21
High-precipitation (HP) supercell thunderstorm in the N. Hemisphere. FFD = forward flank downdraft; RFD = rear flank downdraft. Hatched grey regions indicate updrafts.

Now that we are finished covering the descriptive appearance and types of thunderstorms, the next five sections examine the meteorological conditions needed to form a thunderstorm.

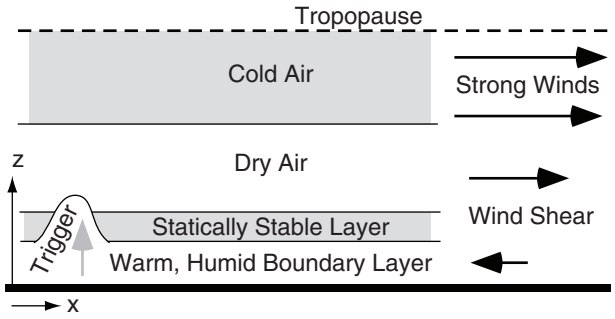

Figure 14.22
An environment conducive to severe thunderstorms.

THUNDERSTORM FORMATION

Convective Conditions

Four environmental (pre-storm) conditions are needed to form the strong **moist convection** that is a severe thunderstorm:

1) **high humidity** in the boundary layer,
2) nonlocal conditional **instability**,
3) strong **wind shear**,
4) a **trigger mechanism** to cause **lifting** of atmospheric boundary-layer air.

Fig. 14.22 illustrates these conditions. Meteorologists look for these conditions in the pre-storm environment to help forecast thunderstorms. We will examine each of these conditions in separate sections. But first, we define key convective altitudes that we will use in the subsequent sections to better understand thunderstorm behavior.

Key Altitudes

The existence and strength of thunderstorms depends partially on layering and stability in the pre-storm environment. Thus, you must first obtain an **atmospheric sounding** from a **rawinsonde balloon** launch, **numerical-model** forecast, aircraft, dropsonde, satellite, or other source. Morning or early afternoon are good sounding times, well before the thunderstorm forms (i.e., **pre-storm**). The environmental sounding data usually includes temperature (T), dew-point temperature (T_d), and wind

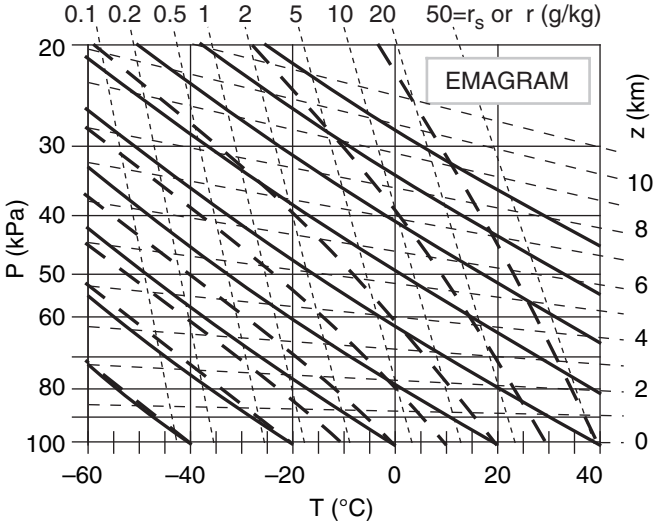

Figure 14.23
Thermo diagram, with approximate height contours (z) added as nearly horizontal thin dashed lines (labeled at right). Sounding data plotted on this diagram will enable you to anticipate storm formation and strength.

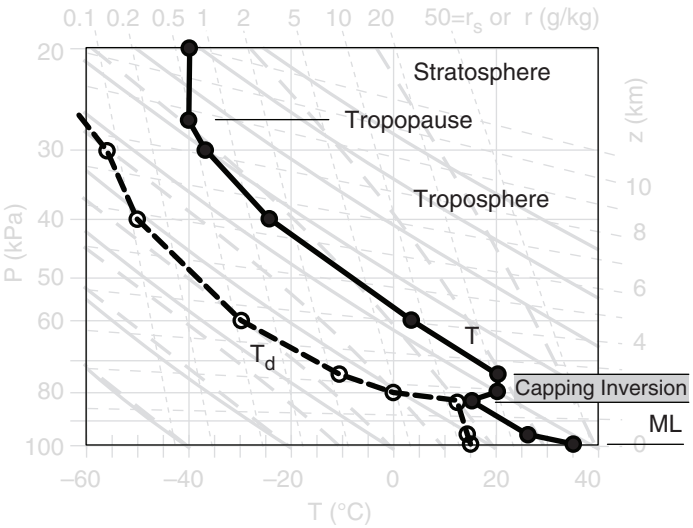

Figure 14.24
Environmental sounding of temperature (T) and dew-point temperature (T_d) plotted on a thermo diagram. The mixed layer (ML), capping inversion (Cap), tropopause, troposphere, and stratosphere are identified. This example shows an early-afternoon pre-storm environment.

speed (M) and direction (α) at various heights (z) or pressures (P).

Plot the environmental sounding on a thermo diagram such as the Emagram of Fig. 14.23, being sure to connect the data points with straight lines. Fig. 14.24 shows a typical pre-storm (early afternoon) sounding, where T is plotted as black-filled circles connected with a thick black solid line, and T_d is plotted as white-filled circles connected with a thick black dashed line. The mixed layer (ML; i.e., the daytime turbulently well-mixed boundary layer), capping inversion, and tropopause are identified in Fig. 14.24 using the methods in Chapter 5.

During the day, the sun heats the ground. The hot ground heats the air and evaporates soil moisture into the air. Air near the surface becomes statically unstable, allowing air parcels from the surface-layer (bottom of the ML) to rise. If we assume each rising air parcel does not mix with the environment, then its temperature decreases dry adiabatically with height initially, and its mixing ratio is constant.

Fig. 14.25 shows how this process looks on a thermo diagram. The parcel temperature starts near the ground from the solid black circle and initially follows a **dry adiabat** (thin black solid line with arrow). The dew point starts near the ground from the open circle and follows the **isohume** (thin black dotted line with arrow).

Typically, the rising parcel hits the statically stable layer at the top of the mixed layer, and stops rising without making a thunderstorm. This temperature-inversion height z_i represents the average **mixed-layer (ML) top**, and is found on a thermo diagram where the dry adiabat of the rising parcel first crosses the environmental sounding (Fig. 14.25). In pressure coordinates, use symbol P_i to represent the ML top.

If the air parcel were to rise a short distance above z_i, it would find itself cooler than the surrounding environment, and its negative buoyancy would cause it sink back down into the mixed layer. On many such days, no thunderstorms ever form, because of this strong lid on top of the mixed layer.

But suppose some external trigger mechanism (described later) forces the air to rise past the boundary-layer top z_i in spite of the negative buoyancy. The rising air parcel continues cooling until it becomes saturated. On a thermo diagram, this saturation point is the **lifting condensation level** (**LCL**), where the dry adiabat first crosses the isohume for the rising parcel.

As the trigger mechanism continues to push the reluctant air parcel above the lifting condensation level (LCL), clouds form and latent heat is added to the air. The temperature of the rising cloudy air parcel now follows a **moist adiabat** (black dashed line

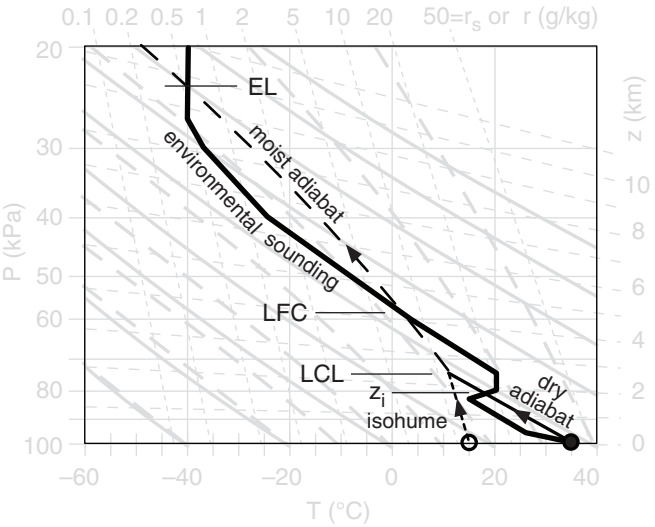

Figure 14.25
Afternoon pre-storm environmental air from near the surface (indicated with the circles), is hypothetically lifted as an air parcel to the top of the thermo diagram. Identified are the average mixed-layer height (z_i), the lifting condensation level (LCL), the level of free convection (LFC), and the equilibrium level (EL).

FOCUS • Cap vs. Capping Inversion

The strongly stable layer at the top of the daytime boundary layer (i.e., at the top of the mixed layer) is called the "**capping inversion,**" as sketched in the figure below (a modification of Fig. 14.25).

The region near the top of the mixed layer where the rising air parcel is colder than the environment is called the "**cap**." It is this region between z_i and the LFC that opposes or inhibits the rise of the air parcel, and which must be overcome by the external forcing mechanism. See the section later in this chapter on "Triggering vs. Convective Inhibition" for more details.

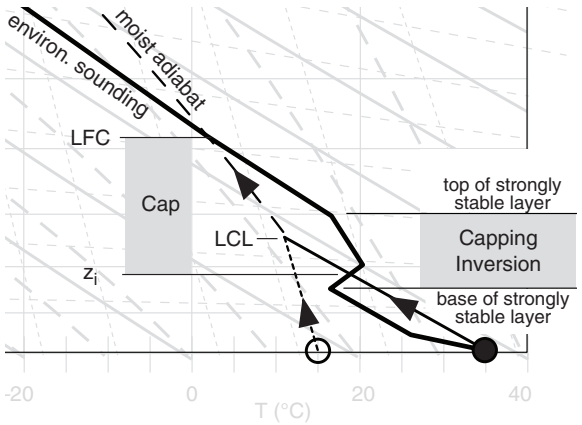

Figure 14.b
Emagram with idealized pre-storm environmental sounding (thick solid line). Circles and lines with arrows show the rise of an air parcel from near the surface.

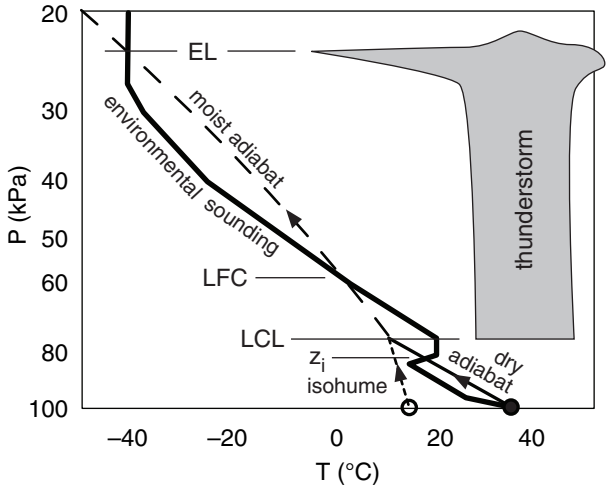

Figure 14.26
From Fig. 14.25, we infer that a thunderstorm could form with cloud top and base as sketched, if successfully triggered.

Solved Example

Plot this sounding on a full-size **skew-T** diagram (Chapter 5), and estimate the pressure altitudes of the ML top , LCL, LFC, and EL for an air parcel rising from near the surface.

P (kPa)	T (°C)	T_d (°C)
100	30	20.
96	25	.
80	10	.
70	15	.
50	–10	.
30	–35	.
20	–35	.

Solution

Given: Data in the table above.

Find: P_i = ? kPa (= ML top), P_{LCL} = ? kPa, P_{LFC} = ? kPa, P_{EL} = ? kPa.

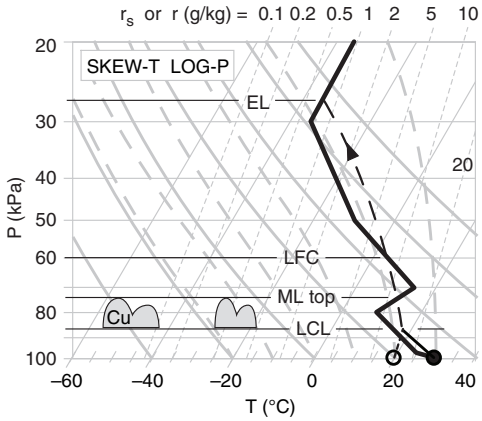

After plotting the air-parcel rise, we find:

P_i = **74 kPa**, P_{LCL} = **87 kPa**,
P_{LFC} = **60 kPa**, P_{EL} = **24 kPa**.

Discussion: The LCL for this case is below the ML top. Thus, the ML contains scattered fair-weather cumulus clouds (cumulus humilis, Cu). If there is no external trigger, the capping inversion prevents these clouds from growing into thunderstorms.

in Fig. 14.25). Even so, this cloudy parcel is still colder than the ambient environment at its own height, and still resists rising due to its negative buoyancy.

If the ambient sounding is conducive to thunderstorm development, as is sketched in Fig. 14.25, and if the trigger mechanism pushes the air parcel sufficiently high, then the cloudy air parcel will reach an altitude where it is again warmer than the environment. This altitude is called the **level of free convection** (**LFC**). On a thermo diagram, it is where the moist adiabat of the rising air parcel crosses back to the warm side of the environmental sounding.

Above the LFC, the air parcel can rise and accelerate under its own buoyancy, while still following the moist adiabat. This positive buoyancy gives the thunderstorm its energy, and if large enough can cause violent updrafts.

Eventually, the rising parcel reaches an altitude where it becomes colder than the environment (Fig. 14.25), and no longer feels an upward buoyancy force. This altitude is called the **equilibrium level** (**EL**) or the **limit of convection** (**LOC**). Often, the EL is near (or just above) the tropopause (Fig. 14.24), because the strong static stability of the stratosphere impedes further air-parcel rise.

Thus, thunderstorm cloud-base is at the LCL, and thunderstorm anvil top is at the EL (Fig. 14.26). In very strong thunderstorms, the rising air parcels are so fast that the inertia of the air in this updraft causes an **overshooting dome** above the EL before sinking back to the EL. The most severe thunderstorms have tops that can penetrate up to 5 km above the tropopause, due to a combination of the EL being above the tropopause (as in Fig. 14.26) and inertial overshoot above the EL.

In the bottom portion of the region between the LFC and the EL, the environment is **conditionally unstable**, as defined in Chapter 5. Recall that this means the environment is statically stable if the air already there is unsaturated, but is unstable if the environment is saturated (cloudy). On a thermo diagram, this is revealed by an environmental lapse rate between the dry- and moist-adiabatic lapse rates.

However, it is not the environmental air between the LFC and EL that becomes saturated and forms the thunderstorm. Instead, it is air rising above the LFC from lower altitudes (from the boundary layer) that forms the thunderstorm. Hence, this process is a **nonlocal conditional instability** (**NCI**).

Frequently the LCL is below z_i. This allows fair-weather cumulus clouds (cumulus humilis) to form in the top of the atmospheric boundary layer (see the solved example at left). But a trigger mechanism is still needed to force this cloud-topped mixed-layer air up to the LFC to initiate a thunderstorm.

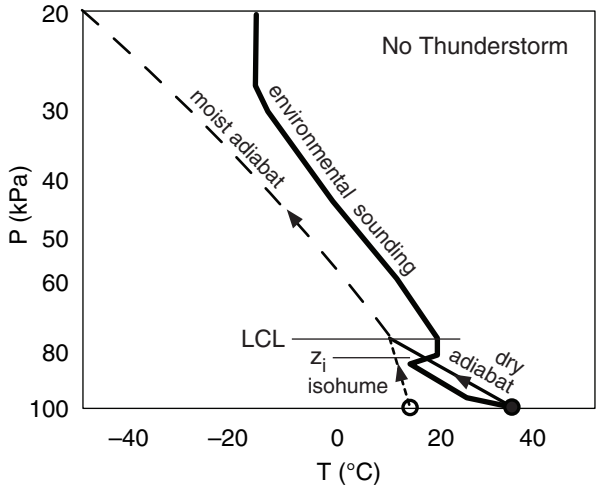

Figure 14.27
An environmental sounding that does not favor thunderstorms, because the environmental air aloft is too warm.

In many situations, no LFC (and also no EL) exists for an air parcel that is made to rise from the surface. Namely, the saturated air parcel never becomes warmer than the environmental sounding (such as Fig. 14.27). Such soundings are NOT conducive to thunderstorms.

HIGH HUMIDITY IN THE ABL

One of the four conditions needed to form **convective storms** such as thunderstorms is high humidity in the atmospheric boundary layer (ABL). Thunderstorms draw in pre-storm ABL air, which rises and cools in the thunderstorm updraft. As water vapor condenses, it releases latent heat, which is the main energy source for the storm (see the solved example). Thus, the ABL is the fuel tank for the storm. **Warmer moister boundary layers** favor more-intense thunderstorms (assuming all other factors are constant, such as the environmental sounding, wind shear, trigger, etc.).

The **dew-point temperature** T_d in the ABL is a good measure of the low-altitude humidity. High dew points also imply high air temperature, because $T \geq T_d$ always (Chapter 4). Thus, larger dew points indicate a warmer moister ABL, implying that copious amounts of sensible and latent heat are available. Thunderstorms in regions with $T_d \geq 16$°C can have heavy precipitation, and those in regions with $T_d \geq 21$°C can have greater severity.

Solved Example

How much **energy does an air-mass thunderstorm** release? Assume it draws in atmospheric boundary layer (ABL, or BL) air of T_d = 21°C & depth Δz_{BL} = 1 km (corresponding roughly to ΔP_{BL} = 10 kPa), and that all water vapor condenses. Approximate the cloud by a cylinder of radius R = 5 km and depth Δz = 10 km with base at P = 90 kPa & top at P = 20 kPa.

Solution

Given: R = 5 km, Δz = 10 km, T_d = 21°C,
Δz_{BL} = 1 km, ΔP_{BL} = 10 kPa,
ΔP_{storm} = 90 – 20 = 70 kPa
Find: ΔQ_E = ? (J)

Use eq. (3.3) with $L_v = 2.5\text{x}10^6$ J/kg, and eq. (4.3)

$$\Delta Q_E = L_v \cdot \Delta m_{water} = L_v \cdot r \cdot \Delta m_{air} \quad \text{(a)}$$

where $r \approx 0.016$ kg_{water}/kg_{air} from thermo diagram.

But eq. (1.8) $\Delta P = \Delta F/A$ and eq. (1.24) $\Delta F = \Delta m \cdot g$ give:

$$\Delta m_{air} = \Delta P \cdot A/g \quad \text{(b)}$$

where A = surface area = πR^2.

For a cylinder of air within the ABL, but of the same radius as the thunderstorm, use eq. (b), then (a):

$\Delta m_{air} = (10\text{ kPa})\cdot\pi\cdot(5000\text{m})^2/(9.8\text{ m/s}^2) = 8\text{x}10^8$ kg_{air}

$\Delta Q_E = (2.5\text{x}10^6\text{ J/kg})(0.016\text{ kg}_{water}/\text{kg}_{air})(8\text{x}10^8\text{ kg}_{air})$
$= 3.2\text{x}10^{15}$ J

Given the depth of the thunderstorm (filled with air from the ABL) compared to the depth of the ABL, we find that $\Delta P_{storm} = 7 \cdot \Delta P_{BL}$ (see Figure).

Thus, $\Delta Q_{E\,storm} = 7\ \Delta Q_{E\,BL}$

$$\Delta Q_{E\,storm} = \underline{\mathbf{2.24x10}}^{16}\text{ J}$$

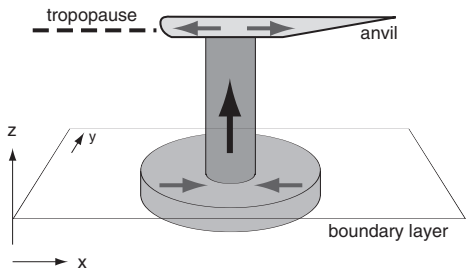

Check: Physics OK. Units OK. Values approximate.
Discussion: A **one-megaton nuclear bomb** releases about $4\text{x}10^{15}$ J of heat. This hypothetical thunderstorm has the power of 5.6 one-megaton bombs.

Actual heat released in a small thunderstorm is about 1% of the answer calculated above. Reasons include: T_d < 21°C; storm entrains non-ABL air; and not all of the available water vapor condenses. However, supercells continually draw in fresh ABL air, and can release more heat than the answer above. Energy released differs from energy available (CAPE). For another energy estimate, see the "Heavy Rain" section of the next chapter.

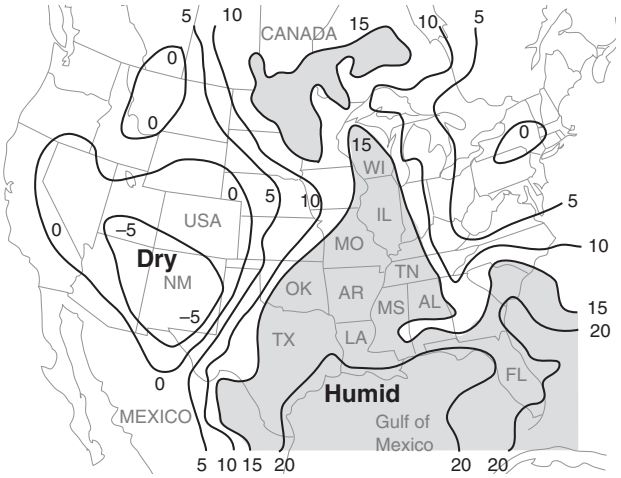

Figure 14.28
Surface weather map valid at 22 UTC on 24 May 2006 showing isodrosotherms (lines of equal dew-point, T_d, in °C) over N. America. Moistest air is shaded, and highlights the greatest fuel supply for thunderstorms. A dry line (sharp decrease in humidity) exists in west Texas (TX) and Oklahoma (OK).

Note, this is a different case study than was used in the previous chapter. The Extratropical Cyclone chapter used a Winter storm case, while here we use an early Spring severe-storm case.

On weather maps, lines of equal dew-point temperature are called **isodrosotherms** (recall Table 1-6). Fig. 14.28 shows an example, where the isodrosotherms are useful for identifying regions having warm humid boundary layers.

Most of the weather maps in this chapter and the next chapter are from a severe weather case on 24 May 2006. These case-study maps are meant to give one example, and do not show average or climatological conditions. The actual severe weather that occurred for this case is described at the end of this chapter, just before the Summary.

An alternative moisture variable is **mixing ratio**, *r*. Large mixing-ratio values are possible only if the air is warm (because warm air can hold more water vapor at saturation), and indicate greater energy available for thunderstorms. For example, Fig. 14.29 shows **isohumes** of mixing ratio.

Wet-bulb temperature T_w , **wet-bulb potential temperature** θ_w , **equivalent potential temperature** θ_e , or **liquid-water potential temperature** θ_L also indicate moisture. Recall from Normand's rule in Chapter 4 that the wet-bulb potential temperature corresponds to the moist adiabat that passes through the LCL on a thermo diagram. Also in Chapter 4 is a graph relating θ_w to θ_e.

For afternoon thunderstorms in the USA, pre-storm boundary layers most frequently have wet-bulb potential temperatures in the θ_w = 20 to 28°C range (or θ_e in the 334 to 372 K range, see example in Fig. 14.30). For supercell thunderstorms, the boundary-layer average is about θ_w = 24°C (or θ_e = 351 K), with some particularly severe storms (strong tornadoes or large hail) having $\theta_w \geq$ 27°C (or $\theta_e \geq$ 366 K).

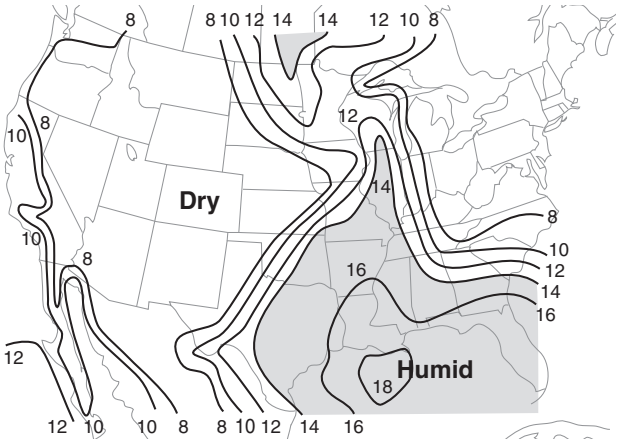

Figure 14.29
Similar to the previous weather map, but for isohumes of mixing ratio (g/kg).

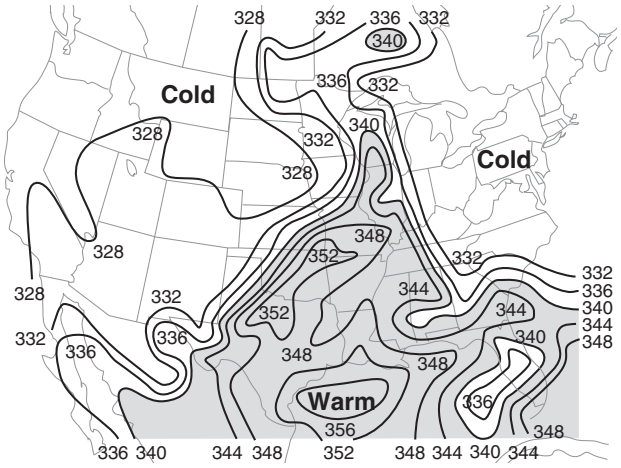

Figure 14.30
Similar to previous figure, but for equivalent potential temperature θ_e in Kelvin. Larger θ_e indicates warmer, moister air.

Precipitable water gives the total water content in a column of air from the ground to the top of the atmosphere (see example in Fig. 14.31). It does not account for additional water advected into the storm by the inflow winds, and thus is not a good measure of the total amount of water vapor that can condense and release energy.

Mean-layer lifting condensation level (**ML-LCL**) is the average of the LCL altitudes for all air parcels starting at heights within the bottom 1 km of atmosphere (i.e., ≈ boundary layer). Lower ML-LCL values indicate greater ABL moisture, and favor stronger storms (Figs. 14.32 & 14.33).

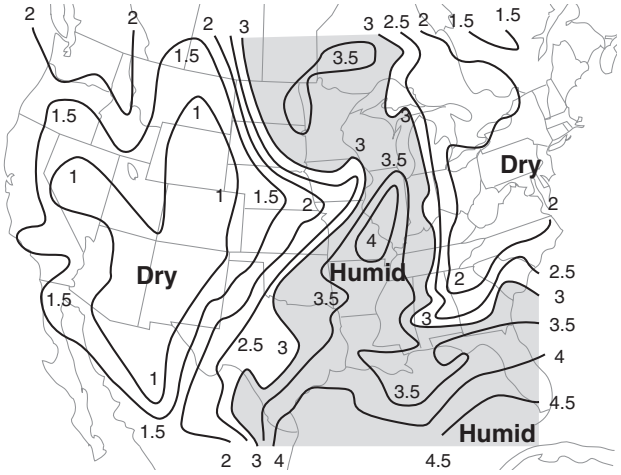

Figure 14.31
Similar to previous figure, but for precipitable water in cm.

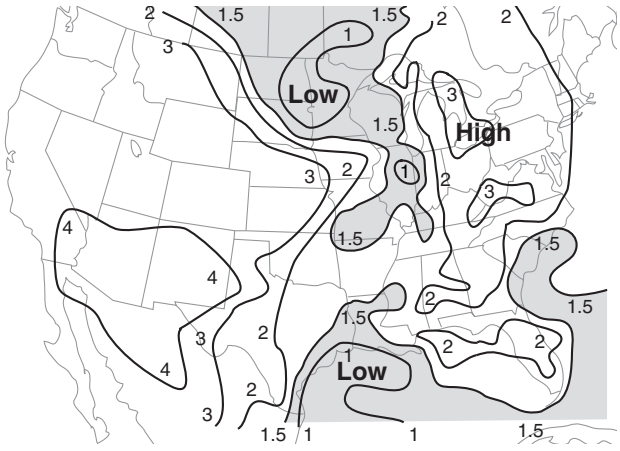

Figure 14.32
Similar to previous figure, but for mean-layer lifting condensation level (ML-LCL) heights in km above ground level. Lower ML-LCL heights (suggesting more intense storms) are shaded.

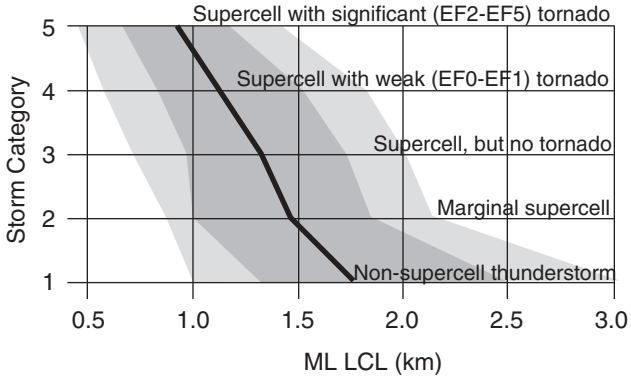

Figure 14.33
Statistical relationship between storm category (as labeled along the horizontal lines) and the mean-layer lifting condensation level (ML-LCL). A marginal supercell is one with weak (< 20 m/s) or short-duration (< 30 min) cyclonic shear. EF is the Enhanced Fujita scale tornado intensity. Thick line is median (50 percentile) of about 500 observed thunderstorms in the central USA. Dark grey spans 25 through 75 percentiles (i.e., the interquartile range), and light grey spans 10 through 90 percentiles. Lower ML-LCL values generally correspond to greater storm intensities. Caution: There is significant overlap of ML-LCLs for all storm categories, implying that ML-LCL cannot sharply discriminate between storm severities.

See the Focus box on the next page to learn about the median, interquartile range, and percentiles.

FOCUS • Median, Quartiles, Percentiles

Median, quartiles, and percentiles are statistical ways to summarize the location and spread of experimental data. They are a robust form of **data reduction**, where hundreds or thousands of data are represented by several summary statistics.

First, **sort** your data from the smallest to largest values. This is easy to do on a computer. Each data point now has a **rank** associated with it, such as 1st (smallest value), 2nd, 3rd, ... n^{th} (largest value). Let $x_{(r)}$ = the value of the r^{th} ranked data point.

The middle-ranked data point [i.e., at $r = (1/2)\cdot(n+1)$] is called the **median**, and the data value x of this middle data point is the median value ($q_{0.5}$). Namely,

$$q_{0.5} = x_{(1/2)\cdot(n+1)} \qquad \text{for } n = \text{odd}$$

If n is an even number, there is no data point exactly in the middle, so use the average of the 2 closest points:

$$q_{0.5} = 0.5\cdot [x_{(n/2)} + x_{(n/2)+1}] \qquad \text{for } n = \text{even}$$

The median is a measure of the **location** or center of the data

The data point with a rank closest to $r = (1/4)\cdot n$ is the **lower quartile** point:

$$q_{0.25} = x_{(1/4)\cdot(n+1)}$$

The data point with a rank closest to $r = (3/4)\cdot n$ is the **upper quartile** point:

$$q_{0.75} = x_{(3/4)\cdot(n+1)}$$

These last 2 equations work well if n is large (≥100, see below). The **interquartile range** (**IQR**) is defined as $IQR = q_{0.75} - q_{0.25}$, and is a measure of the **spread** of the data. (See the solved example nearby.)

Generically, the variable q_p represents any **quantile**, namely the value of the ranked data point having a value that exceeds portion p of all data points. We already looked at $p = 1/4$, 1/2, and 3/4. We could also divide large data sets into hundredths, giving **percentiles**. The lower quartile is the same as the 25th percentile, the median is the 50th percentile, and the upper quartile is the 75th percentile.

These **non-parametric statistics** are **robust** (usually give a reasonable answer regardless of the actual distribution of data) and **resistant** (are not overly influenced by **outlier** data points). For comparison, the mean and standard deviation are NOT robust nor resistant. Thus, for experimental data, you should use the median and IQR.

To find quartiles for a small data set, split the ranked data in half, and look at the lower and upper halves separately.

Lower half of data: If n = odd, consider those data points ranked less than or equal to the median point. For n = even, consider points with values less than the median value. For this subset of data, find its median, using the same tricks as in the previous paragraph. The resulting data point is the **lower quartile**.

Upper half of data: For n = odd, consider those data points ranked greater than or equal to the original median point. For n = even, use the points with values greater than the median value. The median point in this data subset gives the **upper quartile**.

Solved Example (§)

Suppose the z_{LCL} (km) values for 9 supercells (with EF0-EF1 tornadoes) are:

1.5, 0.8, 1.4, 1.8, 8.2, 1.0, 0.7, 0.5, 1.2

Find the median and interquartile range. Compare with the mean and standard deviation.

Solution:

Given: data set listed above.

Find: $q_{0.5}$ = ? km, IQR = ? km,
$Mean_{zLCL}$ = ? km, σ_{zLCL} = ? km

First sort the data in ascending order:

Values (z_{LCL}):	0.5,	0.7,	0.8,	1.0,	1.2,	1.4,	1.5,	1.8,	8.2
Rank (r):	1	2	3	4	5	6	7	8	9
Middle:					^				

Thus, the median point is the 5th ranked point in the data set, and corresponding value of that data point is **median = $q_{0.5}$ = $z_{LCL(r=5)}$ = 1.2 km**.

Because this is a small data set, use the special method at the bottom of the Focus box to find the quartiles.

Lower half:

Values:	0.5,	0.7,	0.8,	1.0,	1.2
Subrank:	1	2	3	4	5
Middle:			^		

Thus, the lower quartile value is $q_{0.25}$ = 0.8 km

Upper half:

Values:	1.2,	1.4,	1.5,	1.8,	8.2
Subrank:	1	2	3	4	5
Middle:			^		

Thus, the upper quartile value is $q_{0.75}$ = 1.5 km

The IQR = $q_{0.75} - q_{0.25}$ = (1.5km – 0.8km) = **0.7 km**

Using a spreadsheet to find the mean and standard deviation:

$Mean_{zLCL}$ = **1.9 km** , σ_{zLCL} = **2.4 km**

Check: Values reasonable. Units OK.

Discussion: The original data set has one "wild" z_{LCL} value: 8.2 km. This is the **outlier**, because it lies so far from most of the other data points.

As a result, the mean value (1.9 km) is not representative of any of the data points; namely, the center of the majority of data points is not at 1.9 km. Thus, the mean is not robust. Also, if you were to remove that one outlier point, and recalculate the mean, you would get a significantly different value (1.11 km). Hence, the mean is not resistant. Similar problems occur with the standard deviation.

However, the median value (1.2 km) is nicely centered on the majority of points. Also, if you were to remove the one outlier point, the median value would change only slightly to a value of 1.1 km. Hence, it is robust and resistant. Similarly, the IQR is robust and resistant.

INSTABILITY, CAPE & UPDRAFTS

The second requirement for convective-storm formation is instability in the pre-storm sounding. **Nonlocal conditional instability** (**NCI**) occurs when warm humid atmospheric boundary layer (ABL) air is capped by a temperature inversion, above which is relatively cold air. The cold air aloft provides an environment that gives more buoyancy to the warm updraft air from below, allowing stronger thunderstorms. The "nonlocal" aspect arises because air from below the cap becomes unstable above the cap. The "condition" is that the ABL air must first be lifted past the cap (i.e., past its LCL and LFC) for the instability to be realized.

The capping inversion traps the warm humid air near the ground, allowing sensible and latent heat energy to build up during the day as the sun heats the ground and causes evaporation. Without this cap, smaller cumulus clouds can withdraw the warm humid air from the boundary layer, leaving insufficient fuel for thunderstorms. Thus, the cap is important — it prevents the fuel from leaking out.

CAPE

Tremendous energy is released in thunderstorms, causing strong updrafts. A measure of the amount of energy available to create such motion is the **Convective Available Potential Energy** (CAPE). **CAPE** is proportional to the shaded area in Fig 14.34; namely, the area between LFC and EL altitudes that is between the environmental sounding and the moist adiabat of the rising air parcel.

At these heights, the air parcel is warmer than the environment, so positive buoyant forces tend to accelerate the parcel upward. Recall from Chapter 5 that the buoyant force per unit mass is $F/m = |g| \cdot (T_{vp} - T_{ve}) / T_{ve}$, where $|g|$ is the magnitude of gravitational acceleration (9.8 m/s^2), T_{vp} is the parcel virtual temperature, and T_{ve} is environmental virtual temperature at the same altitude as the parcel.

Energy (**work**) is force times distance. Thus, the incremental buoyant energy per unit mass ($\Delta E/m$) associated with the rise of an air parcel across some small increment of distance Δz is $\Delta E/m = (F/m) \cdot \Delta z$, or:

$$\frac{\Delta E}{m} \cong \Delta z \cdot |g| \frac{(T_{vp} - T_{ve})}{T_{ve}} \qquad (14.1)$$

Recall from Chapter 1 that virtual temperature includes the effects of both water vapor and liquid water. Water vapor is less dense than air ($T_v > T$), thus increasing the buoyant energy. Liquid- and

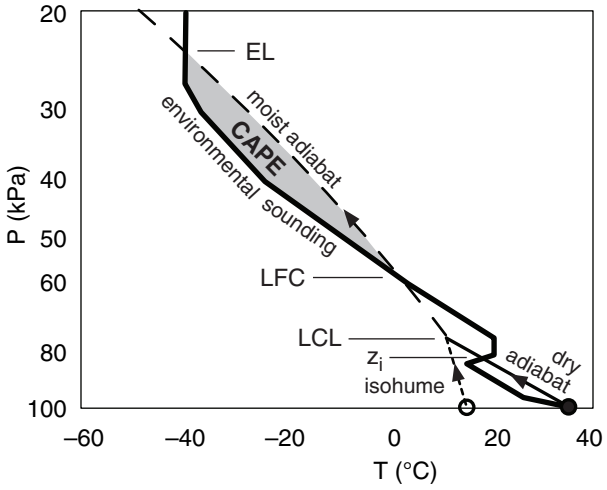

Figure 14.34
Surface-based Convective Available Potential Energy (CAPE) is the grey shaded area for an afternoon pre-storm environment.

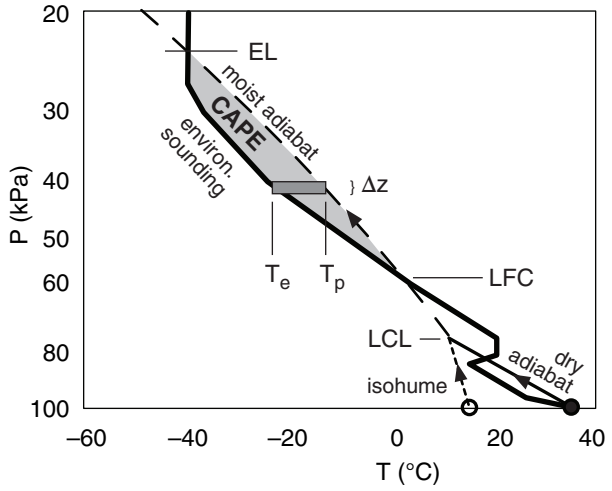

Figure 14.35
Dark shaded rectangle of incremental height Δz and width $T_p - T_e$ shows the portion of total CAPE area associated with just one thin layer of air.

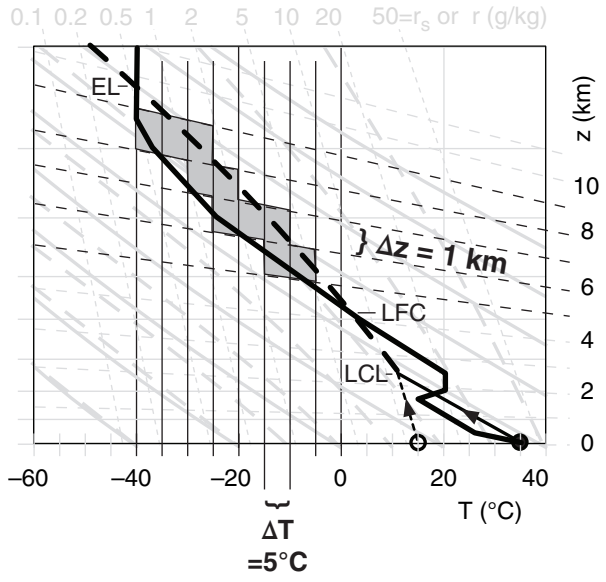

Figure 14.36
Approximating the CAPE area by non-overlapping tiles, each of area Δz by ΔT. In this example, Δz = 1 km, and ΔT = 5°C.

solid-water hydrometeors (cloud droplets, rain, and snow) falling at their terminal velocity are heavier than air ($T_v < T$), thus decreasing the upward buoyant energy. Both are important for thunderstorms, but are often difficult to determine.

Instead, you can use the approximation $T_v \approx T$, which gives:

$$\frac{\Delta E}{m} \cong |g| \frac{\Delta z \cdot (T_p - T_e)}{T_e} \; . \qquad (14.2)$$

where T_p is air-parcel temperature and T_e is environmental temperature. This increment of energy is proportional to the area inside the rectangle plotted in Fig. 14.35. The width of the shaded rectangle is the parcel–environment temperature difference, and the height is Δz.

The total energy is proportional to the total shaded area in Fig. 14.35. Thus, the total convective available potential energy is proportional to the sum of all the incremental rectangles that fill the shaded area:

$$CAPE \cong |g| \cdot (Total \qquad (14.3)$$

or

$$CAPE \cong |g| \sum_{LFC}^{EL} (T_p - T_e) \cdot \Delta z \; / \qquad \bullet (14.4)$$

The units of CAPE are J/kg. These units are equivalent to $m^2 \cdot s^{-2}$; namely, velocity squared. The temperature in the denominator of eqs. (14.3 & 14.4) must be in Kelvin. Both numerator temperatures must have the same units: either Kelvin or °C.

The shape of the CAPE area is usually not simple, so calculating the area is not trivial. At severe-weather forecast centers, computers calculate CAPE automatically based on the pre-storm sounding. By hand, you can use a simple graphical method by first plotting the sounding and the surface-parcel rise on a thermo diagram, and then using whatever height and temperature increments are plotted on the background diagram to define "bricks" or "tiles", each of known size.

Namely, instead of using long narrow rectangles, each of different width, as sketched in Fig. 14.35, you can cover the complex shaded area with smaller, non-overlapping tiles, each of equal but arbitrary size ΔT by Δz (such as ΔT = 5°C and Δz = 1 km, see Fig. 14.36). Count the number of tiles, and multiply the result by the area of each tile ($\Delta T \cdot \Delta z$ = 5 °C·km in this example). When tiling the CAPE area, try to compensate for small areas that are missed by the

Solved Example

For the sounding in Fig 14.36, estimate the CAPE.

Solution

Given: Fig 14.36.
Find: CAPE = ? J/kg

Each tile has size ΔT = 5°C by Δz = 1000 m. The area of each tile is 5,000 °C·m, and there are 10 tiles. The total area is: *Area* = 10 x 5000 °C·m = 50,000 K·m , [where I took advantage of ΔT(°C) = ΔT(K)].

By eye, the average T_e in the CAPE region is about –25°C = 248 K. Use eq. (14.3):

CAPE = [9.8 m·s^{-2} / 248K]·(50,000 K·m) =
= 1976 m^2/s^2 = **1976 J/kg**.

Check: Units OK. Physics OK. Figure OK.
Discussion: This is a moderate value of CAPE that could support supercell storms with tornadoes.

tiles by allowing some of the other tiles to extend slightly beyond the boundaries of the desired shaded area by roughly an equal area (e.g., see the solved example). Smaller-size tiles (such as ΔT = 1°C and Δz = 0.2 km) give a more accurate answer (and are recommended), but are more tedious to count.

On many thermo diagrams such as the emagram of T vs. ln(P) used here, the height contours and isotherms are not perpendicular; hence, the rectangles look like trapezoids (see the solved example that employed Fig. 14.36). Regardless of the actual area within each trapezoid in the plotted graph, each trapezoid represents a contribution of ΔT by Δz toward the total CAPE area.

To replace heights with pressures in the equation for CAPE, use the hypsometric equation from Chapter 1, which yields:

$$CAPE = \Re_d \cdot \sum_{LFC}^{EL} (T_p - T_e) \cdot \ln\left(\frac{P_{bottom}}{P_{top}}\right) \quad \bullet(14.5)$$

where $\Re_d$ = 287.053 J·K^{-1}·kg^{-1} is the gas constant for dry air, P_{bottom} and P_{top} are the bottom and top pressures of the incremental rectangle, and the sum is still over all the rectangles needed to tile the shaded CAPE area on the sounding (Fig. 14.37). Again, the temperature difference in eq. (14.5) in °C is equal to the same value in Kelvin.

All of the CAPE figures up until now have followed a rising air parcel that was assumed to have started from near the surface. This is called **Surface-Based CAPE** (SBCAPE), which is often a good method for the mid-afternoon pre-storm soundings that have been shown so far.

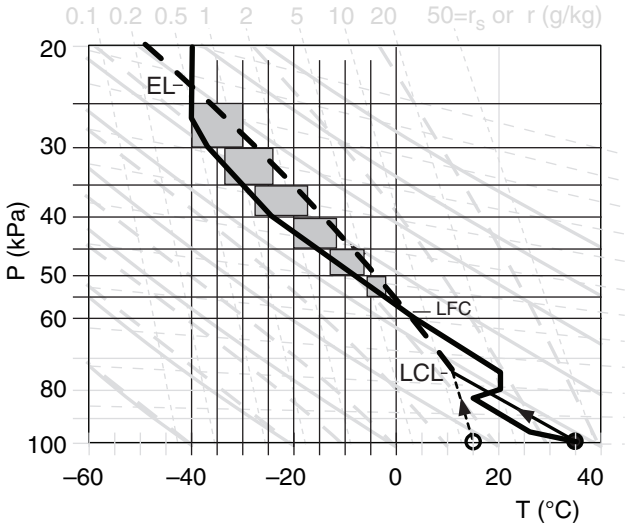

Figure 14.37
Approximating the CAPE area by non-overlapping tiles, each of area ΔP by ΔT. In this example, ΔP = 5 kPa, and ΔT varies.

Solved Example

For the sounding in Fig. 14.37, estimate the CAPE using pressure rather than height increments.

Solution:

Given: Fig. 14.37.
Find: CAPE = ? J/kg

Use eq. (14.5):
CAPE = [287 J/(K·kg)] · {
[–30°C – (–40°C)] · ln(30kPa/25kPa)] +
[–24°C – (–33°C)] · ln(35kPa/30kPa)] +
[–17°C – (–27°C)] · ln(40kPa/35kPa)] +
[–12°C – (–20°C)] · ln(45kPa/40kPa)] +
[–7°C – (–13°C)] · ln(50kPa/45kPa)] +
[–2°C – (–6°C)] · ln(55kPa/50kPa)] }

CAPE = [287 J/(K·kg)] ·
{ 10K · 0.182 + 9.2K · 0.154 + 10K · 0.134 +
8K · 0.118 + 6K · 0.105 + 4K · 0.095 }

CAPE = [287 J/(K·kg)] · 6.53 K = **1874 J/kg** .

Check: Physics OK. Units OK.
Discussion: Theoretically, we should get exactly the same answer as we found in the previous solved example. Considering the coarseness of the boxes that I used in both solved examples, I am happy that the answers are as close as they are. I found the height-tiling method easier than the pressure-tiling method.

CAPE values vary greatly with location and time. By finding the CAPE for many locations in a region (by using rawinsonde observations, or by using forecast soundings from numerical weather prediction models), you can write the CAPE values on a weather map and then draw isopleths connecting lines of equal CAPE, such as shown in Fig. 14.38.

Other parcel-origin assumptions work better in other situations. If the pre-storm sounding is from earlier in the morning, then the forecast max surface temperature for that afternoon (along with the dew point forecast for that time) is a better choice for the rising air-parcel initial conditions (Fig. 14.39). This is also a type of SBCAPE.

Another way is to average the conditions in the bottom 1 km (roughly 10 kPa) of the environmental sounding to better estimate ABL conditions. Thus, the initial conditions for the rising air parcel represents the mean layer (ML) conditions, or the mixed-layer (ML) conditions (Fig. 14.40). CAPE calculated this way is called **Mean Layer CAPE** (MLCAPE). Fig. 14.41 shows a case-study example of MLCAPE.

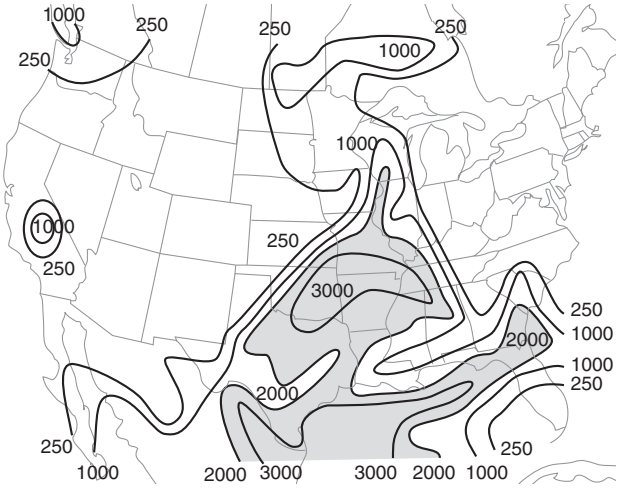

Figure 14.38
Weather map of surface-based CAPE (SBCAPE) in J/kg over N. America. Valid 22 UTC on 24 May 2006. Shaded region highlights larger SBCAPE values, where more intense thunderstorms can be supported.

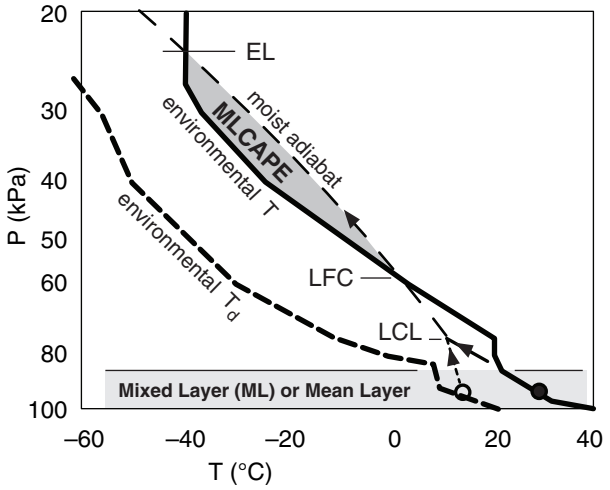

Figure 14.40
Another method for estimating CAPE is to use air-parcel initial conditions equal to the average conditions (filled and open circles) in the boundary layer (shaded). This is called the mean layer CAPE (MLCAPE).

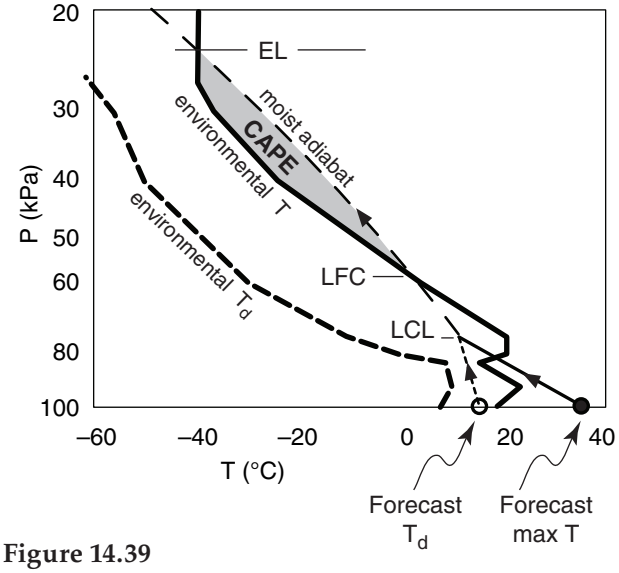

Figure 14.39
Shown is one method for estimating CAPE from an early morning sounding. Instead of using actual surface environmental conditions for the air parcel, you can use the forecast maximum near-surface air temperature (max T) for later that day, and assume no change in environmental conditions above the ML.

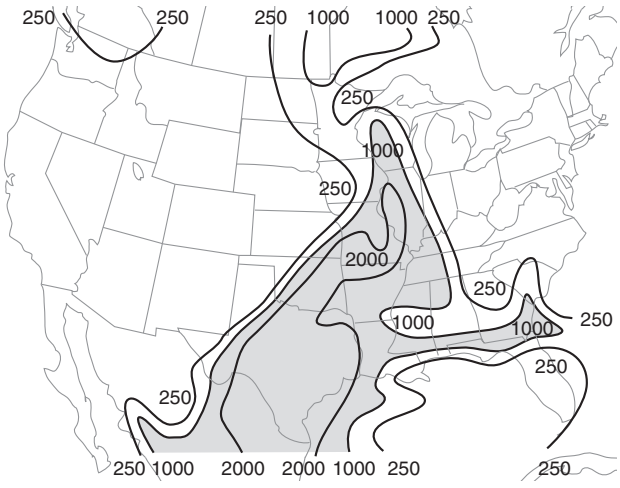

Figure 14.41
Weather map similar to Fig. 14.38, but for mean-layer CAPE (MLCAPE) in J/kg.

Early studies of thunderstorm occurrence vs. MLCAPE lead to forecast guidelines such as shown in Table 14-1. However, MLCAPE is not a sharp discriminator of thunderstorm intensity, as shown by the large overlap of storm categories in Fig. 14.42.

Yet another way is to calculate many different CAPEs for air parcels that start from every height in the bottom 30 kPa of the pre-storm environmental sounding, and then select the one that gives the greatest CAPE values. This is called the **Most Unstable CAPE** (MUCAPE). This method works even if thunderstorm updrafts are triggered by an elevated source, and also works for pre-storm soundings from any time of day. Although it is too tedious to compute these multiple CAPEs by hand, it is easily automated on a computer (Figs. 14.43 & 14.44). MUCAPE is always ≥ SBCAPE.

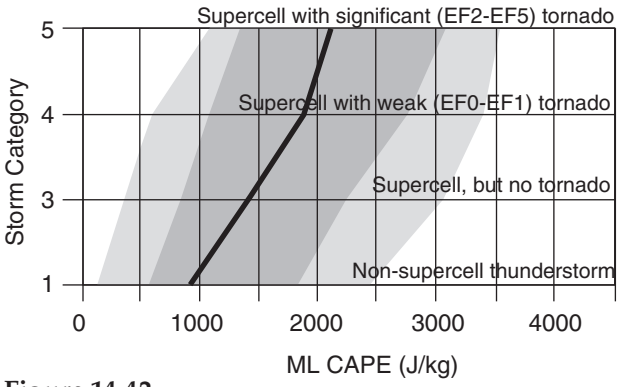

Figure 14.42
Statistics of thunderstorm intensity vs. MLCAPE, based on several hundred paired soundings and thunderstorms in central N. America. Dark line is median (50 percentile); dark shading spans the interquartile range (25 to 75 percentiles); light shading spans the 10 to 90 percentile range.

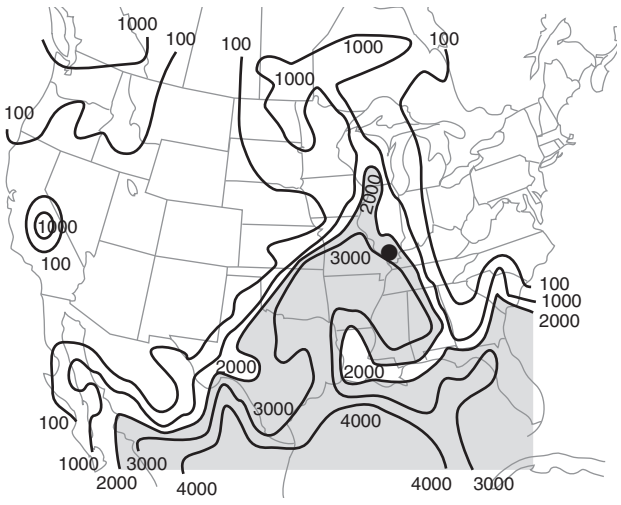

Figure 14.43
Weather map similar to Fig. 14.38 over the USA, but for most-unstable CAPE (MUCAPE) in J/kg.

Table 14-1. Thunderstorm (CB) intensity guide.

MLCAPE (J/kg)	Stability Description	Thunderstorm Activity
0 - 300	mostly stable	little or none
300 - 1000	marginally unstable	weak CB
1000 - 2500	moderately unstable	moderate CB likely; severe CB possible
2500 - 3500	very unstable	severe CB likely, possible tornado
3500 & greater	extremely unstable	severe CB, tornadoes likely

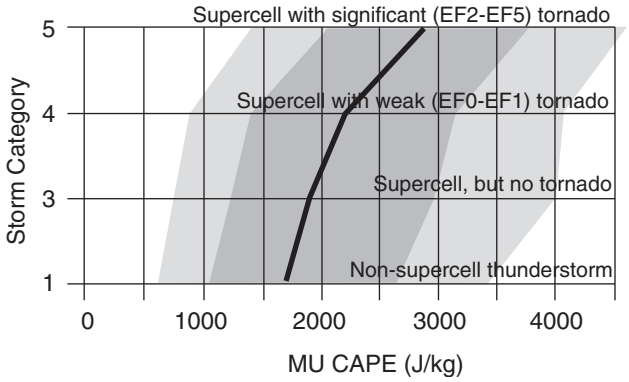

Figure 14.44
Statistics of thunderstorm intensity vs. MUCAPE, similar to Fig. 14.42.

Solved Example

Assume a thunderstorm forms at the dot in Fig. 14.43, where MUCAPE ≈ 2700 J/kg. Estimate the possible intensity of this storm. Discuss the uncertainty.

Solution

Given: MUCAPE ≈ 2,700 J/kg at the dot (•) in Fig. 14.43, located in southern Illinois.

Find: Possible storm intensity. Discuss uncertainty.

Use Fig. 14.44 to estimate intensity. For MUCAPE of 2,700 J/kg, the median line is about half way between "supercell with **weak tornado** (EF0-EF1)", and "supercell with **significant tornado** (EF2-EF5)." So we might predict a supercell with an EF1 - EF2 tornado.

Discussion: Although there is some uncertainly in picking the MUCAPE value from Fig. 14.43, there is even greater uncertainty in Fig 14.44. Namely, within the interquartile range (dark shading) based on hundreds of past storms used to make this figure, there could easily be a supercell with no tornado, or a supercell with a significant tornado. There is even a chance of a non-supercell thunderstorm.

Thus, MUCAPE is not capable of sharply distinguishing thunderstorm intensity.

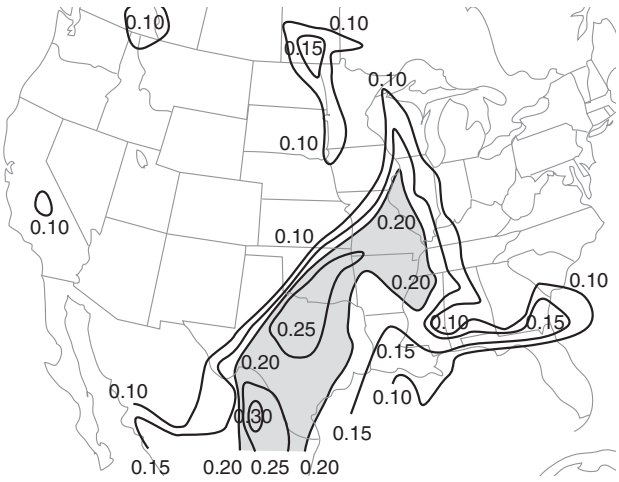

Figure 14.45
Weather map similar to Fig. 14.38 over the USA, but for normalized CAPE (nCAPE) in m·s^{-2}.

Solved Example

For the sounding in Fig. 14.36 (CAPE = 1976 J/kg) find thunderstorm intensity, normalized CAPE, max updraft velocity, and likely updraft velocity.

Solution

Given: Fig. 14.36, with CAPE = 1976 J/kg
Find: Intensity = ? , $nCAPE$ = ? m·s^{-2},
w_{max} & $w_{max\ likely}$ = ? m/s

a) From Table 14-1, **moderate thunderstorms**.

b) By eye using Fig. 14.36, the bottom and top of the CAPE region are $z_{LFC} \approx 4.2$ km, and $z_{EL} = 9.6$ km.
Use eq. (14.6):
$nCAPE$=(1976 J/kg)/[9600−4200m]=**0.37**m/s^2.

c) Use eq. (14.7):
$w_{max} = [2 \cdot (1976\ m^2/s^2)\ ]^{1/2} = w_{max} =$ **63 m/s** .

d) Use eq (14.8):
$w_{max\ likely}$ = (63 m/s)/2 = **31 m/s** .

Check: Units OK. Physics OK. Figure OK.
Discussion: Because the LFC is at such a high altitude, the CAPE area is somewhat short and fat, as indicated by the small value of nCAPE. Thus, strong low-altitude updrafts and tornadoes are possible. This thunderstorm has violent updrafts, which is why aircraft would avoid flying through it.

The shape of the CAPE area gives some information about the storm. To aid shape interpretation, a **normalized CAPE** (**nCAPE**) is defined as

$$nCAPE = \frac{CAPE}{z_{EL} - z_{LFC}} \qquad \bullet(14.6)$$

where z_{EL} is height of the equilibrium level, z_{LFC} is height of the level of free convection, and the units of nCAPE are m·s^{-2} or J/(kg·m). Tall, thin CAPE areas (i.e., nCAPE ≤ 0.1 m·s^{-2}) often suggest heavy precipitation, but unlikely tornadoes. Short, wide CAPE area (i.e., nCAPE ≥ 0.3 m·s^{-2}) in the mid to lower part of the sounding can result in thunderstorms with strong, low-altitude updrafts, which cause vertical stretching of the air, intensification of rotation, and greater chance of tornadoes. See Fig. 14.45.

A word of caution. CAPE gives only an estimate of the strength of a thunderstorm if one indeed forms. It is a necessary condition, but not a sufficient condition. To form a thunderstorm, there must also be a process that triggers it. Often no thunderstorms form, even in locations having large CAPE. If thunderstorms are triggered, then larger CAPE indicates greater instability, stronger updrafts, and a chance for more violent thunderstorms. It is a useful, but not perfect, forecast tool, as evident by the lack of sharpness in the statistics (Figs. 14.42, & 14.44).

Updraft Velocity

You can also use CAPE to estimate the updraft speed in thunderstorms. Define the kinetic energy per unit mass for updrafts as $KE/m = 0.5 \cdot w^2$, where w is the updraft speed. If all of the potential energy were converted into kinetic energy, then KE/m = CAPE. If there were no frictional drag and no mixing of the air parcel as it rises, then the updraft velocity at the EL would be:

$$w_{\max} = \sqrt{2 \cdot CAPE} \qquad (14.7)$$

However, studies of actual thunderstorm updrafts suggest that the most likely max updraft speed is

$$w_{\max\ likely} \approx w_{\max} / 2 \qquad \bullet(14.8)$$

The inertia of the rising air can cause the updraft-top to overshoot above the EL. This is called **penetrative convection**, and is observed in satellite pictures and by eye as a turret or dome of cloud that temporarily overshoots into the lower stratosphere from the top of the thunderstorm anvil. As stated before, such domes give a good clue to storm spotters that the thunderstorm is probably violent, and has strong updrafts. Such strong updrafts are felt as severe or extreme **turbulence** by aircraft.

WIND SHEAR IN THE ENVIRONMENT

Wind shear, the change of horizontal wind speed and/or direction with height, is the third requirement for thunderstorm formation. The wind shear across a layer of air is the vector difference between the winds at the top of the layer and winds at the bottom (Fig. 14.46), divided by layer thickness Δz. Shear has units of (1/s).

Using geometry, shear can be expressed via its components as:

$$\frac{\Delta U}{\Delta z} = \frac{U_2 - U_1}{z_2 - z_1} \tag{14.9}$$

$$\frac{\Delta V}{\Delta z} = \frac{V_2 - V_1}{z_2 - z_1} \tag{14.10}$$

or

$$\text{Shear Magnitude} = \frac{\left[(\Delta U)^2 + (\Delta V)^2\right]^{1/2}}{\Delta z} \tag{14.11a}$$

Shear Direction:

$$\alpha_{shear} = 90° - \frac{360°}{C}\arctan\left(\frac{\Delta V}{\Delta U}\right) + \alpha_o \tag{14.11b}$$

where subscript 2 is the layer top, and subscript 1 is layer bottom. Eq. (1.2) was used to find the direction α of the shear vector, but with ΔU in place of U, and ΔV in place of V. $\alpha_o = 180°$ if $\Delta U > 0$, but is zero otherwise. C is the angular rotation in a circle (360° or 2π radians, depending on the output from "arctan").

For thunderstorm forecasting, meteorologists look at shear across many layers at different heights in the atmosphere. To make this easier, you can use layers of equal thickness, such as $\Delta z = 1$ km. Namely, look at the shear across the bottom layer from $z = 0$ to $z = 1$ km, and the shear across the next layer from $z = 1$ to $z = 2$ km, and so forth.

When studying shear across layers of equal thickness, meteorologists often use the **vector wind difference** (ΔU, ΔV) as a surrogate measure of **vector wind shear**. We will use this surrogate here. This surrogate, and its corresponding **wind-difference magnitude**

$$\Delta M = \left(\Delta U^2 + \Delta V^2\right)^{1/2} \tag{14.12}$$

has units of wind speed (m/s).

Low-altitude wind shear in the storm environment favors long-lasting, intense thunderstorms. With shear, the boundary-layer winds move relative to the storm, and can continuously feed fuel into the storm (Fig. 14.47). Another way to picture this process is that wind shear causes the storm to move away from locations of depleted boundary layers into locations with warm, humid boundary layers.

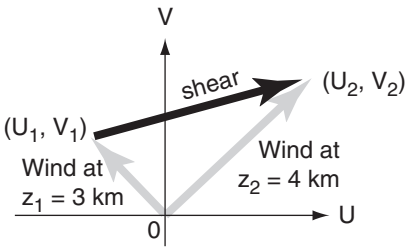

Figure 14.46
Wind difference (black arrow) between two altitudes is the vector difference between wind (long grey arrow) at the top altitude minus wind at the bottom (short grey arrow). We will use vector wind difference as a surrogate for vector wind shear.

Solved Example

Given a horizontal wind of (U, V) = (1, 2) m/s at 2 km altitude, and a wind of (5, –3) m/s at 3 km, what are the wind-difference & shear magnitudes & direction?

Solution:

Given: (U, V) = (1, 2) m/s at z = 2 km
(U, V) = (5, –3) m/s at z = 3 km

Find: ΔM = ? (m/s), α = ? (°)
Shear Magnitude = ? (1/s),

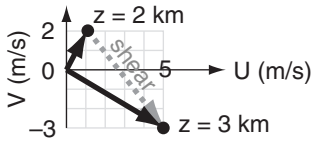

Use eq. (14.12) to find the wind difference magnitude:
$\Delta U = (5 - 1) = 4$ m/s. $\Delta V = (-3 - 2) = -5$ m/s.
$\Delta M = [\ (4\ \text{m/s})^2 + (-5\ \text{m/s})^2\ ]^{1/2} =$
$[16+25\ \text{m}^2/\text{s}^2]^{1/2} =$ **6.4 m/s**

Use eq. (14.11b) to find shear direction:
$\alpha = 90° - \arctan(-5/4) + 180° = 90° - (-51.3°) + 180° =$ **321.3°**
which is the direction that the wind shear is coming from.

Layer thickness is $\Delta z = 3$ km – 2 km = 1 km = 1000 m.
Use eq. (14.11a) to find shear magnitude, rewritten as:
Shear Mag.= $\Delta M/\Delta z$ = (6.4 m/s)/(1000 m) = **0.0064 s^{-1}**

Check: Units OK. Magnitude & direction agree with figure.

Discussion: There is both **speed shear** and **directional shear** in this example. It always helps to draw a figure, to check your answer.

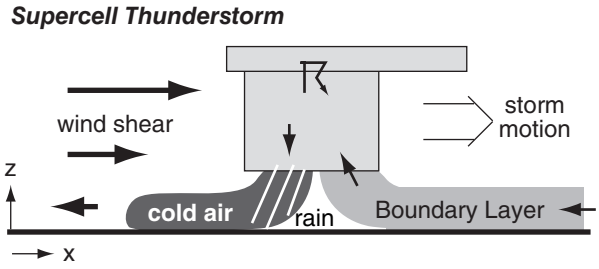

Figure 14.47
Wind shear allows long-lasting strong thunderstorms, such as supercell storms and bow-echo thunderstorm lines.

The storm behaves similar to an upright vacuum cleaner, sucking up fresh boundary layer air as it moves, and leaving behind an exhaust of colder air that is more stable.

Without any shear, the whole environment including the thunderstorm and the boundary layer would move en masse. For this situation the storm consumes the limited fuel supply of boundary-layer air in the neighborhood under it, and then dies after 15 minutes to one hour (Fig. 14.6) after no fuel remains nearby.

Shear can also control the directions that thunderstorms move. As will be shown later, a clockwise turning wind shear vector can create a dynamic vertical pressure gradient that favors thunderstorms that move to the right of the mean steering-level wind direction.

Low-altitude shear can also generate **mesocyclones**, where the whole thunderstorm rotates. Mesocyclones are often a precursor to strong tornadoes, and are discussed in detail in the next chapter. Strong shear also enhances MCSs such as bow-echo thunderstorms. Thus, there are many ways that **upper-air wind** (winds above the surface) and wind shear are important to thunderstorms.

Hodograph Basics

One way to plot upper-air wind vs. height is to draw wind symbols along the side of a thermo diagram (Fig. 14.48). Recall from Chapter 10 that wind direction is from the tail end (with the feathers) toward the other end of the shaft, and more barbs (feathers or pennants) indicate greater speed. The tip of the arrow is at the altitude of that wind.

Another way to plot winds is to collapse all the wind vectors from different heights into a single polar graph, which is called a **hodograph**. For example, Fig. 14.49 shows winds at 1 km altitude blowing from the southeast at 15 m/s, winds at 3 km altitude blowing from the south at 25 m/s, and winds at 5 km altitude blowing from the southwest at 35 m/s. Both **directional shear** and **speed shear** exist.

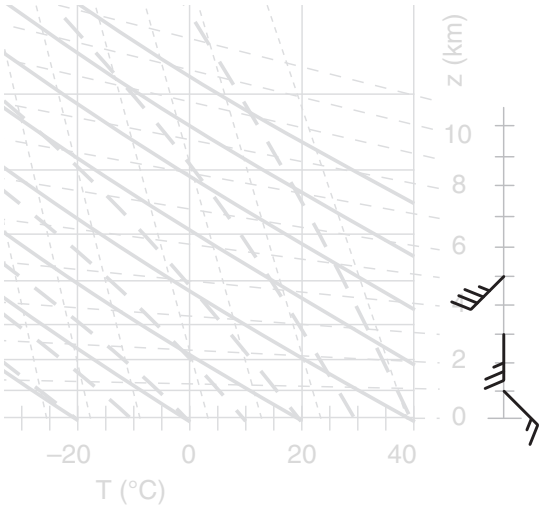

Figure 14.48
Winds at different heights, indicated with wind barbs adjacent to a thermo diagram. The same speeds are indicated by vectors in the next figure. Wind-barb speed units are m/s. (Look back at Table 10-1 for wind-barb definitions.)

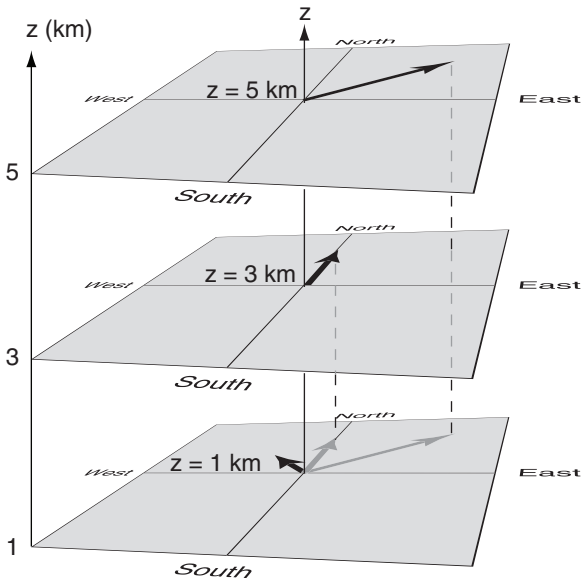

Figure 14.49
Projection of wind vectors (black arrows) from different altitudes onto the bottom plane (grey arrows). These wind vectors correspond to the wind vectors in the previous figure.

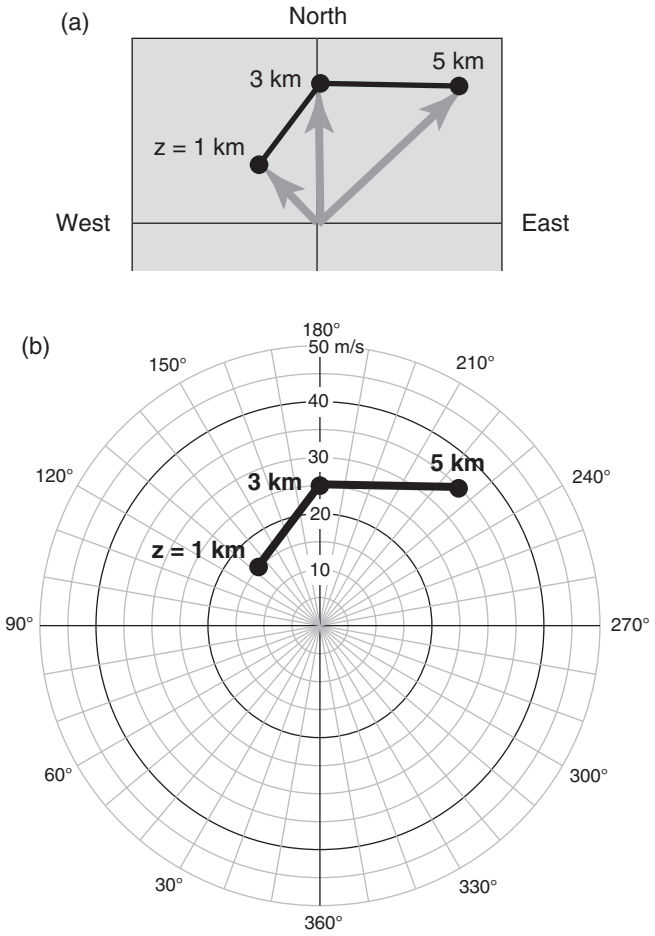

Figure 14.50
(a) Using the projected vectors from the previous figure, draw dots at the end of each vector, and connect with straight lines. When that line and dots are plotted on polar graph paper (b), the result is a hodograph.

If you project those wind vectors onto a single plane, you will get a graph that looks like the bottom of Fig. 14.49. Next, draw a dot at the end of each projected vector (Fig. 14.50a), and connect the dots with straight lines, going sequentially from the lowest to the highest altitude. Label the altitudes above ground level (AGL) next to each dot.

Plot the resulting dots and connecting lines on polar graph paper, but omit the vectors (because they are implied by the positions of the dots). The result is called a **hodograph** (Fig. 14.50b). Fig. 14.51 is a large blank hodograph that you can copy and use for plotting your own wind profiles. Coordinates in this graph are given by radial lines for wind direction, and circles are wind speed.

Solved Example

Use the table of winds below to plot a hodograph.

z (km)	dir. (°)	M (m/s)	z (km)	dir. (°)	M (m/s)
0	0	0	4	190	15
1	130	5	5	220	20
2	150	10	6	240	30
3	170	13			

Solution

Plot these points on a copy of Fig. 14.51, and connect with straight lines. Label each point with its altitude.

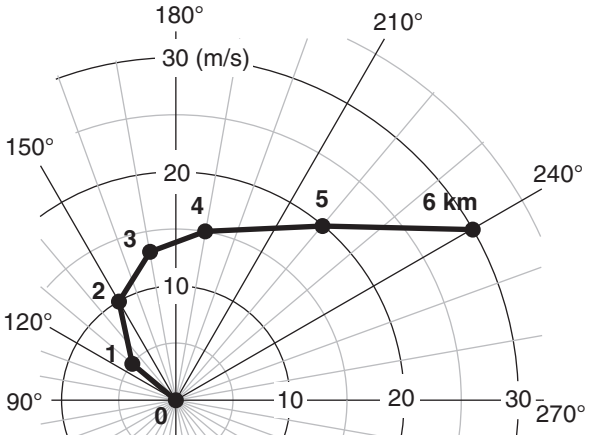

Check: The wind at 6 km, for example, is from the west southwest (240°), implying that the tip of the wind vector would be pointing toward the east northeast. This agrees with the location of the 6 km dot.

Discussion: This profile shows both speed and directional shear. Also, these winds **veer** (turn clockwise) with increasing altitude. From the thermal wind discussion in Chapter 11, recall that veering winds are associated with warm-air advection, which is useful for bringing warmer air into a thunderstorm.

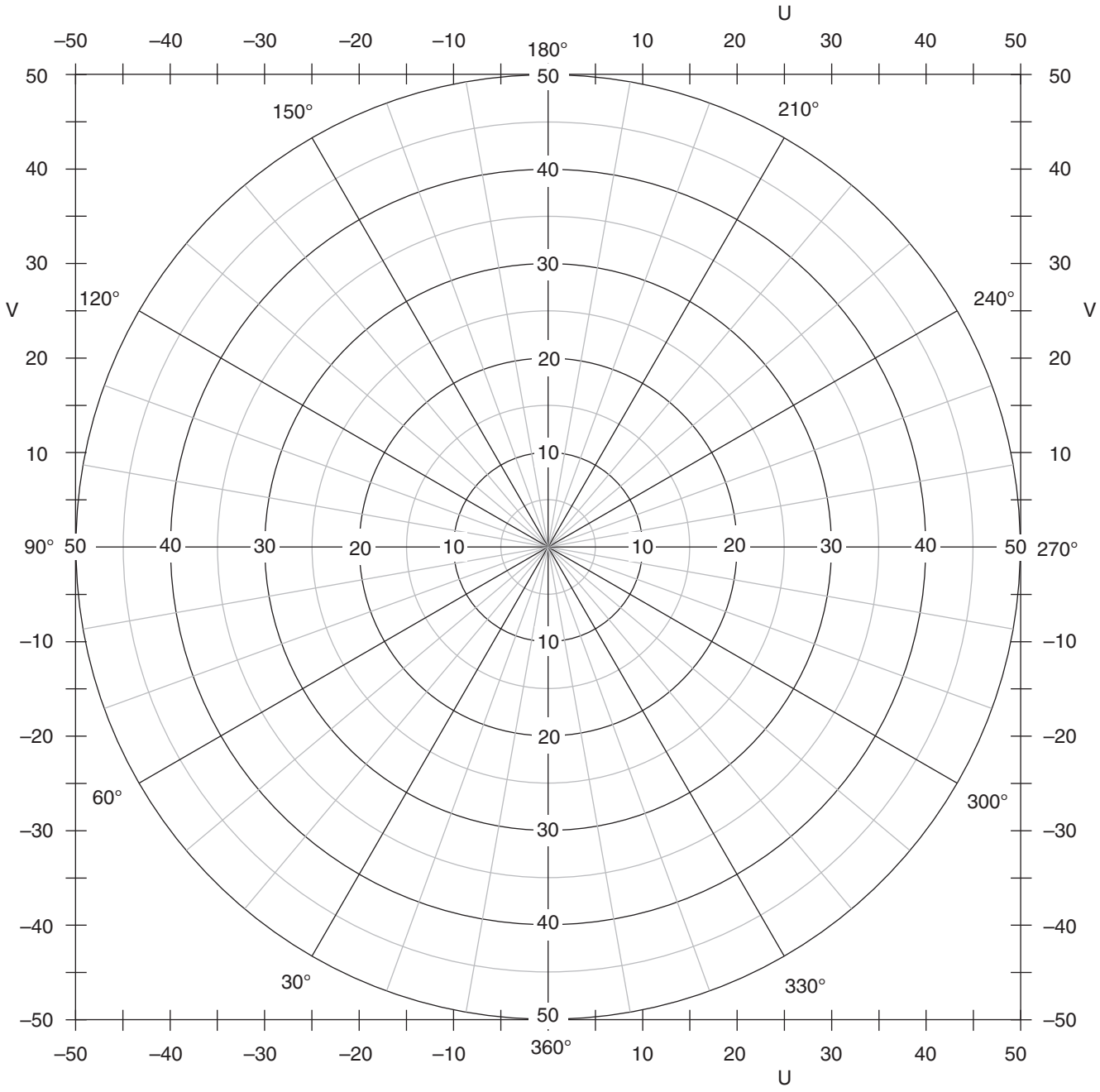

Figure 14.51
Blank hodograph for you to copy and use. Compass angles are direction winds are from. Speed-circle labels can be changed for different units or larger values, if needed.

From "Meteorology for Scientists & Engineers, 3rd Ed."
Copyright © 2011, 2015 by Roland Stull
Free copies of this page permitted.

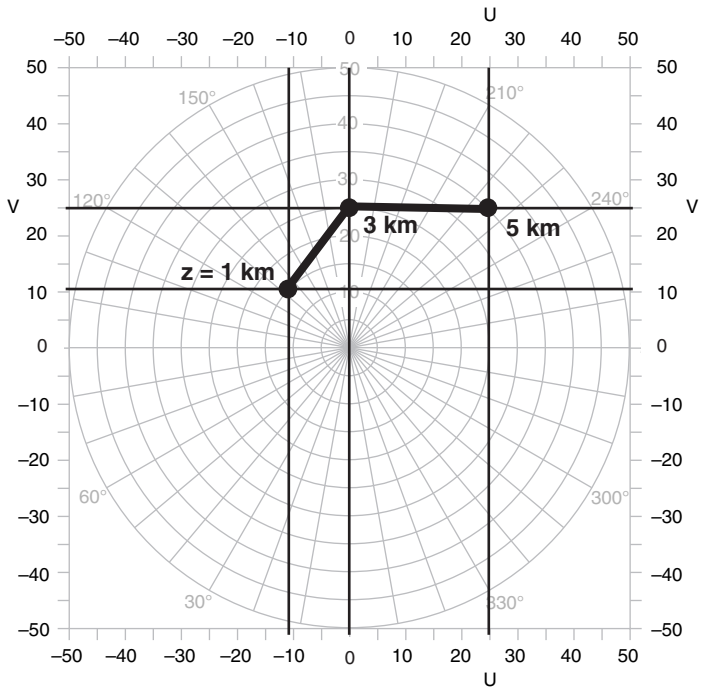

Figure 14.52
Example of determination of U and V Cartesian wind components from a hodograph. Legend: speeds are in (m/s).

Solved Example

For the hodograph of Fig. 14.52, find the (*U*, *V*) Cartesian coordinate for each of the 3 data points.

Solution

Given: Hodograph Fig. 14.52 with data points at z = 1, 3, and 5 km.

Find: (*U*, *V*) = ? (m/s) for each point.

Hint: The hodograph has the *U* velocities labeled at both top and bottom to make it easier to draw perfectly vertical lines thru any data point. For the same reason, *V* velocities are labeled at both left and right.

Method: Draw horizontal and vertical lines through each data point, and then pick off the *U* and *V* values by eye. Results:

For z = 1 km: **U = –11 m/s, V = 11 m/s**
For z = 3 km: **U = 0 m/s, V = 25 m/s**
For z = 5 km: **U = 25 m/s, V = 25 m/s**

Check: Signs and magnitudes are consistent with directions and speeds.

Discussion: Be careful to use the proper units. The legend in the Fig. 14.52 caption tells us the units for wind speed.

CAUTION: Different agencies use different units (m/s, knots, miles/h, km/h) and sometimes forget to state the units in the hodograph legend or caption.

Notice that the compass angles labeled on the blank hodograph appear to be backwards. This is not a mistake. The reason is that winds are specified by where they come from. For example, the wind at 1 km altitude is from the southeast; namely, from a compass direction of 135° (Fig. 14.50). The south wind at 3 km is from 180°, and the southwest wind at 5 km is from 235°. Using the "from" direction and the wind speed to specify a point on the hodograph, the result is a hodograph that implies wind vectors pointing from the origin to the correct directions.

Often you need to use the *U* and *V* wind components to determine thunderstorm characteristics. You could calculate these using eqs. (1.3) and (1.4) from Chapter 1. Alternately, you can pick them off from the coordinates of the hodograph. As demonstrated in Fig. 14.52, for any hodograph point, use a straight-edge to draw a horizontal line from that point to the ordinate to determine *V*, and draw a vertical line from the point to the abscissa to get *U*.

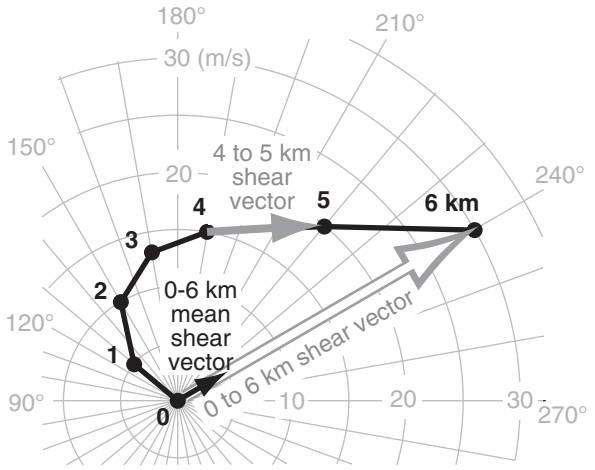

Figure 14.53
Example of mean shear vector between 0 to 6 km, shown by the small black arrow. There are six 1 km layers in this example. Vector wind differences are used as surrogates for shear.

Solved Example

Using data from the previous solved example, mathematically get the mean shear vector coordinates $(\Delta U, \Delta V)_{ms}$, magnitude ($\Delta M_{ms}$), and direction ($\alpha_{ms}$).

Solution

Given: Wind vectors at 6 and 0 km altitude:
M = 30 m/s and α = 240° at z = 6 km,
M = 0 m/s and α = 0° at z = 0 km.
Let: subscript "*ms*" = "mean shear"
Find: $(\Delta U, \Delta V)_{ms}$ = ? (m/s),
ΔM_{ms} = ? (m/s), α_{ms} = ? (°)

First, find (U, V) components from eqs. (1.3) & (1.4):
$U_{6km} = -M\cdot\sin(\alpha) = -(30\text{m/s})\cdot\sin(240°) = 26$ m/s
$V_{6km} = -M\cdot\cos(\alpha) = -(30\text{m/s})\cdot\cos(240°) = 15$ m/s
and
$U_{0km} = -M\cdot\sin(\alpha) = -(0\text{m/s})\cdot\sin(0°) = 0$ m/s
$V_{0km} = -M\cdot\cos(\alpha) = -(0\text{m/s})\cdot\cos(0°) = 0$ m/s

Next, use eqs. (14.13 & 14.14):
$\Delta U_{ms} = (26 - 0\text{ m/s})/6 =$ **4.3 m/s**
$\Delta V_{ms} = (15 - 0\text{ m/s})/6 =$ **2.5 m/s**

Then, use (ΔU, ΔV) in eq. (14.15):
$\Delta M_{ms} = [(\Delta U_{ms})^2 + (\Delta V_{ms})^2]^{1/2}$
$= [(4.3\text{ m/s})^2 + (2.5\text{ m/s})^2]^{1/2}$
$= [24.74\text{ (m/s)}^2]^{1/2} =$ **5 m/s**

Finally, use (ΔU, ΔV) in eq. (14.16):
$\alpha_{ms} = 90° - \arctan(\Delta V_{ms}/\Delta U_{ms}) + 180°$
$= 90° - \arctan(2.5/4.3) + 180°$
$= 90° - 30° + 180° =$ **240°**

Check: Units OK. Agrees with Fig. 14.53 black arrow.
Discussion: The only reason the mean shear direction equaled the wind direction at 6 km was because the surface wind was zero. Normally they differ.

Using Hodographs

Wind and wind-shear between the surface and 6 km altitude affects the dynamics, evolution, and motion of many N. American thunderstorms. You can use a hodograph to determine key wind-related quantities, including the:

- local shear across a single layer of air
- mean wind-shear vector
- total shear magnitude
- mean wind vector (normal storm motion)
- right & left moving supercell motions
- storm-relative winds.

Shear Across a Single Layer

Local shear between winds at adjacent wind-reporting altitudes is easy to find using a hodograph. Comparing Figs. 14.46 with 14.50, you can see that the hodograph line segment between any two adjacent altitudes is equal to the local shear across that one layer. For example, the solid grey arrow in Fig. 14.53 (one of the line segments of the hodograph) shows the local shear across the 4 to 5 km layer.

Mean Wind Shear Vector

The **mean wind-shear vector** across multiple layers of air of equal thickness is the vector sum of the local shear vectors (i.e., all the hodograph line segments for those layers), divided by the number of layers spanned. Namely, it is a vector drawn from the bottom-altitude wind point to the top-altitude wind point (white arrow with grey border in Fig. 14.53), then divided by the number of layers to give the mean (solid black arrow). For Fig. 14.53, the mean 0 - 6 km shear vector is 5 m/s from the west southwest. This graphical method is easy to use.

To find the same mean wind-shear vector mathematically, use the U and V components for the wind at z = 0, and also for the wind at z = 6 km. The mean shear (subscript $_{ms}$) vector coordinates $(\Delta U, \Delta V)_{ms}$ for the 0 to 6 km layer is given by:

$$\Delta U_{ms} = \left(U_{6km} - U_{0km}\right)/6 \qquad \bullet(14.13)$$

$$\Delta V_{ms} = \left(V_{6km} - V_{0km}\right)/6 \qquad \bullet(14.14)$$

You can use these coordinates to plot the mean shear vector on a hodograph. Find the magnitude of this mean shear vector using eq. (14.15), and the direction using eq. (14.16). Namely:

$$\Delta M_{ms} = \left(\Delta U_{ms}{}^2 + \Delta V_{ms}{}^2\right)^{1/2} \qquad (14.15)$$

$$\alpha_{ms} = 90° - \frac{360°}{C}\cdot\arctan\left(\Delta V_{ms}/\Delta U_{ms}\right) + \alpha_o \qquad (14.16)$$

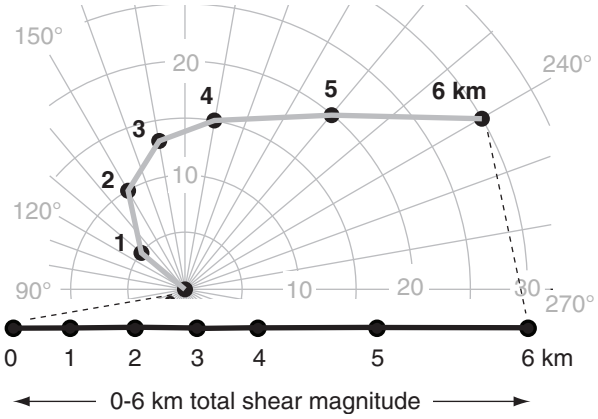

Figure 14.54
Example of total shear magnitude (black line), found as the sum of the shear magnitudes from the individual layers (grey line segments) between 0 to 6 km altitude. Vector wind differences are used as surrogates for shear.

where $C = 360°$ or 2π radians (depending on the units returned by your calculator or spreadsheet), and $\alpha_o = 180°$ if $\Delta U_{ms} > 0$, but is zero otherwise. As before, these wind-difference values are surrogates for the true shear.

Total Shear Magnitude

The **total shear magnitude** (TSM) across many layers, such as between 0 to 6 km, is the algebraic sum of the lengths of the individual line segments in the hodograph. For a simple graphic method that gives a good estimate of TSM, conceptually lay flat the grey line from Fig. 14.54 without stretching or shrinking any of the line segments. The length of the resulting straight line (black line in Fig. 14.54) indicates the total shear magnitude. For this example, the total shear magnitude is roughly 45 m/s, comparing the length of the black line to the wind-speed circles in the graph. Again, wind difference is used as a surrogate for shear.

To find the total shear magnitude mathematically, sum over all the individual layer shear magnitudes (assuming layers of equal thickness):

$$TSM = \sum_{i=1}^{n} \left[(U_i - U_{i-1})^2 + (V_i - V_{i-1})^2 \right]^{1/2} \quad \bullet(14.17)$$

where n is the total number of layers, and subscripts i and i–1 indicate top and bottom of the i^{th} layer. For the Fig. 14.54 example, $n = 6$, and each layer is 1 km thick.

Although two different environments might have the same total wind shear (TSM), the distribution of that shear with height determines the types of storms possible. For example, Fig. 14.55 shows two hodographs with exactly the same total shear

Solved Example(§)

Mathematically calculate the total shear magnitude for the hodograph of Fig. 14.53 (i.e., using data table from the solved example 4 pages ago).

Solution

Given: The data table from 4 pages ago, copied below.
Find: *TSM* = ? m/s

Use a spreadsheet to do these tedious calculations: First, use eqs. (1.3) and (1.4) to find U and V components of the winds. Next, find the wind differences $\Delta U = U_i - U_{i-1}$, and $\Delta V = V_i - V_{i-1}$. Finally, use these in eq. (14.17).

All speed and surrogate-shear units below are (m/s) except for direction α (degrees) and height z (km).

z	α	M	U	V	ΔU	ΔV	Shear
6	240	30	26.0	15.0	13.1	-0.3	13.1
5	220	20	12.9	15.3	10.3	0.5	10.3
4	190	15	2.6	14.8	4.9	2.0	5.2
3	170	13	-2.3	12.8	2.7	4.1	5.0
2	150	10	-5.0	8.7	-1.2	5.4	5.6
1	130	5	-3.8	3.2	-3.8	3.2	5.0
0	0	0	0.0	0.0	**Sum=TSM=**		**44.2**

Check: Units OK.
Discussion: The graphical estimate of 45 m/s by eye from Figure 14.54 was very close to the calculated value here.

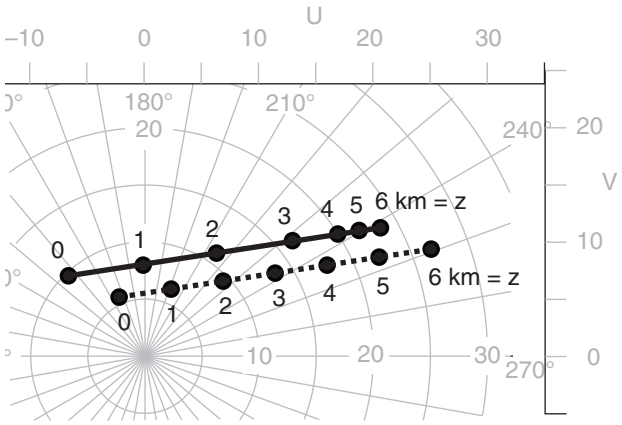

Figure 14.55
Two lines on this hodograph have exactly the same total length which means they have the same total shear magnitude. But that shear distributed differently with depth z for each line.

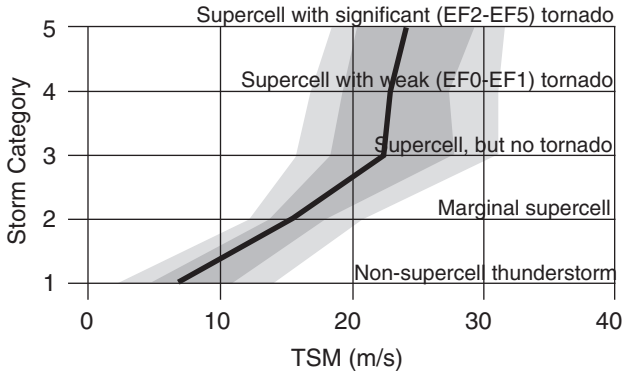

Figure 14.56
Observation frequency of thunderstorms of various intensities vs. environmental total shear magnitude (TSM) in the 0 to 6 km layer of atmosphere. Black line is the median (50 percentile) of several hundred observations in central N. America; dark grey shading spans 25 to 75 percentiles (the interquartile range); and light grey spans 10 to 90 percentiles.

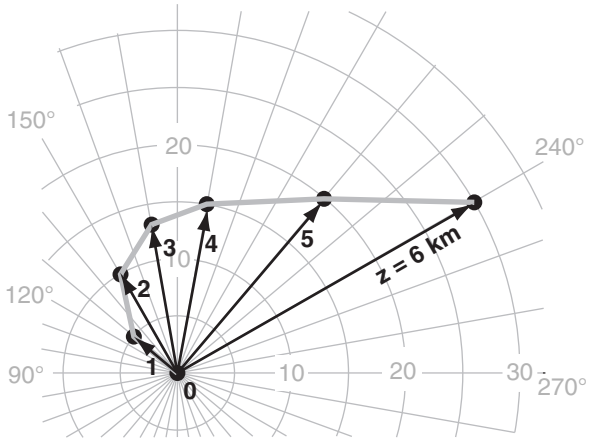

Figure 14.57
Wind vectors (black) associated with points on a hodograph.

Solved Example

How many fence posts are needed to support a straight fence with 6 sections?

Solution: **7** (see figure)

Discussion: Only 6 posts are needed for a closed loop.

magnitude, but the solid line has most of that shear in the bottom 3 km (as seen by the spacing between height (*z*) points along the hodograph), favoring **squall lines** and **bow echoes**. The dashed line has evenly distributed shear through the bottom 6 km, favoring **supercells**. Fig. 14.56 verifies that greater TSM values support supercells.

Mean Environmental Wind (Normal Storm Motion)

Airmass thunderstorms often translate in the direction and speed of the **mean environmental wind** vector in the bottom 6 km of the atmosphere. These are sometimes called **steering-level winds** or **normal winds**. To find the 0 to 6 km **mean wind** (i.e., NOT the shear) first picture the wind vectors associated with each point on the hodograph (Fig. 14.57). Next, vector sum all these winds by moving them tail to head, as shown in Fig. 14.58).

Finally, divide the vector sum by the number of wind points to find the **mean wind vector**, as indicated with the "X". [CAUTION: As you can see in Fig. 14.58, the 6 layers of air are bounded by 7 wind-vector points, not forgetting the zero wind at the ground. Thus, the vector sum in Fig. 14.58 must be divided by 7, not by 6.] For this example, the mean wind (i.e., the location of the "X") is from about 203° at 11 m/s. An arrow from the origin to the "X" gives the forecast **normal motion for thunderstorms**.

An easier way to approximate this mean wind vector without doing a vector addition is to estimate (by eye) the center of mass of the area enclosed by the original hodograph (shaded black in Fig. 14.59;

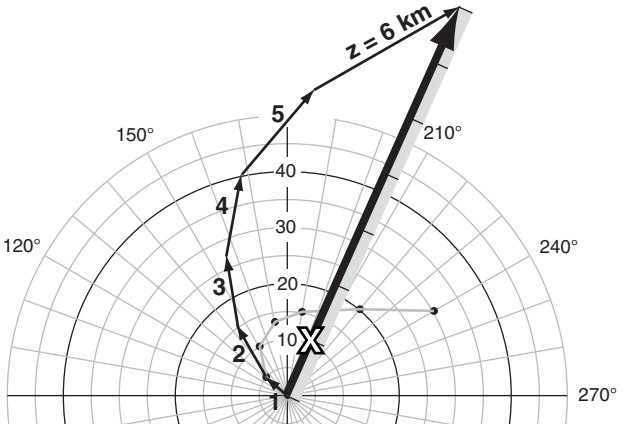

Figure 14.58
Individual wind vectors (thin black arrows), added as a vector sum (thick black arrow), divided by the number of wind vectors (7 in this example, not forgetting the zero wind at the ground), gives the mean wind (X) in the 0 to 6 km layer of air.

NOT the area enclosed by the re-positioned vectors of Fig. 14.58). Namely, if you were to: (1) trace that area onto a piece of cardboard, (2) cut it out, & (3) balance it on your finger tip, then the balance point (shown by the "X" in Fig. 14.59) marks the center of mass. "X" indicates the normal motion of thunderstorms, and is easy to estimate graphically using this center-of-mass estimate.

To mathematically calculate the **mean wind** (indicated with overbars) in the bottom 6 km of the atmosphere, first convert the vectors from speed and direction to their Cartesian components. Then sum the U velocities at all equally-spaced heights, and separately sum all the V velocities, and divide those sums by the number of velocity heights to get the components $(\overline{U}, \overline{V})$ of the mean wind.

$$\overline{U} = \frac{1}{N}\sum_{j=0}^{N} U_j \qquad \bullet(14.18)$$

$$\overline{V} = \frac{1}{N}\sum_{j=0}^{N} V_j \qquad \bullet(14.19)$$

where N is the number of wind levels (not the number of shear layers), and j is the altitude index. For winds every 1 km from $z = 0$ to $z = 6$ km, then $N = 7$. [CAUTION: Don't confuse the mean wind with the mean shear.] Then, use eqs. (1.1) and (1.2) [similar to eqs. (14.15 & 14.16), but for mean wind instead of mean shear] to convert from Cartesian coordinates to mean speed and direction $(\overline{M}, \overline{\alpha})$.

In summary the normal motion of thunderstorms is $(\overline{U}, \overline{V})$, or equivalently $(\overline{M}, \overline{\alpha})$. This corresponds to the center-of-mass "X" estimate of Fig. 14.59.

ON DOING SCIENCE • Be Safe *(part 2)*

Charles Doswell's web page recommends storm-chase guidelines, which I paraphrase here:

The #1 Threat: Being on the Highways

1. Avoid chasing alone.
2. Be very alert to standing water on the roads.
3. Avoid chasing in cities if at all possible.
4. Don't speed.
5. Pull fully off the road when you park.
6. Use your turn signals.
7. Slow down in poor visibility (rain; blowing dust).
8. Plan where to get fuel; don't let your tank get low.
9. Avoid unpaved roads (very slippery when wet).
10. Make your vehicle visible to other vehicles.

(continues in the next chapter).

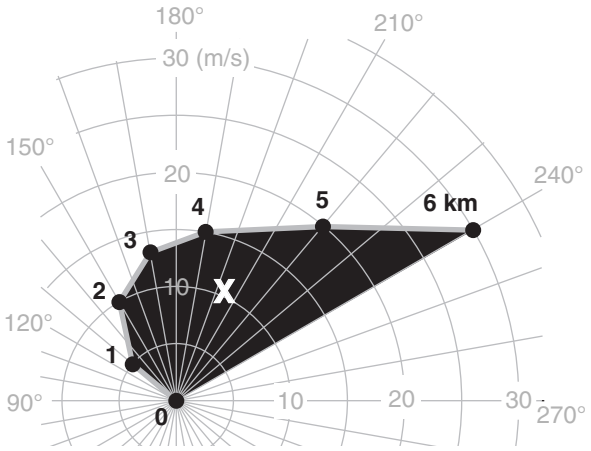

Figure 14.59
Mean wind ("X") in the 0 to 6 km layer of air, estimated as a center of mass of the area (black) enclosed by the hodograph. "X" indicates the normal motion of thunderstorms.

Solved Example

Mathematically calculate the mean wind components, magnitude, and direction for the hodograph of Fig. 14.57 (i.e., using data table from the solved example about 5 pages ago).

Solution:

Given: The data table from 5 pages ago, copied below.
Find: $(\overline{U}, \overline{V})$ = ? (m/s), $(\overline{M}, \overline{\alpha})$ = ? (m/s , °)

Use a spreadsheet to do these tedious calculations: First, use eqs. (1.3) and (1.4) to find U and V components of the winds. Next, average the U's, and then the V's, using eqs. (14.18 & 14.19). Finally, use eqs. (1.1) and (1.2) to covert to speed and direction.

All velocities below are (m/s), direction is in degrees, and height z in km.

z	direction	M	U	V
6	240	30	26.0	15.0
5	220	20	12.9	15.3
4	190	15	2.6	14.8
3	170	13	-2.3	12.8
2	150	10	-5.0	8.7
1	130	5	-3.8	3.2
0	0	0	0.0	0.0
Mean wind components (m/s) =			**4.3**	**10.0**
Mean wind magnitude (m/s) =			**10.9**	
Mean wind direction (°) =			**203.5**	

Check: Units OK. Magnitudes and signs reasonable.
Discussion: The graphical estimate of mean wind speed 11 m/s and direction 203° by eye from Figs. 14.58 and 14.59 were very close to the calculated values here. Namely, expect normal thunderstorms to move from the south southwest at about 10.9 m/s in this environment. Thus, the center-of-mass estimate by eye saves a lot of time and gives a reasonable answer.

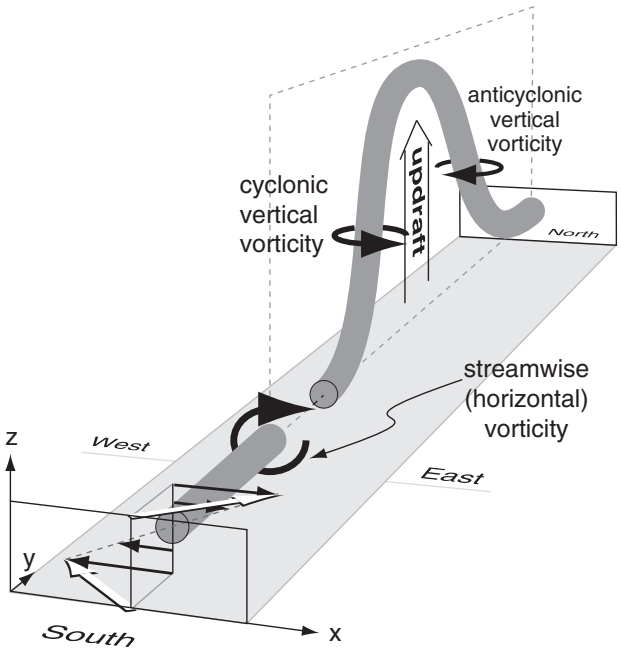

Figure 14.60
Counter-rotating mesocyclones formed when a convective updraft tilts the horizontal vorticity associated with environmental wind shear. Near-surface environmental winds from the southeast, and winds at 6 km altitude from the southwest, are white arrows. Dark cylinders represent vorticity axis.

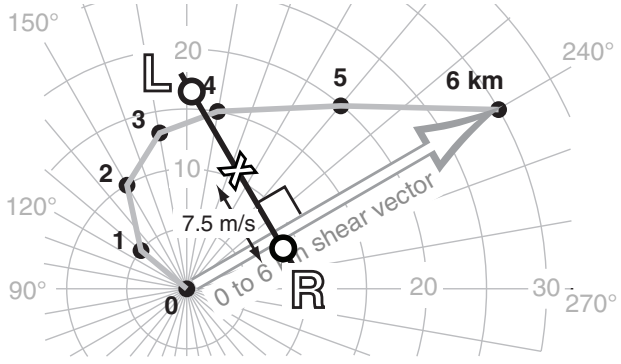

Figure 14.61
Bunker's internal dynamics technique for finding the movement of right-moving (R) and left-moving (L) supercell thunderstorms.

Supercell Storm Motion

Supercell thunderstorms have rotating updrafts, and to get that rotation they need sufficient environmental wind shear. The environmental total shear magnitude typically must be TSM ≥ 25 m/s and be distributed relatively evenly across the lower troposphere (from the surface to 6 km) to support supercells. Total shear magnitudes less than 15 m/s often are too small for supercells. In between those two shears, thunderstorms may or may not evolve into supercells.

One reason that strong shear promotes supercells is that horizontal vorticity associated with vertical shear of the horizontal wind in the environment can be tilted into vertical vorticity by the strong convective updraft of a thunderstorm (Fig. 14.60). This causes counter-rotating vortices (mesocyclones) on the left and right sides of the updraft. These two mesocyclones are deep (fill the troposphere) and have diameters roughly equal to the tropospheric depth. One is cyclonic; the other is anticyclonic.

Sometimes supercell thunderstorms split into two separate storms: **right-moving** and **left-moving supercells**. Namely, the cyclonic and anticyclonic mesocyclones support their own supercells, and move right and left of the "normal" motion as would have been expected from the mean steering-level wind.

Bunker's **Internal Dynamics (ID)** method to forecast the movement of these right and left-moving supercells is:

(1) Find the 0 to 6 km mean wind (see "X" in Fig. 14.61), using methods already described. This would give normal motion for thunderstorms. But supercells are not normal.
(2) Find the 0.25 to 5.75 km layer shear vector (approximated by the 0 to 6 km layer shear, shown with the white arrow in Fig. 14.61).
(3) Through the mean wind point (X), draw a line (black line in Fig. 14.61) perpendicular to the 0 to 6 km shear vector.
(4) On the line, mark 2 points (white in black circles): one 7.5 m/s to the right and the other 7.5 m/s to the left of the "X".
(5) The point that is right (clockwise) from the mean wind "X" gives the average motion forecast for the right (R) moving storm.
(6) The point that is left (counter-clockwise) from the mean wind "X" gives the average forecast motion of the left (L) moving storm.

Not all storms follow this simple rule, but most supercell motions are within a 5 m/s radius of error around the R and L points indicated here. For the example in Fig. 14.61, motion of the right-moving supercell is 8 m/s from 246°, and the left mover is 17 m/s from 182°.

Only for straight hodographs (Fig. 14.62a) are the right and left-moving supercells expected to exist simultaneously with roughly equal strength (Fig. 14.63a). Hodographs that curve clockwise (Fig. 14.62b) with increasing height favor right-moving supercell thunderstorms (Fig. 14.63b). For this situation, the left-moving storm often dissipates, leaving only a right-moving supercell.

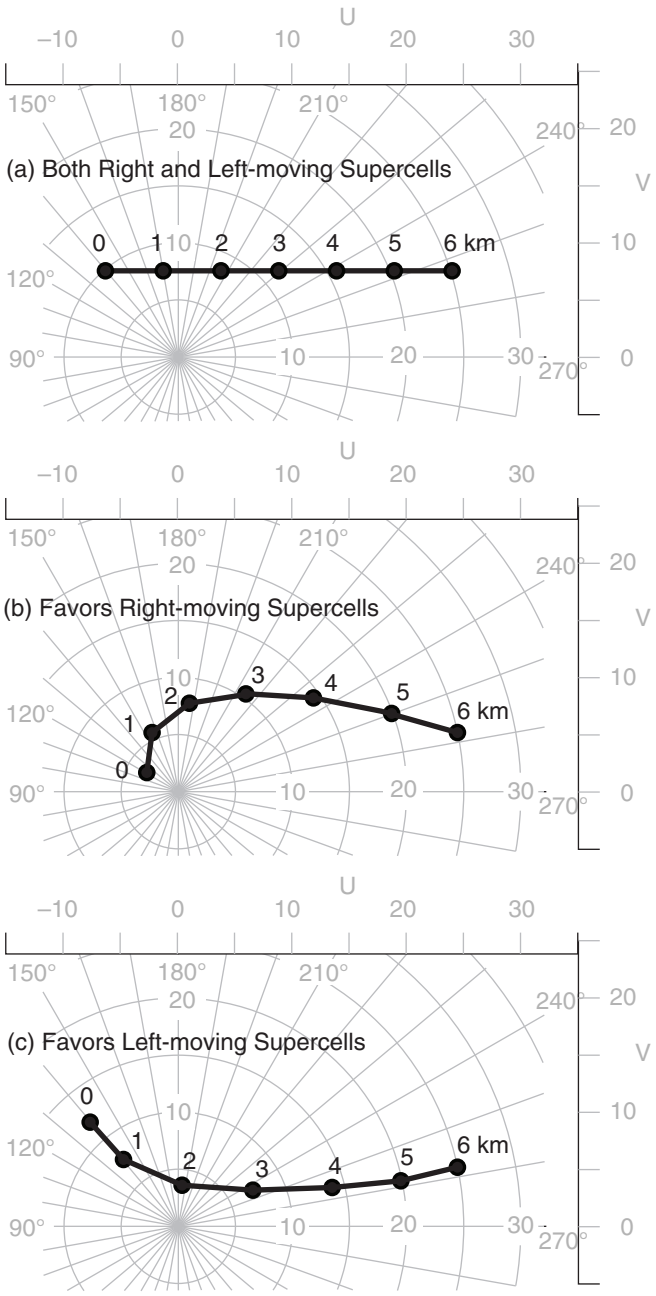

Figure 14.62
Shapes of hodograph that favor right and left-moving supercell thunderstorms: (a) straight hodograph; (b) hodograph showing clockwise curvature with increasing height; (c) hodograph showing counter-clockwise curvature with increasing height.

Hodographs that curve counterclockwise (Fig. 14.62c) favor left-moving supercells (Fig. 14.63c), with the right-moving storm often dissipating. In the plains/prairies of North America, most hodographs curve clockwise (as in Figs. 14.61 and 14.62b), resulting in right-moving supercell thunderstorms that are about ten times more abundant than left-moving storms. The opposite is true in the S. Hemisphere for midlatitude thunderstorms.

In summary, supercell thunderstorms often do **not** move in the same direction as the mean environmental (steering-level) wind, and do not move at the mean wind speed. The methods that were discussed here are useful to forecast movement of storms that haven't formed yet. However, once storms form, you can more accurately estimate their motion by tracking them on radar or satellite. Regardless of the amounts of shear, CAPE, and moisture in the pre-storm environment, thunderstorms won't form unless there is a trigger mechanism. Triggers are discussed in the next main section (after the Bulk Richardson Number subsection).

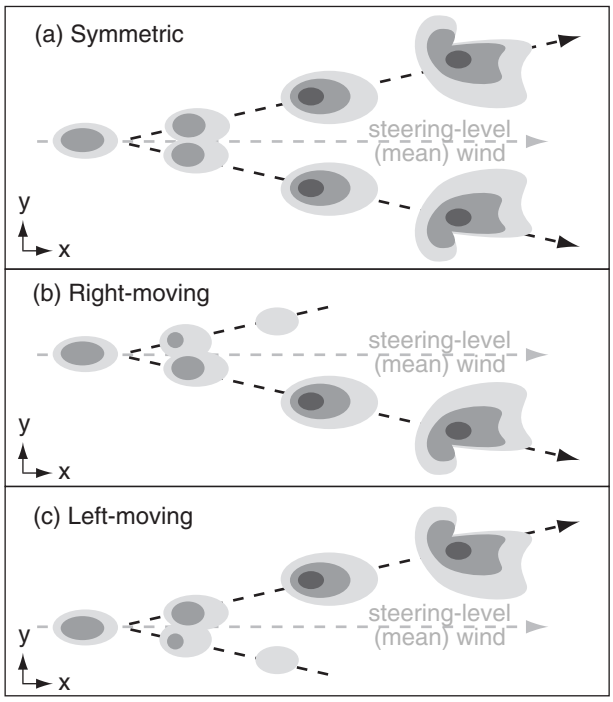

Figure 14.63
Sketch of sequence of radar reflectivity echoes over time (left to right) for: (a) symmetric supercell split; (b) dominant right-moving supercells; and (c) dominant left-moving supercells. Note the different orientation of the hook echo in the left-moving supercell. The steering-level wind is the "normal" wind.

Solved Example

Given the wind profile in the table below:

z (km)	dir. (°)	speed (m/s)	z (km)	dir. (°)	speed (m/s)
0	150	15	4	270	15
1	160	8	5	270	22
2	210	5	6	270	30
3	260	8			

(a) Plot the hodograph;
(b) Graphically find the mean wind-shear vector for the 0 to 6 km layer;
(c) Graphically find the total shear magnitude.
(d) Does this hodograph favor bow echoes or supercells? Why?
(e) Graphically find the 0 to 6 km mean wind.
(f) Graphically find the motions for the right and left-moving supercell thunderstorms.
(g) Which is favored: right or left-moving supercell thunderstorms? Why?

Solution

(a) Plot the hodograph (see curved black line below):

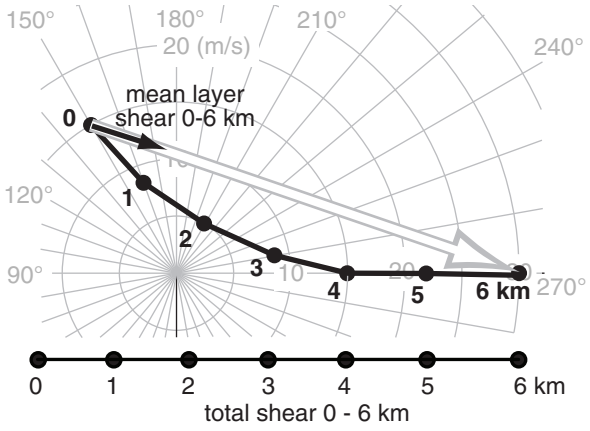

(b) The 0 to 6 km shear vector is shown with the white arrow. Dividing by 6 gives a mean layer shear (black arrow) of about **7 m/s from the west northwest**.

(c) The total shear magnitude, shown at the bottom of the hodograph above, is about **42 m/s**.

(d) **Supercells** are favored, because shear is evenly distributed throughout the bottom 6 km of atmosphere. Also, the total shear magnitude is greater than 25 m/s, as required for supercells.

(e) The answer is a vector, drawn from the origin to the "X" (see hodograph in next column). Namely, the mean wind is from about **250° at 10 m/s**. Vector method roughly agrees with center-of-mass method, done by eye.

(Continues in next column.)

Solved Example *(continuation)*

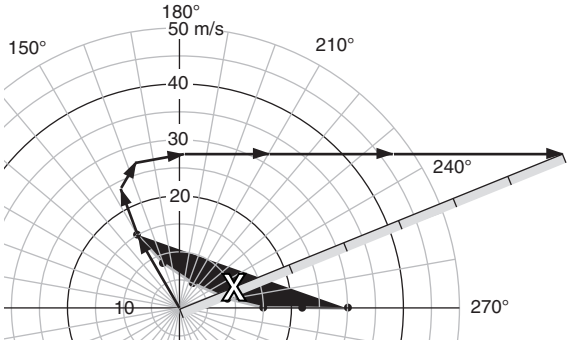

Thus, for normal thunderstorms (and for the first supercell, before it splits into right and left-moving supercells) forecast them to move from the west southwest at about 10 m/s. For both this example and Fig. 14.59, the center-of-mass method gives a better estimate if we look at the hodograph area between z = 0.5 and 5.5 km.

(f) Bunker's Internal Dynamics method is shown graphically on the hodograph below. The left supercell (L) is forecast to move at **16 m/s from 229°**, and the right supercell (R) at **8 m/s from 298°**.

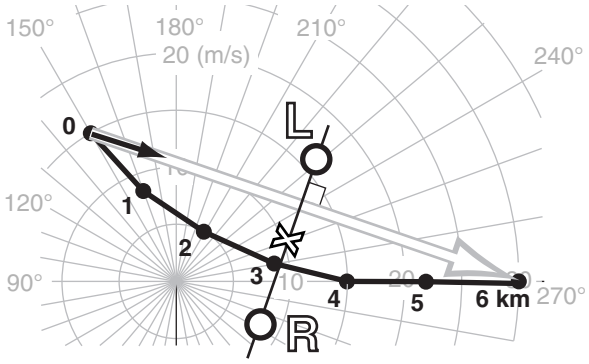

(g) **Left-moving supercells** are favored, because the hodograph curves counterclockwise with increasing height. This storm moves faster than the mean wind (i.e., faster than the "normal" thunderstorm steering-level wind).

Discussion: This hodograph shows **veering winds** (winds turning clockwise with increasing altitude), implying warm-air advection according to the thermal-wind relationship. Even though the wind vectors veer clockwise, the hodograph curvature is counterclockwise (implying dominant left-moving supercell storms), so be careful not to confuse these two characteristics.

Winds alone are not sufficient to forecast whether thunderstorms will occur. Other key ingredients are instability and abundant moisture, as previously discussed. Also needed is sufficient lifting by a trigger mechanism to overcome the capping inversion.

Bulk Richardson Number

Thunderstorm type depends both on the amounts of instability and wind shear in the pre-storm environmental sounding. The **bulk Richardson number** (**BRN**) is the ratio of nonlocal instability (i.e., the CAPE) in the mid to upper part of the troposphere to shear (ΔM) in the lower half of the troposphere:

$$BRN = \frac{CAPE}{0.5 \cdot (\Delta M)^2} \qquad \bullet(14.20)$$

Table 14-2 summarizes the utility of the BRN. The BRN is dimensionless, because the units of CAPE (J/kg) are the same as (m^2/s^2) (see Appendix A).

In the denominator, the shear magnitude (ΔM) is given by:

$$\Delta M = \left[(\Delta U)^2 + (\Delta V)^2 \right]^{1/2} \qquad \bullet(14.21)$$

where

$$\Delta U = \overline{U} - U_{SL} \qquad (14.22a)$$

$$\Delta V = \overline{V} - V_{SL} \qquad (14.22b)$$

Eqs. (14.22) are the shear components between the mean wind ($\overline{U}, \overline{V}$) in the 0 to 6 km layer, and the surface-layer winds (U_{SL}, V_{SL}) estimated as an average over the bottom 0.5 km of the atmosphere. Fig. 14.64 shows how to estimate this shear magnitude from a hodograph.

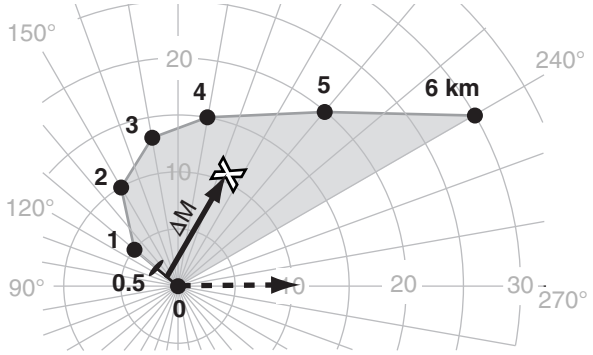

Figure 14.64
Solid black arrow shows shear ΔM between the average winds in the lowest 0.5 km of air, and the mean wind (X) in the lowest 6 km. Dashed arrow is just the solid arrow moved (without stretching) to the origin, so that the speed circles indicate the shear magnitude. ΔM = 11 m/s in this example. ΔM is important in the bulk Richardson number (BRN), and BRN shear.

Table 14-2. Thunderstorm type determination using the bulk Richardson number (BRN)

BRN	Thunderstorm Type
< 10	(unlikely to have severe thunderstorms)
10 - 45	Supercells
45 - 50	Supercells and/or multicells
> 50	Multicells

Solved Example

For the previous solved example, assume the associated CAPE = 3000 J/kg. (a) Find the BRN shear. (b) Find the BRN. (c) Are tornadic supercells likely?

Solution

Given: CAPE = 3000 J/kg
hodograph = previous solved example
Find: BRN shear = ? m^2/s^2
BRN = ? (dimensionless)
Yes/no: thunderstorms? supercells? tornadoes?

(a) On the hodograph from the previous solved example, put the tail of a vector (solid black arrow) a quarter of the way from the z = 0 point to the z = 1 point on the hodograph). Put the arrowhead on the "X" mean wind. Then measure the vector's length (see dashed arrow), which is about ΔM = 18 m/s.

Then use eq. (14.23):

BRN Shear = $0.5 \cdot (18 \text{ m/s})^2$ = **162** m^2/s^2

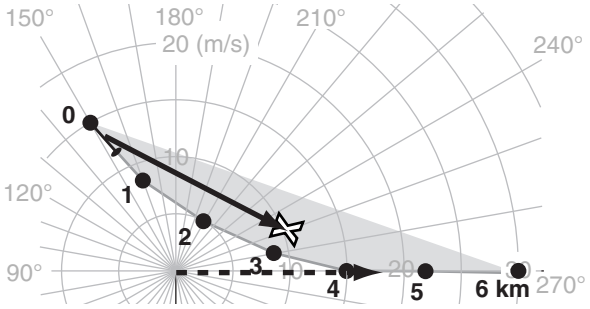

(b) Use eq. (14.20):
BRN = (3000 m^2/s^2) / (162 m^2/s^2) = **18.5**

(c) Assume CAPE ≈ MLCAPE. Then from Table 14-1:
Severe thunderstorms likely, possible tornado.
Next, use Table 14-2: Thunderstorm type = **supercell**.
Finally, use Table 14-3: **Tornadoes are likely**.

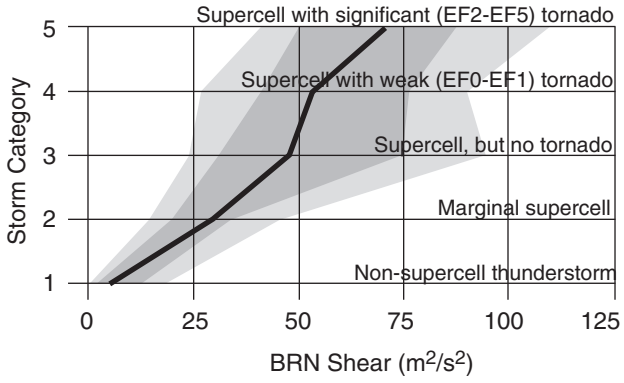

Figure 14.65
Statistics of bulk Richardson number shear (BRN shear) as a discriminator for thunderstorm and tornado intensity, based on several hundred storms in central N. America. Light grey spans 10 to 90 percentiles of the observations; dark grey spans the interquartile range of 25 to 75 percentiles; and the black line is the median (50 percentile).

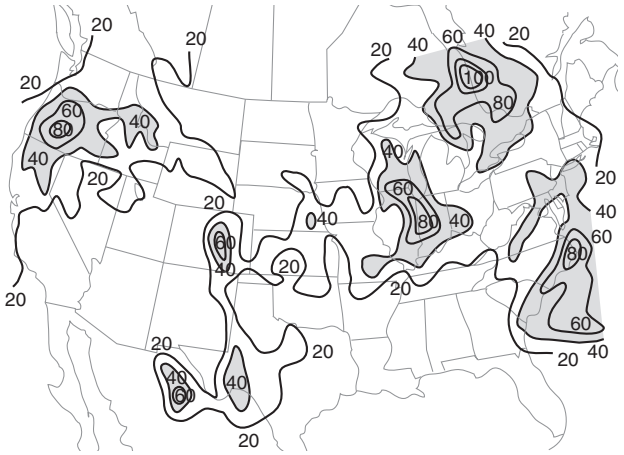

Figure 14.66
Weather map similar to Fig. 14.38, but for bulk Richardson number shear (BRN shear) in m^2/s^2. Unlike the smooth variations in CAPE across N. America, the BRN shear values have a more local structure and are highly variable.

Table 14-3. If supercell thunderstorms form, then the bulk-Richardson-number shear (BRN Shear) suggests whether they might have tornadoes.

BRN Shear (m^2/s^2)	**Tornadoes**
25 - 50	possible, but less likely
50 - 100	more likely

The denominator of the BRN, known as the **bulk-Richardson-number shear** (**BRN Shear**), is

$$\text{BRN Shear} = 0.5 \cdot (\Delta M)^2 \qquad \bullet(14.23)$$

which has units of (m^2/s^2). BRN shear can help indicate which supercells might be tornadic (see Table 14-3). Although BRN shear is statistically sharper in its ability to discriminate between thunderstorms and tornadoes of different severity, there is still significant overlap in thunderstorm/tornado categories as was found by verification against several hundred thunderstorms in central N. America (Fig. 14.65).

A case study weather map of BRN shear is analyzed in Fig. 14.66. As before, you should NOT use BRN shear alone as an indicator of tornado likelihood, because additional conditions must also be satisfied in order to allow tornadic thunderstorms to form. Some of these other conditions are instability, and a trigger mechanism.

TRIGGERING VS. CONVECTIVE INHIBITION

The fourth environmental requirement for thunderstorm formation is a **trigger** mechanism to cause the initial **lifting** of the air parcels. Although the capping inversion is needed to allow the fuel supply to build up (a good thing for thunderstorms), this cap also inhibits thunderstorm formation (a bad thing). So the duty of the external trigger mechanism is to lift the reluctant air parcel from z_i to the LFC. Once triggered, thunderstorms develop their own circulations that continue to tap the boundary-layer air.

The amount of external forcing required to trigger a thunderstorm depends on the strength of the cap that opposes such triggering. One measure of cap strength is convective inhibition energy.

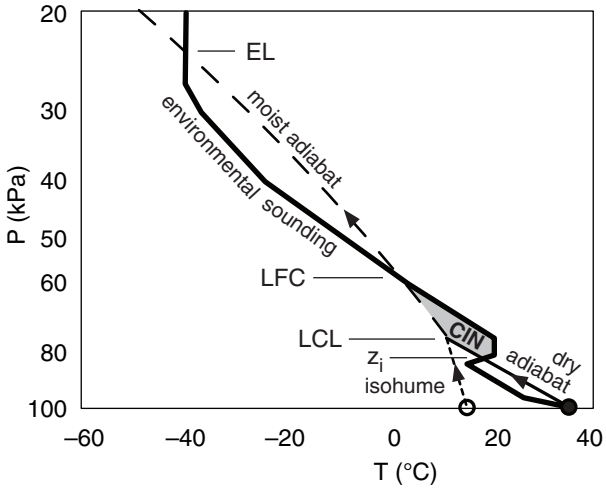

Figure 14.67
Convective Inhibition (CIN) is proportional to the area (shaded) where the rising air parcel is colder than the environment for an early afternoon pre-storm sounding.

Convective Inhibition (CIN)

Between the mixed-layer top z_i and the level of free convection LFC, an air parcel lifted from the surface is colder than the environment. Therefore, it is negatively buoyant, and does not want to rise. If forced by a trigger mechanism to rise above z_i, then the trigger process must do work against the buoyant forces within this cap region.

The total amount of work needed is proportional to the area shaded in Fig. 14.67. This work per unit mass is called the **Convective Inhibition** (**CIN**). The equation for CIN is identical to the equation for CAPE, except for the limits of the sum. Another difference is that CIN values are negative. CIN has units of J/kg.

For the afternoon sounding of Fig. 14.67, CIN corresponds to the area between z_i and LFC. For a morning sounding, a forecast of the afternoon's high temperature provides the starting point for the rising air parcel, where z_i is the corresponding forecast for mixed-layer top (Fig. 14.68). Thus, for both Figs. 14.67 and 14.68, you can use:

$$CIN = \sum_{z_i}^{LFC} \frac{|g|}{T_{ve}} (T_{vp} - T_{ve}) \cdot \Delta z \qquad \bullet(14.24)$$

where T_v is virtual temperature, subscripts p and e indicate the air parcel and the environment, $|g| = 9.8\ m \cdot s^{-2}$ is the magnitude of gravitational acceleration, and Δz is a height increment. Otherwise, CIN is usually found by summing between the surface ($z = 0$) and the LFC (Fig. 14.69).

$$CIN = \sum_{z=0}^{LFC} \frac{|g|}{T_{ve}} (T_{vp} - T_{ve}) \cdot \Delta z \qquad (14.25)$$

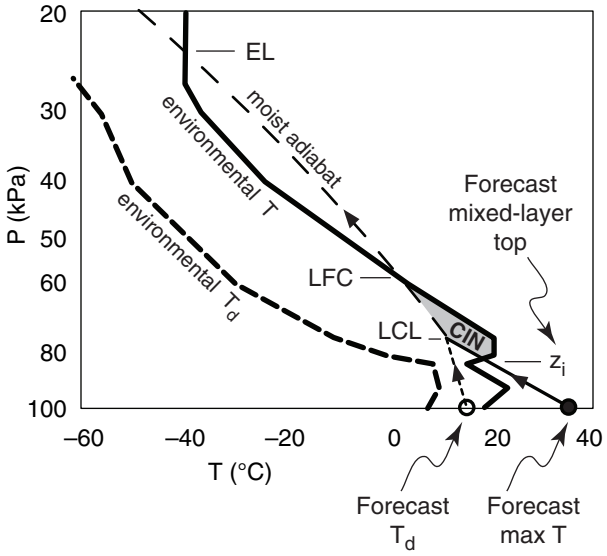

Figure 14.68
CIN based on max surface temperature forecasts and the early morning pre-storm sounding.

Science Graffiti

"Every sin is the result of a collaboration." – Seneca

"Sin is sweet in the beginning, but bitter in the end." – The Talmud

"There is no sin except stupidity." – Oscar Wilde

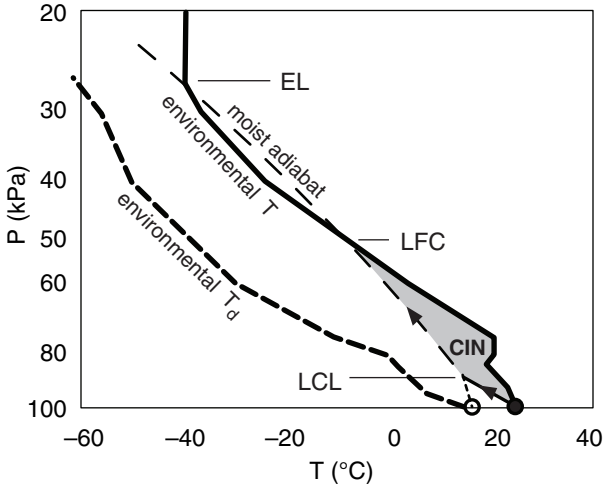

Figure 14.69
CIN between the surface and the LFC, for an early morning pre-storm sounding.

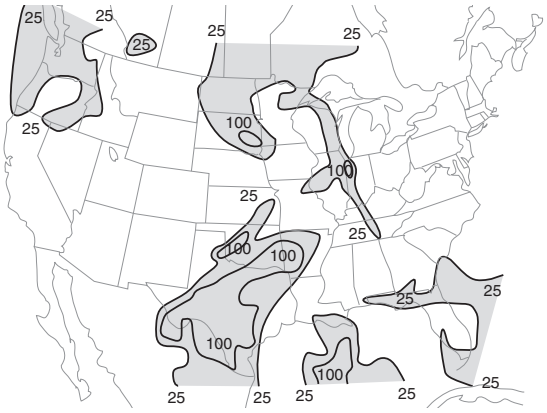

Figure 14.70
Weather map similar to Fig. 14.38 over USA, but for magnitude of mean-layer convective inhibition energy (ML CIN) in J/kg.

Solved Example

Estimate the convective inhibition (CIN) value for the sounding of Fig. 14.25. Are thunderstorms likely?

Solution

Given: Sounding of Fig. 14.25, as zoomed below.
Find: CIN = ? J/kg.

Cover the CIN area with small tiles of size Δz = 500 m and ΔT = –2°C (where the negative sign indicates the rising parcel is colder than the environmental sounding). Each tile has area = $\Delta T \cdot \Delta z$ = –1,000 K·m. I count 12 tiles, so the total area is –12,000. Also, by eye the average environmental temperature in the CIN region is about T_e = 12°C = 285 K.

Use eq. (14.26):
CIN = [(9.8 m/s^2) / (285 K)]·(–12,000 K·m) = **–413 J/kg**.
From Table 14-4, **thunderstorms are unlikely**.

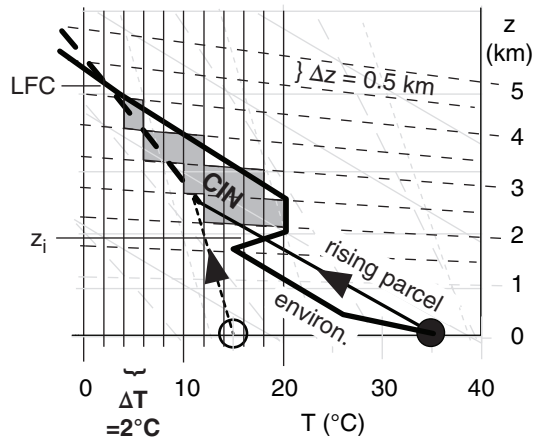

Check: By eye, the CIN area of Fig. 14.25 is about 1/5 the size of the CAPE area. Indeed, the answer above has about 1/5 the magnitude of CAPE (1976 J/kg), as found in previous solved exercises. Units OK too.

Discussion: The negative CIN implies that work must be done ON the air to force it to rise through this region, as opposed to the positive CAPE values which imply that work is done BY the rising air.

Table 14-4. Convective Inhibition (CIN)

CIN Value (J/kg)	Interpretation
> 0	No cap. Allows weak convection.
0 to –20	Weak cap. Triggering easy. Air-mass thunderstorms possible.
–20 to –60	Moderate cap. Best conditions for CB. Enables fuel build-up in boundary layer. Allows most trigger mechanisms to initiate storm.
–60 to –100	Strong cap. Difficult to break. Need exceptionally strong trigger.
< –100	Intense cap. CB triggering unlikely.

As before, if the virtual temperature is not known or is difficult to estimate, then often storm forecasters will use T in place of T_v in eq. (14.24) to get a rough estimate of CIN:

$$CIN = \sum_{z_i}^{LFC} \frac{|g|}{T_e}(T_p - T_e)\cdot\Delta z \qquad \bullet(14.26)$$

although this can cause errors as large as 35 J/kg in the CIN value. Similar approximations can be made for eq. (14.25). Also, a **mean-layer CIN** (**ML CIN**) can be used, where the starting air parcel is based on average conditions in the bottom 1 km of air.

CIN is what prevents, delays, or inhibits formation of thunderstorms. Larger magnitudes of CIN (as in Fig. 14.69) are less likely to be overcome by trigger mechanisms, and are more effective at preventing thunderstorm formation. CIN magnitudes (Table 14-4) smaller than about 60 J/kg are usually small enough to allow deep convection to form if triggered, but large enough to trap heat and humidity in the boundary layer prior to triggering, to serve as the thunderstorm fuel. CIN is the **cap** that must be broken to enable thunderstorm growth.

Storms that form in the presence of large CIN are less likely to spawn tornadoes. However, large CIN can sometimes be circumvented if an elevated trigger mechanism forces air-parcel ascent starting well above the surface.

The area on a thermo diagram representing CIN is easily integrated by computer, and is often reported with the plotted sounding. [**CAUTION: often the magnitude of CIN is reported (i.e., as a positive value).**] CIN magnitudes from many sounding stations can be plotted on a weather map and analyzed, as in Fig. 14.70. To estimate CIN by hand, you can use the same tiling method as was done for CAPE (see the Solved Example at left).

Thunderstorms are more likely for smaller values of the difference $\Delta z_{cap} = z_{LFC} - z_{LCL}$, which is the nonlocally stable region at the bottom of the storm. Namely, a thinner cap on top of the ABL might allow thunderstorms to be more easily triggered.

Trigger Mechanisms

Any external process that forces the boundary-layer air parcels to rise through the statically stable cap can be a trigger. Triggers include:

- Boundaries between airmasses:
  - synoptic fronts,
  - dry lines,
  - sea-breeze fronts,
  - gust fronts from other thunderstorms;
- Other triggers:
  - mountains,
  - atmospheric buoyancy waves,
  - localized regions of excess surface heating.

If one airmass is denser than an adjacent airmass, then any convergence of air toward the dividing line between the airmasses (called an **airmass boundary**) will force the less-dense air to rise over the denser air. For example, advancing cold air can drive under the warmer, ambient boundary-layer air, forcing the warm air upward through the stable layer at z_i (Fig. 14.71).

Cold fronts and **warm fronts** are synoptically-forced examples of airmass boundaries. Upper-level synoptic fronts (with no signature on a surface weather map) can also cause lifting and trigger thunderstorms. Fig. 14.72 shows the frontal analysis for the 24 May 2006 case study that has been presented in many of the preceding sections. These frontal zones could trigger thunderstorms.

Sea-breeze (see the Local Wind chapter) or **lake-breeze fronts** create a similar density discontinuity on the mesoscale at the boundary between the cool marine air and the warmer continental air during daytime, and can also trigger convection. If a cold **downburst** from a thunderstorm hits the ground and spreads out, the leading edge is a **gust front** of cooler, denser air that can trigger other thunderstorms (via the propagation mechanism already discussed). The **dry line** separating warm dry air from warm humid air is also an airmass boundary (Figs. 14.71 & 14.72), because dry air is more dense than humid air at the same temperature (see definition of virtual temperature in Chapter 1).

These airmass boundaries are so crucial for triggering thunderstorms that meteorologist devote much effort to identifying their presence. Lines of thunderstorms can form along them. Synoptic-scale fronts and dry lines are often evident from weather-map analyses and satellite images. Sea-breeze fronts and gust fronts can be seen by radar as convergence

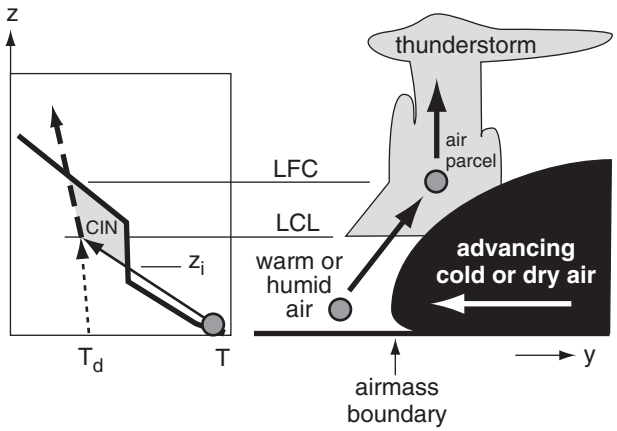

Figure 14.71
Warmer or moister (less-dense) air forced to rise over advancing colder or drier (more-dense) air can trigger thunderstorms if the air parcels forced to rise reach their LFC. The portion of thunderstorm clouds between the LCL and the LFC can have a smooth or laminar appearance. Above the LFC the clouds look much more convective, with rising turrets that look like cauliflower.

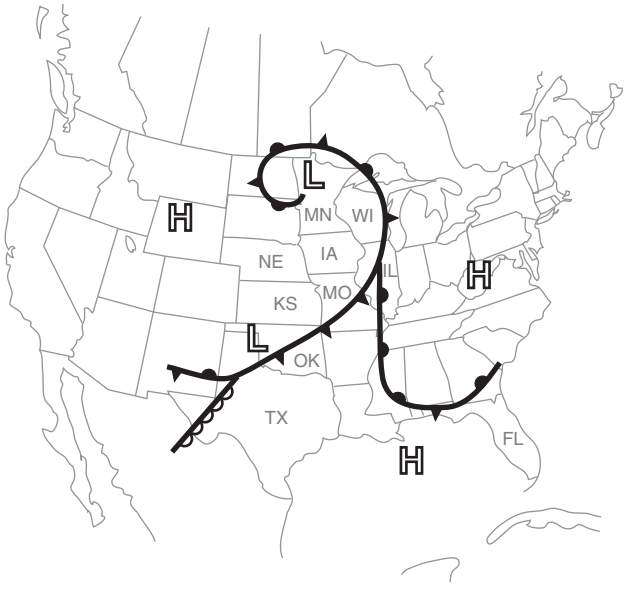

Figure 14.72
Synoptic frontal analysis over N. America at 22 UTC on 24 May 2006. An occluded front extends from a low (𝕃) in Minnesota (MN) into Illinois (IL), where the warm and cold fronts meet. The cold front extends from IL through Oklahoma (OK) and Texas (TX), and merges with a dry line in SW Texas.

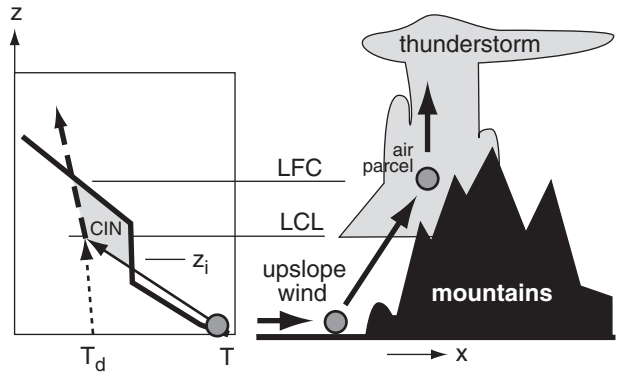

Figure 14.73
Wind hitting a mountain can be forced upslope, triggering thunderstorms called orographic thunderstorms.

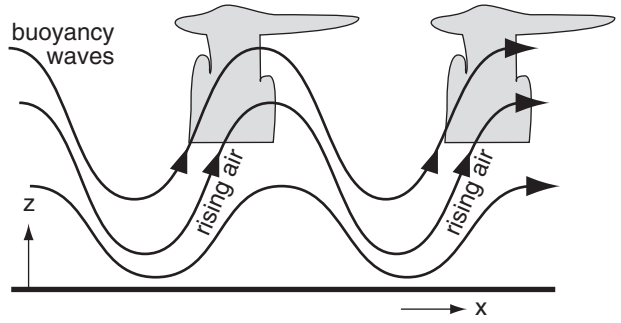

Figure 14.74
Thunderstorms generated in the updraft portions of buoyancy (gravity) waves.

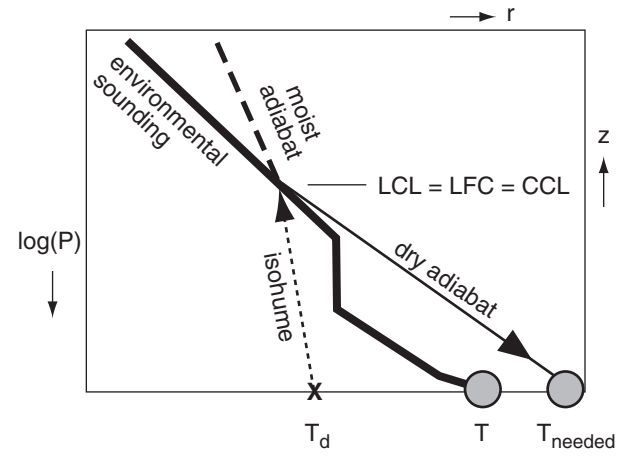

Figure 14.75
The convective temperature needed so that an air parcel has no CIN, and can reach its LFC under its own buoyancy. CCL = convective condensation level.

lines in the Doppler wind field, and as lines of weakly enhanced reflectivity due to high concentrations of insects (converging there with the wind) or a line of small cumulus clouds. When two or more airmass boundaries meet or cross, the chance of triggering thunderstorms is greater such as over Illinois and Texas in the case-study example of Fig. 14.72.

Horizontal winds hitting a mountain slope can be forced upward (Fig. 14.73), and can trigger **orographic thunderstorms**. Once triggered by the mountains, the storms can persist or propagate (trigger daughter storms via their gust fronts) as they are blown away from the mountains by the steering-level winds.

Sometimes when the air flows over mountains or is pushed out of the way by an advancing cold front, vertical oscillations called **buoyancy waves** or **gravity waves** (Fig. 14.74) can be generated in the air (see the Local Winds chapter). If the lift in the updraft portion of a wave is sufficient to bring air parcels to their LFC, then thunderstorms can be triggered by these waves.

Another trigger is possible if the air near the ground is warmed sufficiently by its contact with the sun-heated Earth. The air may become warm enough to rise as a thermal through the cap and reach the LFC under its own buoyancy. The temperature needed for this to happen is called the **convective temperature**, and is found as follows (Fig. 14.75):

(1) Plot the environmental sounding and the surface dew-point temperature.
(2) From T_d, follow the isohume up until it hits the sounding. This altitude is called the **convective condensation level** (**CCL**).
(3) Follow the dry adiabat back to the surface to give the convective temperature needed.

You should forecast airmass thunderstorms to start when the surface air temperature is forecast to reach the convective temperature, assuming the environmental sounding above the boundary layer does not change much during the day. Namely, determine if the forecast high temperature for the day will exceed the convective temperature.

Often several triggering mechanisms work in tandem to create favored locations for thunderstorm development. For example, a jet streak may move across North America, producing upward motion under its left exit region and thereby reducing the strength of the cap as it passes (see the "Layer Method for Static Stability" section in Chapter 5). If the jet streak crosses a region with large values of CAPE at the same time as the surface temperature reaches its maximum value, then the combination of these processes may lead to thunderstorm development.

Solved Example

Use the sounding in Fig. 14.25 to find the convective temperature and the convective condensation level. Are thunderstorms likely to be triggered?

Solution

Given: Fig. 14.25.

Find: P_{CCL} = ? kPa, T_{needed} = ? °C , yes/no Tstorms

Step 1: Plot the sounding (see next column).

Step 2: From the surface dew-point temperature, follow the isohume up until it hits the sounding to find the CCL. Thus: $P_{CCL} \approx$ **63 kPa** (or $z_{CCL} \approx$ **3.7 km**).

Step 2: Follow the dry adiabat down to the surface, and read the temperature from the thermo diagram. $T_{needed} \approx$ **47 °C** is the convective temperature

Check: Values agree with figure.

Discussion: Typical high temperatures in the prairies of North America are unlikely to reach 47°C.

(continues in next column)

Solved Example *(continuation)*

Thus, the **triggering of a thunderstorm by a rising thermal is unlikely** for this case. However, thunderstorms could be triggered by an airmass boundary such as a cold front, if the other conditions are met for thunderstorm formation.

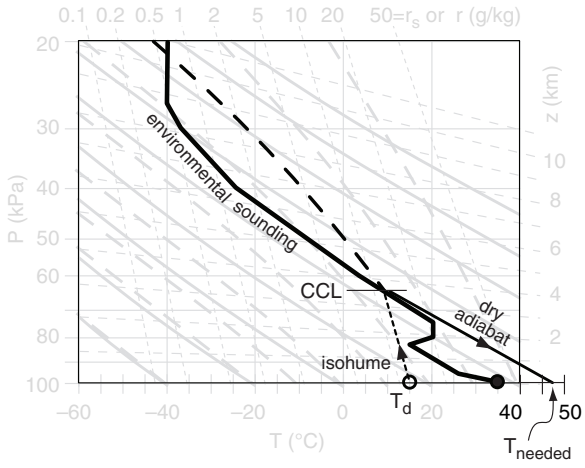

Finally, a word of caution. As with each of the other requirements for a thunderstorm, triggering (lift) by itself is insufficient to create thunderstorms. Also needed are the instability, abundant moisture, and wind shear. To forecast thunderstorms you must forecast all four of the key ingredients. That is why thunderstorm forecasting is so difficult.

THUNDERSTORM FORECASTING

Forecasting thunderstorms is not easy. Thunderstorms are very nonlinear (i.e., they grow explosively), and are extremely dependent on initial conditions such as triggering, shear, and static stability. Individual storms are relatively short lived (15 to 30 min), and are constantly changing in intensity and movement during their lifetimes. Intense thunderstorms also modify their environment, making the relationships between pre-storm environments and storm evolution even more challenging to apply.

Much appears to depend on random chance, since we are unable to observe the atmosphere to the precision needed to describe it fully. Will a boundary-layer thermal or an airmass boundary happen to be strong enough to be the first to break through the capping inversion? Will a previous thunderstorm create a strong-enough downburst to trigger a new

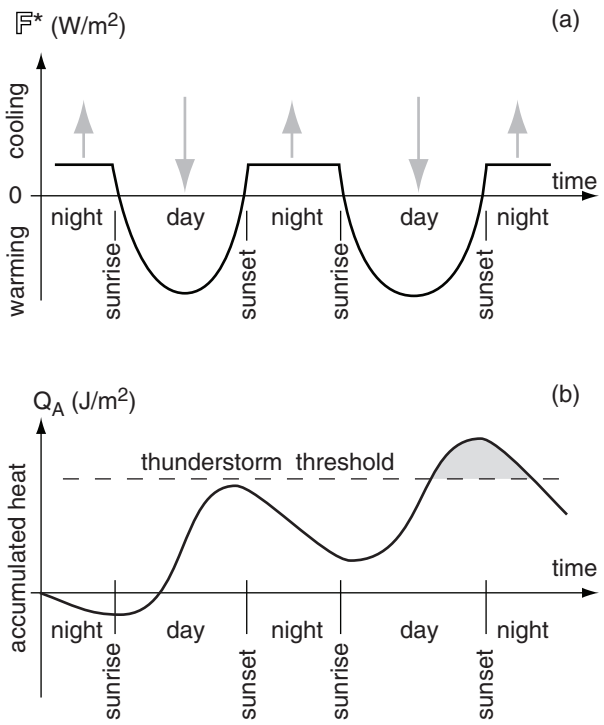

Figure 14.76
(a) Simplification of daily (diurnal) cycle of upward net radiation $\mathbb{F}^*$, which combines solar heating during the day and infrared cooling all the time, for summer over land. Grey arrows represent direction of net flux at the surface. (b) Accumulated (sensible plus latent) heats Q_A in the boundary layer. During summer, days are longer than nights, allowing accumulated heat to increase from day to day. Dash line thunderstorm threshold schematically represents the net effect of all the complex thunderstorm-genesis processes reviewed in this chapter. Grey shading shows that thunderstorms are most likely to form around sunset, plus and minus several hours

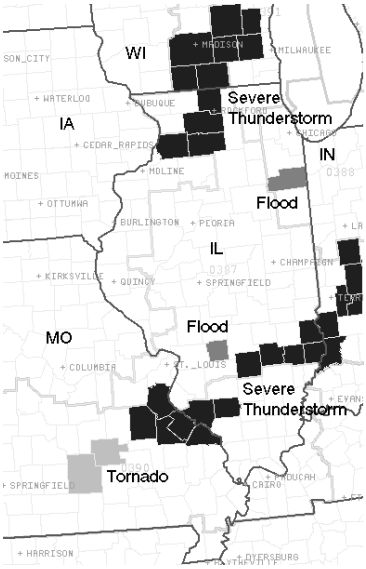

Figure 14.77
Map of tornado (light grey), flood (medium grey), and severe thunderstorm (black) **warnings** *associated with the 24 May 2006 case study in the USA. The shaded boxes indicate which counties were warned. State abbreviations are: IL = Illinois, MO = Missouri, IA = Iowa, IN = Indiana, WI = Wisconsin.*

thunderstorm with its gust front? Will high clouds happen to move over a region, shading the ground and thereby reducing the instability?

Tornadoes, hail, heavy rain, lightning, and strong straight-line wind events may or may not occur, and also vary in intensity, track, and duration within the constraints of the parent thunderstorm. Thunderstorms interact in complex ways with other existing thunderstorms and with the environment and terrain, and can trigger new thunderstorms.

Luckily, most thunderstorms over land have a very marked diurnal cycle, because atmospheric instability is strongly modulated by heating of the ground by the sun. Thunderstorms usually form in mid to late afternoon, are most frequent around sunset, and often dissipate during the night. As sketched in Fig. 14.76, the reason is that the greatest accumulation of heat (and moisture) in the boundary layer occurs not at noon, but about a half hour before sunset.

There are notable exceptions to this daily cycle. For example, thunderstorms can be triggered by the Rocky Mountains in late afternoon, and then propagate eastward all night to hit the Midwest USA with the greatest frequency around midnight to early morning.

Outlooks, Watches & Warnings

A thunderstorm is defined as "**severe**" in the USA if it has one or more of the following:

- tornadoes
- damaging winds (and any winds ≥ 25 m/s)
- hail with diameter ≥ 1.9 cm

Severe weather (thunderstorm caused or not) also includes heavy rain that could cause flash flooding. All thunderstorms have lightning, by definition, so lightning is not included in the list of severe weather elements even though it kills more people than tornadoes, hail, or winds.

In the USA, severe convective weather forecasting is broken into three time spans: outlook, watch, and warning. These are defined as follows:

- **outlook**: 6 to 72 h forecast guidance for broad regions. Types:
  - **convective outlooks**: very technical
  - **public severe weather outlooks**: plain language

- **watch**: 0.5 to 6 h forecast that severe weather is favorable within specific regions called **watch boxes**. Watch types include:
  - **severe thunderstorm watch** (includes tornadoes)
  - **tornado watch**

• **warning:** 0 to 1 h forecast that severe weather is already occurring and heading your way. Warned are specific towns, counties, transportation corridors, and small regions called warning boxes.
Warning types include:
- **severe thunderstorm warning**
- **tornado warning**

Forecast methods for **warnings** are mostly **nowcasts**. Namely, wait until the severe weather is already occurring as observed by human spotters or radar signatures, or find other evidence indicating that severe weather is imminent. Then anticipate its movement in the next few minutes, and warn the towns that are in the path.

These warnings are delivered by activating civil-defense warning sirens and weather-radio alert messages, by notifying the news media, and by talking with local emergency planners, police and fire agencies. Although the warnings are the most useful because of the details about what, where, and when (Fig 14.77), they are also the shortest term forecasts, giving people only a few minutes to seek shelter. The safest tornado and outflow wind shelters are underground in a basement or a ditch, or in a specially designed reinforced-concrete aboveground **safe room**.

Methods for forecasting **watches** are essentially the methods described earlier in this chapter. Namely, short term (0 to 24 h) numerical weather prediction (NWP) model output, soundings from rawinsondes and satellites, and mesoscale analyses of surface weather-station data are analyzed. These analyses focus on the four elements needed for thunderstorm formation later in the day: high humidity in the boundary layer; nonlocal conditional instability; strong wind shear; and a trigger mechanism to cause the initial lifting. The indices and parameters described earlier in this chapter speed the interpretation of the raw data. To handle some of the uncertainty in thunderstorm behavior, probabilistic severe weather forecasts are produced using ensemble methods (see the NWP Chapter).

Nonetheless, watches are somewhat vague, with no ability to indicate which specific towns will be hit and exactly when they will be threatened (the Focus box has an example of a tornado watch and the associated **watch box** graphic). People in the watch area can continue their normal activities, but should listen to weather reports and/or watch the sky in case storms form nearby. Watches also help local officials prepare for events through changes in staffing of emergency-management and rescue organizations (fire departments, ambulance services, hospitals, police), and deploying storm spotters.

FOCUS • A Tornado Watch (WW)

```
Urgent - immediate broadcast requested
   Tornado watch number 387
   NWS Storm Prediction Center, Norman OK
   245 PM CDT Wed May 24 2006

   The NWS Storm Prediction Center has issued
a tornado watch for portions of
          Eastern Iowa
          Central into northeast Illinois
          Far east central Missouri
Effective this Wednesday afternoon and eve-
ning from 245 PM until  1000 PM CDT.

   Tornadoes...Hail to 3 inches in diameter...
Thunderstorm wind gusts to 70 mph...And dan-
gerous lightning are possible in these ar-
eas.

    The tornado watch area is approximately
along and 75 statute miles east and west of a
line from 30 miles east northeast of Dubuque
Iowa to 25 miles southwest of Salem Illinois
[see Fig. below].  For a complete depiction
of the watch see the associated watch outline
update (WOUS64 KWNS WOU7).

   Remember...A tornado watch means conditions
are favorable for tornadoes & severe thunder-
storms in & close to the watch area. Persons
in these areas should be on the lookout for
threatening weather conditions & listen for
later statements and possible warnings.

    Other watch info...Continue...WW 385...WW
386...

   Discussion...50+ knot westerly mid level jet
will spread across far southern Iowa/north-
ern Missouri through the evening and increase
shear atop moderate instability already in
place across WW.  Supercells and organized mul-
ticell clusters/lines are expected to evolve
and shift from west to east through the mid
evening.  Large hail could become quite large
with stronger cores...With additional isolated
tornado threat accompanying more persistent
supercells through the evening.  Wind damage
is also likely.

   Aviation...Tornadoes and a few severe thun-
derstorms with hail surface and aloft to 3
inches. Extreme turbulence and surface wind
gusts to 60 knots. A few cumulonimbi with
maximum tops to 50,000 ft. Mean storm motion
vector from 260° at 25 knots.
```

[Courtesy of the Storm Prediction Center, US National Weather Service, NOAA.]

Figure 14.c *Example of a tornado watch box.*

Table 14-5. Alphabetical listing of some thunderstorm (CB) stability indices, compiled from both this chapter and the next chapter.

Abbr.	Full Name	Use to anticipate
BRN	Bulk Richardson Number	CB type
BRN Shear	Bulk Richardson Number Shear	tornado likelihood
CAPE	Convective Available Potential Energy (SB=surface based; ML = mean layer; MU = most unstable)	CB intensity
CIN	Convective Inhibition	strength of cap
DCAPE	Downdraft CAPE	downburst and gust front intensity
EHI	Energy Helicity Index	supercell intensity tornado intensity
ML LCL	Mean-layer Lifting Condensation Level	moisture availability & CB intensity
S	Swirl Ratio	multi-vortex tornadoes
SCP	Supercell Composite Parameter	supercell & tornado intensity
SHIP	Significant Hail Parameter	large-hail likelihood
SRH	Storm-Relative Helicity	mesocyclone rotation
STP	Significant Tornado Parameter	tornado intensity

Science Graffito

"True genius resides in the capacity for evaluation of uncertain, hazardous, and conflicting information." — Sir Winston Churchill

The **convective outlooks** include a general statement about the level of risk that severe weather will occur in broad regions spanning roughly 350 x 350 km, many hours or days into the future. These risk levels are:

• **Slight** (SLGT): well-organized severe thunderstorms are expected in small numbers and/or low coverage. Specifically: 5 to 29 reports of hail ≥ 2.5 cm, and/or 3 to 5 tornadoes, and/or 5 to 29 wind events.

• **Moderate** (MDT): a greater concentration of severe thunderstorms, and in most situations, greater magnitude of severe weather. Details: ≥ 30 reports of hail ≥ 2.5 cm, or 6 to 19 tornadoes, or numerous wind events (30 that might be associated with a squall line, bow echo or derecho).

• **High** (HIGH): a major severe-weather outbreak is expected, with great coverage of severe weather and enhanced likelihood of extreme weather (i.e., violent tornadoes or extreme convective wind events over a large area). Details: ≥ 20 tornadoes with at least two rated ≥ EF3, or an extreme derecho causing ≥ 50 widespread high wind events with numerous higher winds (≥ 35 m/s) and structural damage reports.

Stability Indices for Thunderstorms

As you have already seen, meteorologists have devised a wide variety of indices and parameters to help forecast thunderstorm existence, strength, and type. Table 14-5 summarizes indices that were discussed in earlier in this chapter as well as indices from the next chapter. Many of these indices integrate over large portions of the environmental sounding or hodograph, and are automatically calculated by computer programs for display next to the computer-plotted sounding.

Because no single index has proved to be the best, new indices are devised, modified, and tested every year. Some day a single best index might be found.

The use of indices to aid severe weather forecasting has a long tradition. Many older indices were devised for calculation by hand, so they use data at a few key altitudes, rather than integrating over the whole sounding. Table 14-6 lists some of the older indices, and Table 14-7 give the associated forecast guidelines.

Table 14-8 compares the values of the different indices with respect to the forecasted weather elements. Beware that this table is highly simplified, and that the boundaries between different severity of storm are not as sharp as the table suggests. Nonetheless, you can use it as a rough guide for interpreting the index values that are often printed with plotted soundings or weather maps.

Table 14-6. Definition of some older thunderstorm stability indices. Notation:
T = environmental temperature (°C);
Td = environmental dew-point temperature (°C);
$Tp_{s->e}$ = final temperature of an air parcel that started with average conditions at height s, and which rose to ending height e following dry adiabat up to LCL, and moist adiabat above. M = wind speed (m/s). α = wind direction (degrees). Subscripts give pressure altitude.

Abbr.	Full Name	Values & Interpretation
K or KI	K Index	$K = T_{85kPa} + Td_{85kPa} + Td_{70kPa} - T_{70kPa} - T_{50kPa}$
LI	Lifted Index	$LI = T_{50kPa} - Tp_{95->50kPa}$
SSI	Showalter Stability Index	$SSI = T_{50kPa} - Tp_{85->50kPa}$
SWEAT	Severe Weather Threat Index	$SWEAT = 12 \cdot Td_{85kPa} + 20 \cdot (TT - 49) + 4 \cdot M_{85kPa} + 2 \cdot M_{50kPa} + 125 \cdot [0.2 + \sin(\alpha_{50kPa} - \alpha_{85kPa})]$ where TT = total totals index. Note: more rules set some terms=0
TT	Total Totals Index	$TT = T_{85kPa} + Td_{85kPa} - 2 \cdot T_{50kPa}$

Table 14-7. Interpretation of older thunderstorm stability indices. Notation: CB = thunderstorms.

Abbr.	Full Name	Values & Interpretation
K or KI	K Index	< 20 CB unlikely 20 to 30 Chance of scattered CB 30 to 40 Many CB; heavy rain > 40 CB; very heavy rain
LI	Lifted Index	> 2 CB unlikely 0 to 2 CB only if strong trigger -3 to 0 Weak CB possible -6 to -3 Moderate CB probable < -6 Severe CB likely
SSI	Showalter Stability Index	> 3 CB unlikely 1 to 3 Weak showers possible -3 to 0 Severe CB possible -6 to -4 Severe CB probable < -6 Severe CB likely
SWEAT	Severe Weather Threat Index	< 300 CB unlikely 300-400 Chance isolated severe CB 400-500 Severe CB likely; & tornado possible 500-800 Severe CB & tornado likely
TT	Total Totals Index	< 45 CB unlikely 45 to 50 Scattered CB possible 50 to 55 CB likely; some severe 55 to 60 Severe CB likely; tornado

Table 14-8. Approximate relationship between storm indices and storm intensity.

	Thunderstorm (CB) & Tornado (EF0 - EF5) Severity						
Index	**No CB**	**Ordinary CB**	**Marginal Supercell**	**Supercell, no tornado**	**Supercell & EF0-EF1**	**Supercell & EF2-EF5**	**Units**
BRN		150	70	30	30	30	
BRN Shear		7	30	45	55	70	m^2/s^2
CAPE (ML)		950	2205	1460	1835	2152	J/kg
CAPE (MU)		1750	1500	1950	2150	2850	J/kg
CIN		18		35	12		J/kg
EHI (ML 0-1km)		0.1	0.5	0.8	1.4	2.1	
K	15	25	35	45			°C
LCL (ML)		1.75	1.47	1.34	1.18	1.00	km
LI	+1.5	–1.5	–4.5	–7.5			°C
SCP		0	1.1	3.5	5.9	11.1	
Shear (0-6km)		8	15	22	23	24	m/s
SRH (0-1km)		20	70	115	155	231	m^2/s^2
SRH-effective		16	60	117	166	239	m^2/s^2
SSI	+4.5	+1.5	–1.5	–4.5	–7.5		°C
STP		0	0	0.4	0.9	2.7	
SWEAT	300	350	400	450	500		
TT	42	47	52	57	62		°C

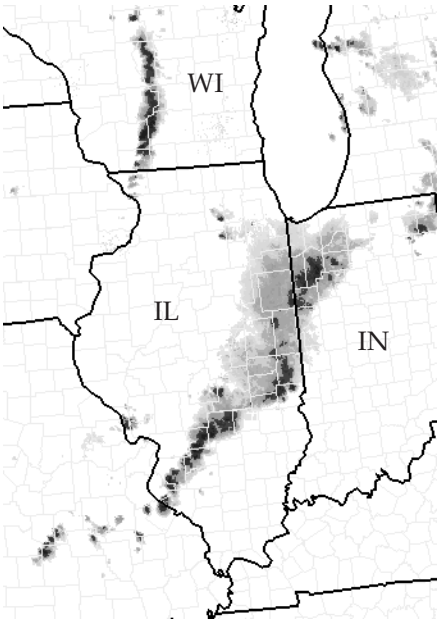

Figure 14.78
Weather radar composite reflectivity image of squall lines in Indiana (IN), Illinois (IL) and Wisconsin (WI), USA, at 2313 UTC on 24 May 2006. Darkest colors correspond to 60 to 65 dBZ reflectivities.

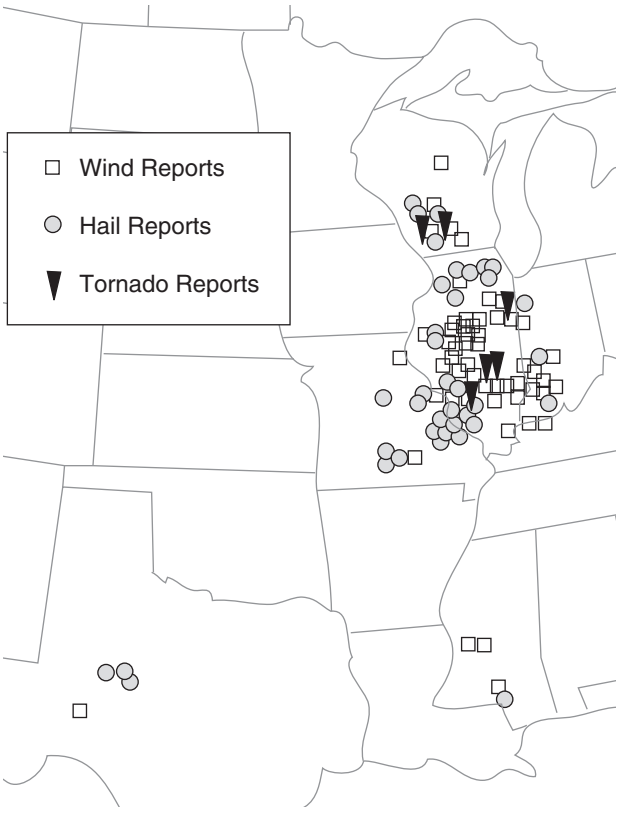

Figure 14.79
All storm reports during 24 May 2006 of damaging wind, hail, and tornadoes in the central USA.

Storm Case Study

Throughout this chapter and the next chapter are examples the weather maps for the severe storm event of 24 May 2006. These maps presented indices and trigger locations that could be used to help forecast severe weather. The weather maps were created by the US National Weather Service and served over the internet in real time on that day, giving up-to-date weather information to meteorologists, public officials, storm chasers, radio and TV stations, and the general public.

On that day, warm humid air from the Gulf of Mexico was streaming northward into the Mississippi Valley, reaching as far north as the Midwest USA. This provided fuel in the boundary layer, ahead of a cold front that was located from Illinois to Texas. An additional trigger was a west-Texas dry line that merged with the cold front. Cold dry air aloft from the west contributed to the instability of the soundings, and wind shear near Illinois enabled supercells to form.

The US Storm Prediction Center anticipated that severe weather would form that afternoon, and issued a series of watches and warnings that successfully covered the severe weather area. Most of the severe weather was expected to occur that day in the Midwest, although there was also a chance of storms in Texas near the dry line.

Fig. 14.78 shows a radar snapshot of the squall line that moved across the Midwest USA at 22 UTC (5 PM local daylight time). Fig. 14.79 shows a map of the resulting **storm reports**, which included:

- 6 tornado reports
- 97 damaging wind reports & 1 wind >32 m/s
- 84 hail reports + 3 reports of hail > 5 cm diam.

A total of 187 reports of severe weather were compiled for this storm case. This was a typical severe weather day.

Now that we are finished with the sections on the formation conditions and characteristics of thunderstorms we will proceed into the next chapter on Thunderstorm Hazards. These include heavy rain, hail, downbursts of wind, gust fronts, lightning, thunder, and tornadoes.

SUMMARY

Thunderstorms (cumulonimbi) are violent convective clouds that fill the depth of the troposphere. Thunderstorms look like mushrooms or anvils. The most violent thunderstorms are called supercells, in which the whole thunderstorm rotates as a

mesocyclone. Other storm organizations include airmass thunderstorms, multicell storms, orographic storms, mesoscale convective systems, squall lines, and bow echoes.

Four conditions are needed to form thunderstorms: high humidity; instability; wind shear, and a trigger to cause lifting. Thermodynamic diagrams and hodographs are used to determine the moisture availability, static stability and shear. A variety of stability and shear indices have been devised to aid thunderstorm forecasting. Trigger mechanisms are often mountains or airmass boundaries such as synoptic fronts, dry lines, sea-breeze fronts, and gust fronts, such as determined from weather radar, satellite, and surface weather analyses.

Thunderstorms are like gigantic engines that convert fuel (moist air) into motion and precipitation via the process of condensation and latent heat release. Once triggered, thunderstorms can often sustain themselves within a favorable environment for 15 minutes to several hours. They are most frequent in the late afternoon and evening over land. The explosive growth of thunderstorms, relatively small diameters, and sensitivity to initial conditions make it difficult to forecast thunderstorms.

Threads

Thunderstorms form in air that has conditionally unstable static stability (Chapter 5), with tops rising to the tropopause (Chapter 1). Solar radiation (Chapter 2) during the day adds heat (Chapter 3) to the boundary layer (Chapter 18), and evaporates water (Chapter 4) from the surface. This warm, humid boundary-layer air serves as the fuel for thunderstorms, which can be triggered by fronts from cyclones (Chapter 13), and by drylines (Chapter 12). Once formed, thunderstorms are steered by mid- and upper-tropospheric winds that make up the jet stream (Chapter 11) in the global circulation.

With fine-enough grid spacing, thunderstorm clouds and winds can be predicted numerically (Chapter 20) by computer. Hurricane (Chapter 16) spiral bands and eye wall consist of lines of thunderstorms. Thunderstorms can transport air pollutants (Chapter 19) vertically from the boundary layer and deposit them higher in the troposphere and lower stratosphere, and thunderstorm rain can scrub out some of the pollutants. Changes in global patterns of aerosol concentrations might alter thunderstorm formation. Climate change (Chapter 21) might alter the atmospheric stability, thereby changing the frequency of thunderstorms.

EXERCISES

Numerical Problems

N1(§). Plot the pressure difference ($\Delta P = P_{MCS} - P_{std.\,atm.}$) vs. height within a mesoscale convective system (MCS), given the temperature differences ($\Delta T = T_{MCS} - T_{std.atm.}$) below. Also plot the given temperature difference vs. height. The surface pressure $P_{MCS\,sfc}$ under the MCS is also given below. For the standard atmosphere (std. atm.), assume the surface pressure is 101.325 kPa. Use a vertical resolution of $\Delta z = 250$ m.

Exercise Part	a.	b.	c.	d.
	ΔT (K)			
$0 \le z < 2$ (km)	–10	–8	–13	–15
$2 \le z < 4$ (km)	0	0	0	0
$4 \le z < 9$ (km)	+6.5	+5	+10	+9
$9 \le z < 11$ (km)	–10	–7.7	–15	–13
$11 \le z \le 12$ (km)	0	0	0	0
$P_{MCS\,sfc}$ (kPa)	101.8	101.7	101.9	102.05

N2. Using your answer for ΔP at 2 km altitude from the previous exercise, calculate the rear-inflow jet (RIJ) speed into the mid-tropospheric meso-low within an MCS. Assume the RIJ is geostrophic, for a latitude of 40°N. Assume the MCS has a horizontal radius (km) of:

a. 80 b. 100 c. 120 d. 140 e. 160
f. 180 g. 200 h. 220 i. 240 j. 260

N3. Given the following sounding. Plot it on a thermo diagram (use a skew-T, unless your instructor specifies a different one). Find the mixed-layer height, tropopause height, lifting condensation level, level of free convection, and equilibrium level, for an air parcel rising from the surface. Use a surface ($P = 100$ kPa) dew-point temperature (°C) of:

a. 22 b. 21 c. 20 d. 19 e. 18 f. 17 g. 16
h. 15 i. 14 j. 13 k. 12 l. 11 m. 10 n. 9
o. 8 p. 7 q. 6 r. 5 s. 4

Sounding:

P (kPa)	T (°C)
20	–45
25	–45
30	–40
40	–30
50	–19
70	+5
80	15
88	21
92	21
98	26
100	30

N4. Using the result from the previous exercise, forecast the intensity (i.e., category) of thunderstorm and possibly tornadoes that are likely, given the lifting condensation level you found.

N5. Find the median and interquartile range for the following data sets:

a. 6 3 9 7 2 1 6 0 8
b. 8 5 9 8 1 1 3 2 6 8 4 9 7 0
c. 3 5 2 7 9 4 7 7
d. 9 6 8 0 9 1 3 2 9 7 8
e. 5 8 2 2 1 6 4 3 7 9
f. 4 5 6 7 8 9 0 1 2 3
g. 1 2 3 4 5 6 7 8 9
h. 9 8 7 6 5 4 3 2 1
i. 0 0 0 0 3 6 8 3 4 8 9 0 6

N6. Find the mean and standard deviation for the data set from the previous exercise.

N7. For the sounding from exercise N3, find the value of surface-based CAPE, using:
(1) the height (z) tiling method.
(2) the pressure (P) tiling method.
Assume $T_v \approx T$. Also, on the plotted sounding, shade or color the CAPE area.

N8. Start with the sounding from exercise N3. Assume that the forecast high temperature for the day is 2°C warmer than the surface temperature from the sounding. Find the value of surface-based CAPE. Assume $T_v \approx T$.

N9. For the sounding from exercise N3, find the value of mean-layer CAPE. Assume $T_v \approx T$. For the air parcel that you conceptually lift, assume its initial temperature equals the average temperature in the bottom 1 km of the sounding, and its initial dew-point is the average dew-point temperature in the bottom 1 km of the sounding (assuming that the mixing ratio is constant with height in this 1 km mixed layer).

N10. Using the result from the previous exercise, forecast the intensity of thunderstorms and possibly tornadoes that are likely, and indicate the uncertainty (i.e., the range of possible storm intensities) in this forecast, given the MLCAPE you found.

N11. Forecast the thunderstorm and/or tornado intensity, and indicate the uncertainty (i.e., the range of possible storm intensities) in this forecast, given a ML CAPE (J/kg) value of:

a. 1000	b. 1250	c. 1500	d. 1750	e. 2000
f. 2250	g. 2500	h. 2750	i. 3000	j. 3250
k. 3500	l. 250	m. 500	n. 750	

N12. Given the sounding from exercise N3, except with a surface temperature of T = 24°C at P = 100 kPa. Assume the surface dew point from exercise N3 defines a mixing ratio that is uniform in the bottom 2 layers of the sounding.

Find the most unstable CAPE considering air parcels that start their rise from just the bottom two levels of the sounding (i.e., for air parcels that start at P = 100 and 98 kPa). Assume $T_v \approx T$.

N13. Using the result from the previous exercise, forecast the intensity (i.e., category) of thunderstorm and possibly tornadoes that are likely, given the MUCAPE you found, and indicate the uncertainty (i.e., the range of possible storm intensities) in this forecast.

N14. Forecast the thunderstorm and/or tornado intensity, and indicate the uncertainty (i.e., the range of possible storm intensities) in this forecast, given a MU CAPE (J/kg) value of:

a. 1000	b. 1250	c. 1500	d. 1750	e. 2000
f. 2250	g. 2500	h. 2750	i. 3000	j. 3250
k. 3500	l. 3750	m. 4000	n. 4250	n. 4500

N15. Using the SBCAPE you found in exercise N7, and the sounding and key altitudes from exercise N3, find the value of normalized CAPE, indicate of the CAPE is tall thin or short wide, and suggest whether thunderstorms would favor heavy precipitation or tornadoes.

N16. Estimate the max likely updraft speed in a thunderstorm, given a SB CAPE (J/kg) value of:

a. 1000	b. 1250	c. 1500	d. 1750	e. 2000
f. 2250	g. 2500	h. 2750	i. 3000	j. 3250
k. 3500	l. 3750	m. 4000	n. 500	n. 750

N17. Given a wind of (U, V) = (10, 5) m/s at z = 1 km. Find the wind difference magnitude, shear direction, and shear magnitude between z = 1 and 2 km, given winds at 2 km of (U, V) (m/s) of:

a. (20, –3)	b. (25, –15)	c. (30, 0)	d. (25, 5)
e. (10, 15)	f. (5, 20)	g. (–15, 15)	h. (–5, 0)
i. (–20, –30)	j. (–5, 8)	k. (–10, –10)	l. (0, 0)

N18. Plot the following wind sounding data on a hodograph. (Make copies of the blank hodograph from Fig. 14.51 to use for all the hodograph exercises.)

Exercise	a	b	c	d
z (km)	In each cell: wind direction (°), speed (m/s)			
0	calm	100, 5	120, 8	150, 10
1	120, 5	120, 10	150, 5	180, 5
2	150, 8	160, 15	210, 5	240, 5
3	180, 12	220, 25	240, 10	260, 10
4	210, 15	240, 30	250, 15	260, 20
5	240, 25	250, 33	258, 25	250, 30
6	260, 40	250, 33	260, 35	240, 40

N19. On your plotted hodograph from the previous exercise, draw wind vectors from the origin to each wind data point. Discuss the relationship between these wind vectors and the original hodograph that connected just the tips of all the vectors.

N20. Using your hodograph plot from exercise N18, use the hodograph (not equations) to find the (U, V) components (m/s) at each altitude in the sounding.

N21. Graphically, using your hodograph plot from exercise N18, plot the local shear vector (m/s) across the z = 2 to 3 km layer.

N22. Same as the previous exercise, except solve for the local shear vector (m/s) mathematically.

N23. Graphically, using your hodograph plot from exercise N18, plot the 0 to 6 km mean shear vector (m/s).

N24. Same as exercise N23, except solve for the 0 to 6 km mean shear vector (m/s) mathematically.

N25. Using your hodograph plot from exercise N18, graphically find the 0 to 6 km total shear magnitude (m/s). Also, predict the likely thunderstorm and possibly tornado intensity based on this parameter, and indicate the uncertainty (i.e., the range of possible storm intensities) in this forecast.

N26(§). Same as the previous exercise, except solve for the 0 to 6 km total shear magnitude (m/s) mathematically. Also, predict the likely thunderstorm and possibly tornado intensity based on this parameter, and indicate the uncertainty (i.e., the range of possible storm intensities) in this forecast.

N27. Predict the thunderstorm and possibly tornado intensity based on the following total shear magnitude (m/s) across the 0 to 6 km layer, and indicate the uncertainty (i.e., the range of possible storm intensities) in this forecast.

a. 4 b. 6 c. 8 d. 10 e. 12 f. 14 g. 16
h. 18 i. 20 j. 22 k. 24 l. 26 m. 28 n. 30

N28. Graphically, using your hodograph plot from exercise N18, find the mean environmental wind direction (°) and speed (m/s), for normal storm motion.

N29(§). Same as the previous exercise, except solve mathematically for the mean environmental wind direction (°) and speed (m/s), for normal storm motion.

N30. Given the hodograph shape from exercise N18, indicate whether right or left-moving supercells would dominate. Also, starting with the "normal storm motion" from exercise N28 (based on hodograph from exercise N18), use the Internal Dynamics method on your hodograph to graphically estimate the movement (i.e., direction and speed) of

(1) Right-moving supercell thunderstorms
(2) Left-moving supercell thunderstorms

N31. Using your result from exercise N28 for normal storm motion (based on exercise N18), and assuming CAPE = 2750 J/kg:

(1) calculate the shear ΔM (m/s) between the mean (0-6 km) environment winds and the average winds at z = 0.5 km.

(2) calculate the bulk Richardson number shear (BRN shear) in m^2/s^2.

(3) calculate the bulk Richardson number (BRN).

(4) forecast the thunderstorm likelihood, thunderstorm type, and tornado intensity.

N32. Given the following value of bulk Richardson number, determine the likely thunderstorm type:

a. 7 b. 12 c. 17 d. 22 e. 27 f. 32 g. 37
h. 42 i. 47 j. 52 k. 57 l. 62 m. 67 n. 72

N33. Given the following value of bulk Richardson number (BRN) shear (m^2/s^2), determine the likely thunderstorm and tornado intensity:

a. 5 b. 10 c. 20 d. 30 e. 40 f. 45 g. 50
h. 55 i. 60 j. 65 k. 70 l. 75 m. 80 n. 90

N34. Given the sounding from exercise N3, calculate the value of the convective inhibition (CIN) in J/kg for an air parcel lifted from the surface. Assume $T_v \approx T$. Also, shade or color the CIN area on the plotted sounding.

N35. Given your answer to the previous exercise, interpret the strength of the cap and how it affects thunderstorm triggering.

N36. Calculate the mean-layer CIN using the sounding from exercise N3. Temperatures in the bottom 10 kPa of atmosphere are as plotted from the sounding, and assume that the mixing ratio is constant over this layer and equal to the mixing ratio that corresponds to the surface dew point.

N37. For the sounding from exercise N3:

(1) To what altitude must a surface air parcel be lifted by an airmass boundary or a mountain, to trigger thunderstorms?

(2) To what temperature must the surface air be heated in order to convectively trigger thunderstorms (i.e., find the convective temperature), and what is the value of the convective condensation level?

N38. What values of K index, Lifted Index, Showalter Stability Index, SWEAT Index, and Total-totals Index would you anticipate for the following intensity of thunderstorm (CB)?

a. no CB
b. ordinary CB
c. marginal supercell
d. supercell with no tornado
e. supercell with EF0 - EF1 tornado
f. supercell with EF2 - EF5 tornado

N39. What value of the Bulk Richardson Number, BRN-Shear, ML CAPE, MU CAPE, CIN, Energy Helicity Index, Lifting Condensation Level, Supercell Composite Parameter, 0-6 km Shear, Storm-Relative Helicity, effective Storm-Relative Helicity, and Significant Tornado Parameter would you anticipate for the following intensity of thunderstorm (CB)?

a. no CB b. ordinary CB
c. marginal supercell
d. supercell with no tornado
e. supercell with EF0 - EF1 tornado
f. supercell with EF2 - EF5 tornado

Understanding & Critical Evaluation

U1. Identify as many thunderstorm features as you can, from the photo below. (Image "wea00106" courtesy of NOAA photo library).

U2. Why does a thunderstorm have a flat (anvil or mushroom) top, instead of a rounded top such as cumulus congestus clouds? (Ignore the overshooting dome for this question.)

U3. Almost all clouds associated with thunderstorms are caused by the lifting of air. List each of these clouds, and give their lifting mechanisms.

U4. Circle the stations in the weather map below that are reporting thunderstorms. (Image courtesy of the Storm Prediction Center, NWS, NOAA.)

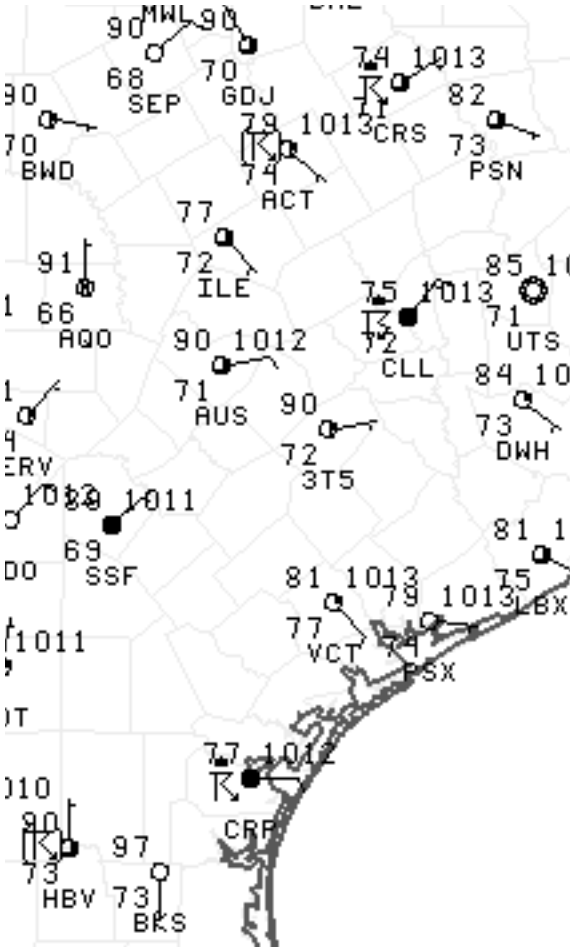

U5. Consider Figs. 14.4a & b. If you were a storm chaser, and were off to the side of the storm as indicated below, sketch which components of the storm and associated clouds would be visible (i.e., could be seen if you had taken a photo). Label the key cloud features in your sketch. Assume you are in the following direction from the storm:

a. northeast b. southwest c. northwest

For example, Fig. 14.4a shows the sketch for the view from southeast of the storm.

U6. Consider Fig. 14.4b. If a Doppler radar were located near the words in that figure given below, then sketch the resulting color patterns on the Doppler PPI wind display for near-surface winds.

a. "FFD" b. "RFD" c. "Anvil Edge" d. "Cu con"
e. "Gust Front" f. "Beaver Tail"
g. "Outflow Boundary Layer Winds"
h. "Inflow Boundary Layer Winds"
i. "Main Updraft" j. "Storm Movement"
k. "Forward Flank Downdraft"

U7. Can a thunderstorm exist without one or more cells? Explain.

U8. For each thunderstorm type or organization, explain which triggered mechanism(s) would have most likely initiated it.

U9. For each thunderstorm type or organization, explain how the phenomenon would differ if there had been no wind shear.

U10. What is a derecho, and what causes it? Also, if strong straight-line winds can cause damage similar to that from a weak tornado, what are all the ways that you could use to determine (after the fact) if a damaged building was caused by a tornado or derecho?

U11. Summarize the different types of supercells, and list their characteristics and differences. Explain what factors cause a supercell to be of a specific type, and where you would most likely find it.

U12. In a thunderstorm, there is often one or more updrafts interspersed with one or more downdrafts. Namely, up- and down-drafts are often adjacent. Do these adjacent up- and down-drafts interfere or support each other? Explain.

U13. List the 4 conditions needed for thunderstorm formation. Then, consider a case where one of the conditions is missing, and explain why thunderstorms would be unlikely, and what would form instead (if anything). Do this for each of the 4 conditions separately.

U14. If thunderstorms normally occur at your town, explain how the 4 conditions needed for thunderstorm formation are satisfied for your region. Namely, where does the humid air usually come from, what conditions contribute to shear, what trigger mechanisms dominate in your region, etc.

U15. If thunderstorms are rare in your region, identify which one or more of the 4 conditions for thunderstorms is NOT satisfied, and also discuss how the other conditions are satisfied for your region.

U16. If the cap inhibits thermals from rising, why is it considered a good thing for thunderstorms?

U17. If your national weather service were to make only one upper-air (rawinsonde) sounding per day, when would you want it to happen, in order to be most useful for your thunderstorm forecasts?

U18. In the section on convective conditions and key altitudes, one thermo diagram was presented with the LCL above z_i (the mixed layer top), while the solved example showed a different situation with the LCL below z_i. Both are frequently observed, and both can be associated with thunderstorms.

Is it possible to have an environment favorable for thunderstorms if:

a. z_i is above the LFC
b. z_i is above the tropopause
c. LCL is at the Earth's surface
d. LFC is at the Earth's surface
e. LCL is above the LFC

U19. The tops of thunderstorms are often near the tropopause.

a. Why is that?
b. Why are thunderstorm tops usually NOT exactly at the tropopause.

U20. Based on tropopause info from earlier chapters, how would you expect thunderstorm depth to vary with:

a. latitude
b. season

U21. Environments favorable for thunderstorms are said to be "unstable" or "convective". Implicit in such a statement is that we are talking about nonlocal instabilities.

For the sounding in Fig. 14.25, use techniques you learned in earlier chapters to determine the layer stability of each of the layers in the environmental sounding. Contrast this with the concept of nonlocal conditional instability, and discuss.

U22. By eye, estimate the temperature and dew point values at each of the data points plotted in Fig. 14.24. Then use this same data to re-plot the sounding on your own:

a. skew-T diagram
b. tephigram
c. Stüve diagram
d. theta-z diagram.
e. emagram

After you have produced this plot, then determine graphically the locations (i.e., pressures) of z_i, LCL, LFC, EL, and the tropopause. Compare these values with the locations from Fig. 14.25, and discuss any differences.

U23. Same as the previous exercise, but for the sounding given in the solved example after Fig. 14.26.

U24. Fig. 14.22 shows schematically the information that is in Fig. 14.25. Explain how these two figures relate to each other.

U25. Consider Fig. 14.22. Why is the following environmental condition conducive to severe thunderstorms?

a. cold air near the top of the troposphere
b. dry air near the middle of the troposphere
c. a stable cap at the top of the boundary layer
d. a warm humid boundary layer
e. wind shear
f. strong winds aloft.

(Hint, consider info from the whole chapter, not just the section on convective conditions.)

U26. Fig. 14.26 shows a nonlocally conditionally unstable environment up to the EL, yet the sounding in the top of that region (i.e., between the tropopause and the EL) is locally statically stable. Explain how that region can be both stable and unstable at the same time.

U27. How much energy does an airmass thunderstorm release (express your answer in units of megatons of TNT equivalent)? Assume all the water vapor condenses. Approximate the cloud by a cylinder of radius 5 km, with base at P = 90 kPa and top at P = 30 kPa. The ABL air has depth 1 km, and dew-point temperature (°C) of:

a. 17 b. 16 c. 15 d. 14 e. 13 f. 12 g. 11
h. 18 i. 19 j. 20 k. 22 l. 23 m. 24 n. 25

U28. Why do thunderstorms have (nearly) flat bases? (Hint, what determines the height of cloud base in a convective cloud?)

U29. Compare the different ways to present information about "high humidity in the boundary layer", such as the different weather maps shown in that section. What are the advantages and disadvantages of each?

Normally, meteorologists need use only one of the humidity metrics to get the info they need on moisture availability. Which one moisture variable would you recommend using, and why?

U30. Look up the definitions of the residual layer and nocturnal stable layer from the atmospheric boundary layer chapter. Consider atmospheric conditions (temperature, humidity) in the residual layer, relative to the conditions in the mixed layer from the afternoon before. Use this information to explain why strong thunderstorms are possible at night, even after the near-surface air temperature has cooled significantly.

U31. Often statistical data is presented on a **box-and-whisker diagram**, such as sketched below.

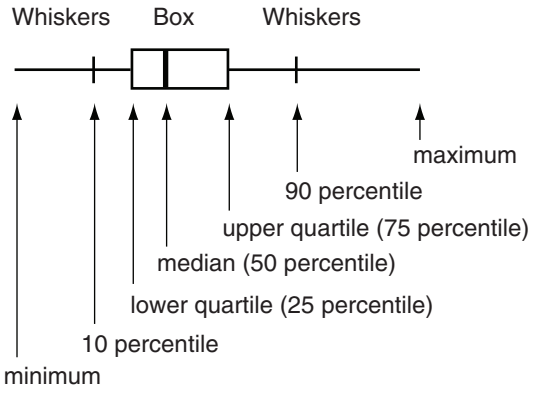

For example, the data such as in Fig. 14.33 is often presented in the journal literature as shown below (where the max and min values are not shown for this illustration, but are often given in the literature).

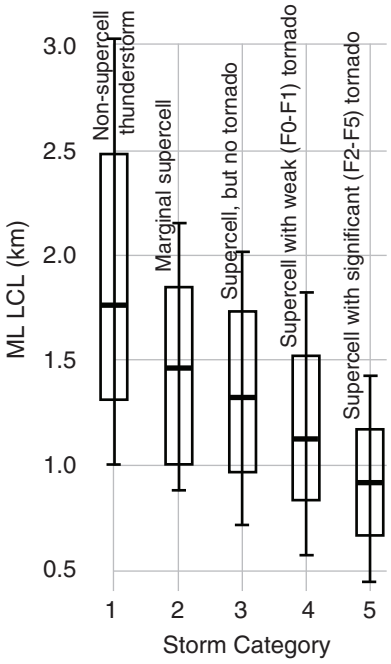

Create box-and-whisker diagrams, using data in this textbook for:

a. ML CAPE

b. MU CAPE
c. TSM
d. BRN Shear
e. 0-1 km SRH
f. 0-1 km EHI

U32. Look at a blank thermo diagram. At colder temperatures, the moist adiabats don't deviate far from the dry adiabats. Use this characteristic to help explain why CAPE is smaller for colder environments, and thus why strong thunderstorms are less likely.

U33. Thunderstorms are much more prevalent in the tropics than near the poles. Use all the info from this chapter to help explain this. Also relate it to info in other chapters, such as: radiation, global circulation, boundary layers etc.

U34. If you were given a file of ASCII text data of temperature and dew point vs. height in a sounding, show schematically (i.e., with a flow chart) a computer program that you could write to compute the CAPE. Don't actually write the program, just show the main steps, procedures, and/or data structures that you would use. (Hint: the method in Fig. 14.35 might be easier than the method in Fig. 14.36, especially for very small Δz.)

a. Do this based on eq. (14.2) [gives an approximate answer]

b. Do this based on eq. (14.1) [this is more accurate]

U35. Describe all the factors in a plotted sounding that could contribute to larger CAPE values.

U36. Compare and contrast the different parcel-origin methods for computing CAPE (SB, forecast SB, ML, and MU). Recommend which methods would be best for different situations.

U37. Derive eq. (14.5) from eq. (14.4) by using the hypsometric equation. Show your steps.

U38. Critically analyze eq. (14.6). Discuss the behavior of the equation as the height difference between the LFC and EL approaches zero.

U39. a. Can thunderstorms fully utilize all the CAPE?

b. What are limitations on use of the CAPE equations?

c. Why might vertical velocity in thunderstorms be not as great as that given by eq. (14.8)?

U40. a. Is wind shear a vector or scalar quantity? Why?

b. Is it possible to have non-zero shear between two altitudes where the winds have the same speed? Explain.

U41. Suppose that Fig. 14.47 gives the winds relative to the ground. Redraw that figure showing the storm-relative winds instead. Also, explain why storm-relative winds are important for thunderstorm dynamics.

U42. On a hodograph, why is it important to list the altitude of the winds next to each wind data point?

U43. Draw a hodograph showing an environment where winds ____ with height. a. veer b. back

U44. On blank hodographs such as Fig. 14.51, why are the printed wind directions 180° out of phase with the normal compass directions?

U45. In Fig. 14.52, notice that the dark vertical and horizontal lines don't look straight. This is an optical illusion caused by the background circles of the hodograph. In fact, they are straight, as you can see by tilting the page so you are looking almost edge-on, sighting down each line. Based in this info, discuss why you should never draw the vertical or horizontal lines by eye, when trying to determine *U* and *V* components of wind.

U46. Three different types (i.e., ways of measuring) of shear vectors are shown in Fig. 14.53. Explain and contrast them.

U47. Create a table listing all the different types of shear that are discussed in this chapter, and add a column to the table that indicates what thunderstorm characteristics can be estimated from each shear type.

U48. A thunderstorm index or parameter is useful only if it can discriminate between different storm types or intensities. Using Fig. 14.56, critically evaluate the utility of TSM in estimating storm and tornado intensity.

U49. Explain the difference between the mean shear vector (as in Fig. 14.53) and the mean wind vector (as in Fig. 14.58), and discuss their significance.

U50. In Fig. 14.59, the mean wind is estimated as the center of mass of the shaded area. Is the actual mean wind exactly at the center of mass of the shaded area, or only close? [Hint, to help think about this

question, create some very simple hodographs with simple shapes for the shaded area [such as a rectangle] for which you can calculate the exact center of mass. Then see if you can extend your argument to more complex, or arbitrary shapes. This scientific approach is called inductive reasoning (see p107).]

U51. Using information from Fig. 14.61, identify where in Fig. 14.60 are the right and left moving mesocyclones.

U52. Although Fig. 14.62c shows a hodograph that is concave up, the whole curve is above the origin. Suppose that, on a different day, the hodograph has the same shape, but is shifted to be all below the origin. Assume N. Hemisphere, mid-latitudes.

Would such a hodograph still favor left-moving supercell storms? Justify your answer.

U53. Both the bulk Richardson number (BRN) and the Supercell Composite Parameter (SCP) include CAPE and shear. However, BRN is CAPE/shear, while SCP is CAPE·shear (times a third factor that we can ignore for this discussion). Which (BRN or SCP) would you anticipate to give the best storm intensity forecasts, and which is most physically justified? Explain.

U54. Figs. 14.67 - 14.69 show 3 different ways to calculate CIN. Discuss the advantages and disadvantages of each, and for which conditions each method is most appropriate.

U55. Table 14-4 relates CIN to the difficulty in triggering thunderstorms. For the "strong" and "intense" cap categories, can you think of a trigger mechanism that would be powerful enough to trigger thunderstorms? Explain.

U56. Figs. 14.71 and 14.73 show how thunderstorms can be triggered by warm, humid air forced to rise over an obstacle (cold air, or a mountain). In both situations, sometimes after the thunderstorms are triggered and develop to maturity, environmental wind shear causes them to move away from the triggering location. After they have moved away, what is needed in order for the supercell thunderstorm to continue to exist (i.e., not to die immediately after moving away from the triggering area)? Do you think this is possible in real life, and if so, can you give an example?

U57. Consider Fig. 14.74. The "Local Wind" chapter states that buoyancy (gravity) waves need statically stable air to exist without damping. But thunderstorms need nonlocally conditionally unstable air to exist. These seems contradictory. Explain how it might be possible.

U58. Fig. 14.75 shows a way to estimate T_{needed} for convection, given T and T_d from a sounding earlier in the day. Although this is an easy method, it has a major flaw. Critically discuss this method. (Hint: what was assumed in order to use this method?)

U59. Step back from the details of thunderstorms, and look at the big picture. After the thunderstorm has occurred, some precipitation has fallen out, and there has been net heating of the air. Explain how these two processes affect the overall stability and entropy (in the sense of randomness) in the troposphere.

U60. Re-draw Fig. 14.76, but for a winter case over mid-latitude land where nocturnal cooling is longer duration than daytime heating, and for which the total accumulated heating during the day (because the sun is lower in the sky) is less than the accumulated cooling at night. Use you resulting figure to discuss the likelihood of thunderstorms in winter.

U61. Recall from other chapters that the ocean has a much large heat capacity than land, and thus has less temperature change during day and night. Redraw Fig. 14.76 for a location at a tropical ocean, and discuss how the resulting figure relates to thunderstorm occurrence there.

U62. Some of the older stability indices in Table 14-6 are very similar in basis to some of the newer indices in Table 14-5, as described throughout this chapter. The main differences are often that the old indices consider meteorological conditions at just a few levels, whereas the newer indices integrate (sum) over many levels. Create a table matching as many old indices to as many new indices as possible.

U63. Based on what you learned so far, which subsets of indices from Table 14-8 would you prefer to utilize in your own storm forecasting efforts, to forecast:

a. hail
b. heavy rain
c. lots of lightning
d. tornadoes
e. strong straight-line winds
f. downbursts

Justify your choices.

Web-Enhanced Questions

W1. Search the web for (and print the best examples of) photographs of:
- a. airmass thunderstorms
- b. multicell thunderstorms
- c. orographic thunderstorms
- d. squall-line thunderstorms
- e. supercell thunderstorms
  - (i) classic
  - (ii) low precipitation
  - (iii) high precipitation
- f. mammatus clouds
- g. wall clouds
- h. beaver tail clouds
- i. flanking lines
- j. tail cloud

(Hint: search on "storm stock images photographs".) Discuss the features of your resulting image(s) with respect to information you learned in this chapter.

W2. Search the web for (and print the best examples of) radar reflectivity images of
- a. airmass thunderstorms
- b. multicell thunderstorms
- c. squall line thunderstorms
- d. mesoscale convective systems
- e. bow echoes

Discuss the features of your resulting image(s) with respect to information you learned in this chapter.

W3. Same as the previous question, but for radar Doppler velocity images.

W4. Search the web for (and print the best examples of) satellite images of:
- a. airmass thunderstorms
- b. multicell thunderstorms
- c. squall line thunderstorms
- d. mesoscale convective systems
- e. dry lines

Do this for visible, IR, and water vapor channels. Discuss the features of your resulting image(s) with respect to information you learned in this chapter.

W5. Search the web for plotted soundings. In particular, find web sites that also list the values of key stability indices and key altitudes along with the sounding. From this site, get a sounding for a location in the pre-storm environment toward which thunderstorms are moving. Print the sounding and the stability indices, and use the sounding and indices to discuss the likelihood and severity of thunderstorms. (Hint: To find a region where thunderstorms are likely, first search the web for a weather radar image showing where the thunderstorms are. Alternately, find via web search the regions where the weather service has issued thunderstorm watches.)

W6. Search the web for plotted hodographs. (Hint: Some sites plot hodographs along with plotted soundings, while others have separate hodograph plots.) Find a web site that also shows key wind-shear parameters associated with the hodograph, and perhaps also gives expected storm motion and/or storm-relative winds. Do this for a location into which thunderstorms are moving (see hint from previous exercise). Print and discuss the results.

W7. Search the web for (and print the best examples of) real-time weather-map analyses or forecasts (from numerical models) showing plotted fields of the four conditions needed for convective storm formation. (Hint, you might find these 4 conditions on 4 separate maps, so you should print and discuss all 4 maps.) Discuss.

W8. Search the web for maps showing real-time thunderstorm and tornado watches. Print and discuss the results. If you also did the previous exercise, then discuss the amount of agreement of the watch areas with the regions that satisfy the conditions for thunderstorms.

W9. Search the web for tutorials on thunderstorms. (Hints: some elementary tutorials are at the "university of Illinois online meteorology guide" site. More advanced tutorials are at the "ucar meted" site. Much miscellaneous info is at the "wikipedia" site.) After reading the tutorial, print and discuss one new aspect of thunderstorms that wasn't in this textbook, but which you find interesting and/or important.

W10. Search the web for newer thunderstorm indices that are not already discussed in this chapter. Summarize and print key information (e.g., definitions for, equations governing, advantages compared to older indices) for one of these new indices, and if possible show a real-time map of the values of this index.

W11. Search the web for a recent sounding close to your present location. Get and print this sounding data in text form. Then manually plot the temperatures and dew points on a thermo diagram, and plot the winds on a hodograph. Manually calculate a few key thunderstorm indices, and make your own forecast about whether thunderstorms are likely.

W12. Same as the previous exercise, but for a sounding just ahead of a severe thunderstorm location.

W13. Search the web for a "storm spotter glossary", and list 10 new thunderstorm-related terms and their definitions that were not discussed in this chapter, but which you feel are important. Justify your choice of terms.

W14. Search the web for (and print the best example of) new research that is being done on thunderstorms or any of the topics discussed in this chapter.

W15. Search the web for (and print and discuss) 4 components that storm spotters look for, to gauge the type of thunderstorm and its development.

W16. Search the web for explanations of the difference between "storm chasers" and "storm spotters".

W17. Search the web to find which agency or agencies within your own country are responsible for making the national forecasts of severe thunderstorms. Print their web address, along with basic information about their mission and location. Also, find and print a list of qualifications they want in new meteorologists that they hire.

W18. From what web site can you get current weather watches and warnings for thunderstorms and tornadoes, for:

a. USA b. Canada c. Europe
d. Japan e. China f. Australia
g. Other country specified by your instructor?

Synthesis Questions

S1. Suppose that thunderstorms were typically 30 km deep. How would the weather and general circulation differ, if at all?

S2. If there were no thunderstorms on Earth, how would the global circulation be different, if at all?

S3. Draw a supercell diagram similar to Fig. 14.4b, but for mid-latitudes in the southern hemisphere.

S4. Why do thunderstorms have flat, anvil-shaped tops, while cumulus congestus do not? Both reach their equilibrium level.

S5. Suppose that N. Hemisphere mid-latitude thunderstorms exist in an environment that usually has the same lower-tropospheric geographic arrangement of heat and humidity relative to the storm as our real atmosphere, but for which the winds aloft are from the east. How would thunderstorms differ, if at all?

S6. Suppose that thunderstorms never move relative to the ground. Could long-lasting supercells form and exist? Explain.

S7. In multicell storms, new cells usually form on the south side of the storm complex, closest to the supply of warm humid boundary-layer air. What changes in the environment or the thunderstorm might allow new cells to form on the north side of the storm? Assume N. Hemisphere.

S8. If orographic thunderstorms need the mountain-triggered lifting to be initiated, why can the storms persist after being blown away from the mountain?

S9. What if there were no mountain ranges on Earth. How would thunderstorm frequency, location, and characteristics be different, if at all? How would it change the local weather at your location, if at all?

S10. Suppose a 100 km diameter circular region of warm humid boundary layer air existed, surrounding by much colder air. If the cold air all around the circle started advancing toward the center of the circle and thunderstorms were triggered along this circular cold front, then describe the evolution of the thunderstorms.

S11. In Fig. 14.14 showing a vertical slice through a mesoscale convective system, the arrows show winds being drawn in toward low pressure in the mid troposphere, and other arrows blowing outward from high-pressure in the upper troposphere. Explain how this could happen, because normally we would expect winds to circulate around highs and lows due to Coriolis force, and not to converge or diverge (assuming no frictional drag because we are not in the boundary layer).

S12. Could a classic supercell change into a low-precipitation or a high-precipitation supercell? Explain what factors might cause this, and how the storm would evolve.

S13. Suppose there was never a cap on the atmospheric boundary layer. Explain how thunderstorms would differ from those in our real atmosphere, if at all.

S14. Start with the sounding in Fig. 14.24. Modify the dew point in the mid troposphere to create a new sounding that would support a layer of altocumulus castellanus (accus) clouds.

S15. Suppose that thunderstorm downdrafts could never penetrate downward through the cap at the

top of the boundary layer. Explain how thunderstorms would differ, if at all?

S16. Suppose that shading of the ground by clouds would cause the Earth's surface to get warmer, not cooler during daytime. How would thunderstorms and climate differ, if at all?

S17. Suppose the atmospheric sounding over your town showed conditions nearly, but not quite, favorable for the existence of thunderstorms. If you could cause the surface energy balance over land to be partitioned differently between sensible and latent heat, how would you partition it in order to generate a thunderstorm? Note that given a fixed input of energy from the sun, increasing either the temperature or the humidity would decrease the other variable.

S18. Suppose that latent heat of condensation cools the air instead of warms it. What would be the characteristics of thunderstorms?

S19. In the discussion of rising air parcels in a nonlocally conditionally unstable environment, we assumed that the surrounding environment was not changing. But if there are many air parcels rising in a thunderstorm updraft, then there must be compensating subsidence in the environment that advects downward the temperature and moisture layers. How would this alter our description of the evolution of thunderstorms?

S20. Under what conditions would the median of a distribution exactly equal the mean? Under what conditions would half the interquartile range exactly equal the standard deviation?

S21. Consider Fig. 14.34. Suppose that when the air parcel is above its LFC, that it entrains environmental air at such a high rate that the air parcel follows a thermodynamic path that is exactly half way between the environment and the moist adiabats that passes through it at each height during its rise. Sketch the resulting path on a copy of Fig. 14.34, and discuss how thunderstorms would differ, if at all.

S22. Consider Fig. 14.34. Suppose that there is no frictional drag affecting the rising air parcel. All of the CAPE would lead to kinetic energy of the updraft. Once the air parcel reaches its EL, inertia would cause it to continue to rise (i.e., overshoot) until its negative potential energy (by being colder than the environment) balanced the initial kinetic energy. Assuming an isothermal sounding above the tropopause in that figure, determine exactly how high the overshooting air parcel would rise. Also, discuss whether such behavior is likely in real thunderstorms.

S23. Suppose that no wind shear existed in the environment. How would thunderstorms differ, if at all?

S24. Suppose that the wind profile of Fig. 14.53 (based on the wind data tabulated in a solved example a couple pages earlier) corresponded to the same environment as the thermodynamic sounding data in Fig. 14.24. Draw "phase-space" plots as follows:

a. T vs. U b. T vs. V c. T vs. M
d. T_d vs. U e. T_d vs. V f. T_d vs. M
g. T vs. T_d

(Hint: "phase-space" plots are explained in the Numerical Weather Prediction chapter as a way to help analyze the chaos of nonlinear-dynamics systems.)

Also, speculate on whether phase-diagram plots of real thunderstorm environments could be used to help forecast different types of thunderstorms.

S25. Suppose that moist adiabats curve concave upward instead of concave downward. How would thunderstorms be different, if at all?

S26. Suppose that the hodograph of Fig. 14.62b were everywhere below the origin of the hodograph. How would thunderstorms differ, if at all?

S27. Suppose that right-moving supercells altered the environment so that it favored left-moving supercells, and left-moving supercells altered the environment to favor right movers. How would thunderstorms differ, if at all?

S28. Suggest 3 or more thunderstorm trigger mechanisms beyond what was already discussed in this chapter.

S29. Suppose that the "cold cloud" process for creating large cloud hydrometeors did not exist. Would thunderstorms exist? If so, what would be their characteristics?

S30. Suppose that accurate thunderstorm (including hail, lightning, and tornado) warnings could be issued 2 days in advance. How would society and commerce change, if at all.

Copyright © 2011, 2015 by Roland Stull. *Meteorology for Scientists and Engineers, 3rd Ed.*

THUNDERSTORM HAZARDS

CONTENTS

Precipitation and Hail 545
- Heavy Rain 545
- Hail 548

Downbursts and Gust Fronts 554
- Characteristics 554
- Precipitation Drag 555
- Evaporative Cooling 556
- Downdraft CAPE (DCAPE) 557
- Pressure Perturbation 559
- Outflow Winds & Gust Fronts 560

Lightning And Thunder 563
- Origin of Electric Charge 564
- Lightning Behavior & Appearance 566
- Lightning Detection 568
- Lightning Hazards and Safety 569
- Thunder 571
  - Shock Front 571
  - Sound 575

Tornadoes 577
- Tangential Velocity & Tornado Intensity 577
- Types of Tornadoes & Other Vortices 582
- Evolution as Observed by Eye 583
- Tornado Outbreaks 583
- Storm-relative Winds 584
- Origin of Tornadic Rotation 586
- Mesocyclones and Helicity 587
- Tornadoes and Swirl Ratio 592

Summary 593
- Threads 593

Exercises 594
- Numerical Problems 594
- Understanding & Critical Evaluation 597
- Web-Enhanced Questions 600
- Synthesis Questions 601

15 The basics of thunderstorms were covered in the previous chapter. Here we cover the dangerous aspects of thunderstorms, including:

- hail and intense precipitation,
- downbursts and gust fronts,
- lightning and thunder, and
- mesocyclones and tornadoes.

Two other hazards were covered in the previous chapter: vigorous updrafts and turbulence.

In spite of their danger, thunderstorms can also produce the large-diameter rain drops that enable beautiful rainbows (Fig. 15.1).

PRECIPITATION AND HAIL

Heavy Rain

Thunderstorms are deep clouds that can create:

- **large raindrops** (2 - 8 mm diameter), in
- **scattered showers** (order of 5 to 10 km diameter rain shafts moving across the ground, resulting in brief-duration rain [1 - 20 min] over any point), of
- **heavy rainfall rate** (10 to over 1000 mm/h rainfall rates).

The Precipitation chapter lists world-record rainfall rates, some of which were caused by thunderstorms.

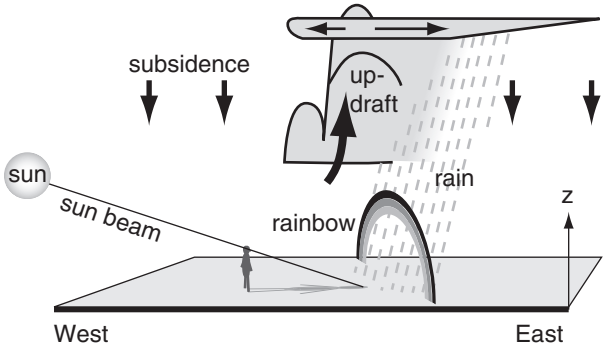

Figure 15.1
Rainbow under an evening thunderstorm. Updraft in the thunderstorm is compensated by weak subsidence around it to conserve air mass, causing somewhat clear skies that allow rays of sunlight to strike the falling large raindrops.

"Meteorology for Scientists and Engineers, 3rd Edition" by Roland Stull is licensed under a Creative Commons Attribution-NonCommercial-ShareAlike 4.0 International License. To view a copy of the license, visit http://creativecommons.org/licenses/by-nc-sa/4.0/ . This work is available at http://www.eos.ubc.ca/books/Practical_Meteorology/ .

Compare this to nimbostratus clouds, that create smaller-size **drizzle drops** (0.2 - 0.5 mm) and **small rain drops** (0.5 - 2 mm diameter) in widespread regions (namely, regions hundreds by thousands of kilometers in size, ahead of warm and occluded fronts) of light to moderate rainfall rate that can last for many hours over any point on the ground.

Why do thunderstorms have large-size drops? Thunderstorms are so tall that their tops are in very cold air in the upper troposphere, allowing cold-cloud microphysics even in mid summer. Once a spectrum of different hydrometeor sizes exists, the heavier ice particles fall faster than the smaller ones and collide with them. If the heavier ice particles are falling through regions of supercooled liquid cloud droplets, they can grow by **riming** (as the liquid water instantly freezes on contact to the outside of ice crystals) to form dense, conical-shaped **snow pellets** called **graupel** (< 5 mm diameter). Alternately, if smaller ice crystals fall below the 0°C level, their outer surface partially melts, causing them to stick to other partially-melted ice crystals and grow into miniature fluffy snowballs by a process called **aggregation** to sizes as large as 1 cm in diameter.

The snow aggregates and graupel can reach the ground still frozen or partially frozen, even in summer. This occurs if they are protected within the cool, saturated downdraft of air descending from thunderstorms (downbursts will be discussed later). At other times, these large ice particles falling through the warmer boundary layer will melt completely into large raindrops just before reaching the ground. These rain drops can make a big splat on your car windshield or in puddles on the ground.

Why scattered showers in thunderstorm? Often large-size, cloud-free, rain-free subsidence regions form around and adjacent to thunderstorms due to air-mass continuity. Namely, more air mass is pumped into the upper troposphere by thunderstorm updrafts than can be removed by in-storm precipitation-laden downdrafts. Much of the remaining excess air descends more gently outside the storm. This subsidence (Fig. 15.1) tends to suppress other incipient thunderstorms, resulting in the original cumulonimbus clouds that are either isolated (surrounded by relatively cloud-free air), or are in a thunderstorm line with subsidence ahead and behind the line.

Why do thunderstorms often have heavy rainfall?

• First, the upper portions of the cumulonimbus cloud is so high that the rising air parcels become so cold (due to the moist-adiabatic cooling rate) that virtually all of the water vapor carried by the air is forced to condense, deposit, or freeze out.

• Second, the vertical stacking of the deep cloud allows precipitation forming in the top of the storm to grow by collision and coalescence or accretion as it falls through the middle and lower parts of the cloud, as already mentioned, thus sweeping out a lot of water in a short time.

• Third, long lasting storms such as supercells or orographic storms can have continual inflow of humid boundary-layer air to add moisture as fast as it rains out, thereby allowing the heavy rainfall to persist. As was discussed in the previous chapter, the heaviest precipitation often falls closest to the main updraft in supercells (see Fig. 15.5).

Rainbows are a by-product of having large numbers of large-diameter drops in a localized region surrounded by clear air (Fig. 15.1). Because thunderstorms are more likely to form in late afternoon and early evening when the sun angle is relatively low in the western sky, the sunlight can shine under cloud base and reach the falling raindrops. In North America, where thunderstorms generally move from the southwest toward the northeast, this means that rainbows are generally visible just after the thundershowers have past, so you can find the rainbow looking toward the east (i.e., look toward your shadow). Rainbow optics are explained in more detail in the last chapter.

Any rain that reached the ground is from water vapor that condensed and did not re-evaporate. Thus, rainfall rate (RR) can be a surrogate measure of the rate of latent-heat release:

$$H_{RR} = \rho_L \cdot L_v \cdot RR \qquad (15.1)$$

where H_{RR} = rate of energy release in the storm over unit area of the Earth's surface ($J \cdot s^{-1} \cdot m^{-2}$), ρ_L is the density of pure liquid water, L_v is the latent heat of vaporization (assuming for simplicity all the precipitation falls out in liquid form), and RR = rainfall rate. Ignoring variations in the values of water density and latent heat of vaporization, this equation reduces to:

$$H_{RR} = a \cdot RR \qquad \bullet(15.2)$$

where $a = 694$ ($J \cdot s^{-1} \cdot m^{-2}$) / ($mm \cdot h^{-1}$) , for rainfall rates in mm/h.

The corresponding warming rate averaged over the tropospheric depth (assuming the thunderstorm fills the troposphere) was shown in the Heat chapter to be:

$$\Delta T/\Delta t = b \cdot RR \qquad (15.3)$$

where $b = 0.33$ K/(mm of rain).

From the Moisture chapter recall that **precipitable water**, d_w, is the depth of water in a rain gauge

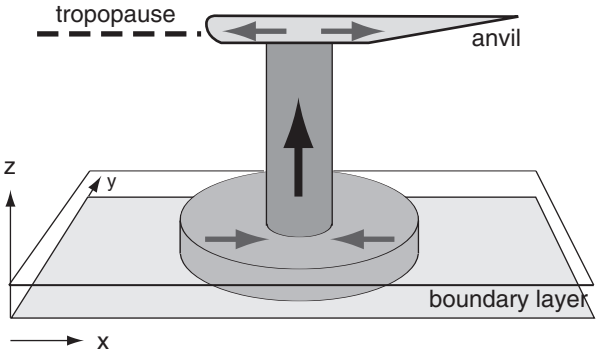

Figure 15.2
The thunderstorm updraft draws in a larger area of warm, humid boundary-layer air, which is fuel for the storm.

if all of the moisture in a column of air were to precipitate out. As an extension of this concept, suppose that pre-storm boundary-layer air of mixing ratio 20 g/kg was drawn up into a column filling the troposphere by the action of convective updrafts (Fig. 15.2). If cloud base was at a pressure altitude of 90 kPa and cloud top was at 30 kPa, and if **half** of the water in the cloudy domain were to condense and precipitate out, then eq. (4.33) says that the depth of water in a rain gauge is expected to be $d_w = 61$ mm.

The ratio of amount of rain falling out of a thunderstorm to the inflow of water vapor is called **precipitation efficiency**, and ranges from 5 to 25% for storms in an environment with strong wind shear to 80 to 100% in weakly-sheared environments. Most thunderstorms average 50% efficiency. Processes that account for the non-precipitating water include anvil outflow of ice crystals that evaporate, evaporation of hydrometeors with entrained air from outside the storm, and evaporation of some of the precipitation before reaching the ground (i.e., **virga**).

Extreme precipitation that produce rainfall rates over 100 mm/h are unofficially called **cloudbursts**. A few cloudbursts or **rain gushes** have been observed with rainfall rates of 1000 mm/h, but they usually last for only a few minutes. As for other natural disasters, the more intense rainfall events occur less frequently, and have **return periods** (average time between occurrence) of order hundreds of years (see the Rainfall Rates subsection in the Precipitation chapter).

For example, a stationary **orographic thunderstorm** over the eastern Rocky Mountains in Colorado produced an average rainfall rate of 76 mm/h for 4 hours during 31 July 1976 over an area of about 11 x 11 km. A total of about 305 mm of rain fell into the catchment of the Big Thompson River, produc-

Solved Example

A thunderstorm near Holt, Missouri, dropped 305 mm of rain during 0.7 hour. How much net latent heat energy was released into the atmosphere over each square meter of Earth's surface, and how much did it warm the air in the troposphere?

Solution

Given: $RR = 305$ mm / 0.7 h = 436 mm/h.
Duration $\Delta t = 0.7$ h.
Find: $H_{RR} \cdot \Delta t$ = ? (J·m^{-2}) ; ΔT = ? (°C)

First, use eq. (15.2):
H_{RR} = [694 (J·s^{-1}·m^{-2})/(mm·h^{-1})]·[436 mm/h]·[0.7 h]·[3600s/h] = **762.5** MJ·m^{-2}

Next, use eq. (15.3):
$\Delta T = b \cdot RR \cdot \Delta t$ = (0.33 K/mm)·(305 mm)
= **101 °C**

Check: Units OK, but values seem too large???
Discussion: After the thunderstorm has finished raining itself out and dissipating, why don't we observe air that is 101°C warmer where the storm used to be? One reason is that in order to get 305 mm of rain out of the storm, there had to be a continual inflow of humid air bringing in moisture. This same air then carries away the heat as the air is exhausted out of the anvil of the storm.

Thus, the warming is spread over a much larger volume of air than just the air column containing the thunderstorm. Using the factor of 5 number as estimated by the needed moisture supply, we get a much more reasonable estimate of (101°C)/5 ≈ 20°C of warming. This is still a bit too large, because we have neglected the mixing of the updraft air with additional environmental air as part of the cloud dynamics, and have neglected heat losses by radiation to space. Also, the Holt storm, like the Big Thompson Canyon storm, were extreme events — many thunderstorms are smaller or shorter lived.

The net result of the latent heating is that the upper troposphere (anvil level) has warmed because of the storm, while the lower troposphere has cooled as a result of the rain-induced cold-air downburst. Namely, the thunderstorm did its job of removing static instability from the atmosphere, and leaving the atmosphere in a more stable state. This is a third reason why the first thunderstorms reduce the likelihood of subsequent storms.

In summary, the **three reasons why a thunderstorm suppresses neighboring storms** are: (1) the surrounding environment becomes stabilized (smaller CAPE, larger CIN), (2) sources of nearby boundary-layer fuel are exhausted, and (3) subsidence around the storm suppresses other incipient storm updrafts. But don't forget about other thunderstorm processes such as the gust front that tend to trigger new storms. Thus, competing processes work in thunderstorms, making them difficult to forecast.

© Gene Moore / chaseday.com

Figure 15.3
Large hailstones and damage to car windshield.

ing a flash flood that killed 139 people in the **Big Thompson Canyon**. This amount of rain is equivalent to a tropospheric warming rate of 25°C/h, causing a total latent heat release of about 9.1×10^{16} J. This **thunderstorm energy** (based only on latent heat release) was equivalent to the energy from 23 one-megaton nuclear bomb explosions (given about 4×10^{15} J of heat per **one-megaton nuclear bomb**).

This amount of rain was possible for two reasons: (1) the continual inflow of humid air from the boundary layer into a well-organized (long lasting) orographic thunderstorm (Fig 14.11), and (2) the weakly sheared environment allowed a precipitation efficiency of about 85%. Comparing 305 mm observed with 61 mm expected from a single troposphere-tall column of humid air, we conclude that the equivalent of about 5 troposphere-thick columns of thunderstorm air were consumed by the storm.

Since the thunderstorm is about 6 times as tall as the boundary layer is thick (in pressure coordinates, Fig. 15.2), conservation of air mass suggests that the Big Thompson Canyon storm drew boundary-layer air from an area about 5·6 = 30 times the cross-sectional area of the storm updraft (or 12 times the updraft radius). Namely, a thunderstorm updraft core of 5 km radius would ingest the fuel supply of boundary-layer air from within a radius of 60 km. This is a second reason why subsequent storms are less likely in the neighborhood of the first thunderstorm. Namely, the "fuel tank" is empty after the first thunderstorm, until the fuel supply can be regenerated locally via solar heating and evaporation of surface water, or until fresh fuel of warm humid air is blown in by the wind.

Hail

Hailstones are irregularly shaped balls of ice larger than 0.5 cm diameter that fall from severe thunderstorms. The event or process of hailstones falling out of the sky is called **hail**. The damage path on the ground due to a moving hail storm is called a **hail swath**.

Most hailstones are in the 0.5 to 1.5 cm diameter range, with about 25% of the stones greater than 1.5 cm. While rare, hailstones are called **giant hail** (or **large** or **severe hail**) if their diameters are between 1.9 and 5 cm. Hailstones with diameters ≥ 5 cm are called **significant hail** or **enormous hail** (Fig. 15.3) One stone of diameter 17.8 cm was found in Nebraska, USA, in June 2003.

Hailstone diameters are sometimes compared to standard size balls (ping-pong ball = 4 cm; tennis ball ≈ 6.5 cm). They are also compared to nonstandard sizes of fruit, nuts, and vegetables. One such classification is the TORRO Hailstone Diameter relationship (Table 15-1).

Table 15-1. TORRO Hailstone Size Classification.

Size Code	Max. Diameter (cm)	Description
0	0.5 - 0.9	Pea
1	1.0 - 1.5	Mothball
2	1.6 - 2.0	Marble, grape
3	2.1 - 3.0	Walnut
4	3.1 - 4.0	Pigeon egg to golf ball
5	4.1 - 5.0	Pullet egg
6	5.1 - 6.0	Hen egg
7	6.1 - 7.5	Tennis ball to cricket ball
8	7.6 - 9.0	Large orange to soft ball
9	9.1 - 10.0	Grapefruit
10	> 10.0	Melon

Hail Damage

Large diameter hailstones can cause severe damage to crops, tree foliage, cars, aircraft, and sometimes buildings (roofs and windows). Damage is often greater if strong winds cause the hailstones to move horizontally as they fall. Most humans are smart enough not to be outside during a hail storm, so deaths due to hail in North America are rare, but animals can be killed. Indoors is the safest place for people to be in a hail storm, although inside a metal-roofed vehicle is also relatively safe (but stay away from the front and rear windows, which can break).

The terminal fall velocity of hail increases with hailstone size, and can reach magnitudes greater than 50 m/s for large hailstones. An equation for hailstone terminal velocity was given in the Precipitation chapter, and a graph of it is shown here in Fig. 15.4. Hailstones have different shapes (smooth and round vs. irregular shaped with protuberances) and densities (average is ρ_{ice} = 900 kg/m^3, but varies depending on the amount of air bubbles). This causes a range of air drags (0.4 to 0.8, with average 0.55) and a corresponding range of terminal fall speeds. Hailstones that form in the updraft vault region of a supercell thunderstorm are so heavy that most fall immediately adjacent to the vault (Fig. 15.5).

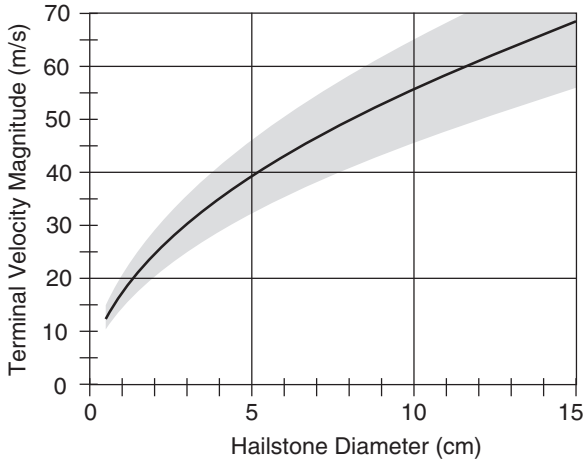

Figure 15.4
Hailstone fall-velocity magnitude relative to the air at pressure height of 50 kPa, assuming an air density of 0.69 kg/m^3.

Hail Formation

Two stages of hail development are embryo formation, and then hailstone growth. A hail **embryo** is a large frozen raindrop or graupel particle (< 5 mm diameter) that is heavy enough to fall at a different speed than the surrounding smaller cloud droplets. It serves as the nucleus of hailstones. Like all normal (non-hail) precipitation, the embryo first rises in the updraft as a growing cloud droplet or ice crystal that eventually becomes large enough (via collision and accretion, as discussed in the Precipitation chapter) to begin falling back toward Earth.

While an embryo is being formed, it is still so small that it is easily carried up into the anvil and out of the thunderstorm, given typical severe thunderstorm updrafts of 10 to 50 m/s. Most potential embryos are removed from the thunderstorm this way, and thus cannot then grow into hailstones.

The few embryos that do initiate hail growth are formed in regions where they are not ejected from the storm, such as: (1) outside of the main updraft in the flanking line of cumulus congestus clouds or in other smaller updrafts, called **feeder cells**; (2) in a side eddy of the main updraft; (3) in a portion of the main updraft that tilts upshear, or (4) earlier in the evolution of the thunderstorm while the main updraft is still weak. Regardless of how it is formed, it is believed that the embryos then move or fall into the main updraft of the severe thunderstorm a second time.

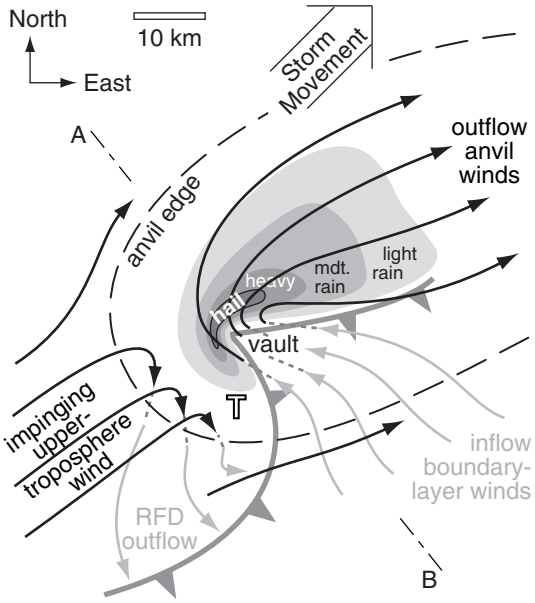

Figure 15.5
Plan view of classic (CL) supercell in the N. Hemisphere (copied from the Thunderstorm chapter). Low altitude winds are shown with light-grey arrows, high altitude with black, and ascending/descending with dashed lines. T indicates tornado location. Precipitation is at the ground. Cross section A-B is used in Fig. 15.10.

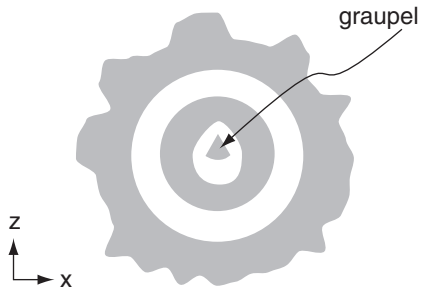

Figure 15.6
Illustration of slice through a hailstone, showing a graupel embryo surrounded by 4 layers of alternating clear ice (indicated with grey shading) and porous (white) ice.

Solved Example

If a supercooled cloud droplet of radius 50 μm and temperature –20°C hits a hailstone, will it freeze instantly? If not, how much heat must be conducted out of the droplet (to the hailstone and the air) for the droplet to freeze?

Solution

Given: $r = 50\ \mu m = 5x10^{-5}$ m, $T = -20°C$
Find: ΔQ_E = ? J , ΔQ_H = ? J,
Is $\Delta Q_E < \Delta Q_H$? If no, then find $\Delta Q_E - \Delta Q_H$.
Use latent heat and specific heat for liquid water, from Appendix B.

Assume a spherical droplet of mass

$$m_{liq} = \rho_{liq} \cdot Vol = \rho_{liq} \cdot (4/3) \cdot \pi \cdot r^3$$
$$= (1000\ kg/m^3) \cdot (4/3) \cdot \pi \cdot (5x10^{-5}\ m)^3 = 5.2x10^{-10}\ kg$$

Use eq. (3.3) to determine how much heat must be removed to freeze the whole droplet ($\Delta m = m_{liq}$):

$$\Delta Q_E = L_f \cdot \Delta m = (3.34x10^5\ J/kg) \cdot (5.2x10^{-10}\ kg)$$
$$= 1.75x10^{-4}\ J .$$

Use eq. (3.1) to find how much can be taken up by allowing the droplet to warm from –20°C to 0°C:

$$\Delta Q_H = m_{liq} \cdot C_{liq} \cdot \Delta T$$
$$= (5.2x10^{-10}\ kg) \cdot [4217.6\ J/(kg \cdot K)] \cdot [0°C - (-20°C)]$$
$$= 0.44x10^{-4}\ J .$$

Thus $\Delta Q_E > \Delta Q_H$, so the sensible-heat deficit associated with –20°C is not enough to compensate for the latent heat of fusion needed to freeze the drop. The droplet will **NOT** freeze instantly.

The amount of heat remaining to be conducted away to the air or the hailstone to allow freezing is:

$$\Delta Q = \Delta Q_E - \Delta Q_H = (1.75x10^{-4}\ J) - (0.44x10^{-4}\ J)$$
$$= \mathbf{1.31x10^{-4}}\ J .$$

Check: Units OK. Physics OK.
Discussion: During the several minutes needed to conduct away this heat, the liquid can flow over the hailstone before freezing, and some air can escape. This creates a layer of clear ice.

The hailstone grows during this second trip through the updraft. Even though the embryo is initially rising in the updraft, the smaller surrounding supercooled cloud droplets are rising faster (because their terminal fall velocity is slower), and collide with the embryo. Because of this requirement for abundant supercooled cloud droplets, hail forms at altitudes where the air temperature is between –10 and –30°C. Most growth occurs while the hailstones are floating in the updraft while drifting relatively horizontally across the updraft in a narrow altitude range having temperatures of –15 to –20°C.

In pockets of the updraft happening to have relatively low liquid water content, the supercooled cloud droplets can freeze almost instantly when they hit the hailstone, trapping air in the interstices between the frozen droplets. This results in a porous, brittle, white layer around the hailstone. In other portions of the updraft having greater liquid water content, the water flows around the hail and freezes more slowly, resulting in a hard clear layer of ice. The result is a hailstone with 2 to 4 visible layers around the embryo (when the hailstone is sliced in half, as sketched in Fig. 15.6), although most hailstones are small and have only one layer. Giant hail can have more than 4 layers.

As the hailstone grows and becomes heavier, its terminal velocity increases and eventually surpasses the updraft velocity in the thunderstorm. At this point, it begins falling relative to the ground, still growing on the way down through the supercooled cloud droplets. After it falls into the warmer air at low altitude, it begins to melt. Almost all strong thunderstorms have some small hailstones, but most melt into large rain drops before reaching the ground. Only the larger hailstones (with more frozen mass and quicker descent through the warm air) reach the ground still frozen as hail (with diameters > 5 mm).

Hail Forecasting

Forecasting large-hail potential later in the day is directly tied to forecasting the maximum updraft velocity in thunderstorms, because only in the stronger updrafts can the heavier hailstones be kept aloft against their terminal fall velocities (Fig. 15.4). CAPE is an important parameter in forecasting updraft strength, as was given in eqs. (14.7) and (14.8) of the Thunderstorm chapter. Furthermore, since it takes about 40 to 60 minutes to create hail (including both embryo and hail formation), large hail would be possible only from long-lived thunderstorms, such as supercells that have relatively steady organized updrafts (which can exist only in an environment with appropriate wind shear).

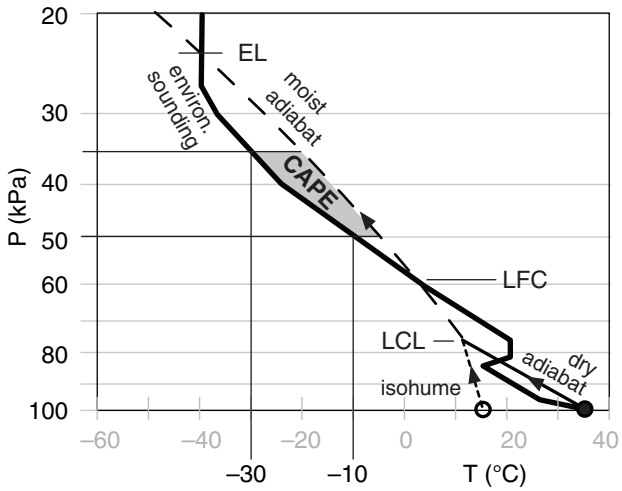

Figure 15.7
Shaded grey is the portion of CAPE area between altitudes where the environment is between –10 and –30°C. Greater areas indicate greater hail likelihood.

However, even if all these conditions are satisfied, hail is not guaranteed. So national forecast centers in North America do not issue specific hail watches, but include hail as a possibility in severe thunderstorm watches and warnings.

To aid in hail forecasting, meteorologists sometimes look at forecast maps of the portion of CAPE between altitudes where the environmental air temperature is $-30 \le T \le -10$°C, such as sketched in Fig. 15.7. Larger values (on the order of 400 J/kg or greater) of this portion of CAPE are associated with more rapid hail growth. Computers can easily calculate this portion of CAPE from soundings produced by numerical forecast models, such as for the case shown in Fig. 15.8. Within the shaded region of large CAPE on this figure, hail would be forecast at only those subsets of locations where thunderstorms actually form.

Weather maps of freezing-level altitude and wind shear between 0 to 6 km are also used by hail forecasters. More of the hail will reach the ground without melting if the freezing level is at a lower altitude. Environmental wind shear enables longer-duration supercell updrafts, which favor hail growth.

Research is being done to try to create a single forecast parameter that combines many of the factors favorable for hail. One example is the **Significant Hail Parameter** (**SHIP**):

$$SHIP = \{ MUCAPE(\text{J/kg}) \cdot r_{MUP}(\text{g/kg}) \cdot \gamma_{70\text{-}50kPa}(\text{°C/km}) \cdot [-T_{50kPa}(\text{°C})] \cdot TSM_{0\text{-}6km}(\text{m/s}) \} \; / \; a \qquad (15.4)$$

Solved Example

What is the largest size hailstone that could be supported in a thunderstorm having CAPE = 1976 J/kg? Also give its TORRO classification.

Solution

Given: CAPE = 1976 J/kg.

Find: d_{max} = ? cm (max hailstone diameter)

From Appendix A, note that units J/kg = m^2/s^2.

First, use eqs. (14.7) and (14.8) from the Thunderstorm chapter to get the likely max updraft speed. This was already computed in a solved example near those eqs:

$$w_{max\ likely} = 31 \text{ m/s}$$

Assume that the terminal fall velocity of the largest hailstone is just balanced by this updraft.

$$w_T = -w_{max\ likely} = -31 \text{ m/s}$$

where the negative sign implies downward motion.

Then use Fig. 15.4 to find the diameter.

$$d_{max} \approx \underline{\textbf{3.1 cm}}$$

From Table 15-1, the TORRO hail **size code is 4**, which corresponds to **pigeon egg to golf ball size**.

Check: Units OK. Physics OK.

Discussion: Hail this size would be classified as large or giant hail, and could severely damage crops.

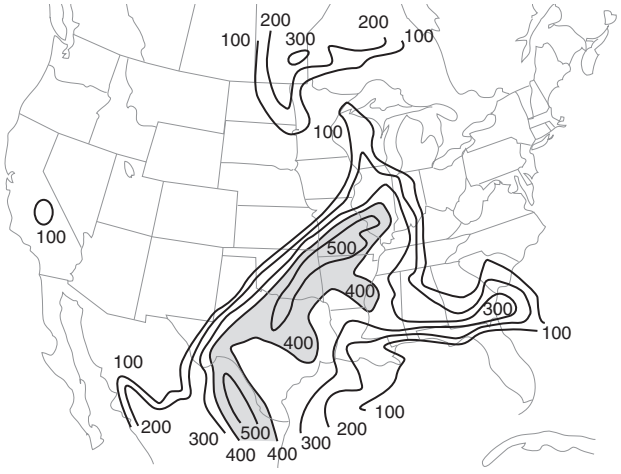

Figure 15.8
Portion of CAPE (J/kg) between altitudes where the environment is between –10 and –30°C. Larger values indicate greater hail growth rates. Case: 22 UTC on 24 May 2006 over the USA and Canada.

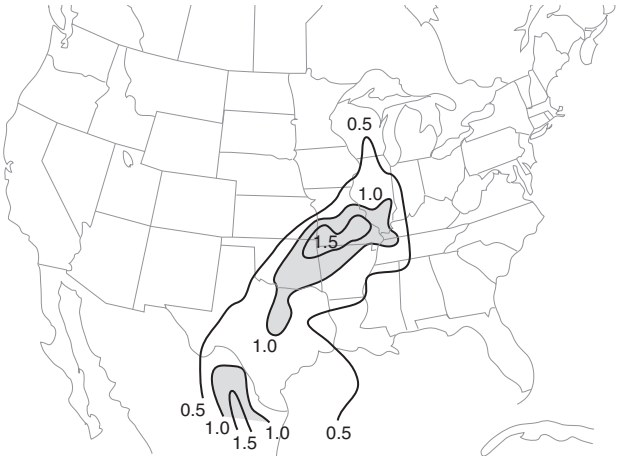

Figure 15.9
Values of significant hail parameter (SHIP) over the USA for the same case as the previous figure. This parameter is dimensionless.

Solved Example
Suppose a pre-storm environmental sounding has the following characteristics over a corn field:
$MUCAPE$ = 3000 J/kg,
r_{MUP} = 14 g/kg,
$\gamma_{70\text{-}50kPa}$ = 5 °C/km,
T_{50kPa} = –10°C
$TSM_{0\text{-}6km}$ = 45 m/s
If a thunderstorm forms in this environment, would significant hail (with diameters ≥ 5 cm) be likely?

Solution
Given: values listed above
Find: $SHIP$ = ? .

Use eq. (15.4):

$$SHIP = [\,(3000\ J/kg)\cdot(14\ g/kg)\cdot(5\ °C/km)\cdot(10°C)\cdot(45\ m/s)\,] / (44x10^6)$$
$$= 99.5x10^6 / (44x10^6) = \underline{\mathbf{2.15}}$$

Check: Units are dimensionless. Value reasonable.
Discussion: Because SHIP is much greater than 1.0, significant (tennis ball size or larger) hail is indeed likely. This would likely totally destroy the corn crop. Because hail forecasting has so many uncertainties and often short lead times, the farmers don't have time to take action to protect or harvest their crops. Thus, their only recourse is to purchase crop insurance.

where r_{MUP} is the water vapor mixing ratio for the most-unstable air parcel, $\gamma_{70\text{-}50kPa}$ is the average environmental lapse rate between pressure heights 70 and 50 kPa, T_{50kPa} is the temperature at a pressure height of 50 kPa, $TSM_{0\text{-}6km}$ is the total shear magnitude between the surface and 6 km altitude, and empirical parameter $a = 44x10^6$ (with dimensions equal to those shown in the numerator of the equation above, so as to leave $SHIP$ dimensionless).

This parameter typically ranges from 0 to 4 or so. If $SHIP > 1$, then the prestorm environment is favorable for significant hail (i.e., hail diameters ≥ 5 cm). Significant hail is frequently observed when $1.5 \le SHIP$. Fig. 15.9 shows a weather map of $SHIP$ for the 22 UTC 24 May 2006 case study.

Nowcasting (forecasting 1 to 30 minutes ahead) large hail is aided with weather radar:
- Large hailstones cause very large radar reflectivity (order of 60 to 70 dBZ) compared to the maximum possible from very heavy rain (up to 50 dBZ). Some radar algorithms diagnose hail when it finds reflectivities ≥ 40 dBZ at altitudes where temperatures are below freezing, with greater chance of hail for ≥ 50 dBZ at altitudes above the –20°C level.
- Doppler velocities can show if a storm is organized as a supercell, which is statistically more likely to support hail.
- Polarimetric methods (see the Remote Sensing chapter) allow radar echoes from hail to be distinguished from echoes from rain or smaller ice particles.
- The updrafts in some supercell thunderstorms are so strong that only small cloud droplets exist, causing weak (<25 dBZ) radar reflectivity, and resulting in a **weak-echo region** (**WER**) on the radar display. Sometimes the WER is surrounded on the top and sides by strong precipitation echoes, causing a **bounded weak-echo region** (**BWER**), also known as an **echo-free vault**. This enables very large hail, because embryos falling from the upshear side of the bounding precipitation can re-enter the updraft, thereby efficiently creating hail (Fig. 15.10).

Hail Locations

The hail that does fall often falls closest to the main updraft (Figs. 15.5 & 15.10), and the resulting **hail shaft** (the column of falling hailstones below cloud base) often looks white or invisible to observers on the ground. Most hail falls are relatively short lived, causing small (10 to 20 km long, 0.5 to 3 km wide) damage tracks called **hailstreaks**. Sometimes long-lived supercell thunderstorms can create longer **hailswaths** of damage 8 to 24 km wide and

160 to 320 km long. Even though large hail can be extremely damaging, the mass of water in hail at the ground is typically only 2 to 3% of the mass of rain from the same thunderstorm.

In the USA, most giant hail reaching the ground is found in the central and southern plains, centered in Oklahoma (averaging 6 to 9 giant-hail days/yr), and extending from Texas north through Kansas and Nebraska (3 or more giant-hail days/yr). Hail is also observed less frequently (1 to 3 giant-hail days/yr) eastward across the Mississippi valley and into the southern and mid-Atlantic states.

Although hail is less frequent in Canada than in the USA, significant hail falls are found in Alberta between the cities of Calgary and Edmonton, particularly near the town of Red Deer. Hail is also found in central British Columbia, and in the southern prairies of Saskatchewan and Manitoba.

In the S. Hemisphere, hail falls often occur over eastern Australia. The 14 April 1999 hailstorm over Sydney caused an estimated AUS$ 2.2 billion in damage, the second largest weather-related damage total on record for Australia. Hailstorms have been observed over North and South America, Europe, Australia, Asia, and Africa.

Hail Mitigation

Attempts at **hail suppression** (mitigation) have generally been unsuccessful, but active hail-suppression efforts still continue in most continents to try to reduce crop damage. Five approaches have been suggested for suppressing hail, all of which involve **cloud seeding** (adding particles into clouds to serve as additional or specialized hydrometeor nuclei), which is difficult to do precisely:

- **beneficial competition** - to create larger numbers of embryos that compete for supercooled cloud water, thereby producing larger numbers of smaller hailstones (that melt before reaching the ground). The methods are cloud seeding with **hygroscopic** (attracts water; e.g., salt particles) cloud nuclei (to make larger rain drops that then freeze into embryos), or seeding with **glaciogenic** (makes ice; e.g., silver iodide particles) ice nuclei to make more graupel.
- **early rainout** - to cause precipitation in the cumulus congestus clouds of the flanking line, thereby reducing the amount of cloud water available before the updraft becomes strong enough to support large hail. The method is seeding with ice nuclei.
- **trajectory altering** - to cause the embryos to grow to greater size earlier, thereby following a lower trajectory through the updraft where the temperature or supercooled liquid water con-

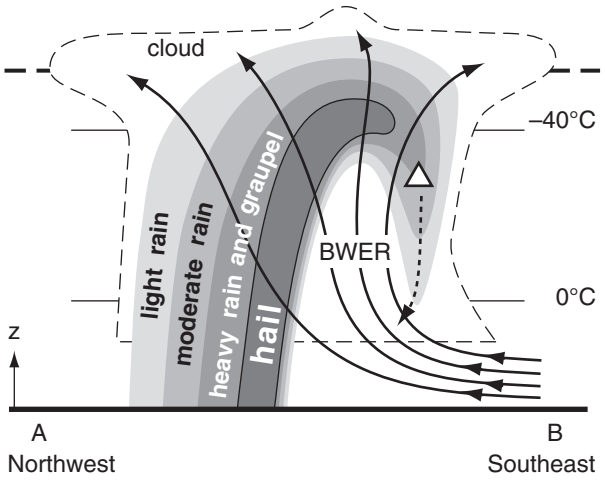

Figure 15.10
Vertical cross section through a classic supercell thunderstorm along slice A-B from Fig. 15.5. Thin dashed line shows visible cloud boundary, and shading indicates intensity of precipitation as viewed by radar. BWER = bounded weak echo region of supercooled cloud droplets. White triangle represents graupel on the upshear side of the storm, which can fall (dotted line) and re-enter the updraft to serve as a hail embryo. Thick dashed line is the tropopause. Isotherms are thin solid lines. Curved thick black lines with arrows show air flow.

FOCUS • Hail Suppression

For many years there has been a very active cloud seeding effort near the town of Red Deer, Alberta, Canada, in the hopes of suppressing hail. These activities were funded by some of the crop-insurance companies, because their clients, the farmers, demanded that something be done.

Although the insurance companies knew that there is little solid evidence that hail suppression actually works, they funded the cloud seeding anyway as a public-relations effort. The farmers appreciated the efforts aimed at reducing their losses, and the insurance companies didn't mind because the cloud-seeding costs were ultimately borne by the farmers via increased insurance premiums.

Solved Example

During cloud seeding, how many silver iodide particles need to be introduced into a thunderstorm to double the number of ice nuclei? Assume the number density of natural ice nuclei is 10,000 per cubic meter.

Solution

Given: $n_{ice\ nuclei}/Volume = 10{,}000\ /m^3$

Find: $N_{total} = ?$ total count of introduced nuclei

To double ice nuclei, the count of introduced nuclei must equal the count of natural nuclei:

$$N_{total} = (n_{ice\ nuclei}/Volume) \cdot Volume$$

Estimate the volume of a thunderstorm above the freezing level. Assume freezing level is at 3 km altitude, and the anvil top is at 12 km. Approximate the thunderstorm by a box of bottom surface area 12 x 12 km, and height 9 km (= 12 – 3).

$$Volume \approx 1300\ km^3 = 1.3x10^{12}\ m^3$$

Thus:

$$N_{total} = (n_{ice\ nuclei}/Volume) \cdot Volume = (10{,}000\ /m^3) \cdot (1.3x10^{12}\ m^3) = \underline{\mathbf{1.3x10}}^{16}$$

Check: Units OK. Physics OK.

Discussion: Cloud seeding is often done by an aircraft. For safety reasons, the aircraft doesn't usually fly into the violent heart of the thunderstorm. Instead, it flies under the rain-free portion of cloud base, releasing the silver iodide particles into the updraft in the hopes that the nuclei get to the right part of the storm at the right time. It is not easy to do this correctly, and even more difficult to confirm if the seeding caused the desired change. Seeding thunderstorms is an uncontrolled experiment, and one never knows how the thunderstorm would have changed without the seeding.

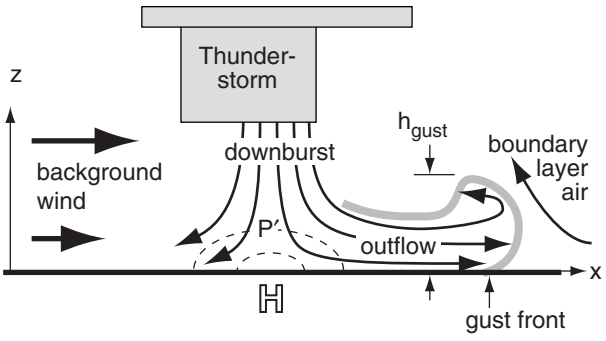

Figure 15.11

Side view illustration of a downburst, also showing the resulting straight-line outflow winds and gust front. H indicates location of meso-high pressure at the surface, and isobars of positive pressure perturbation P′ are dashed lines.

tent is not optimum for large hail growth. This method attempts to increase rainfall (in drought regions) while reducing hail falls.

- **dynamic effects** - to consume more CAPE earlier in the life cycle of the updraft (i.e., in the cumulus congestus stage), thereby leaving less energy for the main updraft, causing it to be weaker (and supporting only smaller hail).
- **glaciation of supercooled cloud water** - to more quickly convert the small supercooled cloud droplets into small ice crystals that are less likely to stick to hail embryos and are more likely to be blown to the top of the storm and out via the anvil. This was the goal of most of the early attempts at hail suppression, but has lost favor as most hail suppression attempts have failed.

DOWNBURSTS AND GUST FRONTS

Characteristics

Downbursts are rapidly descending (w = –5 to –25 m/s) downdrafts of air (Fig. 15.11), found below clouds with precipitation or virga. Downbursts of 0.5 to 10 km diameter are usually associated with thunderstorms and heavy rain. Downburst speeds of order 10 m/s have been measured 100 m AGL. The descending air can hit the ground and spread out as strong **straight-line winds** causing damage equivalent to a weak tornado (up to EF3 intensity). Smaller mid-level clouds (e.g., altocumulus with virga) can also produce downbursts that usually do not reach the ground.

Small diameter (1 to 4 km) downbursts that last only 2 to 5 min are called **microbursts**. Sometimes a downburst area will include one or more imbedded microbursts.

Acceleration of downburst velocity w is found by applying Newton's 2nd law of motion to an air parcel:

$$\frac{\Delta w}{\Delta t} \approx -\frac{1}{\rho}\frac{\Delta P'}{\Delta z} + |g| \cdot \left[\frac{\theta_v'}{\theta_{ve}} - \frac{C_v}{C_p}\frac{P'}{P_e}\right] \qquad \bullet(15.5)$$

Term: (A) (B) (C)

where w is negative for downdrafts, t is time, ρ is air density, $P' = P_{parcel} - P_e$ is pressure perturbation of the air parcel relative to the environmental pressure P_e, z is height, $|g| = 9.8\ m/s^2$ is the magnitude of gravitational acceleration, $\theta_v' = \theta_{v\ parcel} - \theta_{ve}$ is the deviation of the parcel's virtual potential temperature from that of the environment θ_{ve} (in Kelvin), and $C_v/C_p = 0.714$ is the ratio of specific heat of air at constant volume to that at constant pressure.

Remember that the virtual potential temperature (from the Heat chapter) includes liquid-water and ice loading, which makes the air act as if it were colder, denser, and heavier. Namely, for the air parcel it is:

$$\theta_{v\,parcel} = \theta_{parcel} \cdot (1 + 0.61 \cdot r - r_L - r_I)_{parcel} \qquad (15.6)$$

where θ is air potential temperature (in Kelvin), r is water-vapor mixing ratio (in g/g, not g/kg), r_L is liquid water mixing ratio (in g/g), and r_I is ice mixing ratio (in g/g). For the special case of an environment with no liquid water or ice, the environmental virtual potential temperature is:

$$\theta_{ve} = \theta_e \cdot (1 + 0.61 \cdot r)_e \qquad (15.7)$$

Equation (15.5) says that three forces (per unit mass) can create or enhance downdrafts. (A) Pressure-gradient force is caused by a vertical pressure profile that differs from the background hydrostatic pressure profile. (B) Buoyant force combines the effects of temperature in the evaporatively cooled air, precipitation drag associated with falling rain drops or ice crystals, and the relatively lower density of water vapor. (C) Perturbation-pressure buoyancy force is where an air parcel of lower pressure than its surroundings experiences an upward force. Although this last effect is believed to be small, not much is really known about it, so we will neglect it here.

Evaporative cooling and precipitation drag are important for initially accelerating the air downward out of the cloud. We will discuss those factors first, because they can create downbursts. The vertical pressure gradient becomes important only near the ground. It is responsible for decelerating the downburst just before it hits the ground, which we will discuss in the "gust front" subsection.

Precipitation Drag

As rain or ice crystals fall, they tend to drag some air along with it. If the precipitation is falling at its **terminal velocity** relative to the moving air parcel (see the Precipitation chapter) then the pull of gravity on the precipitation particles is balanced by air drag. Because drag acts between air and rain, it not only retards the drop velocity but it enhances the air downdraft velocity. Thus, **precipitation drag** produces a downward force on the air equal to the weight of the precipitation particles.

This effect is also called **liquid-water loading** or **ice loading**, depending on the phase of the hydrometeor. It makes the air parcel behave as if it were colder and more dense, as can be quantified by the virtual temperature T_v (see Chapter 1) or the virtual potential temperature θ_v (see the Heat chapter).

Solved Example

10 g/kg of liquid water exists as rain drops in saturated air of temperature 10°C and pressure 80 kPa. The environmental air has a temperature of 10°C and mixing ratio of 4 g/kg. Find the: (a) buoyancy force per mass associated with air temperature and water vapor, (b) buoyancy force per mass associated with just the precipitation drag, and (c) the downdraft velocity after 1 minute of fall, due to only the sum of (a) and (b).

Solution

Given: Parcel: r_L = 10 g/kg, T = 10°C, P = 80 kPa,
Environ.: r = 4 g/kg, T = 10°C, P = 80 kPa,
Δt = 60 s. Neglect terms (A) and (C).

Find: (a) Term($B_{\text{due to } T \,\&\, r}$) = ? N/kg,
(b) Term($B_{\text{due to } r_L \,\&\, r_I}$) = ? N/kg (c) w = ? m/s

(a) Because the parcel air is saturated, $r_{parcel} = r_s$. Using a thermo diagram (because its faster than solving a bunch of equations), $r_s \approx 9.5$ g/kg at P = 80 kPa and T = 10°C. Also, from the thermo diagram, $\theta_{parcel} \approx 28$°C = 301 K. Thus, using the first part of eq. (15.6):

$\theta_{v\,parcel} \approx (301\text{ K}) \cdot [1 + 0.61 \cdot (0.0095\text{ g/g})] \approx 302.7$ K

For the environment, also θ ≈ 28°C = 301 K, but r = 4 g/kg. Thus, using eq. (15.7):

$\theta_{ve} \approx (301\text{ K}) \cdot [1 + 0.61 \cdot (0.004\text{ g/g})] \approx 301.7$ K

Use eq. (15.5):

$$\text{Term}(B_{\text{due to } T \,\&\, r}) = |g| \cdot [\,(\theta_{v\,parcel} - \theta_{ve})\,/\,\theta_{ve}\,]$$
$$= (9.8\text{ m/s}^2) \cdot [\,(302.7 - 301.7\text{ K})\,/\,301.7\text{ K}\,]$$
$$= 0.032\text{ m/s}^2 = \underline{\mathbf{0.032\ N/kg}}.$$

(b) Because r_I was not given, assume r_I = 0 everywhere, and r_L = 0 in the environment.

$$\text{Term}(B_{\text{due to } r_L \,\&\, r_I}) = -|g| \cdot [\,(r_L + r_I)_{parcel} - (r_L + r_I)_e\,].$$
$$= -(9.8\text{ m/s}^2) \cdot [\,0.01\text{ g/g}\,] = \underline{\mathbf{-0.098\ N/kg}}.$$

(c) Assume initial vertical velocity is zero.

Use eq. (15.5) with only Term B:

$$(w_{final} - w_{initial})/\Delta t = [\text{Term}(B_{T \,\&\, r}) + \text{Term}(B_{r_L \,\&\, r_I})]$$
$$w_{final} = (60\text{ s}) \cdot [\,0.032 - 0.098\text{ m/s}^2\,] \approx \underline{\mathbf{-4\ m/s}}.$$

Check: Units OK. Physics OK.

Discussion: Although the water vapor in the air adds buoyancy equivalent to a temperature **in**crease of 1°C, the liquid-water loading decreases buoyancy, equivalent to a temperature **de**crease of 3°C. The net effect is that this saturated, liquid-water laden air acts 2°C colder and heavier than dry air at the same T.

CAUTION. The final vertical velocity assumes that the air parcel experiences constant buoyancy forces during its 1 minute of fall. This is NOT a realistic assumption, but it did make the exercise a bit easier to solve. In fact, if the rain-laden air descends below cloud base, then it is likely that the rain drops are in an **un**saturated air parcel, not saturated air as was stated for this exercise. We also neglected turbulent drag of the downburst air against the environmental air. This effect can greatly reduce the actual downburst speed compared to the idealized calculations above.

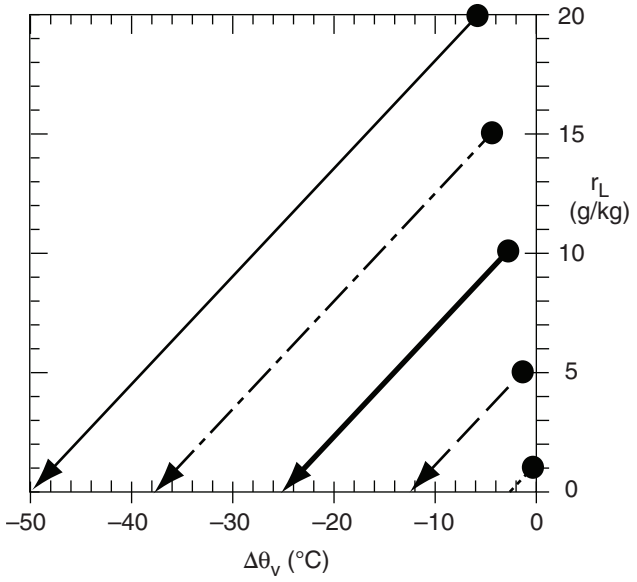

Figure 15.12
Rain drops reduce the virtual potential temperature of the air by both their weight (precipitation drag) and cooling as they evaporate. $\Delta\theta_v$ is the change of virtual potential temperature compared to air containing no rain drops initially. r_L is liquid-water mixing ratio for the drops in air. For any initial r_L along the vertical axis, the black dot indicates the $\Delta\theta_v$ due to only liquid water loading. As that same raindrop evaporates, follow the diagonal line down to see changes in both r_L and $\Delta\theta_v$.

Solved Example

For data from the previous solved example, find the virtual potential temperature of the air if:
a) all liquid water evaporates, and
b) no liquid water evaporates, leaving only the precipitation-loading effect.
c) Discuss the difference between (a) and (b)

Solution

Given: r_L = 10 g/kg initially. r_L = 0 finally.
Find: (a) $\Delta\theta_{parcel}$ = ? K (b) $\Delta\theta_{v\ parcel}$ = ? K

(a) Use eq. (15.8):

$$\Delta\theta_{parcel} = [2.5\ \text{K}\cdot\text{kg}_{\text{air}}\cdot(\text{g}_{\text{water}})^{-1}] \cdot (-10\ \text{g/kg}) = \mathbf{-25\ K}$$

(b) From the discussion section of the previous solved example:

$\Delta\theta_{v\ parcel\ precip.\ drag}$ = –3 K initially.

Thus, the change of virtual potential temperature (between before and after the drop evaporates) is

$$\Delta\theta_{v\ parcel} = \Delta\theta_{v\ parcel\ final} - \Delta\theta_{v\ parcel\ initial}$$
$$= -25\text{K} - (-3\ \text{K}) = \mathbf{-22\ K}.$$

Check: Units OK. Physics OK.
Discussion: (c) The rain is more valuable to the downburst if it all evaporates.

Evaporative Cooling

Three factors can cause the rain-filled air to be unsaturated. One, the rain can fall out of the thunderstorm into drier air (namely, the rain moves through the air parcels, not with the air parcels). Two, as air parcels descend in the downdraft (being dragged downward by the rain), the air parcels warm adiabatically and can hold more vapor. Three, the rain-filled air of the storm can mix with neighboring environmental air that is drier.

The result is raindrop-laden air that is often not saturated, which allows evaporation of water from the raindrops. This evaporation cools the air due to absorption of latent heat, and contributes to its negative buoyancy. The potential temperature change associated with evaporation of Δr_L grams of liquid water per kilogram of air is:

$$\Delta\theta_{parcel} = (L_v/C_p) \cdot \Delta r_L \qquad \bullet(15.8)$$

where (L_v/C_p) = 2.5 $\text{K}\cdot\text{kg}_{\text{air}}\cdot(\text{g}_{\text{water}})^{-1}$, and where $\Delta r_L = r_{L\ final} - r_{L\ initial}$ is negative for evaporation. This parcel cooling enters the downdraft-velocity equation via θ_{parcel} in eq. (15.6).

Evaporative cooling of falling rain is often a much larger effect than the precipitation drag. Fig. 15.12 shows both the precipitation-drag effect for different initial liquid-water mixing ratios (the black dots), and the corresponding cooling and liquid-water decrease as the drops evaporate. For example, consider the black dot corresponding to an initial liquid water loading of 10 g/kg. Even before that drop evaporates, the weight of the rain decreases the virtual potential temperature by about 2.9°C. However, as that drop evaporates, it causes a much larger amount of cooling to due latent heat absorption, causing the virtual-potential-temperature to decrease by 25°C after it has completely evaporated.

In regions such as the western Great Plains of the United States (e.g., near Denver, Colorado), the environmental air is often so dry that evaporative cooling causes dangerous downbursts. This is particularly hazardous to landing and departing aircraft, because this vertical velocity can sometimes exceed aircraft climb rate. Also, when the downburst hits the ground and spreads out, it can create hazardous changes between headwinds and tailwinds for landing and departing aircraft (see the "Downburst and Flight Operations" Focus Box near the end of this section.)

Doppler radars can detect some of the downbursts and their associated surface divergence flows (see the Remote Sensing chapter), as can arrays of wind sensors on the airport grounds, so that warnings can be given to pilots.

Downdraft CAPE (DCAPE)

Eq. (15.5) applies at any one altitude. As precipitation-laden air parcels descend, many things change. The descending air parcel cools and looses some of its liquid-water loading due to evaporation, thereby changing its virtual potential temperature. It descends into surroundings having different virtual potential temperature than the environment where it started. As a result of these changes to both the air parcel and its environment, the θ_v' term in eq. (15.5) changes.

To account for all these changes, find term B from eq. (15.5) at each depth, and then sum over all depths to get the accumulated effect of evaporative cooling and precipitation drag. This is a difficult calculation, with many uncertainties.

An alternative estimate of downburst strength is via the **Downdraft Convective Available Potential Energy** (**DCAPE**, see shaded area in Fig. 15.13):

$$DCAPE = \sum_{z=0}^{z_{LFS}} |g| \cdot \frac{\theta_{vp} - \theta_{ve}}{\theta_{ve}} \cdot \Delta z \qquad \bullet(15.9)$$

where $|g| = 9.8$ m/s^2 is the magnitude of gravitational acceleration, θ_{vp} is the parcel virtual potential temperature (including temperature, water vapor, and precipitation-drag effects), θ_{ve} is the environment virtual potential temperature (Kelvin in the denominator), Δz is a height increment to be used when conceptually covering the DCAPE area with tiles of equal size.

The altitude z_{LFS} where the precipitation laden air first becomes negatively buoyant compared to the environment is called the **level of free sink** (**LFS**), and is the downdraft equivalent of the level of free convection. If the downburst stays negatively buoyant to the ground, then the bottom limit of the sum is at $z = 0$, otherwise the downburst would stop at a **downdraft equilibrium level** (**DEL**) and not be felt at the ground. DCAPE is negative, and has units of J/kg or m^2/s^2.

By relating potential energy to kinetic energy, the downdraft velocity is approximately:

$$w_{max\ down} = -(2 \cdot |DCAPE|)^{1/2} \qquad (15.10)$$

Air drag of the descending air parcel against its surrounding environmental air could reduce the likely downburst velocity w_d to about half this max value (Fig. 15.14):

$$w_d = w_{max\ down} / 2 \qquad \bullet(15.11)$$

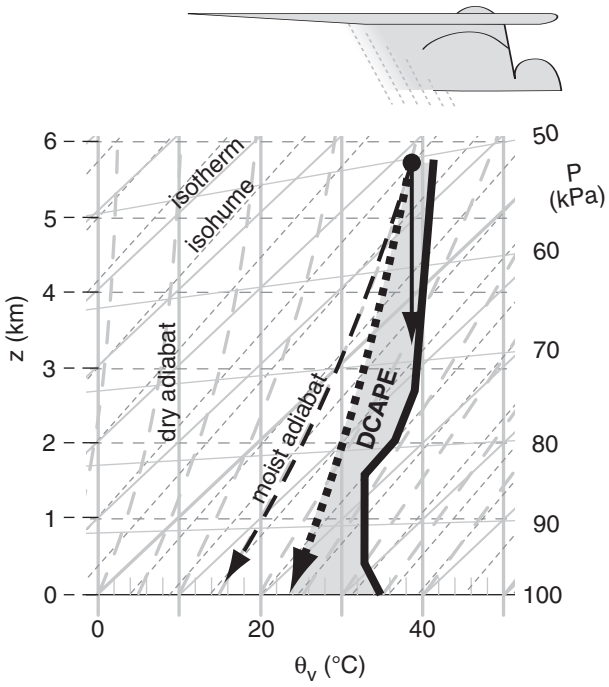

Figure 15.13
Thermo diagram (Theta-z diagram from the Stability chapter) example of Downdraft Convective Available Potential energy (DCAPE, shaded area). Thick solid line is environmental sounding. Black dot shows virtual potential temperature after top of environmental sounding has been modified by liquid-water loading caused by precipitation falling into it from above. Three scenarios of rain-filled air-parcel descent are shown: (a) no evaporative cooling, but only constant liquid water loading (thin solid line following a dry adiabat); (b) an initially saturated air parcel with evaporative cooling of the rain (dashed line following a moist adiabat); and (c) partial evaporation (thick dotted line) with a slope between the moist and dry adiabats.

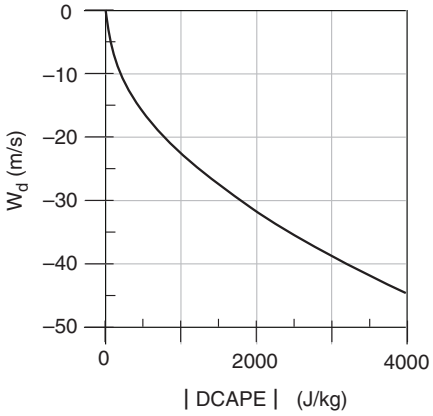

Figure 15.14
Downburst velocity w_d driven by DCAPE

Solved Example

For the shaded area in Fig. 15.13, use the tiling method to estimate the value of DCAPE. Also find the maximum downburst speed and the likely speed.

Solution

Given: Fig. 15.13, reproduced here.

Find: $DCAPE$ = ? m^2/s^2,

$w_{max\ down}$ = ? m/s, w_d = ? m/s

The DCAPE equation (15.9) can be re-written as

$$DCAPE = -[|g|/\theta_{ve}]\cdot(\text{shaded area})$$

Method: Overlay the shaded region with tiles:

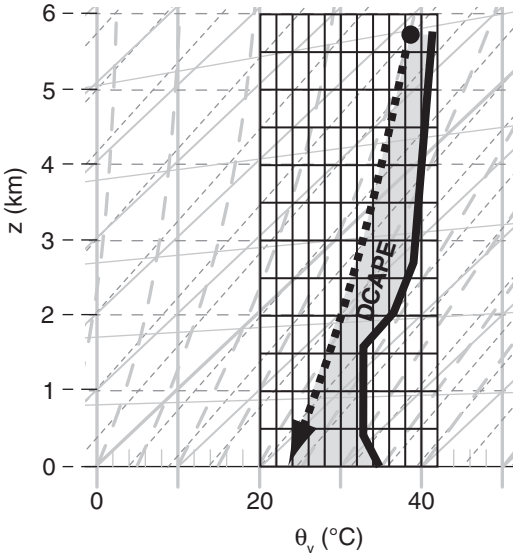

Each tile is 2°C = 2 K wide by 0.5 km tall (but you could pick other tile sizes instead). Hence, each tile is worth 1000 K·m. I count approximately 32 tiles needed to cover the shaded region. Thus:

(shaded area) = 32 x 1000 K·m = 32,000 K·m.

Looking at the plotted environmental sounding by eye, I estimate the average θ_{ve} = 37°C = 310 K.

$$DCAPE = -[(9.8\ m/s^2)/310K]\cdot(32{,}000\ K\cdot m)$$
$$= \underline{\mathbf{-1012}}\ m^2/s^2$$

Next, use eq. (15.10):

$$w_{max\ down} = -[\,2\cdot|-1012\ m^2/s^2\ |]^{1/2}$$
$$= \underline{\mathbf{-45\ m/s}}$$

Finally, use eq. (15.11):

$w_d = w_{max\ down}/2$ = **<u>–22.5 m/s</u>**.

Check: Units OK. Physics OK. Drawing OK.

Discussion: While this downburst speed might be observed 1 km above ground, the speed would diminish closer to the ground due to an opposing pressure-perturbation gradient. Since the DCAPE method doesn't account for the vertical pressure gradient, it shouldn't be used below about 1 km altitude.

Stronger downdrafts and associated straight-line winds near the ground are associated with larger magnitudes of DCAPE. For example, Fig. 15.15 shows a case study of DCAPE magnitudes valid at 22 UTC on 24 May 2006.

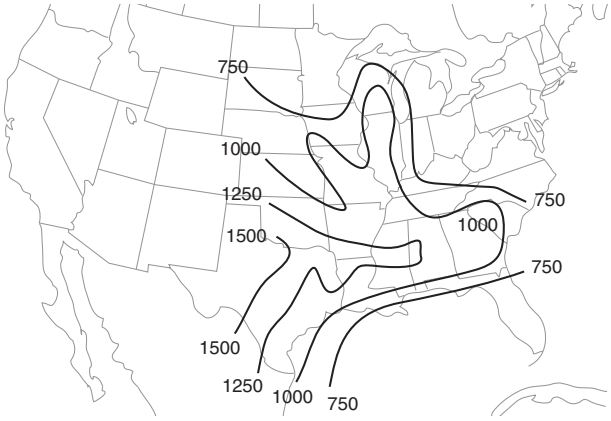

Figure 15.15

Example of downdraft DCAPE magnitude (J/kg) for 22 UTC 24 May 06 over the USA.

FOCUS • CAPE vs. DCAPE

Although DCAPE shares the same conceptual framework as CAPE, there is virtually no chance of practically utilizing DCAPE, while CAPE is very useful. Compare the two concepts.

<u>For CAPE</u>: The initial state of the rising air parcel is known or fairly easy to estimate from surface observations and forecasts. The changing thermodynamic state of the parcel is easy to anticipate; namely, the parcel rises dry adiabatically to its LCL, and rises moist adiabatically above the LCL with vapor always close to its saturation value. Any excess water vapor instantly condenses to keep the air parcel near saturation. The resulting liquid cloud droplets are initially carried with the parcel.

<u>For DCAPE</u>: Both the initial air temperature of the descending air parcel near thunderstorm base and the liquid-water mixing ratio of raindrops are unknown. The raindrops don't move with the air parcel, but pass through the air parcel from above. The air parcel below cloud base is often NOT saturated even though there are raindrops within it. The temperature of the falling raindrops is often different than the temperature of the air parcel it falls through. There is no requirement that the adiabatic warming of the air due to descent into higher pressure be partially matched by evaporation from the rain drops (namely, the thermodynamic state of the descending air parcel can be neither dry adiabatic nor moist adiabatic).

Unfortunately, the exact thermodynamic path traveled by the descending rain-filled air parcel is unknown, as discussed in the Focus box. Fig. 15.13 illustrates some of the uncertainty in DCAPE. If the rain-filled air parcel starting at pressure altitude of 50 kPa experiences no evaporation, but maintains constant precipitation drag along with dry adiabatic warming, then the parcel state follows the thin solid arrow until it reaches its DEL at about 70 kPa. This would not reach the ground as a down burst.

If a descending saturated air parcel experiences just enough evaporation to balance adiabatic warming, then the temperature follows a moist adiabat, as shown with the thin dashed line. But it could be just as likely that the air parcel follows a thermodynamic path in between dry and moist adiabat, such as the arbitrary dotted line in that figure, which hits the ground as a cool but unsaturated downburst.

Pressure Perturbation

As the downburst approaches the ground, its vertical velocity must decelerate to zero because it cannot blow through the ground. This causes the dynamic pressure to increase (P' becomes positive) as the air stagnates.

Rewriting Bernoulli's equation (see the Local Winds chapter) using the notation from eq. (15.5), the maximum stagnation pressure perturbation P'_{max} at the ground directly below the center of the downburst is:

$$P'_{\max} = \rho \cdot \left[\frac{w_d^2}{2} - \frac{|g| \cdot \theta_v' \cdot z}{\theta_{ve}} \right] \qquad \bullet(15.12)$$

Term: (A) (B)

where ρ is air density, w_d is likely peak downburst speed at height z well above the ground (before it feels the influence of the ground), $|g| = 9.8$ m/s^2 is gravitational acceleration magnitude, and virtual potential temperature depression of the air parcel relative to the environment is $\theta_v' = \theta_{v\,parcel} - \theta_{ve}$.

Term (A) is an inertial effect. Term (B) includes the added weight of cold air (with possible precipitation loading) in increasing the pressure [because θ_v' is usually (but not always) negative in downbursts]. Both effects create a mesoscale high (**mesohigh**, $\mathbb{H}$) pressure region centered on the downburst. Fig. 15.16 shows the solution to eq. (15.12) for a variety of different downburst velocities and virtual potential

Solved Example

A downburst has velocity –22 m/s at 1 km altitude, before feeling the influence of the ground. Find the corresponding perturbation pressure at ground level for a downburst virtual potential temperature perturbation of (a) 0, and (b) –5°C.

Solution:

Given: $w_d = -22$ m/s, $z = 1$ km, θ_v' = (a) 0, or (b) –5°C

Find: P'_{max} = ? kPa

Assume standard atmosphere air density at sea level

$\rho = 1.225$ kg/m^3

Assume $\theta_{ve} = 294$ K. Thus $|g|/\theta_{ve} = 0.0333$ m·s^{-2}·K^{-1}

Use eq. (15.12):

(a) $P'_{max} = (1.225 \text{ kg/m}^3)\cdot[\,(-22 \text{ m/s})^2/2 - 0\,]$

$= 296$ kg·m^{-1}·s^{-2} = 296 Pa = **0.296 kPa**

(b) $\theta_v' = -5$°C = –5 K because it represents a temperature difference.

$P'_{max} = (1.225 \text{ kg/m}^3)\cdot$

$[\,(-22 \text{ m/s})^2/2 - (0.0333 \text{ m·s}^{-2}\text{·K}^{-1})\cdot(-5 \text{ K})\cdot(1000 \text{ m})]$

$P'_{max} = [\,296 + 204\,]$ kg·m^{-1}·s^{-2} = 500 Pa = **0.5 kPa**

Check: Units OK. Physics OK. Agrees with Fig. 15.16.

Discussion: For this case, the cold temperature of the downburst causes P′ to nearly double compared to pure inertial effects. Although P'_{max} is small, P' decreases to 0 over a short distance, causing large $\Delta P'/\Delta x$ & $\Delta P'/\Delta z$. These large pressure gradients cause large accelerations of the air, including the rapid deceleration of the descending downburst air, and the rapid horizontal acceleration of the same air to create the outflow winds.

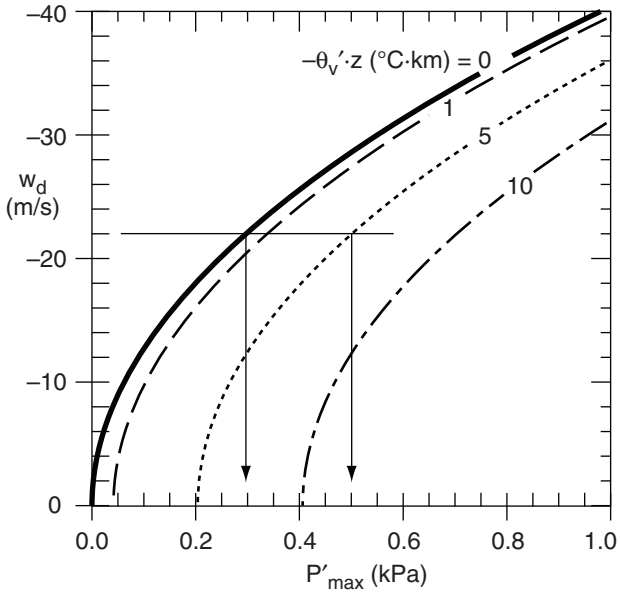

Figure 15.16

Descending air of velocity w_d decelerates to zero when it hits the ground, causing a pressure increase P'_{max} at the ground under the downburst compared to the surrounding ambient atmosphere. For descending air of the same temperature as its surroundings, the result from Bernoulli's equation is plotted as the thick solid line. If the descending air is also cold (i.e., has some a virtual potential temperature deficit $-\theta_v'$ at starting altitude z), then the other curves show how the pressure increases further.

temperature deficits. Typical magnitudes are on the order of 0.1 to 0.6 kPa (or 1 to 6 mb) higher than the surrounding pressure.

As you move away vertically from the ground and horizontally from the downburst center, the pressure perturbation decreases, as suggested by the dashed line isobars in Figs. 15.11 and 15.17. The vertical gradient of this pressure perturbation decelerates the downburst near the ground. The horizontal gradient of the pressure perturbation accelerates the air horizontally away from the downburst, thus preserving air-mass continuity by balancing vertical inflow with horizontal **outflow** of air.

Outflow Winds & Gust Fronts

The near-surface **outflow** air tends to spread out in all directions radially from the downburst, but can be enhanced or reduced in some directions by background winds (Fig. 15.17). These outflow winds are called **straight-line winds**, to distinguish them from rotating tornadic winds. Nevertheless, straight-line winds can cause significant damage — blowing down trees and overturning mobile homes. Wind speeds of 35 m/s or more are possible.

The outflow winds are accelerated by the perturbation-pressure gradient associated with the downburst mesohigh. Considering only the horizontal pressure-gradient force in Newton's 2nd Law (see the Dynamics Chapter), estimate the acceleration from

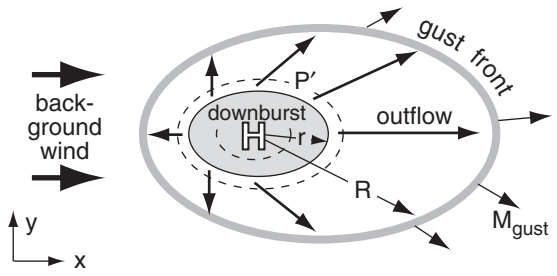

Figure 15.17
Top view of a downburst (grey shading), straight-line outflow winds (thin lines with arrows), and gust front at the ground (corresponding to Fig. 15.11). H shows the location of a meso-high pressure center at the ground, and the thin dashed lines show isobars of positive perturbation pressure P′.

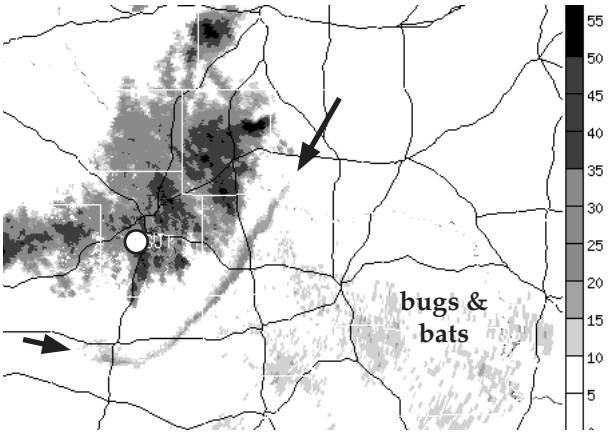

Figure 15.18
Radar reflectivity from the San Angelo (SJT) Texas weather radar. White circle shows radar location. Thunderstorm cells with heavy rain are over and northeast of the radar. Arrows show ends of gust front. Scale at right is dBZ. Elevation angle is 0.5°. Both figs. courtesy of the National Center for Atmospheric Research, based on National Weather Service radar data, NOAA.

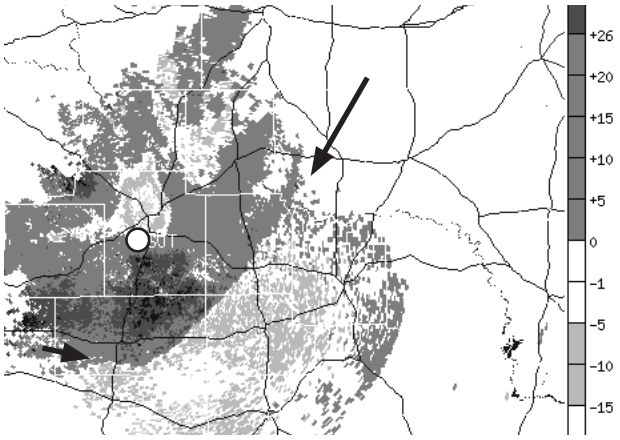

Figure 15.19
Same as 15.18, but for Doppler velocity. Medium and dark greys are winds away from the radar (white circle), and light greys are winds towards. Scale at right is speed in knots.

$$\frac{\Delta M}{\Delta t} = \frac{1}{\rho}\frac{P'_{\max}}{r} \qquad \bullet(15.13)$$

where ΔM is change of outflow wind magnitude over time interval Δt , ρ is air density, P'_{max} is the pressure perturbation strength of the mesohigh, and r is the radius of the downburst (assuming it roughly equals the radius of the mesohigh).

The horizontal **divergence signature** of air from a downburst can be detected by Doppler weather radar by the couplet of "toward" and "away" winds, as was shown in the Remote Sensing chapter. Figs. 15.18 and 15.19 show a downburst divergence signature and gust front.

The intensity of the downburst (Table 15-2) can be estimated by finding the maximum radial wind speed M_{max} observed by Doppler radar in the divergence couplet, and finding the max change of wind speed ΔM_{max} along a radial line extending out from the radar at any height below 1 km above mean sea level (MSL).

The leading edge of the spreading **outflow** air from the downburst is called the **gust front** (Figs. 15.11 & 15.17). Gust fronts can be 100 to 1000 m deep, 5 to 100 kilometers wide, and last for a few minutes to several hours. The longer-lasting gust fronts are often associated with squall lines or supercells, where downbursts of cool air from a sequence of individual cells can continually reinforce the gust front. Gust fronts typically spread with speeds of 5 to 15 m/s.

Because the gust front forms from downdraft air that was chilled by evaporative cooling, a temperature decrease of 1 to 3 °C is often noticed during gust front passage. The leading edge of this cold air acts like a miniature cold front as it progresses away from the downburst. It hugs the surface because of its cold temperature, and plows under the warmer boundary-layer air.

As the boundary-layer air is forced to rise over the advancing gust front (Fig. 15.11), it can reach its LCL and trigger new thunderstorms. Thus, a parent thunderstorm with gust front can spawn offspring storms in a process called **propagation**. The result is a sequence of storms that move across the country, rather than a single long-lived storm.

The speed of advance of the gust front, as well as the gust-front depth, are partly controlled by the continuity equation. Namely, the vertical supply rate of air by the downburst must balance the horizontal removal rate by expansion of outflow air away from the downburst. This can be combined with an empirical expression for depth of the outflow.

The result for gust-front advancement speed M_{gust} in a calm environment is

Solved Example

For a mesohigh of max pressure 0.5 kPa and radius 5 km, how fast will the outflow winds become during 1 minute of acceleration?

Solution

Given: $P'_{max} = 0.5$ kPa, $r = 5$ km, $\Delta t = 60$ s

Find: ΔM = ? m/s

Solve eq. (15.13) for M. Assume $\rho = 1.225$ kg/m^3.

$$\Delta M = \frac{(60\,\text{s})}{(1.225\,\text{kg/m}^3)}\cdot\frac{(0.5\,\text{kPa})}{(5\,\text{km})} = \underline{\textbf{4.9 m/s}}$$

Check: Physics OK. Units OK. Magnitude OK.

Discussion: In real downbursts, the pressure gradient varies rapidly with time and space. So this answer should be treated as only an order-of-magnitude estimate.

Table 15-2. Doppler-radar estimates of thunderstorm-cell downburst intensity based on outflow winds.

Intensity	Max radial-wind speed (m/s)	Max wind difference along a radial (m/s)
Moderate	18	25
Severe	25	40

Solved Example

Given a downburst speed of 5 m/s within an area of radius 0.5 km. If the gust front is 2 km away from the center of the downburst and is 2°C colder than the environment air of 300 K, find the depth and advance rate of the gust front.

Solution

Given: $w_d = -5$ m/s, $r = 0.5$ km, $R = 2$ km,
$\Delta T_v = -2$ K, $T_{ve} = 300$ K.
Find: $M_{gust} = ?$ m/s, $h_{gust} = ?$ m

Use eq. (15.14): $M_{gust} =$

$$\left[\frac{0.2\cdot(600\text{ m})^2\cdot\left|(-4\text{ m/s})\cdot(-9.8\text{ m}\cdot\text{s}^{-2})\cdot(-3\text{ K})\right|}{(2000\text{ m})\cdot(300\text{ K})}\right]^{1/3}$$

$= \underline{\mathbf{2.0\ m/s}}$

Use eq. (15.15): $h_{gust} =$

$$0.85\left[\left(\frac{(-4\text{m/s})\cdot(600\text{m})^2}{(2000\text{ m})}\right)^2\frac{(300\text{ K})}{\left|(-9.8\text{m}\cdot\text{s}^{-2})\cdot(-3\text{K})\right|}\right]^{1/3}$$

$= \underline{\mathbf{181\ m}}$

Check: Units OK. Physics OK.
Discussion: These equations are too simple. As real gust fronts advance, they entrain and mix with boundary layer air. This dilutes the cold outflow, warms it toward the boundary-layer temperature, and retards the gust-advancement velocity.

$$M_{gust} = \left[\frac{0.2\cdot r^2\cdot|w_d\cdot g\cdot\Delta T_v|}{R\cdot T_{ve}}\right]^{1/3} \qquad (15.14)$$

where w_d is the downburst velocity, r is the radius of the downburst, R is the distance of the gust front from the downburst center, ΔT_v is the virtual temperature difference between the environment and the cold outflow air, and T_{ve} is the environmental virtual temperature (in Kelvin). The gust front depth h_{gust} is:

$$h_{gust} \approx 0.85\cdot\left[\frac{T_{ve}}{|g\cdot\Delta T_v|}\left(\frac{w_d\cdot r^2}{R}\right)^2\right]^{1/3} \qquad (15.15)$$

Both equations show that the depth and speed of the gust front decreases as the distance R of the front increases away from the downburst. Also, colder outflow increases the outflow velocity, but decreases its depth.

When the cold outflow winds move over dry soil and stir up dust or sand, the result is a **dust storm** or **sand storm** called a **haboob** (Fig. 15.20). The airborne dust is an excellent tracer to make the gust front visible, which appears as a turbulent advancing wall of brown or ochre color.

In moister environments over vegetated or rain-wetted surfaces, instead of a haboob you might see **arc cloud** (**arcus**) or **shelf cloud** over an advancing gust front. The arc cloud forms when the warm humid environmental air is pushed upward by the undercutting cold outflow air. Sometimes the top and back of the arc cloud are connected or almost connected to the thunderstorm, in which case the cloud looks like a shelf attached to the thunderstorm, and is called a **shelf cloud**.

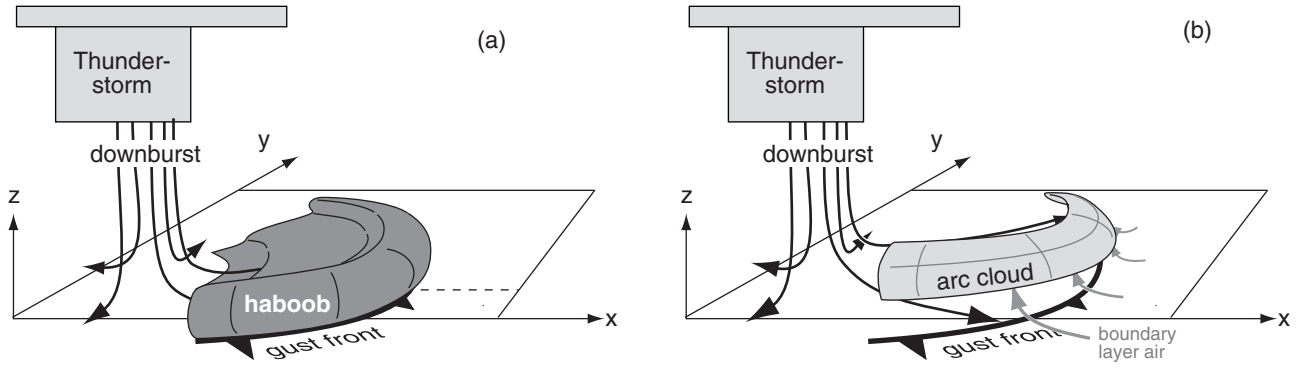

Figure 15.20
Sketches of (a) a haboob (dust storm) kicked up within the outflow winds, and (b) an arc cloud in the boundary-layer air pushed above the leading edge of the outflow winds (i.e., above the gust front). Haboobs occur in drier locations, while arc clouds occur in more humid locations.

When the arc cloud moves overhead, you will notice sudden changes. Initially, you might observe the warm, humid, fragrant boundary-layer air that was blowing toward the storm. After gust-front passage, you might notice colder, gusty, sharp-smelling (from ozone produced by lightning discharges) downburst air.

LIGHTNING AND THUNDER

Lightning (Fig. 15.21) is an electrical discharge (spark) between one part of a cloud and either:

- another part of the same cloud
  [**intracloud** (**IC**) **lightning**],
- a different cloud
  [**cloud-to-cloud (CC) lightning**, or **intercloud lightning**],
- the ground or objects touching the ground
  [**cloud-to-ground** (**CG**) **lightning**], or
- the air
  [**air discharge (CA)**].

Other weak high-altitude electrical discharges (blue jets, sprites and elves) are discussed later.

The lightning discharge heats the air almost instantly to temperatures of 15,000 to 30,000 K in a **lightning channel** of small diameter (2 to 3 cm) but long path (0.1 to 10 km). This heating causes:

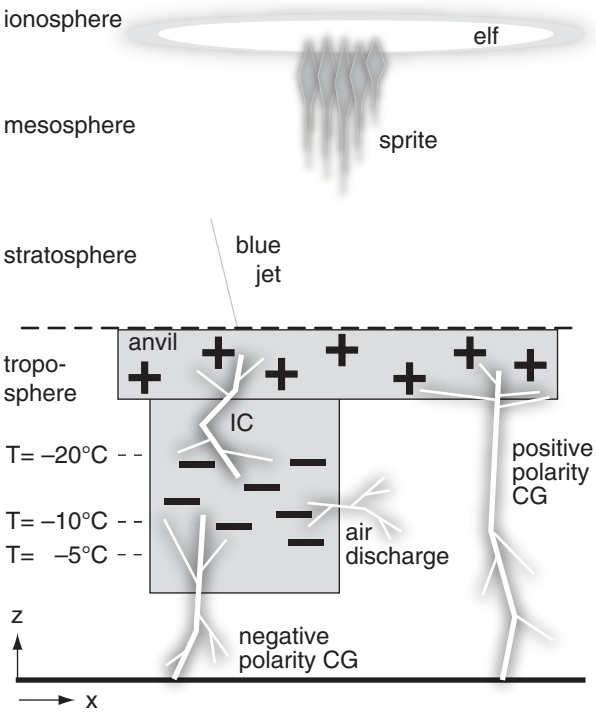

Figure 15.21
Types of lightning. (Vertical axis not to scale.)

FOCUS • Downburst & Flight Operations

In 1975 a jet airliner crashed killing 113 people at JFK airport in New York, while attempting to land during a downburst event. Similar crashes prompted major research programs to understand and forecast downbursts. One outcome is a recommended procedure for pilots to follow, which is counter to their normal reactions based on past flight experience.

Picture an aircraft flying through a downburst while approaching to land, as sketched below. First the aircraft experiences strong headwinds (1) , then the downburst (2) , and finally strong tail winds (3).

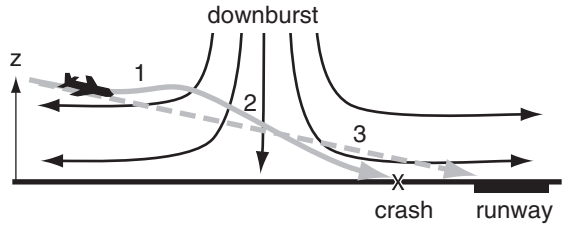

Figure 15.a
Vertical cross section of downburst and aircraft glide slope (dashed grey) and actual path (solid grey).

The dashed grey line shows the desired glideslope, while the solid grey line shows the actual flight path of the aircraft that crashed at JFK. Initially, the aircraft was on the desired glideslope.

Upon reaching point 1, strong headwinds blowing over the aircraft wings increased the lift, causing the aircraft to rise above the glide slope. The pilot reduced pitch and engine power to descend to the glideslope. The aircraft was in a nose-low and reduced-power configuration as it reached point 2, opposite to what was needed to counteract the downburst.

By point 3, strong tailwinds reduced the airflow over the wings, reducing the lift and causing the aircraft to sink faster. The pilot increased pitch and engine power, but the turbine engines took a few seconds to reach full power. The inertia of the heavy aircraft caused its speed to increase too slowly. The slow airspeed and downward force of the downburst caused the aircraft to crash short of the runway.

Since that time, downburst and wind-shear sensors have been (and are continuing to be) deployed at airports to provide warnings to pilots and air-traffic controllers. Also, pilots are now trained to maintain extra airspeed if they fly through an unavoidable downburst event, and to be prepared to make an earlier decision about a **missed approach** (i.e., to climb away from the ground instead of trying to land).

FOCUS • Electricity in a Channel

Electricity is associated with the movement of electrons and ions (charged particles). In metal channels such as electrical wires, it is usually only the electrons (negative charges) that move. In the atmospheric channels such as lightning, both negative and positive ions can move, although electrons can move faster because they are smaller, and carry most of the current. Lightning forms when **static electricity** in clouds discharges as **direct current** (DC).

Each electron carries one elementary negative charge. One **coulomb** (C) is an **amount of charge** (Q) equal to 6.24×10^{18} elementary charges. [Don't confuse C (coulombs) with °C (degrees Celsius).] The **main charging zone** of a thunderstorm is between altitudes where $-20 \le T \le -5$°C (Fig. 15.21), where typical thunderstorms hold 10 to 100 coulombs of static charge.

The movement of 1 C of charge per 1 second (s) is a **current** (I) of 1 A (**ampere**).

$$I = \Delta Q \,/\, \Delta t$$

The median current in lightning is 25 kA.

Most substances offer some **resistance** (R) to the movement of electrical charges. Resistance between two points along a wire or other conductive channel is measured in **ohms** (Ω).

An electromotive force (V, better known as the **electrical potential difference**) of 1 V (**volt**) is needed to push 1 A of electricity through 1 ohm of resistance.

$$V = I \cdot R$$

[We use italicized V to represent the variable (electrical potential), and non-italicized V for its units (volts).]

The **power** P_e (in watts W) spent to push a current I with voltage V is

$$P_e = I \cdot V$$

where 1 W = 1 V · 1 A. For example, lightning of voltage 1×10^9 V and current 25 kA dissipates 2.5×10^{13} W.

A lightning stroke might exist for Δt = 30 μs, so the energy moved is $P_e \cdot \Delta t = (2.5 \times 10^{13}\ \text{W}) \cdot (0.00003\ \text{s}) = 7.5 \times 10^8$ J; namely, about 0.75 billion Joules.

- incandescence of the air, which you see as a bright flash, and
- a pressure increase to values in the range of 1000 to 10,000 kPa in the channel, which you hear as thunder.

On average, there are about 2000 thunderstorms active at any time in the world, resulting in about 45 flashes per second. Worldwide, there are roughly 1.4×10^9 lightning flashes (IC + CG) per year, as detected by optical transient detectors on satellites. Africa has the greatest amount of lightning, with 50 to 80 flashes/(km^2 yr) over the Congo Basin. In North America, the region having greatest lightning frequency is the Southeast, having 20 to 30 flashes/(km^2 yr), compared to only 2 to 5 flashes/(km^2 yr) across most of southern Canada.

On average, only 20% of all lightning strokes are CG, as measured using ground-based lightning detection networks, but the percentage varies with cloud depth and location. The fraction of lightning that is CG is less than 10% over Kansas, Nebraska, the Dakotas, Oregon, and NW California, and is about 50% over the Midwest states, the central and southern Rocky Mountains, and eastern California.

CG lightning causes the most deaths, and causes power surges or disruptions to electrical transmission lines. In North America, the southeastern states have the greatest density of CG lightning [4 to 10 flashes/(km^2 yr)], with Tampa, Florida, having the greatest CG flash density of 14.5 flashes/(km^2 yr).

Most CG lightning causes the transfer of electrons (i.e., negative charge) from cloud to ground, and is called **negative-polarity** lightning. About 9% of CG lightning is **positive-polarity**, and usually is attached to the thunderstorm anvil (Fig. 15.21) or from the extensive stratiform region of a mesoscale convective system. Because positive-polarity lightning has a longer path (to reach between anvil and ground), it requires a greater voltage gradient. Thus, positive CG lightning often transfers more charge with greater current to the ground, with a greater chance of causing deaths and **forest fires**.

Origin of Electric Charge

Large-scale (macroscale) **cloud electrification** occurs due to small scale (microphysical) interactions between individual cloud particles. Three types of particles are needed in the same volume of cloud:

- small ice crystals formed directly by deposition of vapor on to ice nuclei;
- small supercooled liquid water (cloud) droplets;
- slightly larger graupel ice particles.

An updraft of air is also needed to blow the small particles upward relative to the larger ones falling down.

These three conditions can occur in cumulonimbus clouds between altitudes where the temperature is 0°C and –40°C. However, most of the electrical charge generation is observed to occur at heights where the temperature ranges between –5 and –20°C (Fig. 15.21).

The details of how charges form are not known with certainty, but one theory is that the falling graupel particles intercept lots of supercooled cloud droplets that freeze relatively quickly as a glass (i.e., too fast for crystals to grow). Meanwhile, separate ice nuclei allow the growth of ice crystals by direct deposition of vapor. The alignment of water molecules on these two types of surfaces (glass vs. crystal) are different, causing different arrangement of electrons near the surface.

If one of the small ice crystals (being blown upward in the updraft because of its small terminal velocity) hits a larger graupel (falling downward relative to the updraft air), then about 100,000 electrons (i.e., a charge of about 1.5×10^{-14} C) will transfer from the small ice crystal (leaving the ice crystal positively charged) to the larger glass-surfaced graupel particle (leaving it negatively charged) during this one collision (Fig. 15.22). This is the microphysical electrification process.

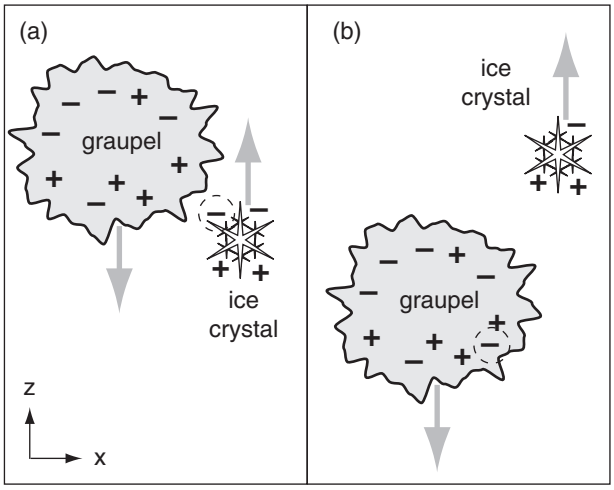

Figure 15.22
Illustration of charge transfer from a small, neutrally-charged, rising ice crystal to a larger, neutrally-charged, falling graupel or hail stone. The electron being transferred during the collision is circled with a dashed line. After the transfer, the graupel has net negative charge that it carries down toward the bottom of the thunderstorm, and the ice crystal has net positive charge that it carries up into the anvil.

FOCUS • Electricity in a Volume

The **electric field strength** (E, which is the magnitude of the **electric field** or the gradient of the **electric potential**) measures the electromotive force (voltage V) across a distance (d), and has units of V/m or V/km.

$$E = V / d .$$

Averaged over the whole atmosphere, $|E| \approx 1.3 \times 10^5$ V/km in the vertical. A device that measures electric field strength is called a **field mill**.

Near thunderstorms, the electric field can increase because of the charge build up in clouds and on the ground surface, yielding electric-potential gradients ($E = 1 \times 10^9$ to 3×10^9 V/km) large enough to ionize air along a narrow channel, causing lightning. When air is ionized, electrons are pulled off of the originally neutral molecules, creating a **plasma** of charged positive and negative particles that is a good conductor (i.e., low resistivity).

Electrical **resistivity** (ρ_e) is the resistance (R) times the cross-section area ($Area$) of the substance (or other conductive path) through which electricity flows, divided by the distance (d) across which it flows, and has units of Ω·m.

$$\rho_e = R \cdot Area / d$$

Air near sea level is not a good electrical conductor, and has a resistivity of about $\rho_e = 5 \times 10^{13}$ Ω·m. One reason why its resistivity is not infinite is that very energetic protons (**cosmic rays**) enter the atmosphere from space and can cause a sparse array of paths of ionized particles that are better conductors. Above an altitude of about 30 km, the resistivity is very low due to ionization of the air by sunlight; this conductive layer (called the **electrosphere**) extends into the ionosphere.

Pure water has $\rho_e = 2.5 \times 10^5$ Ω·m, while seawater is an even better conductor with $\rho_e = 0.2$ Ω·m due to dissolved salts.

Vertical **current density** (J) is the amount of electric current that flows vertically through a unit horizontal area, and has units A/m^2.

$$J = I / Area$$

In clear air, typical background current densities are 2×10^{-12} to 4×10^{-12} A/m^2.

Within a volume, the electric field strength, current density, and resistivity are related by

$$E = J \cdot \rho_e$$

Solved Example

What voltage difference is necessary to create a lightning bolt across the dry air between cloud base (at 2 km altitude) and the ground?

Solution

Given: $\Delta z = 2$ km, $B = 3\text{x}10^9$ V/km

Find: $\Delta V_{lightning} = ?$ V

Use eq. (15.16):

$\Delta V_{lightning} = (3\text{x}10^9 \text{ V/km})\cdot(2 \text{ km}) = 6\text{x}10^9$ V

Check: Units OK. Physics OK.

Discussion: Six billion volts is more than enough to cause cardiac arrest, so it is wise to avoid being struck by lightning. High-voltage electrical transmission lines are often about $3.5\text{x}10^5$ V. Lightning is nearly tied with floods as being the most fatal weather hazard in North America.

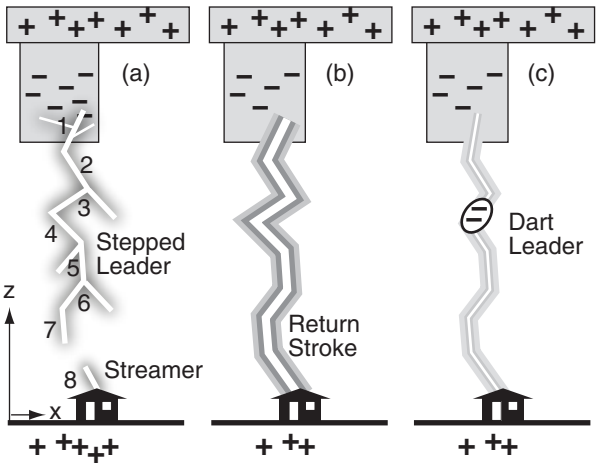

Figure 15.23

Sequence of events during lightning. (a) Stepped leader (1 to 7) moving rapidly downward from thunderstorm, triggers upward streamer (8) from objects on ground. (b) Intense return stroke transferring negative charge from the bottom of the thunderstorm to the ground. (c) Dart leader of negative charge following old ionized path toward ground, followed by another return stroke (not shown).

In 1 km^3 of thunderstorm air, there can be on the order of $5\text{x}10^{13}$ collisions of graupel and ice crystals per minute. The lighter-weight ice crystals carry their positive charge with them as they are blown in the updraft to the top of the thunderstorm, leading to the net positive charge in the anvil. Similarly, the heavier graupel carry their negative charges to the middle and bottom of the storm. The result is a macroscale (Fig. 15.21) charging rate of the thunderstorm cloud of order 1 C km^{-3} min^{-1}. As these charges continue to accumulate, the electric field (i.e., voltage difference) increases between the cloud and the ground, and between the cloud and its anvil.

Air is normally a good insulator in the bottom half of the troposphere. Lightning occurs when the voltage difference is large enough to **ionize** (removing or adding electrons) the air and make it conductive. This voltage difference, called the **breakdown potential**, is $B_{dry} = 3\text{x}10^9$ V/km for dry air (where V is volts), and roughly $B_{cloud} = 1\text{x}10^9$ V/km for cloudy air.

Thus, by measuring the length Δz of any electrical spark, including lightning, you can estimate the voltage difference $\Delta V_{lightning}$ that caused the spark:

$$\Delta V_{lightning} = B\cdot\Delta z \qquad \bullet(15.16)$$

where B is the dry-air or cloudy-air breakdown potential, depending on the path of the lightning.

Lightning Behavior & Appearance

When sufficient charge builds up in the cloud to reach the breakdown potential, an ionized channel called a **stepped leader** starts to form. It steps downward from the cloud in roughly 50 m increments, each of which takes about 1 μs to form, with a pause of about 50 μs between subsequent steps (Fig. 15.23). While propagating down, it may branch into several paths. To reach from the cloud to the ground might take hundreds of steps, and take 50 ms duration. For the most common (negative polarity) lightning from the middle of the thunderstorm, this stepped leader carries about 5 C of negative charge downward.

When it is within about 30 to 100 m of the ground or from the top of any object on the ground, its strong negative charge repels free electrons on the ground under it, leaving the ground strongly positively charged. This positive charge causes ground-to-air discharges called **streamers**, that propagate upward as very brief, faintly glowing, ionized paths from the tops of trees, poles, and tall buildings. When the top of a streamer meets the bottom of a stepped leader, the conducing path between the cloud and ground is complete, and there is a very strong (bright)

return stroke from the ground to the cloud. During this return stroke, electrons drain downward first from the bottom of the stepped leader, and then drain downward from successively higher portions of the channel, producing the flash of light that you see. Taken together, the stepped leader and return stroke are called a lightning **stroke**.

Although thunderstorm winds and turbulence tend to rip apart the ionized channel, if the remaining negative charges in the cloud can recollect within about 20 to 50 ms, then another stroke can happen down the same conducting path. This second stroke (and subsequent strokes) forms as a **dart leader** carrying about 1 C of charge that moves smoothly (not in steps) down the existing channel (with no branches) to the ground, triggering another return stroke. Ten strokes can easily happen along that one ionized channel, and taken together are called a **lightning flash**. The multiple return strokes are what makes a lightning flash appear to flicker.

IC and CG lightning can have different appearances that are sometimes given colloquial names. **Anvil crawlers** or **spider lightning** is IC lightning that propagates with many paths (like spider legs) along the underside of anvils or along the bottom of the stratiform portion of mesoscale convective systems. Some spider lightning is exceptionally long, exceeding 100 km path lengths.

If an IC lightning channel is completely hidden inside a cloud, then often observers on the ground see the whole cloud illuminated as the interior light scatters off the cloud drops (similar to the light emitted from a frosted incandescent light bulb where you cannot see the filament). This is called **sheet lightning**. Lightning from distant thunderstorms may illuminate hazy cloud-free sky overhead, causing dim flashing sky glow called **heat lightning** in the warm, prestorm environment.

A **bolt from the blue** is a form of CG **anvil lightning** that comes out laterally from the side of a storm, and can travel up to 16 km horizontally into clear air before descending to the ground. To people near where this lightning strikes, it looks like it comes from clear blue sky (if they cannot see the thunderstorm that caused it).

Ball lightning has been difficult to study, but has been observed frequently enough to be recognized as a real phenomenon. It is rare, but seems to be caused by a normal CG strike that creates a longer lasting (many seconds to minutes) glowing, hissing plasma sphere that floats in the air and moves.

After the last return stroke of CG lightning, the rapidly dimming lightning channel sometimes exhibits a string of bright spots that don't dim as fast as the rest of the channel, and thus appear as a string of glowing beads, called **bead lightning**.

ON DOING SCIENCE • Be Safe *(part 3)*

More chase guidelines from Charles Doswell III (continued from the previous chapter):

The #2 Threat: Lightning

1. Stay inside your car if cloud-to-ground (CG) lightning is less than 1 mile away.
2. CG threat is high when rain first reaches you.
3. CG can strike well away from the storm. Move to safety. If you can't, then:
   a. Avoid being the tallest object around.
   b. Don't stand close to fences or power poles that are connected to wires going closer to the storm.
   c. Make yourself low (i.e., squat), but don't lay, sit, or kneel on the ground, and don't have your hands touching anything connected to the ground.
   d. You might not have any warning signs (hear thunder, hear hissing or crackling discharges of electricity nearby, or feel your hair stand on end) before you are struck.
   e. You and your chase-team members should be trained on how to do **CPR** (cardiopulmonary resuscitation), and don't be afraid to use it immediately if appropriate.
   f. Non-metalic camera tripods and insulated shoes don't reduce your threat of being struck by lightning.

(continues later in this chapter)

FOCUS • Lightning Burns the Air

The initial high temperature and pressure inside the lightning channel cause the oxygen in the air to react with the other gases.

Nitrogen, which makes up 78% of the atmosphere (see Chapter 1), oxidizes inside the ionized lightning path to become various oxides of nitrogen (NO_x). During rainout, the NO_x can fall as acid rain (nitric acid), which hurts the plants and acidifies streams and lakes on the short term. But over the long term, the NO_x rained out can help fertilize the soil to encourage plant growth.

Even the oxygen molecules (O_2) can be oxidized within the lightning channel to become ozone (O_3), which we smell in the air as a sharp or fresh odor. Sometimes this odor is carried down and out from the thunderstorm by the downburst and outflow winds, which we can smell when the gust front passes just before the thunderstorm arrives.

Because of all this oxidation, we can say that lightning causes the air to burn.

FOCUS • Lightning in Canada

In Canada, lightning currents greater than 100 kA are rare (approximately 1% of all cloud-to-ground CG strokes). Summer is when these large-current flashes occur. Large-current flashes with negative polarity can have 10 or more strokes, and are found mostly in western Canada. First-stroke peak currents are strongest in winter, and strongest in northern Canada.

In eastern Canada, about 11% of the CG flashes have positive polarity, and in western Canada about 17% have positive polarity. In British Columbia and Yukon about 25% of the CG flashes have positive polarity.

In western Canada, 89% of the positive CG lightning flashes had only one stroke, while 48% of the negative CG lightning had only one stroke. The average number of strokes per CG flash is 2 to 2.4 for negative polarity CG lightning flashes, and about 1 stroke for positive CG.

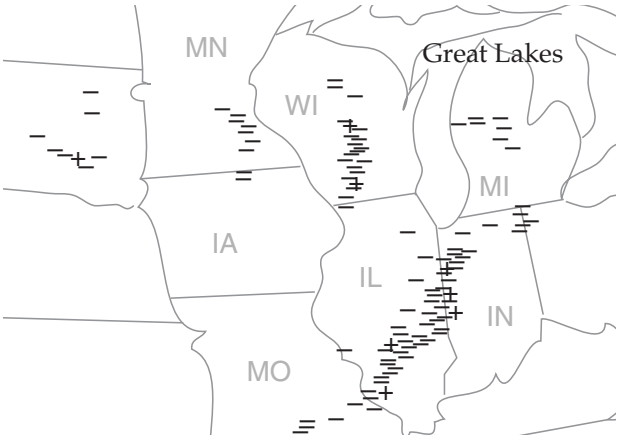

Figure 15.24
Map of negative (–) and positive (+) lightning strikes over the US Midwest from a (simulated) lightning detection network, for the 24 May 2006 case.

When CG multiple return strokes happen along a lightning channel that is blowing horizontally in the wind, the human eye might perceive the flash as a single broad ribbon of light called **ribbon lightning**. Lightning with a very brief, single return stroke is called **staccato lightning**.

Above the top of strong thunderstorms can be very brief, faint, electrical discharges that are difficult to see from the ground, but easier to see from space or a high-flying aircraft (Fig. 15.21). A **blue jet** is a vertical anvil-to-air discharge into the stratosphere. **Red sprites** can spread between cloud top and about 90 km altitude (in the mesosphere), and have diameters of order 40 km. **Elves** are extremely faint glowing horizontal rings of light at 90 km altitude with radii that increases at the speed of light, centered above strong lightning strokes in thunderstorms. Most people never see these.

Lightning Detection

The sudden increase and decrease in electricity through the lightning path in air generates electromagnetic radiation much like a broadcast antenna. A broad range of frequencies is transmitted, including radio waves. The transmitted radio signals are known as **sferics**, and can be heard as snaps or static on AM radio bands. Networks of receiving stations on the ground can measure the time and amplitude of the sferics. Other types of lightning sensors are based on magnetic direction finders.

To pinpoint the location of each lightning strike, a continent-wide array of multiple ground stations observe signals from the same lightning discharge. These ground stations either have direction-finding capability or relative time-of-arrival capability (to infer the range of the strike from the station). Regardless of the station capabilities, the strike is located by triangulating directions or ranges from all the stations that received the signal. All the strike locations during a time interval (5 minutes to a hour) are then plotted on a map (Fig. 15.24). The received amplitude can also be used to estimate lightning-stroke strength. This forms the basis of ground-based **lightning detection networks** (LDN).

Some surface-based networks receive **very low frequency** (**VLF**) radio waves (10 kHz frequency; 30 km wavelength), where the domain between the ground and the ionosphere is a waveguide for these waves. If the ground station can measure the peak electric field E (V/m, see Focus box on "Electricity in a Volume") associated with the VLF wave passage, and if distance D (m) to the lightning can be determined by triangulation, then the peak current I_{max} (A) flowing in the return stroke can be estimated from:

$$I_{\max} = -2\pi \cdot \varepsilon_o \cdot c^2 \cdot E \cdot D / v_L \qquad (15.17)$$

where c = 3.00986 x 10^8 m/s is the speed of light, ε_o = 8.854 x 10^{-12} A·s·(V·m)$^{-1}$ is the permittivity of free space, and v_L = 1.0 to 2.2 x 10^8 m/s is the velocity of the current through the return-stroke path.

Over 29 million CG lightning flashes are detected each year in the USA by the **National Lightning Detection Network** (NLDN). The median peak current is 25 kA, for negative currents. High electrical currents (up to 400 kA) in lightning are less likely than low currents. The average duration of a lightning stroke is about 30 μs, and the average peak power per stroke is about 10^{12} W. Often, lightning flashes consist of one to ten quick return strokes in the same ionized path, with a typical time interval between strokes of 50 to 300 ms.

Satellite systems also detect lightning. Low-light-level video and digital cameras have been on board some satellites and manned space vehicles, and have observed lightning at night from the flashes of light produced. An **optical transient detector** (**OTD**) has also been deployed that measures the changes in light leaving the portion of atmosphere viewed.

Solved Example

What electric field would be measured at a lightning detection station 200 km from a lightning stroke of max intensity 20 kA?

Solution

Given: I_{max} = 20 kA, D = 200 km
Find: E = ? V/m
Assume: v_L = 2.0 x 10^8 m/s

Solve eq. (15.17) for E:

$$E = [-v_L / (2\pi \cdot \varepsilon_o c^2)] \cdot (I_{\max} / D)$$

E = [(20 kA)/200 km)] · [(– 2.0 x 10^8 m/s) / (2π· (8.854 x 10^{-12} A·s·(V·m)$^{-1}$)·(3.00986 x 10^8 m/s)^2)]
= **– 4 V/m**

Check: Units OK. Physics OK. The negative sign means that the direction of current flow is opposite to the voltage gradient. Namely, lightning current flows from high toward low voltage.

Discussion: Lightning detection stations can also determine the polarity of the lightning, and the waveform. Cloud-to-ground lightning has a different waveform and polarity than cloud-to-cloud lightning. Thus, algorithms processing signals from the network of stations can determine lightning type, charge (positive or negative), intensity and location.

Lightning Hazards and Safety

Based on measurements of lightning **surges** (excessive current and voltage in electrical power lines), the probability *Prob* that lightning current will exceed value I (kA) is well approximated by a log-normal distribution:

$$Prob = \exp\left\{-0.5 \cdot \left[\frac{\ln\left((I + I_o)/I_1\right)}{s_1}\right]^2\right\} \qquad (15.18)$$

for $I \geq (I_1 - I_o)$, where I_o = 2 kA, I_1 = 3.5 kA, and s_I = 1.5. As plotted in Fig. 15.25, there is a 50% chance that a lightning current in a power line will exceed about 20 kA.

A standardized wave shape is used by electrical engineers to model the lightning surge in electrical power lines. It is given by

$$e = e_{\max} \cdot a \cdot \left[\exp\left(-\frac{t}{\tau_1}\right) - \exp\left(-\frac{t}{\tau_2}\right)\right] \qquad (15.19)$$

where e and e_{max} can apply to current or voltage. The nominal constants are: τ_1 = 70 μs, τ_2 = 0.15 μs, and a = 1.014. The surge, plotted in Fig. 15.26 reaches a peak in 1 μs, and decreases by half in 50 μs. The actual time constants vary from case to case.

When lightning strikes sandy ground, it can melt and fuse the sand along its path into a long narrow

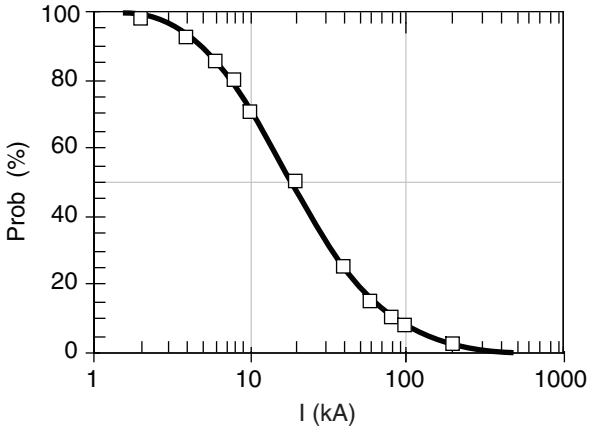

Figure 15.25
Probability (Prob) that lightning current will exceed I in an electrical power line. Data points (observations), curve (eq. 15.18).

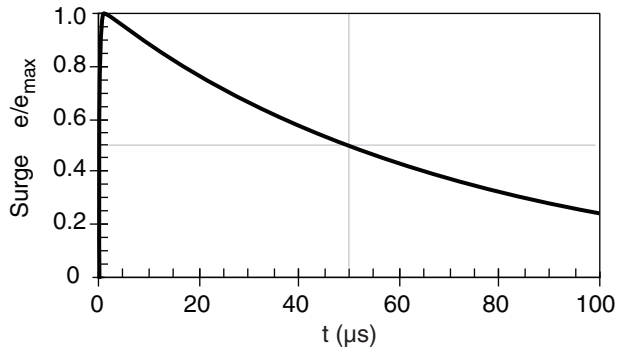

Figure 15.26
Lightning-surge wave shape in an electrical power line.

Solved Example

What is the probability that a lightning strike will cause a current of 80 kA or greater in a power line? How soon after the strike will the current be reduced to 8 kA?

Solution

Given: $I = 80$ kA, $I/I_{max} = 8/80 = 0.1$
Find: $Prob$ = ? %, t = ? μs

Use eq. (15.18):

$$Prob = \exp\left\{-0.5\cdot\left[\frac{\ln((60+2\text{kA})/(3.5\text{kA}))}{1.5}\right]^2\right\}$$

$$= \underline{\mathbf{11\%}}$$

Use eq. (15.19), replacing e/e_{max} with I/I_{max}. For long times the last exponential is negligible compared to the first. Hence we can solve eq. (15.19) for the time:

$$t = -\tau_1 \cdot \ln[(1/a)\cdot e/e_{\max}] = -\tau_1 \cdot \ln[(1/a)\cdot I/I_{\max}]$$

$$= -(70\ \mu\text{s}) \cdot \ln[\ (1/1.014) \cdot 0.1\ ] = \underline{\mathbf{162.2\ \mu s}}$$

Check: Units OK. Physics OK. Agrees with Figs.
Discussion: During the short but intense electrical surge, insulation can be destroyed, power transformers can be melted, and circuit breakers can open. This results in power surges or interruptions that reach homes and businesses, causing comp#ters to go berserk, file$ to be cor@upte#, and #@!*.&%$ #¶£$ #... .. .

FOCUS • The 30-30 Lightning Safety Rule

For the non-storm-chaser, use the 30-30 Rule of lightning safety: If you are outdoors and the time between the lightning flash and thunder is 30 s or less, then seek shelter immediately. Wait 30 minutes after hearing the last thunder clap before going outdoors.

tube called a **fulgurite**. When it strikes trees and flows down the trunk to the ground, it can cause the moisture and sap in the tree to instantly boil, causing the bark to splinter and explode outward as lethal wooden shrapnel. Sometimes the tree trunk will split, or the tree will ignite.

When lightning strikes a metal-skinned vehicle such as a car or aircraft, the electricity flows on the outside of the metal skin, which acts like a **Faraday cage**. If you are inside the vehicle, there is little direct hazard to health from the lightning, other than the surprise of the loud thunder and the temporary blindness by the flash. However, while the electricity flows around the metal skin, it can induce secondary currents within the wires of the car or plane, which can destroy electronic equipment and avionics. Where the lightning attaches to the car or aircraft, a pinhole can be burned through the metal.

Dangerous activities/locations associated with lightning strikes are:

1. Open fields including sports fields.
2. Boating, fishing, and swimming.
3. Using heavy farm or road equipment.
4. Playing golf.
5. Holding a hard-wired telephone.
6. Repairing or using electrical appliances.

You should take precautions to avoid being struck by lightning. Avoid water and metal objects. Get off of high ground. Avoid open fields. Stay away from solitary trees or poles or towers (which might attract lightning). Go indoors or inside a metal-skinned car, van or truck if lightning is within 10 km (i.e., 30 seconds or less between when you see a lightning flash and when you hear its thunder). Even if you don't see lightning or hear thunder, if the hair on your head, neck or arms stands on end, immediately go inside a building or car. If indoors, avoid using hard-wired phones, hair driers, or other appliances, and avoid touching metal plumbing or water in your sink, shower, or tub.

If you are outside and no shelter is available, crouch down immediately in the lowest possible spot with your feet together and your hands over your ears. Do not lie down, because once lightning strikes the ground or a tree, it often spreads out along the surface of the ground and can still hit you. Do not put both your hands and feet on the ground, because then the lightning circuit could go through your heart.

If people near you are struck by lightning and fall down, do not assume they are dead. In many cases, lighting will cause a person to stop breathing or will stop their heart, but they can often be revived. If a person isn't breathing then try performing mouth-to-mouth resuscitation. If a person has no pulse, and

if you have the training, apply cardiopulmonary resuscitation (CPR).

Cardiac arrest (stopped heart) is the main cause of death from a lightning strike. Surprisingly, there is usually very little burning of the skin. Other immediate effects include tinnitus (ringing in the ears due to the loud thunder), blindness, amnesia, confusion, cardiac arrhythmias, and vascular instability. Later problems include sleep disturbances, anxiety attacks, peripheral nerve damage, pain syndromes, fear of storms, personality changes, irritability, short-term memory difficulties, and depression. Lightning injures 800 to 1000 people per year in the USA, and kills 75 to 150 people per year. Support groups exist for lightning survivors.

Thunder

When lightning heats the air to T = 15,000 to 30,000 K, it instantly increases the air pressure to P = 1,000 to 10,000 kPa along the ionized lightning path, creating a **shock front** that moves at speeds up to ten times the speed of sound (i.e., Ma = 10, where Ma is **Mach number**). By 7 μs later, the supersonic shock-front speed has decreased to Mach 5, and has spread only about 1.5 cm from the edge of the lightning channel (Fig. 15.27). By 0.01 s after the lightning, the shock front has spread about 4 m in all directions around the lightning, and has a speed (Ma = 1.008) that is almost equal to the speed of sound (Ma = 1). Namely, it becomes a **sound wave** that continues to spread at the speed of sound, which you hear as thunder. So to understand thunder, we will study shock fronts first, and then sound.

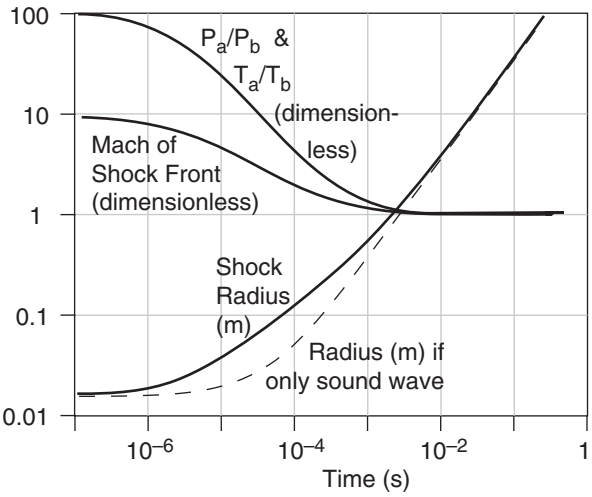

Figure 15.27
Evolution of initial stages of thunder as it propagates as a supersonic shock front. P_a/P_b is the ratio of average pressure behind the shock front to background pressure ahead of the front. T_a/T_b is similar ratio for absolute temperature. Propagation speed of the shock front is given by its Mach number. Radius of the shock front from the lightning axis is compared to radius if only sound waves had been created.

FOCUS • Force of Thunder

One time when I was driving, lightning struck immediately next to my car. The shock wave instantly pushed the car into the next lane, without breaking any windows or causing damage. I was amazed at the power of the shock wave, and happy to be alive.
- R. Stull

Shock Front

A shock front in air is created by a pressure discontinuity or pressure step. The thickness of this pressure step is only a few micrometers. This shock front advances supersonically at speed C through the air toward the lower pressure. It is NOT like a piston that pushes against the ambient air in front of it. Instead it moves THROUGH the background low-pressure air, modifies the thermodynamic and dynamic state of the air molecules it overtakes, and leaves them behind as the front continues on. This modification of the air is irreversible, and causes entropy to increase.

To analyze the shock, picture an idealized vertical lightning channel (Fig. 15.28) of radius r_o. Assume the background air is calm (relative to the speed of the shock) and of uniform thermodynamic state. For simplicity, assume that air is an ideal gas, which is a bad assumption for the temperatures and pressures inside the lightning channel.

Because the shock front will expand as a cylinder of radius r around the axis of the lightning chan-

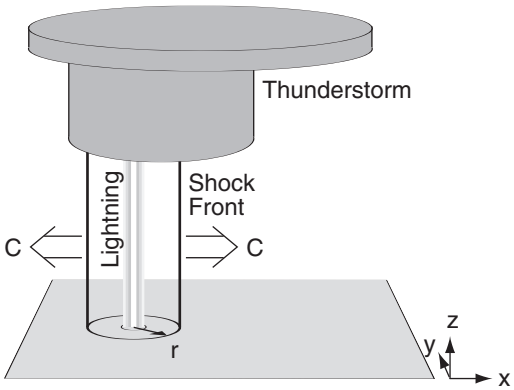

Figure 15.28
Sketch of idealized vertical lightning discharge that generates a cylindrical shock front of radius r that expands at speed C.

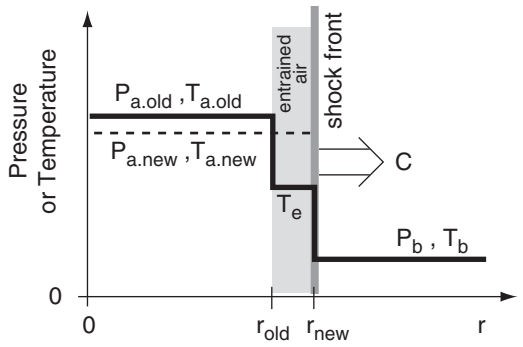

Figure 15.29
Characteristics of the thunder shock front as a function of radial distance r from the lightning-channel axis (at r = 0). P_a and T_a are the average pressure and temperature behind the shock front, relative to background conditions ahead of the front P_b and T_b. As the shock front overtakes background air molecules, their temperature is modified to be T_e, which is assumed to mix with the old conditions behind the front to create new average conditions. $r_{new} - r_{old} \approx$ a few μm.

nel, ignore the vertical (because no net change in the vertical), and use the circular symmetry to treat this as a 1-D **normal-shock** problem in the horizontal. Namely, the movement the shock front across the air molecules is perpendicular to the face of the shock front.

Use subscript $_b$ to indicate background air (not yet reached by the shock), and subscript $_e$ to indicate entrained air (namely, background air that has been modified by the shock-front passage). For simplicity, assume that the entrained air instantly mixes with the rest of the air inside the shock-front circle, and use subscript $_a$ to indicate the resulting average conditions inside that circle (Fig. 15.29).

For a normal-shock, the Mach number (dimensionless) of the shock wave expanding into the background air is

$$Ma = \left[\frac{(P_a / P_b)\cdot(k-1) + k - 1}{2k} \right]^{1/2} \qquad (15.20)$$

where P is pressure, and $k = C_p/C_v$. For air, $k = 1.40$, allowing the previous equation to be simplified to:

$$Ma = \left[\frac{(P_a / P_b)\cdot 6 + 1}{7} \right]^{1/2} \qquad (15.21)$$

One equation for the speed of sound (s) in air is

$$s = (k\cdot\Re\cdot T)^{1/2} \qquad \bullet(15.22)$$

where $\Re = C_p - C_v = 287\ m^2\ s^{-2}\ K^{-1}$ is the gas constant, and T is absolute air temperature. For background air, this simplifies to

$$s_b = a_s \cdot (T_b)^{1/2} \qquad (15.23)$$

where $a_s = 20\ (m/s)\cdot K^{-1/2}$ is a constant for air, and T_b is background air temperature (in Kelvin). For example, if the background air has temperature 27°C (= 300 K), then sound speed is $s_b = 346.41$ m/s.

By definition, the Mach number is the speed of the object (or the shock) divided by sound speed. Thus the speed C of the shock front through the calm background air is

$$C = Ma \cdot s_b \qquad \bullet(15.24)$$

During a small time interval Δt, the radius r of the shock circle expands as:

$$r_{new} = r_{old} + C \cdot \Delta t \qquad (15.25)$$

The thin layer of air immediately behind the shock front is warmed (due to compression) to:

$$T_e = T_b \cdot \frac{[2 + (k-1)\cdot Ma^2][2k\cdot Ma^2 - k + 1]}{(k+1)^2 Ma^2} \qquad (15.26)$$

or

$$T_e = T_b \cdot \frac{[5 + Ma^2][7Ma^2 - 1]}{36Ma^2} \qquad (15.27)$$

where T_b is background air temperature and Ma is the Mach number of the shock front. T_e is the temperature of the air entrained inside the shock circle.

By keeping track of the average temperature T_a of all air enclosed by the shock circle, use geometry to find how that average changes as the entrained air is added

$$T_{a.new} = T_e + \frac{(T_{a.old} - T_e)}{(r_{new} / r_{old})^2} \qquad (15.28)$$

Lightning-formed shocks are quite different from shocks caused by chemical explosives (i.e., bombs). Conventional bombs explosively release large amounts of gas via chemical reactions, which increases the pressure, temperature, and density of the atmosphere by quickly adding gas molecules that were not there before. As the resulting shock front expands, there is a net out rush of gas behind the shock as the gas density decreases toward background values.

Lightning, however, is a constant density (**isopycnal**) process, because no extra air molecules are added to the lightning channel. Namely, lightning starts with existing background air molecules and energizes whichever ones happen to be within the ionized channel. Furthermore, just outside the shock front nothing has changed in the background air (i.e., no density changes, and no movement of molecules toward or away from the shock front).

Therefore, by mass conservation, the average density ρ_a of air enclosed by the shock front is also constant and equal to the original (pre-lightning) background value ρ_b:

$$\rho_a = \rho_b = \text{constant} = P_b / \Re \cdot T_b \qquad \bullet(15.29)$$

using the ideal gas law with P_b as background air pressure, and T_b as background air temperature (in Kelvin). Immediately behind the shock front, the entrained air has higher density and pressure, but this is compensated by lower-density lower-pressure air closer to the lightning axis, resulting in constant average density as shown above.

Finally, the average pressure P_a of all air enclosed by the shock circle is found using the ideal gas law with constant density:

$$P_a / P_b = T_a / T_b \qquad \bullet(15.30)$$

where $T_a = T_{a.new}$. Equations (15.20) through (15.30) can be solved iteratively to find how conditions change as the shock evolves. Namely, P_a can be used back in eq. (15.20), and the calculations repeated. This assumes that the background thermodynamic state T_b and P_b of the undisturbed air is known.

To iterate, you need the initial conditions. Start with r_{old} = radius of the ionized lightning channel, although there is evidence that the incandescent region of air is about 10 to 20 times larger radius than this (so you could try starting with this larger value). Because of the isopycnal nature of lightning, if you know the initial lightning temperature T_a in Kelvin, use eq. (15.30) to find the initial pressure ratio P_a/P_b, as sketched in Fig. 15.30.

An iterative approach is demonstrated in a solved example, the results from which were used to create Fig. 15.27. The background air state was T_b = 300K and P_b = 100 kPa, giving ρ_b = 1.1614 kg/m^3. For the lightning, I used initial conditions of r_{old} = 1.5 cm = 0.015 m, $T_{a.old}$ = 30,000 K, P_a = 10,000 kPa.

Anyone who has been very close (within 1 m or less) of a lightning strike (but not actually hit by the lightning itself) feels a tremendous force that can instantly throw your body (or your car if you are driving) many meters horizontally (as well as rupturing your ear drums). This is the combined effect of the pressure difference across the shock front as it passes your body or your car, and the dynamic effect of a supersonic wind in the thin layer of entrained air immediately behind the shock front.

Assuming a normal shock, the extremely brief, outward-directed wind M_e in the entrained air immediately behind the shock is:

$$M_e = C - [C^2 - 2 \cdot C_p \cdot (T_e - T_b)]^{1/2} \qquad (15.31)$$

Solved Example

Background atmospheric conditions are P_b = 100 kPa, T_b = 300 K, and calm winds. If lightning heats the air in the lightning channel to 15,000 K, what is the initial speed of the shock front, and the initial speed of the air behind the shock front?

Solution

Given: P_b = 100 kPa, T_b = 300 K, M_b = 0 m/s.
T_a = 15,000 K
Find: C = ? m/s , M_e = ? m/s

The shock speed equation requires the Mach speed and the speed of sound, which must be calculated first. Mach speed, in turn, depends on the initial pressure ratio. Use eq. (15.30) to find the pressure ratio:

$P_a/P_b = T_a/T_b$ = (15000 K)/(300 K) = 50

Next, use eq (15.21) to find the Mach speed of the shock front through the background air:

$Ma = \{[(50) \cdot 6 + 1\ ]/\ 7\}^{1/2}$ = 6.56

The background speed of sound from eq. (15.23) is:

s_b = [20 (m/s)·K$^{-1/2}$] · (300 K)$^{1/2}$ = 346.4 m/s

Thus, using eq. (15.24):

C = 6.56 · (346.4 m/s) = **2,271.6 m/s**

The equation for wind speed behind the shock requires the temperature behind the shock. Use eq. (15.27):

T_e = (300 k)· { [5 + 6.56^2]·[7· 6.56^2 – 1] / (36 · 6.56^2) }
= (300 k)·{ 48 · 300 / 1548 } = 2791 K

Finally, using eq. (15.31):

M_e = (2,271.6 m/s) – [(2,271.6 m/s)^2 –
2·(1005 m^2 s^{-2} K^{-1})·(2791K – 300 K)]$^{1/2}$
= 2,271.6 – 392.3 m/s = **1,879.3 m/s**

Check: Units OK. Physics OK.

Discussion: Both the initial shock front and the initial wind behind the shock are supersonic, but the wind is slower than the shock front.

Nonetheless, the initial shock-front speed (about 2.3x10^3 m/s) is still much slower than the speed of light (3x10^8 m/s). Hence, we will see the lightning before we hear the thunder (except if lightning strikes you).

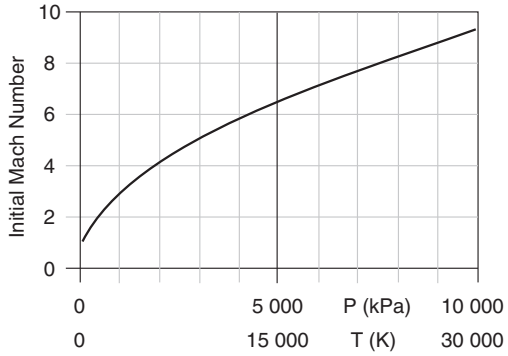

Figure 15.30
Higher temperature T in the lightning channel creates higher pressure P, which generates a shock front that initially moves with greater Mach number. (Mach 1 is the speed of sound).

Solved Example (§)

Background air is calm, with temperature 300 K and pressure 100 kPa. If lightning heats the air to 30,000 K within a vertical lightning channel of radius 1.5 cm, then find and plot the evolution of average temperature inside the shock circle (relative to background temperature), average relative pressure, Mach of the shock front, and shock radius. (Namely, produce the data that was plotted in Fig. 15.27.)

Solution

Given: P_b = 100 kPa, T_b = 300 K, M_b = 0 m/s.
T_a = 30,000 K initially

Find: T_a/T_b = ? , P_a/P_b = ? , Ma = ? , r = ? m
and how they vary with time.

This is easily done with a spreadsheet. Because conditions vary extremely rapidly initially, and vary slower later, I will not use a constant time step for the iterations. Instead, I will use a constant ratio of

$$r_{new}/r_{old} = 1.05 \qquad (a)$$

Namely, I will redo the calculation for every 5% increase in shock radius. Thus,

$$t_{new} = t_{old} + (r_{new} - r_{old})/C_{old} \qquad (b)$$

Procedure: First, enter the given background air values in cells on the spreadsheet, and compute the speed of sound in the background air.

Next, create a table in the spreadsheet that holds the following columns: r, t, T_a, P_a/P_b, Ma, C, and T_e.

In the first row, start with r_{old} = 0.015 m at t_{old} = 0, and initialize with T_a = 30,000 K. Then compute the ratio T_a/T_b, and use that ratio in eq. (15.30) to find P_a/P_b. Use this pressure ratio to find Ma (using eq. 15.21) and C (using eq. 15.24 and knowing background sound speed). Finally, the last column in the first row is T_e found using eq. (15.27).

The second row is similar to the first, except estimate the new r using eq. (a), and the new t using eq. (b). The new T_a can be found using eq. (15.28). The other columns can then be filled down into this second row. Finally, the whole second row can be filled down to as many rows as you want (be careful: do not complete the table by filling down from the first row). Some results from that spreadsheet are shown in the table in the next column.

Fig. 15.27 shows a plot of these results.

Check: Units OK. Physics OK. Some decimal places have been dropped to fit in the table on this page.

Discussion: To check for accuracy, I repeated these calculations using smaller steps (1% increase in shock radius), and found essentially the same answer.

The equations in this section for shock-front propagation are not exact. My assumption of constant density, while correct when averaged over large scales, is probably not correct at the very small scale at the shock front. Thus, my equations are an oversimplification.

(table is in next column)

where C_p = 1005 m^2 s^{-2} K^{-1} is the specific heat of air at constant pressure. Although initially very fast, these winds are slower than the speed of the shock front. Initial supersonic post-shock winds are about 2500 m/s while the shock radius is still small (1.5 cm), but they quickly diminish to subsonic values of about 10 m/s as the shock front expands past 2 m radius.

The resulting sequence of winds at any point not on the lightning axis is: (1) no lightning-created winds prior to shock front passage; (2) near instantaneous increase in outward-directed winds M_e immediately after the shock front passes; which is quickly followed by (3) weaker inward-directed winds (never supersonic) drawn back toward the lower pressure along the lightning axis in order to conserve mass. A similar sequence of events has been observed with shock fronts from atmospheric nuclear-bomb explosions just above ground.

Solved Example *(continuation)*

r (m)	t (s)	T_a (K)	P_a / P_b	Ma	C (m/s)	T_e (K)
0.0150	0	30000	100.0	9.27	3210	5291
0.0158	2.34E-07	27703	92.3	8.90	3085	4908
0.0165	4.89E-07	25584	85.3	8.56	2965	4555
0.0174	7.68E-07	23629	78.8	8.23	2849	4229
0.0182	1.07E-06	21825	72.7	7.91	2739	3928
0.0191	1.41E-06	20161	67.2	7.60	2632	3651
0.0201	1.77E-06	18626	62.1	7.30	2530	3395
0.0211	2.17E-06	17210	57.4	7.02	2433	3159
0.0222	2.60E-06	15904	53.0	6.75	2339	2941
0.0233	3.07E-06	14699	49.0	6.49	2249	2740
0.0244	3.59E-06	13587	45.3	6.24	2162	2555
0.0257	4.16E-06	12561	41.9	6.00	2079	2384
0.0269	4.77E-06	11615	38.7	5.77	2000	2226
0.0283	5.45E-06	10742	35.8	5.55	1924	2081
0.0297	6.18E-06	9937	33.1	5.34	1850	1946
0.0312	6.98E-06	9194	30.6	5.14	1780	1822
• • •						
0.0958	6.73E-05	1729	5.8	2.25	781	572
0.1006	7.35E-05	1621	5.4	2.19	757	553
0.1056	8.01E-05	1522	5.1	2.12	734	536
0.1109	8.73E-05	1430	4.8	2.06	712	520
0.1164	9.51E-05	1346	4.5	2.00	692	506
0.1222	1.03E-04	1268	4.2	1.94	672	492
• • •						
3.5424	0.0094	307	1.02	1.01	350	302
3.7195	0.0099	306	1.02	1.01	350	302
3.9055	0.0105	306	1.02	1.01	349	302
4.1007	0.0110	306	1.02	1.01	349	302
4.3058	0.0116	305	1.02	1.01	349	301
4.5210	0.0122	305	1.02	1.01	349	301
• • •						
35.091	0.100	300	1.00	1.00	347	300
36.845	0.105	300	1.00	1.00	347	300
38.687	0.111	300	1.00	1.00	347	300
• • •						

Sound

By about 0.1 s after the lightning stroke, the shock wave has radius 35 m, and has almost completely slowed into a sound wave. Because this happens so quickly, and so close to the lightning channel, ignore the initial shock aspects of thunder in this subsection, and for simplicity assume that the sound waves are coming directly from the lightning channel.

Sound travels much slower than the speed of light. The sound velocity s relative to the ground depends mostly on absolute temperature T of the background air and wind speed M, according to:

$$s = s_o \cdot \left(\frac{T}{T_o} \right)^{1/2} + M \cdot \cos(\phi) \qquad \bullet(15.32)$$

where ϕ is the angle between wind direction and sound-propagation direction, s_o = 343.15 m/s is a reference sound speed, and T_o = 293 K. At 20°C in calm air, the speed of sound relative to the ground equals s_o. Sound travels faster in warmer air, and when blown by a tail wind.

To estimate the distance to the lightning in kilometers, count the number of seconds between seeing the lightning and hearing the thunder, then divide that time by 3 s/km. This "**3 second rule**" algorithm assumes typical temperatures and calm winds. (If you prefer to use statute miles, divide the number of seconds by 5 s/mile.)

When light waves or sound waves propagate from one medium into another, they **refract** (bend). The amount of bending depends on the **index of refraction** n, which is proportional to the ratio of wave propagation speeds in the different media. This relationship is called **Snell's Law**, and is discussed in more detail in the Optics chapter.

Sound waves refract as they propagate through regions of varying temperature or wind. For calm conditions, the index of refraction for sound is:

$$n = \sqrt{T_o / T} \qquad (15.33)$$

where T_o = 293 K. Snell's law can be written as

$$n \cdot \cos(\alpha) = \text{constant} \qquad (15.34)$$

or

$$\cos(\alpha_2) = \sqrt{T_2 / T_1} \cdot \cos(\alpha_1) \qquad \bullet(15.35)$$

where α is the elevation angle of the path of the sound (called the sound **ray** path), and subscripts 1 and 2 denote "before" and "after" refraction across a sharp change of temperature, respectively.

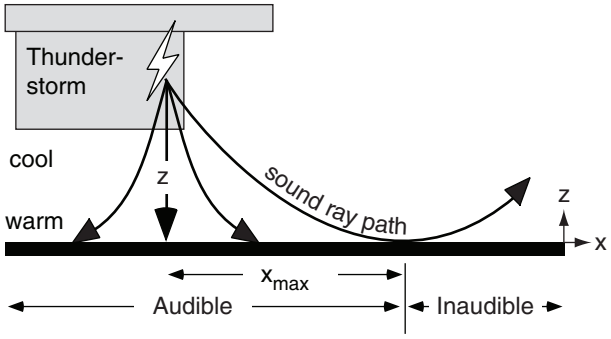

Figure 15.31
Thunder ray paths, and audibility at ground level in calm winds.

Solved Example

A thunderstorm approaching from the northwest creates a visible lightning stroke. There is a 5 m/s wind from the southeast blowing into the storm, and the temperature is 30°C. If you hear thunder 10 s after seeing the lightning, how far away was the stroke?

Solution

Given: T = 30°C = 303 K, M = 5 m/s, ϕ = 180°.
Find: x = ? km

Assume the light reaches you almost instantly. Then the only issue is the speed of sound.
Use eq. (15.32):

$s = (343.15 \text{ m/s}) \cdot [303\text{K}/293\text{K}]^{1/2} + (5 \text{ m/s}) \cdot \cos(180°)$
$= 349 - 5 = 344$ m/s

From basic physics, speed times time equals distance:

$x = s \cdot t = (344 \text{ m/s}) \cdot (10 \text{ s}) =$ **3.44 km**

Check: Units OK. Physics OK.
Discussion: If the wind had been blowing in the opposite direction, the distance estimate would have been 3.54 km. Given typical errors in timing the thunder after the lightning, we see that the winds usually play only a small role.

If we had used the "3 second rule" instead of the full equation, our answer would have been $x \approx$ (10 s) /(3 s/km) = 3.33 km, which is close to the exact answer. Experts recommend that, for your own safety, you should **seek shelter if the thunderstorm is within 10 km of you**. This corresponds to a time difference between the lightning and thunder of 30 s or less.

Solved Example (§)

For the previous solved example (except assume calm winds), if the lapse rate is adiabatic and the lightning altitude was 2 km, find the maximum distance of thunder audibility. Also, plot the path of this sound ray backwards from the location of max audible distance.

Solution

Given: T = 303 K, γ = 9.8 K/km, z = 2 km
Find: x_{max} = ? km, and plot z vs. x

Use eq. (15.38): x_{max} =
$2 \cdot [(303\text{ K})\cdot(2\text{ km}) / (9.8\text{ K/km})]^{1/2}$ = **15.7 km**

Use eq. (15.36): $\Delta\alpha = (9.8\text{ K/km})\cdot(1\text{ km}) / [2\cdot(303\text{K})]$
= 0.01617 radians ≈ constant

Next, use eqs. (15.37) in a spreadsheet, and plot backward from the ground, where initially:
x = 0 km, z = 0 km, and α = 0 radians. This backwards trajectory will allow us to follow the sound ray path back to the lightning that caused it.

x (km)	α (rad)	Δz (km)	z (km)
0	0	0	0
1	0.01617162	0.01617303	0.01617303
2	0.03234323	0.03235452	0.04852754
3	0.04851485	0.04855295	0.09708049
4	etc.		

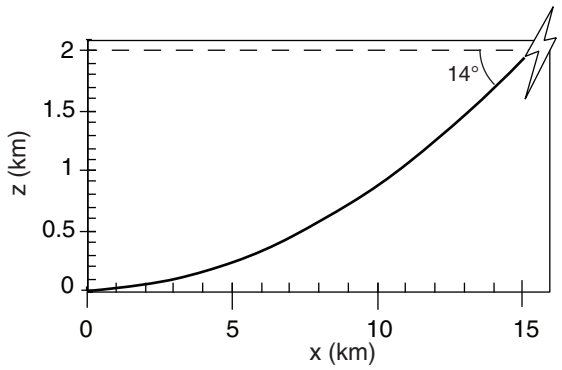

Check: Units OK. Physics OK.
Discussion: The ray path reaches 2 km altitude at a lateral distance slightly greater than 15 km, which agrees with x_{max}. This ray, which is tangent to the ground, happens to leave the cloud at an elevation angle of about 14° (it looks like a greater angle in the figure above because the vertical scale is stretched).

For gradual changes in temperature, the ray path equation is:

$$\Delta\alpha = \frac{\gamma}{2\cdot T}\cdot\Delta x \tag{15.36}$$

where T is the absolute temperature of background air at ground level, $\gamma = -\Delta T/\Delta z$ is the lapse rate (assumed constant with height), and $\Delta\alpha$ is the angle change (radians) of a ray that moves a small increment of distance Δx horizontally. Normally the absolute temperature changes by only a small percentage with height, making $\Delta\alpha$ nearly constant over the interval Δx.

To solve eq (15.36) iteratively, start with a known ray angle α at a known height z and known x location. Next, take a step in the horizontal by solving the following equations sequentially:

$$\begin{aligned} x_{new} &= x_{old} + \Delta x \\ \alpha_{new} &= \alpha_{old} + \Delta\alpha \\ \Delta z &= \Delta x\cdot\tan(\alpha) \\ z_{new} &= z_{old} + \Delta z \end{aligned} \tag{15.37}$$

Repeat for the next increment of Δx. A plot of each pair of z_{new} vs. x_{new} is the ray path (Fig. 15.31).

Sound rays bend toward the colder air. In the atmosphere, temperature usually decreases smoothly with height. Thus, a ray of thunder traveling downward from a cloud will tend to curve upward (Fig 15.31). Those sound rays that are pointed more vertically downward will reach the ground near the storm, allowing you to hear the thunder.

Other rays leaving the cloud at shallower angles will be refracted away from the ground, preventing people on the ground from hearing it. The greatest distance x_{max} away from the storm at which you can still hear thunder (neglecting wind effects) is

$$x_{\max} \cong 2\cdot\sqrt{T\cdot z\,/} \tag{15.38}$$

where z is the height of sound origin.

When wind is included, the ray-path equation from Snell's law is a bit more complicated:

$$\frac{n\cdot(\cos\alpha)\left[1-(Ma\cdot n\cdot\sin\alpha)^2\right]-Ma\cdot(n\cdot\sin\alpha)^2}{1+Ma\cdot n\cdot(\cos\alpha)\left[1-(Ma\cdot n\cdot\sin\alpha)^2\right]^{1/2}-(Ma\cdot n\cdot\sin\alpha)^2} = \text{constant} \tag{15.39}$$

where $Ma = M/s_o$ is the Mach number of the wind.

TORNADOES

Tornadoes are violently rotating, small-diameter columns of air in contact with the ground. Diameters range from 10 to 1000 m, with an average of about 100 m. In the center of the tornado is very low pressure (order of 10 kPa lower than ambient).

Tornadoes are usually formed by thunderstorms, but most thunderstorms do not spawn tornadoes. The strongest tornadoes come from supercell thunderstorms. Tornadoes have been observed with a wide variety of shapes (Fig. 15.32).

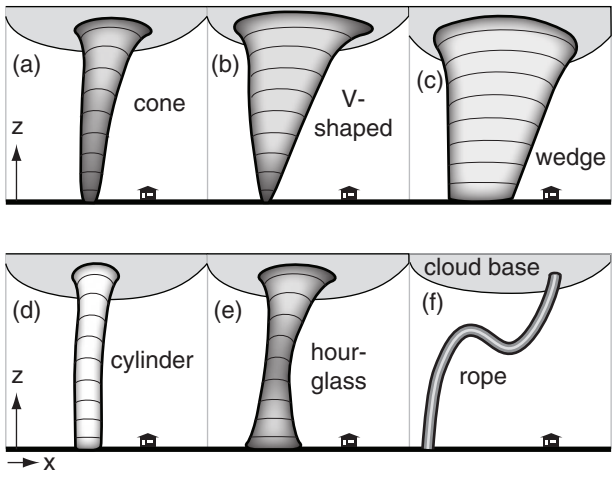

Figure 15.32
Illustration of some of the different tornado shapes observed.

Tangential Velocity & Tornado Intensity

Tangential velocities around tornadoes range from about 18 m/s for weak tornadoes to greater than 140 m/s for exceptionally strong ones. Tornado rotation is often strongest near the ground (15 to 150 m AGL), where upward vertical velocities of 25 to 60 m/s have been observed in the outer wall of the tornado. This combination of updraft and rotation can rip trees, animals, vehicles and buildings from the ground and destroy them. It can also loft trucks, cars, and other large and small objects, which can fall outside the tornado path causing more damage.

Often a two-region model is used to approximate tangential velocity M_{tan} in a tornado, with an internal **core** region of radius R_o surrounded by an external region. R_o corresponds to the location of fastest tangential velocity $M_{tan\ max}$ (Fig. 15.33), which is sometimes assumed to coincide with the outside edge of the visible funnel. Air in the core of the tornado rotates as a solid-body, while air outside the core is irrotational (has no relative vorticity as it moves around the tornado axis), and conserves angular momentum as it is drawn into the tornado. This model is called a **Rankine combined vortex (RCV)**.

The pressure deficit is $\Delta P = P_\infty - P$, where P is the pressure at any radius R from the tornado axis, and P_∞ is ambient pressure far away from the tornado (for $P_\infty \geq P$). At R_o, match the inner and outer tangential wind speeds, and match the inner and outer pressure deficits:

Core Region ($R < R_o$):

$$\frac{M_{\tan}}{M_{\tan \max}} = \frac{R}{R_o} \qquad \bullet(15.40)$$

$$\frac{\Delta P}{\Delta P_{\max}} = 1 - \frac{1}{2}\left(\frac{R}{R_o}\right)^2 \qquad \bullet(15.41)$$

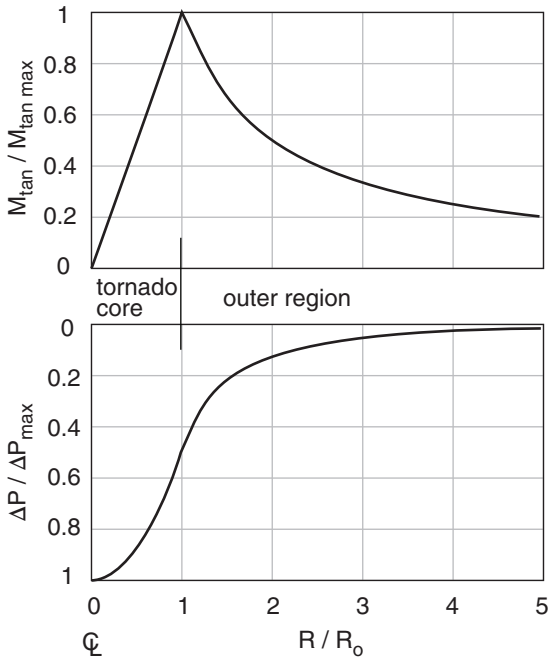

Figure 15.33
A Rankine-combined-vortex (RCV) model for tornado tangential velocity and pressure. The pressure deficit is plotted with reversed ordinate, indicating lower pressure in the tornado core.

Solved Example

If the max pressure deficit in the center of a 20 m radius tornado is 10 kPa, find the max tangential wind speed, and the wind and pressure deficit at R = 50 m.

Solution

Given: R_o = 20 m, ΔP_{max} = 10 kPa, R = 50 m

Find: $M_{tan\ max}$ = ? m/s.

Also M_{tan} = ? m/s and ΔP = ? kPa at R = 50 m.

Assume: ρ = 1 kg/m^3.

Use eq. (15.44):

$M_{tan\ max} = [\Delta P_{max}/\ \rho]^{1/2} =$

$[(10{,}000\ \text{Pa}) / (1\ \text{kg/m}^3)]^{1/2} =$ **100 m/s**

Because $R > R_o$, use outer-region eqs. (15.42 & 15.43):

M_{tan} = (100 m/s) · [(20 m)/(50 m)] = **40 m/s**

ΔP = 0.5·(10 kPa) · [(20 m)/(50 m)]^2 = **0.8 kPa**.

Check: Physics OK. Units OK. Agrees with Fig. 15.33.

Discussion: 10 kPa is quite a large pressure deficit in the core — roughly 10% of sea-level pressure. However, most tornadoes are not this violent. Typical tangential winds of 60 m/s or less would correspond to core pressure deficits of 3.6 kPa or less.

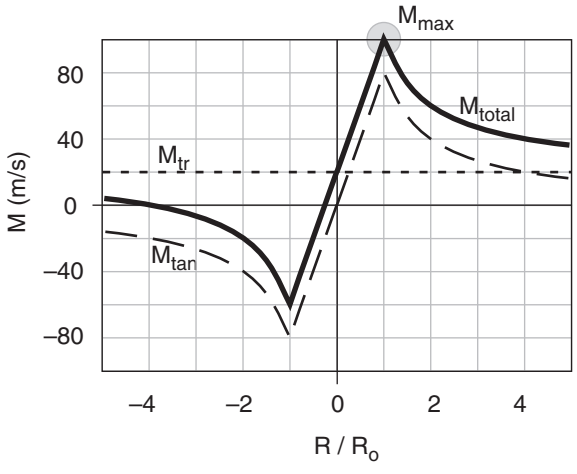

Figure 15.34

Illustration of sum of relative rotational (M_{tan}) wind and tornado translation (M_{tr}) to yield total winds (M_{total}) measured at the ground. Tornado intensity is classified based on the maximum wind speed (M_{max}) anywhere in the tornado.

Outer Region ($R > R_o$):

$$\frac{M_{\tan}}{M_{\tan\max}} = \frac{R_o}{R} \qquad \bullet(15.42)$$

$$\frac{\Delta P}{\Delta P_{\max}} = \frac{1}{2}\left(\frac{R_o}{R}\right)^2 \qquad \bullet(15.43)$$

These equations are plotted in Fig. 15.33, and represent the wind relative to the center of the tornado.

Max tangential velocity (at $R = R_o$) and max **core pressure deficit** (ΔP_{max} , at R = 0) are related by

$$\Delta P_{\max} = \rho\cdot(M_{\tan\max})^2 \qquad \bullet(15.44)$$

where ρ is air density. This equation, derived from the **Bernoulli equation**, is also consistent with **cyclostrophic balance** between pressure-gradient force and centrifugal force (see the Dynamics chapter). Forecasting these maximum values is difficult.

Low pressure in the tornado core tends to suck air into it, but is balanced by centrifugal force that tends to throw air out from the center of rotation. The net result is no radial flow across the tornado perimeter, which acts like the walls of a vacuum-cleaner hose. At the bottom of the tornado, friction near the ground reduces the wind speed, preventing centrifugal force from balancing pressure gradient force. As a result, the low pressure inside the tornado sucks air into it, analogous to air being sucked into the end of a vacuum-cleaner hose.

The previous 5 equations gave tangential wind speed relative to the center of the tornado. But the tornado also moves horizontally (**translates**) with its parent thunderstorm. The total wind M_{total} at any point near the tornado is the vector sum of the rotational wind M_{tan} plus the translational wind M_{tr} (Fig. 15.34). The max wind speed M_{max} associated with the tornado is

$$|M_{max}| = |M_{tan\ max}| + |M_{tr}| \qquad \bullet(15.45)$$

and is found on the right side of the storm (relative to its translation direction) for cyclonically (counterclockwise, in the Northern Hemisphere) rotating tornadoes.

Most tornadoes rotate cyclonically. Less than 2% of tornadoes rotate the opposite direction (anticyclonically). This low percentage is due to two factors: (1) Coriolis force favors mesocyclones that rotate cyclonically, and (2) friction at the ground causes a turning of the wind with increasing height

(Fig. 15.42, presented in a later section), which favors right-moving supercells in the Northern Hemisphere with cyclonically rotating tornadoes.

Either of two **tornado damage scales** can be used to classify the severity of tornadoes. One is the **TORRO** (**T**) scale, developed by the Tornado and Storm Research Organization in Europe. The other is the **Fujita** (**F**) scale, developed by Ted Fujita, and adopted by the US National Weather Service.

The Fujita scale ranges from F0 for slight damage, to F12 for damage caused by wind speeds of Mach 1. Tornadoes of F5 intensity and greater cause nearly total destruction of most buildings and trees, with most of the debris swept away by the wind. So it is virtually impossible to identify tornadoes of F6 or greater based on damage surveys (because they look the same as F5 damage). Thus, the normal range of reported Fujita intensity is F0 to F5. The lower wind speed M_{max} bound for each **F** range (such as F2 or F3) is defined by:

$$M_{max} = a \cdot (2\mathbf{F} + 4)^{1.5} \qquad (15.46)$$

where a = 2.25 m/s.

In 2007 the Fujita scale was revised into the **Enhanced Fujita** (**EF**) scale (Table 15-3), based on better measurements of the relationship between winds and damage for 28 different types of structures. This EF scale was calibrated by shooting (with an air cannon) various objects (such as wood fence slats or 2x4 inch studs) through steel car doors and concrete walls, and by comparing Doppler-radar observations of tornadic winds with damage surveys.

For example, consider modern, well-built single-family homes and duplexes, typically built with wood or steel studs, with plywood roof and outside walls, all covered with usual types of roofing, sidings, or brick. For this structure, use the following damage descriptions to estimate the EF value:

- If threshold of visible damage, then EF0 or less.
- If loss of gutters, or awnings, or vinyl or metal siding, or less than 20% of roof covering material, then EF0 - EF1.
- If broken glass in doors and windows, or roof lifted up, or more than 20% of roof covering missing, or chimney collapse, or garage doors collapse inward, or failure of porch or carport, then EF0 - EF2.
- If entire house shifts off foundation, or large sections of roof structure removed (but most walls remain standing), then EF1 - EF3.
- If exterior walls collapse, then EF2 - EF3.
- If most walls collapse, except small interior rooms, then EF2 - EF4.
- If all walls collapse, then EF3 - EF4.
- If total destruction & floor slabs swept clean, then EF4 - EF5.

Table 15-3. Enhanced Fujita scale for tornado-damage intensity.

Scale	Max. Tangential 3 second Gust Speed (m/s)	Damage Classification Description (from original Fujita scale)	Relative Frequency in USA	Relative Frequency in Canada
EF0	29 – 38	**Light** damage; some damage to chimneys, TV antennas; breaks twigs off trees; pushes over shallow-rooted trees.	29%	45%
EF1	39 – 49	**Moderate** damage; peels surface off roofs; windows broken; light trailer homes pushed or turned over; some trees uprooted or snapped; moving cars pushed off road.	40%	29%
EF2	50 – 60	**Considerable** damage; roofs torn off frame houses leaving strong upright walls; weak buildings in rural areas demolished; trailer houses destroyed; large trees snapped or uprooted; railroad boxcars pushed over; light object missiles generated; cars blown off roads.	24%	21%
EF3	61 – 73	**Severe** damage; roofs and some walls torn off frame houses; some rural buildings completely destroyed; trains overturned; steel-framed hangars or warehouse-type structures torn; cars lifted off of the ground; most trees in a forest uprooted or snapped and leveled.	6%	4%
EF4	74 – 89	**Devastating** damage; whole frame houses leveled leaving piles of debris; steel structures badly damaged; trees debarked by small flying debris; cars and trains thrown some distance or rolled considerable distances; large wind-blown missiles generated.	2%	1%
EF5	≥ 90	**Incredible** damage; whole frame houses tossed off foundation and blown downwind; steel-reinforced concrete structures badly damaged; automobile-sized missiles generated; incredible phenomena can occur.	< 1%	almost 0%

Solved Example
Find Enhanced Fujita & TORRO intensities for M_{max} = 100 m/s.

Solution
Given: M_{max}= 100 m/s.
Find: EF and T intensities

Use Tables 15-3 & 15-4: ≈ **EF5** , **T8** .

Discussion: This is a violent, very destructive, tornado.

Similar damage descriptions for the other 27 types of structures (including trees) are available from the USA Storm Prediction Center.

Tornado intensity varies during the life-cycle of the tornado, so different levels of destruction are usually found along the damage path for any one tornado. Tornadoes of strength EF2 or greater are labeled **significant tornadoes**.

The TORRO scale (Table 15-4) is defined by maximum wind speed M_{max}, but in practice is estimated by damage surveys. The lower wind-speed bound for each **T** range (such as for T3 or T5) is defined approximately by:

$$M_{max} \approx a \cdot (\mathbf{T} + 4)^{1.5} \qquad (15.47)$$

where **T** is a dimensionless TORRO value, and a = 2.365 m/s. The TORRO scale ranges from T0 for a very weak tornado through T10 for a super tornado, with even larger **T** values possible.

Any tornado-damage scale is difficult to use and interpret, because it is uncalibrated (no actual wind measurements) for most events. However, the accumulation of tornado-damage-scale estimates provides valuable statistics over the long term, as individual errors are averaged out.

Table 15-4. TORRO tornado scale.

Scale	Max. Speed (m/s)	Tornado Intensity & Damage Description
T0	17 – 24	**Light**. Loose light litter raised from ground in spirals. Tents, marquees disturbed. Exposed tiles & slates on roofs dislodged. Twigs snapped. Visible damage path through crops.
T1	25 – 32	**Mild**. Deck chairs, small plants, heavy litter airborne. Dislodging of roof tiles, slates, and chimney pots. Wooden fences flattened. Slight damage to hedges and trees.
T2	33 – 41	**Moderate**. Heavy mobile homes displaced. Caravans blown over. Garden sheds destroyed. Garage roofs torn away. Damage to tile and slate roofs and chimney pots. Large tree branches snapped.
T3	42 – 51	**Strong**. Mobile homes overturned & badly damaged. Light caravans destroyed. Garages and weak outbuilding destroyed. Much of the roofing material removed. Some larger trees uprooted or snapped.
T4	52 – 61	**Severe**. Mobile homes airborne & destroyed. Sheds airborne for considerable distances. Entire roofs removed. Gable ends torn away. Numerous trees uprooted or snapped.
T5	62 – 72	**Intense**. Heavy motor vehicles lifted. More house damage than T4. Weak buildings completely collapsed.
T6	73 – 83	**Moderately Devastating**. Strongly built houses lose entire roofs and perhaps a wall. Weaker built structures collapse completely.
T7	84 – 95	**Strongly Devastating**. Wooden-frame houses wholly demolished. Some walls of stone or brick houses collapsed. Steel-framed warehouse constructions buckled slightly. Locomotives tipped over. Noticeable debarking of trees by flying debris.
T8	96 – 107	**Severely Devastating**. Motor cars hurled great distances. Wooden-framed houses destroyed and contents dispersed over large distances. Stone and brick houses irreparably damaged. Steel-framed buildings buckled.
T9	108 – 120	**Intensely Devastating**. Many steel-framed buildings badly damaged. Locomotives or trains hurled some distances. Complete debarking of standing tree trunks.
T10	121 – 134	**Super**. Entire frame houses lifted from foundations, carried some distances & destroyed. Severe damage to steel-reinforced concrete buildings.

Appearance

Two processes can make tornadoes visible: water droplets and debris (Fig. 15.35). Sometimes these processes make only the bottom or top part of the tornado visible, and rarely the whole tornado is invisible. Regardless of whether you can see the tornado, if the structure consists of a violently rotating column of air, then it is classified as a tornado.

Debris can be formed as the tornado destroys things on the Earth's surface. The resulting smaller fragments (dirt, leaves, grass, pieces of wood, bugs, building materials and papers from houses and barns) are drawn into the tornado wall and upward, creating a visible **debris cloud**. (Larger items such as whole cars can be lifted by the more intense tornadoes and tossed outward, some as much as 30 m.) If tornadoes move over dry ground, the debris cloud can include dust and sand. Debris clouds form at the ground, and can extend to various heights for different tornadoes, including some that extend up to wall-cloud base.

The water-condensation funnel is caused by low pressure inside the tornado, which allows air to expand as it is sucked horizontally toward the core. As the air expands it cools, and can reach saturation if the pressure is low enough and the initial humidity of the air great enough. The resulting cloud of water droplets is called a **funnel cloud**, and usually extends downward from the thunderstorm cloud base. Sometimes this condensation funnel cloud can reach all the way to the ground. Most strong tornadoes have both a condensation funnel and a debris cloud (Fig. 15.35).

Because the tornado condensation funnel is formed by a process similar to the lifting condensation level (LCL) for normal convective cloud base, you can use the same LCL equation (see the Moisture chapter) to estimate the pressure P_{cf} at the outside of the tornado condensation funnel, knowing the ambient air temperature T and dew point T_d at ambient near-surface pressure P. Namely, $P_{cf} = P_{LCL}$.

$$P_{cf} = P \cdot \left[1 - b \cdot \left(\frac{T - T_d}{T} \right) \right]^{C_p / \Re} \qquad \bullet(15.48)$$

where $C_p/\Re = 3.5$ and $b = 1.225$, both dimensionless, and where T in the denominator must be in Kelvin.

Because both the condensation funnel and cloud base indicate the same pressure, the isobars must curve downward near the tornado (Fig. 15.36). Thus, the greatest horizontal pressure gradient associated with the tornado is near the ground (near "A" in Fig. 15.36). Drag at the ground slows the wind a bit there, which is why the fastest tangential winds in a tornado are found 15 to 150 m above ground.

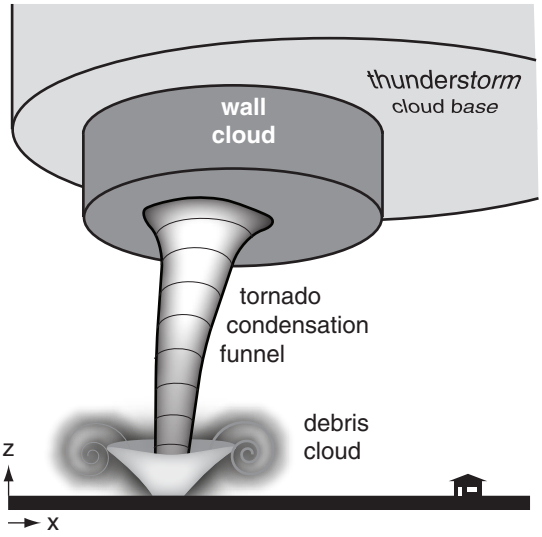

Figure 15.35
Condensation funnel and debris cloud.

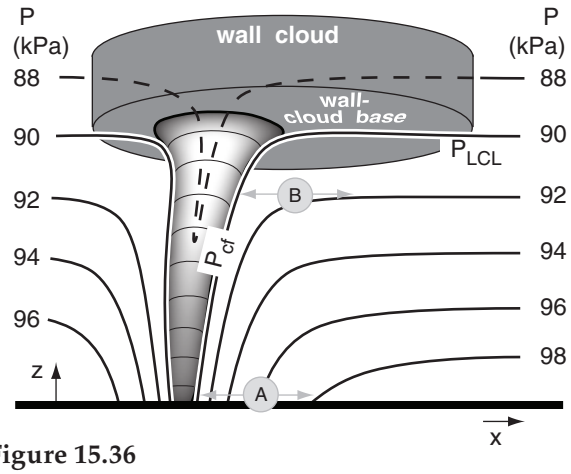

Figure 15.36
Relationship between lifting-condensation-level pressure (P_{LCL}), cloud base, and pressure at the condensation funnel (P_{cf}). Horizontal pressure gradient at point "A" is 4 times that at "B".

Solved Example

Under a tornadic thunderstorm, the temperature is 30°C and dew point is 23°C near the ground where pressure is 100 kPa. Find the near-surface pressure at the outside edge of the visible condensation funnel.

Solution

Given: $T = 30°C = 303K$, $T_d = 23°C$, $P = 100$ kPa
Find: $P_{cf} = ?$ kPa

Use eq. (15.48): $P_{cf} = (100\text{kPa}) \cdot [\, 1 - 1.225 \cdot (30–23)/303]^{3.5}$
$= \underline{\mathbf{90.4\ kPa}}$ at the tornado funnel-cloud edge.

Check: Units OK. Physics OK.
Discussion: The tornado core pressure can be even lower than at the edge of the condensation funnel.

Types of Tornadoes & Other Vortices

We will compare six types of vortices:

- supercell tornadoes
- landspout tornadoes
- waterspouts
- cold-air funnels
- gustnadoes
- dust devils, steam devils, firewhirls

Fig. 15.37 illustrates these vortex types.

Strong tornadoes form when rotation exists on a broad scale in thunderstorms. Recall from the Thunderstorm chapter that long-lived (1 h or more) rotation on the scale of the whole thunderstorm updraft is called a **mesocyclone**, and is approximately 10 to 15 km in diameter for the more-severe, long-lasting thunderstorms called **supercell storms**. By comparison, tornadic circulations have much smaller diameter, averaging about 100 m.

Supercell tornadoes form under (and are attached to) the main updraft of supercell thunderstorms (Figs. 15.32a-c, 15.35, & 15.37) or under a cumulus congestus that is merging into the main supercell updraft from the flanking line. It can be the most violent tornado type — up through EF5 intensity. They move horizontally (i.e., **translate**) at nearly the same speed as the parent thunderstorm (on the order of 5 to 40 m/s). These tornadoes will be discussed in more detail in the next subsections.

Landspouts are weaker tornadoes (EF0 - EF2, approximately) not usually associated with supercell thunderstorms. They are often cylindrical, and look like hollow soda straws (Fig. 15.32d). These short-lived tornadoes form along strong cold fronts. Horizontal wind shear across the frontal zone provides the rotation, and vertical stretching of the air by updrafts in the **squall-line thunderstorms** along the front can intensify the rotation (Fig. 15.37).

Waterspouts (Fig. 15.37) are tornadoes that usually look like landspouts (hollow, narrow, 3 to 100 m diameter cylinders), but form over water surfaces (oceans, lakes, wide rivers, bays, etc.). They are often observed in subtropical regions (e.g., in the waters around Florida), and can form under (and are attached to) cumulus congestus clouds and small thunderstorms. They are often short lived (usually 5 to 10 min) and weak (EF0 - EF1). The waterspout life cycle is visible by eye via changes in color and waves on the water surface: (1) dark spot, (2) spiral pattern, (3) spray-ring, (4) mature spray vortex, and (5) decay. Waterspouts have also been observed to the lee of mountainous islands such as Vancouver Island, Canada, where the initial rotation is caused by wake vortices as the wind swirls around the sides of mountains.

Unfortunately, whenever any type of tornado moves over the water, it is also called a waterspout.

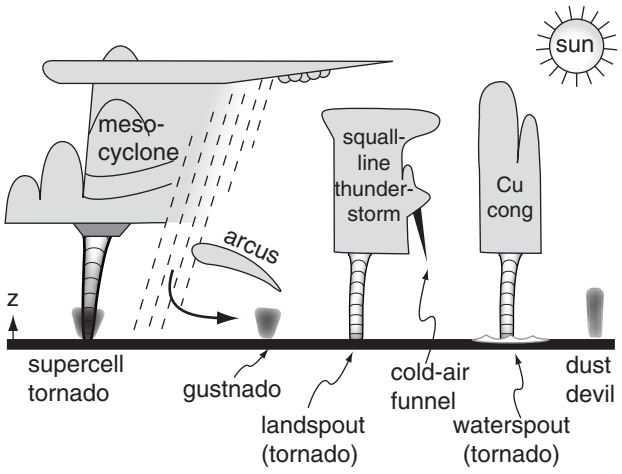

Figure 15.37
Illustration of tornado and vortex types.

Thus, supercell tornadoes (EF3 - EF5) would be called waterspouts if they moved over water. So use caution when you hear waterspouts reported in a weather warning, because without other information, you won't know if it is a weak classical waterspout or a strong tornado.

Cold-air funnels are short vortices attached to shallow thunderstorms with high cloud bases, or sometimes coming from the sides of updraft towers (Fig. 15.37). They are very short lived (1 - 3 minutes), weak, usually don't reach the ground. Hence, they usually cause no damage on the ground (although light aircraft should avoid them). Cold-air funnels form in synoptic cold-core low-pressure systems with a deep layer of unstable air.

Gustnadoes are shallow (order of 100 m tall) debris vortices touching the ground (Fig. 15.37). They form along the gust-front from thunderstorms, where there is shear between the outflow air and the ambient air. Gustnadoes are very weak (EF0 or weaker) and very short lived (a few minutes). The arc clouds along the gust front are not usually convective, so there is little or no updraft to stretch the air vertically, and hence no mechanism for accelerating the vorticity. There might also be rotation or a very small condensation funnel visible in the overlying arc clouds. Gustnadoes translate with the speed of advance of the gust front.

Dust devils are not tornadoes, and are not associated with thunderstorms. They are fair-weather phenomena, and can form in the clear-air thermals of warm air rising from a heated surface (Fig. 15.37). They are weak (less than EF0) debris vortices, where the debris can be dust, sand, leaves, volcanic ash, grass, litter, etc. Normally they form during daytime in high-pressure regions, where the sun heats the ground, and are observed over the desert or oth-

er arid locations. They translate very slowly or not at all, depending on the ambient wind speed.

When formed by arctic-air advection over an unfrozen lake in winter, the resulting **steam-devils** can happen day or night. Smoky air heated by forest fires can create **firewhirls**. Dust devils, steam devils, firewhirls and gustnadoes look very similar.

Evolution as Observed by Eye

From the ground, the first evidence of an incipient supercell tornado is a **dust swirl** near the ground, and sometimes a rotating wall cloud protruding under the thunderstorm cloud base (Fig. 15.38). Stage 2 is the **developing stage**, when a condensation funnel cloud begins to extend downward from the bottom of the wall cloud or thunderstorm base, and the debris cloud becomes larger with well-defined rotation.

Stage 3 is the **mature stage**, when there is a visible column of rotating droplets and/or debris extending all the way from the cloud to the ground. This is the stage when tornadoes are most destructive. During stage 4 the visible tornado weakens, and often has a slender rope-like shape (also in Fig. 15.32f). As it dissipates in stage 5, the condensation funnel disappears up into the cloud base and the debris cloud at the surface weakens and disperses in the ambient wind. Meanwhile, a cautious storm chaser will also look to the east or southeast under the same thunderstorm cloud base, because sometimes new tornadoes form there.

Tornado Outbreaks

A **tornado outbreak** is when many tens to hundreds of tornadoes happen in a period of 1 day to about a week (meteorologists are still debating a more precise definition). Tornado outbreaks have been observed every decade in North America for the past couple hundred years of recorded meteorological history. Sometimes outbreaks occur every year, or multiple times a year.

The following list highlights a small portion of the outbreaks in North America:

- 25 May - 1 June 1917: 63 tornadoes in Illinois killed 383 people.
- 18 March 1925 (tri-state) Tornado: Deadliest tornado(es) in USA, killing 695 people on a 350 km track through Missouri, Illinois & Indiana.
- 1 - 9 May 1930: 67 tornadoes in Texas killed 110.
- 5 - 6 April 1936: 17 tornadoes in Tupelo, Mississippi, and Gainesville, Georgia, killed 454.
- 15 - 24 May 1949: 74 torn. in Missouri killed 66.
- 7 - 11 April 1965 (Palm Sunday): 51 F2 - F5 tornadoes, killed 256.

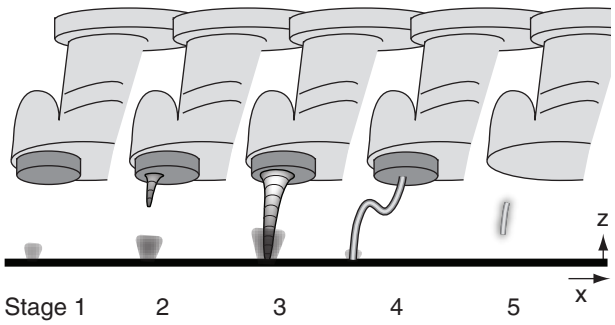

Figure 15.38
Stages in a supercell-tornado life cycle.

ON DOING SCIENCE • Be Safe *(part 4)*

More chase guidelines from Charles Doswell III.

The #3 Threat: The Storm

1. Avoid driving through the heaviest precipitation part of the storm (known as "**core punching**").
2. Avoid driving under, or close to, rotating wall clouds.
3. Don't put yourself in the path of a tornado or a rotating wall cloud.
4. You must also be aware of what is happening around you, as thunderstorms and tornadoes develop quickly. You can easily find yourself in the path of a new thunderstorm while you are focused on watching an older storm. Don't let this happen — be vigilant.
5. For new storm chasers, find an experienced chaser to be your mentor. (Work out such an arrangement ahead of time; don't just follow an experienced chaser uninvited.)
6. Keep your engine running when you park to view the storm.
7. Even with no tornado, straight-line winds can move hail or debris (sheet metal, fence posts, etc.) fast enough to kill or injure you, and break car windows. Move away from such regions.
8. Avoid areas of rotating curtains of rain, as these might indicate that you are in the dangerous center of a mesocyclone (called the "**bear's cage**").
9. Don't be foolhardy. Don't be afraid to back off if your safety factor decreases.
10. Never drive into rising waters. Some thunderstorms such as HP supercell storms can cause flash floods.
11. Always have a clear idea of the structure, evolution, and movement of the storm you are viewing, so as to anticipate safe courses of action.

(continues on next page)

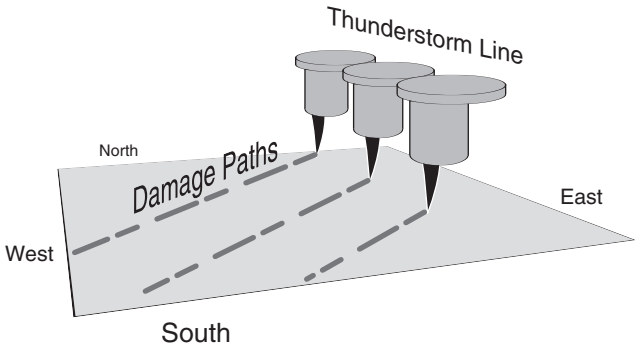

Figure 15.39
Sketch of parallel damage paths from a line of supercell thunderstorms during a tornado outbreak.

ON DOING SCIENCE • Be Safe *(part 5)*

More chase guidelines from Charles Doswell III.

The #3 Threat: The Storm *(continuation)*

12. Plan escape routes in advance.
13. Although vehicles offer safety from lightning, they are death traps in tornadoes. If you can't drive away from the tornado, then abandon your vehicle and get into a ditch or culvert, or some other place below the line-of-fire of all the debris.
14. In open rural areas with good roads, you can often drive away from the tornado's path.
15. Don't park under bridge overpasses. They are not safe places if a tornado approaches.
14. Avoid chasing at night. Some difficulties include:
    a. Don't trust storm movement as broadcast on radio or TV. Often, the media reports the heavy precipitation areas, not the action (dangerous) areas of the mesocyclone and tornado.
    b. Storm info provided via various wireless data and internet services can be several minutes old or older
    c. It is difficult to see tornadoes at night. Flashes of light from lightning & exploding electrical transformers (known as "**power flashes**") are often inadequate to see the tornado. Also, not all power flashes are caused by tornadoes.
    d. If you find yourself in a region of strong inflow winds that are backing (changing direction counterclockwise), then you might be in the path of a tornado.
    e. Flooded roads are hard to see at night, and can cut-off your escape routes. Your vehicle could hydroplane due to water on the road, causing you to lose control of your vehicle.
    f. Even after you stop chasing storms for the day, dangerous weather can harm you on your drive home or in a motel.

On his web site, Doswell offers many more tips and recommendations for responsible storm chasing.

- 3 - 4 April 1974: 147 tornadoes, killed 309 people in Midwest USA, and 8 in Canada.
- 31 May 1985: 41 tornadoes in USA & Canada, killed 88.
- 13 March 1990: 59 tornadoes in central USA, killed 2.
- 3 May 1999: 58 tornadoes in Oklahoma & Kansas, killed 44.
- 3 - 11 May 2003: 366 tornadoes in tornado alley killed 41.
- September 2004 in Hurricanes Francis & Ivan: 240 tornadoes.
- 26 - 31 August 2005 in Hurricane Katrina: 44 tornadoes in southeast USA.
- 5 - 6 February 2008 (Super Tuesday): 84 tornadoes in central USA killed 59
- 22 - 25 May 2008: 234 tornadoes in central USA killed 10
- 25 - 28 April 2011: 336 tornadoes in E. USA, killed 346, causing about $10 billion in damage
- 21 - 26 May 2011: 180 tornadoes in midwest USA killed 177

Outbreaks are often caused by a line or cluster of supercell thunderstorms. Picture a north-south line of storms, with each thunderstorm in the line marching toward the northeast together like troops on parade (Fig. 15.39). Each tornadic supercell in this line might create a sequence of multiple tornadoes (called a **tornado family**), with very brief gaps between when old tornadoes decay and new ones form. The aftermath are parallel tornado damage paths like a wide (hundreds of km) multi-lane highway oriented usually from southwest toward northeast.

Storm-relative Winds

Because tornadoes translate with their parent thunderstorms, the winds that influence supercell and tornado rotation are the environmental wind vectors relative to a coordinate system that moves with the thunderstorm. Such winds are called **storm-relative winds**.

First, find the storm motion vector. If the thunderstorm already exists, then its motion can be tracked on radar or satellite (which gives a vector based on its actual speed and direction of movement). For forecasts of future thunderstorms, recall from the previous chapter that many thunderstorms move in the direction of the mean wind averaged over the 0 to 6 km layer of air, as indicated by the "X" in Fig. 15.40. Some supercell storms split into two parts: a right moving storm and a left moving storm, as was shown in the Thunderstorm chapter. Namely, if tornado formation from a right-moving supercell is of concern, then use a mean storm vector

associated with the "R" in Fig. 14.61 of the previous chapter (i.e., do not use the "X").

Next, to find storm-relative winds, take the vector difference between the actual wind vectors and the storm-motion vector. On a hodograph, draw the storm-relative wind vectors from the storm-motion point to each of the original wind-profile data points. This is illustrated in Fig. 15.40a, based on the hodograph and normal storm motion "X". After (optionally) repositioning the hodograph origin to coincide with the mean storm motion (Fig. 15.40b), the result shows the directions and speed of the storm-relative environmental wind vectors.

The algebraic components (U_j', V_j') of these storm-relative horizontal vectors are:

$$U_j' = U_j - U_s \qquad \bullet(15.49)$$

$$V_j' = V_j - V_s \qquad \bullet(15.50)$$

where (U_j, V_j) are the wind components at height index j, and the storm motion vector is (U_s, V_s). For a supercell that moves with the 0 to 6 km mean wind: $(U_s, V_s) = (\overline{U}, \overline{V})$ from the previous chapter. The vertical component of storm-relative winds $W_j' = W_j$, because the thunderstorm does not translate vertically.

Solved Example

For the right-moving supercell of Fig. 14.61 from the previous chapter plot the storm-relative wind vectors on a hodograph.

Solution

Given: Fig. 14.61. Storm motion indicated by "R".
Find: Hodograph of storm-relative winds.
Method: Copy Fig. 14.61, draw relative vectors on it, and then re-center origin of hodograph to be at R:

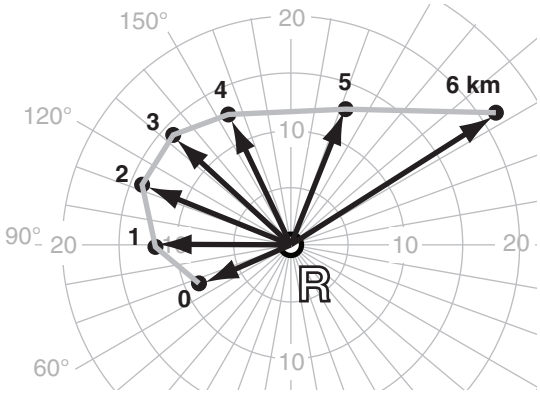

Check: Similar to Fig. 15.40b.
Discussion: Compared to storm X, storm R has less directional shear, but more inflow at middle altitudes.

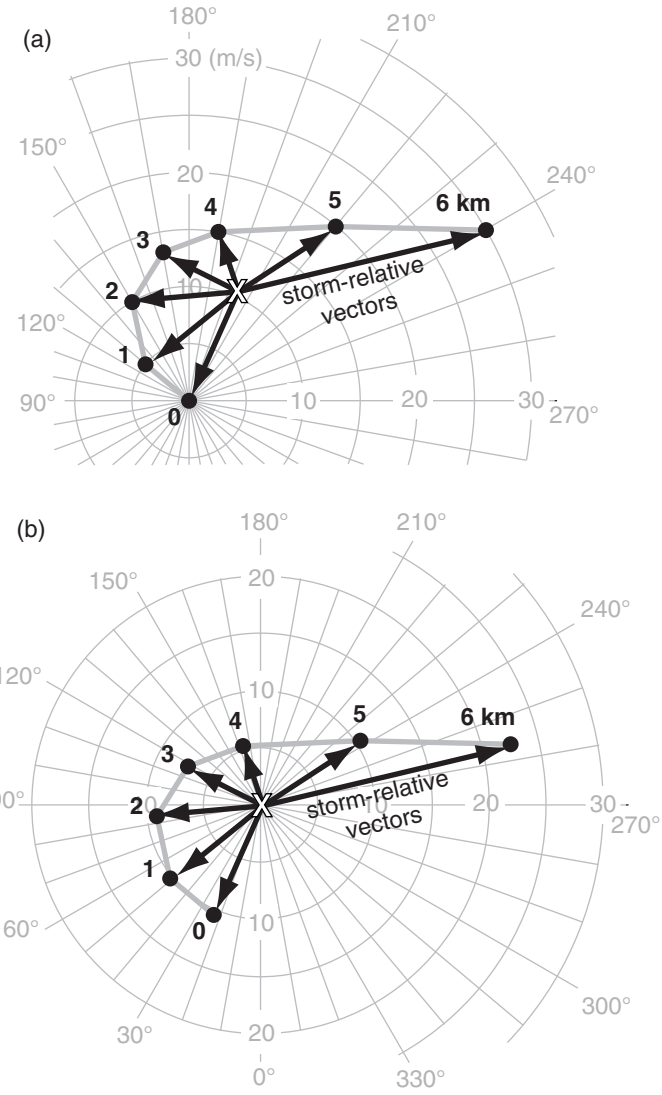

Figure 15.40
(a) Hodograph showing wind vector differences between the winds relative to a fixed coordinate system (grey line hodograph) and the mean storm motion (X), based on the data from Figs. 15.31 & 14.59. (b) Same data, but with the hodograph origin shifted to "X" to give **storm-relative** *wind vectors (black arrows). Some people find version (b) difficult to interpret, so they prefer to use version (a).*

Solved Example

Given storm-relative horizontal wind shear in the environment of $\Delta U'/\Delta z$ of 15 m/s across 3 km of height, find the vorticity spin-up if vertical velocity increases from 0 to 10 m/s across Δy=10 km.

Solution

Given: $\Delta U'/\Delta z = (15\text{ m/s})/(3\text{ km}) = 5\text{x}10^{-3}\text{ s}^{-1}$

$\Delta W/\Delta y = (10\text{ m/s})/(10\text{ km}) = 1\text{x}10^{-3}\text{ s}^{-1}$

Find: $\Delta\zeta_r/\Delta t = ?\ \text{s}^{-2}$

Assume: All other terms in eq. (15.51) are negligible.

$\Delta\zeta_r/\Delta t = (5\text{x}10^{-3}\text{ s}^{-1})\cdot(1\text{x}10^{-3}\text{ s}^{-1}) = \underline{\mathbf{5x10}}^{-6}\text{ s}^{-2}$

Check: Units OK. Physics OK.

Discussion: Tilting by itself might create a mesocyclone, but is too weak to create a tornado.

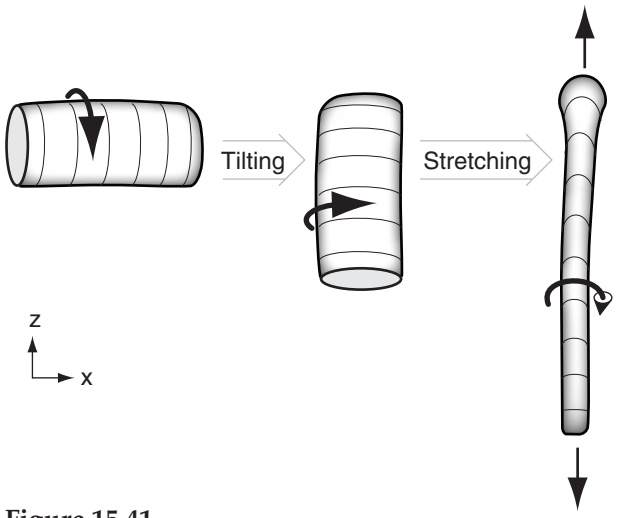

Figure 15.41

Tilting can change rotation about a horizontal axis to rotation about a vertical axis, to create a mesocyclone (a rotating thunderstorm). Stretching can then intensify the rotation into a tornado.

Origin of Tornadic Rotation

Because tornado rotation is around a vertical axis, express this rotation as a **relative vertical vorticity** ζ_r. Relative vorticity was defined in the Global Circulation chapter as $\zeta_r = (\Delta V/\Delta x) - (\Delta U/\Delta y)$, and a forecast (tendency) equation for it was given in the Extratropical Cyclone chapter in the section on cyclone spin-up.

Relative to the thunderstorm, there is little horizontal or vertical advection of vertical vorticity, and the beta effect is small because any one storm moves across only a small range of latitudes during its lifetime. Thus, mesocyclone and tornadic vorticity are affected mainly by tilting, stretching, and turbulent drag:

$$\underset{spin-up}{\frac{\Delta\zeta_r}{\Delta t}} \approx \underset{tilting}{\frac{\Delta U'}{\Delta z}\cdot\frac{\Delta W}{\Delta y} - \frac{\Delta V'}{\Delta z}\cdot\frac{\Delta W}{\Delta x}} \qquad \bullet(15.51)$$

$$+(\zeta_r + f_c)\cdot\underset{stretching}{\frac{\Delta W}{\Delta z}} \; - \; C_d\cdot\underset{turb.drag}{\frac{M}{z_{TornBL}}}\cdot\zeta_r$$

where the storm-relative wind components are (U', V', W), the Coriolis parameter is f_c, the tangential wind speed is approximately M, drag coefficient is C_d, and z_{TornBL} is the depth of the tornado's boundary layer (roughly z_{TornBL} = 100 m).

This simplified vorticity-tendency equation says that rotation about a vertical axis can increase (i.e., **spin up**) if horizontal vorticity is **tilted** into the vertical, or if the volume of air containing this vertical vorticity is **stretched** in the vertical (Fig. 15.41). Also, cyclonically rotating tornadoes (namely, rotating in the same direction as the Earth's rotation, and having positive ζ_r) are favored slightly, due to the Coriolis parameter in the stretching term. Rotation decreases due to **turbulent drag**, which is greatest at the ground in the tornado's boundary layer.

Most theories for tornadic rotation invoke tilting and/or stretching of vorticity, but these theories disagree about the origin of rotation. There is some evidence that different mechanisms might trigger different tornadoes.

One theory assumes that there is weak cyclonic vertical vorticity that already exists in the boundary layer of small synoptic-scale or mesoscale cyclones (**mesocyclone**). This vorticity is spun-up by vortex stretching as the boundary-layer top rises in convective updrafts that form in, or move over, the mesocyclone.

Another theory is that there is a cascade of vertical vorticity from larger to smaller-scale vortices.

For example, weak vorticity from a large, mid-level mesocyclone could cascade to a low-altitude mesocyclone. From there, it cascades to an intensifying tornado vortex aloft, and finally to a tornado that touches the ground.

A third theory is that vertical shear of the horizontal wind ($\Delta U/\Delta z$ in Fig. 15.42) in the boundary layer is responsible, by creating horizontal, **streamwise vorticity.** This is rotation about a horizontal axis that is parallel to an average streamline (V in Fig. 15.42). This vorticity is later tilted into vertical vorticity (rotation about a vertical axis) by convective updrafts from thunderstorms, creating counter-rotating **mesocyclones** (only one of which is shown in Fig. 15.42). Mesocyclones often are precursors to tornadoes. By itself, this mesocyclonic vorticity is too weak to explain the intense tornadoes that can form. Thus, stretching of the weak vertical vortex by convective updrafts (w) is still needed to increase its vorticity.

A fourth theory is that horizontal vorticity is generated baroclinicly by the rain-cooled, downdraft air that hits the ground and spreads out horizontally under the storm. Shear between this cool outflow air and the warmer ambient air that it is under-running creates horizontal vorticity. Observations show that there are many mesoscale frontal boundaries under thunderstorms that can generate horizontal vorticity, and that these vorticity sources are not always under the mesocyclone that is visible by radar. The horizontal vorticity is then tilted into vertical, either by the downdraft, the gust front, or other mesoscale boundary. Once in the vertical, the updraft stretches the vortex to spin-up the vorticity.

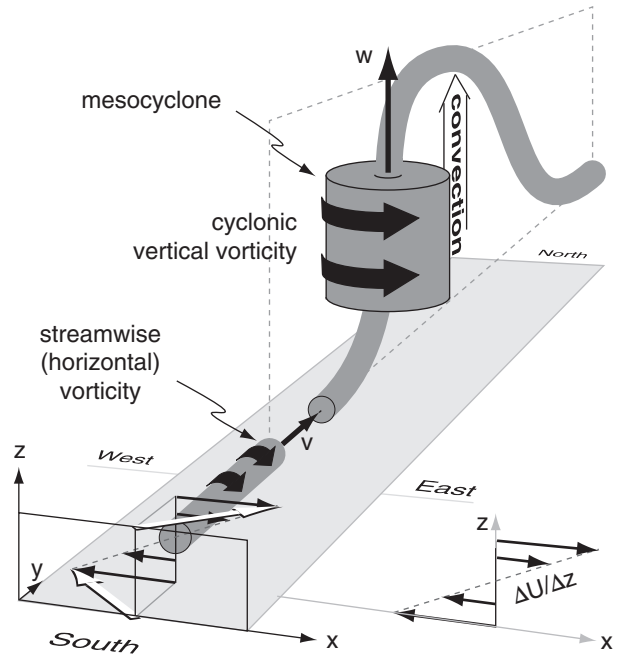

Figure 15.42
Vertical shear of the horizontal wind ($\Delta U/\Delta z$) causes streamwise horizontal vorticity (dark slender horizontal cylinder), which can be tilted by convective updrafts to create mesocyclones (fat vertical cylinder). This wind profile is typical of the prairies in central North America.

Mesocyclones and Helicity

In the mesocyclone, air is both rotating and rising (Fig. 15.43a) resulting in spiral or helical motion (Fig. 15.43b).

Helicity H is a measure of the corkscrew nature of the winds. It is a scalar, defined at any point in the fluid as:

$$H = U_{avg}\cdot\left[\frac{\Delta W}{\Delta y}-\frac{\Delta V}{\Delta z}\right]+V_{avg}\cdot\left[-\frac{\Delta W}{\Delta x}+\frac{\Delta U}{\Delta z}\right]+ W_{avg}\cdot\left[\frac{\Delta V}{\Delta x}-\frac{\Delta U}{\Delta y}\right] \qquad (15.52)$$

where $U_{avg} = 0.5\cdot(U_{j+1} + U_j)$ is the average U-component of wind speed between height indices j and j+1. V_{avg} and W_{avg} are similar. $\Delta U/\Delta z = (U_{j+1} - U_j)/(z_{j+1} - z_j)$, and $\Delta V/\Delta z$ and $\Delta W/\Delta z$ are similar. Helicity units are $m\cdot s^{-2}$, and the differences Δ should be across very small distances.

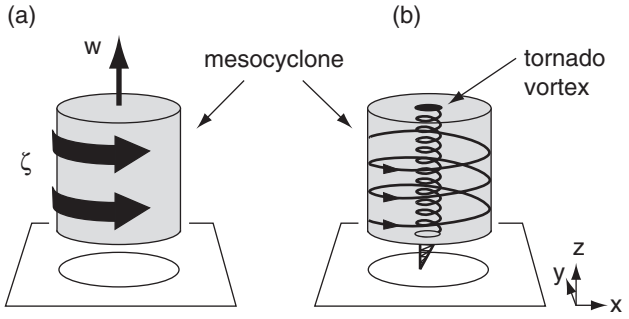

Figure 15.43
(a) Updraft and rotation in a mesocyclone combine to give (b) helical flow. The tornado vortex has a much smaller radius than the mesocyclone. ζ is vorticity, and w is vertical velocity.

Solved Example

(a) Find the streamwise helicity associated with these winds:

z (km)	U (m/s)	V (m/s)
1	0	6
2	4	8

(b) If helicity is preserved when streamwise vorticity is tilted into a mesocyclone with convective updraft 10 m/s, find the vertical vorticity of the mesocyclone.

Solution

Given: (a) see above (b) w = 10 m/s

Find: (a) H = ? m·s^{-2} (b) ζ_r = ? s^{-1}

(a) Use eq. (15.53) with winds averaged between the two heights where needed:

$$H \approx (8\text{m/s})\cdot\frac{(5-1\text{m/s})}{(2000-1000\text{m})} - (3\text{m/s})\cdot\frac{(9-}{(2000-}$$

$$= \underline{\mathbf{0.024\ m\cdot s^{-2}}}$$

(b) Use this helicity in eq. (15.54):

$(0.024\ \text{m}\cdot\text{s}^{-2}) = (10\text{m}\cdot\text{s}^{-1})\cdot\zeta_r$. Thus, $\zeta_r = \underline{\mathbf{0.0024\ s^{-1}}}$

Check: Units OK. Physics OK.

Discussion: This is roughly 100 times the vorticity of a synoptic-scale cyclone. Time-lapse movies of mesocyclone thunderstorms show noticeable rotation.

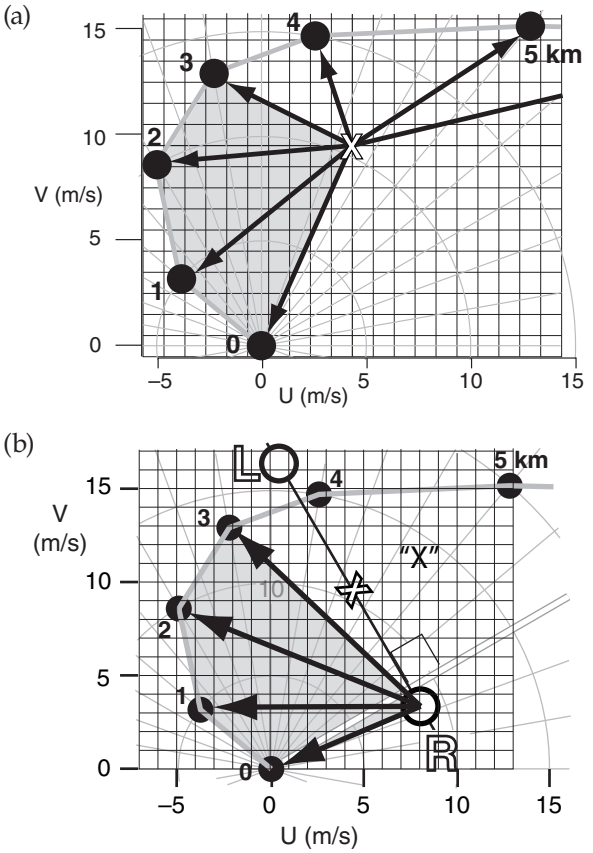

Figure 15.44

Storm-relative helicity (SRH) between the surface and z = 3 km is twice the shaded area. (a) For "normal" storm motion "𝕏", based on hodograph of Figs. 14.61 & 15.40a. (b) For right-moving storm motion "ℝ", based on the hodograph of Fig. 14.61.

For environmental air possessing only vertical shear of the horizontal winds, eq. (15.52) reduces to

$$H \approx V_{avg}\cdot\frac{\Delta U}{\Delta z} - U_{avg}\cdot\frac{\Delta V}{\Delta z} \qquad \bullet(15.53)$$

This is the portion of helicity associated with **streamwise vorticity**, and is easily calculated from the information in a hodograph.

After convection tilts the vortex tube to form the **mesocyclone**, most of the helicity is moved into the last term of eq. (15.52):

$$H = W_{avg}\cdot\left[\frac{\Delta V}{\Delta x} - \frac{\Delta U}{\Delta y}\right] = W_{avg}\cdot\zeta_r \qquad \bullet(15.54)$$

Thus, greater values of streamwise helicity in the environmental flow (eq. 15.53) can lead to larger values of mesocyclone vorticity (eq. 15.54).

More useful for mesocyclone and tornado forecasting is a **storm relative helicity** (**SRH**), which uses storm-relative environmental winds (U', V') to get a relative horizontal helicity contribution H'. Substituting storm-relative winds into eq. (15.53) gives:

$$H' \approx V'_{avg}\cdot\frac{\Delta U'}{\Delta z} - U'_{avg}\cdot\frac{\Delta V'}{\Delta z} \qquad (15.55)$$

where $U'_{avg} = 0.5\cdot(U'_{j+1} + U'_j)$ is the average U'-component of wind within the layer of air between height indices j and j+1, and V'_{avg} is similar.

To get the overall effect on the thunderstorm, SRH then sums H' over all atmospheric layers within the inflow region to the thunderstorm, times the thickness of each of those layers.

$$SRH = \sum H'\cdot\Delta z \qquad \bullet(15.56)$$

$$= \sum_{j=0}^{N-1}\left[(V'_j\cdot U'_{j+1}) - (U'_j\cdot V'_{j+1})\right] \qquad \bullet(15.57)$$

where N is the number of layers. j = 0 is the bottom wind observation (usually at the ground, z = 0), and $j = N$ is the wind observation at the top of the inflow region of air. Normally, the inflow region spans all the atmospheric layers from the ground to 1 or 3 km altitude. Units of SRH are m^2·s^{-2}.

On a hodograph, the SRH is twice the area swept by the storm-relative wind vectors in the inflow region (Fig. 15.44).

SRH is an imperfect indicator of whether thunderstorms are likely to be supercells, and might form tornadoes, hail, and strong straight-line winds. Fig. 15.45 shows the relationship between SRH values and tornado strength. Recent evidence suggests that the 0 to 1 km SRH (Fig. 15.46) works slightly better than SRH over the 0 to 3 km layer.

Solved Example

For the hodograph of Fig. 15.44a, graphically find SRH for the (a) $z = 0$ to 3 km layer, and (b) 0 to 1 km layer. (c, d) Find the SRHs for those two depths using an equation method. (e) Discuss the potential for tornadoes?

Solution:

Given Fig. 15.44a.

Find: 0-3 km & 0-1 km SRH = ? $m^2 \cdot s^{-2}$, both graphically & by eq.

a) Graphical method: Fig. 15.44a is copied below, and zoomed into the shaded region. Count squares in the shaded region of the fig., knowing that each square is 1 m/s by 1 m/s, and thus spans 1 $m^2 \cdot s^{-2}$ of area.

When counting squares, if a shaded area (such as for square #2 in the fig. below) does not cover the whole square, then try to compensate with other portions of shaded areas (such as the small shaded triangle just to the right of square #2).

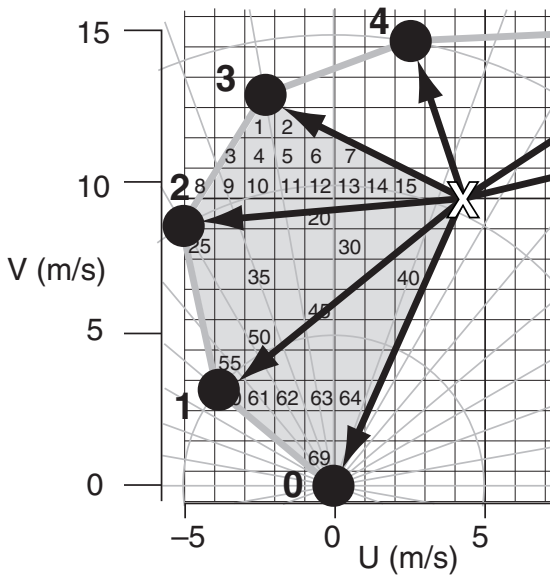

Thus, for 0 to 3 km SRH:

SRH = 2·(# of squares)·(area of each square)

SRH =2 · (69 squares) · (1 $m^2 \cdot s^{-2}$/square) = **138 $m^2 \cdot s^{-2}$**.

(continues in next column)

Solved Example *(SRH continuation)*

b) For 0 to 1 km: SRH:

SRH =2 · (25 squares) · (1 $m^2 \cdot s^{-2}$/square) = **50 $m^2 \cdot s^{-2}$**.

c) Equation method: Use eq. (15.57). For our hodograph, each layer happens to be 1 km thick. Thus, the index j happens to correspond to the altitude in km of each wind observation, for this fortuitous situation.

For the 0-3 km depth, eq. (15.57) expands to be:

$$SRH = V'_0 \cdot U'_1 - U'_0 \cdot V'_1 \quad (\text{for } 0 \le z \le 1 \text{ km})$$
$$+ V'_1 \cdot U'_2 - U'_1 \cdot V'_2 \quad (\text{for } 1 \le z \le 2 \text{ km})$$
$$+ V'_2 \cdot U'_3 - U'_2 \cdot V'_3 \quad (\text{for } 2 \le z \le 3 \text{ km})$$

Because the figure at left shows storm-relative winds, we can pick off the (U', V') values by eye for each level:

z (km)	U′ (m/s)	V′ (m/s)
0	–4.3	–9.5
1	–8.1	–6.2
2	–9.3	–1.0
3	–7.7	+3.3

Plugging these values into the eq. above gives:

$$SRH = (-9.5)\cdot(-8.1) - (-4.3)\cdot(-6.2)$$
$$+ (-6.2)\cdot(-9.3) - (-8.1)\cdot(-1.0)$$
$$+ (-1.0)\cdot(-7.7) - (-9.3)\cdot(+3.3)$$
$$SRH = 76.95 - 26.66 + 57.66 - 8.1 + 7.7 + 30.69$$
$$= \mathbf{138.2\ m^2 \cdot s^{-2}} \text{ for 0 - 3 km}$$

d) 0-1 km SRH = 76.95 – 26.66 = **50.3 $m^2 \cdot s^{-2}$** .

e) Using Fig. 15.45 there is a **good chance of supercells and EF0 to EF1 tornadoes. Slight chance of EF2 tornado.** However, Fig. 15.46 suggests a **supercell with no tornado.**

Check: Units OK. Physics OK. Magnitudes OK.

Discussion: The graphical and equation methods agree amazingly well with each other. This gives us confidence to use either method, whichever is easiest.

The disagreement in tornado potential between the 0-1 and 0-3 km SRH methods reflects the tremendous difficulty in thunderstorm and tornado forecasting. Operational meteorologists often must make difficult decisions quickly using conflicting indices.

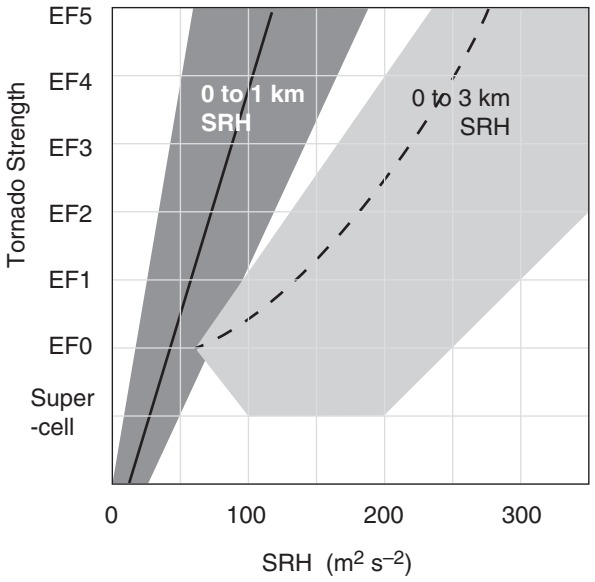

Figure 15.45
Approximate relationship between storm-relative helicity (SRH) and tornado strength on the Enhanced Fujita scale (EF0 to EF5), for North America. "Supercell" indicates a non-tornadic mesocyclonic thunderstorm. Caution: the shaded domain boundaries are not as sharp as drawn. Solid and dashed lines are medians.

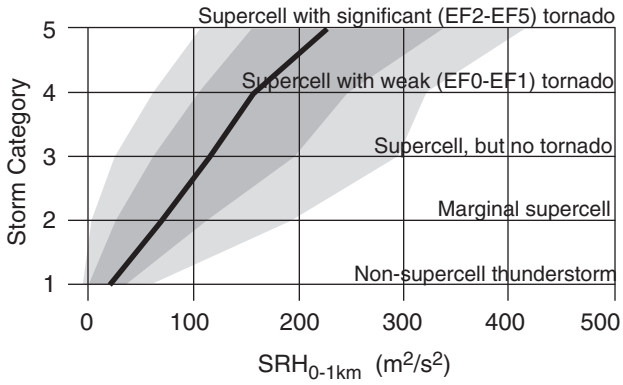

Figure 15.46
Statistics of thunderstorm intensity vs. storm-relative helicity (SRH) across the 0 to 1 km layer of air. For several hundred storms in central N. America, the black line is the median (50 percentile); dark grey shading spans 25 to 75 percentiles (the interquartile range); and light grey spans 10 to 90 percentiles.

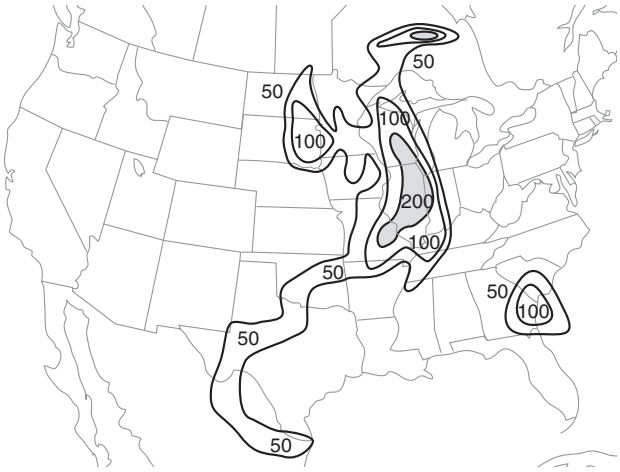

Figure 15.47
A case-study example of effective storm-relative helicity (eSRH) in units of m^2/s^2 at 23 UTC on 24 May 2006, over the USA. Values of eSRH greater than 200 m^2/s^2 are shaded, and indicate locations of greatest likelihood for tornadic supercells.

Because actual thunderstorms do not necessarily draw in air from the 0 to 1 km layer, an **effective Storm Relative Helicity** (**eSRH**) has been proposed that is calculated across a range of altitudes that depends on CAPE and CIN of the environmental sounding. The bottom altitude is found as the lowest starting altitude for a rising air parcel that satisfies two constraints: CAPE ≥ 100 J/kg when lifted to its EL, and CIN ≥ –250 J/kg (i.e., is less negative than –250 J/kg). The top altitude is the lowest starting height (above the bottom altitude) for which rising air-parcel CAPE ≤ 100 J/kg or CIN ≤ –250 J/kg.

The eSRH calculation is made only if the top and bottom layer altitudes are within the bottom 3 km of the atmosphere. eSRH is easily found using computer programs. Fig. 15.47 shows a map of eSRH for the 24 May 2006 case.

eSRH better discriminates between non-tornadic and tornadic supercells than SRH. eSRH values are usually slightly smaller than SRH values. It works even if the residual-layer air ingested into the thunderstorm lies on top of a shallow stable layer of colder air, such as occurs in the evening after sunset.

One difficulty with SRH is its sensitivity to storm motion. For example, hodographs of veering wind as plotted in Fig. 15.44 would indicate much greater SRH for a right moving ("R") storm compared to a supercell that moves with the average 0 to 6 km winds ("X").

As sketched in Fig. 15.43a, both updraft and rotation (vorticity) are important for mesocyclone formation. You might anticipate that the most violent supercells have both large CAPE (suggesting strong updrafts) and large SRH (suggesting strong rotation). A composite index called the **Energy Helicity Index** (**EHI**) combines these two variables:

$$EHI = \frac{CAPE \cdot SRH}{a} \qquad \bullet(15.58)$$

where $a = 1.6 \times 10^5$ m^4·s^{-4} is an arbitrary constant designed to make EHI dimensionless and to scale its values to lie between 0 and 5 or so. Large values of EHI suggest stronger supercells and tornadoes.

CAPE values used in EHI are always the positive area on the sounding between the LFC and the EL. MLCAPE SRH values can be either for the 0 to 1 km layer in the hodograph, or for the 0 to 3 km layer. For this reason, EHI is often classified as 0-1 km EHI or 0-3 km EHI. Also, EHI can be found either from actual rawinsonde observations, or from forecast soundings extracted from numerical weather prediction models.

Table 15-5 indicates likely tornado strength in North America as a function of 0-3 km EHI. Caution: the EHI ranges listed in this table are only approximate. If 0-1 km EHI is used instead, then significant tornadoes can occur for EHI as low as 1 or 2, such as shown in Fig. 15.48. To illustrate EHI, Fig. 15.49 shows a forecast weather map of EHI for 24 May 2006.

Solved Example

Suppose a prestorm environmental sounding is analyzed, and shows that the convective available potential energy is 2000 J/kg, and the storm relative helicity is 150 m^2/s^2 in the bottom 1 km of atmosphere. Find the value of energy helicity index, and forecast the likelihood of severe weather.

Solution:
Given: $CAPE$ = 2000 J/kg = 2000 m^2/s^2,
$SHR_{0\text{-}1km}$ = 150 m^2/s^2
Find: EHI = ? (dimensionless)

Use eq. (15.58):
EHI = (2000 m^2/s^2) · (150 m^2/s^2) / (1.6x10^5 m^4/s^4)
= **1.88**

Check: Units dimensionless. Value reasonable.
Discussion: Using this value in Fig. 15.48, there is a **good chance for a tornadic supercell thunderstorm**, and the tornado could be significant (EF2 - EF5). However, there is a slight chance that the thunderstorm will be non-tornadic, or could be a marginal supercell.

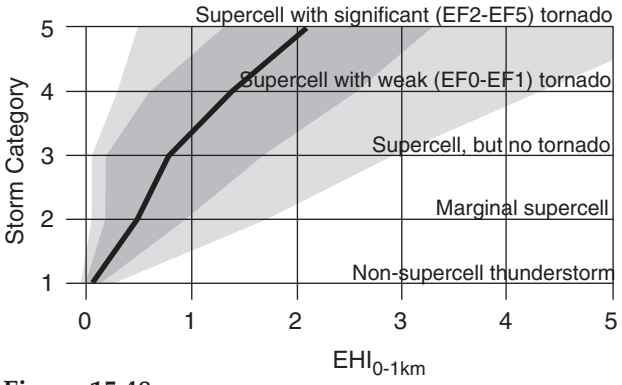

Figure 15.48
Statistics of thunderstorm intensity vs. energy helicity index (EHI) across the 0 to 1 km layer of air. For several hundred storms in central N. America, the black line is the median (50 percentile); dark grey shading spans 25 to 75 percentiles (the interquartile range); and light grey spans 10 to 90 percentiles.

Table 15-5. Energy Helicity Index (0-3 km EHI) as an indicator of possible tornado existence and strength.

EHI	Tornado Likelihood
< 1.0	Tornadoes & supercells unlikely.
1.0 to 2.0	Supercells with weak, short-lived tornadoes possible. Non-supercell tornadoes possible (such as near bow echoes).
2.0 to 2.5	Supercells likely. Mesocyclone-induced tornadoes possible.
2.5 to 3.0	Mesocyclone-induced supercell tornadoes more likely.
3.0 to 4.0	Strong mesocyclone-induced tornadoes (EF2 and EF3) possible.
> 4.0	Violent mesocyclone-induced tornadoes (EF4 and EF5) possible.

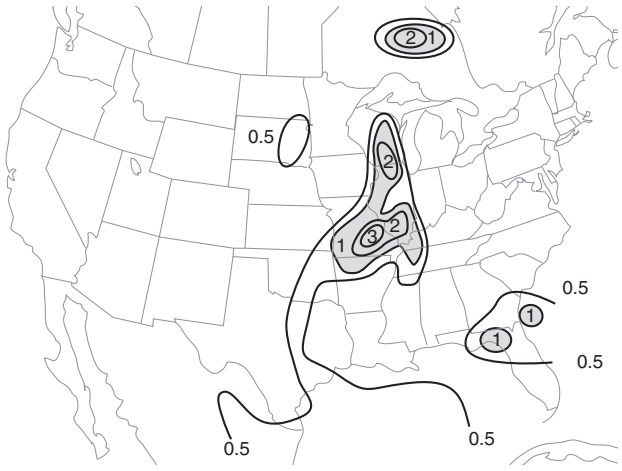

Figure 15.49
Map of energy helicity index (EHI) over the 0 to 1 km layer, for the 23 UTC case on 24 May 2006, over the USA. Dimensionless values greater than 1 are shaded, and suggest stronger supercell storms with greater likelihood of tornadoes.

Science Graffito

Mobile homes and trailers are so vulnerable to thunderstorm and tornadic winds that, to many non-scientists, those homes seem to attract tornadoes. This has led disaster preparedness officers in some towns to suggest putting mobile home parks outside of town, to serve as "tornado bait" to lure tornadoes away from town. (This doesn't work.)

Solved Example

What is the swirl ratio for a mesocyclone with radial velocity 2 m/s, tangential velocity 10 m/s at radius 2000 m in a boundary layer 1 km deep?

Solution

Given: M_{tan} = 10 m/s, M_{rad} = 2 m/s,
R_M = 2000 m, z_i = 1 km
Find: S = ? (dimensionless)

Use eq. (15.60):

$$S = \frac{(2500\ \text{m})\cdot(3\ \text{m/s})}{2\cdot(1500\ \text{m})\cdot(1\ \text{m/s})} = \underline{\mathbf{5.0}}$$

Check: Units OK. Physics OK.
Discussion: A multiple vortex tornado is likely with perhaps 6 vortices moving around the larger parent funnel.

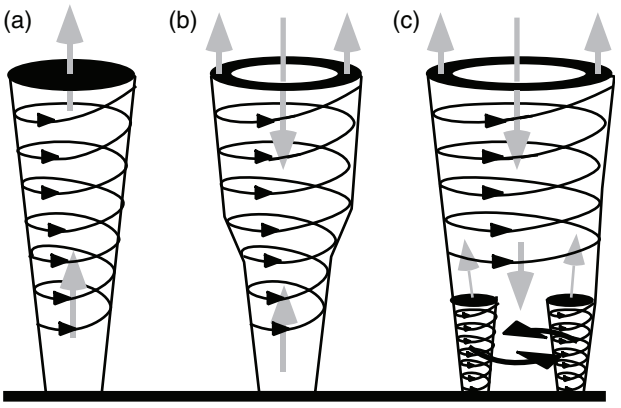

Figure 15.50
Tornadoes with swirl ratios (S) of: (a) S = 0.2 ; (b) S = 0.4 ; and (c) S = 2.0 .

Because none of the forecast parameters and indices give perfect forecasts of supercells and tornadoes, researchers continue to develop and test new indices. One example is the **Supercell Composite Parameter** (**SCP**), which is a normalized product of MUCAPE, eSRH, and effective bulk shear. Non-supercell thunderstorms have SCP values near zero, marginal and elevated supercells have values between 0 and 6, while strong surface-based supercells have values between 2 and 11.

Another experimental parameter is the **Significant Tornado Parameter** (**STP**), which is a normalized product of MLCAPE, surface-based effective bulk shear, eSRH, MLLCL, and MLCIN. Values between 0 and 1 are associated with non-tornadic supercells, while values between 1 and 5 indicate supercells likely to have significant (EF2 - EF5) tornadoes.

Tornadoes and Swirl Ratio

The characteristics of a tornado can vary, depending on the dimensionless **swirl ratio**:

$$S = M_{tan} / \qquad \bullet(15.59)$$

where M_{tan} is the tangential component of velocity around the perimeter of the updraft region, and W is the average updraft velocity. For a cylindrical mesocyclone, this can be rewritten as

$$S = \frac{R_{MC}\cdot M_{tan}}{2z_i\cdot M_{rad}} \qquad \bullet(15.60)$$

where R_M is the mesocyclone radius, z_i is the boundary-layer depth, and M_{rad} is the radial (inflow) component of velocity. Typically, $R_M \approx 2\cdot z_i$; thus,

$$S \approx M_{tan} / M_{rad} . \qquad \bullet(15.61)$$

For small swirl ratios (0.1 to 0.3), tornadoes simulated in laboratories have a single, well-defined funnel (Fig. 15.50a) that looks somewhat smooth (laminar). The tornado core has low pressure, updraft, and has a core radius R_o of 5% to 25% of the mesocyclone updraft radius, R_M.

At larger swirl ratios, a turbulent downdraft begins to form in the top part of the tornado core, which has a much larger diameter than the laminar bottom that still has an updraft (Fig. 15.50b). The updraft and downdraft portions of the core meet at a vertical stagnation point called the **breakdown bubble**.

As the swirl ratio approaches a **critical swirl ratio** of $S^* \approx 0.45$, the turbulent downdraft extends downward, with the breakdown bubble eventually reaching the ground. As the swirl ratio continues to increase, the tornado looks quite turbulent and has a large diameter, with a downdraft core surrounded by a helix of rotating, rising air.

For even larger swirl ratio ($S \geq 0.8$), the large-diameter tornado breaks down into **multiple vortices** that chase each other around the perimeter of the large tornado downdraft (Fig. 15.50c). The process of changing from a single laminar funnel to a turbulent, **multiple-vortex tornado**, is called **tornado breakdown**. As S continues to increase toward 3 and beyond, the number of multiple vortices increases from 2 to 6.

Wind speeds and damage are greatest in these small vortices, sometimes known as **suction vortices**. The individual vortices not only circulate around the perimeter of the parent tornado, but the whole tornado system translates over the ground as the thunderstorm moves across the land. Thus, each vortex traces a cycloidal pattern on the ground, which is evident in post-tornado aerial photographs as cycloidal damage paths to crops (Fig. 15.51).

When single-vortex tornadoes move over a forest, they blow down the trees in a unique pattern that differs from tree blowdown patterns caused by straight-line winds (Fig. 15.52). Sometimes these patterns are apparent only from an aerial vantage point.

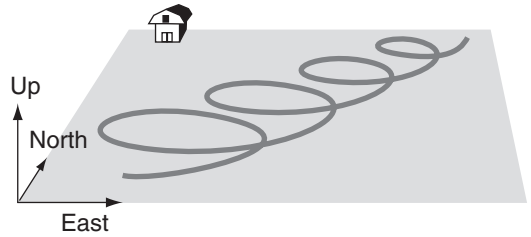

Figure 15.51
Cycloidal damage path in a farm field caused by a tornadic suction vortex imbedded in a larger diameter parent tornado.

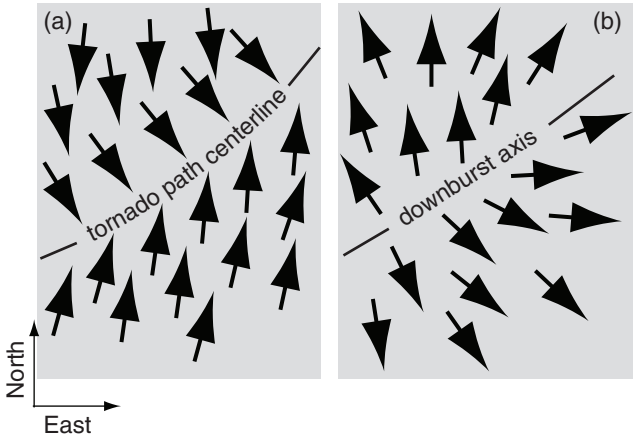

Figure 15.52
Damage signatures of (a) tornadoes and (b) downbursts in a forest, as seen in aerial photographs of tree blowdown.

SUMMARY

Supercell thunderstorms can create tornadic winds, straight-line winds, downbursts, lightning, heavy rain, hail, and vigorous turbulence.

Larger hail is possible in storms with stronger updraft velocities, which is related to CAPE. When precipitation falls into drier air, both precipitation drag and evaporative cooling can cause acceleration of downdraft winds. When the downburst wind hits the ground, it spreads out into straight-line winds, the leading edge of which is called a gust front. Dust storms (haboobs) and arc clouds are sometimes created by gust fronts.

As ice crystals and graupel particles collide they each transfer a small amount of charge. Summed over billions of such collisions in a thunderstorm, sufficient voltage gradient builds up to create lightning. The heat from lightning expands air to create the shock and sound waves we call thunder. Horizontal wind shear can be tilted into the vertical to create mesocyclones and tornadoes.

Threads

Condensation of water vapor in the buoyant, rising air makes the cumulonimbus cloud (Chapter 6), and the cold-cloud ice process in the top of the cloud contributes to rapid precipitation formation (Chapter 7). Thunderstorm rain drops have fairly large diameter, which makes them ideal for contributing to rainbows (Chapter 22). Weather radars can measure both rainfall intensity (Chapter 8) and Doppler velocity.

The downburst and horizontal winds are driven by pressure-gradient and buoyancy forces (Chapter 10), and rotating tornadoes are also influenced by centrifugal force. Boundary-layer wind shear (Chapter 18) creates vorticity (Chapter 11) that can be tilted into the vertical vorticity of mesocyclones. The strong winds hitting buildings creates a damaging dynamic pressure (Chapter 17) that can be estimated with Bernoulli's equations. Bernoulli's equation also relates tornado core pressure to tangential wind speed.

EXERCISES

Numerical Problems

N1. If a thunderstorm cell rains for 0.5 h at the precipitation rate (mm/h) below, calculate both the net latent heat released into the atmosphere, and the average warming rate within the troposphere.

a. 50 b. 75 c. 100 d. 125 e. 150
f. 175 g. 200 h. 225 i. 250 j. 275
k. 300 l. 325 m. 350 n. 375 o. 400

N2. Indicate the TORRO hail size code, and descriptive name, for hail of diameter (cm):

a. 0.6 b. 0.9 c. 1.2 d. 1.5 e. 1.7
f. 2.1 g. 2.7 h. 3.2 i. 3.7 j. 4.5
k. 5.5 l. 6.5 m. 7.5 n. 8.0 o. 9.5

N3. Graphically estimate the terminal fall velocity of hail of diameter (cm):

a. 0.6 b. 0.9 c. 1.2 d. 1.5 e. 1.7
f. 2.1 g. 2.7 h. 3.2 i. 3.7 j. 4.5
k. 5.5 l. 6.5 m. 7.5 n. 8.0 o. 9.5

N4. A supercooled cloud droplet of radius 40 μm hits a large hailstone. Using the temperature (°C) of the droplet given below, is the drop cold enough to freeze instantly (i.e., is its temperature deficit sufficient to compensate the latent heat of fusion released)? Based on your calculations, state whether the freezing of this droplet would contribute to a layer of clear or white (porous) ice on the hailstone.

a. –40 b. –37 c. –35 d. –32 e. –30
f. –27 g. –25 h. –22 i. –20 j. –17
k. –15 l. –13 m. –10 n. –7 o. –5

N5. Given the sounding in exercise N3 of the previous chapter, calculate the portion of SB CAPE between altitudes where the environmental temperature is –10 and –30°C. Also, indicate if rapid hail growth is likely.

N6. Given the table below of environmental conditions, calculate the value of Significant Hail Parameter (SHIP), and state whether this environment favors the formation of hailstone > 5 cm diameter (assuming a thunderstorm indeed forms).

Exercise	a	b	c	d
MUCAPE (J/kg)	2000	2500	3000	3500
r_{MUP} (g/kg)	10	12	14	16
$\gamma_{70\text{-}50kPa}$ (°C/km)	2	4	6	8
T_{50kPa} (°C)	–20	–15	–10	–5
$TSM_{0\text{-}6km}$ (m/s)	20	30	40	50

N7. For the downburst acceleration equation, assume that the environmental air has temperature 2°C and mixing ratio 3 g/kg at pressure 85 kPa. A cloudy air parcel at that same height has the same temperature, and is saturated with water vapor and carries liquid water at the mixing ratio (g/kg) listed below. Assume no ice crystals.

(1) Find portion of vertical acceleration due to the combination of temperature and water vapor effects.

(2) Find the portion of vertical acceleration due to the liquid water loading only.

(3) If all of the liquid water were to evaporate and cool the air parcel, find the change in parcel virtual potential temperature.

(4) If all of the liquid water were to evaporate and cool the air parcel, find the new vertical acceleration.

The liquid water mixing ratios (g/kg) are:

a. 20 b. 18 c. 16 d. 14 e. 12 f. 10 g. 9
h. 8 i. 7 j. 6 k. 5 l. 4 m. 3 n. 2

N8. Given the sounding from exercise N3 of the previous chapter, assume a descending air parcel in a downburst follows a moist adiabat all the way down to the ground. If the descending parcel starts at the pressure (kPa) indicated below, and assuming its initial temperature is the same as the environment there, plot both the sounding and the descending parcel on a thermo diagram, and calculate the value of downdraft CAPE.

a. 80 b. 79 c. 78 d. 77 e. 76 f. 75 g. 74
h. 73 i. 72 j. 71 k. 70 l. 69 m. 68 n. 67

N9. Find the downdraft speed if the DCAPE (J/kg) for a downburst air parcel is:

a. –200 b. –400 c. –600 d. –800 e. –1000
f. –1200 g. –1400 h. –1600 i. –1800 j. –2000
k. –2200 l. –2400 m. –2600 n. –2800 o. –3000

N10. If a downburst has the same potential temperature as the environment, and starts with vertical velocity (m/s, negative for descending air) given below, use Bernoulli's equation to estimate the maximum pressure perturbation at the ground under the downburst.

a. –2 b. –4 c. –6 d. –8 e. –10
f. –12 g. –14 h. –16 i. –18 j. –20
k. –22 l. –24 m. –26 n. –28 o. –30

N11. Same as the previous exercise, but in addition to the initial downdraft velocity, the descending air parcel is colder than the environment by the following product of virtual potential temperature depression and initial altitude (°C·km):

(1) –0.5 (2) –1 (3) –1.5 (4) –2

(5) –2.5	(6) –3	(7) –3.5	(8) –4
(9) –4.5	(10) –5	(11) –5.5	(12) –6
(13) –6.5	(14) –7	(15) –7.5	(16) –8

N12. Find the acceleration (m/s^2) of outflow winds from under a downburst, assuming a maximum mesohigh pressure (kPa) perturbation at the surface as given below, and a radius of the mesohigh of 3 km.

a. 0.1	b. 0.2	c. 0.3	d. 0.4	e. 0.5
f. 0.6	g. 0.7	h. 0.8	i. 0.9	j. 1.0
k. 1.1	l. 1.2	m. 1.3	n. 1.4	o. 1.5

N13. A downburst of radius 0.6 km and speed 8 m/s descends through an environment of 30°C. Find the gust front advancement speed and depth at a distance of 5 km from the downburst center, given a magnitude of temperature deficit (°C) of

a. 1	b. 1.5	c. 2	d. 2.5	e. 3	f. 3.5
g. 4	h. 4.5	i. 5	j. 5.5	k. 6	l. 6.5
m. 7	n. 7.5	o. 8	p. 8.5	q. 9	r. 9.5

N14(§). For the previous problem, plot curves of advancement speed and depth versus gust-front distance from the downburst center.

N15. Given a lightning discharge current (kA) below and a voltage difference between the beginning to end of the lightning channel of 10^{10} V, find (1) the resistance of the ionized lightning channel and (2) the amount of charge (C) transferred between the cloud and the ground during the 20 μs lifetime of the lightning stroke.

a. 2	b. 4	c. 6	d. 8	e. 10	f. 15	g. 20
h. 40	i. 60	j. 80	k. 100	l. 150	m. 200	n. 400

N16. What voltage difference is needed to cause lightning for (1) dry air, and (2) cloudy air, given a lightning stroke length (km) of:

a. 0.2	b. 0.4	c. 0.6	d. 0.8	e. 1	f. 1.2	g. 1.4
h. 1.6	i. 1.8	j. 2.0	k. 2.5	l. 3	m. 4	n. 5

N17. For an electrical potential across the atmosphere of 1.3×10^5 V/km, find the current density if the resistivity (Ω·m) is:

a. 5×10^{13}	b. 1×10^{13}	c. 5×10^{12}	d. 1×10^{12}	e. 5×10^{11}
f. 1×10^{11}	g. 5×10^{10}	h. 1×10^{10}	i. 5×10^{9}	j. 1×10^{9}
k. 5×10^{8}	l. 1×10^{8}	m. 5×10^{7}	n. 1×10^{7}	o. 5×10^{6}

N18. What is the value of peak current in a lightning stroke, as estimated using a lightning detection network, given the following measurements of electrical field E and distance D from the ground station.

	$-E$ (V/m)	D (km)
a.	1	10
b.	1	50
c.	2	10
d.	2	100
e.	3	20
f.	3	80
g.	4	50
h.	4	100
i.	5	50
j.	5	200
k.	6	75
l.	6	300

N19. For a power line struck by lightning, what is the probability that the lightning-generated current (kA) is greater than:

a. 2	b. 4	c. 6	d. 8	e. 10	f. 15	g. 20
h. 40	i. 60	j. 80	k. 100	l. 150	m. 200	n. 400

N20. When, after a lightning strike, will the surge in a power line decay to the following fraction of its peak value:

a. 0.1	b. 0.15	c. 0.2	d. 0.25	e. 0.3
f. 0.35	g. 0.4	h. 0.45	i. 0.5	j. 0.55
k. 0.6	l. 0.65	m. 0.7	n. 0.75	o. 0.8

N21(§). If lightning heats the air to the temperature (K) given below, then plot (on a log-log graph) the speed (Mach number), pressure (as ratio relative to background pressure), and radius of the shock front vs. time given ambient background pressure of 100 kPa and temperature 20°C.

a. 16,000	b. 17,000	c. 18,000	d. 19,000
e. 20,000	f. 21,000	g. 22,000	h. 23,000
i. 24,000	j. 25,000	k. 26,000	l. 27,000
m. 28,000	n. 29,000	o. 30,000	

N22. What is the speed of sound in calm air of temperature (°C):

a. –20	b. –18	c. –16	d. –14	e. –12
f. –10	g. –8	h. –6	i. –4	j. –2
k. 0	l. 2	m. 4	n. 6	o. 8
p. 10	q. 12	r. 14	s. 16	t. 18

N23(§). For calm conditions, draw a curve of range vs. time interval between seeing lightning and hearing thunder. Assume $T_{environment}$ = 290 K. Draw additional curves for head and for tail winds (m/s) of:

a. 2	b. 4	c. 6	d. 8	e. 10	f. 12	g. 14
h. 16	i. 18	j. 20	k. 22	l. 24	m. 26	n. 28

N24(§). For a lightning stroke 2 km above ground in a calm adiabatic environment of average temperature 300 K, plot the thunder ray paths leaving downward from the lightning stroke, given that they arrive at the ground at the following elevation angle (°).

a. 5	b. 6	c. 7	d. 8	e. 9	f. 10	g. 11

h. 12 i. 13 j. 14 k. 15 l. 16 m. 17 n. 18
o. 19 p. 20 q. 21 r. 22 s. 23 t. 24 u. 25

N25. What is the maximum distance you can expect to hear thunder from lightning 5 km high in calm conditions with average temperature 300 K , if the lapse rate (°C/km) is:
a. 9.8 b. 9 c. 8.5 d. 8 e. 7.5 f. 7 g. 6.5
h. 6 i. 5.5 j. 5 k. 4.5 l. 4 m. 3.5 n. 3
o. 2.5 p. 2 q. 1.5 r. 1 s. 0.5 t. 0 u. –1

N26. How low below ambient 100 kPa pressure must the core pressure of a tornado be, in order to support max tangential winds (m/s) of:
a. 20 b. 30 c. 40 d. 50 e. 60 f. 70 g. 80
h. 90 i. 100 j. 110 k. 120 l. 130 m. 140 n. 150

N27(§). For a Rankine Combined Vortex model of a tornado, plot the pressure (kPa) and tangential wind speed (m/s) vs. radial distance (m) out to 125 m, for a tornado of core radius 25 m and core pressure deficit (kPa) of:
a. 0.1 b. 0.2 c. 0.3 d. 0.4 e. 0.5
f. 0.6 g. 0.7 h. 0.8 i. 0.9 j. 1.0
k. 1.1 l. 1.2 m. 1.3 n. 1.4 o. 1.5

N28. If the max tangential wind speed in a tornado is 100 m/s, and the tornado translates at the speed (m/s) given below, then what is the max wind speed (m/s), and where is it relative to the center of the tornado and its track?
a. 2 b. 4 c. 6 d. 8 e. 10 f. 12 g. 14
h. 16 i. 18 j. 20 k. 22 l. 24 m. 26 n. 28

N29. What are the Enhanced Fujita and Torro intensity indices for a tornado of max wind speed (m/s) of
a. 20 b. 30 c. 40 d. 50 e. 60 f. 70 g. 80
h. 90 i. 100 j. 110 k. 120 l. 130 m. 140 n. 150

N30 Find the pressure (kPa) at the edge of the tornado condensation funnel, given an ambient near-surface pressure and temperature of 100 kPa and 35°C, and a dew point (°C) of:
a. 30 b. 29 c. 28 d. 27 e. 26 f. 25 g. 24
h. 23 i. 22 j. 21 k. 20 l. 19 m. 18 n. 17

N31. For the winds of exercise N18 (a, b, c, or d) in the previous chapter, first find the storm movement for a
(1) normal supercell
(2) right-moving supercell
(3) left-moving supercell
Then graphically find and plot on a hodograph the storm-relative wind vectors.

N32. Same as previous exercise, except determine the (U_s, V_s) components of storm motion, and then list the (U_j', V_j') components of storm-relative winds.

N33. A mesocyclone at 38°N is in an environment where the vertical stretching $(\Delta W/\Delta z)$ is (20 m/s) / (2 km). Find the rate of vorticity spin-up due to stretching only, given an initial relative vorticity (s^{-1}) of
a. 0.0002 b. 0.0004 c. 0.0006 d. 0.0008 e. 0.0010
f. 0.0012 g. 0.0014 h. 0.0016 i. 0.0018 j. 0.0020
k. 0.0022 l. 0.0024 m. 0.0026 n. 0.0028 o. 0.0030

N34. Given the hodograph of storm-relative winds in Fig. 15.40b. Assume that vertical velocity increases with height according to $W = a \cdot z$, where a = (5 m/s)/km. Considering only the tilting terms, find the vorticity spin-up based on the wind-vectors for the following pairs of heights (km):
a. 0,1 b. 1,2 c. 2,3 d. 3,4 e. 4,5 f. 5,6 g. 0,2
h. 1,3 i. 2,4 j. 3,5 k. 4,6 l. 1,4 m. 2,5 n. 3,6
o. 1,5 p. 2,6 q. 1,6

N35. Same as the previous exercise but for the storm-relative winds in the hodograph of the solved example in the "Storm-relative Winds" subsection of the tornado section.

N36. Given the hodograph of winds in Fig. 15.40a. Assume $W = 0$ everywhere. Calculate the helicity H based on the wind-vectors for the following pairs of heights (km):
a. 0,1 b. 1,2 c. 2,3 d. 3,4 e. 4,5 f. 5,6 g. 0,2
h. 1,3 i. 2,4 j. 3,5 k. 4,6 l. 1,4 m. 2,5 n. 3,6
o. 1,5 p. 2,6 q. 1,6

N37. Same as the previous exercise, but use the storm-relative winds from Fig. 15.40b to get the storm-relative helicity H'. (Hint, don't sum over all heights for this exercise.)

N38. Given the hodograph of winds in Fig. 15.40a. Assume that vertical velocity increases with height according to $W = a \cdot z$, where a = (5 m/s)/km. Calculate the vertical contribution to helicity (eq. 15.54) based on the wind-vectors for the following pairs of heights (km):
a. 0,1 b. 1,2 c. 2,3 d. 3,4 e. 4,5 f. 5,6 g. 0,2
h. 1,3 i. 2,4 j. 3,5 k. 4,6 l. 1,4 m. 2,5 n. 3,6
o. 1,5 p. 2,6 q. 1,6

N39. Use the storm-relative winds in the hodograph of the solved example in the "Storm-relative Winds" subsection of the tornado section. Calculate the total storm-relative helicity (SRH) graphically for the following height ranges (km):
a. 0,1 b. 0,2 c. 0,3 d. 0,4 e. 0,5 f. 0,6 g. 1,2

h. 1,3 i. 1,4 j. 1,5 k. 1,6 l. 2,3 m. 2,4 n. 2,5
o. 2,6 p. 3,5 q. 3,6

N40. Same as the previous exercise, but find the answer using the equations (i.e., NOT graphically).

N41. Estimate the intensity of the supercell and tornado (if any), given a 0-1 km storm-relative helicity (m^2/s^2) of:
a. 20 b. 40 c. 60 d. 80 e. 100 f. 120 g. 140
h. 160 i. 180 j. 200 k. 220 l. 240 m. 260 n. 280
o. 300 p. 320 q. 340 r. 360 s. 380 t. 400

N42. Given a storm-relative helicity of 220 , find the energy-helicity index if the CAPE (J/kg) is:
a. 200 b. 400 c. 600 d. 800 e. 1000 f. 1200
g. 1400 h. 1600 i. 1800 j. 2000 k. 2200
l. 2400 m. 2600 n. 2800 o. 3000

N43. Estimate the likely supercell intensity and tornado intensity (if any), given an energy-helicity index value of:
a. 0.2 b. 0.4 c. 0.6 d. 0.8 e. 1.0 f. 1.2 g. 1.4
h. 1.6 i. 1.8 j. 2.0 k. 2.2 l. 2.4 m. 2.6 n. 2.8
o. 3.0 p. 3.2 q. 3.4 r. 3.6 s. 3.8 t. 4.0

N44. If the tangential winds around a mesocyclone updraft are 20 m/s, find the swirl ratio of the average updraft velocity (m/s) is:
a. 2 b. 4 c. 6 d. 8 e. 10 f. 12 g. 14
h. 16 i. 18 j. 20 k. 22 l. 24 m. 26 n. 28
o. 30 p. 32 q. 34 r. 36 s. 38 t. 40

N45. Given a mesocyclone with a tangential velocity of 20 m/s around the updraft region of radius 1000 m in a boundary layer 1 km thick. Find the swirl ratio and discuss tornado characteristics, given a radial velocity (m/s) of:
a. 1 b. 2 c. 3 d. 4 e. 5 f. 6 g. 7
h. 8 i. 9 j. 10 k. 11 l. 12 m. 13 n. 14
o. 15 p. 16 q. 17 r. 18 s. 19 t. 20

Understanding & Critical Evaluation

U1. Why cannot hook echoes be used reliably to indicate the presence of a tornado?

U2. Cases of exceptionally heavy rain were discussed in the "Precipitation and Hail" section of this chapter and in the Precipitation chapter section on Rainfall Rates. However, most of those large rainfall rates occurred over exceptionally short durations (usually much less than an hour). Explain why longer-duration extreme-rainfall rates are unlikely.

U3. Use the info in Fig. 15.4 and the relationship between max likely updraft speed and CAPE, to plot a new graph of max possible hailstone diameter vs. total CAPE.

U4. In Fig. 15.7, what is the advantage to ignoring a portion of CAPE when estimating the likelihood of large hail? Explain.

U5. Explain why the various factors in the SHIP equation (15.4) are useful for predicting hail?

U6. Figures 15.5 and 15.10 show top and end views of the same thunderstorm, as might be seen with weather radar. Draw a side view (as viewed from the southeast by a weather radar) of the same thunderstorm. These 3 views give a blueprint (mechanical drawing) of a supercell.

U7. Cloud seeding (to change hail or rainfall) is a difficult social and legal issue. The reason is that even if you did reduce hail over your location by cloud seeding, an associated outcome might be increased hail or reduced rainfall further downwind. So solving one problem might create other problems. Discuss this issue in light of what you know about sensitive dependence of the atmosphere to initial conditions (the "butterfly effect"), and about the factors that link together the weather in different locations.

U8. a. Confirm that each term in eq. (15.5) has the same units.
b. Discuss how terms A and C differ, and what they each mean physically.
c. In term A, why is the numerator a function of $\Delta P'$ rather than ΔP?

U9. a. If there were no drag of rain drops against air, could there still be downbursts of air?
b. What is the maximum vertical velocity of large falling rain drops relative to the ground, knowing that air can be dragged along with the drops as a downburst? (Hint: air drag depends on the velocity of the drops relative to the air, not relative to the ground.)
c. Will that maximum fall velocity relative to the ground be reached at the ground, or at some height well above ground? Why?

U10. What is the name of the temperature to which a raindrop cools when it falls through unsaturated air?

U11. Suppose that an altocumulus (mid-tropospheric) cloud exists within an environment having

a linear, conditionally unstable, temperature profile with height. Rain-laden air descends from this little cloud, warming at the moist adiabatic rate as it descends. Because this warming rate is less than the conditionally unstable lapse rate of the environment, the temperature perturbation of the air relative to the environment becomes colder as it descends.

But at some point, all the rain has evaporated. Descent below this altitude continues because the air parcel is still colder than the environment. However, during this portion of descent, the air parcel warms dry adiabatically, and eventually reaches an altitude where its temperature equals that of the environment. At this point, its descent stops. Thus, there is a region of strong downburst that does NOT reach the ground. Namely, it can be a hazard to aircraft even if it is not detected by surface-based wind-shear sensors.

Draw this process on a thermo diagram, and show how the depth of the downburst depends on the amount of liquid water available to evaporate.

U12. Demonstrate that eq. (15.10) equates kinetic energy with potential energy. Also, what assumptions are implicit in this relationship?

U13. Eqs. (15.12) and (15.13) show how vertical velocities (w_d) are tied to horizontal velocities (M) via pressure perturbations P'. Such coupling is generically called a circulation, and is the dynamic process that helps to maintain the continuity of air (namely, the uniform distribution of air molecules in space). Discuss how horizontal outflow winds are related to DCAPE.

U14. How do gust-front depth and advancement speed vary with:

a. virtual temperature of the outflow air?

b. downburst velocity?

Plot the variation of gust front depth and advancement speed with distance R of the gust front from the center of the downburst.

U15. Fig. 15.21 shows large accumulations of electrical charge in thunderstorm clouds. Why don't the positive and negative charge areas continually discharge against each other to prevent significant charge accumulation, instead of building up such large accumulations as can cause lightning?

U16. At the end of the Focus box about "Electricity in a Channel" is given an estimate of the energy dissipated by a lightning stroke. Compare this energy to:

a. The total latent heat available to the thunderstorm, given a typical inflow of moisture.

b. The total latent heat actually liberated based on the amount of rain falling out of a storm.

c. The kinetic energy associated with updrafts and downbursts and straight-line winds.

d. The CAPE.

U17. Look at both Focus boxes on electricity. Relate:

a. voltage to electrical field strength

b. resistance to resistivity

c. current to current density

d. power to current density and electrical potential.

U18. If the electrical charging process in thunderstorms depends on the presence of ice, then why is lightning most frequently observed in the tropics?

U19. a. What is the probability that lightning current will be exactly 10 kA?

b. What is the probability that lightning current will be between 9 and 11 kPa?

U20. How does the shape of the lightning surge curve change with changes of parameters τ_1 and τ_2?

U21. Show why eqs. (15.22) and (15.32) are equivalent ways to express the speed of sound, assuming no wind.

U22. Do you suspect that nuclear explosions behave more like chemical explosions or like lightning, regarding the resulting shock waves, pressure, and density? Why?

U23. The equations for shock wave propagation from lightning assumed an isopycnal processes. Critique this assumption.

U24. Is it possible for the speed of sound relative to the ground to be zero? Under what conditions would this occur? Are these conditions likely?

U25. If there was no refraction of sound waves in air, then what is the maximum distance from lightning that one could hear thunder?

U26. Show how the expression of Snell's law in an environment with gradually changing temperature (eq. 15.36) is equivalent to, or reduces to, Snell's law across an interface (eq. 15.35).

U27. Show that eq. (15.39) for Snell's Law reduces to eq. (15.34) in the limit of zero wind.

U28. Show how the relationship between core pressure deficit and tangential velocity around a tornado can be found from Bernoulli's equation (see the Local Wind chapter). What assumptions are needed, and what are the resulting limitations?

U29(§). Suppose that the actual tangential velocity in a tornado is described by a **Rankine combined vortex (RCV)**. Doppler radars, however, cannot measure radial velocities at any point, but instead observe velocities averaged across the radar beam width. So the Doppler radar sees a smoothed version of the Rankine combined vortex. It is this smoothed tangential velocity shape that is called a **tornado vortex signature** (**TVS**), and for which the Doppler-radar computers are programmed to recognize. This exercise is to create the tangential velocity curve similar to Fig. 15.34, but for a TVS.

Let ΔD be the diameter of radar beam at some range from the radar, and R_o be the core radius of tornado. The actual values of ΔD and R_o are not important: instead consider the dimensionless ratio $\Delta D/R_o$. Compute the TVS velocity at any distance R from the center of the tornado as the average of all the RCV velocities between radii of $[(R/R_o)–(\Delta D/2R_o)]$ and $[(R/R_o)+(\Delta D/2R_o)]$, and repeat this calculation for many values of R/R_o to get a curve. This process is called a **running average**. Create this curve for $\Delta D/R_o$ of:

a. 1.0 b. 1.5 c. 2.0 d. 2.5 e. 3.0 f. 3.5 g. 4.0
h. 4.5 i. 5.0 j. 0.9 k. 0.8 l. 0.7 m. 0.6 n. 0.5

Hint: Either do this by analytically integrating the RCV across the radar beam width, or by brute-force averaging of RCV values computed using a spreadsheet.

U30(§). For tornadoes, an alternative approximation for tangential velocities M_{tan} as a function of radius R is given by the **Burgers-Rott Vortex** (BRV) equation:

$$\frac{M_{\tan}}{M_{\tan\max}} = 1.398 \cdot \left(\frac{R_o}{R}\right) \cdot \left[1 - e^{-(1.12 \cdot R/R_o)^2}\right] \qquad (15.62)$$

where R_o is the core radius.

Plot this curve, and on the same graph replot the Rankine combined vortex (RCV) curve (similar to Fig. 15.33). Discuss what physical processes in the tornado might be included in the BRV that are not in the RCV, to explain the differences between the two curves.

U31. For the Rankine combined vortex (RCV), both the tangential wind speed and the pressure deficit are forced to match at the boundary between the tornado core and the outer region. Does the pressure gradient also match at that point? If not, discuss any limitations that you might suggest on the RCV.

U32. Suppose a suction vortex with max tangential speed $M_{s\,tan}$ is moving around a parent tornado of tangential speed $M_{p\,tan}$, and the parent tornado is translating at speed M_{tr}. Determine how the max speed varies with position along the resulting cycloidal damage path.

U33. The TORRO scale is related to the **Beaufort** wind scale (**B**) by:

$$\mathbf{B} = 2 \cdot (\mathbf{T} + 4) \qquad (15.63)$$

The Beaufort scale is discussed in detail in the Hurricane chapter, and is used to classify ocean storms and sea state. Create a graph of Beaufort scale vs. TORRO scale. Why cannot the Beaufort scale be used to classify tornadoes?

U34. Can the TORRO scale be used to classify the intensity of winds triggered by meteor strikes and volcanic eruptions? Discuss.

U35. Suppose that tangential winds around a tornado involve a balance between pressure-gradient force, centrifugal force, and Coriolis force. Show that anticyclonically rotating tornadoes would have faster tangential velocity than cyclonic tornadoes, given the same pressure gradient. Also, for anticyclonic tornadoes, are their any tangential velocity ranges that are excluded from the solution of the equations (i.e., are not physically possible)? Assume N. Hem.

U36. Does the outside edge of a tornado condensation funnel have to coincide with the location of fastest winds? If not, then is it possible for the debris cloud (formed in the region of strongest winds) radius to differ from the condensation funnel radius? Discuss.

U37. Given a fixed temperature and dew point, eq. (15.48) gives us the pressure at the outside edge of the condensation funnel.

a. Is it physically possible (knowing the governing equations) for the pressure deficit at the tornado axis to be higher than the pressure deficit at the visible condensation funnel? Why?

b. If the environmental temperature and dew point don't change, can we infer that the central pressure deficit of a large-radius tornado is lower than that for a small-radius tornado? Why or why not?

U38. Gustnadoes and dust devils often look very similar, but are formed by completely different mechanisms. Compare and contrast the processes that create and enhance the vorticity in these vortices.

U39. From Fig. 15.40a, you see that the winds at 1 km above ground are coming from the southeast. Yet, if you were riding with the storm, the storm relative winds that you would feel at 1 km altitude would be from the northeast, as shown for the same data in Fig. 15.40b. Explain how this is possible; namely, explain how the storm has boundary layer inflow entering it from the northeast even though the actual wind direction is from the southeast.

U40. Consider Fig. 15.42.

a. What are the conceptual (theoretical) differences between streamwise vorticity, and the vorticity around a local-vertical axis as is usually studied in meteorology?

b. If it is the streamwise (horizontal axis) vorticity that is tilted to give vorticity about a vertical axis, why don't we see horizontal-axis tornadoes forming along with the usual vertical tornadoes in thunderstorms? Explain.

U41. Compare eq. (15.51) with the full vorticity-tendency equation from the Extratropical Cyclone chapter, and discuss the differences. Are there any terms in the full vorticity equation that you feel should not have been left out of eq. (15.51)? Justify your arguments.

U42. Show that eq. (15.57) is equivalent to eq. (15.56). (Hint: use the average-wind definition given immediately after eq. (15.55).)

U43. Show mathematically that the area swept out by the storm-relative winds on a hodograph (such as the shaded area in Fig. 15.44) is indeed exactly half the storm-relative helicity. (Hint: Create a simple hodograph with a small number of wind vectors in easy-to-use directions, for which you can easily calculate the shaded areas between wind vectors. Then use inductive reasoning and generalize your approach to arbitrary wind vectors.)

U44. What are the advantages and disadvantages of eSRH and EHI relative to SRH?

U45. Suppose the swirl ratio is 1 for a tornado of radius 300 m in a boundary layer 1 km deep. Find the radial velocity and core pressure deficit for each tornado intensity of the

a. Enhanced Fujita scale. b. TORRO scale.

U46. The denominator of the swirl ratio (eq. 15.60) can be interpreted physically as the volume of air flowing in toward the tornado from the ambient environment (per unit crosswind width). What is a physical interpretation of the numerator?

U47. The cycloidal damage sketched in Fig. 15.51 shows a pattern in between that of a true cycloid and a circle. Look up in another reference what the true cycloid shape is, and discuss what type of tornado behavior would cause damage paths of this shape.

Web-Enhanced Questions

W1. Search the web for (and print the best examples of) photographs of:

a. tornadoes
   (i) supercell tornadoes
   (ii) landspouts
   (iii) waterspouts
   (iv) gustnadoes
b. gust fronts and arc clouds
c. hailstones, and hail storms
d. lightning
   (i) CG
   (ii) IC (including spider lightning, also known as lightning crawlers)
   (iii) a bolt from the blue
e. damage caused by intense tornadoes

(Hint: search on "storm stock images photographs".) Discuss the features of your resulting photos with respect to information you learned in this chapter.

W2. Search the web for (and print the best examples of) radar reflectivity images of

a. hook echoes
b. gust fronts
c. tornadoes

Discuss the features of your resulting image(s) with respect to information you learned in this chapter.

W3. Search the web for (and print the best example of) real-time maps of lightning locations, as found from a lightning detection network or from satellite. Print a sequence of 3 images at about 30 minute intervals, and discuss how you can diagnose thunderstorm movement and evolution from the change in the location of lightning-strike clusters.

W4. Search the web for discussion of the health effects of being struck by lightning, and write or print a concise summary. Include information about how to resuscitate people who were struck.

W5. Search the web for, and summarize or print, recommendations for safety with respect to:
a. lightning
b. tornadoes
c. straight-line winds and derechoes
d. hail
e. flash floods
f. thunderstorms (in general)

W6. Search the web (and print the best examples of) maps that show the frequency of occurrence of:
a. tornadoes & tornado deaths
b. lightning strike frequency & lightning deaths
c. hail
d. derechos

W7. Search the web for, and print the best example of, a photographic guide on how to determine Fujita or Enhanced Fujita tornado intensity from damage surveys.

W8. Search the web for (and print the best examples of) information about how different building or construction methods respond to tornadoes of different intensities.

W9. Search the web for, and print and discuss, 5 tips for successful and safe tornado chasing.

W10. Search the web for tornado chaser sites. In particular, look for information from the National Severe Storms Lab (NSSL). List 5 storm-chasing tips that you consider most important.

W11. Search the web to find the probability that any one house will be struck by a tornado during 1 year.

W12. Search the web for private companies that provide storm-chasing tours/adventures/safaris for paying clients. List 5 or more, including their web addresses, physical location, and what they specialize in.

W13. Search the web for information and images of red sprites, blue jets, and elves (electrical discharges visible as fleeting glows in the mesosphere 30 to 90 km above ground, over thunderstorm anvils). Summarize and print info about these discharges, and included some images.

W14. Search the web for, and print one best example of, tornadoes associated with hurricanes.

W15. Search the web for a complete list of tornado outbreaks and/or tornado outbreak sequences. Print 5 additional outbreaks that were large and/or important, but which weren't already included in this chapter in the list of outbreaks. Focus on more-recent outbreaks.

W16. With regard to tornadoes, search the web for info to help you discuss the relative safety or dangers of:
a. being in a storm shelter
b. being in an above-ground tornado safe room
c. being in a mobile home or trailer
d. hiding under bridges and overpasses
e. standing above ground near tornadoes

W17. Search the web for examples of downburst, gust front, or wind-shear sensors and warning systems at airports, and summarize and print your findings.

Synthesis Questions

S1. Since straight-line outflow winds exist surrounding downbursts that hit the surface, would you expect similar hazardous outflow winds where the updraft hits the tropopause? Justify your arguments.

S2. Suppose that precipitation loading in an air parcel caused the virtual temperature to increase, not decrease. How would thunderstorms differ, if at all?

S3. If hailstones were lighter than air, discuss how thunderstorms would differ, if at all.

S4. If all hailstones immediately split into two when they reach a diameter of 2 cm, describe how hail storms would differ, if at all.

S5. Which types of aircraft would likely have greater difficulty with downbursts: large, heavy commercial jet aircraft; or small, light, general-aviation planes? Explain.

S6. Suppose that precipitation did not cause a downward drag on the air, and that evaporation of precipitation did not cool the air. Nonetheless, assume that thunderstorms have a heavy precipitation region. How would thunderstorms differ, if at all?

S7. Suppose that downbursts did not cause a pressure perturbation increase when they hit the ground. How would thunderstorm hazards differ, if at all?

S8. Suppose that downbursts sucked air out of thunderstorms. How would thunderstorms differ, if at all?

S9. Discuss 5 ways to harness the power of lightning.

S10. Suppose air was a much better conductor of electricity. How would thunderstorms differ, if at all?

S11. Suppose that once a lightning strike happened, the resulting plasma path that was created through air persists as a conducting path for 30 minutes. How would thunderstorms differ, if at all.

S12. Suppose that the intensity of shock waves from thunder did not diminish with increasing distance. How would thunderstorm hazards differ, if at all?

S13. Under what atmospheric conditions could sound waves from thunder be focused toward one point on the ground. If those conditions could be made to occur, what would happen at that point? Could this be used as a weapon?

S14. The air outside of the core of a Rankine-combined-vortex (RCV) model of a tornado is moving around the tornado axis. Yet the flow is said to be **irrotational** in this region. Namely, at any point outside the core, the flow has no vorticity. Why is that? Hint: consider aspects of a flow that can contribute to relative vorticity (see the Global Circulation chapter), and compare to characteristics of the RCV.

S15. Is there an upper limit to the tangential speed of tornadoes? If so, what is it, and why? Discuss the dynamics that would be involved.

S16. Do anticyclonically rotating tornadoes have higher or lower core pressure than the surrounding environment? Explain the dynamics.

S17. Consider Fig. 15.36. If the horizontal pressure gradient near the bottom of tornadoes was weaker than that near the top, how would tornadoes be different, if at all?

S18. If a rapidly collapsing thunderstorm (nicknamed a **bursticane,** which creates violent downbursts and near-hurricane-force straight-line winds at the ground) has a rapidly sinking top, could it create a tornado above it due to stretching of the air above the collapsing thunderstorm? Justify your arguments.

S19. Positive helicity forms not only with updrafts and positive vorticity, but also with downdrafts and negative vorticity. Could the latter condition of positive helicity create mesocyclones and tornadoes? Explain.

Copyright © 2011, 2015 by Roland Stull. *Meteorology for Scientists and Engineers, 3rd Ed.*

HURRICANES

CONTENTS

Hurricane Structure 604
Intensity and Geographic distribution 605
- Saffir-Simpson Hurricane Wind Scale 607
- Typhoon Intensity Scales 607
- Other Tropical-Cyclone Scales 607
- Geographic Distribution and Movement 607

Evolution 608
- Requirements for Cyclogenesis 608
- Hurricane Triggers 610
- Life Cycle 613
- Movement/Track 615
- Tropical Cyclolysis 616

Dynamics 617
- Initial Spin Up 617
- Subsequent Development 617
- Inflow and Outflow 618

Thermodynamics 620
- Fuel Creation and Intake 620
- Exhaust 620
- Warm Core 621
- Carnot-cycle Heat Engine 624

A Hurricane Model 626
- Pressure Distribution 626
- Tangential Velocity 626
- Radial Velocity 627
- Vertical Velocity 628
- Temperature 629
- Composite Picture 629

Climatology 630
- Seasonality 630
- Locations of Strongest Cyclones 631
- Natural Cycles & Changes in Activity 631

Hazards 631
- Human Population and Zoning 631
- Storm Surge 632
- Surface Wind-waves 634
- Inland Flooding 637
- Thunderstorms, Lightning & Tornado Outbreaks 637

Hurricane Forecasting 637
- Prediction 637
- Safety 638

Summary 639

Exercises 640

"Meteorology for Scientists and Engineers, 3rd Edition" by Roland Stull is licensed under a Creative Commons Attribution-NonCommercial-ShareAlike 4.0 International License. To view a copy of the license, visit http://creativecommons.org/licenses/by-nc-sa/4.0/ . This work is available at http://www.eos.ubc.ca/books/Practical_Meteorology/ .

16 Intense synoptic-scale cyclones in the tropics are called **tropical cyclones**. As for all cyclones, tropical cyclones have low pressure in the cyclone center near sea level. Also, the low-altitude winds rotate cyclonically (counterclockwise in the N. Hemisphere) around the storm and spiral in towards the center.

Tropical cyclones are called **hurricanes** over the Atlantic, Caribbean, Gulf of Mexico (Fig. 16.1), and eastern Pacific Oceans. They are called **typhoons** over the western Pacific. Over the Indian Ocean and near Australia they are called **cyclones**. Although this chapter is entitled "Hurricanes", the concepts apply to all tropical cyclones.

Hurricanes differ from mid-latitude cyclones in that hurricanes do not have fronts. Hurricanes have warm cores while mid-latitude cyclones have cold cores. Hurricanes can persist two to three times longer than typical mid-latitude cyclones. To help explain this behavior, we start by describing hurricane structure.

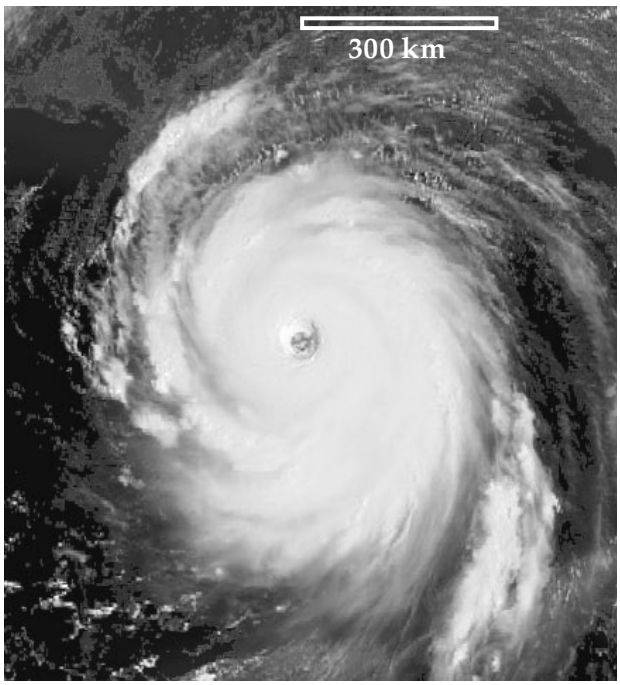

Figure 16.1
Visible satellite image of Hurricane Katrina over the Gulf of Mexico, taken 28 Aug 2005 at 1545 UTC. (GOES image courtesy of US DOC/NOAA.)

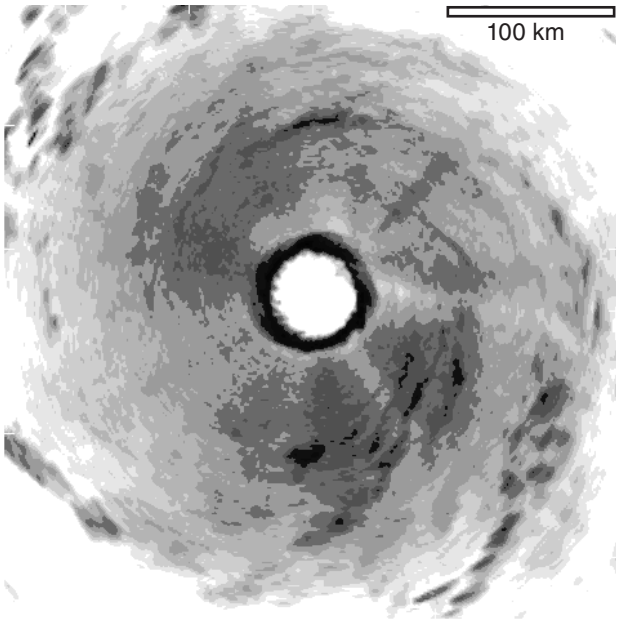

Figure 16.2
Radar reflectivity PPI image of Hurricane Katrina, taken from a research aircraft at altitude 2325 m on 28 Aug 2005 at 1747 UTC while it was over the Gulf of Mexico. Darkest regions in the eyewall correspond to 35 to 40 dBZ radar reflectivity. (Image courtesy of US DOC/NOAA/AOML/ Hurricane Research Division.)

HURRICANE STRUCTURE

Hurricanes are made of thunderstorms. Near the center (**core**) of the hurricane is a ring or circle of thunderstorms called the **eyewall**. This is the most violent part of the storm with the heaviest rain and the greatest radar reflectivity (Fig. 16.2). The tops of these thunderstorms extend into the lower stratosphere — 15 to 18 km high. The thunderstorm bases are very low — in the boundary layer. Thus, hurricanes fill the depth of the tropical troposphere.

The anvils from each of the thunderstorms in the eyewall merge into one large roughly-circular **cloud shield** that is visible by satellite (Fig. 16.1). These anvils spread outward 75 to 150 km away from the eye wall. Hence, hurricane diameters are roughly 10 to 20 times their depth (Fig. 16.3), although the high-altitude outflow from the top of some asymmetric hurricanes can reach 1000s of km (Fig. 16.4).

In the center of this eyewall is a calmer region called the **eye** with warm temperatures, subsiding (sinking) air, and fewer or no clouds. Eye diameter at sea level is 20 to 50 km. The eye is conical, with the larger diameter at the storm top (Fig. 16.5).

Spiraling out from the eye wall can be zero or more bands of thunderstorms called **spiral bands**. Sometimes these spiral **rain bands** will merge to

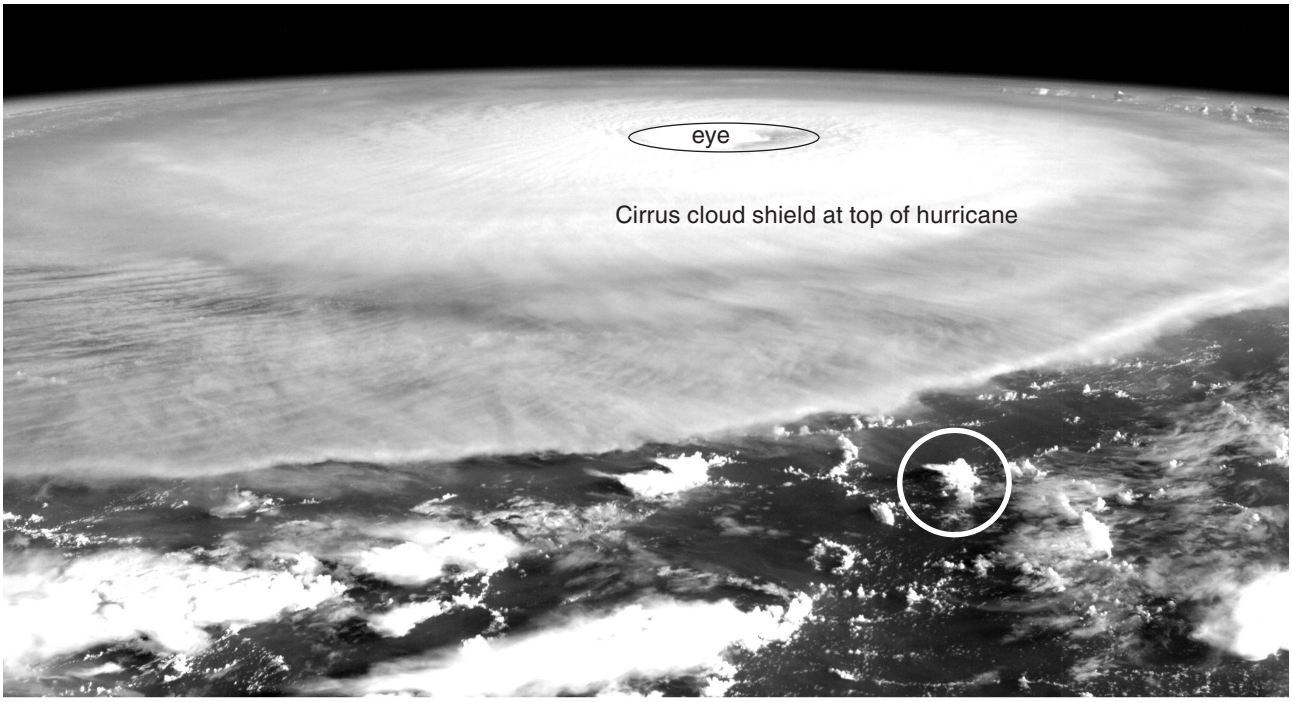

Figure 16.3
Hurricane Isabel as viewed from the International Space Station on 13 Sep 2003. The hurricane eye is outlined with the thin black oval, while the outflow from the eyewall thunderstorms fills most of this image. For scale comparison, the white circle outlines a nearby thunderstorm of depth and diameter of roughly 15 km. [Image courtesy of NASA - Johnson Spaceflight Center.]

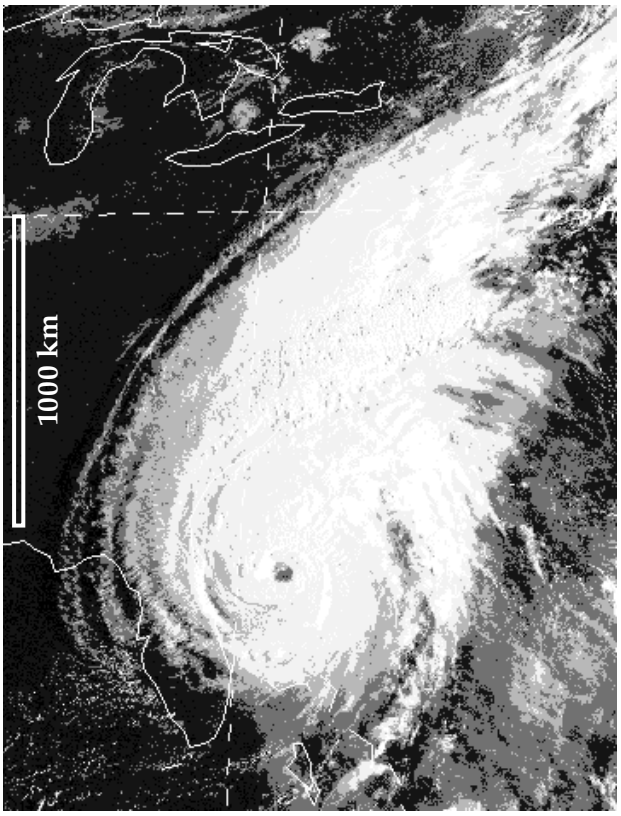

Figure 16.4
Visible satellite image of category 4 hurricane Floyd, at 12 UTC on 15 Sep 1999, showing asymmetric outflow extending 1000s of km. The eye is in the NW Atlantic just east of Florida, and the outflow reaches Canada. [Image courtesy of NOAA.]

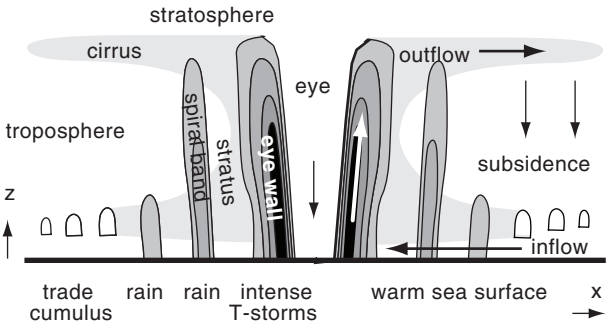

Figure 16.5
Vertical cross-section through an idealized hurricane. Darker shading indicates more intense radar echoes associated with heavy rain in thunderstorms. Lighter shading shows stratiform clouds. The less-intense rain that falls from the lower stratiform cloud deck of real hurricanes is not shown here. Depth ≈ 15 km. Width ≈ 1500 km. Trade cumulus are in the trade winds.

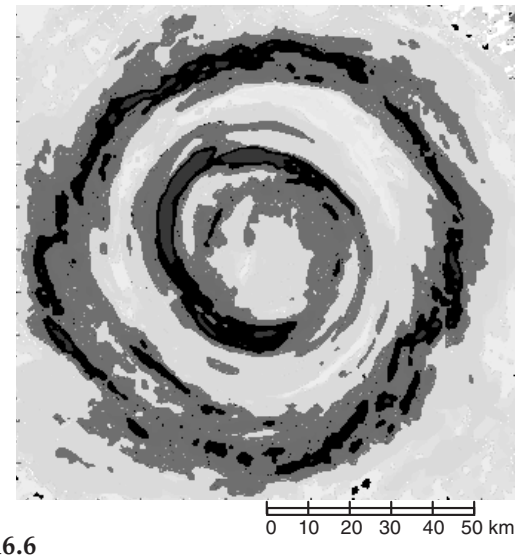

Figure 16.6
Zoomed view of double eyewall in Hurricane Rita, as viewed by airborne radar at 1 km altitude on 22 Sep 2005 at 1801 UTC. Darker greys show two concentric rings of heavier rain. Darkest grey corresponds to roughly 40 dBZ. [Modified from original image by Michael Bell and Wen-Chau Lee.]

form a temporary second eyewall of thunderstorms around the original eye wall (Fig. 16.6). The region of lighter rain between the two eyewalls is called the **moat**.

During an **eyewall replacement cycle**, in very strong hurricanes, the inner eyewall dissipates and is replaced by the outer eyewall. When this happens, hurricane intensity sometimes diminishes temporarily, and then strengthens again when the new outer eyewall diameter shrinks to that of the original eyewall.

INTENSITY AND GEOGRAPHIC DISTRIBUTION

Lower sea-level pressures in the eye and faster winds in the lower troposphere indicate stronger hurricanes. Several different hurricane scales have been devised to classify hurricane strength, as summarized below.

Table 16-1. Saffir-Simpson Hurricane Wind Scale — Definition. Based on max 1-minute sustained wind speed measured at standard anemometer height of 10 m. Applies in the Atlantic Ocean, and in the eastern Pacific from the coast of the Americas to 180°W.

Category	Wind Speed			
	m/s	km/h	knots	miles/h
1	33 - 42	119 - 153	64 - 82	74 - 95
2	43 - 49	154 - 177	83 - 95	96 - 110
3	50 - 58	178 - 209	96 - 113	111 - 130
4	59 - 69	210 - 249	114 - 135	131 - 155
5	> 69	> 249	> 135	> 155

Table 16-2. Saffir-Simpson Hurricane Wind Scale — Description of Expected Damage — *Examples.*

Category	Concise Statement Damage Expected Examples
1	**Very dangerous winds will produce some damage.**
	People, livestock, and pets struck by flying or falling debris could be injured or killed. Older (mainly pre-1994 construction) mobile homes could be destroyed, especially if they are not anchored properly as they tend to shift or roll off their foundations. Newer mobile homes that are anchored properly can sustain damage involving the removal of shingle or metal roof coverings, and loss of vinyl siding, as well as damage to carports, sunrooms, or lanais. Some poorly constructed frame homes can experience major damage, involving loss of the roof covering and damage to gable ends as well as the removal of porch coverings and awnings. Unprotected windows may break if struck by flying debris. Masonry chimneys can be toppled. Well-constructed frame homes could have damage to roof shingles, vinyl siding, soffit panels, and gutters. Failure of aluminum, screened-in, swimming pool enclosures can occur. Some apartment building and shopping center roof coverings could be partially removed. Industrial buildings can lose roofing and siding especially from windward corners, rakes, and eaves. Failures to overhead doors and unprotected windows will be common. Windows in high-rise buildings can be broken by flying debris. Falling and broken glass will pose a significant danger even after the storm. There will be occasional damage to commercial signage, fences, and canopies. Large branches of trees will snap and shallow rooted trees can be toppled. Extensive damage to power lines and poles will likely result in power outages that could last a few to several days.
	Hurricane Dolly (2008) brought Category 1 winds and impacts to South Padre Island, Texas.
2	**Extremely dangerous winds will cause extensive damage.**
	There is a substantial risk of injury or death to people, livestock, and pets due to flying and falling debris. Older (mainly pre-1994 construction) mobile homes have a very high chance of being destroyed and the flying debris generated can shred nearby mobile homes. Newer mobile homes can also be destroyed. Poorly constructed frame homes have a high chance of having their roof structures removed especially if they are not anchored properly. Unprotected windows will have a high probability of being broken by flying debris. Well-constructed frame homes could sustain major roof and siding damage. Failure of aluminum, screened-in, swimming pool enclosures will be common. There will be a substantial percentage of roof and siding damage to apartment buildings and industrial buildings. Unreinforced masonry walls can collapse. Windows in high-rise buildings can be broken by flying debris. Falling and broken glass will pose a significant danger even after the storm. Commercial signage, fences, and canopies will be damaged and often destroyed. Many shallowly rooted trees will be snapped or uprooted and block numerous roads. Near-total power loss is expected with outages that could last from several days to weeks. Potable water could become scarce as filtration systems begin to fail.
	Hurricane Frances (2004) brought Category 2 winds and impacts to coastal portions of Port St. Lucie, Florida.
3	**Devastating damage will occur.**
	There is a high risk of injury or death to people, livestock, and pets due to flying and falling debris. Nearly all older (pre-1994) mobile homes will be destroyed. Most newer mobile homes will sustain severe damage with potential for complete roof failure and wall collapse. Poorly constructed frame homes can be destroyed by the removal of the roof and exterior walls. Unprotected windows will be broken by flying debris. Well-built frame homes can experience major damage involving the removal of roof decking and gable ends. There will be a high percentage of roof covering and siding damage to apartment buildings and industrial buildings. Isolated structural damage to wood or steel framing can occur. Complete failure of older metal buildings is possible, and older unreinforced masonry buildings can collapse. Numerous windows will be blown out of high-rise buildings resulting in falling glass, which will pose a threat for days to weeks after the storm. Most commercial signage, fences, and canopies will be destroyed. Many trees will be snapped or uprooted, blocking numerous roads. Electricity and water will be unavailable for several days to a few weeks after the storm passes.
	Hurricane Ivan (2004) brought Category 3 winds and impacts to coastal portions of Gulf Shores, Alabama.
4	**Catastrophic damage will occur.**
	There is a very high risk of injury or death to people, livestock, and pets due to flying and falling debris. Nearly all older (pre-1994) mobile homes will be destroyed. A high percentage of newer mobile homes also will be destroyed. Poorly constructed homes can sustain complete collapse of all walls as well as the loss of the roof structure. Well-built homes also can sustain severe damage with loss of most of the roof structure and/or some exterior walls. Extensive damage to roof coverings, windows, and doors will occur. Large amounts of windborne debris will be lofted into the air. Windborne debris damage will break most unprotected windows and penetrate some protected windows. There will be a high percentage of structural damage to the top floors of apartment buildings. Steel frames in older industrial buildings can collapse. There will be a high percentage of collapse to older unreinforced masonry buildings. Most windows will be blown out of high-rise buildings resulting in falling glass, which will pose a threat for days to weeks after the storm. Nearly all commercial signage, fences, and canopies will be destroyed. Most trees will be snapped or uprooted and power poles downed. Fallen trees and power poles will isolate residential areas. Power outages will last for weeks to possibly months. Long-term water shortages will increase human suffering. Most of the area will be uninhabitable for weeks or months.
	Hurricane Charley (2004) brought Category 4 winds and impacts to coastal portions of Punta Gorda, Florida.
5	**Catastrophic damage will occur.**
	People, livestock, and pets are at very high risk of injury or death from flying or falling debris, even if indoors in mobile homes or framed homes. Almost complete destruction of all mobile homes will occur, regardless of age or construction. A high percentage of frame homes will be destroyed, with total roof failure and wall collapse. Extensive damage to roof covers, windows, and doors will occur. Large amounts of windborne debris will be lofted into the air. Windborne debris damage will occur to nearly all unprotected windows and many protected windows. Significant damage to wood roof commercial buildings will occur due to loss of roof sheathing. Complete collapse of many older metal buildings can occur. Most unreinforced masonry walls will fail which can lead to the collapse of the buildings. A high percentage of industrial buildings and low-rise apartment buildings will be destroyed. Nearly all windows will be blown out of high-rise buildings resulting in falling glass, which will pose a threat for days to weeks after the storm. Nearly all commercial signage, fences, and canopies will be destroyed. Nearly all trees will be snapped or uprooted and power poles downed. Fallen trees and power poles will isolate residential areas. Power outages will last for weeks to possibly months. Long-term water shortages will increase human suffering. Most of the area will be uninhabitable for weeks or months.
	Hurricane Andrew (1992) brought Category 5 winds and impacts to coastal portions of Cutler Ridge, Florida.

From an online report "The Saffir-Simpson Hurricane Wind Scale", National Hurricane Center, National Weather Service, NOAA. 2010.

Saffir-Simpson Hurricane Wind Scale

In the early 1970's, consulting engineer Herbert Saffir and US National Hurricane Center director Robert Simpson developed a scale to give public-safety officials an estimate of hurricane strength based on max wind speed, sea-level pressure in the eye, and storm-surge (local rise in sea-level). This was the **Saffir-Simpson Hurricane Scale**.

In 2010, the US National Hurricane Center updated this scale (now called the **Saffir-Simpson Hurricane Wind Scale**), and defined hurricane intensity on wind speed only. The scale ranges from category 1 for a weak hurricane to category 5 for the strongest hurricane (Table 16-1). A description of the expected damage for each category is in Table 16-2.

Typhoon Intensity Scales

For typhoons in the western North Pacific Ocean, storm intensity has been classified three different ways by three different organizations: the **Japan Meteorological Agency (JMA)**, the **Hong Kong Observatory (HKO)**, and the **US Joint Typhoon Warning Center (JTWC)**. See Table 16-3.

Other Tropical-Cyclone Scales

Additional tropical cyclone intensity scales (with different wind-speed definitions and category names) have been defined by hurricane agencies in:

- Australia (**Australian Bureau of Meteorology**, for S. Hemisphere east of 90°E),
- India (**Regional Specialized Meteorological Center in New Delhi**, for N. Hemisphere Indian Ocean between 45°E and 100°E), and by
- **Météo-France** (for S. Hemisphere west of 90°E).

Even more confusing, some agencies use 1-minute average (sustained) winds, some use 10-minute average (sustained) winds, and some use gusts.

Geographic Distribution and Movement

Fig. 16.7 outlines the regions of greatest frequency of tropical cyclones and shows typical storm tracks.

Tropical cyclones are steered mostly by the large-scale global circulation. Most tropical cyclones form between 10° and 30° latitude, which is the trade-wind region. Hence, most tropical cyclones are steered from east to west initially.

Later, these storms tend to turn poleward under the influence of monsoon circulations. For example, the Bermuda High (also known as the Azores High) over the North Atlantic Ocean has a clockwise circulation around it (see Fig. 11.31 in the Global Circulation chapter), which turns hurricanes northward in the Western North Atlantic Ocean. The tracks of

Table 16-3. Typhoon (tropical cyclone) intensity scale, based on max sustained winds during 10 minutes. Defined by JMA, unless otherwise noted. Applies between 100°E to 180°E.

Category	Wind Speed		
	m/s	km/h	knots
Tropical Depression	< 17	< 61	< 33
Tropical Storm	17 - 24	62 - 88	35 - 48
Severe Tropical Storm	25 - 32	89 - 117	48 - 63
Typhoon	33 - 41	118 - 149	64 - 79
Severe Typhoon	42 - 51 (HKO)	150 - 184 (HKO)	80 - 99 (HKO)
Super Typhoon	> 51 (HKO) > 67 (JTWC*)	>185 (HKO) > 241 (JTWC*)	>100 (HKO) > 130 (JTWC*)

** Based on 1-minute average max sustained winds.*

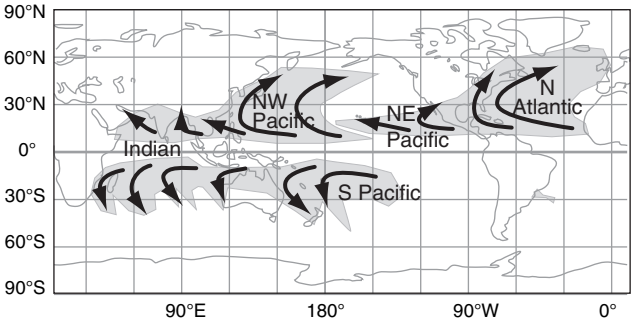

Figure 16.7
Map of tropical-cyclone locations (grey shading), with a general sense of the cyclone tracks (black arrows).

Science Graffito

"The tempest arose and wearied me so that I knew not where to turn; ...[my] eyes never beheld the seas so high, angry and covered by foam. The wind not only prevented our progress, but offered no opportunity to run behind any headland for shelter; hence we were forced to keep out in this bloody ocean, seething like a pot on a hot fire. Never did the sky look more terrible; for one whole day and night it blazed like a furnace, and the lightning broke forth with such violence that each time I wondered if it had carried off my spars and sails; the flashes came with such fury and frightfulness that we all thought this ship would be blasted. All this time the water never ceased to fall from the sky; I don't say it rained, because it was like ...[a] deluge. The people were so worn out that they longed for death to end their dreadful suffering."

– Christopher Columbus, 1502.

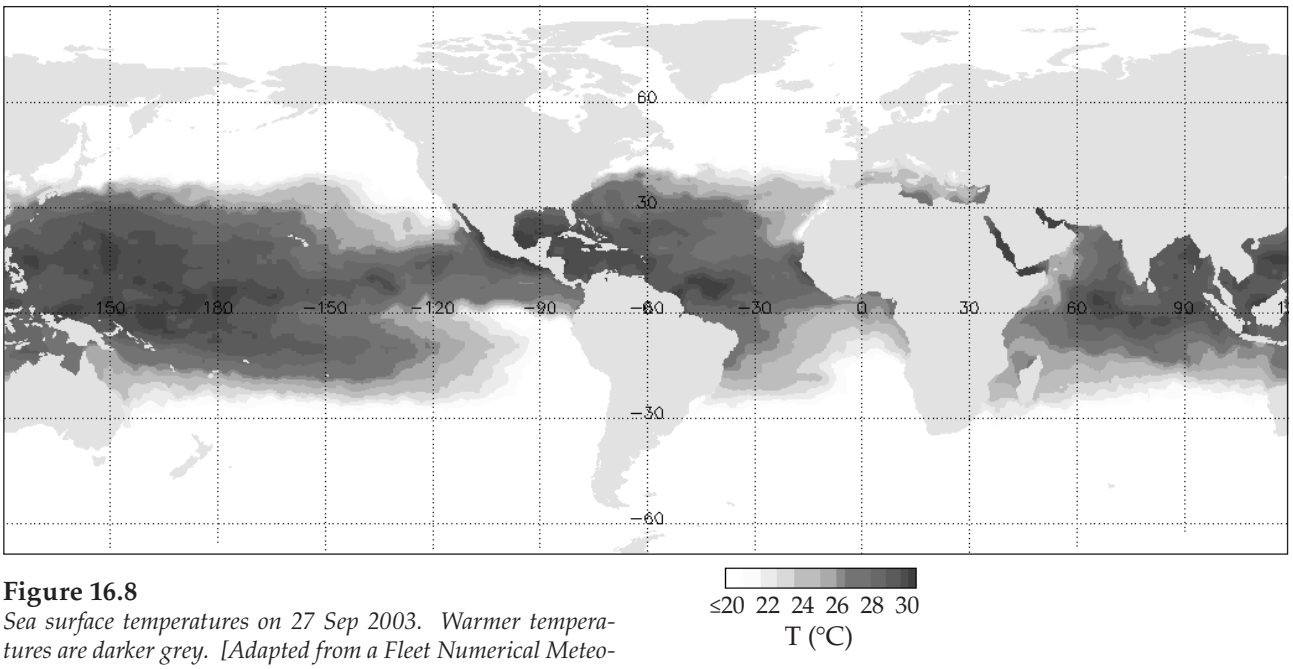

Figure 16.8
Sea surface temperatures on 27 Sep 2003. Warmer temperatures are darker grey. [Adapted from a Fleet Numerical Meteorology and Oceanography Center (FNMOC) image.]

hurricanes and former hurricanes continue to turn toward the northeast as they proceed further into the mid-latitudes and encounter west winds in the global circulation.

A striking observation in Fig. 16.7 is that no tropical cyclones form at the equator. Also, none cross the equator. The next section explains why.

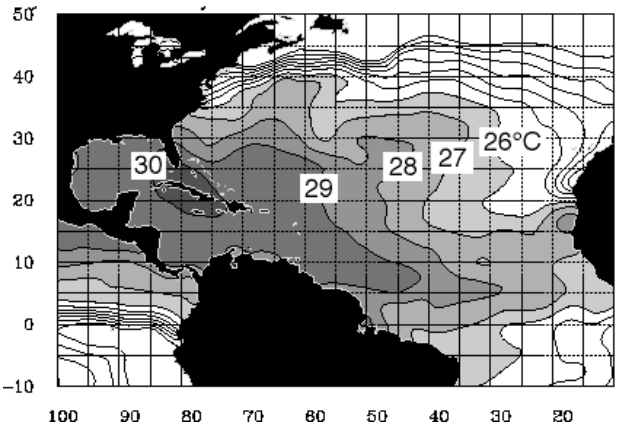

Figure 16.9
Sea surface temperature (°C) in the Atlantic Ocean averaged over the week of 5 to 11 Sep 1999, just prior to hurricane Floyd, a category 4 hurricane. Shaded regions are warmer than 26°C, the isotherm increment is 1°C, and the isotherm range is 20 to 30°C. [Adapted from a National Hurricane Center image.]

EVOLUTION

Requirements for Cyclogenesis

Seven conditions are necessary for tropical cyclones to form: a warm sea surface, non-zero Coriolis force, nonlocal conditional instability, high humidity in the mid troposphere, weak ambient wind shear, enhanced synoptic-scale vorticity, and a trigger.

Warm Sea Surface

The **sea surface temperature** (**SST**) must be approximately 26.5°C or warmer (Figs. 16.8 and 16.9), and the warm surface waters must be at least 50 m deep. This warm temperature is needed to enable strong evaporation and heat transfer from the sea surface into the boundary layer. The warmer, more-humid boundary-layer air serves as the fuel for thunderstorms in the tropical cyclone.

The fast winds in hurricanes create large waves that stir the top part of the ocean. If the warm wa-

ters are too shallow, then this turbulent mixing will stir colder deeper water up to the surface (see Focus Box two pages later). When this happens, the sea-surface temperature decreases below the 26.5°C threshold, and the hurricane kills itself.

Coriolis Force

Tropical cyclones cannot exist within about 500 km of the equator (i.e., ≤ 5° latitude), because Coriolis force is near zero there (and is exactly zero right at the equator). Rarely, very small-diameter tropical cyclones have been observed closer to the equator, but none are observed right at the equator. Not only cannot tropical cyclones form at the equator, but existing cyclones cannot cross the equator (Fig. 16.7).

Without Coriolis force, boundary-layer air would be sucked directly into the eye by the low pressure there. Thus, air molecules would accumulate in the eye, causing pressure to increase towards ambient values. The result is that the low pressure would disappear, winds would die, and the tropical cyclone would cease to exist in less than a day. This is what happens to tropical cyclones that approach the equator (Fig. 16.10).

But with Coriolis force, winds in the bottom half of the troposphere are forced around the eye at gradient- or cyclostrophic-wind speeds. Namely, most of the air is flowing tangentially around the eye rather than flowing radially into it. Only close to the ground does drag change the winds into boundary-layer gradient winds, resulting in a small amount of convergence toward the eye. Thus, the hurricane can persist for many days.

Nonlocal Conditional Instability

Because tropical cyclones are made of thunderstorms, the tropical environment must have sufficient nonlocal conditional instability to support deep thunderstorm convection. Namely, there must be a stable layer (i.e., a cap) above a warm humid boundary layer, and the mid-troposphere must be relatively cool compared to the boundary layer.

The warm humid boundary layer is achieved via strong heat and moisture fluxes from the warm sea surface into the air. The cap is the trade-wind inversion that was discussed in the Global Circulation chapter. These conditions, combined with a cool mid troposphere, lead to large values of convective available potential energy (CAPE), as was thoroughly explained in the Thunderstorm chapter. Hence, large values of CAPE imply sufficient nonlocal conditional instability for tropical cyclones.

High Humidity in the Mid-troposphere

In a deep layer of air centered at roughly 5 km above sea level, humidity must be high. Otherwise, the incipient thunderstorms cannot continue to grow and become organized into tropical cyclones.

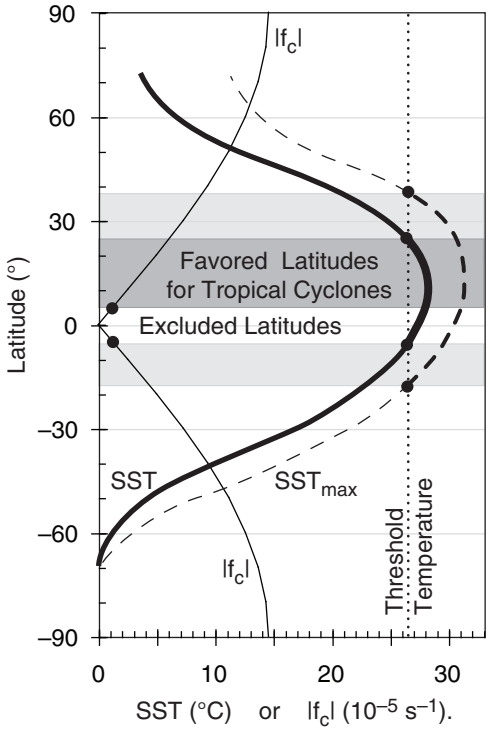

Figure 16.10

Approximate zonal average sea-surface temperature SST (°C, thick solid line) averaged around the globe during 3 Aug 2009. Also shown is the max SST (°C, thin dashed line) on that day at each latitude. The magnitude of the Coriolis parameter f_c (10^{-5} s^{-1}) is the thin solid line. Dotted line is the SST threshold of 26.5°C for tropical cyclones. Those latitudes that exceed the temperature threshold and have Coriolis parameter that is not near zero are favored locations for tropical cyclones (shaded medium grey). Tropical cyclones can also occur in limited regions (shaded light grey) at other latitudes where the max SST exceeds the threshold. "Excluded latitudes" are those for which Coriolis force is too small.

As the seasons progress, the location of peak SST shifts, causing the favored latitudes to differ from this particular August example.

Note that this differs from mid-latitude thunderstorms, where a drier mid-troposphere allows more violent thunderstorms. When dry environmental air is entrained into the sides of mid-latitude thunderstorms, some of the storm's hydrometeors evaporate, causing the strong downdrafts that define supercell storms and which create downbursts, gust fronts, and can help trigger tornadoes.

In the tropics, such downbursts from any one thunderstorm can disrupt neighboring thunderstorms, reducing the chance that neighboring thunderstorms can work together in an incipient eyewall. Also, the cold downburst air accumulates at the bot-

FOCUS • Hurricane-induced Currents

Near-surface winds cause net ocean transport 90° to the right of the wind vector in the N. Hemisphere, as explained later in the Storm Surge section. Given tangential winds that circle a tropical cyclone, we expect the net Ekman transport (average ocean currents induced by the hurricane) to be outward (Fig. 16.a)

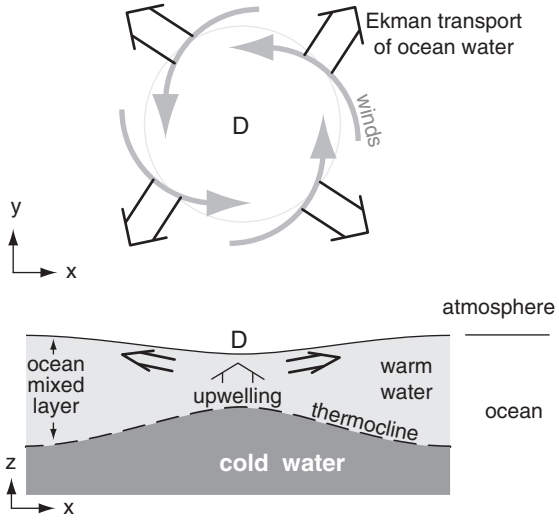

Fig. 16.a. *Ocean currents (double-shaft arrows) induced by hurricane winds (grey arrows).*

Such horizontal divergence (*D*) of the ocean-surface water does three things: (1) lowers the sea surface by removing sea water; (2) causes upwelling of water toward the surface; and (3) causes the colder deep water to be brought closer to the surface (Fig. 16.a-bottom). The **thermocline** is the interface between cold deep water and warmer mixed-layer above.

The hurricane brings cold water closer to the surface, where ocean mixed-layer turbulence caused by breaking waves can further mix the warm and cold waters. Thus, hurricanes will kill themselves by cooling the sea-surface temperature unless the pre-storm warm ocean mixed-layer is deep enough (≥ 50 m).

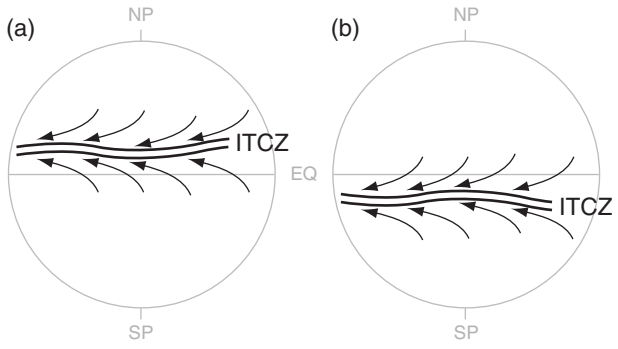

Figure 16.11
Sketch of the Earth showing the Intertropical Convergence Zone (ITCZ, double solid line) for the early Autumn hurricane seasons during (a) August and (b) February. NP = North Pole. SP = South Pole. EQ = equator.

tom of the troposphere, thereby increasing static stability and reducing deep convection.

Weak Ambient Wind Shear

Wind shear within 4° latitude of the incipient storm must be weak (ΔM < 10 m/s between pressure levels 80 and 25 kPa) to enable thunderstorm clusters to form. These clusters are the precursors to tropical cyclones.

If the shear is too strong, the updrafts in the thunderstorms become tilted, and latent heating due to water-vapor condensation is spread over a broader area. This results in less-concentrated warming, and a reduced ability to create a low-pressure center at sea level around which the thunderstorms can become organized into a hurricane.

This requirement differs from that for mid-latitude thunderstorms. At mid-latitudes, strong shear in the ambient environment is good for storms because it encourages the creation of mesocyclones and supercell thunderstorms. Apparently, in the tropics such rotation of individual thunderstorms is bad because it interferes with the collaboration of many thunderstorms to create an eyewall.

Synoptic-scale Vorticity

A relative maximum of relative vorticity in the bottom half of the troposphere can help organize the thunderstorms into an incipient hurricane. Otherwise, any thunderstorms that form would act somewhat independently of each other.

Hurricane Triggers

Even if all six previous conditions are satisfied, a method to trigger the hurricane is also needed. A trigger is anything that creates synoptic-scale horizontal convergence in the atmospheric boundary layer. Such horizontal convergence forces upward motion out of the boundary-layer top as required by mass conservation (see the Dynamics chapter). Synoptic-scale upward motion can initiate and support an organized cluster of thunderstorms — incipient hurricanes.

Some triggers are: the ITCZ, easterly waves, Monsoon trough, mid-latitude fronts that reach the tropics, and Tropical Upper Tropospheric Troughs.

ITCZ

The **Intertropical Convergence Zone** (**ITCZ**, see Global Circulation chapter) is the region where the northeasterly trade winds from the Northern Hemisphere meet the southeasterly trade winds from the Southern Hemisphere. This convergence zone shifts between about 10°N during August and September (end of N. Hemisphere summer, Fig. 16.11), and 10°S during February and March (end of

S. Hemisphere summer). During these months of maximum asymmetry in global heating, the ITCZ is far enough from the equator for sufficient Coriolis force to enable tropical cyclones.

African Easterly Wave

Although equatorial Africa is hot, the Sahara Desert (roughly spanning 15° to 30°N) and Arabian Peninsula are even hotter. This temperature excess is within an atmospheric boundary layer that can reach 5 km depth by late afternoon, although average depth over 24 h is about 3 km. Thus, along the southern edge of the Sahara and the Arabian Peninsula is a strong temperature gradient (Fig. 16.12).

As explained in the thermal-wind section of the Global Circulation chapter, a north-south temperature gradient creates a north-south pressure gradient that increases with altitude (up to the top of the boundary layer for this scenario). For Africa, higher pressure aloft is over the Sahara Desert and lower pressure aloft is further south over the Sudan and Congo.

This pressure gradient drives a geostrophic wind from the east over the African Sahel (at about 15°N). These winds reach maximum speeds of 10 to 25 m/s at an altitude of about 3 km in late summer. This is called the **African Easterly Jet** (**AEJ**).

Like the subtropical and mid-latitude jets, the AEJ is barotropically and baroclinically unstable. This means that the jet tends to meander north and south while blowing from east to west. The mountains in eastern Africa (Ethiopia Highlands and Darfur Mountains) can trigger such oscillations.

The oscillations in this low-altitude jet are called waves, and are known as **Easterly Waves** because the wave troughs and crests move from the east at speeds of 7 to 8 m/s. These waves have wavelength of about 2,000 to 2,500 km, and have a wave period of 3 to 4 days. Although these waves are created over Africa, they continue to propagate west across the tropical North Atlantic, the Caribbean, central America, and finally into the tropical Northeast Pacific (Fig. 16.13).

Easterly waves can trigger hurricanes because of the low-altitude convergence that occurs east of the wave troughs. These waves are found predominantly in a latitude band between 10°N and 30°N, where there is lower pressure to the south and the subtropical high-pressure belt to the north. Thus, a trough of low pressure in an easterly wave corresponds to a region where the isobars meander to the north (Fig. 16.14) in the N. Hemisphere.

Because the pressure gradient is weak and sometimes difficult to analyze from sparsely spaced weather stations in this region, tropical meteorologists will often look at the streamlines instead of iso-

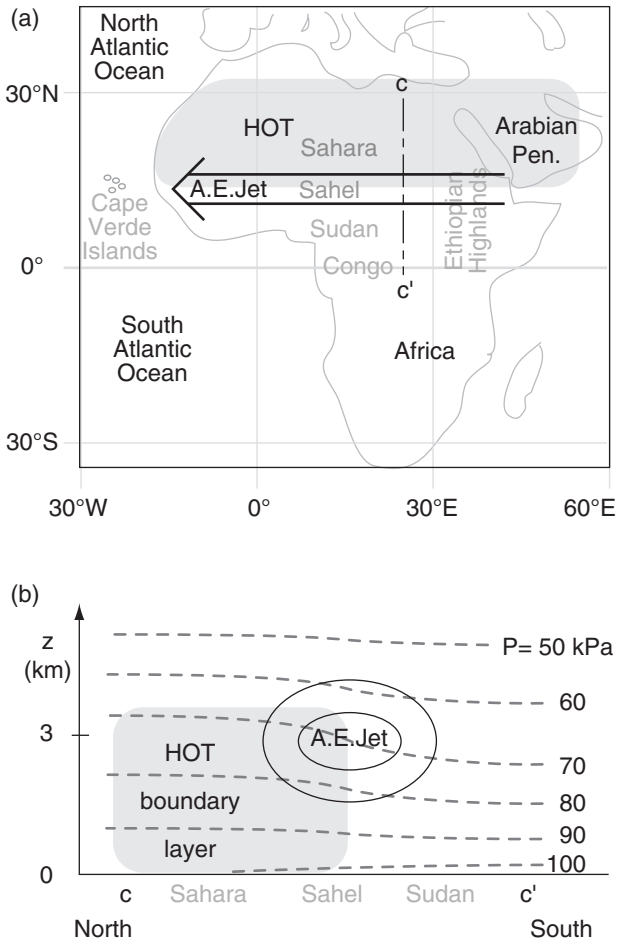

Figure 16.12
African Easterly (A.E.) Jet. (a) Map of Africa. (b) Vertical cross section along c - c′ in (a), where thin black ovals represent isotachs around the core of the AEJ. Grey area indicates hot air. Note the low altitude of this A.E. jet.

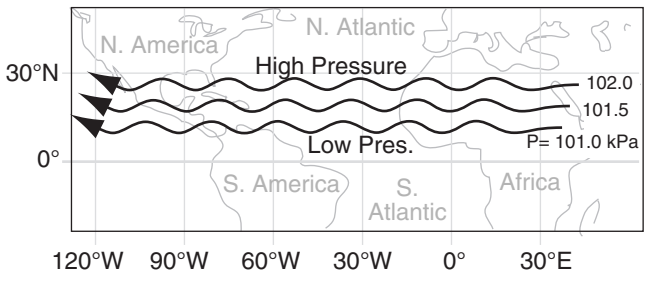

Figure 16.13
Easterly waves near the bottom of the troposphere. Wavelength is roughly 20° to 25° of longitude (≈ 2000 to 2500 km). Isobars of sea-level pressure are solid lines with arrows. Wave troughs propagate toward the west.

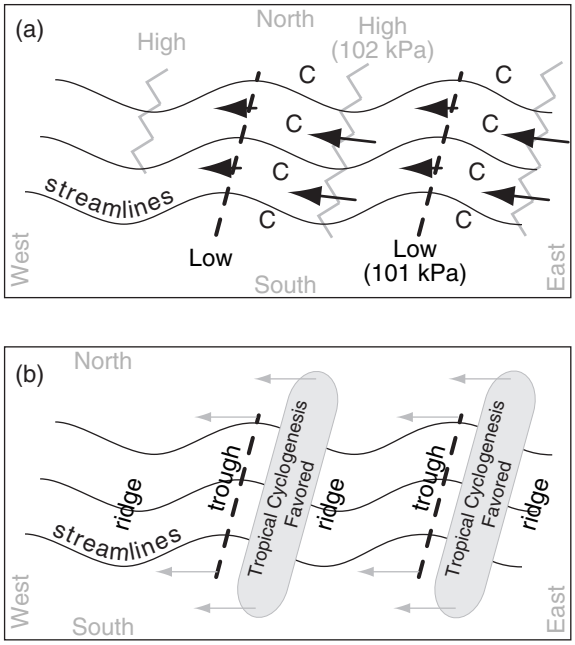

Figure 16.14
Characteristics of easterly waves in lower tropospheric flow over the tropical North Atlantic. (a) Black arrows indicate winds; longer arrows denote faster winds. C = convergence (b) Grey arrows show how the easterly waves and the tropical cyclogenesis regions propagate toward the west.

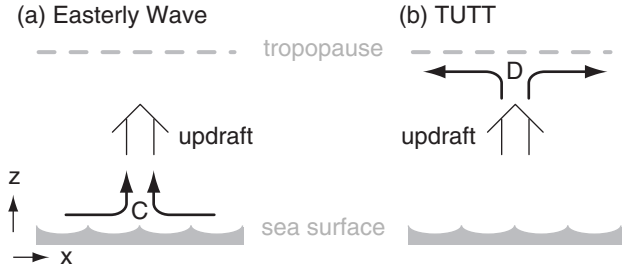

Figure 16.15
Mechanisms that create updrafts to trigger thunderstorm clusters: (a) C = lower-tropospheric horizontal convergence in an easterly wave; (b) D = horizontal divergence aloft in a TUTT.

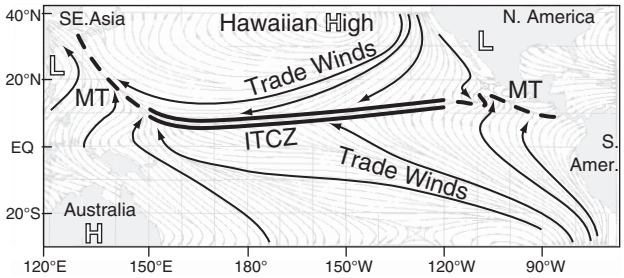

Figure 16.16
Streamline analysis (thin grey & thin black lines with arrows) of near-surface winds, averaged during August. MT denotes Monsoon Trough, shown by the thick dashed lines. 𝕃 and 𝕳 are monsoon lows and highs. [modified from Naval Research Lab. image]

bars. Streamlines are weather-map lines that are everywhere parallel to the flow at any instant in time (see the Local Winds chapter). They more-or-less follow the isobars. Thus, regions where streamlines for low-altitude winds meander to the north can also be used to locate troughs in the easterly waves.

Recall that mid-latitude cyclones are favored in the updrafts under divergence regions in the polar jet (centered at the top of the troposphere). However, for tropical cyclogenesis we also look for updrafts above the convergence regions of the jet near the bottom of the troposphere (Fig. 16.15a).

Where are these convergence regions in easterly waves? According to the Dynamics chapter, winds are slower-than-geostrophic around troughs, and faster around ridges. This rule continues to hold in the tropics and subtropics. Thus, the convergence zone with fast inflow and slow outflow is east of the trough axis (Fig. 16.14a).

Also, since the trough axis often tilts eastward with increasing altitude, it means that a mid-tropospheric trough is often over a lower-troposphere convergence regions. This mid-troposphere trough has the cyclonic vorticity that encourages organization of thunderstorms into incipient hurricanes.

It is these regions east of troughs in easterly waves where the thunderstorms of incipient hurricanes can be triggered (Fig. 16.14b). As the easterly waves propagate from east to west, so move the convergence regions favoring hurricane formation. This convergence mechanism is important for hurricane triggering in both the North Atlantic and Northeast Pacific. Roughly 85% of the intense Atlantic hurricanes are triggered by easterly waves.

Monsoon Trough

A **monsoon trough** (MT) is where the ITCZ merges into a monsoon circulation. For example, Fig. 16.16 shows a monsoon low pressure (𝕃) region over southeast Asia (left side of Fig.), with winds rotating counterclockwise around it. Near the dashed line labeled MT in the western Pacific, monsoon winds from the southwest converge with easterly trade winds from the Hawaiian (Pacific) High.

Thus, the monsoon trough in the western Pacific is a convergence region that can trigger thunderstorms for incipient typhoons. Similar monsoon troughs have been observed in the Indian Ocean and the Eastern Pacific. In Fig. 16.16, the region where the monsoon trough in the western Pacific meets the ITCZ has enhanced convergence, and is a more effective trigger for hurricanes.

Mid-latitude Frontal Boundary

Sometimes cold fronts from midlatitudes can move sufficiently far equatorward to reach the

subtropics. Examples include cold fronts reaching southern Florida (Fig. 16.17). Although these fronts are often weak and slow moving by the time the reach the subtropics, they nonetheless have convergence across them that can trigger hurricane thunderstorms in the Caribbean and the subtropical western North Atlantic.

TUTT

TUTT stands for **Tropical Upper Tropospheric Trough**. This is a high-altitude cold-core low-pressure system that can form in the subtropics. East of the TUTT axis is a region of horizontal divergence aloft, which creates upward motion below it in order to satisfy air mass continuity (Fig. 16.15b). This upward motion can help trigger thunderstorms as precursors to hurricanes.

Life Cycle

At locations where all of the necessary conditions are met (including any one trigger), the incipient hurricanes usually progress through the following intensification stages: tropical disturbance, tropical depression, tropical storm, hurricane.

Tropical Disturbance

The US National Hurricane Center defines a **tropical disturbance** as "a discrete tropical weather system of apparently organized convection - generally 200 to 600 km in diameter — originating in the tropics or subtropics, having a nonfrontal migratory character, and maintaining its identity for 24 hours or more." Namely, it is a cluster of thunderstorms that stay together as they move across the ocean.

This thunderstorm cluster is visible by satellite as consisting distinct thunderstorms with their own anvils and separate precipitation regions. There is no eye, and little or no rotation visible. Some tropical disturbances form out of **Mesoscale Convective Systems** (**MCS**s), particularly those that develop a **Mesoscale Convective Vortex** (**MCV**, see the Thunderstorm chapter). Some are identified as the thunderstorm clusters that move with easterly waves.

Most tropical disturbances do not evolve into tropical cyclones. Hence, tropical disturbances are not usually named or numbered. However, tropical meteorologists watch them carefully as they evolve, as potential future tropical cyclones.

As condensation and precipitation continue in this thunderstorm cluster, more and more latent heat is released in those storms. Namely, the mid-tropospheric air near this cluster becomes warmer than the surrounding ambient air. According to the hypsometric relationship, pressure decreases more slowly with increasing altitude in this warm region.

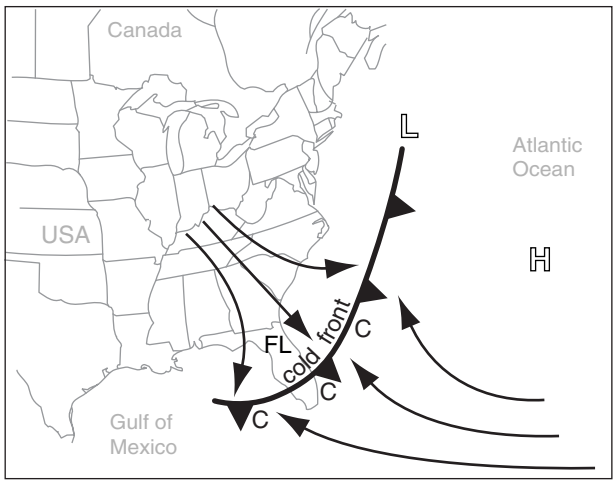

Figure 16.17
Lower tropospheric convergence (C) along a cold front over Florida (FL), USA.

Thus, a synoptic-scale high-pressure starts to form near the top of the troposphere in the region of this cluster.

Tropical Depression (TD)

The high-pressure aloft begins to create a thermal circulation (see Global Circulation chapter), where air aloft is driven horizontally outward — down the pressure gradient toward the lower pressure outside of the cluster. This diverging air aloft also starts to rotate anticyclonically.

The outward moving air aloft removes air molecules from the thunderstorm cluster region of the troposphere, thereby lowering the surface pressure under the cluster. The "depressed" pressure at sea level is why this stage gets its name: **tropical depression**. Tropical depressions are given an identification number, starting with number 1 each year.

As this weak surface low forms, it creates a pressure gradient that starts to suck winds horizontally toward the center of the low. This inflowing air begins rotating cyclonically due to Coriolis force. The surface low pressure is usually too weak to measure directly. However, this tropical depression stage is defined by measurable near-surface winds of 17 m/s or less (Table 16-4) turning cyclonically as a closed circulation around the cluster. There is still no eye at this stage, however the thunderstorms are becoming aligned in spiral rain bands (Fig. 16.18). Most tropical depressions do not strengthen further.

However, for the few storms that do continue to strengthen, the near-surface winds are boundary-layer gradient winds that spiral in towards the center of the cluster. This radial inflow draws in more

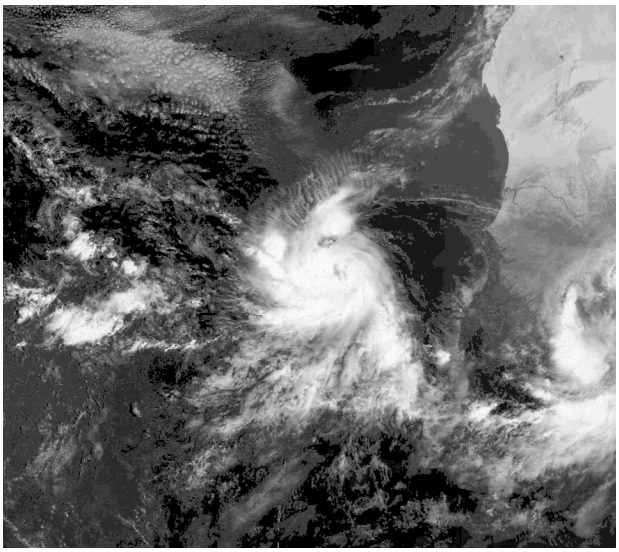

Figure 16.18
Tropical Depression 10 (in center of photo), over the tropical Atlantic Ocean south-southeast of the Cape Verde Islands. Africa is visible in the right quarter of the photo. (Visible satellite image taken 11:45 UTC on 2 Sep 2008, courtesy of NOAA.)

Table 16-4. Stages leading to tropical cyclones. M_{max} = maximum wind speed near the surface. n/a = not applicable.

Stage	M_{max}		
	(m/s)	(km/h)	(knots)
Tropical Disturbance	n/a	n/a	n/a
Tropical Depression	< 17	< 61	≤ 33
Tropical Storm	17 - 32	61 - 118	33 - 63
Hurricane	≥ 33	≥ 119	≥ 64

warm humid boundary-layer air, thereby refueling the thunderstorms and allowing them to persist and strengthen. Condensation and precipitation increase, causing a corresponding increase in latent-heat release.

This warm core of the storm further strengthens the high pressure aloft via the hypsometric relationship, which drives more outflow aloft and removes more air molecules from the troposphere near the cluster. Thus, the surface low pressure can continue to deepen in spite of the boundary-layer inflow. Namely, the high-pressure aloft creates an exhaust system, while the boundary layer is the intake system to the incipient cyclone.

Tropical Storm (TS)

When the surface low is deep enough to drive winds faster than 17 m/s (but less than 33 m/s) in a closed cyclone circulation, then the system is classified as a **tropical storm**. On weather maps, it is indicated with symbol 6.

At this point, the thunderstorm rain bands have nearly completely wrapped into a circle — the future eyewall (Fig. 16.19d). The anvils from the thunderstorms have usually merged in to a somewhat circular **central dense overcast** (**CDO**), which is clearly visible as a large-diameter cold high cloud. There is no eye at this stage. Tropical storms are organized sufficiently to be able to modify their local environment to allow them to persist, without relying so much on a favorable ambient environment.

At this stage the storm is given a name for identification (and its former tropical-depression number is dropped). The same name is used if the storm further strengthens into a tropical cyclone, and for the rest of its life cycle.

Hurricanes (Atlantic and Eastern Pacific) and Cyclones (Indian Ocean and Southwestern Pacific near

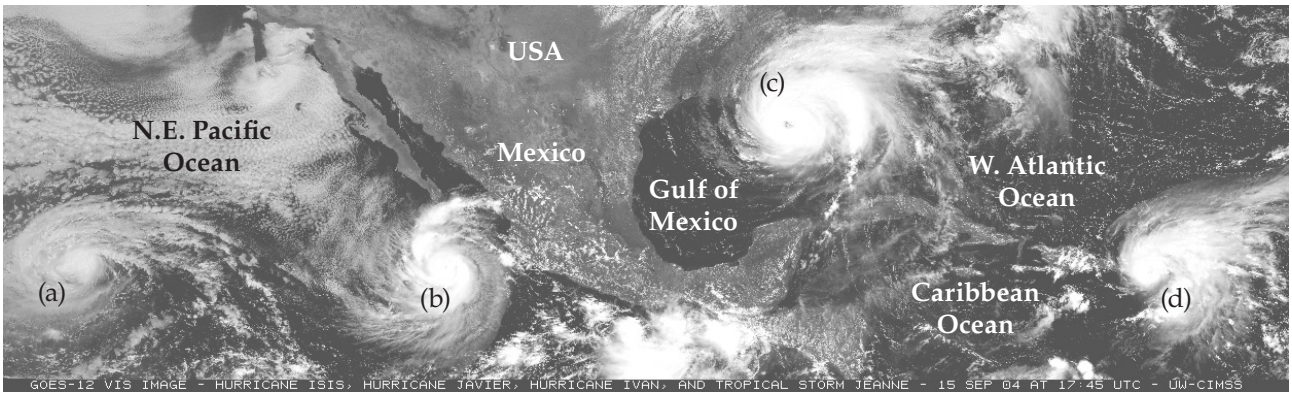

Figure 16.19
Visible satellite image at 17:45 UTC on 15 Sep 2004, showing four tropical systems. From left to right: (a) Hurricane Isis, (b) Hurricane Javier, (c) Hurricane Ivan, (d) Tropical Storm Jeanne. This image covers the eastern N. Pacific Ocean, Central America, Gulf of Mexico, Caribbean Ocean, and western N. Atlantic. (Image courtesy of University of Wisconsin–Madison CIMSS/ SSEC.)

Australia) are usually given names of men or women. These are assigned in alphabetical order according to lists that have been set in advance by the **World Meteorological Organization** (**WMO**). Typhoons are given names of flowers, animals, birds, trees, foods (not in alphabetical order but in an order set by the WMO's Typhoon Committee).

Tropical-storm and tropical-cyclone names are re-used in a six-year cycle. However the names of the strongest, most destructive tropical cyclones are "retired" and never used again (they are replaced with other names starting with the same letter).

Tropical Cyclone (Hurricane, Typhoon)

Roughly half of the tropical storms in the Atlantic continue to strengthen into hurricanes. By this stage there is a well defined eye surrounded by an eyewall of thunderstorms. Max wind speeds are 33 m/s or greater in a closed circulation around the eye. The central dense overcast usually has a cloud-free eye. The weather map symbol for a tropical cyclone is ❦.

There is heavy precipitation from the eyewall thunderstorms, and the core of the storm is significantly warmer than the environment outside the storm. Sea-level pressure decrease in the eye is measurable and significant, and a rise of sea level into a storm surge is possible. The storm organization allows it to persist for days to weeks as it moves across ocean basins (Fig. 16.19a-c).

Movement/Track

Steering by the Global Circulation

Tropical cyclones are moved by the larger-scale winds near them. These winds are variable, causing a wide variety of hurricane tracks and translation speeds. However, by focusing on the climatological average trade winds and the monsoon circulations (Figs. 16.7 & 16.20), we can the anticipate average movement of tropical cyclones.

During late Summer and early Fall, monsoon high-pressure regions form over the oceans, as was discussed in the Global Circulation chapter. Winds rotate (clockwise; counterclockwise) around these highs in the (Northern; Southern) Hemisphere. Equatorward of the high center the monsoon winds are in the same direction as the trade winds — from east to west. Thus, average hurricane tracks in the eastern and central longitudes of an ocean basin are usually zonal — from east to west.

However, near the west sides of the ocean basins, the monsoon winds turn poleward (Fig. 16.20), and thus steer the hurricanes away from the equator. Many of these hurricanes travel along the east coast of continents in a poleward direction. The tracks vary from year to year, and vary within any one year (Fig. 16.20). Some of the tracks in the Atlantic might never hit N. America. Other tracks can be along the East Coast of North America, causing significant damage to coastal cities. Yet other tracks continue further westward across the Caribbean Sea and into the Gulf of Mexico before reaching the mainland.

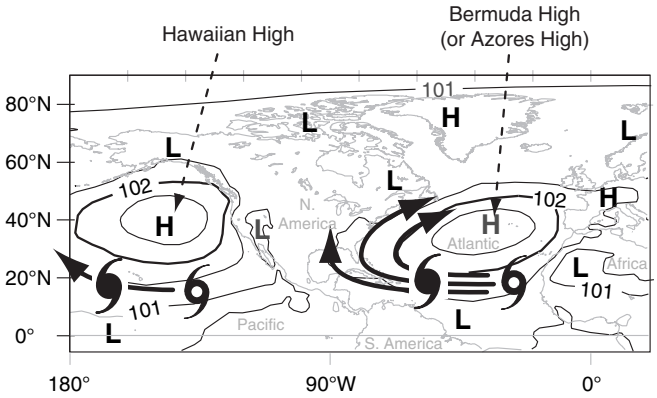

Figure 16.20
Monsoon sea-level pressure (kPa) pattern for July (copied from the Global Circulation chapter), with isobars as thin black lines. Winds and average hurricane tracks (dark arrows) tend to follow the isobars around the monsoon highs, although actual tracks are quite variable.

Extratropical Transition

As the monsoon circulations move the tropical cyclones poleward, the cyclones leave the tropics and subtropics and enter the mid-latitudes. Here, prevailing winds are from the west in the global circulation. Also, winds on the poleward side of the monsoon highs are from the west. Thus, many tropical cyclone tracks eventually turn towards the east at midlatitudes.

Extratropical transition is the name given to the movement of tropical cyclones out of the tropics and into the midlatitudes. At these latitudes the storms are generally moving over colder water, causing them to rapidly die. Nonetheless, these former hurricanes can change into extratropical cyclones and still cause damaging floods, wind, and waves if over coastal areas. Even dying tropical cyclones well away from a coastline can influence mid-latitude weather downwind by pumping copious amounts of moisture into the air. This humid air can later serve as the fuel for mid-latitude cyclones thousands of kilometers downwind, creating heavy rain and possible flooding.

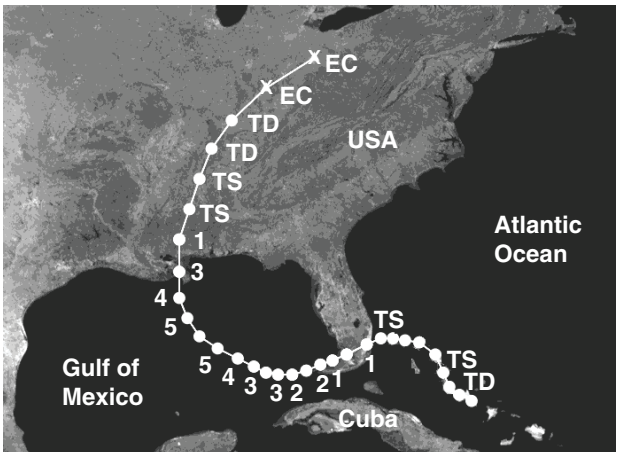

Figure 16.21
Track of hurricane Katrina, showing its intensity during 23 - 31 Aug 2005. 1 to 5 is Saffir-Simpson category. TS = tropical storm. TD = tropical depression. EC = extratropical cyclone.

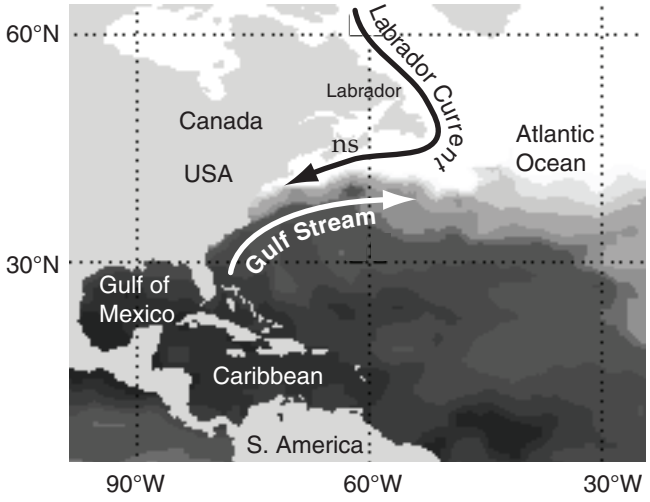

Figure 16.22
Enlargement of part of Fig. 16.8, showing sea-surface temperatures (warm = darker grey fill; cold = white fill). The Labrador Current and Gulf Stream are shown. ns = Nova Scotia.

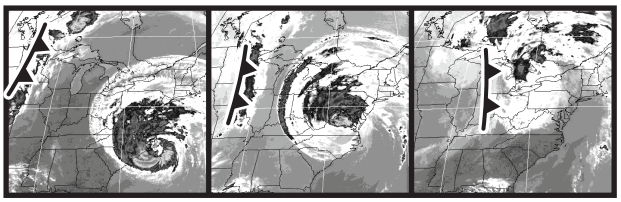

(a) 1615 UTC, 18 Sep (b) 0315 UTC, 19 Sep (c) 1615 UTC, 19 Sep

Figure 16.23
Collision of an extratropical cold front with former Hurricane Isabel in Sep 2003. (a) A cold front is over Minnesota, USA, while the hurricane eye makes landfall on the N. Carolina coast. (b) Later. (c) The front and hurricane collide over the Great Lakes. (IR GOES satellite images courtesy of NOAA.)

Tropical Cyclolysis

Tropical cyclones can exist for weeks because they have the ability to create their own fuel supply of warm humid boundary-layer air. They create this fuel by tapping the heat and water stored in the upper ocean. Tropical cyclones die (**tropical cyclolysis**) when they move to a location where they cannot create their own fuel, or if they are destroyed by larger-scale weather systems, as described next.

Movement over Land

If the global circulation steers a tropical cyclone over land, it begins to die rapidly because it is unable to tap the warm ocean for more fuel (Fig. 16.21). If the land is a small island or narrow isthmus, then the weakened tropical cyclone can possibly re-intensify when it again moves over warm ocean water.

Movement over Cold Water

If the global circulation steers a tropical cyclone over water colder than 26.5°C, then it is unable to create new warm humid air as fast the eyewall thunderstorms consume this fuel. As a result, tropical cyclones quickly weaken over cold water.

This often happens when tropical cyclones are steered poleward toward mid-latitudes, where sea surface temperatures (**SST**) are colder (Fig. 16.8). In the Atlantic, the Gulf Stream of warm ocean water moving north along the east coast of the USA allows hurricanes there to survive. However, further north, the very cold Labrador Current (Fig. 16.22) moving south from the Arctic along the east coast of Canada causes most hurricanes to diminish below hurricane force before making landfall (see Focus Box on next page).

Tropical cyclolysis can also occur if the layer of warm ocean water is too shallow, such that hurricane-induced ocean waves stir colder deep water to the surface. Also, if a hurricane crosses the path of a previous hurricane, the ocean surface along this previous path is often colder due to the wave stirring.

Interaction with Mid-latitude Synoptic System

When tropical cyclones move into mid-latitudes, they can encounter the larger, more powerful mid-latitude cyclones (Fig. 16.23) that were discussed in a previous chapter. Strong mid-latitude cold fronts can inject cold air into the tropical cyclone, causing the tropical cyclone to die. The fronts and associated jet stream aloft often have strong wind shear, and can rip apart the tropical cyclones. Sometimes tropical cyclones will move into the path of a mid-latitude cyclone, allowing the mid-latitude cyclone to capture some of the hurricane's energy and consume the hurricane as the two systems merge.

DYNAMICS

Initial Spin Up

While tornadoes form by tilting of the horizontal wind shear, such is not the case for tropical cyclones. For tropical cyclones, rotation is associated with convergence into a low center. During this convergence, angular momentum associated with the Earth's rotation (related to Coriolis force) is concentrated into angular momentum associated with hurricane winds.

The **absolute angular momentum** AAM is:

$$AAM = M_{\tan} \cdot R + 0.5 \cdot f_c \cdot R^2 \qquad \bullet(16.1)$$

where M_{tan} is the tangential velocity at radius R from the tropical-cyclone center, and f_c is the Coriolis parameter. At latitudes typical of hurricanes (20°), $f_c \approx 0.00005\ s^{-1}$. The adjective "absolute" means that this quantity includes both the relative angular momentum of the tropical cyclone as well as the background angular momentum associated with the Earth's rotation.

If the tropical cyclone were to experience no friction against the surface, then angular momentum would be conserved while air converges. Thus, tangential wind speed M_{tan} at some small radius R_{final} can be created even if the air at some larger initial radius R_{init} possesses no rotation ($M_{tan.initial} = 0$):

$$M_{\tan} = \frac{f_c}{2} \cdot \left(\frac{R_{init}^2 - R_{final}^2}{R_{final}} \right) \qquad (16.2)$$

In real tropical cyclones, frictional drag cannot be neglected. Hence, actual tangential winds are less than those calculated with eq. (16.2).

Subsequent Development

As the winds accelerate in a strengthening tropical cyclone, centrifugal force gains importance. Recall from the Dynamics chapter that the **gradient-wind** equation in cylindrical coordinates (eq. 10.32) is:

$$\frac{1}{\rho} \cdot \frac{\Delta P}{\Delta R} = f_c \cdot M_{\tan} + \frac{M_{\tan}^2}{R} \qquad (16.3)$$

where $\Delta P/\Delta R$ is the radial pressure gradient, and ρ is air density. The last term represents centrifugal force. The gradient wind applies at all radii from the center of the storm, and at all altitudes except near the bottom (in the boundary layer) and near the top (in the anvil or cirrus shield region).

FOCUS • Hurricane Juan Hits Canada

The Canadian East Coast only rarely gets hurricanes — one every 3 to 4 years on average. But it gets many former hurricanes that have weakened to Tropical Storm or lower categories during passage over the cold Labrador current (for Atlantic Canada), or due to passage over land (for Central Canada).

On 29 Sep 2003, Hurricane Juan hit Nova Scotia, Canada, as a category 2 hurricane. Two factors made this possible: (1) warm (but colder than 26.5°C) sea-surface water was relatively close to Nova Scotia; and (2) the hurricane was translating north so quickly that it did not have time to spin down over the narrow cold-water region before making landfall.

This storm began as Tropical Depression #15 about 470 km southeast of Bermuda at noon on 25 Sep. Six hours later it became a Tropical Storm, and by noon 26 Sep it became a Hurricane while 255 km east of Bermuda. During the next 3 days it traveled northward over the Gulf Stream, with intensity of category 2 for most of its journey.

When it reached Canada, it dropped 25 to 40 mm of rain in Nova Scotia. The storm surge was 1.5 m, and the maximum wave height was roughly 20 m. Hundreds of thousands of people lost electrical power due to trees falling on power lines, and 8 people were killed in storm-related accidents.

Before Juan, the most remembered "former hurricane" to strike Canada was Hurricane Hazel. It transitioned into a strong extratropical cyclone before reaching Canada, but caused 81 deaths and severe flooding in southern Ontario in mid October 1954.

Since 1887, there were two hurricanes of category 3, five of category 2, and 26 of category 1. Info about Canadian hurricanes is available from the **Canadian Hurricane Centre**, Halifax, Nova Scotia.

Solved Example

In initially rotationless air at radius 400 km from a tropical-cyclone center, find its tangential velocity after it converges to a radius of 100 km. The cyclone is centered at 10° latitude.

Solution

Given: $\phi = 10°$, $R_{init} = 400$ km, $R_{final} = 100$ km

Find: $M_{tan} = ?$ m/s

First, find the Coriolis parameter:

$f_c = 2 \cdot \omega \cdot \sin(\phi) = (1.458 \times 10^{-4}\ s^{-1}) \cdot \sin(10°)$

$= 0.0000253\ s^{-1}$

Use eq. (16.2): $M_{tan} =$

$$\frac{303 s^{-1})}{2} \cdot \left(\frac{(500\text{km})^2 - (200\text{km})^2}{200\text{km}} \right) = \underline{\textbf{19 m/s}}$$

Check: Units OK. Physics OK.

Discussion: This velocity is already 60% of the 32 m/s required in order for the tropical storm to be reclassified as a hurricane. At the equator, there is no Coriolis force, hence there are no hurricanes.

Solved Example

Given a hurricane with: sea-level pressure difference between the eye and far outside of ΔP_{max} = 11.3 kPa, eyewall outside radius of R_o = 25 km, latitude = 14°N, and ρ = 1 kg/m^3. From the hurricane model presented later in this chapter, assume the pressure gradient is roughly: $\Delta P/\Delta R = (4/5)\cdot\Delta P_{max}/R_o$.
a) Find the magnitude of the gradient wind just outside of the eye wall (i.e., at $R = R_o$) .
b) Compare the relative importance of the Coriolis and centrifugal terms in the gradient wind eq.
c) Compare this gradient wind with the max expected surface wind of 67 m/s, and explain any difference.

Solution

Given: ΔP_{max} = 11.3 kPa, R_o = 25 km,
latitude = 14°N, ρ = 1 kg/m^3.
Find: M_{tan} = ? m/s. Compare terms.

a) Use: $\Delta P/\Delta R = (4/5)\cdot\Delta P_{max}/R_o$
Find $f_c = (1.458\text{x}10^{-4}\ \text{s}^{-1})\cdot\sin(14°) = 3.5\text{x}10^{-5}\ \text{s}^{-1}$.
Use eq. (16.3) and neglect translation speed:

$$\frac{(4/5)}{\rho}\cdot\frac{\Delta P_{\max}}{R_o} = f_c\cdot M_{\tan} + \frac{M_{\tan}^2}{R}$$

Pressure Gradient = Coriolis + Centrifugal

Using trial and error (i.e., trying different values of M_{tan} in a spreadsheet until the left and right sides of the eq balance): M_{tan} = **<u>94.65 m/s</u>**.

b) From my spreadsheet, the terms in the eq. are:

0.361 = 0.003 + 0.358

Pressure Gradient = Coriolis + Centrifugal

Thus, the **<u>Coriolis force is about 2 orders of magnitude smaller than centrifugal force</u>**, at this location of strongest tangential wind just outside the eye wall. At this location, the cyclostrophic assumption (of neglecting Coriolis force) is OK.

c) The max expected <u>surface</u> wind of 67 m/s includes the effect of **<u>drag against the sea surface</u>**, which is why it is smaller than our answer from (a) M_{tan} = 95 m/s.

Check: Units OK. Physics OK.
Discussion: This scenario is similar to the composite hurricane model presented later in this chapter.

Solved Example

Find the cyclostrophic wind at a radius of 50 km. The pressure gradient is 1 kPa/20 km.

Solution

Given: R = 50 km, ΔP = 1 kPa, ΔR = 20 km,
Assume ρ = 1 kg/m^3.
Find: M_{cs} = ? m/s

Use eq. (16.4): $M_{cs} = \sqrt{\dfrac{(60\text{km})}{(1\text{kg}\cdot\text{m}^{-3})}\cdot\dfrac{(1000\text{Pa})}{(15\text{km})}}$ = **<u>50 m/s</u>**

Check: Units OK. Physics OK.
Discussion: This is a category 3 hurricane.

Some researchers find it convenient to neglect Coriolis force closer to the center of the stronger hurricanes where the winds are faster. For this situation, the tangential hurricane winds can be crudely approximated by the **cyclostrophic wind**, M_{cs} (see the Dynamics Chapter):

$$M_{cs} = M_{\tan} = \sqrt{\frac{R}{\rho}\cdot\frac{\Delta P}{\Delta R}} \qquad (16.4)$$

Nonetheless, the gradient-wind equation (16.3) is the most appropriate equation to use for hurricanes, at <u>middle</u> altitudes of the storm.

Inflow and Outflow

At the <u>bottom</u> of the tropical cyclone (Fig. 16.24), drag against the sea surface causes the winds to spiral in towards the eyewall. The **boundary-layer gradient wind** equation (see the Dynamics chapter) describes this flow well. Without this drag-related inflow, the eyewall thunderstorms would not get sufficient warm humid air to survive, causing the hurricane to die.

Explaining the outflow at the <u>top</u> of a tropical cyclone is trickier, because drag forces are so small that we cannot invoke the boundary-layer gradient-wind equation. One important process is that the

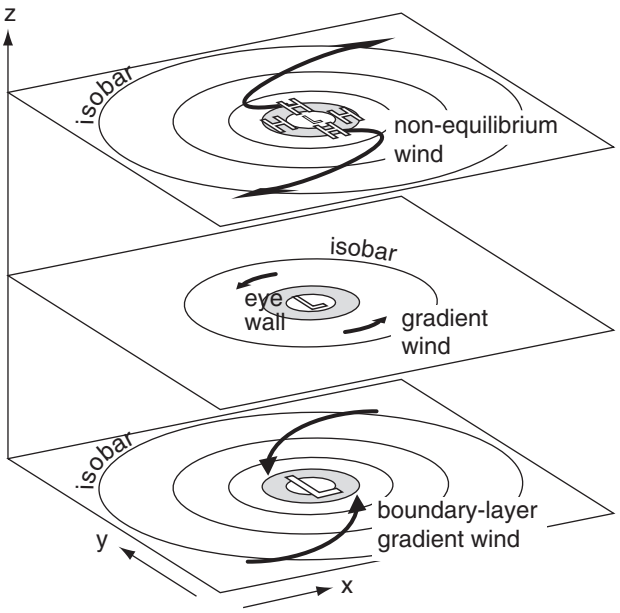

Figure 16.24
Wind dynamics at the bottom, middle and top of a tropical cyclone. Thick arrows represent wind vectors. Low pressure 𝕃 at storm bottom is associated with spiraling inflow winds. High pressure 𝕳 at storm top is associated with outflow winds. Thus, storm top is the exhaust system of the hurricane engine, and storm bottom is the intake system.

thunderstorm updrafts in the eyewall rapidly move air upward and deposit enough air molecules at the top of the storm to contribute to high pressure there. Thus, the outflow is related to two factors.

(1) The cyclonically moving air from the boundary layer is brought to the top of the hurricane by eyewall-thunderstorm updrafts so quickly that its inertia prevents it from instantly changing to anticyclonic outflow. Namely, the outflow is initially moving the wrong way (cyclonically) around the high (Fig. 16.24). The outflow must change direction and accelerate, and thus is not in steady state.

(2) It is physically impossible to create a balanced gradient-wind flow around a high-pressure area that is surrounded by an excessively strong pressure gradient, as was explained in the Dynamics chapter (see Beyond Algebra in the next column). But the thunderstorm updrafts help create such an excessive high pressure at storm top. In this situation, pressure-gradient force exceeds the compensating Coriolis force (Fig. 16.25), resulting in a net outward force that causes the air to accelerate outward from the eyewall as a non-equilibrium wind.

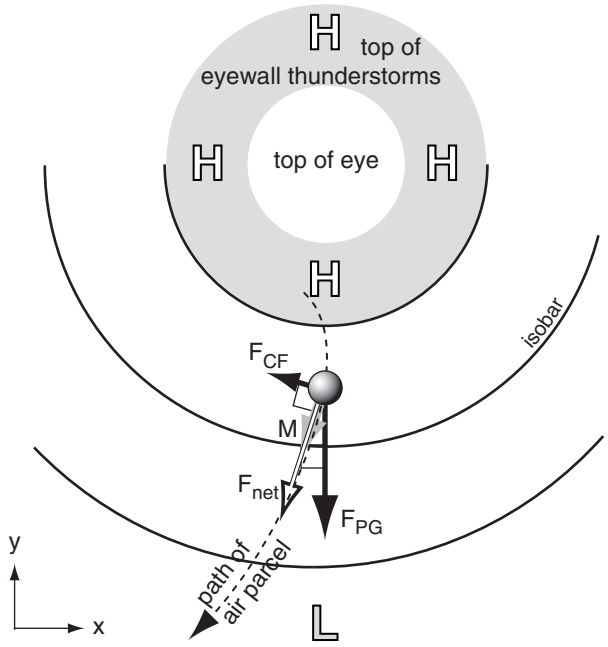

Figure 16.25
Isobars on a constant height surface near the top of a tropical cyclone. Grey ring represents the eyewall thunderstorms. H and L are high and low pressure. M is non-equilibrium wind speed. F_{CF} is Coriolis force, F_{PG} is pressure-gradient force, and F_{net} is the vector sum of forces.

BEYOND ALGEBRA • Non-equilibrium winds at the top of tropical cyclones

Recall from the Dynamics chapter that solutions for the gradient wind around an anticyclone are physically realistic only for curvature Rossby numbers $Ro_c \le 1/4$. But $Ro_c = (\partial P/\partial R)/(\rho \cdot f_c^2 \cdot R)$. Setting $Ro_c = 1/4$, separating variables, and integrating from $P = P_o$ at $R = 0$, to P at R gives:

$$P = P_o - a \cdot R^2 \qquad \text{(a)}$$

where $a = \rho \cdot f_c^2/8$. This equation gives the max change of pressure with radial distance R that is allowed for a gradient wind that is in equilibrium. But real hurricanes can have greater-than-equilibrium pressure gradients at the storm top.

For example, at hurricane top ($z \approx 17$ km) suppose $P_o = 8.8$kPa in the eye and $\rho = 0.14$ kg/m^3. Thus, $a \approx 2.5\text{x}10^{-8}$ kPa/km at 15° latitude. The strongest horizontal pressure gradient possible for a gradient wind around the high-pressure center at the top of the eye is plotted below as the slope of the solid line (from equation a). This is a miniscule pressure gradient, due in part to the very small Coriolis force at 15° latitude.

But actual horizontal pressure gradients can be much stronger (dashed line). Thus, steady-state gradient winds (winds that follow the curved isobars) are not possible at tropical-cyclone top. Instead, the non-equilibrium winds are accelerating outward (crossing this isobars at a large angle) from the high due to the strong pressure gradient, and only gradually develop some anticyclone rotation further from the eye.

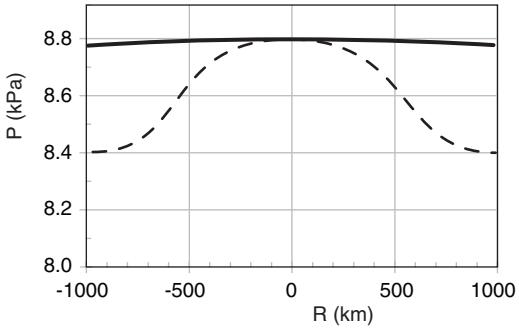

Fig. 16.b. *Horizontal pressure gradients at the top of a tropical cyclone. R = distance from cyclone center, P = atmospheric pressure. The slope of the solid line shows the max pressure gradient that admits a gradient-wind solution. The dashed line is hypothetical and focuses on the pressure gradient from the eyewall outward.*

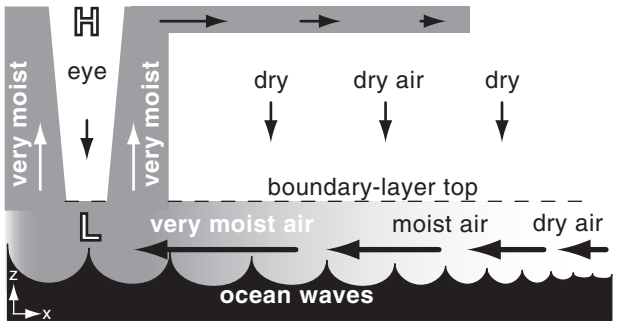

Figure 16.26
The intake system in the bottom of a tropical cyclone. As boundary-layer winds accelerate, they cause larger ocean waves that add more moisture (darker grey indicates higher humidity) to the inflowing air (thick arrows). L is the low-pressure center at sea level. Air is exhausted out of the top of the storm in the central dense overcast composed of thunderstorm anvils.

FOCUS• Hurricane Condensation Energy

One way to estimate the energy of tropical cyclones is by the amount of latent heat released during condensation. Rainfall rate is a measure of the net condensation.

An average Atlantic Hurricane produces about 1.5 cm of rain/day, which when accumulated over the area (of radius 665 km) covered by hurricane rain is equivalent to **2.1x10**^{10} m^3/day.

This converts to **6x10**^{14} W (= 5.2x10^{19} J/day). Namely, it is about 200 times the daily electricity generation capacity of the whole world.

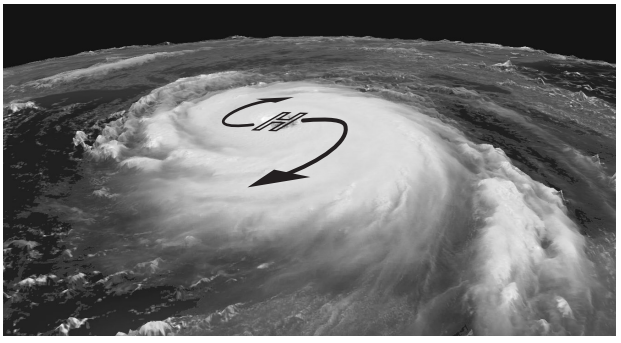

Figure 16.27
Exhaust system at the top of a tropical cyclone, where H is the high-pressure center near the tropopause and arrows are outflow winds. Computer-enhanced 3-D satellite image of Hurricane Katrina over the Gulf of Mexico, taken 28 Aug 2005 at 1545 UTC. Visible satellite imagery is mapped into a 3-D surface of cloud-top altitudes estimated from satellite IR data. (Image courtesy of US DOC/NOAA.)

THERMODYNAMICS

Tropical cyclones work somewhat like engines. There is an intake system (the atmospheric boundary layer) that draws in the fuel (warm, humid air). The engine (thunderstorms) converts heat into mechanical energy (winds and waves). And there is an exhaust system (precipitation fallout for water and anvil blowout for air) for the spent fuel.

Fuel Creation and Intake

In midlatitudes, thunderstorms can last for hours. However, tropical cyclones (which are made of thunderstorms) can last for weeks. Why the difference it longevity?

The main reason is that mid-latitude thunderstorms use warm humid air from only the nearby boundary layer, and after this nearby fuel is consumed the thunderstorms die. Even supercells and squall-line storms rely on an existing fuel supply of warm humid air, which they can utilize as they move across the countryside.

However, tropical cyclones create their own fuel of warm humid boundary-layer air. They do this via the fast near-surface winds that create large ocean waves (Fig. 16.26). These violent waves break and foam, causing rapid evaporation of sea-spray water into the air, and efficient transfer of heat from the ocean surface to the air. By the time this air reaches the base of the eyewall, it has an air temperature nearly equal to the sea-surface temperature and a relative humidity of nearly 100%.

Namely, tropical cyclones extract heat from the ocean. The ocean is a giant heat reservoir that has been absorbing sunlight all Summer and early Fall. This is the reason why warm, deep sea-surface temperatures are needed for tropical cyclones.

Exhaust

The large volume of inflowing boundary-layer air is good and bad for the tropical cyclone. It is good because this air carries the sensible- and latent-heat fuel for the storm. It is bad because it also brings massive amounts of other air molecules (nitrogen, oxygen) into the core of the storm.

The problem is that if these air molecules were to accumulate in the center of the storm, their weight would cause the sea-level air pressure to rise. This would weaken the surface low pressure, which would reduce the radial pressure gradient near sea level, causing the inflow winds and waves to diminish. With reducing inflow, the eyewall thunderstorms would run of fuel and die, causing the tropical cyclone to disintegrate in half a day or so.

However, we know that tropical cyclones can exist for weeks. Thus, there must be some other mechanism that removes air from the hurricane core as fast as it enters. That other mechanism is the strong outflow winds in the thunderstorm anvils at the top of the eyewall. This outflow exists because of high pressure at the top of the troposphere in the eye and eyewall regions (Figs. 16.26 & 16.27), which drives winds outward down the pressure gradient.

But what causes this high pressure aloft? We already discussed a non-hydrostatic process — the air deposited aloft from eyewall thunderstorm updrafts. But another process is hydrostatic — related to the excessive warmth of the center or **core** portion of the tropical cyclone.

Warm Core

The center of tropical cyclones is warmer than the surrounding air, due to latent heat release by the organized convection and adiabatic warming due to subsidence in the eye. Namely, air rises moist adiabatically in the eyewall thunderstorms, but then after losing water due to precipitation from the eyewall, the air descends dry adiabatically in the eye.

While the eye might be only 0 to 4°C warmer than its distant surroundings near the surface, it can be 10 to 16°C warmer at 12 to 16 km altitude (Fig. 16.28). Hence, a tropical cyclone is a **warm core** system (see Focus box) surrounded by cooler air.

This radial temperature gradient causes a radial pressure-gradient reversal with increasing altitude (Fig. 16.29), as is explained by the thermal-wind relationship. To determine this pressure gradient, define the sea-level pressure in the eye as $P_{B\,eye}$, and that of the distant surroundings at sea level as $P_{B\,\infty}$. Near the top of the tropical cyclone, define the core pressure as $P_{T\,eye}$ and that of its distant surroundings as $P_{T\,\infty}$ at the same altitude. Subscripts B and T denote bottom and top of the troposphere.

Suppose a hurricane is approximately $z_{max} \approx 15$ km deep, has a temperature in the eye averaged over the whole hurricane depth of $\overline{T_{eye}} = 273$ K, and has ambient surface pressure distant from the storm of $P_{B\,\infty} = 101.3$ kPa. The pressure difference at the top of the hurricane ($\Delta P_T = P_{T\,\infty} - P_{T\,eye}$) is approximately related to the pressure difference at the bottom ($\Delta P_B = P_{B\,\infty} - P_{B\,eye}$) by:

$$\Delta P_T \approx a \cdot \Delta P_B - b \cdot \Delta T \qquad \bullet(16.5)$$

where $a \approx 0.15$ (dimensionless), $b \approx 0.7$ kPa/K, and $\Delta T = T_{eye} - T_{\infty}$ is the temperature difference averaged over the depth of the troposphere. Note that ΔP_T is negative.

Next, consider the tangential winds. These winds spiral cyclonically around the eye at low al-

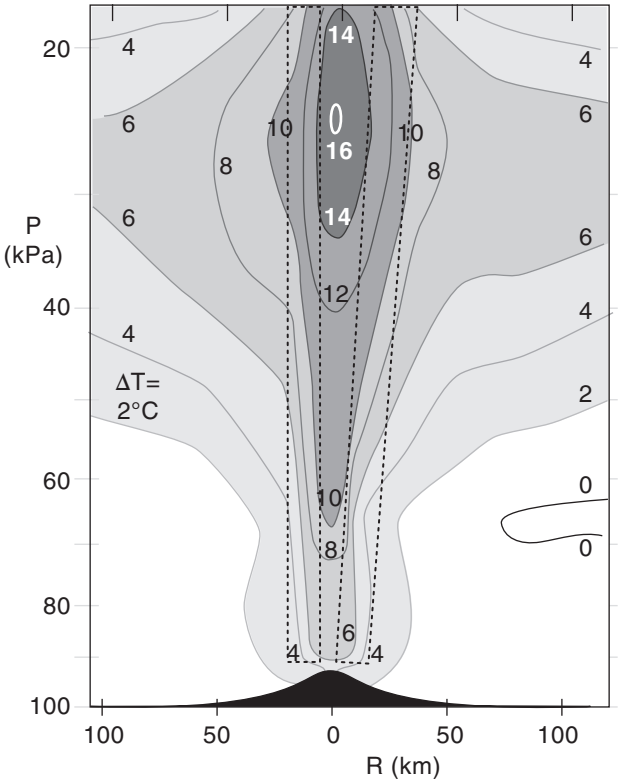

Figure 16.28
The exceptionally warm core of Hurricane Inez. Vertical cross section through the eye, showing the temperature excess ΔT compared to the environmental temperature at the same altitude. The approximate eyewall location is outlined with dotted lines. R is radial distance from the center of the eye, and P is pressure. Inez existed during 22 Sep to 11 Oct 1996 in the eastern Caribbean, and reached category 4 intensity. The black area at the bottom of the figure masks atmospheric pressures that did not exist at sea level, because of the very low surface pressure in and near the eye. (Based on data from Hawkins and Imbembo, 1976.)

Solved Example

The surface pressure in the eye of a hurricane is 90 kPa, while the surrounding pressure is 100 kPa. If the core is 10 K warmer than the surroundings, find the pressure difference at the top of the hurricane between the eye and surroundings.

Solution

Given: $\Delta P_B = 100 - 90 = 10$ kPa, $\Delta T = 10$ K

Find: $\Delta P_T = ?$ kPa

Use eq. (16.5):

$\Delta P_T = (0.15)\cdot(10\text{kPa}) - (0.7\text{kPa/K})\cdot(10\text{K}) =$ **– 5.5 kPa**

Check: Units OK. Physics OK.

Discussion: This answer is negative, meaning that the eye has higher pressure than the surroundings, aloft. This pressure reversal drives the outflow aloft.

FOCUS • Warm vs. Cold Core Cyclones

For a cyclone to survive and intensify, air must be constantly withdrawn from the top. This removal of air mass from the cyclone center (**core**) counteracts the inflow of boundary-layer air at the bottom, which always happens due to surface drag. The net result is low surface pressure in the core, which drives the near-surface winds.

Warm-core cyclones (e.g., hurricanes) and **cold-core cyclones** (e.g., extratropical lows) differ in the way they cause horizontal divergence to remove air from the top of the cyclones [see Fig. 16.c, parts (a) and (b)].

Hurricanes are vertically stacked, with the eye of the hurricane near the top of the tropopause almost directly above the eye near the surface [Fig. 16.c(a)]. Intense latent heating in the hurricane warms the whole depth of the troposphere near the core, causing high pressure aloft because warm layers of air have greater thickness than cold. This high aloft causes air to diverge horizontally at the top of the hurricane, which is why visible and IR satellite loops show cirrus and other high clouds flowing away from the hurricane center.

Extratropical lows are not vertically stacked, but have low pressure that tilts westward with increasing height [Fig 16.c(b)]. As the surface circulation around the cyclone advects in cold, polar, boundary-layer air on the west side of the cyclone, the small thicknesses in that sector cause pressure to decrease more rapidly with height. The net result is an upper-level trough west of, and a ridge east of, the surface low. A jet stream meandering through this trough-ridge system would cause horizontal divergence (D), as was shown in the Extratropical Cyclone chapter.

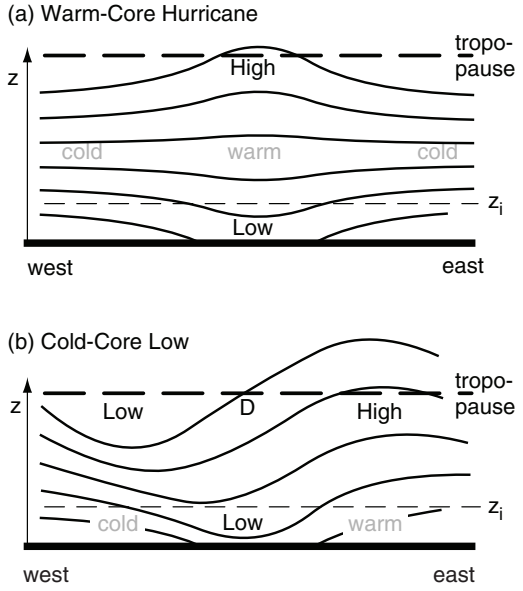

Figure 16.c.
Vertical cross section of (a) warm, and (b) cold core cyclones. Thin lines are isobars, and z_i is ABL top.

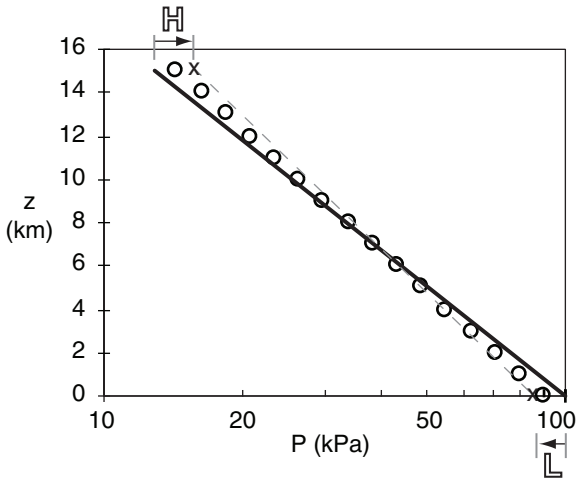

Figure 16.29
Hydrostatic pressure decrease with height in a warm hurricane core (circles) and in a cooler surrounding environment (line). The eye has lower pressure than the surroundings near the surface, but higher pressure than the surroundings aloft. Additional nonhydrostatic P variation (plotted with dashed line between two x's) in the horizontal is due to strong updrafts in eyewall thunderstorms, removing low-altitude air and depositing it at storm top. (This is a semi-log graph.)

titudes, but spiral anticyclonically near the top of the troposphere well away from the eye. Hence, the tangential velocity must decrease with altitude and eventually change sign. The ideal gas law can be used with the gradient wind eq. (16.3) to show how tangential wind component M_{tan} varies with altitude z :

$$\left(\frac{2\cdot M_{\tan}}{R}+f_c\right)\cdot\frac{\Delta M_{\tan}}{\Delta z}=\frac{|g|}{\overline{T}}\cdot\frac{\Delta T}{\Delta R} \qquad \bullet(16.6)$$

Solved Example

Suppose at a radius of 40 km the tangential velocity decreases from 50 m/s at the surface to 10 m/s at 10 km altitude. Find the radial temperature gradient at a latitude where the Coriolis parameter is 0.00005 s^{-1}. Assume $|g|/T = 0.0333\ m\cdot s^{-2}\cdot K^{-1}$.

Solution

Given: R = 40 km, M_{tan} = 50 m/s at z = 0,
M_{tan} = 10 m/s at z = 10 km, f_c = 0.00005 s^{-1} ,
$|g|/T = 0.0333\ m\cdot s^{-2}\cdot K^{-1}$

Find: $\Delta T/\Delta R$ = ? K/km

Use eq. (16.6):

$$\frac{|g|}{\overline{T}}\cdot\frac{\Delta T}{\Delta R}=\left(\frac{2\cdot(30\text{m/s})}{40{,}000\text{m}}+0.00005\text{s}^{-1}\right)\cdot\frac{(10-50\text{m/s})}{(10{,}000\text{m})}$$

$$= -6.2\text{x}10^{-6}\ \text{s}^{-2}\ .$$

Thus, $$\frac{\Delta T}{\Delta R}=\frac{-6.2\times10^{-6}\text{s}^{-2}}{0.0333\text{m}\cdot\text{s}^{-2}\cdot\text{K}^{-1}} = \underline{\textbf{– 0.19 K/km}}.$$

Check: Units OK. Physics OK.

Discussion: From the center of the eye, the temperature decreases about 7.4 K at a radius of 40 km, for this example. Indeed, the core is warm.

BEYOND ALGEBRA • Pressure Reversal

Derivation of eq. (16.5):

Use the hypsometric equation to relate the pressure at the top of the hurricane eye to the pressure at the bottom of the eye. Do the same for the surroundings. Use those equations to find the pressure difference at the top:

$$\Delta P_T = P_{B\infty} \cdot \exp[-|g| \cdot z_{\max} / (\Re \cdot \bar{T}_{\infty})] \; - P_{B.eye} \cdot \exp[-|g| \cdot z_{\max} / (\Re \cdot \bar{T}_{eye})] \quad .$$

Then, using $P_{B.eye} = P_{B\infty} - \Delta P_B$, collecting the exponential terms that are multiplied by $P_{B\infty}$, and finally using a first-order series approximation for those exponentials, one gets eq. (16.5), where

$a = \exp[-|g| \cdot z_{\max} / (\Re \cdot \bar{T}_{eye})] \approx 0.15$,

$b = -(|g| \cdot z_{\max} \cdot P_{B\infty}) / (\Re \cdot \bar{T}_{eye} \cdot \bar{T}_{\infty}) \approx 0.7$ kPa/K,

$|g| = 9.8$ m·s^{-2} is gravitational acceleration magnitude, and

$\Re = 287.04$ m^2·s^{-2}·K^{-1} is the gas constant for dry air.

BEYOND ALGEBRA • Warm Core Winds

Derivation of eq. (16.6):

There are 3 steps: (1) scale analysis; (2) differentiation of eq. (16.3) with respect to height z, and (3) simplification of the pressure term.

(1) Scale Analysis

Differentiate the ideal gas law $P = \rho \Re T$ with respect to z, and use the chain rule of calculus:

$$\frac{\partial P}{\partial z} = \rho \Re \frac{\partial T}{\partial z} + \Re T \frac{\partial \rho}{\partial z}$$

Then divide this by the ideal gas law:

$$\frac{1}{P}\frac{\partial P}{\partial z} = \frac{1}{T}\frac{\partial T}{\partial z} + \frac{1}{\rho}\frac{\partial \rho}{\partial z}$$

Between $z = 0$ to 20 km, typical variations of the variables are: $P = 101$ to 5.5 kPa, $T = 288$ to 216 K, and $\rho = 1.23$ to 0.088 kg/m^3 . Thus, the temperature term in the eq. above varies only 1/4 as much as the other two terms. Based on this scale analysis, we can neglect the temperature term, which leaves:

$$\frac{1}{P}\frac{\partial P}{\partial z} \approx \frac{1}{\rho}\frac{\partial \rho}{\partial z} \qquad \text{(a)}$$

(2) Differentiate eq. (16.3) with respect to z:

$$\frac{\partial}{\partial z}\left[\frac{1}{\rho}\frac{\partial P}{\partial R}\right] = f_c \cdot \frac{\partial M_{\tan}}{\partial z} + \frac{2M_{\tan}}{R} \cdot \frac{\partial M_{\tan}}{\partial z}$$

Upon switching the left and right sides:

$$\left[\frac{2M_{\tan}}{R} + f_c\right] \cdot \frac{\partial M_{\tan}}{\partial z} = \frac{\partial}{\partial z}\left[\frac{1}{\rho}\frac{\partial P}{\partial R}\right] \qquad \text{(b)}$$

(3) Simplify the pressure term:

First, use the chain rule:

$$\frac{\partial}{\partial z}\left[\frac{1}{\rho}\frac{\partial P}{\partial R}\right] = \frac{1}{\rho} \cdot \frac{\partial}{\partial z}\left[\frac{\partial P}{\partial R}\right] + \frac{\partial P}{\partial R} \cdot \frac{\partial}{\partial z}\left[\rho^{-1}\right]$$

R and z are independent, allowing the order of differentiation to be reversed in the first term on the RHS:

(continues in next column)

BEYOND ALGEBRA • Warm Core Winds 2

Derivation of eq. (16.6) *(continuation)*

$$\frac{\partial}{\partial z}\left[\frac{1}{\rho}\frac{\partial P}{\partial R}\right] = \frac{1}{\rho} \cdot \frac{\partial}{\partial R}\left[\frac{\partial P}{\partial z}\right] - \frac{1}{\rho^2}\frac{\partial P}{\partial R} \cdot \frac{\partial \rho}{\partial z}$$

Use the hydrostatic eq. $\partial P/\partial z = -\rho \cdot |g|$ in the first term on the RHS:

$$\frac{\partial}{\partial z}\left[\frac{1}{\rho}\frac{\partial P}{\partial R}\right] = \frac{1}{\rho} \cdot \frac{\partial}{\partial R}\left[-\rho \cdot |g|\right] - \frac{1}{\rho}\frac{\partial P}{\partial R} \cdot \frac{1}{\rho}\frac{\partial \rho}{\partial z}$$

But $|g|$ is constant. Also, substitute (a) in the last term:

$$\frac{\partial}{\partial z}\left[\frac{1}{\rho}\frac{\partial P}{\partial R}\right] = -\frac{|g|}{\rho} \cdot \frac{\partial \rho}{\partial R} - \frac{1}{\rho}\frac{\partial P}{\partial R} \cdot \frac{1}{P}\frac{\partial P}{\partial z}$$

Substitute the ideal gas law in the first term on the RHS:

$$\frac{\partial}{\partial z}\left[\frac{1}{\rho}\frac{\partial P}{\partial R}\right] = -\frac{|g|}{\rho \cdot \Re} \cdot \frac{\partial (P \cdot T^{-1})}{\partial R} - \frac{1}{P}\frac{\partial P}{\partial R} \cdot \frac{1}{\rho}\frac{\partial P}{\partial z}$$

Use the chain rule on the first term on the right, and substitute the hydrostatic eq. in the last term:

$$\frac{\partial}{\partial z}\left[\frac{1}{\rho}\frac{\partial P}{\partial R}\right] = -\frac{P \cdot |g|}{\rho \cdot \Re} \cdot \frac{\partial (T^{-1})}{\partial R} - \frac{|g|}{\rho \cdot \Re \cdot T} \cdot \frac{\partial P}{\partial R} + \frac{|g|}{P}\frac{\partial P}{\partial R}$$

Substitute the ideal gas law in the 2nd term on the right:

$$\frac{\partial}{\partial z}\left[\frac{1}{\rho}\frac{\partial P}{\partial R}\right] = \frac{P \cdot |g|}{\rho \cdot \Re \cdot T^2} \cdot \frac{\partial T}{\partial R} - \frac{|g|}{P} \cdot \frac{\partial P}{\partial R} + \frac{|g|}{P}\frac{\partial P}{\partial R}$$

But the last two terms cancel. Using the ideal gas law in the remaining term leaves:

$$\frac{\partial}{\partial z}\left[\frac{1}{\rho}\frac{\partial P}{\partial R}\right] = \frac{|g|}{T} \cdot \frac{\partial T}{\partial R} \qquad \text{(c)}$$

(4) Completion:

Finally, equate (b) and (c):

$$\boxed{\left[\frac{2M_{\tan}}{R} + f_c\right] \cdot \frac{\partial M_{\tan}}{\partial z} = \frac{|g|}{T} \cdot \frac{\partial T}{\partial R}} \qquad (16.6)$$

which is the desired answer, when converted from derivatives to finite differences.

Science Graffito

"You should call it entropy [because] ... no one really knows what entropy really is, so in a debate you will always have the advantage." — *John von Neumann*.

Table 16-5. Example of thermodynamic states within a hurricane, corresponding to the points (Pt) circled in Fig. 16.30. Reference: T_o = 273 K, P_o = 100 kPa.

Pt	P (kPa)	T (°C)	T_d (°C)	r (g/kg)	s [J/(K·kg)]
1	100	28	–70	≈ 0	98
2	90	28	28	28	361
3	25	–18	–18	3.7	366
4	20	–83	–83	≈ 0	98

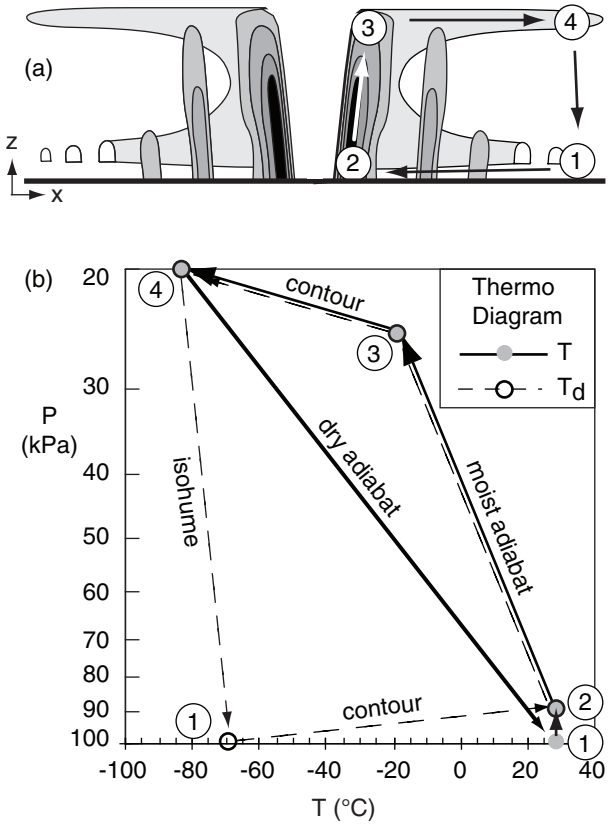

Figure 16.30
(a) Circulation of air through the hurricane. (b) Thermodynamic diagram showing hurricane processes for the same numbered locations as in (a). Solid lines show the temperature changes, dashed lines show dew point temperature changes.

where T is absolute temperature, and the overbar denotes an average over depth. Eqs. (16.5 & 16.6 are overly simplistic because they ignore nonhydrostatic and non-equilibrium effects.

Carnot-cycle Heat Engine

Hurricanes are analogous to **Carnot heat engines** in that they convert thermal energy into mechanical energy. One measure of the energy involved is the **total entropy** s per unit mass of air:

$$s = C_p \cdot \ln\left(\frac{T}{T_o}\right) + \frac{L_v \cdot r}{T} - \Re \cdot \ln\left(\frac{P}{P_o}\right) \qquad \bullet(16.7)$$

where C_p = 1004 J·kg^{-1}·K^{-1} is the specific heat of air at constant pressure, T is absolute temperature, L_v = 2500 J/$g_{\text{water vapor}}$ is the latent heat of vaporization, r is mixing ratio, $\Re$ = 287 J·kg^{-1}·K^{-1} is the gas-law constant, P is pressure. T_o = 273 K and P_o = 100 kPa are arbitrary reference values.

A thermo diagram is used to illustrate hurricane thermodynamics (Fig. 16.30). Because of limitations in range and accuracy of thermo diagrams, you might find slightly different answers than those given here in Table 16-5. For simplicity, assume constant sea surface temperature of T_{SST} = 28°C.

As an initial condition at Point 1 in Fig. 16.30, consider relatively warm (T = 28°C) dry air ($r \approx 0$, T_d = –70°C) in the boundary layer (z = 0; P = 100 kPa), but outside of the hurricane. Using eq. (16.7), the initial entropy is $s_1 \approx 98$ J·kg^{-1}·K^{-1}.

In the first part of the hurricane's Carnot cycle, air in the boundary layer spirals in from Point 1 toward the eye wall of the hurricane (Point 2) isothermally (T = 28°C, because of heat transfer with the sea surface) at constant height (z = 0 = sea level). Pressure decreases to P = 90 kPa as the air approaches the low-pressure eye. Evaporation from the sea surface increases the mixing ratio to saturation ($r \approx 28$ g/kg, $T_d \approx 28$°C), thereby causing entropy to increase to $s_2 \approx 361$ J·kg^{-1}·K^{-1}. This evaporation is the major source of energy for the storm.

From Point 2, air rises moist adiabatically to Point 3 in the thunderstorms of the eye wall. The moist-adiabatic process conserves entropy (s_3 = 366 J·kg^{-1}·K^{-1} , within the accuracy of the thermo diagram, thus $s_2 \approx s_3$). During this process, temperature drops to $T \approx$ –18°C and mixing ratio decreases to about $r \approx 3.7$ g/kg. However, the decrease of pressure (P = 90 to 25 kPa) in this rising air compensates to maintain nearly constant entropy.

Once the cloudy air reaches the top of the troposphere at Point 3, it flows outward to Point 4 at roughly constant altitude. (Sorry, the thermo diagrams at the end of the Stability chapter do not go

high enough to simulate a real hurricane of 15 km depth, so we will use $z \approx 10$ km here.) The divergence of air is driven by a pressure gradient of P = 25 kPa in the eye to 20 kPa outside the hurricane.

During this high-altitude outflow from Points 3 to 4, air rapidly loses heat due to infrared radiation, causing its temperature to decrease from $T = T_d$ = –18°C to – 83°C. The air remains saturated, and mixing ratio decreases from $r \approx 3.7$ to near 0. The cooling also converts more water vapor into precipitation. Entropy drops to 98 J·kg^{-1}·K^{-1}.

Finally, the air subsides dry adiabatically from Points 4 to 1, with no change of mixing ratio ($r \approx 0$; $T_d \approx$ –70°C). Temperature increases adiabatically to T = 28°C, due to compression as the air descends into higher pressure (P = 100 kPa). This dry adiabatic process also preserves entropy, and thus is called an **isentropic** process (and dry adiabats are also known as **isentropes**). The final state of the air is identical to the initial state, at Point 1 in Fig. 16.30.

This Carnot process is a closed cycle – the air can recirculate through the hurricane. However, during this cycle, entropy is gained near the sea surface where the temperature is warm, while it is lost near cloud top where temperatures are much colder.

The gain of entropy at one temperature and loss at a different temperature allows the Carnot engine to produce mechanical energy ME according to

$$ME = (T_B - T_{T.avg}) \cdot (s_{eyewall} - s_\infty)_B \qquad \bullet(16.8)$$

where subscripts B and T denote bottom and top of the troposphere, eyewall denotes boundary-layer air under the eye wall, and ∞ denotes the ambient conditions at large distances from the hurricane (e.g.: $P_\infty \approx 101.3$ kPa). This mechanical energy drives the hurricane-force winds, ocean waves, atmospheric waves, and mixing of both the atmospheric and ocean against buoyant forces.

If all of the mechanical energy were consumed trying to maintain the hurricane force winds against the frictional drag in the boundary layer (an unrealistic assumption), then the hurricane could support the following maximum pressure ratio at the surface:

$$\ln\left(\frac{P_\infty}{P_{eye}}\right)_B = \frac{ME}{T_B \cdot \Re} \qquad (16.9)$$

Solved Example

Suppose air in the eye of a hurricane has the following thermodynamic state: P = 70 kPa, r = 1 g/kg, T = 15°C. Find the entropy.

Solution

Given: P = 70 kPa, r = 1 g/kg, T = 288 K.

Find: s = ? J·kg^{-1}·K^{-1} .

Use eq. (16.7):

$$s = \left(1004 \frac{J}{kg_{air} \cdot K}\right) \cdot \ln\left(\frac{288K}{273K}\right) + \left(2500 \frac{J}{g_{water}}\right) \cdot \left(1 \frac{g_{water}}{kg_{air}}\right) \frac{1}{288K} - \left(287 \frac{J}{kg_{air} \cdot K}\right) \cdot \ln\left(\frac{70kPa}{100kPa}\right)$$

s = **165 J·kg^{-1}·K^{-1}**

Check: Units OK. Physics OK.

Discussion: The actual value of entropy is meaningless, because of the arbitrary constants T_o and P_o. However, the difference between two entropies is meaningful, because the arbitrary constants cancel out.

Solved Example

Find the mechanical energy and minimum possible eye pressure that can be supported by the hurricane of Table 16-5.

Solution

Given: $s_{eyewall}$ = 361 J·kg^{-1}·K^{-1}, s_∞ = 98 J·kg^{-1}·K^{-1}

T_B = 28°C, $T_{T\,avg} \approx$ 0.5·(–18–83) = –50.5°C.

Find: ME = ? kJ/kg, P_{eye} = ? kPa

Use eq. (16.8): ME = (28 + 50.5)(K)·(361–98)(J·kg^{-1}·K^{-1})

= **20.6 kJ/kg**

Use eq. (16.9):

$$\ln\left(\frac{P_\infty}{P_{eye}}\right)_B = \frac{(20,600 J \cdot kg^{-1})}{(301K) \cdot (287 J \cdot kg^{-1} \cdot K^{-1})} = 0.238$$

Solving for P_{eye} gives:

P_{eye} =(101.3kPa)/exp(0.238) = **79.8 kPa**.

Check: Units OK. Physics OK.

Discussion. This eye pressure is lower than the actual eye pressure of 90 kPa. The difference is related to the ME of winds and waves.

FOCUS • The Power of Hurricanes

Another measure of hurricane power is the rate of dissipation of kinetic energy by wind drag against the sea surface. This is proportional to the ABL wind speed cubed, times the sea-surface area over which that speed is valid, summed over all areas under the hurricane. K. A. Emanuel (1999, *Weather*, **54**, 107-108) estimates dissipation rates of 3 x 10^{12} W for a typical Atlantic hurricane (with max winds of 50 m/s at radius 30 km), and 3 x 10^{13} W for a Pacific typhoon (with max winds of 80 m/s at radius 50 km).

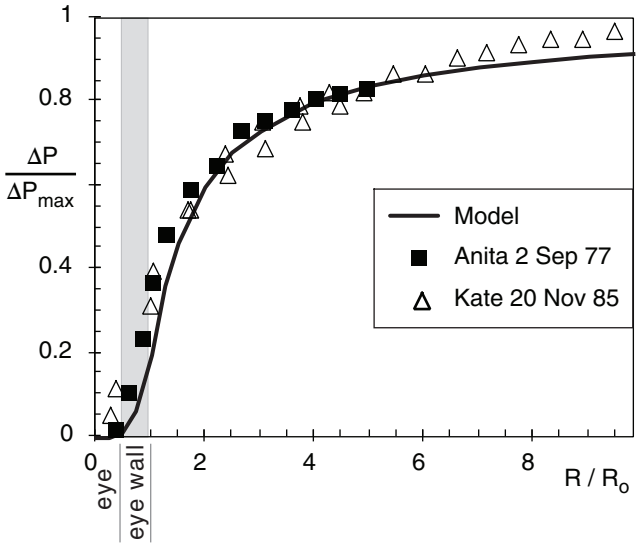

Figure 16.31
Surface pressure distribution across a hurricane. Model is eq. (16.11).

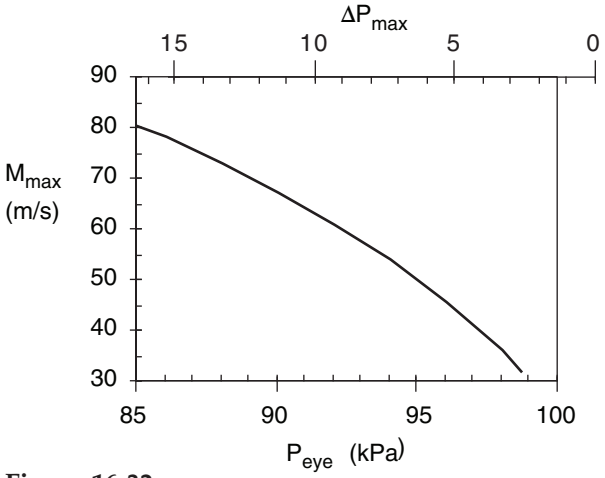

Figure 16.32
Maximum sustained winds around a hurricane increase as sea-level pressure in the eye decreases.

Solved Example

What max winds are expected if the hurricane eye has surface pressure of 95 kPa?

Solution

Given: $P_{B\,eye}$ = 95 kPa, Assume $P_{B\,\infty}$ = 101.3 kPa
Find: M_{max} = ? m/s.
Assume translation speed can be neglected.

Use eq. (16.12):
M_{max} = [20 (m/s)·kPa$^{-1/2}$]·(101.3–95kPa)$^{1/2}$ = **50 m/s**

Check: Units OK. Physics OK.
Discussion: This is a category 3 hurricane on the Saffir-Simpson Hurricane Wind Scale.

A HURRICANE MODEL

Although hurricanes are quite complex and not fully understood, we can build an idealized model that mimics some of the features of real hurricanes.

Pressure Distribution

Eye pressures of 95 to 99 kPa at sea level are common in hurricanes, although a pressure as low as P_{eye} = 87 kPa has been measured. One measure of hurricane strength is the pressure difference ΔP_{max} between the eye and the surrounding ambient environment P_∞ = 101.3 kPa:

$$\Delta P_{\max} = P_\infty - P_{eye} \tag{16.10}$$

The surface pressure distribution across a hurricane can be approximated by:

$$\frac{\Delta P}{\Delta P_{\max}} = \begin{cases} \frac{1}{5}\cdot\left(\frac{R}{R_o}\right)^4 & \text{for } R \le R_o \\ \left[1 - \frac{4}{5}\cdot\frac{R_o}{R}\right] & \text{for } R > R_o \end{cases} \tag{16.11}$$

where $\Delta P = P(R) - P_{eye}$, and R is the radial distance from the center of the eye. This pressure distribution is plotted in Fig 16.31, with data points from two hurricanes.

R_o is the critical radius where the maximum tangential winds are found. In the hurricane model presented here, R_o is twice the radius of the eye. Eyes range from 4 to 100 km in radius, with average values of 15 to 30 km radius. Thus, one anticipates average values of critical radius of: $30 < R_o < 60$ km, with an observed range of $8 < R_o < 200$ km.

Tangential Velocity

To be classified as a hurricane, the sustained winds (averaged over 1-minute) must be 33 m/s or greater near the surface. While most anemometers are unreliable at extreme wind speeds, maximum hurricane winds have been reported in the 75 to 95 m/s range.

As sea-level pressure in the eye decreases, maximum tangential surface winds M_{max} around the eye wall increase (Fig. 16.32). An empirical approximation for this relationship, based on **Bernoulli's equation** (see the Local Winds chapter), is :

$$M_{\max} = a\cdot(\Delta P_{\max})^{1/2} \tag{16.12}$$

where a = 20 (m/s)·kPa$^{-1/2}$.

If winds are assumed to be cyclostrophic (not the best assumption, because drag against the sea surface and Coriolis force are neglected), then the previous approximation for pressure distribution (eq. 16.11) can be used to give a distribution of tangential velocity M_{tan} (relative to the eye) in the boundary layer:

$$\frac{M_{\tan}}{M_{\max}} = \begin{cases} (R / R_o)^2 & \text{for } R \le R_o \\ (R_o / R)^{1/2} & \text{for } R > R_o \end{cases} \qquad (16.13)$$

where the maximum velocity occurs at critical radius R_o. This is plotted in Fig. 16.33, with data points from a few hurricanes.

For the hurricanes plotted in Fig. 16.33, the critical radius of maximum velocity was in the range of R_o = 20 to 30 km. This is a rough definition of the outside edge of the **eye wall** for these hurricanes, within which the heaviest precipitation falls. The maximum velocity for these storms was M_{max} = 45 to 65 m/s.

Winds in Fig. 16.33 are relative to the eye. However, the whole hurricane including the eye is often moving. Hurricane **translation** speeds (movement of the center of the storm) can be as slow as M_t = 0 to 5 m/s as they drift westward in the tropics, and as fast as 25 m/s as they later move poleward. Average translation speeds of the hurricane over the ocean are M_t = 10 to 15 m/s.

The <u>total</u> wind speed relative to the surface is the vector sum of the translation speed and the rotation speed. On the right quadrant of the storm relative to its direction of movement in the Northern Hemisphere, the translation speed adds to the rotation speed. Thus, hurricane winds are fastest in the hurricane's right quadrant (Fig. 16.34). On the left the translation speed subtracts from the tangential speed, so the fastest total speed in the left quadrant is not as strong as in the right quadrant (Fig. 16.35).

Total speed relative to the surface determines ocean wave and surge generation. Thus, the right quadrant of the storm near the eye wall is most dangerous. Also, tornadoes are likely there.

Radial Velocity

For an idealized hurricane, boundary-layer air is trapped below the top of the boundary layer as the air converges horizontally toward the eye wall. Horizontal continuity in cylindrical coordinates requires:

$$M_{rad} \cdot R = \text{constant} \qquad (16.14)$$

where M_{rad} is the radial velocity component, negative for inflow. Thus, starting from far outside the

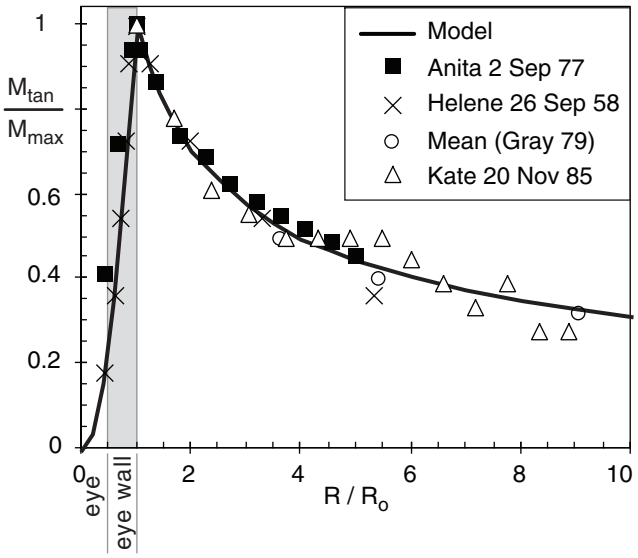

Figure 16.33
Tangential winds near the surface at various radii around hurricanes. Model is eq. (16.13).

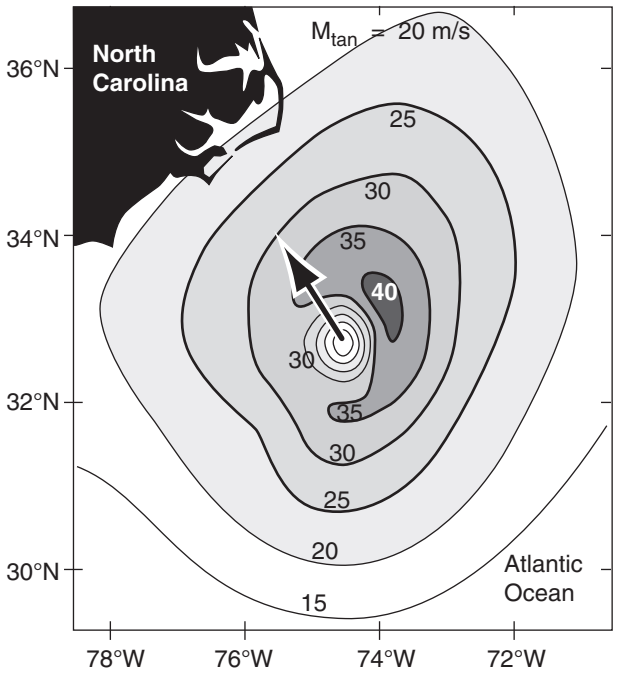

Figure 16.34
Max 1-minute <u>total</u> sustained surface winds (m/s) around Hurricane Isabel, 0730 UTC 18 Sep 2003. $M_{max\ total}$ = 42 m/s, and $P_{eye} \approx$ 95.7 kPa. Arrow shows translation toward 325° at 5.5 m/s. The Saffir-Simpson Hurricane Wind Scale is based on the fastest total sustained wind (rotational + translational) found anywhere in the hurricane.

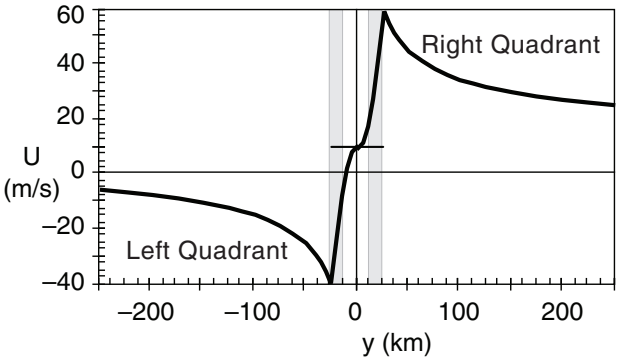

Figure 16.35
Sum of the modeled tangential winds relative to the eye and the translation speed (10 m/s) of the eye, for a hypothetical tropical cyclone. Assumes M_{max} = 50 m/s relative to the eye, R_o = 25 km, and uses a coordinate system with the x-axis aligned in the same direction as the translation vector.

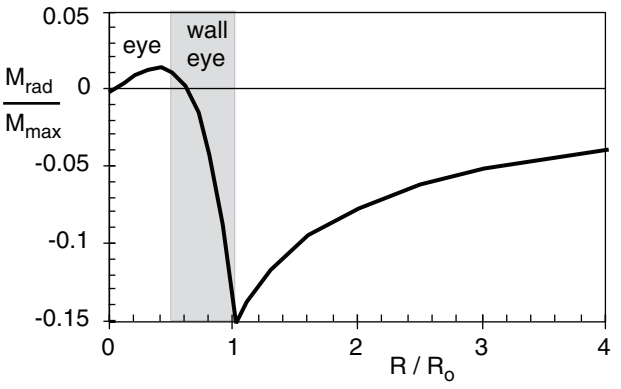

Figure 16.36
Radial winds in a hurricane boundary layer. (Negative values indicate motion inward, converging toward R/R_o = 0.)

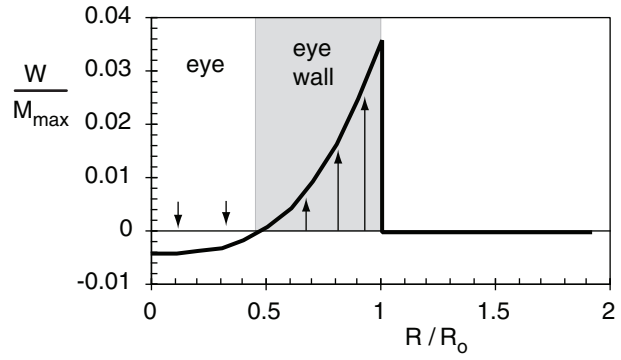

Figure 16.37
Vertical velocity at various radii around hurricanes, out of the top of the boundary layer. W_s = –0.2 m/s in the eye.

hurricane, as R decreases toward R_o, the magnitude of inflow must increase. Inside of R_o, thunderstorm convection removes air mass vertically, implying that horizontal continuity is no longer satisfied.

As wind velocities increase inward toward the eye wall from outside (see previous subsections), wave height and surface roughness also increase. The resulting turbulent drag against the ocean surface tends to couple the radial and tangential velocities, which we can approximate by $M_{rad} \propto M_{tan}{}^2$. Drag-induced inflow such as this eventually converges and forces ascent via the **boundary-layer pumping** process (see the Dynamics chapter).

The following equations utilize the concepts above, and are consistent with the tangential velocity in the previous subsection:

(16.15)

$$\frac{M_{rad}}{M_{\max}} = \begin{cases} -\frac{R}{R_o}\cdot\left[\frac{1}{5}\left(\frac{R}{R_o}\right)^3 + \frac{1}{2}\frac{W_s}{M_{\max}}\frac{R_o}{z_i}\right] & \text{for } R \le R_o \\ -\frac{R_o}{R}\cdot\left[\frac{1}{5} + \frac{1}{2}\cdot\frac{W_s}{M_{\max}}\cdot\frac{R_o}{z_i}\right] & \text{for } R > R_o \end{cases}$$

where W_s is negative, and represents the average subsidence velocity in the eye. Namely, the horizontal area of the eye, times W_s, gives the total kinematic mass flow downward in the eye. The boundary-layer depth is z_i, and M_{max} is still the maximum tangential velocity.

As an example, Fig. 16.36 shows a plot of the equations above, using z_i = 1 km, R_o = 25 km, M_{max} = 50 m/s, and W_s = –0.2 m/s. In the eye, subsidence causes air to weakly diverge (positive M_{rad}) toward the eye wall. Inside the eye wall, the radial velocity rapidly changes to inflow (negative M_{rad}), reaching an extreme value of –7.5 m/s for this example. Outside of the eye wall, the radial velocity smoothly decreases as required by horizontal mass continuity.

Vertical Velocity

At radii less than R_o, the converging air rapidly piles up, and rises out of the boundary layer as thunderstorm convection within the eye wall. The vertical velocity out of the top of the boundary layer, as found from mass continuity, is

(16.16)

$$\frac{W}{M_{\max}} = \begin{cases} \left[\frac{z_i}{R_o}\left(\frac{R}{R_o}\right)^3 + \frac{W_s}{M_{\max}}\right] & \text{for } R < R_o \\ 0 & \text{for } R > R_o \end{cases}$$

For simplicity, we are neglecting the upward motion that occurs in the spiral rain bands at $R > R_o$.

As before, W_s is negative for subsidence. Although subsidence acts only inside the eye for real hurricanes, the relationship above applies it every where inside of R_o for simplicity. Within the eye wall, the upward motion overpowers the subsidence, so our simplification is of little consequence.

Using the same values as for the previous figure, the vertical velocity is plotted in Fig. 16.37. The maximum upward velocity is 1.8 m/s in this case, which represents an average around the eye wall. Updrafts in individual thunderstorms can be much faster.

Subsidence in the eye is driven by the non-hydrostatic part of the pressure perturbation (Fig. 16.29). Namely, the pressure gradient (shown by the dashed line between X's in that Fig.) that pushes air upward is weaker than gravity pulling down. This net imbalance forces air downward in the eye.

Temperature

Suppose that pressure difference between the eye and surroundings at the top of the hurricane is equal and opposite to that at the bottom. From eq. (16.5) the temperature T averaged over the hurricane depth at any radius R is found from:

$$\Delta T(R) = c \cdot \left[\Delta P_{\max} - \Delta P(R) \right] \tag{16.17}$$

where c = 1.64 K/kPa, the pressure difference at the bottom is $\Delta P = P(R) - P_{eye}$, and the temperature difference averaged over the whole hurricane depth is $\Delta T(R) = T_{eye} - T(R)$. When used with eq. (16.11), the result is:

$$\frac{\Delta T}{\Delta T_{\max}} = \begin{cases} 1 - \frac{1}{5} \cdot \left(\frac{R}{R_o} \right)^4 & \text{for } R \le R_o \\ \frac{4}{5} \cdot \frac{R_o}{R} & \text{for } R > R_o \end{cases} \tag{16.18}$$

where $\Delta T_{max} = T_{eye} - T_\infty = c \cdot \Delta P_{max}$, and c = 1.64 K/kPa. This is plotted in Fig. 16.38.

Composite Picture

A coherent picture of hurricane structure can be presented by combining all of the idealized models described above. The result is sketched in Fig. 16.39. For real hurricanes, sharp cusps in the velocity distribution would not occur because of vigorous turbulent mixing in the regions of strong shear.

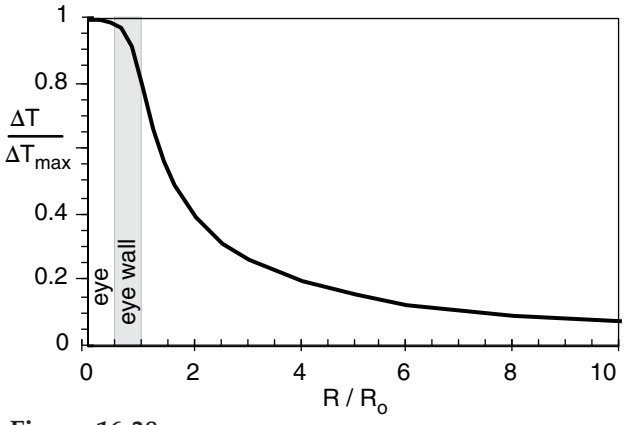

Figure 16.38
Temperature distribution, averaged over a 15 km thick hurricane, showing the warm core.

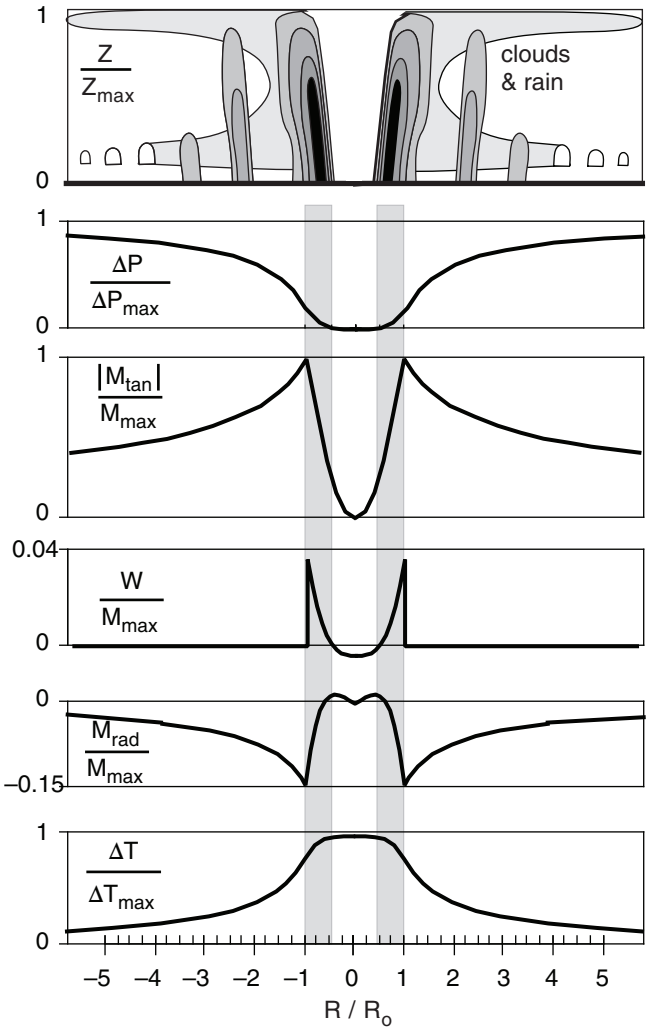

Figure 16.39
Composite hurricane structure based on the idealized model. Pressure differences are at sea level. All horizontal velocities are in the boundary layer, while vertical velocity is across the top of the boundary layer. Temperature differences are averaged over the whole hurricane depth. Grey vertical bands indicate eyewall locations.

Solved Example

A hurricane of critical radius R_o = 25 km has a central pressure of 90 kPa. Find the wind components, vertically-averaged temperature excess, and pressure at radius 40 km from the center. Assume W_s = –0.2 m/s in the eye, and z_i = 1 km.

Solution

Given: $P_{B\,eye}$ = 90 kPa, R_o = 25 km, R = 40 km, W_s = –0.2 m/s, and z_i = 1 km.
Find: P = ? kPa, T = ? °C, M_{tan} = ? m/s, M_{rad} = ? m/s, W = ? m/s
Assume $P_{B\,\infty}$ = 101.3 kPa
Figure: Similar to Fig. 16.39. Note that $R > R_o$.

First, find maximum values:

ΔP_{max} = (101.3 – 90kPa) = 11.3 kPa

Use eq. (16.12):

$M_{max} = [(20\text{m/s})\cdot\text{kPa}^{-1/2}]\cdot(11.3\text{kPa})^{1/2}$ = 67 m/s

$\Delta T_{max} = c\cdot\Delta P_{max}$=(1.64 K/kPa)·(11.3kPa) = 18.5°C

Use eq. (16.11):

$$\Delta P = (11.3\text{kPa})\cdot\left[1-\frac{4}{5}\cdot\frac{25\text{km}}{40\text{km}}\right] = 5.65\text{ kPa}$$

$P = P_{eye} + \Delta P$ = 90 kPa + 5.65 kPa = **95.65 kPa**.

(continues in next column)

Solved Example *(continuation)*

Use eq. (16.18):

$$\Delta T = (18.5°C)\cdot\frac{4}{5}\cdot\frac{(25\text{km})}{(40\text{km})} = \underline{\textbf{9.25°C}}$$

averaged over the whole hurricane depth.

Use eq. (16.13):

$$M_{\tan} = (67\text{m/s})\cdot\sqrt{\frac{25\text{km}}{40\text{km}}} = \underline{\textbf{53 m/s}}$$

Use eq. (16.15):

$$M_{rad} = -(67\text{m/s})\cdot\frac{(25\text{km})}{(40\text{km})}\cdot\left[\frac{1}{5}+\frac{1}{2}\cdot\frac{(-0.2\text{m/s})}{(67\text{m/s})}\cdot\frac{(25\text{km})}{(1\text{km})}\right]$$

M_{rad} = **–6.8 m/s**

Use eq. (16.16): W = **0 m/s**

Check: Units OK. Physics OK.
Discussion: Using P_{eye} in Table 16-7, the approximate Saffir-Simpson category of this hurricane is borderline between levels 4 and 5, and thus is very intense.

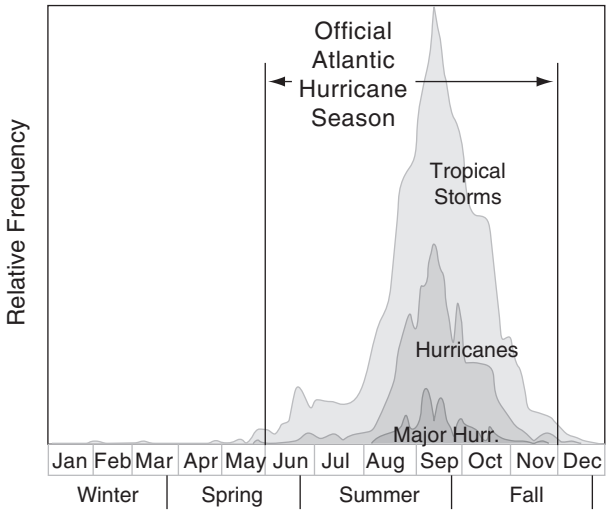

Figure 16.40
Relative frequency of Atlantic Tropical Storms, Hurricanes, and **Major Hurricanes** *(Saffir-Simpson categories 3 - 5).*

CLIMATOLOGY

Seasonality

Tropical cyclones are most frequent in late Summer and Fall of their respective hemisphere. This is because the sun has been highest in the sky, causing the top layers of the tropical ocean to accumulate the most heat. Fig. 16.40 shows the frequency of Atlantic Hurricanes. Table 16-6 shows periods of frequent tropical cyclones in all the ocean basins.

Table 16-6. Tropical Cyclone Seasons. Start and end dates are for the major portion of the storm season, but some storms occur outside the major season.

Location	Start	Peak	End
Atlantic	1 June	mid Sep	30 Nov
NE Pacific	15 May	late Aug /early Sep	30 Nov
NW Pacific*	July	late Aug /early Sep	Nov
N. Indian	Apr	2 peaks: Apr-Jun, & late Sep-early Dec	Dec
S Indian	Oct	2 peaks: mid-Jan, & mid Feb - early Mar	May
Australia & SW Pacific	Oct	late Feb /early Mar	May

** The NW Pacific has typhoons all year.*

Locations of Strongest Cyclones

The largest number of strongest tropical cyclones is in the northwestern Pacific. The reason is that the Pacific is a larger ocean with warmer sea-surface temperatures, allowing typhoons more opportunity to organize and strengthen. Activity ranges from 17 typhoons in a slow year (1998) to 35 in an active year (1971). Also, the larger **fetch** (distance that wind blows over the ocean) allows larger ocean waves, which can cause more destruction (and better surfing further from a Pacific typhoon).

The opposite extreme is the South Atlantic, which has had only 2 recorded hurricanes in the past century. One was Cyclone Catarina, which struck Brazil in March 2004. The other was a Tropical Storm that formed west of Congo in April 1991. There might have been other hurricanes in the South Atlantic that were not recorded historically.

There are two reasons for the dearth of hurricanes in the South Atlantic. One is the weaker and sometimes nonexistent ITCZ, which reduces hurricane triggering because of less convergence and less initial vorticity. The other is strong wind shear in the upper troposphere, which rips apart thunderstorm clusters before they can become hurricanes.

Natural Cycles & Changes in Activity

Atlantic hurricanes have a very large natural variability from year to year. For example, in the Atlantic there were only 4 hurricanes recorded in 1983, and 19 in 1994. An active hurricane year was 2005, with 14 hurricanes and 13 other tropical storms.

Hidden behind this large annual variability are longer-time-period variations of weaker amplitude, making them more difficult to detect and confirm. One is a **natural 40-year cycle** in Atlantic hurricane power (based on wind-speed cubed accumulated over the lifetime of all Atlantic hurricanes). This power was relatively high during the 1950s and 1960s, and was weaker during the 1970s, 1980s, and early 1990s. Since the late 1990s and 2000s the hurricane power has increased again.

Another is the **El Niño/La Niña**, which is an irregular 3 to 5 year cycle. During El Niño, there is a tendency for reduced tropical cyclone activity, and some displacement of these storms closer to the equator. The reason is that stronger west winds aloft during El Niño cause stronger wind shear across the troposphere, thereby inhibiting tropical cyclogenesis. Conversely, tropical cyclone activity is enhanced during La Niña.

Of concern these days is human-caused **global warming**. While most scientists suspect that there will be some effect on tropical cyclones if global warming continues, they have not yet found a clear signal. Debate continues.

HAZARDS

Human Population and Zoning

The most important factor causing increased deaths and destruction from tropical cyclones is the increase in **global population**. As population expands, more people live more densely in coastal areas threatened by tropical cyclones. Even if tropical-cyclone activity remains relatively constant, the human impact increases as population increases.

As more structures are built in vulnerable areas, so increase the property losses caused by hurricane destruction. It also becomes more difficult to evacuate people along inadequate transportation networks. As more people move from farms to cities, there is increased fatalities due to urban flooding caused by heavy tropical-cyclone rainfall.

In highly developed countries, an easy solution would be proper land-use **zoning**. Namely, governments should not let people live and work in threatened areas. Instead, these areas can be used for parks, floodable farmland, wildlife refuges, etc. However, zoning is a political activity that sometimes results in poor decisions in the face of pressure from real-estate developers who want to build more waterfront properties. An example of such a poor decision is the reconstruction of New Orleans, Louisiana, USA, at its original location after being destroyed by hurricane Katrina in 2005.

Also, people are unfortunately encouraged to live in threatened areas because of the existence of hurricane **insurance** and hurricane **disaster relief**. Namely, some individuals choose to make these poor decisions on where to live because they do not have to bear the full costs of reconstruction — instead the cost is borne by all taxpayers.

In less developed, highly populated, low-lying countries such as Bangladesh, an additional problem is an inadequate **warning** system. Even when tropical cyclone tracks are successfully predicted, sometimes the warning does not reach rural poor people, and often there is inadequate transportation to enable their evacuation. Bangladesh has suffered terribly from tropical cyclones: 400,000 deaths in Nov 1970, 140,000 deaths in Apr 1991, and 10,000 deaths in May 1985.

So these aspects of tropical-storm hazards are social (cultural, political, religious, etc.). Do not assume that all problems can be ameliorated by technical solutions (more dams; higher levies). Instead, some tough decisions need to be made on zoning, transportation, and population growth.

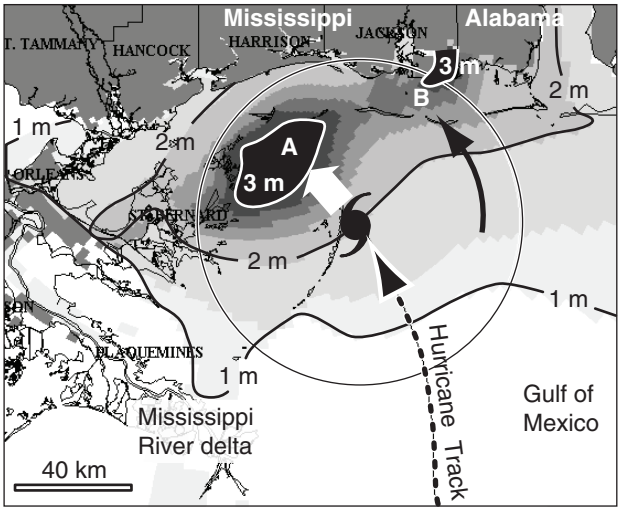

Figure 16.41
Simulated storm surge [rise (m) in sea level] associated with a hypothetical landfalling hurricane. (After NOAA/HRD).

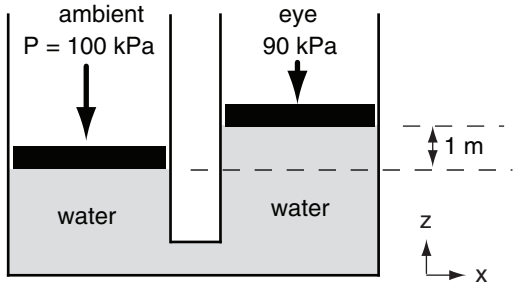

Figure 16.42
Reduced atmospheric pressure in the eye allows sea-level to rise.

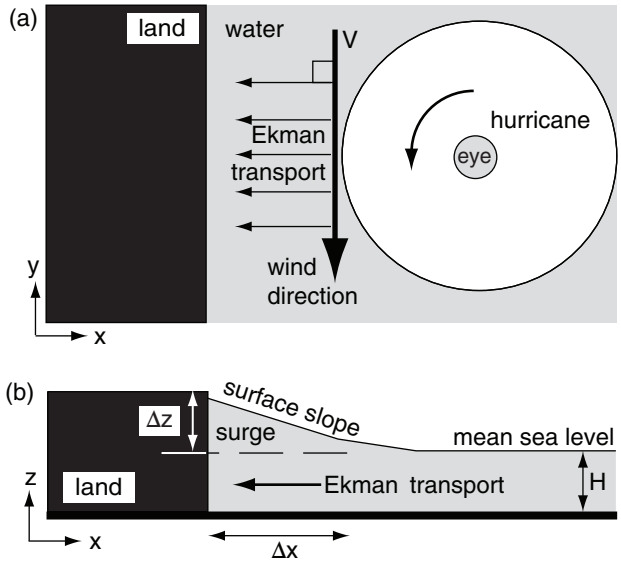

Figure 16.43
Onshore Ekman transport prior to hurricane landfall, in the Northern Hemisphere. (a) Top view. (b) View from south.

Storm Surge

Much of the hurricane-caused damage results from inundation of coastal areas by high seas (Fig. 16.41). The rise in sea level (i.e., the **storm surge**) is caused by the reduced atmospheric pressure in the eye, and by wind blowing the water against the coast to form a large propagating surge called a Kelvin wave. Table 16-7 gives typical storm-surge heights. High tides and high surface-waves can exacerbate the damage.

Atmospheric Pressure Head

In the eye of the hurricane, atmospheric surface pressure is lower than ambient. Hence the force per area pushing on the top of the water is less. This allows the water to rise in the eye until the additional head (weight of fluid above) of water compensates for the reduced head of air (Fig. 16.42).

The amount of rise Δz of water in the eye is

$$\Delta z = \frac{\Delta P_{\max}}{\rho_{liq} \cdot |g|} \qquad \bullet(16.19)$$

where $|g|$ is gravitational acceleration magnitude (9.8 m/s^2), ρ_{liq} = 1025 kg/m^3 is the density of sea water, and ΔP_{max} is the atmospheric surface pressure difference between the eye and the undisturbed environment.

To good approximation, this is

$$\Delta z \approx a \cdot \Delta P_{\max} \qquad (16.20)$$

where a = 0.1 m/kPa. Thus, in a strong hurricane with eye pressure of 90 kPa (causing $\Delta P_{max} \approx$ 10 kPa), the sea level would rise 1 m.

Ekman Transport

Recall from the Global Circulation chapter that ocean currents are generated by wind drag on the sea surface. The Ekman spiral describes how the current direction and speed varies with depth. The net **Ekman transport**, accumulated over all depths, is exactly perpendicular to the surface wind direction.

In the Northern Hemisphere, this net transport of water is to the right of the wind, and has magnitude:

$$\frac{Vol}{\Delta t \cdot \Delta y} = \frac{\rho_{air}}{\rho_{water}} \cdot \frac{C_D \cdot V^2}{f_c} \qquad (16.21)$$

where *Vol* is the volume of water transported during time interval Δt, Δy is a unit of length of coastline parallel to the mean wind, V is the wind speed near the surface (actually at 10 m above the surface), C_D is

the drag coefficient, f_c is the Coriolis parameter, ρ_{air} = 1.225 kg·m^{-3} is the air density at sea level, and ρ_{water} = 1025 kg·m^{-3} is sea-water density.

As a hurricane approaches the eastern coast of continents, the winds along the front edge of the hurricane are parallel to the coast, from north to south in the Northern Hemisphere. Hence, there is net Ekman transport of water directly toward the shore, where it begins to pile up and make a storm surge (Fig. 16.43).

If the hurricane were to hover just offshore for sufficient time to allow a steady-state condition to develop, then the Ekman transport toward the shore would be balanced by downslope sloshing of the surge. The surge slope $\Delta z/\Delta x$ for that hypothetical equilibrium is:

$$\frac{\Delta z}{\Delta x} \approx \frac{\rho_{air}}{\rho_{water}} \cdot \frac{C_D \cdot V^2}{|g| \cdot H} \qquad (16.22)$$

where H is the unperturbed ocean depth (e.g., 50 m) near the coast, and the other variables are the same as for eq. (16.21).

Kelvin Wave

Because the hurricane has finite size, Ekman transport is localized to the region immediately in front of the hurricane. Thus, water is piled higher between the hurricane and the coast than it is further north or south along the coast. When viewed from the East, the surge appears as a long-wavelength wave, called a **Kelvin wave** (Fig. 16.44).

The propagation speed of the wave, called the **phase speed** c, is

$$c = \sqrt{|g| \cdot H} \qquad \bullet(16.23)$$

which is also known as the **shallow-water wave speed**, where $|g|$ is gravitational acceleration magnitude and H is average water depth. Typical phase speeds are 15 to 30 m/s. These waves always travel with the coast to their right in the Northern Hemisphere, so they propagate southward along the east coast of continents, and northward along west coasts.

As the wave propagates south along the East Coast, it will hug the coast and inundate the shore immediately south of the hurricane. Meanwhile, Ekman transport continues to build the surge in the original location. The net result is a continuous surge of high water along the shore that is closest to, and south of, the hurricane. Typical surge depths can be 2 to 10 m at the coast, with extreme values of 13 to 20 m.

Table 16-7. Storm surge height S and sea-level pressure P_{eye}, from the old Saffir-Simpson classification. CAUTION: Actual storm-surge heights can vary significantly from these typical values. This is one of the reasons why the new Saffir-Simpson scale doesn't use S.

Category	P_{eye} (kPa)	S (m)
1	≥ 98.0	1.2 - 1.6
2	97.9 - 96.5	1.7 - 2.5
3	96.4 - 94.5	2.6 - 3.9
4	94.4 - 92.0	4.0 - 5.5
5	< 92.0	> 5.5

Solved Example

For hurricane-force winds of 40 m/s, over a continental shelf portion of ocean of depth 50 m, find the volume transport rate and equilibrium surge slope. Assume C_D = 0.01 .

Solution

Given: ρ_{air} = 1.225 kg·m^{-3} , ρ_{water} = 1025 kg·m^{-3}
M = 40 m/s, H = 50 m, C_D = 0.01
Find: $Vol/(\Delta t \cdot \Delta y)$ = ? m^2/s, and $\Delta z/\Delta x$ = ?
Assume: f_c = 0.00005 s^{-1}

Use eq. (16.21):

$$\frac{Vol}{\Delta t \cdot \Delta y} = \frac{(1.225 \text{kg/m}^3)}{(1025 \text{kg/m}^3)} \cdot \frac{(0.01) \cdot (40 \text{m/s})^2}{(0.00005 \text{s}^{-1})} = \underline{\mathbf{382\ m}}^2/\text{s}$$

Use eq. (16.22):

$$\frac{\Delta z}{\Delta x} \approx \frac{(1.225 \text{kg/m}^3)}{(1025 \text{kg/m}^3)} \cdot \frac{(0.01) \cdot (40 \text{m/s})^2}{(9.8 \text{m/s}^2) \cdot (50 \text{m})} = \underline{\mathbf{3.9x10}}^{-5}$$

Check: Units OK. Physics OK.
Discussion: The flow of water is tremendous. As it starts to pile up, the gradient of sea-level begins to drive water away from the surge, so it does not continue growing. The slope corresponds to 4 cm rise per km distance toward the shore. Over 10s to 100s km, the rise along the coast can be significant.

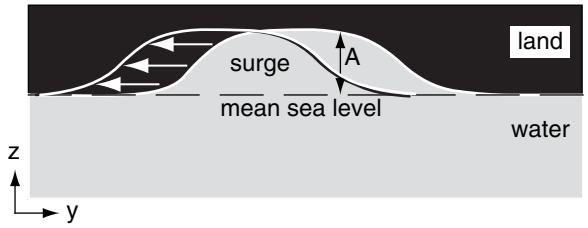

Figure 16.44
The surge, viewed from the east, is a Kelvin wave that propagates south.

Solved Example

Using info from the previous solved example, find the Kelvin wave phase speed, and the growth rate if the hurricane follows the wave southward.

Solution

Given: (same as previous example)
Find: c = ? m/s, $\Delta A/\Delta t$ = ? m/s

Use eq. (16.23):

$$c = \sqrt{(9.8\text{m/s}^2)\cdot(50\text{m})} = \underline{\mathbf{22.1\ m/s}}$$

Use eq. (16.24):

$$\frac{\Delta A}{\Delta t} \approx \frac{(1.225\text{kg/m}^3)}{(1025\text{kg/m}^3)} \cdot \frac{(0.01)\cdot(40\text{m/s})^2}{\sqrt{(9.8\text{m/s}^2)\cdot(50\text{m})}} = \underline{\mathbf{0.00086\ m/s}}$$

Check: Units OK. Physics OK.
Discussion: Luckily, hurricanes usually turn northward. If hurricanes were to translate southward with speed 22.1 m/s, matching the Kelvin wave speed, then an exceptionally dangerous situation would develop with amplification of the surge by over 3 m/hour.

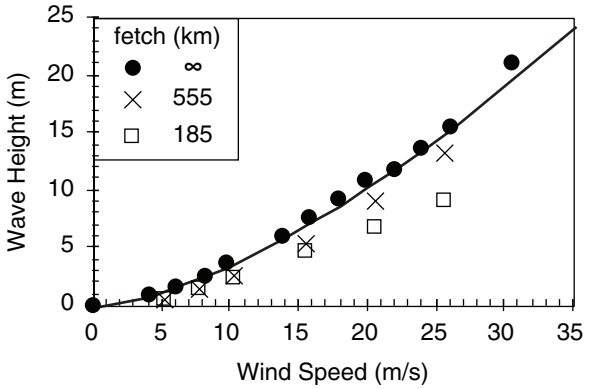

Figure 16.45
Wave height of surface wind-generated waves. Solid line is eq. (16.25) for unlimited fetch and duration. Data points are ocean observations with different fetch.

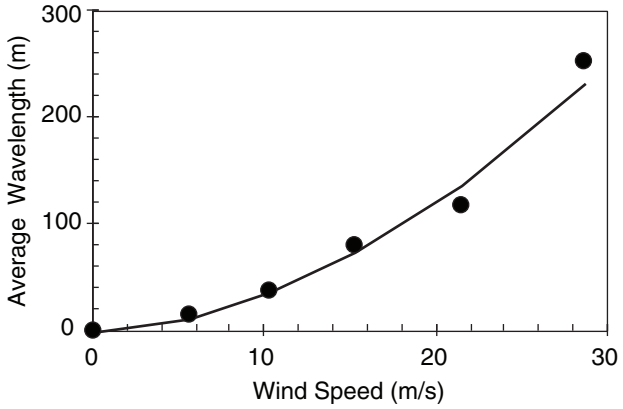

Figure 16.46
Wavelength of wind waves. Solid line is eq. (16.26).

Should the hurricane move southward at a speed nearly equal to the Kelvin wave speed, then Ekman pumping would continue to reinforce and build the surge, causing the amplitude of the wave A to grow according to:

$$\frac{\Delta A}{\Delta t} \approx \frac{\rho_{air}}{\rho_{water}} \cdot \frac{C_D \cdot V^2}{\sqrt{|g|\cdot H}} \qquad (16.24)$$

where the amplitude A is measured as maximum height of the surge above mean sea level, and the other variables are the same as for eq. (16.21).

Surface Wind-waves

Waves are generated on the sea surface by action of the winds. Greater winds acting over longer distances (called **fetch**) for greater time durations can excite higher waves. High waves caused by hurricane-force winds are not only a hazard to shipping, but can batter structures and homes along the coast.

Four coastal hazards of a hurricane are:

- wave scour of the beach under structures,
- wave battering of structures,
- surge flooding, and
- wind damage.

The first two hazards exist only right on the coast, in the beach area. Also, the surge rapidly diminishes by 10 to 15 km inland from the coast.

For wind speeds M up to hurricane force, the maximum-possible wave height (for unlimited fetch and duration) can be estimated from:

$$h = h_2 \cdot \left(\frac{M}{M_2}\right)^{3/2} \qquad (16.25)$$

where h_2 = 4 m and M_2 = 10 m/s. Wave heights are plotted in Fig. 16.45.

As winds increase beyond hurricane force, the wave tops become partially chopped off by the winds. Thus, wave height does not continue to increase according to eq. (16.25). For extreme winds of 70 m/s, the sea surface is somewhat flat, but poorly defined because of the mixture of spray, foam, and chaotic seas that appear greenish white during daytime.

Wavelengths of the wind-waves also increase with wind speed. Average wavelengths λ can be approximated by:

$$\lambda = \lambda_2 \left(\frac{M}{M_2}\right)^{1.8} \qquad (16.26)$$

where λ_2 = 35 m, and M_2 = 10 m/s. Wavelengths are plotted in Fig. 16.46.

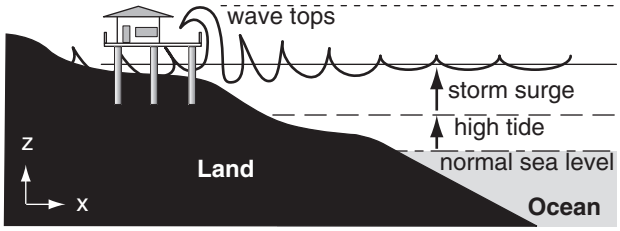

Figure 16.47
Tides, storm surge, and waves are additive.

The longest wavelength waves are called swell, and can propagate large distances, such as across whole oceans. Hence, a hurricane in the middle tropical Atlantic can cause large surf in Florida well before the storm reaches the coast.

Wind and waves as affect mariners are classified according to the Beaufort scale. The Focus Box with Table 16-8 gives an historical description of the Beaufort scale, and the modern description is in Table 16-9.

Tides, storm surges, and wind waves are additive (Fig. 16.47). Namely, if the storm surge and high waves happen to occur during high tide according to routine astronomic tide tables, then the coastal destruction is likely to be greatest.

For safety, houses at coasts threatened with storm surges and tsunami are usually built on top of concrete or steel piles. These piles are driven very deep into the land to survive wave scour and erosion of the land. While the floor deck is above expected storm-surge plus high tide levels in this figure, the waves can still batter and damage the structure.

Solved Example

Find the maximum possible wave height (assuming unlimited fetch) and wavelength for hurricane force winds of 35 m/s.

Solution

Given: $M = 35$ m/s

Find: $h = ?$ m, $\lambda = ?$ m

Use eq. (16.25):

$$h = (4\text{m}) \cdot \left(\frac{35\text{m/s}}{10\text{m/s}} \right)^{3/2} = \underline{\mathbf{26.2\ m}}$$

Use eq. (16.26):

$$\lambda = (35\text{m}) \cdot \left(\frac{35\text{m/s}}{10\text{m/s}} \right)^{1.8} = \underline{\mathbf{334\ m}}$$

Check: Units OK. Physics OK. Agrees with Figs.

Discussion: Wavelengths are much longer than wave heights. Thus, wave slopes are small — less that 1/10. Only when these waves reach shore does wave slope grow until the waves break as surf.

FOCUS • Beaufort Wind-Scale History

In 1805, Admiral Beaufort of the British Navy devised a system to estimate and report wind speeds based on the amount of canvas sail that a full-rigged frigate could carry. It was updated in 1874, as listed in Table 16-8 for historical interest. Modern descriptors for the Beaufort wind scale are in Table 16-9.

Table 16-8. Legend: B = Beaufort number; D = modern classification; M = wind speed in knots (2 knots ≈ 1 m/s), S1 = speed through smooth water of a well-conditioned man-of-war with all sail set, and clean full; S2 = sails that a well-conditioned man-of-war could just carry in chase, full and by; S3 = sails that a well-conditioned man-of-war could scarcely bear.

B	D	M (kt)	Deep Sea Criteria
0	Calm	0 - 1	S1 = Becalmed
1	Light Air	1 - 3	S1 = Just sufficient to give steerageway
2	Slight Breeze	4 - 6	S1 = 1 - 2 knots
3	Gentle Breeze	7 - 10	S1 = 3 - 4 knots
4	Moderate Breeze	11 - 16	S1 = 5 - 6 knots
5	Fresh Breeze	17 - 21	S2 = Royals, etc.
6	Strong Breeze	22 - 27	S2 = Topgallant sails
7	High Wind	28 - 33	S2 = Topsails, jib, etc.
8	Gale	34 - 40	S2 = Reefed upper topsails and courses
9	Strong Gale	41 - 48	S2 = Lower topsails and courses
10	Whole Gale	49 - 55	S3 = lower main topsail and reefed foresail
11	Storm	56 - 65	S3 = storm staysails
12	Hurricane	> 65	S3 = no canvas

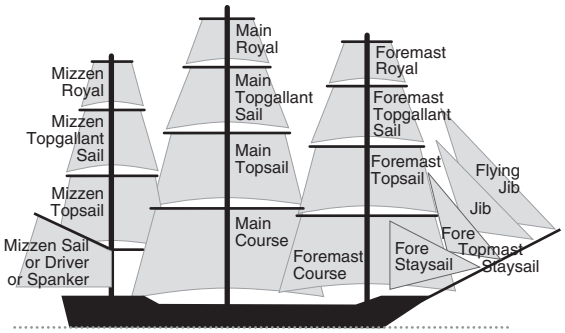

Figure 16.d. *Frigate sails.*

Table 16-9. Beaufort wind scale. B = Beaufort Number. (See Focus Box for historical info.)

B	Description	Wind Speed (km/h)	Wind Speed (m/s)	Wave Height (m)	Sea Conditions (in deep ocean)	Land Conditions
0	Calm	< 1	< 0.3	0	Flat.	Calm. Smoke rises vertically.
1	Light Air	1 - 5	0.3 - 1.5	0 -00.2	Ripples without crests.	Wind motion visible in smoke.
2	Light Breeze	6 - 11	1.5 - 3.3	0.2 - 0.5	Small wavelets. Crests of glassy appearance, not breaking.	Wind felt on exposed skin. Leaves rustle.
3	Gentle Breeze	12 - 19	3.3 - 5.5	0.5 - 1	Large wavelets. Crests begin to break; scattered whitecaps.	Leaves and smaller twigs in constant motion.
4	Moderate Breeze	20 - 28	5.5 - 8.0	1 - 2	Small waves with breaking crests. Fairly frequent white horses.	Dust and loose paper raised. Small branches begin to move.
5	Fresh Breeze	29 - 38	8.0 - 11	2 - 3	Moderate waves of some length. Many white horses. Small amounts of spray.	Branches of a moderate size move. Small trees begin to sway.
6	Strong Breeze	39 - 49	11 - 14	3 - 4	Long waves begin to form. White foam crests are very frequent. Some airborne spray is present.	Large branches in motion. Whistling heard in overhead wires. Umbrella use becomes difficult. Empty plastic garbage cans tip over.
7	High Wind, Moderate Gale, Near Gale	50 - 61	14 - 17	4 - 5.5	Sea heaps up. Some foam from breaking waves is blown into streaks along wind direction. Moderate amounts of airborne spray.	Whole trees in motion. Effort needed to walk against the wind. Swaying of skyscrapers may be felt, especially by people on upper floors.
8	Gale, Fresh Gale	62 - 74	17 - 20	5.5 - 7.5	Moderately high waves with breaking crests forming spindrift. Well-marked streaks of foam are blown along wind direction. Considerable airborne spray.	Some twigs broken from trees. Cars veer on road. Progress on foot is seriously impeded.
9	Strong Gale	75 - 88	21 - 24	7 - 10	High waves whose crests sometimes roll over. Dense foam is blown along wind direction. Large amounts of airborne spray may begin to reduce visibility.	Some branches break off trees, and some small trees blow over. Construction/temporary signs and barricades blow over. Damage to circus tents and canopies.
10	Storm, Whole Gale	89 - 102	25 - 28	9 - 12.5	Very high waves with overhanging crests. Large patches of foam from wave crests give the sea a white appearance. Considerable tumbling of waves with heavy impact. Large amounts of airborne spray reduce visibility.	Trees are broken off or uprooted, saplings bent and deformed. Poorly attached asphalt shingles and shingles in poor condition peel off roofs.
11	Violent Storm	103 - 117	29 - 32	11.5 - 16	Exceptionally high waves. Very large patches of foam, driven before the wind, cover much of the sea surface. Very large amounts of airborne spray severely reduce visibility.	Widespread vegetation damage. Many roofing surfaces are damaged; asphalt tiles that have curled up and/or fractured due to age may break away completely.
12	Hurricane	≥ 118	≥ 33	≥14	Huge waves. Sea is completely white with foam and spray. Air is filled with driving spray, greatly reducing visibility.	Very widespread damage to vegetation. Some windows may break; mobile homes and poorly constructed sheds and barns are damaged. Debris may be hurled about.

Inland Flooding

In developed countries such as the USA, storm-surge warning and evacuation systems are increasingly successful in saving lives of coastal dwellers. However, inland flooding due to heavy rain from decaying tropical storms is increasingly fatal — causing roughly 60% of the hurricane-related deaths in the USA during the past 30 years.

Streams and storm drains overflow, trapping people in cars and on roof tops. For this reason, people should not be complacent about former hurricanes reaching their inland homes, because these dying hurricanes contain so much tropical moisture that they can cause record-setting rainfalls.

The inland flooding hazard can affect people hundreds of kilometers from the coast. Of the 56 people who died in Hurricane Floyd (1999) in the eastern USA, 50 drowned in inland floods caused by heavy rains. Tropical storm Alberto dropped 53 cm of rain over Americus, Georgia, and 33 people drowned in 1994. Over 200 people drowned in Pennsylvania, New York, and New England from Hurricane Diane in 1955.

More recently, many unnecessary drowning deaths are caused by people driving into water of unknown depth covering the road. For people comfortable in driving their usual roads day after day, many find it hard to believe that their roads can become impassable. They unknowingly drive into deep water, causing the engine to stall and the car to stop in the middle of the water. If the water continues to rise, the car and passengers can be carried away. An easy solution is to approach each flooded road with caution, and be prepared to interrupt your journey and wait until the flood waters subside.

Thunderstorms, Lightning & Tornado Outbreaks

Because tropical cyclones are made of thunderstorms, they contain all the same hazards as thunderstorms. These include lightning, downbursts, gust fronts, downpours of rain, and tornadoes (see the Thunderstorm chapter for hazard details). Lightning is somewhat infrequent in the eyewall (about 12 cloud-to-ground strikes per hour), compared to about 1000 strikes per hour for midlatitude MCSs.

Hurricanes can cause **tornado outbreaks**. For example, Hurricanes Cindy and Katrina each spawned 44 tornadoes in the USA in 2005. Hurricane Rita spawned 101 tornadoes in Sep 2005. Hurricanes Frances and Ivan spawned 103 and 127 tornadoes, respectively, in Sep 2004.

Most tornadoes are weak (≤ EF2), and occur in the right front quadrant of tropical cyclones in the N. Hemisphere. Although some form near the eyewall, most tornadoes form in the thunderstorms of outer rain bands 80 to 480 km from the cyclone center.

HURRICANE FORECASTING

Prediction

The most important advance in tropical cyclone prediction is the weather satellite (see the Remote Sensing chapter). Satellite images can be studied to find and track tropical disturbances, depressions, storms, and cyclones. By examining loops of sequential images of tropical-cyclone position, their past track and present translation speed and direction can be determined. Satellites can be used to estimate rainfall intensity and storm-top altitudes.

Research aircraft (**hurricane hunters**) are usually sent into dangerous storms to measure pressure, wind speed, temperature, and other variables that are not easily detected by satellite. Also, they can fly transects through the middle of the tropical storm to precisely locate the eye (Fig. 16.48). The two organizations that do this for Atlantic Hurricanes are the US Air Force Reserves **53rd Reconnaissance Squadron**, and the Aircraft Operations Center of the US **National Oceanic and Atmospheric Administration** (**NOAA**).

Forecasting future tracks and intensity of tropical cyclones is more difficult, and has lots of error. Computer codes (called models) describing atmospheric physics and dynamics (see the Numerical Weather Prediction chapter) are run to forecast the

Figure 16.48
Photo inside the eye of Hurricane Rita on 21 Sep 2005, taken from a NOAA P3 aircraft. Rita was category 5 at max intensity. (Image courtesy of NOAA/AOC.)

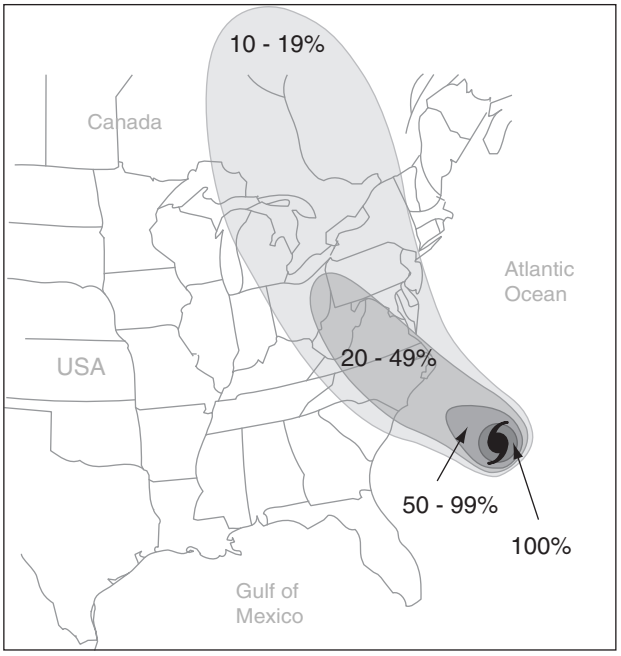

Figure 16.49
Probability forecast that the eye of Hurricane Isabel would pass within 120 km of any point on the map during the 72 h starting 1800 UTC on 17 Sep 2003. The actual location of the hurricane at this time is indicated with the hurricane map symbol.

weather. But different models yield different forecast tracks. So human forecasters consider all the NWP model forecasts, and issue probability forecasts (Fig. 16.49) on the likelihood that any tropical cyclone will strike different sections of coastline. Local government officials and emergency managers then make the difficult (and costly) decision on whether to evacuate any sections of coastline.

Predicting tropical cyclone intensity is even more difficult. Advances have been made based on sea-surface temperatures, atmospheric static stability, ambient wind shear, and other factors. Also, processes such as eyewall replacement and interaction with other tropical and extratropical systems are considered. But much more work needs to be done.

Different countries have their own organizations to issue forecasts. In the USA, the responsible organization is the **National Hurricane Center**, also known as the **Tropical Prediction Center**, a branch of NOAA. This center issues the following forecasts:

- **Tropical Storm Watch** - tropical storm conditions are possible within 36 h for specific coastal areas. (Includes tropical storms as well as the outer areas of tropical cyclones.)
- **Tropical Storm Warning** - tropical storm conditions are expected within 12 h or less for specific coastal areas. (Includes tropical storms as well as the outer areas of tropical cyclones.)
- **Hurricane Watch** - hurricane conditions are possible within 36 h for specific coastal areas.
- **Hurricane Warning** - hurricane conditions are expected within 24 h or less for specific coastal areas. Based on the worst of expected winds, high water, or waves.

In Canada, the responsible organization is the **Canadian Hurricane Center,** a branch of the **Meteorological Service of Canada**.

Safety

The US National Hurricane Center offers these recommendations for a Family Disaster Plan:

- Discuss the type of hazards that could affect your family. Know your home's vulnerability to storm surge, flooding and wind.
- Locate a safe room or the safest areas in your home for each hurricane hazard. In certain circumstances the safest areas may not be your home but could be elsewhere in your community.
- Determine escape routes from your home and places to meet. These should be measured in tens of miles rather than hundreds of miles.
- Have an out-of-state friend as a family contact, so all your family members have a single point of contact.
- Make a plan now for what to do with your pets if you need to evacuate.
- Post emergency telephone numbers by your phones and make sure your children know how and when to call 911.
- Check your insurance coverage — flood damage is not usually covered by homeowners insurance.
- Stock non-perishable emergency supplies and a Disaster Supply Kit.
- Use a NOAA weather radio. Remember to replace its battery every 6 months, as you do with your smoke detectors.
- Take First Aid, cardiopulmonary resuscitation (**CPR**) and disaster-preparedness classes.

If you live in a location that receives an evacuation order, it is important that you follow the instructions issued by the local authorities. Some highways are designated as evacuation routes, and traffic might be rerouted to utilize these favored routes. Get an early start, because the roads are increasingly congested due to population growth. Before you evacuate, be sure to board-up your home to protect it from weather and looters.

Many people who live near the coast have storm shutters permanently installed on their homes,

which they can close prior to hurricane arrival. For windows and storefronts too large for shutters, have large pieces of plywood on hand to screw over the windows.

If a hurricane overtakes you and you cannot escape, stay indoors away from windows. Street signs and corrugated metal roofs are often torn loose by hurricane-force winds. These fast-moving objects can slice through your body like a guillotine.

SUMMARY

Hurricanes are tropical cyclones. They have low-pressure centers, called eyes, and rotation is cyclonic (counterclockwise in the Northern Hemisphere) near the surface. The hurricane core is warm, which causes high pressure to form in the eye near the top of the storm. This high pressure drives diverging, anticyclonic winds out of the hurricane.

Tropical cyclones are born over tropical oceans with temperature ≥26.5°C over 50 m or more depth. Evaporation from the warm ocean into the windy boundary layer increases the energy in the storm, which ultimately drives its circulation similar to a Carnot-cycle heat engine. Hurricanes die over cold water and over land, not due to the extra drag caused by buildings and trees, but due mostly to the lack of strong evaporation from the ocean.

Because hurricanes are born in the trade-wind regions of the global circulation, they are initially blown westward. Many eventually reach the eastern shores of continents where the global circulation turns them poleward. At the equator there is no Coriolis force; hence there is no rotation available to be concentrated into hurricanes. Thus, hurricanes are most likely to form between 10° to 30° latitude during autumn.

Updrafts are strongest in the eye wall of thunderstorms encircling the clear eye. Rotation is initially gathered from the absolute angular momentum associated with the Earth's rotation. As the storm develops and gains speed, centrifugal force dominates over Coriolis force within about 100 km of the eye, causing winds that are nearly cyclostrophic in the bottom third of the troposphere. Simple analytical models can be built to mimic the velocities, temperature, and pressure across a hurricane.

While near the shore, hurricanes can cause damage due to storm-surge flooding, wind-wave battering, beach erosion, wind damage, heavy rain, tornadoes, and lightning. The surge is caused by Ekman transport of water toward shore, and by the reduced atmospheric pressure head.

Threads

Energy for hurricanes comes ultimately from the sun (Chapter 2), which heats the sea surface (Chapter 3). Evaporation of sea water into the boundary layer (Chapter 18) increases the humidity (Chapter 4). Latent heat release during condensation drives the atmosphere like a heat engine. This thermodynamic cycle can be described using a thermodynamic diagram (Chapter 5).

Some of this energy is realized as motions (Chapter 10) that drive the strong winds around the eye of the tropical cyclone. These warm-core cyclones are different from cold-core extratropical cyclones (Chapter 13). The relationship between the warm core temperature, the low pressure at the surface, and the high pressure aloft is described by the hypsometric equation (Chapter 1) and thermal wind effects (Chapter 11). Radial velocity is governed partly by boundary layer turbulence (Chapter 18) and surface drag, and vertical velocity can be described using the continuity equation (Chapter 10).

Once formed in the subtropics, hurricanes move toward the west in the trade winds of the global circulation (Chapter 11). Surrounding the hurricane eye is an eye wall of clouds (Chapter 6), heavy precipitation (Chapter 7), and strong thunderstorms (Chapters 14 and 15). Hurricane frequency of occurrence is modulated by the climate (Chapter 21), and is less frequent during El Niño events. Weather satellites and radar (Chapter 8) are invaluable in locating hurricanes

Science Graffito

In 1989, category 5 hurricane Hugo moved directly over the US. Virgin Islands in the Caribbean Sea. When the hurricane reached the island of St. Croix, it temporarily stopped its westward translation, allowing the intense eye wall to blast the island with violent winds for hours. The following is an eyewitness account.

"It had been many years since St. Croix was in the path of a major storm. Hurricane Hugo reached into the Lesser Antilles with a deliberate vengeance. St. Croix was somewhat prepared. Many hundreds of people had moved into schools and churches to take refuge. But no one was ready for what happened next. By 1800 hours winds were a steady 50 kts [25 m/s] with gusts up to 70 kts [35 m/s] from the northwest. I was on the top floor of the wooden Rectory at the St. Patrick's Church in Frederiksted with my husband and 8 month old son."

"By 2000 hours it was apparent that our comfortable room with a view was not going to provide a safe haven. The electricity had been out for some time and a very big gust from the north blew the air conditioner out of the window, landing at the foot of our bed. We evacuated with only one diaper change and bottle of baby juice, leaving behind the playpen, high chair, and bundles of accessories brought

(continues on next page)

Science Graffito

(continuation)

from home. We followed Fr. Mike down the wooden staircase. Drafts were everywhere and glass doors exploded just as we passed on our way to Fr. O'Connor's main living quarters on the first floor, where the walls were made of thick coral blocks."

"We settled in again in spite of the persistent crashing and banging against the heavy wooden shutters. We had to shout to hear each other across the room and our ears were popping. In the bathroom, the plumbing sounded like a raging sea. The water in the toilet bowl sloshed around and vibrated. Mercifully the baby slept."

"Soon the thick concrete walls and floors were vibrating accompanied by a hum that turned into the 'freight train howl'. The banging intensified and persisted for the next 4 hours. By 0100 hours we were tense and sweaty and wondering if it would ever end and if there was anything left outside. Fr. O'Connor was praying and feared that many people must be dead. He got up to open a closet door and a wall of water flowed into the bedroom. At that point we moved to the dining room with a group of 8 other people trapped in the rectory and waited."

"There was concern that the rest of the roof would go and it was decided we would make a run for the schoolhouse made of 2-foot [0.61 m] thick concrete walls. I held the baby in my arms and with flimsy flip-flops [sandals], just about skated across the cement courtyard dodging flying branches and sheets of galvanized aluminum. The window was opened for us as a big, old mahogany tree blocked the door."

"Shortly after, the eye was over us. The thick wooden shutters were flung open and about 100 people outside climbed in the window. The housing project nearby had been stripped of its north and east walls. The eye remained over us for 2 hours then the wind started up with the same intensity coming from the southwest. Only now the room was packed. Strangers were sharing the same mattresses. People slept in desks and chairs made for elementary children, and it was hot. Toddlers and infants wailed."

"There was no generator, only an occasional flashlight could be seen. Fears of [storm] surges were on everyone's' minds. We were only 200 meters from the west shoreline. Hugo had slowed down its eastward track to 4 mph [1.8 m/s] and the eye passed straight through the middle of the 23-mile [37 km] long island of St. Croix. It seems like the storm was in a fixed permanent position."

"When dawn broke, the winds still howled. By 0800 it was safe to open the windows and the landscape made me burst into tears. There was not a leaf left on a tree, there was not a tree left standing, just tangled branches lying sideways everywhere and not one blade of green grass. The wind had burned the ground and turned everything brown. The gray skies, light rain, and brown landscape persisted for several weeks."

"There were only 2 deaths reported but within weeks several dozen people died from heart attacks, strokes, electrocutions and other accidents associated with reconstruction. The majority of the island residents functioned without power for 3 to 6 months, using generators or candle power and gas stoves."

– Susan Krueger Allick, 1999

EXERCISES

Numerical Problems

N1. At 10° latitude, find the absolute angular momentum (m^2/s) associated with the following radii and tangential velocities:

	R (km)	M_{tan} (m/s)
a.	50	50
b.	100	30
c.	200	20
d.	500	5
e.	1000	0
f.	30	85
g.	75	40
h.	300	10

N2. If there is no rotation in the air at initial radius 500 km and latitude 10°, find the tangential velocity (m/s and km/h) at radii (km):

a. 450 b. 400 c. 350 d. 300
e. 250 f. 200 g. 150 h. 100

N3. Assume $\rho = 1$ kg/m^3, and latitude 20° Find the value of gradient wind (m/s and km/h) for:

	R (km)	$\Delta P/\Delta R$ (kPa/100 km)
a.	100	5
b.	75	8
c.	50	10
d.	25	15
e.	100	10
f.	75	10
g.	50	20
h.	25	25

However, if a gradient wind is not possible for those conditions, explain why.

N4. For the previous problem, find the value of cyclostrophic wind (m/s and km/h).

N5. Plot pressure vs. radial distance for the max pressure gradient that is admitted by gradient-wind theory at the top of a tropical cyclone for the latitudes (°) listed below. Use $z = 17$ km, $P_o = 8.8$ kPa.

a. 5 b. 7 c. 9 d. 11 e. 13 f. 17 g. 19
h. 21 i. 23 j. 25 k. 27 m. 29 n. 31 o. 33

N6. At sea level, the pressure in the eye is 93 kPa and that outside is 100 kPa. Find the corresponding pressure difference (kPa) at the top of the hurricane, assuming that the core (averaged over the hurricane depth) is warmer than surroundings by (°C):

a. 5 b. 2 c. 3 d. 4
e. 1 f. 7 g. 10 h. 15

N7. At radius 50 km the tangential velocity decreases from 35 m/s at the surface to 10 m/s at the altitude (km) given below:

a. 2 b. 4 c. 6 d. 8
e. 10 f. 12 g. 14 h. 16

Find the radial temperature gradient (°C/100km) in the hurricane. The latitude = 10°, and average temperature = 0°C.

N8. Find the total entropy ($J \cdot kg^{-1} \cdot K^{-1}$) for:

	P (kPa)	T (°C)	r (g/kg)
a.	100	26	22
b.	100	26	0.9
c.	90	26	24
d.	80	26	0.5
e.	100	30	25
f.	100	30	2.0
g.	90	30	28
h.	20	–36	0.2

N9. On a thermo diagram of the Stability chapter, plot the data points from Table 16-5. Discuss.

N10. Starting with saturated air at sea-level pressure of 90 kPa in the eye wall with temperature of 26°C, calculate (by equation or by thermo diagram) the thermodynamic state of that air parcel as it moves to:

a. 20 kPa moist adiabatically, and thence to
b. a point where the potential temperature is the same as that at 100 kPa at 26°C, but at the same height as in part (a). Thence to
c. 100 kPa dry adiabatically and conserving humidity. Thence to
d. Back to the initial state.
e to h: Same as a to d, but with initial T = 30°C.

N11. Given the data from Table 16-5, what would be the mechanical energy (J) available if the average temperature at the top of the hurricane were

a. –18 b. –25 c. –35 d. –45
e. –55 f. –65 g. –75 h. –83

N12. For the previous problem, find the minimum possible eye pressure (kPa) that could be supported.

N13. Use P_∞ = 100 kPa at the surface. What maximum tangential velocity (m/s and km/h) is expected for an eye pressure (kPa) of:

a. 86 b. 88 c. 90 d. 92
e. 94 f. 96 g. 98 h. 100

N14. For the previous problem, what are the peak velocity values (m/s and km/h) to the right and left of the storm track, if the hurricane translates with speed (m/s):

(i) 2 (ii) 4 (iii) 6 (iv) 8 (v) 10
(vi) 12 (vii) 14 (viii) 16 (ix) 18 (x) 20

N15. For radius (km) of:

a. 5 b. 10 c. 15 d. 20
e. 25 f. 30 g. 50 h. 100

find the hurricane-model values of pressure (kPa), temperature (°C), and wind components (m/s), given a pressure in the eye of 95 kPa, critical radius of R_o = 20 km, and W_s = –0.2 m/s. Assume the vertically-averaged temperature in the eye is 0°C.

N16. (§) For the previous problem, plot the radial profiles of those variables between radii of 0 to 200 km.

N17. Use P_∞ = 100 kPa at the surface. Find the pressure-head contribution to rise of sea level (m) in the eye of a hurricane with central pressure (kPa) of:

a. 86 b. 88 c. 90 d. 92
e. 94 f. 96 g. 98 h. 100

N18. Find the Ekman transport rate [$km^3/(h \cdot km)$] and surge slope (m/km) if winds (m/s) of:

a. 10 b. 20 c. 30 d. 40
e. 50 f. 60 g. 70 h. 80

in advance of a hurricane are blowing parallel to the shore, over an ocean of depth 50 m. Use C_D = 0.005 and assume a latitude of 30°.

N19. What is the Kelvin wave speed (m/s and km/h) in an ocean of depth (m):

a. 200 b. 150 c. 100 d. 80
e. 60 f. 40 g. 20 h. 10

N20. For the previous problem, find the growth rate of the Kelvin wave amplitude (m/h) if the hurricane tracks south parallel to shore at the same speed as the wave.

N21. Find the wind-wave height (m) and wavelength (m) expected for wind speeds (m/s) of:

a. 10 b. 15 c. 20 d. 25
e. 30 f. 40 g. 50 h. 60

N22. For the previous problem, give the:

(i) Beaufort wind category, and give a modern description of the conditions on land and sea
(ii) Saffir-Simpson Hurricane Wind category, its corresponding concise statement, and describe the damage expected.

Understanding & Critical Evaluation

U1. In Fig. 16.2, if the thin ring of darker shading represents heavy precipitation from the eyewall thunderstorms, what can you infer is happening in

most of the remainder of the image, where the shading is lighter grey? Justify your inference.

U2. Thunderstorm depths nearly equal their diameters. Explain why hurricane depths are much less than their diameters. (Hint, consider Fig. 16.3)

U3. If you could see movie loops of satellite images for the same storms shown in Figs. 16.1 and 16.4 in the Northern Hemisphere, would you expect these satellite loops to show the hurricane clouds to be rotating clockwise or counterclockwise? Why?

U4. Speculate on why hurricanes can have eyes, but mid-latitude supercell thunderstorms do not?

U5. If a hurricane with max sustained wind speed of 40 m/s contains tornadoes that do EF4 damage, what Saffir-Simpson Wind Scale category would you assign to it? Why?

U6. Why don't hurricanes or typhoons hit the Pacific Northwest coast of the USA and Canada?

U7. The focus box on Hurricane-induced Currents in the ocean shows how Ekman transport can lower sea level under a tropical cyclone. However, we usually associate rising sea level with tropical cyclones. Why?

U8. Consider Fig. 16.12. Should there also be a jet along the north edge of the hot Saharan air? If so, explain its characteristics. If not, explain why.

U9. Fig. 16.14a shows wind moving from east to west through an easterly wave. Fig. 16.14b shows the whole wave moving from east to west. Can both these figures be correct? Justify your answer.

U10. In the Extratropical Cyclone chapter, troughs were shown as southward meanders of the polar jet stream. However, in Fig. 16.14 the troughs are shown as northward meanders of the trade winds. Explain this difference. Hint, consider the Global Circulation.

U11. Compare and contrast a TUTT with mid-latitude cyclone dynamics as was discussed in the Extratropical Cyclone chapter.

U12. Consider Fig. 16.16. If a typhoon in the Southern Hemisphere was blown by the trade winds toward the Northern Hemisphere, explain what would happen to the hurricane as it approaches the equator, when it is over the equator, and when it reaches the Northern Hemisphere. Justify your reasoning.

U13. Fig. 16.17 suggests that a cold front can help create a tropical cyclone, while Fig. 16.23 suggests that a cold front will destroy a tropical cyclone. Which is correct? Justify your answer. If both are correct, then how would you decide on tropical cyclogenesis or cyclolysis?

U14. In the life cycle of tropical cyclones, Mesoscale Convective Systems (MCSs) are known to be one of the possible initial stages. But MCSs also occur over the USA, as was discussed in the Thunderstorm chapter. Explain why the MCSs over the USA don't become hurricanes.

U15. Based on the visible satellite image of Fig. 16.19, compare and contrast the appearance of the hurricane at (c) and the tropical storm at (d). Namely, what clues can you use from satellite images to help you decide if the storm has reached full hurricane strength, or is likely to be only a tropical storm?

U16. What are the other large cloud areas in Fig. 16.19 that were not identified in the caption? Hint, review the Remote Sensing chapter.

U17. The Bermuda High (or Azores High) as shown in Fig. 16.20 forms because the ocean is cooler than the surrounding continents. However, tropical cyclones form only when the sea-surface temperature is exceptionally warm. Explain this contradiction.

U18. If global warming allowed sea-surface temperatures to be warmer than 26.5°C as far north as 60°N, could Atlantic hurricanes reach Europe? Why?

U19. Could a tropical cyclone exist for more than a month? Explain.

U20. a. What is the relationship between angular momentum and vorticity?

b. Re-express eq. (16.1) as a function of vorticity.

U21. From the Dynamics chapter, recall the equation for the boundary-layer gradient wind. Does this equation apply to hurricane boundary layers? If so what are it's limitations and characteristics.

U22. The top of Fig. 16.24 shows weak low pressure in the eye surrounding by high pressure in the eyewall at the top of the storm. Explain why the storm cannot have high pressure also in the eye.

U23. Fig. 16.25 shows the wind vector M parallel to the acceleration vector F_{net}. Is that realistic? If not, sketch the likely vectors for M and F_{net}. Explain.

U24. The words "**supergradient winds**" means winds faster that the gradient wind speed. Are the outflow winds at the top of a tropical cyclone supergradient? Justify your answer.

U25.(§) Using relationships from Chapter 1, plot an environmental pressure profile vs. height across the troposphere assuming an average temperature of 273 K. Assume the environmental sea-level pressure is 100 kPa. On the same graph, plot the pressure profile for a warm hurricane core of average temperature (K): a. 280 b. 290 c. 300 assuming a sea-level pressure of 95 kPa. Discuss.

U26. Suppose that the pressure-difference magnitude between the eye and surroundings at the hurricane top is only half that at the surface. How would that change, if at all, the temperature model for the hurricane? Assume the sea-level pressure distribution is unaltered.

U27. Create a table that has a column listing attributes of mid-latitude cyclones, and another column listing attributes of tropical cyclones. Identify similarities and differences.

U28. The circles in Fig. 16.29 illustrate the hypsometric situation applied to the warm core of a tropical cyclone. Why cannot the hypsometric equation explain what drives subsidence in the eye?

U29. In Fig. 16.30b, why does the T_d line from Point 1 to Point 2 follow a contour that slopes upward to the right, even though the air parcel in Fig 16.30a is moving horizontally, staying near sea level?

U30. a. Re-express eq. (16.7) in terms of potential temperature.

b. Discuss the relationship between entropy and potential temperature.

U31. What factors might prevent a tropical cyclone from being perfectly efficient at extracting the maximum possible mechanical energy for any given thermodynamic state?

U32. For the hurricane model given in this chapter, describe how the pressure, tangential velocity, radial velocity, vertical velocity, and temperature distribution are consistent with each other, based on dynamic and thermodynamic relationships. If they are not consistent, quantify the source and magnitude of the discrepancy, and discuss the implications and limitations. Consider the idealizations of the figure below. (ABL = atmos. boundary layer.)

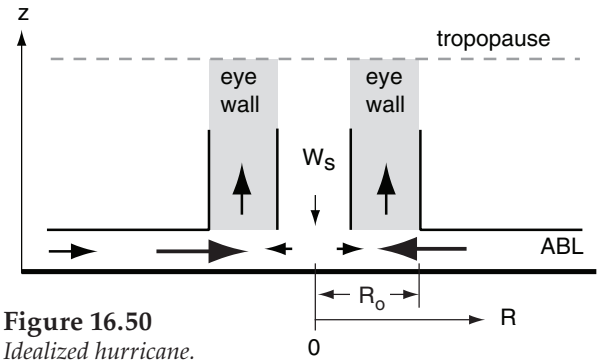

Figure 16.50
Idealized hurricane.

Hints: a. Use the cyclostrophic relationship to show that tangential velocity is consistent with the pressure distribution.

b. Use mass conservation for inflowing air trapped within the boundary layer to show how radial velocity should change with R, for $R > R_o$.

c. Assuming wave drag causes radial velocity to be proportional to tangential velocity squared, show that the radial velocity and tangential velocity equations are consistent. For $R < R_o$, use the following alternate relationship based on observations in hurricanes: $M_{tan}/M_{max} = (R/R_o)^2$.

d. Rising air entering the bottom of the eye wall comes from two sources, the radial inflow in the boundary layer from $R > R_o$, and from the subsiding air in the eye, which hits the ground and is forced to diverge horizontally in order to conserve mass. Combine these two sources of air to compute the average updraft velocity within the eye wall.

e. Use mass continuity in cylindrical coordinates to derive vertical velocity from radial velocity, for $R < R_o$. (Note, for $R > R_o$, it was already assumed in part (a) that air is trapped in the ABL, so there is zero vertical velocity there.)

f. Use the hypsometric relationship, along with the simplifications described in the temperature subsection of the hurricane model, to relate the radial temperature distribution (averaged over the whole hurricane depth) to the pressure distribution.

U33. An article by Willoughby and Black (1996: Hurricane Andrew in Florida: dynamics of a disaster, *Bull. Amer. Meteor. Soc.*, **77**, 543-549) shows tangential wind speed vs. radial distance.

a. For their Figs. 3b and 3d, compare their observations with the hurricane model in this chapter.

b. For their Figs. 3e - 3g, determine translation speed of the hurricane and how it varied with time as the storm struck Florida.

U34. To reduce fatalities from tropical cyclones, argue the pros and cons of employing better mitigation technology and the pros and cons of population control. Hint: Consider the whole world, including issues such as carrying capacity (i.e., the finiteness of

natural resources and energy), sustainability, politics and culture.

U35. In Fig. 16.41, one relative maximum (A) of storm-surge height is directly in front of the storm's path, while the other (B) is at the right front quadrant. Explain what effects could cause each of these surges, and explain which one might dominate further from shore while the other might dominate when the hurricane is closer to shore.

U36. Fig. 16.43 for a storm surge caused by Ekman transport is for a hurricane just off the east coast of a continent. Instead, suppose there was a hurricane-force cyclone just off the west coast of a continent at mid-latitudes.

a. Would there still be a storm surge caused by Ekman transport?

b. Which way would the resulting Kelvin wave move (north or south) along the west coast?

U37. Devise a mathematical relationship between the Saffir-Simpson Hurricane Wind scale, and the Beaufort wind scale.

Web-Enhanced Questions

W1. a. Search for satellite images and movies for a few recent tropical cyclones. Discuss similarities and differences of the hurricane appearance.

b. Same, but for radar images during landfall.

c. Same, but for photos from hurricane hunters.

W2. Search for web sites that show hurricane tracks for: a. the current hurricane season.

b. past hurricane seasons.

W3. What names will be used for tropical cyclones in the next tropical cyclone season, for the ocean basin assigned by your instructor?

W4. How many NWP models are available for forecasting hurricane track, & how are they used?

W5. What is the long range forecast for the number of tropical cyclones for the upcoming season, for an ocean basin assigned by your instructor. (Or, if the season is already in progress, how are actual numbers and intensities comparing to the forecast.)

W6. Find maps of "hurricane potential", "tropical cyclone energy", "intensity", or "sea-surface temperature". What are these products based on, and how are they used for hurricane forecasting?

W7. Search the web for photos and info on **hot convective towers**. How do they affect hurricanes?

Synthesis Questions

S1. What if the Earth rotated twice as fast. Describe changes to hurricane characteristics, if any.

S2. What if the average number of hurricanes tripled. How would the momentum, heat, and moisture transport by hurricanes change the global circulation, if at all?

S3. Some science fiction novels describe "supercanes" with supersonic wind speeds. Are these physically possible? Describe the dynamics and thermodynamics necessary to support such a storm in steady state, or use the same physics to show why they are not possible.

S4. Suppose the tropical tropopause was at 8 km altitude, instead of roughly 16 km altitude. How would hurricane characteristics change, if at all?

S5. What if the Earth's climate was such that the tropics were cold and the poles were hot, with sea surface temperature greater than 26°C reaching from the poles to 60° latitude. Describe changes to hurricane characteristics, if any.

S6. Suppose that the sea surface was perfectly smooth, regardless of the wind speed. How would hurricane characteristics change, if at all?

S7. Is it possible to have a hurricane without a warm core? Be aware that in the real atmosphere, there are hurricane-force cyclones a couple times a year over the northern Pacific Ocean, during winter.

S8. Suppose that the thermodynamics of hurricanes were such that air parcels, upon reaching the top of the eye wall clouds, do not loose any heat by IR cooling as they horizontally diverge away from the top of the hurricane. How would the Carnot cycle change, if at all, and how would that affect hurricane intensity?

S9. Is it possible for two tropical cyclones to merge into one? If so, explain the dynamics and thermodynamics involved. If so, is it likely that this could happen? Why?

Copyright © 2011, 2015 by Roland Stull. *Meteorology for Scientists and Engineers, 3rd Ed.*

LOCAL WINDS

CONTENTS

Wind Frequency 645
- Wind-speed Frequency 645
- Wind-direction Frequency 646

Wind-Turbine Power Generation 647

Thermally Driven Circulations 648
- Thermals 648
- Cross-valley Circulations 649
  - Anabatic Wind 649
  - Katabatic Wind 652
- Along-valley Winds 653
- Sea breeze 654

Open-Channel Hydraulics 657
- Wave Speed 658
- Froude Number - Part 1 659
- Conservation of Air Mass 660
- Hydraulic Jump 660

Gap Winds 661
- Basics 661
- Short-gap Winds 661
- Long-gap Winds 662

Coastally Trapped Low-level (Barrier) Jets 664

Mountain Waves 666
- Natural Wavelength 666
- Lenticular Clouds 666
- Froude Number - Part 2 667
- Mountain-wave Drag 668

Streamlines, Streaklines, and Trajectories 668

Bernoulli's Equation 669
- Principles 669
- Some Applications 672
  - Dynamic & Static Pressure & Temperature 672
  - Venturi Effect 674

Downslope Winds 675
- Bora 675
- Foehns and Chinooks 676

Canopy Flows 677
- Forests and Crops 677
- Cities 678

Summary 679

Exercises 680

"Meteorology for Scientists and Engineers, 3rd Edition" by Roland Stull is licensed under a Creative Commons Attribution-NonCommercial-ShareAlike 4.0 International License. To view a copy of the license, visit http://creativecommons.org/licenses/by-nc-sa/4.0/ . This work is available at http://www.eos.ubc.ca/books/Practical_Meteorology/ .

17 Each locale has a unique landscape that creates or modifies the wind. These local winds affect where we choose to live, how we build our buildings, what we can grow, and how we are able to travel.

During synoptic high pressure (i.e., fair weather), some winds are generated locally by temperature differences. These gentle circulations include thermals, anabatic/katabatic winds, and sea breezes.

During synoptically windy conditions, mountains can modify the winds. Examples are gap winds, boras, hydraulic jumps, foehns/chinooks, and mountain waves.

WIND FREQUENCY

Wind-speed Frequency

Wind speeds are rarely constant. At any one location, wind speeds might be strong only rarely during a year, moderate many hours, light even more hours, and calm less frequently (Fig. 17.1). The number of times that a range ΔM of wind speeds occurred in the past is the **frequency** of occurrence. Dividing the frequency by the total number of wind measurements gives a **relative frequency**. The expectation that this same relative frequency will occur in the future is the **probability** (*Pr*).

The probability distribution of mean wind speeds M is described by the **Weibull distribution**:

$$Pr = \frac{\alpha \cdot \Delta M \cdot M^{\alpha-1}}{M_o{}^{\alpha}} \cdot \exp\left[-\left(\frac{M}{M_o}\right)^{\alpha}\right] \qquad (17.1)$$

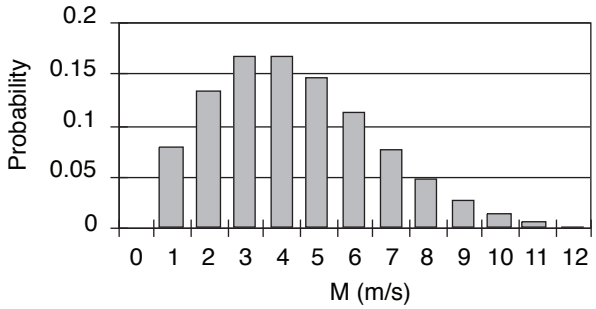

Figure 17.1
Wind-speed M probability (relative frequency) for a Weibull distribution with parameters $\alpha = 2$ *and* $M_o = 5$ *m/s.*

Solved Example

Given M_o = 5 m/s and α = 2, what is the probability that the wind speed will be between 5.5 and 6.5 m/s?

Solution

Given: M_o = 5 m/s, α = 2, ΔM = 6.5 – 5.5 m/s = 1 m/s, M= 6 m/s

Find: Pr = ? (dimensionless)

Use eq. (17.1):

$$Pr = \frac{2\cdot(1\text{m/s})\cdot(6\text{m/s})^{2-1}}{(5\text{m/s})^2}\cdot\exp\left[-\left(\frac{6\text{m/s}}{5\text{m/s}}\right)^2\right]$$

= 0.114 = **11.4%**

Check: Units OK. Physics OK.

Discussion: This agrees with Fig. 17.1 at M = 6 m/s, which had the same parameters as this example. To get a sum of probabilities that is very close to 100%, use a smaller bin size ΔM and be sure not to cut off the tail of the distribution at high wind speeds.

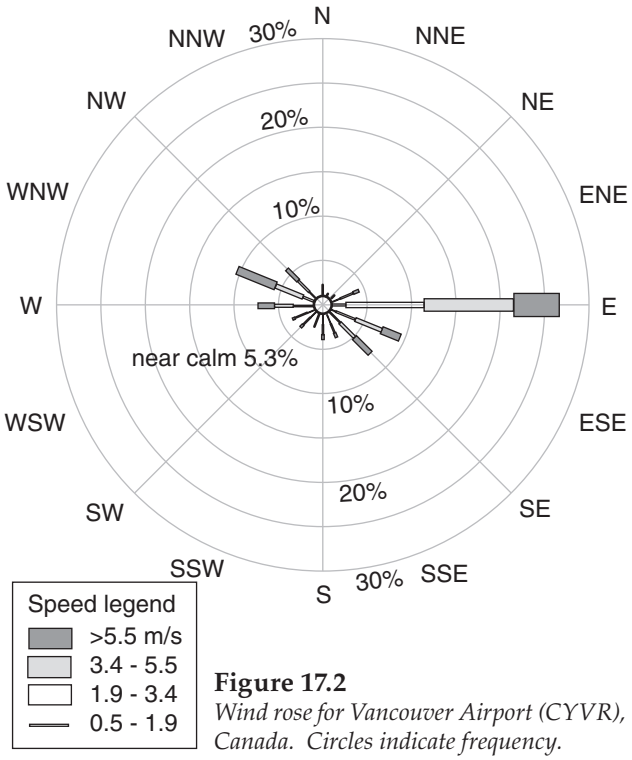

Figure 17.2
Wind rose for Vancouver Airport (CYVR), Canada. Circles indicate frequency.

Solved Example

How frequent are east winds at Vancouver airport?

Solution

Use Fig. 17.2. Frequency ≈ **26%** .

Discussion: This is the sum of 2% for 0.5 < M ≤ 1.9, plus 9% for 1.9 < M ≤ 3.4, plus 10% for 3.4 < M ≤ 5.5, plus 5% for M > 5.5 m/s.

where Pr is the probability (or relative frequency) of wind speed M± 0.5·ΔM. Such wind-speed variations are caused by synoptic, mesoscale, local and boundary-layer processes.

Location parameter M_o is proportional to the mean wind speed. For **spread parameter** α, smaller α causes wider spread of winds about the mean. Values of the parameters and the corresponding distribution shape vary from place to place.

The **bin size** or **resolution** is ΔM. For example, the column plotted in Fig. 17.1 for M = 3 m/s is the probability that the wind is between 2.5 and 3.5 m/s. The width of each column in the histogram is ΔM = 1 m/s. The sum of probabilities for all wind speeds should equal 1, meaning there is a 100% chance that the wind speed is between zero and infinity. Use this to check for errors. Eq. (17.1) is only approximate, so the sum of probabilities almost equals 1.

Use wind-speed distributions when estimating electrical-power generation by wind turbines, and when designing buildings and bridges to withstand extreme winds.

You can express extreme-wind likelihood as a **return period** (RP), which is equal to the total period of measurement divided by the number of times the wind exceeded a threshold. For example, if winds exceeding 30 m/s occurred twice during the last century, then the return period for 30 m/s winds is RP = (100 yr)/2 = 50 years. Faster winds occur less frequently, and have greater return periods.

Wind-direction Frequency

By counting the frequency of occurrence that winds came from each compass direction (N, NNE, NE, etc.) over a period such as 10 years, and then plotting that frequency on a polar graph, the result is called a **wind rose**. For example, Fig. 17.2 shows the wind rose for Vancouver Airport (CYVR).

The total length of each wind line gives the total frequency of any wind speed from that direction, while the width (or color) of the line subdivides that frequency into the portions associated with various wind speeds. (Not all wind roses are subdivided by wind speed.) The frequency of calm winds is usually written in the center of the circle if it fits, or is indicated off to the side. The sum of all the frequencies (including calm) should total 100%. At a glance, the longest lines indicate the predominant wind directions for any location.

For example, at Vancouver Airport, East (E) winds (winds from the east) are most frequent, followed by winds from the WNW and then from the ESE. Aircraft take-offs and landings are safer — and require shorter distances — if they are done into the wind. Hence, airports are built with their runways aligned parallel to the predominant wind directions (within

reason, as dictated by property boundaries and obstacles).

Fig. 17.3 shows that the runways at Vancouver Airport are appropriate for the wind climatology of the previous figure. The end of each runway is labeled with the magnetic compass direction (in tens of degrees; e.g., 12 means 120° magnetic) towards which the aircraft is flying when approaching that end of the runway from outside the airport. Thus, aircraft will use runway 30 for winds from 300°. Parallel runways are labeled as left (L) or right (R).

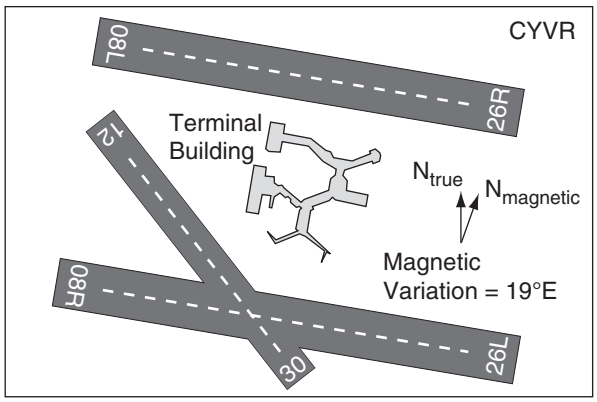

Figure 17.3
Plan view of runways at Vancouver International Airport (CYVR), Canada.

WIND-TURBINE POWER GENERATION

Kinetic energy of the wind is proportional to air mass times wind-speed squared. The rate at which this energy is blown through a wind turbine equals the wind speed. Thus, the theoretical power available from the wind is proportional to speed cubed:

$$Power = (\pi / 2) \cdot \rho \cdot E \cdot R^2 \cdot M_{in}{}^3 \qquad (17.2)$$

where R is the turbine-blade radius, M_{in} is incoming wind speed, and ρ is air density. Turbine efficiencies are E = 30% to 45%.

Faster winds and larger radii turbines allow greater power generation. Modern large wind turbines have a hub height (center of the turbine) of 80 m or more, to reach the faster winds higher above the surface. Turbines with radius of 30 m can generate up to 1.5 MW (mega Watts) of electricity, while blades of 40 m radius can generate up to 2.5 MW.

To see how a wind turbine works, consider Fig. 17.4 with an incoming wind speed M_{in}. Even before the wind reaches the disk swept out by the turbine blades, it feels the increased drag (higher pressure) from the turbine and begins to slow. It slows further while passing through the turbine (because the turbine is extracting energy from the wind), and slows more just behind the turbine due to the suction drag. Because the exit speed M_{out} is slower than the entrance speed, and because air-volume flow rate (= M · cross-section area) is conserved, the diameter of the air that feels the influence of the turbine must increase as wind speed decreases.

Zero exit speed is impossible, because the exited air would block subsequent in-flow, preventing power production. Also, if the exit speed equals the entrance speed, then power production is zero because no energy is extracted from the wind. Thus, wind turbines are designed to have an optimum wind-speed decrease of M_{out}/M_{in} = 1/3 (see Beyond Algebra box on **Betz' Law**). Albert Betz showed that the theoretical maximum turbine efficiency at

Solved Example

A wind turbine at sea level uses a 30 m radius blade to convert a 10 m/s wind into electrical power at 40% efficiency. What is the theoretical power output?

Solution

Given: ρ = 1.225 kg·m^{-3}, R= 30 m, M_{in} = 10 m/s, E = 0.4
Find: *Power* = ? kW (Appendix A defines Watt, W)

Use eq. (17.2):
Power = (π/2)·(1.225 kg·m^{-3})·(0.4)·(30m)^2·(10m/s)^3
= 6.93x10^5 kg·m^2·s^{-3} = **693 kW**

Check: Units OK. Physics OK.
Discussion: To estimate annual wind turbine power, use the Weibull distribution to find the power for each wind speed separately, and add all these power increments. Do not use the annual average wind speed.

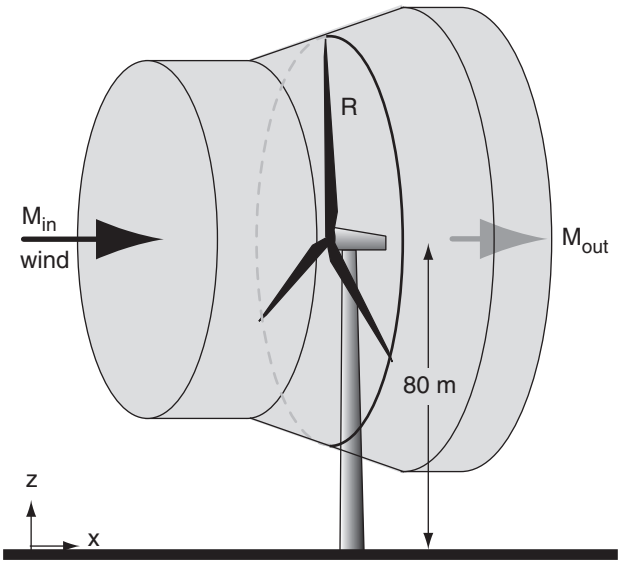

Figure 17.4
Wind turbine for electrical-power generation. Grey region shows the air that transfers some of its energy to the wind turbine.

BEYOND ALGEBRA • Betz' Law

In 1919 Albert Betz reasoned that the energy extracted by the turbine is the difference between incoming and outgoing kinetic energies:

$$Energy = 0.5 \cdot m \cdot M_{in}^2 - 0.5 \cdot m \cdot M_{out}^2 \quad (1)$$

where m is air mass and M is wind speed. The amount of air mass moving through the disk swept by the turbine during time interval Δt is the air density ρ times disk area ($A = \pi R^2$) times average speed:

$$m = \rho \cdot A \cdot 0.5(M_{in} + M_{out}) \cdot \Delta t \quad (2)$$

Plug this into the previous eq. and divide by Δt to get the power that the turbine can produce:

$$Power = 0.25 \cdot \rho \cdot A \cdot (M_{in} + M_{out}) \cdot (M_{in}^2 - M_{out}^2) \quad (3)$$

Divide this power by the power of the incoming wind $0.5 \cdot \rho \cdot A \cdot M_{in}^3$ to get a theoretical efficiency E_o:

$$E_o = (1/2) \cdot [1 - (M_{out}/M_{in})^2] \cdot [1 + (M_{out}/M_{in})] \quad (4)$$

Solve eq. (4) on a spreadsheet and plot E_o vs. M_{out}/M_{in} (see Fig. below) The peak in the curve gives

$$E_{max} = \underline{\mathbf{0.593}} \quad \text{at} \quad M_{out}/M_{in} = \underline{\mathbf{1/3}}.$$

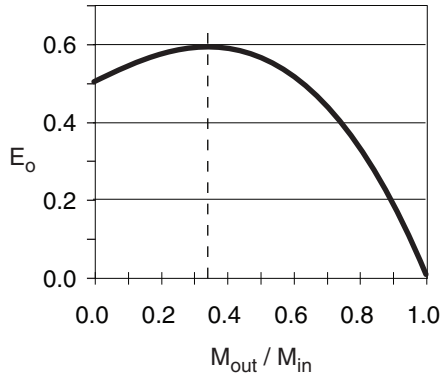

Fig. 17.a *Theoretical turbine efficiencies using Betz' Law.*

We can get the precise answer using calculus. Let the ratio of wind speeds be $r = M_{out}/M_{in}$, to simplify the notation. Use r in eq. (4):

$$E_o = (1/2) \cdot (1 - r^2) \cdot (1 + r) = (1/2) \cdot [1 + r - r^2 - r^3] \quad (5)$$

Differentiate E_o and set $dE_o/dr = 0$ to find the value of r at max E_o: $3r^2 + 2r - 1 = 0$ (6)

Solving this quadratic eq for r gives $r = 1/3$ and $r = -1$, for which the only physically reasonable answer is

$$r = M_{out}/M_{in} = \underline{\mathbf{1/3}} .$$

Finally, plug this r into eq. (5) to get the max E_o:

$$E_{max} = (1/2) \cdot [1 + (1/3) - (1/9) - (1/27)] \quad (7)$$

Using a common denominator of 27, we find

$$E_{max} = (1/2) \cdot [32/27] = 16/27 = 0.593 = \underline{\mathbf{59.3\%}}.$$

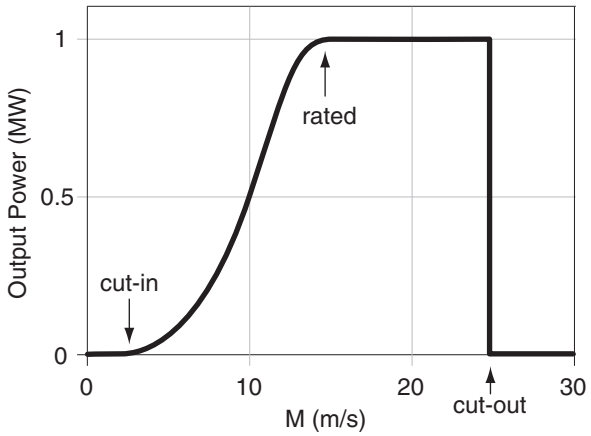

Figure 17.5
Typical power-output curve for a 1 MW wind turbine as a function of wind speed M.

this optimum speed is $E_{max} = 16/27 = 59.3\%$, which is known as **Betz' Limit**.

Wind turbines need a wind speed of at least 3 to 5 m/s to start turning. This is called the **cut-in** speed. As wind speed increases, so increases the amount of power generated. At its **rated** wind speed (8 to 15 m/s), the turbine is producing the maximum amount of electricity that the generators can handle. As wind speeds increase further, the aerodynamics of the blades are designed to change (via feathering the blades to reduce their pitch, or causing aerodynamic stalling) to keep the shaft rotation rate and electrical power generation nearly constant. Namely, the efficiency is intentionally reduced to protect the equipment. Finally, for wind speeds at or above a **cut-out** wind speed (25 - 30 m/s), turbine rotation is stopped to prevent damage. Fig. 17.5 shows the resulting idealized power output curve for a wind turbine.

THERMALLY DRIVEN CIRCULATIONS

Thermals

Thermals are warm updrafts of air, rising due to their buoyancy. Thermal diameters are nearly equal to their depth, z_i (Fig. 17.6).

A rising thermal feels drag against the surrounding environmental air (not against the ground). This drag is proportional to the square of the thermal updraft velocity relative to its environment. Neglecting advection and pressure deviations, the equation of vertical velocity W from the Dynamics chapter reduces to:

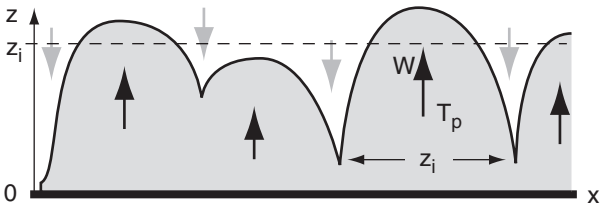

Figure 17.6
Thermals in a convective mixed layer of depth z_i. Black arrows show W updrafts in each thermal, and T_p is temperatue of the thermal. Grey arrows show free-atmosphere air being entrained down into the convective mixed layer between the thermals.

$$\frac{\Delta W}{\Delta t} = \frac{\theta_{vp} - \theta_{ve}}{\overline{T}_{ve}} \cdot |g| - C_w \frac{W^2}{z_i} \qquad (17.3)$$

tendency *buoyancy* *turb. drag*

where z_i is the mixed-layer (boundary-layer) depth, $C_w \approx 5$ is vertical drag coefficient, θ_v is virtual potential temperature, subscripts p and e indicate the air parcel (the thermal) and the environment, $\overline{T_{ve}}$ is average absolute virtual temperature of the environment, and $|g| = 9.8$ m·s^{-2} is gravitational acceleration.

At steady state, the acceleration is near zero ($\Delta W/\Delta t \approx 0$). Eq. (17.3) can be solved for the updraft speed of buoyant thermals (i.e., of warm air parcels):

$$W = \sqrt{\frac{|g| \cdot z_i}{C_w} \frac{(\theta_{vp} - \theta_{ve})}{\overline{T}_{ve}}} \qquad (17.4)$$

Thus, warmer thermals in deeper boundary layers have greater updraft speeds.

This equation also applies to deeper convection at the synoptic and mesoscales, such as weak updrafts in thunderstorms that rise to the top of the troposphere. For that case, z_i is the depth of the troposphere, and the temperature difference is that between the mid-cloud and the surrounding environment at the same height. For stronger updrafts and downdrafts in thunderstorms, the pressure deviation term of the equation of vertical motion must also be included (see the Thunderstorm chapters).

Cross-valley Circulations

(Circulations perpendicular to the valley axis.)

Anabatic Wind

During daytime in synoptically calm conditions (high-pressure center) with mostly clear skies, the sunlight heats mountain slopes. The warm mountain surface heats the neighboring air, which then rises. However, instead of rising vertically like thermals, the rising air hugs the slope as it rises. This warm turbulent air rising upslope is called an **anabatic**

Solved Example

Find the steady-state updraft speed in the middle of (a) a thermal in a boundary layer that is 1 km thick; and (b) a thunderstorm in a 11 km thick troposphere. The virtual temperature excess is 2°C for the thermal and 5°C for the thunderstorm, and $|g|/\overline{T_{ve}} = 0.0333$ m·s^{-2}·K^{-1} .

Solution

Given: $|g|/\overline{T_{ve}} = 0.0333$ m·s^{-2}·K^{-1} ,
(a) $z_i = 1000$ m, $T_{vp} - T_{ve} = 2$°C
(b) $z_i = 11{,}000$ m, $T_{vp} - T_{ve} = 5$°C,
Find: W = ? m/s

Use eq. (17.4): (a) For the thermal:

$$W = \sqrt{\frac{(0.0333\text{m}\cdot\text{s}^{-2}\text{K}^{-1})(1000\text{m})(2\text{K})}{5}} = \underline{\textbf{3.65 m/s}}$$

(b) For the thunderstorm:

$$W = \sqrt{\frac{(0.0333\text{m}\cdot\text{s}^{-2}\text{K}^{-1})(11000\text{m})(5\text{K})}{5}} = \underline{\textbf{19.1 m/s}}$$

Check: Units OK. Physics OK.

Discussion: Actually, neither thermal nor thunderstorm updrafts maintain a constant speed. However, this gives us an order-of-magnitude estimate. In convection, these updrafts must have downdrafts between them, but usually of larger diameter and slower speeds. Air-mass continuity requires that mass flow up must balance mass flow of air down, across any arbitrary horizontal plane. This would cause quite a bumpy ride in an airplane, which is why most aircraft pilots try to avoid areas of **convection** (regions filled with thermal or thunderstorm up- and downdrafts).

When I pilot a small plane, I try to stay above the atmospheric boundary layer for the whole flight (except take-off and landing) to have a smooth ride, and I avoid thunderstorms by flying around them.

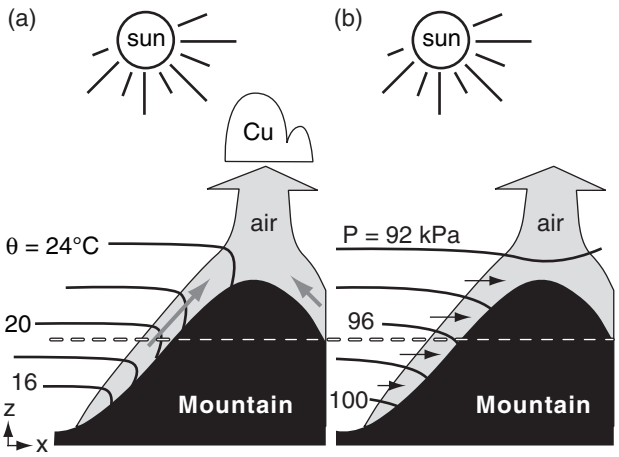

Figure 17.7
Anabatic winds (shaded grey). (a) Isentropes. (b) Isobars. Cu = cumulus cloud. θ = potential temperature. P = pressure.

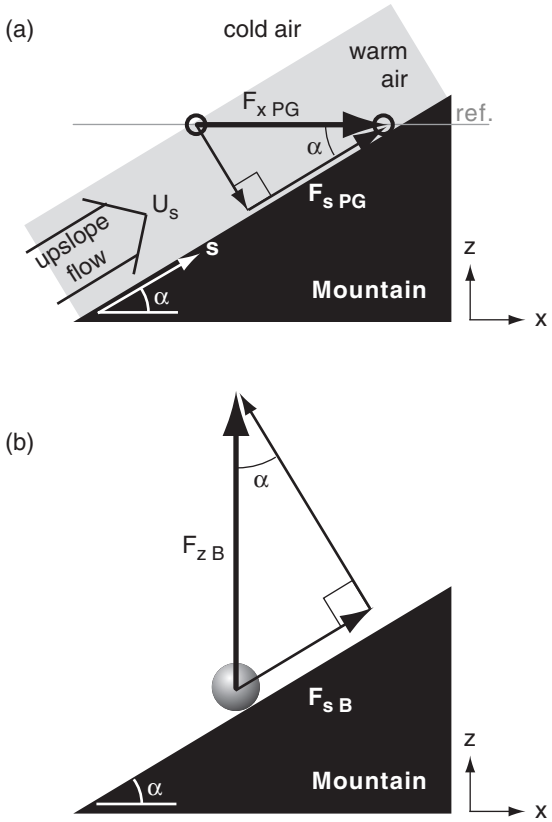

Figure 17.8
Geometry of anabatic (upslope) flows. F is force, subscript s is in the up-slope direction, subscript PG is pressure gradient, and subscript B is buoyancy. $F_{sB} = F_{sPG}$.

Solved Example

Anabatic flow is 5°C warmer than the ambient environment of 15°C. Find the horizontal and along-slope pressure-gradient forces/mass, for a 30° slope.

Solution

Given: T_e = 15°C + 273 = 288 K, ΔT = 5 K, $\alpha = 30°$
Find: (a) F_{xPG}/m = ? m·s^{-2}, (b) F_{sPG}/m = ? m·s^{-2}

$|g|\cdot\Delta T/T_e$ = (9.8m·s^{-2})·(5K)/(288K) = 0.17 m·s^{-2}

Use eq. (17.5):
$F_{x\,PG}/m$ = (0.17 m·s^{-2})·tan(30°) = **0.098 m·s**$^{-2}$

Use eq. (17.6):
$F_{s\,PG}/m$ = (0.17 m·s^{-2})·sin(30°) = **0.085 m·s**$^{-2}$

Check: Units OK, because m·s^{-2} = N/kg.
Discussion: Glider and hang-glider pilots use the anabatic updrafts to soar along mountain slopes and mountain tops.

wind (Fig. 17.7). Typical speeds are 3 to 5 m/s, and depths are hundreds of meters. The anabatic wind is the rising portion of a **cross-valley circulation**.

When the warm air reaches ridge top, it breaks away from the mountain and rises vertically, often joined by the updraft from the other side of the same mountain. Cumulus clouds called **anabatic clouds** can form just above ridge top in this updraft.

The dashed line in Fig. 17.7 is at a constant height above sea level. Following the line from left to right in Fig. 17.7a, potential temperatures of about 19°C are constant until reaching anabatic air near the mountain, where the potential temperature rises to about 21°C in this idealized illustration.

The temperature difference between the warmed air near the mountain and the cooler ambient air creates a small horizontal pressure gradient force (exaggerated in Fig. 17.7b) that holds the warm rising air against the mountain. To find this horizontal pressure-gradient force per unit mass m, use the hypsometric equation (see Focus box on next page):

$$\frac{F_{x\,PG}}{m} = -\frac{1}{\rho}\frac{\Delta P}{\Delta x} = |g|\frac{\Delta T}{T_e}\cdot\tan(\alpha) \qquad (17.5)$$

where Δx is horizontal distance (positive in the uphill direction), $|g| = 9.8$ m·s^{-2} is gravitational acceleration magnitude, $\Delta T = T_p - T_e$ is temperature difference between the air near and far from the slope, T_p is temperature of the warm near-mountain air, T_e is temperature of the cooler environmental air, and α is the mountain slope angle. Use absolute temperature in the denominator of the equation above.

The horizontal pressure difference across the anabatic flow is very small compared to the vertical pressure difference of air in hydrostatic balance. However, the horizontal pressure difference occurs across a short horizontal distance (tens of meters), yielding a modest pressure gradient that drives a measurable anabatic wind.

The portion of this pressure-gradient force in the along-slope direction (s) is $F_{s\,PG} = F_{x\,PG}\cdot\cos(\alpha)$, as can be seen from Fig. 17.8a. Combining this with the previous equation, and using the trigonometric identity $\tan(\alpha)\cdot\cos(\alpha) = \sin(\alpha)$, gives:

$$\frac{F_{s\,PG}}{m} = |g|\frac{\Delta T}{T_e}\cdot\sin(\alpha) \qquad (17.6)$$

But recall from the vertical equation of motion that the vertical buoyancy force is $F_{zB}/m = |g|\cdot(\Delta T/T_e)$. Thus, eq. (17.6) can also be interpreted as the component of vertical buoyancy force in the up-slope direction (s), as can be seen from Fig. 17.8b.

FOCUS • Anabatic Slope Flow

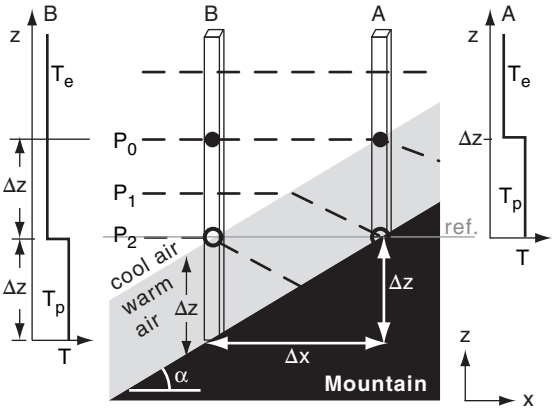

Fig. 17.b. *Dashed lines are isobars. Soundings at left and right correspond to columns of air B and A.*

Derivation of Horizontal Pressure Gradient

Consider an idealized situation of isothermal environmental air of temperature T_e and warmer near-mountain air (shaded grey) of temperature T_p with uniform vertical depth Δz, as sketched in Fig. 17.b. Consider two air columns: A and B. If a reference height *ref* is set at the base of column A (thin grey line), then place column B such that the same *ref* height is at the top of the warm-air layer.

For both columns A and B, start at the same pressure (P_o, at the solid black dots in Fig. 17.b). As you descend distance Δz, the pressure P increase depends on air temperature T, as given by the hypsometric equation (from Chapter 1):

$$\ln(P) = \ln(P_o) + \frac{\Delta z}{a \cdot T} \qquad (1)$$

where $a = \Re_d / |g| = 29.3$ m/K. Thus, the ln(P) increases linearly with decreasing altitude (Fig. 17.c).

In column B, the temperature is uniformly cool between the solid black dot and the reference height, so pressure increases rapidly as you descend (Fig. 17.c). However, in column A, the temperature is uniformly

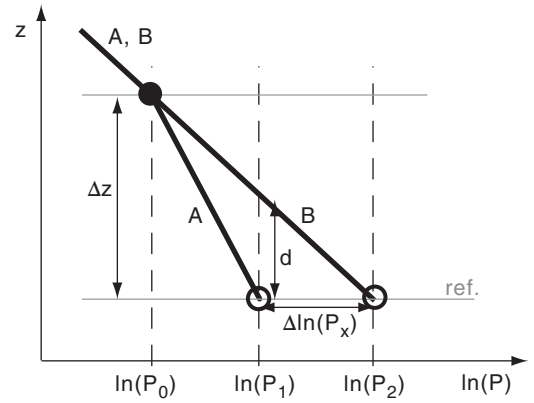

Fig. 17.c. *Change of pressure with height, as given by the hypsometric equation for cool air in column B and warm air in column A. (not to scale)*

(continues in next column)

FOCUS • Anabatic (continuation)

warmer, so the pressure doesn't increase as fast. By the time you have descended distance Δz from the black dot to the reference height, the pressure in the cold air has increased to P_2, but in the warm air has increased a smaller amount to P_1. Thus, at the reference height, there is a horizontal pressure difference $\Delta P = P_2 - P_1$ pointing toward the mountain slope.

To quantify this effect, start with the hypsometric equation, separately for columns A and B:

Col. B at ref.: $\ln(P_2) = \ln(P_o) + \Delta z/(a \cdot T_e)$

Col. A at ref: $\ln(P_1) = \ln(P_o) + \Delta z/(a \cdot T_p)$

where $a = \Re_d / |g| = 29.3$ m/K from Chapter 1. Subtract equation A from B

$$\ln(P_2) - \ln(P_1) = \frac{\Delta z}{a} \cdot \left(\frac{1}{T_e} - \frac{1}{T_p} \right)$$

Create a common denominator in the parentheses, and combine the ln() terms:

$$\ln\left(\frac{P_2}{P_1} \right) = \frac{\Delta z}{a} \cdot \left(\frac{T_p - T_e}{T_e \cdot T_p} \right)$$

Take the exponential of both sides, solve for P_1:

$$P_1 = P_2 \cdot \exp\left(-\frac{\Delta z}{a} \cdot \frac{\Delta T}{T_e^2} \right)$$

where $\Delta T = T_p - T_e$, and where $T_e^2 \approx T_e \cdot T_p$ because both are absolute temperatures. Next, subtract P_2 from both sides, and let $\Delta P = P_1 - P_2$ be the pressure change in the positive x-direction at the reference height:

$$\Delta P = -P_2 \cdot \left[1 - \exp\left(-\frac{\Delta z}{a} \cdot \frac{\Delta T}{T_e^2} \right) \right]$$

But $\exp(-y) \approx 1 - y + y^2/2 - \ldots$ Thus, the pressure decrease along the *ref.* height from B to A is

$$\Delta P \approx -P_B \cdot \left[\frac{\Delta z}{a} \cdot \frac{\Delta T}{T_e^2} \right] \qquad (2)$$

Expanding a and using the ideal gas law gives:

$$-\frac{\Delta P}{\rho} \approx |g| \cdot \Delta z \cdot \frac{\Delta T}{T_e}$$

Divide both sides by Δx to give the horizontal pressure-gradient force per unit mass $F_{x\,PG}/m$:

$$\boxed{\frac{F_{x\,PG}}{m} = -\frac{1}{\rho} \frac{\Delta P}{\Delta x} = |g| \cdot \frac{\Delta T}{T_e} \cdot \frac{\Delta z}{\Delta x}}$$

Substituting $\Delta z/\Delta x = \tan(\alpha)$ gives the desired eq. (17.5), where α is the mountain slope angle.

$$\frac{F_{x\,PG}}{m} = -\frac{1}{\rho} \frac{\Delta P}{\Delta x} = |g| \frac{\Delta T}{T_e} \cdot \tan(\alpha) \qquad (17.5)$$

Also, in Fig. 17.c, $d = z(P_{1\ at\ B}) - z(P_{1\ at\ A})$ is the deflection distance of the near-mountain end of isobar P_1 in Fig. 17.b.

Solved Example

For the scenario in the previous solved example, suppose a steady-state is reached where the only two forces are buoyancy and drag. Find the anabatic wind speed, assuming an anabatic flow depth of 50 m and drag coefficient of 0.05.

Solution

Given: buoyancy term = 0.085 $m \cdot s^{-2}$ from previous solved example. $C_D = 0.05$, $\Delta z = 50$m

Find: U_s = ? m/s

Solve eq. (17.7) for U_s, considering only buoyancy and drag terms:

$$U_s = [(\Delta z / C_D) \cdot \text{buoyancy term})\,]^{1/2}$$

$$= [\,((50\text{m})/(0.05)) \cdot (0.085\ m \cdot s^{-2})\,]^{1/2} = \underline{\mathbf{9.2\ m/s}}$$

Check: Units OK. Magnitude too large.

Discussion: In real anabatic flows, the temperature excess (5°C in this example) exists only close to the ground, and decreases to near zero by 50 to 100 m away from the mountain slope. If we had applied eq. (17.7) over the 5 m depth of the temperature excess, then a more-realistic answer of 2.9 m/s is found.

A better approach is to use the average temperature excess over the depth of the anabatic flow, not the maximum temperature excess measured close to the mountain slope.

Turbulence is strong during convective conditions such as during anabatic winds, which increases the turbulent drag against the ground.

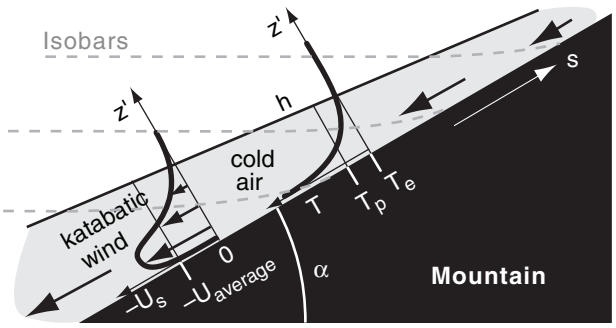

Figure 17.9

Katabatic winds (shaded light gray). Superimposed (thick black lines) are the along-slope wind-speed profile (U_s vs. z′) and temperature profile (T vs z′), where z′ is normal to the surface s. T_p is the average temperature in the katabatic-flow air, and T_e is the ambient environmental temperature just outside of the katabatic flow. The katabatic wind is indicated with the large arrows. Isobars (dashed grey lines) tilt upward in the cold air.

To forecast the speed of the upslope flow, apply the equation of horizontal motion to a sloping surface and use the approximation above:

$$\frac{\Delta U_s}{\Delta t} = -U_s \frac{\Delta U_s}{\Delta s} - V \frac{\Delta U_s}{\Delta y} + |g| \frac{\Delta \theta_v}{T_{ve}} \sin(\alpha) + f_c \cdot V - C_D \frac{U_s^{\,2}}{\Delta z} \qquad (17.7)$$

tendency advection buoyancy Coriolis drag

where U_s is along-slope (up- or down-slope) flow, V is across-slope flow, $\Delta\theta_v$ is virtual potential temperature difference between the slope-flow air and the environment (where $\Delta\theta_v = \Delta\theta = \Delta T$ for dry air), T_v is absolute virtual temperature, $f_c = 2\Omega \cdot \sin(latitude)$ is the Coriolis parameter, $2\Omega = 1.458423 \times 10^{-4}\ s^{-1}$, C_D is a drag coefficient against the ground, and Δz is the vertical depth of the slope flow.

Katabatic Wind

During anticyclonic conditions of calm or light synoptic-scale winds at night, air adjacent to a cold mountain slope can become colder than the surrounding air. This cold, dense air flows downhill under the influence of gravity (buoyancy), and is called a **katabatic wind** (Fig. 17.9). It can also form in the daytime over snow- or ice-covered slopes.

The katabatic wind is shallowest at the top of the slope, and increases in thickness and speed further downhill. Typical depths are 10 to 100 m, where the depth is roughly 5% of the vertical drop distance from the hill top. Typical speeds are 3 to 8 m/s. Katabatic flows are shallower and less turbulent than anabatic flows.

Equation (17.7) also applies for katabatic flows, but with negative $\Delta\theta_v$. A horizontal pressure gradient drives the katabatic wind, but with hydrostatic air pressure increasing near the slope due to the cold dense air. Namely, isobars bend upward near the mountain during katabatic flows (Fig. 17.9).

The virtual potential temperature in a katabatic flow is generally coldest at the ground, and smoothly increases with height (Fig. 17.9). For the difference $\Delta\theta_v = (\theta_{vp} - \theta_{ve})$, use the <u>average</u> temperature in the katabatic flow θ_{vp} minus the environmental temperature at the same altitude θ_{ve}.

If there were no friction against the surface, then the fastest downslope winds would be where the air is the coldest; namely, closest to the ground. However, winds closest to the ground are slowed due to turbulent drag, leaving a nose of fast winds just above ground level (Fig. 17.9).

In Antarctica where downslope distances are hundreds of kilometers, the katabatic wind speeds are 3 to 20 m/s with extreme cases up to 50 m/s, and durations are many days. These attributes are sufficiently large that Coriolis force turns the equilibrium wind direction 30 to 50° left of the fall line.

However, for most smaller valleys and slopes you can neglect Coriolis force and the *V*-wind, allowing eq. (17.7) to be solved for some steady-state situations, as shown next.

Initially the wind (averaged over the depth of the katabatic flow) is influenced mostly by buoyancy and advection. It accelerates with distance *s* downslope:

$$|U_{average}| = \left[\left| g \cdot \frac{\Delta\theta_v}{T_{ve}} \cdot s \cdot \sin(\alpha) \right| \right]^{1/2} \qquad (17.8)$$

where $|g|$ = 9.8 m·s^{-2}, T_{ve} is absolute temperature in the environment at the height of interest, α is the mountain slope angle, and *s* is distance downslope.

The average katabatic wind eventually approaches an equilibrium where drag balances buoyancy:

$$|U_{eq}| = \left[\left| g \cdot \frac{\Delta\theta_v}{T_{ve}} \cdot \frac{h}{C_D} \cdot \sin(\alpha) \right| \right]^{1/2} \qquad (17.9)$$

where C_D is the total drag against both the ground and against the slower air aloft, and *h* is depth of the katabatic flow.

Solved Example (§)

Air adjacent to a 10° slope averages 10°C cooler over its 20 m depth than the surrounding air of virtual temperature 10°C. Find and plot the wind speed vs. downslope distance, and the equilibrium speed. C_D = 0.005 .

Solution

Given: $\Delta\theta_v$= –10°C, T_{ve}=283 K, α= 10°, C_D= 0.005

Find: U (m/s) vs. x (km), where $s \approx x$.

Use eq. (17.9) to find final equilibrium value:

$$|U_{eq}| = \left[\left| \frac{(9.8\text{m}\cdot\text{s}^{-2})\cdot(-10°\text{C})}{283\text{K}} \cdot \frac{(20\text{m})}{0.005} \cdot \sin(10°) \right| \right]^{1/2}$$

$|U_{eq}|$ = **15.5 m/s**

Use eq. (17.8) for the initial variation.

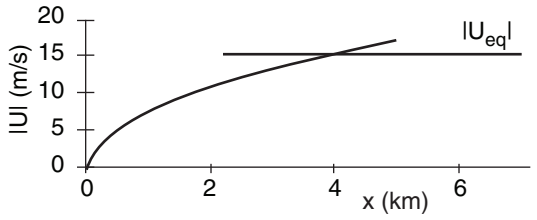

Check: Units OK. Physics OK.

Discussion: Although these two curves cross, the complete solution to eq. (17.7) smoothly transitions from the initial curve to the final equilibrium value.

Along-valley Winds

Katabatic and anabatic winds are part of larger circulations in the valley.

Night

At night, the katabatic winds from the bottom of the slopes drain into the valley, where they start to accumulate. This pool of cold air is often stratified like a layer cake, with the coldest air at the bottom and less-cold air on top. Katabatic winds that start higher on the slope often do not travel all the way to the valley bottom (Fig. 17.10). Instead, they either spread out at an altitude where they have the same buoyancy as the stratified pool in the valley, or they end in a turbulent eddy higher above the valley floor. This leads to a relatively mild **thermal belt** of air at the mid to upper portions of the valley walls — a good place for vineyards and orchards because of fewer frost days.

Meanwhile, the cold pool of air in the valley bottom flows along the valley axis in the same direction that a stream of water would flow. As this cold air drains out of the valley onto the lowlands, it is known as a **mountain wind**. This is part of an **along-valley circulation**. A weak return flow aloft (not drawn), called the **anti-mountain wind**, flows up-valley, and is the other part of this along-valley circulation.

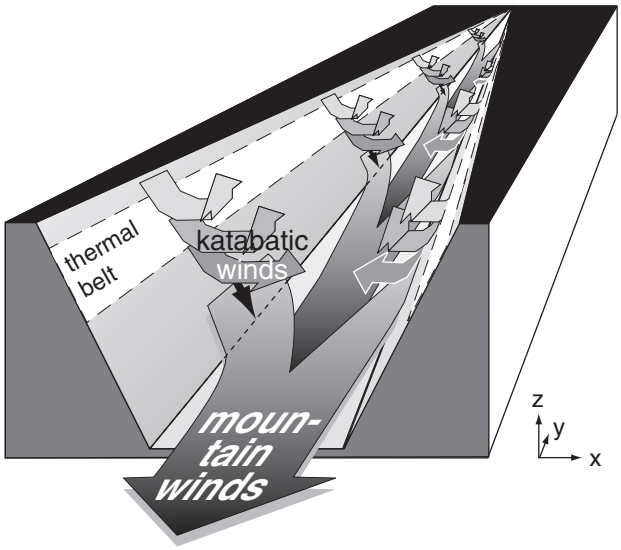

Figure 17.10
Katabatic winds are cross-valley flows that merge into the along-valley mountain winds draining down valley. Relatively warm air can exist in the "thermal belt" regions.

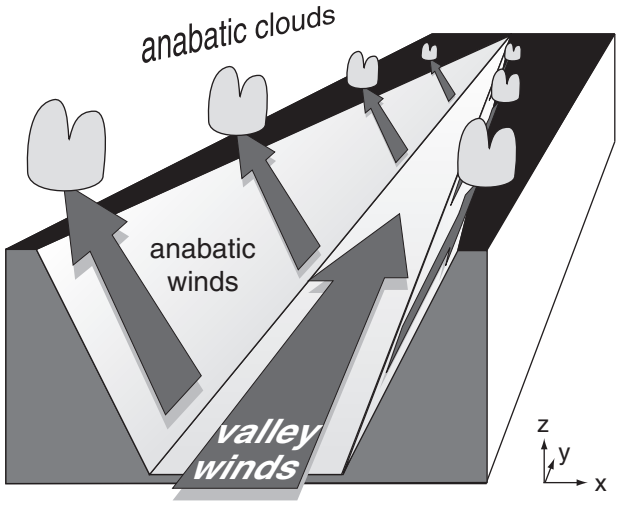

Figure 17.11
Anabatic winds are warm upslope flows that are resupplied with air by valley winds flowing upstream.

FOCUS • On Naming Local Winds

Local winds are often named by where they come from. Winds from the mountains are called mountain winds. Winds from the valley are called valley winds. A breeze from the sea is called a sea-breeze. The opposite is a land breeze.

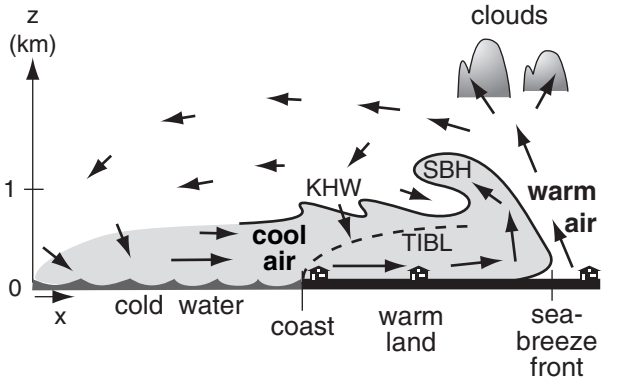

Figure 17.12
Vertical cross section through a sea-breeze circulation. KHW = Kelvin-Helmholtz waves. SBH = sea-breeze head. TIBL = thermal internal boundary layer.

Day

During anabatic conditions, there is often a weak **cross-valley horizontal circulation** (not drawn) from the tops of the anabatic updrafts back toward the center of the valley. Some of this air sinks (**subsides**) over the valley center, and helps trap air pollutants in the valley.

During daytime, the upslope anabatic winds along the valley walls remove air from the valley floor. This lowers the pressure very slightly near the valley floor, which creates a pressure gradient that draws in replacement air from lower in the valley. These upstream flowing winds are called **valley winds** (Fig. 17.11), and are part of an **along-valley circulation**. A weak return flow aloft (heading down valley; not drawn in Fig. 17.11) is called the **anti-valley wind**.

Transitions

Because the sun angle relative to the mountain slope determines the solar heating rate of that slope, the anabatic winds on one side of the valley are often stronger than on the other. At low sun angles near sunrise or sunset, the sunny side of the valley might have anabatic winds while the shady side might have katabatic winds.

Sea breeze

A **sea breeze** is a shallow cool wind that blows onshore (from sea to land) during daytime (Fig. 17.12). It occurs in large-scale high-pressure regions of weak or calm geostrophic wind under mostly clear skies. Similar flows called **lake breezes** form along lake shorelines, and **inland sea breezes** form along boundaries between adjacent land regions with different land-use characteristics (e.g., irrigated fields of crops adjacent to drier land with less vegetation).

The sea breeze is caused by a 5 °C or greater temperature difference between the sun-heated warm land and the cooler water. It is a surface manifestation of a thermally driven mesoscale circulation called the **sea-breeze circulation**, which often includes a weak return flow aloft from land to sea.

For warm air over land, the hypsometric equation states that hydrostatic pressure does not decrease as rapidly with increasing height as it does in the cooler air over the sea (Fig. 17.13). This creates a pressure gradient aloft between higher pressure over land and lower pressure over the sea, which initiates a wind aloft. This wind moves air molecules from over land to over sea, causing surface pressure over the warm land to decrease because fewer total molecules in the warm-air column cause less weight of air at the base of the column. Similarly, the surface pressure over the water increases due to mol-

ecules added to the cool-air column. This creates a pressure gradient near the surface that drives the bottom portion of the sea-breeze circulation. Such **hydrostatic thermal circulations** were explained in the Global Circulation chapter.

A **sea-breeze front** marks the leading edge of the advancing cool marine air and behaves similarly to a weak advancing cold front or a thunderstorm gust front. If the updraft ahead of the front is humid enough, a line of cumulus clouds can form along the front, which can grow into a line of thunderstorms if the atmosphere is convectively unstable.

The raised portion of cool air immediately behind the front, called the **sea-breeze head**, is analogous to the head at the leading edge of a gust front. The sea-breeze head is roughly twice as thick as the subsequent portion of the **feeder** cool onshore flow (which is 0.5 to 1 km thick). The top of the sea-breeze head often curls back in a large horizontal roll eddy over warmer air from aloft.

Vertical wind shear at the density interface between the low-level sea breeze and the return flow aloft can create **Kelvin-Helmholtz (KH) waves**. These breaking waves in the air have wavelength of 0.5 to 1 km. The KH waves increase turbulent drag on the sea breeze by entraining low-momentum air from above the interface. A slowly subsiding return flow occurs over water and completes the circulation as the air is again cooled as it blows landward over the cold water.

As the cool marine air flows over the land, a **thermal internal boundary layer** (**TIBL**) forms just above the ground (Fig. 17.12). The TIBL grows in depth z_i with the square root of distance x from the shore as the marine air is modified by the heat flux F_H (in kinematic units K·m/s) from the underlying warm ground:

$$z_i = \left[\frac{2 \cdot F_H}{\gamma \cdot M} \cdot x \right]^{1/2} \qquad (17.10)$$

where $\gamma = \Delta\theta/\Delta z$ is the gradient of potential temperature in the air just before reaching the coast, and M is the wind speed.

In early morning, the sea-breeze circulation does not extend very far from the coast, but progresses further over land and water as the day progresses. Advancing cold air behind the sea-breeze front behaves somewhat like a **density current** or **gravity current** in which a dense fluid spreads out horizontally beneath a less dense fluid. When this is simulated in water tanks, the speed M_{SBF} of advance of the sea-breeze front, is

$$M_{SBF} = k \cdot \sqrt{|g| \cdot \frac{\Delta\theta_v}{T_v} \cdot d} \qquad (17.11)$$

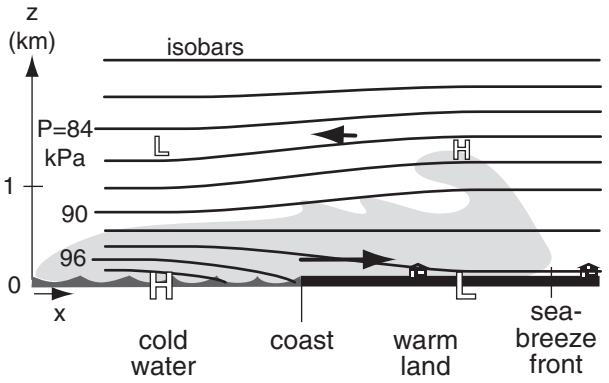

Figure 17.13
Vertical cross section through a sea-breeze circulation, showing isobars. H and L at any one altitude indicate relatively higher or lower pressure. The horizontal pressure gradient is greatly exaggerated in this illustration. Thick arrows show the coast-normal component of horizontal winds.

Solved Example

What horizontal pressure difference is needed in the bottom part of the sea-breeze circulation to drive a onshore wind that accelerates from 0 to 6 m/s in 6 h?

Solution

Given: $\Delta M/\Delta t = (6 \text{ m/s})/(6 \text{ h}) = 0.000278 \text{ m·s}^{-2}$
Find: $\Delta P/\Delta x = ?$ kPa/km

Neglect all other terms in the horiz. eq. of motion:

$$\Delta M/\Delta t = -(1/\rho)\cdot\Delta P/\Delta x \qquad (10.23a)$$

Assume air density is $\rho = 1.225 \text{ kg/m}^3$ at sea level.
Solve for $\Delta P/\Delta x$:

$\Delta P/\Delta x = -\rho \cdot (\Delta M/\Delta t) = -(1.225 \text{kg/m}^3)\cdot(0.000278 \text{m·s}^{-2})$
$= -0.00034 \text{ kg·m}^{-1}\text{·s}^{-2}/\text{m} = -0.00034 \text{ Pa/m}$
$= \underline{\mathbf{-0.00034 \text{ kPa/km}}}$

Check: Units OK. Magnitude OK.
Discussion: Only a small pressure gradient is needed to drive a sea breeze.

Solved Example

For a surface kinematic heat flux of 0.2 K m/s, wind speed of 5 m/s, and $\gamma = 3$K/km, find the TIBL depth 5 km from shore.

Solution

Given: $F_H = 0.2$ K·m/s, $M = 5$ m/s, $\gamma = 3$K/km, $x = 5$ km
Find: $z_i = ?$ m

Use eq. (17.10):

$z_i = [2\cdot(0.2\text{K·m/s})\cdot(5\text{km}) / \{(3\text{K/km})\cdot(5\text{m/s})\}]^{1/2}$
$= \underline{\mathbf{0.365 \text{ km}}}$

Check: Units OK. Magnitude reasonable.
Discussion: Above this height, the air still feels the marine influence, and not the warmer land.

Solved Example

Marine-air of thickness 500 m and virtual temperature 16°C is advancing over land. The displaced continental-air virtual temperature is 20°C. Find the sea-breeze front speed, and the sea-breeze wind speed.

Solution

Given: $\Delta\theta_v = \Delta T_v = 20 - 16°C = 4°C$, $d = 500$ m
$T_{v\ average} = (16+20°C)/2 = 18°C = 291K$
Find: M_{SBF} = ? m/s, M = ? m/s

For speed-of-advance of the front, use eq. (17.11):
$M_{SBF} = (0.62) \cdot [(9.8 m \cdot s^{-2}) \cdot (4K) \cdot (500m)/(291K)]^{1/2}$
$= \underline{\mathbf{5.1\ m/s}}$

For the sea-breeze wind speed, use eq. (17.12):
$M = 1.15 \cdot (5.1 m/s) = \underline{\mathbf{5.9\ m/s}}$

Check: Units OK. Magnitude OK.
Discussion: Because the sea-breeze circulation extends 20 to 250 km over the sea, mariners used these reliable breezes to sail north-south along the Atlantic coasts of Europe and Africa centuries ago. Upon reaching the latitude of the easterly trade winds in the tropical global circulation, they then sailed west towards the Americas. Upon reaching the Americas, they again used the sea-breezes to sail north and south along the East Coasts of North and South America. For the return trip to Europe, they sailed in the mid-latitude westerlies. Thus, by using both local sea-breeze winds and the global circulation, they achieved an effective commercial trade route.

Solved Example

Assuming calm synoptic conditions (i.e., no large-scale winds that oppose or enhance the sea-breeze), what maximum distance inland would a sea-breeze propagate. Use data from the previous solved example, for a latitude of 45°N.

Solution:

Given: $M_{SBF} = 5.1$ m/s from previous example.
latitude = 45°N.
Find: L = ? km

First, find the Coriolis parameter:
$f_c = (1.458 \times 10^{-4}\ s^{-1}) \cdot \sin(45°) = 1.03 \times 10^{-4}\ s^{-1}$
Use eq. (17.13):
$L = (5.1\ m/s) / [(7.27 \times 10^{-5}\ s^{-1})^2 - (1.03 \times 10^{-4}\ s^{-1})^2]^{1/2}$
$= \underline{\mathbf{70\ km}}$

Check: Units OK. Magnitude reasonable.
Discussion: At 30° latitude the denominator of eq. (17.13) is zero, causing $L = \infty$. But this is physically unreasonable. Thus, we expect eq. (17.13) to not be reliable at latitudes near 30°.

where $\Delta\theta_v$ is the virtual potential temperature difference between the cool marine sea-breeze air and the warmer air over land that is being displaced, T_v is an absolute average virtual temperature, $|g| = 9.8\ m \cdot s^{-2}$ is gravitational acceleration magnitude, d is depth of the density current, and constant $k \approx 0.62$.

When fully developed, surface (10 m height) wind speeds in the marine, inflow portion of the sea breeze at the coast are 1 to 10 m/s with typical values of 6 m/s. The relationship between sea-breeze wind speed M at the coast and speed of the sea-breeze front is:

$$M \approx 1.15 \cdot M_{SBF} \qquad (17.12)$$

The sea-breeze front can advance L = 10 to 200 km inland by the end of the day, although typical advances are L = 20 to 60 km unless inhibited by mountains or by opposing synoptic-scale winds. Even without mountain barriers, the sea breeze will eventually turn away from its advance due to Coriolis force. For latitudes ≠ 30°, L is roughly

$$L \approx \frac{M_{SBF}}{\left|\omega^2 - f_c^2\right|^{1/2}} \qquad (17.13)$$

where M_{SBF} is given by the previous equation, $\omega = 2\pi/day = 7.27 \times 10^{-5}\ s^{-1}$ is the frequency of the daily heating/cooling cycle, and $f_c = (1.458 \times 10^{-4}\ s^{-1}) \cdot \sin(latitude)$ is the Coriolis parameter. As the front advances, prefrontal waves may cause wind shifts ahead of the front.

At the end of the day, the sea-breeze circulation dissipates and a weaker, reverse circulation called the **land-breeze** forms in response to the nighttime cooling of the land surface relative to the sea. Sometimes, the now-disconnected sea-breeze front from late afternoon continues to advance farther inland during the night as a **bore** (the front of dense fluid advancing under less-dense fluid; also described as a propagating solitary wave with characteristics similar to the **hydraulic jump**). In Australia, such a bore and its associated cloud along the wave crest are known as the **Morning Glory**.

In the vertical cross section normal to the coastline (as in Fig. 17.12), the surface wind oscillates back and forth between onshore and offshore, reversing directions during the morning and evening hours. The Coriolis force induces an oscillating along-shore wind component that lags the onshore-offshore component by 6 h (or 1/4 of a daily cycle). Hence, the horizontal wind vector rotates throughout the course of the day. Rotation is clockwise in the northern hemisphere and counterclockwise in the southern hemisphere.

The idealized sea-breeze hodograph has an elliptical shape (Fig. 17.14). For example, along a me-

ridional coastline with the ocean to the west in the Northern Hemisphere, the diurnal component of the surface wind tends to be westerly (onshore) during the mid-day, northerly (alongshore) during the evening, easterly near midnight, and southerly (alongshore) near sunrise.

The sea-breeze wind and the mean (24 h average) synoptic-scale surface wind are additive. If the synoptic-scale wind in the above example is blowing, say, from the north, the surface wind speed will tend to be higher around sunset when the mean wind and the diurnal component are in the same direction, than around sunrise when they oppose each other.

Many coasts have complex shaped coastlines with bays or mountains, resulting in a myriad of interactions between local flows that distort the sea breeze and create regions of enhanced convergence and divergence. The sea breeze can also interact with boundary-layer thermals, and urban circulations, causing complex dispersion of pollutants emitted near the shore. If the onshore synoptic-scale geostrophic wind is too strong, only a TIBL develops with no sea-breeze circulation.

In regions such as the west coast of the Americas, where major mountain ranges lie within a few hundred kilometers of the coast, sea breezes and terrain-induced winds appear in combination.

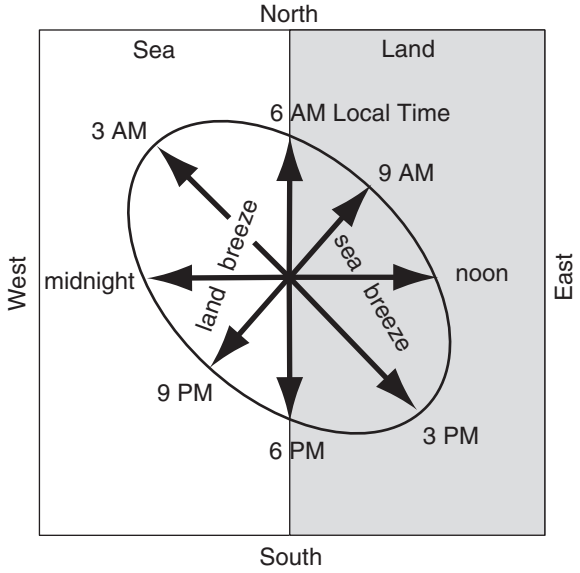

Figure 17.14
Idealized hodograph of surface (z = 10 m) wind vectors during a diurnal cycle for a sea breeze. Assumes Northern Hemisphere latitude of Europe, and fair-weather anticyclonic conditions of light to calm large-scale winds. (In this hodograph, compass directions show the direction toward which the wind blows. Also, the vectors are for different times, not different altitudes.)

OPEN-CHANNEL HYDRAULICS

Sometimes a dense cold-air layer lies under a less-dense warmer layer, with a relatively sharp temperature discontinuity ($\Delta T = \Delta\theta$) between the two layers (Fig. 17.15a and b). This temperature jump marks the **density interface** between the two layers. Examples of such a **two-layer system** include arctic air advancing behind a cold front and sliding under warmer air, cold gust fronts from thunderstorms, and cool marine air moving inland under warmer continental air.

These two-layer systems behave similarly to water in an **open channel** — a two layer system of dense water under less-dense air. Hence, you can apply **hydraulics** (applications of liquid flow based on its mechanical properties) to the atmosphere, for cases where air compressibility is not significant.

Sometimes the cold air can be stably stratified (Figs. 17.15c & d) as idealized here with constant lapse rate, where $\Delta\theta/\Delta z = \Delta T/\Delta z + \Gamma_d$, using the dry adiabatic lapse rate Γ_d = 9.8 °C/km. You can use modified hydraulic theory for these cases.

Hydraulic theory depends on the speed of waves on the interface between cold and warm air.

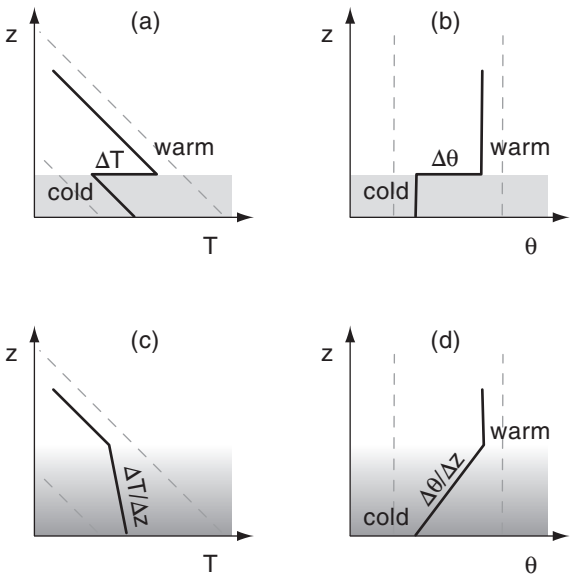

Figure 17.15
Idealized stratification situations in the atmosphere. The dashed lines indicate dry adiabats (lines of constant potential temperature θ) (a) and (b) are two ways of plotting the same situation: two-layers each having uniform potential temperature θ, and with a temperature jump between them. (c) and (d) both show a different situation: a linear change of T with height (i.e., constant stratification) instead of a temperature jump.

Because hydraulics depends on density, it is more accurate to use virtual temperature instead of temperature, to include the effect of humidity on air density. Namely, use T_v instead of T, use ΔT_v instead of ΔT, and $\Delta\theta_v$ instead of $\Delta\theta$.

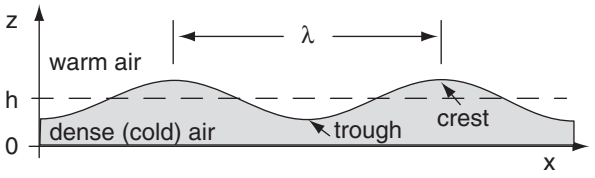

Figure 17.16
Sketch of waves on the interface between cold and warm air layers. λ is wavelength, and h is average depth of cold air.

Solved Example

For a two-layer air system with 5°C virtual potential temperature difference across the interface and a bottom-layer depth of 20 m, find the intrinsic group speed, and compare it to the speed of a water wave.

Solution

Given: $\Delta\theta_v = 5°C = 5K$, $h = 20$ m. Assume $T_v = 283$ K
Find: c_g = ? m/s, for air and for water

For a 2-layer air system, use eqs. (17.15 & 17.16):
$c_g = c_o = [(9.8\ m{\cdot}s^{-2}){\cdot}(5K){\cdot}(20m)/(283K)]^{1/2} =$ **1.86 m/s**

For water under air, use eq. (17.14 & 17.16)):
$c_g = c_o = [(9.8\ m{\cdot}s^{-2}){\cdot}(20m)]^{1/2} =$ **14 m/s**

Check: Units OK. Magnitude OK.
Discussion: Atmospheric waves travel much slower than channel or ocean waves, and have much longer wavelengths. This is because of the reduced gravity $|g'|$ for air, compared to the full gravity $|g|$ for water.

Solved Example

Find the internal-wave horizontal group speed in air for a constant virtual potential-temperature gradient of 5°C across a stable-layer depth of 20 m.

Solution

Given: $\Delta\theta_v = 5°C = 5K$, $\Delta z = h = 20$ m. Let $T_v = 283$ K
Find: u_g = ? m/s

Use eq. (17.17):
$u_g = [(9.8\ m{\cdot}s^{-2}){\cdot}(5K)/(283K \cdot 20m)]^{1/2} \cdot (20m) =$ **1.86 m/s**

Check: Units OK. Magnitude OK.
Discussion: For the example here with $\Delta z = h$, the equation for u_g in a stably-stratified fluid is identical to the equation for c_g in a two layer system. This is one of the reasons why we can often use hydraulics methods for a stably-stratified atmosphere.

Wave Speed

Waves (vertical oscillations that propagate horizontally on the density interface) can exist in air (Fig. 17.16), and behave similarly to water waves. For hydraulics, if water in a channel is shallow, then long-wavelength waves on the water surface travel at the intrinsic "shallow-water" **phase speed** c_o of:

$$c_o = \sqrt{|g| \cdot h} \qquad (17.14)$$

where $|g| = 9.8\ m/s^2$ is gravitational acceleration magnitude, and h is average water depth. **Phase speed** is the speed of propagation of any wave crest. **Intrinsic** means relative to the mean fluid motion. **Absolute** means relative to the ground.

For a two-layer air system, the **reduced gravity** $|g'| = |g| \cdot \Delta\theta_v / T_v$ accounts for the cold-air buoyancy relative to the warmer air. For a shallow bottom layer, the resulting intrinsic phase speed of **surface waves** on the interface between the cold- and warm-air layers is:

$$c_o = \sqrt{|g'| \cdot h} \ = \ \left(|g| \cdot \frac{\Delta\theta_v}{T_v} \cdot h \right)^{1/2} \qquad (17.15)$$

where $\Delta\theta_v$ is the virtual potential temperature jump between the two air layers, T_v is an average absolute virtual temperature (in Kelvin), h is the depth of the cold layer of air, and $|g| = 9.8\ m{\cdot}s^{-2}$ is gravitational acceleration magnitude.

The speed that wave energy travels through a fluid is the **group speed** c_g. Group speed is the speed that hydraulic information can travel relative to the mean flow velocity, and it determines how the upstream flow reacts to downstream flow changes. For a two-layer system with bottom-layer depth less than 1/20 the wavelength, the group speed equals the phase speed

$$c_g = c_o \qquad (17.16)$$

For a statically-stable atmospheric system with constant lapse rate, there is no surface (no interface) on which the waves can ride. Instead, **internal waves** can exist that propagate both horizontally and vertically inside the statically-stable region. Internal waves reflect from solid surfaces such as the ground, and from statically neutral layers.

For internal waves, the horizontal component of group velocity u_g depends on both vertical and horizontal wavelength λ. To simplify this complicated situation, focus on infinitely-long waves in the horizontal (which propagate the fastest in the horizontal), and focus on a wave for which the vertical wavelength is proportional to the depth h of the statically stable layer of air. Thus:

$$u_g = N_{BV} \cdot h \ = \ \left(\frac{|g|}{T_v} \cdot \frac{\Delta\theta_v}{\Delta z} \right)^{1/2} \cdot h \qquad (17.17)$$

where N_{BV} is the Brunt-Väisälä frequency, and $\Delta\theta_v/\Delta z$ is the vertical gradient of virtual potential temperature (a measure of static-stability strength).

Froude Number - Part 1

The ratio of the fluid speed (M) to the wave group velocity (c_g , the speed that energy and information travels) is called the **Froude number** Fr.

$$Fr = M / c_g \tag{17.18}$$

At least three different Froude numbers can be defined, depending on the static stability and the flow situation. We will call these Fr_1, Fr_2, and Fr_3, the last of which will be introduced in a later section.

For surface (interfacial) waves in an idealized atmospheric two-layer system where $c_g = c_o = (|g'|\cdot h)^{1/2}$, the Froude number is $Fr_1 = M/c_o$:

$$Fr_1 = \frac{M}{\left(|g|\cdot\frac{\Delta\theta_v}{T_v}\cdot h\right)^{1/2}} \tag{17.19}$$

where h is the depth of the bottom (cold) air layer, $\Delta\theta_v$ is the virtual potential temperature jump between the two air layers, T_v is an average absolute virtual temperature (in Kelvins), and $|g| = 9.8\ \text{m}\cdot\text{s}^{-2}$ is gravitational acceleration magnitude.

For the other situation of a statically stable region supporting internal waves, the Froude number is $Fr_2 = M/u_g$:

$$Fr_2 = \frac{M}{\left(\frac{|g|}{T_v}\cdot\frac{\Delta\theta_v}{\Delta z}\right)^{1/2}\cdot h} \tag{17.20}$$

The nature of the flow is classified by the value of the Froude number:

- **subcritical (tranquil)** for $Fr < 1$
- **critical** for $Fr = 1$
- **supercritical (rapid)** for $Fr > 1$

For subcritical flow, waves and information travel upstream faster than the fluid is flowing downstream, thus allowing the upstream flow to "feel" the effect of both upstream conditions and downstream conditions such as flow constrictions. For supercritical flow, the fluid is moving so fast that no information can travel upstream (relative to a fixed location); hence, the upstream fluid does not "feel" the effects of downstream flow constrictions until it arrives at the constriction. For airflow, the words (upwind, downwind) can be used instead of (upstream, downstream).

Solved Example

For a two-layer air system with 5°C virtual potential temperature difference across the interface and a bottom-layer depth of 20 m, find the Froude number if the average flow speed is 5 m/s. Discuss whether the flow is critical.

Solution

Given: $\Delta\theta_v = 5°C = 5K$, $h = 20$ m. $M = 5$ m/s.
Assume $T_v = 283$ K
Find: Fr_1 = ? (dimensionless)

For a 2-layer air system, use eq. (17.19):
$Fr_1 = (5\ \text{m/s}) / [(9.8\ \text{m}\cdot\text{s}^{-2})\cdot(5\text{K})\cdot(20\text{m})/(283\text{K})]^{1/2}$
$= (5\ \text{m/s}) / (1.86\ \text{m/s}) =$ **2.69**

Check: Units OK. Magnitude OK.
Discussion: This flow is supercritical. Hence, the air blows the wave downwind faster than it can propagate upwind against the mean flow.

Solved Example

For a smooth virtual potential-temperature gradient of 5°C across a stable-layer depth of 20 m, find the Froude number if the average flow speed is 5 m/s. Discuss whether the flow is critical.

Solution

Given: $\Delta\theta_v = 5°C = 5K$, $\Delta z = h = 20$ m.
Assume $T_v = 283$ K
Find: Fr_2 = ? (dimensionless)

Use eq. (17.20). But since $\Delta z = h$, this causes eq. (17.20) to reduce to eq. (17.19). Hence, we get the same answer as in the previous solved example:
$Fr_2 =$ **2.69**

Check: Units OK. Magnitude OK.
Discussion: This flow is also supercritical. Although this example was contrived to give the same virtual potential temperature gradient across the whole fluid depth as before, often this is not the case. So always use eq. (17.20) for a constant stable stratification flow, and don't assume that it always reduces to eq. (17.19).

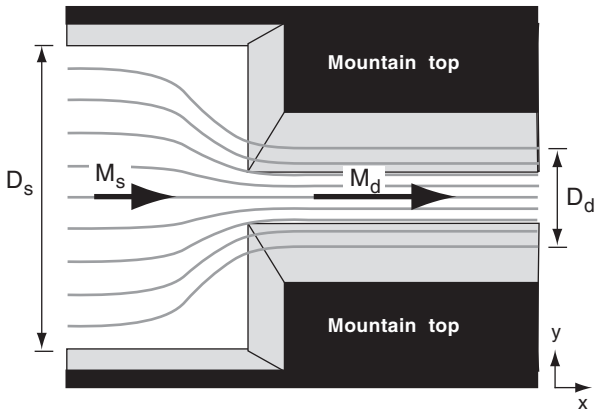

Figure 17.17
Acceleration of air through a constriction. View looking down from above.

Solved Example

If a 20 km wide band of winds of 5 m/s must contract to pass through a 2 km wide gap, what is the wind speed in the gap.

Solution

Given: D_s = 20 km, D_d = 2 km, M_s = 5 m/s.
Find: M_d = ? m/s

Use eq. (17.23): M_d = [(20km)/(2km)]·(5m/s) = **50 m/s**

Check: Units OK. Physics OK.
Discussion: The actual winds would be slower, because turbulence would cause significant drag.

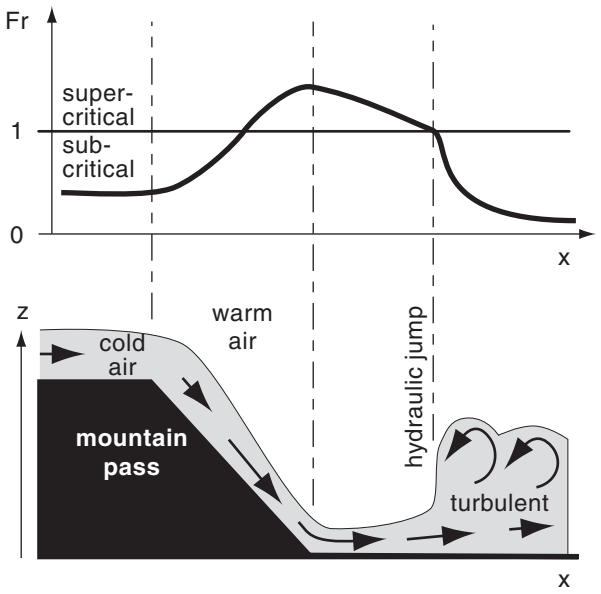

Figure 17.18
Variation of Froude number (Fr) with downwind distance (x), showing a hydraulic jump where the flow changes from supercritical to subcritical.

Conservation of Air Mass

Consider a layer of well-mixed cold air flowing at speed M_s along a wide valley of width D_s. If it encounters a constriction where the valley width shrinks to D_d (Fig. 17.17), the winds will accelerate to M_d to conserve the amount of air mass flowing. If the depth h of the flow is constant (not a realistic assumption), then **air-mass conservation** gives:

$$\textit{mass flowing } \underline{\text{out}} \;=\; \textit{mass flowing } \underline{\text{in}} \qquad (17.21)$$

$$\rho \cdot \textit{volume flowing out} \;=\; \rho \cdot \textit{volume flowing in}$$

$$\rho \cdot M_d \cdot h \cdot D_d \;=\; \rho \cdot M_s \cdot h \cdot D_s \qquad (17.22)$$

Thus,

$$M_d = \frac{D_s}{D_d} \cdot M_s \qquad \bullet(17.23)$$

under the assumptions of negligible changes in air density ρ. Thus, the flow must become faster in the narrower valley.

Similarly, suppose air is flowing downhill through a valley of constant-width D. Cold air of initial speed M_s might accelerate due to gravity to speed M_d further down the slope. Air-mass conservation requires that the depth of the flow h_d in the high speed region be less than the initial depth h_s in the lower-speed region.

$$h_d = \frac{M_s}{M_d} \cdot h_s \qquad (17.24)$$

Hydraulic Jump

Consider a layer of cold air flowing supercritically in a channel or valley. If the valley geometry or slope changes at some downstream location and allows wind speed M to decrease to its critical value (Fr = 1), there often occurs a sudden increase in flow depth h and a dramatic increase in turbulence. This transition is called an **hydraulic jump**. Downstream of the hydraulic jump, the wind speed is slower and the flow is subcritical.

In Fig. 17.18, you can consider the hydraulic jump as a wave that is trying to propagate upstream. However, the cold air flowing downslope is trying to wash this wave downstream. At the hydraulic jump, the wave speed exactly matches the opposing wind speed, causing the wave to remain stationary relative to the ground.

For example (Fig. 17.18), consider cold air flowing down a mountain slope. It starts slowly, and has Fr < 1. As gravity accelerates the air downslope and causes its depth to decrease, the Froude can eventually reach the critical value Fr = 1. As the air continues to accelerate downhill the flow can become supercritical (Fr > 1). But once this supercritical flow

reaches the bottom of the slope and begins to decelerate due to turbulent drag across the lowland, its velocity can decrease and the flow depth gradually increases. At some point downstream the Froude number again reaches its critical value $Fr = 1$. An hydraulic jump can occur at this point, and turbulent drag increases. If this descending cold air is foggy or polluted, the hydraulic jump can be visible.

GAP WINDS

Basics

During winter in mountainous regions, sometimes the synoptic-scale weather pattern can move very cold air toward a mountain range. The cold air is denser than the warm overlying air, so buoyancy opposes rising motions in the cold air. Thus, the mountain range is a barrier that dams cold air behind it (Fig. 17.20).

However, river valleys, fjords, straits, and passes (Fig. 17.19) are mountain gaps through which the cold air can move as **gap winds** (Fig. 17.20). Gap wind speeds of 5 to 25 m/s have been observed, with gusts to 40 m/s. Temperature jumps at the top of the cold-air layer in the 5 to 10°C range are typical, while extremes of 15°C have been observed. Gap flow depths of 500 m to over 2 km have been observed. In any locale, the citizens often name the gap wind after their town or valley.

The cold airmass dammed on one side of the mountain range often has high surface pressure (H), as explained in the Hydrostatic Thermal Circulation section of the Global Circulation chapter. When synoptic low-pressure centers (L) approach the opposite side of the mountain range, a pressure gradient of order (0.2 kPa)/(100 km) forms across the range that can drive the gap wind. Gap winds can also be driven by gravity, as cold air is pulled downslope through a mountain pass.

Divide gap flow into two categories based on the gap geometry: (1) short gaps, and (2) long gaps. Long gaps are ones with a gap width (order of 2 - 20 km) that is much less than the gap length (order of 100 km). Coriolis force is important for flow through long gaps, but is small enough to be negligible in short gaps.

Short-gap Winds

Use open-channel hydraulics for short gaps, and neglect Coriolis force. Although the gap-wind speed could range from subcritical to supercritical, observations suggest that one or more hydraulic jumps (Fig. 17.21) are usually triggered in the supercritical

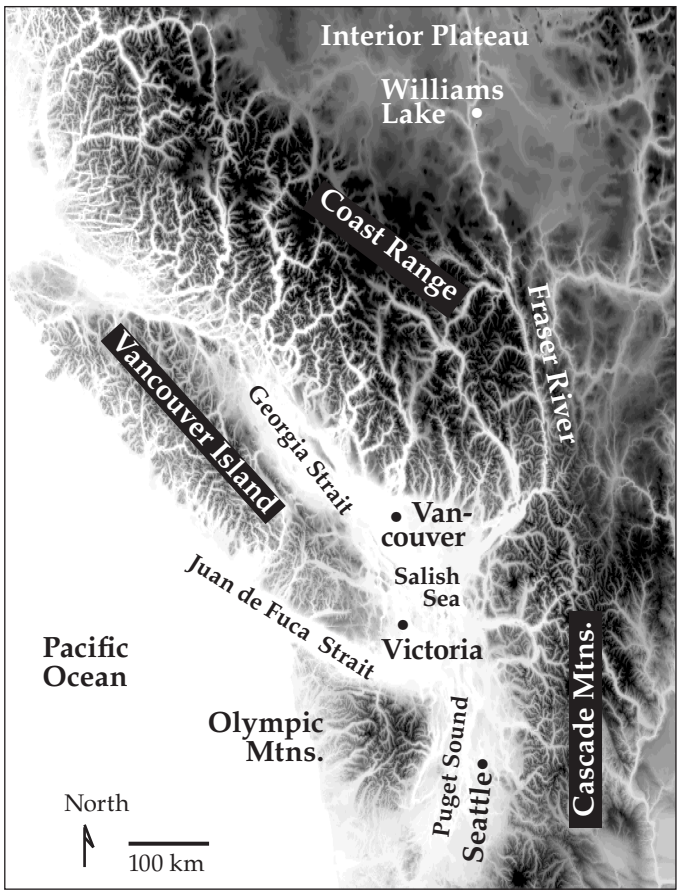

Figure 17.19
Geography of southwestern British Columbia, Canada, and northwestern Washington, USA, illustrating mountain gaps. Higher elevations are shown as darker greys, with the highest peaks 3,000 to 4,000 m above sea level. Ocean and very-low-elevation-land areas are white. Lower-elevation fjords, straits, and river valleys (i.e., gaps) appear as filaments of white or light-grey across the dark-shaded mountain range. In winter, sometimes very cold arctic air can pool in the Interior Plateau northeast of the Coast Mountains.

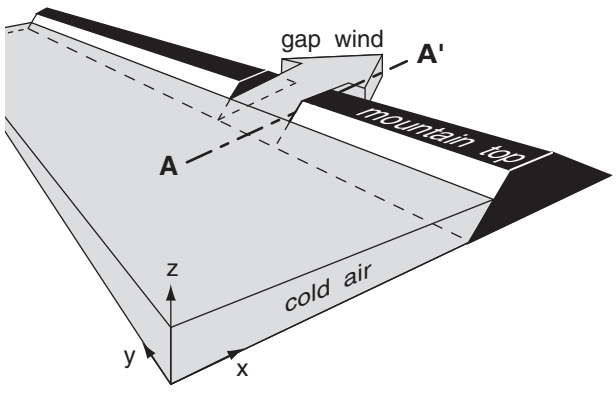

Figure 17.20
Cold air flow through a short gap.

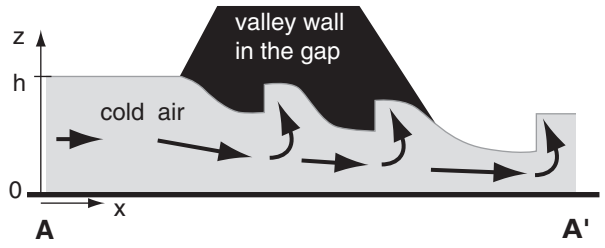

Figure 17.21
Cold air flow through a short gap. Vertical slice inside the gap, along section **A** - **A′** *from the previous figure. A series of 3 hydraulic jumps are shown in this idealization.*

Solved Example

Cold winter air of virtual potential temperature –5°C and depth 200 m flows through an irregular short mountain pass. The air above has virtual potential temperature 10°C. Find the max likely wind speed through the short gap.

Solution

Given: $\Delta\theta_v = 15°C = 15K$, $h = 200$ m.
Find: $M_{gap\ max}$ = ? m/s

For a 2-layer air system, use eq. (17.25):

$M_{gap\ max} = [(9.8\ m{\cdot}s^{-2}){\cdot}(15K){\cdot}(200m)/(267K)]^{1/2}$
$= \underline{\mathbf{10.5}}$ m/s

Check: Units OK. Magnitude OK.
Discussion: Because of the very strong temperature jump across the top of the cold layer of air and the correspondingly faster wave group speed, faster gap flow speeds are possible. Speeds any faster than this would cause an hydraulic jump, which would increase turbulent drag and slow the wind back to this wind speed.

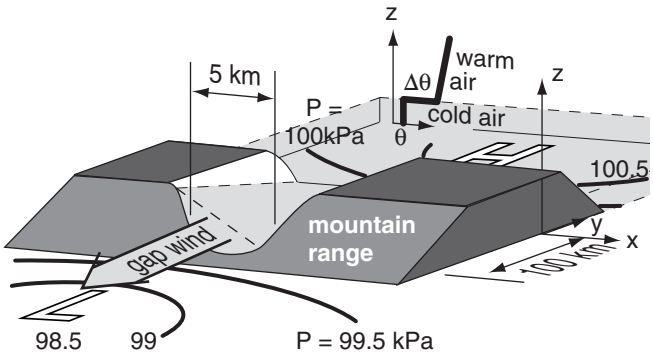

Figure 17.22
Scenario for gap winds in the N. Hemisphere in long valleys, with cold air (light grey) dammed behind a mountain range (dark grey). High pressure (H) is in the cold air, and low pressure (L) is at the opposite side of the mountains. Thick curved lines are sea-level isobars around the synoptic-scale pressure centers. The vertical profile of potential temperature θ is plotted.

regions due to irregularities in the valley shape, or by obstacles. The resulting turbulence in the hydraulic jumps causes extra drag, slowing the wind to its critical value.

The net result is that many gap winds are likely to have maximum speeds nearly equal to their critical value: the speed that gives $Fr = 1$. Using this in the definition of the Froude number allows us to solve for the likely maximum gap wind speed through gaps short enough that Coriolis force is not a factor:

$$M_{gap\ max} = \left[|g| \cdot \frac{\Delta\theta_v}{T_v} \cdot h \right]^{1/2} \qquad (17.25)$$

Long-gap Winds

For long gaps, examine the horizontal forces (including Coriolis force) that act on the air. Consider a situation where the synoptic-scale isobars are nearly parallel to the axis of the mountain range (Fig. 17.22), causing a pressure gradient across the mountains.

For long narrow valleys this synoptic-scale cross-mountain pressure gradient is unable to push the cold air through the gap directly from high to low pressure, because Coriolis force tends to turn the wind to the right of the pressure gradient. Instead, the cold air inside the gap shifts its position to enable the gap wind, as described next.

Fig. 17.23 idealizes how this wind forms in the N. Hemisphere. Cold air (light grey in Fig. 17.23a) initially at rest in the gap feels the synoptically imposed pressure-gradient force F_{PGs} along the valley axis, and starts moving at speed M (shown with the short dark-grey arrow in Fig. 17.23a′) toward the imposed synoptic-scale low pressure (L) on the opposite side of the gap. At this slow speed, both Coriolis force (F_{CF}) and turbulent drag force (F_{TD}) are correspondingly small (Fig. 17.23a′). The sum (black-and-white dotted arrow) of all the force vectors (black) causes the wind to turn slightly toward its right in the N. Hemisphere and to accelerate into the gap.

This turning causes the cold air to "ride up" on the right side of the valley (relative to the flow direction, see Fig. 17.23b). It piles up higher and higher as the gap wind speed M increases. But cold air is denser than warm. Thus slightly higher pressure (small dark-grey H) is under the deeper cold air, and slightly lower pressure (small dark-grey L) is under the shallower cold air. The result is a cross-valley mesoscale pressure-gradient force F_{PGm} per unit mass m (Fig. 17.23b′) at the valley floor of:

$$\frac{F_{PGm}}{m} = -\frac{1}{\rho} \cdot \frac{\Delta P_m}{\Delta x} = -|g| \cdot \frac{\Delta\theta_v}{T_v} \cdot \frac{\Delta z}{\Delta x} \qquad (17.26)$$

where $\Delta z/\Delta x$ is the cross-valley slope of the top of the cold-air layer, $\Delta P_m/\Delta x$ is the mesoscale pressure gradient across the valley, $\Delta\theta_v$ is the virtual potential temperature difference between the cold and warm air, T_v is an average virtual temperature (Kelvin), $|g| = 9.8$ m·s^{-2} is the magnitude of gravitational acceleration, and ρ is the average air density.

When this new pressure gradient force is vector-added to the larger drag and Coriolis forces associated with the moderate wind speed M, the resulting vector sum of forces (dotted white-and-black vector; Fig. 17.23b′) begins to turn the wind to become almost parallel to the valley axis.

Gap-wind speed M increases further down the valley (Fig. 17.23c and c′), with the gap-wind cold air hugging the right side of the valley. In the along-valley direction (the $-y$ direction in Figs. 17.23), the synoptic pressure gradient force F_{PGs} is often larger than the opposing turbulent drag force F_{TD}, allowing the air to continue to accelerate along the valley, reaching its maximum speed near the valley exit. The **antitriptic wind** results from a balance of drag and synoptic-scale pressure-gradient forces. Similar gap winds are sometimes observed in the Juan de Fuca Strait (Fig. 17.19), with the fastest gap winds near the west exit region of the strait.

In the cross-valley direction, Coriolis force F_{CF} nearly balances the mesoscale pressure gradient force F_{PGm}. These last two forces define a mesoscale "**gap-geostrophic wind**" speed G_m parallel to the valley axis:

$$G_m = \left| \frac{g}{f_c} \cdot \frac{\Delta\theta_v}{T_v} \cdot \frac{\Delta z}{\Delta x} \right| \qquad (17.27)$$

The actual gap wind speeds are of the same order of magnitude as this gap-geostrophic wind.

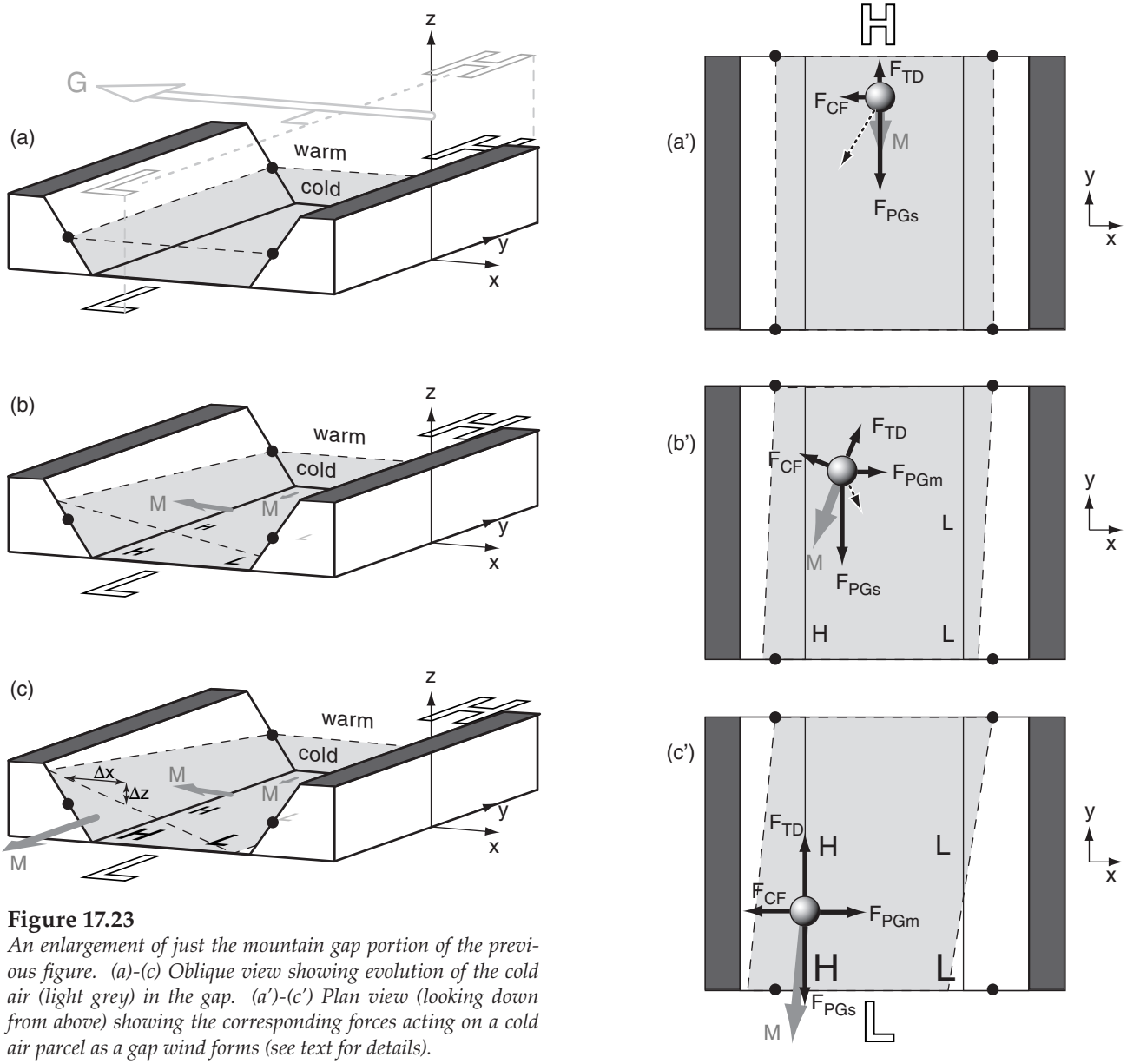

Figure 17.23
An enlargement of just the mountain gap portion of the previous figure. (a)-(c) Oblique view showing evolution of the cold air (light grey) in the gap. (a′)-(c′) Plan view (looking down from above) showing the corresponding forces acting on a cold air parcel as a gap wind forms (see text for details).

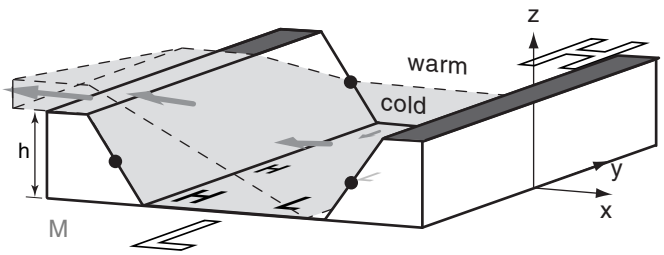

Figure 17.24
Gap winds can overtop the valley side walls if these walls are too low, or if the temperature difference between cold and warm layers of air is too small.

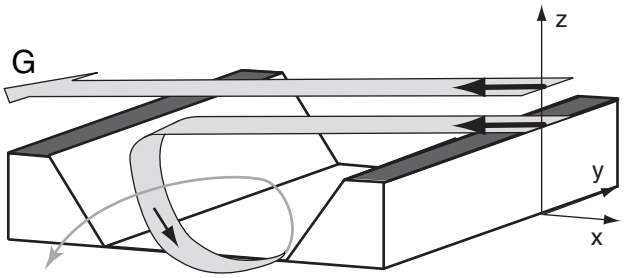

Figure 17.25
Without a layer of cold air near the surface, the cross-valley component of synoptic-scale geostrophic wind can create turbulent corkscrew motions and channeling of wind in the valley.

Solved Example

What long-gap wind speed can be supported in a strait 10 km wide through mountains 0.5 km high? The cold air is 4°C colder than the overlying 292 K air.

Solution

Given: $h = \Delta z = 0.5$ km, $\Delta x = 10$ km, $\Delta\theta_v = 4°C = 4$ K,
$T_v = 0.5 \cdot (288K + 292K) = 290K$.
Find: $G_m = ?$ m/s

Assume: $f_c = 10^{-4}$ s^{-1}.
Use eq. (17.27):
$G_m = |(9.8 \text{ m}\cdot\text{s}^{-2} / 10^{-4} \text{ s}^{-1}) \cdot (4K/290K) \cdot (0.5km/10km)|$
$= \underline{\mathbf{67 \text{ m/s}}}$.

Check: Units OK. Magnitude seems too large.
Discussion: The unrealistically large magnitude might be reached if the strait is infinitely long. But in a finite-length strait, the accelerating air would exit the strait before reaching this theoretical wind speed.

We implicitly assumed that the air was relatively dry, allowing $T_v \approx T$, and $\Delta\theta_v \approx \Delta\theta$. If humidity is larger, then you should be more accurate when calculating virtual temperatures. Also, as the air accelerates within the valley, mass conservation requires that the air depth Δz decreases, thereby limiting the speed according to eq. (17.27).

The synoptic-scale geostrophic wind on either side of the mountain range is nearly equal to the synoptic-scale geostrophic wind well above the mountain (*G*, in Fig. 17.23a). These synoptic winds are at right angles to the mesoscale gap-geostrophic wind.

The maximum possible gap wind speed is given by the equation above, but with Δz replaced with the height *h* of the valley walls above the valley floor. If either *h* or $\Delta\theta_v$ are too small, then some of the cool air can ride far enough up the valley wall to escape over top of the valley walls (Fig. 17.24), and the resulting gap winds are weaker. Gap winds occur more often in winter, when cold valley air causes large $\Delta\theta_v$.

For a case where $\Delta\theta_v$ is near zero (i.e., near-neutral static stability), the synoptic-scale geostrophic wind dominates. The vector component of *G* along the valley axis can appear within the valley as a **channeled wind** parallel to the valley axis. However, the cross-valley component of *G* can create strong turbulence in the valley (due to cavity, wake, and mountain-wave effects described later in this chapter). These components combine to create a turbulent corkscrew motion within the valley (Fig. 17.25).

COASTALLY TRAPPED LOW-LEVEL (BARRIER) JETS

Coriolis force is also important in locations such as the eastern Pacific Ocean, where low-altitude wind jets form parallel to the west coast of N. America. The dynamics describing these jets are very similar to the dynamics of long-gap winds.

Consider situations where synoptic-scale low-pressure systems reach the coast of N. America and encounter mountain ranges. Behind the approaching cyclone is cold air, the leading edge of which is the cold front (Fig. 17.26a). The cold air stops advanc-

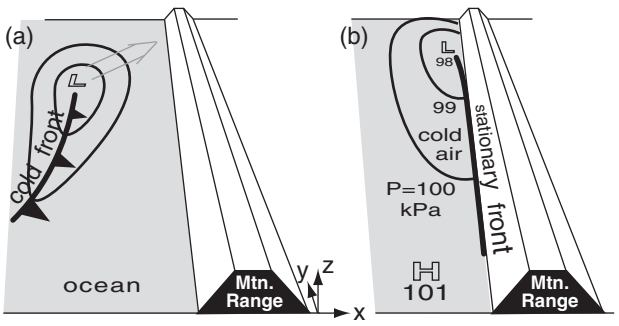

Figure 17.26
(a) Precursor synoptic conditions, as a low 𝕃 center approaches a coastal mountain (Mtn.) range in the N. Hemisphere. Curved lines are isobars at sea level. (b) Conditions later when the low reaches the coast, favoring coastally trapped low-level jets.

ing eastward when it hits the mountains, causing a stationary front along the ocean side of the mountain range (Fig. 17.26b).

A pressure gradient forms parallel to the mountain range (Fig. 17.26b), between the low (𝕃) center to the north and higher pressure (ℍ) to the south. Fig. 17.27 shows a zoomed view of the resulting situation close to the mountains. The isobars are approximately perpendicular to the mountain-range axis, not parallel as was the case for gap winds.

As the synoptic-scale pressure gradient (*PGs*) accelerates the cold air from high towards low, Coriolis force (*CF*) turns this air toward the right (in the N. Hem.) causing the cold air to ride up along the mountain range. This creates a mesoscale pressure gradient (*PGm*) pointing down the cold-air slope (Fig. 17.28). Eventually an equilibrium is reached where turbulent drag (TD) nearly balances the synoptic pressure-gradient force, and Coriolis force is balanced by the mesoscale pressure gradient.

The end result is a low-altitude cold wind parallel to the coast, just west of the mountain range. The jet-core height is centered about 1/3 of the distance from the ocean (or lowland floor) to the ridge top. Jet core altitudes of 50 to 300 m above sea level have been observed along the west coast of N. America, while altitudes of about 1 km have been observed in California west of the Sierra-Nevada mountain range. Maximum speeds of 10 to 25 m/s have been observed in the jet core.

Width of the coastal jet is on the order of 100 to 150 km. This width is roughly equal to the **Rossby radius of deformation**, λ_R, which is a measure of the upstream region of influence of the mountain range on a flow that is in geostrophic balance. For a cold marine layer of air capped by a strong inversion as sketched in Fig. 17.28, the **external Rossby radius of deformation** is

$$\lambda_R = \frac{\sqrt{|g| \cdot h \cdot \Delta\theta_v / T_v}}{f_c} \qquad (17.28)$$

where $|g|$ = 9.8 m·s^{-2} is gravitational acceleration magnitude, h is mountain range height, f_c is the Coriolis parameter, $\Delta\theta_v$ is the jump of virtual potential temperature at the top of the marine air layer, and T_v is an average absolute virtual temperature of the air. For a statically-stable layer of air having a linear increase of potential temperature with height instead of a step discontinuity, an **internal Rossby radius of deformation** is

$$\lambda_R = \frac{N_{BV} \cdot h}{f_c} \qquad (17.29)$$

where $N_{BV} = [(|g|/T_v) \cdot \Delta\theta_v/\Delta z]^{1/2}$ is the Brunt-Väisälä frequency.

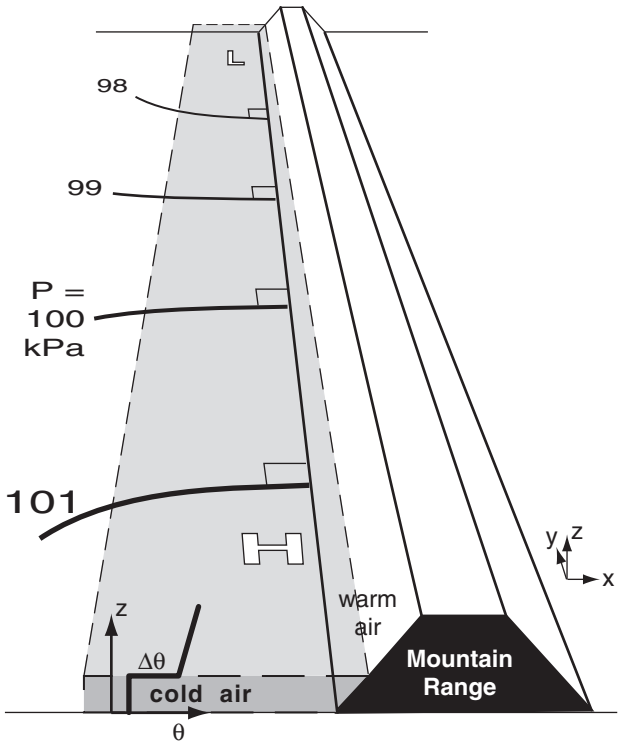

Figure 17.27
Synoptic conditions that favor creation of a mesoscale low-level jet parallel to the coast. Curved lines are isobars, ℍ and 𝕃 are high and low-pressure centers, and θ is potential temperature.

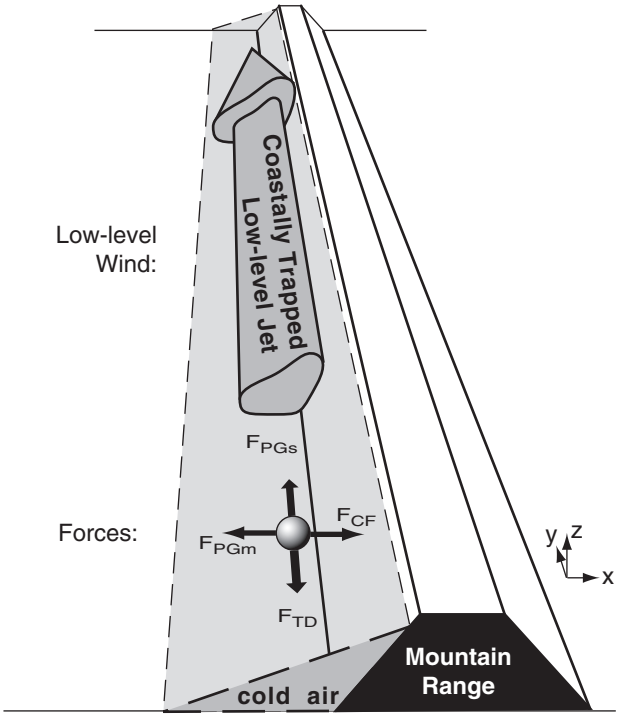

Figure 17.28
Final force (F) balance and cold-air location during a coastally trapped low-level jet (fast winds parallel to the coast). Vertical scale is stretched roughly 100:1 relative to the horizontal scale

Solved Example

The influence of the coast mountains extends how far to the west of the coastline in Fig. 17.28? The cold air has virtual potential temperature 8°C colder than the neighboring warm air. The latitude is such that the Coriolis parameter is 10^{-4} s^{-1}. Mountain height is 2000 m.

Solution

Given: h = 2000 m, $\Delta\theta_v$ = 8°C = 8 K, $f_c = 10^{-4}$ s^{-1} .
Find: λ_R = ? km, external Rossby deformation radius

Assume: $|g|/T_v$ = 0.03333 m·s^{-2}·K^{-1}
The region of influence extends a distance equal to the Rossby deformation radius. Thus, use eq. (17.28):

λ_R = [(0.03333 m·s^{-2}·K^{-1})·(2000 m)·(8 K)]$^{1/2}$ /(10^{-4} s^{-1})
= 231,000 m = **231 km**

Check: Units OK. Magnitude OK.
Discussion: Even before fronts and low-pressure centers hit the coastal mountains, the mountains are already influencing these weather systems hundreds of kilometers offshore.

Solved Example (§)

Find and plot the path of air over a mountain, given: z_1 = 500 m, M = 30 m/s, b = 3, $\Delta T/\Delta z$ = –0.005 K/m, T = 10°C, and T_d = 8°C for the streamline sketched in Fig. 17.29.

Solution

Given: (see above). Thus T = 283 K
Find: N_{BV} = ? s^{-1}, λ = ? m, and plot z vs. x

From the Stability chapter:

$$N_{BV} = \left[\frac{9.8\text{m}\cdot\text{s}^{-2}}{283\text{K}}\cdot(-0.005+0.0098)\right]^{1/2}$$

= 0.0129 s^{-1}

Use eq. (17.30)

$$\lambda = \frac{2\pi\cdot(30\text{m/s})}{0.0129\text{s}^{-1}} = 14.62 \text{ km}$$

Solve eq. (17.31) on a spreadsheet to get the answer:

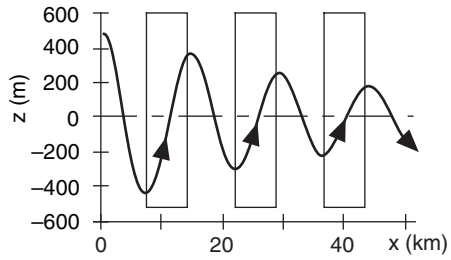

Check: Units OK. Physics OK. Sketch OK.
Discussion: Glider pilots can soar in the updraft portions of the wave, highlighted with white boxes.

MOUNTAIN WAVES

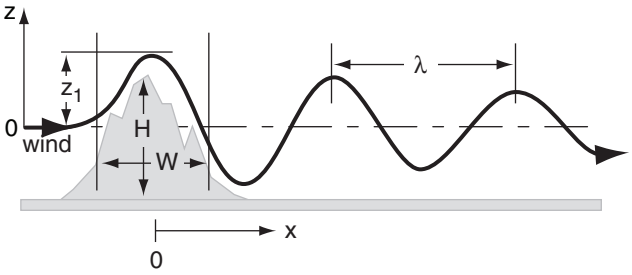

Figure 17.29
Mountain-wave characteristics.

Natural Wavelength

When statically stable air flows with speed M over a hill or ridge, it is set into oscillation at the Brunt-Väisälä frequency, N_{BV}. The natural wavelength λ is

$$\lambda = \frac{2\pi\cdot M}{N_{BV}} \qquad \bullet(17.30)$$

Longer wavelengths occur in stronger winds, or weaker static stabilities.

These waves are known as **mountain waves**, **gravity waves**, **buoyancy waves**, or **lee waves**. They can cause damaging winds, and interesting clouds (see the Cloud chapter).

Friction and turbulence damp the oscillations with time (Fig. 17.29). The resulting path of air is a damped wave:

$$z = z_1\cdot\exp\left(\frac{-x}{b\cdot\lambda}\right)\cdot\cos\left(\frac{2\pi\cdot x}{\lambda}\right) \qquad (17.31)$$

where z is the height of the air above its starting equilibrium height, z_1 is the initial amplitude of the wave (based on height of the mountain), x is distance downwind of the mountain crest, and b is a damping factor. Wave amplitude reduces to 1/e at a downwind distance of b wavelengths (that is, $b\cdot\lambda$ is the e-folding distance).

Lenticular Clouds

In the updraft portions of mountain waves, the rising air cools adiabatically. If sufficient moisture is present, clouds can form, called **lenticular clouds**. The first cloud, which forms over the mountain crest, is usually called a **cap cloud** (see Cloud chapter).

The droplet sizes in these clouds are often quite uniform, because of the common residence times of air in the clouds. This creates interesting optical

phenomena such as **corona** and **iridescence** when the sun or moon shines through them (see the Optics chapter).

Knowing the temperature and dew point of air at the starting altitude before blowing over the mountain, a lifting condensation level (LCL) can be calculated using equations from the Moisture chapter. Clouds will form in the crests of those waves for which $z > z_{LCL}$.

Froude Number - Part 2

For individual hills not part of a continuous ridge, some air can flow around the hill rather than over the top. When less air flows over the top, shallower waves form.

The third variety of **Froude Number** Fr_3 is a measure of the ability of waves to form over hills. It is given by

$$Fr_3 = \frac{\lambda}{2 \cdot W} \qquad \bullet(17.32)$$

where W is the hill width, and λ is the natural wavelength. Fr_3 is dimensionless.

For strong static stabilities or weak winds, $Fr_3 << 1$. The natural wavelength of air is much shorter than the width of the mountain, resulting in only a little air flowing over the top of the hill, with small waves (Fig. 17.30a). If H is the height of the hill (Fig. 17.29), then wave amplitude $z_1 < H/2$ for this case. Most of the air is **blocked** in front of the ridge, or flows around the sides for an isolated hill.

For moderate stabilities where the natural wavelength is nearly equal to twice the hill width, $Fr_3 \approx 1$. The air **resonates** with the terrain, causing very intense waves (Fig. 17.30b). These waves have the greatest chance of forming lenticular clouds, and pose the threat of violent turbulence to aircraft. Extremely fast near-surface winds on the downwind (lee) side of the mountains cause **downslope wind storms** that can blow the roofs off of buildings. Wave amplitude roughly equals half the hill height: $z_1 \approx H/2$. Sometimes rotor circulations and **rotor clouds** will form near the ground under the wave crests (Fig. 17.30b; also see the Cloud chapter).

For weak static stability and strong winds, the natural wavelength is much greater than the hill width, $Fr_3 >> 1$. Wave amplitude is weak, $z_1 < H/2$. A turbulent **wake** will form downwind of the mountain, sometimes with a **cavity** of reverse flow near the ground (Fig. 17.30c). The cavity and rotor circulations are driven by the wind like a bike chain turning a gear.

For statically neutral conditions, $Fr = \infty$. A large turbulent wake occurs (Fig. 17.30d). These wakes are hazardous to aircraft.

Solved Example (§)

Replot the results from the previous solved example, indicating which waves have lenticular clouds.

Solution

Given: (see previous solved example).
Find: z_{LCL} = ? m.

From the Moisture chapter: $z_{LCL} = a \cdot (T - T_d)$.

z_{LCL} = (125m/°C)·(10°C – 8°C) = **250 m**

above the reference streamline altitude. From the sketch below, we find 1 cap cloud and 2 lenticular clouds.

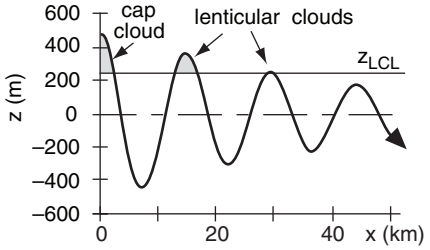

Check: Units OK. Physics OK. Sketch OK.

Discussion: Most clouds are blown with the wind, but **standing-lenticular clouds** are stationary while the wind blows through them!

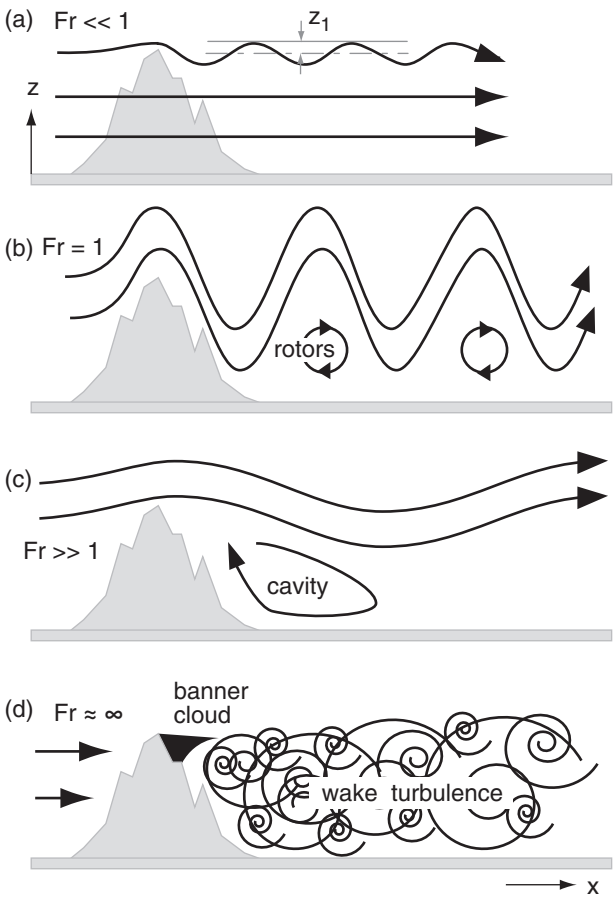

Figure 17.30
Mountain wave behavior vs. Froude number, Fr_3.

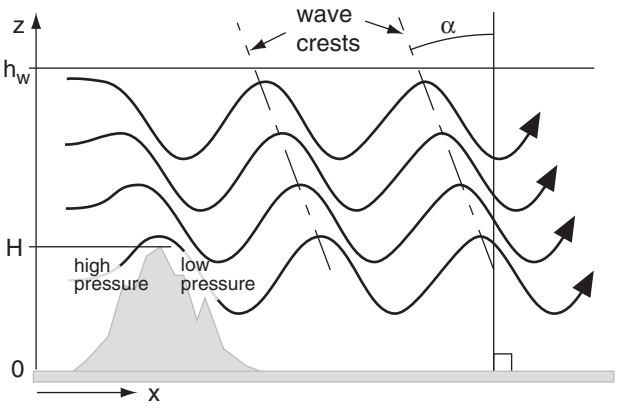

Figure 17.31
Vertical wave propagation, tilting crests, and wave drag.

Solved Example

For $Fr_3 = 0.8$, find the angle of the wave crests and the wave drag force over a hill of height 800 m. The Brunt-Väisälä frequency is 0.01 s^{-1}, and the waves fill the 11 km thick troposphere.

Solution

Given: $Fr_3 = 0.8$, $H = 800$ m, $N_{BV} = 0.01\ s^{-1}$.
Find: $\alpha = ?°$, $F_{x\,WD}/m = ?\ m{\cdot}s^{-2}$

Use eq. (17.33): $\alpha = \cos^{-1}(0.8) = \underline{\mathbf{36.9°}}$
Use eq. (17.34):

$$\frac{F_{xWD}}{m} = -\frac{[(800\text{m})\cdot(0.01\text{s}^{-1})]^2}{8\cdot(11,000\text{m})}\cdot 0.8\cdot[1-(0.8)^2]^{1/2}$$

$$= \underline{\mathbf{3.5x10}}^{-4}\ \text{m}\cdot\text{s}^{-1}\ .$$

Check: Units OK. Physics OK.
Discussion: This is of the same order of magnitude as the other forces in the equations of motion.

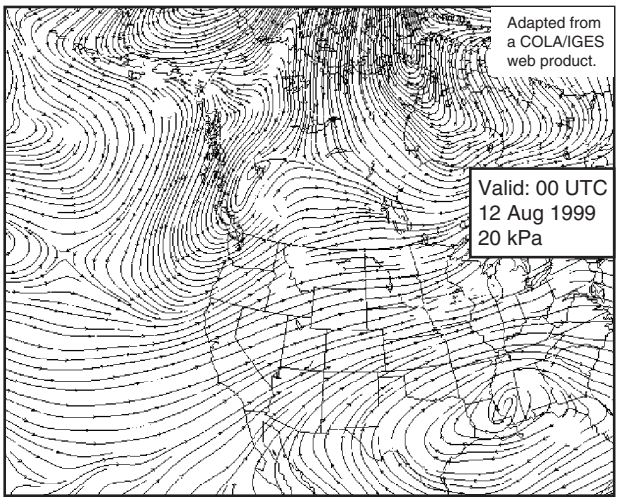

Figure 17.32
Streamlines near the tropopause, over N. America.

Solved Example

For a natural wavelength of 10 km and a hill width of 15 km, describe the type of waves.

Solution

Given: $\lambda = 10$ km, $W = 15$ km.
Find: $Fr = ?$ (dimensionless)

Use eq. (17.32): $Fr_3 = (10\text{km})/[2\cdot(15\text{km})] = \underline{\mathbf{0.333}}$

Check: Units OK. Magnitude OK.
Discussion: Waves as in Fig. 17.30a form off the top of the hill, because $Fr_3 < 1$. Some air also flows around sides of hill.

Mountain-wave Drag

For $Fr_3 < 1$, wave crests tilt upwind with increasing altitude (Fig. 17.31). The angle α of tilt relative to vertical is

$$\cos(\alpha) = Fr_3 \qquad (17.33)$$

For this situation, slightly lower pressure develops on the lee side of the hill, and higher pressure on the windward side. This pressure gradient opposes the mean wind, and is called wave drag. Such wave drag adds to the skin drag. The **wave drag** (*WD*) force per unit mass near the ground is:

$$\frac{F_{xWD}}{m} = -\frac{H^2\cdot {N_{BV}}^2}{8\cdot h_w}\cdot Fr_3\cdot\left[1-{Fr_3}^2\right]^{1/2} \qquad (17.34)$$

where h_w is the depth of air containing waves.

Not surprisingly, higher hills cause greater wave drag. The whole layer of air containing these waves feels the wave drag, not just the bottom of this layer that touches the mountain.

STREAMLINES, STREAKLINES, AND TRAJECTORIES

Streamlines are conceptual lines that are everywhere parallel to the flow at some instant (i.e., a snapshot). This is an Eulerian point of view. Fig. 17.32 shows an example of streamlines on a weather map. Streamlines never cross each other except where the speed is zero, and the wind never crosses streamlines. Streamlines can start and end anywhere, and can change with time. They are often not straight lines.

Streaklines are lines deposited in the flow during a time interval by continuous emission of a tracer from a fixed point. Examples can be seen in aerial photographs of smoke plumes emitted from smokestacks, or volcanic ash clouds.

Trajectories, also called **path lines**, trace the route traveled by an air parcel during a time interval. This is the Lagrangian point of view. For **stationary** (not changing with time) flow, streamlines, streaklines, and trajectories are identical.

For nonstationary flow (flow that changes with time), there can be significant differences between them. For example, suppose that initially the flow is steady and from the north. Later, the wind suddenly shifts to come from the west.

Fig. 17.33 shows the situation shortly after this wind shift. Streamlines (thin solid lines in this figure) are everywhere from the west in this example. The streakline caused by emission from a smokestack is the thick grey line. The black dashed line shows the path followed by one air parcel in the smoke plume.

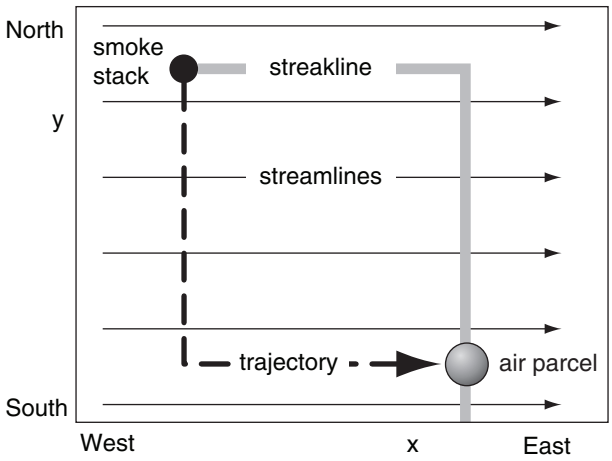

Figure 17.33
Streamlines, streaklines (smoke plumes), and trajectories (path lines) in nonstationary flow.

BERNOULLI'S EQUATION

Principles

Consider a **steady-state** flow (flow that does not change with time), but which can have different velocities at different locations. If we follow an air parcel as it flows along a streamline, its velocity can change as it moves from one location to another. For wind speeds $M \le 20$ m/s at constant altitude, the air behaves as if it is nearly incompressible (namely, constant density ρ).

Incompressible Flow

For the special case of incompressible, steady-state, **laminar** (nonturbulent) motion with no drag, the equations of motion for an air parcel following a streamline can be simplified into a form known as **Bernoulli's equation**:

$$\frac{1}{2}M^2 + \frac{P}{\rho} + |g| \cdot z = C_B \qquad \bullet(17.35)$$

energy: kinetic + flow + potential = constant

where M is the total velocity along the streamline, P is static air pressure, ρ is air density, $|g| = 9.8\ \text{m}\cdot\text{s}^{-2}$ is gravitation acceleration magnitude, and z is height above some reference.

C_B is an arbitrary constant called **Bernoulli's constant** or **Bernoulli's function**. C_B is constant

Science Graffito

"With four parameters I can fit an elephant, and with five I can make him wiggle his trunk."
– *John von Neumann* (attributed by Enrico Fermi)

Solved Example
Environmental air outside a hurricane has sea-level pressure 100 kPa. Find the rise in sea level at the eye, where sea-level pressure is 90 kPa. Neglect currents and wind waves.

Solution
Given: $P_{env} = 100$ kPa, $z_{env} = 0$ m, $P_{eye} = 90$ kPa, $M \approx 0$
Find: $z_{eye} = ?$ m , where z is height of sea level.

Consider a streamline in the water at the sea surface.
$\rho = 1025\ \text{kg/m}^3$ for sea water.

Use Bernoulli's eq. (17.35) to find C_B for the environment, then use it for the eye:

Env: $0.5\cdot(0\text{m/s})^2 + (100{,}000\text{Pa})/(1025\text{kg/m}^3) + (9.8\ \text{m/s}^2)\cdot(0\text{m}) = C_B = 97.6\ \text{m}^2/\text{s}^2$

Eye: $0.5\cdot(0\text{m/s})^2 + (90{,}000\text{Pa})/(1025\text{kg/m}^3) + (9.8\ \text{m/s}^2)\cdot(z_{eye}) = C_B = 97.6\ \text{m}^2/\text{s}^2$

$z_{eye} = \{(97.6\ \text{m}^2/\text{s}^2) - [(90{,}000\text{Pa})/(1025\text{kg/m}^3)]\}/(9.8\ \text{m/s}^2)$
$= \underline{\mathbf{1.0\ m}}$.

Check: Units OK. Magnitude OK.
Discussion: Such a rise in sea level is a hazard called the **storm-surge**.

BEYOND ALGEBRA • Bernoulli Derivation

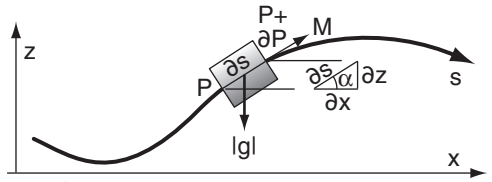

Fig. 17.d. *Forces on air parcel following streamline.*

To derive Bernoulli's equation, apply Newton's second law ($a = F/m$) along a streamline s: Acceleration is the total derivative of wind speed: $a = dM/dt = \partial M/\partial t + M\cdot\partial M/\partial s$. Consider the special case of flow that is steady at any location ($\partial M/\partial t = 0$) even though the flow can be different at different locations ($\partial M/\partial s \neq 0$). Thus

$$M\cdot\partial M/\partial s = F/m$$

The forces per unit mass F/m acting on a fluid parcel along the direction of the streamline are pressure-gradient force and the component of gravity along the streamline [$|g|\cdot\sin(\alpha) = |g|\cdot\partial z/\partial s$]:

$$M\cdot\partial M/\partial s = -(1/\rho)\cdot\partial P/\partial s - |g|\cdot\partial z/\partial s$$

or

$$(1/2)\, dM^2 + (1/\rho)\cdot dP + |g|\cdot dz = 0$$

For incompressible flow, ρ = constant. Integrate the equation above to get Bernoulli's equation:

$$(1/2)\, M^2 + P/\rho + |g|\cdot z = C_B$$

where C_B is the constant of integration.

This result applies only to steady incompressible flow along a streamline. Do not use it for situations where additional forces are important, such as turbulent drag, or across wind turbines or fans.

Solved Example

Cold-air flow speed 10 m/s changes to 2 m/s after passing a hydraulic jump. This air is 10°C colder than the surroundings. How high can the hydraulic-jump jump?

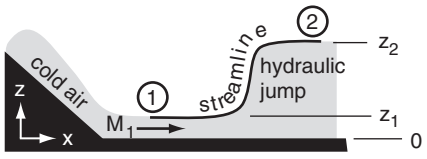

Solution

Given: $M_1 = 10$ m/s, $M_2 = 2$ m/s, $\Delta T = 10$K, $z_1 = 0$.
Find: z_2 = ? m above the initial z.

Assume: $\Delta\theta_v = \Delta T$ and $|g|/T_v = 0.0333$ m·s^{-2}·K^{-1}. $P \approx$ constant on a streamline along the top of the cold air.

Use eq. (17.36), noting that $C_B - P/\rho$ is constant :

- At point 1: $0.5\cdot(10\text{m/s})^2 + 0 = C_B - P/\rho = 50$ m^2/s^2
- At 2: $0.5\cdot(2\text{m/s})^2 + (0.0333\text{m}\cdot\text{s}^{-2}\cdot\text{K}^{-1})\cdot(10\text{K})\cdot z_2 = 50$ m^2/s^2

Solve for z_2: $z_2 = [M_1^2 - M_2^2]\cdot T_v/(2\cdot|g|\cdot\Delta\theta_v) =$ **144 m**

Check: Units OK. Magnitude OK.

Discussion: Hydraulic jumps are very turbulent and would dissipate some of the mechanical energy into heat. So the actual jump height would be less.

along any one streamline, but different streamlines can have different C_B values.

Bernoulli's equation focuses on **mechanical-energy** conservation along a streamline. The first term on the left is the **kinetic energy** per unit mass. The middle term is the work done on the air (sometimes called **flow energy** per unit mass) that has been stored as pressure. The last term on the left is the **potential energy** per mass. Along any one streamline, energy can be converted from one form to another, provided the sum of these energies is constant.

In hydraulics, the gravity term is given by the change in depth of the water, especially when considering a streamline along the water surface. In meteorology, a similar situation occurs when cold air rises into a warmer environment; namely, it is a dense fluid rising against gravity. However, the gravity force felt by the rising cold air is reduced because of its buoyancy within the surrounding air. To compensate for this, the gravity factor in Bernoulli's equation can be replaced with a **reduced gravity** $g' = |g|\cdot\Delta\theta_v/T_v$, yielding:

$$\frac{1}{2}M^2 + \frac{P}{\rho} + |g|\frac{\Delta\theta_v}{T_v}\cdot z = C_B \qquad \bullet(17.36)$$

where $\Delta\theta_v$ is the virtual potential temperature difference between the warm air aloft and the cold air below, and T_v is absolute virtual air temperature (K). Thus, the gravity term is nonzero when the streamline of interest is surrounded by air of different virtual potential temperature, for air flowing up or down.

To use eq. (17.36), first measure all the terms in the left side of the equation at some initial (or upstream) location in the flow. Call this point 1. Use this to calculate the initial value of C_B. Then, at some downstream location (point 2) along the same streamline use eq. (17.36) again, but with the known value of C_B from point 1. The following equation is an expression of this procedure of equating final to initial flow states:

$$\frac{1}{2}M_2^2 + \frac{P_2}{\rho} + |g|\frac{\Delta\theta_v}{T_v}\cdot z_2 = \frac{1}{2}M_1^2 + \frac{P_1}{\rho} + |g|\frac{\Delta\theta_v}{T_v}\cdot z_1 \qquad \bullet(17.37)$$

Another way to consider eq. (17.36) is if any one or two terms increase in the equation, the other term(s) must decrease so that the sum remains constant. In other words, the sum of changes of all the terms must equal zero:

$$\Delta\left[\frac{1}{2}M^2\right]+\Delta\left[\frac{P}{\rho}\right]+\Delta\left[|g|\cdot\frac{\Delta\theta_v}{T_v}\cdot z\right]=0 \qquad \bullet(17.38)$$

Caution: $\Delta[(0.5)\cdot M^2] \neq (0.5)\cdot[\Delta M]^2$.

The Bernoulli equations above do NOT work:

- anywhere the flow is turbulent
- behind obstacles that create turbulent wakes or which cause sudden changes in the flow
- at locations of heat input or loss
- at locations of mechanical-energy input (such as a fan) or loss (such as a wind turbine)
- near the ground where drag slows the wind
- where flow speed > 20 m/s
- where density is not approximately constant

Hence, there are many atmospheric situations for which the above equations are too simplistic.

Compressible Flow

For many real atmospheric conditions where winds can be any speed, you should use a more general form of the Bernoulli equation that includes thermal processes.

For an **isothermal** process, the equation becomes:

$$\frac{1}{2}M^2+\Re_d\cdot T_v\cdot\ln(P)+|g|\frac{\Delta\theta_v}{T_v}\cdot z=C_B \qquad (17.39)$$

where $\Re_d$ = 287 $m^2\cdot s^{-2}\cdot K^{-1}$ is the ideal gas constant for dry air, and where C_B is constant during the process (i.e., initial C_B = final C_B).

For **adiabatic** (isentropic; no heat transfer) flow, the Bernoulli equation is

$$\frac{1}{2}M^2+\left(\frac{C_p}{\Re}\right)\frac{P}{\rho}+|g|\frac{\Delta\theta_v}{T_v}\cdot z=C_B \qquad (17.40)$$

where C_p is the specific heat at constant pressure, and $\Re$ is the ideal gas constant. For dry air, $C_{pd}/\Re_d$ = 3.5 (dimensionless).

Using the ideal gas law, this last equation for adiabatic flow along a streamline becomes

$$\frac{1}{2}M^2+C_p\cdot T+|g|\frac{\Delta\theta_v}{T_v}\cdot z=C_B \qquad \bullet(17.41)$$

kinetic energy + sensible heat + potential energy = constant

where $C_p\cdot T$ is the **enthalpy** (also known as the **sensible heat** in meteorology), and C_p = 1004 $m^2\cdot s^{-2}\cdot K^{-1}$ for dry air. In other words:

Solved Example

Wind at constant altitude decelerates from 15 to 10 m/s while passing through a wind turbine. What opposing net pressure difference would have caused the same deceleration in laminar flow?

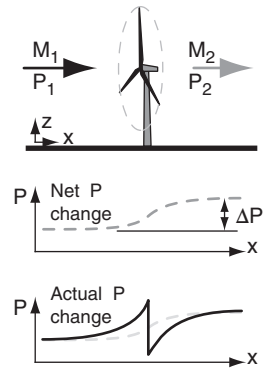

Solution

Given: Δz = 0,
M_1 = 15 m/s , M_2 = 10 m/s.
Find: ΔP = ? Pa

Assume ρ = 1 kg/m^3 = constant.
Solve eq. (17.38) for ΔP: $\Delta P = -\rho\cdot\Delta[(0.5)\cdot M^2]$
$\Delta P = -(1\ kg/m^3)\cdot(0.5)\cdot[(10m/s)^2-(15m/s)^2]$ = **62.4 Pa**

Check: Units OK. Magnitude OK.
Discussion: The process of extracting mechanical energy from the wind has the same affect as an opposing pressure difference. This pressure difference is small compared to ambient atmospheric pressure P = 100,000 Pa.

The actual pressure change across a wind turbine is shown in bottom figure.

Solved Example

Air with pressure 100 kPa is initially at rest. It is accelerated over a flat 0°C snow surface as it is sucked toward a household ventilation system. If the final speed is 10 m/s, what is the air pressure at the fan entrance?

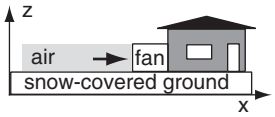

Solution

Given: P_1 = 100 kPa, M_1 = 0, M_2 = 10 m/s, Δz = 0 .
Find: P_2 = ? kPa

Assume the snow keeps their air at constant T_v = 0°C.
Use eq. (17.39) for an isothermal process:
$[0.5M_2^2-0]+\Re_d\cdot T_v\cdot[\ln(P_2)-\ln(P_1)]=0$
Use $\ln(a)-\ln(b)=\ln(a/b)$. Then take exp of both sides, and rearrange: $P_2=P_1\cdot\exp[-0.5M_2^2/(\Re_d\cdot T_v)]$
$P_2=(100kPa)\cdot\exp[-0.5(10m/s)^2/\{(287m^2\cdot s^{-2}\cdot K^{-1})\cdot(273K)\}]$
$=(100kPa)\cdot\exp[-0.000638]=(100kPa)\cdot(0.9994)$
= **99.94 kPa**.

Check: Units OK. Magnitude OK.
Discussion: This decrease of about 0.06 kPa is small compared to ambient P = 100 kPa. The air-pressure decrease is expected because of the suction caused by the fan.

Solved Example

A short distance behind the engine of a jet aircraft flying in level flight, the exhaust temperature is 400 °C and the jet-blast speed is 200 m/s. After the jet exhaust decelerates to zero, what is the final exhaust air temperature, neglecting conduction & turbulent mixing.

Solution

Given: M_1 = 200 m/s, T_1 = 400°C = 673K, M_2 = 0, Δz=0
Find: T_2 = ? °C. Assume adiabatic process.

Rearrange eq. (17.42): $T_2 = T_1 + M_1^2/(2C_p)$
T_2 = (673K) + (200m/s)^2/(2· 1004 m^2·s^{-2}·K^{-1})
= 673K + 19.9K = 693 K = **420°C**

Check: Units OK. Magnitude OK.
Discussion: Jet exhaust is turbulent and mixes quickly with the cooler ambient air, so it is not appropriate to use Bernoulli's equation. See the "dynamic warming" section later in this chapter for more info.

Solved Example

A 75 kW electric wind machine with a 2.5 m radius fan is used in an orchard to mix air to reduce frost damage on fruit. The fan horizontally accelerates air from 0 to 5 m/s. Find the temperature change across the fan, neglecting mixing with environmental air.

Solution

Given: *Power* = 75 kW = 75000 kg·m^2·s^{-3}, R = 2.5 m,
M_1 = 0, M_2 = 5 m/s, Δz = 0
Find: ΔT = ? °C

Assume that all the electrical energy used by the fan motor goes into a combination of heat and shaft work.
The mass flow rate through this fan is:
$\rho \cdot M_2 \cdot \pi \cdot R^2$ = (1.225kg/m^3)·(5m/s)·π·(2.5m)^2 = 120 kg/s
Thus: $\Delta q + \Delta SW$ = *Power*/(*Mass Flow Rate*) = 624 m^2·s^{-2}
Use eq. (17.45): $\Delta T = (1/C_p)\cdot[\Delta q + \Delta SW - 0.5\cdot(M_2^2 - M_1^2)]$
= (1/1004 m^2·s^{-2}·K^{-1})·[(624 m^2·s^{-2}) – 0.5·(5m/s)^2]
= 0.61 K = **0.61°C**

Check: Units OK. Magnitude OK.
Discussion: In spite of the large energy consumption of the electric motor, the heating is spread into a very large volume of air that passes through the fan. Hence, the amount of temperature change is small.

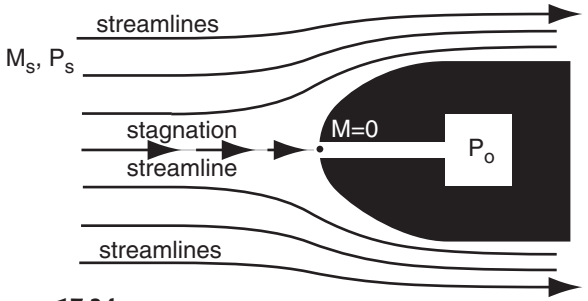

Figure 17.34
Streamlines, showing stagnation as air approaches the obstacle.

(•17.42)

$$\frac{1}{2}M_2^2 + C_p \cdot T_2 + |g|\frac{\Delta\theta_v}{T_v}\cdot z_2 = \frac{1}{2}M_1^2 + C_p \cdot T_1 + |g|\frac{\Delta\theta_v}{T_v}\cdot z_1$$

where subscript 2 denotes final state, and subscript 1 denotes initial state. Equation (17.41) is also sometimes written as

$$\frac{1}{2}M^2 + C_v \cdot T + \frac{P}{\rho} + |g|\frac{\Delta\theta_v}{T_v}\cdot z = C_B \qquad (17.43)$$

energy: kinetic + internal + flow + potential = constant

Again, C_B is constant during the adiabatic process.

Energy Conservation

Because these several previous equations also consider temperature, we cannot call them Bernoulli equations. They are **energy conservation equations** that consider mechanical and thermal energies following a streamline.

If we extend this further into an **energy budget equation**, then we can add the effects of net addition of **thermal energy** (heat per unit mass) Δq via radiation, condensation or evaporation, conduction, combustion, etc. We can also include **shaft work per unit mass** ΔSW done on the air by a fan, or work extracted from the air by a wind turbine.

(17.44)

$$\Delta\left[\frac{1}{2}M^2\right] + \Delta\left[\frac{P}{\rho}\right] + \Delta\left[C_v \cdot T\right] + \Delta\left[|g|\cdot\frac{\Delta\theta_v}{T_v}\cdot z\right] = \Delta q + \Delta SW$$

or

•(17.45)

$$\Delta\left[\frac{1}{2}M^2\right] + \Delta\left[C_p \cdot T\right] + \Delta\left[|g|\cdot\frac{\Delta\theta_v}{T_v}\cdot z\right] = \Delta q + \Delta SW$$

Some Applications

Dynamic & Static Pressure & Temperature

Free-stream atmospheric pressure away from any obstacles is called the **static pressure** P_s. Similarly, let T be the free stream (initial) temperature.

When the wind approaches an obstacle, much of the air flows around it, as shown in Fig. 17.34. However, for one streamline that hits the obstacle, air decelerates from an upstream speed of $M_{initial} = M_s$ to an ending speed of $M_{final} = 0$. This ending point is called the **stagnation point**.

As air nears the stagnation point, wind speed decreases, and both the air pressure and temperature increase. The increased pressure is called the **dynamic pressure** P_{dyn}, and the increased tempera-

ture is called the **dynamic temperature** T_{dyn}. At the stagnation point where velocity is zero, the final dynamic pressure is called the **stagnation pressure** P_o, and the associated dynamic temperature is given the symbol T_o. Think of subscript "*o*" as indicating zero wind speed relative to the obstacle.

To find the dynamic effects at stagnation, use the energy conservation equation (17.42) for wind blowing horizontally (i.e., no change in *z*), and assume a nearly adiabatic process:

$$C_p \cdot T_o = \frac{1}{2} M_s^2 + C_p \cdot T \qquad (17.46)$$

Solving for the dynamic temperature T_o gives:

$$T_o = T + \frac{M_s^2}{2 \cdot C_p} \qquad \bullet(17.47)$$

where C_p = 1004 $m^2 \cdot s^{-2} \cdot K^{-1}$ for dry air. Eq. (17.47) is valid for subsonic speeds (see Focus box).

This effect is called **dynamic warming** or **dynamic heating**, and must be avoided when deploying thermometers in the wind, because the wind stagnates when it hits the thermometer. As shown in Fig. 17.35, dynamic warming ($\Delta T = T_o - T$) is negligible ($\Delta T \le 0.2$°C) for flow speeds of $M_s \le 20$ m/s.

However, for thermometers on an aircraft moving 100 m/s relative to the air, or for stationary thermometers exposed to tornadic winds of M_s = 100 m/s, the dynamic warming is roughly $\Delta T \approx 5$°C. For these extreme winds you can correct for dynamic warming by using the dynamic temperature T_o measured by the thermometer, and using the measured wind speed M_s, and then solving eq. (17.47) for free-stream temperature *T*.

In the Heat chapter is a relationship between temperature and pressure for an adiabatic, compressible process. Using this with the equation above allows us to solve for the **stagnation pressure**:

$$P_o = P_s \cdot \left(\frac{T_o}{T} \right)^{c_p / \Re} \qquad (17.48)$$

or

$$P_o = P_s \cdot \left(1 + \frac{0.5 \cdot M_s^2}{C_p \cdot T} \right)^{c_p / \Re} \qquad (17.49)$$

where $C_p/\Re \approx C_{pd}/\Re_d = 3.5$ for air, P_s is static (free-stream) pressure, M_s is free-stream wind speed along the streamline, $C_p \approx C_{pd}$ = 1004 $J \cdot kg^{-1} \cdot K^{-1}$, *T* is free-stream temperature, and subscript *d* denotes dry air. Fig. 17.35 shows stagnation-pressure increase.

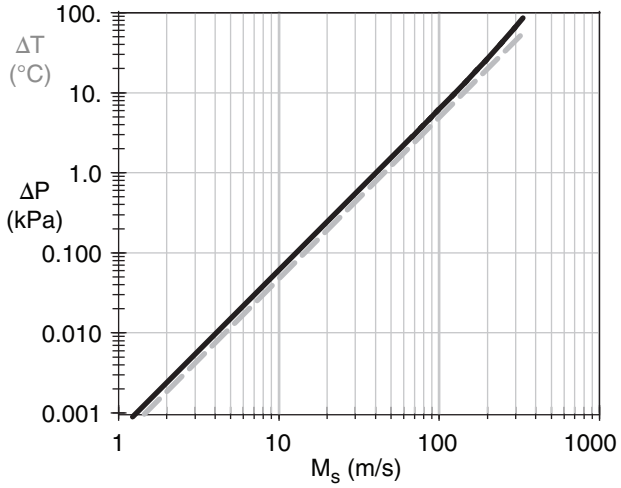

Figure 17.35
Increase in pressure (ΔP, black solid line) and temperature (ΔT, grey dashed line) due to dynamic warming when air of speed M_s hits an obstacle and stagnates. Ambient free-stream conditions for this calculation are T = 290K and P_s = 100 kPa, giving a speed of sound of c = 341 m/s.

Solved Example

Tornadic winds of 100 m/s and 30°C blow into a garage and stagnate. Find stagnation *T* & *P*. What net force pushes against a 3 x 5 m garage wall?

Solution

Given: M_s =100 m/s, *T*=30°C, Wall area *A*=3x5 = 15 m^2
Find: F_{net} = ? N. Assume: ρ = 1.2 kg/m^3, *P* = 100 kPa.

Use eq. (17.47):
T_o = (30°C)+[(100m/s)^2/(2 · 1004$m^2 \cdot s^{-2} \cdot K^{-1}$) = **35°C**.

Use eq. (17.48):
P_o = (100 kPa)·[(35+273)/(30+273)]$^{3.5}$ = **105.9 kPa**.

Compare with eq. (17.50): P_o = (100kPa) + [(0.5 · 1.2kg/m^3)·(100m/s)^2]·(1 kPa/1000Pa)= **106 kPa**

$F_{net} = \Delta P \cdot A$ = (6 kN/m^2)·(15 m^2) = **90 kN**

Check: Units OK. Physics OK.
Discussion: This force is equivalent to the weight of more than 1000 people, and acts on all walls and the roof. It is strong enough to pop the whole roof up off of the house. Then the walls blow out, and the roof falls back down onto the floor.

Hide in the basement. Quickly.

FOCUS • Speed of Sound

The speed c of sound in air is

$$c = [\, k \cdot \Re \cdot T \,]^{1/2} \qquad (17.42)$$

where $k = C_p/C_v$ is the ratio of specific heats for air, $\Re$ is the ideal gas law constant, and T is absolute temperature. For dry air, the constants are: $k = C_{pd}/C_{vd} = 1.4$, and $\Re_d = 287.053\ (m^2/s^2)\cdot K^{-1}$. Thus, the speed of sound increases with the square root of absolute temperature.

The speed M of any object such as an aircraft or an air parcel can be compared to the speed of sound:

$$Ma = M / c \qquad (17.43)$$

where Ma is the dimensionless **Mach number**. Thus, an object moving at Mach 1 is traveling at the speed of sound.

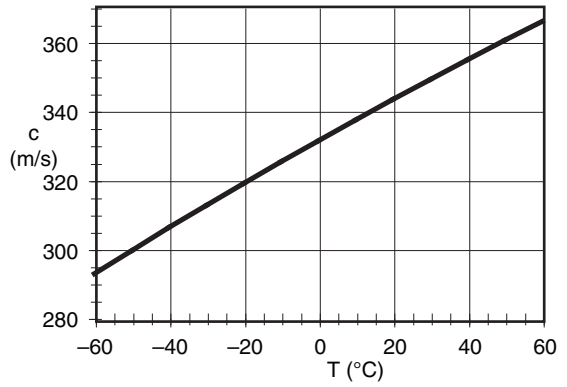

Fig. 17.e. *Speed of sound in dry air.*

Solved Example

If a 20 km wide band of winds of 5 m/s must contract to pass through a 2 km wide gap, what is the pressure drop in the gap compared to the non-gap flow?

Solution

Given: $D_s = 20$ km, $D_d = 2$ km, $M_s = 5$ m/s.
Find: $M_d = ?$ m/s.

Assume: $\rho = 1.2\ kg/m^3$.

Use eq. (17.52):

$\Delta P = (1.2\ kg\cdot m^{-3}/2)\cdot(5 m/s)^2\cdot[1 - ((20\ km)/(2\ km))^2]$
$= -1485\ kg\cdot m^{-1}\cdot s^{-2} =$ **–1.5 kPa**

Check: Units OK. Physics OK.

Discussion: This is a measurable drop in atmospheric pressure. The pressure measured at weather stations in such gaps should be compensated for this venturi effect to calculate the effective static pressure, such as could be used in analyzing weather maps.

For wind speeds of $M_s < 100$ m/s, the previous equation is very well approximated by the simple Bernoulli equation for incompressible flow:

$$P_o = P_s + \frac{\rho}{2} M_s^2 \qquad \bullet(17.50)$$

where ρ is air density. Do not use eq. (17.50) to find dynamic heating when combined with the ideal gas law, because it neglects the large density changes that occur in high-speed flows that stagnate.

The previous 3 equations show that the pressure increase due to stagnation ($\Delta P = P_o - P_s$) is small ($\Delta P < 0.25$ kPa) compared to ambient atmospheric pressure ($P_s = 100$ kPa) for wind speeds of $M_s < 20$ m/s.

Dynamic effects make it difficult to measure static pressure in the wind. When the wind hits the pressure sensor, it decelerates and causes the pressure to increase. For this reason, static pressure instruments are designed to minimize flow deceleration and dynamic errors by having pressure ports (holes) along the sides of the sensor where there is no flow toward or away from the sensor.

Dynamic pressure can be used to measure wind speed. An instrument that does this is the **pitot tube**. Aircraft instruments measure stagnation pressure with the pitot tube facing forward into the flow, and static pressure with another port facing sideways to the flow to minimize dynamic effects. The instrument then computes an "indicated airspeed" from eq. (17.49 or 17.50) using the **pitot – static** pressure difference.

During tornadoes and hurricanes, if strong winds encounter an open garage door or house window, the wind trying to flow into the building causes pressure inside the building to increase dynamically. As is discussed in a solved example, the resulting pressure difference across the roof and walls of the building can cause them to blow out so rapidly that the building appears to explode.

Venturi Effect

Bernoulli's equation says that if velocity increases in the region of flow constriction, then pressure decreases. This is called the **Venturi effect**.

For gap winds of constant depth, eq. (17.37) can be written as

$$\frac{1}{2} M_s^2 + \frac{P_s}{\rho} = \frac{1}{2} M_d^2 + \frac{P_d}{\rho} \qquad (17.51)$$

which can be combined with eq. (17.23) to give the Venturi pressure decrease:

$$P_d - P_s = \frac{\rho}{2} \cdot M_s^2 \cdot \left[1 - \left(\frac{D_s}{D_d} \right)^2 \right] \qquad (17.52)$$

Unfortunately, gap flows are often not constant depth, because the temperature inversion that caps these flows are not rigid lids.

DOWNSLOPE WINDS

Consider a wintertime situation of a layer of cold air under warm, with a synoptic weather pattern forcing strong winds toward a mountain range. Flow over ridge-top depends on cold-air depth, and on the strength of the temperature jump between the two layers. If conditions are right, fast winds, generically called **fall winds**, can descend along the lee slope. Sometimes these downslope winds are fast enough to cause significant destruction to buildings, and to affect air and land transportation. **Downslope wind storms** can be caused by mountain waves (previously discussed), bora winds, and foehns.

Bora

If the fast-moving cold air upstream is deeper than the ridge height H (Fig. 17.36), then very fast (hurricane force) cold winds can descend down the lee side. This phenomena is called a **Bora**. The winds accelerate in the constriction between mountain and the overlying inversion, and pressure drops according to the Venturi effect. The lower pressure upsets hydrostatic balance and draws the cold air layer downward, causing fast winds to hug the slope.

The overlying warmer air is also drawn down by this same pressure drop. Because work must be done to lower this warm air against buoyancy, Bernoulli's equation tells us that the Bora winds decelerate slightly on the way down. Once the winds reach the lowland, they are still destructive and much faster than the winds upstream of the mountain, but are slower than the winds at ridge top. See the Solved Example for the application of Bernoulli's equation.

Boras were originally named for the cold fall wind along the Dalmatian coast of Croatia and Bosnia in winter, when cold air from Russia crosses the mountains and descends southwest toward the Adriatic Sea. The name Bora is used generally now for any cold fall wind having similar dynamics.

For situations where the average mountain ridge height is greater than z_i but the mountain pass is lower than z_i, boras can start in the pass (as a gap wind) and continue down the lee slope.

The difference between katabatic and Bora winds is significant. Katabatic winds are driven by the local thermal structure, and form during periods of weak synoptic forcing such as in high-pressure ar-

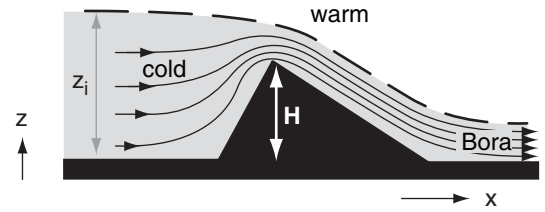

Figure 17.36
Cold Bora winds, during synoptic weather patterns where strong winds are forced toward the ridge from upstream. Thin lines are streamlines. Thick dashed line is a temperature inversion.

Solved Example

For the Bora situation of Fig. 17.36, the inversion of strength 6°C is 1200 m above the upstream lowland. Ridge top is 1000 m above the valley floor. If upstream winds are 10 m/s, find the Bora wind speed in the lee lowlands.

Solution

Given: $H = 1$ km, $z_i = 1.2$ km, $\Delta\theta_v = 6$°C,
$M_s = 10$ m/s. Assume $|g|/T_v = 0.0333$ m·s^{-2}·K^{-1}
Find: M_{Bora} = ? m/s

Volume conservation similar to eq. (17.23) gives ridge top winds M_d:

$$M_d = \frac{z_i}{z_i - H} \cdot M_s = 60 \text{ m/s}$$

Assume Bora thickness = constant = $z_i - H$.
Follow the streamline indicated by the thick dashed line in Fig. 17.36. Assume ending pressure equals starting pressure on this streamline.

Use Bernoulli's eq. (17.37):

$$\left[\frac{1}{2}M^2 + |g|\frac{\Delta\theta_v}{T_v}\cdot z\right]_{ridgetop} = \left[\frac{1}{2}M^2 + |g|\frac{\Delta\theta_v}{T_v}\cdot z\right]_{Bora}$$

Combine the above eqs. Along the streamline, $z_{ridgetop} = z_i$, and $z_{Bora} = z_i - H$. Thus $\Delta z = H$. Solve for M_{Bora}:

$$\boxed{M_{Bora} = \left[\left(\frac{z_i}{z_i - H}\right)^2 \cdot M_s{}^2 - 2\cdot\frac{|g|}{T_v}\cdot\Delta\theta_v\cdot H\right]^{1/2}}$$

Finally, we can plug in the numbers: $M_{Bora} =$

$$\sqrt{\left(\frac{1.2\text{km}}{0.2\text{km}}\right)^2\left(10\frac{\text{m}}{\text{s}}\right)^2 - 2\cdot\left(0.033\frac{\text{m}}{\text{s}^2\text{K}}\right)\cdot(6\text{K})\cdot(1000\text{m})}$$

$$= \sqrt{(3600 - 400)\text{m}^2\text{s}^{-1}} \quad = \quad \underline{\mathbf{56.6\ m/s}}$$

Check: Units OK. Physics OK.
Discussion: Winds at ridge top were 60 m/s. Although the Bora winds at the lee lowlands are weaker than ridge top, they are still strong and destructive. Most of the wind speed up was due to volume conservation, with only a minor decrease given by Bernoulli's equation. This decrease is because kinetic energy associated with wind speed must be expended to do work against gravity by moving warm inversion air downward.

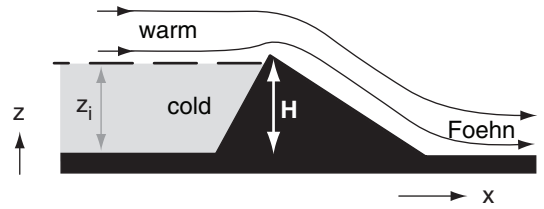

Figure 17.37
One mechanism for creating warm Foehn winds, given synoptic weather patterns where strong winds are forced toward the mountain ridge from upstream. Thin lines are streamlines. Thick dashed line is a temperature inversion.

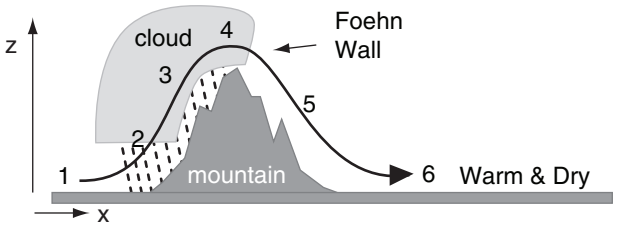

Figure 17.38
Another mechanism for creating warm Foehn winds, where net heating occurs due to formation and fallout of precipitation (dashed lines). Black curved line shows one streamline.

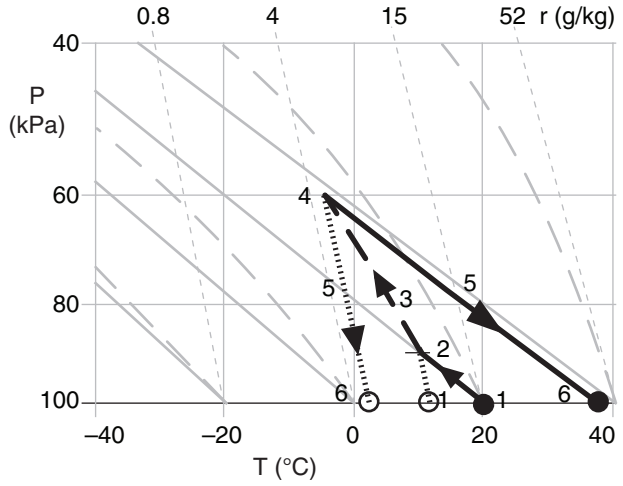

Figure 17.39
Foehn thermodynamics, plotted on a Stüve thermo diagram. P is pressure, T is temperature, r is water-vapor mixing ratio. Black dots and thick black lines indicate air temperature, while dashed lines and open circles indicate humidity. The numbers 1 - 6 correspond to the numbered locations in the previous figure.

eas of fair weather and light winds. Over mid-latitude land, katabatic winds exist only at night and are usually weak, while on the slopes of Antarctica they can exist for days and can become strong. Boras are driven by the inertia of strong upstream winds that form in regions of low pressure and strong horizontal pressure gradient. They can last for several days. Although both phenomena are cold downslope winds, they are driven by different dynamics.

Foehns and Chinooks

One mechanism for creating Foehn winds does not require clouds and precipitation. If the mountain height H is greater than the thickness z_i of cold air upstream, then the cold air is dammed behind the mountain and does not flow over (Fig. 17.37). The strong warm winds aloft can flow over the ridge top, and can warm further upon descending adiabatically on the lee side. The result is a warm, dry, downslope wind called the **Foehn**.

Foehn winds were originally named for the southerly winds from Italy that blow over the Alps and descend in Austria, Germany, and Switzerland. A similar downslope wind is called the **chinook** just east of the Rocky Mountains in the USA and Canada. Other names in different parts of the world are **zonda** (Argentina), **austru** (Romania), **aspre** (France). The onset of foehn winds in winter can be accompanied with a very rapid temperature increase at the surface. If the warm and very dry air flows over snowy ground, it rapidly melts and sublimes the snow, and is nicknamed "snow eater".

Another Foehn mechanism is based on net latent heating associated with condensation and precipitation on the upwind side of the mountain range. Consider an air parcel before it flows over a mountain, such as indicated at point (1) in Fig. 17.38. Suppose that the temperature is 20°C and dew point is 10°C initially, as indicated by the filled and open circles at point (1) in Fig. 17.39. This corresponds to about 50% relative humidity.

As the air rises along the windward slopes, it cools dry-adiabatically while conserving mixing ratio until the lifting condensation level (LCL) is reached (2). Further lifting is moist adiabatic (3) within the **orographic cloud** (a cloud caused by the terrain). Suppose that most of the condensed water falls out as precipitation on the windward slopes.

Over the summit (4), suppose that the air has risen to a height where the ambient pressure is 60 kPa. The air parcel now has a temperature of about –8°C. As it begins to descend down the lee side, any residual cloud droplets will quickly evaporate in the adiabatically warming air. The trailing edge of the orographic cloud is called a **Foehn wall**, because

it looks like a wall of clouds when viewed from the lowlands downwind.

Continued descent will be dry adiabatic (5) because there are no liquid water drops to cause evaporative cooling. By the time the air reaches its starting altitude on the lee side (6), its temperature has warmed to about 35°C, with a dew point of about –2°C. This is roughly 10% relative humidity.

The net result of this process is: clouds and precipitation form on the windward slopes of the mountain, a Foehn wall forms just downwind of the mountain crest, and there is warming and drying in the lee lowlands.

Solved Example

Air from the Pacific Ocean (T =5°C, T_d = 3°C, z = 0) flows over the Coast Mountains ($z \approx 3000$ m), and descends toward the interior plateau of British Columbia, Canada ($z \approx 1000$ m). Fig. 17.19 shows the topography of this region. Find the final T and T_d.

Solution

Given: T = 5 °C, T_d = 3 °C, z = 0 m initially.
Find: T = ? °C, T_d = ? ° at z = 1000 m finally.

Use the thermo diagram from chapter 5:

Use the thermo diagram to find that the initial mixing ratio is $r \approx 5$ g/kg. Clouds form as the air rises over the mountains, with base at z_{LCL} = (0.125 km/°C)·(5–3°C) = 0.25 km. From there to z = 3000 m, the air follows a moist adiabat, reaching $T = T_d \approx$ –17°C.

Assuming all condensate falls out as precipitation on the windward side, the air then descends dry-adiabatically to the town of Williams Lake. The final state is: $T \approx$ **4°C** at z = 1000 m, and $T_d \approx$ **–13°C**.

Check: Units OK. Physics OK.
Discussion: The air is much drier ($RH \approx 25\%$) on the lee side, but nearly the same temperature as initially. This is typical of a foehn wind.

CANOPY FLOWS

Forests and Crops

The leaf or needle layer of a crop or forest is called a **canopy**. Individual plants or trees in these crops or forests each cause drag on the wind. The average winds in the air space between these **plant-canopy** or **forest-canopy** obstacles is the canopy flow.

Just above the top of the canopy, the flow is approximately logarithmic with height (Fig. 17.40a), as is described in more detail in the Boundary-Layer chapter for statically neutral conditions in the surface layer:

$$M = \frac{u_*}{k} \ln\left(\frac{z-d}{z_o}\right) \qquad \text{for } z \geq h_c \quad (17.53)$$

where M is wind speed, z is height above ground, u_* is the **friction velocity** (a measure of the drag force per unit surface area of the ground), $k \approx 0.4$ is the **von Kármán constant**, d is the **displacement distance** ($0 \leq d \leq h_c$), and z_o is the **roughness length**, for an average canopy-top height of h_c.

If you can measure the actual wind speed M at 3 or more heights z within 20 m above the top of the canopy, then you can use the following procedure to find d, z_o, and u_*: (1) use a spreadsheet to plot your M values on a linear horizontal axis vs. their $[z–d]$ values on a logarithmic vertical axis; (2) experiment with different values of d until you find the one that aligns your wind points into a straight line; (3) extrapolate that straight line to M = 0, and note the resulting intercept on the vertical axis, which gives the roughness length z_o. (4) Finally, pick any point exactly on the plotted line, and then plug in its M and z values, along with the d and z_o values just found, to calculate u_*. using eq. (17.53).

If you do not have measurements of wind speed above the canopy top, you can use the following

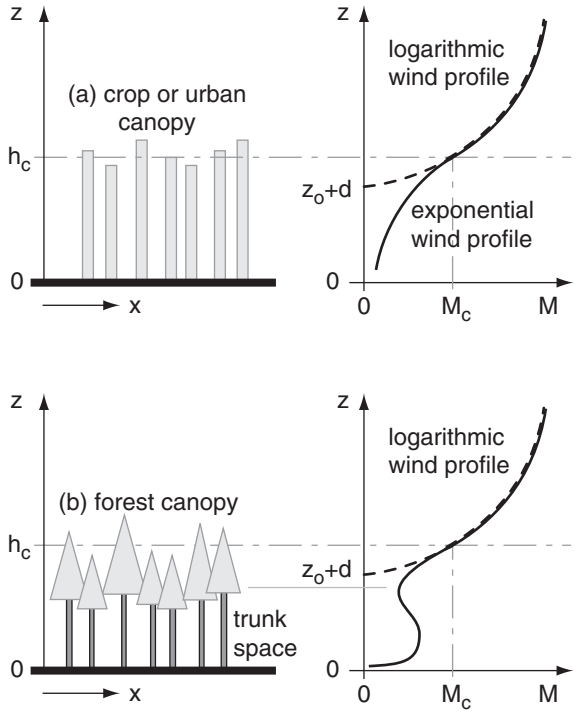

Figure 17.40
Canopy flows for (a) crops or urban canopies, and (b) forest canopies having a relatively open trunk space. Left: sketch of the canopy objects. Right: wind profile (solid line). The dashed black line shows a logarithmic profile extrapolated to zero wind speed M. Average top of the canopy is at height h_c.

Solved Example (§)

Given these wind measurements over a 2 m high corn crop: [z (m), M (m/s)] = [5, 3.87] , [10, 5.0] , [20, 6.01]. Find the displacement distance, roughness length, and friction velocity. If the attenuation coefficient is 2.5, plot wind speed M vs. height over $0.5 \text{ m} \le z \le 5$ m.

Solution

Given: h_c =2m, [z (m), M (m/s)] as listed above, a = 2.5.
Find: d = ? m, z_o = ? m, u_* = ? m/s, and plot M vs. z.

Guess d = 0, and plot M vs. log(z–d) on a spreadsheet. This d is too small (see graph below), because the curve is concave up. Guess d = 4, which is too large, because curve is concave down. After other guesses (some not shown), I find that **d = 1.3 m** gives the straightest line.

Next, extrapolate on the semi-log graph to M = 0, which gives an intercept of **z_o = 0.2 m**.

Solve eq. (17.53) for $u_* = k \cdot M / \ln[(z–d)/z_o]$
u_* = 0.4(5m/s)/ln[(10–1.3)/0.2] = **0.53 m/s**

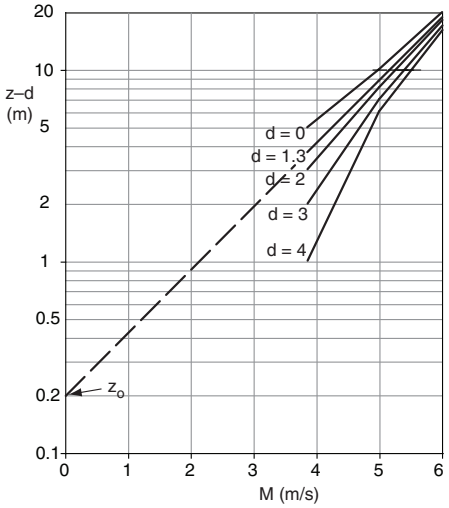

Solve eq. (17.53) for M_c at $z = h_c$ = 2 m:
M_c = [(0.53m/s)/0.4] · ln[(2–1.3m)/0.2] = 1.66 m/s

Use eq. (17.54) to find M for a range of heights below h_c, and use eq. (17.53) for heights above h_c:

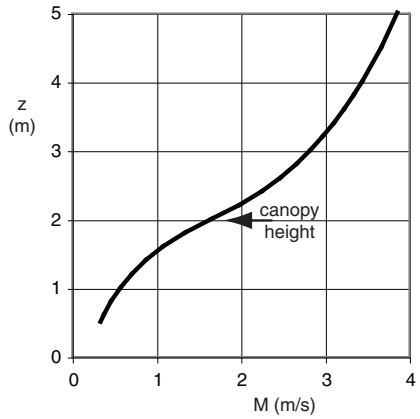

Check: Shape of curve looks reasonable.
Discussion: For this exercise, $z_o = 0.1\ h_c$, and $d = 0.65\ h_c$. Namely, the crude approximations are OK.

crude approximations to estimate the needed parameters: $d \approx 0.65 \cdot h_c$ and $z_o \approx 0.1 \cdot h_c$. Methods to estimate u_* are given in the Boundary-Layer chapter.

The average wind speed at the average canopy-top height is M_c. For the crude approximations above, we find that $M_c \approx 3.13\ u_*$.

Within the top 3/4 of canopy, an exponential formula describes the average wind-speed M profile:

$$M = M_c \cdot \exp\left[a \cdot \left(\frac{z}{h_c} - 1 \right) \right] \qquad \text{for } 0.5 h_c \le z \le h_c \qquad (17.54)$$

where a is an **attenuation coefficient** that increases with increasing leaf area and decreases as the mean distance between individual plants increases. Typical values are $a \approx$ 2.5 - 2.8 for oats and wheat; 2.0 - 2.7 for mature corn; 1.3 for sunflowers, 1.0 - 1.1 for larch and small evergreen trees, and 0.4 for a citrus orchard. The exponential and log-wind speeds match at the average canopy top h_c.

For a forest with relatively open trunk space (i.e., only the tree trunks without many leaves, branches, or smaller underbrush), the previous equation fails. Instead, a weak relative maximum wind speed can occur (Fig. 17.40b). In such forests, if the canopy is very dense, then the sub-canopy (trunk space) flow can be relatively disconnected from the flow above the tree tops. Weak katabatic flows can exist in the trunk space day and night.

Cities

The collection of buildings and trees that make up a city is sometimes called an **urban canopy**. These obstacles cause an average canopy-flow wind similar to that for forests and crops (Fig. 17.40a).

However, winds at any one location in the city can be quite different. For example, the street corridors between tall buildings can channel flow similar to the flow in narrow valleys. Hence these corridors are sometimes called **urban canyons**. Also, taller buildings can deflect down to the surface some of the faster winds aloft. This causes much greater wind speeds and gusts near the base of tall buildings than near the base of shorter buildings.

Cities can be 2 - 12°C degrees warmer than the surrounding rural countryside — an effect called the **urban heat island** (UHI, Fig. 17.41). Reasons include the abundance of concrete, glass and asphalt, which capture and store the solar heat during daytime and reduce the IR cooling at night. Also, vegetated areas are reduced in cities, and rainwater is channeled away through storm drains. Hence, there is less evaporative cooling. Also, fuel and electrical consumption by city residents adds heat via heating, air conditioning, industry, and transportation.

The city–rural temperatue difference ΔT_{UHI} is greatest during clear calm nights, because the city stays warm while rural areas cool considerably due to IR radiation to space. Temperature difference is much smaller during daytime. The largest ΔT_{UHI} values occur near the city center, at the greatest density of high buildings and narrow streets. Max ΔT_{UHI} increases with city population N (Fig. 17.42). When averaged over a year (including windy and cloudy periods of minimal UHI), the average ΔT_{UHI} at the city center is only 1 to 2°C.

During periods of fair weather and light synoptic-scale winds, the warm city can generate circulations similar to sea breezes, with inflow of low-altitude rural air toward the city, and rising air over the hottest parts of town. These circulations can enhance clouds, and trigger or strengthen thunderstorms over and downwind of the city. With light to moderate winds, the UHI area is asymmetric, extending much further from the city in the downwind direction (Fig. 17.41), and the effluent (heat, air pollution, odors) from the city can be observed downwind as an **urban plume** (Fig. 17.43).

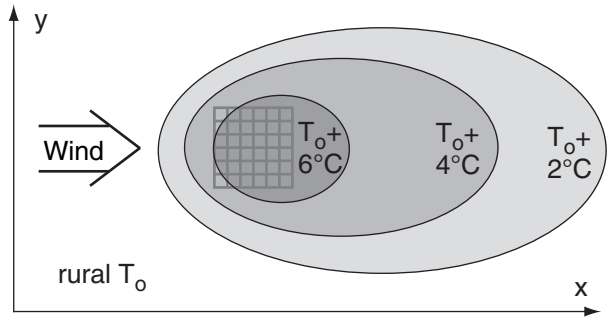

Figure 17.41
An urban heat island at night, where T_o is the rural air temperature. The grid represents city streets.

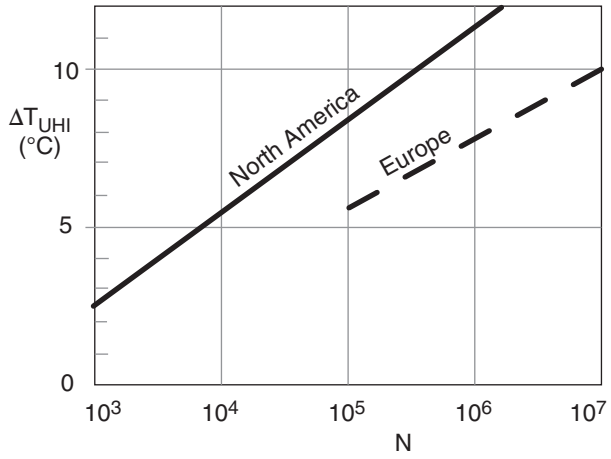

Figure 17.42
Urban-heat-island temperature difference ΔT_{UHI} increases with city population N.

SUMMARY

The probability of any wind speed can be described by a Weibull distribution, and the distribution of wind directions can be plotted on a wind rose. Regions with greater probability of strong winds are ideal for siting wind turbines to generate electrical power.

During weak synoptic forcing (weak geostrophic winds), local circulations can be driven by thermal forcings. Examples include anabatic (warm upslope) and katabatic (cold downslope) winds, mountain and valley winds, and sea breezes near coastlines.

During strong synoptic forcing, winds can be channeled through gaps, can form downslope windstorms, and can create mountain waves and wave drag. The winds in short gaps can be well described by open-channel hydraulics and Bernoulli's equation. Winds in longer gaps and fjords are influenced by Coriolis force.

The Bora is a cold downslope wind — driven dynamically by the synoptic scale flow. Foehn winds are also driven dynamically, but are warm, and can be enhanced by orographic precipitation and latent heating. Hydraulic jumps occur downstream of bora winds and in some gap flows as the flow re-adjusts to hydrostatic equilibrium.

Wind and temperature instruments are constructed to minimize dynamic pressure and heating errors. Wind speed is reduced inside plant and ur-

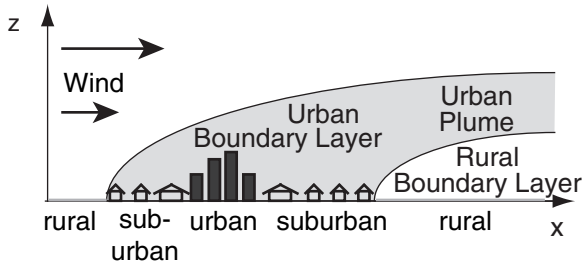

Figure 17.43
Sketch of an urban plume blowing downwind.

ban canopies. The urban-heat-island effect of cities can induce local circulations.

Threads

Winds in this chapter were mostly mesoscale and smaller, as described by Newton's second law of motion (Chapter 10). Positions of synoptic-scale low and high-pressure centers (Chapter 13) and fronts (Chapter 12) drives gap winds, coastal jets, and mountain waves.

Mountain waves, Boras, and Foehns require a statically stable environment (Chapter 5) such as is in the standard atmosphere (Chapter 1). Warm foehn winds can occur by latent heating (Chapters 4 and 5), or by adiabatic warming (Chapter 3) of downslope air. Clouds (Chapter 6) can be created in the updrafts near mountains.

Wind turbines are often sited near hilly regions where wind speed increases. Turbines are designed to withstand the wind shear and gusts typical of the atmospheric boundary layer (Chapter 18).

ON DOING SCIENCE • Simple is Best

Fourteenth century philosopher William of Occam suggested that "the simplest scientific explanation is the best". This tenant is known as **Occam's Razor**, because with it you can cut away the bad theories and complex equations from the good.

But why should the simplest or most elegant be the best? There is no law of nature that says it must be so. It is just one of the philosophies of science, as is the scientific method of Descartes. Ultimately, like any philosophy or religion, it is a matter of faith.

I suggest an alternative tenant: "**a scientific relationship should not be more complex than needed**." This is motivated by the human body — an amazingly complex system of hydraulic, pneumatic, electrical, mechanical, chemical, and other physical processes that works exceptionally well. In spite of its complexity, the human body is not more complex than needed (as determined by evolution).

Although this alternative tenant is only subtly different from Occam's Razor, it admits that sometimes complex mathematical solutions to physical problems are valid. This tenant is used by a data-analysis method called **computational evolution** (or **gene-expression programming**). This approach creates a population of different algorithms that compete to best fit the data, where the best algorithms are allowed to persist with mutation into the next generation while the less-fit algorithms are culled via computational natural selection.

EXERCISES

Numerical Problems

N1.(§) Plot the probability of wind speeds using a Weibull distribution with a resolution of 0.5 m/s, and M_o = 8 m/s, for α =

a. 1.0 b. 1.5 c. 2.0 d. 2.5 e. 3.0 f. 3.5 g. 4.0
h. 4.5 i. 5.0 j. 5.5 k. 6.0 m. 7 n. 8 o. 9

N2. A wind turbine of blade radius 25 m runs at 35% efficiency. At sea level, find the theoretical power (kW) for winds (m/s) of:

a. 1 b. 2 c. 3 d. 4 e. 5 f. 6 g. 7 h. 8
i. 9 j. 10 k. 11 m. 12 n. 13 o. 14 p. 15

N3. Find the equilibrium updraft speed (m/s) of a thermal in a 2 km boundary layer with environmental temperature 15°C. The thermal temperature (°C) is: a. 16 b. 16.5 c. 17 d. 17.5 e. 18 f. 18.5
g. 19 h. 19.5 i. 20 j. 20.5 k. 21 m. 21.5

N4. Anabatic flow has a temperature excess of 4°C. Find the buoyant along-slope pressure gradient force per unit mass for a slope of angle (°):

a. 10 b. 15 c. 20 d. 25 e. 30 f. 35 g. 40
h. 45 i. 50 j. 55 k. 60 m. 65 n. 70 o. 75

N5(§). Plot katabatic wind speed (m/s) vs. downslope distance (m) if the environment is 20°C and the cold katabatic air is 15°C. The slope angle (°) is:

a. 10 b. 15 c. 20 d. 25 e. 30 f. 35 g. 40
h. 45 i. 50 j. 55 k. 60 m. 65 n. 70 o. 75

N6. Find the equilibrium downslope speed (m/s) for the previous problem, if the katabatic air is 5 m thick and the drag coefficient is 0.002.

N7. Find the depth (m) of the thermal internal boundary layer 2 km downwind of the coastline, for an environment with wind speed 8 m/s and γ = 4 K/km. The surface kinematic heat flux (K·m/s) is

a. 0.04 b. 0.06 c. 0.08 d. 0.1 e. 0.12
f. 0.14 g. 0.16 h. 0.18 i. 0.2 j. 0.22

N8. Assume T_v = 20°C. Find the speed (m/s) of advance of the sea-breeze front, for a flow depth of 700 m and a temperature excess $\Delta\theta$ (K) of:

a. 1.0 b. 1.5 c. 2.0 d. 2.5 e. 3.0 f. 3.5 g. 4.0
h. 4.5 i. 5.0 j. 5.5 k. 6.0 m. 7 n. 8 o. 9

N9. For the previous problem, find the sea-breeze wind speed (m/s) at the coast.

N10. For a sea-breeze frontal speed of 5 m/s, find the expected maximum distance (km) of advance of the sea-breeze front for a latitude (°) of

a. 10 b. 15 c. 20 d. 25 e. 80 f. 35 g. 40
h. 45 i. 50 j. 55 k. 60 m. 65 n. 70 o. 75

N11. What is the shallow-water wave phase speed (m/s) for a water depth (m) of:

a. 2 b. 4 c. 6 d. 8 e. 10 f. 15 g. 20
h. 25 i. 30 j. 40 k. 50 m. 75 n. 100 o. 200

N12. Assume $|g|/T_v = 0.0333$ m·s^{-2}·K^{-1}. For a cold layer of air of depth 50 m under warmer air, find the surface (interfacial) wave phase speed (m/s) for a virtual potential temperature difference (K) of:

a. 1.0 b. 1.5 c. 2.0 d. 2.5 e. 3.0 f. 3.5 g. 4.0
h. 4.5 i. 5.0 j. 5.5 k. 6.0 m. 7 n. 8 o. 9

N13. For the previous problem, find the value of the Froude number Fr_1. Also, classify this flow as subcritical, critical, or supercritical. Given $M = 15$ m/s.

N14. Assume $|g|/T_v = 0.0333$ m·s^{-2}·K^{-1}. Find the internal wave horizontal group speed (m/s) for a stably stratified air layer of depth 400 m, given $\Delta\theta_v/\Delta z$ (K/km) of:

a. 1.0 b. 1.5 c. 2.0 d. 2.5 e. 3.0 f. 3.5 g. 4.0
h. 4.5 i. 5.0 j. 5.5 k. 6.0 m. 7 n. 8 o. 9

N15. For the previous problem, find the value of the Froude number Fr_2. Also, classify this flow as subcritical, critical, or supercritical.

N16. Winds of 10 m/s are flowing in a valley of 10 km width. Further downstream, the valley narrows to the width (km) given below. Find the wind speed (m/s) in the constriction, assuming constant depth flow.

a. 1.0 b. 1.5 c. 2.0 d. 2.5 e. 3.0 f. 3.5 g. 4.0
h. 4.5 i. 5.0 j. 5.5 k. 6.0 m. 7 n. 8 o. 9

N17. Assume $|g|/T_v = 0.0333$ m·s^{-2}·K^{-1}. For a two-layer atmospheric system flowing through a short gap, find the maximum expected gap wind speed (m/s). Flow depth is 300 m, and the virtual potential temperature difference (K) is:

a. 1.0 b. 1.5 c. 2.0 d. 2.5 e. 3.0 f. 3.5 g. 4.0
h. 4.5 i. 5.0 j. 5.5 k. 6.0 m. 7 n. 8 o. 9

N18. Find the long-gap geostrophic wind (m/s) at latitude 50°, given $|g|/T_v = 0.0333$ m·s^{-2}·K^{-1} and $\Delta\theta_v$ = 3°C, and assuming that the slope of the top cold-air surface is given by the height change (km) below across a valley 10 km wide.

a. 0.3 b. 0.4 c. 0.5 d. 0.6 e. 0.7
f. 0.8 g. 0.9 h. 1.0 i. 1.1 j. 1.2
k. 2.4 m. 2.6 n. 2.8 o. 3

N19. Find the external Rossby radius of deformation (km) for a coastally trapped jet that rides against a mountain range of 2500 m altitude at latitude (°) given below, for air that is colder than its surroundings by 10°C. Assume $|g|/T_v = 0.0333$ m·s^{-2}·K^{-1}.

a. 80 b. 85 c. 20 d. 25 e. 30 f. 35 g. 40
h. 45 i. 50 j. 55 k. 60 m. 65 n. 70 o. 75

N20. Assume $|g|/T_v = 0.0333$ m·s^{-2}·K^{-1}. Find the natural wavelength of air, given

a. $M = 2$ m/s, $\Delta T/\Delta z = 5$ °C/km
b. $M = 20$ m/s, $\Delta T/\Delta z = -8$ °C/km
c. $M = 5$ m/s, $\Delta T/\Delta z = -2$ °C/km
d. $M = 20$ m/s, $\Delta T/\Delta z = 5$ °C/km
e. $M = 5$ m/s, $\Delta T/\Delta z = -8$ °C/km
f. $M = 2$ m/s, $\Delta T/\Delta z = -2$ °C/km
g. $M = 5$ m/s, $\Delta T/\Delta z = 5$ °C/km
h. $M = 2$ m/s, $\Delta T/\Delta z = -8$ °C/km

N21. For a mountain of width 25 km, find the Froude number Fr_3 for the previous problem. Draw a sketch of the type of mountain waves that are likely for this Froude number.

N22. For the previous problem, find the angle of the wave crests, and the wave-drag force per unit mass. Assume $H = 1000$ m and $h_w = 11$ km.

N23(§). Plot the wavy path of air as it flows past a mountain, given an initial vertical displacement of 300 m, a wavelength of 12.5 km, and a damping factor of

a. 1.0 b. 1.5 c. 2.0 d. 2.5 e. 3.0 f. 3.5 g. 4.0
h. 4.5 i. 5.0 j. 5.5 k. 6.0 m. 7 n. 8 o. 9

N24(§) Given a temperature dew-point spread of 1.5°C at the initial (before-lifting) height of air in the previous problem, identify which wave crests contain lenticular clouds.

N25. Cold air flow speed 12 m/s changes to 3 m/s after a hydraulic jump. Assume $|g|/T_v = 0.0333$ m·s^{-2}·K^{-1}. How high can the hydraulic jump rise if the exit velocity (m/s) is

a. 1.0 b. 1.5 c. 2.0 d. 2.5 e. 3.0 f. 3.5 g. 4.0
h. 4.5 i. 5.0 j. 5.5 k. 6.0 m. 7 n. 8 o. 9

N26. Assuming standard sea-level density and streamlines that are horizontal, find the pressure change given the following velocity (m/s) change:

a. 1.0 b. 1.5 c. 2.0 d. 2.5 e. 3.0 f. 3.5 g. 4.0
h. 4.5 i. 5.0 j. 5.5 k. 6.0 m. 7 n. 8 o. 9

N27. Wind at constant altitude decelerates from 12 m/s to the speed (m/s) given below, while passing through a wind turbine. What opposing net pressure difference (Pa) would have caused the same deceleration in laminar flow?
a. 1.0 b. 1.5 c. 2.0 d. 2.5 e. 3.0 f. 3.5 g. 4.0
h. 4.5 i. 5.0 j. 5.5 k. 6.0 m. 7 n. 8 o. 9

N28. Air with pressure 100 kPa is initially at rest. It is accelerated isothermally over a flat 0°C snow surface as it is sucked toward a household ventilation system. What is the final air pressure (kPa) just before entering the fan if the final speed (m/s) through the fan is:
a. 1 b. 2 c. 3 d. 4 e. 5 f. 6 g. 7 h. 8
i. 9 j. 10 k. 11 m. 12 n. 13 o. 14 p. 15

N29. A short distance behind the jet engine of an aircraft flying in level flight, the exhaust temperature is 500°C. After the jet exhaust decelerates to zero, what is the final exhaust air temperature (°C), neglecting conduction and mixing, assuming the initial jet-blast speed (m/s) is:
a. 100 b. 125 c. 150 d. 175 e. 200 f. 210 g. 220
h. 230 i. 240 j. 250 k. 260 m. 270 n. 280 o. 290

N30. An 85 kW electric wind machine with a 3 m radius fan blade is used in an orchard to mix air so as to reduce frost damage on fruit. The fan horizontally accelerates the air from calm to the speed (m/s) given below. Find the temperature change (°C) across the fan, neglecting mixing with the environmental air.
a. 6 b. 6.5 c. 7 d. 7.5 e. 8 f. 8.5 g. 9
h. 9.5 i. 10 j. 10.5 k. 11 m. 12 n. 13 o. 14

N31. Tornadic air of temperature 25°C blows with speed (m/s) given below, except that it stagnates upon hitting a barn. Find the final stagnation temperature (°C) and pressure change (kPa).
a. 100 b. 125 c. 150 d. 175 e. 200 f. 210 g. 220
h. 230 i. 240 j. 250 k. 260 m. 270 n. 280 o. 290

N32. Find the speed of sound (m/s) and Mach number for M_{air} = 100 m/s, given air of temperature (°C):
a. –50 b. –45 c. –40 d. –35 e. –30
f. –25 g. –20 h. –15 i. –10 j. –5
k. 0 m. 5 n. 10 o. 15 p. 20

N33. Water flowing through a pipe with speed 2 m/s and pressure 100kPa accelerates to the speed (m/s) given below when it flows through a constriction. What is the fluid pressure (kPa) in the constriction? Neglect drag against the pipe walls.
a. 6 b. 6.5 c. 7 d. 7.5 e. 8 f. 8.5 g. 9
h. 9.5 i. 10 j. 10.5 k. 11 m. 12 n. 13 o. 14

N34. For the bora solved example, redo the calculation assuming that the initial inversion height (km) is: a. 1.1 b. 1.15 c. 1.25 d. 1.3 e. 1.35
f. 1.4 g. 1.45 h. 1.5 i. 1.55 j. 1.6
k. 1.65 m. 1.7 n. 1.75 o. 1.8 p. 1.85

N35. Use a thermodynamic diagram. Air of initial temperature 10°C and dew point 0°C starts at a height where the pressure (kPa) is given below. This air rises to height 70 kPa as it flows over a mountain, during which all liquid and solid water precipitate out. Air descends on the lee side of the mountain to an altitude of 95 kPa. What is the temperature, dew point, and relative humidity of the air at its final altitude? How much precipitation occurred on the mountain? [Hint: use a thermo diagram.]
a. 104 b. 102 c. 100 d. 98 e. 96 f. 94 g. 92
h. 90 i. 88 j. 86 k. 84 m. 82 n. 80

N36. Plot wind speed vs. height, for heights between 0.25 h_c and 5 h_c, where h_c is average plant canopy height. Given:

	Plant	h_c(m)	u_*(m/s)	attenuation coef.
a.	Wheat	1.0	0.5	2.6
b.	Wheat	1.0	0.75	2.6
c.	Soybean	1.0	0.5	3.5
d.	Soybean	1.0	0.75	3.5
e.	Oats	1.5	0.5	2.8
f.	Oats	1.5	0.75	2.8
g.	Corn	2.0	0.5	2.7
h.	Corn	2.0	0.75	2.7
i.	Corn	2.5	0.5	2.2
j.	Corn	2.5	0.75	2.2
k.	Sunflower	2.75	0.5	1.3
m.	Sunflower	2.75	0.75	1.3
n.	Pine	3.0	0.5	1.1
o.	Pine	3.0	0.25	1.1
p.	Orchard	4.0	0.5	0.4
q.	Orchard	4.0	0.25	0.4
r.	Forest	20.	0.5	1.7
s.	Forest	20.	0.25	1.7

N37. Estimate the urban heat island temperature excess compared to the surrounding rural countryside, for a N. American city of population
a. 2000 b. 5000 c. 7000 d. 10,000 e. 20,000
f. 50k g. 70k h. 100k i. 200k j. 500k k. 700k
m. 1M n. 2M

Understanding & Critical Evaluation

U1. For a Weibull distribution, what is the value of the probability in any one bin as the bin size becomes infinitesimally small? Why?

U2(§). Create a computer spreadsheet with location and spread parameters in separate cells. Create and plot a Weibull frequency distribution for winds by referencing those parameters. Then try changing the parameters to see if you can get the Weibull distribution to look like other well-known distributions, such as Gaussian (symmetric, bell shaped), exponential, or others.

U3. Why was an asymmetric distribution such as the Weibull distribution chosen to represent winds?

U4. What assumptions were used in the derivation of Betz' Law, and which of those assumptions could be improved?

U5. To double the amount of electrical power produced by a wind turbine, wind speed must increase by what percentage, or turbine radius increase by what percentage?

U6. For the Weibull distribution as plotted in Fig. 17.1, find the total wind power associated with it.

U7. In Fig. 17.5, what determines the shape of the wind-power output curve between the cut-in and rated points?

U8. List and explain commonalities among the equations that describe the various thermally-driven local flows.

U9. If thermals with average updraft velocity of W = 5 m/s occupy 40% of the horizontal area in the boundary layer, find the average downdraft velocity.

U10. What factors might affect rise rate of the thermal, in addition to the ones already given in this chapter?

U11. Anabatic and lenticular clouds were described in this chapter. Compare these clouds and their formation mechanisms. Is it possible for both clouds to occur simultaneously over the same mountain?

U12. Is the equation describing the anabatic pressure gradient force valid or reasonable in the limits of 0° slope, or 90° slope. Explain.

U13. Explain in terms of Bernoulli's equation the horizontal pressure gradient force acting on anabatic winds.

U14. What factors control the shape of the katabatic wind profile, as plotted in Fig. 17.9?

U15. The solved example for katabatic wind shows the curves from eqs. (17.8) and (17.9) as crossing. Given the factors that appear in those equations, is a situation possible where the curves never cross? Describe.

U16. Suppose a mountain valley exits right at a coastline. For synoptically weak conditions (near zero geostrophic wind), describe how would the mountain/valley circulation and sea-breeze circulation interact. Illustrate with drawings.

U17. The thermal internal boundary layer can form both during weak- and strong-wind synoptic conditions. Why?

U18. For stronger land-sea temperature contrasts, which aspects of the sea-breeze would change, and which would be relatively unchanged? Why?

U19. At 30° latitude, can the sea-breeze front advance an infinite distance from the shore? Why?

U20. In the Southern Hemisphere, draw a sketch of the sea-breeze-vs.-time hodograph, and explain it.

U21. For what situations would open-channel hydraulics NOT be a good approximation to atmospheric local flows? Explain.

U22. Interfacial (surface) wave speed was shown to depend on average depth of the cold layer of air. Is this equation valid for any depth? Why?

U23. In deriving eq. (17.17) for internal waves, we focused on only the fastest wavelengths. Justify.

U24. In what ways is the Froude number for incompressible flows similar to the Mach number for compressible flows?

U25. If supercritical flows tend to "break down" toward subcritical, then why do supercritical flows exist at all in the atmosphere?

U26. Is it possible to have supercritical flow in the atmosphere that does NOT create an hydraulic jump when it changes to subcritical? Explain?

U27. Contrast the nature of gap winds through short and long gaps. Also, what would you do if the gap length were in between short and long?

U28. For gap winds through a long gap, why are they less likely to form in summer than winter?

U29. Can coastally trapped jets form on the east coast of continents in the N. Hemisphere? If so, explain how the process would work.

U30. It is known from measurements of the ionosphere that the vertical amplitude of mountain waves increases with altitude. Explain this using Bernoulli's equation.

U31. What happens to the natural wavelength of air for statically unstable conditions?

U32. Why are lenticular clouds called **standing lenticular**?

U33. Compare and contrast the 3 versions of the Froude number. Do they actually describe the same physical processes? Why?

U34. Is there any max limit to the angle a of mountain wave crests (see Fig. 17.31)? Comment.

U35. If during the course of a day, the wind speed is constant but the wind direction gradually changes direction by a full 360°, draw a graph of the resulting streamline, streakline, and path line at the end of the period. Assume continuous emissions from a point source during the whole period.

U36. Identify the terms of Bernoulli's equation that form the hydrostatic approximation. According to Bernoulli's equation, what must happen or not happen in order for hydrostatic balance to be valid?

U37. Describe how the terms in Bernoulli's equation vary along a mountain-wave streamline as sketched in Fig. 17.29.

U38. If a cold air parcel is given an upward push in a warmer environment of uniform potential temperature, describe how the terms in Bernoulli's equation vary with parcel height.

U39. For compressible flow, show if (and how) the Bernoulli equations for isothermal and adiabatic processes reduce to the basic incompressible Bernoulli equation under conditions of constant density.

U40. In the solved example for the pressure variation across a wind turbine, hypothesize why the actual pressure change has the variation that was plotted.

U41. In Fig. 17.34, would it be reasonable to move the static pressure port to the top center of the darkly shaded block, given no change to the streamlines drawn? Comment on potential problems with a static port at that location.

U42. Design a thermometer mount on a fast aircraft that would not be susceptible to dynamic warming. Explain why your design would work.

U43. In Fig. 17.34, speculate on how the streamlines would look if the approaching flow was supersonic. Draw your streamlines, and justify them.

U44. Comment on the differences and similarities of the two mechanisms shown in this Chapter for creating Foehn winds.

U45. For Bora winds, if the upwind cold air was over an elevated plateau, and the downwind lowland was significantly lower than the plateau, how would Bora winds be different, if at all? Why?

U46. If the air in Fig. 17.38 went over a mountain but there was no precipitation, would there be a Foehn wind?

U47. Relate the amount of warming of a Foehn wind to the average upstream wind speed and the precipitation rate in mm/h .

U48. How sensitive is the solution for wind speed above a plant canopy? [Hint: see the solved example in the canopy flow section.] Namely, if you have a small error in estimating displacement distance d, are the resulting errors in friction velocity u_* and roughness length z_0 relatively small or large?

Web-Enhanced Questions

W1. Search the web for wind-rose graphs for a location (weather station or airport) near you, or other location specified by your instructor.

W2. Search the web for wind-speed distributions for a weather station near you. Relate this distribution to extreme or record-breaking winds.

W3. Find on the web climatological maps giving locations of persistent, moderate winds. These are favored locations for wind turbine farms. Also search the web for locations of existing turbine farms.

W4. Search the web for a weather map showing vertical velocities over your country or region. Sometimes, these vertical velocities are given as omega (ω) rather than w, where ω is the change of pressure

with time experienced by a vertically moving parcel, and is defined in the Extratropical Cyclone chapter. What is the range of vertical velocities on this particular day, in m/s?

W5. Search the web for the highest resolution (hopefully 0.5 km or better resolution) visible satellite imagery for your area. Which parts of the country have rising thermals, based on the presence of cumulus clouds at the top of the thermals?

W6. Search the web for lidar (laser radar) images of thermals in the boundary layer.

W7. Search the web for the highest resolution (hopefully 0.5 km or better resolution) visible satellite imagery for your area. Also search for an upper-air sounding (i.e., thermo diagram) for your area. Does the depth of the mixed layer from the thermo diagram agree with the diameter of thermals (clouds) visible in the satellite image? Comment.

W8. Access IR high resolution satellite images over cloud-free regions of the Rocky Mountains (or Cascades, Sierra-Nevada, Appalachians, or other significant mountains) for late night or early morning during synoptic conditions of high pressure and light winds. Identify those regions of cold air in valleys, as might have resulted from katabatic winds. Sometimes such regions can be identified by the fog that forms in them.

W9. Search the web for weather station observations at the mouth of a valley. Plotted meteograms of wind speed and direction are best to find. See if you can find evidence of mountain/valley circulations in these station observations, under weak synoptic forcing.

W10. Same as the previous problem, but to detect a sea breeze for a coastal weather station.

W11. Search the web for satellite observations of the sea breeze, evident as changes in cloudiness parallel to the coastline.

W12. Search the web for information on how tsunami on the ocean surface travel at the shallow-water wave speed as defined in this chapter, even when the waves are over the deepest parts of the ocean. Explain.

W13. Search the web for images of hydraulic jump in the atmosphere. If you can't find any, then find images of hydraulic jump in water instead.

W14. Access images from digital elevation data, and find examples of short and long gaps through mountain ranges for locations other than Western Canada.

W15. Search the web for news stories about dangerous winds along the coast, but limit this search to only coastally-trapped jets. If sufficient information is given in the news story, relate the coastal jet to the synoptic weather conditions.

W16. Access visible high-resolution satellite photos of mountain wave clouds downwind of a major mountain range. Measure the wavelength from these images, and compare with the wind speed accessed from upper air soundings in the wave region. Use those data to estimate the Brunt-Väisälä frequency.

W17. Access from the web photographs taken from ground level of lenticular clouds. Also, search for **iridescent** clouds on the web, to find if any of these are lenticular clouds.

W18. Access from the web pilot reports of turbulence, chop, or mountain waves in regions downwind of mountains. Do this over several days, and show how these reports vary with wind speed and static stability.

W19. Access high-resolution visible satellite images from the web during clear skies, that show the smoke plume from a major source (such as Gary, Indiana, or Sudbury, Ontario, or a volcano, or a forest fire). Assume that this image shows a streakline. Also access the current winds from a weather map corresponding roughly to the altitude of the smoke plume, from which you can infer the streamlines. Compare the streamlines and streaklines, and speculate on how the flow has changed over time, if at all. Also, draw on your printed satellite photo the path lines for various air parcels within the smoke plume.

W20. From the web, access weather maps that show streamlines. These are frequently given for weather maps of the jet stream near the tropopause (at 20 to 30 kPa). Also access from the web weather maps that plot the actual upper air winds from rawinsonde observations, valid at the same time and altitude as the streamline map. Compare the instantaneous winds with the streamlines.

W21. From the web, access a sequence of weather maps of streamlines for the same area. Locate a point on the map where the streamline direction has

changed significantly during the sequence of maps. Assume that smoke is emitted continuously from that point. On the last map of the sequence, plot the streakline that you would expect to see. (Hint, from the first streamline map, draw a path line for an air parcel that travels until the time of the next streamline map. Then, using the new map, continue finding the path of that first parcel, as well as emit a new second parcel that you track. Continue the process until the tracks of all the parcels end at the time of the last streamline map. The locus of those parcels is a rough indication of the streakline.)

W22. Access from the web information for aircraft pilots on how the pitot tube works, and/or its calibration characteristics for a particular model of aircraft.

W23. Access from the web figures that show the amount of destruction for different intensities of tornado winds. Prepare a table giving the dynamic pressures and forces on the side of a typical house for each of those different wind categories.

W24. Access from the web news stories of damage to buildings or other structures caused by Boras, mountain waves, or downslope windstorms.

W25. Access from the web data or images that indicate typical height of various mature crops (other than the ones already given at the end of the Numerical exercises).

W26. Access from the web the near-surface air temperature at sunrise in or just downwind of a large city, and compare with the rural temperature.

Synthesis Questions

S1. Suppose that in year 2100 everyone is required by law to have their own wind turbine. Since wind turbines take power from the wind, the wind becomes slower. What effect would this have on the weather and climate, if any?

S2. If fair-weather thermals routinely rose as high as the tropopause without forming clouds, comment on changes to the weather and climate, if any.

S3. Suppose that katabatic winds were frictionless. Namely, no turbulence, no friction against the ground, and no friction against other layers of air. Speculate on the shape of the vertical wind profile of the katabatic winds, and justify your arguments.

S4. If a valley has two exists, how would the mountain and valley winds behave?

S5. Suppose that katabatic winds flow into a bowl-shaped depression instead of a valley. Describe how the airflow would evolve during the night.

S6. If warm air was not less dense than cold, could sea breezes form? Explain.

S7. Why does the cycling in a sea-breeze hodograph not necessarily agree with the timing of the pendulum day?

S8. What local circulations would disappear if air density did not vary with temperature? Justify.

S9. Can a Froude number be defined based on deep-water waves rather than shallow-water waves? If so, write an equation for the resulting Froude number, and suggest applications for it in the atmosphere.

S10. What if waves could carry no information and no energy. How would the critical nature of the flow change, if at all?

S11. If the Earth did not rotate, compare the flow through short and long gaps through mountains.

S12. If no mountains existing along coasts, could there ever be strong winds parallel to the coast?

S13. If mountain-wave drag causes the winds to be slower, does that same drag force cause the Earth to spin faster? Comment.

S14. Suppose that mountain-wave drag worked oppositely, and caused winds to accelerate aloft. How would the weather & climate be different, if at all?

S15. Is it possible for a moving air parcel to not be traveling along a streamline? Comment.

S16. Suppose that Bernoulli's equation says that pressure decreases as velocity decreases along a streamline of constant height. How would the weather and climate be different, if at all? Start by commenting how Boras would be different, if at all.

S17. Suppose you are a 2 m tall person in a town with average building height of 8 m. How would the winds that you feel be different (if at all) than the winds felt by a 0.2 m tall cat in a young corn field of average height 0.8 m?

S18. If human population continued to grow until all land areas were urban, would there be an urban heat island? Justify, and relate to weather changes.

Copyright © 2011, 2015 by Roland Stull. *Meteorology for Scientists and Engineers, 3rd Ed.*

ATMOSPHERIC BOUNDARY LAYER

CONTENTS

Static Stability — A Review 687
- Explanation 687
- Rules of Thumb for Stability in the ABL 689

Boundary-layer Formation 689
- Tropospheric Constraints 689
- Synoptic Forcings 690

ABL Structure and Evolution 692

Temperature 693
- Cumulative Heating or Cooling 693
- Stable-ABL Temperature 696
- Mixed-Layer (ML) Temperature 697

Wind 699
- Wind Profile Evolution 699
- Drag, Stress, Friction Velocity, and Roughness Length 700
- Log Profile in the Neutral Surface Layer 702
- Log-Linear Profile in Stable Surf. Layer 702
- Profile in the Convective Radix Layer 703

Turbulence 705
- Mean and Turbulent Parts 705
- Variance and Standard Deviation 706
- Isotropy 707
- Turbulence Kinetic Energy 708
- Free and Forced Convection 710
- Turbulent Fluxes and Covariances 711
- Turbulence Closure 713

Summary 716

Exercises 717
- Numerical Problems 717
- Understanding & Critical Evaluation 719
- Web-Enhanced Questions 721
- Synthesis Questions 722

"Meteorology for Scientists and Engineers, 3rd Edition" by Roland Stull is licensed under a Creative Commons Attribution-NonCommercial-ShareAlike 4.0 International License. To view a copy of the license, visit http://creativecommons.org/licenses/by-nc-sa/4.0/ . This work is available at http://www.eos.ubc.ca/books/Practical_Meteorology/ .

18 Sunrise, sunset, sunrise. The daily cycle of radiative heating causes a daily cycle of sensible and latent heat fluxes between the Earth and the air, during clear skies over land. These fluxes influence only the bottom portion of the troposphere — the portion touching the ground (Fig. 18.1).

This layer is called the **atmospheric boundary layer** (ABL). It experiences a **diurnal** (daily) cycle of temperature, humidity, wind, and pollution variations. Turbulence is ubiquitous in the ABL, and is one of the causes of the unique nature of the ABL.

Because the boundary layer is where we live, where our crops are grown, and where we conduct our commerce, we have become familiar with its daily cycle. We perhaps forget that this cycle is not experienced by the rest of the atmosphere above the ABL. This chapter examines the formation and unique characteristics of the ABL.

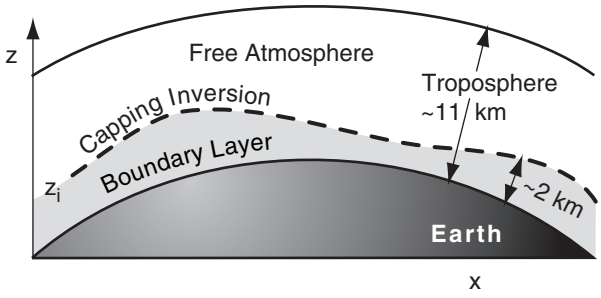

Figure 18.1
Location of the boundary layer, with top at z_i.

STATIC STABILITY — A REVIEW

Explanation

Static stability controls formation of the ABL, and affects ABL wind and temperature profiles. Here is a quick review of information from the Stability chapter.

If a small blob of air (i.e., an **air parcel**) is warmer than its surroundings at the same height or pressure, the parcel is positively buoyant and rises. If cooler, it is negatively buoyant and sinks. A parcel

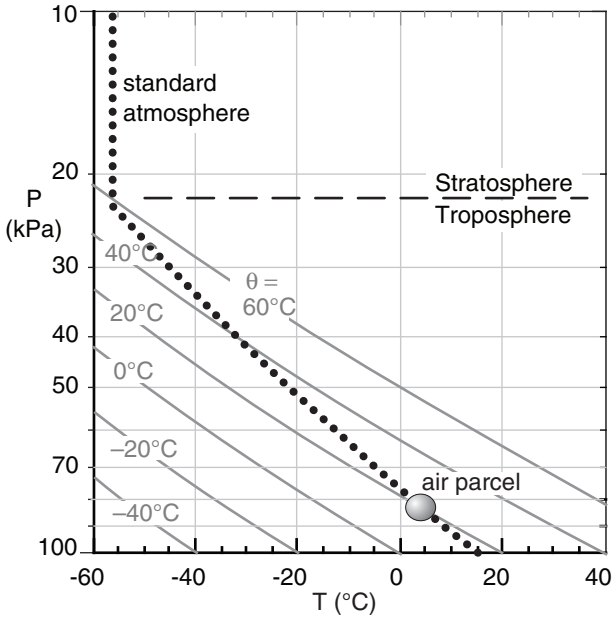

Figure 18.2
Standard atmosphere (dotted black line) plotted on a thermodynamic diagram. The circle represents a hypothetical air parcel. Diagonal grey lines are dry adiabats.

Solved Example

Find the vertical gradient of potential temperature in the troposphere for a standard atmosphere.

Solution

Given: $\Delta T/\Delta z = -6.5$°C/km from Chapter 1 eq. (1.16)
Find: $\Delta\theta/\Delta z$ = ? °C/km

Use eq. (3.11) from the Heat chapter:

$$\theta(z) = T(z) + \Gamma_d \cdot z \qquad (3.11)$$

where the dry adiabatic lapse rate is Γ_d = 9.8°C/km
Apply this at heights z_1 and z_2, and then subtract the z_1 equation from the z_2 equation:

$$\theta_2 - \theta_1 = T_2 - T_1 + \Gamma_d \cdot (z_2 - z_1)$$

Divide both sides of the equation by $(z_2 - z_1)$. Then define $(z_2 - z_1) = \Delta z$, $(T_2 - T_1) = \Delta T$, and $(\theta_2 - \theta_1) = \Delta\theta$ to give the algebraic form of the answer:

$$\Delta\theta/\Delta z = \Delta T/\Delta z + \Gamma_d$$

This eq. applies to <u>any</u> vertical temperature profile.

If we plug in the temperature profile for the standard atmosphere:

$\Delta\theta/\Delta z$ = (–6.5°C/km) + (9.8°C/km) = **<u>3.3°C/km</u>**

Check: Units OK. Agrees with Fig. 18.2, where θ increases from 15°C at the surface to 51.3°C at 11 km altitude, which gives (51.3–15°C)/(11km) = 3.3°C/km.
Discussion: θ gradually <u>in</u>creases with height in the troposphere, which as we will see tends to gently oppose vertical motions. Although the standard-atmosphere (an engineering specification similar to an average condition) troposphere is statically stable, the real troposphere at any time and place can have layers that are statically stable, neutral, or unstable.

with the same temperature as its surrounding environment experiences zero buoyant force.

Figure 18.2 shows the standard atmosphere from Chapter 1, plotted on a thermodynamic diagram from the Stability chapter. Let the standard atmosphere represent the environment or the background air. Consider an air parcel captured from one part of that environment (plotted as the circle). At its initial height, the parcel has the same temperature as the surrounding environment, and experiences no buoyant forces.

To determine static stability, you must ask what would happen to the air parcel if it were forcibly displaced a small distance up or down. When moved from its initial capture altitude, the parcel and environment temperatures could differ, thereby causing buoyant forces.

If the buoyant forces on a displaced air parcel push it back to its starting altitude, then the environment is said to be **statically stable**. In the absence of any other forces, statically stable air is **laminar**. Namely, it is smooth and non-turbulent.

However, if the displaced parcel is pulled further away from its starting point by buoyancy, the portion of the atmosphere through which the air parcel continues accelerating is classified as **statically unstable**. Unstable regions are **turbulent** (gusty).

If the displaced air parcel has a temperature equal to that of its new surroundings, then the environment is **statically neutral**.

When an air parcel moves vertically, its temperature changes adiabatically, as described in previous chapters. Always consider such adiabatic temperature change before comparing parcel temperature to that of the surrounding environment. The environment is usually assumed to be **stationary**, which means it is relatively unchanging during the short time it takes for the parcel to rise or sink.

If an air parcel is captured at P = 83 kPa and T = 5°C (as sketched in Fig. 18.2), and is then is forcibly lifted dry adiabatically, it cools following the θ = 20°C adiabat (one of the thin diagonal lines in that figure). If lifted to a height where the pressure is P = 60 kPa, its new temperature is about T = –20°C.

This air parcel, being colder than the environment (thick dotted line in Fig. 18.2) at that same height, feels a downward buoyant force toward its starting point. Similarly if displaced downward from its initial height, the parcel is warmer than its surroundings at its new height, and would feel an upward force toward its starting point.

Air parcels captured from any initial height in the environment of Fig. 18.2 always tend to return to their starting point. Therefore, <u>the standard atmosphere is statically stable</u>. This stability is critical for ABL formation.

Rules of Thumb for Stability in the ABL

Because of the daily cycle of radiative heating and cooling, there is a daily cycle of static stability in the ABL. ABL static stability can be anticipated as follows, without worrying about air parcels for now.

Unstable air adjacent to the ground is associated with light winds and a surface that is warmer than the air. This is common on sunny days in fair-weather. It can also occur when cold air blows over a warmer surface, day or night. In unstable conditions, thermals of warm air rise from the surface to heights of 200 m to 4 km, and turbulence within this layer is vigorous.

At the other extreme are **stable** layers of air, associated with light winds and a surface that is cooler than the air. This typically occurs at night in fair-weather with clear skies, or when warm air blows over a colder surface day or night. Turbulence is weak or sometimes nonexistent in stable layers adjacent to the ground. The stable layers of air are usually shallow (20 - 500 m) compared to the unstable daytime cases.

In between these two extremes are **neutral** conditions, where winds are moderate to strong and there is little heating or cooling from the surface. These occur during overcast conditions, often associated with bad weather.

BOUNDARY-LAYER FORMATION

Tropospheric Constraints

Because of buoyant effects, the vertical temperature structure of the troposphere limits the types of vertical motion that are possible. The standard atmosphere in the troposphere is not parallel to the dry adiabats (Fig. 18.2), but crosses the adiabats toward warmer potential temperatures as altitude increases.

That same standard atmosphere is replotted as the thick dotted grey line in Fig. 18.3, but now in terms of its potential temperature (θ) versus height (z). The standard atmosphere slopes toward warmer potential temperatures at greater altitudes. Such a slope indicates statically stable air; namely, air that opposes vertical motion.

The ABL is often turbulent. Because turbulence causes mixing, the bottom part of the standard atmosphere becomes homogenized. Namely, within the turbulent region, warmer potential-temperature air from the standard atmosphere in the top of the ABL is mixed with cooler potential-temperature air from near the bottom. The resulting mixture has a

FOCUS • Engineering Boundary Layers

In wind tunnel experiments, the layer of air that turbulently "feels" frictional drag against the bottom wall grows in depth indefinitely (Fig. 18.a). This engineering boundary-layer thickness h grows proportional to the square root of downstream distance x, until hitting the top of the wind tunnel.

On an idealized rotating planet, the Earth's rotation imposes a dynamical constraint on ABL depth (Fig. 18.b). This maximum depth is proportional to the ratio of wind drag (related to the friction velocity u_*, which is a concept discussed later in this chapter) to Earth's rotation (related to the Coriolis parameter f_c, as discussed in the Dynamics chapter). This dynamic constraint supersedes the turbulence constraint.

For the real ABL on Earth, the strong capping inversion at height z_i makes the ABL unique (Fig. 18.c) compared to other fluid flows. It constrains the ABL thickness and the eddies within it to a maximum size of order 200 m to 4 km. This stratification (thermodynamic) constraint supersedes the others. It means that the temperature structure is always very important for the ABL.

(a) Engineering Boundary Layers:

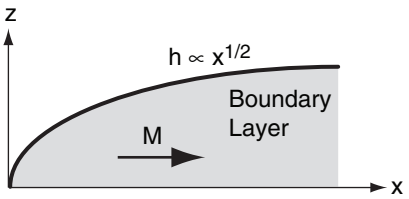

(b) Boundary Layers on a Rotating Planet:

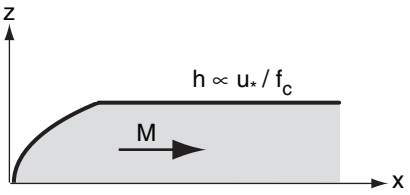

(c) Boundary Layers in Earth's Stratified Atmosphere:

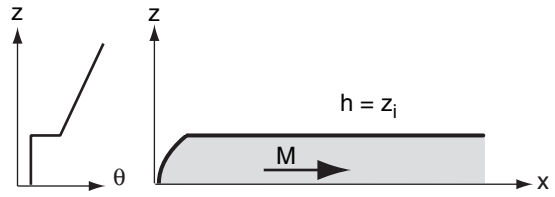

Figure 18.a-c
Comparison of constraints on boundary layer thickness, h. M is mean wind speed away from the bottom boundary, θ is potential temperature, z is height, and x is downwind distance.

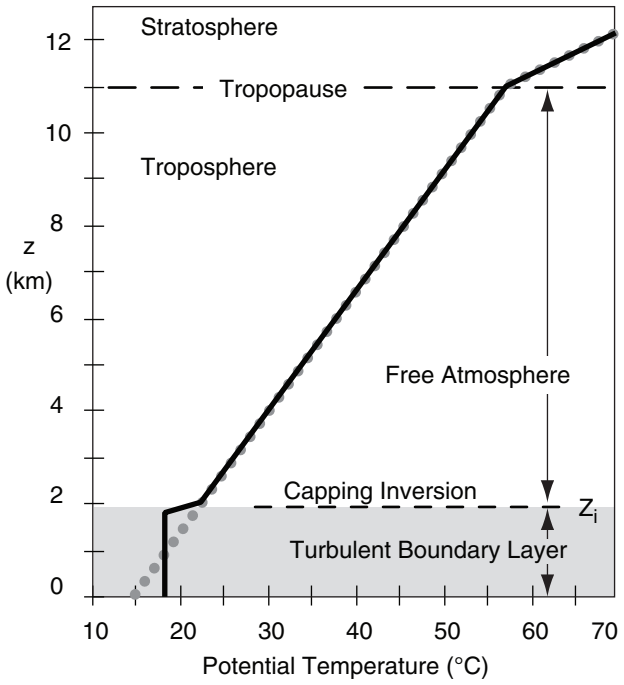

Figure 18.3
Restriction of ABL depth by tropospheric temperature structure during fair weather. The standard atmosphere is the grey dotted line. The thick black line shows an idealized temperature profile after the turbulent boundary layer modifies the bottom part of the standard atmosphere.

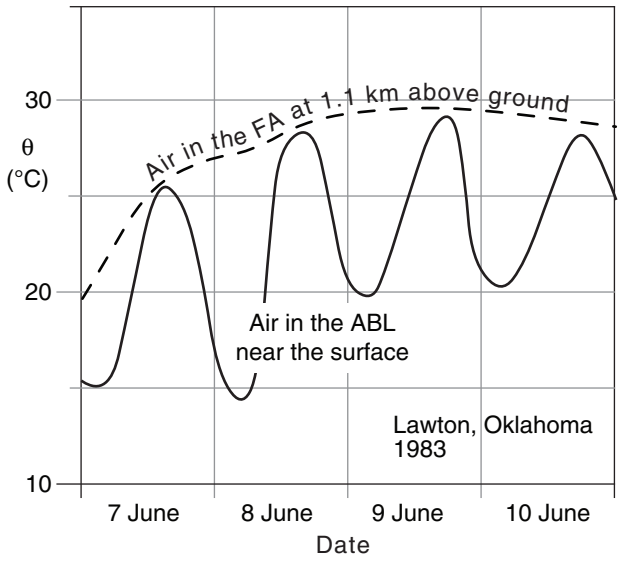

Figure 18.4
Observed variations of potential temperature in the ABL (solid line) and the free atmosphere (FA) (dashed line). The daily heating and cooling cycle that we are so familiar with near the ground does not exist above the ABL.

medium potential temperature that is uniform with height, as plotted by the thick black line in Fig. 18.3. In situations of vigorous turbulence, the ABL is also called the **mixed layer** (**ML**).

Above the mixed layer, the air is usually unmodified by turbulence, and retains the same temperature profile as the standard atmosphere in this idealized scenario. This tropospheric air above the ABL is known as the **free atmosphere** (**FA**).

As a result of a turbulent mixed layer being adjacent to the unmixed free atmosphere, there is a sharp temperature increase at the mixed layer top. This transition zone is very stable, and is often a **temperature inversion**. Namely, it is a region where temperature increases with height. The altitude of the middle of this inversion is given the symbol z_i, and is a measure of the depth of the turbulent ABL.

The temperature inversion acts like a lid or cap to motions in the ABL. Picture an air parcel from the mixed layer in Fig. 18.3. If turbulence were to try to push it out of the top of the mixed layer into the free atmosphere, it would be so much colder than the surrounding environment that a strong buoyant force would push it back down into the mixed layer. Hence, air parcels, turbulence, and any air pollution in the parcels, are trapped within the mixed layer.

There is always a strong stable layer or temperature inversion capping the ABL. As we have seen, turbulent mixing in the bottom of the statically-stable troposphere creates this cap, and in turn this cap traps turbulence below it.

The capping inversion breaks the troposphere into two parts. Vigorous turbulence within the ABL causes the ABL to respond quickly to surface influences such as heating and frictional drag. However, the remainder of the troposphere does not experience this strong turbulent coupling with the surface, and hence does not experience frictional drag nor a daily heating cycle. Fig. 18.4 illustrates this.

In summary, the bottom 200 m to 4 km of the troposphere is called the atmospheric boundary layer. ABL depth is variable with location and time. Turbulent transport causes the ABL to feel the direct effects of the Earth's surface. The ABL exhibits strong diurnal (daily) variations of temperature, moisture, winds, pollutants, turbulence, and depth in response to daytime solar heating and nighttime IR cooling of the ground. The name "boundary layer" comes from the fact that the Earth's surface is a boundary on the atmosphere, and the ABL is the part of the atmosphere that "feels" this boundary during fair weather.

Synoptic Forcings

Weather patterns such as high (𝕳) and low (𝕷) pressure systems that are drawn on weather maps

are known as **synoptic** weather. These large diameter (≥ 2000 km) systems modulate the ABL. In the N. Hemisphere, ABL winds circulate clockwise and spiral out from high-pressure centers, but circulate counterclockwise and spiral in toward lows (Fig. 18.6). See the Dynamics chapter for details on winds.

The outward spiral of winds around highs is called **divergence**, and removes ABL air horizontally from the center of highs. Conservation of air mass requires **subsidence** (downward moving air) over highs to replace the horizontally diverging air (Fig. 18.5). Although this subsidence pushes free atmosphere air downward, it cannot penetrate into the ABL because of the strong capping inversion. Instead, the capping inversion is pushed downward closer to the ground as the ABL becomes thinner. This situation traps air pollutants in a shallow ABL, causing air stagnation and air-pollution episodes.

Similarly, horizontally converging ABL air around lows is associated with upward motion (Fig. 18.5). Often the synoptic forcings and storms associated with lows are so powerful that they easily lift the capping inversion or eliminate it altogether. This allows ABL air to be deeply mixed over the whole depth of the troposphere by thunderstorms and other clouds. Air pollution is usually reduced during this situation as it is diluted with cleaner air from aloft, and as it is washed out by rain.

Because winds in high-pressure regions are relatively light, ABL air lingers over the surface for sufficient time to take on characteristics of that surface. These characteristics include temperature, humidity, pollution, odor, and others. Such ABL air is called an **airmass**, and was discussed in the chapter on Airmasses and Fronts. When the ABLs from two different high-pressure centers are drawn toward each other by a low center, the zone separating those two airmasses is called a **front**.

At a frontal zone, the colder, heavier airmass acts like a wedge under the warm airmass. As winds blow the cold and warm air masses toward each other, the cold wedge causes the warm ABL to peel away from the ground, causing it to ride up over the colder air (Figs. 18.7a & b). Also, thunderstorms can vent ABL air away from the ground (Figs. 18.7a & b). It is mainly in these stormy conditions (statically stable conditions at fronts, and statically unstable conditions at thunderstorms) that ABL air is forced away from the surface.

Although an ABL forms in the advancing airmass behind the front, the warm humid air that was pushed aloft is not called an ABL because it has lost contact with the surface. Instead, this rising warm air cools, allowing water vapor to condense and make the clouds that we often associate with fronts.

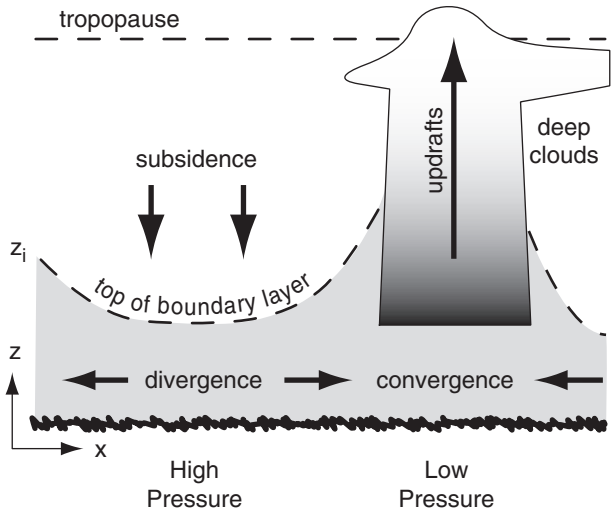

Figure 18.5
Influence of synoptic-scale vertical circulations on the ABL.

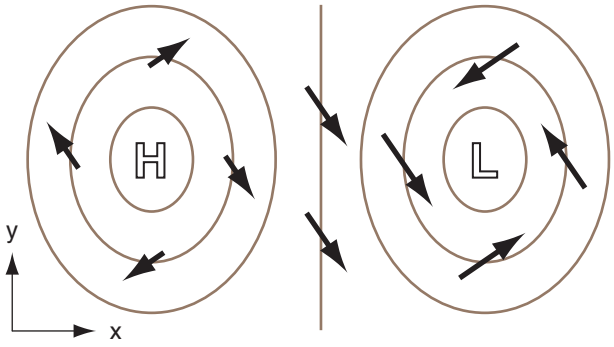

Figure 18.6
Synoptic-scale horizontal winds (arrows) in the ABL near the surface. Thin lines are isobars around surface high (H) and low (L) pressure centers.

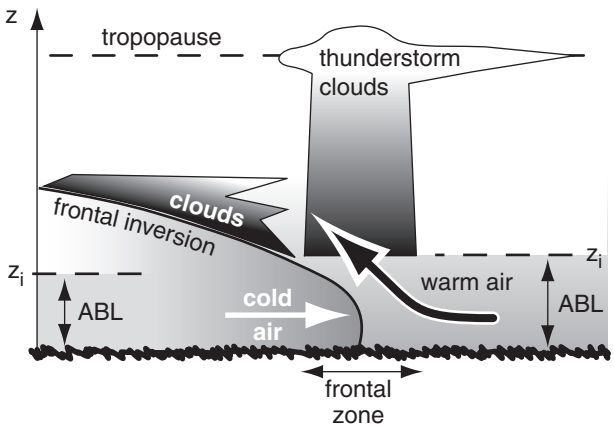

Figure 18.7a
Idealized ABL modification near a frontal zone.

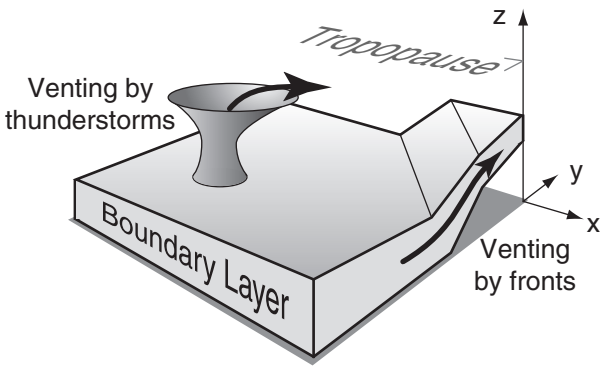

Figure 18.7b
Idealized venting of ABL air away from the surface during stormy weather.

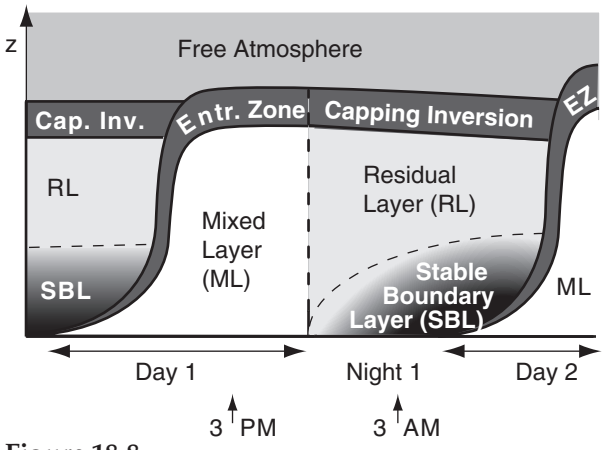

Figure 18.8
Components of the boundary layer during fair weather in summer over land. White indicates nonlocally statically unstable air, light grey (as in the RL) is neutral stability, and darker greys indicate stronger static stability.

For synoptic-scale low-pressure systems, it is difficult to define a separate ABL, so boundary-layer meteorologists study the air below cloud base. The remainder of this chapter focuses on fair-weather ABLs associated with high-pressure systems.

ABL STRUCTURE AND EVOLUTION

The fair-weather ABL consists of the components sketched in Fig. 18.8. During daytime there is a statically-unstable **mixed layer** (**ML**). At night, a statically **stable boundary layer** (**SBL**) forms under a statically neutral **residual layer** (**RL**). The residual layer contains the pollutants and moisture from the previous mixed layer, but is not very turbulent.

The bottom 20 to 200 m of the ABL is called the **surface layer** (SL, Fig. 18.9). Here frictional drag, heat conduction, and evaporation from the surface cause substantial variations of wind speed, temperature, and humidity with height. However, turbulent fluxes are relatively uniform with height; hence, the surface layer is known as the **constant flux layer**.

Separating the **free atmosphere** (FA) from the mixed layer is a strongly stable **entrainment zone** (**EZ**) of intermittent turbulence. Mixed-layer depth z_i is the distance between the ground and the middle of the EZ. At night, turbulence in the EZ ceases, leaving a nonturbulent layer called the **capping inversion** (**CI**) that is still strongly statically stable.

Typical vertical profiles of temperature, potential temperature, humidity mixing ratio, and wind speed are sketched in Fig. 18.9. The "day" portion of Fig. 18.9 corresponds to the 3 PM time indicated in Fig. 18.8, while "night" is for 3 AM.

Next, look at ABL temperature, winds, and turbulence in more detail.

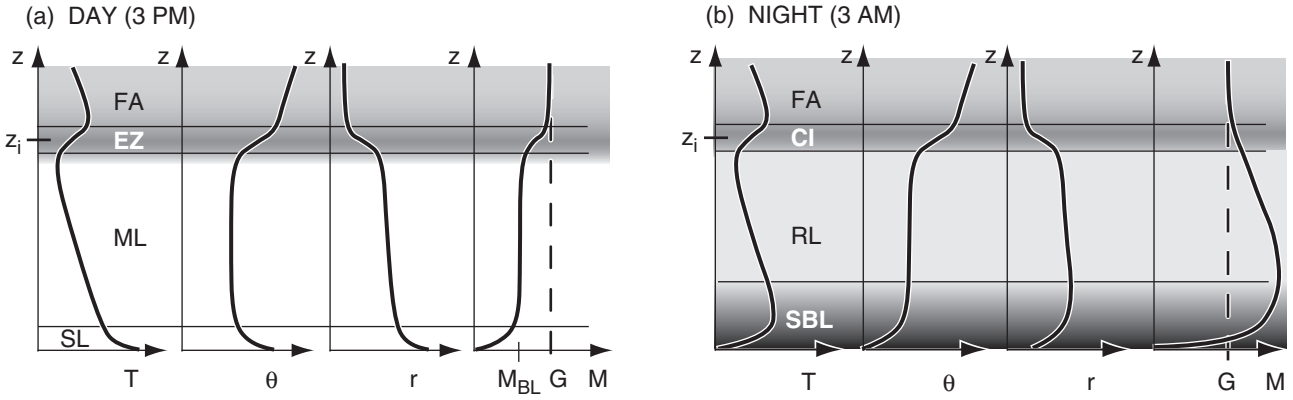

Figure 18.9
Typical vertical profiles of temperature (T), potential temperature (θ), mixing ratio (r, see the Moisture chapter), and wind speed (M) in the ABL. The dashed line labeled G is the geostrophic wind speed (a theoretical wind in the absence of surface drag, see the Dynamics chapter). M_{BL} is average wind speed in the ABL. Shading corresponds to shading in Fig. 18.8, with white being statically unstable, and black very stable.

TEMPERATURE

The capping inversion traps in the ABL any heating and water evaporation from the surface. As a result, heat accumulates within the ABL during day, or whenever the surface is warmer than the air. Cooling (actually, heat loss) accumulates during night, or whenever the surface is colder than the air. Thus, the temperature structure of the ABL depends on the accumulated heating or cooling.

Cumulative Heating or Cooling

The cumulative effect of surface heating and cooling is more important on ABL evolution than the instantaneous heat flux. This cumulative heating or cooling Q_A equals the area under the curve of heat flux vs. time (Fig. 18.10). We will examine cumulative nighttime cooling separately from cumulative daytime heating.

Nighttime

During clear nights over land, heat flux from the air to the cold surface is relatively constant with time (dark shaded portion of Fig. 18.10). If we define t as the time since cooling began, then the accumulated cooling per unit surface area is:

$$Q_A = \mathbb{F}_{H\ night} \cdot t \qquad (18.1a)$$

For night, Q_A is a negative number because $\mathbb{F}_H$ is negative for cooling. Q_A has units of J/m^2.

Dividing eq. (18.1a) by air density and specific heat ($\rho_{air} \cdot C_p$) gives the kinematic form

$$Q_{Ak} = F_{H\ night} \cdot t \qquad (18.1b)$$

where Q_{Ak} has units of K·m.

For a night with variable cloudiness that causes a variable surface heat flux (see the Radiation chapter), use the average value of $\mathbb{F}_H$ or F_H.

Daytime

On clear days, the nearly sinusoidal variation of solar elevation and downwelling solar radiation (Fig. 2.13 in the Radiation chapter) causes nearly sinusoidal variation of surface net heat flux (Fig. 3.9 in the Heat chapter). Let t be the time since $\mathbb{F}_H$ becomes positive in the morning, D be the total duration of positive heat flux, and $\mathbb{F}_{H\ max}$ be the peak value of heat flux (Fig. 18.10). These values can be found from data such as in Fig. 3.9. The accumulated daytime heating per unit surface area (units of J/m^2) is:

$$Q_A = \frac{\mathbb{F}_{H\max} \cdot D}{\pi} \cdot \left[1 - \cos\left(\frac{\pi \cdot t}{D}\right)\right] \qquad (18.2a)$$

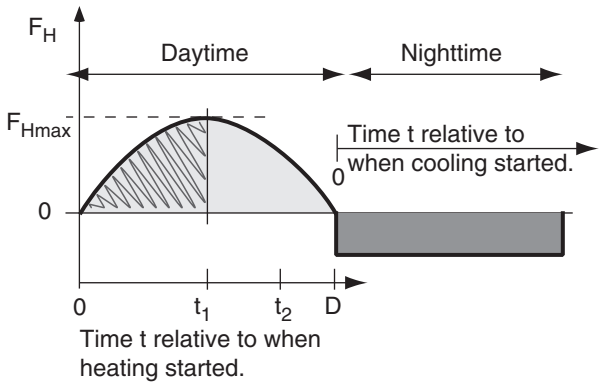

Figure 18.10
Idealization of the heat flux curve over land during fair weather, from Fig. 3.9 of the Heat chapter. Light shading shows total accumulated heating during the day, while the hatched region shows the portion of heating accumulated up to time t_1 after heating started. Dark shading shows total accumulated cooling during the night.

BEYOND ALGEBRA • Cumulative Heating

Derivation of Daytime Cumulative Heating

Assume that the kinematic heat flux is approximately sinusoidal with time:

$$F_H = F_{H\max} \cdot \sin(\pi \cdot t / D)$$

with t and D defined as in Fig. 18.10 for daytime. Integrating from time $t = 0$ to arbitrary time t :

$$Q_{Ak} = \int_{t'=0}^{t} F_H dt' = F_{H\max} \cdot \int_{t'=0}^{t} \sin(\pi \cdot t' / D) dt'$$

where t' is a dummy variable of integration.

From a table of integrals, we find that:

$$\int \sin(a \cdot x) = -(1/a) \cdot \cos(a \cdot x)$$

Thus, the previous equation integrates to:

$$Q_{Ak} = \frac{-F_{H\max} \cdot D}{\pi} \cdot \cos\left(\frac{\pi \cdot t}{D}\right)\Bigg|_0^t$$

Plugging in the two limits gives:

$$Q_{Ak} = \frac{-F_{H\max} \cdot D}{\pi} \cdot \left[\cos\left(\frac{\pi \cdot t}{D}\right) - \cos(0)\right]$$

But the cos(0) = 1, giving the final answer (eq. 18.2b):

$$Q_{Ak} = \frac{F_{H\max} \cdot D}{\pi} \cdot \left[1 - \cos\left(\frac{\pi \cdot t}{D}\right)\right]$$

Solved Example

Use Fig. 3.9 from the Heat chapter to estimate the accumulated heating and cooling in kinematic form over the whole day and whole night.

Solution

By eye from Fig. 3.9:

Day: $\mathbb{F}_{H\,max} \approx$ 150 W·m^{-2} , D = 8 h

Night: $\mathbb{F}_{H\,night} \approx$ –50 W·m^{-2} (averaged)

Given: Day: $t = D$ = 8 h = 28800. s

Night: t = 24h – D = 16 h = 57600. s

Find: Q_{Ak} = ? K·m for day and for night

First convert fluxes to kinematic form by dividing by $\rho_{air}\cdot C_p$:

$F_{H\,max} = \mathbb{F}_{H\,max} / \rho_{air}\cdot C_p$

= (150 W·m^{-2}) / [1231(W·m^{-2})/(K·m/s)]

= 0.122 K·m/s

$F_{H\,night}$ = (–50W·m^{-2})/[1231(W·m^{-2})/(K·m/s)]

= –0.041 K·m/s

Day: use eq. (18.2b):

$$Q_{Ak} = \frac{(0.122\ \mathrm{K\cdot m/s})\cdot(28800\ \mathrm{s})}{3.14159}\cdot\left[1-\cos(\pi)\right]$$

= **2237 K·m**

Night: use eq. (18.1b):

Q_{Ak} = (–0.041 K·m/s)·(57600. s) = **–2362 K·m**

Check: Units OK. Physics OK.

Discussion: The heating and cooling are nearly equal for this example, implying that the daily average temperature is fairly steady.

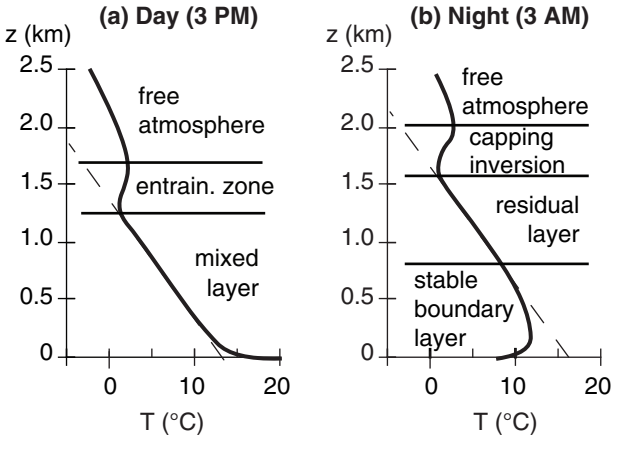

Figure 18.11

Examples of boundary-layer temperature profiles during day (left) and night (right) during fair weather over land. Adiabatic lapse rate is dashed. The heights shown here are illustrative only. In the real ABL the heights can be greater or smaller, depending on location, time, and season.

In kinematic form (units of K·m), this equation is

$$Q_{Ak} = \frac{F_{H\,\max}\cdot D}{\pi}\cdot\left[1-\cos\left(\frac{\pi\cdot t}{D}\right)\right] \qquad (18.2b)$$

Temperature-Profile Evolution

Idealized Evolution

A typical afternoon temperature profile is plotted in Fig. 18.11a. During the daytime, the environmental lapse rate in the mixed layer is nearly adiabatic. The unstable surface layer (plotted but not labeled in Fig. 18.11) is in the bottom part of the mixed layer. Warm blobs of air called **thermals** rise from this surface layer up through the mixed layer, until they hit the temperature inversion in the entrainment zone. Fig. 18.12a shows a closer view of the surface layer (bottom 5 - 10% of ABL).

These thermal circulations create strong turbulence, and cause pollutants, potential temperature, and moisture to be well mixed in the vertical (hence the name **mixed layer**). The whole mixed layer, surface layer, and bottom portion of the entrainment zone are statically unstable.

In the entrainment zone, free-atmosphere air is incorporated or **entrained** into the mixed layer, causing the mixed-layer depth to increase during the day. Pollutants trapped in the mixed layer cannot escape through the EZ, although cleaner, drier free atmosphere air is entrained into the mixed layer. Thus, the EZ is a one-way valve.

At night, the bottom portion of the mixed layer becomes chilled by contact with the radiatively-cooled ground. The result is a stable ABL. The bottom portion of this stable ABL is the surface layer (again not labeled in Fig. 18.11b, but sketched in Fig. 18.12b).

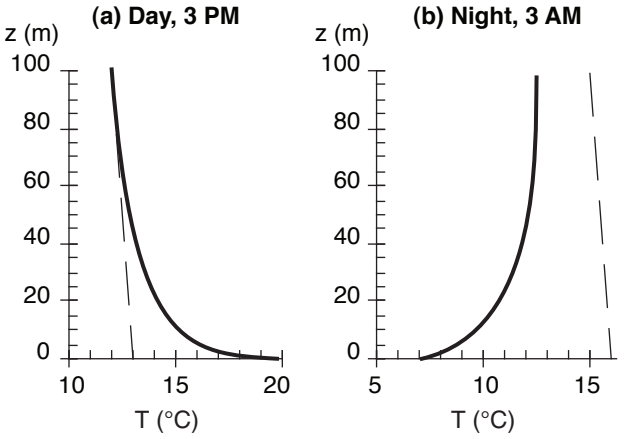

Figure 18.12

Examples of surface-layer temperature profiles during day (left) and night (right). Adiabatic lapse rate is dashed. Again, heights are illustrative only. Actual heights might differ.

Above the stable ABL is the residual layer. It has not felt the cooling from the ground, and hence retains the adiabatic lapse rate from the mixed layer of the previous day. Above that is the capping temperature inversion, which is the nonturbulent remnant of the entrainment zone.

Seasonal Differences

During summer at mid- and high-latitudes, days are longer than nights during fair weather over land. More heating occurs during day than cooling at night. After a full 24 hours, the ending sounding is warmer than the starting sounding as illustrated in Figs. 18.13 a & b. The convective mixed layer starts shallow in the morning, but rapidly grows through the residual layer. In the afternoon, it continues to rise slowly into the free atmosphere. If the air contains sufficient moisture, cumuliform clouds can exist. At night, cooling creates a shallow stable ABL near the ground, but leaves a thick residual layer in the middle of the ABL.

During winter at mid- and high-latitudes, more cooling occurs during the long nights than heating during the short days, in fair weather over land. Stable ABLs dominate, and there is net temperature decrease over 24 hours (Figs. 18.13 c & d). Any nonfrontal clouds present are typically stratiform or fog. Any residual layer that forms early in the night is quickly overwhelmed by the growing stable ABL.

Fig. 18.14 shows the corresponding structure of the ABL. Although both the mixed layer and residual layer have nearly adiabatic temperature profiles, the mixed layer is nonlocally unstable, while the residual layer is neutral. This difference causes pollutants to disperse at different rates in those two regions.

If the wind moves ABL air over surfaces of different temperatures, then ABL structures can evolve in space, rather than in time. For example, suppose the numbers along the abscissa in Fig. 18.14b represent distance x (km), with wind blowing from left to right over a lake spanning $8 \le x \le 16$ km. The ABL

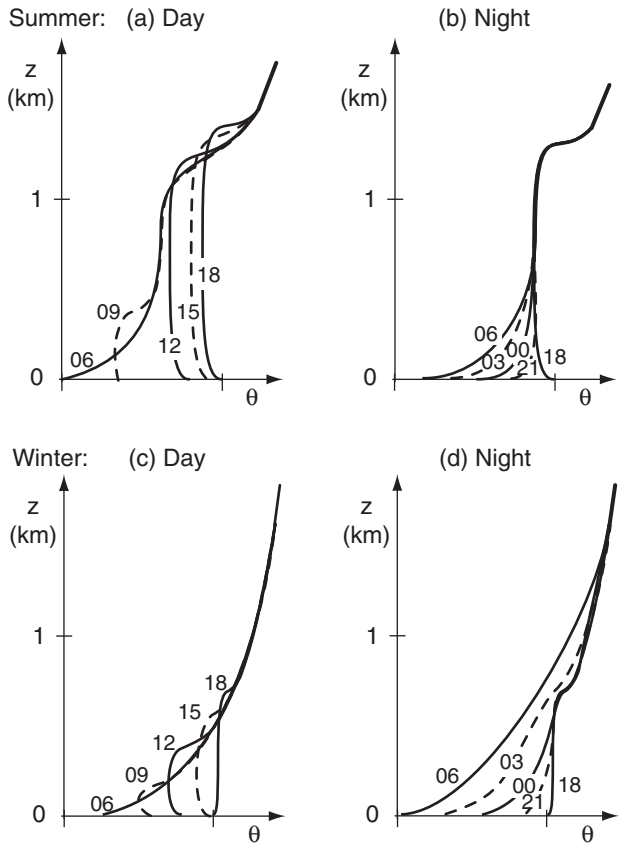

Figure 18.13
Evolution of potential temperature θ profiles for fair-weather over land. Curves are labeled with local time in hours. The nighttime curves begin at 18 local time, which corresponds to the ending sounding from the previous day.

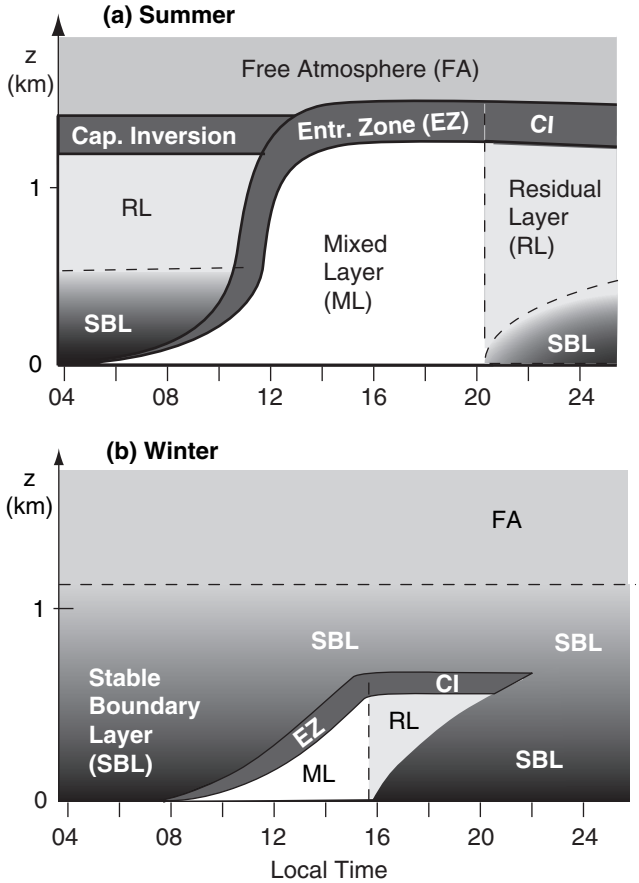

Figure 18.14
Daily evolution of boundary-layer structure by season, for fair weather over land. CI = Capping Inversion. Shading indicates static stability: white = unstable, light grey = neutral (as in the RL), darker greys indicate stronger static stability.

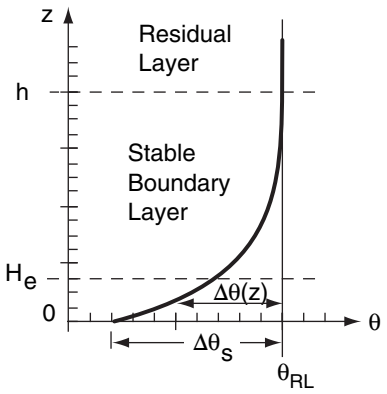

Figure 18.15
Idealized exponential-shaped potential temperature profile in the stable (nighttime) boundary layer.

Solved Example (§)

Estimate the potential temperature profile at the end of a 12-hour night for two cases: windy (10 m/s) and less windy (5 m/s). Assume $Q_{Ak} = -1000$ K·m.

Solution

Given: $Q_{Ak} = -1000$ K·m, $t = 12$ h
(a) $M_{RL} = 10$ m/s, (b) $M_{RL} = 5$ m/s
Find: θ vs. z

Assume: flat prairie. To plot profile, need H_e & $\Delta\theta_s$.
Use eq. (18.4):

$$H_e \approx (0.15\text{m}^{1/4}\cdot\text{s}^{1/4})\cdot(10\text{m}\cdot\text{s}^{-1})^{3/4}\cdot(43200\text{s})^{1/2}$$

(a) $H_e = 175$ m

$$H_e \approx (0.15\text{m}^{1/4}\cdot\text{s}^{1/4})\cdot(5\text{m}\cdot\text{s}^{-1})^{3/4}\cdot(43200\text{s})^{1/2}$$

(b) $H_e = 104$ m

Use eq. (18.5):
(a) $\Delta\theta_s = (-1000\text{K·m})/(175) = -5.71$ °C
(b) $\Delta\theta_s = (-1000\text{K·m})/(104) = -9.62$ °C
Use eq. (18.3) in a spreadsheet to compute the potential temperature profiles, using H_e and $\Delta\theta_s$ from above:

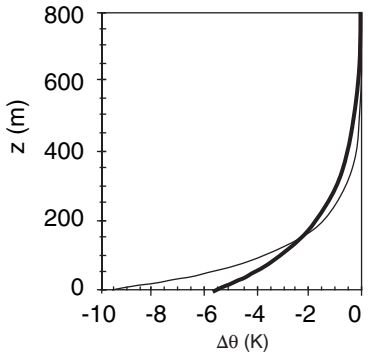

Check: Units OK, Physics OK. Graph OK.
Discussion: The windy case (thick line) is not as cold near the ground, but the cooling extends over a greater depth than for the less-windy case (thin line).

structure in Fig. 18.14b could occur at midnight in mid-latitude winter for air blowing over snow-covered ground, except for the unfrozen lake in the center. If the lake is warmer than the air, it will create a mixed layer that grows as the air advects across the lake.

Don't be lulled into thinking the ABL evolves the same way at every location or at similar times. The most important factor is the temperature difference between the surface and the air. If the surface is warmer, a mixed layer will develop regardless of the time of day. Similarly, colder surfaces will create stable ABLs.

Stable-ABL Temperature

Stable ABLs are quite complex. Turbulence can be intermittent, and coupling of air to the ground can be quite weak. In addition, any slope of the ground causes the cold air to drain downhill. Cold, downslope winds are called **katabatic winds**, as discussed in the Local Winds chapter.

For a simplified case of a contiguously-turbulent stable ABL over a flat surface during light winds, the potential temperature profile is approximately exponential with height (Fig. 18.15):

$$\Delta\theta(z) = \Delta\theta_s \cdot e^{-z/H_e} \tag{18.3}$$

where $\Delta\theta(z) = \theta(z) - \theta_{RL}$ is the potential temperature difference between the air at height z and the air in the residual layer. $\Delta\theta(z)$ is negative.

The value of this difference near the ground is defined to be $\Delta\theta_s = \Delta\theta(z{=}0)$, and is sometimes called the **strength** of the stable ABL. H_e is an **e-folding height** for the exponential curve. The actual **depth** h of the stable ABL is roughly $h = 5{\cdot}H_e$.

Depth and strength of the stable ABL grow as the cumulative cooling Q_{Ak} increases with time:

$$H_e \approx a \cdot M_{RL}{}^{3/4} \cdot t^{1/2} \tag{18.4}$$

$$\Delta\theta_s = \frac{Q_{Ak}}{H_e} \tag{18.5}$$

where $a = 0.15\ \text{m}^{1/4}\cdot\text{s}^{1/4}$ for flow over a flat prairie, and where M_{RL} is the wind speed in the residual layer. Because the cumulative cooling is proportional to time, both the depth $5{\cdot}H_e$ and strength $\Delta\theta_s$ of the stable ABL increase as the square root of time. Thus, fast growth of the SBL early in the evening decreases to a much slower growth by the end of the night.

Mixed-Layer (ML) Temperature

The shape of the potential temperature profile in the mixed layer is simple. To good approximation it is uniform with height. Of more interest is the evolution of mixed-layer average θ and z_i with time.

Use the potential temperature profile at the end of the night (early morning) as the starting sounding for forecasting daytime temperature profiles. In real atmospheres, the sounding might not be a smooth exponential as idealized in the previous subsection. The method below works for arbitrary shapes of the initial potential temperature profile.

A graphical solution is easiest. First, plot the early-morning sounding of θ vs. z. Next, determine the cumulative daytime heating Q_{Ak} that occurs between sunrise and some time of interest t_1, using eq. (18.2b). This heat warms the air in the ABL; thus the area under the sounding equals the accumulated heating (and also has units of K·m). Plot a vertical line of constant θ between the ground and the sounding, so that the area (hatched in Fig. 18.16a) under the curve equals the cumulative heating.

This vertical line gives the potential temperature of the mixed layer $\theta_{ML}(t_1)$. The height where this vertical line intersects the early-morning sounding defines the mixed-layer depth $z_i(t_1)$. As cumulative heating increases with time during the day ($Area_2$ = total grey-shaded region at time t_2), the mixed layer becomes warmer and deeper (Fig. 18.16a). The resulting potential temperature profiles during the day are sketched in Fig. 18.16b. This method of finding mixed layer growth is called the **encroachment method**, or **thermodynamic method**, and explains roughly 90% of typical mixed-layer growth on sunny days with winds less than 10 m/s.

Entrainment

As was mentioned earlier, the turbulent mixed layer grows by entraining non-turbulent air from the free atmosphere. One can idealize the mixed layer as a **slab model** (Fig. 18.17a), with constant potential temperature in the mixed layer, and a jump of potential temperature (Δθ) at the EZ.

Entrained air from the free atmosphere has warmer potential temperature than air in the mixed layer. Because this warm air is entrained downward, it corresponds to a negative heat flux $F_{H\,zi}$ at the top of the mixed layer. The heat-flux profile (Fig. 18.17b) is often linear with height, with the most negative value marking the top of the mixed layer.

The entrainment rate of free atmosphere air into the mixed layer is called the **entrainment velocity**, w_e, and can never be negative. The entrainment velocity is the volume of entrained air per unit horizontal area per unit time. In other words it is a volume flux, which has the same units as velocity.

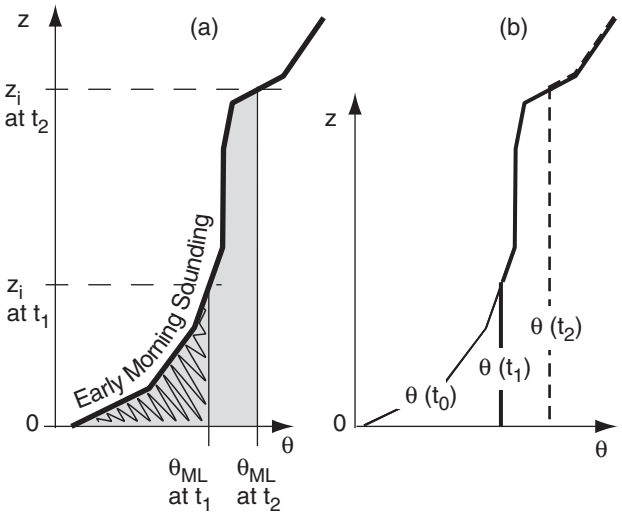

Figure 18.16
Evolution of the mixed layer with time, as cumulative heating increases the areas under the curves.

Solved Example

Given an early morning sounding with surface temperature 5°C and lapse rate Δθ/Δz = 3 K/km. Find the mixed-layer potential temperature and depth at 10 AM, when the cumulative heating is 500 K·m.

Solution

Given: θ_{sfc} = 5°C, Δθ/Δz = 3 K/km,
Q_{Ak} =0.50 K·km
Find: θ_{ML} = ? °C, z_i = ? km
Sketch:

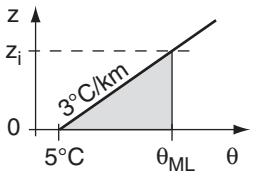

The area under this simple sounding is the area of a triangle: $Area = 0.5\cdot[base]\cdot(height)$,
$Area = 0.5\cdot[(\Delta\theta/\Delta z)\cdot z_i]\cdot(z_i)$
$0.50\ \text{K·km} = 0.5\cdot(3\ \text{K/km})\cdot z_i^2$
Rearrange and solve for z_i:
z_i = **0.577 km**

Next, use the sounding to find the θ_{ML}:
$\theta_{ML} = \theta_{sfc} + (\Delta\theta/\Delta z)\cdot z_i$
θ_{ML} = (5°C) + (3°C/km)·(0.577 km) = **6.73 °C**

Check: Units OK. Physics OK. Sketch OK.
Discussion: Arbitrary soundings can be approximated by straight line segments. The area under such a sounding consists of the sum of areas within trapezoids under each line segment. Alternately, draw the early-morning sounding on graph paper, count the number of little grid boxes under the sounding, and multiply by the area of each box.

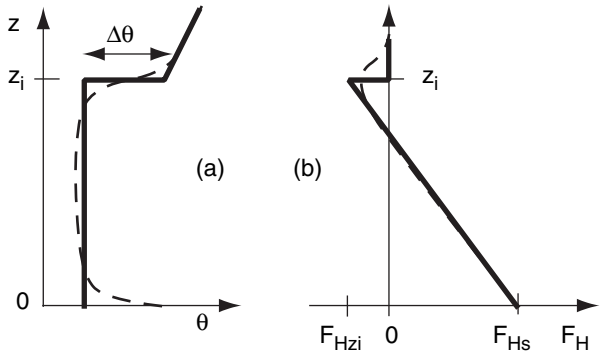

Figure 18.17
(a) Slab idealization of the mixed layer (solid line) approximates a more realistic potential temperature (θ) profile (dashed line). (b) Corresponding real and idealized heat flux (F_H) profiles.

Solved Example

The mixed layer depth increases at the rate of 300 m/h in a region with weak subsidence of 2 mm/s. If the inversion strength is 0.5°C, estimate the surface kinematic heat flux.

Solution

Given: $w_s = -0.002$ m/s, $\Delta z_i/\Delta t = 0.083$ m/s, $\Delta\theta = 0.5$°C
Find: $F_{H\,sfc} = ?$ °C·m/s

First, solve eq. (18.6) for entrainment velocity:
$w_e = \Delta z_i/\Delta t - w_s = [0.083 - (-0.002)]$ m/s = 0.085 m/s

Next, use eq. (18.7):
$F_{Hzi} = (-0.085$ m/s)·(0.5°C) = −0.0425 °C·m/s

Finally, rearrange eq. (18.8):
$F_{H\,sfc} = -F_{Hzi}/A = -(-0.0425$ °C·m/s)/0.2 = **0.21°C·m/s**

Check: Units OK. Magnitude and sign OK.
Discussion: Multiplying by $\rho \cdot C_P$ for the bottom of the atmosphere gives a dynamic heat flux of $\mathbb{F}_H$ = 259 W/m^2. This is roughly half of the value of max incoming solar radiation from Fig. 2.13 in the Radiation chapter.

Solved Example

Find the entrainment velocity for a potential temperature jump of 2°C at the EZ, and a surface kinematic heat flux of 0.2 K·m/s.

Solution

Given: $F_{H\,sfc} = 0.2$ K·m/s, $\Delta\theta = 2$ °C = 2 K
Find: $w_e = ?$ m/s

Use eq. (18.9):

$$w_e \cong \frac{A \cdot F_{H\,sfc}}{\Delta\theta} = \frac{0.2 \cdot (0.2\,\mathrm{K \cdot m/s})}{(2\,\mathrm{K})} = \mathbf{0.02\ m/s}$$

Check: Units OK. Physics OK.
Discussion: While 2 cm/s seems small, when applied over 12 h of daylight works out to z_i = 864 m, which is a reasonable mixed-layer depth.

The rate of growth of the mixed layer during fair weather is

$$\frac{\Delta z_i}{\Delta t} = w_e + w_s \qquad \bullet(18.6)$$

where w_s is the synoptic scale vertical velocity, and is negative for the subsidence that is typical during fair weather (recall Fig. 18.5).

The kinematic heat flux at the top of the mixed layer is

$$F_{Hzi} = -w_e \cdot \Delta\theta \qquad \bullet(18.7)$$

where the sign and magnitude of the temperature jump is defined by $\Delta\theta$ = θ(just above z_i) − θ(just below z_i). Greater entrainment across stronger temperature inversions causes greater heat-flux magnitude. Similar relationships describe entrainment fluxes of moisture, pollutants, and momentum as a function of jump of humidity, pollution concentration, or wind speed, respectively. As for temperature, the jump is defined as the value above z_i minus the value below z_i. Entrainment velocity has the same value for all variables.

During free convection (when winds are weak and thermal convection is strong), the entrained kinematic heat flux is approximately 20% of the surface heat flux:

$$F_{H\,zi} \cong -A \cdot F_{H\,sfc} \qquad (18.8)$$

where $A = 0.2$ is called the **Ball ratio**, and $F_{H\,sfc}$ is the surface kinematic heat flux. This special ratio works only for heat, and does not apply to other variables. During windier conditions, A can be greater than 0.2. Eq. (18.8) was used in the Heat chapter to get the vertical heat-flux divergence (eq. 3.40 & 3.41), a term in the Eulerian heat budget.

Combining the two equations above gives an approximation for the entrainment velocity during free convection:

$$w_e \cong \frac{A \cdot F_{H\,sfc}}{\Delta\theta} \qquad \bullet(18.9)$$

Combining this with eq. (18.6) gives a mixed-layer growth equation called the **flux-ratio method**. From these equations, we see that stronger capping inversions cause slower growth rate of the mixed layer, while greater surface heat flux (e.g., sunny day over land) causes faster growth. The flux-ratio method and the thermodynamic methods usually give equivalent results for mixed layer growth during free convection.

For stormy conditions near thunderstorms or fronts, the ABL top is roughly at the tropopause. Alternately, in the Dynamics chapter (Mass Conservation section) are estimates of z_i for bad weather.

WIND

For any given weather condition, there is a theoretical equilibrium wind speed, called the **geostrophic wind** *G*, that can be calculated for frictionless conditions (see the Dynamics chapter). However, steady-state winds in the ABL are usually slower than geostrophic (i.e., **subgeostrophic**) because of frictional and turbulent drag of the air against the surface, as was illustrated in Fig. 18.9a.

Turbulence continuously mixes slower air from close to the ground with faster air from the rest of the ABL, causing the whole ABL to experience drag against the surface and to be subgeostrophic. This vertically averaged steady-state ABL wind M_{BL} is derived in the Dynamics chapter. The actual ABL winds are nearly equal to this theoretical M_{BL} speed over a large middle region of the ABL.

Winds closer to the surface (in the **surface layer, SL**) are even slower (Fig. 18.9a). Wind-profile shapes in the SL are empirically found to be similar to each other when scaled with appropriate length and velocity scales. This approach, called **similarity theory**, is described later in this section.

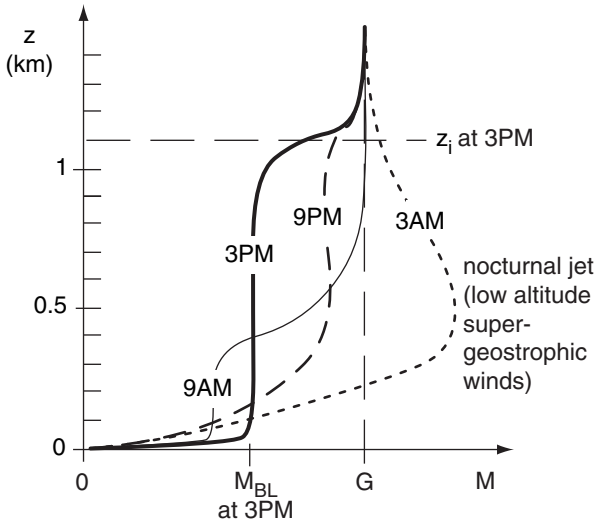

Figure 18.18
Typical ABL wind-profile evolution during fair weather over land. G is geostrophic wind speed. M_{BL} is average ABL wind speed and z_i is the average mixed-layer depth at 3 PM local time. The region of **supergeostrophic** *(faster-than-geostrophic: M > G) winds is called a nocturnal jet.*

Wind Profile Evolution

Over land during fair weather, the winds often experience a diurnal cycle as illustrated in Fig. 18.18. For example, a few hours after sunrise, say at 9 AM local time, there is often a shallow mixed layer, which is 300 m thick in this example. Within this shallow mixed layer the ABL winds are uniform with height, except near the surface where winds approach zero.

As the day progresses, the mixed layer deepens, so by 3 PM a deep layer of subgeostrophic winds fills the ABL. Winds remain moderate near the ground as turbulence mixes down faster winds from higher in the ABL. After sunset, turbulence intensity usually diminishes, allowing surface drag to reduce the winds at ground level. However, without turbulence, the air in the mid-ABL no longer feels drag against the surface, and begins to accelerate.

By 3 AM, the winds a few hundred meters above ground can be supergeostrophic, even though the winds at the surface might be calm. This low-altitude region of supergeostrophic winds is called a **nocturnal jet**. This jet can cause rapid horizontal transport of pollutants, and can feed moisture into thunderstorms. Then, after sunrise, turbulence begins vertical mixing again, and mixes out the jet with the slower air closer to the ground.

For measurements made at fixed heights on a very tall tower, the same wind-speed evolution is shown in Fig. 18.19. Below 20 m altitude, winds are often calmer at night, and increase in speed during

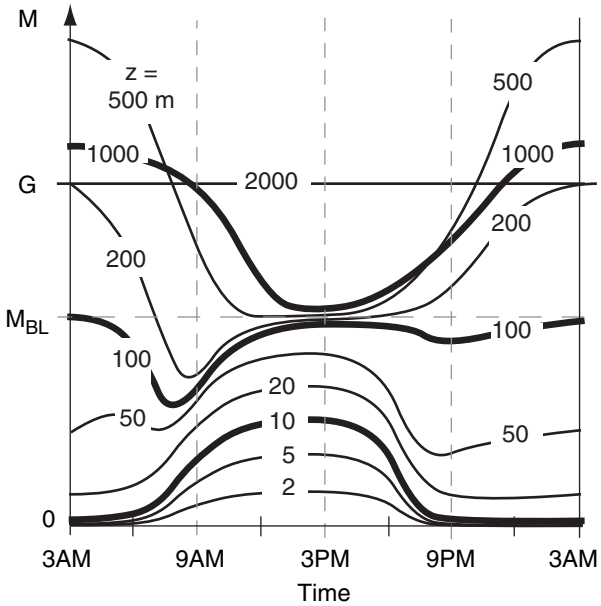

Figure 18.19
Typical ABL wind speed evolution at different heights. G is geostrophic wind speed, M_{BL} is average ABL wind, and the vertical time lines correspond to the profiles of Fig. 18.18.

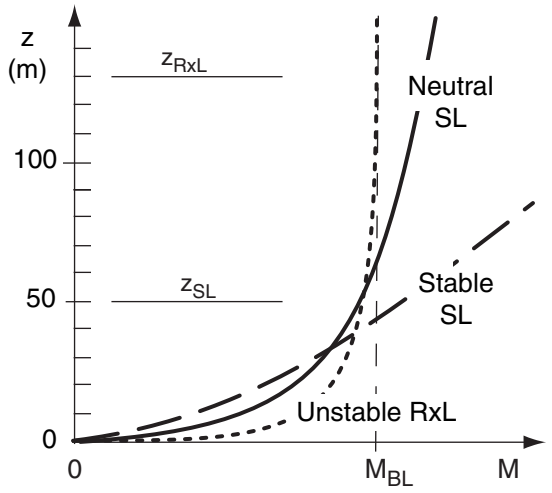

Figure 18.20
Typical wind speed profiles in the surface layer (SL, bottom 5% of the ABL) and radix layer (RxL, bottom 20% of the ABL), for different static stabilities. z_{RxL} and z_{SL} give order-of-magnitude depths for the radix layer and surface layer.

Table 18-1. The Davenport-Wieringa roughness-length z_o (m) classification, with approximate drag coefficients C_D (dimensionless).

z_o (m)	Classification	C_D	Landscape
0.0002	sea	0.0014	sea, paved areas, snow-covered flat plain, tide flat, smooth desert
0.005	smooth	0.0028	beaches, pack ice, morass, snow-covered fields
0.03	open	0.0047	grass prairie or farm fields, tundra, airports, heather
0.1	roughly open	0.0075	cultivated area with low crops & occasional obstacles (single bushes)
0.25	rough	0.012	high crops, crops of varied height, scattered obstacles such as trees or hedgerows, vineyards
0.5	very rough	0.018	mixed farm fields and forest clumps, orchards, scattered buildings
1.0	closed	0.030	regular coverage with large size obstacles with open spaces roughly equal to obstacle heights, suburban houses, villages, mature forests
≥ 2	chaotic	≥0.062	centers of large towns and cities, irregular forests with scattered clearings

daytime. The converse is true above 1000 m altitude, where winds are reduced during the day because of turbulent mixing with slower near-surface air, but become faster at night when turbulence decays.

At the ABL bottom, near-surface wind speed profiles have been found **empirically** (i.e., experimentally). In the bottom 5% of the statically neutral ABL is the **surface layer**, where wind speeds increase roughly logarithmically with height (Fig. 18.20).

For the statically stable surface layer, this logarithmic profile changes to a more linear form (Fig. 18.20). Winds close to the ground become slower than logarithmic, or near calm. Winds just above the surface layer are often not in steady state, and can temporarily increase to faster than geostrophic (**supergeostrophic**) in a process called an **inertial oscillation** (Figs. 18.9b and 18.20).

The bottom 20% of the convective (unstable) ABL is called the **radix layer** (RxL). Winds in the RxL have an exponential power-law relationship with height. The RxL has faster winds near the surface, but slower winds aloft than the neutral logarithmic profile. After a discussion of drag at the ground, these three wind cases at the bottom of the ABL will be described in more detail.

Drag, Stress, Friction Velocity, and Roughness Length

The frictional force between two objects such as the air and the ground is called **drag**. One way to quantify drag is by measuring the force required to push the object along another surface. For example, if you place your textbook on a flat desk, after you first start it moving you must continue to push it with a certain force (i.e., equal and opposite to the drag force) to keep it moving. If you stop pushing, the book stops moving.

Your book contacts the desk with a certain surface area. Generally, larger contact area requires greater force to overcome friction. The amount of friction force per unit surface contact area is called **stress**, τ, where for stress the force is parallel to the area. Contrast this with pressure, which is defined as a force per unit area that is perpendicular to the area. Units of stress are N/m^2, and could also be expressed as Pascals (Pa) or kiloPascals (kPa).

Stress is felt by both objects that are sliding against each other. For example, if you stack two books on top of each other, then there is friction between both books, as well as between the bottom book and the table. In order to push the bottom book in one direction without moving the top book, you must apply a force to the top book in the opposite direction as the bottom book.

Think of air within the ABL as a stack of layers of air, much like a stack of books. Each layer feels

stress from the layers above and below it. The bottom layer feels stress against the ground, as well as from the layer of air above. In turn, the surface tends to be pushed along by air drag. Over the ocean, this **wind stress** drives the **ocean currents**.

In the atmosphere, stress caused by turbulent motions is many orders of magnitude greater than stress caused by molecular viscosity. For that reason, we often speak of **turbulent stress** instead of frictional stress, and **turbulent drag** rather than frictional drag. This turbulent stress is also called a **Reynolds stress**, after Osborne Reynolds who related this stress to turbulent gust velocities in the late 1800s.

Because air is a fluid, it is often easier to study the stress per unit density ρ of air. This is called the **kinematic stress**. The kinematic stress against the Earth's surface is given the symbol u_*^2, where u_* is called the **friction velocity**:

$$u_*^2 = |\tau / \rho| \qquad \bullet(18.10)$$

Typical values range from $u_* = 0$ during calm winds to $u_* = 1$ m/s during strong winds. Moderate-wind values are often near $u_* = 0.5$ m/s.

For fluid flow, turbulent stress is proportional to wind speed squared. Also stress is greater over rougher surfaces. A dimensionless **drag coefficient** C_D relates the kinematic stress to the wind speed M_{10} at $z = 10$ m.

$$u_*^2 = C_D \cdot M_{10}^2 \qquad \bullet(18.11)$$

The drag coefficient ranges from $C_D = 2\text{x}10^{-3}$ over smooth surfaces to $2\text{x}10^{-2}$ over rough or forested surfaces (Table 18-1). It is similar to the bulk heat-transfer coefficient of the Heat chapter.

The surface roughness is usually quantified as an **aerodynamic roughness length** z_o. Table 18-1 shows typical values of the roughness length for various surfaces. Rougher surfaces such as sparse forests have greater values of roughness length than smoother surfaces such as a frozen lake. Roughness lengths in this table are not equal to the heights of the houses, trees, or other roughness elements.

For statically neutral air, there is a relationship between drag coefficient and aerodynamic roughness length:

$$C_D = \frac{k^2}{\ln^2(z_R / z_o)} \qquad (18.12)$$

where $k = 0.4$ is the **von Kármán constant**, and $z_R = 10$ m is a reference height defined as the standard anemometer height for measuring "**surface winds**". The drag coefficient decreases as the air becomes

Solved Example

Find the drag coefficient in statically neutral conditions to be used with standard surface winds of 5 m/s, over (a) villages, and (b) grass prairie. Also, find the friction velocity and surface stress.

Solution

Given: $z_R = 10$ m for "standard" winds
Find: C_D = ? (dimensionless), u_* = ? m/s, τ = ? N/m^2

Use Table 18-1:
(a) $z_o = 1$ m for villages. (b) $z_o = 0.03$ m for prairie

Use eq. (18.12) for drag coefficient:

(a) $C_D = \dfrac{0.4^2}{\ln^2(10\text{m} / 1\text{m})}$ = **0.030** (dimensionless)

(b) $C_D = \dfrac{0.4^2}{\ln^2(10\text{m} / 0.03\text{m})}$ = **0.0047** (dimensionless)

Use eq. (18.11) for friction velocity:
(a) $u_*^2 = C_D \cdot M_{10}^2 = 0.03 \cdot (5\text{m/s})^2 = 0.75\ \text{m}^2\cdot\text{s}^{-2}$
Thus u_* = **0.87 m/s.**
(b) Similarly, u_* = **0.34 m/s**.

Use eq. (18.10) for surface stress, and assume $\rho = 1.2\ \text{kg/m}^3$:
(a) $\tau = \rho \cdot u_*^2 = (1.2\ \text{kg/m}^3)\cdot(0.75\text{m}^2/\text{s}^2) =$
$\tau = 0.9\ \text{kg}\cdot\text{m}^{-1}\cdot\text{s}^{-2}$ = **0.9 Pa** (using Appendix A)
(b) $\tau = 0.14\ \text{kg}\cdot\text{m}^{-1}\cdot\text{s}^{-2}$ = **0.14 Pa**

Check: Units OK. Physics OK.
Discussion: The drag coefficient, friction velocity, and stress are smaller over smoother surfaces.

In this development we examined the stress for fixed wind speed and roughness. However, in nature, greater roughness and greater surface drag causes slower winds (see the Dynamics chapter).

Solved Example

If the wind speed is 20 m/s at 10 m height over an orchard, find the friction velocity.

Solution

Given: M_{10} = 20 m/s at z_R = 10 m, z_o = 0.5 m
Find: u_* = ? m/s

Use eq. (18.13):
u_* = (0.4)·(20 m/s)/ln(10m/0.5m) = **2.67 m/s**

Check: Units OK. Magnitude OK.
Discussion: This corresponds to a large stress on the trees, which could make the branches violently move, causing some fruit to fall.

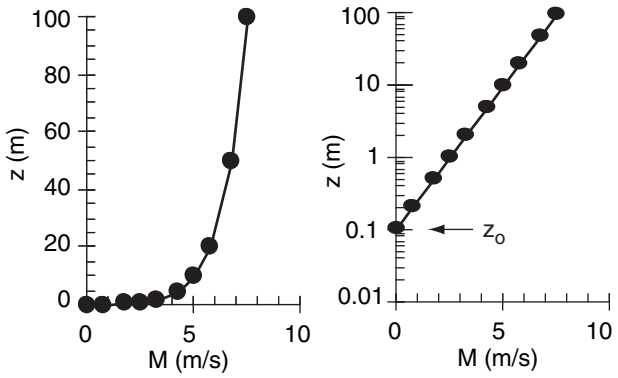

Figure 18.21
Wind-speed (M) profile in the statically-neutral surface layer, for a roughness length of 0.1 m. (a) linear plot, (b) semi-log plot.

Solved Example

On an overcast day, a wind speed of 5 m/s is measured with an anemometer located 10 m above ground within an orchard. What is the wind speed at the top of a 25 m smoke stack?

Solution

Given: M_1 = 5 m/s at z_1 = 10 m
Neutral stability (because overcast)
z_o = 0.5 m from Table 18-1 for an orchard
Find: M_2 = ? m/s at z_2= 25 m

Sketch:

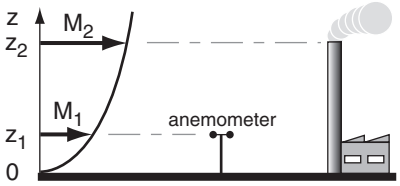

Use:
eq. (18.14b):

$$M_2 = 5(\text{m/s}) \cdot \frac{\ln(25\text{m}/0.5\text{m})}{\ln(10\text{m}/0.5\text{m})} = \underline{\textbf{6.53 m/s}}$$

Check: Units OK. Physics OK. Sketch OK.
Discussion: Hopefully the anemometer is situated far enough from the smoke stack to measure the true undisturbed wind.

more statically stable. For unstable air, roughness is less important, and alternative approaches are given in the Heat chapter and the Dynamics chapter.

Combining the previous two equations gives an expression for friction velocity in terms of surface wind speed and roughness length:

$$u_* = \frac{k \cdot M_{10}}{\ln[z_R / z_o]} \qquad (18.13)$$

The physical interpretation is that faster winds over rougher surfaces causes greater kinematic stress.

Log Profile in the Neutral Surface Layer

Wind speed M is zero at the ground (more precisely, at a height equal to the aerodynamic roughness length). Speed increases roughly logarithmically with height in the statically-neutral surface layer (bottom 50 to 100 m of the ABL), but the shape of this profile depends on the surface roughness:

$$M(z) = \frac{u_*}{k} \ln\left(\frac{z}{z_o}\right) \qquad \bullet(18.14a)$$

Alternately, if you know wind speed M_1 at height z_1, then you can calculate wind speed M_2 at any other height z_2 :

$$M_2 = M_1 \cdot \frac{\ln(z_2 / z_o)}{\ln(z_1 / z_o)} \qquad (18.14b)$$

Many weather stations measure the wind speed at the standard height z_1 = 10 m.

An example of the **log wind profile** is plotted in Fig. 18.21. A perfectly logarithmic wind profile (i.e., eq. 18.14) would be expected only for **neutral** static stability (e.g., overcast and windy) over a uniform surface. For other static stabilities, the wind profile varies slightly from logarithmic.

On a semi-log graph, the log wind profile would appear as a straight line. You can determine the roughness length by measuring the wind speeds at two or more heights, and then extrapolating the straight line in a semi-log graph to zero wind speed. The z-axis intercept gives the roughness length.

Log-Linear Profile in Stable Surf. Layer

During statically stable conditions, such as at nighttime over land, wind speed is slower near the ground, but faster aloft than that given by a logarithmic profile. This profile in the surface layer is empirically described by a **log-linear profile** formula with both a logarithmic and a linear term in z:

$$M(z) = \frac{u_*}{k}\left[\ln\left(\frac{z}{z_o}\right) + 6\frac{z}{L}\right] \qquad \bullet(18.15)$$

where M is wind speed at height z, $k = 0.4$ is the von Kármán constant, z_o is the aerodynamic roughness length, and u_* is friction velocity. As height increases, the linear term dominates over the logarithmic term, as sketched in Fig. 18.20.

An **Obukhov length** L is defined as:

$$L = \frac{-u_*^3}{k \cdot (|g| / T_v) \cdot F_{Hsfc}} \qquad \bullet(18.16)$$

where $|g| = 9.8$ m/s^2 is gravitational acceleration magnitude, T_v is the absolute virtual temperature, and F_{Hsfc} is the kinematic surface heat flux. L has units of m, and is positive during statically stable conditions (because F_{Hsfc} is negative then). The Obukhov length can be interpreted as the height in the stable surface layer below which shear production of turbulence exceeds buoyant consumption.

Profile in the Convective Radix Layer

For statically unstable ABLs with vigorous convective thermals, such as occur on sunny days over land, wind speed becomes uniform with height a short distance above the ground. Between that uniform wind-speed layer and the ground is the **radix layer** (RxL). The wind speed profile in the radix layer is:

$$M(z) = M_{BL} \cdot \left(\zeta_*^D\right)^A \cdot \exp\left[A \cdot \left(1 - \zeta_*^D\right)\right] \quad \text{for } 0 \le \zeta_* \le 1.0 \qquad \bullet(18.17a)$$

and

$$M(z) = M_{BL} \quad \text{for } 1.0 \le \zeta_* \qquad (18.17b)$$

where $\zeta_* = 1$ defines the top of the radix layer. In the bottom of the RxL, wind speed increases faster with height than given by the log wind profile for the neutral surface layer, but becomes tangent to the uniform winds M_{BL} in the mid-mixed layer (Fig. 18.20).

The dimensionless height in the eqs. above is

$$\zeta_* = \frac{1}{C} \cdot \frac{z}{z_i} \cdot \left(\frac{w_*}{u_*}\right)^B \qquad (18.18)$$

where w_* is the **Deardorff velocity**, and the empirical coefficients are $A = 1/4$, $B = 3/4$, and $C = 1/2$. $D = 1/2$ over flat terrain, but increases to near $D = 1.0$ over hilly terrain.

The Deardorff velocity (eq. 3.39) is copied here:

$$w_* = \left[\frac{|g|}{T_v} \cdot z_i \cdot F_{Hsfc}\right]^{1/3} \qquad \bullet(18.19a)$$

Solved Example (§)

For a friction velocity of 0.3 m/s, aerodynamic roughness length of 0.02 m, average virtual temperature of 300 K, and kinematic surface heat flux of –0.05 K·m/s at night, plot the wind-speed profile in the surface layer. (Compare profiles for statically stable and neutral conditions.)

Solution

Given: $u_* = 0.3$ m/s, $z_o = 0.02$ m,
$T_v = 300$ K, $F_{Hsfc} = -0.05$ K·m/s
Find: $M(z) = ?$ m/s

Use eq. (18.16):
$L = -(0.3\text{m/s})^3/[0.4 \cdot (9.8\text{m}\cdot\text{s}^{-2}) \cdot (-0.05\text{K}\cdot\text{m/s})/(300\text{K})]$
= **41.3 m**

Use eq. (18.14a) for M in a neutral surface layer.
For example, at $z = 50$ m:
$M = [(0.3\text{m/s})/0.4] \cdot \ln(50\text{m}/0.02\text{m})$ = **5.9 m/s**

Use eq. (18.15) for M in a stable surface layer.
For example, at $z = 50$ m: $M = [(0.3\text{m/s})/0.4] \cdot [\ln(50\text{m}/0.02\text{m}) + 6 \cdot (50\text{m}/41.3\text{m})]$ = **11.3 m/s**

Use a spreadsheet to find M at the other heights:

z (m)	M(m/s)$_{neutral}$	M (m/s)$_{stable}$
0.02	0.0	0.0
0.05	0.7	0.7
0.1	1.2	1.2
0.2	1.7	1.7
0.5	2.4	2.5
1	2.9	3.0
2	3.5	3.7
5	4.1	4.7
10	4.7	5.7
20	5.2	7.4
50	5.9	11.3
100	6.4	17.3

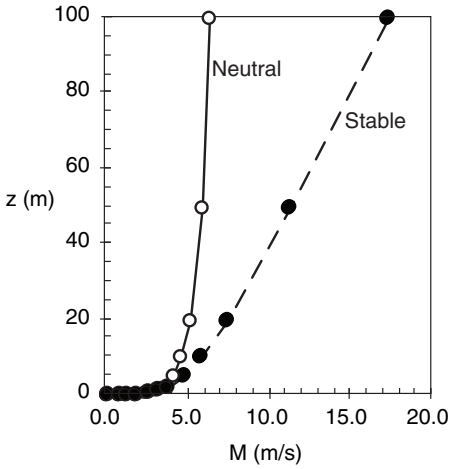

Check: Units OK. Physics OK. Plot OK.
Discussion: Open circles are for neutral, solid are for statically stable. The linear trend is obvious in the wind profile for the stable boundary layer.

Solved Example (§)

For a 1 km deep mixed layer with surface heat flux of 0.3 K·m/s and friction velocity of 0.2 m/s, plot the wind speed profile using a spreadsheet. Terrain is flat, and mid-ABL wind is 5 m/s.

Solution

Given: F_{Hsfc} =0.3 K·m/s, $u_* = 0.2$ m/s,
$z_i = 1000$ m, $M_{BL} = 5$ m/s, $D = 0.5$.
Find: $M(z)$ = ? m/s .

The ABL is statically unstable, because F_{Hsfc} is positive.
First, find w_* = ? m/s using eq. (18.19a).
Assume: $|g|/T_v = 0.0333$ m·s^{-2}·K^{-1} (typical).

$$w_* = \left[\left(0.0333\frac{\text{m}}{\text{s}^2\text{K}}\right)\cdot(1000\text{m})\cdot\left(0.3\frac{\text{K}\cdot\text{m}}{\text{s}}\right)\right]^{1/3}$$

$$= (10\ \text{m}^3/\text{s}^3)^{1/3} = 2.15\ \text{m/s}$$

Use eq. (18.18) in a spreadsheet to get ζ_* at each z, then use eq. (18.17) to get each M. For example, at z = 10 m: $\zeta_* = 2\cdot(10\text{m}/1000\text{m})\cdot[(2.15\text{m/s})/(0.2\text{m/s})]^{3/4} =$ **0.1187** , & $M = (5\text{m/s})\cdot(0.119^{1/2})^{1/4}\cdot\exp[0.25\cdot(1-0.119^{1/2})] =$ **4.51m/s**

z (m)	ζ_*	M (m/s)
0	0.000	0.00
0.1	0.001	2.74
0.2	0.002	2.98
0.5	0.006	3.32
1.0	0.012	3.59
2	0.024	3.87
5	0.059	4.24
10	0.119	4.51
15	0.178	4.66
20	0.237	4.75

etc.

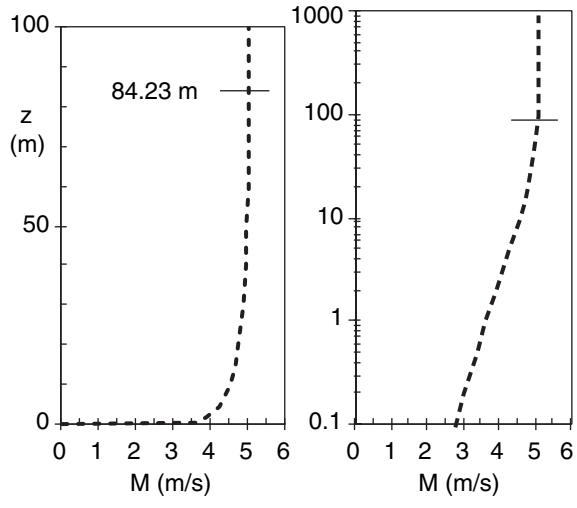

Check: Units OK. Physics OK. Sketch OK.
Discussion: This profile smoothly merges into the uniform wind speed in the mid-mixed layer, at height $\zeta_* = 1.0$, which is at $z = C\cdot z_i\cdot(u_*/w_*)_B = 84.23$ m from eq. (18.18).

where $|g| = 9.8$ m/s^2 is gravitational acceleration magnitude, T_v is absolute virtual temperature, z_i is depth of the ABL (= depth of the mixed layer), and F_{Hsfc} is the kinematic sensible heat flux (units of K·m/s) at the surface. Typical values of w_* are on the order of 1 m/s. The Deardorff velocity and buoyancy velocity w_B (defined in the Heat chapter) are both convective velocity scales for the statically unstable ABL, and are related by:

$$w_* \approx 0.08\ w_B \qquad (18.19b)$$

To use eq. (18.17) you need to know the average wind speed in the middle of the mixed layer M_{BL}, as was sketched in Fig. 18.9. The Dynamics chapter shows how to estimate this if it is not known from measurements.

For both the free-convection radix layer and the forced-convection surface layer, turbulence transports momentum, which controls wind-profile shape, which then determines the shear (Fig. 18.22). However, differences between the radix layer and surface layer are caused by differences in feedback.

In the neutral surface layer (Fig. 18.22a) there is strong feedback because wind shear generates the

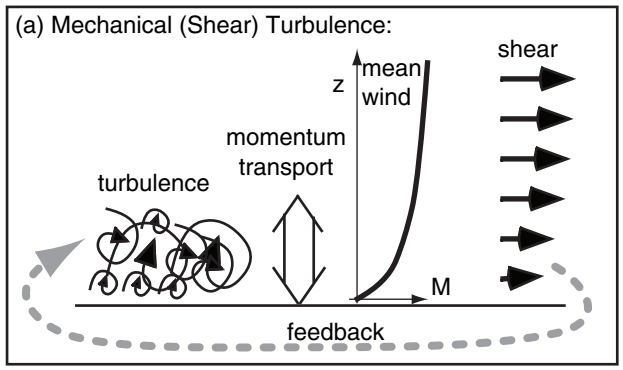

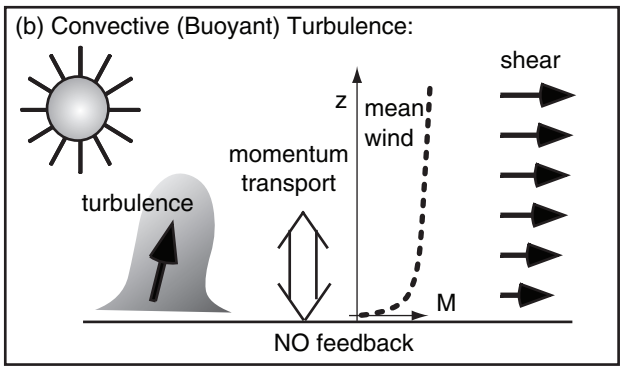

Figure 18.22
(a) Processes important for the log-wind profile in the surface layer dominated by mechanical turbulence (forced convection; neutral stability). (b) Processes important for the radix-layer wind profile during convective turbulence (free convection; statically unstable).

turbulence, which in turn controls the wind shear. However, such feedback is broken for convective turbulence (Fig. 18.22b), because turbulence is generated primarily by buoyant thermals, not by shear.

TURBULENCE

Mean and Turbulent Parts

Wind can be quite variable. The total wind speed is the superposition of three types of flow:

- **mean wind** – relatively constant, but varying slowly over the course of hours
- **waves** – regular (linear) oscillations of wind, often with periods of ten minutes or longer
- **turbulence** – irregular, quasi-random, non-linear variations or gusts, with durations of seconds to minutes

These flows can occur individually, or in any combination. Waves are discussed in the Local Winds chapter. Here, we focus on mean wind and turbulence.

Let $U(t)$ be the x-direction component of wind at some instant in time, t. Different values of $U(t)$ can occur at different times, if the wind is variable. By averaging the **instantaneous wind** measurements over a time period, P, we can define a **mean wind** $\overline{U}$, where the overbar denotes an average. This mean wind can be subtracted from the instantaneous wind to give the **turbulence** or gust part u' (Fig. 18.23).

Similar definitions exist for the other wind components (U, V, W), temperature (T) and humidity (r):

$$u'(t) = U(t) - \overline{U} \qquad (18.20a)$$

$$v'(t) = V(t) - \overline{V} \qquad (18.20b)$$

$$w'(t) = W(t) - \overline{W} \qquad (18.20c)$$

$$T'(t) = T(t) - \overline{T} \qquad (18.20d)$$

$$r'(t) = r(t) - \overline{r} \qquad (18.20e)$$

Thus, the wind can be considered as a sum of mean and turbulent parts (neglecting waves for now).

The averages in eq. (18.20) are defined over time or over horizontal distance. For example, the mean temperature is the sum of all individual temperature measurements, divided by the total number N of data points:

$$\overline{T} = \frac{1}{N}\sum_{k=1}^{N} T_k \qquad \bullet(18.21)$$

Science Graffito

"I am an old man now, and when I die and go to heaven there are two matters on which I hope for enlightenment. One is quantum electrodynamics, and the other is the turbulent motion of fluids. And about the former I am rather optimistic."
– *Sir Horace Lamb* (1932)

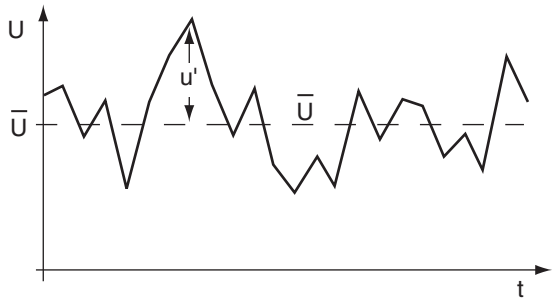

Figure 18.23
The instantaneous wind speed U shown by the zigzag line. The average wind speed $\overline{U}$ is shown by the thin horizontal dashed line. A gust velocity u' is the instantaneous deviation of the instantaneous wind from the average.

Solved Example

Given the following measurements of total instantaneous temperature, T, find the average $\overline{T}$. Also, find the T' values.

t (min)	T (°C)	t (min)	T (°C)
1	12	6	13
2	14	7	10
3	10	8	11
4	15	9	9
5	16	10	10

Solution

As specified by eq. (18.21), adding the ten temperature values and dividing by ten gives the average $\overline{T}$ = 12.0°C. Subtracting this average from each instantaneous temperature gives:

t (min)	T '(°C)	t (min)	T '(°C)
1	0	6	1
2	2	7	–2
3	–2	8	–1
4	3	9	–3
5	4	10	–2

Check: The average of these T' values should be zero, by definition, useful for checking for mistakes.

Discussion: If a positive T' corresponds to a positive w', then warm air is moving up. This contributes positively to the heat flux.

where k is the index of the data point (corresponding to different times or locations). The averaging time in eq. (18.21) is typically about 0.5 h. If you average over space, typical averaging distance is 50 to 100 km.

Short term fluctuations (described by the primed quantities) are associated with small-scale swirls of motion called **eddies**. The superposition of many such eddies of many sizes makes up the **turbulence** that is imbedded in the mean flow.

Molecular viscosity in the air causes friction between the eddies, tending to reduce the turbulence intensity. Thus, turbulence is NOT a conserved quantity, but is **dissipative**. Turbulence decays and disappears unless there are active processes to generate it. Two such production processes are **convection**, associated with warm air rising and cool air sinking, and **wind shear**, the change of wind speed or direction with height.

Normally, weather forecasts are made for mean conditions, not turbulence. Nevertheless, the net effects of turbulence on mean flow must be included. Idealized average turbulence effects are given in the chapters on Heat, Moisture, and Dynamics.

Meteorologists use statistics to quantify the net effect of turbulence. Some statistics are described next. In this chapter we will continue to use the overbar to denote the mean conditions. However, we drop the overbar in most other chapters in this book to simplify the notation.

Solved Example (§)

(a) Given the following V-wind measurements. Find the mean wind speed, and standard deviation. (b) If the standard deviation of vertical velocity is 1 m/s, is the flow isotropic?

t (h)	V (m/s)
0.1	2
0.2	–1
0.3	1
0.4	1
0.5	–3
0.6	–2
0.7	0
0.8	2
0.9	–1
1.0	1

Solution

Given: Velocities listed at right
$\sigma_w = 1$ m/s.

Find: $\bar{V}$ = ? m/s, σ_v = ? m/s, isotropy = ?

(a) Use eq. (18.21), except for V instead of T:

$$\bar{V}(z) = \frac{1}{n}\sum_{i=1}^{n} V_i(z) = \frac{1}{10}(0) \quad = \underline{\mathbf{0\ m/s}}$$

Use eq. (18.22), but for V:

$$\sigma_v^2 = \frac{1}{n}\sum_{i=1}^{n} (V_i - \bar{V})^2$$

$\sigma_v^2 = (1/10)\cdot(4+1+1+1+9+4+0+4+1+1) = 2.6\ m^2/s^2$

Finally, use eq. (18.23), but for v:

$$\sigma_v = \sqrt{2.6 m^2 \cdot s^{-2}} \quad = \underline{\mathbf{1.61\ m/s}}$$

Check: Units OK. Physics OK.

Discussion: (b) Anisotropic, because $\sigma_v > \sigma_w$ (see next subsection). This means that an initially spherical smoke puff would become elliptical in cross section as it disperses more in the horizontal than the vertical.

Variance and Standard Deviation

The **variance** σ^2 of vertical velocity is an overall statistic of gustiness:

$$\sigma_w^2 = \frac{1}{N}\sum_{k=1}^{N} (W_k - \bar{W})^2 = \frac{1}{N}\sum_{k=1}^{N} (w_k')^2 = \overline{w'^2} \qquad \bullet(18.22)$$

Similar definitions can be made for σ_u^2 , σ_v^2 , σ_θ^2 , etc. Statistically, these are called "biased" variances. Velocity variances can exist in all three directions, even if there is a mean wind in only one direction.

The **standard deviation** σ is defined as the square-root of the variance, and can be interpreted as an average gust (for velocity), or an average turbulent perturbation (for temperatures and humidities, etc.). For example, standard deviations for vertical velocity, σ_w, and potential temperature, σ_θ , are:

$$\sigma_w = \sqrt{\sigma_w^2} = \overline{(w')^2}^{1/2} \qquad (18.23a)$$

$$\sigma_\theta = \sqrt{\sigma_\theta^2} = \overline{(\theta')^2}^{1/2} \qquad (18.23b)$$

Larger variance or standard deviation of velocity means more intense turbulence.

For statically **stable** air, standard deviations in an ABL of depth h have been empirically found to vary with height z as:

$$\sigma_u = 2 \cdot u_* \cdot [1 - (z/h)]^{3/4} \qquad (18.24a)$$

$$\sigma_v = 2.2 \cdot u_* \cdot [1 - (z/h)]^{3/4} \qquad (18.24b)$$

$$\sigma_w = 1.73 \cdot u_* \cdot [1 - (z/h)]^{3/4} \qquad (18.24c)$$

where u_* is friction velocity. These equations work when the stability is weak enough that turbulence is not suppressed altogether.

For statically **neutral** air:

$$\sigma_u = 2.5 \cdot u_* \cdot \exp(-1.5 \cdot z/h) \qquad (18.25a)$$

$$\sigma_v = 1.6 \cdot u_* \cdot [1 - 0.5 \cdot (z/h)] \qquad (18.25b)$$

$$\sigma_w = 1.25 \cdot u_* \cdot [1 - 0.5 \cdot (z/h)] \qquad (18.25c)$$

For statically **unstable** air:

$$\sigma_u = 0.032 \cdot w_B \cdot \left(1 + [1 - (z/z_i)]^6\right) \qquad (18.26a)$$

$$\sigma_v = 0.032 \cdot w_B \qquad (18.26b)$$

$$\sigma_w = 0.11 \cdot w_B \cdot (z/z_i)^{1/3} \cdot [1 - 0.8 \cdot (z/z_i)] \qquad (18.26c)$$

where z_i is the mixed-layer depth, w_B is buoyancy velocity (eq. 3.38 or 18.19b). These relationships are important for air-pollution dispersion, and are used in the Air Pollution chapter. These equations are valid only within the boundary layer (i.e., from z = 0 up to h or z_i).

Isotropy

If turbulence has nearly the same variance in all three directions, then turbulence is said to be **isotropic**. Namely:

$$\sigma_u^2 = \sigma_v^2 = \sigma_w^2 \qquad \bullet(18.27)$$

Solved Example (§)

Plot the vertical profiles of standard deviation of vertical velocity for statically stable and neutral situations for which the friction velocity is 0.5 m/s. The boundary-layer depth is 300 m.

Solution

Given: u_* = 0.5 m/s, h = 300 m

Find: σ_w = ? vs. z for neutral and stable conditions

Use eqs. (18.24c and 18.25c). For example, for z = 100m:

Stable:

$\sigma_w = 1.73 \cdot (0.5\text{m/s}) \cdot [1 - (100\text{m}/300\text{m})]^{0.75}$ = **0.638 m/s**

Neutral:

$\sigma_w = 1.25 \cdot (0.5\text{m/s}) \cdot [1 - 0.5 \cdot (100\text{m}/300\text{m})$ = **0.521 m/s**

Using a spreadsheet with a range of heights yields:

	sigma w (m/s)	
z (m)	Stable	Neut.
0.0	0.865	0.625
1.0	0.863	0.624
10	0.843	0.615
100	0.638	0.521
150	0.514	0.469
200	0.379	0.417
250	0.266	0.365
300	0.0	0.313

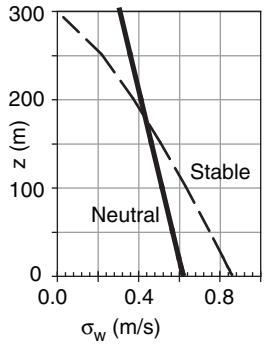

Check: Units OK. Magnitudes OK.

Discussion: Turbulence diminishes rapidly with increasing height for statically stable conditions.

Solved Example (§)

For a 1 km thick unstable boundary layer, compare the vertical profiles of σ_u & σ_w. Assume w_B = 30 m/s.

Solution

Given: z_i = 1000 m , w_B = 30 m/s

Find: σ_u & σ_w vs. z .

Use eqs. (18.26a and 18.26c) in a spreadsheet, and plot.

	sigma (m/s)	
z (m)	σ_u	σ_w
0	0.865	0.625
50	0.863	0.624
100	0.843	0.615
200	0.638	0.521
300	0.514	0.469
500	0.379	0.417
800	0.266	0.365
1000	0.0	0.313

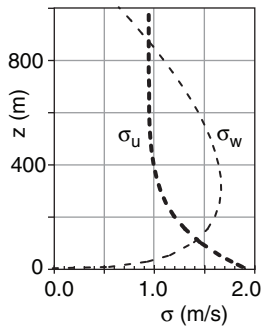

Check: Units OK. Magnitude reasonable.

Discussion: The flow is anisotropic at most heights. Near both the surface and z_i, horizontal turbulence is greater than vertical. But in the middle of the mixed layer, vertical turbulence is greater than horizontal.

Solved Example

Find u_*, the velocity standard deviations, and *TKE* in statically stable air at height 50 m in an ABL that is 200 m thick. Assume $C_D = 0.002$, and the winds at height 10 m are 5 m/s.

Solution

Given: $z = 50$ m, $h = 200$ m, $C_D = 0.002$,
$M = 5$ m/s. Statically stable.
Find: u_*, σ_u, σ_v, σ_w = ? m/s. TKE = ? m^2/s^2.

Use eq. (18.11):

$u_*^2 = 0.002 \cdot (5 m/s)^2 = 0.05\ m^2/s^2$. $u_* =$ **0.22 m/s**

Use eqs. (18.24a-c):

$\sigma_u = 2 \cdot (0.22 m/s) \cdot [1 - (50m/200m)]^{3/4} =$ **0.35 m/s**

$\sigma_v = 2.2 \cdot (0.22 m/s) \cdot [1 - (50m/200m)]^{3/4} =$ **0.39 m/s**

$\sigma_w = 1.73 \cdot (0.22 m/s) \cdot [1 - (50m/200m)]^{3/4} =$ **0.31 m/s**

Use eq. (18.28b):

$TKE = 0.5 \cdot [0.35^2 + 0.39^2 + 0.31^2] =$ **0.185** m^2/s^2.

Check: Units OK. Physics OK.
Discussion: In statically stable air, vertical turbulence is generally less than horizontal turbulence. Also, turbulence intensity increases with wind speed. If the atmosphere is too stable, then there will be no turbulence (see "dynamic stability" in the Stability chapter).

Science Graffito

"Big whirls have little whirls that feed on their velocity, and little whirls have lesser whirls and so on to viscosity – in the molecular sense."
– *L.F. Richardson*, 1922: "Weather Prediction by Numerical Process". p66.

[CAUTION: Do not confuse this word with "isentropic", which means adiabatic or constant entropy.]

Turbulence is **anisotropic** (not isotropic) in many situations. During the daytime over bare land, rising thermals create stronger vertical motions than horizontal. Hence, a smoke puff becomes **dispersed** (i.e., spread out) in the vertical faster than in the horizontal. At night, vertical motions are very weak, while horizontal motions can be larger. This causes smoke puffs to **fan** out horizontally with only little vertical dispersion in statically stable air.

Turbulence Kinetic Energy

An overall measure of the intensity of turbulence is the **turbulence kinetic energy** per unit mass (*TKE*):

$$TKE = 0.5 \cdot \left[\overline{(u')^2} + \overline{(v')^2} + \overline{(w')^2} \right] \qquad \bullet(18.28a)$$

$$TKE = 0.5 \cdot \left[\sigma_u^2 + \sigma_v^2 + \sigma_w^2 \right] \qquad \bullet(18.28b)$$

TKE is usually produced at the scale of the boundary-layer depth. The production is made mechanically by wind shear and buoyantly by thermals.

Turbulent energy cascades through the **inertial subrange**, where the large-size eddies drive medium ones, which in turn drive smaller eddies. Molecular viscosity continuously damps the tiniest (**microscale**) eddies, dissipating *TKE* into heat. *TKE* is not conserved.

The tendency of *TKE* to increase or decrease is given by the following *TKE* budget equation:

$$\frac{\Delta TKE}{\Delta t} = A + S + B + Tr - \varepsilon \qquad \bullet(18.29)$$

where A is advection of *TKE* by the mean wind, S is shear generation, B is buoyant production or consumption, Tr is transport by turbulent motions and pressure, and ε is viscous dissipation rate. For **stationary** (steady-state) turbulence, the tendency term on the left side of eq. (18.29) is zero.

Mean wind blows *TKE* from one location to another. The **advection** term is given by:

$$A = -U \cdot \frac{\Delta TKE}{\Delta x} - V \cdot \frac{\Delta TKE}{\Delta y} - W \cdot \frac{\Delta TKE}{\Delta z} \qquad (18.30)$$

Thus, turbulence can increase (or decrease) at any location if the wind is blowing in greater (or lesser) values of TKE from somewhere else.

Wind shear generates turbulence near the ground according to:

$$S = u_*^2 \cdot \frac{\Delta M}{\Delta z} \qquad (18.31a)$$

in the surface layer, where u_* is the friction velocity, and $\Delta M/\Delta z$ is the wind shear. To good approximation for near-neutral static stability:

$$S \approx a \cdot M^3 \qquad (18.31b)$$

where $a = 2\text{x}10^{-4}$ m^{-1} for wind speed M measured at a standard height of $z = 10$ m. Greater wind speeds near the ground cause greater wind shear, and generate more turbulence.

Buoyancy can either increase or decrease turbulence. When thermals are rising from a warm surface, they generate *TKE*. Conversely, when the ground is cold and the ABL is statically stable, buoyancy opposes vertical motion and consumes *TKE*.

The rate of **buoyant production or consumption** of *TKE* is:

$$B = \frac{|g|}{T_v} \cdot F_{H\ sfc} \qquad (18.32)$$

where $|g| = 9.8$ m·s^{-2} is gravitational acceleration magnitude, T_v is the absolute virtual air temperature near the ground, and $F_{H\ sfc}$ is the kinematic effective surface heat flux (positive when the ground is warmer than the air). Over land, $F_{H\ sfc}$ and B are usually positive during the daytime, and negative at night.

Turbulence can advect or **transport** itself. For example, if turbulence is produced by shear near the ground (in the **surface layer**), then turbulence motions will tend to move the excess *TKE* from the surface layer to locations higher in the ABL. Pressure fluctuations can have a similar effect, because turbulent pressure forces can generate turbulence motions. This pressure term is difficult to simplify, and will be grouped with the turbulent transport term, *Tr*, here.

Molecular viscosity dissipates turbulent motions into heat. The amount of heating is small, but the amount of damping of *TKE* is large. The **dissipation** is always a loss:

$$\varepsilon \approx \frac{(TKE)^{3/2}}{L_\varepsilon} \qquad (18.33)$$

where $L_\varepsilon \approx 50$ m is a **dissipation length scale**.

The ratio of buoyancy to shear terms of the *TKE* equation is called the **flux Richardson number**, R_f:

$$R_f = \frac{-B}{S} \approx \frac{-(|g|/T_v)\cdot F_{H\ sfc}}{u_*^2 \cdot \frac{\Delta M}{\Delta z}} \qquad (18.34a)$$

BEYOND ALGEBRA • Shear Generation

To get *TKE* shear-generation eq. (18.31b), start with eq. (18.31a):

$$S = u_*^2 \cdot (\partial M/\partial z) \qquad (18.31a)$$

But

$$(\partial M/\partial z) = u_*/(k\cdot z) \quad \text{from eq. (18.14a).}$$

Thus,

$$S = u_*^3 \,/\, (k\cdot z)$$

But

$$u_*^2 = C_D \cdot M^2 \qquad \text{from eq. (18.11)}$$

which gives

$$u_*^3 = C_D^{3/2} \cdot M^3$$

Thus:

$$S = [C_D^{3/2}/(k\cdot z)] \cdot M^3$$

or

$$S = a \cdot M^3 \qquad (18.31b)$$

where

$$a = [C_D^{3/2}/(k\cdot z)]$$

For $C_D \approx 0.01$, $k = 0.4$ is von Kármáns constant, and $z = 10$ m, the result is $a = 2.5\text{x}10^{-4}$ m^{-1}, but which can vary by an order of magnitude depending on the drag coefficient and height.

Solved Example

Assume steady state, and neglect advection and transport. What equilibrium TKE is expected in the surface layer with a mean wind of 5 m/s and surface heat flux of –0.02 K·m/s? The ambient temperature is 25°C, and the air is dry.

Solution

Given: $M = 5$ m/s, $F_{H\ sfc} = -0.02$ K·m/s, $A = 0$, $Tr = 0$, $\Delta TKE/\Delta t = 0$ for steady state, $T_v = 298$ K.

Find: $TKE = ?$ m^2/s^2 .

Rearrange eq. (18.29).

$$\varepsilon = S + B$$

But ε depends on *TKE*, thus, we can rearrange eq. (18.33) to solve for $TKE = (L_\varepsilon \cdot [\varepsilon])^{2/3}$ and then plug in the eq. above:

$$TKE = \{ L_\varepsilon \cdot [S + B] \}^{2/3}$$

Use eqs. (18.31b and 18.32) to find S and B, and plug into the equation above:

$$TKE = \left\{ L_\varepsilon \cdot \left[a \cdot M^3 + (|g|/T_v)\cdot F_{H\ sfc} \right] \right\}^{2/3} = \left\{ (50\text{m}) \cdot \left[\left(2\times10^{-4}\text{m}^{-1}\right)\left(5\frac{\text{m}}{\text{s}}\right)^3 + \frac{9.8\text{ms}^{-2}}{298\text{K}}(-0.02\text{Km/s}) \right] \right\}^{2/3}$$

$$= \{1.25 - 0.033\ \text{m}^3/\text{s}^3\}^{2/3} = \underline{\mathbf{1.14}}\ \text{m}^2/\text{s}^2$$

Check: Units OK. Physics OK.

Discussion: This turbulence intensity is weak, as is typical at night when heat fluxes are negative. Also, eq. (18.31b) for S is not accurate for statically stable conditions.

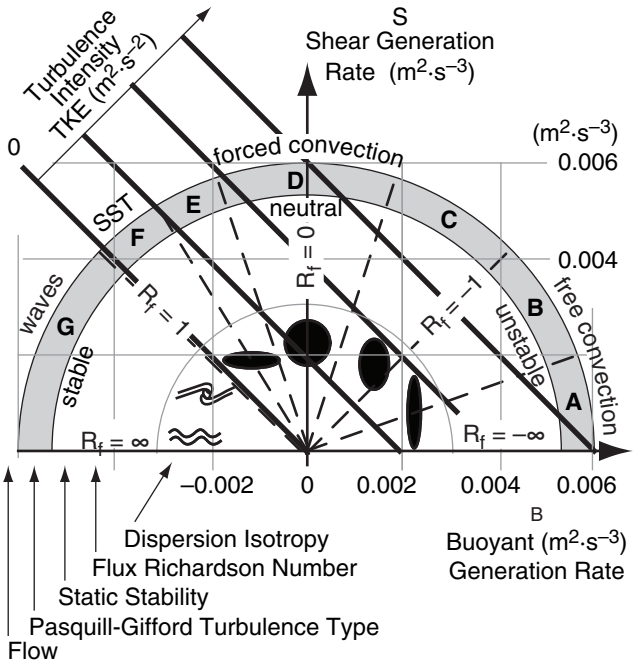

Figure 18.24
Rate of generation of TKE by buoyancy (abscissa) and shear (ordinate). Shape and rates of plume dispersion (dark spots or waves). Dashed lines separate sectors of different Pasquill-Gifford turbulence type (A - G). Isopleths of TKE intensity (dark diagonal lines). R_f is flux Richardson number. SST is stably-stratified turbulence.

Solved Example

For the previous solved example, determine the nature of convection (free, forced, etc.), the Pasquill-Gifford (PG) turbulence type, and the flux Richardson number. Assume no clouds.

Solution

Given: (see previous solved example)
Find: S = ? m²/s³ , B = ? m²/s³ , R_f = ? , PG = ?

Use eq. (18.31b):

$$S \approx \left(2\times10^{-4}\,\mathrm{m^{-1}}\right)\left(5\,\frac{\mathrm{m}}{\mathrm{s}}\right)^3 = 0.025\ \mathrm{m^2/s^3}$$

Use eq. (18.32):

$$B = \frac{9.8\mathrm{ms^{-2}}}{298\mathrm{K}}(-0.02\mathrm{Km/s}) = -0.00066\ \mathrm{m^2/s^3}$$

Because the magnitude of B is less than a third of that of S, we conclude convection is **forced**.

Use eq. (18.34): R_f = −(−0.00066) / 0.025 = **0.0264** and is dimensionless.

Use Fig. 18.24. Pasquill-Gifford Type = **D** (but on the borderline near E).

Check: Units OK. Physics OK.
Discussion: The type of turbulence is independent of the intensity. Intensity is proportional to *S*+*B*.

$$R_f \approx \frac{-(|g|/T_v)\cdot F_{H\ sfc}}{a\cdot M^3} \qquad (18.34b)$$

with $a \approx 2\text{x}10^{-4}$ m^{-1}. R_f is approximately equal to the **gradient or bulk Richardson number**, discussed in the Stability chapter. Generally, turbulence dies if $R_f > 1$.

Free and Forced Convection

The nature of turbulence, and therefore the nature of pollutant dispersion, changes with the relative magnitudes of terms in the *TKE* budget. Two terms of interest are the shear S and buoyancy B terms.

When $|B| < |S/3|$, the atmosphere is said to be in a state of **forced convection** (Fig. 18.24). These conditions are typical of windy overcast days, and are associated with near **neutral static stability**. Turbulence is nearly **isotropic**. Smoke plumes disperse at nearly equal rates in the vertical and lateral, which is called **coning**. The sign of B is not important here — only the magnitude.

When B is positive and $|B| > |3{\cdot}S|$, the atmosphere is said to be in a state of **free convection**. **Thermals** of warm rising air are typical in this situation, and the ABL is **statically unstable** (in the nonlocal sense; see the Stability chapter). These conditions often happen in the daytime over land, and during periods of cold-air advection over warmer surfaces. Turbulence is **anisotropic**, with more energy in the vertical, and smoke plumes loop up and down in a pattern called **looping**.

When B is negative and $|B| > |S|$, static stability is so strong that turbulence cannot exist. During these conditions, there is virtually no dispersion while the smoke blows downwind. **Buoyancy waves** (**gravity waves**) are possible, and appear as waves in the smoke plumes. For values of $|B| \approx |S|$, breaking **Kelvin-Helmholtz waves** can occur (see the Stability chapter), which cause some dispersion.

For B negative but $|B| < |S|$, weak turbulence is possible. These conditions can occur at night. This is sometimes called **stably-stratified turbulence** (**SST**). Vertical dispersion is much weaker than lateral, causing an **anisotropic** condition where smoke spreads horizontally more than vertically, in a process called **fanning**.

Fig. 18.24 shows the relationship between different types of convection and the terms of the *TKE* equation. While the ratio of B/S determines the nature of convection, the sum $S + B$ determines the intensity of turbulence. A Pasquill-Gifford turbulence type (Fig. 18.24) can also be defined from the relative magnitudes of S and B, and is used in the Air Pollution to help estimate pollution dispersion rates.

Turbulent Fluxes and Covariances

Rewrite eq. (18.22) for variance of w as

$$\text{var}(w) = \frac{1}{N}\sum_{k=1}^{N}(W_k - \bar{W})\cdot(W_k - \bar{W}) \qquad (18.35)$$

By analogy, a **covariance** between vertical velocity w and potential temperature θ can be defined as:

$$\begin{aligned}\text{covar}(w,\theta) &= \frac{1}{N}\sum_{k=1}^{N}(W_k - \bar{W})\cdot(\theta_k - \bar{\theta}) \\ &= \frac{1}{N}\sum_{k=1}^{N}(w_k')\cdot(\theta_k') \qquad \bullet(18.36) \\ &= \overline{w'\theta'}\end{aligned}$$

where the overbar still denotes an average. Namely, one over N times the sum of N terms (see middle line of eq. 18.36) is the average of those items. Comparing eqs. (18.35) with (18.36), we see that variance is just the covariance between a variable and itself.

Covariance indicates the amount of common variation between two variables. It is positive where both variables increase or decrease together. Covariance is negative for opposite variation, such as when one variable increases while the other decreases. Covariance is zero if one variable is unrelated to the variation of the other.

The **correlation coefficient** $r_{a,b}$ is defined as the covariance between a and b normalized by the standard deviations of the two variables a and b. Using vertical velocity and potential temperature for illustration:

$$r_{w,\theta} = \frac{\overline{w'\theta'}}{\sigma_w \cdot \sigma_\theta} \qquad \bullet(18.37)$$

By normalized, we mean that $-1 \le r_{a,b} \le 1$. A correlation coefficient of +1 indicates a perfect correlation (both variables increase or decrease together proportionally), –1 indicates perfect opposite correlation, and zero indicates no correlation. Because it is normalized, $r_{a,b}$ gives no information on the absolute magnitudes of the variations.

In the ABL, many turbulent variables are correlated. For example, in the statically unstable ABL (Fig. 18.25a), parcels of warm air rise and while other cool parcels sink in convective circulations. Warm air (θ′ = +) going up (w' = +) gives a positive product [$(w'\theta')_{up}$ = +]. Cool air (θ′ = –) going down (w' = –) also gives a positive product [$(w'\theta')_{down}$ = +].

The average of those two products is also positive [$\overline{w'\theta'} = 0.5\cdot(\,(w'\theta')_{up} + (w'\theta')_{down}\,) = +$]. The result gives positive correlation coefficients $r_{w,\theta}$ during free convection, which is typical during daytime.

Science Graffito

Seen on a bumper sticker:
"**Lottery**: A tax on people who are bad at math."

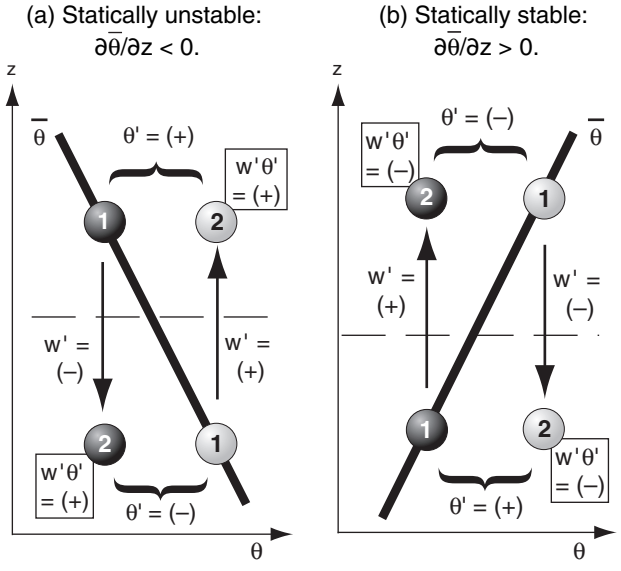

Figure 18.25
(a) Relationship between turbulent potential temperature θ and vertical velocity w for a statically unstable environment (e.g., daytime over land with clear skies) . (b) Same, but for a statically stable environment (e.g., nighttime over land with clear skies). In both figures, the thick line represents the ambient environment, circles represent air parcels, with light grey being the warm air parcel and dark gray being cool. Numbers 1 and 2 indicate starting and ending positions of each air parcel during time interval Δt.

Solved Example (§)

Fast-response measurements of potential temperature θ, water-vapor mixing ratio *r*, and *u* and *w* components of wind are given below as a function of time *t*. For θ and *w*, find their means, variances, and standard deviations. Also find the covariance, correlation coefficient, kinematic heat flux, and the heat flux (W/m^2).

Columns C and D are not used in this example, but will be used in some of the homeworks.

	A	B	C	D	E
1	Given:				
2	t (s)	θ (°C)	r (g/kg)	U (m/s)	W (m/s)
3	0	21	6.0	10	-5
4	0.1	28	9.5	6	4
5	0.2	29	10.0	7	3
6	0.3	25	8.0	3	4
7	0.4	22	6.5	5	0
8	0.5	28	9.5	15	-5
9	0.6	23	7.0	12	-1
10	0.7	26	8.5	16	-3
11	0.8	27	9.0	10	2
12	0.9	24	7.5	8	-4
13	1.0	21	6.0	14	-4
14	1.1	24	7.5	10	1
15	1.2	25	8.0	13	-2
16	1.3	27	9.0	5	3
17	1.4	29	10.0	7	5
18	1.5	22	6.5	11	2
19	1.6	30	10.5	2	6
20	1.7	23	7.0	15	-1
21	1.8	28	9.5	13	3
22	1.9	21	6.0	12	-3
23	2.0	22	6.5	16	-5
24	**avg =**	**25**			**0**

Solution:

Given: Data above in rows 2 through 23.

Find: $\overline{W}$ =? m/s , $\overline{\theta}$ = ? °C , σ_w^2 = ? m^2/s^2, σ_θ^2 = ? °C^2, σ_w =? m/s, σ_θ = ? °C, $\overline{w'\theta'}$ = ? K·m/s, $r_{w,\theta}$ = ? (dimensionless) F_H = ? K·m/s, $\mathbb{F}_H$ = ? W/m^2 .

First, use eq. (18.21) to find the mean values. These answers are already shown in row 24 above.

$\overline{\theta}$ = **25 °C** , $\overline{W}$ = **0 m/s**

Next, use eqs. (18.20) to find the deviation from the mean, for each of the observations. The results are tabulated in columns G and H on the next page. Then square each of those perturbation (primed) values, as tabulated in columns I and J on the next page.

Use eq. (18.22), averaging the squared perturbations to give the variances (row 24, columns I and J):

σ_θ^2 = **8.48 °C**^{2} , σ_w^2 = **12.38** m^2/s^2.

The square root of those answers (eq. 18.23) gives the standard deviations in row 25, columns I and J:

σ_θ = **2.91 °C** , σ_w = **3.52 m/s** .

(continues on next page)

Similarly, for statically stable conditions (Fig. 18.25b) where wind-shear-induced turbulence drives vertical motions against the restoring buoyant forces (see the Stability chapter), one finds cold air moving up, and warm air moving down. (Parcel warmness or coldness is measured relative to the ambient mean potential temperature $\overline{\theta}$ at the same ending height as the parcel.) This gives $\overline{w'\theta'} = -$, which is often the case during night.

More important than the statistics are the physical processes they represent. Covariances represent fluxes. Look at the air parcels crossing the horizontal dashed line in Fig. 18.25a. Pretend that the dashed line is an edge view of a horizontal area that is 1 m^2.

During time interval Δt, the warm (light-grey shaded) air parcel moves warm air upward through that area in Fig. 18.25a. Heat flux is defined as heat moved per area per time. Thus this rising warm air parcel contributes to a positive heat flux. Similarly, the cold sinking air parcel (shaded dark grey) contributes to a positive heat flux through that area (because negative w' times negative θ' is positive). Both parcels contribute to a positive heat flux.

This implies that covariance between vertical velocity and potential temperature is a turbulent kinematic heat flux, F_H [= $F_{z\ turb}(\theta)$ in the notation of the Heat chapter]:

$$\overline{w'\theta'} = F_H \qquad \bullet(18.38a)$$

Similarly, the covariance between vertical velocity w and water vapor mixing ratio, r (see the Moisture chapter), is a kinematic moisture flux, $F_{z\ turb}(r)$:

$$\overline{w'r'} = F_{z\ turb}(r) \qquad \bullet(18.38b)$$

Momentum flux is even more interesting. Recall from physics that **momentum** is mass times velocity. Units would be kg·m·s^{-1}. Therefore, momentum flux (momentum per area per time) would have units of (kg·m·s^{-1})·m^{-2}·s^{-1} = (kg·m·s^{-2})·m^{-2} = N·m^{-2}. Appendix A was used to find the equivalent units for a force of 1 Newton (N). But N·m^{-2} is a force per unit area, which is the definition of stress, τ. Thus, stress and momentum flux are physically the same in a fluid such as air.

A kinematic momentum flux is the momentum flux divided by air density ρ, which from the paragraph above is equal to τ/ρ. But this is just the definition of friction velocity squared u_*^2 (eq. 18.10).

As in Fig. 18.25, if vertically moving air parcels (w') transport air with different horizontal velocities (u') across a horizontal area per unit time, then the covariance between vertical velocity and horizontal velocity is a kinematic momentum flux. From the

paragraph above, the magnitude is also equal to the friction velocity squared. Thus:

$$\left|\overline{w'u'}\right| = \left|F_{z\ turb}(\text{momentum})\right| = \left|\tau / \rho\right| = u_*^2 \qquad \bullet(18.38c)$$

where $\overline{w'u'}$ is called a **Reynolds stress**.

In Fig. 18.25, air mass is conserved. Namely, each rising air parcel is compensated by a descending air parcel with the same air mass. Thus, as seen from the discussion above, turbulence can cause a net vertical transport of heat, moisture, and momentum, even though there is no net transport of air mass.

Turbulent fluxes given by eqs. (18.38) are called **eddy-correlation fluxes**. They can be measured with fast response velocity, humidity, and temperature sensors, sampling at about 10 Hz for 30 minutes. Turbulent fluxes can also be parameterized, as discussed next.

Turbulence Closure

To forecast the weather (see the NWP chapter), we need to solve the Eulerian conservation equations for temperature, humidity, and wind:

- temperature forecasts ← heat conservation eq. ← First Law of Thermodynamics (see the Heat chapter)
- humidity forecasts ← water conservation eq. ← Eulerian water-budget equation (see the Moisture chapter)
- wind forecasts ← momentum conservation eq. ← Newton's Second Law (see the Dynamics chapter)

For example, the Eulerian net heat-budget equation from the Heat chapter (eq. 3.51) is:

$$\frac{\Delta T}{\Delta t} = Advection + Radiation + LatentHeat - \frac{\Delta F_{z\ turb}(\theta)}{\Delta z} \qquad (18.39a)$$

where the last term is the turbulence term. But from eq. (18.38a), we recognize the turbulent heat flux as a covariance. Thus, eq. (18.39a) can be rewritten as:

$$\frac{\Delta \overline{T}}{\Delta t} = (otherPhysics) - \frac{\Delta \overline{w'\theta'}}{\Delta z} \qquad (18.39b)$$

The derivation of this equation is shown in the Beyond Algebra box on the next page.

Because the heat flux $\overline{w'\theta'}$ is needed in eq. (18.39b), we need to get a forecast equation for it:

$$\frac{\Delta \overline{w'\theta'}}{\Delta t} = (otherPhysics) - \frac{\Delta \overline{w'w'\theta'}}{\Delta z} \qquad (18.40)$$

Solved Example (§) *(continuation)*

Use eq. (18.36) and multiply each w' with θ' to give in column K the values of $w'\theta'$. Average those to get the covariance: $\overline{w'\theta'} = F_H =$ **6.62 K·m/s**, which is the kinematic heat flux by definition.

Use eq. (18.37) and divide the covariance by the standard deviations to give the correlation coef: $r_{w,\theta} =$ **0.65** (dimensionless).

Use eq. (2.11) to give heat flux, with $\rho \cdot C_p$ =1231 (W/m^2)/(°C·m/s) from Appendix B, yielding $\mathbb{F}_H = \rho \cdot C_p \cdot F_H$ = **8150 W/m^2** .

	G	H	I	J	K	L
1	θ'	w'	θ'^{2}	w'^{2}	w'θ'	
2	(°C)	(m/s)	(°C^2)	(m/s)^2	°C·(m/s)	
3	–4	–5	16	25	20	
4	3	4	9	16	12	
5	4	3	16	9	12	
6	0	4	0	16	0	
7	–3	0	9	0	0	
8	3	–5	9	25	–15	
9	–2	–1	4	1	2	
10	1	–3	1	9	–3	
11	2	2	4	4	4	
12	–1	–4	1	16	4	
13	–4	–4	16	16	16	
14	–1	1	1	1	–1	
15	0	–2	0	4	0	
16	2	3	4	9	6	
17	4	5	16	25	20	
18	–3	2	9	4	–6	
19	5	6	25	36	30	
20	–2	–1	4	1	2	
21	3	3	9	9	9	
22	–4	–3	16	9	12	
23	–3	–5	9	25	15	
24	**0**	**var.=**	8.48	12.38	**6.62=**	**covar**
25		**st.dev.=**	2.61	3.52	**0.65=**	**$r_{w,\theta}$**

Check: The average is zero of the singled primed values, as they always should be. Units OK.

Discussion: The magnitude of $\mathbb{F}_H$ is unrealistically big for this contrived data set.

Solved Example

If $\overline{w'\theta'}$ = 0.2 K·m/s at the surface, and is 0 at the top of a 1 km thick layer, find the warming rate.

Solution

Given: $\overline{w'\theta'}$ = 0.2 K·m/s at z = 0, $\overline{w'\theta'}$ = 0 at z = 1km

Find: $\Delta \overline{T} / \Delta t$ = ? K/h

Use eq. (18.39b): $\Delta \overline{T} / \Delta t$ = – (0 – 0.2 K·m/s) /(1000m – 0)
= 2x10^{-4} K/s = **0.72 K/h**.

Check: Units OK. Magnitude small.

Discussion: Over 12 hours of daylight, this surface flux would warm the thick layer of air by 8.6°C.

BEYOND ALGEBRA • Turbulence Terms

Why does a turbulence covariance term appear in the forecast equation for average temperature, $\overline{T}$? To answer, consider the vertical advection term (3.31) in the heat-budget equation (3.17) as an example:

$$\frac{\partial T}{\partial t} = \cdots - W\frac{\partial \theta}{\partial z}$$

For each dependent variable (T, W, θ), describe them by their mean plus turbulent parts:

$$\frac{\partial(\overline{T}+T')}{\partial t} = \cdots - (\overline{W}+w')\frac{\partial(\overline{\theta}+\theta')}{\partial z}$$

or

$$\frac{\partial \overline{T}}{\partial t} + \frac{\partial T'}{\partial t} = \cdots - \overline{W}\frac{\partial \overline{\theta}}{\partial z} - \overline{W}\frac{\partial \theta'}{\partial z} - w'\frac{\partial \overline{\theta}}{\partial z} - w'\frac{\partial \theta'}{\partial z}$$

Next, average the whole equation. But the average of a sum is the same as the sum of the averages:

$$\overline{\frac{\partial \overline{T}}{\partial t}} + \overline{\frac{\partial T'}{\partial t}} = \cdots - \overline{\overline{W}\frac{\partial \overline{\theta}}{\partial z}} - \overline{\overline{W}\frac{\partial \theta'}{\partial z}} - \overline{w'\frac{\partial \overline{\theta}}{\partial z}} - \overline{w'\frac{\partial \theta'}{\partial z}}$$

[**Aside**: Let A be any variable. Expand into mean and turbulent parts: $A = \overline{A} + a'$, then average the whole eq: $\overline{A} = \overline{\overline{A}} + \overline{a'}$. But the average of an average is just the original average: $\overline{A} = \overline{A} + \overline{a'}$. This equation can be valid only if $\overline{a'} = 0$. Thus, the average of any term containing a single primed variable (along with any number of unprimed variables) is zero.]

Thus the heat budget becomes:

$$\frac{\partial \overline{T}}{\partial t} = \cdots - \overline{\overline{W}\frac{\partial \overline{\theta}}{\partial z}} - \overline{w'\frac{\partial \theta'}{\partial z}}$$

The term on the left and the first term on the right are average of averages, and can be rewritten by just the original averages. The last term can be transformed into **flux form** using the turbulent continuity equation (which works if you apply it to the turbulent advection in all 3 directions, but which is not shown here). The end result is:

$$\frac{\partial \overline{T}}{\partial t} = \cdots - \overline{W}\frac{\partial \overline{\theta}}{\partial z} - \frac{\partial \overline{w'\theta'}}{\partial z}$$

This says that to forecast the average temperature, you need to consider not only the average advection by the mean wind (first term on the right), but you also need to consider the turbulence flux divergence (last term on the right).

Similar terms appear for advection in the x and y directions. Also, similar terms appear in the forecast equations for moisture and wind. Thus, the effects of turbulence cannot be neglected.

To simplify the notation in almost all of this book, the overbar is left off of the terms for mean temperature, mean wind, etc. Also, earlier in this chapter, and in other chapters, the turbulence flux divergence term has already been parameterized directly as a function of non-turbulent (average) wind, temperature, humidity, etc. Such parameterizations are turbulence closure approximations.

But this contains yet another unknown $\overline{w'w'\theta'}$. A forecast equation for $\overline{w'w'\theta'}$ would yield yet another unknown. Hence, we need an infinite number of equations just to forecast air temperature. Or, if we use only a finite number of equations, then we have more unknowns than equations.

Hence, this set of equations is mathematically not closed, which means they cannot be solved. To be a **closed system of equations**, the number of unknowns must equal the number of equations.

One reason for this **closure problem** is that it is impossible to accurately forecast each swirl and eddy in the wind. To work around this problem, meteorologists **parameterize** the net effect of all the eddies; namely, they use a finite number of equations, and approximate the unknowns as a function of known variables. Such an approximation is called **turbulence closure**, because it mathematically closes the governing equations, allowing useful weather forecasts and engineering designs.

Turbulence Closure Types

For common weather situations with mean temperature, wind and humidity that are nearly horizontally uniform, turbulent transport in any horizontal direction nearly cancels transport in the opposite direction, and thus can be neglected. But vertical transport is significant. Medium and large size turbulent eddies can transport air parcels from many different source heights to any destination height within the turbulent domain, where the smaller eddies mix the parcels together.

Different approximations of turbulent transport consider the role of small and large eddies differently. **Local closures**, which neglect the large eddies, are most common. This gives turbulent heat fluxes that flow down the local gradient of potential temperature, analogous to molecular diffusion or conduction (see the Heat and Air Pollution chapters). One such turbulence closure is called **K-theory**.

A **nonlocal closure** alternative that accounts for the superposition of both large and small eddies is called **transilient turbulence theory** (T3). While this is more accurate, it is also more complicated. There are many other closures that have been proposed. K-theory is reviewed here.

K-Theory

One approximation to turbulent transport considers only small eddies. This approach, called **K-theory**, **gradient transport theory**, or **eddy-diffusion theory**, models turbulent mixing analogous to molecular diffusion Using heat flux F_H for example:

$$F_H = \overline{w'\theta'} = -K\cdot\frac{\Delta\overline{\theta}}{\Delta z} \qquad \bullet(18.41a)$$

This parameterization says that heat flows down the gradient of potential temperature, from warm to cold. The rate of this turbulent transfer is proportional to the parameter K, called the **eddy viscosity** or **eddy diffusivity**, with units $m^2 \cdot s^{-1}$.

Similar expressions can be made for moisture flux as a function of the mean mixing-ratio (r) gradient, or momentum flux as a function of the shear in horizontal wind components (U, V):

$$\overline{w'r'} = -K \frac{\Delta \bar{r}}{\Delta z} \qquad (18.41b)$$

$$\overline{w'u'} = -K \frac{\Delta \overline{U}}{\Delta z} \qquad (18.41c)$$

$$\overline{w'v'} = -K \frac{\Delta \overline{V}}{\Delta z} \qquad (18.41d)$$

K is expected to be larger for more intense turbulence. In the surface layer, turbulence is generated by wind shear. **Prandtl** made a **mixing-length** suggestion that:

$$K = k^2 \cdot z^2 \cdot \left| \frac{\Delta \overline{M}}{\Delta z} \right| \qquad (18.42)$$

where $k = 0.4$ is von Kármán's constant (dimensionless), z is height above ground, and $\Delta M/\Delta z$ is mean shear of the horizontal wind M.

When K-theory used in the Eulerian heat budget equation, neglecting all other terms except turbulence, the result gives the heating rate of air at height z due to **turbulent flux divergence** (i.e., change of flux with height):

$$\frac{\Delta \bar{\theta}(z)}{\Delta t} = K \cdot \left[\frac{\bar{\theta}(z + \Delta z) - 2\bar{\theta}(z) + \bar{\theta}(z - \Delta z)}{(\Delta z)^2} \right] \qquad (18.43)$$

{For those of you who like calculus, the ratio in square brackets is an approximation to the second derivative $[\partial^2 \bar{\theta} / \partial z^2]$. Namely, it is equal to the curvature of the potential temperature vertical profile.} Although the example above was for heat flux, you can also use it for moisture or momentum flux by substituting $\bar{r}$ or $\overline{U}$, $\overline{V}$ in place of $\bar{\theta}$.

K-theory works best for windy surface layers, where turbulent eddy sizes are relatively small. Fig. 18.26 shows that heat flux flows "down" the temperature gradient from warm to colder potential temperature, which gives a negative (downward) heat flux in the statically stable surface layer. Fig. 18.25 is also a small-eddy (K-theory-like) illustration.

K-theory does not apply at the solid ground, but only within the air where turbulence exists. For heat fluxes at the surface, use approximations given in earlier in this chapter, and in the Heat chapter.

ON DOING SCIENCE • Parameterization Rules

For some situations in science and engineering, the governing equations are not known or are so complicated as to be unwieldy. Nonetheless, an approximation might be good enough to give useful answers.

A **parameterization** is an approximation to an unknown term, made using one or more known terms or factors. Because these approximations do not come from first principles, one or more fudge factors are often included in the substitute term to make it have the correct behavior or order-of-magnitude. These fudge factors are called **parameters**, and are not known from first principles. They must be found **empirically** (from field or laboratory experiments, or from numerical simulations).

Different scientists and engineers can invent different parameterizations for the same unknown term. While none are perfect, each would have different advantages and disadvantages. However, every parameterization must follow certain rules.

The parameterization should:

(1) be physically reasonable,
(2) have the same dimensions as the unknown term,
(3) have the same scalar or vector properties,
(4) have the same symmetries,
(5) be invariant under an arbitrary transformation of coordinate system,
(6) be invariant under an **inertial** or **Newtonian transformation** (e.g., a coordinate system moving at constant speed and direction),
(7) satisfy the same constraints & budget equations.

Even if the parameterization satisfies the above rules, it often will be successful for only a limited range of conditions. An example from this book is the transport velocity, w_T. One parameterization was developed for statically neutral boundary layers, while a different one worked better for statically unstable mixed layers. Thus, every parameterization should state the limitations on its use, including accuracy and range of validity.

In summary, parameterizations only approximate nature. As a result, they will never work perfectly. But they can be designed to work satisfactorily.

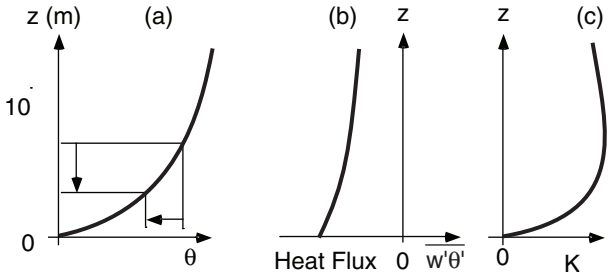

Figure 18.26
Typical profiles of (a) potential temperature; (b) heat flux; and (c) eddy diffusivity in the statically stable surface layer.

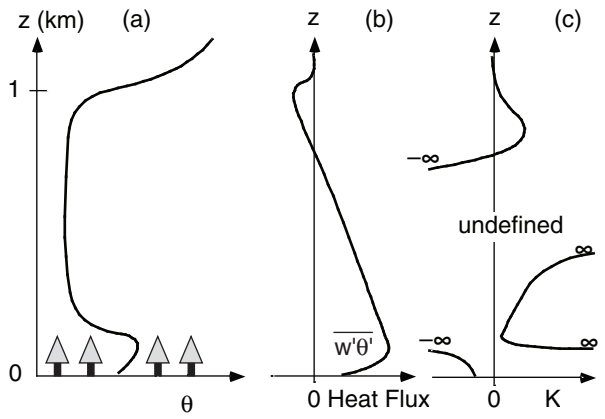

Figure 18.27
The value (c) of K needed to get (b) the observed heat flux F_H from (a) the observed potential temperature θ over a forest for an unstable (convective) ABL.

Solved Example

Instruments on a tower measure θ = 15°C and M = 5 m/s at z = 4 m, and θ = 16°C and M = 8 m/s at z = 10 m. What is the vertical heat flux?

Solution:

Given:	z (m)	θ (°C)	M (m/s)
	10	16	8
	4	15	5

Find: F_H = ? K·m/s

First, use eq. (18.42), at average z = (10+4)/2 = 7 m

$$K = k^2 \cdot z^2 \cdot \left|\frac{\Delta M}{\Delta z}\right| = [0.4\cdot(7\text{m})]^2 \left|\frac{(8-5)\text{m/s}}{(10-4)\text{m}}\right| = 3.92\ \text{m}^2/\text{s}$$

Next, use eq. (18.41):

$F_H = -K(\Delta\theta/\Delta z) = -(3.92\ \text{m}^2/\text{s})\cdot(16–15°\text{C})/(10–4\text{m})$

$= \underline{\mathbf{-0.65\ K\cdot m/s}}$

Check: Units OK. Physics OK.

Discussion: The negative sign means a downward heat flux, from hot to cold. This is typical for statically stable ABL.

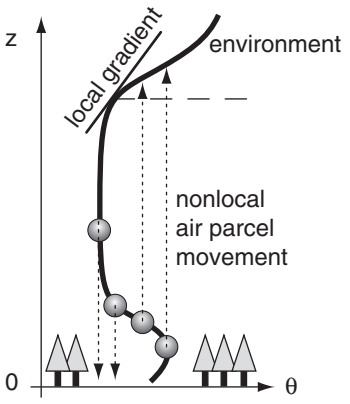

Figure 18.28
Typical potential temperature θ profile in the ABL over a forest, showing nonlocal convective movement of some of the air parcels that are moving across relatively large vertical distances during free convection.

K-theory has difficulty for convective ABLs and should not be used there. Figs. 18.27a and b illustrate these difficulties, giving typical values in the atmosphere, and the resulting K values backed out using eq. (18.42). Negative and infinite K values are unphysical.

Nonlocal Closure

Instead of looking at local down-gradient transport as was done in K-theory, you can look at all ranges of distances across which air parcels move during turbulence (Fig. 18.28). This is an approach called **nonlocal closure**, and is useful for a statically unstable ABL having free convection.

For heat flux at the altitude of the dashed line in Fig. 18.28, K-theory (small-eddy theory) would utilize the local gradient of θ at that altitude, and conclude that the heat flux should be downward and of a certain magnitude. However, if the larger-size eddies are also included (as in nonlocal closure), such as the parcel rising from tree-top level, we see that it is bringing warm air upward (a positive contribution to heat flux). This could partially counteract, or even overwhelm, the negative contribution to flux caused by the local small eddies.

As you can probably anticipate, a better approach would be to consider all size eddies and nonlocal air-parcel movement. One such approach is called **transilient turbulence theory** (T3). This approach uses arrays to account for eddies of each different size, and combines them to find the average effect of all eddy sizes. It is more complex, and will not be described here.

SUMMARY

We live in a part of the atmosphere known as the boundary layer (ABL), the bottom 200 m to 4 km of the troposphere. Tropospheric static stability and turbulence near the Earth's surface combine to create this ABL, and cap it with a temperature inversion.

Above the boundary layer is the free atmosphere, which is not turbulently coupled with the ground (except during stormy weather such as near low pressure centers, fronts, and thunderstorms). Thus, the free atmosphere does not normally experience a strong diurnal cycle.

Within the ABL there are significant daily variations of temperature, winds, static stability, and turbulence over land under mostly clear skies. These variations are driven by the diurnal cycle of radiative heating of the ground during daytime and cooling at night.

During daytime under fair weather (i.e., in anticyclonic or high-pressure regions), vigorous turbulence mixes potential temperature, humidity, wind speed, and pollutants to be nearly uniform with height. This turbulence creates a well-mixed layer that grows due to entrainment of free atmosphere air from above.

At night in fair weather, there is a shallow stable boundary layer near the ground, with a nearly neutral residual layer above. Turbulence is weak and sporadic. Winds often become calm near the surface, but can be very fast a few hundred meters above ground.

The bottom 5 to 10% of the ABL is called the surface layer. Surface drag causes the wind to be zero near the ground, and to increase with height. The shape of this wind profile is somewhat logarithmic, but depends on the roughness of the surface, and on convection.

Turbulence is a quasi-random flow phenomenon that can be described by statistics. Covariance of vertical velocity with another variable represents the vertical kinematic flux of that variable. Heat fluxes, moisture fluxes, and stress can be expressed as such an eddy-correlation statistic.

Velocity variances represent components of turbulent kinetic energy (*TKE*) per unit mass, a measure of the intensity of turbulence. *TKE* is produced by wind shear and buoyancy, is advected from place to place by the mean and turbulent winds, and is dissipated into heat by molecular viscosity.

The relative magnitudes of the shear and buoyant production terms determine whether convection is free or forced. The sum of those terms is proportional to the intensity of turbulence. The ratio gives the flux Richardson number for determining whether turbulence can persist.

Turbulence is so complex that it cannot be solved exactly for each swirl and eddy. Instead, parameterizations are devised to allow approximate solutions for the net statistical effect of all turbulent eddies. Parameterizations, while not perfect, are acceptable if they satisfy certain rules.

One type of local parameterization, called K-theory, neglects the large eddies, but gives good answers for special regions such as the surface layer in the bottom 10% of the atmospheric boundary layer. It is popular because of its simplicity. Another type of parameterization is called transilient turbulence theory (T3), which is a nonlocal closure that includes all eddy sizes. It is more accurate, more complicated, and works well for free convection.

Threads

Formation and evolution of the ABL is intimately tied to the temperature structure of the troposphere, such as described with the standard atmosphere (Chapter 1). The diurnal cycle in the ABL is created by the radiation and heat budgets at the surface (Chapters 2 and 3).

Turbulence causes dispersion of air pollutants (Chapter 19). It mixes boundary-layer air down to the ground where it takes on temperature and humidity characteristics of the underlying surface, thereby creating an airmass (Chapter 12). The border between two such boundary layers is a front (Chapter 12).

The ABL throttles the flow of heat (Chapter 2) and moisture (Chapter 4) from the surface into the troposphere, thereby controlling the formation of clouds and precipitation (Chapters 6 and 7). The resulting sensible and latent heat can fuel mid-latitude cyclones (Chapter 13), thunderstorms (Chapters 14 & 15) and hurricanes (Chapter 16). The creation of tornado rotation (Chapter 15) is believed to be due to wind shear in the ABL. Thunder propagation depends on ABL temperature.

The north-south temperature gradient that drives the jet stream (Chapter 11) is created by heat fluxes through the boundary layer. Mirages (Chapter 22) form in ABL temperature gradients.

Additional boundary-layer results and equations are presented in the chapters covering budgets of heat (Chapter 3), moisture (Chapter 4), and momentum (Chapter 10). Many of the aspects of atmospheric dispersion (Chapter 19) are applications of boundary layers and turbulence. Thermals and katabatic winds of Chapter 17 are also boundary-layer phenomena.

EXERCISES

Numerical Problems

N1(§). Calculate and plot the increase of cumulative kinematic heat (cooling) during the night, for a case with kinematic heat flux (K·m/s) of:

a. –0.02 b. –0.05 c. – 0.01 d. –0.04 e. –0.03
f. – 0.06 g. – 0.07 h. –0.10 i. –0.09 j. –0.08

N2 (§). Calculate and plot the increase of cumulative kinematic heat during the day, for a case with daytime duration of 12 hours, and maximum kinematic heat flux (K·m/s) of:

a. 0.2 b. 0.5 c. 0.1 d. 0.4 e. 0.3
f. 0.6 g. 0.7 h. 1.0 i. 0.9 j. 0.8

N3(§). For a constant kinematic heat flux of –0.02 K·m/s during a 12-hour night, plot the depth and

strength of the stable ABL vs. time. Assume a flat prairie, with a residual layer wind speed (m/s) of:
a. 2 b. 5 c. 8 d. 10 e. 12
f. 15 g. 18 h. 20 i. 22 j. 25

N4(§). For the previous problem, plot the vertical temperature profile at 1-h intervals.

N5. Find the entrained kinematic heat flux at the top of the mixed layer, given a surface kinematic heat flux (K·m/s) of
a. 0.2 b. 0.5 c. 0.1 d. 0.4 e. 0.3
f. 0.6 g. 0.7 h. 1.0 i. 0.9 j. 0.8

N6. Find the entrainment velocity for a surface heat flux of 0.2 K·m/s, and a capping inversion strength of (°C): a. 0.1 b. 0.2 c. 0.3 d. 0.5 e. 0.7
f. 1.0 g. 1.2 h. 1.5 i. 2.0 j. 2.5

N7. For the previous problem, calculate the increase in mixed-layer depth during a 6 h interval, assuming subsidence of – 0.02 m/s.

N8. Calculate the surface stress at sea level for a friction velocity (m/s) of:
a. 0.1 b. 0.2 c. 0.3 d. 0.4 e. 0.5
f. 0.6 g. 0.7 h. 0.8 i. 0.9 j. 1.0

N9. Find the friction velocity over a corn crop during wind speeds (m/s) of:
a. 2 b. 3 c. 4 d. 5 e. 6 f. 7 g. 8
h. 9 i. 10 j. 12 k. 15 m. 18 n. 20 o. 25

N10. Find the roughness length and standard drag coefficient over: a. sea b. beach
c. tundra d. low crops e. hedgerows
f. orchards g. village h. city center

N11. Same as previous problem, but find the friction velocity given a 10 m wind speed of 5 m/s.

N12(§). Given M_1 = 5 m/s at z_1 = 10 m, plot wind speed vs. height, for z_o (m) =
a. 0.001 b. 0.002 c. 0.005 d. 0.007 e. 0.01
f. 0.02 g. 0.05 h. 0.07 i. 0.1 j. 0.2
k. 0.5 m. 0.7 n. 1.0 o. 2.0 p. 2.5

N13. Find the drag coefficients for problem N12.

N14(§). For a neutral surface layer, plot wind speed against height on linear and on semi-log graphs for friction velocity of 0.5 m/s and aerodynamic roughness length (m) of:
a. 0.001 b. 0.002 c. 0.005 d. 0.007 e. 0.01
f. 0.02 g. 0.05 h. 0.07 i. 0.1 j. 0.2
k. 0.5 m. 0.7 n. 1.0 o. 2.0 p. 2.5

N15. An anemometer on a 10 m mast measures a wind speed of 8 m/s in a region of scattered hedgerows. Find the wind speed at height (m):
a. 0.5 b. 2 c. 5 d. 30
e. 1.0 f. 4 g. 15 h. 20

N16. The wind speed is 2 m/s at 1 m above ground, and is 5 m/s at 10 m above ground. Find the roughness length. State all assumptions.

N17. Over a low crop with wind speed of 5 m/s at height 10 m, find the wind speed (m/s) at the height (m) given below, assuming overcast conditions:
a. 0.5 b. 1.0 c. 2 d. 5 e. 15 f. 20
g. 25 h. 30 i. 35 j. 40 k. 50 m. 75

N18. Same as previous problem, but during a clear night when friction velocity is 0.1 m/s and surface kinematic heat flux is –0.01 K·m/s. Assume $|g|/T_v$ = 0.0333 m·s^{-2}·K^{-1}.

N19(§). Plot the vertical profile of wind speed in a stable boundary layer for roughness length of 0.2 m, friction velocity of 0.3 m/s, and surface kinematic heat flux (K·m/s) of:
a. –0.02 b. –0.05 c. – 0.01 d. –0.04 e. –0.03
f. – 0.06 g. – 0.07 h. –0.10 i. –0.09 j. –0.08
Assume $|g|/T_v$ = 0.0333 m·s^{-2}·K^{-1}.

N20. For a 1 km thick mixed layer with $|g|/T_v$ = 0.0333 m·s^{-2}·K^{-1}, find the Deardorff velocity (m/s) for surface kinematic heat fluxes (K·m/s) of:
a. 0.2 b. 0.5 c. 0.1 d. 0.4 e. 0.3
f. 0.6 g. 0.7 h. 1.0 i. 0.9 j. 0.8

N21§). For the previous problem, plot the wind speed profile, given u_* = 0.4 m/s, and M_{BL} = 5 m/s.

N22(§). For the following time series of temperatures (°C): 22, 25, 21, 30, 29, 14, 16, 24, 24, 20
a. Find the mean and turbulent parts
b. Find the variance
c. Find the standard deviation

N23(§). Using the data given in the long solved example in the "Turbulent Fluxes and Covariances" section of this Chapter:
a. Find the mean & variance for mixing ratio *r*.
b. Find the mean and variance for *U* .
c. Find the covariance between *r* and *W*.
d. Find the covariance between *U* and *W*.
e. Find the covariance between *r* and *U*.
f. Find the correlation coefficient between *r* & *W*.
g. Find the correlation coef. between *u* & *W*.
h. Find the correlation coefficient between *r* & *U*.

N24(§). Plot the standard deviations of U, V, and W with height, and determine if and where the flow is nearly isotropic, given $u_* = 0.5$ m/s, $w_B = 40$ m/s, $h = 600$ m, and $z_i = 2$ km, for air that is statically:
a. stable b. neutral c. unstable
Hint: Use only those "given" values that apply to your stability.

N25(§). Same as exercise N24, but plot *TKE* vs. z.

N26(§). Plot wind standard deviation vs. height, and determine if and where the flow is nearly isotropic, for all three wind components, for
a. stable air with $h = 300$ m, $u_* = 0.1$ m/s
b. neutral air with $h = 1$ km, $u_* = 0.2$ m/s
c. unstable air with $z_i = 2$ km, $w_B = 0.3$ m/s

N27(§). Plot the turbulence kinetic energy per unit mass vs. height for the previous problem.

N28. Given a wind speed of 20 m/s, surface kinematic heat flux of –0.1 K·m/s, *TKE* of 0.4 m^2/s^2, and $|g|/T_v = 0.0333$ $m \cdot s^{-2} \cdot K^{-1}$, find
a. shear production rate of *TKE*
b. buoyant production/consumption of *TKE*
c. dissipation rate of *TKE*
d. total tendency of *TKE* (neglecting advection and transport)
e. flux Richardson number
f. the static stability classification?
g. the Pasquill-Gifford turbulence type?
h. flow classification

N29. Given the following initial sounding

z (m)	θ (°C)	M (m/s)
700	21	10
500	20	10
300	18	8
100	13	5

Compute the
a. value of eddy diffusivity at each height.
b. turbulent heat flux in each layer, using K-theory
c. the new values of θ after 30 minutes of mixing.
d. turbulent kinematic momentum flux $\overline{w'u'}$ in each layer, using K-theory. (Hint, generalize the concepts of heat flux. Also, assume $M = U$, and $V = 0$ everywhere.)
e. the new values of M after 30 minutes of mixing.

Understanding & Critical Evaluation

U1. Can the ABL fill the whole troposphere? Could it extend far into the stratosphere? Explain.

U2. Estimate the static stability near the ground now at your location?

U3. If the standard atmosphere was statically neutral in the troposphere, would there be a boundary layer? If so, what would be its characteristics.

U4. It is nighttime in mid winter with snow on the ground. This air blows over an unfrozen lake. Over the lake, what is the static stability of the air, and what type of ABL exists there.

U5. It is daytime in summer during a solar eclipse. How will the ABL evolve during the eclipse?

U6. Given Fig. 18.3, if turbulence were to become more vigorous and cause the ABL depth to increase, what would happen to the strength of the capping inversion? How would that result affect further growth of the ABL?

U7. The ocean often has a turbulent boundary layer within the top tens of meters of water. During a moderately windy, clear, 24 h period, when do you think stable and unstable (convective) ocean boundary layers would occur?

U8. Fig. 18.4 shows the free-atmosphere line touching the peaks of the ABL curve. Is it possible during other weather conditions for the FA curve to cross through the middle of the ABL curve, or to touch the minimum points of the ABL curve? Discuss.

U9. It was stated that subsidence cannot penetrate the capping inversion, but pushes the inversion down in regions of high pressure. Why can subsidence not penetrate into the ABL?

U10. Fig. 18.7a shows a cold front advancing. What if it were retreating (i.e., if it were a warm front). How would the ABL be affected differently, if at all?

U11. Draw a sketch similar to Fig. 18.8, except indicating the static stabilities in each domain.

U12. Copy Fig. 18.9, and then trace the nighttime curves onto the corresponding daytime curves. Comment on regions where the curves are the same, and on other regions where they are different. Explain this behavior.

U13. Use the solar and IR radiation equations from the Radiation chapter to plot a curve of daytime radiative heat flux vs. time. Although the resulting curve looks similar to half of a sine wave (as in Fig.

18.10), they are theoretically different. How would the actual curve change further from a sine curve at higher or lower latitudes? How good is the assumption that the heat flux curve is a half sine wave?

U14. Similar to the previous question, but how good is the assumption that nighttime heat flux is constant with time?

U15. In the explanation surrounding Fig. 18.10, the accumulated heating and cooling were referenced to start times when the heat flux became positive or negative, respectively. We did not use sunrise and sunset as the start times because those times did not correspond to when the surface heat flux changes sign. Use all of the relevant previous equations in the chapter (and in the Radiation chapter) to determine the time difference today at your town, between:

a. sunrise and the time when surface heat flux first becomes positive.
b. sunset and the time when surface heat flux first becomes negative.

U16. At nighttime it is possible to have well-mixed layers if wind speed is sufficiently vigorous. Assuming a well-mixed nocturnal boundary layer over a surface that is getting colder with time, describe the evolution (depth and strength) of this stable boundary layer. Also, for the same amount of cooling, how would its depth compare with the depth of the exponentially-shaped profile?

U17. Derive an equation for the strength of an exponentially-shaped nocturnal inversion vs. time, assuming constant heat flux during the night.

U18. Use eq. (18.3) and the definition of potential temperature to replot Fig. 18.15 in terms of actual temperature T vs. z. Discuss the difference in heights between the relative maximum of T and relative maximum of θ.

U19. For a linear early morning sounding (θ increases linearly with z), analytically compare the growth rates of the mixed layer calculated using the thermodynamic and the flux-ratio methods. For some idealized situations, is it possible to express one in terms of the other? Were any assumptions needed?

U20. Given an early morning sounding as plotted in Fig. 18.16a. If the daytime heat flux were constant with time, sketch a curve of mixed-layer depth vs. time, assuming the thermodynamic method. Comment on the different stages of mixed layer growth rate.

U21. Use the early-morning (6 AM) sounding given below with surface temperature 5°C. Find the mixed-layer potential temperature and depth at 11 AM, when the cumulative heating is 800 K·m. Assume the early-morning potential temperature profile is: a. $\Delta\theta/\Delta z$ = 2 K/km = constant
b. $\Delta\theta(z)$ = (8°C)·exp(–z/150m)
Hint: Use the encroachment method.

U22. If the heating rate is proportional to the vertical heat-flux divergence, use Fig. 18.17b to determine the heating rate at each z in the mixed layer. How would the mixed-layer T profile change with time?

U23. Assume that equations similar to eq. (18.7) applies to moisture fluxes as well as to heat fluxes, but that eq. (18.9) defines the entrainment velocity based only on heat. Combine those two equations to give the kinematic flux of moisture at the top of the mixed layer as a function of potential temperature and mixing ratio jumps across the mixed-layer top, and in terms of surface heat flux.

U24. If the ABL is a region that feels drag near the ground, why can the winds at night accelerate, as shown in Fig. 18.18?

U25. Use eqs. (18.11) and (18.14a) to show how eq. (18.12) is derived from the log wind profile.

U26. Given the moderate value for u_* that was written after eq. (18.10), what value of stress (Pa) does that correspond to? How does this stress compare to sea-level pressure?

U27. Derive eq. (18.14b) from (18.14a).

U28. Given the wind-speed profile of the solved example in the radix-layer subsection, compare the bottom portion of this profile to a log wind profile. Namely, find a best fit log-wind profile for the same data. Comment on the differences.

U29. Using eq. 18.21, find the average value (or simplify the notation) of $c{\cdot}T$, where c is a constant.

U30. Abbreviation "rms" means "root mean square". Explain why "rms" can be used to describe eq. (18.23).

U31. For fixed w_B and z_i, plot eqs. (18.26) with z, and identify those regions with isotropic turbulence.

U32. Using eqs. (18.24 – 18.26), derive expressions for the TKE vs. z for statically stable, neutral, and unstable boundary layers.

U33. Derive an expression for the shear production term vs. z in the neutral surface layer, assuming a log wind profile.

U34. Knowing how turbulent heat flux varies with z (Fig. 18.17b) in a convective mixed layer, comment on the *TKE* buoyancy term vs. z for that situation.

U35. Given some initial amount of *TKE*, and assuming no production, advection, or transport, how would *TKE* change with time, if at all? Plot a curve of *TKE* vs. time.

U36. Use K-theory to relate the flux Richardson number to the gradient Richardson number ($R_i = [(|g|/T_v)\cdot\Delta\theta\cdot\Delta z] \,/\, \Delta M^2$, see the Stability chapter).

U37. If shear production of *TKE* increases with time, how must the buoyant term change with time in order to maintain a constant Pasquill-Gifford stability category of E?

U38. Create a figure similar to Fig. 18.25, but for the log wind profile. Comment on the variation of momentum flux with z in the neutral surface layer.

U39. A negative value of eddy-correlation momentum flux near the ground implies that the momentum of the wind is being lost to the ground. Is it possible to have a positive eddy-correlation momentum flux near the surface? If so, under what conditions, and what would it mean physically?

Web-Enhanced Questions

W1. Access the upper-air soundings every 6 or 12 h for a rawinsonde station near you (or other site specified by your instructor). For heights every 200 m (or every 2 kPa) from the surface, plot how the temperature varies with time over several days. The result should look like Fig. 18.4, but with more lines. Which heights or pressure levels appear to be above the ABL?

W2. Same as the previous question, but first convert the temperatures to potential temperatures at those selected heights. This should look even more like Fig. 18.4.

W3. Access temperature profiles from the web for the rawinsonde station closest to you (or for some other sounding station specified by your instructor). Convert the resulting temperatures to potential temperatures, and plot the resulting θ vs z. Can you identify the top of the ABL? Consider the time of day when the sounding was made, to help you anticipate what type of ABL exists (e.g., mixed layer, stable boundary layer, neutral layer.)

W4. Access a weather map with surface wind observations. Find a situation or a location where there is a low pressure center. Draw a hypothetical circle around the center of the low, and find the average inflow velocity component across this circle. Using volume conservation, and assuming a 1 km thick ABL, what vertical velocity to you anticipate over the low?

W5. Same as previous question, but for a high-pressure center.

W6. Access a number of rawinsonde soundings for stations more-or-less along a straight line that crosses through a cold front. Identify the ABL top both ahead of and behind the front.

W7. Access the current sunrise and sunset times at your location. Estimate a curve such as in Fig. 18.10.

W8. Find a rawinsonde station in the center of a clear high pressure region, and access the soundings every 6 h if possible. If they are not available over N. America, try Europe. Use all of the temperature, humidity, and wind information to determine the evolution of the ABL structure, and create a sketch similar to Fig. 18.8, but for your real conditions. Consider seasonal affects, such as in Figs. 18.13 & 18.14.

W9. Access a rawinsonde sounding for nighttime, and find the best-fit parameters (height, strength) for an exponential potential temperature profile that best fits the sounding. If the exponential shape is a poor fit, explain why.

W10. Get an early morning sounding for a rawinsonde site near you. Calculate the anticipated accumulated heating, based on the eqs. in the Radiation & Heat chapters, and predict how the mixed layer will warm & grow in depth as the day progresses.

W11. Compare two sequential rawinsonde soundings for a site, and estimate the entrainment velocity by comparing the heights of the ABL. What assumptions did you make in order to do this calculation?

W12. Access the wind information from a rawinsonde site near you. Compare the wind speed profiles between day and night, and comment on the change of wind speed in the ABL.

W13. Access the "surface" wind observations from a weather station near you. Record and plot the wind speed vs. time, using wind data as frequent as are available, getting a total of roughly 24 to 100 observations. Use these data to calculate the mean wind, variance, and standard deviation.

W14. Same as the previous exercise, but for *T*.

W15. Same as the previous exercise, except collect both wind and temperature data, and find the covariance and correlation coefficient.

W16. Search the web for **eddy-correlation sensors**, **scintillometers**, **sonic anemometers**, or other instruments used for measuring vertical turbulent fluxes, and describe how they work.

W17. Search the web for eddy viscosity, eddy diffusivity, or K-theory values for *K* in the atmosphere.

Synthesis Questions

S1. At the end of one night, assume that the stable ABL profile of potential temperature has an exponential shape, with strength 10°C and e-folding depth of 300 m. Using this as the early-morning sounding, compute and plot how the potential temperature and depth of the mixed layer evolve during the morning. Assume that D = 12 hr, and F_{Hmax} = 0.1 K·m/s. (Hint: In the spirit of the "Seek Solutions" box in a previous chapter, feel free to use graphical methods to solve this without calculus. However, if you want to try it with calculus, be very careful to determine which are your dependent and independent variables.)

S2. Suppose that there was no turbulence at night. Assume, the radiatively-cooled surface cools only the bottom 1 m of atmosphere by conduction. Given typical heat fluxes at night, what would be the resulting air temperature by morning? Also describe how the daytime mixed layer would evolve from this starting point?

S3. On a planet that does not have a solid core, but has a gaseous atmosphere that increases in density as the planet center is approached, would there be a boundary layer? If so, how would it behave?

S4. What if you were hired by an orchard owner to tell her how deep a layer of air needs to be mixed by electric fans to prevent frost formation. Create a suite of answers based on different scenarios of initial conditions, so that she can consult these results on any given day to determine the speed to set the fans (which we will assume can be used to control the depth of mixing). State and justify all assumptions.

S5. What if the Earth's surface was a perfect conductor of heat, and had essentially infinite heat capacity (as if the Earth were a solid sphere of aluminum, but had the same albedo as Earth). Given the same solar and IR radiative forcings on the Earth's surface, describe how ABL structure and evolution would differ from Fig. 18.8, if at all?

S6. What if all the air in the troposphere were saturated & cloudy. How would the ABL be different?

S7. Suppose that for some reason, the actual 2 km thick ABL in our troposphere was warm enough to have zero capping inversion on one particular day, but otherwise looked like Fig. 18.3. Comment on the evolution of the ABL from this initial state. Also, how might this initial state have occurred?

S8. If the ABL were always as thick as the whole troposphere, how would that affect the magnitude of our diurnal cycle of temperature?

S9. It was stated in this chapter that entrainment happens one way across the capping inversion, from the nonturbulent air into the turbulent air. Suppose that the capping inversion was still there, but that both the ABL below the inversion and the layer of air above the inversion were turbulent. Comment on entrainment and the growth of the mixed layer.

S10. Suppose that *TKE* was not dissipated by viscosity. How would that change our weather and climate, if at all?

S11. Suppose that wind shear destroyed *TKE* rather than generated it. How would that change our weather and climate, if at all?

S12. Suppose there were never a temperature inversion capping the ABL. How would that change our weather and climate, if at all?

S13. Suppose that the winds felt no frictional drag at the surface of the Earth. How would that change our weather and climate, if at all?

S14. Verify that K-theory satisfies the rules of parameterization.

S15. Positive values of *K* imply down-gradient transport of heat (i.e., heat flows from hot to cold, a process sometimes called the Zeroth Law of Thermodynamics). What is the physical interpretation of negative values of *K*?

Copyright © 2011, 2015 by Roland Stull. *Meteorology for Scientists and Engineers, 3rd Ed.*

AIR POLLUTION DISPERSION

CONTENTS

Dispersion Factors 724
Air Quality Standards 725
Turbulence Statistics 726
- Review of Basic Definitions 726
- Isotropy (again) 727
- Pasquill-Gifford (PG) Turbulence Types 728

Dispersion Statistics 728
- Snapshot vs. Average 728
- Center of Mass 729
- Standard Deviation – Sigma 729
- Gaussian Curve 730
- Nominal Plume Edge 730

Taylor's Statistical Theory 731
- Passive Conservative Tracers 731
- Dispersion Equation 731
- Dispersion Near & Far from the Source 732

Dispersion In Neutral & Stable Boundary Layers 732
- Plume Rise 732
  - Neutral Boundary Layers 733
  - Stable Boundary Layers 733
- Gaussian Concentration Distribution 734

Dispersion In Unstable Boundary Layers (Convective Mixed Layers) 735
- Relevant Variables 735
  - Physical Variables: 735
  - Mixed-Layer Scaling Variables: 735
  - Dimensionless Scales: 736
- Plume Centerline 736
- Crosswind Integrated Concentration 736
- Concentration 737

Summary 737
- Threads 738

Exercises 739
- Numerical Problems 739
- Understanding & Critical Evaluation 741
- Web-Enhanced Questions 742
- Synthesis Questions 743

"Meteorology for Scientists and Engineers, 3rd Edition" by Roland Stull is licensed under a Creative Commons Attribution-NonCommercial-ShareAlike 4.0 International License. To view a copy of the license, visit http://creativecommons.org/licenses/by-nc-sa/4.0/ . This work is available at http://www.eos.ubc.ca/books/Practical_Meteorology/ .

19 Every living thing pollutes. Life is a chemical reaction, where input chemicals such as food and oxygen are converted into growth or motion. The reaction products are waste or pollution.

The only way to totally eliminate pollution is to eliminate life — not a particularly appealing option. However, a system of world-wide population control could stem the increase of pollution, allowing residents of our planet to enjoy a high quality of life.

Is pollution bad? From an anthropocentric point of view, we might say "yes". To do so, however, would deny our dependence on pollution. In the Earth's original atmosphere, there was very little oxygen. Oxygen is believed to have formed as pollution from plant life. Without this pollutant, animals such as humans would likely not exist now.

However, it is reasonable to worry about other **chemicals that threaten our quality of life**. We call such chemicals **pollutants**, regardless of whether they form naturally or **anthropogenically** (man-made). Many of the natural sources are weak emissions from large area sources, such as forests or swamps. Anthropogenic sources are often concentrated at points, such as at the top of smoke stacks (Fig. 19.1). Such high concentrations are particularly hazardous, and been heavily studied.

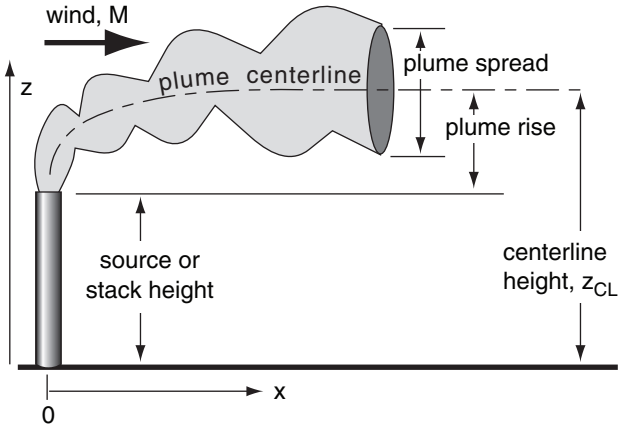

Figure 19.1
Pollutant plume characteristics.

FOCUS • Pollutant Concentration Units

The amount of a pollutant in the air can be given as a **fraction** or **ratio**, q. This is the amount (moles) of pollution divided by the total amount (moles) of all constituents in the air. For air quality, the ratios are typically reported in **parts per million** (**ppm**). For example, 10 ppm means 10 parts of pollutant are contained within 10^6 parts of air. For smaller amounts, **parts per billion** (**ppb**) are used.

Although sometimes the ratio of masses is used (e.g., **ppmm** = parts per million by mass), usually the ratio of volumes is used instead (**ppmv** = parts per million by volume).

Alternately, the amount can be given as a **concentration**, c, which is the mass of pollutant in a cubic meter of air. For air pollution, units are often micrograms per cubic meter ($\mu g/m^3$). Higher concentrations are reported in milligrams per cubic meter, (mg/m^3), while lower concentrations can be in nanograms per cubic meter (ng/m^3).

The conversion between fractions and concentrations is

$$q(\text{ppmv}) = \frac{a \cdot T}{P \cdot M_s} \cdot c(\mu g/m^3)$$

where T is absolute temperature (Kelvin), P is total atmospheric pressure (kPa), M_s is the molecular weight of the pollutant, and $a = 0.008314$ kPa·K^{-1}·(ppmv)·($\mu g/m^3$)$^{-1}$.

For a standard atmosphere at sea level, where temperature is 15°C and pressure is 101.325 kPa, the equation above reduces to

$$q(\text{ppmv}) = \frac{b}{M_s} \cdot c(\mu g/m^3)$$

where $b = 0.02363$ (ppmv) / ($\mu g/m^3$).

For example, nitrogen dioxide (NO_2) has a molecular weight of $M_s = 46.01$ (see Table 1-2 in Chapter 1). If concentration $c = 100$ $\mu g/m^3$ for this pollutant, then the equation above gives a volume fraction of $q = (0.02363/46.01) \cdot (100) = 0.051$ ppmv.

Science Graffito

"**The solution to pollution is dilution.**"
– Anonymous.

This aphorism was accepted as common sense during the 1800s and 1900s. By building taller smoke stacks, more pollutants could be emitted, because the pollutants would mix with the surrounding clean air and become dilute before reaching the surface.

However, by 2000, society started recognizing the global implications of emitting more pollutants. Issues included greenhouse gases, climate change, and stratospheric ozone destruction. Thus, government regulations changed to include total emission limits.

DISPERSION FACTORS

The stream of polluted air downwind of a smoke stack is called a **smoke plume**. If the plume is buoyant, or if there is a large effluent velocity out of the top of the smoke stack, the center of the plume can rise above the initial emission height. This is called **plume rise**.

The word "plume" in air pollution work means a long, slender, nearly-horizontal region of polluted air. However, the word "plume" in atmospheric boundary-layer (ABL) studies refers to the relatively wide, nearly vertical updraft portion of buoyant air that is convectively overturning. Because smoke plumes emitted into the boundary layer can be dispersed by convective plumes, one must take great care to not confuse the two usages of the word "plume".

Dispersion is the name given to the spread and movement of pollutants. Pollution dispersion depends on

- wind speed and direction
- plume rise, and
- atmospheric turbulence.

Pollutants disperse with time by mixing with the surrounding cleaner air, resulting in an increasingly dilute mixture within a spreading smoke plume.

Wind and **turbulence** are characteristics of the ambient atmosphere, as were described in earlier chapters. While emissions out of the top of the stack often have strong internal turbulence, this quickly decays, leaving the ambient atmosphere to do the majority of the dispersing.

The direction that the effluent travels is controlled by the local, synoptic, and global-scale winds. Pollutant destinations from known emission sources can be found using a **forward trajectory** along the mean wind, while source locations of polluted air that reach receptors can be found from a **backward trajectory**.

The goal of calculating dispersion is to predict or diagnose the pollutant concentration at some point distant from the source. **Concentration** c is often measured as a mass per unit volume, such as $\mu g/m^3$. It can also be measured as volume ratio of pollutant gas to clean air, such as parts per million (**ppm**). See the Focus box for details about units.

A **source - receptor** framework is used to relate emission factors to predicted downwind concentration values. We can examine pollutants emitted at a known rate from a **point source** such as a **smoke stack**. We then follow the pollutants as they are blown downwind and mix with the surrounding air. Eventually, the mixture reaches a receptor such as a sensor, person, plant, animal or structure, where we can determine the expected concentration.

In this chapter, we will assume that the mean wind is known, based on either weather observations, or on forecasts. We will focus on the plume rise and dispersion of the pollutants, which allows us to determine the concentration of pollutants downwind of a known source.

AIR QUALITY STANDARDS

To prevent or reduce health problems associated with air pollutants, many countries set air quality standards. These standards prescribe the maximum average concentration levels in the ambient air, as allowed by law. Failure to satisfy these standards can result in fines, penalties, and increased government regulation.

In the USA, the standards are called **National Ambient Air Quality Standards (NAAQS)**. In Canada, they are called National Ambient Air Quality Objectives & Guidelines. In the Great Britain, they are called UK Air Quality Objectives. Other countries have similar names for such goals. Table 19–1 lists standards for a few countries. Governments can change these standards.

In theory, these average concentrations are not to be exceeded anywhere at ground level. In practice, meteorological events sometimes occur, such as light winds and shallow ABLs during anticyclonic conditions, that trap pollutants near the ground and cause concentration values to become undesirably large.

Also, temporary failures of air-pollution control measures at the source can cause excessive amounts of pollutants to be emitted. Regulations in some of the countries allow for a small number of concentration **exceedances** without penalty.

To avoid expensive errors during the design of new factories, smelters, or power plants, **air pollution modeling** is performed to determine the likely pollution concentration based on expected emission rates. Usually, the greatest concentrations happen near the source of pollutants. The procedures presented in this chapter illustrate how concentrations at receptors can be calculated from known emission and weather conditions.

By comparing the predicted concentrations against the air quality standards of Table 18–1, engineers can modify the factory design as needed to ensure compliance with the law. Such modifications can include building taller smoke stacks, removing the pollutant from the stack effluent, changing fuels or raw materials, or utilizing different manufacturing or chemical processes.

Table 19-1. Air quality concentration standards for the USA (US), Canada (CAN), and Great Britain (UK) for some of the commonly-regulated chemicals, as of Feb 2010. Concentrations represent averages over the time periods listed. For Canada, listed are the **maximum acceptable** levels. For UK, listed are standards for protection of human health.

Avg. Time	US	CAN	UK
Sulfur Dioxide (SO_2)			
1 yr	0.03 ppm	0.023 ppm	
1 day	0.14 ppm	0.115 ppm	125 μg/m^3
3 h	1300 μg/m^3 or 0.5 ppm		
1 h		0.334 ppm	350 μg/m^3
15 min			266 μg/m^3
Nitrogen Dioxide (NO_2)			
1 yr	100 μg/m^3 or 0.053 ppm	0.053 ppm	40 μg/m^3
1 day		0.106 ppm	
1 h	0.100 ppm	0.213 ppm	200 μg/m^3
Carbon Monoxide (CO)			
8 h	10,000 μg/m^3 or 9 ppm	13 ppm	10,000 μg/m^3
1 h	40,000 μg/m^3 or 35 ppm	31 ppm	
Ozone (O_3)			
1 yr		0.015 ppm	
1 day		0.025 ppm	
8 h	0.075 ppm	0.065 ppm	100 μg/m^3
1 h	0.12 ppm	0.082 ppm	
Fine Particulates, diameter < 10 μm (PM_{10})			
1 yr		70 μg/m^3	40 μg/m^3
1 day	150 μg/m^3	120 μg/m^3	50 μg/m^3
Very Fine Particulates, diam. < 2.5 μm ($PM_{2.5}$)			
1 yr	15 μg/m^3		25 μg/m^3
1 day	35 μg/m^3	30 μg/m^3	
Lead (Pb)			
1 yr			0.25 μg/m^3
3 mo	0.15 μg/m^3		
Benzene (C_6H_6)			
1 yr			3.25 μg/m^3
1,3-Butadiene (CH_2=CHCH=CH_2)			
1 yr			2.25 μg/m^3
PAH (Polycyclic Aromatic Hydrocarbons)			
1 yr			0.25 ng/m^3

Science Graffito

"If I had only one day left to live, I would live it in my statistics class — it would seem so much longer."

– Anonymous. [from C.C Gaither (Ed.), 1996: *Statistically Speaking: A Dictionary of Quotations*, Inst. of Physics Pub., 420 pp].

Solved Example (§)

Given an x-axis aligned with the mean wind U = 10 m/s, and the y-axis aligned in the crosswind direction, V. Listed at right are measurements of the V-component of wind.

a. Find the V mean wind speed and standard deviation.

b. If the vertical standard deviation is 1 m/s, is the flow isotropic?

t (h)	V (m/s)
0.1	2
0.2	–1
0.3	1
0.4	1
0.5	–3
0.6	–2
0.7	0
0.8	2
0.9	–1
1.0	1

Solution

Given: V speeds above, σ_w = 1 m/s, $\overline{U}$ = 10 m/s

Find: $\overline{V}$ = ? m/s, σ_v = ? m/s, isotropic (yes/no) ?

Assume V wind is constant with height.

Use eq. (19.2), except for V instead of M:

$$\overline{V}(z) = \frac{1}{N}\sum_{i=1}^{N} V_i(z) = (1/10)\cdot(0) = \mathbf{0\ m/s}$$

Use eq. (19.5), but for V: $\sigma_V{}^2 = \frac{1}{N}\sum_{k=1}^{N}(V_k - \overline{V})^2$

$= (1/10)\cdot[4 + 1 + 1 + 1 + 9 + 4 + 0 + 4 + 1 + 1]$

$= 2.6\ m^2/s^2$

Use eq. (19.6)

$\sigma_v = [2.6\ m^2/s^2]^{1/2} = \mathbf{1.61\ m/s}$

Use eq. (19.7): (σ_v = 1.61 m/s) > (σ_w = 1.0 m/s), therefore **Anisotropic** in the y-z plane (but no info on σ_u here).

Check: Units OK. Physics OK.

Discussion: The sigma values indicate the rate of plume spread. In this example is greater spread in the crosswind direction than in the vertical direction, hence dispersion looks like the "statically stable" case plotted in Fig. 19.2. By looking at the spread of a smoke plume, you can estimate the static stability.

TURBULENCE STATISTICS

For air pollutants emitted from a point source such as the top of a smoke stack, mean wind speed and turbulence both affect the pollutant concentration measured downwind at ground level. The mean wind causes pollutant transport. Namely it blows or advects the pollutants from the source to locations downwind. However, while the plume is advecting, turbulent gusts acts to spread, or **disperse**, the pollutants as they mix with the surrounding air. Hence, we need to study both mean and turbulent characteristics of wind in order to predict downwind pollution concentrations.

Review of Basic Definitions

Recall from the Atmospheric Boundary-Layer (ABL) chapter that variables such as velocity components, temperature, and humidity can be split into mean and turbulent parts. For example:

$$M = \overline{M} + M' \tag{19.1}$$

where M is instantaneous speed in this example, $\overline{M}$ is the mean wind speed [usually averaged over time (≈ 30 min) or horizontal distance (≈ 15 km)], and M' is the instantaneous deviation from the mean value.

The mean wind speed at any height z is

$$\overline{M}(z) = \frac{1}{N}\sum_{i=1}^{N} M_i(z) \tag{19.2}$$

where M_i is the wind speed measured at some time or horizontal location index i, and N is the total number of observation times or locations. Use similar definitions for mean wind components $\overline{U}$, $\overline{V}$, and $\overline{W}$.

Smoke plumes can spread in the vertical direction. Recall from the ABL chapter that the ABL wind speed often varies with height. Hence, the wind speed that affects the pollutant plume must be defined as an average speed over the vertical thickness of the plume.

If the wind speeds at different, equally spaced layers, between the bottom and the top of a smoke plume are known, and if k is the index of any layer, then the average over height is:

$$\overline{\overline{M}} = \frac{1}{K}\sum_{k=1}^{K} \overline{M}(z_k) \tag{19.3}$$

where the sum is over only those layers spanned by the plume. K is the total number of layers in the plume.

This works for nearly horizontal plumes that have known vertical thickness. For the remainder of this chapter, we will use just one overbar (or sometimes no overbar) to represent an average over both time (index i), and vertical plume depth (index k).

The coordinate system is often chosen so that the x-axis is aligned with the mean wind direction, averaged over the whole smoke plume. Thus,

$$\bar{M} = \bar{U} \tag{19.4}$$

There is no lateral (crosswind) mean wind ($\bar{V} \approx 0$) in this coordinate system. The mean vertical velocity is quite small, and can usually be neglected ($\bar{W} \approx 0$, except near hills) compared to plume dispersion rates. However, $u' = U - \bar{U}$, $v' = V - \bar{V}$, and $w' = W - \bar{W}$ can be non-zero, and are all important.

Recall from the ABL chapter that **variance** σ_A^2 of any quantity A is defined as

$$\sigma_A{}^2 = \frac{1}{N}\sum_{k=1}^{N}(A_k - \bar{A})^2 = \frac{1}{N}\sum_{k=1}^{N}(a'^2) = \overline{a'^2} \tag{19.5}$$

The square root of the variance is the **standard deviation**:

$$\sigma_A = \left(\sigma_A{}^2\right)^{1/2} \tag{19.6}$$

The ABL chapter gives estimates of velocity standard deviations.

Isotropy (again)

Recall from the ABL chapter that turbulence is said to be **isotropic** when:

$$\sigma_u{}^2 = \sigma_v{}^2 = \sigma_w{}^2 \tag{19.7}$$

As will be shown later, the rate of smoke dispersion depends on the velocity variance. Thus, if turbulence is isotropic, then a smoke puff would tend to expand isotropically, as a sphere; namely, it would expand equally in all directions.

There are many situations where turbulence is **anisotropic** (not isotropic). During the daytime over bare land, rising thermals create stronger vertical motions than horizontal. Hence, a smoke puff would **loop** up and down and disperse more in the vertical. At night, vertical motions are very weak, while horizontal motions can be larger. This causes smoke puffs to **fan** out horizontally at night, and for other stable cases.

Similar effects operate on smoke plumes formed from continuous emissions. For this situation, only the vertical and lateral velocity variances are relevant. Fig. 19.2 illustrates how isotropy and anisotropy affect average smoke plume cross sections.

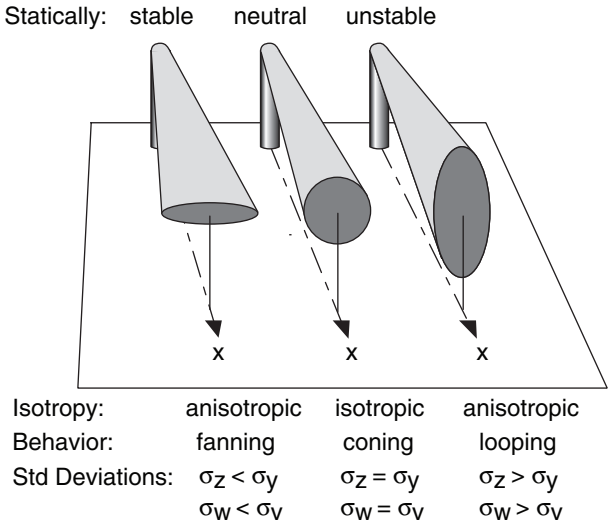

Figure 19.2
Isotropic and anisotropic dispersion of smoke plumes. The shapes of the ends of these smoke plumes are also sketched in Fig. 19.3, along the arc labeled "dispersion isotropy".

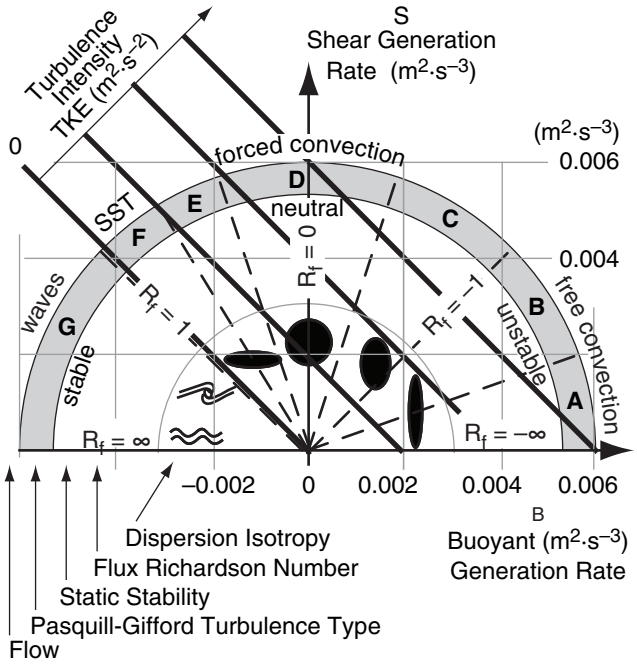

Figure 19.3
Rate of generation of TKE by buoyancy (abscissa) and shear (ordinate). Shape and rates of plume dispersion (dark spots or waves). Dashed lines separate sectors of different Pasquill-Gifford turbulence type. Isopleths of TKE intensity (dark diagonal lines). R_f is flux Richardson number. SST is stably-stratified turbulence. (See the Atmospheric Boundary Layer chapter for turbulence details.)

Table 19-2a. Pasquill-Gifford turbulence types for **Daytime**. *M* is wind speed at *z* = 10 m.

M (m/s)	**Insolation** (incoming solar radiation)		
	Strong	**Moderate**	**Weak**
< 2	A	A to B	B
2 to 3	A to B	B	C
3 to 4	B	B to C	C
4 to 6	C	C to D	D
> 6	C	D	D

Table 19-2b. Pasquill-Gifford turbulence types for **Nighttime**. *M* is wind speed at *z* = 10 m.

M (m/s)	**Cloud Coverage**	
	≥ 4/8 low cloud or thin overcast	**≤ 3/8**
< 2	G	G
2 to 3	E	F
3 to 4	D	E
4 to 6	D	D
> 6	D	D

Solved Example

Determine the PG turbulence type during night with 25% cloud cover, and winds of 5 m/s.

Solution

Given: *M* = 5 m/s, clouds = 2/8 .
Find: PG = ?
Use Table 18–2b. **PG = "D"**

Check: Units OK. Physics OK.
Discussion: As wind speeds increase, the PG category approaches "D" (statically neutral), for both day and night conditions. "D" implies "forced convection".

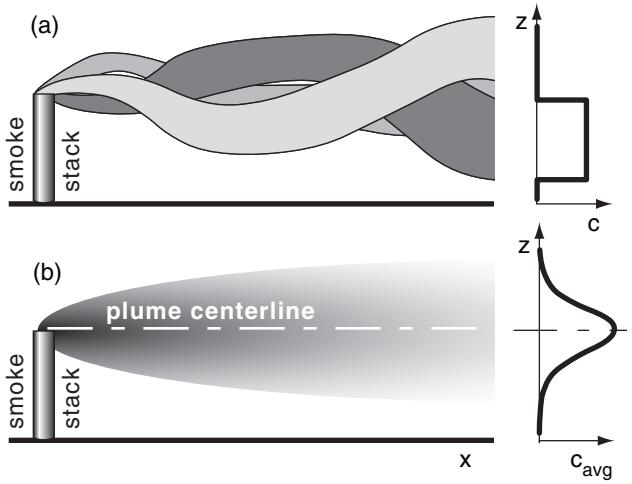

Figure 19.4
(a) Snapshots showing an instantaneous smoke plume at different times, also showing a concentration c profile for the dark-shaded plume. (b) Average over many plumes, with the average concentration c_{avg} profile shown at right.

Pasquill-Gifford (PG) Turbulence Types

During weak advection, the nature of convection and turbulence are controlled by the wind speed, incoming solar radiation (**insolation**), cloud shading, and time of day or night. Pasquill and Gifford (PG) suggested a practical way to estimate the nature of turbulence, based on these forcings.

They used the letters "A" through "F" to denote different turbulence types, as sketched in Fig. 19.3 (reproduced from the ABL chapter). "A" denotes free convection in statically unstable conditions. "D" is forced convection in statically neutral conditions. Type "F" is for statically stable turbulence. Type "G" was added later to indicate the strongly statically stable conditions associated with meandering, wavy plumes in otherwise nonturbulent flow. PG turbulence types can be estimated using Tables 19-2.

Early methods for determining pollutant dispersion utilized a different plume spread equation for each Pasquill-Gifford type. One drawback is that there are only 7 discrete categories (A – G); hence, calculated plume spread would suddenly jump when the PG category changed in response to changing atmospheric conditions.

Newer air pollution models do not use the PG categories, but use the fundamental meteorological conditions (such as shear and buoyant TKE generation, or values of velocity variances that are continuous functions of wind shear and surface heating), which vary smoothly as atmospheric conditions change.

DISPERSION STATISTICS

Snapshot vs. Average

Snapshots of smoke plumes are similar to what you see with your eye. The plumes have fairly-well defined edges, but each plume wiggles up and down, left and right (Fig. 19.4a). The concentration *c* through such an instantaneous smoke plume can be quite variable, so a hypothetical vertical profile is sketched in Fig. 19.4a.

A time exposure of a smoke-stack plume might appear as sketched in Fig. 19.4b. When averaged over a time interval such as an hour, most of the pollutants are found near the centerline of the plume. Average concentration decreases smoothly with distance away from the centerline. The resulting profile of concentration is often bell shaped, or Gaussian. Air quality standards in most countries are based on averages, as was listed in Table 18–1.

Center of Mass

The **plume centerline** height z_{CL} can be defined as the location of the **center of mass** of pollutants. In other words, it is the average height of the pollutants. Suppose you measure the concentration c_k of pollutants at a range of equally-spaced heights z_k through the smoke plume. The center of mass is a weighted average defined by:

$$z_{CL} = \bar{z} = \frac{\sum_{k=1}^{K} c_k \cdot z_k}{\sum_{k=1}^{K} c_k} \qquad \bullet(19.8)$$

where K is the total number of heights, and k is the height index, and the overbar denotes a mean.

For passive tracers with slow exit velocity from the stack, the plume centerline is at the same height as the top of the stack. For buoyant plumes in hot exhaust gases, and for smoke blown at high speed out of the top of the stack, the centerline rises above the top of the stack.

A similar center of mass can be found for the crosswind (lateral) location, assuming measurements are made at equal intervals across the plume. Passive tracers blow downwind. Thus, the center of mass of a smoke plume, when viewed from above such as from a satellite, follows a mean wind trajectory from the stack location (see the discussion of streamlines, streaklines, and trajectories in the Local Winds chapter).

Standard Deviation – Sigma

For time-average plumes such as in Figs. 19.4b and 19.5, the plume edges are not easy to locate. They are poorly defined because the bell curve gradually approaches zero concentration with increasing distance from the centerline. Thus, we cannot use edges to measure plume spread (depth or width).

Instead, the standard deviation σ_z of pollutant location is used as a measure of plume spread, where standard deviation is the square root of the variance σ_z^2 . The vertical-position deviations must be weighted by the pollution concentration to find sigma, as shown here:

$$\sigma_z = \left[\frac{\sum_{k=1}^{K} c_k \cdot (z_k - \bar{z})^2}{\sum_{k=1}^{K} c_k} \right]^{1/2} \qquad \bullet(19.9)$$

where $\bar{z} = z_{CL}$ is the average height found from the previous equation.

A similar equation can be defined for lateral standard deviation σ_y. The vertical and lateral dis-

ON DOING SCI. • Data Misinterpretation

Incomplete data can be misinterpreted, leading to expensive erroneous conclusions. Suppose an air-pollution meteorologist/engineer erects a tall tower at the site of a proposed 75 m high smoke stack. On this tower are electronic thermometers at two heights: 50 and 100 m. On many days, these measurements give temperatures that are on the same adiabat (Fig. a).

Regarding static stability, one interpretation (Fig. b) is that the atmosphere is statically neutral. Another interpretation (Fig. c) is that it is a statically unstable convective mixed layer. If neutral stability is erroneously noted on a day of static instability, then the corresponding predictions of dispersion rate and concentrations will be embarrassingly wrong.

To resolve this dilemma, the meteorologist/engineer needs additional info. Either add a third thermometer near the ground, or add a net radiation sensor, or utilize manual observations of sun, clouds, and wind to better determine the static stability.

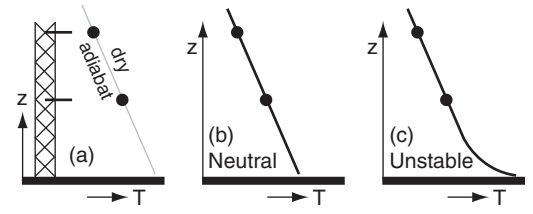

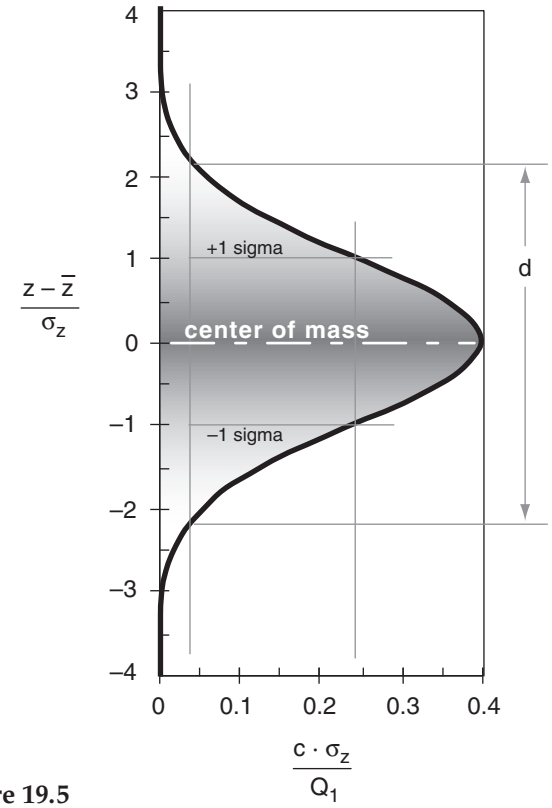

Figure 19.5
Gaussian curve.
Each unit along the ordinate corresponds to one standard deviation away from the center. Nominal 1-D plume width is d.

Solved Example (§)

Given the following 1-D concentration measurements. Find the plume centerline height, standard deviation of height, and nominal plume depth. Plot the best-fit curve through these data points.

z (km)	c(μg/m)
2.0	0
1.8	1
1.6	3
1.4	5
1.2	7
1.0	6
0.8	2
0.6	1
0.4	0
0.2	0
0.0	0

Solution

Given: Δz = 0.2 km, with concentrations above

Find: $\bar{z}$ = ? km, σ_z = ? km, Q_1 = ? km·μg/m, d = ? km, and plot $c(z)$ = ? μg/m

Use eq. (19.8) to find the plume centerline height:

$\bar{z}$ = (30.2 km·μg·m^{-1}) / (25 μg·m^{-1}) = **1.208 km**

Use eq. (19.9):

σ_z^2 = (1.9575 km^2·μg·m^{-1})/(25 μg·m^{-1}) = 0.0783 km^2

σ_z = [σ_z^2]$^{1/2}$ = [0.0783 km^2]$^{1/2}$ = **0.28 km**

Use eq. (19.12):

d = 4.3 · (0.28 km) = **1.2 km**

Use eq. (19.11):

Q_1 = (0.2 km) · (25 μg·m^{-1}) = **5.0 km·μg/m**

Use eq. (19.10) to plot the best-fit curve:

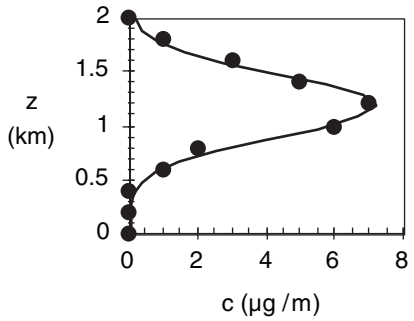

Check: Units OK. Physics OK. Sketch OK.

Discussion: The curve is a good fit to the data. Often the measured data will have some scatter due to the difficulty of making concentration measurements, but the equations in this section are able to find the best-fit curve. This statistical curve-fitting method is called the **method of moments**, because we matched the first two statistical moments (mean & variance) of the Gaussian distribution to the corresponding moments calculated from the data.

persion need not be equal, because the dispersive nature of turbulence is not the same in the vertical and horizontal when turbulence is anisotropic.

When the plume is compact, the standard deviation and variance are small. These statistics increase as the plume spreads. Hence we expect sigma to increase with distance downwind of the stack. Such spread will be quantified in the next main section.

Gaussian Curve

The **Gaussian** or "**normal**" curve is bell shaped, and is given in one-dimension (1-D) by:

$$c(z) = \frac{Q_1}{\sigma_z \sqrt{2\pi}} \cdot \exp\left\{ -0.5 \left[\frac{z - \bar{z}}{\sigma_z} \right]^2 \right\} \qquad \bullet(19.10)$$

where $c(z)$ is the one-dimensional concentration (g/m) at any height z, and Q_1 (g) is the total amount of pollutant emitted.

This curve is symmetric about the mean location, and has tails that asymptotically approach zero as z approaches infinity (Fig. 19.5). The area under the curve is equal to Q_1, which physically means that pollutants are conserved. The **inflection points** in the curve (points where the curve changes from concave left to concave right) occur at exactly one σ_z from the mean. Between $\pm 2 \cdot \sigma_z$ are 95% of the pollutants; hence, the Gaussian curve exhibits strong central tendency.

Eq. (19.10) has three parameters: Q_1, $\bar{z}$, and σ_z. These parameters can be estimated from measurements of concentration at equally-spaced heights through the plume, in order to find the best-fit Gaussian curve. The last two parameters are found with eqs. (19.8) and (19.9). The first parameter is found from:

$$Q_1 = \Delta z \cdot \sum_{k=1}^{K} c_k \qquad \bullet(19.11)$$

where Δz is the height interval between neighboring measurements.

Nominal Plume Edge

For practical purposes, the edge of a Gaussian plume is defined as the location where the concentration is 10% of the centerline concentration. This gives a plume spread (e.g., depth from top edge to bottom edge) of

$$d \approx 4.3 \cdot \sigma_z \qquad \bullet(19.12)$$

TAYLOR'S STATISTICAL THEORY

Statistical theory explains how plume dispersion statistics depend on turbulence statistics and downwind distance.

Passive Conservative Tracers

Many pollutants consist of gases or very fine particles. They passively ride along with the wind, and trace out the air motion. Hence, the rate of dispersion depends solely on the air motion (wind and turbulence) and not on the nature of the pollutant. These are called **passive tracers**. If they also do not decay, react, fall out, or stick to the ground, then they are also called **conservative tracers,** because all pollutant mass emitted into the air is conserved.

Some pollutants are not passive or conservative. Dark soot particles can adsorb sunlight to heat the air, but otherwise they might not be lost from the air. Thus, they are active because they alter turbulence by adding buoyancy, but are conservative. Radioactive pollutants are both nonconservative and active, due to radioactive decay and heating.

For passive conservative tracers, the amount of dispersion (σ_y or σ_z) depends not only on the intensity of turbulence (σ_v or σ_w , see the ABL chapter), but on the distribution of turbulence energy among eddies of different sizes. For a plume of given spread, eddies as large as the plume diameter cause much greater dispersion than smaller-size eddies. Thus, dispersion rate increases with time or downwind distance, as shown below.

Dispersion Equation

G.I. Taylor theoretically examined an individual passive tracer particle as it moved about by the wind. Such an approach is **Lagrangian**, as discussed in the Heat chapter. By averaging over many such particles within a smoke cloud, he derived a statistical theory for turbulence.

One approximation to his result is

•(19.13a)

$$\sigma_y^2 = 2 \cdot \sigma_v^2 \cdot t_L^2 \cdot \left[\frac{x}{M \cdot t_L} - 1 + \exp\left(- \frac{x}{M \cdot t_L} \right) \right]$$

•(19.13b)

$$\sigma_z^2 = 2 \cdot \sigma_w^2 \cdot t_L^2 \cdot \left[\frac{x}{M \cdot t_L} - 1 + \exp\left(- \frac{x}{M \cdot t_L} \right) \right]$$

where x is distance downwind from the source, M is wind speed, and t_L is the Lagrangian time scale.

BEYOND ALGEBRA • Diffusion Equation

The Gaussian concentration distribution is a solution to the diffusion equation, as is shown here.

For a conservative, passive tracer, the budget equation says that concentration c in a volume will increase with time t if greater tracer flux F_c enters a volume than leaves. In one dimension (z), this is:

$$\frac{dc}{dt} = -\frac{\partial F_c}{\partial z} \qquad \text{(a)}$$

If turbulence consists of only small eddies, then turbulent flux of tracer flows down the mean tracer gradient:

$$F_c = -K \frac{\partial c}{\partial z} \qquad \text{(b)}$$

where K, the eddy diffusivity, is analogous to a molecular diffusivity (see K-Theory in the Atmospheric Boundary Layer chapter), and F_c is in kinematic units (concentration times velocity).

Plugging eq. (b) into (a), and assuming constant K, gives the 1-D **diffusion equation**:

$$\boxed{\frac{dc}{dt} = K \frac{\partial^2 c}{\partial z^2}} \qquad \text{(c)}$$

This parabolic differential equation can be solved with initial conditions (IC) and boundary conditions (BC). Suppose a smoke puff of mass Q grams of tracer is released in the middle of a vertical pipe that is otherwise filled with clean air at time $t = 0$. Define the vertical coordinate system so that $z = 0$ at the initial puff height (and $\bar{z} = 0$). Dispersion up and down the pipe is one-dimensional.

IC: $c = 0$ at $t = 0$ everywhere except at $z = 0$.

BC1: $\int c \, dz = Q$, at all t, where integration is $-\infty$ to ∞

BC2: c approaches 0 as z approaches $\pm \infty$, at all t .

The solution is:

$$c = \frac{Q}{(4\pi K t)^{1/2}} \exp\left(\frac{-z^2}{4Kt} \right) \qquad \text{(d)}$$

You can confirm that this is a solution by plugging it into eq. (c), and checking that the LHS equals the RHS. It also satisfies all initial & boundary conditions.

Comparing eq. (d) with eq. (19.10), we can identify the standard deviation of height as

$$\sigma_z = \sqrt{2Kt} \qquad \text{(e)}$$

which says that tracer spread increases with the square root of time, and greater eddy-diffusivity causes faster spread rate. Thus, the solution is Gaussian:

$$\boxed{c = \frac{Q}{\sqrt{2\pi} \cdot \sigma_z} \exp\left[-\frac{1}{2} \left(\frac{z}{\sigma_z} \right)^2 \right]} \qquad (19.10)$$

Finally, using **Taylor's hypothesis** that $t = x/M$, we can compare eq. (e) with the σ_z version of eq. (19.15), and conclude that:

$$K = \sigma_w^2 \cdot t_L \qquad \text{(f)}$$

showing how K increases with turbulence intensity.

Solved Example (§)

Plot vertical and horizontal plume spread σ_z and σ_y vs. downwind distance x, using a Lagrangian time scale of 1 minute and wind speed of 10 m/s at height 100 m in a neutral boundary layer of depth 500 m. There is a rough surface of varied crops.

a) Plot on both linear and log-log graphs.

b) Also plot the short and long-distance limits of σ_y on the log-log graph.

Solution

Given: z = 100 m, M = 10 m/s, t_L = 60 s, h = 500 m

Find: σ_z and σ_y (m) vs. x (km).

Refer to Boundary Layer chapter to calculate the info needed in the eqs. for Taylor's statistical theory.

Use Table 18-1 for rough surface of varied crops:

aerodynamic roughness length is z_o = 0.25 m

Use this z_o in eq. (18.13) to get the friction velocity:

u_* = [0.4·(10m/s)] / ln(100m/0.25m) = 0.668 m/s

Use this u_* in eq. (18.25b) to get the velocity variance

σ_v = 1.6·(0.668m/s) ·[1 – 0.5·(100m/500m)] = 0.96 m/s

Similarly, use eq. (18.25c): σ_w = 0.75 m/s

Use σ_v and σ_w in eqs. (19.13a & b) in a spreadsheet to calculate σ_y and σ_z , and plot the results on graphs:

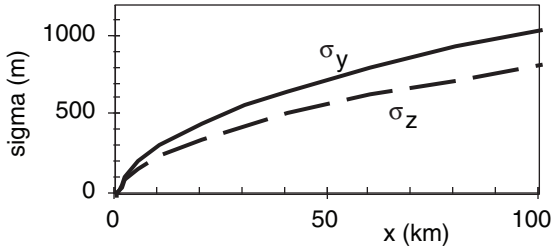

A linear graph is shown above, and log-log below.

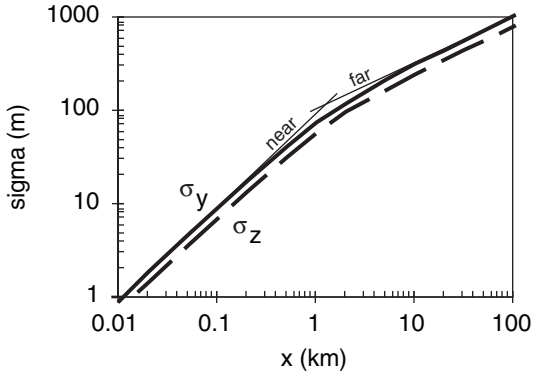

Eqs. (19.14) & (19.15) for the near and far approximations are plotted as the thin solid lines.

Check: Units OK. Physics OK. Sketch OK.

Discussion: Plume spread increases with distance downwind of the smoke stack. $\sigma_y \approx \sigma_z$ at any x, giving the nearly isotropic dispersion expected for statically neutral air. The cross-over between short and long time limits is at $x \approx 2 \cdot M \cdot t_L$ = 1.2 km.

Thus, the spread (σ_y and σ_z) of passive tracers increases with turbulence intensity (σ_v and σ_w) and with downwind distance x.

The **Lagrangian time scale** is a measure of how quickly a variable becomes uncorrelated with itself. For very small-scale atmospheric eddies, this time scale is only about 15 seconds. For convective thermals, it is on the order of 15 minutes. For the synoptic-scale high and low pressure systems, the Lagrangian time scale is on the order of a couple days. We will often use a value of $t_L \approx 1$ minute for dispersion in the boundary layer.

Dispersion Near & Far from the Source

Close to the source (at small times after the start of dispersion), eq. (19.13a) reduces to

$$\sigma_y \approx \sigma_v \cdot \left(\frac{x}{M} \right) \qquad \bullet(19.14)$$

while far from the source it can be approximated by:

$$\sigma_y \approx \sigma_v \cdot \left(2 \cdot t_L \cdot \frac{x}{M} \right)^{1/2} \qquad \bullet(19.15)$$

There are similar equations for σ_z as a function of σ_w.

Thus, we expect plumes to initially spread linearly with distance near to the source, but change to square-root with distance further downwind.

DISPERSION IN NEUTRAL & STABLE BOUNDARY LAYERS

To calculate pollutant concentration at the surface, one needs to know both the height of the plume centerline, and the spread of pollutants about that centerline. **Plume rise** is the name given to the first issue. **Dispersion** (from Taylor's statistical theory) is the second. When they are both used in an expression for the average spatial distribution of pollutants, pollution concentrations can be calculated.

Plume Rise

Ground-level concentration generally decreases as plume-centerline height increases. Hence, plume rise above the physical stack top is often desirable. The centerline of plumes can rise above the stack top due to the initial momentum associated with exit velocity out of the top of the stack, and due to buoyancy if the effluent is hot.

Neutral Boundary Layers

Statically neutral situations are found in the residual layer (not touching the ground) during light winds at night. They are also found throughout the bottom of the boundary layer (touching the ground) on windy, overcast days or nights.

The height z_{CL} of the plume centerline above the ground in neutral boundary layers is:

$$z_{CL} = z_s + \left[a \cdot {l_m}^2 \cdot x + b \cdot l_b \cdot x^2 \right]^{1/3} \qquad \bullet(19.16)$$

where a = 8.3 (dimensionless), b = 4.2 (dimensionless), x is distance downwind of the stack, and z_s is the physical stack height. This equation shows that the plume centerline keeps rising as distance from the stack increases. It ignores the capping inversion at the ABL top, which would eventually act like a lid on plume rise and upward spread.

A momentum length scale, l_m, is defined as:

$$l_m \approx \frac{W_o \cdot R_o}{M} \qquad \bullet(19.17)$$

where R_o is the stack-top radius, W_o is stack-top exit velocity of the effluent, and M is the ambient wind speed at stack top. l_m can be interpreted as a ratio of vertical emitted momentum to horizontal wind momentum.

A buoyancy length scale, l_b, is defined as:

$$l_b \approx \frac{W_o \cdot {R_o}^2 \cdot |g|}{M^3} \cdot \frac{\Delta\theta}{\theta_a} \qquad \bullet(19.18)$$

where $|g|$ = 9.8 m/s^2 is gravitational acceleration magnitude, $\Delta\theta = \theta_p - \theta_a$ is the temperature excess of the effluent, θ_p is the initial stack gas potential temperature at stack top, and θ_a is the ambient potential temperature at stack top. l_b can be interpreted as a ratio of vertical buoyancy power to horizontal power of the ambient wind.

Stable Boundary Layers

In statically stable situations, the ambient potential temperature increases with height. This limits the plume-rise centerline to a final equilibrium height z_{CLeq} above the ground:

$$z_{CLeq} = z_s + 2.6 \cdot \left(\frac{l_b \cdot M^2}{{N_{BV}}^2} \right)^{1/3} \qquad \bullet(19.19)$$

where the Brunt-Väisälä frequency N_{BV} is used as a measure of static stability (see the Stability chapter).

Solved Example (§)

At stack top, effluent velocity is 20 m/s, temperature is 200°C, emission rate is 250 g/s of SO_2. The stack is 75 m high, and has a radius of 2 m at the top. At stack top, the ambient wind is 5 m/s, and ambient potential temperature is 20°C. For a neutral boundary layer, plot plume centerline height vs. downwind distance.

Solution

Given: W_o = 20 m/s, Q = 250 g/s, z_s = 75 m, M = 5 m/s
θ_p =473K +(9.8K/km)·(0.075 km) = 474 K, θ_a = 293 K
Find: $z_{CL}(x)$ = ? m.

Use eq. (19.17): l_m = (20m/s)·(2m) / (5m/s) = 8 m
Use eq. (19.18):

$$l_b \approx \frac{(20\text{m/s}) \cdot (2\text{m})^2 \cdot (9.8\text{m}\cdot\text{s}^{-2})}{(5\text{m/s})^3} \cdot \frac{(474 - 293\text{K})}{293\text{K}} = 3.87 \text{ m}$$

Use eq. (19.16):

$$z_{CL} = (75\text{m}) + \left[8.3 \cdot (8\text{m})^2 \cdot x + 4.2 \cdot (3.87\text{m}) \cdot x^2 \right]^{1/3}$$

This is shown as the solid line on the plot below:

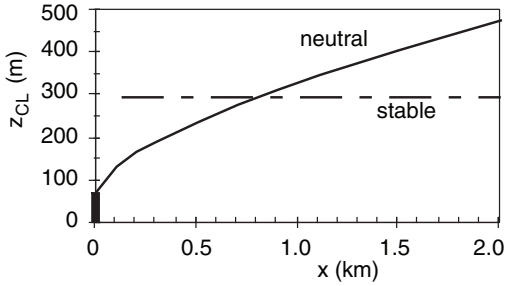

Check: Units OK. Physics OK. Sketch OK.

Discussion: In neutral conditions, the plume continues to rise with downwind distance. However, real plumes usually hit an elevated inversion & stop rising. Use a thermo diagram to locate the inversions aloft.

Solved Example

Same as previous example, but for a stable boundary layer with $\Delta\theta_a/\Delta z$ = 5°C/km. Find z_{CLeq} .

Solution

Given: W_o = 20 m/s, Q = 250 g/s, z_s = 75 m, M = 5 m/s
θ_p = 474 K, θ_a = 293 K, $\Delta\theta_a/\Delta z$ = 5°C/km
Find: Δz_{CLeq} = ? m , then plot z_{CLeq} vs. x

Use eq. (5.4b) to find the Brunt-Väisälä frequency^2:
N_{BV}^2 = [(9.8m·s^{-2})/293K]·[5K/1000m] =1.67x10^{-4} s^{-2}
Use eq. (19.19):

$$z_{CLeq} = (75\text{m}) + 2.6 \cdot \left(\frac{(3.87\text{m}) \cdot (5\text{m/s})^2}{1.67 \times 10^{-4}\,\text{s}^{-2}} \right)^{1/3}$$

$z_{CLeq} = z_s + \Delta z_{CL\,eq}$ = 75 m + 216.7 m = **291.75 m**
See dashed line in the previous solved example.

Check: Units OK. Physics OK. Sketch OK.

Discussion: The actual plume centerline does not reach the equilibrium height instantly. Instead, it approaches it a bit slower than the neutral plume rise curve plotted in the previous solved ex.

Solved Example (§)

Given a "surface" wind speed of 10 m/s at 10 m above ground, neutral static stability, boundary layer depth 800 m, surface roughness length 0.1 m, emission rate of 300 g/s of passive, non-buoyant SO_2, wind speed of 20 m/s at plume centerline height, and Lagrangian time scale of 1 minute.

Plot isopleths of concentration at the ground for plume centerline heights of: (a) 100m, (b) 200m

Solution

Given: M = 10 m/s at z = 10 m, z_o = 0.1 m,
M = 20 m/s at z = 100 m = z_{CL}, neutral,
Q = 300 g/s of SO_2, t_L = 60 s, h = 800 m
Find: c (μg/m^3) vs. x (km) and y (km), at z = 0.
Assume z_{CL} is constant.

Use eq. (18.13) from the Boundary Layer (BL) chapter:
$u_* = 0.4 \cdot (10 \text{ m/s}) / \ln(10 \text{ m}/0.1 \text{ m}) = 0.869$ m/s

(a) Use eqs. (18.25b) & (18.25c) from the BL chapter:
$\sigma_v = 1.6 \cdot (0.869 \text{m/s}) \cdot [1 - 0.5(100/800)] = 1.3$ m/s
$\sigma_w = 1.25 \cdot (0.869 \text{m/s}) \cdot [1 - 0.5(100/800)] = 1.02$ m/s

Use eq. (19.13a & b) in a spreadsheet to get σ_y and σ_z vs. x. Then use eq. (19.21) to find c at each x and y:

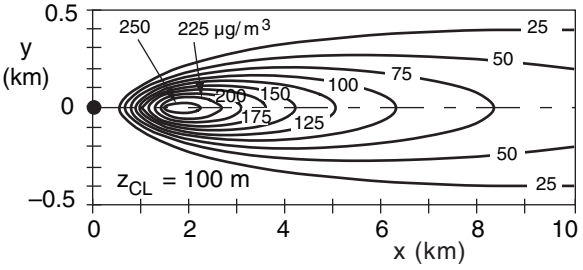

(b) Similarly, for a higher plume centerline:

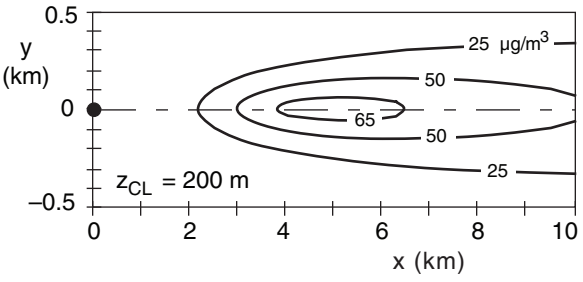

Check: Units OK. Physics OK.

Discussion: These plots show the pollutant **footprints**. Higher plume centerlines cause lower concentrations at the ground. That is why engineers design tall smoke stacks, and try to enhance buoyant plume rise.

Faster wind speeds also cause more dilution. Because faster winds are often found at higher altitudes, this also favors tall stacks for reducing surface concentrations.

Gaussian Concentration Distribution

For neutral and stable boundary layers (PG types C through F), the sizes of turbulent eddies are relatively small compared to the depth of the boundary layer. This simplifies the problem by allowing turbulent dispersion to be modeled analogous to molecular diffusion. For this situation, the average concentration distribution about the plume centerline is well approximated by a 3-D Gaussian bell curve:

•(19.20)

$$c = \frac{Q}{2\pi\sigma_y\sigma_z M} \cdot \exp\left[-0.5 \cdot \left(\frac{y}{\sigma_y}\right)^2\right] \cdot \left\{\exp\left[-0.5 \cdot \left(\frac{z - z_{CL}}{\sigma_z}\right)^2\right] + \exp\left[-0.5 \cdot \left(\frac{z + z_{CL}}{\sigma_z}\right)^2\right]\right\}$$

where Q is the source emission rate of pollutant (g/s), σ_y and σ_z are the plume-spread standard deviations in the crosswind and vertical, y is lateral (crosswind) distance of the receptor from the plume centerline, z is vertical distance of the receptor above ground, z_{CL} is the height of the plume centerline above the ground, and M is average ambient wind speed at the plume centerline height.

For receptors at the ground (z = 0), eq. (19.20) reduces to:

•(19.21)

$$c = \frac{Q}{\pi\sigma_y\sigma_z M} \cdot \exp\left[-0.5 \cdot \left(\frac{y}{\sigma_y}\right)^2\right] \cdot \exp\left[-0.5 \cdot \left(\frac{z_{CL}}{\sigma_z}\right)^2\right]$$

The pattern of concentration at the ground is called a **footprint**.

The above two equations assume that the ground is flat, and that pollutants that hit the ground are "reflected" back into the air. Also, they do not work for dispersion in statically unstable mixed layers.

To use these equations, the turbulent velocity variances σ_v^2 and σ_w^2 are first found from the equations in the Boundary Layer chapter. Next, plume spread σ_y and σ_z is found from Taylor's statistical theory (eqs. 19.13). Plume centerline heights z_{CL} are then found from the previous subsection. Finally, they are all used in eqs. (19.20) or (19.21) to find the concentration at a receptor.

Recall that Taylor's statistical theory states that the plume spread increases with downwind distance. Thus, σ_y , σ_z, and z_{CL} are functions of x, which makes concentration c a strong function of x, in spite of the fact that x does not appear explicitly in the two equations above.

DISPERSION IN UNSTABLE BOUNDARY LAYERS (CONVECTIVE MIXED LAYERS)

During conditions of light winds over an underlying warmer surface (PG types A & B), the boundary layer is **statically unstable** and in a state of **free convection**. Turbulence consists of thermals of warm air that rise from the surface to the top of the mixed layer. These vigorous updrafts are surrounded by broader areas of weaker downdraft. The presence of such large turbulent structures and their asymmetry causes dispersion behavior that differs from the usual Gaussian plume dispersion.

As smoke is emitted from a point source such as a smoke stack, some of the emissions are by chance emitted into the updrafts of passing thermals, and some into downdrafts. Thus, the smoke appears to **loop** up and down, as viewed in a snapshot. However, when averaged over many thermals, the smoke disperses in a unique way that can be described deterministically. This description works only if variables are normalized by free-convection scales.

The first step is to get the meteorological conditions such as wind speed, ABL depth, and surface heat flux. These are then used to define the ABL convective scales such as the Deardorff velocity w_*. Source emission height, and downwind receptor distance are then normalized by the convective scales to make dimensionless distance variables.

Next, the dimensionless (normalized) variables are used to calculate the plume centerline height and vertical dispersion distance. These are then used as a first guess in a Gaussian equation for cross-wind-integrated concentration distribution, which is a function of height in the ABL. By dividing each distribution by the sum over all distributions, a corrected cross-wind-integrated concentration can be found that has the desirable characteristic of conserving pollutant mass.

Finally, the lateral dispersion distance is estimated. It is used with the cross-wind-integrated concentration to determine the dimensionless Gaussian concentration at any lateral distance from the plume centerline. Finally, the dimensionless concentration can be converted into a dimensional concentration using the meteorological scaling variables.

Although this procedure is complex, it is necessary, because non-local dispersion by large convective circulations in the unstable boundary layer works completely differently than the small-eddy dispersion in neutral and stable ABLs. The whole procedure can be solved on a spreadsheet, which was used to produce Figs. 19.7 and 19.8.

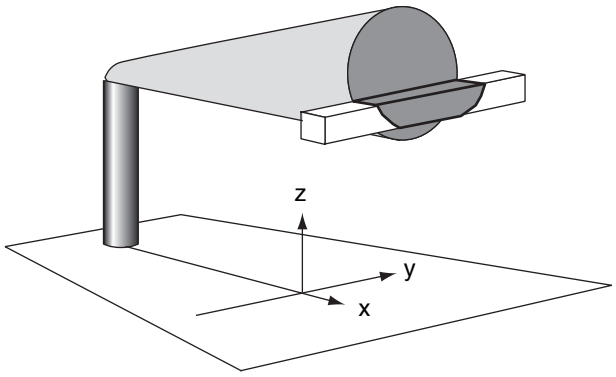

Figure 19.6
Crosswind integrated concentration c_y is the total amount of pollutants in a thin conceptual box (1 m^2 at the end) that extends crosswind (y-direction) across the smoke plume. This concentration is a function of only x and z.

Relevant Variables

Physical Variables:

c = concentration of pollutant (g/m^3)

c_y = **crosswind-integrated concentration** (g/m^2), which is the total amount of pollutant within a long-thin box that is 1 m^2 on each end, and which extends laterally across the plume at any height z and downwind location x (see Fig. 19.6)

Q = emission rate of pollutant (g/s)

x = distance of a receptor downwind of the stack (m)

z = height of a receptor above ground (m)

z_{CL} = height of the plume centerline (center of mass) above the ground (m)

z_s = source height (m) after plume-induced rise

σ_y = lateral standard deviation of pollutant (m)

σ_z = vertical standard deviation of pollutant (m)

σ_{zc} = vertical standard deviation of crosswind-integrated concentration of pollutant (m)

Mixed-Layer Scaling Variables:

F_H = effective surface kinematic heat flux (K·m/s), see Surface Fluxes section of Heat chapter.

M = mean wind speed (m/s)

$$w_* = \left[\frac{|g|\cdot z_i \cdot F_H}{T_v}\right]^{1/3} = \textbf{Deardorff velocity (m/s)} \quad (19.22)$$

$\approx 0.08 \cdot w_B$, where w_B is the buoyancy velocity.

z_i = depth of the convective mixed layer (m)

Dimensionless Scales:

These are usually denoted by uppercase symbols (except for M and Q, which have dimensions).

$$C = \frac{c \cdot z_i^2 \cdot M}{Q} = \text{dimensionless concentration} \bullet (19.23)$$

$$C_y = \frac{c_y \cdot z_i \cdot M}{Q} = \text{dimensionless crosswind-integrated concentration} \quad (19.24)$$

$$X = \frac{x \cdot w_*}{z_i \cdot M} = \text{dimensionless downwind distance of receptor from source} \bullet (19.25)$$

$$Y = y / z_i = \text{dimensionless crosswind (lateral) distance of receptor from centerline} \quad (19.26)$$

$$Z = z / z_i = \text{dimensionless receptor height} \quad (19.27)$$

$$Z_{CL} = z_{CL} / z_i = \text{dimensionless plume centerline height} \quad (19.28)$$

$$Z_s = z_s / z_i = \text{dimensionless source height} \quad (19.29)$$

$$\sigma_{yd} = \sigma_y / z_i = \text{dimensionless lateral standard deviation} \quad (19.30)$$

$$\sigma_{zdc} = \sigma_{zc} / z_i = \text{dimensionless vertical standard deviation of crosswind-integrated concentration} \quad (19.31)$$

As stated in more detail earlier, to find the pollutant concentration downwind of a source during convective conditions, three steps are used: (1) Find the plume centerline height. (2) Find the crosswind integrated concentration at the desired x and z location. (3) Find the actual concentration at the desired y location.

Plume Centerline

For neutrally-buoyant emissions, the dimensionless height of the center of mass (= centerline Z_{CL}) varies with dimensionless distance downwind X :

$$Z_{CL} \approx 0.5 + \frac{0.5}{1 + 0.5 \cdot X^2} \cdot \cos\left[2\pi \frac{X}{\lambda} + \cos^{-1}\left(2 \cdot Z_s - 1\right)\right] \bullet (19.32)$$

where Z_s is the dimensionless source height, and the dimensionless wavelength parameter is $\lambda = 4$.

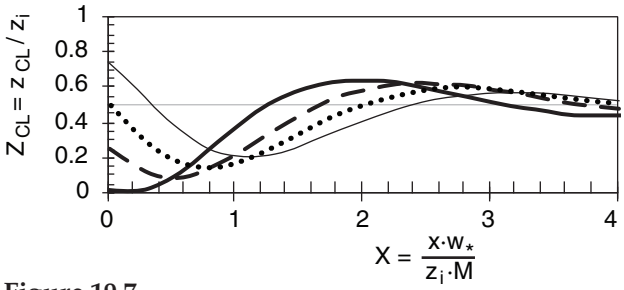

Figure 19.7

Height of the averaged pollutant centerline z_{CL} with downwind distance x, normalized by mixed-layer scales. Dimensionless source heights are $Z_s = z_s/z_i = 0.025$ (thick solid line); 0.25 (dashed); 0.5 (dotted); and 0.75 (thin solid). The plume is neutrally buoyant.

The centerline tends to move down from elevated sources, which can cause high concentrations at ground level (see Fig. 19.7). Then further downwind, they rise a bit higher than half the mixed-layer depth, before reaching a final height at $0.5 \cdot z_i$. For buoyant plumes, the initial downward movement of the centerline is much weaker, or does not occur.

Crosswind Integrated Concentration

The following algorithm provides a quick approximation for the crosswind integrated concentration. Find a first guess dimensionless C_y' as a function of dimensionless height Z using a Gaussian approach for vertical dispersion:

$$C_y' = \exp\left[-0.5 \cdot \left(\frac{Z - Z_{CL}}{\sigma_{zdc}'}\right)^2\right] \bullet (19.33)$$

where the prime denotes a first guess, and where the vertical dispersion distance is:

$$\sigma_{zdc}' = a \cdot X \quad (19.34)$$

with $a = 0.25$. This calculation is done at K equally-spaced heights between the ground to the top of the mixed layer.

Next, find the average over all heights $0 \le Z \le 1$:

$$\overline{C_y'} = \frac{1}{K}\sum_{k=1}^{K} C_y' \quad (19.35)$$

where index k corresponds to height z . Finally, calculate the revised estimate for dimensionless crosswind integrated concentration at any height:

$$C_y = C_y' / \overline{C_y'} \bullet (19.36)$$

Examples are plotted in Fig. 19.8 for various source heights.

Concentration

The final step is to assume that lateral dispersion is Gaussian, according to:

$$C = \frac{C_y}{(2\pi)^{1/2} \cdot \sigma_{yd}} \exp\left[-0.5 \cdot \left(\frac{Y}{\sigma_{yd}} \right)^2 \right] \qquad \bullet(19.37)$$

The dimensionless standard deviation of lateral dispersion distance from an elevated source is

$$\sigma_{yd} \approx b \cdot X \qquad (19.38)$$

where $b = 0.5$.

At large downwind distances (i.e., at $X \geq 4$), the dimensionless crosswind integrated concentration always approaches $C_y \rightarrow 1.0$, at all heights. Also, directly beneath the plume centerline, $Y = 0$.

SUMMARY

Pollutants emitted from a smoke stack will blow downwind and disperse by turbulent mixing with ambient air. By designing a stack of sufficient height, pollutants at ground level become sufficiently dilute as to not exceed local environmental air-quality standards. Additional buoyant plume rise above the physical stack top can further reduce ground-level concentrations.

Air-quality standards do not consider instantaneous samples of pollutant concentration. Instead, they are based on averages over time. For such averages, statistical descriptions of dispersion must be used, including the center of mass (plume centerline) and the standard deviation of location (proportional to plume spread).

For emissions in the boundary layer, the amount of dispersion depends on the type of turbulence. This relationship can be described by Taylor's statistical theory.

During daytime conditions of free convection, thermals cause a peculiar form of dispersion that often brings high concentrations of pollutants close to the ground. At night, turbulence is suppressed in the vertical, causing little dispersion. As pollutants remain aloft for this case, there is often little hazard at ground level. Turbulent dispersion is quite anisotropic for these convective and stable cases.

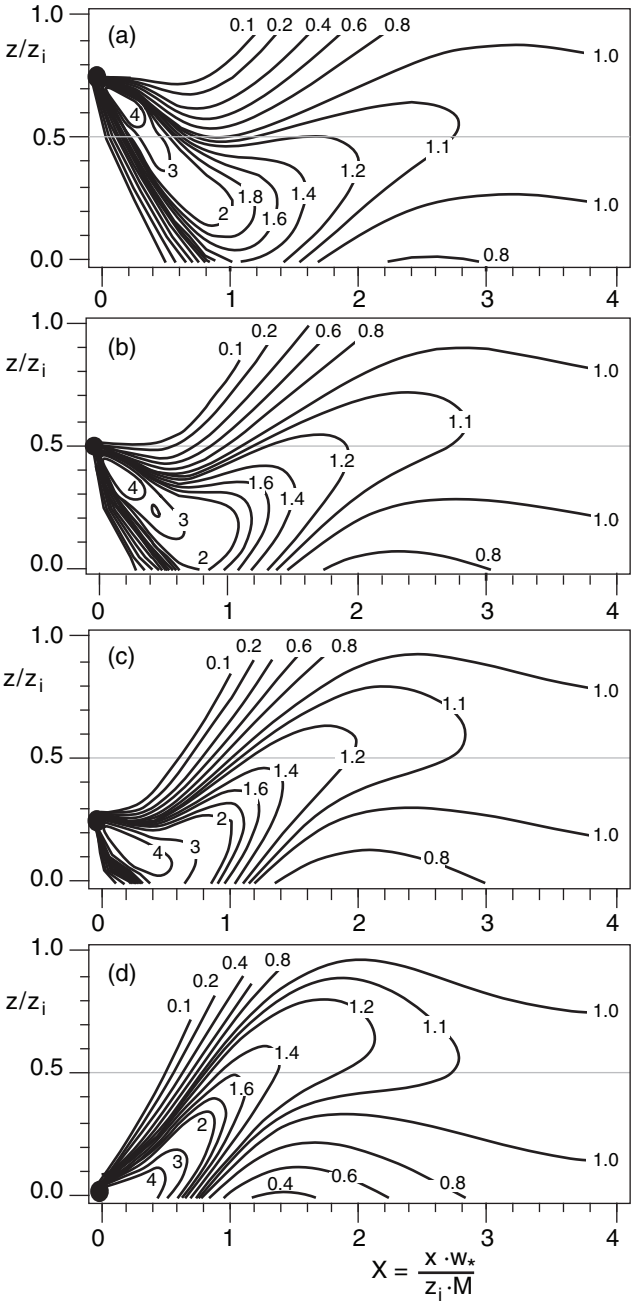

Figure 19.8 (at right)
Isopleths of dimensionless crosswind-integrated concentration $C_y = c_y \cdot z_i \cdot M / Q$ in a convective mixed layer, where c_y is crosswind integrated concentration, z_i is depth of the mixed layer, M is mean wind speed, and Q is emission rate of pollutants. Source heights are $Z_s = z_s/z_i =$ (a) 0.75, (b) 0.5, (c) 0.25, (d) 0.025, and are plotted as the large black dot at left.

Science Graffito

"The service we render to others is really the rent we pay for our room on the Earth."

– Sir Wilfred Grenfell.

Solved Example

Source emissions of 200 g/s of SO_2 occur at height 150 m. The environment is statically unstable, with a Deardorff convective velocity of 1 m/s, a mixed layer depth of 600 m, and a mean wind speed of 4 m/s.

Find the concentration at the ground 3 km downwind from the source, directly beneath the plume centerline.

Solution

Given: $Q = 200$ g/s, $z_s = 150$ m, $z_i = 600$ m, $M = 4$ m/s, $w_* = 1$ m/s

Find: c (μg/m^3) at $x = 3$ km, $y = z = 0$.

Use eq. (19.25):

$$X = \frac{(3000\text{m})\cdot(1\text{m/s})}{(600\text{m})\cdot(4\text{m/s})} = 1.25$$

Use eq. (19.29): $Z_s = (150\text{m}) / (600\text{m}) = 0.25$

From Fig. 19.8c, read $C_y \approx 0.9$ at $X = 1.25$ and $Z = 0$.

Use eq. (19.38): $\sigma_{yd} \approx 0.5 \cdot (1.25) = 0.625$

Use eq. (19.37) with $Y = 0$:

$$C = \frac{0.9}{\sqrt{2\pi}\cdot 0.625} = 0.574$$

Finally, use eq. (19.23) rearranging it first to solve for concentration in physical units:

$$c = \frac{C\cdot Q}{z_i^2\cdot M} = \frac{(0.574)\cdot(200\text{g/s})}{(600\text{m})^2\cdot(4\text{m/s})} = 79.8\ \mu\text{g/m}^3$$

Check: Units OK. Physics OK.

Discussion: We were lucky that the dimensionless source height was 0.25, which allowed us to use Fig. 19.8c. For other source heights not included in that figure, we would have to create new figures using equations (19.33) through (19.36).

ON DOING SCIENCE • Citizen Scientist

Scientists and engineers have at least the same responsibilities to society as do other citizens. Like our fellow citizens, we ultimately decide the short-term balance between environmental quality and material wealth, by the goods that we buy and by the government leaders we elect. Be informed. Take a stand. Vote.

Perhaps we have more responsibility, because we can also calculate the long-term consequences of our actions. We have the ability to evaluate various options and build the needed technology. Take action. Discover the facts. Design solutions.

In statically neutral conditions of overcast and strong winds, turbulence is more isotropic. Smoke plumes disperse at roughly equal rates in the vertical and lateral directions, and are well described by Gaussian formulae.

Various classification schemes have been designed to help determine the appropriate turbulence and dispersion characteristics. These range from the detailed examination of the production of turbulence kinetic energy, through examination of soundings plotted on thermo diagrams, to look-up tables such as those suggested by Pasquill and Gifford.

Finally, although we used the words "smoke" and "smoke stack" in this chapter, most emissions in North America and Europe are sufficiently clean that particulate matter is not visible. This clean-up has been expensive, but commendable.

Threads

Because most pollutants are emitted from near the surface, and most receptors are at the surface, the mean transport and turbulent dispersion of pollutants are primarily controlled by atmospheric boundary layer characteristics (Chapter 18). The nature of the turbulence depends on the radiatively driven (Chapter 2) heating (Chapter 3), and the dynamic forces and winds (Chapters 10 through 17). Many emissions, particularly from fuel combustion, contain water vapor (Chapter 4) as a combustion product, which can condense and form billowy white emission plumes.

Once emitted, the dispersion depends partly on the static stability (Chapter 5) of the ambient atmosphere. Cumulus clouds (Chapter 6) can withdraw pollutants out of the top of the ABL, and precipitation (Chapter 7) can scrub out some pollutants. The transport and dispersion of pollutants, and their interaction with weather (Chapters 12 and 13) and clouds, can be included as part of numerical weather forecasts (Chapter 20).

However, not all pollutants are immediately scrubbed out of the smoke plume, and can be carried by the global circulation (Chapter 11) to the whole globe, which could affect the climate (Chapter 21). As pollution concentrations increase, the visibility and color of the air is affected (Chapter 22) via the scattering and absorption of light.

EXERCISES

Numerical Problems

N1. Given the following pollutant concentrations in $\mu m/m^3$, convert to volume fraction units ppmv assuming standard sea-level conditions:

a. SO_2 1300	b. SO_2 900	c. SO_2 365
d. SO_2 300	e. SO_2 80	f. SO_2 60
g. NO_2 400	h. NO_2 280	i. NO_2 200
j. NO_2 150	k. NO_2 40	m. CO 40,000
n. CO 35,000	o. CO 20,000	p. CO 15,000
q. O_3 235	r. O_3 160	s. O_3 157
t. O_3 100	u. O_3 50	v. O_3 30

N2. Same as previous exercise, but for a summer day in Denver, Colorado, USA, where T = 25°C and P = 82 kPa.

N3. Create a table similar to Table 19-1, but where all the ppm values of volume fraction have been converted into concentration units of $\mu g/m^3$.

N4. Given wind measurements in the table below.
- a. Find the mean wind speed component in each direction
- b. Create a table showing the deviation from the mean at each time for each wind component.
- c. Find the velocity variance in each direction.
- d. Find the standard deviation of velocity for each wind direction.
- e. Determine if the turbulence is isotropic.
- f. Speculate on the cross-section shape of smoke plumes as they disperse in this atmosphere.

t (min)	U (m/s)	V (m/s)	W (m/s)
1	8	1	0
2	11	2	–1
3	12	0	1
4	7	–3	1
5	12	0	–1

N5. Determine the Pasquill-Gifford turbulence type
- a. Strong sunshine, clear skies, winds 1 m/s
- b. Thick overcast, winds 10 m/s, night
- c. Clear skies, winds 2.5 m/s, night
- d. Noon, thin overcast, winds 3 m/s.
- e. Cold air advection 2 m/s over a warm lake.
- f. Sunset, heavy overcast, calm.
- g. Sunrise, calm, clear.
- h. Strong sunshine, clear skies, winds 10 m/s.
- i. Thin overcast, nighttime, wind 2 m/s
- j. Thin overcast, nighttime, wind 5 m/s
- k. Thin overcast, 9 am, wind 3.5 m/s

N6. Given turbulence kinetic energy (TKE) buoyant generation (B) and shear generation (S) rates in this table (both in units of $m^2 \cdot s^{-3}$), answer questions (i) - (vi) below.

	B	S		B	S
a.	0.004	0.0	k.	0.0	0.004
b.	0.004	0.002	m.	0.0	0.006
c.	0.004	0.004	n.	–0.002	0.0
d.	0.004	0.006	o.	–0.002	0.002
e.	0.002	0.0	p.	–0.002	0.004
f.	0.002	0.002	q.	–0.002	0.006
g.	0.002	0.004	r.	–0.004	0.0
h.	0.002	0.006	s.	–0.004	0.002
i.	0.0	0.0	t.	–0.004	0.004
j.	0.0	0.002	u.	–0.004	0.006

(i) Specify the nature of flow/convection
(ii) Estimate the Pasquill-Gifford turbulence type.
(iii) Classify the static stability (from strongly stable to strongly unstable)
(iv) Estimate the **flux Richardson number** $R_f = -B/S$
(v) Determine the dispersion isotropy
(vi) Is turbulence intensity (*TKE*) strong or weak?

N7. Given the table below with pollutant concentrations c ($\mu g/m^3$) measured at various heights z (km), answer these 5 questions.
(i) Find the height of center of mass.
(ii) Find the vertical height variance.
(iii) Find the vertical height standard deviation.
(iv) Find the total amount of pollutant emitted.
(v) Find the nominal plume spread (depth)

z (km)	c ($\mu g/m^3$)				
Question:	a	b	c	d	e
1.5	0	0	0	0	0
1.4	0	10	0	86	0
1.3	5	25	0	220	0
1.2	25	50	0	430	0
1.1	20	75	0	350	0.04
1.0	45	85	0	195	0.06
0.9	55	90	2	50	0.14
0.8	40	93	8	5	0.18
0.7	30	89	23	0	0.13
0.6	10	73	23	0	0.07
0.5	0	56	7	0	0.01
0.4	0	30	3	0	0
0.3	0	15	0	0	0
0.2	0	5	0	0	0
0.1	0	0	0	0	0

N8.(§) For the previous problem, find the best-fit Gaussian curve through the data, and plot the data and curve on the same graph.

N9. Using the data from question N7, find the nominal plume width from edge to edge.

N10. Given lateral and vertical velocity variances of 1.0 and 0.5 m^2/s^2, respectively. Find the variance of plume spread in the lateral and vertical, at distance 3 km downwind of a source in a wind of speed 5 m/s. Use a Lagrangian time scale of:

a. 15 s	b. 30 s	c. 1 min	d. 2 min
e. 5 min	f. 10 min	g. 15 min	h. 20 min
i. 5 s	j. 45 s	m. 12 min	n. 30 min

N11.(§) For a Lagrangian time scale of 2 minutes and wind speed of 10 m/s, plot the standard deviation of vertical plume spread vs. downwind distance for a vertical velocity variance (m^2/s^2) of:

a. 0.1	b. 0.2	c. 0.3	d. 0.4	e. 0.5
f. 0.6	g. 0.8	h. 1.0	i. 1.5	j. 2
k. 2.5	m. 3	n. 4	o. 5	p. 8

N12.(§) For the previous problem, plot σ_z if
(i) only the near-source equation
(ii) only the far source equation
is used over the whole range of distances.

N13. Given the following emission parameters:

	W_o (m/s)	R_o (m)	$\Delta\theta$ (K)
a.	5	3	200
b.	30	1	50
c.	20	2	100
d.	2	2	50
e.	5	1	50
f.	30	2	100
g.	20	3	50
h.	2	4	20

Find the momentum and buoyant length scales for the plume-rise equations. Assume $|g|/\theta_a \approx 0.0333$ $m{\cdot}s^{-2}{\cdot}K^{-1}$, and $M = 5$ m/s for all cases.

N14.(§) For the previous problem, plot the plume centerline height vs. distance if the physical stack height is 100 m and the atmosphere is statically neutral.

N15. For buoyant length scale of 5 m, physical stack height 10 m, environmental temperature 10°C, and wind speed 2 m/s, find the equilibrium plume centerline height in a statically stable boundary layer, given ambient potential temperature gradients of $\Delta\theta/\Delta z$ (K/km):

a. 1	b. 2	c. 3	d. 4	e. 5	f. 6	g. 7
h. 8	i. 9	j. 10	k. 12	m. 15	n. 18	o. 20

N16. Given $\sigma_y = \sigma_z = 300$ m, $z_{CL} = 500$ m, $z = 200$ m, $Q = 100$ g/s, $M = 10$ m/s. For a neutral boundary layer, find the concentration at y (km) =

a. 0	b. 0.1	c. 0.2	d. 0.3	e. 0.4	f. 0.5	g. 0.7
h. 1	i. 1.5	j. 2	k. 3	m. 4	n. 5	o. 6

N17(§). Plot the concentration footprint at the surface downwind of a stack, given: $\sigma_v = 1$ m/s, $\sigma_w = 0.5$ m/s, $M = 2$ m/s, Lagrangian time scale = 1 minute, $Q = 400$ g/s of SO_2, in a stable boundary layer. Use a plume equilibrium centerline height (m) of:

a. 10	b. 20	c. 30	d. 40	e. 50	f. 60	g. 70
h. 15	i. 25	j. 35	k. 45	m. 55	n. 65	o. 75

N18. Calculate the dimensionless downwind distance, given a convective mixed layer depth of 2 km, wind speed 3 m/s, and surface kinematic heat flux of 0.15 K·m/s. Assume $|g|/T_v \approx 0.0333$ $m{\cdot}s^{-2}{\cdot}K^{-1}$. The actual distance x (km) is:

a. 0.2	b. 0.5	c. 1	d. 2	e. 3	f. 4
g. 5	h. 7	i. 10	j. 20	k. 30	m. 50

N19. If $w_* = 1$ m/s, mixed layer depth is 1 km, wind speed is 5 m/s, $Q = 100$ g/s, find the
a. dimensionless downwind distance at $x = 2$ km
b. dimensionless concentration if $c = 100$ μg/m^3
c. dimensionless crosswind integrated concentration if $c_y = 1$ mg/m^2

N20.(§) For a convective mixed layer, plot dimensionless plume centerline height with dimensionless downwind distance, for dimensionless source heights of:

a. 0	b. 0.01	c. 0.02	d. 0.03	e. 0.04
f. 0.05	g. 0.06	h. 0.07	i. 0.08	j. 0.09
k. 0.1	m. 0.12	n. 0.15	o. 0.2	p. 0.22

N21.(§) For the previous problem, plot isopleths of dimensionless crosswind integrated concentration, similar to Fig. 19.8, for convective mixed layers.

N22. Source emissions of 300 g/s of SO_2 occur at height 200 m. The environment is statically unstable, with a Deardorff convective velocity of 1 m/s, and a mean wind speed of 5 m/s.

Find the concentration at the ground at distances 1, 2, 3, and 4 km downwind from the source, directly beneath the plume centerline. Assume the mixed layer depth (km) is:

a. 0.5	b. 0.75	c. 1.0	d. 1.25	e. 1.5	f. 1.75
g. 2.0	h. 2.5	i. 3.0	j. 3.5	k. 4.0	m. 5.0

(Hint: Interpolate between figures if needed, or derive your own figures.)

Understanding & Critical Evaluation

U1. Compare the two equations for variance: (19.5) and (19.9). Why is the one weighted by pollution concentration, and the other not?

U2. To help understand complicated figures such as Fig. 19.3, it helps to separate out the various parts. Using the info from that figure, produce a separate sketch of the following on a background grid of B and S values:

a. TKE (arbitrary relative intensity)
b. R_f c. Flow type d. Static stability
e. Pasquill-Gifford turbulence type
f. Dispersion isotropy (plume cross section)
g. Suggest why these different variables are related to each other.

U3. Fig. 19.3 shows how dispersion isotropy can change as the relative magnitudes of the shear and buoyancy TKE production terms change. Also, the total amount of spread increases as the TKE intensity increases. Discuss how the shape and spread of smoke plumes vary in different parts of that figure, and sketch what the result would look like to a viewer on the ground.

U4. Eq. (19.8) gives the center of mass (i.e., plume centerline height) in the vertical direction. Create a similar equation for plume center of mass in the horizontal, using a cylindrical coordinate system centered on the emission point.

U5. In eq. (19.10) use Q_1 = 100 g/m and $\bar{z} = 0$. Plot on graph paper the Gaussian curve using σ_z (m) =
a. 100 b. 200 c. 300 d. 400
Compare the areas under each curve, and discuss the significance of the result.

U6. Why does a "nominal" plume edge need to be defined? Why cannot the Gaussian distribution be used, with the definition that plume edge happens where the concentration becomes zero. Discuss, and support your arguments with results from the Gaussian distribution equation.

U7. The Lagrangian time scale is different for different size eddies. In nature, there is a superposition of turbulent eddies acting simultaneously. Describe the dispersion of a smoke plume under the influence of such a spectrum of turbulent eddies.

U8. While Taylor's statistical theory equations give plume spread as a function of downwind distance, x, these equations are also complex functions of the Lagrangian time scale t_L. For a fixed value of downwind distance, plot curves of the variation of plume spread (eq. 19.13) as a function of t_L. Discuss the meaning of the result.

U9. a. Derive eqs. (19.14) and (19.15) for near-source and far-source dispersion from Taylor's statistical theory equations (19.13).

b. Why do the near and far source dispersion equations appear as straight lines in a log-log graph (see the solved example near eq. (19.15)?

U10. Plot the following sounding on the boundary-layer $\theta - z$ thermo diagram from the Stability chapter. Determine the static stability vs. height. Determine boundary-layer structure, including location and thickness of components of the boundary layer (surface layer, stable BL or convective mixed layer, capping inversion or entrainment zone, free atmosphere). Speculate whether it is daytime or nighttime, and whether it is winter or summer. For daytime situations, calculate the mixed-layer depth. This depth controls pollution concentration (shallow depths are associated with periods of high pollutant concentration called **air-pollution episodes**, and during calm winds to **air stagnation events**). [Hint: Review how to nonlocally determine the static stability, as given in the ABL and Stability chapters.]

z (m)	a. T (°C)	b. T (°C)	c. T (°C)	d. T (°C)
2500	–11	8	–5	5
2000	–10	10	–5	0
1700	–8	8	–5	3
1500	–10	10	0	5
1000	–5	15	0	10
500	0	18	5	15
100	4	18	9	20
0	7	15	10	25

U11. For the ambient sounding of the previous exercise, assume that a smoke stack of height 100 m emits effluent of temperature 6°C with water-vapor mixing ratio 3 g/kg. (Hint, assume the smoke is an air parcel, and use a thermo diagram.)

(i). How high would the plume rise, assuming no dilution with the environment?
(ii). Would steam condense in the plume?

U12. For plume rise in statically neutral conditions, write a simplified version of the plume-rise equation (19.16) for the special case of:

a. momentum only b. buoyancy only

Also, what are the limitations and range of applicability of the full equation and the simplified equations?

U13. For plume rise in statically stable conditions, the amount of rise depends on the Brunt-Väisälä fre-

quency. As the static stability becomes weaker, the Brunt-Väisälä frequency changes, and so changes the plume centerline height. In the limit of extremely weak static stability, compare this plume rise equation with the plume rise equation for statically neutral conditions. Also, discuss the limitations of each of the equations.

U14. In eq. (19.20), the "reflected" part of the Gaussian concentration equation was created by pretending that there is an imaginary source of emissions an equal distance underground as the true source is above ground. Otherwise, the real and imaginary sources are at the same horizontal location and have the same emission rate.

In eq. (19.20), identify which term is the "reflection" term, and show why it works as if there were emissions from below ground.

U15. In the solved example in the Gaussian Concentration Distribution subsection, the concentration footprints at ground level have a maximum value neither right at the stack, nor do concentrations monotonically increase with increasing distances from the stack. Why? Also, why are the two figures in that solved example so different?

U16. Show that eq. (19.20) reduces to eq. (19.21) for receptors at the ground.

U17. For Gaussian concentration eq. (19.21), how does concentration vary with:

a. σ_y b. σ_z c. M

U18. Give a physical interpretation of crosswind integrated concentration, using a different approach than was used in Fig. 19.6.

U19. For plume rise and pollution concentration in a statically unstable boundary layer, what is the reason for, or advantage of, using dimensionless variables?

U20. If the Deardorff velocity increases, how does the dispersion of pollutants in an unstable boundary layer change?

U21. In Fig. 19.8, at large distances downwind from the source, all of the figures show the dimensionless concentration approaching a value of 1.0. Why does it approach that value, and what is the significance or justification for such behavior?

Web-Enhanced Questions

W1. Search the web for the government agency of your country that regulates air pollution. In the USA, it is the Environmental Protection Agency (EPA). Find the current air pollution standards for the chemicals listed in Table 19-1.

W2. Search the web for an air quality report for your local region (such as town, city, state, or province). Determine how air quality has changed during the past decade or two.

W3. Search the web for a site that gives current air pollution readings for your region. In some cities, this pollution reading is updated every several minutes, or every hour. If that is the case, see how the pollution reading varies hour by hour during a typical workday.

W4. Search the web for information on health effects of different exposures to different pollutants.

W5. Air-pollution models are computer codes that use equations similar to the ones in this chapter, to predict air-pollution concentration. Search the web for a list of names of a few of the popular air-pollution models endorsed by your country or region.

W6. Search the web for inventories of emission rates for pollutants in your regions. What are the biggest polluters?

W7. Search the web for an explanation of **emissions trading**. Discuss why such a policy is or is not good for industry, government, and people.

W8. Search the web for information on **acid rain**. What is it? How does it form? What does it do?

W9. Search the web for information on **forest death** (**waldsterben**) caused by pollution or acid rain.

W10. Search the web for instruments that can measure concentration of the chemicals listed in Table 19-1.

W11. Search the web for "web-cam" cameras that show a view of a major city, and discuss how the visibility during fair weather changes during the daily cycle on a workday.

W12. Search the web for information of plume rise and/or concentration predictions for complex (mountainous) terrain.

W13. Search the web for information to help you discuss the relationship between "good" ozone in the stratosphere and mesosphere, vs. "bad" ozone in the boundary layer.

W14. For some of the major industry in your area, search the web for information on control technologies that can, or have, helped to reduce pollution emissions.

W15. Search the web for satellite photos of emissions from major sources, such as a large industrial complex, smelter, volcano, or a power plant. Use the highest-resolution photographs to look at lateral plume dispersion, and compare with the dispersion equations in this chapter.

W16. Search the web for information on forward or backward trajectories, as used in air pollution. One example is the Chernobyl nuclear accident, where radioactivity measurements in Scandinavia were used with a back trajectory to suggest that the source of the radioactivity was in the former Soviet Union.

W17. Search the web for information on chemical reactions of air pollutants in the atmosphere.

W18. Search the web for satellite photos and other information on an **urban plume** (the pollutant plume downwind of a whole city).

W19. To simplify the presentation of air-quality data to the general public, many governments have created an **air-quality index** that summarizes with a simple number how clean or dirty the air is. For your national government (or for the USA if your own government doesn't have one), search the web for info about the air-quality index. How is it defined in terms of concentrations of different pollutants? How do you interpret the index value in terms of visibility and/or health hazards?

Synthesis Questions

S1. Suppose that there was not a diurnal cycle, but that the atmospheric temperature profile was steady, and equal to the standard atmosphere. How would local and global dispersion of pollutants from tall smoke stacks be different, if at all?

S2. In the present atmosphere, larger-size turbulent eddies often have more energy than smaller size one. What if the energy distribution were reversed, with the vigor of mixing increasing as eddy sizes decrease. How would that change local dispersion, if at all?

S3. What if tracers were not passive, but had a special magnetic attraction only to each other. Describe how dispersion would change, if at all.

S4. What if a plume that is rising in a statically neutral environment has buoyancy from both the initial temperature of the effluent out of the top of the stack, and also from additional heat gained while it was dispersing.

A real example was the black smoke plumes from the oil well fires during the Gulf War. Sunlight was strongly absorbed by the black soot and unburned petroleum in the smoke, causing solar warming of the black smoke plume.

Describe any resulting changes to plume rise.

S5. Suppose that smoke stacks produced smoke rings, instead of smoke plumes. How would dispersion be different, if at all?

S6. When pollutants are removed from exhaust gas before the gas is emitted from the top of a smoke stack, those pollutants don't magically disappear. Instead, they are converted into water pollution (to be dumped into a stream or ocean), or solid waste (to be buried in a dump or landfill). Which is better? Why?

S7. Propose methods whereby life on Earth could produce zero pollution. Defend your proposals.

S8. What if the same emission rate of pollutions occurs on a fair-weather day with light winds, and an overcast rainy day with stronger winds. Compare the dispersion and pollution concentrations at the surface for those situations. Which leads to the least concentration at the surface, locally? Which is better globally?

S9. Suppose that all atmospheric turbulence was extremely anisotropic, such that there was zero dispersion in the vertical , but normal dispersion in the horizontal.

a. How would that affect pollution concentrations at the surface, for emissions from tall smoke stacks?

b. How would it affect climate, if at all?

S10. What if ambient wind speed was exactly zero. Discuss the behavior of emission plumes, and how the resulting plume rise and concentration equations would need to be modified.

S11. What if pollutants that were emitted into the atmosphere were never lost or removed from the

atmosphere. Discuss how the weather and climate would be different, if at all?

S12. If there were no pollutants in the atmosphere (and hence no cloud and ice nuclei), discuss how the weather and climate would be different, if at all.

S13. Divide the current global pollutant emissions by the global population, to get the net emissions per person. Given the present rate of population increase, discuss how pollution emissions will change over the next century, and how it will affect the quality of life on Earth, if at all.

Copyright © 2011, 2015 by Roland Stull. *Meteorology for Scientists and Engineers, 3rd Ed.*

NUMERICAL WEATHER PREDICTION (NWP)

CONTENTS

Scientific Basis of Forecasting 746
- The Equations of Motion 746
- Approximate Solutions 749
- Dynamics, Physics and Numerics 749
- Models 751

Grid Points 752
- Nested and Variable Grids 752
- Staggered Grids 753

Finite-Difference Equations 754
- Notation 754
- Approximations to Spatial Gradients 754
- Grid Computation Rules 756
- Time Differencing 757
- Discretized Equations of Motion 758

Numerical Errors & Instability 759
- Round-off Error 759
- Truncation Error 760
- Numerical Instability 760

The Numerical Forecast Process 762
- Balanced Mass and Flow Fields 763
- Data Assimilation and Analysis 765
- Forecast 768
- Case Study: 22-25 Feb 1994 768
- Post-processing 770

Nonlinear Dynamics And Chaos 773
- Predictability 773
- Lorenz Strange Attractor 773
- Ensemble Forecasts 776
- Probabilistic Forecasts 777

Forecast Quality & Verification 777
- Continuous Variables 777
- Binary / Categorical Events 780
- Probabilistic Forecasts 782
- Cost / Loss Decision Models 784

Summary 786
- Threads 786

Exercises 787
- Numerical Problems 787
- Understanding & Critical Evaluation 789
- Web-Enhanced Questions 790
- Synthesis Questions 791

"Meteorology for Scientists and Engineers, 3rd Edition" by Roland Stull is licensed under a Creative Commons Attribution-NonCommercial-ShareAlike 4.0 International License. To view a copy of the license, visit http://creativecommons.org/licenses/by-nc-sa/4.0/ . This work is available at http://www.eos.ubc.ca/books/Practical_Meteorology/ .

20 Most weather forecasts are made by computer, and some of these forecasts are further enhanced by humans. Computers can keep track of myriad complex nonlinear interactions among winds, temperature, and moisture at thousands of locations and altitudes around the world — an impossible task for humans. Also, data observation, collection, analysis, display and dissemination are mostly automated.

Fig. 20.1 shows an automated forecast for the case-study cyclone from the Extratropical Cyclone chapter. Produced by computer, this **meteogram** (graph of weather vs. time) is easier for non-meteorologists to interpret than weather maps. But to produce such forecasts, the equations describing the atmosphere must first be solved.

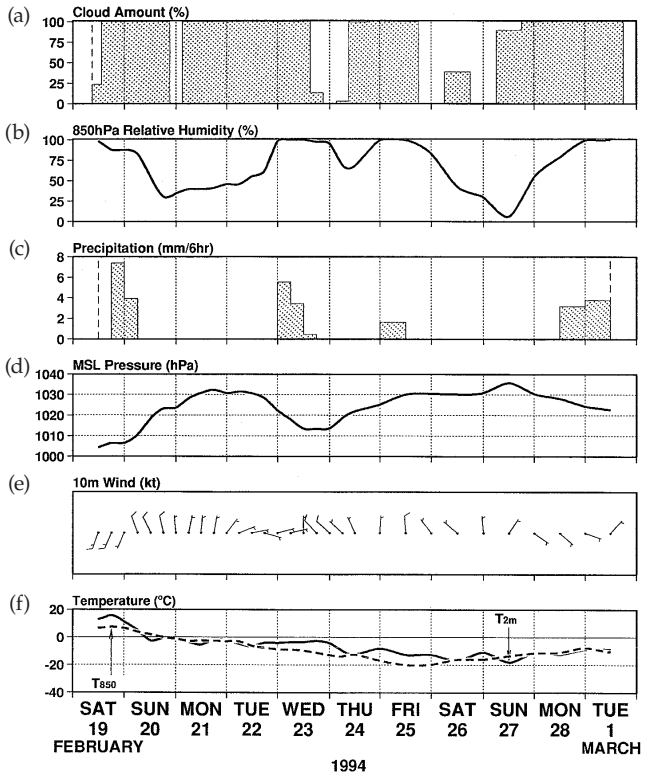

Figure 20.1
Ten-day weather forecast for Des Moines, Iowa, plotted as a meteogram (time series), based on initial conditions observed at 12 UTC on 19 Feb 94. (a) Cloud amount (%), (b) relative humidity (%) at 85 kPa, (c) precipitation (mm/6 hours), (d) mean sea-level (MSL) pressure (10^{-1} kPa), (e) wind at 10 m (full barb = 10 kt ≈ 5 m/s), (f) temperature (°C) at 2 m (solid) and 85 kPa (dashed). Produced by ECMWF.

FOCUS • Alternative Vertical Coordinate

Eqs. (20.1-20.7) use z as a vertical coordinate, where z is height above mean sea level. But local terrain elevations can be higher than sea level. The atmosphere does not exist underground; thus, it makes no sense to solve the meteorological equations of motion at heights below ground level.

To avoid this problem, define a **terrain-following coordinate** σ (**sigma**). One definition for σ is based on the hydrostatic pressure $P_{ref}(z)$ at any height z relative to the hydrostatic pressure difference between the earth's surface ($P_{ref\ bottom}$) and a fixed pressure ($P_{ref\ top}$) representing the top of the atmosphere:

$$\sigma = \frac{P_{ref}(z) - P_{ref\ top}}{P_{ref\ bottom} - P_{ref\ top}}$$

$P_{ref\ bottom}$ varies in the horizontal due to terrain elevation (see Fig. 20.A) and varies in space and time due to changing surface weather patterns (high- and low-pressure centers). The new vertical coordinate σ varies from 1 at the earth's surface to 0 at the top of the domain.

The figure below shows how this **sigma coordinate** varies over a mountain. **Hybrid coordinates** (Fig. 20.5) are ones that are terrain following near the ground, but constant pressure aloft.

If σ is used as a vertical coordinate, then (U, V) are defined as winds along a σ surface. The vertical advection term in eq. (20.1) changes from $W{\cdot}\Delta U/\Delta z$ to $\dot{\sigma}{\cdot}\Delta U / \Delta\sigma$, where sigma dot is analogous to a vertical velocity, but in sigma coordinates. Similar changes must be made to most of the terms in the equations of motion, which can be numerically solved within the domain of $0 \le \sigma \le 1$.

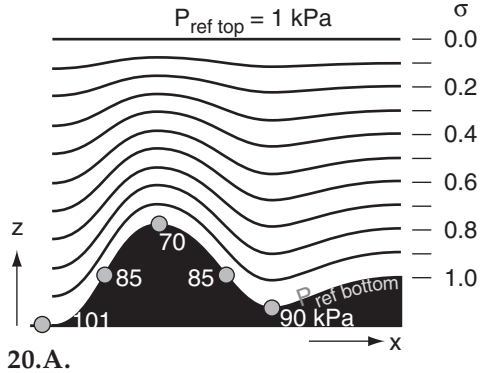

Figure 20.A.
Vertical cross section through the atmosphere (white) and earth (black). White numbers represent surface air pressure at the weather stations shown by the grey dots. For the equation above, $P_{ref\ bottom}$ = 70 kPa at the mountain top, which differs from $P_{ref\ bottom}$ = 90 kPa in the valley.

Although sigma coordinates avoid the problem of coordinates that go underground, they create problems for advection calculations due to small differences between large terms. To reduce this problem, stair-step terrain-following coordinates have been devised — known as **eta coordinates** (η).

SCIENTIFIC BASIS OF FORECASTING

The Equations of Motion

Numerical weather forecasts are made by solving Eulerian equations for U, V, W, T, r_T, ρ and P.

From the Dynamics chapter are forecast equations for the three wind components (U, V, W) (modified from eqs. 10.23a & b, and eq. 10.59):

$$\frac{\Delta U}{\Delta t} = -U\frac{\Delta U}{\Delta x} - V\frac{\Delta U}{\Delta y} - W\frac{\Delta U}{\Delta z} - \frac{1}{\rho}\cdot\frac{\Delta P}{\Delta x} + f_c \cdot V - \frac{\Delta F_{z\ turb}(U)}{\Delta z} \tag{20.1}$$

$$\frac{\Delta V}{\Delta t} = -U\frac{\Delta V}{\Delta x} - V\frac{\Delta V}{\Delta y} - W\frac{\Delta V}{\Delta z} - \frac{1}{\rho}\cdot\frac{\Delta P}{\Delta y} - f_c \cdot U - \frac{\Delta F_{z\ turb}(V)}{\Delta z} \tag{20.2}$$

$$\frac{\Delta W}{\Delta t} = -U\frac{\Delta W}{\Delta x} - V\frac{\Delta W}{\Delta y} - W\frac{\Delta W}{\Delta z} - \frac{1}{\bar{\rho}}\frac{\Delta P'}{\Delta z} + \frac{\theta_{vp} - \theta_{ve}}{\bar{T}_{ve}}\cdot|g| - \frac{\Delta F_{z\ turb}(W)}{\Delta z} \tag{20.3}$$

From the Heat chapter is a forecast equation for temperature T (modified from eq. 3.51):

$$\frac{\Delta T}{\Delta t} = -U\frac{\Delta T}{\Delta x} - V\frac{\Delta T}{\Delta y} - W\left[\frac{\Delta T}{\Delta z} + \Gamma_d\right] - \frac{1}{\rho\cdot C_p}\frac{\Delta \mathbb{F}^*_{z\ rad}}{\Delta z} + \frac{L_v}{C_p}\frac{\Delta r_{condensing}}{\Delta t} - \frac{\Delta F_{z\ turb}(\theta)}{\Delta z} \tag{20.4}$$

From the Moisture chapter is a forecast equation (4.44) for total-water mixing ratio r_T in the air:

$$\frac{\Delta r_T}{\Delta t} = -U\frac{\Delta r_T}{\Delta x} - V\frac{\Delta r_T}{\Delta y} - W\frac{\Delta r_T}{\Delta y} + \frac{\rho_L}{\rho_d}\frac{\Delta Pr}{\Delta z} - \frac{\Delta F_{z\ turb}(r_T)}{\Delta z} \tag{20.5}$$

From the Dynamics chapter is the continuity equation (10.60) to forecast air density ρ:

$$\frac{\Delta\rho}{\Delta t} = -U\frac{\Delta\rho}{\Delta x} - V\frac{\Delta\rho}{\Delta y} - W\frac{\Delta\rho}{\Delta z} - \rho\left[\frac{\Delta U}{\Delta x} + \frac{\Delta V}{\Delta y} + \frac{\Delta W}{\Delta z}\right] \tag{20.6}$$

For pressure P, use the equation of state (ideal gas law) from Chapter 1 (eq. 1.23):

$$P = \rho\cdot\Re_d\cdot T_v \tag{20.7}$$

In these seven equations: f_c is Coriolis parameter, P' is the deviation of pressure from its hydrostatic value, θ_{vp} and θ_{ve} are virtual potential temperatures of the air parcel and the surrounding environment, T_{ve} is virtual temperature of the environment, $|g|$ = 9.8 m/s^2 is the magnitude of gravitational acceleration, Γ_d = 9.8 K/km is the dry adiabatic lapse rate, $\mathbb{F}^*_{z\ rad}$ is net radiative flux, $L_v \approx 2.5\text{x}10^6$ J/kg is the latent heat of vaporization, $C_p \approx 1004$ J·kg^{-1}·K^{-1} is the specific heat of air at constant pressure, $\Delta r_{condensing}$ is the increase in liquid-water mixing ratio associated with water vapor that is condensing, $\rho_L \approx 1000$ kg·m^{-3} and ρ_d are the densities of liquid water and dry air, Pr is precipitation rate (m/s) of water accumulation in a rain gauge at any height z, $\Re_d$ = 287 J·kg^{-1}·K^{-1} is the gas constant for dry air, and T_v is the virtual temperature. For more details, see the chapters cited with those equations.

Notice the similarities in eqs. (20.1 - 20.6). All have a **tendency term** (rate of change with time) on the left. All have **advection** as the first 3 terms on the right. Eqs. (20.1 - 20.5) include a **turbulence flux divergence** term on the right. The other terms describe the special forcings that apply to individual variables. Sometimes the hydrostatic equation (Chapter 1, eq. 1.25b) is also included in the set of forecast equations:

$$\frac{\Delta P_{ref}}{\Delta z} = -\rho \cdot |g| \qquad (20.8)$$

to serve as a reference state for the definition of $P' = P - P_{ref}$, as used in eq. (20.3).

Equations (20.1) - (20.7) are the **equations of motion**. They are also known as the **primitive equations**, because they forecast fundamental (primitive) variables rather than derived variables such as vorticity. The first six equations are **budget equations**, because they forecast how variables change in response to inputs and outputs. Namely, the first three equations describe **momentum conservation** per unit mass of air. Eqs. (20.4 - 20.5) describe **heat conservation** and **moisture conservation** per unit mass of air. Eq. (20.6) describes **mass conservation**.

The first six equations are **prognostic** (i.e., forecast the change with time), and the seventh (the ideal gas law) is **diagnostic** (not a function of time). The third equation includes **non-hydrostatic** processes, the fourth equation includes **diabatic** processes (non-adiabatic heating), and the sixth equation includes **compressible** processes.

These equations of motion are **nonlinear**, because many of the terms in these equations consist of products of two or more dependent variables. Also, they are **coupled** equations, because each equation contains variables that are forecast or diagnosed

FOCUS • Alternative Horizontal Coord.

Spherical Coordinates

For the Cartesian coordinates used in eqs. (20.1-20.8), the coordinate axes are straight lines. However, on Earth we prefer to define x to follow the Earth's curvature toward the East, and define y to follow the Earth's curvature toward the North. If U and V are defined as velocities along these spherical coordinates, then add the following terms to the right side of the horizontal momentum equations (20.1-20.3):

$$+\frac{U \cdot V \cdot \tan(\phi)}{R_o} - \frac{U \cdot W}{R_o} - \left[2 \cdot \Omega \cdot W \cdot \cos(\phi)\right] \qquad (20.1b)$$

$$-\frac{U^2 \cdot \tan(\phi)}{R_o} - \frac{V \cdot W}{R_o} \qquad (20.2b)$$

$$+\frac{U^2 + V^2}{R_o} + \left[2 \cdot \Omega \cdot U \cdot \cos(\phi)\right] \qquad (20.3b)$$

where $R_o \approx 6371$ km is the average Earth radius, ϕ is latitude, and $\Omega = 0.7292\text{x}10^{-4}$ s^{-1} is Earth's rotation rate. The terms containing R_o are called the **curvature terms**. The terms in square brackets are small components of Coriolis force (recall the Focus Box "Coriolis Force in 3-D" from the Dynamics chapter).

Map Factors

Suppose we pick (x, y) to represent horizontal coordinates on a map projection, such as shown in the Focus Box on the next page. Let (U, V) be the horizontal components of winds in these (x, y) directions. [Vertical velocity W applies unchanged in the z (up) direction.] One reason why meteorologists use such map projections is to avoid singularities, such as near the Earth's poles where meridians converge.

The equations of motion can be rewritten for any map projection. For example, eq. (20.1) can be written for a **polar stereographic projection** as:

$$\frac{\Delta U}{\Delta t} = -m_o \cdot U \frac{\Delta U}{\Delta x} - m_o \cdot V \frac{\Delta U}{\Delta y} - W \frac{\Delta U}{\Delta z} - m_x \cdot V^2 + m_y \cdot U \cdot V - \frac{U \cdot W}{R_o} + [Cor] - \frac{m_o}{\rho} \cdot \frac{\Delta P}{\Delta x} + f_c \cdot V - \frac{\Delta F_{z\,turb}(U)}{\Delta z} \qquad (20.1c)$$

where $[Cor]$ is a 3-D Coriolis term, and the **map factors** (m) are:

$$m_o = \frac{1 + \sin(\phi_o)}{1 + \sin(\phi)} = \frac{L^2 + x^2 + y^2}{2 \cdot R_o \cdot L}$$

and

$$m_x = x / (R_o \cdot L) \quad , \quad m_y = y / (R_o \cdot L) \ ,$$

where $L = R_o \cdot [1 + \sin(\phi_o)]$, $R_o \approx 6371$ km is the average Earth radius, ϕ is latitude, and ϕ_o is the reference latitude for the map projection (see Focus Box).

Thus, the equation has extra terms, and many of the terms are scaled by a map factor. Eqs. (20.2 - 20.6) have similar changes when cast on a map projection.

Solved Example (§)

Plot the given coordinates: (a) on a lat-lon grid, and (b) on a polar stereographic grid with $\phi_o = 60°$.

Solution

Given: Latitudes (ϕ) & longitudes (λ) of N. America				
Each column holds [ϕ(°) λ(°)]. λ is positive eastward				
50 -125	9 -76	38 -77	55 -82	0 0
40 -125	11 -84	46 -65	58 -95	0 180
23 -110	15 -84	43 -66	68 -82	
24 -110	15 -88	46 -60	70 -140	0 -45
30 -115	22 -87	45 -65	73 -157	0 135
32 -114	22 -90	50 -65	65 -168	
22 -106	18 -91	50 -60	58 -158	0 45
20 -106	18 -96	53 -56	53 -170	0 -135
7 -80	22 -98	48 -59	60 -146	
9 -78	27 -97	47 -52	60 -140	0 0
4 -76	30 -85	53 -56	50 -125	0 10
0 -80	28 -83	60 -65		0 20
	25 -81	58 -68		0 30
0 -48	26 -80	64 -78	0 -90	0 etc.
10 -63	30 -82	52 -79	0 90	0 350
12 -73	35 -76	53 -83		0 360

Hint: In Excel, copy these numbers into 2 long columns: the first for latitudes and the second for longitudes. Leave blank rows in Excel corresponding to the blank lines in the table, to create discontinuous plotted lines.

(a) Lat-Lon Grid: To save space, only the portion of the grid near North America is plotted.

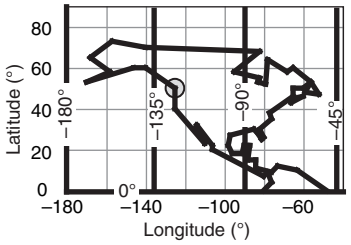

Fig. 20.B1.

(b) Polar Stereographic Grid:

Hint: In Excel, don't forget to convert from (°) to (radians).

To demonstrate the Excel calculation for the first coordinate (near Vancouver): $\phi = 50°$, $\lambda = -125°$:

L = (6371 km)·[1 + sin(60°·π/180°)] = 11,888 km.

r = (11888 km)·tan[0.5·(90°– 50°)·π/180°] = 4327 km

x = (4327 km)·cos(–125°·π/180°) = **– 2482 km**

y = (4327 km)·sin(–125°·π/180°) = **– 3545 km**

That point is circled on the maps above and below:

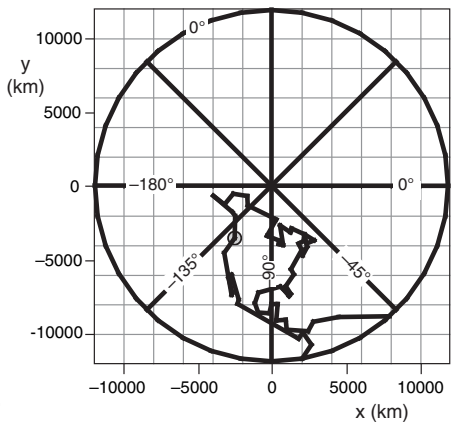

Fig. 20.B2

FOCUS • Map Projections

A map displays the 3-D Earth's surface on a 2-D plane. On maps you can also: (1) create perpendicular (x, y) coordinates; and (2) rewrite the equations of motion within these map coordinates. You can then solve these eqs. to make numerical weather forecasts.

Create a map by projecting the spherical Earth on to a plane (**stereographic** projection), a cylinder (**Mercator** projection), or a cone (**Lambert** projection), where the cylinder and cone can be "unrolled" after the projection to give a flat map. Although other map projections are possible, the 3 listed above are **conformal**, meaning that the angle between two intersecting curves on the Earth is equal to the angle between the same curves on the map.

For stereographic projections, if the projector is at the North or South Pole, then the result is a **polar stereographic** projection (Fig. 20.C). For any latitude (ϕ) longitude (λ, positive eastward) coordinates on Earth, the corresponding (x, y) map coordinates are:

$$x = r \cdot \cos(\lambda) \quad , \quad y = r \cdot \sin(\lambda) \qquad \text{(F20.1)}$$

$$r = L \cdot \tan[0.5 \cdot (90° - \phi)] \ , \ L = R_o \cdot [1 + \sin(\phi_o)] \qquad \text{(F20.2)}$$

R_o = 6371 km = Earth's radius, and ϕ_o is the latitude intersected by the projection plane. The Fig. below has $\phi_o = 60°$, but often $\phi_o = 90°$ is used instead.

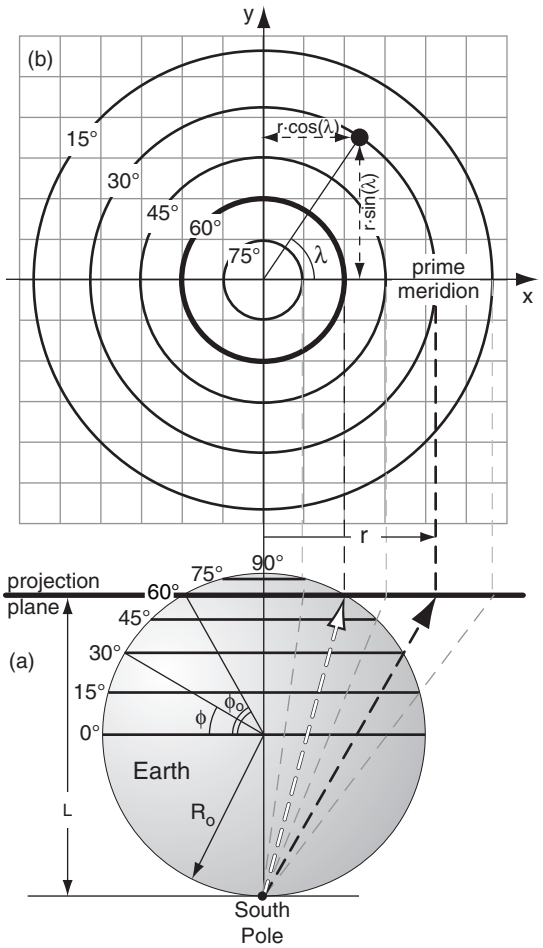

Fig. 20.C. *Polar stereographic map projection.*

from one or more of the other equations. Hence, all 7 equations must be solved together.

Unfortunately, no one has yet succeeded in solving the full governing equations analytically. An **analytical solution** is itself an algebraic equation or number that can be applied at every location in the atmosphere. For example, the equation $y^2 + 2xy = 8x^2$ has an analytical solution $y = 2x$, which allows you to find y at any location x.

Approximate Solutions

To get around this difficulty of no analytical solution, three alternatives are used. One is to find an exact analytical solution to a simplified (approximate) version of the governing equations. A second is to conceive a simplified physical model, for which exact equations can be solved. The third is to find an approximate **numerical solution** to the full governing equations (the focus of this chapter).

(1) An atmospheric example of the first method is the geostrophic wind, which is an exact solution to a highly simplified equation of motion. This is the case of steady-state (equilibrium) winds above the boundary layer where friction can be neglected, and for regions where the isobars are nearly straight.

(2) Early **numerical weather prediction** (**NWP**) efforts used the 2nd method, because of the limited power of early computers. Rossby derived simplified equations by modeling the atmosphere as if it were one layer of water surrounding the Earth. Charney, von Neumann, and others extended this work and wrote a program for a one-layer **barotropic** atmosphere (Fig. 20.2a) for the ENIAC computer in 1950. These earliest programs forecasted only vorticity and geopotential height at 50 kPa.

(3) Modern NWP uses the third method. Here, the full primitive equations are solved using finite-difference approximations for full **baroclinic** scenarios (Fig. 20.2b), but only at discrete locations called **grid points**. Usually these grid points are at regularly-spaced intervals on a map, rather than at each city or town.

Dynamics, Physics and Numerics

If computers had infinite power, then we could: forecast the movement of every air molecule, forecast the growth of each snowflake and cloud droplet, precisely describe each turbulent eddy, consider atmospheric interaction with each tree leaf and blade of grass, diagnose the absorption of radiation for an infinite number of infinitesimally fine spectral bands, account for every change in terrain elevation, and could even include the movement and activities of each human as they affect the atmosphere. But it might be a few years before we can do that. At pres-

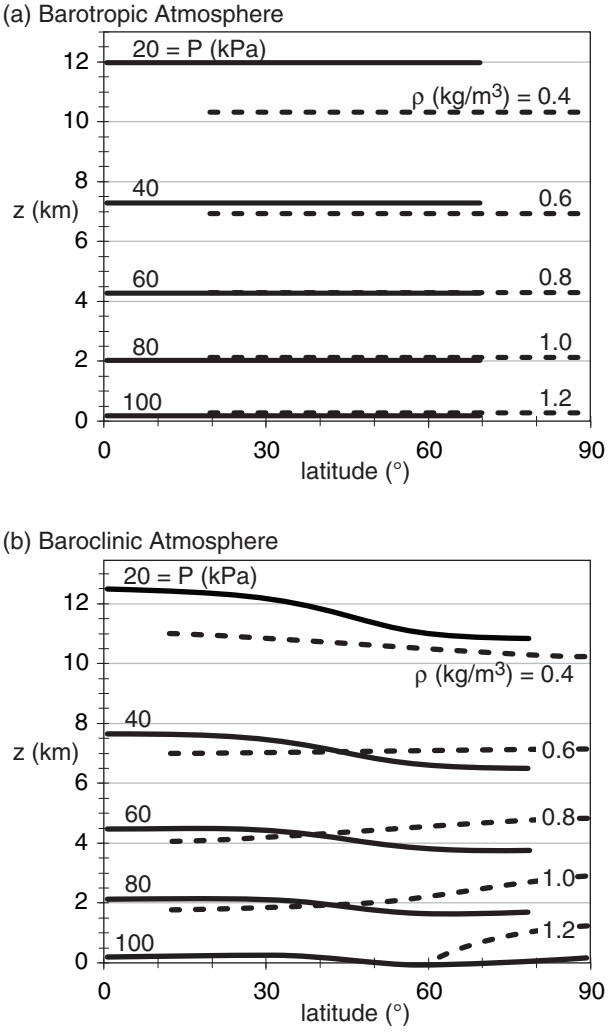

Figure 20.2
(a) Barotropic idealization, based on the standard atmosphere from Chapter 1. (b) Baroclinic example, based on data from the Global Circulation chapter.

FOCUS • Barotropic vs. Baroclinic

In a **barotropic** atmosphere (Fig. 20.2a), the **isobars** (lines of equal pressure) do not cross the **isopycnics** (lines of equal density). This would occur for a situation where there are no variations of temperature in the horizontal. Hence, there could be no thermal-wind effect.

In a **baroclinic** atmosphere (Fig. 20.2b), isobars can cross isopycnics. Horizontal temperature gradients contribute to the tilt of the isopycnics. These temperature gradients also cause changing horizontal pressure gradients with increasing altitude, according to the thermal-wind effect.

The real atmosphere is baroclinic, due to differential heating by the sun (see the Global Circulation chapter). In a baroclinic atmosphere, potential energy associated with temperature gradients can be converted into the kinetic energy of winds.

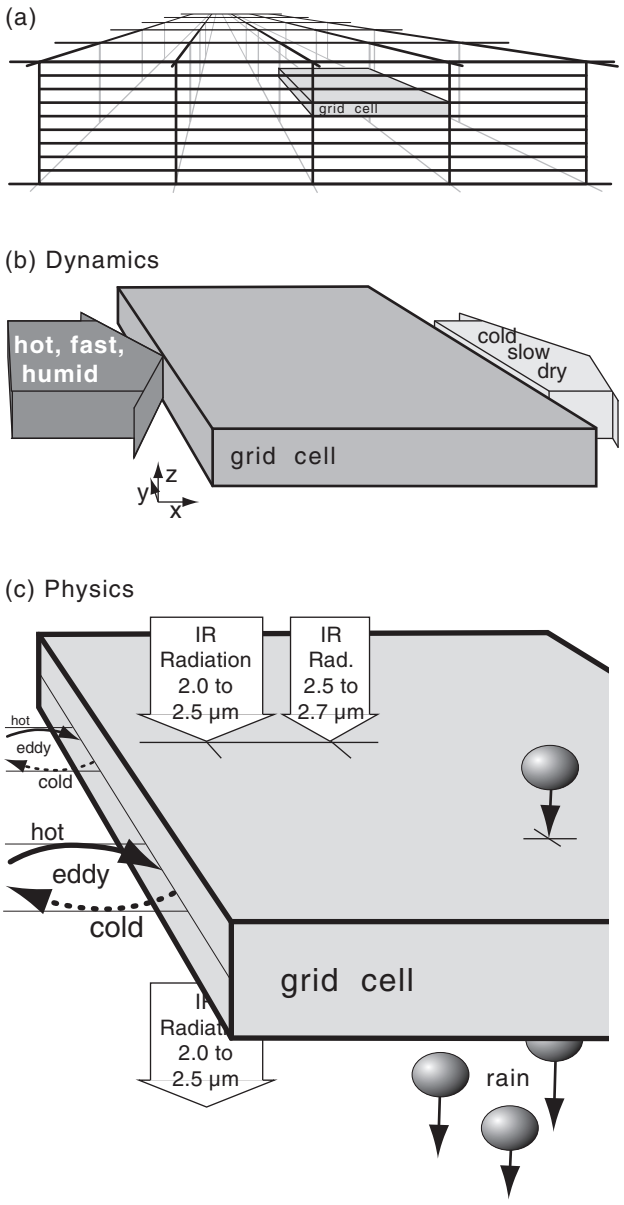

Figure 20.3
(a) The forecast **domain** *(the portion of atmosphere we wish to forecast) is split into discrete grid cells, such as the shaded one. The 3-D grid cells are relatively thin, with sizes on the order of 10s m in the vertical, and 10s km in the horizontal. (b) Enlargement of the shaded grid cell, illustrating one* **dynamics** *process (advection in the x-direction). Namely, the resolved U wind is blowing in hot, fast, humid air from the upwind neighboring grid cell, and is blowing out colder, slower, drier air into the downwind neighboring cell. Simultaneously, advection could be occurring by the V and W components of wind (not shown). Not shown are other resolved forcings, such as Coriolis and pressure-gradient forces. (c) Further enlargement, illustrating* **physics** *such as turbulence, radiation, and precipitation. Turbulence is causing a net heat flux into the left side of the grid cell in this example, even though the turbulence has no net wind (i.e., the wind-gust arrows moving air into the grid cell are balanced by gusts moving the same amount of air out of the grid cell). Two of the many radiation bands are shown, where infrared (IR) wavelengths in the 2.0 to 2.5 μm "window" band shine through the grid cell, while wavelengths in the 2.5 to 2.7 band are absorbed by water vapor and carbon dioxide (see the Remote Sensing chapter), causing warming in the grid cell. Some liquid water is falling into the top of the grid cell from the cell above, but even more is falling out the bottom into the grid cell below, suggesting a removal of water and net latent heating due to condensation.*

ent, we must make compromises to our description of the atmosphere.

Numerics: The main compromise is the process of **discretization**, where:
(1) we split the continuum of space into a finite number of small volumes called **grid cells** (Fig. 20.3a), within which we forecast average conditions;
(2) we approximate the smooth progression of time with finite **time steps**; and
(3) we replace the elegant equations of motion with **numerical approximations**.
These topics are generically known as **numerics**, as will be discussed in detail later. Numerics also include the **domain** being forecast, the mapping and coordinate systems, and the representation of data.

The word "**dynamics"** refers to the **governing equations.** It applies to only the resolved portions of motions, thermodynamic states, and moisture states (Fig. 20.3b) for the particular discretization used. A variable or process is said to be **resolved** if it can be represented by the average state within a grid cell. The dynamics described by eqs. (20.1 - 20.7) depend on sums, differences, and products of these resolved grid-cell average values.

The word "**physics"** refers to other processes (Fig. 20.3c and Table 20-1) that:
(1) are not forecast by the equations of motion, or
(2) are not well understood even though their effects can be measured, or
(3) involve motions or particles that are too small to resolve (called **subgrid scale**), or
(4) have components that are too numerous (e.g., individual cloud droplets or radiation bands), or
(5) are too complicated to compute in finite time.
However, unresolved processes can combine to produce resolved forecast effects. Because we cannot neglect them, we parameterize them instead.

A **parameterization** is a physical or statistical approximation to a physical process by one or more known terms or factors. Parameterization rules are given in an "On Doing Science" box in the Atmos. Boundary Layer chapter. In NWP, the "knowns" are the resolved state variables in the grid cells, and any imposed boundary conditions such as solar radiation, surface topography, land use, ice coverage, etc. Empirically estimated factors called **parameters** tie the knowns to the approximated physics.

Solved Example

Suppose subgrid-scale cloud coverage C is parameterized by

$$C = 0 \quad \text{for } RH \le RH_o$$
$$C = [(RH - RH_o) / (1 - RH_o)]^2 \quad \text{for } RH_o \le RH < 1$$
$$C = 1 \quad \text{for } RH \ge 1$$

RH is the grid-cell average relative humidity. Parameter $RH_o \approx 0.8$ for low and high clouds, and $RH_o \approx 0.65$ for mid-level cloud. Plot parameterized cloud coverage vs. resolved relative humidity.

Solution

Given: info above
Find: C vs. RH

Spreadsheet solution is graphed at right Grey curve: mid-level clouds. Black curve: low and high clouds.

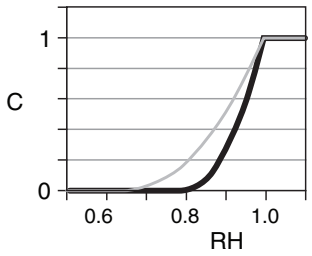

Check: Coverage bounded between clear & overcast.
Discussion: Partial cloud coverage is important for computing how much radiation reaches the ground.

Because parameterizations are only approximations, no single parameterization is perfectly correct. Different scientists might propose different parameterizations for the same physical phenomenon. Different parameterizations might perform better for different weather situations.

Models

The computer code that incorporates one particular set of dynamical equations, numerical approximations, and physical parameterizations is called a **numerical model** or **NWP model**. People developing these extremely large sets of computer code are called **modelers**. It typically takes teams of modelers (meteorologists, physicists, chemists, and computer scientists) several years to develop a new numerical weather model.

Different forecast centers develop different numerical models containing different dynamics, physics and numerics. These models are given names and acronyms, such as the Weather Research and Forecasting (**WRF**) model, the Global Environmental Multiscale (**GEM**) model, or the Global Forecast System (**GFS**). Different models usually give slightly different forecasts.

Table 20-1. Some physics parameterizations in NWP.

Process	Approximation Methods
Cloud Coverage	• Subgrid-scale cloud coverage as a function of resolved relative humidity. Affects the radiation budget.
Precipitation & Cloud Microphysics	Considers conversions between water vapor, cloud ice, snow, cloud water, rain water, and graupel + hail. Affects large-scale condensation, latent heating, and precipitation based on resolved supersaturation. Methods: • bulk (assumes a size distribution of hydrometeors); or • bin (separate forecasts for each subrange of hydrometeor sizes).
Deep Convection	• Approximations for cumuliform clouds (including thunderstorms) that are narrower than grid-cell width but which span many grid layers in the vertical (i.e., are unresolved in the horizontal but resolved in the vertical), as function of moisture, stability and winds. Affects vertical mixing, precipitation, latent heating, & cloud coverage.
Radiation	• Impose solar radiation based on Earth's orbit and solar emissions. Include absorption, scattering, and reflection from clouds, aerosols and the surface. • Divide IR radiation spectrum into small number of wide wavelength bands, and track up- and down-welling radiation in each band as absorbed and emitted from/to each grid layer. Affects heating of air & Earth's surface.
Turbulence	Subgrid turbulence intensity as function of resolved winds and buoyancy. Fluxes of heat, moisture, momentum as function of turbulence and resolved temperature, water, & winds. Methods: • local down-gradient eddy diffusivity; • higher-order local closure; or • nonlocal (transilient turb.) mixing.
Atmospheric Boundary Layer (ABL)	Vertical profiles of temperature, humidity, and wind as a function of resolved state and turbulence, based on forecasts of ABL depth. Methods: • bulk; • similarity theory.
Surface	• Use albedo, roughness, etc. from statistical average of varied land use. • Snow cover, vegetation greenness, etc. based on resolved heat & water budget.
Sub-surface heat & water	• Use climatological average. Or forecast heat conduction & water flow in rivers, lakes, glaciers, subsurface, etc.
Mountain-wave Drag	• Vertical momentum flux as function of resolved topography, winds and static stability.

FOCUS • Moore's Law & Forecast Skill

Gordon E. Moore co-founded the **integrated-circuit** (computer-chip) manufacturer Intel. In 1965 he reported that the maximum number of transistors that were able to be inexpensively manufactured on integrated circuits had doubled every year. He predicted that this trend would continue for another decade.

Since 1970, the rate slowed to about a doubling every two years. This trend, known as **Moore's Law**, has continued for over 4 decades.

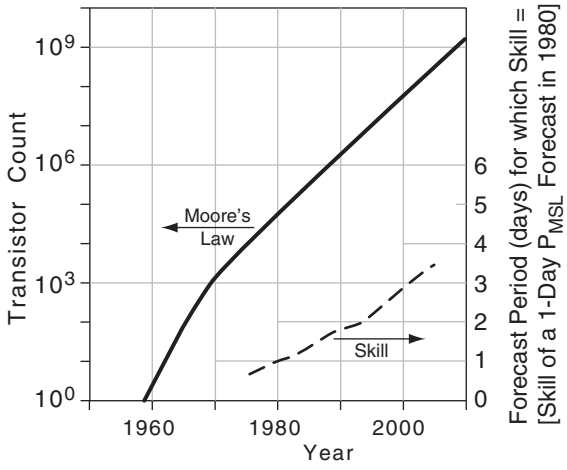

Fig. 20.D. *Moore's Law and forecast skill vs. time.*

GRID POINTS

Define the size of a grid cell in the three Cartesian directions as ΔX, ΔY, and ΔZ (Fig. 20.6A). Typical values are $\Delta X = \Delta Y$ = one to hundreds of kilometers, while ΔZ = one to hundreds of meters. Small-size grid cells give **fine-resolution** (or **high-resolution**) forecasts, and large-size cells give **coarse-resolution** (or **low-resolution**) forecasts.

Because we forecast only the average condition of weather variables at each grid cell, we can represent these average values as being physically located at a **grid point** (Fig. 20.6A) in each cell. The distance between grid points is the same as the grid-cell size: ΔX, ΔY, ΔZ. More closely spaced grid points have finer resolution (see a later Focus Box on Resolution).

Finer resolution requires more grid cells to span your forecast domain. Each cell requires a certain number of numerical calculations to make the forecast. Thus, more cells require more total calculations. Hence, finer resolution forecasts take longer to compute, but often give more accurate forecasts.

Thus, your choice of domain and grid size is a compromise between forecast timeliness and accuracy, based on the computer power available. As computer power has improved over the past 6 decades, so have weather-forecast resolution and skill (see Focus Box on Moore's Law and Forecast Skill). **Skill** is the forecast improvement relative to some reference such as climatology.

Nested and Variable Grids

Alternatives exist to the domain-size vs. resolution trade off. In the horizontal, use a fast-running coarse-grid over a large domain to span large-scale weather systems, and nest inside that a smaller-horizontal-domain finer-mesh grid (Fig. 20.4a). Such **nested grids** reduce overall run time while capturing finer-scale features where they are needed most. Typically, the fine mesh has a horizontal grid size (ΔX) of 1/3 of the coarse-mesh grid size, although ratios of 1/5 have sometimes been used. Nesting can continue with successively finer nests. The author's research team has run nested grids with grid sizes ΔX = 108, 36, 12, 4, 1.33, and 0.44 km.

Nested grids can employ **one-way nesting**, where the coarse grid is solved first, and its output is applied as time-varying boundary conditions to the finer grid. For **two-way nesting**, both grids are solved together, and features from each grid are fed into the other at each time step. Two-way nesting often gives better forecasts, but are more complicated to implement.

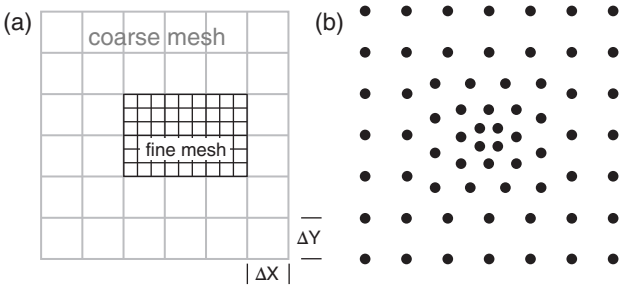

Figure 20.4
Horizontally nested grids. (a) Discrete meshes (shown as grid cells). (b) Variable mesh (shown as grid points).

Science Graffito

"Prediction is very difficult, especially of the future."
- Niels Bohr

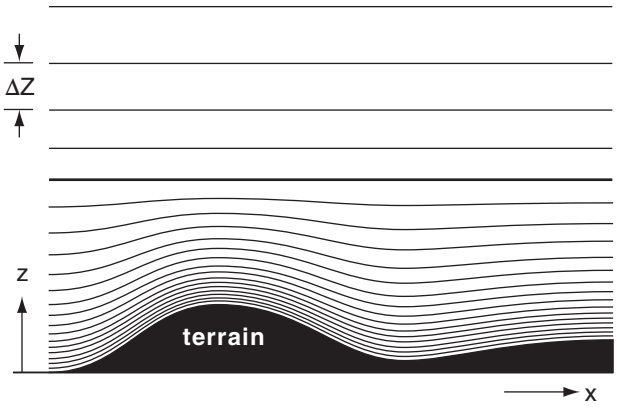

Figure 20.5
Illustration of variable grid increments (ΔZ) in the vertical.

An alternative to discrete nested grids in the horizontal is a **variable-mesh grid** (Fig. 20.4b), which uses smoothly varying grid spacings. Again, the finer mesh is positioned over the region of interest.

In the vertical, fine resolution (i.e., small ΔZ) is needed near the Earth's surface and in the boundary layer, because of important small-scale motions and strong vertical gradients. To reduce the computation time, coarse resolution (i.e., larger ΔZ) is acceptable higher above the surface — in the stratosphere and upper troposphere. Variable mesh vertical grids (i.e., smoothly changing ΔZ values) are often used for this reason (Fig. 20.5). For models using pressure or sigma as a vertical coordinate, ΔP or $\Delta\sigma$ varies smoothly with height. As an alternative, some NWP models use discrete vertical nests.

Staggered Grids

You could represent all the cell-average variables at the same grid point, as in Fig. 20.6A (called an A-Grid). But this has some undesirable characteristics: wavy motions do not disperse properly, some wave energy gets stuck in the grid, and some weather variables oscillate about their true value.

Instead, grid points are often arranged in a **staggered grid** arrangement within the cell, with different variables being represented by points at different locations in the grid (Fig. 20.6 Grids B - E). Staggered Grid D has many of the same problems as unstaggered Grid A. Grids B and C have fewer problems.

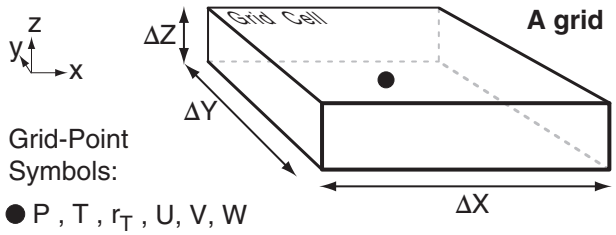

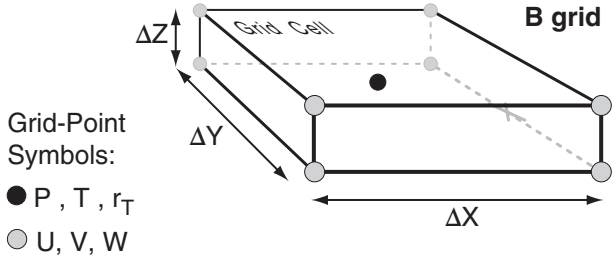

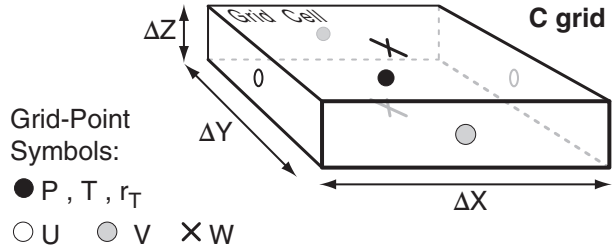

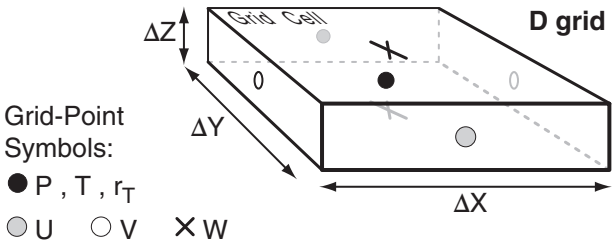

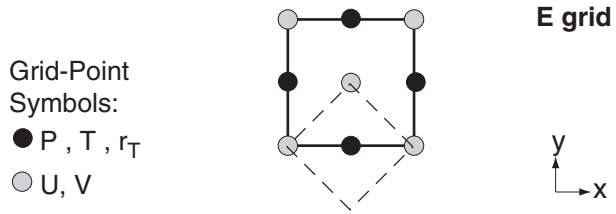

Figure 20.6 (in right column)
Akio Arakawa (1972) identified 5 grid arrangements. Grid A is an unstaggered grid (where all variables are at the same grid point). All the others are staggered grids. Only 2 dimensions are shown for grid E, which is a rotated version of Grid B. Grids C and D differ in their locations of the U and V winds.

Science Graffito

"Nature's rules are refreshingly free of human prejudice."

Jim Al-Khalili, from the 2009 BBC TV series *Science and Islam*. Episode 3: *The Power of Doubt*.

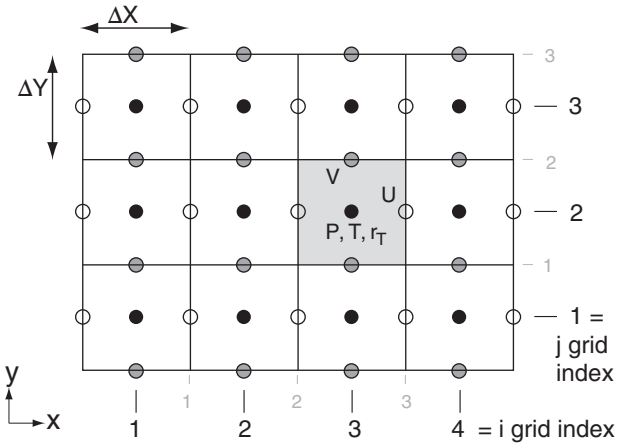

Figure 20.7
Arrangement and indexing of grid cells for a 2-dimensional C-Grid. Each variable in the shaded cell has indices i = 3, j = 2. For variables located at grid-cell edges, some models use whole-index numbering, as shown by the grey numbers. Other models use half indices, as in Fig. 20.9.

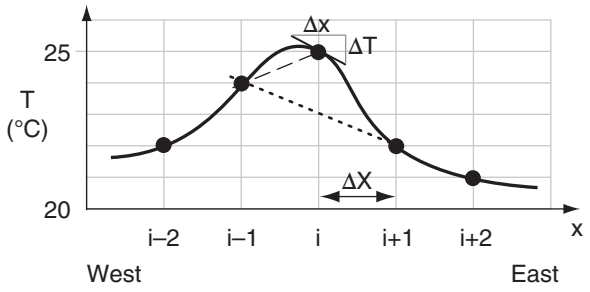

Figure 20.8
The slope (thin unbroken black line) of the temperature (T) curve (thick black line) at grid point i is represented by ΔT/Δx. The lower-case "x" is used in Δx to represent an infinitesimally small increment of distance, while upper-case "X" is used in ΔX to indicate the spacing between grid points (black dots), where i is a grid-point index. Thin dashed and dotted lines are various finite-difference approximations to the slope at i.

FINITE-DIFFERENCE EQUATIONS

Here we see how to find discrete numerical approximations to the equations of motion (20.1 - 20.7) as applied to grid cells.

Notation

Cells are identified by a set of indices (i, j, k) that indicate their (x, y, z) positions within the domain. Fig. 20.7 shows a two-dimensional example. By using these indices as subscripts, we can specify any variable at any grid-point location. For example, $T_{3,2}$ is the temperature in the center of the shaded grid cell, at x-location $i = 3$, and y-location $j = 2$. For a 3-D grid, you can use 3 indices or subscripts.

*[**CAUTION**: Throughout this book, we have used ratios of differences (such as $\Delta T/\Delta x$) instead of derivatives ($\partial T/\partial x$) to represent the local slope or local gradient of a variable. While this allowed us to avoid calculus, it causes problems in this chapter because Δx now has two conflicting meanings: (1) Δx is an infinitesimal increment of distance, such as used to find the local slope of a curve at point i in Fig. 20.8. (2) ΔX is a finite distance between grid points, such as between points i and i+1 in Fig. 20.8.*

To artificially discriminate between these two meanings, we will use lower-case "x" in Δx to represent an infinitesimal distance increment, and upper-case "X" in ΔX to represent a finite distance between grid points.]

Approximations to Spatial Gradients

The equations of motion (20.1 - 20.6) contain many terms involving local gradients, such as the horizontal temperature gradient $\Delta T/\Delta x$. So to solve these equations, we need a way to approximate the local gradients as a function of things that we know — e.g., values of T at the discrete grid points.

But when the local gradient of an analytical variable is represented at one grid point as a function of its values at other grid points, the result is an infinite sum of terms — each term of greater power of ΔX or Δt. This is a **Taylor series** (see the Beyond Algebra box). The most important terms in the series are the first ones — the ones of lowest power of ΔX (said to be of **lowest order**).

However, the **higher-order** terms do slightly improve the accuracy. For practical reasons, the numerical forecast can consider only the first few terms from the Taylor series. Such a series is said to be **truncated**; namely, the highest-order terms are cut from the calculation. For example, a second-order approximation to T' (= $\Delta T/\Delta x$) has an error of about $\pm T'/6$, while a third-order approximation has an error of about $\pm T'/24$.

Different approximations to the local gradients have different **truncation errors**. Such approximations can be applied to the local gradient of any weather variable — the illustrations below focus on temperature (T) gradients. Assuming a mean wind from the west, an **upwind first-order difference** approximation is:

$$\left.\frac{\Delta T}{\Delta x}\right|_i \approx \frac{(T_i - T_{i-1})}{\Delta X} \tag{20.9}$$

which applies at grid point i. But first-order approximations to the gradient (shown by slope of the dashed line in Fig. 20.8) can have large errors relative to the actual gradient (shown by the slope of the thin black line).

A **centered second-order difference** gives a better approximation to the gradient at i:

$$\left.\frac{\Delta T}{\Delta x}\right|_i \approx \frac{(T_{i+1} - T_{i-1})}{2\Delta X} \tag{20.10}$$

as sketched by the dotted line in Fig. 20.8.

An even-better **centered fourth-order difference** for the gradient at i is:

$$\left.\frac{\Delta T}{\Delta x}\right|_i \approx \frac{1}{12\Delta X}\left[8(T_{i+1} - T_{i-1}) - (T_{i+2} - T_{i-2})\right] \tag{20.11}$$

as shown by the thin solid line in Fig. 20.8.

Use similar equations for gradients of other variables (U, V, W, r_T, ρ). Orders higher than fourth-order are also used in some numerical models.

Solved Example
Find $\Delta T/\Delta x$ at grid point i in Fig. 20.8 using 1, 2, & 4th order gradients, for a horizontal grid spacing of 5 km.

Solution
Given: $T_{i-2} = 22$, $T_{i-1} = 24$, $T_i = 25$, $T_{i+1} = 22$, $T_{i+2} = 21$°C from the data points in Fig. 20.8. $\Delta X = 5$ km.
Find: $\Delta T/\Delta x$ = ? °C/km

For Upwind 1st-order Difference, use eq. (20.9):
$\Delta T/\Delta x \approx (25 - 24°C)/(5\text{ km}) =$ **0.2 °C/km**

For Centered 2nd-order Difference, use eq. (20.10):
$\Delta T/\Delta x \approx (22 - 24°C)/[2\cdot(5\text{ km})] =$ **–0.2 °C/km**

For Centered 4th-order Difference, use eq. (20.11):
$\Delta T/\Delta x \approx [8\cdot(22–24°C) – (21–22°C)]/[12\cdot(5\text{ km})]$
$\approx [(–16 + 1)°C]/(60\text{ km}) =$ **–0.25 °C/km**

Check: Units OK. Agrees with lines in Fig. 20.8.
Discussion: Higher-order differences are better approximations, but none give the true slope exactly.

BEYOND ALGEBRA • Taylor Series

The equations of motion have terms such as $U\cdot\partial T/\partial x$. We can use a Taylor series to approximate derivative $\partial T/\partial x$ as a function of discrete grid-point values. [Notation: use T' for $\partial T/\partial x$, use T'' for $\partial^2 T/\partial x^2$.]

Any analytic function such as temperature vs. distance $T(x)$ can be expanded into an infinite series called a **Taylor series** if the derivatives (T', T'', etc.) are well behaved near x. To find the value of T at $(x + \Delta X)$, where ΔX is a small finite distance from x, use a Taylor series of the form: (20.BA1)

$$T(x+\Delta X) \approx T(x) + \frac{(\Delta X)^1}{1!}\cdot T'(x) + \frac{(\Delta X)^2}{2!}\cdot T''(x) + \frac{(\Delta X)^3}{3!}\cdot T'''(x) + \frac{(\Delta X)^4}{4!}\cdot T''''(x) + \ldots$$

Apply the Taylor series to grid points (Fig. 20.8), where the spatial position is indicated by an index i: (20.BA2)

$$T_{i+1} \approx T_i + \Delta X\cdot T_i' + \frac{(\Delta X)^2}{2}\cdot T_i'' + \frac{(\Delta X)^3}{6}\cdot T_i''' + \frac{(\Delta X)^4}{24}\cdot T_i'''' + \ldots$$

Similarly, by using $-\Delta X$ in the Taylor expansion, you can estimate T upwind, at grid index i–1: (20.BA3)

$$T_{i-1} \approx T_i - \Delta X\cdot T_i' + \frac{(\Delta X)^2}{2}\cdot T_i'' - \frac{(\Delta X)^3}{6}\cdot T_i''' + \frac{(\Delta X)^4}{24}\cdot T_i'''' - \ldots$$

For practical reasons, **truncate** the series to a finite number of terms. The more terms you keep, the smaller the **truncation error**. The lowest power of the ΔX term not used defines the **order** of the truncation. Higher-order truncations have less error.

• For a simple upwind difference (with poor, first-order error in ΔX), solve eq (20.BA3) for T':

$$T_i' = \frac{(T_i - T_{i-1})}{\Delta X} + O(\Delta X) \tag{20.BA4}$$

where the last term indicates the truncation error. This T' value gives the dashed-line slope in Fig. 20.8.

• For a centered difference (with moderate, second-order error in ΔX), subtract eq. (20.BA3) from (20.BA2) and solve the result for T':

$$T_i' = \frac{(T_{i+1} - T_{i-1})}{2\Delta X} + O(\Delta X)^2 \tag{20.BA5}$$

This T' value gives the dotted-line slope in Fig. 20.8.

• For an even-better, 4th-order, centered difference, use: (20.BA6)

$$T_i' = \frac{1}{12\Delta X}\left[8(T_{i+1} - T_{i-1}) - (T_{i+2} - T_{i-2})\right] + O(\Delta X)^4$$

which is a slightly better fit to the true slope at i.

In this chapter, we use $\Delta T/\Delta x$ in place of T'. Hence, the bullets above give approximations to $\Delta T/\Delta x$.

Grid Computation Rules

(1) When multiplying or dividing any two variables, both of those variables must be at the same point in space. The result applies at that same point.

(2) When adding, averaging, or subtracting any two variables, if both those variables are at the same point in space, then the result applies at the same point.

(3) However, when adding, averaging, or subtracting two variables at different locations in space, the sum, average, or difference applies at a physical location halfway between the locations of the original variables.

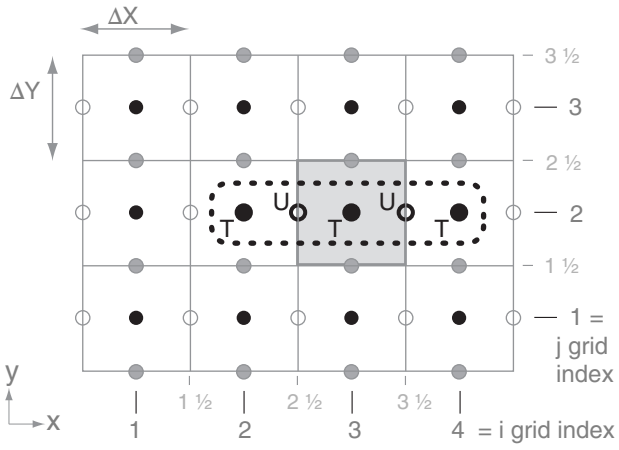

Figure 20.9
Sketch of a two-dimensional C grid. Consider the computation of temperature advection by the U wind, as contributes to the temperature tendency at the one grid point centered in the shaded cell. The grid points needed to make that calculation are outlined with the dotted line, and their arrangement is called a stencil.

Solved Example
What is the warming rate at grid point (i=3, j=2) in Fig. 20.9 due to temperature advection in the x-direction, given $T_{2,2}$ = 22°C, $T_{3,2}$ = 23°C, $T_{4,2}$ = 24°C, $U_{2½,2}$ = –5 m/s, $U_{3½,2}$ = –7 m/s, ΔX = 10 km?

Solution
Given: T and U values above. ΔX = 10 km
Find: $\Delta T/\Delta t = -U\cdot\Delta T/\Delta x$ = ? °C/h .

Use eq. (20.12):
$\Delta T/\Delta t \approx -0.5\cdot(-7-5\text{ m/s})\cdot[\,0.5\cdot(24-22°\text{C})/(10^4\text{m})\,]$
$\approx (6\text{ m/s})\cdot[\,1°\text{C}/(10^4\text{m})\,]\cdot(3600\text{ s/h}) =$ **2.16 °C/h**

Check: Units OK. Sign OK. Magnitude OK.
Discussion: Winds are advecting in warmer air from the East, causing advective warming.

NWP Corollary 1: The forecast at any one point is affected by ALL other points in the forecast domain.

Grid Computation Rules

For mathematical and physical consistency, the grid computation rules at left must be obeyed when making calculations with grid-point values. Rule 3 is handy because you can use it to "move" values to locations where you can then multiply by other variables while obeying Rule 1.

For example, consider the temperature forecast equation (20.4) for grid point (i = 3, j = 2), for the C-grid in Fig. 20.9. The first term on the right side of eq. (20.4) is temperature advection in the x-direction. If we choose to use second-order difference eq. (20.10) at location (i,j) = (3,2), we have a mismatch because we do not have wind at that same location. Rule 1 says we can not multiply the wind times the T gradient.

However, we can use Rule 3 to average the U-winds from the right and left of the temperature point, knowing that this average applies halfway between the two U points. The average thus spatially coincides with the temperature gradient, so we can multiply the two factors together.

For that one grid point (i,j) = (3,2), the result is:

(20.12)
$$\left\{-U\cdot\frac{\Delta T}{\Delta x}\right\}_{3,2} \approx -\left(\frac{U_{3½,2}+U_{2½,2}}{2}\right)\cdot\left[\frac{T_{4,2}-T_{2,2}}{2\cdot\Delta X}\right]$$

where the ½ grid index numbering method was used for values at the edges of the grid cell (Fig. 20.9). The parentheses hold the average U, and the square brackets hold the centered second-order difference approximation for the local T gradient.

Similarly, for any grid point (i,j), the result is:

(20.13)
$$\left\{-U\cdot\frac{\Delta T}{\Delta x}\right\}_{i,j} \approx -\left(\frac{U_{i+½,j}+U_{i-½,j}}{2}\right)\cdot\left[\frac{T_{i+1,j}-T_{i-1,j}}{2\cdot\Delta X}\right]$$

The spatial arrangement of all grid points used in any calculation is called a **stencil**. Fig. 20.9 shows the stencil for eq. (20.13). Different grid arrangements (Grids A - E) and different approximation orders will result in different stencils.

Significantly, the forecast for any one grid point (such as i,j) depends on the values at other nearby grid points [such as (i–1,j) , (i–½,j) , (i+½,j) , (i+1,j)]. In turn, forecasts at each of these points depends on values at their neighbors. This interconnectivity is summarized as NWP Corollary 1, at left.

For grid points near the edges of the domain, special stencils using one-sided difference approximations must be used, to avoid referencing grid points that don't exist because they are outside of the domain. Alternately, a **halo** of **ghost-cell** grid points outside the forecast domain can be specified using values found from a larger coarser domain or from imposed **boundary conditions** (**BCs**; i.e., the state of the air along the edges of the forecast domain).

Time Differencing

The smooth flow of time implied by the left side of the equations of motion can be approximated by a sequence of discrete time steps, each of duration Δt. For example, the temperature tendency term on the left side of eq. (20.4) can be written as a centered time difference:

$$\frac{\Delta T}{\Delta t} \approx \frac{T(t+\Delta t) - T(t-\Delta t)}{2 \cdot \Delta t} \qquad (20.14)$$

When combined with the right side of eq. (20.4), the result gives the temperature at some future time as a function of the temperatures and winds at earlier times:

$$T_{3,2}(t+\Delta t) = T_{3,2}(t-\Delta t) + 2\Delta t \cdot [\text{RHS of eq. } 20.4] \qquad (20.15)$$

Typical time-step durations Δt are on the order of a few seconds to tens of minutes, depending on the grid size (see the section on numerical stability).

The equation above is a form of the **leapfrog** scheme. It gets its name because the forecast starts from the previous time step (t–Δt) and leaps over the present step (t) to make a forecast for the future (t+Δt). Although it leaps over the present step, it utilizes the present conditions to determine the future conditions. Fig. 20.10 shows a sketch of this scheme.

The two leapfrog solutions (one starting at t–Δt and the other starting at t, illustrated above and below the time line in Fig. 20.10) sometimes diverge from each other, and need to be occasionally averaged together to yield a consistent forecast. Without such averaging the solution would become unstable, and would numerically blow up (see next section).

There are other numerical solutions that work better than the leapfrog method. One example is the **Runge-Kutta** method, described in the Focus Box.

By combining eqs. (20.12 & 20.15), we get a temperature forecast equation that includes only the U-advection forcing:

$$T_{3,2}(t+\Delta t) = T_{3,2}(t-\Delta t) + \frac{\Delta t}{\Delta X} \cdot \left\{ (U_{3\frac{1}{2},2} + U_{2\frac{1}{2},2}) \cdot \tfrac{1}{2} \left[T_{4,2} - T_{2,2} \right] \right\}_t \qquad (20.16)$$

where the subscript t at the very right indicates that all of the terms inside the curly brackets are evaluated at time t. So the future temperature (at t+Δt), depends on the current temperature and winds (at t) and on the past temperature (at t–Δt). The concept of a **stencil** can be extended to include the 4-D arrangement of locations and times needed to forecast one aspect of physics for any grid point.

Generalizing the previous equation, and recalling NWP Corollary 1, we infer that: the forecast Δt

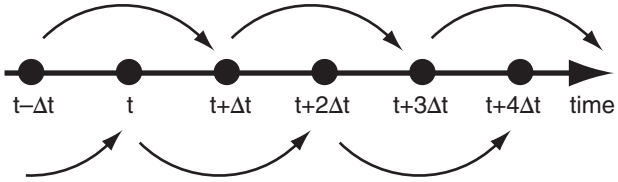

Figure 20.10
Time line illustrating the "leapfrog" time-differencing scheme.

FOCUS • Time Differencing Methods

The prognostic equations of motion (20.1 - 20.6) can be written in a generic form:

$$\Delta A/\Delta t = f[A, x, t] ,$$

where A = any dependent variable (e.g., U, V, W, T, etc.), f is a function that describes all the dynamics and physics of the equations of motion, and x represents all other independent variables (x, y, z) as indicated by grid-point indices (i, j, k). Knowing present (at time t) and all past values at the grid points, how do we make a small time step Δt into the future?

One of the simplest methods is called the **Euler method** (also known as the Euler-forward method):

$$A(t+\Delta t) = A(t) + \Delta t \cdot f[A(t), x, t]$$

But this is only first-order accurate, and is never used because errors accumulate so quickly that the numerical forecast often **blows up** (forecasts values of ± infinity) causing the computer to **crash** (premature termination due to computation errors).

The **leapfrog method** was already given in the text, and is second-order accurate.

$$A(t+\Delta t) = A(t-\Delta t) + 2\Delta t \cdot f[A(t), x, t]$$

Higher-order accuracy has less error.

Also popular is the **fourth-order Runge-Kutta method**, which has even less error, but requires intermediate steps done in the order listed:

(1) $k_1 = f[\, A(t) \,,\, x \,,\, t \,]$

(2) $k_2 = f[\, A(t)+\tfrac{1}{2}\Delta t \cdot k_1 \,,\, x \,,\, t+\tfrac{1}{2}\Delta t \,]$

(3) $k_3 = f[\, A(t)+\tfrac{1}{2}\Delta t \cdot k_2 \,,\, x \,,\, t+\tfrac{1}{2}\Delta t \,]$

(4) $k_4 = f[\, A(t)+\Delta t \cdot k_3 \,,\, x \,,\, t+\Delta t \,]$

(5) $A(t+\Delta t) = A(t) + (\Delta t/6) \cdot [\, k_1 + 2k_2 + 2k_3 + k_4 \,]$

Solved Example (§)
Given a 1-D array consisting of 10 grid points in the x-direction with the following initial temperatures (°C):
$T_i\,(t = 0)$ = 21.76 22.85 22.85 21.76 20.00 18.24 17.15 17.15 18.24 20.00 for i = 1 to 10.
Assume that the lateral boundaries are cyclic, so that this number sequence repeats outside this primary domain. Grid spacing is 3 km and wind speed from the west is 10 m/s. For a 250 s time step, forecast the temperature at each point for the first 6 time steps, using leapfrog temporal and 4th-order centered spatial differences.

Solution
Given: ΔX = 3 km , Δt = 250 s , U = 10 m/s. Initially:

i =	1	2	3	4	5	6	7	8	9	10
T =	21.76	22.85	22.85	21.76	20.00	18.24	17.15	17.15	18.24	20.00

Find: T_i at t = 250 s, 500 s, etc. out to 1500 s

We can use leapfrog for every time step except the first step, because for the first step we have no temperatures before time zero. So I will use an Eulerian time difference for the first step. The resulting eqs. are:
For 1st time step:

$$T_i(t+\Delta t) = T_i(t=0) - \frac{\Delta t \cdot U}{\Delta X \cdot 12}\left[8\cdot(T_{i+1} - T_{i-1}) - (T_{i+2} - T_{i-2})\right]_{t=0}$$

For all other time steps:

$$T_i(t+\Delta t) = T_i(t-\Delta t) - \frac{\Delta t \cdot U \cdot 2}{\Delta X \cdot 12}\left[8\cdot(T_{i+1} - T_{i-1}) - (T_{i+2} - T_{i-2})\right]_{t}$$

Solving these in a spreadsheet gives, the following, where each row is a new time step and each column is a different grid point:

t(s)	[i = 1	2	3	4	5	6	7	8	9	10]
0	[21.76	22.85	22.85	21.76	20.00	18.24	17.15	17.15	18.24	20.00]
250	[20.50	22.37	23.34	23.03	21.56	19.50	17.63	16.66	16.97	18.44]
500	[18.28	20.34	22.27	23.34	23.13	21.72	19.66	17.73	16.66	16.87]
750	[17.43	18.83	20.68	22.27	22.99	22.57	21.17	19.32	17.73	17.01]
1000	[16.66	17.46	19.22	21.29	22.86	23.34	22.54	20.78	18.71	17.14]
1250	[17.15	16.56	17.29	19.05	21.17	22.85	23.44	22.71	20.95	18.83]
1500	[18.67	17.34	17.02	17.84	19.49	21.33	22.66	22.98	22.16	20.51]

These are plotted as Fig. 20.11b, showing a temperature pattern that is advected by the wind toward the East.

Check: Units OK. Fig. 20.11b looks reasonable
Discussion: The **Courant Number** [$\Delta t \cdot U/\Delta x$] is (250 s) · (10 m/s) / (3000 m) = 0.833 (dimensionless). Since this number is less than 1, it says that the solution could be numerically stable (see the Numerical Error section).

The boxes in the table above show which numbers are used in the calculation. For example, the temperature forecast at i = 4 and t = 1500 s used data from the grey boxes near it, based on leapfrog in time and 4th-order centered in space. For i = 4 and t = 250 s, the Euler forward time difference was used. For i = 9 and t = 750 s, one of the grey boxes wrapped around, due to the cyclic boundary conditions.

into the future of any one variable at one location can depend on the current state of ALL other variables at ALL other locations. Thus, ALL other variable at ALL other locations must be stepped forward the same one Δt into the future, based on current values. Only after they all have made this step can we proceed to the next step, to get to time $t + 2\Delta t$ into the future. This characteristic is summarized as NWP Corollary 2:

NWP Corollary 2: ALL variables at ALL grid points must march in step into the future*.

**Some terms (e.g., for acoustic waves) and some parameterizations require very short time steps for numerical stability. They can be programmed to take many "baby" steps for each "adult" time step Δt in the model, to enable them to remain synchronized (holding hands) as they advance toward the future.*

To start the whole NWP, we need **initial conditions** (**ICs**). These ICs are estimated by merging weather observations with past forecasts (see the Data Assimilation section). ICs are often named by the **synoptic time** when most of the observations were made, such as the "00 UTC analysis", the "00 UTC initialization", or the "00 UTC model run". Modern assimilation schemes can also incorporate **asynoptic** (off-hour) observations.

Discretized Equations of Motion

In summary, the physical equations of motion, which are essentially smooth analytical functions, must be discretized to work at grid points. For example, if we use leapfrog time differencing with second-order spatial differencing on a C-grid, the temperature forecast equation (20.4) becomes:

(20.17)

$$\begin{aligned} T_{i,j,k}(t+\Delta t) = T_{i,j,k}(t-\Delta t) + 2\Delta t\cdot\Bigg\{ & \\ & -\left(\frac{U_{i+\frac{1}{2},j,k} + U_{i-\frac{1}{2},j,k}}{2}\right)\cdot\left[\frac{T_{i+1,j,k} - T_{i-1,j,k}}{2\cdot\Delta X}\right] \\ & -\left(\frac{V_{i,j+\frac{1}{2},k} + V_{i,j-\frac{1}{2},k}}{2}\right)\cdot\left[\frac{T_{i,j+1,k} - T_{i,j-1,k}}{2\cdot\Delta Y}\right] \\ & -\left(\frac{W_{i,j,k+\frac{1}{2}} + W_{i,j,k-\frac{1}{2}}}{2}\right)\cdot\left[\frac{T_{i,j,k+1} - T_{i,j,k-1}}{2\cdot\Delta Z}\right] \\ & -\frac{\Re\cdot T_{i,j,k}}{P_{i,j,k}\cdot C_p}\cdot\left[\frac{\mathbb{F}_{z\ rad\ i,j,k+\frac{1}{2}} - \mathbb{F}_{z\ rad\ i,j,k-\frac{1}{2}}}{\Delta Z}\right] \\ & +\frac{L_v}{C_p}\cdot\left[\frac{r_{cond\ i,j,k}(t+\Delta t) - r_{cond\ i,j,k}(t-\Delta t)}{2\Delta t}\right] \\ & -\left[\frac{F_{z\ turb\ i,j,k+\frac{1}{2}} - F_{z\ turb\ i,j,k-\frac{1}{2}}}{\Delta Z}\right] \quad \Bigg\} \end{aligned}$$

Finite-difference equations that are used to forecast winds and humidity are similar. If we had used higher-order differencing, and included the curvature terms and mapping factors, the result would have contained even more terms.

Although the equation above looks complicated, it is trivial for a digital computer to solve because it is just algebra. Computing this equation takes a finite time — perhaps a few microseconds. Similar computation time must be spent for all the other grid points in the domain. These computations must be repeated for a succession of short time steps to reach forecast durations of several days. Thus, for many grid points and many time steps, the total computer run-time accumulates and can take many minutes to several hours on powerful computers.

NUMERICAL ERRORS & INSTABILITY

Causes of NWP errors include **round-off error**, **truncation error**, **numerical instability**, and **dynamical instability**. Dynamical instability related to initial-condition errors will be discussed later in the section on chaos. Additional errors not considered in this section are coding bugs, computer viruses, user errors, numerical or physical approximations, simplifications and parameterizations.

Round-off Error

Round-off error exists because computers represent numbers by a limited number of binary bits (e.g., 32, 64, 128 bits). As a result, some real decimal numbers can be only approximately represented in the computer. For example, a 32-bit computer can resolve real numbers that are different from each other by about 3×10^{-8} or greater. Any finer differences are missed.

To demonstrate, I wrote a computer program to start with $x = 0.0$, and then repeatedly add 0.1 to x (printing x at each step) until it reaches $x = 3.0$, at which point I programmed it to stop. When I used single precision (32-bits), my program never stopped. After 30 additions it had found $x = 2.9999993$, but since this was not exactly equal to 3.0, the program kept adding 0.1 in an **infinite loop** (i.e., ran forever). When I tried it again using double precision (64 bits) it also never stopped, getting only as close to 3.0 as $x = 3.0000000000000013$.

Namely, the slight error between decimal and binary representations of a number can accumulate, or can cause unexpected outcomes of conditional tests ("if" statements). Most modern computers use many bits to represent numbers. Nonetheless, always consider round-off errors when you write programs.

FOCUS • Early History of NWP

The first equations of fluid mechanics were formulated by Leonhard Euler in 1755, using the differential calculus invented by Isaac Newton in 1665, Gottfried Wilhelm Leibniz in 1675, and using partial derivatives devised by Jean le Rond d'Alembert in 1746.

Terms for molecular viscosity were added by Claude-Louis Navier in 1827 and George Stokes in 1845. The equations describing fluid motion are often called the **Navier-Stokes equations**. These primitive equations for fluid mechanics were refined by Herman von Helmholtz in 1888.

About a decade later Vilhelm Bjerknes in Norway suggested that these same equations could be used for the atmosphere. He was a very strong proponent of using physics, rather than empirical rules, for making weather forecasts.

In 1922, Lewis Fry Richardson in England published a book describing the first experimental numerical weather forecast — which he made by solving the primitive equations with mechanical desk calculators. His book was very highly regarded and well received as one of the first works that combined physics and dynamics in a thorough, interactive way.

It took him 6 weeks to make a 6 h forecast. Unfortunately, his forecast of surface pressure was off by an order of magnitude compared to the real weather. Because of the great care that Richardson took in producing these forecasts, most of his peers concluded that NWP was not feasible. This discouraged further work on NWP until two decades later.

John von Neumann, a physicist at Princeton University's Institute for Advanced Studies, and Vladimir Zworykin, an electronics scientist at RCA's Princeton Laboratories and key inventor of television, proposed in 1945 to initiate NWP as a way to demonstrate the potential of the recently-invented electronic computers. Their goal was to simulate the global circulation. During the first few years they could not agree on how to approach the problem.

Von Neumann formed a team of theoretical meteorologists including Carl-Gustav Rossby, Arnt Eliassen, Jule Charney, and George Platzman. They realized the need to simplify the full primitive equations in order to focus their limited computer power on the long waves of the global circulation. So Charney and von Neumann developed a simple one-layer barotropic model (conservation of absolute vorticity).

Their first electronic computer, the ENIAC, filled a large room at Princeton, and used vacuum tubes that generated tremendous heat and frequently burned out. The research team had to translate the differential equations into discrete form, write the code in machine language (FORTRAN and C had not yet been invented), decide how large a forecast domain was necessary, and do many preliminary calculations using slide rules and mechanical calculators.

Their first ENIAC forecasts were made in March-April 1950, for three weather case studies over North America. This was the start of modern NWP.

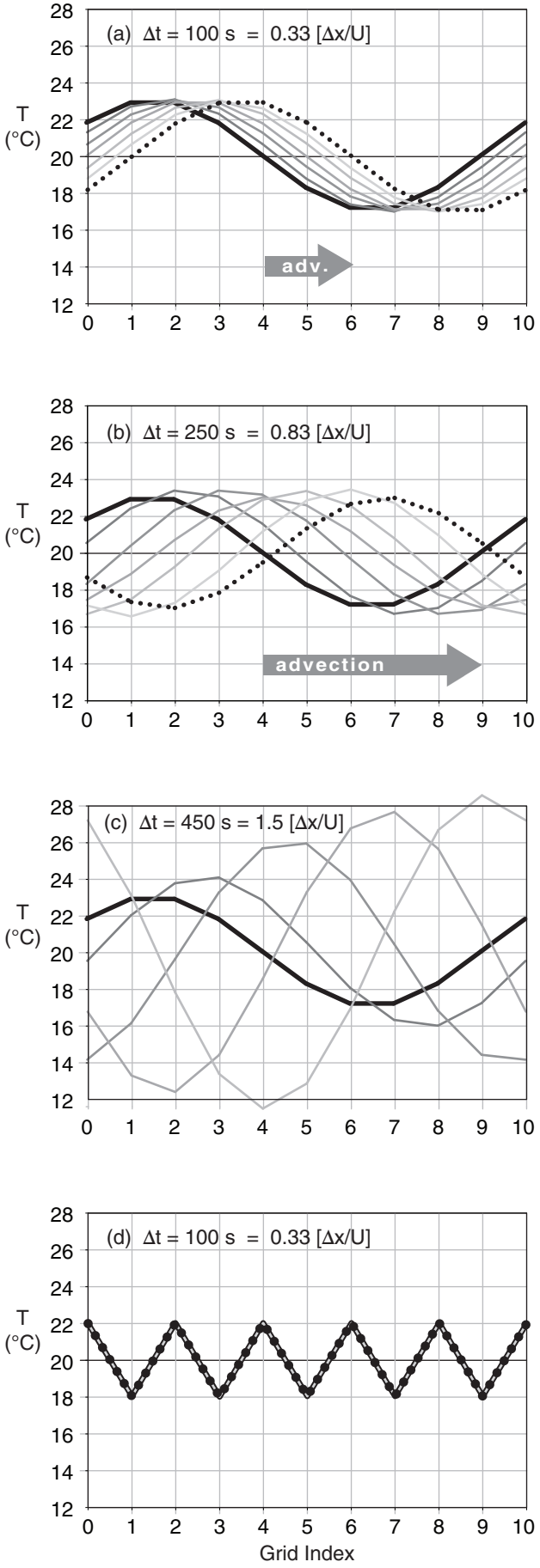

Truncation Error

Truncation error was already discussed, and refers to the neglect (i.e., truncation) of higher-order terms in a Taylor series approximation to local gradients. If we retain more terms in the Taylor series, then the result is a higher-order solution that is more accurate, but which takes longer to run because there are more terms to compute. If we truncate the series at lower order, the numerical solution is faster but less accurate. In NWP, time and space difference schemes are chosen as a compromise between accuracy and speed.

Numerical Instability

Numerical instability causes forecasts to **blow up**. Namely, the numerical solution rapidly diverges from the true solution, can have incorrect sign, and can approach unphysical values (±∞). Truncation error is one cause of numerical instability.

Numerical instability can also occur if the wind speeds are large, the grid size is small, and the time step is too large. For example, eq. (20.16) models advection by using temperature in neighboring grid cells. But what happens if the wind speed is so strong that temperature from a more distant location in the real atmosphere (beyond the neighboring cell) can arrive during the time step Δt? Such a physical situation is not accounted for in the numerical approximation of eq. (20.16). This can create numerical errors that amplify, causing the model to blow up (see Fig. 20.11).

Such errors can be minimized by taking a small enough time step. The specific requirement for stability of advection processes in one dimension is

$$\Delta t \leq \frac{\Delta X}{|U|} \qquad \bullet(20.18)$$

with similar requirements in the y and z directions. This is known as the **Courant-Friedrichs-Lewy** (**CFL**) **stability criterion**, or the **Courant condition**. When modelers use finer mesh grids with smaller ΔX values, they must also reduce Δt to preserve numerical stability. The combined effect greatly increases model run time on the computer. For example, if ΔX and ΔY are reduced by half, then

Figure 20.11 (at left)
Examples of numerical stability for advection, with ΔX = 3 km and U = 10 m/s. Thick black line is initial condition, and the forecast after each time step is shown as lighter grey, with the last (6^{th}) step dotted. A temperature signal of wavelength $10{\cdot}\Delta X$ is numerically stable for time steps Δt of (a) 100 s and (b) 250 s, but (c) = 450 s exceeds the CFL criterion, and the solution blows up (i.e., the wave amplitude increases without bound).
(d) A $2{\cdot}\Delta X$ wave does not advect at all (i.e., is unphysical).

FOCUS • Resolution vs. Grid Spacing

Theoretically, the smallest horizontal wavelength you can resolve with data at discrete grid points is $2{\cdot}\Delta X$. However, the finite-difference equations that are used to describe advection and other dynamics in NWP models are unable to handle $2{\cdot}\Delta X$ waves. Namely, these waves either do not advect at all (Fig. 20.11d), or they are numerically unstable.

To avoid such unphysical behavior, small wavelength waves are numerically filtered out of the model. As a result, the smallest waves that are usually retained in NWP models are about 5 to $7{\cdot}\Delta X$.

Hence, the actual **resolution** (i.e., the smallest weather features that can be modeled) are about 7 times the **grid spacing**. Stated another way, if you know the size of the smallest weather system or terrain-related flow that you want to be able to forecast, then you need to design your NWP model with horizontal grid spacing ΔX smaller than 1/7 of that size.

so must Δt, thereby requiring 8 times as many computations to complete the forecast.

For other physical processes such as diffusion and wave propagation, there are other requirements for numerical stability. To preserve overall stability in the model, one must satisfy the most stringent condition; that is, the one requiring the smallest time step. Some high-resolution NWP models use time steps of Δt = 5 s or less.

For advection, one way to avoid the time-step limitation above is to use a **semi-Lagrangian** method. This scheme uses the wind at each grid point to calculate a **backward trajectory**. The backward trajectory indicates the source location for air blowing into the grid cell of interest. This source location need not be adjacent to the grid-cell of interest. By carrying the values of meteorological variables from the source to the destination during the time step, advection can be successfully modeled (i.e., be numerically stable) even for long time steps.

FOCUS • Lipschitz Continuity

A semi-Lagrangian numerical approach can be numerically stable if the velocity and advected variables A are limited in how fast they vary along the back trajectory path s. Namely, a graph of A vs. s must not cross into the grey shaded cone of Fig. 20.E, for a double cone centered anywhere along s.

This smoothness requirement is called the **Lipschitz condition**. In the example shown in Fig. 20.E, the curve at (1) is OK, but at (2) is bad because the curve crosses the grey cone.

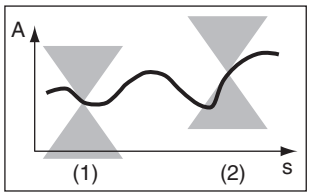

Fig. 20.E

Solved Example

What grid size, domain size, number of grid points, and time steps would you use for a numerical model of a hurricane, and how many computations would be needed to make a 3-day forecast? How fast should your computer be? [Hint: Use info from the Hurricane chapter.]

Solution

This is an example of how you **design an NWP system**, including both the software and hardware.

Assume the smallest feature you want to resolve is a thunderstorm in the eyewall. If tropical thunderstorms are about 14 km in diameter, then you would want **ΔX** = (14 km)/7 = **2 km** to horizontally resolve it.

Hurricanes can be 300 km in diameter. To model the whole hurricane and a bit of its surrounding environment, you might want a horizontal **domain of 500 km by 500 km**. This works out to (500 km / 2 km) = 250 grid points in each of the x and y directions, giving $(250)^2$ = 62,500 grid points in the horizontal. If you want a model with 50 vertical levels, then you need (50) · (62,500) = **3,125,000 grid points total**.

If you want to be able to forecast hurricanes up through category 5 (wind speed > 69 m/s), then design for a max wind of 80 m/s. The CFL criterion (eq. 20.18) gives Δt = (2000 m)/(80 m/s) = 25 s. Thus, a 3-day forecast would require (72 h) · (3600 s/h) / (25 s) = **10,368 time steps**.

The temperature forecast eq (20.17) has about 43 arithmetic operations (adds, subtracts, multiplies, divides). We have 7 equations of motion, so this gives about (7 ·43 ≈) 300 operations. You must do these operations at each grid point for each time step, giving a total = 3,125,000 x 10,368 x 300 ≈ 10^{13} operations.

But we haven't included the calculations for all the other physics (clouds, turbulence, precipitation, radiation, etc.) that must be done at each grid point. As a quick estimate, round up to 10^{15} **floating-point** (real-number) operations.

But you need to complete all these calculations quickly, in order to be useful as a forecast to warn people to evacuate. Suppose you design the model to finish within 3 h (=10,800 s) of computer run time. Thus, your computer must be powerful enough to compute at the rate of (10^{15} operations)/(10,800 s) ≈ 10^{11} = **100 Giga flops** (where 1 **flops** = 1 **floating-point operation per second**).

Check: Units OK. Physics OK.

Discussion: The number of calculations needed to make a hurricane forecast is tremendous, and requires a powerful computer. As computer power increases, NWP modelers strive for finer horizontal and vertical resolution spanning larger domains, and including more accurate (and complex) physics parameterizations.

Namely, NWP modelers always tend to fully use all the computer power available, and dream of even more powerful computers.

ON DOING SCIENCE • Mathematics

"To have to translate one's verbal statement into mathematical formulae compels one to scrutinize the ideas therein expressed. Next the possession of formulae makes it much easier to deduce the consequences. In this way absurd implications, which might have passed unnoticed in a verbal statement, are brought clearly into view & stimulate one to amend the formula.

Mathematical expressions have, however, their special tendencies to pervert thought: the definiteness may be spurious, existing in the equation but not in the phenomena to be described; and the brevity may be due to the omission of the more important things, simply because they cannot be mathematized. Against these faults we must constantly be on our guard."

– L.F. Richardson, 1919

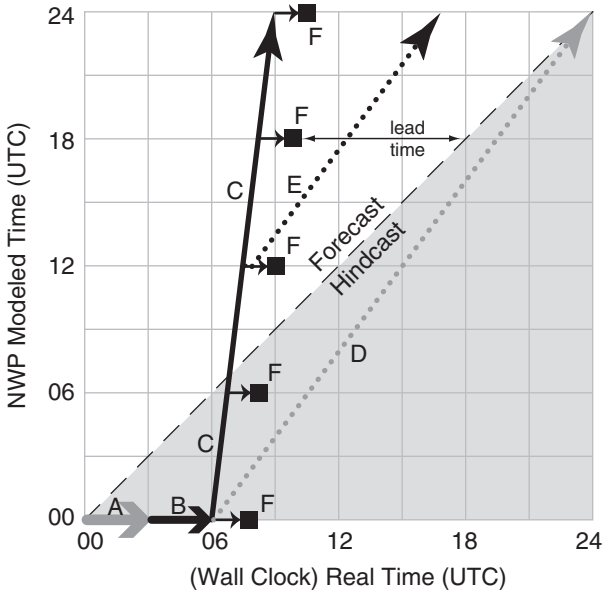

Figure 20.12
Hypothetical forecast schedule, for a 00 UTC initialization.
A: wait for weather observations to arrive.
B: data assimilation to produce the analysis (ICs).
C: coarse-mesh forecast.
D: fine-mesh forecast, initialized from 00 UTC.
E: fine-mesh forecast initialized from coarse forecast at 12 h.
F: postprocessing and creation of products (e.g., weather maps).

THE NUMERICAL FORECAST PROCESS

Weather forecasting is an **initial value problem**. As shown in eq. (20.17), you must know the **initial conditions** on the right hand side in order to forecast the temperature at later times ($t + \Delta t$). Thus, to make forecasts of real weather, you must start with observations of real weather.

Weather-observation platforms and instruments were already discussed in the Weather Reports chapter. Data from these instruments are communicated to central locations. Government forecast centers use these weather data to make the forecasts.

There are three phases of this forecast process. First is pre-processing, where weather observations from various locations and times around the world are assimilated into a regular grid of initial conditions known as an **analysis**. Second is the actual computerized NWP forecast, where the finite-difference approximations of the equations of motion are iteratively stepped forward in time. Finally, **post-processing** is performed to refine and correct the forecasts, and to produce additional secondary products tailored for specific users.

Fig. 20.12 shows a hypothetical forecast schedule, for a weather forecast initialized from 00 UTC synoptic observations. First, it takes a few hours (timeline A in Fig. 20.12) for all the data to be communicated from around the world to the weather forecast center (WFC). This step includes quality control, and rejection of suspected bad data.

Next, the data assimilation programs run for a few hours (B) to create a gridded analysis field. This is the optimum initial condition for the NWP model. At this point, we are ready to start making the forecast, but the initial conditions are already 6 h old compared to the present weather.

So the first part of forecast (C) is spent trying to catch up to "present". This wasted initial forecast period is not lamented, because startup problems associated with the still-slightly-imbalanced initial conditions yield preliminary results that should be discarded anyway. Forecasts that occur AFTER the weather has already happened are known as **hindcasts**, as shown by the shaded area in Fig. 20.12.

The computer continues advancing the forecast (C) by taking small time steps. As the NWP forecast reaches key times, such as 6, 12, 18, and 24 (=00) UTC, the forecast fields are saved for post-processing and display (F). **Lead time** is how much the forecast is ahead of real time. For example, for coarse-mesh model (C), weather-map products (F) that are produced for a **valid time** of 18 UTC appear with a lead time of about 8 h before 18 UTC actually happens, in this hypothetical illustration.

Fig. 20.12 shows a coarse-mesh model (C) that takes 3 h of computation for each 24 h of forecast, as indicated by the slope of line (C). A finer-mesh model might take longer to run (with gentler slope). Model (D) takes 18 h to make a 24 h forecast, and if initialized from the 00 UTC initial conditions, might never catch up to the real weather during Day 1. Hence, it would be useless as a forecast — it would never escape from the hindcast domain.

But for one-way nesting, a fine-mesh forecast (E) could be initialized from the 12 UTC coarse-mesh forecast. This is analogous to a multi-stage rocket, where the coarse mesh (C) blasts the forecast from the past to the future, and then the finer-mesh (E) can remain in the future even though E has the same slope as D.

NWP meteorologists always have the need for speed. Faster computers allow most phases of the forecast process to run faster, allowing finer-resolution forecasts over larger domains with more accuracy and greater lead time. Speed-up can also be achieved computationally by making the dynamics and physics subroutines run faster, by utilizing more processor cores, and by utilizing special computer chips such as **Graphics Processing Units** (**GPU**s). However, tremendous speed-up of a few subroutines might cause only a small speed-up in the overall run time of the NWP model, as explained by **Amdahl's Law** (see Focus Box).

The actual duration of phases (A) through (F) vary with the numerical forecast center, depending on their data-assimilation method, model numerics, domain size, grid resolution, and computer power. Details of the forecast phases are explained next.

Balanced Mass and Flow Fields

Over the past few decades it was learned by hard experience that numerical models give bad forecasts if they are initialized with the raw observed data. One reason is that the in-situ observation network has large gaps, such as over the oceans and in much of the Southern Hemisphere. Also, while there are many observations at the surface, there are fewer in-situ observations aloft. Remote sensors on satellites do not observe many of the needed dynamic variables (U, V, W, T, r_T, ρ) directly, and have very poor vertical resolution. Observations can also contain errors, and local flow around mountains or trees can cause observations that are not representative of the larger-scale flow.

The net effect of such gaps, errors, and inconsistencies is that the numerical representation of this initial condition is **imbalanced**. By imbalanced, we mean that the observed winds disagree with the theoretical winds, where theoretical winds such as

FOCUS • Amdahl's Law

Computer architect Gene Amdahl described the overall speedup factor S_{ALL} of a computer program as a function of the speedup S_i of individual subroutines, where P_i is the portion of the total computation done by subroutine i:

$$S_{ALL} = \left[\sum (P_i / S_i)\right]^{-1}$$

and where $\Sigma P_i = 1$.

Special programs called **profilers** can find how much time it takes to run each component of an NWP model, such as for the implementation of the WRF model shown below.

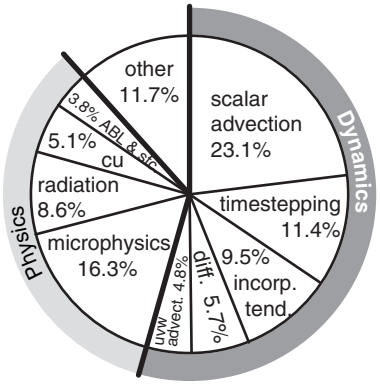

Fig. 20.F. *Portion of total run time of the WRF model for some of the major components.*
"incorp. tend." = incorporation of tendencies.
"diff." = diffusion.
"uvw advect." = advection of U, V, and W wind components.
"microphysics" = hydrometeor parameterizations.
"cu" = parameterizations for convective clouds.
"ABL & sfc." = boundary layer and surface parameterizations.

For example, if **graphics-processing units** (**GPUs**) speed-up the microphysics 20 times and speedup scalar advection by 1.8 times (i.e., an 80% speedup), and the remaining 60.6% of WRF has no speedup, then overall:

$$S_{ALL} = [0.163/20 + 0.231/1.8 + 0.606/1]^{-1} = \underline{\mathbf{1.35}}$$

Namely, even though the microphysics portion of the model is sped up 2000%, the overall speedup of WRF is 35% in this hypothetical example.

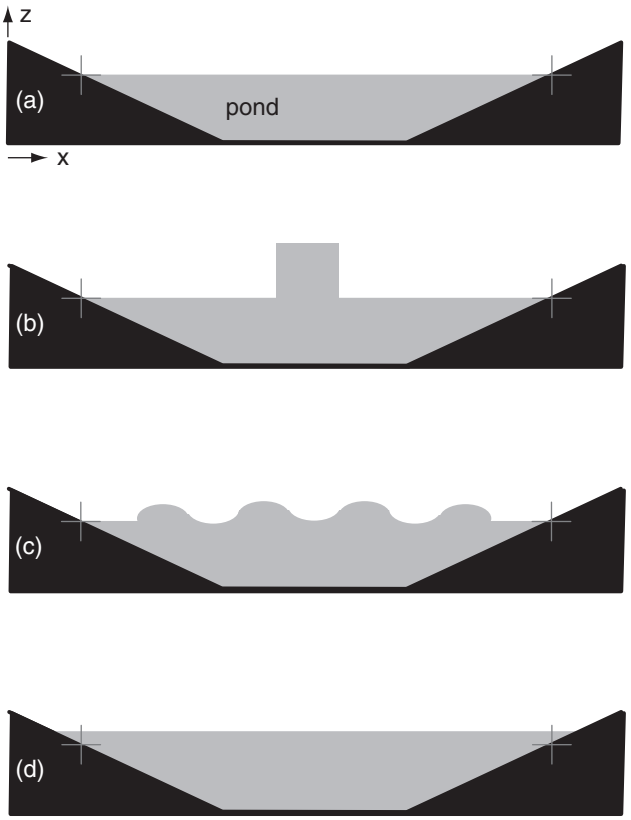

Figure 20.13
Demonstration of a dynamic system becoming balanced. (a) Balanced initial state of a pond of water (shaded grey), with no waves and no currents. (b) Extra water added in center of pond, causing the water-mass distribution to not be in equilibrium with the waves and currents. (c) Wave generation as the pond adjusts itself toward a new balanced state. (d) Final balanced state with slightly higher water everywhere, but no waves and no currents.

Science Graffito

"The scheme is complicated because the atmosphere is complicated."
– L.F. Richardson, 1922: *Weather Prediction by Numerical Process*. Cambridge University Press.

the geostrophic wind are based on temperature and pressure fields via atmospheric dynamics.

Balanced and imbalanced flows can be illustrated with a pond of water. Suppose initially the water-level is everywhere level, and the water currents and waves are zero (Fig. 20.13a). This flow system is **balanced**, because with a level pond surface we indeed expect no currents or waves. Next, add extra water to the center of the pond (Fig. 20.13b). This **mass field** (i.e., the distribution of water mass in the pond) is not balanced with the **flow field** (i.e., the motions or circulations within the pond, which for Fig. 20.13b are assumed to be zero). This imbalance causes waves and currents to form (Fig. 20.13c), which help to redistribute mass. These transient waves and currents decay, leaving the pond in a new balanced state (i.e., level water surface, no waves, no currents), but with slightly greater water depth.

Consider what happens to a numerical model of the pond if observation errors are incorporated into the initial conditions. Suppose that the water level in the center of the numerical pond is erroneously "observed" to be 1 m higher than the level everywhere else (Fig. 20.13b). Namely, the "true" initial conditions might be like Fig. 20.13a, but observation errors might cause the "modeled" initial conditions to be like Fig. 20.13b.

A well-designed numerical model of a pond would simulate the dynamical behavior of an actual pond. Hence, the modeled pond would respond as in Figs. 20.13c & d, even though the actual pond would remain motionless as in Fig. 20.13a.

The transient waves and currents are an artifact of the poor initial conditions in the model, and are not representative of the true flow in the real pond. Hence, the forecast results are not to be trusted during the first few minutes of the forecast period while the model is adjusting itself to a balanced state.

Numerical forecasts of the atmosphere have the same problem, but on a longer time scale than a pond. Namely, the first 0.5 to 3 hours of a weather forecast are relatively useless while the model adjusts to imbalances in the initial conditions (see the Data Assimilation section). During this startup period, simulated atmospheric waves are bouncing around in the model, both vertically and horizontally.

After the first 3 to 12 h of forecast, the dynamics are fairly well balanced, and give essentially the same forecast as if the fields were balanced from the start. However, spurious waves in the model might also cause unjustified rejection of good data during data assimilation (see next subsection).

Also, the erroneous waves can generate erroneous clouds that cause erroneous precipitation, etc. The net result could be an unrealistic loss of water from the model that could reduce the chance of future cloud formation and precipitation. Change of

water content is just one of many **irreversible processes** that can permanently harm the forecast.

In summary, initialization problems cause a transient period of poor forecast quality, and can permanently degrade longer-term forecast skill or cause rejection of good data. Hence, data-assimilation methods to reduce startup imbalances, such as described next, are highly desirable.

Data Assimilation and Analysis

The technique of incorporating observations into the model's initial conditions is called **data assimilation**. Most assimilation techniques capitalize on the tendency of NWP models to create a balanced state during their forecasts.

One can utilize the balanced state from a previous forecast as a **first guess** of the initial conditions for a new forecast. When new weather observations are incorporated with the first guess, the result is called a weather **analysis**.

To illustrate the initialization process, suppose a forecast was started using initial conditions at 00 UTC, and that a 6-hour forecast was produced, valid at 06 UTC. This 06 UTC forecast could serve as the first guess for new initial conditions, into which the new 06 UTC weather observations could be incorporated. The resulting 06 UTC analysis could then be used as the initial conditions to start the next forecast run. The process could then be repeated for successive forecasts started every 6 h.

Although the analysis represents current or recent-past weather (not a forecast), the analyzed field is usually not exactly equal to the raw observations because the analysis has been smoothed and partially balanced. Observations are used as follows.

First, an automated initial screening of the raw data is performed. During this **quality control** phase, some observations are rejected because they are unphysical (e.g., negative humidities), or they disagree with most of the surrounding observations. In locations of the world where the observation network is especially dense, neighboring observations are averaged together to make a smaller number of statistically-robust observations.

When incorporating the remaining weather observations into the analysis, the raw data from various sources are not treated equally. Some sources have greater likelihood of errors, and are weighted less than those observations of higher quality. Also, observations made slightly too early or too late, or made at a different altitude, are weighted less. In some locations such as the tropics where Coriolis force and pressure-gradients are weak, more weight can be given to the winds than to the pressures.

We focus on two data-assimilation methods here: optimum interpolation and variational. Both are

FOCUS • The Pacific Data Void

One hazard of data assimilation is that the resulting analysis does not represent truth, because the analysis includes a previous forecast as a first guess. If the previous forecast was wrong, then the subsequent analysis is poor.

Even worse are situations where there are little or no observation data. For data-sparse regions, the first-guess from the previous forecast dominates the "analysis". This means that future forecasts start from old forecasts, not from observations. Forecast errors tend to accumulate and amplify, causing very poor forecast skill further downstream.

One such region is over the N.E. Pacific Ocean. From Fig. 9.23 in the Weather Reports & Map Analysis chapter, there are no rawinsonde observations (RAOBs) in that region to provide data at the dynamically important mid-tropospheric altitudes. Ships and buoys provide some surface data, and aircraft and satellites provide data near the tropopause, but there is a sparsity of data in the middle. This is known as the **Pacific data void**.

Poor forecast skill is indeed observed downstream of this data void, in British Columbia, Canada, and Washington and Oregon, USA. The weather-forecast difficulty there is exacerbated by the complex terrain of mountains and shoreline.

FOCUS • Giving a Weather Briefing

NWP forecast maps make up an important part of most weather briefings, but they should not be the only part. Bosart (2003), Snelling (1982), West (2011), and others recommend the following:

Your discussion should answer 6 questions:
- What has happened?
- Why has it happened?

- What is happening?
- Why is it happening?

- What will happen?
- Why will it happen?

Identify forecast issues throughout your briefing:
- Difficult/tricky forecast details.
- Significant/interesting weather.

Go from the large-scale to the smaller scales.
Verify your previous forecast.
Encourage questions, discussion, and debate.

For the past and current weather portions of the briefing, show satellite images/animations, radar images/animations, soundings, and weather analyses.

Speak clearly, concisely, loudly, and with confidence. No forecast is perfect, but do the best you can. Your audience will appreciate your sincerity.

Table 20-2.
Standard deviation σ_o of observation errors.

Sensor Type	σ_o
Wind errors in the lower troposphere:	(m/s)
Surface stations and ship obs	3 to 4
Drifting buoy	5 to 6
Rawinsonde, wind profiler	0.5 to 2.7
Aircraft and satellite	3
Pressure errors:	(kPa)
Surface weather stations & Rawinsonde	0.1
Ship and drifting buoy	0.2
S. Hemisphere manual analysis	0.4
Geopotential height errors:	(m)
Surface weather stations	7
Ship and drifting buoy	14
S. Hemisphere manual analysis	32
Rawinsonde	13 to 26
Temperature errors:	(°C)
ASOS surface automatic weather stn.	0.5 to 1.0
Rawinsonde upper-air obs at $z < 15$ km	0.5
at altitudes near 30 km	< 1.5
Humidity errors:	
ASOS surface weather stations: T_d (°C)	0.6 to 4.4
Rawinsonde in lower troposph. RH (%)	5
near tropopause: RH (%)	15

Solved Example

A drifting buoy observes a wind of M = 10 m/s, while the first guess for the same location gives an 8 m/s wind with 2 m/s likely error. Find the analysis wind speed.

Solution

Given: M_O = 10 m/s, M_F = 8 m/s, σ_f = 2 m/s
Find: M_A = ? m/s

Use Table 20-2 for Wind Errors: Drifting buoy:
σ_o = 6 m/s

Use eq. (20.20) for wind speed M:

$$M_A = M_F \cdot \frac{\sigma_o^2}{\sigma_f^2 + \sigma_o^2} + M_O \cdot \frac{\sigma_f^2}{\sigma_f^2 + \sigma_o^2}$$

$$M_A = (8\text{m/s}) \cdot \frac{(6\text{m/s})^2}{(2\text{m/s})^2 + (6\text{m/s})^2} + (10\text{m/s}) \cdot \frac{(2\text{m/s})^2}{(2\text{m/s})^2 + (6\text{m/s})^2}$$

= (8 m/s)·(36/40) + (10 m/s)·(4/40) = **8.2 m/s**

Check: Units OK. Physics OK.
Discussion: Because the drifting buoy has such a large error, it is given very little weight in producing the analysis. If it had been given equal weight as the first guess, then the average of the two would have been 9 m/s. It might seem disconcerting to devalue a real observation compared to the artificial value of the first guess, but it is needed to avoid startup problems.

objective analysis methods in the sense that they are calculated by computer based on equations, in contrast to a "subjective analysis" by a human (such as was demonstrated in the Map Analysis chapter).

Objective optimum interpolation

Let σ_o be the standard deviation of raw-observation errors from a sensor such as a rawinsonde (Table 20-2). Larger σ indicates larger errors.

Let σ_f be the standard deviation of errors associated with the **first guess** from a previous forecast. These are also known as **background errors**. Generally, error increases with increasing forecast range. For example, some global NWP models have the following errors for geopotential height Z of the 50-kPa isobaric surface:

$$\sigma_{Zf} = a \cdot t \qquad (20.19)$$

where $a \approx 11$ m/day and t is forecast time range. Namely, a first guess from a 2-day forecast is less accurate (has greater error) than a first guess from a 1-day forecast.

An **optimum interpolation** analysis weights the first guess F and the observation O according to their errors to produce an analysis field A:

$$A = F \cdot \frac{\sigma_o^2}{\sigma_f^2 + \sigma_o^2} + O \cdot \frac{\sigma_f^2}{\sigma_f^2 + \sigma_o^2} \qquad (20.20)$$

where A, F, O , and σ all apply to the same one weather element, such as pressure, temperature, or wind. If the observation has larger errors than the first guess, then the analysis weights the observation less and the first-guess more.

The equation above can be used to define a **cost function** J:

$$J(A) = \frac{1}{2}\left[\frac{(F-A)^2}{\sigma_f^2} + \frac{(O-A)^2}{\sigma_o^2}\right] \qquad (20.21)$$

where the optimum analysis from eq. (20.20) gives the minimum cost for eq. (20.21).

Optimum interpolation is "local" in the sense that it considers only the observations near a grid point when producing an analysis for that point. Optimum interpolation is not perfect, leaving some imbalances that cause atmospheric gravity waves to form in the subsequent forecast. A **normal-mode initialization** modifies the analysis further by removing the characteristics that might excite gravity waves.

Variational data assimilation

Another scheme, called **variational analysis**, attempts to match secondary characteristics calculated from the analysis field to observations so as to minimize the cost function. For example, the radiation emitted by air of the analyzed temperature is compared to radiance measured by satellite, allowing corrections to be made to the temperature analysis as appropriate.

Eq. (20.21) can be modified to utilize such secondary observations:

$$J(A) = \frac{1}{2}\left[\frac{(F-A)^2}{\sigma_f^2} + \frac{(Y-H(A))^2}{\sigma_{yo}^2} \right] \qquad (20.22)$$

where H is an operator that converts from the analysis variable A to the secondary observed variable Y, and σ_{yo} is the standard deviation of observation errors for variable Y. The "best" analysis A is the one that minimizes the value of the cost function J. This minimum can be found by an iterative approach, or by trial and error.

For example, suppose a satellite radiometer looks toward Paris, and measures the upwelling radiance L for an infrared wavelength λ corresponding to the water-vapor channel of Fig. 8.8 in the Remote Sensing chapter. This channel has the strongest returns at about 8 km altitude. For this example, Y is the measured radiance L. $H(A)$ is the Planck blackbody radiance function (eq. 8.1), and A is the analysis temperature at 8 km over Paris. To find the best analysis: guess different values of A, calculate the associated cost function values, and iterate towards the value of A that yields the lowest value of cost function.

The variational approach allows you to consider all worldwide observations at the same time — a method called **3DVar**. To do this, the first-guess (F), analysis (A), and observation (O) factors in eq. (20.22) must be replaced by vectors (arrays of numbers) containing all grid points in the whole 3-D model domain, and all observations worldwide made at the analysis time. Also, the first-guess and observation error variances must be replaced by covariance matrices. Although the resulting matrix-equation version of (20.22) contains millions of elements, large computers can iterate towards a "best" analysis.

An extension is **4DVar**, where the additional dimension is time. This allows off-time observations to be incorporated into the variational analysis. 4DVar is even more computationally expensive than 3DVar. Although the role of any analysis method is to create the initial conditions for an NWP forecast, often it takes more computer time and power to create the optimum initial conditions than to run the subsequent numerical forecast.

Solved Example

The water vapor channel of a satellite observes a radiance of 1.53 $W{\cdot}m^{-2}{\cdot}\mu m^{-1}{\cdot}sr^{-1}$ over Paris. On average, this channel has an error standard deviation of 0.05 $W{\cdot}m^{-2}{\cdot}\mu m^{-1}{\cdot}sr^{-1}$. Output from a previous NWP run gives a temperature of –35°C at altitude 8 km over Paris, which we can use as a balanced first guess for the new analysis. This forecast has an error standard deviation of 1°C. The upper troposphere over Paris is very humid. For your analysis, find the "best" estimate of the temperature at 8 km over Paris.

Solution

Given: L_o = 1.53 $W{\cdot}m^{-2}{\cdot}\mu m^{-1}{\cdot}sr^{-1}$, T_F = –35°C at 8 km σ_{Lo} = 0.05 $W{\cdot}m^{-2}{\cdot}\mu m^{-1}{\cdot}sr^{-1}$, σ_{Tf} = 1°C , water-vapor channel: λ = 6.7 μm from the Remote Sensing chapter with peak weighting function at $z \approx 8$ km. High humidity implies blackbody emissions.

Find: T_A = ? °C at 8 km altitude over Paris.

Use eq. (20.22), & use Planck's Law eq. 8.1 for $H(T_A)$

$$J(T_A) = \frac{1}{2}\left\{ \frac{(T_F - T_A)^2}{\sigma^2_{Tf}} + \frac{1}{\sigma^2_{Lo}}\left[L_o - \frac{c_{1B}\cdot\lambda^{-5}}{\exp\left(\frac{c_2}{\lambda\cdot T_A}\right) - 1} \right]^2 \right\}$$

with c_{1B} = 1.191043x10^8 $W{\cdot}m^{-2}{\cdot}\mu m^4{\cdot}sr^{-1}$ and c_2 = 14387.75 μm K from near eq. (8.1) in The Remote Sensing chapter. [Hint: don't forget to convert T_A in Kelvin to use in Planck's Law.]

Calculate $J(T_A)$ for various values of T_A. I will start with a std. atmosphere guess of T_A = –37°C at 8 km.

$J = 0.5 \cdot \{ [(-35°C)-(-37°C)]^2/(1°C)^2 +$
$(1/(0.05u)^2 \cdot [1.53u - (8822u/(\exp(9.09926) - 1))]^2 \}$
$J = 0.5 \cdot \{ 4 + 118.4 \} = 61.2$ (dimensionless)

where u are units of $W{\cdot}m^{-2}{\cdot}\mu m^{-1}{\cdot}sr^{-1}$.

Repeating the calculation in a spreadsheet for other values of T_A in the range of –37 to –25°C gives:

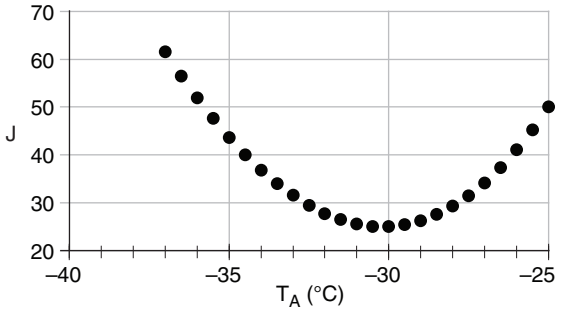

The best analysis is at minimum cost J, near T_A= **–30°C**

Check: Units OK. T_A value reasonable.

Discussion: The satellite radiance corresponds to a brightness temperature of –25°C. An error propagation calculation (see Appendix A) for eq. (8.1) shows that a radiance error of σ_{Lo} = 0.05 $W{\cdot}m^{-2}{\cdot}\mu m^{-1}{\cdot}sr^{-1}$ corresponds to a brightness-temperature error of 1°C. Thus, both the first guess and the observed radiance have the same effective error, giving T_A equally weighted between the satellite value –25°C and the first-guess value –35°C. Try different error values in the spreadsheet to see how T_A varies between –35 & –25°C.

Table 20-3. Hierarchy of operational numerical weather prediction (NWP) models.

Forecast Type	Fcst. Duration & (Fcst. Cycle)	Domain & (ΔX)
nowcasts	0 to 3 h (re-run every few minutes)	local: town, county (100s of m)
short-range	3 h to 3 days (re-run every few hours)	regional: state, national, continental (1 to 5 km)
medium-range	3 to 7 days (re-run daily)	continental to global (5 to 25 km)
long-range	7 days to 1 month (re-run daily or weekly)	global (25 to 100 km)
seasonal	1 to 12 months (re-run monthly)	global (100 to 500 km)
GCM*	1 to 1000 years [non-operational (not run routinely); focus instead on case studies & hypothetical scenarios.]	global (100 to 500 km)

** GCM = Global Climate Model -or- General Circulation Model.*

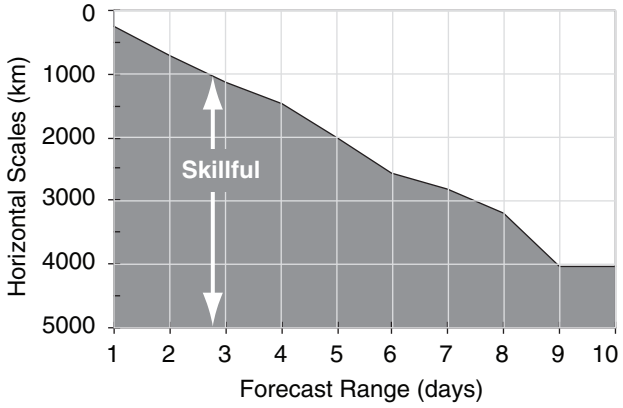

Figure 20.14
Range of horizontal scales having reasonable forecast skill (shaded) for various forecast durations. [from the European Centre for Medium Range Weather Forecasts (ECMWF), 1999]

Forecast

The next phase of the forecast process is the running of the NWP models. Recall that weather consists of the superposition of many different scales of motion (Table 10-6), from small turbulent eddies to large Rossby waves. Different NWP models focus on different time and spatial scales (Table 20-3).

Unfortunately, the forecast quality of the smaller scales deteriorates much more rapidly than that for the larger scales. For example, cloud forecasts might be good out to 2 to 12 hours, frontal forecasts might be good out to 12 to 36 hours, while the Rossby-wave forecasts might be useful out to several days. Fig. 20.14 indicates the ranges of horizontal scales over which the forecast is reasonably skillful.

Don't be deceived when you look at a weather forecast, because all scales are superimposed on the weather map regardless of the forecast duration. Thus, when studying a 5 day forecast, you should try to ignore the small features on the weather map such as thunderstorms or frontal positions. Even though they exist on the map, they are probably wrong. Only the positions of the major ridges and troughs in the jet stream might possess any forecast skill at this forecast duration. Maps in the next section illustrate such deterioration of small scales.

Case Study: 22-25 Feb 1994

Figures 20.15 show the weather valid at 00 UTC on 24 February 1994 — same case study used in the Extratropical Cyclone chapter. Fig. 20.15a gives the

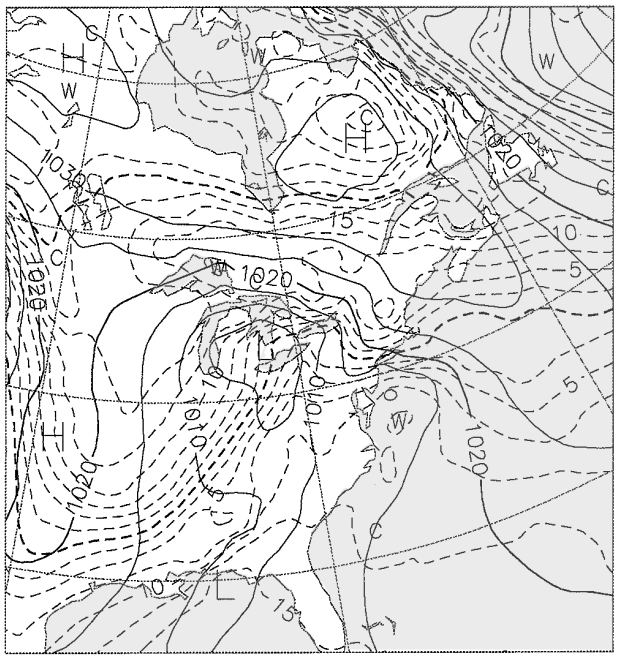

Figure 20.15a
Analysis of 85 kPa temperature and mean-sea-level pressure, valid 00 UTC 24 Feb 94. (Courtesy of ECMWF.)

verifying analysis; namely, a smoothed fit to the actual weather measured at 00 UTC on 24 Feb 1994.

Figs. 20.15b-e give the weather forecasts valid for the same time, but initialized 1.5, 3.5, 5.5, and 7.5 days earlier. For example, Fig. 20.15b was initialized with weather observations from 12 UTC on 22 Feb 94, and the resulting 1.5 day forecast valid at 00 UTC on 24 Feb 94 is shown in the figure. Fig. 20.15c was initialized from 12 UTC on 20 Feb 94, and the resulting 3.5 day forecast is shown in the figure. Thus, each succeeding figure is the result of a longer-range forecast, which started with earlier observations, but ended at the same time.

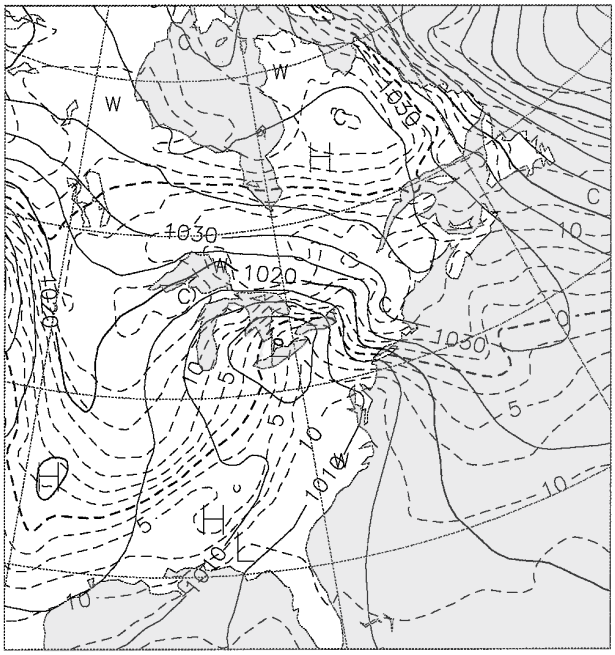

Figure 20.15b
1.5-day forecast, valid 00 UTC 24 Feb 94, started from initialization data at 12 UTC on 22 Feb 94. (From ECMWF.)

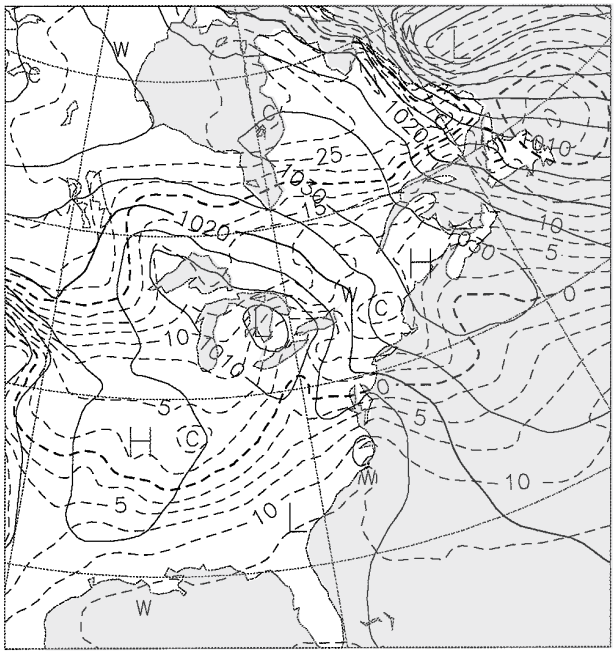

Figure 20.15d
5.5-day forecast, valid 00 UTC 24 Feb 94, started from initialization data at 12 UTC on 18 Feb 94. (From ECMWF.)

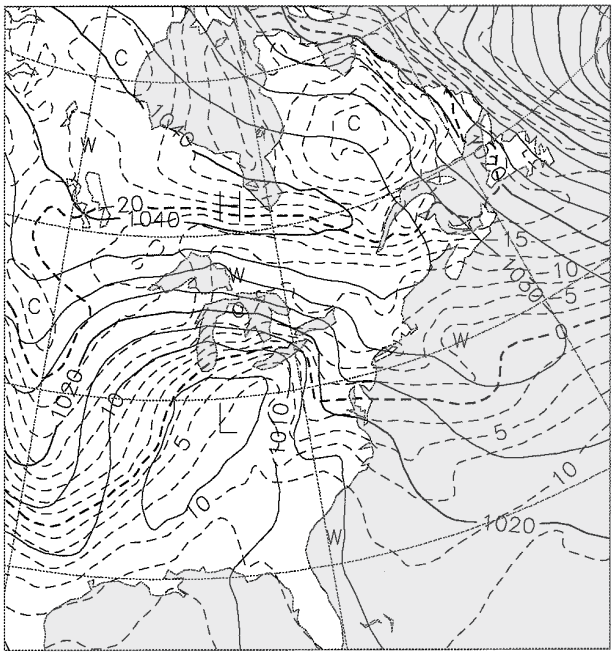

Figure 20.15c
3.5-day forecast, valid 00 UTC 24 Feb 94, started from initialization data at 12 UTC on 20 Feb 94. (From ECMWF.)

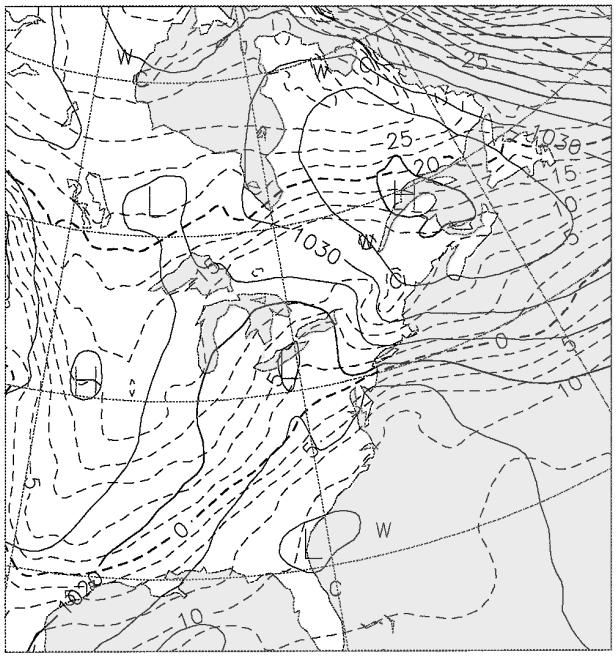

Figure 20.15e
7.5-day forecast, valid 00 UTC 24 Feb 94, started from initialization data at 12 UTC on 16 Feb 94. (From ECMWF.)

FOCUS • Linear Regression

Suppose that y represents a weather element observed at a weather station. Let x be the corresponding forecast by a NWP model. Over many days, you might accumulate many (N) data points (x_i, y_i) of forecasts and corresponding observations, where i is the data-point index.

If you anticipate that the relationship between x and y is linear, then that relationship can be described by:

$$y = a_o + a_1 \cdot x$$

where a_o is an unknown bias (called the **intercept**), and a_1 is an unknown trend (called the **slope**).

The best-fit (in the **least-squared** error sense) coefficients are:

$$a_o = \frac{\left(\overline{x}\right)\cdot\overline{xy} - \overline{x^2}\cdot\left(\overline{y}\right)}{\left(\overline{x}\right)^2 - \overline{x^2}} \qquad a_1 = \frac{\left(\overline{x}\right)\cdot\overline{y} - \overline{xy}}{\left(\overline{x}\right)^2 - \overline{x^2}}$$

The overbar indicates an average over all data points of the quantity appearing under the overbar; e.g.:

$$\overline{x} = \frac{1}{N}\sum_{i=1}^{N} x_i \qquad \overline{xy} = \frac{1}{N}\sum_{i=1}^{N}\left(x_i \cdot y_i\right) \qquad \overline{x^2} = \frac{1}{N}\sum_{i=1}^{N}\left(x_i{}^2\right)$$

FOCUS • Kalman Filter (KF)

Rudolf Kalman suggested a method that we can modify to estimate the bias x in tomorrow's forecast. It uses the observed bias y in today's forecast, and also uses yesterday's estimate for today's bias x_{old}:

$$x = x_{old} + \beta\cdot\left(y - x_{old}\right)$$

The **Kalman gain** β depends on ratio $r = \sigma^2_{PL}/\sigma^2_{NWP}$, where σ^2_{PL} is the "predictability-limit" error variance associated with the chaotic nature of a "perfect" weather-forecast model, and σ^2_{NWP} is the error variance of the operational NWP model. If those error variances are steady, then $\beta = 0.5\cdot[(r^2+4r)^{1/2} - r]$. The e-folding response time (days) is $\tau = -1/[\ln(1-\beta)]$.

Midlatitude weather is more variable and less predictable in winter. As a result, useful values are:

- Winter: $r \approx 0.06$, $\beta = 0.217$, $\tau = 4$ days.
- Summer: $r \approx 0.02$, $\beta = 0.132$, $\tau = 7$ days.

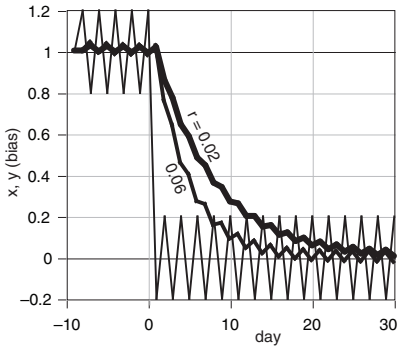

This Fig. shows a noisy input y (thin line) and KF responses x (thicker lines) for different values of the ratio r. The KF adapts to changes, and is recursive.

Fig. 20.G

Solid isobars are MSL pressure in mb (1000 mb = 100 kPa), plotted every 5 mb. Dashed isotherms are 85-kPa temperatures, plotted every 2.5°C, with the 0°C line darker. The map domain covers eastern North America, and is centered on Lake Ontario.

These figures demonstrate the inconsistency of forecasts started at different times with different initial conditions. Such inconsistency is inherent in all forecasts, and illustrates the limits of predictability. The analysis (Fig. 20.15a) shows a low centered near Detroit, Michigan, with a cold front extending southwest toward Arkansas. The 1.5-day forecast (Fig. 20.15b) is reasonably close, but the 3.5-day forecast (Fig. 20.15c) shows the low too far south and the cold front too far west. The 5.5 and 7.5-day forecasts (Fig. 20.15d & e) show improper locations for the fronts and lows, but the larger scales are good.

Post-processing

After the dynamical computer model has completed its forecast, additional **post-processing** computations can be made with the saved output. Postprocessing can include:

- forecast refinement to correct biases,
- calculation of secondary weather variables,
- drawing of weather maps and other graphics,
- compression into databases & climatologies, &
- verification (see the Forecast Quality section).

Forecast Refinement

Forecasts often contain **biases** (systematic errors; see Appendix A), due to: the NWP model formulation; the initial conditions used; and characteristics of different locales. For example, towns might be located in valleys or near coastlines. These are landscape features that can modify the local weather, but which might not be captured by a coarse-mesh numerical model. A number of automated statistical techniques (e.g., **linear regression**, **Kalman filtering**) can be applied as post-processing to reduce the biases and to tune the model output toward the climatologically-expected or observed local weather.

Two classical statistical methods are the **Perfect Prog Method** (**PPM**) and **Model Output Statistics** (**MOS**). Both methods use a best-fit statistical regression (see Focus boxes) to relate input fields (**predictors**) to different output fields (**predictands**). An example of a predictand is surface temperature at a weather station, while predictors for it might include values interpolated from the nearest NWP grid points. PPM uses observations as predictors to determine regression coefficients, while MOS uses model forecast fields. Once the regression coefficients are found, both methods then use the model forecast fields as the predictors to find the surface-temperature forecast for that weather station.

Best fit regressions are found using multi-year sets of predictors and predictands. The parameters of the resulting best fit regression equations are held constant during their subsequent usage.

The PPM method has the advantage that it does not depend on the particular forecast model, and can be used immediately after changing the forecast model. The PPM produces best predictand values only when the model produces perfect predictor forecasts, which is rare.

The MOS advantage is that any systematic model errors can be compensated by the statistical regression. A disadvantage of MOS is that a multi-year set of model output must first be collected and statistically fit, before the resulting regression can be used for future forecasts. Both MOS and PPM have a disadvantage that the statistical parameters are fixed.

Alternative methods include the **Kalman Filter** (KF; see Focus box) and **Updateable MOS**, which continually refine their statistical parameters each day. They share the advantage of MOS in that they use model output for the predictors. They learn from their mistakes (i.e., are adaptive), and can automatically and quickly retune themselves after any changes in the numerical model or in the synoptic conditions. They are recursive (tomorrow's bias correction depends on today's bias correction, not on many years of past data), which significantly reduces the data-storage requirements. A disadvantage is that the KF cannot capture rare, extreme events.

Calculation of Secondary Variables

Fundamental output from the NWP forecast include winds, temperature, pressure or height, mixing ratio, and precipitation. Additional weather variables can be created for human forecasters, for the general public, and for specific industries such as agriculture, transportation, and utilities. Some of these secondary variables (such as relative humidity) can be calculated directly from the primary fields using their defining equations. Other secondary variables (such as visibility) can be estimated statistically via regression.

Secondary thermodynamic variables include: potential temperature, virtual potential temperature, liquid-water or equivalent potential temperature, wet-bulb temperature, near-surface (z = 2 m) temperature, surface skin temperature, surface heat fluxes, surface albedo, wind-chill temperature, static stability, short- and long-wave radiation, and various storm-potential indices such as CAPE.

Secondary moisture variables include: relative humidity, cloudiness (altitudes and coverage), precipitation type and amount, visibility, near-surface dew-point (z = 2 m), soil wetness, and snowfall.

Solved Example (§)

Given the following set of past data (T_{fcst} vs. T_{obs}):
(a) Find the best-fit straight line. Namely, train MOS using linear regression (see Focus box).
(b) If the NWP forecast for tomorrow is T_{fcst} = 15°C, then post-process it to estimate the bias-corrected T ?

Solution

Given: The first 3 columns of data below.
Find: a_o = ? °C, a_1 = ? , T_{fcst} = ? °C
(a) Train MOS using past data to find the coefficients.

i	$x=T_{fcst}$	$y=T_{obs}$	$x \cdot y$	x^2
1	-10	-11.4	114.0	100
2	-8	-7.9	62.8	64
3	-6	0.7	-4.0	36
4	-4	-2.7	10.9	16
5	-2	-1.4	2.8	4
6	0	3.8	0.0	0
7	2	5.0	10.1	4
8	4	3.8	15.2	16
9	6	6.7	40.0	36
10	8	14.7	117.5	64
11	10	13.9	139.1	100
12	12	17.9	214.3	144
13	14	17.7	247.8	196
14	16	24.8	397.0	256
15	18	22.0	396.4	324
16	20	28.4	568.0	400
17	22	27.2	599.5	484
18	24	34.3	822.0	576
19	26	34.7	902.7	676
20	28	29.7	831.1	784
21	30	36.7	1100.3	900
avg=	10.0	14.2	313.7	246.7

$a_o = (10 \cdot 313.7 - 246.7 \cdot 14.2) \,/\, (10^2 - 246.7) =$ **2.52 °C**
$a_1 = (\,10 \cdot 14.2 - 313.7\,) \,/\, (10^2 - 246.7) =$ **1.17** (dim'less)

The original data points and the best-fit line are:

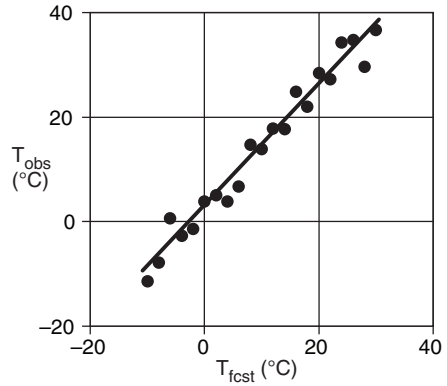

(b) Use MOS to correct the forecast: $T = a_o + a_1 \cdot T_{fcst}$.
T = (2.52°C) + 1.17·(15°C) = **20.1 °C**.

Check: Units OK. Line fits data nicely.
Discussion: The predictor (x) and predictand (y) need not have the same units. For example, MOS could be trained to use model forecasts of relative humidity (%) to estimate observed values of visibility (km).

If you draw a vertical line from each data point to the regressed line, then the length of each line is a measure of the error between the data and the regression. Square each error value and sum them to give the total error. Linear regression is a "best fit" in the sense of finding the "least squared error".

Solved Example

Given the following simplified MOS regression:

$$T_{min} = -295 + 0.4 \cdot T_{15} + 0.25 \cdot \Delta TH + 0.6 \cdot T_d$$

for daily minimum temperature (K) in winter at Madison, Wisconsin, where T_{15} = observed surface temperature (K) at 15 UTC, ΔTH = model forecast of 100-85 kPa thickness (m), and T_d = model fcst. dew point (K). Predict T_{min} given NWP model forecasts of: T_{15} = 273 K, ΔTH = 1,200 m, and T_d = 260 K.

Solution

Given: T_{15} = 273 K, ΔTH = 1,200 m, and T_d = 260 K.
Find: T_{min} = ? K

$$T_{min} = -295 + 0.4 \cdot (273) + 0.25 \cdot (1{,}200) + 0.6 \cdot (260)$$
$$= 270.2 \approx \underline{\mathbf{-3°C}}.$$

Check: Units OK. Physics OK.
Discussion: Chilly, but typical for winter in Madison. Note that MOS regressions can be made for any variables in any units. Thus, (1) units might not be consistent from term to term in the regression, but (2) you MUST use the same units for each variable as was used when the MOS regression was created.

FOCUS • Human Contributions

NWP forecasts are rarely perfect. Thus, humans have the opportunity to improve the forecasts.

By comparing the current model forecast to recent observations, you can discover biases early in the forecast that you can use to correct future forecasts. For example, if the NWP forecast for your location was 2 °C too cold during the past few hours, perhaps it will continue to be 2 °C too cold in the next few hours. Errors in timing or position of fronts and cyclones early in the forecast can be extrapolated to anticipate what corrections are needed for wind and precipitation forecasts later.

You can incorporate knowledge of local effects that might not be resolved by the model — such as the effects of local terrain, coastlines, land use, and urban centers. You may have noticed that some NWP models do not perform well in certain weather patterns, so you can anticipate similar errors when those same weather patterns happen in the future.

Humans can also tailor the weather forecasts to individual users and industries. Examples are forecasts for road or rail transportation, aviation, shipping/fishing/recreational boating, servicing of offshore oil platforms, electrical utility companies (including hydro and wind-energy), air-quality regulatory agencies, avalanche forecast centers, flood and landslide prediction, forest-fire fighting, ski resorts, emergency services, etc.

Humans are also rarely perfect. Nonetheless, studies have shown that the best forecasts are achieved by a combination of NWP and human experience.

Secondary dynamic variables include streamlines, trajectories, absolute vorticity, potential vorticity, isentropic potential vorticity, dynamic tropopause height, vorticity advection, Richardson number, dynamic stability, near-surface winds (z = 10 m), surface stress, surface roughness, mean-sea-level pressure, and turbulence.

While many of the above variables are computed at central numerical-computing facilities, additional computations can be made by separate organizations. Local forecast offices of National Weather Services can tailor the numerical guidance to produce local forecasts of maximum and minimum temperature, precipitation, cloudiness, and storm and flood warnings for the neighboring counties.

Consulting firms, broadcast companies, utility companies, and airlines, for example, acquire the fundamental and secondary fields via data networks such as the internet. From these fields they compute products such as computerized flight plans for aircraft, crop indices and threats such as frost, hours of sunshine, and heating- or cooling-degree days for energy consumption.

Universities also acquire the primary and secondary output fields, to use for teaching and research. Some of the applications result in weather maps that are put back on the internet.

Weather Maps and Other Graphics

The fundamental and secondary variables that are output from the NWP and from forecast refinement are arrays of numbers. To make these data easier to use and interpret by humans, the numbers can be converted into weather-map graphics and animations, **meteograms** (plots of a weather variable vs. time), sounding profiles, cross-sections, text forecasts, and other output forms. Computation of these outputs can take hours, depending on the graphical complexity and the number of products, and thus cannot be neglected in the forecast schedule.

Some visualization programs for NWP output include: GrADS, Vis5D, MatLab, NCAR RIP, GEMPAK, unidata IDV, AWIPS, and NinJo.

Compression into Databases and Climatologies

It is costly to save the terabytes of output produced by operational NWP models every day for every grid point, every level, and every time step. Instead, only key weather fields at RAOB **mandatory levels** in the atmosphere are saved. These WMO **standard isobaric surfaces** are: surface, 100, 92.5, 85, 70, 50, 40, 30, 25, 20, 15, 10, 7, 5, 3, 2, & 1 kPa. Output files can be converted from model-specific formats to standard formats (NetCDF, Vis5D, SQL, GRIB). Forecasts at key locations such as weather stations can be accumulated into growing climatologies.

NONLINEAR DYNAMICS AND CHAOS

Predictability

Recall that NWP is an initial-value problem, where these initial values are partially based on observed weather conditions. Unfortunately, the observations include instrumentation, sampling, and representativeness errors. We have already examined how such errors cause startup problems due to imbalanced flow conditions. How do these errors affect the long-range predictability?

Lorenz suggested that the equations of motion (which are **nonlinear** because they contain products of dependent variables, such as U and T in $U{\cdot}\Delta T/\Delta x$) are **sensitive to initial conditions**. Such sensitivity means that small differences in initial conditions can grow into large differences in the forecasts.

This is unfortunate. Initial conditions will always have errors. Thus our forecasts will always become less accurate with increasing forecast time. Thus, there is a **limit to the predictability of weather** that is related to **instability of the dynamics**.

A simple physical illustration of **sensitive dependence to initial conditions** is a toy balloon. Inflate one with air and then let it go to fly around the room. Repeat the experiment, being careful to inflate the balloon the same amount and to point it in the same direction. You probably know from experience that the path and final destination of the balloon will differ greatly from flight to flight. In spite of how simple a toy balloon seems, the dynamical equations describing its flight are extremely sensitive to initial conditions, making predictions of flight path virtually impossible.

Lorenz Strange Attractor

Another illustration of sensitive dependence to initial conditions was suggested by Lorenz. Suppose we examine 2-D convection within a tank of water, where the bottom of the tank is heated (Fig. 20.16). The vertical temperature gradient from bottom to top drives a circulation of the water, with warm fluid trying to rise. The circulation can modify the temperature distribution within the tank.

A very specialized, highly-simplified set of equations that approximates this flow is:

$$\frac{\Delta C}{\Delta t} = \sigma \cdot (L - C)$$

$$\frac{\Delta L}{\Delta t} = r \cdot C - L - C \cdot M \qquad (20.23)$$

$$\frac{\Delta M}{\Delta t} = C \cdot L - b \cdot M$$

ON DOING SCIENCE • Scientific Revolutions

In the late 1950s and early 1960s, Ed Lorenz was making numerical forecasts of convection to determine if statistical forecasts were better than NWP forecasts using the nonlinear dynamical equations. One day he re-ran a numerical forecast, but entered slightly different initial data. He got a strikingly different answer.

He was curious about this effect, and allowed himself to become sidetracked from his original investigations. This lead to his description of chaos, discovery of a strange attractor, and realization of the sensitive dependence of some equations to initial conditions.

He published his results in 1963 ("Deterministic non-periodic flow". *J. Atmos. Sci.*, **20**, p 130-141). From 1963 to about 1975, this innovative paper was rarely cited by other scientists — a clue that it was not yet accepted by his colleagues. However, between 1975 to 1980, researchers were becoming increasingly aware of his work. From 1980 to present, this paper has been cited on the order of 100 times per year.

About a decade and a half elapsed before this new theory gained wide acceptance, which is typical of many paradigm shifts. Namely, it takes about one human generation for a scientific revolution to mature, because typically the older scientists (who hold the power) are not willing to make the shift. The scientific revolution occurs when this group retires and younger scientists (with the newer ideas) take their place.

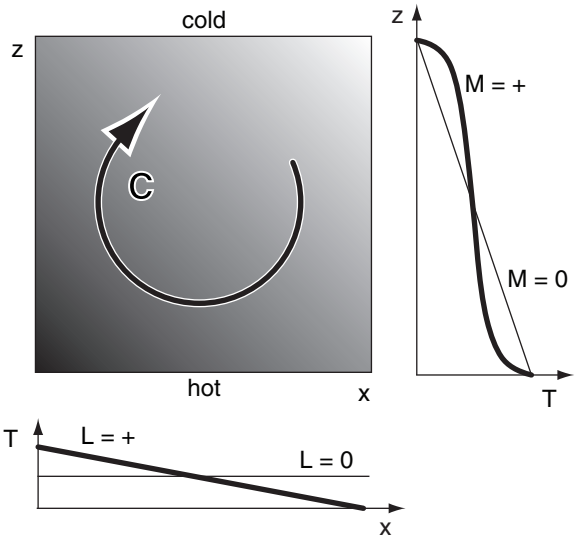

Figure 20.16
Tank of fluid (shaded), showing circulation C. The vertical M and horizontal L distributions of temperature are also shown.

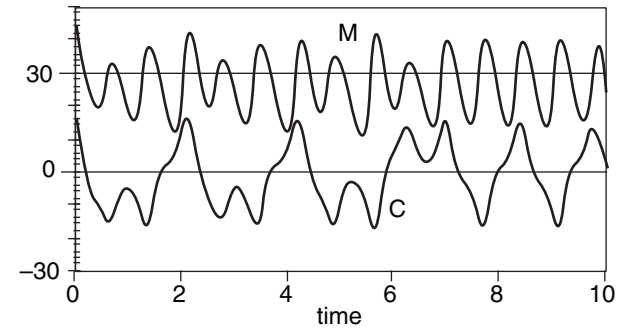

Figure 20.17
Time evolution of circulation C and mixing M.

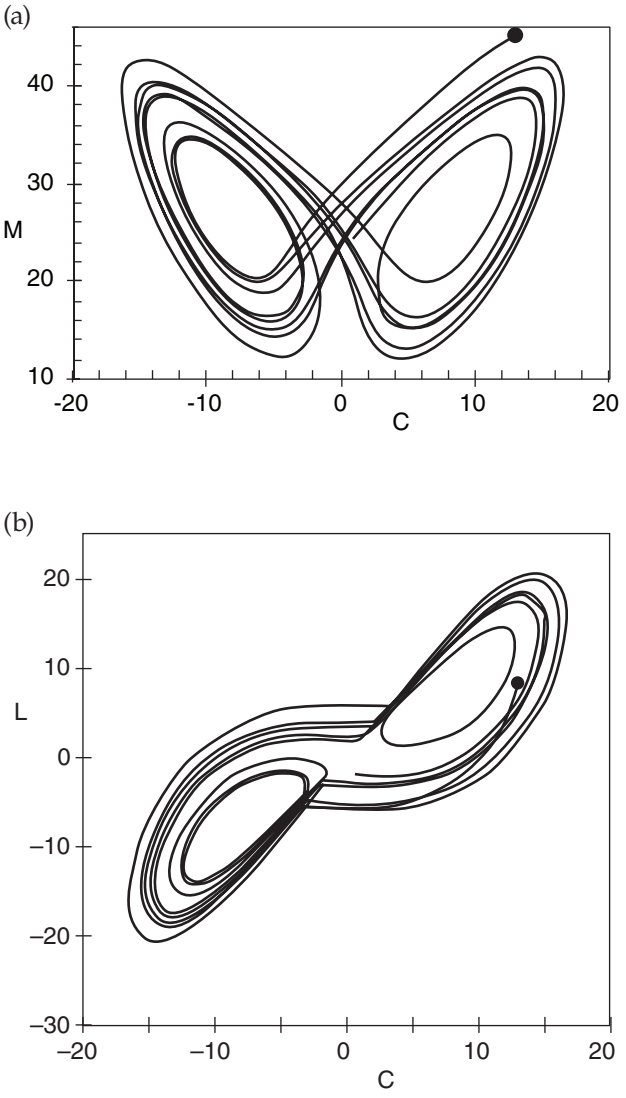

Figure 20.18
"Butterfly" showing evolution of the solution to the Lorenz equations in phase space. Solid dot indicates initial condition. (a) M vs. C. (b) L vs. C.

where C gives the circulation (positive for clockwise, and greater magnitude for a more vigorous circulation), L gives the left-right distribution of temperature (positive for warm water on the left), and M indicates the amount of vertical mixing (0 for a linear temperature gradient, and positive when temperature is more uniformly mixed within the middle of the tank). Each of these dependent variables is dimensionless. Terms $C{\cdot}M$ and $C{\cdot}L$ are nonlinear.

Fig. 20.17 shows forecasts of C and M vs. time, made with parameter values:

$$\sigma = 10.0, \quad b = 8/3, \quad \text{and } r = 28$$

and initial conditions:

$$C(0) = 13.0, \quad L(0) = 8.1, \quad \text{and } M(0) = 45.$$

Note that all three variables were forecast together, even though L was not plotted to reduce clutter. From Fig. 20.17 it is apparent that the circulation changes direction chaotically, as indicated by the change of sign of C. Also, the amount of mixing in the interior of the tank increases and decreases, as indicated by chaotic fluctuations of M.

When one dependent variable is plotted against another, the result is a **phase-space** plot of the solution. Because the Lorenz equations have three dependent variables, the phase space is three-dimensional. Figs. 20.18 shows two-dimensional views of the solution, which looks like a butterfly.

This solution exhibits several important characteristics that are similar to the real atmosphere. First, it is irregular or chaotic, meaning that it is impossible to guess the solution in the future. Second, the solution is bounded within a finite domain:

$$-20 < C < 20, \qquad -30 < L < 30, \qquad 0 \le M < 50.$$

which implies that the solution will always remain physically reasonable. Third, the solution (M vs. C) appears to flip back and forth between two favored regions, (i.e., the separate wings of the butterfly). These wings tend to attract the solution toward them, but in a rather strange way.

Hence, they are called **strange attractors**. Fourth, the exact solution is very dependent on the initial conditions, as illustrated in the solved examples next. Yet, the eventual solution remains attracted to the same butterfly.

The atmosphere has many more degrees of freedom (i.e., is more complex) than the simple Lorenz model. So we anticipate that the atmosphere is **intrinsically unpredictable** due to its nonlinear chaotic nature. In other words, **there is a limit to how well we can predict the weather**.

Solved Example (§)

Solve the Lorenz equations for the parameters and initial conditions listed previously in this chapter. Use a dimensionless time step of $\Delta t = 0.01$, and forecast from $t = 0$ to $t = 10$.

Solution

Given: $C(0) = 13.0$, $L(0) = 8.1$, and $M(0) = 45$,
and $\sigma = 10.0$, $b = 8/3$, and $r = 28$.
Find: $C(t) = ?$, $L(t) = ?$, $M(t) = ?$

First, rewrite eqs. (20.23) in the form of a forecast:

$$C(t+\Delta t) = C(t) + \Delta t \cdot [\sigma \cdot (L(t) - C(t))]$$

$$L(t+\Delta T) = L(t) + \Delta t \cdot [r \cdot C(t) - L(t) - C(t) \cdot M(t)]$$

$$M(t+\Delta T) = M(t) + \Delta t \cdot [C(t) \cdot L(t) - b \cdot M(t)]$$

As an example, for the 1st step:

$C(0.01) = 13.0 + 0.01 \cdot [10.0 \cdot (8.1 - 13.0)] = 12.51$

Next, set this up on a spreadsheet, a portion of which is reproduced below.

t	C	L	M
0.00	13.00	8.1	45.00
0.01	12.51	5.809	44.85
0.02	11.84	3.643	44.38
0.03	11.02	1.666	43.63
0.04	10.08	-0.07	42.65
0.05	9.069	-1.55	41.51
0.06	8.007	-2.76	40.26
0.07	6.931	-3.71	38.96
0.08	5.866	-4.44	37.67
0.09	4.836	-4.96	36.4
0.10	3.856	-5.32	35.19

Note that your answers might be different than these, due to different round-off errors and mathematical libraries on the spreadsheets.

Plots. These answers are already plotted in Figs. 20.17 - 20.18.

Check: Units dimensionless. Physics OK.
Discussion: The forecast equations above use an Euler time-differencing scheme, which is the least accurate. Nevertheless, it illustrates the Lorenz attractor.

Solved Example (§)

Repeat the previous solved example, but for a slightly different initial condition: $M(0) = 44$.

Solution

Given: $C(0) = 13.0$, $L(0) = 8.1$, and $M(0) = 44$,
and $\sigma = 10.0$, $b = 8/3$, $r = 28$.
Find: $C(t) = ?$, $L(t) = ?$, $M(t) = ?$

As in the previous solved example.

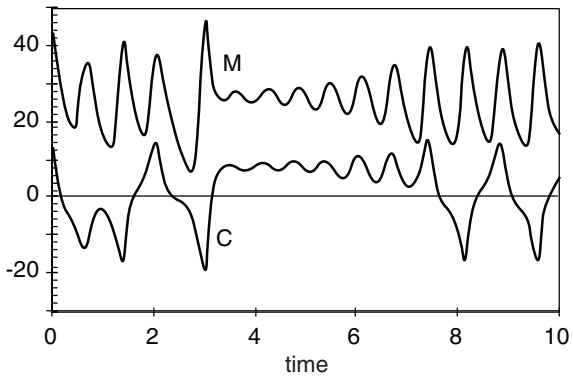

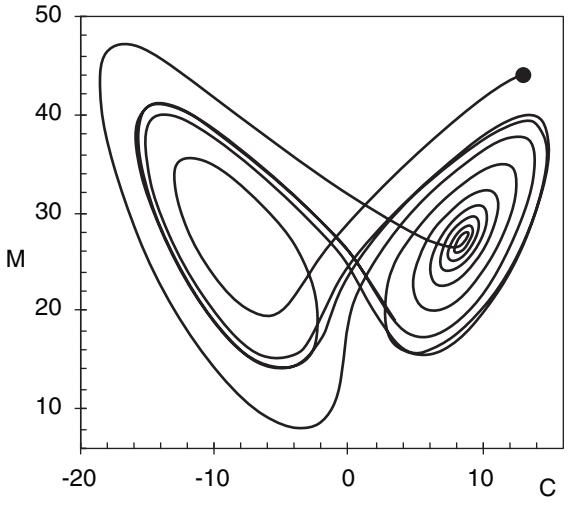

Check: Units OK. Physics OK.
Discussion: These are quite different from Figs. 20.17 & 20.18, demonstrating sensitive dependence to initial conditions.

Science Graffiti

Sensitive Dependence on Initial Conditions

"Does the flap of a butterfly's wings in Brazil set off a tornado in Texas?" – E. Lorenz & P. Merilees, 1972.

"Can a man sneezing in China cause a snow storm in New York? – George R. Stewart, 1941: *Storm*.

"Did the death of a prehistoric butterfly change the outcome of a US presidential election?" – Ray Bradbury, 1952, 1980, *A Sound of Thunder.*

Science Graffito

"Computations indicate that a perfect model should produce:
• three-day forecasts ... which are generally good;
• one-week forecasts ... which are occasionally good;
• and two-week forecasts ... which, although not very good, may contain some useful information"
– E. Lorenz, 1993: *The Essence of Chaos*.
Univ. of Washington Press, Seattle. 227 pp.

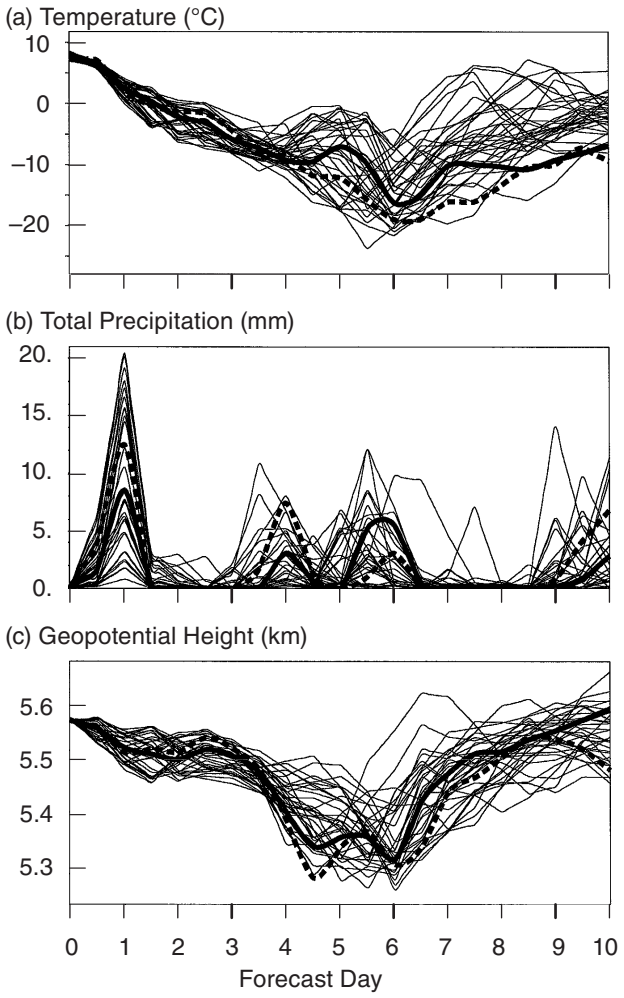

Figure 20.19
Ten-day ensemble forecasts for Des Moines, Iowa, starting from 19 Feb 1994. (a) Temperature (°C) at 85 kPa. (b) Total precipitation (mm). (c) Geopotential height (km) of the 50 kPa surface. Thick solid line is a coarse-resolution forecast that was started from the analyzed initial conditions. Thin lines are course-resolution forecasts, each started from a slightly different initial condition created by adding a different small perturbation to the analysis. The thick dotted line shows a single high-resolution forecast started from the analyzed initial conditions. (Courtesy of ECMWF, 1999).

Ensemble Forecasts

Some forecast centers repeatedly forecast the same time period, but for different conditions. These differences can be created by using different initial conditions, physical parameterizations, numerics, and/or NWP models. Such a procedure yields an **ensemble** of forecasts, which reveal the sensitive dependence of weather forecasts on those different conditions. Fig. 20.19 shows 10-day ensemble forecasts of 85-kPa temperature, precipitation, and 50-kPa geopotential heights at Des Moines, Iowa, for the same case-study period as discussed previously.

The heavy dotted line in these figures shows the single forecast run made with the high-resolution model, starting from the "best" initial conditions. This is the "official" forecast produced by ECMWF. The thick solid line starts from the same initial conditions, but is made with a coarser grid resolution to save forecast time. Note that the forecast changes substantially when the grid resolution changes.

The thin lines are forecasts from slightly different initial conditions. To save computer time, these multiple forecasts are also made with the lower grid-resolution. The forecasts of temperature and geopotential height start out quite close, and diverge slowly during the first 3.5 days. At that time (roughly when the cyclone reaches Des Moines late 22 Feb 94), the solution rapidly diverges, signaling a sudden loss in forecast skill that is never regained.

The spread of the ensemble members informs you about the **uncertainty** of the forecast. Unfortunately, you have no way of knowing which of the ensemble members will be closest to reality.

By averaging all the ensemble members together, you can find an **ensemble average** forecast that is usually more skillful than any individual member. This is one of the strengths of ensemble forecasting.

After several days into the forecast (Fig. 20.19), the ensemble forecasts seem chaotic. Yet this chaotic solution is bounded within a finite region — perhaps a "strange attractor" such as studied by Lorenz.

Studies of chaos often focus on the eventual state of the solution, at times far from the initial condition. At these long times, the dynamics have forgotten the initial state. Although this eventual state is somewhat useless as a weather forecast, it can provide some insight into the range of possible climatic conditions that are allowed by the dynamical equations in the model (i.e., the **model's climate**).

Ensemble forecasts can also suggest which conditions are unlikely — valuable information for some users. For example, if none of the ensemble forecasts give temperatures below freezing on a particular day, then a categorical "no freeze" forecast could be made. Better **confidence** in such forecasts is possible by calibrating the ensemble spread into a probabilistic forecast, discussed next.

Probabilistic Forecasts

Due to the inherent unpredictability of the atmosphere, we cannot confidently make **deterministic forecasts** such as "the temperature tomorrow at noon will be exactly 19.0°C". However, it is possible to routinely create **probabilistic forecasts** similar to "there is a 60% chance the temperature tomorrow at noon will be between 17°C and 21°C, and an 80% chance the it will be between 14 and 24°C."

Ensemble forecasts are increasingly used to create probabilistic forecasts. Various methods can be used to convert the distribution of ensemble members into calibrated probabilistic forecasts, such as illustrated in Fig. 20.20.

The **spread** of the probability distribution (i.e., the **uncertainty** in the forecast) depends on the season (greater spread in winter), the location (greater spread downwind of data-void regions), the climate (greater spread in parts of the globe where weather is more variable), and on the accuracy of the NWP models. A perfect forecast would have no spread.

Often probability forecasts are given as a cumulative probability *CP* that some **threshold** will be met. In Fig. 20.20, the lowest solid line represents a cumulative probability of *CP* = 10% (there is a 10% chance that the observed temperature will be colder than this forecast temperature) and the highest solid black line is for *CP* = 90% (there is a 90% chance that the observation will be colder than this forecast).

For example, using Fig. 20.20 we could tell a farmer that there is 35% chance the low temperature will be below freezing ($T_{threshold}$ = 0°C) on 6 - 7 Jan 2011.

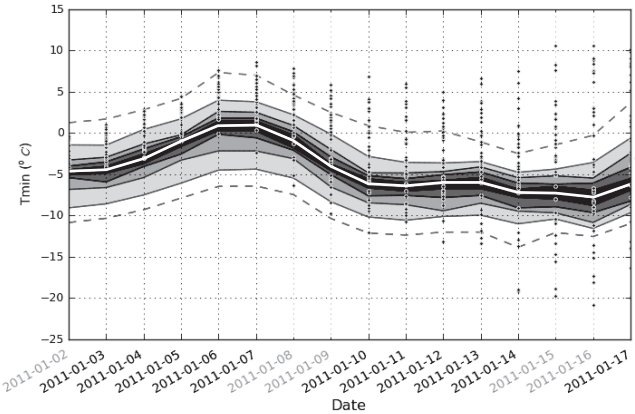

Figure 20.20

Calibrated probabilistic forecast for the minimum temperature (T_{min} °C) at Vancouver Airport (CYVR) for 2 to 17 Jan 2011. The thin white line surrounded by black is the median (50% of the observations should fall below this line, and 50% above). The black, dark grey, medium grey, and light grey regions span ±10%, 20%, 30%, and 40% of cumulative probability around the median. The dashed lines are ±49% around the median — namely, 98% of the time the observations should fall between the dashed lines. The dots are the raw forecasts from each of the 42 members of the North American Ensemble Forecast System.

FORECAST QUALITY & VERIFICATION

NWP forecasts can have both **systematic error** and **random error** (see Appendix A). By making ensemble forecasts you can reduce random errors caused by the chaotic nature of the atmosphere. By postprocessing each ensemble member using Model Output Statistics, you can reduce systematic errors (biases) before computing the ensemble average. After making these corrections, the forecast is still not perfect. How good is the forecast?

Verification is the process of determining the quality of a forecast. Quality can be measured in different ways, using various statistical definitions.

One of the least useful measures of quality is forecast **accuracy**. For example, in Vancouver, Canada, clouds are observed 327 days per year, on average. If I forecast clouds every day of the year, then my accuracy (= number of correct forecasts / total number of forecasts) will be 327/365 = 90% on the average. Although this accuracy is quite high, it shows no skill. To be skillful, I must beat climatology to successfully forecast which days will be cloudless.

Skill measures forecast improvement above some reference such as the climatic average, persistence, or a random guess. On some days the forecast is better than others, so these measures of skill are usually averaged over a long time (months to years) and over a large area (such as all the grid points in the USA, Canada, Europe, or the world).

Methods to calculate verification scores and skills for various types of forecasts are presented next.

Continuous Variables

An example of a continuous variable is temperature, which varies over a wide range of values. Other variables are bounded continuous. For example, precipitation is bounded on one side — it cannot be less than zero. Relative humidity is bounded on two sides — it cannot be below 0% nor greater than 100%, but otherwise can vary smoothly in between.

First, define the terms. Let:

A = initial analysis (based on observations)
V = verifying analysis (based on later obs.)
F = deterministic forecast
C = climatological conditions
n = number of grid points being averaged

An **anomaly** is defined as the difference from climatology at any instant in time. For example

$F - C$ = predicted anomaly
$A - C$ = persistence anomaly
$V - C$ = verifying anomaly

A **tendency** is the change with time:
$F - A$ = predicted tendency
V – A = verifying tendency

An **error** is the difference from the observations (i.e., from the verifying analysis):
F – V = forecast error
$A - V$ = persistence error
The first error is used to measure forecast accuracy. Note that the persistence error is the negative of the verifying tendency.

As defined earlier in this book, the overbar represents an average. In this case, the average can be over n times, over n grid points, or both:

$$\bar{X} = \frac{1}{n}\sum_{k=1}^{n} X_k \qquad \bullet(20.24)$$

where k is an arbitrary grid-point or time index, and X represents any variable.

Mean Error

The simplest quality statistic is the **mean error** (**ME**):

$$ME = \overline{(F - V)} = \bar{F} - \bar{V} \qquad \bullet(20.25)$$

This statistic gives the mean **bias** (i.e., a mean difference) between the forecast and verification data. [CAUTION: For precipitation, sometimes the bias is given as a ratio $\bar{F} / \bar{V}$.]

A **persistence forecast** is a forecast where we say the future weather will be the same as the current or initial weather (A) — namely, the initial weather will persist. Persistence forecasts are excellent for very short range forecasts (minutes), because the actual weather is unlikely to have changed very much during a short time interval. The quality of persistence forecasts decreases exponentially with increasing lead time, and eventually becomes worse than climatology. Analogous to mean forecast error, we can define a **mean persistence error**:

$$\overline{(A - V)} = \bar{A} - \bar{V} \ = \text{mean persistence error} \qquad (20.26)$$

Other persistence statistics can be defined analogous to the forecast statistics defined below, by replacing F with A.

For forecast ME, positive errors at some grid points or times can cancel out negative errors at other grid points or times, causing ME to give a false impression of overall error.

Mean Absolute Error

A better alternative is the **mean absolute error** (**MAE**):

$$MAE = \overline{|F - V|} \qquad \bullet(20.27)$$

Thus, both positive and negative errors contribute positively to this error measure.

Mean Squared Error and RMSE

Another way to quantify error that is independent of the sign of the error is by the **mean squared error** (**MSE**)

$$MSE = \overline{(F - V)^2} \qquad (20.28)$$

A similar mean squared error for climatology (MSEC) can be defined by replacing F with C in the equation above. This allows a **mean squared error skill score** (**MSESS**) to be defined as

$$MSESS = 1 - \frac{MSE}{MSEC} \qquad (20.29)$$

which equals 1 for a perfect forecast, and equals 0 for a forecast that is no better than climatology. Negative skill score means the forecast is worse than climatology.

The MSE is easily converted into a **root mean square error** (**RMSE**):

$$RMSE = \sqrt{\overline{(F - V)^2}} \qquad \bullet(20.30)$$

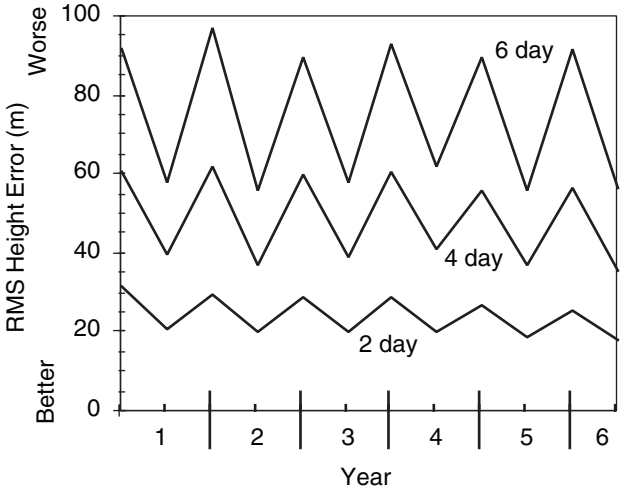

Figure 20.21
Maximum (winter) and minimum (summer) RMS error of 50-kPa heights over the Northern Hemisphere, for forecast durations of 2, 4, and 6 days. (a hypothetical case)

This statistic not only includes contributions from each individual grid point or time, but it also includes any mean bias error.

RMSE increases with forecast duration (i.e., lead time, or forecast range). It is also greater in winter than summer, because summer usually has more quiescent weather. Fig. 20.21 shows the maximum (winter) and minimum (summer) RMS errors of the 50 kPa heights in the Northern Hemisphere, for hypothetical forecasts.

Correlation Coefficient

To discover how well the forecast and verification vary together (e.g., hotter than average on the same days, colder than average on the same days), you can use the Pearson product-moment **correlation coefficient**, r:

$$r = \frac{\overline{F'V'}}{\sqrt{\overline{(F')^2}} \cdot \sqrt{\overline{(V')^2}}} \qquad \bullet(20.31)$$

where

$$F' = F - \overline{F} \quad \text{and} \quad V' = V - \overline{V} \qquad (20.32)$$

The correlation coefficient is in the range $-1 \le r \le 1$. It varies from +1 when the forecast varies perfectly with the verification (e.g., forecast hot when verification hot), to –1 for perfect opposite variation (e.g., forecast hot when verification cold), and is zero for no common variation.

Anomaly Correlation

Anomaly correlations indicate whether the forecast (or persistence) is varying from climatology in the same direction as the observations. For example, if the forecast is for warmer-than-normal temperatures and the verification confirms that warmer-than-normal temperatures were observed, then there is a positive correlation between the forecast and the weather. At other grid points where the forecast is poor, there might be a negative correlation. When averaged over all grid points, one hopes that there are more positive than negative correlations, giving a net positive correlation.

By dividing the correlations by the standard deviations of forecast and verification anomalies, the result is normalized into an **anomaly correlation coefficient**. This coefficient varies between 1 for a perfect forecast, to 0 for an awful forecast. (Actually, for a really awful forecast the correlation can reach a minimum of –1, which indicates that the forecast is opposite to the weather. Namely, the model forecasts warmer-than-average weather when colder weather actually occurs, and vice-versa.)

Solved Example (§)

Given the following synthetic analysis (A), NWP forecast (F), verification (V), and climate (C) fields of 50-kPa height (km). Each field represents a weather map (North at top, East at right).

Analysis:

5.3	5.3	5.3	5.4
5.4	5.3	5.4	5.5
5.5	5.4	5.5	5.6
5.6	5.5	5.6	5.7
5.7	5.6	5.7	5.7

Forecast:

5.5	5.2	5.2	5.3
5.6	5.4	5.3	5.4
5.6	5.5	5.4	5.5
5.7	5.6	5.5	5.6
5.7	5.7	5.6	5.6

Verification:

5.4	5.3	5.3	5.3
5.5	5.4	5.3	5.4
5.5	5.5	5.4	5.5
5.6	5.6	5.5	5.6
5.6	5.7	5.6	5.7

Climate:

5.4	5.4	5.4	5.4
5.4	5.4	5.4	5.4
5.5	5.5	5.5	5.5
5.6	5.6	5.6	5.6
5.7	5.7	5.7	5.7

Find the mean error of the forecast and of persistence. Find the forecast MAE and MSE. Find MSEC and MSESS. Find the correlation coefficient between the forecast and verification. Find the RMS errors and the anomaly correlations for the forecast and persistence.

Solution

Use eq. (20.25): $ME_{forecast}$ = 0.01 km = **10 m**
Use eq. (20.26): $ME_{persistence}$ = **15 m**
Use eq. (20.27): MAE = **40 m**
Use eq. (20.28): $MSE_{forecast}$ = 0.004 km^2 = **4000 m**^{2}
Use eq. (20.28): $MSEC$ = 0.0044 km^2 = **4500 m**^{2}
Use eq. (20.29): $MSESS$ = 1 – (4000/4500) = **0.11**
Use eq. (20.30): $RMSE_{forecast}$ = **63 m**
Use eq. (20.30): $RMSE_{persistence}$ = **87 m**
Use eq. (20.31): r = **0.92** (dimensionless)
Use eq. (20.33): forecast anomaly correlation = **81.3%**
Use eq. (20.34): persist. anomaly correlation = **7.7%**

Check: Units OK. Physics OK.

Discussion: Analyze (i.e., draw height contour maps for) the analysis, forecast, verification, and climate fields. The analysis shows a Rossby wave with ridge and trough, and the verification shows this wave moving east. The forecast amplifies the wave too much. The climate field just shows the average of higher heights to the south and lower heights to the north, with all transient Rossby waves averaged out.

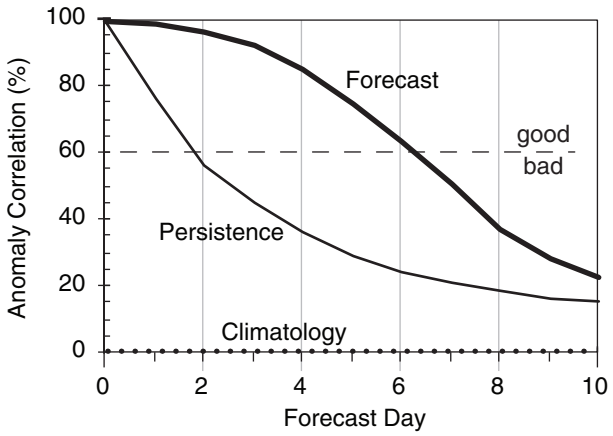

Figure 20.22
NWP forecast skill (thick line) of 50-kPa heights for a hypothetical forecast model. A persistence forecast (thin line) is one where the weather is assumed not to change with time from the initial conditions. A value of 100% is a perfect forecast, while a value of 0 is no better than climatology (dotted line).

(a)

Forecast \ Observation	Yes	No
Yes	Hit	False Alarm
No	Miss	Correct Rejection or Correct Negative

(b)

Forecast \ Observation	Yes	No
Yes	a	b
No	c	d

(c)

Forecast \ Observation	Yes	No
Yes	Mitigated Loss (C)	Cost (C)
No	Loss (L)	No Cost (0)

Figure 20.23
Contingency table for a binary (Yes/No) situation. "Yes" means the event occurred or was forecast to occur. (a) Meaning of cells. (b) Counts of occurrences, where $a + b + c + d = n$. (c) Expense matrix, where C = cost for taking protective action (i.e., for mitigating the loss), and L = loss due to an unmitigated event.

The definitions of these coefficients are:

anomaly correlation coef. for the forecast =

$$\frac{\overline{\left[(F-C)-\overline{(F-C)}\right]\cdot\left[(V-C)-\overline{(V-C)}\right]}}{\sqrt{\overline{\left[(F-C)-\overline{(F-C)}\right]^2}\cdot\overline{\left[(V-C)-\overline{(V-C)}\right]^2}}} \quad (20.33)$$

anomaly correlation coef. for persistence =

$$\frac{\overline{\left[(A-C)-\overline{(A-C)}\right]\cdot\left[(V-C)-\overline{(V-C)}\right]}}{\sqrt{\overline{\left[(A-C)-\overline{(A-C)}\right]^2}\cdot\overline{\left[(V-C)-\overline{(V-C)}\right]^2}}} \quad (20.34)$$

Fig. 20.22 compares hypothetical persistence and NWP-forecast anomaly correlations for 50-kPa geopotential height. One measure of forecast skill is the vertical separation between the forecast and persistence curves in Fig. 20.22.

This figure shows that the forecast beats persistence over the full 10 days of forecast. Also, using 60% correlation as an arbitrary measure of quality, we see that a "good" persistence forecast extends out to only about 2 days, while a "good" NWP forecast is obtained out to about 6 days, for this hypothetical case for 50 kPa geopotential heights. For other weather elements such as precipitation or surface temperature, both solid curves decrease more rapidly toward climatology.

Binary / Categorical Events

A binary event is a yes/no event, such as snow or no snow. Continuous variables can be converted into binary variables by using a **threshold**. For example, is the temperature below freezing (0°C) or not? Does precipitation exceed 25 mm or not?

A **contingency table** (Fig. 20.23a) has cells for each possible outcome of forecast and observation. "Hit" means the event was successfully forecast. "Miss" means it occurred but was not forecast. "False Alarm" means it was forecast but did not happen. "Correct Rejection" means that the event was correctly forecast not to occur.

After making a series of categorical forecasts, the forecast outcomes can be counted into each cell of a contingency table. Let *a*, *b*, *c*, *d* represent the counts of all occurrences as shown in Fig. 20.23b. The total number of forecasts is *n*:

$$n = a + b + c + d \quad (20.35)$$

The **bias score** B indicates over- or under-prediction of the frequency of event occurrence:

$$B = \frac{a+b}{a+c} \tag{20.36}$$

The **portion correct** PC (also known as **portion of forecasts correct** PFC) is

$$PC = \frac{a+d}{n} \tag{20.37}$$

But perhaps a portion of PC could have been due to random-chance (dumb but lucky) forecasts. Let E be this "random luck" portion, assuming that you made the same ratio of "YES" to "NO" forecasts:

$$E = \left(\frac{a+b}{n}\right)\cdot\left(\frac{a+c}{n}\right) + \left(\frac{d+b}{n}\right)\cdot\left(\frac{d+c}{n}\right) \tag{20.38}$$

We can now define the portion of correct forecasts that was actually skillful (i.e., not random chance), which is known as the **Heidke skill score** (HSS):

$$HSS = \frac{PC - E}{1 - E} \tag{20.39}$$

The **hit rate** H is the portion of actual occurrences (obs. = "YES") that were successfully forecast:

$$H = \frac{a}{a+c} \tag{20.40}$$

It is also known as the **probability of detection** POD.

The **false-alarm rate** F is the portion of non-occurrences (observation = "NO") that were incorrectly forecast:

$$F = \frac{b}{b+d} \tag{20.41}$$

Don't confuse this with the **false-alarm ratio** FAR, which is the portion of "YES" forecasts that were wrong:

$$FAR = \frac{b}{a+b} \tag{20.42}$$

A **true skill score** TSS (also known as **Peirce's skill score** PSS, and as **Hansen and Kuipers' score**) can be defined as

$$TSS = H - F \tag{20.43}$$

which is a measure of how well you can discriminate between an event and a non-event, or a measure of how well you can detect an event.

A **critical success index** CSI (also known as a **threat score** TS) is:

$$CSI = \frac{a}{a+b+c} \tag{20.44}$$

Science Graffito

"Consumers...have often been satisfied with forecasts that meteorologists...have judged to be of little or no value."

– Frederik Nebeker, 1995.

Solved Example

Given the following contingency table, calculate all the binary verification statistics.

		Observation	
		Yes	No
Forecast	Yes:	90	50
	No	75	150

Solution:

Given: $a = 90$, $b = 50$, $c = 75$, $d = 150$

Find: B, PC, HSS, H, F, FAR, TSS, CSI, GSS

First, use eq. (20.35): $n = 90 + 50 + 75 + 150 = 365$

So apparently we have daily observations for a year.

Use eq. (20.36): $B = (90 + 50) / (90 + 75) =$ **0.85**

Use eq. (20.37): $PC = (90 + 150) / 365 =$ **0.66**

Use eq. (20.38):

$E = [(90+50)\cdot(90+75) + (150+50)\cdot(150+75)]/(365^2)$

$E = 68100 / 133225 =$ **0.51**

Use eq. (20.39): $HSS = (0.66 - 0.51) / (1 - 0.51) =$ **0.**31

Use eq. (20.40): $H = 90 / (90 + 75) =$ **0.55**

Use eq. (20.41): $F = 50 / (50 + 150) =$ **0.25**

Use eq. (20.42): $FAR = 50 / (90 + 50) =$ **0.36**

Use eq. (20.43): $TSS = 0.55 - 0.25 =$ **0.30**

Use eq. (20.44): $CSI = 90 / (90 + 50 + 75) =$ **0.42**

Use eq. (20.45): $a_r = [(90+50)\cdot(90+75)]/365 = 63.3$

Use eq. (20.46):

$GSS = (90-63.3) / (90-63.3+50+75) =$ **0.18**

Check: Values reasonable. Most are dimensionless.

Discussion: No verification statistic can tell you whether the forecast was "good enough". That is a subjective decision to be made by the end user. One way to evaluate "good enough" is via a cost/loss model (see next section).

Solved Example (§)

Given the table below of k = 1 to 31 forecasts of the probability p_k that the temperature will be below threshold 20°C, and the verification o_k = 1 if indeed the observed temperature was below the threshold.

(a) Find the Brier skill score. (b) For probability bins of width Δp = 0.2, plot a reliability diagram, and find the reliability Brier skill score.

k	p_k	o_k	BN	j	k	p_k	o_k	BN	j
1	0.43	0	0.18	2	16	0.89	1	0.01	4
2	0.98	1	0.00	5	17	0.13	0	0.02	1
3	0.53	1	0.22	3	18	0.92	1	0.01	5
4	0.33	1	0.45	2	19	0.86	1	0.02	4
5	0.50	0	0.25	3	20	0.90	1	0.01	5
6	0.03	0	0.00	0	21	0.83	0	0.69	4
7	0.79	1	0.04	4	22	0.00	0	0.00	0
8	0.23	0	0.05	1	23	1.00	1	0.00	5
9	0.20	1	0.64	1	24	0.69	0	0.48	3
10	0.59	1	0.17	3	25	0.36	0	0.13	2
11	0.26	0	0.07	1	26	0.56	1	0.19	3
12	0.76	1	0.06	4	27	0.46	0	0.21	2
13	0.17	0	0.03	1	28	0.63	0	0.40	3
14	0.30	0	0.09	2	29	0.10	0	0.01	1
15	0.96	1	0.00	5	30	0.40	1	0.36	2
					31	0.73	1	0.07	4

Solution

Given: The white portion of the table above.
Find: BSS = ? , $BSS_{reliability}$ = ?, and plot reliability.

(a) Use eq. (20.47). The grey-shaded column labeled BN shows each contribution to the numerator $(p_k - o_k)^2$ in that eq. The sum of BN = 4.86. The sum of o_k = 16. Thus, the eq is: BSS = 1 – [4.86 / {16 ·(31–16)}] = **0.98**

(b) There are J = 6 bins, with bin centers at p_j = 0, 0.2, 0.4, 0.6, 0.8, and 1.0. (Note, the first and last bins are one-sided, half-width relative to the nominal "center" value.) I sorted the forecasts into bins using j = round($p_k/\Delta p$, 0), giving the grey j columns above.

For each j bin, I counted the number of forecasts n_j falling in that bin, and I counted the portion of those forecasts that verified n_{oj}. See table below:

j	p_j	n_j	n_{oj}	n_{oj}/n_j	num
0	0	2	0	0	0
1	0.2	6	1	0.17	0.04
2	0.4	6	2	0.33	0.16
3	0.6	6	3	0.50	0.36
4	0.8	6	5	0.83	0.04
5	1.0	5	5	1	0

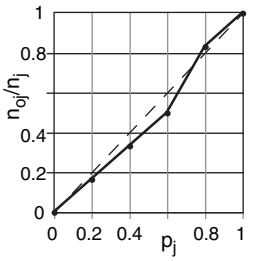

The observed relative frequency n_{oj}/n_j plotted against p_j is the **reliability diagram** :

Use eq. (20.48). The contribution to the numerator from each bin is in the num column above, which sums to 0.6 . Thus: $BSS_{reliability}$ = 0.6/ {16 ·(31–16)} = **0.0025**

Check: Small $BSS_{reliability}$ agrees with the reliability diagram where the curve nearly follows the diagonal.
Discussion: N = 31 is small, so these statistics are not very robust. Large BSS suggests good probability forecasts. Also, the forecasts are very reliable.

which is the portion of hits given that the event was forecast, or observed, or both. This is often used as a forecast-quality measure for rare events.

Suppose we consider the portion of hits that might have occurred by random chance a_r:

$$a_r = \frac{(a+b)\cdot(a+c)}{n} \qquad (20.45)$$

Then we can subtract this from the actual hit count to modify CSS into an **equitable threat score** ETS, also known as **Gilbert's skill score** GSS:

$$GSS = \frac{a - a_r}{a - a_r + b + c} \qquad (20.46)$$

which is also useful for rare events.

For a perfect forecasts (where $b = c = 0$), the values of these scores are: B = 1, PC = 1, HSS = 1, H = 1, F = 0, FAR = 0, TSS = 1, CSS = 1, GSS = 1.

For totally wrong forecasts (where $a = d = 0$): B = 0 to ∞, PC = 0, HSS = negative, H = 0, F = 1, FAR = 1, TSS = –1, CSS = 0, GSS = negative.

Probabilistic Forecasts

Brier Skill Score

For calibrated probability forecasts, a **Brier skill score** (BSS) can be defined relative to climatology as

$$BSS = 1 - \frac{\sum_{k=1}^{N} (p_k - o_k)^2}{\left(\sum_{k=1}^{N} o_k\right)\cdot\left(N - \sum_{k=1}^{N} o_k\right)} \qquad \bullet(20.47)$$

where p_k is the forecast probability ($0 \le p_k \le 1$) that the threshold will be exceeded (e.g., the probability that the precipitation will exceed a precipitation threshold) for any one forecast k, and N is the number of forecasts. The verifying observation o_k = 1 if the observation exceeded the threshold, and is set to zero otherwise.

BSS = 0 for a forecast no better than climatology. BSS = 1 for a perfect deterministic forecast (i.e., the forecast is p_k = 1 every time the event happens, and p_k = 0 every time it does not). For probabilistic forecasts, $0 \le BSS \le 1$. Larger BSS values are better.

Reliability

How **reliable** are the probability forecasts? Namely, when we forecast an event with a certain probability, is it observed with the same relative frequency? To determine this, after you make each forecast, sort it into a forecast probability bin (j) of probability width Δp, and keep a tally of the number of forecasts (n_j) that fell in this bin, and count how

many of the forecasts verified (n_{oj}, for which the corresponding observation satisfied the threshold).

For example, if you use bins of size $\Delta p = 0.1$, then create a table such as:

bin index	bin center	fcst. prob. range	n_j	n_{oj}
$j = 0$	$p_j = 0$	$0 \le p_k < 0.05$	n_0	n_{o0}
$j = 1$	$p_j = 0.1$	$0.05 \le p_k < 0.15$	n_1	n_{o1}
$j = 2$	$p_j = 0.2$	$0.15 \le p_k < 0.25$	n_2	n_{o2}
etc.	. . .	. . .	. . .	. . .
$j = 9$	$p_j = 0.9$	$0.85 \le p_k < 0.95$	n_9	n_{o9}
$j = 10 = J$	$p_j = 1.0$	$0.95 \le p_k \le 1.0$	n_{10}	n_{o10}

A plot of the observed relative frequency (n_{oj}/n_j) on the ordinate vs. the corresponding forecast probability bin center (p_j) on the abscissa is called a **reliability diagram**. For perfect reliability, all the points should be on the 45° diagonal line.

A Brier skill score for **relative reliability** ($BSS_{reliability}$) is:

$$BSS_{reliability} = \frac{\sum_{j=0}^{J}\left[(n_j \cdot p_j) - n_{oj}\right]^2}{\left(\sum_{k=1}^{N} o_k\right)\cdot\left(N - \sum_{k=1}^{N} o_k\right)} \qquad (20.48)$$

where $BSS_{reliability} = 0$ for a perfect forecast.

ROC Diagram

A **Relative Operating Characteristic** (**ROC**) diagram shows how well a probabilistic forecast can **discriminate** between an event and a non-event. For example, an event could be heavy rain that causes flooding, or cold temperatures that cause crops to freeze. The probabilistic forecast could come from an ensemble forecast, as illustrated next.

Suppose that the individual NWP models of an $N = 10$ member ensemble made the following forecasts of 24-h accumulated rainfall R for Day 1:

NWP model	R (mm)	NWP model	R (mm)
Model 1	8	Model 6	4
Model 2	10	Model 7	20
Model 3	6	Model 8	9
Model 4	12	Model 9	5
Model 5	11	Model 10	7

Consider a precipitation threshold of 10 mm. The ensemble above has 4 models that forecast 10 mm or more, hence the forecast probability is $p_1 = 4/N = 4/10 = 40\%$. Supposed that 10 mm or more of precipitation was indeed observed, so the observation flag is set to one: $o_1 = 1$.

On Day 2, three of the 10 models forecast 10 mm or more of precipitation, hence the forecast probability is $p_2 = 3/10 = 30\%$. On this day precipitation did NOT exceed 10 mm, so the observation flag is set to zero: $o_2 = 0$. Similarly, for Day 3 suppose the forecast probability is $p_3 = 10\%$, but heavy rain was observed, so $o_3 = 1$. After making ensemble forecasts every day for a month, suppose the results are as listed in the left three columns of Table 20-4.

An end user might need to make a decision to take action. Based on various economic or political reasons, the user decides to use a probability threshold of $p_{threshold} = 40\%$; namely, if the ensemble model forecasts a 40% or greater chance of daily rain exceeding 10 mm, then the user will take action. So we can set forecast flag $f = 1$ for each day that the ensemble predicted 40% or more probability, and $f = 0$ for the other days. These forecast flags are shown in Table 20-4 under the $p_{threshold} = 40\%$ column.

Other users might have other decision thresholds, so we can find the forecast flags for all the other probability thresholds, as given in Table 20-4. For an N member ensemble, there are only $(100/N) + 1$ discrete probabilities that are possible. For our example with $N = 10$ members, we can consider only 11 different probability thresholds: 0% (when no members exceed the rain threshold), 10% (when 1 out of the 10 members exceeds the threshold), 20% (etc.), . . . 90%, 100%.

For each probability threshold, create a 2x2 contingency table with the elements a, b, c, and d as shown in Fig. 20.23b. For example, for any pair of observation and forecast flags (o_j, f_j) for Day j, use

a = count of days with hits $(o_j, f_j) = (1, 1)$.
b = count of days with false alarms $(o_j, f_j) = (0, 1)$.
c = count of days with misses $(o_j, f_j) = (1, 0)$.
d = count of days: correct rejection $(o_j, f_j) = (0, 0)$.

For our illustrative case, these contingency-table elements are shown near the bottom of Table 20-4.

Next, for each probability threshold, calculate the hit rate $H = a/(a+c)$ and false alarm rate $F = b/(b+d)$, as defined earlier in this chapter. These are shown in the last two rows of Table 20-4 for our example. When each (F, H) pair is plotted as a point on a graph, the result is called a **ROC diagram** (Fig. 20.24).

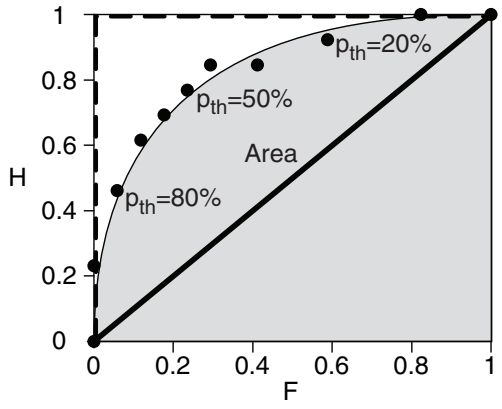

Figure 20.24
ROC diagram plots hit rate (H) vs. false-alarm rate (F) for a range of probability thresholds (p_{th}).

Table 20-4. Sample calculations for a ROC diagram. Forecast flags *f* are shown under the probability thresholds.

Day	*o*	*p* (%)	Probability Threshold $p_{threshold}$ (%)										
			0	10	20	30	40	50	60	70	80	90	100
1	1	40	1	1	1	1	1	0	0	0	0	0	0
2	0	30	1	1	1	1	0	0	0	0	0	0	0
3	1	10	1	1	0	0	0	0	0	0	0	0	0
4	1	50	1	1	1	1	1	1	0	0	0	0	0
5	0	60	1	1	1	1	1	1	1	0	0	0	0
6	0	30	1	1	1	1	0	0	0	0	0	0	0
7	0	40	1	1	1	1	1	0	0	0	0	0	0
8	1	80	1	1	1	1	1	1	1	1	1	0	0
9	0	50	1	1	1	1	1	1	0	0	0	0	0
10	1	20	1	1	1	0	0	0	0	0	0	0	0
11	1	90	1	1	1	1	1	1	1	1	1	1	0
12	0	20	1	1	1	0	0	0	0	0	0	0	0
13	0	10	1	1	0	0	0	0	0	0	0	0	0
14	0	10	1	1	0	0	0	0	0	0	0	0	0
15	1	70	1	1	1	1	1	1	1	1	0	0	0
16	0	70	1	1	1	1	1	1	1	1	0	0	0
17	1	60	1	1	1	1	1	1	1	0	0	0	0
18	1	90	1	1	1	1	1	1	1	1	1	1	0
19	1	80	1	1	1	1	1	1	1	1	1	0	0
20	0	80	1	1	1	1	1	1	1	1	1	0	0
21	0	20	1	1	1	0	0	0	0	0	0	0	0
22	0	10	1	1	0	0	0	0	0	0	0	0	0
23	0	0	1	0	0	0	0	0	0	0	0	0	0
24	0	0	1	0	0	0	0	0	0	0	0	0	0
25	1	70	1	1	1	1	1	1	1	1	0	0	0
26	0	10	1	1	0	0	0	0	0	0	0	0	0
27	0	0	1	0	0	0	0	0	0	0	0	0	0
28	1	90	1	1	1	1	1	1	1	1	1	1	0
29	0	20	1	1	1	0	0	0	0	0	0	0	0
30	1	80	1	1	1	1	1	1	1	1	1	0	0
Contingency Table Values		*a* =	13	13	12	11	11	10	9	8	6	3	0
		b =	17	14	10	7	5	4	3	2	1	0	0
		c =	0	0	1	2	2	3	4	5	7	10	13
		d =	0	3	7	10	12	13	14	15	16	17	17
Hit Rate: $H = a/(a+c)$ =			1.00	1.00	0.92	0.85	0.85	0.77	0.69	0.62	0.46	0.23	0.00
False Alarm Rate: $F=b/(b+d)$			1.00	0.82	0.59	0.41	0.29	0.26	0.18	0.12	0.06	0.00	0.00

The area A under a ROC curve (shaded in Fig. 20.24) is a measure of the overall ability of the probability forecast to discriminate between events and non-events. Larger area is better. The dashed curve in Fig. 20.24 illustrates perfect discrimination, for which $A = 1$. A random probability forecast with no ability to discriminate between events has a curve following the thick diagonal line, for which $A = 0.5$. Since this latter case represents no skill, a **ROC skill score** SS_{ROC} can be defined as

$$SS_{ROC} = (2 \cdot A) - 1 \qquad (20.49)$$

where $SS_{ROC} = 1$ for perfect skill, and $SS_{ROC} = 0$ for no discrimination skill.

Although a smooth curve is usually fit through the data points in a ROC diagram, we can nonetheless get a quick estimate of the area by summing the trapezoidal areas under each pair of data points. For our illustration, $A \approx 0.84$, giving $SS_{ROC} \approx 0.68$.

Cost / Loss Decision Models

Weather forecasts are often used to make decisions. For example, a frost event might cause L dollars of economic loss to a citrus crop in Florida. However, you could save the crop by deploying orchard fans and smudge pots, at a cost of C dollars.

Another example: A hurricane or typhoon might sink a ship, causing L dollars of economic loss. However, you could save the ship by going around the storm, but the longer route would cost C dollars in extra fuel and late-arrival fees.

No forecast is perfect. Suppose the event is forecast to happen. If you decide to spend C to mitigate the loss by taking protective action, but the forecast was bad and the event did not happen, then you wasted C dollars. Alternately, suppose the event is NOT forecast to happen, so you decide NOT to take protective action. But the forecast was bad and the event actually happened, causing you to lose L dollars. How do you decide which action to take, in consideration of this forecast uncertainty?

Suppose you did NOT have access to forecasts of future weather, but did have access to climatological records of past weather. Let o be the climatological (base-rate) frequency ($0 \le o \le 1$) that the event occurred in the past, where $o = 0$ means it never happened, and $o = 1$ means it always happened.

Assume this same base rate will continue to occur with that frequency in the future. If your $C \le o \cdot L$, then it would be most economical to always mitigate, at cost C. Otherwise, it would be cheaper to never mitigate, causing average losses of $o \cdot L$. The net result is that the expense based only on climate data is

$$E_{climate} = \min(C, o \cdot L) \tag{20.50}$$

But you can possibly save money if you use weather forecasts instead of climatology. The expected (i.e., average) expense associated with a sometimes-incorrect deterministic forecast $E_{forecast}$ is the sum of the cost of each contingency in Fig. 20.23c times the relative frequency that it occurs in Fig. 20.23b:

$$E_{forecast} = \frac{a}{n}C + \frac{b}{n}C + \frac{c}{n}L \tag{20.51}$$

This assumes that you take protective action (i.e., try to mitigate the loss) every time the event is forecast to happen. For some of the individual events the forecast might be bad, causing you to respond inappropriately (in hindsight). But in the long run (over many events) your taking action every time the event is forecast will result in a minimum overall expense to you.

If forecasts were perfect, then you would never have any losses because they would all be mitigated, and your costs would be minimal because you take protective action only when needed. On average you would need to mitigate at the climatological frequency o, so the expenses expected with perfect forecasts are

$$E_{perfect} = o \cdot C \tag{20.52}$$

Combine these expenses to find the **economic value** V of deterministic forecasts relative to climatology:

$$V = \frac{E_{climate} - E_{forecast}}{E_{climate} - E_{perfect}} \tag{20.53}$$

V is an economic skill score, where $V = 1$ for a perfect forecast, and $V = 0$ if the forecasts are no better than using climatology. V can be negative if the forecasts are worse than climatology, for which case your best course of action is to ignore the forecasts and choose a response based on the climatological data, as previously described.

Define a **cost/loss ratio** r_{CL} as

$$r_{CL} = C / L \tag{20.54}$$

Different people and different industries have different protective costs and unmitigated losses. So you should estimate your own cost/loss ratio for your own situation.

The economic-value equation can be rewritten using hit rate H, false-alarm rate F, and the cost/loss ratio r_{CL}:

$$V = \frac{\min(r_{CL}, o) - \left[F \cdot r_{CL} \cdot (1-o)\right] + \left[H \cdot (1 - r_{CL}) \cdot o\right] - o}{\min(r_{CL}, o) - o \cdot r_{CL}} \tag{20.55}$$

You can save even more money by using probabilistic forecasts. If the probabilistic forecasts are perfectly calibrated (i.e., are reliable), then you should take protective action whenever the forecast probability p of the event exceeds your cost/loss ratio:

$$p > r_{CL} \tag{20.56}$$

The forecast probability of the event is the portion of cumulative probability that is beyond the event-threshold condition. For the frost example, it is the portion of the cumulative distribution of Fig. 20.20 below a $T_{threshold} = 0°C$.

Solved Example

Given forecasts having the contingency table from the solved example 4 pages ago. Protective cost is \$75k to avoid a loss of \$200k. Climatological frequency of the event is 40%. Find the value of the forecast.

Solution:

Given: a=90, b=50, c=75, d=150, C=\$75k, L=\$200k, o=0.4

Find: E_{clim} = \$?, E_{fcst} = \$?, E_{perf} = \$?, V = ?

Use eq. (20.50): E_{clim} = min(\$75k, 0.4·\$200k) = \$75k.

Use eq. (20.35): n = 90+50+75+150 = 365.

Use eq. (20.51):

E_{fcst} =(90+50)·\$75k/365 + (75/365)·\$200k = \$70k

Use eq. (20.52): E_{perf} = 0.4 · \$75k = \$30k.

Use eq. (20.53): V = (\$75k – \$70k)/(\$75k – \$30k) = **0.11**

Check: Units are OK. Values are consistent.

Discussion: The forecast is slightly more valuable than climatology.

r_{CL} = \$75k/\$200k = **0.375** from eq. (20.54).

If you are lucky enough to receive probabilistic forecasts, then based on eq. (20.56) you should take protective action when $p > 0.375$.

SUMMARY

The atmosphere is a fluid. It obeys the laws of fluid mechanics, thermodynamics, and conservation of mass and water. If we can solve these equations, then we can forecast the weather.

Unfortunately, no one has yet found an analytical solution to these equations. Instead, we can approximate these continuous differential equations with finite-difference equations (i.e., algebra) that we can solve on a computer. One approach is to divide the spatial domain into finite-size grid cells, and to forecast the average conditions for a grid point within each cell.

If we know (or can approximate) the initial condition of each grid point by assimilating new observations into past forecasts, then we can make an iterative forecast by taking finite-size time steps into the future. To do this, all grid points must be marched together one step at a time.

Some aspects of atmospheric physics cause resolvable changes to the forecast, even though the grid resolution is not fine enough to resolve all the physical details. Hence, physical processes such as turbulence, radiation, clouds, and precipitation must be parameterized as a simplified function of variables that can be resolved in the model (winds, temperature, etc.).

The finite-difference equations suffer from truncation, round-off, numerical instability, and dynamic instability errors. Round-off errors are smaller when more bits are used to represent numbers in a computer. Truncation errors are smaller when more of the higher-order terms are retained in Taylor-series approximations of derivatives. Numerical instability is reduced when the time step is sufficiently small relative to the grid size. Dynamic instability refers to the sensitive dependence of the forecast on initial conditions and model parameters. Dynamic instability can be reduced with better weather analyses, but it cannot be eliminated.

No numerical forecast is perfect. For any specific location, forecasts might have a consistent bias or systematic error. Most of these biases can be removed by using statistics such as model output statistics (MOS) to post-process the NWP output. Random errors associated with the chaotic nonlinear-dynamic nature of the atmosphere can be estimated and/or reduced by making multiple forecasts (called ensemble forecasts) with different initial conditions or parameterizations. The ensemble forecasts can be averaged to give a deterministic forecast, and they can be used to make probabilistic forecasts.

Unfortunately, we have not discovered a way to reduce all errors. Thus, forecast error usually increases with increasing forecast time (i.e., how far into the future you forecast). Often forecast skill is defined relative to some baseline or reference, such as climatology. Short-range (out to 3 days) forecasts show significant skill, while medium-range forecasts show modest skill out to about 10 days. In addition to deterministic forecasts, NWP is increasingly used to make probabilistic forecasts. Methods exist to verify deterministic, binary, and probabilistic forecasts.

The resulting forecasts can be analyzed and graphed to reveal cyclones, fronts, airmasses, and other weather systems. Of all the tools (satellites, radar, weather balloons, etc.) that meteorologists use to forecast the weather, only NWP gives the future weather with a skill that is better than persistence.

Threads

The equations of motion (i.e., the "dynamics" portion of NWP models) come from the conservation equations for heat (Chapter 3), moisture (Chapter 4), momentum and mass (Chapter 10), and from the ideal gas law (Chapter 1). Physical parameterizations are made for radiation (Chapter 2), clouds (Chapters 6), precipitation (Chapter 7), and the atmospheric boundary layer (Chapter 18). Forecasts are started from initial conditions assimilated using data from radars and satellites (Chapter 8) and from other weather observations (Chapter 9).

NWP models are able to forecast a range of scales (Chapter 10), from global-scale climate (Chapter 21) and global circulation (Chapter 11) through synoptic-scale cyclones (Chapter 13) and fronts (Chapter 12), down to mesoscale hurricanes (Chapter 16) and individual thunderstorms (Chapters 14 and 15). Higher-resolution NWP models can forecast local-scale winds (Chapter 17), and extremely-fine resolution models can make **large-eddy simulations** of thermals in the atmospheric boundary layer (Chapter 18). Output from NWP models can be used as input to air-pollution (Chapter 19) models.

EXERCISES

Numerical Problems

N1. An NWP model has a bottom hydrostatic pressure of 95 kPa over the mountains, and a top pressure of 5 kPa. Find the sigma coordinate value for a height where the pressure (kPa) is:

a. 90 b. 85 c. 80 d. 75 e. 70 f. 65 g. 60 h. 55
i. 50 j. 45 k. 40 m. 35 n. 30 o. 25 p 20

N2. For a polar stereographic map projection with a reference latitude of 60°, find the (x, y) coordinates on the map that corresponds to the lat & lon at:

a. Montreal b. Boston c. New York City
d. Philadelphia e. Baltimore f. Washington DC
g. Atlanta h. Miami i. Toronto j. Chicago
k. St. Louis m. New Orleans n. Minneapolis
o. Kansas City p. Oklahoma City q. Dallas
r. Denver s. Phoenix t. Vancouver
u. Seattle v. San Francisco w. Los Angeles
x. A location specified by your instructor

N3. For a polar stereographic map projection with a reference latitude of 90°, find the map factors m_o, m_x, and m_y for latitudes (°) of:

a. 90 b. 85 c. 80 d. 75 e. 70 f. 65 g. 60 h. 55
i. 50 j. 45 k. 40 m. 35 n. 30 o. 25 p 20

N4. Estimate subgrid-scale cloud coverage of low and high clouds for a grid-average RH (%) of:

a. 70 b. 75 c. 80 d. 85 e. 90 f. 95 g. 100

N5. Given the following temperature T values (°C) at the indicated grid-point indices (i) for ΔX = 10 km:

i:	1	2	3	4	5	6	7	8	9	10
T:	30	27	26	28	24	20	18	23	25	25

Find the gradient $\Delta T/\Delta x$ for upwind first-order difference, centered second-order difference, and centered fourth-order difference, at grid index i:

a. 3 b. 4 c. 5 d. 6 e. 7 f. 8

N6. Same as the previous exercise, except find the advection term $-U{\cdot}\Delta T/\Delta x$ for a C grid with U values (m/s) of:

i:	1.5	2.5	3.5	4.5	5.5	6.5	7.5	8.5	9.5
U:	3	3	4	5	7	10	14	19	25

N7(§). Suppose that an equation of motion in some strange universe has the form $\Delta U/\Delta t = U{\cdot}t^2/\tau_o^3$ where constant τ_o = 1 min, and variable wind U = 1 m/s initially (t = 0). With time steps of Δt = 1 min, use the (a) Euler method, (b) leapfrog method, and (c) fourth-order Runge-Kutta method to forecast the value of U at t = 5 min. Compare your results to the analytical solution of $U = U_o \cdot \exp[\ (1/3){\cdot}(t/\tau_o)^3]$ where U_o = 1 m/s is the initial condition. [Hint: for the leapfrog method, you will need to use the Euler forward method for the first step.] Show your work and the results at each time step.

N8(§). Given a 1-D array consisting of 12 grid points in the x-direction with the following initial temperatures (°C). $T_i(t{=}0)$ =

20 24 20 16 20 24 20 16 20 24 20 16 20

for i = 1 to 12. Assume that the lateral boundaries are cyclic, so that the number sequence repeats outside this primary domain. Grid spacing is 5 km, and wind speed is from the west at 10 m/s. Use the leapfrog time-step method (except for the first time step) and 4th-order spatial differencing. Make enough time steps to forecast out to t = 5000 s. Use time steps of size Δt (s) =

a. 100 b. 200 c. 300 d. 400 e. 500 f. 600

Plot the temperature graph at each time step, and comment on the numerical stability.

N9. Given the following pairs of [grid spacings (km), wind speeds (m/s)], find the largest time step that satisfies the CFL criterion.

a. [0.1, 50] b. [0.2, 30] c. [0.5, 75] d. [1.0, 50]
e. [2, 40] f. [3, 80] g. [5, 50] h. [10, 100]
i. [15, 75] j. [20, 20] k. [33, 50] m. [50, 75]

N10. A program has 3 subprograms that each take 1/3 of the running time of the whole program. If the first subprogram is sped up 10 times, the second subprogram is sped up 40%, and the third one is sped up as indicated, what is the total speedup of the program?

a. 10% b. 50% c. 75% d. 100% e. 3 times
f. 5 times g. 10 times h. 20 times i. 50 times

N11. A surface weather station reports a temperature of 20°C with an observation error of σ_T = 1°C. An NWP model forecasts temperature of 24°C at the same point. For optimum interpolation, find the analysis temperature and the cost function if the NWP forecast error (°C) is

a. 0.2 b. 0.4 c. 0.6 d. 0.8 e. 1.0 f. 1.2
g. 1.5 h. 2.0 i. 3 j. 4 k. 5

N12. Suppose the first guess pressure in an optimum interpolation is 100 kPa, with an error of 0.2 kPa. Find the analysis pressure if an observation of P = 102 kPa was observed by:

a. surface weather station b. ship
c. Southern Hemisphere manual analysis

N13(§). A surface weather station at P = 100 kPa reports a dew-point temperature of T_d = 10°C with an observation error of σ_{Td} = 3°C. An NWP model forecasts a mixing ratio of r = 12 g/kg at the same point.

For variational data assimilation, find the analysis mixing ratio (in g/kg, and plot the variation of the cost function with mixing ratio) if the NWP mixing-ratio forecast error (g/kg) is:

a. 0.1 b. 0.2 c. 0.4 d. 0.5 e. 0.7 f. 1.0
g. 1.2 h. 1.5 i. 2 j. 2.5 k. 3 m. 4 n. 5

[Hint: Use (4.15b) from the Moisture chapter as your "*H*" function to convert from r to T_d.]

N14. Using Fig. 20.14 estimate at what forecast range (days) do we lose the ability to forecast:

a. tornadoes b. hurricanes
c. fronts d. cyclones
e. Rossby waves f. thunderstorms
g. Boras h. lenticular clouds

N15. Given the following pairs of x, y values. Use linear regression to find the slope and intercept of the best-fit straight line.

	x=	1	2	3	4	5	6	7	8	9
a.	y=	0.1	0.4	0.2	0.6	0.3	0.3	0.5	0.8	0.7
b.	y=	2	4	7	7	10	12	16	14	18
c.	y=	7	9	12	12	15	17	21	19	23
d.	y=	–3	–1	2	2	5	7	11	9	13
e.	y=	10	7	9	8	6	3	3	3	2
f.	y=	–20	–25	–30	–35	–40	–45	–50	–55	–60

N16. Given the forecast bias input (y, thin line) in Fig. 20.G, plot the Kalman filter estimate x of tomorrow's bias for error variance ratios (r) of:

a. 0.001 b. 0.002 c. 0.005 d. 0.01 e. 0.03
f. 0.04 g. 0.05 h. 0.07 i. 0.08 j. 0.09 k. 0.1

N17. Using the MOS regression from the solved example in this chapter, calculate the predictand if each of the predictors based on forecast-model output increased by

a. 1% b. 2%. c. 3% d. 4% e. 5%
f. 6%. g. 7% h. 8% i. 9% j. 10%

N18.(§) For the Lorenz equations, with the same parameters and initial conditions as used in this chapter, reproduce the results similar to the first solved example, except for all 1000 time steps. Also:

a. Plot L and C on the same graph vs. time.
b. Plot M vs. L c. Plot L vs C.

N19.(§) Given the following fields of 50-kPa height (km). Find the:

a. mean forecast error
b. mean persistence error
c. mean absolute forecast error
d. mean squared forecast error
e. mean squared climatology error
f. mean squared forecast error skill score
g. RMS forecast error
h. correlation coefficient between forecast and verification
i. forecast anomaly correlation
j. persistence anomaly correlation
k. Draw height contours by hand for each field, to show locations of ridges and troughs.

Each field (i.e., each weather map) below covers an area from North to South and West to East.

Analysis:

5.2	5.3	5.4	5.3
5.3	5.4	5.5	5.4
5.4	5.5	5.6	5.5
5.5	5.6	5.7	5.6
5.6	5.7	5.8	5.7

Forecast:

5.3	5.4	5.5	5.4
5.5	5.4	5.5	5.6
5.6	5.6	5.6	5.6
5.8	5.7	5.6	5.7
5.9	5.8	5.7	5.8

Verification:

5.3	5.3	5.3	5.4
5.4	5.3	5.4	5.5
5.5	5.4	5.5	5.5
5.7	5.5	5.6	5.6
5.8	5.7	5.6	5.6

Climate:

5.4	5.4	5.4	5.4
5.4	5.4	5.4	5.4
5.5	5.5	5.5	5.5
5.6	5.6	5.6	5.6
5.7	5.7	5.7	5.7

N20. Given the following contingency table, calculate all the binary verification statistics.

		Observation	
		Yes	No
Forecast	Yes:	150	65
	No:	50	100

N21. Given forecasts having the contingency table of exercise N20. Protective cost is \$5k to avoid a loss of \$50k. Climatological frequency of the event is 50%. (a) Find the value of the forecast. (b) If you can get probabilistic forecasts, then what probability would you want in order to decide to take protective action?

N22. Given the table below of k = 1 to 20 forecasts of probability p_k that 24-h accumulated precipitation will be above 25 mm, and the verification o_k = 1 if the observed precipitation was indeed above this threshold. (a) Find the Brier skill score. (b) For probability bins of width Δp = 0.2, plot a reliability diagram, and (c) find the reliability Brier skill score.

k	p_k	o_k	k	p_k	o_k
1	0.9	1	11	0.4	0
2	0.85	1	12	0.35	0
3	0.8	0	13	0.3	1
4	0.75	1	14	0.25	0
5	0.7	1	15	0.2	0
6	0.65	1	16	0.15	1
7	0.6	0	17	0.1	0
8	0.55	1	18	0.05	0
9	0.5	0	19	0.02	0
10	0.45	1	20	0	0

N23. For any <u>one</u> part of this exercise (Ex a to Ex d) of this problem, a 10-member ensemble forecast system forecasts probabilities that 24-h accumulated rainfall will exceed 5 mm. The observation flags (o) and forecast probabilities (p) are given below for a 30-day period. Calculate the hit rate and false-alarm rate for the full range of allowed probability thresholds, and plot the result as a ROC diagram. Also find the area under the ROC curve and find the ROC skill score.

Data for calculations of a ROC diagram:

		(Ex a)	(Ex b)	(Ex c)	(Ex d)			(Ex a)	(Ex b)	(Ex c)	(Ex d)
Day	o	p(%)	p(%)	p(%)	p(%)	Day	o	p(%)	p(%)	p(%)	p(%)
1	1	50	10	100	0	16	0	60	30	20	40
2	0	20	0	0	10	17	1	70	60	60	50
3	1	20	30	90	20	18	1	90	70	60	60
4	1	60	40	90	30	19	1	80	80	60	70
5	0	50	30	0	40	20	0	70	70	30	80
6	0	20	40	0	50	21	0	10	80	30	90
7	0	30	50	10	60	22	0	10	90	30	100
8	1	90	80	80	70	23	0	0	0	40	10
9	0	40	70	10	80	24	0	0	10	40	20
10	1	30	100	80	90	25	1	80	40	50	30
11	1	100	100	70	100	26	0	0	30	40	40
12	0	10	0	10	0	27	0	0	40	0	50
13	0	0	0	20	10	28	1	100	70	50	60
14	0	10	10	20	20	29	0	10	60	0	70
15	1	80	40	70	30	30	1	90	10	50	0

Understanding & Critical Evaluation

U1. Use the meteogram of Fig. 20.1.
- a. After 20 Feb, when does the low pass closest to Des Moines, Iowa?
- b. During which days does it rain, and which does it snow?
- c. During which days is there cold-air advection?
- d. Based on the wind direction, does the low center pass north or south of Des Moines.
- e. After 20 Feb, when does the cold front pass Des Moines?
- f. What is the total amount of precipitation that fell during the midweek storm?
- g. How does this forecast, which was initialized with data from 19 Feb, compare with the actual observations (refer to a previous chapter)?

U2(§). Reproduce the polar stereographic map from the solved example for map projections. Then add:
a. Greenland b. Europe c. Asia
d. your location if in the N. Hemisphere.

U3. If Moore's law continues to hold, and if forecast skill continues to improve as it has in the past, then estimate the transistor count on an integrated circuit, and the skillful forecast period (days) for the year: a. 2010 b. 2015 c. 2020 d. 2025 e. 2030 Also, comment on what factors might cause errors in your estimate.

U4. Speculate on the capability of weather forecasting if digital computers had not been invented.

U5. Critique the validity of a statement that "A variable mesh grid is analogous to a number of discrete nested grids."

U6. What procedure (i.e., what equations and how they are manipulated) would you use to create the 4^{th}-order centered difference of eq. (20.BA6).

U7. If NWP Corollaries 1 and 2 did not exist, describe tricks that you could use to increase the speed of numerical weather forecasts.

U8. Write a finite-difference equation similar to eq. (20.13) for the shaded grid cell of Fig. 20.9, but for:
- a. vertical advection
- b. advection in the y-direction

U9. Draw the stencil of grid points used for computing horizontal advection, but for the ___ grid for 2^{nd}-order spatial differencing.
a. A b. B c. D

U10. If the atmosphere is balanced, and if observations of the atmosphere are perfectly accurate, why would numerical models of the atmosphere start out imbalanced?

U11. For the case study forecast of Figs. 20.15, first photocopy the figures. Then, on each map
- a. Draw the likely location for fronts.
- b. Indicate the locations of low centers
- c. Comment on the forecast accuracy for fronts, cyclones, and the large-scale flow for this case.

U12. Suppose you are making weather forecasts for Pittsburgh, Pennsylvania, which is close to the intersection of the 40°N parallel and 80°W meridian, shown by the intersection of latitude and longitude lines in Figs. 20.15 just south of Lake Erie. During

the 7.5 days prior to 00 UTC 24 Feb 94, your temperature forecasts for 00 UTC 24 Feb would likely change as you received newer updated forecast maps.

What is your temperature forecast for 00 UTC 24 Feb, if you made it ___ days in advance from the ECMWF forecast charts of Fig. 20.15?

a. 7.5 b. 5.5 c. 3.5 d. 1.5

e. and which forecast was closest to the actual verifying analysis?

U13.(§) Suppose the Lorenz equations were modified by assuming that $C = L$. For the second two Lorenz equations, replace every C with L, and recalculate for the first 1000 time steps.

a. Plot L and M vs. time on the same graph.

b. Plot M vs. L.

Note that the solution converges to a steady-state solution. On the graph of M vs. L, this is called a **fixed point**. This fixed point is an **attractor**, but not a strange attractor.

c. Describe what type of physical circulation is associated with this solution.

U14. Experiment with the Lorenz equations on a spreadsheet. Over what range of values of the parameters σ, b, and r, do the solutions still exhibit chaotic solutions similar to that shown in Fig. 20.18?

U15. A pendulum swings with a regular oscillation.

a. Plot the position of the pendulum vs. time.

b. Plot the velocity of the pendulum vs. time.

c. Plot the position vs. velocity. This is a called a **phase diagram** according to chaos theory. How does it differ from the phase diagram (i.e., the butterfly) of the Lorenz strange attractor?

U16. Use the ensemble forecast for Des Moines in Fig. 20.19.

a. What 85-kPa temperature forecast, and with what reliability, would you make for forecast day: 1, 3, 5, 7, and 9 ?

b. Which temperature ranges would you be confident to forecast would NOT occur, for day: 1, 3, 5, 7, and 9 ?

c. In spite of the forecast uncertainty, are you confident about the general trends in temperature?

d. Could you confidently forecast when rain is most likely? If so, how much rain would you predict?

U17. Fit an exponential curve to the persistence data of Fig. 20.22. What is the e-folding time?

U18. In what order are weather maps presented in the weather briefing given by your favorite local TV meteorologist? What are the advantages and disadvantages of this approach compared to the order suggested in this chapter?

Web-Enhanced Questions

W1. Search the web for info about each of the following operational weather forecast centers. Describe the full title, location, computers that they use, and models that they run. Also answer any special questions indicated below for these forecast centers.

a. CMC (and list the branches of CMC).

b. NCEP (and list the centers that make up NCEP)

c. ECMWF

d. FNMOC

e. UK Met Office

W2. Search the web for the government forecast centers in Germany, Japan, China, Australia, or any other country specified by your instructor. Describe the NWP models they run.

W3. Based on web searches for each of the numerical models listed below:

a. Define the full title.

b. At which centers or universities are they run?

c. Find the max forecast duration for each run.

d. Find the domain (i.e., world, N. Hem. N. America, Canada, Oklahoma, etc.).

e. What is the finest horizontal grid resolution?

f. How many model layers are in the vertical?

g. Which type of grid arrangement (A, B, etc.) is used?

h. What order spatial and time differencing schemes are used?

GEM
NAM
GFS
AVN
NOGAPS
COAMPS
ECMWF
MC2
UW-NMS
MM5
RAMS
ARPS
WRF-NMM
WRF-ARW

W4. Search the web for models in addition to those listed in the previous exercise, which are being run

operationally. Describe the basic characteristics of these models.

W5. Search the web for a discussion of MOS. What is it, and why is it useful to forecasting?

W6. Find on the web different forecast models that produce precipitation forecasts for Vancouver, Canada (or other city specified by your instructor). Do this for as many models as possible that are valid at the same time and place. Specify the date/time for your discussion. Try to pick an interesting day when precipitation is starting or ending, or a storm is passing. Compare the forecasts from the different models, and if possible search the web for observation data of precipitation against which to validate the forecasts.

W7. At which web sites can you find forecast sea states (e.g., wave height, etc.)?

W8. Based on results of a web search, discuss different ways that ensemble forecasts can be presented via images and graphs.

W9. What types of publicly available daily forecasts are being made by a university (not a government operational center) closest to your location?

W10. What are the broad categories of observation data that are used to create the analyses (the starting point for all forecasts). Hint, see the ECMWF data coverage web site, or similar sites from NCEP or the Japanese forecast agency.

W11. Search the web for verification scores for the national weather forecast center that forecasts for your location. How have the scores changed by season, by year? How do the anomaly correlation scores vary with forecast day, compared to the results from ECMWF shown in this chapter?

W12. Find a web site that shows plots of the Lorenz "butterfly", similar to Fig. 20.18. Even better, search the web for a 3-D animation, showing how the solution chaotically shifts from wing to wing.

W13. Search the web for other equations that have different strange attractors. Discuss how the equations and attractors differ from those of Lorenz.

W14. Examine from the web the forecast maps that are produced by various forecast centers. Instead of looking at the quality of the forecasts, look at the quality of the weather map images that are served on the web. Which forecast centers produce the maps that are most attractive? Which are easiest to understand? Which are most useful? What geographic map projections are used for your favorite maps?

W15. Search the web for a meteogram of the weather forecast for your town (or for a town near you, or a town specified by the instructor). What are the advantages and disadvantages of using meteograms to present weather forecasts, rather than weather maps?

W16. Search the web for a summary of different options that are used for physics parameterizations in WRF, or other model selected by your instructor.

W17. Search the web for images/photos of some of the earliest computers used in weather forecasting, such as the ENIAC computer. Discuss how computers have changed.

W18. Find examples of probabilistic forecasts on the web. Print a few examples and discuss.

W19. Computational fluid dynamics (CFD) is the name for numerical methods used to solve fluid dynamics equations in engineering. Search the web for images of CFD forecasts for the finest grid resolution that you can find. What flow situation is it solving? What are the grid spacings and time steps?

Synthesis Questions

S1. Learn what an analog computer is, and how it differs from a digital computer. If automated weather forecasts were made with analog rather than digital computers, how would forecasts be different, if at all?

S2. a. Suppose that there were no weather observations in the western half of N. America. How would the forecast quality over Washington, DC, and Ottawa, Canada, be different, if at all? Given that national legislators live in those cities, speculate on the changes that they would require of the national weather services in the USA and Canada in order to improve the forecasts.

b. Extending the discussion from part (a), suppose that weather observations are back to normal in N. America, but the seats of government were moved to Seattle and Vancouver. Given what you know about the Pacific data void, speculate on the changes that they would require of the national weather services in the USA and Canada in order to improve the forecasts.

S3. How many grid points are needed to forecast over the whole world with roughly 1-m grid spacing? When do you anticipate computer power will have the capability to do such a forecast? What, if any, are the advantages to such a forecast?

S4. Design a grid arrangement different from that in Fig. 20.9, but which is more efficient (i.e., involves fewer calculations) or utilizes a smaller stencil.

S5. a. Suppose one person developed and ran a NWP model that gave daily forecasts with twice the skill as those produced by any other NWP model run operationally around the world. What power and wealth could that person accumulate, and how would they do it? What would be the consequences, and who would suffer?

b. Same question as part (a), but for one country rather than one person.

S6. Look up the Runge-Kutta finite-difference method in a book or internet site on numerical methods. Find equations for a Runge-Kutta method that is higher order than fourth-order. Can you implement this method on a computer spreadsheet? Try it.

S7. Suppose that there was not a CFL numerical stability criterion that restricted the time step that can be used for NWP. How would NWP be different, if at all? Even without a numerical stability criterion, would there be any other restrictions on the time step? If so, discuss.

S8. Speculate on the ability of national forecast centers to make timely weather forecasts if a computer hacker destroyed the internet and other world-wide data networks.

S9. If greater spread of ensemble members in an ensemble forecast means greater uncertainty, then is greater spread desirable or undesirable in an ensemble forecast?

S10. Which would likely give more-accurate forecasts: a categorical model with very fine grid spacing, or an average of ensemble runs where each ensemble member has coarse grid spacing? Why?

S11. Same as the previous question, but specifically for over steep mountainous terrain. Discuss.

S12. Finite-difference equations are approximations to the full, differential equations that describe the real atmosphere. However, such finite-difference equations can also be thought of as exact representations of a numerical atmosphere that behaves according to different physics. How is this numerical atmosphere different from the real atmosphere? How would physical laws differ for this numerical atmosphere, if at all? When the NWP model runs for a long time, if it approaches steady state, is this state equal to the real climate or to the **"model" climate**?

S13. Suppose that electricity did not exist. How would you make numerical weather forecasts? Also, how would you disseminate the results to customers?

S14. How good must a numerical forecast be, to be good enough? Should the quality and value of a weather forecast be determined by meteorologists, computer scientists, or end users? Discuss.

S15. Lorenz suggested that there is a limit to predictability. Is that a "hard" limit, or might it be possible to make skillful forecasts beyond that limit? Discuss.

S16. Comment on the interconnectivity of the atmosphere, as expressed by NWP corollary 1 and by the first Science Graffiti box in the Lorenz attractor section.

Copyright © 2011, 2015 by Roland Stull. *Meteorology for Scientists and Engineers, 3rd Ed.*

NATURAL CLIMATE PROCESSES

CONTENTS

Radiative Equilibrium 793
- Greenhouse Effect 795
- Atmospheric Window 796
- Average Energy Budget 797

Astronomical Influences 797
- Milankovitch Theory 797
- Solar Output 803

Tectonic Influences 804
- Continent Movement 804
- Volcanism 804

Feedbacks 806
- Concept 806
- Idealized Example 807
- Infrared Radiative (IR) Feedback 810
- Water-vapor Feedback 810
- Lapse-rate Feedback 810
- Cloud Feedback 811
- Ice–albedo (Surface) Feedback 811
- Ocean CO_2 Feedback 812
- Biological CO_2 Feedback 812

Daisyworld 813
- Physics 813
- Equilibrium and Homeostasis 815

GCMs 815

Present Climate 816
- Definition 816
- Köppen Climate Classification 817

Natural Oscillations 818
- El Niño - Southern Oscillation (ENSO) 818
- Pacific Decadal Oscillation (PDO) 820
- North Atlantic Oscillation (NAO) 824
- Arctic Oscillation (AO) 824
- Madden-Julian Oscillation (MJO) 824
- Other Oscillations 824

Summary 825
- Threads 826

Exercises 826
- Numerical Problems 826
- Understanding & Critical Evaluation 828
- Web-Enhanced Questions 831
- Synthesis Questions 832

"Meteorology for Scientists and Engineers, 3rd Edition" by Roland Stull is licensed under a Creative Commons Attribution-NonCommercial-ShareAlike 4.0 International License. To view a copy of the license, visit http://creativecommons.org/licenses/by-nc-sa/4.0/ . This work is available at http://www.eos.ubc.ca/books/Practical_Meteorology/ .

21 Earth's average surface temperature has been surprisingly steady over millennia. Factors that control the temperature are solar output, Earth orbital characteristics, ocean currents, atmospheric circulations, plate tectonics, volcanoes, clouds, ice caps, gas emissions, particulates, aerosols, and life.

Some of these factors tend to reduce climate change, and are classified as negative feedbacks. Others amplify change, and are positive feedbacks. The steadiness of Earth's surface temperature suggests that negative feedbacks dominate.

Idealized models of climate processes are presented next. These "toy models" are oversimplifications of nature, yet they serve to illustrate fundamental climatic controls and responses.

RADIATIVE EQUILIBRIUM

The Earth is heated by shortwave radiation from the sun, and is cooled by longwave (infrared, IR) radiation to space (Fig. 21.1). Geological records show that the Earth's surface has had nearly constant annual-average temperature (less than 4% change of absolute temperature over the past 100 million years), suggesting a balance between radiation inflow and outflow.

Incoming minus reflected sunlight, times the interception area, gives the total radiative input to Earth:

$$Radiation\ In = (1 - A) \cdot S_o \cdot \pi \cdot R_{Earth}^2 \qquad \bullet(21.1)$$

where A = 0.30 is **global albedo** (see Focus Box), S_o = 1366 W·m^{-2} is the annual average **total solar irradiance** (**TSI**) over all wavelengths as measured

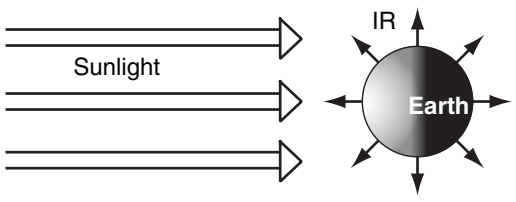

Figure 21.1
Solar input (white arrows) and infrared output (dark arrows) from Earth.

FOCUS • Albedo

The average global reflectivity (portion of incoming sunlight that is reflected back to space) for Earth is called the **albedo**, *A*. But the exact value of *A* is difficult to measure, due to natural variability of cloud and snow cover, and due to calibration errors in the satellite radiation sensors.

Trenberth, Fasullo & Kiehl (2009, *Bul. Amer. Meteor. Soc.*) report a range of values of $27.9\% \le A \le 34.2\%$. They suggest $A = 29.8\%$. We use $\boldsymbol{A \approx 30\%}$ here.

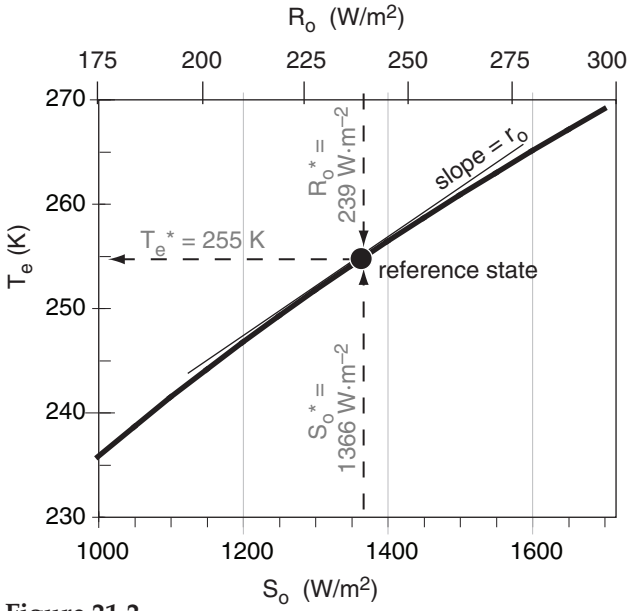

Figure 21.2

Thick curved line shows the variation of Earth effective radiation temperature T_e with solar irradiance S_o , assuming an albedo of $A = 0.30$. Dashed lines show present conditions, which will be used as a reference point or reference state (R_o, T_e*). Thin black straight line shows the slope r_o of the curve at the reference point. $R_o = (1–A)\cdot S_o/4$ is net solar input for each square meter of the Earth's surface (see Focus Box, next page).*

Solved Example

Find the radiative equilibrium temperature of the Earth-atmosphere system.

Solution:

Given: $S_o = 1366\ \text{W}\cdot\text{m}^{-2}$ solar irradiance
$A = 0.30$ global albedo (reflectivity)
Find: $T_e = ?\ \text{K}$ radiative equilibrium temp.

Use eq. (21.3):

$$T_e = \left[\frac{(1-0.3)\cdot(1366\ \text{W}\cdot\text{m}^{-2})}{4\cdot(5.67\times10^{-8}\ \text{W}\cdot\text{m}^{-2}\cdot\text{K}^{-4})}\right]^{1/4}$$

$$= 254.8\ \text{K} \approx 255\ \text{K} = \underline{\mathbf{-18°C}}$$

Check: Units OK. Physics OK.

Discussion: The effective radiation temperature does not depend on the radius of the planet.

by satellites, and R_{Earth} is the Earth radius. The area of a disk πR^2 rather than the surface area of a sphere $4\pi R^2$ is used because the area of intercepted solar radiation is equivalent to the area of the shadow cast behind the Earth. The TSI has fluctuated about ±0.5 $\text{W}\cdot\text{m}^{-2}$ (the thickness of the dashed line in Fig. 21.2) during the past 33 years due to the average sunspot cycle. See the Radiation chapter for TSI details.

Assume the Earth is a black body in the infrared, and that it emits IR radiation from its whole surface area (continents and oceans). Multiplying the Stefan-Boltzmann law (eq. 2.15), which gives the emissions per unit area, times surface area of the Earth (assumed spherical here) gives:

$$\textit{Radiation Out} = 4\pi\cdot R_{Earth}^2\cdot\sigma_{SB}\cdot T_e^4 \qquad \bullet(21.2)$$

where $\sigma_{SB} = 5.67\text{x}10^{-8}\ \text{W}\cdot\text{m}^{-2}\cdot\text{K}^{-4}$ is the Stefan-Boltzmann constant, and T_e is the **effective radiation emission temperature**.

The real Earth is quite heterogeneous, with oceans, continents, forests, clouds and ice caps of differing temperatures. Each of these regions emits different amounts of radiation. Also, some radiation is emitted from the Earth's surface, some from various heights in the atmosphere, and some from clouds. The effective radiation temperature is defined so that the total emissions from the actual Earth-ocean-atmosphere system equal the theoretical emissions from a uniform Earth of temperature T_e.

For a steady-state climate (i.e., no temperature change with time), outputs must balance the inputs. Thus, equate outgoing and incoming radiation from eqs. (21.1 and 21.2), and then solve for T_e :

$$T_e = \left[\frac{(1-A)\cdot S_o}{4\cdot\sigma_{SB}}\right]^{1/4} = \left[\frac{R_o}{\sigma_{SB}}\right]^{1/4} \qquad \bullet(21.3)$$

$$\approx 254.8\ \text{K} \approx -18°\text{C}$$

where $R_o = (1–A)\cdot S_o/4$. Fig. 21.2 shows this reference state and shows how the effective temperature varies with total solar irradiance, assuming constant albedo. This effective temperature is too cold compared to the observed surface temperature of 15°C. Hence, this simple model must be missing some important physics.

This radiation balance is a **negative feedback**. Namely, increases of incoming solar radiation are mostly compensated by increases in outgoing IR, yielding only small temperature changes.

Because the radiative feedback dominates over all others, the Earth's climate is relatively stable, as geological records demonstrate (Fig. 21.3). Fifty million years ago, the average surface temperature

was about 6°C warmer than now. During the past ten thousand years, the climate has oscillated about ±1°C about the recent 15°C average. Although these temperature changes are small (range of ΔT is of order 10°C) relative to the Earth's absolute temperature, they can cause dramatic changes in sea level and glaciation.

Greenhouse Effect

You can increase the sophistication of the previous model by adding a layer of atmosphere (see Fig. 21.4) that is opaque to infrared radiation, but transparent to visible. Sunlight heats the Earth's surface. Radiation from the surface heats the opaque atmosphere. Radiation from the top of the atmosphere is lost to space, while radiation from the bottom of the atmosphere heats the Earth.

The incoming radiation from the sun must balance the outgoing radiation from the atmosphere, in order for the Earth-atmosphere system to remain in radiative equilibrium. Hence

$$T_A = T_e = 255\ \text{K} = -18°\text{C} \qquad (21.4)$$

as before, where T_e is the effective emission temperature of the whole Earth-atmosphere system, and T_A is the temperature of the atmosphere. For this case, the two temperatures are equal, because the atmosphere is opaque.

Other energy balances can be made for the atmosphere separately, and for the Earth's surface separately, with output from one system being the input to the other. The opaque atmosphere is assumed to emit as much IR radiation upward to space, as downward toward the Earth. The amount emitted both up and down from the atmosphere is given by the Stefan-Boltzmann law as $\sigma_{SB} \cdot T_A^4$. Incoming IR radiation from the Earth's surface is $\sigma_{SB} \cdot T_s^4$, where T_s is the Earth-surface temperature. If the atmosphere is at **steady state**, then absorbed IR equals emitted IR:

$$\sigma_{SB} \cdot T_s^4 = 2 \cdot \sigma_{SB} \cdot T_e^4 \qquad (21.5)$$

The sum of atmospheric and solar radiation reaching the Earth's surface is exactly twice that of the solar radiation alone. This extra heating from the atmosphere causes the Earth to warm until it emits exactly twice the radiation as before. This allows the Earth's surface temperature to be estimated by:

$$T_s = 2^{1/4} \cdot T_e \qquad \bullet(21.6)$$

$$= 303\ \text{K} = 30°\text{C}$$

Warming of the Earth's surface due to radiation emitted from the atmosphere is known as the **Greenhouse effect**. Water vapor is a greenhouse gas.

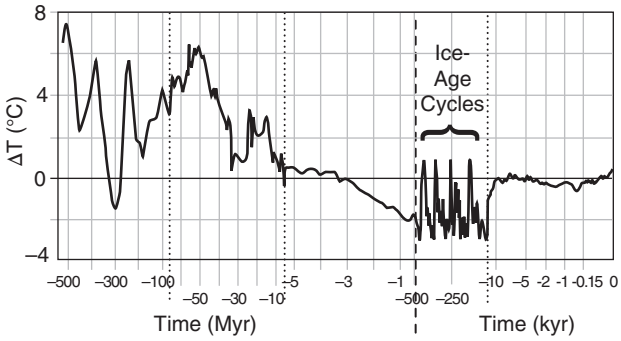

Figure 21.3
Paleotemperature estimate (smoothed) as a difference ΔT from the 1961 to 1990 temperature average. Time is relative to calendar year 2000. Scale breaks at the dotted and dashed lines. Glacial/interglacial oscillations (i.e., ice-age cycles) prior to 500,000 yr ago have been smoothed out.

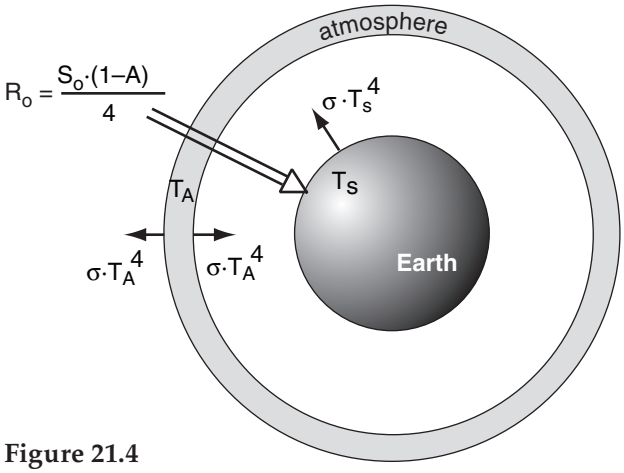

Figure 21.4
Greenhouse effect with an idealized one-layer atmosphere. Distance between Earth and atmosphere is exaggerated. Assume that the radius of the Earth approximately equals the radius at the top of the atmosphere. R_o is the net solar input, and σ is the Stefan-Boltzmann constant.

FOCUS • Why does $R_o = (1-A) \cdot S_o / 4$?

In Figs. 21.4 and 21.5, the **net solar input** R_o is given as $(1-A) \cdot S_o/4$ instead of S_o. The $(1-A)$ factor is because any sunlight reflected back to space is not available to heat the Earth system. But why also divide by 4? The reason is due to geometry.

Of the radiation streaming outward from the sun, the shadow cast by the Earth indicates how much radiation was intercepted. The shadow is a circle with radius equal to the Earth's radius R_{Earth}, hence the interception area is $\pi \cdot R_{Earth}^2$.

But we prefer to study the energy fluxes relative to each square meter of the Earth's surface. The surface area of a sphere is $4 \cdot \pi \cdot R_{Earth}^2$. Namely, the surface area is four times the area intercepted by the sun.

Hence, the average net solar input that we allocate to each square meter of the Earth's surface is:
$R_o = (1-A) \cdot S_o/4 = (1-0.3) \cdot (1366\ \text{W} \cdot \text{m}^{-2})/4 =$ **239 W·m^{-2}**.

Solved Example

For the previous solved example, find the Earth surface temperature under a one-layer atmosphere.

Solution

Given: T_e = 255 K

Find: T_s = ? K

Use eq. (21.6): $T_s = 1.189 \cdot (255\text{K}) = 303\text{ K} = 30°\text{C}$

Check: Units OK. Physics OK.

Discussion: Although the radiation reaching the Earth's surface doubles, the surface temperature increases by a smaller portion.

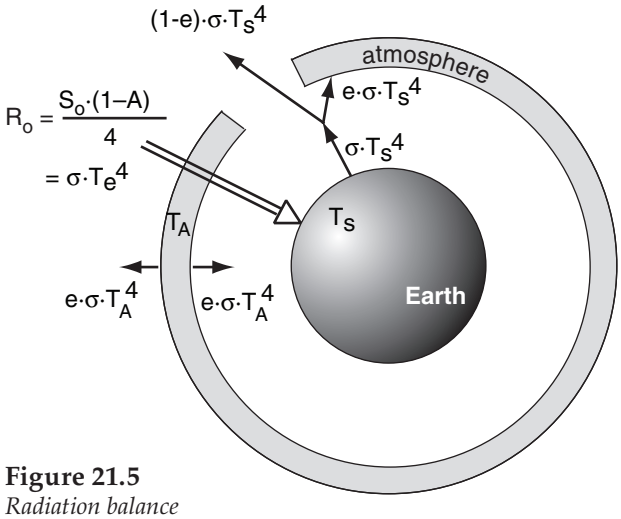

Figure 21.5
Radiation balance in a hypothetical one-layer atmosphere with an IR window.

Solved Example

For the previous solved example, assume $e_\lambda = 0.899$. Find the surface and atmosphere temperatures.

Solution

Given: T_e = 255 K, $e_\lambda = 0.899$

Find: T_s = ? K

Use eq. (21.10):

$$T_s = \left(\frac{2}{2-0.899}\right)^{1/4} \cdot (254.8\text{K} = 296\text{ K} = \underline{\mathbf{23°C}}$$

From Eq. (21.7) we see that the effective emission temperature of the atmosphere is:

$$T_A = (0.5)^{1/4} \cdot T_s = 0.84 \cdot (296\text{ K}) = 249\text{ K} = \underline{\mathbf{-24°C}}$$

Check: Units OK. Physics OK.

Discussion: This model is more sophisticated than the previous one, and gives a result closer to the observed temperature of 15°C. But the wrong temperature suggests that some important physics is missing.

But 30°C is too warm compared to the observed average surface temperature of 15°C. Hence, we infer that some important physics are still missing.

Atmospheric Window

Between 8 and 14 μm wavelengths, the atmosphere is semi-transparent to infrared (IR) radiation (see the Remote Sensing chapter). This is the **atmospheric window**. Suppose this window allows 10.1% of the IR radiation from the Earth to be lost directly to space, without first being absorbed by the atmosphere. Using Kirchhoff's law from the Radiation chapter, this gives an absorptivity = emissivity (e_λ) = 89.9% for this hypothetical atmosphere.

As before, the incoming fluxes must balance the outgoing, for an equilibrium atmosphere. The same holds for the Earth's surface. As before, the flux output from one system is often an input to another.

For a one-layer atmosphere with a window as sketched in Fig. 21.5, the equilibrium energy balance (input = output) of the atmosphere is:

$$e_\lambda \cdot \sigma_{SB} \cdot T_s^{\,4} = 2 \cdot e_\lambda \cdot \sigma_{SB} \cdot T_A^{\,4} \qquad (21.7)$$

For the Earth's surface, the corresponding balance is:

$$R_o + e_\lambda \cdot \sigma_{SB} \cdot T_A^{\,4} = \sigma_{SB} \cdot T_s^{\,4} \qquad (21.8)$$

Solving these coupled equations for the atmosphere and surface temperatures yields:

$$T_A^4 = \frac{T_e^4}{2 - e_\lambda} \qquad \bullet(21.9)$$

$$T_s^4 = \frac{2 \cdot T_e^4}{2 - e_\lambda} \qquad \bullet(21.10)$$

Thus:

$$T_s = 296\text{ K} = 23°\text{C} \quad \text{and} \quad T_A = 249\text{ K} = -24°\text{C} \qquad (21.11)$$

This surface temperature is closer to realistic, but is still slightly too warm.

If **anthropogenic greenhouse gases** carbon dioxide (CO_2), nitrous oxide (N_2O), methane (CH_4), and freon CFC-12 ($C\,Cl_2\,F_2$) accumulate in the atmosphere, they can close the atmospheric window by absorbing and re-emitting more IR radiation emitted from Earth. This could cause surface temperatures to warm toward those of the previous solved example. This is the threat of **global warming**.

Finally, be assured that Fig. 21.5 is just a cartoon designed to illustrate that some IR radiation from Earth can escape to space through a translucent atmosphere. A spatial hole in the atmosphere does not really exist (although a hole of ozone has sometimes existed over the Earth's poles).

Average Energy Budget

Radiation is not the only physical process that transfers energy. Between the Earth and bottom layer of the atmosphere can also be sensible-heat transfer via conduction (see the Heat chapter), and latent-heat transfer via evapotranspiration (see the Moisture chapter). Once this heat and moisture are in the air, they can be transported further into the atmosphere by the mean wind, by deep convection such as thunderstorms, by shallow convection such as thermals, and by smaller turbulent eddies in the atmospheric boundary layer.

One estimate of the annual mean of energy fluxes between all these components, when averaged over the surface area of the globe, is sketched in Fig. 21.6. According to the Stefan-Boltzmann law, the emitted IR radiation from the Earth's surface (396 W·m^{-2}) corresponds to an average surface temperature of 16°C, which is close to observed temperature of 15°C.

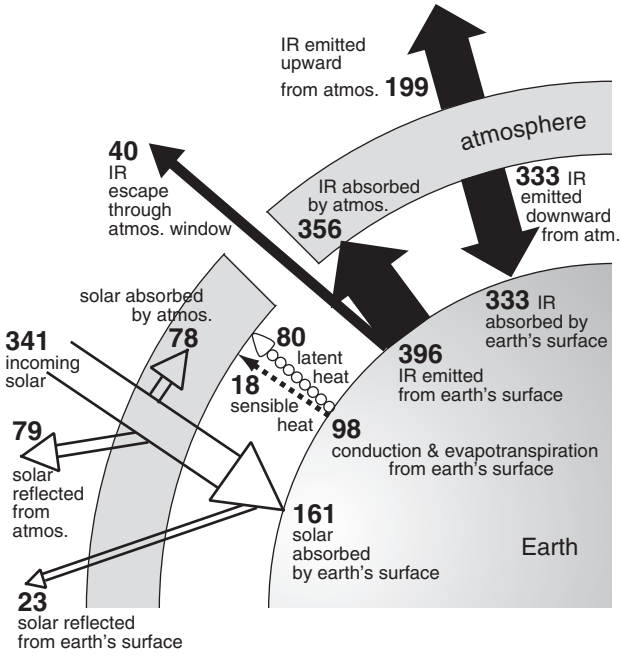
IR emitted upward from atmos. 199
atmosphere
40 IR escape through atmos. window
IR absorbed by atmos. 356
333 IR emitted downward from atm.
solar absorbed by atmos. 78
341 incoming solar
80 latent heat
18 sensible heat
333 IR absorbed by earth's surface
396 IR emitted from earth's surface
79 solar reflected from atmos.
98 conduction & evapotranspiration from earth's surface
161 solar absorbed by earth's surface
Earth
23 solar reflected from earth's surface

Figure 21.6
Global annual mean energy budget for the Earth system, based on data from 2000-2004. The "atmosphere" component includes the air, clouds, and particles in the air. Numbers are approximate energy fluxes in units of W·m^{-2}. Errors are of order 3% for fluxes at the top of the atmosphere, and errors are 5 to 10% for surface fluxes. The incoming solar radiation, when averaged over all the Earth's surface, is $S_o/4$ = 341 W·m^{-2}. After subtracting the outgoing (reflected) solar radiation (341 − 79 − 23 = 239 W·m^{-2}), the result is the same R_o that we used before. (Based partially on info from Trenberth, Fasullo and Kiehl, 2009, Bull. Amer. Meteor. Soc.)

ASTRONOMICAL INFLUENCES

If the incoming solar radiation (**insolation**) changes, then the radiation budget of the Earth will adjust, possibly altering the climate. Two causes of average-daily-insolation $\overline{E}$ change at the top of the atmosphere are changes in solar output S_o and changes in Earth-sun distance R (recall eq. 2.21).

Milankovitch Theory

In the 1920s, astrophysicist Milutin Milankovitch proposed that slow fluctuations in the Earth's orbit around the sun can change the sun-Earth distance. Distance changes alter insolation due to the inverse square law (eq. 2.16), thereby contributing to climate change. Ice-age recurrence (inferred from ice and sediment cores) was later found to be correlated with orbital characteristics, supporting his hypothesis. Milankovitch focused on three orbital characteristics: eccentricity, obliquity, and precession.

Eccentricity

The shape of Earth's elliptical orbit around the sun (Fig. 21.7a) slowly fluctuates between nearly circular (**eccentricity** $e \approx 0.0034$) and slightly elliptical ($e \approx 0.058$). For comparison, a perfect circle has $e = 0$. Gravitational pulls by other planets (mostly Jupiter and Saturn) cause these eccentricity fluctuations.

Earth's eccentricity at any time (past or future) can be approximated by a sum of cosine terms:

Solved Example
Confirm that energy flows in Fig. 21.6 are balanced.

Solution

Solar: incoming = [reflected] + (absorbed)
341 = [79 + 23] + (78 + 161)
341 = 341 W·m^{-2}

Earth's surface: incoming = outgoing
(161 + 333) = (98 + 396)
494 = 494 W·m^{-2}

Atmosphere: incoming = outgoing
(78 + 18 + 80 + 356) = (199 + 333)
532 = 532 W·m^{-2}

Earth System: in from space = out to space
341 = (23 + 79 + 40 + 199)
341 = 341 W·m^{-2}

Check: Yes, all budgets are balanced.
Discussion: The solar budget must balance because the Earth-atmosphere system does not create/emit solar radiation. However, IR radiation is created by the sun, Earth, and atmosphere; hence, the IR fluxes by themselves need not balance.

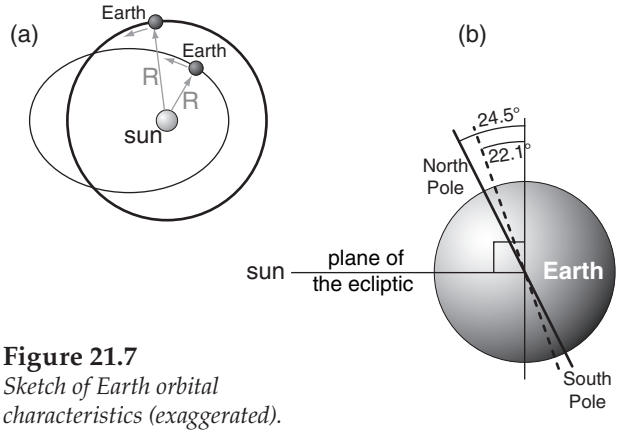

Figure 21.7
Sketch of Earth orbital characteristics (exaggerated). (a) Eccentricity variations. (b) Obliquity variations.

$$e \approx e_o + \sum_{i=1}^{N} A_i \cdot \cos\left[C \cdot \left(\frac{t}{P_i} + \frac{\phi_i}{360°} \right) \right] \qquad \bullet(21.12)$$

where e_o = 0.0275579, A_i are amplitudes, t is time in years relative to calendar year 2000, P_i are oscillation periods in years, ϕ_i are phase shifts in degrees, and i is an index that counts the 1 to N terms. C should be either 360° or 2·π radians, depending on the type of trigonometric argument required by your calculator, spreadsheet, or programming language.

Table 21-1 shows values for these orbital factors for N = 5 terms in this series. [CAUTION: *A more accurate description requires N =20 or more terms. The first 10 terms are listed in Table 21-1b near exercise U9 at the end of this chapter.*] I used a spreadsheet to solve these 5 terms for times ranging from 1 million years in the past to 1 million years into the future (see results in Fig. 21.8).

By eye, we see two superimposed oscillations of eccentricity with periods of about 100 and 400 kyr (where "kyr" = kilo years = 1000 years). The first oscillation correlates very well with the roughly 100 kyr period for cool events associated with **ice ages**. The present eccentricity is about 0.0167. Short-term forecast: eccentricity will change little during the next 100,000 years. Variations in e affect Earth-sun distance R via eq. (2.4) in the Radiation chapter.

Solved Example
Plot ellipses for eccentricities of 0, 0.005, 0.058 & 0.50.
Hints: the (x, y) coordinates are given by $x = a \cdot \cos(t)$, and $y = b \cdot \sin(t)$, where t varies from 0 to 2π radians. Assume a semi-major axis of a = 1, and get the semi-minor axis from $b = a \cdot (1 - e^2)^{1/2}$.

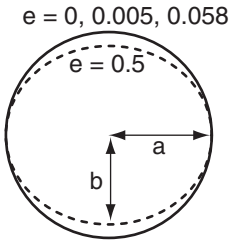

Solution
Plotted at right:

Discussion. The first 3 curves (solid lines) look identical. Thus, for the full range of Earth's eccentricities (0.0034 ≤ e ≤ 0.58), we see that Earth's orbit is nearly circular (e = 0).

Solved Example.
Find the Earth-orbit eccentricity 600,000 years ago (i.e., 600,000 years before year 2000).

Solution.
Given: t = –600,000 years (negative sign for past).
Find: e (dimensionless).

Use eq. (21.12) with data from Table 21-1:
$e \approx$ 0.0275579
+ 0.010739·cos[2π·(–600000yr/405091yr + 170.739°/360°)]
+ 0.008147·cos[2π·(–600000yr/ 94932yr + 109.891°/360°)]
+ 0.006222·cos[2π·(–600000yr/123945yr – 60.044°/360°)]
+ 0.005287·cos[2π·(–600000yr/ 98857yr – 86.140°/360°)]
+ 0.004492·cos[2π·(–600000yr/130781yr + 100.224°/360°)]

$e \approx$ 0.0275579 + 0.0107290 + 0.0081106 + 0.0062148
– 0.0019045 – 0.0016384 ≈ **0.049** (dimensionless)

Check: 0.0034 ≤ e ≤ 0.058, within the expected eccentricity range for Earth. Agrees with Fig. 21.8.
Discussion: An **interglacial** (non-ice-age) period was ending, & a new **glacial** (ice-age) period was starting.

Table 21-1. Factors in orbital series approximations.

index	A	P (years)	ϕ (degrees)
Eccentricity:			
i= 1	0.010739	405,091.	170.739
2	0.008147	94,932.	109.891
3	0.006222	123,945.	–60.044
4	0.005287	98,857.	–86.140
5	0.004492	130,781.	100.224
Obliquity:			
j= 1	0.582412°	40,978.	86.645
2	0.242559°	39,616.	120.859
3	0.163685°	53,722.	–35.947
4	0.164787°	40,285.	104.689
Climatic Precession:			
k= 1	0.018986	23,682.	44.374
2	0.016354	22,374.	–144.166
3	0.013055	18,953.	154.212
4	0.008849	19,105.	–42.250
5	0.004248	23,123.	90.742

*Simplified from Laskar, Robutel, Joutel, Gastineau, Correia & Levrard, 2004: A long-term numerical solution for the insolation quantities of the Earth. "Astronomy & Astrophysics", **428**, 261-285.*

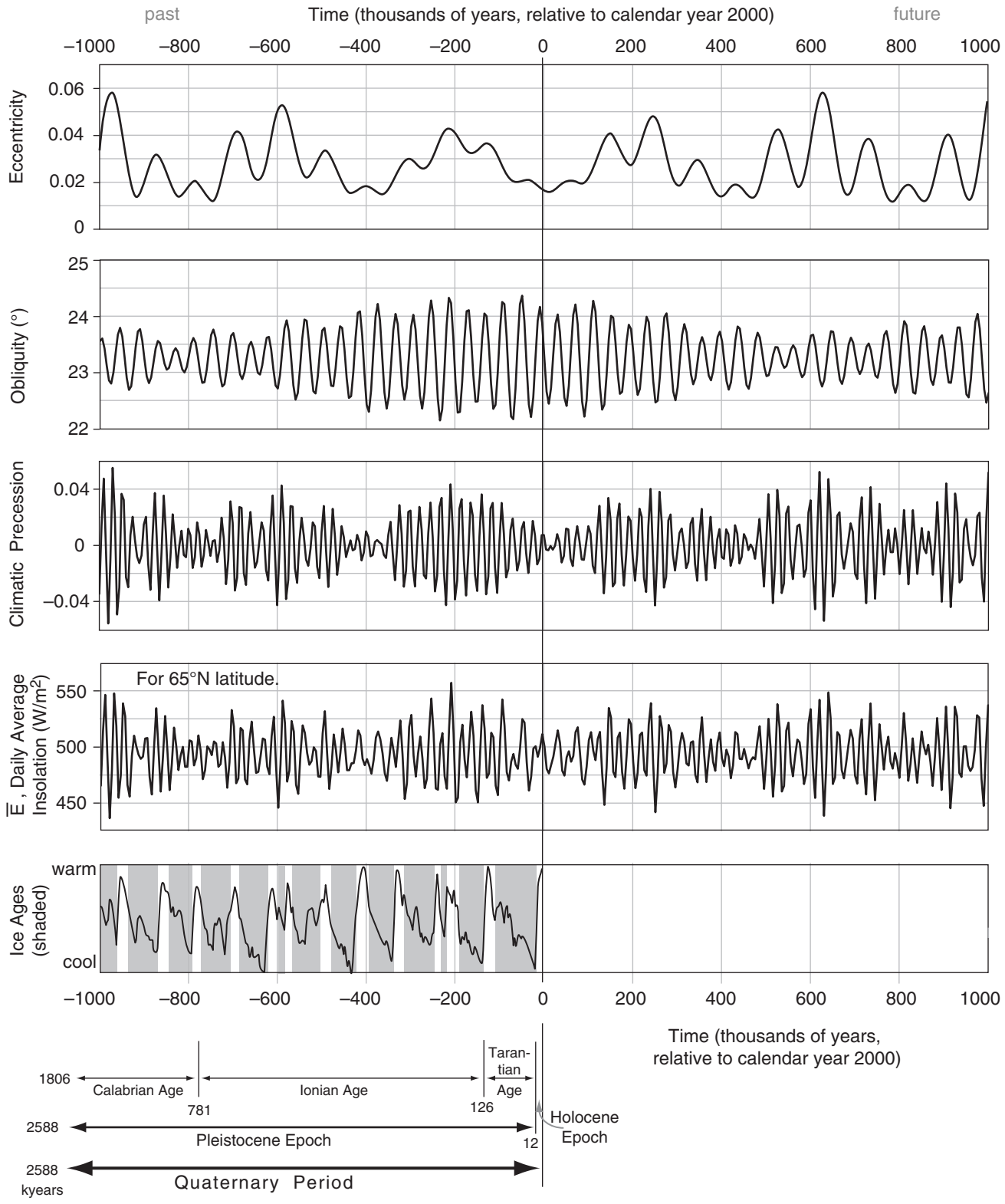

Figure 21.8

Past and future orbital characteristics in Milankovitch theory, as calculated using only the 4 or 5 highest-order terms (see Table 21-1) in the series approximations of eqs. (21.12 - 21.20). Bottom curve shows relative temperature changes estimated from ice and sediment cores. Ice ages (glacial periods) are shaded grey. Precession is for the summer solstice (i.e., only the e·sin(ϖ) term is used).

Solved Example
Estimate Earth's obliquity 90,000 yrs in the future (relative to calendar year 2000).

Solution
Given: t = 90,000 yr (positive sign indicates future)
Find: ε = ?°

Use eq. (21.13) with coefficients from Table 21-1.

$$\varepsilon = 23.2545° + 0.582412°\cdot[2\pi\cdot(90000\text{yr}/40978\text{yr} + 86.645°/360°)] + 0.242559°\cdot[2\pi\cdot(90000\text{yr}/39616\text{yr} + 120.859°/360°)] + 0.163685°\cdot[2\pi\cdot(90000\text{yr}/53722\text{yr} - 35.947°/360°)] + 0.164787°\cdot[2\pi\cdot(90000\text{yr}/40285\text{yr} + 104.689°/360°)]$$

$$\varepsilon = 23.2545° - 0.537349° - 0.189273° - 0.145639° - 0.162777° = \underline{\mathbf{22.219°}}$$

Check: Units OK. Within Earth range 22.1°≤ ε ≤24.5°.
Discussion: Agrees with Fig. 21.8. At this small obliquity, seasonal contrasts are smaller than at present, allowing glaciers to grow due to cooler summers.

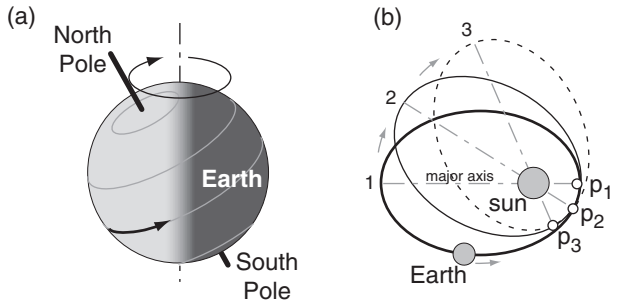

Figure 21.9
Sketch of additional Earth orbital characteristics. (a) Precession of Earth's axis. (b) Precession of the orbit-ellipse major axis (aphelion precession) at successive times 1 - 3. Small white dots p_1, p_2, p_3 show locations of the perihelion (point on Earth's orbit closest to sun). All the orbit ellipses are in the same plane.

Obliquity

The tilt (obliquity) of Earth's axis slowly fluctuates between 22.1° and 24.5°. This tilt angle is measured from a line perpendicular to Earth's orbital plane (the ecliptic) around the sun (Fig. 21.7b).

A series approximation for obliquity ε is:

$$\varepsilon = \varepsilon_o + \sum_{j=1}^{N} A_j \cdot \cos\left[C \cdot \left(\frac{t}{P_j} + \frac{\phi_j}{360°} \right) \right] \qquad \bullet(21.13)$$

where ε_o = 23.254500°, and all the other factors have the same meaning as for the eq. (21.12). Table 21-1 shows values for these orbital factors for N = 4 terms in this series.

Fig. 21.8 shows that obliquity oscillates with a period of about 41,000 years. The present obliquity is 23.439° and is gradually decreasing.

Obliquity affects insolation via the solar declination angle (eq. 2.5 in the Radiation chapter, where a different symbol Φ_r was used for obliquity). Recall from the Radiation chapter that Earth-axis tilt is responsible for the seasons, so greater obliquity would cause greater contrast between winter and summer. One hypothesis is that ice ages are more likely during times of lesser obliquity, because summers would be cooler, causing less melting of glaciers.

Precession

Various precession processes affect climate.

Axial Precession. Not only does the tilt magnitude (obliquity) of Earth's axis change with time, but so does the tilt direction. This tilt direction rotates in space, tracing one complete circle in 25,680 years (Fig. 21.9a) relative to the fixed stars. It rotates opposite to the direction the Earth spins. This precession is caused by the gravitational pull of the sun and moon on the Earth, because the Earth is an oblate spheroid (has larger diameter at the equator than at the poles). Hence, the Earth behaves somewhat like a spinning toy top.

Aphelion Precession. The direction of the major axis of Earth's elliptical orbit also precesses slowly (with a 174,000 to 304,00 year period) relative to the fixed stars (Fig. 21.9b). The rotation direction is the same as the axial-precession, but the precession speed fluctuates due to the gravitational pull of the planets (mostly Jupiter and Saturn).

Equinox Precession. Summing axial and aphelion precession rates (i.e., adding the inverses of their periods) gives a total precession with fluctuating period of about 22,000 years. This combined precession describes changes to the angle (measured at the sun) between Earth's orbital positions at the perihelion (point of closest approach) and at the moving vernal (Spring) equinox (Fig. 21.10). This

fluctuating angle (ϖ, a math symbol called "variant pi") is the equinox precession.

For years when angle ϖ is such that the winter solstice is near the perihelion (as it is in this century), then the cooling effect of the N. Hemisphere being tilted away from the sun is slightly moderated by the fact that the Earth is closest to the sun; hence winters and summers are not as extreme as they could be. Conversely, for years with different angle ϖ such that the summer solstice is near the perihelion, then the N. Hemisphere is tilted toward the sun at the same time that the Earth is closest to the sun — hence expect hotter summers and colder winters. However, seasons near the perihelion are shorter duration than seasons near the aphelion, which moderates the extremes for this latter case.

Climatic Precession. ϖ by itself is less important for insolation than the combination with eccentricity e: $e\cdot\sin(\varpi)$ and $e\cdot\cos(\varpi)$. These terms, known as the climatic precession, can be expressed by series approximations, where both terms use the same coefficients from Table 21-1, for $N = 5$.

$$e\cdot\sin(\varpi) \approx \sum_{k=1}^{N} A_k \cdot \sin\left[C\cdot\left(\frac{t}{P_k}+\frac{\phi_k}{360°}\right)\right] \qquad \bullet(21.14)$$

$$e\cdot\cos(\varpi) \approx \sum_{k=1}^{N} A_k \cdot \cos\left[C\cdot\left(\frac{t}{P_k}+\frac{\phi_k}{360°}\right)\right] \qquad (21.15)$$

Other factors are similar to those in eq. (21.12).

A plot of eq. (21.14), labeled "climatic precession", is shown in Fig. 21.8. It shows high frequency (22,000 year period) waves with amplitude modulated by the eccentricity curve from the top of Fig. 21.8. Climatic precession affects sun-Earth distance, as described next.

Insolation Variations

Eq. (2.21) from the Radiation chapter gives average daily insolation $\bar{E}$. It is repeated here:

$$\bar{E} = \frac{S_o}{\pi}\cdot\left(\frac{a}{R}\right)^2 \cdot\left[h_o'\cdot\sin(\phi)\cdot\sin(\delta_s) + \cos(\phi)\cdot\cos(\delta_s)\cdot\sin(h_o)\right] \qquad \bullet(21.16)$$

where S_o =1366 W/m^2 is the solar irradiance, a = 149.457 Gm is the semi-major axis length, R is the sun-Earth distance for any day of the year, h_o' is the hour angle in radians., ϕ is latitude, and δ_s is solar declination angle. Factors in this eq. are given next.

Instead of solving this formula for many latitudes, climatologists often focus on one key latitude: ϕ = 65°N. This latitude crosses Alaska, Canada,

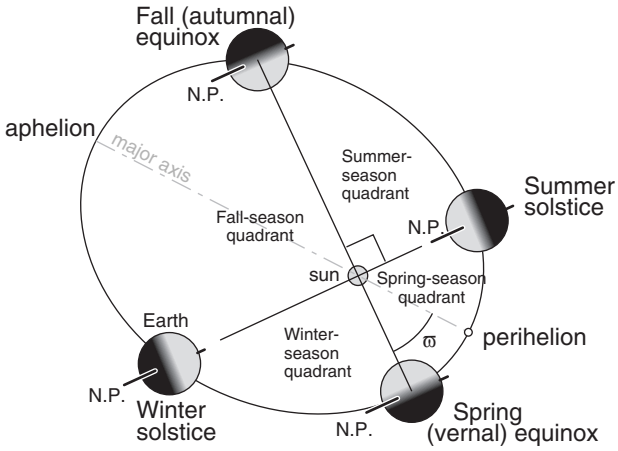

Figure 21.10
Illustration for sometime in the future, showing the angle (ϖ) of the perihelion from the moving vernal equinox. N.P. = North Pole. Seasons are for the N. Hemisphere.

Solved Example
Estimate the climatic precession (sine term) for year 2000.

Solution
Given: $t = 0$
Find: $e\cdot\sin(\varpi)$ = ? (dimensionless)

Use eq. (21.14) with coefficients from Table 21-1.

$e\cdot\sin(\varpi)$ =
+ 0.018986·[2π·(0yr/23682yr + 44.374°/360°)]
+ 0.016354·[2π·(0yr/22374yr – 144.166°/360°)]
+ 0.013055·[2π·(0yr/18953yr + 154.212°/360°)]
+ 0.008849·[2π·(0yr/19105yr – 42.250°/360°)]
+ 0.004248·[2π·(0yr/23123yr + 90.742°/360°)]

$e\cdot\sin(\varpi)$ = 0.0132777 – 0.0095743 + 0.0056795 – 0.0059498 + 0.0042476 = **0.00768**

Check: Agrees with curve plotted in Fig. 21.8.
Discussion: The small eccentricity in year 2000 (i.e., almost at present) causes small climatic precession.

Table 21-2. Key values of λ, the angle between the Earth and the moving vernal equinox. Fig. 21.10 shows that solstices and equinoxes are exactly 90° apart.

Date	λ (radians, °)	sin(λ)	cos(λ)
Vernal (Spring) equinox	0 , 0	0	1
Summer solstice	π/2 , 90°	1	0
Autumnal (Fall) equinox	π , 180°	0	–1
Winter solstice	3π/2 , 270°	–1	0

Solved Example

For the summer solstice at 65°N latitude, find the average daily insolation for years 2000 and 2200.

Solution

Given: $\lambda = \pi/2$, $\phi = 65°N$, (a) $t = 0$, (b) $t = 200$ yr
Find: $\bar{E}$ = ? W/m^2 (Assume $S_o = 1366$ W/m^2)

(a) From previous statements and solved examples:
$e = 0.0167$, $\delta_s = \varepsilon = 23.439°$, $e{\cdot}\sin(\varpi) = 0.00768$
Use eq. (21.17): $h_o = \arccos[-\tan(65°){\cdot}\tan(23.439°)]$
$= 158.4° = 2.7645$ radians $= h_o'$.
Eq. (21.20): $(a/R) = (1+0.00768)/[1-(0.0167)^2] = 1.00796$
Plugging all these into eq. (21.16):
$\bar{E}$ = [(1366 W/m^2)/π] ·(1.00796)^2 · [2.7645 ·sin(65°)
·sin(23.439°) + cos(65°)·cos(23.439°)·sin(158.4°)]
$\bar{E}$ = **503.32 W/m**^{2} for $t = 0$.

(b) Eq. (21.12) for $t = 200$: $e \approx 0.0168$
Eq. (21.13): $\varepsilon = 23.2278°$. Eq. (21.14): $e{\cdot}\sin(\varpi) = 0.00730$
Eq. (21.20): $a/R = 1.00758$. Eq. (21.16): $\bar{E}$ = **499.3 W/m**^{2}

Check: Units OK. Magnitude ≈ that in Fig. 2.11 (Ch2).
Discussion: Milankovitch theory indicates that insolation will decrease slightly during the next 200 yr.

FOCUS • Sun-Earth Distance

Recall from Chapter 2 (eq. 2.4) that the sun-Earth distance R is related to the semi-major axis a by:

$$\frac{a}{R} = \frac{1+e\cdot\cos(\nu)}{1-e^2} \qquad (21.19)$$

where ν is the true anomaly (position of the Earth from the perihelion), and e is the eccentricity from eq. (21.12). By definition, $\nu = \lambda - \varpi$ (21.a) where λ is position of the Earth from the moving vernal equinox, and ϖ is position of the perihelion from the moving vernal equinox. Thus,

$$\frac{a}{R} = \frac{1+e\cdot\cos(\lambda-\varpi)}{1-e^2} \qquad (21.b)$$

Using trigonometric identities, the cosine term is:

$$\frac{a}{R} = \frac{1+\cos(\lambda)\cdot[e\cdot\cos(\varpi)]+\sin(\lambda)\cdot[e\cdot\sin(\varpi)]}{1-e^2} \qquad (21.c)$$

The terms in square brackets are the **climatic precessions** that you can find with eqs. (21.14) and (21.15).

To simplify the study of climate change, researchers often consider a special time of year; e.g., the summer solstice ($\lambda = \pi/2$ from Table 21-2). This time of year is important because it is when glaciers may or may not melt, depending on how warm the summer is. At the summer solstice, the previous equation simplifies to:

$$\frac{a}{R} = \frac{1+[e\cdot\sin(\varpi)]}{1-e^2} \qquad (21.20)$$

Also, during the summer solstice, the solar declination angle from eq. (21.18) simplifies to: $\delta_s = \varepsilon$

Greenland, Iceland, Scandinavia, and Siberia, and is representative of genesis zones for ice caps.

The hour angle h_o at sunrise and sunset is given by the following set of equations:

$$\alpha = -\tan(\phi)\cdot\tan(\delta_s) \qquad (21.17a)$$

$$\beta = \min[1,(\max(-1,\alpha)] \qquad (21.17b)$$

$$h_o = \arccos(\beta) \qquad (21.17c)$$

Although the hour angle h_o can be in radians or degrees (as suits your calculator or spreadsheet), the hour angle marked with the prime (h_o') must be in radians.

The solar declination angle, used in eq. (21.16), is

$$\delta_s = \arcsin[\sin(\varepsilon)\cdot\sin(\lambda)] \approx \varepsilon\cdot\sin(\lambda) \qquad (21.18)$$

where ε is the obliquity from eq. (21.13), and λ is the **true longitude** angle (measured at the sun) between the position of the Earth and the position of the moving vernal equinox. Special cases for λ are listed in Table 21-2.

Recall from the Radiation chapter (eq. 2.4) that the sun-Earth distance R is related to the semi-major axis a by:

$$\frac{a}{R} = \frac{1+e\cdot\cos(\nu)}{1-e^2} \qquad (21.19)$$

where ν is the true anomaly (position of the Earth from the perihelion), and e is the eccentricity. For the special case of the summer solstice (see the Sun-Earth Distance Focus Box), this becomes:

$$\frac{a}{R} = \frac{1+[e\cdot\sin(\varpi)]}{1-e^2} \qquad (21.20)$$

where e is from eq. (21.12) and $e{\cdot}\sin(\varpi)$ is from eq. (21.14)

I used all the information above to solve eq. (21.16) on a spreadsheet for average daily insolation at latitude 65°N during the summer solstice for 1 Myr in the past to 1 Myr in the future. This results in the curve for $\bar{E}$ plotted in Fig. 21.8. This is the climatic signal resulting from Milankovitch theory. Some scientists have found a good correlation between it and the historical temperature curve plotted at the bottom of Fig. 21.8, although the issue is still being debated.

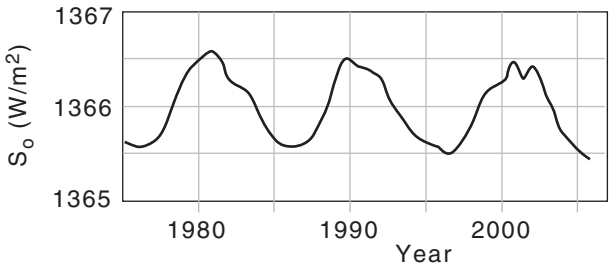

Figure 21.11
Variation of annual average total solar irradiance S_o at the top of Earth's atmosphere during 3 recent sunspot cycles.

Solar Output

The average total solar irradiance (TSI) currently reaching the top of Earth's atmosphere is S_o = 1366 W·m^{-2}, but the magnitude fluctuates daily due to solar activity, with extremes of 1362 and 1368 W·m^{-2} measured by satellite since 1975. Satellite observations have calibration errors on the order of ±7 W·m^{-2}.

Sunspot Cycle

When averaged over each year, the resulting smoothed curve of TSI varies with a noticeable 11-yr cycle (Fig. 21.11), corresponding to the 9.5 to 11-yr sunspot cycle (Fig. 21.12) as observed by telescope. Because the TSI variation is only about 0.1% of its total magnitude, the sunspot cycle is believed to have only a minor (possibly negligible) effect on recent climate change.

Longer-term Variations in Solar Output

To get solar output information for the centuries before telescopes were invented, scientists use **proxy** measures. Proxies are measurable phenomena that vary with solar activity, such as beryllium-10 concentrations in Greenland ice cores, or carbon-14 concentration in tree rings (**dendrochronology**). Radioactive carbon-14 dating suggests solar activity for the past 1,000 years as plotted in Fig. 21.13. Noticeable is the 200-yr cycle in solar-activity minima.

Going back 11,000 yr in time, Fig. 21.14 shows a highly-smoothed carbon-14 estimate of solar/sunspot activity. There is some concern among scientists that Earth-based factors might have confounded the proxy analysis of tree rings, such as extensive volcanic eruptions that darken the sky and reduce tree growth over many decades.

Even further back (3 to 4 Myr ago), the sun was younger and weaker, and emitted only about 70% of what it currently emits. About 5 billion years into the future, the sun will grow into a red-giant star (killing all life on Earth), and later will shrink into a white dwarf star.

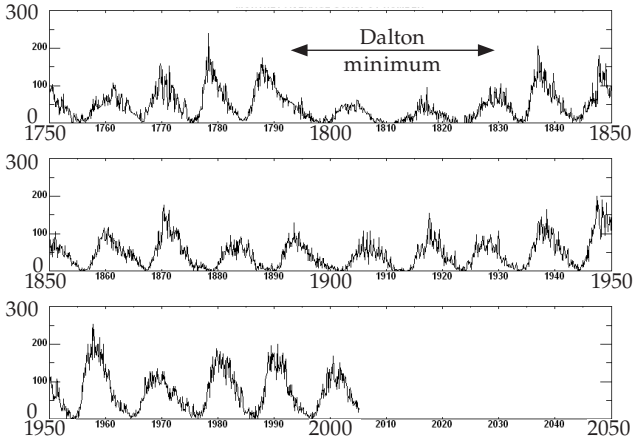

Figure 21.12
Monthly average sunspot number during 1750 - 2005. NASA.

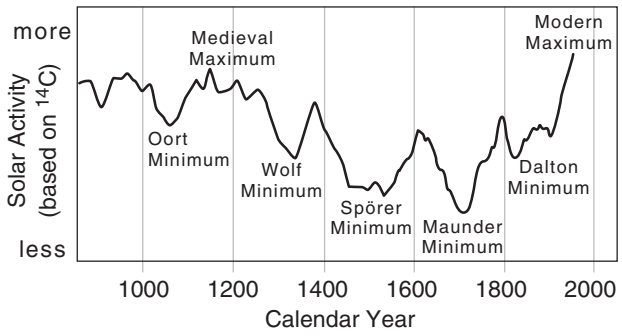

Figure 21.13
Carbon 14 concentration as a proxy for solar activity. Approximate dates for these minima: **Oort Minimum:** *1040 - 1080,* **Wolf Minimum:** *1280 - 1350,* **Spörer Minimum:** *1450 - 1550,* **Maunder Minimum:** *1645 - 1715, and* **Dalton Minimum:** *1790 - 1830. The 11-year sunspot cycle still exists during this time span, but was smoothed out for this plot.*

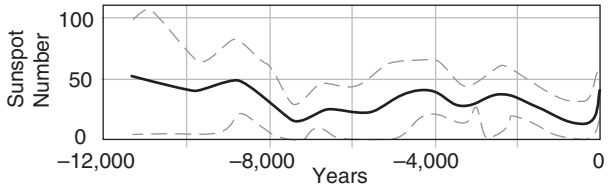

Figure 21.14
Smoothed proxy estimate of sunspots. Time is relative to calendar year 2000. Dashed lines show envelope of fluctuations.

Figure 21.15
Location of continents about 225 million years ago to form the supercontinent Pangea (also spelled as Pangaea and Pangæa). This supercontinent spanned north-south from pole to pole.

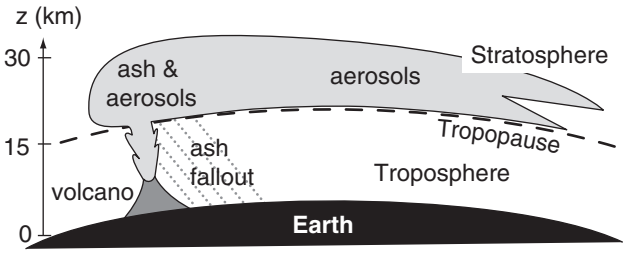

Figure 21.16
Eruption of volcanic ash and aerosols into the stratosphere. Average times for particles to fall 1 km are: 36 yr for 0.1 μm diameter particles, 3.2 yr for 0.5 μm, 328 days for 1 μm, 89 days for 2 μm, 14.5 days for 5 μm, and 3.6 days for 10 μm.

Science Graffito

"The most important fact about Spaceship Earth: an instruction book didn't come with it."
– R. Buckminster Fuller.

TECTONIC INFLUENCES

Continent Movement

As Earth-crust tectonic plates move, continents form, change, merge and break apart. About 225 million years ago the continents were merged into the **Pangea** supercontinent (Fig. 21.15). The interior of such large continents are sufficiently far from the moderating influence of oceans that extreme daily and seasonal temperature variations can occur. Large monsoon circulations can form due to the temperature contrasts between continent and ocean. The more recent (200 million years ago) supercontinents of Gondwanaland and Laurasia would likely have had similar monsoon circulations, and extreme temperature variations in their interiors.

Colliding tectonic plates can cause **mountain building** (**orogenesis**). Large mountain ranges can block portions of the global circulation, changing the Rossby waves in the jet stream, and altering cyclogenesis regions. Mountains can partially block the movement of airmasses, changing temperature and precipitation patterns.

Changes in continent location and ocean depths cause changes in ocean circulations. **Thermohaline** circulations are driven by water-density differences caused by temperature and salt-concentration variations. These large, slow circulations connect deep water and surface waters of all oceans, and are important for redistributing the excess heat from the equator toward the poles. Climatic changes in ocean-surface temperatures can alter atmospheric temperature, humidity, winds, cloudiness, and precipitation distribution.

Volcanism

When volcanoes erupt explosively, the eruptive heat and vertical momentum ejects tons of tiny rock particles called **volcanic ash** into the upper troposphere and lower stratosphere (Fig. 21.16). During the few weeks before this ash falls out of the air, it can block some sunlight from reaching the surface.

Gases such as **sulfur dioxide** (SO_2) are also emitted in large volumes (0.1 to 6000 Mtons from the larger eruptions), and are much more important for climate change. SO_2 oxidizes in the atmosphere to form sulfuric acid and sulfate **aerosols**, tiny droplets that fall so slowly they seem suspended in the air.

Those sulfate particles in the stratosphere can remain suspended in the atmosphere for a few years as they are spread around the world by the winds. The sulfates absorb and reflect some of the incoming solar radiation, allowing less to be transmitted

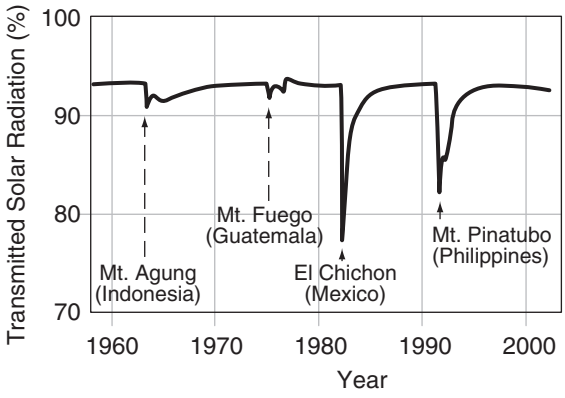

Figure 21.17
Reduction in transmitted shortwave radiation from the sun due to aerosols and particulates erupted into the atmosphere from volcanoes, as observed at Muana Loa.

toward the ground (Fig. 21.17). Also, these aerosols absorb upwelling IR radiation from the Earth and troposphere.

The net result for aerosol particle diameters less than 0.5 μm is that the stratosphere warms while the Earth's surface and lower troposphere cool. This cooling causes short-term (2 - 3 yr) climate change known as **volcanic winter** (analogous to the effects of nuclear winter). The surface cooling can be so great as to ruin vegetation and crops around the world, as was experienced throughout history (Table 21-3). For a brief explosive eruption, the stratospheric effects are greatest initially and gradually diminish over a 3-year period as the aerosols fall out. For violent continuous eruptions, the climatic effects can last decades to millennia.

Volcanoes also erupt hundreds of millions tons of **greenhouse gases** (gases that absorb IR radiation as can alter the global heat budget), including carbon dioxide (CO_2) and water vapor (H_2O). These gases can cause longer term global warming after the aerosol-induced cooling has ended.

After the large eruptions, you can see amazingly beautiful sunsets and sunrises with a bright **red glow** in the sky. Sometimes you can see a **blue moon** at night. These phenomena are due to scattering of sunlight by sulfate aerosols with diameters ≤ 0.5 μm (see the Optics Chapter).

Table 21-3. Some notable volcanic eruptions.

Volcano (Date, Location) • Effect
Siberian Traps, creating floods of basaltic lava (~250 Myr ago, Russia) - Lasted a million years, emitting tremendous volumes of sulfates and greenhouse gases into the atmosphere that caused a mass extinction at the **Permian-Triassic** geological-period boundary. Known as the "**Great Dying**", where 96% of all marine species and 70 percent of terrestrial vertebrate species disappeared. Major volcanic eruptions likely contributed to other mass extinctions: End-Ordovician (~450 Myr ago) and Late Devonian (~375 Myr ago).
Deccan Traps, creating floods of basaltic lava (~65.5 Myr ago, India) • The Cretaceous–Paleogene extinction event (K–Pg event, formerly known as Cretaceous–Tertiary or **K-T event**) was when the **dinosaurs** disappeared (except for those that evolved into modern-day birds). The sulfate and greenhouse-gas emissions from this massive eruption are believed to be a contributing factor to the K-T event, which was exacerbated by a massive asteroid impact in Mexico.
Yellowstone Caldera (640 kyr ago, USA) • Emissions reduced N. Hem. temperatures by about 5°C
Lake Toba (~90 kyr ago, Indonesia) • Emissions killed most of the humans on Earth, possibly causing a **genetic bottleneck** of reduced genetic diversity. Stratospheric aerosol load ≈ 1000 Mtons. Optical depth $\tau \approx 10$ (see Optics chapter for definition of τ).
Mt. Tambora (1815, Indonesia) • Emissions caused so much cooling in the N. Hemisphere that 1816 is known as the "**Year Without Summer**". Widespread famine in Europe and N. America due to crop failure and livestock deaths. Followed by an exceptionally cold winter. Stratospheric aerosol load ≈ 200 Mtons. Optical depth $\tau \approx 1.3$.
Krakatau (1883, Indonesia) • Violent explosion heard 3,500 km away. Ash reached 80 km altitude. Global temperature decrease ≈ 0.3 - 1.2°C. 50 Mtons of aerosols into stratosphere. $\tau \approx 0.55$.

Science Graffito

Darkness

"I had a dream, which was not all a dream.
The bright sun was extinguish'd, and the stars
Did wander darkling in the eternal space,
Rayless, and pathless, and the icy Earth
Swung blind and blackening in the moonless air;
Morn came and went — and came, and
brought no day,
And men forgot their passions in the dread
Of this their desolation; and all hearts
Were chill'd into a selfish prayer for light."

- Lord Byron (1816 –the Year Without Summer.)

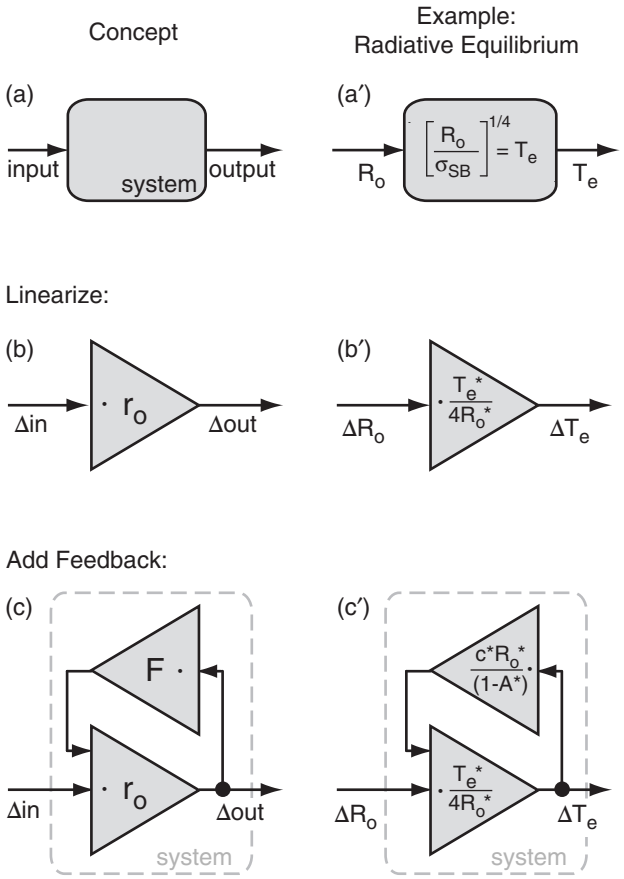

Figure 21.18
Left column: feedback concepts. Right column: example of ice-albedo feedback within the radiative-equilibrium process, as described by nonlinear eq. (21.3). The reference state is (R_o, T_e*, A*, c*).*

Solved Example

Suppose r_o = 0.1 and F = –3. Find the feedback factor, gain, and compare system responses with and without feedback.

Solution

Given: F = –3, no-feedback system response r_o = 0.1
Find: f = ? , G = ? , r = ? = response with feedback

Use eq. (21.24):
$f = (0.1) \cdot (-3)$ = **–0.3** is the feedback factor
Use eq. (21.26):
$G = 1 / [1 - (-0.3)]$ = **0.77** is the gain
Use eq. (21.28):
$r = (0.77)\cdot(0.1)$ = **0.077** is the system response with feedback, compared to r_o = 0.1 without.

Check: Units all dimensionless. Magnitudes OK.
Discussion: This system is damped. It has negative feedback. This feedback diminishes the response. For many systems, the output units differ from the input units, in which case r_o , F, and r would have units.

FEEDBACKS

Concept

Consider a system or physical process with an input and output (Fig. 21.18a). This system might be **linear** (described by a straight line when output is plotted vs. input) or **nonlinear** (described by a curved line). Various values of input give various values of output.

Choose one particular set of input and output values as a **reference state** of the system. Find the slope r_o of the line at this reference point. This slope describes the **response** of the output (Δout) to a small change of input (Δin). Namely,

$$\Delta\text{out} = r_o \cdot \Delta\text{in} \qquad (21.21)$$

as sketched in Fig. 21.18b. The slope is a straight line. Thus, even if the original system is nonlinear, this slope describes a **linearized approximation** to the system response at the reference point.

Feedback (Fig. 21.18c) is where the output signal is added to the input via some feedback process F:

$$\Delta\text{out} = r_o \cdot [\,\Delta\text{in} + F \cdot \Delta\text{out}] \qquad (21.22)$$

A linear approximation is also used for this feedback. The feedback is internal to the system (Fig. 21.18c). Thus the amount of feedback responds to changes in the system. Contrast that to inputs, which are considered **external forcings** that do not respond to changes within the system.

The previous feedback equation can be rewritten as

$$\Delta\text{out} = r_o \cdot \Delta\text{in} + f \cdot \Delta\text{out} \qquad \bullet(21.23)$$

where the **feedback factor** f is given by

$$f = r_o \cdot F \qquad (21.24)$$

Solving this equation for Δout gives:

$$\Delta\text{out} = \frac{1}{(1-f)} \cdot r_o \cdot \Delta\text{in} \qquad (21.25)$$

Eq. (21.25) looks similar to eq. (21.21) except for the new factor $1/(1–f)$. In electrical engineering, this factor is called the **gain**, G:

$$G = \frac{1}{(1-f)} \qquad (21.26)$$

[*CAUTION: Some climate researchers use a different definition of gain than electrical engineers. See the Focus Box on the next page.*]

If we rewrite eq. (21.25) as

$$\Delta \text{out} = r \cdot \Delta \text{in} \tag{21.27}$$

then we see that the linearized process WITH feedback (eq. 21.27) looks identical to that without (eq. 21.21) but with a different **response**:

$$r = G \cdot r_o \tag{21.28}$$

If $f \geq 1$, then the feedback is so strong that the response increases without limit (i.e., a **runaway** response), and no equilibrium exists. If $0 < f < 1$, then there is **positive feedback** with gain $G > 1$ that leads to an amplified but stable new equilibrium. If $f < 0$, then there is **negative feedback** with gain $G < 1$ that damps the response toward a different stable equilibrium.

For N feedback processes that are independent of each other and additive, the total gain is

$$G = \left[1 - \sum_{i=1}^{N} f_i \right]^{-1} \tag{21.29}$$

where f_i is the feedback factor for any one process i.

Idealized Example

To illustrate feedback, use the simple no-atmosphere blackbody radiative-equilibrium system of Fig. 21.1. The net solar input per square meter of the Earth's surface is

$$R_o = (1 - A) \cdot S_o \,/\, 4 \tag{21.30}$$

(see the Focus box on the 3rd page of this chapter). The IR-radiation output is described by the Stefan-Boltzmann law, resulting in the following energy balance of input = output:

$$R_o = \sigma_{SB} \cdot T_e^4 \tag{21.31}$$

as indicated in Fig. 21.18a'.

The dashed lines in Fig. 21.2 show how an input of $R_o = 239$ W/m^2 ($S_o = 1366$ W/m^2) results in an output $T_e \approx 255$ K. Use this blackbody Earth-equilibrium condition as the **reference state**, and denote the reference values with asterisks (R_o^*, T_e^*). The thick curved line in Fig. 21.2 shows how T_e varies nonlinearly for different inputs of R_o, assuming $A = 0.3$ is constant (i.e., no feedback other than the background outgoing IR).

No Feedback

Focus on this no-feedback example first (Fig. 21.18b'). For small solar-input variations ΔR_o about its reference state, the corresponding temperature

FOCUS • Gain — Different Definitions

Some climate researchers define the **gain** g as

$$g = \frac{\Delta out - \Delta out_o}{\Delta out}$$

where Δout_o is the background response with NO feedbacks. Thus:

$$g = \frac{G \cdot r_o \cdot \Delta in - r_o \cdot \Delta in}{G \cdot r_o \cdot \Delta in} = 1 - \frac{1}{G}$$

But $G = 1/(1-f)$ from eq. (21.26). Thus

$$g = f$$

Namely, the "gain" used in some climate studies is the feedback factor used in this chapter and in electrical engineering.

Science Graffito

"There are no great people in this world, only great challenges which ordinary people rise to meet."

Admiral William F. Halsey, Jr.

BEYOND ALGEBRA • No-feedback Response

Start with no feedback, as described by the energy balance of eq. (21.31).

$$R_o = \sigma_{SB} \cdot T_e^4$$

Take the derivative:

$$dR_o = 4\, \sigma_{SB} \cdot T_e^3 \; dT_e$$

Rearrange to find the change of output with input (dT_e/dR_o),

$$\frac{\partial T_e}{\partial R_o} = \frac{1}{4 \cdot \sigma_{SB} \cdot T_e^3}$$

Finally, convert to finite differences:

$$r_o = \frac{\Delta T_e}{\Delta R_o} = \frac{1}{4 \cdot \sigma_{SB} \cdot T_e^3} \tag{21.33}$$

Another form of this answer can be found by multiplying the numerator and denominator by T_e, and then substituting eq. (21.31) in the denominator:

$$r_o = \frac{T_e}{4 \cdot R_o}$$

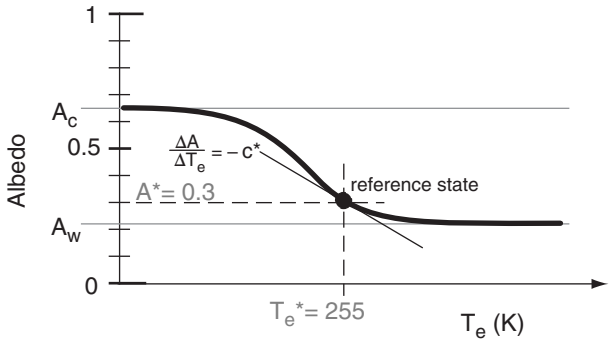

Figure 21.19
Thick line is a sketch of response of Earth's albedo to changes in radiative equilibrium temperature T_e , associated with changes in snow- and ice-cover. The thin line of slope $-c^*$ corresponds to the slope of the thick line at the reference point. Values for A_c and A_w are not accurate — only for illustration.

Solved Example

For ice-albedo radiative-equilibrium with a blackbody-Earth reference state, find the feedback factor and gain. Compare system responses with and without feedback.

Solution

Given: T_e^*= 255 K, R_o^*= 239 W/m^2, A^*= 0.3, c^*= 0.01 K^{-1}
Find: r_o = ? (K/W·m^{-2}), f = ? , G = ? , r = ? (K/W·m^{-2})

Use eq. (21.33) for the no-feedback system response:
r_o = (255K)/(4 · 239W/m^2) = **0.267** K/(W·m^{-2})

Use eq. (21.36) for the feedback factor:
f = (0.01 K^{-1})·(255K) / [4 · (1 – 0.3)] = **0.91** (dim'less)

Use eq. (21.26): G = 1/(1 – 0.91) = **11.1** (dimensionless)

Use eq. (21.28):
r = (11.1) · [0.267 K/(W·m^{-2})] = **2.96** K/(W·m^{-2})

Check: Response is reasonable. Units OK.
Discussion: This illustrates positive feedback; namely, the response is **amplified** by the feedback. As an example, $\Delta S_o \approx 1$ W/m^2 due to sunspot cycle (Fig. 21.11) implies ΔR_o = 0.175 W/m^2, giving $\Delta T_e = r \cdot \Delta R_o$ = 0.52°C variation in equilibrium radiation temperature due to sunspots.

change ΔT_e can be approximated by a straight line tangent to the curve at the reference point (Fig. 21.2), as defined by

$$r_o = \Delta T_e / \Delta R_o \tag{21.32}$$

Based on eq. (21.31) the slope r_o of this straight line is (see Beyond Algebra box on the previous page):

$$r_o = \frac{1}{4 \cdot \sigma_{SB} \cdot T_e{}^{*3}} = \frac{T_e{}^*}{4 \cdot R_o{}^*} = 0.267 \text{ K/(W·m}^{-2}) \tag{21.33}$$

Ice Albedo Feedback

Next, add **ice-albedo feedback** by allowing the albedo to vary with temperature. Changes in temperature T_e alter the areal extent of highly reflective ice caps and glaciers, thereby changing the albedo (A) between two extremes (Fig. 21.19). A warm limit A_w assumes 0% snow cover, and is based on the reflectivities of the ground, crops, cities, and oceans. A cold-limit A_c represents 100% snow cover, causing a highly reflective Earth. The blackbody Earth state is useful as a reference point (T_e^* = 255 K, A^* = 0.3).

Use the slope (thin line in Fig. 21.19) of the A vs. T_e curve at the reference point as a **linear approximation** of the nonlinear feedback (thick line). Numerical simulations of the global climate suggest this slope is:

$$\frac{\Delta A}{\Delta T} = -c^* \tag{21.34}$$

where c^* = 0.01 K^{-1} is the magnitude of the slope at the reference point. The ice-albedo feedback described here is highly oversimplified, for illustrative purposes.

For this idealized ice-albedo radiative-equilibrium case, the feedback equation (21.23) becomes:

$$\Delta T_e = r_o \cdot \Delta R_o + f \cdot \Delta T_e \tag{21.35}$$

where r_o was given in eq. (21.33), and where

$$f = \frac{c^* \cdot T_e{}^*}{4 \cdot (1 - A^*)} \tag{21.36}$$

(see the Beyond Algebra box on the next page).

The resulting gain is

$$G = \frac{4 \cdot (1 - A^*)}{4 \cdot (1 - A^*) - c^* \cdot T_e{}^*} \tag{21.37}$$

After multiplying r_o by the gain to give r, we find that the temperature response to solar-input variations (when feedbacks ARE included) is:

$$r = \frac{(1 - A^*) \cdot T_e{}^*}{R_o{}^* \cdot [4 \cdot (1 - A^*) - c^* \cdot T_e{}^*]} \tag{21.38}$$

Fig. 21.20 shows how the total response r with feed-

BEYOND ALGEBRA • Feedback Example

For ice-albedo feedback, infinitesimal variations in solar irradiance dS_o and albedo dA cause infinitesimal changes in equilibrium temperature dT_e :

$$dT_e = \frac{\partial T_e}{\partial S_o} dS_o + \frac{\partial T_e}{\partial A} dA \qquad (21.a)$$

To find the factors that go into this equation, start with a simple radiative-equilibrium balance:

$$T_e = \left[\frac{(1-A)\cdot S_o}{4\cdot \sigma_{SB}} \right]^{1/4} : \qquad (21.3)$$

and take the derivative $\partial T_e / \partial S_o$:

$$\frac{\partial T_e}{\partial S_o} = \frac{1}{4}\left[\frac{(1-A)\cdot S_o}{4\cdot \sigma_{SB}} \right]^{-3/4} \cdot \left[\frac{1-A}{4\cdot \sigma_{SB}} \right]$$

Substituting eq. (21.3) into this gives:

$$\frac{\partial T_e}{\partial S_o} = \frac{1}{4}\left[T_e \right]^{-3} \cdot \left[\frac{1-A}{4\cdot \sigma_{SB}} \right]$$

which we can rewrite as:

$$\frac{\partial T_e}{\partial S_o} = \frac{1}{4}\cdot T_e \cdot \left[\frac{1-A}{4\cdot \sigma_{SB} \cdot {T_e}^4} \right]$$

Solve (21.3) for S_o and substituting into the eq. above :

$$\frac{\partial T_e}{\partial S_o} = \frac{1}{4}\cdot T_e \cdot \left[\frac{1}{S_o} \right]$$

You can similarly find $\partial T_e / \partial A$ from eq. (21.3) to be:

$$\frac{\partial T_e}{\partial A} = \frac{-T_e}{4\cdot(1-A)}$$

When these derivatives are plugged into eq. (21.a) and applied at the reference point (S_o*, T_e*, A*), the result is:

$$dT_e = \frac{T_e *}{4\cdot S_o *} dS_o - \frac{T_e *}{4\cdot(1-A*)} dA$$

Albedo decreases when Earth's temperature increases, due to melting snow and retreating glacier coverage:

$$dA = -c^* \cdot dT_e$$

where c^* is the magnitude of this variation at the reference point. Plugging this into the previous eq. gives:

$$dT_e = \frac{T_e *}{4\cdot S_o *} dS_o + \frac{c^* \cdot T_e *}{4\cdot(1-A*)} dT_e \qquad (21.b)$$

(continues in next column)

BEYOND ALGEBRA • Feedback (continued)

Next, take the derivative of eq. (21.30):

$$dR_o = [(1-A)/4] \cdot dS_o$$

Dividing this by eq. (21.30) shows that:

$$\frac{dR_o}{R_o} = \frac{dS_o}{S_o}$$

Plug this into eq. (21.b), and convert from calculus to finite differences:

$$\boxed{\Delta T_e = \frac{T_e *}{4\cdot {R_o}*} \cdot \Delta R_o + \frac{c^* \cdot T_e *}{4\cdot(1-A*)} \cdot \Delta T_e}$$

Compare this with eq. (21.23) to realize that:

$$r_o = \frac{T_e *}{4\cdot R_o *} \quad \text{(eq. 21.33)} \quad \text{and} \quad f = \frac{c^* \cdot T_e *}{4\cdot(1-A*)}$$

Thus,

$$F = \frac{f}{r_o} = \frac{c^* \cdot R_o *}{(1-A*)} \quad \text{and} \quad G = \frac{4\cdot(1-A*)}{4\cdot(1-A*) - c^* \cdot T_e *}$$

For the idealized (toy model) example in this section, the reference values are:

T_e* = 255 K = radiative equilibrium temperature
S_o* = 1366 W/m^2 = solar irradiance
R_o* = 239 W/m^2 = solar input / m^2 Earth's surface
A* = 0.3 (dimensionless) = albedo
c* = 0.01 K^{-1} =albedo response to temperature change

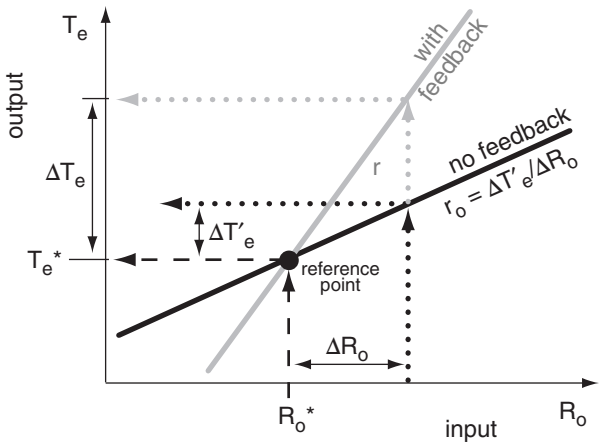

Figure 21.20
Response of system with feedback (grey) and without (black). The prime ' denotes the no-feedback response.

Table 21-4. Feedbacks affecting Earth's climate.
(+) = positive, (–) = negative feedbacks.
F = Feedback parameter $(W \cdot m^{-2})/K$.
f = feedback factor (dimensionless)
G = Gain (dimensionless)
r = system response $K/(W \cdot m^{-2})$. This is also known as the **sensitivity**, λ.

Processes for gradual climate change:				
Feedback	**F**	**f** = $r_o \cdot F$	**G** = 1/(1–f)	**r** = $G \cdot r_o$
IR Radiative (–) • blackbody Earth • realistic Earth				r_o = 0.27 0.31
Water-vapor (+)	1.8 ±0.18	0.48	1.93	0.51
Lapse-rate (–)	–0.84 ±0.26	–0.22	0.82	0.22
Cloud (+)	0.69 ± 0.38	0.18	1.2	0.33
Surface albedo (+)	0.26 ±0.08	0.07	1.1	0.29
Ocean CO_2 (+)				
Biological (–)				
Processes for Abrupt climate change:				
• Meridional Overturning Ocean Circulation • Fast Antarctic & Greenland Ice-sheet Collapse • Volcanoes • Methane Release (Hydrate Instability & Permafrost) • Biogeochemical				

Based on IPCC AR4, 2007.

Solved Example

Given the feedbacks listed in Table 21-4, what is the total response.

Solution

Given: Table 21-4. Use realistic Earth for r_o.
Find: r = ? $K/(W \cdot m^{-2})$.
Assume: total response is based on only those feedback processes for which numbers are given in the table.

Use eq. (21.29): $G = 1 / [1 - \Sigma f]$
$G = 1 / [1 - (0.48 - 0.22 + 0.18 + 0.07)]$
$G = 1 / [1 - 0.51] = 2.04$

Use eq. (21.28): $r = G \cdot r_o$
$r = 2.04 \cdot 0.31 =$ **0.63** $K/(W \cdot m^{-2})$.

Check: Units OK. Physics OK.
Discussion: For each ΔR = 1 W/m^2 change in solar input, the Earth-system response with all feedbacks is ΔT = 0.63 K, which is twice the response (0.31 K) without feedback (other than the background IR feedback). {CAUTION: The total response is NOT equal to the sum of the individual responses *r*. Instead, use the sum of feedback factors *f* to get the net feedback.]

back differs from the r_o without. With feedback, eq. (21.32) becomes:

$$\Delta T_e = r \cdot \Delta R_o \qquad (21.39)$$

Table 21-4 lists some feedbacks that can affect Earth's climate. These are briefly discussed next.

Infrared Radiative (IR) Feedback

IR is the strongest feedback — it dominates all others. It was already discussed as the "radiation out" term in eq. (21.2). This important negative feedback allows the Earth to have an equilibrium state. Even a small change in Earth's temperature results in a strong compensating energy loss because IR radiation is to the 4th power of T_e in the Stefan-Boltzmann equation. This strong damping keeps Earth's climate relatively steady.

As we have seen, the reference response to changes in net solar input is r_o = 0.267 $K/(W \cdot m^{-2})$. Global climate models that include more realistic atmospheric absorption and emission of IR radiation find r_o = 0.30 to 0.32 $K/(W \cdot m^{-2})$.

Water-vapor Feedback

Warmer air can hold more water vapor, which absorbs and re-radiates more IR radiation back to the surface and reduces the atmospheric window sketched in Fig. 21.5. The warmer surface warms the air, resulting in a very strong positive feedback (see Table 21-4). The upper troposphere is where this feedback is most effective.

Water vapor is an important natural greenhouse gas. If the climate warms and the upper tropospheric water-vapor content increases to the point where the atmospheric window is mostly closed (net atmospheric emissivity $e \approx 1$), then we return to the negative feedback sketched in Fig. 21.4 and steady Earth temperature of T_s = 30°C from eq. (21.6).

Lapse-rate Feedback

The simple model of Fig. 21.4 uses the same air temperature T_A to determine IR radiation both up to space and down toward the Earth. However, in the real atmosphere the temperature varies with altitude — decreasing with lapse rate 6.5 °C/km in the troposphere. Thus, colder temperatures at the top of the troposphere emit less upward IR radiation to space than is emitted downward from the warmer bottom of the troposphere. This difference in upward and downward IR radiation is part of our normal climate, causing our normal temperatures.

Global warming tends to reduce the lapse rate. Namely, the temperature difference diminishes between the top and bottom of the troposphere. Rela-

tive to each other, IR radiation out to space will increase and IR radiation down toward the Earth will decrease. The net effect is to cool the Earth system. Thus, lapse-rate feedback is negative (Table 21-4).

Water-vapor and lapse-rate feedbacks are closely related, and are often considered together. Their combined effect is a modest positive feedback.

Cloud Feedback

Cloud feedback is likely important, but the details are poorly understood. Relative to clear skies, clouds at all heights cause cooling by reflecting incoming solar radiation. But clouds also cause warming by trapping (absorbing and re-radiating back towards the surface) upwelling IR radiation. The small difference between these large opposing forcings can have very large error, depending on cloud type and altitude. For our present climate, the net effect of clouds is cooling.

Table 21-4 indicates a positive feedback for clouds, based on global climate modeling. Namely, an increase in radiative input to the Earth system would decrease the cloud cover, thus causing less cooling. But much more research must be done to gain more confidence in cloud-feedback processes.

Sometimes **aerosol feedback** is grouped with cloud feedback. Aerosols (microscopic solid or liquid particles in the air) can have similar effects as cloud droplets. However, some aerosols such as sulfates are darker than pure water droplets, and can absorb more solar radiation to cause atmospheric warming. As already discussed, volcanoes can inject sulfate aerosols into the stratosphere. **Phytoplankton** (microscopic plant life) in the ocean can release into the atmospheric boundary layer a chemical called dimethyl sulfide, which can later be oxidized into sulfate aerosols.

Ice–albedo (Surface) Feedback

This positive feedback was discussed earlier in the idealized feedback example, where we found a response of $r = 2.96$ K/(W·m^{-2}). More realistic estimates from Global Climate Model simulations are $r = 0.27$ to 2.97 K/(W·m^{-2}). At our current reference temperature, this feedback mostly affects the climate at high latitudes.

This positive-feedback sensitivity applies only over the limited range of Fig. 21.19 for which albedo can vary with temperature. At the cold extreme of a completely snow covered Earth (**snowball Earth**), the albedo is constant at its cold-limit value A_c. At the warm extreme the Earth has no ice caps or snow cover, and albedo is constant at A_w.

At these two extremes, the negative feedback of IR radiation again dominates, leading to steady

Solved Example

Use Table 21-4 to estimate the combined water-vapor and lapse-rate response, $r_{wv.lr}$.

Solution

Given Table 21-4: $f_{water.vapor} = 0.48$, $f_{lapse.rate} = -0.22$
Find: $r_{wv.lr}$ = ? K/(W·m^{-2})
Assume: $r_o = 0.267$ K/(W·m^{-2}) from eq. (21.33)

For multiple feedbacks, we must use eq. (21.29):

$G = 1 / [1 - (0.48 - 0.22)] = 1.35$

Use eq. (21.28):

$r_{wv.lr} = 1.35 \cdot [0.267$ K/(W·m^{-2})] = **0.361 K/(W·m^{-2})**

Check: Units OK. Magnitude OK.
Discussion: This response is midway between water vapor alone ($r = 0.51$) and lapse-rate alone ($r = 0.22$).

FOCUS • Greenhouse Gases

A **greenhouse gas** is an atmospheric gas that absorbs and emits IR radiation. Of particular concern are gases that absorb and emit within the 8 to 14 μm wavelength range of the **atmospheric window**. As the concentrations of such gases increase, the atmospheric window can close due to the increased atmospheric emissivity (Fig. 21.5), resulting in global warming.

Greenhouse gases, ranked by importance, are:
(1) water vapor (H_2O),
(2) carbon dioxide (CO_2),
(3) methane (CH_4),
(4) nitrous oxide (N_2O),
(5) ozone (O3),
(6) halocarbons [e.g., freon CFC-12 (C Cl_2 F_2)]

Except for (6), most greenhouse gases have both natural and **anthropogenic** (man-made) sources. CO_2 is of particular concern because it is released by humans burning fossil fuels for energy.

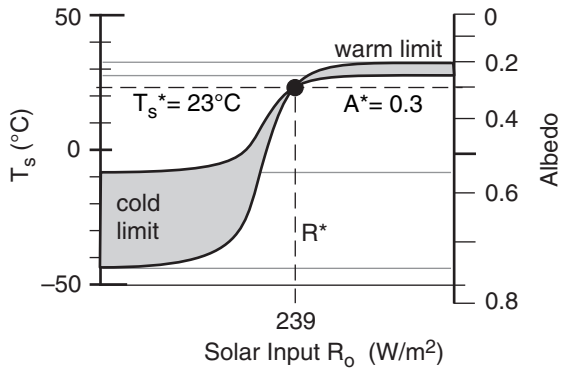

Figure 21.21
Illustration of how Earth surface temperature is bounded once the Earth becomes fully snow covered (cold limit) or fully snow-free (warm limit). Grey shading shows temperature uncertainty due to uncertainty in the limiting albedo values.

FOCUS • Effervescence and CO_2

Carbonated beverages retain their tart flavor when cold. The tartness or sourness comes from carbonic acid (H_2CO_3) due to CO_2 dissolved in water (H_2O). But as the beverage warms, it cannot hold as much dissolved CO_2, forcing some of the CO_2 to **effervesce** (bubble out). Namely, the beverage loses its fizz, causing it to taste "flat".

The same phenomenon happens to the oceans. If oceans warm, they lose some of their fizz.

FOCUS • Climate Sensitivity

The Intergovernmental Panel on Climate Change (**IPCC**) states that **climate sensitivity** is "a measure of the climate system response to sustained radiative forcing. It is defined as the equilibrium global average surface warming" (ΔT_s) "following a doubling of CO_2 concentration."

Based on research by international teams using global climate models, IPCC suggests in their 4th Assessment Report (AR4, 2007) that "this sensitivity is likely to be in the range of" ΔT_s = "2 to 4.5°C with a best estimate of 3°C" for a doubling of the greenhouse gas CO_2. This temperature rise would be equivalent to a **radiative forcing** (ΔR_o in Fig. 21.18b′ and c′; abbreviated as *RF* by IPCC) of 3.7 to 4.0 W/m^2.

But CO_2 has not doubled yet. What are the actual forcings so far. The IPCC is particularly concerned about anthropogenic forcings, because these can be mitigated by people. Based on estimates of anthropogenic changes between years 1750 (the start of the industrial age) and 2005, they find that people have inadvertently altered the net radiative forcing of the Earth system as follows:

Process	ΔR_o or RF (W/m^2)
CO_2 increase	1.66
CH_4 increase	0.48
N_2O increase	0.16
Halocarbons	0.34
O_3 in stratosphere	–0.05
O_3 in troposphere	0.35
H_2O from CH_4 in stratosphere	0.07
Surface albedo/land use	–0.2
Surface albedo/carbon on snow	0.1
Aerosols/ direct	-0.5
Aerosols/ via cloud albedo	-0.7
Jet contrails	0.01
Total anthropogenic	**1.6**
	range [0.6 to 2.4]

Compare this to a natural process:

Solar irradiance change	**0.12**

The large anthropogenic effect relative to the natural solar variations is what motivates policy makers to take action.

Earth temperatures. For snowball Earth, cold-limit albedo estimates are in the range of $0.55 \le A_c \le 0.75$. When used in the radiation balance of eq. (21.3) the cold-limit blackbody temperature is 197 K $\le T_e \le$ 228K, yielding a surface temperature ($T_s = 1.161 \cdot T_e$, from eq 21.10) of –44°C $\le T_s \le$ –8°C.

For the warm limit (assuming that clouds having 37% albedo still cover roughly 70% of the Earth) $0.20 \le A_w \le 0.25$, and the equilibrium blackbody temperature is 259 K $\le T_e \le$ 263 K. This corresponds to a surface-temperature of 28°C $\le T_s \le$ 33°C using eq. (21.10). Thus, runaway global warming or cooling is not possible beyond these bounds (see Fig. 21.21).

Ocean CO_2 Feedback

Warmer seawater can hold less dissolved carbon dioxide (CO_2) than colder water. Hence global warming will cause oceans to release CO_2 into the atmosphere. Greater atmospheric CO_2 concentrations reduce the atmospheric window due to an increase in net atmospheric emissivity *e*, and thus cause the atmosphere to re-radiate more IR radiation back toward the Earth surface. The net result is positive feedback.

Biological CO_2 Feedback

As plants grow, they consume CO_2 to make hydrocarbons and carbohydrates via photosynthesis. As a result, the carbon is **sequestered** (stored) as the body of the plant. Some of the carbohydrates (e.g., sugars) are consumed by the plant, and are converted back to CO_2 and **transpired** (exhaled by the plant) into the atmosphere.

When plants die and decay, or when they burn in a **wild fire**, they release their remaining carbon as CO_2 back to the atmosphere. If plants are buried under sediment before they decay or burn, their carbon can be fossilized into coal, oil, natural gas (**fossil fuels**). Carbonate rocks can also sequester carbon from the atmosphere, but the carbon can later be released through weathering of the rocks.

The change of carbon from CO_2 to other forms is called the **global carbon cycle**. It is extremely difficult to model the global carbon cycle, which leads to large uncertainty in estimates of climate feedback. Also, anthropogenic effects of fossil-fuel and biomass burning affect the cycle. At present, it is believed that biological CO_2 causes a positive feedback. Namely, global warming will cause more CO_2 to be released than sequestered.

Processes of **abrupt climate change** in Table 21-4 are left to the reader to explore (via an Understanding and Critical Evaluation exercise). But next we introduce the intriguing gaia hypothesis.

DAISYWORLD

Does life on Earth merely respond and adapt to changes of climate? James Lovelock suggested that life controls the climate in a way that favors continuance of life (**homeostasis**). This theory is called the **gaia** hypothesis, after the Greek word for "mother Earth".

To illustrate such "biological homeostasis of the global environment", Lovelock and Andrew Watson presented a simple hypothetical model called **Daisyworld**. On daisyworld, only two types of plants exist: black daisies and white daisies. These daisies grow and die depending on the temperature. However, as their populations increase, they alter the global albedo due to their color, and thus alter the global radiation temperature (Fig. 21.22).

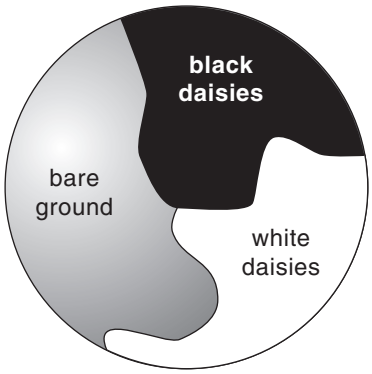

Figure 21.22
Coverage of daisies on a Daisyworld Earth.

Physics

A highly simplified and parameterized set of equations were suggested by Lovelock to illustrate biological homeostasis. We will present the equations in an order and with modifications that aid spreadsheet computations.

First, there are two constants. One is the Stefan-Boltzmann constant $\sigma_{SB} = 5.67 \times 10^{-8}$ W·m^{-2}·K^{-4}. The other is the solar irradiance, $S_o = 1366$ W/m^2. A solar luminosity parameter, $L \approx 1$, provides a convenient way to experiment with increases or decreases in solar output. From these quantities, a solar forcing ratio is defined as

$$q = \frac{L \cdot S_o}{4 \cdot \sigma_{SB}} \tag{21.40}$$

Parameters are:
$A_W = 0.75$ albedo of white daisies
$A_B = 0.25$ albedo of black daisies
$A_G = 0.5$ albedo of bare ground.
$D = 0.3$ daisy death rate (equal for black and white).
$Tr = 0.6$ horizontal transport parameter (varies between 0 for no transport, to 1 for total mixing in the horizontal). When $Tr = 0$, the temperature in a daisy patch is controlled locally by the albedo of that patch. For $Tr = 1$, the average global albedo determines the local temperature.

The areas of the globe covered by daisies are:
C_W = fractional area covered by white daisies
C_B = fractional area covered by black daisies.
Our initial condition will be no daisies: $C_W = C_B = 0$. Also

$$C_G = 1 - C_B - C_W \tag{21.41}$$

is the fractional area of bare ground.

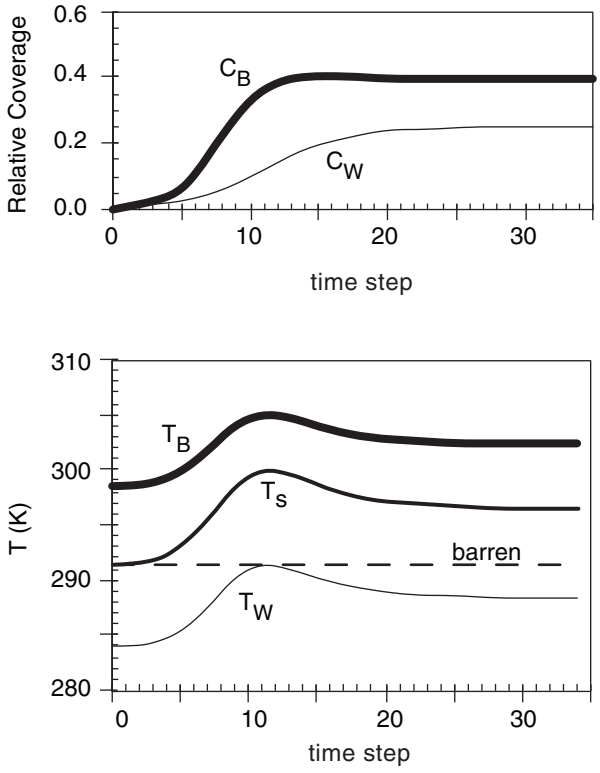

Figure 21.23
Sample Daisyworld forecast as it evolves toward an equilibrium, for L = 1.2.

Solved Example (§)

Use the parameter values of the previous page, along with L = 1.2, to make a Daisyworld forecast.

Solution

Given: L=1.2, Tr=0.6, D=0.3, A_W=0.75, A_B=0.25, A_G=0.5
Find: C_B = ?, C_W = ? , T_s = ? K, T_B = ? K, T_W = ? K

First use eq. (21.40):

$$q = \frac{1.5 \cdot (1366 \text{W} \cdot \text{m}^{-2})}{4 \cdot (5.67 \times 10^{-8} \text{W} \cdot \text{m}^{-2} \cdot \text{K}^{-4})} = 7.24\text{x}10^9 \text{ K}^4$$

Initialize with $C_B = C_W = 0$, but seed with $C_s = 0.01$.

Iterate, solving eqs. (21.41) through (21.46) on a spreadsheet:

t	C_B	C_W	C_G	A	T_s (K)	T_B (K)	T_w (K)	β_B	β_W
0	0.00	0.00	1.00	0.50	291.6	298.7	284.1	0.97	0.57
1	0.01	0.01	0.98	0.50	291.6	298.7	284.1	0.97	0.57
2	0.02	0.01	0.97	0.50	291.8	298.8	284.2	0.96	0.58
3	0.03	0.02	0.96	0.50	292.0	299.0	284.4	0.96	0.60
4	0.04	0.02	0.94	0.49	292.5	299.3	284.8	0.95	0.63
5	0.07	0.03	0.90	0.49	293.2	299.9	285.4	0.94	0.67
. . . etc. . .									
98	0.39	0.25	0.36	0.46	296.7	302.5	288.5	0.84	0.84

Check: Units OK. Physics OK.

Discussion: Because of the "seed" coverage, values of C_W and C_B of 0.01 actually correspond to no daisies.

At steady state, the growth parameters should be equal: $\beta_B = \beta_W$. This is a good check to see if steady state has been obtained.

The temperature of a barren planet happens to equal the value of T_s from the first iteration (before any daisies). Thus, T_s barren = 291.6 K.

These answers are plotted in Fig. 21.23.

The planetary albedo (A) is an average of the albedoes (A_i) of the daisies, weighted by their relative coverage (C_i):

$$A = C_G \cdot A_G + C_D \cdot A_D + C_L \cdot A_L \tag{21.42}$$

The effective radiation temperature (Kelvin) is:

$$T_e^{\,4} = q \cdot (1 - A) \tag{21.43}$$

and the surface temperature under a one-layer windowless atmosphere is

$$T_s^{\,4} = 2 \cdot T_e^{\,4} \tag{21.44}$$

Surface temperatures of individual daisy patches are:

$$T_D^{\,4} = (1 - Tr) \cdot q \cdot (A - A_D) + T_s^{\,4} \tag{21.45a}$$

and

$$T_L^{\,4} = (1 - Tr) \cdot q \cdot (A - A_L) + T_s^{\,4} \tag{21.45b}$$

for black and white daisies, respectively.

These daisies grow fastest at an optimum temperature of T_o = 22.5°C = 295.5 K. Growth rate is less for warmer or colder temperature, and growth ceases altogether at temperatures colder than 5°C or warmer than 40°C. The growth rate β is:

$$\beta_D = 1 - b \cdot (T_o - T_D)^2 \tag{21.46a}$$

$$\beta_L = 1 - b \cdot (T_o - T_L)^2 \tag{21.46b}$$

where parameter b = 0.003265 K^{-2}, and subject to the constraint that $\beta \geq 0$.

This biological homeostasis model is a prognostic model. It forecasts how daisy coverage changes with time as populations of black and white daisies grow and interact. The population equation for daisy coverage is

$$C_{D\,new} = C_D + \Delta t \cdot C_D \cdot (C_G \cdot \beta_D - D \tag{21.47a}$$

$$C_{L\,new} = C_L + \Delta t \cdot C_L \cdot (C_G \cdot \beta_L - D) \tag{21.47b}$$

which gives the new values after a time step of Δt. We use Δt = 1. The daisy coverages are constrained such that $C_{B\,new} \geq C_s$ and $C_{W\,new} \geq C_s$, where C_s = 0.01 is the seed coverage. Without such seeding of the planet, no daisies could grow.

These new coverages are then used back in eq. (21.41), and the computation process is repeated for many time steps. After sufficient steps, the model approaches a stable equilibrium.

Equilibrium and Homeostasis

For $L = 1.2$ from the solved example, daisy populations reach equilibrium values of $C_B = 0.39$ and $C_W = 0.25$ (Fig. 21.23). The equilibrium surface temperature is $T_s = 296.75$ K, which is warmer than the corresponding temperature of a barren planet of 291.65 K. This latter quantity is found using $A = A_G$ in eqs. (21.43 and 21.44).

By rerunning the model for various values of luminosity, we can discover the equilibrium states that are possible. These are plotted in Fig. 21.24. **Homeostasis** is evident in that the fecund planet maintains a nearly-steady surface temperature conducive to life, for a wide range of luminosities. It does this by producing predominantly black daisies for low luminosity, in order to maximize absorption of the solar energy. Alternately, white daisies dominate for high luminosity to reflect the excess solar energy and maintain temperate conditions.

Although this conceptual model is too simplistic to describe the real Earth, it makes us think about new possibilities.

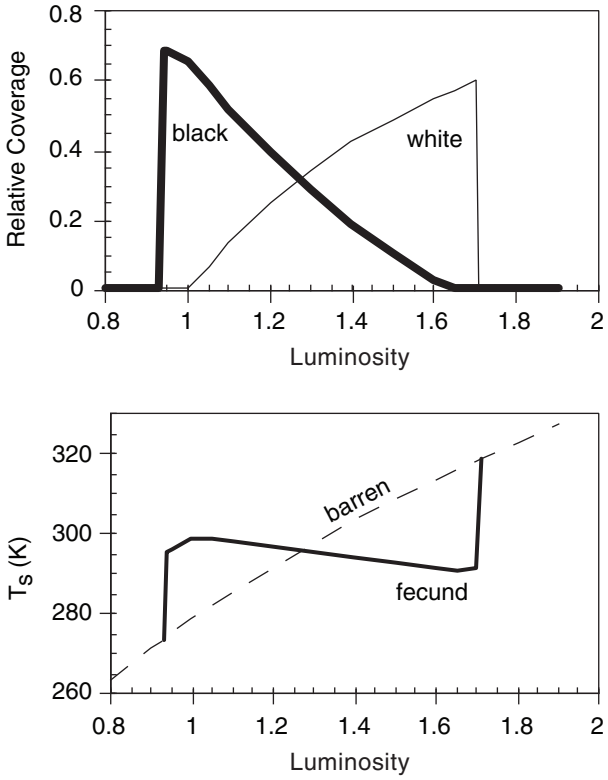

Figure 21.24
Equilibrium conditions in Daisyworld for various solar luminosities. Top: areal coverage of white and black daisies. Bottom, surface temperature for the lushly flowered (fecund) and unflowered (barren) worlds.

GCMS

Global climate models (**GCM**s) are special types of numerical weather prediction (NWP) models (see the NWP chapter). A regular grid of nodes (grid points) covers the globe, and climate simulations are made at each node for each time step by numerically solving sets of finite-difference equations that describe the governing equations for heat, momentum, mass, moisture, etc. Some GCMs use spectral rather than grid-point numerics in the horizontal, where a sum of sine waves of various wavelengths are used to approximate the spatial structure of the climate.

Climate feedback processes are explicitly included via the dynamics, thermodynamics, and physics in the model. Other feedback processes must be approximated and parameterized. Many climate models couple atmosphere, ocean, biosphere, cryosphere (ice) and soil forecasts. The net result is a model that includes many but not all of the complex interactions that exist in the real atmosphere.

To simulate the climate, the run duration must be long enough to model years to decades to centuries. For these models to run on present-day computers, sacrifices must be made in horizontal grid resolution to reduce the run time. **Coarse horizontal resolutions** of about 1° to 5° latitude are used on the whole globe, and only a limited number of vertical grid layers are used.

The coarse resolution is a drawback in that much of the important physics (boundary layers, turbu-

Science Graffito

"We tend to predict impacts on people by assuming a static human society. But humans are adapting quickly, and time scales of human change are faster than the climate change. There's no unique perfect temperature at which human societies operate. Run them a little warmer, and they'll be fine; run them a little cooler, they'll be fine. People are like roaches — hard to kill. And our technology is changing rapidly, and we're getting richer, internationally and individually, at an absurd rate. We're rapidly getting less and less sensitive to climatic variations."

– David Keith

(from an interview published in *Discover*, Sep 2005.)

Table 21-5. Comparison of global climate models (GCMs) and short-range operational forecast models (OFM). Both are numerical weather prediction models.

Attribute	GCM	OFM
duration	years	days
grid resolution	coarse	fine
ICs	less important	important
BCs	important	less important
parameterized	heavily	some
forecast quality	statistical	deterministic

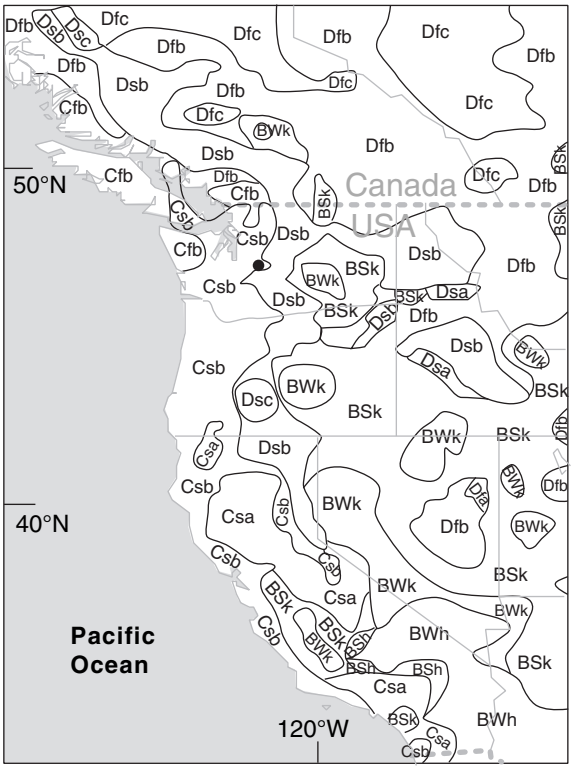

Figure 21.25
Köppen climate map for western North America. See Table 21-6 for explanations of the climate code letters. [Color maps of Köppen climate classification for the whole world are available on the internet.]

lence, radiation, cloud physics) are **subgrid scale**, and cannot be resolved. For example, clouds of diameter less than about 7° of latitude (≈ 777 km) would be missed (see a focus box on Resolution, in the NWP chapter). Instead, these subgrid physical processes must be **parameterized** (approximated).

The nature of interactions between processes can be studied fairly successfully using GCMs. For example, two hypothetical climate forecasts could be made: one with mountains and another without. By comparing the two forecasts, the sensitivity of climate to topography can be documented. Similarly, the sensitivities of climate to other processes can also be examined (e.g., hypothetical doubling of CO_2 concentration), by making appropriate model runs.

All numerical models need initial (ICs) and boundary (BCs) conditions (Table 21-5). While short-term weather forecast models rely heavily on initial conditions (an analysis of what the weather is now), climate models mostly forget their initial conditions after several weeks into the forecast.

Conversely, boundary conditions are critical for climate models, and less important for short-term forecast models. In order for climate forecasts to not drift from the true climate, the models need very accurate parameterizations of the heat, moisture, and momentum budgets at the Earth's surface. GCMs that use these parameterizations are validated against observations of the real climate (recent past and present) before they are used to study hypothetical climates in the future.

Operational forecast models attempt to accurately forecast synoptic features, such as the location and intensity of cyclones. Forecast quality rapidly deteriorates with forecast duration, as shown in the NWP chapter.

GCM modelers, however, do not even attempt to forecast the precise nature of individual storms. Instead, they want the overall statistics of cyclone intensity and location to agree with observed statistics. They want the net effect of many storms to be accurate, even though the individual storms in the forecast match nothing in the observations.

PRESENT CLIMATE

So far, we focused on processes that create and modify global climate. But before we leave this chapter, let's briefly summarize current climate.

Definition

Climate describes the slowly varying characteristics of the atmosphere, as part of the atmosphere/

Table 21-6. Köppen climate codes and defining criteria. *(Peel et al, 2007)*

1st	2nd	3rd	Description	Criteria*
A			Tropical	$T_{cold} \le 18$
	f		Rainforest	$P_{dry} \ge 60$
	m		Monsoon	[not Af] and [$P_{dry} \ge (100 - MAP/25)$]
	w		Savannah	[not Af] and [$P_{dry} < (100 - MAP/25)$]
B			Arid	$MAP < [10 \cdot P_{threshold}]$
	W		Desert	$MAP < [5 \cdot P_{threshold}]$
	S		Steppe	$MAP \ge [5 \cdot P_{threshold}]$
		h	Hot	$MAT \ge 18$
		k	Cold	$MAT < 18$
C			Temperate	$[T_{hot} \ge 10]$ and $[0 < T_{cold} < 18]$
	s		Dry summer	$[P_{sdry} < 40]$ and $[P_{sdry} < (P_{wwet}/3)]$
	w		Dry winter	$P_{wdry} < [P_{swet}/10]$
	f		Without dry season	[not Cs] and [not Cw]
		a	Hot summer	$T_{hot} > 22$
		b	Warm summer	[not a] and $[N_{monT10} \ge 4]$
		c	Cold summer	[not (a or b)] and $[1 \le N_{monT10} < 4]$
D			Cold	$[T_{cold} \le 0]$ and $[T_{hot} > 10]$
	s		Dry summer	$[P_{sdry} < 40]$ and $[P_{sdry} < (P_{wwet}/3)]$
	w		Dry winter	$P_{wdry} < [P_{swet}/10]$
	f		Without dry season	[not Ds] and [not Dw]
		a	Hot summer	$T_{hot} \ge 22$
		b	Warm summer	[not a] and $[T_{mon10} \ge 4]$
		c	Cold summer	[not (a or b or d)]
		d	Very cold winter	[not (a or b)] and $T_{cold} < -38$
E			Polar	$T_{hot} < 10$
	T		Tundra	$T_{hot} > 0$
	F		Frost	$T_{hot} \le 0$

Table 21-6 (*continuation*). *Footnotes

MAP = mean annual precipitation (mm/yr)
MAT = mean annual temperature (°C)
N_{monT10} = number of months where the temperature is above 10 (°C)
P_{dry} = precipitation of the driest month (mm/month)
P_{sdry} = precipitation of the driest month in summer (mm/month)
P_{swet} = precipitation of the wettest month in summer (mm/month)
P_{wdry} = precipitation of the driest month in winter (mm/month)
P_{wwet} = precipitation of the wettest month in winter (mm/month)
T_{hot} = average temperature of the hottest month (°C)
T_{cold} = average temperature of the coldest month (°C)

$P_{threshold}$ (mm) = is given by the following rules:
If (70% of MAP occurs in winter) then
$P_{threshold} = (2 \cdot MAT)$
Elseif (70% of MAP occurs in summer) then
$P_{threshold} = (2 \cdot MAT) + 28$
Else $P_{threshold} = (2 \cdot MAT) + 14$

Summer (winter) is defined as the warmer (cooler) six month period of [October through March] and [April through September].

hydrosphere/cryosphere/biosphere/land-surface system. Climate is found by averaging or filtering the hourly or daily weather data over 30 years, with the last year ending in zero (e.g., 1971-2000, or 1981-2010). Mean values of weather, temporal and spatial variability, and extremes are the statistics that are recorded as components of the climate signal.

Köppen Climate Classification

In 1884, Wladimir Köppen used temperature and precipitation to define different types of climate. He drew maps, classifying every point on land according to these climates. The climate at each location controls the dominant type of plants that naturally grow there. The Köppen climate map was modified by Rudolf Geiger in the early 1900s, and was significantly updated in 2007 by Peel, Finlayson and McMahon (*Hydrol. Earth Syst. Sci.*, **11**, 1633-1644) using modern weather data.

A two-or-three-letter code is used to identify each climate type. The criteria used to classify the climate types are in Table 21-6. Fig. 21.25 shows a small portion of the global climate map.

Table 21-7. Climate oscillations. SST = sea-surface temperature, SLP = sea-level pressure.

Name	Period (yr)	Key Place	Key Variable
El Niño (EN)	2 to 7	Tropical E. Pacific	SST
Southern Oscillation (SO)	2 to 7	Tropical Pacific	SLP
Pacific Decadal Oscillation (PDO)	20 to 30	Extratrop. NE Pacific	SST
North Atlantic Oscillation (NAO)	variable	Extratrop. N. Atlantic	SLP
Arctic Oscillation (AO)	variable	N. half of N. hem.	Pressure
Madden-Julian Oscillation (MJO)	30 to 60 days	Tropical Indian & Pacific	Convective Precipitation

FOCUS • What is an Oscillation?

Oscillations are regular, repeated variations of a measurable quantity such as temperature (T) in space x and/or time t. They can be described by sine waves: $T = A \cdot \sin[C \cdot (t - t_o) / \tau]$
where A is a constant **amplitude** (signal strength), τ is a constant **period** (duration one oscillation), t_o is a constant **phase shift** (the time delay after $t = 0$ for the signal to first have a positive value), and C is 2π radians or 360° (depending on your calculator).

True oscillations are **deterministic** — the signal T can be predicted exactly for any time in the future. The climate "oscillations" discussed here are not deterministic, cannot be predicted far in the future, and do not have constant amplitude, period, or phase.

NATURAL OSCILLATIONS

The 30-year-average climate is called the **normal climate**. Any shorter-term (e.g., monthly) average weather that differs or varies from the climate norm is called an **anomaly**. Natural climate "oscillations" are recurring, multi-year anomalies with irregular amplitude and period, and hence are not true oscillations (see the Focus Box).

Table 21-7 lists these oscillations, and their major characteristics. Although each oscillation is associated with, or defined by, a location or place on Earth (Fig. 21.26), most of these oscillations affect climate over the whole world. At the defining place(s), a combination of key weather variables is used to define an "**index**", which is the varying climate signal. Fig. 21.27 shows these oscillation indices.

El Niño - Southern Oscillation (ENSO)

(**El Niño**; **La Niña**) occurs when the tropical sea-surface temperature (**SST**) in the central and eastern Pacific ocean is (warmer; cooler) than the multi-decadal climate average.

The El Niño index plotted in Fig. 21.27a is the Pacific SST anomaly in the tropics (averaged within ±20° latitude of the equator) minus the Pacific SST anomaly outside the tropics (averaged over more poleward latitudes). Alternative El Niño indices are also useful.

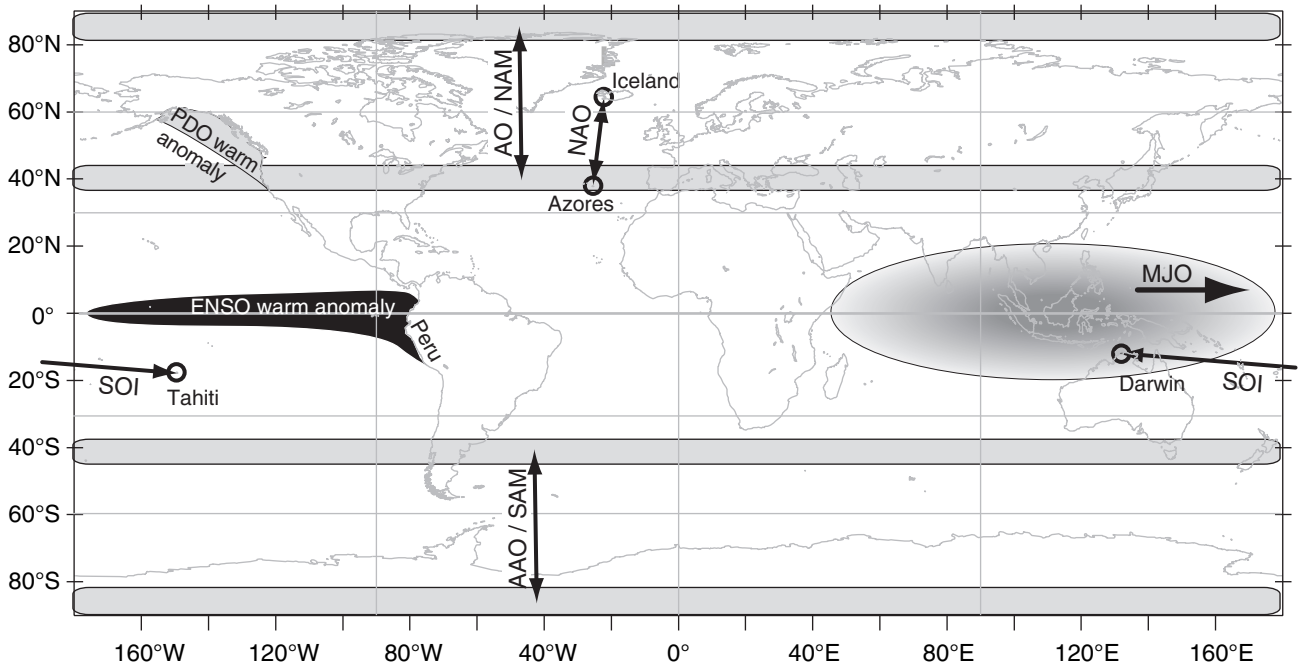

Figure 21.26 *Places and key variables that define some climate oscillations. Acronyms are defined in the text.*

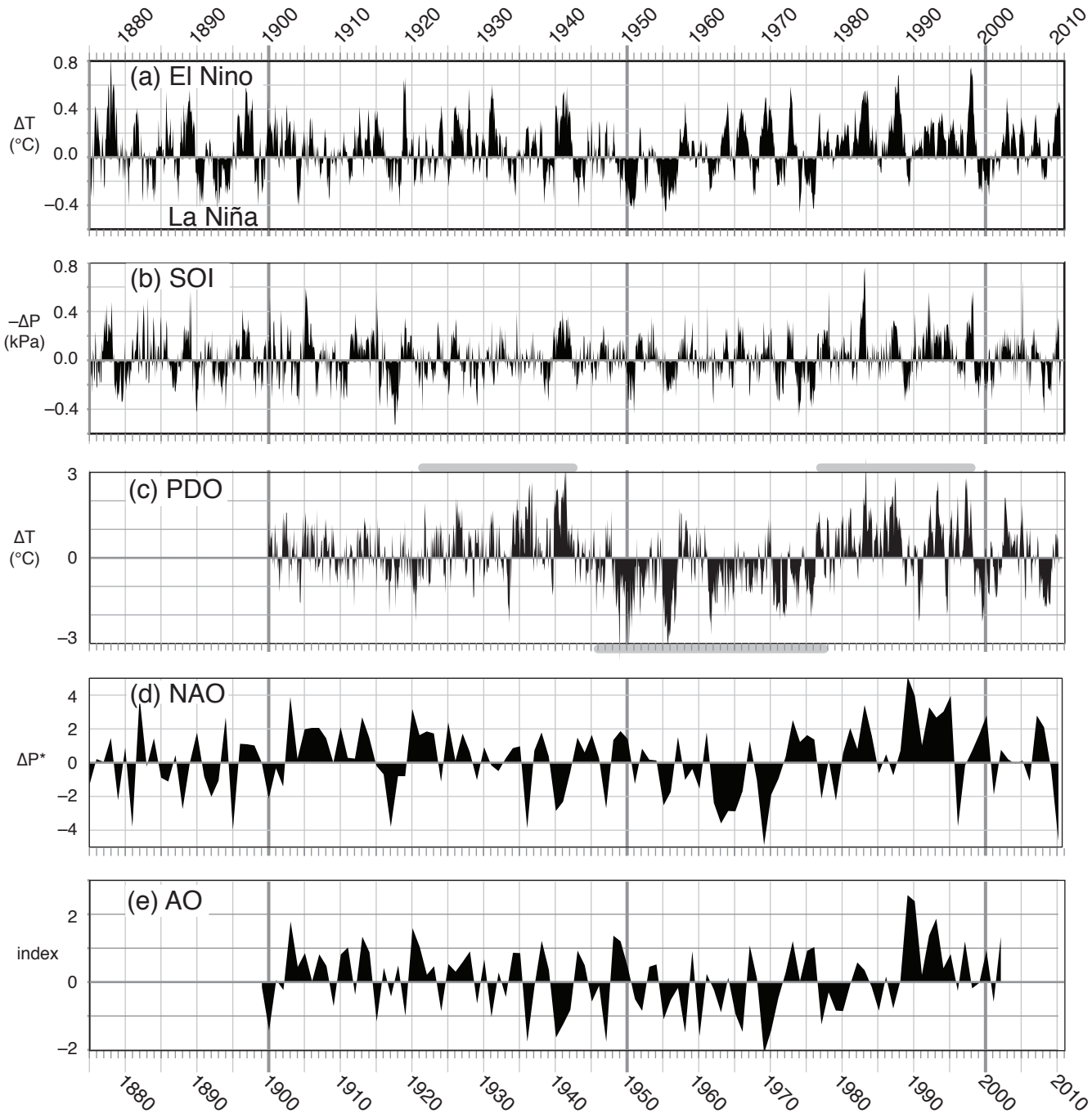

Figure 21.27
Natural oscillations of some climate indices.
(a) **El Niño** *index, based on average sea-surface temperature (SST) anomalies ΔT [data courtesy of Todd Mitchell of the Univ. of Washington Joint Inst. for Study of the Atmosphere and Ocean (US JISAO)].*
(b) Negative of the **Southern Oscillation index** *(***SOI***), based on sea-level pressure (SLP) difference:* $-\Delta P = P_{Darwin} - P_{Tahiti}$ *[data courtesy of the Climate Analysis Section of the National Center for Atmospheric Research's (NCAR) Climate and Global Dynamics Division (NCAR/CGD/CAS)].*
(c) **Pacific Decadal Oscillation** *(***PDO***) index, based on the leading principal component for monthly Pacific SST variability north of 20° latitude [data courtesy of Nate Mantua and Steven Hare of UW JISAO]. Grey bands show warm and cool phases.*
(d) **North Atlantic Oscillation** *(***NAO***) index, based on the difference of normalized SLP:* $\Delta P^* = P^*_{Azores} - P^*_{Iceland}$ *for winter (Dec - Mar) [data courtesy of Jim Hurrell, NCAR/CGD/CAS].*
(e) **Arctic Oscillation** *(***AO***), based on the leading principal component of winter SLP in the N. Hemisphere for winter (Jan-Mar) [courtesy of Todd Mitchell of UW JISAO].*

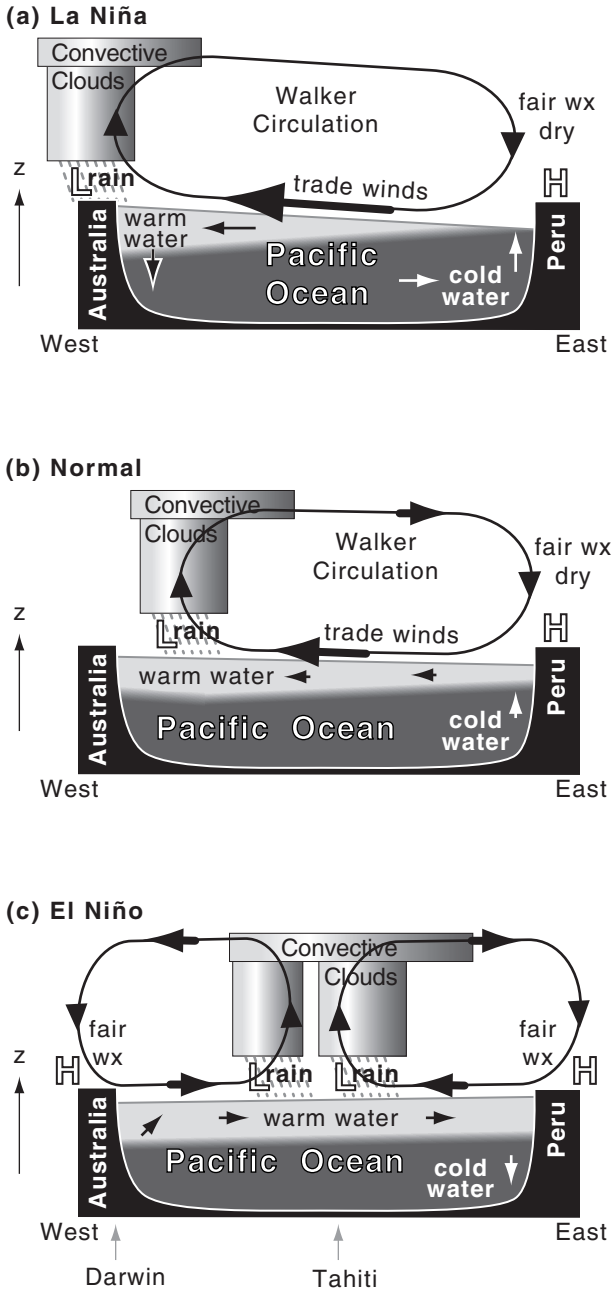

Figure 21.28
Processes that drive ENSO. (a) La Niña conditions, where cold upwelling nutrient-rich water off the coast of Peru enables increases in fish populations. Also, cool equatorial water upwells near the central Pacific. Strong trade winds. (b) Normal conditions, with modest trade winds. (c) El Niño conditions, associated with a warm-water anomaly in the eastern Pacific, and a decline in fish stocks there. H and L indicate centers of high and low atmospheric pressure, respectively.

The **Southern Oscillation** refers to a change in sign of the east-west atmospheric pressure gradient across the tropical Pacific and Indian Oceans. One indicator of this pressure gradient is the sea-level pressure difference between Tahiti (an island in the central equatorial Pacific, Fig. 21.26) and Darwin, Australia (western Pacific). This indicator ($\Delta P = P_{Tahiti} - P_{Darwin}$) is called the **Southern Oscillation index** (**SOI**).

The negative of the SOI, plotted in Fig. 21.27b, agrees with the El Niño index (Fig. 21.27a). The reason for this agreement is that El Niño (EN) and the Southern Oscillation (SO) are the ocean and atmospheric signals of the same coupled phenomenon, abbreviated as **ENSO**.

During normal and La Niña conditions, the east-to-west decrease in air pressure drives the easterly trade winds, which drag much of the warm ocean-surface waters to the west side of the Pacific basin (Fig. 21.28a). The trade winds are part of the **Walker Circulation**, which includes cloudy rainy updrafts over the warm SST anomaly in the western tropical Pacific, a return flow aloft, and fair-weather (fair wx) dry downdrafts. Heavy rain can fall over Australia. Other changes are felt around the world, including cool winters over northern North America, with drier warmer winters over the southern USA.

During El Niño, this pressure gradient breaks down, causing the trade winds to fail, and allowing anomalously warm western Pacific waters to return to the eastern Pacific (Fig. 21.28c). Thunderstorms and rain tend to be strongest over the region of warmest SST. As the SST anomaly shifts eastward, droughts (allowing wild fires) occur in Australia, and heavy rains (causing floods and landslides) occur in Peru. Other changes are felt around the world, including warm winters over northern N. America and cool, wet winters over southern N. America.

Pacific Decadal Oscillation (PDO)

The PDO is a 20 to 30 year variation in the extratropical SST near the American coast in the NE Pacific. It has a warm or positive phase (i.e., warm in the key place sketched in Fig. 21.26) and a cool or negative phase. Phase durations are highlighted by the thick grey lines in Fig. 21.27c. The PDO signal is found using a statistical method called **principal component analysis** (**PCA**, also called **empirical orthogonal function analysis**, **EOF**; see the Focus box on the next three pages.)

The PDO affects weather in northwestern North America as far east as the Great Lakes, and affects the salmon production between Alaska and the Pacific Northwest USA. There is some debate among scientists whether the PDO is a statistical artifact associated with the ENSO signal.

FOCUS • PCA and EOF

Principal Component Analysis (**PCA**) and **Empirical Orthogonal Function** (**EOF**) analysis are two names for the same statistical analysis procedure. It is a form of data reduction designed to tease out dominant patterns that naturally occur in the data. Contrast that with Fourier analysis, which projects the data onto sine waves regardless of whether the data naturally exhibits wavy patterns or not.

You can use a spreadsheet for most of the calculations, as is illustrated here with a contrived example.

1) The Meteorological Data to be Analyzed

Suppose you have air temperature T measurements from different locations over the North Pacific Ocean. Although PCA works for any number of locations, we will use just 4 locations for simplicity:

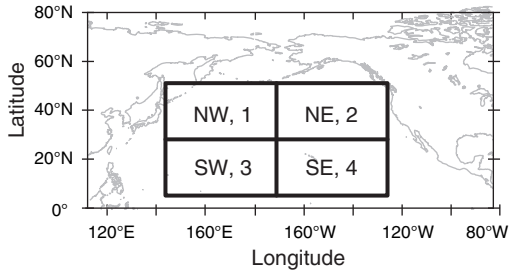

Fig. 21.a. *Locations for weather data.*

These 4 locations might have place names such as Northwest quadrant, Northeast quadrant, etc., but we will index them by number: j = 1 to 4. You can number your locations in any order.

For each location, suppose you have annual average temperature for N = 10 years, so your raw input data on a spreadsheet might look this:

Location Index:	j = 1	2	3	4
Location:	NW	NE	SW	SE
Year	Air Temperature (°C)			
i = 1	0	3	8	5
2	4	7	6	8
3	0	6	6	7
4	4	9	5	8
5	0	8	5	6
6	0	9	6	6
7	4	2	10	4
8	0	4	9	4
9	4	6	8	5
10	0	7	5	5
Average:	1.6	6.1	6.8	5.8

(continues)

FOCUS • PCA and EOF *(continuation)*

These meteorological data are plotted below:

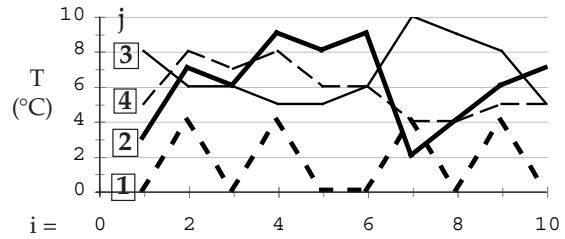

Fig. 21.b. *Graphs of raw data at each of 4 locations, where numbers in boxes indicate the j index for each line.*

Looking at this data by eye, we see that location 2 has a strong signal. Location 4 varies somewhat similarly to 2 (i.e., has positive correlation); location 3 varies somewhat oppositely (negative correlation). Location 1 looks uncorrelated with the others.

2) Preliminary Statistical Computations

Next, use your spreadsheet to find the average temperature at each location (shown at the bottom of the previous table). Then subtract the average from the individual temperatures at the same locations, to make a table of temperature **anomalies** T':

$$T'_i = T_i - T_{avg} \tag{21.48}$$

Location	j= 1	2	3	4
Year	Air Temperature Anomalies T′ (°C)			
i= 1	-1.6	-3.1	1.2	-0.8
2	2.4	0.9	-0.8	2.2
3	-1.6	-0.1	-0.8	1.2
4	2.4	2.9	-1.8	2.2
5	-1.6	1.9	-1.8	0.2
6	-1.6	2.9	-0.8	0.2
7	2.4	-4.1	3.2	-1.8
8	-1.6	-2.1	2.2	-1.8
9	2.4	-0.1	1.2	-0.8
10	-1.6	0.9	-1.8	-0.8

[Check: The average of each T′ column should = 0.]

The covariance between variables A and B is:

$$\text{covar}(A,B) = \frac{1}{N}\sum_{i=1}^{N} A'_i \cdot B'_i \tag{21.49}$$

where covar(A,A) is the variance. Use a spreadsheet to compute a table of covariances, where T1 are the temperatures at location j=1, T2 are from location 2, etc.:

covar(T1,T1)	covar(T1,T2)	covar(T1,T3)	covar(T1,T4)
covar(T1,T2)	**covar(T2,T2)**	covar(T2,T3)	covar(T2,T4)
covar(T1,T3)	covar(T2,T3)	**covar(T3,T3)**	covar(T3,T4)
covar(T1,T4)	covar(T2,T4)	covar(T3,T4)	**covar(T4,T4)**

(continues)

FOCUS • PCA and EOF *(continuation)*

The numbers in that table are symmetric around the main diagonal, so you need to compute the covariances for only the black cells, and then copy the appropriate covariances into the grey cells.

This table is called a **covariance matrix**. When I did it in a spreadsheet, I got the values below:

3.84	-0.16	0.72	0.72
-0.16	**5.29**	-3.48	2.22
0.72	-3.48	**2.96**	-1.74
0.72	2.22	-1.74	**1.96**

The underlined values along the main diagonal are the variances. The sum of these diagonal elements (known as the **trace of the matrix**) is a measure of the total variance of our original data (= 14.05 °C^2).

3) More Statistical Computations

Next, find the **eigenvalues** and **eigenvectors** of the covariance matrix. You cannot do that in most spreadsheets, but other programs can do it for you.

I used a website: http://www.arndt-bruenner.de/mathe/scripts/engl_eigenwert.htm where I copied my covariance matrix into the web page. It gave back the following info, which I pasted into my spreadsheet. Under each eigenvalue is the corresponding eigenvector.

k=	1	2	3	4
	Eigenvalues (largest first)			
	8.946	4.118	0.740	0.247
	Eigenvectors (columns under evalues)			
j=1	-0.049	0.959	-0.144	-0.238
2	0.749	0.031	-0.579	0.323
3	-0.548	0.126	-0.267	0.782
4	0.369	0.251	0.757	0.477

The sum of all eigenvalues = 14.05 °C^2 = the total variance of the original data. Those eigenvectors with the largest eigenvalues explain the most variance. Eigenvectors are dimensionless.

4) Find the Principal Components

Next, compute the **principal components** (PCs) — one for each eigenvector (*evect*). The number of eigenvectors ($K = 4$ in our case) equals the number of raw variables ($J = 4$ in our case).

Each PC will be a column of N numbers ($i = 1$ to 10 in our case) in our spreadsheet. Compute each of these N numbers in your spreadsheet using:

$$PC(k,i) = \sum_{j=1}^{J} [evect(k,j) \cdot T(j,i)] \qquad (21.50)$$

For each data table (T data; eigenvectors; PCs) used in eq. (21.50), the first index indicates the column and the second indicates the row.

(continues)

FOCUS • PCA and EOF *(continuation)*

Namely:
- k indicates which PC it is ($k = 1$ for the first PC, $k = 2$ for the second PC, up through $k = 4$ in our case) and also indicates the eigenvector (*evect*).
- i is the observation index ($i = 1$ to 10 yrs in our case), and indicates the corresponding element in any PC.
- j is the data variable index (1 for NW quadrant, etc.), and indicates an element within each eigenvector.

For example, focus on the first PC (i.e., $k = 1$); i.e., the first column in the table below. The first row ($i = 1$) is computed as:

PC(1,1) = –0.049·0 + 0.749·3 –0.548·8 + 0.369·5 = –0.29

For the second row ($i = 2$), it is:

PC(1,2) = –0.049·4 + 0.749·7 –0.548·6 + 0.369·8 = 4.71

Each PC element has the same units as the original data (°C) in our case. The resulting PCs are:

k =	1	2	3	4
	PC1	PC2	PC3	PC4
i=1	-0.29	2.36	-0.08	9.61
2	4.71	6.82	-0.17	9.81
3	3.79	2.70	0.23	9.97
4	6.76	6.75	-1.06	9.68
5	5.46	2.38	-1.42	9.35
6	5.66	2.54	-2.26	10.46
7	-2.70	6.16	-1.37	9.42
8	-0.46	2.26	-1.68	10.24
9	1.76	6.29	-2.39	9.63
10	4.34	2.10	-1.60	8.55
evalue:	8.946	4.118	0.740	0.247

Each PC applies to the whole data set, not just to one location. These PCs, plotted below, are like alternative T data:

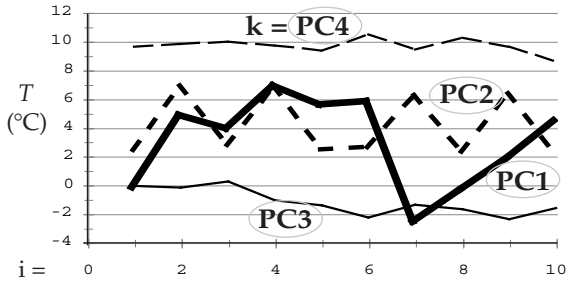

Fig. 21.c. *PCs.*

- PC1 captures the dominant pattern that is in the raw data for locations 2, 3, and 4. This 1st PC explains 8.946/14.05 = 63.7% of the original total variance.
- PC2 captures the oscillation that is in the raw data for location 1. Since location 1 was uncorrelated with the other locations, it couldn't be captured by PC1, and hence needed its own PC. The 2nd PC explains 4.118/14.05 = 29.3% of the variance.
- PC3 captures a nearly linear trend in the data.
- PC4 captures a nearly constant offset.

(continues)

FOCUS • PCA and EOF *(continuation)*

5) Synthesis

Now that we've finished computing the PCs, we can see how well each PC explains the original data. Let T_k be an approximation to the original data, reconstructed using only the k^{th} single principal component. Such reconstruction is known as **synthesis**.

$$T_k(j,i) = evect(k,j) \cdot PC(k,i) \qquad (21.51)$$

using the same (column, row) notation as before.

For k = 1 (the dominant PC), the reconstructed T_1 data is:

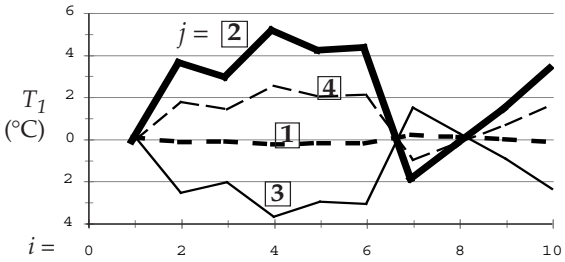

Fig. 21.d. *Reconstruction of temperature for each geographic location j = 1 to 4 (boxed numbers), but using only the 1st PC.*

It is amazing how well just one PC can capture the essence (including positive and negative correlations) of the signal patterns in the raw data.

The spatial pattern associated with PC1 can be represented on a map by the elements of the first eigenvector (arbitrarily scaled by 100 here & rounded):

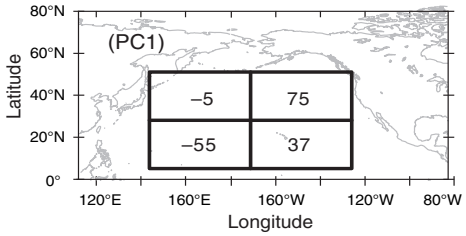

Fig. 21.e. *Geographic pattern of influence of PC1.*

6) Interpretation:

A dominant pattern in the NE quadrant extends in diminished form to the SE quadrant, with the SW quadrant varying oppositely. But this pattern is not experienced very much in the NW quadrant. Similar maps can be created for the other eigenvectors. When data from more than 4 stations are used, you can contour the eigenvector data when plotted on a map.

Eq. (21.51) can also be used to partially reconstruct the data based on only PC2 (i.e., k = 2). As shown in Fig. 21.f, you won't be surprised to find that it almost completely captures the signal in the NW quadrant (j = 1), but doesn't explain much in the other regions.

(continues)

FOCUS • PCA and EOF *(continuation)*

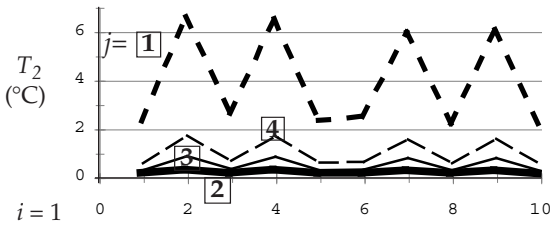

Fig. 21.f. *Similar to Fig. 21.d, but using only PC2.*

Plotting the elements of the second eigenvector scaled by 100 on a map at their geographic locations:

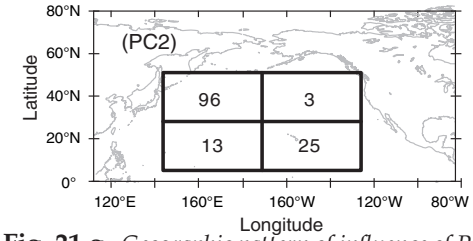

Fig. 21.g. *Geographic pattern of influence of PC2.*

7) Data Reduction

Suppose that you compute graphs similar to Figs. 21.d & 21.f for the other PCs, and then add all location 1 curves from each PC. Similarly, add all location 2 curves together, etc. The result would have perfectly synthesized the original data as was plotted in Fig. 21.a. Although the last 2 PCs don't explain much of the variance (fluctuations of the raw data), they are important to get the mean temperature values.

But what happens if you synthesize the temperature data with only the first 2 PCs (see plot below). These first 2 PCs explain 93% of the total variance. Indeed, the graph below captures most of the variation in the original signals that were in Fig. 21.a, including positive, negative, and near-zero correlations. This allows data reduction: We can use only the dominant 2 PCs to explain most of the signals, instead of using all 4 columns of raw data.

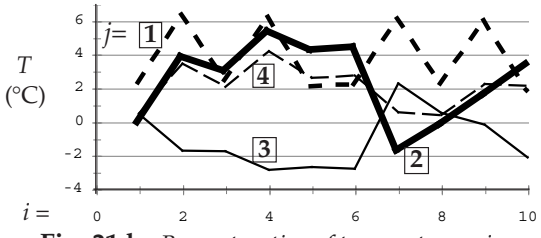

Fig. 21.h. *Reconstruction of temperature using only the first 2 PCs.*

8) Conclusions

For our small data set, the data reduction might not seem like much, but for larger data sets with hundreds of geographic points, this can be an important way to find dominant patterns in noisy data, and to describe these patterns efficiently. For this reason, PCA/EOF is valued by climate researchers.

North Atlantic Oscillation (NAO)

In the Global Circulation chapter (Fig. 11.31) we identified an Iceland low and Azores (or Bermuda) high on the map of average sea-level pressure (SLP). The NAO is a variation in the strength of the pressure difference between these two pressure centers (Fig. 21.26).

Greater differences (called the positive phase of the NAO) correspond to stronger north-south pressure gradients that drive stronger west winds in the North Atlantic — causing mid-latitude cyclones and associated precipitation to be steered toward N. Europe. Weaker differences (negative phase) cause weaker westerlies that tend to drive the extratropical cyclones toward southern Europe.

An NAO index is defined as $\Delta P^* = P^*_{Azores} - P^*_{Iceland}$, where $P^* = (P - P_{clim})/\sigma_P$ is a normalized pressure that measures how many standard-deviations (σ_P) the pressure is from the mean (P_{clim}). The winter average (Dec - Mar) is often most relevant to winter storms in Europe, as plotted in Fig. 21.27d.

Arctic Oscillation (AO)

The AO is also known as the **Northern Annular Mode** (**NAM**). It is based on the leading PCA mode for sea-level pressure in the N. Hemisphere, and varies over periods of weeks to decades. Fig. 21.27e shows the winter (Jan-Mar) averages.

The AO acts over the whole tropospheric depth, and is associated with the **polar vortex** (a belt of mid-troposphere through lower-stratosphere westerly winds circling the pole over the polar front). It compares the average pressure anomaly over the whole Arctic with pressure anomaly averaged around the 37 to 45°N latitude band. Thus, the AO pattern is zonal, like a bulls-eye centered on the N. Pole (Fig. 21.26). You can think of the NAO as a regional portion of the AO.

The positive, high-index, warm phase corresponds to greater pressure difference between mid-latitudes and the North Pole. This is correlated with faster westerly winds, warmer wetter conditions in N. Europe, warmer drier winters in S. Europe, and warmer winters in N. America. The negative, low-index, cool phase has weaker pressure gradient and winds, and opposite precipitation and temperature patterns.

Madden-Julian Oscillation (MJO)

The MJO is 45-day variation (±15 days) between enhanced and reduced convective (CB) precipitation in the tropics. It is the result of a region of enhanced convection (sketched as the grey shaded oval in Fig. 21.26) that propagates toward the east at roughly 5 to 10 m/s.

The region of enhanced tropical convection consists of thunderstorms, rain, high anvil cloud tops (cold, as seen by satellites), low SLP anomaly, convergent U winds in the boundary layer, and divergent U winds aloft. MJO can enhance tropical cyclone and monsoonal-rain activity. Outside of this region is reduced convection, clearer skies, subsiding air, less or no precipitation, divergent U winds in the boundary layer, convergent U winds aloft, and reduced tropical-cyclone activity.

The convective regions are strongest where they form over the Indian Ocean and as they move eastward over the western and central Pacific Ocean. By the time they reach the eastern Pacific and the Atlantic Oceans, they are usually diminished, although they can still have observable effects.

For example, when the thunderstorm region approaches Hawaii, the moist storm outflow can merge with a southern branch of the jet stream to feed abundant moisture toward the Pacific Northwest USA and SW Canada. This moist river of air is known as the **Pineapple Express**, and can cause heavy rains, flooding, and landslides due to orographic uplift of the moist air over the coastal mountains (see the Extratropical Cyclone chapter).

A useful analysis method to detect the MJO and other propagating phenomena is to plot key variables on a **Hovmöller diagram** (see Focus box). Eastward propagating weather features would tilt down to the right in such a diagram. Westward moving ones would tilt down to the left. The slope of the tilt indicates the zonal propagation speed.

Other Oscillations

Other climate oscillations have been discovered:

- **Antarctic Oscillation** (**AAO**, also known as the **Southern Annular Mode** (**SAM**) in S. Hem. SLP (sketched in Fig. 21.26). 2 - 7 yr variation.
- **Arctic Dipole Anomaly** (ADA), 2 - 7 yr variation with high SLP over northern Canada and low SLP over Eurasia.
- **Atlantic Multi-decadal Oscillation** (**AMO**), 30 - 40 yr variations in SST over the N. Atlantic
- **Indian Ocean Dipole** (**IOD**). 7.5 yr oscillation between warm east and warm west SST anomaly in the Indian Ocean.
- **Interdecadal Pacific Oscillation** (**IDPO** or **IPO**) for SST in the N. and S. Hemisphere extratropics. 15-30 yr periods.
- **Pacific North American Pattern** (**PNA**) in SLP and in 50 kPa geopotential heights.
- **Quasi-biennial Oscillation** (**QBO**) in stratospheric equatorial zonal winds
- **Quasi-decadal Oscillation** (**QDO**) in tropical SST, with 8-12 yr periods.

Other climate variations may also exist.

SUMMARY

Climate is weather averaged over 30 yr. Earth's climate is controlled by both external and internal processes. External processes include the balance between incoming solar radiation and outgoing infrared (IR) radiation. Internal processes include changes to the composition or structure of the atmosphere that alter how energy is distributed within the Earth-ocean-atmosphere-cryosphere-biosphere system.

Externally, changes in Earth's orbit around the sun as predicted by Milankovitch can alter the amount of sunlight reaching Earth, and changes in the tilt of Earth's axis can alter the severity of the seasons. Solar output can also vary. Changes in Earth's average albedo (via snow cover, cloud cover, or coverage of vegetation) can modulate the amount of IR radiation lost from the Earth system.

Internally, normal chemicals (water vapor, carbon dioxide, etc.) in the atmosphere absorb IR radiation, causing the air to become warmer and re-radiate a large amount of IR radiation back toward the Earth's surface. This greenhouse effect does not have perfect efficiency, because some wavelength bands of IR radiation can escape directly to space through the so-called "atmospheric window." Anthropogenic and natural changes to these greenhouse gases can alter the greenhouse efficiency and shift the climate equilibrium — an effect called "climate change."

Natural internal processes such as volcanic eruptions can also change the climate via emission of sulfates into the stratosphere. Movement of tectonic plates can shift the locations of continents and oceans relative to the equator, altering global-scale and continental-scale circulations and climate.

Some processes in the atmosphere cause negative feedbacks that tend to stabilize the climate, while other positive-feedback processes tend to amplify climate variations. Many of these feedbacks apply to external, internal, natural, and anthropogenic forcings. Overall, our climate is remarkable steady.

Short-term (few years to few decades) variations in Earth's climate are also observed. El Niño is one example out of many such "oscillations" in the climate signal.

Researchers have classified the current climate (Köppen). They also utilize tools including global climate models (GCMs), principal component analysis (PCA), Hovmöller diagrams, and conceptual models (Daisyworld) to study climate variability.

FOCUS • Hovmöller Diagram

A Hovmöller diagram is a plot of a meteorological variable as a function of date and longitude. Usually date is along the ordinate — increasing downward. Longitude is along the abscissa. The meteorological variable is contoured with grey or color fill. The latitude or latitude band of these meteorological observations is fixed, and is specified in the figure legend. These diagrams are useful for detecting the zonal movement of weather features over time.

For example, suppose that on 1 January you flew an airplane around the world along the equator (0° latitude), and remotely measured the sea surface temperature (SST). After subtracting the average SST, you would be left with a temperature anomaly T' at each point around the equator. Suppose the first graph below shows what you measured.

Later, on 15 January, make the same flight, and plot your measurements (second graph below). Repeat the flights for many different dates.

Instead of plotting each circumnavigation on a separate graph, we can write all the T' numbers on the same diagram of time vs. longitude. Then analyze the result as you learned in the Map Analysis chapter, by drawing isotherms of T'. The result is a Hovmöller diagram (third diagram below). You can use any meteorological variable, not just T'.

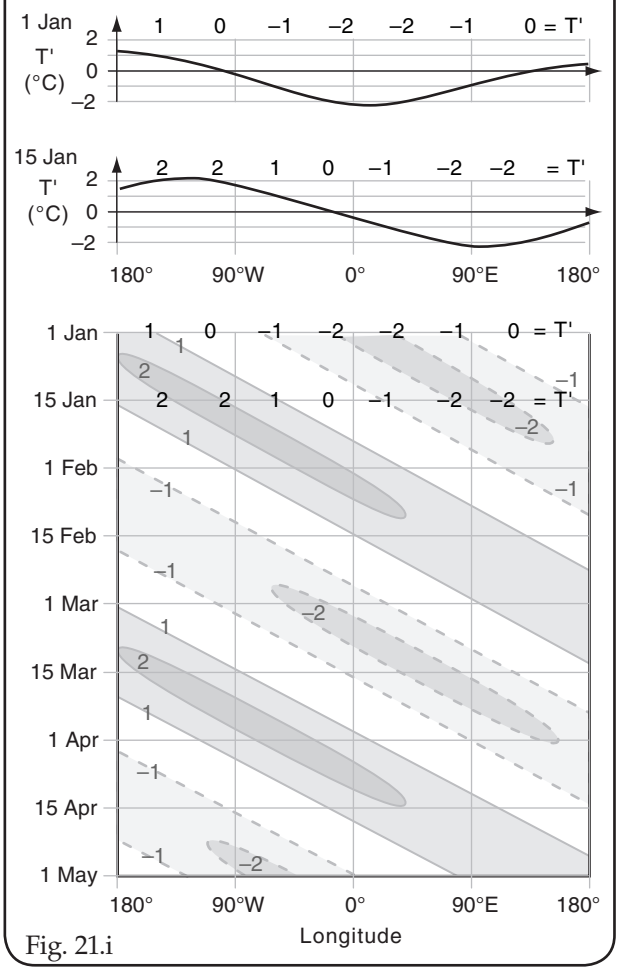

Fig. 21.i

Threads

Many of the climate-change issues relate to radiation (Chapter 2) within the setting of our existing atmospheric structure (Chapter 1). The radiative input alters the heat budget (Chapter 3), which controls water evaporation (Chapter 4), clouds (Chapter 6) and precipitation (Chapter 7).

Climate is partly governed by, and in turn alters, the global circulation (Chapter 11), which can affect the frequency, intensity, and track of cyclones (Chapters 13 and 16) and thunderstorms (Chapters 14 and 15).

Much of the concern about climate change is related to pollutants (Chapter 19) emitted into the atmosphere by people in the boundary layer (Chapter 18). Venting of greenhouse gases out of the boundary layer, and longevity of these tracers in the upper atmosphere depends, in part, on the vertical stability of the atmosphere (Chapter 5).

Global climate models (GCMs) are forms of numerical weather prediction models (Chapter 20).

ON DOING SCI. • Ethics & Data Abuse

In the race to reach scientific conclusions, and with the natural human desire to be successful, scientists sometimes inappropriately manipulate their data. The following are considered to be unethical in science:

"• **Massaging** – performing extensive transformations... to make inconclusive data appear to be conclusive;

• **Extrapolating** – developing curves [or proposing theories] based on too few data points, or predicting future trends based on unsupported assumptions about the degree of variability measured;

• **Smoothing** [or **trimming**] – discarding data points too far removed from expected or mean values;

• **Slanting** [or **cooking**]– deliberately emphasizing and selecting certain trends in the data, ignoring or discarding others which do not fit the desired or preconceived pattern;

• **Fudging** [or **forging**]– creating data points to augment incomplete data sets or observations; and

• **Manufacturing** – creating entire data sets de novo, without benefit of experimentation or observation."

[from C. J. Sindermann, 1982: *Winning the Games Scientists Play*. Plenum. 290 pp.; and Sigma Xi, 1984: *Honor in Science*. Sigma Xi Pubs., 41 pp.]

EXERCISES

Numerical Problems

N1. Find the radiation input to the Earth system for an albedo of:

a. 0.1 b. 0.15 c. 0.2 d. 0.25 e. 0.35 f. 0.4
g. 0.45 h. 0.5 i. 0.55 j. 0.6 k. 0.65 m. 0.7

N2. Find the Earth effective radiation temperature for the albedoes in the previous exercise.

N3. For a global albedo of 0.3, find the radiation input to the Earth system for total solar irradiance values (W/m^2) of:

a. 1350 b. 1352 c. 1354 d. 1356 e. 1358
f. 1360 g. 1362 h. 1364 i 1365 j. 1367
k. 1368 m. 1370 n. 1372 o. 1374

N4. For a global albedo of 0.3, find the Earth effective radiation temperature for solar constant values of the previous exercise.

N5. Find the net radiation out from the Earth system, for an Earth effective radiation emission temperature (°C) of

a. –19 b. –17 c. –15 d. –13 e. –11
f. –9 g. –7 h. –5 i. –3 j. –1
k. 1 m. 3 n. 5 o. 10 p. 15

N6. Calculate the effective radiation temperature for the following planets and dwarf planets.

Planet	Albedo	Planet	Albedo
a. Mercury	0.12	b. Venus	0.75
c. Mars	0.25	d. Jupiter	0.34
e. Saturn	0.34	f. Uranus	0.30
g. Neptune	0.29	h. Pluto	0.40

N7. For an idealized one-layer atmosphere that is opaque to all IR radiation, find the surface temperature for:

(i) exercise N2 (ii) exercise N4 (iii) exercise N6

N8. For an atmosphere with a window in the IR, find Earth's surface temperature under a one-layer atmosphere with emissivity:

a. 0.70 b. 0.73 c. 0.76 d. 0.80 e. 0.83
f. 0.86 g. 0.88 h. 0.91 i. 0.93 j. 0.95
k. 0.97 m. 0.99

Assume an effective emission temperature of 255 K.

N9. Use Fig. 21.6 to answer these questions:

a. What fraction of energy absorbed at the Earth's surface comes from solar radiation?

b. What fraction of energy leaving the Earth's surface consists of (latent + sensible) heat?

c. What is the net flux of IR radiation between the Earth's surface and the atmosphere, and how does this compare to the flux of (latent + sensible) heat?

d. What is the total amount of upwelling energy (solar, IR, sensible, latent) that reaches the bottom of the idealized atmosphere in that figure?

e. Why is the 79 W/m^2 of "solar reflected from atmos." not included in the energy budget of the atmosphere as one of the outgoing fluxes (Hint: See the Solved Example after that figure)?

f. Why is the (sensible + latent) heat flux upward from the top of the atmosphere not shown?

N10(§). On a very large graph, carefully plot two ellipses. One has eccentricity of 0.0 (i.e., is a circle), and the other has an eccentricity of:

a. 0.05 b. 0.1 c. 0.15 d. 0.2 e. 0.25 f. 0.3
g. 0.35 h. 0.4 i. 0.6 j. 0.7 k. 0.8 m. 0.9

N11(§). Using the data from Table 21-1, find the Earth-orbit eccentricity for the following time:

a. 400 kyr ago b. 1.1 Myr ago c. 1.2 Myr ago
d. 1.4 Myr ago e. 1.6 Myr ago f. 2 Myr ago
g. 625 kyr in the future h. 1.1 Myr in future
i. 1.3 Myr in future j. 2 Myr in future

N12.(§). Same as for N11, but find the obliquity (°).

N13.(§). Same as for N11, but find the climatic precession at the summer solstice (i.e., the $e \cdot \sin(\varpi)$ term).

N14(§). Same as for N11 (and N13), but find the ratio of semi-major axis to sun-Earth distance: a/R .

N15(§). Same as N11 (and using your results from N12 - N14), but find the average daily insolation at 65°N during the summer solstice.

N16. Find the sun-Earth distance R (Gm) given an eccentricity of 0.05 and a climatic precession value of: a. –0.05 b. –0.04 c. –0.03 d. –0.02 e. –0.01
f. 0.01 g. 0.02 h. 0.03 i. 0.04 j. 0.05

N17. Use the definition of optical depth from the Beer's Law section of the Radiation chapter to estimate the optical depth for background "clean" air, which transmits about 94% of incident solar radiation. Also, use data from Fig. 21.17 on recent volcanic eruptions, and compare the "clean" optical depth to the optical depth for:

a. Mt. Agung (Indonesia)
b. Mt. Fuego (Guatemala)
c. El Chichon (Mexico)
d. Mt. Pinatubo (Philippines)

N18. Find the feedback factor, gain, and system response, given a no-feedback response of $r_o = 0.2$, and a feedback value (F) of:

a. –8 b. –6 c. –4 d. –2 e. 1 f. 2 g. 3
h. 4 i. 5 j. 6 k. 7 m. 8 n. 9 o. 10

N19. Based on the answer to N18, is the feedback negative, stable positive, or run-away positive?

N20. For a no-feedback reference state for Earth, find the no-feedback climate response r_o for a blackbody Earth equilibrium radiative temperature of T_e* (K):

a. 200 b. 210 c. 220 d. 230 e. 240 f. 250
g. 260 h. 270 i. 280 j. 290 k. 300 m. 310

N21. Given a reference Earth blackbody radiative temperature of T_e* = 255 K and a reference albedo of A* = 0.3 . Find the feedback factor, gain, and total system response if ice-albedo feedback behaves such that the change of Earth albedo (associated with ice coverage changes) with surface temperature ($\Delta A/\Delta T = -c$), where c (K^{-1}) has a value of:

a. 0.002 b. 0.005 c. 0.008 d. 0.012 e. 0.015
f. 0.02 g. 0.03 h. 0.05 i. 0.10 j. 0.2

N22. Suppose that doubling of CO_2 in the global atmosphere had the same effect as increasing the incoming solar radiation by $\Delta R_o = 4$ W/m^2 (due to the increased absorption of solar radiation, as explained in the Focus box on Climate Sensitivity). Given Table 21-4, how much would Earth's equilibrium temperature change (i.e., find ΔT_e in °C) for a reference response with no feedbacks, and for the following feedback process:

a. water-vapor only b. lapse-rate only
c. cloud only d. surface-albedo only
e. all of a - d combined

N23(§). Program the Daisyworld equations into your spreadsheet. Calculate the surface temperature (K), coverage of white daisies, and coverage of black daisies, for luminosity of:

a. 0.9 b. 1.0 c. 1.1 d. 1.2 e. 1.3
f. 1.4 g. 1.5 h. 1.6 i. 1.7 j. 1.8

N24. Describe the climate at

a. Oregon coast
b. Olympic Mtns (NW corner of Washington)
c. central Vancouver Island (British Columbia)
d. at the USA-Canada border labels in Fig. 21.25
e. north-central California
f. north-central Idaho
g. western Nevada
h. extreme SE California
i. central part of Alberta (portion shown in map)
j. south central Idaho

Understanding & Critical Evaluation

U1. If the atmosphere can be idealized as having two layers, each opaque to IR, extend the results from the Greenhouse section to find an equation for surface temperature as a function of effective radiation temperature.

U2. After a major (hypothetical) volcanic eruption, assume that the ash in the atmosphere quickly spreads evenly around the globe. This dirty air absorbs 25% of any sunlight that shines through the atmosphere. For simplicity, assume that IR absorption/emission is not affected by the ash, and that the albedo of the Earth's surface has not changed by ash deposits. Using a simplified climate model with a one-layer atmosphere with no atmospheric window, what is the new temperature of the Earth's surface (averaged over the whole globe)?

U3. For the last 2 million years the global climate is believed to have been 1.5 to 3 degrees colder than now. For the 100 million years before that, the climate ranged from 2 to 5 degrees warmer than now. If our climate is presently warming, does that mean we are approaching or diverging from "normal"?

U4. Explain how the "atmospheric window" in Fig. 21.5 relates to Figs. 8.3 and 8.4 in the Remote Sensing chapter.

U5. Given a single layer atmosphere with no window. Suppose that initially the Earth-atmosphere system is in equilibrium. Then, suddenly, the sun becomes hotter and the insolation doubles. Describe how the fluxes and energy budgets of Fig. 21.6 would change while the Earth and atmosphere adjust toward their new equilibrium. Also, which of the fluxes would change the quickest; and which the slowest?

U6. In music there is a concept of "**beat frequency**". Namely, when two sounds are produced that have nearly the same tone (frequency), you can hear a third tone that depends on the difference between the two frequencies. Look-up the definition of "beat frequency", and use that info to explain why the Climatic Precession curve in Fig. 21.8 looks the way it does.

U7. a. Given the max and min values of climatic precession plotted in Fig. 21.8, what are the max and min of values of (a/R); namely, the ratio of semi-major axis to sun-Earth distance?

b. Simplify the equation (21.18) for the solar declination angle for the special case of the summer solstice.

c. Given the max and min of obliquities plotted in Fig. 21.8, what are the max and min of solar declination angles (°) for the summer solstice?

d. Combine the info in Figs. 21.11 - 21.13 to estimate the max and min values of solar irradiance (W/m^2) during the past 1000 years.

e. Given your answers to (a) - (d) above, which has the largest effect on the value of daily-average insolation at 65°N during the summer equinox: climatic precession, obliquity, eccentricity, or solar irradiance?

U8. In Fig. 21.8, the Daily Average Insolation graph is based on a combination of the previous three graphs in that figure. Looking at the nature of the signals in all four top graphs in Fig. 21.8, which of the top 3 graphs best explains the Insolation, and which of the top 3 least explain the Insolation? Why?

U9(§). Table 21-1 shows only the first $N = 4$ or 5 terms for Earth's orbital factors. Use the first $N = 10$ terms (in Table 21-1b, on the next page) to more accurately re-calculate the first 3 graphs in Fig. 21.8. [The original paper by Laskar et al has over 20 terms for each orbital series.]

U10. Use the orbital data for Earth to answer the following. How many years in the future is the first time when the perihelion will coincide with the summer solstice? This is important because it means that summers will be hotter and winters colder in the N. Hemisphere, because the N. Hemisphere will be tilted toward the sun at the same date that the Earth is closest to the sun.

U11 Show that the right-hand approximation in eq. (21.18) for the solar declination is the same as eq. (2.5). [Hints: Consider that in summer, Earth is 90° further along its orbit than it was in Spring. Use trig identities that relate sines to cosines. Consider the definitions of various orbital angles, as summarized in the Focus box on Sun-Earth Distance.]

U12. Explain why Pangea's climate would be different than our present climate. [Hint: Consider global circulations and monsoonal circulations, as discussed in the Global Circulation chapter.]

U13. a. Use the definitions of optical depth and visual range from the Beer's Law section of the Radiation chapter to find a relationship for visibility (km) as a function of optical depth τ.

b. Use your answer from (a) with the data from Table 21-3 to estimate the atmospheric visibilities associated with the following volcanic eruptions:

(i) Lake Toba (ii) Mt. Tambora (iii) Krakatau

Table 21-1b. Factors in orbital series approximations.

index	A	P (years)	ϕ (degrees)
Eccentricity:			
i= 1	0.010739	405,091.	170.739
2	0.008147	94,932.	109.891
3	0.006222	123,945.	−60.044
4	0.005287	98,857.	−86.140
5	0.004492	130,781.	100.224
6	0.002967	2,373,298.	-168.784
7	0.002818	977,600.	57.718
8	0.002050	105,150.	49.546
9	0.001971	486,248.	148.744
10	0.001797	688,038.	137.155
Obliquity:			
j= 1	0.582412°	40,978.	86.645
2	0.242559°	39,616.	120.859
3	0.163685°	53,722.	−35.947
4	0.164787°	40,285.	104.689
5	0.095382°	41,697.	-112.872
6	0.094379°	41,152.	60.778
7	0.087136°	9,572,151.	39.928
8	0.064348°	29,842.	-15.13
9	0.072451°	28,886.	-155.175
10	0.080146°	40,810.	-70.983
Climatic Precession:			
k= 1	0.018986	23,682.	44.374
2	0.016354	22,374.	−144.166
3	0.013055	18,953.	154.212
4	0.008849	19,105.	−42.250
5	0.004248	23,123.	90.742
6	0.002742	19,177.	61.600
7	0.002386	19,025.	74.660
8	0.001796	22,570.	−145.502
9	0.001908	19,260.	119.333
10	0.001496	16,465.	141.244

*Simplified from Laskar, Robutel, Joutel, Gastineau, Correia & Levrard, 2004: A long-term numerical solution for the insolation quantities of the Earth. "Astronomy & Astrophysics", **428**, 261-285.*

U14. For every type of climate feedback, explain why runaway climate change is not possible. [Or if it is possible, show how runaway climate changes applies for only a limited change of Earth temperatures before a new stable climate equilibrium is reached. Can you recall any Hollywood movies that showed runaway climate change, with or without reaching a stable equilibrium?]

U15. For the feedback interconnections shown in Fig. 21.18, the feedback outcomes are only: negative (damped), positive (amplified), or runaway (increasing without limit). Can you think of a different type of interconnection or process that could cause the system response to oscillate? Explain.

U16. Ice-albedo processes were used for an idealized illustration of feedback. Try to develop your own feedback concepts that account for the following (and ignores all other feedbacks except the fundamental radiative feedback). Suppose there is a CO_2 feedback process whereby warmer Earth temperatures cause the oceans to release more CO_2 into the air. But more CO_2 in the air acts to partially close the IR window sketched in Fig. 21.5.

a. What info or what relationships do you need to be able to figure out the feedback? [Just list what info you need here — do not actually try to find these relationships.]

b. If you are good at calculus and if assigned by your instructor, then try to create a governing equation similar to that used for ice-albedo feedback, then take the derivatives as was done in the Beyond Algebra Feedback Example box. There is no single correct answer — many different approximations and solutions might be reasonable. Justify your methods.

U17. For feedbacks in the Earth climate system, use error-propagation methods as discussed in Appendix A, to propagate the errors listed in the feedback (*F*) column of Table 21-4 into the other columns for feedback factor (*f*), gain (*G*), & system response (*r*).

U18. Do outside readings to explain how the following abrupt climate-change processes work (Table 21-4). Also, explain if feedback is positive or negative.

a. meridional overturning ocean circulation
b. fast Antarctic & Greenland ice-sheet collapse
c. volcanoes
d. methane release due to hydrate instability and permafrost)
e. biogeochemical

U19.(§) For a daisyworld

a. Redo the calculation shown in this chapter.

b. What happens to the temperature over black and white daisies if the transport parameter changes to 0 or 1?

c What happens if you start with initial conditions of 100% coverage by white or black daisies?

d. What happens if you take a time step increment of 2, 4, or 8?

e. What parameter values prevent homeostasis from occurring (i.e., eliminate the nearly constant temperature conditions on a fecund daisyworld?

f. Is it possible for homeostasis to occur on Earth, given the large fraction of area covered by oceans?

U20(§). In Fig. 21.24 for Daisyworld, the daisies are able to control the climate only over a limited range of luminosities. What changes to the growth

Table 21-8. Names of Köppen climate classes.

Exercise	Code	Name
a	Af	equatorial climate
b	Am	monsoon climate
c	Aw	tropical savanna climate
d	BWh	warm desert climate
e	BWk	cold desert climate
f	BSh	warm semi-arid climate (warm steppe clim.)
g	BSk	cold semi-arid climate (cold steppe climate)
h	Csa	warm mediterranean climate
i	Csb	temperate mediterranean climate
j	Cwa	warm humid subtropical climate
k	Cwb	temperate humid subtropical climate
l	Cwc	cool humid subtropical climate
m	Cfa	warm oceanic/marine; or humid subtropical
n	Cfb	temperate oceanic/marine climate
o	Cfc	cool oceanic/marine climate
p	Dsa	warm continental (mediterranean continental)
q	Dsb	temperate continental (mediter. continental)
r	Dsc	cool continental climate
s	Dsd	cold continental climate
t	Dwa	warm humid continental climate
u	Dwb	temperate humid continental climate
v	Dwc	cool continental clim.; cool subarctic climate
w	Dwd	cold continental clim.; cold subarctic climate
x	Dfa	warm humid continental climate
y	Dfb	temperate humid continental climate
z	Dfc	cool continental clim.; cool subarctic climate
aa	Dfd	cold continental clim.; cold subarctic climate
ab	ET	tundra climate
ac	EF	ice cap climate

characteristics of the daisies would allow control of the climate over a wider range of luminosities (and thus would allow greater chance of survival of an extreme luminosity change event)? Check your theory by modifying the growth equations accordingly, and performing the calculation on a spreadsheet or other program.

U21. Where in the world (but NOT in any region plotted in Fig. 21.25) would you expect to find the climate in Table 21-8 above. (Hint, consider info in the Global Circulation chapter, and also use the Köppen climate definitions in Table 21-6.)

U22(§-difficult). Find the covariance matrix, the eigenvectors and eigenvalues (using some other resource such as a web-based eigenvector calculator), leading 2 principal components (PCs), interpret the results, and reconstruct (synthesize) the original data as approximated using the dominant 2 PCs, given time series in Table 21-9. Assume that the locations for these time series correspond to the geographic locations shown in Fig. 21.a of the **PCA** Focus box.

U23. Given the Hovmöller diagram in Fig. 21.29, determine the zonal speed and direction that features move.

Table 21-9. Time series for PCA exercise.

Location Index:	j = 1	2	3	4
Location:	NW	NE	SW	SE
Year	Air Temperature (°C)			
i = 1	9	1	1	8
2	7	2	1	8
3	5	3	2	7
4	7	4	5	6
5	9	5	9	5
6	7	6	9	5
7	5	5	5	5
8	7	4	5	6
9	9	3	4	7
10	7	2	1	8

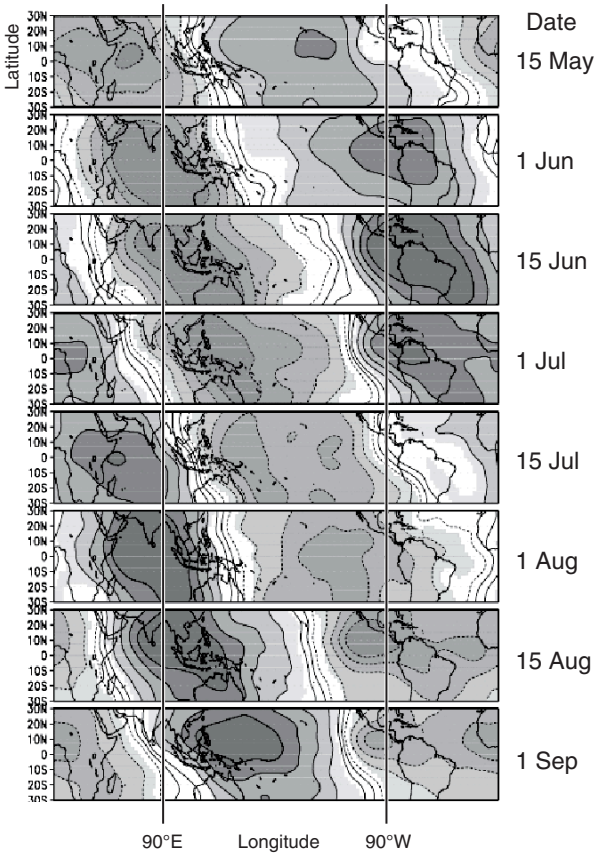

Figure 21.29
Hovmöller Diagram showing 20 kPa winds. (Shading is arbitrary for this exercise.) Modified from data courtesy of the Climate Prediction Center, National Weather Service, National Oceanic and Atmospheric Admin.

Web-Enhanced Questions

W1. Search the web for graphs comparing different satellite measurements of the solar irradiance (i.e., the solar constant). Discuss the relative magnitudes of the variation of solar irradiance with time vs. the errors associated with measuring solar irradiance. [Hint: Recall info about accuracy and precision from Appendix A.]

W2. Search the web for maps showing the ice cover on Earth, and how ice cover has changed during the past decades. Discuss these changes in relation to ice-albedo feedback.

W3. Use info from the web to discuss the difference between **Bond albedo** and **geometric albedo**. Which one of these albedos is most appropriate to use for studying the radiation budget of other planets?

W4. Search the web for animations or graphs showing/predicting the changes in eccentricity, obliquity, and precession of the Earth over time. Discuss the simplifications made in these diagrams/animations to communicate this info to the general public.

W5. Search the web for more accurate Earth orbital parameters, to improve and expand the data that were in Tables 21-1 and 21-1b. Save and print this table.

W6. Search the web for accurate graphs of ice ages. Discuss what ice-age details are missing or poorly resolved in the ice-age graph in Fig. 21.8.

W7. Search the web for graphs of solar activity or sunspot number, going as far back in time as you can find. Discuss the regular and irregular components of the sunspot cycle.

W8. Search the web for animations or a sequence of still-frames showing how the continents moved to create Pangea, and how they continued to move into their current configuration. Discuss how monsoonal circulations change and alter the continental climates as the continents move.

W9. Search the web for photos of one recent volcanic eruptions that show: (a) ash fallout close to the volcano, and (b) the plume of aerosols injected into the stratosphere, showing their track around the Earth. Discuss the relative amount of global impact due to the one volcanic eruption.

W10. Search the web for photos of beautiful sunsets that were enhanced by volcanic aerosols in the stratosphere. Read ahead in the Optics chapter to see why you can see red skies and blue moons after some volcanic eruptions.

W11. Search the web for info about other major volcanic eruptions that were not listed in Table 21-3. Discuss the impacts of these eruptions on species.

W12. Search the web for the most recent Assessment Report from the Intergovernmental Panel on Climate Change (IPCC), and identify new information and understanding that updates information in this Chapter.

W13. Search the web for additional climate feedback processes that were not listed in Table 21-4, and discuss their relative importance to the ones already listed.

W14. Search the web for data on actual amounts of global warming during the past two decades, and compare to the predictions presented in older IPCC reports. How accurate are climate predictions?

W15. Search the web for animations of Daisyworld evolution. Enjoy.

W16. Lovelock, the inventor of Daisyworld, wrote a more recent book called "The Revenge of Gaia." If you don't have time to read the book, search the web for a summary of its key points, and argue either for or against his thesis.

W17. Search the web (particularly IPCC Assessment Reports) that summarize the attributes of the various global climate models (GCMs) that were used for the most recent IPCC climate report. Summarize the commonalities and differences between these various GCMs.

W18. Search the web for color maps showing Köppen climate classification for the whole world. Focus on where you live, and discuss how the climate classification does or does not agree with the climate you observed in your area.

W19. Search the web for color diagrams illustrating the processes involved in these climate oscillations:

a. El Niño or ENSO, including the relationship between trade winds, upwelling water, and SST
b. PDO c. NAO d. AO e. MJO

W20. What is meant by an "anomaly map" (for example, of sea surface temperature (SST))? Find ex-

amples of such maps or animations on the web for ENSO, and compare to the actual SST map. How are the SST anomalies associated with rainfall shifts, cloud coverage changes, etc.?

W21. Search the web for maps showing the geographic distribution of dominant principal components for any one of the climate oscillations.

W22. Search the web for a Hovmöller diagram for climate oscillations such as MJO in the most recent 6 or 12 months, and analyze it to explain the direction and movement of features.

W23. Use the web to find what is meant by **teleconnections**.

W24. Search the web to find the worldwide weather consequences a recent major El Niño event.

W25. Use the web to learn about the US government agency NCDC. How might it be useful to you? What similar agencies exist in other countries?

W26. Search the web graphs showing observed changes in many of the greenhouse gases.

Synthesis Questions

S1. What if emitted IR radiation were constant — not a function of temperature. How would Earth's climate be different, if at all?

S2. Create an energy balance to determine T_s and T_e for an atmosphere with:
a. 2 opaque atmospheric layers (no window)
b. 3 opaque atmospheric layers (no window)
c. extrapolate your theory so it works with a large number of windows

S3. What if the Earth did not rotate, the atmosphere did not move, and there was no conduction from the warm side to the cold side of the Earth. Create an energy balance (and justify your assumptions) for:
a. a single-layer atmosphere with no atmospheric window.
b. a single-layer atmosphere with an atmospheric window.

S4. What if Earth had an internal heat source that created as much excess heat as the insolation at the top of the atmosphere. Describe the resulting energy balances of all relevant systems, and find the final equilibrium temperatures of the Earth's surface and the atmosphere (assume single layer with no window), and discuss feedbacks.

S5. Estimate the variation in insolation if Earth's orbit were to have eccentricity of 0.8.

S6. Suppose that transparent windows in the atmosphere opened over the north and south pole, similar to the ozone hole. Given that these spatial windows are over only the colder parts of the Earth's surface, calculate the resulting energy balances for all relevant systems, and compute the average Earth surface and atmosphere temperatures. State all assumptions.

S7. What if solar radiation from the sun ionized the sunny side of the atmosphere resulting in complete closure of the IR atmospheric window there. But assume that the shady side remains un-ionized, and a window can exist. Calculate the resulting energy budgets, and the equilibrium temperatures of the Earth and the atmosphere. State all assumptions.

S8. Re-derive the Daisyworld equations, but for a situation where daisies always cover the whole Earth. The relative coverages of black and white daisies can vary, but there is never any bare ground. How do the results differ, both in equilibrium and sensitivity to disturbances, from the Daisyworld described in this chapter?

S9. If runaway climate change caused the Earth to reach a new equilibrium, how difficult would it be to return to our present equilibrium? Would there also be a positive feedback to return to our present climate?

S10. Would global warming alter:
a. the global circulation?
b. thunderstorm severity?
c. hurricane severity?
Explain how.

S11. Discuss the scientific accuracy of recent Hollywood movies where the theme was weather or climate disasters.

S12. Repeat the principal component analysis from the focus box, but when you calculate the table of principal components (PC), use the temperature anomaly T' in eq. (21.50) instead of T. Then finish all the remaining calculations using these new PCs.

What is the sum of elements in each PC (i.e., the sum of each column in the PC table)? What is the relationship between your plotted PCs and Fig. 21.c? When you synthesize the signal using only PC1, how does your result compare to Fig. 21.d?

Outcome: you are synthesizing T' and not T. Most researchers use PCA to focus on the anomaly.

Copyright © 2011, 2015 by Roland Stull. *Meteorology for Scientists and Engineers, 3rd Ed.*

OPTICS

CONTENTS

Ray Geometry 833
- Reflection 833
- Refraction 834
- Huygens' Principle 837
- Critical Angle 837

Liquid-Drop Optics 837
- Primary Rainbow 839
- Secondary Rainbow 840
- Alexander's Dark Band 841
- Other Rainbow Phenomena 841

Ice Crystal Optics 842
- Parhelic Circle 844
- Subsun 844
- 22° Halo 845
- 46° Halo 846
- Halos Associated with Pyramid Crystals 847
- Circumzenith & Circumhorizon Arcs 848
- Sun Dogs (Parhelia) 850
- Subsun Dogs (Subparhelia) 851
- Tangent Arcs 851
- Other Halos 853

Scattering 856
- Background 856
- Rayleigh Scattering 857
- Geometric Scattering 857
- Mie Scattering 858

Diffraction & Interference 858
- Corona, Iridescence and Glory 859
- Supernumerary Bows 860

Mirages 861

Summary 863
- Threads 863

Exercises 863
- Numerical Problems 863
- Understanding & Critical Evaluation 865
- Web-Enhanced Questions 867
- Synthesis Questions 868

"Meteorology for Scientists and Engineers, 3rd Edition" by Roland Stull is licensed under a Creative Commons Attribution-NonCommercial-ShareAlike 4.0 International License. To view a copy of the license, visit http://creativecommons.org/licenses/by-nc-sa/4.0/ . This work is available at http://www.eos.ubc.ca/books/Practical_Meteorology/ .

22 Light can be considered as photon particles or electromagnetic waves, either of which travel along paths called **rays**. To first order, light rays are straight lines within a uniform transparent medium such as air or water, but can **reflect** (bounce back) or **refract** (bend) at an interface between two media. Gradual refraction (curved ray paths) can also occur within a single medium containing a smooth variation of optical properties.

The beauty of nature and the utility of physics come together in the explanation of rainbows, halos, and myriad other atmospheric optical phenomena.

RAY GEOMETRY

When a **monochromatic** (single color) light ray reaches an interface between two media such as air and water, a portion of the incident light from the air can be reflected back into the air, some can be refracted as it enters the water (Fig. 22.1), and some can be absorbed and changed into heat (not sketched). Similar processes occur across an air-ice interface.

Reflection

The angle θ_3 of the reflected ray always equals the angle θ_1 of the incident ray, measured with respect to a line normal (perpendicular) to the interface:

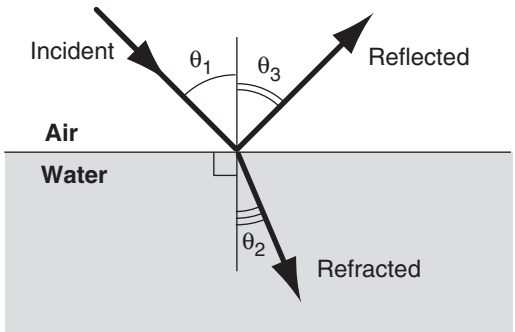

Figure 22.1
Geometric optics at an air-water interface. Black arrows are light-ray paths.

Solved Example

Rays of red and violet light in air strike a water surface, both with incident angle of 60°. Find the angle of refraction for each color, given T = 20°C, P = 101 kPa?

Solution

Given: $\theta_1 = 60°$, $T = 20°C$, $P = 101$ kPa
Find: $\theta_2 = ?°$ for red (λ=0.7 μm) and violet (λ=0.4 μm).

Use eq. (22.5):
$\theta_2 = \arcsin[(n_1/n_2)\cdot\sin(\theta_1)] = \arcsin[\mu_{12}\cdot\sin(\theta_1)]$
with μ_{12} from eq. (22.3) and refractive indices from Table 22-1.

For red: $\mu_{12} = n_1/n_2 = 1.0002704/1.3305 = 0.7518$
$\theta_2 = \arcsin[0.7518\cdot\sin(60°)]$
$\theta_2 = \underline{\mathbf{40.62°}}$
Similarly for violet: $\theta_2 = \underline{\mathbf{40.15°}}$

Check: Units OK. Physics OK.
Discussion: Had there been no bending, then both answers would have been 60°. Angles closer to 60° for this example correspond to less bending. The answers above confirm the statement that red light is bent less than violet. The **amount of bending** (difference between incident and refracted angles) is large: 60° – 40° = 20°.

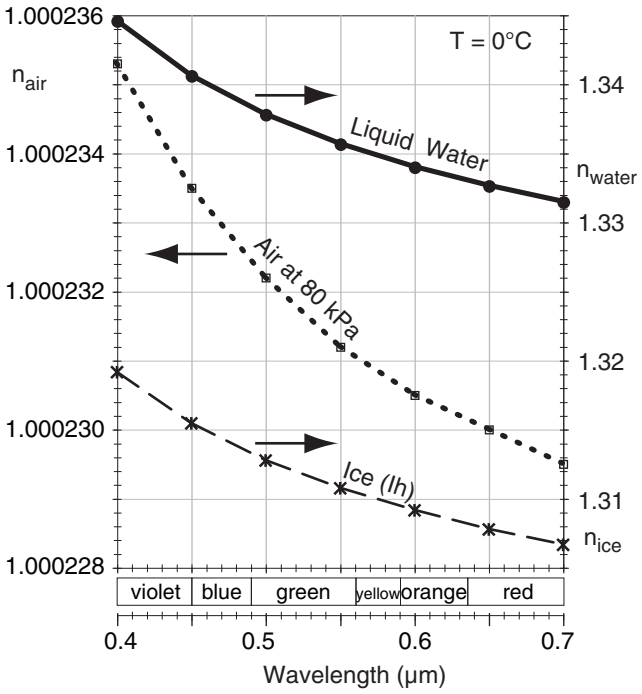

Figure 22.2
Refractive index n for various wavelengths of visible light at T = 0°C. See Table 22-1 for details. The wavelength bands that we perceive as different **colors** *is approximate, and is slightly different for each person. In this chapter we will use red ≈ 0.7 μm, orange ≈ 0.62 μm, yellow ≈ 0.58 μm, green ≈ 0.53 μm, blue ≈ 0.47 μm, and violet ≈ 0.4 μm wavelength.*

$$\theta_1 = \theta_3 \qquad \bullet(22.1)$$

The reflected angle does not depend on color (i.e., is not a function of the wavelength of light).

Refraction

Refractive index

The **refractive index** n_i for medium i relative to a vacuum is defined as:

$$n_i = \frac{c_o}{c_i} \qquad \bullet(22.2)$$

where c_i is the speed of light through medium i and $c_o = 3 \times 10^8$ m/s is the speed of light in a vacuum.

The ratio of refractive indices is sometimes defined as

$$\mu_{12} = \frac{n_1}{n_2} \qquad \bullet(22.3)$$

where subscripts 1 and 2 refer to the media containing the incident ray and refracted rays, respectively. Different colors and different media have different refractive indices, as indicated in Table 22-1 and Fig. 22.2.

Snell's Law

The relationship between the incident angle θ_1 and refracted angle θ_2 (Fig. 22.1) is called **Snell's Law**:

$$\frac{\sin\theta_1}{\sin\theta_2} = \frac{c_1}{c_2} = \frac{n_2}{n_1} = \frac{1}{\mu_{12}} \qquad \bullet(22.4)$$

Incident and refracted rays are always in the same plane. This plane includes the line that is normal to the surface. It is the plane that gives the smallest angle between the incident ray and the surface.

Solving Snell's Law for the refracted ray angle gives:

$$\theta_2 = \arcsin[\mu_{12}\cdot\sin(\theta_1)] \qquad (22.5)$$

Red light is bent less than violet light as it passes through an interface. Thus, refraction causes white light to be spread into a **spectrum** of colors. This phenomenon is called **dispersion**.

A viewer looking toward the incoming light ray (Fig. 22.3) would see a **light point** in the celestial sphere overhead at angle θ_2 from normal.

Table 22-1a. Refractive index (n_{air}) for **air** with pressure P = 101.325 kPa and relative humidity RH = 75%. *From NIST.*

λ (μm)	Temperature (°C)				
	–40	**–20**	**0**	**20**	**40**
0.4 violet	1.0003496	1.0003219	1.0002982	1.0002773	1.0002583
0.45	1.0003469	1.0003194	1.0002958	1.0002751	1.0002562
0.5	1.0003450	1.0003176	1.0002942	1.0002736	1.0002548
0.55	1.0003436	1.0003163	1.0002930	1.0002725	1.0002537
0.6	1.0003425	1.0003154	1.0002921	1.0002716	1.0002529
0.65	1.0003417	1.0003146	1.0002914	1.0002710	1.0002523
0.7 red	1.0003410	1.0003140	1.0002908	1.0002704	1.0002518

Table 22-1b. Refractive index (n_{air}) for **air** with P = 80 kPa and RH = 75%. *Based on data from NIST modified Edlen Eq. calculator.*

λ (μm)	Temperature (°C)				
	–40	**–20**	**0**	**20**	**40**
0.4 violet	1.0002760	1.0002541	1.0002353	1.0002188	1.0002036
0.45	1.0002738	1.0002521	1.0002335	1.0002171	1.0002019
0.5	1.0002723	1.0002507	1.0002322	1.0002158	1.0002008
0.55	1.0002712	1.0002497	1.0002312	1.0002150	1.0001999
0.6	1.0002704	1.0002489	1.0002305	1.0002143	1.0001993
0.65	1.0002697	1.0002483	1.0002300	1.0002138	1.0001988
0.7 red	1.0002692	1.0002479	1.0002295	1.0002134	1.0001984

Table 22-1c. Refractive index (n_{air}) for **air** with P = 40 kPa and RH = 75%. *Based on data from NIST modified Edlen Eq. calculator.*

λ (μm)	Temperature (°C)				
	–40	**–20**	**0**	**20**	**40**
0.4 violet	1.0001379	1.0001270	1.0001176	1.0001091	1.0001009
0.45	1.0001369	1.0001260	1.0001166	1.0001082	1.0001000
0.5	1.0001361	1.0001253	1.0001160	1.0001076	1.0000994
0.55	1.0001355	1.0001248	1.0001155	1.0001071	1.0000990
0.6	1.0001351	1.0001244	1.0001151	1.0001068	1.0000987
0.65	1.0001348	1.0001241	1.0001149	1.0001066	1.0000985
0.7 red	1.0001346	1.0001239	1.0001147	1.0001064	1.0000983

Table 22-1d. Refractive index (n_{water}) for **liquid water**. *Based on data from IAPWS 1997 release and CRC Handbook.*

λ (μm)	Temperature (°C)				
	–40	**–20**	**0**	**20**	**40**
0.4 violet	(values below	1.3429	1.3446	1.3436	1.3411
0.45	0°C are for	1.3390	1.3406	1.3396	1.3371
0.5	supercooled	1.3362	1.3378	1.3368	1.3344
0.55	water)	1.3341	1.3357	1.3347	1.3323
0.6		1.3324	1.3340	1.3330	1.3306
0.65		1.3310	1.3326	1.3317	1.3293
0.7 red		1.3299	1.3315	1.3305	1.3281
density (kg/m^3):		**993.547**	**999.840**	**998.207**	**992.200**

Table 22-1e. Refractive index (n_{ice}) for **ice (Ih)**. *Based on data from S.G. Warren (1984) and V.F. Petrenko & R.W. Whitworth (1999).*

λ (μm)	Temperature (°C)				
	–40	**–20**	**0**	**20**	**40**
0.4 violet	1.3206	1.3199	1.3192	(values at 0°C were extrapolated)	
0.45	1.3169	1.3162	1.3155		
0.5	1.3142	1.3135	1.3128	(See Focus Box in Precipitation	
0.55	1.3122	1.3115	1.3108	chapter for info on ice phases	
0.6	1.3106	1.3099	1.3092	such as Ih.)	
0.65	1.3092	1.3085	1.3078		
0.7 red	1.3081	1.3074	1.3067		

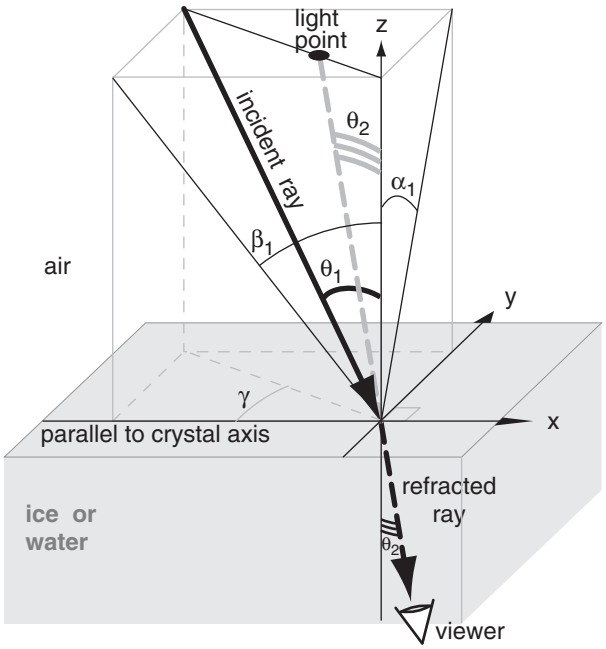

Figure 22.3
Components of refraction geometry. Incident ray is heavy solid arrow. Refracted ray is heavy dashed arrow. The tail (thick grey dashed line) of the refracted ray is extended to show that it lies in the same plane as the incident ray.

Solved Example

A ray of red light in air strikes a water surface, with incidence angle components of $\alpha_1 = 45°$ and $\beta_1 = 54.74°$. What are the corresponding component angles of the refracted ray? Assume $T = 20°C$ and $P = 101.325$ kPa.

Solution

Given: $\alpha_1 = 45°$, $\beta_1 = 54.74°$.
Find: $\alpha_2 = ?°$, $\beta_2 = ?°$

From Table 22-1 for red light:
$\mu_{12}^2 = (1.0002704/1.3305)^2 = (0.7518)^2 = 0.5652$
Also: $\tan(45°) = 1$, and $\tan(54.74°) = 1.414$
Next, solve eq. (22.8):

$$b_{\alpha\beta} = \frac{0.5652}{1+(1-0.5652)\cdot(1+2)} = 0.2453$$

Then use eqs. (22.7):
$\tan^2(\alpha_2) = 0.2453\cdot[\tan^2(45°)] = 0.2453$
$\tan^2(\beta_2) = 0.2453\cdot[\tan^2(54.74°)] = 0.4906$

Thus: $\alpha_2 = \arctan[(0.2453)^{0.5}] =$ **26.35°**
$\beta_2 = \arctan[(0.4906)^{0.5}] =$ **35.01°**

Check: Units OK. Physics OK.
Discussion: Using eq. (22.6) with the incident angle components of 45° and 54.74°, we find that the incident ray angle is $\theta_1 = \arctan[(1+2)^{0.5}] = 60°$. This is the same as a previous solved example. Using eq. (22.6) on the answers above, we find $\theta_2 = \arctan[(0.2453+0.4906)^{0.5}] =$ **40.62°**. This is also the same as a previous solved example, which verifies eqs. (22.6 - 22.9).

Solved Example

Find the speed of red light through liquid water and through air at $T = 20°C$ and $P = 101.325$ kPa.

Solution

Given: $\lambda = 0.7$ μm, $T = 20°C$ and $P = 101.325$ kPa.
Find: $c_{air} = ?$ m/s , $c_{water} = ?$ m/s

Use eq. (22.2) with refractive indices from Table 22-1:
$c_{air} = c_o/n_{air} = (3\text{x}10^8\text{m/s})/1.0002704 =$ **2.999x10^8 m/s**
$c_{water} = c_o/n_{water} = (3\text{x}10^8\text{m/s})/1.3305 =$ **2.255x10^8 m/s**

Check: Speeds reasonable. Units OK.
Discussion: The difference in speeds of light is useful for understanding Huygens' principle.

Snell's Law in 3 Dimensions

Sometimes it is easier to work with x and y components of the incident ray, where the x-axis might be aligned with the axis of a columnar ice crystal, for example, and the y-axis might be on the crystal prism surface (Fig. 22.3). The relationship between the component angles and the incident angle is:

$$\tan^2\theta_1 = \tan^2\alpha_1 + \tan^2\beta_1 \qquad (22.6)$$

This relationship also applies to refracted angles (θ_2, α_2, β_2), and will be used extensively later in this chapter to discuss ice-crystal optics.

Component angles α and β of the refracted and incident rays do NOT individually obey Snell's law (eq. 22.4). Nevertheless, Snell's law can be reformulated in terms of components as follows:

$$\tan^2\alpha_2 = b_{\alpha\beta}\cdot\tan^2\alpha_1 \qquad (22.7a)$$

$$\tan^2\beta_2 = b_{\alpha\beta}\cdot\tan^2\beta_1 \qquad (22.7b)$$

where α_2 and β_2 are the components of the refracted ray (analogous to α_1 and β_1), and

$$b_{\alpha\beta} = \frac{{\mu_{12}}^2}{1+(1-{\mu_{12}}^2)\cdot\left\{\tan^2\alpha_1+\tan^2\beta_1\right\}} \qquad (22.8)$$

These equations are abbreviated as

$$\alpha_2 = S_\alpha(\alpha_1,\beta_1,,\mu_{12}) = \arctan\left[\left(b_{\alpha\beta}\cdot\tan^2\alpha_1\right)^{1/2}\right] \qquad \bullet(22.9b)$$

$$\beta_2 = S_\beta(\alpha_1,\beta_1,,\mu_{12}) = \arctan\left[\left(b_{\alpha\beta}\cdot\tan^2\beta_1\right)^{1/2}\right] \qquad \bullet(22.9b)$$

where S represents Snell's law for components.

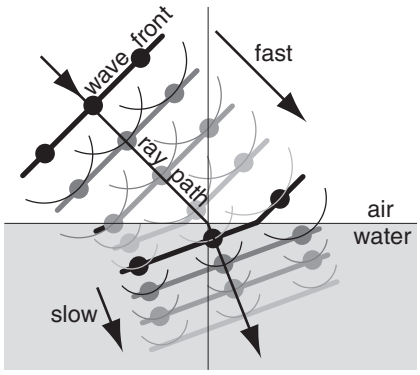

Figure 22.4
Propagation of wave fronts across an interface.

Huygens' Principle

Huygens suggested that every point along a wave front acts like a generator of new spherical secondary wavelets. Wave-front position after some time interval is located at the tangent to all of the new wavelets. Thus, when a portion of a wave front encounters a medium with a slower light velocity, then that portion of the wave slows, causing the whole wave front to turn into the medium (Fig. 22.4).

Critical Angle

When Snell's law is applied to light rays moving from a denser medium (having slower light velocity) to a less-dense medium (having faster light velocity), there is a **critical angle** at which light is bent so much that it follows the interface. At angles greater than this critical incidence angle, light cannot refract out of the dense medium at all. Instead, all of the light reflects (Fig. 22.5).

The critical angle θ_c is found from:

$$\sin(\theta_c) = \frac{n_2}{n_1} \qquad \bullet(22.10)$$

where n_1 is the refractive index for the incident ray (i.e., in the denser medium with slower light velocity). An example is a light ray moving out of water and into air (i.e., $n_2 < n_1$). For red light the critical angle is about 48.7°, while for violet light the it is about 48.1°. There is no critical angle for light moving into a denser medium (i.e., $n_2 > n_1$).

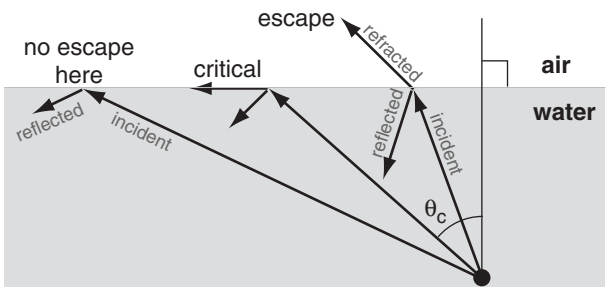

Figure 22.5
Angles greater than critical θ_c do not allow light to escape from a dense to less dense medium.

Solved Example

Find the critical angle for red light going from a cirrus-cloud ice crystal to air, where the air state is T = –20°C & P = 40 kPa.

Solution

Given: red light λ = 0.7 μm, T = –20°C & P = 40 kPa.
Find: θ_c = ? °

From Table 22-1: n_{ice} = 1.3074 and n_{air} = 1.0001239.
Use eq. (22.10):
θ_c = arcsin(1.0001239/1.3074) = **49.9°**.

Check: Magnitude OK. Units OK.
Discussion: This critical angle is close to that for liquid water, because the refractive indices for liquid and solid water are nearly the same.

LIQUID-DROP OPTICS

Most rain-drop water optics are found by looking away from the sun. **Rainbows** are circles or portions of circles (Fig. 22.6) that are centered on the **antisolar** point, which is the point corresponding to the shadow of your head or camera. (As viewed

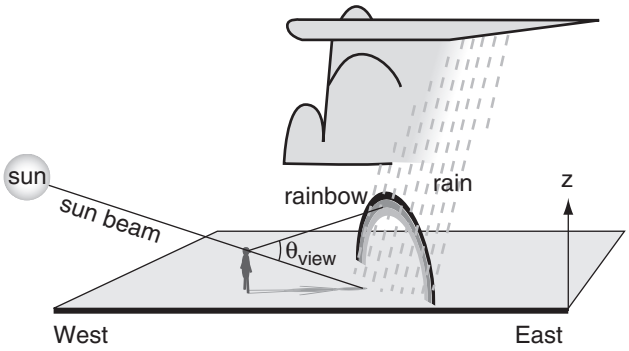

Figure 22.6
Orientation of rainbows relative to the observer and the sun.

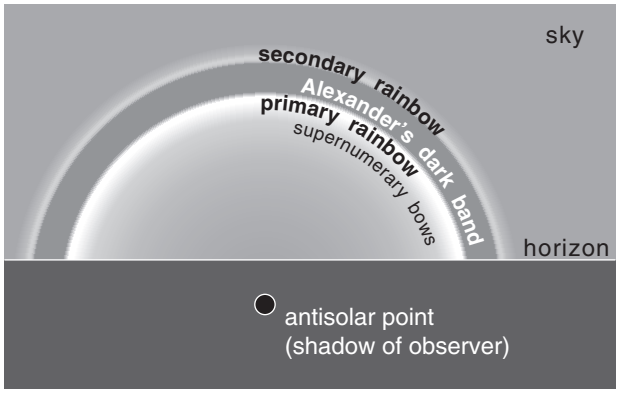

Figure 22.7
Rainbows.

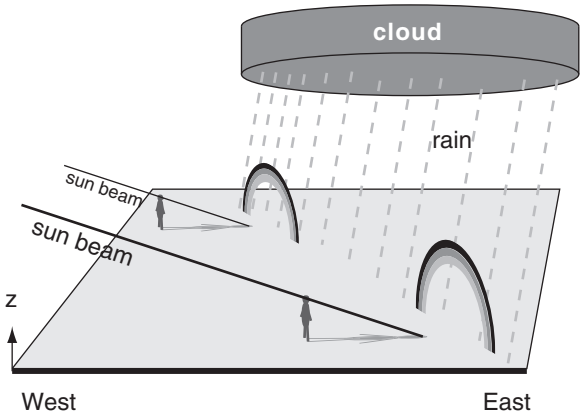

Figure 22.8
Different observers see different rainbows.

by the observer, the antisolar point is also called the sun's **antipodal point**.)

Primary rainbows have red on the outside of the circle, and are the brightest and most easily seen (Fig. 22.7). The **viewing angle** (θ_{view} = angle between two lines: the line from your eye to the rainbow and the line from your eye and the antisolar point) is about 42°. **Secondary rainbows** have red on the inside at viewing angle of about 50°. **Supernumerary bows** are very faint, and touch the inside of the primary rainbow — these will be discussed in the Diffraction and Interference section.

At any one time for any one rain storm, different observers see different rainbows caused by different light rays interacting with different rain drops (Fig. 22.8). Hence, one observer in a region of bright sun and large drops might see a vivid rainbow, while another observer a half kilometer away might see only a weak or partial rainbow in light rain with smaller drops.

We can explain these rainbow phenomena using geometric optics, assuming spherical rain drops. First, we will consider the portion of incident sunlight that is lost due to reflection off the outside of the drop. Then we will look at the remainder that is refracted and reflected in the drop to make the rainbow.

Reflection from Water

Rays of light that hit a water surface at a shallow angle are reflected more than those hitting straight on. Reflectivity r vs. elevation angle Ψ above the water surface is approximately:

$$r = r_o + r_1 \cdot e^{-\Psi/a} \qquad (22.11)$$

where $r_o = 0.02$, $r_1 = 0.98$, and $a = 9.3°$. This is plotted in Fig. 22.9.

Solved Example

Just after sunrise, sunlight hits a smooth lake surface at elevation angle 5°. Find the reflectivity.

Solution

Given: $\Psi = 5°$

Find: r = ? (dimensionless)

Use eq. (22.11):

$r = 0.02 + 0.98 \cdot \exp(-5°/9.3°) =$ **0.59**

Check: Units dimensionless. Magnitude agrees with Fig. 22.9.

Discussion: 59% of incident sunshine in this case is reflected away, and is not available to heat the lake.

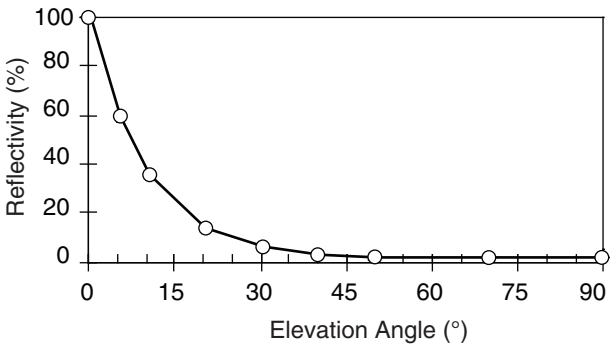

Figure 22.9
Reflectivity from a water surface as a function of ray elevation angle.

Solved Example

For a light ray hitting a spherical rain drop at a distance from the center of 90% of the drop radius, find the elevation angle and the fraction of light reflected.

Solution:
Given: $x/R = 0.9$
Find: Ψ = ?°, and r = ? dimensionless

Use eq. (22.12): $\Psi = \arccos(0.9) = 25.8°$
Use eq. (22.11): $r = 0.02 + 0.98 \cdot \exp(-25.8°/9.3°) =$ **0.081**

Check: Units OK. Magnitude agrees with Fig. 22.9.
Discussion: Even at this large impact parameter, only 8% of the light is reflected off the outside.

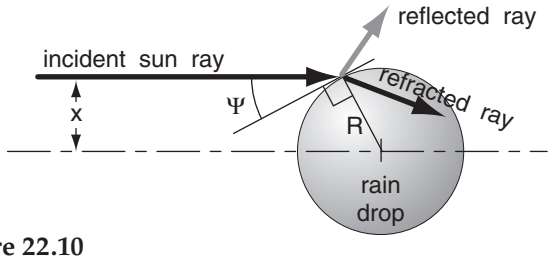

Figure 22.10
Fate of incident ray after first impact with drop.

Rays of sunlight can enter a spherical drop at any distance x from the centerline (Fig. 22.10). The ratio of this distance to the drop radius R is called the **impact parameter** (x/R). Because of curvature of the drop surface, rays arriving at larger impact parameters strike the drop at smaller elevation angles:

$$\psi = \arccos\left(\frac{x}{R}\right) \qquad \bullet(22.12)$$

Thus, the amount of reflected light from a drop increases with increasing impact parameter.

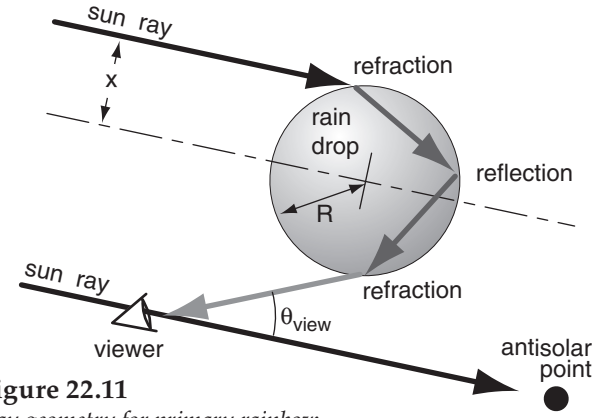

Figure 22.11
Ray geometry for primary rainbow.

Primary Rainbow

Rays that are not reflected from the outside of the drop can make zero or more reflections inside the drop before leaving. Those entering rays that make one reflection (in addition to the two refractions during entry and exit) cause the **primary rainbow** (Fig. 22.11). White light is dispersed by the refractions such that reds are bent less and appear on the outside of the rainbow circle, while violets are bent more and appear on the inside (Fig. 22.12).

Variations of impact parameter cause a range of output viewing angles θ_{view} according to:

$$\theta_{view} = 4 \cdot \arcsin\left(\frac{n_{air}}{n_{water}} \cdot \frac{x}{R}\right) - 2 \cdot \arcsin\left(\frac{x}{R}\right) \qquad \bullet(22.13)$$

where x/R is the impact parameter, and n is refractive index. In other words, there is not a single magic angle of 42° for the primary rainbow. Instead, there is a superposition of many rays of different colors with a wide range of viewing angles.

To learn how these rays interact to form the rainbow, we can solve eq. (22.13) on a spreadsheet for a large number of evenly spaced values of the impact parameter, such as intervals of 0.02 for x/R. Output

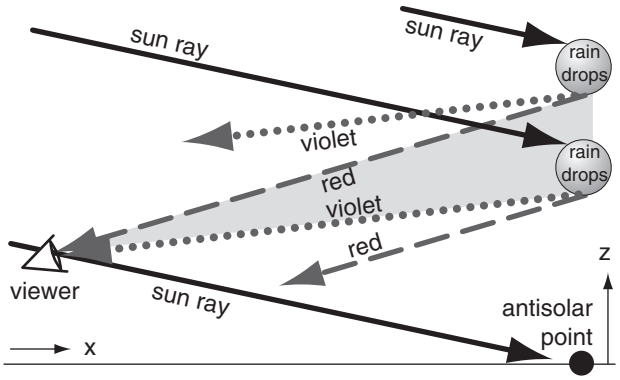

Figure 22.12
Viewer sees primary rainbow (shaded) with red light coming from drops further from the antisolar point than for violet. Thus, the different colors you see come from different drops.

Solved Example

For red light calculate the primary-rainbow viewing angle for x/R= 0.70 in air of P= 80 kPa and T= 0°C.

Solution
Given: $x/R = 0.70$
$n_{air} = 1.0002295$, $n_{water} = 1.3315$ from Table 22-1.
Find: θ_{view} = ?°
Use eq. (22.13) for the primary rainbow:
$\theta_{view} = 4 \cdot \arcsin(0.7512 \cdot 0.70) - 2 \cdot \arcsin(0.70) =$ **38.05°**

Check: Units OK. Physics OK. Agrees with Fig. 22.13.
Discussion: This lights inside the primary rainbow.

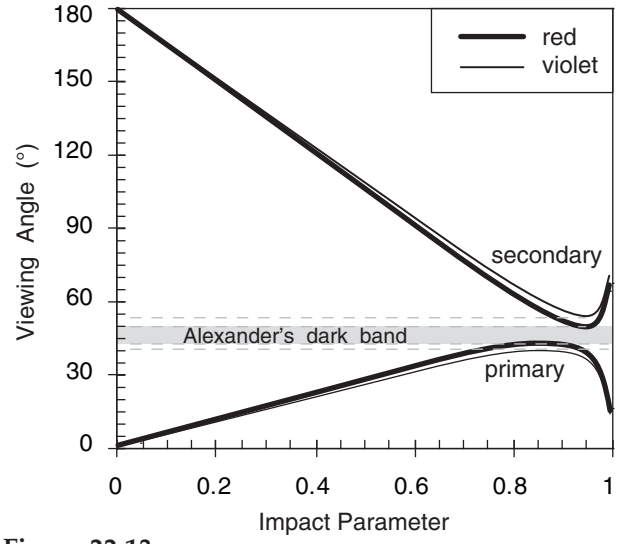

Figure 22.13a
Viewing angles for rainbow rays.

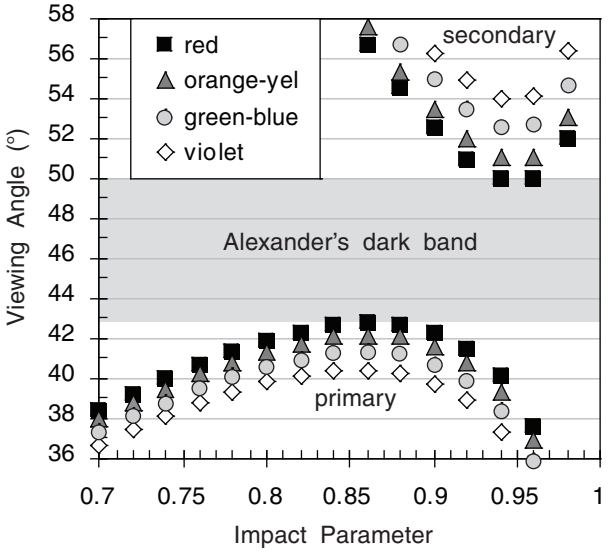

Figure 22.13b
Viewing angles for rainbow rays (expanded version).

Solved Example

For red light calculate the secondary-rainbow viewing angle for x/R= 0.90, with P= 80 kPa and T= 0°C.

Solution

Given: $x/R = 0.90$

$n_{air} = 1.0002295$, $n_{water} = 1.3315$ from Table 22-1.

Find: $\theta_{view} = ?°$

Use eq. (22.14) for the primary rainbow:

$\theta_{view} = 180° + 2\cdot\arcsin(0.90) - 6\cdot\arcsin(0.7512 \cdot 0.90)$

$= \underline{\mathbf{53.09°}}$

Check: Units OK. Physics OK.

Discussion: This almost agrees with Fig. 22.13, which was created for a slightly different T and P.

viewing angles, measured from the antisolar point, range between 0° and 42.7°, as plotted in Fig. 22.13a. This is why the sky is brighter inside the primary rainbow (i.e., for viewing angles of 0 to 42.7°), than just outside of it.

Fig. 22.13b is a blow-up of Fig. 22.13a. Three of the data points have a viewing angle of about 42.5°, and these all correspond to rays of red light. Hence, the primary rainbow looks red at that viewing angle. At 42.0°, there are mostly orange-yellow data points, and just a couple red points. Hence, at this angle the rainbow looks orange. Similar arguments explain the other colors. Inside the primary rainbow the sky looks white, because roughly equal amounts of all colors are returned at each viewing angle.

Secondary Rainbow

Entering light rays can also make two reflections before leaving the raindrop, as sketched in Fig. 22.14. The extra reflection reverses the colors, putting red on the inside of the circle of a **secondary rainbow**. At each internal reflection some light is lost (refracted) out of the drop. Thus, the secondary rainbow is faint -- only 43% as bright as the primary rainbow.

The relationship between impact parameter and viewing angle for a secondary rainbow is:

•(22.14)

$$\theta_{view} = 180° + 2\cdot\arcsin\left(\frac{x}{R}\right) - 6\cdot\arcsin\left(\frac{n_{air}}{n_{water}}\cdot\frac{x}{R}\right)$$

where x/R is the impact parameter, and n is refractive index. Again, a range of output viewing angles occurs because light enters over the full range of impact parameters. In this case, the sky is dark inside of the secondary rainbow (about 50° viewing angle), and bright outside, as sketched in Figs. 22.13a & b, based on spreadsheet calculations.

Higher-order rainbows (having more internal reflections) are theoretically possible, but are rarely seen because they are so faint:

- **Tertiary Rainbow**:
  3 internal reflections
  $\theta_{view} = 137.52°$
  intensity ≈ 24% as bright as the primary
- **Quaternary Rainbow**:
  4 internal reflections
  $\theta_{view} = 137.24°$
  intensity ≈ 15% as bright as the primary
- **5th Order Rainbow**:
  5 internal reflections
  $\theta_{view} = 52.9°$
  very faint

Viewing angles for tertiary and quaternary rainbows are 43° from the sun (i.e., not from the antisolar point). Hence, their faint presence is washed out

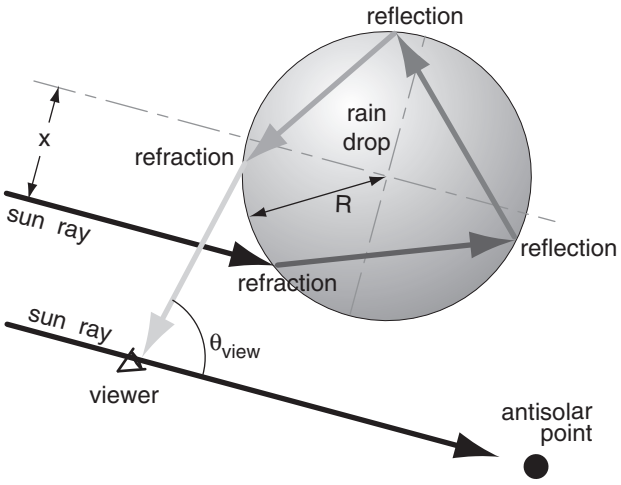

Figure 22.14
Ray geometry for secondary rainbow.

by the intense zero-order glow from the sun. **Zero-order glow** is light from the sun passing through a raindrop with no internal reflections while en route to the observer.

Alexander's Dark Band

Neither the primary nor secondary rainbows return light in the viewing-angle range between 42.7° and 50°. Hence, the sky is noticeably darker between these rainbows (Figs. 22.7 & 22.13). This dark region is called **Alexander's dark band**, after Greek philosopher Alexander of Aphrodisias who described it during the third century A.D.

Other Rainbow Phenomena

Larger diameter raindrops cause more vivid, colorful rainbows. But as discussed in the Remote Sensing chapter, large raindrops are often not spherical. A mixture of large non-spherical drops (oblate spheroids the shape of hamburger buns) and moderate size spherical drops causes cause **twinned rainbows**, where the top of the rainbow circle splits into two rainbows (Fig. 22.15a).

Sea-spray rainbows are about 0.8° smaller radius than normal rainbows, because of greater refraction by salt water. Near sunset, the blue-diminished sunlight illuminates raindrops with reddish light, creating **red bows** with enhanced red and orange bands. Faint rainbows (**moon bows**) can also be created by moonlight at night.

Reflection rainbows form when the incident sunlight bounces off a lake before hitting the raindrops (Fig. 22.15b). This bow is centered on the **anthelic point**, which is as high above the horizon as the antisolar point is below, but at the same azimuth.

FOCUS • Rainbows and the Renaissance

German monk Theodoric von Freiberg created a physical model of rainbow physics in 1304 by filling a glass sphere with water. By carefully shining light through it at different impact parameter values, he could measure the various output angles. However, the physics behind these observations were not explained until the renaissance, after Willebrod Snell van Royen had discovered the law for refraction in the early 1600's.

Twenty years after Snell's discovery, Descartes used it to demonstrate the capabilities of his scientific method by mathematically solving the rainbow problem. His calculations were very similar to our spreadsheet calculations, except that he manually performed calculations for a large number of different impact parameters. Through these repetitive "brute-force" calculations he verified the magic number of 42° for the brightest returned light, and 50° for the secondary rainbow.

About 30 years later, Newton applied his knowledge of color dispersion to explain why the rainbow has colors. Also, he was able to use his invention of calculus to elegantly derive the magic angle of 42°.

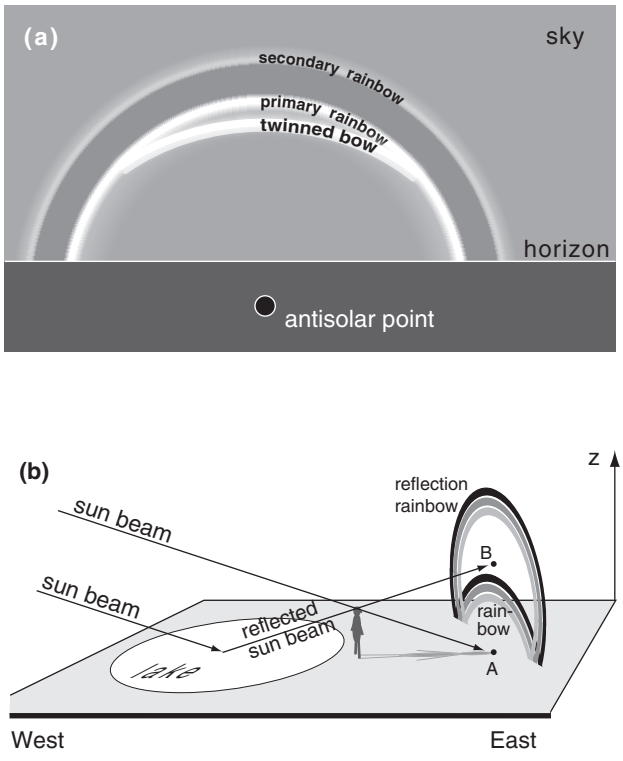

Figure 22.15
(a) Twinned primary rainbow (twinned bow) inside the normal primary rainbow, caused by large oblate rain drops. (b) Reflection rainbow caused by sunlight reflecting from a lake or ocean before reaching the falling raindrops. The reflection bow is a circle centered on the anthelic point (B), while the normal primary rainbow circle is centered on the antisolar point (A).

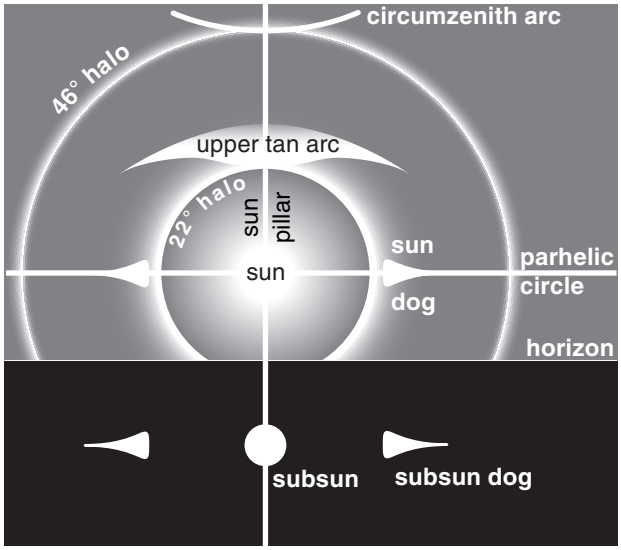

Figure 22.16
Some of the more common halos and other optical phenomena associated with ice crystals in air.

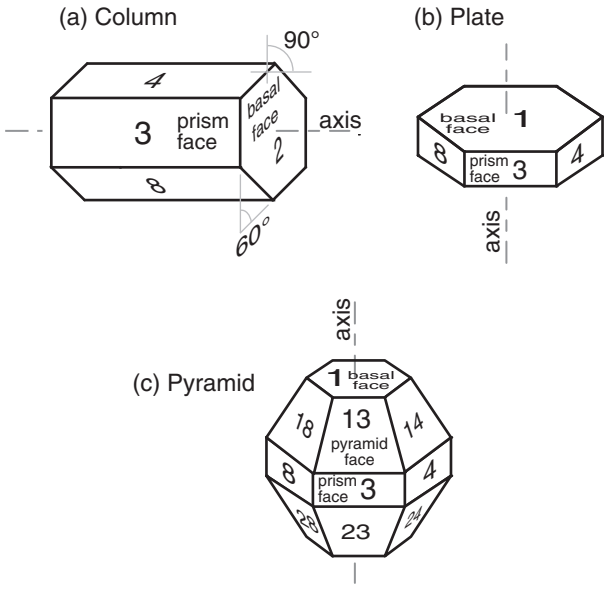

Figure 22.17
Ice-crystal geometry relevant to atmospheric optics. The angles highlighted in (a) are known as **wedge angles**, β_c, *which correspond to the angles of a prism that would yield the refraction as discussed in this section. There are many different wedge angles (not shown here) between different faces of the pyramid.*

ICE CRYSTAL OPTICS

Most of the common ice-crystal optical phenomena are seen by looking more-or-less toward the sun (Fig. 22.16). To observe them, shield your eyes from the direct rays of the sun to avoid blinding yourself. Also, wear sunglasses so your eyes are not dazzled by the bright sky close to the sun.

Subsuns, sun pillars, and parhelic circles are caused by simple reflection from the outside surface of ice crystals. Reflections from inside the ice crystal can also contribute to the intensity of these phenomena.

Sundogs, halos, circumzenith arcs, and tangent arcs are caused by refraction through the ice crystals, with the red color closest to the sun.

Subsun dogs are caused by both refraction and reflection in the ice. There are many other optical phenomena related to ice crystals, only a few of which we cover here.

Ice crystals (types of snow) can form as high-altitude cirrus clouds, can be naturally seeded within and fall from the base of mid-altitude water-droplet clouds, can grow within low- or mid-altitude cloudless cold air of high relative humidity, or can be stirred up by the wind from fresh surface snow. For all these situations, the best optical displays occur with a diffuse concentration of crystals in the air. Namely, the air looks mostly or partially clear, except for sparkles of light reflected from the sparsely spaced crystals (nicknamed **diamond dust**).

The crystals have a variety of shapes, most with hexagonal cross section (see Figs. 7.12 and 7.13 in the Precipitation chapter). The two shapes most important for atmospheric optical phenomena are the **hexagonal column** and **hexagonal plate** (Fig. 22.17). The plate is just a very short column. **Hexagonal pyramid**-capped columns cause rarer halos.

Plates or columns, if larger than about 30 μm, gently fall through the air with the **orientation** relative to horizontal as sketched in Fig. 22.17. Namely, the crystal axis of large columns is nearly parallel to the ground, and the axis of large plates is nearly vertical. Surprisingly, this natural orientation is associated with relatively high aerodynamic drag on the falling crystal. Smaller crystals tend to tumble as they fall, giving random orientations.

Crystal faces are numbered as shown in Fig. 22.17, where **basal faces** numbered 1 and 2 mark the ends of the hexagonal column, and **prism faces** 3 - 8 wrap sequentially around the sides. In naming the relative positions of prism faces: 4 and 3 are examples of **adjacent** faces, 4 and 8 are **alternate** faces, while 4 and 7 are **opposite** faces. **Pyramid faces** are numbered as double digits, where the first

digit indicates the number of the adjacent basal face, and the second digit indicates the number of the adjacent prism face. The numbering is useful to track ray paths.

As shown in Fig. 22.17, the most important **wedge angles** (β_c) of plate and column crystals are 60° (such as between faces 3 and 7, or 4 and 8) and 90° (such as between faces 3 and 1, or between 4 and 2). Angles for pyramids are discussed later.

Sun Pillar

A sun pillar is a vertical column of light that appears to come out of the top (and sometimes the bottom) of the sun (Fig. 22.16). It forms when sunlight reflects off the outside of any of the following nearly-horizontal faces:

- prism faces of large oriented column ice crystals (such as off of face 8 in Fig. 22.18a),
- basal faces of fluttering large oriented plates (such as off face 2 in Fig. 22.18b), or
- basal faces of large oriented **dendrites** (6-armed snowflake plates) (such as off the bottom of the snowflake in Fig. 22.18d).

These crystals act like myriad tiny mirrors.

Internal reflections can contribute to the intensity of sun pillars. In the example of Fig. 22.18c, light enters the ice crystal (with refraction) through face 5, then reflects from the inside of the crystal at face 1, and leaves (with refraction) from face 8.

An end view of this phenomenon for reflection from oriented hexagonal columns is sketched in Fig. 22.19. Column crystals are free to rotate about their column axis as they gently fall to Earth, and flat plates and dendrites have random wobble of their axes causing them to flutter like leafs when they fall. As a result, some of the ice crystals have faces that by chance reflect the sunlight to your eye, while other ice crystals reflect the sunlight elsewhere.

Relatively few sunbeams reflect to your eye, causing the sun pillar to be very faint. The best time to observe sun pillars is at sunrise or sunset when the sun is hidden just below the horizon, but is still able to illuminate the ice precipitation. Sun pillars often appear to be red not because of refraction in the crystal, but because light from the rising or setting sun has lost much of its blue components due to scattering from air molecules before it reaches the ice crystals.

Similar pillars can form above and below:

- bright street lights
- the moon and bright planets (e.g., Venus) and
- other bright lights, such as aircraft lights,

and these pillars often have the same color as the light source.

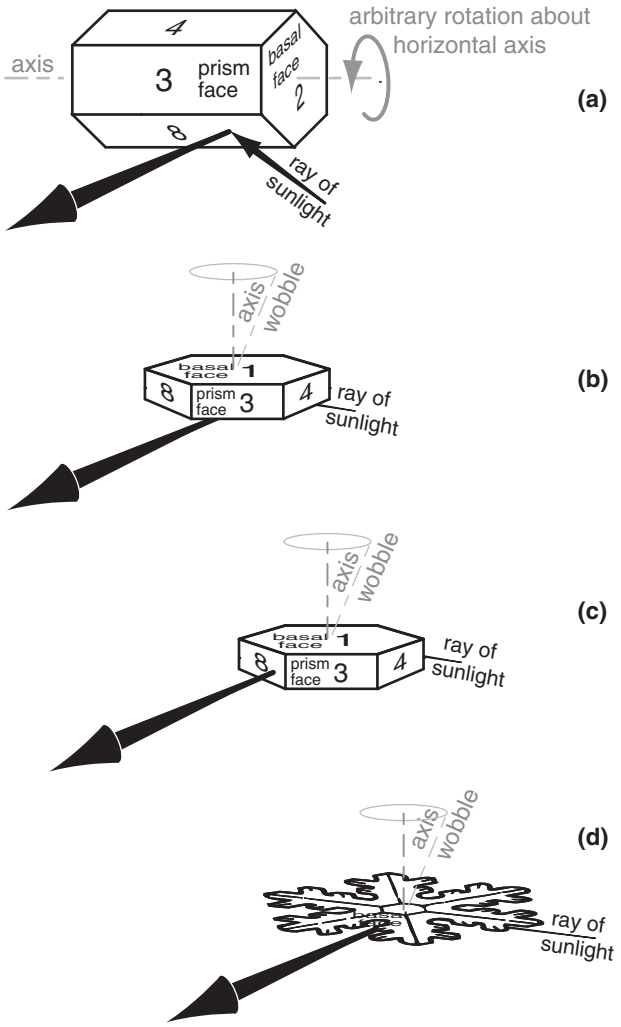

Figure 22.18
Sun-pillar optics caused by reflection of sunlight off the faces of large (a) oriented ice columns, (b & c) oriented plates, and (d) oriented dendrites.

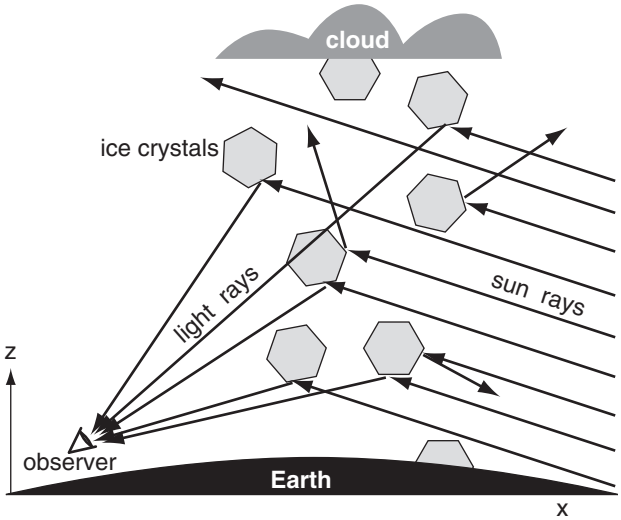

Figure 22.19
Geometry of sun pillar optics (end view) reflecting from oriented large hexagonal-column ice crystals (size is exaggerated).

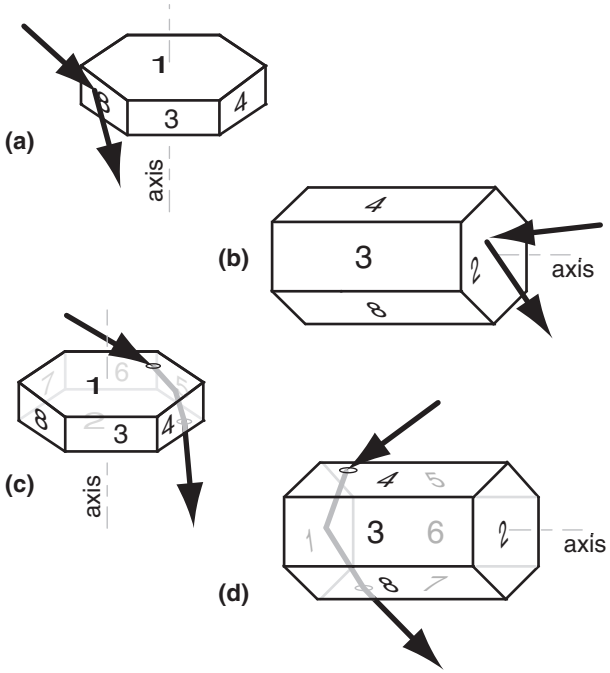

Figure 22.20
Ray geometry of parhelic-circle optics, showing some of the possible external and internal reflections. Small ovals indicate points where light rays enter or leave the ice crystal.

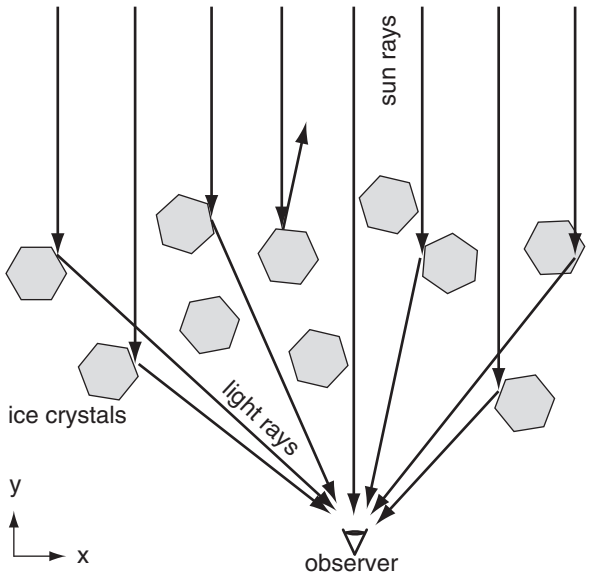

Figure 22.21
Reflection from many large hexagonal plates (size is exaggerated) to form a parhelic circle (top or plan view).

Parhelic Circle

The parhelic circle is a horizontal band of white light extending left and right through the sun (Fig. 22.16). It can be formed by external reflection off of the vertical faces of large hexagonal plates (e.g., face 8 in Fig. 22.20a) or large hexagonal columns (e.g., face 2 in Fig. 22.20b). It can also be formed by internal reflection off of similar vertical faces, such as the ray path touching faces 1 5 2 in Fig. 22.20c, or the path touching faces 4 1 7 in Fig. 22.20d.

These crystals can have any rotation orientation about their axis, causing reflections from many different ice crystals to reach your eye from many different angles left and right from the sun (Fig. 22.21). In other words, they act as a large number of small mirrors.

Subsun

The subsun is a spot of white light seen below the horizon (Fig. 22.16), as viewed looking down from a bridge, mountain, or aircraft. It forms by external reflection of sunlight off of the top surfaces of large hexagonal plates (face 1 in Fig. 22.22a), and by internal reflection (face 2 in Fig. 22.22b; namely, the ray touches faces 7 2 4). If all the hexagonal plates are oriented horizontally, they act as mirrors to produce a simple reflection of the sun (Fig. 22.23). As given by eq. (22.1), the subsun appears the same angle θ_3 below the horizon that the sun is above θ_1.

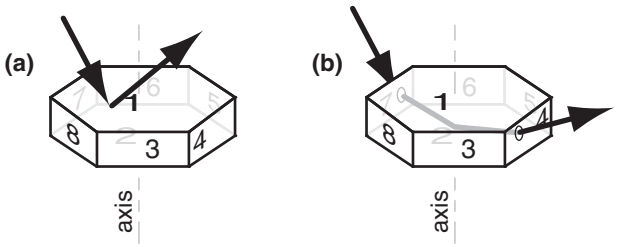

Figure 22.22
Ray geometry of subsun optics. Small ovals indicate points where light rays enter or leave the ice crystal.

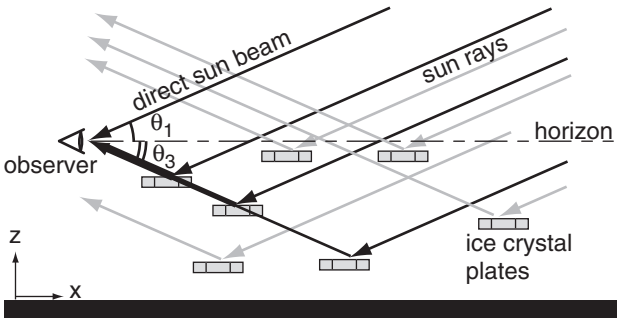

Figure 22.23
Reflection from many ice-crystal plates to form a subsun (side view). Grey rays reach someone else's eyes.

22° Halo

Optics for 22° halos (Fig. 22.16) are not as simple as might be expected. Small ice-crystal columns are free to tumble in all directions. As a result, light rays can enter the crystal at a wide range of angles, and can be refracted over a wide range of sky.

The brightest light that we identify as the halo is caused by refraction through those ice crystals that happen to be oriented with their column axis perpendicular to the sun rays (Fig. 22.24). We will study this special case. Different crystals can nevertheless have different rotation angles about their axis (the dark point in the center of the ice crystal of Fig. 22.24). As a result, the angle of incidence θ_1 can vary from crystal to crystal, thereby causing different viewing (output) angle θ_2 values.

For hexagonal crystals (for which the **wedge angle** is $\beta_c = 60°$) and for the special case of light rays approaching normal to the column axis, Snell's law yields:

$$\theta_2 = \theta_1 - \beta_c + \arcsin\left\{\frac{n_{ice}}{n_{air}} \cdot \sin\left[\beta_c - \arcsin\left(\frac{n_{air}}{n_{ice}} \cdot \sin\theta_1\right)\right]\right\} \quad \bullet(22.15)$$

where n is refractive index.

The 22° halo observed by a person is the result of superposition of rays of light from many ice crystals possessing many different rotation angles. Hence, it is not obvious why 22° is a magic number for θ_2. Also, if refraction is involved, then why are the red to yellow colors seen most vividly, while the blues and violets are fading to white?

To answer these questions, suppose ice crystals are randomly rotated about their axes. There would be an equal chance of finding an ice crystal having any incidence angle θ_1. We can simulate this on a computer spreadsheet by doing calculations for a large number of evenly-spaced incidence angles (for example, every 2°), and then calculating the set of θ_2 angles as an outcome. The result is plotted in Fig. 22.25 for two of the colors (because n_{air}/n_{ice} varies with color).

Colors and angles of a 22° halo can be explained using Fig. 22.26 (which is a zoomed view of Fig. 22.25). For viewing (output) angles less than about 21.6°, there is no refracted light of any color; hence, the halo is dark inside (the edge closest to the sun).

In the range of viewing angles averaging 22° (i.e., from 21.6° to 22.6°), there are 29 data points plotted in Fig. 22.26, which cause the bright ring of light we call the halo. There are also data points at larger angles, but they are more sparse — causing the brightness of the halo to gradually fade at greater viewing angles from the sun.

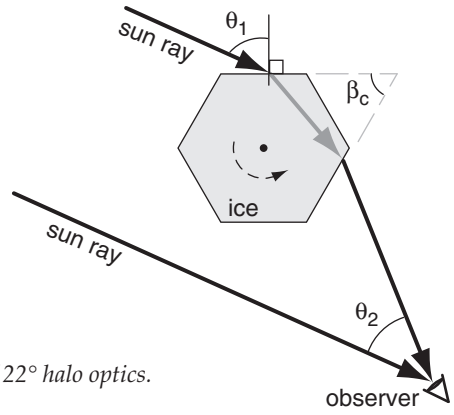

Figure 22.24
Ray geometry of 22° halo optics.

Solved Example

What is θ_2 if $\theta_1 = 80°$ and $\beta_c = 60°$ for red light in a 22° halo? $T = -20°C$, $P = 80$ kPa, $RH = 75\%$.

Solution

Given: $\theta_1 = 80°$. $\beta_c = 60°$. $\lambda = 0.7$ μm for red light.
$n_{air} = 1.0002479$, $n_{ice} = 1.3074$ from Table 22-1.
Find: $\theta_2 = ?°$

Use eq. (22.15) with $\beta_c = 60°$ for hexagonal crystal:

$$\theta_2 = 80° - 60° + \text{asin}\left\{\frac{1.3074}{1.0002479} \cdot \sin\left[60° - \text{asin}\left(\frac{1.0002479}{1.3074} \cdot \sin 80°\right)\right]\right\}$$

$$= 80° - 60° + 14.59° = \underline{\mathbf{34.59°}}$$

Check: Units OK. Physics OK.
Discussion: Quite different from 22°, but agrees with Fig. 22.25. Namely, this is one of the light rays that contributes to the bright glow outside the 22° halo, as sketched in Fig. 22.16.

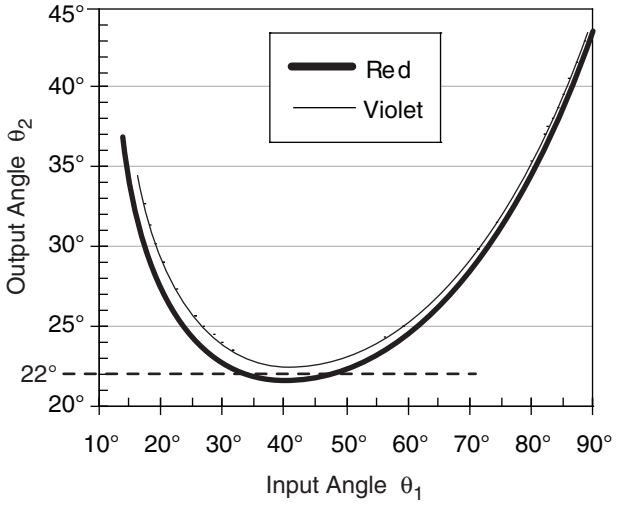

Figure 22.25
Viewing (output) angles θ_2 from hexagonal ice crystals in a 22° halo, for various incident angles θ_1 of sunlight.

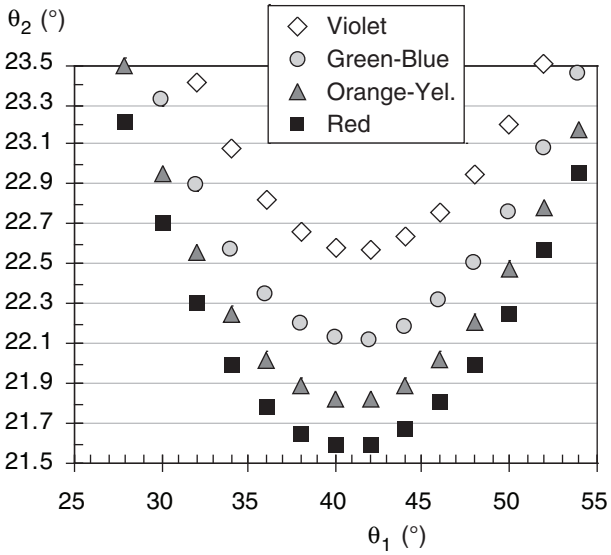

Figure 22.26
Blow-up of viewing (output) angles θ_2 from hexagonal ice crystals in a 22° halo, for various incident angles θ_1.

Solved Example
Find $\theta_{2\min}$ for green-blue light for wedge angle 60°.

Solution
Given: $\beta_c = 60°$, $n_{ice} = 1.3135$ for blue-green (λ=0.5 μm).
Find: $\theta_{2\min} = ?\,°$. (Assume $T = -20°C$ & $n_{air} \approx 1.0$.)

Use eq. (22.16): $\theta_{2\min} = 2\cdot\arcsin[1.3135\cdot\sin(30°)] - 60°$
$= 82.10° - 60° = \underline{\mathbf{22.10°}}$

Check: Agrees with Table 22-2.
Discussion: The different colors of the 22° halo are not all at exactly 22°.
CAUTION: If you do these angle calculations on a spreadsheet, don't forget to convert to/from radians for the sine/arcsine terms.

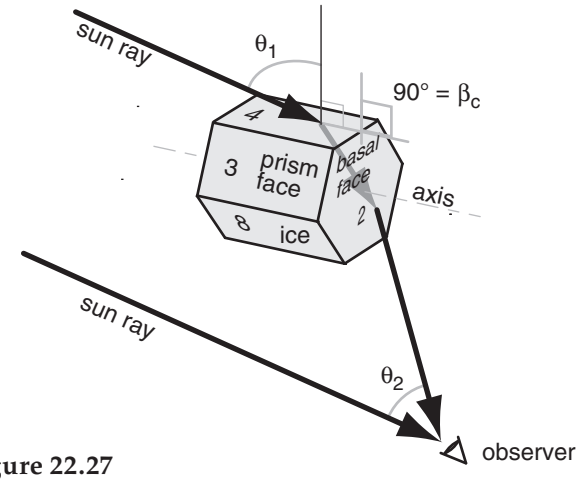

Figure 22.27
Ray geometry for 46° halo.

For a viewing angle range of $\theta_2 = 21.5°$ to 21.7°, we see four "red light" data points in Fig. 22.26, but no other colors. Thus, the portion of the halo closest to the sun looks bright red. In the next range of viewing angles (21.7° - 21.9°), we see four "yellow-orange" and two "red" data points. Thus, in this range of viewing angles we see bright orange light.

In the angle range 22.1 - 22.3°, there are four blue-green data points, and two orange-yellows and two reds. These colors combine to make a bluish white color. By an angle of 23° , there are roughly equal portions of all colors, creating white light. Thus, the colors of a 22° halo can have bright reds, oranges, and yellows on the inside, fading to light green and bluish-white further away from the sun.

The **minimum viewing angle** is the angle for which the halo gets its name, and can be found from:

$$\theta_{2\,\min} = 2\cdot\arcsin\left[\frac{n_{ice}}{n_{air}}\cdot\sin\left(\frac{\beta_c}{2}\right)\right] - \beta_c \qquad (22.16)$$

where β_c is wedge angle and n is refractive index. This is at the bottom of the curves in Fig. 22.26.

46° Halo

The 46° halo (Fig. 22.16) forms by sun rays shining through a prism face and a basal end of short hexagonal columns (Fig. 22.27). Equations (22.15 and 22.16) apply, but with an ice wedge angle β_c = 90°. The resulting viewing angles θ_2 are shown in Fig. 22.28 for a variety of input angles θ_1. Except for the different radius, this halo has visual characteristics similar to those of the 22° halo. But it is faint, and less frequently seen.

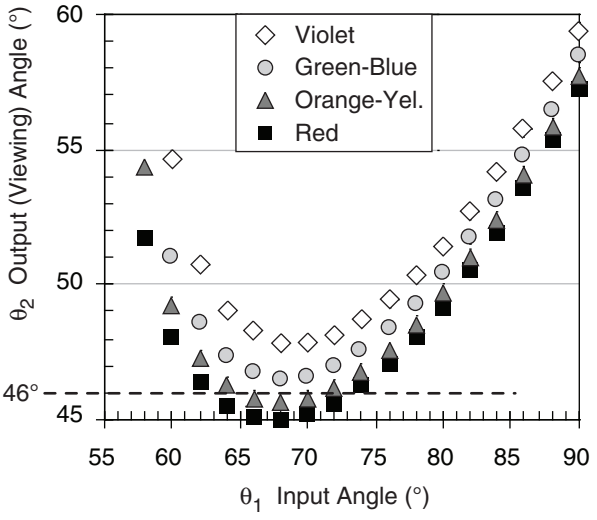

Figure 22.28
Viewing (output) angles for a 46° halo.

Solved Example

Find the viewing angle θ_2 for a 46° halo, given input angle $\theta_1 = 80°$ and $\beta_c = 90°$ for red light.

Solution

Given: $\theta_1 = 80°$, $\beta_c = 90°$. $\lambda = 0.7$ μm for red light.
Find: $\theta_2 = ?°$
Assume: $n_{air} = 1.0002479$, $n_{ice} = 1.3074$ from Table 22-1.

Use eq. (22.15):

$$\theta_2 = 80° - 90° + \text{asin}\left\{\frac{1.3074 \cdot \sin}{1.0002479}\left[90° - \text{asin}\left(\frac{1.0002479}{1.3074} \cdot \sin 80°\right)\right]\right\}$$

$$= \underline{\mathbf{49.25°}}$$

Check: Units OK. Physics OK.
Discussion: This agrees with Fig. 22.28.

Halos Associated with Pyramid Crystals

Ice crystals with pyramid ends (Fig. 22.17c) have a wide variety of wedge angles depending on the path of the light ray through the crystal. This can cause additional halos of differing radii centered on the sun (Fig. 22.29).

Table 22-2 lists the ray path, wedge angle, and minimum viewing angle (from eq. 22.16) for some of these odd-radius halos. The 9° halo is often hard to see against the glare close to the sun, while the 18°, 20°, 23°, and 24° halos might be mis-reported as 22° halos unless accurate measurements are made. Nonetheless, most of the rare halos have been observed and photographed.

Table 22-2. Halo viewing angles (θ_{2min}) found from eq. (22.16). Ray paths refer to the face numbers in the Fig. at right. β_c = wedge angle of ice crystal (from *W. Tape & J. Moilanen, 2006: "Atm. Halos & the Search for Angle x"*. $n_{air} \approx 1.0$

	color =	red	yellow orange	green blue	violet
	wavelength (μm) =	0.7	0.6	0.5	0.4
	(For T = –20°C) n_{ice} =	1.3074	1.3099	1.3135	1.3199

Halo Name	β_c (°)	Ray Path	Minimum **Halo Viewing Angles** (°)			
9°	25	18 · 5	8.88	8.95	9.06	9.24
18°	52.4	18 · 24	18.11	18.27	18.49	18.89
20°	56	18 · 15	19.73	19.90	20.14	20.58
22°	60	8 · 4	21.64	21.83	22.10	22.59
23°	62	18 · 7	22.65	22.85	23.14	23.66
24°	63.8	18 · 4	23.60	23.81	24.11	24.65
35°	80.2	18 · 14	34.53	34.87	35.37	36.26
46°	90	1 · 3	45.18	45.71	46.49	47.91

Science Graffito

"The skipper he stood beside the helm,
His pipe was in his mouth,
And he watched how the veering flaw did blow
The smoke now West, now South.
Then up and spake an old Sailor
Had sailed to the Spanish Main,
'I pray thee, put into yonder port,
For I fear a Hurricane.
Last night **the moon had a golden ring**,
And tonight no moon we see!'
The skipper he blew a whiff from his pipe,
And a scornful laugh laughed he."
– by Henry Wadsworth Longfellow, from
The Wreck of the Hesperus.

FOCUS • Estimating 22° Angles

For most people, if you extend your arm fully and open your hand as widely as possible, then the angle that you see subtended by your hand is about 22°. This works for people of different sizes, because hand size and arm length are often proportional.

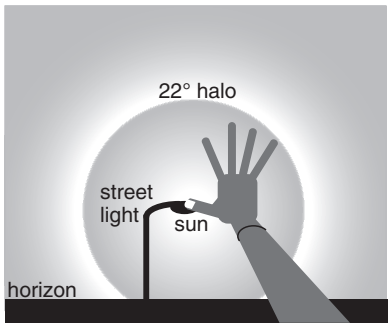

Fig. 22.a

To view halos, first move so that the sun is hidden behind an obstacle such as a street light, stop sign, or a corner of a building, so you don't blind yourself. Then extend your arm and stretch your hand, and position the tip of your thumb over the location where the center of the sun would be (hidden behind the obstacle). The tip of your little finger should just touch the halo if it is indeed a 22° halo.

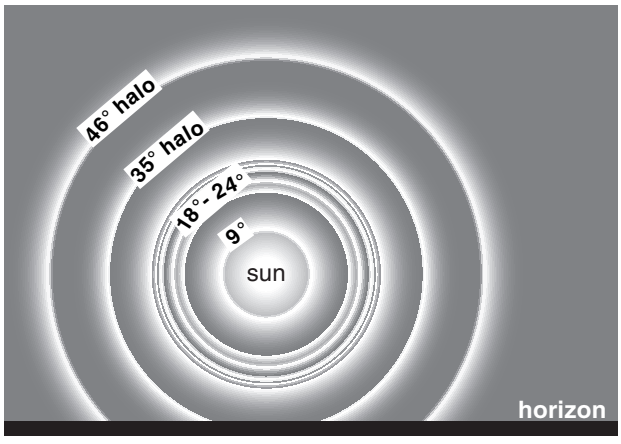

Figure 22.29
Halos. (It is unusual to see all these halos at the same time.)

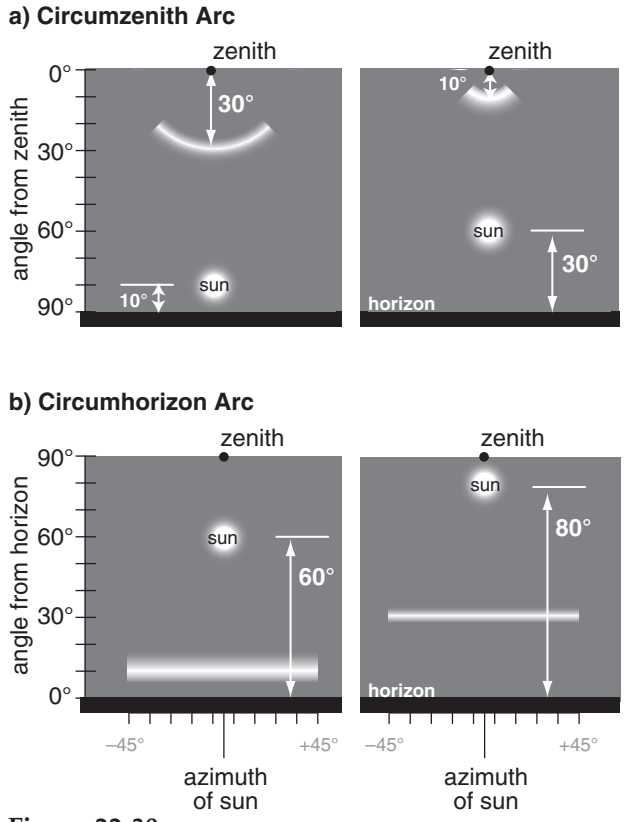

Figure 22.30
Although both circumzenith and circumhorizon arcs are portions of circles around the zenith and both are parallel to the horizon, we perceive them differently. Circumzenith arcs look like a part of a circle around the zenith point, as sketched in (a). Circumhorizon arcs look like horizontal lines just above the horizon, as sketched in (b). Angles above are approximate.

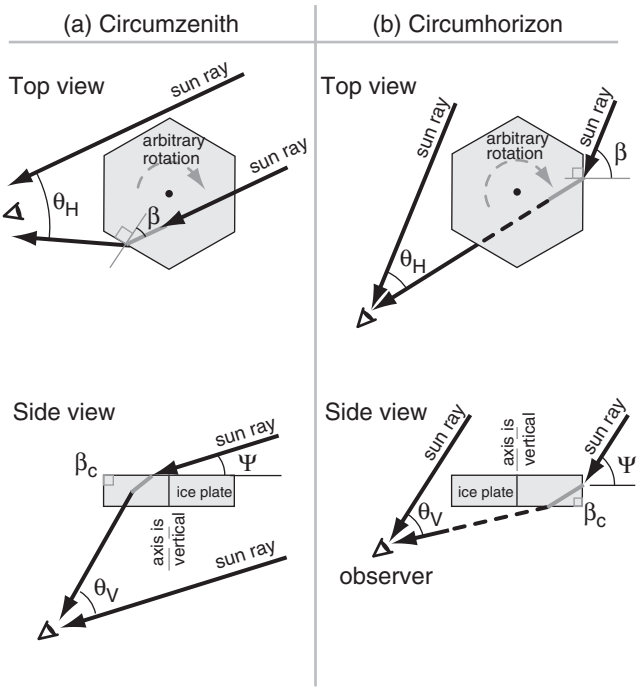

Figure 22.31
Ray geometry for (a) circumzenith & (b) circumhorizon arcs.

Circumzenith & Circumhorizon Arcs

Circumzenith arcs and circumhorizon arcs are similar (Fig. 22.30). They are both portions of circles at constant viewing angle above the horizon, and thus at constant viewing angle from the zenith (the point directly above the viewer). They are lines parallel to the horizon that partially encircle the viewer. Only the portion of the circle within about ±45° azimuth of the sun's azimuth from the viewer are visible; hence, they are seen as arcs, not circles.

Both arcs are caused by light refracted through the $\beta_c = 90°$ wedge angle of large oriented hexagonal plates (Fig. 22.31). For circumzenith arcs the light ray enters the top of the plate (through basal face 1) and exits through the side (such as through prism face 8 in Fig. 22.17b). For circumhorizon arcs the ray enters a side (such as face 5) and exits the bottom (face 2). Because refraction is involved, these arcs can be colorful, with red closest to the sun.

The arc's viewing-angle from the zenith (i.e., the apparent radius of the arc) varies with solar elevation (Fig. 22.32). The circumzenith arc is seen high in the sky (above the sun) only when the sun is low in the sky (for solar elevation angles of $0° < \Psi < 32°$). The circumzenith arc is always outside the 46° halo (Fig. 22.16).

The circumhorizon arc is seen low in the sky (below the sun) only when the sun is high in the sky ($58° < \Psi \leq 90°$). At high latitudes the circumhorizon arc is never visible because the sun never gets high enough in the sky.

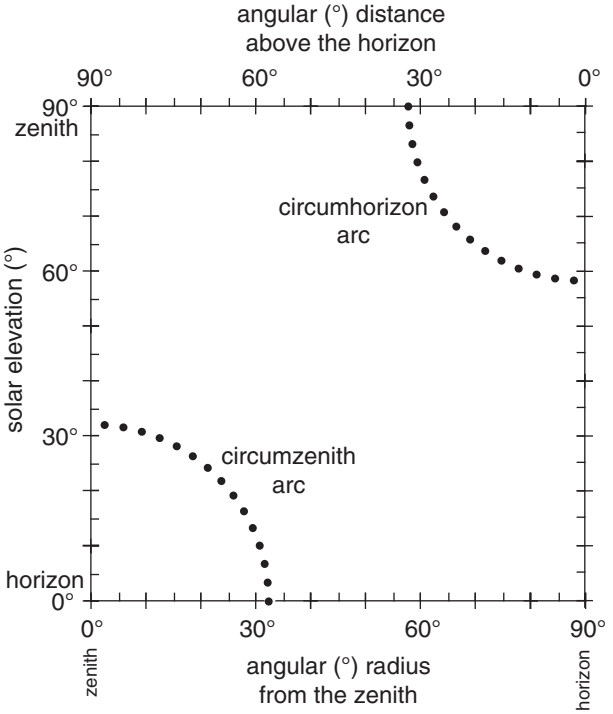

Figure 22.32
Radius of circumzenith and circumhorizon arcs about the zenith point, as viewed from the ground.

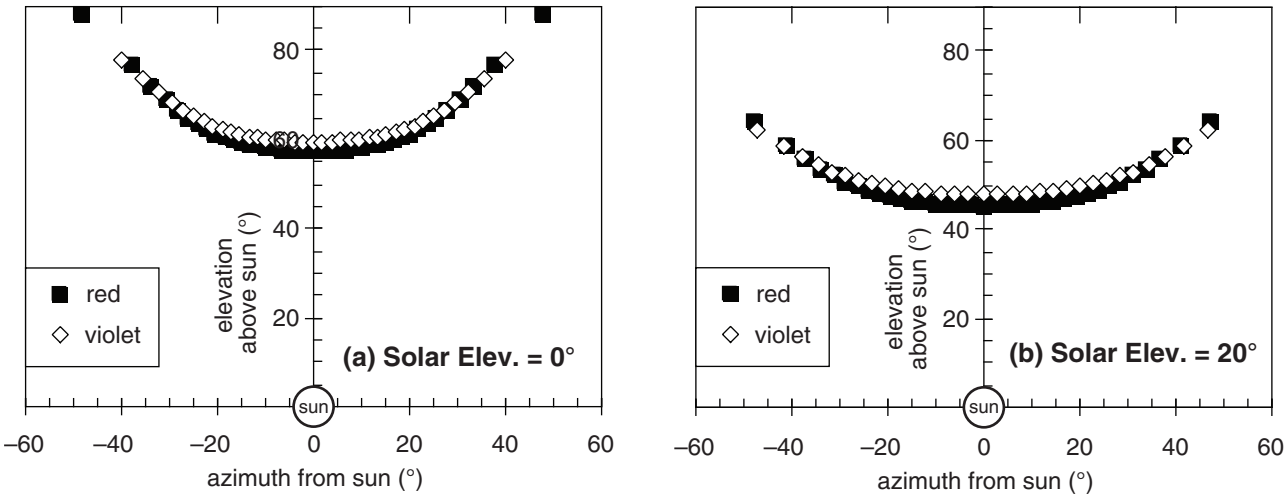

Figure 22.33
Circumzenith arcs found by solving eq. (22.17) for a variety of crystal rotation angles β, *at solar elevation angles of (a) 0°, at left, and (b) 20°, above.*

To illustrate how these arcs form, we will focus on just one of them — the circumzenith arc. The large hexagonal plates can assume any rotation angle β about their vertically-oriented column axis. At different times and locations, there are different solar elevation angles ψ. The ray equations for vertical viewing angle θ_V (elevation above the sun) and horizontal angle θ_H (azimuth from the sun) are:

$$\theta_V = S_\alpha[\arccos(\mu_{ai}\cdot\cos\psi),\beta,\mu_{ia}] - \psi$$
$$\theta_H = S_\beta[\arccos(\mu_{ai}\cdot\cos\psi),\beta,\mu_{ia}] - \beta \qquad (22.17)$$

Subscripts "*ai*" are for rays going from air to ice (e.g.; $\mu_{ai} = n_{air}/n_{ice}$), while subscripts "*ia*" are from ice to air (e.g.; $\mu_{ia} = n_{ice}/n_{air}$).

A spreadsheet can be used with a large number of evenly spaced values of β to simulate the superposition of rays from a large number of randomly-rotated ice plates. The resulting locus of output viewing angles traces the circumzenith arc in Fig. 22.33.

Eq. (22.17) does not include reflection of some or all of the rays from the outside of the crystal as a function of incidence angle, nor does it include the critical angle for rays already inside the crystal. Thus, some of the points plotted in Fig. 22.33 might not be possible, because the sun rays corresponding to those points either cannot enter the crystal, or cannot leave it.

Science Graffito

"It is clear and cold... And all about is snow and silence. And in the sky are three suns, and all the air is flashing with the dust of diamonds."
– Jack London, on a trip down the Yukon River in search of gold in Alaska.

Solved Example

For a circumzenith arc, what are the elevation and azimuth viewing angles (relative to the sun)? Solar elevation is 10°. Rotation angle is β = 20°. Assume nearly red light with: $n_{air} = 1.0002753$ and $n_{ice} = 1.307$.

Solution

Given: Ψ = 10°, β = 20°, $n_{air} = 1.0002753$, $n_{ice} = 1.307$
Find: θ_V = ?°, and θ_H = ?°

First, find the refraction parameters:
$\mu_{ai} = n_{air}/n_{ice} = 0.7653$, and $\mu_{ia} = 1/\mu_{ai} = 1.3067$

Next: $\arccos[\mu_{ai}\cos(\Psi)] = \arccos(0.7653\cdot\cos 10°) = 41.09°$

Then, use eqs. (22.17):
$\theta_V = S_\alpha[41.09°,\ 20°,\ 1.3067] - 10°$
$\theta_H = S_\beta[41.09°,\ 20°,\ 1.3067] - 20°$.

To find the *S* values, we first need to use eq. (22.8):

$$b_{\alpha\beta} = \frac{(1.3067)^2}{1+[1-(1.3067)^2]\cdot\left\{[\tan(41.09°)]^2+[\tan(20°)]^2\right\}} = 4.634$$

Then use eq. (22.9):

$$S_\alpha(\alpha_1,\beta_1,,\mu_{12}) = \arctan\left[\left\{4.634\cdot[\tan(41.09)]^2\right\}^{1/2}\right]$$

$S_\alpha = 61.95°$

Similarly: $S_\beta = 38.08°$
Finally: $\theta_V = 61.95° - 10° = \underline{\mathbf{51.95°}}$
$\theta_H = 38.08° - 20° = \underline{\mathbf{18.08°}}$

Check: Units OK. Physics OK.
Discussion: This answer agrees with Fig. 22.33b. Obviously this calculation is tedious for more than one ray, but it is easy on a spreadsheet.

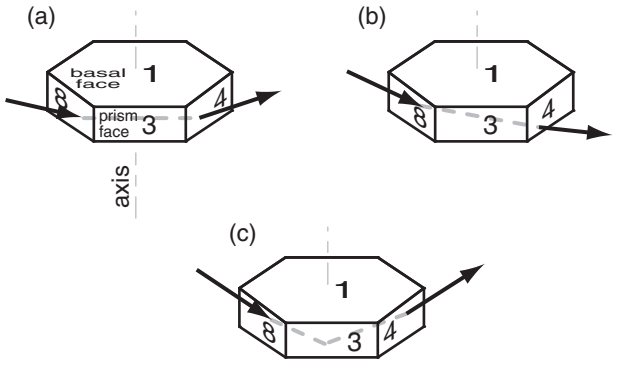

Figure 22.34
Geometry of sun dog optics (oblique side view), for (a) low sun elevation angle, (b) higher sun angle, and for (c) subsun dogs.

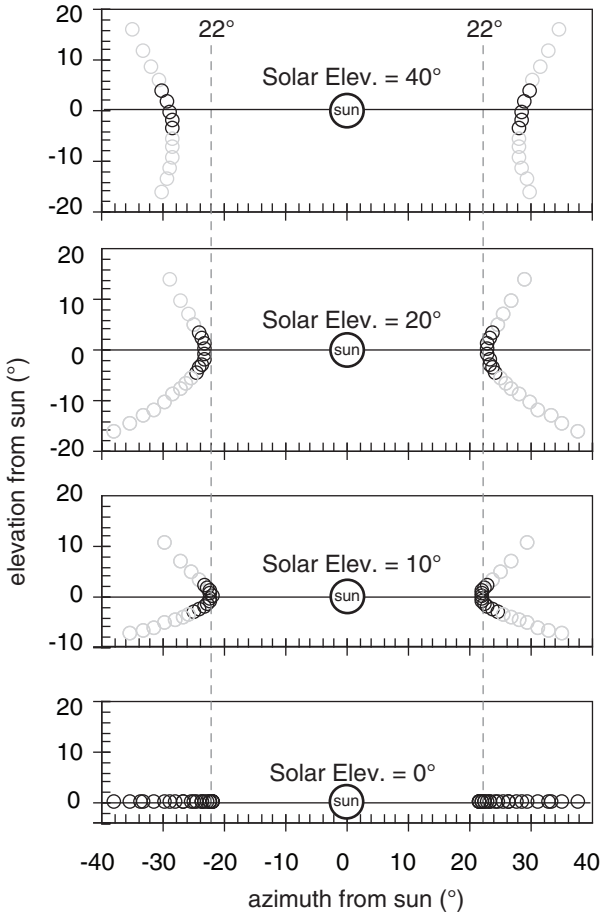

Figure 22.35
Variation of parhelia (sun-dog) appearance with solar elevation angle. Vertical dashed lines are 22° from sun. Greater density of data points indicates brighter parhelia. Grey data points, although solutions to eqs. (22.18), are unphysical because those equations don't consider the finite size of the ice crystals.

Sun Dogs (Parhelia)

Parhelia are bright spots of light to the right and left of the sun, roughly 22° from the sun (Fig. 22.16). As the sun moves through the sky, the parhelia move with the sun as faithful companions — earning their nickname **sun dogs**.

They are formed when light shines through the sides (prism faces) of large horizontal ice-crystal plates that gently fall through the air with their column axes vertical. The crystals are free to rotate about their column axes, so there is no favored rotation angle.

Because of the preferred orientation of the column axis, sun-dog optics depend on the solar elevation angle. When the sun is on the horizon, sun rays shine through the crystal as sketched in Fig. 22.34a, with a nearly horizontal path through prism faces such as 8 4. This causes the parhelia at a viewing angle of 22° from the sun. If a 22° halo is also present due to other smaller ice crystals in the air, then each parhelion appears as a bright spot on the halo to the right or left of the sun.

For higher sun angles (Fig. 22.34b), ice-crystal geometry causes the sun dogs to move horizontally further away from the sun. For example, at a solar elevation angle of $\Psi = 47°$, the sun dogs are at a horizontal viewing angle of 31° from the sun; namely, they are found outside the 22° halo. As the solar elevation angle becomes greater than about 60°, the sun dog is so faint and so far from the 22° halo that it effectively ceases to exist.

For a single ray input from the sun, let β be the rotation angle of the ice-crystal plate about its column axis. The ray equation for a sun dog is:

(22.18)

$$\theta_V = S_\alpha[S_\alpha(\psi,\beta,\mu_{ai}),\ \ 60° - S_\beta(\psi,\beta,\mu_{ai}),\ \ \mu_{ia}] - \psi$$

$$\theta_H = S_\beta[S_\alpha(\psi,\beta,\mu_{ai}),\ \ 60° - S_\beta(\psi,\beta,\mu_{ai}),\ \ \mu_{ia}] + \beta - 60°$$

where θ_V is the viewing angle of the output ray (elevation above the sun), and θ_H is the viewing angle (azimuth to the right of the sun).

The sun dog as viewed by an observer is the superposition of rays from many ice crystals having a variety of rotation angles. For randomly rotated crystals, there is an equal chance of any β between 0° and 90°. This is simulated on a spreadsheet by solving the sun-dog equation for a large number of equally-spaced β angles. The results are plotted in Fig. 22.35. For a finite size ice crystal with aspect ratio typical of hexagonal plates, ray paths with large vertical viewing angle are not physically possible because the light ray would exit or reflect from a basal face before reaching the required prism face.

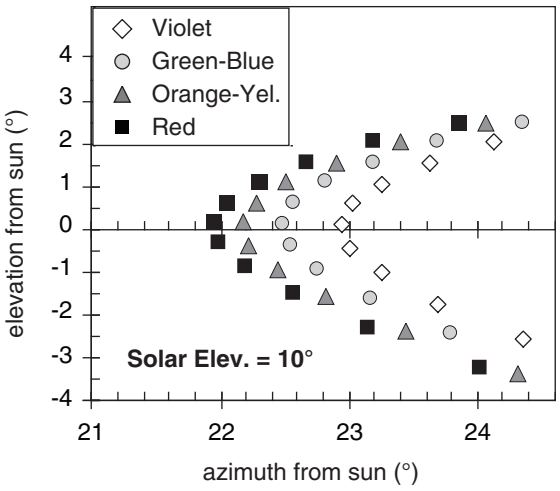

Figure 22.36
Dispersion of colors in a sun dog.

Sun dog colors are similar to the halo, with bright red on the inside (closest to the sun), then orange and yellow, but with green, blue, and violet fading to white (Fig. 22.36 is an expanded view of Fig. 22.35.)

Subsun Dogs (Subparhelia)

Subparhelia (spots of light to the left and right of the subsun) are sketched in Fig. 22.16. Ray geometry for a subsun dog is identical to that for a sun dog, except that the ray within the ice reflects from the inside of the bottom (basal) face (face 2 in Fig. 22.34c), in addition to refractions through prism faces when entering and exiting the crystal.

Tangent Arcs

Tangent arcs are caused when light rays are refracted through large hexagonal column ice crystals, which often fall with their column axis nearly horizontal (Fig. 22.17a). Three phenomena in this tangent-arc category include the **upper-tangent arc**, the **lower-tangent arc**, and the **circumscribed halo**. We will examine the optics of upper-tangent arcs in detail, and then briefly discuss the others.

Upper-Tangent Arc

In Fig. 22.16, the upper tangent arc is just above (and is tangent to) the 22° halo. The shape of this arc changes with solar elevation angle, Ψ.

In the absence of wind shear, the ice-crystal column axes can point in any compass direction within that horizontal plane. Thus, the crystal axis can have any directional orientation γ with respect to the compass direction of the incoming sun ray. The crystal can also have any rotation angle α_1 about the column axis (see Fig. 22.37).

Solved Example

Find the vertical and horizontal viewing angles of a sun-dog ray of red light for solar elevation 40° and crystal rotation $\beta = 45°$.

Solution

Given: $\Psi = 40°$, $\beta = 45°$

Assume for red light: $n_{air} \approx 1.0002753$, $n_{ice} \approx 1.307$

Find: $\theta_V = ?°$, $\theta_H = ?°$

Use eq. (22.18), with $\mu_{ai} = 0.7653$ from before:

$$\theta_V = S_\alpha[S_\alpha(40°, 45°, 0.7653), 60° - S_\beta(40°, 45°, 0.7653), \ 1.3067] - 40°$$

$$\theta_H = S_\beta[S_\alpha(40°, 45°, 0.7653), \{60° - S_\beta(40°, 45°, 0.7653)\}, \ 1.3067] + 45° - 60°$$

For the S_α and S_β inside the square brackets:
$b_{\alpha\beta} = 0.3433$, $S_\alpha = 26.18°$, $S_\beta = 30.37°$

For outside the square brackets: $b_{\alpha\beta} = 2.8448$, because
$S_\alpha[26.18°, (60°–30.37°), 1.3067] =$
$S_\alpha[26.18°, 29.63°, 1.3067] = 39.67°$

$S_\beta[26.18°, 29.63°, 1.3067] = 43.81°$

Finally:
$\theta_V = 39.67° - 40° = \underline{\mathbf{-0.332°}}$
$\theta_H = 43.81° - 15° = \underline{\mathbf{28.81°}}$

Check: Units OK. Physics OK.
Discussion: This portion of the sun dog is nearly at the same elevation as the sun, but is 28.81° to the side of the sun. This is 6.81° outside of the 22° halo.

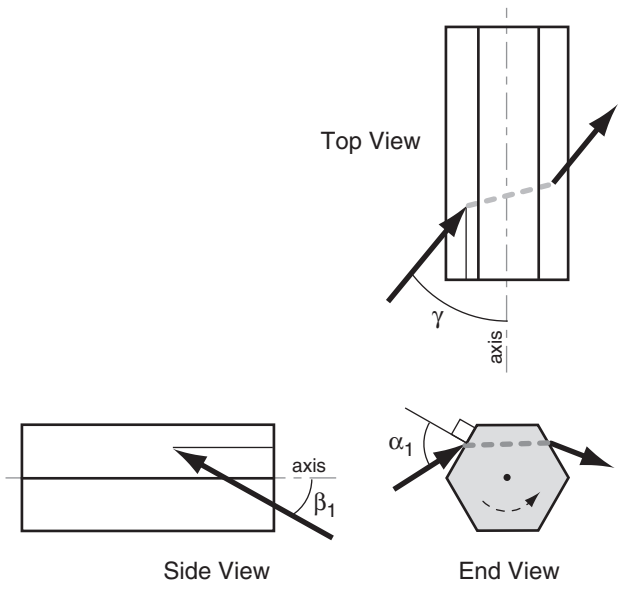

Figure 22.37
Ice crystal geometry associated with upper-tangent arcs.

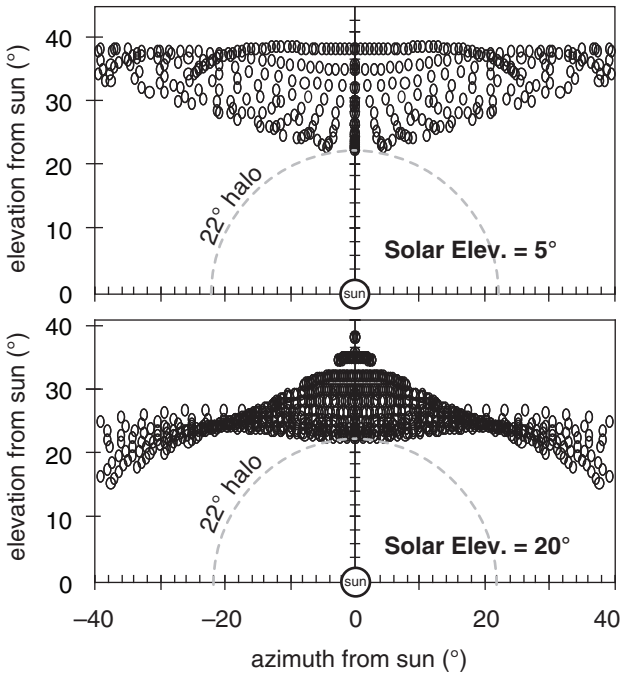

Figure 22.38
The locus of data points (from the solution of eqs. 22.19) shows the upper tangent arc for low solar elevation angles. Data points that were sparser (corresponding to fainter illumination) have been removed to clarify this illustration.

Solved Example

Find the vertical and horizontal viewing angles of a ray of red light in an upper tangent arc for solar elevation $\Psi = 10°$, crystal rotation $\alpha_1 = 76°$, and crystal axis direction $\gamma = 45°$.

Solution

Given: $\Psi = 10°$, $\alpha_1 = 76°$, $\gamma = 45°$.
Assume: $n_{air} \approx 1.0002753$, $n_{ice} \approx 1.307$
Find: $\theta_V = ?°$, $\theta_H = ?°$

Use eqs. (22.19). Various intermediate results are:
$\beta_1 = 76°$
$b_{\alpha\beta} = 0.0402$ (1st calculation)
$\alpha_3 = 21.2°$, $\beta_3 = 38.8°$
$b_{\alpha\beta} = 3.9142$ (2nd calculation)
$\alpha_5 = 22.50°$, $\beta_5 = 57.84°$
$G = 2.701$, $\varepsilon = 75.4°$, $\phi = -30.4°$

Finally:
θ_V = **25.20°**
θ_H = **39.25°**

Check: Units OK. Physics OK.
Discussion: This one data point within the upper tangent arc is above the sun and above the top of the 22° halo, but is off to the right. These calculations would need to be repeated for many other values of input angles to create an image similar to Fig. 22.38

Because there are three input angles for this case, the solution of ray paths is quite nasty. The equations below show how one can calculate the ray output vertical viewing angle θ_V (elevation above the sun), and the horizontal viewing angle θ_H (azimuth from the sun), for any input ray. All other variables below show intermediate steps.

As before, one must examine rays entering many crystals having many angles in order to generate the locus of points that is the upper tangent arc. Even on a spreadsheet, this solution is tedious. Again, no consideration was made for the finite size of the crystal, or rays that cannot enter the crystal due to reflection, or rays that are trapped inside because of the critical angle.

Given: Ψ, α_1, and γ:

$$\beta_1 = \arctan\left[\cos(\gamma)\cdot\tan(90° - \psi)\right] \qquad (22.19)$$

$$\alpha_3 = 60° - S_\alpha(\alpha_1, \beta_1, \mu_{ai})$$

$$\beta_3 = S_\beta(\alpha_1, \beta_1, \mu_{ai})$$

$$\alpha_5 = 60° - S_\alpha(\alpha_3, \beta_3, \mu_{ia}) - \alpha_1 + \arctan\left[\sin(\gamma)\cdot\tan(90° - \psi)\right]$$

$$\beta_5 = S_\beta(\alpha_3, \beta_3, \mu_{ia})$$

$$G = [\tan(\alpha_5)]^2 + [\tan(\beta_5)]^2$$

$$\varepsilon = \arctan\left[\frac{\tan(\beta_5)}{\tan(\alpha_5)}\right]$$

$$\phi = 90° - \gamma - \varepsilon$$

$$\theta_V = 90° - \psi - \arctan\left[G^{1/2}\cdot\cos(\phi)\right]$$

$$\theta_H = \arctan\left[\sin(\phi)\cdot\left(\frac{G}{1 + G\cdot[\cos(\phi)]^2}\right)^{1/2}\right]$$

To keep the spreadsheet calculations to a finite size, we used γ in the range of 55° to 90°, and α_1 in the range of 0° to 90°. The results for two solar elevations are shown in Fig. 22.38.

The locus of points of the upper tangent arc looks like the wings of a bird. For low solar elevations, the wings are up in the air. As the sun rises in the sky, the wings gently lower. At solar elevations of about 45° or more the wings are wrapped closely around the 22° halo. Above about 60° solar elevation, there is no solution to the upper tangent arc that is physically realistic.

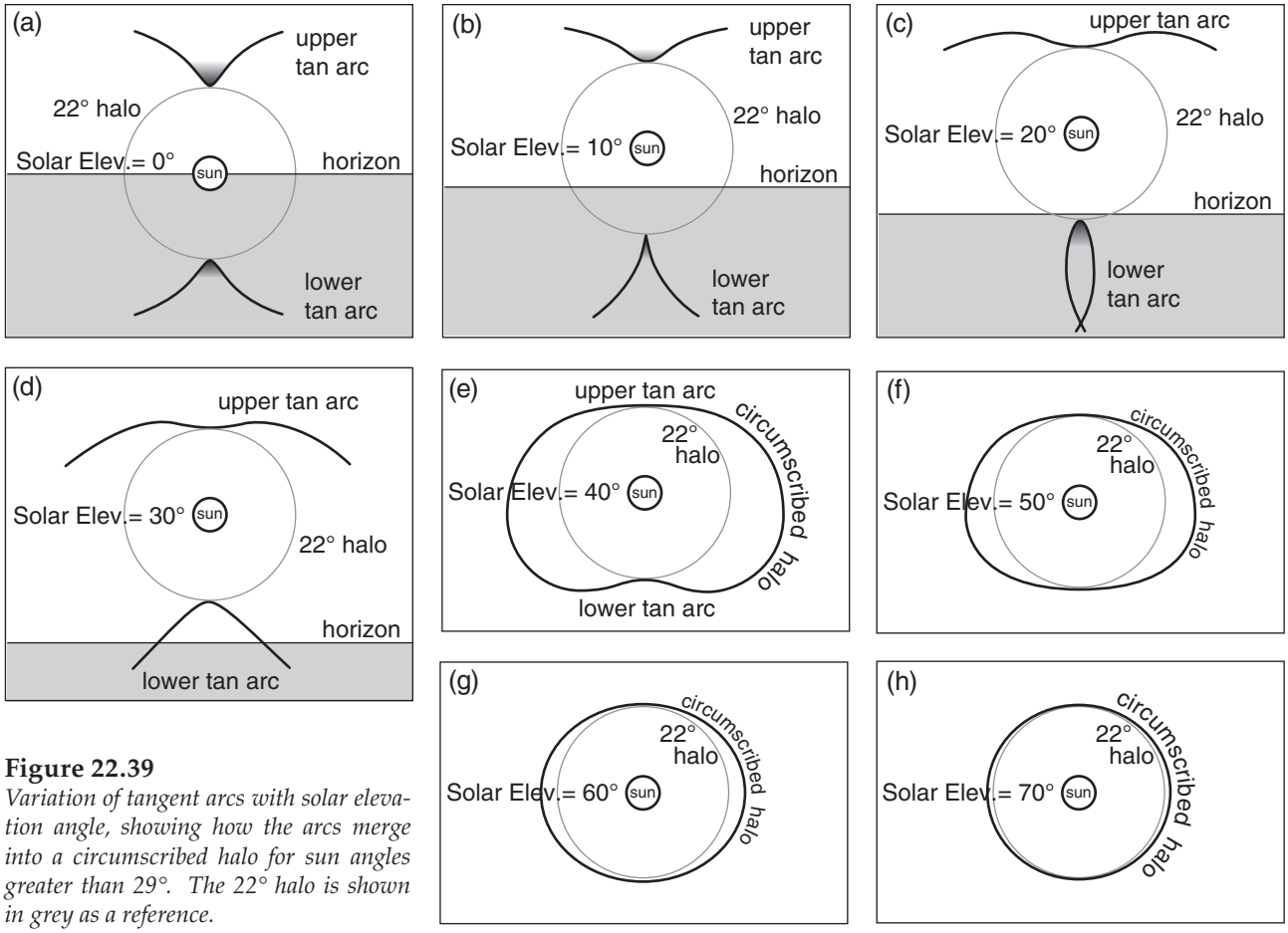

Figure 22.39
Variation of tangent arcs with solar elevation angle, showing how the arcs merge into a circumscribed halo for sun angles greater than 29°. The 22° halo is shown in grey as a reference.

Lower Tangent Arcs

Figs. 22.39 show lower tangent arcs, which occur during the same conditions as upper tangent arcs. Lower tangent arcs are tangent to the bottom of the 22° halo. Upper and lower tangent arcs have similar ray paths (Fig. 22.40) through large hexagonal column ice crystals. Eqs. (22.19) also apply to lower tangent arcs.

For solar elevations of 22° or less, you cannot see the lower tangent arc unless you look down into ice-crystal filled air. You can have such a view from aircraft, mountain peaks, bridges or tall buildings.

Circumscribed Halo

At solar elevations of 29° and greater, the upper and lower tangent arcs merge to form a circumscribed halo (Figs. 22.39). At solar elevations above 70°, the circumscribed halo is so tight around the 22° halo that they are often indistinguishable.

Other Halos

Fig. 22.41 and Table 22-3 show most of the halos and arcs.

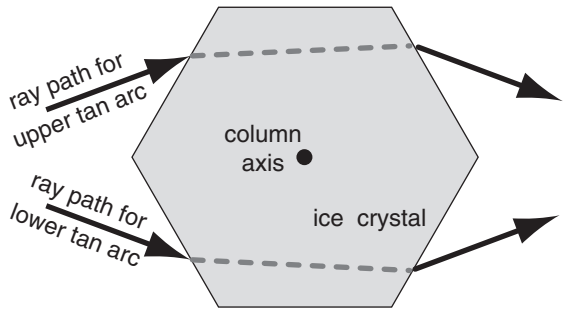

Figure 22.40
Ray paths for upper and lower tangent arcs. This is an end view of a hexagonal column ice crystal oriented with its column axis horizontal (out of the page).

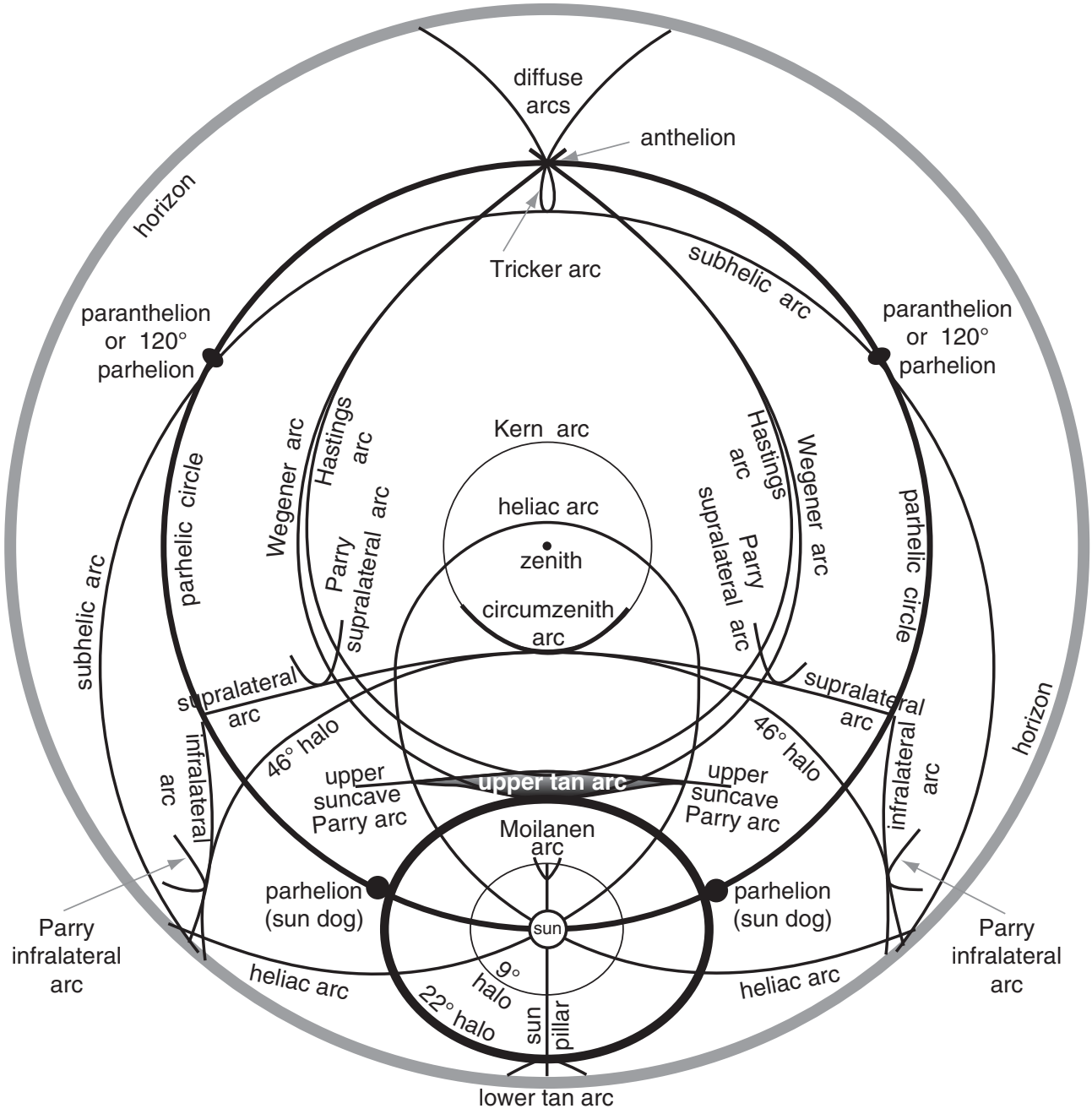

Figure 22.41
Halos in the sky, for a solar elevation of 26°. This view is looking straight up toward the zenith, as what could be photographed using an all-sky camera (with a fish-eye lens). The outermost thick grey circle represents the horizon, and the zenith point is marked as a dot in the center of this circle. Some of these halos are extremely rare. Most would not be seen at the same time, because they require ice crystals of different shapes and having perfect orientation. This fish-eye view distorts the 9°, 22°, and 46° halos, which would appear as circles to the observer. The halos of other diameters (including the 28° Scheiner's halo) are not plotted. [Based on data from Les Cowley's website (viewed Jan 2010) http://www.atoptics.co.uk/ , and from W. Tape, 1994: "Atmospheric Halos", and W. Tape and J. Moilanen, 2006: "Atmospheric Halos and the Search for Angle x", published by AGU.]

Table 22-3. Alphabetical catalog of halos. Fig. 22.41 shows most of these halos.

Legend:

Ice crystals:
- A = large oriented hexagonal pyramid
- a = small hex. pyramid (random orientations)
- C = large hexagonal column (col. axis horiz.)
- c = small hex. column (random orientations)
- L = Lowitz large hex. plate (see Focus Box)
- P = large hexagonal plate (col. axis vertical)

Angles:
- 22° ≈ angle of phenomenon from sun, associated with 60° ice wedge angle.
- 46° ≈ angle of phenomenon from sun, associated with 90° ice wedge angle.

Optics:
- m = (mirror) = one or more reflections
- r = one or more refractions

9° halo, a, r
9° Parry arc, A, r
18° halo, a, r
20° halo, a, r
22° halo, c, r
22° Lowitz arcs (upper & lower), L, r (rare)
22° Parry arcs (upper & lower; suncave & sunvex), C, r
23° halo, a, r
24° halo, a, r
35° halo, a, r
44° parhelia (sun dogs of sun dogs, formed when light passes through 2 hex. plates), 2P, 22°, r
46° halo, c, r
46° Lowitz arcs, L, r (extremely rare)
46° Parry arcs (infralateral, supralateral), C, r
120° parhelia (left & right), P, r, m
Anthelic arc, C, r, m (= Antisolar arc)
Anthelion (a crossing point of diffuse & anthelic arcs)
Antisolar arc, C, r, m (= Anthelic arc)
Circumhorizon arc, P, 46°, r (also Parry)
Circumscribed halo, C, 22°, r
Circumzenith arc, P, 46°, r (also Parry)
Diffuse arcs, C, r, m
Halos (see 9° through 46° halos above)
Hastings arcs (of upper suncave Perry arc; and of lower suncave Perry arc), r, m
Heliac arc, C, m or (r, m)
Infralateral arc, C, 46°, r (also Parry)
Kern arc, P, 46°, r, m (rare)
Lower suncave Parry arc, C, 22°, r
Lower sunvex Parry arc, C, 22°, r
Lower tangent arc, C, 22°, r
Lower Wegener arc, C, r, m
Lowitz arcs (upper & lower), L, 22°, r (rare)
Moilanen arc (rare; seen in ice crystals from snow-making machines)
Paranthelia (= 120° parhelia, left & right), P, r, m
Parhelia (sun dogs) (left & right), P, 22°, r
Parhelic circle, [P, m or (r, m)] or [C, m or (r, m)] (also Parry)
Parry arcs (Many arcs. See separate listings for: 9°, upper suncave, upper sunvex, lower suncave, lower sunvex, circumzenith, circumhorizon, infralateral, supralateral, Hastings, helic, subhelic, anthelic, subanthelic)
Scheiner's 28° halo (from cubic Ic ice crystals), r
Subanthelic arc, C, r, m
Subcircumzenith arc, P, 46°, r, m (not yet observed)
Subhelic arc, C, r, m
Subhorizon halo (halos and arcs below the horizon, including portions of diffuse, Tricker, subhelic, lower Wegener, and lower tangent arcs)
Subparhelia (subsun dogs) (left & right), P, 22°, r, m
Subparhelic circle, [P, r, m] or [C, r, m]
Subsun, P, r
Subsun dogs (subparhelia) (left & right), P, 22°, r, m
Sun dogs (parhelia) (left & right), P, 22°, r
Sun pillar, C or P, r
Supralateral arc, C, 46°, r (also Parry)
Tangent arc (upper & lower), C, 22°, r
Tricker arc, C, r, m
Upper suncave Parry arc, C, 22°, r
Upper sunvex Parry arc, C, 22°, r
Upper tangent arc, C, 22°, r
Upper Wegener arc, C, r, m
Wegener arcs (upper & lower), C, r, m

FOCUS • Special Crystal Orientations

A **Parry oriented column** crystal has both a horizontal column axis and horizontal top and bottom prism faces (see Fig. at right). Resulting **Parry arcs** (Fig. 22.41) are observed 1% as frequently as 22° halos.

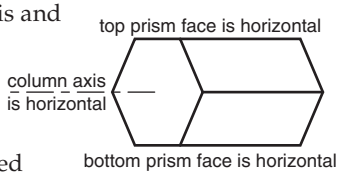

Fig. 22.b

A **Lowitz** oriented plate crystal has an unusual orientation. **Lowitz arcs** are extremely rare & faint (not shown in Fig. 22.41).

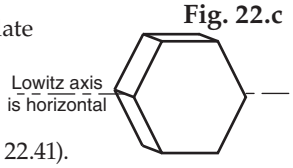

Fig. 22.c

FOCUS • Scheiner's Halo

In year 1629, Christopher Scheiner observed a rare 28° halo, which has been observed only about 6 times since then. One explanation is that sun rays pass through an octahedral crystal made of cubic ice Ic. Cubic ice is discussed in a Focus Box in the Precipitation chapter. The Fig. below shows a ray path through a truncated octahedron.

The wedge angle of 70.528° yields a minimum viewing angle of 27.46° according to eq. (22.16), assuming a refractive index of 1.307. But this cubic-ice explanation is still being debated.

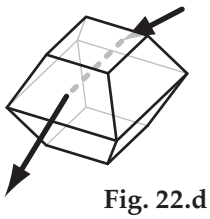

Fig. 22.d

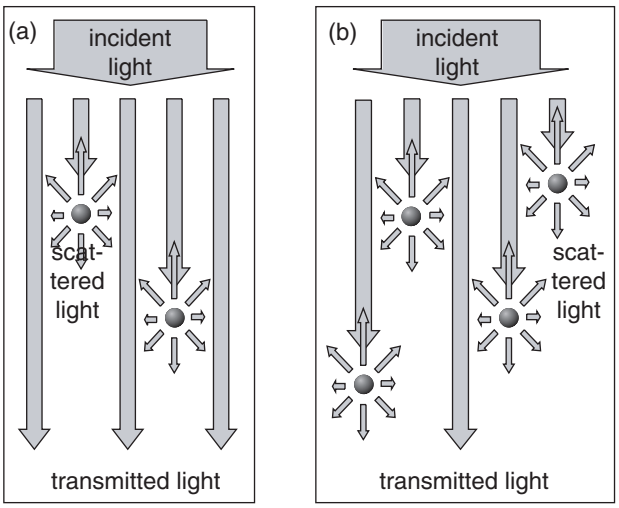

Figure 22.42
Incident light (long downward arrows) can be scattered (small arrows in all directions) by particles (black dots) that are in the path of the light. Paths with few particles (a) scatter less light and transmit more light than paths with many particles (b).

Solved Example
What fraction of light is scattered for $\tau = 2$?

Solution
Given: $\tau = 2$
Find: $I_{scat}/I_o = ?$

Use eq. (22.21): $I_{scat}/I_o = 1 - e^{-2} = 0.865 = \underline{\mathbf{86.5\%}}$

Check: Units OK. Magnitudes agree with text.
Discussion: A large portion of light is scattered. This optical depth can occur in polluted air.

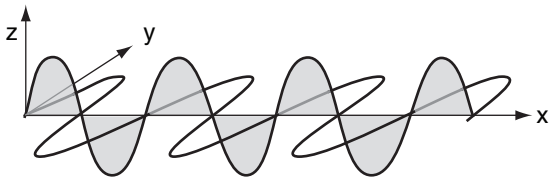

Figure 22.43
Unpolarized light consists of two cross-polarized parts.

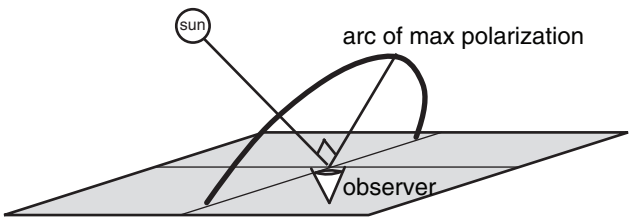

Figure 22.44
Arc of max polarization in the sky due to Rayleigh scattering.

SCATTERING

Background

Optical thickness

Light can scatter off of air molecules, pollutant particles, dust, and cloud droplets. More particles in the air cause more of the light to be scattered (Fig. 22.42). The ratio of transmitted (I_{tran} , non-scattered) to incident (I_o) light can be quantified using the **optical thickness** or **optical depth** τ (dimensionless) in Beer's Law:

$$\frac{I_{tran}}{I_o} = e^{-\tau} \qquad (22.20)$$

Thus, the relative amount of light scattered (I_{scat}) is:

$$\frac{I_{scat}}{I_o} = 1 - \frac{I_{tran}}{I_o} = 1 - e^{-\tau} \qquad (22.21)$$

Zero optical thickness means no light is scattered, while $\tau > 5$ implies that virtually all the light is scattered. Optical thickness increases for longer paths and for higher particle concentrations. Examples are $\tau = 0.03$ to 0.3 for a clean dry atmosphere, and $\tau > 10$ for thick clouds.

Polarization

Light propagating in the *x*-direction can be thought of as having oscillations in the *y* and *z* directions (Fig. 22.43). This is unpolarized light. Polarizing filters eliminate the oscillations in one direction (for example, the shaded curve) while passing the other oscillations. What remains is **polarized** light, which has half the intensity of the unpolarized ray.

Sunlight becomes polarized when it is scattered from air molecules. The maximum amount of polarization occurs along an arc in the sky that is 90° from the sun, as viewed from the ground (Fig. 22.44).

If the sky scatters light with one polarity, and a polarizing camera filter or polarized sunglasses are rotated to eliminate it, then virtually no sky light reaches the camera or observer. This makes the sky look very deep blue, providing a very striking background in photographs of clouds or other objects. If you want to maximize this effect, pick a camera angle looking toward the 90° arc from the sun.

Scattering by small dust particles in ice also explains why glaciers are often magnificently blue.

Types of Scattering

The type and efficiency of scattering depends on the ratio of particle diameter *D* to the wavelength λ of the light. Table 22-4 summarizes the types of scattering. Actual size ranges of cloud droplets and aerosols are wider than indicated in this table.

Table 22-4. Scattering of visible light. D = particle diameter. λ = wavelength of light.					Scattering Varies with		
D / λ	**Particles**	**Diameter, D (μm)**	**Type**	**Phenomena**	**λ**	**Direction**	**Polarization**
< 1	air molecules	0.0001 to 0.001	Rayleigh	blue sky, red sunsets	X		X
≈ 1	aerosols (smog)	0.01 to 1.0	Mie	brown smog	X	X	X
> 1	cloud droplets	10 to 100	geometric	white clouds		X	

Rayleigh Scattering

Air molecules have sizes of $D \approx 0.0001$ to 0.001 μm, which are much smaller than the wavelength of light (λ = 0.4 to 0.7 μm). These particles cause **Rayleigh scattering**. The ratio of scattered intensity of radiation I_{scat} to the incident radiation intensity I_o is:

$$\frac{I_{scat}}{I_o} \approx 1 - \exp\left[-\frac{a \cdot (n_{air} - 1)^2}{\rho \cdot \lambda^4} \cdot x \right] \qquad (22.22)$$

where a = 1.59x10^{-23} kg, ρ is air density, n_{air} is the refractive index, and x is the path length of light through the air.

Fig. 22.45a shows the relative amount of scattering vs. wavelength. Because of the λ^{-4} dependence, shorter wavelengths such as blue and violet are scattered much more (about a factor of 10) than red light, which makes the **sky blue**. For light shining vertically through a clean dry atmosphere, τ = 0.3 for violet light and 0.03 for red.

Sunlight intensity varies according to Planck's law (Fig. 22.45b and the Radiation chapter). The product of the top 2 curves shows the amount of sunlight that is scattered in the atmosphere (Fig. 22.45c). All curves have been normalized to have a maximum of 1.0.

The curve in Fig. 22.45c peaks in the ultraviolet portion of the spectrum. Although this is not visible to the naked eye, the scattered ultraviolet light can affect photographic films to produce a picture that looks hazier than the view by eye. Haze filters on cameras can filter out this unwanted scattered ultraviolet light.

Geometric Scattering

For large particles such as cloud droplets, light reflects from them according to geometric optics. Because all wavelengths are reflected equally, **clouds look white** when illuminated by white sunlight.

There is, however, a directional dependence. Light that is scattered in the same direction that the incident ray is pointing is called **forward scattering**. The opposite is **backward scattering**. For clouds, forward scattering is usually greater than backscattering. Thus, clouds you see in the direction of the sun look bright white, while those in the direction of your shadow look slightly more grey.

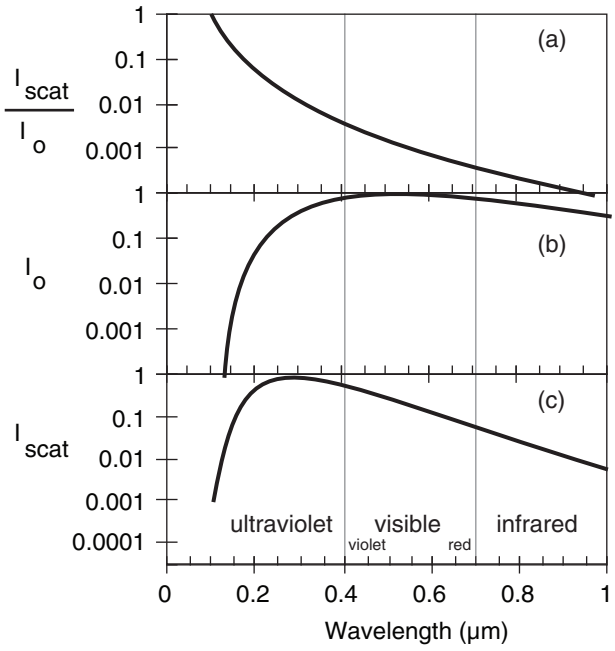

Figure 22.45
Top: Relative Rayleigh scattering. Middle: Planck spectrum for the sun. Bottom: product of the top two curves, indicating the amount of sunlight scattered in clean air.

Solved Example

What fraction of incident violet light is scattered by air molecules along a 20 km horizontal ray path near the Earth?

Solution

Given: $x = 5\text{x}10^6$ m, $\lambda = 4\text{x}10^{-7}$ m for violet
Find: I_{scat}/I_o = ?
Assume: ρ = 1 kg·m^{-3} for simplicity.

Use eq. (22.22): $I_{scat}/I_o =$

$$1 - \exp\left[-\frac{(1.59\times10^{-23}\,\text{kg})\cdot(0.0002817)^2}{(1\ \text{kg}\cdot\text{m}^{-3})\cdot(4\times10^{-7}\,\text{m})^4} \cdot (2\times10^4\,\text{m}) \right]$$

$$= \underline{\mathbf{0.627}} = 62.7\% \text{ scattered}$$

Check: Units OK. Physics OK.
Discussion: Looking toward the horizon, distant objects are difficult to see because some of the light is lost. Vertical rays experience less scattering, because air density decreases with height.

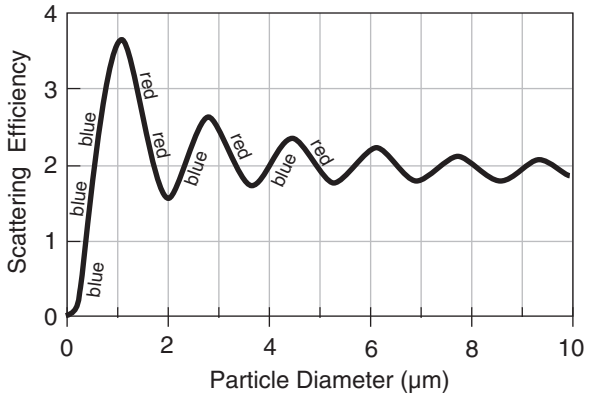

Figure 22.46
Mie scattering efficiency and dominant color scattered out of white light for various particle diameters.

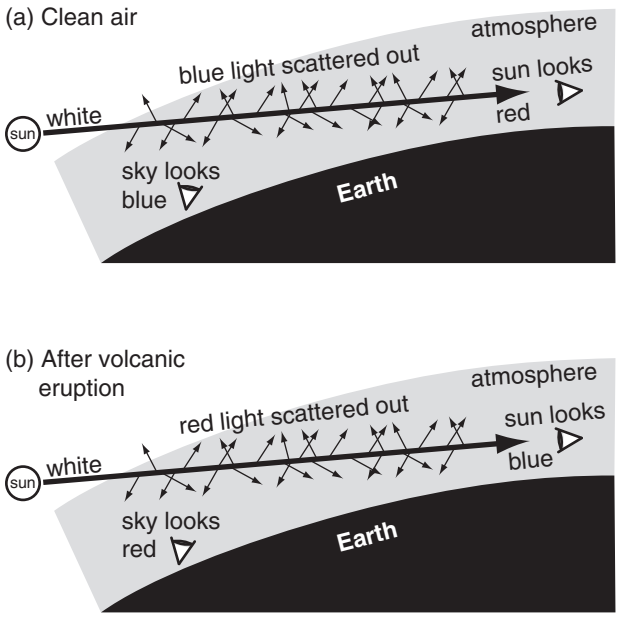

Figure 22.47
Scattering of sunlight as it travels through a long path through the atmosphere. (a) Clear skies. (b) Air hazy due to tiny sulfuric-acid aerosol droplets suspended in the stratosphere after a volcanic eruption.

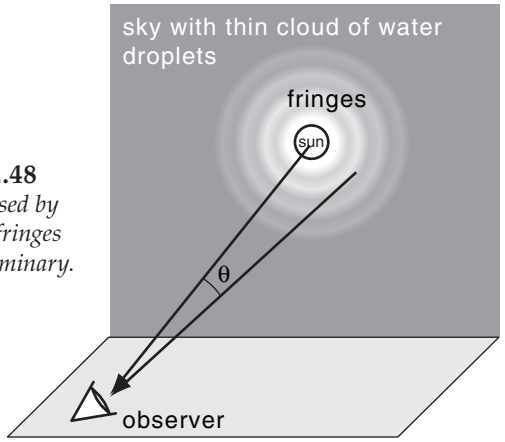

Figure 22.48
Corona caused by diffraction fringes around a luminary.

Mie Scattering

Gustov Mie proposed a comprehensive theory that describes reflection, scattering, polarization, absorption, and other processes for all size particles. The theory reduces to Rayleigh scattering for particles smaller than the wavelength, and to geometric scattering for larger particles. Aerosol particles are middle size, so no simplification of Mie theory is possible.

Fig. 22.46 shows that aerosols with diameters greater than about 0.1 μm are 10 to 1000 times more efficient light scatterers than air molecules, which is why polluted air looks hazy and has low visibility. Uniform aerosol smog particles can produce bluish or reddish-brown colors, depending on the dominant aerosol diameter.

Most aerosol particles have diameters smaller than 1 μm. Fig. 22.46 shows that these aerosols still scatter more blue light than red, causing blue haze. When the sun is low in the sky, the light rays travel through a very long path of air en route to the observer. For this situation, so much blue light is scattered out (making the **sky blue**) by these small aerosols and air molecules that it leaves more red in the remaining direct beam — giving a beautiful **red sun** at sunrise or sunset (Fig. 22.47a).

However, some acid droplet aerosols have diameters of about 1.5 μm, which scatters more red than blue. In some polluted regions where combustion processes emit SO_2 and NO_2 into the air, these pollutants can react with water in the air to form sulfuric acid and nitric acid. Scattering in this condition creates a **brown cloud** haze.

Another source of 1.5 μm diameter acid aerosols is volcanic eruptions, where sulfur emissions change into sulfuric acid droplets in the stratosphere. When the sun is low in the sky, so much red light is scattered out that beautiful **crimson sunset skies** are often observed after volcanic eruptions (Fig. 22.47b). Also, this leaves the remaining direct beam of sunlight in the setting sun slightly blue, which is hard to see because it is so bright. However, direct moonlight from a rising or setting moon can often be blue — causing a **blue moon** after a volcanic eruption.

For aerosols, forward scattering is usually greater than backscattering. Scattering can be polarized.

DIFFRACTION & INTERFERENCE

When sunlight or moonlight passes through a thin cloud of water droplets, diffraction and interference can produce a disk of bright sky centered on the luminary, surrounded by one or more colored rings or **fringes** (Fig. 22.48).

Recall from physics that when wave fronts hit the edge of an object, part of the wave bends around the edge — a process called **diffraction**. This is consistent with Huygens' principle, where every point on an incident wave front can be thought of as a source of new wavelets radiating away, and that the subsequent position of the wave front depends on the superposition of the wavelets.

Fig. 22.49a sketches cloud droplets and the wave fronts of incident light from the sun or moon. The edge of each droplet is marked with an "x". Consider the wavelets generated from each edge, sketched as the thin grey concentric circles. Superposition of these wavelets, indicated with the thick black wavy line, can **constructively interfere** to create a new wave train. Fig. 22.49a shows one of the resulting wave trains — the one for light that is transmitted straight through the cloud to the observer. Other angles have **destructive interference**.

However, there are many other angles where the wavelet fronts constructively interfere, one of which is sketched in Fig. 22.49b. This has the net effect of producing an additional train of wave fronts that leaves the cloud at a different angle. Because this angle of light leaving the cloud is the same as the angle observed by the observer, the observer sees the constructive interference (i.e., bright light) from all those different drops that happen to be the same viewing angle away from the sun. The different angles that can be produced from a set of drops produces many rings of different radii, called fringes.

The angle θ to each ring depends on the radius R of the droplet and the wavelength λ of light:

$$\theta = \arcsin\left(\frac{m \cdot \lambda}{R}\right) \qquad (22.23)$$

where m is a dimensionless diffraction parameter given in Table 22-5.

For any one color, there are faint rings of light separated by darker gray background. The different colors of the spectrum have different fringe radii, causing the fringes of any one color (e.g. blue-green) to appear in the dark spaces between fringes of another color (e.g., red). Fringes further from the sun (with higher fringe index) are less bright, as given in Table 22-5 and plotted in Fig. 22.50.

Corona, Iridescence and Glory

Wave clouds (standing **lenticular** clouds) have extremely uniform drop sizes. This means that all the drops in the cloud produce the same fringe angles, for any one color. Hence, the diffraction from all the droplets reinforce each other to produce bright colorful fringes (rings) called **corona**. Most

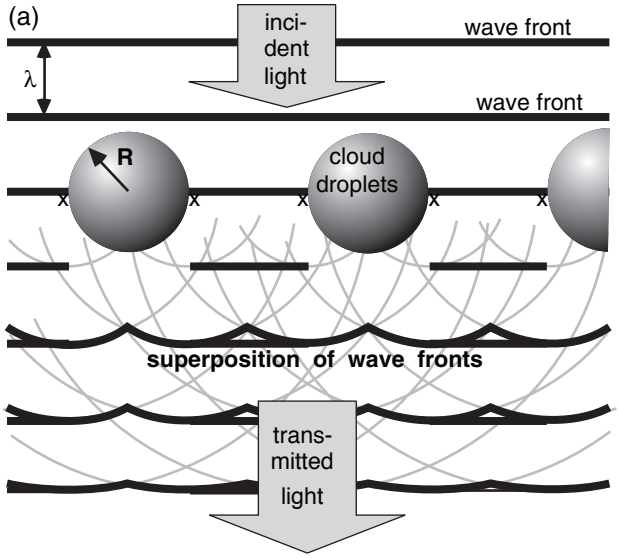

Figure 22.49a
Diffraction of light from edges of cloud droplets.

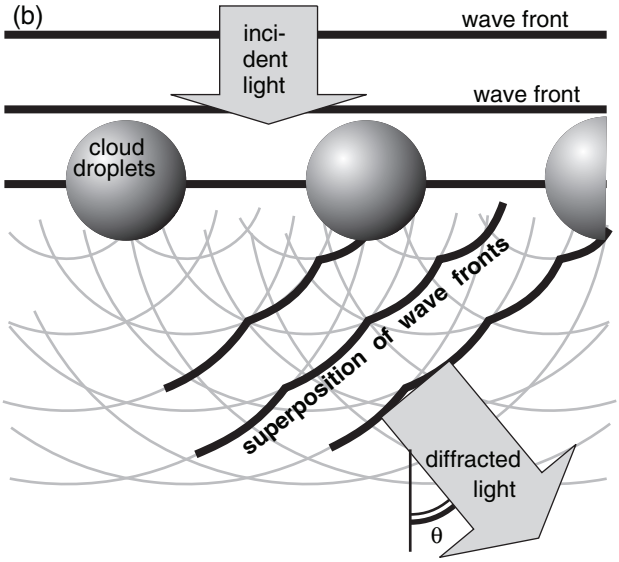

Figure 22.49b
Another direction where constructive interference happens.

Table 22-5. Diffraction fringes.

Fringe Index	m	Relative Intensity
1	0	1.0
2	0.819	0.01745
3	1.346	0.00415
4	1.858	0.00165
5	2.362	0.00078
6	2.862	0.00043
7	3.362	0.00027
8	3.862	0.00018

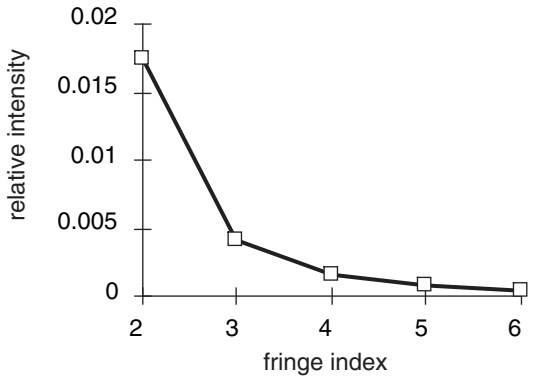

Figure 22.50
Diffraction fringe brightness. Larger indices indicate fringes that are further from the luminary.

Solved Example

The first visible fringe (index = 2) of red is 10° from the moon. What is the cloud drop radius?

Solution

Given: $\theta = 10°$, $\lambda = 0.7$ μm.
$m = 0.819$ from Table 19-3 for fringe #2.
Find: $R = ?$ μm
Assume $n_{air} \approx 1.0002753$ for red light.

Rearrange eq. (22.23):

$$R = \frac{m \cdot \lambda}{\sin\theta} = \frac{0.819 \cdot (0.7\mu m)}{\sin(10°)} = \underline{\mathbf{3.3\ \mu m}}$$

Check: Units OK. Physics OK.
Agrees with Fig. 22.51.
Discussion: Smaller than typical cloud-droplet size, perhaps associated with a wave cloud.

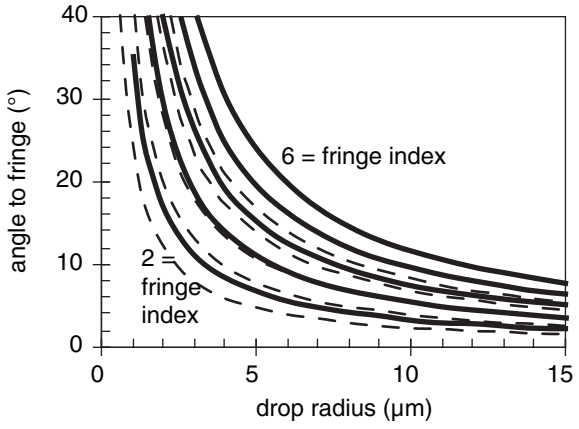

Figure 22.51
Viewing angle vs. cloud droplet size, for red (solid) and blue-green (dashed) diffraction fringes.

other clouds contain drops with a wide range of sizes, causing the colors to smear together to form a whitish disk (called an **aureole**) touching the sun or moon.

Eq. (22.23) can be solved on a spreadsheet for various cloud droplet sizes and colors. The results in Fig. 22.51 show that smaller droplets produce larger-diameter fringes. For reference, typical cloud droplets have 10 μm radii, and the viewing angle subtended by the sun is 0.534°.

To help discriminate between corona and halos, remember that corona are bright disks of light that touch the sun or moon, while halos have a dark region between the luminary and the halo ring. Also, corona are formed from liquid water droplets, while halos are formed from ice crystals.

Droplets near the edges of clouds (particularly wave clouds) can be very small as they form or evaporate, and can cause fringes of very large angular radius. As a result, the edges of clouds near the sun or moon are often colorful, a phenomenon called **iridescence**.

When looking down from above a cloud, diffraction patterns are sometimes seen around the shadow of the observer. This is called **glory**, and is associated with both diffraction and reflection from the cloud droplets. When viewed from an aircraft flying above the clouds, the glory is a circle of light centered on the shadow of the airplane.

Supernumerary Bows

As sketched in Fig. 22.7, supernumerary bows are closely spaced faint pinkish-purple and turquoise diffraction arcs touching the inside of the primary rainbow arc. The viewing-angle width of this bow (containing 2 to 4 sequences of fringes) is 1 to 2°. Supernumerary bows are most visible when the rain drop diameter is smaller than about 1 mm, during a rain shower when most of the falling drops have nearly the same size (i.e., a narrow drop-size distribution).

When the rain shower has a wider drop-size distribution, the greater flattening of the larger drops causes many drops to have nearly the same vertical thickness, even though their horizontal diameters vary widely. Thus, supernumerary bows are often most visible inside the top of the rainbow arc, and less visible inside the sides. Rainbows and supernumerary bows are also visible when the sun shines on dew drops on grass, and in water sprays from irrigation systems. Very faint supernumerary bows can sometimes be seen outside the secondary rainbow.

To explain the optics, look at Fig. 22.13b and consider red light at viewing angle 40°, for example. We see that light at this viewing angle comes from two different paths through the rain drop: one at impact

parameter 0.74 and the other at impact parameter 0.94. These two different paths travel different distances through the drop, hence their wave fronts can get out of phase with each other. At certain angles for certain colors the wave fronts interfere with each other, canceling to yield no light of that color. At other angles for other colors, the wave fronts are in phase and reinforce each other, yielding a bright color. This **constructive and destructive interference** of wave fronts creates supernumeraries.

MIRAGES

Refractive index n_{air} varies with air density ρ:

$$n_{air} - 1 \approx (n_{ref} - 1) \cdot \rho / \rho_{ref} \qquad (22.24)$$

where *ref* denotes a reference condition (such as given for air at any of the T and P values in Table 22-1). Knowing T and P, you can use the ideal gas law to find density [$\rho = P/(\Re T)$ for $\Re = 0.287$ (kPa/K)·(m^3/kg); see Chapter 1 for details]. Thus, you can rewrite eq. (22.24) as:

$$n_{air} - 1 = (n_{ref} - 1) \cdot \frac{T_{ref}}{T} \cdot \frac{P}{P_{ref}} \qquad (22.25)$$

A sharp change in density between two media causes a sharp kink in the ray path (Fig. 22.1). A gradual change of density causes a smoothly curving ray path (Fig. 22.52). The radius of curvature R_c (positive for concave up) is:

$$R_c \approx \frac{\rho_{ref}}{(n_{ref} - 1) \cdot (\cos\alpha) \cdot (\Delta\rho / \Delta z)} \qquad (22.26)$$

where α is the angle of the ray above horizontal, and the gradient of density $\Delta\rho/\Delta z$ is assumed to be perpendicular to the Earth's surface.

Substituting the ideal gas law and the hydrostatic relationship into eq. (22.26) yields

$$R_c \approx \frac{-(T / T_{ref}) \cdot (P_{ref} / P)}{(n_{ref} - 1) \cdot (\cos\alpha) \cdot \left\{ \frac{1}{T} \left[\frac{\Delta T}{\Delta z} + a \right] \right\}} \qquad (22.27)$$

where $a = 0.0342$ K·m^{-1} .

Because average density decreases with height in the atmosphere (see Chapter 1), eq. (22.27) gives a negative radius of curvature in the presence of weak temperature gradients. In other words, the ray is bent downward in a standard atmosphere. This

Solved Example
During winter with cold (T = –30°C) high-pressure (P = 104 kPa), find the refractive index for violet light.

Solution
Given: T = –30°C = 243 K, P = 104 kPa, λ = 0.4 μm.
Find: n_{air} = ? (dimensionless)

Use Table 22-1: For T_{ref} = –20°C = 253K & P_{ref} = 101.325 kPa, the table gives n_{ref} = 1.0003219, assuming RH=75%.

Use eq. (22.25):
$n_{air} = 1 + (0.0003219) \cdot (253/243) \cdot (104/101.325)$
$= \underline{\mathbf{1.0003440}}$

Check: Value reasonable compared to Table 22-1.
Discussion: By the ideal gas law, air density increases when temperature decreases and pressure increases. Higher density gives greater refractive index.

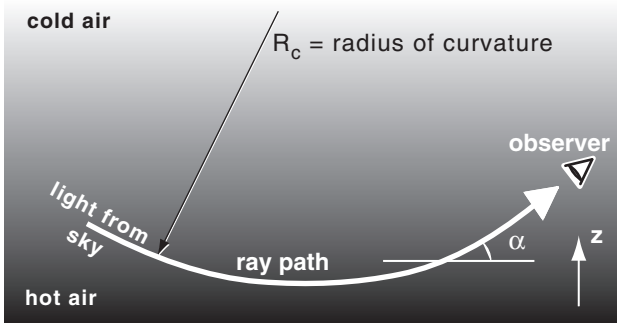

Figure 22.52
Ray curvature within a vertical gradient of density, creating an inferior mirage.

Solved Example
What is the radius of curvature of a horizontal indigo (λ ≈ 0.45 μm from Table 2-3 in the Radiation chapter) ray near the ground in a standard atmosphere?

Solution
Given: z = 0, α = 0°,
n_{air} ≈ 1.00028 from Table 22-1 for indigo light.
Find: R_c = ? km

Assume T = 288K and P = 101.3 kPa in a standard atmosphere near the ground. Assume the vertical temperature gradient is negligible. Rearrange eq. (22.27):

$$R_c \approx \frac{-1}{(0.00028) \cdot (\cos 0°) \cdot (0.0342\text{K} \cdot \text{m}^{-1} / 288\text{K})}$$
$$= \underline{\mathbf{-30{,}000\ km}}$$

Check: Units OK. Physics OK.
Discussion: The large negative radius implies very weak downward curvature, which agrees with the small angle of the **apparent sunrise** (Table 2-2).

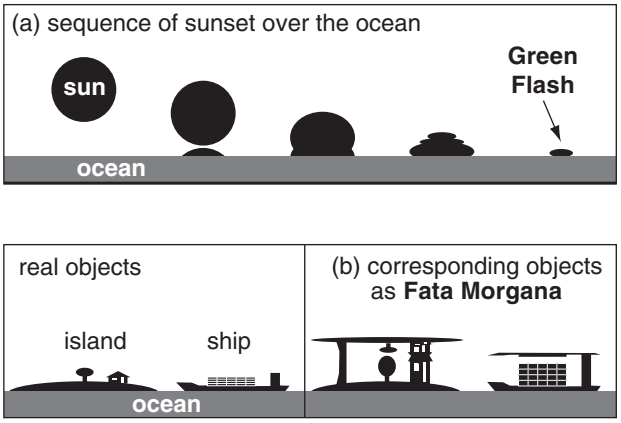

Figure 22.53
(a) Appearance of the sun setting over the ocean in inferior mirage conditions. (b) Distortion of distant objects during Fata Morgana mirage.

FOCUS • Newton and Colors

To confirm his laws of motion, Isaac Newton wanted to view the motions of the planets. He built his own telescopes for this purpose. However, the images he observed through his lenses were blurry. For example, images of stars were spread (**dispersed**) into a streak of colors.

After experimenting with different lenses, he concluded that neither the glass nor the construction was flawed. He realized that there must be some unknown physics causing this optical phenomenon. Like many great scientists, he allowed himself to get side-tracked to study this phenomenon in detail.

One of his experiments was to obtain a triangular prism, and to allow sunlight to pass through it. He observed that the white sunlight is composed of a spectrum of colors: red, orange, yellow, green, blue, indigo, and violet. Newton must have had a unique sense of color, because most people cannot discriminate between indigo and violet in the spectrum.

Newton concluded that the refraction of light through a lens inevitably causes color **dispersion**. Thus, a pinpoint of white starlight would be spread into a smear of colors. His solution to the telescope problem was to design a telescope without glass lenses. Instead he invented a reflecting telescope using curved mirrors, because reflection does not cause separation of light into colors.

agrees with Huygens' principle, that says light rays are bent toward media of higher density.

For ray paths near horizontal, the total bending through the whole atmosphere is about 0.567°, which is why **apparent sunrise** occurs before geometric sunrise (see the Radiation chapter). In everyday life, we rarely notice refraction associated with the standard atmosphere. However, in the presence of strong temperature gradients we can see mirages.

For rays to bend up instead of down, the term in square brackets in eq. (22.27) must be negative. This is possible when $\Delta T/\Delta z < -a$. A temperature decrease of at least 3.5°C per 10 cm height rise is necessary. Such a strong gradient is possible on hot sunny days in the air touching strongly-absorbing (black) surfaces. This condition of warm air under cold causes **inferior mirages**, where the objects appear lower than they really are. Warm under cold air is statically unstable (see the Stability chapter), causing turbulence that makes these mirages shimmer.

Inferior mirages are common above black roads on hot sunny days. Looking down toward the road, you see light rays refracted from the sky (Fig. 22.52). As these shimmer in the convective turbulence, the mirages look similar to reflections from the surface of water puddles.

Inferior mirages can also form over the ocean, if a thin layer of warm air is created by heat conduction from a warm sea surface, but colder air exists aloft. As the sun sets over the ocean, the base of the sun sometimes appears to spread out (Fig. 22.53a), causing the shape of the sun's outline to look like the Greek letter omega (Ω). Later, just as the top of the sun sets, the inferior-mirage effect causes the top of the sun to briefly appear emerald green just before it disappears below the horizon. This phenomenon is called **green flash**. *[CAUTION: to avoid damaging your eyes, do not look directly at the sun.]*

Cold air under warm air (as during early morning over land, or in arctic regions over ice, or where warm air flows over cold seas) causes **superior mirages**, where objects appear higher than they are. This accentuates the downward bending of rays, causing the image of the object to **loom** or stretch vertically upward.

The **Fata Morgana** mirage is caused by light rays passing through one or more elevated temperature inversions (a sharp interface between cold air below and warmer air aloft). Some ray paths bend as in superior mirages, and others bend as in inferior mirages. This causes portions of normal objects to appear stretched in the vertical, and other portions to appear compressed (Fig. 22.53b).

The results are fanciful images of mountains, ramparts, and castle turrets (some of which appear to float above ground) where none exist in reality.

The name of this mirage comes from Fairy Morgan (or Fata Morgana in Italian) of the King Arthur legend, an enchantress/magician who could create illusions of floating castles, etc.

SUMMARY

Atmospheric optical phenomena can be caused by reflection, refraction, scattering, diffraction and interference. Some of these processes are caused by the difference in density between hydrometeors (liquid and solid water particles) and air.

Common ice-crystal optical phenomena include the sun pillar, parhelic circle, subsun, 22° halo, 46° halo, circumzenith arc, sun dogs, subsun dogs and tangent arcs. They are usually found by looking toward the sun. The hexagonal column shape of many ice crystals creates 60° and 90° prismatic effects. The somewhat random orientation of these crystals causes sunlight to be returned in different directions from different crystals. The phenomena we see are the superposition from many crystals. Many other rarer halos can occur, some of which are associated with hexagonal pyramid crystals.

Rain-drop phenomena are a bit easier to describe, because the approximate spherical shape eliminates orientational dependence. Rainbows are seen by looking away from the sun. Cloud droplets produce corona, iridescence, glory, and aureole. Air molecules cause blue sky and red sunsets. Refraction in air causes amazing mirages.

Threads

This brings you to the end of this book. Along the way, you examined the physics of atmospheric pressure, wind, temperature, and humidity. You saw how these threads weave together to make cyclones, precipitation, thunderstorms, fronts, and hurricanes that we experience as weather. You have the quantitative wherewithal to critically evaluate weather-related issues, and to make sound decisions that affect society and the future of our planet.

If this is your last course on meteorology, be confident that you have the background to delve into the meteorology journals to learn the latest details that might help you in your engineering or scientific work. If you plan to continue your study of meteorology, the overview that you have gained here will help you put into context the advanced material that you will soon be learning.

As the Irish might bless: "May the wind be always at your back, may the sun shine warm upon your face, and may the rains fall soft upon your fields." Sincerely, *Roland Stull*

ON DOING SCIENCE • Great Scientists Can Make Big Mistakes Too

Isaac Newton explained many atmospheric optical phenomena in his books on optics. Not all his theories were correct. One of his failures was his explanation of the blue sky.

He thought that the sky was blue for the same reason that soap bubbles or oil slicks have colors. For blue sky, he thought that there is interference between light reflecting from the backs of small water droplets and the light from the front of the drops.

Although Newton's theory was accepted for about 175 years, eventually observations were made of the polarization of sky light that were inconsistent with the theory. Lord Rayleigh proposed the presently accepted theory in 1871.

Like Newton, many great scientists are not afraid to propose radical theories. Although most radical theories prove to be wrong, the few correct theories are often so significant as to eventually create **paradigm shifts** (radical changes) in scientific thought. Unfortunately, "publish or perish" demands on modern scientists discourage such "high risk, high gain" science.

Science Graffito

"The right to fail [is] as liberating as the right to succeed." W. Zinsser, 1998: *On Writing Well, 6 Ed*.

EXERCISES

Numerical Problems

N1. Calculate the angle of reflection, given the following angles of incidence:

a. 10° b. 20° c. 30° d. 40° e. 45
f. 50° g. 60° h. 70° i. 80° j. 90°

N2. Find the refractive index for the following (medium, color) for $T = 0°C$ and $P = 80$ kPa.

a. air, red	b. air, orange	c. air, yellow
d. air, green	e. air, blue	f. air, violet
g. water, red	h. water, orange	i. water, yellow
j. water, green	k. water, blue	
m. ice, red	n. ice, orange	o. ice, yellow
p. ice, green	q. ice, blue	r. ice, violet

N3. Find the speed of light for the medium and color of the previous exercise.

N4. Find the ratio μ of refractive indices for the following pairs of medium from exercise N2:

a. (a, g) b. (a, m) c. (g, m) d. (b, h) e. (b, n)

f. (h, n) g. (c, i) h. (c, o) i. (i, o) j. (d, j)
k. (d, p) m. (j, p) n. (e, k) o. (e, q) p. (k, q)

N5. For the conditions in Fig. 22.2, find the angle of refraction in water, given an incident angle of 45° in air for λ (μm) of
a. 0.4 b. 0.45 c. 0.5 d. 0.55 e. 0.6
f. 0.65 g. 0.7 h. 0.42 i. 0.47 j. 0.52
k. 0.57 m. 0.62 n. 0.67

N6. For green light, calculate the angle of refraction for: (i) water, and (ii) ice, given the following incident angles in air, for conditions in Fig. 22.2:
a. 5° b. 10° c. 15° d. 20° e. 25° f. 30° g. 35°
h. 40° i. 45° j. 50° k. 55° m. 60° n. 65° o. 70°
p. 75° q. 80° r. 85°

N7. For Snell's law in 3-D, given the following component angles in degrees (α_1, β_1), find the total incident angle (θ_1) in degrees.
a. 5, 20 b. 5, 35 c. 5, 50 d. 5, 65 e. 5, 80
f. 20, 35 g. 20, 50 h. 20, 65 i. 20, 80 j. 35, 50
k. 35, 65 m. 35, 80 n. 50, 65 o. 50, 80 p. 65, 80

N8. Using the incident components in air from the previous problem, find the refraction components of blue-green light in ice. Check your answers using Snell's law for the total refraction angle. Assume the refractive index in air is 1.0 and in ice is 1.31 .

N9. Use the data in Fig. 22.2 to calculate the critical angles for light moving from ice to air, for λ (μm) of
a. 0.4 b. 0.45 c. 0.5 d. 0.55 e. 0.6
f. 0.65 g. 0.7 h. 0.42 i. 0.47 j. 0.52
k. 0.57 m. 0.62 n. 0.67

N10. Same as the previous exercise, but for light moving from water to air.

N11. Find the reflectivity from spherical rain drops, given impact parameters of:
a. 0.0 b. 0.1 c. 0.2 d. 0.3 e. 0.4 f. 0.5
g. 0.6 h. 0.7 i. 0.75 j. 0.8 k. 0.85 m. 0.9
n. 0.95 o. 0.98

N12. What value(s) of the impact parameter gives a primary-rainbow viewing angle of $\theta_1 = 42.0°$ for light of the following wavelength (μm)?
a. 0.4 b. 0.45 c. 0.5 d. 0.55 e. 0.6
f. 0.65 g. 0.7 h. 0.42 i. 0.47 j. 0.52
k. 0.57 m. 0.62 n. 0.67

N13. Find the output viewing angle for a primary rainbow with the conditions in Fig. 22.2 for green light and the following impact parameters.
a. 0.5 b. 0.55 c. 0.6 d. 0.65 e. 0.7 f. 0.75
g. 0.8 h. 0.85 i. 0.9 j. 0.95

N14.(§) Use a spreadsheet to calculate and plot primary-rainbow viewing angles for a full range of impact parameters from 0 to 1, for the conditions in Fig. 22.2. Do this for light of wavelength (μm):
a. 0.4 b. 0.45 c. 0.5 d. 0.55 e. 0.6
f. 0.65 g. 0.7 h. 0.42 i. 0.47 j. 0.52
k. 0.57 m. 0.62 n. 0.67

N15.(§) Same as previous exercise but for a secondary rainbow.

N16. For yellow light in a 22° halo, what is the viewing angle for the following input angles? Use the conditions in Fig. 22.2.
a. 15° b. 20° c. 25° d. 30° e. 35°
f. 40° g. 45° h. 50° i. 55° j. 60°
k. 65° m. 70° n. 75° o. 80° p. 85°

N17. Same as the previous exercise, but for blue light.

N18.(§) Use a spreadsheet to generate curves for green light, similar to those drawn in Fig. 22.25 for the 22° halo. Use the conditions in Fig. 22.2.

N19.(§) Same as previous exercise, but for the 46° halo.

N20. For yellow light in a 46° halo, find the viewing angle for the following input angles. Use the conditions in Fig. 22.2.
a. 58° b. 60° c. 62° d. 64° e. 66° f. 68° g. 70°
h. 72° i. 74° j. 76° k. 78° m. 80° n. 82°
o. 84° p. 86° q. 88°

N21. Same as the previous exercise, but for blue light.

N22. Find the minimum viewing angle (i.e., the nominal halo angle) for green light using the conditions in Fig. 22.2 for the following ice-crystal wedge angle:
a. 25° b. 52.4° c. 56° d. 60° e. 62° f. 63.8°
g. 70.5° h. 80.2° i. 90° j. 120° k. 150°

N23. For a solar elevation of 10° and conditions as in Fig. 22.2, calculate the viewing angle components for a circumzenith arc for red light with a crystal rotation of β =
a. 10° b. 12° c. 14° d. 16° e. 18° f. 20°
g. 22° h. 24° i. 26° j. 28° k. 30°
m. 32° n. 34°

N24.(§) For conditions as in Fig. 22.2, calculate and plot circumzenith arcs similar to Fig. 22.33 for red and violet light, but for solar elevation angles of

a. 10° b. 12° c. 14° d. 16° e. 18° f. 20°
g. 22° h. 24° i. 26° j. 28° k. 30° m. 0°
n. 2° o. 4° p. 6° q. 8°

N25. For a solar elevation of 10°, calculate the viewing angle components for a sun dog for red light with the following crystal rotations β. Use the conditions in Fig. 22.2.

a. 15° b. 20° c. 25° d. 30° e. 35°
f. 40° g. 45° h. 50° i. 55° j. 60°
k. 65° m. 70° n. 75° o. 80° p. 85°

N26.(§) Calculate and plot sun dog arcs similar to Fig. 22.35, but for the following solar elevation angles. Use the conditions of Fig. 22.2 for green light.

a. 5° b. 15° c. 25° d. 30°
e. 35° f. 45° g. 50° h. 55° i. 60°

N27.(§) For $\gamma = 80°$, plot upper tangent arc elevation and azimuth angles for a ray of orange-yellow light, for a variety of evenly-space values of rotation angle. Use a solar elevation of:

a. 10° b. 12° c. 14° d. 16° e. 18° f. 8°
g. 22° h. 24° i. 26° j. 28° k. 30°
m. 32° n. 34° o. 36° p. 38° q. 40°

N28. Find the fraction of incident light that is scattered for an optical thickness of:

a. 0.01 b. 0.02 c. 0.05 d. 0.10 e. 0.2
f. 0.5 g. 1. h. 2 i. 3 j. 4
k. 5 m. 7 n. 10 o. 20 p. 50

N29. What fraction of incident red light is scattered from air molecules along a horizontal path near the Earth's surface, with path length (km) of

a. 0.5 b. 1 c. 2 d. 5 e. 10 f. 20 g. 50
h. 100 i. 200 j. 500 k. 1000 m. 2000

N30.(§) Calculate and plot the relative fraction of scattering as a function of wavelength, for Rayleigh scattering in air.

N31. For cloud droplets of 5 μm radius, find the corona fringe viewing angles for the 2nd through 8th fringes, for light of the following wavelength (μm):

a. 0.4 b. 0.45 c. 0.5 d. 0.55 e. 0.6
f. 0.65 g. 0.7 h. 0.42 i. 0.47 j. 0.52
k. 0.57 m. 0.62 n. 0.67

N32.(§) Calculate and plot the viewing angle vs. wavelength for the:

a. second corona fringe.
b. third corona fringe.
c. fourth corona fringe.

N33. (§) Calculate and plot the ratio of refractive index in air to a reference refractive index in air, for a variety of values of ratio of air density to reference air density.

N34. If the temperature decreases 10°C over the following altitude, find the mirage radius of curvature of a light ray. Assume a standard atmosphere at sea level.

a. 1 mm b. 2 mm c. 3 mm d. 4 mm
e. 5 mm f. 6 mm g. 7 mm h. 8 mm
i. 9 mm j. 1 cm k. 2 cm m. 3 cm
n. 4 cm o. 5 cm p. 10 cm q. 20 cm

Understanding & Critical Evaluation

U1. If light is coming from the water towards the air in Fig. 22.1 (i.e., coming along the θ_2 path but in the opposite direction), then sketch any incident and reflected rays that might occur.

U2. Salt water is more dense than fresh water. Sketch how light wave fronts behave as they approach the salt-water interface from the fresh water side.

U3. Is it possible for a material to have a refractive index less than 1.0 ? Explain.

U4. In general, how does the refractive index vary with temperature, pressure, and density?

U5. Use geometry and trig to derive eq. (22.6).

U6. Consider Fig. 22.5. If you were in a boat near the words "no escape here" and were looking into the water towards an object in the water at the black dot near the bottom of that figure, what would you see?

U7. Speculate on why rainbows are common with rain from cumulonimbus clouds (thunderstorms) but not with rain from nimbostratus clouds.

U8. If you were standing on a mountain top in a rain shower, and the sun was so low in the sky that sun rays were shining at a small angle upward past your position, could there be a rainbow? If so, where would it be, and how would it look?

U9. Use the relationship for reflection of light from water to describe the variations of brightness of a wavy sea surface during a sunny day.

U10. How does the intensity and color of light entering the rain drop affect the brightness of colors you see in the rainbow?

U11. Draw a sketch of a sun ray shining through a rain drop to make a primary rainbow. If red light is bent less than violet as a sun ray refracts and reflects through a rain drop, why isn't red on the inside of the primary rainbow instead of the outside?

U12. Use geometry to derive eq. (22.13).

U13. Use geometry to derive eq. (22.14).

U14. Draw a sketch of a sun ray path through a raindrop for a:
a. Tertiary rainbow b. Quaternary rainbow.
Your sketch must be consistent with the viewing angle listed for these rainbows.

U15. During the one reflection or two reflections of light inside a raindrop for primary and secondary rainbows, what happens to the portion of light that is not reflected? Who would be able to see it, and where must they look for it?

U16. Why are higher-order rainbows fainter than lower-order ones?

U17. If neither the primary or secondary rainbows return light within Alexander's dark band, why is it not totally black?

U18. Compare and contrast a twinned rainbow and supernumerary bows.

U19. Often hexagonal column ice crystals in the real atmosphere have indentations in their basal faces. These are known as hollow columns. How might that affect ice-crystal optical phenomena?

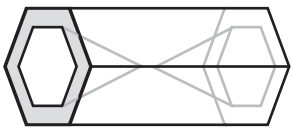

U20. For hexagonal columns, what other crystal angles exist besides 60° and 90°? For these other crystal angles, at what viewing angles would you expect to see light from the crystal?

U21. In Fig. 22.18, why are plate-crystal wobble and column-crystal rotation necessary to explain a sun pillar?

U22. Fig. 22.18d shows a dendrite ice crystal. In addition to the sun pillar, for what other halos & optical phenomena might such dendrites be important?

U23. Fig. 22.22a has only reflection while Fig. 22.22b also has two refractions. How might this affect the color of subsuns?

U24. Eq. (22.15) does not consider the finite size of a hexagonal column. What range of input angles would actually allow rays to exit from the face sketched in Fig. 22.24 for 22° halos?

U25. Use geometry to derive eq. (22.15) for the 22° halo.

U26. Derive equation (22.16) for the minimum viewing angle for halos. (You might need calculus for this).

U27.(§) Suppose a halo of 40° was discovered. What wedge angle β_c for ice would cause this?

U28. When the sun is on the horizon, what is the angle between the 22° halo and the bottom of the circumzenith arc?

U29. Is it possible to see both a circumzenith and a circumhorizon arc at the same time? Explain.

U30 Why might only one of the sun dogs appear?

U31. Using geometry, derive the minimum thickness to diameter ratio of hexagonal plates that can create sun dogs, as a function of solar elevation angle.

U32. For both sun dogs and rainbows, the red color comes via a path from the sun to your eyes that does not allow other colors to be superimposed. However, for both phenomena, as the wavelength gets shorter, wider and wider ranges of colors are superimposed at any viewing angle. Why, then, do rainbows have bright, distinct colors from red through violet, but sundogs show only the reds through yellows, while the large viewing angles yield white color rather than blue or violet?

U33. Why are the tangent arcs always tangent to the 22° halo?

U34. Sometimes it is possible to see multiple phenomena in the sky. List all of the optical phenomena associated only with
a. large hexagonal plates
b. large hexagonal columns
c. small hexagonal columns
d. small hexagonal plates
e. large hexagonal pyramids

U35. If optical depth is defined as the optical thickness measured vertically from the top of the atmosphere, then sketch a graph of how optical depth might vary with height above ground for a standard atmosphere.

U36. If you take photographs using a polarizing filter on your camera, what is the angle between a line from the subject to your camera, and a line from the subject to his/her shadow, which would be in the proper direction to see the sky at nearly maximum polarization? By determining this angle now, you can use it quickly when you align and frame subjects for your photographs.

U37 In the Radiation chapter, Beer's law was introduced, which related incident to transmitted light. Assume that transmitted light is 1 minus scattered light.

a. Relate the Rayleigh scattering equation to Beer's law, to find the absorption coefficient associated with air molecules.

b. If **visibility** is defined as the distance traveled by light where the intensity has decreased to 2% of the incident intensity, then find the visibility for clean air molecules.

c. Explain the molecular scattering limit in the atmospheric transmittance curve of Fig. 8.4a in the Remote Sensing chapter.

U38. Discuss the problems and limitations of using visibility measurements to estimate the concentration of aerosol pollutants in air.

U39. For atmosphere containing lots of 1.5 μm diameter sulfuric acid droplets, describe how the sky and sun would look during a daily cycle from sunrise past noon to sunset.

U40. To see the brightest fringes furthest from the sun during a corona display, what size cloud droplets would be best?

U41. If you were flying above a cloud during daytime with no other clouds above you, describe why you might not be able to see glory for some clouds.

U42. Contrast and compare the refraction of light in mirages, and refraction of sound in thunder (see the Thunderstorm chapter). Discuss how the version of Snell's law in the Thunderstorm chapter can be applied to light in mirages.

U43. Microwaves are refracted by changes in atmospheric humidity. Use Snell's law or Huygens' principle to describe how ducting and trapping of microwaves might occur, and how it could affect weather radar and air-traffic control radar.

U44. What vertical temperature profile is needed to see the Fata Morgana mirage?

U45. Green, forested mountains in the distance sometimes seem purple or black to an observer. Also, the mountains sometimes seem to loom higher than they actually are. Discuss the different optical processes that explain these two phenomena.

U46. Paint on traffic signs and roadway lines is often sprinkled with tiny glass spheres before the paint dries, in order to make the signs more reflective to automobile headlights at night. Explain how this would work. Also, would it be possible to see other optical phenomena from these glass spheres, such as rainbows, halos, etc? Justify your answer.

Web-Enhanced Questions

W1. Search the web for images of the following atmospheric optical phenomena:

a. 22° halo b. 46° halo
c. sun dogs d. sub sun dogs
e. sub sun f. sun pillar
g. supersun h. upper tangent arc
i. parhelic circle j. lower tangent arc
k. white clouds l. circumzenith arc
m. Parry arcs n. primary rainbow
o. red sunset p. secondary rainbow
q. blue sky r. Alexander's dark band
s. corona t. crepuscular rays
u. iridescence v. anti-crepuscular rays
w. glory x. fata morgana
y. green flash z. mirages
aa. halos other than 22° and 46°
ab. circumhorizon arc ac. circumscribed halo
ad. Lowitz arcs ae. Scheiner's halo
af. Moilanen arc ag. Hastings arc
ah. Wegener arc ai. supralateral arc
aj. infralateral arcs ak. subhelic arc
am. heliac arc an. diffuse arcs
ao. Tricker arc ap. 120° parhelia (120° sun dogs)
aq. various subhorizon arcs
ar. fog bow as. blue moon
at. reflection rainbow au. twinned rainbow
av. supernumerary bows

W2. Search the web for images and descriptions of additional atmospheric phenomena that are not listed in the previous question.

W3. Search the web for microphotographs of ice crystals for ice Ih. Find images of hexagonal plates, hexagonal columns, and hexagonal pyramids.

W4. Search the web for diagrams or microphotographs of ice crystals for cubic ice Ic.

W5. Search the web for lists of indices of refraction of light through different materials.

W6. Search the web for highway camera or racetrack imagery, showing inferior mirages on the roadway.

W7. Search the web for computer programs to simulate atmospheric optical phenomena. If you can download this software, try running it and experimenting with different conditions to produce different optical displays.

W8. Search the web for images that have exceptionally large numbers of atmospheric optical phenomena present in the same photograph.

W9. Search the web for information on linear vs. circular polarization of sky light. Polarizing filters for cameras can be either circular or linear polarized. The reason for using circular polarization filters is that many automatic cameras loose the ability to auto focus or auto meter light through a linear polarizing filter. Compare how clear sky would look in a photo using circular vs. linear polarization filters.

W10. Search the web for literature, music, art, or historical references to atmospheric optical phenomena, other than the ones already listed in this chapter.

W11. Search the web for info on the history of scientific understanding of atmospheric optical phenomena. (E.g., Snell's law, etc.)

Synthesis Questions

S1. Suppose atmospheric density were (a) constant with height; or (b) increasing with height. How would optical phenomena be different, if at all?

S2. How would optical phenomena be different if ice crystals were octagonal instead of hexagonal?

S3. Suppose the speed of light through liquid and solid water was faster than through air. How would optical phenomena be different, if at all?

S4. After a nuclear war, if lots of fine Earth debris were thrown into the atmosphere, what optical phenomena would cockroaches (as the only remaining life form on Earth) be able to enjoy?

S5. Using the data in Fig. 22.2, fit separate curves to the refractive index variation with wavelength for air, water, and ice. Can you justify any or all of the resulting equations for these curves based on physical principles?

S6. Knowing the relationship between optical phenomena and the cloud (liquid or water) microphysics, and the relationship between clouds and atmospheric vertical structure, cyclones and fronts, create a table that tells what kind of weather would be expected after seeing various optical phenomena.

S7. If large raindrops were shaped like thick disks (short cylinders) falling with their cylinder axis vertical, how would rainbows be different, if at all?

S8. If large ice crystals were shaped like cylinders falling with their cylinder axis horizontal, how would ice-crystal optics be different, if at all?

S9. Consider Fig. 22.5. Could a thin layer of different fluid be floated on the liquid water to allow all light ray angles to escape from liquid to air? Justify your proposal.

S10. If there were two suns in the sky, each with light rays going to the same raindrop but arriving from different angles, is there a special angle between the arriving sun rays such that the two separate rainbows reinforce each other to make a single brighter rainbow?

S11. Design an ice-crystal shape that would cause:
a. different halos and arcs than exist naturally.
b. a larger number of natural halo and arcs to occur simultaneously.

S12. Suppose rain drops and ice crystals could cause refraction but not reflection or diffraction. What atmospheric optical phenomena could still exist? Justify your answers.

S13. Suppose that spacecraft landing on other planets can photograph optical phenomena such as halos, arcs, bows, etc. Describe how you could analyze these photographs to determine the chemicals and/or temperature of these planetary atmospheres.

S14. Design equipment to be used in the Earth's atmosphere that could determine the vertical temperature profile by measuring the characteristics of mirages.

Copyright © 2011, 2015 by Roland Stull. *Meteorology for Scientists and Engineers, 3rd Ed.*

FUNDAMENTALS OF SCIENCE

CONTENTS

Dimensions and Units 870
- Standards 870
- Unit Conversion 871

Functions and Finite Difference 872

Relationships and Graphs 873
- Linear 873
- Logarithmic 873
- Power 874

Errors 875
- Systematic Error & Accuracy 875
- Random Error & Precision 875
- Reporting Observations 875
- Error Propagation 876

On Doing Science 877

Summary 878

Exercises 878
- Numerical Problems 878
- Understanding & Critical Evaluation 878
- Web Enhanced Questions 878
- Synthesis Questions 878

Science Graffito

"When you make the finding yourself — even if you're the last person on Earth to see the light — you'll never forget it." — *Carl Sagan*.

"Meteorology for Scientists and Engineers, 3rd Edition" by Roland Stull is licensed under a Creative Commons Attribution-NonCommercial-ShareAlike 4.0 International License. To view a copy of the license, visit http://creativecommons.org/licenses/by-nc-sa/4.0/ . This work is available at http://www.eos.ubc.ca/books/Practical_Meteorology/ .

Many physical sciences including atmospheric science share the same fundamental definitions and analysis techniques. These fundamentals include problem-solving methods, standard units, ways of expressing relationships, formats for plotting the results, measurement uncertainty, and error propagation. The fundamentals reviewed here are used throughout this book.

ON DOING SCIENCE • Problem Solving

The following method aids understanding the problem, speeds solution, and helps to avoid errors. This method is used throughout the book in the various solved examples.

1) List the "Given" variables with their symbols, values and units.
2) List the unknown variables to "Find", with units.
3) Sketch the objects, velocities, etc. if appropriate.
4) Determine which equation(s) contains the unknown variable as a function of the knowns. This equation might need to be rearranged to solve for the unknown. If the solution equation contains more unknowns, find additional equations for them.
5) Make assumptions, if necessary, for any of the unknowns for which you have no equations. Clearly state your assumptions, and justify them.
6) Solve the equations using the known or assumed values, being sure to carry along the units. Show your intermediate steps.
7) Identify the final answer by putting a box around it, underlining it, or making it bold face.
8) Check your answer. If the solved units don't match the desired units of the unknown, then either a mistake was made, or unit conversion might be needed (e.g., convert from knots to m/s). Also, certain functions such as "ln" and "exp" require arguments that are dimensionless, while trig functions like "sine" need an argument in degrees or radians. These are clues to help catch mistakes. Also, compare your answer with your sketch, to check if it is physically reasonable. Check other physical constraints (e.g., humidities cannot be negative, speeds cannot be infinite).
9) Discuss the significance of the answer.

Table A-1. Basic dimensions and their SI units.

Dimension	Unit	Abbrev.
length	meter	m
mass	kilogram	kg
time	second	s
electrical current	ampere	A
temperature (thermodynamic)	kelvin	K
amount of substance	mole	mol
luminous intensity	candela	cd

Table A-2. Some derived dimensions & their SI units.

Dimension	Unit (Abbrev.)	Composition
force	newton (N)	$kg{\cdot}m{\cdot}s^{-2}$
energy	joule (J)	$kg{\cdot}m^2{\cdot}s^{-2}$
power	watt (W)	$kg{\cdot}m^2{\cdot}s^{-3}$
pressure, stress	pascal (Pa)	$kg{\cdot}m^{-1}{\cdot}s^{-2}$
temperature	degree Celsius (°C)	T(K) – 273.15
frequency	hertz (Hz)	s^{-1}
electric charge	coulomb (C)	s·A
electric potential	volt (V)	$m^2{\cdot}kg{\cdot}s^{-3}{\cdot}A^{-1}$
electric resistance	ohm (Ω)	$m^2{\cdot}kg{\cdot}s^{-3}{\cdot}A^{-2}$
plane angle	radian (rad)	$m{\cdot}m^{-1}$
solid angle	steradian (sr)	$m^2{\cdot}m^{-2}$

Table A-3. Prefixes. (*Size is in terms of USA "short scale" designations. Some international "long scale" designations are shown in *italics*, if different.)

Multiplier	Size*	Unit	Abbrev.
10^{24}	septillion (*quadrillion*)	yotta	Y
10^{21}	sextillion (*trilliard*)	zetta	Z
10^{18}	quintillion (*trillion*)	exa	E
10^{15}	quadrillion (*billiard*)	peta	P
10^{12}	trillion (*billion*)	tera	T
10^{9}	billion (*milliard*)	giga	G
10^{6}	million	mega	M
10^{3}	thousand	kilo	k
10^{2}	hundred	hecto	h
10^{1}	ten	deka	da
10^{-1}	tenth	deci	d
10^{-2}	hundredth	centi	c
10^{-3}	thousandth	milli	m
10^{-6}	millionth	micro	μ
10^{-9}	billionth	nano	n
10^{-12}	trillionth	pico	p
10^{-15}	quadrillionth	femto	f
10^{-18}	quintillionth	atto	a
10^{-21}	sextillionth	zepto	z
10^{-24}	septillionth	yocto	y

DIMENSIONS AND UNITS

Standards

There are seven basic dimensions in science, from which all other dimensions are derived (Table A-1). The first letters of the first three units are 'm, k, s'; hence, this system of units is sometimes called the **MKS system**. It has been adopted as the international system (**SI**) of units.

Derived units are formed from combinations of basic units. Examples of derived units that are used frequently in meteorology are listed in Table A-2.

A **prefix** can be added in front of these units to indicate larger or smaller values, such as kilometer (km), which is 1000 meters. The most commonly used prefixes are given in Table A-3. In this book, units and prefixes are NOT italicized, while *variables are italicized*. Other units are listed in Table A-4.

When we quantify things in nature, the value has four parts (but magnitude and prefix are optional):

•(A.1)

value = number · magnitude · prefix · units

A **scientific notation** example is:

distance value = $5x10^2$ km

where number = 5, magnitude = 10^2 (= 100), prefix = k (=1000), and units = m. This is equivalent to 500,000 m. The value must include the units (except for a few things that are truly dimensionless). The number can include a negative sign (–) if needed.

Table A-4. Some other units. (* unofficial symbol)

Name	Symbol	Value in SI units
minute	min	1 min = 60 s
hour	h	1 h = 60 min = 3600 s
day	d	1 d = 24 h = 86,400 s
degree (angle)	°	1° = (π/180) rad
liter (or litre)	L	1 L = 10^{-3} m^3
metric ton (or tonne)	t	1 t = 10^3 kg
astronomical unit	ua	1 ua ≈ 1.49598 x 10^{11} m
ångström	Å	1 Å = 10^{-10} m
nautical mile	nm*	1 naut. mile = 1852 m
knot	kt*	1 knot = (1852 m / 3600 s)
hectare	ha	1 ha = 10^4 m^2
bar	bar	1 bar = 100 kPa = 10^5 Pa

FOCUS • Binary multiples

The IEEE Standards Board officially adopted the SI units of Table A-3. For example, 1 kilobit = 1000 bits.

CAUTION: Historically, manufacturers have called 2^{10} bits (=1,024 bits) as 1 kilobit (NOT SI standard), 2^{20} bits (=1,048,576) as 1 megabit (NOT SI standard), 2^{30} bits (=1,073,741,824) as 1 gigabit (NOT SI std.).

Unit Conversion

Create ratios of equivalent values to enable easy unit conversion. For example, a velocity of 1 knot equals 0.51 m/s. Because these two values equal, their ratio must be one:

$$1 = \frac{(1 \text{ knot})}{(0.51 \text{ m/s})} \qquad \text{(A.2)}$$

[*CAUTION: Although the numbers 1 and 0.51 do NOT equal each other (and their ratio does NOT equal 1), the values include the units, and hence the ratio of values does equal 1.*]

The inverse of 1 is 1, thus, it makes no difference which value appears in the numerator. For example:

$$1 = \frac{(0.51 \text{ m/s})}{(1 \text{ knot})} \qquad \text{(A.3)}$$

When any quantity is multiplied by 1, its value does not change. Hence, by multiplying a velocity by the ratio in eqs. (A.2) or (A.3), we can change the units without changing the physics or the value.

Even if a conversion relationship is not known, you can sometimes figure it out if you know equivalent values that apply to a situation. For example, what is the conversion between pressure in "pounds per square inch" (PSI) and in "inches of mercury" (in Hg). Perhaps you might already know that the average pressure at sea level is 14.7 PSI. You might also know that standard sea-level pressure is 29.92 in Hg. Thus, these two values are equivalent at sea level, and their ratio gives the conversion between them:

$$1 = \frac{(14.7 \text{ PSI})}{(29.92 \text{ in Hg})} = 0.49 \frac{(\text{PSI})}{(\text{in Hg})}$$

or 1 in Hg = 0.49 PSI.

Ratios can also be formed to add or remove prefixes and magnitudes to units. For example, 1 milligram (mg) equals 0.001 grams, by definition. Thus their ratio is one. We can use this ratio to find 5×10^7 mg in units of kg. For example:

$$(5 \times 10^7 \cancel{\text{mg}}) \cdot \frac{0.001 \cancel{\text{g}}}{1 \cancel{\text{mg}}} \cdot \frac{1 \text{ kg}}{1000 \cancel{\text{g}}} = 50 \text{ kg}$$

This trick of forming ratios to do conversions works only when both units have the same zero point. In the example above, 0 PSI = 0 inHg. Similarly, 0 m/s = 0 knots. This trick fails for temperature conversions, because °F, °C, and K all have different zero points. For temperature conversions, you must use special conversion formulae, as described in the "Relationships and Graphs" section.

Solved Example

Convert a wind speed of 10 knots into m/s.

Solution:

Given: $M = 10$ kt wind speed

Find: $M =$? m/s

Multiply wind speed by 1 in the form of eq. (A.3):

$$M = 10 \text{ kt} = (10 \text{ kt}) \cdot 1$$

$$= (10 \text{ kt}) \cdot \left(\frac{0.51 \text{ m/s}}{1 \text{ kt}} \right)$$

$$= \left(\frac{10 \cdot 0.51}{1} \right) \cdot \left(\frac{\cancel{\text{kt}} \cdot (\text{m/s})}{\cancel{\text{kt}}} \right) \quad \text{grouping}$$

$$= \underline{\mathbf{5.1 \text{ m/s}}}$$

Check: Units OK. Physically reasonable.

Discussion: Note how we grouped the numbers separately from the units. You can calculate the number group using your calculator. You can reduce the units group by canceling identical units in the numerator and denominator (such as knots, in this example).

How do you know whether to use (A.2) or (A.3)? Given a value with knots in the numerator, we want to multiply it by a ratio that has knots in the denominator, so that the knots will cancel. Eq. (A.3) will work.

Solved Example

Sometimes you can use units to guess the form of an equation. For example, metabolic heat-production rate by humans sitting quietly is about 100 watts. Find the number of calories produced in half a day.

Solution

Given: $C = 100$ W, $\Delta t = 0.5$ d

Find: $B =$? cal heat production

Eqs: From tables of unit conversion in other books

1 W = 14.3353 cal/min, 1 h = 60 min, & 1 d = 24 h

By forming each of these equivalences as ratios, you can convert from watts into calories, and then from minutes into hours into days:

$$C = (100 \cancel{\text{W}}) \cdot \left(\frac{14.3353 \text{ cal/}\cancel{\text{min}}}{1 \cancel{\text{W}}} \right) \cdot \left(\frac{60 \cancel{\text{min}}}{1 \cancel{\text{h}}} \right) \cdot \left(\frac{24 \cancel{\text{h}}}{1 \text{ d}} \right)$$

$$= 2.06 \times 10^6 \text{ cal/d}$$

By looking at the units of the last line it is obvious that if we multiply it by the time Δt in days, then we will be left with our desired units of calories. Thus, the final equation is:

B(cal) = C(cal/day) $\cdot$ Δt(day)

$$= (2.06 \times 10^6 \text{ cal/d}) \cdot (0.5 \text{ d}) = \underline{\mathbf{1.03 \times 10^6 \text{ cal}}}$$

Check: Units OK. Physically reasonable.

Discussion: Over a million calories of heat is given off by a human sitting still for half a day. The number of calories of food we eat should be sufficient to replace those calories burned metabolically. Caution: "calories" listed on food packages are really kilocalories.

Solved Example

Suppose the air at the ground has a temperature of 20°C, while the air at height 500 m is 15 °C. Find the vertical temperature gradient.

Solution

Given:

z_2 = 500 m top altitude
z_1 = 0 m ground altitude
$T_2 = T(z_2)$ = 15 °C temperature at 500 m altitude
$T_1 = T(z_1)$ = 20 °C temperature at ground

Find: $\Delta T/\Delta z$ = ? °C/m
temperature gradient

Sketch:

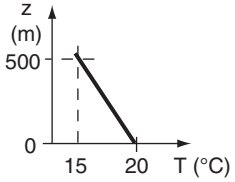

Use definition of a gradient:

$\Delta T/\Delta z = (T_2 - T_1) / (z_2 - z_1)$
= (15°C – 20°C) / (500 m – 0 m)
= (– 5 °C) / (500 m) = **– 0.01°C/m**

Check: Units OK. Sketch OK. Sign negative.

Discussion: If this gradient is constant with height, then the temperature at your head is 0.02°C colder than at your toes, assuming you are roughly 2m tall.

CAUTION: Suppose you erroneously had computed the gradient as (20 – 15°C) / (500 – 0 m). Then your answer would have had the wrong sign, because you had erroneously computed $(T_1–T_2)/(z_2–z_1)$ instead of the desired $(T_2–T_1)/(z_2–z_1)$. Always form your differences in the same order (point 2 – point 1) in both the numerator and denominator.

BEYOND ALGEBRA • Calculus

In theoretical meteorology, the physics of the atmosphere is described by differential equations. Outside of these "Beyond Algebra" boxes, we utilize the following approximations to avoid calculus.

A derivative can be approximated as:

$$\frac{\partial T}{\partial z} \approx \frac{\Delta T}{\Delta z} \qquad \text{for small } \Delta z$$

A total derivative:

$$\frac{dT}{dt} = \frac{\partial T}{\partial t} + U\frac{\partial T}{\partial x} + V\frac{\partial T}{\partial y} + W\frac{\partial T}{\partial z}$$

is approximated as:

$$\approx \frac{\Delta T}{\Delta t} + U\frac{\Delta T}{\Delta x} + V\frac{\Delta T}{\Delta y} + W\frac{\Delta T}{\Delta z}$$

Also, you can approximate an integral by a sum:

$$\int T\ dz \approx \sum T(z)\cdot\Delta z$$

where T is temperature, z is height, t is time, (U, V, W) are wind components in the (x, y, z) directions, which are positive toward the (east, north, up).

FUNCTIONS AND FINITE DIFFERENCE

As in other fields of science and engineering, functional relationships describe how one variable (the **dependent** variable) changes when one or more other variables (the **independent** variables) change. Suppose that P_2 is the pressure at time t_2, and P_1 is the pressure at time t_1. Pressure "varies" with time, or "is a function of time". Such functional dependence is written generically as $P(t)$. For a single value of pressure that occurs at specific time, such as at t = 50 s, the notation P(50 s) is used.

The symbol Δ means change or difference. Differences must always be taken in the same direction relative to the independent variable. For example, if temperature T and pressure P both vary with time t, then ΔT and ΔP are defined as their values at the later time minus their values at the earlier time. For example, $\Delta T = T(t_2) - T(t_1)$, and $\Delta P = P(t_2) - P(t_1)$, where t_2 is later than t_1. The notation is sometimes simplified to be $\Delta T = T_2 - T_1$ and $\Delta P = P_2 - P_1$ for $\Delta t = t_2 - t_1$.

In a different example, let temperature T depend on independent variable height z. Then

$$\Delta T = T(z_2) - T(z_1) = T_2 - T_1$$

and

$$\Delta z = z_2 - z_1$$

where z_2 is higher than z_1. Furthermore, a ratio such as $\Delta T/\Delta z$ is equivalent to $(T_2 - T_1)/(z_2 - z_1)$, or $[T(z_2) - T(z_1)]/(z_2 - z_1)$, where the differences in the numerator and denominator must always be taken in the same direction (e.g., point 2 – point 1). Don't be deceived into subtracting the smaller value from the larger one when you compute a finite difference, because if you do, the sign of your answer might be wrong (see the Solved Example on this page).

The change of something with distance is called a **gradient**. Thus, $\Delta T/\Delta z$ is a **vertical temperature gradient**.

Although calculus is a useful mathematical tool for studying the physics of the atmosphere, this book is designed for an audience who might not have had calculus. In the place of differential calculus we will use finite differences, Δ. In place of integral calculus, we will use sums or graphically examine the area under curves.

However, for those students with a calculus background, "Beyond Algebra" boxes are scattered here and there in the book to provide a taste of theoretical meteorology. These "Beyond Algebra" boxes are surrounded by a double line as shown at left, and may be safely skipped by students wishing to avoid calculus.

RELATIONSHIPS AND GRAPHS

Although $T(z)$ says that there is some functional relationship between temperature T and height z, it does not specify what that relationship is. Temperature could increase as height increases. It could decrease as height increases. It could increase with the square of height. It could vary logarithmically with height. It could be invariant with height.

The particular form of the function might be governed by some underlying physics, and have a fixed functional form that is sometimes called a physical "law" or a mathematical definition. Other relationships can be found by plotting observational data.

Linear, **semi-log** and **log-log** graphs are frequently used to discover and display relationships between dependent and independent variables.

Linear

A **linear** relationship yields a straight line on a **linear graph** (values along both axes increase at constant rates with distance from the origin).

For example, the relationship between temperature in degrees Celsius and Fahrenheit is linear; namely, temperature in Fahrenheit is proportional to the first power of temperature in Celsius

$$T_{\circ F} = a \cdot T_{\circ C} + b \qquad \bullet(A.4)$$

where the parameters in this equation are a = 9/5 (°F/°C) and b = 32 °F, see Fig. A.1.

The slope (change in values along the vertical axis per change of values along the horizontal axis) of the line equals the factor a, which is 9/5 in this case. As shown in Fig. A.1, the nonzero parameter b causes the plotted line to cross the vertical axis not at the origin $(T_{\circ C}, T_{\circ F}) = (0, 0)$, but at an intercept of T = 32°F [i.e., at point (0°C, 32°F].

The relationship between temperature in degrees Celsius and absolute temperature in kelvins is also linear:

$$T(\text{K}) = T(\text{°C}) + 273 \qquad \bullet(A.5)$$

If plotted on a linear graph, the slope would be 1 and the intercept is 273 K. Most equations using temperature require the use of absolute temperature.

Logarithmic

An **exponential** or **logarithmic** relationship gives a straight line when plotted on a **semi-log graph** (one axis is linear, the other is logarithmic).

For example, the decrease of pressure with height is logarithmic in atmospheres where the temperature is constant with height:

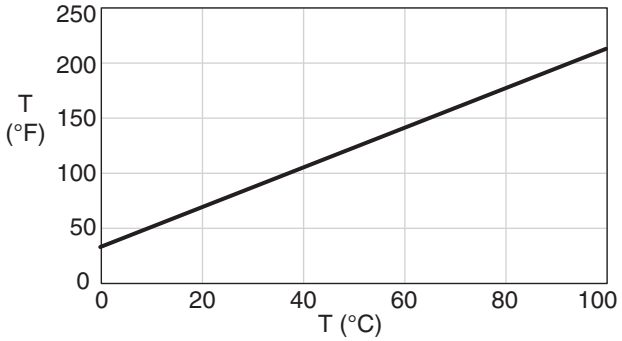

Figure A.1
Relationship between Celsius (°C) and Fahrenheit (°F) temperature (T), plotted on a linear graph.

Solved Example
Convert 10°C to Fahrenheit.

Solution:
Given: $T_{\circ C}$ = 10°C. Find: $T_{\circ F}$ = ? °F

Sketch: (see Fig A.1). Use eq. (A.4):
$T_{\circ F} = a \cdot T_{\circ C} + b$
= (9/5 °F/°C)·(10°C) + 32°F
= 18°F + 32°F = **50°F**

Check: Units OK. Sketch OK. Physics OK.
Discussion: As the temperature in Celsius increases by equal amounts of 10°C, the corresponding Fahrenheit values increase in equal amounts of 18°F. Such a constant rate of increase of the dependent variable for a constant rate of increase of independent variable indicates a linear relationship.

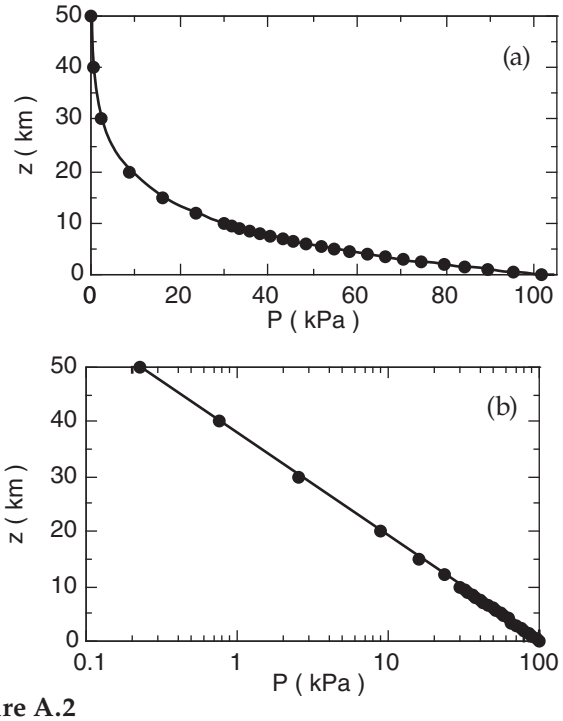

Figure A.2
Height z vs. pressure P in the atmosphere, plotted on (a) linear; and (b) semi-log graphs. (Copied from Chapter 1.)

Solved Example

At what height does P = 50 kPa, given T = 0°C?

Solution

Given: P = 50 kPa, T = 0 + 273.15 = 273.15 K.
Find: z = ? km

Solve eq. (A.6) for z: $z = (T/a) \cdot \ln(P_o/P)$
z = [(273.15K) / (0.0342 K/m)] · ln(101.3kPa/50kPa)
= (7987 m) · ln(2.026) = 5639 m = **5.6 km**.

Check: Units OK. Agrees with Fig. A.2.
Discussion: At this height the air is so thin that people would die of **hypoxia** (lack of oxygen) unless they breath pressurized oxygen.

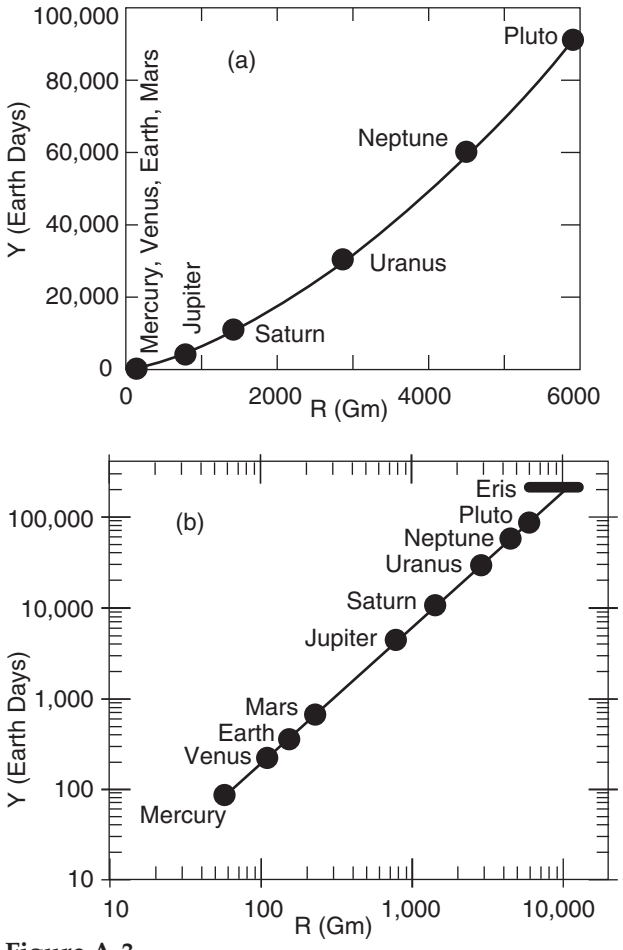

Figure A.3
Plot of planetary orbital periods in Earth days versus distance from sun in billions of meters, on (a) linear, (b) log-log graphs.

Solved Example

Find the orbital period of Mercury (R = 58 Gm).

Solution

Given: R = 58 Gm. Find: Y = ? d
Use eq.(A.7): Y = [0.1996 d·(Gm)$^{-3/2}$] · (58 Gm)$^{3/2}$ = **88d**
Check: Units OK. Agrees with Fig. A.3
Discussion: 4 orbits of Mercury per each Earth orbit.

$$\ln\left(\frac{P}{P_o}\right) = \frac{-a}{T} \cdot z \qquad \text{(A.6)}$$

where a = 0.0342 K/m, P_o = 101.3 kPa for Earth, and average temperature T must be in Kelvin.

[CAUTION: symbol a in this equation has a different value than in the previous equation. I often re-use symbols in this book, because there are not enough symbols for all the variables.]

Fig. A.2 plots the relationship between P and z in both linear and semi-log graphs, for T = 280 K. Pressure decreases rapidly with height near the ground, but decreases more slowly at higher altitude.

From Fig. A.2a we see that the portion of the curve in the lowest 3 km of the atmosphere is almost a straight line, and conclude that the variation of pressure with height is nearly linear in that region. Near the ground, the pressure decreases roughly 10 kPa with each 1 km height gain.

Fig. A.2b plots P with a logarithmic scale along the bottom axis, and plots z with a linear scale on the vertical axis. All of the data points at all heights fall on a straight line on this graph. This is evidence that the logarithm of P is proportional to z.

Power

If the dependent variable is proportional to a **power** of the independent variable, then the data will appear as a straight line on a **log-log graph** (both axes are logarithmic).

For example, Johannes Kepler, the 17th century astronomer, discovered that planets in the solar system have elliptical orbits around the sun, and that the time period Y of each orbit is related to the average distance R of the planet from the sun by:

$$Y = a \cdot R^{3/2} \qquad \text{(A.7)}$$

Parameter $a \approx 0.1996$ d·(Gm)$^{-3/2}$, where d is the abbreviation for Earth days and Gm is gigameters (= 10^6 km).

Using a table of the average distance of the planets from the sun (see Numerical Exercise N1 in the Radiation chapter), you can calculate orbital period using eq. (A.7). These are plotted in Fig. A.3a on a linear-linear graph, and in Fig. A.3b on a log-log graph (copied from the Radiation chapter).

The slope of the straight line on the log-log graph (Fig. A.3b) equals the power of the exponent. Namely, the range of orbital periods between Mercury and Pluto is about 3 decades (i.e., 100 to 1,000 to 10,000 to 100,000), while the range of distances from the sun is 2 decades. Thus, the slope is 3 to 2, as indicated in eq. (A.7).

ERRORS

Error is the difference between a measured (or estimated) value and the true (or reference) value.

Systematic Error & Accuracy

If part of the error is **systematic** or **repeatable** (namely, you get the same error each time you make a measurement), then the difference between the average measurement and the true value is called the **bias**. Smaller bias magnitude (i.e., lower systematic errors) corresponds to greater **accuracy**. Namely, accuracy indicates how close your **average** observations are to truth (Fig. A4).

Systematic errors can be due to **errors in instrument calibration**, **personal errors** (such as parallax error in reading a dial), **erroneous experimental conditions** (such as not shielding a thermometer from sunlight), and **imperfect technique** (such as breathing on a thermometer before you read it).

If you can calculate or otherwise know the bias, then you can remove this bias from your observations to correct for systematic error. Namely, you can easily make your corrected observations more accurate.

Random Error & Precision

After removing systematic errors, you might find that your observations still have some unexplained variability from measurement to measurement. These are called **random errors** (Fig. A.4). Experiments with smaller random errors are said to have higher **precision**; namely, are more precise. The **standard deviation** (or spread) of your observations is a measure of the random error — greater standard deviation indicates greater random error and lower precision.

Random errors can be due to **errors in judgement** (such as by manually reading a dial with poor resolution), **fluctuating conditions** (such as trying to determine sea level on a wavy ocean), **small disturbances** (such mechanical vibrations of an instrumented tower in high winds), and **errors in definition** (such as measuring the dimension of a fractal-shaped cloud, which depends on the size of the measuring stick).

Unfortunately, the probabilistic nature of random errors makes them difficult to remove after the fact. Often, the only recourse is to repeat the experiment under better controlled conditions and with higher quality instruments, and be sure to take a large number of observations to improve the statistical robustness of your results.

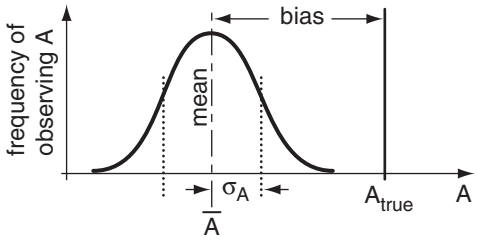

Figure A.4
The dark curve is the frequency that different A values are observed. Accuracy is related to bias. Precision is related to spread of curve (described by standard deviation σ_A). $\overline{A}$ is the mean.

Reporting Observations

For any variable A that you have measured N times to yield a **data set** (A_1, A_2, A_3, ..., A_N), let $\overline{A}$ be the **mean value**, and σ_A be the **standard deviation**. These are defined as:

$$\overline{A} = \frac{1}{N}\sum_{i=1}^{N} A_i \qquad \bullet(A.8)$$

and

$$\sigma_A = \left[\frac{1}{(N-1)}\sum_{i=1}^{N}(A-\overline{A})^2\right]^{1/2} \qquad \bullet(A.9)$$

where i is a **dummy index** that points to a single **data element** A_i in your data set.

After removing any known biases, the resulting observation is usually reported or written as a mean (average) value plus or minus (±) the standard deviation:

$$A = \overline{A} \pm \sigma_A \qquad \bullet(A.10)$$

where the precision or **standard uncertainty** is given by the standard deviation σ_A.

Solved Example

Given these T observations: (15, 13, 20, 12, 10, 17, 18)°C. T_{true} = 8°C. Find the mean, bias & std dev.

Solution

Given: T_{true} = 8°C, and the data set above.
Find: $\overline{T}$ = ? °C, σ_T = ? °C, bias = ? °C.

Use eq. (A.8): $\overline{T}$ = (1/7)(15+13+20+12+10+17+18) = **15°C**
Define the deviation from mean as: $T' = T - \overline{T}$
Thus, our observation have T' = (0, –2, 5, –3, –5, 2, 3)°C
Use eq. (A.9), rewritten as $\sigma_T = [(N-1)^{-1}\,\Sigma(A'^2)]^{1/2}$
Thus: $\sigma_T = [(1/6)\cdot(0+4+25+9+25+4+9)(°C)^2]^{1/2}$ = **3.56°C**
From the raw observations: **T = 15 ± 3.56 °C** .
Bias = $\overline{T} - T_{true}$ = 15 – 8 °C = **7°C** .

Check: Units OK. We seem to have a warm bias.
Discussion: Our observations are **not accurate** (large bias) and are **not precise** (large σ_T).

BEYOND ALGEBRA • Error Propagation

Suppose D is a function of A , B and C, where C is not a constant. Namely: $D(A, B, C)$.

If the error standard deviations σ_A, σ_B, and σ_C for A, B & C are known, then the **propagation of errors** into the standard deviation σ_D of variable D is:

$$\sigma_D = \left[\left(\frac{\partial D}{\partial A}\right)^2 \cdot \sigma_A^2 + \left(\frac{\partial D}{\partial B}\right)^2 \cdot \sigma_B^2 + \left(\frac{\partial D}{\partial C}\right)^2 \cdot \sigma_C^2 + 2r_{AB} \cdot \left(\frac{\partial D}{\partial A}\right) \cdot \left(\frac{\partial D}{\partial B}\right) \cdot \sigma_A \cdot \sigma_B + 2r_{AC} \cdot \left(\frac{\partial D}{\partial A}\right) \cdot \left(\frac{\partial D}{\partial C}\right) \cdot \sigma_A \cdot \sigma_C + 2r_{BC} \cdot \left(\frac{\partial D}{\partial B}\right) \cdot \left(\frac{\partial D}{\partial C}\right) \cdot \sigma_B \cdot \sigma_C \right]^{1/2} \quad \text{(A.a)}$$

The correlation coefficients r are defined as

$$r_{AB} = \frac{1}{(N-1) \cdot \sigma_A \cdot \sigma_B} \cdot \sum_{i=1}^{N} \left[(A_i - \overline{A}) \cdot (B_i - \overline{B}) \right]$$

and correlations r_{BC} and r_{AC} are defined similarly. If A and B are independent, the $r_{AB} = 0$, and similarly for the other correlation coefficients.

For example, suppose you measure air density ($\rho = \overline{\rho} \pm \sigma_\rho$) and temperature ($T = \overline{T} \pm \sigma_T$), and calculate pressure (P) using the ideal gas law $P = \rho \cdot \Re \cdot T$, where $\Re$ is a constant. Thus, from calculus: $\partial P/\partial \rho = \Re \cdot T$, and $\partial P/\partial T = \rho \cdot \Re$. Assume ρ and T are independent, thus the correlation coefficient $r_{\rho T} = 0$.

Our best estimate of pressure is

$$\overline{P} = \overline{\rho} \cdot \Re \cdot \overline{T} \, .$$

To estimate the pressure error σ_P, use eq. (A.a) to propagate the other errors into the pressure error:

$$\sigma_P = \left[\left(\frac{\partial P}{\partial \rho}\right)^2 \cdot \sigma_\rho^2 + \left(\frac{\partial P}{\partial T}\right)^2 \cdot \sigma_T^2 \right]^{1/2}$$

$$\sigma_P = \left[(\Re \cdot T)^2 \cdot \sigma_\rho^2 + (\Re \cdot \rho)^2 \cdot \sigma_T^2 \right]^{1/2}$$

Multiply the right side by 1 in the form of $\overline{P} / \left(\overline{\rho} \cdot \Re \cdot \overline{T}\right)$

$$\sigma_P = \overline{P} \cdot \left[\left(\frac{1}{\overline{\rho}}\right)^2 \cdot \sigma_\rho^2 + \left(\frac{1}{\overline{T}}\right)^2 \cdot \sigma_T^2 \right]^{1/2}$$

or

$$\sigma_P = \overline{P} \cdot \left[(\sigma_\rho / \overline{\rho})^2 + (\sigma_T / \overline{T})^2 \right]^{1/2}$$

where we use the averages as our best estimates of P, ρ, and T. This last result looks like eq. (A.14). In fact, we could have used eq. (A.14) directly and avoided all the calculus.

Thus, we would report our calculated pressure as:

$$P = \overline{P} \pm \sigma_P$$

Similarly, the mean and standard deviation of some other variable B would be $\overline{B}$ and σ_B.

For example, Newton's constant of gravitation G is reported (CODATA 2006) as:

$$G = 6.67428 \times 10^{-11} \pm 0.00067 \times 10^{-11} \ \text{m}^3 \, \text{kg}^{-1} \, \text{s}^{-2} \, .$$

Error Propagation

Error propagation tells us how the errors in A and B affect the error of D, where D depends on A and B according to some equation. Namely, how can we estimate σ_D knowing σ_A and σ_B. Assume the errors in A and B are independent of each other.

For a simple sum or difference (e.g., $D = A + B$, or $D = A - B$), then

$$\sigma_D = [\sigma_A^2 + \sigma_B^2]^{1/2} \quad \text{(A.11)}$$

For $D = c \cdot A$ where c is a constant, then

$$\sigma_D = c \cdot \sigma_A \quad \text{(A.12)}$$

Similarly, if $D = c_A \cdot A \pm c_B \cdot B$ where c_A and c_B are different constants, then

$$\sigma_D = [c_A^2 \cdot \sigma_A^2 + c_B^2 \cdot \sigma_B^2]^{1/2} \quad \text{(A.13)}$$

For a simple product $D = c \cdot A \cdot B$ or quotient $D = c \cdot A / B$, then

$$\sigma_D = \overline{D} \cdot [\, (\sigma_A / \overline{A} \,)^2 + (\sigma_B / \overline{B} \,)^2 \,]^{1/2} \quad \text{(A.14)}$$

where $\overline{D}$ is the average of D, $\overline{A}$ is the average of A, and $\overline{B}$ is the average of B.

For a simple power relationship $D = c \cdot A^m$ where m is a fixed constant, then

$$\sigma_D = \overline{D} \cdot m \cdot (\sigma_A / \overline{A} \,) \quad \text{(A.15)}$$

For the general case of a product of factors raised to various fixed (errorless) powers $D = c \cdot A^m \cdot B^q$, then

$$\sigma_D = \overline{D} \cdot [\, m^2 \cdot (\sigma_A / \overline{A} \,)^2 + q^2 \cdot (\sigma_B / \overline{B} \,)^2 \,]^{1/2} \quad \text{(A.16)}$$

For a logarithm such as $D = \ln(c \cdot A)$, where c is a constant, then

$$\sigma_D = (\sigma_A / \overline{A} \,) \quad \text{(A.17)}$$

For an exponential such as $D = e^{c \cdot A}$ where c is a constant, then

$$\sigma_D = c \cdot \overline{D} \cdot \sigma_A \quad \text{(A.18)}$$

For more complicated relationships, the rules above can be combined or used sequentially (or see the Beyond Algebra box).

Solved Example

Observations give $P_1 = 100 \pm 0.1$ kPa, $P_2 = 50 \pm 0.5$ kPa, and $\overline{T_v} = 260 \pm 5$ K. Use hypsometric eq. to find Δz.

Solution

Given: $\overline{P}_1 = 100$ kPa, $\sigma_{P1} = 0.1$ kPa, $\overline{P}_2 = 50$ kPa, $\sigma_{P2} = 0.5$ kPa, $\overline{T_v} = 260$ K, $\sigma_T = 5$ K.

Hyp. eq.(1.26a): $\Delta z = a \cdot \overline{T_v} \cdot \ln(P_1/P_2)$, a=29.3m/K.

Find: $\Delta z = ? \pm ?$ m. Namely, find $\overline{\Delta z} = ?$m, $\sigma_{\Delta Z} = ?$ m

Method: Use error propagation rules sequentially.

For (P_1/P_2): *Average(P/P)* = (100kPa)/(50kPa) = 2

Use eq. (A.14): $\sigma_{P/P} = 2 \cdot [(0.1/100)^2 + (0.5/50)^2]^{1/2} = 0.02$

For $a \cdot \ln(P_1/P_2)$: *Average* = (29.3m/K)· ln(2) = 20.31 m/K

Use eq. (A.17): $\sigma_{a \cdot ln} = (29.3\text{m/K}) \cdot (0.02/2) = 0.293$ m/K

For $\overline{T_v} \cdot a \cdot \ln(P_1/P_2)$: *Average*=(20.31m/K)·(260K)= **5281m**

Use eq. (A.14): $\sigma_{\Delta Z} = (5281\text{m}) \cdot [(5/260)^2 + (0.293/20.31)^2]^{1/2}$

= **127 m**

Thus: **$\Delta z = 5281 \pm 127$ m**

Discussion: Notice that error-propagation eqs. (A.11 - A.18) are dimensionally consistent. A good check.

ON DOING SCIENCE

Science is a philosophy. It is faith in a set of principles that guide the actions of scientists. It is a faith based on observation. Scientists try to explain what they observe. Theories not verified by observations are discarded. This philosophy applies to **atmospheric science**, also known as **meteorology**.

A good theory is one that works anywhere, anytime. Such a theory is said to be **universal**. Engineers utilize universal theories with the expectation they will continue working in the future. The structures, machines, circuits, and chemicals designed by engineers that we use in every-day life are evidence of the success of this philosophy.

But we scientists and engineers are people, and share the same virtues and foibles as others. Those of you planning to become scientists or engineers might appreciate learning some of the pitfalls so that you can avoid them, and learning some of the tools so that you can use them to good advantage.

For this reason, scattered throughout the book are boxes called "On Doing Science", summarized in Table A–5. These go beyond the mathematical preciseness and objective coldness that is the stereotype of scientists. These boxes cover issues and ideas that form the fabric of the philosophy of science. As such, many are subjective. While they give you one scientist's (my) perspectives, I encourage you to discuss and debate these issues with other scientists, colleagues, and teachers.

ON DOING SCIENCE • Have Passion

The best scientists and engineers need more than the good habits of diligence and meticulousness. They need passion for their field, and they need creativity. In this regard, they are kindred spirits to artists, composers, musicians, authors, and poets.

While an observation is something that can usually be quantified, the explanation or theory for it comes from the minds of people. For example, does light consist of particles (photons) or waves? Probably it consists of neither, but those are two theories from the creative imagination of scientists that have proved useful in explaining the observations.

The joy that a scientist feels after successfully explaining an observation, and pride that an engineer feels for making something work within the constraints of physics and economics, are no less intense than the joy and pride felt by an artist who has just completed his or her masterpiece.

Approach your work with passion, evaluate your result objectively, and enjoy your travel through life as you help society.

Table A-5. Guidelines and issues for scientists. Locations and topics of the "On Doing Science" boxes.

Chapter	Issues	Page
1	Descartes and the Scientific Method	2
1	Check for Errors	16
1	Be Meticulous	20
1	Give Credit	24
2	Scientific Laws — The Myth	38
2	Seek Solutions	46
3	Expert vs. Novice	72
4	Look for Patterns	107
6	Cargo Cult Science	167
7	Consequences	218
9	Creativity in Engineering	288
10	Be Creative	293
11	Toy Models	330
11	Residuals	340
11	The Scientific Method Revisited	343
11	Model Sensitivity	350
12	Math Clarity	393
13	Truth vs. Uncertainty	470
14	Be Safe (many parts)	485, 517
15	Be Safe (continuation)	567, 583, 584
17	Simple is Best	680
18	Parameterization Rules	715
19	Data Misinterpretation	729
19	The Citizen Scientist	738
20	Mathematics	762
20	Scientific Revolutions	773
21	Ethics and Data Abuse	826
22	Great Scientists Make Big Mistakes Too	863
A	Problem Solving	869
A	Have Passion	877

SUMMARY

SI units are used by atmospheric scientists. Functional relationships between variables can sometimes be discerned when the data is plotted on linear, semi-log, or log-log graphs. An organized approach to problem solving is recommended, including error propagation. The philosophy of science blends the passions of people with the objective analysis of observations. These principles are used throughout this book.

EXERCISES

Numerical Problems

N1. Convert the values on the left to the units at right, using a table of conversions.

a. 50 miles =? km
b. 15 knots = ? m/s
c. 30 lb/in^2 =? kPa
d. 5000 kW =? horsepower
e. 150 lb$_{Mass}$ =? kg
f. 150 lb$_{Force}$ =? N
g. 12 ft = ? m
h. 50 km/h = ? m/s

N2. Solve the expression on the left, and give the answer in the units at right, using a table of conversions, and the basic definitions of units:

a. (55. knots) x (36. inches) =? m^2·s^{-1}
b. (14. lb$_F$/in^2) x (2.5 m)^2 = ? N
c. (120. lb$_M$) x (3. knots) / day =? mN
d. (15. inHg) x (2. ft^3) = ? J
e. (500. mb) x (3. knots) x (5. in)^2 =? kW
f. (9.8 m·s^{-2}) x (6 kg) / (ft^2) = ? mb
g. (4200 J·kg^{-1}·K^{-1}) x (5°C) x (3.3 g) = ? ergs
h. (2 ha)$^{1/2}$ / 3 weeks = ? m/s

N3. Find $\Delta T/\Delta z$ between the height at assigned letter (a - e) and the height immediately above it?

	z(m)	T(°C)
	1000	10
e.	500	15
d.	200	17
c.	100	17
b.	50	15
a.	0	10

N4. Convert the following temperatures:

a. 15°C = ? K
b. 50°F = ? °C
c. 70 °F =? K
d. 48°C = ? °F
e. 400 K = ? °F
f. 250 K=?°C

N5(§). Plot the following relationships on linear, semi-log, and log-log graphs. Use a spreadsheet (§) on a personal computer to make this easier. Any variable with subscript "o" represents a constant.

a. $I = I_o \cdot (R_o/R)^2$
b. $U = U_o \cdot \ln(z/z_o)$
c. $E = E_o \cdot \exp(-z/z_o)$
d. $f = c_o / \lambda$
e. $q = e / e_o$
f. $c = c_o \cdot \exp[-(z/z_o)^2]$
g. $w = [2\cdot(F/m)_o\cdot z]^{1/2}$
h. $\Delta P/\Delta P_o = (1/5)\cdot(R/R_o]^4$

N6. Given: A = 4000±20 m, B = 300±5 K, C = 80±2 m Also, k = 5 is a constant. Find $D = \overline{D} \pm \sigma_D$ for:

a. $D = A + C$
b. $D = A - C$
c. $D = 3C + A$
d. $D = k\cdot B$
e. $D = k^2\cdot A$
f. $D = A/B$
g. $D = A\cdot C$
h. $D = A\cdot B/C$
i. $D = (C+A)/B$
j. $D = A^k$
k. $D = B^{-k}$
m. $D = C^k\cdot B^{1/3}$
n. $D = k\cdot\ln(A/25\text{m})$
o. $D = k\cdot(C-A)/\ln(B/273\text{K})$

Understanding & Critical Evaluation

U1. Is anything dimensionally wrong with the following equations, given: P = 100 kPa, z = 2 km, T = 30°C, W = 0.5 m/s? If so, why?

a. $\log(P) = z$
b. $\sin(T) = W$
c. $\arccos(P) = T$
d. $\exp(-P/z) = 1$
e. $\cos(W) = 2$
f. $\ln(0) = z$
g. $\ln(-10) = T$
h. $\exp(0) = 1$

U2. What is the difference between a good assumption and a bad one? What can you do to detect bad assumptions?

Web Enhanced Questions

W1. Search the web for recommended units to use in meteorology, and list 3 that were not given in this chapter. [Hint, on the American Meteorological Society web site, search for a "Guide for Authors".]

W2. For 5 of the universal constants listed in Appendix B, search the web to find their precision (i.e., the ± σ value). [Hint: try NIST (U.S. National Institute of Standards and Technology.]

Synthesis Questions

S1. Suppose that you discovered a new physical characteristic of nature, and that you devised a new dimension to explain it. However, also assume that the list of basic dimensions in Table A–1 is still valid, which means that your new dimension must be able to be described in terms of the basic dimensions. Describe the steps that you could take to determine the relationship between your new physical dimension and the basic units.

S2. Suppose science did not involve human creativity. What physical "laws" might have been described differently than they are now, or might have not been discovered at all?

Copyright © 2011, 2015 by Roland Stull. *Meteorology for Scientists and Engineers, 3rd Ed.*

CONSTANTS & CONVERSION FACTORS

B

CONTENTS

Universal Constants 879
Math Constants 879
Earth Characteristics 879
Air and Water Characteristics 880
Conversion Factors & Combined Parameters 880

UNIVERSAL CONSTANTS

[from US National Institute of Standards and Technology (NIST), based on 2006 CODATA]

c_o = 299,792,458 m/s = speed of light in a vacuum

c_1 = 3.741 771 18 x10^{8} W ·m^{-2} ·μm^{4} = first radiation constant (in Planck's law)

c_{1B} = 1.191 042 759 x10^{8} W ·m^{-2} ·μm^{4} ·sr^{-1} = first radiation constant for spectral radiance

c_2 = 1.438 775 2 x10^{4} μm ·K = second radiation constant (in Planck's law)

G = 6.674 28 x10^{-11} m^{3} ·s^{-2} ·kg^{-1} = Newtonian gravitational constant

h = 6.626 068 96 x10^{-34} J ·s = Planck constant

k_B = 1.380 650 4 x10^{-23} J ·K^{-1} ·molecule^{-1} = Boltzmann constant

N_A = 6.022 141 79 x10^{23} mol^{-1} = Avogadro constant

σ_{SB} = 5.670 400 x10^{-8} W ·m^{-2} ·K^{-4} = Stefan-Boltzmann constant

T = –273.15°C = 0 K = absolute zero (not considered a true universal constant)

MATH CONSTANTS

[from *CRC Handbook of Chemistry and Physics*]

e = 2.718 281 828 459 = base of natural logarithms

1/e = 0.367 879 441 = e-folding ratio

π = 3.141 592 653 589 793 238 462 643 = pi

sqrt(2) = 1.414 213 562 373 095

"Meteorology for Scientists and Engineers, 3rd Edition" by Roland Stull is licensed under a Creative Commons Attribution-NonCommercial-ShareAlike 4.0 International License. To view a copy of the license, visit http://creativecommons.org/licenses/by-nc-sa/4.0/ . This work is available at http://www.eos.ubc.ca/books/Practical_Meteorology/ .

EARTH CHARACTERISTICS

1° latitude = 111 km = 60 nautical miles (nm) [Caution: This relationship does NOT hold for degrees longitude.]

a = 149.60 Gm = semi-major axis of Earth orbit

A = 0.306 = Bond albedo (NASA 2009)

A = 0.367 = visual geometric albedo (NASA 2009)

b = 149.090 Gm = semi-minor axis of Earth orbit

d = 149.59787 Gm = average sun-Earth distance = 1 Astronomical Unit (AU)

$d_{aphelion}$ = 152.10 Gm = furthest sun-Earth distance, which occurs about 4 July (NASA 2009)

$d_{perihelion}$ = 147.09 Gm = closest sun-Earth distance, which occurs about 3 January (NASA 2009)

d_r = 173 = 22 June = approx. day of summer solstice

e = 0.0167 = eccentricity of Earth orbit around sun

g = –9.798 m ·s^{-2} = average gravitational acceleration on Earth at sea level (negative = downward). (from NASA)

$|g| = g_o \cdot [1 + A \cdot \sin^2(\phi) - B \cdot \sin^2(2\phi)] - C \cdot H$ = variation of gravitational-acceleration magnitude with latitude ϕ and altitude H(m) above mean sea level. g_o = 9.780 318 4 m·s^{-2}, A = 0.005 3024, B = 0.000 0059, C = 3.086x10^{-6} s^{-2}.

M = 5.9736 x10^{24} kg = mass of Earth (from NASA)

P_{earth} = 365.254 63 days = Earth orbital period

P_{moon} = 27.32 days = lunar orbital period

$P_{sidereal}$ = 23.934 469 6 h = sidereal day = period for one revolution of the Earth about its axis, relative to fixed stars

R_{earth} = 6371.0 km = volumetric average Earth radius (from NASA)
= 6378.1 km = Earth radius at equator
= 6356.8 km = Earth radius at poles

S = 1366 W ·m^{-2} = solar irradiance (solar constant) at top of atmosphere
≈ 1.125 K ·m ·s^{-1} = kinematic solar constant (based on mean sea-level density)

T_e = 254.3 K = effective radiation emission black-body temperature of the Earth system (NASA)

Φ_r = 23.45° = 0.409 radians = tilt of Earth axis = obliquity relative to the orbital plane

Ω = 0.729 211 6 x10^{-4} s^{-1} = rotation frequency of Earth

2·Ω = 1.458 423 x10^{-4} s^{-1} = Coriolis factor

2·Ω / R_{earth} = 2.294 285 x10^{-11} m^{-1} ·s^{-1} = beta factor

AIR AND WATER CHARACTERISTICS

$a = 0.0337$ (mm/day) $\cdot(W/m^2)^{-1}$ = water depth evaporation per latent heat flux

$B = 3 \times 10^9$ V/km = breakdown potential for dry air

$C_{vd} = 717$ J $\cdot kg^{-1} \cdot K^{-1}$ = specific heat for dry air at constant volume

$C_{pd} = 1003$ J $\cdot kg^{-1} \cdot K^{-1}$ = specific heat for dry air at constant pressure at –23°C

$C_{pd} = 1004$ J $\cdot kg^{-1} \cdot K^{-1}$ = specific heat for dry air at constant pressure at 0°C

$C_{pd} = 1005$ J $\cdot kg^{-1} \cdot K^{-1}$ = specific heat for dry air at constant pressure at 27°C

$C_{pv} = 1850$ J $\cdot kg^{-1} \cdot K^{-1}$ = specific heat for water vapor at constant pressure at 0°C

$C_{pv} = 1875$ J $\cdot kg^{-1} \cdot K^{-1}$ = specific heat for water vapor at constant pressure at 15°C

$C_{liq} = 4217.6$ J $\cdot kg^{-1} \cdot K^{-1}$ = specific heat of liquid water at 0°C

$C_{ice} = 2106$ J $\cdot kg^{-1} \cdot K^{-1}$ = specific heat of ice at 0°C

$D = 2.11 \times 10^{-5}$ $m^2 \cdot s^{-1}$ = molecular diffusivity of water vapor in air in standard conditions

$e_o = 0.611$ kPa = reference vapor pressure at 0°C

$k = 0.0253$ W $\cdot m^{-1} \cdot K^{-1}$ = molecular conductivity of air at sea level in standard conditions

$L_d = 2.834 \times 10^6$ J $\cdot kg^{-1}$ = latent heat of deposition at 0°C

$L_f = 3.34 \times 10^5$ J $\cdot kg^{-1}$ = latent heat of fusion at 0°C

$L_v = 2.501 \times 10^6$ J $\cdot kg^{-1}$ = latent heat of vaporization at 0°C

$n = 3.3 \times 10^{28}$ molecules $\cdot m^{-3}$ for liquid water at 0°C

$n_{air} \approx 1.000\,277$ = index of refraction for air

$n_{water} \approx 1.336$ = index of refraction for liquid water

$n_{ice} \approx 1.312$ = index of refraction for ice

$P_{STP} = 101.325$ kPa = standard sea-level pressure (STP = Standard Temperature & Pressure)

$\Re_d = 0.287\,053$ kPa $\cdot K^{-1} \cdot m^3 \cdot kg^{-1} = C_{pd} - C_{vd}$
$= 287.053$ J $\cdot K^{-1} \cdot kg^{-1}$ = gas constant for dry air

$\Re_v = 461.5$ J $\cdot K^{-1} \cdot kg^{-1}$ = water-vapor gas constant
$= 4.61 \times 10^{-4}$ kPa $\cdot K^{-1} \cdot m^3 \cdot g^{-1}$

$Ri_c = 0.25$ = critical Richardson number

$s_o = 343.15$ m/s = sound speed in standard, calm air

$T_{STP} = 15$°C = standard sea-level temperature

$\varepsilon = 0.622\ g_{water} \cdot g_{air}^{-1} = \Re_d / \Re_v$ = gas-constant ratio

$\gamma = 0.0004\ (g_{water} \cdot g_{air}^{-1}) \cdot K^{-1} = C_p / L_v$
$= 0.4\ (g_{water} \cdot kg_{air}^{-1}) \cdot K^{-1}$ = psychrometric constant

$\Gamma_d = 9.75$ K $\cdot km^{-1} = |g|/C_p$ = dry adiabatic lapse rate

$\rho_{STP} = 1.225$ kg $\cdot m^{-3}$ = standard sea-level air density

$\rho_{avg} = 0.689$ kg $\cdot m^{-3}$ = air density averaged over the troposphere (over z = 0 to 11 km)

$\rho_{liq} = 999.84$ kg $\cdot m^{-3}$ = density of liquid water at 0°C
$= 1000.0$ kg $\cdot m^{-3}$ = density of liquid water at 4°C
$= 998.21$ kg $\cdot m^{-3}$ = density of liquid water at 20°C
$= 992.22$ kg $\cdot m^{-3}$ = density of liquid water at 40°C
$= 983.20$ kg $\cdot m^{-3}$ = density of liquid water at 60°C
$= 971.82$ kg $\cdot m^{-3}$ = density of liquid water at 80°C
$= 958.40$ kg $\cdot m^{-3}$ = density of liquid water at 100°C

$\rho_{sea\text{-}water} = 1025$ kg $\cdot m^{-3}$ = avg. density of sea water, (sea water contains 34.482 g of salt ions per kg of water, on average)

$\rho_{ice} = 916.8$ kg $\cdot m^{-3}$ = density of ice at 0°C

$\sigma = 0.076$ N $\cdot m^{-1}$ = surface tension of pure water 0°C

CONVERSION FACTORS & COMBINED PARAMETERS

$C_{pd} / C_{vd} = k = 1.400$ (dimensionless)
= specific heat ratio

$C_{pd} / |g| = 102.52$ m $\cdot K^{-1}$

$C_{pd} / L_v = 0.0004\ (g_{water} \cdot g_{air}^{-1}) \cdot K^{-1} = \gamma$
$= 0.4\ (g_{water} \cdot kg_{air}^{-1}) \cdot K^{-1}$
= psychrometric constant

$C_{pd} / \Re_d = 3.50$ (dimensionless)

$C_{vd} / C_{pd} = 1/k = 0.714$ (dimensionless)

$|g|/C_{pd} = \Gamma_d = 9.8$ K $\cdot km^{-1}$ = dry adiabatic lapse rate

$|g|/\Re_d = 0.0342$ K $\cdot m^{-1}$ = 1/(hypsometric constant)

$L_v / C_{pd} = 2.5$ K / $(g_{water} \cdot kg_{air}^{-1})$

$L_v / \Re_v = 5423$ K = Clausius-Clapeyron parameter for vaporization

$\Re_d / C_{pd} = 0.28571$ (dimensionless) = potential-temperature constant

$\Re_d / \Re_v = \varepsilon = 0.622\ g_{water} \cdot g_{air}^{-1}$ = gas-constant ratio

$\Re_d / |g| = 29.29$ m $\cdot K^{-1}$ = hypsometric constant

$\rho_{air} \cdot C_{pd\ air} = 1231$ (W $\cdot m^{-2}$) / (K $\cdot m \cdot s^{-1}$) at sea level
$= 12.31$ mb $\cdot K^{-1}$ at sea level
$= 1.231$ kPa $\cdot K^{-1}$ at sea level

$\rho_{air} \cdot |g| = 12.0$ kg $\cdot m^{-2} \cdot s^{-2}$ at sea level
$= 0.12$ mb $\cdot m^{-1}$ at sea level
$= 0.012$ kPa $\cdot m^{-1}$ at sea level

$\rho_{air} \cdot L_v = 3013.5$ (W $\cdot m^{-2}$) / $[(g_{water} \cdot kg_{air}^{-1}) \cdot (m \cdot s^{-1})]$ at sea level

$\rho_{liq} \cdot C_{liq} = 4.295 \times 10^6$ (W $\cdot m^{-2}$) / (K $\cdot m \cdot s^{-1}$)

1 megaton nuclear explosion $\approx 4 \times 10^{15}$ J

2π radians = 360°

$(1-\varepsilon)/\varepsilon = 0.61$ = virtual-temperature constant

Copyright © 2011, 2015 by Roland Stull. *Meteorology for Scientists and Engineers, 3rd Ed.*

INDEX

1-D normal shock, 572-574
1-leucine, 195
1-tryptophan, 195
1,3-butadiene, 725
1,5-dihydroxynaphlene, 195
1.5 PVU line, 364, 441, 443
2 Δx waves, 760-761
2 layer system of fluids, 657-661
3 second rule between lightning and thunder, 575
3DVar data assimilation, 273
4DVar data assimilation, 273
5-D nature of weather, 436
5th order rainbow, 840
9 degree
  halo, 847, 854-855
  Parry arc, 855
18 degree halo, 847, 855
20 degree halo, 847, 855
22 degree
  angles, estimating, 847
  halo, 842, 845-846, 854-855
  Lowitz arc, 855
  Parry arc (upper, lower, suncave, sunvex), 854-855
23 degree halo, 847, 855
24 degree halo, 847, 855
30-30 rule for lightning safety, 570
35 degree halo, 847, 855
40-year natural hurricane cycle, 631
44 degree parhelia, 855
46 degree
  halo, 842, 846, 854-855
  Lowitz arc, 855
  Parry arc (infralateral, supralateral), 854-855
53rd Reconnaissance Squadron (hurricane hunters), 637
100-50 kPa thickness charts, 345-349, 436, 439, 442
120° parhelia (or paranthelia), 854-855

A

A-grid, 753
abbreviations for
  airmasses, 392
  chemicals, 7
  clouds, 168-170
  METARs and SPECIs, 208, 270
  states and provinces, 431
  time zones, 5
  weather-map symbols, 168-170, 208, 274-279, 614-615
abrupt climate change processes, 810-812
abscissa - defined, 3
absolute
  angular momentum for hurricanes, 617
  circulation, 366
  humidity, 91
    definition, 14, 91
    measurement, 97, 111
    saturated, 91
  phase speed, 658
  stability, 140
  temperature, 7
  virtual temperature, 14-15
  vorticity, 363, 448
    advection of, 448
  zero, 879
absolutely stable or unstable, 140
absorptance, 225
absorption
  bands, 221
  hygrometer, 111
  lines, 221
  of light, 833
  of radiation, 41-43, 219-226
  window, 43, 220, 796
absorptivity, 41
  and Beer's Law, 43
  and Kirchhoff's Law, 41, 220
  of atmosphere, 41-43
ac (altocumulus clouds), 168
ACARS (aircraft communication & reporting system), 272
accas (altocumulus castellanus clouds), 168
acceleration
  definition, 292
  gravitational, 15
  in Newton's second law, 292, 301, 314, 746-749
    vertical, 315, 554, 746
accessory clouds, 168-169
accretion (or riming), 205
accumulated heating or cooling, 394-395, 693-694
  calculation of, 693-694
  in fogs, 176-177
  role in thunderstorm formation, 528
accumulation
  mode for CCN, 188
  storm-total rainfall, 257
accuracy
  error definition, 875
  of forecasts, 777
achieved heat transport globally, 339
acid rain, 567, 742
actinometers (radiometers), 45-47
action, take protective, 785
activated
  droplets, 191-192
  nuclei, 192-196
active
  clouds, 162
  remote sensors, 219
  tracers, 731
adaptive, 771
adiabat, 17
  dry, 63, 119-158, 497
  moist (saturated), and on thermo diagrams, 119-158
adiabatic
  cooling, 60-64, 101-106
    to create clouds, 159-161
  effects in frontogenesis, 408-411
  excess water variation, 187
  lapse rate, 60-64, 101-106, 140, 880
  dry (unsaturated), 60-64
  moist (saturated), 101-106
  process, 60, 121
    on thermo diagrams, 121, 129
  vertical movement, 60
  warming, 60
    in downslope winds, 676-677
adjacent faces of ice crystal, 842
adjustment
  geostrophic, 343-349
    part 1, 344
    part 2, 349
    part 3, 404-407
  moist convective, 70
Admiral Beaufort, 635
Adriatic Sea, bora winds, 675
ADT, Atlantic daylight time, defined, 5
advection, 65
  adiabatic, 411
  cold air, 349
  differential, and castellanus clouds, 164
  definition, 65-67
  flux, 34-35, 65-67, 107
  fog, 173-177
  force, 294-295
  heat, 65-67, 714
  of TKE by mean wind, 708
  mass, 317-318, 465
  max, as found on weather maps, 458
  moisture, 107
  momentum, 294-295
  numerical stability, 760-761
  related to pressure tendency, 465
  role in katabatic wind, 653
  temperature, 65-67
    self-development of cyclones, 468-469
  turbulence, 708
  turbulent heat, 714
  term, 747
  vorticity, 447-451
    by thermal wind (cyclogenesis), 456-462
  warm air, 349
  water, 107
advective
  clouds (stratiform), 94, 164
  flux, 34-35, 65, 107, 294
  force, 294
aerodynamic
  drag on falling
    cloud droplets, 202
    hailstones, 204
    ice crystals, 842
    rain drops, 203
  roughness length, 677-678, 700-703
    typical values, 700
aerosol(s)
  definition, 188
  feedbacks for climate change, 811
  haze, 193
  scattering of radiation by, 221, 856-858
  stratospheric, and climate change, 805, 856-858
  swelling, 193
African easterly jet (AEJ) and waves, 611-612
age
  Calabrian, 799
  ice, 795, 798-799
  Ionian, 799
  Tarantian, 799
ageostrophic
  definition, 304, 314, 343, 454
  during approach to geostrophy, 304
  flow, 343, 462, 454-462
    dynamic frontogenesis, 412
  right-hand rule, 455
  wind , 304, 314, 454-462
    direction of, 455
    equations, 314, 454
aggregation
  in cold clouds, 205
  in thunderstorms, 546
  of ice crystals into snowflakes, 200, 202, 206-207
  processes, 204-205
air
  characteristics, constants & parameters, 880
  composition, 7
  conditioning, 116
  denisty, 10
    forecast equation for, 746
    standard (STP), 880
  drag, 700-702
  mass (see airmass), 389-399
    conservation, 317-319, 660
  mass of, 10
  molecular weight, 7
  molecule, scattering of light by, 220-222, 856-858
  parcel, 57, 59, 687-688
    adiabatic movement, 58-64
    angular momentum of, 360-361
    buoyancy, 135, 649, 687-688
    definition, 11, 57

"Meteorology for Scientists and Engineers, 3rd Edition" by Roland Stull is licensed under a Creative Commons Attribution-NonCommercial-ShareAlike 4.0 International License. To view a copy of the license, visit http://creativecommons.org/licenses/by-nc-sa/4.0/ . This work is available at http://www.eos.ubc.ca/books/Practical_Meteorology/ .

A

follows isentropes, 144
rise, 129-130, 648-649
temperature and humidity, 128
static stability method, 138-139, 687-689
vs. environment, 59, 134-141
water in, 99-106
pollution dispersion (see also pollution), 7, 723-744
brown cloud, 857-858
episodes, 741
events, 725, 741
exceedences, 725
thermo diagrams for, 151, 157-158
trapped in highs, 390
pressure, 7-10
quality standards, 7, 725
for individual gases, 7, 725
index, 743
USA, Canada, and UK, 7, 725
refractive index, 834-835
specific heats, 53-56, 880
stagnation (events), 559, 741
aircraft
airspeed, using pitot-static system, 674
commercial, weather observations by, 272
communications & reporting sys. (ACARS), 272
glory, 860
hurricane hunter, 637
radars, 243
severe-weather hazards, 529, 556, 563
downbursts and gustfronts, 556, 563
sounding, 134, 496
turbulence experienced by
boundary layer, 649
clear-air, 141-142, 165
convective, 483, 498, 508
mountain wave, 667
wind shear; gust fronts at airports, 560-563
wings, flow over, 88
AIREPS, 272
airmass(es), 389-399
abbreviations for, 392
arctic vs. Antarctic, 392, 396
atmospheric boundary layers are, 691
blocking/damming by mountains, 397
boundary layers are, 393-397
boundaries = fronts, drylines, 397, 416
thunderstorm triggers, 525-526
channeling by mountains, 397
characteristics of, 391
classification, 391-392
codes for, 391-392
continental polar, 392
creation, 392-397
definition, 391
depth of cold air, 404-406
formation region map, 392
fronts at boundaries of, 397
genesis, 392-397
growth rate, 394-397
locations, 392
maritime tropical, 392
modification, 397-399
via flow over mountains, 398-399
via surface heat fluxes, 397-398
movement, 397
residence times, 392
temperature at distance from origin, 398
thickness, 394-397, 404-406
thunderstorms, 481-482, 486
energy released by, 499
triggering. Convective temperature., 526-527
airplane
bumpy ride in, 649, 667
mass of air inside, 23
pitot-static system for airspeed, 674
shadow, white disk centered on (glory), 860
window, pressure against, 21
airport
CYVR (Vancouver Internat. Airport in Canada), 647
KJFK (JFK Airport in New York), 563
routine meteorological report (METAR), 268-279
runway visual range (RVR), 270
runways vs. wind direction, 646-647
special meteorological report (SPECI), 268-279
wind-shear sensors, 563
AIRS (atmospheric infrared sounding), 273
airspeed, using pitot-static system, 674
AKDT & AKST, Alaska daylight & standard times, 5
Alaska, 431
current, 175
time zone, 5
albedo, 42, 44, 793-794
average global, 42, 793-794
Bond, 831, 879
geometric, 831, 879
ice-albedo feedback, 808-812
in daisyworld, 813-815
Moon, 42
typical values, 42, 794
Alembert, Jean le Rond d', 759
Aleutian
low, 354-356
time zone, 5
Alexander of Aphrodisias, 841
Alexander's dark band, 841
aligned coordinate, 727
Al-Khalili, Jim, 754
Allick, Susan Krueger, 639-640
along
shore coastal low-level jet, 664-665
valley winds, 653-654
alpha time zone (Europe), 5
alphanumeric weather codes, 268-269
alpine ski snow, 209
alternative coordinates, horizontal & vertical, 746-747
alternate faces of ice crystal, 842
altitude
cooking time vs, 90
key, for thunderstorms, 496-499
pressure change with (see height), 3, 8-9, 12-13, 16-17
alto prefix, 163
weather-map symbols for, 277
altocumulus, 134, 162-163, 168
castellanus, 162, 164-165
altostratus, 134, 162-164, 168
AM
radio, static on, 568
satellite, 229
ambient air-quality standards, 725
Amdahl, Gene, 763
Amdahl's Law, 763
AMDAR (aircraft meteorological data relay) code, 269, 272
American geography, 431
amino acids as ice nuclei, 195
ammonium sulfate, 190-192
amount of
clouds, 170
substance, 870
flowing through area, 34-35
units, 870
ampere, 564, 870
amplified response (positive feedback), 806-808
amplitude of
Kelvin wave, 634
meridional displacement, 373-374
mountain lee waves, 666-668
oscillations, 818
Rossby waves in lee of mountains, 444
AMSU (advanced microwave sounding unit), 273
anabatic
cumulus clouds, 649-650
horizontal pressure gradient force, 650-652
wind, 649-652
high-pressure associated with, 391, 650-651
anafront, 404
analysis
data assimilation, 762, 765-767
definition, 267, 280-281, 762
in case study, 768-770
field, 763-765
initial conditions, 293, 762
objective methods, 280, 766-767
3DVar and 4DVar, 273, 767
optimum interpolation, 766
variational, 273, 767
verifying, 769
weather map, 274-281, 425-470
hand (subjective; manual), 279-281, 402
methods, 274-281, 402
numerical, 762
surface, 267, 402
analytical solution, 749
anemometers, 219, 321-322
aneroid barometer, 19
angle
azimuth, 4
solar, 33
between
Earth and perihelion (=true anomaly), 28-30, 802
Earth and vernal equinox (=true longitude), 801
perihelion and vernal equinox, 801
component, 836
conventions in math & meteorology, 2
critical, 837
elevation, 4-5
solar, 32
hour, 40-41, 801-802
incidence, 833
mean anomaly, 29
of turbine blades, 647-648
plane, definition of units, 870
refraction, 833-834
solar declination, 30-31
solar aximuth & elevation, 32-33
solid, definition of units, 870
true anomaly, 29
wedge, 843, 845-847, 855
zenith, 4-5
ångström unit of distance, 870
angular
frequency, 36
momentum, 360-361
conservation of, 360-361
equation, 360
of hurricane, 617
of tornado, 577
Rossby wave transport, 375
subtropical jet, effects on, 360-361
rotation rate of Earth, 297
anisotropic, 708
turbulence, 708, 710, 727
annual
mean global energy budget, 797
precipitation worldwide, 209
anomalous propagation of radar beam, 244-245
anomaly, 777
climate, 818, 821
correlation, 779-780
mean & true, for orbit of earth, 29
warm sea surface (for ENSO and PDO), 818-820
weather, 777
Antarctic
airmass
code, 392
katabatic winds (downslope flow), 396, 652, 676
circle, 31
oscillation (AAO), 824
antenna dish, radar, 240
anthelic
arc, 855
point, 841
anthelion, 855
anthropogenic, 723, 811
climate change, 812
clouds, 166
greenhouse gases, 796, 811-812
pollutants, 723
anticyclones (see also highs, H), 389-391
airmass creation within, 389-399
aloft in hurricane core, 613
atmospheric boundary layer within, 690-692
convergence at top of, 391
definition, 390
divergence at bottom of, 390, 691
dynamics, 391
formation locations, 391
isobars around, 390
maximum height/pressure variation nearby, 306-307
mesoscale, 391
midlatitude, 331, 390-391
polar, 391
ridges, relationship to, 390
structure , 390-391
subsidence within, 390, 691
subtropical, 391
tilt with altitude, 390
vertical structure, 391
weather associated with, 390, 691
winds around, 305-307, 390, 691
anticyclonic
radius of curvature, 304-306
winds, 306-307, 311
antimountain wind, 653
antipodal point, 838
antisolar
arc, 855
point, 837
antitriptic wind, 312-313, 663

A

antivalley wind, 654
anvil
  cloud, 482-484
    conditions, 489
    debris stage of evolution, 485
    hurricane central dense overcast, 604, 614, 620, 624
    lightning from, 564
    thunderstorms, 481-602
  crawlers (lightning), 567
  lightning, 564, 567
apex method (static stability), 139
aphelion, Earth orbit, 28-30
  precession, 800-801
apparent
  force, 299
  sunrise and sunset, 33-34, 861-862
  temperature, 76-78, 117
    heat index, 77-78, 117
    humidex, 77-78, 117
    wind chill, 76-77
appearance of thunderstorms, 482
applications of thermo diagrams, 127-133
applied meteorology, 2
approach to
  airports, 563
  geostrophy, 303-304
approximate solution, 749
approximations to spatial gradients, 754-755
Aqua satellite, 273
Arakawa, Akio, 753
  NWP grids A - E, 753
arbitrary vertical cross section (AVCS) radar display, 242
arc
  catalog & diagram of most arcs, 854-855
  circumhorizon (optical phenomenon), 848-849, 855
  circumzenith (optical phenomenon), 848-849, 854-855
  (arcus) clouds, 169, 482, 562
  coloring, 848-849
  of maximum polarization, 856
  tangent, 851-853
Archimedes, 135, 150
Arctic
  aerosols and CCN at, 188
  airmass
    code for, 392
    formation, 396
  circle, 31
  dipole anomaly, 824
  oscillation (AO), 818-819, 824
arcus, 482, 562
area in a sounding, for CAPE & DCAPE, 503-508, 557-558
ARFOR code, 269
argon, Ar, 7
Aristotle, 2, 26
arrangement of clouds, 169
as (altostratus clouds), 168
ascending
  air parcels, 129-130
  motion in cyclones (lows), 356
  node, 228-229
ASDAR (aircraft to satellite data relay), 272
ash, volcanic, 170
ASOS (Automated Surface Observing System), 271
aspect ratio, 485
  of ice crystals, 200
  of thunderstorm cells, 485
aspirated psychrometer, 94
assimilation, data, 765-767
AST, Atlantic standard time, defined, 5
astronomical
  influences on climate variability, 797
    Milankovitch theory, 797
  twilight, 33-34
  unit (au or ua), 28, 870
asynoptic observation data, 758
Atlantic
  multi-decadal oscillation (AMO), 824
  North Atlantic oscillation (NAO), 818-819, 824
  time zone, 5
atlas of clouds, 168
atm, atmospheres, a pressure unit, defined, 7
atmosphere, 1-26
  one-layer, 795
  radiative models for climate, 795-797
  standard, 11-13, 688-690
atmospheric
  attenuation factor in the radar eq., 245-246
  bending of light, 861-863
  composition, 7
  density, 10-12
  dynamics, 289-328
  heat transfer globally, 339
  gases, 7
  layers, defined, 13, 563, 565
  optics, 833-868
  physics, 872
  pressure head, 632
  radiation emissions, climate, 795-797
  radiative transfer, 220-226
  refraction of light, 861-863
  science, 205, 877
  sounding, pre thunderstorm, 496-499
  spectrum of transmittance, 222-223
  structure (in the vertical), 11-13
  window, 796, 811
    "closed", 796, 811
atmospheric boundary layer (ABL), 13, 68, 687-722
  accumulated cooling or heating, 693-694
  aerosols within, 188
  African Sahara, 611
  airmasses are, 393-396, 691
  air parcels in, 687
  anticyclones, relationship to, 390, 690-692
  Ball ratio, 698
  buoyancy velocity, 704
  capping inversion, 496-499, 522-525, 687-692
  constant flux layer, 692
  convection: free vs. forced, 704
  convective
    boundary layer (CBL), 109, 649, 692
    velocity scales, 704
  cyclolysis, role in, 432
  daytime (convective), 692
    accumulated heating, 693-694
  Deardorff velocity, 69, 703-704
  defined, 13
  depth estimate from soundings, 143
  depth and strength over time, 110, 649
    during airmass genesis, 394-395
  depth within an anticyclone, 690-692
  depth within a cyclone, 319, 690-692
  dispersion of smoke within, 723-744
    neutral and stable ABLs, 732-734
    unstable ABLs, 735-737
  diurnal cycle, 687
  drag, 300-301, 699-702
    coefficients, 700-701
    in hurricane, 625
  encroachment method for ML growth, 697-698
  entrainment
    velocity, 697-698
    zone, 692
  fair weather, 69-70, 690-692
  flux-ratio method for entrainment, 698
  fogs within, 159, 173-177
  formation, 13, 689-692
  free atmosphere above top of ABL, 687-692
  free convection, 704
  friction velocity, 677-678, 700-713
  fuel tank for thunderstorms, 499-502, 547-548
  gradient (BLG) wind, 309-311
  heat flux profiles, 698
  highs, relationship to, 390
  hurricane, 618-620
    triggering by easterly wave, 611-612
  internal, thermal (TIBL), 654-657
  inversion at top of, 496-499, 522-525, 687-692
  jet, nocturnal (low-level), 699-700
  katabatic winds at night, 696
  kinematic heat flux, 698
  location, thickness, 13
  log profiles of wind, 702-703
  mixed layer (ML), 690, 692
    growth rate, 697-698
    kinematic heat flux profile, 698
    smoke dispersion within, 735-737
  modification near frontal zone, 70-71, 691-692
  neutral, statically, 300, 308, 319
    smoke dispersion within, 732-733
    smoke plume rise within, 732-733
    standard deviations for, 707
    winds, 702
  nighttime/nocturnal (stable), 692
    accumulated cooling, 693
    jet, 699-700
  Obukhov length, 703
  parameterizations, 714-716
    in NWP models, 751
  potential temperature vs. height, 690, 692
    standard deviations for, 707
  profiles of variables, 692, 702-705
  pumping, 319-320
    cyclolysis, role in, 432, 465
    in hurricanes, 628
  radiative forcings, 687
  radix layer, 700-705
  residual layer, 692-696
  response to heating and frictional drag, 687-705
  roughness length, 677-678, 700-703
    Davenport-Wieringa classification, 700
  rural, 677-679
  seasonal variations, 695-696
  slab model, 697-698
  stable boundary layer (SBL), 692, 696
    depth and e-folding height, 696
    smoke dispersion within, 732-734
    smoke plume rise within, 732-733
    standard deviations for, 707
    strength, 696
    winds, 702-703
  static stability, 687
  stormy, 691
  stress, 700-701, 712-715
  strength of stable boundary layer, 696
  structure and evolution, 692
    layers within, 692
  subgeostrophic winds, 699-700
  summer, 695-696
  supergeostrophic winds, 699-700
  surface layer, 692
    thickness, 700
    wind profiles, 700-703
  synoptic forcings, 690-692
  temperature, 13, 693-698
    cumulative heating or cooling, 693-694
    inversion, 690-695
    mixed-layer temperature, 697-698
    stable-boundary-layer temperature, 696
    temperature-profile evolution, 694-696
  temperature profiles, 688-698
  thermal-internal (TIBL), 654-657
  thermals, 648-649
  thermo diagrams for, 151, 157-158
  thermodynamic method for ML growth, 697-698
  thickness, 13, 300, 649
  top of, 496-499, 522-525, 689
  tropospheric constraints, 13, 689-692
  turbulence, 13, 687-690
    airmass, 393-396
    drag, 300-301
    free and forced convection, 704, 710
    isotropy, 707-708
    mean and turbulent parts, 705-706
    transport velocity, 300
    turbulence kinetic energy (TKE), 708-709
    turbulent fluxes and covariances, 711-713
    variance and standard deviation, 706-708
  unstable (convective), 648-649, 704, 710
    mixed layer, 692
    smoke dispersion within, 735-737
    smoke plume centerline, 736
    standard deviations for, 707
    static stability, 300, 308
    winds in radix layer, 703-705
  urban, 678-679
  vertical velocity at top of, 319-320
  wind, 307-309, 699-705
    diurnal evolution, 699-700
    log profile in the neutral surface layer, 700-702
    log-linear profile in the stable surface layer, 700-703
    low-level nocturnal jet, 699-700
    profile evolution, 699-700
    profile in convective radix layer, 699-705
    shear, 300
    subgeostrophic, 699
    supergeostrophic, 699-700
    wind profile evolution, 699-700
  winter, 695-696
atmospheres (a pressure unit), 7
atomic clock, 51
attenuation
  coefficient in exponential wind profile, 678
  factor in the radar equation, 245-246
  radar energy, 241
  rain gauges, 210
atto (10^{-18}), 870
attractor, 790
  fixed point, 790
  strange, 773-776
audibility distance of thunder, 575-576
aureole, 860
aurora, 11

A, B

Australian Bureau of Meteorology, 607
author, about the, XIV
automated weather
  forecasts (NWP), 745-792
  map analysis, 765-767
  station METAR report, 270
autumnal (Fall) equinox, 30-31, 800
availability of water for droplet formation, 186-187
available
  energy, 503-508, 557-558
  potential energy, 356
    convective (CAPE), 503-508
    downdraft (DCAPE), 557-558
  supersaturation, 187
average, 502, 705, 726
  daily insolation, 40-41, 336, 799-802
  energy budget, global, 797
  ensemble, 776
  jet stream speeds, winter, 357-361
  meridional kinematic heat flux, 338-339, 375, 378
  observations, 875
  running, 599
  total water mixing ratio, 98
  wavelength of wind waves, 634
  winds in global circulation, 330-331
averaging, 502, 705, 726
  distance, 706
  time, 706
aviation (also see aircraft and airplanes)
  boundary layer turbulence, 649
  runways vs. wind directions, 646-647
  severe weather hazards, 529
Avogadro constant, 879
AWIPS, 772
AWOS (Automated Weather Observing System), 271

axes of graphs (defined, and switching of), 3
axial precession of Earth, 799-801
axis of
  contraction, 320-321
  dilation, 320-321, 410
  tilt of earth, 30, 798-802
  ridges and troughs, 281, 367, 399
azimuth angle, 4-5
  defined, 4
Azores high, 354-356
  role in steering hurricanes, 607-608

B

B-grid, 753
background state, mean, 316
  errors, 766
backing of wind, due to cold air advection, 349
backscatter cross-section, 245
backward scattering, 219, 857
backward trajectory, 724
  in semi-Lagrangian NWP, 761
  of pollutant emissions, 724
bacteria as ice nuclei, 195
bad-weather regions (extratropical cyclones), 425-480
  local winds modified by terrain, 645
balance of
  forces to make winds, 302-314
  heat, 64
    globally, 338-339
balanced mass and flow fields, 763-765
balloons, weather, 134
  pilot, 322
  rawinsonde, 134, 322, 496
ball
  lightning, 567
  ratio, 698
bands
  cumuliform cloud, 425-428
  radar, 242-243
  radiation absorption, 221
  rain, 401, 604
  spiral (in hurricanes), 604-605
Bangladesh vs. hurricanes, 631
banks of clouds, 168
banner clouds, 165, 667
barbs for wind, on a weather map, 278
baroclinic, 343, 749
  atmosphere, 343, 349, 359, 749
    circulation in, 366
    Bjerknes circulation theorem for, 366
  instability, 371
    in African easterly jet, causing waves, 611
  vs. barotropic, 749
  wave (Rossby), 371-374
    idealized structure, 374
    qualitative model, 371
    quantitative approach, 372-374
  zones and cyclone self-development, 469-471
    strengthening, 469-470
baroclinicity, 359
  polar jet driven by, 359-360
  role in tornado formation, 587
barogaph, 19, 278
barometer, 7, 19, 219
  aneroid, contra, digital, electronic, mercury, 19
  Torricelli (U-tube), 19
barometric
  pressure (see pressure), 7-19, 267, 270, 275
  tendency, weather map symbols, 278
barotropic, 749
  atmosphere, 366, 749
    circulation in, 366
    Kelvin's circulation theorem for, 366
  instability, 367-370
    easterly waves in African jet caused by, 611
    Rossby waves caused by, 367-370
  vs. baroclinic, 749
  wave, 367-370
barren daisyworld, 815
barrier to ice formation, 194
bar(s), unit of pressure, 7, 870
barycenter, 27
basal face, 842
base
  cloud height, 93, 130, 162, 278
  fog, 177
  of natural logarithms, 879
  rain-free, 483
basic
  dimensions, 870
  thunderstorms, 486-487
basis, scientific, for weather forecasting, 746-751
BATHY code, 269
battering of structures by waves, 634-635
be creative, 293
be safe, 485, 517, 567, 570, 583-584
beach erosion by ocean waves, 634-635
bead lightning, 567
beam, radar, 240
  propagation
    equation, 244
    path, 243-245
  width, 240
bears's cage (region in supercell thunderstorm), 495, 583
beaver tail cloud, 483, 492, 494-495
Beaufort wind scale number, 635-636
  related to tornado intensity, 599
Beer's Law, 43, 856
bell curve, Gaussian, 729-730, 875
bending of light (refraction), 833-868
beneficial competition (cloud seeding), 553
benzene, 725
Bergen School of Meteorology, 399
Bergeron, T., 201-202, 399
Bermuda high, 354-356
  role in steering hurricanes, 607-608
Bernoulli's
  constant, 669-672
  equation, 559, 669-674
    applications, 672-675
    derivation, 670
    downbursts and gust fronts, 559
    downslope winds - Bora and Foehn, 675-677
    dynamic vs. static pressure, 672-674
    for compressible flow, 671-672
    for incompressible flow, 669-671
    hurricanes, 626
    hydraulic jump, 670
    limitations, 671
    principles, 669-672
    reduced gravity in, 670
    requirements, 671
    tornadoes, 578
    venturi effect and gap winds, 674-675
  function, 669-672
Berra, Yogi, quotations, 5, 132, 228
beryllium-10, 803
beta
  effect on
    lee cyclogenesis, 444
    tornadoes, 586
    vorticity tendency, 447-451
  plane, 369
  term, 447-449, 586
Betz
  Albert, 647
  law, 647-648
  limit, 648
Beyond Algebra boxes, 11
  Adiabatic Lapse Rate, 60
  Advection Fog, 173
  Apparent Forces, 299
  Bernoulli [Equation] Derivation, 670
  Beta Plane, The, 369
  Betz' Law, 648
  Brunt-Väisälä Frequency, 137
  Calculus, 872
  Clausius-Clapeyron Equation, 89
  Critical Radius, 193
  Cumulative Heating, 693
  Diffusion Equation, 731
  Error Propagation, 876
  Explanation of purpose of these boxes, 11
  Feedback Example, 809
  Geopotential Height, 11
  Geostrophic Adjustment, 406
  Hypsometric Equation, 18
  Incremental Changes, 38
  Info Projection, 239
  Laplacian, The, 450
  No-feedback Response, 807
  Non-equilibrium Winds [at hurricane top], 619
  Omega Equation, The, 458
  Physical Interpretation of Equations, 16
  Pressure Reversal, 623
  Q-vector Omega Equation, 462
  Taylor Series, 755
  Temperature Gradient, 336
  Thermal Wind Effect, 346
  Turbulence Terms, 714
  Vorticity of a Wave, 368
  Warm Core Winds, 623
bias (mean error; systematic error), 770, 778, 875
  score, 781
Big Thompson Canyon flash flood, 487, 547-548
big whirls have little whirls (eddies), 708
billow clouds, 142, 165
bimetalic strip thermometer, 78
bin size, 646
binary
  bits, 759, 870
  event verification, 780-782
biogeochemical climate-change processes, 810
biological
  climate change process, 810-812
  homeostasis & daisyworld, 813-815
bits, binary, 759, 870
Bjerknes
  circulation theorem, 366
  Jacob, 399, 450
  Vilhelm, 399, 759
bkn (broken) cloud cover, 170
blackbody, 36, 39, 794
  radiance, 221, 224-225
blades of wind turbines, 647
blank diagrams that you can copy
  hodograph, 512
  thermo diagrams, 151-158
blanket-shaped clouds (see stratus), 162-163
blessing, 863
blizzard, 208-209
  associated with extratropical cyclones, 425, 434-435
blocking of airmass movement by mountains, 397, 667
blow up (of numerical weather forecast), 757, 760
blowing snow, weather-map symbol for, 275-276
blue
  color defined (also see optics chapter), 37, 834
  haze, 858
  jet, 563, 568
  moon, 805, 858
  sky, 857-858
    Rayleigh vs. Newton theories, 863
  sun, 858
Bohr, Niels, 745
boiling, 90
bolometer, 46
bolt
  from the blue, 567
  lightning (see return stroke), 556-567
Boltzmann constant, 37, 118, 189, 879
bomb
  cyclone, 426
  nuclear, 499, 548
Bond albedo, 831, 879
bookend vortices, 490-491
Bora winds vs. katabatic winds, 675-676
bore: Morning Glory, 656

Bosart, 765
Bosnia, bora winds, 675
boundary
  airmass, 525-526
    drylines, 416, 525
    fronts, 399-415, 525
    thunderstorm trigger, 525
  conditions, 731, 756, 816
  currents in oceans, 431
boundary-layer (see atmospheric boundary layer, ABL), 13, 687-722
  gradient wind, 309-311
    in hurricanes, 609, 618-619
    in tropical depression, 613
  growth, 689
  parameterizations in NWP models, 751
  pre-storm, 496, 499-503
  pumping, 319-320, 432
    cyclolysis, role in, 432, 465
    in hurricanes, 628
  thermal internal (TIBL), 654-657
  total water, 99
  urban, 678-679
  wind, 307-309
    profilers, 259
    tunnels, 689
bounded weak echo region (BWER), 552-553
bounds on climate change, 811
Boussinesq approximation, 316
bow echo, 490-491, 516
Bowen ratio, 74-76
  measurement, 75
  method of estimating surface fluxes, 75
bows (rainbows, moon bows, supernumerary), 837-841, 860-861
box
  and whisker diagram (statistics), 538
  counting (fractal dimension), 172
Bradbury, Ray, 775
branched star ice crystal shapes, 199
breakdown
  bubble in tornado, 592-593
  of zonal flow, 367-376
  potential for lightning, 566, 880
breaking the cap of thunderstorm inhibition, 522-527
breaking waves in the atmosphere (K-H waves), 142, 165
breath, condensation within, 160
breeze, 635-636
  lake, 654-657
  sea, 654-657
    inland, 654
  urban, 679
briefing, weather, 765
Brier skill score, 782
bright band, 248
brightness temperature, 211, 221-224
British Commonwealth (thermo diagrams used by), 121
broken (bkn) cloud cover, 170, 279
brown cloud, 857-858
Brunt-Väisälä frequency, 136-137, 658-659, 666-668
  use in baroclinic wave equation, 372-373
  use in group velocity for waves, 658-659
  use in mountain lee waves, 666-668
  use in Rossby radius of deformation, 344
  use in smoke plume rise, 733-734
bubble, updraft, 482
budget
  equation(s), 713, 746-747
  energy, global annual mean, 797
  heat , 57-76, 713, 746-747
  mass, 746-747
  momentum, 746-747
  net heat, 72-73
  radiation, 42, 44-45
    global annual mean, 797
  surface heat, 73-76
  water, 99-111, 746-747
BUFR = binary universal form for representation of data, 268
bugs
  computer coding, 759
  radar observations of, 248-249
bulb, wet or dry, 78, 94-96
bulk
  heat transfer coefficient, 68, 397-398
    airmass modification, 397-398
  moisture transfer coefficient, 109
  Richardson number
    dynamic stability, 141-142
    shear, 522, 530-531
    thunderstorm, 521-522, 530-531
bullet shaped ice crystals, 199
bumpy ride in aircraft, 649, 667
Bunker's internal dynamics method, storm motion, 518-520
BUOY code, 269, 271
buoy, cycloidal paths of, 312
buoyancy, 62, 135-136
  definition, 135-136, 316-317
  generated turbulence, 709
  length scale, 733
  negative (downward), 554-563
  neutral, 135
  on thermo diagram, 135
  positive (upward; also see CAPE), 503-508
  pressure-perturbation, 555
  role in katabatic wind, 653
  velocity, 68-69, 110, 300, 704
    scale, 68-69, 110, 300, 394-395, 704
  virtual potential temperature, 62
  waves, 666-668, 710
    thunderstorm triggering, 526
buoyant
  consumption of turbulence, 709
  force, 135-136, 316-317, 554
    along mountain slope, 650-651
    in neutral and stable regions, 135-136
    of rain laden air, 554-563
    pressure-couplets caused by, 341
  forcings, 135, 315-317, 341, 403, 496-499, 503-508, 554-559, 649-653
  production of turbulence, 709
  thermals, 648-649
  turbulence, 704
Burgers-Rott vortex, 599
burning the air (by lightning), 567
bursticane, 602
bursts of rain, 547
butterfly, Lorenz attractor, 774-775
Byron, Lord, 805

C

C and C++ programming languages, trig conventions, 3
C band radar, 242
C, degrees Celsius or centigrade, 7
C-grid, 753
cadmium iodide, 195-196
cal (calvus), 168
Calabrian age, 799
calculation of
  weather (numerical), 745-792
  secondary variables, 771-772
calculus, 11, 16, 18, 293, 872
calibrated probabilistic forecasts, 777
calibration errors, 875
California (advection) fog, 173-175
calm winds, weather-map symbol for, 278
calvus (cumulonimbus), 168, 482
camera filters
  haze, 858
  polarizing, 857
Canada/Canadian
  air quality standards, 725
  geography & province abbreviations, 431
  Hurricane Centre, 617, 638
  hurricanes, 617
  Vancouver, British Columbia, 32-33, 472, 646-647
Cancer, Tropic of, 31
candela, 870
canopy flows, 677-679
  forest or plant, 677-678
  urban or city, 678-679
  winds at canopy top, 678
canyon, urban, 678
cap
  and nonlocal conditional instability, 503
  breaking, 524-527
  clouds, 165, 666-667
  convective inhibition (CIN), 522-527
  definition (inhibiting thunderstorms), 496-499, 522-524
  strength reduction by jet streak, 526
  traps humid-air fuel for thunderstorms, 503
  vs. capping inversion, 497
CAPE (convective available potential energy), 503-508, 530-531
  downdraft (DCAPE), 530-531, 557-559
    vs. CAPE, 558
  energy helicity index (EHI), 591-592
  hail forecasting, 550-552
  in hurricanes, 609
Cape Verde Islands, 611
capillatus/cap (cumulonimbus), 168, 482
capped column ice-crystal shapes, 199
CAPPI radar displays, 242
capping temperature inversion, 496-499, 522-527, 687-698
Capricorn, 31
carbon
  14 isotope, 803
  cycle, global, 812
  dioxide (also see CO2), 7, 805
    effervescence from oceans, 812
    greenhouse gas, 811-812
  film hygrometer, 111
  monoxide, CO, 7, 725
cardiopulmonary resuscitation (CPR), 567, 571
cargo-cult science, 167
Carnot cycle, 624-625
Carnot, S., 89
Cartesian coordinate system, 2, 293
  framework, 293
cartography, 4
cas (castellanus), 168
cascade of vertical vorticity, 586
case study
  cyclone, 433-443, 448-456, 459-463, 466, 745, 768-770, 776
  forecast, 745, 768-770, 776
  thermal wind, 348-349
  thunderstorm, 500-501, 506-508, 522-525, 528-529, 532, 551-552, 558, 568, 590-591
castellanus clouds, 162, 164, 168
castle-like mirages: Fata Morgana, 862-863
CAT = clear air turbulence, 142, 165
  L band radar to view, 242
categorical event verification, 780-782
categories of
  clouds, 168-169
  hurricane intensities, 605-607
  tornado intensities, 579-580
cats and dogs, raining, 206
cavity of reverse flow, 667
cauliflower-shaped clouds (see cumulus), 161-162
CB (cumulonimbus, thunderstorm), 481
cc (cirrocumulus clouds), 168
CCD, 46
CCN (see cloud condensation nuclei), 188-189
CDT, Central daylight time (Americas), 5
ceiling, 170
  change criterion for SPECI, 270
celestial sphere, 834, 854
cell
  closed-cell clouds, 167
  direct and indirect circulation, 377
  Ferrel, 332-333, 357, 377
  grid, 750-758
  Hadley, 329, 332-333, 350-351, 377-378
  open-cell clouds, 167
  polar, 329, 332-333, 352, 378
  solar, 46
  thunderstorm, 484-487, 492-495
Celsius, degrees, unit of temperature, 7, 870
center
  of mass
    hodograph, for normal storm motion, 516-517
    pollutant, 729, 736
  Storm Prediction Center (SPC), 532
centered finite difference scheme, 755-757
  spatial (2nd & 4th orders), 755
  temporal (leapfrog), 757
centerline height, 723, 729, 736
centi (10^{-2}), 870
centigrade = celsius, 7
central
  dense overcast (CDO), 614
  limit theorem, 184
  European time (CET), 5
  time zone (Americas), 5
centrifugal force, 296, 301
  explanation of Coriolis force, 298-299
  in hurricane, 617-618
  sign coefficient, 296
centripetal force, 296, 301
  related to BLG wind, 309-311
  related to cyclostrophic wind, 311-312
  related to gradient wind, 304-307
  related to hurricanes, 617-619
  related to inertial wind, 312
CET (Central European Time), 5
CFC-12 (freon; halocarbons), 796, 811-812
CFL criterion for numerical stability, 760-761

C

channel(ed)
  flow, open-hydraulics, 657-661
  of lightning, 563
  winds, 664
channeling of airmasses by mountains, 397
channels on satellites, 222-223, 230
chaos, 1, 773
  theory & nonlinear dynamics, 773-776
characteristic soundings for clouds, 162, 496-499, 503-508
charge, electric, 564
  transfer to/from ice crystals, 565
charge-coupled devics (CCDs), 46
charging rate & zone of thunderstorm, 564-566
Charney, Jule, 749, 759
charts, weather
  analysis methods, 274-281
  case-study examples, 433-466
  multi-field, utility of, 443
chaser, storm, 583
chasing storms, 484, 583
  core punching, 583
  safety, 485, 517, 567, 570, 583-584
chemical energy, 54
chemicals & chemical symbols, 7, 725
  equilibria, 132
  gases/pollutants in the atmosphere, 7, 725
chill, wind, 76-77
chilled mirror (dew-point) hygrometer, 97, 111
Chinooks , 676-677
Churchill, Winston, 530
ci (cirrus clouds), 168
CIN (convective inhibition, of thunderstorms), 522-525, 530-531
  cap on convection, 524
  mean-layer, 524
cinnamon roll shape of occluding cyclones, 472
Circles
  Arctic and Antarctic, 31
  of light in the sky (see optics), 833-868
circular
  frequency, 36
  orbits, 27
  symmetry, 572
circulation
  absolute, 366
  ageostrophic, 410, 455-456
  along-valley, 653-654
  atmospheric and oceanic, 339, 378
  baroclinic & barotropic atmospheres, in, 366
  Bjerknes theorem, 366
  cells
    direct vertical, 351
    Ferrel, 333, 357
    Hadley, 350-351
    indirect vertical, 333, 357
    polar, 352
  cross
    frontal, 412
    valley, 649-653
  defined, 365-366, 377
  direct, 351, 376-377, 456
  driven by pressure perturbations, 340-341
  general, 329-388
  global, 329-388
    explaining, 350-356
  Hadley, 329, 332-333, 350-351
  horizontal, 365-366
  hurricane, 620-625
  indirect, 456
  Kelvin's theorem, 366
  lake breeze, 654-657
  monsoon, 333-334, 356
  mountain/valley, 649-654, 660-670, 675-677
  relative, 366
  Sawyer-Eliassen, 412
  sea-breeze, 654-657
  secondary, 412, 455-456
  thermal (hydrostatic), 341-342, 648-657
  thermally direct, 351, 412
  three-band general, 329, 376-378
  through hurricane, 620-625
  transverse frontal, 412
  urban, 679
  vertical, 332-333, 377-378
  vorticity, relationship to, 366
  Walker, 820
circumhorizon arc, 848-849, 855
circumpolar trough, 432
circumscribed halo, 851, 853-855
circumzenith arc , 848-849, 854-855
cirro prefix, 163
cirrocumulus, 162-163, 168
  satellite images of, 234
cirroform clouds, weather-map symbol for, 276
cirrostratus, 162-163, 168
  satellite images of, 234
cirrus, 162-163, 168
  satellite images of, 234
citing the work of others (giving credit where due), 24
citizen scientist, 738
city (urban) canopy, 678-679
  temperature excess relative to rural, 679
civil
  defense sirens for storm warning, 529
  twilight, 33-34
Clapeyron, B.-P.-E., 89
classes of stability, 138-141
classic supercell, 482-483, 486, 492-494, 549
classification of
  clouds, 168-169
  snow grains, 199
  thunderstorm types, 486
  winds, 302, 314
Clausius, R., 89
Clausius-Clapeyron equation, 88-92
  as affects mixing and saturation, 160-161
clay (kaolinite), 195
Clean Air Act, 7
clear
  air scans; returns on radar, 249
  air turbulence (CAT), 142, 165
    L band radar to view, 242
  sky, 170, 279
CLIMAT codes (SHIP, TEMP, TEMP SHIP), 269
climate, 793-832
  abrupt-change causes, 810
  anomaly, 818-819, 821
    warm (ENSO and PDO), 818-820
  anthropogenic vs. natural effects, 812
  Arctic Oscillation (AO), 818-819, 824
  astronomical influences, 797-803
  atmospheric window, 796, 811
  averaging time, 817
  change
    abrupt, 810
    bounds, 811
    effects of pollutants on, 724
    gradual, 810
    natural vs. human-caused, 812
  classification (Köppen), 816-817
  clouds, and condensation, 810-811
  codes & criteria, 816-817
  daisyworld, 813-815
  definition, 816-817
  El Niño - Southern Oscillation (ENSO), 818-820
  feedbacks, 806-812
  global climate models (GCMs), 815-816
  gradual-change causes, 810
  greenhouse effect, 795-796
  ice-albedo feedback, 808-812
  IPCC (Intergovernmental Panel on Climate Change), 812
  Köppen classification, 816-817
  La Niña, 818-820
  Madden-Julian oscillation (MJO), 818-819, 824
  Milankovitch theory, 797-803
  natural processes, 793-832
  normal, 818
  North Atlantic oscillation (NAO), 818-819, 824
  of NWP model, 776
  orbital effects, 797-803
  oscillations, 818-824
  Pacific decadal oscillation (PDO), 818-820
  present, 816-817
  radiative equilibrium, 793-797
    astronomical influences, 797-803
    reference state, 794
  sea-surface temperature variations, 818-820
  sensitivity, 810-812
    definition, 810-812
    factor & usage, 812
    magnitudes & processes, 812
  southern oscillation, 818-820
  variability
    astronomical influences, 797-803
    continent movement, 804
    tectonic influences, 804-805
    volcanism, 804-805
  water-vapor and cloud feedbacks, 810-811
climatic precession, 799-802
climatological average, 330
  highs, 354-356
  lows, 354-356
  pressure patterns globally, 354-355
  storm (extratropical cyclone) tracks, 430-431
  vertical cross section of atmosphere, 359
  winds near tropopause, 358
climatology/climatologies of
  hurricanes, typhoons, tropical cyclones, 630-631
  lightning, 564
  numerical weather forecasts, 772, 776
  reference for verification, 780
CLINP code, 269
CLISA code, 269
clock
  24 hour, 6
  mechanical & sundial, 34
  time correction (eq. of time), 34
clockwise, 2
closed
  cellular convection, 167
  system of equations, 714
closure, turbulence
  K-theory & other local, 714-716
  mathematical, 714
  parameterization types, 714-716
  problem, 713-714
  transilient theory & other nonlocal, 716
cloud(s), 159-184
  accessory, 168-169
  active, 162
  advective, 94, 164
  airmass, 393-397
  altocumulus, 134, 162-163, 168
    castellanus, 164-165
  altostratus, 134, 162-164, 168
  anabatic cumulus, 162, 649-650
  anthropogenic, 166
  anvil (incus), 169, 482-484, 604, 614, 620, 624
    debris, 485
  arc/arcus or shelf, 169, 482, 562
  arrangement, 169
  aspect ratio of, 485
  associated with thunderstorms, 482-484
  atlas, 168
  banks, 168
  banner, 165, 667
  base
    estimation of height, 93, 130, 162
    for descending air, 130
    on thermo diagram, 130, 134, 496-499
    rain-free, 483
    height, weather-map symbols for, 277-278
    thunderstorm, 496-506
  beaver tail, 483
  billow, 142, 165
  broken, 170
  brown, 857-858
  buoyancy within, 159
  bursts, 547
  calvus, 168
  cap, 165
  capillatus, 168
  castellanus, 162, 164-165, 168
  categories, 168-169
  ceiling, 170
    thunderstorm, 484-485
    closed, 167
    open, 167
  central dense overcast (CDO), 614
  change criterion for SPECI, 270
  cirro prefix, 163
  cirrocumulus, 162-163, 168
  cirrostratus, 162-163, 168
  cirrus, 162-163, 168, 485
  classification, 168-169
  clear, 170
  climate feedbacks, 810-811
  cold
    frontal cumuliform clouds, 162, 400, 404
    process of precipitation formation, 201-202
  colors in, 856-861
  condensation nuclei (CCN), 185, 188-189
    airmass characteristics of, 391
    density equation, 189
    giant, 206
    Junge distribution of, 189
    number density, 188-189
    sources, 188
  congestus, 162, 168
  contrails, 160, 166
    climate change effects, 812
  convective, 93, 161-162
  cooling in, 101-106
  coverage/cover fraction, 170
    parameterization in NWP models, 751
    total, weather map symbol, 279

vs. PG turbulence type, 728
creation processes, 159-161
cumuliform, 93, 161-162, 170, 482-484
cumulonimbus (cb), 161-162, 168, 481-602
cumulus (cu), 161-162, 168
anabatic, 162
castellanus, 164-165
congestus (cu con), 161-162, 483
fair-weather (humilis), 161, 498
fractus (scud), 165-166, 483
humilis, 161, 498
mediocris (cu med), 161-162, 483
towering (tcu), 161-162, 483
decks, 164
destabilization and cloud formation, 162
determination from soundings, 164
development, 161-166
active-cumuliform, 161-162
passive-stratiform, 162-164
stratocumulus, 164
dimensions, 168
dome (overshooting thunderstorm top), 483
droplets, 159, 185-218
fall velocities, 159, 202
distance between, 194
scattering of light by, 856-859
typical sizes, 185
duplicatus, 169
dust (haboob), 562
electrification, 564-566
eyewall, 604-605, 618-620, 624-629, 637
feedbacks for climate, 810-811
few, 170
fibratus, 168
filaments, 168
flanking line, 483
floccus, 168
foehn wall, 676-677
fog, 159
forecasts
formation, 98, 159-161
in anabatic flows, 162
in cold air advection, 162
orographic, 168
via cooling, 159
via adding moisture, 160
via mixing, 160-161
forms, 168
fractus, 165-166, 168, 483
-free air around thunderstorms, 546
frontal
cold front and cumuliform, 162, 400, 404
occluded fronts, 413
warm front and stratiform, 162-164, 401, 404
fumulus, 166
funnel (also see tornado), 169, 483
genera, 168
glaciated, 485
haboob, 562
hat, 165
horizontal roll vortices, 167
humilis, 161, 168
hurricane, 603-644
ice-crystal, in arctic airmasses, 393-397
identification, 161-169
incus, 169
intortus, 169
K-H wave, 142, 165
lacunosus, 169
Lagrangian heat budget within, 159
lapse rate inside, 101-106
layers, 168
as reported in METAR, 270
lee-wave, 165, 666-668
lenticular/lenticularis, 165, 168, 666-668, 684-685
optical phenomena, 859-860
lines, 167
mammatus/mamma, 169, 484
man-made, 166
mesoscale cellular convection, 167
mesoscale convective complex, 486, 491
mediocris, 161-162, 168
mesocyclone, 483
mesoscale cellular convection (MCC), 167
METAR, 270
meteors, 168-169
microphysics, 185-218
parameterization in NWP models, 751
(in) midlatitude cyclones, 425-428, 472
morphology, 168
mother, 168-169
-of-pearl, 166
mountain-related (orographic), 162, 165-168, 649-650, 676-677
mountain-wave, 165
movement, 483
nacreous, 166
names, 161-169
NAT, 166
nebulosis, 168
nimbostratus, 162-163, 168
noctilucent, 166
obscured, 170
observation from satellite, 220
occluded frontal clouds, 413
opacus, 169
organization, 167
orographic, 162, 165-168, 649-650, 676-677
overcast, 170
pannus, 169
passive, 163
perlucidus, 169
photographic tips, 180, 484
pileus, 165, 169, 483
polar, 166
mesospheric (PMC), 166
stratospheric (PSC), 166
praecipitatio, 169
radiatus, 169
rain, 482-483, 486
rain-free base of, 483
roll, 169
rotor, 165, 667
sand, 562
satellite images of, 232-234
saturation within, 159-161
scarf, 165
scattered, 170
scattering of light from, 856-858
scud (cumulus fractus), 483
seeding, 195-196, 218, 553-554
shapes, 171
sheets, 168
shelf, 482, 562
shield
from hurricanes, 604
from thunderstorms, 488
warm-frontal, 425-428
sizes, 170
snow-banner, 165
species, 168
spissatus, 168
standing lenticular, 165, 666-668, 684-685
optical phenomena, 859-860
static stability within, 159
stratiform/stratiformis, 94, 162-164, 168
stratocumulus, 164, 168
stratus, 162-163, 168
streets, 167
striations, 483
structure, 168
STS clouds, 166
subcategories, 168-169
supercell, 482-483
supplementary features, 168-169
surface-turbulence related, 165-166
symbols on weather maps, 168
tail, 483
thermo diagram (detection using), 134
thickness, 161-162
thunderstorm, 481-602
-to-air lightning (air discharge; CA), 563
-to-cloud lightning (CC), 563
-to-ground lightning (CG), 563
top, 162
track winds, 321-322
trade cumulus, 351
translucidus, 169
transparency, 169
triggering mechanisms
cold fronts, 162
mountains, 162
tuba, 169
turbulence and mixing, 132, 165-166
types, 168-169
uncinus, 168
undulatus, 169
urban, 162
varieties, 168-169
veils, 168
velum, 169
vertebratus, 169
virga, 169
wall, 483, 581-583
warm frontal, stratiform clouds, 162-164, 401, 404
wave (see lenticular), 165, 168, 666-668, 684-685, 859
weather map symbols for, 168, 277
white color of, 857
cloudiness
airmass characteristics of, 391
constant (isoneph), 18
feedback factor for climate change, 810
related to albedo, 44, 811
cloud-radiation interaction, 131-132
clusters of ice crystals, 199
CO, carbon monoxide, 7, 725
CO2, carbon dioxide, 7
biological climate feedback, 810-812
doubling, 812
fossil fuels vs. global cycle, 812
greenhouse gas, 811-812
ocean, feedback for climate, 810-812
effervescence, 812
sequestered, 812
transpired and release during wild fires, 812
coagulation, 188
coalescence, 202-207
efficiency, 204-205
coarse
mode CCN formation, 188
resolution NWP & GCMs, 752, 815
coastal
breezes, 654-657
fogs (advection fog), 173-175
hazards of hurricanes, 634
jets, 664-665
waves and surf, 634-636
winds, 654-657, 661-665
coastally trapped low-level barrier jets, 664-665
cockroach, 151, 815
CODAR code, 269
CODATA, 876, 879
codes for
airmasses, 391-392
weather reports, 268-273
coefficient
drag, 700-701
extinction, 43
cold
air
advection and backing of wind, 349
advection and cloud formation, 162
aloft in pre-storm environment, 496, 503
pool from thunderstorms, 488-489
pool at night, 653
sector, 425-428
airmass, 392
depth, 404-406
genesis, 393-397
cloud
precipitation aggregation, 202, 205
process of precipitation formation, 201-202, 205-206, 546
seeding, 196
tops in thunderstorms, 206
core systems, 426, 622
vs. warm core, 622
frontogenesis, 281, 399
frontolysis, 281, 399
front, 399-404
aloft, map symbol for, 281, 399
cumuliform clouds, 162, 400, 425-428
definition, 404
deformation behind, 470-471
descent and diffluence behind, 433, 470-471
depth, 405
extratropical cyclone, attached to, 425-428
horizontal structure, 400
occlusion, 413
propagation, found using Q-vectors, 470-471
radar observations of, 248-249
thunderstorms along, 400
trigger for hurricanes, 612-613
trigger for thunderstorms, 525
weather map symbols for, 281
high-pressure centers, 341-342
katafront, 404
mode rainfall estimates, 257
sector of extratropical cyclones, 425-428
vs. warm core cyclones, 622
collection, 202-207
and aggregation processes, 204-205
efficiency, 205
collision efficiency, 204
collision and collection, 202-207
of hydrometeors, 185, 202-207
droplet size distributions, 207

C

processes, 202-207
terminal velocity of droplets, 202-204
colors
angles of 22 degree halo, 845
defined, 37, 834-835, 862
dispersion of, 834, 862
Newton's work on, 862
of halos and arcs, 845-851
of rainbow, 838-840
of sky, 857-858
of sunset, 858
scattered vs. particle diameter, 858
wavelengths of, 37, 834-835, 862
Columbus, Christopher, 607
column
ice crystals, 198-199, 842
hollow, 198-199, 866
optics caused by, 842-855
of air in closed cylinder, 55, 463-465
combined parameters and conversion factors, 880
commercial aircraft, 563
compass direction, 2, 646
complete thermo diagrams, 121, 151-158
complexity of the atmosphere, 1
component angles of refraction geometry, 833-836
components of the atmosphere, 7
composition of atmosphere, 7
compressible flow, 671-672
adiabatic, 671-672
isothermal, 671
numerical weather prediction model for, 747
compression, 8
of NWP output into databases & climatologies, 772
computational
evolution, 680
natural selection, 680
computer
Amdahl's Law, 763
blowing up, 757, 760
chips, 752
crash, 757
ENIAC, 749, 759
Moore's Law, 752
profilers, 763
speed-up, 763
vs. human contributions to forecasts, 772
computerized (numerical) weather forecasts, 745-792
concentration, 724-725
of pollutant, 725
crosswind-integrated, 735-737
Gaussian distribution, 729-730, 734, 737
of pollutant downwind, 724,
units for pollution, 724
condensation, 56, 88
amount in rising air parcels, 130
convective condensation level (CCL), 526-527
freezing, 195
funnel of tornado, 581-583
energy in hurricanes, 620
latent heat of, 56
lifting condensation level (LCL), 93-94, 496-506
nuclei (see also CCN), 188
on to snow, 110
role in frontal strengthening, 411
role in self development of cyclone, 465-471
trail (contrail), 160, 166
conditional instability, 140-141
nonlocal, in hurricane environment, 609
nonlocal, in thunderstorm environment, 140, 496-499, 503-508
conditionally unstable, 140-141
conditions favoring thunderstorms, 496-499
conduction, 67-69
contribution to airmass genesis, 393
contribution to frontolysis, 411
from cloud droplets, 185, 197
(and) turbulence on windy days, 68
conductive heat flux, 67-69
at surface, 73-76
conductivity, molecular, 67-68, 880
cone shaped tornadoes, 577
confidence in NWP forecasts, 776
confluence, 409-410
frontogenesis, 409-410
conformal map projections, 748
congestus/con, cumulus, 161-162, 168, 483
pileus clouds created by, 165
coning, pollutant plume, 710, 727
consequences of doing science, 218
conservation of
angular momentum, 360-361
breakdown of, 361
energy along a streamline, 671-672
heat, 1, 59, 64, 746-747
isentropic potential vorticity, 364-365
mass, 317-320, 660, 746-747
momentum, 392-393, 746-747
potential vorticity, 363-364, 445
total water, 1, 107, 746-747
conservative tracers, 731
conserved variable, 61, 104
constant
altitude plan position indicator (radar), 242
flux layer, 692
gases in the atmosphere, 7
height map (such as mean-sea level), 436
case-study cyclone examples, 434, 438
vs. isobaric map, 290-291, 436
potential temperature map, 437
potential vorticity map, 437
pressure map, 436
pressure difference (giving thickness charts), 436
solar (total solar irradiance), 39
von Kármán, 677, 701
constants and conversion factors, 879-880
Earth, 879
math, 879
universal, 879
constantan, 78
constituents (gases) in the atmosphere, 7
constructive interference, 859-861
contact freezing, 194-195
continental
airmass code, 392
arctic airmasses, 396
polar (cP) airmass, 392
genesis, 393-397
scale circulations (monsoons), 333-334
continent(s)
aerosols and CCN over, 188, 194
movement, 804
ocean circulations (monsoons), 333-334, 356
super, 804
contingency table, 780
continuity, 317-318
effects, 340-341
downburst & gust fronts, 561-562
driving vertical velocity, 452-456
equation, 317-318
flux form, 714
sign convention, 320
pressure perturbations related to, 340-341
continuous variables, verification of, 777-780
contours, 17, 121, 151
contraction, axis of, 320-321
contrails (condensation trails), 160, 166
climate change effects, 812
controlling the weather, 218
convection
deep (i.e., thunderstorms), 481-601
parameterizations in NWP, 751
definition, 66, 649
forced vs. free, 704, 710, 727
free, 704, 710
smoke dispersion within, 735-737
level of free (LFC), 496-506
limit of (LOC), 498
moist (i.e., thunderstorms), 496, 649
organized, in tropical disturbance, 613
parameterizations in NWP models, 751
penetrative, 508
convective
adjustment, moist, 70
available potential energy (CAPE), 503-508, 530-531
boundary layer, 68, 109-110
circulations, 134-139, 161-162, 332, 341-342, 350-351, 357, 376-378, 481-544, 648-657, 704
clouds (including thunderstorms), 93, 138, 161-162, 481-601
formation regions, 162
condensation level (CCL), 526-527
conditions for thunderstorm formation, 68, 496-499
inhibition (CIN), 522-525, 530-531
instability (nonlocal conditional), 498, 503-508
mixed layer, 648-649, 692, 695, 697-698
airmass, 393-396
depth, 649, 695, 697-698
humid. Role in thunderstorms., 497-501
smoke dispersion within, 735-737
winds in radix layer, 703-705
mixing, 301
outlooks, 528-530
radix layer, 703-705
temperature, 526-527
towers, hot, 644
transport coefficient, 68, 110
for heat, 68, 110
for moisture, 110
turbulence, 508, 527-530, 704
generation, 706
velocity scales, 68-69, 704
vortex, mesoscale, 492
winds in boundary layer, 703-705
conventions - mathematical and meteorological, 2
convergence, 318-321
evolution vs. cyclone evolution, 467
of air at bottom of cyclones (lows), 309, 331, 691
of air at top of anticyclones (highs), 391
of air in certain jet streak quadrants, 454-456
of air in easterly waves, 612
of mass, 318-321, 340-341
of Q-vectors, 460-462, 469-471
radar observations of, 252-253
zone
intertropical (ITCZ), 330-332
Olympic Mtn. & Puget Sound, 472
conversion
constants and conversion factors, 879-880
factors and combined parameters, 880
of pollutant concentration units, 724
of units, 871
of wind components, 3
conveyor belt of warm air, 433
cooking
boiling temperature vs altitude, 90, 115
data, 826
cooling
accumulated in boundary layer, 693
evaporative, in downbursts, 556
process to make clouds, 159
tower clouds, 166
coordinate system, 2
aligned with mean wind, 727
alternative
horizontal, 747
vertical, 746
Cartesian (rectangular), 2
cylindrical, 2, 627
eta, 746
hybrid, 746
map-projection, 747-748
polar, 2
stererographic, 747-748
sigma, 746
spherical, 747
terrain-following, 746, 753
Coordinated Universal Time (UTC), 5, 268
co-polar correlation coefficient, 256-257
copper-constantan thermocouple, 78
core
cold, 426, 622
of cyclone, 426. 622
of hurricane, 604, 614, 618-625
of jet stream, 357-361
of tornado, 577-578
pressure deficit in
hurricane, 621-624, 626, 633
tornado, 577-578
punching, 583
warm, 426, 614, 621-622
vs. cold, 622
Coriolis force, 297-299, 301
acting on
Antarctic winds, 652
katabatic winds, 652-653
as a component of centrifugal force, 298-299
derivation of equations for, 299
direction, 297
explanation of, 298-299, 301
factor, 879
in gap winds, 662-664
in hurricane, 609, 617-619
in 3D, 297
contributing to wind, 302
boundary layer, 307
boundary-layer gradient, 309
geostrophic, 302
gradient, 304
inertial, 312
magnitude, 297-299, 301
near equator, 297
on objects moving east/west, 298-299
on objects moving north/south, 299
role in cyclogenesis, 426, 443-450, 609

sign convention, 297
vertical component, 297
Coriolis, Gaspar Gustave, 298
Coriolis parameter, 297
rate of change (beta) with latitude, 297, 369, 879
corkscrew (helical) motion, 587-592
corollaries
numerical weather prediction, 756, 758
satellite sounding retrieval, 235-239
corona, 858-860
clouds that cause, 163, 667, 859
igneous meteors, 205
vs. halos, 860
correct negative or correct rejection, 780
correction of temperature for dynamic warming, 673
correlation coefficient, 711, 779
anomaly, 779-780
cosine law of radiation (see sine law), 40
cosmic rays, 565
cost, 780
function, 766-767
loss
decision model, 784-785
ratio, 785
cotton-ball shaped clouds (see cumulus), 161-162
coulombs, C, unit of electric charge, 7, 564, 870
counter-clockwise, 2
counter-rotating mesocyclones, 490-491, 587
coupled equations in math, 393, 747
coupled heat and moisture budgets, 108
couplet
wind, 253, 561
pressure, 340-341
Courant
condition, 760
number, 758
Friedrichs-Lewy (CFL) stability criterion, 760-761
courses on meteorology/atmospheric science, 863
covariance, 711-713, 821
matrix, 821-822
coverage of clouds, total, 279
Cp vs. Cv, 55
CPR (cardiopulmonary resuscitation), 567, 571, 638
crash
aircraft, due to bad weather, 563
computer, 757
CRC Handbook of Chemistry and Physics, 879
creativity in
engineering, 288
science, 293
crests of waves, 658, 668
tilt with altitude, 668
Cretaceous-
Paleogene extinction event, 805
Tertiary (KT) extinction event, 805
CREX = character form for the representation of data, 268
crimson sunset skies, 858
critical
angle, 837
evaluation exercises explained, 22
flows, 659
Froude number, 659
radius, 192
derivation, 193
Richardson number, 142, 880
success index, 781
supersaturation, 192
swirl ratio, 593
Croatia, bora winds, 675
crop
canopy flows/winds, 677-678
damage from hail, 549
cross
equatorial flow
in Hadley cell, 332-333
in monsoon circulations, 356
frontal circulation, 412
jet-stream flow, 415
isobaric flow, 307-311, 314, 318-320, 454, 691
product vector operator, 299
section in
baroclinic atmosphere, 373
extinction, 43
fronts, 403-416
global circulation cells, 332
hurricane, 605, 618-624, 629
jet streams, 357
valley circulation, 649-653
wind
direction definition (i.e., lateral), 727
integrated concentration, 735-737
crystal (see ice crystal)
liquid-crystal thermometer, 78
cs (cirrostratus clouds), 168
CST, Central standard time (Americas), 5
cu (cumulus clouds), 168
cubic ice (Ic), 198
cumulative
daytime heating, 693-694
seasonal differences, 695
nighttime cooling, 693
seasonal differences, 695
probabilities, 777
cumuliform clouds
along cold fronts, 425-428
altitude of bases, 93
formed by adiabatic cooling in updrafts, 160
formed by turbulence near surface, 165-166
typical sizes, 170
cumulonimbus (see thunderstorm), 161-162, 168, 481-602
calvus, 482
capillatus, 482
cumulus, 161-162, 168
anabatic, 162, 649-650
castellanus, 164-165
congestus (cu con), 161-162, 483
triggering pileus clouds, 165
fair-weather, 161, 498
fractus, 165-166, 483
frontal, 400, 404, 413
humilis, 161, 498
mediocris (cu med), 161-162, 483
mixing caused by, 301
stage of thunderstorm evolution, 485
towering (tcu), 483
trade, 351
weather-map symbols for, 277
cup
anemometer, 321
shaped ice crystals, 199
cupric sulfide, 195-196
current
density, 565, 655-656
direct electric, 564
units, 564
gravity, 655-656
induced by lightning, 570
lightning, 564, 568-569
ocean, 339, 378, 431, 610, 701
Gulf Stream, 616
Labrador, 616
curvature , 375
Earth's, 244
effect, 189-192
jet stream, driving updrafts and cyclogenesis, 453
Laplacian, as a measure of, 450
of a line, 450
radius of light ray, 861
Rossby number, 306
Rossby wave, 375
terms in equations of motion, 747
vorticity, 362
cut
in wind speed for turbines, 648
out wind speed for turbines, 648
Cv or Cvd, 55, 880
cyan color defined (also see optics chapter), 37
cycle, global carbon, 812
cyclogenesis, 426-433
attributes, 446
characterized by, 426, 446
sea-level pressure decrease, 463-467
upward motion increase, 451-462
cyclonic vorticity increase, 446-450
evolution, 467
explosive, 426
favored regions, 426, 431-431, 450, 456
feedbacks, favoring self-development, 468-471
hurricane, 608-615
lee side, 430-431, 443-446
isentropic potential vorticity conservation, 364-365
potential vorticity conservation, 364-365, 445
omega equation, 456-462
Q-vectors, 460-462
rapid, 426
self-development, 468-471
Sutcliffe development theorem, 456
Trenberth omega equation, 458
tilt of trough with altitude, role of, 432
cycloidal paths of
damage from multi-vortex tornadoes, 593
drifting buoys, 312
cyclolysis, 426-433
evolution, 467
cyclone
atmospheric boundary layer within, 690-692
bomb, 426
Catarina, 631
case study, 433-443
characteristics, 426-433
cold vs. warm core, 622
convergence of horizontal winds, 691
deepening, 463
evolution, 427-429
filling, 463
glyphs (symbols) on weather maps, 426
graveyard, 431, 472
landfalling, at Pacific Northwest coast, 472
lifetime, 431
propagation and self-development, 469
self-development, 468-471
spin-up, 446-451
tracks and propagation, 425-426, 430, 469
Q-vectors, 469-471
warm vs. cold core, 622
cyclone types/names
comparison of, 425-426
cyclones (tropical or extratropical), 425-426
extratropical cyclones (lows), 425-480
hurricanes, 603-644
low-pressure centers (see extratrop. cyclones), 425-480
lows (see extratropical cyclones chapter), 331, 425-480
mesocyclones (see thunderstorm chapters), 481-602
midlatitude cyclones (see extratrop. cyclones), 425-480
polar cyclones (see extratrop. cyclones chap.), 425-480
storm systems (see extratrop. cyclones chap.), 425-480
tropical cyclones (see hurricane chapter), 603-644
typhoons (see hurricane chapter), 603-644
cyclonic
rotation direction of most tornadoes, 578, 586
vorticity, 446-450
spin-up, 446-450, 586-587
cyclonic winds, 306-307, 331
convergence in the boundary layer, 309, 691
definition, 425
cyclostrophic balance, 311-312, 578
cyclostrophic wind, 311-312
in hurricane, 609, 618
in tornadoes and waterspouts, 311, 578
cylindrical
coordinates - defined, 3
for hurricanes, 627
shaped tornadoes, 577
CYVR (Vancouver International Airport), 646-647

D

D-grid, 753
daily cycle (diurnal), 687
of thunderstorms, 528
daily solar effects, 32, 40, 687
daisyworld , 813-815
Dalton minimum in solar activity, 803
damage
paths
cycloidal vs. divergent, 593
parallel, 584
scales
hurricane, 605-607
tornado, 579-580
wind, by hurricanes, 634-636
damming of cold air behind mountains, 661-665
damped
inertial oscillation, 311
response (negative feedback), 806
dark
band, Alexander's, 841
spot (waterspout evolution), 582
Darkness, by Lord Byron, 805
dart leader (lightning), 567
data
abuse, 826
analysis methods
on weather maps , 280, 765-768

D

(also see statistical methods)
assimilation and analysis, 765-768
element, 875
empirical orthogonal function (EOF), 820-823
ethics and abuse, 826
extrapolating, 826
fudging, 826
manufacturing, 826
massaging, 826
misinterpretation, 729
outliers, 502
principal component analysis (PCA), 820-823
reduction, 502, 823
reporting, 875
set, 875
slanting, 826
smoothing, 826
statistical (see statistical methods)
void, Pacific, 287-288, 765
databases, 772
date line, international, 5
daughter storm, 485
Davenport-Wieringa roughness-length classification, 700
day
duration, change of, 376
sidereal, 297
unit, 870
winds (anabatic; valley; sea-breeze), 649-657
daylight
duration of, 32-33, 40
time (DT) = daylight savings time, 5, 6
daytime (convective) boundary layer, 692
dazzled by bright sunlight sky, 842
dB (decibels), 246
dBZ (decibels of radar reflectivity factor), 246-247
hail, 247-248, 552
DCAPE (see downdraft CAPE), 557-558
Deardorff velocity, 69, 703-704, 736
deaths caused by
downbursts of air and aircraft crashes, 563
downpours of rains and flash floods, 548
hurricanes and storm surge, 606, 617, 631, 637
lightning, 564
tornado outbreaks, 583-584
winter storms, 434-435
debris cloud, tornado, 581-583
decade on logarithmic graph axis, 215
Deccan traps, 805
deci (10^{-1}), 870
decibels, 246-247
decision model, cost/loss, 784-785
decks of clouds, 164
declination angle, solar, 30-31
decoding a METAR or SPECI, 270-279
decreasing, weather-map symbol for, 276
deductive reasoning, 107-109
deep convection (see thunderstorms), 481-601
parameterizations in NWP models, 751
deepening of lows (cyclones), 463
definition errors, 875
deformation, 320-321
internal Rossby radius of, 319-320, 344, 665
use in coastally trapped jets, 664-665
use in Rossby waves, 372-373
external Rossby radius of, 405-406, 665
frontal, 410, 433
shearing, 320-321
stretching, 320-321
total, 321
degrees
angle unit, 870
Celsius (°C), unit of temperature, 870
latitude & longitude, 4
temperature symbols (°C, °F, K), 7
deka (10), 870
del operator, 458
deluge, 607
dendrite snowflake/ice-crystal, 198-199, 843
optics caused by, 842-843
dendrochronology (tree ring dating), 803
density
at sea level, 10
change with height, 10, 316
constant (isopycnic), 18
current, 655-656
definition, 10
forecast equation for, 746
hailstone, 549
ice, 209
interface, 657-661
of average tropospheric air, 72, 880
of droplet laden air, 14-15, 202
of liquid water vs. temperature, 835, 880
sea water, 880
mean background state, 316
partial, 91
scale height, 10
snow, 209
specific volume, 10
standard (STP), 880
units, 10
dependent variable, 3, 872
deposition
latent heat of, 56, 88
nucleation, 194-195
depression
tropical, 613-614
wet-bulb, 94-96
depth
Ekman layer in ocean, 378
evaporation rate, 108
liquid-water equivalent, 107, 208, 210
of atmospheric boundary layer, 144, 319, 687-705, 716
of the troposphere, 143, 163, 357-360, 414-415
optical, 43, 805, 856
parameter (Ekman) in ocean, 378
precipitable water, 98-99, 211, 501
precipitation rate, 108
derecho, 489, 491, 494
derivative
finite-difference approximation, 16, 872
total, 872
derived dimensions, 870
Des Moines, Iowa, 745, 776
Descartes, Rene, 2, 90, 680, 841
descending air (see subsidence)
descending node of satellite orbits, 228-229
description of global circulation, simplified, 330-334
descriptor on weather maps, 276
desert
Gobi, 397
oasis effect, 74
subtropical, 351
suface heat flux at, 74
design of an NWP system, 761
destabilization
of air to make cumulus clouds, 162
of well-mixed fog, 176-177
to maintain a circulation, 342
destructive interference, 859-861
detection networks, lightning, 568-569
deterministic forecasts, 777, 816, 818
detrainment of air, 57
development
clouds, 161-166
hurricanes, 617-618
theorem for cyclogenesis (Sutcliffe), 456
tornadoes, 583
dew, 93
dew-point
depression, 93
hygrometers, 111
temperature, 89, 92-93
constant (isodrosotherm), 18
definition, 92-93
in thunderstorm environment, 499-502
measurement, 111-112
plotted on weather maps, 275, 438, 500
reported in METAR, 270
diabatic
effects in frontogenesis, 411
excess water variation, 187
heating, 131
role in cyclone evolution, 465-466
numerical weather prediction model, 747
process, 61, 131
warming rate for frontogenesis, 411
diagnostic equations, 747
diagrams
Hovmöller, 824-825, 830
reliability, 782-783
ROC, 783-784
thermo, 63, 119-158
DIAL (differential absorption lidar), 112
diameter of rain drops, radar observed, 247-248
diamond dust (ice crystals), 276, 396, 842, 849
dice, 184
difference, finite, 872
differential
absorption lidar (DIAL), 112
advection (see also castellanus clouds), 164
equation, 16, 137, 872
heating, 329, 334-339
heat transport by global circulation, 338-339
meridional temperature gradient, 335-336
radiative forcings, 329, 334-339
reflectivity, 256-257
diffraction, 858-861
fringe, 858-860
diffuse arcs, 854-855
diffusion, 185, 196-197
definition, 196-197
equation, 196-197, 731
of water molecules, 185, 196-197
diffusive growth of
droplets, 196-197
ice crystals, 198-202
diffusive moisture flux, 196
diffusivity, 196-197
eddy (turbulent), 715
molecular, 196-200, 880
diffusometer, 46
difluence, 410, 433
behind cold front, 433
dilation, axis of, 320-321, 410
dimensionless ratios
Froude number, 659, 667
Richardson number, 141-142, 521
Rossby number, 313
curvature, 306
scales for pollutant dispersion, 736
dimensions, 870
basic & derived, 870
fractal, 171
units, 870
conversions, 871
dimethyl sulfide, 188, 811
dinosaurs, 805
dipoles
Arctic, 824
Indian Ocean, 824
pressure couplets, 340
direct
cell, 377
circulations, 351, 376-377, 462
frontal, 412, 462
climatic response, 806-812
current (DC), 564
instruments (in situ), 219
sense, 332-333, 357, 377, 456
vertical circulation cells, 351, 376-377
vs. indirect heating, 73
direction of
scattered light, 857
wind, 2, 3
frequency; wind rose, 646-647
isogon, 18
directional shear, 509-510
directions of up and down, 298
dirt, 188
dirty window, 220-223
disaster
plan, 638
relief, 631
supply kit, 638
discomfort indices (humidity), 117
Discours de la Méthod (book), 2
discretization, 750
equations of motion, 758-759
discriminate between event and non-event, 783
discriminator, statistical, for thunderstorm forecasts, 507
disdrometer, 210
dispersion, 723-744
color, 834-835, 862
equation, 731-732
Deardorff method for unstable ABLs, 735-737
factors of pollutants, 724-725
atmospheric turbulence, 724-728
plume rise, 724
wind speed and direction, 724-727
far from source, 732
fog, of, 175-177
in neutral and stable boundary layers, 708, 732-734
in unstable boundary layer, 708, 735-737
isotropy, 727
near pollution source, 732
of light into colors, 834-835, 862
Newton's work on, 862
of pollutants and smoke, 708, 723-744
Pasquill-Gifford turbulence type, 727-728
relation of waves, 369
baroclinic; planetary, 372
barotropic; Rossby, 369
statistics, 728-730

displacement
distance, 677
of fluid, causing buoyancy, 135
dissipation
length scale, 709
of fogs, 175-177
of turbulence, 315, 706, 709
rate, 709
stage of thunderstorm-cell evolution, 485
stage of tornadoes, 583
subrange, 315
dissipative turbulent behaviour, 706
distance
between cloud droplets, 194
between crest and trough (jet stream), 367-374, 453
between sun and earth, 30, 797-802
displacement, 677
distribution
Junge, 188-189
lognormal
cloud sizes, 170
drop sizes, 207
of pressure in hurricane, 618-633
of radiation, 39
of smoke concentrations, 734, 737
Weibull, for wind speed, 645
disturbance
tropical, 613
upper-level, 433
diurnal (daily) cycle, 27, 356, 687
heat, 73-76, 528, 687-698
of dry line, 416
of thunderstorms, 528
radiative fluxes, 27, 44, 687
winds, 699-704
divergence, 318, 320-321
airmass formation, role of, 393-394
aloft in
low-pressure region, 432, 452-459, 463-467
tropical upper tropospheric trough, 612-613
at surface in a high-pressure region, 331, 390, 691
evolution vs. cyclone evolution, 467
in pressure systems, 340-341, 467
jet-stream winds, role in cyclogenesis, 427-428, 432, 452-459
of flux, 64, 109-110, 715
of mass, 318-321, 340
of Q-vectors, 460-462, 469-471
outflow straight-line thunderstorm winds, 252-253, 560-561
plotted on a weather map, 441, 449
pressure tendency at MSL, role in, 463-467
radar observations of, 252-253, 560-561
term in vertical vorticity eqn., 447-448
upward motion driven by, 452-459
DMSP (defense meteorological satellite program), 273
dogs, sun, 842, 850-851, 854-855
doing science, 877
doldrums, 331
domain of NWP, 750
dome (overshooting thunderstorm top), 483
dominant wavelength of lee Rossby waves, 444
Doppler
dilemma, 251
displays, 250-254
dual radars, 249, 253
maximum unambiguous velocity, 250-251
phase shift, 250
radar (see also radar), 241, 249-254, 552
downburst & gust-front detection, 556-560
locations worldwide, 272
radial wind speed (isodop), 18
thunderstorm diagram, 493
shift, 241, 249-250
Doswell III, Charles, 517, 567, 583-584
dot product, 239
doubling of carbon dioxide, 812
down, direction defined, 298
downbursts and gust fronts, 482-483, 554-563
bursticane, 602
causes, 555-556
evaporative cooling, 556
precipitation drag, 555
characteristics and definition, 554-555
downdraft CAPE (DCAPE), 557-559
pressure perturbation, 559-550
geographic locations, 556
intensity estimates from radar, 561
outflow straight-line winds, 560-563
radar observations of, 253, 560-561
triggering new thunderstorms, 525, 561
vertical velocities, 557-559
downdraft
CAPE (DCAPE), 530-531, 557-559
dangerously fast (downbursts), 554-563
equilibrium level (DEL), 557
forward-flank (FFD), 483
rear-flank (RFD), 482
speed, 554, 557-559
downslope winds , 652-653, 667, 675-677
Antarctic, 676
Bora, 675-676
Foehn, 676-677
katabatic, 652-653
mountain waves, 667
storms, 667, 675
downwelling radiation, 44-45
downwind mountain process, 443-446, 666-668
drag
atmospheric boundary layer, 699-702
coefficient, 300, 700-701
range, 300, 700-701
force, 300-301
related to antitriptic wind, 312-313
related to BL & BLG wind, 307-311
sign convention, 300
on air by falling rain, 202, 555
on falling
cloud droplets, 202
hailstones, 204
ice crystals, 842
rain drops, 203
on tornado rotation, 586
precipitation, 555
role in katabatic wind, 653
skin, 668
Stokes law, 202-203
wave, 668
parameterization in NWP, 751
drainage winds (see katabatic winds), 397
drawing weather maps by hand, 280-281
drifting snow, weather-map symbols for, 275-276
drizzle, 207-208
area coverage, 546
drops, 546
rate and symbols on weather maps, 208, 275-276
warm frontal, 401
drop (see also droplet)
deformed, 203, 255, 841, 860
diameter as affects radar returns, 247-248
flattening, 203, 255, 841, 860
number in cubic meter of air, 188, 194, 201, 207, 245-246
optics, 837-841, 856-861
radius, 185
shapes, 203, 255, 545-546, 841, 860
size distribution, 185, 545-546
terminal velocity, 203
typical sizes, 185
volumes, 185
droplet, 185-218
curvature and solute effects, 198-192
growth effects, 189
growth by diffusion, 196-197
growth rate, 196-197
max droplet radius via diffusion, 187
nucleation, 188-194
optics, 837-841, 856-861
radius, 185
equivalent, 203
increase with time, 197
maximum via diffusion, 187, 197
size distributions, 185, 207
lognormal, 207
Marshall-Palmer distribution, 207
terminal velocity, 202
typical sizes, 185
dropsonde sounding, 134, 322, 496
locations worldwide, 272
drowning due to
hurricane rain and storm surge, 632-637
thunderstorm flash floods, 547-548
dry (see also unsaturated), 57
absolutely unstable, 140
adiabatic lapse rate, 59-64, 880
to determine static stability, 139-141
adiabatic process
adiabats, 63
labeled by potential temp, 63
on thermo diagram, 119-158, 497
air
gas constant, 880
in highs, 390
in thunderstorm, 497
specific heat, 880
bulb temperature, 94, 111
lifting of air parcels, 129
lines, 416-417
airmass boundary, 416
distance moved over time, 416-417
radar observations of, 248-249
triggering thunderstorms, 525
weather-map symbols for, 281, 399
neutral stability, 140
tongue of air in cyclone, 429
drying in downslope winds, 676-677
dual Doppler radar, 249, 253
ducting of radar beam, 244-245
dummy index, 875
duplicatus, 169
dust, 151, 170
airmass characteristics, 391
lithometeors, 205
storm (Haboob), 562
weather-map symbols for, 275-276
swirl, 583
dynamic
frontogenesis, 411-412
hail mitigation methods, 554
heating, 672-674
numerical stability, 759, 773-777
pressure, 559, 672-674
stability, 141
Richardson number, 141
turbulence determination, 142
temperature, 672-674
warming, 672-674
dynamical instability, 141-142
dynamics, 289-328
frontal strengthening, 411-412, 469-470
hurricane, 617
nonlinear, 773-776
numerical weather prediction, 749-750
topics, 1-2

E

e, base of natural logarithms, 9
E-grid, 753
early rainout, 553
Earth
albedo, 793-794
angular rotation rate, 297
average
global energy budget, annual, 797
surface temperature, 12, 793-797
axis, 34, 798-801
blackbody radiation emitted, 37, 39, 794
buldge of Earth at equator, 3-4
characteristics, 3-4, 879
climate
precession, 798-803
processes, natural, 793-832
constants, 879
daisyworld, 813-815
eccentricity, 28, 34, 797-802
variations and climate, 797-803
effective radiation emission temperature, 794, 879
emission of radiation, 37-39
energy budget, annual average, 797
frameworks, 3-4
gravity, 227
greenhouse effect, 795-797
mass, 28
moon barycenter, 27
obliquity (tilt of axis), 34, 797-802, 879
variations and climate, 797-803
orbital factors, 27-34, 797-802, 879
plastic, 298
precession (axial, aphelion, equinox, climate), 799-801
radiation balance, 793-797
radius, 3-4, 11, 879
average volume; at poles; at equator, 879
rotation rate, 34, 227, 297
change of, 376
controlling sub-tropical jet latitude, 350
satellite observations of, 228-234
shape, 3-4, 298, 879
snowball, 811
sun distance, 30, 802, 879
aphelion, average, perihelion, 879
surface
parameterizations, 751

E

temperature, 793-797
tectonic plates, movement of, 804
tilt of axis (obliquity), 30, 797-802, 879
viewed from space, 220, 228, 232-233
volcanism, 804-805
easterlies, easterly
African jet and wave, 611-612
polar, 352
tropical trade wind, 330-332, 351
wave and hurricane triggering, 611-612
low-altitude convergence, 612
Eastern
Hemisphere defined, 4
time zone, 5
eccentricity of Earth's orbit, 28, 797-803
echo
-free vault, 493, 552-553
hook, 494
intensity (=dBZ), 246
radar, 493
weak region, 493, 552-553
ecliptic, 30
ECMWF (Europ. Ctr. for Med.-range Weather Fcsts.), 271
locations of weather data worldwide, 271-273
economic value of forecasts, 784-785
EDT, Eastern daylight time, defined, 5
eddy, eddies, 706
-correlation fluxes, 713
-diffusion theory, 714-716
diffusivity (K), 715, 731
large, 716
microscale, 708
motions, 69, 705-706
planetary scale, heat transport by, 378
size in ABL, 706
turbulent, 138
viscosity, 715
whirls, 708
edge of smoke plume, 730
EF (enhanced Fujita) scale for tornadoes, 579-580
effective
gravity, 298
radiation emission temperature, 794
variation with temperature, 794
storm relative helicity (eSRH), 590
surface heat flux, 68, 110
surface mixing ratio, 109
surface turbulent heat flux, 68
surface water vapor flux, 110
temperature, 117
vertical circulation, 377
effervescence, 812
efficiency of
droplet coalescence, collision, collection, 204-205
thunderstorms, 547
wind turbines, 647-648
e-folding
definition, 9, 879
distance, 9
Rossby radius of deformation, 344
sunlight through cloud top, 131-132
height, 8-9
of stable boundary layer, 696
ratio, 879
time, 9
airmass formation, 393-396
EHI (energy helicity index), 530-531, 591-592
eigenvalues and eigenvectors, 822
Einstein, Albert (quotations), 54, 99, 235
Ekman
layer depth, 378
pumping, 319
spiral in the ocean, 378
transport, 378, 610, 632-633
Ekman, V.W., 399
EL (equilibrium level), 483
El Chichon, 805
El Niño, 818-820
cyclone track, influence on, 430
southern oscillation (ENSO), 818-820
electric
charge, 564, 870
origin in thunderstorms, 564-566
field, 255, 565
strength, 565
electrical
charge & units, 870
current, 564, 870
units, 870
energy, 564
potential, 564, 870
gradient, 565
units, 870
power, 564
generation by wind turbines, 647-648
surges in electric lines, 569-570
raindrop growth affected by lightning, 206
resistance, 564, 870
units, 870
voltage, 564
electricity
generation by wind turbines, 647-648
in a channel, 564
lightning, 564
in a volume, 565
electric field, 565
static, 564
electrification of clouds, 564-566
electromagnetic
radiation speed, 243-245, 834
spectrum, 220-223, 834-835
upwelling radiation, 220
waves, 219-226, 833, 837, 856-863
electrometeors, 205
electron
charge of, 565
movement in a lightning channel, 565
electrosphere, 565
elements
data, 875
of a good weather briefing, 765
elephant, 669
elevation angle, 4-5
defined, 4
of sun and radiative flux, 40
of sun vs. time, 32
elf, 563, 568
Eliassen, Arnt, 759
ellipsoid, Earth shape, 298
elliptical orbits, 27-28
eccentricity variations, 797-803
elves, 563, 568
emagram (a thermo diagram), 119-152
pre-storm soundings plotted on, 496-499
full, 152
simplified, 127
Emanuel, K. A., 625
embryo, hail, 549-553
emerald green sun during green flash, 862
emission(s)
limits for pollutants, 724
of radiation, 36-38, 41-42, 219
blackbody, 36-38
Earth temperature, 794
trading, 742
emissivity, 37, 41-42
and Kirchhoff's Law, 41, 220
infrared (table of typical values), 42
surface, 45
with water vapor feedback, 810
emittance, 36
empirical, 700, 715
orthogonal function (EOF) analysis methods, 820-823
wind profiles, 699-705
encroachment method of ABL growth, 394-395, 697-698
energy
balances, Earth climate, 795-797
budget
equation, 672
global annual mean, 797
chemical, 54
conservation along streamline, 671-672
convective available potential (CAPE), 503-508, 530-531
dimension of, 870
flow, 669-672
flux density, 221
heat, 53-86
helicity index (EHI), 530-531, 591-592
internal, 54, 672
kinetic, 150, 647, 669-672
dissipation in hurricanes, 625
turbulence, 708-709
latent, 54
lightning, 564
mechanical, 625, 670
nuclear, 54
bomb, 499, 548
-per-unit-mass diagram (emagram), 122
potential, 150, 503-508, 669-672
propagation via waves, 658
released in a
hurricane, 620, 625
thunderstorm, 499
sensible, 54
thermal, 672
thunderstorm, 499, 546-548
turbulence, 708-709
units, 870
wave, 658
wind, 647-648
work, 503
shaft, 672
engine, hurricane as, 620-625
engineering
boundary layers in wind tunnels, 689
creativity in, 288
enhanced Fujita (EF) scale for tornadoes, 579-580
ENIAC computer, 749, 759
enormous hail, 548
ensemble, 776
average, 776-777
calibrated probability forecasts from, 777
forecasts, 776-777
prediction system (EPS), 776
spread vs. skill, 777
uncertainty forecasts, 777
ENSO (El Niño Southern Oscillation), 818-820
enthalpy, 53, 58, 671
entrainment
at high-pressure regions, 390
flux-ratio method to estimate, 698
of dry air
into boundary layers and clouds, 57, 111, 649, 694
behind thunder shock front, 572
velocity or rate into ABL top, 394-395, 697-698
zone, 692
entrance region of jet streaks, 454-456
entropy
adiabat, 18
hurricane, 624-625
isentrope, 18
on thermo diagrams, to define tephigram, 122
thunder, 571
total, 624-625
environment
Canada, 284
Hurricane Centre, 617, 638
Meteorological Service of Canada, 638
on a thermo diagram, 134
thunderstorm (pre-storm), 496-499
environmental
lapse rate, 59, 134
in mixed layer, 692, 697-698
Protection Agency (EPA), air-quality standards, 7
sounding, 59, 134
pre-thunderstorm, 496-499
temperature profile, 59
wind (and thunderstorm motion), 516-520
EOF (empirical orthogonal function) analysis methods, 820-823
EPA, Environmental Protection Agency, air qual. Stds., 7
episodes, air pollution, 741
epitaxial substances, 195
epoch
Holocene, 799
Pleistocene, 799
equation(s)
Bernoulli's, 559
coupled, 747
diagnostic, 747
error propagation through, 876-877
forecast, 293
hypsometric, 17
Navier-Stokes, 759
nonlinear, 747
of motion, 293, 301-302, 314-317, 713, 746-749
anabatic winds, 649-652
analytical solution, 749
boundary-layer winds, 307-308
discretized, 757-758
for slope flows, 652
horizontal, 301-302, 314, 652
katabatic winds, 652-653
typical magnitudes for terms, 301
vertical velocity, 315-317, 508, 554-558, 649
of state, ideal gas law, 14-15, 746
of time, 34
primitive, 747
prognostic, 747
scalar, 746
Young-Laplace, 215

equator, 4, 330
-to-pole temperature gradient, 335-336
equatorial, 330
airmass code, 392
heating excess, 338-339
high-pressure belt aloft, 350-351
trough, 331, 350-351
winds, 343
equatorward propagation of cyclones, 446
equilibrium
geostrophic adjustment, 405
conditions in daisyworld: homeostasis, 813-815
earth's heating, 334-339, 793-797
height (or level), 483, 733
humidity, 87-96
level (EL), 483, 496-506
relative humidities, 190-193
saturation, 87
supersaturation, 88, 191
vapor pressure, 87-90
equinox, Spring (vernal) and Fall (autumnal), 30-31, 800
precession, 800-801
equipment factor in the radar equation, 245-246
equitable threat score, 782
equivalent potential temperature, 104-106
on weather maps, 500
equivalent radius of drops, 203
erosion (scour) of beaches by ocean waves, 634-635
error(s), 875-877
accuracy, 875
anomaly correlation, 779
background, 766
bias, 770, 778, 875
calibration, 875
check for, 15
correlation coefficient, 779
definition, 875
experimental conditions, 875
first guess, 766
fluctuating conditions, 875
forecast , 777-785
imperfect technique, 875
instrument calibration, 875
judgement, 875
mean, 778, 875
absolute, 778
squared, 778
measurement, 875-877
numerical (round-off, truncation, etc.), 759-761
observation, 766
personal, 875
precision, 875
probabilistic forecast, 782-784
propagation, 876-877
random, 777, 875-877
repeatable, 875
root mean square (RMS), 778
small disturbances, 875
standard deviation, 875-877
systematic, 770, 777, 875
uncertainty, 875-877
verification, 778
escape velocity, 6
eSRH (effective storm-relative helicity, 590
EST, Eastern standard time, defined, 5
estimating 22 degree angles, 847
eta coordinates for NWP, 746
ethical issues, 218, 826
Euclidian geometry & dimensions, 171
Euler, Leonhard, 759
Euler method of finite differencing, 757
Eulerian
definition, 53
equations of motion, 713, 746-749
framework, 34-35, 53
heat budget, 64-73, 746
advection, 65-67
conduction and surface fluxes, 67-69
cooling and heating of air parcels, 60-64, 159-160
equation, 64-65, 73
first law of thermodynamics, 64-65
latent heat, 72
net heat budget, 73
radiation, 71
turbulence, 69-71
unsaturated, 64-73
momentum budget, 293, 314-315, 746
streamlines, 668
water budget, 107-111, 746
horizontal advection, 107
precipitation, 107-108
surface moisture flux, 108-109
turbulent transport, 109-111
EUMETSAT, 228
Europe, airmasses in, 397
European centre for medium-range weather forecasts, 271
(ECMWF), 271
evacuation, 638-639
evaporation, 88
of water from droplets, 189-193, 556
net, 92
rate from the surface, 108
rate of solutions, 190-193
zonally-averaged, vs. precipitation, 210
evaporative
cooling of falling rain, 556
rain gauge, 210
events
air pollution, 725, 741
binary/categorical, verification of, 780-782
evolution
computational, 680
of
atmospheric boundary layer, 692-699
cyclones (extratropical lows), 427-429
fogs, 173-177
hurricanes, typhoons, tropical cyclones, 608-616
mixed layer, 692-698
thunderstorm cells, 484-485
tornadoes, 583
wind profile in boundary layer, 699-700
exa (10^{18}), 870
exceedences of pollution concentration, 725
excess water mixing ratio, 186-187
exercises, explained
numerical problems, 21
synthesis questions, 25
tips for doing homework exercises, 20
understanding & critical evaluation, 23
web-enhanced questions, 24
exhaust system of hurricane, 614, 618-621
exit region of jet streaks, 454-456
exitance, radiant, 36
exosphere, 6
exothermal chemical reactions, 64
experimental-condition errors, 875
expert vs. novice scientists, 72
explained variance (square of correl. coefficient), 779
explosive
cyclogenesis , 426
growth of thunderstorms, 527
pressure increase, due to
air stagnation, 674
lightning, 571-574
exponential
curve of the wind profile, 677-678
relationships and semi-log graphs, 873-874
external
forcings (inputs) to feedback processes, 806
Rossby-radius of deformation, 405-406, 665
trigger mechanism for thunderstorms, 496-499, 525-526
extinction (coefficients, cross-section), 43
extrapolating data, 826
extratropical cyclones, 330, 425-480
atmospheric boundary layer within, 690-692
baroclinic zone support, 427-429
birth and growth (cyclogenesis), 426-432
bomb, 426
case study , 433-443
100-50 kPa thickness chart, 439
overview and storm track, 433-434
storm data, 434-435
surface weather, 438, 466
vertical cross section, 441
upper-level charts, 439-441, 443, 448-449, 451-452, 455-456, 459-463, 466
central-pressure evolution, 435
clouds, 400-401, 425-428, 691-692
convergence of horizontal winds, 691
death (cyclolysis), 426-432
deepening, 427, 463-467
definition, 425-426
descending air in cold sector, 433
development, rapid, 426
diffluence behind cold front, 433
direction of movement, 430-433
evolution, 427-429
explosive cyclogenesis, 426
graveyard, 431
lifetime, 431
meso (see mesocyclone), 492, 518, 586-592
midlatitude (lows), 331, 425-480
movement, 429-430
sea-level pressure tendency, 463-467
diabatic heating, 465
mass budget, 463
net pressure tendency, 466-467
Southern Hemisphere, 426, 430-432
spin-up, 427, 446-450
application to typical weather patterns, 450
quasi-geostrophic approximation, 449
vorticity tendency, 447
tilt of trough axis, 622
transition of hurricanes into, 615
translation speed, 431
upward motion, 451-462, 691
continuity effects, 452-456
omega equation, 456-459
Q-vector estimates of, 460-462
vigor, 446
warm-air sector, 425-428
winds around, 305-307, 690-692
extreme
rainfall rates, 208
turbulence for aircraft in thunderstorms, 529
eye of hurricane, 604-605, 618-619
eyewall, 604-605, 618-619
replacement cycle/double eyewall, 605

F

faces of ice crystals, 842
factor (of)
attenuation, in the radar eq., 245-246
beta, 368-369, 879
Coriolis, 297-299, 879
equipment, 245-246
feedback, 806-807
reflectivity, Z, 245-246
Fahrenheit, degrees, defined, 7
fair weather (synoptic high pressure), 645
cumulus (humilis), 161, 498
turbulent heat flux, 69-70
winds generated thermally, 645
Fairy Morgan (Fata Morgana), 862-863
faith, 680, 877
Fall (autumnal) equinox, 30-31, 801
fall
line (downslope direction), 652
velocities of cloud droplets, 159
winds, 675
falling pressure, 463
symbol on weather map, 278
false alarm, 780
rate, 781, 783-784
ratio, 781
family
disaster plan, 638
of tornadoes, 584
fan/fanning, pollutant plume, 708, 710, 727
far
field pollutant dispersion, 732
infrared and ultraviolet, 222-223
Faraday cage, 570
farads, F, 7
fast-response weather instruments, 112
Fata Morgana, 862-863
fatalities (see deaths)
favored latitudes for hurricane formation, 609
features of clouds, 168-169
fecund daisyworld, 815
Federal Meteorological Handbook No. 1, USA, 268
Federation of Atomic Scientists/American Scientists, 218
feedback, 793, 806-812
aerosol, 811
amplification (positive feedback), 807-809
atmospheric processes, 1
biological
CO2 feedback, 812
homeostasis, 813-815
climate change, 810-812
biological CO2, 812
cloud, 811
ice-albedo (surface), 808-812
infrared radiation, 810
lapse-rate, 810-811
ocean CO2, 812
water-vapor, 810
cloud, 811
concepts/basics, 806-807
daisyworld, 813-815

F

damping (negative feedback), 807-808
equation, 808-809
example, idealized, 807-810
blackbody radiative equilibrium, 807-808
ice-albedo feedback, 808-810
external inputs and forcings, 806
factor, 806-807
forces and winds, 302
gain, 806-810
different definitions, 807
ice-albedo, 808-810
infrared radiation, 810
internal, 806
lapse rate, 810-811
linear, 806
approximation to ice-albedo process, 808
approximation to nonlinear system, 806
multiple processes, 807
negative (damped), 793-794, 807
nonlinear, 806
ocean CO2, 812
positive (amplified), 807
reference state, 806-809
response, 806-810
ice-albedo, 808-810
negative (damped), 807
no-feedback, 807, 809
positivie (amplified), 807, 809
runaway, 807
sensitivity, 810
turbulence, 704-705
water vapor, 810
feeder
cells for hail, 549
feeder flow in sea breeze, 655
femto (10^{-15}), 870
Fengyun weather satellite, 228
Fermi, Enrico, 669
Ferrel Cell, 332-333, 357, 377
fetch, 631, 634
few clouds (coverage), 170, 279
Feynman, Richard (quotations), 132, 167
FFD (forward-flank downdraft), 483
fibratus/fib, 168
field, 280
mill, 565
of height, mass, pressure, wind, 343, 359
of temperature, 280, 343, 359
filling of lows, 429, 432-433, 463-467
filter
camera
haze, 857
polarizing, 856
Kalman, 770
Findeisen, 201-202
Finlayson, 817
fine particulates (PM10) and aerosols, 188, 725
fine-resolution grids, 752
fine-scale turbulence, 315
finite curve, 9
finite-difference
approximations, 872
spatial gradients, 754-755
temporal gradients, 757-758
equations, 754-759
numerical weather prediction (NWP), 745-792
fires (forest, wild, bush) caused by lightning, 564
CO2 release, 812
firn snow, 209
first
guess, 766
NWP analyses, 765-767
satellite retrievals, 239
law of thermodynamics, 53, 58-59, 64-65
power, 873
fitting an elaphant, 669
fixed point attractor, 790
fjord winds (gap winds), 661-664
flanking line, 482-483, 492, 494-495
flash(es)
floods, 487, 547-548
green, 862
lightning, 567-569
flat surface of water, vapor pressure over, 87-90
flattened rain drops, 203, 255, 841, 860
flight operations near downbursts, 563
floating, 135
point operations per second (flops), 761
floccus/flo, 168
floods/flooding associated with
coastal, 632-635
extratropical cyclones, 425, 434-435
hurricane caused storm surge, 632-635
inland, 637
thunderstorm caused flash floods, 487, 547-548
urban, 637
flops (floating point operations per second), 761
flow
adiabatic compressible, 671-672
along a streamline, 669-672
around hills
balanced with mass fields, 763-765
canopy, 677-679
classification: subcritical, critical, supercritical, 659-661
compressible, 671-672
energy, 669-672
field in forecast models, 764
incompressible, 669-671
isothermal compressible, 671
laminar, 669
meridional, defined, 330
stability, 138-142
steady state, 669
through a constriction, 660
zonal, defined, 330
fluctuation-condition errors, 875
fluid
air, 1
mechanics, 1
object immersed in, 135
flux
advective, 35
conduction, 73-76
constant flux layer, 692
covariance vs., 710-713
defined, 34
density, 34
divergence, 64, 109-110, 715
dynamic , 35
eddy-correlation, 713
effective surface turbulent heat, 68
energy, 221
form of turbulent continuity eq., 714
gradients, 64
ground heat, 73-76
heat , 34-35, 711-712
kinematic, 35, 698, 711-713
latent heat at surface, 73-76
longwave radiative, net, 45
mass, 34-35
moisture, 108
momentum, 712-713
vs. Reynolds stress, 712-713
radiative, 35, 221
-ratio method, 698
Richardson number, 709-710, 739
related to PG types, 710
sensible heat at surface, 73-76
sign of, 74
surface heat, 73-76
surface moisture, 108
turbulent , 35, 698, 711-713
FNMOC (Fleet Numerical Meteorology & Ocean. Ctr.), 608
Focus boxes
30 - 30 Rule (for lightning safety), 570
A Holistic Approach to Stability, 139
Ageostrophic Right-hand Rule, 455
Albedo, 794
Alternative Horizontal Coordinates, 747
Alternative Vertical Coordinates, 746
Amdahl's Law, 763
Anabatic Slope Flow, 651
Approach to Geostrophy, 303-304
Astronomical Values for Time, 34
Barotropic vs. Baroclinic, 749
Beaufort Wind Scale History, 635
Bergen School of Meteorology, 399
Binary Multiples, 870
Boiling, 90
Cap vs. Capping Inversion, 497
CAPE vs. DCAPE, 558
Climate Sensitivity, 812
Coriolis Force in 3-D, 297
Cp vs. Cv, 55
Cubic Ice, 198
Derecho, 494
Deriving the Radar Equation, 245
Downbursts and Flight Operations, 563
Droplet Growth, 191
E-folding Distance, 9
Early History of NWP, 759
Effervescence and CO2, 812
Electricity in a Channel, 564
Electricity in a Volume, 565
Engineering Boundary Layers, 689
Enthalpy vs. Heat, 58
Eötvös Effect, 317
Escape Velocity, 6
Estimating 22° Angles, 847
Force of Thunder, 571
Gain — Different Definitions, 807
Geostrophic Paradox, 459
Giving a Weather Briefing, 765
Greenhouse Gases, 811
Hail Suppression, 553
Human Contributions (to Forecasts), 772
Hurricane Condensation Energy, 620
Hurricane-induced [Ocean] Currents, 610
Hurricane Juan Hits Canada, 617
In Newton's Own Words, 292
Internal Energy, 54
Isosurfaces & Their Utility, 436-437
Jet Stream Aspect Ratio, 357
Kalman Filter, 770
Landfalling Pacific Cyclones, 472
LeChatelier's Principle, 132
Lightning Burns the Air, 567
Lightning in Canada, 568
Linear Regression, 770
Lipschitz Continuity, 761
Mandatory and Significant Levels, 135
Map Projections, 748
Maximum Advection on Weather Maps, 458
Median, Quartiles, Percentiles, 502
Meteors and Meteorology, 205
Moore's Law and Forecast Skill, 752
Multi-field Charts, 443
Newton and Colors, 862
North American Geography, 431
On Naming Local Winds, 654
Pacific Data Void, 765
PCA and EOF, 821-823
Polar Front, 408
Pollution Concentration Units, 724
Power of Hurricanes, 625
Rainbows and the Renaissance, 841
Resolution and Grid Spacing, 761
Rossby Number, The, 313
Satellite Retrieval Difficulties, 239
Scheiner's Halo, 855
Snow Grain Classification, 199
Solid-body Relative Vorticity, 363
Solution by Iteration, 310
Some Other Satellite Systems, 230
Southern Hemisphere Lows, 426
Special Crystal Orientations, 855
Specific Heat Cp for Air, 56
Speed of Sound, 674
Spreadsheet Thermodynamics, 63, 103
Stratospheric & Mesospheric Clouds, 166
Sun-Earth Distance, 802
Sutcliffe Development Theorem, 456
Time Differencing Methods, 757
Time of Max Airmass Thickness, 395
Tornado Watch, 529
Torques on the Earth, 376
Trade Inversion, 351
Warm Airmass Genesis, 394
Warm vs. Cold Core Cyclones, 622
What is an Oscillation, 818
What is Coriolis Force?, 298-299
Why Does Ro = (1-A)·So/4, 795
Why So Many Moisture Variables?, 96-97
Why So Many Thermo Diagrams?, 121
Why Use Isobaric Maps?, 291
Foehn winds, 676-677
wall (cloud), 676-677
fog
channel on satellites, 231
dissipation, 175-177
in satellite images, 234
nuclei, 177
processes, 173
types, 173
fogs, 170, 173-177
advection, 173-175
atmospheric boundary layer, 159, 173-177
dissipation of well-mixed fogs, 173-177
formation, 98, 173-177
frontal, 173
models, 173-177
radiation, 173-177
steam, 173
stratified, 175-177
upslope, 173
vs. clouds, 159, 173
weather-map symbols, 275-276

folds in tropopause, 364, 414-415
isentropic potential vorticity, 364, 443
radionuclide injection at, 364
footprint, 734
forced convection, 710
related to PG types, 710
force(s), 295-302
advection, 294-295, 301
apparent, 299
balance of, 302-314
buoyancy, 135-136, 316-317, 554
negative, 554-559
centrifugal, 296-297, 301
centripetal , 296-297, 301
convection (buoyant), 135-136, 317, 503-508, 648
Coriolis, 297-299, 301
dimension of, 870
driving horizontal winds, 289-328
driving vertical winds, 554-559
horizontal, 295-302, 301
imbalance of (causing centripetal force), 305-312
in Netwon's 2nd law, 292, 294
net, 292, 294
pressure-gradient, 295-296, 301
summary table, 301
thunder, 571-574
turbulent drag , 300-301
units, 7, 292, 294, 870
vertical, 301, 554-555
forcing (radiative) and responses (fluxes), 74
forecast, weather
accuracy, 777
blow up, 760
case study, 433-443, 448-456, 459-463, 466, 745, 768-770, 776
clouds, to aid in, 166
confidence, 776
cost/loss decisions, 784-785
difficulties, 527
equations
Eulerian, 293
relative vorticity, 447
wind velocity, 293
error, 777-785
vs. time into future, 775, 780
hurricane, 637-639
max surface temperature, for thunderstorms, 506, 523
models, 637, 751
nowcasts, 552
numerical, 745-792
outlooks, 528-530
persistence, 778-780
post-processing, 770-772
probabilistic, 777
verification, 782-784
probability of hurricanes, 638
quality, 777-785
ranges issued: outlook, watch, warning, 528-530
nowcast, short, medium, long, seasonal, climate, 768
refinement, 770-771
Kalman filter, 770
model output statistics (MOS), 770
schedule, 762
scientific basis for, 746-751
short-range (nowcasts), 552
skill, 752, 777-784
vs. time into future, 775, 780
thunderstorm intensity, 501, 507, 516, 521-522, 524, 527-531
tornadoes, 530-531, 588-592
uncertainty, 776
verification, 777-784
watches & warnings, 528-530, 638
forest
canopy, 677-678
death (waldsterben), 742
fire
clouds, 166
CO2 release, 812
lightning causing, 564
nuclei from, 195
forging data, 826
formation and growth of
airmasses, 389-399
atmospheric boundary layer, 689-692
fogs, 173-177
highs (anticyclones), 391
thunderstorms, 496-499
forward
-flank downdraft (FFD), 483, 492-495
-flank precipitation area, 483
problem, 235
scattering, 219, 857
trajectory, 724
fossil fuels and climate, 812
Fourier-transform spectrometers, 47
fractals
definition, dimensions and cloud shapes, 171
errors in measuring, 875
vs. Euclidean geometry, 171
fraction of
pollutants in air, 724
sky covered by clouds, 277-279
fractus/fra, cumulus, 165-166, 168, 483
scud, weather-map symbols for, 277
frame of reference, 2-4
on Earth, 3-4
framework: source-receptor, 724
free
atmosphere, 687, 690-695
convection, 704, 710
level of (LFC), 497-506
related to PG types, 710, 727-730
smoke dispersion during, 735-737
sink level (LFS), 557
freezing
crops, 653
level altitude and hail formation, 551
nucleation, 194-195
precipitation change criterion for SPECI, 270
rain, 195
weather-map symbols, 276
freon, 796, 811
frequency
angular, 36
beat, 828
Brunt-Väisälä, 136-137
circular, 36
dimension of, 870
of light, 36
of occurrence of wind
directions (plotted as wind rose), 646-647
speeds, 645-646
of oscillation, 136-137
of tornadoes in USA & Canada, 579
relative, 645
vs. probability, 645
shift (Doppler), 249
units, 870
friction
molecular, 301
velocity, u*, 677, 700-713
typical values, 701
for air, 378, 700-713
for water, 378
frictional drag
in hurricane boundary layer, 625
on oscillating air parcel, 136-137
vs. stress, 700-702
frigate sails, 635
fringes, 858-861
index, 859-860
front(s), 280-281, 399-424, 389
adiabatic processes, 408-410
aloft, 281, 413-414
ana-, 404
analyzing, 280-281, 402
attributes of, 399
between two boundary layers, 691
cold, 399-400, 525
aloft, 399
genesis, 399
triggering hurricanes, 612
depth, 403
drawing, rules, 280-281
drylines, 399, 525
dynamics, 411-412
formation, 408-413
geostrophic adjustment, 404-406, 412
glyphs (lines) on weather maps, 399
gust, 482, 525
horizontal structure, 400-402
kata-, 404
kinematics, 408-410
labeled by temperature, 281
lake-breeze, 525
layer stability affected by, 140
locating, 280-281
lows associated with, 389
occluded, 281, 399, 413-414
over-riding air, 407
polar, 352
rotation around lows, 389
sea-breeze, 525, 654-657
squall line, 400
stationary, 281, 399, 404
strength, 408-412
structure, 400-417
horizontal, 400-402
vertical, 403-407
surface, 399-412
thermodynamics, 411
thunderstorm triggers, 525-526
upper-level (upper-tropospheric), 414-415
vertical structure, 403-404
warm, 399-401, 525
aloft, 399
genesis, 399
weather-map symbols for, 280-281, 399
winds above, 407
frontal
analysis, 280-281, 402
baroclinic zones, 427, 469-471
boundary on weather maps, 280-281
clouds
cumuliform at cold fronts, 162
stratiform at warm fronts, 162-164
fog, 173
forecasts, 427-429, 768
inversion, 403-404, 691
jets, 357-359, 407, 472
lifting of air layers, 140
line on weather maps, 280-281, 399
pre-frontal waves, 400, 656
propagation using Q-vectors, 470-471
scale, 315
shear, 407
slope, 403-405
strength, 408-412, 469-470
symbols, 281, 399
thunderstorms, 400
tilting, 412
venting of boundary layer air, 691-692
vorticity, 407
wave (early cyclogenesis), 427-428
winds aloft, 407
zone(s)
deformation at, 410
drawing on weather maps, 280-281
identification, 280-281, 403
relationship to frontal inversion, 403-407
strength, 408-412
strengthening, 469-471
frontogenesis, 407-412
definition, 407-408
dynamics, 411-412
kinematics, 408-410
Q-vectors, 469-471
thermodynamics, 411
vorticity and updrafts, 407
weather-map symbols for, 281, 399
frontogenetic, 408
frontolysis, 409
weather-map symbols for, 281, 399
frost as affects growing crops, 653
frostbite, 77
frost-point
hygrometer, 111
temperature, 92
Froude number, 659-661
1. For surface or interfactial waves, 659
2. For internal waves, 659
3. For flow over hills, 667-668
fudging data, 826
fuel
for hurricanes, 620
for thunderstorms, 99, 499-502, 547-548
fossil: climate change issues, 812
Fujita (F) scale for tornadoes, 579-580
fulgurite, 570
Fuller, R. Buckminster, 804
fumulus, 166
functions , 872
fundamentals of
science, 869-878
weather radar, 240-245
funnel cloud, 483, 581-583
weather-map symbols for, 276
fusion, latent heat of, 56

G

gaia hypothesis, 813-815
gain, feedback, 806-811
different definitions of, 807
gale, 635-636

G, H

Galileo, 315
gamma rays, 222
gap winds/flows (for long and short gaps), 661-664
gas
  anthropogenic greenhouse, 796, 811-812
  constant
    for dry air, 14, 572, 880
    for water vapor, 14, 88, 880
    ratio, epsilon, 91, 554, 880
  ideal gas law, 14-15, 572
  natural greenhouse, 805, 811-812
gases
  atmospheric (constant and variable), 7
    water vapor, 87-118
  greenhouse, 811-812
  on other planets in the solar system, 22
gauges, rain and snow, 210-211
Gaussian
  curve, 184, 729-730, 875
  plume dispersion, 729-731
    distribution of concentrations, 729, 737
    parameters, 729-730
    profile, 729
GCMs (global climate models -or-, 815-816
  general circulation models), 768
Geiger, Rudolf, 817
GEM (global environ. multiscale) model, 751
GEM-PAK, 772
gene expression programming, 680
genera (clouds), 168
general circulation (see global circulation), 329-388
  models, 379, 768
  three-band, 329, 376-378
generation of electricity by wind, 647-648
genesis of
  airmasses, 392-397
  anticyclones (highs), 390-391
genetic
  bottleneck, 805
  programming, 680
geographic information systems, 274
geography of
  lightning, 564
  North America, 431
  Pacific Northwest (USA & Canada), 661
geomagnetic effects on Earth's rotation, 376
geometric
  albedo, 831, 879
  height, 11
    measurement by GPS, 291
  optics, 833
  scattering, 857
  sunrise and sunset, 33-34
geometry
  of atmospheric optics, 833-868
  of light rays, 833-868
geopotential, 11, 304
  height, 11
    errors, 766
    global map example, 355
    N. American map examples, 433-442
  measurement errors, 766
geostationary satellites, 227-228
  GOES, 228-229
  METEOSAT, 228-229
  weather observation locations from, 272
geostrophic
  adjustment, 343-344, 406, 412
    part 1, 344
    part 2, 349
    part 3, 404-407
  approach to geostrophy, 303-304
  balance, 302-304
  departure, 314
  paradox, 459, 462
  relative vorticity, 319
  vorticity, 319
    Laplacian form, 450
  wind, 302-304, 343-349
    at cold front, 405-407
    at equator, 343
    at mountains, 662-664
    changes with altitude, 345-349
    changes with latitude, 303
    for atmospheric boundary layer, 699
    gap, 663-664
    related to thermal wind, 345-349
    temperature advection, 458
    vs. actual wind, 303
  wind speed, 303
    related to isobar packing, 303
    related to tilt in isobaric surfaces, 359
geostrophy, approach to, 303-304
GFS (global forecast system) model, 751
ghost grid cells, 756
giant
  CCN, 206
  hail, 247, 548, 553
giants, on the shoulders of, 294
Gibbs free energy, 217
Gifford-Pasquill turbulence types, 727-728
giga (10^9), 870
gigabit, 870
Gilbert's skill score, 782
GIS (geographic information systems), 274
giving a weather briefing, 765
glacial/interglacial (ice age) periods, 795, 799
glaciated clouds, 482, 485
glacier ice, 209
glaciogenic, 553
Gladwell, Malcolm, 924
glass windows, transparency of, 45
global
  albedo, 793-794
  carbon cycle, 812
  climate models (GCMs), 379, 768, 815-816
  circulation, 329-388
    anticyclones (highs), formation locations, 391
    explaining, for various latitudes, 350-356
    heat transport by, 338-339
    steering hurricanes, 607-608, 615
    three-band, 329, 376-378
  environmental multiscale (GEM) model
  geopotential height patterns, 355
  heat
    budget, 166
    transport, 338-339
  insolation, 41, 336-337, 793
  nomenclature, 330
  population vs. hurricane disasters, 631
  positioning system (GPS), 112, 291
  pressure patterns, 354-355
  radiative forcings, 41, 793-794
  telecommunication system (GTS), 268
  temperatures, 335
  warming, 150, 796
    influence on hurricanes, 631
glory, 859-860
  Morning, 656
glow, zero-order, 841
glyphs (symbols) plotted on weather maps, 275-279, 614-615
GMT (Greenwich Mean Time) defined, see UTC, 5
Gobi desert, 397
GOES satellite, 226-228
  channels for imager and sounder, 222-223
  orbits, 227-228
Goethe, 249
GOMS satellite, 228
Gondwana; Gondwanaland, 804
governing equations, 746-750
GPS (Global Positioning System), 112, 291
GPU (graphics processing unit, on computers), 763
gradient
  definition, 15, 295, 872
  of flux, 64
  of pressure, 295-296
  of temperature, vertical, 872
  of wind or momentum, 295
  Richardson number, 710
  supergradient wind, 643
  transport theory, 714-716
  wind, 304-307
    imbalanced, 619
    in anticyclones, 306-307, 391
    in cyclones, 306-307, 432
    in hurricanes, 609, 617-619
    subgeostrophic, 304
    supergeostrophic, 304
    supergradient, 643
GrADS, 772
GRAF code, 269
graffito (the singular of graffiti) (see Science Graffiti)

grain size of snow, 199
granddaughter storm, 485
graphics processing unit (GPU), 762
graphing, 873-874
  abscissa, 3
  axes, 3, 873-874
  linear, 9, 873
  log-log, 215, 874
    slope, 215
  meteorological variables, 3, 9
  ordinate (vertical) axis, 3
  power, 874
  pressure as height variable, 9-10,
  relationships, 873-874
  semi-log, 9, 873-874
graupel(n), 199, 205, 546-554
  lightning, role in creating, 564-566
  weather-map symbols for, 276
graveyard for extratropical cyclones, 430-432
gravitation law (Newton's), 11
gravitational
  acceleration on Earth, 15, 879
    variation with latitude & altitude, 879
  constant, Newtonian, 6, 15, 879
  force, 15, 301
gravity, 14-15
  current, 355-656
  Earth's, 227, 298
  effective, 298
  Eötvös effect, 317
  force, 301
  measurement, 317
  Newton's discover of, 293
  reduced, 135-136, 316, 658, 670
  waves, 658-661, 666-668, 710
    thunderstorm triggering, 526
great dying, 805
Greeks, 205, 444
green
  color defined (also see optics chapter), 37, 834
  flash, 862
  sun, 862
greenhouse effect, 795-797
greenhouse gas(es), 724, 796, 805, 811-812
  from volcanoes, 805
Greenland, 396
  ice cores, 803
Greenwich Mean Time (GMT), 5
Greenwich Meridian, 4, 28
Gregorian calendar, 31
Grenfell, Sir Wilfred, 737
GRIB = gridded binary, 268
GRID code, 269
grid(s)
  Arakawa A to E, 753
  box, 750
  cell, 750
    ghost, 756
  computation rules for NWP, 756
  nested, one-way and two way, 752-753
  points, 749-756
  resolution, 750, 752, 761, 816
  staggered, 753
  variable, 752-753
  volume, 750
grooming machines for snow trails, 209
ground
  clutter in radar returns, 243-245, 254
  subsurface heat and moisture parameterizations, 751
growing days for crops, 653
growth
  rates for ice crystals, 200
  rate of daisies (daisyworld), 814
  rate of droplets, 196-197
GTS = global telecommunications system, 268
Gulf Stream current, 431, 616
gust
  1 to 10 minute average, for hurricanes, 607
  3-second, for tornado speeds, 579
gust fronts (related to downbursts), 482, 494, 554-563

  arc & shelf clouds along, 532
  depth of, 562
  dust storm (haboob), 562
  speed of, 562
  radar observations of, 253, 556, 560
  triggering new thunderstorms, 525
gustnado, 582

H

habits, ice crystal, 198-200
haboob (sand storm), 562
Hadley cell, 329, 332-333, 350-351, 357, 377-378
  influence on worldwide rain distribution, 209
  heat transport in tropics, 339, 378
  mixing caused by, 335-336
hail, 199, 205, 548-554
  change criterion for SPECI, 270
  damage from, 532, 549-554
  embryo, 549-554
  forecasting, 530-531, 550-552

formation, 549-550
giant, 548, 553
location climatology, 552-553
mitigation, 553-554
nucleus, 549
radar observations of, 247-248, 552-553
shaft, 552
significant hail parameter (SHIP), 530-531, 551-552
streak, 552
suppression, 553-554
swath on the ground, 163, 548, 552
weather map symbols for, 276
hailstones, 185, 548-554
fall speeds, 204, 549
layers, 550
size classification (TORRO scale), 548
hair hygrometer, 111
halo, 845-855
22 degree, 842, 845-846, 854-855
46 degree, 842, 846, 854-855
arctic airmass ice-cloud, 396
associated with pyramid crystals, 847
circumscribed, 851, 853-855
clouds that enable, 163
luminous meteors, 205
numerical computation, 756
others, 853-855
rare halos: 9, 18, 20, 23, 24, 35°, 847, 854-855
viewing angles, 846-847
vs. corona, 860
halocarbons (e.g., freon; CFC-12 & others), 796, 811-812
Halsey Jr., Admiral William F. , 807
hand analysis of weather maps, 279-281
Handbook on Chemistry and Physics, 879
Hansen and Kuiper's score, 781
Hastings arcs, 854-855
Hawaii time zone, 5
Hawaiian high, 354-356
hazards
coastal, 634-635
hurricane, 631-637
lightning, 569-571
thunderstorm, 545-602
haze, 170, 191-193
filters for cameras, 857
lithometeors, 205
scattering of light in, 856-858
weather map symbols for, 276
HDT, Hawaii daylight time, 5
head, sea-breeze, 655
headwinds, aircraft, 563
heat, 53-86
adiabatic process, 60-64
balance, 64, 94
budget, 64
closure problem, 713-714
equation, 64, 73, 713, 746-747
Eulerian, 64-76, 713, 746-747
Lagrangian - saturated, 101-106
Lagrangian - unsaturated, 57-64
net, 73, 713
surface, 73-76
capacity changes due to precipitation, 121
conservation equation, 58, 64-76, 746
engine, 624-625
enthalpy, 58, 671
flux, 34-35
airmass modification by, 397
at top of mixed layer, 698
bottom of ABL, 693-698
curvature, 375-377
effective surface turbulent, 68
kinematic, 34-35, 698
sinusoidal variation, 693
top of ABL, 698
turbulent, 711-715
vs. height, 698
vs. time, 693
index, 77-78, 117
internal sources, 64
island, urban, 678-679
latent, 53-56, 72, 101-106, 546, 880
condensation, vaporization, 56, 880
deposition, sublimation, 56, 880
fusion, melting, 56, 880
lightning, 567
net budget, 72
released in thunderstorms, 546-548
sensible, 53-56, 671
specific, 53, 55
stress, 77-78
stroke, 78
surface budget of, 73-76
thermodynamics, 1, 53-86
transfer coefficient, bulk, 68
transferred, 58, 672
transport
achieved, 338-339, 378
by jet stream (Rossby waves), 374-375, 378
global, 338-339, 378
needed, 338-339
to compensate radiative differences, 338-339
vs. latitude, 329, 335-336, 339, 378
urban heat island, 678-679
heating
cumulative, 693-694
differential, 329, 334-339
dynamic, 672-674
heavy rain, 207-208, 545-548, 637
weather map symbols for, 276
hectare unit of area, 870
hecto (10^2), 870
Pascals, defined, 7, 8
Heidke skill score, 781
height
cloud-base, 130, 278
constant, map at, 436
contours on an isobaric map, 18, 121, 151, 290-291
errors, 766, 778
field, 343
geopotential, defined, 11
isohypse, 18
of smoke plume centerline, 723, 729, 733-734, 736
of temperature inversion, 144, 496-499
on weather maps, 436-437
on isobaric charts, 439-441
tendency (isallohypse), 18
tiling method for CAPE, 504-505
vs. pressure, 8, 9
relative maximum/minimum of height, 290
relative minimum/minimum of temperature, 138
scale heights for pressure and density, 8-10
tendency forecast equation, 463-467
variation of weather variables, 11-13
vs. pressure, 290-291
heirarchy of operational forecast models, 768
heliac arc, 854-855
helicity, 587-592
energy helicity index (EHI), 530-531, 591-592
hodograph, determination using, 588-589
mesocyclone, 587-592
storm relative (SRH), 530-531, 588-592
effective, 590
tornado indices, 588-592
helium, He, 7
Helmholtz, Herman von, 759
Helprin, Mark, quotations, 13, 171
Hemispheres
Eastern & Western defined, 4
Northern & Southern defined, 4
hemispheric weather maps, 441
hertz (Hz), unit of frequency, 870
heterogeneous nucleation
freezing, 194-196
liquid water, 188-194
heuristic approach , 371
heuristic (toy) models, 280, 330, 793
hexagonal ice crystals, 198, 842-843
columns, 198-199, 842-843
dendrites, 198-199, 843
hollow columns and needles, 198-199
needles, 198-199
optics, 842-855
plates, 198-199, 842-843
pyramids, 198-199, 842
sheaths, 198-199
Hg (see mercury), 7, 19
high
altitude
clouds (stratospheric & mesospheric), 166
winds (upper-tropospheric), 331-332
clouds, 162-163, 168
height variation with latitude, 163
weather-map symbols for, 168, 277
Earth orbit satellites, 227-228
humidity needed for formation of
hurricanes, 609-610
thunderstorms, 496, 499-502
latitudes, defined, 330
global circulation, 352
monsoon, 333-334, 354, 391, 615
order truncation finite-difference scheme, 754-755
plateaus, influence on drylines, 416-417
precipitation supercell, 495
pressure center (H, see also anticyclones), 389-391
airmass creation within, 389-399
aloft, in hurricane core, 613
boundary layer within, 390, 690-692
convergence at top of, 391
descending (subsiding) air in, 356, 390
divergence at bottom of, 390
formation locations, 391
isobars around, 390
meso-, 391, 488, 554, 559
mid-latitude, 331, 389-391
monsoon-related, 333-334
named (Bermuda, Pacific, etc.), 354-356
polar, 331, 352, 391
ridges, relationship to, 390
subtropical, 391
thermal (cold), 341-342
tilt with altitude, 390
vertical structure, 391
weather associated with, 390
winds around, 305-307, 390-391
resolution, 752
risk, high gain science, 863
thunderstorm risk, 530
highs (see high pressure centers), 354, 390-391
highways, as threat to safety, 517
hills, flow over, 397-398, 472, 487, 526, 649-676
Himalaya mountains, 397
hindcast, 762
history of
Beaufort wind scale, 635
numerical weather prediction, 759
hit, 780
rate, 781, 783-784
hodograph, 510-522
basics, 510-513
blank, which you can copy, 512
using for thunderstorm prediction, 514-522
sea-breeze, 656-657
storm-relative
helicity, 588-589
winds, 585
hollow ice crystals (needles, columns), 198-199, 866
Holocene epoch, 799
Holt, MO, 547
homeostasis, 813-815
homeothermic, 76
homework exercises (at end of each chapter)
answers (see Solved Examples)
tips and explanations, 20-26
homogeneous
freezing nucleation, 194
nucleation of liquid water droplets, 188-191
homogenization, 109, 689
Hong Kong Observatory (HKO), 607
hook echo, 494
horizontal
advection
of heat, 65-67
of momentum, 294-295
of total water, 107
of vorticity, 447-449
circulation, 365-366
method for finding, 365-366
convergence, 252-253, 318-321, 340-341
coordinates, alternative, 747
divergence, 318-321, 340-341
aloft, 449, 452-459
equations of motion, 301-302, 314
forces, 294-302
advection, 294
centrifugal & centripetal, 296-297
Coriolis, 297-299
in slope flows, 650-651
pressure-gradient, 295-296, 619, 650-651
turbulent drag, 300
IR flux gradient, 71
local, 4
motions, scales of, 315
plates (ice crystal), 198-199, 842-855
roll vortices, 167
scales vs.
forecast skill, 768
time scales, 315
structure of fronts, 400-402
turbulent transport , 71-72
velocities, 314
vorticity (streamwise), 518, 586-587
advection of, 447-451

H

tilting of, 586-587
winds, 302-314
horse latitudes, 331
hot
convective towers, 644
film anemometer, 321
wire anemometer, 321
hour
angle, 41, 801-802
glass shaped tornadoes, 577
unit, 870
Hovmöller diagram, 824-825, 830
Howard, Luke, 168
HP (high-precipitation supercell), 495
hPa (hectoPascal) definition, 7-8
HST, Hawaii standard time, 5
hub height, 647
human
contributions to forecasting, 772
population & zoning for hurricanes, 631
humidex, 77-78, 117
humidity, 87-118
absolute, 14, 91
airmass, 391-392
comfort indices, 77-78
constant (isohume), 18
dew-point temperature, 92-93, 499-500
equivalent potential temperature, 500
errors, 766
gradient, 196-197
high (needed for thunderstorms), 499-502
hurricane cyclogensis conditions, 609-610
indices of discomfort, 117
instruments, 97, 111-112
isohume, 18
lifting condensation level (LCL), 93-94, 501
mean-layer, 501
liquid water potential temperature, 500
mixing ratio, 91, 95, 500
precipitable water, 98, 501
relationships between moisture variables, 87-97
relative , 92, 95
satellite observations of, 226, 234, 273
saturation, 87-96
saturation level, 93-94
sensors, 97, 111-112
specific, 91
thunderstorm convective conditions, 496, 499-502
variables, 91-96
vs. dew point temperature, 95
weather maps of, 500-501
wet-bulb temperature, 94-95, 104, 500
humilis/hum (cumulus), 161, 168
humisery, 117
humiture, 117
hunter, hurricane, 637
hurricane(s), typhoons & tropical cyclones, 330, 603-644
along coastlines, 631-635
Andrew, 606, 643
bands, spiral rain, 604
boundary layer flow, 618-619
Canadian Hurricane Centre, 617, 638
Carnot cycle, 624-625
category, 605-606
Charley, 606
circulation of air through, 620-625
classification, 605-607
cloud shield, 604
cold water, movement over, 616
composite picture, 629
condensation energy, 620-621
core, 604, 615, 618-625
Coriolis force, 609
cyclone, 426
cyclogenesis (birth), 608-610
cyclolysis (death), 615-616
damage scales, 605-607
dangerous portions, 627
disaster relief, 631
Dolly, 606
drag against the sea surface, 625
dynamics, 617-619
inflow and outflow, 618-619
initial spin-up, 617
subsequent development, 617-618
easterly jet and waves (from Africa), 611-612
Ekman transport, 610
El Niño/La Niña effects, 631
energy, 620, 625
entropy, 624-625
evacuation, 638-639
evolution, 608-616
exhaust system of, 614, 618-621
extratropical
cold fronts, triggering by, 613
systems, collision with, 616
transition, 615
eye, 604, 615, 621
downdrafts in, 605, 620, 628-629
photo inside, 637
eyewall, 604, 615
double, 605
replacement cycle, 605
second, 605
Floyd, 605, 608
force winds (Beaufort scale), 635-636
forecasting, 637-639
formation requirements, 608-606
Frances, 606
frequency, 630
fronts from midlatitude, interaction with, 612-613
fuel creation, 620
geographic distribution, 605-609, 615
global warming effects, 631
glyph (symbol) on weather maps, 426, 614-615
hazards, 631-637
Hazel, 617
heat engine, 624-625
hot convective towers, 644
Hugo, 639-670
human population and zoning, 631
humidity needed, 609-610
hunters, 637
idealized, 605
identification (ID) number, 613-614
incipient, 612-615
-induced ocean currents, 610
Inez, 621
inflow, 618-619
initial spin-up, 617
instability (nonlocal conditional) & CAPE, 609
insurance, 631
intake system of, 614, 618-620
intensity, 605-607
Isabel, 604, 616, 627
Isis, 614
ITCZ, 610-611
Ivan, 606, 614
Javier, 614
Juan, 617
Katrina, 603-604, 616, 620
kinetic energy dissipation, 625
latent heat release, 620-624
latitude of formation, 608-615
life-cycle, 613-615
moat, 605
model, 626-629
composite picture, 629
pressure distribution, 626
radial velocity, 624-628
tangential velocity, 626-627
temperature, 629
vertical velocity, 628-629
monsoon trough, 612
movement (translation), 607-608, 615
names for, 426, 614-615
retired, 615
National Hurricane Center (NHC), 638
natural 40-year cycle, 631
non-equilibrium winds, 619
-ocean interactions, 610
outflow, 618-619
over land, movement, 616
Pacific, 631
power, 620, 625
precipitation, 615
prediction, 637-638
pressure, 618-623, 626, 633
reversal with altitude, 621-623
probability of threat, 638
radar observations of, 254
radial winds, 627-628
rain bands, 604, 613-615
rainfall rate, 620
research aircraft, 637
right quadrant (most dangerous), 627
Rita, 605, 637
safety, 637-638
Saffir-Simpson hurricane wind scale, 605-606
satellite observations of, 603-605, 608, 614, 616, 620, 637
sea-surface temperature (SST), 608, 616
season, 630
social issues, 631
spiral bands, 604
stages in life cycle, 613-615
steered by global circulation & monsoons, 607-608, 615
Azores high, 607-608, 615
Bermuda high, 607-608, 615
Hawaiian high, 615
trade winds, 607-608, 615
storm surge, 632-634
atmospheric pressure head, 632
Ekman transport, 632-633
Kelvin wave, 633-634
structure, 604-605
surface wind-waves, 634-636
symbols on weather maps, 614-615
temperature (air), 621-622, 624, 629
thermodynamics, 620-625
Carnot cycle, 624-625
diagram, 624
warm core, 621-623
thunderstorms, 609
hazards, 637
tornadoes and tornado outbreaks in, 584, 627, 637
total entropy, 624-625
tracks (translation speeds & directions), 607-608, 615, 627
triggers, 610-613
tropical
cyclone, 426, 615
depression, 613-614
disturbance, 613
Prediction Center, 638
storm, 614
TUTT (tropical upper tropospheric trough), 613
typhoon, 426
intensity scales, 607
vertical
cross section, 605, 618, 620-622, 624, 629
velocity, 629
vorticity in environment, 610
warm core, 614-615, 618-625
warning, 631, 638
watch, 638
weak wind shear in environment needed, 610
winds
gust averaging time, 605
vs. geostrophic adjustment, 384
shear in hurricane environment, 610
tangential, 622-623
total (tangential + translational), 627
zoning and landuse, 631
Huxley, Aldous (quotations), 38, 236
Huygens, Christiaan, 837
Huygens' Principle, 837, 859
hybrid
coordinates in NWP model, 746
supercell thunderstorm, 492
HYDRA code, 269
hydrate, methane, 810
hydraulic(s)
jump, 656, 660-662
open-channel, 657-661
hydrogen, H2, 7
hydrogen peroxide, 190-192
hydrometeor(s), 185
definitions, 205
graupel, 205
hail, 205
number, 187
radius, 187
size, 187
terminal velocities, 202-204
hydrometeorologists, 257
hydrometer(s), 111
hydrophilic, 188
hydrophobic, 218
hydrostatic
assumption/definition, 15-16
balance, 15-16, 316
equation, 15-16, 316
use of, for isobaric surfaces, 296
equilibrium, 15-16
thermal circulations, 341-342, 655
HYFOR code, 269
hygrometers, 75, 97, 111-112, 219
hygroscopic
cloud seeding, 553
pollutants, 191
hypothermia, 77
hypoxia, 874
hypsometric

constant, 17, 880
equation, 17-18
sea-level-pressure reduction, 267
use in explaining anabatic flow, 650-651
H2, hydrogen gas, 7
H2O, (see water), 7

I

IAC code, 269
FLEET, 269
ICAO = international civial aviation organization, 149
weather station ID or code, 270
ice
ages, 795, 798-799
aggregation into snowflakes, 200, 202
albedo climate feedback, 808-810
cores, 803
crystal, 185,
clouds (cirrus clouds), 163
columns, 842, 866
electrification of clouds, role in, 564-566
faces, 842
fall speeds, 206
fogs in arctic airmasses, 393-397
geometry, 198-199, 842
habits, 198-199, 842-843
halos, 842-855
hollow columns, 198-199, 866
lattice, 194-195, 198
lightning creating, role in, 564-566
mass, 200
nucleation, 194-196
optics (also see Optics chapter), 163, 842-855
plates, 842
pyramids & pyramid optics, 842, 847
rotation angles, 843, 845-846
shapes, 198-199, 842-843
weather-map symbols for, 276
cubic (Ic), 198, 855
density, 209, 880
embryo, 194, 549-550, 553
fallout from arctic airmass, 396
formation on aircraft wings, 130
growth by diffusion, 198-202
growth rates, 200-202
ice crystal habits, 198
Wegener-Bergeron-Findeisen (WBF), 201-202
hail, 199
hexagonal (Ih), 198, 834-835
index of refraction, 834-835
loading, 14, 555
melting into rain, 206
mixing ratio, 97, 186
needles, 199, 276
nucleation, 194-196, 202
nuclei, 185, 194-195
particles, 185, 546
pellets (sleet), 199
weather-map symbols for, 276
phases, 198
refractive index, 834-835
saturation vapor pressure over, 88
snowflakes, 198-200
specific heat, 880
ICEAN code, 269
Icelandic low, 356
ideas, 99
ideal gas law, 14-15
gas constant, 14, 880
idealized
feedback example, 807-810
fog models, 173-177
hurricane model, 626-629
winds, 302
identification of
clouds, 161-169
hurricanes, using numbers and names, 613-615
lines (isopleths) on thermo diagrams, 126-127
different types of thermo diagrams, 126-127
identity matrix
IEEE standards board, 870
igneous meteors, 205
image(s)
interpretation of satellite photos, 231-233
radar reflectivity, 243, 246, 248, 254
imager, 230
channels on satellites, 222-223, 230
imbalanced
forces (causing a centripetal force), 305
initial conditions, 304
mass and flow fields, 763
systems, tendency to reach new balance, 329
immersion
buoyancy of objects, 135
freezing, 194-195
impact parameter, 839-841
imperfect-technique errors, 875
inaudible thunder, 575-576
incandescence, lightning, 564
inches of mercury (in. Hg), 7
incident
angle, 833
light, 833-863
radiation, 41-47, 334-339, 793-803, 833-863
INCLI code, 269
inclination of satellite orbits, 228
incoming solar radiation (insolation), 40-41, 334-337
incompressible
continuity equation, 318-319
flow, 669-671
increased water vapor, 810
increasing, weather-map symbol for, 276
incremental changes, beyond algebra box, 38
incus, 169, 482
independent
observations, 236-239
variable, 3, 872
index
air quality, 743
discomfort, 117
dummy, 875
heat, 77-78, 117
humidex, 77-78
livestock weather safety, 117
of thermal stress, 77-78, 117
of refraction
light, 834-835, 880
radar, 243-244
sound, 575-576
summer-simmer, 117
temperature-humidity, 77-78, 117
thunderstorm-forecast, 530-531, 551-552
wind-chill, 76-77
India
monsoon, 356
Regional Specialized Meteorological Center, 607
Indian Ocean dipole (IOD), 824
indices for thunderstorm forecasting, 530-531
indigo color defined (also see optics chapter), 37
indirect
sense, 455-456
sunlight, 33-34, 46
vertical circulation cells, 377
induced electric currents, 570
inductive reasoning, 107-109
industrial centers, clouds forming over, 162
inefficient coalescence, 205
inertia, 292
inertial
forcing, 367-371
motion, 312
in downbursts, 559
oscillation, 304, 311-312, 700
damped, 311
subrange, 708
subrange turbulence scale, 315
transformation, 715
wind, 312
inferior mirages, 83, 861-862
infinite
loop, 759
number of equations, 714
inflection points, 730
inflow winds into thunderstorms, 483
info projection, 239
infralateral arc, 854-855
infrared (IR) radiation (see also longwave), 27, 37-39, 222-223, 793-794
emissions from Earth system, 220, 334, 337, 794
emissivity (table of typical values), 42
feedback, for climate, 810
fog formation, role in, 173-177
hygrometer, 111
in troposphere, 71
rain drop growth affected by, 206
satellite images (photos), 230-233
satellite sensors, 46-47, 226, 230-232
scattering in atmosphere, 857
thermometer, 78
inhibition, convective (CIN), 523-524, 530-531
initial
conditions, 731, 758, 762, 816
sensitivity, 773
spin-up of hurricane, 617
value problem, 293, 762
initialization
objective optimum interpolation, 766
normal mode, 766
variational analysis, 767
inland
flooding, 637
sea breeze, 654
input, net solar, 795
external forcings to feedback processes, 806
inquisition, 470
INSAT, 228
insects, 151
in situ (direct) sensors, 219
insolation (incoming solar radiation), 334-337
average annual, 336-337
average daily, 40-41, 336, 799-802
latitude variation of, 337
related to PG types, 727-728
variations vs. climate variability, 799-802
instability
baroclinic, 353, 371-374
barotropic, 353, 367-370
CAPE & thunderstorm updrafts, 503-508
dynamic
and chaos, 773-776
and the Richardson number, 141-142
nonlocal conditional (thunderstorm), 496, 503-508
nonlocal conditional (hurricane), 609
numerical, 759-761
instantaneous
smoke plume, 728
wind part, 705-706
instrument calibration error, 875
instrumented tower, 75
instruments (see weather instruments)
insurance
hail/crop, 553
hurricane/disaster, 631
intake system of hurricanes, 608-620
integral/integration, approximation for, 872
integrated circuits (computer chips), 752
intensity
of rain, 207-208
of hurricanes, 605-607
of thunderstorms, 528-531
of tornadoes, 579-580
of turbulence, 503-508
of typhoons, 607
weather-map symbols for, 276
intercept, 770
intercloud lightning, 563
interdecadal Pacific oscillation (IDPO), 824
interface, density, 657-661
light refraction across, 833
interfacial waves, 658-661
interference, 858-861
constructive and destructive, 859
fringes, 858-861
interferometers, interferometry, 46-47
interglacial/glacial (ice age) periods, 795, 799
Intergovernmental Panel on Climate Change (IPCC), 811
intermittent
turbulence in entrainment zone, 692
weather-map symbol for, 276
internal
boundary layer, thermal (TIBL), 654-657
dynamics (Bunker's) method for storm motion, 518-520
energy, 54, 672
feedback processes, 806
heat sources, 64, 72
Rossby radius of deformation, 319-320, 344, 665
international
civil aviation organization (ICAO), 149
cloud atlas, 168
date line, 5
long scale number prefixes, 870
space station (obs. of hurricane & thunderstorms), 604
system of units (SI), 7, 870
interpretation of
hodographs, 510-522
METARs and SPECIs, 270-279
satellite images, 231-233
weather maps, 436-472
interquartile range (IQR), 502
intertropical convergence zone (ITCZ), 233, 330-332,

I, J, K

350-351
intortus, 169
intracloud lightning, 563
intrinsic
phase speed, 369, 658
unpredictability, 774
inundation, 632-637
invariance, rotational, 320
inverse problem, 237-239
inverse square law of radiation, 39-40
inversion
capping, 143-144, 496-499, 687-690
vs. thunderstorm cap, 497
frontal, 403-404, 691
lapse rate, 140
passat, 351
surfaces, 403, 687, 691, 695
temperature, 139, 687-691
trade, 351
iodide (cadmium, lead, silver), 195
Ionian age, 799
ionized air, lightning, 565-566
ionosphere, 565
ions, 564
IPCC (Intergovernmental Panel on Climate Change), 812
IR (also infrared, terrestrial, or longwave radiation), 37-39
thermometer, 78
iridescence, 165, 667, 685, 859-860
irradiance (see also radiation), 36
irregular ice crystal shapes, 199
irreversible processes, 121, 131, 765
irrotational winds, 385
in tornado, 577, 602
isallobar, 17
isallohypse, 17
isallotherm, 17
isanabat, 17
isanomal, 17
isentrope, 17, 63, 103-105, 122-123, 143-144, 156, 365, 373, 403, 407-410, 414, 437, 624-625
on case-study weather maps, 438
on vertical cross section, 441
isentropic
analysis, 144, 364, 437, 441, 443
chart, 437, 441
compressible flow, 671-672
potential vorticity (IPV), 364-365, 441-443
conservation, 364
lee cyclogenesis due to, 365
tropopause folds visible by, 364, 414-415
units (PVU), 364, 441
upper-level fronts, 414-415
processes in hurricanes, 625
surfaces, 437
in fronts, 403, 414-415
on weather maps, 437
Islam, 754
island, urban heat, 678-679
isobar, 17
for barotropic vs. baroclinic atmospheres, 749
frontal, 400-401
on thermo diagram, 63, 100, 119-158
packing vs. wind speed, 303, 307
rules for drawing on weather maps, 280-281
tornado, 581
isobaric
charts, 290-291
for case-study cyclone, 433-466
definition, 17, 290, 436
maps/charts, 290-291, 436
reason for using, 291, 436-437, 442
20 kPa, 440-443, 452, 455-456
50 kPa, 433, 442, 448, 451
70 kPa, 439, 442
85 kPa, 439, 442, 449, 459-462
100 kPa, 438, 463
surfaces, 290-291, 345-349
mandatory, 772
on weather maps, 290-291, 436-442
vs. constant height maps, 290-291
isobath, 17
isobathytherm, 17
isoceraunic, 17
isochrone, 17
isodop, 17, 250
isodrosotherm, 17
map of pre-thunderstorm environment, 500
isoecho, 17
isogon, 17
isogram, 17
isohel, 17
isohume, 17, 100-101
on thermo diagram, 100-101, 119-158
pre-storm environment, 497-499
on weather maps
rules for drawing, 280-281
pre-storm environment, 499-501
isohyet, 17
isohypse, 17
isoline, 17
isoneph, 17
isopleth, 17
hand analysis and drawing on maps, 280-281
of pollution concentration, 734, 737
isopycnic, 17
for baroclinic vs. barotropic atmospheres, 749
process behind thunder shock front, 572
isoshear, 17
isostere, 17
iso-surfaces, utility of, 436-437
isotach, 17, 358-359
weather map of, 440, 443
isotherm, 17
frontal, 400-401
on cross sections of atmosphere, 359
on thermo diagram, 63, 100, 119-158
on weather maps, 280, 400-402, 427, 439-440, 608, 768-769
rules of drawing, 280-281
isothermal
compressible flow, 671
lapse rate, 140
isotropic, 8, 221, 315
defined, 8, 707-708, 727
force, 8
motions and scales, 315, 707
radiation, 221
turbulence, 707-708, 727
isotropy, 707-708, 727
ITCZ (intertropical convergence zone), 233, 330-332, 350-351
hurricane trigger, 610-612
thunderstorms, 331-332
iterative techniques, 103, 238, 308, 310, 394-395, 573-576

J

Japan Meteorological Agency (JMA), 607
jet
barrier, 664-665
blue, 563, 568
coastally trapped low-level barrier, 664-665
contrails, 160
climate change effects, 812
easterly, 611-612
low-level
coastal barrier, 664-665
nocturnal, 699-700
nocturnal, 699-700
prefrontal, 407, 433, 472
rear inflow (RIJ), 489
jet-streak, 454
driving updrafts and cyclogenesis, 454-456, 467
entrance and exit regions, 455-456
four quadrants, 455-456
of cyclone case study, 455-456
thunderstorm triggering , 526
jet-stream(s), 357-361
African easterly, 611-612
angular momentum, 360-361
aspect ratio, 357
axis, 362
baroclinicity, 359-360
core, 357-359, 414-415
circulation around the globe, 357-358
curvature, 453
driving updrafts and cyclogenesis, 453
cyclogenesis, role in, 427-429, 432
easterly, 611-612
equation, 359-361
exit region, 454-456
frontal zones, at, 407
maximum, 357-362, 454-456
meanders (Rossby waves), 329, 357, 367-376
polar, 233, 331-332, 352-353, 357-360
secondary circulations, 455-456
speed, 357-361
vs. season, 357-358
streaks of max winds, 454-456
subtropical, 233, 331-332, 350-351, 357-361
angular momentum effects, 360-361
Joint Polar Satellite Systems, 229
Joint Typhoon Warning Center (US), 607
joule, unit of energy, 870
JPSS, 229
Juan
de Fuca Strait, 661-663
Hurricane, 617
judgement errors, 875
Julian day, 29
jump
hydraulic, 660-661
potential temperature, 110, 690-698
Junge distribution of cloud condensation nuclei, 189

K

K (degrees), 7
K band radar (including Ka and Ku bands), 242
K index (KI), 531
K-Pg event (mass extinctions), 805
K-T event (mass extinctions), 805
K theory, 714-716
Kalman filter & gain, 770
kaolinite, 195
Kármán, von, 677, 701
katabatic wind
equilibrium speed, 653
high pressure associated with, 391
in Antarctic airmass formation, 396, 676
in Antarctic cyclone formation, 432
in fog formation, 177
in forest trunk space, 678
in stable (nocturnal) boundary layer, 696
vs. Bora winds, 675-676
katafront, 404
Keith, David, 815
Kelvin
circulation theorem, 366
equation, 189-191
Helmholtz (K-H) waves, 142, 165, 654-655, 710
temperature units, defined, 7, 870
wave, 633-634
Kepler, Johannes, 27
Kepler's second law, 29
Kern arc, 854-855
key altitudes for thunderstorms, 496-499
K-H waves, 142, 165, 654-655
clouds, 165
kilo (10^3), 870
kilobit, 870
kilograms, 870
force
mass , 870
kiloPascals, defined, 7-8
kinematic
definition, 320-321
effective surface water-vapor flux, 110
flux of total water, 109-110
flux of water vapor, 108-110
frontogenesis, 408-410
heat flux profiles in ABL, 698
mass flux, 34-35
momentum flux, 704, 715
stress, 701
surface heat flux, 73-76
kinematics, 320-321
circulation, 365-366
convergence and divergence, 320-321
deformation, 320-321
vorticity, 320-321
kinetic energy
in Richardson number, 150
of flow, 669-672
of global circulation, 356
of molecules, 6
of wind, 150
turbulence, 708-709
King Arthur legend, 863
Kirchhoff's Law, 41, 220
klystron vacuum tubes in radar, 240
Knollenberg probe, 210
knot unit of speed, 278, 291, 870
knowledge, organizing, 72
Köhler
curves, 191
equation, 190
Köppen climate classification, 816-817
Köppen, Wladimir, 817
kPa (kiloPascals) defined, 7-8
Krakatau, 805
krypton hygrometer, 111
Kuiper's and Hansen's skill score, 781

Kuroshio ocean current, 431

L

L band radar, 242
Labrador current, 616
lacunosus, 169
Lagrangian
  definition, 53
  heat budget-saturated, 101-106
    liquid-water, wet-bulb, & equivalent potential temperatures, 104-106
    saturated adiabatic lapse rate, 101
    thermo diagrams, 102-103
  heat budget-unsaturated, 57-64
    adiabatic lapse rate, 60
    first law of thermodynamics, 58-59, 64-65
    potential temperature, 61-62
    thermodynamic diagrams, 63
  momentum budget, 292
    Bernoulli's equation, 670
  net source of water, 99
  pollutant dispersion, 731
  time scale, 732
  trajectories, 669
  water budget, 99-106
    thermo diagrams, 100-101
    water conservation, 99
lake
  breeze, 654
    fronts, 525, 655-657
    high pressure, 391, 655
  steam fog, 173
  Toba, 805
Lamb, Sir Horace, 705
Lambert map projection, 748
laminar air flow, 138, 140, 669-671, 688
land
  breeze, 656
  surface observation from satellite, 234
landfalling Pacific cyclones, 472
landscape vs. roughness length, 700
landspout tornadoes, 582
land-use observation from satellite, 220
La Niña, 818-820
  cyclone track influence on, 430
Laplacian, 450, 458
  form for geostrophic vorticity, 450
lapse rate, 59-64, 139-140
  adiabatic, 139-140
  environmental, 59, 134, 140-141
  feedback in climate, 810-811
  inversion, 140
  isothermal, 140
  moist vs dry, 104-106
  names, 140
  process, 59-64
  saturated (moist), 101-106
  standard atmosphere, 11-12, 70
  subadiabatic, 139-140
  superadiabatic, 139-140
  thunderstorm environment, 496-499, 503-508
  unsaturated (dry), 60-64
  vs. static stability, 139
large
  eddy simulation models, 786
  scale (global) circulation, 329-388
laser radar (lidar), 112, 322
latent heat
  condensation, 56, 465-467
  cyclogenesis, 465-471
  deposition, 56, 88, 880
  energy, 54
  Eulerian heat budget, 72
  evaporation, 54
  factor, 56
  flux at surface, 73-76
  fusion, 56, 880
  hurricanes, fuel for, 620
  internal energy source, 64, 72
  melting, 54, 56
  on thermo diagrams, 130-131
  precipitation, measure of net heating, 465-466
  rate, 72, 465-466
  release in
    hurricanes, 613, 620
    thunderstorms, 72, 465-466, 499-502, 546-548
  self-development of cyclones, 468-471
  sign convention, 56
  sublimation, 56
  thunderstorms, fuel for, 499-502
  vaporization, 56, 88, 880
  variation with temperature, 90, 880
  water, 54
lateral direction, defined, 727
latitude(s)
  belts, 329-330, 350-355
    radiative forcings, 338-339
  change with distance north, 336
  degrees of, 4, 330, 879
  elevation angle of sun as function of, 32, 801-802
  excluded, for hurricane formation, 609
  high-, 330
  horse, 331
  hurricane, favored & excluded, 609
  lines, 4
  low-, 330
  mid-, 330
  of strongest jet-stream, 359-361
Laurasia, 804
Laws
  Amdahl's, 763
  Beer's, 43, 856
  first law of thermodynamics, 53,58-59, 64-65
  inverse square law of radiaion, 39-40
  Kirchhoff's, 41
  gravitation (Netwon's), 11
  Moore's, 752
  motion (Newton's), 292
  myth of, 38
  Newton's, 11, 292
  sine law of radiation, 40
  Snell's, 834-837
  Stefan-Boltzmann, 37-38
  Planck's, 36
  Wien's, 37
large hail, 548
layer, 147
  atmospheric boundary, 687-722
  clouds, 162-164, 168
  method for static stability, 140-141
    triggering of thunderstorms, 526
  radix, 703-705
  stability classes, 140-141
layers of the atmosphere, 12-13, 563, 565, 692, 700-705

LCL (see lifting condensation level)
LDN (lightning detection network), 568
lead (Pb), the chemical, 725
  iodide, 195-196
lead time in forecasting, 762
leaders
  dart, 567
  stepped, 566
leap
  day, 31
  -frog (time-differencing) scheme, 757
  year, 31
least squares, 770
LeChatelier's Principle, 132, 141, 329, 344, 383, 429
lee cyclogenesis, 430-431, 443-446
  conservation of potential vorticity, 364-365, 445
    isentropic, 364-365
  equatorward propagation along the lee side, 446
  stationary planetary waves, 443
lee waves, 666-668
left
  moving supercells, 518-520
  quadrants of jet streak, 454-456
Leibniz, Gottfried Wilhelm, 759
length, 870
  buoyancy scale, 733
  mixing (Prandtl), 715
  momentum-scale, 733
  Obukhov , 703
  path (radiative), 43
  roughness, 677, 700-703
  scales, 315
    buoyancy, 733
    dissipation, 709
    momentum, 733
  units, 870
lenticular/lenticularis/len clouds, 165, 168, 666-668, 684-685
  optical phenomena caused by, 859-860
LEO (low Earth orbiting) satellites, 227
levels
  mandatory, 134, 772
  significant, 134, 147
  radar echo intensity, 247
level of
  downdraft equilibrium (DEL), 557
  equilibrium (EL), 483, 497-506
  free convection (LFC), 497-506
  free sink (LFS), 557
  lifting condensation (LCL), 93-94, 496-499
lidar (laser radar, including DIAL), 112, 219
  anemometer, 322
life
  controls on climate, 813
  cycle of
    hurricane, 613-615
    thunderstorm, 484-485
    tornado, 583
lifted index (LI), 531
lifting
  condensation level (LCL), 93-96, 105-107, 130, 138, 162, 164, 483, 496-501, 530-531
    cumuliform cloud base, 162
    height change with precipitation, 130-131, 398, 676-677
    mean-layer, 501, 530-531
    of chinooks and foehns, 676-677
    of lenticular clouds, 666-668
    of upslope fog, 173
    on thermo diagram, 129-130, 497-499
    pre-thunderstorm, 497-501
    pressure at, 93
    stratiform cloud base (not related to), 164
    temperature at, 96
    tornado funnel cloud, 581
  fog, 177
  trigger for thunderstorms, 496, 522-526, 530-531
light, 222
  bending, 833
  colors, 37, 834-835, 862
  diffraction, 858-861
  electromagnetic waves, 833
  ice-crystal optics, 842-855
  liquid drop optics, 837-841
  mirages, 861-863
  monochromatic, 833
  optics in the atmosphere, 833-868
  photon particles, 833
  point, 834-835
  polarization, 856-857
  rainfall rate, 207-208
    weather-map symbols for, 276
  rays, 833-837
  reflection, 833-844
  refraction, 833-855
  scattering, 856-857
  spectrum, 37, 222, 834-835, 862
  speed of, 36, 240, 243, 834-837, 879
  transmission of, 73, 805, 856
  ultraviolet, 222, 857
  waves, 833
lightning, 563-571
  30-30 safety rule, 570
  air discharge (cloud-to-air, CA), 563
  anvil, lightning from, 564
  ball, 567
  bead, 567
  behavior and appearance, 566-568
  blue jet, 563, 568
  bolt (see return stroke), 566-567
    from the blue, 567
  breakdown potential, 566
  burning the air, 567
  Canadian, 568
  channel, 563-567
  climatology, 564
  cloud-to-cloud (CC), 563
  cloud-to-ground (CG), 563
  creation by micropysical processes, 564-566
  currents, peak, 568-569
  deaths caused by, 564, 571
  detection networks (LDN), 568-569
    satellite low-light cameras, 569
    satellite optical transient detectors, 569
  duration, 569
  electrometeors, 205
  elf / elves, 563, 568
  fatalities from lightning strikes, 571
  fires (forest, wild) caused by, 564
  flashes, 567
  flickering, 567
  hazards, 569-571, 607
  heat, 567
  hurricane, 637
  igneous meteors, 205
  incandescence, 564
  intercloud, 563
  intracloud (IC), 563
  jet, 563, 568
  median peak current, 564
  negative (polarity), 563-564
  odor, 567

L, M

plasma, 567
polarity, 563-564
positve (polarity), 563-564
power, peak, 569
pressure wave in thunder, 564, 571-574
red sprite, 563, 568
ribbon, 568
safety & warning signs, 567, 569-571
sferics, 568
sheet, 567
size, 563
spider, 567
sprite, 563, 568
staccato, 568
storm (see Thunderstorms), 481-602, 564
strike sequence, 566-568
temperature, 563
thunder, 571-576
types, 563
weather-map symbol for, 276
likelihood of tornadoes, 591
likely velocity
downburst in thunderstorm, 557-559
updraft in thunderstorm, 508
limit of
convection, 498
predictability, 773-776
line(s)
absorption, 221
clouds, 167
end vortices, 490
dry, 399
flanking, 482-483
path, 668-669
squall, 399
streak, 668-669
stream, 611-612, 668-669
thunderstorms (squall line), 399, 490
linear
depolarization ratio, 256-257
feedback processes, 806
approximation to nonlinear process, 806-809
graph, 873
regression, 770-771
relationship, 873
Lipschitz condition/continuity/smoothness, 761
liquid-crystal thermometers, 78
liquid drop optics, 837-841
Alexander's dark band, 841
primary rainbow, 839-840
reflection from water, 838
secondary rainbow, 840-841
liquid droplet nucleation, 188-194
liquid-in-glass thermometers, 78
liquid-water
content (LWC), 97
measurement, 210
density vs. temperature, 835, 880
equivalent, 107, 208
loading, 15, 555
mixing ratio, 97-98, 186
on thermo diagram, 130
potential temperature, 104-106
on thermo diagram, 103-106
on weather maps, 500
specific heat, 880
liter (or litre) unit of volume, 870
lithometeors, 205
litre (or liter) unit of volume, 870
livestock weather safety index, 117
loading, liquid water or ice, 15, 555
local
closure, 714-716
elevation angle of sun, 32
horizontal, 4, 5
shear across one layer, 514
winds, 645-686
naming, 654
location parameter, Weibull distribution, 646
median as, 502
locations of
hail, 552-553
strongest hurricanes, typhoons, trop. Cyclones, 631
weather observations worldwide, 271-273
logarithmic
relationships and semi-log graphs, 873-874
wind profile, 677
logarithms, base of natural, 879
log-linear wind profile, 702-703
log-log graph, 215, 874
slope, meaning of, 215
lognormal distribution
clouds, 170
lightning surge probabilities, 569-570
rain-drop size, 207
log wind profile, 677, 702-703
London, Jack, 849
long
gap winds, 662-664
range forecast models, 768
scale number prefixes (international), 870
waves
Rossby; planetary waves, 369
radiation, 37-39
Longfellow, Henry Wadsworth, 847
longitude, 4, 802
longwave radiation (see infrared), 37-39, 220, 793-794

loom, optically, 862
looping of smoke plumes, 727-728, 735-737
loops
radar, 241
satellite, 227
Lord Byron, 805
Lorenz strange attractor, 773-775
Lorenz, Ed, 773, 775
loss, 780
vs. cost, 785
lottery, 711
Lovelock, James, 813
low
clouds (see also fog), 162, 168
height variation with latitude, 163
scud, 483
weather-map symbols for, 168, 277
Earth orbit (LEO) satellites, 227
latitudes, defined, 330
global circulation, 350-351
level jet
coastal barrier, 664-665
nocturnal, 699-700
light level cameras for lightning detection, 569
order truncation finite difference schemes, 754-755
precipitation supercell (LP), 495
pressure
boundary-layer pumping, 319-320, 432
meso-lows, 489
mountain lee, 165
systems (see extratropical cyclones), 330, 425
pressure-centers (extratropical cyclones; lows; L), 425-480
fronts rotating around, 389, 425-426
glyph (symbol) on weather maps, 426
hurricane eye, 613-615
midlatitude, 331, 425-480
monsoon-related, 333-334
named (Aleutian, Islandic, etc.), 354-356
rising air in, 356, 451-462
thermal, 341-342
tracks, 429-431
winds around, 305-307, 446-450
resolution NWP, 752
lower
quartile, 502
suncave Parry arc, 854-855
sunvex Parry arc, 854-855
tangent arc, 851-852, 854-855
Wegener arc, 854-855
Lowitz
arcs, 855
oriented crystal, 855
lows (see extratropical cyclone chapter), 425-480
midlatitude cyclones, 330-331, 425-480
Southern Hemisphere, 426, 430-432
subpolar, 331
LP (low-precipitation supercell), 495
luminary, 858
luminous
intensity units, 870
meteors, 205
lumpy cloud shapes, 161-164
lunar tides, 376
Lyman-alpha hygrometer, 111

M

Mach number, 571-576, 579, 674
one, 579, 674
macroscale cloud electrification, 564-566
Madden-Julian oscillation (MJO), 818, 824
Maddox, Bruno, 54
MAFOR code, 269
magnetic
direction finders, 568
field, 255
variation, 647
magnetron vacuum tube in radar, 240
magnitude
component of scientific notation, 870
of total shear, 515-516
main updraft tower, 482-483
major Hadley cell, 332-333
mammatus/mamma clouds, 169, 484
mandatory levels for RAOBs & NWP output, 134-135, 772
Manhattan project, 218
man-made clouds, 166
manual (hand) analysis of weather maps, 279-281
Manual on Codes No. 306, WMO, 268
manufacturing data, 826
map, 274-281
factors, 747
polar stereographic, 747
NWP output, 772
projections, 747-748
conformal, 748
Lambert, 748
Mercator, 748
polar stereographic, 747-748
stereographic, 748
weather
airmass locations, 392
analysis methods, 274-281, 402
CAPE, 506-508
surface, 267
marine air, 656
maritime
airmass code, 392
cloud condensation nuclei, 194
fogs, 173-174
tropical airmass, 392
Marshall-Palmer distribution, 207
mass, 870
air, in a column, or between pressure levels, 10, 464, 466
airmass, 389-399
budget, 317-318, 746-747
of air column (for MSL pressure), 463
center of, for
pollutants, 729
wind vector, 516-517
conservation, 317-318, 660, 746-747
boundary-layer pumping, 318-319
continuity equation, 317-318
incompressible continuity equation, 318
thunderstorm, 545-546
density, 10-13
Earth, 28, 879
extinction events, 805
field, 343
adjustment to wind field, 343-344
balanced with flow fields, 763-765
in forecast models, 764
flux (dynamic & kinematic), 34-35, 317-318
in Newton's second law, 292
inflow vs. outflow, 317-319
moon, 28
of air in column, 10
of air parcel mixture, 160
of solute in droplet, 190-193
of water vapor, 91
planets in the solar system, 22
units, 870
massaging data, 826
mathematical
closure, 714
constants, 879
framework, 2
mathematics, 315, 711, 762
clarity, 393
matrix, 822
covariance, 821-822
eigenvalues and eigenvectors of, 822
trace, 822
mature stage of
waterspout spray vortex, 582
thunderstorm cell evolution, 485
tornadoes, 583
Maunder minimum in sunspots, 39, 803
maximum
acceptable levels of air pollutants, 725
advection on weather maps, 458
likely
downdraft speed in thunderstorms, 557-559
updraft speed in thunderstorms, 508

precipitation for WBF process, 201-202
solar output, 803
surface temperature for thunderstorms, 506, 523
tangential winds around eye wall, 605, 622, 626-627
theoretical pressure ratio of hurricane, 625-626
unambiguous range, for radar, 240-241
unambiguous velocity, for Doppler radar, 250-251
updraft speed in thunderstorms, 508
vorticity advection, 458
wave-height, 634-636
winds through short mountain-gaps, 662
mb, millibar, definition, 7-8
MCC (mesoscale convective complex), 491
McMahon, 817
MCS (mesoscale convective system), 488-492
role of wind shear, 510
MCV (mesoscale convective vortex), 492
MDT, Mountain daylight time, defined, 5
mean, 502, 705, 726, 875
absolute error (MAE), 778
and turbulent parts of wind, 705-706, 726
anomaly, 29
background state, 316
bias, 778, 875
condition for air, 7
environmental wind (normal storm motion), 516-518
error, 778, 875
layer
CAPE, 506-507
CIN, 524
lifting condensation level (ML-LCL), 501, 530-531
persistence error, 778
running average, 599
sea level (MSL) pressure, 267, 275
forecast equation, 464-467
maps, 354
reduction from station pressure, 267
shear vector, 514-515
squared error (MSE), 778
skill score, 778
statistical definition (=average), 502, 705, 726
wind, 705, 726
radar observations of, 252-253
shear vector, 514-515
vector, 516-518
measurement of
fractal dimension, 172
humidity, 111-112
radiation, 45-47
rainfall, 210-211
soundings, 134-135
temperatures, 78-79
winds, 249-254, 321-322
mechanical
clocks & time, 34
energy, 625, 670
turbulent production, 704
Medawar, Sir Peter, 343
median, statistical definition, 502
medical symptoms for people struck by lightning, 571
medieval maximum in solar output, 803
mediocris/med, cumulus, 161-162, 168, 483
Mediterranean airmasses, 397
medium-range weather forecast models, 768
mega (10^6), 870
megabit, 870
megaton bomb, energy of, 499, 548, 880
melting
ice crystals, as seen by radar, 248
latent heat of, 56
Mercator map projection, 748
mercury
barometer, 7, 19
inches of, 7
millimeters of, 7
meridians, 4, 330
defined, 4, 330
prime, 4, 28
meridional
displacement, 372
flow, defined, 330
gradient (MG) of zonal momentum, 376
kinematic heat flux, 374
overturning ocean circulation, 810
propagation of baroclinic waves, 372-374
temperature gradient, 335-336, 352
transport by Rossby waves, of, 374-376
heat, 374-375
momentum, 375-376
wave flux, 375
Merilees, Phil, 775
mesocyclone (see thunderstorm), 481, 483, 492-495, 586-592
counter-rotating, 490-491, 587
radar observations of, 253
wind shear, importance for, 510
as affects storm-center motion, 518-520
tornadoes, relationship to, 582, 586-592
meso-high, 488, 554, 559-563
meso-low (also see mesocyclone), 489
mesopause, 12-13
mesoscale, 315
cellular convection (MCC), 167
convective
complex (MCC), 140, 491
system (MCS), 488-492, 613
system, lightning from, 564
vortex (MCV), 492, 613
forces in gap winds, 662-664
gap geostrophic wind, 663
high pressure (see meso-high), 488, 554, 559-563
mesosphere, 12-13
polar clouds in, 166
MET (Middle European time), 5
metabolism, 76
metaldehyde, 195-196
metamorphosis of snow crystals, 209
METAR = aviation routine weather report , 170, 268-271, 275-279
abbreviations for precipitation, 208
Météo-France, 607
meteogram, 117, 745, 772
meteoroids, 205
Meteorologica (book by Aristotle), 26
meteorological
aviation report (METAR), 270-279
conventions, 2
Meteorological Service of Canada (MSC), 243, 638
meteorology, 205
applied, 2
Bergen School of, 399
definition, 1, 205, 877
disciplines or components of, 1, 353
forecasting, 745-792
synoptic, 353
theoretical, 872
meteorite dust, seeding clouds, 166
meteoroids, 205
meteors, 11, 168-169, 205
hydrometeors, 205
other meteorological meteors, 205
meteosat, 228-229
meter, 870
methane, CH4, 7
greenhouse gas, 811
hydrates in ocean & permafrost, 810
sulfonic acid, 188
method of
moments, 730
problem solving, 869
meticulous, 19
metric
(SI) units, 7, 870
ton (or tonne), 870
Mexico time zone (MEX), 5
Michelson interferometer, 46
micro (10^{-6}), 870
microbursts, 554
microphysics (of clouds and precipitation), 185-218, 546
parameterizations in NWP models, 751
microscale, 315, 708
processes creating cloud electrification, 564-566
microwave
bands, 223
energy from radars, 240
ovens, 243
radiation, 220
rain sensors, 211
refractometer, 111
satellite sensors, 211
wind profilers, 112
middle
clouds (prefix: alto), 162-163, 168
height variation with latitude, 163
satellite images of, 234
weather-map symbols for, 168, 277
European time (MET), 5
midlatitude, 330
anticyclones, 331, 390-391
cyclones, 331, 425-480
Southern Hemisphere, 426
highs, 331, 390-391
lows, 331, 425-480
system collision with hurricanes, 616
troughs and ridges, 367-376
baroclinic instability and planetary waves, 371-374
barotropic instability and Rossby waves, 367-370
heat transport , 374-375
momentum transport, 375-376
ridge axis, 367
weather
cloud heights, 163
tropopause heights, 163
variability, 353, 425-480
midlatitudes, defined, 330
global circulation, 352-355
mid-level vertical velocity, 452-462
mid-tropospheric fronts, 413-414
Mie scattering, 857-858
haze, 858
Mie, Gustov, 858
Milankovitch, Milutin, 797
theory, 797-803, 829
miles, nautical, 4
military , 218
polar orbiting weather satellite, 273
twilight, 33-34
milli (10^{-3}), 870
millibars, defined, 7
minima in solar activity, 803
minimum
viewing angle, 846
visibility (in METAR), 270
minor Hadley cell, 332-333
minute unit, 870
mirages, 861-863
Fata Morgana, 862-863
green flash, 862
inferior, 83, 861-863
superior, 862
mirrors, ice crystals acting like, 843-844
misinterpretation of data, 729
miss, 780
missed approach to airports, 563
mist, 170
weather-map symbol for, 276
mitigated loss, 780
mixed-layer (see atmospheric boundary layer), 68, 692
airmass, 393-396
CAPE, 506-507
convective, 649, 692
Deardorff velocity for, 703-704
depth, 144, 649
determination of, 143-144
entrainment into, 649, 697-698
growth, 695
associated with airmasses, 393-395
associated with dry lines, 416
rate, 698
lifting condensation level (ML-LCL), 501
ocean, 610
scaling variables, 735-736
temperature profile, 692
thunderstorm environment, 496-497
top, 143-144, 497-499
transport coefficient, 68
unstable, 692
winds in radix layer, 703-705
mixing
length theory, Prandtl, 715
of air parcels to create clouds & contrails, 160-161
ratio, 91
average total water, 97-99
definition, 91
excess water, 186-187
gradient, 196
ice, 97, 186
liquid-water, 97-98, 186
pollutant, 724
saturated, 91
thermo diagram, 100
total water, average, 97-99
total-water, 97, 186
vs. RH and temp, 92
water vapor, 56, 89-98
weather maps of, 500
wet-bulb, 94-95
in middle of mixed layer, 109-110
turbulent, effects on frontolysis, 411

M, N

mixture of air parcels, 160-161
MJO (Madden-Julian oscillation), 818, 824
MKS units (see International System of Units), 7, 870

ML (see mixed layer)
  CAPE, 506-507
moat, 605
mode of CCN growth, 188
Model Output Statistics (MOS), 770-771
modelers, 751
model(s), 751
  climate, 792
  fog, 173-177
  GCM (Global Climate), 768
  general circulation, 330-388
  heuristic (also see toy models), 280, 330, 793
  hurricane, 626-629, 637-638
  numerical weather prediction, 751
    current, 751
    history of, 759
  output statistics (MOS), 770-771
    updateable, 771
  pollution, 725
  primitive equation, 747
  sensitivity, 350
  toy (simplified), 330
moderate
  rainfall rate, 207-208
    weather-map symbol for, 276
  thunderstorm risk, 530
modern maximum in solar activity, 803
modification of airmass (see airmass), 397
  via flow over mountains, 398-399
  via surface fluxes, 397-398
Moilanen arc, 854-855
moist, 57
  adiabatic lapse rate (saturated), 101-103
    for determining static stability, 139
  adiabats, 101-106, 497
    on thermo diagrams, 102-106, 119-158
    thunderstorms, 497-499
  convection (thunderstorms), 496-499
  convective adjustment, 70
  process, 130
moisture, 87-118
  budget at surface, 107-110
  cyclogenesis, 426
  flux, 108, 110
    diffusive, 197
  forecast equations for, 746
  instruments, 111-112
  transfer coefficient, bulk, 109
  variables, 87-99
moisturizing process to form clouds, 159-160
mole, 870
  molecular weights (g/mole), 7
  ratio of pollutants, 724
molecular
  compression, 7-10
  conduction flux, 67-69, 73
  conductivity, 67-68, 880
  diffusivity (see also diffusivity), 196-200, 880
  energy, 118
  friction, 301
  rotation lines in spectra, 221
  scale, 315
  scattering of radiation, 220-222
  speed & temperature, 6-7
  vibration lines in spectra, 221
  viscosity, 709
  weight, 7
    of air, 7
    of atmospheric gases, 7, 724
    of solute in CCN, 190
moments, method of, 730
momentum, 292
  advection, 294
  angular, 360, 375
    subtropical jet, 360-361
  budget, 292-293
    Eulerian, 293, 746-747
    Lagrangian, 292
  definition, 292
  forecast equations for, 746
  flux, 375-376
    turbulent, 712-713
    vs. stress, 712-713
  gradient, 294
  length scale, 733
  reservoirs, 375
  specific, 294
  transport, 294
    by Rossby waves, 375-376
Monin-Obukhov length, 703
monochromatic , 36
  irradiance, 36
  light ray, 833
monodisperse distribution, 197
monotonic, defined, 9, 290
monsoon
  airmass code, 392
  circulations, 333-334, 343, 356
  highs associated with, 333-334, 354, 391, 615
    steering hurricanes, 615
  Indian, 356
  trough hurricane trigger, 612
Moon, 27
  albedo, 42
  bows, 841
  mass, 28
  optical phenomena around, 163
  orbital period & direction, 27-28, 879
Moore, Gordon E., 752
Moore's Law, 752
moral issues of doing science, 218
Morgana, Fata, 862-863
morning
  Glory, 656
  satellite, 229
morphology (shape) of
  clouds, 168
  ice crystals, 198-199
MOS (model output statistics), 770-771
most-unstable CAPE, 507
mother
  clouds, 168-169
  Earth (gaia), 813
  of-pearl clouds, 166
  storm, 485
motion
  cyclone translation, 425, 429-431, 433-435
  eddy, 35, 750, 704-716
  equations of, 746-749
  horizontal, 314
    equations of, 301-302, 314, 746
    scales of, 315
  laws, 292
  thunderstorm translation, 487, 492, 516-520
  vertical, 315-320
    boudary layer pumping, 319-320
    equations of, 315-320, 746
    in extratropical cyclones, 451-462
    in hurricanes, 605, 612, 628-629
    in thermals, 648-649, 694, 703-708, 711-716
    in thunderstorms, 482, 485-498, 503-508
mountain
  anabatic (upslope) flow, 649-652
  blocking of airmass & high pressure formation, 391
  building (orogenesis), 804
  clouds, 165, 649-650
  convergence zones, 472
  cyclogenesis (lee), 364-365, 443-446
  downslope (katabatic) flow, 652-653
  gap winds, 661-664
  high pressure formation near, 391
  katabatic (downslope) flow, 652-653
  pass winds, 661-664
  precipitation, 398-399, 472
  ranges, 397, 661
  slope
    angle, 650-653
    flows, 649-653
  time zone, 5
  -related clouds, 165
  triggering of
    easterly waves, 611
    Rossby waves, 364-367, 443-445
    thunderstorms, 487, 526
  upslope
    flow (anabatic), 649-652
    rain (orographic), 398-399, 472
  wave(s)
    behavior, 666-668
    clouds, 165, 667
    drag, 301, 668, 751
    Froude number, 668-668
    high-pressure regions in, 391
    lenticular clouds, 165, 667
    natural wavelength, 666
    turbulence, 667
  winds, 649-654, 660-670, 675-676
movement of
  airmasses, 397
  lows (extratropical cyclones), 429-431
MSL (see mean sea level)
  pressure, case-study maps, 438
    forecasts for cyclogenesis, 463-467
  reduction to, 267
MST, Mountain standard time, defined, 5
Mt. Agung, 805
Mt. Fuego, 805
Mt. Pinatubo, 805
MT-SAT, 228
Mt. Tambora, 805
Muana Loa, 805
MU-CAPE, 507
multicell thunderstorms, 486-487
multi-field charts, utility of, 443
multiple vortex tornadoes, 592-593
mushroom cloud (thunderstorm appearance) , 482, 532

N

n-CAPE, 508
NAAQS (national ambient air quality standards), 7, 725
NACLI code, 269
nacreous clouds, 166
names of
  clouds, 161-169
  cyclones, 425-426
  hurricanes (tropical cyclones & typhoons), 614-615
    retired, 615
  local winds, 654
nano (10^{-9}), 870
NAO (North Atlantic oscillation), 430, 818-819, 824
NAT clouds, 166
National
  ambient air quality standards (NAAQS), 7, 725
  ambient air quality objectives & guidelines, 725
  Centers for Environmental Prediction (NCEP), 279, 283
  Hurricane Center (NHC), 608, 638
  Institute of Standards and Technology (NIST), 51, 879
  Lightning Detection Network (NLDN), 569
  Oceanic & Atmospheric Admin. (NOAA), 637
  Weather Service (NWS), 532
  radar used by, 243
natural
  climate processes, 793-832
  cycles & changes in hurricane activity, 631
  greenhouse gas, 811-812
  logarithms, base of, 879
  oscillations in climate, 818-824
  selection, computational, 680
  wavelength, 666
nature of convection , 481, 704, 710, 716
nautical miles, 4, 870
Navier, Claude-Louis, 759
Navier-Stokes equations, 293, 301-302, 314-317, 759
NCAR-RIP, 772
NDT, Newfoundland daylight time, 5
nebulosis/neb, 168
needed heat transport globally, 338-339
needle ice crystals, 198-199
neon, Ne, 7
near
  infrared and ultraviolet, 222-223
  source pollutant dispersion, 732
  surface (see also surface)
    global circulation, 330-331
    temperature, 330-331
    winds, 330-331
Nebeker, Frederik, 781
negative
  buoyancy, 556
  feedbacks, 807
  flux divergence (=convergence), 64
  polarity lightning, 563-564
  sign in scientific notation, 870
  vorticity advection (NVA), 447-448
nested grids (one-way and two-way), 752-753
net
  actinometer, 45-47
  Ekman transport, 378, 610, 632-633
  evaporation, 92
  force, 292-294
  heat budget (Eulerian), 72-73
  heating, 72-73, 131-132, 336-339, 465, 546
  longwave flux, 45, 337
  meridional transport of zonal momentum, 375-376
  pressure tendency, 466-467
  pyranometer, 45-47

pyrgeometer, 45-47
pyrheliometer, 45-47
radiation, 27, 44-45
global distribution, 337-338
radiometer, 45-47
sea level pressure tendency equation, 466
sky transmissivity, 44
solar input, 795
spring force, 136
total water (Eulerian), 107
neutral static stability, 139-140, 688-689
neutral stability, 138, 140
air standard deviations of velocity, 707
boundary-layer wind, 308-310
boundary layers, 688-689
determination of, 139-140
dispersion within, 733-734
drag, turbulent, 701
dry, 140
plume rise within, 733
saturated, 140
surface-layer wind, 702
neutrally buoyant, 135
névé snow, 209
Newfoundland time zone, 5
Newton, Isaac, 292-294, 759, 841, 862-863
great scientists and big mistakes, 863
reflecting telescope, 862
work on colors, 862-863
newton (unit of force), 8, 870
Newtonian
physics, 1
transformation, 715
Newton's Law of Gravitation, 11
gravitational constant, 879
Newton's Laws of Motion , 1, 292
second law, 1, 292, 301, 314-315, 554, 560-561, 670, 746-749
Eulerian momentum budget, 293
Lagrangian momentum budget, 292
in his own words, 292
Newtons per square meter, 7, 8
NEXRAD (weather surveillance radar WSR-88D), 243
locations, 272
nightime (nocturnal)
boundary layer (stable), 692
clouds visible during, 166
cooling, 690, 692-696
winds (katabatic; mountain; land-breeze), 649-657
nimbo prefix, 163
nimbostratus, 162-163
nimbus suffix, 163
NinJo, 772
NIST (National Institute of Standards and Technology), 51, 879
nitric acid, 190-192, 858
trihydrate (NAT) clouds, 166
nitrogen, 7
oxides (NOx), 7, 725, 796, 811-812
lightning produced, 567
nitrogen dioxide, NO2, 7, 725, 858
nitrous oxide, N2O, 7, 811
NOAA (National Oceanographic and Atmos. Admin.), 637
satellites, 229, 273
weather radio, 529, 638
noctilucent clouds, 166
nocturnal
boundary layer (stable), 692
jet, 311, 699-700
nodes of satellite orbits, 228-229
nomenclature (global), 330
nominal plume edge (depth), 730
non-equilibrium wind (at hurricane top), 618-619
nonhydrostatic, 316
global circulation components, 351
hurricane vertical motions, 622, 629
numerical weather prediction model, 747
nonlinear
dynamics
and chaos, 773-776
causing T-storm forecast difficulties, 527
forecast equations, 747, 773-776
feedback processes, 806
linear approximation to, 806
nonlocal
air-parcel movement, 497-499, 503-508, 557-558, 716
closure, 714, 716
conditional instability
for hurricanes, 609
for thunderstorms, 496-499, 503-508
flux, 716
stability, 138-139, 142-144
non-parametric statistics, 502
nonstationary flow, 669
nonturbulent (see laminar), 138, 140, 669-671, 688
nordic ski snow, 209
normal
climate, 818
curve (Gaussian), 729-730
mode initialization, 766
shock (1-D) from thunder, 572-574
storm motion, 516-518
normalized CAPE, 508
Normand's Rule, 96, 105-106, 500
North American geography, 431
North Atlantic oscillation (NAO), 430, 818-819, 824
north direction, 2-4, 30, 298-299, 330, 646-647, 797-802
North Pole, 4, 30, 298-299, 330, 646-647, 797-802
north-south (also see meridional), 4, 330
displacement of baroclinic wave, 371-376, 452-453
temperature gradient (see baroclinicity), 329, 334-336, 359, 749
Northern
annular mode (NAM), 824
Hemisphere, 4, 330
defined, 4
direction of geostrophic wind, 303, 314
sign of Coriolis force, 297-301
sign of centrifugal force, 296
Nova Scotia, 617
novice vs. expert, 72
nowcasting (short-range forecasting), 552, 768
ns (nimbostratus clouds), 168
NST, Newfoundland standard time, defined, 5
nuclear
bomb, 499, 548, 574, 880
energy, 54
winter, 151, 805
nucleation, 188
definition, 185
deposition, 194-195
freezing, 194-195
heterogeneous, 188-194
homogeneous, 188-194
ice crystals, 194-196
nuclei, 194-195
processes, 198-201
liquid droplets, 188-194
activated nuclei, 193
cloud condensation nuclei (CCN), 188
critical radius, 192
curvature and solute effects, 189-191
haze, 192
nuclei (see also cloud condensation nuclei, CCN), 188-195
number, 870
Ball ratio, 698
density of
CCN, 187
hydrometeors, 187
ice nuclei, 195-196
Froude number, 659, 667
hydrometers, 187
Mach, 571-576, 579, 674
prefixes, 870
Richardson, 141, 521, 709-710, 739
Rossby, 306, 313
scientific notation for, 870
swirl ratio, 592
value, 870
numerical
approximations to eqs. of motion, 749-750
instability, 759-761
model (see num. weather pred. model), 496, 751
parameterizations (numerics), 749-751
problems, explained, 21
solutions to atmospheric equations, 749
stability, 759-761
value, 870
numerical forecast models (see numerical weather prediction)
numerical weather prediction (NWP), 745-792
accuracy, 777
Amdahl's Law vs. NWP speed-up, 763
analysis/assimilation of data, 762, 765-767
verifying, 769
Arakawa grids A to E, 753
backward trajectory for semi-Lagrangian, 761
balanced mass and flow fields, 763-765
blowing up of solution, 757
boundary conditions, 756
ghost cell or halo grid points, 756
calculation of secondary variables, 771-772
calibrated probabilistic forecasts, 777
case study, 768-770
climate, 768, 815-816
climatology (as a skill reference), 780
computation rules, 756
confidence in the forecast, 776
coordinate systems, 746-748
eta, 746
hyrid, 746
polar stereographic, 747
sigma, 746
spherical, 747
terrain-following, 746, 753
corollaries, 756, 758
cost/loss decisions, 784-785
Courant number, 758
data assimilation and analysis, 765-767
design, 761
deterministic, 777
differencing schemes - spatial, 755
centered fourth order, 755
centered second order, 755
upwind first order, 755
differencing schemes - temporal, 757-758
Euler (first order), 757
leapfrog (second order), 757
Runge-Kutta (4th order), 757
discretization, 750
equations of motion, 758-759
domain, 750
dynamics, 749-750
economic value, 784-785
ensemble, 776
calibrated, 777
spread vs. skill, 777
equations of motion, 746-749
compressible, 747
diagnostic, 747
discritized, 758-759
non-hydrostatic, 747
primitive, 747
prognostic, 747
errors
bugs in the code, 759
dynamic instability, 759, 773-777
numerical, 759-761
numerical instability, 760-761
random, 777
round-off, 759
systematic, 770, 777
truncation, 754-755, 760
verification & error measures, 777-785
viruses, 759
file formats for output, 772
finite-difference equations, 754-759
applications to spatial gradients, 754-755
differencing schemes of various orders, 755
notation, 754
spatial differencing, 754-755
Taylor series, 754-755
time differencing, 757-758
truncation vs. order of terms, 754-755
first guess, 765-767
flops (floating point operations per second), 761
forecast quality, 780
accuracy vs. skill, 777
verification scores, 777-785
forecast refinement, 770-771
forecast stage of NWP, 768
GCMS (global climate models -or-), 768, 815-816
(general circulation models), 768
governing equations (see eqs of motion), 746-750
GPUs, 763
graphical outputs, 772
grid
A - E, Arakawa, 753
cells, 750
computation rules, 756
nested, 752
notation, 754
points, 749, 752-753, 761
resolution, 752
spacing, 761
staggered, 753
variable, 752
heirarchy of operational forecast models, 768
hindcasts, 762
history, early, 759
human contributions to the forecast, 772
initial conditions, 758, 762

N, O

sensitive dependence, 773-776
synoptic vs. asynoptic data, 758
initial value problem, 762
initialization of NWP models, 763
instabilities
dynamic, 773-777
numerical, 759-761
lead time, 762
limit of predictability, 773-776
Lipschitz condition/continuity, 761
long-range forecasts, 768
Lorenz, 773-776
map
factors, 747
output graphics, 772
projections, 748
medium-range forecasts, 768
meteograms, 745, 772
models, 496, 751
GEM (global environ. multiscale), 751
GFS (global forecast system), 751
heirarchy, 768
WRF (weather research & forecasting), 751
moisture, 746
Moores' Law vs. NWP skill, 752
MOS (model output statistics), 770-771
nests, one-way and two-way, 752
non-linear dynamics and chaos, 773-777
ensemble & probability forecasts, 776-777
Lorenz strange attractor, 773-775
predictability, 773
notation for grid points, 754
nowcasts, 768
numerical stability, 759-761
numerics, 749-750
operational short-range vs. GCMs, 816
output graphics
compression and storage into databases, 772
graphics, 772
parameterizations (numerics), 749-751
perfect prog method (PPM), 770
persistence skill, 780
physics, 749-751
subgrid-scale, 750
post-processing, 762, 770-772
predictability limit, 773-776
probabilistic, 777
calibrated, 777
verification, 782-784
process, 762-772
balanced mass and flow fields, 763-764
case study, 768-769
data assimilation and analysis, 764-767
forecast refinement, 770-771
forecasts, 768
post-processing, 770-772
quality
control of input data, 765
of forecast, 777-785
resolution, 750, 752, 761
vs. grid spacing, 761
scale vs. skill, 768
schedule, 762
scientific basis for, 746-751
seasonal forecasts, 768
semi-Lagrangian, 761
sensitive dependence to initial conditions, 773-776
short-range forecasts, 768
skill, 777-784
vs. forecast time, 775, 780
vs. scale, 768
solutions to atmospheric equations, 749
spatial gradients, approximations, 754-755
spread (of ensembles) vs. skill, 777
staggered grids, 753
statistics, 777-785
stencil, 756
strange attractors, 773-776
temperature, 746
temporal gradients, approximations, 757-758
thunderstorm sounding forecasts, 496
time steps, 750, 761
uncertainty in the forecast, 776
valid time, 762
verification statistics, 777-785
visualization programs, 772
winds, 746
numerics, in numerical weather prediction models, 749-750
NVA (negative vorticity advection), 447-448
NWP (see numerical weather prediction), 745-792

O

O2, oxygen, 7
O3, ozone, 7
oasis effect, 74
object immersed in a fluid, 135
objective analysis method, 280, 766-767
objective optimum interpolation analysis, 766
oblate
rain drop shape, 255-257
spheriod of revolution (Earth is), 3
obliquity, Earth axis tilt, 30, 879
variations and climate, 798-803
obscuration, weather map symbols, 276
obscured sky, 170, 279
observations
errors, 766, 875-877
locations worldwide, 271-273
reporting, 875
synoptic, 268
weather, 268-273
observers of atmospheric optics, 833-868
observing system simulation experiment (OSSE), 236
Obukhov length, L, 703
Occam, William of, 680
Occam's Razor, 680
occluded fronts, 413-414, 428-429
weather-map symbol for, 281, 399
occluding low, 428
at landfall in Pacific Northwest , 472
occlusion process, 428-429
ocean
aerosols and CCN over, 188
CO2
effervescence, 812
feedback process for climate, 810-812
continent circulations (monsoons), 333-334, 356
circulations, 804
meridional overturning, 810
thermohaline, 804
currents, 431, 610, 632-633, 701
Gulf Stream, 431
heat transport by, 339, 378
hurricane-induced, 610
Kuroshio, 431
wind-driven, 701
divergence of ocean water, 610
drag, 701
Ekman
spiral, 378
transport, 610
meridional overturning circulation, 810
methane hydrate release, 810
mixed layer, 610
storm surge, 632-635
surf, 635
thermocline, 610
thermohaline, 804
upwelling during hurricane, 610
waves during hurricane, 633-636
odor characteristics of airmasses, 391
ohm, unit of electrical resistance, 564-565, 870
oktas, 170, 279
Olympic Mountain convergence zone, 472
omega (vertical velocity in P coordinates), 451
equation, 456-459, 462
Q-vector, 462
Sutcliffe development theorem, 456
Trenberth, 456-458
shape of setting sun, 862
On Doing Science (see summary in Appendix A), 877
Be Creative, 288, 293
Be Meticulous, 20
Be Safe, 485, 517, 567, 570, 583-584
Cargo Cult Science, 167
Check for Errors, 16
Citizen Scientist, 738
Consequences, 218
Creativity in Engineering, 288
Data Misinterpretation, 729
Descartes and the Scientific Method, 2, 343
Ethics and Data Abuse, 826
Expert vs. Novice, 72
Give Credit, 24
Great Scientists Make Big Mistakes, 863
Have Passion, 877
Look for Patterns, 107-109
Mathematics & Math Clarity, 393, 762
Model Sensitivity, 350
Parameterization Rules, 715
Problem Solving, 869
Residuals, 340
Scientific Laws - The Myth, 38
Scientific Method, 2, 343
Scientific Revolutions, 773
Seek Solutions, 46
Simple is Best, 680
Toy Models, 330
Truth vs. Uncertainty, 470
U.S. Supreme Court Quotation, 470
one-layer atmosphere, 795
one-way nesting of NWP grids, 752
Oort minimum in solar activity, 803
opacus, 169
opaque
atmosphere, 220
surface, 42
open
cellular convective clouds, 167
channel hydraulics, 657-661
operational numerical weather forecast models (OFMs), 751
heirarchy, 758
opposite faces of ice crystal, 842
optical
depth, 43, 856
due to volcanic eruptions, 805, 858
hygrometer, 111
thickness, 43, 856
transient (lightning) detectors, satellite borne, 569
optically thick fog, 176-177
optics, atmospheric, 833-868
arcs, 847-855
diffraction & interference, 858-860
halos, 842-855
ice crystal, 396, 842-855
liquid droplets, 837-841
mirages, 861-863
scattering, 856-858
optimium
interpolation analysis, 766
wind-speed decrease in wind turbine, 647-648
orange color defined (also see optics chapter), 37
orbit
geostationary satellite, 227
planetary, 28, 293
polar orbiting satellite, 227-228
satellite, 227-229
orbital factors of Earth, 27-34
climate variability, 797-803, 829
daily effects, 32
Milankovitch theory, 797-803, 829
orbit of earth, 27
period of satellites, 227-229
seasonal effects, 30
sunrise, sunset, and twilight, 33
orbital period of planets, 27-28, 872
orbital plane, 30-31, 799-802
ordinate (defined; and use of pressure as), 3
organization of
clouds, 167
thunderstorms, 486-495
organized convection in tropical disturbance, 613
organizing knowledge, 72
orientation of falling ice crystals, 842, 855
origin of tornadic rotation, 586-587
orogenesis (mountain building), 804
orographic (related to mountains)
cloud, 165, 168, 676-677
high-pressure formation near, 391
lee-side cyclogenesis, 443-446
lift and cloud formation, 162
precipitation modifying airmasses, 398-399
thunderstorms, 487, 526, 547-548
winds, 649-654, 660-670, 675-676
oscillation(s), 136-137
amplitude, 818
climate, natural, 818-824
damped, 666
inertial, 304, 311-312, 700
period, 137, 304, 818
phase shift, 818
TRUE, 818
waves
mountain lee, 666-668
Rossby, 367-376
what is an oscillation, 818
out of phase light waves, causing interference, 858-861
outbreaks of tornadoes, 583-584
outer space, 234
outflow winds from thunderstorm, 483, 554, 560-563

outgoing
radiation, 337
radiation from opaque atmosphere, 220
radiative flux, 337
terrestrial radiation, 337
transmitted radiative flux, 220-223
outlier data points, 502
outlook forecasts of severe weather, 528-530
overcast (ovc) cloud cover, 170, 279
over-pressure from thunder shock front, 571-574
over-riding air at fronts, 407
overshooting top (of thunderstorm), 483, 498, 508
oxides of nitrogen (also see nitrogen oxides), 193
oxygen, O2, 7, 723
ozone, O3, 7, 193
air-quality standards for, 725
greenhouse gas, 811-812
lightning produced, 567
odor, 567
tropopause folds, injection at, 364

P

P (Newfoundland time zone) defined, 5
Pacific, 431
airmass modification, 398-399
data void, 287-288, 765
decadal oscillation (PDO), 818-820
high, 356
landfalling cyclones, 472
North American pattern (PNA), 824
Northwest
geography & topography, 661
weather, 288, 397-399, 472, 765
oscillations in climate, 818-824
time zone, defined, 5
tropical cyclones, 631
packing of
height contours, 290-291
isentropes & relationship to stability, 143
isobars, 290-291, 307
PAH (polycyclic aromatic hydrocarbons), 725
paleotemperature estimates, 795, 803
Pangea, Pangaea, Pangæa, 388, 804
pannus, 169
Papa, Station, 288
paradigm shift, 773, 863
paradox, geostrophic, 459, 462
parallel damage paths, 584
parallels, defined, 4, 330
parameterization, 715
and models, 751, 816
physical and numerical, 750-751
rules, 715
turbulence closure, 714-716
parameters, 646, 669, 715, 750
combined, 880
physical, 879-880
paranthelia, 854-855
parcel (see also air parcel), 57, 59
lapse rate (see also lapse rate), 59-64
method to determine stability, 138-139
vs. environment (on thermo diagram), 134
parhelia (sun dogs), 842, 850-851, 854-855
120°, 854-855
sub, 842, 851, 854-855
parhelic circle , 842, 844, 854-855
Parry
arcs, 854-855
oriented ice-crystal columns, 855
partial
absorption, 220-223
density, 91
pressure, 14, 87, 115
weather-map symbol for, 276
particles in air, 188, 725
particulate matter (air pollution)
fine (PM10), 725
very fine (PM2.5), 725
volcanic eruptions, from, 804-805
parts of wind: mean, waves, turbulence, 705
parts per billion (ppb), 724
parts per million (ppm), 724
pascals (Pa), unit of pressure and stress, 7, 8, 870
Pasquill-Gifford (PG) turbulence types, 727-728
pass, winds through mountain gap, 661-664
passat (trade) inversion, 351
passion, scientists should have, 877
passive
clouds, 163
microwave sensors of rain, 211
sensors, 219
tracers, 731
past weather, as plotted on weather maps, 275
patchy, weather-map symbol for, 276
path length, Beer's Law, 43
path of
radar beam, 243-245
Rossby wave, 368-374
patterns, 107
dominant pattern finding via PCA, 821-823
Pauling, Linus, 99
PCA (principal component analysis) method, 820-823
PDO (Pacific Decadal Oscillation), 818-820
PDT, Pacific daylight time, defined, 5, 6
peak current in lightning, 568-569
Peel, 817
Peirce's skill score, 781
pellets, ice (sleet), 199, 276
snow (graupel), 199, 276, 546
pendulum day, 304, 312
penetrative convection, 483, 498, 508
pennant wind-speed symbol on weather maps, 278
percentiles, 502
perfect prog method (PPM), 770-771
perihelion, Earth orbit
angle relative to vernal equinox, 34, 801
climatic variation, 799-801
Earth orbit, 28-30
period
earth and moon rotation, 879
of oscillation, 137, 818
of satellite orbits, 227-229
Quaternary, 799
perlucidus, 169
permafrost, 810
Permian-Triassic boundary, 805
permittivity of free space, 569
persistence forecast, 778
error, 778
skill, 780
personal errors, 875
perspiration, 76
Persson, Anders, 298
perturbation pressure, 340-341, 554, 559-563
peta (10^{15}), 870
Watt, 339
PG (Pasquill-Gifford) turbulence type, 728
phase
change, 56
condensation, 56
deposition, 56
fusion, 56
melting, 56
sublimation, 56
vaporization, 56
water, 54
diagram for
attractors and strange attractors, 774, 790
water, 198
shift, 250-251
in high-pressure regions, 390-391
of deterministic oscillations, 818
space, 774, 790
specific differential, 256-257
speed
of Rossby wave, 369
intrinsic, 369
relative to ground, 369-372
shallow-water, 633, 658
space plot ("butterfly"), 774-775
warm and cool (of ENSO and PDO), 818-820
phased-array radar, 257-258
phases of water, 198
phenomena, optical, 833-868
philosophers, 2
philosophy of science, 877
phloroglucinol, 195
photo-detector in dew-point hygrometer, 111
photoelectric effect, 46
photographic tips, clouds, 180, 484
photometer, 46
photons, 833
photoresistor, 46
photovoltaic cells (solar cells), 46
physical
meteorology, 1
parameterization (physics), 749-751
physics
atmospheric, 872
parameterizations in NWP models, 749-751
Newtonian, 1
phytoplankton, 188, 811
pi (π = 3.14159265358979323846264), 879
variant, 801
pico (10^{-12}), 870
pileus clouds, 165-166, 169, 483
pillar (sun, moon, Venus, street light), 843
pillow, snow, 210
PILOT code, 269, 272
MOBIL, 269
SHIP, 269
pilot balloons (PIBALs), 272, 322
pilots - weather issues, 165, 166
altimeter setting, 275
METAR weather reports, 268-279
pineapple express, 472, 824
piste, 209
pitfalls, scientific, 877
pitot tube, 321, 674
pitot-static pressure difference for air speed, 674
plagiarism, 24
Planck
constant, 879
curve, 36-39, 224
function, linear approximations to, 239
Planck's Law, 36-38, 221-224
constants, 879
plane angle, dimension and units, 870
planetary
boundary layer (see atmospheric boundary layer), 13
data, 22, 47
orbits, 27, 293, 874
scale, 315
general circulation, 329-388
shear, 368
vorticity, 363-364, 367-372, 447-449
wavelength, 329, 367-376, 427, 468
waves (also see Rossby waves), 367-376
definition, 367
highs associated with, 391
horizontal, midlatitude, 367-376
path taken, 372-374
phase speed, 369, 372
stationary (lee side), 443-444
typical wavelength, 367
planets in the solar system, data for, 22, 27, 874
plan-position indicator (PPI), 242
plant canopy, 677-678
plasma, 565
plateaus, 397
plates, ice crystal, 198-199, 842
optics caused by, 842-855
Platzman, George, 759
Pleistocene epoch, 799
plotting
by hand, 280-281
station model, 274-279
weather maps, 280-281
winds, 210-513
plume
average, 728
center of mass, 729
centerline, 723, 729, 736
centerline height, 723, 733-734, 736
concentration, crosswind-integrated, 737
coning, 727
convective, 724
definition, 724
dispersion, 723-744
edge, nominal, 730
fanning, 727
footprint, 734
Gaussian concentration distribution, 729-730
instantaneous (snapshot), 728
looping, 727
rise, 648-649, 723-724, 732-737
smoke, 723-744
spread, 723-744
thermal, 648-649, 654, 704, 724
urban, 679, 743
PM (particulate matter) air pollutants, 725
2.5 (very fine particulates, air pollution), 725
10 (fine particulates, air pollution), 725
PMC (polar mesospheric clouds), 166
POES satellites, 229
point source, 724
polar, 330
airmass code, 392
cell , 329, 332-333, 352, 357, 378
cloud heights, 163
coordinate, 2, 646
cyclones, 425
easterlies, 352
front, 352, 357, 367, 408

P

graph used as a hodograph, 510-513
heat deficit, 338-339
highs (anticyclones), 331, 352, 391
jet stream, 233, 331-332, 353, 357-360
low, 332
mesospheric clouds (PMC), 166
orbiting satellites, 227-229
regions, 330
stereographic map projection, 748
stratospheric clouds (PSC), 166
tropopause height, 163
upper-tropospheric low, 352
vortex, 352, 397, 824
polarity of lightning, 563-564
polarimetric radar, 241, 255-257
dual polarization, 255
polarization diversity, 255
polarization(s)
circular, 255
horizontal, 255-257
vertical, 255-257
polarized light, 856-857
polarizing sunglasses, or filters for cameras, 856
Poles (North & South), 4
poleward transport of heat and momentum, 374-376

police radar, 243
pollen characteristics of airmasses, 391
pollution/pollutants, 7, 725
air quality standards, 7, 725
airmass characteristics, 391
brown cloud, 857-858
concentration units, 724
ppmm, 724
ppmv, 724
µg/m3, 724
conservative, 731
conversion between units, 724
crosswind-integrated concentration, 735-737
dispersion, 723-744
factors, 724-725
forecast equations, 731-732
dispersion in neutral & stable boundary-layers, 732
Gaussian concentration distribution, 729-730
plume rise, 732
dispersion in unstable boundary layers, 735-737
concentration, 737
crosswind integrated concentration, 736
plume centerline, 736
relevant variables, 735-736
dispersion statistics, 728-730
center of mass, 729
Gaussian curve, 729-730
nominal plume edge, 730
snapshot vs. average, 728
standard deviation - sigma, 729-730
episodes, events, exceedences, 725
footprint, 733
framework: source-receptor, 724
Gaussian concentration distribution, 729-730
in highs and airmasses, 390, 691
in lows, 691
mixing ratio, 724
modeling, 725
passive, 731
point source, 724
smoke stack, 724
solution, 724
source
height, 723
receptor framework, 724
spread of pollutants, 729
stack height, 723
standards for air quality, 725
Taylor's statistical theory, 731-732
dispersion equation, 731-732
dispersion near and far from source, 732
passive conservative tracers, 731
trapping, 390
in valleys, 654
turbulence statistics, 726-728
Pasquill-Gifford (PG) turbulence types, 727-728
pool of cold air, 653
population vs.
air pollution, 723
hurricane disasters, 631
urban heat-island temperature excess, 679
portion
correct, 781
of forecasts corect, 781
positive
feedback, 807
polarity lightning, 563-564
vorticity advection (PVA), 447-448
post-processing of numerical forecast, 762, 770-772
postal abbreviations for US states & Canadian provinces, 431
potential
breakdown lightning, 566
difference, electrical, 564
energy, 150
associated with horizontal temperature gradient, 406
convective available (CAPE), 503-508, 530-531
of flow, 669-672
temperature, 61-64
constant (see adiabatic or isentropic), 61-64
definition, 61
diurnal evolution, 690-698
equivalent, 104-106, 500
in atmospheric boundary layer, 689-698
in buoyancy, 136
in vertical cross section of front, 403, 405, 407-409, 414
isentrope, 17-18, 63, 103-105, 122-123, 143-144, 156, 365, 373, 403, 407-410, 414, 437, 624-625
liquid water, 103-106, 500
maps of constant, 437, 443
mixed layer, 689-698
on weather maps, 437-438, 441
profile in boundary layer, 110, 690, 692, 695-698
substitute for advection, 67
thermo diagram, 135-136
vertical profile, 135-136, 689-698
virtual, 61-62
vs. height, 61-63, 104-106
wet-bulb, 103-106, 500
vorticity, 363-364
conservation of, 363-365, 397, 445
isentropic, 364-365
units (PVU) definition and maps of, 364, 437, 441
pounds-force per square inch, pressure units, 7
powder snow, 209
power
curve for wind turbines, 648
dimension of, 870
electrical by wind turbines, 647-648
electricity, 564
flashes, 584
lines, electrical surges caused by lightning, 569-570
of hurricanes, 620, 625
of lightning electricity, 569
output curve for wind turbines, 647-648
relationships on log-log graphs, 874
surge by lightning, 569-570
units, 870
PPI radar scans, 242
ppm (parts per million), 724
(perfect prog method), 770
praecipitatio, 169
Prandtl mixing length theory, 715
precession of
Earth's orbit, 28, 798-803
aphelion, 800
axial, 800
climate, 801
equinox, 800-801
satellite orbits around Earth, 229
precipitable water , 98-99, 501, 546
on weather maps, 501
precipitating clouds, 163
precipitation, 185-218
accumulation
isohyet, 18
weather-map symbols for, 278
amount, 18, 107-108
annual distribution worldwide, 209
characteristics, 207-210
cloudless ice
cold-cloud process, 201-202, 206
distribution worldwide, 209
drag, 555
efficiency of thunderstorms, 547
extreme, 207-208, 545-548
fog, 173
formation, 205-207
growth, 202-207
hail, 548-554
heavy rain, 207-208, 545-548
ice, from arctic airmasses, 396
in water budget, 107-108, 746
intensity, 208
laden air, unsaturated, 555
likelihood or probability (POP), 782-784
loading of air, 555, 559
measurement, 210-211
METAR code, 208
midlatitude cyclones, associated with, 425-428, 435, 438, 466, 472
on thermo diagrams, 121, 130-131
orographic, 398-399, 676-677
parameterization in NWP models, 751
radar, 486
rate, 107-108, 207-208
as affects cyclone evolution, 465-467
and latent heating of an air column, 465-467
snow fall, 131
symbols on weather maps, 208, 275-276
terminal velocity, 202-204
thunderstorm, 206-207, 482, 486, 545-548
intensity forecasting using n-CAPE, 508
time for start or end, weather map symbols, 278
unknown type (weather-map symbol for), 276
visibility within, 208-209
vs. evaporation, 210
warm-cloud processes, 204-206
water equivalent, 208
WBF process, 201-202
weather-map symbols, 275-276
zonal average, 210
precision and random errors, 875-877
predictability
limit, 773
nonlinear dynamics & chaos, 773-776
predicting (see forecasting;
or numerical weather prediction), 745-792
predictands, 770
predictors, 770
prefix component of scientific notation, 870
prefrontal
jet, 407, 433, 472
pineapple express, 472
waves, 656
present
climate, 816-817
weather, as plotted on weather maps, 275-276
pressure, 8-10,
background state, 316
change with height, 8-9, 316
monotonic, 9
weather-map symbols for, 277-278
charts, 436-442
constant, 17, 55-56, 290, 439-441
cooker, 115
coordinates, 290-291, 451
couplets, non-hydrostatic, 340-341
deepening, 463
deficit in tornado, 577
definition, 7, 870
difference, as indicates mass of air, 10
dimension of, 870
distribution in hurricane, 626
driving the global circulation, 340-342
dynamic, 559, 672-674
errors, 766
evolution, for MSL, 467
falls, 463
field, 343, 359
filling, 463
free stream, 672-674
forecast equation for, at MSL, 463-467
global patterns, 331, 350-355
gradient, 295-296
horizontal, 295-296, 559-561
gradient force, 295-296, 301
cross-mountain, 662
horizontal, for anabatic flow, 650-652
near center of pressure region, 306-307
on isobaric surfaces, 296
related to packing of isobars, 303
sign convention, 295-296
winds driven by, 302
vertical, 15-16, 18, 315-317, 554
head, 632
height
as vertical axis on graphs, 9-10,
increments, 103
tendency, 463
high (anticyclone), 354-355, 390-391
meso-, 554, 559-563
hurricane, 621-623, 626, 633

hydrostatic balance, 15-16, 316, 340, 622
hypsometric equation, 16-17
in eye of hurricane, 618-620, 622, 624, 626, 629, 632-633
instruments for measuring, 19
isallobar, 18
isobar, isobaric, 18
isotropic nature, 8
latent heating causing falls of, 466-467
lightning, 564
maps on surfaces of constant, 436-442
mass of air above, 10, 464-466
mean background state, 316
meso-high, 554, 559-563
mesoscale variations in thunderstorms, 488-489, 554-563
METAR, 270
non-hydrostatic couplets, 340-341, 622
observation errors, 267, 766
omega, 451
on weather maps, 275
partial, 87
perturbation
buoyancy force, 555
downburst and gustfront, 554, 559-563
profile in the vertical, 8-9, 340-342
reduction to sea level, 267
reversal in hurricane, 618-623
rises, 463
scale height, 8
sea level, 7
reduction method, 267
sensors, 19
shock front, 571-574
stagnation, 672-674
standard, 7
STP, 7, 107, 880
static, 7, 559, 672-674
tendency
cyclogenesis, 463-467
forecast equation for, 463-467
isallobar, 18
net, 466-467
rainfall-rate relationships for, 465-467
weather-map symbols for, 277-278
tendency equation, 463-467
thermo diagram, 63, 100, 103-106, 119-131, 151-158
thunder, 571-574
tiling method for CAPE, 505
tornado, core, 577-578
trough, 367-376, 399, 432-433, 443
units, 7, 870
vapor, 87
saturation, 87-90
vertical gradient, 8, 9
in hurricane, 622
pre-storm environments, 496-527
prevailing visibility (in METAR), 270
primary rainbow , 838-840
prime meridian, 4, 5, 28
primed variables, 368-376, 705-716, 726-729
primitive equations of motion (see also equations), 747
vs. quasi-geostrophic equations, 449
principal component
analysis (PCA) method, 820-823
of Pacific Decadal and Arctic Oscillations, 819-820, 824
Principle, Le Chatelier's, 132, 141, 329
principles of radiation, 36
prism
face, 842
shaped ice crystals, 199, 842
probabilistic forecasts, 777
calibrated, 777
cumulative, 777
verification, 782-784
probability
forecasts of hurricane threat, 638
of detection, 781
wind speed, 645-646
vs. relative frequency, 645
problem-solving methods, 72, 869
forward, 236
inverse, 236-239
process(es)
adiabatic, 17, 60
causing saturation, 159-161
cold cloud, 201, 205-206
cooling, 44-45, 59-76, 129-133, 393-397, 693, 793-797
diabatic, 61, 411, 465, 624, 648-657
isobaric, 17, 55
isohume, 100-101
isothermal, 100
lapse rate, 59
names, 17
nucleation of ice crystals, 194
saturation causing, 159-161
terminology, 17
thermo diagrams, 100-101
warm cloud, 204-205
WBF (Wegener-Bergeron-Findeisen), 201
profile, vertical
of pressure, 8, 9
profilers
computer code, 763
wind, 112
prognostic equations (also see numerical weather fcst), 747
projections
map, 748
vector or info, 239
propagation
anomalous, 244
equation for radar beam, 244
of cold fronts (using Q-vectors), 470-471
of errors through equations, 876-877
of radar beam path, 243-245
of radiaion, 36
of thunderstorms, 485, 561
propellor anemometer, 321
prop-vane anemometer (propellor), 321
provinces in Canada, 431
proximity symbols on weather maps, 276
proxy measures of climate information, 803
pseudoadiabatic diagrams, 121-123, 126-127, 153
PSI, pounds-force per square inch, pressure unit, 7
PST, Pacific standard time, defined, 5
psychrometer, 111
aspirated, 94, 111
sling, 94, 111
psychrometric
constant, 75, 108, 880
graphs, 95
tables, 95-96
publish or perish, 863
Puget Sound convergence zone, 472
pulse
duration & length, radar, 240
repetition frequency (PRF) of radar, 240
thunderstorm, 486
pumping, boundary layer, 319-320
PVA (positive vorticity advection), 447-448
PVU (potential vorticity units), 364
tropopause identification, 364
example on weather map, 364, 441
pyramid
face, 842
ice-crystal optics/halos, 847
pyranometer, 45-47, 219
pyrgeometer, 46-47
pyrheliometer, 46-47

Q

Q time zone (Atlantic), defined, 5
Q-vectors, 460-462, 469-471
cold-front propagation, 470-471
convergence, 460-462, 469-471
cyclone propagation, 469-470
frontal intensification & propagation, 469-471
omega equation, 462
vertical velocity & cyclogenesis, 460-462
weather maps, case study cyclone, 461-462
quadrants of jet streak, 454-456
quality-control, 765
quality of
air, 725
forecasts, 777-786
life, 723
quantiles, 502
quartiles and interquartile range, 502
quasi-
biennial oscillation (QBO), 824
decadal oscillation (QDO), 824
quasi-geostrophic, 449
approximation, 449-451
vorticity, 449-451
equation for, 449
Laplacian form, 450
quaternary
period, 799
rainbow, 840

R

r (correlation coefficient), 779
R time zone (Eastern), defined, 5
radar , 219, 240-260
antenna, 250
AVCS display, 242
bands (electromagnetic), 223, 242
beam, 240
propagation equation, 244
propagation paths, 243-245
width, 240
bounded weak echo region (BWER), 552-553
bright band, 248
C band, 242
CAPPI display, 242
defined, 219
difficulties, 254
Doppler, 241, 249-254, 493, 556, 560
downburst observations, 560
ducting and trapping, 244-245
echo intensity, 240
inside thunderstorms, 486, 560
isoecho, 18
weather maps, 438
echo-free vault, 552-553
energy
attenuation, 241
scattered (reflected) back, 240-241
equation, 245-246
derivation of, 245
false echo, 251
fundamentals, 240-244
gust front observations, 560
hail observations, 247-248, 552-553
hook echo, 494
humidity measurement using, 112
hurricane images, 604-605
image interpretation, 253-254
insect returns, 248-249, 560
klystron tubes, 240
laser (lidar), 112
loop, 241
magnetron tubes, 240
max unambiguous range (MUR), 240-241, 251
max unambiguous velocity , 250-251
NEXRAD WSR-88D radar (in USA), 240-243
plan-position indicator (PPI), 242
phased array, 257
polarimetric, 241, 255-256
power, 240, 245
precipitation observation, 211
pulse
duration, 240
length, 240
repetition frequency (PRF), 240, 250
radome, 253
rainfall rate measurement, 211, 247, 257
range
height indicator (RHI), 242
measurement, 240-241
reflectivity (the name for scattered energy), 245-248
equation for, 245-246
factor, 245-246
isoecho, 18
returns, 240
S band, 242
sample volume, 240
scans, 241-242
shadows, 241
spectrum width, 254
standard refraction of beam, 244
thunderstorm images & diagrams, 482-483, 486-488, 490-493, 532, 560
right- and left-moving supercells, 519
tornado vortex signature (TVS), 251, 253
volume scans, 241, 249-254, 493
wind profilers, 257
WSR-88D weather surveillance radar, 240-243
Z-R relationships, 247
radial
component, 249
distance, 240-241, 296-301, 304-314, 319, 362-371, 453, 511-513, 560-562, 571-574, 577-578, 617-618, 622-623, 626-630, 837-855, 861
radar-, 242, 249
shear, 362-364
velocity, 249-254, 310, 318, 321, 560-562, 572-574, 627-628
wind in hurricane, 627-628

R

wind speed, 18
isodop, 18
radian, unit of plane angle, 870, 880
radiance
blackbody, 221-226
from atmospheric layers, 224-225
locations of satellite observations, 273
radiant energy (see also radiation)
radiant exitance (emittance), 36
radiation, radiative, 27-52
absorption in clouds, 131-132
airmass genesis, role in, 393-397
average annual, 336-337
average daily insolation, 40-41, 336
balance, 43
of the whole Earth, 793-797
blackbody, 36, 794
budget, 42
global, 793-797
surface, 44
climate-change issues, 806-815
cloud processes, 131-132
constants in Plancks's law, 36, 221, 879
cooling / heating, 131
front strengthening, 411
of hurricane top, 624-625
of well-mixed fog, 175-177
daisyworld, 813-815
differential heating, 329, 334-339
distribution, 39
downwelling, 43-44
Earth-atmosphere system, 793-797
effect on circulation, 377
emission
emissivity, 36
temperature, effective, 794
equilibrium of whole Earth-atmosphere system, 793-797
exitance, 36
flux
gradient, 71
net at surface, 45, 74, 336-339, 528, 693-694, 793-797, 801-803, 807-815
fog, 173-177
forcings, 329, 334-339
by latitude belt, 338-339
climate-change, 793-815
incoming solar (insolation), 336-337
net, 337-338
outgoing terrestrial, 337
zonally integrated, 338-339
frontal effects, 411
global
albedo, 793
climate equilibrium, 794, 806-815
forcings, 329, 334-339, 793-797
heating, 70, 687
incoming, 793, 797
infrared (longwave), 27, 37
insolation, 40-41, 336-337, 797, 801-802
instruments for measuring, 45-47
inverse square law, 39-41, 245-246, 801
irradiance, 36
longwave (or terrestrial or IR), 37, 131, 793-794
net, at surface, 27, 797
outgoing, 794
parameterizations in NWP models, 751
principles, 36-45
absorption, reflection & transmission, 36
average daily insolation, 40
Beer's Law, 43
blackbody emission, 36-38
distribution, 39-40
emission definition, 36-37
emission temperature of Earth, 37
emissivity (IR) table, 42
propagation, 36
Stefan-Boltzmann Law, 37
transmittance windows, 43
Wien's Law, 37
rain drop growth affected by, 206
sensors, 45-47
solar (shortwave), 37, 793
constant (total solar irradiance), 793
up/downwelling, 44, 131-132
terrestrial (longwave or IR), 37
thermo diagram process, 131-132
warming of air, 71-73, 795-797
windows, 43, 220-223, 796, 811
radiative transfer equation, 224-225, 237-238
forward problem, 236
inverse problem, 236-239
radiatus, 169
radio
acoustic sounding system, 78, 266, 272
detection and ranging (radar), 219
NOAA weather, 529, 638
severe weather reporting, 529-532
radioactive decay, 364
radioactivity characteristics of airmasses, 391
radiometers, 45-47
satellite borne, 220
radionuclide injection at tropopause folds, 364
radiosondes (also see rawinsonde), 111, 134, 143, 291
radius
critical, 192
deformation, Rossby
external, 405-406
internal, 319-320, 344
droplet, 187, 202-204
Earth, 879
earth orbit, 879
equivalent, droplet, 203
hydrometeor, 187
of curvature, 445
of light rays in mirages, 861-863
in jet stream, 367-373
lee cyclogenesis, 445
of planets in the solar system, 22
radix layer, 700-705
radome, 253
RADOB code, 269
RADOF code, 269
RADREP code, 269
rain (also see precipitation), 185-218, 482-484
accumulation, storm total, 257
weather map symbols for, 278
acid, 742
bands
at warm fronts, 401
in tropical depressions & hurricanes, 604-605, 613-615
clouds
cumuliform, 162-163
stratiform, 164
drop
shape, 203, 545-546
size distribution, 207
velocity, 203
evaporating (virga), 482-484
gauges, 98, 210-211, 219
heavy, 207-208, 545-548, 637
hurricane, 604-605, 607, 637
in tropics, 209
leaving an air parcel, 130-131
mid-latitude thunderstorm, 206
orographic (upslope), 472
scattered showers, 545-546
shadow, 397, 472
thunderstorm, 545-548
weather map symbols, 275-276
rainbow(s), 837-841
5th order, 840
Alexander's dark band, 841
colors, 839-840
luminous meteors, 205
moon bows, 841
optics, 837-841
orientation, 837
primary, 839-840
quaternary, 840
red bows, 841
reflection, 841
renaissance, 841
sea-spray, 841
secondary, 840-841
supernumerary, 838, 860-861
tertiary, 840
thunderstorm conditions for, 545-546
twinned, 841
raindrop (see also drop, or precipitation)
drizzle, 546
growth processes, 205-207
optics, 837-841, 856-861
shapes, 255, 545-546
terminal fall speeds, 203
typical sizes, 185, 545-546, 857-861
from stratiform clouds, 546
from thunderstorms, 545
rainfall , 99
accumulations, storm total, 257
categories, 247
coverage, 545-546
distribution worldwide, 209
intensity, 207-208, 247
levels, 247
likelihood, 782-784
radar observations, 245-257
rate, 72, 108, 207-208, 545-548
and cyclogenesis, 465-467
and latent heating, 72, 465
definition, 208
polarimetric radar estimates of, 257
radar Z-R estimates of, 247
records, 208, 545-548
storm-total accumulations, 257
thunderstorm, 482
raining cats and dogs, frogs, fish, nuts, animals, etc., 206
rain-free cloud base, 483
random
errors and precision, 777, 875-877
number generator, 184
range
factor in the radar equation, 245-246
-height indicator (RHI), 242
mountain, 397
radar, 240-241
ranked data, 502
Rankine combined vortex (RCV) for tornadoes, 577-578, 599
RAOBs= Radiosonde Observations (see rawinsonde), 272
rapid
changes in weather due to short waves, 370
cyclogenesis, 426
baroclinicity, 426
conditions needed, 426
static stability, 426
flow classification, 659
RASS (Radio acoustic sounding systems), 78, 266, 272
rate
of buoyant production/consumption of TKE, 709
of molecular diffusion, 196-202
of earth's rotation, 227, 297-299
of growth of mixed layer, 697-698
rated wind speed for turbines, 648
ratio
Bowen, 74-76
of gas constants, 91, 880
raw data, 765
rawinsonde (radiosonde) , 134, 272
balloon, 322, 496
code for reporting (TEMP), 269-271
data, 134
frontal structure using, 403
mandatory levels, 134, 772
significant levels, 134, 147
sites for launching, 271
ray
curved, in air, 575-576, 861
equations for air, ice, and water optics, 833-868
geometry, 833-837
critical angle, 837
for halos (ice crystals), 842-855
for rainbows (liquid water drops), 837-841
Huygens' Principle, 837, 859
reflection, 833-837
refraction, 833-837
Snell's law, 834-837
light, 833-868
path, 833-861
equation for sound refraction, 575-576
equation for light refraction, 861
sound, 575-576
Rayleigh scattering
haze, 856-858
of microwaves from radar, 245
of light, 857
blue sky and red sunsets, 857
Rayleigh, Lord, 863
read, how to
METARs and SPECIs weather reports, 270-279
weather maps, 274-279
rear-flank downdraft (RFD), 482-483, 492-495
rear inflow jet (RIJ), 488-491
reasoning, inductive and deductive, 107-109
recency symbols on weather maps, 276
receptor, pollutant, 724
record rainfall rates, 208, 545-548, 637
rectangular (Cartesian) coordinate system, 2
recursive techniques, 103, 771
red
bows, 841
color defined (also see optics chapter), 37, 834
Deer, Alberta, 553

giant star, 803
glow sunsets, 805, 858
sky, 858
sprite, 563, 568
sun, 858
sunsets, 857-858
reduced gravity, 135-136, 316, 658
in Bernoulli's equation, 670
reduction
data (also see statistical methods), 823
method to sea-level pressure, 267
reference
height for surface wind measurement, 701
state, 316
Earth climate/radiative equilibrium, 794, 807-808
feedback-processes, 806-807
vapor pressure, 88, 880
reflected pollutants, 734
reflecting telescope, 293, 862
reflection
definition, 833
from ice crystals, 842-844
from water, 838-839
of radiation, 41, 219, 833-844
rainbows, 841
reflectivity, 41-42
albedo, 42, 793-794
differential, 256
equation for radar, 245-246
factor for radar, Z, 245-248
for water, 838
radar (the name for scattered energy), 240-241
table of,, 42
unit factor for radar, 245-246
refract
radar beam, 244-245
refraction, 833-855
atmospheric, 861-863
light, 33, 833
components in 3-D, 836
refractive index, 834-835
for radar, 243-244
Snell's Law, 575-576, 834-837
sound waves, 575-576
standard (for radar beams), 244
sub-, 244-245
sunrise & sunset effects, 33, 862
super-, 244-245
refractive index, 834-835, 861
light, through air, ice, and water, 834-835, 861, 880
magnitude of radar targets, 245-246
radar, 243-244
sound, 575-576
varying with air density, 243-244, 575-576, 861
refractivity, radar, 243-244
refractometer, microwave, 111
regression, linear, 770
relationships and graphs, 873
linear, 873
logarithmic, 873-874
power, 874
relative
circulation, 366
frequency of wind speeds, 645-646
helicity, 588-591
humidity, 92
definition, 92
equation, 92
in clouds, 189
measurement of, 76-79, 111
reduction of, in WBF, 201-202
saturation, 92
supersaturation, 186
thermo diagram, 133-134
maxima and minima, 138-139
operating characteristic (ROC) curve, 783-784
vorticity, 320-321, 362-363
geostrophic, 319
sign convention, 320, 362
south /north side changes, 446
tornadic, 586-591
typical order of magnitude, 362
variation with distance in planetary wave, 368
winds, 584
reliable, 782
reliability, 782-783
diagram, 782-783
relative, 783
remote sensors, 134, 219-266
on ground, 240-260
radar (see radar), 240-260
satellites (see satellites), 219-239
renaissance and rainbows, 841
Rene Descartes, 2, 841
repeatable errors, 875
replacement cycle for hurricane eyewalls, 605
reporting observations, 875
reports, weather, 267-273
of storm damage, 532
research aircraft, 135
reservoirs of momentum, 375
residence times of air in airmasses, 392-397
residual layer (RL), 692-696
drylines, relationship to, 416-417
temperature, 416-417
residuals, finding unknowns as, 340
resistant statistics, 502
resistance, electrical, 564
resistivity, 565
resolution
coarse, 752, 815
fine, 752
frequency-distribution, 646
numerical weather prediction, 750, 752, 761, 816
subgrid scale (unresolved), 750, 816
vs. grid spacing, 761, 816
resolving the geostrophic paradox, 459, 462
resonating air in lee wave, 667
response, feedback, 806-810
ice-albedo, 808-810
negative (damped), 807
no-feedback, 807, 809
positive (amplified), 807-809
runaway, 807
restoring force, 136-137, 367-374
retired hurricane names, 615
retrieval of soundings by satellite, 235-239
corollaries 1, 2, 3, 235, 236, 239
return
flow
antimountain, 653
antivalley, 654
sea-breeze, 654-655
periods of disasters vs. intensity, 547, 646
stroke(s) of lightning, 567, 569
returned energy from radar, 245-246
returning airmass code, 392
returns from radar, 240
reverse flow in cavity, 667
reversible process, 121
revolutions, scientific, 773
Reynolds stress, 701, 712-713
vs. turbulent momentum flux, 712-713
Reynolds, Osborne, 701
RFD (rear-flank downdraft), 482-483
RHI radar scan, 242
ribbon lightning, 568
Richardson number
bulk, 141, 710
dynamic stability, 141-142
shear, 522, 530-531
thunderstorm, 521, 530-531
critical, 142, 880
flux, 709-710
gradient, 710
Richardson, Lewis Fry, 708, 759, 762, 764
ridges (see also midlatitude), 332
axis symbols on weather maps, 281, 367, 391, 399
formation and characteristics, 367-376, 391
highs, relationship to, 390
in Easterly waves, 611-612
in Rossby waves, 353, 367-376
right
hand rule for ageostrophic wind direction, 455
moving supercells, 518-520
quadrant of
hurricane, 627
jet streak, 454-456
RIJ (rear inflow jet), 488-491
riming of ice crystals, 199, 202, 546
rings of light in the sky (see optics), 833-868
rising
air parcels, 129
motion in cyclones (lows), 356
pressure in cyclones, 463
symbol on weather map, 278
risk of severe weather (convective outlook), 528-530

roads, as threat during storm chasing, 517
mirages on, 862
robust statistics, 502
ROC curve and diagram, 783-784
skill score, 784
rocketsonde, 134
Rocky Mountains, chinook winds, 676-677
ROCOB code, 269
SHIP, 269
ROFOR code, 269
roll vortices, horizontal, 167
root-mean-square (RMS) error, 778-779
of 50 kPa geopotential heights, 778
rope shaped tornado, 577, 583
rosette shaped ice crystals, 199
Rossby
deformation radius, 344
and geostrophic adjustment, 344
external radius of deformation, 405-406, 665
internal radius of deformation, 319-320, 344, 665
use in baroclinic waves, 372-373
ise in coastal jets, 664-665
number, 306
curvature, 306
defined, 313
frontogenesis issues, 411
vs. geostrophy, 306
wave(s) (also called planetary waves), 332, 353, 367-376
characteristics, 373-374
definition, 367
forecasts, 370
heat transport, 339, 374-375, 378
highs associated with, 391
instability, 367-376
momentum transport, 375-376
size (wavelength; wavenumber), 367, 369
stationary (lee side), 443-444
Rossby, Carl-Gustav, 399, 749, 759
rotating
planet; boundary layer growth on, 689
storms (also see vortices)
cyclones, extratropical lows, 425-480
hurricanes, typhoons, tropical cyclones, 603-644
mesocyclones (thunderstorms), 492-495, 587-592
tornadoes, 577-592
rotation
angular momentum, 360-361, 617
forces, 296-299
hurricane, 617-619, 626-629
lines in spectra, 221
rate of Earth, 297, 879
changes of, 376
solid body, 363, 577
supercell thunderstorms, 483, 586-587
tornadic origin of, 586-587
wind-vector, in sea breeze, 656-657
rotational invariance, 320
rotation-angle of Earth, 229, 268-299
rotor circulations, 165, 667
rotor clouds, 165, 667
roughness length, 677, 700-702
Davenport-Wieringa classification, 700
round-off error, 759
rule(s) for
determining static stability, 138, 688-689
determining unstable regions, 138
drawing isopleths on weather maps, 280-281
runaway feedback, 807
Runge-Kutta method, 757
running average, 599
runway
direction, 646-647
visual range (RVR), 270
change criterion for SPECI, 270
in METAR, 270

S

S band radar, 242
S time zone (Central & Mexico), defined, 5
safe room (above-ground tornado shelter), 529
safety
hurricane, 638-639
index, livestock weather, 117
lightning, 567-571
when storm chasing, 485, 517, 567, 570, 583-584
Saffir, Herbert, 607
Saffir-Simpson hurricane wind scale, 605-607
Sagan, Carl, 415, 869
sails on frigate, 635
salt, 188, 190-192
sample volume, radar, 240
sand, 170

S

lithometeors, 205
storm (haboob), 562
weather-map symbols for, 275-276
San Francisco (advection) fog, 173-175
SAR (synthetic aperture radar), 230
SARAD code, 269
SAREP code, 269
satellites, 219-239
channels, 222-223, 230-233
geostationary (GOES), 227
humidity observation from, 112
hurricane tracking, 637
image interpretation, 231-235
imager, 230-235
locations of weather observations from, 272-273
loop (of images), 227
low-light-level cameras, 569
observed Total Solar Irradiance, 39
observations of hurricanes, 603-605, 608, 614, 616, 620
optical transient detectors, 569
orbits, 227-229
photos of Earth, 228, 232-233
polar orbiting (POES), 228-229
radiative transfer, concepts for, 220-226
remote sensing from, 219
retrievals, 235-239
difficulties, 239
sensors, 273
sounder, 235-239
sounding pre-thunderstorm, 496
triangulation, 291
types, 227-229
SATEM code, 269, 273
SATOB code, 269, 272-273
SATRAD observation locations, 273
saturated (see also moist)
adiabat on thermo diagrams, 119-158
adiabatic lapse rate, 101-106
plot using spreadsheet, 103
for determining static stability, 139-141
air, 87-98
air parcels, 130
absolutely unstable, 140
neutral stability, 140
saturation (see also equilibrium), 87-90
absolute humidity, 91
humidity, 87-96
vs. air temperature, 88, 92, 100
in clouds, 159-161
level (also see Lifting Condensation Level), 93-94, 130
mixing ratio, 91-92
processes causing, 159-161
cooling, 159
moisture addition, 160
mixing, 160-161
relative humidity, 92
specific humidity, 91
vapor pressure, 87-90
ice vs. water, 88, 201-202
savings time, daylight, 5, 6
sawtooth shape of Rossby waves, 374-376
Sawyer-Eliassen circulation, 412, 415
SB-CAPE, 503-505
sc (stratocumulus clouds), 168
scalar equation, 293
scale
analysis, 623
height
for density, 10
for pressure, 8
length
buoyancy, 733
dissipation, 709
momentum, 733
velocity
buoyancy, 68-69, 109, 703-704
mechanical turbulence, 701-703
scales of motion, 315
vs. forecast skill, 768
scan strategies and angles for radar, 241-242
scattered
cloud cover, 170, 279
light, 33, 219-222, 856-858
rain showers, 545-546
scattering, 856-858
backward, forward, 219, 857-858
blue sky, 857
by aerosols, 221, 805, 857-858
from volcanic SO2 in stratosphere, 805, 858
by air molecules, 220-222, 857
directional variation (forward vs. backward), 219, 857
geometric, 857
Mie, 858
of energy from radar, 240-241
of radiation, 219-222, 856-858
of visible light, 856-858
optical depth/thickness, 805, 856
polarization, 856
Rayleigh, 857
transmitted light, 856
twilight, 857-858
types, 856-858
visibility, 856-858
vs. wavelength, 857-858
white clouds, 857
scatterometer sensors on satellites, 230
locations of observations, 272
schedule, forecast, 762
Scheiner, Christopher, 855
Scheiner's 28° halo, 855
Schwarzchild's equation for radiative transfer, 224-225
Science Graffito and Graffiti, scattered in most chapters
anonymous, 16, 31
science
atmospheric, 205, 877
fundamentals, 869-878
high-risk, high-gain, 863
on doing, 877
philosophies, 877
scientific
basis for numerical weather forecasts, 746-751
laws (see Laws)
method, 2, 26, 343, 680
mistakes & pitfalls, 863, 877
notation for numbers or values, 870
paradigm shifts, 863
paradox, 293
philosophies, 167, 293, 680, 877
problem solving methods, 72
revolutions, 26, 773, 863
thought, expert vs. novice, 72
tools, 877
scientists, 877
mistakes made by great scientists, 863
passion, 877
responsibilities as a citizen, 738
young, 293
score, forecast skill, 777-785
scour of beaches by ocean waves, 634-635
screen, Stevenson, 115
scrolls on ice crystal plates, 199
sct (scattered) cloud cover, 170
scud (cumulus fractus), 483
weather-map symbol for, 277
sea breeze, 654-657
front, 655-656
radar observations of, 249
thunderstorms triggered by, 525, 654-655
head, 655
high-pressure associated with, 391, 654-655
sea-level
density, 10
pressure
change, as plotted on weather maps, 277-278
cyclone-intensity measure, 426, 463-467
in various units, 7
mean, 267
METAR, 270
on weather maps, 275, 434
reduction methods, 267
tendency, 277-278, 463-467
rise due to hurricane, 632-634
temperature (average), 7
sea-spray rainbow, 841
sea surface temperature (SST), 608-609, 616
climate variations, 818
role of cold temperatures in hurricane death, 616
warm anomaly, 818
ENSO, 818-820
PDO, 818-820
sea water density, 880
season(s)
Earth, 30, 797-802, 879
hurricane, 630
seasonal
averages (months used for), 330, 333
differences in atmospheric boundary layer, 695-696
forecast models, 768
heating cycle, 30-33, 40-41, 332-333, 354-358
seasonality of hurricanes, 630
second, 870
secondary
circulation (Sawyer-Eliassen) at fronts, 412
associated with jet streaks, 455-456
fields, 772
rainbow, 838, 840-841
variables in NWP, 771-772
wavelets, 859
sector plate ice crystals, 198-199
seeding of clouds, 195-196, 218, 553-554
self development of cyclones, 468-471
semi-
Lagrangian method of NWP, 761
log graph, 873-874
major axis of Earth's orbit, 28, 800-802
precession, 800
minor axis of Earth's orbit, 28
transparent (=translucent), 42, 169, 220
Seneca, 523
sense (direction) of circulation, 456, 377-378
sensible heat (enthalpy), 58, 671
flux at the surface, 73-76
sensitive dependence to initial conditions, 773-776
sensitivity, 350, 810
climate, 810, 812
definition, 350, 810
factor, 812
magnitudes, 812
studies, 350
sensors (see weather instruments)
in situ (direct)
definition, 219
list of, 219
remote, 219-266
definition, 219
radar, 240-260
satellites, 220-239
separation of variables, 89
sequestered carbon dioxide (CO2), 812
set of data, reporting, 875
setting sun, shape of, 862
severe
hail, 548
thunderstorm
definition, 528
environment, 496
intensity forecasting, 501, 507, 516, 521-522, 524, 530-531
probabilistic forecasts, 529
watches and warnings, 528-530
weather
forecasting & risks, 528-530
Storm Prediction Center (SPC), 532
SWEAT index, 531
SFAZI code, 269
SFAZU code, 269
sferics, 568
SFLOC code, 269
shadows
aircraft, glory optical phenomena around, 860
radar, 241
rain, 397, 472
shaft
hail-, 553
work, 672
shallow, weather-map symbol for, 276
shallow water wave speed, 633
shapes of
clouds, 171
tornadoes, 577
shear (also see wind shear), 509-522
bulk Richardson number, 522, 530-531
components, 509
direction, 509
frontal, 407-412
frontogenesis, 407-412
generation of TKE, 708-710, 727
geostrophic wind, caused by thermal wind, 345-349
hodograph usage to determine, 509-522
isoshear, 18
local (single layer), 514
magnitude, 509, 515-516
mean vector, 514
production of turbulence, 704, 710
single-layer, 514
speed, 509-510
surrogate using wind difference, 509
total magnitude, 515-516
turbulence production, 704, 710
units, 509

vorticity, 362
wind, 706
radar observations of, 254
hurricane environment, 610
thunderstorm environment, 496, 509-522
shearing deformation, 320-321
sheath ice crystals, 198-199
sheet lightning, 567
sheets of clouds, 168
shelf clouds, 562
shield of stratiform clouds, 425-428
from hurricanes, 604
from thunderstorm MCS, 488
shifting winds, 349, 400-401
shimmering mirages, 862
SHIP
code, 269, 271
parameter, 530-531
shock
front, from lightning, 571-574
1-D normal, 572
wave, 571-574
short
gap winds, 661-662
range weather forecast models, 768
scale number prefixes (for USA), 870
waves (see also planetary waves), 369-370, 372
short-wave
radiation (see also radiation, solar), 37, 220, 793
Rossby, 369-370
transmitted, 805
shoulder region of window, 220-223
Showalter stability index (SSI), 531
showers, symbols on weather maps, 275-276
SI (Système Internationale) - international system of units, 8, 870
Siberian
high, 354-356
traps, 805
sidereal (relative to the stars)
day, 227, 297
Earth year period, 29
moon orbital period, 27
sigma (s)
coordinates, 746
model, 746
plume spread standard deviation, 729
velocity standard deviation, 727
sign
coefficient (centrifugal force), 296
positive or negative, in scientific notation, 870
signals, 219-220
signal strength from radar, 245-246
signature
damage to crops and forests, 593
horizontal divergence (downburst outflow), 253, 561
tornado vortex (TVS), 253
significant
hail, 548
parameter (SHIP), 530-531, 551-552
levels, 134-135, 147
tornadoes, 501, 507, 516, 522, 530-531, 580
parameter (STP), 530-531, 592
silicon window on IR radiometers, 45
silver iodide, 195-196, 553-554
similarity theory, 699-704
simple is best (Occam's razor), 680
simplified (toy) models, 330
of global circulation, 330-334
of hurricanes, 626-629
Simpson, Robert, 607
sine law of radiation, 40
single-cell thunderstorms, 486
single-layer shear, 514
sink, level of free (LFS), 557
sinking, 135
sirens, civil-defense, 529
sizes of
clouds, 170
hydrometeors, 187
skc (sky clear), 170
skeletal shaped ice crystals, 199
skew-T log -P diagram, 121-158
components, 124
creation of , 124-125
skewness factor, 125
ski runs, 209
skill
climatology, 780
forecast (NWP), 752, 777-785
persistence, 780
scores, 777-785
vs. forecast time, 775, 780
vs. scale of event, 768
vs. spread of ensemble forecasts, 777
skin of air parcel, 57
sky
color, 857-858
cover, 170
weather-map symbols for, 279
transmissivity, net, 44
slab model, 697-698
slalom ski snow, 209
slanting data, 826
sleet (ice pellets), 199, 276
slight thunderstorm risk, 530
sling psychrometer, 94
slope
definition, 396
on log-log graph, 215
flows (anabatic, katabatic), 649-653
force of katabatic winds, 396, 651-653
of storm surge, 633
statistical calculation, 770
SLP, sea-level pressure, units, 7
small
disturbance errors, 875
nuclei, 188
smog (see also pollution), 193
brown cloud, 857-858
smoke, 170
concentration distribution, 734, 737
dispersion, 710, 723-744
lithometeors, 205
plumes, 710, 724
edge, 730
footprint, 733
stack, 723-724
clouds, 166
weather-map symbol for, 276
smoothing data, 826
smoothness, Lipschitz, 761
snapshot of smoke plume, 728
Snell, Willebrod van Royen, 841
Snell's Law
for light, 834-837
3-D, 836
for sound, 575
Snelling, 765
snow
accumulation and liq. water equivalent, 107, 208-209
banner cloud, 165
capped mountains, viewed from satellite, 234
characteristics, 209
condensation onto, 110
dendrites, 198-199
density, 209
depth sensor, 210
eater, 676
formation in cold clouds, 201-202
grain classification, 199, 209
weather-map symbols for, 276
melting into rain, 206
optics (ice-crystal optics), 163, 842-855
pellets (graupel), 199, 546
weather-map symbols for, 276
pillow, 210
powder, 209
shapes, 198-199
strength, 209
swath on the ground, 163
symbols on weather maps, 208, 275-279
thunder-, 207
snowball Earth, 811
snowfall rates, 208-209
snowflakes as aggregates of many crystals, 200
SO (Southern Oscillation), 818-819, 824
social aspects of hurricane hazards , 631
sodar, 219
sodium chloride (salt), 190-192
SOI (Southern Oscillation Index), 818-819, 824
solar
activity variations, 803
azimuth angle, 33
blackbody radiation emitted, 37, 39
cells (photovoltaics), 46
constant (total solar irradiance), 39, 793-794, 879
kinematic, 879
variations, 803
declination angle, 30-31, 802
downwelling radiation, 793
elevation angle, 32
vs. latitude, 40, 334
emission of radiation, 37-39
forcing ratio, 813-815
heating and cloud formation, 162
incoming radiation, 39, 334-337, 793, 797, 801-802
input, net, 795
insolation, 40, 336, 793, 797, 801-802
irradiance, 37-39, 793-794, 879
luminosity parameter, 813-815
net input to Earth, 795
output variations, 803
radiation, 37-39, 220
astronomical influences, 797-803
driving the global circulation, 329, 334-339
transmitted, 805
radiative forcing, 40
radius, 33
tides, 376
total solar irradiance (TSI), 39, 793-794, 803, 879
upwelling radiation, 44-47, 220-226, 230-239, 797
variability, 39
wind, 376
zenith angle, 33
Solberg, H., 399
solenoid
on weather maps, giving max advection, 458
term, in the circulation equation, 366
solid
angle, dimension and units, 870
body rotation
in tornado core, 577-578
quasi-geostrophic vorticity, 449
relative vorticity, 363
solitary wave (bore), 656
solstice, summer and winter, 30-31, 801, 879
solute, 190-192
solute effect, 189-193
solution to pollution, 724
solutions
in water droplets, 190
to atmospheric equations, 749
solving problems, 72, 869
sonde (instrument to make soundings), 134
dropsonde, 134
radiosonde, 134
rawinsonde, 134
rocketsonde, 134
weather balloon, 134
sonic
anemometer, 321
thermometer, 78
soot, 151
sound
rays in air, 575-576
refraction of, 575-576
speed/velocity, 572, 575-576, 674, 880
supersonic thunder shock wave, 571-574
waves, 571, 575-576
transition from shock waves, 571
sounder
channels on satellites, 222-223, 226, 235
operation on satellites, 235-239
soundings, 119
environmental, 59, 134
locations worldwide, 271
mandatory levels, 134, 772
methods, 134-135, 496
pre-thunderstorm, 496-499, 503-508
retrieval by satellite, 235-239
significant levels, 134, 147
to determine boundary layer depth, 143
to determine CAPE, 503-508
to determine clouds, 162-164
to determine tropopause height, 143, 496
source
height of pollutant emissions, 723
latitudes for angular momentum, 361, 375
location for parcels, 360-361, 711
of pollution, 724
of turbulence, 69-71, 138-142, 666-668, 705-715
of weather data, 271-273
point, 724
receptor framework, 724
south direction (opposite north), 2
South Pole, 4
Southern
annular mode (SAM), 824
Hemisphere, 4
defined, 4
global circulation, 332, 339, 343, 350-358
midlatitude cyclones (lows), 426, 430-432
sign of Coriolis force, 297, 301
sign of centrifugal force, 296
oscillation index (SOI), 818-819, 824
SO2, sulfur dioxide, 7, 725, 804, 858

S

space
  dust, 376
  outer, satellite images of, 234
Space Science and Engineering Center (SSEC), 232
spatial
  distribution of pressure /temperature, 280, 343, 359
  gradients; finite-difference approximations, 754-755
SPCLI code, 269
special crystal orientations, 855
species of clouds, 168
SPECI code (special meteor. aviation report), 269-271, 275-279
  criteria that trigger issuance of, 270
specific
  differential phase, 256
  heat
    air, 53, 55-56, 58, 880
    at constant pressure, Cp, 53-56, 880
    at constant volume, Cv, 55, 880
    of humid air, 56
    of liquid water, 54, 56, 880
    of water vapor, 880
    ratio, 880
  humidity, 91
    saturation value of, 91
  volume, 11, 121
    isostere, 18
  work, 121
spectral
  absorption, 222-223
    hygrometer, 111
    lines, 221
  dispersion, 834
  radiance constants, 221, 879
  transmittance, 222-223
spectrometer, 46-47
spectrum
  electromagnetic, 220-223
  light (colors), 37, 222, 834-835, 862
  width, 254
speed (see also velocity)
  airspeed, indicated with pitot-static system, 674
  constant (isotach), 18
  equation, 2-3, 314-315, 746
  difference in jet stream, 450-453
  group, 658
  of dry line movement, 417
  of electromagnetic radiation, 243
  of light, 36, 240, 243, 834-837, 879
  of rain drops (see terminal velocity), 202-204
  of sea-breeze front, 655-656
  of sound, 572, 575-576, 674, 880
  of wind, 2, 3, 302-314
    around highs and lows, 307
    Beaufort scale, 635-636
    in hurricanes, 605-607, 626-629
    in tornadoes, 577-580
    total (rotation + translation), 578, 627-628
  phase, 369-370, 658
  shear (shear magnitude), 509-510
  updraft, 649
  wave, 658
spheres, layers in atmosphere (e.g., troposphere), 12-13, 563
  electrosphere and ionosphere, 565
spherical
  coordinates, 747
  cow, 330
spider lightning, 567
spin (see vorticity), 320-321
spin down
  of cyclone, 429
  of Earth, 376
  of global circulation, 388
spin-up
  rate of cyclones, 446-451, 617
  of global circulation, 388
  of hurricanes, 617
  of tornadoes, 586-587
  of vorticity, 446-451, 586-587
spinning forces, 296-299
spiral
  bands in tropical depressions & hurricanes, 604-605, 613-615
  Ekman (in ocean), 378
  pattern (waterspout evolution), 582
spissatus/spi, 168
Spörer minimum in solar activity, 803
spotters, storm, 529
spray, 170, 276
  ring (waterspout evolution), 582
spread
  parameter, Weibull distribution, 646
    interquartile range (IQR), 502
  smoke plume, 729-730
  temperature-dew-point, 92
  vs. skill, 777
spreadsheet
  programs and samples, 20-21
  thermodynamics, 63, 103
  thermo diagrams, 63, 100, 103, 125
Spring (vernal) equinox, 30-31, 801
sprite, red, 563, 568
squall, weather-map symbol for, 276
squall line of thunderstorms, 488, 490-491
  predicting, by using total shear magnitude, 516
  radar image of, 243
  tornadoes (landspouts) from, 582
  weather-map symbols for, 281
SRH (storm relative helicity), 530-531, 588-592
SSM/I (Special Sensor Microwave Imager), 230, 273

SST (sea surface temperature), 608-610, 616
st (stratus clouds), 168
stability, 119-158
  absolute, 140
  airmass, 391-396
  cloud type vs., 161-164
  conditionally unstable, 140
  cyclogenesis, impact of stability on, 426
  dry absolutely unstable, 140
  dry neutral, 140
  dynamic, 141-142
  flow, 138-142
  in stratosphere, 143-144
  in troposphere, 143-144, 688-690
  indices for thunderstorm & tornado forecasting, 530-531
  neutral, 138-140
  nonlocally unstable, 138-139
  numerical, 759-761
  Paquill-Gifford classification, 727-728
  rules for determining, 138-141
  saturated absolutely unstable, 140
  saturated neutral, 140
  smoke dispersion, vs., 732-737
  static, 138-141
  turbulence determination, 142
  unstable, 138
stable
  absolutely, 140
  air, 138-142
  boundary layer (SBL), 692, 696
    cold airmass genesis, 393
    depth, 696
    e-folding height, 696
    smoke plume rise within, 733
    strength, 696
    temperature, 692-696
    turbulence, 707-710
    velocity standard deviations, 707
  Brunt-Väisälä frequency, 136-137
  definition, in flow stability, 138
  equilibrium of droplets, 191
  regions, 138-140
  surface-layer wind, 702-703
stably-stratified
  flow, 657-661, 688-689
  turbulence related to PG types, 710
staccato lightning, 568
stack height, smoke emission, 723
stacking of pressure characteristics
  hurricane, warm core, 622
  low-pressure, role in cyclolysis, 432-433
stages of evolution of
  thunderstorm cells, 485
  tornadoes, 583
staggered arrangement of grid points, 753
  Arakawa grids, 753
stagnation
  events for air pollution, 741
  point, 672
  pressure, 673
  streamline, 672-675
standard
  atmosphere, 11-13, 688-690
    definition, 11-13
    density, 10-13
    in thermo diagram, 135, 688-690
    lapse rate, 11-13, 70, 688-690
    static stability, 688-690
    temperature, 11-13, 688
  deviation, 706-707, 727, 875-877
    of pollutant location, 729-730
    of wind components, 706-708, 727
    propagation in equations, 876-877
    variation with height, 707
  isobaric surfaces (upper air), 772
  pressure, 7, 107, 880
    levels (mandatory), 772
  refraction of radar beam, 244-245
  scientific notation, 870
  STP, 7, 107, 880
  temperature, 7, 107, 880
  time, 5
  uncertainty, 875
standardized wave shape for lightning surge, 569-570
standards, air-quality, 725
standing lenticular clouds, 165, 666-668, 684-685
  optical phenomena caused by, 859-860
start shaped ice crystals, 199
star(s)
  red giant, 803
  visible at night, 33
  white dwarf, 803
state
  equation of, defined, 14-15
  of air, 2
  of parcel, 128
  thermodynamic, defined, 2, 6
  on a thermo diagram, 100, 128
  USA, in, 431
static
  AM radio, 568
  definition, 16
  electricity, 564
  hydrostatic, 15-16, 340, 651, 747
  instabilities and circulations, 132
    cumulus cloud formation, 162
  -pitot system for air speed, 674
  pressure, 7, 672-674
  stability, 138-141, 687-689
    airmass, 391-396
    air parcel method, 138-139, 687-688
    apex method for determining, 138-139
    atmospheric boundary layer, 687-689
    cloud formation within, 162-163
    estimation, 728-729
    forced vs. free convection, 710
    frontal, 414
    layer method for determining, 140-141
    misinterpretation, 729
    neutral, 139-140, 688-689, 710
    nonlocal, 138-139
    parcel method for determining, 138-139
    rules for determining, 138-139, 688-689
    smoke dispersion in, 710, 723-744
    stable, 136-137, 139-140, 688-689, 710
    thunderstorm, 496-499, 503-508
    unstable, 138-139, 688-689, 710
  temperature, 672-674
statically stable air, 136-140
  clouds that form in, 163, 165
  mirages in, 861-863
statically unstable air, 128-142
  clouds that form in, 161-162, 164
  mirages in, 861-863
  smoke plume dispersion in, 735-737
station
  ID or weather station code (ICAO), 270
  Papa, 288
  plot model on weather maps, 274-279
stationary
  environment, 688
  flow, 669
    turbulence, 708
  front(s), 404
    weather-map symbols for, 281, 399
  mountain waves & lenticular clouds, 666-668
  planetary waves (& lee cyclogenesis), 443-444
    north-south amplitude & wavelength, 444
statistical methods
  adaptive, 771
  average (mean), 502, 705, 726, 875
    running, 599
  bell curve, 729-730
  biases (mean, systematic errors), 770, 778
  binary event verification, 780-782
  box-and-whisker diagram, 538
  calibrated ensemble forecasts, 777
  categorical event verification, 780-782
  central-limit theorem, 184
  correlation coefficient, 711, 779
    anomaly, 779-780
  cost function, 766-767

covariance, 711, 821-822
matrix, 822
cumulative probability threshold, 777
data reduction, 502
dice, 184
discriminator of thunderstorm intensity, 507
eigenvalues and eigenvectors, 822
empirical orthogonal function (EOF) analysis, 820-823
error, 778, 875-877
propagation, 876-877
forecasts, 816
Gaussian distribution, 184, 729-730, 875
intercept, 770
interquartile range (IQR), 502
Kalman filtering & gain, 770
least squared error, 770
linear regression, 770
matrix, 822
mean (average), 502, 726, 875
absolute error (MAE), 778
error (ME), 778, 875
squared error (MSE), 778
squared error skill score (MSESS), 778
median, 502
method of moments, 730
model output statistics, 770-771
updateable, 771
normal distribution, 729-730
outliers, 502
percentiles, quartiles, 502
predictands and predictors, 770
perfect prog method (PPM), 770-771
principal component analysis (PCA) methods, 820-823
probabilistic forecasts, 777
propagation of errors, 876-877
random number generator, 184
rank, 502
recursive, 771
regression, 770
root mean square error (RMSE), 778
running average, 599
slope, 770
standard
deviation, 502, 706-708, 727, 875-877
uncertainty, 875
thunderstorm & tornado likelihood, 501-502, 507, 516, 522, 538, 588-592
trace of matrix, 822
variance, 706-708, 727, 821
verification of weather forecasts, 777-785
statistical theory (Taylor's) for pollutant dispersion, 731-732
statistics
dispersion, pollutant, 728-730
non-parametric, 502
resistant & robust, 502
turbulence, 706-708, 726-728
verification of forecasts, 777-785
vs. life, 726
Steadman, R.G. Heat Index, 77, 117
steady pressure symbol on weather map, 278
steady state
atmosphere (radiative equilibrium), 795
definition, 302
flow, 669
radiation balance of Earth system, 794
winds, 302-314
in ABL, 699
steam
engines, 89
fog, 173
steering winds
hurricanes, 607-608
thunderstorm (normal storm motion), 487, 516-518
Stefan-Boltzmann
constant, 37, 337, 879
law, 37-39, 337, 794
stellar shaped ice crystals, 199
stencil, 757-758
stepped leader, 566
steps for problem solving, 869
steradian, unit of solid angle, 221-224, 870
stereographic map projections, 748
Stevenson screen, 115
Stewart, George R., 775
Stokes Drag Law, 202-203
Stokes, George, 759
Stone, Alex, 315
storm (also see thunderstorms, cyclones or hurricanes)
case-study of extratropical cyclone, 433-466
cells, 485
chasing, 484, 532
core punching, 583
safety, 485, 517, 567, 570, 583-584
convective (see Thunderstorms), 496-499
damage scales (tornado), 579-580
data for case-study cyclone, 434-435
downslope wind, 667, 675-677
dust, 562
evolution, 484-485
hazards, for thunderstorms, 545-602
hail, 548-554
helicity, 587-592
hurricanes, 603-644
intensity forecasting (indices for), 530-531, 588-592
lghtning, 563-571
motion/movement of thunderstorms, 483, 488, 510
normal, 516-518
left- and right-moving, 518-520
winds relative to, 584-585
movement of hurricanes, 615
Prediction Center (SPC), 532, 580
pre-storm environment, 496-499
radar identification and observations of, 248
relative
effective helicity (eSRH), 590
helicity (SRH), 530-531, 588-592
winds, 584-585
reports, 532
rotation, origin of, 586-587
sand (haboob), 562
spotters, 529
strength, indices for forecasting, 530-531
surge, 615, 632-634, 669
heights, 633
supercell, 483, 492-495
system, 426
thunderstorms, 481-602
total rainfall accumulations, 257
track
hurricanes, 607-608, 615
extratropical cyclones (Lows), 429-431
thunderstorms and tornadoes, 483, 516-520, 584, 593
tropical, 614-615, 635-636
typhoons, 603-644
weather-map symbols for, 276, 426, 614-615
winds (Beaufort scale), 635-636
downslope, 667, 675-677
stormy-weather heat flux, 70-71
STP, standard temperature & pressure, 7, 107, 880
straight-line winds (also see derecho), 489, 491, 494, 554, 560-563
downburst generated, 554-563
radar observations of, 253, 560-561
strange attractors , 773-776
stratified
air layers at night, 653
fogs, 176-177
system, 657-661
stratiform/stratiformis (advective) clouds, 94, 162-164, 168
clouds in thunderstorm MCS, 488
drizzle from, 546
formed at frontal boundaries, 160, 425-428
radiative effects in, 132, 160
shield at warm fronts, 425-426
stratocumulus, 161, 164
stratopause, 12-13
stratosphere, 12-13, 143
isentropic potential vorticity in, 415
pressure gradient in, 359
temperature reversal in, 359
tight packing of isentropes, 143, 414
winds in, 359
stratospheric
aerosols, 804-805, 858
air, 414-415
clouds, 166
ozone, 364
destruction, 724
stratus, 162-163
in satellite images, 234
streaklines, 668-669
streaks
hail, 552
jet, 454
role in upward motion & cyclogenesis, 454-456
streamer (lightning), 566
streamlines, 611-612, 668-675
stagnation, 672-674
streamwise vorticity, 518, 587-592
streets
clouds, 167
urban, 678-679
strength of
fronts, 408-412
stable boundary layer, 696
stress, 700-702, 712-715
dimension of, 870
kinematic, 701, 712-713
Reynolds, 701, 712-713
vs. momentum flux, 712-713
units, 870
stretching
deformation, 320-321
in typical weather patterns, 447-451
self-development of cyclones, 468-471
term in vertical vorticity eqn, 447-451, 586-587
striations, cloud, 483
strokes, lightning, 567-568
structure of
atmosphere, 11-13
boundary layer, 13, 692
hurricanes, 604
Stull, Roland - about the author, XIV
Stüve diagrams, 121-158
subadiabatic
lapse rate, 140
region, 144
subanthelic arc, 855
subcategories of clouds, 168-169
subcircumzenith arc, 855
subcritical flow, 659
subgeostrophic wind, 304, 455, 699-700
subgrid scale, 750, 816
subhelic arc, 854-855
subhorizon halos, 855
subjective (hand) analysis of weather maps, 279-281
sublimation, latent heat of, 56
subparhelia (subsun dogs), 842, 851, 854-855
subparhelic circle, 855
subpolar
lows, 331
zone, 330
subranges of turbulence, 315, 708
subrefraction of radar beam, 244-245
subsidence
air pollution episodes and exceedences, 691
around clouds including thunderstorms, 161, 545-546
at top of atmospheric bounary layer, 691
by Ekman or boundary layer pumping, 319-320
in anticyclones (highs), 356, 390-396, 691
in Hadley cell, 351
in hurricanes, 629
in troposphere of high, 390
on weather maps, 433, 437, 448, 451, 471
estimated from convergence/diverg., 441, 449, 452, 455-456, 461-462
radar estimates of, 252-253
trapping of air pollutants, 691
subsun , 842, 844, 854-855
subsun dog, 842, 851, 854-855
subsurface heat and water parameterizations for NWP, 751
subtropical, 330
deserts, 351
highs (anticyclones), 331, 351, 391
jet, 233, 331-332, 350-351, 357-361
angular momentum, 360-361
latitude dependence on Earth rotation, 351
zone, 330
suction vortices, 593
sulfates, 188, 811, 858
sulfur dioxide, SO2, 7, 725, 858
aerosols and emissions from volcanoes, 804-805, 858
stratospheric, 804-805, 858
sulfuric acid, 188, 190-192
sultriness, 77
summer, 330
atmospheric boundary layer, 695-696
simmer index, 117
solstice, 30, 801-802, 879
year without (1816), 805
sun (also see solar)
apparent
rise and setting times, 33, 861-862
shape during rise and set, 862
azimuth angle, 33

S, T

blackbody radiation emitted, 37, 39
blue, 858
crimson, 858
distance to earth, 30, 802, 879
aphelion, average, and perihelion, 879
dog, 842, 850-851, 854-855
sub, 842, 851, 854-855
elevation angle, 32
emission of radiation, 37-39
evolution: red-giant start; white dwarf star, 803
green flash, 862
halos around, 842-855
optical phenomena around, 163
output variations, 803
pillar, 842-843, 854-855
radius angle as viewed from Earth, 33
red, 858
shape when rising or setting, 862
subsun, 842, 844, 854-855
synchronous orbit, 227-229
younger, 803
zenith angle, 33
sundial time, 34
sunlight, 131-132
sunrise
apparent & geometric, 33-34, 861-862
time, 33-34
sunset
apparent & geometric, 33-34, 861-862
blue color, 858
red color, 858
time, 33-34
sunshine, constant (isohel), 18
and cloud formation, 162
sunspot
activity or cycle, 39, 803
number, 803
superadiabatic lapse rate, 139-140
supercell
thunderstorm, 482-484, 492-495
classic (CL), 492-494, 549, 553
composite parameter (SCP), 530-531, 592
high-precipitation (HP), 495
hybrid, 492
indices for forecasting, 530-531, 588-592
intensity forecasting, 501, 507, 516, 521-522, 524, 530-531
likelihood, 516, 530-531
low-precipitation (LP), 495
motion, 518-520
normal storm motion, 516-518
right- and left-moving, 518-520
rotation (as a mesocyclone), 586-592
tornadoes, 577, 582, 588-592
supercontinents (Pangea, Gondwana, Laurasia), 804
supercooled liquid water, 88, 98, 186, 194-195, 201-202
glaciation of, 554
lightning creating, role in, 564-566
supercritical flow, 659
supergeostrophic wind, 304, 311, 455, 699-700
supergradient wind, 643
superior
airmass code, 392
mirages, 862-863
supernumerary bows, 838, 860-861
superposition of light rays, 845
superrefraction of radar beam, 244-245
supersaturated, 88
air, 88
supersaturation, 185-187
activating nuclei, 195
available, 187
background, 197
critical, 192
droplet growth rate, 190-192
fraction, 186, 196-197
gradient, 196-197
percentage, 186, 196-197
reduction of, in WBF, 201-202
water availability to make droplets, 186-187
supersonic
flight, 88
shock waves in thunder, 571-574
supplementary cloud features, 168-169
suppression of hail, 553
supralateral arc, 854-855
surf, 635
surface (also see near-surface)
albedo feedback (snow & ice cover), 810-812
based CAPE, 503-506
budget of radiation, 44-45, 797
drag, 300-301, 319, 447-448, 625, 632-634, 700-701
emissivity, 42
energy budget, global, 797
fluxes, 67-69
front, 399-412
attributes, 399
glyphs (lines) on weather maps, 399
horizontal structure, 400-402
vertical structure, 403-407
heat budget, 73-76, 797
Bowen ratio, 74-76
daily variation of, 74
units, 74
heat flux
airmass modification by, 397-398
bulk transfer relationships, 397-398
calm days, 68
effective turbulent, 68
measurement, 75
isobaric, 290-291
latent heat flux, 108
layer, 308, 692, 700
depth, 308, 692
log wind profiles, 702-705
neutral, 702
stable, 702-703
temperature profile, 692-694
turbulence, 705, 709
unstable, 703-705
winds, 692, 700-705
moisture flux, 108-111
observations, 270-271
automatic (ASOS and AWOS), 271
parameterizations in NWP models, 750
radiation budget, 44-45
longwave (IR), 45
net radiation, 45, 797
solar, 44
roughness, 677-678, 700-703
sensible heat flux, 73-76, 797
skin temperature, 67-68
solar radiation, 44
temperature
gradients, 66-75, 872
max, for thunderstorms, 506, 523
tension of pure water, 189, 215, 880
weather maps, 435, 437-438, 466
waves (in open channel hydraulics), 658-661
winds, 701
wind-waves, 634-636
surfaces of constant
height above ground (= 0 for surface maps), 437
height above mean sea level (= 0 at MSL), 436
potential temperature, 437
potential vorticity, 437
pressure, 436
thickness, 436
surge(s)
power, due to lightning, 569-570
probabilities, 569
storm, due to hurricanes, 632-634
surplus radiation, 338
surrogate vertical velocity, for mass budget, 463-464
Sutcliffe development theorem (for cyclogenesis), 456
Sverdrup, H.U., 399
swamp coolers, 116
swaths of hail or snow, 163, 548, 552
sweat, 93
index (severe weather threat), 531
swell, 635
swirl ratio, 530-531, 592-593
switching axes of graphs, 3
symbols and notation, 481
for ice crystals, 199
for fronts, 399
for weather maps, 168-170, 208, 274-279, 614-615
SYNOP code, 269, 271
MOBIL, 269
synoptic
definition, 268, 274
observations, 268-273
meteorology, 353, 444
scale, 315, 444
cross-mountain pressure gradient, 661-664
divergence, 393-396
vorticity needed for hurricanes, 610
weather, 274, 444
times for NWP forecasts, 758
weather maps, 274-281, 444
synopticians, 444
synoptics, the field of, 444
synthesis
PCA reconstruction of data, 823
questions at end of each chapter, explained, 25
synthetic aperture radar (SAR), 230
Syracuse, 150
systematic errors (biases), 770, 777, 875

T

T time zone (Mountain), defined, 5
T-phi thermo diagram (tephigram), 122
table-driven code formats (TDCF), 268
TAF (terminal aerodrome forecast) code, 269
tail
beaver, 483
cloud, 483
winds, aircraft, 563
tailored weather forecasts, 772
Talmud, 523
Tambora, Mt., 805
tangent arcs, 851-855
lower, 851-8532, 854-855
upper, 842, 851-852-854-855
tangential
component, 249, 304-312, 320-321, 362-364, 577-581, 626-627
velocity
hurricane model, 626-627
hurricane winds, 622-623
of earth, 298-299, 360-361
tornado, 577-580
winds near surface, 622-623
winds varying with altitude, 618-623
Tarantian age, 799
tax, 711
Taylor, G.I., 731
Taylor series, 754-755
finite differencing schemes, 754-755
truncation order, 754-755
Taylor's hypothesis, 731
Taylor's statistical theory for pollutant dispersion, 731
TCU (see towering cumulus, or cumulus congestus), 161-162, 165-166, 168, 482-485, 582
tectonic influences on climate, 804-805
teleconnections, 832
telescope, reflecting, 293, 862
TEMP code, 269, 271
DROP, 269
MOBIL, 269
SHIP, 269
temperature, 6-7, 54, 870
absolute, 7
absolute virtual, 14-15
absolute zero, 7
advection, 65-67
in grid cells, 750, 754-761
role in self development of cyclones, 468-469
airmass, 391-397
apparent, 76-78
brightness, 211, 221-224
Celsius, Centegrade, defined, 7
change with height, 11-13, 129-144
city (urban heat island), 678-679
climate, radiative balance, 794-797
constant (isotherm), 18
contrasts between land and water, 356
convective condensation , 526-527
conversion formulae , 7
correction for dynamic warming, 673-674
definition, 6-7
dew-point, 92-93
isodrosotherm, 18
distribution over hurricane depth, 621-625, 629
dynamic, 672-674
Earth effective radiative, 794, 879
equivalent potential, 104-106
errors, 766
evolution, 72-73, 746
excess in cities, vs. population, 649
Fahrenheit, defined, 7
field, 280, 343, 359
forecast equations, 746
frost-point, 92
global warming, 796
gradient
derivation of equation, 336
equator to pole, 336
horizontal; meridional, 335
in troposphere, 335-336
near the ground, 335-336
heat index, 77-78, 117

humidex, 77-78, 117
humidity index, 77-78, 117
hurricane model, 621-622, 629
ice-albedo feedback, 808-812
instruments, 78-79
correction for dynamic warming, 673
inversion, 139, 144, 687-691
isotherm, isothermal, 18
Kelvin, defined, 7
lapse rate, 59-60
latitude variation of, 335
layers of atmosphere, 12
lightning, of, 563
liquid-water potential, 104, 500
max surface, for thunderstorms, 506, 523
measurement, 78-79
correction for dynamic warming, 673
meridional gradient, 335-336
METAR, 270
mixed layer, 692-698
modification in airmasses, 397-399
molecular velocity, 6
of planets in the solar system, 22
potential, 61-64, 500
profile, 3
evolution of boundary layer, 694-696
hypothetical, 3
vs. geopotential height, 11-12
radiative
emission, effective, 794
equilibrium, 794-797
reversal in stratosphere, 359
sea-level, 7
sensible energy, 54
sensors, 78-79
sounding locations from satellite, 273
stable boundary layer, 696
standard, 7
STP, 7, 107, 880
static, 672-674
stratospheric, 359
surface, 12, 794-797
tendency, 64, 72, 746
thermo diagram, 119-158
threshold for ice nucleation, 195
units, defined, 7, 870
urban-rural difference, 679
variation of saturation humidity, 88-90
virtual, 14-15
constant, 880
virtual potential, 61-62
vs. height, 11-12, 127-145
near surface, 335
weather maps, 274-275, 438-440
wet-bulb, 94-96, 500
wind chill, 76-77
zonally averaged, 335-336
temperature influence on albedo (modeled), 808
temperature-dew-point spread, 92
temperature-humidity index (THI), 77-78
tempest, 607
tendency, 18
height, 463
in forecast verification, 778
pressure, at MSL, 463-467
term, 747
temperature, 746
tephigrams (also see thermo diagrams), 121-158
tera (10^{12}), 870
terminal velocity of, 202-204
cloud droplets, 202
hydrometeors, 202-204
rain drops, 203, 555
causing downbursts, 555
hailstones, 204, 549
terminology, process, 18
terrain (also see mountains), 365, 397-398
following coordinate system, 746, 753
influence on cyclogenesis, 443-446
terrestrial radiation (or IR or longwave), 37-39, 223
tertiary rainbow, 840
TESAC code, 269
Tetens' formula, 90
Texas, USA, 416, 431, 560
theoretical
meteorology, 872
winds, 302-313
thermal(s)
belt for crops on mountain slopes, 653
circulations, 341-342, 356, 648-657
in hurricanes, 613
in local winds (e.g., sea breezes), 655
clouds, in, 162
convective, 649, 694, 710
diameters, 648-649
drag, felt by, 648-649
energy transferred, 58, 672
internal boundary layer (TIBL), 654-657
low, 341-342, 356, 430-431
rise, 649, 710
scales of motion, 315
stress index, 117
updraft, 648-649
upside-down, cold-air sinking, 177, 396
wind, 345-348
African easterly jet, creation by, 611
advection of vorticity (cyclogenesis), 456-462
case study, 348-349
components, 347
cyclone propagation direction, 469
direction, 347-348
effect, 345-346, 352
magnitude, 347
wind relationship, 345-349
in hurricanes, 621-623
thermal wind, 346-348
thickness, 345-346, 436
thermally driven circulations, 341-342, 648-657
anabatic wind, 649-652
direct, 351, 412
hydrostatic, 341-342
katabatic wind, 652-653
monsoons, 356
sea-breeze, 654-657
thermals, 68, 648-649
thermister, 78
thermocline, 610
thermocouple, 78
thermo diagram (see thermodynamic diagram), 119-158
thermodynamic diagram, 63, 119-158
airmass modification over mountains, 398-399
applications, 127-133
chinook and foehn winds, 676-677
blanks, 151-158
boundary layer, for, 144, 157-158
building/creating, 119
cloud base height, 130, 162, 164, 496-498
cloud diagnosis, 134
cloud top, 162, 164, 496-498
complete/full/large, 121, 151-158
components, 119-121
adiabats, 63, 103
buoyancy, 135-136, 498, 503-508
cloud base, 130, 162, 164, 496-498
dry adiabats, 63, 119-128
environmental lapse rate, 134-136, 138, 496-498, 503-508
height contours, 121
isentrope, 63
isobar, 63, 100, 119-128
isohume, 100-102, 119-128
isotherm, 63, 100, 119-128
lifting condensation level, 93-96, 105-107, 130, 138, 162, 164, 483, 496-501, 522-527, 530-531
moist adiabats, 102-106, 119-128, 496-499, 503-506, 522-527
convective inhibition (CIN) determination, 523-526
dew-point temperature, 128
dry (unsaturated) processes, 129
environment, 134
excess water, 186
for boundary layer, 157-158
humidity, 128
hurricane thermodynamics, 624-625
identifying different types of, 126-127
isohumes of mixing ratio, 100-101
locate stable layers, 733-734
masters, 151-158
misinterpretation, 729
mixing ratio, 128
moist (saturated) processes and liquid water, 101-106, 129
mountains, lifting over, 398-399
parcels vs environment, 134
partial water fallout from clouds, 130-131
plotting on, 128
pressure, 128
processes, 100-106, 121, 129-133
dry (unsaturated) lifting/lowering, 129
moist (saturated) lifting/lowering, 130
precipitation, 130-131
radiative heating/cooling, 131-132
pseudoadiabatic assumption, 121
relative humidity, 133
saturated adiabats, 102-106
saturated (cloudy or foggy) air, 128, 130
saturation mixing ratio, 128
soundings, 134-135
spreadsheet construction of, 63, 103
state, 100, 121
temperature, 128
thunderstorm thermodynamics, 496-526, 557-558
total water mixing ratio, 128
types, 121-123
emagram, 119-123, 127, 152
P vs. alpha diagram, 121
pseudoadiabatic diagram, 121-123, 153
skew-T log-P diagram, 121-125, 154, 157
Stüve diagram, 121-123, 153
tephigram, 121-123, 155
T - log P (emagram), 119-123, 127, 152
theta-height diagram, 121-123, 156, 158
unsaturated air, 128
wind, plotted on, 510
thermodynamic
method of mixed layer growth, 394-395, 697-698
state, defined, 6
density, 10
on a thermo diagram, 128
pressure, 7
temperature, 6
within a hurricane, 624-625
thermodynamics
first law of, 53, 58-59, 64-65
frontogenesis, 411
heat, 53-86
hurricane, 620-625
thunderstorm, 496-508, 522-526
topics, 1
thermohaline circulations in ocean, 804
thermometers, 75, 78-79, 219
thermosphere, 12-13
thermostat, 78
theta (q) - (potential temperature), 61-63, 103-106
theta-height (z) thermodynamic diagram, 121-158
theta-w vs theta-e, 105
thickness, 17
100 to 50 kPa chart, 346-348, 436, 439, 442
contours, 346-348, 458
definition, 17, 345-346
in high pressure center, 390-391
of clouds, 161-162
on weather maps, 346-348, 436, 439
optical, 43, 805, 856
related to thermal wind, 345-349, 436
temperature relationship for, 79
threads (see end of each chapter)
threat score, 781-782
equitable, 782
three-band general circulation, 329, 376-378
threshold
for binary/categorical forecasts, 780
for probability forecasts, 777
temperatures for ice nucleation, 195
thunder, 571-576
3-second rule, 575
audibility, 575-576
creation mechanism by lightning, 571
distance away, 576
force of, 571
ray paths, 575-576
shock wave, 571-574
sound wave, 575-576
thunderhead, 482
thundersnow, 207
thunderstorm(s), 481-602
airmass, 486
altitudes, 496-499
appearance, 482
aspect ratio of, 485
attributes, 481-495
base at LCL, 497-498
basic, 486-487
bear's cage, 495
beaver-tail cloud, 492, 494-495
bookend vortex, 490-491
bow echo, 490-491
bursticane, 602
CAPE, 503-508, 530-531
cells, 484-485
change criterion for SPECI, 270
chasing, 484
safety, 485, 517, 567, 570, 583-584
CIN (convective inhibition), 522-526

T

classic supercell, 492-494, 549, 553
cloud shield, 488
clouds associated with, 482, 488, 494
cold-pool of air, 488
conditional instability, 141, 498, 503-508
convective available potential energy (CAPE), 503-508, 530-531
convective conditions, 496-499, 530-531
  high humidity in the ABL, 499-502
  instability (nonlocal conditional), 503-508
  trigger mechanisms causing lifting, 522-526
  wind shear in the environment, 509-521
convective inhibition (CIN), 522-526, 530-531
Coriolis force, effect on, 490-492
cumulonimbus cloud, 161-162
daily cycle, 528
damage scales, tornado, 579-580
derecho, 491, 494
development, 484-485
difficulties in forecasting, 527-528, 547
direction (see movement), 516-520
downbursts and gust fronts, 554-562
  downdraft CAPE, 530-531, 557-559
  evaporative cooling, 556
  gust fronts, 560-563
  precipitation drag, 555
  pressure perturbation, 559-560
  radar observations of, 253
downdraft CAPE (DCAPE), 530-531, 557-559
downdrafts, 483, 492-494
duration/lifetime, 486
echo-free vault, 493
energy helicity index, 530-531
energy released by, 499
environment, 141, 496-499
  pre-storm, 496-531
equilibrium level (EL; storm top), 497-506
evolution, 484-485
flanking line, 492, 494
flow stability, causing, 138
forecasting, 527-532, 547
formation conditions, 496-527
forward-flank downdraft (FFD), 483, 492-493
frequency/activity (isoceraunic), 18
frontal, 400, 525
graupel, 493
gust fronts, 494, 554-562
hail, 493, 548-553
  significant hail parameter (SHIP), 530-531
hazards, 481, 545-602
heat
  flux profile, 70-71
  released, 546-548
helicity, 587-592
  storm-relative (SRH), 530-531
high-precipitation (HP) supercell, 492, 495
highs (anticyclones) associated with, 391
hook echo, 494
humidity, 499-502
hurricanes, in, 604, 613-615, 620-621, 637
hybrid supercell, 492
in cold fronts, 400, 525
indices for forecasting, 530-531
inflow of humid air from ABL, 546-547
influence on mixed layer, 510
instability, 496-508
intensity forecasting, 501, 507, 516, 521-522, 524, 530-531
key altitudes, 496-499
latent heating inside, 546-548
level of free convection (LFC), 497-506
lifting condensation level (LCL; storm base), 497-506, 530-531
lifting needed to trigger, 522-527
lightning and thunder, 563-576
limit of convection (LOC; see equil. level), 498
line-end vortices, 490
long-lasting, 509-510
low-precipitation (LP) supercell, 492, 495
main updraft, 483, 492, 495
MCC (see mesoscale convective complex), 491
MCS (see mesoscale convective system), 488-492
mesocyclone, 481, 483, 492-495, 510, 582, 586-591
meso-high, 391, 488
meso-low, 489
mesoscale convective
  complex (MCC), 491
  systems (MCS), 488-492
  vortex (MCV), 492
midlatitude-cyclone related, 425-428, 434, 438, 466
mixed layer, 496-503
movement, 483, 510
  normal storm motion, 516-518
  left- and right-moving, 518-520
multicell, 486-487
nonlocal conditional instability (NCI), 498, 503-508
organization, 486-495
orographic, 487, 526, 547-548
outflow winds, 560-562
outlook forecasts of convection, 528-530
overshooting dome (penetrative convection), 498
parameterization in NWP models, 751
path (see movement), 516-520
precipitation, 206, 486, 493, 495, 545-554
precursor clouds (altocumulus castellanus), 165

pressure perturbations, 559
propagation of, 485
pulse, 486
radar images of, 243, 248, 253-254, 482-483, 486-488, 490-495, 552-553
radiative effects, 131-133, 624-625
rain, heavy, 545-548
rainfall rate, 546
random effects in thunderstorm development, 527
rear-flank downdraft (RFD), 492-494
rear inflow jet (RIJ), 489
risk of, 528-530
rotation, 586-591
safety, 485, 517, 567, 570, 575, 583-584
satellite images of, 234
sequence of events, 484
severe thunderstorm
  definition, 528
  environment, 496-502
  watches and warnings, 528-530
severity forecasting, 501, 507, 516, 521-522, 524, 530-531
significant hail parameter (SHIP), 530-531
significant tornado parameter (STP), 530-531
single-cell, 486
size, 481-498
soundings, pre-storm environmental, 496-499
squall line, 243, 488, 490, 582
stability indices, 530-531
stages of evolution, 485
storm-relative helicity (SRH), 530-531
straight-line winds, 489-490, 554, 560-563
  derecho, 491, 494
stratiform clouds, 488-489, 492
strength forecasting, 501, 507, 516, 521-522, 524, 530-531
supercell, 482-484, 492-495, 549, 553
  composite parameter (SCP), 530-531
  tornadoes, 577, 582
steering-level winds, 487
suppression of neighboring storms, 547
swirl ratio, 530-531, 592-593
symbols on weather maps, 275-276, 481
thunder, 571-576
timing, 528, 546
  effect of mountains on, 528
top
  cold, 546
  equilibrium level (EL), 498
tornadoes, 494, 577-593
  significant tornado parameter (STP), 530-531
triggering, 496, 522-526
tropical, 331-332, 350-351
tropopause vs. storm top, 496-506
turbulence (see updrafts & downbursts), 111, 508, 527-530
types, 486-495
unfavorable conditions for, 499
updrafts, 483, 498, 503-508, 649
upslope, 526
vault (echo-free), 493
venting of boundary layer air, 691-692
violent, 492, 498
warming rate due to condensation, 546
warnings and watches, 528-530
watch-box, 528-529
weak echo region (WER), 493
weather-map symbols, 275-276, 481
wind shear in pre-storm environment, 509-521
Tibetan low, 354-356
TIBL (thermal internal boundary layer), 654-657
tidal bulge of solid earth, 229
tides, lunar and solar, 376, 635
tight packing of isopleths, 143
tiling method for finding CAPE & CIN areas, 504-505, 524
tilt of
  earth axis (obliquity), 30, 798-803, 879
    variations and climate, 798-803
  high pressure with altitude, 390-391
  low-pressure with altitude, 432
  mountain waves with altitude, 668
  troughs with altitude, 432
tilted
  coordinate system, 124-125, 650-653
  isobars, 345-349, 359
tilting
  effect on frontal zone strength, 409
  of cold-core cyclone, 622
  of front, 412
  of tropopause, 415
  of trough, role in cyclogenesis, 432, 622
  of vertical temp gradient, 409
  of wave crests with altitude, 668
  term in vertical vorticity eqn, 447-448, 586-587
time, 870
  airmass thickness, max, 395
  astronomical values that determine time, 34
  constant (isochrone), 18
  daylight (summer), 5
  differencing in NWP, 757
  e-folding, 9, 393-396
  equation of, 34
  GMT, 5
  isochrone, 18
  lead, 762
  line, numerical, 757
  scales, 315
    Lagrangian turbulence, 732
  standard, defined, 5
  step, 750
  sunrise & sunset, 33-34
  twilight starts and ends, 33-34
  units, 870
  UTC, defined, 5
  valid, 762
  zones, defined, 5
  Zulu, defined, 5
tipping bucket rain gauge, 210
tips for doing homework exercises, 20-26
TIROS (Television and Infrared Operational System), 273
TKE (see turbulence kinetic energy), 708-710
Toba, Lake, 805
tongue, dry air, 429
tonne mass units (or metric ton), 870
tools, scientific, 877
top of
  atmosphere, observations of, 220
  clouds, 162
  mixed layer, 497
  thunderstorm (equilibrium level, EL), 497
topographic formation of highs, 391
tornado, 483, 494, 577-593
  appearance, 581-583
  bait, 592
  blowdown of trees, 593
  boundary layer of, 586
  breakdown bubble, 592-593
  bulk Richardson number shear, 522
  Burgers-Rott vortex (BRV), 599
  change criterion for SPECI, 270
  cold-air funnels, 582
  cone shape, 577
  core pressure deficit, 577-578
  cylinder shaped, 577
  damage
    exploding houses, 674
    paths, 584
    scales, 579-580
  debris cloud, 581-583
  developing stage, 583
  dissipating, 583
  dust swirl, 583
  evolution, 583
  family, 584
  forecasting, indices for, 530-531, 588-592
  frequency in USA & Canada, 579
  funnel cloud, 483, 581-583
  hourglass shaped, 577
  in hurricanes, 584, 627, 637
  intensity scales, 579-580
    enhanced Fujita (EF) scale, 578-580
    forecasting, 501, 507-508, 516, 522, 530-531
    Fujita (F) scale, 579
    Torro (T) scale, 579-580
  irrotational winds around, 385
  landspouts, 582
  life cycle, 583

likelihood, 591
mature stage, 583
mesocyclones and helicity, 582, 587-592
multiple vortex, 592-593
origin of rotation, 586-587
outbreaks, 583-584
in hurricanes, 637
intensity scales, 579-580
origin of rotation, 586-587
pressure
decrease in core, 577-578
increase due to wind stagnation, 672-674
Rankine combined vortex wind model, 577-578, 599
reports, 532
rope shape/stage, 577, 583
rotation, 577-578
direction, 578-579, 586
origin, 586-587
safety, 583-584
scales, 579-580
shapes, 577
significant vs. weak, 501, 507-508, 516, 522, 530-531, 580
significant tornado parameter (STP), 530-531, 592
spin-up, 586-587
stages in evolution, 583
suction vortices, 592-593
supercell, 582
swirl ratio, 530-531, 592-593
tangential velocity vs. intensity, 577-580
thunderstorms, relationship to, 577
total speed, 578
translation speed, 578, 582
types, 582-583
V-shaped, 577
vortex signature, 251, 253, 599
vortices that are not tornadoes, 582-583
dust devils, 582
gustnadoes, 582
steam devils, 583
firewhirls, 583
wall cloud, 483
watches and warnings, 528-530
waterspouts, 582
weather-map symbols, 276
wedge, 577
winds
cyclostrophic, 311-312
dynamic warming, 673
exploding houses, 674
irrotational, 385, 577
torque on
atmosphere, 366
Earth, 376
satellite orbit, 229
Torr, 7
TORRO scale for
hailstone diameter, 548
tornado intensity (T), 579-580
total
deformation, 321
derivative, 872
entropy, 624-625
meridional heat transport, 378
shear magnitude, 515-516
distribution of, 515
solar irradiance (TSI), 39, 793-794
variations, 803
totals index (TT), 531
water, 94, 97-99
conservation of, 99-111
content in a column of air, 211
fallout from cloud, 108
in fogs, 176
in thermo diagram, 128-133
mixing ratio, 97-99, 186
reduction in thermo diagrams, 130-133, 397-398, 676
TOVS (TIROS Operational vertical sounder), 273
tower
hot convective, 644
updraft, 482
towering cumulus (tcu), 162, 168, 483
stage of thunderstorm-cell evolution, 485
toy model(s) of, 330
airmass formation, 393-396
climate processes, 793-796
differential heating (global), 334-339
extratropical cyclone, 450-451
global circulation, 330-334
hurricanes, 626-629
jet stream, 359-360
MSL pressure tendency, 464-467
transmittance of radiation, 225-226
trace
matrix, 822
rainfall rate, 208
tracers, passive, conservative, 731
TRACKOB code, 269
tracks
extratropical cyclones (lows), 429-431
tropical cyclones (hurricanes), 607-608, 615
thunderstorms and tornadoes, 483, 516-520, 584, 593
trade
inversion, 351
winds, 330-332, 351
cumuli, 351
role in steering hurricanes, 607-608, 615
role in triggering hurricanes, 610-612
Walker circulation, 820
trading, emissions, 742
trajectories, 668-669
backward, 724
forward, 724
of hailstones, altering, 553-554
path lines, 669
transfer of electric charge, 564-566
transformations: inertial or Newtonian, 715
transilient turbulence theory (T3), 714, 716
transition
hurricane extratropical, 615
winds: anabatic vs. katabatic, 654
translation of
hurricanes, 627-628
thunderstorms, 516-520
tornadoes, 578, 582
translucent, 42
translucidus, 169
transistors, 752
transmission of radiation, 41-43
transmissivity, 42
net sky, 44
transmittance of atmosphere, 220-226
profiles, 225-226
transmitted solar radiation, 805, 856-858
transparency of
atmosphere, 220-223
reduction due to volcanic eruptions, 805
clouds, 169
windows on radiometers, 45
transpired (CO2 from plants), 812
transport
coefficients
bulk heat, 68
bulk moisture, 109
convective coefficient, 68, 109
Ekman, hurricane, 610, 633-634
energy, 53, 499-502, 708-709
heat, 68
global, 338-339
planetary waves, by, 374-375
mixed layer coefficient, 68
momentum, global, 375-376
turbulent, 709
of heat, 67-71
of moisture, 109-111
velocity of turbulence, 300
transverse (cross-frontal) circulation, 412, 415
trapped low-level barrier jet, 664-665
trapping of
pollutants, 725
radar beam, 244-245
tree
blowdown by downbursts & tornadoes, 593
ring dating (dendrochronology), 803
Trenberth omega equation (see omega equation), 456-458
Trenberth, Kevin, 339, 458, 797
omega equation, 458
triangle shaped ice crystals, 199
Tricker arc, 854-855
trigger mechanisms for
hurricanes, 610-613
thunderstorms, 485, 496, 522-526
trigonometric conversions, 650
trimming data, 826
triple point, 414
trof (see trough)
trop (see tropopause)
Tropic of
Cancer, 31
Capricorn, 31
tropical
airmass
code, 392
genesis, 393-395
cloud heights, 163
convection variations due to ENSO & PDO, 820
convergence
in easterly waves, 611-612
zone (ITCZ), 330-332, 351, 610-612
cyclogenesis (birth of hurricanes), 608-610
cyclolysis (death of hurricanes), 616
cyclones (see hurricanes), 330, 427, 603-644
cumulus, 351
depression, 613-614
disturbance, 613
easterly jet and waves, 611-612
forecasters/meteorologists, 343, 611, 613
geostrophic & gradient winds, 611-612
hurricane, 603-644
monsoon, 333-334, 356, 612
Prediction Center, 638
rainfall, 209-211, 351
storm, 614-615, 635-636
watches & warnings, 638
streamlines, 611-612
thunderstorms, 331-332, 351-352
trade inversion, 351
trade winds, 331, 351, 358, 376, 610, 612, 615
tropopause, 163
typhoon (see hurricanes), 603-644
upper tropospheric trough (TUTT), 612-613
winds, 611-612
year, 31
tropics, 330
tropopause, 12-13, 414-415
folding
fronts, upper-level, 414-415
isentropic potential vorticity, 364, 441-443
of cyclone case study, 441-443
on weather maps, 364, 441-443
ozone injection by, 364, 414-415
radionuclide injection by, 364, 414-415
satellite observations of, 234
height, 143
determination, 143, 496
variation with latitude, 163, 353
pressure, 163
thunderstorm tops near, 497-498
winds near (also see jet stream), 331-332, 357-362
troposphere, 12-13
average density, 72
average depth, 12
coupling with daily heating cycle, 687-692
depth, 12, 143
variation with latitude, 163
folds, 364, 414-415
upper trough, tropical (TUTT), 612-613
tropospheric constraints on atmos. boundary layer, 689-690
trough(s) (see also midlatitude), 332
axis, 281, 367
of cyclone case study, 433
symbols on weather map, 281, 399
circumpolar, 432
formation & characteristics, 367-376
in tropical easterly waves, 611-612
in Rossby waves, 353, 367-376
monsoon (MT), 612
tilt with altitude, 432
tropical upper-tropospheric (TUTT), 612-613
upper-level disturbance, 433
TROWAL (trough of warm air aloft), 413-414
true
anomaly, 29, 802
longitude, 802
skill score, 781
truncation error, 754-755, 760
trunk space, 677-678
TSI = total solar irradiance, 39
tuba, 169
tumble of small falling ice crystals, 842
turbine, wind
efficiencies, 647-648
pressure change across, 671
turbulence, 705-716
atmospheric boundary layer (ABL), 687, 705-716
above ABL, 110, 687
airmass characteristics of, 391-396
role in evolution, 393-396
buoyant, 704, 705
generation, 709-710
cascade, 315
clear-air (CAT), 141-142, 165
closure, 713-716

T, U

closure types, 714-716
K-theory, 714-716
transilient turbulence theory, 716
clouds created by, 165-166
conservation, 706, 708-709
covariances, 711-713
convection
forced, 710
free, 710
convective, 705
mixed-layer, 704
thunderstorm, 508, 527-530
correlation coefficients, 711-713
defined, 705
determination, 138-142
dispersion of pollutants, caused by, 723-744
dissipation, 706, 709
existence, 142
fair-weather, 69-70
flux
as a covariance, 711-713
from advection terms, 714
divergence terms, 747
gradient, 65, 67-71, 107-111, 698, 711-716, 746-747
heat, 711-714
momentum, 713
forced convection, 710
free convective/convection, 704, 710
heat budget, in, 69, 713-716
heat flux, 711-712
in air masses, 397-398, 691-692
in cloud
rotor clouds, 165
thunderstorms, 481-602
in neutral static stability
inertial subrange of, 708
intensity, 710
intermittent, 692
isotropy, 707, 710
kinetic energy (TKE), 708
advection, 708
budget equation, 708
buoyant production or consumption, 709
cascade, 315
dissipation, 709
generation, 708-709
shear generation, 708-709
tendency, 708
mean and turbulent parts, 705-706
mechanical, 704, 705
microscale, 708
momentum flux, 713
mountain wave, 667
onset, 142
parameterization in NWP models, 751
production, 708-709
scales of motion, 315
radar observations of CAT, 242
radar spectrum width in, 254
raindrop growth affected by, 206
scales of motion, 315
shear, 704, 705
generation, 708-710
stability dependence, 119, 138-142, 688, 707-708, 710
stably-stratified (SST), 710
stationary, 708
statistics, 706-708, 726-728
stormy-weather, 70-71
terms, derivation, 714
thermal, 134-140, 144, 648-657, 704, 708-710, 716
thunderstorm, 111, 508, 527-530
transilient, 714-716
transport, 300, 709
types, Pasquill-Gifford, 727-728
velocity scales, 68-69
wake, behind mountains, 667
turbulent
continuity equation, in flux form, 714
convective mixing, 69-71, 108-111, 138-139, 144, 704, 710, 735-737
dispersion of pollutants, 724
drag, 300
above the boundary layer, 300, 687-690
atmospheric boundary layer, 300, 699-701
force, 300-301
term in vertical vorticity equation, 447-448, 586
eddies, 706, 708
flow, 660, 705
heat flux, effective, 68
flux
divergence, 715
variation with height, 70, 698, 715-716
gusts, 705-706
kinematic moisture flux, 108-109
kinematic heat flux, 68
mixing
frontolysis, 411
by thunderstorms, 70-71, 111
parts, 705-706
Reynolds stress, 701
stress, 701
surface layer, 709
transport, 709
of heat, 67-71
of moisture, 109-111
transport velocity, 300
velocity variances, 706-708
vertical heat flux divergence, 64-65, 69-71, 698, 711-716
wake, 165, 667
whirls (eddies), 708
turret (shaped clouds), 168
TUTT (tropical upper tropospheric trough), 612-613

TV (television), severe weather reporting, 529-532
TVS = tornado vortex signature, 253, 599
twilight, 11, 33-34
astronomical, civil & military, 33-34
twinned rainbows, 841
twister (see tornado), 577-593
two-layer system of fluids, 657-661
two-way nesting of NWP grids, 752
types of
clouds, 168-169
fog, 173
thunderstorms, 486-495
typhoons (see hurricanes), 330, 426, 603-644
international forecast organizations, 607
intensity scales, 607

U

U time zone (Pacific), defined, 5
u* (see friction velocity), 378, 700-704, 709
U velocity definition, 2, 3
determination using hodographs, 513
UHF = ultra high frequencies, 259
UK air quality objectives, 725
ultrafine aerosols, 188
ultrasonic snow depth sensor, 210
ultraviolet light (see also radiation), 222, 857
haze filters for cameras, 857
uncertainty in weather forecasts, 776
uncinus/unc, 168
uncontrolled experiments, 554
understanding & critical evaluation, exercises explained, 23
undulatus, 169
unidata IDV, 772
United Nations, 268
units, 870
component of scientific notation, 870
concentration of pollutants, 724
conversion, 871
density, 10
force per mass, 292-300
metric (SI), 7, 870
MKS system, International System (SI), 7, 870
potential vorticity (PVU), 364
pressure, 7, 19
scientific, 8, 870
temperature, 7, 870
water vapor pressure, 87
universal
constants, 879
observation codes, 268
theories, 107, 877
universities and NWP, 772
unsaturated (see also dry), 57, 87, 92
air, 87
air parcel, 128-129
definition, 87
heat budget, 57
humidity, 87-96
lapse rate, 60, 129
unstable
absolutely, 140
air (regions), 138-139, 688-689
clouds in, 161-162, 164-165
dispersion of smoke in, 710
determining, 138-139
velocity standard deviations, 707
atmospheric boundary layer (ABL), 692
turbulence, 707-710
baroclinically, 371
barotropically, 368
boundary-layer wind, 308
conditionally, 140-141, 498
nonlocal, 496-499, 503-508
drag, turbulent, 300
dry absolutely, 140
equilibrium of droplets, 191
flow, definition, 138
mixed layer, 692
nonlocally, 138-144
conditionally, 496-499, 503-508
saturated absolutely, 140
statically, 138, 688-689
cumulus cloud formation in, 162
up, definition of, 4, 298
updateable MOS (model output statistics), 771
updraft(s)
bubble, 482
cloud, 162
main, 483
rotating, 492
, instability & CAPE in thunderstorms, 503-508
thermals, 648-649
tower, 482
velocity in
cyclones, 446, 451-462
easterly waves, 612
hurricanes, 605, 612, 620, 628
of buoyant thermals, 648-649
thunderstorms, 508, 649
upper-air
jet
streaks, 454-456
streams, 357-361, 405-407, 414-415, 452-453
mandatory levels, 134, 772
significant levels, 134, 147
soundings, 134
locations worldwide, 271
Pacific data void, 288
weather maps and charts, 291
winds vs. thunderstorm strength, 510
upper-level
charts, in case-study of cyclone, 433-466
reason for using, 291, 436-437, 442
20 kPa, 440-443, 452, 455-456
50 kPa, 433, 442, 448, 451
70 kPa, 439, 442
85 kPa, 439, 442, 449, 459-462
100 kPa, 438, 463
disturbance, 433
divergence
due to jet streak ageostrophic flow, 454-456
due to jet stream curvature, 453
related to pressure tendency, 464-467
fronts, 414-415
trough, position that causes cyclogenesis, 432, 450-453, 467
winds, 331-332
upper
quartile, 502
suncave Parry arc, 854-855
sunvex Parry arc, 854-855
tangent arcs, 842, 851-855
tropospheric
fronts, 414-415
winds, 331-332
Wegener arc, 855
upside-down cold thermals, 177
upslope
flow (anabatic), 649-652
fog, 173
rain, 398-399
thunderstorms, 526
upward motion
at cold fronts, 470-471
in extratropical cyclones, 425, 451-462
upward velocity in extratropical cyclones, 425, 426, 451-462
upwelling
ocean water in hurricanes, 610
radiation, 44-45, 220
urban
breezes, 679
canopy, 678-679
canyon, 678-679
cloud formation over, 162
heat island, 678-679
plume, 678-679, 742
smog, 193
U.S. (USA)

air quality standards, 725
geography, 431
Joint Typhoon Warning Center, 607
National Hurricane Center (NHC), 608, 638
National Inst. for Standards & Tech. (NIST), 51, 879
national lightning detection network (NLDN), 568-569
National Oceanic & Atmos. Admin. (NOAA), 637
National Weather Service (NWS), 532
short scale number prefixes, 870
standard atmosphere, 11-13
states & their postal abbreviations, 431
Storm Prediction Center, 532
Supreme Court, quotation, 470
symbols for clouds on weather maps, 168
Tropical Prediction Center, 638
UTC (Coordinated Universal Time), 5, 268
uv (see ultraviolet), 222

V

V shaped tornado, 577
V time zone (Alaska), defined, 5
V-velocity definition, 2, 3
determination using hodographs, 513
vacuum, 19
speed of light in, 834
VAD = velocity azimuth display, 252-253
Väisälä (in Brunt-Väisälä frequency), 136-137
valid time, 762
valley
circulations, 649-654, 660-670, 675-676
fog, 177
gap winds, 661-664
pollutants trapped in, 654
subsidence into, 654
winds, 649-654, 660-670, 675-676
value
components in scientific notation, 870
of forecasts, economic, 784-785
Vancouver
International Airport (CYVR), 646-647
solar azimuth & elevation, 32-33
vanes, wind, 219, 321
van't Hoff factor, 190
vapor pressure, 14, 87
definition, 87
over curved droplets, 189-192
over flat surface of water, 87-90
reference, 88, 880
saturation, 87-90
supersaturation, 186
units, 87
variation with temperature, 14, 88
vapor, water feedback, climate, 810
vaporization, latent heat of, 54, 56, 88-90, 108, 880
variance, 706, 727
smoke plume spread, 726-732, 735-737
velocity, 706-708, 727
variable(s)
conserved, 61
continuous, verification of, 777-780
dependent, 872
independent, 872
gases in the atmosphere, 7
grids and grid meshes, 752-753
italicized notation for, 870
variant pi, 801
variational data assimilation (3DVar & 4DVar), 273, 767
varieties of clouds, 168-169
vault, echo-free, 493, 552-553
vector
equation, 292
force , 292
operators
cross product, 299
dot product, 239
sum, 292
wind
difference (surrogate for shear), 509
shear, 509
velocity, 292, 509
veering wind, due to warm-air advection, 349, 511, 520
vegetation
greenness, 230, 751
parameterizations, 749-751
veils of clouds, 168
velocity (see also speed), 2-3
azimuth display, 252-253
buoyancy scale, 68-69, 110, 704
components, 2-3, 293, 314-315, 746
convective, 68-69, 704
Deardorff, 69, 703-704
downburst, 554-557
entrainment, 697-698
friction, 378, 677, 700-713
group, 658
horizontal, 2-3
scales, buoyant, 68-69, 109, 300, 703-704
scales, mechanical, 68-69, 109, 700-703, 708-709
hurricane
radial, 627-628
tangential, 605-607, 622-623, 626-627
vertical, 628-629
mean wind, 705-706, 726-727
of air parcel relative to earth, 360-361
phase, 658
radial, 249-254
standard deviation, 706-708, 727, 731-732
tangential
in hurricane, 605-607, 622-623, 626-627
in tornado, 577-580
terminal, 202-204, 555
thermals, 649
thunderstorm updrafts, 508
tornado, 577-580
turbulent transport, 68-69, 109, 300, 703-704
variance, 706-708, 727, 731-732
vertical, 2-3, 252, 448, 451-462, 628-629, 746
max up- and down-drafts, 508, 557-559
omega, 451, 456-462
Q-vectors, 460-462, 469-471
wave, 658
winds, summary of, 314
velum, 169
venting of atmos. boundary layer air, 691-692
venturi effect , 674-675
verification of forecasts, 777-785
binary variables, 780-782
categorical events, 780-782
continuous variables, 777-780
cost-loss decision models, 784-785
probabilistic forecasts, 782-784
scores, 752, 777-785
verifying analysis, 769, 777
vernal equinox (Spring), 30-31, 801-802
angle from perihelion, variation of, 799-801
angle from Earth, 802
vertebratus, 169
vertical
advection of
heat, 67, 72, 714
mass, 317-318
momentum, 295, 315
vorticity, 447-448
axis on graphs, 3
cell circulation, 377
circulations (global), 332-333, 377-378
effective, 377-378
component of the equations of motion, 315-317
coordinates, alternative, 746
cross section of
atmosphere, 143-144, 332, 357, 359, 373, 432
cyclone (case study), 441
dry line, 416
fronts, 403-407, 412-416
hurricanes, 605, 618, 620-621, 624, 629
storm surge, 632-635
thunderstorms, 482-490, 496, 510, 525-526, 553-554, 563, 566, 575
troughs, 432
density profile, 10
direction, 4
equation of motion, 315-317, 746
applied to thunderstorms, 649, 554
for thermals, 649
flux divergence, 65-73, 109-110, 746
flux of water vapor, 108
during free convection , 109-110
forces as cause vertical motion, 315-317
frontal structure, 403-404
gradient, 872
geostrophic wind (thermal wind), 345-349
IR flux, 71
mixing ratio, 75, 110, 692
potential temperature, 67, 75, 110, 688, 690, 692, 695-698
pressure, 8-9, 12-13, 15-17, 554, 621-623
mean temperature advection, 72
motion, 66, 451-462
omega, 451, 456-462
pressure gradient, 15
profiles, 119
pressure, 9
potential temperature, 67, 75, 110, 688, 690, 692, 695-698
weather variables, 119, 134
shear, 509-521, 699-704
structure
anticyclone (highs), 391
atmosphere, 11-13
cold front, 403-404
warm front, 403-404
temperature gradient definition, 872
turbulent flux, 67-71, 108-111, 711-716
velocity, 2-3, 252, 448, 451-462, 628-629, 746
constant, 17
continuity effects that drive, 452-459
cyclones, in extratropical, 446, 451-462
downbursts, in, 554-562
equations for, 315-320
hurricane model, 628-629
omega, 451, 456-459, 462
Q-vectors, 460-462, 469-471
radar, 252-253
standard deviation, 706-711, 731-732
subsidence, 545-546
synoptic scale, 448
thermals, in, 649
thunderstorms, in, 508, 545-546, 557-559
top of boundary layer, 319-320
top of hurricane, 612, 618, 628
typical, 318
vorticity, effect of, 448
weather map of, 448
visibility, 170
wave propagation, 668
wind speed, 318, 451-462
Ekman pumping, 319-320
isanabat, 18
thermals, 648-649
very
fine particulate matter (PM2.5), 725
low frequency (VLF) radio waves, 568
VHF = very high frequencies, 258-259
vibration lines is spectra, 221
vicinity, weather map symbol for, 276
viewing angle, 838, 846
for rainbow rays, 839-840
minimum, 846
vs. cloud droplet for diffraction fringes, 858-860
violent stage of thunderstorms, 485
violet color defined (also see optics chapter), 37
virga, 169, 185, 482-484, 547
weather-map symbol for, 276
virtual
potential temperature, 61-62
in buoyancy, 135-136
in downbursts & DCAPE, 555-563
in katabatic flow, 649-653
temperature
average, as measure of thickness, 17-18
constant, 14-15, 880
defined, 14-15
in buoyancy, 135-136
in CAPE, 503-504
in gust fronts, 562-563
vis5D, 772
viscosity, eddy, 715
viscous dissipation rate of TKE, 315, 709
scales, 315
visibility, 43, 170, 270, 275, 867
airmass characteristics, 391
change criterion for SPECI, 270
definition, 43, 867
haze, 193, 856-858
in precipitation, 208-209
METAR, 270
minimum (in METAR), 270
reduced, 170, 193, 270, 275
runway visual range (RVR), 270
weather-map codes, 275
vertical, 170
visible
light, 220, 222
satellite images (photos), 230-233
visual
geometric albedo, 879
range (also see runway visual range, RVR), 43
visualization programs for NWP output, 772
void, Pacific data, 287-288
volatile hydrocarbons, 193
volcanic

ash & aerosols, 170, 276, 804-805, 858
climate change processes, 804-805, 810
eruption(s), 804-805
change criterion for SPECI, 270
Deccan traps, 805
Krakatau, 805
Lake Toba, 805
Mt. Tambora, 805
Siberian traps, 805
Yellowstone caldera, 805
red skies caused by, 858
winter, 805
The Year Without Summer, 805
volcanism influences on climate, 804-805, 810
volt, unit of electric potential, 564, 870
voltage breakdown potential in air, 566
voltage difference, 564-566
volume
density, 10
extinction coefficient, 43
fraction of gases in air, 7
grid, 750-756
sampled by radar, 240
scans by radar, 241
specific, 10
isostere, 18
von
Freiberg, Theodoric, 841
Goethe, 249
Kármán constant, 677, 701
Neumann, John, 624, 669, 749, 759
vort max (see also vorticity maximum), 457
vortex / vortices
book-end, 490-491
Burgers-Rott (BRV), 599
cold-air funnels, 582
debris cloud, 581
dust devil, 582
firewhirl, 582
funnel cloud, 581
gustnado, 582
landspouts, 582
line-end, 490
mountain-lee, 165
multiple-vortex tornadoes, 592-593
polar, 397, 824
Rankine combined, 577-578, 599
roll, horizontal, 167
spray, 582
steam devil, 582
stretching, 447-451, 586
suction, 593
tornado, 577-593
signature (TVS) on Doppler radar, 253, 599
supercell, 582
tube, 166, 447, 518, 586-587
waterspouts, 582
wing-tip, 166
vorticity, 320-321, 362-365
absolute vorticity, 363, 448
advection, 447-451, 458
PVA & NVA, 447-448, 459
beta effect, 447-451
cascade, 586
charts, for case-study cyclone, 439-441, 448
circulation, 365-366
conservation, 363, 397, 445
curvature-induced, 362
cyclogenesis indicator, 426
cyclonic, along fronts, 407
definition, 320-321, 362-365
divergence effect, 447-449
drag effect, 447-449
forecast equation for, 447-449
frontal, 407
geostrophic, 319, 449-451
relative, 319
helicity, 587-592
horizontal (streamwise), 518
advection, 447-449
circulation, 365-366
hurricane environment, 610
isentropic potential vorticity, 364-365
maximum (vort max), 457
of cyclone case study, 459
on weather maps, 457-458
negative advection (NVA), 447-448
planetary, 363-364
positive advection (PVA), 447-448, 459
potential vorticity, 363-365, 397
conservation, 445
isentropic, 364-365
quasigeostrophic approx., 449-451
relative vorticity, 319-321, 362-363, 577, 586-588
shear-induced, 362
solid body, 363
spin-up, 447-449
streamwise, 518, 587-592
stretching, 447-451, 586-590
swirl ratio, 592-593
tendency equation, 447-449, 586
tilting effect, 447-449, 586-588
tornado, 577-578, 586-588
turbulent drag, 447-449, 586
vertical advection, 447-449
wave, 368

V, W

W

W time zone (Hawaii, Aleutian), defined, 5
w* (see Deardorff velocity), 69, 110, 703-704, 736
W-velocity definition, 2, 451
wake turbulence behind mountains, 667
waldsterben (forest death), 742
Walker circulation, 820
wall
cloud (tornadic), 483, 581-583
Foehn, 676-677
warm
air
advection (& veering wind), 66, 349, 511, 520
conveyor belt, 433
rises, 135
sector of extratropical cyclone, 425-428
airmass formation (genesis), 393-395
anafront, 404
cloud precipitation processes, 204-206
conveyor belt, 433
core system, 426
of hurricanes, 614, 621-625
vs. cold core, 426, 622
frontogenesis, 281, 399
frontolysis, 281, 399
fronts, 399-401
aloft, weather-map symbol for, 281, 399
clouds at, 162-164
definition, 404
drizzle from, 546
extratropical cyclones, attached to, 425-428
halos , 401, 842
horizontal structure, 401
horizontal winds, 401
occlusion, 413-414
rain from, 546
stratiform clouds, 162-164, 401, 425-428
sundogs, 401, 842
thunderstorm triggers, 525
weather map symbol, 281, 399
wind shifts, 401
low-pressure centers, 621-623
mode rainfall estimates, 257
rain, 115
sector, 425-428
vs. cold core cyclones, 622
winds, 66, 349, 511, 520, 676
warming
dynamic, 672-674
global (climate), 150, 796
thunderstorm latent heat release, 546-548
warnings (forecasts)
hurricane, 631, 638
thunderstorm/severe-storm, 528-530
tropical storm, 638
watches (forecasts), 528-530, 638
water, 87-118
availability for droplet formation, 186-187
barometer, 7
budget, 99-111
at surface, 108-109
Eulerian, 107-111
Lagrangian, 99-101
thunderstorm, 547
total water, 99-100
zonally averaged, 210
characteristics, constants, and parameters, 880
conservation, 99-101
content, 97
density vs. temperature, 835, 880
depth, constant (isobath), 18
depth of constant temperature (isobathytherm), 18
droplet clouds, 163
in cold airmasses, 393-397
index of refraction, 834-835
latent heats, 54
liquid
content, 97
depth, 210-211
depth vs pressure, 7
loading, 15, 555
mixing ratio, 15, 97-98
specific heat, 880
mixing ratio, 15, 75, 91, 97-98
molecular arrangement & electric charge transfer, 565
molecule content, 188-189
phases, 198
precipitable, 98
reflection from, 838
saturation vapor pressure, 87-90
specific heats, 54, 880
supercooled, 186
surface tension, 189, 880
thermo diagram, 99-105
total, 97-100
vapor, 7, 87-118
absorption of radiation, 221-223
channel on satellites, 112, 226, 231
cloud feedbacks, 810-811
density, 91
density excess, 198
feedback, 810
gas constant, 88-92, 880
greenhouse gas, 811
holding capacity, 87-90
in air, 7
mixing ratio, 89-98
molecular weight, 7
pressure, 87
specific heats, 880
vertical flux, 108-110
volcanic eruptions of, 805
waterspout tornadoes, 582
change criterion for SPECI, 270
cyclostrophic winds, 311-312
life cycle, 582
weather-map symbol for, 276
Watson, Andrew, 813
watt, unit of power, 870
wave, 705
African easterly wave, 611-612
amplitude, 368-374, 443-444, 634, 666-668
atmospheric, 705, 710
battering of structures by ocean waves, 634-635
bore, 656
boundary layer, 710
buoyancy, 666-668, 710
thunderstorm triggering, 526
clouds (see lenticular, or standing lenticular), 165, 168, 666-667
optics caused by, 859-860
crests, 658, 668
tilt with altitude, 668
curvature, 375
definition, 705
drag, 668
parameterization in NWP, 751
easterly, 611-612
electromagnetic, 219
energy, 658
equations, 368-374, 634, 666
flux of heat meridionally, 375
effect on circulation, 377
formation in jet stream, 357, 367-376, 443-445
fronts/frontal, 427-428, 837, 859
gravity, 666-668, 710
thunderstorm triggering, 526
group speed, 658
heat transport by Rossby waves, 374-375, 378
height of ocean waves, 634-636
interfacial (surface), 658
internal, 658
intrinsic phase speed, 658
jet stream (Rossby), 367-376
Kelvin, in ocean, 633-634
Kelvin-Helmholtz, 142, 165, 710
lee, 666-668
long, IR, 37-39, 45, 220-226, 230-239, 751, 794-797, 810
long Rossby, 369
mountain, 666-668
drag parameterization in NWP, 751
momentum
effect on circulation, 377
transport by Rossby waves, 375-376
or density current (bore), 655-656
phase speed, 658-661

planetary (see Rossby waves), 367-376
prefrontal, 656
propagation, 36, 369-370, 611-612
for remote sensing, 219-226
ridge, 443
Rossby, 329, 332, 353, 367-376
amplitude & other characteristics, 373-374
scour by ocean waves, 634-635
shallow-water, 658
shape of lightning surge, 569-560
short Rossby, 369
short, solar, 37-46, 220-223, 230-234, 334-339, 693, 793-815
solitary (bore), 656
sound, 219
speed (see phase speed), 367-374, 611, 834-837
shallow-water, 633, 658
stationary lee-side Rossby, 443-444
surf, 635
surface, 658
swell, 635
tilt, 372-376, 611, 668
tops sheared off by hurricane winds, 634
trough, 443, 658
vapor, 87-118
channel of satellites, 226
feedback in climate, 810
thunderstorm environment, 499-502
velocity, 658
vorticity, 368
westward propagation of, 369-372, 611-612
wind-driven ocean, 634-636
wavelength(s), 36-37, 221-226, 230, 242-243, 329, 367-376, 427, 468
bands of visible and IR sensors, 45
bands for satellite sensors, 222-223, 230
natural, 666
of easterly waves, 611
of electromagnetic radiation, 222-223
of light, 36, 222, 834-857
for different colors, 37, 834-835, 862
of max growth rate for Rossby waves, 372
of mountain waves, 666
of planetary Rossby waves, 367, 369
of planetary stationary lee waves, 444
of wind waves, ocean, 634-636
wavelets, 837
wavenumber, 36
of Rossby waves, 367, 369
WAVEOB code, 269
WBF (Wegener-Bergeron-Findeisen) process, 201-202
weak
echo region (WER), 493
tornadoes vs. significant, 501, 507, 516, 522, 530-531
weather, 1
altitudes, 143
analysis
hand (manual; subjective), 280-281
objective (automated), 765-767
anomaly (isanomal), 18
anticyclonic, 390
associated with warm katafront, 404
balloon, 134
briefing procedure, 765
codes & code modifiers, 268-273, 276
control, 218
data sources, 271-273
definition, 1
forecast(s)
agencies (Nat. Weather Service NWS), 532
computerized (see numerical), 745-792
medium-range, 768, 775
numerical, 745-792
topics, 2
forecast models, 751
heirarchy, 768
frontal, 400-401
glyphs (symbols on weather maps), 276, 282
highs, in, 390
instruments for measuring
errors of, 875
humidity, 97, 111-112, 219
precipitation, 219
pressure, 19, 219
temperature, 78-79, 219
radiation, 45-47
remotely, 219-266
soundings, 134-135
wind, 219, 321-322
map(s)
airmass codes, 391-392
analysis methods, 274-281, 402
CAPE, 506-508
case-study examples of, 433-466
global pressure patterns, 354-355
humidity, pre-storm, 500-501
max advection, finding, 458
NWP output, 772
solenoids, finding, 458
station plot model, 274-279
symbols for cloud genera, 168
symbols for hurricanes, 614-615
symbols for precipitation rate, 208
synoptic, 274-281
thunderstorm environment, 500-501, 506-508, 522-525, 532
vorticity advection, 459
winds on, 290-291
METAR, 270
observations, 268-273
at airports , 268-271
locations, 271-273
METARS, 268-271
using satellites, 227-239, 272-273
Pacific Northwest, 288, 398, 472, 765
past and present, as plotted on maps, 275-276
predictability limit, 773-775
prediction, numerical, 745-792
Richardson's 1922 book, 764
radar, 211, 240-260, 322
radio, NOAA, 529, 638
reports, 267-273
station
ID or code (ICAO), 270
plot model on weather maps, 274-279
satellites, 112, 219-239
locations of weather obs. From, 272-273
sensors, 273
services, radars used by, 243
symbols (glyphs) on weather maps, 276, 282
web-enhanced questions, explained, 24
wedge angles, 843, 845-847, 855
Wegener arc, 854-855
Wegener-Bergeron-Findeisen (WBF) process, 201-202, 546
Weibull distribution for wind speeds, 645-646
weighing rain gauge, 210
weighting functions for radiative transfer, 226, 237-239
weights, 15
air, 8
person, 8, 15
pressure, 7
well-mixed fog, 176-177
WER (weak echo region), 493
west
Coast weather, 288, 397-399, 472, 765
direction, 2
Gregory, 765
westerlies (winds in global circulation), 331, 353
Western Hemisphere, 4
defined, 4
westward tilt, 432
wet-bulb, 94
depression, 94
globe temperature, 117
mixing ratio, 95
potential temperature, 103-106
in fogs, 176
weather maps of, 500
temperature, 94, 96, 111
weather maps of, 500
what scientists do, 470
whirls, big and little, 708
white, 862
clouds, 856-858
dwarf star, 803
out (in blowing snow), 208
Wien's Law, 37
Wieringa, Davenport - roughness length classification, 700
wild fire and CO2 release, 812
Wilde, Oscar, 523
wind(s), 302-314
ageostrophic, 304, 343, 454-456
anabatic, 649-652
anemometer, 321-322
anticyclonic, 306
antitriptic, 312-313, 663
aspre, 676
austru, 676
average, global circulation, 330-334, 358
barbs on station-plot model, 278, 291
Beaufort scale, 635-636
Bora, 675-676
boundary-layer gradient (BLG) wind, 309-311, 613-615, 618-619
boundary-layer wind, 307-309
breeze, 635-636
canopy, 677-679
ceaseless, 329
channeled, 664
chill temperature index, 76-77
Chinook, 675-676
circulation, 329-388
coastal, 654-657, 661-665
cold-air drainage, 177, 652-653
components (U, V, W), 2, 3
conversion to speed and direction, 2
graphical determination (hodograph), 513
conversion, 3
cyclonic, 306
cyclostrophic wind, 311-312, 618
damage by
downbursts of air and gust fronts, 554-563
downslope windstorms, 667, 675-677
hurricanes, 605, 626-636
tornadoes, 579-580, 592-593
wind waves and coastal flooding, 631-637
difference (surrogate for shear), 509
magnitude, 509
vector, 509
direction, 2, 314
change criterion for SPECI, 270
constant (isogon), 18
conversion to components, 3
defined, 2
frequency, 646-647
instruments to measure, 219
naming, 2, 513
radar observations of, 252-253
rose, 646
variability in METAR, 270
dispersion of pollutants, 724
Doppler-radar measured, 249-254, 322
downburst, 554-563
downslope, 652-653, 675-677
storm, 667, 675-677
driven
by forces, 289-328
ocean currents, 610, 632-633, 701
easterlies, 330-332
jet (African), 611
electrical generation by, 647-648
equations of motion, 301, 314-315, 554, 746-749
equatorial, 343
errors, 766
exponential profile, 678
extratropical cyclonic, 425
field, 343
adjustment to mass field, 344
Foehn, 676-677
forces that drive, 302
forecast equations, 746
forest canopy, 677-678
frontal, 400-407
gale, 635-636
gap, 661-664
geostrophic, 663
long, 662-664
short, 661-662
general circulation, 330-334
geostrophic wind, 302-304, 343-349
African easterly jet, 611
global circulation, 330-334
gradient wind, 304-307, 617-618
gust duration, 605, 607
gust-front, 560-563
high-altitude (upper-tropospheric), 330-331
hodograph, for plotting winds, 510-513
horizontal, 302-314
hurricane
exploding houses, 674
force winds (Beaufort scale), 635-636
radial, 627-628
stages of life cycle, 614
tangential, 614, 622, 626-627
idealized, 302-314
inertial, 312
oscillation, 304, 311-312, 700
inflow, 618-619
instruments for measuring, 321-322
pitot-static system, 674
irrotational, 385
jet stream, 357-362
low level, 664-665
katabatic, 652-653

W, X, Y, Z

local, 645-686
log wind profile, 677, 702-703
magnitudes, 314
mean vs. instantaneous (turbulent), 705-706, 726
measuring, 321-322
  height, 701
METAR, 270
mountain, 649-654, 660-670, 675-676
names of (at steady state), 302, 314, 654
near-surface, global, 330-331
non-equilibrium, 618-619
outflow, 554, 560-563, 618-619
plotting on weather maps, 291
power, 647-648
  average, 647
  theoretical available, 647-648
  vs. wind speed, 647-648
profile
  convective radix layer, 703-705
  exponential, 678
  instruments to measure, 134, 321-322, 701
  logarithmic, 677, 702-703
  stable surface layer, 702-703
  neutral surface layer, 677, 702
  unstable radix layer, 703-705
profilers, 257-258, 322
  locations worldwide, 272
reports of damage from, 532
rose, 646-647
Saffir-Simpson hurricane scale, 605-607
scale, Beaufort, 635-636
sensors for measuring, 321-322
  arrays for airport wind shear, 556, 563
shear (also see shear), 509-522
  components, 509
  constant (isoshear), 18
  definition, 509, 706
  direction, 509
  frontal, 404-407
  in hurricane environment, 610
  in thunderstorm environment, 496-499, 509-522, 586-592
  magnitude, 509
  radar observations of, 254
  sensors at airports, 563
  thermal-wind effect, causing, 345-349
  tornado formation, role in, 586-592
  turbulence generation, 706, 708-709
  units, 509
  vs. stability, 141
shield around rain gauges, 210
shift in fronts, 349, 400-401
slope, 649-653
speed, 2, 3, 314
  around highs and lows, 307
  constant or equal, 17
  conversion to components, 3
  decrease across a wind turbine, 647-648
  defined, 3
  Doppler radar measurement of, 252-253
  for gap winds at constant depth, 661-663
  frequency, 645-646
  instruments to measure, 219, 321-322
  isotach, 17
  latitude, variation with, 359
  mean, 705, 726-727
  probability, 645
  probability distribution - Weibull, 645-646
  profile, 702-705
  radial speed, 249-253
  relative frequency, 645-646
  weather-map symbols, 278
  Weibull distribution, 645-646
speed profile, 699-705
storm
  downslope, 667, 675-677
  force winds (Beaufort scale), 635-636
storm-relative, 584-585
straight-line (also see derecho), 489, 491, 494, 554, 560-563
stress, 700-713
  ocean currents driven by, 701
subgeostrophic, 304, 455, 699
summary of, horizontal, 302, 313-314
supergeostrophic, 304, 455, 699-700
supergradient, 643
superposition of mean, waves & gusts, 705-706
surface
  layer, 699-705
  measuring height, 701
thermal, 345-349
  African easterly jet, 611
  derived, 346
thunder shock front, associated, 572-574
 -torn clouds (fractus), 165-166
tornadic, 385, 577-580
  exploding houses, 674
total (rotational + translational), 578, 627-628
trade, 330-331
tropopause (jet stream), 357-362
tunnels, boundary-layer growth in, 689
turbines and power generation, 647-648
  efficiency, 647-648
  power output curve, 648
  pressure change across, 671
turbulent part, 705-706
upper-tropospheric, global, 331-332
upslope, 649-652
urban canopy, 678-679
valley winds, 649-654, 660-670, 675-676
vane, 219, 321-322
variance of, 706-711, 727
vector weather map case study, 438, 440
veering, 349, 511, 520
vertical speed
  downburst, 554-559
  in extratropical cyclones, 451-462
  in hurricanes, 628-629
  in thunderstorms, 508, 557
  omega, 451, 456-459
waves on ocean, 634-636
weather maps, 290-291, 440
westerlies, 331-332
zonally averaged at 20 kPa, 358
zonda, 676
window
  absorption, 43
  atmospheric, 43, 796-797
  dirty, 220-223
  radiative, 43, 220-221, 796-797
  transmittance, 220-221
  visible and IR radiometers, 45
wing(s)
  aircraft, 88
  tip vortices, 166
WINTEM code, 269
winter, 330
  atmospheric boundary layer, 695-696
  nuclear, 151
  solstice, 30-31, 801
WMO = world meteorological organization, 149, 268, 615
Wolf minimum in solar activity, 803
work, 54, 58, 503, 526
  shaft, 672
World Meteorological Organization (WMO), 149, 268
  cloud classification, 168-169
  cloud height definitions, 163
  cloud symbols on weather maps, 168
  hurricane and typhoon names, 615
  identification of upper-air stations, 149
  mandatory (upper-air) levels, 772
world
  circulations (global), 329-388
  climate processes (natural), 793-832
  map of annual precipitation, 209
  record rainfall rates, 208, 545-548
Wreck of the Hesperus, 847
WRF (weather research & forecasting) model, 751
WSR-88D weather surveillance radar, 243
wstar (w*, see Deardorff velocity), 69, 110, 703-704, 736

X

X band radar, 242
x direction definition, 2
  change to match mean wind direction, 649-653, 727
xenon, Xe, 7
x rays, 222

Y

y-direction definition, 2
year
  leap, 31
  sidereal, 29
  tropical, 31
  without summer, 1816, 805
yellow color defined (also see optics chapter), 37
Yellowstone caldera, 805
yocto (10^{-24}), 870
Yogi Berra (see Berra)
yotta (10^{24}), 870
Young-Laplace equation, 215

Z

z direction definition, 2
Z (radar reflectivity factor), 245-246
Z time zone, defined (see UTC), 5
Z-R relationship, 247
zenith
  angle defined, 4-5
  circumzenith arcs, 848-849
  point, 854
zepto (10^{-21}), 870
zero
  absolute, 879
  buoyancy, 135, 688
  isodop, 250, 253-254
  set, 171
zetta (10^{21}), 870
zi = mixed layer depth, 143-144
Zinsser, William, 863
zo = roughness length, 677-678
zonal
  average
    heat transport, 339, 378
    insolation, radiation, 336-338
    temperature, 335
  flow, 330
    breakdown, 367
    defined, 330
    perturbed, 367-368
  propagation of baroclinic waves, 369-374
  velocity from source latitudes, 361
  wavenumber, 367
zonally averaged
  evaporation vs. precipitation, 210
  radiative forcings, 338-339
  winds at 20 kPa, 358
zonda wind, 676
zone, frontal, 280-281, 400-412
zones, time, 5
zoning for hurricanes, 631
Zulu Time, Z, defined (see UTC), 5
Zworykin, Vladimir, 759

Science Graffito

"We have come to confuse information with understanding."
— Malcolm Gladwell, *Blink. The Power of Thinking Without Thinking.* 2005, 2007.